

# Advanced Organic Chemistry

FIFTH  
EDITION

Part A: Structure and Mechanisms

# Advanced Organic Chemistry

---

PART A: Structure and Mechanisms

PART B: Reactions and Synthesis

# Advanced Organic Chemistry

FIFTH  
EDITION

Part A: Structure and Mechanisms

FRANCIS A. CAREY  
and RICHARD J. SUNDBERG

*University of Virginia  
Charlottesville, Virginia*

 Springer

Francis A. Carey  
Department of Chemistry  
University of Virginia  
Charlottesville, VA 22904

Richard J. Sundberg  
Department of Chemistry  
University of Virginia  
Charlottesville, VA 22904

Library of Congress Control Number: 2006939782

ISBN-13: 978-0-387-44897-8 (hard cover)      e-ISBN-13: 978-0-387-44899-3  
ISBN-13: 978-0-387-68346-1 (soft cover)

Printed on acid-free paper.

©2007 Springer Science+Business Media, LLC

All rights reserved. This work may not be translated or copied in whole or in part without the written permission of the publisher (Springer Science+Business Media, LLC, 233 Spring Street, New York, NY 10013, USA), except for brief excerpts in connection with reviews or scholarly analysis. Use in connection with any form of information storage and retrieval, electronic adaptation, computer software, or by similar or dissimilar methodology now known or hereafter developed is forbidden.

The use in this publication of trade names, trademarks, service marks and similar terms, even if they are not identified as such, is not to be taken as an expression of opinion as to whether or not they are subject to proprietary rights.

9 8 7 6 5 4 3 2 1

springer.com

# Preface

This Fifth Edition marks the beginning of the fourth decade that *Advanced Organic Chemistry* has been available. As with the previous editions, the goal of this text is to allow students to build on the foundation of introductory organic chemistry and attain a level of knowledge and understanding that will permit them to comprehend much of the material that appears in the contemporary chemical literature. There have been major developments in organic chemistry in recent years, and these have had a major influence in shaping this new edition to make it more useful to students, instructors, and other readers.

The expanding application of computational chemistry is reflected by amplified discussion of this area, especially density function theory (DFT) calculations in Chapter 1. Examples of computational studies are included in subsequent chapters that deal with specific structures, reactions and properties. Chapter 2 discusses the principles of both configuration and conformation, which were previously treated in two separate chapters. The current emphasis on enantioselectivity, including development of many enantioselective catalysts, prompted the expansion of the section on stereoselective reactions to include examples of enantioselective reactions. Chapter 3, which covers the application of thermodynamics and kinetics to organic chemistry, has been reorganized to place emphasis on structural effects on stability and reactivity. This chapter lays the groundwork for later chapters by considering stability effects on carbocations, carbanions, radicals, and carbonyl compounds.

Chapters 4 to 7 review the basic substitution, addition, and elimination mechanisms, as well as the fundamental chemistry of carbonyl compounds, including enols and enolates. A section on the control of regiochemistry and stereochemistry of aldol reactions has been added to introduce the basic concepts of this important area. A more complete treatment, with emphasis on synthetic applications, is given in Chapter 2 of Part B.

Chapter 8 deals with aromaticity and Chapter 9 with aromatic substitution, emphasizing electrophilic aromatic substitution. Chapter 10 deals with concerted pericyclic reactions, with the aromaticity of transition structures as a major theme. This part of the text should help students solidify their appreciation of aromatic stabilization as a fundamental concept in the chemistry of conjugated systems. Chapter 10 also considers

the important area of stereoselectivity of concerted pericyclic reactions. Instructors may want to consider dealing with these three chapters directly after Chapter 3, and we believe that is feasible.

Chapters 11 and 12 deal, respectively, with free radicals and with photochemistry and, accordingly, with the chemistry of molecules with unpaired electrons. The latter chapter has been substantially updated to reflect the new level of understanding that has come from ultrafast spectroscopy and computational studies.

As in the previous editions, a significant amount of specific information is provided in tables and schemes. These data and examples serve to illustrate the issues that have been addressed in the text. Instructors who want to achieve a broad coverage, but without the level of detail found in the tables and schemes, may choose to advise students to focus on the main text. In most cases, the essential points are clear from the information and examples given in the text itself.

We have made an effort to reduce the duplication between Parts A and B. In general, the discussion of basic mechanisms in Part B has been reduced by cross-referencing the corresponding discussion in Part A. We have expanded the discussion of specific reactions in Part A, especially in the area of enantioselectivity and enantioselective catalysts.

We have made more extensive use of abbreviations than in the earlier editions. In particular, EWG and ERG are used throughout both Parts A and B to designate electron-withdrawing and electron-releasing substituents, respectively. The intent is that the use of these terms will help students generalize the effect of certain substituents such as C=O, C≡N, NO<sub>2</sub>, and RSO<sub>2</sub> as electron withdrawing and R (alkyl) and RO (alkoxy) as electron releasing. Correct use of this shorthand depends on a solid understanding of the interplay between polar and resonance effects in overall substituent effects. This matter is discussed in detail in Chapter 3 and many common functional groups are classified.

Several areas have been treated as “Topics”. Some of the Topics discuss areas that are still in a formative stage, such as the efforts to develop DFT parameters as quantitative reactivity indices. Others, such as the role of carbocations in gasoline production, have practical implications.

We have also abstracted information from several published computational studies to present three-dimensional images of reactants, intermediates, transition structures, and products. This material, including exercises, is available at the publishers web site, and students who want to see how the output of computations can be applied may want to study it. The visual images may help toward an appreciation of some of the subtle effects observed in enantioselective and other stereoselective reactions. As in previous editions, each chapter has a number of problems drawn from the literature. A new feature is solutions to these problems, which are also provided at the publisher’s website at [springer.com/carey-sundberg](http://springer.com/carey-sundberg)

Our goal is to present a broad and fairly detailed view of the core area of organic reactivity. We have approached this goal by extensive use of both the primary and review literature and the sources are referenced. Our hope is that the reader who works through these chapters, problems, topics, and computational studies either in an organized course or by self-study will be able to critically evaluate and use the current literature in organic chemistry in the range of fields in which is applied, including the pharmaceutical industry, agricultural chemicals, consumer products, petroleum chemistry, and biotechnology. The companion volume, Part B, deals extensively with organic synthesis and provides many more examples of specific reactions.

# Acknowledgment and Personal Statement

The revision and updating of *Advanced Organic Chemistry* that appears as the Fifth Edition spanned the period September 2002 through December 2006. Each chapter was reworked and updated and some reorganization was done, as described in the Prefaces to Parts A and B. This period began at the point of conversion of library resources to electronic form. Our university library terminated paper subscriptions to the journals of the American Chemical Society and other journals that are available electronically as of the end of 2002. Shortly thereafter, an excavation mishap at an adjacent construction project led to structural damage and closure of our departmental library. It remained closed through June 2007, but thanks to the efforts of Carol Hunter, Beth Blanton-Kent, Christine Wiedman, Robert Burnett, and Wynne Stuart, I was able to maintain access to a few key print journals including the *Journal of the American Chemical Society*, *Journal of Organic Chemistry*, *Organic Letters*, *Tetrahedron*, and *Tetrahedron Letters*. These circumstances largely completed an evolution in the source for specific examples and data. In the earlier editions, these were primarily the result of direct print encounter or search of printed *Chemical Abstracts* indices. The current edition relies mainly on electronic keyword and structure searches. Neither the former nor the latter method is entirely systematic or comprehensive, so there is a considerable element of circumstance in the inclusion of specific material. There is no intent that specific examples reflect either priority of discovery or relative importance. Rather, they are interesting examples that illustrate the point in question.

Several reviewers provided many helpful corrections and suggestions, collated by Kenneth Howell and the editorial staff of Springer. Several colleagues provided valuable contributions. Carl Trindle offered suggestions and material from his course on computational chemistry. Jim Marshall reviewed and provided helpful comments on several sections. Michal Sabat, director of the Molecular Structure Laboratory, provided a number of the graphic images. My co-author, Francis A. Carey, retired in 2000 to devote his full attention to his text, *Organic Chemistry*, but continued to provide valuable comments and insights during the preparation of this edition. Various users of prior editions have provided error lists, and, hopefully, these corrections have

been made. Shirley Fuller and Cindy Knight provided assistance with many aspects of the preparation of the manuscript.

This Fifth Edition is supplemented by the *Digital Resource* that is available at [springer.com/carey-sundberg](http://springer.com/carey-sundberg). The *Digital Resource* summarizes the results of several computational studies and presents three-dimensional images, comments, and exercises based on the results. These were developed with financial support from the Teaching Technology Initiative of the University of Virginia. Technical support was provided by Michal Sabat, William Rourk, Jeffrey Hollier, and David Newman. Several students made major contributions to this effort. Sara Fitzgerald Higgins and Victoria Landry created the prototypes of many of the sites. Scott Geyer developed the dynamic representations using IRC computations. Tanmaya Patel created several sites and developed the measurement tool. I also gratefully acknowledge the cooperation of the original authors of these studies in making their output available. *Problem Responses* have been provided and I want to acknowledge the assistance of R. Bruce Martin, David Metcalf, and Daniel McCauley in helping work out some of the specific kinetic problems and in providing the attendant graphs.

It is my hope that the text, problems, and other material will assist new students to develop a knowledge and appreciation of structure, mechanism, reactions, and synthesis in organic chemistry. It is gratifying to know that some 200,000 students have used earlier editions, hopefully to their benefit.

Richard J. Sundberg  
Charlottesville, Virginia  
March 2007

# Introduction

This volume is intended for students who have completed the equivalent of a two-semester introductory course in organic chemistry and wish to expand their understanding of *structure and reaction mechanisms* in organic chemistry. The text assumes basic knowledge of physical and inorganic chemistry at the advanced undergraduate level.

Chapter 1 begins by reviewing the familiar Lewis approach to structure and bonding. Lewis's concept of electron pair bonds, as extended by adding the ideas of hybridization and resonance, plus fundamental atomic properties such as electronegativity and polarizability provide a solid foundation for *qualitative* descriptions of trends in reactivity. In polar reactions, for example, the molecular properties of acidity, basicity, nucleophilicity, and electrophilicity can all be related to information embodied in Lewis structures. The chapter continues with the more *quantitative* descriptions of molecular structure and properties that are obtained by quantum mechanical calculations. Hückel, semiempirical, and *ab initio* molecular orbital (MO) calculations, as well as density functional theory (DFT) are described and illustrated with examples. This material is presented at a level sufficient for students to recognize the various methods and their ranges of application. Computational methods can often provide insight into reaction mechanisms by describing the structural features of intermediates and transition structures. Another powerful aspect of computational methods is their ability to represent electron density. Various methods of describing electron density, including graphical representations, are outlined in this chapter and applied throughout the remainder of the text. Chapter 2 explores the two structural levels of stereochemistry—*configuration* and *conformation*. Molecular conformation is important in its own right, but can also influence reactivity. The structural relationships between stereoisomers and the origin and consequences of molecular chirality are discussed. After reviewing the classical approach to resolving racemic mixtures, modern methods for chromatographic separation and kinetic resolution are described. The chapter also explores how stereochemistry affects reactivity with examples of *diastereoselective* and *enantioselective* reactions, especially those involving addition to carbonyl groups. Much of today's work in organic chemistry focuses on enantioselective reagents and catalysts. The enantioselectivity of these reagents usually involves rather small and sometimes subtle differences in intermolecular interactions. Several of the best-understood enantioselective

reactions, including hydrogenation, epoxidation of allylic alcohols, and dihydroxylation of alkenes are discussed. Chapter 3 provides examples of structure-stability relationships derived from both experimental thermodynamics and computation. Most of the chapter is about the effects of substituents on reaction rates and equilibria, how they are measured, and what they tell us about reaction mechanisms. The electronic character of the common functional groups is explored, as well as substituent effects on the stability of carbocations, carbanions, radicals, and carbonyl addition intermediates. Other topics in this chapter include the Hammett equation and related linear free-energy relationships, catalysis, and solvent effects. Understanding how thermodynamic and kinetic factors combine to influence reactivity and developing a sense of structural effects on the energy of reactants, intermediates and transition structures render the outcome of organic reactions more predictable.

Chapters 4 to 7 relate the patterns of addition, elimination, and substitution reactions to the general principles developed in Chapters 1 to 3. A relatively small number of reaction types account for a wide range of both simple and complex reactions. The fundamental properties of carbocations, carbanions, and carbonyl compounds determine the outcome of these reactions. Considerable information about reactivity trends and stereoselectivity is presented, some of it in tables and schemes. Although this material may seem overwhelming if viewed as individual pieces of information, taken in the context of the general principles it fills in details and provides a basis for recognizing the relative magnitude of various structural changes on reactivity. The student should strive to develop a sufficiently broad perspective to generate an intuitive sense of the effect of particular changes in structure.

Chapter 4 begins the discussion of specific reaction types with an examination of *nucleophilic substitution*. Key structural, kinetic, and stereochemical features of substitution reactions are described and related to reaction mechanisms. The limiting mechanisms  $S_N1$  and  $S_N2$  are presented, as are the “merged” and “borderline” variants. The relationship between stereochemistry and mechanism is explored and specific examples are given. Inversion is a virtually universal characteristic of the  $S_N2$  mechanism, whereas stereochemistry becomes much more dependent on the specific circumstances for borderline and  $S_N1$  mechanisms. The properties of carbocations, their role in nucleophilic substitution, carbocation rearrangements, and the existence and relative stability of bridged (nonclassical) carbocations are considered. The importance of carbocations in many substitution reactions requires knowledge of their structure and reactivity and the effect of substituents on stability. A fundamental characteristic of carbocations is the tendency to rearrange to more stable structures. We consider the mechanism of carbocation rearrangements, including the role of bridged ions. The case of nonclassical carbocations, in which the bridged structure is the most stable form, is also discussed.

Chapter 5 considers the relationship between mechanism and regio- and stereoselectivity. The reactivity patterns of electrophiles such as protic acids, halogens, sulfur and selenium electrophiles, mercuric ion, and borane and its derivatives are explored and compared. These reactions differ in the extent to which they proceed through discrete carbocations or bridged intermediates and this distinction can explain variations in regio- and stereochemistry. This chapter also describes the E1, E2, and E1cb mechanisms for elimination and the idea that these represent specific cases within a continuum of mechanisms. The concept of the variable mechanism can explain trends in reactivity and regiochemistry in elimination reactions. Chapter 6 focuses on the fundamental properties and reactivity of *carbon nucleophiles*, including

organometallic reagents, enolates, enols, and enamines. The mechanism of the aldol addition is discussed. The acidity of hydrocarbons and functionalized molecules is considered. Chapter 7 discusses the fundamental reactions of carbonyl groups. The reactions considered include hydration, acetal formation, condensation with nitrogen nucleophiles, and the range of substitution reactions that interconvert carboxylic acid derivatives. The relative stability and reactivity of the carboxylic acid derivatives is summarized and illustrated. The relationships described in Chapters 6 and 7 provide the broad reactivity pattern of carbonyl compounds, which has been extensively developed and is the basis of a rich synthetic methodology.

Chapter 8 discusses the concept of *aromaticity* and explores the range of its applicability, including annulenes, cyclic cations and anions, polycyclic hydrocarbons, and heterocyclic aromatic compounds. The criteria of aromaticity and some of the methods for its evaluation are illustrated. We also consider the *antiaromaticity* of cyclobutadiene and related molecules. Chapter 9 explores the mechanisms of *aromatic substitution* with an emphasis on electrophilic aromatic substitution. The general mechanism is reviewed and the details of some of the more common reactions such as nitration, halogenation, Friedel-Crafts alkylation, and acylation are explored. Patterns of position and reactant selectivity are examined. Recent experimental and computational studies that elucidate the role of aromatic radical cations generated by electron transfer in electrophilic aromatic substitution are included, and the mechanisms for nucleophilic aromatic substitution are summarized. Chapter 10 deals with *concerted pericyclic reactions*, including *cycloaddition*, *electrocyclic reactions*, and *sigmatropic rearrangements*. This chapter looks at how *orbital symmetry* influences reactivity and introduces the idea of aromaticity in transition structures. These reactions provide interesting examples of how stereochemistry and reactivity are determined by the structure of the transition state. The role of Lewis acids in accelerating Diels-Alder reactions and the use of chiral auxiliaries and catalysts to achieve enantioselectivity are explored.

Chapter 11 deals with *free radicals* and their reactions. Fundamental structural concepts such as substituent effects on bond dissociation enthalpies (BDE) and radical stability are key to understanding the mechanisms of radical reactions. The patterns of stability and reactivity are illustrated by discussion of some of the absolute rate data that are available for free radical reactions. The reaction types that are discussed include halogenation and oxygenation, as well as addition reactions of hydrogen halides, carbon radicals, and thiols. Group transfer reactions, rearrangements, and fragmentations are also discussed.

Chapter 12 ventures into the realm of *photochemistry*, where structural concepts are applied to following the path from initial excitation to the final reaction product. Although this discussion involves comparison with some familiar intermediates, especially radicals, and offers mechanisms to account for the reactions, photochemistry introduces some new concepts of *reaction dynamics*. The excited states in photochemical reactions traverse energy surfaces that have small barriers relative to most thermal reactions. Because several excited states can be involved, the mechanism of conversion between excited states is an important topic. The nature of *conical intersections*, the transition points between excited state energy surfaces is examined.

Fundamental concepts of structure and its relationship to reactivity within the context of organic chemistry are introduced in the first three chapters, and thereafter the student should try to relate the structure and reactivity of the intermediates and transition structures to these concepts. Critical consideration of bonding, stereochemistry, and substituent effects should come into play in examining each of the basic

reactions. Computational studies frequently serve to focus on particular aspects of the reaction mechanism. Many specific reactions are cited, both in the text and in schemes and tables. The purpose of this specific information is to illustrate the broad patterns of reactivity. As students study this material, the goal should be to look for the underlying relationships in the broad reactivity patterns. Organic reactions occur by a combination of a relatively few reaction types—substitution, addition, elimination, and rearrangement. Reagents can generally be classified as electrophilic, nucleophilic, or radical in character. By focusing on the fundamental character of reactants and reagents, students can develop a familiarity with organic reactivity and organize the vast amount of specific information on reactions.

# Contents

<b>Preface</b> .....	<b>v</b>
<b>Acknowledgment and Personal Statement</b> .....	<b>vii</b>
<b>Introduction</b> .....	<b>ix</b>
<b>Chapter 1. Chemical Bonding and Molecular Structure</b> .....	<b>1</b>
Introduction .....	1
1.1. Description of Molecular Structure Using Valence Bond Concepts .....	2
1.1.1. Hybridization .....	4
1.1.2. The Origin of Electron-Electron Repulsion .....	7
1.1.3. Electronegativity and Polarity .....	8
1.1.4. Electronegativity Equalization.....	11
1.1.5. Differential Electronegativity of Carbon Atoms.....	12
1.1.6. Polarizability, Hardness, and Softness .....	14
1.1.7. Resonance and Conjugation .....	18
1.1.8. Hyperconjugation.....	22
1.1.9. Covalent and van der Waals Radii of Atoms .....	24
1.2. Molecular Orbital Theory and Methods.....	26
1.2.1. The Hückel MO Method .....	27
1.2.2. Semiempirical MO Methods .....	32
1.2.3. Ab Initio Methods.....	32
1.2.4. Pictorial Representation of MOs for Molecules .....	35
1.2.5. Qualitative Application of MO Theory to Reactivity: Perturbational MO Theory and Frontier Orbitals .....	41
1.2.6. Numerical Application of MO Theory.....	50
1.3. Electron Density Functionals.....	54
1.4. Representation of Electron Density Distribution .....	57
1.4.1. Mulliken Population Analysis .....	60
1.4.2. Natural Bond Orbitals and Natural Population Analysis.....	61

1.4.3. Atoms in Molecules .....	63
1.4.4. Comparison and Interpretation of Atomic Charge Calculations .....	70
1.4.5. Electrostatic Potential Surfaces .....	73
1.4.6. Relationships between Electron Density and Bond Order .....	76
Topic 1.1. The Origin of the Rotational (Torsional) Barrier in Ethane and Other Small Molecules .....	78
Topic 1.2. Heteroatom Hyperconjugation (Anomeric Effect) in Acyclic Molecules .....	81
Topic 1.3. Bonding in Cyclopropane and Other Small Ring Compounds .....	85
Topic 1.4. Representation of Electron Density by the Laplacian Function .....	92
Topic 1.5. Application of Density Functional Theory to Chemical Properties and Reactivity .....	94
T.1.5.1. DFT Formulation of Chemical Potential, Electronegativity, Hardness and Softness, and Covalent and van der Waal Radii .....	95
T.1.5.2. DFT Formulation of Reactivity—The Fukui Function .....	97
T.1.5.3. DFT Concepts of Substituent Groups Effects .....	100
General References .....	106
Problems .....	106
<b>Chapter 2. Stereochemistry, Conformation, and Stereoselectivity .....</b>	<b>119</b>
Introduction .....	119
2.1. Configuration .....	119
2.1.1. Configuration at Double Bonds .....	119
2.1.2. Configuration of Cyclic Compounds .....	121
2.1.3. Configuration at Tetrahedral Atoms .....	122
2.1.4. Molecules with Multiple Stereogenic Centers .....	126
2.1.5. Other Types of Stereogenic Centers .....	128
2.1.6. The Relationship between Chirality and Symmetry .....	131
2.1.7. Configuration at Prochiral Centers .....	133
2.1.8. Resolution—The Separation of Enantiomers .....	136
2.2. Conformation .....	142
2.2.1. Conformation of Acyclic Compounds .....	142
2.2.2. Conformations of Cyclohexane Derivatives .....	152
2.2.3. Conformations of Carbocyclic Rings of Other Sizes .....	161
2.3. Molecular Mechanics .....	167
2.4. Stereoselective and Stereospecific Reactions .....	169
2.4.1. Examples of Stereoselective Reactions .....	170
2.4.2. Examples of Stereospecific Reactions .....	182
2.5. Enantioselective Reactions .....	189
2.5.1. Enantioselective Hydrogenation .....	189
2.5.2. Enantioselective Reduction of Ketones .....	193
2.5.3. Enantioselective Epoxidation of Allylic Alcohols .....	196
2.5.4. Enantioselective Dihydroxylation of Alkenes .....	200
2.6. Double Stereodifferentiation: Reinforcing and Competing Stereoselectivity .....	204

Topic 2.1. Analysis and Separation of Enantiomeric Mixtures .....	208
T.2.1.1. Chiral Shift Reagents and Chiral Solvating Agents.....	208
T.2.1.2. Separation of Enantiomers .....	211
Topic 2.2. Enzymatic Resolution and Desymmetrization.....	215
T.2.2.1. Lipases and Esterases.....	216
T.2.2.2. Proteases and Acylases .....	222
T.2.2.3. Epoxide Hydrolases.....	224
Topic 2.3. The Anomeric Effect in Cyclic Compounds .....	227
Topic 2.4. Polar Substituent Effects in Reduction of Carbonyl Compounds .....	234
General References.....	239
Problems .....	240
<b>Chapter 3. Structural Effects on Stability and Reactivity .....</b>	<b>253</b>
Introduction.....	253
3.1. Thermodynamic Stability.....	254
3.1.1. Relationship between Structure and Thermodynamic Stability for Hydrocarbons .....	256
3.1.2. Calculation of Enthalpy of Formation and Enthalpy of Reaction .....	257
3.2. Chemical Kinetics .....	270
3.2.1. Fundamental Principles of Chemical Kinetics.....	270
3.2.2. Representation of Potential Energy Changes in Reactions.....	273
3.2.3. Reaction Rate Expressions .....	280
3.2.4. Examples of Rate Expressions .....	283
3.3. General Relationships between Thermodynamic Stability and Reaction Rates.....	285
3.3.1. Kinetic versus Thermodynamic Control of Product Composition.....	285
3.3.2. Correlations between Thermodynamic and Kinetic Aspects of Reactions .....	287
3.3.3. Curtin-Hammett Principle.....	296
3.4. Electronic Substituent Effects on Reaction Intermediates .....	297
3.4.1. Carbocations.....	300
3.4.2. Carbanions .....	307
3.4.3. Radical Intermediates .....	311
3.4.4. Carbonyl Addition Intermediates .....	319
3.5. Kinetic Isotope Effects.....	332
3.6. Linear Free-Energy Relationships for Substituent Effects.....	335
3.6.1. Numerical Expression of Linear Free-Energy Relationships .....	335
3.6.2. Application of Linear Free-Energy Relationships to Characterization of Reaction Mechanisms .....	342
3.7. Catalysis .....	345
3.7.1. Catalysis by Acids and Bases.....	345
3.7.2. Lewis Acid Catalysis.....	354

3.8. Solvent Effects .....	359
3.8.1. Bulk Solvent Effects .....	359
3.8.2. Examples of Specific Solvent Effects .....	362
Topic 3.1. Acidity of Hydrocarbons .....	368
General References .....	376
Problems .....	376
<b>Chapter 4. Nucleophilic Substitution .....</b>	<b>389</b>
Introduction .....	389
4.1. Mechanisms for Nucleophilic Substitution .....	389
4.1.1. Substitution by the Ionization ( $S_N1$ ) Mechanism .....	391
4.1.2. Substitution by the Direct Displacement ( $S_N2$ ) Mechanism .....	393
4.1.3. Detailed Mechanistic Description and Borderline Mechanisms .....	395
4.1.4. Relationship between Stereochemistry and Mechanism of Substitution .....	402
4.1.5. Substitution Reactions of Alkyldiazonium Ions .....	405
4.2. Structural and Solvation Effects on Reactivity .....	407
4.2.1. Characteristics of Nucleophilicity .....	407
4.2.2. Effect of Solvation on Nucleophilicity .....	411
4.2.3. Leaving-Group Effects .....	413
4.2.4. Steric and Strain Effects on Substitution and Ionization Rates .....	415
4.2.5. Effects of Conjugation on Reactivity .....	417
4.3. Neighboring-Group Participation .....	419
4.4. Structure and Reactions of Carbocation Intermediates .....	425
4.4.1. Structure and Stability of Carbocations .....	425
4.4.2. Direct Observation of Carbocations .....	436
4.4.3. Competing Reactions of Carbocations .....	438
4.4.4. Mechanisms of Rearrangement of Carbocations .....	440
4.4.5. Bridged (Nonclassical) Carbocations .....	447
Topic 4.1. The Role Carbocations and Carbonium Ions in Petroleum Processing .....	454
General References .....	459
Problems .....	459
<b>Chapter 5. Polar Addition and Elimination Reactions .....</b>	<b>473</b>
Introduction .....	475
5.1. Addition of Hydrogen Halides to Alkenes .....	476
5.2. Acid-Catalyzed Hydration and Related Addition Reactions .....	482
5.3. Addition of Halogens .....	485
5.4. Sulfenylation and Selenenylation .....	497
5.4.1. Sulfenylation .....	498
5.4.2. Selenenylation .....	500
5.5. Addition Reactions Involving Epoxides .....	503
5.5.1. Epoxides from Alkenes and Peroxidic Reagents .....	503
5.5.2. Subsequent Transformations of Epoxides .....	511

5.6. Electrophilic Additions Involving Metal Ions.....	515
5.6.1. Solvomercuration.....	515
5.6.2. Argentation—the Formation of Silver Complexes.....	520
5.7. Synthesis and Reactions of Alkylboranes.....	521
5.7.1. Hydroboration.....	522
5.7.2. Reactions of Organoboranes.....	526
5.7.3. Enantioselective Hydroboration.....	529
5.8. Comparison of Electrophilic Addition Reactions.....	531
5.9. Additions to Alkynes and Allenes.....	536
5.9.1. Hydrohalogenation and Hydration of Alkynes.....	538
5.9.2. Halogenation of Alkynes.....	540
5.9.3. Mercuration of Alkynes.....	544
5.9.4. Overview of Alkyne Additions.....	544
5.9.5. Additions to Allenes.....	545
5.10. Elimination Reactions.....	546
5.10.1. The E2, E1 and E1cb Mechanisms.....	548
5.10.2. Regiochemistry of Elimination Reactions.....	554
5.10.3. Stereochemistry of E2 Elimination Reactions.....	558
5.10.4. Dehydration of Alcohols.....	563
5.10.5. Eliminations Reactions Not Involving C–H Bonds.....	564
General References.....	569
Problems.....	569
<b>Chapter 6. Carbanions and Other Carbon Nucleophiles.....</b>	<b>579</b>
Introduction.....	559
6.1. Acidity of Hydrocarbons.....	579
6.2. Carbanion Character of Organometallic Compounds.....	588
6.3. Carbanions Stabilized by Functional Groups.....	591
6.4. Enols and Enamines.....	601
6.5. Carbanions as Nucleophiles in $S_N2$ Reactions.....	609
6.5.1. Substitution Reactions of Organometallic Reagents.....	609
6.5.2. Substitution Reactions of Enolates.....	611
General References.....	619
Problems.....	619
<b>Chapter 7. Addition, Condensation and Substitution Reactions of Carbonyl Compounds.....</b>	<b>629</b>
Introduction.....	629
7.1. Reactivity of Carbonyl Compounds toward Addition.....	632
7.2. Hydration and Addition of Alcohols to Aldehydes and Ketones.....	638
7.3. Condensation Reactions of Aldehydes and Ketones with Nitrogen Nucleophiles.....	645
7.4. Substitution Reactions of Carboxylic Acid Derivatives.....	654
7.4.1. Ester Hydrolysis and Exchange.....	654
7.4.2. Aminolysis of Esters.....	659
7.4.3. Amide Hydrolysis.....	662
7.4.4. Acylation of Nucleophilic Oxygen and Nitrogen Groups.....	664

7.5. Intramolecular Catalysis of Carbonyl Substitution Reactions .....	668
7.6. Addition of Organometallic Reagents to Carbonyl Groups.....	676
7.6.1. Kinetics of Organometallic Addition Reactions.....	677
7.6.2. Stereoselectivity of Organometallic Addition Reactions.....	680
7.7. Addition of Enolates and Enols to Carbonyl Compounds: The Aldol Addition and Condensation Reactions .....	682
7.7.1. The General Mechanisms.....	682
7.7.2. Mixed Aldol Condensations with Aromatic Aldehydes.....	685
7.7.3. Control of Regiochemistry and Stereochemistry of Aldol Reactions of Ketones.....	687
7.7.4. Aldol Reactions of Other Carbonyl Compounds.....	692
General References.....	698
Problems .....	698

## **Chapter 8. Aromaticity .....** 713

Introduction .....	713
8.1. Criteria of Aromaticity.....	715
8.1.1. The Energy Criterion for Aromaticity.....	715
8.1.2. Structural Criteria for Aromaticity .....	718
8.1.3. Electronic Criteria for Aromaticity .....	720
8.1.4. Relationship among the Energetic, Structural, and Electronic Criteria of Aromaticity .....	724
8.2. The Annulenes .....	725
8.2.1. Cyclobutadiene.....	725
8.2.2. Benzene.....	727
8.2.3. 1,3,5,7-Cyclooctatetraene .....	727
8.2.4. [10]Annulenes—1,3,5,7,9-Cyclodecapentaene Isomers.....	728
8.2.5. [12], [14], and [16]Annulenes .....	730
8.2.6. [18]Annulene and Larger Annulenes .....	733
8.2.7. Other Related Structures.....	735
8.3. Aromaticity in Charged Rings.....	738
8.4. Homoaromaticity.....	743
8.5. Fused-Ring Systems.....	745
8.6. Heteroaromatic Systems .....	758
General References .....	760
Problems .....	760

## **Chapter 9. Aromatic Substitution .....** 771

Introduction .....	771
9.1. Electrophilic Aromatic Substitution Reactions .....	771
9.2. Structure-Reactivity Relationships for Substituted Benzenes.....	779
9.2.1. Substituent Effects on Reactivity .....	779
9.2.2. Mechanistic Interpretation of the Relationship between Reactivity and Selectivity.....	787
9.3. Reactivity of Polycyclic and Heteroaromatic Compounds.....	791

9.4. Specific Electrophilic Substitution Reactions .....	796
9.4.1. Nitration.....	796
9.4.2. Halogenation.....	800
9.4.3. Protonation and Hydrogen Exchange .....	804
9.4.4. Friedel-Crafts Alkylation and Related Reactions.....	805
9.4.5. Friedel-Crafts Acylation and Related Reactions .....	809
9.4.6. Aromatic Substitution by Diazonium Ions .....	813
9.4.7. Substitution of Groups Other than Hydrogen .....	814
9.5. Nucleophilic Aromatic Substitution.....	816
9.5.1. Nucleophilic Aromatic Substitution by the Addition-Elimination Mechanism.....	817
9.5.2. Nucleophilic Aromatic Substitution by the Elimination-Addition Mechanism.....	821
General References .....	824
Problems.....	824
<b>Chapter 10. Concerted Pericyclic Reactions.....</b>	<b>833</b>
Introduction .....	833
10.1. Cycloaddition Reactions .....	834
10.2. The Diels-Alder Reaction .....	839
10.2.1. Stereochemistry of the Diels-Alder Reaction.....	839
10.2.2. Substituent Effects on Reactivity, Regioselectivity and Stereochemistry .....	843
10.2.3. Catalysis of Diels-Alder Reactions by Lewis Acids.....	848
10.2.4. Computational Characterization of Diels-Alder Transition Structures.....	851
10.2.5. Scope and Synthetic Applications of the Diels-Alder Reaction.....	860
10.2.6. Enantioselective Diels-Alder Reactions .....	865
10.2.7. Intramolecular Diels-Alder Reactions .....	868
10.3. 1,3-Dipolar Cycloaddition Reactions.....	873
10.3.1. Relative Reactivity, Regioselectivity, Stereoselectivity, and Transition Structures .....	874
10.3.2. Scope and Applications of 1,3-Dipolar Cycloadditions.....	884
10.3.3. Catalysis of 1,3-Dipolar Cycloaddition Reactions .....	886
10.4. [2 + 2] Cycloaddition Reactions .....	888
10.5. Electrocyclic Reactions .....	892
10.5.1. Overview of Electrocyclic Reactions .....	892
10.5.2. Orbital Symmetry Basis for the Stereospecificity of Electrocyclic Reactions.....	894
10.5.3. Examples of Electrocyclic Reactions .....	903
10.5.4. Electrocyclic Reactions of Charged Species .....	906
10.5.5. Electrocyclization of Heteroatomic Trienes .....	910
10.6. Sigmatropic Rearrangements .....	911
10.6.1. Overview of Sigmatropic Rearrangements.....	911
10.6.2. [1,3]-, [1,5]-, and [1,7]-Sigmatropic Shifts of Hydrogen and Alkyl Groups.....	912

10.6.3. Overview of [3,3]-Sigmatropic Rearrangements .....	919
10.6.4. [2,3]-Sigmatropic Rearrangements.....	939
Topic 10.1. Application of DFT Concepts to Reactivity and Regiochemistry of Cycloaddition Reactions .....	945
Problems .....	951
<b>Chapter 11. Free Radical Reactions .....</b>	<b>965</b>
Introduction .....	965
11.1. Generation and Characterization of Free Radicals.....	967
11.1.1. Background .....	967
11.1.2. Long-Lived Free Radicals .....	968
11.1.3. Direct Detection of Radical Intermediates .....	970
11.1.4. Generation of Free Radicals .....	976
11.1.5. Structural and Stereochemical Properties of Free Radicals.....	980
11.1.6. Substituent Effects on Radical Stability.....	986
11.1.7. Charged Radicals .....	988
11.2. Characteristics of Reactions Involving Radical Intermediates .....	992
11.2.1. Kinetic Characteristics of Chain Reactions.....	992
11.2.2. Determination of Reaction Rates.....	995
11.2.3. Structure-Reactivity Relationships .....	1000
11.3. Free Radical Substitution Reactions.....	1018
11.3.1. Halogenation .....	1018
11.3.2. Oxygenation .....	1024
11.4. Free Radical Addition Reactions.....	1026
11.4.1. Addition of Hydrogen Halides .....	1026
11.4.2. Addition of Halomethanes.....	1029
11.4.3. Addition of Other Carbon Radicals.....	1031
11.4.4. Addition of Thiols and Thiocarboxylic Acids .....	1033
11.4.5. Examples of Radical Addition Reactions.....	1033
11.5. Other Types of Free Radical Reactions.....	1037
11.5.1. Halogen, Sulfur, and Selenium Group Transfer Reactions .....	1037
11.5.2. Intramolecular Hydrogen Atom Transfer Reactions .....	1040
11.5.3. Rearrangement Reactions of Free Radicals.....	1041
11.6. $S_{RN}1$ Substitution Processes.....	1044
11.6.1. $S_{RN}1$ Substitution Reactions of Alkyl Nitro Compounds.....	1045
11.6.2. $S_{RN}1$ Substitution Reactions of Aryl and Alkyl Halides.....	1048
Topic 11.1. Relationships between Bond and Radical Stabilization Energies.....	1052
Topic 11.2. Structure-Reactivity Relationships in Hydrogen Abstraction Reactions.....	1056
General References.....	1062
Problems .....	1063
<b>Chapter 12. Photochemistry .....</b>	<b>1073</b>
Introduction.....	1073
12.1. General Principles .....	1073

12.2. Photochemistry of Alkenes, Dienes, and Polyenes .....	1081
12.2.1. <i>cis-trans</i> Isomerization .....	1081
12.2.2. Photoreactions of Other Alkenes .....	1091
12.2.3. Photoisomerization of 1,3-Butadiene .....	1096
12.2.4. Orbital Symmetry Considerations for Photochemical Reactions of Alkenes and Dienes .....	1097
12.2.5. Photochemical Electrocyclic Reactions .....	1100
12.2.6. Photochemical Cycloaddition Reactions .....	1109
12.2.7. Photochemical Rearrangements Reactions of 1,4-Dienes .....	1112
12.3. Photochemistry of Carbonyl Compounds .....	1116
12.3.1. Hydrogen Abstraction and Fragmentation Reactions .....	1118
12.3.2. Cycloaddition and Rearrangement Reactions of Cyclic Unsaturated Ketones .....	1125
12.3.3. Cycloaddition of Carbonyl Compounds and Alkenes .....	1132
12.4. Photochemistry of Aromatic Compounds .....	1134
Topic 12.1. Computational Interpretation of Diene and Polyene Photochemistry .....	1137
General References .....	1145
Problems .....	1146
<b>References to Problems .....</b>	<b>1155</b>
<b>Index .....</b>	<b>1171</b>

# Chemical Bonding and Molecular Structure

## Introduction

In this chapter we consider *molecular structure* and the concepts of *chemical bonding* that are used to interpret molecular structure. We will also begin to see how information about molecular structure and ideas about bonds can be used to interpret and predict physical properties and chemical reactivity. *Structural formulas* are a key tool for describing both structure and reactivity. At a minimum, they indicate *molecular constitution* by specifying the *connectivity* among the atoms in the molecule. Structural formulas also give a rough indication of electron distribution by representing electron pairs in bonds by lines and unshared electrons as dots, although the latter are usually omitted in printed structures. The reader is undoubtedly familiar with structural formulas for molecules such as those shown in Scheme 1.1.

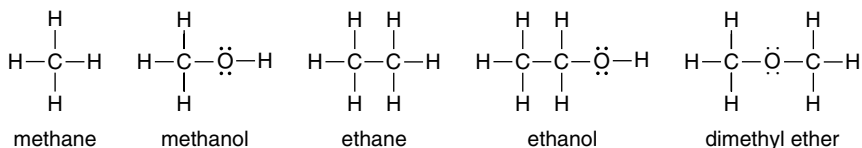
In quantitative terms, molecular structure specifies the relative position of all atoms in a molecule. These data provide the bond lengths and bond angles. There are a number of experimental means for precise determination of molecular structure, primarily based on spectroscopic and diffraction methods, and structural data are available for thousands of molecules. Structural information and interpretation is also provided by *computational chemistry*. In later sections of this chapter, we describe how molecular orbital theory and density functional theory can be applied to the calculation of molecular structure and properties.

The *distribution of electrons* is another element of molecular structure that is very important for understanding chemical reactivity. It is considerably more difficult to obtain experimental data on *electron density*, but fortunately, in recent years the rapid development of both structural theory and computational methods has allowed such calculations. We make use of computational electron density data in describing molecular structure, properties, and reactivity. In this chapter, we focus on the minimum energy structure of individual molecules. In Chapter 2, we consider other elements of molecular geometry, including dynamic processes involving *conformation*, that is, the variation of molecular shape as a result of bond rotation. In Chapter 3, we discuss

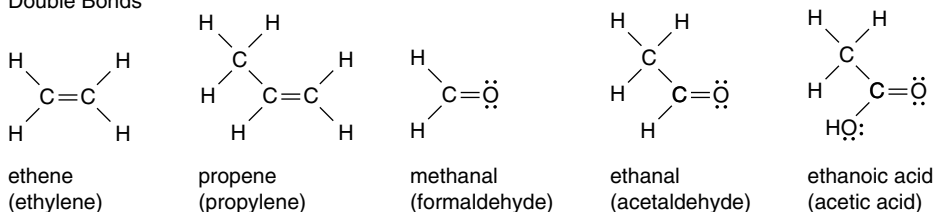
## CHAPTER 1

Chemical Bonding  
and Molecular Structure

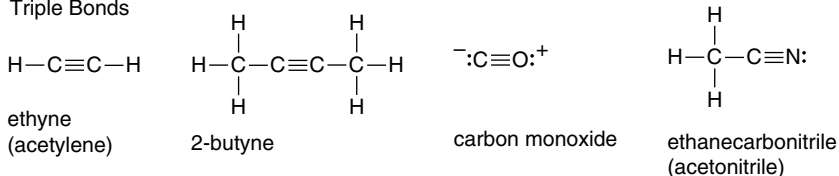
## Single Bonds



## Double Bonds



## Triple Bonds

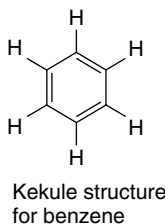


how structure effects the energy of *transition structures* and *intermediates* in chemical reactions. The principal goal of this chapter is to discuss the concepts that chemists use to develop relationships between molecular structure and reactivity. These relationships have their foundation in the fundamental physical aspects of molecular structure, that is, nuclear position and electron density distribution. Structural concepts help us see, understand, and apply these relationships.

## 1.1. Description of Molecular Structure Using Valence Bond Concepts

Introductory courses in organic chemistry usually rely primarily on the valence bond description of molecular structure. Valence bond theory was the first structural theory applied to the empirical information about organic chemistry. During the second half of the nineteenth century, correct structural formulas were deduced for a wide variety of organic compounds. The concept of “valence” was recognized. That is, carbon almost always formed four bonds, nitrogen three, oxygen two, and the halogens one. From this information, chemists developed structural formulas such as those in Scheme 1.1. Kekule’s structure for benzene, published in 1865, was a highlight of this period. The concept of *functional groups* was also developed. It was recognized that structural entities such as hydroxy (–OH), amino (–NH<sub>2</sub>), carbonyl (C=O), and

carboxy ( $\text{CO}_2\text{H}$ ) groups each had characteristic reactivity that was largely independent of the hydrocarbon portion of the molecule.



These structural formulas were developed without detailed understanding of the nature of the *chemical bond* that is represented by the lines in the formulas. There was a key advance in the understanding of the origin of chemical bonds in 1916, when G.N. Lewis introduced the concept of electron-pair bonds and the “rule of 8” or *octet rule*, as we now know it. Lewis postulated that chemical bonds were the result of sharing of electron pairs by nuclei and that for the second-row atoms, boron through neon, the most stable structures have eight valence shell electrons.<sup>1</sup> Molecules with more than eight electrons at any atom are very unstable and usually dissociate, while those with fewer than eight electrons at any atom are usually highly reactive toward electron donors. The concept of bonds as electron pairs gave a fuller meaning to the traditional structural formulas, since the lines then specifically represent single, double, and triple bonds. The dots represent unshared electrons. Facility with Lewis structures as a tool for accounting for electrons, bonds, and charges is one of the fundamental skills developed in introductory organic chemistry.

Lewis structures, however, convey relatively little information about the details of molecular structure. We need other concepts to deduce information about relative atomic positions and, especially, electron distribution. *Valence bond theory* provides one approach to deeper understanding of molecular structure. Valence bond (VB) theory has its theoretical foundation in quantum mechanics calculations that demonstrated that electrons hold nuclei together, that is, form bonds, when shared by two nuclei. This fact was established in 1927 by calculations on the hydrogen molecule.<sup>2</sup> The results showed that an energy minimum occurs at a certain internuclear distance if the electrons are free to associate with either nucleus. Electron density accumulates between the two nuclei. This can be depicted as an electron density map for the hydrogen molecule, as shown in Figure 1.1a. The area of space occupied by electrons is referred to as an *orbital*. A fundamental concept of VB theory is that there is a concentration of electron density between atoms that are bonded to one another. Figure 1.1b shows that there is *electron density depletion* relative to spherical atoms outside of the hydrogen nuclei. Nonbonding electrons are also described by orbitals, which are typically more diffuse than bonding ones. The mathematical formulation of molecular structure by VB theory is also possible. Here, we emphasize qualitative concepts that provide insight into the relationship between molecular structure and properties and reactivity.

<sup>1</sup> G. N. Lewis, *J. Am. Chem. Soc.*, **38**, 762 (1916).

<sup>2</sup> W. Heitler and F. London, *Z. Phys.*, **44**, 455 (1927).

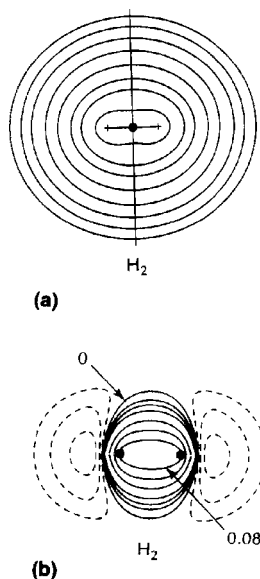
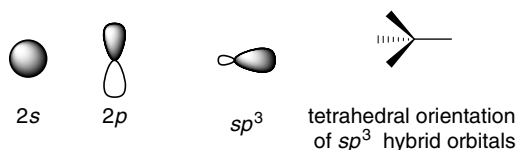


Fig. 1.1. Contour maps of (a) total electron density and (b) density difference relative to the spherical atoms for the  $\text{H}_2$  molecule. Reproduced with permission from R. F. W. Bader, T. T. Nguyen, and Y. Tal, *Rep. Prog. Phys.*, **44**, 893 (1981).

### 1.1.1. Hybridization

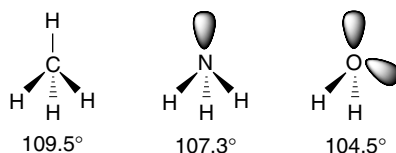
Qualitative application of VB theory to molecules containing second-row elements such as carbon, nitrogen, and oxygen involves the concept of *hybridization*, which was developed by Linus Pauling.<sup>3</sup> The atomic orbitals of the second-row elements include the spherically symmetric  $2s$  and the three  $2p$  orbitals, which are oriented perpendicularly to one another. The sum of these atomic orbitals is equivalent to four  $sp^3$  orbitals directed toward the corners of a tetrahedron. These are called  $sp^3$  hybrid orbitals. In methane, for example, these orbitals overlap with hydrogen  $1s$  orbitals to form  $\sigma$  bonds.



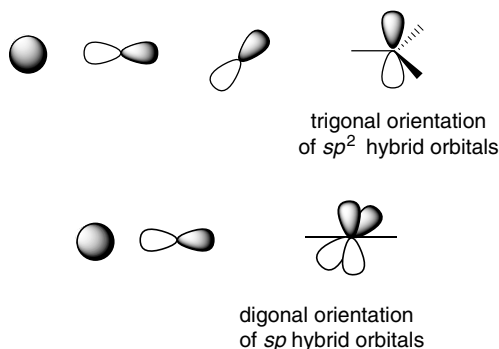
The valence bond description of methane, ammonia, and water predicts tetrahedral geometry. In methane, where the carbon valence is four, all the hybrid orbitals are involved in bonds to hydrogen. In ammonia and water, respectively, one and two nonbonding (unshared) pairs of electrons occupy the remaining orbitals. While methane

<sup>3</sup> L. Pauling, *J. Am. Chem. Soc.*, **53**, 1367 (1931).

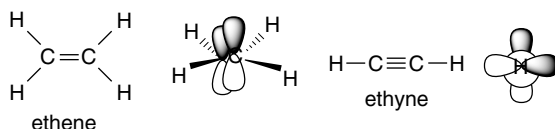
is perfectly tetrahedral, the bond angles in ammonia and water are somewhat reduced. This suggests that the electron-electron repulsions between unshared pairs are greater than for electrons in bonds to hydrogen. In other words, the unshared pairs occupy somewhat larger orbitals. This is reasonable, since these electrons are not attracted by hydrogen nuclei.



The hybridization concept can be readily applied to molecules with double and triple bonds, such as those shown in Scheme 1.1. Second-row elements are described as having  $sp^2$  or  $sp$  orbitals, resulting from hybridization of the  $s$  orbital with two or one  $p$  orbitals, respectively. The double and triple bonds are conceived as arising from the overlap of the unhybridized  $p$  orbitals on adjacent atoms. These bonds have a nodal plane and are called  $\pi$  bonds. Because the overlap is not as effective as for  $sp^3$  orbitals, these bonds are somewhat weaker than  $\sigma$  bonds.



The prototypical hydrocarbon examples of  $sp^2$  and  $sp$  hybridization are ethene and ethyne, respectively. The total electron density between the carbon atoms in these molecules is the sum from the  $\pi$  and  $\sigma$  bonds. For ethene, the electron density is somewhat elliptical, because the  $\pi$  component is not cylindrically symmetrical. For ethyne, the combination of the two  $\pi$  bonds restores cylindrical symmetry. The electron density contours for ethene are depicted in Figure 1.2, which shows the highest density near the nuclei, but with net accumulation of electron density between the carbon and hydrogen atoms.



The hybridization concept also encompasses empty antibonding orbitals, which are designated by an asterisk (\*). These orbitals have nodes between the bound atoms. As discussed in Section 1.1.8,  $\sigma^*$  and  $\pi^*$  orbitals can interact with filled orbitals and contribute to the ground state structure of the molecule. These empty orbitals are also

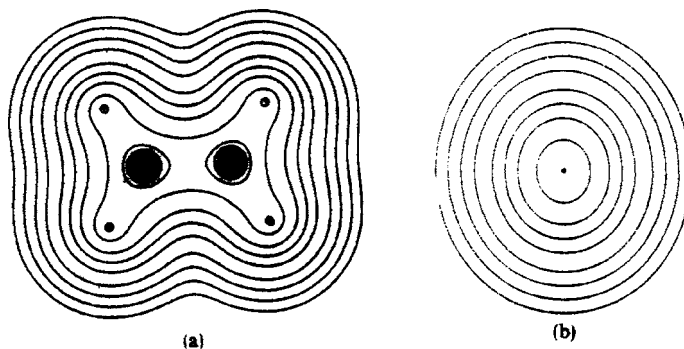
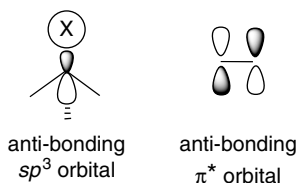
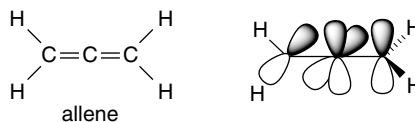


Fig. 1.2. (a) Contour map of electron density in the plane of the ethene molecule. (b) Contour map of electron density perpendicular to the plane of the ethene molecule at the midpoint of the C=C bond. Reproduced with permission from R. F. W. Bader, T. T. Nguyen-Dang, and Y. Tal, *Rep. Prog. Phys.*, **44**, 893 (1981).

of importance in terms of reactivity, particularly with electron-donating *nucleophilic* reagents, since it is the empty antibonding orbitals that interact most strongly with approaching nucleophiles.

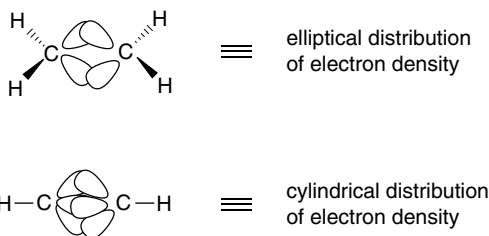


The hybridization concept indicates some additional aspects of molecular structure. The tetrahedral, trigonal, and digonal natures of  $sp^3$ ,  $sp^2$ , and  $sp$  carbon atoms provide an approximation of bond angles. The idea that  $\pi$  bonds are formed by the overlap of  $p$  orbitals puts some geometrical constraints on structure. Ethene, for example, is planar to maximize  $p$ -orbital overlap. Allene, on the other hand, must have the terminal  $\text{CH}_2$  groups rotated by  $90^\circ$  to accommodate two  $\pi$  bonds at the central  $sp$  carbon.



It is important to remember that hybridization is a *description* of the observed molecular geometry and electron density. Hybridization does not *cause* a molecule to have a particular shape. Rather, the molecule adopts a particular shape because it maximizes bonding interactions and minimizes electron-electron and other repulsive interactions. We use the hybridization concept to recognize similarities in structure that have their origin in fundamental forces within the molecules. The concept of hybridization helps us to see how molecular structure is influenced by the number of ligands and electrons at a particular atom.

It is worth noting at this point that a particular hybridization scheme *does not provide a unique description of molecular structure*. The same fundamental conclusions about geometry and electron density are reached if ethene and ethyne are described in terms of  $sp^3$  hybridization. In this approach, the double bond in ethene is thought of as arising from two overlapping  $sp^3$  orbitals. The two bonds are equivalent and are called *bent bonds*. This bonding arrangement also predicts a planar geometry and elliptical electron distribution, and in fact, this description is mathematically equivalent to the  $sp^2$  hybridization description. Similarly, ethyne can be thought of as arising by the sharing of three  $sp^3$  hybrid orbitals. The fundamental point is that there is a single real molecular structure defined by atomic positions and electron density. Orbitals partition the electron density in specific ways, and it is the *sum of the orbital contributions that describes the structure*.



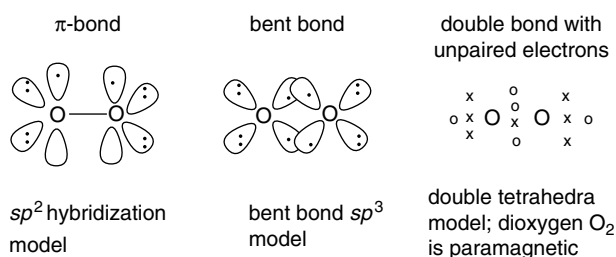
### 1.1.2. The Origin of Electron-Electron Repulsion

We have already assumed that electron pairs, whether in bonds or as nonbonding pairs, repel other electron pairs. This is manifested in the tetrahedral and trigonal geometry of tetravalent and trivalent carbon compounds. These geometries correspond to maximum separation of the electron-pair bonds. Part of this repulsion is electrostatic, but there is another important factor. The *Pauli exclusion principle* states that only two electrons can occupy the same point in space and that they must have opposite spin quantum numbers. Equivalent orbitals therefore maintain maximum separation, as found in the  $sp^3$ ,  $sp^2$ , and  $sp$  hybridization for tetra-, tri-, and divalent compounds of the second-row elements. The combination of Pauli exclusion and electrostatic repulsion leads to the *valence shell electron-pair repulsion rule* (VSEPR), which states that bonds and unshared electron pairs assume the orientation that permits maximum separation.

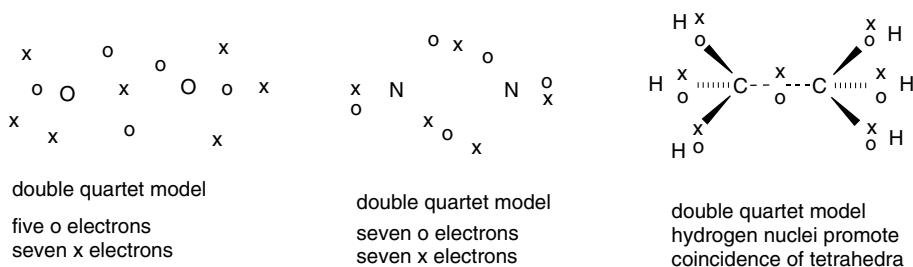
An important illustration of the importance of the Pauli exclusion principle is seen in the  $O_2$  molecule. If we were to describe  $O_2$  using either the  $sp^2$  hybridization or bent bond model, we would expect a double bond with all the electrons paired. In fact,  $O_2$  is *paramagnetic*, with two unpaired electrons, and yet it does have a double bond. If we ask how electrons would be distributed to maintain maximum separation, we arrive at two tetrahedral arrays, with the tetrahedra offset by the maximum amount.<sup>4</sup> Electronic spin can be represented as x and o. The structure still has four bonding electrons between the oxygen atoms, that is, a double bond. It also obeys the octet rule for each oxygen and correctly predicts that two of the electrons are unpaired.

<sup>4</sup> J. W. Linnett, *The Electronic Structure of Molecules*, Methren Co. LTD, London, 1964, pp. 37–42; R. J. Gillespie and P. L. A. Popelier, *Chemical Bonding and Molecular Geometry*, Oxford University Press, New York, 2001, pp 102–103.

This structure minimizes electron-electron repulsions and obeys the Pauli principle by maximizing the separation of electrons having the same spin.



A similar representation of  $N_2$  with offset of the tetrahedral of electrons correctly describes the molecule as having a triple bond, but it is diamagnetic, since there are equal numbers of electrons of each spin. For ethane, all the electrons are bonding and are attracted toward the hydrogen nuclei, and the tetrahedra of electrons of opposite spin both occupy a region of space directed toward a hydrogen nucleus.



For most of the molecules and reactions we want to consider, the Pauling hybridization scheme provides an effective structural framework, and we use VB theory to describe most of the reactions and properties of organic compounds. However, we have to keep in mind that it is *neither a unique nor a complete description of electron density*, and we will find cases where we need to invoke additional ideas. In particular, we discuss *molecular orbital theory* and *density functional theory*, which are other ways of describing molecular structure and electron distribution.

### 1.1.3. Electronegativity and Polarity

The VB concept of electron-pair bonds recognizes that the sharing of electrons by the nuclei of two different elements is unequal. Pauling defined the concept of unequal sharing in terms of *electronegativity*,<sup>5</sup> defining the term as “the power of an atom in a molecule to attract electrons to itself.” Electronegativity depends on the number of protons in the nucleus and is therefore closely associated with position in the periodic table. The metals on the left of the periodic table are the least electronegative elements, whereas the halogens on the right have the highest electronegativity in each row. Electronegativity decreases going down the periodic table for both metals and nonmetals.

The physical origin of these electronegativity trends is *nuclear screening*. As the atomic number increases from lithium to fluorine, the nuclear charge increases, as does

<sup>5</sup> L. Pauling, *J. Am. Chem. Soc.*, **54**, 3570 (1932).

the number of electrons. Each successive electron “feels” a larger nuclear charge. This charge is partially screened by the additional electron density as the shell is filled. However, the screening, on average, is less effective for each electron that is added. As a result, an electron in fluorine is subject to a greater effective nuclear charge than one in an atom on the left in the periodic table. As each successive shell is filled, the electrons in the valence shell “feel” the effective nuclear charge as screened by the filled inner shells. This screening is more effective as successive shells are filled and the outer valence shell electrons are held less tightly going down the periodic table. As we discuss later, the “size” of an atom also changes in response to the nuclear charge. Going across the periodic table in any row, the atoms become *smaller* as the shell is filled because of the higher effective nuclear charge. Pauling devised a numerical scale for electronegativity, based on empirical interpretation of energies of bonds and relating specifically to electron sharing in covalent bonds, that has remained in use for many years. Several approaches have been designed to define electronegativity in terms of other atomic properties. Allred and Rochow defined electronegativity in terms of the electrostatic attraction by the effective nuclear charge  $Z_{\text{eff}}$ <sup>6</sup>:

$$\chi_{\text{AR}} = \frac{0.3590Z_{\text{eff}}}{r^2} + 0.744 \quad (1.1)$$

where  $r$  is the covalent radius in Å. This definition is based on the concept of nuclear screening described above. Another definition of electronegativity is based explicitly on the relation between the number of valence shell electrons,  $n$ , and the effective atomic radius  $r$ :<sup>7</sup>

$$V = n/r \quad (1.2)$$

As we will see shortly, covalent and atomic radii are not absolutely measurable quantities and require definition.

Mulliken found that there is a relationship between *ionization potential* (IP) and *electron affinity* (EA) and defined electronegativity  $\chi$  as the average of those terms:<sup>8</sup>

$$\chi_{\text{abs}} = \frac{\text{IP} + \text{EA}}{2} \quad (1.3)$$

This formulation, which turns out to have a theoretical justification in density functional theory, is sometimes referred to as *absolute electronegativity* and is expressed in units of eV.

A more recent formulation of electronegativity, derived from the basic principles of atomic structure, has led to a *spectroscopic scale for electronegativity*.<sup>9</sup> In this formulation, the electronegativity is defined as the average energy of a valence electron in an atom. The lower the average energy, the greater the electron-attracting power (electronegativity) of the atom. The formulation is

$$\chi_{\text{spec}} = \frac{(a\text{IP}_s + b\text{IP}_p)}{a + b} \quad (1.4)$$

<sup>6</sup> A. L. Allred and E. G. Rochow, *J. Inorg. Nucl. Chem.*, **5**, 264 (1958).

<sup>7</sup> Y.-R. Luo and S. W. Benson, *Acc. Chem. Res.*, **25**, 375 (1992).

<sup>8</sup> R. S. Mulliken, *J. Chem. Phys.*, **2**, 782 (1934); R. S. Mulliken, *J. Chem. Phys.*, **3**, 573 (1935).

<sup>9</sup> L. C. Allen, *J. Am. Chem. Soc.*, **111**, 9003 (1989); L. C. Allen, *Int. J. Quantum Chem.*, **49**, 253 (1994); J. B. Mann, T. L. Meek, and L. C. Allen, *J. Am. Chem. Soc.*, **122**, 2780 (2000).

where  $IP_s$  and  $IP_p$  are the ionization potentials of the  $s$  and  $p$  electrons and  $a$  and  $b$  are the number of  $s$  and  $p$  electrons, respectively.

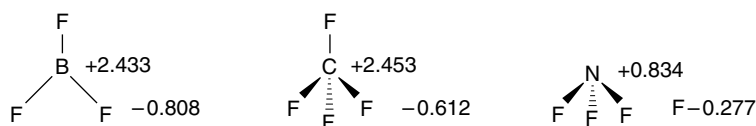
The values on this scale correlate well with the Pauling and Allred-Rochow scales. One feature of this scale is that the IP values can be measured accurately so that electronegativity becomes an *experimentally measured* quantity. When the same concepts are applied to atoms in molecules, the atom undergoes an electronegativity adjustment that can be related to the energy of its orbitals (as expressed by molecular orbital theory). The average adjusted energy of an electron is called the *energy index* (EI). The EI values of two bound atoms provide a measure of bond polarity called the *bond polarity index*<sup>10</sup> (BPI), formulated as

$$BPI_{AB} = (EI_A - EI_A^{\text{ref}}) - (EI_B - EI_B^{\text{ref}}) \quad (1.5)$$

where  $EI^{\text{ref}}$  are parameters of A–A and B–B bonds.

These approaches, along with several others, give electronegativity scales that are in good relative agreement in assessing the electron-attracting power of the elements. Each scale is based on fundamental atomic properties. However, they are in different units and therefore not directly comparable. Table 1.1 gives the values assigned by some of the electronegativity scales. The numerical values are scaled to the original Pauling range. At this point, we wish to emphasize the broad consistency of the values, not the differences. We use the *order of the electronegativity of the elements* in a qualitative way, primarily when discussing *bond polarity*. It should be noted, however, that the concept of electronegativity has evolved from an empirical scale to one with specific physical meaning. We pursue the relationship between these scales further in Topic 1.5.3.

The most obvious consequence of differential electronegativity is that covalent bonds between different elements are *polar*. Each atom bears a partial charge reflecting the relative electronegativity of the two elements sharing the bond. These charges can be estimated, and the values found for  $BF_3$ ,  $CF_4$ , and  $NF_3$  are shown below.<sup>11</sup> Note that the negative charge on fluorine becomes smaller as the electronegativity of the central atom increases.



The individual polar bonds contribute to the polarity of the overall molecule. The overall molecular polarity is expressed as the dipole moment. For the three molecules shown, the overall molecular dipole moment is 0 for  $BF_3$  (planar) and  $CF_4$  (tetrahedral), because of the symmetry of the molecules, but  $NF_3$  has a dipole moment of 0.235 D, since the molecule is pyramidal.<sup>12</sup>

<sup>10</sup> L. C. Allen, D. A. Egolf, E. T. Knight, and C. Liang, *J. Phys. Chem.*, **94**, 5603 (1990); L. C. Allen, *Can. J. Chem.*, **70**, 631 (1992).

<sup>11</sup> R. J. Gillespie and P. L. A. Popelier, *Chemical Bonding and Molecular Geometry*, Oxford University Press, New York, 2001, p. 47.

<sup>12</sup> Dipole moments are frequently expressed in Debye (D) units;  $1\text{ D} = 3.335641 \times 10^{-30}\text{ C m}$  in SI units.

Table 1.1. Electronegativity Scales<sup>a</sup>

Atom	Original Pauling <sup>b</sup>	Modified Pauling <sup>c</sup>	Allred-Rochow <sup>d</sup>	Luo-Benson <sup>e</sup>	Mulliken <sup>f</sup>	Allen <sup>g</sup>
H	2.1	2.20	2.20		2.17	2.30
Li	1.0	0.98	0.97	0.93	0.91	0.91
Be	1.5	1.57	1.47	1.39	1.45	1.58
B	2.0	2.04	2.01	1.93	1.88	2.05
C	2.5	2.55	2.50	2.45	2.45	2.54
N	3.0	3.04	3.07	2.96	2.93	3.07
O	3.5	3.44	3.50	3.45	3.61	3.61
F	4.0	3.98	4.10	4.07	4.14	4.19
Na	0.9	0.93	1.01	0.90	0.86	0.87
Mg	1.2	1.31	1.23	1.20	1.21	1.29
Al	1.5	1.61	1.47	1.50	1.62	1.61
Si	1.8	1.90	1.74	1.84	2.12	1.92
P	2.1	2.19	2.06	2.23	2.46	2.25
S	2.5	2.58	2.44	2.65	2.64	2.59
Cl	3.0	3.16	2.83	3.09	3.05	2.87
Ge	1.8	2.01	2.02	1.79	2.14	1.99
As	2.0	2.18	2.20	2.11	2.25	2.21
Se	2.4	2.55	2.48	2.43	2.46	2.42
Br	2.8	2.96	2.74	2.77	2.83	2.69
Sn	1.8	1.96	1.72	1.64	2.12	1.82
I	2.5	2.66	2.21	2.47	2.57	2.36

a. All numerical values are scaled to the original Pauling scale.

b. L. Pauling, *The Nature of the Chemical Bond*, 3rd Edition, Cornell University Press, Ithaca, NY, 1960.

c. A. L. Allred, *J. Inorg. Nucl. Chem.*, **17**, 215 (1961).

d. A. L. Allred and E.G. Rochow, *J. Inorg. Nucl. Chem.*, **5**, 264 (1958).

e. Y. R. Luo and S.W. Benson, *Acc. Chem. Res.*, **25**, 375 (1992).

f. D. Bergman and J. Hinze, *Angew. Chem. Int. Ed. Engl.*, **35**, 150 (1996).

g. L. C. Allen, *Int. J. Quantum Chem.*, **49**, 253 (1994).

SECTION 1.1

Description of Molecular  
Structure Using Valence  
Bond Concepts

#### 1.1.4. Electronegativity Equalization

The concept of *electronegativity equalization* was introduced by R. T. Sanderson.<sup>13</sup> The idea is implicit in the concept of a molecule as consisting of nuclei embedded in an electronic cloud and leads to the conclusion that the electron density will reach an equilibrium state in which there is no net force on the electrons. The idea of electronegativity equalization finds a theoretical foundation in *density functional theory* (see Section 1.3). Several numerical schemes have been developed for the assignment of charges based on the idea that electronegativity equalization must be achieved. Sanderson's initial approach averaged all atoms of a single element, e.g., carbon, in a molecule and did not distinguish among them. This limitation was addressed by Hercules and co-workers,<sup>14</sup> who assigned electronegativity values called SR' values to specific groups within a molecule. For example, the methyl and ethyl groups, respectively, were derived from the number of C and H atoms in the group:

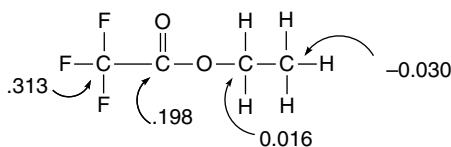
$$SR'_{\text{CH}_3} = (SR_{\text{C}} \times SR_{\text{H}}^3)^{1/4} \quad (1.6)$$

$$SR'_{\text{C}_2\text{H}_5} = [(SR_{\text{C}} \times SR_{\text{H}}^2)(SR_{\text{C}} \times SR_{\text{H}}^3)^{1/4}]^{1/4} \quad (1.7)$$

<sup>13</sup>. R. T. Sanderson, *Chemical Bonds and Bond Energies*, Academic Press, New York, 1976;  
R. T. Sanderson, *Polar Covalence*, Academic Press, New York, 1983.

<sup>14</sup>. J. C. Carver, R. C. Gray, and D. M. Hercules, *J. Am. Chem. Soc.*, **96**, 6851 (1974).

This approach was extended by M. Sastry to a variety of organic compounds.<sup>15</sup> For example, the charges calculated for the carbon atoms in  $\text{CF}_3\text{CO}_2\text{C}_2\text{H}_5$  are as shown below. We see that the carbon of the methyl group carries a small negative charge, whereas the carbons bound to more electronegative elements are positive.



The calculated charge on carbon for a number of organic molecules showed good correlation with the core atomic binding energies, as measured by X-ray photoemission spectroscopy. We discuss other methods of assigning charges to atoms based on computational chemistry in Section 1.4. We also find that all these methods are in some sense arbitrary divisions of molecules. The concept of electronegativity equalization is important, however. It tells us that electron density shifts in response to bonding between atoms of different electronegativity. This is the basis of *polar substituent effects*. Furthermore, as the data above for ethyl trifluoroacetate suggest, a highly electronegative substituent induces a net positive charge on carbon, as in the  $\text{CF}_3$  and  $\text{C}=\text{O}$  carbons in ethyl trifluoroacetate. Electronegativity differences are the origin of *polar bonds*, but electronegativity equalization suggests that there will also be an *inductive effect*, that is, the propagation of changes in electron distribution to adjacent atoms.

### 1.1.5. Differential Electronegativity of Carbon Atoms

Although carbon is assigned a single numerical value in the Pauling electronegativity scale, its effective electronegativity depends on its hybridization. The qualitative relationship is that carbon electronegativity toward other bound atoms increases with the extent of  $s$  character in the bond, i.e.,  $sp^3 < sp^2 < sp$ . Based on the atomic radii approach, the carbon atoms in methane, benzene, ethene, and ethyne have electronegativity in the ratio 1:1.08:1.15:1.28. A scale based on bond polarity measures gives values of 2.14, 2.34, and 2.52 for  $sp^3$ ,  $sp^2$ , and  $sp$  carbons, respectively.<sup>16</sup> A scale based on NMR coupling constants gives values of 1.07 for methyl, 1.61 for ethenyl, and 3.37 for ethynyl.<sup>17</sup> If we use the density functional theory definition of electronegativity (see Topic 1.5.1) the values assigned to methyl, ethyl, ethenyl, and ethynyl are 5.12, 4.42, 5.18, and 8.21, respectively.<sup>18</sup> Note that by this measure methyl is significantly more electronegative than ethyl. With an *atoms in molecules* approach (see Section 1.4.3), the numbers assigned are methyl 6.84; ethenyl 7.10, and ethynyl 8.23.<sup>19</sup> Table 1.2 converts each of these scales to a relative scale with methyl equal to 1. Note that the various definitions *do not* reach a numerical consensus on the relative electronegativity of  $sp^3$ ,  $sp^2$ , and  $sp$  carbon, although the order is consistent. We are

<sup>15</sup> M. Sastry, *J. Electron Spectros.*, **85**, 167 (1997).

<sup>16</sup> N. Inamoto and S. Masuda, *Chem. Lett.*, 1003, 1007 (1982).

<sup>17</sup> S. Marriott, W. F. Reynolds, R. W. Taft, and R. D. Topsom, *J. Org. Chem.*, **49**, 959 (1984).

<sup>18</sup> F. De Proft, W. Langenaeker, and P. Geerlings, *J. Phys. Chem.*, **97**, 1826, (1995).

<sup>19</sup> S. Hati and D. Datta, *J. Comput. Chem.*, **13**, 912 (1992).

**Table 1.2. Ratio of Electronegativity for Carbon of Different Hybridization**

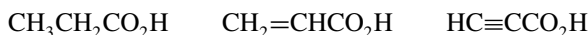
Comparison	Methyl	Ethenyl	Ethynyl
Atomic radii	1.0	1.15	1.28
Bond polarity	1.0	1.09	1.18
NMR coupling	1.0	1.50	3.15
Density function theory	1.0	1.01	1.60
Atoms in molecules	1.0	1.04	1.20

SECTION 1.1

Description of Molecular  
Structure Using Valence  
Bond Concepts

not so concerned with the precise number, but rather with the trend of increasing electronegativity  $sp^3 < sp^2 < sp$ . It is also important to note that the range of carbon electronegativities is close to that of hydrogen. While  $sp^3$  carbon and hydrogen are similar in electronegativity,  $sp^2$  and  $sp$  carbon are more electronegative than hydrogen.

If we compare the  $pK_a$  values of propanoic acid (4.87), propenoic acid (4.25), and propynoic acid (1.84), we get some indication that the hybridization of carbon does exert a substantial polar effect. The acidity increases with the electronegativity of the carbon group.



Orbitals of different hybridization on the same carbon are also thought of as having different electronegativities. For example, in strained hydrocarbons such as cyclopropane the C–H bonds are more acidic than normal. This is attributed to the additional  $s$  character of the C–H bonds, which compensates for the added  $p$  character of the strained C–C bonds.<sup>20</sup>

It is also possible to assign electronegativity values to groups. For alkyl groups the numbers are:  $\text{CH}_3$ , 2.52;  $\text{C}_2\text{H}_5$ , 2.46;  $(\text{CH}_3)_2\text{CH}$ , 2.41;  $(\text{CH}_3)_3\text{C}$ , 2.38;  $\text{C}_6\text{H}_5$ , 2.55;  $\text{CH}_2=\text{CH}$ , 2.55;  $\text{HC}\equiv\text{C}$ , 2.79.<sup>21</sup> The order is in accord with the general trend that *more-substituted alkyl groups are slightly better electron donors than methyl groups*. The increased electronegativity of  $sp^2$  and  $sp$  carbons is also evident. These values are based on bond energy data by a relationship first explored by Pauling and subsequently developed by many other investigators. The original Pauling expression is

$$D[\text{A} - \text{B}] = 1/2(D[\text{A} - \text{A}] + D[\text{B} - \text{B}]) + 23(\Delta\chi)^2 \quad (1.8)$$

where  $\Delta\chi$  is the difference in electronegativity of A and B.

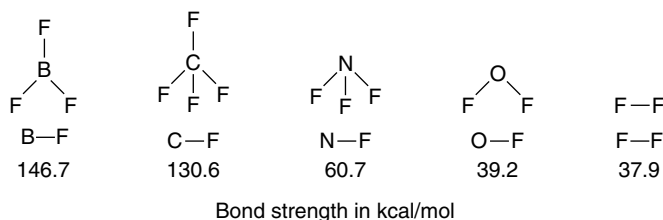
Thus the bond strength (in kcal/mol) can be approximated as the average of the two corresponding homonuclear bonds and an increment that increases with the difference in electronegativity. For any bond, application of this equation suggests a “covalent” and “polar” term. The results for the series  $\text{CH}_3\text{F}$ ,  $\text{CH}_3\text{OH}$ ,  $\text{CH}_3\text{NH}_2$ , and  $\text{CH}_3\text{CH}_3$  is shown below.

<sup>20</sup> J. N. Shoolery, *J. Chem. Phys.*, **31**, 1427 (1959); N. Muller and D. E. Pritchard, *J. Chem. Phys.*, **31**, 1471 (1959); K. B. Wiberg, R. F. W. Bader, and C. D. H. Lau, *J. Am. Chem. Soc.*, **109**, 1001 (1987).

<sup>21</sup> N. Matsunaga, D. W. Rogers, and A. A. Zavitsas, *J. Org., Chem.*, **68**, 3158 (2003).

	D(A – A)	$\chi$	$(\Delta\chi)^2$	Covalent	Polar	% Covalent	% Polar
CH <sub>3</sub>	89.8	2.525					
–F	38.0	3.938	1.189	63.90	27.35	70	30
–OH	56.1	3.500	0.987	72.95	22.70	76	24
–NH <sub>2</sub>	61.1	3.071	0.749	75.45	17.23	81	19
–CH <sub>3</sub>	89.8	2.525	0.000	89.8	0.0	100	0

An important qualitative result emerges from these numbers. *Bond strength is increased by electronegativity differences.* This is illustrated, for example, by the strength of the bonds of fluorine with the other second-row elements.



### 1.1.6. Polarizability, Hardness, and Softness

The interaction of valence shell electrons with the nucleus and intervening filled shells also affects the *polarizability* of the valence shell electrons. Polarizability can be described in terms of *hardness* and *softness*. A relatively large atom or ion with a small effective nuclear charge is relatively easily distorted (polarized) by an external charge and is called *soft*. A more compact electron distribution resulting from a higher net nuclear charge and less effective screening is called *hard*. The hard-soft-acid-base (HSAB) theory of stability and reactivity, introduced by Pearson,<sup>22</sup> has been extensively applied to qualitative reactivity trends,<sup>23</sup> and has been theoretically justified.<sup>24</sup> The qualitative expression of HSAB is that hard-hard and soft-soft reaction partners are preferred to hard-soft combinations. As for electronegativity, numerical scales of hardness and softness have been devised. One definition, like the Mulliken definition of absolute electronegativity, is based on ionization potential and electron affinity:

$$\text{Hardness} = \eta = \frac{1}{2}(\text{IP} - \text{EA}) \quad \text{and} \quad \text{Softness} = \sigma = \frac{1}{\eta} \sim 2(\text{IP} + \text{EA}) \quad (1.9)$$

Hardness increases with electronegativity and with positive charge. Thus, for the halogens the order is  $\text{F}^- > \text{Cl}^- > \text{Br}^- > \text{I}^-$ , and for second-row anions,  $\text{F}^- > \text{HO}^- > \text{H}_2\text{N}^- > \text{H}_3\text{C}^-$ . For cations, hardness decreases with size and increases with positive charge, so that  $\text{H}^+ > \text{Li}^+ > \text{Na}^+ > \text{K}^+$ . The proton, lacking any electrons, is infinitely hard. In solution it does not exist as an independent entity but contributes to the hardness of some protonated species. Metal ion hardness increases with oxidation state as the electron cloud contracts with the removal of each successive electron. All these as

<sup>22</sup> R. G. Pearson and J. Songstad, *J. Am. Chem. Soc.*, **89**, 1827 (1967); R. G. Pearson, *J. Chem. Educ.*, **45**, 581, 643 (1968).

<sup>23</sup> R. G. Pearson, *Inorg. Chim. Acta*, **240**, 93 (1995).

<sup>24</sup> P. K. Chattaraj, H. Lee, and R. G. Parr, *J. Am. Chem. Soc.*, **113**, 1855 (1991).

well as other hardness/softness relationships are consistent with the idea that hardness and softness are manifestations of the influence of nuclear charge on polarizability.

For polyatomic molecules and ions, hardness and softness are closely related to the HOMO and LUMO energies, which are analogous to the IP and EA values for atoms. The larger the HOMO-LUMO gap, the greater the hardness. Numerically, hardness is approximately equal to half the energy gap, as defined above for atoms. In general, chemical reactivity increases as LUMO energies are lower and HOMO energies are higher. The implication is that softer chemical species, those with smaller HOMO-LUMO gaps, tend to be more reactive than harder ones. In qualitative terms, this can be described as the ability of nucleophiles or bases to donate electrons more readily to electrophiles or acids and begin the process of bond formation. Interactions between harder chemical entities are more likely to be dominated by electrostatic interactions. Table 1.3 gives hardness values for some atoms and small molecules and ions. Note some of the trends for cations and anions. The smaller  $\text{Li}^+$ ,  $\text{Mg}^{2+}$ , and  $\text{Na}^+$  ions are harder than the heavier ions such as  $\text{Cu}^+$ ,  $\text{Hg}^{2+}$ , and  $\text{Pd}^{2+}$ . The hydride ion is quite hard, second only to fluoride. The increasing hardness in the series  $\text{CH}_3^- < \text{NH}_2^- < \text{OH}^- < \text{F}^-$  is of considerable importance and, in particular, correlates with nucleophilicity, which is in the order  $\text{CH}_3^- > \text{NH}_2^- > \text{OH}^- > \text{F}^-$ .

Figure 1.3 shows the IP-EA gap ( $2\eta$ ) for several neutral atoms and radicals. Note that there is a correlation with electronegativity and position in the periodic table. The halogen anions and radicals become progressively softer from fluorine to iodine. Across the second row, softness decreases from carbon to fluorine. The cyanide ion is a relatively soft species.

The HSAB theory provides a useful precept for understanding Lewis acid-base interactions in that hard acids prefer hard bases and soft acids prefer soft bases. The principle can be applied to chemical equilibria in the form of the *principle of maximum hardness*,<sup>25</sup> which states that “molecules arrange themselves so as to

**Table 1.3. Hardness of Some Atoms, Acids, and Bases<sup>a</sup>**

Atom	$\eta$	Cations	$\eta$	Anions	$\eta$
H	6.4	$\text{H}^+$		$\text{H}^-$	6.8
Li	2.4	$\text{Li}^+$	35.1	$\text{F}^-$	7.0
C	5.0	$\text{Mg}^{2+}$	32.5	$\text{Cl}^-$	4.7
N	7.3	$\text{Na}^+$	21.1	$\text{Br}^-$	4.2
O	6.1	$\text{Ca}^{2+}$	19.7	$\text{I}^-$	3.7
F	7.0	$\text{Al}^{3+}$	45.8	$\text{CH}_3^-$	4.0
Na	2.3	$\text{Cu}^+$	6.3	$\text{NH}_2^-$	5.3
Si	3.4	$\text{Cu}^{2+}$	8.3	$\text{OH}^-$	5.6
P	4.9	$\text{Fe}^{2+}$	7.3	$\text{SH}^-$	4.1
S	4.1	$\text{Fe}^{3+}$	13.1	$\text{CN}^-$	5.3
Cl	4.7	$\text{Hg}^{2+}$	7.7		
		$\text{Pb}^{2+}$	8.5		
		$\text{Pd}^{2+}$	6.8		

a. From R. G. Parr and R. G. Pearson, *J. Am. Chem. Soc.*, **105**, 7512 (1983).

<sup>25</sup> R. G. Pearson, *Acc. Chem. Res.*, **26**, 250 (1993); R. G. Parr and Z. Zhou, *Acc. Chem. Res.*, **26**, 256 (1993); R. G. Pearson, *J. Org. Chem.*, **54**, 1423 (1989); R. G. Parr and J. L. Gazquez, *J. Phys. Chem.*, **97**, 3939 (1993).

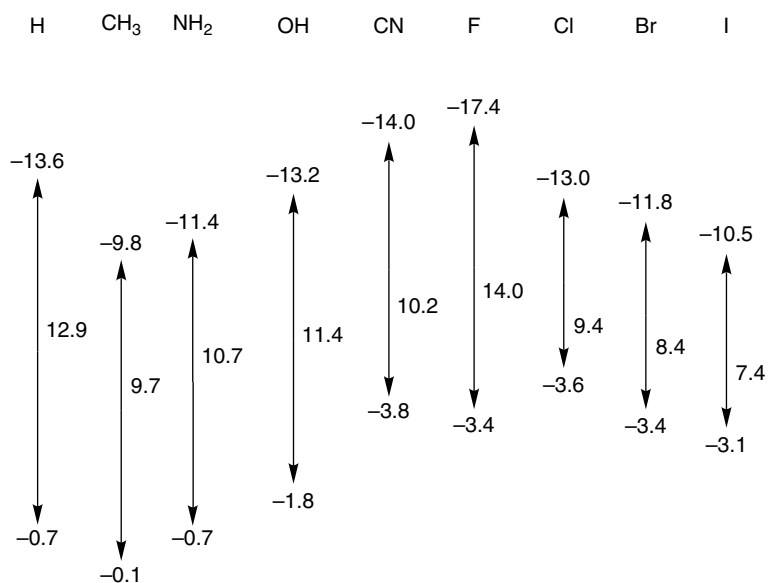
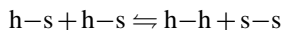


Fig. 1.3. Ionization (IP) and electron affinity (EA) gaps in eV for neutral atoms and radicals. Adapted from R. G. Pearson, *J. Am. Chem. Soc.*, **110**, 7684 (1988).

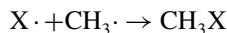
be as hard as possible.” Expressed in terms of reaction energetics,  $\Delta E$  is usually negative for



The hard-hard interactions are dominated by electrostatic attraction, whereas soft-soft interactions are dominated by mutual polarization.<sup>26</sup> Electronegativity and hardness determine the extent of electron transfer between two molecular fragments in a reaction. This can be approximated numerically by the expression

$$\Delta N = \frac{\chi_x - \chi_y}{2(\eta_x + \eta_y)} \quad (1.10)$$

where  $\chi$  is absolute electronegativity and  $\eta$  is hardness for the reacting species. For example, we can calculate the degree of electron transfer for each of the four halogen atoms reacting with the methyl radical to form the corresponding methyl halide.



X <sup>·</sup>	$\chi_x$	$\eta_x$	$\Delta N$	$\eta_{\text{CH}_3\text{X}}$
F <sup>·</sup>	10.4	7.0	0.23	9.4
Cl <sup>·</sup>	8.3	4.7	0.17	7.5
Br <sup>·</sup>	7.6	4.2	0.14	5.8
I <sup>·</sup>	6.8	3.7	0.10	4.7

<sup>26</sup> R. G. Pearson, *J. Am. Chem. Soc.*, **85**, 3533 (1963); T. L. Ho, *Hard and Soft Acids and Bases in Organic Chemistry*, Academic Press, New York, 1977; W. B. Jensen, *The Lewis Acid-Base Concept*, Wiley-Interscience, New York, 1980, Chap. 8.

According to this analysis, the C–X bond is successively both more polar and harder in the order  $I < Br < Cl < F$ . This result is in agreement with both the properties and reactivities of the methyl halides. When bonds are compared, reacting pairs of greater hardness result in a larger net charge transfer, which adds an increment to the exothermicity of bond formation. That is, bonds formed between two hard atoms or groups are stronger than those between two soft atoms or groups.<sup>27</sup> This is an example of a general relationship that recognizes that there is an increment to bond strength resulting from added ionic character.<sup>28</sup>

*Polarizability* measures the response of an ion or molecule to an electric field and is expressed in units of volume, typically  $10^{-24} \text{ cm}^3$  or  $\text{\AA}^3$ . Polarizability increases with atomic or ionic radius; it depends on the effectiveness of nuclear screening and increases as each valence shell is filled. Table 1.4 gives the polarizability values for the second-row atoms and some ions, molecules, and hydrocarbons. Methane is the least polarizable hydrocarbon and polarity increases with size. Polarizability is also affected by hybridization, with ethane  $>$  ethene  $>$  ethyne and propane  $>$  propene  $>$  propyne.

It should be noted that polarizability is *directional*, as illustrated in Scheme 1.2 for the methyl halides and halogenated benzenes.

Polarizability is related to the *refractive index* ( $n$ ) of organic molecules, which was one of the first physical properties to be carefully studied and related to molecular structure.<sup>29</sup> As early as the 1880s, it was recognized that the value of the refractive index can be calculated as the sum of atomic components. Values for various groups were established and revised.<sup>30</sup> It was noted that some compounds, in particular compounds with conjugated bonds, had higher (“exalted”) polarizability. Polarizability is also directly related to the dipole moment *induced by an electric field*. The greater the polarizability of a molecule, the larger the induced dipole.

**Table 1.4. Polarizability of Some Atoms, Ions, and Molecules<sup>a</sup>**

Atoms	Ions		Molecules		Hydrocarbons	
H	0.67		H <sub>2</sub> O	1.45	CH <sub>4</sub>	2.59
Li	24.3		N <sub>2</sub>	1.74	C <sub>2</sub> H <sub>6</sub>	4.47
Be	5.6		CO	1.95	CH <sub>2</sub> =CH <sub>2</sub>	4.25
B	3.0		NH <sub>3</sub>	2.81	HC≡CH	3.93
C	1.8		CO <sub>2</sub>	2.91	C <sub>3</sub> H <sub>8</sub>	6.29
N	1.1		BF <sub>3</sub>	3.31	CH <sub>3</sub> CH=CH <sub>2</sub>	6.26
O	0.8				CH <sub>3</sub> C≡CH	6.18
F	0.06	F <sup>-</sup>	1.2		<i>n</i> -C <sub>4</sub> H <sub>10</sub>	8.20
Ne	1.4	Na <sup>+</sup>	0.9		<i>i</i> -C <sub>4</sub> H <sub>10</sub>	8.14
Cl	2.2	Cl <sup>-</sup>	3		<i>n</i> -C <sub>5</sub> H <sub>12</sub>	9.99
Ar	3.6	K <sup>+</sup>	2.3		Neopentane	10.20
Br	3.1	Br <sup>-</sup>	4.5		<i>n</i> -C <sub>6</sub> H <sub>14</sub>	11.9
Kr	4.8				Cyclohexane	10.9
I	5.3	I <sup>-</sup>	7		C <sub>6</sub> H <sub>6</sub>	10.3
Xe	6.9					

a. T. M. Miller, in *Handbook of Chemistry and Physics*, 83rd Edition, pp. 10-163–10-177, 2002.

b. A. Dalgano, *Adv. Phys.*, **11**, 281 (1962), as quoted by R. J. W. Le Fevre, *Adv. Phys. Org. Chem.*, **3**, 1 (1965).

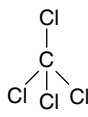
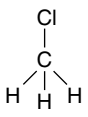
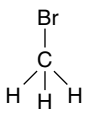
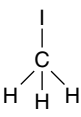
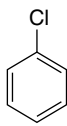
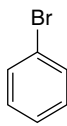
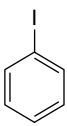
<sup>27</sup> P. K. Chattaraj, A. Cedillo, R. G. Parr, and E.M. Arnett, *J. Org. Chem.*, **60**, 4707 (1995).

<sup>28</sup> P. R. Reddy, T. V. R. Rao, and R. Viswanath, *J. Am. Chem. Soc.*, **111**, 2914 (1989).

<sup>29</sup> R. J. W. Le Fevre, *Adv. Phys. Org. Chem.*, **3**, 1 (1965).

<sup>30</sup> K. von Auwers, *Chem. Ber.*, **68**, 1635 (1935); A. I. Vogel, *J. Chem. Soc.*, 1842 (1948); J. W. Brühl, *Liebigs Ann.Chem.*, **235**, 1 (1986); J. W. Brühl, *Liebigs Ann.Chem.*, **236**, 233 (1986).

Scheme 1.2. Molecular Polarizability<sup>a</sup>

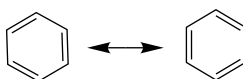
					
x		1.026	.411	.499	.657
y		1.026	.411	.499	.657
z		1.026	.509	.656	.872
					
x		1.12	1.255	1.301	1.588
y		.736	.821	.892	.996
z		1.12	1.478	1.683	1.971

a. From R J. W. Le Fevre, *Adv. Phys. Org. Chem.*, **3**, 1 (1965).

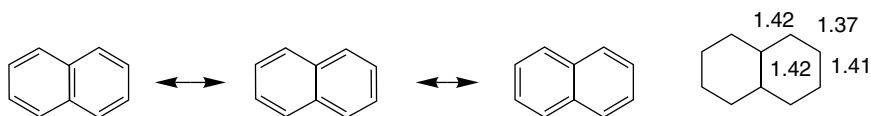
The concepts of electronegativity, polarizability, hardness, and softness are all interrelated. For the kind of qualitative applications we make in discussing reactivity, the concept that initial interactions between reacting molecules can be dominated by either partial electron transfer and bond formation (soft reactants) or by electrostatic interaction (hard reactants) is an important generalization.

### 1.1.7. Resonance and Conjugation

Qualitative application of VB theory makes use of the concept of *resonance* to relate structural formulas to the description of molecular structure and electron distribution. The case of benzene is a familiar and striking example. Two equivalent Lewis structures can be drawn, but the actual structure is the average of these two *resonance structures*. The double-headed arrow is used to specify a resonance relationship.



What structural information does this symbolism convey? Resonance structures imply that the true molecular structure is a weighted average of the individual structures. In the case of benzene, since the two structures are equivalent, each contributes equally. The *resonance hybrid* structure for benzene indicates hexagonal geometry and that the bond lengths are intermediate between a double and a single bond, since a bond order of 1.5 results from the average of the two structures. The actual structure of benzene is in accord with these expectations. It is perfectly hexagonal in shape and the carbon-carbon bond length is 1.40 Å. On the other hand, naphthalene, with three neutral resonance structures, shows bond length variation in accord with the predicted 1.67 and 1.33 bond orders.



Another important property of benzene is its thermodynamic stability, which is greater than expected for either of the two resonance structures. It is much more stable than noncyclic polyenes of similar structure, such as 1,3,5-hexatriene. What is the origin of this additional stability, which is often called *resonance stabilization* or *resonance energy*? The resonance structures imply that the  $\pi$  electron density in benzene is equally distributed between the sets of adjacent carbon atoms. This is not the case in acyclic polyenes. The electrons are evenly spread over the benzene ring, but in the polyene they are more concentrated between alternating pairs of carbon atoms. Average electron-electron repulsion is reduced in benzene. The difference in energy is called the *delocalization energy*. The resonance structures for benzene describe a particularly favorable bonding arrangement that leads to greater thermodynamic stability. In keeping with our emphasis on structural theory as a means of describing molecular properties, resonance *describes, but does not cause*, the extra stability.

Figure 1.4 shows electron density contours for benzene and 1,3,5-hexatriene. Note that the contours show completely uniform electron density distribution in benzene, but significant concentration between atoms 1,2; 3,4; and 5,6 in hexatriene, as was argued qualitatively above.

Resonance is a very useful concept and can be applied to many other molecules. Resonance is associated with delocalization of electrons and is a feature of *conjugated systems*, which have alternating double bonds that permit overlap between adjacent  $\pi$  bonds. This permits delocalization of electron density and usually leads to stabilization of the molecule. We will give some additional examples shortly.

We can summarize the applicability of the concept of resonance as follows:

1. When alternative Lewis structures can be written for a molecule and they differ only in the assignment of electrons among the nuclei, with nuclear positions being constant, then the molecule is not completely represented by a single Lewis structure, but has weighted properties of all the alternative Lewis structures.
2. Resonance structures are restricted to the maximum number of valence electrons that is appropriate for each atom: two for hydrogen and eight for second-row elements.

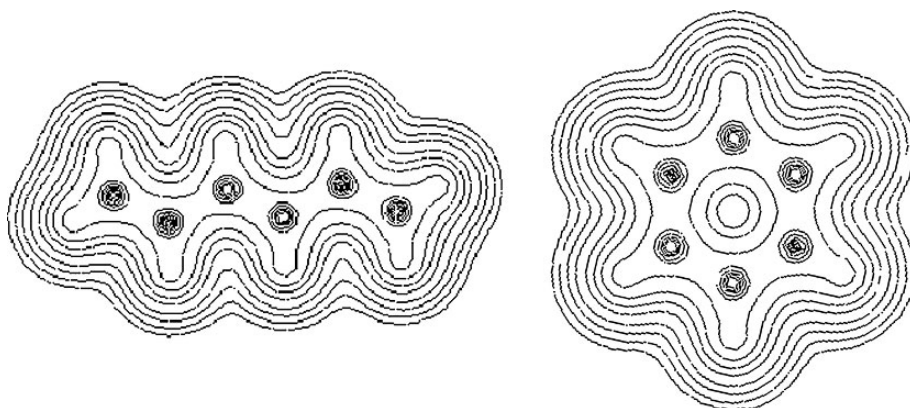
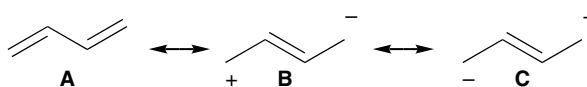


Fig. 1.4. Contour maps of electron density for 1,3,5-hexatriene and benzene in the planes of the molecules. Electron density was calculated at the HF/6-311G level. Electron density plots were created by applying the AIM2000 program; F.Biegler-Koenig, J.Shoenbohm and D.Dayles, *J. Compt. Chem.*, **22**, 545-559 (2001).

3. The more stable Lewis structures make the largest contribution to the weighted composite structure. Structures that have the following features are more stable and make the largest contribution: (a) maximum number of bonds, (b) minimum separation of opposite charges, and (c) charge distribution that is consistent with relative electronegativity.

Resonance structures are used to convey the structural and electron distribution consequences of conjugation and delocalization. Let us look specifically at 1,3-butadiene, 1,3,5-hexatriene, prop-2-enal (acrolein), methoxyethene (methyl vinyl ether), and ethenamine (vinylamine) to illustrate how resonance can help us understand electron distribution and reactivity. The hybridization picture for 1,3-butadiene suggests that there can be overlap of the  $p$  orbitals. Thermodynamic analysis (see Section 3.1.2.3) indicates that there is a net stabilization of about 3–4 kcal/mol, relative to two isolated double bonds. The electron density profile in Figure 1.5 shows some enhancement of  $\pi$ -electron density between C(2) and C(3).

Resonance structures portray increased electron density between C(2) and C(3), but only in structures that have fewer bonds and unfavorable charge separation.



In the diagram above there are two identical structures having opposite charge distributions and there is no net separation of charge. The importance of resonance structures to the composite structure increases with the stability of the individual structures, so structures **B** and **C** are less important than **A**, as they have separation of charge and only one rather than two  $\pi$  bonds. By applying resonance criteria 3a and 3b, we conclude that these two structures contribute less stabilization to butadiene than the two equivalent benzene resonance structures. Therefore, we expect the enhancement of electron density between C(2) and C(3) to be small.

For propenal (acrolein), one uncharged and two charged structures analogous to 1,3-butadiene can be drawn. In this case, the two charged structures are not equivalent.

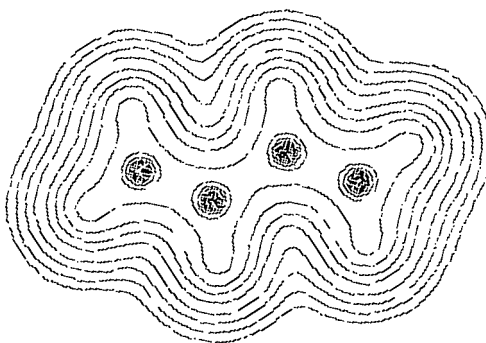
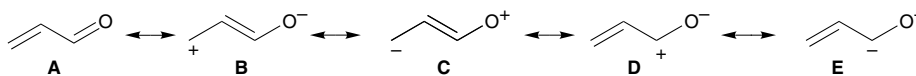
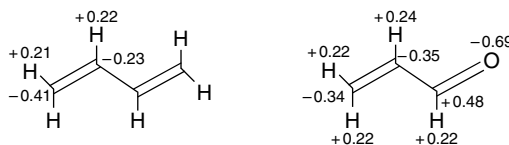


Fig. 1.5. Contour map of electron density for 1,3-butadiene in the plane of the molecule. Electron density was calculated at the HF/6-311G level. Electron density plots were created by applying the AIM2000 program; F.Biegler-Koenig, J.Shoenbohm and D.Dayles, *J. Compt. Chem.*, **22**, 545-559 (2001).

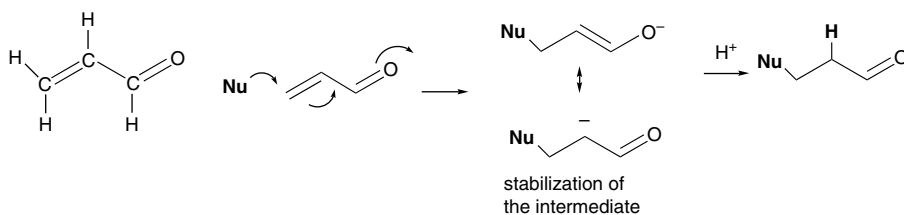
Structure **B** is a better structure than **C** because it places the negative charge on a more electronegative element, oxygen (resonance criteria 3c). Structure **D** accounts for the polarity of the C=O bond. The real molecular structure should then reflect the character of **A** > **B** ~ **D** > **C** ~ **E**. The composite structure can be qualitatively depicted by indicating weak partial bonding between C(1) and C(2) and partial positive charges at C(1) and C(3).



The electronic distributions for butadiene and propenal have been calculated using molecular orbital methods and are shown below.<sup>31</sup> Butadiene shows significantly greater negative charge at the terminal carbons. In propenal there is a large charge distortion at the carbonyl group and a decrease in the electron density at the terminal carbon C(3).

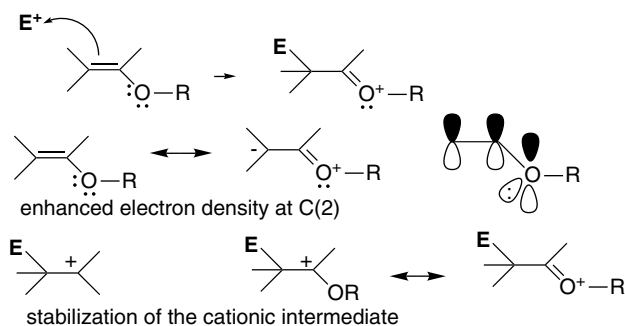


The chemical reactivity of propenal is representative of  $\alpha, \beta$ -unsaturated carbonyl compounds. The conjugation between a carbon-carbon double bond and a carbonyl group leads to characteristic reactivity, which includes reduced reactivity of the carbon-carbon double bond toward electrophiles and enhanced susceptibility to the addition of nucleophilic reagents at the  $\beta$  carbon. The anion formed by addition is a delocalized enolate, with the negative charge shared by oxygen and carbon. The topic of nucleophilic addition to enals and enones is considered further in Section 2.6, Part B.



Methoxyethene (methyl vinyl ether) is the prototype of another important class of compounds, the *vinyl ethers*, which have an alkoxy substituent attached directly to a double bond. Such compounds have important applications in synthesis, and the characteristic reactivity is toward electrophilic attack at the  $\beta$ -carbon.

<sup>31</sup> M. A. McAllister and T. T. Tidwell, *J. Org. Chem.*, **59**, 4506 (1994).



Why does an alkoxy group enhance reactivity and direct the electrophile to the  $\beta$  position? A resonance structure can be drawn that shows an oxygen unshared pair in conjugation with the double bond. More importantly, the same conjugation strongly stabilizes the cation formed by electrophilic attack. This conjugation provides an additional covalent bond in the intermediate and is strongly stabilizing (resonance criterion 3a). Taking the ethyl cation for comparison, there is a stabilization of nearly 30 kcal, according to PM3 MO semiempirical computations (see Section 1.2.2).<sup>32</sup> Stabilization relative to the methyl cation is as follows:

$\text{CH}_3^+$	$\text{CH}_3\text{CH}_2^+$	$\text{CH}_3\text{CH}=\text{O}^+\text{R}$	$\text{CH}_3\text{CH}=\text{N}^+\text{H}_2$
0	29.0 kcal/mol	57.6 kcal/mol	80.2 kcal/mol

Vinyl amines (also called enamines) are even more reactive than vinyl ethers toward electrophiles. The qualitative nature of the conjugation is the same as in vinyl ethers, both for the neutral vinyl amine and for the cationic intermediate. However, nitrogen is an even better electron donor than oxygen, so the stabilizing effect is stronger. The stabilization for the cation is calculated to be around 80 kcal/mol relative to the methyl cation.

These molecules, propenal, methoxyethene, and etheneamine, show how we can apply VB theory and resonance to questions of reactivity. We looked at how structure and conjugation affect *electron density* and *bond formation* in both the reactant and the intermediate. When VB theory indicates that the particular disposition of function groups will change the electron distribution relative to an unsubstituted molecule, we can expect to see those differences reflected in altered reactivity. For propenal, the *electron withdrawal* by the formyl group causes decreased reactivity toward electrophiles and increased reactivity toward nucleophiles. For methoxyethene and ethenamine, the *electron release* of the substituents is reflected by increased reactivity toward electrophiles with strong *selectivity* for the  $\beta$ -carbon.

### 1.1.8. Hyperconjugation

All the examples of resonance cited in the previous section dealt with conjugation through  $\pi$  bonds. VB theory also incorporates the concept of hyperconjugation, which is the idea that there can be electronic interactions between  $\sigma$  and  $\sigma^*$  bonds and between  $\sigma$  and  $\pi^*$  bonds. In alkenes such as propene or 2-methylpropene, the electron-releasing effect of the methyl substituents can be represented by hyperconjugated

<sup>32</sup> A. M. El-Nahas and T. Clark, *J. Org. Chem.*, **60**, 8023 (1995).

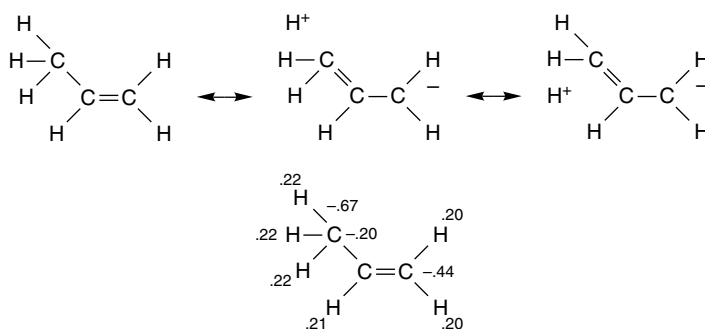
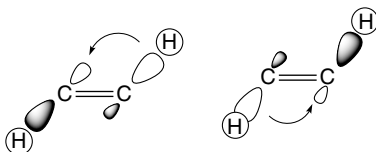


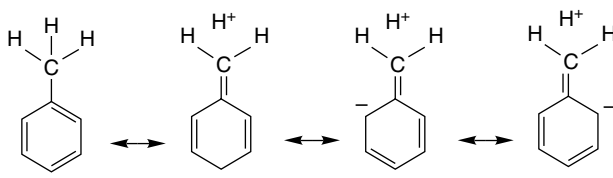
Fig. 1.6. Electron density distribution for propene.

(no-bond) resonance structures. The implication of these resonance structures is that some electron density is transferred from the C–H  $\sigma$  bond to the empty  $\pi^*$  orbital. This is in accord with the calculated electron density distribution for propene shown in Figure 1.6. Carbon-1, which is negatively charged in the resonance structure, has a higher electron density than carbon-2, even though the latter carries the methyl substituent.

There is also hyperconjugation *across* the double bond. Indeed, this interaction may be even stronger because the double bond is shorter than a corresponding single bond, permitting better orbital overlap.<sup>33</sup> Because these resonance structures show equivalent compensating charge transfer, there is no net charge separation, but structural features, such as bond length, and spectroscopic properties are affected.



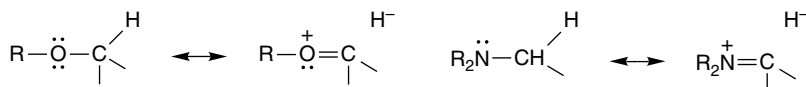
Hyperconjugation also can describe the electron-releasing effect of alkyl groups on aromatic rings.



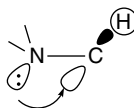
While part of the electron-releasing effect of alkyl groups toward double bonds and aromatic rings can be attributed to the electronegativity difference between  $sp^3$  and  $sp^2$  carbon, the fact that the  $\beta$ -carbon of alkenes and the *ortho* and *para* positions of aromatic rings are selectively affected indicates a resonance component.

<sup>33</sup>. I. V. Alabugin and T. A. Zeidan, *J. Am. Chem. Soc.*, **124**, 3175 (2002).

Heteroatoms with unshared electron pairs can also interact with adjacent  $\sigma^*$  bonds. For example, oxygen and nitrogen substituents substantially weaken an adjacent (geminal) C–H bond.



This interaction is readily apparent in spectroscopic properties of amines. The C–H bond that is antiperiplanar to a nitrogen unshared electron pair is lengthened and weakened.<sup>34</sup> Absorptions for C–H bonds that are *anti* to nitrogen nonbonded pairs are shifted in both IR and NMR spectra. The C–H vibration is at higher frequency (lower bond energy) and the <sup>1</sup>H signal is at higher field (increased electron density), as implied by the resonance structures. There is a *stereoelectronic* component in hyperconjugation. The optimal alignment is for the  $\sigma$  C–H bond that donates electrons to be aligned with the  $\sigma^*$  orbital. The heteroatom bond-weakening effect is at a maximum when the electron pair is antiperiplanar to the C–H bond, since this is the optimal alignment for the overlap of the  $n$  and  $\sigma^*$  orbitals (see Topic 1.2 for further discussion).



Population of  $\sigma^*$  orbital  
weakens anti C–H bond

### 1.1.9. Covalent and van der Waals Radii of Atoms

Covalent and van der Waals radii are other fundamental properties of atoms in molecules that are influenced by nuclear charge and electron distribution. A glance at a molecular model or graphic suggests that most atoms have several different dimensions. There is the distance between each bound atom and also a dimension in any direction in which the atom is not bonded to another atom. The former distance, divided between the two bonded atoms, is called the *covalent radius*. The nonbonded dimension of an atom or group in a molecule is called the *van der Waals radius*. This is the distance at which nonbonded atoms begin to experience mutual repulsion. Just short of this distance, the interatomic forces are weakly attractive and are referred to as *dispersion* or *London* forces and are attributed to mutual *polarization* of atoms.

There are several definitions and values assigned to covalent radii. Pauling created an early scale using bond lengths in simple homonuclear compounds as the starting point. An extended version of this scale is listed as “covalent” in Table 1.5. A related, but more comprehensive, approach is to examine structural data to determine covalent radii that best correlate with observed bond distances. This approach was developed by Slater.<sup>35</sup> An extensive tabulation of bond lengths derived from structural data was published in 1987.<sup>36</sup> These values are labeled “structural” in Table 1.5. A set of

<sup>34</sup> A. Pross, L. Radom, and N. V. Riggs, *J. Am. Chem. Soc.*, **102**, 2253 (1980).

<sup>35</sup> J. C. Slater, *J. Chem. Phys.*, **39**, 3199 (1964); J. C. Slater, *Quantum Theory of Molecules and Solids*, McGraw-Hill, New York, 1965, Vol. 2.

<sup>36</sup> F. H. Allen, O. Kennard, D. G. Watson, L. Brammer, A. G. Opren and R. Taylor, *J. Chem. Soc., Perkin Trans. 2*, Supplement S1–S19 (1987).

Table 1.5. Covalent Radii in Å

	Covalent <sup>a</sup>	Structural <sup>b</sup>	Alcock <sup>c</sup>	Carbon <sup>d</sup>
H	0.37	0.25	0.30	0.327
Li	1.34	1.45		1.219
Be	0.90	1.05	1.06	0.911
B	0.82	0.85	0.83	0.793
C ( <i>sp</i> <sup>3</sup> )	0.77	0.70	0.77	0.766
C ( <i>sp</i> <sup>2</sup> )	0.67			
C ( <i>sp</i> )	0.60			
N	0.75	0.65	0.70	0.699
O	0.73	0.60	0.66	0.658
F	0.71	0.50	0.62	0.633
Al	1.18	1.25	1.18	1.199
Si	1.11	1.10	1.09	1.123
P	1.06	1.00	1.09	1.110
S	1.02	1.00	1.05	1.071
Cl	0.99	1.00	1.02	1.039
Se	1.19	1.15	1.20	1.201
Br	1.14	1.15	1.20	1.201
I	1.33	1.4	1.40	1.397

a. L. E. Sutton, ed., *Tables of Interatomic Distances and Configuration in Molecules and Ions*, Suppl., 1956–1959, Chemical Society Special Publication No. 18, 1965.

b. J. C. Slater, *J. Chem. Phys.*, **39**, 3199 (1964).

c. N. W. Alcock, *Bonding and Structure*, Ellis Horwood, Chichester, 1990.

d. C. H. Suresh and N. Koga, *J. Phys. Chem. A*, **105**, 5940 (2001).

## SECTION 1.1

Description of Molecular  
Structure Using Valence  
Bond Concepts

numbers that may be particularly appropriate for organic compounds was introduced by Alcock, who examined carbon compounds and subtracted the carbon covalent radii to obtain the covalent radii of the bound atoms.<sup>37</sup> This definition was subsequently applied to a larger number of compounds using computational bond length data.<sup>38</sup> These values are listed as “carbon” in Table 1.5. The covalent radii given for *sp*<sup>3</sup>, *sp*<sup>2</sup>, and *sp* carbon are half of the corresponding C–C bond lengths of 1.55, 1.34, and 1.20 Å. Note that the covalent radii shorten somewhat going to the right in the periodic table. This trend reflects the greater nuclear charge and the harder character of the atoms on the right and is caused by the same electronic shielding effect that leads to decreased polarizability, as discussed in Section 1.1.6. Covalent radii, of course, increase going down the periodic table.

Van der Waals radii also require definition. There is no point at which an atom ends; rather the electron density simply decreases to an infinitesimal value as the distance from the nucleus increases. There are several approaches to assigning van der Waals radii. A set of numbers originally suggested by Pauling was refined and extended by Bondi.<sup>39</sup> These values were developed from nonbonded contacts in crystal structures and other experimental measures of minimum intermolecular contact. A new set of data of this type, derived from a much larger structural database, was compiled somewhat more recently.<sup>40</sup> The latter values were derived from a search of nearly 30,000 crystal structures. Table 1.6 gives both sets of radii.

<sup>37</sup>. N. W. Alcock, *Bonding and Structure*, Ellis Horwood, Chichester, 1990.

<sup>38</sup>. C. H. Suresh and N. Koga, *J. Phys. Chem. A*, **105**, 5940 (2001).

<sup>39</sup>. A. Bondi, *J. Phys. Chem.*, **68**, 441 (1964).

<sup>40</sup>. R. S. Rowland and R. Taylor, *J. Phys. Chem.*, **100**, 7384 (1996).

**Table 1.6. Van der Waals Radii in Å**

	Bondi <sup>a</sup>	Structural <sup>b</sup>
H	1.20	1.09
C	1.70	1.75
N	1.55	1.61
O	1.52	1.56
F	1.47	1.44
S	1.80	1.79
Cl	1.75	1.74
Br	1.85	1.85
I	1.98	2.00

a. A. Bondi, *J. Phys. Chem.*, **68**, 441 (1964).

b. R. S. Rowland and R. Taylor, *J. Phys. Chem.*, **100**, 7384 (1996).

Van der Waals dimensions are especially significant in attempts to specify the “size” of molecules, for example, in computational programs that attempt to “fit” molecules into biological receptor sites. In the next chapter, we discuss the effects of van der Waals interactions on molecular shape (conformation). These effects can be quantified by various *force fields* that compute the repulsive energy that molecules experience as *nonbonded repulsion*.

## 1.2. Molecular Orbital Theory and Methods

Molecular orbital (MO) theory is an alternative way of describing molecular structure and electron density. The fundamental premise of MO theory is that the orbitals used to describe the molecule are not necessarily associated with particular bonds between the atoms but can encompass all the atoms of the molecule. The properties of the molecule are described by the sum of the contributions of all orbitals having electrons. There are also empty orbitals, which are usually at positive (i.e., antibonding) energies. The theoretical foundation of MO theory lies in quantum mechanics and, in particular, the Schrödinger equation, which relates the total energy of the molecule to a wave function describing the electronic configuration:

$$E = \int \psi H \psi d\tau \quad \text{when} \quad \int \psi^2 d\tau = 1 \quad (1.11)$$

where  $H$  is a Hamiltonian operator.

The individual MOs are described as linear combinations of the atomic orbitals  $\{\varphi_x\}$  (LCAO):

$$\psi_\rho = c_{1\rho}\varphi_1 + c_{2\rho}\varphi_2 + c_{3\rho}\varphi_3 \dots c_{n\rho}\varphi_n \quad (1.12)$$

The atomic orbitals that are used constitute what is known as the *basis set* and a minimum basis set for compounds of second-row elements is made up of the  $2s$ ,  $2p_x$ ,  $2p_y$ , and  $2p_z$  orbitals of each atom, along with the  $1s$  orbitals of the hydrogen atoms. In MO calculations, an initial molecular structure and a set of approximate MOs are chosen and the molecular energy is calculated. Iterative cycles of calculation of a self-consistent electrical field (SCF) and geometry optimization are then repeated until a

minimization of total energy is reached. It is not possible to carry out these calculations exactly, so various approximations are made and/or parameters introduced. Particular sets of approximations and parameters characterize the various MO methods. We discuss some of these methods shortly.

The output of an MO calculation includes atomic positions and the fractional contribution of each basis set orbital to each MO, that is, the values of  $c_{kp}$ . The energy of each MO is calculated, and the total binding energy of the molecule is the sum of the binding energies of the filled MOs:

$$E = \sum f_{ii} + h_{ii} \quad (1.13)$$

The electronic charge at any particular atom can be calculated by the equation

$$q_r = \sum n_j c_{jr}^2 \quad (1.14)$$

where  $c_{jr}$  is the contribution of the atom to each occupied orbital. Thus, MO calculations give us information about molecular structure (from the nuclear positions), energy (from the total binding energy), and electron density (from the atomic populations).

The extent of approximation and parameterization varies with the different MO methods. As computer power has expanded, it has become possible to do MO calculations on larger molecules and with larger basis sets and fewer approximations and parameters. The accuracy with which calculations can predict structure, energy, and electron density has improved as better means of dealing with the various approximations have been developed. In the succeeding sections, we discuss three kinds of MO calculations: (1) the Hückel MO method, (2) semiempirical methods, and (3) ab initio methods, and give examples of the application of each of these approaches.

### 1.2.1. The Hückel MO Method

The Hückel MO (HMO) method was very important in introducing the concepts of MO theory into organic chemistry. The range of molecules that the method can treat is quite limited and the approximations are severe, but it does provide insight into a number of issues concerning structure and reactivity. Furthermore, the mathematical formulation is simple enough that it can be used to illustrate the nature of the calculations. The HMO method is restricted to planar conjugated systems such as polyenes and aromatic compounds. The primary simplification is that only the  $2p_z$  orbitals are included in the construction of the HMOs. The justification is that many of the properties of conjugated molecules are governed by the  $\pi$  orbitals that arise from the  $p_z$  atomic orbitals. A further approximation of the HMO calculations is that only adjacent  $p_z$  orbitals interact. This allows construction of mathematical formulations for the  $\pi$  MOs for such systems as linear and branched-chain polyenes, cyclic polyenes, and fused-ring polyenes. For conjugated linear polyenes such as 1,3,5-hexatriene, the energy levels are given by the equation

$$E = \alpha + m_j \beta \quad (1.15)$$

where  $m_j = 2 \cos(j\pi/n + 1)$  for  $j = 1, 2, 3, \dots, n$ , with  $n$  being the number of carbon atoms in the conjugated polyene.

The quantity  $\alpha$  is called the *Coulomb integral*; it represents the binding of an electron in a  $2p_z$  orbital and is considered to be constant for all  $sp^2$  carbon atoms. The

quantity  $\beta$  is called the *resonance integral* and represents the energy of an electron distributed over two or more overlapping  $2p_z$  orbitals. For linear polyenes, this equation generates a set of HMOs distributed symmetrically relative to the energy  $\alpha$  associated with an isolated  $2p_z$  orbital. The contribution of each atomic orbital to each HMO is described by a coefficient:

$$C_{rj} = \left( \frac{2}{n+1} \right)^{1/2} \sin \left( \frac{rj\pi}{n+1} \right) \quad (1.16)$$

Figure 1.7 gives the resulting HMOs for  $n = 2$  to  $n = 7$ . Table 1.7 gives the coefficients for the HMOs of 1,3,5-hexatriene. From these coefficients, the overall shape of the orbitals can be deduced and, in particular, the location of nodes is determined. Nodes represent an antibonding contribution to the total energy of a particular orbital. Orbitals with more nodes than bonding interactions are *antibonding* and are above the reference  $\alpha$  energy level. The spacing between orbitals decreases with the length of the polyene chain, and as a result, the gap between the HOMO and LUMO decreases as the conjugated chain lengthens.

These coefficients give rise to the pictorial representation of the 1,3,5-hexatriene molecular orbitals shown in Figure 1.8. Note in particular the increase in the energy of the orbital as the number of nodes goes from 0 to 5. The magnitude of each atomic coefficient indicates the relative contribution at that atom to the MO. In  $\psi_1$ , for example, the central atoms C(3) and C(4) have larger coefficients than the terminal atoms C(1) and C(6), whereas for  $\psi_3$  the terminal carbons have the largest coefficients.

The equation for the HMOs of completely conjugated monocyclic polyenes is

$$E = \alpha + m_j\beta \quad (1.17)$$

where  $m_j = 2 \cos(2j\pi/n)$  for  $j = 0, \pm 1, \pm 2, \dots, (n-1)/2$  for  $n = \text{odd}$  and  $(n/2)$  for  $n = \text{even}$ . This gives rise to the HMO diagrams shown in Figure 1.9 for cyclic polyenes with  $n = 3$  to  $n = 7$ . Table 1.8 gives the atomic coefficients for benzene,  $n = 6$ , and Figure 1.10 gives pictorial representations of the MOs.

There is an easy way to remember the pattern of MOs for monocyclic systems. Figure 1.11 shows Frost's circle.<sup>41</sup> A polygon corresponding to the ring is inscribed

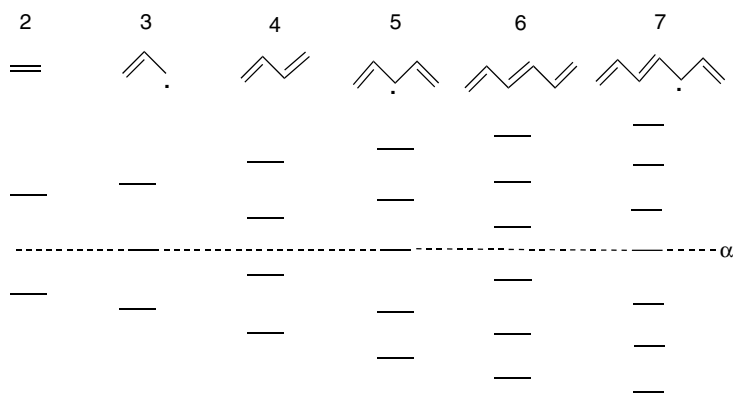


Fig. 1.7. HMO orbital diagram for polyenes  $n = 2$  to  $n = 7$ .

<sup>41</sup> A. A. Frost and B. Musulin, *J. Chem. Phys.*, **21**, 572 (1953).

**Table 1.7. Energy Levels and Atomic Coefficients for HMOs of 1,3,5-Hexatriene**

$\pi$ orbital $m_j$	$c_1$	$c_2$	$c_3$	$c_4$	$c_5$	$c_6$
$\Psi_1$	1.802	0.2319	0.4179	0.5211	0.5211	0.4179
$\Psi_2$	1.247	0.4179	0.5211	0.2319	-0.2319	-0.5211
$\Psi_3$	0.445	0.5211	0.2319	-0.4179	-0.4179	0.2319
$\Psi_4$	-0.445	0.5211	-0.2319	-0.4179	0.4179	0.2319
$\Psi_5$	-1.247	0.4179	-0.5211	0.2319	0.2319	-0.5211
$\Psi_6$	-1.802	0.2319	-0.4179	0.5211	-0.5211	0.4179

SECTION 1.2

*Molecular Orbital  
Theory and Methods*

in a circle with one point of the polygon at the bottom. The MO pattern corresponds to each point of contact of the polygon and circle. If the circle is given a radius of  $2\beta$ , the point of contact gives the coefficient of  $\beta$  in the expression for the energy of the MO. Compilations of HMO energy levels and atomic coefficients are available for a number of conjugated systems.<sup>42</sup>

What do we learn about molecules such as 1,3,5-hexatriene and benzene from the HMO description of the  $\pi$  orbitals?

1. *The frontier MOs are identified and described.* The frontier orbitals are the *highest occupied MO (HOMO)* and the *lowest unoccupied MO (LUMO)*. These orbitals are intimately involved in chemical reactivity, because they are the most available to electrophiles and nucleophiles, respectively. From the atomic coefficients, which can be represented graphically, we see the symmetry and relative atomic contribution

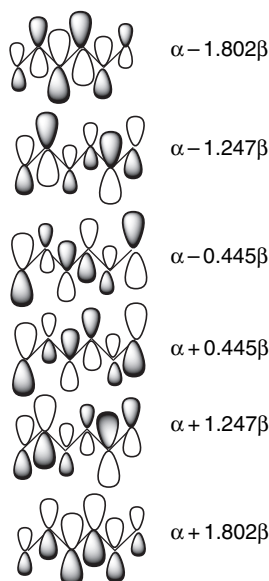
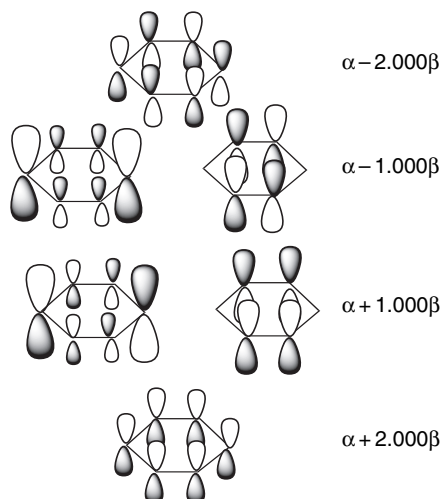


Fig. 1.8.  $\pi$  Molecular orbitals for 1,3,5-hexatriene.

<sup>42</sup> E. Heilbronner and P. A. Straub, *Hückel Molecular Orbitals*, Springer Verlag, New York, 1966; C. A. Coulson, A. Streitwieser, Jr., and J. I. Brauman, *Dictionary of  $\pi$ -Electron Calculations*, W H. Freeman, San Francisco, 1965.



Fig. 1.10.  $\pi$  Molecular orbitals for benzene.

not support this result (see Section 3.1.1). Relative to three ethene double bonds, 1,3,5-hexatriene is stabilized by about 8 kcal,<sup>43</sup> whereas for benzene the stabilization is around 30 kcal/mol. Furthermore, the HMO DE for polycyclic aromatic hydrocarbons such as anthracene and phenanthrene continues to increase with molecular size. This is contrary to chemical reactivity and thermodynamic data, which suggest that on a per atom basis, benzene represents the optimum in stabilization. Thus, the absolute value of the DE does not seem to be a reliable indicator of stabilization.

On the other hand, the *difference in stabilization* between acyclic and cyclic polyenes turns out to be a very useful indicator of the extra stabilization associated with cyclic systems. This extra stabilization or *aromaticity* is well represented by the difference in the DE of the cyclic compound and the polyene having the same number of conjugated double bonds.<sup>44</sup> For 1,3,5-hexatriene and benzene, this difference is  $1.012\beta$ . For comparison of molecules of different sizes, the total stabilization energy is divided by the number of  $\pi$  electrons.<sup>45</sup> We will see in Chapter 9 that this value gives a very useful estimate of the stability of cyclic conjugated systems.

For monocyclic conjugated polyenes, high stabilization is found for systems with  $(4n + 2)$   $\pi$  electrons but not for systems with  $(4n)$   $\pi$  electrons. The relationship is formulated as *Hückel's rule*, which states that completely conjugated planar hydrocarbons are strongly stabilized (aromatic) when they have  $(4n + 2)$   $\pi$  electrons. Benzene (6  $\pi$  electrons) is aromatic but cyclobutadiene (4  $\pi$  electrons) and cyclooctatetraene (8  $\pi$  electrons) are not.

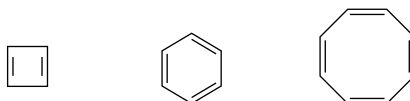


Fig. 1.11. Frost's circle mnemonic for HMOs of cyclic polyenes.

<sup>43</sup> W. Fang and D. W. Rogers, *J. Org. Chem.*, **57**, 2294 (1992).

<sup>44</sup> M. J. S. Dewar and C. de Llano, *J. Am. Chem. Soc.*, **91**, 789 (1969).

<sup>45</sup> B. A. Hess, Jr., and L. J. Schaad, Jr., *J. Am. Chem. Soc.*, **93**, 305, 2413 (1971).



Hückel's rule also pertains to charged cyclic conjugated systems. The cyclopropenyl ( $2\pi$  electrons), cyclopentadienyl anion ( $6\pi$  electrons), and cycloheptatrienyl (tropylium) cation ( $6\pi$  electrons) are examples of stabilized systems. We say much more about the relationship between MO configuration and aromaticity in Chapter 9.



### 1.2.2. Semiempirical MO Methods

Beginning in the 1960s, various more elaborate MO methods were developed and applied to organic molecules. Among those that are historically significant are extended Hückel theory (EHT),<sup>46</sup> complete neglect of differential overlap (CNDO),<sup>47</sup> and modified neglect of differential overlap (MNDO).<sup>48</sup> In contrast to HMO theory, these methods include all the valence shell electrons in the calculation. Each of these methods incorporates various approximations and parameters. The parameters are assigned values based on maximizing the agreement for a set of small molecules. The CNDO findings were calibrated with higher-level computational results, while MNDO was calibrated to experimental stability data. These parameters are then employed for computations on more complex molecules. The output provides molecular geometry, atomic coefficients, and orbital energies. Each method had both strengths and limitations with respect to the range of molecules and properties that could be adequately described. At the present time, the leading semiempirical methods, called AM1<sup>49</sup> and PM3,<sup>50</sup> are incorporated into various MO computational programs and are widely employed in the interpretation of structure and reactivity. In Section 1.2.6, we illustrate some of the problems that can be addressed using these methods.

### 1.2.3. Ab Initio Methods

Ab initio computations are based on iterative calculations of a self-consistent electronic field (SCF), as is the case in the semiempirical methods just described, but do not use experimental data to calibrate quantities that appear in the calculations. These methods are much more computationally demanding than semiempirical methods, but their reliability and range of applicability has improved greatly as more powerful computers have permitted more sophisticated approaches and have enabled handling of more complex molecules. The computations are carried out by successive series of calculations minimizing the energy of the electron distribution and the molecular geometry. The cycle of the calculations is repeated until there is no further improvement (convergence).

<sup>46</sup> R. Hoffmann, *J. Chem. Phys.*, **39**, 1397 (1963).

<sup>47</sup> J. A. Pople and G. A. Segal, *J. Chem. Phys.*, **44**, 3289 (1966).

<sup>48</sup> M. J. S. Dewar and W. Thiel, *J. Am. Chem. Soc.*, **99**, 4907 (1977).

<sup>49</sup> M. J. S. Dewar, E. G. Zoebisch, E. F. Healy, and J. P. Stewart, *J. Am. Chem. Soc.*, **109**, 3902 (1985).

<sup>50</sup> J. P. Stewart, *J. Comput. Chem.*, **10**, 209, 221 (1989).

Specific ab initio methods are characterized by the form of the wave function and the nature of the basis set functions that are used. The most common form of the wave function is the single determinant of molecular orbitals expressed as a linear combination of basis functions, as is the case with semiempirical calculations. We describe alternatives later in this section. Early calculations were often done with Slater functions, designated STO for Slater-type orbitals. Currently most computations are done with Gaussian basis functions, designated by GTOs. A fairly accurate representation of a single STO requires three or more GTOs. This is illustrated in Figure 1.12, which compares the forms for one, two, and three GTOs. At the present time most basis sets use a six-Gaussian representation, usually designated 6G. The weighting coefficients for the  $N$  components of a STO-NG representation are not changed in the course of a SCF calculation.

A basis set is a collection of basis functions. For carbon, nitrogen, and oxygen compounds, a minimum basis set is composed of a  $1s$  function for each hydrogen and  $1s$ ,  $2s$ , and three  $2p$  functions for each of the second-row atoms. More extensive and flexible sets of basis functions are in wide use. These basis sets may have two or more components in the outer shell, which are called *split-valence* sets. Basis sets may include  $p$  functions on hydrogen and/or  $d$  and  $f$  functions on the other atoms. These are called *polarization functions*. The basis sets may also include *diffuse functions*, which extend farther from the nuclear center. Split-valence bases allow description of tighter or looser electron distributions on atoms in differing environments. Polarization permits changes in orbital shapes and shifts in the center of charge. Diffuse functions allow improved description of the outer reaches of the electron distribution.

People developed a system of abbreviations that indicates the composition of the basis sets used in ab initio calculations. The series of digits that follows the designation 3G or 6G indicates the number of Gaussian functions used for each successive shell. The combination of Gaussian functions serves to improve the relationship between electron distribution and distance from the nucleus. Polarization functions incorporate additional orbitals, such as  $p$  for hydrogen and  $d$  and/or  $f$  for second-row atoms. This permits changes in orbital shapes and separation of the centers of charge. The inclusion of  $d$  and  $f$  orbitals is indicated by the asterisk (\*). One asterisk signifies  $d$  orbitals on second-row elements; two asterisks means that  $p$  orbitals on hydrogen are also included. If diffuse orbitals are used they are designated by a plus sign (+), and the

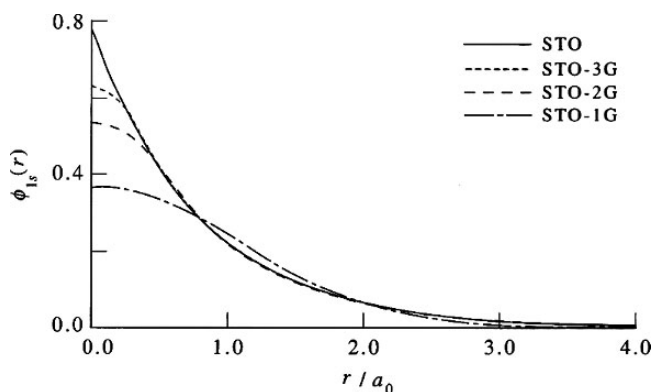


Fig. 1.12. Comparison of electron distribution for STO, G, 2G, and 3G expressions of orbitals.

designation double plus (++) means that diffuse orbitals are present on both hydrogen and the second-row elements. Split-valence sets are indicated by a sequence defining the number of Gaussians in each component. Split-valence orbitals are designated by primes, so that a system of three Gaussian orbitals would be designated by single, double, and triple primes (' , '' , and '''). For example 6-311 + G(*d*, *p*) conveys the following information:

- 6: Core basis functions are represented as a single STO-6G expression.
- 311: The valence set is described by three sets of STO-NG functions; each set includes an *s* orbital and three *p* orbitals. In the 6-311+G(*d*) basis there are three such sets. One is composed of three Gaussians (STO-3G expression of one *s*-type and three *p*-type forms) and the other two are represented by a single Gaussian (STO-1G) representation of the *s-p* manifold. The collection of components of the split-valence representation can be designated by a series of primes.
- +: A STO-1G diffuse *s-p* manifold is included in the basis set for each nonhydrogen atom; ++ implies that diffuse functions are also included for the hydrogen atoms.
- *p*: A set of *p* functions placed on each nonhydrogen atom and specifies the composition.
- *d*: A set of STO-1G *d*-functions is placed on each nonhydrogen atom for which *d* functions are not used in the ground state configuration. If *d* functions are so used, polarization is effected by a manifold of *f* functions.

The composition of several basis sets is given in Table 1.9.

An important distinguishing feature among *ab initio* calculations is the extent to which they deal with *electron correlation*. Correlation is defined as the difference between the exact energy of a molecular system and the best energy obtainable by a SCF calculation in which the wave function is represented by a single determinant. In single-determinant calculations, we consider that each electron experiences an averaged electrostatic repulsion defined by the total charge distribution, a *mean field* approximation. These are called *Hartree-Fock* (HF) calculations. Correlation corrections arise from fluctuations of the charge distribution. Correlations energies can be estimated by including effects of admixtures of excited states into the Hartree-Fock determinant.

**Table 1.9. Abbreviations Describing Gaussian Basis Sets<sup>a</sup>**

Designation	H	C	Functions on second-row atoms
3-21G	2	9	1 <i>s</i> ' ; 2 <i>s</i> ' , 3 2 <i>p</i> ' ; 2 <i>s</i> ''' , 3 2 <i>p</i> ''
3-21+G	2	13	1 <i>s</i> ' ; 2 <i>s</i> ' , 3 2 <i>p</i> ' ; 2 <i>s</i> '' , 3 2 <i>p</i> '' ; 2 <i>s</i> + , 3 2 <i>p</i> +
6-31G* or 6-31G( <i>d</i> )	2	15	1 <i>s</i> ; 2 <i>s</i> ' , 3 2 <i>p</i> ' ; 2 <i>s</i> '' , 3 2 <i>p</i> '' ; 5 3 <i>d</i>
6-31G** or 6-31( <i>d</i> , <i>p</i> )	5	18	1 <i>s</i> ; 2 <i>s</i> ' , 3 2 <i>p</i> ' ; 2 <i>s</i> '' , 3 2 <i>p</i> '' ; 2 <i>s</i> ''' ; 3 2 <i>p</i> ''' ; 5 3 <i>d</i>
6-31+G* or 6-31+( <i>d</i> )	3	19	1 <i>s</i> ; 2 <i>s</i> ' , 3 2 <i>p</i> ' ; 2 <i>s</i> '' , 3 2 <i>p</i> '' ; 5 3 <i>d</i> ; 2 <i>s</i> + , 3 2 <i>p</i> +
6-311G** or 6-311( <i>d</i> , <i>p</i> )	6	18	1 <i>s</i> ; 2 <i>s</i> ' , 3 2 <i>p</i> ' ; 2 <i>s</i> '' , 3 2 <i>p</i> '' ; 2 <i>s</i> ''' ; 3 2 <i>p</i> ''' ; 5 3 <i>d</i>
6-311G( <i>d</i> , <i>f</i> , <i>p</i> )	6	25	1 <i>s</i> ; 2 <i>s</i> ' , 3 2 <i>p</i> ' ; 2 <i>s</i> '' , 3 2 <i>p</i> '' ; 2 <i>s</i> ''' ; 3 2 <i>p</i> ''' ; 5 3 <i>d</i> ; 7 4 <i>f</i>
6-311G(3 <i>d</i> , <i>f</i> ,3 <i>p</i> <i>d</i> )	17	35	1 <i>s</i> ; 2 <i>s</i> ' , 3 2 <i>p</i> ' ; 2 <i>s</i> '' , 3 2 <i>p</i> '' ; 2 <i>s</i> ''' 3 <i>p</i> ''' ; 5 3 <i>d</i> , 7 4 <i>f</i>

a. From E. Lewars, *Computational Chemistry*, Kluwer Academic Publishers, Boston, 2003, pp. 225–229.

This may be accomplished by perturbation methods such as *Moeller-Plesset* (MP)<sup>51</sup> or by including excited state determinants in the wave equation as in *configurational interaction* (CISD)<sup>52</sup> calculations. The excited states have electrons in different orbitals and reduced electron-electron repulsions.

The output of *ab initio* calculations is analogous to that from HMO and semiempirical methods. The atomic coordinates at the minimum energy are computed. The individual MOs are assigned energies and atomic orbital contributions. The total molecular energy is calculated by summation over the occupied orbitals. Several schemes for apportioning charge among atoms are also available in these programs. These methods are discussed in Section 1.4. In Section 1.2.6, we illustrate some of the applications of *ab initio* calculations. In the material in the remainder of the book, we frequently include the results of computational studies, generally indicating the type of calculation that is used. The convention is to list the treatment of correlation, e.g., HF, MP2, CISDT, followed by the basis set used. Many studies do calculations at several levels. For example, geometry can be minimized with one basis set and then energy computed with a more demanding correlation calculation or basis set. This is indicated by giving the basis set used for the energy calculation followed by parallel lines (*//*) and the basis set used for the geometry calculation. In general, we give the designation of the computation used for the energy calculation. The information in Scheme 1.3 provides basic information about the nature of the calculation and describes the characteristics of some of the most frequently used methods.

#### 1.2.4. Pictorial Representation of MOs for Molecules

The VB description of molecules provides very useful generalizations about molecular structure and properties. Approximate molecular geometry arises from hybridization concepts, and qualitative information about electron distribution can be deduced by applying the concepts of polarity and resonance. In this section we consider how we can arrive at similar impressions about molecules by using the underlying principles of MO theory in a qualitative way. To begin, it is important to remember some fundamental relationships of quantum mechanics that are incorporated into MO theory. The *Aufbau principle* and the *Pauli exclusion principle*, tell us that electrons occupy the MOs of lowest energy and that any MO can have only two electrons, one of each spin. The MOs must also conform to molecular symmetry. Any element of symmetry that is present in a molecule must also be present in *all the corresponding MOs*. Each MO must be either *symmetric* or *antisymmetric* with respect to each element of molecular symmetry. To illustrate, the  $\pi$  MOs of *s-cis*-1,3-butadiene in Figure 1.13 can be classified with respect to the plane of symmetry that dissects the molecule between C(2) and C(3). The symmetric orbitals are identical (exact reflections) with respect to this plane, whereas the antisymmetric orbitals are identical in shape but

<sup>51</sup> W. J. Hehre, L. Radom, P. v. R. Schleyer, and J. A. Pople, *Ab Initio Molecular Orbital Theory*, Wiley-Interscience, New York, 1986, pp. 38–40; A. Bondi, *J. Phys. Chem.*, **68**, 441 (1964); R. S. Rowland and R. Taylor, *J. Phys. Chem.*, **100**, 7384 (1996); M. J. S. Dewar and C. de Llano, *J. Am. Chem. Soc.*, **91**, 789 (1969); R. Hoffmann, *J. Chem. Phys.*, **39**, 1397 (1963); J. A. Pople and G. A. Segal, *J. Chem. Phys.*, **44**, 3289 (1966); M. J. S. Dewar and W. Thiel, *J. Am. Chem. Soc.*, **99**, 4907 (1977); M. J. S. Dewar, E. G. Zoebisch, E. F. Healy, and J. P. Stewart, *J. Am. Chem. Soc.*, **109**, 3902 (1985); J. P. Stewart, *J. Comput. Chem.*, **10**, 209, 221 (1989); ; J. A. Pople, M. Head-Gordon, and K. Raghavachari, *J. Phys. Chem.*, **87**, 5968 (1987).

<sup>52</sup> J. A. Pople, M. Head-Gordon, and K. Raghavachari, *J. Phys. Chem.*, **87**, 5968 (1987).

Scheme 1.3. Characteristics of *ab Initio* MO Methods

**STO-3G.** STO-3G is a minimum basis set consisting of 1s orbitals for hydrogen and 2s and 2p orbitals for second-row elements, described by Gaussian functions.

**Split-Valence Gaussian Orbitals.** (3-21G, 4-31G, 6-31G) Split-valence orbitals are described by two or more Gaussian functions. Also in this category are Dunning-Huzinaga orbitals.

**Polarized Orbitals.** These basis sets add further orbitals, such as *p* for hydrogen and *d* for carbon that allow for change of shape and separation of centers of charge. Numbers in front of the *d*, *f* designations indicate inclusion of multiple orbitals of each type. For example, 6-311(2*df*, 2*pd*) orbitals have two *d* functions and one *f* function on second-row elements and two *p* functions and one *d* function on hydrogen.

**Diffuse Basis Sets.** (6-31+G\*, 6-31++G\*) Diffuse basis sets include expanded orbitals that are used for molecules with relatively loosely bound electrons, such as anions and excited states. 6-31+G\* have diffuse *p* orbitals on second-row elements. 6-31++G\* orbitals have diffuse orbitals on both second-row elements and hydrogen.

**Correlation Calculations**

**MP2, MP4.** MP (Moeller-Plesset) calculations treat correlation by a perturbation method based on adding excited state character. MP2 includes a contribution from the interaction of doubly excited states with the ground state. MP4 includes, single, double, and quadruple excited states in the calculation.

**CISD.** CISD (configuration interaction, single double) are LCAO expressions that treat configuration interactions by including one or two excited states. The designations CISDT and CISDTQ expand this to three and four excitations, respectively.

**CAS-SCF.** CAS-SCF (complete active space self-consistent field) calculations select the chemically most significant electrons and orbitals and apply configuration interactions to this set.

**Composite Calculations**

**G1, G2, G2(MP2), and G3** are composite computations using the 6-311G\*\* basis set and MP2/6-31G\* geometry optimization. The protocols are designed for efficient calculation of energies and electronic properties. The G2 method calculates electron correlation at the MP4 level, while G2(MP2) correlation calculations are at the MP2 level. A scaling factor derived from a series of calibration molecules is applied to energies.

**CBS.** CBS protocols include CBS-4, CBS-Q, and CBS-APNO. The objectives are the same as for G1 and G2. The final energy calculation (for CBS-Q) is at the MP4(SQD)/6-31G(*d*, *p*) level, with a correction for higher-order correlation. A scaling factor is applied for energy calculations.

**References to Scheme 1.3**

STO-3G: W. J. Hehre, R. F. Stewart, and J. A. Pople, *J. Phys. Chem.*, **51**, 2657 (1969).

3-21G, 4-21G, and 6-31G: R. Ditchfield, W. J. Hehre, and J. A. Pople, *J. Chem. Phys.*, **54**, 724 (1971); W. J. Hehre and W. A. Lathan, *J. Chem. Phys.*, **56**, 5255 (1972); W. J. Hehre, R. Ditchfield, and J. A. Pople, *J. Chem. Phys.*, **56**, 2257 (1972); M. M. Francl, W. J. Pietro, W. J. Hehre, J. S. Binkley, M. S. Gordon, D. J. DeFrees, and J. A. Pople, *J. Chem. Phys.*, **77**, 3654 (1982).

Dunning-Huzinaga Orbitals: T. H. Dunning, Jr., and P. J. Hay, in *Modern Theoretical Chemistry*, Vol. 3, H. F. Schaefer, ed., Plenum Publishing, New York, 1977, pp 1–27.

MP: J. S. Binkley and J. A. Pople, *Int. J. Quantum Chem.*, **9**, 229 (1975).

G1, G2, G3: J. A. Pople, M. Head-Gordon, D. J. Fox, K. Raghavachari, and L. A. Curtiss, *J. Chem. Phys.*, **90**, 5622 (1989); L. A. Curtiss, C. Jones, G. W. Trucks, K. Raghavachari, and J. A. Pople, *J. Chem. Phys.*, **93**, 2537 (1990); L. A. Curtiss, K. Raghavachari, G. W. Trucks, and J. A. Pople, *J. Chem. Phys.*, **94**, 7221 (1991); L. A. Curtiss, K. Raghavachari, and J. A. Pople, *J. Chem. Phys.*, **98**, 1293 (1993); M. Head-Gordon, *J. Chem. Phys.*, **100**, 13213 (1996); L. A. Curtiss and K. Raghavachari, *Theor. Chem. Acc.*, **108**, 61 (2002).

CBS-Q: J. W. Ochterski, G. A. Petersson, and J. A. Montgomery, *J. Chem. Phys.*, **104**, 2598 (1996); G. A. Petersson, *Computational Thermochemistry*, ACS Symposium Series, Vol. 677, pp 237–266 (1998).

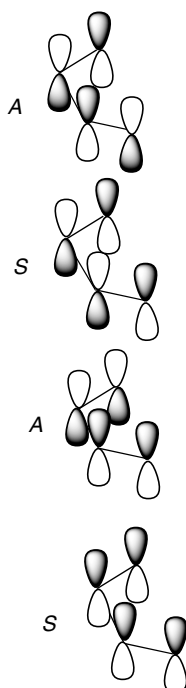


Fig. 1.13. Symmetry characteristics of butadiene HMOs with respect to a plane bisecting the molecule in the *s-cis* conformation perpendicular to the plane of the molecule.

*change phase at all locations.* Although these formal symmetry restrictions can ignore nonconjugated substituents, the symmetry pattern of the MOs must conform to the symmetry of the conjugated system.

What do the MOs of other small molecules look like? Let us consider methane. A convenient frame of reference is a cube with the four hydrogens at alternate corners and the carbon at the center. This orientation of the molecule reveals that methane possesses three twofold symmetry axes, one each along the  $x$ ,  $y$ , and  $z$  axes. There are also planes of symmetry diagonally across the cube. Because of this molecular symmetry, the MOs of methane must possess symmetry with respect of these same axes. There are two possibilities: the orbital may be unchanged by  $180^\circ$  rotation about the axis (symmetric), or it may be transformed into an orbital of identical shape but opposite phase by the symmetry operation (antisymmetric). The minimum basis set orbitals are the hydrogen  $1s$  and the carbon  $2s$ ,  $2p_x$ ,  $2p_y$ , and  $2p_z$  atomic orbitals. The combinations that are either symmetric or antisymmetric with respect to the diagonal planes of symmetry are shown in Figure 1.14. These give rise to four bonding MOs. One has no nodes and bonds between all the atoms. The other three consist of two boomerang-shaped lobes, with a node at carbon corresponding to the node in the basis set  $p$  orbital.

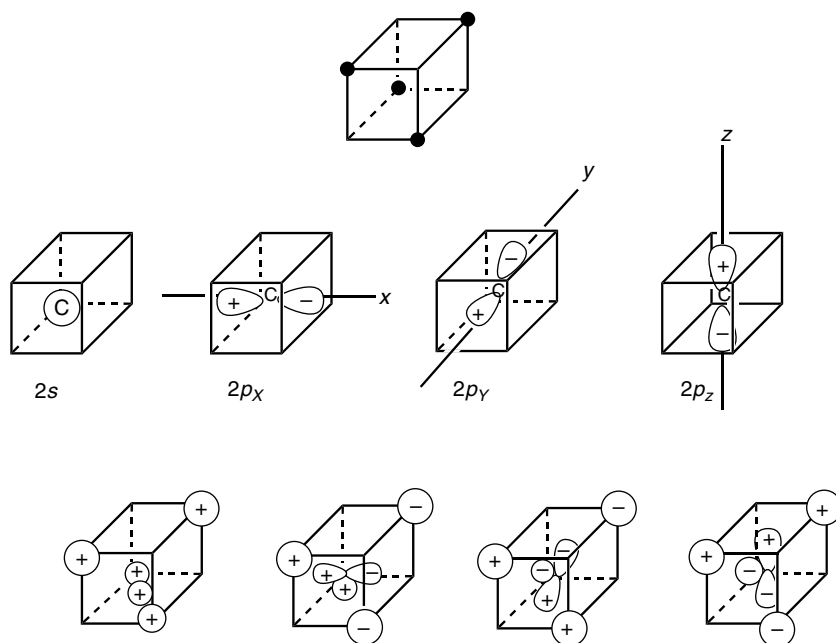


Fig. 1.14. Combinations of atomic orbitals leading to the methane molecular orbitals.

The carbon  $2s$  orbital is symmetric with respect to each axis but the three  $2p$  orbitals are each antisymmetric to two of the axes and symmetric with respect to one. The combinations that give rise to molecular orbitals that meet these symmetry requirements are shown in the lower part of Figure 1.14. The bonding combination of the carbon  $2s$  orbital with the four  $1s$  hydrogen orbitals leads to a molecular orbital that encompasses the entire molecule and has no nodes. Each of the MOs derived from a carbon  $2p$  orbital has a node at carbon. The three combinations are equivalent, but higher in energy than the MO with no nodes. The four antibonding orbitals arise from similar combinations, but with the carbon and hydrogen orbitals having opposite phases in the region of overlap. Thus the molecular orbital diagram arising from these considerations shows one bonding MO with no nodes and three degenerate (having the same energy) MOs with one node. The diagram is given in Figure 1.15.

There is experimental support for this MO pattern. The ESCA spectrum of methane is illustrated in Figure 1.16. It shows two peaks for valence electrons at 12.7 and 23.0 eV, in addition to the band for the core electron at 291.0 eV.<sup>53</sup> Each band

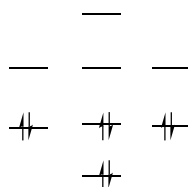


Fig. 1.15. Molecular orbital diagram for methane.

<sup>53</sup> U. Gelius, in *Electron Spectroscopy*, D. A. Shirley, ed., American Elsevier, New York, 1972, pp. 311–344.

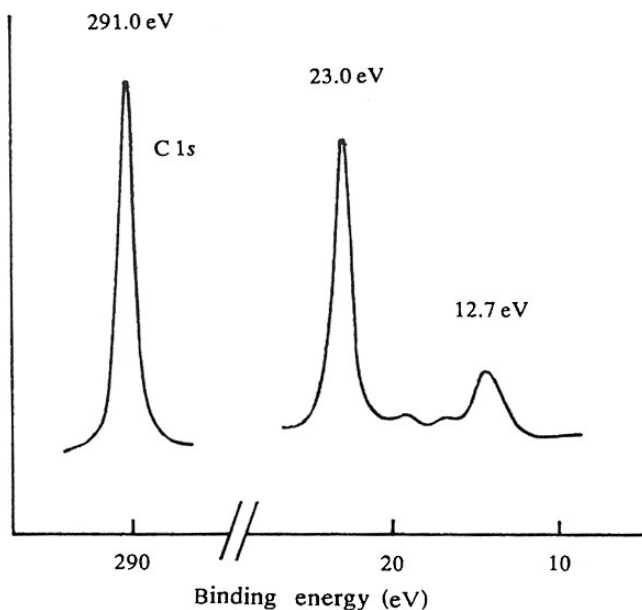
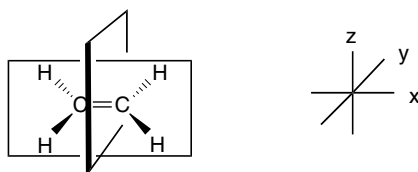


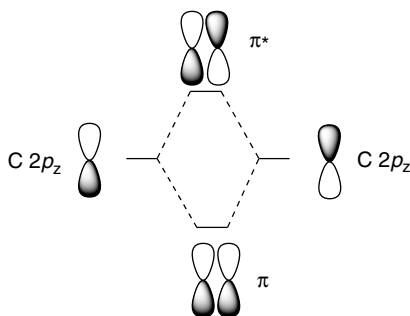
Fig. 1.16. ESCA spectrum of methane.

corresponds to the binding energy for the removal of a particular electron, not the successive removal of one, two, and three electrons. The presence of two bands in the valence region is consistent with the existence of two different molecular orbitals in methane.

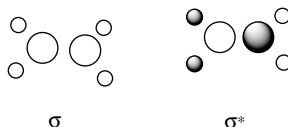
The construction of the MOs of ethene is similar to the process used for methane, but the total number of atomic orbitals is greater: twelve instead of eight. We must first define the symmetry of ethene, which is known from experiment to be a planar molecule.



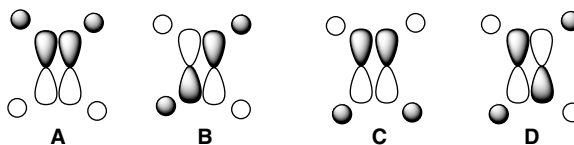
This geometry possesses three important elements of symmetry, the molecular plane and two planes that bisect the molecule. All MOs must be either symmetric or antisymmetric with respect to each of these symmetry planes. With the axes defined as in the diagram above, the orbitals arising from carbon  $2p_z$  have a node in the molecular plane. These are the  $\pi$  and  $\pi^*$  orbitals. Because the two  $p_z$  atomic orbitals are perpendicular (orthogonal) to all the other atomic orbitals and the other orbitals lie in the nodal plane of the  $p_z$  orbitals, there is no interaction of the  $p_z$  with the other C and H atomic orbitals. The  $\pi$  orbital is symmetric with respect to both the  $x$ - $z$  plane and the  $y$ - $z$  plane. It is antisymmetric with respect to the molecular ( $x$ - $y$ ) plane. On the other hand,  $\pi^*$  is antisymmetric with respect to the  $y$ - $z$  plane.



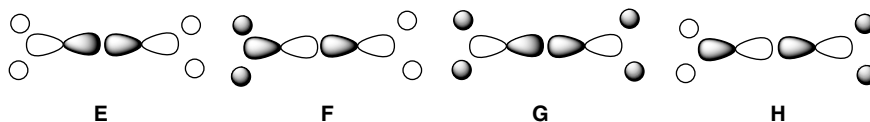
The orbitals that remain are the four hydrogen  $1s$ , two carbon  $1s$ , and four carbon  $2p$  orbitals. All lie in the molecular plane. The combinations using the carbon  $2s$  and hydrogen  $1s$  orbitals can take only two forms that meet the molecular symmetry requirements. One,  $\sigma$ , is bonding between all atoms, whereas  $\sigma^*$  is antibonding between all nearest-neighbor atoms. No other combination corresponds to the symmetry of the ethene molecule.



Let us next consider the interaction of  $2p_y$  with the four hydrogen  $1s$  orbitals. There are four possibilities that conform to the molecular symmetry.



Orbital **A** is bonding between all nearest-neighbor atoms, whereas **B** is bonding within the  $\text{CH}_2$  units but antibonding with respect to the two carbons. The orbital labeled **C** is C–C bonding but antibonding with respect to the hydrogens. Finally, orbital **D** is antibonding with respect to all nearest-neighbor atoms. Similarly, the  $2p_x$  orbitals must be considered. Again, four possible combinations arise. Note that the nature of the overlap of the  $2p_x$  orbitals is different from the  $2p_y$  case, so the two sets of MOs have different energies.



The final problem in construction of a qualitative MO diagram for ethene is the relative placement of the orbitals. There are some useful guidelines. The relationship between the relative energy and the number of nodes has already been mentioned. The more nodes, the higher the energy of the orbital. Since  $\pi$ -type interactions are normally weaker than  $\sigma$ -type, we expect the separation between  $\sigma$  and  $\sigma^*$  to be greater than between  $\pi$  and  $\pi^*$ . Within the sets

**ABCD** and **EFGH** we can order  $A < B < C < D$  and  $E < F < G < H$  on the basis that C–H bonding interactions outweigh C–C antibonding interactions arising from weaker  $p$ - $p$  overlaps. Placement of the set **ABCD** in relation to **EFGH** is not qualitatively obvious. Calculations give the results shown in Figure 1.17.<sup>54</sup> Pictorial representations of the orbitals are given in Figure 1.18.

The kinds of qualitative considerations that we used to construct the ethene MO diagram do not give any indication of how much each atomic orbital contributes to the individual MOs. This information is obtained from the coefficients provided by the MO calculation. Without these coefficients we cannot specify the shapes of the MOs very precisely. However, the qualitative ideas do permit conclusions about the *symmetry* of the orbitals. As will be seen in Chapter 10, just knowing the symmetry of the MOs provides very useful insight into many chemical reactions.

### 1.2.5. Qualitative Application of MO Theory to Reactivity: Perturbational MO Theory and Frontier Orbitals

The construction of MO diagrams under the guidance of the general principles and symmetry restrictions that we have outlined can lead to useful insights into molecular structure. Now we want to consider how these concepts can be related to reactivity. In valence bond terminology, structure is related to reactivity in terms of the electronic nature of the substituents. The impact of polar and resonance effects on the electron

$D$	———	0.892
$\sigma^*$	———	0.845
$H$	———	0.640
$G$	———	0.621
$C$	———	0.587
$\pi^*$	———	0.243
$\pi$	———	-0.371
$B$	———	-0.506
$F$	———	-0.562
$A$	———	-0.644
$E$	———	-0.782
$\sigma$	———	-1.01

Fig. 1.17. Ethene molecular orbital energy levels. Energies are in atomic units. From W. L. Jorgensen and L. Salem, *The Organic Chemists Book of Orbitals*, Academic Press, New York, 1973.

<sup>54</sup> W. L. Jorgensen and L. Salem, *The Organic Chemist's Book of Orbitals*, Academic Press, New York, 1973.

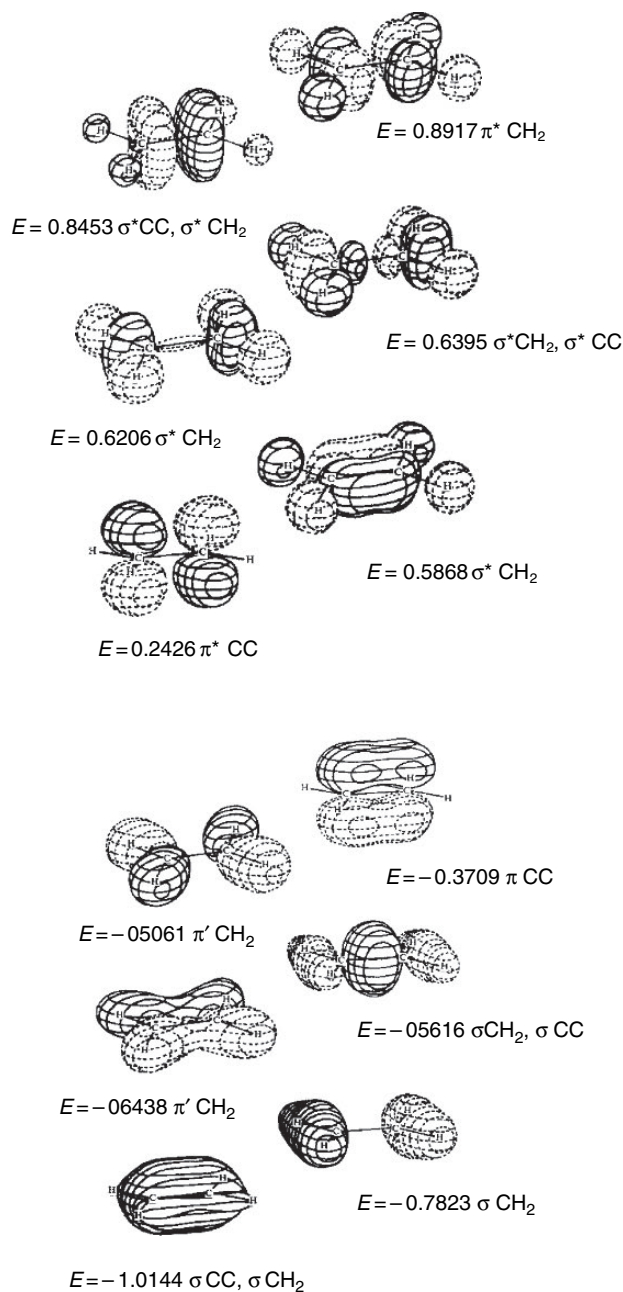


Fig. 1.18. Pictorial representation of ethene MOs. Reproduced with permission from W. L. Jorgensen and L. Salem, *The Organic Chemist's Book of Orbitals*, Academic Press, New York, 1973.

distribution and stability of reactants, transition structures, intermediates, and products is assessed and used to predict changes in reactivity. In MO theory, reactivity is related to the relative energies and shapes of the orbitals that are involved as the reactants are transformed into products. Reactions that can take place through relatively stable

intermediates and transition structures are more favorable than reactions that involve less stable ones. The *symmetry of the molecular orbitals* is a particularly important feature of many analyses of reactivity based on MO theory. The shapes of orbitals also affect the energy of reaction processes. Orbital shapes are defined by the atomic coefficients. The strongest interactions (bonding when the interacting orbitals have the same phase) occur when the orbitals have high coefficients on those atoms that undergo bond formation.

The qualitative description of reactivity in molecular orbital terms begins with a basic understanding of the MOs of the reacting systems. At this point we have developed a familiarity with the MOs of ethene and conjugated unsaturated systems from the discussion of HMO theory and the construction of the ethene MOs from atomic orbitals. To apply these ideas to new systems, we have to be able to understand how a change in structure will affect the MOs. One approach is called *perturbation molecular orbital theory* or PMO for short.<sup>55</sup> The system under analysis is compared to another related system for which the MO pattern is known. In PMO theory, the MO characteristics of the new system are deduced by analyzing how the change in structure affects the MO pattern. The type of changes that can be handled in a qualitative way include substitution of atoms by other elements, with the resulting change in electronegativity, as well as changes in connectivity that alter the pattern of direct orbital overlap. The fundamental thesis of PMO theory is that the resulting changes in the MO energies are relatively small and can be treated as adjustments (perturbations) on the original MO system.

Another aspect of qualitative application of MO theory is the analysis of interactions of the orbitals in reacting molecules. As molecules approach one another and reaction proceeds there is a mutual perturbation of the orbitals. This process continues until the reaction is complete and the product (or intermediate in a multistep reaction) is formed. The concept of *frontier orbital control* proposes that the most important interactions are between a particular pair of orbitals.<sup>56</sup> These orbitals are the highest filled orbital of one reactant (the HOMO) and the lowest unfilled (LUMO) orbital of the other reactant. We concentrate attention on these two orbitals because they are the closest in energy. A basic postulate of PMO theory is that *interactions are strongest between orbitals that are close in energy*. Frontier orbital theory proposes that these strong initial interactions guide the course of the reaction as it proceeds to completion. A further general feature of MO theory is that only MOs of matching symmetry can interact and lead to bond formation. Thus, analysis of a prospective reaction path focuses attention on the *relative energy* and *symmetry* of the frontier orbitals.

These ideas can be illustrated by looking at some simple cases. Let us consider the fact that the double bonds of ethene and formaldehyde have quite different chemical reactivities. Formaldehyde reacts readily with nucleophiles, whereas ethene does not. The  $\pi$  bond in ethene is more reactive toward electrophiles than the formaldehyde C=O  $\pi$  bond. We have already described the ethene MOs in Figures 1.17 and 1.18. How do those of formaldehyde differ? In the first place, the higher atomic number of

<sup>55</sup> C. A. Coulson and H. C. Longuet-Higgins, *Proc. R. Soc. London Ser. A*, **192**, 16 (1947); L. Salem, *J. Am. Chem. Soc.*, **90**, 543, 553 (1968); M. J. S. Dewar and R. C. Dougherty, *The PMO Theory of Organic Chemistry*, Plenum Press, New York, 1975; G. Klopman, *Chemical Reactivity and Reaction Paths*, Wiley-Interscience, New York, 1974, Chap. 4.

<sup>56</sup> K. Fukui, *Acc. Chem. Res.*, **4**, 57 (1971); I. Fleming, *Frontier Orbital and Organic Chemical Reactions*, Wiley, New York, 1976; L. Salem, *Electrons in Chemical Reactions*, Wiley, New York, 1982, Chap. 6.

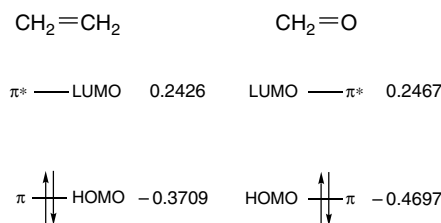


Fig. 1.19. Relative energy of the  $\pi$  and  $\pi^*$  orbitals in ethene and formaldehyde. Energies values in au are from W. L. Jorgensen and L. Salem, *The Organic Chemists Book of Orbitals*, Academic Press, New York, 1973.

oxygen provides two additional electrons, so that in place of the  $\text{CH}_2$  group of ethene, the oxygen of formaldehyde has two pairs of nonbonding electrons. This introduces an additional aspect to the reactivity of formaldehyde. The oxygen atom can form a bond with a proton or a Lewis acid, which increases the effective electronegativity of the oxygen.

Another key change has to do with the frontier orbitals, the  $\pi$  (HOMO) and  $\pi^*$  (LUMO) orbitals. These are illustrated in Figure 1.19. One significant difference between the two molecules is the lower energy of the  $\pi$  and  $\pi^*$  orbitals in formaldehyde. These are lower in energy than the corresponding ethene orbitals because they are derived in part from the lower-lying (more electronegative)  $2p_z$  orbital of oxygen. Because of its lower energy, the  $\pi^*$  orbital is a better acceptor of electrons from the HOMO of any attacking nucleophile than is the LUMO of ethene. We also see why ethene is more reactive to electrophiles than formaldehyde. In electrophilic attack, the HOMO acts as an electron donor to the approaching electrophile. In this case, because the HOMO of ethene lies higher in energy than the HOMO of formaldehyde, the electrons are more easily attracted by the approaching electrophile. The unequal electronegativities of the oxygen and carbon atoms also distort electron distribution in the  $\pi$  molecular orbital. In contrast to the symmetrical distribution in ethene, the formaldehyde  $\pi$  MO has a higher atomic coefficient at oxygen. This results in a net positive charge on the carbon atom, which is favorable for an approach by a nucleophile. One method of charge assignment (see Section 1.4.1) estimates that the  $\pi$  orbital has about 1.2 electrons associated with oxygen and 0.8 electrons associated with carbon, placing a positive charge of  $+0.2e$  on carbon. This is balanced by a greater density of the LUMO on the carbon atom.

One principle of PMO theory is that the degree of perturbation is a function of the degree of overlap of the orbitals. Thus in the qualitative application of MO theory, it is important to consider the shape of the orbitals (as indicated quantitatively by their atomic coefficients) and the proximity that can be achieved by the orbitals within the limits of the geometry of the reacting molecules. Secondly, the strength of an interaction depends on the relative energy of the orbitals. The closer in energy, the greater the mutual perturbation of the orbitals. This principle, if used in conjunction with reliable estimates of relative orbital energies, can be of value in predicting the relative importance of various possible interactions.

Let us illustrate these ideas by returning to the comparisons of the reactivity of ethene and formaldehyde toward a nucleophilic species and an electrophilic species.

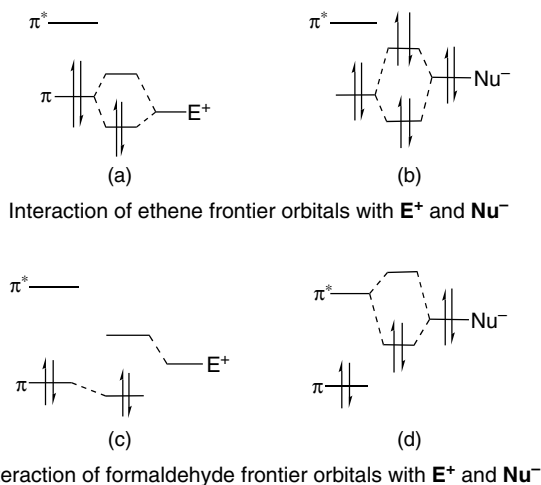


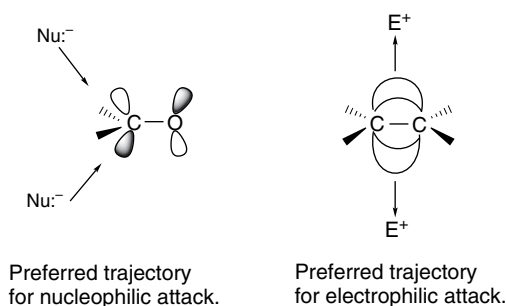
Fig. 1.20. PMO description of interaction of ethylene and formaldehyde with an electrophile ( $E^+$ ) and a nucleophile ( $Nu^-$ ).

The perturbations that arise as a nucleophile and an electrophile approach are sketched in Figure 1.20.

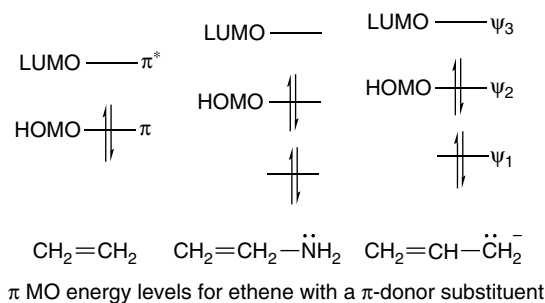
The electrophilic species  $E^+$  must have a low-lying empty orbital. The strongest interaction will be with the ethene  $\pi$  orbital and this leads to a stabilizing effect on the complex since the electrons are located in an orbital that is stabilized (Figure 1.20a). The same electrophilic species would lie further from the  $\pi$  orbital of formaldehyde since the formaldehyde orbitals are shifted to lower energy. As a result the mutual interaction with the formaldehyde HOMO will be weaker than in the case of ethene (Figure 1.20c). The conclusion is that an electrophile will undergo a greater stabilizing attraction on approaching ethene than it will on approaching formaldehyde. In the case of  $Nu^-$ , a strong bonding interaction with  $\pi^*$  of formaldehyde is possible (Figure 1.20d). In the case of ethene, the strongest interaction is with the HOMO of the nucleophile, but this is a destabilizing interaction since both orbitals are filled and the lowering of one orbital is canceled by the raising of the other (Figure 1.20b). Thus we conclude that a nucleophile with a high-lying HOMO will interact more favorably with formaldehyde than with ethene.

The representations of nucleophilic attack on formaldehyde as involving the carbonyl LUMO and electrophilic attack on ethene as involving the HOMO also make a prediction about the trajectory of the approach of the reagents. The highest LUMO density is on carbon and it is oriented somewhat away from the oxygen. On the other hand, the ethene HOMO is the  $\pi$  orbital, which has maximum density at the midpoint above and below the molecular plane. Calculations of the preferred direction of attack of electrophilic and nucleophilic reagents are in accord with this representation, as shown below.<sup>57</sup>

<sup>57</sup>. H. B. Bürgi, J. D. Dunitz, J. M. Lehn, and G. Wipff, *Tetrahedron*, **30**, 1563 (1974); H. B. Bürgi, J. M. Lehn, and G. Wipff, *J. Am. Chem. Soc.*, **96**, 1956 (1974); K. N. Houk, M. N. Paddon-Row, N. G. Rondan, Y. D. Wu, F. K. Brown, D. C. Spellmeyer, J. T. Metz, Y. Li, and R. J. Loncarich, *Science*, **231**, 1108 (1986).



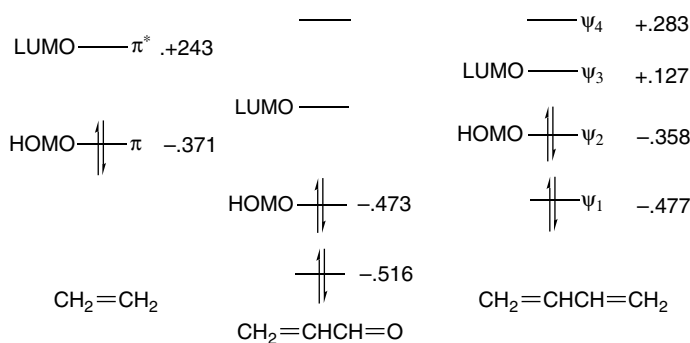
The ideas of PMO theory can also be used to describe substituent effects. Let us consider, for example, the effect of a  $\pi$ -donor substituent and a  $\pi$ -acceptor substituent on the MO levels and reactivity of substituted ethenes. We can take the amino group as an example of a  $\pi$ -donor substituent. The nitrogen atom adds one additional  $2p_z$  orbital and two electrons to the  $\pi$  system. The overall shape of the  $\pi$  orbitals for ethenamine is very similar to those of an allyl anion. The highest charge density is on the terminal atoms, i.e. the nitrogen atom and the  $\beta$ -carbon, because the HOMO has a node at the center carbon. The HOMO in ethenamine resembles  $\psi_2$  of the allyl anion and is higher in energy than the HOMO of ethene. It is not as high as the allyl  $\psi_2$  because ethenamine is neutral rather than anionic and because of the greater electronegativity of the nitrogen atom. Thus we expect ethenamine, with its higher-energy HOMO, to be more reactive toward electrophiles than ethene. Furthermore, the HOMO has the highest coefficient on the terminal atoms so we expect an electrophile to become bonded to the  $\beta$ -carbon or nitrogen, but not to the  $\alpha$ -carbon. The LUMO corresponds to the higher-energy  $\psi_3$  of the allyl anion, so we expect ethenamine to be even less reactive toward nucleophiles than is ethene.



An example of a  $\pi$ -acceptor group is the formyl group as in propenal (acrolein).



In this case, the  $\pi$  MOs resemble those of butadiene. Relative to butadiene, however, the propenal orbitals lie somewhat lower in energy because of the more electronegative oxygen atom. This factor also increases the electron density at oxygen at the expense of carbon.

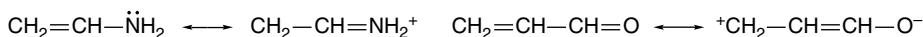


π MO energy levels in au for ethylene with a π-acceptor substituent. From Ref 54.

The LUMO, which is the frontier orbital in reactions with nucleophiles, has a larger coefficient on the β-carbon atom, whereas the two occupied orbitals are distorted in such a way as to have larger coefficients on the oxygen. The overall effect is that the LUMO is relatively low lying and has a high coefficient on the β-carbon atom. Frontier orbital theory therefore predicts that nucleophiles will react preferentially at the β-carbon atom.

MO orbital calculations at the HF/6-31G\*\* level have been done on both propenal and ethenamine. The resulting MOs were used to calculate charge distributions. Figure 1.21 gives the electron densities calculated for butadiene, propenal, and aminoethylene.<sup>58</sup> We see that the C(3) in propenal has a less negative charge than the terminal carbons in butadiene. On the other hand, C(2), the β-carbon in ethenamine, is more negative.

The MO approach gives the same qualitative picture of the substituent effect as described by resonance structures. The amino group is pictured by resonance as an electron donor, indicating a buildup of electron density at the β-carbon, whereas the formyl group is an electron acceptor and diminishes electron density at the β-carbon.



The chemical reactivity of these two substituted ethenes is in agreement with the MO and resonance descriptions. Amino-substituted alkenes, known as enamines, are very reactive toward electrophilic species and it is the β-carbon that is the site of attack. For example, enamines are protonated on the β-carbon. Propenal is an electrophilic alkene, as predicted, and the nucleophile attacks the β-carbon.

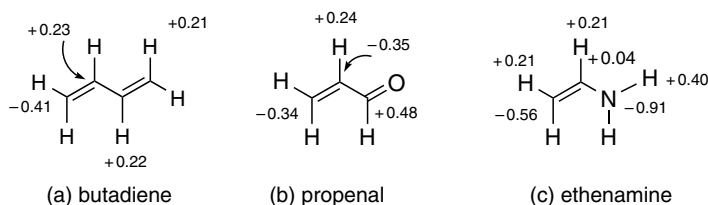
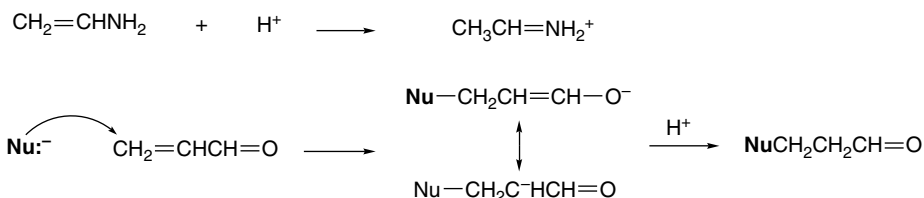
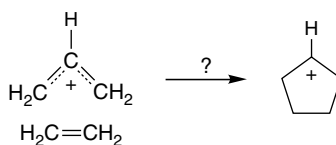


Fig. 1.21. Charge distribution in butadiene, acrolein, and aminoethylene based on HF/6-31G\* calculations. From *J. Org. Chem.*, **59**, 4506 (1994).

<sup>58</sup>. M. A. McAllister and T. T. Tidwell, *J. Org. Chem.*, **59**, 4506 (1994).



Frontier orbital theory also provides the framework for analysis of the effect that the orbital symmetry has on reactivity. One of the basic tenets of PMO theory is that the symmetries of two orbitals must match to permit a strong interaction between them. This symmetry requirement, used in the context of frontier orbital theory, can be a very powerful tool for predicting reactivity. As an example, let us examine the approach of an allyl cation and an ethene molecule and ask whether the following reaction is likely to occur:



The positively charged allyl cation would be the electron acceptor in any initial interaction with ethene. Therefore to consider this reaction in terms of frontier orbital theory, the question we have to ask is: “Do the ethene HOMO and allyl cation LUMO interact favorably as the reactants approach one another?” The orbitals that are involved are shown in Figure 1.22. If we assume that a symmetrical approach is necessary to simultaneously form the two new bonds, we see that the symmetries of the two orbitals do not match. Any bonding interaction developing at one end is canceled by an antibonding interaction at the other end. The conclusion drawn from this analysis is that this particular reaction process is not favorable. We would need to consider other modes of approach to examine the problem more thoroughly, but this analysis

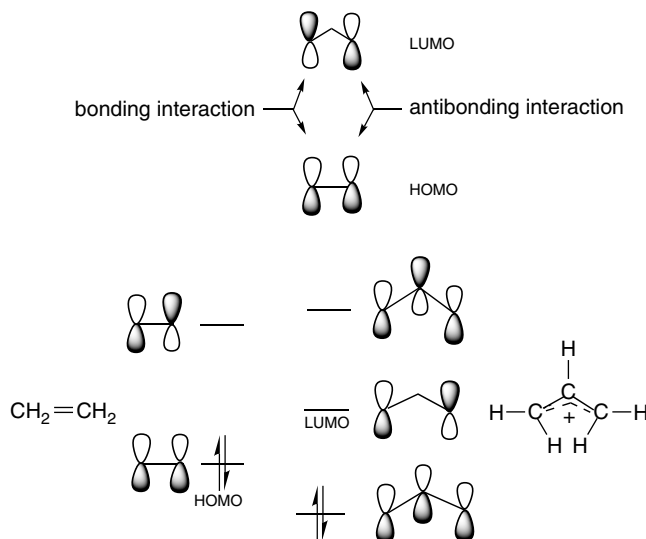


Fig. 1.22. MOs for ethene and allyl cation.

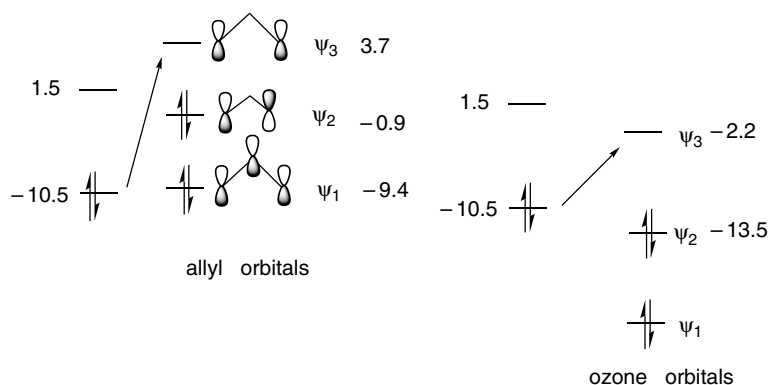
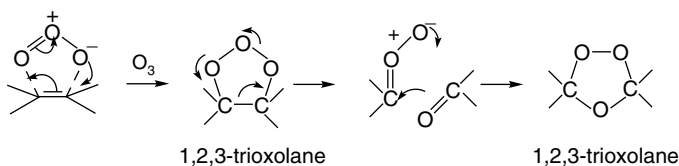


Fig. 1.23. Comparison of FMO interactions of ethene with an allyl anion and ozone.

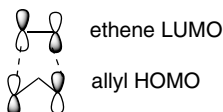
indicates that simultaneous (concerted) bond formation between ethene and an allyl cation to form a cyclopentyl cation will not occur.

Another case where orbital symmetry provides a useful insight is ozonolysis, which proceeds through a 1,2,3-trioxolane intermediate to a 1,2,4-trioxolane (ozonide) product.



Each step in this reaction sequence is a *concerted reaction* and therefore requires matching of orbital symmetry. The first step is a *cycloaddition reaction*, the second is a *cycloreversion*, and the third is another cycloaddition.<sup>59</sup> Furthermore, because of the electronegative character of  $O_3$  relative to a  $C=C$  double bond, we anticipate that  $O_3$  will furnish the LUMO and the alkene the HOMO. The  $\pi$  orbitals of ozone are analogous to those of an allyl anion, although much lower in energy, and contain four  $\pi$  electrons. We see that concerted bond formation is possible. Because of the large shift in the placement of the orbitals, the strongest interaction is between the ethene HOMO and the  $O_3$  LUMO. The approximate energies (eV) shown in Figure 1.23 are from CNDO calculations.<sup>60</sup>

In contrast to the reaction of ethene with ozone, which is very fast, the reaction with an allyl anion itself is not observed, even though the reaction does meet the symmetry requirement.



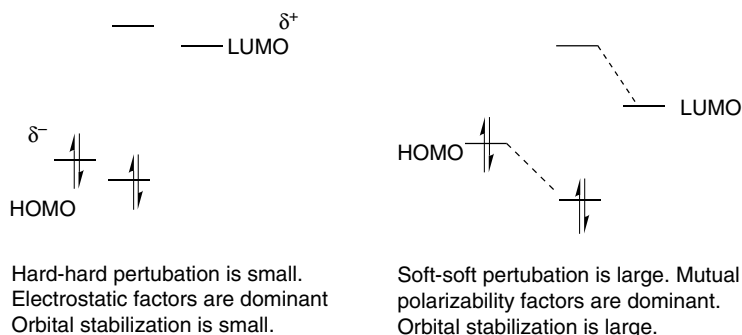
A major factor is the absence of an electrophilic component, that is, a species with a low-lying LUMO. The energy of  $\psi_3$  for of allyl anion lies well above the  $\pi$  orbital of ethene.<sup>61</sup>

<sup>59</sup> R. C. Kuczkowski, *Chem. Soc. Rev.*, **21**, 79 (1992).

<sup>60</sup> K. N. Houk, J. Sims, C. R. Watts, and L. J. Luskus, *J. Am. Chem. Soc.*, **95**, 7301 (1973).

<sup>61</sup> R. R. Sauer, *Tetrahedron Lett.*, **37**, 7679 (1996).

The concepts of PMO and frontier orbital theory can be related to the characteristics of hard-hard and soft-soft reactions. Recall that hard-hard reactions are governed by electrostatic attractions, whereas soft-soft reactions are characterized by partial bond formation. The hard-hard case in general applies to situations in which there is a large separation between the HOMO and LUMO orbitals. Under these conditions the stabilization of the orbitals is small and the electrostatic terms are dominant. In soft-soft reactions, the HOMO and LUMO are close together, and the perturbational stabilization is large.



### 1.2.6. Numerical Application of MO Theory

Molecular orbital computations are currently used extensively for calculation of a range of molecular properties. The energy minimization process can provide detailed information about the most stable structure of the molecule. The total binding energy can be related to thermodynamic definitions of molecular energy. The calculations also provide the total electron density distribution, and properties that depend on electron distribution, such as dipole moments, can be obtained. The spatial distribution of orbitals, especially the HOMO and LUMO, provides the basis for reactivity assessment. We illustrate some of these applications below. In Chapter 3 we show how MO calculations can be applied to intermediates and transition structures and thus help define reaction mechanisms. Numerical calculation of spectroscopic features including electronic, vibrational, and rotational energy levels, as well as NMR spectra is also possible.

Most MO calculations pertain to the *gas phase*. The effect of solvent can be probed by examining the effect of the dielectric constant on the structure and energy of molecules. The most common treatment of solvation effects is by one of several *continuum models*, which describe the change in energy as a result of *macroscopic solvation effects*. They describe averaged effects of the solvent, rather than specific interactions. The calculations require information about the shape of the molecule and its charge distribution, which are available from the MO computation. The molecule is represented as a surface reflecting van der Waals radii and point charges corresponding to charge separation. The solvent is characterized by a dielectric constant chosen to correspond to the solvent of interest. The calculations take into account electrostatic, polarization, and repulsive interactions with the solvent. A commonly used procedure is the polarizable continuum model (PCM).<sup>62</sup> The application of a solvation model

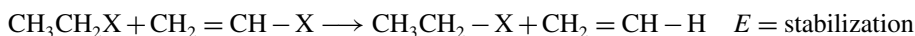
<sup>62</sup> J. Tomasi and M. Persico, *Chem. Rev.*, **94**, 2027 (1994); V. Barone, M. Cossi, and J. Tomasi, *J. Phys. Chem.*, **107**, 3210 (1997).

can adjust the relative energy of molecules. Species with substantial charge separation will be stabilized most strongly.

Current *ab initio* methods give computed molecular structures that are in excellent agreement with experimental results. Quite good agreement is obtained using relatively small basis sets, without the need for correlation corrections. Scheme 1.4 compares the bond lengths for some small compounds calculated at the MP2/6-31G\* level with experimental values.

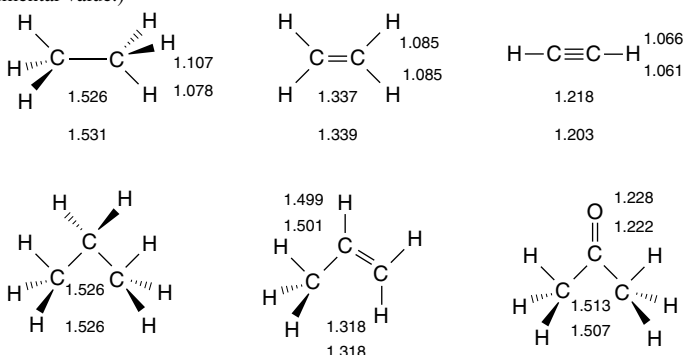
Quite good energy comparisons can also be obtained. The MO calculations pertain to a rigid molecule at 0 K, so corrections for zero-point energy and temperature effects must be made for comparison with thermodynamic data (see Section 3.1). The various computational methods differ in their scope of application and reliability. All give good results for most small hydrocarbons. A particularly challenging area is small ring compounds and other strained molecules. Table 1.10 gives some data comparing agreement for some small hydrocarbons and also for some strained molecules.

A common numerical application of MO calculations is to compare the stability of related compounds. For example, in the discussion of both resonance and qualitative MO theory, we stated that “stabilization” results from attachment of conjugating substituents to double bonds. We might ask, “How much stabilization?” One way to answer this question is to compare the total energy of the two compounds, but since they are not isomers, simple numerical comparison is not feasible. We discuss various ways to make the comparison, and some of the pitfalls, in Chapter 3, but one method is to use *isodesmic reactions*. These are hypothetical reactions in which *the number of each kind of bond is the same on each side of the equation*. For the case of substituents on double bonds the isodesmic reaction below estimates the added stabilization, since it is balanced with respect to bond types. Any extra stabilization owing to substituents will appear as an energy difference.



**Scheme 1.4. Comparison of Computed and Experimental Bond Lengths<sup>a</sup>**

(Upper number is MP2/6-31G\* computed bond length. Lower number is experimental value.)



a. From E. Lewars, *Computational Chemistry*, Kluwer Academic Publishers, Boston 2003, pp. 255–260.

**Table 1.10. Comparison of Differences in kcal/mol between Computed and Experimental  $\Delta H_f$  for Some Hydrocarbons**

	MNDO <sup>a</sup>	AM1 <sup>b</sup>	PM3 <sup>c</sup>	HF/6-31G <sup>*a</sup>	G2 <sup>d</sup>
Methane	5.9	9.0	4.9	-0.5	0.7
Ethane	0.3	2.6	2.1	0.9	-0.2
Butane	0.7	-0.7	1.3	-0.8	-0.6
Pentane	0.7	-2.8	0.6	-0.5	
Cyclopentane	-11.9	-10.4	-5.6	4.0	-0.4
Cyclohexane	-5.3	-9.0	-1.5	3.1	3.9
Cyclopropane					-1.6
Cyclobutane					-1.5
Bicyclo[1.1.0]butane					-1.5
Bicyclo[2.2.1]heptane	2.1	-2.0	-1.3	8.8	
Bicyclo[2.2.2]octane	-2.2	-11.9	-3.7	10.7	
Ethene	3.1	4.0	4.2	-2.4	0.3
Allene	-1.6	0.6	1.5	-6.8	0.0 <sup>e</sup>
1,3-Butadiene	2.7	3.6	5.0	-2.9	0.5 <sup>f</sup>
Benzene	1.5	2.2	3.6		4.0 <sup>g</sup>

a. M. J. S. Dewar, E. G. Zoebisch, E. F. Healy, and J. J. P. Stewart, *J. Am. Chem. Soc.*, **107**, 3902 (1985).

b. M. J. S. Dewar and D. M. Storch, *J. Am. Chem. Soc.*, **107**, 3898 (1985).

c. J. J. P. Stewart, *J. Comput. Chem.*, **10**, 221 (1989).

d. J. A. Pople, M. Head-Gordon, D. J. Fox, K. Raghavachari, and L. A. Curtiss, *J. Chem. Phys.*, **90**, 5622 (1989); L. A. Curtiss, K. Raghavachari, G. W. Trucks, and J. A. Pople, *J. Chem. Phys.*, **94**, 7221 (1991); L. A. Curtiss, K. Raghavachari, P. C. Redfern, and J. Pople, *J. Phys. Chem.*, **106**, 1063 (1997).

e. D. W. Rogers and F. W. McLafferty, *J. Phys. Chem.*, **99**, 1375 (1993).

f. M. N. Glukhovtsev and S. Laiter, *Theor. Chim. Acta*, **92**, 327 (1995).

g. A. Nicolaidis and L. Radom, *J. Phys. Chem.*, **98**, 3092 (1994).

The results using HF/4-31G<sup>63</sup> and HF/6-31G<sup>\*\*64</sup> for some common substituents are given below. They indicate that both electron-donating groups, such as amino and methoxy, and electron-withdrawing groups, such as formyl and cyano, have a stabilizing effect on double bonds. This is consistent with the implication of resonance that there is a stabilizing interaction as a result of electron delocalization.

#### Stabilization (kcal/mol)

Substituent	HF/4-31G	HF/6-31G <sup>**</sup>
CH <sub>3</sub>	3.2	3.05
NH <sub>2</sub>	11.2	7.20
OH	6.6	6.43
OCH <sub>3</sub>	6.1	
F		0.99
Cl		-0.54
CH=O	4.5	
CN	2.4	
CF <sub>3</sub>	-2.5	

The dipole moments of molecules depend on both the molecular dimensions and the electron distribution. For example, *Z*-1,2-dichloroethene has a dipole moment of 1.90 D, whereas, owing to its symmetrical structure, the *E* isomer has no molecular dipole.

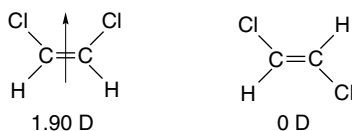
<sup>63</sup> A. Greenberg and T. A. Stevenson, *J. Am. Chem. Soc.*, **107**, 3488 (1985).

<sup>64</sup> K. B. Wiberg and K. E. Laidig, *J. Org. Chem.*, **57**, 5092 (1992).

**Table 1.11. Comparison of Computed and Experimental Molecular Dipoles<sup>a</sup>**

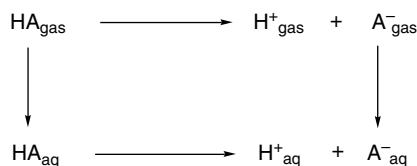
	HF/6-31G*	MP2/6-31G*	Experimental
CH <sub>3</sub> C≡CH	0.64	0.66	0.75
CH <sub>3</sub> OCH <sub>3</sub>	1.48	1.60	1.30
CH <sub>3</sub> OH	1.87	1.95	1.70
CH <sub>3</sub> Cl	2.25	2.21	1.87
(CH <sub>3</sub> ) <sub>2</sub> SO	4.50	4.63	3.96

a. From E. Lewars, *Computational Chemistry*, Kluwer Academic Publishers, Boston, 2003, pp 296–300.



MO calculations of molecular dipoles involves summing the electron distribution in the filled orbitals. Although they calculating the order correctly, both HF/6-31G\* and MP2/6-31G\* calculations seem to overestimate the dipole moments of small polar molecules (Table 1.11).

MO calculations can also be applied to reactions. The effect of substituents on the acidity ( $pK_a$ ) of carboxylic acids is a well-studied area experimentally. Shields and co-workers used several of the ab initio protocols to calculate the aqueous acidity of some substituted carboxylic acids relative to acetic acid,<sup>65</sup> which represented quite a challenging test of theory. The dissociation of a carboxylic acid involves formation of ions, and solvation is a major component of the free energy change. Furthermore, solvation introduces both enthalpy and entropy components. The calculations were approached using a thermodynamic cycle that includes the energies of solvation of the neutral acids and the anion. Since the calculation is relative to acetic acid, the energy of solvation of the proton cancels out.

**Calculated Solvation Energies CPCM/HF/6-31+G(d) (kcal/mol)**

X-CO <sub>2</sub> H	HA	Exp	A <sup>-</sup>	Experimental
H	-8.23		-77.10	
CH <sub>3</sub>	-7.86	-6.69	-77.58	-77
ClCH <sub>2</sub>	-10.61		-70.57	
NCCH <sub>2</sub>	-14.52		-69.99	
(CH <sub>3</sub> ) <sub>3</sub> C	-6.70		-72.42	

<sup>65</sup>. A. M. Toth, M. D. Liptak, D. L. Phillips, and G. C. Shields, *J. Chem. Phys.*, **114**, 4595 (2001).

Table 1.12. Calculated  $pK_a$  Relative to Acetic Acid<sup>a</sup>

CHAPTER 1	X-CO <sub>2</sub> H	CBS-4	CBS-QB3	G-2	G2(MP2)	G3	Experimental
<i>Chemical Bonding and Molecular Structure</i>	H	2.46	3.10	3.83	3.88	4.02	3.75
	CH <sub>3</sub> <sup>b</sup>	[4.75]	[4.75]	[4.75]	[4.75]	[4.75]	4.75
	ClCH <sub>2</sub>	3.30	2.92	3.37	3.37	3.18	2.85
	NCCH <sub>2</sub>	1.38	1.90	2.31	2.32	1.90	2.45
	(CH <sub>3</sub> ) <sub>3</sub> C	5.08	4.75	6.28	6.24	6.20	5.03

a. CPCMHF/6-31+G(d) continuum solvent model

b. Reference standard.

The differences in ionization energies are only a small fraction (1–5 kcal/mol) of the total gas phase ionization energies (325–350 kcal/mol), and the solvation terms for the anions are quite large (70–80 kcal/mol). The results from CBS-4, CBS-QB3, G2, G2(MP), and G3, along with the experimental results are shown in Table 1.12. The calculation reproduces the electron-withdrawing and acid-strengthening effect of substituents such as Cl and CN and the acid-weakening effect of the *t*-butyl group. The mean errors ranged between 0.4 and 1.2 kcal/mol for the various methods.

### 1.3. Electron Density Functionals

Another means of calculating molecular properties is based on *density functional theory* (DFT),<sup>66</sup> which focuses on the total electron density of a molecule. The introduction of efficient versions of density functional theory in the 1990s profoundly altered computational chemistry. Computational study of medium-sized organic and organometallic systems is currently dominated by density functional methods. DFT methods are founded on a theorem by Hohenberg and Kohn that states that the exact energy for a ground state system is defined entirely by the electron density and the functional of that density that links it to the energy.<sup>67</sup> This means that the density functional contains all the information on electron correlation. The invention of useful approximations to the functional has made DFT powerful and popular.

DFT calculations describe the electron density  $\rho$  at a point in a particular field, designated  $n(\mathbf{r})$ . The external potential operating on this field, symbolized by  $v(\mathbf{r})$ , is generated by the atomic nuclei. The electron distribution is specified by  $\rho(\mathbf{r})$ , which is the measure of electron density per unit volume at any point  $\mathbf{r}$ . Integration over space provides the information needed to describe the structure and electron distribution of molecules. The calculation involves the construction of an expression for the electron density. The energy of the system is expressed by the Kohn-sham equation.<sup>68</sup>

$$E = T + v_{\text{en}} + J_{\text{ee}} + v_{\text{xc}} \quad (1.18)$$

where  $T$  is the kinetic energy,  $v_{\text{en}}$  and  $J_{\text{ee}}$  are electrostatic electron-nuclear and electron-electron interactions, respectively, and  $v_{\text{xc}}$  are electron correlation and exchange effects.

The energy function  $F$  contains terms for kinetic energy, electrostatic interactions, and exchange and correlation energy:

<sup>66</sup> R. G. Parr and W. Yang, *Density Functional Theory of Atoms and Molecules*, Oxford University Press, Oxford, 1989; W. Kohn, A. D. Becke, and R. G. Parr, *J. Phys. Chem.*, **100**, 12974 (1996).

<sup>67</sup> P. Hohenberg and W. Kohn, *Phys. Rev. A*, **136**, 864 (1964); M. Levy, *Proc. Natl. Acad. Sci. USA*, **76**, 6062 (1979).

<sup>68</sup> W. Kohn and L. J. Shan *Phys. Rev. A*, **140**, 1133 (1965).

$$F[n(\mathbf{r})] = T_s[n(\mathbf{r})] + 1/2 \int \frac{n(\mathbf{r})n(\mathbf{r}')}{|\mathbf{r} - \mathbf{r}'|} d\mathbf{r}d\mathbf{r}' + E_{xc}[n(\mathbf{r})] \quad (1.19)$$

The energy of the system is given by integration:

$$E = \sum_j^0 \varepsilon_j - \frac{1}{2} \int \frac{n(\mathbf{r})n(\mathbf{r}')}{|\mathbf{r} - \mathbf{r}'|} d\mathbf{r}d\mathbf{r}' - \int v_{xc}(\mathbf{r})n(\mathbf{r})d\mathbf{r} + E_{xc}[n(\mathbf{r})] \quad (1.20)$$

In principle, these equations provide an exact description of the energy, but the value  $E_{xc}[n(\mathbf{r})]$  is not known. Although  $E_{xc}[n(\mathbf{r})]$  cannot be formulated exactly, Kohn and Sham developed equations that isolate this term:

$$h_i^{KS} \chi_i = \varepsilon_i \chi_i$$

$$h_i^{KS} = -\frac{1}{2} \nabla_i^2 - \sum \frac{Z_A}{|\mathbf{r}_i - \mathbf{R}_A|} + \int \frac{\rho(\mathbf{r}')}{|\mathbf{r}_i - \mathbf{r}'|} d\mathbf{r}' + V_{xc}[\rho]$$

Various approximations have been developed and calibrated by comparison with experimental data and MO calculations. The strategy used is to collect the terms that can be calculated exactly and parameterize the remaining terms. Parameters in the proposed functionals are generally selected by optimizing the method's description of properties of a training set of molecular data. The methods used most frequently in organic chemistry were developed by A. D. Becke.<sup>69</sup> Lee, Yang, and Parr<sup>70</sup> (LYP) developed a correlation functional by a fit to exact helium atom results. Combining such "pure DFT" functionals with the Hartree-Fock form of the exchange is the basis for the hybrid methods. Becke's hybrid exchange functional called "B3," combined with the LYP correlation functional, is the most widely applied of the many possible choices of exchange and correlation functionals. This is called the B3LYP method. Much of the mechanics for solution of the Kohn-Sham equations is analogous to what is used for solution of the SCF (Hartree-Fock) equations and employs the same basis sets. That is, a guess is made at the orbitals; an approximation to the Kohn-Sham Hamiltonian  $h_i^{KS}$  is then reconstructed using the guess. Revised orbitals are recovered from the Kohn-Sham equations, the Hamiltonian is reconstructed, and the process continued until it converges.

DFT computations can be done with less computer time than the most advanced ab initio MO methods. As a result, there has been extensive use of B3LYP and other DFT methods in organic chemistry. As with MO calculations, the minimum energy geometry and total energy are calculated. Other properties that depend on electronic distribution, such as molecular dipoles, can also be calculated.

A number of DFT methods and basis sets have been evaluated for their ability to calculate bond distances in hydrocarbons.<sup>71</sup> With the use of the B3LYP functionals, the commonly employed basis sets such as 6-31G\* and 6-31G\*\* gave excellent correlations with experimental values but overestimated C-H bond lengths by about 0.1 Å, while C-C bond lengths generally were within 0.01 Å. Because of the systematic variation, it is possible to apply a scaling factor that predicts C-H bond lengths with high accuracy. Ground state geometries have also been calculated (B3LYP) for molecules such as formaldehyde, acetaldehyde, and acetone.

<sup>69</sup> A. D. Becke, *Phys. Rev. A*, **38**, 3098 (1988); A. D. Becke, *J. Chem. Phys.*, **96**, 2155 (1992); A. D. Becke, *J. Chem. Phys.*, **97**, 9173 (1992); A. D. Becke, *J. Chem. Phys.*, **98**, 5648 (1993).

<sup>70</sup> C. Lee, W. Yang and R. G. Parr, *Phys. Rev. B*, **37**, 785 (1988).

<sup>71</sup> A. Neugebauer and G. Häflinger, *Theochem*, **578**, 229 (2002).

Basis set	CH <sub>2</sub> =O		CH <sub>3</sub> CH=O		(CH <sub>3</sub> ) <sub>2</sub> C=O		
	C–H	C=O	C–H	C=O	C–C	C=O	C–C
Experiment	1.108	1.206	1.106	1.213	1.504	1.222	1.507
311 + +G** <sup>a</sup>	1.105	1.201	1.109	1.205	1.502	1.211	1.514
aug-CCPVDZ <sup>b</sup>	1.114	1.207					

a. W. O. George, B. F. Jones, R. Lewis, and J. M. Price, *J. Molec. Struct.*, **550**, 281 (2000).

b. B. J. Wang, B. G. Johnson, R. J. Boyd, and L. A. Eriksson, *J. Phys. Chem.*, **100**, 6317 (1996).

In Chapter 3, we compare the results of DFT calculations on the relative thermodynamic stability of hydrocarbons with those from MO methods. There is some indication that B3LYP calculations tend to underestimate the stability of hydrocarbons as the size of the molecule increases. For example, with the 6-311 + +G(3*df*, 2*p*) basis set, the error calculated for propane (−1.5 kcal/mol), hexane (−9.3), and octane (−14.0) increased systematically.<sup>72</sup> Similarly, when the effect of successive substitution of methyl groups on ethane on the C–C bond energy was examined, the error increased from 8.7 kcal/mol for ethane to 21.1 kcal/mol for 2,2,3,3-tetramethylbutane (addition of six methyl groups, B3LYP/6-311 + +G(*d*, *p*)). The trend for the MP2/6-311 + +G(*d*, *p*) was in the same direction, but those were considerably closer to the experimental value.<sup>73</sup> The difficulty is attributed to underestimation of the C–C bond strength. As we study reactions, we will encounter a number of cases where DFT calculations have provided informative descriptions of both intermediates and transition structures.<sup>74</sup> In these cases, there is presumably cancellation of these kinds of systematic errors, because the comparisons that are made among reactants, intermediates, and product compare systems of similar size. Use of isodesmic reactions schemes should also address this problem.

DFT calculations have been used to compute the gas phase acidity of hydrocarbons and compare them with experimental values, as shown in Table 1.13. The

**Table 1.13. Gas Phase Enthalpy of Ionization of Hydrocarbons in kcal/mol by B3LYP/6-311++G\*\* Computation**

Compound	$\Delta H_{\text{calc}}$	$\Delta H_{\text{exp}}$
CH <sub>4</sub> <sup>a</sup>	416.8	416.7
C <sub>2</sub> H <sub>6</sub> <sup>a</sup>	419.4	420.1
CH <sub>3</sub> CH <sub>2</sub> CH <sub>3</sub> ( <i>pri</i> ) <sup>a</sup>	416.5	419.4
CH <sub>3</sub> CH <sub>2</sub> CH <sub>3</sub> ( <i>sec</i> ) <sup>a</sup>	414.4	415.6
(CH <sub>3</sub> ) <sub>3</sub> CH ( <i>tert</i> ) <sup>a</sup>	410.2	413.1
Cyclopropane <sup>b</sup>	411.5	411.5
Bicyclo[1.1.0]butane <sup>b</sup>	396.7	399.2
Bicyclo[1.1.1]pentane <sup>b</sup>	407.7	–
Cubane <sup>b</sup>	406.7	404.0
CH <sub>2</sub> =CH <sub>2</sub> <sup>a</sup>	405.8	407.5
HC≡CH <sup>a</sup>	375.4	378.8

a. P. Burk and K. Sillar, *Theochem*, **535**, 49 (2001).

b. I. Alkorta and J. Elguero, *Tetrahedron*, **53**, 9741 (1997).

<sup>72</sup> L. A. Curtiss, K. Ragahavachari, P. C. Redfern and J. A. Pople, *J. Chem. Phys.*, **112**, 7374 (2000).

<sup>73</sup> C. E. Check and T. M. Gilbert, *J. Org. Chem.*, **70**, 9828 (2005).

<sup>74</sup> T. Ziegler, *Chem. Rev.*, **91**, 651 (1991).

**Table 1.14. Gas Phase Ionization Energies in kcal/mol for Some Strong Acids<sup>a</sup>**

Acid	DFT	Experimental		DFT
H <sub>2</sub> SO <sub>4</sub>	306	302.2	ClSO <sub>3</sub> H	292.6
FSO <sub>3</sub> H	295.9	299.8	HClO <sub>4</sub>	298.5
CF <sub>3</sub> SO <sub>3</sub> H	297.7	299.5	HSbF <sub>6</sub>	293.1
CH <sub>3</sub> SO <sub>3</sub> H	317.0	315.0	H <sub>2</sub> S <sub>2</sub> O <sub>7</sub>	280.2
CF <sub>3</sub> CO <sub>3</sub> H	316.0	316.3		262.4

a. From B3LYP/6-311+G\*\* computations. Ref. 75.

agreement with experimental values is quite good. The large differences associated with hybridization changes are well reproduced. The increased acidity of strained hydrocarbons such as cyclopropane, bicyclo[1.1.1]butane, and cubane is also reproduced. For acyclic alkanes, the acidity order is *tert*-H > *sec*-H > *pri*-H, but methane is more acidic than ethane. We discuss the issue of hydrocarbon acidity further in Topic 3.1.

DFT computations can be extended to considerably larger molecules than advanced ab initio methods and are being used extensively in the prediction and calculation of molecular properties. A recent study, for example, examined the energy required for ionization of very strong acids in the gas phase.<sup>75</sup> Good correlations with experimental values were observed and predictions were made for several cases that have not been measured experimentally, as shown in Table 1.14.

Apart from its computational application, the fundamental premises of DFT lead to a theoretical foundation for important chemical concepts such as electronegativity and hardness-softness. The electron density distribution should also be capable of describing the structure, properties, and reactivity of a molecule. We explore this aspect of DFT in Topic 1.5.

## 1.4. Representation of Electron Density Distribution

The total electron density distribution is a physical property of molecules. It can be approached experimentally by a number of methods. Electron density of solids can be derived from X-ray crystallographic data.<sup>76</sup> However, specialized high-precision measurements are needed to obtain information that is relevant to understanding chemical reactivity. Gas phase electron diffraction can also provide electron density data.<sup>77</sup> The electron density is usually depicted as a comparison of the observed electron density with that predicted by spherical models of the atoms and is called *deformation electron density*. For example, Figure 1.24 is the result of a high-precision determination of the electron density in the plane of the benzene ring.<sup>78</sup> It shows an accumulation of electron density in the region between adjacent atoms and depletion of electron density in the center and immediately outside of the ring. Figure 1.25

<sup>75</sup> I. A. Koppel, P. Burk, I. Koppel, I. Leito, T. Sonoda, and M. Mishima, *J. Am. Chem. Soc.*, **122**, 5114 (2000).

<sup>76</sup> P. Coppens, *X-ray Charge Densities and Chemical Bonding*, Oxford University Press, Oxford, 1997.

<sup>77</sup> S. Shibata and F. Hirota, in *Stereochemical Applications of Gas-Phase Electron Diffraction*, I. Hargittai and M. Hargittai, eds., VCH Publishers, New York, 1988, Chap. 4.

<sup>78</sup> H.-B. Burgi, S. C. Capelli, A. E. Goeta, J. A. K. Howard, M. A. Sparkman, and D. S. Yufit, *Chem. Eur. J.*, **8**, 3512 (2002).

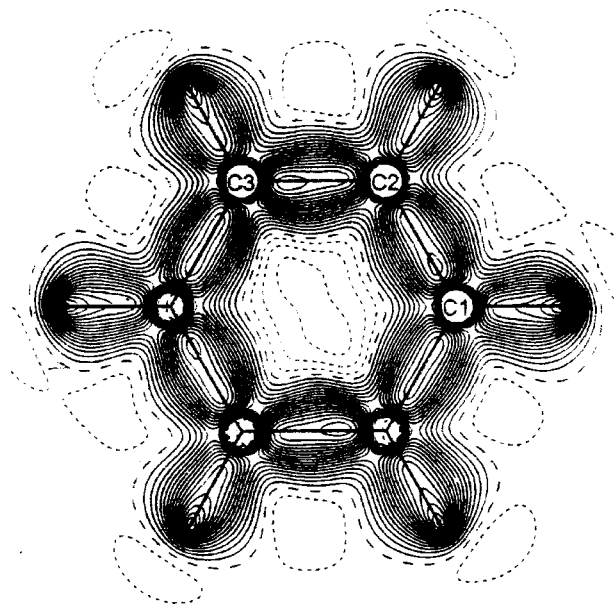


Fig. 1.24. Deformation electron density in the molecular plane of benzene. Contours at  $0.05e\text{\AA}^{-3}$  intervals. Positive contours are solid; negative contours are dashed. From *Chem. Eur. J.*, **8**, 3512 (2002).

shows electron density difference maps for benzene in and perpendicular to the molecular plane. The latter representation shows the ellipsoidal distribution owing to the  $\pi$  bond. These experimental electron density distributions are consistent with our concept of bonding. Electron density accumulates between the carbon-carbon and carbon-hydrogen bond pairs and constitutes both the  $\sigma$  and  $\pi$  bonds. The density above and below the ring is ellipsoid, owing to the  $\pi$  component of the bonding.

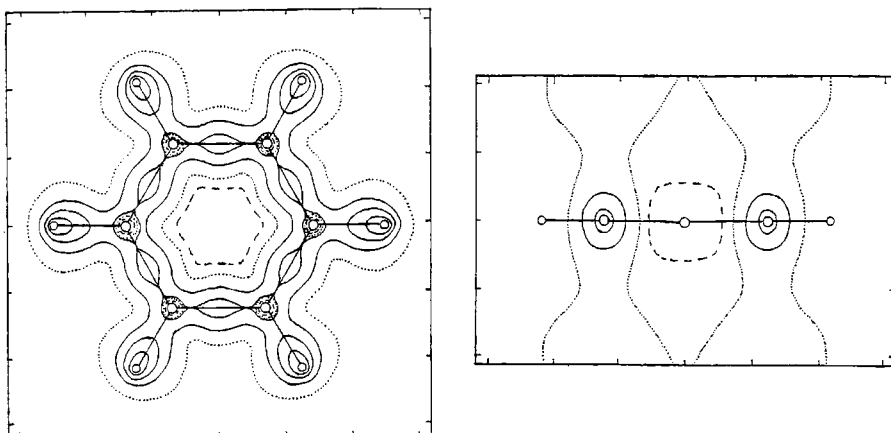


Fig. 1.25. Deformation electron density maps for benzene. (a) In the plane of the ring. (b) Perpendicular to the ring and intersecting a C–C bond. The positive contours (solid lines) are in steps of  $0.2e\text{\AA}^{-3}$  and negative contours (dashed lines) in steps of  $0.1e\text{\AA}^{-3}$ . From S. Shibata and F. Hirota, in *Stereochemical Applications of Gas-Phase Electron Diffraction*, I. Hargittai and M. Hargittai, eds., VCH Publishers, Weinheim, 1988, Chap. 4.

Figure 1.26 presents data for formaldehyde. Panel (a) is the theoretical electron density in the molecular plane. It shows the expected higher electron density around oxygen. The hydrogen atoms are represented by the small peaks extending from the large carbon peak. The electron density associated with the C–H bonds is represented by the ridge connecting the hydrogens to carbon. Panels (b) and (c) are difference maps. Panel (b) shows the accumulation of electron density in the C–H bonding regions and that corresponding to the oxygen unshared electrons. Panel (c) shows the net accumulation of electron density between the carbon and oxygen atoms, corresponding to the  $\sigma$  and  $\pi$  bonds. The electron density is shifted toward the oxygen.

These experimental electron density distributions are in accord with the VB, MO, and DFT descriptions of chemical bonding, but are not easily applied to the determination of the relatively small differences caused by substituent effects that are of primary interest in interpreting reactivity. As a result, most efforts to describe electron density distribution rely on theoretical computations. The various computational approaches to molecular structure should all arrive at the same “correct” *total electron distribution*, although it might be partitioned among orbitals differently. The issue we discuss in this section is how to interpret information about electron density in a way that is chemically informative, which includes efforts to partition the total electron density among atoms. These efforts require a definition (model) of the atoms, since there is no inherent property of molecules that partitions the total electron density among individual atoms.

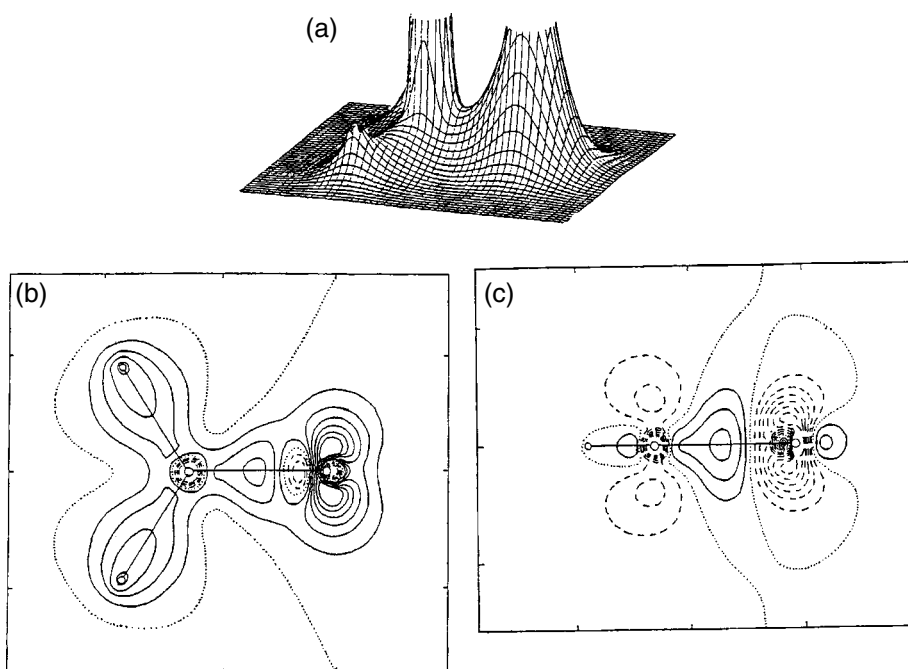
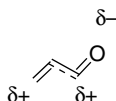


Fig. 1.26. Comparison of electron density of formaldehyde with a spherical atom model: (a) total electron density in the molecular plane; (b) the electron density difference in the molecular plane; (c) the electron density difference in a plane perpendicular to the molecular plane. The contours in (b) and (c) are in steps of  $0.2e\text{\AA}^{-3}$ . The solid contours are positive and the dashed contours are negative. From S. Shibata and F. Hirota, in *Stereochemical Applications of Gas-Phase Electron Diffraction*, I. Hargittai and M. Hargittai, eds., VCH Publishers, Weinheim, 1988, Chap. 4.

Qualitative VB theory uses resonance structures and bond polarity relationships to arrive at an indication of relative charge distribution. For example, in propanal the combination of a preferred resonance structure and the higher electronegativity of oxygen relative to carbon leads to the expectation that there will be a net negative charge on oxygen and compensating positive charges on C(1) and C(3) (see p. 21). How much the hydrogen atoms might be affected is not clear. As a first approximation, they are unaffected, since they lie in the nodal plane of the conjugated  $\pi$  system, but because the electronegativity of the individual carbons is affected, there are second-order adjustments.



Numerical expression of atomic charge density in qualitative VB terminology can be obtained by use of the electronegativity equalization schemes discussed in Section 1.1.4. The results depend on assumptions made about relative electronegativity of the atoms and groups. The results are normally in agreement with chemical intuition, but not much use is made of such analyses at the present time. MO calculations give the total electron density distribution as the sum of the electrons in all the filled molecular orbitals. The charge distribution for individual atoms must be extracted from the numerical data. Several approaches to the goal of numerical representation of electron distribution have been developed.<sup>79</sup>

#### 1.4.1. Mulliken Population Analysis

In MO calculations, the total electron density is represented as the sum of all populated MOs. The electron density at any atom can be obtained by summing the electron density associated with the basis set orbitals for each atom. Electron density shared by two or more atoms, as indicated by the overlap integral, is partitioned equally among them. This is called a *Mulliken population analysis*.<sup>80</sup>

$$P = 2 \sum_{\substack{\mu=1 \\ \mu\nu}}^{N_{\text{occ}}} c_{i\mu} c_{i\nu} X_{\mu} X_{\nu} \quad (1.21)$$

$$P_A = \sum c_{i\mu} c_{i\nu} X_{\mu} X_{\nu} \text{ for } \mu, \nu \text{ on } A \quad (1.22)$$

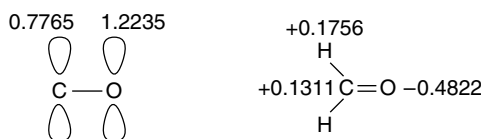
The Mulliken population analysis, and all other schemes, depend on the definition used to assign charges to atoms. For example, the  $\pi$  orbital in formaldehyde has two electrons, and according to HF/3-21G calculations they are assigned as shown at the left below. When all the basis set orbitals are considered, the charge distribution is as shown on the right.<sup>81</sup> Output from typical MO calculations can provide this kind of atomic charge distribution. No great significance can be attached to the specific numbers, since they are dependent on the particular basis set that is used. The qualitative trends in redistribution

<sup>79</sup> S. M. Bachrach, *Rev. Comput. Chem.*, **5**, 171 (1994).

<sup>80</sup> R. S. Mulliken, *J. Chem. Phys.*, **36**, 3428 (1962).

<sup>81</sup> W. J. Hehre, L. Radom, P. v. R. Schleyer, and J. A. Pople, *Ab Initio Molecular Orbital Theory*, Wiley-Interscience, New York, 1986, pp. 118–121; A. Szabo and N. S. Ostlund, *Modern Quantum Chemistry: Introduction to Advanced Electronic Structure Theory*, Macmillan, New York, 1982.

of electron density are more meaningful. The charge distribution of formaldehyde is in accord with its fundamental chemical reactivity, that is, susceptibility to reactions with nucleophiles at carbon and with Lewis acids at oxygen.



#### 1.4.2. Natural Bond Orbitals and Natural Population Analysis

Another approach for assignment of atomic charges, known as the *natural population analysis* (NPA) method, developed by F. Weinhold and collaborators,<sup>82</sup> involves formulating a series of hybrid orbitals at each atom. *Natural bond orbitals* (NBO) describe the molecule by a series of localized bonding orbitals corresponding to a Lewis structure. Another set of orbitals describes combinations in which electron density is transferred from filled to antibonding orbitals. These interactions correspond to *hyperconjugation* in VB terminology. The total energy of the molecule is given by the sum of these two components:

$$E = E_{\sigma,\sigma} + E_{\sigma,\sigma^*} \quad (1.23)$$

Typically the  $E_{\sigma,\sigma^*}$  term accounts for only a small percentage of the total binding energy; however, as it represents a perturbation on the localized structure, it may be particularly informative at the level of chemical structure and reactivity. The charges found by NPA are illustrated below by the methyl derivatives of the second-row elements. Note that the hydrogens are assigned quite substantial positive charges ( $\sim 0.2e$ ), even in methane and ethane. The total positive charge on the hydrogen *decreases* somewhat as the substituent becomes more electronegative. The carbon atom shows a greater shift of electron density to the substituent as electronegativity increases, but remains slightly negative, even for fluoromethane. The protocol for the NPA method is incorporated into MO computations and is used frequently to represent electron distribution.

NPA Populations for  $\text{CH}_3\text{-X}$  (6-31G\*)<sup>a</sup>

X	$\delta\text{C}$	$\delta\text{H}_3^{\text{b}}$	$\delta\text{X}$
H	-0.867	+0.650	+0.217
Li	-1.380	+0.576	+0.805
BeH	-1.429	+0.689	+0.740
BH <sub>2</sub>	-1.045	+0.712	+0.333
CH <sub>3</sub>	-0.634	+0.643	0.000
NH <sub>2</sub>	-0.408	+0.586	-0.178
OH	-0.225	+0.547	-0.322
F	-0.086	+0.513	-0.427

a. From A. E. Reed, R. B. Weinstock and F. Weinhold, *J. Chem. Phys.*, **83**, 735 (1985).

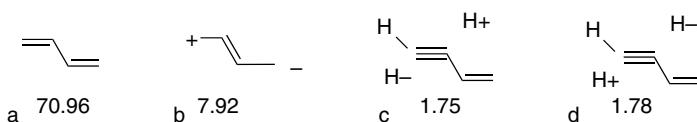
b. Total charge on the three hydrogens of the methyl group.

<sup>82</sup>. A. E. Reed, R. B. Weinstock, and F. Weinhold, *J. Chem. Phys.*, **83**, 735 (1985); A. E. Reed, L. A. Curtiss, and F. Weinhold, *Chem. Rev.*, **88**, 899 (1988); F. Weinhold and J. Carpenter, in R. Naaman and Z. Vager, eds., *The Structure of Small Molecules and Ions*, Plenum Press, New York, 1988.

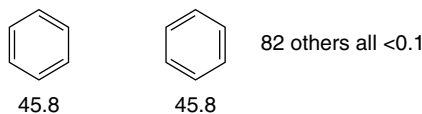
## CHAPTER 1

Chemical Bonding  
and Molecular Structure

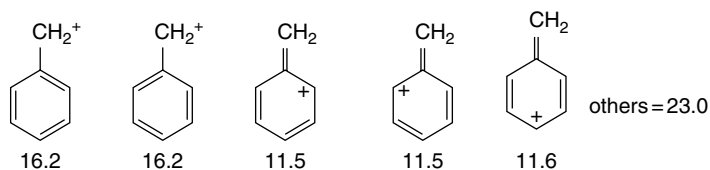
## Butadiene



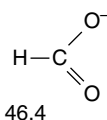
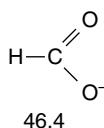
## Benzene



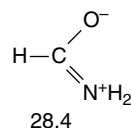
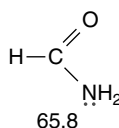
## Benzyl Cation



## Formate Anion



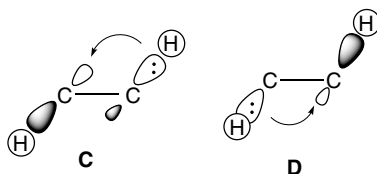
## Formamide



a. E. D. Glendening and F. Weinhold, *J. Comput. Chem.*, **19**, 593, 610 (1998).

The NPA electron distribution can be related to the VB concept of resonance structures. The orbitals corresponding to localized structures and those representing delocalization can be weighted. For example, Scheme 1.5 shows the relative weighting of the most important resonance structures for 1,3-butadiene, benzene, the benzyl cation, formamide, and the formate anion. These molecules are commonly used examples of the effect of conjugation and resonance on structure and reactivity.

Resonance structure **b** is commonly used to describe delocalization of  $\pi$  electrons in butadiene. Resonance structures **c** and **d** describe hyperconjugation. The structures represent electron transfer between *anti* hydrogens by  $\sigma$ - $\sigma^*$  interactions. Note that the hydrogen atoms act as both electron donors and acceptors. As the two hydrogens are in very similar chemical environments, we expect little net transfer of charge, but the delocalization affects such properties as NMR spin coupling constants. We will see in Topic 1.1 that this kind of delocalization is also important for hydrogens bonded to  $sp^3$  carbon atoms.



The NBO resonance structures for benzyl cation reveals the importance of charge delocalization to the *ortho* and *para* positions. The resonance structures shown for formate ion and formamide represent the important cases of carboxylate anions and amides and coincide with the qualitative ideas about the relative importance of resonance structures discussed on pp. 19–20.

### 1.4.3. Atoms in Molecules

Chemists have long thought of a molecule as the sum of its constituent atoms and groups. The homologous hydrocarbons, for example, have closely related properties, many of which can be quantitatively expressed as the sum of contributions from the  $\text{CH}_3$ ,  $\text{CH}_2$ ,  $\text{CH}$ , and  $\text{C}$  groups in the molecule. The association of properties with constituent atoms is also inherent in the concept of functional groups and its implication that a particular combination of atoms, such as a hydroxy group, has properties that are largely independent of the remainder of the molecule. There is now a vast amount of both experimental and computational data on nuclear positions and electron distribution in molecules. The question is whether these data can be interpreted as being the sum of atomic properties and, if so, how one would go about “dividing” a molecule into its constituent atoms.

R. F. W. Bader and associates at Canada’s McMaster University have derived a means of describing the electron distribution associated with specific atoms in a molecule, called the *atoms in molecules* (AIM) method.<sup>83</sup> The foundation of this approach is derived from quantum mechanics and principles of physics. It uses the methods of topology to identify atoms within molecules. The electron density of a molecule is depicted by a series of contours. *Bond paths* are the paths of maximum electron density between any two atoms. The *critical point* is a point on the bond path where the electron density is a maximum or a minimum with respect to dislocation in any direction. The bond critical point is defined by the equation

$$\bar{\nabla}\rho(\mathbf{r}) \cdot \bar{N}(\mathbf{r}) = 0 \quad (1.24)$$

The critical point is the point at which the gradient vector field for the charge density is zero, that is, either a maximum or minimum along  $\bar{N}$ . The condition  $\bar{\nabla}\rho(\mathbf{r}) \cdot \bar{N}(\mathbf{r}) = 0$  applied to other paths between two atoms defines a unique surface that can represent the boundary of the atoms within the molecule. The electron density within these boundaries then gives the atomic charge. The combination of electron density contours, bond paths, and critical points defines the *molecular graph*. This analysis can be applied to electron density calculated by either MO or DFT methods. For a very simple molecule such as  $\text{H}_2$ , the bond path is a straight line between the nuclei. The

<sup>83</sup> R. F. W. Bader, *Atoms in Molecules: A Quantum Theory*, Oxford University Press, Oxford, 1990. For an introductory discussion of the AIM method for describing electron density, see C. F. Matta and R. J. Gillespie, *J. Chem. Ed.*, **79**, 1141 (2002).

electron density accumulates between the two nuclei, relative to electron distribution in spherical atoms, as indicated earlier in Figure 1.1. Although there is an electron density *minimum* on the bond path midway between the two hydrogens, this minimum is a *maximum* with respect to displacement perpendicular to the bond path.

Bond paths are generally *not* linear in more complex molecules. They are particularly strongly curved in strained molecules, such as those containing small rings. Figure 1.27 gives the molecular graphs for ethane, propane, butane, pentane, and hexane, showing subdivision of the molecule into methyl and methylene groups. Note that the CH<sub>2</sub> units become increasingly similar as the chain is lengthened. Bader's work gives a theoretical foundation to the concept that the properties of a molecule are the sum of the properties of the constituent atoms or groups.

The total electron density graphs for molecules such as methyl cation, ethane, and ethene show strong peaks around the nuclear positions. Figure 1.28a illustrates the electron density  $\rho(\mathbf{r})$  for the methyl cation, and Figure 1.28b gives the corresponding gradients, showing the surfaces that partition the ion into C and H atoms. Note that there are peaks in the electron density corresponding to the nuclear positions. The existence of bonds is indicated by the ridge of electron density between the C and H atoms. The arrow in Figure 1.28a indicates the location of the bond critical point, which occurs at a *saddle point*, that is, the electron density is at a minimum along the bond path, but a maximum with respect to any other direction. Figure 1.28b shows the gradient and the zero flux surface that divides the ion into C and H atoms. The dots show the location of the bond critical points.

The electron density can also be characterized by its *ellipticity*, the extent to which it deviates from cylindrical symmetry, reflecting the contribution of  $\pi$  orbitals. While the C $\equiv$ C bond in ethyne is cylindrically symmetrical, the C–C bonds in ethene and benzene have greater extension in the direction of the  $\pi$  component.<sup>84</sup> Ellipticity is defined by

$$E = \lambda_1/\lambda_2 - 1 \quad (1.25)$$

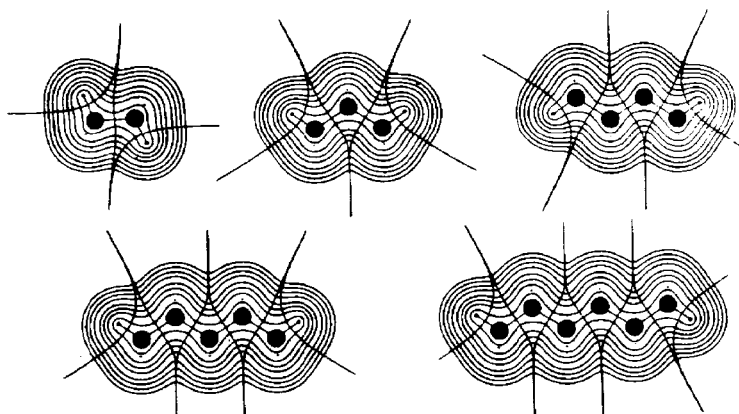


Fig. 1.27. Molecular graphs for ethane, propane, butane, pentane, and hexane. Reproduced with permission from R. F. W. Bader, in *The Chemistry of Alkanes and Cycloalkanes*, S. Patai and Z. Rappoport, eds., John Wiley & Sons, New York, 1992, Chap. 1.

<sup>84</sup> R. F. W. Bader, T. S. Slee, D. Cremer, and E. Kraka, *J. Am. Chem. Soc.*, **105**, 5061 (1983); D. Cremer and E. Kraka, *J. Am. Chem. Soc.*, **107**, 3800 (1985).

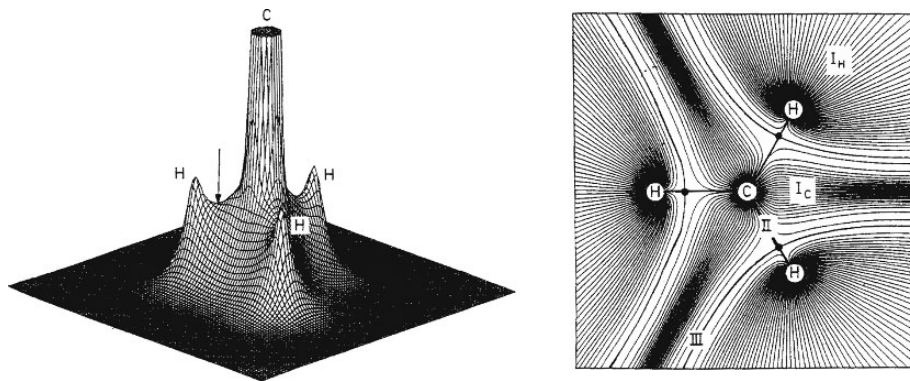
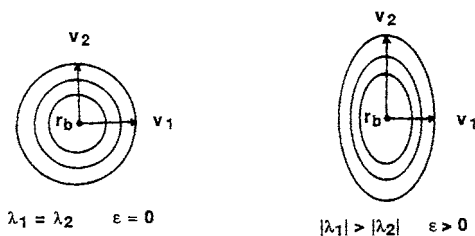


Fig. 1.28. (a) Electron density of the methyl cation in the plane of the atoms (truncated at C); (b) gradient vector field  $\nabla\rho(\mathbf{r})$  of the electron density distribution terminating at H ( $I_H$ ), C ( $I_C$ ); the bond path and critical point (II); and the zero flux surfaces (III) partitioning the ion into C and H atoms. From E. Kraka and D. Cremer, in *Theoretical Models of Chemical Bonding*, Part 2, Z. B. Maksic, ed., Springer Verlag, Berlin, 1990, pp. 459, 461.

where  $\lambda_1$  and  $\lambda_2$  are vectors to a specified electron density in the two dimensions perpendicular to the bond path at the bond critical point.



The ellipticity of the electron density in benzene is 0.23, while that in ethene is 0.45 using HF/6-31G\* electron density. Ellipticity can provide structural insight as an indicator of  $\pi$  character. For example, the ellipticity of the C(2)–C(3) bond in 1,3-butadiene is about one-seventh that of the 1,2-bond, indicating a modest contribution from the  $\pi$  bond. Bond ellipticity can also indicate delocalization through hyperconjugation. For example, the C(2)–C(3) bond in propene has an ellipticity of 0.03, reflecting the  $\sigma - \pi^*$  interactions in the molecule (see pp. 22–23).

We would expect the electron density to respond to the electronegativity of the atoms forming the bond. This relationship has been examined for the hydrogen compounds of the second-row elements. Table 1.15 gives the AIM radius for each of the second-row elements in its compound with hydrogen. Note that the bond critical point moves closer to the hydrogen as the other element becomes more electronegative. That is, the *hydrogen gets smaller* as electron density shifts to the more electronegative element. The charge density at the bond critical point,  $\rho_{(c)}$ , rises rapidly at first, but then levels off going toward the right in the periodic table. The initial increase reflects the increasing covalent character of the bond. The bonds to Li and Be are largely ionic in character, whereas the other bonds have increasing covalent character.

These relationships are depicted in Figure 1.29. Note that the hydrogen changes from hydridelike character in LiH to the much diminished electron density in H–F. There is steadily greater sharing of electron density from Li to C, as indicated by the

**Table 1.15. Charge Density and Its Location at Bond Critical Points for Hydrogen Compounds of the Second-Row Elements (6-31G<sup>\*\*</sup>)<sup>a</sup>**

Compound	$r_X$ (au)	$r_H$ (au)	$\rho_{(c)}$
LiH	1.358	1.656	0.0369
BeH <sub>2</sub>	1.069	1.416	0.0978
BH <sub>3</sub>	0.946	1.275	0.1871
CH <sub>4</sub>	1.252	0.801	0.2842
NH <sub>3</sub>	1.421	0.492	0.3495
OH <sub>2</sub>	1.460	0.352	0.3759
FH	1.454	0.279	0.3779

a. K. E. Edgecombe and R. J. Boyd, *Int. J. Quantum Chem.*, **29**, 959 (1986).

increased prominence of the nonspherical valence (shared) electron density. Beginning at N, the electron density associated with unshared electron pairs becomes a prominent feature.

Although not so dramatic in character, the same trends can be seen in carbon atoms of different hybridization. The “size” of hydrogen shrinks as the electronegativity of carbon increases in the sequence  $sp^3 < sp^2 < sp$  (Figure 1.30).

Wiberg and co-workers looked at how electron density changes as substituents on methane change from very electropositive (e.g., lithium) to very electronegative (e.g., fluorine).<sup>85</sup> This is a question of fundamental relevance to reactivity, since we know that compounds such as methyllithium are powerful bases and nucleophiles, whereas the methyl halides are electrophilic in character. The results illustrate how fundamental characteristics of reactivity can be related to electron density. Table 1.16 Gives the methyl group “radius” and  $\rho_{(c)}$ , the electron density at the bond critical point for several substituted methanes.

Going across the second row, X = Li, BeH, CH<sub>3</sub>, F, we see that the bond critical point moves closer to C as the C “shrinks” in response to the more electronegative substituents. This is particularly evident in the value of  $R$ , which gives the ratio of the

**Table 1.16. Bond Critical Points, Charge Density, and Bond Angles for Substituted Methanes<sup>a</sup>**

X	$r_C$	$r_X$	$R$	$\rho_{(c)}C-X$	$\angle H-C-X^\circ$
Li	1.2988	0.7025	0.541	0.0422	112.6
BeH	1.1421	0.5566	0.487	0.1030	112.1
CH <sub>3</sub>	0.7637	0.7637	1.000	0.2528	111.2
H	0.6605	0.4233	1.560	0.2855	109.5
CN	0.6263	0.8421	1.344	0.2685	109.8
O <sup>-</sup>	0.4417	0.8781	1.988	0.3343	116.5
O-Li	0.4425	0.9181	2.075	0.2872	112.5
F	0.4316	0.9331	2.162	0.2371	109.1
CF <sub>3</sub>	0.6708	0.8286	1.235	0.2871	109.4
NH <sub>3</sub> <sup>+</sup>	0.4793	1.0278	2.144	0.2210	108.1
N <sub>2</sub> <sup>+</sup>	0.4574	1.0522	2.301	0.1720	105.0

NOTE:  $r_C$  and  $r_X$  are distances to bond critical point in Å.  $R$  is the ratio at these distances.  $\rho_{(c)}$  is the electron density at the bond critical point and  $\angle H-C-X$  is the bond angle.

a. K. B. Wiberg and C. M. Breneman, *J. Am. Chem. Soc.*, **112**, 8765 (1990).

<sup>85</sup> K. B. Wiberg and C. M. Breneman, *J. Am. Chem. Soc.*, **112**, 8765 (1990).

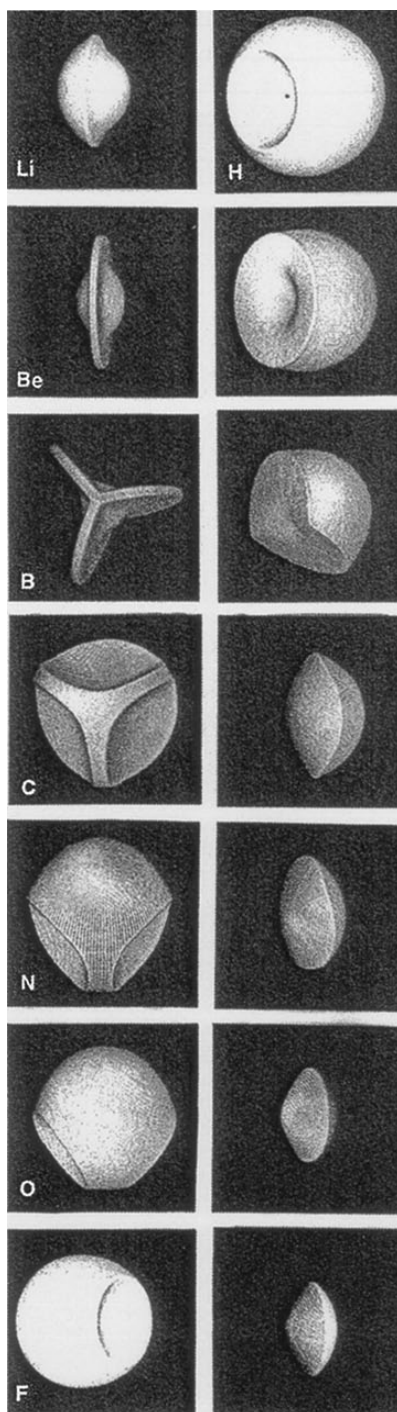


Fig. 1.29. Representation of the atoms in the second-row hydrides. The hydrides of Li, Be, and B consist primarily of a core of decreasing radius and a small, but increasing, shared density. The form of the atoms changes markedly at methane. No core is visible on the C atom, and the H atoms are reduced in size and lie on the convex interatomic surface. The increasing polarity of the remaining molecules is reflected in the decreasing size of the H atom and the increasing convexity of the interatomic surface. Reproduced from R. F. W. Bader, *Angew. Chem. Int. Ed. Engl.*, **33**, 620 (1994), by permission of Wiley-VCH.

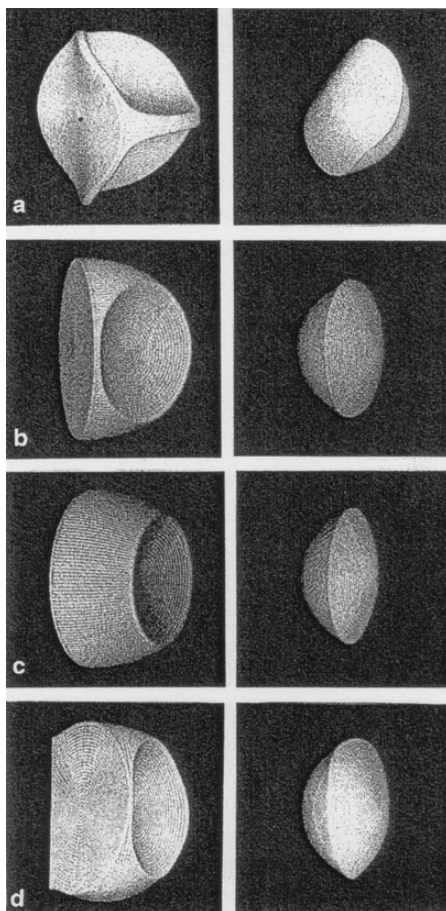
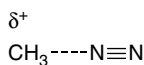


Fig. 1.30. The carbon and hydrogen atoms in: (a) ethane, (b) ethene, (c) ethyne, and (d) benzene. Note that the hydrogen is largest in ethane and smallest in ethyne. Reproduced from *Angew. Chem. Int. Ed. Engl.*, **33**, 620 (1994), by permission of Wiley-VCH.

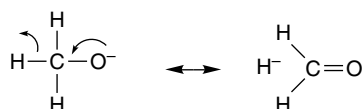
C radius to the radius of the substituent X in the C–X bond. The charge density  $\rho_{(c)}$  is very low for the largely ionic C–Li bond. It is also worth noting that there is a trend in bond angles: they become smaller as the substituent becomes more electronegative. This can be attributed to the C–X bond having more  $p$  character as the substituent becomes more electronegative. The net atomic charges are shown in Table 1.17.

The methyldiazonium ion  $[\text{CH}_3\text{--N}\equiv\text{N}]^+$  is interesting. Later (Section 4.1.5) we will learn that  $\text{N}\equiv\text{N}$  is a very reactive leaving group and indeed it is the best there is, at least of those routinely used in solution chemistry. The computed structure of  $[\text{CH}_3\text{--N}\equiv\text{N}]^+$  shows a weak bond (low value of  $\rho$ ) and a high net positive charge (+0.840) on the methyl group. This structural information suggests that  $[\text{CH}_3\text{--N}\equiv\text{N}]^+$  is a methyl cation weakly bound to  $\text{N}_2$ , and poised to release  $\text{N}_2$ .



There is a remarkable difference in the stability of methyl and ethyldiazonium ions.<sup>86</sup> The affinity of  $\text{CH}_3^+$  for  $\text{N}_2$  (C–N bond strength) based on thermodynamic data is  $45 \pm 7$  kcal/mol. Computational results give values of  $43.5 \pm 1$  kcal/mol. The ethyldiazonium ion is much less stable and the computed bond strength is only 11.5 kcal/mol, some 32 kcal/mol less than for methyldiazonium ion. Two aspects of this comparison are worth remembering for future reference: (1) The very unstable methyldiazonium ion is the *most stable* of the alkyl diazonium ions by a considerable margin. Later (Section 11.2.1, Part B) we will examine aryldiazonium ions and find that they are substantially more stable. (2) The indication that because it is better able to disperse the positive charge, an ethyl group binds nitrogen even more weakly than a methyl group presages the major differences in carbocation stability (methyl < *pri* < *sec* < *tert*) that we explore in Chapters 3 and 4.

The methoxide ion  $\text{CH}_3\text{O}^-$  is another important and familiar reagent. We know it to be a strong base and a good nucleophile. These characteristics are consistent with the high charge density on oxygen. Less well appreciated is the reactivity of methoxide as a hydride donor. We see that potential chemical reactivity reflected in the high negative charge on hydrogen in the methoxide ion given in Table 1.17.



The AIM method provides a means of visualizing the subdivision of molecules into atoms. However, its definition of atoms differs from that used for the MPA and NPA methods, and it gives distinctly different numerical values for atomic charges. The distortion of charge toward the more electronegative atom is greater than in the MPA and NPA methods. The magnitude of these charge distributions often overwhelm resonance contributions in the opposite direction. Another feature of AIM charges is that they assign small negative charge to hydrogen and positive charge to carbon in hydrocarbons. This is the reverse of the case for MPA and NPA charges and is also counter to the electronegativity scales, which assign slightly greater electronegativity to carbon than hydrogen.

**Table 1.17. Net AIM Charges for Methyl Derivatives**

X	$\delta\text{C}$	$\delta\text{X}$	$\delta\text{H}_3^a$
Li	-0.506	+0.903	-0.397
BeH	-0.669	+0.876	-0.207
$\text{CH}_3$	+0.237	0	-0.237
CN	+0.343	-0.362	+0.018
$\text{O}^-$	+1.206	-1.475	-0.732
F	+0.867	-0.743	-0.123
$\text{NH}_3^+$	+0.504	+0.337	+0.159
$\text{N}_2^+$	+0.390	+0.160	+0.450

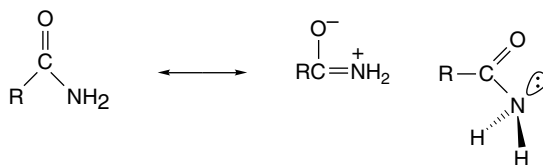
<sup>a</sup>.  $\delta\text{C}$  = total electron density for carbon in the methyl group;  $\delta\text{X}$  = total electron density for substituent X;  $\delta\text{H}$  = net electron density on the three hydrogens in the methyl group. From K. B. Wiberg and C. M. Breneman, *J. Am. Chem. Soc.*, **112**, 8765 (1990).

<sup>86</sup>. R. Glaser, G. S.-C. Choy, and M. K. Hall, *J. Am. Chem. Soc.*, **113**, 1109 (1991).

## 1.4.4. Comparison and Interpretation of Atomic Charge Calculations

While the total electron density is a real physical property that can be measured or calculated, atomic charge distribution is not a physically observable quantity. Rather, the values depend on the definition and procedures used to define atoms and assign charges. Moreover, with some methods, the charge found is dependent on the basis set orbitals that are used. For these reasons, the actual numerical values of charge should not be taken literally, but useful information about the trends in electron distribution within a molecule and qualitative comparisons can be made.<sup>87</sup> For example, Table 1.18 gives the total charge on carbon and oxygen in formaldehyde using several different basis sets by the MPA, NPA, and AIM methods. Each of the methods shows the expected shift of electron density from carbon to oxygen, but the shift is considerably more pronounced for the AIM analysis.

Atomic charges have been used to analyze the nature of the interaction between the nitrogen and carbon groups in amides. In VB language this interaction is described in terms of resonance. These resonance structures account for the most characteristic properties of amides. They are quite polar and react with protons and Lewis acids at oxygen, but not at nitrogen. The partial C=N double bond character also accounts for the observed rotational barrier of about 18 kcal/mol.



There has been a NPA analysis of the delocalization in amides.<sup>88</sup> Both the planar and rotated forms of formamide and its =S, =Se, and =Te analogs were studied by NPA and natural resonance theory. HF/6-31+G\*, MP2/6-31+G\*, and B3LYP/6-31+G\* calculations were employed. At the MP2/6-31+G\* level, the transfer of charge noted on going from the planar to rotated form of formamide was +0.105 at N, -0.088 at O, and -0.033 at C. This charge transfer is consistent with the resonance formulation. The shifts were in the same direction but somewhat larger for the heavier elements,

**Table 1.18. Atomic Populations in Formaldehyde Calculated Using Various Methods and Basis Sets<sup>a</sup>**

Basis set	Oxygen population			Carbon population		
	MPA	NPA	AIM	MPA	NPA	AIM
STO-3G	8.188	8.187	8.935	5.925	5.833	4.999
4-31G	8.485	8.534	8.994	5.824	5.778	5.069
3-21G	8.482	8.496	8.935	5.869	5.782	5.124
6-31G*	8.416	8.578	9.295	5.865	5.668	4.742
6-31G**	8.432	8.577	9.270	5.755	5.676	4.701
6-311+G**	8.298	8.563	9.240	5.892	5.606	4.755

<sup>a</sup> From S. M. Bachrach, *Rev. Comp. Chem.*, **5**, 171 (1994).

<sup>87</sup> S. M. Bachrach, *Rev. Comp. Chem.*, **5**, 171 (1994).

<sup>88</sup> E. D. Glendening and J. A. Hrabal, II, *J. Am. Chem. Soc.*, **119**, 12940 (1997).

**Table 1.19. AIM Charge Distribution and Bond Order in Planar and 90° Formamide<sup>a</sup>**

A. Charge Distribution						
	Planar			90°		
	$\sigma$	$\pi$	Total	$\sigma$	$\pi$	Total
O	5.682	1.710	9.394	5.736	1.604	9.344
N	4.626	1.850	8.476	4.852	1.370	8.222
C	1.632	1.710	4.020	1.854	0.390	4.240

B. Bond Order						
	Planar			90°		
	$\sigma$	$\pi$	Total	$\sigma$	$\pi$	Total
C=O	0.458	0.668	1.127	0.571	0.677	1.248
C–N	0.229	0.655	0.884	0.046	0.844	0.891

<sup>a</sup> K. B. Wiberg and K. E. Laidig, *J. Am. Chem. Soc.*, **109**, 5935 (1987). K. B. Wiberg and C. M. Breneman, *J. Am. Chem. Soc.*, **114**, 831 (1992).

evidently reflecting the increasing ability of S, Se, and Te to accept electron density by *polarization*. As indicated earlier in Scheme 1.3, formamide shows a considerable contribution from the dipolar resonance structure when analyzed by natural resonance theory. At the MP2/6-31G+\* level, the weightings of the two dominant structures are 58.6 and 28.6%. The C=N bond order is 1.34 and the C=O bond order is 1.72. The specific numbers depend on the computational method, but this analysis corresponds closely to the traditional description of amide resonance.

An AIM electron distribution analysis was also performed by comparing the planar structure with a 90° rotated structure that would preclude resonance. The charges,  $\pi$ , and total bond orders are given in Table 1.19. Although the O charge does not change much, the C–N bond order does, consistent with the resonance formulation. The charge buildup on oxygen suggested by the dipolar resonance structure is largely neutralized by a compensating shift of  $\sigma$  electron density from carbon to nitrogen.

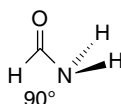
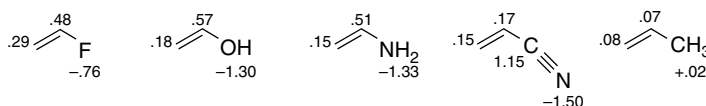


Table 1.20 gives data by which we can compare the output of several methods of charge assignment for substituted ethenes. If we compare ethene and ethenamine as an example of a double bond with an electron-releasing group (ERG) substituent, we see evidence of the conjugation (resonance) effects discussed on p. 22. The MPA and NPA methods show an increase in negative charge at the terminal CH<sub>2</sub> group, as indicated by resonance. There is a smaller, although still negative, charge on this carbon in the compounds with electron-withdrawing groups (EWG), e.g., CH=O, CF<sub>3</sub>, CN, and NO<sub>2</sub>. The AIM charges present a quite different picture, with *inductive effects* resulting from differences in electronegativity playing a dominant role. The shift of electron density to more electronegative atoms overwhelms other factors. Compare, for example, the fluoro, hydroxy, amino, cyano, and methyl substituents. The dominant factor in the charge distribution here is accumulation of negative charge on the more electronegative atoms. Note that the calculated charge at the terminal C is the same for NH<sub>2</sub> and CN substituents, which have opposing influences on reactivity.





AIM charges on substituted ethenes.

There are, as indicated at the beginning of this section, not necessarily “right” and “wrong” charge densities, since they are determined by the definitions of the models that are used, not by a physical measurement. That circumstance should be kept in mind when using atomic charge densities in evaluating structural and reactivity features. We encounter all three (MPA, NPA, AIM) of the methods for charge assignment in specific circumstances. The MPA and NPA methods, which are based on orbital occupancy partitions, seem to parallel qualitative VB conceptions more closely. In Table 1.20, for example, C(1) is less negative with the EWG cyano and nitro groups than with propene. For the ERG amino and hydroxyl, the carbon is more negative. The AIM charges minimize these resonance effects by compensating adjustments in the  $\sigma$  electron distribution. The tendency of the AIM charges to emphasize polar effects can be seen in nitroethene and cyanoethene. The AIM charges are more positive at C(2) than at C(1). These characteristic shifts of charge toward the more electronegative element are due, at least in part, to an inherent tendency of the AIM analysis to derive larger sizes for the more electronegative elements.<sup>89</sup>

#### 1.4.5. Electrostatic Potential Surfaces

While atomic charges must be assigned on the basis of definitions that depend on the method, the *electrostatic potential surface* (EPS) of a molecule is both a theoretically meaningful and an experimentally determinable quantity. The mathematical operation in constructing the electronic potential surface involves sampling a number of points external to the van der Waals radii of atoms in the molecule. A positive charge is attracted to regions of high electron density (negative potential) and repelled in regions of low electron density (positive potential). The calculations then give a contour map or color representation of the molecule’s charge distribution. Several approaches have been developed, one of which is called CHELPG.<sup>90</sup>

Figure 1.31 shows electrostatic potential maps for the planar (conjugated) forms butadiene, ethenamine, and propenal.<sup>91</sup> The diagrams on the left are in the plane of the molecule, and those on the right are perpendicular to the plane of the molecule and depict effects on the  $\pi$  orbital. Solid and dashed lines represent positive and negative potentials, respectively. The electrostatic potential for butadiene is positive at all locations in the plane of the molecule. For propenal (b) the potential becomes negative in the area of the oxygen unshared electron pairs. For ethenamine there is a negative potential external to the  $\text{CH}_2$  group. There are regions of negative potential above and below the molecular plane in butadiene, reflecting the  $\pi$  electron density. This area is greatly diminished and shifted toward oxygen in propenal. For ethenamine the negative potential is expanded on C(2) and also includes the plane of the molecule. This is consistent with an increase in the electron density at C(2). Table 1.21 gives

<sup>89</sup> C. L. Perrin, *J. Am. Chem. Soc.*, **113**, 2865 (1991).

<sup>90</sup> A. C. M. Breneman and K. B. Wiberg, *J. Comput. Chem.*, **11**, 361 (1990).

<sup>91</sup> K. B. Wiberg, R. E. Rosenberg, and P. R. Rablen, *J. Am. Chem. Soc.*, **113**, 2890 (1991).

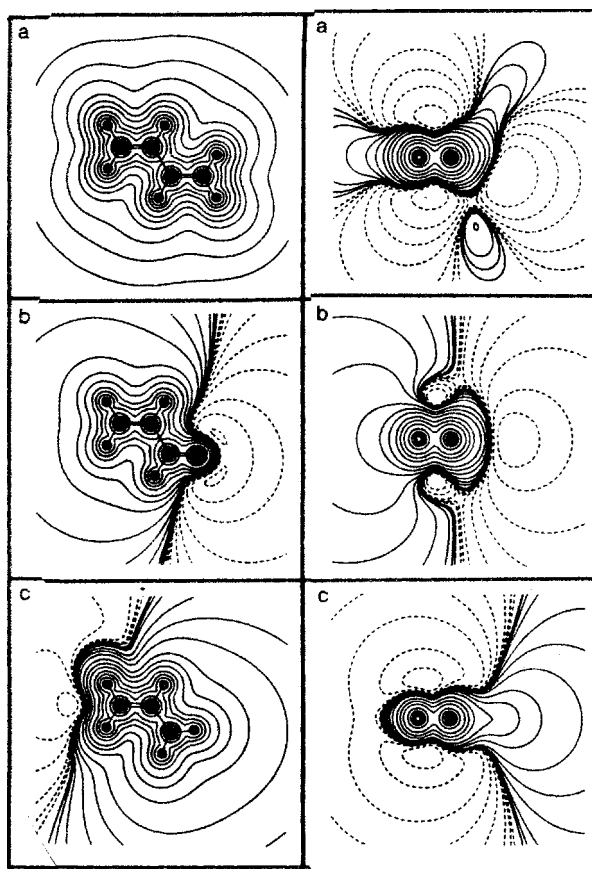


Fig. 1.31. Electrostatic potential contours for: (a) butadiene, (b) propenal, and (c) ethenamine. Solid lines are positive potential and dashed lines are negative. Left. In the plane of the molecule. Right. In the plane of the  $\pi$  electrons. Reproduced from *J. Am. Chem. Soc.*, **113**, 2890 (1991), by permission of the American Chemical Society.

the effective atomic charges derived from electrostatic potential at the  $\text{CH}_2$ , CH, and a substituent group comparable to propenal.

These charges are in accord with the resonance (pp. 20–22) and qualitative MO (pp. 46–48) descriptions of electron density in these molecules. The  $\text{CH}_2=\text{CH}-$  bond in ethenamine is seen to be strongly polarized, with the  $\pi$ -donor effect of the nitrogen unshared pair increasing electron density at C(2), while the polar effect makes C(1) substantially positive. The effects on the double bond in propenal are much less

**Table 1.21. Atomic Charges for Butadiene, Propenal, and Ethenamine Derived from Electrostatic Potentials**

X	$\text{CH}_2$	CH	X	
$-\text{CH}=\text{CH}_2$	-0.097	+0.097	CH + 0.097	$\text{CH}_2 - 0.097$
$-\text{CH}=\text{O}$	+0.024	-0.065	CH + 0.579	O - 0.538
$-\text{NH}_2$	-0.292	+0.438	N - 0.950	H + 0.178

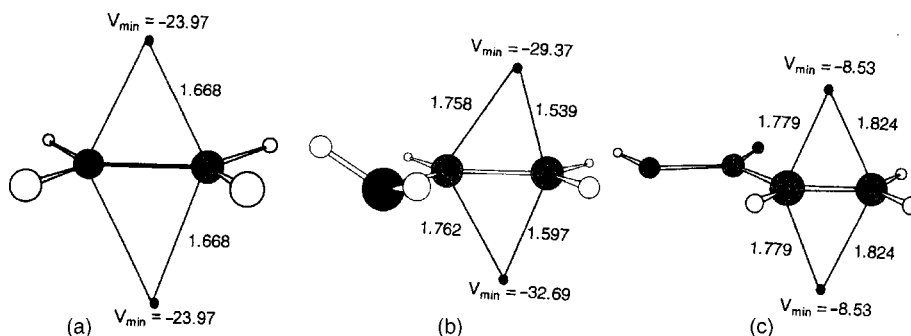


Fig. 1.32. Location and magnitude of points of most negative potential for: (a) ethene, (b) ethenamine, and (c) propenoic acid. Potentials are in kcal/mol. From *J. Org. Chem.*, **66**, 6883 (2001).

dramatic. Most of the charge separation is in the formyl group. However, the charge at the terminal  $\text{CH}_2$  changes from slightly negative to slightly positive.

The effect of substituents on ethene on the location and magnitude of the most negative potential has been calculated (HF/6-31G\*\*).<sup>92</sup> Figure 1.32 compares the position and magnitude for ethene, ethenamine, and propenoic acid, which has an electron-withdrawing carbonyl group comparable to propenal. Table 1.22 gives the same data for several other substituted ethenes.

The  $V_{\text{neg}}$  data give an order of  $\text{NH}_2 > \text{OH}, \text{OCH}_3 > \text{CH}_3 > \text{CH}_2=\text{CH} > \text{HC}\equiv\text{C} > \text{F} > \text{CO}_2\text{H} > \text{CH}=\text{O} > \text{NO}_2$ . This corresponds well with substituent effects that are discussed in Chapter 3. Note that the order  $\text{CH}_3 > \text{CH}_2=\text{CH} > \text{HC}\equiv\text{C}$  reflects the electronegativity differences of the carbon substituents. The location of the point of most negative potential (cp) also shifts with substituents. It is closer to the terminal carbon C(2) for electron-releasing groups, but slightly closer to C(1) for electron-withdrawing groups. The cp is closer to the molecular plane for electron-releasing groups. This information can be translated into predictions about reactivity toward electrophiles. Donor substituents both increase the negative potential and move it toward C(2), consistent with preferred attack by the electrophile at the more electron-rich carbon (Markovnikov's rule, see Chapter 5). Electron-withdrawing groups such

**Table 1.22. Magnitude and Location of Most Negative Potential in Substituted Ethenes**

Substituent	$V_{\text{neg}}$	C(1)-cp	C(2)-cp
$\text{NH}_2$	-33.07	1.758	1.539
OH	-26.54	1.795	1.606
$\text{CH}_3\text{O}$	-25.98	1.790	1.628
$\text{CH}_3$	-25.04	1.696	1.618
H	-23.97	1.668	1.669
$\text{CH}_2=\text{CH}$	-21.90	1.724	1.682
$\text{HC}\equiv\text{C}$	-15.94	1.769	1.773
F	-13.99	1.850	1.689
$\text{HO}_2\text{C}$	-8.53	1.779	1.824
$\text{HC}=\text{O}$	-5.08	1.790	1.839
$\text{O}_2\text{N}$	+5.90	2.205	2.223

<sup>92</sup> C. H. Suresh, N. Koga, and S. R. Gadre, *J. Org. Chem.*, **66**, 6883 (2001).

as CH=O and NO<sub>2</sub> decrease the negative potential (in fact it is positive for NO<sub>2</sub>) and increase the distance from the double bond. This results in a weaker attraction to the approaching electrophile and reduced reactivity.

#### 1.4.6. Relationships between Electron Density and Bond Order

We would expect there to be a relationship between the electron density among nuclei and the bond length. There is a correlation between bond length and bond order. Bonds get shorter as bond order increases. Pauling defined an empirical relationship for bond order in terms of bond length for C–C, C=C, and C≡C bond lengths.<sup>93</sup> For carbon, the parameter  $a$  is 0.3:

$$n_{\text{BOND}} = \exp\left(\frac{r_0 - r}{a}\right) \quad (1.26)$$

The concept of a bond order or bond index can be particularly useful in the description of transition structures, where bonds are being broken and formed and the bond order can provide a measure of the extent of reaction at different bonds. It has been suggested that the parameter in the Pauling relationship (1.26) should be 0.6 for bond orders < 1.<sup>94</sup>

MO calculations can define bond order in terms of atomic populations. Mayer developed a relationship for the bond order that is related to the Mulliken population analysis<sup>95</sup>:

$$B_{AB} = \sum_{\lambda \in A} \sum_{\omega \in B} (PS)_{\omega\lambda} (PS)_{\lambda\omega} \quad (1.27)$$

Wiberg applied a similar expression to CNDO calculations, where  $\mathbf{S} = 1$ , to give the bond index, BI<sup>96</sup>:

$$\text{BI}_{AB} = \sum_{\lambda \in A} \sum_{\omega \in B} P_{\omega\lambda} P_{\lambda\omega} \quad (1.28)$$

In these treatments, the sum of the bond order for the second-row elements closely approximates the valence number, 4 for carbon, 3 for nitrogen, and 2 for oxygen. As with the Mulliken population analysis, the Mayer-Wiberg bond orders are basis-set dependent.

The NPA orbital method of Weinhold (Section 1.4.2) lends itself to a description of the bond order. When the NPAs have occupancy near 2.0, they correspond to single bonds, but when delocalization is present, the occupancy (and bond order) deviates, reflecting the other contributing resonance structures. There have also been efforts to define bond orders in the context of AIM. There is a nearly linear relationship between the  $\rho_{(c)}$ , and the bond length for the four characteristic bond orders for carbon 1, 1.5 (aromatic), 2, and 3.<sup>97</sup>

<sup>93</sup> L. Pauling, *J. Am. Chem. Soc.*, **69**, 542 (1947).

<sup>94</sup> Ref. 30 in K. N. Houk, S. N. Gustafson, and K. A. Black, *J. Am. Chem. Soc.*, **114**, 8565 (1992).

<sup>95</sup> I. Mayer, *Chem. Phys. Lett.*, **97**, 270 (1983).

<sup>96</sup> K. B. Wiberg, *Tetrahedron*, **24**, 1083 (1968).

<sup>97</sup> R. F. W. Bader, T. T. Nguyen-Dang, and Y. Tal, *Rep. Prog. Phys.*, **44**, 893 (1981); For 6-31G\* values see X. Fadera, M. A. Austen, and R. F. W. Bader, *J. Phys. Chem. A*, **103**, 304 (1999).

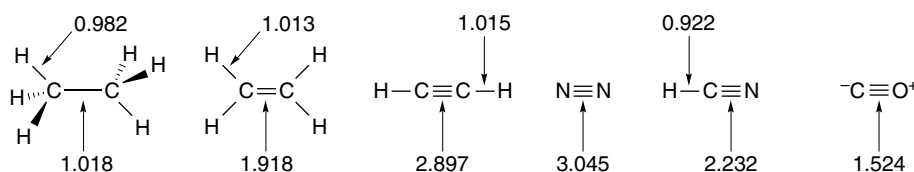
	$r$ (au)	$\rho$ (au)
$C_2H_6$	2.906	0.241
$C_6H_6$	2.646	0.291
$C_2H_4$	2.468	0.329
$C_2H_2$	2.207	0.368

This linear relationship exists for a variety of other C–C bonds, including those in strained ring molecules and even in carbocations.<sup>98</sup> There is also a high-precision correlation ( $r = -0.998$ ) for a series of bond lengths in aromatic compounds having differing bond orders,<sup>99</sup> but it does not appear to hold for C–O or C–N bonds.<sup>100</sup>

Bond order in the AIM context has also been defined as:<sup>101</sup>

$$\rho_{AB} = 2 \sum_i \langle i/i \rangle_A \langle i/i \rangle_B \quad (1.29)$$

For hydrocarbons, this treatment gives bond orders closely corresponding to the Lewis structures, but there is a reduction of the bond order for polar bonds, owing to the ionic portion of the bond.



## Chapter Summary

In this chapter we have reviewed the basic concepts of chemical bonding and their relationship to molecular structure. We have also introduced the two major computational approaches based on both molecular orbital (MO) and density functional theory (DFT) methods. These computational methods are powerful complements to experimental methods for describing molecular structure and properties. The orbital and electron density representations these computations provide can help interpret structure, properties, and reactivity. We must, however, remember to distinguish between the parts of this information that represent physically measurable properties (e.g., molecular dimensions and total electron distribution) and those that depend on definition (e.g., individual orbital shapes, atomic charge assignments). Our goal is to grasp the fundamental structural consequences of nuclear positions and electron distribution. Three key concepts, *electronegativity*, *delocalization*, and *polarizability*, allow us to make qualitative judgments about structure and translate them into a first approximation of expected properties and reactivity.

<sup>98</sup>. R. F. W. Bader, T. H. Tang, Y. Tal, and F. W. Biegler-König, *J. Am. Chem. Soc.*, **104**, 946 (1982).

<sup>99</sup>. S. T. Howard and T. M. Krygowski, *Can. J. Chem.*, **75**, 1174 (1997).

<sup>100</sup>. S. T. Howard and O. Lamarcke, *J. Phys. Org. Chem.*, **16**, 133 (2003).

<sup>101</sup>. J. Cioslowski and S. T. Mixon, *J. Am. Chem. Soc.*, **113**, 4142 (1991).

## Topic 1.1. The Origin of the Rotational (Torsional) Barrier in Ethane and Other Small Molecules

One of the most general structural features of saturated hydrocarbons is the preference for staggered versus eclipsed conformations. This preference is seen with the simplest hydrocarbon with a carbon-carbon bond—ethane. The staggered conformation is more stable than the eclipsed by 2.9 kcal/mol, as shown in Figure 1.33.<sup>102</sup>

The preference for the staggered conformation continues in larger acyclic and also cyclic hydrocarbons, and is a fundamental factor in the conformation of saturated hydrocarbons (see Section 2.2.1). The origin of this important structural feature has been the subject of ongoing analysis.<sup>103</sup> We consider here the structural origin of the energy barrier. A first step in doing so is to decide if the barrier is the result of a destabilizing factor(s) in the eclipsed conformation or a stabilizing factor(s) in the staggered one. One destabilizing factor that can be ruled out is van der Waals repulsions. The van der Waals radii of the hydrogens are too small to make contact, even in the eclipsed conformation. However, there is a repulsion between the bonding electrons. This includes both electrostatic and quantum mechanical effects (exchange repulsion) resulting from the Pauli exclusion principle, which requires that occupied orbitals maintain maximum separation (see Section 1.1.2). There is also a contribution from nuclear-nuclear repulsion, since the hydrogen nuclei are closer together in the eclipsed conformation. The main candidate for a stabilizing interaction is  $\sigma$  delocalization (hyperconjugation). The staggered conformation optimizes the alignment of the  $\sigma$  and  $\sigma^*$  orbitals on adjacent carbon atoms.

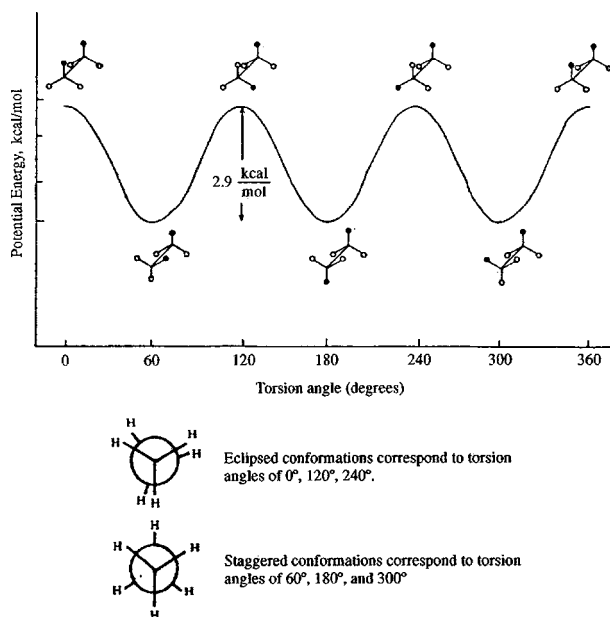
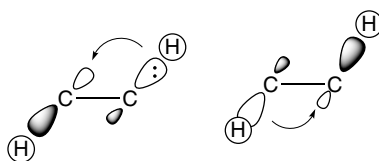


Fig. 1.33. Potential energy as a function of rotation angle for ethane.

<sup>102</sup> K. S. Pitzer, *Disc. Faraday Soc.*, **10**, 66 (1951); S. Weiss and G. E. Leroi, *J. Chem. Phys.*, **48**, 962 (1968); E. Hirota, S. Saito, and Y. Endo, *J. Chem. Phys.*, **71**, 1183 (1979).

<sup>103</sup> R. M. Pitzer, *Acc. Chem. Res.*, **16**, 207 (1983).



The repulsive electronic interactions were emphasized in early efforts to understand the origin of the rotational barrier.<sup>104</sup> In particular the  $\pi$  character of the  $\pi_z$ ,  $\pi_y$ ,  $\pi'_z$ , and  $\pi'_y$  (see Figure 1.34) was emphasized.<sup>105</sup> The repulsive interactions among these orbitals are maximized in the eclipsed conformation.

Efforts have been made to dissect the contributing factors within an MO framework. The NPA method was applied to ethane. Hyperconjugation was found to contribute nearly 5 kcal/mol of stabilization to the staggered conformation, whereas electron-electron repulsion destabilized the eclipsed conformation by 2 kcal/mol.<sup>106</sup> These two factors, which favor the staggered conformation, are partially canceled by other effects. The problem is complicated by adjustments in bond lengths and bond angles that minimize repulsive interactions. These deformations affect the shapes and energies of the orbitals. When the effects of molecular relaxation are incorporated into

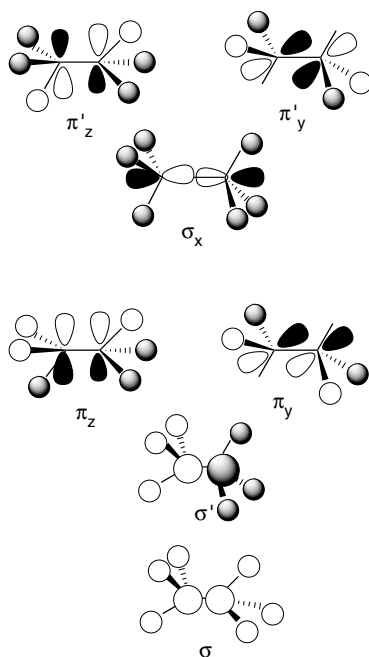


Fig. 1.34. Molecular orbitals of ethane revealing  $\pi$  character of  $\pi_z$ ,  $\pi_y$ ,  $\pi'_z$ , and  $\pi'_y$  orbitals. Only filled orbitals are shown.

<sup>104</sup>. J. P. Lowe, *J. Am. Chem. Soc.*, **92**, 3799 (1970); J. P. Lowe, *Science*, **179**, 527 (1973).

<sup>105</sup>. E. T. Knight and L. C. Allen, *J. Am. Chem. Soc.*, **117**, 4401 (1995).

<sup>106</sup>. J. K. Badenhop and F. Weinhold, *Int. J. Quantum Chem.*, **72**, 269 (1999).

the analysis, the conclusion reached is that delocalization (hyperconjugation) is the principal factor favoring the staggered conformation.<sup>107</sup>

When methyl groups are added, as in butane, two additional conformations are possible. There are two staggered conformations, called *anti* and *gauche*, and two eclipsed conformations, one with methyl-methyl eclipsing and the other with two hydrogen-methyl alignments. In the methyl-methyl eclipsed conformation, van der Waals repulsions come into play. The barrier for this conformation increases to about 6 kcal/mol, as shown in Figure 1.35. We pursue the conformation of hydrocarbons further in Section 2.2.1.

Changing the atom bound to a methyl group from carbon to nitrogen to oxygen, as in going from ethane to methylamine to methanol, which results in shorter bonds, produces a regular *decrease* in the rotational barrier from 2.9 to 2.0 to 1.1 kcal/mol, respectively. The NPA analysis was applied to a dissection of these barriers.<sup>108</sup> The contributions to differences in energy between the eclipsed and staggered conformations were calculated for four factors. These are effects on the localized bonds ( $E_{\text{Lewis}}$ ), hyperconjugation ( $E_{\text{deloc}}$ ), van der Waals repulsions ( $E_{\text{steric}}$ ), and exchange ( $E_{2 \times 2}$ ). The dominant stabilizing terms are the  $\Delta E_{\text{deloc}}$  and  $\Delta E_{2 \times 2}$ , representing hyperconjugation and exchange, respectively, but

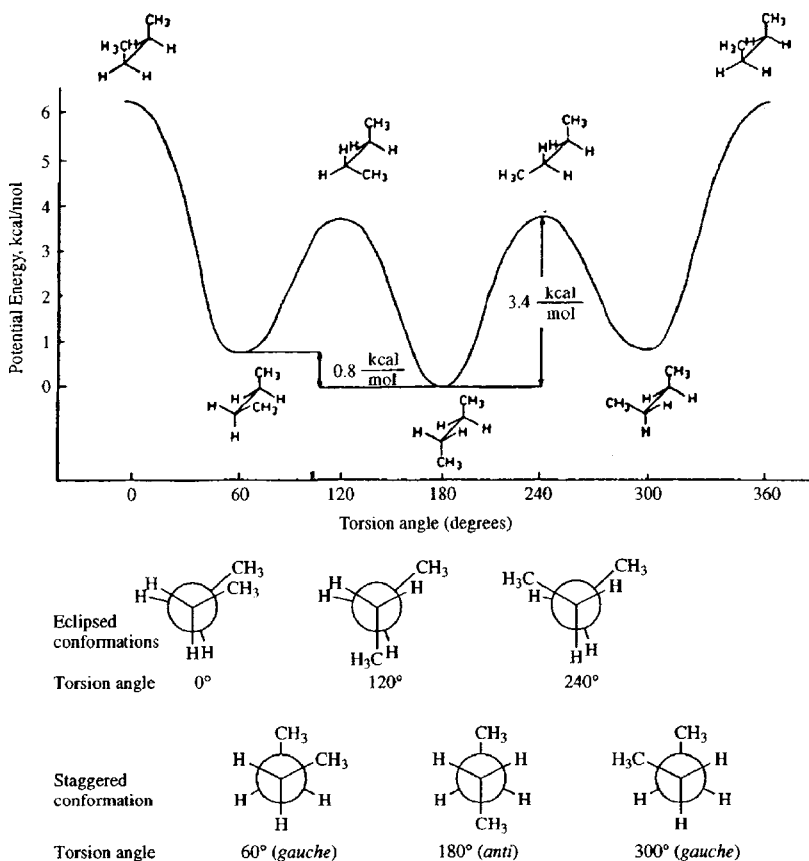


Fig. 1.35. Potential energy diagram for rotation about the C(2)–C(3) bond in butane.

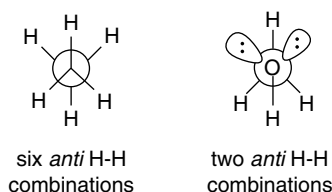
<sup>107</sup> V. Pophristic and L. Goodman, *Nature*, **411**, 565 (2001); F. Weinhold, *Angew. Chem. Int. Ed. Engl.*, **42**, 4188 (2003).

<sup>108</sup> J. K. Badenhop and F. Weinhold, *Int. J. Quantum Chem.*, **72**, 269 (1999).

this analysis indicates that the overall barrier results from compensating trends in the four components. These results pertain to a fixed geometry and do not take into account bond angle and bond length adjustments in response to rotation.

	CH <sub>3</sub> CH <sub>3</sub>	CH <sub>3</sub> NH <sub>2</sub>	CH <sub>3</sub> OH
$\Delta E_{\text{Lewis}}$	-1.423	-0.766	-0.440
$\Delta E_{\text{deloc}}$	+4.953	+2.920	+1.467
$\Delta E_{\text{steric}}$	-0.827	-0.488	-1.287
$\Delta E_{2 \times 2}$	+2.009	+1.483	+0.475
$\Delta E_{\text{total}}$	+4.712	+3.149	+0.215

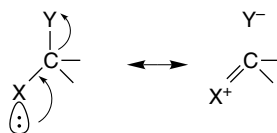
The methanol rotational barrier was further explored, using the approach described above for ethane.<sup>109</sup> The effect of changes in molecular structure that accompany rotation were included. The approach taken was to systematically compare the effect on the rotational barrier of each specific interaction, e.g., hyperconjugation and exchange repulsion, and to determine the effect on molecular geometry, i.e., bond lengths and angles. The analysis of electrostatic forces (nuclear-nuclear, electron-electron, and nuclear-electron) showed that it was the nuclear-electron forces that are most important in favoring the staggered conformation, whereas the other two actually favor the eclipsed conformation. The structural response to the eclipsed conformation is to lengthen the C–O bond, destabilizing the molecule. The more favorable nuclear-electron interaction in the staggered conformation is primarily a manifestation of hyperconjugation. In comparison with ethane, a major difference is the number of hyperconjugative interactions. The oxygen atom does not have any antibonding orbitals associated with its unshared electron pairs and these orbitals cannot act as acceptors. The oxygen unshared electrons function only as donors to the adjacent *anti* C–H bonds. The total number of hyperconjugative interactions is reduced from six in ethane to two in methanol.



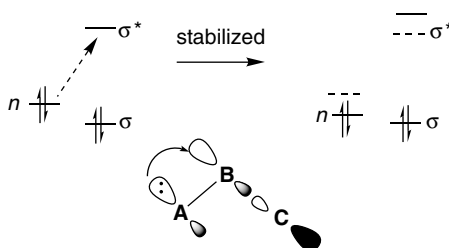
## Topic 1.2. Heteroatom Hyperconjugation (Anomeric Effect) in Acyclic Molecules

It is expected that hyperconjugation would be enhanced in certain systems containing heteroatoms. If one atom with an unshared electron pair is a particularly good electron donor and another a good  $\sigma^*$  acceptor, the  $n \rightarrow \sigma^*$  contribution should be enhanced. This is represented by a charged, “no-bond” resonance structure.

<sup>109</sup> V. Pophristic and L. Goodman, *J. Phys. Chem. A*, **106**, 1642 (2002).



Heteroatom hyperconjugation can also be expressed in MO terms. The  $n$ ,  $\sigma$ , and  $\sigma^*$  orbitals are involved, as depicted below. If the **A** atom is the donor and **C** the acceptor, the MO perturbation indicates a stabilization of the **A**  $n$  orbital by partial population of the **B–C**  $\sigma^*$  orbital.



This stereoelectronic interaction has a preference for an *anti* relationship between the donor electron pair and the acceptor  $\sigma^*$  orbital. Such interactions were first recognized in carbohydrate chemistry, where the term *anomeric effect* originated. We use the more general term *heteroatom hyperconjugation* in the discussion here. The  $n \rightarrow \sigma^*$  interaction should be quite general, applying to all carbon atoms having two heteroatom substituents. Such compounds are generally found to be stabilized, as indicated by the results from an HF/3-21G level calculations given in Table 1.23.

A study of the extent of hyperconjugation in disubstituted methanes using B3LYP/6-31G\*\* calculations and NPA analysis found that  $\sigma^*$  acceptor capacity increases with electronegativity, i.e., in the order  $C < N < O < F$  for the second row.<sup>110</sup> However, acceptor  $\sigma^*$  capacity also increases going down the periodic table for the halogens,  $F < Cl < Br < I$ . The electronegativity trend is readily understood, but the trend with size had not been widely recognized. The effect is attributed to the lower energy of the  $\sigma^*$  orbitals with the heavier elements. Donor ability also appears to increase going down the periodic table. This trend indicates that *softness* (polarizability) is a factor in hyperconjugation. The stabilizations for substituted methylamines according to these B3LYP/6-31G\*\* calculations are as follows:

**Table 1.23. Calculated Stabilization in kcal/mol for Disubstituted Methanes<sup>a</sup>**

X(donor)	Y(acceptor)		
	NH <sub>2</sub>	OH	F
NH <sub>2</sub>	10.6	12.7	17.6
OH		17.4	16.2
F			13.9

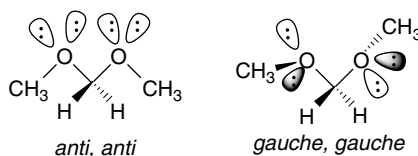
a. P. v. R. Schleyer, E. D. Jemmis, and G. W. Spitznagel, *J. Am. Chem. Soc.*, **107**, 6393 (1985).

<sup>110</sup> I. V. Alabugin and T. A. Zeidan, *J. Am. Chem. Soc.*, **124**, 3175 (2002).

$\text{H}_2\text{N}-\text{CH}_2-\text{X} \leftrightarrow \text{H}_2\text{N}^+=\text{CH}_2 \text{X}^-$	
X	kcal/mol
H	8.07
F	20.49
Cl	22.55
Br	29.87

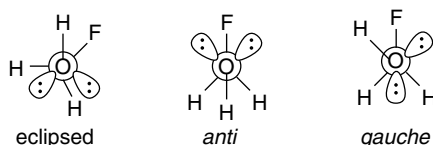
Heteroatom hyperconjugation favors the *anti* alignment of the interacting orbitals. One way to estimate the magnitude of the stabilization is to compare the conformations of individual molecules that are or are not properly aligned for hyperconjugation. Hyperconjugative stabilization is expected to have at least three interrelated consequences: (1) altered bond lengths; (2) enhanced polarity, as represented by the charged resonance structure; and (3) an energetic preference for the conformation that optimizes hyperconjugation. These issues have been examined for many small molecules, and we illustrate the analysis by considering a few, such as dimethoxymethane, fluoromethanol, fluoromethylamine, and diaminomethane.

Dimethoxymethane prefers a conformation that allows alignment of an unshared pair on each oxygen (donor) with a C–O  $\sigma^*$  orbital on the other. This condition is met in the conformation labeled *gauche, gauche*. In contrast, the extended hydrocarbon-like *anti, anti* conformation does not permit this alignment.



Calculations using the 6-31\* basis set found the *gauche, gauche* conformation to be about 5 kcal/mol more stable than the *anti, anti*.<sup>111</sup> Later MP2/6-311++G\*\* and B3LYP/6-31G\*\* calculations found the *gauche, gauche* arrangement to be about 7 kcal/mol more stable than *anti, anti*. There are two other conformations that have intermediate (3–4 kcal/mol) energies.<sup>112</sup> Dissecting these conformational preferences to give an energy for the anomeric effect is complicated, but there is general agreement that in the case of dimethoxymethane it accounts for several kcal/mol of stabilization.

Fluoromethanol also shows a preference for the *gauche* conformation. At the HF/6-31G\*\* level it is 4.8 kcal/mol more stable than the *anti* conformation and 2.4 kcal/mol more stable than the eclipsed conformation.<sup>113</sup> Only the *gauche* conformation aligns an unshared pair *anti* to the C–F bond.



NPA analysis was used to isolate the  $n \rightarrow \sigma^*$  component and placed a value of 18 kcal/mol on the heteroatom hyperconjugation. This is about 11 kcal/mol higher than

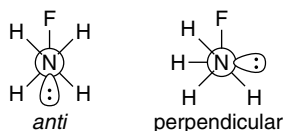
<sup>111</sup> K. B. Wiberg and M. A. Murcko, *J. Am. Chem. Soc.*, **111**, 4821 (1989).

<sup>112</sup> J. R. Kneisler and N. L. Allinger, *J. Comput. Chem.*, **17**, 757 (1996).

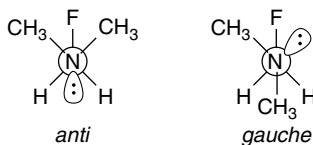
<sup>113</sup> U. Salzner and P. v. R. Schleyer, *J. Am. Chem. Soc.*, **115**, 10231 (1993).

the same component in the *anti* and eclipsed conformations, so other factors must contribute to reducing the total energy difference.

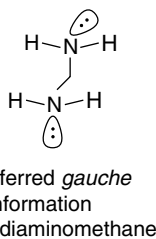
Another molecule that has received attention is fluoromethylamine. From MP2/6-31G\*\* calculations the *anti* arrangement of the nitrogen unshared pair and the C–F bond is found to be the most stable conformation by 7.5 kcal/mol.<sup>114</sup> Some of the structural effects expected for hyperconjugation, such as lengthening of the C–F bond are seen, but are not dramatic.<sup>115</sup>



Experimental structural data (electron diffraction) is available for *N*-fluoromethyl-*N,N*-dimethylamine.<sup>116</sup> The only conformation observed is the *anti* arrangement of the unshared pair and C–F bond. MP2/6-311G(2*d*,*p*) calculations suggest that the *gauche* alignment is about 5 kcal/mol less stable.



Diaminomethane would also be expected to be stabilized by an anomeric effect. Overall, there is a rather small preference for the *gauche*, *gauche* conformation, but NPA analysis suggests that there is an  $n \rightarrow \sigma^*$  component of 5–6 kcal/mol that is offset by other factors.<sup>117</sup>



We should conclude by emphasizing that the *stabilization of these compounds does not mean that they are unreactive*. In fact,  $\alpha$ -halo ethers and  $\alpha$ -halo amines are highly reactive toward solvolysis. The hyperconjugation that is manifested in net stabilization *weakens* the carbon-halogen bond and the molecules dissociate readily in polar solvents. Methoxymethyl chloride is at least  $10^{14}$  times as reactive a methyl

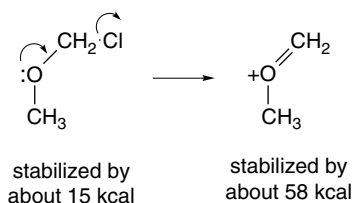
<sup>114</sup>. J. J. Irwin, T. K. Ha, and J. Dunitz, *Helv. Chim. Acta*, **73**, 1805 (1990).

<sup>115</sup>. K. B. Wiberg and P. R. Rablen, *J. Am. Chem. Soc.*, **115**, 614 (1993).

<sup>116</sup>. D. Christen, H. G. Mack, S. Rudiger, and H. Oberhammer, *J. Am. Chem. Soc.*, **118**, 3720 (1996).

<sup>117</sup>. L. Carballeira and I. Perez-Juste, *J. Comput. Chem.* **22**, 135 (2001).

chloride toward solvolysis in ethanol,<sup>118</sup> owing to the fact that the cationic intermediate is stabilized even more, 57.6 kcal/mol, according to the computational results on p. 22.

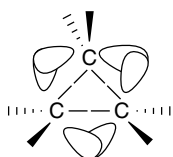


As indicated at the beginning of this section, heteroatom hyperconjugation was first recognized in carbohydrates. The anomeric effect has been particularly well studied in cyclic systems, such as found in carbohydrates. We return to the anomeric effect in cyclic systems in Topic 2.3.

### Topic 1.3. Bonding in Cyclopropane and Other Small Ring Compounds

Molecules such as cyclopropane that are forced by geometry to have nonideal bond angles are said to be *strained*. This means that the bonds are not as strong as those in comparable molecules having ideal bond angles and results in both lower thermodynamic stability and increased reactivity. The increased reactivity has at least two components. (1) Typically, reactions lead to a less strained product and partial relief of strain lowers the energy barrier. (2) Strained molecules require orbital rehybridization, which results in electrons being in higher energy orbitals, so they are more reactive.<sup>119</sup> There have been many experimental and computational studies aimed at understanding how strain affects structure and reactivity.

The simplest VB description of cyclopropane is in terms of bent bonds. If the carbons are considered to be  $sp^3$  hybrid, in accordance with their tetravalent character, the bonding orbitals are not directed along the internuclear axis. The overlap is poorer and the bonds are “bent” and weaker.



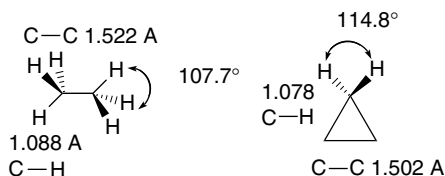
The overlap can be improved somewhat by adjustment of hybridization. Increased  $p$  character in the C–C bonds reduces the interorbital angle and improves overlap, which means that the C–H bonds must have increased  $s$  character. Compared to ethane or propane, cyclopropane has slightly shorter C–C and C–H distances and an open  $\text{CH}_2$  bond angle,<sup>120</sup> which is consistent with rehybridization. The C–H bonds in cyclopropane are significantly stronger than those in unstrained hydrocarbons, owing

<sup>118</sup>. P. Ballinger, P. B. de la Mare, G. Kohnstam, and B. M. Prestt, *J. Chem. Soc.*, 3641 (1955).

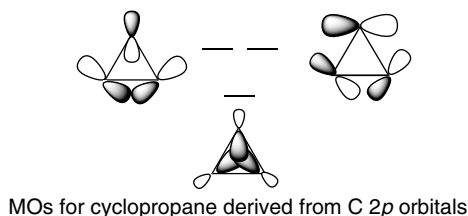
<sup>119</sup>. A. Sella, H. Basch, and S. Hoz, *J. Am. Chem. Soc.*, **118**, 416 (1996).

<sup>120</sup>. J. Gauss, D. Cremer, and J. F. Stanton, *J. Phys. Chem. A*, **104**, 1319 (2000).

to the greater  $s$  character in the carbon orbital. Proponents of VB description argue that the properties of cyclopropane are well described by the bent bond idea and that no other special characteristics are needed to explain bonding in cyclopropane.<sup>121</sup> There is, however, an unresolved issue. Cyclopropane has a total strain energy of 27.5 kcal/mol. This is only slightly greater than that for cyclobutane (26.5 kcal/mol), which suggests that there might be some special stabilizing feature present in cyclopropane.



In MO terms, cyclopropane can be described as being formed from three  $sp^2$ -hybridized methylene groups. The carbon-carbon bonds in the plane of the ring are then considered to be derived from six unhybridized carbon  $2p$  orbitals. This leads to a delocalized molecular orbital with maximum overlap *inside* the ring and two other degenerate orbitals that have maximum density *outside* the ring. According to this picture, the orbital derived from lobes pointing to the center of the ring should be particularly stable, since it provides for delocalization of the electrons in this orbital.



Schleyer and co-workers made an effort to dissect the total bonding energy of cyclopropane into its stabilizing and destabilizing components.<sup>122</sup> Using C-H bond energies to estimate the strain in the three-membered ring relative to cyclohexane, they arrived at a value of 40.4 kcal/mol for total strain. The stronger C-H bonds (108 kcal/mol), contribute 8.0 kcal/mol of stabilization, relative to cyclohexane. Using estimates of other components of the strain, such as eclipsing, they arrived at a value of 11.3 kcal/mol as the stabilization owing to  $\sigma$  delocalization. The concept of  $\sigma$  delocalization is also supported by the NMR spectrum and other molecular properties that are indicative of a ring current. (See Section 8.1.3 for a discussion of ring current as an indicator of electron delocalization.) The Laplacian representation (see Topic 1.4) of the electron density for cyclopropane shown in Figure 1.36 shows a peak at the center of the ring that is not seen in cyclobutane.<sup>123</sup> The larger cross-ring distances in cyclobutane would be expected to reduce overlap of orbitals directed toward the center of the ring.

<sup>121</sup> J. G. Hamilton and W. E. Palke, *J. Am. Chem. Soc.*, **115**, 4159 (1993); P. Karadakov, J. Gerratt, D. L. Cooper, and M. Raimondi, *J. Am. Chem. Soc.*, **116**, 7714 (1994); P. B. Karadakov, J. Gerratt, D. L. Cooper, and M. Raimondi, *Theochem*, **341**, 13 (1995).

<sup>122</sup> K. Exner and P. v. R. Schleyer, *J. Phys. Chem. A*, **105**, 3407 (2001).

<sup>123</sup> D. Cremer and J. Gauss, *J. Am. Chem. Soc.*, **108**, 7467 (1986).

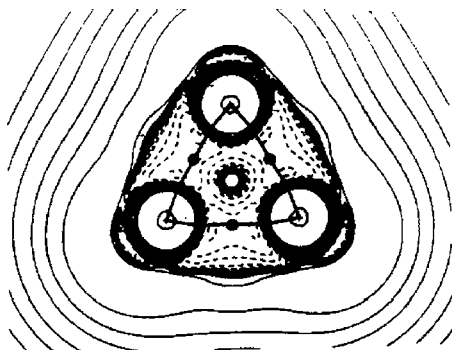
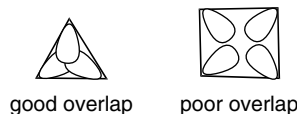
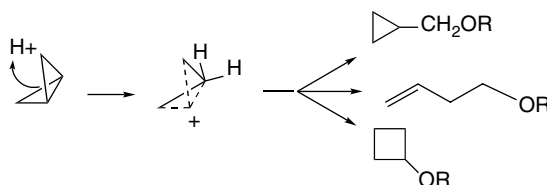


Fig. 1.36. Contours of the Laplacian for cyclopropane in the plane of the rings. Dots are bond critical points. Reproduced with permission from R. F. W. Bader, in *Chemistry of Alkanes and Cycloalkanes*, S. Patai and Z. Rappoport, eds., John Wiley & Sons, New York, 1992, Chap. 1.

Bicyclo[1.1.0]butane, bicyclo[1.1.1]pentane, [1.1.1]propellane, and spiro[2.2]pentane are other molecules where strain and rehybridization affect molecular properties. The molecules show enhanced reactivity that can be attributed to characteristics of the rehybridized orbitals. The structures are shown in Scheme 1.6, which also shows calculated AIM charge distributions and strain energy.

The strain in bicyclo[1.1.0]butane results in decreased stability and enhanced reactivity.<sup>124</sup> The strain energy is 63.9 kcal/mol; the central bond is nearly pure *p* in character,<sup>125</sup> and it is associated with a relatively high HOMO.<sup>126</sup> These structural features are reflected in enhanced reactivity toward electrophiles. In acid-catalyzed reactions, protonation gives the bicyclobutonium cation (see Section 4.4.5) and leads to a characteristic set of products.



<sup>124</sup> S. Hoz, in *The Chemistry of the Cyclopropyl Group*, Part 2, S. Patai and Z. Rappoport, eds., Wiley, Chichester, 1987, pp 1121–1192; M. Christl, *Adv. Strain Org. Chem.*, **4**, 163 (1995).

<sup>125</sup> J. M. Schulman and G. J. Fisanick, *J. Am. Chem. Soc.*, **92**, 6653 (1970); R. D. Bertrand, D. M. Grant, E. L. Allred, J. C. Hinshaw, and A. B. Strong, *J. Am. Chem. Soc.*, **94**, 997 (1972); D. R. Whitman and J. F. Chiang, *J. Am. Chem. Soc.*, **94**, 1126 (1972); H. Finkelmeier and W. Lüttke, *J. Am. Chem. Soc.*, **100**, 6261 (1978).

<sup>126</sup> K. B. Wiberg, G. B. Ellison, and K. S. Peters, *J. Am. Chem. Soc.*, **99**, 3941 (1977).

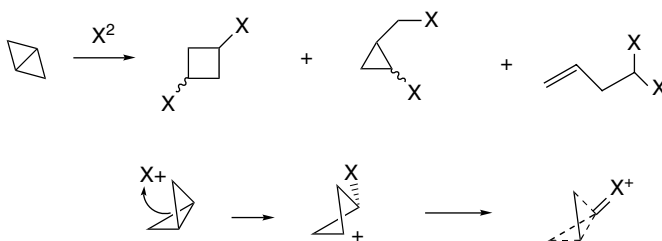
## Scheme 1.6. AIM Charge Distribution and Strain Energy (kcal/mol) for Cyclic Hydrocarbons

Monocyclic				
				
Charge:	C -0.010 H +0.005	C +0.06 H -0.03	C +0.08 H -0.04	C +0.08 H -0.04
Strain:	27.5	26.5	6.2	0
Bicyclic				
		C(5) -0.03 H(5) +0.002		C(2) -0.059 H(2) -0.030
	C(2) +0.072 H(2) -0.002		C(2) +0.082 H(2) -0.025	
C(1) -0.12 H(1) +0.054 63.9		C(1) -0.043 H(1) +0.011 54.7		C(1) +0.030 H(1) -0.028 51.8
	C(2) +0.043 H(2) -0.030		C(7) 0.036 H(7) -0.034 C(2) +0.058 H(2) -0.036	
C(1) +0.036 H(1) -0.011 68.0		C(1) +0.074 H(1) -0.033 14.4		C(1) +0.101 H(1) -0.044 7.4
Propellanes				
	C(2) +0.026 H(2) +0.023		C(5) +0.036 H(5) +0.019 C(2) 0.0103 H(2) -0.014	
C(1) -0.107 98		C(1) -0.149 104		C(7) +0.042 H(7) +0.013 C(2) +0.099 H(2) -0.020 C(1) -0.152 105
				
				C(2) +0.051 H(2) -0.023 C(1) = -0.016 89
Others				
	C(2) = +0.003 H(2) = +0.007			
C(1) = -0.072 63.2		C(1) = -0.111 H(1) = +0.111 140		C(1) = +0.003 H(1) = -0.003 154.7

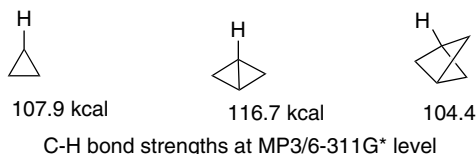
a. R. F. W. Bader in *The Chemistry of Alkanes and Cycloalkanes*, S. Patai and Z. Rappoport, eds., John Wiley & Sons, New York, 1992, p. 51.

Bicyclo[1.1.0]butane also reacts with the halogens. With  $I_2$ , the main product is 1,3-diiodocyclobutane (5:1 *cis:trans*). With  $Br_2$  and  $Cl_2$ , cyclopropylcarbinyl and butenyl products are also formed.<sup>127</sup> The initial attack occurs from the *endo* face of the molecule and the precise character of the intermediate appears to be dependent on the halogen.

<sup>127</sup> K. B. Wiberg, G. M. Lampman, R. P. Ciula, D. S. Connor, P. Schertler, and J. Lavanish, *Tetrahedron*, **21**, 2749 (1968); K. B. Wiberg and G. J. Szejmies, *J. Am. Chem. Soc.*, **92**, 571 (1970).



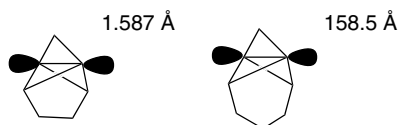
The bridgehead C–H bond in tricyclo[1.1.1]pentane is not quite as strong as the C–H bond in cyclopropane. A value of 104.4 kcal/mol is calculated at the MP3/6-31G\* level.<sup>128</sup> The total strain energy is 68 kcal/mol.



The alignment of the two bridgehead bonds is such that there is strong interaction between them. As a result of this interaction, there is hyperconjugation between the two bridgehead substituents. For example, the <sup>19</sup>F chemical shifts are effected by  $\sigma \rightarrow \sigma^*$  donation to the C–F  $\sigma^*$  orbital.<sup>129</sup>



[1.1.1]Propellane has a very unusual shape. All four bonds at the bridgehead carbons are directed toward the same side of the nucleus.<sup>130</sup> There have been many computational studies of the [1.1.1]propellane molecule. One of the main objectives has been to understand the nature of the bridgehead-bridgehead bond and the extension of the orbital external to the molecule. The distance between the bridgehead carbons in [1.1.1]propellane is calculated to be 1.59 Å. The molecule has been subjected to AIM analysis. The  $\rho_{(c)}$  value for the bridgehead-bridgehead bond is  $0.173a_0^{-3}$ , which indicates a bond order of about 0.7.<sup>131</sup> There is a low-temperature X-ray crystal structure of [1.1.1]propellane. Although it is not of high resolution, it does confirm the length of the bridgehead bond as 1.60 Å.<sup>132</sup> Higher-resolution structures of related tetracyclic compounds give a similar distance and also show electron density external to the bridgehead carbons.<sup>133</sup>



<sup>128</sup>. K. B. Wiberg, C. M. Hadad, S. Sieber, and P. v. R. Schleyer, *J. Am. Chem. Soc.*, **114**, 5820 (1992).

<sup>129</sup>. W. Adcock and A. N. Abeywickrema, *J. Org. Chem.*, **47**, 2957 (1982); J. A. Koppel, M. Mishima, L. M. Stock, R. W. Taft, and R. D. Topsom, *J. Phys. Org. Chem.*, **6**, 685 (1993).

<sup>130</sup>. L. Hedberg and K. Hedberg, *J. Am. Chem. Soc.*, **107**, 7257 (1985).

<sup>131</sup>. K. B. Wiberg, R. F. W. Bader, and C. D. H. Lau, *J. Am. Chem. Soc.*, **109**, 985 (1987); W. Adcock, M. J. Brunger, C. I. Clark, I. E. McCarthy, M. T. Michalewicz, W. von Niessen, E. Weigold, and D. A. Winkler, *J. Am. Chem. Soc.*, **119**, 2896 (1997).

<sup>132</sup>. P. Seiler, *Helv. Chim. Acta*, **73**, 1574 (1990).

<sup>133</sup>. P. Seiler, J. Belzner, U. Bunz, and G. Szeimies, *Helv. Chim. Acta*, **71**, 2100 (1988).



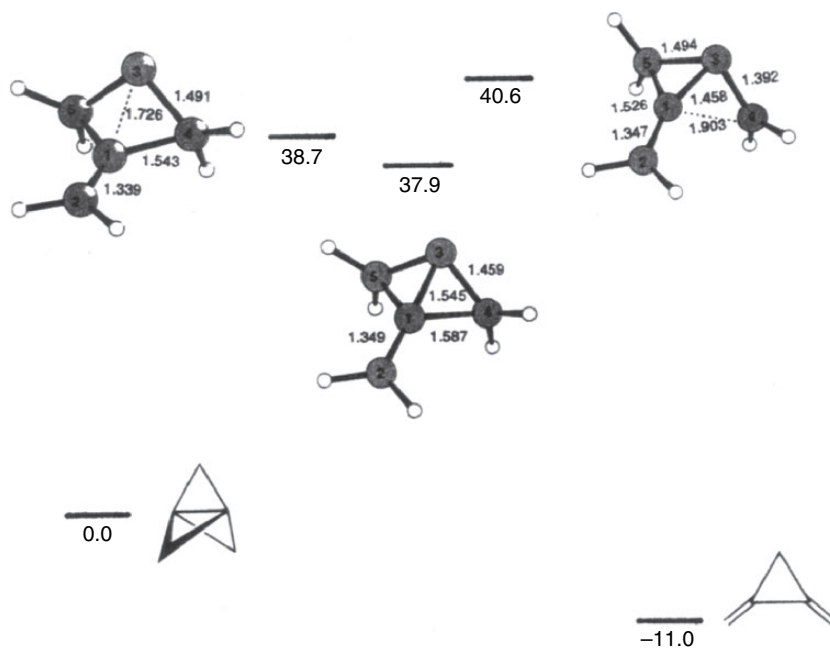
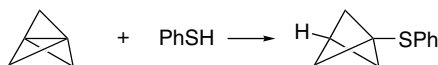


Fig. 1.37. DFT (B3PW91/D95(*d,p*)) representation of the thermal isomerization of [1.1.1]propellane to 1,2-dimethylenecyclopropane. Adapted from O. Jarosch, R. Walsh, and G. Szeimies, *J. Am. Chem. Soc.*, **122**, 8490 (2000).

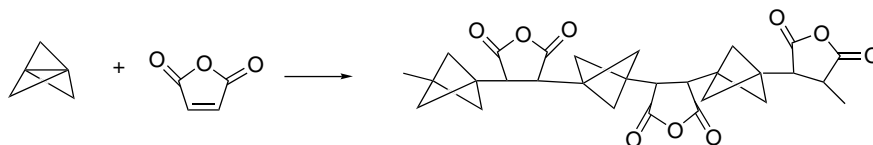
Both radicals and electrophiles react at the bridgehead bond of [1.1.1]propellane. The reactivity toward radicals is comparable to that of alkenes, with rates in the range of  $10^6$  to  $10^8$   $M^{-1} s^{-1}$ , depending on the particular radical.<sup>138</sup> For example, [1.1.1]propellane reacts with thiophenol at room temperature.<sup>139</sup>



Reaction with the halogens breaks the bridgehead bond and leads to 1,3-dihalobicyclo[1.1.1]butanes. When halide salts are included, mixed dihalides are formed, suggesting an ionic mechanism.<sup>140</sup>



[1.1.1]Propellane and maleic anhydride copolymerize to an alternating copolymer.<sup>141</sup>



Each of these reactions indicates the high reactivity of the bridgehead-bridgehead bond.

<sup>138</sup>. P. F. McGarry and J. C. Scaiano, *Can. J. Chem.* **76**, 1474 (1998).

<sup>139</sup>. K. B. Wiberg and S. T. Waddell, *J. Am. Chem. Soc.*, **112**, 2194 (1990).

<sup>140</sup>. I. R. Milne and D. K. Taylor, *J. Org. Chem.*, **63**, 3769 (1998).

<sup>141</sup>. J. M. Gosau and A.-D. Schlüter, *Chem. Ber.*, **123**, 2449 (1990).

## Topic 1.4. Representation of Electron Density by the Laplacian Function

Electron distribution in molecules can be usefully represented by the *Laplacian* of the electron density. The Laplacian is defined by the equation

$$\nabla^2\rho = \frac{\partial^2\rho}{\partial x^2} + \frac{\partial^2\rho}{\partial y^2} + \frac{\partial^2\rho}{\partial z^2} \quad (1.30)$$

which is a measure of the curvature of the electron density. The negative of  $\nabla^2\rho$ , called  $L$ , depicts regions of electron concentration as maxima and regions of electron depletion as minima. The Laplacian function can distinguish these regions more easily than the total electron density contours. It also depicts the concentric shells corresponding to the principal quantum numbers. Figure 1.38 shows the  $L$  functions for water, ammonia, and methane. The diagrams show concentration of valence shell electron density in the region of bonds. The water and ammonia molecules also show maxima corresponding to the nonbonding electrons.

Figure 1.39 shows  $L$  for ethane, ethene, and ethyne.<sup>142</sup> Note the regions of bonding associated with the two shells of carbon between the two carbons and between carbon and hydrogen. Figure 1.40 shows a perspective view of ethene indicating the saddle point between the carbon atoms. The ridge with a saddle point corresponds to electron density in the nodal plane of the  $\pi$  bond.

Figure 1.41 compares the Laplacian of the experimental electron density from a low-temperature crystallographic study of ethane with the computed  $L$  using the 6-311G\*\* basis set.<sup>143</sup> This serves to make a connection between computed and experimental electron density.

The electron density for small molecules corresponds to expectations based on electronegativity. Figure 1.42 gives  $L(\mathbf{r})$  for  $\text{N}_2$  (a),  $\text{CO}$  (b), and  $\text{H}_2\text{C}=\text{O}$  (c, d). The diagram for nitrogen shows the concentric shells and accumulation of electron density between the nitrogen nuclei. The distribution, of course, is symmetrical. For  $\text{C}\equiv\text{O}$  there is a substantial shift of electron density toward carbon, reflecting the polar character of the  $\text{C}\equiv\text{O}$  bond. Figure 1.42c is  $L(\mathbf{r})$  in the molecular plane of formaldehyde. In

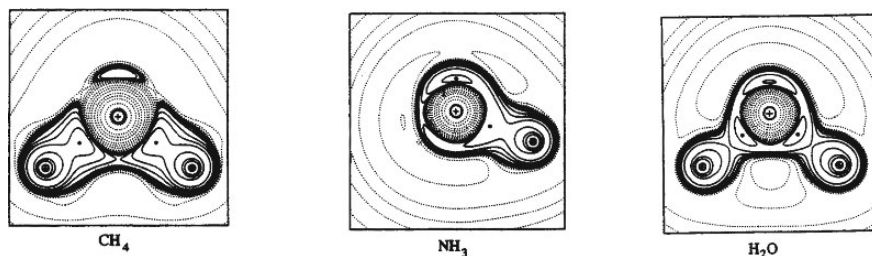


Fig. 1.38. Contour maps of  $L$  for methane, ammonia, and water. For water, the contours are in the plane of the molecule. For ammonia and methane the contours are in the plane that bisects the molecule with a hydrogen above and below the plane. Reproduced with permission from R. J. Gillespie and P. L. A. Popelier, *Chemical Bonding and Molecular Geometry*, Oxford University Press, Oxford, 2001, p. 172.

<sup>142</sup> R. F. W. Bader, S. Johnson, T.-H. Tang and P. L. A. Popelier *J. Phys. Chem.*, **100**, 15398 (1996).

<sup>143</sup> V. G. Tsirelson, *Can. J. Chem.*, **74**, 1171 (1996).

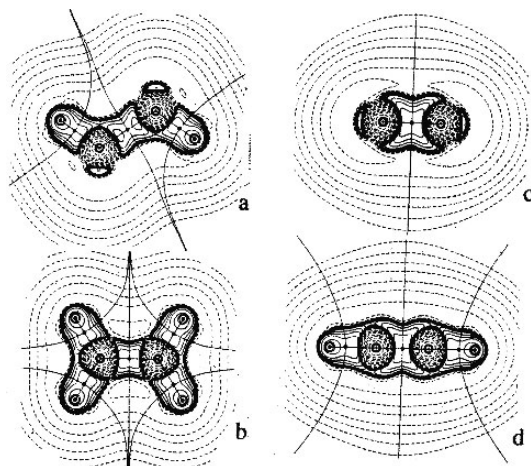


Fig. 1.39. Contour maps of  $L(r)$  for: (a) ethane in a plane bisecting *anti*-hydrogens; (b) ethene in the molecular plane; (c) ethene perpendicular to the molecular plane, and (d) ethyne. The solid lines depict the zero-flux surfaces of the C and H atoms. From *J. Phys. Chem.* **100**, 15398 (1996).

addition to the C-H bonds, the contours indicate the electron density associated with the unshared pairs on oxygen. Figure 1.42d, shows  $L$  perpendicular to the plane of the molecule and is influenced by the  $\pi$  component of the C=O bond. It shows greater electron density around oxygen, which is consistent with the expectation that carbon would have a partial positive charge.

These diagrams can help to visualize the electron density associated with these prototypical molecules. We see that most electron density is closely associated with

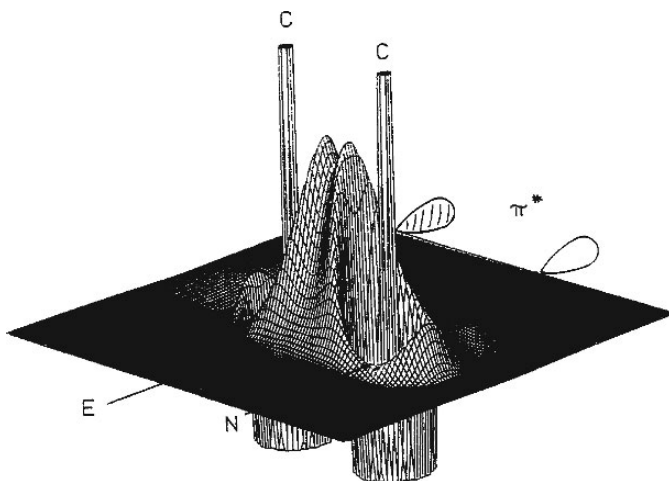


Fig. 1.40. Perspective of Laplacian  $-\nabla^2\rho_e(r)$  of ethene in a plane perpendicular to the molecular plane. From E. Kraka and D. Cremer in *The Concept of the Chemical Bond*, Z. B. Maksic, ed., Springer-Verlag 1990, p. 533.

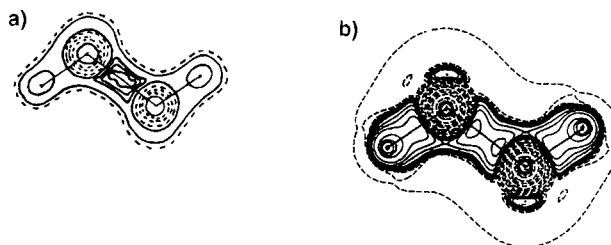


Fig. 1.41. Comparison of experimental (a) and theoretical (b) Laplacian of the electron density of ethane. From *Can. J. Chem.*, **74**, 1171 (1996).

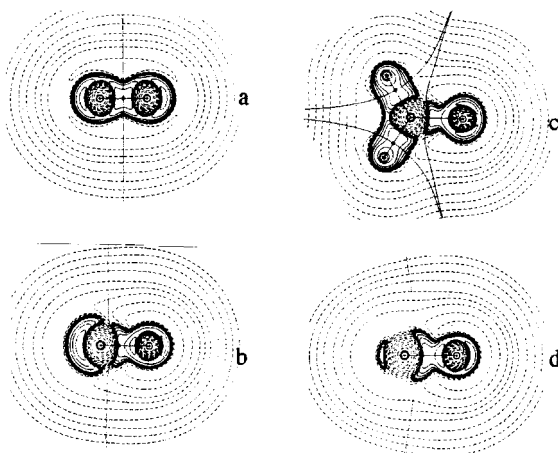


Fig. 1.42. Contour plots of  $L(\mathbf{r})$  for  $\text{N}_2$  (a),  $\text{CO}$  (b), and  $\text{H}_2\text{C}=\text{O}$  in (c) and perpendicular to (d) the plane of the molecule. From *J. Phys. Chem.*, **100**, 15398 (1996).

the nuclei, but that regions of increased electron density corresponding to chemical bonds can be recognized. Most of the electron density diagrams that are available are the results of computation. Where experimental data are available, there is excellent correspondence with the computational data.

### Topic 1.5. Application of Density Functional Theory to Chemical Properties and Reactivity

The qualitative ideas of valence bond (VB) theory provide a basis for understanding the relationships between structure and reactivity. Molecular orbital (MO) theory offers insight into the origin of the stability associated with delocalization and also the importance of symmetry. As a central premise of density functional theory (DFT) is that the electron density distribution determines molecular properties, there has been an effort to apply DFT to numerical evaluation of the qualitative concepts such as electronegativity, polarizability, hardness, and softness. The sections that follow explore the relationship of these concepts to the description of electron density provided by DFT.

DFT suggests quantitative expressions and interrelation of certain properties such as electronegativity and polarizability, and the related concepts of hardness and softness introduced in Sections 1.1.3 through 1.1.6.<sup>144</sup> DFT calls the escaping tendency of an electron from a particular field its *chemical potential*,<sup>145</sup>  $\mu$ , defined by

$$\mu = (\partial E / \partial N)_v \quad (1.31)$$

which is the slope of a curve for the energy of the system as a function of the change in the number of electrons.

A stable system, such as a molecule, attains a common chemical potential among its components. That is, there is no net force to transfer electron density from one point to another. The idea that chemical potential is equivalent throughout a molecule, and specifically between bonded atoms, accords with the concept of *electronegativity equalization* (see Section 1.1.4).<sup>146</sup> Chemical potential is related to electrophilicity and nucleophilicity. A system with an attraction toward electrons is electrophilic, whereas a system that can donate electrons is nucleophilic. Chemical potential is considered to be the opposite of absolute (Mulliken) electronegativity and can be approximated by

$$\mu = -\frac{\text{IP} + \text{EA}}{2} \quad (1.32)$$

which is negative of the Mulliken absolute electronegativity:

$$\chi = \frac{\text{IP} + \text{EA}}{2} \quad (1.33)$$

Since  $\mu$  is the slope of electronic energy as a function of the change in the number of electrons, the Mulliken equation gives the energy for the +1 (IP) and -1 (EA) ionization states. This is illustrated in Figure 1.43, which shows that  $(\text{IP} + \text{EA})/2$  is the average slope over the three points and should approximate the slope at the midpoint, where  $N = 0$ .<sup>147</sup>

The Luo-Benson expression for electronegativity<sup>148</sup>

$$V = n/r \quad (1.34)$$

which relates electronegativity to the number of valence shell electrons  $n$  and the atomic radius  $r$  is both theoretically related<sup>149</sup> and empirically correlated<sup>150</sup> with the Mulliken

<sup>144</sup>. P. W. Chattaraj and R. G. Parr, *Structure and Bonding*, **80**, 11 (1993); G.-H. Liu and R. G. Parr, *J. Am. Chem. Soc.*, **117**, 3179 (1995).

<sup>145</sup>. R. G. Parr, R. A. Donnelly, M. Levy, and W. E. Palke, *J. Chem. Phys.*, **68**, 3801 (1978).

<sup>146</sup>. R. T. Sanderson, *J. Am. Chem. Soc.*, **105**, 2259 (1983); R. T. Sanderson, *Polar Covalence*, Academic Press, New York, 1983.

<sup>147</sup>. R. G. Pearson, *Chemical Hardness*, Wiley-VCH, Weinheim, 1977, p. 33; see also R. P. Iczkowski and J. L. Margrave, *J. Am. Chem. Soc.*, **83**, 3547 (1961).

<sup>148</sup>. Y. R. Luo and S. W. Benson, *J. Phys. Chem.*, **92**, 5255 (1988); Y.-R. Luo and S. W. Benson, *J. Am. Chem. Soc.*, **111**, 2480 (1989); Y. R. Luo and S. W. Benson, *J. Phys. Chem.*, **94**, 914 (1990); Y. R. Luo and S. W. Benson, *Acc. Chem. Res.*, **25**, 375 (1992).

<sup>149</sup>. P. Politzer, R. G. Parr, and D. R. Murphy, *J. Chem. Phys.*, **79**, 3859 (1983).

<sup>150</sup>. Y. R. Luo and P. D. Pacey, *J. Am. Chem. Soc.*, **113**, 1465 (1991).

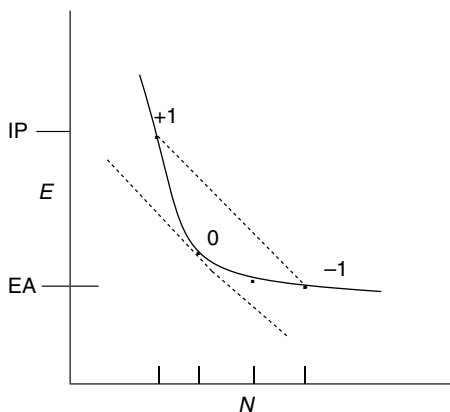


Fig. 1.43. Diagram showing that  $(EA + IP)/2$  provides an approximation of the slope of  $E$  for the neutral atoms. Adapted from R. G. Pearson, *Chemical Hardness*, Wiley-VCH, Weinheim, 1997, p. 33.

absolute electronegativity  $(IP + EA)/2$ . The principle of maximum hardness<sup>151</sup> (p. 16) can be derived as a consequence of DFT, as can the concepts of hardness and softness.<sup>152</sup>

In DFT, hardness is defined as

$$2\eta = (\partial\mu/\partial N)_v \quad (1.35)$$

which is the curvature of the plot of  $E$  versus  $N$  and is approximated by

$$\eta \cong (IP - EA)/2 \quad (1.36)$$

and softness,  $S = 1/\eta$  is

$$(\partial N/\partial\mu)_v \cong 2/(IP - EA) \quad (1.37)$$

There is a linear correlation between the empirical electronegativity (Pauling scale) and hardness and the absolute electronegativity (Mulliken electronegativity) for the nontransition metals<sup>153</sup>:

$$\chi = 0.44\eta + 0.044\chi_{abs} + 0.04 \quad (1.38)$$

This correlation is illustrated in Figure 1.44. Polarizability is related to softness. Expressed as  $\alpha^{1/3}$ , it is proportional to softness, approximated by  $2/(IP - EA)$ .<sup>154</sup>

DFT also suggests explicit definitions of covalent and van der Waals radii. The covalent radius in the AIM context is defined by the location of the bond critical point

<sup>151</sup> R. G. Parr and P. K. Chattaraj, *J. Am. Chem. Soc.*, **113**, 1854 (1991); T. K. Ghanty and S. K. Ghosh, *J. Phys. Chem.*, **100**, 12295 (1996).

<sup>152</sup> P. K. Chattaraj, H. Lee, and R. G. Parr, *J. Am. Chem. Soc.*, **113**, 1855 (1991).

<sup>153</sup> R. G. Pearson, *Chemical Hardness*, Wiley-VCH, Weinheim, Germany, 1997, p. 44; J. K. Nagle, *J. Am. Chem. Soc.*, **112**, 4741 (1990).

<sup>154</sup> T. K. Ghanty and S. K. Ghosh, *J. Phys. Chem.*, **97**, 4951 (1993); S. Hati and D. Datta, *J. Phys. Chem.*, **98**, 10451 (1994).

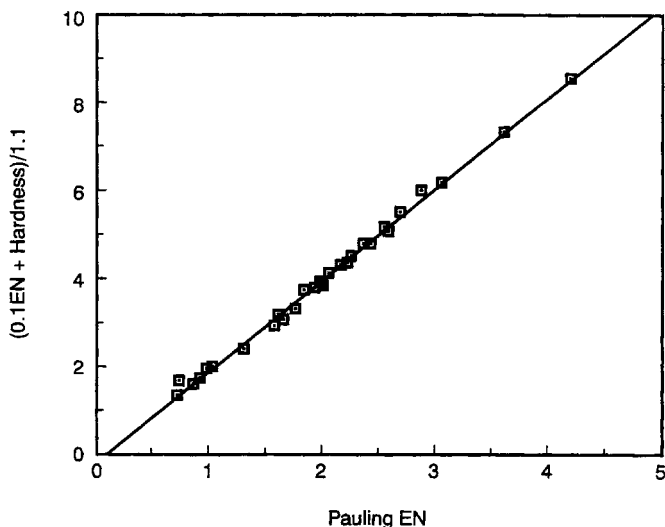


Fig. 1.44. Correlation between empirical (Pauling) electronegativity, ( $\chi_{\text{Pauling}}$ ), hardness ( $\eta$ ), and absolute (Mulliken) electronegativity ( $\chi_{\text{abs}}$ ). From R. G. Pearson, *Chemical Hardness*, Wiley-VCH, Weinheim, 1997, p. 54.

and depends on the other element in the bond. The covalent radii of atoms can also be defined theoretically within DFT,<sup>155</sup> and are equated with the distance at which the chemical potential equals the total electrostatic potential calculated for the atom. This is the point at which the electrostatic potential crosses from negative to positive and where the sum of the kinetic energy and exchange and correlation functionals is zero. Using the approximation  $-(\text{IP} + \text{EA})/2 = \mu$ , one finds  $\varphi_r$ , the distance at which this equality holds<sup>156</sup>:

$$\text{at } r_c \quad V_c = \mu \cong -\frac{\text{IP} + \text{EA}}{2} \quad (1.39)$$

The values derived in this way are shown in Table 1.24.

The AIM treatment defines van der Waals radii in terms of a particular electron density contour. It has been suggested that the 0.002 au contour provides a good representative of the van der Waals dimension of a molecule.<sup>157</sup>

### T.1.5.2. DFT Formulation of Reactivity—The Fukui Function

The electron density  $\rho(\mathbf{r})$  can provide information about the *reactivity* of a molecule. MO theory can assess reactivity in terms of frontier orbitals and, in particular, the energy and atomic distribution and symmetry of the HOMO and LUMO. DFT provides a representation of total electron distribution and extracts indicators of

<sup>155</sup>. P. Ganguly, *J. Am. Chem. Soc.*, **115**, 9287 (1993).

<sup>156</sup>. P. Politzer, R. G. Parr, and D. R. Murphy, *J. Chem. Phys.*, **79**, 3859 (1983).

<sup>157</sup>. R. F. W. Bader, W. H. Henneker, and P. D. Cade, *J. Chem. Phys.* **46**, 3341 (1967); R. F. W. Bader and H. J. T. Preston, *Theor. Chim. Acta*, **17**, 384 (1970).

**Table 1.24. Covalent Radii from DFT**

Atom	Covalent radius (au) <sup>a</sup>
Li	1.357
B	1.091
C	0.912
N	0.814
O	0.765
F	0.671
Na	1.463
Al	1.487
Si	1.296
P	1.185
S	1.120
Cl	0.999
Se	1.209
Br	1.116
I	1.299

a. P. Politzer, R. G. Parr, and D. R. Murphy, *J. Chem. Phys.*, **79**, 3859 (1983); M. K. Harbola, R. G. Parr, and C. Lee, *J. Chem. Phys.*, **94**, 6055 (1991).

reactivity. The *responsiveness* of this electron distribution to a perturbing external field, e.g., an approaching reagent, must be evaluated. This responsiveness is described by the *Fukui function*,<sup>158</sup> which is a reactivity indicator is defined by

$$f(\mathbf{r}) = [n(\mathbf{r})/N] \left[ \frac{\delta\mu}{\delta v(\mathbf{r})} \right]_N = \left( \frac{\partial \rho(\mathbf{r})}{\partial N} \right)_{v(\mathbf{r})} \quad (1.40)$$

where  $N$  is the change in the number of electrons in the system.

Fukui functions are defined for electrophilic ( $f^-$ ), nucleophilic ( $f^+$ ), and radical ( $f^\circ$ ) reactions by comparing the electron density  $\rho(\mathbf{r})$ , with one fewer electron, one more electron, and the average of the two<sup>159</sup>:

$$f^-(\mathbf{r}) = \rho_N(\mathbf{r}) - \rho_{N-1}(\mathbf{r}) \quad (1.41)$$

$$f^+(\mathbf{r}) = \rho_{N+1}(\mathbf{r}) - \rho_N(\mathbf{r}) \quad (1.42)$$

$$f^\circ(\mathbf{r}) = \frac{\rho_{N+1}(\mathbf{r}) - \rho_{N-1}(\mathbf{r})}{2} \quad (1.43)$$

The Fukui function describes interactions between two molecules in terms of the electron transfer between them. The extent of electron transfer is related to chemical potential (and electronegativity) and hardness (and polarizability).

$$\Delta N = \frac{|\mu_B^\circ - \mu_A^\circ|}{\eta_B^\circ + \eta_A^\circ} \quad (1.44)$$

The responsiveness of the electron density to interaction with another field is nonuniform over the molecule. The electron density can be further partitioned among

<sup>158</sup> R. G. Parr and W. Yang, *J. Am. Chem. Soc.*, **106**, 4049 (1984).

<sup>159</sup> C. Lee, W. Yang, and R. G. Parr, *Theochem*, **40**, 305 (1988).

the atoms of a molecule by *condensed Fukui* functions. These calculations must use a scheme, such as Mulliken population analysis (see Section 1.4.1) for dividing the electron density among the atoms. The condensed Fukui functions identify regions of space that are electron-rich ( $f^-$ ) and electron-poor ( $f^+$ ).<sup>160</sup> Reactivity at individual atoms can also be expressed as *local softness*, which is the product of the Fukui function and global softness  $S$ .<sup>161</sup> As with the Fukui function, these are defined for electrophilic, nucleophilic, and radical reactants.

$$s^- = [\rho_{(N)} - \rho_{(N-1)}]S \quad (1.45)$$

$$s^+ = [\rho_{(N+1)} - \rho_{(N)}]S \quad (1.46)$$

and

$$s^\circ = \frac{1}{2}[\rho_{(N+1)} - \rho_{(N-1)}]S \quad (1.47)$$

The idea that *frontier orbitals* control reactivity introduced in the context of MO theory has an equivalent in DFT. The electron density distribution should have regions of differing susceptibility to approach by nucleophiles and electrophiles. Reactivity should correspond to the ease of distortion of electron density by approaching reagents. This response to changes in electron distribution is expressed in terms of the Fukui function, which describes the ease of displacement of electron density in response to a shift in the external field. Since the electron distribution should respond differently to interaction with electron acceptors (electrophiles) or electron donors (nucleophiles), there should be separate  $f^+$  and  $f^-$  functions. Reaction is most likely to occur at locations where there is the best match (overlap) of the  $f^+$  function of the electrophile and the  $f^-$  function of the nucleophile.<sup>162</sup> For example, the  $f^+$  and  $f^-$  functions for formaldehyde have been calculated and are shown in Figure 1.45.<sup>163</sup> The  $f^+$  function, describing interaction with a nucleophile, has a shape similar to the  $\pi^*$  MO. It has a higher concentration on carbon than on oxygen and the maximum value is perpendicular to the molecular plane. The  $f^-$  function is similar in distribution to the nonbonding ( $n$ ) electron pairs of oxygen. This treatment, then, leads to predictions about the reactivity toward nucleophiles and electrophiles that are parallel to those developed from MO theory (see p. 45). A distinction to be made is that in the MO formulation the result arises on the basis of a particular orbital combination—the HOMO and LUMO. The DFT formulation, in contrast, comes from the total electron density. Methods are now being developed to compute Fukui functions and other descriptors of reactivity derived from total electron density.

DFT can evaluate properties and mutual reactivity from the electron distribution. These relationships between qualitative concepts in chemistry, such as electronegativity and polarizability, suggest that DFT does incorporate fundamental relationships between molecular properties and structure. At this point, we want to emphasize the conceptual relationships between the electron density and electronegativity and polarizability. We can expect electrophiles to attack positions with relatively high electron density and polarizability. Nucleophiles should attack positions of relatively

<sup>160</sup> Y. Li and J. N. S. Evans, *J. Am. Chem. Soc.*, **117**, 7756 (1995).

<sup>161</sup> W. Yang and W. J. Mortier, *J. Am. Chem. Soc.*, **108**, 5708 (1986).

<sup>162</sup> R. F. Nalewajski, *Top. Catal.*, **11/12**, 469 (2000).

<sup>163</sup> A. Michalak, F. De Proft, P. Geerlings, and R. F. Nalewajski, *J. Phys. Chem. A*, **103**, 762 (1999); F. Gilardoni, J. Weber, H. Chermette, and T. R. Ward, *J. Phys. Chem. A*, **102**, 3607 (1998).

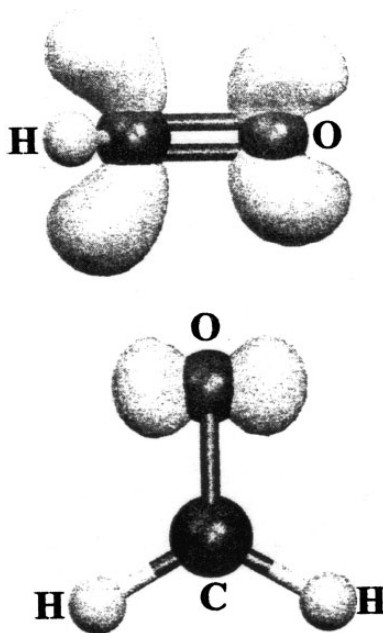


Fig. 1.45. Fukui function  $f^+$  and  $f^-$  isosurfaces for  $\text{CH}_2=\text{O}$  (0.001 au). Reproduced with permission from F. Gilardoni, J. Weber, H. Chermette, and T. R. Ward, *J. Phys. Chem. A*, **102**, 3607 (1998).

low electron density. The hard-soft concept also states that *reactant and reagent should match* with respect to these properties. The methods for exploiting this potential are currently under development.

### T.1.5.3. DFT Concepts of Substituent Groups Effects

The interpretation and correlation of information about organic compounds depends on the concept of *substituent effects*, which is the idea that a particular group of atoms will affect structure and reactivity in a predictable way. This is a long-standing and fundamental concept in organic chemistry. Recent developments, particularly in DFT, have provided new theoretical foundations and interpretations. Substituent groups can be classified as electron-releasing (ERG) or electron-withdrawing (EWG). There is an approximate ordering of such groups that is related in a general way to electronegativity. We discuss substituent effects in detail in Chapter 3, but here we want to introduce some broad concepts concerning the ways that substituents affect structure and reactivity.

Traditionally, the focus has been on polar and resonance effects, based on VB ideas about structure, and the emphasis is on partial charges arising from polar bonds and resonance/hyperconjugation. However, in MO theory, we use the idea of *perturbations*. The question asked is, "How does a substituent affect the energy and shapes of the orbitals, with particular attention to the HOMO and LUMO, the *frontier orbitals*. Ultimately, substituents affect structure and reactivity by changing the electron density distribution. From the concept of electronegativity, we know that bonds have dipoles,

which influence interactions with approaching reagents and thus affect reactivity. We also discussed the concept of *polarizability*, which refers to the ease of distortion of the electron density distribution of an atom or an ion and can be described as *hardness* or *softness*. Since chemical reactions involve the reorganization of electrons by breaking and forming bonds, polarizability also has a major influence on reactivity.

There have been a number of efforts to assign numerical values to electronegativity of substituent groups, analogous to the numbers assigned to atoms (see Section 1.1.3). These have been based on structural parameters, charge distribution, thermodynamic relationships and or MO computations.<sup>164</sup> More recently, as DFT descriptions of electron density have developed and these, too, have been applied to organic functional groups. DFT suggests quantitative expressions of some of the qualitative concepts such as electronegativity, polarizability, hardness, and softness.<sup>165</sup> DFT describes a molecule as an electron density distribution, in which the nuclei are embedded, that is subject to interaction with external electrical fields, such as that of an approaching reagent. Several approaches are currently being explored to find correlations and predictions based on DFT concepts that were introduced in Section 1.3.

De Proft, Langenaeker, and Geerlings applied the DFT definitions of electronegativity, hardness, and softness to calculate group values, which are shown in Table 1.25. These values reveal some interesting comparisons. The electronegativity values calculated for  $C_2H_5$ ,  $CH_2=CH$ , and  $HC\equiv C$  are in accord with the relationship with hybridization discussed in Section 1.1.5. The methyl group is significantly more electronegative and harder than the ethyl group. This is consistent with the difference noted between methyl and ethyl diazonium ions in Section 1.4.3. Typical EWGs such as  $CH=O$ ,  $C\equiv N$ , and  $NO_2$  show high electronegativity. Hardness values are more difficult to relate to familiar substituent effects. The acetyl, carboxamide, and nitro groups, for example, are among the softer substituents. This presumably reflects the electron density of the unshared electron pairs on oxygen in these groups.

AIM results from methyl compounds were also used to develop a group electronegativity scale. Boyd and Edgecombe defined a quantity  $F_A$  in terms of  $r_H$ , the location of the bond critical point to hydrogen,  $N_A$  the number of valence electrons of the atom A, and  $\rho_{(c)}$ , the electron density at the bond critical point<sup>166</sup>:

$$F_n = r_H/N_A\rho(r_c)r_{AH} \quad (1.48)$$

These were then scaled to give numerical comparability with the Pauling electronegativity scale.<sup>167</sup> In another approach, the charge on the methyl group was taken as the indicator of the electronegativity of the group X and the results were scaled to the Pauling atomic electronegativity scale.<sup>168</sup> It was also noted that the electronegativity value correlated with the position of the bond critical point relative to the bond length:

$$r_c/R = 0.785 - 0.042\chi_x^0 \quad (1.49)$$

As the group becomes more electronegative, the critical point shifts toward the substituent. Table 1.26 compares two of the traditional empirical electronegativity

<sup>164</sup>. A. R. Cherkasov, V. I. Galkin, E. M. Zueva, and R. A. Cherkasov, *Russian Chem. Rev.* (Engl. Transl.), **67**, 375 (1998).

<sup>165</sup>. P. W. Chattaraj and R. G. Parr, *Struct. Bonding*, **80** 11 (1993); G.-H. Liu and R. G. Parr, *J. Am. Chem. Soc.*, **117**, 3179 (1995).

<sup>166</sup>. R. J. Boyd and K. E. Edgecombe, *J. Am. Chem. Soc.*, **110**, 4182 (1988).

<sup>167</sup>. R. J. Boyd and S. L. Boyd, *J. Am. Chem. Soc.*, **114**, 1652 (1992).

<sup>168</sup>. S. Hati and D. Datta, *J. Comput. Chem.*, **13**, 912 (1992).

Table 1.25. Properties of Substituent Groups<sup>a</sup>

CHAPTER 1  
*Chemical Bonding  
 and Molecular Structure*

Group	$\chi$ (eV)	$\eta$ (eV)	$S(10^{-2} \text{ eV}^{-1})$
CH <sub>3</sub>	5.12	5.34	9.36
CH <sub>3</sub> CH <sub>2</sub>	4.42	4.96	10.07
CH <sub>2</sub> =CH	5.18	4.96	10.07
HC≡C	8.21	5.77	8.67
HC=O	4.55	4.88	10.25
CH <sub>3</sub> C=O	4.29	4.34	11.51
CO <sub>2</sub> H	5.86	4.71	10.61
CO <sub>2</sub> CH <sub>3</sub>	5.48		
CONH <sub>2</sub>	4.67	4.42	11.32
CN	8.63	5.07	9.86
NH <sub>2</sub>	6.16	6.04	8.28
NO <sub>2</sub>	7.84	4.89	10.22
OH	6.95	5.69	8.79
CH <sub>3</sub> O	5.73	4.39	10.28
F	10.01	7.00	7.14
CH <sub>2</sub> F	4.97	5.31	9.41
CHF <sub>2</sub>	5.25	5.42	9.22
CF <sub>3</sub>	6.30	5.53	9.05
SH	5.69	3.96	12.62
CH <sub>3</sub> S	4.99	3.71	13.49
Cl	7.65	4.59	10.89
CH <sub>2</sub> Cl	4.89	4.71	10.61
CHCl <sub>2</sub>	5.12	4.38	11.42
CCl <sub>3</sub>	5.53	4.10	12.21

a. F. De Proft, W. Langemaeker, and P. Geerlings, *J. Phys. Chem.*, **97**, 1826 (1993).

scales with these two sets calculated on a theoretical basis. Figure 1.46 is a plot that provides an indication of the scatter in the numerical values in comparison with an empirical scale.

The broad significance of the correlation shown in Figure 1.46 is to cross-validate the theoretical and empirical views of functional groups that have developed in organic chemistry. The two theoretical scales are based entirely on measures of electron density. As to more specific insights, with reference to Table 1.26, we see the orders  $\text{CCl}_3 > \text{CHCl}_2 > \text{CH}_2\text{Cl}$  in electronegativity. This accords with the expectation for cumulative effects and is consistent with polar effects, as observed, for example, in the acidities of the corresponding carboxylic acids shown in Table 1.27. Note from Table 1.25 that the hardness and softness of the fluoro and chloro groups differ. Each additional fluoro substituent makes the group harder, but each chlorine makes it softer. This difference reflects the greater polarizability of the chlorine atoms.

If we compare the F, NO<sub>2</sub>, CN, and CF<sub>3</sub> substituents, representing familiar EWGs, we see that they are in the upper range of group electronegativity in Table 1.25 (10.01, 7.84, 8.63, and 6.30, respectively). With the exception of F, however, these substituents are not particularly hard.

The values for ethyl, vinyl, and ethynyl are noteworthy. Quite high electronegativity and hardness are assigned to the ethynyl group. This is in reasonable accord with the empirical values in Table 1.25. The methyl group also deserves notice. We will see in other contexts that the methyl group is harder than other primary alkyl groups. The theoretical treatments suggest this to be the case. It is not clear that the empirical scales reflect much difference between a methyl and ethyl group. This may be because

**Table 1.26. Empirical and Theoretical Electronegativity Scales for Some Functional Groups**

Group	Wells <sup>a</sup>	Inamoto and Masuda <sup>b</sup>	Boyd and Boyd <sup>c</sup>	Hati and Datta <sup>d</sup>
CH <sub>3</sub>	2.3	2.47	2.55	2.09
CH <sub>2</sub> Cl	2.75	2.54	2.61	
CHCl <sub>2</sub>	2.8	2.60	2.66	
CCl <sub>3</sub>	3.0	2.67	2.70	
CF <sub>3</sub>	3.35	2.99	2.71	2.49
CH <sub>2</sub> = CH	3.0	2.79	2.58	2.18
HC≡C	3.3	3.07	2.66	2.56
Ph	3.0	2.72	2.58	
N≡C	3.3	3.21	2.69	3.61
H	2.28	2.18		2.20
NH <sub>2</sub>	3.35	2.99	3.12	2.96
N <sup>+</sup> H <sub>3</sub>	3.8	3.71	3.21	3.52
N≡N <sup>+</sup>		3.71		4.06
NO <sub>2</sub>	3.4	3.42	3.22	3.44
OH	3.7	3.47	3.55	3.49
F	3.95		3.95	3.75
Cl	3.03		3.05	2.68
Br	2.80		2.75	
I	2.28			

a. P. R. Wells, *Prog. Phys. Org. Chem.*, **6**, 111 (1968).

b. N. Inamoto and S. Masuda, *Chem. Lett.*, 1003 (1982).

c. R. J. Boyd and S. L. Boyd, *J. Am. Chem. Soc.*, **114**, 1652 (1992).

d. S. Hati and D. Datta, *J. Comput. Chem.*, **13**, 912 (1992).

TOPIC 1.5

*Application of Density  
Functional Theory  
to Chemical Properties  
and Reactivity*

the theoretical results pertain to isolated molecules, whereas the empirical values are derived from measurements in solution. The smaller size of the methyl group makes it less polarizable than larger alkyl groups. This difference is maximized in the gas phase, where there are no compensating solvent effects.

Let us now consider a few simple but important systems that can illustrate the application of these ideas. We know that the acidity of the hydrides of the second-row elements increases sharply going to the right in the periodic table. The same trend is true for the third row and in each case the third-row compound is more acidic than its second-row counterpart. This is illustrated by the gas phase ionization enthalpy data in Table 1.28.

The gas phase data from both the second- and third-row compounds can be correlated by an expression that contains terms both for electronegativity ( $\chi$ ) and hardness ( $\mu$ ). The sign is negative for hardness:

$$\Delta G_{\text{acid}} = 311.805 - 18.118\chi + 33.771\mu \quad (1.50)$$

**Table 1.27. Gas Phase and Aqueous  $pK_a$  Values**

	$pK_a$		$pK_a$
FCH <sub>2</sub> CO <sub>2</sub> H	2.59	ClCH <sub>2</sub> CO <sub>2</sub> H	2.87
CHF <sub>2</sub> CO <sub>2</sub> H	NA	CHCl <sub>2</sub> CO <sub>2</sub> H	1.35
CF <sub>3</sub> CO <sub>2</sub> H	0.52	CCl <sub>3</sub> CO <sub>2</sub> H	0.66

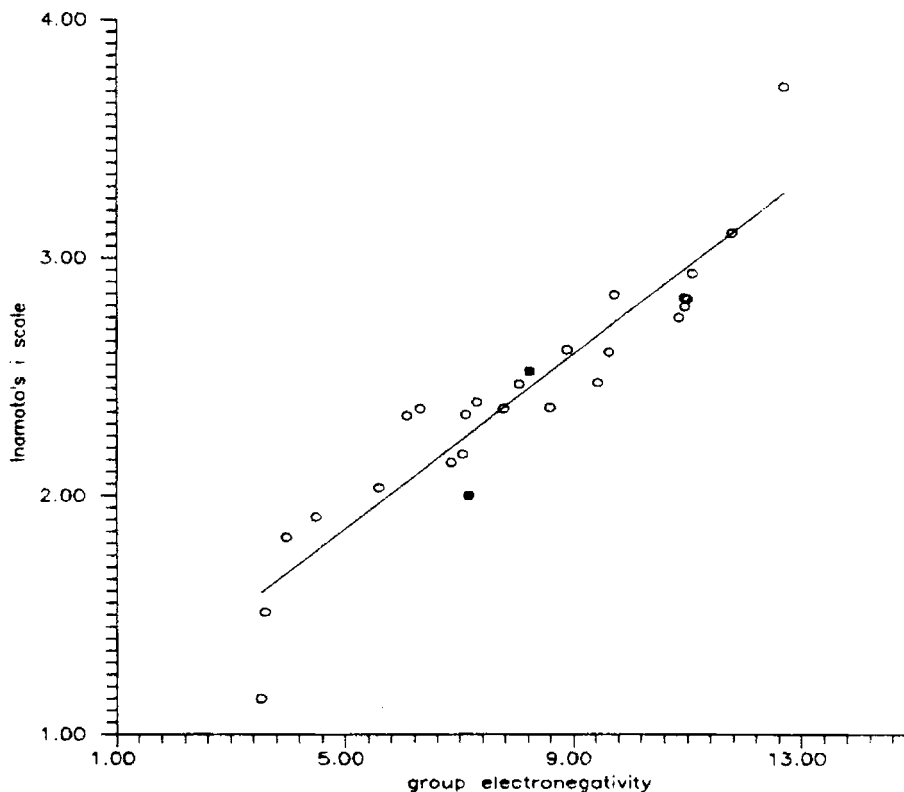


Fig. 1.46. Correlation between AIM electronegativity  $\chi$  (in eV) with Inamoto  $i$  empirical group electronegativity scale. Correlation coefficient is 0.938. Reproduced with permission from S. Hati and D. Datta, *J. Comput. Chem.*, **13**, 912 (1992).

The implication is that both increased electronegativity and polarizability (or softness) contribute to acidity. The increasing acidity can be interpreted in terms of the ability of the anion to accommodate the negative charge left by the removal of a proton. The more electronegative and the more polarizable (softer) the anion, the better it can accept the additional charge. There is a related trend going down the periodic table, i.e.,  $\text{HI} > \text{HBr} > \text{HCl} > \text{HF}$ . The order reflects the increasing bond strength from HI to HF, which is probably due to a combination of overlap and electronegativity effects.

Turning to an analogous group of organic compounds, we know that the order of acidity of alcohols in aqueous media is  $\text{CH}_3\text{OH} > \text{CH}_3\text{CH}_2\text{OH} > (\text{CH}_3)_2\text{CHOH} >$

**Table 1.28. Gas Phase and Aqueous pK Values<sup>a</sup>**

Second row	$\Delta H$	pK	Third row	$\Delta H$	pK
$\text{CH}_4$	416.8	48	$\text{SiH}_4$	372.4	
$\text{NH}_3$	403.7	38	$\text{PH}_3$	369.0	29
$\text{H}_2\text{O}$	390.8	15.7	$\text{H}_2\text{S}$	351.3	7.0
HF	371.4	3.2	HCl	333.4	-7

a. F. De Proft, W. Langenaeker, and P. Geerlings, *Int J. Quantum Chem.*, **55**, 459 (1995).

(CH<sub>3</sub>)<sub>3</sub>COH, but the order is exactly the opposite in the gas phase.<sup>169</sup> The reverse order in the gas phase attracted a good deal of interest when it was discovered, since it is contrary to the general expectation that more highly substituted alkyl groups are better electron donors than methyl and primary groups. Both qualitative<sup>170</sup> and quantitative<sup>171</sup> treatments have identified polarizability, the ability to accept additional charge, as the major factor in the gas phase order. Note also that the order is predicted by the HSAB relationship since the softer (more substituted) alkoxides should bind a hard proton more weakly than the harder primary alkoxides.

Another study examined the acidity of some halogenated alcohols. The gas phase acidity order is ClCH<sub>2</sub>OH > BrCH<sub>2</sub>OH > FCH<sub>2</sub>OH > CH<sub>3</sub>OH. The same Cl > Br > F order also holds for the di- and trihalogenated alcohols.<sup>172</sup> The order reflects competing effects of electronegativity and polarizability. The electronegativity order F > Cl > Br is reflected in the size of the bond dipole. The polarizability order Br > Cl > F indicates the ability to disperse the negative charge. The overall trend is largely dominated by the polarizability order. These results focus attention on the importance of polarizability, especially in the gas phase, where there is no solvation to stabilize the anion. The intrinsic ability of the substituent group to accommodate negative charge becomes very important.

The role of substituents has been investigated especially thoroughly for substituted acetic and benzoic acids. Quantitative data are readily available from pK<sub>a</sub> measurements in aqueous solution. Considerable data on gas phase acidity are also available.<sup>173</sup> EWG substituents increase both solution and gas phase acidity. In the gas phase, branched alkyl groups slightly enhance acidity. In aqueous solution, there is a weak trend in the opposite direction, which is believed to be due to poorer solvation of the more branched anions. Geerling and co-workers have applied DFT concepts to substituent effects on acetic acids.<sup>174</sup> The Fukui functions and softness descriptors were calculated using electron density and Mulliken population analysis (see Topic 1.5.2). The relative correlation of these quantities with both solution and gas phase acidity was then examined. In both cases, the best correlations were with the Mulliken charge. In the case of gas phase data, the correlations were improved somewhat by inclusion of a second parameter for group softness. The picture that emerges is consistent with the qualitative concepts of HSAB. The reactions in question are hard-hard interactions, the transfer of a proton (hard) to an oxygen base (also hard). The reactions are largely controlled by electrostatic relationships, as modeled by the Mulliken charges. The involvement of softness in the gas phase analysis suggests that polarizability makes a secondary contribution to anionic stability in the gas phase.

<sup>169</sup> J. I. Brauman and L. K. Blair, *J. Am. Chem. Soc.*, **92**, 5986 (1976).

<sup>170</sup> W. M. Schubert, R. B. Murphy, and J. Robins, *Tetrahedron*, **17**, 199 (1962); J. E. Huheey, *J. Org. Chem.*, **36**, 204 (1971).

<sup>171</sup> F. De Proft, W. Langenaeker, and P. Geerlings, *Tetrahedron*, **51**, 4021 (1995); P. Pérez, *J. Phys. Chem. A*, **105**, 6182 (2001).

<sup>172</sup> S. Damoun, W. Langenaeker, G. Van de Woude, and P. Geerlings, *J. Phys. Chem.*, **99**, 12151 (1995).

<sup>173</sup> C. Jinfeng, R. D. Topsom, A. D. Headley, I. Koppel, M. Mishima, R. W. Taft, and S. Veji, *Theochem*, **45**, 141 (1988).

<sup>174</sup> F. De Proft, S. Amira, K. Choho, and P. Geerlings, *J. Phys. Chem.*, **98**, 5227 (1994).

## CHAPTER 1

*Chemical Bonding  
and Molecular Structure*

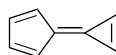
- T. A. Albright, J. K. Burdett, and M. H. Whangbo, *Orbital Interactions in Chemistry*, John Wiley & Sons, New York, 1985.
- R. F. W. Bader, *Atoms in Molecules: A Quantum Theory*, Clarendon Press, Oxford, 1990.
- W. T. Borden, *Modern Molecular Orbital Theory for Organic Chemists*, Prentice-Hall, Englewood Cliffs, NY, 1975.
- I. Fleming, *Frontier Orbital and Organic Chemical Reactions*, John Wiley & Sons, New York, 1976.
- W. J. Hehre, L. Radom, P. v. R. Schleyer, and J. Pople, *Ab Initio Molecular Orbital Theory*, Wiley-Interscience, New York, 1986.
- F. Jensen, *Introduction to Computational Chemistry*, John Wiley & Sons, Chichester, 1999.
- W. Koch and M. C. Holthausen, *A Chemist's Guide to Density Functional Theory*, Wiley-VCH, Chichester, 2000.
- E. Lewars, *Computational Chemistry*, Kluwer Academic Publishers, Boston, 2003.
- R. G. Parr and W. Yang, *Density Functional Theory of Atoms and Molecules*, Oxford University Press, Oxford, 1989.
- L. Salem, *Electrons in Chemical Reactions*, John Wiley & Sons, New York, 1982.
- P. v. R. Schleyer, ed., *Encyclopedia of Computational Chemistry*, John Wiley & Sons, New York, 1998.
- H. E. Zimmerman, *Quantum Mechanics for Organic Chemists*, Academic Press, New York, 1975.

## Problems

(References for these problems will be found on page 1155.)

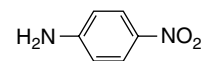
1.1. Suggest an explanation for the following observations:

- a. Although the hydrocarbon calicene has so far defied synthesis, but it has been estimated that it would have a dipole moment as large as 5.6 D.



calicene

- b. The measured dipole moment of 4-nitroaniline (6.2 D) is larger than the value calculated using standard group dipoles (5.2 D).



4-nitroaniline

- c. The dipole moments of furan and pyrrole are in opposite directions.

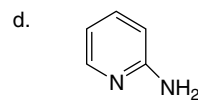
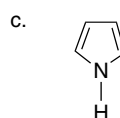
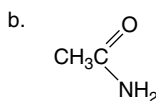
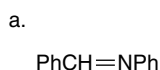


furan

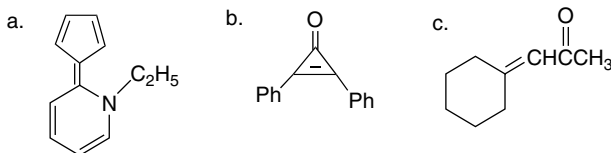


pyrrole

1.2. Predict the preferred site of protonation for each of the following molecules and explain the basis of your prediction.

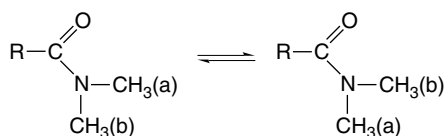


1.3. What physical properties, such as absorption spectra, bond lengths, dipole moment, etc., could be examined to obtain evidence of resonance interactions in the following molecules. What deviation from “normal” physical properties would you expect?



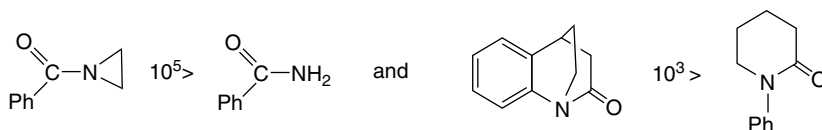
1.4. Consider each of the following physical characteristics of certain amides.

a. Carboxamides have rotational barriers on the order of 20 kcal/mol for the process:



Develop a structural explanation for the barrier both in resonance and MO terminology.

- b. The gas phase rotational barrier of *N,N*-dimethylformamide is about 19.4 kcal/mol, which is about 1.5 kcal/mol less than in solution. Is this change consistent with the explanation you presented in part (a)? Explain.
- c. Account for the substantial differences in relative rates of alkaline hydrolysis for the following pairs of carboxamides.



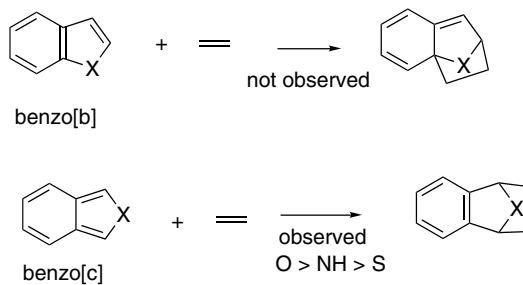
1.5. The AM1 semiempirical MO method was used to calculate structure, HOMO-LUMO orbital coefficients, and charge distribution for several substituted cyclopropanones. The results for 2-phenylcyclopropanone, 2-phenyl-3-methylcyclopropanone, and 2,3-diphenylcyclopropanone are given in Table 1.P5a. Based on this information, make predictions about the following reactions:

- a. What will be the site of protonation of a cyclopropanone?
- b. What will be the site of reaction of a cyclopropanone with a hard nucleophile, such as  $\text{OH}^-$ ?
- c. Is an alkyl or aryl substituent most effective in promoting reaction with a soft nucleophile?

**Table 1.P5a. Orbital Coefficients and Energies**

R	LUMO Coefficients				HOMO coefficients				Energy(kcal/mol)	
	C(1)	C(2)	C(3)	O	C(1)	C(2)	C(3)	O	HOMO	LUMO
C(2)=Ph	-0.088	0.445	-0.494	0.074	-0.058	-0.240	-0.444	0.275	-9.54	-0.82
C(3)=H										
C(2)=Ph	-0.079	0.439	-0.501	0.066	0.071	-0.298	-0.436	0.290	-9.29	-0.76
C(3)=CH <sub>3</sub>										
C(2)=Ph	0.000	0.455	-0.455	0.000	-0.084	-0.348	-0.348	.270	-8.90	-1.14
C(3)=Ph										
Charges	C(1)	C(2)	C(3)	O						
C(2)=Ph	0.28	-0.11	-0.19	-0.27						
C(3)=H										
C(2)=Ph	0.28	-0.11	-0.14	-0.27						
C(3)=CH <sub>3</sub>										
C(2)=Ph	0.28	-0.11	-0.11	-0.27						
C(3)=Ph										

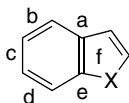
1.6. It is observed that benzo[c] derivatives of furan, pyrrole, and thiophene are less stable and much more reactive than the corresponding benzo[b] derivatives. The differences are apparent for example in [4 + 2] cycloadditions, which are facile with the benzo[c] but not the benzo[b] derivatives. Some MO properties from AM1 calculations are given in Tables 1.P6a, 1.P6b and 1.P6c. What features of the results are in accord with the experimental observations? Do you find any features of the results that run counter to the observations.

**Table 1.P6a. Enthalpy of Reactants and Transition Structures**

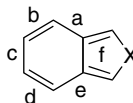
	O	NH	S
$\Delta H_f$ (kcal/mol)			
Benzo[b]	20.8	55.2	42.4
Benzo[c]	27.9	61.7	49.4
$\Delta H_f$ for 4 + 2 TS			
Benzo[b]	75.7	115.3	110.8
Benzo[c]	64.5	104.8	102.4
$\Delta H^\ddagger$ for 4 + 2 TS			
Benzo[b]	38.4	43.6	51.9
Benzo[c]	20.1	26.6	36.5

**Table 1.P6b. Bond Orders in Carbocyclic Rings**

Benzo[b]heterocycles



Benzo[c]heterocycles

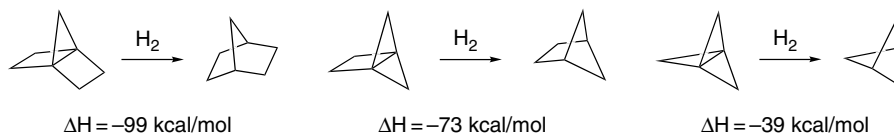


	O	NH	S		O	NH	S
a	1.34	1.30	1.30	a	1.12	1.16	1.15
b	1.46	1.50	1.51	b	1.71	1.66	1.67
c	1.37	1.33	1.32	c	1.15	1.19	1.18
d	1.45	1.50	1.51	d	1.71	1.66	1.67
e	1.45	1.28	1.30	e	1.12	1.16	1.15
f	1.30	1.27	1.32	f	1.14	1.20	1.20

**Table 1.P6c. Orbital Energies in eV**

	O	NH	S
HOMO:benzo[b]	-9.010	-8.403	-8.430
HOMO:benzo[c]	-8.263	-7.796	-8.340
LUMO:benzo[b]	-0.063	0.300	-0.166
LUMO:benzo[c]	-0.396	0.142	-0.592

- 1.7. (Old 1.16) The propellanes are highly reactive in comparison with unstrained hydrocarbons and readily undergo reactions that result in the rupture of the central bond. For example, it has been suggested that the polymerization of propellanes occurs by initial dissociation of the center bond. Perhaps surprisingly, it has been found that [1.1.1]propellane is considerably *less reactive* than either [2.2.1]propellane or [2.1.1]propellane. Use the computational enthalpy data below to estimate the energy required to break the center bond in each of the three propellanes. Assume that the bridgehead C-H bonds in each of the bicycloalkanes has a bond enthalpy of  $-104$  kcal/mol. How might the results explain the relative reactivity of the propellanes.

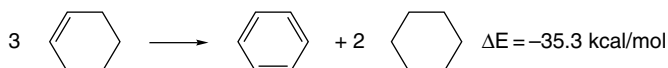


- 1.8. Examine the heats of hydrogenation shown for unsaturated eight-membered ring hydrocarbons. (a) Discuss the differences among the different compounds in comparison with the standard  $\Delta H_{H_2}$  for an unstrained *cis* double bond, which is  $27.4$  kcal/mol. (b) Assigning a strain energy of  $9.3$  kcal/mol to cyclooctane, calculate the relative strain of each of the other compounds. (c) What role does conjugation play in relation to the observed  $\Delta H_{H_2}$ ? (d) What conclusion do these

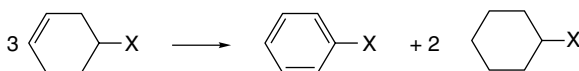
data permit as to whether cyclooctatetraene is stabilized or destabilized by cyclic conjugation.

Compound	$\Delta H_{H_2}$ (kcal/mol)
Z, Z, Z, Z-1,3,5,7-Cyclooctatetraene	97.06
Z, Z, Z-1,3,5-Cyclooctatriene	76.39
Z, Z, Z-1,3,6-Cyclooctatriene	79.91
Z, Z-1,3-Cyclooctadiene	48.96
Z, Z-1,4-Cyclooctadiene	52.09
Z, Z-1,5-Cyclooctadiene	53.68
Z-Cyclooctene	22.98
E-Cyclooctene	32.24

- 1.9. An isodesmic reaction suitable for calculating the resonance stabilization of benzene relative to cyclohexene is



A similar calculation can be done with substituent groups in place. The results for several substituents by G3(MP2) computations are as follows:



X	$\Delta E$ (kcal/mol)
H	-35.3
CH <sub>3</sub>	-35.8
CH <sub>3</sub> CH <sub>2</sub>	-36.1
CH <sub>2</sub> =CH	-38.1
HC≡C	-37.3
H <sub>2</sub> N	-39.5

How do the calculated effects of substituents compare with the qualitative expectations on the basis of resonance concepts? How do the calculated stabilizations for the individual substituents compare with those calculated for double bonds and given on p. 52.

- 1.10. The explanation of substituent effects on the acidity of substituted carboxylic acids usually focuses on two factors: (a) The ability of the substituent to stabilize the negative charge; and (b) the effect of solvation on the anion. However, there will also be substituent effects on the stability and solvation of the undissociated acid. The studies described on p. XXX resulted in the following values for the gas phase energy (in hartrees) of the acids and anions and the resulting  $\Delta G$  for gas phase ionization. Using this information and the solvation energies on p. 53,

analyze the relative importance of intrinsic anion stabilization and solvation on the observed acidity.

X	Acid, $E_{\text{gas}}$	Anion, $E_{\text{gas}}$	$\Delta G$ (kcal/mol)
H	-189.551612	-189.005818	342.49
CH <sub>3</sub>	-228.792813	-228.241528	345.94
ClCH <sub>2</sub>	-687.945725	-687.414262	333.50
NCCH <sub>2</sub>	-320.909115	-320.386960	327.66
(CH <sub>3</sub> ) <sub>3</sub> C	-346.481196	-345.936639	341.71

- 1.11. Cyclic amines such as piperidine and its derivatives show substantial differences in the properties of the axial C(2) and C(6) bonds. The axial C–H bonds are *weaker* than the equatorial C–H bonds, as indicated by a shifted C–H stretching frequency in the IR spectrum. The axial hydrogens also appear at higher field in <sup>1</sup>H-NMR spectra. Axial C(2) and C(6) methyl groups *lower* the ionization potential of the unshared pair of electrons on nitrogen more than equatorial C(2) and C(6) methyl groups. Discuss the structural basis of these effects in MO terminology.
- 1.12. Construct a qualitative MO diagram for the following systems and discuss how the  $\pi$  MOs are modified by addition of the substituent.
- vinyl fluoride, compared to ethene
  - propenal, compared to ethene
  - acrylonitrile, compared to ethene
  - propene, compared to ethene
  - benzyl cation, compared to benzene
  - fluorobenzene, compared to benzene
- 1.13. Given below are the  $\Delta E$  for some isodesmic reactions. Also given are the AIM and NPA charges at the carbon atoms of the double bond. Provide an explanation for these results in terms of both resonance structure and MO terminology.
- Draw resonance structures and qualitative MO diagrams that indicate the stabilizing interaction.
  - Explain the order of stabilization  $\text{N} > \text{O} > \text{F}$  in both resonance and MO terminology.
  - Interpret the AIM and NPA charges in relationship to the ideas presented in (a) and (b).



X	$\Delta E$	$\delta\text{C}(1)^{\text{a}}$	$\delta\text{C}(2)^{\text{a}}$	$\delta\text{C}(1)^{\text{b}}$	$\delta\text{C}(2)^{\text{b}}$
H	0	+0.08	+0.08	-0.25	-0.25
CH <sub>3</sub>	-3.05	+0.02	+0.08	-0.09	-0.29
NH <sub>2</sub>	-7.20	+0.51	+0.15	+0.14	-0.36
OH	-6.43	+0.58	+0.18	+0.26	-0.39
F	-0.99	+0.48	+0.29	+0.30	-0.36

- AIM charges
- NPA charges

- 1.14. In the Hückel MO treatment, orbitals on nonadjacent atoms are assumed to have no interaction. The concept of *homoconjugation* suggests that such orbitals may interact, especially in rigid structures in which the orbitals are directed toward one another. Consider, e.g., norbornadiene, (bicyclo[2.2.1]hepta-2,5-diene).



- Construct an MO diagram according to HMO theory and assign orbital energies.
- Construct the qualitative MO diagram that would result from significant overlap between the C(3) and C(5) and C(2) and C(6) orbitals.
- The ionization potentials (IP) of some 2-substituted norbornadienes are given below. The two IP values pertain to the  $\pi$  system. Use PMO theory to analyze the effect these substituents have on the IP. Use a qualitative MO diagram to show how the substituents interact with the two double bonds and how this affects the IP. Discuss the effect the substituents have on the IP.

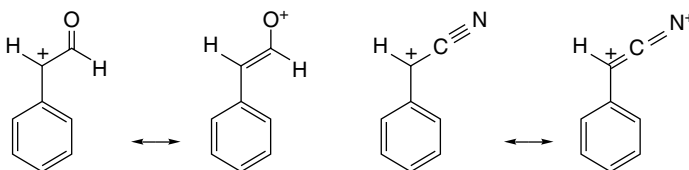
X	IP <sub>1</sub>	IP <sub>2</sub>
H	8.69	9.55
CH <sub>3</sub> O	8.05	9.27
CN	9.26	10.12

- 1.15. a. Sketch the nodal properties of the Hückel HOMO orbital of the pentadienyl cation.
- b. The orbital coefficients of two of the  $\pi$  MOs of pentadienyl are given below. Specify which is of lower energy; classify each orbital as bonding, nonbonding, or antibonding; and specify whether each orbital is *S* or *A* with respect to a plane bisecting the molecule perpendicular to the plane of the structure.

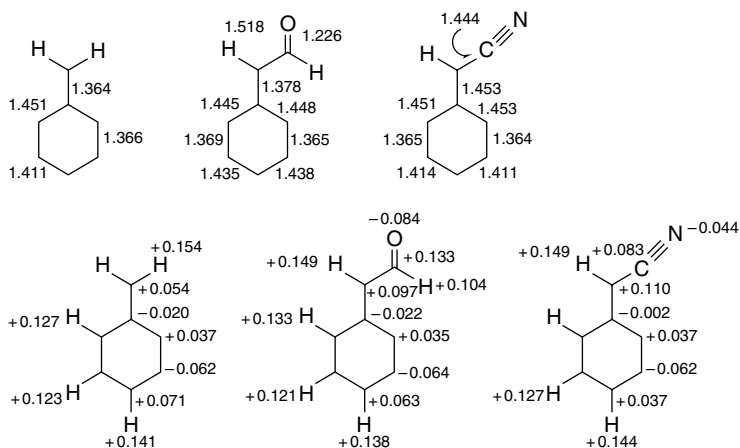
$$\psi_x = 0.50\phi_1 + 0.50\phi_2 - 0.50\phi_4 - 0.50\phi_5$$

$$\psi_y = 0.58\phi_1 - 0.58\phi_3 + 0.58\phi_5$$

- 1.16. There has been discussion as to whether unsaturated EWGs such as formyl or cyano stabilize or destabilize carbocations.



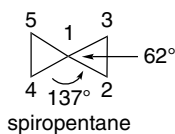
The diagrams below give STO-3G bond lengths and Mulliken charge densities for the benzyl cation and for its  $\alpha$ -formyl and  $\alpha$ -cyano derivatives. Analyze the effect of the substituents on the carbocation.



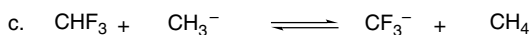
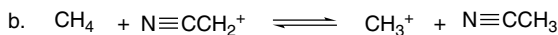
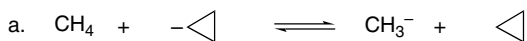
- 1.17 a. Calculate the HMO energy levels and atomic orbital coefficients for 1,3-butadiene.
- b. Estimate the delocalization energy, in units of  $\beta$ , of the cyclobutadienyl dication  $C_4H_4^{2+}$  from HMO theory.
- c. Estimate, in units of  $\beta$ , the energy associated with the longest-wavelength UV-VIS absorption of 1,3,5,7-octatetraene. Does it appear at a longer or shorter wavelength than the corresponding absorption in 1,3,5-hexatriene?
- 1.18. Spiropentane has unusual strain and hybridization. Consider the following facets of its structure.
- a. The strain energy of spiropentane (62.5 kcal/mol) is considerably more than twice that of cyclopropane (27.5 kcal/mol). Suggest an explanation.
- b. The structure of spiropentane has been determined by X-ray crystallography. The endocyclic angles at the spiro carbon are about  $62^\circ$ , and the bond angles between C-C bonds in the adjacent rings are about  $137^\circ$ . How would you relate the strain to the hybridization of each carbon in spirocyclopentane based on these bond angles?
- c. The fractional  $s$  character in a C-C bond can be estimated from  $^{13}C$ - $^{13}C$  coupling constants using the equation

$$J_{C_i-C_j} = K(s_i)(s_j)$$

where  $K$  is a constant = 550 Hz and  $s$  is the fractional  $s$  character of each atom. In spiropentane, the  $J$  for coupling between C(1) and C(3) is 20.2 Hz. The  $J$  between C(2) and C(3) is about 7.5 Hz. Calculate the  $s$  character of the C(1)-C(3) and C(2)-C(3) bonds.



1.19. Predict whether the following gas phase reactions will be thermodynamically favorable or unfavorable. Explain your answer.

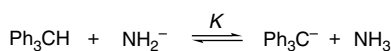


1.20. For each reaction, predict which compound would react faster ( $k$ ) or give the more complete ( $K$ ) reaction. Explain the basis for your prediction.

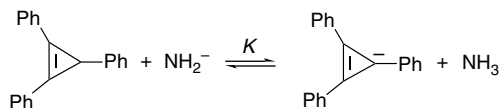
a.



b.



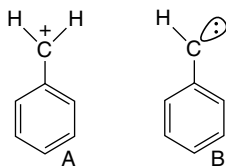
OR



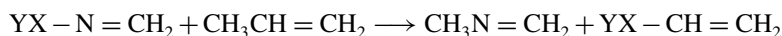
c.



1.21. Computational comparison of the structures of the benzyl cation (**A**) and singlet phenyl carbene (**B**) indicate a much greater degree of double-bond character for the exocyclic bond in **A** than in **B**. Provide a rationale for this difference, both in VB and MO terminology.



1.22. Interesting stability and structural trends have been found with MP2/6-31G\* calculations on substituted imines. The data below give the  $\Delta E$  for the isodesmic reaction:



The data suggest that  $\Delta E$  increases with  $\chi_{\text{XY}}$ , the group electronegativity of the substituent. The X-N=CH<sub>2</sub> bond angle also decreases with  $\chi_{\text{AB}}$ . The NPA

charges on the various atoms are given at the right of the table below. Discuss these trends, with particular attention to the interaction between the unshared electron pair on nitrogen and the C=N bond with the substituents.

Substituent	$\chi_{XY}$	$\Delta E$	XN = CH <sub>2</sub> (°)	$\delta(X)^a$	$\delta(Y)^b$	$\delta(N)$	$\delta(C)$	$\delta(H)_{av}$
H	2.20	+4.1	110	+0.36	–	–0.66	–0.04	+0.17
CH <sub>3</sub>	2.55	0.0	116	–0.44	+0.20(H) <sub>2</sub>	–0.47	–0.06	+0.17
CH=O	2.66	–3.6	114	+0.65	–0.63 (=O)	–0.63	+0.07	+0.20
CN	2.69	–4.8	117	+0.47	–0.39 (N)	–0.55	+0.07	+0.20
CF <sub>3</sub>	2.71	–4.7	118	+1.41	–0.42(F) <sub>3</sub>	–0.59	+0.03	+0.20
NO <sub>2</sub>	3.22	–10.0	111	+0.77	–0.44(O) <sub>2</sub>	–0.38	+0.04	+0.22
NH <sub>2</sub> <sup>c</sup>	3.12	–12.4	117	–0.71	+0.38(H) <sub>2</sub>	–0.26	–0.15	+0.18
OH	3.55	–20.5	110	–0.64	+0.51 (H)	–0.14	–0.13	+0.20
F	4.00	–29.0	108	–0.31	–	0.00	–0.12	+0.22
H <sub>3</sub> Si	1.90	+13.2	120	+1.29	–0.24(H) <sub>3</sub>	–0.92	+0.03	+0.16

a. The charge on atom x.

b. The average charge on each atom Y.

c. The nitrogen in pyramidal in the lowest energy structure.

1.23. Table 1.P23a shows NPA charges for planar and twisted (C–N rotation) for formamide, 3-aminoacrolein and squaramide. Table 1.P23b gives computed <sup>17</sup>O chemical shifts for the planar and twisted forms. Figures 1.P23A–F are maps showing the potential for interaction with a particle of charge +0.5e. The barriers

**Table 1.P23a. NPA Charges**

	Planar	Twisted
Formamide		
O	–0.710	–0.620
C	+0.690	+0.695
N	–0.875	–0.929
NH <sub>2</sub>	–0.080	–0.182
CH	+0.789	+0.812
3-Aminoacrolein		
O	–0.665	–0.625
C(1)	+0.512	+0.506
C(2)	–0.456	–0.351
C(3)	+0.198	+0.144
N	–0.832	–0.884
NH <sub>2</sub>	–0.060	–0.149
Squaramide		
O(1)	–0.655	–0.609
C(1)	+0.519	+0.530
O(2)	–0.631	–0.626
C(2)	+0.554	+0.548
C(3)	+0.162	+0.088
C(4)	+0.258	+0.348
N(3)	–0.819	–0.851
NH <sub>2</sub>	–0.001	–0.095
O(4)	–0.711	–0.687

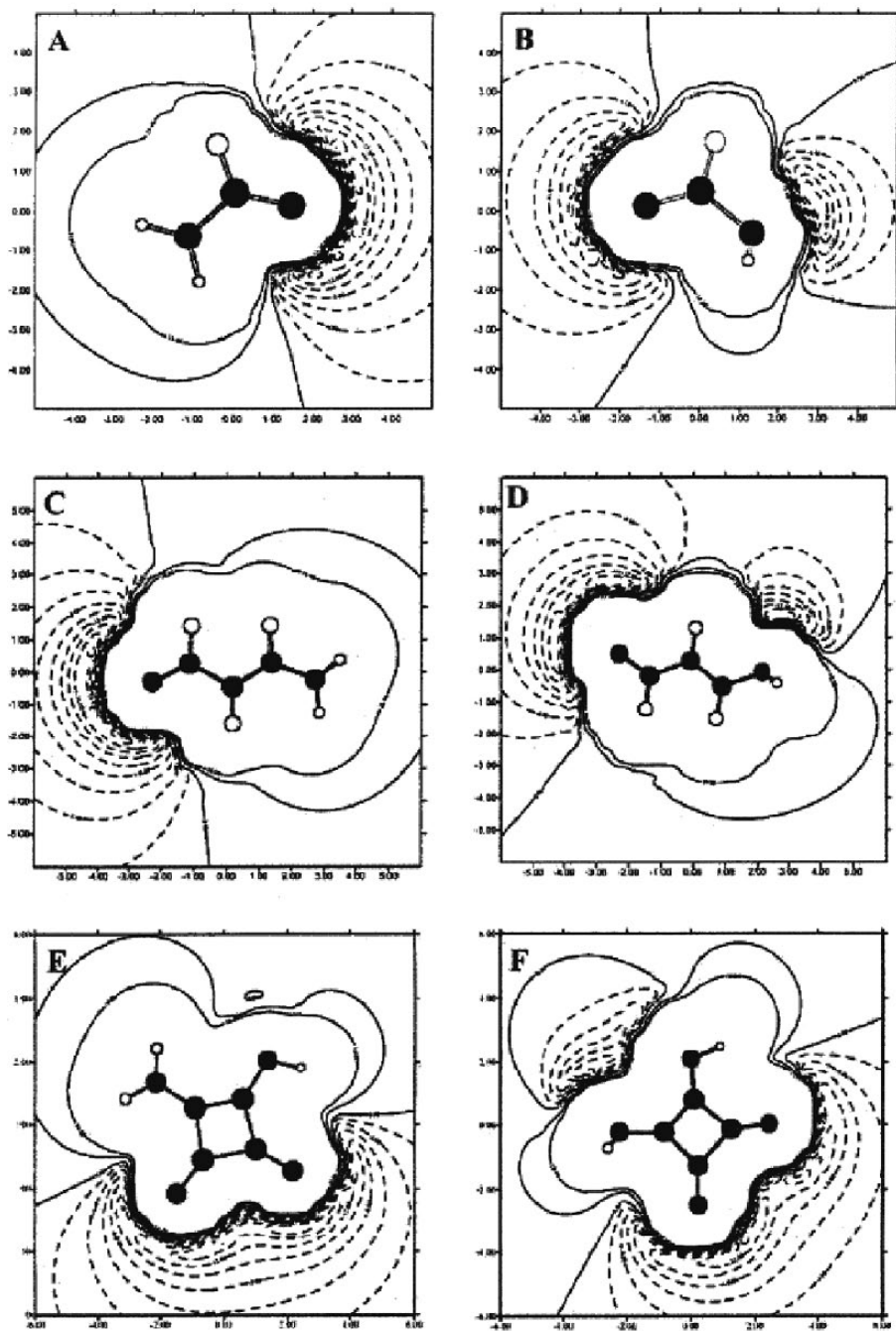
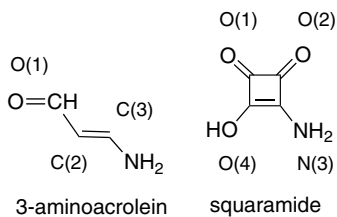


Fig. 1.P23. Molecular interaction potential maps for planar (left) and twisted (right) conformations of formamide, 3-aminoacrolein and squaramide.

**Table 1.P23b. Calculated  $^{17}\text{O}$  Chemical Shifts in ppm**

	Planar	Twisted	$\Delta$
Formamide	390	602	212
3-Aminoacrolein	568	630	62
Squaramide O(1)	446	526	80

to rotation of the three molecules are 14.9, 8.8, and 9.9 kcal/mol, respectively. On the basis of these data, discuss the extent of resonance interaction in each compound.



# Stereochemistry, Conformation, and Stereoselectivity

## Introduction

In the discussion of the structural features of carbon compounds in the Chapter 1, we emphasized some fundamental principles of molecular geometry. Except in strained rings,  $sp^3$  carbon is nearly tetrahedral in shape. Double bonds involving  $sp^2$  carbon are trigonal and planar and have a large barrier to rotation. The  $sp$  hybridization, e.g., in alkynes, leads to a linear (digonal) geometry. *Stereochemistry* in its broadest sense describes how the atoms of a molecule are arranged in three-dimensional space. In particular, *stereoisomers* are molecules that have identical connectivity (constitution) but differ in three-dimensional structure. Stereoisomers differ from one another in *configuration* at one or more atoms. *Conformations* are the various shapes that are available to molecules by single-bond rotations and other changes that do not involve bond breaking. Usually, conformational processes have relatively low energy requirements. The stereochemical features of a molecule, both configuration and conformation, can influence its reactivity. After discussing configuration and conformation, we consider *stereoselectivity*, the preference of a reaction for a particular stereoisomeric product.

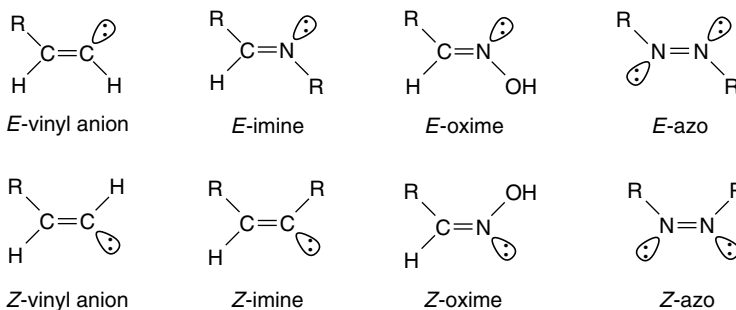
## 2.1. Configuration

### 2.1.1. Configuration at Double Bonds

The  $sp^2$  hybridization in the carbon atoms in a double bond and the resulting  $\pi$  bond favor a planar arrangement of the two carbon atoms and the four immediate

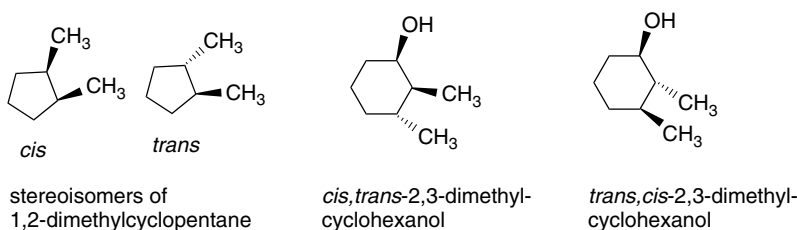


Certain atoms have an unshared electron pair rather than a substituent. Electron pairs are assigned the lowest priority in the Cahn-Ingold-Prelog convention, so assignment the *Z*- or *E*-configuration to compounds such as imines and oximes follows the same rules with R or H >:

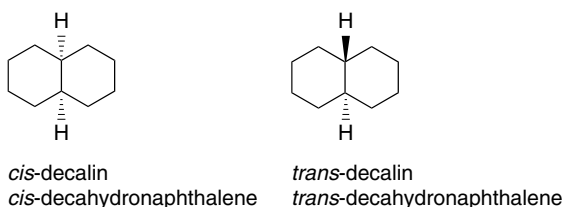


### 2.1.2. Configuration of Cyclic Compounds

Just as substituents can be on the same or opposite side of a double bond, they can be on the same or opposite side in cyclic compounds. The two arrangements are different *configurations* and cannot be interchanged without breaking and reforming at least one bond. Here the terms *cis* (for the same side) and *trans* (for the opposite side) are unambiguous and have been adopted as the designation of configuration. The stereochemistry is specified *relative to the group that takes precedence in the naming of the molecule*, as illustrated for 2,3-dimethylcyclohexanol.

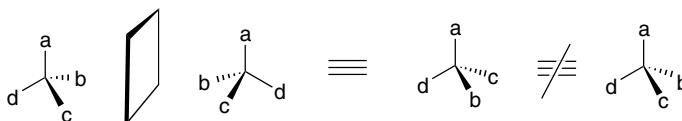


Stereoisomers also arise when two rings share a common bond. In the *cis* isomer both branches of the fused ring are on the same side. In the *trans* isomer they are on opposite sides.



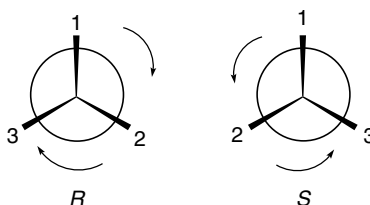
## 2.1.3. Configuration at Tetrahedral Atoms

Carbon and other atoms with  $sp^3$  hybridization have approximately tetrahedral geometry. With the exception of small deviations in bond angles, each of the substituents is in a geometrically equivalent position. Nevertheless, there is an important stereochemical feature associated with tetrahedral centers. If all four substituents are different, they can be arranged in two different ways. The two different arrangements are mirror images of one another, but they cannot be superimposed.

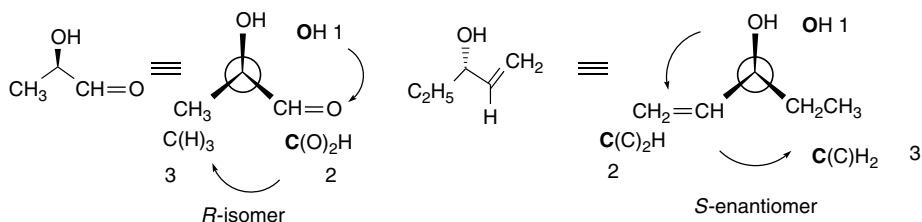


Any object that cannot be superimposed on its mirror image is called *chiral*, that is, it has the property of being right-handed or left-handed. Molecules (or other objects) that are not chiral are described as being *achiral*, which is the opposite of chiral. Tetrahedral atoms with four nonidentical substituents, then, give rise to two stereoisomers. Such atoms are called *stereogenic centers*, sometimes shortened to *stereocenters*. An older term applied specifically to carbon is *asymmetric carbon*.

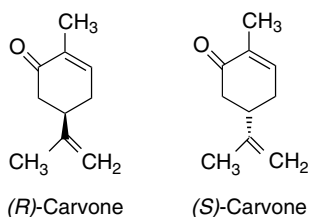
The chirality (or handedness) at stereogenic centers is specified by application of the Cahn-Ingold-Prelog priority rules, as described for double bonds. The four nonidentical ligand atoms are assigned a decreasing priority  $1 > 2 > 3 > 4$ . The molecule is then viewed opposite from the lowest-priority group, that is, the group is placed behind the stereocenter and away from the viewer. Two arrangements are possible for the other three substituents. The groups can decrease in priority in either a clockwise or a counterclockwise direction. The clockwise direction configuration is assigned *R* (for *rectus*) and the counterclockwise direction is assigned *S* (for *sinistre*).



## Example 2.2



The two nonsuperimposable mirror image molecules are called an *enantiomeric pair* and each is the *enantiomer* of the other. The separated enantiomers have identical properties with respect to achiral environments. They have the same solubility, physical, and spectroscopic properties and the same chemical reactivity toward achiral reagents. However, they have different properties in chiral environments. The enantiomers react at different rates toward chiral reagents and respond differently to chiral catalysts. Usually enantiomers cause differing physiological responses, since biological receptors are chiral. For example, the odor of the *R*- (spearmint oil) and *S*- (caraway seed oil) enantiomers of carvone are quite different.



The activity of enantiomeric forms of pharmaceuticals is often distinctly different.

Enantiomers also differ in a specific physical property, namely the rotation of plane polarized light. The two enantiomers rotate the light in equal, but opposite directions. The property of rotating plane polarized light is called *optical activity*, and the magnitude of rotation can be measured by instruments called polarimeters. The observed rotation, known as  $\alpha$ , depends on the conditions of measurement, including concentration, path length, solvent, and the wavelength of the light used. The rotation that is characteristic of an enantiomer is called the *specific rotation* and is symbolized by  $[\alpha]_{589}$ , where the subscript designates the wavelength of the light. The observed rotation  $\alpha$  at any wavelength is related to  $[\alpha]_{\lambda}$  by the equation

$$[\alpha]_{\lambda} = \frac{100\alpha}{cl} \quad (2.1)$$

where  $c$  is the concentration in g/100 mL and  $l$  is the path length in decimeters.

Depending on how it was obtained, a sample of a chiral compound can contain only one enantiomer or it can be a mixture of both. Enantiomerically pure materials are referred to as *homochiral* or *enantiopure*. The 1:1 mixture of enantiomers has zero net rotation (because the rotations caused by the two enantiomers precisely cancel each other) and is called a *racemic mixture* or *racemate*. A racemic mixture has its own characteristic properties in the solid state. It differs in melting point and solubility from the pure enantiomers, owing to the fact that the racemic mixture can adopt a different crystalline structure from that of the pure enantiomers. For example, Figure 2.1 shows the differing intermolecular hydrogen-bonding and crystal-packing arrangements in (+/−) and (−) 2,5-diazabicyclo[2.2.2]octa-3,6-dione.<sup>1</sup>

The composition of a mixture of enantiomers is given by the *enantiomeric excess*, abbreviated e.e., which is the percentage excess of the major enantiomer over the minor enantiomer:

$$\text{e.e.} = \% \text{ Major} - \% \text{ Minor} \quad (2.2)$$

<sup>1</sup> M.-J. Birenne, J. Gabard, M. Leclercq, J.-M. Lehn, M. Cesario, C. Pascard, M. Cheve, and G. Dutruc-Rosset, *Tetrahedron Lett.*, **35**, 8157 (1994).

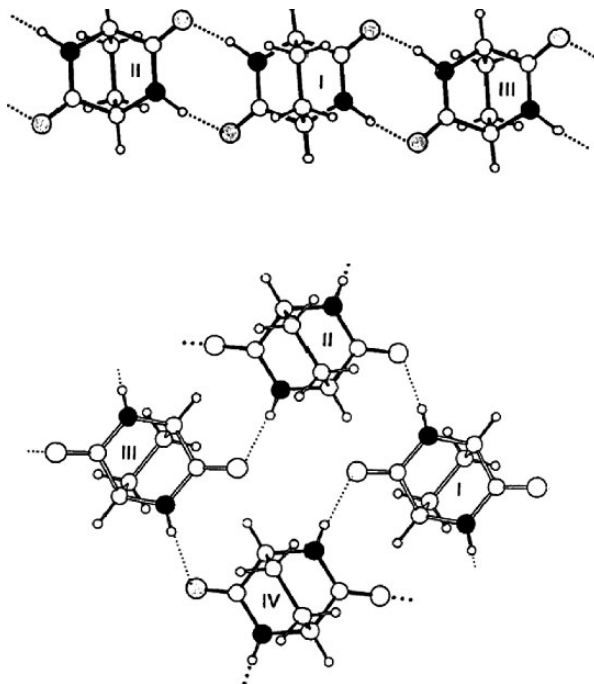


Fig. 2.1. Alternative hydrogen-bonding and crystal-packing arrangements for racemic (top) and (-) (bottom) forms of 2,5-diazabicyclo[2.2.2]octane-3,6-dione. Reproduced from *Tetrahedron Lett.*, **35**, 8157 (1994), by permission of Elsevier.

Alternatively, e.e. can be expressed in terms of the mole fraction of each enantiomer:

$$\text{e.e.} = (\text{Mole fraction}_{\text{major}} - \text{Mole fraction}_{\text{minor}}) \times 100 \quad (2.3)$$

The *optical purity*, an older term, is numerically identical. It represents the observed rotation, relative to the rotation of the pure enantiomer. Since the two enantiomers cancel each other out, the observed rotation is the product of (% Major – % Minor)  $\times$   $[\alpha]_{\lambda}$ . If  $[\alpha]_{\lambda}$  is known, measurement of  $\alpha$  allows the optical purity and enantiomeric excess to be determined:

$$\text{e.e.} = \frac{\alpha_{\text{obs}} \times 100}{[\alpha]_{\lambda}} \quad (2.4)$$

There are several other ways of measuring e.e., including NMR spectroscopy, chromatography, and capillary electrophoresis (see Topic 2.1).

Measurement of rotation as a function of wavelength is useful in structural studies aimed at determining the configuration of a chiral molecule. This technique is called *optical rotatory dispersion* (ORD),<sup>2</sup> and the resulting plot of rotation against wavelength is called an ORD curve. The shape of the ORD curve is determined by the

<sup>2</sup> P. Crabbe, *Top. Stereochem.* **1**, 93 (1967); C. Djerassi, *Optical Rotatory Dispersion*, McGraw-Hill, New York, 1960; P. Crabbe, *Optical Rotatory Dispersion and Circular Dichroism in Organic Chemistry*, Holden Day, San Francisco, 1965; E. Charney, *The Molecular Basis of Optical Activity. Optical Rotatory Dispersion and Circular Dichroism*, Wiley, New York, 1979.

configuration of the molecule and its absorption spectrum. In many cases, the ORD curve can be used to determine the configuration of a molecule by comparison with similar molecules of known configuration. Figure 2.2 shows the UV, ORD, and CD spectra of an enantiomerically pure sulfonium ion salt.<sup>3</sup>

Chiral substances also show differential absorption of circularly polarized light. This is called *circular dichroism* (CD) and is quantitatively expressed as the molecular ellipticity  $\theta$ , where  $\epsilon_L$  and  $\epsilon_R$  are the extinction coefficients of left and right circularly polarized light:

$$\theta = 3330(\epsilon_L - \epsilon_R) \quad (2.5)$$

Molecular ellipticity is analogous to specific rotation in that two enantiomers have exactly opposite values at every wavelength. Two enantiomers also show CD spectra having opposite signs. A compound with several absorption bands may show both positive and negative bands. Figure 2.3 illustrates the CD curves for both enantiomers of 2-amino-1-phenyl-1-propanone.<sup>4</sup>

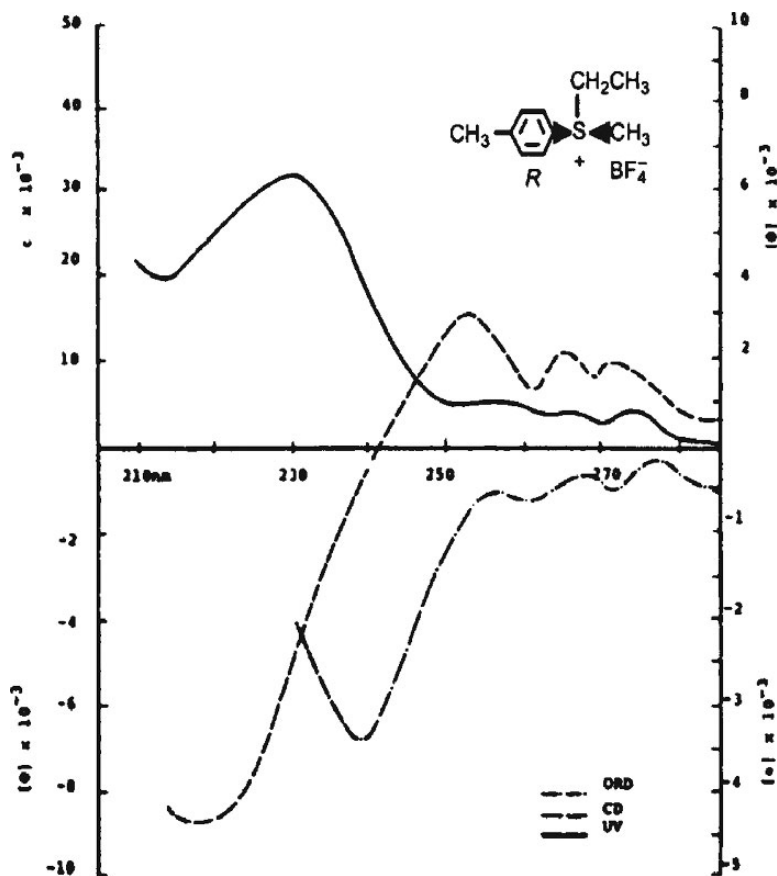


Fig. 2.2. UV absorption, ORD, and CD curves of (*R*)-ethyl methyl *p*-tolyl sulfonium tetrafluoroborate. Reproduced from *J. Org. Chem.*, **41**, 3099 (1976), by permission of the American Chemical Society.

<sup>3</sup>. K. K. Andersen, R. L. Caret, and D. L. Ladd, *J. Org. Chem.*, **41**, 3096 (1976).

<sup>4</sup>. J.-P. Wolf and H. Pfander, *Helv. Chim. Acta*, **69**, 1498 (1986).

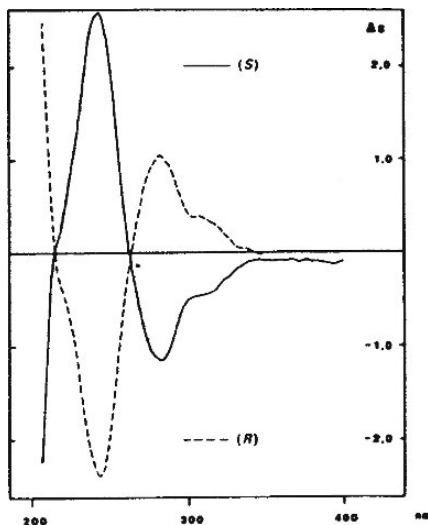


Fig. 2.3. CD spectra of (*S*)- and (*R*)-2-amino-1-phenyl-1-propanone hydrochloride. Reproduced from *Helv. Chim. Acta*, **69**, 1498 (1986), by permission of Wiley-VCH.

#### 2.1.4. Molecules with Multiple Stereogenic Centers

Molecules can have several stereogenic centers, including double bonds with *Z* or *E* configurations and asymmetrically substituted tetrahedral atoms. The maximum number of stereoisomers that can be generated from  $n$  stereogenic centers is  $2^n$ . There are several ways of representing molecules with multiple stereogenic centers. At the present time, the most common method in organic chemistry is to depict the molecule in an extended conformation with the longest chain aligned horizontally. The substituents then point in or out and up or down at each tetrahedral site of substitution, as represented by wedged and dashed bonds. The four possible stereoisomers of 2,3,4-trihydroxybutanal are shown in this way in Figure 2.4. The configuration at each center is specified as *R* or *S*. The isomers can also be characterized as *syn* or *anti*. Two

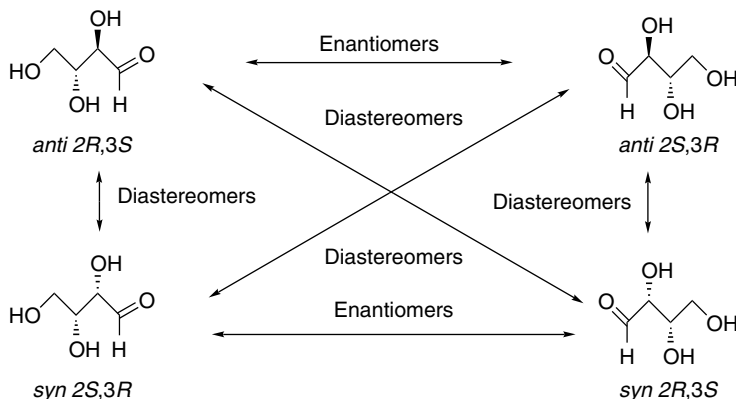
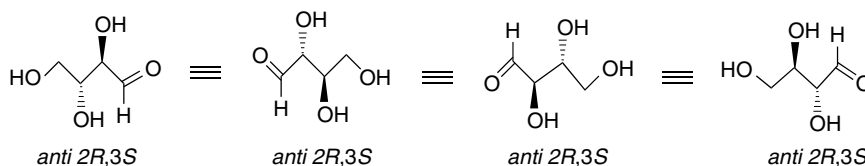


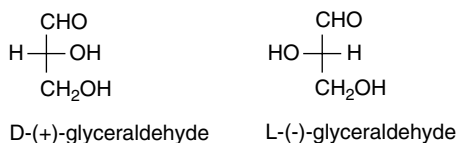
Fig. 2.4. Extended chain representation of all stereoisomers of 2,3,4-trihydroxybutanal.

adjacent substituents pointed in the same direction (in or out) are *syn*, whereas those pointed in opposite directions are *anti*.

For molecules with more than one stereogenic center, the *enantiomeric pair must have the opposite configuration at each center*. The two enantiomeric relationships are shown in Figure 2.4. There are four other pairings that do not fulfill this requirement, but the structures are still stereoisomeric. Molecules that are stereoisomeric but are not enantiomeric are called *diastereomers*, and four of these relationships are pointed out in Figure 2.4. Molecules that are diastereomeric have the same *constitution* (connectivity) but differ in *configuration* at one or more of the stereogenic centers. The positions in two diastereomers that have different configurations are called *epimeric*. For example, the *anti-2R,3R* and *syn-2R,3S* stereoisomers have the same configuration at C(2), but are epimeric at C(3). There is nothing unique about the way in which the molecules in Figure 2.4 are positioned, except for the conventional depiction of the extended chain horizontally. For example, the three other representations below also depict the *anti-2R,3S* stereoisomer.



Another means of representing molecules with several stereocenters is by *Fischer projection formulas*. The main chain of the molecule is aligned vertically, with (by convention) the most oxidized end of the chain at the top. The substituents that are shown horizontally project toward the viewer. Thus the vertical carbon-carbon bonds point away from the viewer at all carbon atoms. Fischer projection formulas represent a *completely eclipsed conformation* of the vertical chain. Because the horizontal bonds project from the plane of the paper, any reorientation of the structures must not change this feature. *Fischer projection formulas may be reoriented only in the plane of the paper*. Fischer projection formulas use an alternative system for specifying chirality. The chirality of the highest-numbered chiral center (the one most distant from the oxidized terminus, that is, the one closest to the bottom in the conventional orientation), is specified as D or L, depending on whether it is like the D- or L-enantiomer of glyceraldehyde, which is the reference compound. In the conventional orientation, D-substituents are to the right and L-substituents are to the left.



The *relative configuration* of adjacent substituents in a Fischer projection formula are designated *erythro* if they are on the same side and *threo* if they are on the opposite side. The stereochemistry of adjacent stereocenters can also be usefully represented

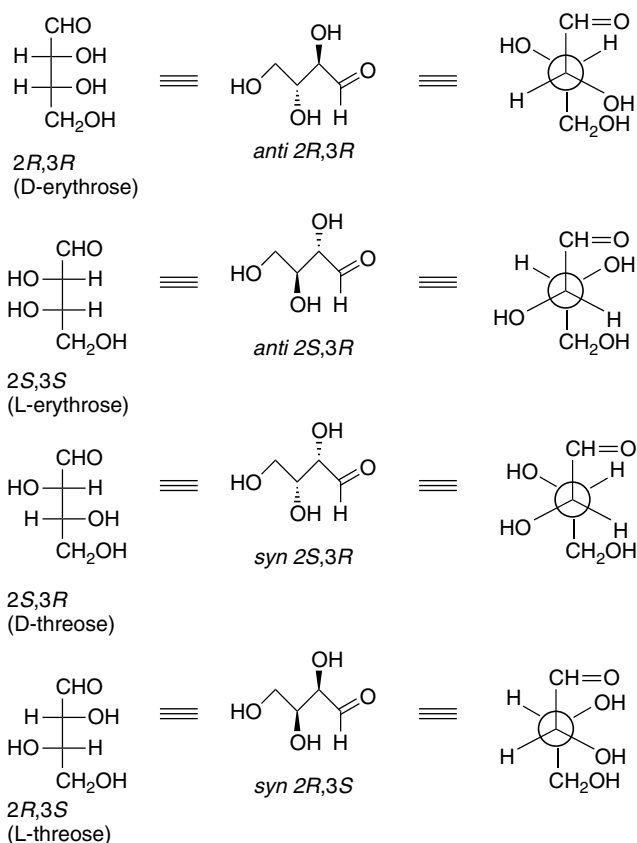


Fig. 2.5. Fischer, extended, and Newman projection representations of the stereoisomers of 2,3,4-trihydroxybutanal.

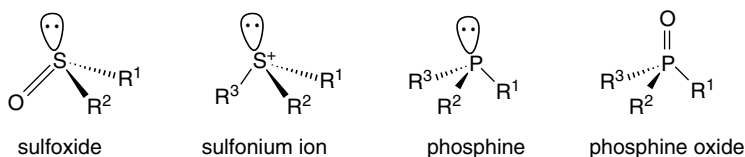
by *Newman projection formulas*. Figure 2.5 shows 2,3,4-trihydroxybutanal (now also with its carbohydrate names, erythrose and threose) as Fischer projection formulas as well as extended and Newman representations.

Because the Fischer projection formulas represent an eclipsed conformation of the carbon chain, the relative orientation of two adjacent substituents is opposite from the extended staggered representation. Adjacent substituents that are *anti* in an extended representation are on the same side of a Fischer projection formula, whereas adjacent substituents that are *syn* in an extended representation are on opposite sides in a Fischer projection. As with extended representations, an enantiomeric pair represented by Fischer projection formulas has the opposite configuration at *all stereogenic centers* (depicted as left or right.)

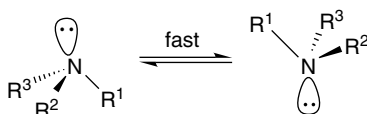
### 2.1.5. Other Types of Stereogenic Centers

Although asymmetrically substituted carbon atoms are by far the most common type of stereogenic center in organic compounds, several other kinds of stereogenic centers are encountered. Tetravalent nitrogen (ammonium) and phosphorus (phosphonium) ions are obvious extensions. Phosphine oxides are also tetrahedral and are chiral if all three substituents (in addition to the oxygen) are different. Not quite

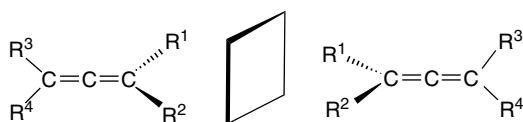
so evident are the cases of *trivalent* sulfur and phosphorus compounds, including sulfonium salts, sulfoxides, and phosphines. The heteroatom in these structures is approximately tetrahedral, with an electron pair occupying one of the tetrahedral positions. Because there is a relatively high energy barrier to inversion of these tetrahedral molecules, they can be obtained as pure enantiomers.



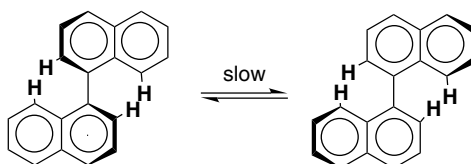
Trivalent nitrogen compounds are also approximately tetrahedral in shape. In this case, however, the barrier to inversion is small and the compounds cannot be separated as pure enantiomers at normal temperatures.



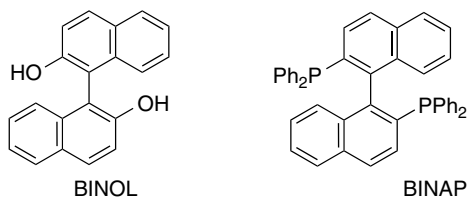
Allenes (see p. 6 for a discussion of bonding in allenes) can be chiral. An allene having nonidentical substituents at both  $sp^2$  carbons gives nonsuperimposable mirror images.



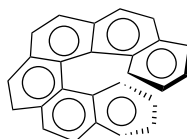
Molecules with shapes analogous to screws are also chiral, since they can be right-handed or left-handed. There are several kinds of molecules in which steric factors impose a screwlike shape. A very important case is 1, 1'-binaphthyl compounds. Steric interactions between the 2 and 8' hydrogens prevent these molecules from being planar, and as a result, there are two nonsuperimposable mirror image forms.



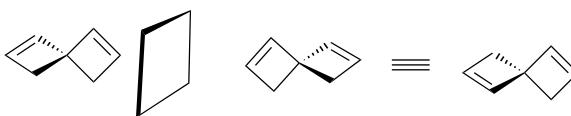
A particularly important example is the 2, 2'-diol, which is called BINOL. Another important type includes 1, 1'-binaphthyl diphosphines, such as BINAP.<sup>5</sup> BINOL and BINAP are useful chiral ligands in organometallic compounds that serve as catalysts for hydrogenations and other reactions. In Section 2.5.1.1, we discuss how compounds such as BINOL and BINAP have been used to develop *enantioselective hydrogenation catalysts*.



A spectacular example of screw-shaped chirality is hexahelicene, in which the six fused benzene rings cannot be planar and give rise to right-handed and left-handed enantiomers. The specific rotation  $[\alpha]_{589}$  is about 3700.<sup>6</sup> Hexahelicene can be racemized by heating. The increased molecular vibration allows the two terminal rings to slip past one another. The activation energy required is 36.2 kcal/mol.<sup>7</sup>



Many *spiro* compounds are chiral. In *spiro* structures, two rings share a common atom. If neither ring contains a plane of symmetry, *spiro* compounds are chiral. An example is *S*-(+)-*spiro*[3,3]hepta-1,5-diene.<sup>8</sup>



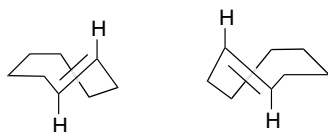
The *E*-cycloalkenes are also chiral. *E*-cyclooctene is a good example. Examination of the structures below using molecular models demonstrates that the two mirror images cannot be superimposed.

<sup>5</sup>. A. Noyori and H. Takaya, *Acc. Chem. Res.*, **23**, 345 (1990).

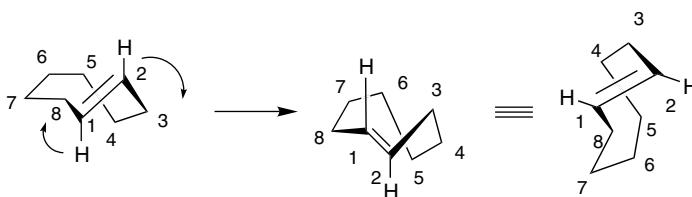
<sup>6</sup>. M. S. Newman and D. Lednicer, *J. Am. Chem. Soc.*, **78**, 4765 (1956).

<sup>7</sup>. R. H. Martin and M. J. Marchant, *Tetrahedron*, **30**, 347 (1974).

<sup>8</sup>. L. A. Hulshof, M. A. McKervey, and H. Wynberg, *J. Am. Chem. Soc.*, **96**, 3906 (1974).

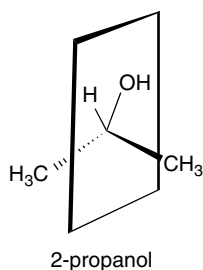


*E*-cyclooctene is subject to thermal racemization. The molecular motion allows the double bond to slip through the ring, giving the enantiomer. The larger and more flexible the ring, the easier the process. The rates of racemization have been measured for *E*-cyclooctene, *E*-cyclononene, and *E*-cyclododecene. For *E*-cyclooctene the half-life is 1 h at 183.9° C. The activation energy is 35.6 kcal/mol. *E*-cyclononene, racemizes much more rapidly. The half-life is 4 min at 0° C, with an activation energy of about 20 kcal/mol. *E*-cyclododecene racemizes immediately on release from the chiral platinum complex used for its preparation.<sup>9</sup>



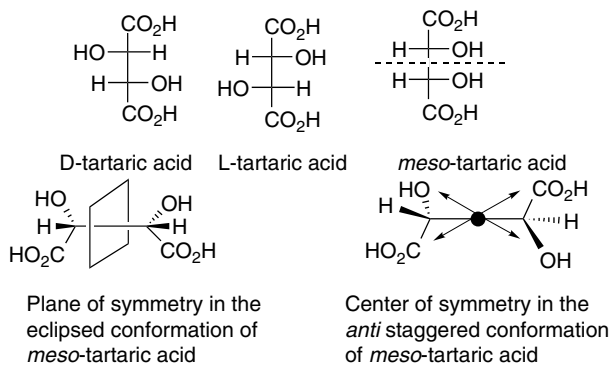
### 2.1.6. The Relationship between Chirality and Symmetry

Molecules that possess certain elements of symmetry are not chiral, because the element of symmetry ensures that the mirror image forms are superimposable. The most common example is a *plane of symmetry*, which divides a molecule into two halves that have identical placement of substituents on both sides of the plane. A trivial example can be found at any tetrahedral atom with two identical substituents, as, for example, in 2-propanol. The plane subdivides the 2-H and 2-OH groups and the two methyl groups are identical.

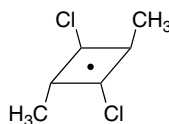


<sup>9</sup> A. C. Cope and B. A. Pawson, *J. Am. Chem. Soc.*, **87**, 3649 (1965); A. C. Cope, K. Banholzer, H. Keller, B. A. Pawson, J. J. Whang, and H. J. S. Winkler, *J. Am. Chem. Soc.*, **87**, 3644 (1965).

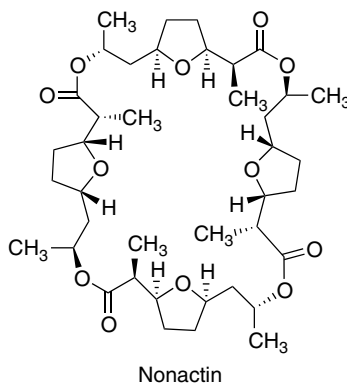
More elaborate molecules can also have a plane of symmetry. For example, there are only three stereoisomers of tartaric acid (2,3-dihydroxybutanedioic acid). Two of these are chiral but the third is achiral. In the achiral stereoisomer, the substituents are located with respect to each other in such a way as to generate a plane of symmetry. Compounds that contain two or more stereogenic centers but have a plane of symmetry are called *meso forms*. Because they are achiral, they do not rotate plane polarized light. Note that the Fischer projection structure of *meso*-tartaric acid reveals the plane of symmetry.



A less common element of symmetry is a *center of symmetry*, which is a point in a molecule through which a line oriented in any direction encounters the same environment (structure) when projected in the opposite direction. For example, *trans, trans, cis*-2,4-dichloro-1,3-dimethylcyclobutane has a center of symmetry, but no plane of symmetry. It is achiral.

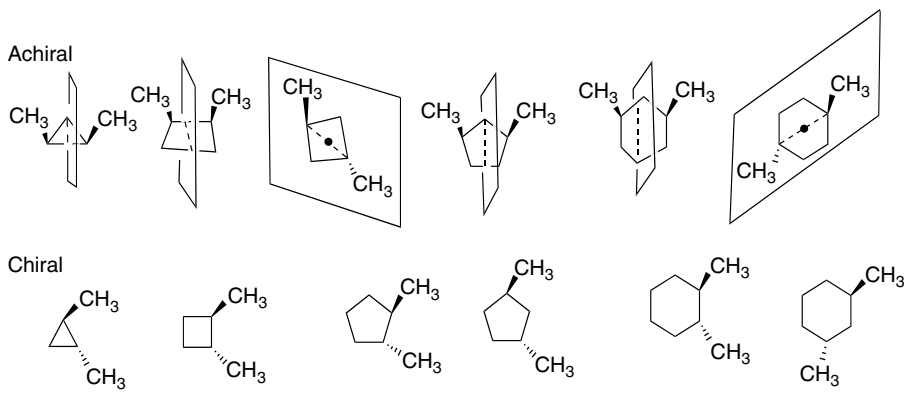


Another very striking example is the antibiotic nonactin. Work out problem 2.15 to establish the nature of the of symmetry in nonactin.



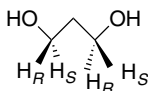
Various di- and polysubstituted cyclic compounds provide other examples of molecules having planes of symmetry. Since chirality depends on *configuration*, not *conformation*, cyclic molecules can be represented as planar structures to facilitate recognition of symmetry elements. These planar structures clearly convey the *cis* and *trans* relationships between substituents. Scheme 2.1 gives some examples of both chiral and achiral dimethylcycloalkanes. Note that in several of the compounds there is both a center and a plane of symmetry. Either element of symmetry ensures that the molecule is achiral.

Scheme 2.1. Chiral and Achiral Disubstituted Cycloalkanes

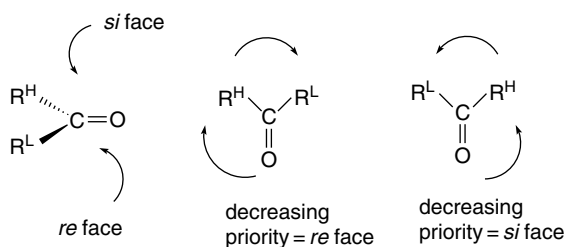


### 2.1.7. Configuration at Prochiral Centers

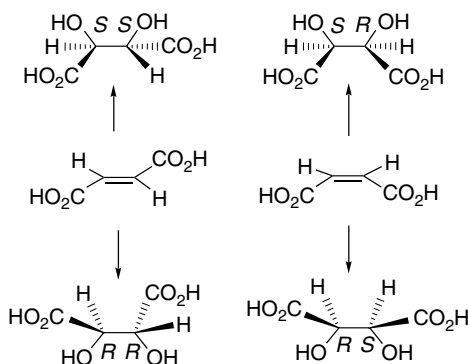
*Prochiral centers* have two identical ligands, such as two hydrogens, and are achiral. In many situations, however, these identical ligands are *topologically nonequivalent* or *heterotopic*. This occurs when the other two substituents are different. If either of the identical groups is replaced by a different ligand, a stereogenic center is created. The two positions are called *enantiotopic*. The position, which if assigned a higher priority, gives an *R* configuration is called *pro-R*. The position, which if assigned a higher priority, gives an *S* configuration is called *pro-S*. Propane-1,3-diol is an example of a prochiral molecule. The C(1) and C(3) positions are prochiral, but the C(2) is not, because its two hydroxymethyl ligands are identical.



Unsymmetrically substituted carbonyl groups are prochiral centers, since addition of a fourth ligand generates a stereogenic center. These are designated by determining the Cahn-Ingold-Prelog priority order. The carbonyl group is said to have an *re* face and an *si* face.



Achiral reagents do not distinguish between the two faces, but chiral reagents do and give unequal amounts of enantiomeric products. Other trigonal centers, including carbon-carbon double bonds, present two prochiral faces. For example, *E*- and *Z*-butenedioic acid (maleic and fumaric acid) generate different stereoisomers when subjected to *syn*-dihydroxylation. If the reagent that is used is chiral, the *E*-isomer will generate different amounts of the *R,R* and *S,S* products. The *S,R* and *R,S* forms generated from the *Z*-isomer are *meso* forms and will be achiral, even if they are formed using a chiral reagent.



The concept of heterotopic centers and faces can be extended to diastereotopic groups. If one of two equivalent ligands in a molecule is replaced by a test group, the ligands are diastereotopic when the resulting molecules are diastereomers. Similarly, if a transformation at opposite faces of a trigonal center generates two different diastereomers, the faces are diastereotopic. There is an important difference between enantiotopic and diastereotopic centers. Two identical ligands at enantiotopic centers are in *chemically equivalent environments*. They respond identically to probes, including chemical reagents, that are achiral. They respond differently to chiral probes, including chiral reagents. Diastereotopic centers are *topologically nonequivalent*. That is, their environments in the molecule are different and they respond differently to achiral, as well as to chiral probes and reagents. As a consequence of this nonequivalence, diastereotopic protons, as an example, have different chemical shifts and are distinguishable in NMR spectra. Enantiotopic protons do not show separate NMR signals. Two diastereotopic protons give rise to a more complex NMR pattern. Because of their chemical shift difference, they show a geminal coupling. An example of this effect can be seen in the proton NMR spectra of 1-phenyl-2-butanol, as shown in

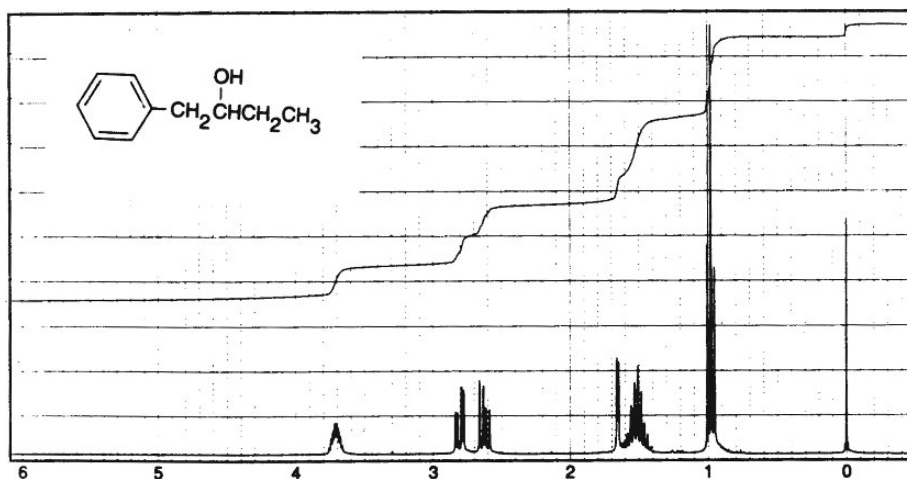
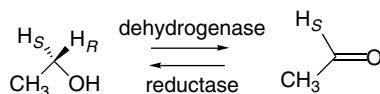


Fig. 2.6. NMR spectrum of 1-phenyl-2-butanol showing the diastereotopic nature of C(1) protons. Reproduced from *Aldrich Library of  $^{13}\text{C}$  and  $^1\text{H}$  NMR Spectra*, Vol. 2, 1993, p. 386.

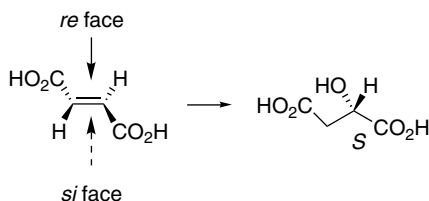
Figure 2.6. The C(1)  $\text{CH}_2$  group appears as a quartet near 2.8 ppm with further coupling to the C(2) proton. The C(1) hydrogens are diastereotopic. The C(3) hydrogens are also diastereotopic, but their nonidentity is not obvious in the multiplet at about 1.6 ppm.

Because biological reactions involve chiral enzymes, enantiotopic groups and faces typically show different reactivity. For example, the two methylene hydrogens in ethanol are enantiotopic. Enzymes that oxidize ethanol, called *alcohol dehydrogenases*, selectively remove the pro-*R* hydrogen. This can be demonstrated by using a deuterated analog of ethanol in the reaction.



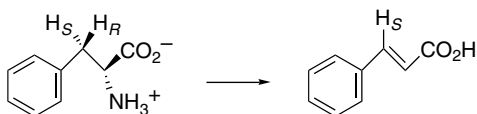
Conversely, *reductases* selectively reduce acetaldehyde from the *re* face.

Fumaric acid is converted to L-malic acid (*S*-2-hydroxybutanedioic acid) by the enzyme *fumarase*. The hydroxyl group is added stereospecifically from the *si* face of the double bond.



Enzymes also distinguish between diastereotopic groups and faces. For example, L-phenylalanine is converted to cinnamic acid by the enzyme *phenylalanine ammonia*

lyase. The reaction occurs by an *anti* elimination involving the amino group and the 3-*pro-R* hydrogen.

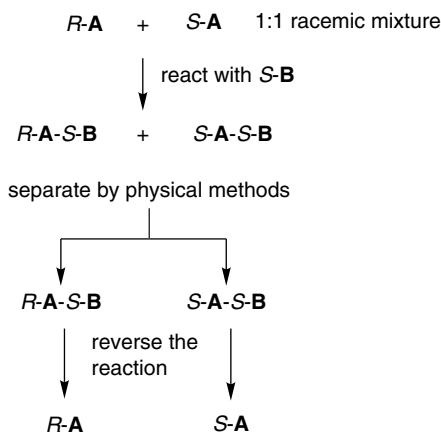


### 2.1.8. Resolution—The Separation of Enantiomers

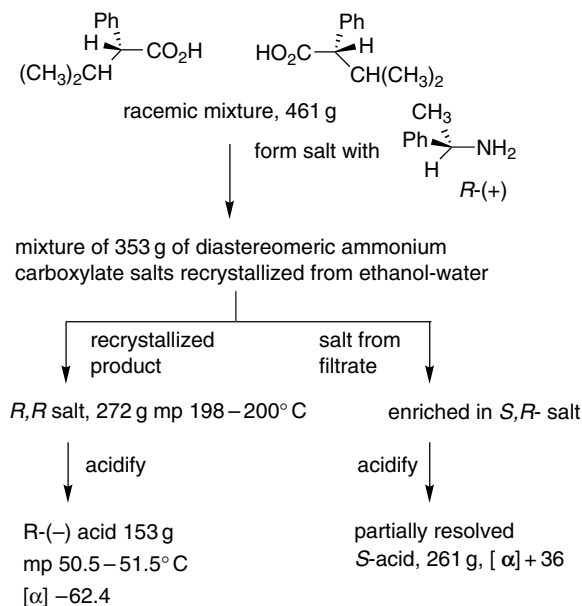
Since all living cells and organisms involve reactions of enantiomerically pure materials such as carbohydrates, proteins, and DNA, most naturally occurring chiral compounds exist in enantiomerically pure form. Chemical reactions, however, often produce racemic mixtures. This is *always* the case if only racemic and/or achiral reactants, reagents, catalysts, and solvents are used. The products of chemical reactions can be enantiomerically enriched or enantiopure only if chiral starting materials, reagents, catalysts or solvents are used. (See Section 2.5 for a discussion of enantioselective reactions.) Racemic mixtures can be separated into the two enantiomeric forms. The process of separating a racemic mixture into its enantiomers is called *resolution*, and it can be accomplished in several different ways.

Historically, the usual method was to use an existing enantiomerically pure compound, often a naturally occurring material, as a *resolving agent*. When a racemic mixture of **A** (*R,S*-**A**) reacts with a pure enantiomer (*S*-**B**), the two products are *diastereomeric*, namely *R,S*-**AB** and *S,S*-**AB**. As diastereomers have differing physical properties, they can be separated by such means as crystallization or chromatography. When the diastereomers have been separated, the original reaction can be reversed to obtain enantiomerically pure (or enriched) samples. The concept is summarized in Scheme 2.2. Scheme 2.3 describes an actual resolution.

#### Scheme 2.2. Conceptual Representation of Resolution through Separation of Diastereomeric Derivatives



**Scheme 2.3. Resolution of 3-Methyl-2-Phenylbutanoic Acid<sup>a</sup>**



\* a. C. Aaron, D. Dull, J. L. Schmiegel, D. Jaeger, Y. Ohahi, and H. S. Mosher, *J. Org. Chem.*, **32**, 2797 (1967).

Another means of resolution is to use a chiral material in a physical separation. Currently, many resolutions are done using medium- or high-pressure chromatography with chiral column-packing materials. Resolution by chromatography depends upon differential adsorption of the enantiomers by the chiral stationary phase. Differential adsorption occurs because of the different “fit” of the two enantiomers to the chiral adsorbent. Figure 2.7 shows such a separation. Topic 2.1 provides additional detail on several types of chiral stationary phases.

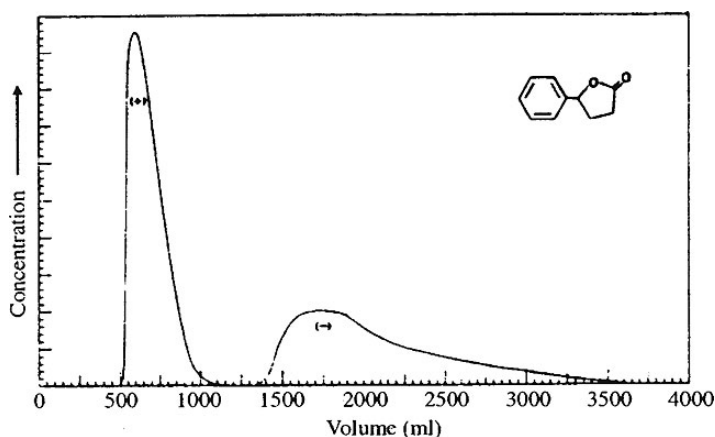
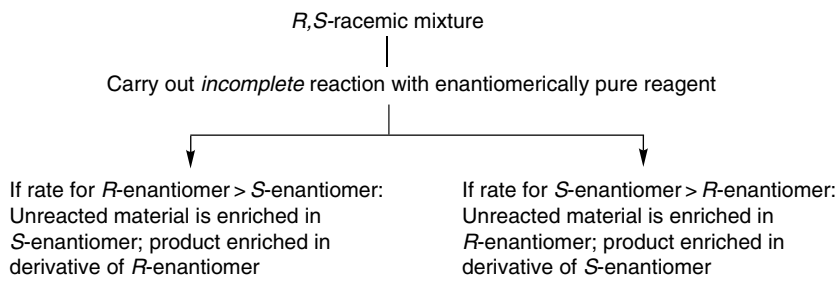


Fig. 2.7. Preparative chromatographic resolution of 5 g of  $\gamma$ -phenyl- $\gamma$ -butyrolactone on 480 g of cellulose triacetate (column 5 cm  $\times$  60 cm). Reproduced from *Helv. Chim. Acta*, **70**, 1569 (1987), by permission of Wiley-VCH.



Another means of resolution depends on the difference in rates of reaction of two enantiomers with a chiral reagent. The rates of reaction of each enantiomer with a single enantiomer of a chiral reagent are different because the transition structures and intermediates (*R*-substrate...*R*-reagent) and (*S*-substrate...*R*-reagent) are *diastereomeric*. *Kinetic resolution* is the term used to describe the separation of enantiomers on the basis of differential reaction rates with an enantiomerically pure reagent. Scheme 2.4 summarizes the conceptual basis of kinetic resolution.

Because the separation is based on differential rates of reaction, the degree of resolution that can be achieved depends on both the *magnitude of the rate difference and the extent of reaction*. The greater the difference in the two rates, the higher the enantiomeric purity of both the reacted and unreacted enantiomer. The extent of enantiomeric purity can be controlled by controlling the degree of conversion. As the extent of conversion increases, the enantiomeric purity of the *unreacted enantiomer increases*.<sup>10</sup> The relationship between the relative rate of reaction, extent of conversion, and enantiomeric purity of the unreacted enantiomer is shown graphically in Figure 2.8.

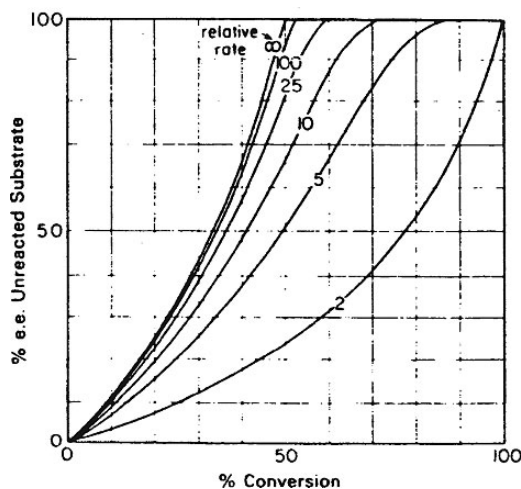


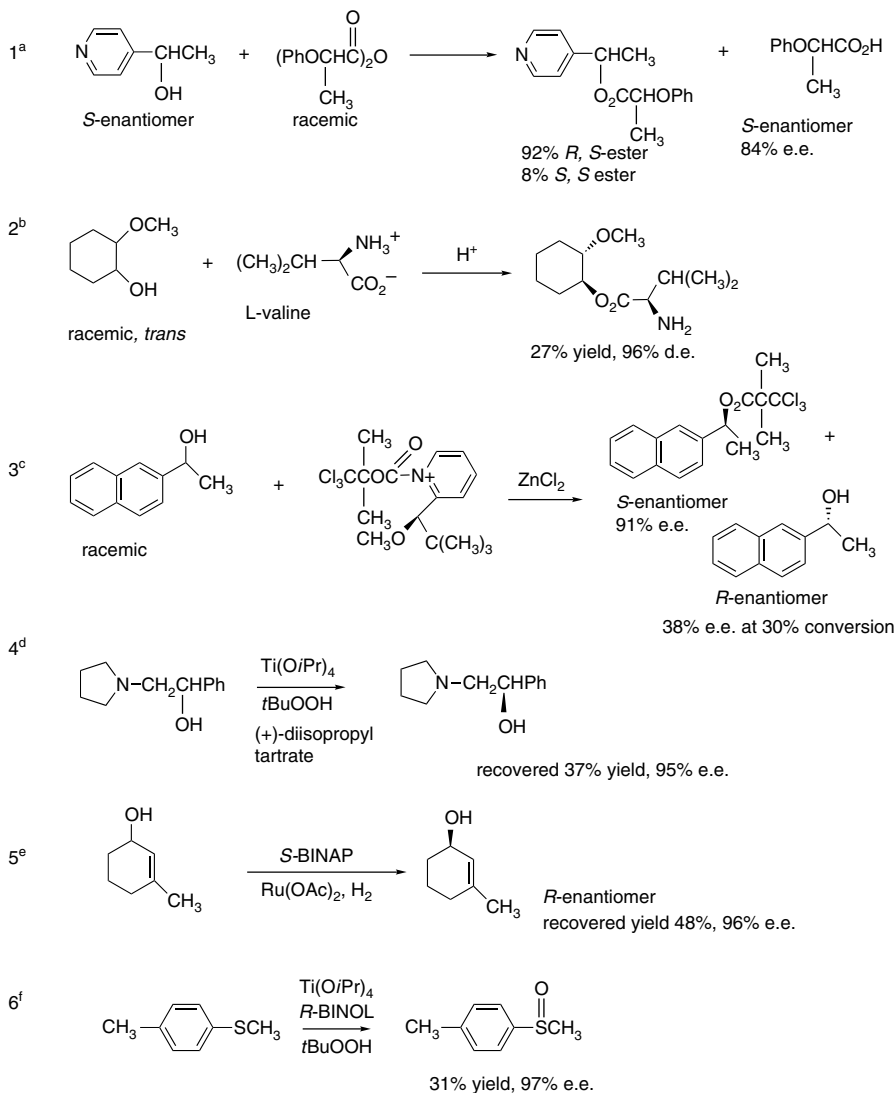
Fig. 2.8. Dependence of enantiomeric excess on relative rate of reaction and extent of conversion with a chiral reagent in kinetic resolution. Reproduced from *J. Am. Chem. Soc.*, **103**, 6237 (1981), by permission of the American Chemical Society.

<sup>10</sup> V. S. Martin, S. S. Woodard, T. Katsuki, Y. Yamada, M. Ikeda, and K. B. Sharpless, *J. Am. Chem. Soc.*, **103**, 6237 (1981).

Of course, the high conversion required for high enantiomeric purity when the relative reactivity difference is low has a serious drawback. The *yield of the unreacted substrate is low* if the overall conversion is high. Relative reactivity differences of  $< 10$  can achieve high enantiomeric purity only at the expense of low yield.

Scheme 2.5 gives some specific examples of kinetic resolution procedures. Entries 1 to 3 in Scheme 2.5 are acylation reactions in which esters are formed. Either the

**Scheme 2.5. Examples of Kinetic Resolution**



a. U. Salz and C. Rüchardt, *Chem. Ber.*, **117**, 3457 (1984).

b. P. Stead, H. Marley, M. Mahmoudian, G. Webb, D. Noble, Y. T. Ip, E. Piga, S. Roberts, and M. J. Dawson, *Tetrahedron: Asymmetry*, **7**, 2247 (1996).

c. E. Vedejs and X. Chen, *J. Am. Chem. Soc.*, **118**, 1809 (1996).

d. S. Miyano, L. D. Lu, S. M. Viti, and K. B. Sharpless, *J. Org. Chem.*, **48**, 3608 (1983).

e. M. Kitamura, I. Kasahara, K. Manabe, R. Noyori, and H. Takaya, *J. Org. Chem.*, **53**, 708 (1988).

f. N. Komatsu, M. Hashizuma, T. Sugita, and S. Uemura, *J. Org. Chem.*, **58**, 7624 (1993).

alcohol or the acylation reagent is enantiopure. The enantioselectivity is a result of differential interactions in the TS (transition structure) and the reactions are carried to partial conversion to achieve kinetic resolution. These reactions presumably proceed via the typical addition-elimination mechanism for acylation (see Section 7.4) and do not have the benefit of any particular organizing center such as a metal ion. The observed enantioselectivities are quite high, and presumably depend primarily on steric differences in the diastereomeric TSs. Entries 4 and 5 involve enantioselective catalysts. Entry 4, is an oxidative cleavage that involves a complex of Ti(IV) with the chiral ligand, diisopropyl tartrate. It is sufficiently selective to achieve 95% e.e. at the point of about 67% completion. The other enantiomer is destroyed by the oxidation. Entry 5 uses a hydrogenation reaction with the chiral BINAP ligand (see p. 130 for structure). The *S*-enantiomer is preferentially hydrogenated and the *R*-enantiomer is obtained in high e.e. In both of these examples, the reactant coordinates to the metal center through the hydroxy group prior to reaction. The relatively high e.e. that is observed in each case reflects the high degree of order and discrimination provided by the chiral ligands at the metal center. Entry 6 is the oxidative formation of a sulfoxide, using BINOL (see p. 130) as a chiral ligand and again involves a metal center in a chiral environment. We discuss enantioselective catalysis further in Section 2.5.

Enzymes constitute a particularly important group of enantioselective catalysts,<sup>11</sup> as they are highly efficient and selective and can carry out a variety of transformations. Enzyme-catalyzed reactions can be used to resolve organic compounds. Because the enzymes are derived from L-amino acids, they are chiral and usually one enantiomer of a reactant (substrate) is much more reactive than the other. The interaction with each enantiomer is diastereomeric in comparison with the interaction of the enzyme with the other enantiomer. Since enzymatic catalysis is usually based on a specific fit to an “active site,” the degree of selectivity between the two enantiomers is often very high. For enzymatic resolutions, the enantioselectivity can be formulated in terms of two reactants in competition for a single type of catalytic site.<sup>12</sup> Enzymatic reactions can be described by *Michaelis-Menten kinetics*, where the key parameters are the equilibrium constant for binding at the active site,  $K$ , and the rate constant,  $k$ , of the enzymatic reaction. The rates for the two enantiomers are given by

$$v_R = k_R[R]/K_R \text{ and } v_S = k_S[S]/K_S \quad (2.6)$$

In a resolution with the initial concentrations being equal,  $[S] = [R]$  the enantiomeric selectivity ratio  $E$  is the relative rate given by

$$E = \frac{k_S/K_S}{k_R/K_R} \quad (2.7)$$

Figure 2.9 shows the relationship between the e.e. of unreacted material and product as a function of the extent of conversion and the value of  $E$ .

The most generally useful enzymes catalyze hydrolysis of esters and amides (esterases, lipases, peptidases, acylases) or interconvert alcohols with ketones and aldehydes (oxido-reductases). Purified enzymes can be used or the reaction can be done by incubating the reactant with an organism (e.g., a yeast) that produces an

<sup>11</sup> J. B. Jones, *Tetrahedron*, **42**, 3351 (1986); J. B. Jones, in *Asymmetric Synthesis*, J. D. Morrison, ed., Vol. 5, Academic Press, Chap. 9; G. M. Whitesides and C.-H. Wong, *Angew. Chem. Int. Ed. Engl.*, **24**, 617 (1985).

<sup>12</sup> C.-S. Chen, Y. Fujimoto, G. Girdaukas, and C. J. Sih, *J. Am. Chem. Soc.*, **104**, 7294 (1982).

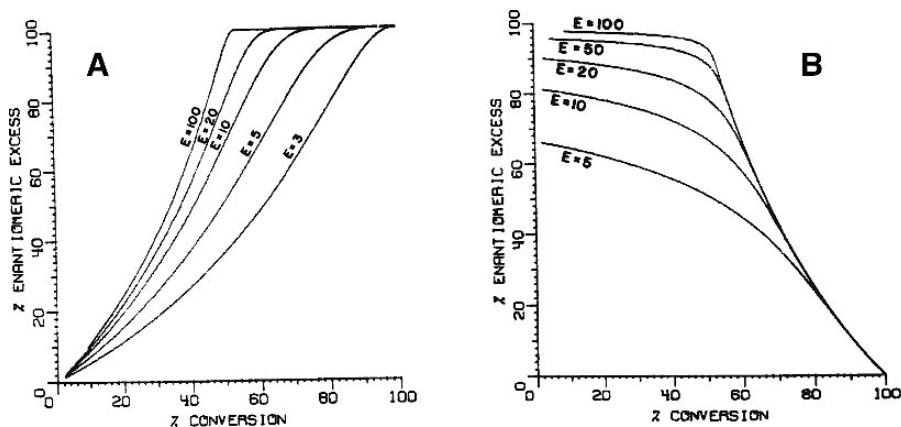
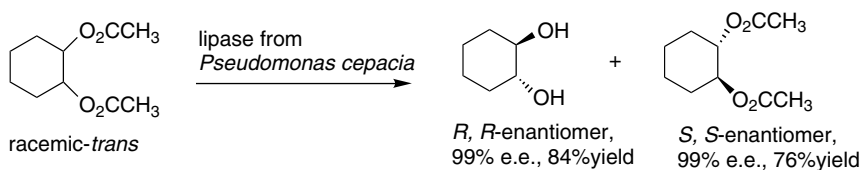
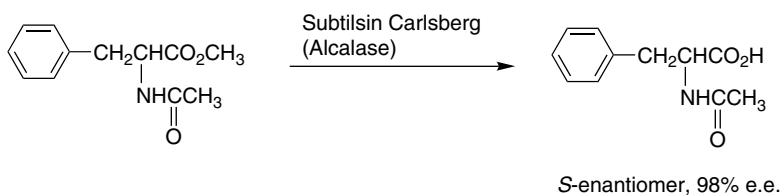


Fig. 2.9. Plots of enantiomeric excess as a function of extent of conversion for various values of  $E$ : (A) unreacted starting material; (B) product. Reproduced from *J. Am. Chem. Soc.*, **104**, 7294 (1982), by permission of the American Chemical Society.

appropriate enzyme during fermentation. Two examples are shown below. The main restriction on enzymatic resolution is the relatively limited range of reactions and substrates to which it is applicable. Enzymes usually have high substrate specificity, that is, they show optimal reactivity for compounds that are similar in structure to the natural substrate. Topic 2.2 gives further information about the application of enzymatic resolution.



Ref. 13



Ref. 14

13. G. Caron and R. J. Kazlauskas, *J. Org. Chem.*, **56**, 7251 (1991).

14. J. M. Roper and D. P. Bauer, *Synthesis*, 1041 (1983).

The structural aspects of stereochemistry discussed in the previous section are the consequences of *configuration*, the geometric arrangement fixed by the chemical bonds within the molecule. Now, we want to look at another level of molecular structure, *conformation*. Conformations are the different shapes that a molecule can attain without breaking any covalent bonds. They differ from one another as the result of rotation at one or more single bond. The energy barrier for rotation of carbon-carbon single bonds is normally small, less than 5 kcal/mol, but processes that involve several coordinated rotations can have higher energy requirements. *Conformational analysis* is the process of relating conformation to the properties and reactivity of molecules.

### 2.2.1. Conformation of Acyclic Compounds

Ethane is a good molecule with which to begin. The two methyl groups in ethane can rotate with respect to one another. There are two unique conformations, called *staggered* and *eclipsed*. The eclipsed conformation represents the maximum energy and the staggered is the minimum. The difference between the two is 2.88 kcal/mol, as shown in Figure 2.10. As a result, any individual molecule is likely to be in the

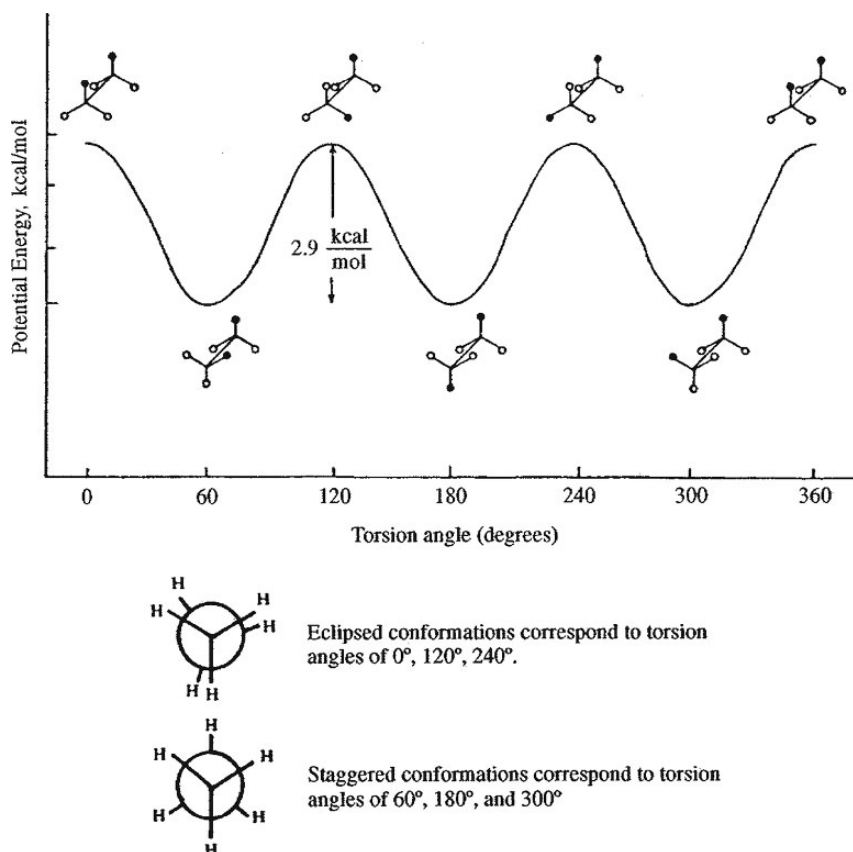
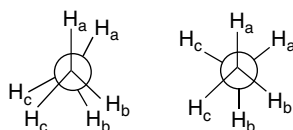
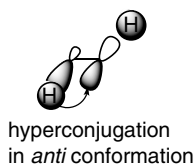


Fig. 2.10. Potential energy as a function of torsion angle for ethane.

staggered conformation at any given instant, but each molecule can rapidly traverse through the eclipsed conformation. The rate of rotation is about  $6 \times 10^9 \text{ s}^{-1}$  at  $25^\circ \text{ C}$ .



Shortly, we will learn that for some hydrocarbon molecules, van der Waals repulsions are a major factor in conformational preferences and energy barriers, but that is not the case for ethane. Careful analysis of the van der Waals radii show that the hydrogens do not come close enough to account for the barrier to rotation.<sup>15</sup> Furthermore, the barrier of just under 3 kcal is applicable to more highly substituted single bonds. The barrier becomes significantly larger only when additional steric components are added, so the barrier must be an intrinsic property of the bond and not directly dependent on substituent size. The barrier to rotation is called the *torsional barrier*. There are analogous (although smaller) barriers to rotation about C–N and C–O bonds. Topic 1.3 probes further into the origin of the torsional barrier in small molecules. The conclusion reached is that the main factor responsible for the torsional barrier is  $\sigma$ - $\sigma^*$  delocalization (hyperconjugation), which favors the staggered conformation.



The interplay between the torsional barrier and nonbonded (van der Waals) interactions can be illustrated by examining the conformations of *n*-butane. The relationship between energy and the torsion angle for rotation about the C(2)–C(3) bond is presented in Figure 2.11. The potential energy diagram of *n*-butane resembles that of ethane in having three maxima and three minima, but differs in that one of the minima is lower than the other two and one of the maxima is of higher energy than the other two. The minima correspond to staggered conformations. Of these, the *anti* is lower in energy than the two *gauche* conformations. The energy difference between the *anti* and *gauche* conformations in *n*-butane is about 0.6 kcal/mol.<sup>16</sup> The maxima correspond to eclipsed conformations, with the highest-energy conformation being the one with the two methyl groups eclipsed with each other.

The rotational profile of *n*-butane can be understood as a superimposition of van der Waals repulsion on the ethane rotational energy profile. The two *gauche* conformations are raised in energy relative to the *anti* by an energy increment resulting from the van der Waals repulsion between the two methyl groups of 0.6 kcal/mol. The

<sup>15</sup> E. Eliel and S. H. Wilen, *Stereochemistry of Organic Compounds*, Wiley, New York, 1994, p. 599.

<sup>16</sup> G. J. Szasz, N. Sheppard, and D. H. Rank, *J. Chem. Phys.*, **16**, 704 (1948); P. B. Woller and E. W. Garbisch, Jr., *J. Am. Chem. Soc.*, **94**, 5310 (1972).

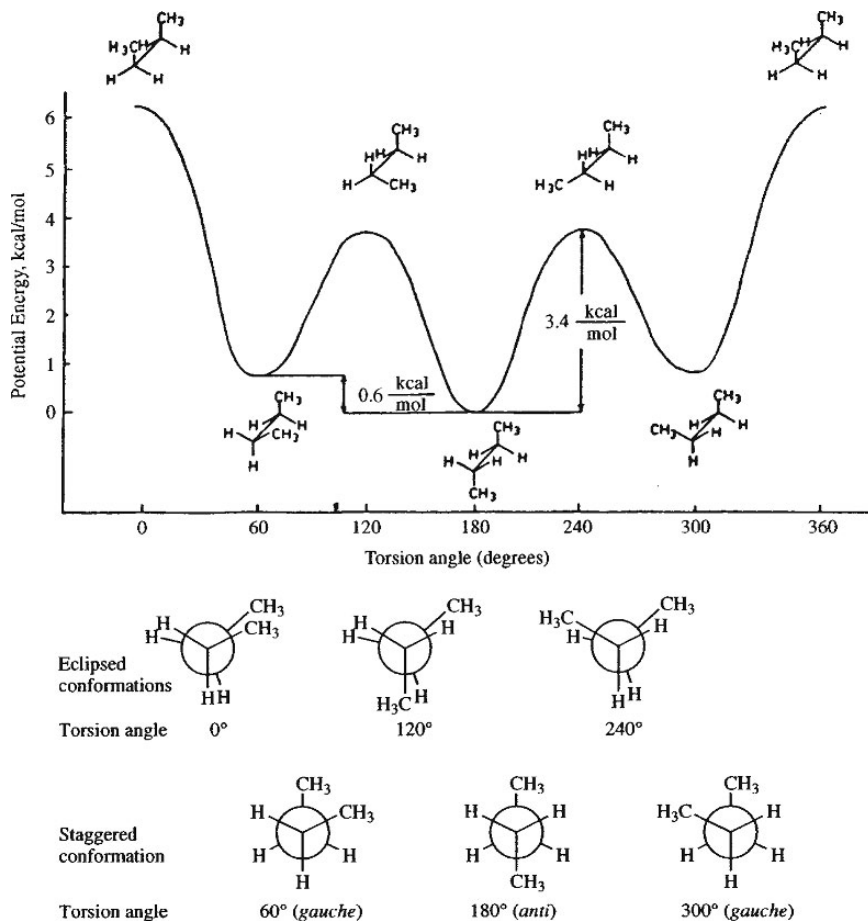


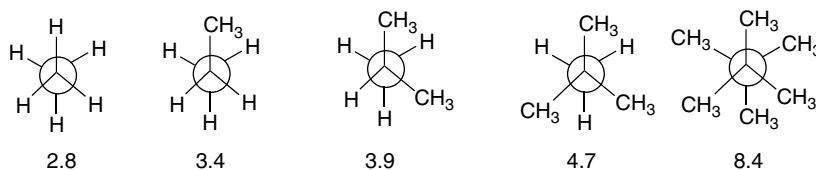
Fig. 2.11. Potential energy diagram for rotation about the C(2)–C(3) bond in *n*-butane.

eclipsed conformations all incorporate 2.8 kcal/mol of torsional strain relative to the staggered conformations, just as in ethane. The methyl-methyl eclipsed conformation is further strained by the van der Waals repulsion between the methyl groups. The van der Waals repulsion between methyl and hydrogen is smaller in the other eclipsed conformations. The methyl/methyl eclipsed barrier is not known precisely, but the range in experimental and theoretical values is between 4.0 and 6.6 kcal/mol, with the most recent values being at the low end of the range.<sup>17</sup>

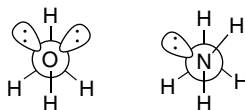
The conformation of other simple hydrocarbons can be interpreted by extensions of the principles illustrated in the analysis of rotational barriers in ethane and *n*-butane. The staggered conformations correspond to torsional minima and the eclipsed conformations to torsional maxima. Of the staggered conformations, *anti* forms are more stable than *gauche*. Substitution of a methyl group for hydrogen on one of the carbon atoms produces an increase of 0.4–0.6 kcal/mol in the height of the rotational energy barrier. The barrier in ethane is 2.88 kcal/mol. In propane, the barrier is 3.4 kcal/mol, corresponding to an increase of 0.5 kcal/mol for methyl-hydrogen eclipsing. When

<sup>17</sup> N. L. Allinger, R. S. Grev, B. F. Yates, and H. F. Schaefer, III, *J. Am. Chem. Soc.*, **112**, 114 (1990); W. A. Herrebout, B. J. van der Veken, A. Wang, and J. R. Durig, *J. Phys. Chem.*, **99**, 578 (1995).

two methyl-hydrogen eclipsing interactions occur, as in 2-methylpropane, the barrier is raised to 3.9 kcal/mol. The increase in going to 2,2-dimethylpropane, in which the barrier is 4.7 kcal/mol, is 1.8 kcal/mol for the total of three methyl-hydrogen eclipsing interactions. For 2,2,3,3-tetramethylbutane, in which there are three methyl-methyl interactions, the barrier is 8.4 kcal/mol. Rotational barriers in kcal/mol are shown below.



The magnitudes of the barriers to rotation of many small organic molecules have been measured.<sup>18</sup> The experimental techniques used to study rotational processes include microwave spectroscopy, electron diffraction, ultrasonic absorption, and infrared spectroscopy.<sup>19</sup> Some representative barriers are listed in Table 2.1. As with ethane, the barriers in methylamine and methanol appear to be dominated by *hyperconjugative stabilization* of the *anti* conformation. The barrier decreases (2.9  $\rightarrow$  2.0  $\rightarrow$  1.1) in proportion to the number of anti H–H arrangements (3  $\rightarrow$  2  $\rightarrow$  1). (See Topic 1.1 for further discussion.)<sup>20</sup>



The conformation of simple alkenes can be considered by beginning with propene. There are two families of conformations available to terminal alkenes: *eclipsed* and *bisected* conformations, as shown below for propene. The eclipsed conformation is preferred by about 2 kcal/mol and represents a barrier to rotation of the methyl group.<sup>21,22</sup> A simple way to relate the propene rotational barrier to that of ethane is to regard the  $\pi$  bond as a “banana bond” (see p. 7). The bisected conformation of propene is then seen to correspond to the eclipsed conformation of ethane, while the more stable eclipsed conformation corresponds to the staggered conformation of ethane.<sup>23</sup>

<sup>18</sup> For reviews, see (a) J. P. Lowe, *Prog. Phys. Org. Chem.*, **6**, 1 (1968); (b) J. E. Andersen, in *The Chemistry of Alkenes and Cycloalkenes*, S. Patai and Z. Rappoport, eds., Wiley, Chichester, 1992, Chap. 3II. D.

<sup>19</sup> Methods for determination of rotational barriers are discussed in Ref. 18a and by E. Wyn-Jones and R. A. Pethrick, *Top. Stereochem.*, **5**, 205 (1969).

<sup>20</sup> J. K. Badenhop and F. Weinhold, *Int. J. Quantum Chem.*, **72**, 269 (1999); V. Pophristic and L. Goodman, *J. Phys. Chem. A.*, **106**, 1642 (2002).

<sup>21</sup> J. R. Durig, G. A. Guirgis, and S. Bell, *J. Phys. Chem.*, **93**, 3487 (1989).

<sup>22</sup> Detailed analysis of the rotation shows that it is coupled with vibrational processes. L. Goodman, T. Kundu, and J. Leszczynski, *J. Phys. Chem.*, **100**, 2770 (1996).

<sup>23</sup> K.-T. Lu, F. Weinhold, and J. C. Weisshaar, *J. Chem. Phys.*, **102**, 6787 (1995).

Table 2.1. Rotational Barriers of Compounds of Type  $\text{CH}_3 - \text{X}^a$ 

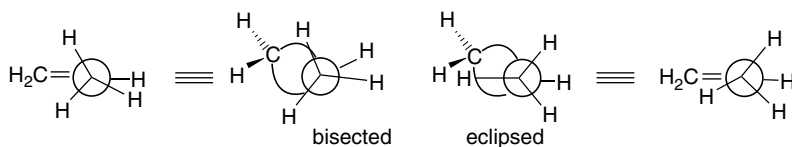
Alkanes <sup>a</sup>	Barrier (kcal/mol)	Heteroatom compounds	Barrier (kcal/mol)
$\text{CH}_3 - \text{CH}_3$	2.9	$\text{CH}_3 - \text{NH}_2^c$	2.0
$\text{CH}_3 - \text{CH}_2\text{CH}_3$	3.4	$\text{CH}_3 - \text{NHCH}_3^c$	3.0
$\text{CH}_3 - \text{CH}(\text{CH}_3)_2$	3.9	$\text{CH}_3 - \text{N}(\text{CH}_3)_2^c$	4.4
$\text{CH}_3 - \text{C}(\text{CH}_3)_3$	4.7	$\text{CH}_3 - \text{OH}^d$	1.1
$(\text{CH}_3)_3\text{C} - \text{C}(\text{CH}_3)_3$	8.4 <sup>b</sup>	$\text{CH}_3 - \text{OCH}_3^d$	4.6

a. Taken from the compilation of J. P. Lowe, *Prog. Phys. Org. Chem.*, **6**, 1 (1968).

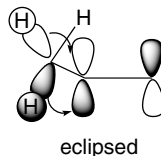
b. Footnote 9, J. E. Andersen, A. de Meijere, S. I. Kozhushkov, L. Lunazzi, and A. Mazzanti, *J. Org. Chem.*, **68**, 8494 (2003).

c. M. L. Senent and Y. G. Meyers, *J. Chem. Phys.*, **105**, 2789 (1996).

d. V. Pophristic, L. Goodman, and N. Guchhait, *J. Phys. Chem. A*, **101**, 4290 (1997).



The conformation of propene is influenced by hyperconjugation. The methyl substituent has an overall stabilizing effect (2.7 kcal) on the double bond, as can be concluded from the less negative heat of hydrogenation compared to ethene (see Section 3.1.1). This stabilization arises from  $\sigma - \pi^*$  interactions. The major effect is a transfer of electron density from the methyl  $\sigma \text{ C-H}$  bonds to the empty  $\pi^*$  orbital.

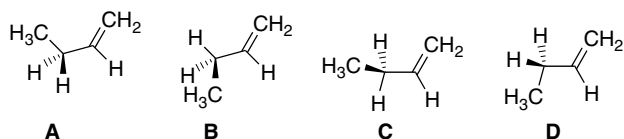


Computational approaches can provide an indication of the magnitude of the interaction. A “block-localized” wave function calculation estimates a stabilization of about 5.4 kcal/mol at the 6-31G\*\* level.<sup>24</sup> The computation also shows a shortening of the C(2)–C(3) single bond as the result of the  $\sigma - \pi^*$  delocalization. Because the extent of hyperconjugation differs between the two unique conformers, this factor contributes to the energy difference between them. The energy difference between the eclipsed and bisected conformations has been broken into components, as described for ethane in Topic 1.3. The hyperconjugation component is the major factor. At the MP2/6-311(3d,2p) level of computation, the  $\text{CH}_3 - \text{C} =$  bond length is 1.4952 Å, versus 1.5042 Å in the staggered conformation. The corresponding difference in energy is the largest component of the energy barrier and results from adjustments in the bond length in response to the rotation.<sup>25</sup>

<sup>24</sup> The block-localized calculations are conceptually similar to NBO analysis (see Section 1.4.2) in that they compare a calculation in which the orbitals are strictly localized with the unrestricted calculation to estimate the effect of delocalization. Y. Mo and S. D. Peyerimhoff, *J. Chem. Phys.*, **109**, 1687 (1998).

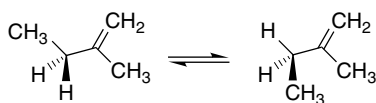
<sup>25</sup> T. Kundu, L. Goodman, and J. Leszczynski, *J. Chem. Phys.*, **103**, 1523 (1995).

With more highly substituted terminal alkenes, additional conformations are available, as indicated for 1-butene.

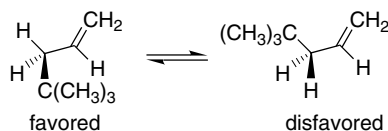


Conformations **A** and **B** are of the eclipsed type, whereas **C** and **D** are bisected. It has been determined by microwave spectroscopy that the eclipsed conformations are more stable than the bisected ones and that **B** is about 0.15 kcal more stable than **A**.<sup>26</sup> MO calculations at the HF/6-31G\* level found relative energies of 0.00, -0.25, 1.75, and 1.74 kcal/mol, respectively, for **A**, **B**, **C**, and **D**.<sup>27</sup> More recently, experimental far-IR spectroscopy and MP2/6-31G++(3df,3pd) computations indicate a difference of about 0.2 kcal (favoring **B**).<sup>28</sup>

Further substitution can introduce van der Waals repulsions that influence conformational equilibria. For example, methyl substitution at C(2), as in 2-methyl-1-butene, introduces a methyl-methyl *gauche* interaction in the conformation analogous to **B**, with the result that in 2-methyl-1-butene the two eclipsed conformations are of approximately equal energy.<sup>29</sup>



Increasing the size of the group at C(3) increases the preference for the eclipsed conformation analogous to **B** at the expense of **A**. 4,4-Dimethyl-1-pentene exists mainly in the hydrogen-eclipsed conformation.



This interaction is an example of *1,3-allylic strain*.<sup>30</sup> This type of steric strain arises in eclipsed conformations when substituents on the double bond and the C(3) group, which are coplanar, are large enough to create a nonbonded repulsion. The conformation of alkenes is an important facet with regard to the stereoselectivity of addition

<sup>26</sup> S. Kondo, E. Hirota, and Y. Morino, *J. Mol. Spectrosc.*, **28**, 471 (1968).

<sup>27</sup> W. J. Hehre, J. A. Pople, and A. J. P. Devaquet, *J. Am. Chem. Soc.*, **98**, 664 (1976).

<sup>28</sup> S. Bell, B. R. Drew, G. A. Guirgis, and J. R. During, *J. Mol. Struct.*, **553**, 199 (2000).

<sup>29</sup> T. Shimanouchi, Y. Abe, and K. Kuchitsu, *J. Mol. Struct.*, **2**, 82 (1968).

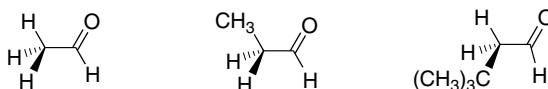
<sup>30</sup> R. W. Hoffmann, *Chem. Rev.*, **89**, 1841 (1989).

reactions of alkenes. Allylic strain and other conformational factors contribute to the relative energy of competing TSs, and can lead to a preference for a particular stereoisomeric product.

The preferred conformations of carbonyl compounds, like 1-alkenes, are eclipsed rather than bisected, as shown below for ethanal and propanal. The barrier for methyl group rotation in ethanal is 1.17 kcal/mol.<sup>31</sup> Detailed analysis has indicated that small adjustments in molecular geometry, including  $\sigma$ -bond lengthening, must be taken into account to quantitatively analyze the barrier.<sup>32</sup> The total barrier can be dissected into nuclear-nuclear, electron-electron, nuclear-electron, and kinetic energy ( $\Delta t$ ), as described in Topic 1.3 for ethane. MP2/6-311+G (3df,2p) calculations lead to the contributions tabulated below. The total barrier found by this computational approach is very close to the experimental value. Contributions to the ethanal energy barrier in kcal/mol are shown below.

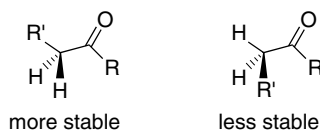
$\Delta V_{nn}$	-10.621
$\Delta V_{ee}$	-5.492
$\Delta V_{ne}$	+18.260
$\Delta t$	-0.938
$\Delta$ total	+1.209

In propanal, it is the methyl group, rather than the hydrogen, that is eclipsed with the carbonyl group in the most stable conformation. The difference in the two eclipsed conformations has been determined by microwave spectroscopy to be 0.9 kcal/mol.<sup>33</sup> A number of other aldehydes have been studied by NMR and found to have similar rotameric compositions.<sup>34</sup> When the alkyl substituent becomes too sterically demanding, the hydrogen-eclipsed conformation becomes more stable. This is the case with 3,3-dimethylbutanal.



preferred conformations for ethanal, propanal, and 3,3-dimethylbutanal

Ketones also favor eclipsed conformations. The preference is for the rotamer in which the alkyl group, rather than a hydrogen, is eclipsed with the carbonyl group because this conformation allows the two alkyl groups to be *anti* rather than *gauche* with respect to the other carbonyl substituent.



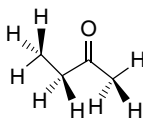
<sup>31</sup> I. Kleiner, J. T. Hougen, R. D. Suenram, F. J. Lovas, and M. Godefroid *J. Mol. Spectros.*, 153, 578 (1992); S. P. Belov, M. Y. Tretyakov, I. Kleiner, and J. T. Hougen, *J. Mol. Spectros.*, 160, 61 (1993).

<sup>32</sup> L. Goodman, T. Kundu, and J. Leszczynski, *J. Am. Chem. Soc.*, 117, 2082 (1995).

<sup>33</sup> S. S. Butcher and E. B. Wilson, Jr., *J. Chem. Phys.*, 40, 1671 (1964).

<sup>34</sup> G. J. Karabatsos and N. Hsi, *J. Am. Chem. Soc.*, 87, 2864 (1965).

The conformational profile for 2-butanone has been developed from analysis of its infrared spectrum.<sup>35</sup> The dominant conformation is *anti* with a C(1)H and the C(4) methyl group eclipsed with the carbonyl.



The C(3)–C(4) rotational barrier is 2.48 kcal/mol, similar to the ethane barrier, while the C(1)–C(2) rotational barrier is 0.67 kcal/mol. Figure 2.12 shows the rotational potential energy diagram for 2-butanone as calculated at the HF/6-31G level. The preferred conformation of 3-methyl-2-butanone is similar.<sup>36</sup>

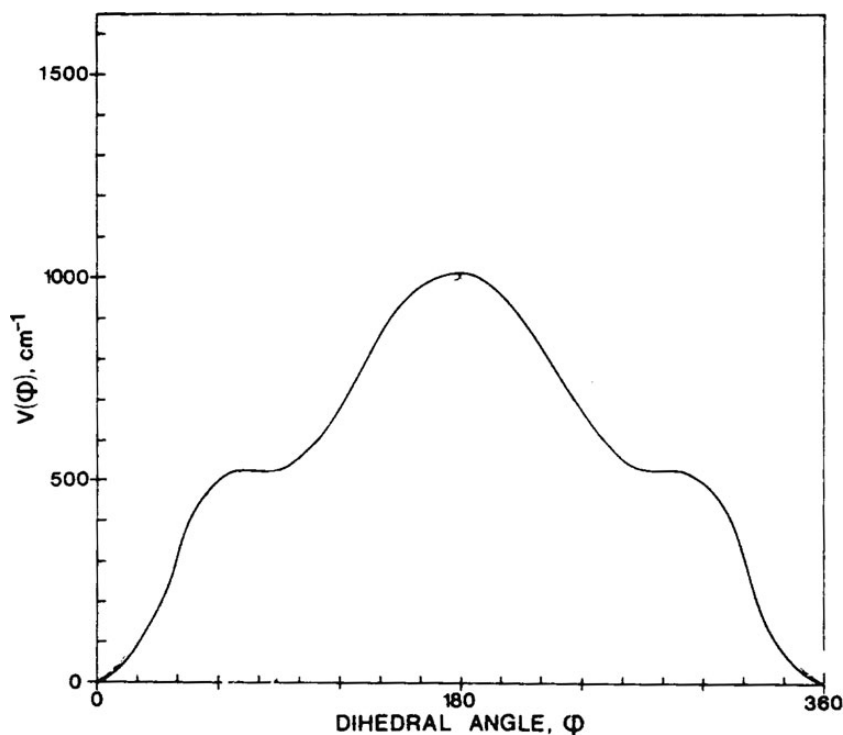
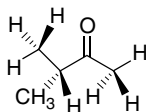


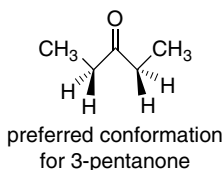
Fig. 2.12. Calculated potential energy diagram (HF/6-31G) for rotation about C(2)–C(3) bond of 2-butanone. Reproduced from *Can. J. Chem.* **69**, 1827 (1991), by permission of the National Research Council Press.

<sup>35</sup> J. R. Durig, F. S. Feng, A. Y. Wang, and H. V. Phan, *Can. J. Chem.*, **69**, 1827 (1991).

<sup>36</sup> T. Sakurai, M. Ishiyama, H. Takeuchi, K. Takeshita, K. Fukushi, and S. Konaka, *J. Mol. Struct.*, **213**, 245 (1989); J. R. Durig, S. Shen, C. Zeng, and G. A. Guirgis, *Can. J. Anal. Sci. Spectrosc.* **48**, 106 (2003).

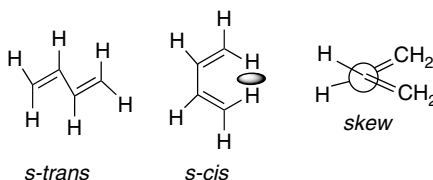


Moreover, electron diffraction studies of 3-pentanone indicate the methyl-eclipsed conformation shown below to be the most stable rotamer.<sup>37</sup>



The pattern, then, is that methyl and unbranched alkyl groups prefer to be eclipsed with the carbonyl group.

1,3-Dienes adopt conformations in which the double bonds are coplanar, so as to permit optimum  $\pi$ -orbital overlap and electron delocalization. The two alternative planar conformations for 1,3-butadiene are referred to as *s-trans* and *s-cis*. In addition to the two planar conformations, there is a third conformation, referred to as the *skew* conformation, which is cisoid but not planar. Various types of structural studies have shown that the *s-trans* conformation is the most stable one for 1,3-butadiene.<sup>38</sup> A small amount of the skew conformation is also present in equilibrium with the major conformer.<sup>39</sup> The planar *s-cis* conformation incorporates a van der Waals repulsion between the hydrogens on C(1) and C(4), which is relieved in the skew conformation.



The barrier for conversion of the skew conformation to the *s-trans* is 3.9 kcal/mol. The energy maximum presumably refers to the conformation in which the two  $\pi$  bonds are mutually perpendicular. The height of this barrier gives an approximation of the stabilization provided by conjugation in the planar *s-trans* conformation. Various MO calculations find the *s-trans* conformation to be 2–5 kcal/mol lower in energy than either the planar or skew cisoid conformations.<sup>40</sup> Most high-level MO calculations

<sup>37</sup> C. Romers and J. E. G. Creutzberg, *Rec. Trav. Chim.*, **75**, 331 (1956).

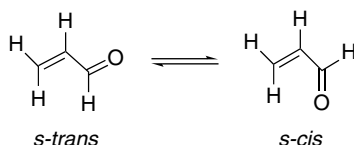
<sup>38</sup> A. Almendingen, O. Bastiansen, and M. Traetteburg, *Acta Chem. Scand.*, **12**, 1221 (1958); K. K. Kuchitsu, T. Fukuyama, and Y. Morino, *J. Mol. Struct.*, **1**, 643 (1967); R. L. Lipnick and E. W. Garbisch, Jr., *J. Am. Chem. Soc.*, **95**, 6370 (1973).

<sup>39</sup> K. B. Wiberg and R. E. Rosenberg, *J. Am. Chem. Soc.*, **112**, 1509 (1990).

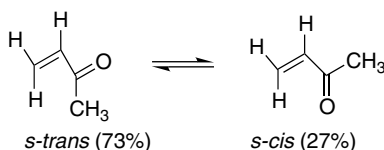
<sup>40</sup> A. J. P. Devaquet, R. E. Townshend, and W. J. Hehre, *J. Am. Chem. Soc.*, **98**, 4068 (1976); K. B. Wiberg, P. R. Rablen, and M. Marquez, *J. Am. Chem. Soc.*, **114**, 8654 (1992); M. Head-Gordon and J. A. Pople, *J. Phys. Chem.*, **97**, 1147 (1993).

favor the skew conformation over the planar *s-cis*, but the energy differences found are quite small.<sup>39,41</sup>

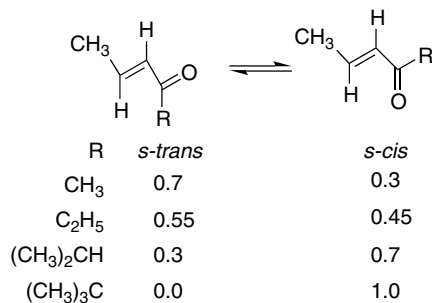
The case of  $\alpha,\beta$ -unsaturated carbonyl compounds is analogous to that of 1,3-dienes, in that conjugation favors coplanarity of the  $C=C-C=O$  system. The rotamers that are important are the *s-trans* and *s-cis* conformations. Microwave data indicate that the *s-trans* form is the only conformation present in detectable amounts in 2-propenal (acrolein).<sup>42</sup>



The equilibrium distribution of *s-trans* and *s-cis* conformations of substituted  $\alpha,\beta$ -unsaturated ketones depends on the extent of van der Waals interaction between the C(1) and the C(4) substituents.<sup>43</sup> Methyl vinyl ketone has the minimal unfavorable van der Waals repulsions and exists predominantly as the *s-trans* conformer.



When larger alkyl groups are substituted for methyl, the ratio of the *s-cis* form progressively increases as the size of the alkyl group increases.<sup>44</sup>



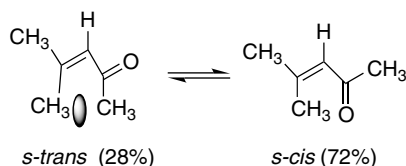
An unfavorable methyl-methyl interaction destabilizes the *s-trans* conformation of 4-methylpent-3-en-2-one (mesityl oxide) relative to the *s-cis* conformation, and the equilibrium favors the *s-cis* form.

<sup>41</sup> J. Breulet, T. J. Lee, and H. F. Schaefer, III, *J. Am. Chem. Soc.*, **106**, 6250 (1984); D. Feller and E. R. Davidson, *Theor. Chim. Acta*, **68**, 57 (1985).

<sup>42</sup> E. A. Cherniak and C. C. Costain, *J. Chem. Phys.* **45**, 104 (1966).

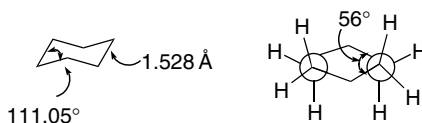
<sup>43</sup> G. Montaudo, V. Librando, S. Caccamese, and P. Maravigna, *J. Am. Chem. Soc.*, **95**, 6365 (1973).

<sup>44</sup> A. Bienvenue, *J. Am. Chem. Soc.*, **95**, 7345 (1973).



### 2.2.2. Conformations of Cyclohexane Derivatives

The conformational analysis of six-membered ring compounds is particularly well developed. Cyclohexane and its derivatives lend themselves to thorough analysis because they are characterized by a small number of energy minima. The most stable conformations are separated by barriers that are somewhat higher and more easily measured than rotational barriers in acyclic compounds or other ring systems. The most stable conformation of cyclohexane is the chair. Electron diffraction studies in the gas phase reveal a slight flattening of the chair, compared with the geometry obtained using tetrahedral molecular models. The torsion angles are  $55.9^\circ$ , compared with  $60^\circ$  for the “ideal” chair conformation, and the axial C–H bonds are not perfectly parallel, but are oriented outward by about  $7^\circ$ . The C–C bonds are  $1.528 \text{ \AA}$ , the C–H bonds are  $1.119 \text{ \AA}$ , and the C–C–C angles are  $111.05^\circ$ .<sup>45</sup>

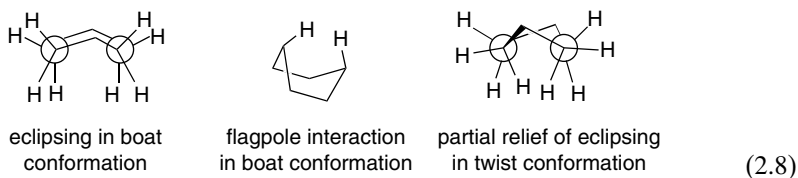


Two nonchair conformations of cyclohexane that have normal bond angles and bond lengths are the *twist* and the *boat*,<sup>46</sup> both of which are less stable than the chair. A direct measurement of the chair-twist energy difference has been made using low-temperature IR spectroscopy.<sup>47</sup> The chair was determined to be  $5.5 \text{ kcal/mol}$  lower in energy than the twist. The twist and the boat conformations are more flexible than the chair, but are destabilized by torsional strain, as the bonds along the “sides” of the boat are eclipsed. In addition, the boat conformation is further destabilized by a van der Waals repulsion between the “flagpole” hydrogens. Both this van der Waals repulsion and the torsional strain are somewhat reduced in the twist conformation.

<sup>45</sup> H. J. Geise, H. R. Buys, and F. C. Mijlthoff, *J. Mol. Struct.*, **9**, 447 (1971).

<sup>46</sup> For a review of nonchair conformations of six-membered rings, see G. M. Kellie and F. G. Riddell, *Top. Stereochem.* **8**, 225 (1974).

<sup>47</sup> M. Squillacote, R. S. Sheridan, O. L. Chapman, and F. A. L. Anet, *J. Am. Chem. Soc.*, **97**, 3244 (1975).



Interconversion of chair forms is known as *conformational inversion*, and occurs by rotation about the carbon-carbon bonds. For cyclohexane, the first-order rate constant for ring inversion is  $10^4$ – $10^5$   $\text{sec}^{-1}$  at  $27^\circ\text{C}$ . The enthalpy of activation is  $10.8$  kcal/mol.<sup>48</sup> Calculation of the geometry of the transition state by *molecular mechanics* (see Section 2.3) suggests a half-twist form lying  $12.0$  kcal/mol above the chair. According to this analysis, the half-twist form incorporates  $0.2$  kcal/mol of strain from bond length deformation,  $2.0$  kcal/mol of bond angle strain,  $4.4$  kcal/mol of van der Waals strain, and  $5.4$  kcal/mol of torsional strain.<sup>49</sup> Figure 2.13 presents a two-dimensional energy diagram illustrating the process of conformational inversion in cyclohexane. The boat form is not shown in the diagram because the chair forms can interconvert without passing through the boat. The boat lies  $1$ – $2$  kcal/mol above the twist conformation and is a transition state for interconversion of twist forms.<sup>50</sup>

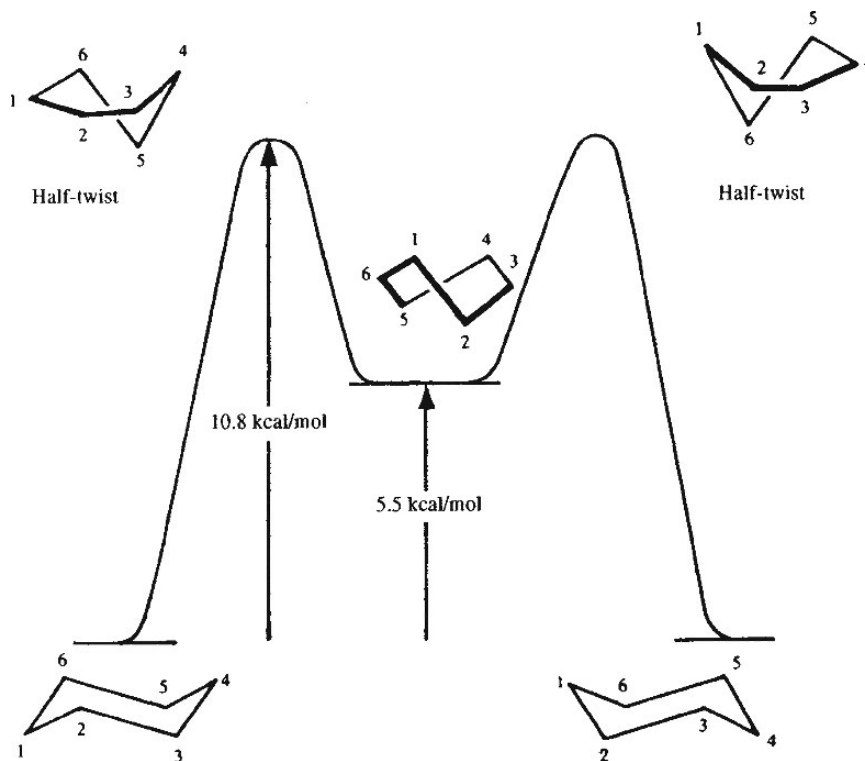


Fig. 2.13. Energy diagram for ring inversion of cyclohexane.

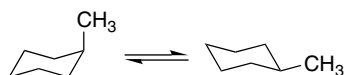
<sup>48</sup> F. A. L. Anet and A. J. R. Bourn, *J. Am. Chem. Soc.*, **89**, 760 (1967).

<sup>49</sup> N. L. Allinger, M. A. Miller, F. A. van Catledge, and J. A. Hirsch, *J. Am. Chem. Soc.*, **89**, 4345 (1967); N. L. Allinger, *J. Am. Chem. Soc.*, **99**, 8127 (1977).

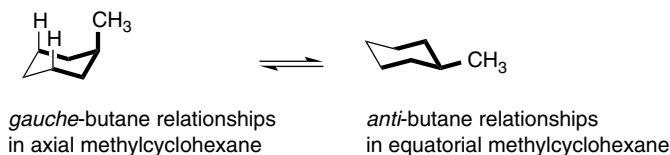
<sup>50</sup> N. Leventis, S. B. Hanna, and C. Sotiriou-Leventis, *J. Chem. Educ.* **74**, 813 (1997); R. R. Sauers, *J. Chem. Educ.* **77**, 332 (2000).

Visual models, additional information and exercises on Cyclohexane Conformations can be found in the Digital Resource available at: [Springer.com/carey-sundberg](http://Springer.com/carey-sundberg).

Substitution on a cyclohexane ring does not greatly affect the rate of conformational inversion, but does change the equilibrium distribution between alternative chair forms. All substituents that are axial in one chair conformation become equatorial on ring inversion, and vice versa. For methylcyclohexane,  $\Delta G$  for the equilibrium is  $-1.8$  kcal/mol, corresponding to a composition with 95% of the equatorial methyl conformation.



Two factors contribute to the preference for the equatorial conformation. The equatorial methyl conformation corresponds to an *anti* arrangement with respect to the C(2)–C(3) and C(6)–C(5) bonds, whereas the axial methyl group is in a *gauche* relationship to these bonds. We saw earlier that the *gauche* conformation of *n*-butane is 0.5–0.6 kcal/mol higher in energy than the *anti* conformation. In addition, there is a van der Waals repulsion between the axial methyl group and the axial hydrogens at C(3) and C(5). Interactions of this type are called *1,3-diaxial interactions*.



Energy differences between conformations of substituted cyclohexanes can be measured by several methods, as can the kinetics of the ring inversion processes. NMR spectroscopy is especially valuable for both thermodynamic and kinetic studies.<sup>51</sup> Depending on the rate of the process, the difference in chemical shift between the two sites and the field strength of the spectrometer, the observed spectrum will be either a weighted average spectrum (rapid site exchange,  $k > 10^5$  sec<sup>-1</sup>) or a superposition of the spectra of the two conformers reflecting the equilibrium composition (slow site exchange,  $k < 10^3$  sec<sup>-1</sup>). At intermediate rates of exchange, broadened spectra are observed. Analysis of the temperature dependence of the spectra can provide the activation parameters for the conformational process. Figure 2.14 illustrates the change in appearance of a simple spectrum.

For substituted cyclohexanes, the slow-exchange condition is met at temperatures below about  $-50^\circ\text{C}$ . Data for the half-life for conformational equilibration of

<sup>51</sup> G. Binsch, *Top. Stereochem.* **3**, 97 (1968); F. G. Riddell, *Nucl. Magn. Reson.*, **12**, 246 (1983); J. Sandstrom, *Dynamic NMR Spectroscopy*, Academic Press, New York, 1982; J. L. Marshall, *Nuclear Magnetic Resonance*, Verlag Chemie, Deerfield Beach, FL, 1983; M. Oki, *Applications of Dynamic NMR to Organic Chemistry*, VCH Publishers, Deerfield Beach, FL, 1985; Y. Takeuchi and A. P. Marchand, eds., *Applications of NMR Spectroscopy in Stereochemistry and Conformational Analysis*, VCH Publishers, Deerfield Beach, FL, 1986.

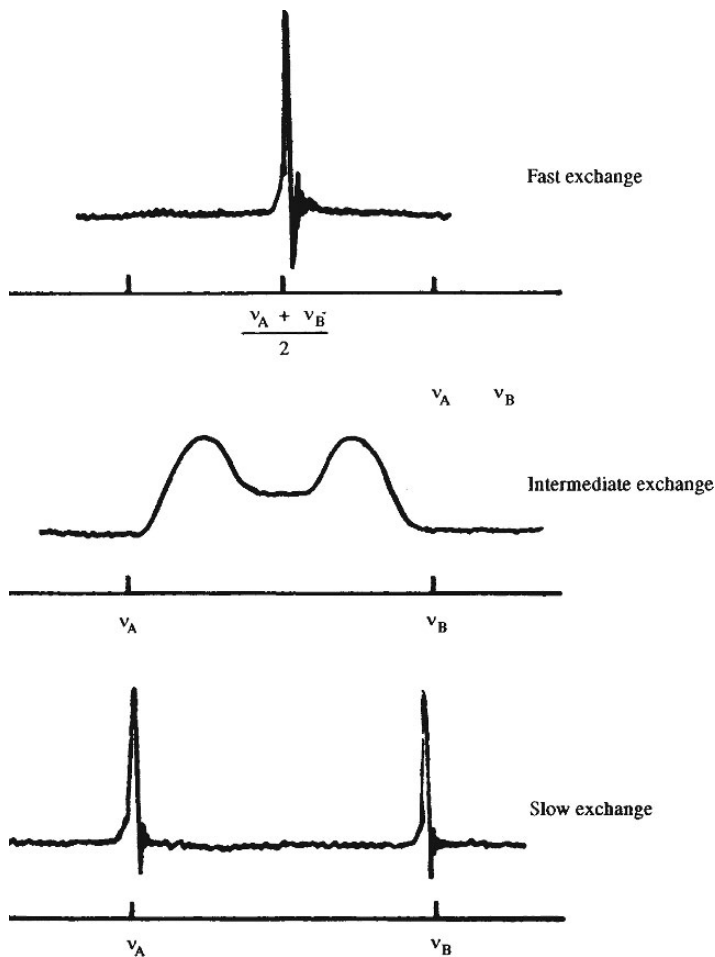


Fig. 2.14. Appearance of NMR spectra for system undergoing site exchange at various rates.

chlorocyclohexane as a function of temperature is shown below. From these data, it can be seen that conformationally pure solutions of equatorial chlorocyclohexane can be maintained at low temperature.<sup>52</sup>

**Half-Life for Conformation Inversion  
for Chlorocyclohexane at Various  
Temperatures**

Temperature (°C)	Half-Life
25	$1.3 \times 10^{-5}$ s
-60	$2.5 \times 10^{-2}$ s
-120	23 min
-160	22 yr

<sup>52</sup> F. R. Jensen and C. H. Bushweller, *J. Am. Chem. Soc.*, **91**, 3223 (1969).

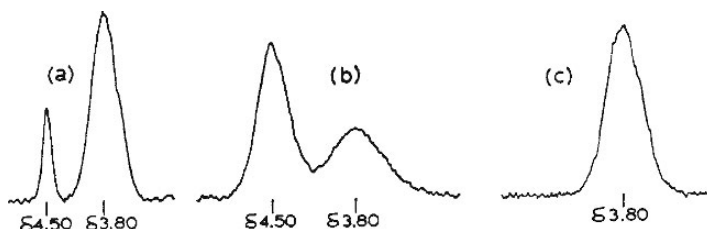


Fig. 2.15. 60-MHz  $^1\text{H}$ -NMR spectrum for the C(1)H in chlorocyclohexane: (a) axial-equatorial equilibrium at  $-115^\circ\text{C}$ ; (b) axial-enriched mixture at  $-150^\circ\text{C}$ ; (c) pure equatorial conformer at  $-150^\circ\text{C}$ . Reproduced from *J. Am. Chem. Soc.*, **91**, 3223 (1969), by permission of the American Chemical Society.

Crystallization of chlorocyclohexane at low temperature provided crystals containing only the equatorial isomer. When the solid is dissolved at  $-150^\circ\text{C}$ , the NMR spectrum of the solution exhibits only the signal characteristic of the equatorial conformer. When the solution is warmed to  $-115^\circ$ , the conformational equilibrium is reestablished. The appearance of the 60-MHz spectrum of the  $\text{H-C-Cl}$  hydrogen is shown in Figure 2.15.

The free-energy difference between conformers is referred to as the *conformational free energy*. For substituted cyclohexanes it is conventional to specify the value of  $-\Delta G_c$  for the equilibrium:



As  $\Delta G_c$  is negative when the equatorial conformation is more stable than the axial, the value of  $-\Delta G_c$  is positive for groups that favor the equatorial position. The larger the  $-\Delta G_c$ , the greater the preference for the equatorial position.

The case of iodocyclohexane provides an example of the use of NMR spectroscopy to determine the conformational equilibrium constant and the value of  $-\Delta G_c$ . At  $-80^\circ\text{C}$ , the NMR shows two distinct peaks in the area of the  $\text{CHI}$  signal as shown in Figure 2.16.<sup>53</sup> The multiplet at higher field is a triplet of triplets with coupling constants of 3.5 and 12 Hz. This pattern is characteristic of a hydrogen in an axial position with two axial-axial couplings and two axial-equatorial couplings. The broader peak at lower field is characteristic of a proton at an equatorial position and reflects the four equatorial-equatorial couplings of such a proton. The relative area of the two peaks is 3.4:1 in favor of the conformer with the axial hydrogen. This corresponds to a  $-\Delta G_c$  value of 0.47 kcal/mol for the iodo substituent.

Another method for measuring conformational free energies involves establishing an equilibrium between diastereomers differing only in the orientation of the designated substituent group. The equilibrium constant can then be determined and used to calculate the free-energy difference between the isomers. For example, *cis*- and *trans*-*t*-butylcyclohexanol can be equilibrated using a nickel catalyst in refluxing benzene to give a mixture containing 28% *cis*-4-*t*-butylcyclohexanol and 72% *trans*-*t*-butylcyclohexanol.<sup>54</sup>

<sup>53</sup> F. R. Jensen, C. H. Bushweller, and B. H. Beck, *J. Am. Chem. Soc.*, **91**, 334 (1969).

<sup>54</sup> E. L. Eliel and S. H. Schroeter, *J. Am. Chem. Soc.*, **87**, 5031 (1965).

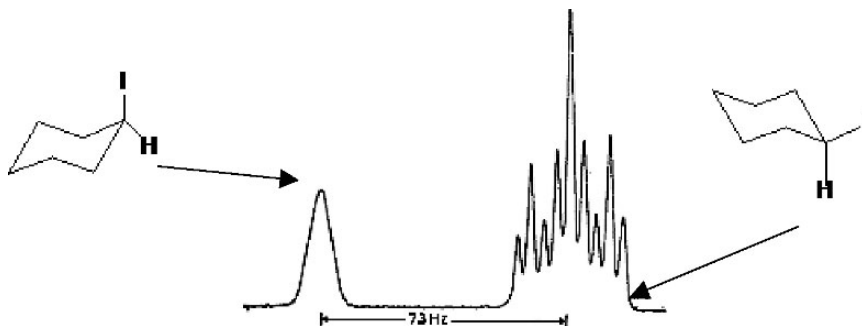
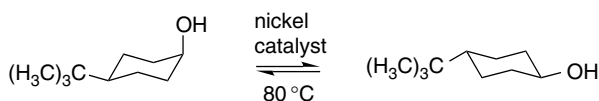


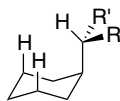
Fig. 2.16. NMR spectrum of iodocyclohexane at  $-80^{\circ}\text{C}$ . Only the low field CHI signal is shown (100 MHz). Reproduced from *J. Am. Chem. Soc.*, **91**, 344 (1969), by permission of the American Chemical Society.



Assuming that only conformations that have the *t*-butyl group equatorial are significant, the free-energy change for the equilibration is equal to the free-energy difference between an axial and equatorial hydroxy group. The equilibrium constant leads to a value of  $-\Delta G_c = 0.7\text{kcal/mol}$  for the hydroxy substituent. This approach also assumes that the *t*-butyl group does not distort the ring or interact directly with the hydroxy group.

There are several other methods available for determining conformational free energies.<sup>55</sup> Values for many substituents in addition to those listed in Table 2.2 have been compiled.<sup>56</sup>

The methyl, ethyl, and isopropyl groups have similar conformational energies, with isopropyl being only slightly greater than methyl and ethyl. The similar values for the three substituents reflects the fact that rotation about the bond between the substituent and the ring allows each group to adopt a conformation that minimizes the effect of the additional methyl substituent in the ethyl and isopropyl groups.



methyl: R, R' = H  
 ethyl R = H, R' = CH<sub>3</sub>  
*i*-propyl R, R' = CH<sub>3</sub>

A *t*-butyl substituent in the axial orientation experiences a strong van der Waals repulsion with the *syn*-axial hydrogens that cannot be relieved by rotation about the bond to the ring. As a result, the  $-\Delta G_c$  value for *t*-butyl group is much larger than for the other alkyl groups. A value of about 5 kcal/mol has been calculated by *molecular*

<sup>55</sup> F. R. Jensen and C. H. Bushweller, *Adv. Alicyclic Chem.*, **3**, 139 (1971).

<sup>56</sup> E. L. Eliel, S. H. Wilen, and L. N. Mander *Stereochemistry of Organic Compounds*, Wiley, New York, 1993, pp. 696–697.

**Table 2.2. Conformational Free Energies ( $-\Delta G_c$ ) for Some Substituent Groups<sup>a</sup>**

Substituent	$-\Delta G_c$	Substituent	$-\Delta G_c$
F	0.26 <sup>b</sup>	C <sub>6</sub> H <sub>5</sub>	2.9 <sup>c</sup>
Cl	0.53 <sup>b</sup>	CN	0.2 <sup>b</sup>
I	0.47 <sup>b</sup>	CH <sub>3</sub> CO <sub>2</sub>	0.71 <sup>b</sup>
CH <sub>3</sub>	1.8 <sup>c</sup>	HO <sub>2</sub> C	1.35 <sup>d</sup>
CH <sub>3</sub> CH <sub>2</sub>	1.8 <sup>c</sup>	C <sub>2</sub> H <sub>5</sub> O <sub>2</sub> C	1.1–1.2 <sup>d</sup>
(CH <sub>3</sub> ) <sub>2</sub> CH	2.1 <sup>c</sup>	HO (aprotic solvent)	0.52 <sup>d</sup>
(CH <sub>3</sub> ) <sub>3</sub> C	> 4.7 <sup>d</sup>	HO (protic solvent)	0.87 <sup>d</sup>
CH <sub>2</sub> =CH	1.7 <sup>e</sup>	CH <sub>3</sub> O	0.60 <sup>d</sup>
HC≡C	0.5 <sup>f</sup>	O <sub>2</sub> N	1.16 <sup>b</sup>

a. For a more extensive compilation see E. L. Eliel, S. H. Wilen, and L. N. Mander, *Stereochemistry of Organic Compounds*, Wiley, New York, 1993, pp. 696–697.

b. F. R. Jensen and C. H. Bushweller, *Adv. Alicyclic Chem.*, **3**, 140 (1971).

c. N. L. Allinger and L. A. Freiburg, *J. Org. Chem.*, **31**, 804 (1966).

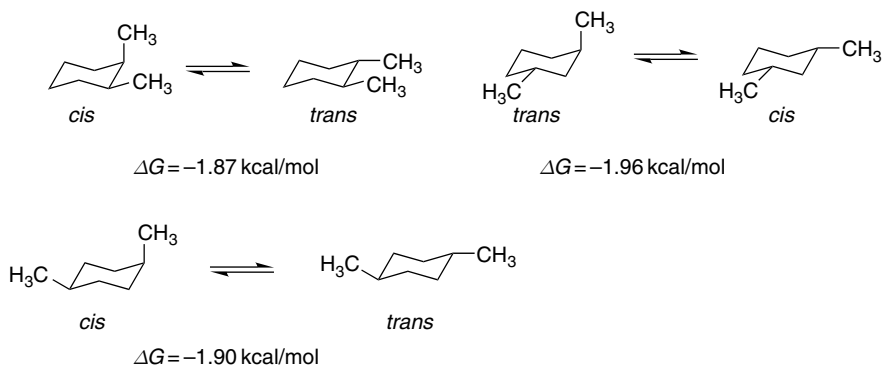
d. J. A. Hirsch, *Top. Stereochem.*, **1**, 199 (1967).

e. E. L. Eliel and M. Manoharan, *J. Org. Chem.*, **46**, 1959 (1981).

*mechanics*.<sup>57</sup> Experimental attempts to measure the  $-\Delta G_c$  value for *t*-butyl have provided only a lower limit, because very little of the axial conformation is present and the energy difference is similar to that between the chair and twist forms of the cyclohexane ring.

The strong preference for a *t*-butyl group to occupy the equatorial position makes it a useful group for the study of *conformationally biased systems*. A *t*-butyl substituent ensures that the conformational equilibrium lies heavily to the side having the *t*-butyl group equatorial but does not stop the process of conformational inversion. It should be emphasized that “conformationally biased” is not synonymous with “conformationally locked.” Because ring inversion can still occur, it is incorrect to think of the systems being “locked” in a single conformation.

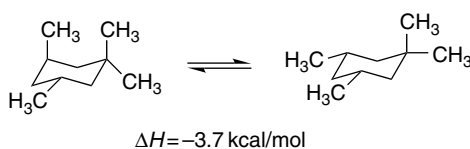
When two or more substituents are present on a cyclohexane ring, the interactions between the substituents must be included in the analysis. The dimethylcyclohexanes provide a case in which a straightforward interpretation is in good agreement with the experimental data. The  $\Delta G$  of the equilibrium for the *cis*  $\rightleftharpoons$  *trans* isomerization is given for 1,2-, 1,3-, and 1,4-dimethylcyclohexane.<sup>49</sup>



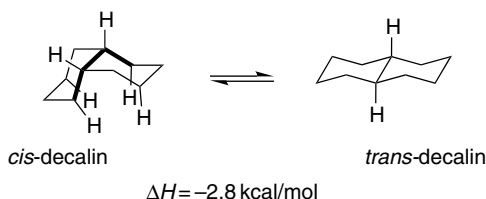
<sup>57</sup> N. L. Allinger, J. A. Hirsch, M. A. Miller, I. J. Tyminski, and F. A. VanCatledge, *J. Am. Chem. Soc.*, **90**, 1199 (1968); B. van de Graf, J. M. A. Baas, and B. M. Wepster, *Recl. Trav. Chim. Pays-Bas*, **97**, 268 (1978); J. M. A. Baas, A. van Veen, and B. M. Wepster, *Recl. Trav. Chim. Pays-Bas*, **99**, 228 (1980); S. Antunez and E. Juaristi, *J. Org. Chem.*, **61**, 6465 (1996).

The more stable diastereomer in each case is the one in which both methyl groups are equatorial. The  $\Delta G$  difference favoring the diequatorial isomer is about the same for each case (about 1.9 kcal/mol) and is very close to the  $-\Delta G_c$  value of the methyl group (1.8 kcal/mol). This implies that there are no important interactions present that are not also present in methylcyclohexane. This is reasonable since in each case the axial methyl group interacts only with the 3,5-diaxial hydrogens, just as in methylcyclohexane. Moreover, both of the 1,2-dimethyl isomers have similar *gauche* interactions between the two methyl groups.

Conformations in which there is a 1,3-diaxial interaction between substituent groups *larger than hydrogen* are destabilized by van der Waals repulsion. Equilibration of *cis*- and *trans*-1,1,3,5-tetramethylcyclohexane, for example, results in a mixture favoring the *cis* isomer by 3.7 kcal/mol.<sup>58</sup> This provides a value for a 1,3-diaxial methyl-methyl interaction that is 1.9 kcal/mol higher than the 1,3-methyl-hydrogen interaction.



The decalin (decahydronaphthalene) ring provides another important system for the study of conformational effects in cyclohexane rings. Equilibration of the *cis* and *trans* isomers favors the *trans* isomer by about 2.8 kcal/mol. Note that this represents a change in configuration, not conformation. The energy difference can be analyzed by noting that the *cis* isomer has an inter-ring *gauche*-butane interaction that is not present in the *trans* isomer. There are also cross-ring interactions between the axial hydrogens on the concave surface of the molecule.

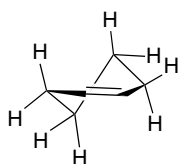


There is an important difference between the *cis*- and *trans*-decalin systems with respect to their conformational flexibility. Owing to the nature of its ring fusion, *trans*-decalin is incapable of chair-chair inversion; *cis*-decalin is conformationally mobile and undergoes ring inversion at a rate only slightly slower than cyclohexane ( $\Delta G^\ddagger = 12.3\text{--}12.4 \text{ kcal/mol}$ ).<sup>59</sup> The *trans*-decalin system is a “conformationally locked” system and can be used to compare properties and reactivity of groups in axial or equatorial environments.

<sup>58</sup> N. L. Allinger and M. A. Miller, *J. Am. Chem. Soc.*, **83**, 2145 (1961).

<sup>59</sup> F. R. Jensen and B. H. Beck, *Tetrahedron Lett.*, 4523 (1966); D. K. Dalling, D. M. Grant, and L. F. Johnson, *J. Am. Chem. Soc.*, **93**, 367 (1971); B. E. Mann, *J. Magn. Resonance*, **21**, 17 (1976).

The effect of introducing  $sp^2$ -hybridized atoms into acyclic molecules was discussed in Section 2.2.1, and it was noted that torsional barriers in 1-alkenes and aldehydes are somewhat smaller than in alkanes. Similar effects are seen when  $sp^2$  centers are incorporated into six-membered rings. Whereas the energy barrier for ring inversion in cyclohexane is 10.3 kcal/mol, it is reduced to 7.7 kcal/mol in methylenecyclohexane<sup>60</sup> and to 4.9 kcal/mol in cyclohexanone.<sup>61</sup> The conformation of cyclohexene is described as a half-chair. Structural parameters determined on the basis of electron diffraction and microwave spectroscopy reveal that the double bond can be accommodated into the ring without serious distortion. The C(1)–C(2) bond length is 1.335 Å, and the C(1)–C(2)–C(3) bond angle is 123°. <sup>62</sup> The substituents at C(3) and C(6) are tilted from the usual axial and equatorial directions and are referred to as *pseudoaxial* and *pseudoequatorial*.



half-chair conformation  
of cyclohexene

There have been both experimental and theoretical studies of the conformational process. According to NMR studies, the  $E_a$  for ring inversion is 5.3 kcal/mol.<sup>63</sup> An IR study gave a significantly higher barrier of about 10 kcal/mol.<sup>64</sup> A more recent theoretical study using both MO and DFT calculations found the barrier to be about 5.5–6.0 kcal/mol.<sup>65</sup> The preference for equatorial orientation of a methyl group in cyclohexene is less than in cyclohexane, because of the ring distortion and the removal of one 1,3-diaxial interaction. A value of 1 kcal/mol has been suggested for the  $-\Delta G_c$  value for a methyl group in 4-methylcyclohexene.<sup>66</sup>

Alkylidenecyclohexanes bearing alkyl groups of moderate size at C(2) tend to adopt the conformation with the alkyl group axial, in order to relieve unfavorable interactions with the alkylidene group. This results from van der Waals repulsion between the alkyl group in the equatorial position and *cis* substituents on the exocyclic

<sup>60</sup> J. T. Gerig, *J. Am. Chem. Soc.*, **90**, 1065 (1968).

<sup>61</sup> F. R. Jensen and B. H. Beck, *J. Am. Chem. Soc.*, **90**, 1066 (1968).

<sup>62</sup> J. F. Chiang and S. H. Bauer, *J. Am. Chem. Soc.*, **91**, 1898 (1969); L. H. Scharpen, J. E. Wollrab, and D. P. Ames, *J. Chem. Phys.*, **49**, 2368 (1968).

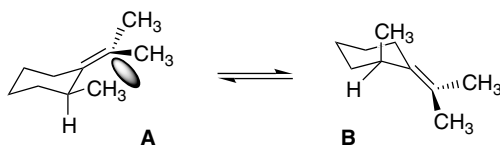
<sup>63</sup> F. A. L. Anet and M. Z. Haq, *J. Am. Chem. Soc.*, **87**, 3147 (1965).

<sup>64</sup> V. E. Rivera-Gaines, S. J. Leibowitz, and J. Laane, *J. Am. Chem. Soc.*, **113**, 9735 (1991).

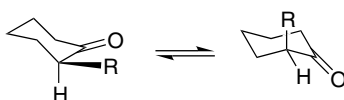
<sup>65</sup> S. V. Shishkina, O. V. Shiskin, and J. Leszczynski, *Chem. Phys. Lett.*, **354**, 428 (2002).

<sup>66</sup> B. Rickborn and S.-Y. Lwo, *J. Org. Chem.*, **30**, 2212 (1965).

double bond, and is an example of 1,3-allylic strain.<sup>67</sup> The repulsive energy is small for methylenecyclohexanes, but molecular mechanics calculations indicate that the axial conformation **B** is 2.6 kcal/mol more stable than **A** with an exocyclic isopropylidene group.<sup>68</sup>



An alkyl group at C(2) of a cyclohexanone ring is more stable in the equatorial than in the axial orientation. The equatorial orientation is eclipsed with the carbonyl group and corresponds to the more stable conformation of open-chain ketones (see p. 148). This conformation also avoids 3,5-diaxial interactions with *syn*-diaxial hydrogens. Conformational free energies ( $-\Delta G_c$ ) for 2-alkyl substituents in cyclohexanones have been determined by equilibration studies. The value for the methyl group is similar to cyclohexanes, whereas the values for ethyl and isopropyl are somewhat smaller. This is attributed to a compensating repulsive steric interaction with the carbonyl oxygen for the larger substituents.<sup>69</sup>



The  $-\Delta G_c$  of an alkyl group at C(3) of cyclohexanone is less than that of a alkyl group in cyclohexane because of reduced 1,3-diaxial interactions. A C(3) methyl group in cyclohexanone has a  $-\Delta G_c$  of 1.3–1.4 kcal/mol.<sup>54</sup>

### 2.2.3. Conformations of Carbocyclic Rings of Other Sizes

The most important structural features that influence the conformation and reactivity of cycloalkanes differ depending on whether small (cyclopropane and cyclobutane), common (cyclopentane, cyclohexane, and cycloheptane), medium (cyclooctane through cycloundecane), or large (cyclododecane and up) rings are

<sup>67</sup>. F. Johnson, *Chem. Rev.* **68**, 375 (1968); R. W. Hoffmann, *Chem. Rev.*, **89**, 1841 (1989).

<sup>68</sup>. N. L. Allinger, J. A. Hirsch, M. A. Miller, and I. J. Tyminski, *J. Am. Chem. Soc.*, **90**, 5773 (1968); P. W. Rabideau, ed., *The Conformational Analysis of Cyclohexenes, Cyclohexadiene and Related Hydroaromatic Compounds*, VCH Publishers, Weinheim, 1989.

<sup>69</sup>. N. L. Allinger and H. M. Blatter, *J. Am. Chem. Soc.*, **83**, 994 (1961); B. Rickborn, *J. Am. Chem. Soc.*, **84**, 2414 (1962); E. L. Eliel, N. L. Allinger, S. J. Angyal, and G. A. Morrison, *Conformational Analysis*, Interscience, New York, 1965, pp. 113–114.

**Table 2.3. Strain Energies for Cycloalkanes<sup>a</sup>**

Cycloalkane	Strain energy (kcal/mol)
Cyclopropane	28.1 <sup>b</sup>
Cyclobutane	26.3
Cyclopentane	7.3
Cyclohexane	1.4
Cycloheptane	7.6
Cyclooctane	11.9
Cyclononane	15.5
Cyclodecane	16.4
Cyclododecane	11.8

a. Values taken from E. M. Engler, J. D. Andose, and P. v. R. Schleyer, *J. Am. Chem. Soc.*, **95**, 8005 (1973).

b. P. v. R. Schleyer, J. E. Williams, and K. R. Blanchard, *J. Am. Chem. Soc.*, **92**, 2377 (1970).

considered. The small rings are dominated by angle and torsional strain. The common rings are relatively unstrained and their conformations are most influenced by torsional factors. Medium rings exhibit conformational equilibria and chemical properties indicating that cross-ring van der Waals repulsions play an important role. Large rings become increasingly flexible and possess a large number of low-energy conformations. The combination of all types of strain for a given ring results in a total *strain energy* for that ring. Table 2.3 presents data on the strain energies of cycloalkanes up to cyclodecane.

The cyclopropane ring is planar and the question of conformation does not arise. The C–C bond lengths are slightly shorter than normal, at 1.50 Å, and the H–C–H angle of 115° C is opened somewhat from the tetrahedral angle.<sup>70</sup> These structural features and the relatively high reactivity of cyclopropane rings are explained by the concept of “bent bonds,” in which the electron density is displaced from the internuclear axis (see Topic 1.3).

Cyclobutane adopts a puckered conformation in which substituents can occupy axial-like or equatorial-like positions.<sup>71</sup> 1,3-Disubstituted cyclobutanes show small energy preferences for the *cis* isomer, which places both substituents in equatorial-like positions.<sup>72</sup> The energy differences and the barrier to inversion are both smaller than in cyclohexane.



There is minimal angle strain in cyclopentane, but considerable torsional strain is present. Cyclopentane is nonplanar and the two minimum energy geometries are the envelope and the half-chair.<sup>73</sup> In the envelope conformation, one carbon atom is

<sup>70</sup> O. Bastiansen, F. N. Fritsch, and K. Hedberg, *Acta Crystallogr.*, **17**, 538 (1964).

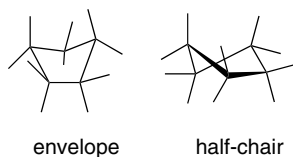
<sup>71</sup> A. Almenningen, O. Bastiansen, and P. N. Skancke, *Acta Chem. Scand.*, **15**, 711 (1961).

<sup>72</sup> (a) K. B. Wiberg and G. M. Lampman, *J. Am. Chem. Soc.*, **88**, 4429 (1966);

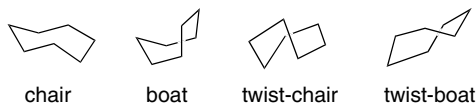
(b) N. L. Allinger and L. A. Tushaus, *J. Org. Chem.*, **30**, 1945 (1965).

<sup>73</sup> A. C. Legon, *Chem. Rev.*, **80**, 231 (1980); B. Fuchs, *Top. Stereochem.*, **10**, 1 (1978).

displaced from the plane of the other four. In the half-chair conformation, three carbons are coplanar, with one of the remaining two being above the plane and the other below. The planar portions of both conformations have torsional strain owing to C–H and C–C bond eclipsing. The energy differences between the conformers are small and there is rapid interconversion of conformers.<sup>74</sup> All of the carbon atoms move rapidly through planar and nonplanar positions, owing to a process called *pseudorotation*.



As ring size increases, there are progressively more conformations that have to be considered. For cycloheptane, four conformations have been calculated to be particularly stable.<sup>75</sup> NMR investigations indicate that the twist-chair is the most stable.<sup>76</sup> Various derivatives adopt mainly twist-chair conformations.<sup>77</sup> The individual twist-chair conformations interconvert rapidly by pseudorotation.<sup>78</sup> The most recent MM4 and CCSD/6-311++G\*\* computations (see Section 2.3) indicate the following relative energies.<sup>79</sup> Figure 2.17 shows the conformations.



	MM4	CCSD/6-311++G**
Twist-chair	0	0
Chair	1.4	0.9
Boat	3.8	3.3
Twist-boat	3.5	3.3

Relative energy in kcal/mol

<sup>74</sup> W. J. Adams, H. J. Geise, and L. S. Bartell, *J. Am. Chem. Soc.*, **92**, 5013 (1970); J. B. Lambert, J. J. Papay, S. A. Khan, K. A. Kappauf, and E. S. Magyar, *J. Am. Chem. Soc.*, **96**, 6112 (1974).

<sup>75</sup> J. B. Hendrickson, *J. Am. Chem. Soc.*, **89**, 7036 (1967); D. F. Bocian and H. L. Strauss, *J. Am. Chem. Soc.*, **99**, 2866 (1977); P. M. Iavanov and E. Osawa, *J. Comput. Chem.*, **5**, 307 (1984).

<sup>76</sup> J. B. Hendrickson, R. K. Boeckman, Jr., J. D. Glickson, and E. Grunwald, *J. Am. Chem. Soc.*, **95**, 494 (1973).

<sup>77</sup> F. H. Allen, J. A. K. Howard, and N. A. Pitchard, *Acta Crystallog.*, **B49**, 910 (1993).

<sup>78</sup> D. F. Bocian, H. M. Pickett, T. C. Rounds, and H. L. Strauss, *J. Am. Chem. Soc.*, **97**, 687 (1975).

<sup>79</sup> K. B. Wiberg, *J. Org. Chem.*, **68**, 9322 (2003).

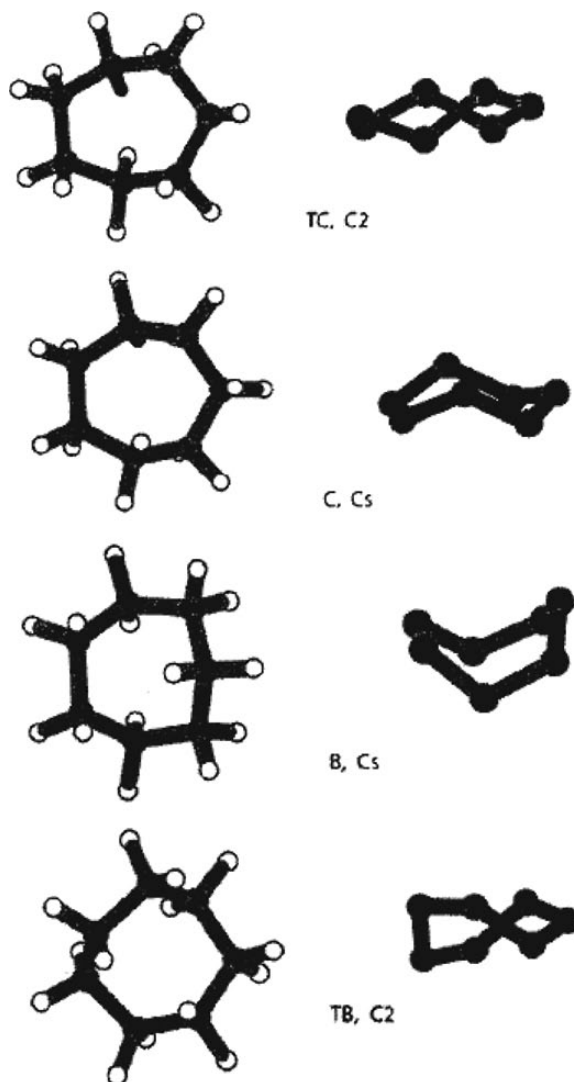


Fig. 2.17. The four most favorable conformations of cycloheptane. Reproduced from *J. Org. Chem.*, **68**, 9322 (2003), by permission of the American Chemical Society.

For cyclooctane, a total of 11 conformations have been suggested for consideration and their relative energies calculated. According to MM<sup>80</sup> and CCSDT/6-311++G\*\*<sup>79</sup> computations, there are five other conformations that are energy minima, of which the boat-chair is calculated to be the most stable. This result is in agreement with analyses of the temperature dependence of the <sup>19</sup>F NMR spectra of fluorocyclooctanes.<sup>81</sup> The activation energy for interconversion of conformers is 5–8 kcal/mol.

<sup>80</sup>. I. Kolossvary and W. C. Guida, *J. Am. Chem. Soc.*, **115**, 2107 (1993).

<sup>81</sup>. J. E. Anderson, E. S. Glazer, D. L. Griffith, R. Knorr, and J. D. Roberts, *J. Am. Chem. Soc.*, **91**, 1386 (1969); see also F. A. Anet and M. St. Jacques, *J. Am. Chem. Soc.*, **88**, 2585, 2586 (1966).

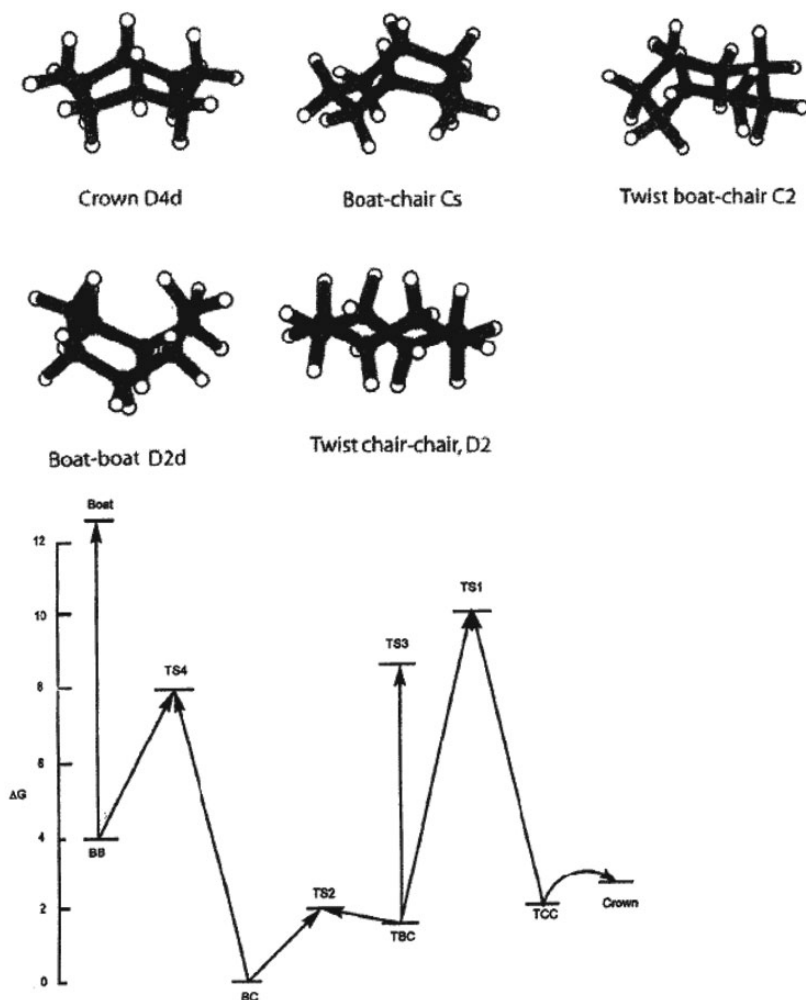


Fig. 2.18. Structures of the low-energy conformations of cyclooctane and the energy barriers separating them. Reproduced from *J. Org. Chem.*, **68**, 9322 (2003), by permission of the American Chemical Society.

Figure 2.18 illustrates the low-energy conformations and the barriers separating them. The crown and twist-chair-twist conformations are quite similar.

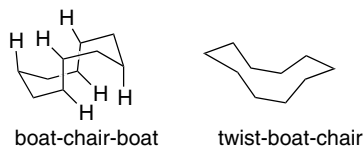
The number of conformations rapidly increases with ring size. For cyclodecane there are 18 conformers that are found as minima in MM3 calculations.<sup>82</sup> The lowest four are within 1 kcal/mol of one another. Low-temperature NMR studies indicate that the boat-chair-boat is the lowest in energy,<sup>83</sup> and studies of cyclodecane derivatives by X-ray crystallography showed that the boat-chair-boat conformation is adopted in the solid state.<sup>84</sup> As was indicated in Table 2.3, cyclodecane is significantly more

<sup>82</sup> N. Weinberg and S. Wolfe, *J. Am. Chem. Soc.*, **116**, 9860 (1994).

<sup>83</sup> D. M. Pawar, S. V. Smith, H. L. Mark, R. M. Odom, and E. A. Noe, *J. Am. Chem. Soc.*, **120**, 10715 (1998).

<sup>84</sup> J. D. Dunitz, in *Perspectives in Structural Chemistry*, Vol II, J. D. Dunitz and J. A. Ibers, eds., Wiley, New York, 1968, pp. 1–70.

strained than cyclohexane. Examination of the boat-chair-boat conformation reveals that the source of most of this strain is the close van der Waals contacts between two sets of three hydrogens on either side of the molecule, as indicated in the drawing below. Distortion of the molecule to twist forms relieves this interaction but introduces torsional strain.



The conformational possibilities for larger rings quickly become very large, but an interesting simplifying concept has emerged. The diamond lattice, which consists of a continuous array of chair cyclohexane rings, is the most stable arrangement for a large array of  $sp^3$  carbon atoms. There are both theoretical and experimental results that show that complex polycyclic saturated hydrocarbons are most stable in diamond-type structures. Adamantane is a familiar example of this type of structure.



It might be anticipated that large flexible rings would adopt similar structures incorporating the chair cyclohexane conformation. Conformations for  $C_{10}$  through  $C_{24}$  cycloalkanes corresponding to diamond lattice sections have been identified by systematic topological analysis using models and molecular mechanics computations.<sup>85</sup> This type of relationship is illustrated in Figure 2.19 for cyclodecane. Molecular

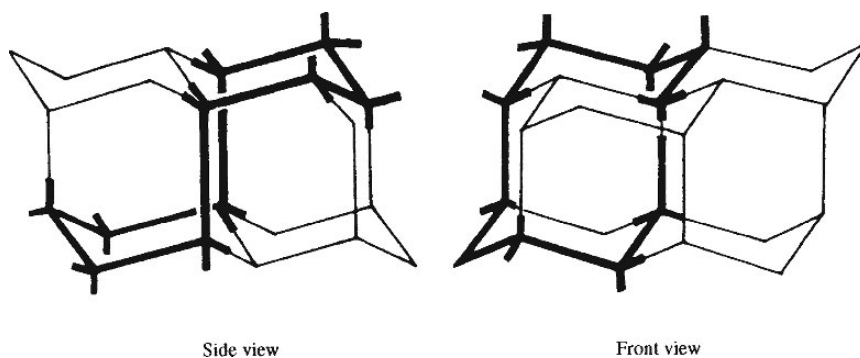


Fig. 2.19. Equivalent diamond lattice conformations of cyclodecane (boat-chair-boat).

<sup>85</sup> J. Dale, *J. Chem. Soc.*, 93 (1963); M. Saunders, *Tetrahedron*, **23**, 2105 (1967); J. Dale, *Top. Stereochem.*, **9**, 199 (1976).

mechanics computations indicate that this is indeed the minimum energy conformation for cyclododecane.<sup>80,86</sup>

As the ring size increases, the number of possible conformations increases further so that many alternative diamond lattice conformations are available.<sup>87</sup>

### 2.3. Molecular Mechanics

The analysis of molecular conformation can be systematically and quantitatively approached through molecular mechanics.<sup>88</sup> A molecule adopts the geometry that minimizes its total strain energy. The minimum energy geometry is strained (destabilized) to the extent that its structural parameters deviate from their ideal values. The energy for a particular kind of distortion is a function of the amount of distortion and the opposing force. The total strain energy is the sum of several contributions:

$$E_{\text{strain}} = E(r) + E(\theta) + E(\varphi) + E(d) \quad (2.9)$$

where  $E(r)$  is the energy associated with stretching or compression of bonds,  $E(\theta)$  is the energy of bond angle distortion,  $E(\varphi)$  is the torsional strain, and  $E(d)$  are the energy increments that result from nonbonded interactions between atoms.

Molecular mechanics calculations involve summation of the force fields for each type of strain. The original mathematical expressions for the force fields were derived from classical mechanical potential energy functions. The energy required to stretch a bond or to bend a bond angle increases as the square of the distortion:

$$\text{Bond stretching : } E(r) = 0.5k_r(r - r_0)^2 \quad (2.10)$$

where  $k_r$ , is the stretching force constant,  $r$  the bond length, and  $r_0$  the normal bond length.

$$\text{Bond angle bending : } E(\theta) = 0.5k_\theta(\Delta\theta)^2 \quad (2.11)$$

where  $k_\theta$  is the bending force constant and  $\Delta\theta$  is the deviation of the bond angle from its normal value. The torsional strain is a sinusoidal function of the torsion angle. Torsional strain results from the barrier to rotation about single bonds, as described for ethane on p. 142–143. For molecules with a threefold barrier such as ethane, the form of the torsional barrier is:

$$E(\varphi) = 0.5V_0(1 + \cos 3\varphi) \quad (2.12)$$

where  $V_0$  is the rotational energy barrier and  $\varphi$  is the torsional angle. For hydrocarbons,  $V_0$  can be taken as being equal to the ethane barrier (2.9 kcal/mol).

Nonbonded interaction energies, which may be attractive or repulsive, are the most difficult contributions to evaluate. When two uncharged atoms approach each other, the interaction between them is very small at large distances, becomes slightly

<sup>86</sup>. M. Saunders, *J. Comput. Chem.*, **12**, 645 (1991).

<sup>87</sup>. M. Saunders, *J. Am. Chem. Soc.*, **109**, 3150 (1987); V. L. Shannon, H. L. Strauss, R. G. Snyder, C. A. Elliger, and W. L. Mattice, *J. Am. Chem. Soc.*, **111**, 1947 (1989); M. Saunders, K. N. Houk, Y. D. Wu, W. C. Still, M. Lipton, G. Chang, and W. C. Guida, *J. Am. Chem. Soc.*, **112**, 1419 (1990).

<sup>88</sup>. For general reviews see: W. Gans, A. Amann, and J. C. A. Boeyens, *Fundamental Principles of Molecular Modeling*, Plenum Press, New York, 1996; A. K. Rappe and C. J. Casewitt, *Molecular Mechanics Across Chemistry*, University Science Books, Sausalito, CA, 1997; J. C. A. Boeyens and P. Comba, *Coordn. Chem. Rev.*, **212**, 3 (2001).

attractive as the separation approaches the sum of their van der Waals radii, but then becomes strongly repulsive as the separation becomes less than the sum of their van der Waal radii. The attractive interaction results from a mutual polarization of the electrons of the atoms. Such attractive forces are called *London forces* or *dispersion forces* and are relatively weak interactions. London forces vary inversely with the sixth power of internuclear distance and become negligible as internuclear separation increases. At distances smaller than the sum of the van der Waals radii, the much stronger electron-electron repulsive forces are dominant. Electrostatic forces must take into account bond dipoles and their orientation. Bond dipoles also have a polarizing effect on adjacent groups.<sup>89</sup>

The separation of the total strain energy into component elements of bond length strain, bond angle strain, torsional strain, and nonbonded interactions is useful for analysis of structural and steric effects on equilibria and reactivity. Minimization of the total strain energy of a molecule, expressed by a parameterized equation for each of the force fields, can be accomplished by iterative computation. The quantitative application of molecular mechanics for calculation of minimum energy geometries, heats of formation, and strain energies has been developed to a high level of reliability. The method has been refined to the point that geometries of saturated hydrocarbons can be calculated to an accuracy of 0.005 Å in bond length and 1° in bond angle.<sup>90</sup> Similar accuracy can be obtained for unsaturated hydrocarbons<sup>91</sup> and molecules with oxygen functional groups.<sup>92</sup> Molecular mechanics calculations can also be applied to unstable reactive intermediates such as carbocations.<sup>93</sup>

The molecular mechanics computations can be done using commercially available programs. The parameters used in the programs determine the range of applicability and reliability of the results. Several systems of parameters and equations for carrying out the calculations have been developed. The most frequently used methods in organic chemistry are those developed by N. L. Allinger and co-workers and is frequently referred to as MM (molecular mechanics) calculations.<sup>94</sup> The most recent version is called MM4.<sup>95</sup> The computations involve iterations to locate an energy minimum. Precautions must be taken to establish that a true (“global”) minimum, as opposed to a local minimum energy, has been achieved. This can be accomplished by using a number of different initial geometries and comparing the structures and energies of the minima that are located. In addition to comparing the relative energy of various conformations of an individual molecule, MM computations can be used to calculate total molecular energy (enthalpy of formation) to a high level of accuracy. Heats of formation for most hydrocarbons are accurate to  $\pm 0.5$  kcal/mol. This application of MM is discussed further in Section 3.1.2.4.

<sup>89</sup> L. Dosen-Micovic, D. Jeremic, and N. L. Allinger, *J. Am. Chem. Soc.*, **105**, 1716, 1723 (1983); B. Mannfors, K. Palmo, and S. Krimm, *J. Mol. Struct.*, **556**, 1 (2000).

<sup>90</sup> N. L. Allinger, Y. H. Yuh, and J.-H. Lii, *J. Am. Chem. Soc.*, **111**, 8551 (1989); N. L. Allinger, K. Chen, and J.-H. Lii, *J. Comput. Chem.*, **17**, 642 (1996).

<sup>91</sup> N. Nevins, K. Chen, and N. L. Allinger, *J. Comput. Chem.*, **17**, 669 (1996); N. Nevins, J.-H. Lii, and N. L. Allinger, *J. Comput. Chem.*, **17**, 695 (1996); N. Nevins and N. L. Allinger, *J. Comput. Chem.*, **17**, 730 (1996).

<sup>92</sup> C. H. Langley, J. H. Lii, and N. L. Allinger, *J. Comput. Chem.*, **22**, 1396, 1426, 1451 (2001).

<sup>93</sup> B. Reindl, T. Clark, and P. v. R. Schleyer, *J. Comput. Chem.*, **17**, 1406 (1996); B. Reindl and P. v. R. Schleyer, *J. Comput. Chem.*, **18**, 28 (1997); B. Reindl, T. Clark, and P. v. R. Schleyer, *J. Comput. Chem.*, **18**, 533 (1997); B. Reindl, T. Clark, and P. v. R. Schleyer, *J. Phys. Chem. A*, **102**, 8953 (1998).

<sup>94</sup> N. L. Allinger, Y. H. Yuh and J.-H. Lii, *J. Am. Chem. Soc.*, **111**, 8551 (1989).

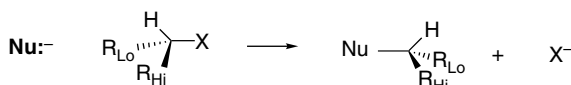
<sup>95</sup> N. L. Allinger, K. S. Chen, and J. H. Lii, *J. Comput. Chem.*, **17**, 642 (1996).

Molecular mechanics can also be used in connection with MO or DFT calculations in computations on transition structures. Because transition structures have partial bonds that vary from case to case, no general set of parameters is applicable. One approach is to apply MO or DFT calculations to the reacting portion of the molecule to obtain structural information. This portion of the structure can then be incorporated into an MM computation involving the remainder of the molecule.<sup>96</sup> It is also possible to use several levels of computations. For example, high-level MO or DFT calculations can be applied to the reaction core, intermediate level calculations to the part of the system immediately adjacent to the reaction core, and MM calculations for the remainder of the molecule.<sup>97</sup> Two examples of these approaches are given in Section 2.5.4, where large catalytic molecules have been examined using combined approaches.

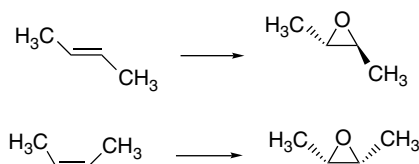
## 2.4. Stereoselective and Stereospecific Reactions

In this section we discuss relationships between reactivity and stereochemistry. Many reactions can produce two or more stereoisomeric products. If a reaction shows a preference for one of the stereoisomers, it is *stereoselective*. Throughout the sections on individual reactions in Parts A and B, we discuss the stereoselectivity associated with particular reactions. In this chapter, we use a few examples to illustrate the fundamental concepts of stereoselectivity.

Stereoselectivity is intimately related to the mechanism of the reaction. Some reactions are *stereospecific*, that is reactions in which *stereoisomeric reactants each provide stereoisomeric products*. For example, the  $S_N2$  substitution reaction results in an inversion of the configuration. It is a stereospecific reaction. The *R*-reactant gives the *S*-product and the *S*-reactant gives the *R*-product (assuming the priority order remains unchanged).



As another example, epoxidation of *E*-2-butene gives *trans*-2,3-dimethyloxirane, whereas *Z*-2-butene gives *cis*-2,3-dimethyloxirane.



<sup>96</sup> J. E. Eksterowicz and K. N. Houk, *Chem. Rev.*, **93**, 2439 (1993); F. Maseras and K. Morokuma, *J. Comput. Chem.*, **16**, 1170 (1995).

<sup>97</sup> M. Svensson, S. Humbel, R. D. J. Froese, T. Matsubara, S. Sieber, and K. Morokuma, *J. Phys. Chem.*, **100**, 19357 (1996).

We discuss several examples to illustrate how reactant structure and mechanism can lead to stereoselectivity, including stereospecificity. We also consider *enantioselective* and *enantiospecific* reactions, which are reactions that favor one enantiomer of a reaction product.

### 2.4.1. Examples of Stereoselective Reactions

Scheme 2.6 gives some examples of the types of stereoselective reactions that are discussed. The first three examples in the scheme are catalytic hydrogenations. Usually such reactions favor *syn* addition of hydrogen from the less hindered face of the double bond; that is, both hydrogens are added to the same face of the  $\pi$  bond. The second entry illustrates another aspect of catalytic hydrogenation: the tendency of hydroxy groups to be *syn*-directive, that is, to favor addition from the same side that is occupied by the hydroxy group. These features are believed to be related to the interaction of the alkene with the catalytic surface during hydrogenation and are discussed further in Section 2.4.2.1. As can be seen from the variable degree of stereoselectivity in Entries 1 and 2, as well as the exception in Entry 3, *catalytic hydrogenation is not always highly stereoselective*.

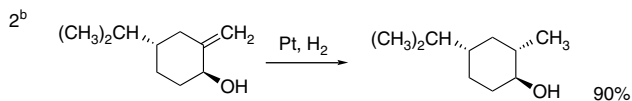
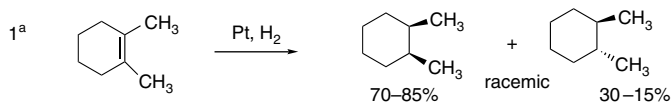
Entries 4 through 6 are examples of stereoselective reduction of cyclic ketones. Comparing entries 4 and 5 shows that stereoselectivity can be controlled by the choice of reagents. As we discuss further in Section 2.4.1.2, some hydride donors, e.g.,  $\text{NaBH}_4$ , approach from the axial direction to give equatorial alcohol. More bulky reducing agents favor the equatorial approach and give axial alcohol. Entry 6 illustrates the tendency of reagents to attack the norbornane ring from the *exo* direction. Entry 7 is an example of diastereoselective addition of a Grignard reagent adjacent to a stereocenter. This is an example of *1,2-asymmetric induction*, in which the configuration at the adjacent stereocenter establishes a preference for the direction of addition to the carbonyl group. This kind of reaction has been studied extensively and is discussed in Section 2.4.1.3. One of the issues that must be considered in this case is the conformation of the reactant. Although the preferred conformation of ring compounds is often evident, the flexibility of acyclic compounds introduces additional variables. Entry 8 is another example in which the configuration of the  $\alpha$ -oxy substituent controls the direction of addition of hydride to the carbonyl group.

**2.4.1.1. Substituent Directing Effects in Heterogeneous and Homogeneous Hydrogenation** The hydrogenation of carbon-carbon double bonds is a very general reaction. Except for very sterically hindered cases, the reaction usually proceeds rapidly and cleanly. Hydrogenation can be carried out using either finely dispersed metal (heterogeneous) or soluble (homogeneous) metal complexes. The heterogeneous catalysts are transition metals, particularly platinum, palladium, rhodium, ruthenium, and nickel. The metals are used as finely dispersed solids or adsorbed on inert supports such as charcoal or alumina. Homogeneous catalysts are usually complexes of rhodium, ruthenium, or iridium. Phosphine ligands are common in these catalytic complexes. Depending upon the conditions and the catalyst, other functional groups may also be subject to catalytic hydrogenation, but for now we focus on double bonds.



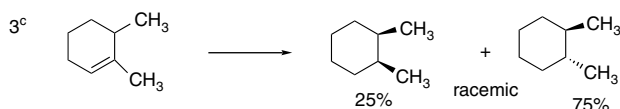
## A. Catalytic Hydrogenation. (See section 2.4.1.1)

Unfunctionalized alkene usually reacts by preferential *syn* delivery of hydrogen from the less hindered face of the double bond. The degree of stereoselectivity is dependent on the reactant structure, catalysts and reaction conditions. Donor functional groups, particularly hydroxy and amino can be *syn* directive.



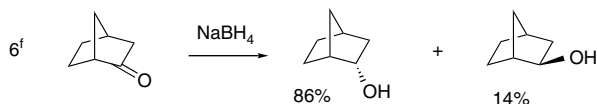
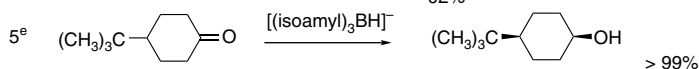
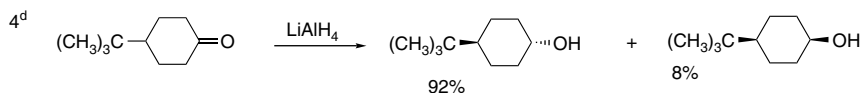
(The same article also sites other examples with low stereoselectivity.)

## A representative exception.



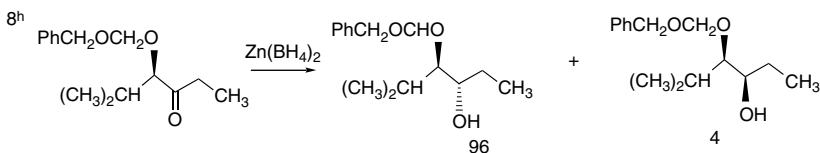
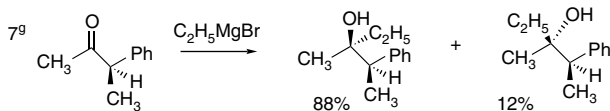
## B. Hydride Reduction of Cyclic Ketones (see Section 2.4.1.2)

Unhindered cyclohexanones normally react with  $\text{NaBH}_4$  and  $\text{LiAlH}_4$  by preferential reagent approach from the axial direction forming mainly the equatorial alcohol. The presence of axial substituents or use of more sterically demanding reagents, such as alkylborohydrides leads to selective equatorial approach and formation of axial alcohols. Bicyclic ketones are generally reduced by hydride approach from the less hindered face of the carbonyl group.



## C. Nucleophilic Addition to Acyclic Ketones (see Section 2.4.1.3)

Adjacent stereocenters influence the mode of addition of nucleophiles such as hydrides and organometallic reagents to acyclic ketones. The Felkin-Ahn transition state provides a predictive model that is general when steric effects are dominant. Other factors must be considered when polar or chelating substituents are present.



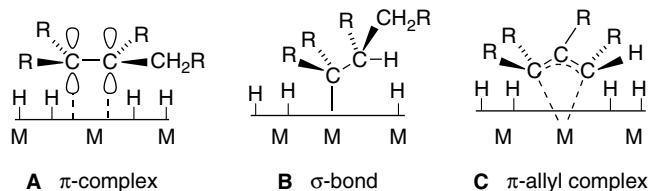
(Continued)

## CHAPTER 2

Stereochemistry,  
Conformation,  
and Stereoselectivity

- a. C. A. Brown, *J. Am. Chem. Soc.*, **91**, 5901 (1969).  
 b. M. C. Dart and H. B. Henbest, *J. Chem. Soc.*, 3563 (1960).  
 c. S. Siegel and G. V. Smith, *J. Am. Chem. Soc.*, **82**, 6082, 6087 (1960).  
 d. H. C. Brown and W. C. Dickason, *J. Am. Chem. Soc.*, **92**, 709 (1970).  
 e. S. Krishnamurthy and H. C. Brown, *J. Am. Chem. Soc.*, **98**, 3383 (1976).  
 f. H. C. Brown and J. Muzzio, *J. Am. Chem. Soc.*, **88**, 2811 (1966).  
 g. O. Arjona, R. Perez-Ossorio, A. Perez-Rubalcaba, and M. L. Quiroga, *J. Chem. Soc., Perkin Trans. 2*, 597 (1981);  
 C. Alvarez-Ibarra, O. Arjona P. Perez-Ossorio, A. Perez-Rubalcaba, M. L. Quiroga, and M. J. Santesmases, *J. Chem. Soc., Perkin Trans. 2*, 1645 (1983).  
 h. G. J. McGarvey and M. Kimura, *J. Org. Chem.*, **47**, 5420 (1982).

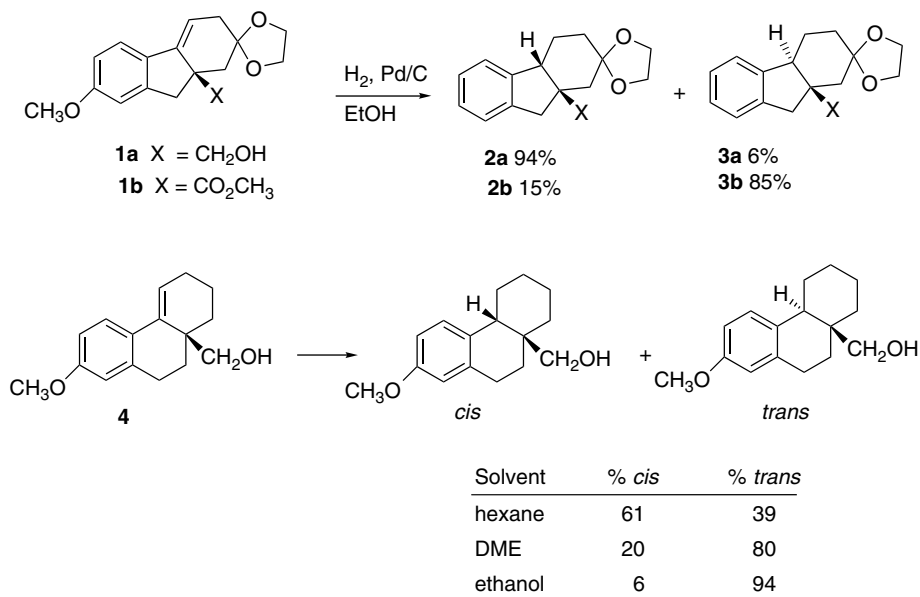
The mechanistic description of heterogeneous hydrogenation is somewhat vague, partly because the reactive sites on the metal surface are not as precisely described as small molecule reagents in solution. As understanding of the chemistry of homogeneous hydrogenation catalysts has developed, it has become possible to extrapolate those mechanistic concepts to heterogeneous catalysts. It is known that hydrogen is adsorbed onto the metal surface, forming metal-hydrogen bonds similar to those found in transition metal hydride complexes. Alkenes are also adsorbed on the catalyst surface and at least three types of intermediates have been implicated in hydrogenation. The initially formed intermediate is pictured as attached at both carbon atoms of the double bond by  $\pi$ -type bonding, as shown in **A**. The bonding involves the alkene  $\pi$  and  $\pi^*$  orbitals interacting with acceptor and donor orbitals of the metal. A hydrogen can be added to the adsorbed group, leading to **B**, which involves a carbon-metal  $\sigma$  bond. This species can react with another hydrogen to give the alkane. Alkanes have little affinity for the catalyst surface, so this reaction is effectively irreversible. A third intermediate species, shown as **C**, accounts for double-bond isomerization and the exchange of hydrogen that sometimes accompanies hydrogenation. This intermediate is equivalent to an allyl group bound to the metal surface by  $\pi$  bonds. It can be formed from adsorbed alkene by abstraction of an allylic hydrogen atom by the metal. Formation of the allyl species is reversible and can lead to alkene isomerization. Analogous reactions take place at single metal ions in homogeneous catalysis. A major uncertainty in heterogeneous catalysis is whether there are cooperative interactions involving several metal centers.



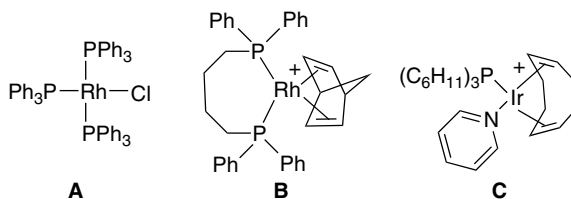
In most cases, both hydrogen atoms are added to the same side of the reactant (*syn* addition). If hydrogenation occurs by addition of hydrogen in two steps, as implied by the mechanism above, the intermediate must remain bonded to the metal surface in such a way that the stereochemical relationship is maintained. Adsorption to the catalyst surface normally involves the less sterically congested face of the double bond, and as a result, hydrogen is added from the less hindered face of the molecule. There are many cases of hydrogenations where hydrogen addition is not entirely *syn* and independent corroboration of the stereochemistry is normally necessary.

The facial stereoselectivity of hydrogenation is affected by the presence of polar functional groups that can influence the mode of adsorption to the catalyst surface. For

instance, there are many of examples where the presence of a hydroxy group results in the hydrogen being introduced from the same side of the molecule occupied by the hydroxy group. This *syn*-directive effect suggests that the hydroxy group interacts with the catalyst surface. This behavior can be illustrated with the alcohol **1a** and the ester **1b**.<sup>98</sup> Although the overall shapes of the two molecules are similar, the alcohol gives mainly the product with a *cis* ring juncture (**2a**), whereas the ester gives mainly a product with *trans* stereochemistry (**3b**). The stereoselectivity of hydroxy-directed hydrogenation is a function of solvent and catalyst as indicated for alcohol **4**.<sup>99</sup> The *cis* isomer is the main product in hexane. This result implies that the hydroxy group directs the molecule to the catalyst surface. In ethanol, the competing interaction of the solvent molecules evidently swamps out the directive effect of the hydroxymethyl group in **4** and the *trans* product is formed.



Substituent directive effects are also observed with soluble (homogeneous) hydrogenation catalysts. A number of transition metal complexes function as homogeneous hydrogenation catalysts. Three important examples are shown below.

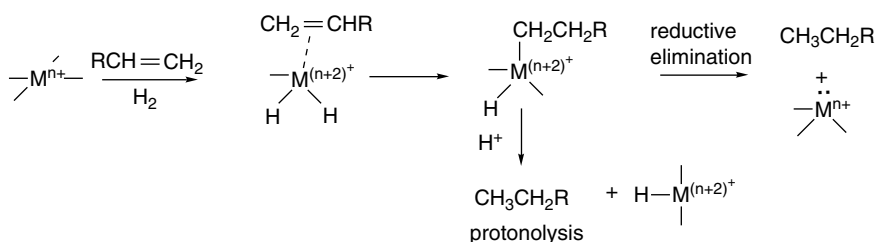


<sup>98</sup>. H. W. Thompson, *J. Org. Chem.*, **36**, 2577 (1971).

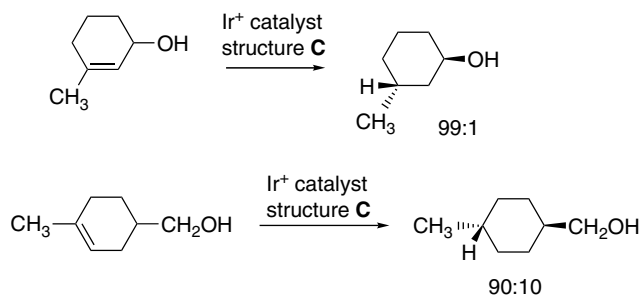
<sup>99</sup>. H. W. Thompson, E. McPherson, and B. L. Lences, *J. Org. Chem.*, **41**, 2903 (1976).

Compound **A** is known as Wilkinson's catalyst and was one of the first of the homogeneous catalysts to be developed.<sup>100</sup> The cationic rhodium complex **B** is a useful catalyst for hydrogenations that involve a chelated structure between the reactant and the catalyst, such as allylic alcohols.<sup>101</sup> The catalyst is activated by the hydrogenation of the norbornadiene ligand, which opens two binding sites at the catalytic metal. The iridium complex **C** (Crabtree catalyst) functions in a similar manner.<sup>102</sup> The cyclooctadiene ligand is removed on exposure to hydrogen, providing two open positions. The  $\text{Rh}^+$  and  $\text{Ir}^+$  metal centers in these catalysts have eight electrons in their valence shells and are able to accommodate up to five additional donor pairs. We will encounter other examples of homogeneous catalysts in Section 2.5.1.1 when we discuss enantioselective hydrogenation.

The mechanism of homogeneous catalysis involves the same steps as heterogeneous catalysis. An initial  $\pi$  complex is formed with the reactant. Metal-hydride bonds then react with the complexed alkene to form a C–H bond and  $\sigma$  bond between the metal and alkyl group. There can be variation in the timing of formation of the M–H bonds. The metal carbon bond can be broken by either *reductive elimination* or *protonolysis*. Note that reductive elimination changes the metal oxidation state, whereas protonolysis does not. The catalytic cycle proceeds by addition of alkene and hydrogen.



As in heterogeneous hydrogenation, substituents can affect the stereoselectivity of the reduction by forming an additional bond to the metal center. This requires that there be sufficient ligand positions to accommodate binding by the substituent. Stereoselective hydrogenation based on substituent directive effects is particularly prevalent for cyclic compounds. The iridium catalyst  $[\text{Ir}(\text{cod})_2\text{py}(\text{PCy}_3)]^+\text{PF}_6^-$  (structure **C** above) has been used frequently. Cyclohexenols and cyclohexenylmethanols exhibit good stereoselectivity, with delivery of the hydrogen *syn* to the hydroxy group.<sup>103</sup>



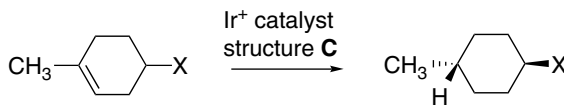
<sup>100</sup> J. A. Osborn, F. H. Jardine, J. F. Young, and G. Wilkinson, *J. Chem. Soc. A*, 1711 (1966).

<sup>101</sup> J. M. Brown, B. A. Chaloner, A. G. Kent, B. A. Murrer, P. N. Nicholson, D. Parker, and P. J. Sidebottom, *J. Organomet. Chem.*, **216**, 263 (1981); D. A. Evans and M. M. Morrissey, *J. Am. Chem. Soc.*, **106**, 3866 (1984).

<sup>102</sup> R. H. Crabtree, H. Felkin, and G. E. Morris, *J. Organomet. Chem.*, **141**, 205 (1977).

<sup>103</sup> R. M. Crabtree and M. W. Davis, *J. Org. Chem.*, **51**, 2655 (1986).

In contrast to the results seen with heterogeneous catalysts, the methoxy, ester, and acetyl groups are also strongly directive in the 4-methylcyclohex-3-enyl system. The effect of amido substituents is greater than the ester substituent.<sup>104</sup> This result indicates that the carbonyl oxygen is a strong donor group toward the Ir<sup>+</sup> catalyst, whereas carbonyl groups are not effective as directing groups with the heterogeneous catalysts.

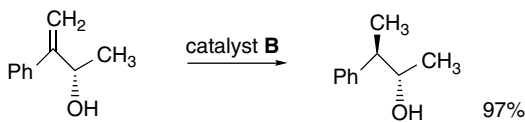


X	product yield %		ref.
	directed	nondirected	
-CO <sub>2</sub> CH <sub>3</sub>	95	1.7	a
-COCH <sub>3</sub>	99.2	0.8	a
-OCH <sub>3</sub>	>99.9	0.1	a
-C(=O)-N<img alt="pyrrolidine ring" data-bbox="235 340 335 375"/>	>99	<1	b
-CH <sub>2</sub> CO <sub>2</sub> CH <sub>3</sub>	50	50	b

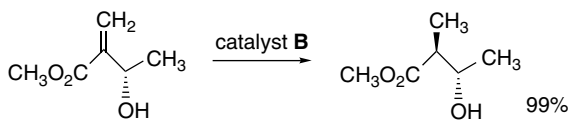
a. R. M. Crabtree and M.W. Davis, *J. Org. Chem.*, **51**, 2685 (1986).

b. A. G. Schultz and P. J. McCloskey, *J. Org. Chem.*, **50**, 5905(1985).

The flexibility of acyclic systems adds another element to the analysis of substituent directive effects. Some of the best examples of stereoselective reductions involve allylic alcohols and the rhodium catalyst **B**.



Ref. 105



Ref. 106

Stereoselectivity is also observed for homoallylic alcohols.



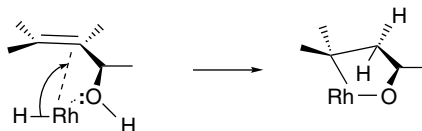
Ref. 105

<sup>104</sup>. A. G. Schultz and P. J. McCloskey, *J. Org. Chem.*, **50**, 5905 (1985).

<sup>105</sup>. J. M. Brown and R. G. Naik, *J. Chem. Soc. Chem. Commun.*, 348 (1982).

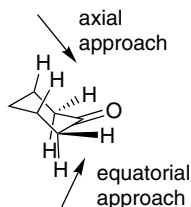
<sup>106</sup>. J. M. Brown and I. Cutting, *J. Chem. Soc., Chem. Commun.*, 578 (1985).

The stereoselectivity for allylic and homoallylic alcohols is attributed to a chelated complex with delivery of the hydrogen *syn* with respect to the hydroxy group.<sup>107</sup>



The general principles that emerge from these examples are the following: (1) The choice of catalyst must be appropriate. In particular, it must have sufficient exchangeable coordination sites to accommodate the directive group and still support the hydrogenation mechanism. (2) The structure of the reactant determines the nature of the coordination and the degree and direction of stereoselectivity. For cyclic systems, this usually results in *syn* delivery of hydrogen. For acyclic systems, the conformation of the coordinated reagent will control stereoselectivity. (3) In the examples cited above, the phosphine ligands were not explicitly considered, but their presence is crucial to the stability and reactivity of the metal center. When we consider enantioselective hydrogenation in Section 2.5.1.1, we will see that chiral phosphine ligands can also be used to establish a chiral environment at the metal center.

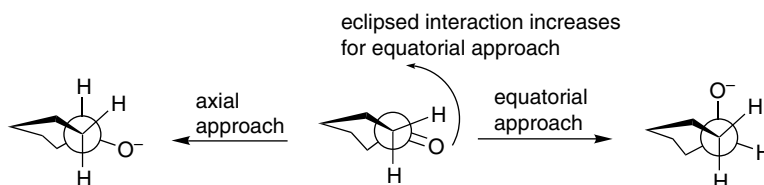
**2.4.1.2. Hydride Reduction of Cyclic Ketones** Section B of Scheme 2.6 gives some examples of hydride reduction of cyclic ketones. The stereoselectivity of nucleophilic additions to cyclic ketones has been studied extensively. The stereoselectivity in cyclohexanones is determined by the preference for approach of reactants from the axial or equatorial direction. The chair conformation of cyclohexanone places the carbonyl group in an unsymmetrical environment. The axial face has C(2, 6) – H<sub>eq</sub> bonds that are nearly eclipsed with the C=O bond and the C(3,5)-diaxial hydrogens point toward the trajectory for reagent approach. In contrast, the equatorial face has axial C–H bonds at an angle of roughly 120° to the carbonyl plane. There is more steric bulk, including the 3,5-axial hydrogens, on the axial face. Remember also that the reagent interaction is with the LUMO and that the optimal trajectory is at an angle somewhat greater than 90° to the carbonyl plane.



It is observed that small nucleophiles prefer to approach the carbonyl group of cyclohexanone from the axial direction, even though this is a more sterically

<sup>107</sup> J. M. Brown, *Angew. Chem. Int. Ed. Engl.*, **26**, 190 (1987).

congested approach.<sup>108</sup> For example,  $\text{NaBH}_4$  and  $\text{LiAlH}_4$  deliver hydride by axial approach to form mainly the equatorial alcohol. How do the differences in the C–C bonds (on the axial side) as opposed to the C–H bonds (on the equatorial side) influence the stereoselectivity of cyclohexanone reduction? Torsional effects are believed to play a major role in the preference for axial approach. In the reactant conformation, the carbonyl group is almost eclipsed by the equatorial C(2) and C(6) C–H bonds. This torsional strain is relieved by axial attack, whereas equatorial approach increases strain because the oxygen atom must move through a fully eclipsed arrangement.<sup>109</sup>



The stereoselectivity can be reversed by using more sterically demanding reagents. More bulky reducing agents usually approach the cyclohexanone carbonyl from the equatorial direction. This is called *steric approach control* and is the result of van der Waals repulsions with the 3,5-axial hydrogens. Alkylborohydride reagents are used instead of  $\text{NaBH}_4$ , and alkoxy derivatives can be used in place of  $\text{LiAlH}_4$ . The bulkier nucleophiles encounter the 3,5-axial hydrogens on the axial approach trajectory and therefore prefer the equatorial approach.<sup>110</sup> A large amount of data has been accumulated on the stereoselectivity of reduction of cyclic ketones.<sup>111</sup> Table 2.4 compares the stereochemistry of reduction of several ketones by hydride donors of increasing steric bulk. The trends in the data illustrate the increasing importance of steric approach control as both the hydride reagent and the ketone become more highly substituted. For example, the axial methyl group in 3,3,5-trimethylcyclohexanone favors an equatorial approach. The alkyl-substituted borohydrides have especially high selectivity for the less hindered direction of approach.

The factors controlling the direction of reagent approach have also been studied in norbornan-2-ones. The stereochemistry of a number of reactions of the parent system and the 7,7-dimethyl derivative have been examined.<sup>112</sup> Some of the results are included in Table 2.4. These compounds reveal a reversal of the preferred direction of attack with the introduction of the 7,7-dimethyl substituents. In the parent system the *exo* direction of attack is preferred because the single  $\text{CH}_2$  group at C(7) offers less steric resistance than the  $-\text{CH}_2\text{CH}_2-$  unit on the *endo* side of the molecule. The *endo*

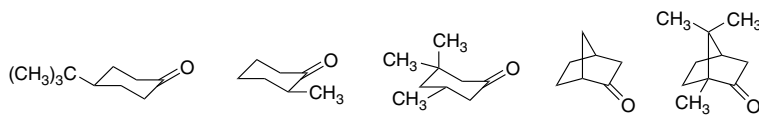
<sup>108</sup>. B. W. Gung, *Tetrahedron*, **52**, 5263 (1996).

<sup>109</sup>. M. Cherest, H. Felkin, and N. Prudent, *Tetrahedron Lett.*, 2199 (1968); M. Cherest and H. Felkin, *Tetrahedron Lett.*, 2205 (1968); Y. D. Wu and K. N. Houk, *J. Am. Chem. Soc.*, **109**, 906, 908 (1987); Y. D. Wu, K. N. Houk, and M. N. Paddon-Row, *Angew. Chem. Int. Ed. Engl.*, **31**, 1019 (1992).

<sup>110</sup>. W. G. Dauben, G. Fonken, and D. S. Noyce, *J. Am. Chem. Soc.*, **78**, 2579 (1956); H. C. Brown and W. C. Dickason, *J. Am. Chem. Soc.*, **92**, 709 (1970); D. C. Wigfield, *Tetrahedron*, **35**, 449 (1979); T. Wipke and P. Gund, *J. Am. Chem. Soc.*, **98**, 8107 (1976).

<sup>111</sup>. D. C. Wigfield, *Tetrahedron*, **35**, 449 (1979); D. C. Wigfield and D. J. Phelps, *J. Org. Chem.*, **41**, 2396 (1976).

<sup>112</sup>. H. C. Brown, J. H. Kawakami, and K.-T. Liu *J. Am. Chem. Soc.*, **95**, 2209 (1973).

**Table 2.4. Stereoselectivity of Hydride Reducing Agents toward Cyclic Ketones<sup>a</sup>**


Reductant	% equat.	% equat.	% equat.	% <i>exo</i>	% <i>endo</i>
NaBH <sub>4</sub>	20 <sup>b</sup>	25 <sup>c</sup>	58 <sup>c</sup>	86 <sup>d</sup>	86 <sup>d</sup>
LiAlH <sub>4</sub>	8	24	83	89	92
LiAl(OMe) <sub>3</sub> H	9	69		98	99
LiAl(O- <i>t</i> -Bu) <sub>3</sub> H	9 <sup>e</sup>	36 <sup>f</sup>	95	94 <sup>f</sup>	94 <sup>f</sup>
LiBH( <i>s</i> -Bu) <sub>3</sub>	93 <sup>g</sup>	98 <sup>g</sup>	99.8 <sup>g</sup>	99.6 <sup>g</sup>	99.6 <sup>g</sup>
LiBH( <i>siam</i> ) <sub>3</sub> <sup>h</sup>	> 99 <sup>i</sup>	> 99 <sup>i</sup>	> 99 <sup>i</sup>	NR <sup>i</sup>	

a. Except where noted otherwise, the data are those given by H. C. Brown and W. C. Dickason, *J. Am. Chem. Soc.*, **92**, 709 (1970). Data for many other cyclic ketones and reducing agents are given by A. V. Kamernitzky and A. A. Akhrem, *Tetrahedron*, **18**, 705 (1962) and W. T. Wipke and P. Gund, *J. Am. Chem. Soc.*, **98**, 8107 (1976).

b. P. T. Lansbury and R. E. MacLeay, *J. Org. Chem.*, **28**, 1940 (1963).

c. B. Rickborn and W. T. Wuesthoff, *J. Am. Chem. Soc.*, **92**, 6894 (1970).

d. H. C. Brown and J. Muzzio, *J. Am. Chem. Soc.*, **88**, 2811 (1966).

e. J. Klein, E. Dunkelblum, E. L. Eliel, and Y. Senda, *Tetrahedron Lett.*, 6127 (1968).

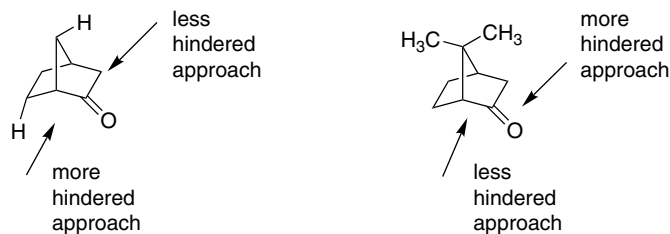
f. E. C. Ashby, J. P. Sevenair, and F. R. Dobbs, *J. Org. Chem.*, **36**, 197 (1971).

g. H. C. Brown and S. Krishnamurthy, *J. Am. Chem. Soc.*, **94**, 7159 (1972).

h. (*siam*) is an abbreviation for 1,2-dimethylpropyl.

i. S. Krishnamurthy and H. C. Brown, *J. Am. Chem. Soc.*, **98**, 3383 (1976).

hydrogens are in a relationship to the reaction site that is similar to the 1,3-diaxial interaction in a chair cyclohexane ring. When a *syn*-7-methyl group is present, the relative steric bulk of the two bridges is reversed.<sup>113</sup>

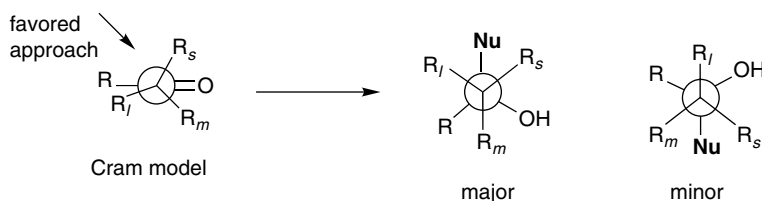


This relatively straightforward combination of torsional and steric effects as the source of stereoselectivity becomes more complicated when *polar* substituents are introduced into the picture. Polar effects are discussed in Topic 2.4.

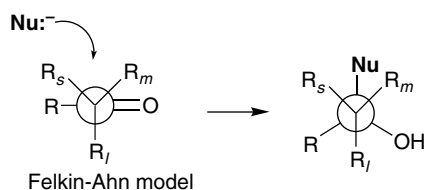
**2.4.1.3. Stereoselective Nucleophilic Additions to Acyclic Carbonyl Groups** The stereochemistry of nucleophilic addition to acyclic aldehydes and ketones is influenced by nearby substituents. A particularly important case occurs when there is a stereogenic center adjacent to the carbonyl group. As a result of the adjacent substituent, two diastereomers can be formed, depending on the direction of the approach of the nucleophile. The stereoselectivity of addition can be predicted on the basis of a conformational model of the TS. The addition reaction has been studied with several kinds

<sup>113</sup> H. C. Brown and J. Muzzio, *J. Am. Chem. Soc.*, **88**, 2811 (1966).

of nucleophiles; we use data from hydride addition and organometallic compounds in our discussion. The initial data were analyzed some time ago by D. J. Cram and co-workers,<sup>114</sup> who observed that the *major* product was correctly predicted by a model in which the largest  $\alpha$  group was eclipsed with the other carbonyl substituent. This empirical relationship became known as *Cram's rule*.



As chemists considered the origin of this diastereoselectivity, the reactant conformation that is considered to be the most important one has changed. The currently preferred *Felkin-Ahn model* places the largest substituent perpendicular to the carbonyl group.<sup>115</sup> The major product results from the nucleophile approaching opposite to the largest substituent. This is the same product as predicted by the Cram model, although the interpretation is different.



The Felkin-Ahn model invokes a combination of steric and stereoelectronic effects to account for the observed stereoselectivity. An approach from the direction of the smallest substituent minimizes steric interaction with the groups  $R_l$  (largest group) and  $R_m$  (medium group). Another key idea is that the nucleophile approaches from above or below the carbonyl group on a trajectory that makes an angle of about  $107^\circ$  to the plane of the carbonyl group.<sup>116</sup> This reflects the fact that the primary interaction of the approaching nucleophile is with the antibonding LUMO. However, it is also proposed that there is a stereoelectronic (hyperconjugation) effect, which involves the interaction between the approaching nucleophile and the LUMO of the carbonyl group. This orbital, which accepts the electrons of the incoming nucleophile, is stabilized when the  $R_l$  group is perpendicular to the plane of the carbonyl group.<sup>117</sup> This conformation permits a stabilizing interaction between the developing bond to the nucleophile and the antibonding  $\sigma^*$  orbital associated with the  $C-R_l$  bond. Because this is a  $\sigma \rightarrow \sigma^*$  interaction, it should increase in importance with the electron-acceptor capacity of X.

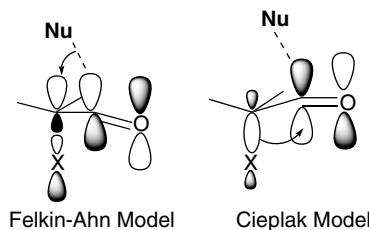
<sup>114</sup> D. J. Cram and F. A. Abd Elhafez, *J. Am. Chem. Soc.*, **74**, 5828 (1952).

<sup>115</sup> M. Cherest, H. Felkin, and N. Prudent, *Tetrahedron Lett.*, 4199 (1968).

<sup>116</sup> H. B. Burgi, J. D. Dunitz, and E. Shefter, *J. Am. Chem. Soc.*, **95**, 5065 (1973).

<sup>117</sup> N. T. Ahn, *Top. Current Chem.*, **88**, 145 (1980).

The *Cieplak model* emphasizes an alternative interaction, between the  $\sigma$  orbital of the C–X bond and the antibonding orbital to the nucleophile.<sup>118</sup> In this case, a better donor X should be the most stabilizing. Li and le Noble pointed out that *both of these hyperconjugative interactions will be present in the transition structure*.<sup>119</sup> There is also general agreement that addition of reactive nucleophiles have *early transition states*, which would suggest that substituent effects might best be examined in the *reactant*.



One broad generalization is that when steric interactions are dominant the Felkin-Ahn model is predictive. Thus *steric approach control*, the idea that the approaching nucleophile will approach the carbonyl group from the least hindered direction, is the first guiding principle.<sup>120</sup>

The TS model emphasizing steric effects must be elaborated when there is a polar substituent in the vicinity of the carbonyl group. At least three additional factors may then be involved. There are stereoelectronic effects associated with heteroatom substituents. Electronegative substituents such as halogen are assigned to the I position in the Felkin-Ahn TS on the basis of presumed stronger stereoelectronic interactions with the C=O bond. According to this analysis, the  $\sigma^*$  bond to the halogen stabilizes the TS. An *anti*-periplanar arrangement maximizes this interaction. It is likely that there are also electrostatic effects involved in controlling nucleophilic addition reactions, since compounds such as decalones,<sup>121</sup> norbornan-7-ones,<sup>122</sup> and adamantanones,<sup>123</sup> which have remote substituents that cannot directly interact with the reaction site, nevertheless influence the stereoselectivity. It remains a point for discussion as to whether these substituent effects are electrostatic in nature or are transmitted by hyperconjugation. (See Topic 2.4 for further discussion.)

It should also be emphasized that the *metal counterions* associated with the nucleophiles are active participants in carbonyl addition reactions. There are strong interactions between the carbonyl oxygen and the metal ions in the TSs and intermediates. This effect can be recognized, for example, in the reactivity of borohydrides, where the  $\text{Li}^+$ ,  $\text{Ca}^{2+}$ , and  $\text{Zn}^{2+}$  salts are more reactive than the standard  $\text{NaBH}_4$  reagent because of the greater Lewis acid strength of these cations.

The examples just discussed pertain to substituents that are on the carbon adjacent to the carbonyl center and the stereoselectivity is referred to as 1,2-asymmetric

<sup>118</sup> A. S. Cieplak, *J. Am. Chem. Soc.*, **103**, 4540 (1981).

<sup>119</sup> H. Li and W. J. le Noble, *Recl. Trav. Chim. Pays-Bas*, **111**, 199 (1992).

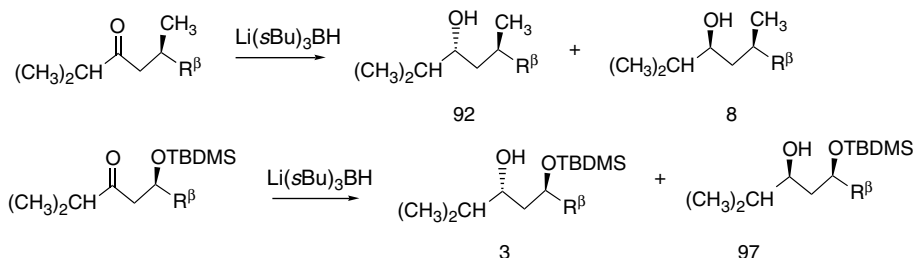
<sup>120</sup> W. G. Dauben, G. J. Fonken, and D. S. Noyce, *J. Am. Chem. Soc.*, **78**, 2579 (1956); H. C. Brown and H. R. Deck, *J. Am. Chem. Soc.*, **87**, 5620 (1965).

<sup>121</sup> Y.-D. Wu, J. A. Tucker, and K. N. Houk, *J. Am. Chem. Soc.*, **113**, 5018 (1991).

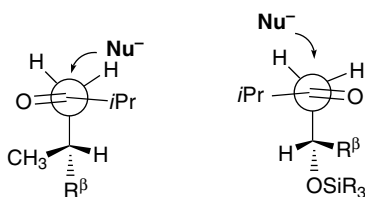
<sup>122</sup> G. Mehta and F. A. Khan, *J. Am. Chem. Soc.*, **112**, 6140 (1990); H. Li, G. Mehta, S. Padma, and W. J. le Noble, *J. Org. Chem.*, **56**, 2006 (1991); G. Mehta, F. A. Khan, B. Ganguly, and J. Chandrasekhan, *J. Chem. Soc., Perkin Trans.*, **2**, 2275 (1994).

<sup>123</sup> C. K. Cheung, L. T. Tseng, M.-H. Lin, S. Srivastava, and W. J. le Noble, *J. Am. Chem. Soc.*, **108**, 1598 (1986); J. M. Hahn and W. J. le Noble, *J. Am. Chem. Soc.*, **114**, 1916 (1992).

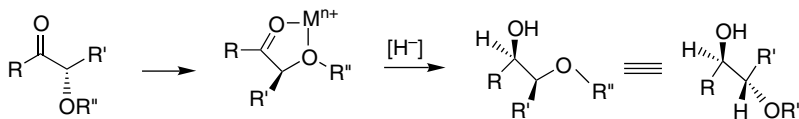
induction. More remote substituents can also affect the stereoselectivity of addition to the carbonyl group. For example, both  $\beta$ -methyl and  $\beta$ -siloxy substituents result in highly stereoselective reductions in ketones by trialkylborohydrides, but their directive effects are opposite.<sup>124</sup> This is a case of 1,3-asymmetric induction.



These results are attributed to alternative conformations of the reactant, with hydride attack being *anti* to the largest alkyl substituent in the methyl case and *anti* to the siloxy group in that case. The corresponding TSs are both of the Felkin-Ahn type in the sense that the large substituent is aligned perpendicularly with respect to the carbonyl group. In the methyl case, the favored TS minimizes the steric interaction of the isopropyl group with the  $\beta$  substituents. In the siloxy case, the favored TS has a stabilizing arrangement of the C=O and C–O dipoles and also avoids a steric interaction between the isopropyl group and  $\text{R}^\beta$ .



Another factor that affects stereoselectivity of carbonyl addition reactions is *chelation*.<sup>125</sup> If an  $\alpha$  or  $\beta$  substituent can form a chelate with a metal ion involving the carbonyl oxygen, the stereoselectivity is usually governed by the chelated conformation. Complexation between a donor substituent, the carbonyl oxygen, and the Lewis acid can establish a preferred conformation for the reactant, which then controls reduction. Usually hydride is delivered from the less sterically hindered face of the chelate.



For example,  $\alpha$ -hydroxy<sup>126</sup> and  $\alpha$ -alkoxyketones<sup>127</sup> are reduced to *anti* 1,2-diols by  $\text{Zn}(\text{BH}_4)_2$  via chelated TSs. This stereoselectivity is consistent with the preference for

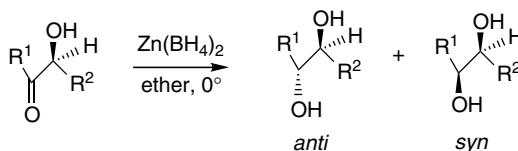
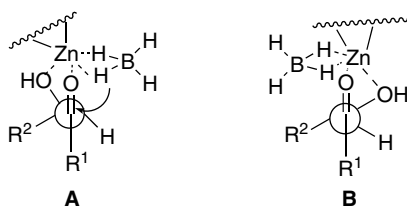
<sup>124</sup>. D. A. Evans, M. J. Dart, and J. L. Duffy, *Tetrahedron Lett.*, **35**, 8541 (1994).

<sup>125</sup>. D. J. Cram and K. R. Kopecky, *J. Am. Chem. Soc.*, **81**, 2748 (1959); D. J. Cram and D. R. Wilson, *J. Am. Chem. Soc.*, **85**, 1245 (1983).

<sup>126</sup>. T. Nakata, T. Tanaka, and T. Oishi, *Tetrahedron Lett.*, **24**, 2653 (1983).

<sup>127</sup>. G. J. McGarvey and M. Kimura, *J. Org. Chem.*, **47**, 5420 (1982).

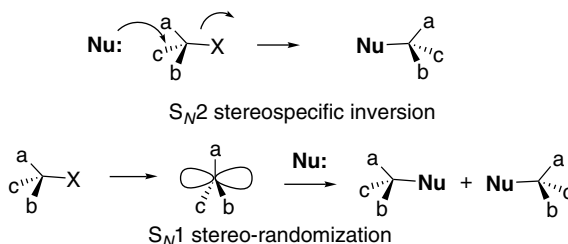
TS **A** over **B**. The stereoselectivity increases with the bulk of substituent  $R^2$ .  $\text{LiAlH}_4$  shows a similar trend, but with reduced selectivity.



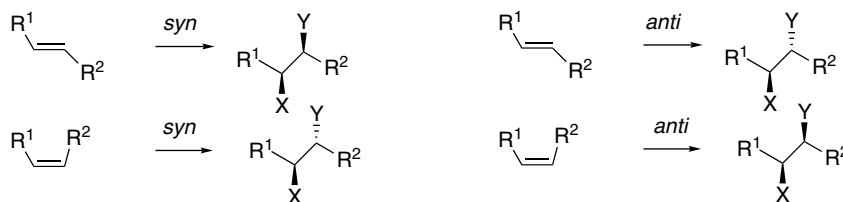
$R^1$	$R^2$	$\text{Zn}(\text{BH}_4)_2$ <i>anti</i> : <i>syn</i>	$\text{LiAlH}_4$ <i>anti</i> : <i>syn</i>
$n\text{-C}_5\text{H}_{11}$	$\text{CH}_3$	77:23	64:36
$\text{CH}_3$	$n\text{-C}_5\text{H}_{11}$	85:15	70:30
$i\text{-C}_3\text{H}_7$	$\text{CH}_3$	85:15	58:42
$\text{CH}_3$	$i\text{-C}_3\text{H}_7$	96:4	73:27
Ph	$\text{CH}_3$	98:2	87:13
$\text{CH}_3$	Ph	90:10	80:20

## 2.4.2. Examples of Stereospecific Reactions

In stereospecific reactions the configuration of the product is directly related to the configuration of the reactant and is determined by the reaction mechanism. Stereoisomeric reactants give different, usually stereoisomeric, products. The reaction mechanism determines the stereochemical relationship between the reactants and products. For any given reaction, stereospecificity may be lost or altered if there is a change in the mechanism. For example, the  $S_N2$  reaction occurs with stereospecific inversion. However, when the mechanism shifts to  $S_N1$  because of a change in reactants or reaction conditions, stereospecificity is lost.

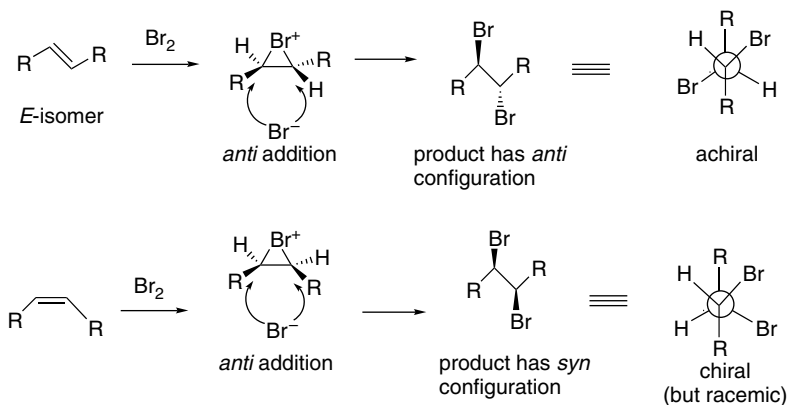


Another familiar and important example is *syn* and *anti* addition to double bonds. There are many examples of stereospecific reactions involving additions to carbon-carbon double bonds. Addition can be *anti* or *syn*, depending on the mechanism. If the mechanism specifies *syn* or *anti* addition, different products will be obtained from the *E*- and *Z*-isomers.

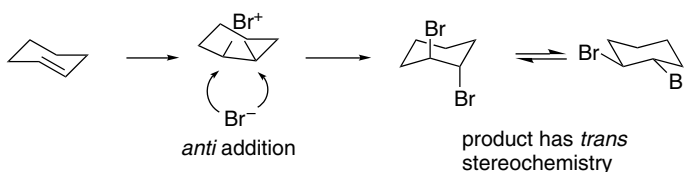


The examples in Scheme 2.7 include bromination, epoxidation and dihydroxylation, and hydroboration-oxidation of alkenes.

**2.4.2.1. Bromination of Alkenes** The bromination of substituted alkenes provides a number of examples of stereospecific reactions. These can be illustrated by considering the *Z*- and *E*-stereoisomers of disubstituted alkenes. The addition of bromine is usually stereospecifically *anti* for unconjugated disubstituted alkenes and therefore the *Z*- and *E*-alkenes lead to *diastereomeric products*. When both substituents on the alkene are identical, as in 2-butene, the product from the *Z*-alkene is chiral, whereas the product from the *E*-alkene is the achiral *meso* form (see p. 132).



The preference for *anti* addition is also evident from the formation of the *trans* product from cyclic alkenes.



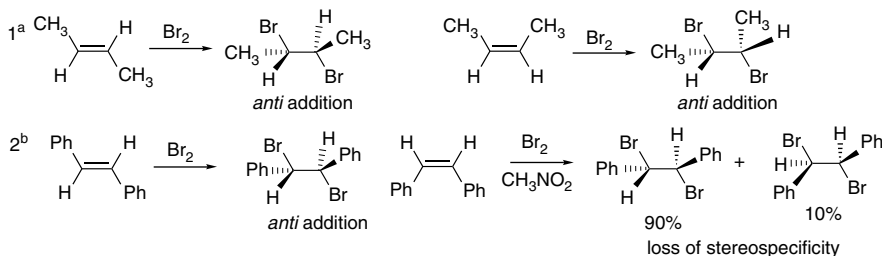
## Scheme 2.7. Examples of Stereospecific Reactions

## CHAPTER 2

Stereochemistry,  
Conformation,  
and Stereoselectivity

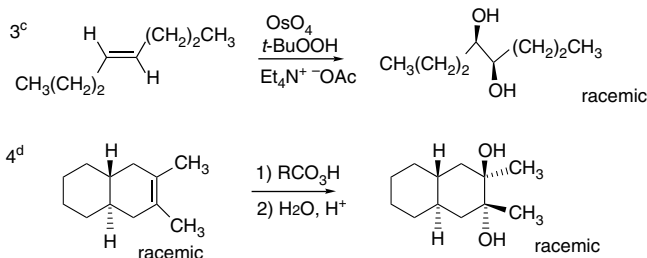
## A. Bromination of Alkenes (see Section 2.4.2.1 for additional discussion)

Bromination of simple alkenes normally proceeds via a bromonium ion and is stereospecifically *anti*. Exceptions occur when the bromonium ion is in equilibrium with a corresponding carbocation.



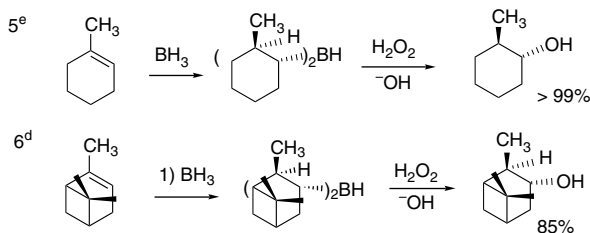
## B. Dihydroxylation and Epoxidation-Hydrolysis of Alkenes (see Section 2.4.2.2 for additional discussion)

Dihydroxylation of epoxides can be carried out with *syn* stereospecificity using  $\text{OsO}_4$  as the active oxidant. The reaction occurs by a cycloaddition mechanism. Epoxidation is also a stereospecific *syn* addition. Ring opening of epoxides by hydrolysis also leads to diols. This is usually an *anti* addition with inversion of configuration at the site of nucleophilic attack, leading to overall *anti* dihydroxylation.



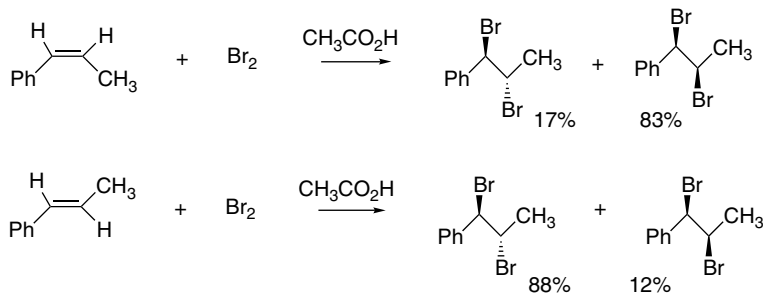
## C. Hydroboration-Oxidation (see Section 2.4.2.3 for additional discussion)

Hydroboration-oxidation occurs by *syn* addition. The reagents are borane or an alkyl or dialkyl derivative, followed by oxidation, usually with  $\text{H}_2\text{O}_2$  and  $\text{OH}^-$ . The oxidation occurs with *retention of configuration of the alkyl group*. The regioselectivity favors addition of the boron at the less-substituted carbon of the double bond. As a result, the reaction sequence provides a stereospecific *syn*, anti-Markovnikov hydration of alkenes.

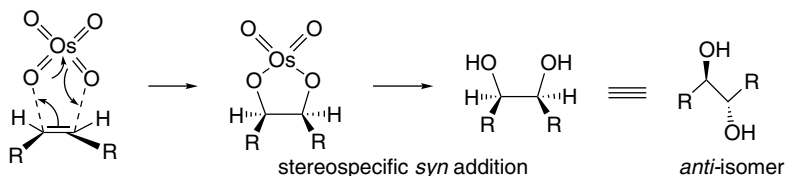


- a. J. H. Rolston and K. Yates, *J. Am. Chem. Soc.*, **91**, 1469, 1477 (1969).  
 b. R. E. Buckles, J. M. Bader, and R. L. Thurmaier, *J. Org. Chem.*, **27**, 4523 (1962).  
 c. K. Akashi, R. E. Palermo, and K. B. Sharpless, *J. Org. Chem.*, **43**, 2063 (1978).  
 d. B. Rickborn and D. K. Murphy, *J. Org. Chem.*, **34**, 3209 (1969).  
 e. H. C. Brown and G. Zweifel, *J. Am. Chem. Soc.*, **83**, 2544 (1961).  
 f. G. Zweifel and H. C. Brown, *Org. Synth.*, **52**, 59 (1972).

The mechanism of bromination is discussed more fully in Section 5.3, but the fundamental cause of the stereospecificity is the involvement of the positively charged bromonium ion intermediate. The bromonium ion is opened by an *anti* approach of the bromide, leading to net *anti* addition. Entry 1 in Scheme 2.7 illustrates this behavior. Stereoisomeric products are obtained from the *E*- and *Z*-isomers, both as the result of *anti* addition. Stereospecificity is diminished or lost when the bromonium ion is not the *only intermediate in the reaction*. Entry 2 in Scheme 2.7 shows this behavior for *cis*-stilbene in nitromethane, where most of the product is the result of *syn* addition. The addition is *anti* in less polar solvents such as cyclohexane or carbon tetrachloride. The loss of *anti* stereospecificity is the result of a change in mechanism. The polar solvent permits formation of a carbocation intermediate. If the bromonium ion can open to a carbocation, a mixture of *syn* and *anti* products is formed. In the stilbene case, the more stable *anti* product is formed. Some loss of stereospecificity is also observed with 1-phenylpropene, where the phenyl group provides stabilization of an open carbocation intermediate.<sup>128</sup> Part of the product from both isomers is the result of *syn* addition.

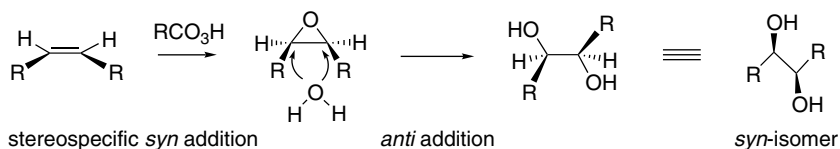


**2.4.2.2. Epoxidation and Dihydroxylation of Alkenes** There are several ways to convert alkenes to diols. Some of these methods proceed by *syn* addition, but others lead to *anti* addition. An important example of *syn* addition is osmium tetroxide-catalyzed dihydroxylation. This reaction is best carried out using a catalytic amount of  $\text{OsO}_4$ , under conditions where it is reoxidized by a stoichiometric oxidant. Currently, the most common oxidants are *t*-butyl hydroperoxide, potassium ferricyanide, or an amine oxide. The two oxygens are added from the same side of the double bond. The key step in the reaction mechanism is a [3 + 2] cycloaddition that ensures the *syn* addition.

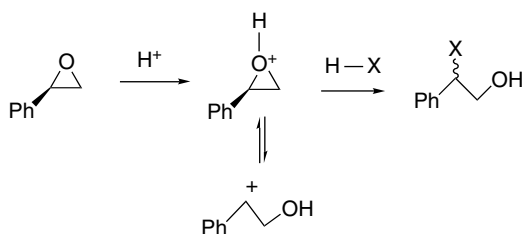


<sup>128</sup>. R. C. Fahey and H.-J. Schneider, *J. Am. Chem. Soc.*, **90**, 4429 (1968).

Alkenes can be converted to diols with overall *anti* addition by a two-step sequence involving epoxidation and hydrolysis. The epoxidation is a *syn* addition that occurs as a single step. When epoxidation is followed by hydrolytic ring opening, the configuration of the diols is determined by the configuration of the alkene, usually with net *anti* dihydroxylation. The hydrolysis reaction proceeds by back-side epoxide ring opening.



Nucleophilic ring opening of epoxides usually occurs with *anti* stereochemistry, with nucleophilic attack at the less substituted carbon.<sup>129</sup> On the other hand, the acid-catalyzed epoxidation-hydrolysis sequence is not always stereospecific. In the case of (*S*)-1-phenyloxirane (styrene oxide), the acid-catalyzed ring opening is regioselective and proceeds through the more stable (benzylic) carbocation; there is extensive racemization because of the involvement of a carbocation.<sup>130</sup>



The ring opening of  $\beta$ -methylstyrene oxide also leads to extensive stereorandomization at the benzylic position.<sup>131</sup>

As summarized in Scheme 2.8, these reactions provide access to three different overall stereochemical outcomes for alkene dihydroxylation, *syn* addition, *anti* addition, or stereorandom addition, depending on the reaction mechanism. In Section 2.5.4 we will discuss enantioselective catalyst for alkene dihydroxylation. These reactions provide further means of controlling the stereochemistry of the reaction.

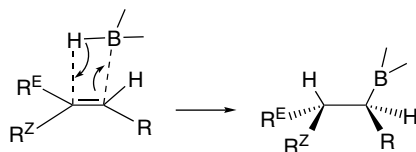
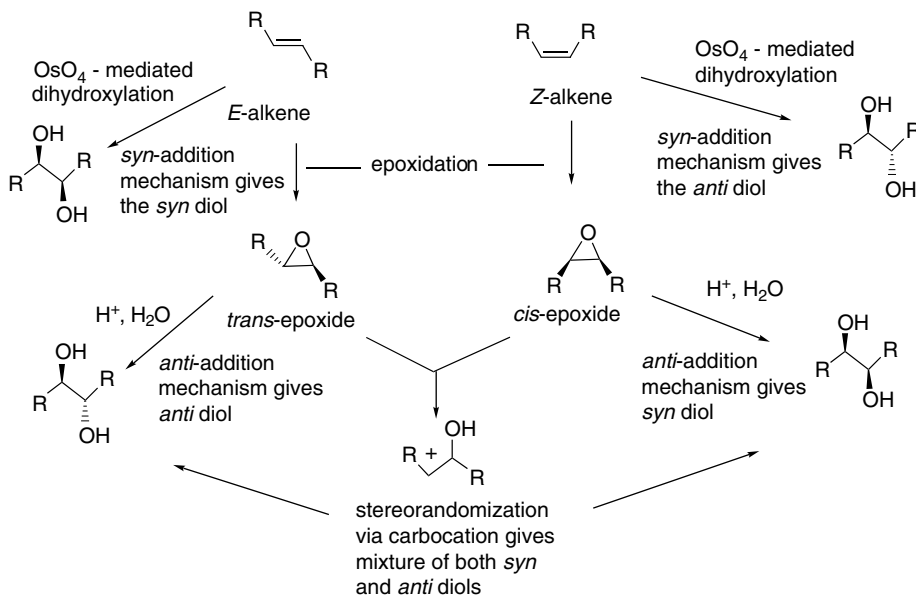
**2.4.2.3. Hydroboration-Oxidation** Hydroboration is a stereospecific *syn* addition. Hydroboration is covered in further detail in Section 5.7. The reaction occurs by an electrophilic attack by borane or alkylborane on the double bond with a concerted shift of hydrogen.

<sup>129</sup> R. E. Parker and N. S. Isaacs, *Chem. Rev.*, **59**, 737 (1959).

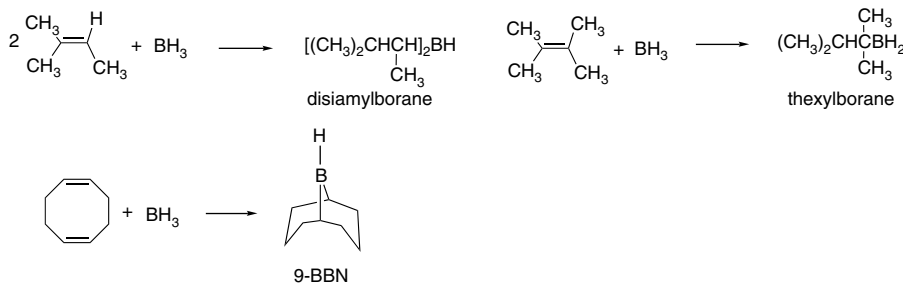
<sup>130</sup> G. Berti, F. Bottari, P. L. Ferrarini, and B. Macchia, *J. Org. Chem.*, **30**, 4091 (1965); B. Lin and D. L. Whalen, *J. Org. Chem.*, **59**, 1638 (1994).

<sup>131</sup> R. S. Mohan and D. L. Whalen, *J. Org. Chem.*, **58**, 2663 (1993).

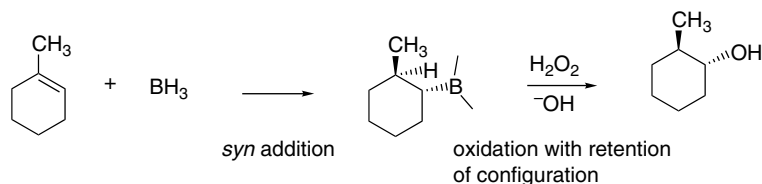
**Scheme 2.8. Summary of Stereochemistry of Alkene Dihydroxylation by OsO<sub>4</sub>-Catalysis and Epoxide Ring Opening**



When the reaction is done with borane it is usually carried to the trialkylborane stage, but by controlling the stoichiometry the dialkyl or monoalkylborane can be obtained, especially from highly substituted alkenes such as 2-methyl-2-butene or 2,3-dimethylbutene. The resulting dialkyl and monoalkyl boranes are known as disiamylborane and thexylborane. Another useful dialkyl borane is 9-borabicyclo[3.3.1]nonane, known as 9-BBN.



When hydroboration is done in a synthetic context it is usually followed by a secondary reaction, most frequently oxidation by hydrogen peroxide and a base, which gives the corresponding alcohol *with retention of configuration*. The stereospecificity is very high. The regioselectivity is also usually excellent for the addition of the borane at the less substituted carbon of the double bond. This is illustrated in Entry 5 of Scheme 2.7, where 1-methylcyclohexene gives *trans*-2-methylcyclohexanol as a result of *syn* addition, followed by oxidation with retention of configuration. The stereospecificity is higher than 99% and none of the *cis* isomer is detected.



There is also an element of stereoselectivity associated with the hydroboration. The borane approaches from the less hindered face of the alkene. For 3-methylcyclohexene, a mixture of products is formed because the 3-methyl substituent has only weak influence on the regiochemistry and the steric approach. This stereoselectivity is accentuated by use of the larger dialkyl and alkyl boranes, as is illustrated by the data for 7,7-dimethylnorbornene in Table 2.5. All of the stereoselectivity and regioselectivity elements are illustrated by Entry 6 in Scheme 2.7. The boron adds at the less substituted end of the double bond and *anti* to the larger dimethyl bridge. Note that this forces the C(2) methyl into proximity of the larger bridge. After oxidation, the hydrogen and hydroxyl that were added are *syn*.

Each of the stereoselective reactions that were considered in Section 2.4 are discussed in more detail when the reaction is encountered in subsequent chapters. The key point for the present is that *reaction mechanism determines stereochemical outcome*. Knowledge about the mechanism allows the prediction of stereochemistry, and conversely, information about stereochemistry provides insight into the mechanism. As we consider additional reactions, we will explore other examples of the relationships between mechanism and stereochemistry.

**Table 2.5. Stereoselectivity of Hydroboration**

Reagent	3-Methylcyclohexene <sup>a</sup>				Norbornene <sup>b</sup>		7,7-Dimethyl-norbornene <sup>b</sup>	
	<i>cis</i> -2	<i>trans</i> -2	<i>cis</i> -3	<i>trans</i> -3 <sup>a</sup>	<i>exo</i>	<i>endo</i> <sup>b</sup>	<i>exo</i>	<i>endo</i> <sup>c</sup>
B <sub>2</sub> H <sub>6</sub>	16	34	18	32	99.5	0.5	22	78
Disiamylborane	18	30	27	25	87	13		
9-BBN	0	20	40	40	99.5	0.5	3	97

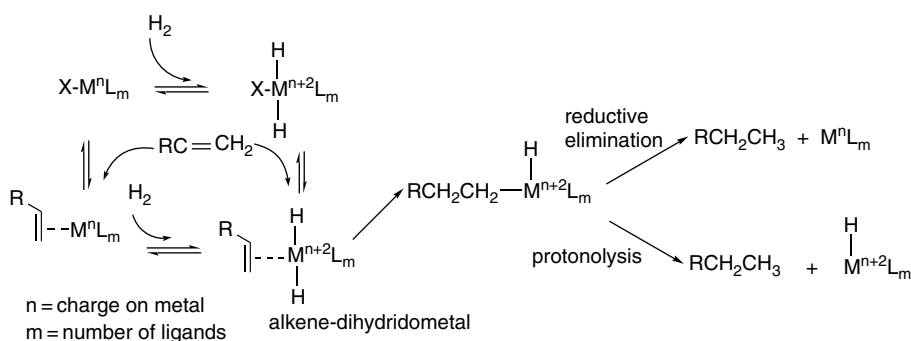
a. H. C. Brown, R. Liotta, and L. Brener, *J. Am. Chem. Soc.*, **99**, 3427 (1977).

b. H. C. Brown, J. H. Kawakami, and K.-T. Liu, *J. Am. Chem. Soc.*, **95**, 2209 (1973).

*Enantioselective reactions* are a particular case of stereoselective reactions that show a preference for one of a pair of enantiomers. As noted in Section 2.1.8, no reaction can produce an excess of one enantiomer unless there is at least one chiral component involved. *Enantiospecific reactions* are a special case of stereoselective reactions in which the mechanism ensures that the configuration of reactant, reagent, or catalyst determines that of the product. A simple example is  $S_N2$  substitution, where the back-side displacement mechanism dictates inversion of configuration. In the next several subsections, we discuss examples of enantioselective and enantiospecific reactions.

### 2.5.1. Enantioselective Hydrogenation

Most catalytic hydrogenations are carried out under heterogeneous conditions using finely dispersed transition metals as catalysts. Such reactions take place on the catalyst surface (heterogeneous hydrogenation) and are not normally enantioselective, although they may be stereoselective (see Section 2.4.1.1). In addition, certain soluble transition metal complexes are active hydrogenation catalysts.<sup>132</sup> Many of these catalysts include phosphine ligands, which serve both to provide a stable soluble complex and to adjust the reactivity of the metal center. Hydrogenation by homogeneous catalysts is believed to take place through a  $\pi$  complex of the unsaturated compound. The metals also react with molecular hydrogen and form metal hydrides. The addition of hydrogen to the metal can occur before or after complexation of the alkene. An alkylmetal intermediate is formed by transfer of hydrogen from the metal to the carbon. This intermediate can break down to alkane by reductive elimination or in some cases by reaction with a proton source.

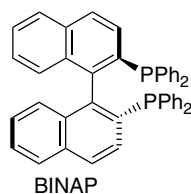


The process of homogeneous catalytic hydrogenation can be made enantioselective by establishing a chiral environment at the catalytic metal center. Most of the successful cases of enantioselective hydrogenation involve reactants having a potential

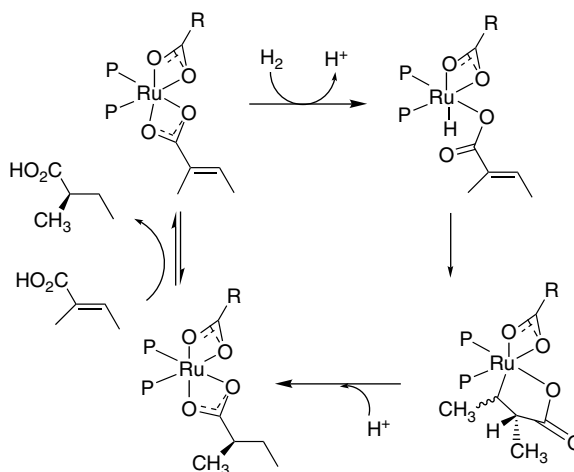
<sup>132</sup> A. J. Birch and D. H. Williamson, *Org. Reactions*, **24**, 1 (1976); B. R. James, *Homogeneous Hydrogenation*, Wiley, New York, 1973; B. R. James, in *Comprehensive Organometallic Chemistry*, G. Wilkinson, F. G. A. Stone, and E. W. Abel, eds., Pergamon Press, Oxford, 1982, Vol. 8, Chap. 51; P. A. Chaloner, M. A. Esteruelas, F. Joo, L. A. Oro, *Homogeneous Hydrogenation*, Kluwer Academic, Dordrecht, 1994.

coordinating group. For example,  $\alpha$ ,  $\beta$ -unsaturated acids and esters, as well as allylic alcohols, are among the reactants that give good results. The reason for this is that the functional group can complex with the metal center, increasing the overall degree of structural organization. Scheme 2.9 provides some examples of enantioselective hydrogenations. Entries 1 and 2 involve acrylic acid derivatives with rhodium catalysts containing chiral phosphine ligands. Entry 3 involves an unsaturated diester. The reactants in Entries 4 and 5 are  $\alpha$ -amido acrylic acids.

A number of chiral ligands have been explored in order to develop enantioselective hydrogenation catalysts.<sup>133</sup> Some of the most successful catalysts are derived from chiral 1,1'-binaphthylidiphosphines such as BINAP.<sup>134</sup> These ligands are chiral by virtue of the sterically restricted rotation of the two naphthyl rings (see Section 2.1.5). Scheme 2.10 gives the structures and common names of some other important chiral diphosphine ligands.



$\alpha$ ,  $\beta$ -Unsaturated acids can be reduced enantioselectively with ruthenium and rhodium catalysts having chiral phosphine ligands. The mechanism of such reactions using  $\text{Ru}(\text{BINAP})(\text{O}_2\text{CCH}_3)_2$  is consistent with the idea that coordination of the carboxy group establishes the geometry at the metal ion.<sup>135</sup> The configuration of the product is established by the hydride transfer from ruthenium to the  $\alpha$ -carbon that occurs on formation of the alkyl-metal intermediate. The second hydrogen is introduced by protonolysis.



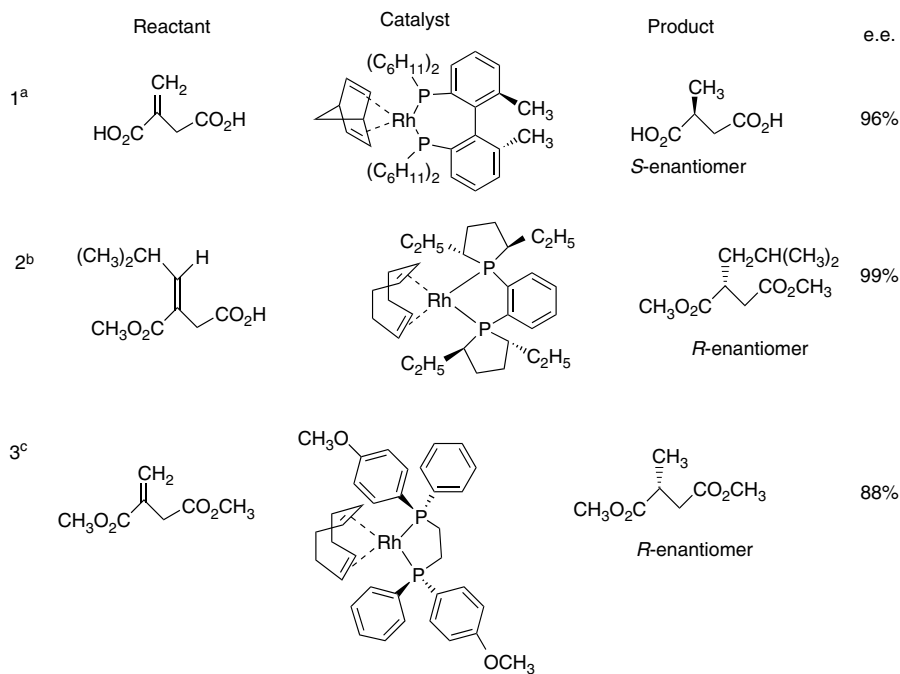
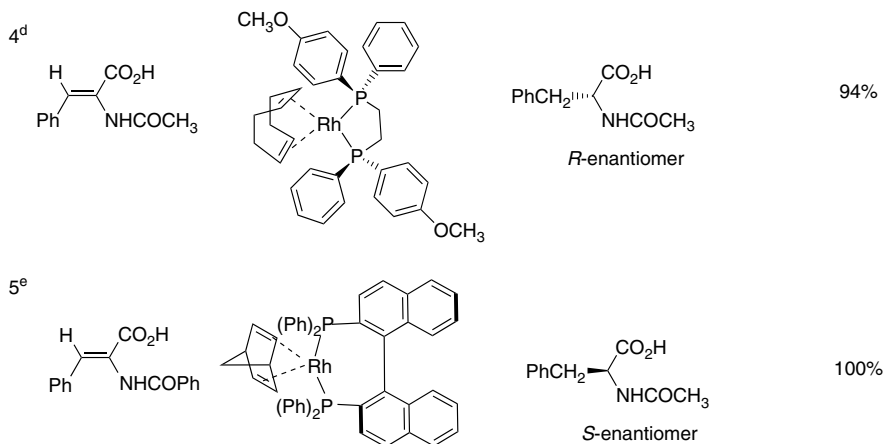
<sup>133</sup> B. Bosnich and M. D. Fryzuk, *Top. Stereochem.*, **12**, 119 (1981); W. S. Knowles, W. S. Chrisopfel, K. E. Koenig, and C. F. Hobbs, *Adv. Chem. Ser.*, **196**, 325 (1982); W. S. Knowles, *Acc. Chem. Res.*, **16**, 106 (1983).

<sup>134</sup> R. Noyori and H. Takaya, *Acc. Chem. Res.*, **23**, 345 (1990).

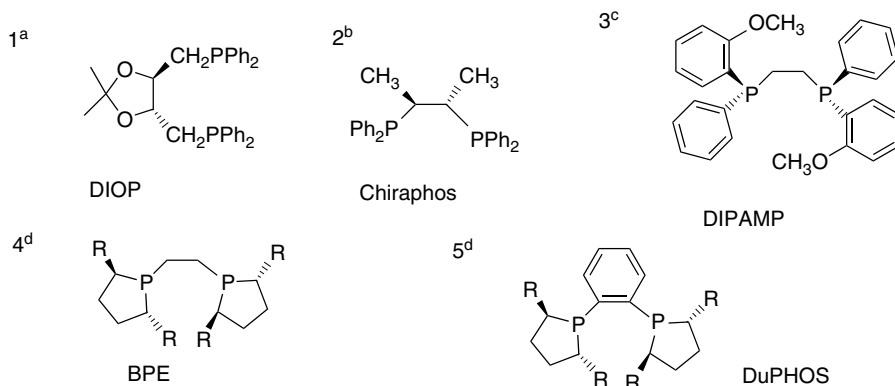
<sup>135</sup> M. T. Ashby and J. T. Halpern, *J. Am. Chem. Soc.*, **113**, 589 (1991).

## A. Acrylic acid and esters.

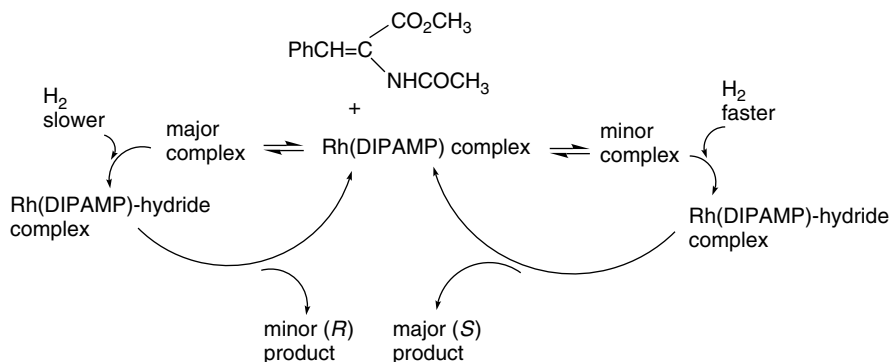
## SECTION 2.5

Enantioselective  
ReactionsB.  $\alpha$ -Amidoacrylic acids.a. T. Chiba, A. Miyashita, H. Nohira, and H. Takaya, *Tetrahedron Lett.*, **32**, 4745 (1991).b. M. J. Burk, F. Bienewald, M. Harris, and A. Zanotti-Gerosa, *Angew. Chem. Int. Ed. Engl.*, **37**, 1931 (1998).c. W. C. Chrispfel and B. D. Vineyard, *J. Am. Chem. Soc.*, **101**, 4406 (1979).d. B. D. Vineyard, W. S. Knowles, M. J. Sabacky, G. L. Bachman, and D. J. Weinkauff, *J. Am. Chem. Soc.*, **99**, 5946 (1977).e. A. Miyashita, H. Takaya, T. Souchi, and R. Noyori, *Tetrahedron*, **40**, 1245 (1984).

## CHAPTER 2

Stereochemistry,  
Conformation,  
and Stereoselectivitya. H. B. Kagan and T.-P. Dang, *J. Am. Chem. Soc.*, **94**, 6429 (1972).b. M. D. Fryzuk and B. Bosnich, *J. Am. Chem. Soc.*, **100**, 5491 (1978).c. W. S. Knowles, *Acc. Chem. Res.*, **16**, 106 (1983).d. M. J. Burk, J. E. Feaster, W. A. Nugent, and R. L. Harlow, *J. Am. Chem. Soc.*, **115**, 10125 (1993).

An especially important case is the enantioselective hydrogenation of  $\alpha$ -amidoacrylic acids, which leads to  $\alpha$ -aminoacids.<sup>136</sup> A particularly detailed study was carried out on the mechanism of reduction of methyl *Z*- $\alpha$ -acetamidocinnamate by a rhodium catalyst with the chiral diphosphine ligand DIPAMP.<sup>137</sup> It was concluded that the reactant can bind reversibly to the catalyst to give either of two complexes. Addition of hydrogen at rhodium then leads to a reactive rhodium hydride intermediate and eventually to product. Interestingly, the addition of hydrogen occurs most rapidly in the *minor isomeric complex* and the enantioselectivity is due to this kinetic preference. The major isomer evidently encounters greater steric repulsions if hydrogenation proceeds and is therefore less reactive.<sup>138</sup>



<sup>136</sup> J. M. Brown, *Chem. Soc. Rev.*, **22**, 25 (1993). A. Pfaltz and J. M. Brown in *Stereoselective Synthesis*, G. Helmchen, R. W. Hoffmann, J. Mulzer and E. Schauman, eds., Thieme, New York, 1996, Part D, Sec. 2.5.1.2; U. Nagel and J. Albrecht, *Top. Catal.*, **5**, 3 (1998).

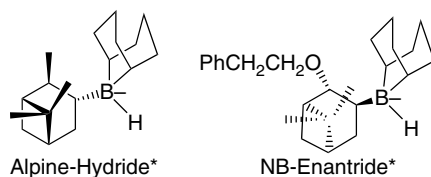
<sup>137</sup> C. R. Landis and J. Halpern, *J. Am. Chem. Soc.*, **109**, 1746 (1987).

<sup>138</sup> S. Feldgus and C. R. Landis, *J. Am. Chem. Soc.*, **122**, 12714 (2000).

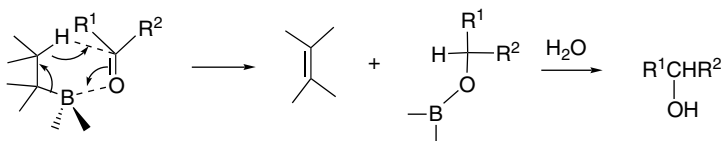
These examples illustrate the factors that are usually involved in successful enantioselective hydrogenation. The first requirement is that the metal center have the necessary reactivity toward both molecular hydrogen and the reactant alkene. The metal center must retain this reactivity in the presence of the chiral ligands. Furthermore, because most of the ligands are bidentate, there must be sufficient coordination sites to accommodate the ligand, as well as hydrogen and the reactant. In particular, there must be at least one remaining coordination site for the functional group. As we can see from the detailed mechanisms of the  $\alpha$ -amido acrylates, the Rh center proceeds through a hexacoordinate dihydride intermediate to a pentacoordinate  $\sigma$ -alkyl intermediate. The reductive elimination frees two coordination sites (including the dissociation of the product). This coordinatively unsaturated complex can then proceed through the catalytic cycle by addition of reactant and hydrogen.

### 2.5.2. Enantioselective Reduction of Ketones

Hydride reducing agents convert ketones to secondary alcohols. Unsymmetrical ketones lead to chiral secondary alcohols. The common hydride reducing agents  $\text{NaBH}_4$  and  $\text{LiAlH}_4$  are achiral and can only produce racemic alcohol. Let us look at some cases where the reaction can be enantioselective. A number of alkylborohydride derivatives with chiral substituents have been prepared. These reagents are generally derived from naturally occurring terpenes.<sup>139</sup> Two examples of the alkylborohydride group have the trade names Alpine-Hydride<sup>®</sup> and NB-Enantride<sup>®</sup>.<sup>140</sup> NB-Enantride achieves 76% e.e. in the reduction of 2-butanone.<sup>141</sup>



Trialkylboranes and dialkylchloroboranes are also useful for reduction of aldehydes and ketones.<sup>142</sup> These reactions involve the coordination of the carbonyl oxygen to boron and transfer of a  $\beta$ -hydrogen through a cyclic TS.



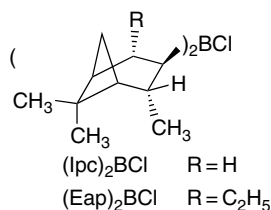
<sup>139</sup>. M. M. Midland, *Chem. Rev.*, **89**, 1553 (1989).

<sup>140</sup>. Alpine-Hydride and NB-Enantride are trade names of the Sigma Aldrich Corporation.

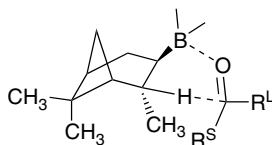
<sup>141</sup>. M. M. Midland, A. Kazubski, and R. E. Woodling, *J. Org. Chem.*, **56**, 1068 (1991).

<sup>142</sup>. M. M. Midland and S. A. Zderic, *J. Am. Chem. Soc.*, **104**, 525 (1982).

When the borane is chiral, these reactions can be enantioselective. The most highly developed of the chiral boranes are derived from  $\alpha$ -pinene. The dialkylborane is known as diisopinocampheylborane,  $\text{Ipc}_2\text{BH}$ . Both enantiomers are available.<sup>143</sup> The corresponding *B*-alkyl and chloroborane derivatives act as enantioselective reductants toward ketones. For example the BBN derivative of isopinocampheylborane is enantioselective in the reduction of acetophenone.<sup>144</sup> The degree of enantioselectivity of alkylchloroboranes depends on the alkyl substituent, increasing from methyl (14% e.e. *S*), ethyl (33% e.e. *S*) through isopropyl (81% e.e. *S*), but then completely reversing with the *t*-butyl derivative (96% e.e. *R*).<sup>145</sup> Di-(isopinocampheyl)chloroborane,<sup>146</sup>  $(\text{Ipc})_2\text{BCl}$ , and *t*-butylisopinocampheylchloroborane<sup>147</sup> achieve high enantioselectivity for aryl and hindered dialkyl ketones. Diiso-2-ethylapopinocampheylchloroborane,  $(\text{Eap})_2\text{BCl}$ , shows good enantioselectivity toward an even wider range of ketones.<sup>148</sup>



In most cases, the enantioselectivity can be predicted by a model that places the smaller carbonyl substituent toward the isopinocampheyl methyl group.<sup>149</sup>



The origin of the enantioselectivity has been examined using semiempirical (AM1) computations.<sup>145c</sup> The main differences in stability arise at the stage of formation of the borane-ketone complex, where the boron changes from  $sp^2$  to  $sp^3$  hybridization. The boron substituents introduce additional steric compressions. Table 2.6 gives some typical results for enantioselective reduction of ketones.

An even more efficient approach to enantioselective reduction of ketones is to use a chiral catalyst. One of the most successful is the oxazaborolidine **D**, which is

<sup>143</sup> H. C. Brown, P. K. Jadhav, and A. K. Mandal, *Tetrahedron*, **37**, 3547 (1981); H. C. Brown and P. K. Jadhav, in *Asymmetric Synthesis*, J. D. Morrison, ed., Academic Press, New York, 1983, Chap. 1.

<sup>144</sup> M. M. Midland, S. Greer, A. Tramontano, and S. A. Zderic, *J. Am. Chem. Soc.*, **101**, 2352 (1979).

<sup>145</sup> (a) M. M. Rogic, *J. Org. Chem.*, **61**, 1341 (1996); (b) M. M. Rogic, P. V. Ramachandran, H. Zinnen, L. D. Brown, and M. Zheng, *Tetrahedron: Asymmetry*, **8**, 1287 (1997); (c) M. M. Rogic, *J. Org. Chem.*, **65**, 6868 (2000).

<sup>146</sup> H. C. Brown, J. Chandrasekharan, and P. V. Ramachandran, *J. Am. Chem. Soc.*, **110**, 1539 (1988); M. Zhao, A. O. King, R. D. Larsen, T. R. Verhoeven, and P. J. Reider, *Tetrahedron Lett.*, **38**, 2641 (1997).

<sup>147</sup> H. C. Brown, M. Srebnik, and P. V. Ramachandran, *J. Org. Chem.*, **54**, 1577 (1989).

<sup>148</sup> H. C. Brown, P. V. Ramachandran, A. V. Teodorovic, and S. Swaminathan, *Tetrahedron Lett.*, **32**, 6691 (1991).

<sup>149</sup> M. M. Midland and J. L. McLoughlin, *J. Org. Chem.*, **49**, 1316 (1984).

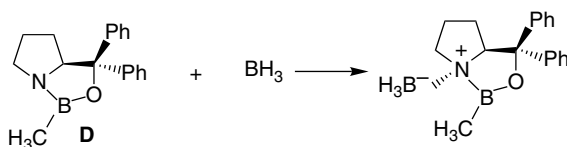
Table 2.6. Enantioselective Reduction of Ketones

Reagent	Ketone	% e.e.	Configuration
Alpine-Borane <sup>ⓐ</sup>	3-Methyl-2-butanone	62	S
NB-Enantride <sup>ⓑ</sup>	2-Octanone	79	S
Eapine-Hydrider <sup>ⓒ</sup>	2-Octanone	78	S
(Ipc) <sub>2</sub> BCl <sup>ⓓ</sup>	2-Acetylnaphthalene	94	S
(Ipc)( <i>t</i> -Bu)BCl <sup>ⓔ</sup>	Acetophenone	96	R
(Ipc) <sub>2</sub> BCl <sup>ⓕ</sup>	2,2-Dimethylcyclohexanone	91	S
(Eap) <sub>2</sub> BCl <sup>ⓖ</sup>	3-Methyl-2-butanone	95	R

NOTE: © Trademark of Sigma Aldrich Corporation.

- H. C. Brown and G. G. Pai, *J. Org. Chem.*, **50**, 1384 (1985).
- M. M. Midland and A. Kazubski, *J. Org. Chem.*, **47**, 2495 (1982).
- P. Ramachandran, R. Veeraghavan, H. C. Brown, and S. Swaminathan, *Tetrahedron: Asymmetry*, **1**, 433 (1990).
- M. Zhao, A. O. King, R. D. Larsen, T. R. Verhoeven, and P. J. Reider, *Tetrahedron Lett.*, **38**, 2641 (1997).
- H. C. Brown, M. Srebnik, and P. V. Ramachandran, *J. Org. Chem.*, **54**, 1577 (1989).
- H. C. Brown, J. Chandrasekharan, and P. V. Ramachandran, *J. Am. Chem. Soc.*, **110**, 1539 (1988).
- H. C. Brown, P. V. Ramachandran, A. V. Teodorovic, and S. Swaminathan, *Tetrahedron Lett.*, **32**, 6691 (1991).

derived from the amino acid proline.<sup>150</sup> The enantiomer is also available. An adduct of borane and **D** is the active reductant. This adduct can be prepared, stored, and used as a stoichiometric reagent, if so desired.<sup>151</sup>



A catalytic amount (5–20 mol %) of this reagent, along with additional BH<sub>3</sub> as the reductant, can reduce ketones such as acetophenone and pinacolone in > 95% e.e. There are experimental data indicating that the steric demand of the boron substituent influences enantioselectivity.<sup>152</sup> The enantioselectivity and reactivity of these catalysts can be modified by changes in substituent groups to optimize selectivity toward a particular ketone.<sup>153</sup>

Computational studies have explored the mechanism and origin of the enantioselectivity of these reactions. Based on semiempirical MO calculations (MNDO), it has

- E. J. Corey, R. K. Bakshi, S. Shibata, C.-P. Chen, and V. K. Singh, *J. Am. Chem. Soc.*, **109**, 7925 (1987); E. J. Corey and C. J. Helal, *Angew. Chem. Int. Ed. Engl.*, **37**, 1987 (1998).
- D. J. Mahre, A. S. Thompson, A. W. Douglas, K. Hoogsteen, J. D. Carroll, E. G. Corley, and E. J. J. Grabowski, *J. Org. Chem.*, **58**, 2880 (1993).
- E. J. Corey and R. K. Bakshi, *Tetrahedron Lett.*, **31**, 611 (1990); T. K. Jones, J. J. Mohan, L. C. Xavier, T. J. Blacklock, D. J. Mathre, P. Sohar, E. T. T. Jones, R. A. Reamer, F. E. Roberts, and E. J. J. Grabowski, *J. Org. Chem.*, **56**, 763 (1991).
- A. W. Douglas, D. M. Tschaen, R. A. Reamer, and Y.-J. Shi, *Tetrahedron: Asymmetry*, **7**, 1303 (1996).

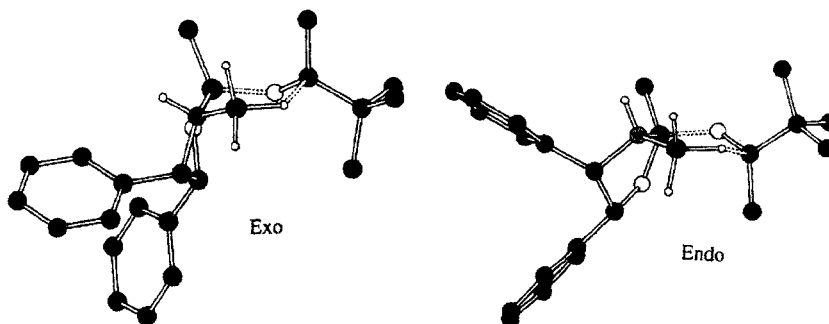
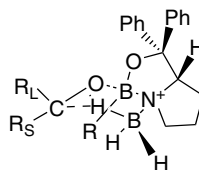
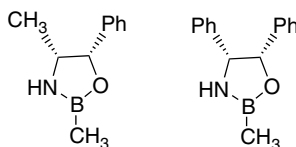


Fig. 2.20. Optimized (HF/3-21G) structures of the *exo* and *endo* transition states for reduction of *t*-butyl methyl ketone by a model catalyst. The *exo* structure is favored by 2.1 kcal, in accord with an experimental e.e of 88%. Reproduced from *J. Am. Chem. Soc.*, **116**, 8516 (1994), by permission of the American Chemical Society.

been suggested that the enantioselectivity in these reductions arises from a chair-like TS in which the governing steric interaction is the one with the alkyl substituent on boron.<sup>154</sup>



There also have been ab initio studies of the transition structure using several model catalysts and calculations at the HF/3-21G, HF/6-31G(*d*), and MP2/6-31G(*d*) levels.<sup>155</sup> The enantioselectivity is attributed to the preference for an *exo* rather than an *endo* approach of the ketone, as shown in Figure 2.20.



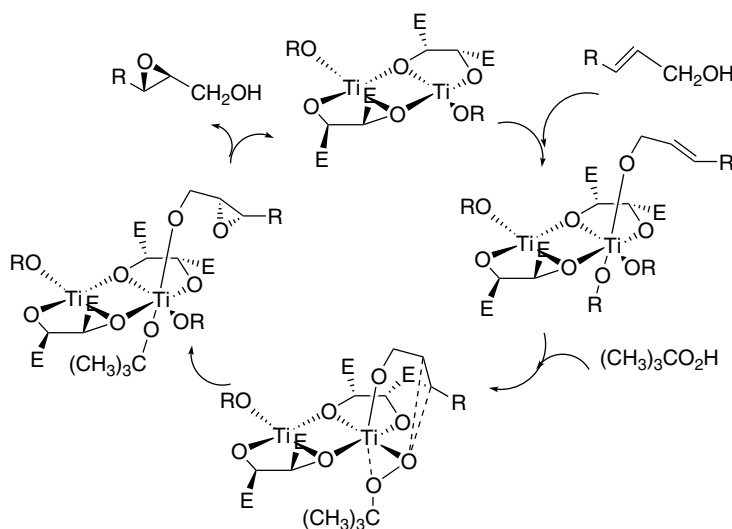
### 2.5.3. Enantioselective Epoxidation of Allylic Alcohols

Certain transition metal complexes catalyze oxidation of allylic alcohols to the corresponding epoxides. The most useful procedures involve *t*-butyl hydroperoxide as

<sup>154</sup> D. K. Jones, D. C. Liotta, I. Shinkai, and D. J. Mathre, *J. Org. Chem.*, **58**, 799 (1993); L. P. Linney, C. R. Self, and T. H. Williams, *J. Chem. Soc., Chem. Commun.* 1651 (1994).

<sup>155</sup> G. J. Quallich, J. F. Blake, and T. M. Woodall, *J. Am. Chem. Soc.*, **116**, 8516 (1994).

the stoichiometric oxidant in combination with titanium catalysts. When enantiomerically pure tartrate esters are included in the system, the reaction is highly enantioselective and is known as *Sharpless asymmetric epoxidation*.<sup>156</sup> Either the (+) or (-) tartrate ester can be used, so either enantiomer of the desired product can be obtained. The allylic hydroxyl group serves to coordinate the reactant to titanium. The mechanism involves exchange of the allylic alcohol and *t*-butyl hydroperoxide for another ligand at the titanium atom. In the TS an oxygen atom from the peroxide is transferred to the double bond.<sup>157</sup> The electrophilic metal polarizes the weak O—O bond of the hydroperoxide to effect the transfer of oxygen to the alkene  $\pi$  bond. Both kinetic data and consideration of the energetics of the monomeric and dimeric complexes suggest that the active catalyst is dimeric.<sup>158</sup>



The orientation of the reactants is governed by the chirality of the tartrate ester.<sup>159</sup> The enantioselectivity can be predicted in terms of the model shown below.<sup>160</sup>

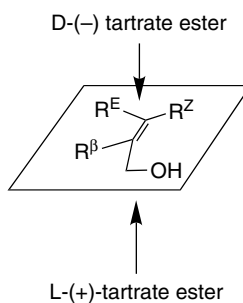
<sup>156</sup> R. A. Johnson and K. B. Sharpless, in *Catalytic Asymmetric Synthesis*, I. Ojima, ed., VCH Publishers, New York, 1993, pp. 103–158.

<sup>157</sup> M. G. Finn and K. B. Sharpless in *Asymmetric Synthesis*, Vol. 5, J. D. Morrison, ed., Academic Press, New York, 1985, Chap 8; B. H. McKee, T. H. Kalantar, and K. B. Sharpless, *J. Org. Chem.*, **56**, 6966 (1991); For an alternative description of the origin of enantioselectivity, see E. J. Corey, *J. Org. Chem.*, **55**, 1693 (1990).

<sup>158</sup> M. G. Finn and K. B. Sharpless, *J. Am. Chem. Soc.*, **113**, 113 (1991).

<sup>159</sup> V. S. Martin, S. S. Woodard, T. Katsuki, Y. Yamada, M. Ikeda, and K. B. Sharpless, *J. Am. Chem. Soc.*, **103**, 6237 (1981); K. B. Sharpless, S. S. Woodard, and M. G. Finn, *Pure Appl. Chem.*, **55**, 1823 (1983); M. G. Finn, and K. B. Sharpless, *J. Am. Chem. Soc.*, **113**, 113 (1996); B. H. McKee, T. H. Kalantar, and K. B. Sharpless, *J. Org. Chem.*, **56**, 6966 (1991).

<sup>160</sup> M. G. Finn and K. B. Sharpless in *Asymmetric Synthesis*, J. D. Morrison, ed., Vol 5, Academic Press, New York, 1985, Chap. 5.



There has been a DFT (BLYP/HW3) study of the TS and its relationship to the enantioselectivity of the reaction.<sup>161</sup> The strategy used was to build up the model by successively adding components. First the titanium coordination sphere, including the allylic alcohol and peroxide group, was modeled (Figure 2.21a). The diol ligand and allylic alcohol were added to the coordination sphere (Figure 2.21b). Then the steric bulk associated with the hydroperoxide was added (Figure 2.21c). Finally the tartrate esters were added (using formyl groups as surrogates; Figure 2.21d). This led successively to TS models of increasingly detailed structure. The energies of the added components were minimized to identify the most stable structure at each step. The key features of the final TS model are the following: (1) The peroxide-titanium interaction has a spiro rather than planar arrangement in the TS for oxygen transfer. (2) The breaking O–O bond is nearly perpendicular to the plane of the C=C bond to meet the stereoelectronic requirement for electrophilic attack. (3) The orientation of the alkyl group of the peroxide plays a key role in the enantioselectivity, which is consistent with the experimental observation that less bulky hydroperoxides give much lower enantioselectivity. (4) This steric effect leads to an arrangement in which the C–O bond of the allylic alcohol bisects the O–Ti–O bonds in the favored TS. (5) The tartrate ester groups at the catalytically active titanium center are in equatorial positions and do not coordinate to titanium, which implies a conformation flip of the diolate ring as part of the activation process, since the ester groups are in axial positions in the dimeric catalyst. (6) This conformation of the tartrate ligands places one of the ester groups in a position that blocks one mode of approach and determines the enantioselectivity.

**Visual models, additional information and exercises on the Sharpless Epoxidation can be found in the Digital Resource available at: [Springer.com/carey-sundberg](http://Springer.com/carey-sundberg).**

As with enantioselective hydrogenation, we see that several factors are involved in the high efficacy of the  $Ti(OiPr)_4$ -tartrate epoxidation catalysts. The metal ion has two essential functions. One is the assembly of the reactants, the allylic alcohol, and the hydroperoxide. The second is its Lewis acid character, which assists in the rupture of the O–O bond in the coordinated peroxide. In addition to providing the reactive oxidant, the *t*-butyl hydroperoxide contributes to enantioselectivity through its steric bulk. Finally, the tartrate ligands establish a chiral environment that leads to a preference for one of the diastereomeric TSs and results in enantioselectivity.

<sup>161</sup> Y.-D. Wu and D. K. W. Lai, *J. Am. Chem. Soc.*, **117**, 11327 (1995).

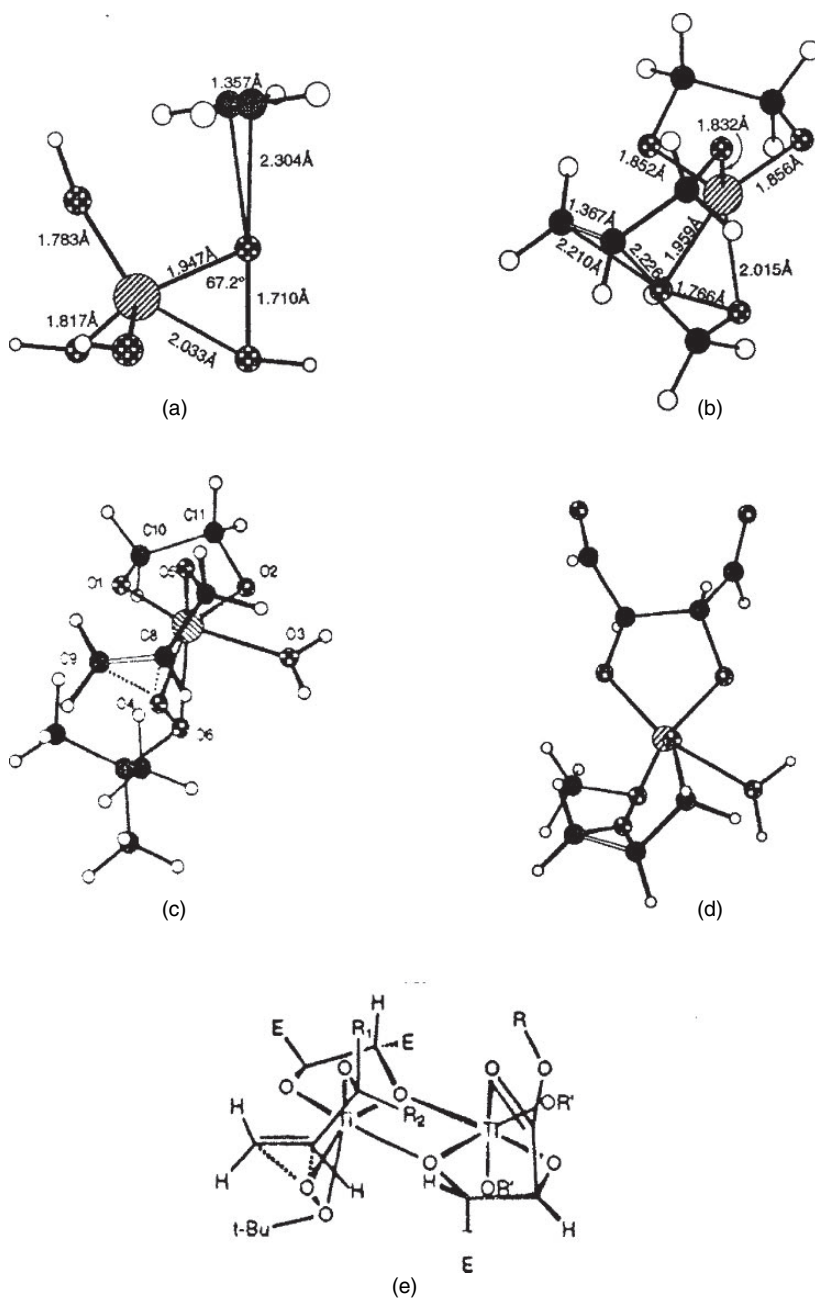
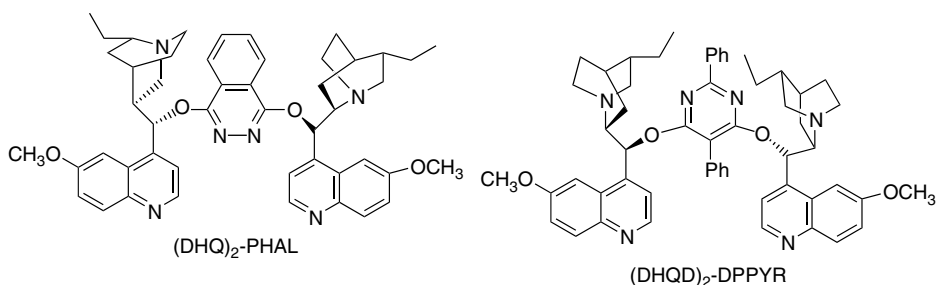


Fig. 2.21. Successive models of the transition structures for Sharpless epoxidation: (a) the hexacoordinate Ti core with hydroxide and hydroperoxide ligand and a coordinated alkene; (b) Ti with methylhydroperoxide, allyl alcohol, and ethanediol as ligands; (c) monomeric catalytic center incorporating *t*-butylhydroperoxide as oxidant; (d) monomeric catalytic center with formyl groups added; (e) representation of the active dimeric catalyst. Reproduced from *J. Am. Chem. Soc.*, **117**, 11327 (1995), by permission of the American Chemical Society.

## 2.5.4. Enantioselective Dihydroxylation of Alkenes

Osmium tetroxide is a stereospecific oxidant that produces diols from alkenes by a *syn*-addition.<sup>162</sup> Currently, the reaction is carried out using a catalytic amount of OsO<sub>4</sub>, with a stoichiometric oxidant such as *t*-butyl hydroperoxide,<sup>163</sup> potassium ferricyanide,<sup>164</sup> or morpholine-*N*-oxide.<sup>165</sup> Osmium tetroxide oxidations can be highly enantioselective in the presence of chiral ligands. The most highly developed ligands are derived from the cinchona alkaloids dihydroquinine (DHQ) and dihydroquinidine (DHQD).<sup>166</sup> The most effective ligands are dimeric derivatives of these alkaloids such as (DHQ)<sub>2</sub>-PHAL and (DHQD)<sub>2</sub>-DDPYR,<sup>167</sup> in which the alkaloid units are linked by heterocyclic ethers. These ligands not only induce high enantioselectivity, but they also *accelerate the reaction*.<sup>168</sup> Optimization of the reaction conditions permits rapid and predictable dihydroxylation of many types of alkenes.<sup>169</sup> The premixed catalysts are available commercially and are referred to by the trade names AD-mix™.



From extensive studies, a consensus has been reached about some aspects of the catalytic mechanism and enantioselectivity: (1) The amine ligands, in particular the quinuclidine nitrogen, are important in activating and stabilizing the osmium intermediate.<sup>170</sup> (2) From the kinetics of the reaction, it is also evident that the *binding of the*

<sup>162</sup> M. Schroeder, *Chem. Rev.*, **80**, 187 (1980).

<sup>163</sup> K. B. Sharpless and K. Akashi, *J. Am. Chem. Soc.*, **98**, 1986 (1976); K. Akashi, R. E. Palermo, and K. B. Sharpless, *J. Org. Chem.*, **43**, 2063 (1978).

<sup>164</sup> M. Minato, K. Yamamoto and J. Tsuji, *J. Org. Chem.*, **55**, 766 (1990); K. B. Sharpless, W. Amberg, Y. L. Bennani, G. A. Crispino, J. Hartung, K.-S. Jeong, H.-L. Kwong, K. Morikawa, Z.-M. Wang, D. Xu, and X.-L. Zhang, *J. Org. Chem.*, **57**, 2768 (1992); J. Eames, H. J. Mitchell, A. Nelson, P. O'Brien, S. Warren, and P. Wyatt, *Tetrahedron Lett.*, **36**, 1719 (1995).

<sup>165</sup> V. VanRheenen, R. C. Kelly, and D. Y. Cha, *Tetrahedron Lett.*, 1973 (1976).

<sup>166</sup> H. C. Kolb, M. S. Van Nieuwenhze, and K. B. Sharpless, *Chem. Rev.*, **94**, 2483 (1994).

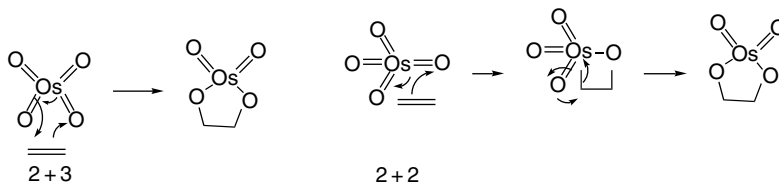
<sup>167</sup> G. A. Crispino, K.-S. Jeong, H. C. Kolb, Z.-M. Wang, D. Xu, and K. B. Sharpless, *J. Org. Chem.*, **58**, 3785 (1993); G. A. Crispino, A. Makita, Z.-M. Wang, and K. B. Sharpless, *Tetrahedron Lett.*, **35**, 543 (1994); K. B. Sharpless, W. Amberg, Y. L. Bennani, G. A. Crispino, J. Hartung, K. S. Jeong, H.-C. Kwong, K. Morikawa, Z. M. Wang, D. Xu, and X. L. Zhang, *J. Org. Chem.*, **57**, 2768 (1992); W. Amberg, Y. L. Bennani, R. K. Chadha, G. A. Crispino, W. D. Davis, J. Hartung, K. S. Jeong, Y. Ogino, T. Shibata, and K. B. Sharpless, *J. Org. Chem.*, **58**, 844 (1993); H. Becker, S. B. King, M. Taniguchi, K. P. M. Vanhessche, and K. B. Sharpless, *J. Org. Chem.*, **60**, 3940 (1995).

<sup>168</sup> P. G. Anderson and K. B. Sharpless, *J. Am. Chem. Soc.*, **115**, 7047 (1993).

<sup>169</sup> H.-L. Kwong, C. Sorato, Y. Ogino, H. Chen, and K. B. Sharpless, *Tetrahedron Lett.*, **31**, 2999 (1990); T. Gobel and K. B. Sharpless, *Angew. Chem. Int. Ed. Engl.*, **32**, 1329 (1993).

<sup>170</sup> D. W. Nelson, A. Gypser, P. T. Ho, H. C. Kolb, T. Kondo, H.-L. Kwong, D. V. McGrath, A. E. Rubin, P.-O. Norrby, K. P. Gable, and K. B. Sharpless, *J. Am. Chem. Soc.*, **119**, 1840 (1997).

reactant is a distinct step in the mechanism and that there are *attractive interactions* between the catalyst ligands and the reactant.<sup>171</sup> The ligands do not function only by steric exclusion, but contribute to the net stabilization of the TS. (3) The aromatic linker groups determine the size of the binding pocket; the ethyl groups on the quinuclidine ring have differing orientations in the DHQD and DHQD catalysts and are a more integral part of the pocket in the DHQD system. (4) The concerted [2+3]cycloaddition mechanism for the actual oxidation step is energetically preferable to an alternative two-step mechanism involving [2+2]cycloaddition.<sup>172</sup>



Within these general terms, the interpretation and prediction of enantioselectivity depends on the binding of the particular reactant in the catalyst pocket. A wide range

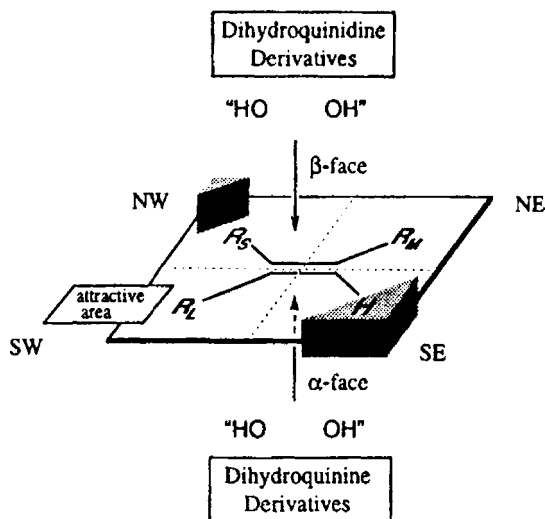


Fig. 2.22. Predictive schematic model for enantioselectivity of AD-mix dihydroxylation catalysts. Reproduced from *Chem. Rev.*, **94**, 2483 (1994), by permission of the American Chemical Society.

- <sup>171</sup>. H. C. Kolb, M. S. Van Nieuwenhze, and K. B. Sharpless, *Chem. Rev.*, **94**, 2483 (1994); E. J. Corey and M. C. Noe, *J. Am. Chem. Soc.*, **118**, 319 (1996); E. J. Corey and M. C. Noe, *J. Am. Chem. Soc.*, **118**, 11038 (1996); P.-O. Norrby, H. Becker, and K. B. Sharpless, *J. Am. Chem. Soc.*, **118**, 35 (1996). H. C. Kolb, P. G. Andersson, and K. B. Sharpless, *J. Am. Chem. Soc.*, **116**, 1278 (1994); B. B. Lohray and V. Bhushan, *Tetrahedron Lett.*, **33**, 5113 (1992).
- <sup>172</sup>. S. Dapprich, G. Ujaque, F. Maseras, A. Lledos, D. G. Musaev, and K. Morokuma, *J. Am. Chem. Soc.*, **118**, 11660 (1996); U. Pidun, C. Boehme, and G. Frenking, *Angew. Chem. Int. Ed. Engl.*, **35**, 2817 (1996); M. Torrent, L. Deng, M. Duran, M. Sola, and T. Ziegler, *Organometallics*, **16**, 13 (1997).

of reactants have been examined, and an empirical model for predicting orientation has been developed from the data.<sup>173</sup> This model is shown in Figure 2.22. Note that the DHQD and DHQ ligands have opposite enantioselectivity because they are of opposite absolute configuration.

There have been a several efforts aimed at theoretical modeling and analysis of the enantioselectivity of osmium-catalyzed dihydroxylation. The system is too large to be amenable to ab initio approaches, but combinations of quantum chemical (either MO or DFT) and molecular mechanics make the systems tractable. A hybrid investigation based on DFT (B3LYP/6-31G) computation and MM3 was applied to the (DHQD)<sub>2</sub>PYDZ catalyst (PYDZ = 3, 5-pyridazinyl).<sup>174</sup> This study examined a number of possible orientations of styrene within the complex and computed their relative energy. The energies were obtained by combining DFT calculations on the reaction core of OsO<sub>4</sub> and the double bond, with MM3 calculations on the remainder of the molecule. Two orientations were found to be very close in energy and these were 2.5–10 kcal/mol more favorable than all the others examined. Both led to the observed enantioselectivity. The two preferred TS structures are shown in Figure 2.23.

Most of the differences in energy among the various orientations are due to differences in the MM portion of the calculation, pointing to nonbonded interactions as the primary determinant of the binding mode. Specifically, attractive interaction with quinoline ring A ( $\pi - \pi$  stacking, 6.1 kcal/mol), quinoline ring B (2.3 kcal/mol), and a perpendicular binding interaction with the pyridazine ring (1.3 kcal/mol) offset the energy required to fit the reactant molecule to the catalytic site. This is consistent with the view that there is an *attractive interaction with the ligand system*.

Norrby, Houk, and co-workers approached the problem by deriving a molecular mechanics type of force field from quantum chemical calculations.<sup>175</sup> This model, too, suggests that there are two possible bonding arrangements and that either might be preferred, depending on the reactant structure. This model was able

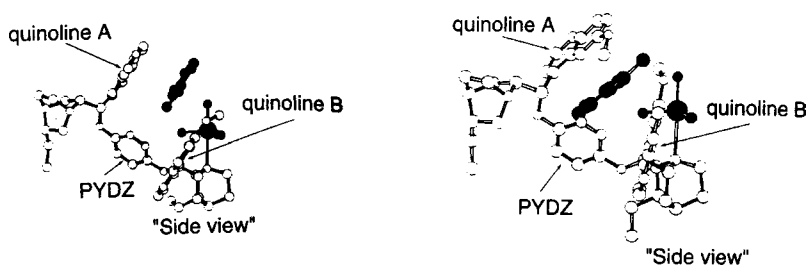


Fig. 2.23. Two most favored orientations of styrene for enantioselective dihydroxylation by (DHQD)<sub>2</sub>PYDZ catalyst. The bridging structure is 3,5-pyridazinyl. Reproduced from *J. Am. Chem. Soc.*, **121**, 1317 (1999), by permission of the American Chemical Society.

<sup>173</sup> H. C. Kolb, P. G. Andersson, and K. B. Sharpless, *J. Am. Chem. Soc.*, **116**, 1278 (1994).

<sup>174</sup> G. Ujaque, F. Maseras, and A. Lledos, *J. Am. Chem. Soc.*, **121**, 1317 (1999).

<sup>175</sup> P.-O. Norrby, T. Rasmussen, J. Haller, T. Strassner, and K. N. Houk, *J. Am. Chem. Soc.*, **121**, 10186 (1999).

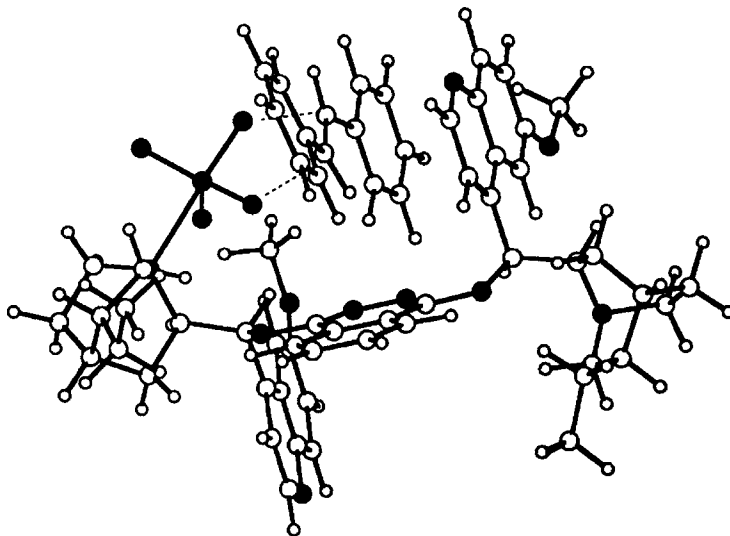


Fig. 2.24. Preferred orientation of stilbene with the (DHQD)<sub>2</sub>PHAL catalyst. Reproduced from *J. Am. Chem. Soc.*, **121**, 10186 (1999), by permission of the American Chemical Society.

to predict the observed enantioselectivity for several styrene derivatives with the PHAL linker. Figure 2.24 shows the optimum TS for the reaction with stilbene. A noteworthy feature of this model is that it uses *both* the binding modes identified for styrene.

**Visual models, additional information and exercises on Enantioselective Dihydroxylation can be found in the Digital Resource available at: [Springer.com/carey-sundberg](http://Springer.com/carey-sundberg).**

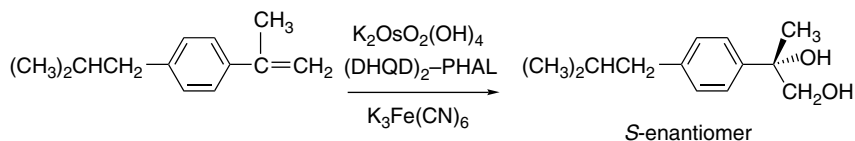
The cases we have considered involve aryl rings as the governing structural feature for enantioselectivity. The AD systems also show excellent enantioselectivity toward functionalized alkenes, especially allylic and homoallylic systems with oxygen substituents.<sup>176</sup> In these systems, another important structural variable comes into play, that is, the conformation of the allylic substituent and its possible interaction with the reaction site.<sup>177</sup>

The asymmetric dihydroxylation has been applied in many synthetic sequences and is discussed further in Part B, Chapter 12. For example the dihydroxylation was the starting point for enantioselective synthesis of *S*-ibuprofen and a similar route was used to prepare *S*-naproxen, which contains a methoxynaphthalene ring.<sup>178</sup> Ibuprofen and naproxen are examples of the NSAID class of analgesic and anti-inflammatory agents.

<sup>176</sup> J. K. Cha and N. S. Kim, *Chem. Rev.*, **95**, 1761 (1995); For additional recent example see: A. Bayer and J. S. Svendsen, *Eur. J. Org. Chem.*, 1769 (2001); L. F. Tietze and J. Grolitzer, *Synthesis*, 877 (1997).

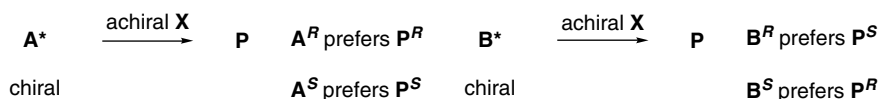
<sup>177</sup> E. Vedejs, W. H. Dent, III, D. M. Gapinski, and C. K. McClure, *J. Am. Chem. Soc.*, **109**, 5437 (1987).

<sup>178</sup> H. Ishibashi, M. Maeki, J. Yagi, M. Ohba, and T. Kanai, *Tetrahedron*, **55**, 6075 (1999).

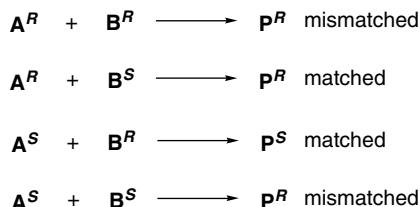


## 2.6. Double Stereodifferentiation: Reinforcing and Competing Stereoselectivity

Up to this point, we have considered cases in which there is a single major influence on the stereo- or enantioselectivity of a reaction. We saw examples of reactant control of facial selectivity, such as 1,2- and 1,3-asymmetric induction in carbonyl addition reactions. In the preceding section, we considered several examples in which the chirality of the catalyst controls the stereochemistry of achiral reagents. Now let us consider cases where there may be two or more independent influences on stereoselectivity, known as *double stereodifferentiation*.<sup>179</sup> For example, if a reaction were to occur between two carbonyl compounds, each having an  $\alpha$ -stereocenter, one carbonyl compound would have an inherent preference for *R* or *S* product. The other would have also have an inherent preference. These preferences would be expressed even toward achiral reagents.



If  $\mathbf{A}^*$  and  $\mathbf{B}^*$  were then to react with one another to create a product with a new chiral center, there would be a two (enantiomeric) matched pairs and two (enantiomeric) mismatched pairs.



In the matched cases the preference of one compound is reinforced by the other. In the mismatched case, they are competing. The concept of matched and mismatched TSs

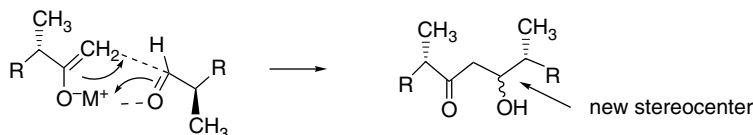
<sup>179</sup> C. H. Heathcock and C. T. White, *J. Am. Chem. Soc.*, **101**, 7076 (1979); S. Masamune, W. Choy, J. S. Petersen, and L. R. Sita, *Angew. Chem. Int. Ed. Engl.*, **24**, 1 (1985).

can be expressed in terms of the free-energy differences resulting from the individual preferences  $\Delta\Delta G^*_1$  and  $\Delta\Delta G^*_2$  plus any incremental change resulting from the combination  $\Delta G^*_{12}$ .

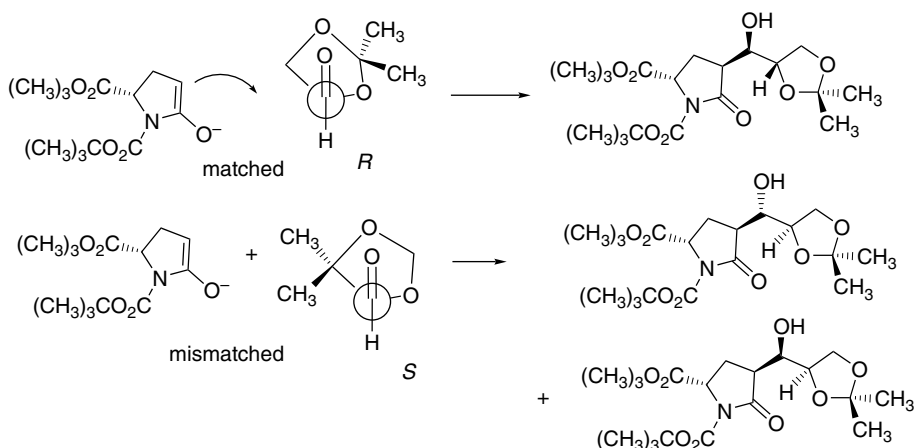
$$\Delta G^*_{\text{matched}} = \Delta\Delta G^*_1 + \Delta\Delta G^*_2 + \Delta G^*_{12}$$

$$\Delta G^*_{\text{mismatched}} = \Delta\Delta G^*_1 - \Delta\Delta G^*_2 + \Delta G^*_{12}$$

An example of such a situation is an aldol addition reaction in which one carbonyl compound acts as the nucleophile and the other as the electrophile.

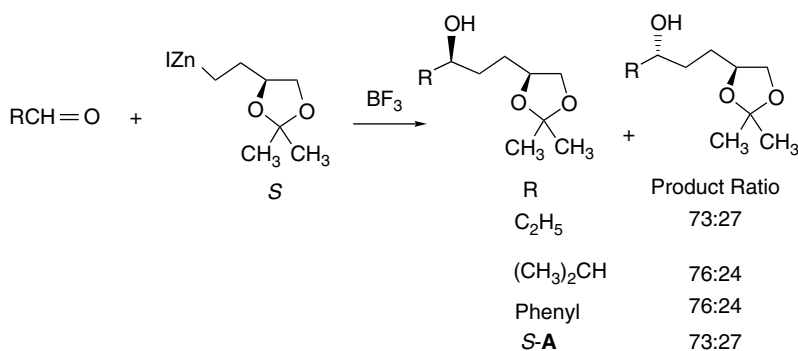


In fact, this case has been extensively studied and we consider it in more detail in Part B, Chapter 2. An example is the condensation of the enolate of a derivative of pyroglutamic acid and a protected form of glyceraldehyde. In the case of the (*R*)-aldehyde a single enantiomer is formed, whereas with the (*S*)-aldehyde a 1:1 mixture of two diastereomers is formed, along with a small amount of a third diastereomer.<sup>180</sup> The facial preference of the enolate is determined by the steric effect of the *t*-butoxycarbonyl group, whereas in the aldehyde the Felkin-Ahn TS prefers an approach *anti* to the  $\alpha$ -oxygen.

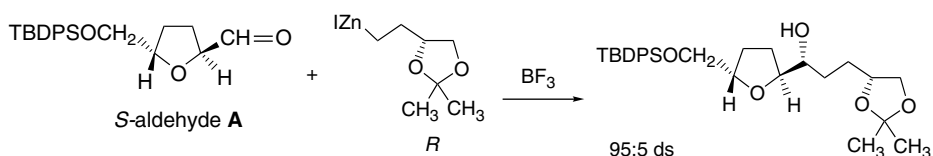


Another example involves addition of an organozinc reagent to a tetrahydrofuran aldehyde. With achiral aldehydes, only a small preference for formation of one enantiomer is seen.

<sup>180</sup> P. B. Hitchcock, B. A. Starkmann, and D. W. Young, *Tetrahedron Lett.*, **42**, 2381 (2001).

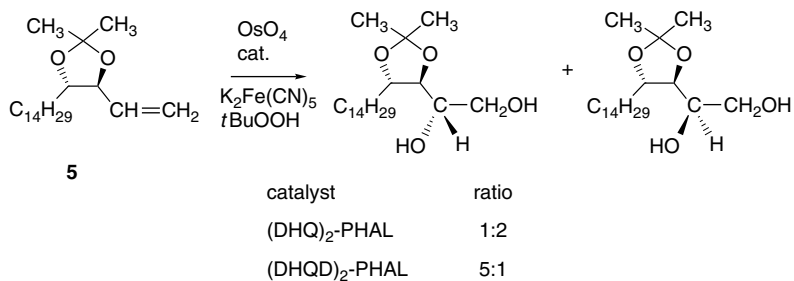


When a chiral aldehyde is used, the matched combination gives a 95:5 stereoselectivity.<sup>181</sup>



In this case, it is the stereocenter in the aldehyde that has the dominant influence on the diastereoselectivity.

In the analysis of multiple stereochemical influences, it is useful to classify the stereoselectivity as *substrate (reactant) controlled* or *reagent controlled*. For example, in the dihydroxylation of the chiral alkene **5**, the product is determined primarily by the choice of hydroxylation catalyst, although there is some improvement in the diastereoselectivity with one pair.<sup>182</sup> This is a case of *reagent-controlled* stereoselection.

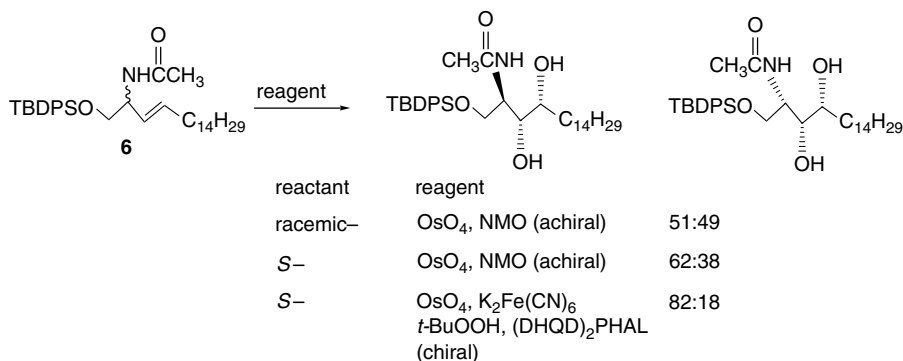


Similarly with the internal alkene **6**, the use of racemic reactant and achiral catalyst gives racemic product. Use of enantiopure *reactant* causes a modest degree of diastereoselectivity to arise from the stereocenter in the reactant. However, when a chiral catalyst is used this is reinforced by the *reagent-control*.<sup>183</sup>

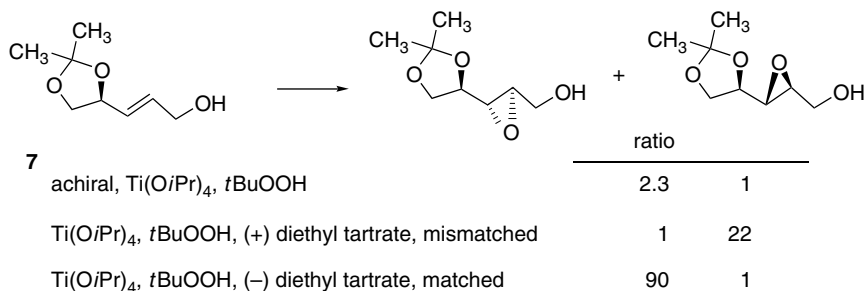
<sup>181</sup> U. Koert, H. Wagner, and U. Pindun, *Chem. Ber.*, **127**, 1447 (1994).

<sup>182</sup> R. A. Fernandes and P. Kumar, *Tetrahedron Lett.*, **41**, 10309 (2001).

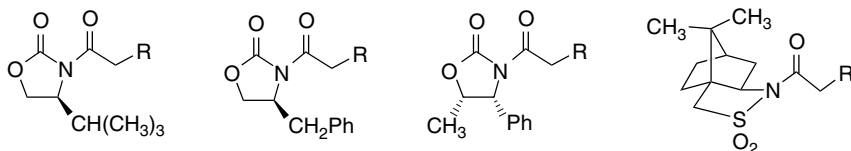
<sup>183</sup> C. Martin, W. Prunck, M. Bortolussi, and R. Bloch, *Tetrahedron: Asymmetry*, **11**, 1585 (2000).



Another example of reagent control can be found in the Sharpless epoxidation of **7**. With achiral reagents in the absence of a tartrate ligand, there is weak stereoselection. The tartrate-based catalysts control the enantioselectivity, although there is a noticeable difference between the matched and mismatched pairs.



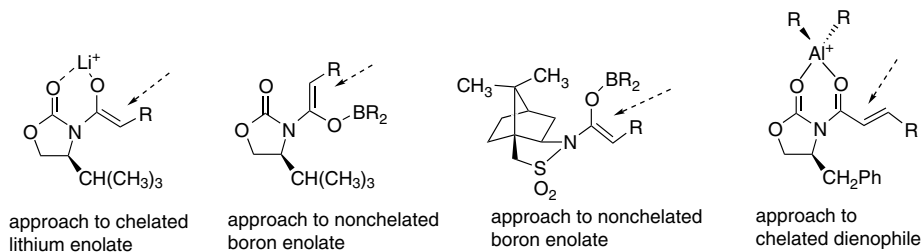
An important strategy for achieving *substrate control* is the use of *chiral auxiliaries*, which are structures incorporated into reactants for the purpose of influencing the stereochemistry. Two of the most widely used systems are oxazolidinones<sup>184</sup> derived from amino acids and sulfams<sup>185</sup> derived from camphorsulfonic acid. These groups are most often used as carboxylic acid amides. They can control facial stereoselectivity in reactions such as enolate alkylation, aldol addition, and Diels-Alder cycloadditions, among others. The substituents on the chiral auxiliary determine the preferred direction of approach.



<sup>184</sup>. D. J. Ager, I. Prakash and D. R. Schaad, *Chem. Rev.*, **96**, 835 (1996).

<sup>185</sup>. W. Oppolzer, J. Blagg, I. Rodriguez, and E. Walther, *J. Am. Chem. Soc.*, **112**, 2767 (1990).

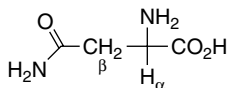
Depending upon the particular system, there may or may not be chelation between a metal cation or Lewis acid and the auxiliary. A change from a chelated to a nonchelated structure can lead to a change in the direction of approach. The configuration at the  $\alpha$ -carbon can be controlled in this way. We will see many examples of the implementation of this strategy in subsequent chapters.



## Topic 2.1. Analysis and Separation of Enantiomeric Mixtures

### 2.1.1. Chiral Shift Reagents and Chiral Solvating Agents

There are several techniques for determination of the enantiomeric purity of a chiral compound. As discussed in Section 2.1.3, the measured rotation can provide this information if the specific rotation  $[\alpha]$  is known. However, polarimetry is not very sensitive, especially if  $[\alpha]$  is relatively low. Several other methods for determining enantiomeric purity have been developed. One of the most frequently used in organic chemistry involves NMR spectroscopy with *chiral shift reagents*, which are complexes of a lanthanide metal and a chiral ligand. The reagents also have labile ligand positions that can accommodate the substance being analyzed. The lanthanides have strong affinity for oxygen and nitrogen functional groups that act as Lewis bases. The lanthanides also have the property of inducing large chemical shifts without excessive broadening of the lines.<sup>186</sup> Shift reagents can be used with both  $^1\text{H}$  and  $^{13}\text{C}$  NMR spectra. For small organic molecules the most frequently used shift reagents are  $\text{Eu}[\text{tfc}]_3$  and  $\text{Eu}[\text{nfc}]_3$  (see Scheme 2.11).<sup>187</sup> The scheme also shows some chiral shift reagents that have proven successful for analysis of amino acids and oligopeptides. Figure 2.25 shows a comparison of the NMR spectrum of asparagine with and without the chiral shift reagent.

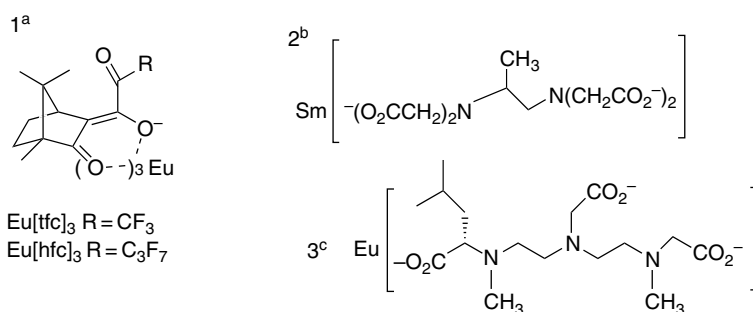


There are also several reagents that can be used to derivatize alcohols, amines, or carboxylic acids to give diastereomeric compounds. The diastereomers then give distinct NMR spectra that can be used to determine the enantiomeric ratio. Typically these compounds have at least an aryl substituent, which leads to strong shifts of signals owing to the anisotropic shielding of aromatic rings. Examples of such compounds are given in Scheme 2.12.

<sup>186</sup> D. Parker, *Chem. Rev.*, **91**, 1441 (1991); R. Rothchild, *Enantiomer*, **5**, 457 (2000).

<sup>187</sup> H. L. Goering, J. N. Eikenberry, G. S. Koerner, and C. J. Lattimer, *J. Am. Chem. Soc.*, **96**, 1493 (1974).

## Scheme 2.11. Chiral Shift Reagents



- a. H. L. Goering, J. Eikenberry, G. Koerner, and C. J. Lattimer, *J. Am. Chem. Soc.*, **96**, 1493 (1974).  
 b. A. Inamoto, K. Ogasawara, K. Omata, K. Kabuto, and Y. Sasaki, *Org. Lett.*, **2**, 3543 (2000).  
 c. M. Watanabe, T. Hasegawa, H. Miyake, and Y. Kojima, *Chem. Lett.*, **4** (2001).

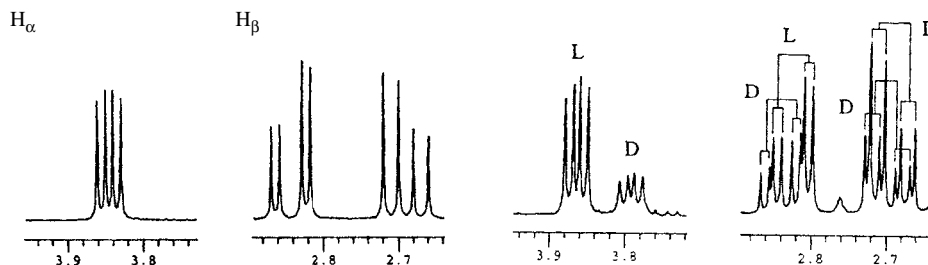
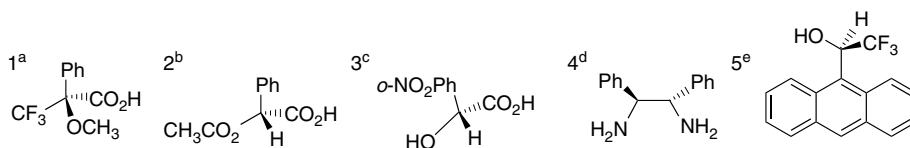


Fig. 2.25. NMR spectrum of 1:2 D:L asparagine mixture with NMR chiral shift reagent: (a) without shift reagent; (b) with shift reagent. Reproduced from *Org. Lett.*, **2**, 3543 (2000), by permission of the American Chemical Society.

## Scheme 2.12. Chiral Derivatizing and Solvating Agents



- a. J. A. Dale, D. L. Dull, and H. S. Mosher, *J. Org. Chem.*, **34**, 2543 (1969); J. A. Dale and H. S. Mosher, *J. Am. Chem. Soc.*, **95**, 512 (1973).  
 b. D. Parker, *J. Chem. Soc., Perkin Trans. 2*, 83 (1983).  
 c. M. A. Haiza, A. Sanyal, and J. K. Snyder, *Chirality*, **9**, 556 (1997).  
 d. R. Fulwood and D. Parker, *Tetrahedron: Asymmetry*, **3**, 25 (1992); R. Fulwood and D. Parker, *J. Chem. Soc., Perkin Trans. 2*, 57 (1994).  
 e. W. H. Pirkle and S. D. Beare, *J. Am. Chem. Soc.*, **91**, 5150 (1969); W. H. Pirkle and D. J. Hoover, *Top. Stereochem.*, **13**, 263 (1982).

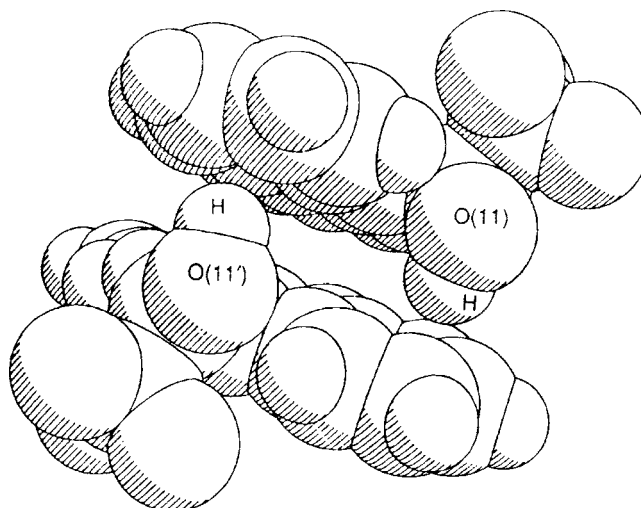


Fig. 2.26. Space-filling model of crystallographic structure of *S*-enantiomer 2,2,2-trifluoro-1-(9-anthryl)ethanol showing hydrogen bonding to the A-ring of anthracene. Reproduced from *J. Chem. Soc., Chem. Commun.*, 765 (1991), by permission of the Royal Society of Chemistry.

Chemical shifts sufficient for analysis can sometimes be achieved without the need for covalent bonding. If solvation is strong enough, the chiral additive induces sufficiently different chemical shifts in the two enantiomeric complexes to permit analysis. One such compound is called the *Pirkle alcohol* (Entry 5 in Scheme 2.12).<sup>188</sup> The structurally important features of this compound are the trifluoroethanol group, which provides a strong hydrogen bond acceptor, and the anthracene ring, which generates anisotropic shielding. In some cases, there may also be  $\pi$ - $\pi$  stacking interactions. The structure of the compound has been determined in both the crystalline state and solution. Figure 2.26 shows an intermolecular hydrogen bond between the hydroxyl group and the anthracene ring for the *S*-enantiomer.<sup>189</sup>

Various amines and amides that can serve as hydrogen bond donors are used as chiral solvating agents for carboxylic acids and alcohols. One example is 1,2-diphenylethane-1,2-diamine (Entry 4 in Scheme 2.12).<sup>190</sup> The alkaloid quinine also shows enantioselective solvation with certain alcohols.<sup>191</sup> It is also possible to design molecules to act as chiral receptors, such as structure **8**, which incorporates a binding environment for the carboxylic acid group and gives good NMR resolution of chiral and prochiral carboxylic acids.<sup>192</sup>

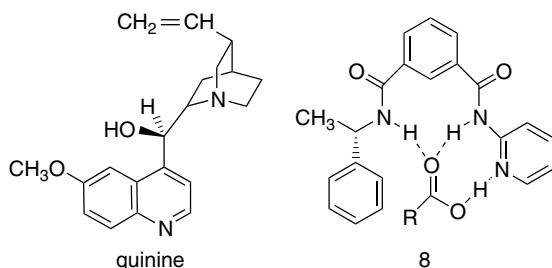
<sup>188</sup> W. H. Pirkle and S. D. Beare, *J. Am. Chem. Soc.*, **91**, 5150 (1969); W. H. Pirkle and D. J. Hoover, *Top. Stereochem.*, **13**, 263 (1982).

<sup>189</sup> H. S. Rzepa, M. L. Webb, A. M. Z. Slawin, and D. J. Williams, *J. Chem. Soc., Chem. Commun.*, 765 (1991); M. L. Webb and H. S. Rzepa, *Chirality*, **6**, 245 (1994).

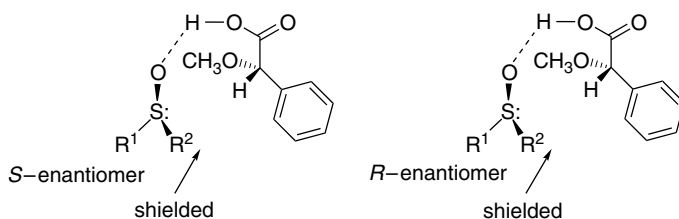
<sup>190</sup> R. Fulwood and D. Parker, *Tetrahedron: Asymmetry*, **3**, 25 (1992); R. Fulwood and D. Parker, *J. Chem. Soc., Perkin Trans.*, **2**, 57 (1994); S. E. Yoo and S. I. Kim, *Bull. Kor. Chem. Soc.*, **17**, 673 (1996).

<sup>191</sup> C. Rosini, G. Uccello-Barretta, D. Pini, C. Abete, and P. Salvadori, *J. Org. Chem.*, **53**, 4579 (1988).

<sup>192</sup> T. Stork and G. Helmchen, *Rec. Trav. Chim. Pays-Bas*, **114**, 253 (1995).



Sulfoxides form hydrogen-bonded complexes with  $\alpha$ -methoxyphenylacetic acid, which results in differential shielding of the two substituents.<sup>193</sup>



### T.2.1.2 Separation of Enantiomers

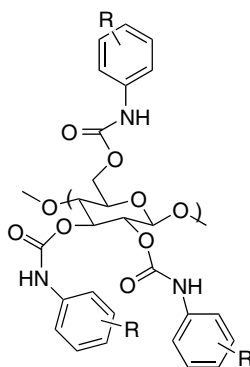
The classical method for separating enantiomers is to form diastereomeric compounds using a stoichiometric amount of a *resolving agent*. This method was described in Section 2.1.8. In this section, we discuss methods of resolution based on physical separations, including chromatography with chiral packing materials and capillary electrophoresis.

**T.2.1.2.1. Separation by Chromatography.** Chromatography is an important means of separating enantiomers on both an analytical and preparative scale. These separations are based on use of a *chiral stationary phase* (CSP). Chromatographic separations result from differential interactions of the enantiomers with the solid column packing material. The differential adsorption arises from the diastereomeric nature of the interaction between the enantiomers and the CSP. Hydrogen bonding and aromatic  $\pi$ - $\pi$  interactions often contribute to the binding.

One important type of chiral packing material is derivatized polysaccharides, which provide a chiral lattice, but separation is improved by the addition of structural features that enhance selectivity. One group of compounds includes aroyl esters and carbamates, which are called Chiralcels (also spelled Chiracel)<sup>194</sup>; two of the most important examples are the 4-methylbenzoyl ester, called Chiralcel OJ, and the 3,5-dimethylphenyl carbamate, called Chiralcel OD. There is a related series of materials derived from amylose rather than cellulose, which have the trade name Chiralpak.

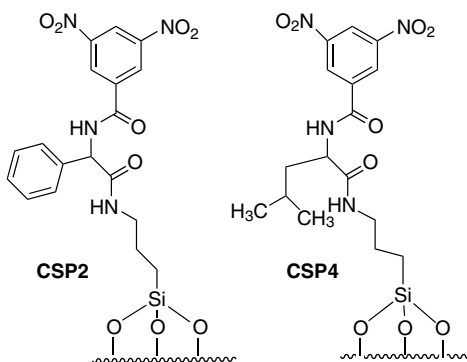
<sup>193</sup>. P. H. Buist, D. Marecak, H. L. Holland, and F. M. Brown, *Tetrahedron: Asymmetry*, **6**, 7 (1995).

<sup>194</sup>. Y. Okamoto and E. Yashima, *Angew. Chem.*, **37**, 1021 (1998).

repeating unit for *tris*-carbamoyl  
derivatives of cellulose

Related materials can be prepared in which the polysaccharides are linked to a silica support by covalently bound tether groups. For example, silica derivatized by 3-aminopropyl groups can be linked to polysaccharides using diisocyanates.<sup>195</sup> These materials seem to adopt organized structural patterns on the surface, and this factor is believed to contribute to their resolving power. The precise structural basis of the chiral recognition and discrimination of derivatized polysaccharides has not been elucidated, but it appears that in addition to polar interactions,  $\pi$ - $\pi$  stacking is important for aromatic compounds.<sup>196</sup>

Other types of CSPs, known as *brush type*, have been constructed synthetically. A chiral structure, usually an amide, is linked to silica by a tether molecule. This approach has the potential for design of the chiral recognition elements. The ability to synthetically manipulate the structures also permits investigation of the role of specific structural elements in chiral selectivity. Several synthetic CSPs were developed by W. H. Pirkle and co-workers at the University of Illinois. An important example is the 3,5-dinitrobenzoyl (3,5-DNB) derivative of *R*-phenylglycine, which is attached to silica by aminopropyl tethers (**CSP 2**). The 3,5-DNB derivatives of several other amino acids (e.g., **CSP 4**) and diamines have also been explored.<sup>197</sup>

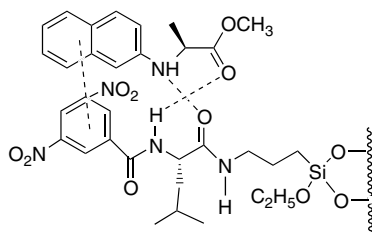
dinitrobenzoyl derivatives of amino acids  
as chiral stationary phases

<sup>195</sup> E. Yashima, H. Fukaya, and Y. Okamoto, *J. Chromatogr. A*, **677**, 11 (1994).

<sup>196</sup> C. Yamamoto, E. Yashima, and Y. Okamoto, *Bull. Chem. Soc. Jpn.*, **72**, 1815 (1999).

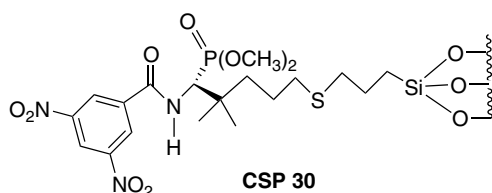
<sup>197</sup> C. J. Welch, *J. Chromatogr. A*, **666**, 3 (1994); C. J. Welch, *Adv. Chromatogr.*, **35**, 171 (1995).

These materials generally show good resolving power toward compounds that have aromatic rings and polar groups. A combination of  $\pi$ - $\pi$  interactions and hydrogen bonding is believed to be the basis of chiral recognition.<sup>198</sup> The relative electronic character of the aromatic rings is important. Complementary donor-acceptor capacity enhances selectivity.<sup>199</sup>

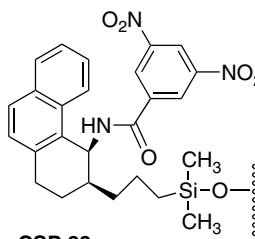


suggested recognition mechanism for  
resolution of *N*-(2-naphthyl)amino acids  
on dinitrobenzoylamino acid CSP

Several variations of these CSPs have been developed, such as the phosphonate ester **CSP 30** and the tetrahydrophenanthryl amide **CSP 33**. These compounds are used in pharmaceutical studies. The former CSP is a good resolving agent for the  $\beta$ -adrenergic blocker class of compounds, such as propranolol,<sup>200</sup> whereas the latter is a good CSP for separation of NSAIDs, such as naproxen and ibuprofen.<sup>201</sup>



**CSP 30**



**CSP 33**

**T.2.1.2.2. Resolution by Capillary Electrophoresis.** Another methodology that has been adapted to analysis of enantiomers is *capillary electrophoresis*.<sup>202</sup> The principle of electrophoretic separation is differential migration of a charged molecule in a

<sup>198</sup> W. H. Pirkle and T. C. Pochapsky, *J. Am. Chem. Soc.*, **108**, 5627 (1986); W. H. Pirkle and T. C. Pochapsky, *J. Am. Chem. Soc.*, **109**, 5975 (1987); W. H. Pirkle, J. A. Burke, III, and S. R. Wilson, *J. Am. Chem. Soc.*, **111**, 9222 (1989); M. H. Hyun, J.-J. Ryoo, and W. H. Pirkle, *J. Chromatogr. A*, **886**, 47 (2000).

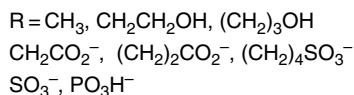
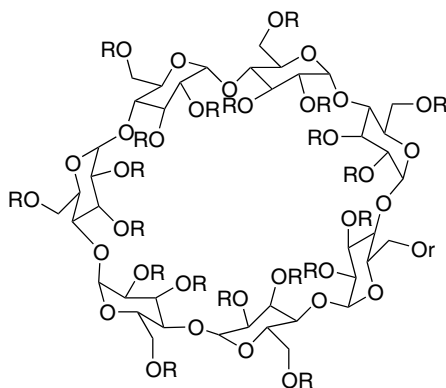
<sup>199</sup> W. H. Pirkle, T. C. Pochapsky, G. S. Mahler, D. E. Corey, D. S. Reno, and D. M. Alessi, *J. Org. Chem.*, **51**, 4991 (1986).

<sup>200</sup> W. H. Pirkle and J. A. Burke, *Chirality*, **1**, 57 (1989).

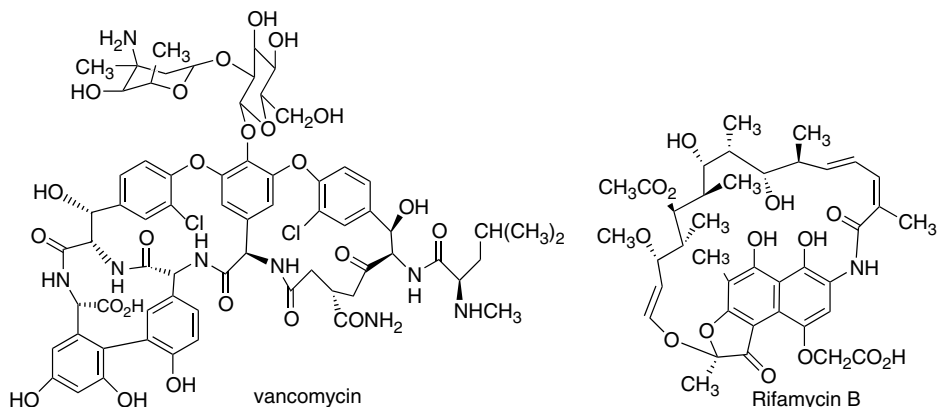
<sup>201</sup> W. H. Pirkle, C. J. Welch, and B. Lamm, *J. Org. Chem.*, **57**, 3854 (1992).

<sup>202</sup> A. Rizzi, *Electrophoresis*, **22**, 3079 (2001); G. Gubitza and M. G. Schmid, *J. Chromatogr. A*, **792**, 179 (1997).

polymer matrix under the influence of an electric field. Gel electrophoresis, a very important bioanalytical technique, is done in a polyacrylamide gel and depends on molecular size and charge differences to achieve differential migration. This method is primarily applied to macromolecules, such as polypeptides and oligonucleotides. Capillary electrophoresis (CE) has been developed as a technique for analysis of small chiral molecules, especially drugs. The most widely applied method of analysis is *capillary zone electrophoresis*, in which a *chiral selector* is added to the electrolyte buffer. The difference in binding between the chiral selector and the two enantiomers being analyzed then determines the rate of migration. Among the most commonly used chiral selectors are cyclodextrins, which are cyclic oligosaccharides. The cyclodextrins can be modified to incorporate polar, anionic, or cationic groups.



Macrocyclic antibiotics such as vancomycin and rifamycin B are also used as chiral selectors.



Another approach to chiral electrophoresis involves covalent attachment of the chiral selector to either the capillary wall or the packing material.<sup>203</sup> For open columns, where the packing material is attached to the capillary wall, a completely methylated  $\beta$ -cyclodextrin is linked to the surface through a polysiloxane (Chirasil-Dex 1). The packed columns use silica bound to the methylated cyclodextrin (Chirasil-Dex 2).

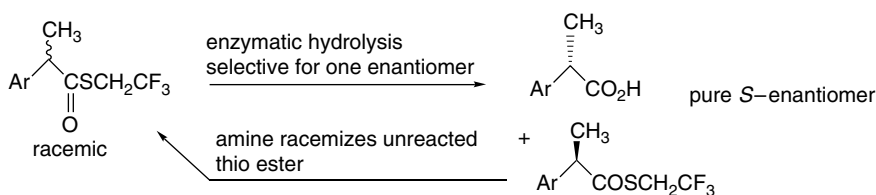
<sup>203</sup> V. Schurig and D. Wistuba, *Electrophoresis*, **20**, 2313 (1999).

The strength of CE as an analytical tool is the very high degree of enantioselection that can be achieved, along with high speed and sensitivity. It is more difficult to use CE on a preparative scale, although successful separation has been reported on the milligram scale.<sup>204</sup>

We have seen that in each of these means of enantiomeric separation, chiral recognition depends upon a combination of intermolecular forces, including electrostatic attractions, hydrogen bonding, and  $\pi$ - $\pi$  stacking. These differential interactions then lead to distinctions between the properties of the two enantiomers, such as chemical shifts in NMR methods or relative mobility in chiral chromatography and electrophoresis. There is much current interest in both the analysis of these interactions and manipulation of structure to increase selectivity.

## Topic 2.2. Enzymatic Resolution and Desymmetrization

Enzymatic resolution is based on the ability of enzymes (catalytic proteins) to distinguish between *R*- and *S*-enantiomers or between enantiotopic pro-*R* and pro-*S* groups in prochiral compounds.<sup>205</sup> The selective conversion of pro-*R* and pro-*S* groups is often called *desymmetrization* or *asymmetrization*.<sup>206</sup> Note that in contrast to enzymatic resolution, which can at best provide half the racemic product as resolved material, prochiral compounds can be completely converted to a single enantiomer, provided that the selectivity is high enough. Complete conversion of a racemic mixture to a single enantiomeric product can sometimes be accomplished by coupling an enzymatic resolution with another reaction (chemical or enzymatic) that racemizes the reactant. This is called *dynamic resolution*,<sup>207</sup> and it has been accomplished for several  $\alpha$ -arylpropanoic acids via the thioesters, using an amine to catalyze racemization.<sup>208</sup> Trifluoroethyl thioesters are advantageous because of their enhanced rate of exchange and racemization.



The criterion for a successful enzymatic resolution is that one enantiomer be a preferred substrate for the enzyme. Generally speaking, the enantioselectivity is quite high, since enzyme-catalyzed reactions typically involve a specific fit of the reactant (substrate) into the catalytically active site. The same necessity for a substrate fit, however, is the primary limitation on enzymatic resolution. The compound to be

<sup>204</sup>. F. Glukhovskiy and G. Vigh, *Electrophoresis*, **21**, 2010 (2000); A. M. Stalcup, R. M. C. Sutton, J. V. Rodrigo, S. R. Gratz, E. G. Yanes, and P. Painuly, *Analyst*, **125**, 1719 (2000).

<sup>205</sup>. C. J. Sih and S. H. Wu, *Top. Stereochem.*, **19**, 63 (1989).

<sup>206</sup>. E. Schoffers, A. Golebiowski, and C. R. Johnson, *Tetrahedron*, **52**, 3769 (1996).

<sup>207</sup>. S. Caddick and K. Jenkins, *Chem. Soc. Rev.*, **25**, 447 (1996); H. Stecher and K. Faber, *Synthesis*, **1** (1997).

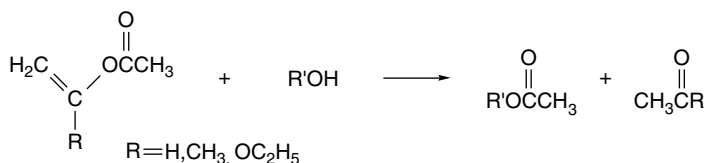
<sup>208</sup>. L. S. Chang, S. W. Tsai, and J. Kuo, *Biotechnol Bioeng.*, **64**, 120 (1999); C. Y. Chen, Y. S. Chang, S. A. Lin H.-I. Wen, Y.-C. Cheng, and S.-W. Tsai, *J. Org. Chem.*, **67**, 3323 (2002); P.-J. Um and D. G. Drueckhammer, *J. Am. Chem. Soc.*, **120**, 5605 (1998).

resolved must be an acceptable substrate for the enzyme. If not, there will be no reaction with either enantiomer. The types of reactions that are suitable for enzymatic resolutions are somewhat limited. The most versatile enzymes—*esterases* and *lipases*—catalyze formation or hydrolysis of esters. There are also enzymes that catalyze amide formation and hydrolysis, which can be broadly categorized as *acylases* or *amidases*. We also discuss *epoxide hydrolases*, which open epoxide rings. Another important family is the *oxido-reductases*, which interconvert alcohols and carbonyl compound by oxidation and reduction.

### T.2.2.1. Lipases and Esterases

The most widely applied enzymes for resolution are lipases and esterases, which can catalyze either the hydrolysis or the formation of esters.<sup>209</sup> The natural function of these enzymes is to catalyze hydrolysis of fatty acid esters of glycerol. There are a number of such enzymes that are commercially available. A very important property of these esterases and lipases is that they can accept a fairly wide variety of molecules as substrates. They are also adaptable for use in organic solvents, which further enhances their practical utility.<sup>210</sup>

The esterases and lipases are members of a still larger group of enzymes that catalyze acyl transfer, either in the direction of solvolysis or by acylation of the substrate. Both types of enzymes are called *hydrolases*. In water, hydrolysis occurs, but in the presence of alcohols, transesterification can occur. Reactions in the acylation direction are done in the presence of acyl donors. Esters of enols such as vinyl acetate or isopropenyl acetate are often used as sources of the acyl group. These enol esters are more reactive than alkyl esters, and the enol that is displaced on acyl transfer is converted to acetaldehyde or acetone. To avoid side products arising from these carbonyl compounds, one can use 1-ethoxyvinyl esters, which give ethyl acetate as the by-product.<sup>211</sup>



The esterases, lipases, and other enzymes that catalyze acyl transfer reactions share a common mechanism. The active site in these enzymes involves a *catalytic triad* consisting of the imidazole ring from a histidine, the hydroxyl group of a serine, and a carboxy group from an aspartic acid.<sup>212</sup> The three moieties, working together, effect transfer of an acyl group to the serine. In solvolysis, this acyl group is then transferred to the solvent, whereas in acylation it is transferred to the substrate. The mechanism is outlined in Figure 2.27. We discuss the catalytic mechanisms of these triads in more detail in Section 7.5.

<sup>209</sup> P. Andersch, M. Berger, J. Hermann, K. Laumen, M. Lobell, R. Seemayer, C. Waldinger, and M. P. Schneider, *Meth. Enzymol.*, **286**, 406 (1997).

<sup>210</sup> A. M. Klibanov, *Acc. Chem. Res.*, **23**, 114 (1990); G. Carrea and S. Riva, *Angew. Chem. Int. Ed. Engl.*, **39**, 2227 (2000).

<sup>211</sup> Y. Kita, Y. Takebe, K. Murata, T. Naka, and S. Akai, *J. Org. Chem.*, **65**, 83 (2000).

<sup>212</sup> R. J. Kazlauskas and H. K. Weber, *Curr. Opinion Chem. Biol.*, **2**, 121 (1998).

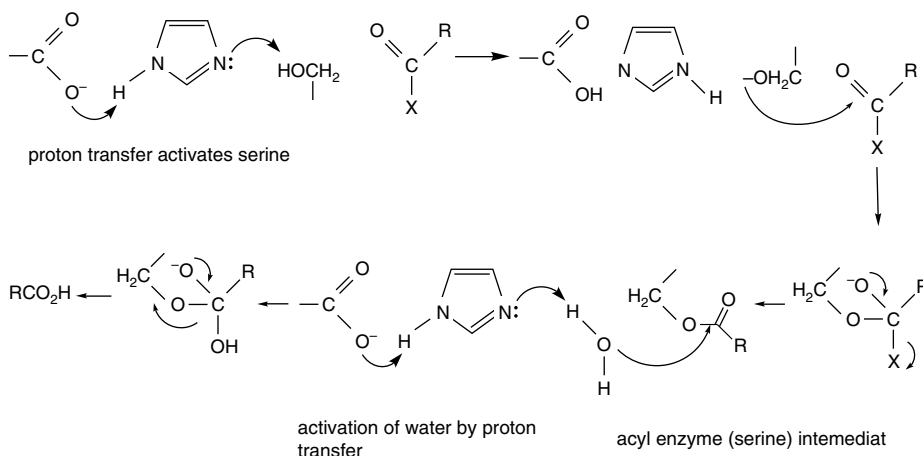


Fig. 2.27. Mechanism for carboxylate-histidine-serine triad catalysis of acyl transfer.

The most commonly used of the hydrolytic enzymes is *pig liver esterase* (PLE). The natural function of this enzyme is to hydrolyze esters during digestion and it has a fairly broad range of substrate reactivity. It has been used to resolve chiral alcohols and esters by acylation or hydrolysis, respectively. *Meso*-derivatives of succinic and glutaric acid diesters are generally good substrates for PLE and are good examples of substrates for desymmetrization. A predictive model for the stereoselectivity of PLE was developed by analysis of many cases.<sup>213</sup> The model pictures two hydrophobic pockets, one larger ( $H_L$ ) and one smaller ( $H_S$ ) and two polar pockets, one front ( $P_F$ ) and one back ( $P_B$ ). These pockets are specifically located in relation to the catalytic serine, and the fit of the substrate then determines the enantioselectivity. Alkyl and aryl groups fit into either the  $H_L$  or  $H_S$  sites based on size. The  $P_F$  site can accommodate moderately polar groups, such as the ester substituent in diesters, whereas the  $P_B$  site accepts more polar groups, including hydroxy and carbonyl groups, and excludes nonpolar groups. This model successfully correlates and predicts the results for a variety of esters and diesters. For example, Figure 2.28 shows the fit of an  $\alpha$ -sulfinyl ester into the catalytic site.<sup>214</sup>

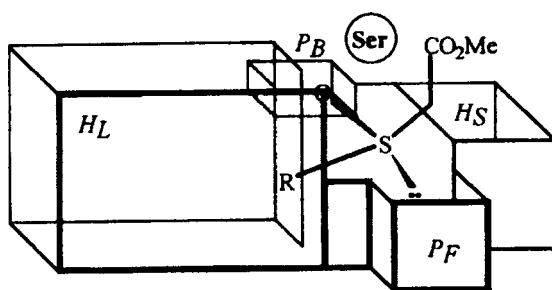


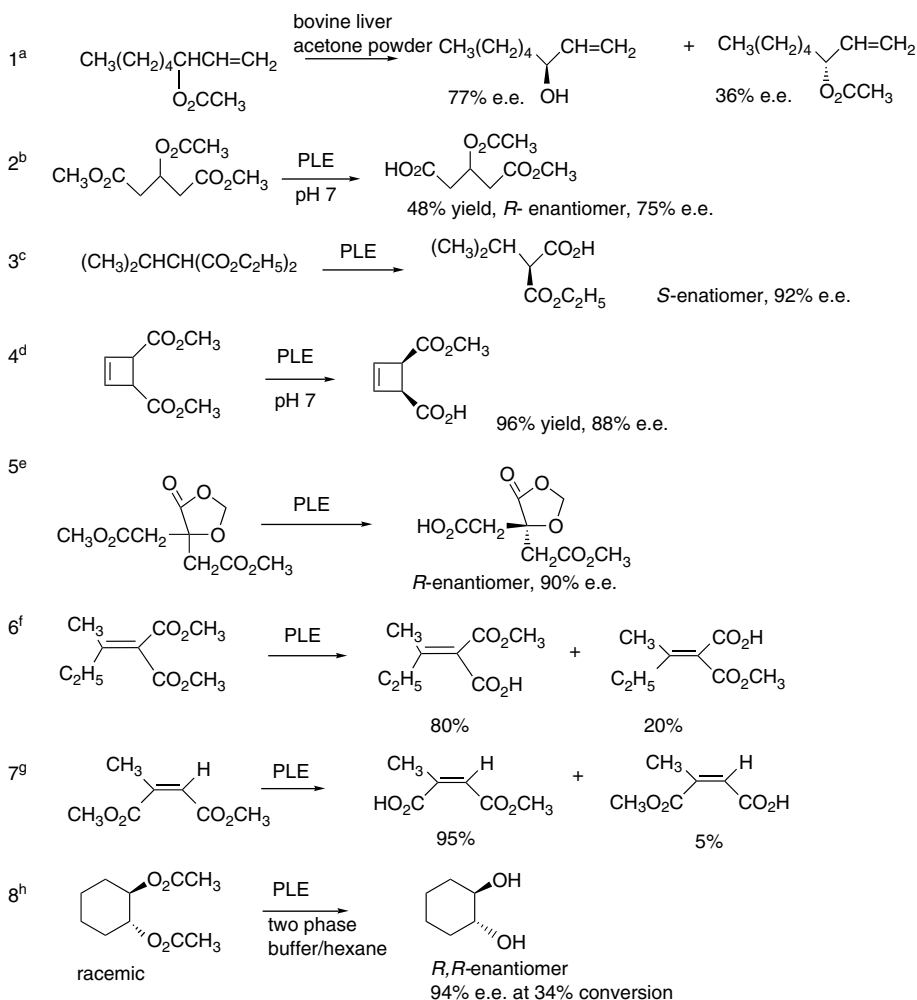
Fig. 2.28. Accommodation of preferred *S*-enantiomer of  $\alpha$ -sulfinylacetate esters in the Jones model of a PLE active site. Reproduced from *Tetrahedron: Asymmetry*, **11**, 911 (2000), by permission of Elsevier.

<sup>213</sup> E. J. Toone, M. J. Werth, and J. B. Jones, *J. Am. Chem. Soc.*, **112**, 4946 (1990); L. Provencher, H. Wynn, J. B. Jones, and A. Krawczyk, *Tetrahedron: Asymmetry*, **4**, 2025 (1993); L. Provencher and J. B. Jones, *J. Org. Chem.*, **59**, 2729 (1994).

<sup>214</sup> P. Kielbasinski, *Tetrahedron Asymmetry* **11**, 911 (2000).

Scheme 2.13 shows a few examples of resolutions and desymmetrization using esterases. Entry 1 shows the partial resolution of a chiral ester using a crude enzyme source. The enantioselectivity is only moderate. Entries 2 to 5 are examples of desymmetrization, in which prochiral ester groups are selectively hydrolyzed. Entries 6 and 7 are examples of selective hydrolysis of unsaturated esters that lead to isomeric monoesters. These cases are examples of diastereoselectivity. In Entry 8, the *R,R*-enantiomer of a racemic diester is selectively hydrolyzed. In all these cases, the

### Scheme 2.13. Representative Resolutions and Desymmetrizations Using Esterases



- a. D. Basavaiah and S. B. Raju, *Tetrahedron*, **50**, 4137 (1994).  
 b. B. Loubinoux, J.-L. Sinnes, A. C. O'Sullivan, and T. Winkler, *Tetrahedron*, **51**, 3549 (1995).  
 c. B. Klotz-Berendes, W. Kleemis, U. Jegelka, H. J. Schaefer, and S. Kotila, *Tetrahedron: Asymmetry*, **8**, 1821 (1997).  
 d. I. Harvey and D. H. G. Crout, *Tetrahedron: Asymmetry*, **4**, 807 (1993).  
 e. R. Chenevert, B. T. Ngatcha, Y. S. Rose, and D. Goupil, *Tetrahedron: Asymmetry*, **9**, 4325 (1998).  
 f. T. Schirmeister and H. H. Otto, *J. Org. Chem.*, **58**, 4819 (1993).  
 g. R. Schmid, V. Partali, T. Anthonsen, H. W. Anthonsen, and L. Kvittingen, *Tetrahedron Lett.*, **42**, 8543 (2001).  
 h. G. Caron and R. J. Kazlauskas, *J. Org. Chem.*, **56**, 7251 (1991).

stereoselectivity of the reaction is determined by the relative fit in the binding site of the esterases.

Lipases are another important group of hydrolases. The most commonly used example is porcine pancreatic lipase (PPL). Lipases tend to function best at or above the solubility limit of the hydrophobic substrate. In the presence of water, the substrate forms an insoluble phase (micelles); the concentration at which this occurs is called the *critical micellar concentration*. The enzyme is activated by a conformational change that occurs in the presence of the micelles and results in the opening of the active site. Lipases work best in solvents that can accommodate this activation process.<sup>215</sup> PPL is often used as a relatively crude preparation called “pancreatin” or “steapsin.” The active site in PPL has not been as precisely described as the one for PLE. There are currently two different models, but they sometimes make contradictory predictions.<sup>216</sup> It has been suggested that the dominant factors in binding are the hydrophobic and polar pockets (sites B and C in Figure 2.29), but that the relative location of the catalytic site is somewhat flexible and can accommodate to the location of the hydrolyzable substituent.<sup>217</sup>

A more refined model of stereoselectivity has been proposed on the basis of the X-ray structure of PPL<sup>218</sup> and the stereoselectivity toward several aryl-substituted diols. This model proposes an important  $\pi$ - $\pi$  stacking interaction between the aryl

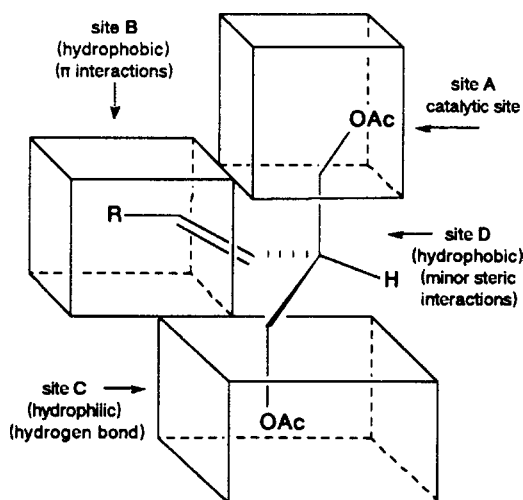


Fig. 2.29. Preferred accommodation of 2-*E*-alkenyl-1,3-propanediol diacetates in an active site model for PPL. Reproduced from *J. Org. Chem.*, **57**, 1540 (1992), by permission of the American Chemistry Society.

- <sup>215</sup> B. Rubin, *Nature Struct. Biol.*, **1**, 568 (1994); R. D. Schmid and R. Verger, *Angew. Chem. Intl. Ed. Engl.*, **37**, 1609 (1998).
- <sup>216</sup> J. Ehrler and D. Seebach, *Liebigs Ann. Chem.*, 379 (1990); P. G. Hultin and J. B. Jones, *Tetrahedron Lett.*, **33**, 1399 (1992); Z. Wimmer, *Tetrahedron*, **48**, 8431 (1992).
- <sup>217</sup> A. Basak, G. Bhattacharya, and M. H. Bdour, *Tetrahedron*, **54**, 6529 (1998). A. Basak, K. R. Rudra, H. M. Bdour, and J. Dasgupta, *Biorg. Med. Chem. Lett.*, **11**, 305 (2001); A. Basak, K. R. Rudra, S. C. Ghosh, and G. Bhattacharya, *Ind. J. Chem. B.*, **40**, 974 (2001).
- <sup>218</sup> J. Hermoso, D. Pignol, B. Kerfelec, I. Crenon, C. Chapus, and J. C. Fontecilla-Camps, *J. Biol. Chem.*, **271**, 18007 (1996); J. Hermoso, D. Pignol, S. Penel, M. Roith, C. Chapus, and J. C. Fontecilla-Camps, *EMBO J.*, **16**, 5531 (1997).

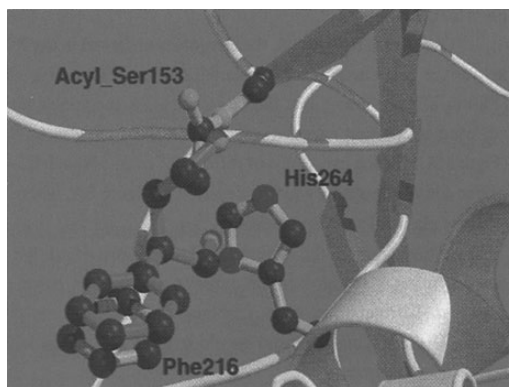
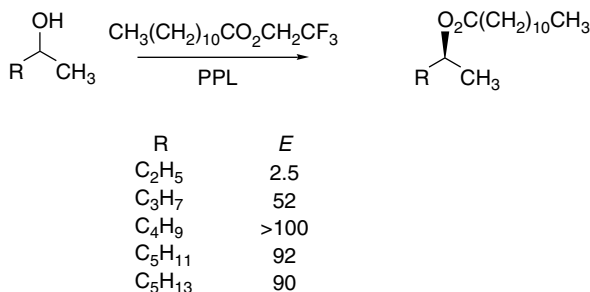


Fig. 2.30. Active site model of PPL showing the binding of 2-phenylpentane-1,4-diol in an active site. Note the  $\pi - \pi$  stacking with Phe-216 and placement of the C(4) hydroxyl near the acyl serine-153 residue. Reproduced from *Tetrahedron*, **55**, 14961 (1999), by permission of Elsevier. (See also color insert.)

group and a phenylalanine residue near the active site.<sup>219</sup> Based on the detailed protein structure, this model is consistent with the model proposed by Guanti et al.<sup>220</sup> The model (Figure 2.30) suggests a hydrophilic site and a rather selective hydrophobic site. The D site is considered to be quite flexible, whereas the B site is particularly favorable for unsaturated groups.

The enantioselectivity of PPL depends on discrimination in binding of the substrate. In the case of acylation of simple secondary alcohols, there is poor discrimination for 2-butanol, but 2-hexanol exhibits the maximal *E* value, and larger alcohols show good enantioselectivity.<sup>221</sup> (The definition of *E* is given on p. 140.)



Two other lipases of microbiological origin are also used frequently in organic chemistry. A lipase from *Pseudomonas cepacia* (formerly identified as *Pseudomonas fluorescens*) is often referred to as *lipase PS*. The binding site for this enzyme is narrower than those of the other commonly used lipases, and it often has excellent

<sup>219</sup> I. Borreguero, J. V. Sinisterra, A. Rumero, J. A. Hermoso, M. Martinez-Ripoll, and A. R. Alcantara, *Tetrahedron*, **55**, 14961 (1999).

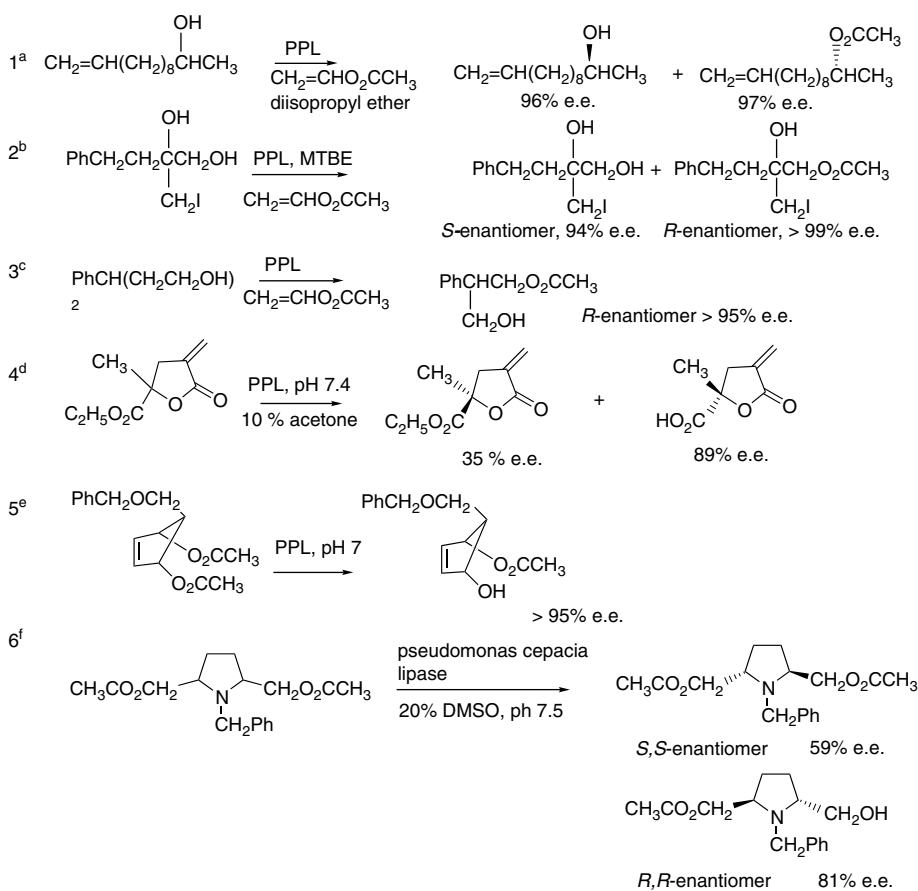
<sup>220</sup> G. Guanti, L. Banfi, and E. Narisano, *J. Org. Chem.*, **57**, 1540 (1992).

<sup>221</sup> B. Morgan, A. C. Oehschlager, and T. M. Stokes, *Tetrahedron*, **47**, 1611 (1991).

selectivity. Lipases from *Candida rugosa* (formerly *Candida cylindracea*), *C. antarctica*, and *C. lipolytica* are also used frequently.<sup>222</sup> Like the esterases, lipases can act as hydrolysis catalysts toward esters or as acylation catalysts toward alcohols. Unlike PLE, the lipases have a specific type of natural substrate, namely triacyl glycerides. They are somewhat more selective in terms of substrate than PLE. Generally, neither  $\alpha,\alpha$ -disubstituted carboxylates nor esters of tertiary alcohols are accepted as substrates. As with PLE, either kinetic resolution or desymmetrization of prochiral reactants can be achieved. The enantioselectivity of lipases depends upon discrimination between the enantiomeric substrates at the active site. A large hydrophobic site acts as the receptor for the largest nonpolar substituent.

Some examples of some lipase-catalyzed reactions are given in Scheme 2.14. The first three examples in Scheme 2.14 are acylations. Entries 1 and 2 are enantioselective

**Scheme 2.14. Representative Resolutions Using Various Lipases**



a. A. Sharma, S. Sankaranarayanan, and S. Chattopadhyay, *J. Org. Chem.*, **61**, 1814 (1996).

b. S.-T. Chen and J.-M. Fang, *J. Org. Chem.*, **62**, 4349 (1997).

c. A. Rumbero, I. Borroguero, J. V. Sinisterra, and A. R. Alcantara, *Tetrahedron*, **55**, 14947 (1999).

d. G. Pitacco, A. Sessanta, O. Santi, and E. Valentin, *Tetrahedron: Asymmetry*, **11**, 3263 (2000).

e. I. C. Cotterill, P. B. Cox, A. F. Drake, D. M. LeGrand, E. J. Hutchinson, R. Latouche, R. B. Pettman, R. J. Pryce,

S. M. Roberts, G. Ryback, V. Sik, and J. O. Williams, *J. Chem. Soc., Perkin Trans. 1*, 3071 (1991).

f. Y. Kawanami, H. Moriya, Y. Goto, K. Tsukao, and M. Hashimoto, *Tetrahedron*, **52**, 565 (1996).

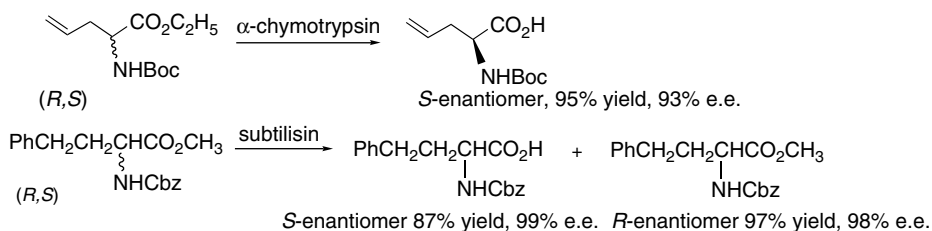
<sup>222</sup> F. Theil, *Chem. Rev.*, **95**, 2203 (1995).

acylations of a chiral secondary alcohol. Entry 3 is a desymmetrization of a 3-phenylpentane-1,5-diol. Entry 4 is a resolution of an ester group attached to a methylene- $\gamma$ -lactone. Entries 5 and 6 are desymmetrizations of diesters.

### T.2.2.2. Proteases and Acylases

*Proteases* and *acylases* have the capacity to catalyze hydrolysis and formation of amide bonds. Proteases find extensive application in analytical biochemistry.<sup>223</sup> The proteases are used to break down large proteins into polypeptides. Various proteases exhibit selectivity for particular sequences in peptides and proteins. Many of the proteases are digestive enzymes and in general they have much more stringent structural requirements for substrates than esterases and lipases. For example, chymotrypsin is selective for hydrolysis at the carboxy group of aromatic amino acids, while trypsin cleaves at the carboxy group of the basic (protonated) amino acids lysine and arginine. The proteases, like the esterases and lipases, function on the basis of a catalytic triad involving a serine, histidine, and aspartic acid.<sup>224</sup> They can catalyze formation and hydrolysis of esters as well as amides.<sup>225</sup>

Considerable attention has also been given to enantioselective enzymatic hydrolysis of esters of  $\alpha$ -amino acids. This is of particular importance as a means of preparing enantiopure samples of unusual (non-proteinaceous)  $\alpha$ -amino acids.<sup>226</sup> The readily available proteases  $\alpha$ -chymotrypsin (from bovine pancreas) and subtilisin (from *Bacillus licheniformis*) selectively hydrolyze the L-esters, leaving D-esters unreacted. These enzymatic hydrolysis reactions can be applied to *N*-protected amino acid esters, such as those containing *t*-Boc<sup>227</sup> and Cbz<sup>228</sup> protecting groups.



Much of the interest in acylases originated from work with the penicillins. Structurally modified penicillins can be obtained by acylation of 6-aminopenicillamic acid. For example, the semisynthetic penicillins such as amoxicillin and ampicillin are obtained using enzymatic acylation.<sup>229</sup> Acylases are used both to remove the phenylacetyl group from the major natural penicillin, penicillin G, and to introduce the modified acyl substituent.

<sup>223</sup> A. J. Barrett, N. D. Rawlings, and J. F. Woessner, eds., *Handbook of Proteolytic Enzymes*, 2nd Edition, Elsevier, 2004.

<sup>224</sup> L. Polgar in *Mechanisms of Protease Action*, CRC Press, Boca Raton, FL, Chap. 3, 1989; J. J. Perona and C. S. Craik, *Protein Sci.*, 4 337 (1995).

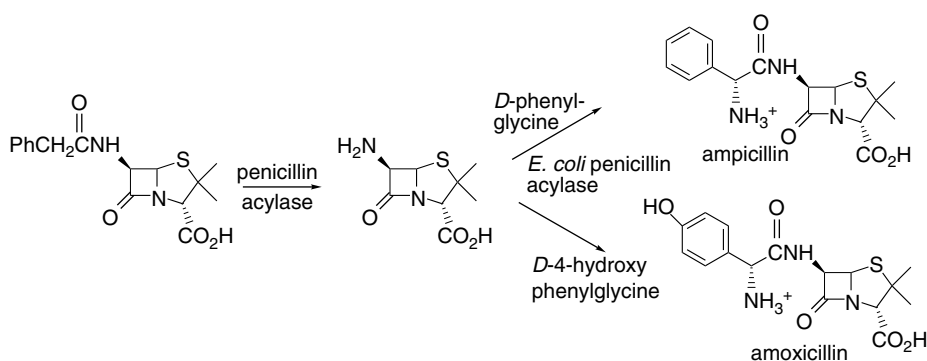
<sup>225</sup> K. Watanabe and S. Ueji, *J. Chem. Soc., Perkin Trans. 1*, 1386 (2001); T. Ke, C. R. Westcott, and A. M. Klivanov, *J. Am. Chem. Soc.*, **118**, 3366 (1996).

<sup>226</sup> T. Miyazawa, *Amino Acids*, **16**, 191 (1999).

<sup>227</sup> B. Schricker, K. Thirring, and H. Berner, *Biorg. Med. Chem. Lett.*, **2**, 387 (1992).

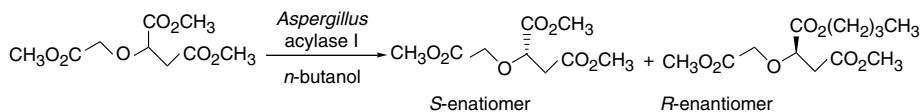
<sup>228</sup> S.-T. Chen, S.-Y. Chen, S.-C. Hsiao, and K.-T. Wang, *Biotechnol. Lett.*, **13**, 773 (1991).

<sup>229</sup> A. Bruggink, E. C. Roos, and E. de Vroom, *Org. Process Res. Dev.*, **2**, 128 (1998).

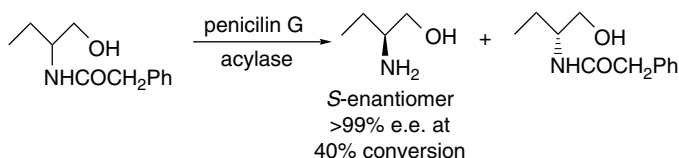


Similar reactions are used in preparation of the related cephalosporin antibiotics.

A related group of acylases catalyzes amide formation and hydrolysis. *Aspergillus* is one source of such enzymes. One class of substrates is made up of di- and triesters with  $\alpha$ -heteroatom substituents. Such substrates show selectivity for the carboxy group that is  $\alpha$  to the heteroatom, which is the position analogous to the amide bond in peptides.

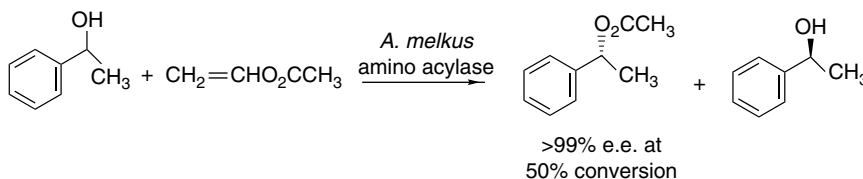


Ref. 230



Ref. 231

Acylases can be used to catalyze esterification of alcohols. These reactions are usually carried out by using vinyl esters. The selectivity (*E*) values for such reactions can be quite high.



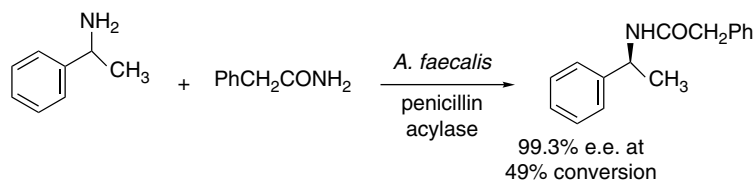
Ref. 232

<sup>230</sup> A. Liljeblad, R. Aksela, and L. T. Kanerva, *Tetrahedron: Asymmetry*, **12**, 2059 (2001).

<sup>231</sup> N. W. Fadnavis, M. Sharfuddin, and S. K. Vadivel, *Tetrahedron: Asymmetry*, **10**, 4495 (1999).

<sup>232</sup> M. Bakker, A. S. Spruijt, F. van Rantwijk, and R. A. Sheldon, *Tetrahedron: Asymmetry*, **11**, 1801 (2000).

Enantioselective acylation of amines is generally more challenging and less explored, although good results have been reported in some cases. A number of 1-phenylethylamines and 4-phenylbutane-2-amine were resolved using an acylase from *Alcaligenes faecalis*.



Ref. 233

### T.2.2.3. Epoxide Hydrolases

Epoxide hydrolases (EH) catalyze the hydrolytic ring opening of epoxides to diols. The natural function of the epoxide hydrolases seems to be to detoxify epoxides, and they have a fairly broad range of acceptable substrates. The epoxide hydrolases use a catalytic triad active site, reminiscent of the lipases and esterases. In the hydrolases, however, an aspartate carboxylate, rather than a serine hydroxy, functions as the nucleophile to open the epoxide ring. The glycol monoester intermediate is then hydrolyzed, as shown in Figure 2.31. According to this mechanism, and as has been experimentally confirmed, the oxygen that is introduced into the diol originates in the aspartate carboxylate group.<sup>234</sup>

There are several forms of EHs that have been used to effect enantioselective opening of epoxides. One commonly used form is isolated as a crude microsomal preparation from rodent livers. EH can also be isolated from bacteria, fungi, and yeasts.<sup>235</sup> The structure of the EH from *Agrobacterium radiobacter* AD1 has been solved by X-ray crystallography.<sup>236</sup> In this enzyme, the catalytic triad involves His-275, Asp-107, and Tyr-152 and/or Tyr-215. The tyrosine functions as a general acid

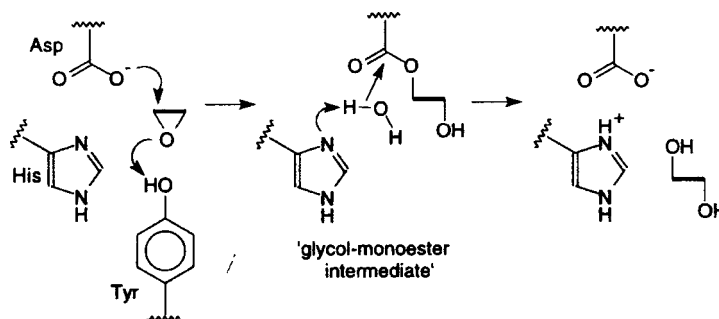


Fig. 2.31. Proposed mechanism of microsomal epoxide hydrolase.

- <sup>233</sup> D. T. Guranda, L. M. van Langen, F. van Rantwijk, R. A. Sheldon, and V. K. Svedas, *Tetrahedron: Asymmetry*, **12**, 1645 (2001).
- <sup>234</sup> G. M. Lacourciere and R. N. Armstrong, *J. Am. Chem. Soc.*, **115**, 10466 (1993); B. Borhan, A. D. Jones, F. Pinot, D. F. Grant, M. J. Kurth, and B. D. Hammock, *J. Biol. Chem.*, **270**, 26923 (1995).
- <sup>235</sup> C. A. G. M. Weijers and J. A. M. de Bont, *J. Mol. Catal. B, Enzymes*, **6**, 199 (1999).
- <sup>236</sup> M. Nardini, I. S. Ridder, H. J. Rozeboom, K. H. Kalk, R. Rink, D. B. Janssen, and B. W. Dijkstra, *J. Biol. Chem.*, **274**, 14579 (1999); M. Nardini, R. B. Rink, D. B. Janssen, and B. W. Dijkstra, *J. Mol. Catal. B, Enzymatic*, **11**, Spec. Issue, 1035 (2001).

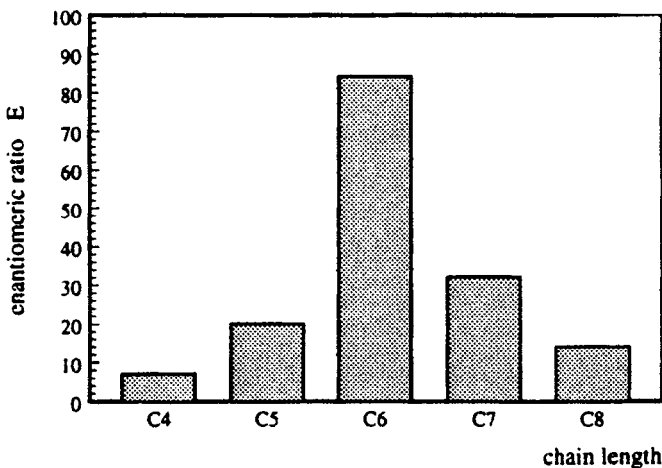


Fig. 2.32. Effect of chain length on enantioselectivity ratio  $E$  for unbranched monosubstituted epoxides. Reproduced from *Tetrahedron: Asymmetry*, **9**, 467 (1998), by permission of Elsevier.

catalyst. A crystal structure has also been determined for the *Aspergillus niger* EH.<sup>237</sup> The essential amino acids in these and other EHs have been identified by site-specific mutagenesis experiments.<sup>238</sup>

One of the more extensively investigated EHs is from the fungus *Aspergillus niger*.<sup>239</sup> The best studied of the yeast EH is from *Rhodotorula glutina*,<sup>240</sup> which can open a variety of mono-, di-, and even trisubstituted epoxides. The  $E$  values for simple monosubstituted epoxides show a sharp maximum in selectivity for the hexyl substituent, as can be seen in Figure 2.32. This indicates that there is a preferential size for binding of the hydrophobic groups.

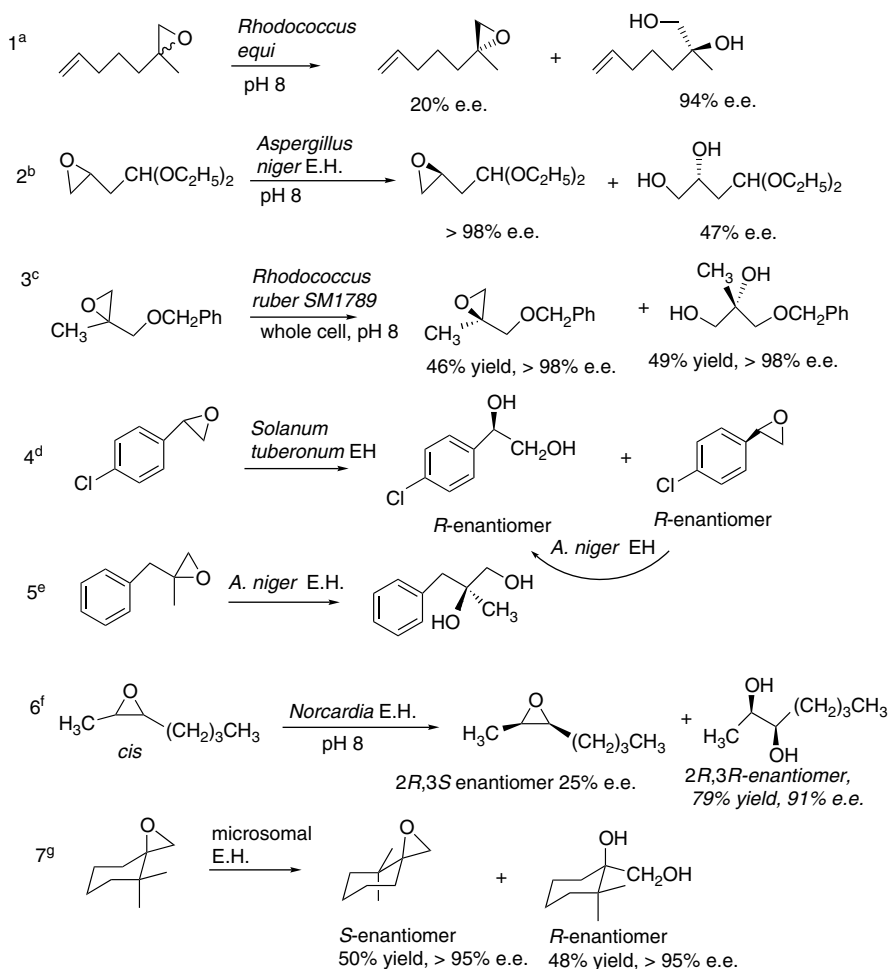
Scheme 2.15 gives some examples of the use of epoxide hydrolases in organic synthesis. Entries 1 to 3 are kinetic resolutions. Note that in Entry 1 the hydrolytic product is obtained in high e.e., whereas in Entry 2 it is the epoxide that has the highest e.e. In the first case, the reaction was stopped at 18% conversion, whereas in the second case hydrolysis was carried to 70% completion. The example in Entry 3 has a very high  $E$  ( $> 100$ ) and both the unreacted epoxide and diol are obtained with high e.e. at 50% conversion. Entry 4 shows successive use of two separate EH reactions having complementary enantioselectivity to achieve nearly complete

<sup>237</sup> J. Y. Zou, B. M. Halberg, T. Bergfors, F. Oesch, M. Arnold, S. L. Mowbry, and T. A. Jones, *Structure with Folding and Design*, **8**, 111 (2000).

<sup>238</sup> H. F. Tzeng, L. T. Laughlin, and R. N. Armstrong, *Biochemistry*, **37**, 2905 (1998); R. Rink, J. H. L. Spelberg, R. J. Pieters, J. Kingma, M. Nardini, R. M. Kellogg, B. K. Dijkstra, and D. B. Janssen, *J. Am. Chem. Soc.*, **121**, 7417 (1999); R. Rink, J. Kingma, J. H. L. Spelberg, and D. B. Janssen, *Biochemistry*, **39**, 5600 (2000).

<sup>239</sup> S. Pedragosa-Moreau, A. Archelas, and R. Furstoss, *J. Org. Chem.*, **58**, 5533 (1993); S. Pedragosa-Moreau, C. Morisseau, J. Zylber, A. Archelas, J. Baratti, and R. Furstoss, *J. Org. Chem.*, **61**, 7402 (1996); S. Pedragosa-Moreau, A. Archelas, and R. Furstoss, *Tetrahedron*, **52**, 4593 (1996).

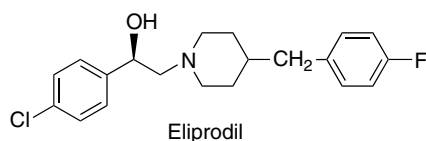
<sup>240</sup> C. A. G. M. Weijers, *Tetrahedron: Asymmetry*, **8**, 639 (1997); C. A. G. M. Weijers, A. L. Botes, M. S. van Dyk, and J. A. M. de Bont, *Tetrahedron: Asymmetry*, **9**, 467 (1998).



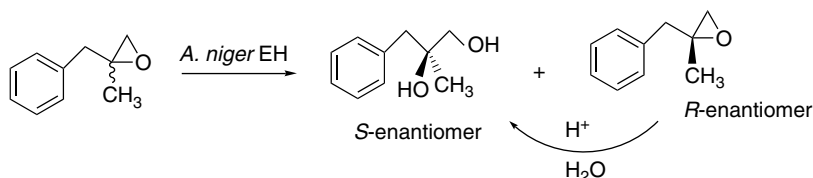
- a. W. Kroutil, I. Osprian, M. Mischitz, and K. Faber, *Synthesis*, 156 (1997).  
 b. C. Guerard, F. Alphand, A. Archelas, C. Demuyneck, L. Hecquet, R. Furstoss, and J. Bolte, *Eur. J. Org. Chem.*, 3399 (1999).  
 c. A. Steinreiber, H. Hellstrom, S. F. Mayer, R. V. A. Orru, and K. Faber, *Synlett*, 111 (2001).  
 d. K. B. Manoj, A. Archelas, J. Baratti, and R. Furstoss, *Tetrahedron*, **57**, 695 (2001).  
 e. R. V. A. Orru, I. Osprian, W. Kroutil, and K. Faber, *Synthesis*, 1259 (1998).  
 f. W. Kroutil, M. Mischitz, and K. Faber, *J. Chem. Soc., Perkin Trans. 1*, 3629 (1997).  
 g. G. Bellucci, C. Chiappe, G. Ingrosso, and C. Rosini, *Tetrahedron: Asymmetry*, **6**, 1911 (1995).

conversion of 4-chlorophenyloxirane to the *R*-enantiomer, which is used to prepare the drug Eliprodil.<sup>241</sup> This compound is a glutamate antagonist that has promising neuro-protective activity in the treatment of stroke. First, an EH from *Solanum tuberosum* that hydrolyzes the *S*-enantiomer was used, leaving the *R*-enantiomer unchanged. When the reaction is complete, *Aspergillus niger* EH converts the *R*-enantiomer to the *R*-3-diol, which can be converted to the *R*-epoxide by chemical means.

<sup>241</sup> K. M. Manoj, A. Archelas, J. Baratti, and P. Furstoss, *Tetrahedron*, **57**, 695 (2001).



Entry 5 is an interesting example that entails both enzymatic and hydrolytic epoxide conversion. In the first step, an enzymatic hydrolysis proceeds with *retention* of the configuration at the tertiary center. This reaction is selective for the *S*-epoxide. The remaining *R*-epoxide is then subjected to acid-catalyzed hydrolysis, which proceeds with *inversion* at the center of chirality (see p. 186). The combined reactions give an overall product yield of 94%, having 94% e.e.<sup>242</sup>



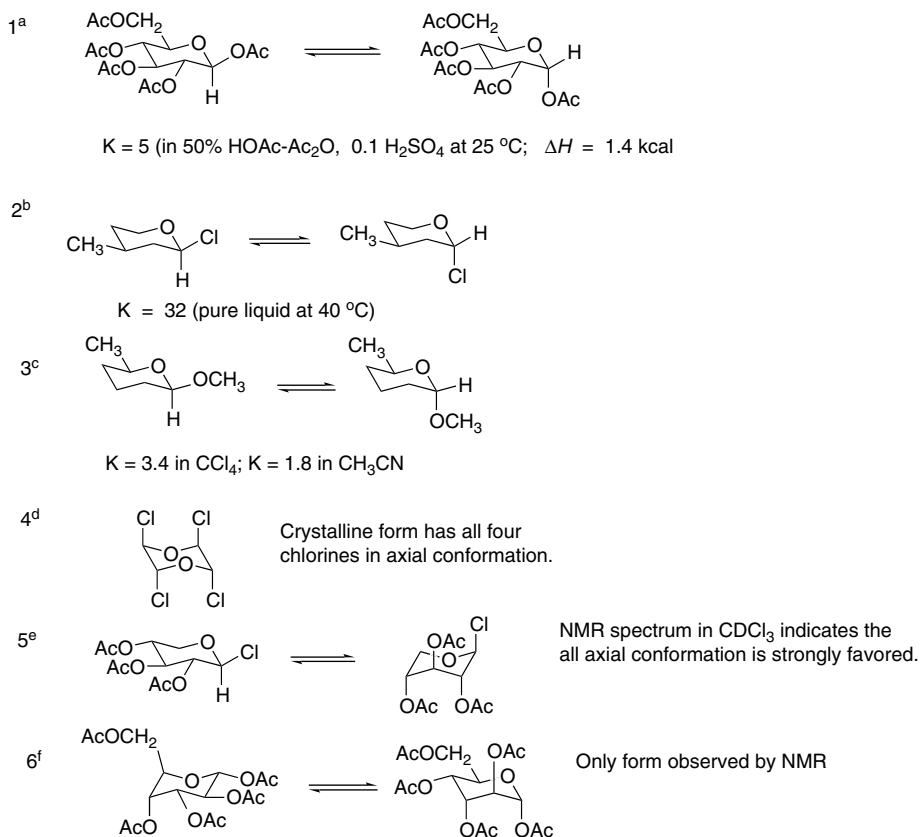
Entry 6 is one of several examples demonstrating enantioselectivity for both the *cis* and *trans* isomers of heptane-2,3-epoxide. Entry 7 shows the kinetic resolution of an exocyclic cyclohexane epoxide. The two stereoisomeric monomethyl analogs were only partially resolved and the 3-methyl isomer showed no enantioselectivity. This shows that the steric or hydrophobic effect of the dimethyl substituents is critical for selective binding.

### Topic 2.3. The Anomeric Effect in Cyclic Compounds

The incorporation of heteroatoms into rings can result in stereoelectronic effects that significantly affect conformation and, ultimately, reactivity. It is known from many examples in carbohydrate chemistry that pyranose (six-membered oxygen-containing rings) sugars substituted with an electron-withdrawing group such as halogen or alkoxy at C(2) are often more stable when the substituent has an axial rather than an equatorial orientation. This tendency is not limited to carbohydrates but carries over to simpler ring systems such as 2-substituted tetrahydropyrans. The phenomenon is known as the *anomeric effect*, since it involves a substituent at the anomeric position in carbohydrate pyranose rings.<sup>243</sup> Scheme 2.16 lists several compounds that exhibit the anomeric effect, along with some measured equilibrium compositions. In Entries 1 to 3, the

<sup>242</sup>. R. V. Orru, I. Osprian, W. Kroutil, and K. Faber, *Synthesis*, 1259 (1998).

<sup>243</sup>. For reviews, see R. U. Lemieux, *Pure Appl. Chem.* **25**, 527 (1971); W. A. Szarek and D. Horton, eds., *Anomeric Effects*, ACS Symposium Series, No. 87, American Chemical Society, Washington, DC, 1979; A. J. Kirby, *The Anomeric Effect and Related Stereoelectronic Effects at Oxygen*, Springer-Verlag, Berlin, 1983; P. Deslongchamps, *Stereoelectronic Effects in Organic Chemistry*, Pergamon Press, Oxford, 1983; M. L. Sinot, *Adv. Phys. Org. Chem.*, **24**, 113 (1988); P. R. Graczyk and M. Mikolajczyk, *Top. Stereochem.*, **21**, 159 (1994); E. Juraisti and G. Cuevas, *The Anomeric Effect*, CRC Press, Boca Raton, FL, 1995; C. J. Cramer, *Theochem*, **370**, 135 (1996).



a. W. A. Bonner, *J. Am. Chem. Soc.*, **73**, 2659 (1951).

b. C. B. Anderson and D. T. Tepp, *J. Org. Chem.*, **32**, 607 (1967).

c. E. L. Eliel and C. A. Giza, *J. Org. Chem.*, **33**, 3754 (1968).

d. E. W. M. Rutten, N. Nibbering, C. H. MacGillavry, and C. Romers, *Rec. Trav. Chim. Pays-Bas*, **87**, 888 (1968).

e. C. V. Holland, D. Horton, and J. S. Jewell, *J. Org. Chem.*, **32**, 1818 (1967).

f. B. Coxon, *Carbohydrate Res.*, **1**, 357 (1966).

equilibria are between diastereoisomers and involve reversible dissociation of the 2-substituent. In all cases, the more stable isomer is written on the right. The magnitude of the anomeric effect depends on the nature of the substituent and decreases with increasing dielectric constant of the medium.<sup>244</sup> The effect of the substituent can be seen by comparing the related 2-chloro- and 2-methoxy substituted tetrahydropyrans in Entries 2 and 3. The 2-chloro compound exhibits a significantly greater preference for the axial orientation than the 2-methoxy. Entry 3 also provides data relative to the effect of solvent polarity, where it is observed that the equilibrium constant is larger in carbon tetrachloride ( $\epsilon = 2.2$ ) than in acetonitrile ( $\epsilon = 37.5$ ).

Compounds in which conformational, rather than configurational, equilibria are influenced by the anomeric effect are depicted in Entries 4 to 6. X-ray diffraction studies have unambiguously established that all the chlorine atoms of *trans*, *cis*, *trans*-2,3,5,6-tetrachloro-1,4-dioxane occupy axial sites in the crystal (Entry 4). Each chlorine

<sup>244</sup> K. B. Wiberg and M. Marquez, *J. Am. Chem. Soc.*, **116**, 2197 (1994).

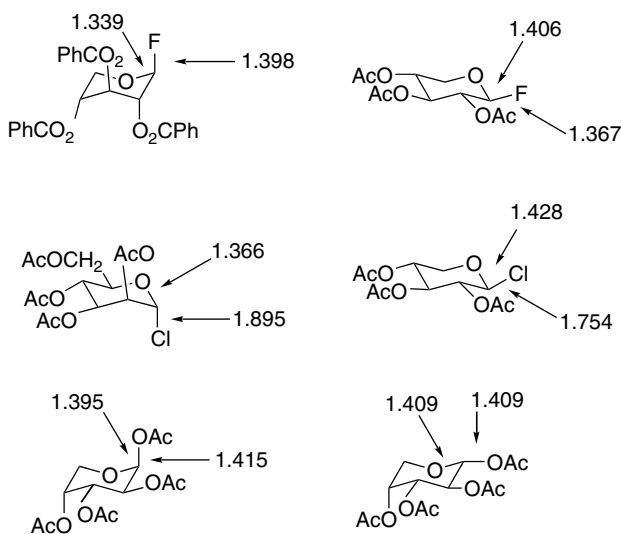
in the molecule is bonded to an anomeric carbon and is subject to the anomeric effect. Equally striking is the observation that all the substituents of the tri-*O*-acetyl- $\beta$ -D-xylopyranosyl chloride shown in Entry 5 are in the axial orientation *in solution*. Here, no special crystal packing forces can favor the preferred conformation. The anomeric effect of a single chlorine is sufficient to drive the equilibrium in favor of the conformation that puts the three acetoxy groups in axial positions.

Changes in bond lengths are also frequently observed in connection with the anomeric effect. The exocyclic bond is shortened and the ring C–O bond to the anomeric center is lengthened. Scheme 2.17 shows some comparisons.

In 2-alkoxytetrahydropyran derivatives there is a correlation between the length of the exocyclic C–O bond and the nature of the oxygen substituent. Figure 2.33 shows bond length data for a series of monocyclic and bicyclic 2-aryloxytetrahydropyran derivatives. The more electron withdrawing the group, the longer the bond to the exocyclic oxygen and the shorter the ring C–O bond. This indicates that the extent of the anomeric effect *increases with the electron-accepting capacity of the exocyclic oxygen*.<sup>245</sup>

Several structural factors have been considered as possible causes of the anomeric effect. In localized valence bond terminology, there is a larger dipole-dipole repulsion between the polar bonds at the anomeric carbon in the equatorial conformation.<sup>246</sup> This dipole-dipole interaction is reduced in the axial conformation and this factor contributes to the solvent dependence of the anomeric effect. The preference for the axial orientation is highest in nonpolar solvent effects, where the effect of dipolar

Scheme 2.17. Bond Distances in Å at Anomeric Carbons<sup>a</sup>



a. From H. Paulsen, P. Luger, and F. P. Heiker, *Anomeric Effect: Origin and Consequences*, W. A. Szarek and D. Horton, eds., ACS Symposium Series No. 87, American Chemical Society, 1979, Chap.5.

<sup>245</sup>. A. J. Briggs, R. Glenn, P. G. Jones, A. J. Kirby, and P. Ramaswamy, *J. Am. Chem. Soc.* **106**, 6200 (1984).

<sup>246</sup>. J. T. Edward, *Chem. Ind.* (London), 1102 (1955).

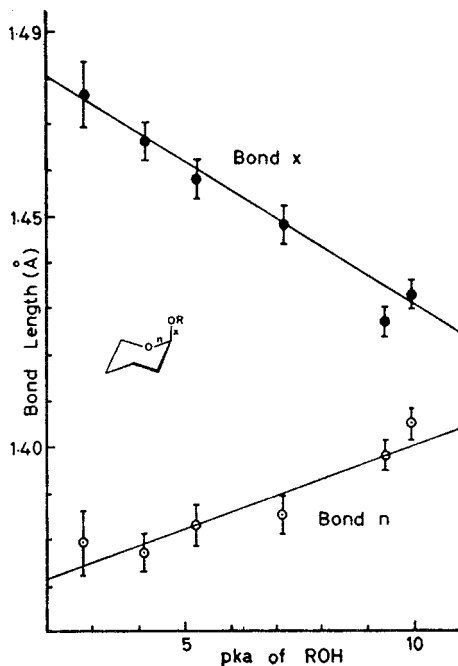
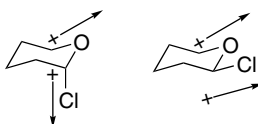


Fig. 2.33. Relationship between  $pK_a$  of alkoxy substituents and bond lengths in anomeric systems. The points represented are (left to right) 2,4-dinitrophenyl, 3,5-dinitrophenyl, 2,5-dinitrophenyl, 4-nitrophenyl\*, 4-chlorophenyl\*, and phenyl\*. For the groups marked with an asterisk, the data are from a bicyclic structure. Reproduced from *J. Am. Chem. Soc.*, **106**, 6200 (1984), by permission of the American Chemical Society.

interactions would be strongest. For example, Table 2.7 shows the solvent dependence of 2-methoxytetrahydropyran.<sup>247</sup>



In general, electrostatic interactions alone do not seem to be sufficient to account for the magnitude of the anomeric effect and do not directly explain the bond length changes that are observed.<sup>248</sup> These factors led to the proposal that the anomeric effect is, at least in part, due to  $\sigma \rightarrow \sigma^*$  hyperconjugation effects.<sup>249</sup> From the molecular orbital viewpoint, the anomeric effect is expressed as resulting from an interaction

<sup>247</sup> R. U. Lemieux, A. A. Pavia, J. C. Martin, and K. A. Watanabe, *Can. J. Chem.*, **47**, 4427 (1969).

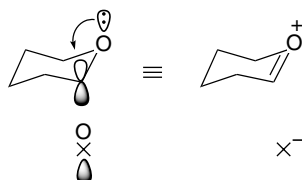
<sup>248</sup> C. Altona, C. Knobler, and C. Romers, *Acta Cryst.*, **16**, 1217 (1963); C. Altona and C. Romers, *Acta Cryst.*, **16**, 1225 (1963).

<sup>249</sup> C. Romers, C. Altona, H. R. Buys, and E. Havinga, *Top. Stereochem.*, **4**, 39 (1969).

**Table 2.7. Solvent Dependence of Conformational Equilibrium for 2-Methoxytetrahydropyran**

Solvent	Dielectric constant	% Axial conformer
CCl <sub>4</sub>	2.2	83
Benzene	2.3	82
Chloroform	4.7	71
Acetone	20.7	72
Methanol	32.6	69
Acetonitrile	37.5	68
Water	78.5	52

between the lone-pair electrons on the pyran oxygen and the  $\sigma^*$  orbital associated with the bond to the electronegative substituent.<sup>250</sup> When the C–X bond is axial, an interaction between an occupied  $p$ -type orbital on oxygen (unshared electrons) and the antibonding  $\sigma^*$  orbital of the C–X combination is possible. This interaction permits delocalization of the unshared electrons and would be expected to shorten and strengthen the C–O bond while lengthening and weakening the C–X bond, as is observed. These are the same structural factors identified in Topic 1.2, where the effect of hyperconjugation on conformation of acyclic compounds is discussed.



There have been various studies aimed at determining the energy differences associated with the anomeric effect. Temperature-dependent <sup>13</sup>C-NMR chemical shift studies of 2-methoxytetrahydropyran determined  $\Delta G$  values ranging from 0.5 to 0.8 kcal/mol, depending on the solvent.<sup>251</sup> Wiberg and Marquez measured a difference of 1.2 kcal/mol between the axial and equatorial methoxy group in the conformationally biased 3,5-dimethyltetrahydropyran ring.<sup>244</sup> The energy difference decreased in more-polar solvents; the equatorial isomer is preferred in water.

There have also been a number of computational investigations into the nature of the anomeric effect. The axial-equatorial conformational equilibria for 2-fluoro and 2-chlorotetrahydropyran have been investigated with several MO calculations, including the MP2/6-31G\* level. The MP2/6-31G\* calculations give values of 3.47 and 2.84 kcal/mol, respectively, for the energy favoring the axial conformer.<sup>252</sup> Solvent effects were also explored computationally and show the usual trend of reduced stability for the axial conformation as solvent polarity increases. Salzner and Schleyer applied

<sup>250</sup>. S. Wolfe, A. Rauk, L. M. Tel, and I. G. Csizmaida, *J. Chem. Soc. B*, 136 (1971); S. O. David, O. Eisenstein, W. J. Hehre, L. Salem, and R. Hoffmann, *J. Am. Chem. Soc.* **95**, 306 (1973); F. A. Van-Catledge, *J. Am. Chem. Soc.*, **96**, 5693 (1974).

<sup>251</sup>. H. Booth, J. M. Dixon, and S. A. Readshaw, *Tetrahedron*, **48**, 6151 (1992).

<sup>252</sup>. I. Tvaroska and J. P. Carver, *J. Phys. Chem.*, **98**, 6452 (1994).

**Table 2.8. Calculated Energy Differences for Tetrahydropyrans (kcal/mol)**

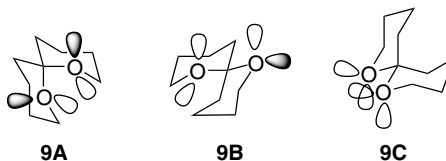
Substituent	$\Delta E_{\text{total}}$	$\Delta E_{\text{local}}$	$\Delta E_{\text{deloc}}$
F	2.8	-1.2	4.0
CH <sub>3</sub> O	1.5	-0.3	1.8
HO	1.3	-0.5	1.8
H <sub>2</sub> N	-2.8	-6.4	3.6
H <sub>3</sub> N <sup>+</sup>	-3.0	-15	12
Cl	2.5	-5.4	7.9

an NBO analysis (see Section 1.4.2) to separate steric, polar, and other localized effects from the delocalization components of the anomeric effect.<sup>253</sup> Using MP2/6-31G\* level calculations, they arrived at the results in Table 2.8.

According to this analysis, the  $\sigma \rightarrow \sigma^*$  ( $\Delta E_{\text{deloc}}$ ) interaction is stabilizing for all substituents. However, opposing electrostatic and steric effects ( $\Delta E_{\text{local}}$ ) are larger for the NH<sub>2</sub> and NH<sub>3</sub><sup>+</sup> groups. Cortes and co-workers carried out a similar analysis for 1,3-dioxanes using B3LYP/6-31G(*d,p*) computations. The results are shown in Table 2.9

The B3LYP computations arrive at much larger values than found for the tetrahydropyrans, especially for the Cl and H<sub>3</sub>N<sup>+</sup> substituents, although there are also large compensating localization effects. These theoretical efforts provide support for  $\sigma \rightarrow \sigma^*$  delocalization as a component of the anomeric effect, although leaving uncertainty as to the relative energies that are involved.

In bicyclic systems such as **9**, the dominant conformation is the one with the maximum anomeric effect. In the case of **9**, only conformation **9A** provides the preferred *anti*-periplanar geometry for both oxygens.<sup>254</sup> *Anti* periplanar relationships are indicated by the shaded oxygen orbitals. Other effects, such as torsional strain and nonbonded repulsion contribute to the conformational equilibrium, of course.

**Table 2.9. Calculated Energy Differences in 1,3-Dioxanes (kcal/mol)**

Substituent	$\Delta E_{\text{total}}$	$\Delta E_{\text{local}}$	$\Delta E_{\text{deloc}}$
F	4.0	1.66	2.34
CH <sub>3</sub> O	2.30	5.17	2.87
HO	-0.98	2.06	3.04
H <sub>2</sub> N	1.75	6.01	-4.26
H <sub>3</sub> N <sup>+</sup>	-1.32	-52.67	51.36
Cl	6.79	-12.69	19.45

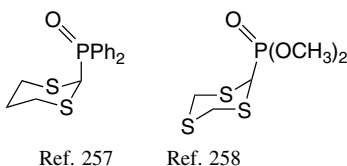
<sup>253</sup> U. Salzner and P. v. R. Schleyer, *J. Org. Chem.*, **59**, 2138 (1994).

<sup>254</sup> P. Deslongchamps, D. D. Rowan, N. Pothier, G. Sauve, J. K. Saunders *Can. J. Chem.*, **59**, 1132 (1981).

Anomeric effects are also observed for elements in the heavier rows of the periodic table. For example, *trans*-2,3-dichloro-1,4-dithiane exists in the diaxial conformation.<sup>255</sup>



Tetravalent phosphorus groups prefer axial orientations in 1,3-dithianes and 1,3,5-trithianes. NMR studies have indicated a preference of about 1 kcal for the diphenylphosphoryl group. When combined with the conformational energy in a cyclohexane ring, this suggests an anomeric effect of around 3 kcal.<sup>256</sup>



The anomeric effect is not limited to six-membered ring compounds. In five-membered rings the anomeric effect can affect both ring and substituent conformation. The 1,3-dioxole ring adopts a puckered conformation as a result of an anomeric effect.<sup>259</sup> Similar effects are observed, although attenuated, in 1,3-benzodioxoles.<sup>260</sup>



The anomeric effect is also believed to be an important factor in the conformation of ribonucleosides. The anomeric effect with the exocyclic nitrogen is stronger when the heterocyclic base is in the pseudoaxial position. Steric factors, on the other hand, favor the pseudoequatorial conformation. By analysis of the pH-dependent conformational equilibria, a contribution from the anomeric effect of as much as 5.6 kcal for adenosine and 9.0 kcal for guanosine has been suggested.<sup>261</sup>

<sup>255</sup> H. T. Kalf and C. Romers, *Acta Cryst.*, **18**, 164 (1965).

<sup>256</sup> E. Juaristi, N. A. Lopez-Nunez, R. S. Glass, A. Petsom, R. O. Hutchins, and J. P. Stercho, *J. Org. Chem.*, **51**, 1357 (1986).

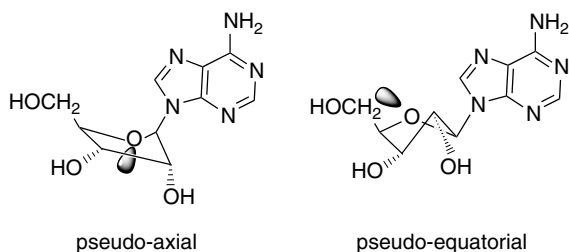
<sup>257</sup> E. Juaristi, L. Valle, C. Mora-Uzeta, B. A. Valenzuela, P. Joseph-Nathan, and M. Fredrich, *J. Org. Chem.*, **47**, 5038 (1982).

<sup>258</sup> M. Mikolajczyk, M. Balczewski, K. Wroblewski, J. Karolak-Wojciechowska, A.J. Miller, M. W. Wiczorek, M. Y. Antipin, and Y. T. Struchkov, *Tetrahedron*, **40**, 4885 (1984).

<sup>259</sup> D. Suarez, T. L. Sordo, and J. A. Sordo, *J. Am. Chem. Soc.*, **118**, 9850 (1996).

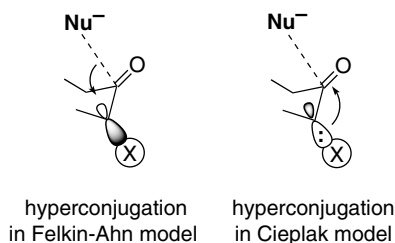
<sup>260</sup> S. Sakurai, N. Meinander, K. Morris, and J. Laane, *J. Am. Chem. Soc.*, **121**, 5056 (1999).

<sup>261</sup> J. Plavec, C. Thibaudeau, and J. Chattopadhyaya, *Pure Appl. Chem.*, **68**, 2137 (1996); I. Luyten, C. Thibaudeau, and J. Chattopadhyaya, *J. Org. Chem.*, **62**, 8800 (1997).



### Topic 2.4. Polar Substituent Effects in Reduction of Carbonyl Compounds

The stereoselectivity of hydride reduction was discussed in terms of steric approach and torsional effects in Section 2.4.1.2. Two additional factors have to be considered when polar substituents are present. The polar substituents enhance the importance of hyperconjugation involving  $\sigma$  and  $\sigma^*$  orbitals. Polar substituents also introduce bond dipoles and the potential for electrostatic interactions. Both the hyperconjugative and dipolar interactions depend on the equatorial or axial orientation of the substituent. There are two contrasting views of the nature of the hyperconjugative effects. One is the *Felkin-Ahn model*, which emphasizes stabilization of the developing negative charge in the forming bond by interaction with the  $\sigma^*$  orbital of the substituent. The preferred alignment for this interaction is with an axial position and the strength of the interaction should increase with the electron-accepting capacity of the substituent.<sup>262</sup> The Cieplak model<sup>263</sup> emphasizes an alternative interaction in which the  $\sigma$  orbital of the C–X bond acts as a donor to the developing antibonding orbital.<sup>264</sup> It has been pointed out that both of these interactions can be present, since they are not mutually exclusive, although one should dominate.<sup>265</sup> Moreover, hydride reductions involve *early transition states*. The electronic effects of substituents on the reactant should be more prominent than effects on the TS.



There have been computational efforts to understand the factors controlling axial and equatorial approaches. A B3LYP/6-31G\* calculation of the TS for addition of lithium hydride to cyclohexanone is depicted in Figure 2.34.<sup>266</sup> The axial approach is

<sup>262</sup> N. T. Ahn, *Top. Current Chem.*, **88**, 145 (1980).

<sup>263</sup> A. S. Cieplak, *J. Am. Chem. Soc.*, **103**, 4540 (1981).

<sup>264</sup> Both the Felkin-Ahn and Cieplak models are also applied to alkyl substituents.

<sup>265</sup> H. Li and W. J. le Noble, *Recl. Trav. Chim. Pays-Bas*, **111**, 199 (1992).

<sup>266</sup> T. Senju, and S. Tomoda, *Chem. Lett.*, 431 (1997).

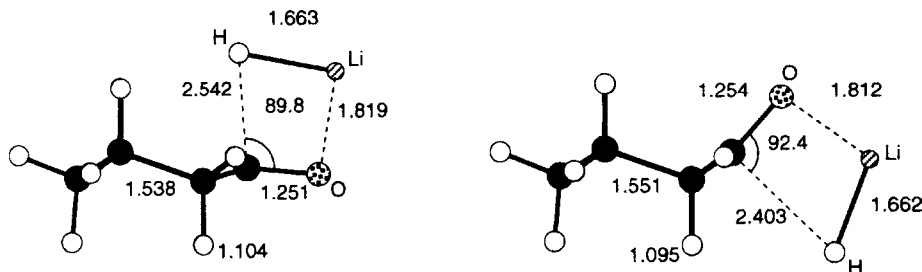
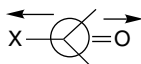


Fig. 2.34. B3LYP/6-31G\* transition structures for axial and equatorial addition of LiH to cyclohexanone. Reproduced from *Chem. Lett.*, 431 (1997).

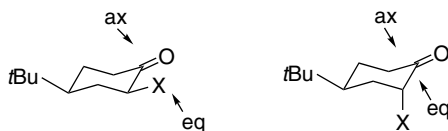
found to be 1.7 kcal more stable, in good agreement with the experimental ratio of 9:1. About half of the energy difference between the two TSs can be attributed to the torsional effect (see p. 177). An NBO analysis was applied to search for hyperconjugative interactions. The Felkin-Ahn interactions were minimal. The Cieplak effect was evident, but was similar in both the axial and equatorial approach TSs, raising doubts that it could determine the stereoselectivity.

Polar substituents may also affect stereoselectivity through an electrostatic effect that depends on the size and orientation of the bond dipole. These are relatively easy to determine for the ground state molecule but may be altered somewhat in the TS. The dipole from an electronegative substituent prefers to be oriented *anti* to the carbonyl substituent.



Rosenberg and co-workers approached the problem of separating the hyperconjugative and electrostatic interactions by examining the product ratios for NaBH<sub>4</sub> reduction of both axially and equatorially oriented substituents in 4-*t*-butylcyclohexanones.<sup>267</sup> The product ratios were used to calculate the energy difference,  $\Delta\Delta G$  (kcal/mol), for axial and equatorial approach. The results are given in Table 2.10.

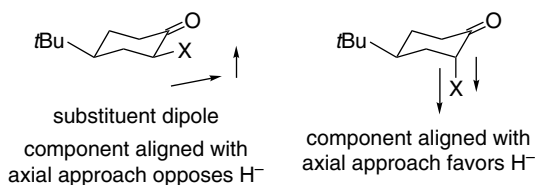
**Table 2.10. Percent Axial and Equatorial Approach in Reduction of 2-Substituted 4-*t*-Butylcyclohexanones**



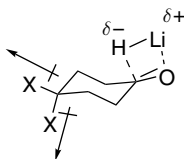
Substituent	% Equatorial	% Axial	$\Delta\Delta G$ (kcal/mol)	% Equatorial	% Axial	$\Delta\Delta G$ (kcal/mol)
H	9	91	0	9	91	0
CH <sub>3</sub>	11	89	0.12	5	95	-0.35
OCH <sub>3</sub>	67	33	1.64	8	92	-0.08
F	40	60	1.04	9	91	0
Cl	34	66	0.90	0.9	99.1	-1.30
Br	29	71	0.77	1.4	98.6	1.05

<sup>267</sup> R. E. Rosenberg, R. L. Abel, M. D. Drake, D. J. Fox, A. K. Ignatz, D. M. Kwiat, K. M. Schaal, and P. R. Virkle, *J. Org. Chem.*, **66**, 1694 (2001).

The equatorial substituents all shift the ratio toward an increased equatorial approach in the order  $\text{CH}_3\text{O} \gg \text{F} > \text{Cl} > \text{Br} \gg \text{CH}_3$ . All axial substituents except F, which has no effect, favor increasing axial attack in the order  $\text{F} < \text{CH}_3\text{O} < \text{CH}_3 < \text{Br} < \text{Cl}$ . These results can be at least partially explained in terms of an electrostatic interaction between the dipole of the substituent and the approaching nucleophile. In the case of the equatorial substituents, the fraction of the dipole that is *opposed* to an approaching negative charge in the TS increases in the order  $\text{Cl}$  (0.28) <  $\text{F}$  (0.43) <  $\text{OCH}_3$  (0.98), which agrees with the substituent effect. The dipole for axial substituents *favours axial attack*. Here, the fractional alignment of the dipoles is  $\text{OCH}_3$  (0.49) <  $\text{Cl}$  (0.97) <  $\text{F}$  (0.98). There is an inherent preference for an axial approach in the case of the *trans* (axial) substituents, which is reinforced by Cl and Br but not by F or  $\text{OCH}_3$ . In these cases some other factor(s) must be operating.



The role of orientation of substituent dipoles is also considered to be a major factor in 3- and 4-substituted cyclohexanones. Shi and Boyd used an AIM analysis to examine stereoselectivity in 3- and 4-substituted cyclohexanones.<sup>268</sup> Little difference in charge depletion was found for the two faces of the cyclohexanone ring. Addition TSs for LiH, similar to those in Figure 2.34, were studied. Energies and charge distributions were obtained from HF/6-31G(d) and MP2/6-31G(d) calculations. Polar F and Cl substituents at C(4) reduce the TS barrier, which is in accord with experimental results. The effect for axial substituents was larger than for equatorial, so that the axial substituents are predicted to have a greater preference for axial approach. The authors suggest that the effect has its origins in the C–X bond dipoles. The axial dipole has a larger component perpendicular to the carbonyl group and favors axial approach by the hydride.

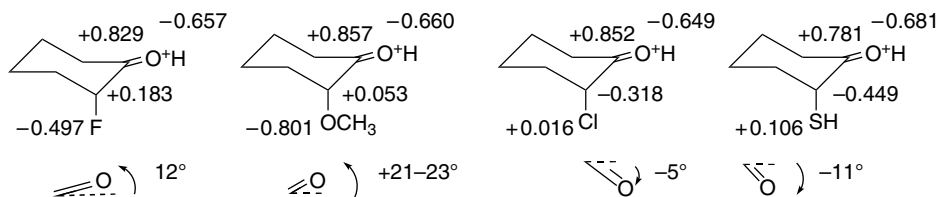


Another computational study<sup>269</sup> examined how cyclohexanone substituent electronic effects respond to Lewis acid complexation. The metal cation was modeled by a  $\text{H}^+$  (which represents the hard extreme of a Lewis acid). It was found that the complexation amplifies the effect of the  $\alpha$ -donor substituents. The computations indicate that the electron-donor substituents cause pyramidalization at the carbonyl carbon and that this then controls the direction of nucleophile approach. The results

<sup>268</sup> Z. Shi and R. J. Boyd, *J. Am. Chem. Soc.*, **115**, 9614 (1993).

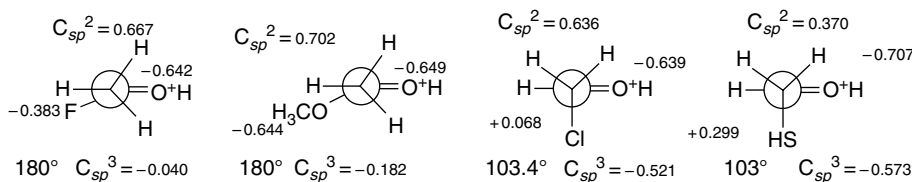
<sup>269</sup> V. K. Yadav, D. A. Jeyaraj, and R. Balamurugan, *Tetrahedron*, **56**, 7581 (2000).

are summarized below. According to NPA charge analysis, the Cl and SH substituents are significant  $\sigma$  donors and lead to movement of oxygen to the equatorial direction, favoring axial approach by the nucleophile. The oxygen and fluoro substituents have the opposite effects and favor equatorial approach. Experimental data are available for the SH, Cl, and  $\text{OCH}_3$  substituents and are in accord with these predictions. Looking at the data in Table 2.10, we see that axial  $\text{OCH}_3$  and F have little effect, whereas Cl and Br favor axial approach. These results are in agreement with the better donor capacity attributed to third-row elements in the discussion of heteroatom hyperconjugation (Topic 1.2). This study concludes that the substituents effects operate in the ground state molecule and are accentuated by coordination of a cation at oxygen.



Angle quoted is change in pyramidalization upon protonation.

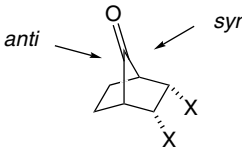
Yadav and co-workers also reported calculations aimed at comparing the relative donor ability of some heteroatom substituents.<sup>268</sup> The preferred orientation of the substituent with respect to a carbonyl group was examined using substituted acetaldehydes as the model. The calculations were done at the MP2/6-31G(*d*) level and charges were assigned by the NPA method. According to these results, methoxy and fluoro substituents are poor  $\sigma$  donors and maintain a dihedral angle of  $180^\circ$  with respect to the carbonyl, presumably reflecting the strong opposing polarity of the  $\text{C}=\text{O}$  and  $\text{C}-\text{F}$  (or  $\text{C}-\text{O}$ ) bonds. This orientation was also found for the protonated carbonyl group. On the other hand, when the carbonyl group is protonated, Cl and SH substituents assume nearly perpendicular angles that maximize hyperconjugation. They become positively charged, reflecting  $\sigma \rightarrow \pi^*$  electron donation (Cieplak model).



In contrast to the case of cyclic ketones, there is not much experimental data for polar  $\alpha$ -substituents for acyclic ketones. Moreover, in some cases, such as  $\alpha$ -methoxy, chelation effects are the dominant factor.

Electronic effects have been examined using *endo,endo*-disubstituted norbornan-7-ones. The *endo* substituents are located so that there are no direct steric interactions with the reaction site. The amount of *anti* versus *syn* approach by  $\text{NaBH}_4$  has been determined,<sup>270</sup> and the results are given in Table 2.11

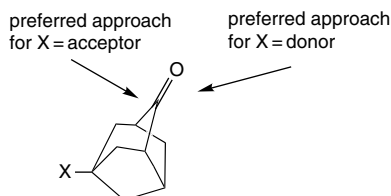
<sup>270</sup> G. Mehta, F. A. Khan, *J. Am. Chem. Soc.*, **112**, 6140 (1990); H. Li, G. Mehta, S. Padma, and W. J. le Noble, *J. Org. Chem.*, **56**, 2006 (1991); G. Mehta, F. A. Khan, B. Ganguly, and J. Chandrasekhan, *J. Chem. Soc., Perkin Trans. 2*, 2275 (1994).

**Table 2.11. Stereoselectivity in NaBH<sub>4</sub> Addition to Norbornan-7-ones**


Substituent	% <i>syn</i>	% <i>anti</i>
CH <sub>3</sub>	45	55
C <sub>2</sub> H <sub>5</sub>	20	80
CH <sub>2</sub> =CH	36	64
CH <sub>3</sub> OCH <sub>2</sub>	40	60
CH <sub>3</sub> O <sub>2</sub> C	84	16

The trend in the data is that electron-donor substituents favor *anti* addition, whereas acceptor substituents favor *syn* addition. A particularly intriguing point is that the 2,3-diethyl compound is more *anti* selective than the 2,3-dimethyl derivative. This is puzzling for any interpretation that equates the electronic effects of the methyl and ethyl groups. Two explanations have been put forward for the overall trend in the data. According to an orbital interaction (hyperconjugation) model, electron-withdrawing substituents decrease the stabilization of the LUMO (Cieplak model) and favor *syn* addition. An electrostatic argument focuses on the opposite direction of the dipole resulting from electron-releasing and electron-withdrawing substituents.<sup>271</sup> The dipoles of the electron-withdrawing groups will facilitate *syn* approach. Several levels of theory have been applied to these results.<sup>272</sup> Most recently, Yadav examined the effect using B3LYP/6-31G\*-level calculations on both the neutral and the protonated ketones.<sup>273</sup> The *anti*-periplanar orbital stabilization found for the diethyl compound was about 0.5 kcal/mol higher than for the dimethyl derivative. In this model, the resulting greater pyramidalization of the reactant accounts for the enhanced selectivity.

Adamantanone is another ketone where interesting stereoselectivity is noted. Reduction by hydride donors is preferentially *syn* to acceptor substituents at C(5) and *anti* to donor substituents.<sup>274</sup> These effects are observed even for differentially substituted phenyl groups.<sup>275</sup> As the substituents are quite remote from the reaction center, steric effects are unlikely to be a factor.



<sup>271</sup> G. Mehta, F. A. Khan, and W. Adcock, *J. Chem. Soc. Perkin Trans.*, **2**, 2189 (1995).

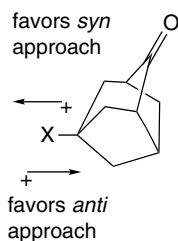
<sup>272</sup> M. N. Paddon-Row, Y.-D. Wu, and K. N. Houk, *J. Am. Chem. Soc.*, **114**, 10638 (1992); R. Ganguly, J. Chandrasekhan, F. A. Khan, and G. Mehta, *J. Org. Chem.*, **58**, 1734 (1993); G. M. Keseru, Z. Kovari, and G. Naray-Szabo, *J. Chem. Soc. Perkin Trans.*, **2**, 2231 (1996).

<sup>273</sup> V. K. Yadav, *J. Org. Chem.*, **66**, 2501 (2001); V. K. Yadav and R. Balmurugan, *J. Chem. Soc. Perkin Trans.*, **2**, 1 (2001).

<sup>274</sup> C. K. Cheung, L. T. Tseng, M.-H. Lin, S. Srivastava and W. J. Le Noble, *J. Am. Chem. Soc.*, **108**, 1598 (1986); J. M. Hahn and W. J. Le Noble, *J. Am. Chem. Soc.*, **114**, 1916 (1992).

<sup>275</sup> I. H. Song and W. J. Le Noble, *J. Org. Chem.*, **59**, 58 (1994).

These effects are attributed to differences in the  $\sigma$ -donor character of the C–C bonds resulting from the substituent (Cieplak model). Electron-attracting groups diminish the donor capacity and promote *syn* addition. An alternative explanation invokes a direct electrostatic effect arising from the C–X bond dipole.<sup>276</sup>



The arguments supporting the various substituent effects on stereoselectivity in cyclic ketones have been discussed by some of the major participants in the field in a series of review articles in the 1999 issue of *Chemical Reviews*.<sup>277</sup> While many of the details are still subject to discussion, several general points are clear. (1) For cyclohexanones, in the absence of steric effects, the preferred mode of attack by small hydride reducing agents is from the axial direction. Torsional effects are a major contributing factor to this preference. (2) When steric factors are introduced, either by adding substituents to the ketone or using bulkier reducing agents, equatorial approach is favored. Steric approach control is generally the dominant factor for bicyclic ketones. (3) In bicyclic ketones, electron donor substituents favor an *anti* mode of addition and acceptor substituents favor a *syn* approach.

The issues that remain under discussion are: (1) the relative importance of the acceptor (Felkin-Ahn) or donor (Cieplak) hyperconjugation capacity of  $\alpha$  substituents; (2) the relative importance of electrostatic effects; and (3) the role of reactant pyramidalization in transmitting the substituent effects. Arguments have been offered regarding the importance of electrostatic effects in all the systems we have discussed. Consideration of electrostatic effects appears to be important in the analysis of stereoselective reduction of cyclic ketones. Orbital interactions (hyperconjugation) are also involved, but whether they are primarily ground state (e.g., reactant pyramidalization) or transition state (e.g., orbital stabilization) effects is uncertain.

## General References

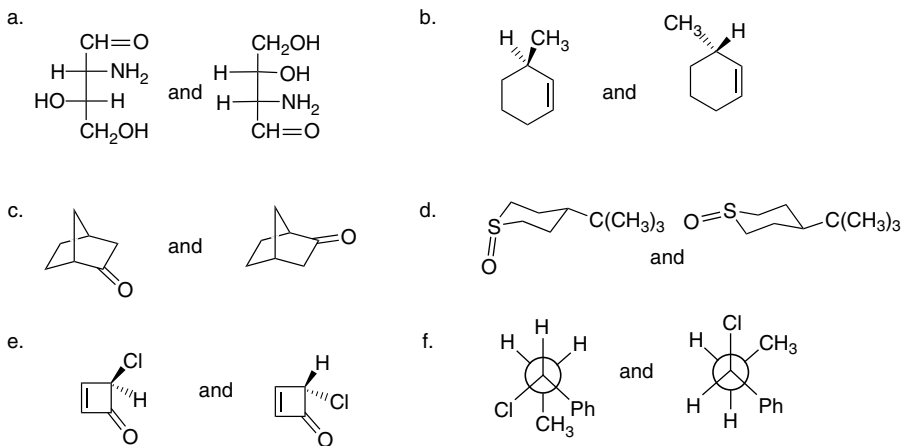
- D. Ager and M. B. East, *Asymmetric Synthetic Methodology*, CRC Press, Boca Raton, FL, 1996.  
 R. S. Atkinson, *Stereoselective Synthesis*, John Wiley & Sons, New York, 1995.  
 J. Dale, *Stereochemistry and Conformational Analysis*, Verlag Chemie, New York, 1978.  
 E. L. Eliel, N. L. Allinger, S. J. Angyal, and G. A. Morrison, *Conformational Analysis*, Wiley-Interscience, New York, 1965.  
 E. L. Eliel, S. H. Wilen, and L. N. Mander, *Stereochemistry of Organic Compounds*, John Wiley & Sons, New York, 1993.  
 E. Juaristi and G. Cuevas, *The Anomeric Effect*, CRC Press, Boca Raton, FL, 1995.  
 A. J. Kirby, *Stereoelectronic Effects*, Oxford University Press, Oxford, 1996.

<sup>276</sup> W. Adcock, J. Cotton, and N. A. Trout, *J. Org. Chem.*, **59**, 1867 (1994).

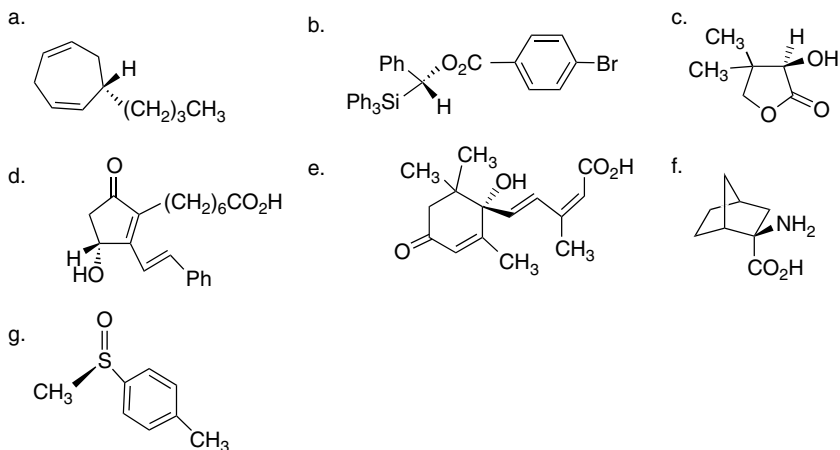
<sup>277</sup> B. W. Gung and W. G. le Noble, eds., Thematic Issue on Diastereoselection, *Chemical Reviews*, **99**, No. 5, 1999.

(References for these problems will be found on page 1156.)

2.1. Indicate whether the following pairs of compounds are identical, enantiomers, diastereomers, or structural isomers.



2.2. Use the sequence rule to specify the configuration of the stereogenic center in each of the following molecules.



2.3. Draw structural formulas for each of the following compounds, clearly showing all aspects of the stereochemistry.

- E*-3,7-dimethyl-2,6-octadien-1-ol (geraniol)
- R*-4-methyl-4-phenylcyclohex-2-enone
- L*-*erythro*-2-(methylamino)-1-phenylpropan-1-ol [(-)-ephedrine]
- 7*R*,8*S*-7,8-epoxy-2-methyloctadecane (dispalure, a pheromone of the female gypsy moth)

- e. methyl 1*S*-cyano-2*R*-phenylcyclopropanecarboxylate
- f. *Z*-2-methyl-2-buten-1-ol
- g. *E*-(3-methyl-2-pentenylidene)triphenylphosphorane

2.4. Draw the structures of the product(s) described for each reaction. Specify all aspects of the stereochemistry.

- a. stereospecific *anti* addition of bromine to *cis*- and *trans*-cinnamic acid.
- b. methanolysis of *S*-3-bromooctane with 6% racemization.
- c. stereospecific *syn* thermal elimination of acetic acid from 1*R*,2*S*-diphenylpropyl acetate
- d. stereoselective epoxidation of bicyclo[2.2.1]hept-2-ene proceeding 94% from the *exo* face.

2.5. The preferred conformation of 1-methyl-1-phenylcyclohexane has the phenyl group in the axial orientation ( $\Delta G = -0.32$  kcal/mol) even though its conformational free energy (2.9 kcal/mol) is greater than that of methyl (1.8 kcal/mol). Explain.

2.6. The computed (HF/6-31G\*) rotational profiles for acetone (2-propanone), 2-butanone, and 3-methyl-2-butanone are given in Figure 2.6P. Draw Newman projections corresponding to each clear maximum and minimum in the curves for each compound. Analyze the factors that stabilize/destabilize each conformation and discuss the differences among them.

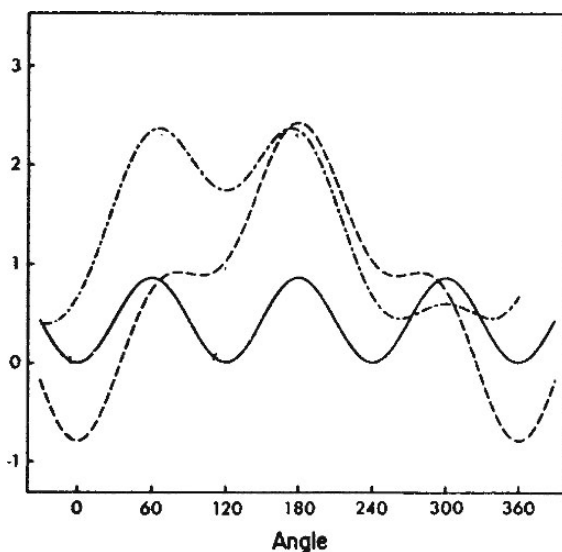
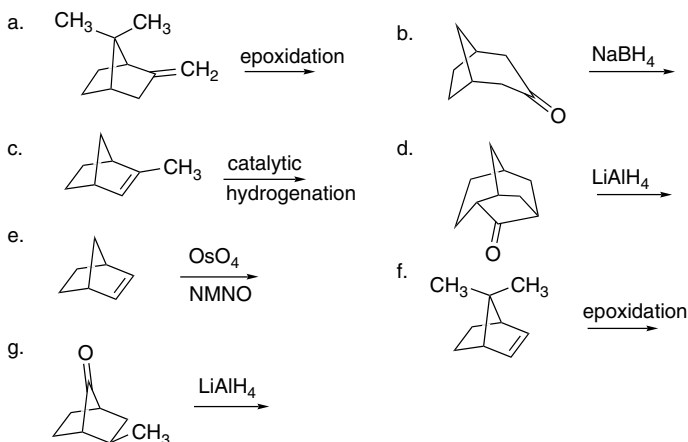
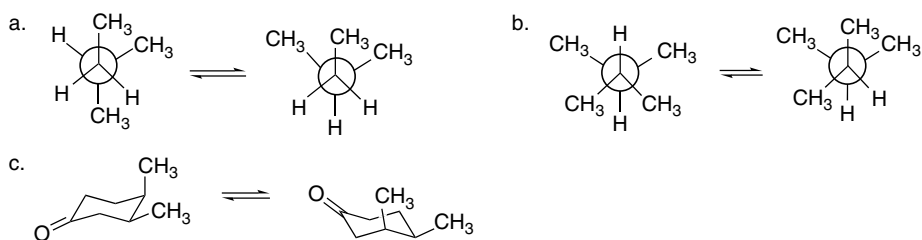


Fig. 2.6P. Rotational profile for acetone (A, solid line), 2-butanone (B, dashed line), and 3-methyl-2-butanone (C, dot-dashed line). Reproduced by permission of the American Chemical Society.

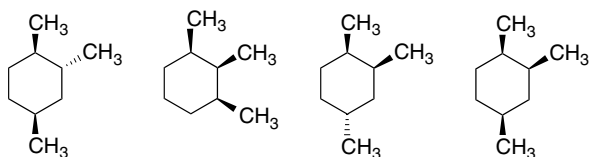
2.7. Predict the stereochemical outcome of the following reactions:



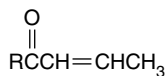
2.8. Estimate  $\Delta H$  for each of the following conformational equilibria.



2.9. Estimate the free-energy difference between the stable and unstable chair conformations of the following trimethylcyclohexanes.

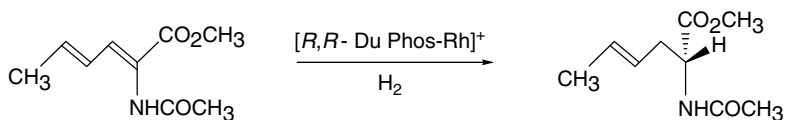


2.10. Predict the preferred conformation of the stereoisomeric *E*-enones **10-A**. How would you expect the conformational equilibrium to change as R becomes progressively larger?

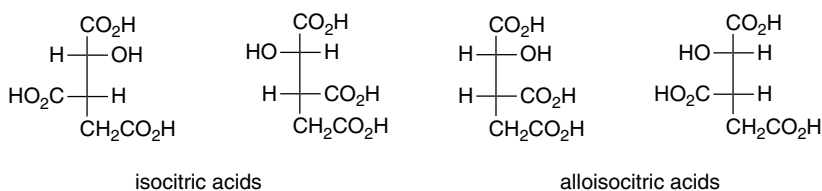


**10-A**

- 2.11. 1,2-Diphenyl-1-propanol can be prepared by hydride reduction of 1,2-diphenyl-1-propanone or by addition of phenylmagnesium bromide to 2-phenylpropanal. Predict the stereochemistry of the major product in each case.
- 2.12. What is the basis of the *chemoselectivity* observed between the two different double bonds in the following reaction?

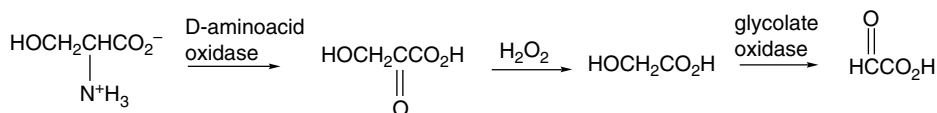
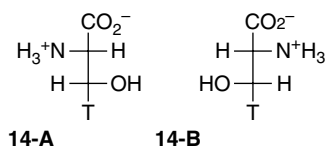


- 2.13. Assign configuration, using the sequence rule, to each stereocenter in the stereoisomers citric acids shown below and convert the Fischer projections to extended chain representations.



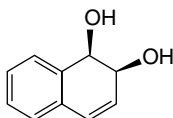
- 2.14. The following questions illustrate how stereochemical considerations can be used to elucidate aspects of biological mechanisms and reactions.

- a. A mixture of  $^3\text{H}$ -labeled **14-A** and **14-B** was carried through the reaction sequence shown:

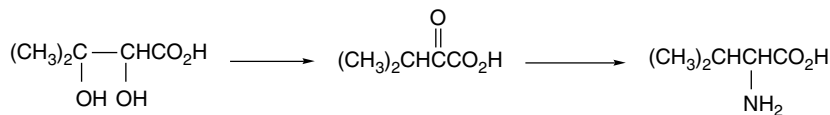


D-amino acid oxidase will oxidize only serine having *R* configuration at C(2). Glycolate oxidase will remove only the *pro-R* hydrogen of glycolic acid. Does the product ( $\text{O}=\text{CHCO}_2\text{H}$ ) contain tritium? Explain your reasoning.

- b. Enzymatic oxidation of naphthalene by bacteria proceeds by way of the intermediate *cis*-diol shown. Which prochiral face of C(1) and C(2) of naphthalene is hydroxylated in this process?

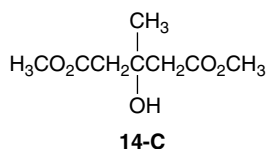


- c. The biosynthesis of valine by bacteria involves the following sequence:

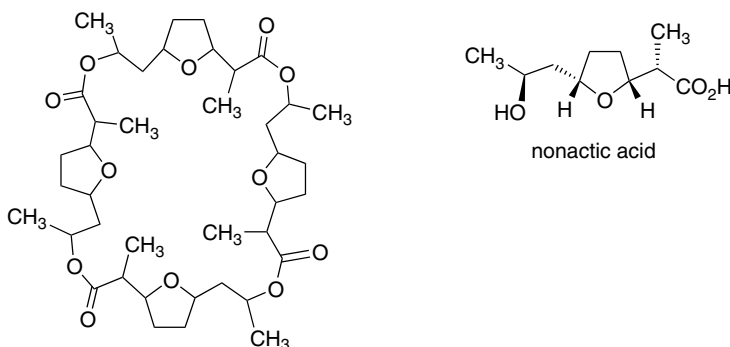


The stereochemistry of the reaction has been examined using the starting diol in which each methyl group was separately replaced by  $\text{CD}_3$ . The diol- $d_3$  of the  $2R,3R$  configuration produces  $2S,3S$ -valine- $d_3$ , whereas the  $2R,3S$  diol- $d_3$  produces  $2S,3R$ -valine- $d_3$ . From this information deduce whether the C(2) and C(3) hydroxy are replaced with inversion or retention of configuration. Show the basis for your conclusion.

- d. A synthesis of the important biosynthetic intermediate mevalonic acid starts with the enzymatic hydrolysis of the diester **14-C** by pig liver esterase. The *pro-R* ester group is selectively hydrolyzed. Draw a three-dimensional structure of the product.



- 2.15. The structure of nonactin is shown below without any specification of stereochemistry. It is isolated as a pure substance from natural sources and gives no indication of being a mixture of stereoisomers. Although it is not optically active, it does not appear to be a racemic mixture, because it does not yield separate peaks on chiral HPLC columns. When completely hydrolyzed, it yields racemic nonactic acid. Deduce the stereochemical structure of nonactin from this information.



- 2.16. (a) The signals for the benzylic hydrogens in the  $^1\text{H}$  NMR spectra of the *cis* and *trans* isomers of 1-benzyl-2,6-dimethylpiperidine have distinctly different appearances, as shown in Figure 2.16Pa. Answer the following questions about these spectra: (a) Which isomer corresponds to which spectrum and why do they have the appearances they do? (b) Only one isomer shows a multiplet corresponding to ring C–H hydrogens adjacent to nitrogen near 3 ppm. Why are these signals not visible in the other partial spectrum? (b) The partial  $^1\text{H}$  NMR spectra corresponding to each benzyl ether of the diastereomeric 2,6-dimethylcyclohexanols are shown in Figure 2.16Pb. Assign the stereochemistry of each isomer.

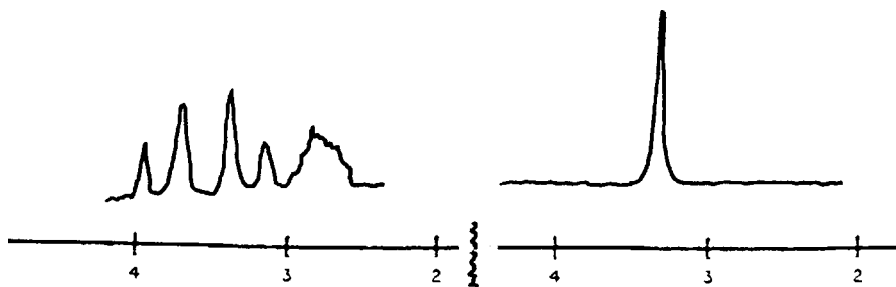


Fig. 2.16Pa. Partial  $^1\text{H}$  NMR spectra of *cis* and *trans* isomers of 1-benzyl-2,6-dimethylpiperidine. Reproduced by permission of Elsevier.

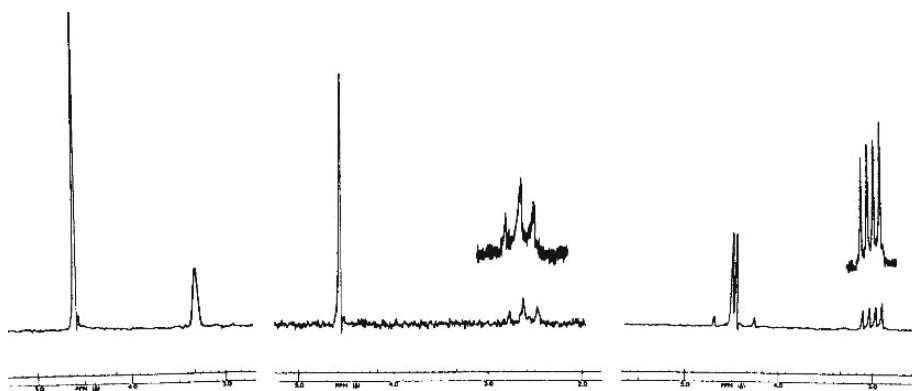


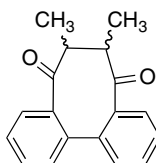
Fig. 2.16Pb. Partial  $^1\text{H}$  NMR spectra of three stereoisomeric benzyl ethers of 2,6-dimethylcyclohexanol. Reproduced by permission of the American Chemical Society.

- 2.17. The *trans*:*cis* ratio of equilibrium for 4-*t*-butylcyclohexanol has been determined in several solvents near  $80^\circ\text{C}$ . From the data, calculate the conformational free energy,  $-\Delta G_c$ , for the hydroxy group in each solvent. What correlation do you find between the observed conformational equilibria and properties of the solvent?

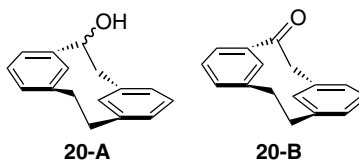
Solvent	<i>trans</i> (%)	<i>cis</i> (%)
Cyclohexane	70.0	30.0
Benzene	72.5	27.5
1,2-Dimethoxyethane	71.0	29.0
Tetrahydrofuran	72.5	27.5
<i>t</i> -Butyl alcohol	77.5	22.5
<i>i</i> -Propyl alcohol	79.0	21.0

- 2.18. *Trans*-3-alkyl-2-chlorocyclohexanones (alkyl=methyl, ethyl, isopropyl) exist with the substituents in the diequatorial conformation. In contrast, the corresponding *E*-*O*-methyloximes exist in the diaxial conformation. Explain the preference for the diaxial conformation of the oxime ethers.
- 2.19. The two stereoisomers (**19-A** and **19-B**) of the structure shown below have distinctly different NMR spectra. Isomer **19-A** shows single signals for the methyl

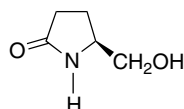
(doublet at 1.25) and methine (broad quartet at 2.94 ppm). Isomer **19-B** shows two methyl peaks (doublets at 1.03 and 1.22 ppm) and two quartets (2.68 and 3.47 ppm) for the methine hydrogens. Both spectra are temperature dependent. For isomer **19-A**, at  $-40^{\circ}\text{C}$  the methyl doublet splits into two doublets of unequal intensity (1.38 and 1.22 ppm in the ratio of 9:5). The methine signal also splits into two broad signals at 3.07 and 2.89 ppm, also in the ratio of 9:5. For isomer **19-B**, pairs of doublets and quartets become single signals (still doublet and quartet, respectively) at  $95^{\circ}\text{C}$ . The spectrum shows no change on going to  $-40^{\circ}\text{C}$ . Assign the stereochemistry of **19-A** and **19-B** and explain how the characteristics of the spectra are related to the stereochemistry.

**19-A**

- 2.20. Compound **20-A** can be resolved to give an enantiomerically pure substance with  $[\alpha]_{\text{D}} = -124$ . Oxidation gives an enantiomerically pure ketone **20-B**,  $[\alpha]_{\text{D}} = -439$ . Heating **20-A** establishes an equilibrium with a stereoisomer with  $[\alpha]_{\text{D}} = +22$ . Oxidation of this compound gives the enantiomer of **20-B**. Heating either enantiomer of **20-B** leads to racemization with  $\Delta G^{\ddagger} = 25 \text{ kcal/mol}$ . Deduce the stereochemical relationship between these compounds.

**20-A****20-B**

- 2.21. When partially resolved samples of *S*-5-(hydroxymethyl)pyrrolidin-2-one are allowed to react with benzaldehyde in the presence of an acid catalyst, two products **21-A** ( $\text{C}_{12}\text{H}_{13}\text{NO}_2$ ) and **21-B** ( $\text{C}_{24}\text{H}_{26}\text{N}_2\text{O}_4$ ) are formed. The ratio of **21-A**:**21-B** depends on the enantiomeric purity of the starting material. When it is enantiomerically pure, only **21-A** is formed, but if it is racemic only **21-B** is formed. Partially resolved samples give **21-A** and **21-B** in a ratio corresponding to the e.e. The rotation of **21-A** is  $[\alpha]_{\text{D}} = +269.6$ , but **21-B** is not optically active. Develop an explanation for these observations including likely structures for **21-A** and **21-B**. Assign the configuration of all the stereogenic centers in the products you propose.

*S*-5-(hydroxymethyl)-  
pyrrolidinone

2.22. Figure 2.22Pa,b shows energy as a function of rotation for a series of 2-substituted acetaldehydes, with  $\theta = 0^\circ$  in the *syn* conformation and  $\theta = 180^\circ$  in the *anti* conformation. The calculations were done by the PM3 method. Figure 2.P22a represents the isolated molecule, while Figure 2.P22b represents an elliptical solvent cavity with a dielectric constant of 4.7, approximating  $\text{CHCl}_3$ . The Table 2.22P gives the calculated rotational barriers. Discuss the following aspects of the data. (a) Rationalize the  $\text{Br} > \text{Cl} > \text{F}$  order of preference for *anti* conformation in the gas phase; (b) Why does the polar medium shift the equilibrium to favor more of the *syn* conformation?

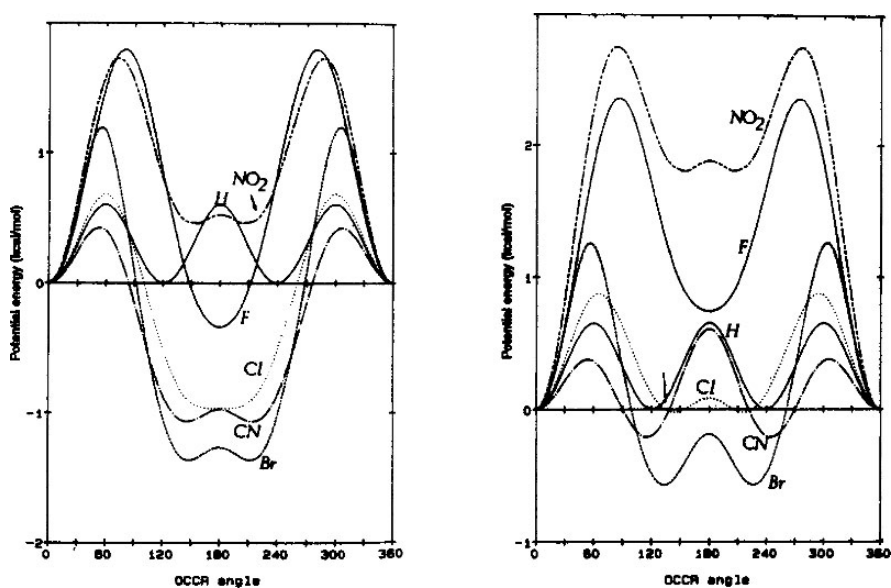
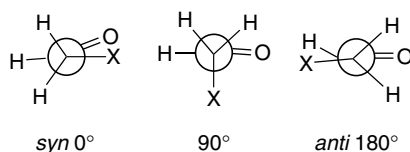
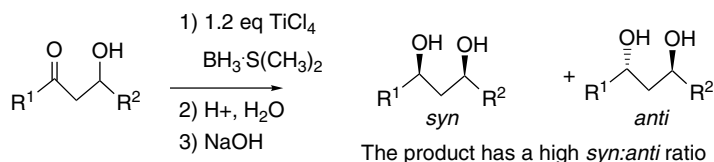


Fig. 2.22P. (a) Rotational profile of the isolated molecules. (b) Rotational profile in solvent cavity with dielectric constant 4.7. Reproduced by permission of Elsevier.

2.23. Provide a mechanistic explanation, including proposed transition structure(s), to account for the stereoselectivity observed in the following reactions:

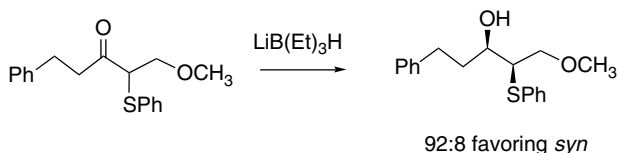
a.



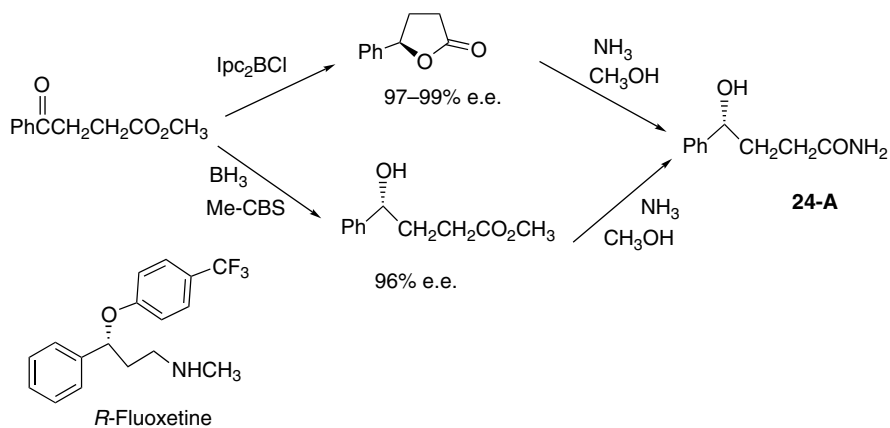
**Table 2.22P. Energy Difference between *syn* and *anti* Conformations**

Substituent	$E_{syn} - E_{anti}$ (kcal/mol)	
	Vacuum	$\epsilon = 4.7$
H	+0.60	+0.65
F	-0.34	+0.74
Cl	-0.97	-0.02
Br	-1.36	-0.57
CN	-1.07	-0.21
NO <sub>2</sub>	+0.46	+1.85

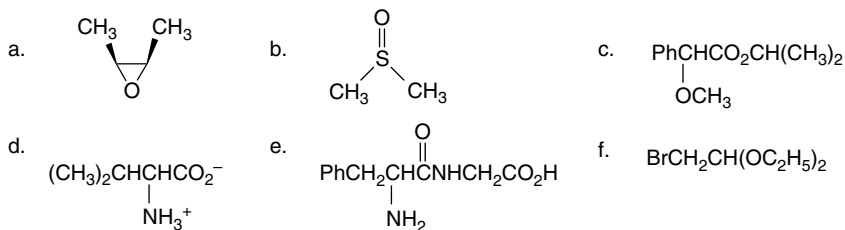
b.



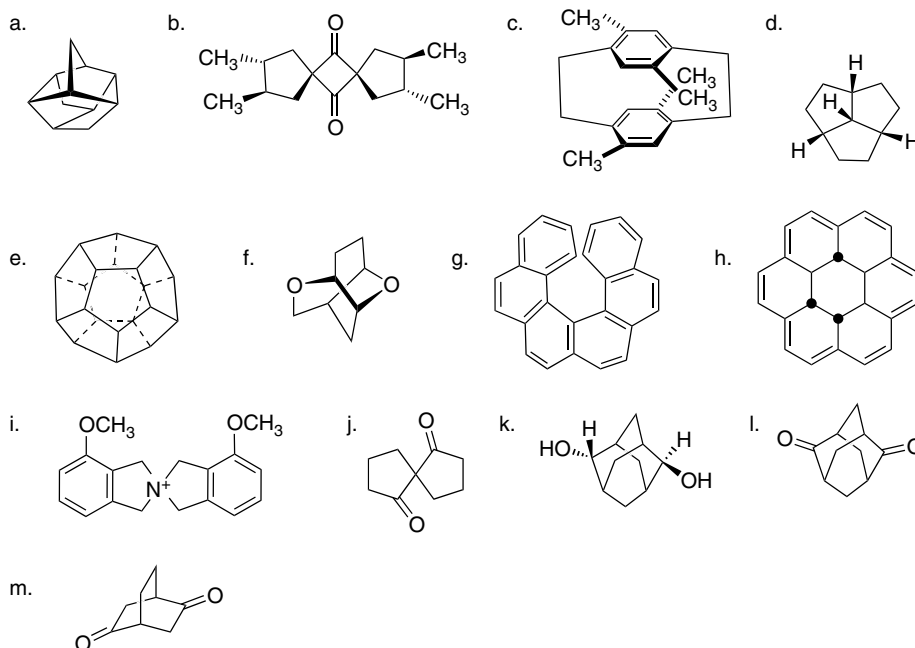
2.24. Either oxaborazolidine-catalysis (Me-CBS) or (Ipc)<sub>2</sub>BCl reductions can be used to prepare **24-A** a precursor of Fluoxetine (Prozac)<sup>®</sup> in good yield and high e.e. Suggest transition structures that account for the observed enantioselectivity.



2.25 Some of the compounds shown below contain enantiotopic or diastereotopic atoms or groups. Which possess this characteristic? For those that do, indicate the atoms or groups that are diastereotopic and assign the groups as *pro-R* and *pro-S*.



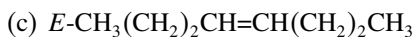
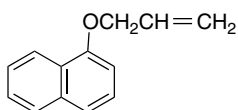
2.26. Indicate which of the following structures are chiral. For each molecule that is achiral, indicate an element of symmetry that is present in the molecule.



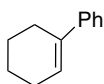
2.27. Predict the absolute configuration of the diols obtained from each of the following alkenes using either a dihydroquinidine or a dihydroquinine type dihydroxylation catalysts.



(b)



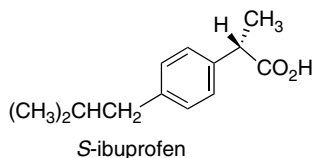
(d)



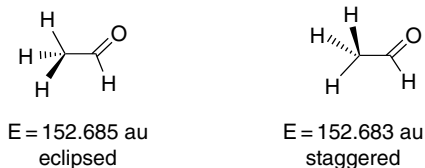
2.28. Based on the standard transition state models, predict the absolute configuration of the products of the following reactions:

- Reduction of 1-phenyl-1-propanone by  $\text{BH}_3\text{-THF}$  using the oxaborazolidine catalyst derived from (*S*)- $\alpha$ ,  $\alpha$ -diphenylpyrrolidine-2-methanol.
- Reduction of 1,1,1-trifluorodec-3-yn-one by (*S*)-Alpine borane.
- Sharpless asymmetric epoxidation of *E*-hex-2-en-1-ol using (+)-diethyl tartrate.

- 2.29. Ibuprofen, an example of an NSAID, is the active ingredient in several popular over-the-counter analgesics. In the United States, it is sold in racemic form, even though only the *S*-enantiomer is pharmacologically active. Suggest methods that might be used to obtain or prepare ibuprofen in enantiomerically pure form, based on processes and reactions discussed in chapter 2.



- 2.30. Ab initio MO calculations (HF/4-31G) indicate that the eclipsed conformation of acetaldehyde is about 1.1 kcal more stable than the staggered conformation. Provide an explanation of this effect in terms of MO theory. Construct a qualitative MO diagram and point out the significant differences that favor the eclipsed conformation. Identify the interactions that are stabilizing and those that are destabilizing. Identify other factors that need to be considered to analyze the origin of the rotational barrier.

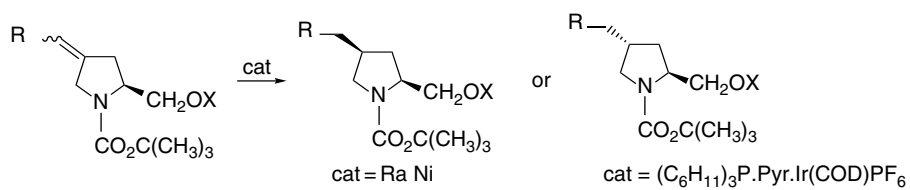


- 2.31. Treatment of alkylphosphoryl dichlorides with 1 equiv. of *L*-proline ethyl ester in the presence of 1-methylimidazole (acting as an acid-scavenger) leads to formation of a monophosphoramidate with low (< 20% diastereoselectivity). Addition of 0.25 equiv. of 4-nitrophenol then gives a 4-nitrophenylphosphoramidate with high (98%) diastereoselectivity, which in turn can be treated with methanol to isolate the methyl 4-nitrophenylphosphonate ester in high enantiomeric purity. This constitutes a kinetic resolution process. Write a mechanistic scheme that accounts for this series of transformations.
- 2.32. Use an appropriate computation program to compare the TS energies for hydroboration of the following alkenes by  $(\text{CH}_3)_2\text{BH}$ . Predict the *exo:endo* ratio for each compound. What factor might complicate the interpretation of the *exo:endo* ratio?



- 2.33. 9-BBN exhibits a high degree of stereoselectivity toward 1,3-dimethyl cycloalkenes such as 1,3-dimethylcyclopentene and 1,3-dimethylcyclohexene, giving exclusively the *trans*, *trans*-2,6-dimethyl cycloalkanols. Offer an explanation.
- 2.34. Diastereoselective reduction of a number of 4-alkylideneprolinols has been accomplished. With a silyl protecting group in place, using Raney nickel, the

*cis* isomers are formed in ratio of about 15:1. When the unprotected alcohols are used with the Crabtree catalyst, quite high selectivity for the *trans* isomer is found. Explain these results.



R	X = <i>t</i> -Butyldimethylsilyl	X = H
C <sub>2</sub> H <sub>5</sub>	13:1	>40:1
Ph	15:1	>40:1
CH <sub>3</sub> O <sub>2</sub> C	15:1	16:1

# Structural Effects on Stability and Reactivity

## Introduction

The concepts of *stability* and *reactivity* are fundamental to understanding chemistry. In this chapter we consider first the *thermodynamic* definition of chemical stability. We then consider *chemical kinetics* (Section 3.2) and how it can provide information about reactivity. We also explore how structure influences stability and reactivity. We want to learn how to make predictions about reactivity based on the structure of the reactants and intermediates. We begin by reviewing the principles of thermodynamics and kinetics, which provide the basis for understanding the relationship of structure to stability and reactivity.

Reactions are usefully described in terms of potential energy diagrams such as shown in Figure 3.1, which identify the potential energy changes associated with the reacting molecules as they proceed to products. The diagram plots the free energy of the system as a function of the progress of the reaction. For each individual step in the reaction there is a *transition state* representing the highest energy arrangement of the molecules for that step. The successive *intermediates* are the molecules that are formed and then react further in the course of the overall reaction. The energies of the transition states relative to the reactants determine the rate of reaction. The energy difference between the reactants and products is  $\Delta G$ , the free-energy change associated with the reaction. The free energy of a chemical reaction is defined by the equation

$$\Delta G = \Delta H - T\Delta S \quad (3.1)$$

where  $\Delta H$  is the *enthalpy change* and  $\Delta S$  is the *entropy change* for the reaction. The enthalpy term is a measure of the stability of the molecule and is determined by the strength of the chemical bonds in the structure. The entropy term specifies the change

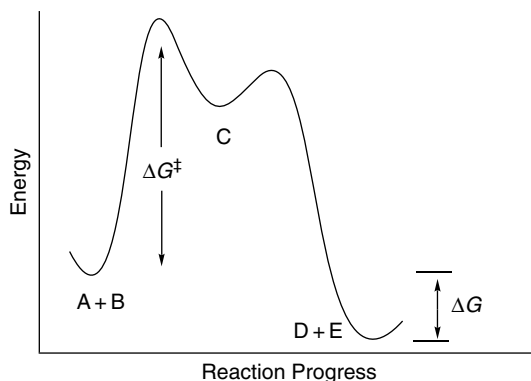


Fig. 3.1. Reaction potential energy profile showing transition states and intermediate for a reaction  $A + B \rightarrow C \rightarrow D + E$ .

in the order (probability) associated with the reaction. The *free energy* of the reaction,  $\Delta G$ , determines the position of the equilibrium for the reaction:

$$\Delta G = -RT \ln K \quad (3.2)$$

where  $K$  is the equilibrium constant for the reaction:

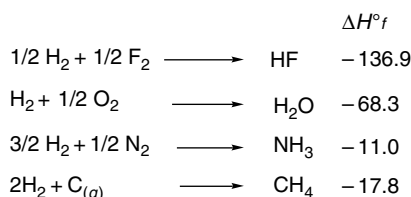
$$K = \frac{[D][E]}{[A][B]}$$

The energy required to proceed from reactants to products is  $\Delta G^\ddagger$ , the *free energy of activation*, which is the energy at the transition state relative to the reactants. We develop the theoretical foundation for these ideas about reaction rates in Section 3.2. We first focus attention on the methods for evaluating the inherent thermodynamic stability of representative molecules. In Section 3.3, we consider general concepts that interrelate the thermodynamic and kinetic aspects of reactivity. In Section 3.4, we consider how substituents affect the stability of important intermediates, such as carbocations, carbanions, radicals, and carbonyl addition (tetrahedral) intermediates. In Section 3.5, we examine quantitative treatments of substituent effects. In the final sections of the chapter we consider catalysis and the effect of the solvent medium on reaction rates and mechanisms.

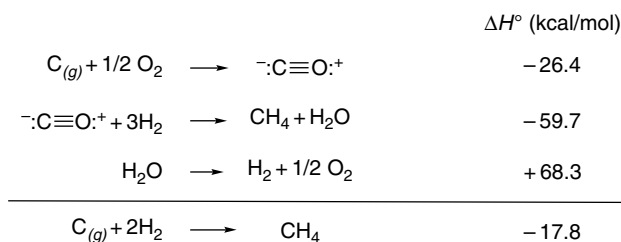
### 3.1. Thermodynamic Stability

Thermodynamic data provide an unambiguous measure of the stability of a particular compound under specified conditions. The thermodynamic measure of molecular stability is  $\Delta H_f^\circ$ , the *standard enthalpy of formation*, which gives the enthalpy of the compound relative to the reference state of its constituent elements under standard conditions of 1 atm and 298 K. For each element a particular form is assigned an enthalpy (potential energy content) of 0. For example, for hydrogen, nitrogen, oxygen, and fluorine, the gaseous diatomic molecules are the reference states. For carbon, 0 energy is assigned to graphite ( $C_{(g)}$ ), which consists entirely of  $sp^2$

carbon atoms. The  $\Delta H_f^\circ$  of compounds can be measured directly or indirectly. The  $\Delta H_f^\circ$  in kcal/mol of HF, H<sub>2</sub>O, NH<sub>3</sub>, and CH<sub>4</sub> are found to be as follows:



The  $\Delta H_f^\circ$  of a given compound is a physical constant and is independent of the process by which the compound is formed. Therefore,  $\Delta H_f^\circ$  values are additive and can be calculated precisely for balanced chemical equations if all the necessary data are available. For example, it might be experimentally impossible to measure the  $\Delta H_f^\circ$  of methane directly by calorimetry, but it can be calculated as the sum of the enthalpy for an equivalent reaction sequence, e.g.:



The  $\Delta H_f^\circ$  for many compounds has been determined experimentally and the data tabulated.<sup>1</sup> In the sections that follow, we discuss approaches to computing  $\Delta H_f^\circ$  when the experimental data are not available. It is important to note that direct comparison of the  $\Delta H_f^\circ$  values for nonisomeric compounds is not meaningful. The  $\Delta H_f^\circ$  for methane through hydrogen fluoride, for example, gives us no comparative information on stability, because the reference points are the individual elements. Other information is needed to examine relative stability. For example, as is discussed in the next section, it is possible to assign *bond energies* to the bonds in CH<sub>4</sub>, NH<sub>3</sub>, H<sub>2</sub>O, and HF. This is the energy required to break a C–H, N–H, O–H, or H–F bond. These numbers do begin to provide some basis for comparison of the properties of nonisomeric compounds, as we now see that the X–H bonds become stronger as we go from C to F in the second-row compounds with hydrogen.

Compound	X–H bond energy (kcal/mol)
CH <sub>4</sub>	105.0
NH <sub>3</sub>	108.2
H <sub>2</sub> O	119.3
HF	136.4

<sup>1</sup> J. B. Pedley, R. D. Naylor, and S. P. Kirby, *Thermochemical Data of Organic Compounds*, 2nd Edition, Chapman and Hall, London, 1986; H. Y. Afeefy, J. F. Liebman, and S. E. Stein, in *NIST Chemistry Webbook*, NIST Standard Reference Database Number 69, P. J. Linstrom and W. G. Mallard, eds., 2001 (<http://webbook.nist.gov>).

### 3.1.1. Relationship between Structure and Thermodynamic Stability for Hydrocarbons

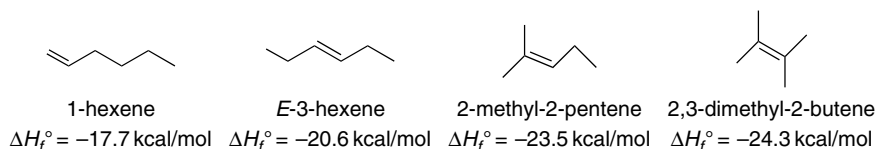
Extensive thermodynamic data are available for the major classes of hydrocarbons. Table 3.1 gives data for the C<sub>4</sub>–C<sub>6</sub> and C<sub>8</sub> alkanes and the C<sub>4</sub>–C<sub>6</sub> alkenes, and several general relationships become apparent. One is that *chain branching increases the stability of alkanes*. This relationship is clear, for example, in the data for the C<sub>6</sub> alkanes, with a total enthalpy difference of nearly 4 kcal/mol between the straight-chain hexane and the tetra-substituted 2,2-dimethylbutane. There is a similar range of 4.5 kcal/mol between the least stable (octane) and most stable

**Table 3.1. Standard Enthalpy of Formation of Some Hydrocarbons  
(in kcal/mol)<sup>a</sup>**

Alkanes (liquid)			
C <sub>4</sub>		C <sub>8</sub>	
Butane	–35.0	Octane	–59.8
2-Methylpropane	–36.7	2-Methylheptane	–60.9
		3-Methylheptane	–60.3
C <sub>5</sub>		4-Methylheptane	–60.1
Pentane	–41.5	2,2-Dimethylhexane	–62.6
2-Methylbutane	–42.7	2,3-Dimethylhexane	–60.4
2,2-Dimethylpropane	–45.5	2,4-Dimethylhexane	–61.4
		2,5-Dimethylhexane	–62.2
C <sub>6</sub>		3,4-Dimethylhexane	–60.2
Hexane	–47.5	3,3-Dimethylhexane	–61.5
2-Methylpentane	–48.9	2,2,3-Trimethylpentane	–61.4
3-Methylpentane	–48.4	2,2,4-Trimethylpentane	–62.0
2,3-Dimethylbutane	–49.6	2,3,4-Trimethylpentane	–60.9
2,2-Dimethylbutane	–51.1	2,3,3-Trimethylpentane	–60.6
		3-Ethyl-2-methylpentane	–59.7
		3-Ethyl-3-methylpentane	–60.4
		2,2,3,3-Tetramethylbutane	–64.3
B. Alkenes (liquid)			
C <sub>4</sub>		C <sub>6</sub>	
1-Butene	–4.90	1-Hexene	–17.7
<i>E</i> -2-Butene	–7.89	<i>E</i> -2-Hexene	–20.4
<i>Z</i> -2-Butene	–7.10	<i>Z</i> -2-Hexene	–20.1
2-Methylpropene	–8.96	<i>E</i> -3-Hexene	–20.6
		<i>Z</i> -3-Hexene	–18.9
C <sub>5</sub>		2-Methyl-1-pentene	–21.5
1-Pentene	–11.2	3-Methyl-1-pentene	–18.7
<i>E</i> -2-Pentene	–13.9	4-Methyl-1-pentene	–19.1
<i>Z</i> -2-Pentene	–12.8	2-Methyl-2-pentene	–23.5
2-Methyl-1-butene	–12.3	3-Methyl-2-pentene	–22.6
3-Methyl-1-butene	–16.4	<i>E</i> -3-Methyl-2-pentene	–22.6
		<i>Z</i> -3-Methyl-2-pentene	–22.6
		<i>E</i> -4-Methyl-2-pentene	–21.9
		<i>Z</i> -4-Methyl-2-pentene	–20.8
		2,3-Dimethyl-1-butene	–22.3
		3,3-Dimethyl-1-butene	–20.9
		2-Ethyl-1-butene	–20.8
		3,3-Dimethyl-1-butene	–20.9
		2,3-Dimethyl-2-butene	–24.3

a. From *Thermochemical Data of Organic Compounds*, 2nd Edition, J. B. Pedley, R. O. Naylor, and S. P. Kirby, Chapman and Hall, London, 1986.

(2,2,3,3-tetramethylbutane) of the  $C_8$  isomers. For alkenes, substitution on the double bond is stabilizing. There is a range of nearly 7 kcal/mol for the  $C_6H_{12}$  isomers. The data for  $C_6$  alkenes, for example show:



These relationships are a result of the stabilizing effect of branching and double-bond substitution and hold quite generally, except when branching or substitution results in van der Waals repulsions (see Section 2.3), which have a destabilizing effect.

### 3.1.2. Calculation of Enthalpy of Formation and Enthalpy of Reaction

In Chapter 1, we introduced various concepts of structure and the idea that the properties of molecules are derived from the combination of the properties of the atoms. One of the qualitative conclusions from these considerations is that the properties of  $CH_3$ ,  $CH_2$ ,  $CH$ , and  $C$  groups in hydrocarbons are expected to be similar from molecule to molecule, as long as they are not perturbed by a nearby functional group. Several methods for the calculation of thermodynamic data based on summation of group properties have been developed and are discussed in the next two sections.

#### 3.1.2.1. Calculations of Enthalpy of Reaction Based on Summation of Bond Energies.

The computation of molecular energy by MO or DFT methods gives the *total binding energy* of a molecule. This is a very large number, since it includes all the electron-nuclei forces in the atoms, not just the additional attractive forces of the bonding electrons. The total energy can be converted to an energy representing all bonding between atoms by subtracting the energy of the individual atoms. This difference in energy is called the *energy of atomization*. This quantity still represents an energy that is far larger than the change involved in chemical reactions, which is of primary interest to chemists. The focus of chemical reactivity is on the bonds that are being formed and broken in the reaction. Useful relationships between structure and reactivity can be developed by focusing on *bond dissociation energies* (BDE). The most completely developed information pertains to *homolytic bond dissociation*,<sup>2</sup> which is the energy required to break a specific bond in a molecule with one electron going to each of the atoms. From the general bond energies in Part A of Table 3.2 we can discern several trends. One is that C–C bonds are considerably stronger than the other homonuclear bonds for the second-row elements (compare with O–O and N–N bonds). We can also note that the bonds in the dihalogens are relatively weak, with a somewhat irregular trend with respect to position in the periodic table:  $F_2 < Cl_2 > Br_2 > I_2$ . The bonds to hydrogen are also slightly irregular:  $N < C < O < F$ . For the hydrogen halides, there is a sharp drop going down the periodic table.

It is known that the immediate molecular environment significantly affects the bond energy, as is illustrated by the data in Part B of Table 3.2. For hydrocarbons the C–H bond dissociation energy depends on the degree of substitution and hybridization

<sup>2</sup> For a discussion of the measurement and application of bond dissociation energies, see S. J. Blanksby and G. B. Ellison, *Acc. Chem. Res.*, **36**, 255 (2003).

Table 3.2. Bond Energies (in kcal/mol)

CHAPTER 3		A. Some Generalized Bond Energies <sup>a</sup>				
Structural Effects on Stability and Reactivity	C–C	81	C–H	98	C=C	145
	N–N	65	N–H	92	C≡C	198
	O–O	34	O–H	105	N≡N	225
	F–F	38	F–H	136	C=O	173
	Cl–Cl	57	Cl–H	102	C–O	79
	Br–Br	45	Br–H	87	C–N	66
	I–I	36	I–H	71		
	B. Some Specific Bond Dissociation Energies <sup>b</sup>					
	CH <sub>3</sub> –H	105.0	H <sub>3</sub> C–CH <sub>3</sub>	90.2	H <sub>3</sub> C–F	110.0
	CH <sub>3</sub> CH <sub>2</sub> –H	100.5	H <sub>3</sub> C <sub>2</sub> –CH <sub>3</sub>	88.5	H <sub>3</sub> C–Cl	83.7
(CH <sub>3</sub> ) <sub>2</sub> CH–H	98.1	(CH <sub>3</sub> ) <sub>2</sub> CH–CH <sub>3</sub>	88.2	H <sub>3</sub> C–Br	70.3	
(CH <sub>3</sub> ) <sub>3</sub> C–H	95.7	H <sub>5</sub> C <sub>2</sub> –C <sub>2</sub> H <sub>5</sub>	86.8	H <sub>3</sub> C–I	57.1	
H <sub>2</sub> C=CH–H	111.2	(CH <sub>3</sub> ) <sub>2</sub> CH–CH(CH <sub>3</sub> ) <sub>2</sub>	84.1	CH <sub>3</sub> CH <sub>2</sub> –F	113.1	
HC≡C–H	132.8	H <sub>2</sub> C=CHCH <sub>2</sub> –CH <sub>3</sub>	75.9	CH <sub>3</sub> CH <sub>2</sub> –Cl	84.2	
H <sub>2</sub> C=CHCH <sub>2</sub> –H	88.2	H <sub>2</sub> C=CH–CH=CH <sub>2</sub>	116.9	CH <sub>3</sub> CH <sub>2</sub> –Br	70.0	
Ph–H	112.9	H <sub>2</sub> C=CH <sub>2</sub>	174.1	CH <sub>3</sub> CH <sub>2</sub> –I	55.8	
PhCH <sub>2</sub> –H	88.5	HC≡CH	229.5	(CH <sub>3</sub> ) <sub>2</sub> CH–F	115.4	
HC≡CHCH <sub>2</sub> –H	88.9	Ph–CH <sub>3</sub>	102.0	(CH <sub>3</sub> ) <sub>2</sub> CH–Cl	84.6	
H <sub>2</sub> N–H	108.2	PhCH <sub>2</sub> –CH <sub>3</sub>	76.4	(CH <sub>3</sub> ) <sub>2</sub> CH–Br	71.5	
CH <sub>3</sub> NH–H	101.6			(CH <sub>3</sub> ) <sub>2</sub> CH–I	56.1	
CH <sub>3</sub> O–H	104.2			H <sub>3</sub> C–OH	92.0	

a. From Table 1, G. J. Janz, *Thermodynamic Properties of Organic Compounds*, Academic Press, New York, 1967.

b. Y. R. Luo, *Handbook of Bond Dissociation Energies in Organic Compounds*, CRC Press, Boca Raton, FL, 2002

of the carbon atom. Primary, secondary, and tertiary  $sp^3$  C–H,  $sp^2$  C–H, and  $sp$  C–H bonds have characteristic values that are significantly different from one another. The variation in bond strengths is related to the stability of the resulting radicals. For C–H bonds, for example, the decrease in bond strength methane  $> pri > sec > tert$  reflects the increasing stability of the more highly substituted carbon radicals. The extra strength of the C–H bond to  $sp^2$  and  $sp$  carbons, as reflected by ethene, ethyne, and benzene, is due in part to the poor stability of ethenyl, ethynyl, and phenyl radicals. The relatively weak primary C–H bonds in propene and methylbenzene reflect conjugative stabilization of the resulting allyl and benzyl radicals (see Section 3.4.3).

A direct approach to estimation of the  $\Delta H$  for a reaction is to apply the fundamental thermodynamic relationship,

$$\Delta H = \Delta H_f^\circ \text{ reactants} - \Delta H_f^\circ \text{ products} \quad (3.3)$$

This equation is exact, but can be applied only if the thermodynamic data pertaining to the actual reaction conditions are available. Thermodynamic manipulations can be used to account for changes in temperature or pressure, but solvation energies are often uncertain (see Section 3.8). The relationship in Equation (3.3) can be approximated by

$$\Delta H = \text{BDE}_{\text{bonds formed}} - \text{BDE}_{\text{bonds broken}} \quad (3.4)$$

For example, data from Table 3.2 can be used to calculate the  $\Delta H$  for reaction of each of the halogens with ethane. The strong trend in exothermicity of  $F_2 > Cl_2 > Br_2 > I_2$  is evident:

X	Break		Form		
	$\text{CH}_3\text{CH}_2-\text{H}$	$\text{X}_2$	$\text{CH}_3\text{CH}_2-\text{X}$	$\text{H-X}$	$\Delta H$
F	100.5	38	113.1	109	-83.6
Cl	100.5	57	84.2	102	-28.7
Br	100.5	45	70.0	87	-11.5
I	100.5	36	55.8	71	+9.7

While bonds of similar type, e.g., C–C, C–O, C–Cl, are of approximately the same strength, the precise value depends on both hybridization and the degree of substitution. For instance, as can be seen in Table 3.2, there is a range from 105.0 to 95.7 kcal/mol for the C–H bonds in methane, ethane, propane (C(2)–H), and isobutane (C(2)–H). The differences between C–H bonds for  $sp^3$ ,  $sp^2$ , and  $sp$  carbon is even greater, as can be seen from the significantly different C–H BDE values for ethane, ethene, ethyne, and benzene. Similarly, C–C bonds between  $sp^2$  carbons are considerably stronger than those between two  $sp^3$  carbons, as is indicated by the C(2)–C(3) BDE of 116.9 kcal/mol for 1,3-butadiene. For estimation of reaction enthalpy using Equation (3.4), the most appropriate BDE must be chosen.

*3.1.2.2. Relationships between Bond Energies and Electronegativity and Hardness.* In his efforts to correlate important chemical properties, Pauling recognized that the difference in electronegativity between two bonded atoms contributes to bond strength. He proposed the empirical relationship

$$\text{BDE}_{\text{AB}} = 1/2(\text{BDE}_{\text{AA}} + \text{BDE}_{\text{BB}}) + 23(\Delta\chi)^2 \quad (3.5)$$

where  $\Delta\chi$  is the difference in electronegativity of the two atoms. A related expression is

$$\text{BDE}_{\text{AB}} = (\text{BDE}_{\text{AA}} \times \text{BDE}_{\text{BB}})^{1/2} + 30(\Delta\chi)^2 \quad (3.6)$$

Both relationships propose that BDE is a function of the strength of the two homonuclear bonds and an increment for electronegativity differences.<sup>3</sup> Although the quantitative reliability of the relationships in Equations (3.5) and (3.6) is limited, the equations do indicate that there is an increment to bond strength that is related to electronegativity differences. Subsequently, many investigators have probed the accuracy, scope, and theoretical foundation of these relationships and have suggested other formulations that improve the accuracy.<sup>4</sup> A refinement of the empirical relationship that includes a term for polarizability gives the equation

$$\text{BDE}_{\text{AB}} = [\text{BDE}_{\text{AA}} \times \text{BDE}_{\text{BB}}]^{1/2} + |2.883(\Delta\chi)|^{[\alpha(\text{A})+\alpha(\text{B})]} \quad (3.7)$$

where  $\alpha$  are polarizability parameters for each element.<sup>5</sup> The polarizability parameters particularly improve the relationship for third-row atoms and other highly polarizable groups.

<sup>3</sup> L. Pauling, *J. Am. Chem. Soc.*, **54**, 3570 (1932); L. Pauling, *The Nature of the Chemical Bond*, 3rd Edition, Cornell University Press, Ithaca, NY, 1960, Chap. 3.

<sup>4</sup> R. R. Reddy, T. V. R. Rao, and R. Viswanath, *J. Am. Chem. Soc.*, **111**, 2914 (1989).

<sup>5</sup> J. W. Ochterski, G. A. Petersson, and K. B. Wiberg, *J. Am. Chem. Soc.*, **117**, 11299 (1995).

The original Pauling equation was reexamined recently by Zavitsas and co-workers.<sup>6</sup> The equation was shown to give quite good agreement with thermochemical data. Furthermore, it permitted assignment of electronegativity and *stabilization energy* to important radicals. The stabilization energy SE is assigned as

$$SE = 1/2(BDE_{[CH_3-CH_3]} - BDE_{[X-X]}) \quad (3.8)$$

Some values are given in Table 3.3. For future reference, note the order of radical stabilization: alkyl > alkenyl > alkynyl and allyl > benzyl > tertiary > secondary > primary. In Section 3.4.3, we discuss the structural basis of these relationships.

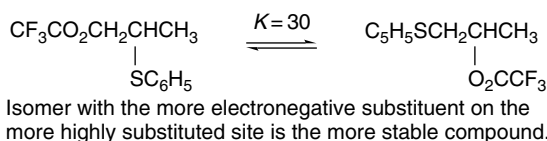
Another idea underlying the nature of bond formation is the concept of *electronegativity equalization*<sup>7</sup> or *electronegativity equilibration*<sup>8</sup> (see Section 1.1.4). This concept states that electron density flows from the less electronegative partner in a bond (making it more positive and therefore more electronegative) to the more electronegative atom (making it more negative and therefore less electronegative) until both atoms have the same effective electronegativity. At that point, there is no net attractive force on the electrons in the bond. This intuitively compelling idea has a theoretical foundation in DFT, which states that the chemical potential  $\mu$  is uniform throughout a molecule. It is observed that the apparent bond strength for several series of compounds increases in the order  $CH_3 - X < pri - X < sec - X, tert - X$ .<sup>9</sup> The differences *increase* with the electronegativity of the substituent X. These electronegativity relationships lead to some qualitative trends. For alkyl groups with electronegative substituents, such as halogens, oxygen, or nitrogen, the trend is *tert* > *sec* > *pri* >  $CH_3$ . On the other hand, for organometallics, alanes, and boranes, the order is reversed. Compounds that can readily interconvert can isomerize in response to these stability relationships.<sup>10</sup>

**Table 3.3. Group Electronegativity and Stabilization Energies (in kcal/mol) Based on the Pauling Equation<sup>a</sup>**

Group	$\chi$	SE	Group	$\chi$	SE
CH <sub>3</sub>	2.525	0.0	HO	3.500	
C <sub>2</sub> H <sub>5</sub>	2.462	1.2	CH <sub>3</sub> O	3.439	26.0
<i>i</i> -C <sub>3</sub> H <sub>7</sub>	2.411	1.4	PhO	3.376	43.1
<i>t</i> -C <sub>4</sub> H <sub>9</sub>	2.378	3.7	CH <sub>3</sub> NH	3.018	13.5
CH <sub>2</sub> =CHCH <sub>2</sub>	2.488	14.3	(CH <sub>3</sub> ) <sub>3</sub> Si	1.838	5.9
PhCH <sub>2</sub>	2.506	11.7	F	3.938	25.9
Ph		-13.1	Cl	3.174	15.9
CH <sub>2</sub> =CH		-11.6			
HC≡C		-32.1			
CH <sub>3</sub> C=O		7.9			

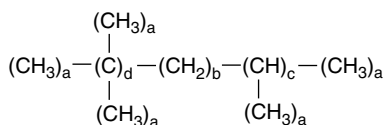
a. N. Matsunaga, D. W. Rogers, and A. A. Zavitsas, *J. Org. Chem.*, **68**, 3158 (2003).

- <sup>6</sup> N. Matsunaga, D. W. Rogers, and A. A. Zavitsas, *J. Org. Chem.*, **68**, 3158 (2003).  
<sup>7</sup> S. G. Bratsch, *J. Chem. Educ.*, **61**, 588 (1984); R. T. Sanderson, *Polar Covalence*, Academic Press, New York, 1983.  
<sup>8</sup> D. W. Smith, *J. Chem. Educ.*, **67**, 559 (1990).  
<sup>9</sup> Y. R. Luo and S. W. Benson, *J. Phys. Chem.*, **92**, 5255 (1988); Y. R. Luo and S. W. Benson, *Acc. Chem. Res.*, **25**, 375 (1992); N. Laurencelle and P. D. Pacey, *J. Am. Chem. Soc.*, **115**, 625 (1993).  
<sup>10</sup> J. N. Harvey and H. G. Viehe, *J. Prakt. Chem. Chem. Zeitung*, **337**, 253 (1995).

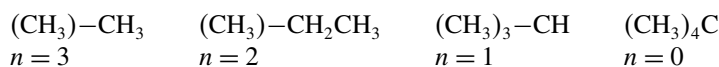


These treatments of bond energies illustrate that there are fundamental relationships between bond strengths and atomic properties such as electronegativity and polarizability. The crucial point is that bond strength *is increased by electronegativity differences in a given row of the periodic table* as a result of an increment that is due to electrostatic attraction.

**3.1.2.3. Calculation of  $\Delta H_f$  Using Transferable Group Equivalents.** The idea that the properties of molecules are the sum of its component atoms and groups has led to the development of schemes by which thermodynamic properties can be calculated as the sum of contributions from all structural units.<sup>11</sup> The most highly developed is that of S. W. Benson and co-workers.<sup>12</sup> The molecule is divided into its component groups. For example, isooctane (which incidentally is the standard for 100 in octane ratings) consists of five C-(C)(H)<sub>3</sub> (a), one C-(C)<sub>2</sub>(H)<sub>2</sub> (b), one C-(C)<sub>3</sub>(H) (c), and one C-(C)<sub>4</sub> (d), as labeled on the structure.



The four groups designated above are sufficient to describe all alkanes. Finer distinctions can be made if these groups are subdivided further, depending on the number of hydrogens on the adjacent carbon. For example, a CH<sub>3</sub> group might be found in four different environments:



Modified increments are also assigned to carbons adjacent to double or triple bonds or benzene rings. The enthalpy of formation of a molecule can then be calculated as the sum of the contributions of the component groups. The main limitation of this method is that it does not explicitly consider long-range nonbonded interactions. The group equivalents refer to *strain-free molecules*. Further refinement can be incorporated by taking account of nonbonded interactions. For example, *gauche* interactions can be counted and applied as a correction to the sum of group equivalents.<sup>13</sup>

<sup>11</sup>. For a discussion of the pioneering efforts in this field, see J. D. Cox and G. Pilcher, *Thermochemistry of Organic and Organometallic Compounds*, Academic Press, New York, 1970, Chap. 7.

<sup>12</sup>. N. Cohen and S. W. Benson, *Chem. Rev.*, **93**, 2419 (1993).

<sup>13</sup>. N. Cohen and S. W. Benson, *The Chemistry of Alkanes and Cycloalkanes*, S Patai and Z. Rappoport, eds., Wiley, 1992, Chap. 6; S. W. Benson and N. Cohen, in *Computational Thermodynamics*, K. K. Irikura and D. J. Frurip, eds., *ACS Symposium Series*, **677**, 20 (1996).

## CHAPTER 3

Structural Effects on  
Stability and Reactivity

5 C-(C)(H <sub>3</sub> ) <sub>a</sub>	-10.00	-50.00
1 C(C) <sub>2</sub> (H <sub>2</sub> ) <sub>b</sub>	-5.00	-5.00
1 C(C) <sub>3</sub> (H) <sub>c</sub>	-2.40	-2.40
1 3C(C) <sub>4</sub>	-0.10	-0.10
3 <i>gauche</i> correction	-0.80	+2.40
Calculated value		-55.10

Group equivalent methods can be extended to functionalized compounds by assigning the enthalpy components of the substituent groups.<sup>14</sup>

Various other methods for making calculations based on bond dissociation energies more precise have been developed. A method developed by G. Leroy and co-workers is based on extensive thermochemical data, as well as energies calculated by MO methods.<sup>15</sup> The heat of atomization of unstrained hydrocarbons is equated to the number of C–C and primary, secondary and tertiary C–H bonds. The heat of atomization is given by

$$\Delta H_{\text{atom}} = N_{\text{cc}}(E_{\text{cc}}) + N_{\text{pri}}(E_{\text{C-H}_{\text{pri}}}) + N_{\text{sec}}(E_{\text{C-H}_{\text{sec}}}) + N_{\text{tert}}(E_{\text{CH}_{\text{tert}}}) \quad (3.9)$$

For stable compounds with known  $\Delta H_{\text{atom}}$  the stabilization (or destabilization) is then the difference between  $\Delta H_{\text{atom}}$  and the calculated sum of standard bond energies:

$$\text{SE} = \Delta H_{\text{atom}} - \Sigma \text{BE}_{\text{standard}} \quad (3.10)$$

Leroy and co-workers developed an extensive series of standard bond energy terms. Terms for specific substituent effects were also assigned, e.g., the  $\Delta(\text{C}_d\text{--C})$  and  $\Delta(\text{C--H})^{\text{O}}$  terms are adjustments for bonds between double bonds and having oxygen substituents, respectively. Comparison of the sum of the standard BE with the actual  $\Delta H_{\text{atom}}$  gives the extra stabilization present in the compound. Calculations for butadiene stabilization (conjugation) and dimethoxymethane (anomeric effect) are given below.

	Butadiene		Dimethoxymethane	
Bond energies:	$2E(\text{C}=\text{C})$	2(137.23)	Bond energies	$4E(\text{C--O})$ 4(91.66)
	$4E(\text{C}_d\text{--H})_2$	4(100.30)		$2E(\text{C--H})_s$ 2(97.53)
	$2E(\text{C}_d\text{--H})_1$	2(99.78)		$4\Delta(\text{C--H})_s^{\text{O}}$ 4(-2.05)
	$E(\text{C--C})$	85.44		$6E(\text{C--H})_p^{\text{O}}$ 6(95.87)
	$2\Delta(\text{C}_d^c\text{--C})$	2(3.88)		
	$\Sigma N_{\text{AB}} B_{\text{AB}} =$	968.42 kcal/mol <sup>-1</sup>		$\Sigma N_{\text{AB}} B_{\text{AB}} =$ 1128.72 kcal/mol <sup>-1</sup>
$\Delta H_{\text{atom}}$		971.5	$\Delta H_{\text{atom}}$	1133.06
	SE	3.08 kcal/mol	SE	4.34 kcal/mol

The enthalpy change of a homolytic bond dissociation is expressed as the difference in stabilization of the products and reactants. A virtue of this approach is

<sup>14</sup> J. B. Pedley, R. D. Naylor, and S. P. Kirby, *Thermochemical Data of Organic Compounds*, 2nd Edition, Chapman and Hall, London, 1986, Chap. 2.

<sup>15</sup> G. Leroy, M. Sana, and C. Wilante, *J. Mol. Structure: Theochem.*, **234**, 303 (1991).

that it recognizes that there may be special stabilization, e.g., conjugation and anomeric effects, in the reactants as well as in the dissociated radicals.

$$\text{BDE} = \sum_{\text{R-Z}} \cdot \text{BE}_{\text{standard}} - \sum_{\text{R}\cdot} \text{BE}_{\text{standard}} - \sum_{\text{Z}\cdot} \text{BE} + \text{SE}_{\text{R-Z}} - \text{SE}_{\text{R}\cdot} - \text{SE}_{\text{Z}\cdot} \quad (3.11)$$

Table 3.4 gives some representative results.

According to this analysis, the weakening of the C–H bonds in isobutane and toluene is largely due to the stabilization of the resulting radicals. However, even though trichloromethyl radicals are quite stable, there is also considerable stabilization in the starting material chloroform, and the C–H bond in chloroform is not weakened as much as that in isobutane. More is said about separating structural effects in reactant and intermediate radicals in Topic 11.1.

The calculation of  $\Delta H_f^\circ$  is now usually done by computational chemistry, but the success of the group equivalent approaches makes an important point. The properties of groups are very similar from molecule to molecule, similar enough to make additivity schemes workable. However, *specific interactions*, e.g., nonbonded interactions, that depend on the detailed structure of the molecule are not accounted for. Whenever interactions that are not accounted for by the group equivalents exist, there will be a discrepancy between the calculated and actual properties of the molecule. Analyses such as that of Leroy can provide valuable insights and concepts. In particular, they provide a means for recognizing stabilization effects present in reactants, as demonstrated by the calculations for 1,3-butadiene and dimethoxymethane.

**3.1.2.4. Calculation of Enthalpy of Formation by Molecular Mechanics.** Molecular mechanics (MM) is a systematic approach to the calculation of molecular energy based on the summation of bond properties and nonbonding (e.g., van der Waals) interactions (review Section 2.4). MM provides a means for analyzing the energy differences between molecules and among various geometries of a particular molecule.<sup>16</sup> Several systems of parameters and equations for carrying out the calculations have been developed. The method most frequently used in organic chemistry is the one developed by N. L. Allinger and co-workers.<sup>17</sup> In the most recent version of MM calculations

**Table 3.4. Calculation of the C–X Bond Dissociation Energies (in kcal/mol; 298.15 K)**

R–X	$\Delta \sum N_{\text{AB}} E_{\text{AB}}$	$\text{SE}_0(\text{R–X})$	$\text{SE}_0(\text{R}\cdot)$	BDE(R–X)
Et–H	99.8	0	0	100.3
t-Bu–H	96.8	0.8	3.7	93.9
Et–Cl	83.3	0	–0.5	83.8
t-Bu–Cl	85.6	0	3.7	81.9
C <sub>6</sub> H <sub>5</sub> CH <sub>2</sub> –H	99.8	–1.0	11.6	87.1
(t-Bu) <sub>2</sub> CH–H	98.2	–6.0	–5.9	98.2
Cl <sub>3</sub> C–H	93.9	–16.3	–18.0	95.7

<sup>16</sup> F. H. Westheimer, in *Steric Effects in Organic Chemistry*, M. S. Newman, ed., Wiley, New York, 1956, Chap. 12; J. E. Williams, P. J. Stang, and P. v. R. Schleyer, *Annu. Rev. Phys. Chem.*, **19**, 531 (1968); D. B. Boyd and K. P. Lipkowitz, *J. Chem. Educ.*, **59**, 269 (1982); P. J. Cox, *J. Chem. Ed.*, **59**, 275 (1982); N. L. Allinger, *Adv. Phys. Org. Chem.*, **13**, 1 (1976); E. Osawa and H. Musso, *Top. Stereochem.*, **13**, 117 (1982); U. Burkett and N. L. Allinger, *Molecular Mechanics*, ACS Monograph 177, American Chemical Society, Washington, DC, 1982.

<sup>17</sup> N. L. Allinger, Y. H. Yuh, and J. -H. Li, *J. Am. Chem. Soc.*, **111**, 8551 (1989).

for organic molecules, known as MM4,<sup>18</sup> the computations involve iterations to locate an energy minimum. Precautions must be taken to establish that a true (“global”) minimum, as opposed to a local minimum energy, is found. This can be accomplished by using a number of different initial geometries and comparing the structures of the minima that are located. As with the group equivalent approach, MM calculations of  $\Delta H_f^\circ$  are grounded in experimental measurements of a limited number of molecules that were used to optimize the parameters. The original parameters pertained to hydrocarbons, but as the method has developed, the parameters have been extended to many functional groups. MM calculations specifically take molecular geometry into account, including nonbonded and dipolar interactions. Van der Waals interactions are described in terms of energy functions and parameters that describe the interaction of the approaching atoms. Polar interactions are modeled as electrostatic interactions.

Heats of formation are calculated as a sum of the bond energies and other stabilizing and destabilizing (e.g., strain) increments for the structure. MM4 calculations include terms for contributions of higher-energy conformations.<sup>19</sup> For a set of hydrocarbons ranging from methane and ethane to adamantane and bicyclo[2.2.2]octane, the heats of formation are calculated with a standard deviation of 0.353 kcal/mol. The MM4 system has also been applied to alkenes,<sup>20</sup> aldehydes,<sup>21</sup> and ketones.<sup>22</sup>

*3.1.2.5. Thermodynamic Data from MO and DFT Computations.* MO and DFT calculations provide another approach to obtaining thermodynamic data. The accuracy with which the various computational methods reproduce molecular energies varies. Of the semiempirical methods only MINDO,<sup>23</sup> MNDO<sup>24</sup>, AM1,<sup>25</sup> and PM3<sup>26</sup> provide reliable estimates of energies and the range of applicability is open to some discussion.<sup>27</sup> Among the ab initio methods the level of accuracy generally increases with larger basis sets and treatment of correlation effects. G1, G2, and G3 computations can achieve a level of accuracy that permits comparison of energy data among related molecules. DFT calculations have also been applied to various compounds.<sup>28</sup> Users of computational thermochemical data must critically assess the reliability of the method being applied in the *particular case* under study.

A large series of compounds, including hydrocarbon derivatives, was studied at the G2 and G2(MP2,SVP) levels and compared with results from the B3LYP method.<sup>29</sup> Another group carried out a similar comparison on a smaller set of molecules.<sup>30</sup>

<sup>18</sup> N. L. Allinger, K. Chen, and J. -H. Lii, *J. Comput. Chem.*, **17**, 642 (1996).

<sup>19</sup> N. L. Allinger, L. R. Schmitz, I. Motoc, C. Bender, and J. Labanowski, *J. Phys. Org. Chem.*, **3**, 732 (1990); N. L. Allinger, L. R. Schmitz, I. Motoc, C. Bender, and J. Labanowski, *J. Am. Chem. Soc.*, **114**, 2880 (1992).

<sup>20</sup> N. Nevins, K. Chen, and N. L. Allinger, *J. Comput. Chem.*, **17**, 695 (1996).

<sup>21</sup> C. H. Langley, J. H. Lii, and N. L. Allinger, *J. Comput. Chem.*, **22**, 1396 (2001).

<sup>22</sup> C. H. Langley, J. H. Lii, and N. L. Allinger, *J. Comput. Chem.*, **22**, 1426, 1451, 1476 (2001).

<sup>23</sup> R. C. Bingham, M. J. S. Dewar, and D. H. Lo, *J. Am. Chem. Soc.*, **97**, 1294 (1975).

<sup>24</sup> M. J. S. Dewar and G. P. Ford, *J. Am. Chem. Soc.*, **101**, 5558 (1979).

<sup>25</sup> M. J. S. Dewar, E. G. Zoebisch, E. F. Healy, and J. J. P. Stewart, *J. Am. Chem. Soc.*, **107**, 3902 (1985).

<sup>26</sup> J. J. P. Stewart, *J. Comput. Chem.*, **10**, 221 (1989).

<sup>27</sup> J. A. Pople, *J. Am. Chem. Soc.*, **97**, 5307 (1975); T. A. Halgren, D. A. Kleier, J. H. Hall, Jr., L. D. Brown, and W. L. Lipscomb, *J. Am. Chem. Soc.*, **100**, 6595 (1978); M. J. S. Dewar and D. M. Storch, *J. Am. Chem. Soc.*, **107**, 3898 (1985).

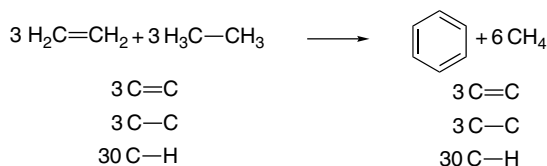
<sup>28</sup> K. Raghavachari, B. B. Stefanov, and L. A. Curtiss, *Molec. Phys.*, **91**, 555 (1997); B. S. Jursic, *Theochem*, **391**, 75 (1997); B. S. Jursic, *Theochem*, **417**, 99 (1997); J. Andzelm, J. Baker, A. Scheiner, and M. Wrinn, *Int. J. Quantum Chem.*, **56**, 733 (1995).

<sup>29</sup> L. A. Curtiss, K. Raghavachari, P. C. Redfern, and J. A. Pople, *J. Chem. Phys.*, **106**, 1063 (1997).

<sup>30</sup> J.-W. Pan, D. W. Rogers, and F. J. McLafferty, *Theochem.*, **468**, 59 (1999).

Table 3.5 includes the B3LYP/6-311 + G(3df,2p) results for some small hydrocarbons. MO and DFT calculations pertain to molecules at 0 K without any molecular motion. In order to make comparisons with thermodynamic data at 298 K, corrections for both zero-point energy (ZPE) and the difference in thermal energy must be made. The corrections are normally incorporated into calculations intended for thermochemical comparisons. The corrections are based on calculation of the vibrations and rotations that contribute to ZPE and thermal energy. Table 3.5 gives a comparison of some calculated  $\Delta H_f$  with experimental values for some simple hydrocarbons. The absolute errors are small for methods such as G2, CBS-Q, and CBS-QB. There are some indications that B3LYP calculations tend to underestimate the stability of hydrocarbons as the size of the molecule increases. For example, using the 6-311 + G(3df,2p) basis set, the error increased systematically from propane (-1.5 kcal/mol) to hexane (-9.3) and octane (-14.0).<sup>31</sup> Similarly, the effect of successively adding methyl groups to ethane resulted in an error of 21.1 kcal/mol for 2,2,3,3-tetramethylbutane.<sup>32</sup>

MO methods can also be used to calculate *heats of reaction* by comparing the heats of formation of reactants and products. The *total energy* calculated for even a small hydrocarbon, relative to the separate nuclei and electrons, is enormous (typically 50,000 and 100,000 kcal/mol for C<sub>2</sub> and C<sub>4</sub> compounds, respectively) relative to the energy of reaction. Sometimes the energy is tabulated as the *energy of atomization*, corresponding to the difference in total energy of the molecule and that of the separate atom, which is the energy required to break all the bonds. These values, too, are very large in comparison with the heat of reaction. The energy differences that are of principal chemical interest, such as  $\Delta H$  for a reaction, are likely to be in the range of 0–30 kcal/mol. A very small error relative to the total energy in an MO calculation becomes a very large error in a calculated  $\Delta H$ . Fortunately, the absolute errors for compounds of similar structure are likely to be comparable and tend to cancel in calculation of the *energy differences* between related molecules. Calculation of heats of formation and heats of reaction is frequently done on the basis of *isodesmic reactions*,<sup>33</sup> in order to provide for maximum cancellation of errors in total binding energies. An isodesmic reaction is defined as a process in which the number of formal bonds of each type is kept constant; that is, there are the same number of C–H, C=C, C=O, etc., bonds on each side of the equation.<sup>34</sup> For example, an isodesmic reaction to evaluate the stability of benzene would be:



The comparison can be further refined by use of *homodesmotic reactions* in which there is matching not only of bond types, but also of hybridization. Thus in the reaction

<sup>31</sup>. L. A. Curtiss, K. Raghavachari, P. C. Redfern, and J. A. Pople, *J. Chem. Phys.*, **112**, 7374 (2000).

<sup>32</sup>. C. E. Check and T. M. Gilbert, *J. Org. Chem.*, **70**, 9828 (2005).

<sup>33</sup>. W. J. Hehre, R. Ditchfield, L. Radom, and J. A. Pople, *J. Am. Chem. Soc.*, **92**, 4796 (1970).

<sup>34</sup>. D. A. Ponomarev and V. V. Takhistov, *J. Chem. Ed.*, **74**, 201 (1997).

Table 3.5. Comparison of Differences between Calculated and Experimental  $\Delta H_f$  in kcal/mol for some Hydrocarbons.<sup>a</sup>

Hydrocarbon	MNDO <sup>a</sup>	AMI <sup>b</sup>	PM3 <sup>c</sup>	HF/3-21G <sup>a</sup>	HF/6-31G <sup>a</sup>	G2 <sup>d</sup>	CBS-Q <sup>e</sup>	CBS-QB3 <sup>f</sup>	MP4/QCI <sup>g</sup>	B3LYP/6-311+G(3d,f,2,p) <sup>h</sup>
Methane	5.9	9.0	4.9	-0.9	-0.5	0.7	-0.2	-0.4	-0.6	-1.6
Ethane	0.3	2.6	2.1	0.2	0.9	-0.2	-0.6	-0.6	-0.7	0.0
Butane	0.7	-0.7		-0.8	-0.8	0.6				-0.8
Pentane	0.7	-2.8		-0.5	-0.5					
Cyclopropane	-1.5	5.1	3.5	-2.4	-2.4		-1.7			-0.6
Cyclobutane	-18.7	0.2	-10.6				-3.4			1.2
Cyclopentane	-12.0	-10.5	-5.6		-6.1			-0.1		4.5
Cyclohexane	-5.3	-9.0	-1.5		-9.1	3.9		-0.1		
Ethene	3.1	4.0	4.2	-1.6	-2.4	0.3	-1.0	0.0	0.1	-0.5
Allene	-1.6	0.6	1.5	-2.5	-6.8	0.0 <sup>i</sup>	1.3	0.0		-2.4
1,3-Butadiene	2.7	3.6	5.0	-4.7	-2.9	0.5 <sup>j</sup>		0.7		-1.5 <sup>d</sup>
Benzene		1.5	2.2	3.6		4.0 <sup>k</sup>	1.5	-0.2		-4.0 <sup>d</sup>
Bicyclo[2.2.1]heptane	2.1	-2.0	-1.3		8.8					
Bicyclo[2.2.2]octane	-2.2	-11.9	-3.7		10.7					

a. M. J. S. Dewar, E. G. Zoebisch, E.F. Healy, and J. J. P. Stewart, *J. Am. Chem. Soc.*, **107**, 3902 (1985).

b. M. J. S. Dewar and D. M. Storch, *J. Am. Chem. Soc.*, **107**, 3898 (1985).

c. J. J. P. Stewart, *J. Comput. Chem.*, **10**, 221 (1989).

d. J. A. Pople, M. Head-Gordon, D. J. Fox, K. Raghavachari, and L. A. Curtiss, *J. Chem. Phys.*, **90**, 5622 (1989); L. A. Curtiss, K. Raghavachari, G. W. Trucks, and J. A. Pople, *J. Phys. Chem.*, **94**, 7221 (1991); L. A. Curtiss, K. Raghavachari, P. C. Redfern, and J. Pople, *J. Chem. Phys.*, **106**, 1063 (1997).

e. L. A. Curtiss, K. Raghavachari, P. C. Redfern, and B. B. Stefanov, *J. Chem. Phys.*, **108**, 692 (1998).

f. M. Saeys, M.-F. Reyniers, G. B. Marin, V. Van Speybroeck, and M. Waroquier, *J. Phys. Chem. A*, **107**, 9147 (2003).

g. M. Sana and M. T. Nguyen, *Chem. Phys. Lett.*, **196**, 390 (1992).

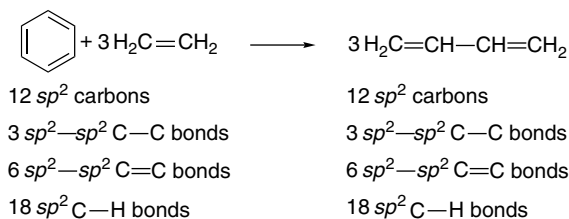
h. J.-W. Pan, D. W. Rogers, and F. J. McLafferty, *Theochem*, **468**, 59 (1999).

i. D. W. Rogers and F. J. McLafferty, *J. Phys. Chem.*, **99**, 1375 (1995).

j. M. N. Glukhovtsev and S. Laiter, *Theor. Chim. Acta*, **92**, 327 (1995).

k. A. Nicolaidis and L. Raddom, *J. Phys. Chem.*, **98**, 3092 (1994).

below, the number of  $sp^3$ ,  $sp^2$ , and  $sp$  C–H bonds and the hybridization types of the C–C bonds are balanced.<sup>35</sup>



Further refinements are possible. For example, in evaluating cyclic compounds, use of matching ring sizes can be specified so as to cancel errors resulting from ring strain.<sup>36</sup> Although the reaction may not correspond to any real chemical process, the calculation can test the reliability of the computation methods because of the additivity of  $\Delta H_f^\circ$  data.

The accuracy of the computational  $\Delta H$  can be judged by comparison with  $\Delta H$  obtained by summation of tabulated  $\Delta H_f^\circ$  for reactants and products. Table 3.6 compares some  $\Delta H_f^\circ$  values calculated at the G2 level of theory from atomization energies and isodesmic reactions. For molecules of this size, the use of isodesmic reactions can usually achieve  $\Delta H_f^\circ$  data within 0.5 kcal/mol.<sup>37</sup> A study of a series of hydrocarbons, including somewhat larger molecules, comparing G2 and G3 calculations is also available.<sup>38</sup>

For larger molecules that are outside the range of ab initio calculations, the semiempirical methods can be used. For example, the AM1 and PM3 methods have been used for a series of polycyclic aromatic hydrocarbons. Some results are shown in Table 3.7. The average errors were 9.1 kcal/mol for AM1 and 5.9 for PM3. Both methods can be internally calibrated by least-squares correlations, which improve the average error to 1.3 kcal/mol for AM1 and 2.1 for PM3.

**Table 3.6. Comparison of Differences from Experimental  $\Delta H_f^\circ$  in kcal/mol for G2 Calculations Using Atomization Energy versus Isodesmic Reactions<sup>a</sup>**

	$\Delta H_f^\circ$ (exp)	G2 (atomization)	G2 (isodesmic)
Propane	-25.0	0.4	0.1
Cyclopropane	66.0	-2.9	-1.6
Butane	-30.0	0.4	0.2
Cyclobutane	37.4	-2.9	-1.5
Bicyclo[1.1.0]butane	51.9	-3.0	-1.5
Cyclopentane	-18.3	-1.1	-0.4
Benzene	19.7	-3.9	-0.8

a. K. Raghavachari, B. Stefanov, and L. A. Curtiss, *J. Chem. Phys.*, **106**, 6764 (1997).

<sup>35</sup> P. George, M. Trachtman, C. W. Bock, and A. M. Brett, *Tetrahedron*, **32**, 317 (1976).

<sup>36</sup> P. v. R. Schleyer, P. K. Freeman, H. Jiao, and B. Goldfuss, *Angew. Chem. Int. Ed. Engl.*, **34**, 337 (1995); M. K. Cyranski, P. v. R. Schleyer, T. M. Krygowski, H. Jiao, and G. Hohlneicher, *Tetrahedron*, **59**, 1657 (2003).

<sup>37</sup> K. Raghavachari, B. B. Stefanov, and L. A. Curtiss, *J. Chem. Phys.*, **106**, 6764 (2000).

<sup>38</sup> R. Notario, O. Castano, J. -L. M. Abboud, R. Gomperts, L. M. Frutos, and R. Palmeiro, *J. Org. Chem.*, **64**, 9011 (1999); R. Notario, O. Castano, R. Gomperts, L. M. Frutos, and R. Palmeiro, *J. Org. Chem.*, **65**, 4298 (2000).

**Table 3.7. Comparison of Experimental  $\Delta H_f^\circ$  (kcal/mol) and Semiempirical Values for Polycyclic Aromatic Hydrocarbons**

Molecule <sup>a</sup>	Experimental $\Delta H_f^\circ$	AM1 <sup>b</sup>	PM3 <sup>c</sup>
Benzene	20.0	22.0	23.5
Naphthalene	36.0	40.6	40.7
Phenanthrene	49.7	57.4	55.0
Anthracene	55.2	62.5	61.7
Pyrene	54.0	67.4	64.1
Triphenylene	66.5	75.5	68.3
Chrysene	66.0	76.2	70.9
Benz[a]anthracene	70.3	78.3	74.5
Benzo[c]phenanthrene	69.6	81.2	77.6
Perylene	78.4	89.3	82.0
Tetracene	72.3	86.9	84.3

a. For structures of the polycyclic aromatic hydrocarbons, see Scheme 8.2, p. 746.

b. W. C. Herndon, P. C. Nowak, D. A. Connor, and P. Lin, *J. Am. Chem. Soc.*, **114**, 41 (1992).

c. D. M. Camaioni, S. T. Autrey, T. B. Salinas, and J. A. Franz, *J. Am. Chem. Soc.*, **118**, 2013 (1996)

Any set of computed energies can be used for calculation of reaction enthalpies by comparing the energy of reactants and products. Table 3.8 gives some data for hydrogenation, hydrogenolysis, and isomerization reactions at several levels of theory, including data for small ring compounds, which represent a particularly challenging test of the accuracy of the computational methods.

The relative merits of various computational methods have been discussed in the literature.<sup>39</sup> In general, the ab initio types of calculations are more reliable but

**Table 3.8. Comparison of Calculated and Observed  $\Delta H$  for Some Reactions<sup>a</sup>**

Reaction	HF/6-31G*	MP2/6-311*	B3LYP/6-31G*	Observed
$\text{CH}_2=\text{CH}_2 + \text{H}_2 \rightarrow \text{C}_2\text{H}_6$	-36.0	-32.2	-31.7	-30.8
$\text{CH}_2=\text{CHCH}=\text{CH}_2 + 2\text{H}_2 \rightarrow \text{C}_4\text{H}_{10}$	-62.5	-55.6	-52.4	-53.3
 + 3H <sub>2</sub> → C <sub>6</sub> H <sub>12</sub>	-53.8	-41.1	-38.1	-44.0
$\text{C}_2\text{H}_6 + \text{H}_2 \rightarrow 2\text{CH}_4$	-18.8	-10.4	-16.5	-15.5
 + H <sub>2</sub> → C <sub>3</sub> H <sub>8</sub>	-41.8	-35.6	-38.6	-35.9
 → CH <sub>2</sub> =CHCH <sub>3</sub>	-8.9	-6.2	-10.5	-8.5
 + H <sub>2</sub> → C <sub>4</sub> H <sub>10</sub>	-40.3	-34.1	-37.3	-35.9
 + H <sub>2</sub> → 	-53.2	-44.0	-47.0	-44.4
 → CH <sub>2</sub> =CHCH=CH <sub>2</sub>	-20.9	-22.4	-31.9	-26.2

a. In kcal/mol; K. B. Wiberg and J. W. Ochlerski, *J. Comput. Chem.*, **18**, 108 (1997).

<sup>39</sup> J. A. Pople, *J. Am. Chem. Soc.*, **97**, 5306 (1975); W. J. Hehre, *J. Am. Chem. Soc.*, **97**, 5308 (1975); T. A. Halgren, D. A. Kleier, J. H. Hall, Jr., L. D. Brown, and W. N. Lipscomb, *J. Am. Chem. Soc.*, **100**, 6595 (1978); M. J. S. Dewar and G. P. Ford, *J. Am. Chem. Soc.*, **101**, 5558 (1979); W. J. Hehre, *Acc. Chem. Res.*, **9**, 399 (1976); M. J. S. Dewar, E.G. Zoebisch, E. F. Healy, and J. J. P. Stewart,

the semiempirical calculations are much faster in terms of computer time. The time requirement for an ab initio calculation increases rapidly as the number of atoms in the molecule increases. The C<sub>8</sub> hydrocarbons represent the current practical limit for high-level ab initio computations. DFT computations are faster than ab initio computations and the amount of computer time required does not increase as rapidly with molecular size. The choice of basis set orbitals influences the outcome, and often several basis sets are checked to determine which are adequate. A choice of computational method is normally made on the basis of evidence that the method is suitable for the problem at hand and the availability of appropriate computer programs and machine time. Results should be subjected to critical evaluation by comparison with experimental data or checked by representative calculations using higher-level methods.

*3.1.2.6. Limitations on Enthalpy Data for Predicting Reactivity.* Whether  $\Delta H$  for a projected reaction is based on tabulated thermochemical data, bond energy, equivalent group additivity, or on MO or DFT computations, fundamental issues that prevent a final conclusion about a reaction's feasibility remain. In the first place, most reactions of interest occur in solution, and the enthalpy, entropy, and free energy associated with any reaction depend strongly on the solvent medium. There is only a limited amount of tabulated thermochemical data that are directly suitable for the treatment of reactions in organic solvents.<sup>40</sup> MO and DFT calculations usually refer to the isolated (gas phase) molecule. Estimates of solvation effects on reactants, products, intermediates, and transition states must be made in order to apply either experimental or computational thermochemical data to reactions occurring in solution. There may be substantial differences between solvation energies of reactants, transition states, intermediates, and products. If so, these solvation differences become a major factor in determining reactivity.

An even more fundamental limitation is that  $\Delta H$  data give no information about the *rate of a chemical reaction*. It is the energy of the transition state relative to the reactants that determines the reaction rate. To be in a position to make judgments on reactivity, we have to see how structure is related to *reactivity*. To do this, we need information about the energy of transition states and intermediates, but because transition states are transitory, we have no physical means of determining their structure. We can, however, determine their energy relative to reactants on the basis of reaction kinetics. We address this topic in the next sections by first examining the principles of chemical kinetics. We can also obtain information about transition states and intermediates by studying the effect of substituents on the rate of reaction. In Section 3.4, we look at how key intermediates such as carbocations, carbanions, and radicals respond to substituents.

Theoretical descriptions of molecules have been applied to the structure of transition states and unobservable intermediates. By applying MO or DFT methods, structures can be calculated for successive geometries that gradually transform the reactants into products. Exploration of a range of potential geometries and calculation of the energy of the resulting ensembles can, in principle, locate and describe

*J. Am. Chem. Soc.*, **107**, 3902 (1985); J. N. Levine, *Quantum Chemistry*, 3rd Edition, Allyn and Bacon, 1983, pp. 507–512; W. Hehre, L. Radom, P. v. R. Schleyer, and J. A. Pople, *Ab Initio Molecular Orbital Calculations*, John Wiley & Sons, 1986, Chap. 6; B. H. Besler, K. M. Merz, Jr., and P. Kollman, *J. Comput. Chem.*, **11**, 431 (1990); M. Sana and M. T. Nguyen, *Chem. Phys. Lett.*, **196**, 390 (1992).

<sup>40</sup> Guthrie has explored the use of a group equivalent scheme to compute  $\Delta G_f$  for aqueous solutions. J. P. Guthrie, *Can. J. Chem.*, **70**, 1042 (1992).

the minimum energy pathway. To the extent that the calculations accurately reflect the molecular reality, this provides a structural description of the reaction path and transition state. Thus we can refer to the *transition structure*, that is, the structural description of the reacting ensemble at the transition state.<sup>41</sup> We use the abbreviation TS to refer to transition structures. We use the term *transition state* in the context of energetic analysis where there is no explicit consideration of the structure. In Section 3.7 we focus attention on another aspect of reactivity—the use of catalysts to accelerate reaction.

## 3.2. Chemical Kinetics

### 3.2.1. Fundamental Principles of Chemical Kinetics

Thermodynamic data give us a means of quantitatively expressing *stability*. Now we need to explore the relationship between *structure* and *reactivity*. The quantitative description of reactivity is called *chemical kinetics*. A fundamental thermodynamic equation relates the equilibrium constant for a reaction to the free-energy change associated with the reaction:

$$\Delta G = -RT \ln K \quad (3.12)$$

The free energy contains both enthalpy and entropy terms:

$$\Delta G = \Delta H - T\Delta S \quad (3.13)$$

Thus we see that thermodynamic stability, as measured by free energy, places a limit on the *extent of a chemical reaction*. However, it does not directly determine the rate of the reaction.

The nature of the *rate constants*  $k_r$  for individual steps in a chemical reaction can be discussed in terms of *transition state theory*, which is a general approach for analyzing the energetic and entropic components of a reaction process. In transition state theory, a reaction is assumed to involve the attainment of an *activated complex* that goes on to product at an extremely rapid rate. The rate of decomposition of the activated complex has been calculated from the assumptions of the theory to be about  $6 \times 10^{12} \text{ s}^{-1}$  at room temperature. The observed rate constant  $k_r$  is given by the expression<sup>42</sup>

$$k_r = \frac{\kappa k_B T}{h} (e^{-\Delta H^\ddagger/RT})(e^{\Delta S^\ddagger/R}) \quad (3.14)$$

<sup>41</sup>. Although the terms transition state and transition structure are often used interchangeably, if the transition state is taken as defined by transition state theory, it may differ in structure from the maximum energy obtained by computation; K. N. Houk, Y. Li, and J. D. Evansck, *Angew. Chem. Int. Ed. Engl.*, **31**, 682 (1992).

<sup>42</sup>. For a more complete development of these relationships, see M. Boudart, *Kinetics of Chemical Processes*, Prentice-Hall, Englewood Cliffs, NJ, 1968, pp. 35–46; or I. Amdur and G. G. Hammes, *Chemical Kinetics: Principles and Selected Topics*, McGraw-Hill, New York, 1966, pp. 43–58; J. W. Moore and R. G. Pearson, *Kinetics and Mechanism*, Wiley, New York, 1981, pp. 159–169; M. M. Kreevoy and D. G. Truhlar, in C. F. Bernasconi, *Investigation of Rates and Mechanisms of Reaction: Techniques of Organic Chemistry*, 4th Edition, Vol. VI, Part 1, Interscience, New York, 1986.

in which  $\kappa$  is the transmission coefficient, which is usually taken to be 1,  $k_B$  is Boltzmann's constant,  $h$  is Planck's constant,  $R$  is the gas constant, and  $T$  is the absolute temperature. If the activated complex is considered to be in equilibrium with its component molecules, the attainment of the transition state ( $TS$ ) can be treated as being analogous to a bimolecular reaction:

$$K^\ddagger = \frac{[TS]}{[A][B]} \quad (3.15)$$

The position of this equilibrium is related to the free energy required for attainment of the transition state. The symbol ( $^\ddagger$ ) is used to specify that it is a transition state or "activated complex" that is under discussion:

$$\Delta G^\ddagger = -RT \ln K^\ddagger \quad (3.16)$$

The free energy  $\Delta G^\ddagger$  is called as the *free energy of activation*. The rate of a reaction step is then given by

$$\text{Rate} = \frac{\kappa k_B T}{h} [TS] \quad (3.17)$$

$$\text{Rate} = \frac{\kappa k_B T}{h} e^{-\Delta G^\ddagger/RT} [A][B] \quad (3.18)$$

Comparison with the form of the expression for the rate of any single reaction step reveals that the magnitude of  $\Delta G^\ddagger$  is the factor that determines the magnitude of  $k_r$  at any given temperature:

$$\text{Rate} = k_r [A][B] \quad (3.19)$$

The temperature dependence of reaction rates permits evaluation of the enthalpy and entropy components of the free energy of activation. The terms in Equation (3.14) can be rearranged to examine the temperature dependence:

$$k_r = \frac{\kappa k_B T}{h} \left( e^{-\Delta H^\ddagger/RT} \right) \left( e^{\Delta S^\ddagger/R} \right) \quad (3.20)$$

The term  $(\kappa k_B T/h)e^{\Delta S^\ddagger/R}$  varies only slightly with  $T$  compared to  $e^{-\Delta H^\ddagger/RT}$  because of the exponential nature of the latter. To a good approximation, then:

$$\frac{k_r}{T} = C e^{-\Delta H^\ddagger/RT} \quad (3.21)$$

$$\ln \frac{k_r}{T} = \frac{-\Delta H^\ddagger}{RT} + C' \quad (3.22)$$

A plot of  $\ln(k_r/T)$  versus  $1/T$  is a straight line, and its slope is  $-\Delta H^\ddagger/R$ . After  $\Delta H^\ddagger$  is determined in this manner,  $\Delta S^\ddagger$  is available from the relationship

$$\Delta S^\ddagger = \frac{\Delta H^\ddagger}{T} + R \ln \frac{h k_r}{\kappa k_B T} \quad (3.23)$$

which can be obtained by rearranging Equation (3.14).

The temperature dependence of reactions is frequently expressed in terms of the Arrhenius equation:

$$k_r = Ae^{-E_a/RT} \quad \text{or} \quad \ln k_r = -E_a/RT + \ln A \quad (3.24)$$

The  $E_a$  can be determined experimentally by measuring the reaction rate at several temperatures over as wide a range as practical. A plot of  $\ln k_r$  against  $1/T$  then gives a line of slope equal to  $-E_a/R$ . The value of  $E_a$  incorporates the  $\Delta H$  term and the value of  $A$  reflects the entropy term. At constant pressure,  $E_a$  and  $\Delta H$  are related by the expression

$$\Delta H^\ddagger = E_a - RT \quad (3.25)$$

and  $\Delta S^\ddagger$  is related to  $A$  by

$$\Delta S^\ddagger = R[\ln(h/k_B T) + \ln A - 1] \quad (3.26)$$

The magnitude of  $\Delta H^\ddagger$  and  $\Delta S^\ddagger$  reflect transition state structure. Atomic positions in the transition state do not correspond to their positions in the ground state. In particular, the reacting bonds are partially formed or partially broken. The energy required for bond reorganization is reflected in the higher energy content of the activated complex and corresponds to the enthalpy of activation  $\Delta H^\ddagger$ . The entropy of activation,  $\Delta S^\ddagger$ , is a measure of the degree of organization resulting from the formation of the activated complex. If translational, vibrational, or rotational degrees of freedom are lost in going to the transition state, there is a decrease in the total entropy of the system. Conversely, an increase of translational, vibrational, or rotational degrees of freedom results in a positive entropy of activation. For reactions in solution, the organization of solvent contributes to the entropy of activation.

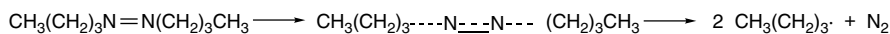
Wide variation in enthalpy and entropy of activation for different reaction systems is possible, as illustrated by the following two reactions.



$$\Delta H^\ddagger = 15.5 \text{ kcal/mol}$$

$$\Delta S^\ddagger = -34 \text{ eu}$$

Ref. 43



$$\Delta H^\ddagger = 52 \text{ kcal/mol}$$

$$\Delta S^\ddagger = +19 \text{ eu}$$

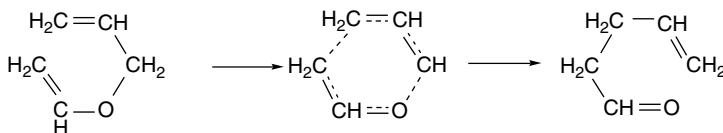
Ref. 44

The relatively low  $\Delta H^\ddagger$  term for the dimerization of cyclopentadiene is characteristic of concerted reactions (see Chapter 10), in which bond making accompanies

<sup>43</sup>. A. Wassermann, *Monatsch. Chem.*, **83**, 543 (1952).

<sup>44</sup>. A. U. Blackham and N. L. Eatough, *J. Am. Chem. Soc.*, **84**, 2922 (1962).

bond breaking. It differs markedly from  $\Delta H^\ddagger$  for the thermal decomposition of 1,1'-azobutane, in which the rate-determining step is a homolytic cleavage of a C–N bond, with little new bond making to compensate for the energy cost of the bond breaking. The entropy of activation, on the other hand, is more favorable in the 1,1'-azobutane decomposition, since a translational degree of freedom is being gained in the TS as the molecular fragments separate. The dimerization of cyclopentadiene is accompanied by a very negative entropy of activation because of the loss of translational and rotational degrees of freedom in formation of the highly ordered cyclic TS. The two reacting molecules must attain a specific orientation to permit the bonding interactions that occur as the TS is approached. Unimolecular reactions that take place by way of cyclic transition states also typically have negative entropies of activation because of the loss of rotational degrees of freedom associated with the highly ordered TS. For example, thermal isomerization of vinyl allyl ether to 4-pentenal has  $\Delta S^\ddagger = -8 \text{ cal/mol-deg}^{-1}$ .<sup>45</sup>



It is important to remember that the enthalpy and entropy of activation reflect the response of the *reacting system as a whole* to formation of the activated complex. As a result, the interpretation of these parameters is more complicated for reactions taking place in solution than for gas phase reactions. This is particularly true for processes involving formation or destruction of charged species. The solvolysis of *t*-butyl chloride in 80% aqueous ethanol, for example, has as its rate-determining step unimolecular ionization of the carbon-chlorine bond to form chloride and *t*-butyl cations. One might think that this ionization would lead to a positive entropy of activation, since two independent particles are being generated. In fact, the entropy of activation is  $-6.6 \text{ cal/mol-deg}^{-1}$ . Owing to its polar character, the TS requires a greater ordering of solvent molecules than the nonpolar reactant.<sup>46</sup> Reactions that generate charged species usually exhibit negative entropies of activation in solution. The reverse is true for reactions in which charged reactants lead to a neutral transition state.

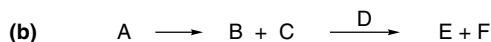
### 3.2.2. Representation of Potential Energy Changes in Reactions

**3.2.2.1. Reaction Energy Profiles.** It is often useful to describe reactions in terms of an energy profile that traces the potential energy of the reacting ensemble of molecules as they proceed from reactants to products, such as shown in Figure 3.1 (page 254). Thermodynamic stability establishes the relative energy of the reactants and the products, but does not provide any information about the intervening stages of the process. It is these intervening stages that determine how fast (or slow) a reaction will be. If a large  $\Delta G^\ddagger$  is required, the reaction will be slow. Reactions often proceed through a sequence of steps involving formation of a series of intermediates that eventually lead to the products. Interpretation of the kinetic characteristics of a reaction can provide information about the intervening steps by providing information about *intermediates*

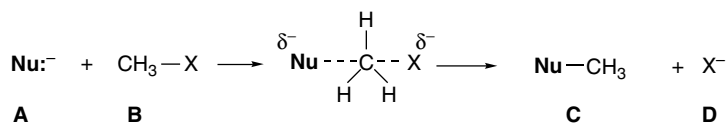
<sup>45</sup> F. W. Schuler and G. W. Murphy, *J. Am. Chem. Soc.*, **72**, 3155 (1950).

<sup>46</sup> E. Grunwald and S. Winstein, *J. Am. Chem. Soc.*, **70**, 846 (1948).

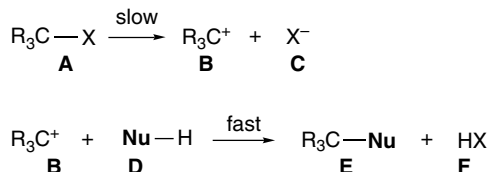
that exist along the reaction pathway. The sequence of reaction steps and intermediates involved in the overall transformation is the *reaction mechanism*. Reactants, intermediates, and products correspond to energy minima on the energy diagram and are separated by *activated complexes or transition states*, which are the molecular arrangements having the maximum energy for each successive step of the reaction mechanism. Figure 3.2 gives reaction energy diagrams for hypothetical reactions that proceed in one, two, or three steps through zero, one, or two intermediates. For the example in Figure 3.2, these are:



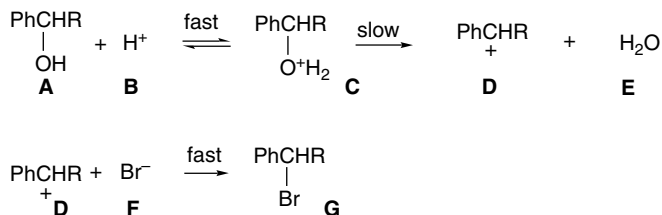
The diagram in (a), for example, might correspond to an  $S_N2$  displacement reaction.



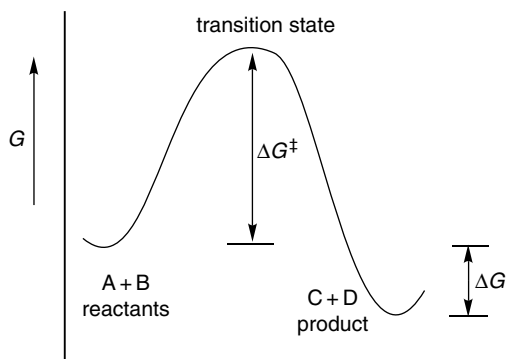
The diagram in (b) could pertain to an  $S_N1$  reaction with a solvent **D** proceeding through a carbocation intermediate (**B**).



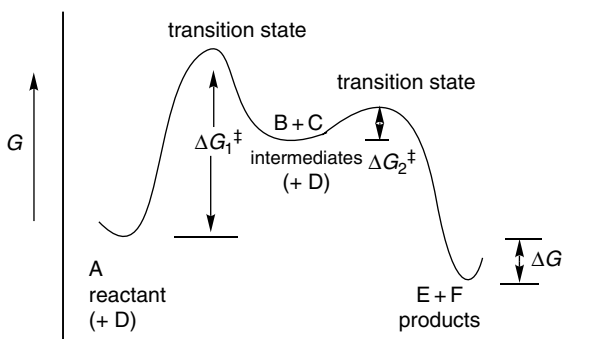
The diagram in (c) might apply to an acid-catalyzed ionization mechanism, such as might occur in a reaction of a secondary benzylic alcohol with HBr.



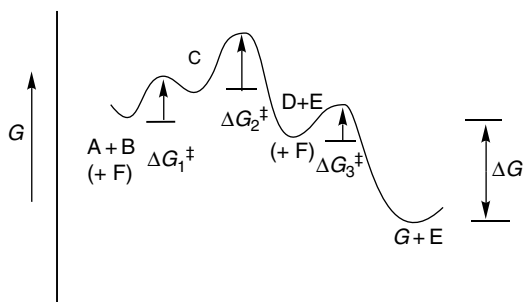
Such diagrams make clear the difference between an intermediate and a transition state. An intermediate lies in a depression on the potential energy curve. Thus, it has a finite lifetime, which depends on the depth of the depression. A shallow depression implies a low activation energy for the subsequent step, and therefore a short lifetime. The deeper the depression, the longer the lifetime of the intermediate. The situation at a transition state is quite different. This arrangement has only fleeting existence and represents an energy maximum on the reaction path.



(a) Energy diagram for a single-step reaction.



(b) Energy diagram for a two-step reaction.



(c) Energy diagram for a three-step reaction.

Fig. 3.2. Reaction energy profiles for one-, two-, and three-step reactions showing successive transition states and intermediates.

There is one path between reactants and products that has a lower energy maximum than any other and is the pathway that the reaction will follow. *The curve in a potential energy plot represents this lowest energy pathway.* It corresponds to a path across an energy surface describing energy as a function of the spatial arrangement of the atoms involved in the reaction. The progress of the reaction is called the *reaction coordinate*, and is a measure of the structural changes taking place as reaction occurs. The *principle of microscopic reversibility* arises directly from transition state theory. *The same pathway that is traveled in the forward direction of a*



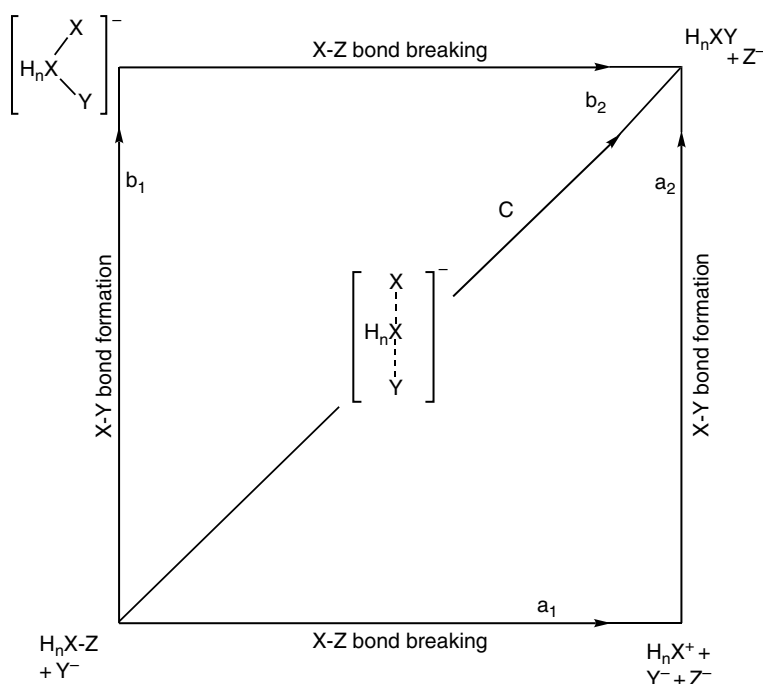
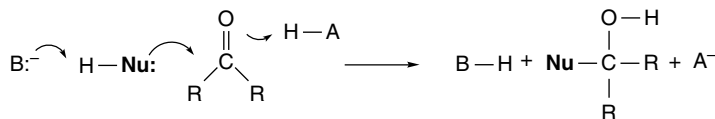


Fig. 3.3. Two-dimensional reaction energy diagram showing (a) dissociative, (b) associative, and (c) concerted mechanisms for a substitution reaction.

O’Ferrall-Jencks diagrams.<sup>47</sup> Energy is not explicitly shown in such diagrams, but it is a third dimension. We use such diagrams in the discussions of several reaction types, including elimination reactions (Section 5.10.1) and carbonyl addition reactions (Section 7.1). When the energy dimension is added, the diagram takes the form of a contour plot as shown in Figure 3.4. The preferred reaction pathway is over the lowest barrier.

Reactions involving changes at three bonds require a reaction cube and those with more bonding changes require cubes within cubes.<sup>48</sup> Figure 3.5 is a general representation of a reaction cube, and Figure 3.6 shows the cube corresponding to a reaction involving deprotonation of a nucleophile and protonation of a carbonyl oxygen in a carbonyl addition reaction.



Diagrams such as these can summarize the conclusions of kinetic and other studies of reaction mechanisms. Whether the diagram is in one, two, or three dimensions, it can specify the sequence of steps in the overall reaction.

<sup>47</sup> W. J. Albery, *Prog. React. Kinetics*, **4**, 353 (1967); R. A. More O’Ferrall, *J. Chem. Soc. B*, 274 (1970); W. P. Jencks, *Chem. Rev.*, **72**, 705 (1972).

<sup>48</sup> E. Grunwald, *J. Am. Chem. Soc.*, **107**, 4715 (1985); P. H. Scudder, *J. Org. Chem.*, **55**, 4238 (1990); J. P. Guthrie, *J. Am. Chem. Soc.*, **118**, 12878 (1996).

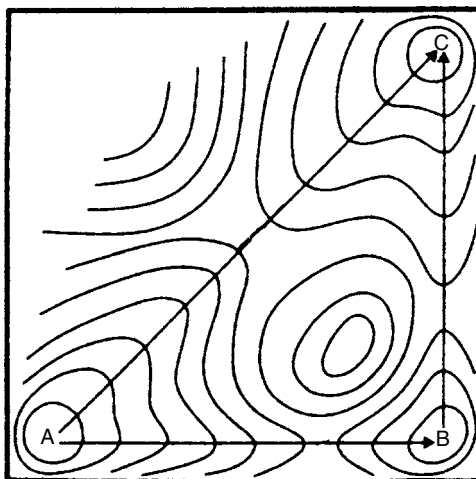


Fig. 3.4. Two-dimensional energy diagram showing energy contours for stepwise ( $A \rightarrow B \rightarrow C$ ) and concerted ( $A \rightarrow C$ ) reaction pathways.

**3.2.2.3. Computation of Reaction Potential Energy Surfaces.** As transition states cannot be observed, there is no experimental means of establishing their structure. Computational methods can be applied for descriptions of intermediates and transition structures. Structural attributes such as bond lengths, bond orders, electron density distribution, and orbital occupancy can be found for transition structures and intermediates, as was described in Sections 3.1.2.5 for stable molecules. The evaluation of a

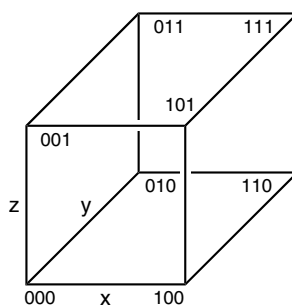


Fig. 3.5. Three-dimensional reaction coordinate diagram:  $x$ ,  $y$ , and  $z$  are the three edge coordinates;  $[0,0,0]$  is the starting point;  $[1,1,1]$  is the product;  $[1,0,0]$ ,  $[0,1,0]$ , and  $[0,0,1]$  are the corner intermediates corresponding to reaction along only one edge coordinate; and  $[1,1,0]$ ,  $[1,0,1]$ , and  $[0,1,1]$  are the corner intermediates corresponding to the reaction along two edge coordinates. Reproduced with permission from *Can. J. Chem.*, **74**, 1283 (1996).

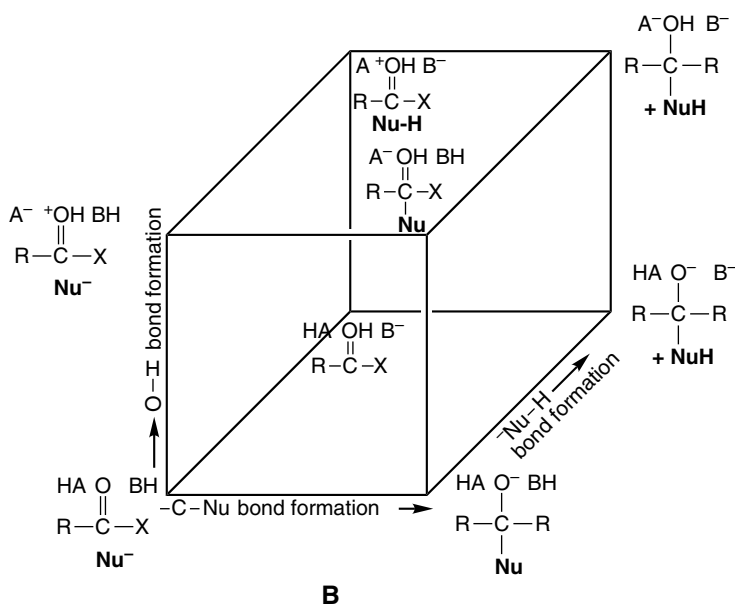


Fig. 3.6. Reaction progress cube showing possible intermediates for nucleophilic addition to a carbonyl group involving HA, B<sup>-</sup>, and Nu-H. Adapted from *J. Org. Chem.*, **55**, 4238 (1990).

reaction mechanism typically involves the comparison of the energy of potential TSs. The expectation is that the reaction will proceed through the lowest energy TS, so if this can be reliably computed, the reaction mechanism can be defined. In the evaluation of stereoselectivity, for example, a comparison of the energies of the alternative TSs can predict the product ratio.

A very large number of structural variations can be conceived, but the structures of interest are the transition structures and intermediates that connect the reactants and products. The mathematics involved in characterizing a potential energy surface involves evaluation of energy gradients as a function of structural change. A *transition state* is a minimum in energy with respect to all changes in molecular dimensions except along the reaction coordinate, where it is a maximum on the energy surface. The transition state is a *saddle point*; that is, it is an energy minimum relative to change in any coordinate except in the direction of reaction. It is an energy maximum relative to that motion so the force constant is negative because there is no barrier to movement in that direction. A property of transition structures is that they have a *single imaginary vibrational frequency*, corresponding to the structural change in the direction of the reaction process. Because there are ordinarily many possible structural variations, the potential energy surface is a multidimensional hypersurface,<sup>49</sup> which can be described mathematically in terms of all the dimensions being explored. Because the reaction coordinate corresponds to the lowest-energy path, it can be located mathematically by minimization of the energy in all dimensions except that corresponding to the progress of the reaction. The computed minimum-energy path is called the *intrinsic reaction coordinate*.<sup>50</sup>

<sup>49</sup>. P. N. Skancke, *Acta Chem. Scand.*, **47**, 629 (1993).

<sup>50</sup>. K. Fukui, *J. Phys. Chem.*, **74**, 4161 (1970); S. Kato and K. Fukui, *J. Am. Chem. Soc.*, **98**, 6395 (1976).

The calculation of the properties of transition structures is more problematic than for stable molecules because TSs involve bond breaking. Thus computations based on the concept of electron pairing may not be applicable, especially for species with radical character. Nevertheless, computational studies have provided insight into many reactions and we frequently use the results of these studies, as well as experimental work, in developing the details of reaction mechanisms.

### 3.2.3. Reaction Rate Expressions

Experimental kinetic data can provide detailed insight into reaction mechanisms. The rate of a given reaction can be determined by following the disappearance of a reactant or the appearance of a product. The extent of reaction is often measured spectroscopically, because spectroscopic techniques provide a rapid, continuous means of monitoring changes in concentration. Numerous other methods are available and may be preferable in certain cases. For example, continuous pH measurement or acid-base titration can be used to follow the course of reactions that consume or generate an acid or a base. Conductance measurements provide a means for determining the rate of reactions that generate ionic species; polarimetry can be used to follow reactions involving optically active materials. In general, any property that can be measured and quantitatively related to the concentration of a reactant or a product can be used to determine a reaction rate.

The goal of a kinetic study is to establish the quantitative relationship between the concentration of reactants and catalysts and the observed rate of the reaction. Typically, such a study involves rate measurements at enough different concentrations of each reactant to determine the *kinetic order* with respect to each reactant. A complete investigation allows the reaction to be described by a *rate expression* or *rate law*, which is an algebraic formula containing one or more *rate constants*, as well as terms for the concentration of all reactant species that are involved in the rate-determining and prior steps. Each concentration has an exponent called the *order of the reaction* with respect to that component. The overall kinetic order of the reaction is the sum of all the exponents in the rate expression. The mathematical form of the rate expression for a reaction depends on the order of the reaction. Using  $[A_0]$ ,  $[B_0]$ ,  $[C_0]$ , etc. for the initial ( $t = 0$ ,  $t_0$ ) concentrations and  $[A]$ ,  $[B]$ ,  $[C]$ , etc. as the reactant concentrations at time  $t$ , give the following expressions<sup>51</sup>:

FIRST ORDER: Rate =  $k[A]$

$$\ln \frac{[A_0]}{[A]} = kt \quad \text{or} \quad [A] = [A]_0 e^{-kt} \quad (3.27)$$

SECOND ORDER/ONE REACTANT: Rate =  $k[A]^2$

$$kt = \frac{1}{A} - \frac{1}{A_0} \quad (3.28)$$

SECOND ORDER/TWO REACTANTS: Rate =  $k[A][B]$

$$kt = \frac{1}{[B_0] - [A_0]} \ln \frac{[A_0][B]}{[B_0][A]} \quad (3.29)$$

<sup>51</sup>. J. W. Moore and R. G. Pearson, *Kinetics and Mechanism*, 3rd Edition, John Wiley & Sons, New York, 1981, Chap. 2.

THIRD ORDER/ONE REACTANT: Rate =  $k[A]^3$

$$kt = \frac{1}{2} \left( \frac{1}{[A]^2} - \frac{1}{[A_0]^2} \right) \quad (3.30)$$

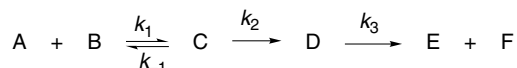
THIRD ORDER/TWO REACTANTS: Rate =  $k[A]^2[B]$

$$kt = \frac{2}{(2[B_0] - [A_0])} \left( \frac{1}{[A]} - \frac{1}{[A_0]} \right) + \frac{2}{(2[B_0] - [A_0])^2} \ln \frac{[B_0][A]}{[A_0][B]} \quad (3.31)$$

Integrated expressions applicable to other systems are available.<sup>52</sup>

The kinetic data available for a particular reaction are examined to determine if they fit a simple kinetic expression. For example, for a first-order reaction, a plot of  $\log [A]$  versus  $t$  yields a straight line with a slope of  $-k/2.303$ . For second-order reactions, a plot of  $1/[A]$  versus  $t$  is linear with a slope of  $k$ . Figure 3.7 shows such plots. Alternatively, the value of  $k$  can be calculated from the integrated expression over a sufficient time range. If the value of  $k$  remains constant, the data are consistent with that rate expression.

Many organic reactions consist of a series of steps involving several intermediates. The overall rate expression then depends on the relative magnitude of the rate constants for the individual steps. The relationship between a kinetic expression and a reaction mechanism can be appreciated by considering the several individual steps that constitute the overall reaction mechanism. The expression for the rate of any *single step* in a reaction mechanism contains a term for the concentration for each reacting species. Thus, for the reaction sequence:



the rates for the successive steps are:

$$\text{STEP 1: } \frac{d[C]}{dt} = k_1[A][B] - k_{-1}[C]$$

$$\text{STEP 2: } \frac{d[D]}{dt} = k_2[C]$$

$$\text{STEP 3: } \frac{d[E]}{dt} = \frac{d[F]}{dt} = k_3[D]$$

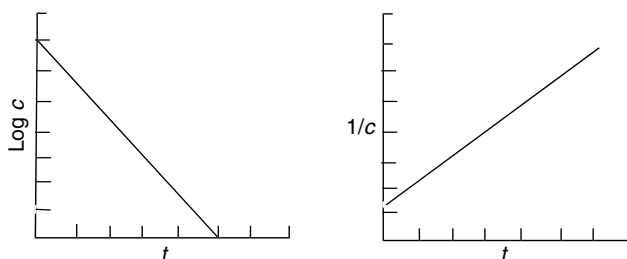


Fig. 3.7. Linear plots of  $\log c$  versus  $t$  for a first-order reaction (a) and  $1/c$  versus  $t$  for a second-order reaction.

<sup>52</sup> C. Capellos and B. N. J. Bielski, *Kinetic Systems*, Wiley-Interscience, New York, 1972.

If we specify that the first step is a very rapid but unfavorable equilibrium, and that  $k_2 \ll k_3$ , then the second step is rate determining. Under these circumstances, the overall rate of the reaction will depend on the rate of the second step. In the reaction under consideration, the final step follows the rate-determining step and does not affect the rate of the overall reaction;  $k_3$  does not appear in the overall rate expression. The rate of the reaction is governed by the second step, which is the bottleneck in the process. The rate of this step is equal to  $k_2$  multiplied by the molar concentration of intermediate **C**, which is small and may not be measurable. It is therefore necessary to express the rate in terms of the concentration of reactants. In the case under consideration, this can be done by recognizing that **[C]** is related to **[A]** and **[B]** by an equilibrium constant:

$$K = \frac{[\text{C}]}{[\text{A}][\text{B}]}$$

Furthermore,  $K$  is related to  $k_1$  and  $k_{-1}$  by the requirement that no net change in composition occur at equilibrium

$$k_{-1}[\text{C}] = k_1[\text{A}][\text{B}]$$

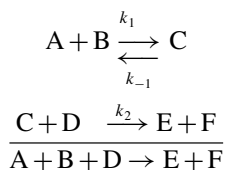
$$[\text{C}] = \frac{k_1}{k_{-1}}[\text{A}][\text{B}]$$

The rate of Step 2 can therefore be written in terms of **[A]** and **[B]**:

$$\frac{d[\text{D}]}{dt} = k_2[\text{C}] = k_2 \frac{k_1}{k_{-1}}[\text{A}][\text{B}] = k_{\text{obs}}[\text{A}][\text{B}]$$

Experimentally, it would be observed that the reaction rate would be proportional to both **[A]** and **[B]**. The reaction will be first order in each reactant and second order overall.

A useful approach that is often used in analysis and simplification of kinetic expressions is the *steady state approximation*, which can be illustrated by a hypothetical reaction scheme:



If **C** is a reactive, unstable species, its concentration will never be very large. It must be consumed at a rate that closely approximates the rate at which it is formed. Under these conditions, it is a valid approximation to set the rate of formation of **C** equal to its rate of destruction:

$$k_1[\text{A}][\text{B}] = k_2[\text{C}][\text{D}] + k_{-1}[\text{C}]$$

Rearrangement of this equation provides an expression for **[C]**:

$$\frac{k_1[\text{A}][\text{B}]}{(k_2[\text{D}] + k_{-1})} = [\text{C}]$$

By substituting into the rate for the second step, we obtain the following expression:

$$\text{Rate} = k_2[C][D] = k_2 \frac{k_1[A][B]}{(k_2[D] + k_{-1})} [D]$$

If  $k_2[D]$  is much greater than  $k_{-1}$ , the rate expression simplifies to

$$\text{Rate} = \frac{k_2 k_1 [A][B][D]}{k_2 [D]} = k_1 [A][B]$$

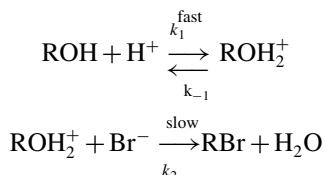
On the other hand, if  $k_2[D]$  is much less than  $k_{-1}$ , the observed rate expression becomes

$$\text{Rate} = \frac{k_1 k_2 [A][B][D]}{k_{-1}}$$

The first situation corresponds to the first step being rate determining; in the second case, it is the second step, with the first step being a pre-equilibrium.

### 3.2.4. Examples of Rate Expressions

The normal course of a kinetic investigation involves the postulation of likely mechanisms and comparison of the observed rate expression with those expected for the various mechanisms. Those mechanisms that are incompatible with the observed kinetics can be eliminated as possibilities. One common kind of reaction involves proton transfer occurring as a rapid equilibrium preceding the rate-determining step, for example, in the reaction of an alcohol with hydrobromic acid to give an alkyl bromide:

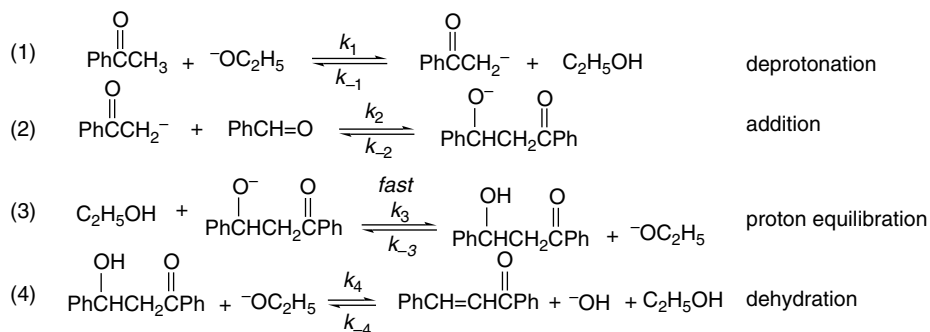


The overall rate being measured is that of Step 2, but there may be no means of directly measuring  $[\text{ROH}_2^+]$ . The concentration of the protonated intermediate  $\text{ROH}_2^+$  can be expressed in terms of the concentration of the starting material by taking into consideration the equilibrium constant, which relates  $[\text{ROH}]$ ,  $[\text{Br}^-]$ , and  $[\text{H}^+]$ :

$$\begin{aligned} K &= \frac{[\text{ROH}_2^+]}{[\text{ROH}][\text{H}^+]} \\ [\text{ROH}_2^+] &= K[\text{ROH}][\text{H}^+] \\ \text{Rate} &= k_2 K [\text{ROH}][\text{H}^+][\text{Br}^-] = k_{\text{obs}} [\text{ROH}][\text{H}^+][\text{Br}^-] \end{aligned}$$

To illustrate the development of a kinetic expression from a postulated reaction mechanism, let us consider the base-catalyzed reaction of benzaldehyde and acetophenone. Based on general knowledge of base-catalyzed reactions of carbonyl compounds, a reasonable sequence of steps can be written, but the relative rates of the steps is an open question. Furthermore, it is known that reactions of this type

are reversible, so the potential reversibility of each step must be taken into account. A completely reversible mechanism is as follows:



Because proton transfer reactions between oxygen atoms are usually very fast, Step 3 can be assumed to be a rapid equilibrium. With the above mechanism assumed, let us examine the rate expression that would result, depending upon which of the steps is rate determining. If Step 1 is rate controlling the rate expression would be

$$\text{Rate} = k_1[\text{PhCOCH}_3][^-\text{OC}_2\text{H}_5]$$

Under these conditions the concentration of the second reactant, benzaldehyde, would not enter into the rate expression. If Step 1 is an equilibrium and Step 2 is rate controlling, we obtain the rate expression

$$\text{Rate} = k_2[\text{PhCOCH}_2^-][\text{PhCHO}]$$

which on substituting in terms of the prior equilibrium gives

$$\text{Rate} = k_2K_1[\text{PhCOCH}_3][^-\text{OC}_2\text{H}_5][\text{PhCHO}]$$

since

$$[\text{PhCOCH}_2^-] = K_1[\text{PhCOCH}_3][^-\text{OC}_2\text{H}_5]$$

where  $K_1$  is the equilibrium constant for the deprotonation in the first step. If the final step is rate controlling the rate is

$$\text{Rate} = k_4[\text{PhCH(OH)CH}_2\text{COPh}][^-\text{OC}_2\text{H}_5]$$

The concentration of the intermediate  $\text{PhCHOHCH}_2\text{COPh}$  (**I**) can be expressed in terms of the three prior equilibria. Using **I** for the intermediate and  $\text{I}^-$  for its conjugate base and neglecting  $[\text{EtOH}]$ , since it is the solvent and will remain constant, gives the following relationships:

$$K_3 = \frac{[\text{I}][^-\text{OEt}]}{[\text{I}^-]} \quad \text{and} \quad [\text{I}] = K_3 \frac{[\text{I}^-]}{[^-\text{OEt}]}$$

Substituting for  $[\text{PhCOCH}_2^-]$  from the equilibrium expression for Step 1 gives

$$[\mathbf{I}] = \frac{K_3 K_2 [\text{PhCHO}]}{[\text{OEt}]} K_1 [\text{PhCOCH}_3] [\text{OEt}] = K' [\text{PhCHO}] [\text{PhCOCH}_3]$$

This provides the final rate expression:

$$\text{Rate} = k_{\text{obs}} [\text{OC}_2\text{H}_5] [\text{PhCHO}] [\text{PhCOCH}_3]$$

Note that the form of this third-order kinetic expression is identical to that in the case where the second step was rate determining and would not distinguish between the two possibilities.

Experimental studies of this base-catalyzed condensation have revealed that it is third order, indicating that either the second or fourth step must be rate determining. Studies on the intermediate **I** obtained by an alternative synthesis have shown that  $k_4$  is about four times as large as  $k_3$  so that about 80% of **I** goes on to product. These reactions are faster than the overall reaction under the same conditions, so the second step must be rate controlling.<sup>53</sup>

These examples illustrate the relationship between kinetic results and the determination of the reaction mechanism. Kinetic results can exclude from consideration all mechanisms that require a rate law different from the observed one. It is often true, however, that related mechanisms give rise to identical predicted rate expressions. In that case, the mechanisms are *kinetically equivalent* and a choice between them is not possible solely on the basis of kinetic data. A further limitation on the information that kinetic studies provide should also be recognized. Although the data can give the *composition* of the activated complex for the rate-determining and preceding steps, it provides no information about the *structure* of the activated complex or any intermediates. Sometimes the structure can be inferred from related chemical experience, but it is never established solely by kinetic data.

### 3.3. General Relationships between Thermodynamic Stability and Reaction Rates

We have considered the fundamental principles of thermodynamics and reaction kinetics. Now we would like to search for relationships between stability, as defined by thermodynamics, and reactivity, which is described by kinetics. Reaction potential energy diagrams are key tools in making these connections.

#### 3.3.1. Kinetic versus Thermodynamic Control of Product Composition

Product composition at the end of the reaction may be governed by the equilibrium thermodynamics of the system. When this is true, the product composition is governed by *thermodynamic control* and the stability difference between the competing products, as given by the free-energy difference, determines the product composition. Alternatively, product composition may be governed by competing rates of formation of

<sup>53</sup> E. Coombs and D. P. Evans, *J. Chem. Soc.*, 1295 (1940); D. S. Noyce, W. A. Pryor, and A. H. Bottini, *J. Am. Chem. Soc.*, **77**, 1402 (1955).

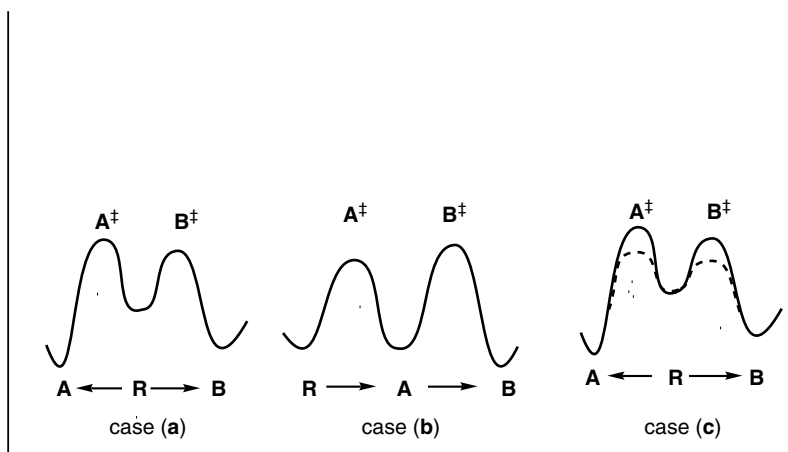


Fig. 3.8. Examples of reactions under kinetic and thermodynamic control. (a)  $\Delta G_B^\ddagger < \Delta G_A^\ddagger$ ; (b)  $\Delta G_A^\ddagger < \Delta G_B^\ddagger$ ; (c) alternative mechanism for product equilibrium.

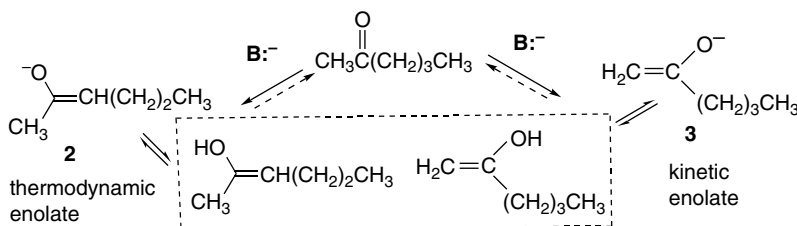
products, which is called *kinetic control*. Let us consider cases (a) to (c) in Figure 3.8. In case (a), the  $\Delta G^\ddagger$ 's for formation of the competing transition states  $A^\ddagger$  and  $B^\ddagger$  from the reactant R are substantially less than the  $\Delta G^\ddagger$ 's for formation of  $A^\ddagger$  and  $B^\ddagger$  from A and B, respectively. If the latter two  $\Delta G^\ddagger$ 's are sufficiently large that the competitively formed products B and A do not return to R, the ratio of the products A and B at the end of the reaction will not depend on their relative stabilities, but only on the *relative rates of formation*. The formation of A and B is effectively irreversible in these circumstances. The reaction energy profile in case (a) corresponds to this situation and is a case of kinetic control. The relative amounts of products A and B depend on the relative activation barriers  $\Delta G_A^\ddagger$  and  $\Delta G_B^\ddagger$  and not on the relative stability of products A and B. The diagram shows  $\Delta G_B^\ddagger < \Delta G_A^\ddagger$ , so the major product will be B, even though it is less stable than A.

Case (b) represents a situation of two successive reactions. The lowest  $\Delta G^\ddagger$  is that for formation of  $A^\ddagger$  from R. But, the  $\Delta G^\ddagger$  for formation of  $B^\ddagger$  from A is not much larger. The system in (b) might be governed by either kinetic or thermodynamic factors. Conversion of R to A will be only slightly faster than conversion of A to B. If the reaction conditions are carefully adjusted it will be possible for A to accumulate and not proceed to the more stable product B. Under such conditions, A will be the dominant product and the reaction will be under kinetic control. Under somewhat more energetic conditions, for example, at a higher temperature, A will be transformed into B. Under these conditions the reaction will be under thermodynamic control. A and B will equilibrate and the product ratio will depend on the equilibrium constant determined by  $\Delta G$  for the reaction  $A \rightleftharpoons B$ .

In case (c), the solid reaction energy profile represents the same situation of kinetic control as shown in (a), with product B (which is thermodynamically less stable) being formed because  $\Delta G_B^\ddagger < \Delta G_A^\ddagger$ . The dashed energy profile represents a different set of conditions for the same transformation, such as addition of a catalyst or change of solvent, that substantially reduces the energy of  $A^\ddagger$  and  $B^\ddagger$  such that interconversion of A and B is fast. This will result in formation of the more stable product A, even though the barrier to formation of B remains lower. Under these circumstances, the reaction is under *thermodynamic control*.

Thus, whenever competing or successive reaction products can come to equilibrium, the product composition will reflect relative stability and be subject to thermodynamic control. If product composition is governed by competing rates, the reaction is under kinetic control. A given reaction may be subject to either thermodynamic or kinetic control, depending on the conditions.

The idea of kinetic versus thermodynamic control can be illustrated by a brief discussion of the formation of enolate anions from unsymmetrical ketones. This is a very important matter for synthesis and is discussed more fully in Chapter 6 and in Section 1.1.2 in Part B. Most ketones can give rise to more than one enolate. Many studies have shown that the ratio among the possible enolates that are formed depends on the reaction conditions.<sup>54</sup> This can be illustrated for the case of 2-hexanone. If the base chosen is a strong, sterically hindered one, such as lithium diisopropylamide, and the solvent is aprotic, the major enolate formed is **3** in the diagram below. If a protic solvent or a weaker base (one comparable in basicity to the ketone enolate) is used, the dominant enolate is **2**. Under these latter conditions, equilibration can occur by reversible formation of the enol. Enolate **3** is the kinetic enolate, but **2** is thermodynamically favored.



The structural and mechanistic basis for the relationships between kinetic versus thermodynamic control and the reaction conditions is as follows. The  $\alpha$ -hydrogens of the methyl group are less sterically hindered than the  $\alpha$ -hydrogens of the butyl group. As a result, removal of a methyl hydrogen as a proton is faster than removal of a butyl hydrogen. This effect is magnified when the base is sterically bulky and is particularly sensitive to the steric environment of the competing hydrogens. If the base is very strong, the enolate will not be reconverted to the ketone because the enolate is too weak a base to regain the proton. These conditions correspond to (a) in Figure 3.8 and represent a case of kinetic control. If a weaker base is used or if the solvent is protic, protons can be transferred reversibly between the isomeric enolates and the base (because the base strengths of the enolate and the base are comparable). Under these conditions the more stable enolate will be dominant because the enolates are in equilibrium. The more substituted enolate **2** is the more stable of the pair, just as more substituted alkenes are more stable than terminal alkenes. This corresponds to case (c) in Figure 3.8, and product (enolate) equilibration occurs through rapid proton exchange. In protic solvents this exchange can occur through the enols.

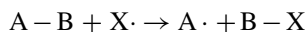
### 3.3.2. Correlations between Thermodynamic and Kinetic Aspects of Reactions

Is there any inherent relationship between the free energy of a reaction,  $\Delta G$ , and the rate of reaction, which is governed by  $\Delta G^\ddagger$ ? Are more exothermic reactions

<sup>54</sup> J. d'Angelo, *Tetrahedron*, **32**, 2979 (1976); H. O. House, *Modern Synthetic Reactions*, 2nd Edition, W. A. Benjamin, Menlo Park, CA, 1972.

faster? These questions raise the issue of a relationship between the thermodynamic and kinetic aspects of reactivity. It turns out that there frequently are such relationships *in series of closely related reactions*, although there is no fundamental requirement that this be the case. The next several sections discuss examples of such relationships.

**3.3.2.1. Bell-Evans-Polyani Relationship.** The Bell-Evans-Polyani formula deals with the relationship between reaction rate and exothermicity for a series of related single-step reactions.<sup>55</sup> Evans and Polyani pointed out that for a series of homolytic atom transfer reactions of the general type

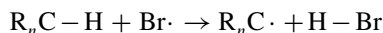


there was a relationship between the activation energy and the reaction enthalpy, which can be expressed as

$$E_a = E_0 + \alpha\Delta H \quad (3.32)$$

where  $E_0$  is the activation energy of the reference reaction and  $\Delta H$  is the enthalpy of each reaction in the series. In terms of reaction energy diagrams, this indicates that for reactions having similar energy profiles, the height of the barrier will decrease as the reaction becomes more exothermic (and vice versa), as illustrated in Figure 3.9.

This relationship can be explored, for example, by considering the rates of hydrogen abstraction reactions. For example, the  $E_a$  for hydrogen abstraction from simple hydrocarbons<sup>56</sup> shown below can be compared with the  $\Delta H$  of the reaction, as derived from the bond energy data in Table 3.2. The plot is shown in Figure 3.10.



Alkane	$E_a$	$\Delta H$
CH <sub>3</sub> -H	18.3	+18.0
C <sub>2</sub> H <sub>5</sub> -H	13.4	+13.5
(CH <sub>3</sub> ) <sub>2</sub> CH-H	10.2	+11.1
C <sub>2</sub> H <sub>5</sub> CH(CH <sub>3</sub> )-H	10.2	+11.3
(CH <sub>3</sub> ) <sub>3</sub> C-H	7.5	+8.7

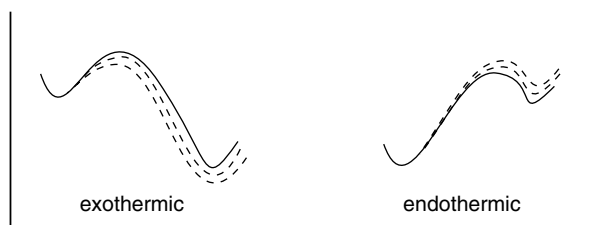


Fig. 3.9. Energy profiles for series of related reactions illustrating the Bell-Evans-Polyani relationship.

<sup>55</sup> M. G. Evans and M. Polanyi, *Trans. Faraday Soc.*, **34**, 11 (1938).

<sup>56</sup> G. C. Fettes and A. F. Trotman-Dickenson, *J. Am. Chem. Soc.*, **81**, 5260 (1959).

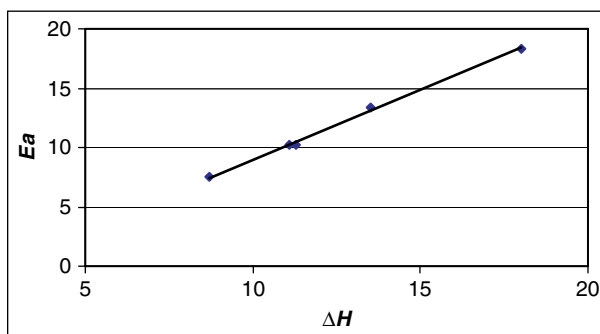


Fig. 3.10. Plot of  $E_a$  for abstraction of hydrogen from alkanes by bromine atom versus  $\Delta H$ .

Another example of data of this type pertains to the reaction of *t*-butoxy radicals with hydrocarbons.<sup>57</sup> The *t*-butoxy radical is more reactive and less selective than bromine atoms and the  $E_a$  are quite low. There is a correlation corresponding to Equation (3.32), with  $\alpha = 0.3$  for hydrocarbons with C–H bond strengths greater than  $\sim 90$  kcal/mol. For weaker bonds, the  $E_a$  levels off at about 2 kcal/mol. We say more about the relationship between  $E_a$  for hydrogen abstraction and the enthalpy of the reaction in Topic 11.2.

Hydrocarbon	BDE (kcal/mol)	$E_a$ (kcal/mol)
Triphenylmethane	81	1.9
Diphenylmethane	84	2.4
3-Phenylpropene	82	2.5
Toluene	90	3.5
Cyclopentane	97	3.5
Cyclohexane	99	4.4
<i>t</i> -Butylbenzene	101	6.1

**3.3.2.2. Hammond's Postulate.** Because the rates of chemical reactions are controlled by  $\Delta G^\ddagger$ , information about the structure of TSs is crucial to understanding reaction mechanisms. However, because TSs have only transitory existence, it is not possible to make experimental measurements that provide direct information about their structure. Hammond pointed out the circumstances under which it is valid to relate transition state structure to the structure of reactants, intermediates, or products.<sup>58</sup> His statement is known as *Hammond's postulate*. Discussing individual steps in a reaction mechanism, Hammond's postulate states: "If two states, as, for example, a transition state and an unstable intermediate, occur consecutively during a reaction process and have nearly the same energy content, their interconversion will involve only a small reorganization of molecular structure."

This statement can be discussed with reference to potential energy diagrams. Case (a) in Figure 3.11 represents a very exothermic step with a low activation energy. It follows from Hammond's postulate that in this step, the TS will resemble the reactant, because the two are close in energy and interconverted by a small structural

<sup>57</sup> M. Finn, R. Fridline, N. K. Suleman, C. J. Wohl, and J. M. Tanko, *J. Am. Chem. Soc.*, **126**, 7578 (2004).

<sup>58</sup> G. S. Hammond, *J. Am. Chem. Soc.*, **77**, 334 (1955).

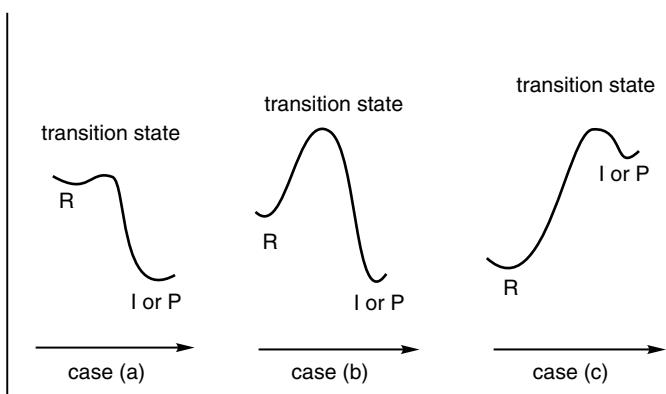


Fig. 3.11. Reaction energy diagram illustrating Hammond's postulate: (a) early transition structure resembles reactant, (b) midpoint transition structure resembles neither reactant or product, (c) late transition structure resembles intermediate or product.

change. This is depicted in the potential energy diagram as a small displacement toward product along the reaction coordinate. This means that comparisons between closely related series of reactants should depend primarily on *structural features present in the reactant*. Case (b) describes a step in which the energy of the TS is a good deal higher than either the reactant or the product. In this case, neither the reactant nor the product is a good model of the TS. Independent information is needed to postulate the characteristics of the TS. Comparison among a series of reactants should focus primarily on TS structure. Case (c) illustrates an endothermic step, such as might occur in the formation of an unstable intermediate. In this case the energy of the TS is similar to that of the intermediate and the TS should be similar in structure to the intermediate. Structural and substituent effects can best be interpreted in terms of their effect on the stability of the intermediate.

The significance of the concept incorporated in Hammond's postulate is that in appropriate cases it permits discussion of TS structure in terms of the reactants, intermediates, or products in a multistep reaction sequence. The postulate indicates that the cases where such comparison is appropriate are those in which the TS energy is close to that of the reactant, intermediate, or product. Chemists sometimes speak of an "early" or "late" TS. An "early" TS is reactant-like, whereas a "late" TS is intermediate- (or product-) like.

Electrophilic aromatic substitution is a situation in which it is useful to discuss TS structure in terms of a reaction intermediate. The *ortho*, *para*, and *meta* directing effects of aromatic substituents were among the first structure-reactivity relationships to be developed in organic chemistry. Certain functional groups activate aromatic rings toward substitution and direct the entering electrophile to the *ortho* and *para* positions, whereas others are deactivating and lead to substitution in the *meta* position. The bromination of methoxybenzene (anisole), benzene, and nitrobenzene can serve as examples for discussion.



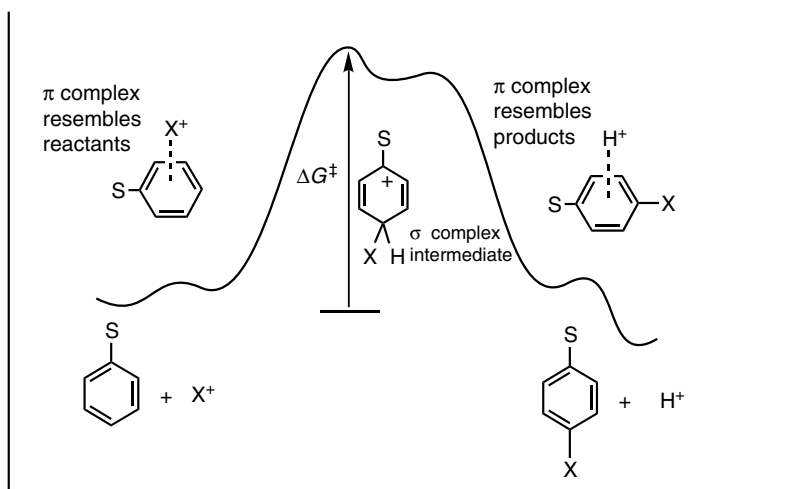
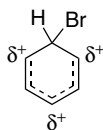


Fig. 3.12. Potential energy diagram for electrophilic aromatic substitution.

It can be demonstrated that the reactions are kinetically controlled; that is, there is no isomerization among the *ortho*, *meta*, and *para* products after they are formed. It is therefore the  $\Delta G^\ddagger$  values that hold the key to the connection between the rate effects and the substituent-directing effects. However, to discuss the effect of substituents on  $\Delta G^\ddagger$ , we must know something about the reaction mechanism and the nature of the competing TS. Electrophilic aromatic substitution is dealt with in detail in Chapter 9. Evidence presented there indicates that electrophilic aromatic substitution involves a distinct intermediate and two less well-defined states. The potential energy diagram in Figure 3.12 is believed to be a good representation of the energy changes that occur during bromination. By application of the Hammond postulate, we conclude that the rate-determining step involves formation of a TS that closely resembles the intermediate, which is called the “ $\sigma$  complex.” It is therefore appropriate to discuss the effect of substituents on the TS in terms of the structure of this intermediate.

Because the product composition is kinetically controlled, the isomer ratio is governed by the relative magnitudes of  $\Delta G_o^\ddagger$ ,  $\Delta G_m^\ddagger$ , and  $\Delta G_p^\ddagger$ , the energies of activation for the *ortho*, *meta*, and *para* transition states, respectively. Figure 3.13 shows a qualitative comparison of these  $\Delta G^\ddagger$  values. At the TS, a positive charge is present on the benzene ring, primarily at positions 2, 4, and 6 in relation to the entering bromine.



The electron-releasing methoxy group interacts directly to delocalize the charge and stabilize the intermediates leading to *o*- and *p*-bromination, but does not stabilize the intermediate leading to *m*-substitution product.

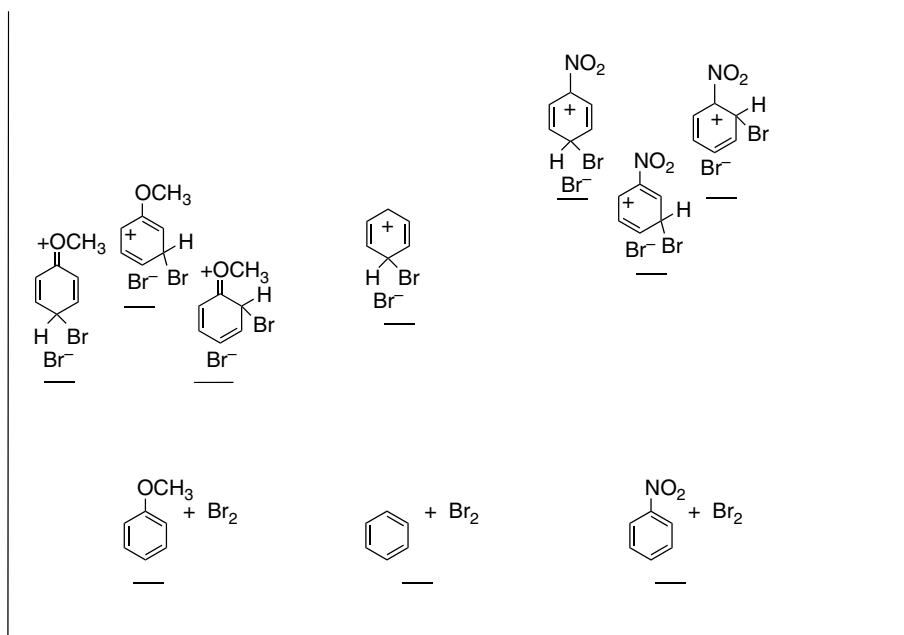
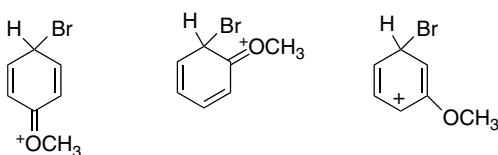
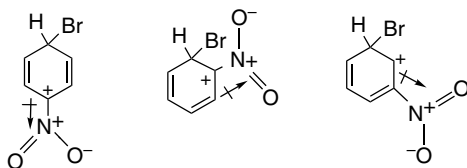


Fig. 3.13. Relative energies of intermediates for bromination of methoxybenzene, benzene, and nitrobenzene indicating the effect of substituents on energy of intermediates.



The *o*- and *p*-intermediates are therefore stabilized relative to benzene but the *m*-intermediate is not, as is illustrated in Figure 3.13. As a result, methoxybenzene reacts faster than benzene and the product is mainly the *o*- and *p*-isomers.

In the case of nitrobenzene, the electron-withdrawing nitro group cannot stabilize the positive charge in the  $\sigma$ -complex intermediate. In fact, it strongly destabilizes the intermediate as a result of an unfavorable polar interaction. This destabilization is greatest in the *o*- and *p*-intermediates, which place a partial positive charge on the nitro-substituted carbon. The *meta*-TS is also destabilized relative to benzene, but not as much as the *ortho*- and *para*-TS. As a result nitrobenzene is less reactive than benzene and the product is mainly the *meta*-isomer



The substituent effects in aromatic electrophilic substitution are dominated by *resonance effects*. In other systems, stereoelectronic or steric effects might be more

important. Whatever the nature of the substituent effects, the Hammond postulate recognizes that structural discussion of transition states in terms of reactants, intermediates, or products is valid only when their structures and energies are similar.

**3.3.2.3. The Marcus Equation.** The *Marcus equation* provides a means for numerical evaluation of the relationship between  $\Delta G^\circ$  and  $\Delta G^\ddagger$ . The Marcus equation proposes that for a single-step reaction process there is a relationship involving the net exo- or endothermicity of the reaction and an energy associated with the activation process called the *intrinsic barrier*.<sup>59</sup> The Marcus equation proposes that for a series of related reactions, there is a predictable relationship between  $\Delta G^\ddagger$  and  $\Delta G^\circ$ , the free energy of reaction. The energies of the reactants, transition state, and products can be described by intersecting parabolic potential energy functions. The relationship can be expressed by the following equation:

$$\Delta G^\ddagger = \tilde{G}[1 + (\Delta G^\circ/4\tilde{G})]^2 \quad (3.33)$$

where  $\tilde{G}$  is the intrinsic barrier of the reaction and  $\Delta G^\circ$  and  $\Delta G^\ddagger$  are free energy and energy of activation for the reaction under consideration.

The Marcus equation (3.33), like the Bell-Evans-Polyani relationship, indicates that for a related series of reactions, the activation energy (and therefore the rate) is related to the net free-energy change. It is based on assumption of a parabolic shape of the potential energy curve and breaks down at certain limits. The range of the equation can be extended by other formulations of the shape of the potential energy functions.<sup>60</sup> Figure 3.14 plots a series of reaction energy profiles with  $\tilde{G} = 25$  kcal and  $\Delta G^\circ$  varying

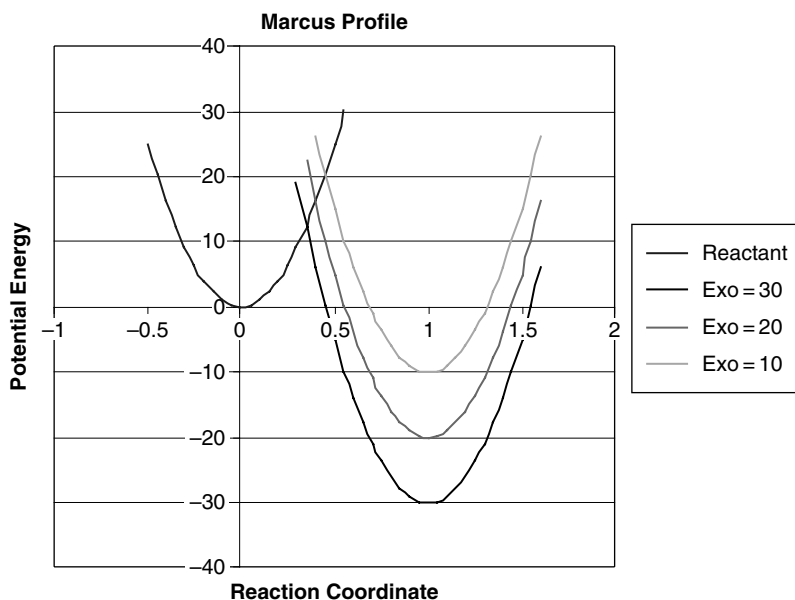


Fig. 3.14. Marcus equation plots for a hypothetical reaction series with an intrinsic barrier of 25 kcal/mol and exothermicities of 10, 20, and 30 kcal/mol.

<sup>59</sup> R. A. Marcus, *J. Phys. Chem.*, **72**, 891 (1968); R. A. Marcus, *J. Am. Chem. Soc.*, **91**, 7224 (1969).

<sup>60</sup> E. S. Lewis, C. S. Shen, and R. A. More O'Ferrall, *J. Chem. Soc., Perkin Trans.*, **2**, 1084 (1981).

from 0 to  $-30$  kcal/mol, and it illustrates that we can indeed expect a correlation between reaction exothermicity (or endothermicity) and rate. The Marcus equation makes another prediction that is quite surprising—that the barrier will increase again for very exothermic reactions. This is called the *inverted region*. This aspect of Marcus theory is not widely applied in organic chemistry, but is of considerable importance in electron transfer reactions.

The Marcus equation can be modified to Equation (3.34) to take account of other energy changes, for example, the desolvation and electrostatic interactions that are involved in bringing together the ensemble of reacting molecules. These energies contribute to the observed activation energy. Similarly, there may be residual interactions in the product ensemble that differ from the independent molecules.<sup>61</sup> Guthrie proposed the following equations:

$$\Delta G_{\text{corr}} = \tilde{G} \left( 1 + \frac{\Delta G_{\text{corr}}^{\circ}}{4\tilde{G}} \right)^2 \quad (3.34)$$

$$\Delta G_{\text{corr}}^{\ddagger} = \Delta G_{\text{obs}}^{\ddagger} - W_R \quad (3.35)$$

$$\Delta G_{\text{corr}}^{\circ} = \Delta G_{\text{obs}}^{\circ} + W_R - W_P \quad (3.36)$$

where  $W_R$  is work to bring reactants together and  $W_P$  is work to bring products together. In this formulation, the assignment of  $W_R$  and  $W_P$  terms, which includes solvation, requires careful consideration. Figure 3.15 shows a reaction energy diagram including the  $W_R$  and  $W_P$  terms.

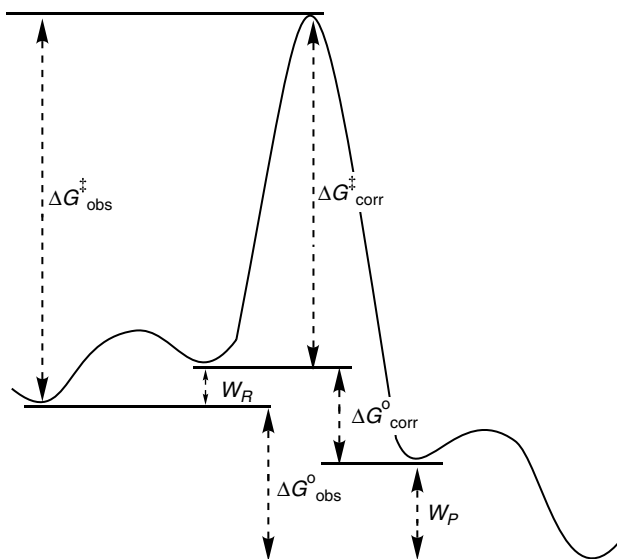
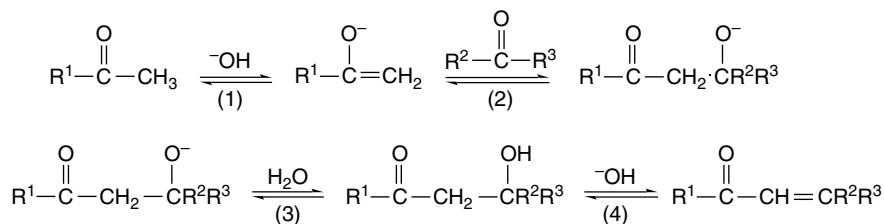


Fig. 3.15. Model for a reaction,  $A + B \rightleftharpoons A \cdot B \rightleftharpoons C \cdot D \rightleftharpoons C + D$  used in applying the Marcus theory. The reactants come together in an encounter complex (A,B) at a free-energy cost  $W_R$  and react within this complex to form (C,D), the encounter complex of products, which then separate, releasing free energy  $W_P$ . The Marcus theory applies to reactions within the encounter complex where  $\Delta G_{\text{corr}}^{\ddagger}$  is determined by  $\Delta G_{\text{corr}}^{\circ}$  and the intrinsic barrier  $\tilde{G}$ . Reproduced from *Can. J. Chem.*, **74**, 1283 (1996), by permission from National Research Council Press.

<sup>61</sup> J. P. Guthrie, *Can. J. Chem.*, **74**, 1283 (1996).

With these two relationships, if reliable values of  $W_R$  and  $W_P$  can be determined and  $\tilde{G}$  established for a reaction series, the activation barriers can be calculated from the thermodynamic data that provide  $\Delta G^\circ$ . Relationships of this kind have been shown to occur in many different organic reactions, so the principles appear to have considerable generality. For example, Guthrie investigated both the addition (Step 2) and elimination (Step 4) parts of the aldol condensation reaction (see p. 283–285).<sup>62</sup> Steps (1) and (3) are proton transfers that are fast under the reaction conditions.



A series of acceptors [ $\text{CH}_2=\text{O}$ ,  $\text{CH}_3\text{CH}=\text{O}$ ,  $\text{PhCH}=\text{O}$ ,  $(\text{CH}_3)_2\text{C}=\text{O}$ ] and a series of enolates ( $^-\text{CH}_2\text{CH}=\text{O}$ ,  $^-\text{CH}_2\text{COCH}_3$ ,  $^-\text{CH}_2\text{COPh}$ ) were examined and good correlations of both the addition and elimination steps were found, as shown in Figure 3.16. The potential value of the Marcus equation is the ability it provides to make predictions of reaction rates based on equilibrium data (which can be obtained from computation as well as experiment).

The Bell-Evans-Polanyi relationship, Hammond's postulate, and the Marcus equation are all approaches to analyzing, understanding, and predicting relationships between the thermodynamics and kinetics of a series of closely related reactions. This is an important issue in organic chemistry, where series of reactions differing only in peripheral substituents are common. Each of these approaches provides a sound basis for the intuitive expectation that substituents that favor a reaction in a thermodynamic

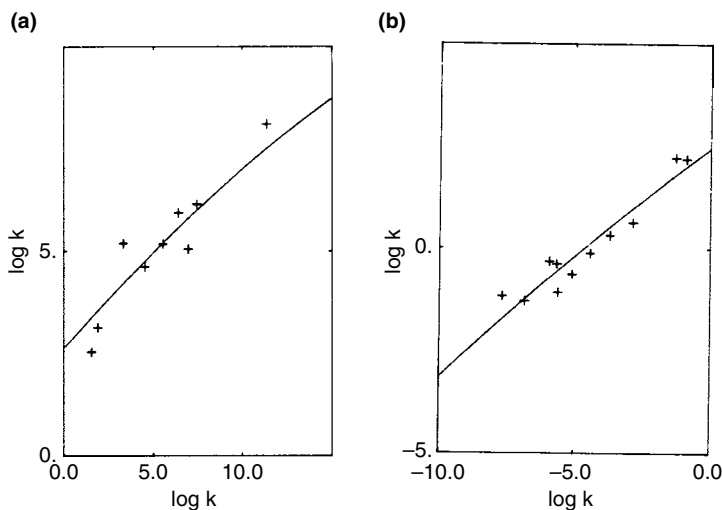


Fig. 3.16. Marcus correlations for (a) addition and (b) elimination steps of an aldol reaction. The values of the intrinsic barrier  $\tilde{G}$  are (a)  $13.8 \pm 0.8$  kcal/mol and (b)  $14.1 \pm 0.5$  kcal/mol. Adapted from *J. Am. Chem. Soc.*, **113**, 7249 (1991).

<sup>62</sup> J. P. Guthrie, *J. Am. Chem. Soc.*, **113**, 7249 (1991).



However, from Figure 3.17,

$$\Delta G_b^\ddagger - \Delta G_a^\ddagger + \Delta G_c = G_b^\ddagger - G_a^\ddagger \quad (3.40)$$

The product ratio is therefore not determined by  $\Delta G_c$  but by the relative energy of the two transition states  $A^\ddagger$  and  $B^\ddagger$ . The conclusion that the ratio of products formed from conformational isomers is not determined by the conformational equilibrium ratio is known as the *Curtin-Hammett principle*.<sup>63</sup> Although the rate of the formation of the products is dependent upon the relative concentration of the two conformers, because  $\Delta G_b^\ddagger$  is decreased relative to  $\Delta G_a^\ddagger$  to the extent of the difference in the two conformational energies, the conformational preequilibrium is established rapidly, relative to the two competing product-forming steps.<sup>64</sup> The position of the conformational equilibrium cannot control the product ratio. The reaction can proceed through a minor conformation if it is the one that provides access to the lowest-energy transition state.

The same arguments can be applied to other energetically facile interconversions of two potential reactants. For example, some organic molecules can undergo rapid proton shifts (tautomerism) and the chemical reactivity of the two isomers may be quite different. However, it is not valid to deduce the ratio of two tautomers on the basis of subsequent reactions that have activation energies greater than that of the tautomerism. Just as in the case of conformational isomerism, the ratio of products formed in subsequent reactions is not controlled by the position of the facile equilibrium, but by the  $E_a$  of the competing steps.

### 3.4. Electronic Substituent Effects on Reaction Intermediates

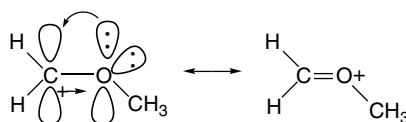
It is often observed that the introduction of substituents changes the rate of organic reactions, even if the substituent is not directly involved in the reaction. Changes that affect the  $\Delta G^\ddagger$  for the rate-determining, or preceding, steps will cause a change in the observed reaction rate. The difference can result from energy changes in the reactant(s) or transition state, or both. Shifts in product composition can result from changes in the relative  $\Delta G^\ddagger$  of competing reaction paths. In the broadest terms, there are three kinds of substituent effects, resulting from electronic, steric, and structure-specific interactions. *Steric effects* have their origin in nonbonding interactions. *Structure-specific interactions* include, for example, intramolecular hydrogen bonding and neighboring-group participation that depend on location of the substituents that are involved. In this section, we focus on *electronic effects*. Electronic substituent effects can be further subdivided. Substituents can operate by delocalization of electrons by *resonance* or *hyperconjugation*, including  $\sigma - \sigma^*$  and  $\sigma - \pi^*$ , as well as  $\pi - \pi$  delocalization. Resonance and hyperconjugation operate through specific orbital interactions and therefore impose particular *stereoelectronic* requirements; that is, interacting orbitals must be correctly aligned. *Polar effects* are electrostatic and include both the effect of proximate charges owing to bond dipoles and the effects of more distant centers of charge. Polar effects also may have a geometric component. For example, the orientation of a particular bond dipole determines how it interacts with a developing charge at a reaction center elsewhere in the molecule. Polar effects are

<sup>63</sup> D. Y. Curtin, *Rec. Chem. Prog.*, **15**, 111 (1954); E. L. Eliel, *Stereochemistry of Carbon Compounds*, McGraw-Hill, New York, 1962, pp. 151–152, 237–238.

<sup>64</sup> For a more complete discussion of the relationship between conformational equilibria and reactivity, see J. I. Seeman, *Chem. Rev.*, **83**, 83 (1983).

sometimes subdivided into *inductive* and *field effects*. Effects attributed to proximate electronic changes owing to bond dipoles are called inductive effects and those that are due to dipole interaction through space are called field effects. *Polarizability effects*, which result from distortion of electronic distribution of a group, provide another mechanism of substituent interaction, and can be particularly important in the gas phase.

The broad classification of substituents into electron-releasing groups (ERGs) and electron-withdrawing groups (EWGs) is useful. However, to achieve further refinement, we must make two additional distinctions. *The electronic effects of substituents resulting from delocalization and polar interactions are not necessarily in the same direction.* A methoxy substituent on a carbocation is a good example. The oxygen atom is strongly stabilizing by resonance because it permits a  $\pi$  bond to form between oxygen and carbon, thereby delocalizing the positive charge. However, the C–O bond dipole is destabilizing, since it increases the positive charge at carbon. In this case the resonance stabilizing effect is dominant and the carbocation is strongly stabilized (see p. 21–22).



We also have to recognize that the relative importance of delocalization and polar effects depends on the nature of the charge that develops in the TS or the intermediate. The delocalization effects of most substituents are in opposite directions, depending on whether a negative or a positive charge is involved, but there are exceptions. Phenyl and vinyl groups can stabilize either negative or positive charges by delocalization. In Section 3.6, we discuss *linear free-energy relationships*, which permit the quantitative description of substituent effects. At this point, however, we want to make a qualitative assessment. Scheme 3.1 lists a number of common substituent groups and indicates whether the group is an ERG or an EWG substituent. The effects of substituents are shown separately for resonance and polar interactions. In the discussions of substituent effects in future chapters, we frequently make reference to the electronic effects of ERG and EWG substituents.

We can quickly note some of the general features of the various types of substituents. Alkyl groups are electron releasing by virtue of  $\sigma$  delocalization (hyperconjugation) and small polar effects. The  $\pi$  and  $\pi^*$  orbitals of vinyl, phenyl, and ethynyl groups allow them to delocalize both positive and negative charges. Because of the greater electronegativity of  $sp^2$  and especially  $sp$  carbon, relative to  $sp^3$  carbon, the unsaturated groups are weakly electron attracting from the polar perspective. (See p. 12–13 to review carbon electronegativity trends.) Oxygen and nitrogen substituents having unshared electron pairs are strong electron donors by resonance. Alkoxy, acyloxy, amino, and acylamido are common examples of this kind of group. On the other hand, because of the higher electronegativity of oxygen and nitrogen relative to carbon, they are EWGs through polar interactions. This is especially true of the acyloxy and acylamido groups because of the dipole associated with the carbonyl group. All the various carbonyl functional groups are EWG through both resonance and polar contributions. The C=O bond dipole and the higher electronegativity of the carbonyl carbon both contribute to the latter effect.

The halogens are an interesting group. They act as electron donors by resonance involving the unshared pairs, but this is opposed by a polar effect resulting from their

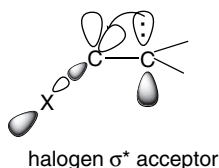
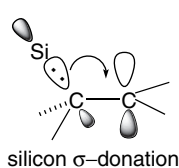
Scheme 3.1. Classification of Substituent Groups

Substituent	Resonance	Polar
<u>Alkyl</u>		
CH <sub>3</sub> , C <sub>2</sub> H <sub>5</sub> , (CH <sub>3</sub> ) <sub>3</sub> C, etc	ERG	ERG (small)
<u>Vinyl and aryl</u>		
CH <sub>2</sub> =CH, C <sub>6</sub> H <sub>5</sub> , etc	ERG or EWG	EWG (small)
<u>Ethynyl</u>		
HC≡C, etc	ERG or EWG	EWG
<u>Alkoxy, Acyloxy, Amino, Acylamido</u>		
RO, RCO <sub>2</sub> , R <sub>2</sub> N, RCONH, etc	ERG	EWG
<u>Carbonyl</u>		
HC=O, RC=O, ROC=O, R <sub>2</sub> NC=O, etc.	EWG	EWG
<u>Halogens</u>		
F, Cl, Br, I	ERG	EWG
<u>Polyhaloalkyl</u>		
CF <sub>3</sub> , CCl <sub>3</sub> , etc.	EWG	EWG
<u>Other Nitrogen Groups</u>		
CN, NO <sub>2</sub> , R <sub>3</sub> N <sup>+</sup> , etc.	EWG	EWG
<u>Sulfur Groups</u>		
RS	ERG	EWG
RSO	ERG	EWG
RSO <sub>2</sub>	EWG	EWG
<u>Silyl Groups</u>		
R <sub>3</sub> Si	ERG	ERG

SECTION 3.4

*Electronic Substituent  
Effects on Reaction  
Intermediates*

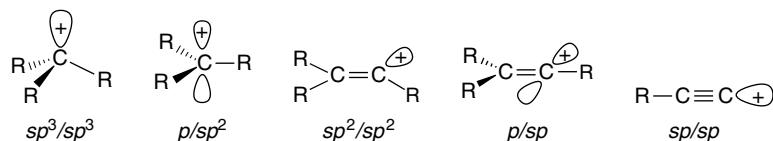
higher electronegativity. Moreover, the resonance and polar effects both weaken going down the periodic table. Resonance weakens because of longer bonds and poorer orbital overlap with carbon, whereas the polar effect decreases as the electronegativity diminishes. As a result, the halogens often exhibit unusual trends resulting from a changing balance between the resonance and polar effects. Halogen substituent effects are also affected by polarizability, which increases from fluorine to iodine. When halogen is placed on a carbon, as in trifluoromethyl or trichloromethyl, the groups are EWG by both polar and resonance mechanisms. The resonance component is associated with  $\sigma^*$  orbitals. The sulfur substituents RS, RSO, and RSO<sub>2</sub> show a shift from being resonance donors to strong polar acceptors, as the sulfur unshared pairs are involved in bonding to oxygen. Trialkylsilyl groups are slightly better ERGs than alkyl, since the silicon is less electronegative than carbon. Trialkylsilyl groups are very good electron donors by hyperconjugation.



There are many types of reaction intermediates that are involved in organic reactions. In this section we consider substituent effects on four important examples—carbocations, carbanions, radicals, and carbonyl addition (tetrahedral) intermediates—which illustrate how substituent effects can affect reactivity. Carbocation and carbanions are intermediates with positive and negative charge, respectively, and we will see that they have essentially opposite responses to most substituent groups. We also discuss substituent effects on neutral radical intermediates, where we might not, at first glance, expect to see strong electronic effects, since there is no net charge on the intermediate. The fourth case to be considered is the important class of carbonyl addition reactions, where substituent effects in the *reactant* often have the dominant effect on reaction rates.

### 3.4.1. Carbocations

Carbocations have a vacant orbital that bears a positive charge. Within the standard hybridization framework, there are five possible hybridization types if all the electrons are paired.

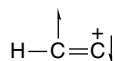


The approximate relative energies of these structures are illustrated in Figure 3.18. For trivalent carbon, the preferred hybridization is for the positive charge to be located in an unhybridized *p* orbital. Similarly, the *p/sp* hybridization is preferred for alkenyl carbocations. These hybridizations place the charge in a less electronegative *p*

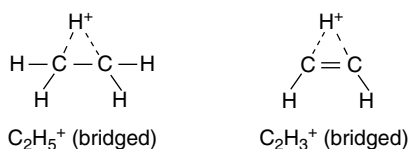
	MP4(SDQ)/6-31G**	MP2/6-31G*
HC≡C <sup>+</sup>		+ 55.3
CH <sub>3</sub> <sup>+</sup>	-----0.0 Reference-----	
C <sub>6</sub> H <sub>5</sub> <sup>+</sup>		-26.5
C <sub>2</sub> H <sub>3</sub> <sup>+</sup> (bridged)		-25.6
CH <sub>3</sub> CH <sub>2</sub> <sup>+</sup> (bridged)	-33.8	-40.8
CH <sub>3</sub> CH <sub>2</sub> <sup>+</sup> (open)	-39.0	-34.4
CH <sub>2</sub> =C <sup>+</sup> CH <sub>3</sub>	-42.9	-46.5
CH <sub>2</sub> =CHCH <sub>2</sub> <sup>+</sup>	-54.5	-60.0
(CH <sub>3</sub> ) <sub>2</sub> C <sup>+</sup> H	-58.5	-58.9
C <sub>6</sub> H <sub>5</sub> CH <sub>2</sub> <sup>+</sup>		-74.5
(CH <sub>3</sub> ) <sub>3</sub> C <sup>+</sup>		-75.0

Fig. 3.18. Gas phase carbocation stabilities relative to methyl cations in kcal/mol. Data from Y. Apeloig and T. Müller, in *Dicoordinated Carbocations*, Z. Rapoport and P. J. Stang, eds., John Wiley & Sons, New York, 1997, Chap.2.

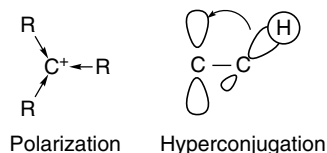
orbital. The  $sp^3/sp^3$  and  $sp^2/sp^2$  arrangements are not energy minima, but lie at least 20–30 kcal above the  $p/sp^2$  and  $p/sp$  arrangements.<sup>65</sup> The very high relative energy of terminal ethynyl carbocations reflects the fact that the positive charge is associated with a more electronegative  $sp$  orbital if the triple bond is retained. Various MO computations indicate that the ethynyl cation adopts an alternative electronic configuration which places the positive charge in a  $\pi$  orbital, but the cation is nevertheless very unstable.<sup>66</sup>



Certain carbocations, especially in the gas phase, appear to be *bridged*. This is true for ethyl and vinyl cations. More will be said about bridging in Section 4.4.



The carbocation stability order  $\text{CH}_3 < \textit{pri} < \textit{sec} < \textit{tert}$  is due to the electron-releasing effect of alkyl substituents. The electron release is a combination of a polar effect that is due to the greater electronegativity of the  $sp^2$  carbon and a hyperconjugative effect through which the electrons in  $\sigma$  C–H and C–C bonds of the alkyl group are delocalized to the empty  $p$  orbital. The delocalization has a stereoelectronic aspect, since alignment of a C–H (or C–C) bond with the empty  $p$  orbital maximizes electron delocalization. Gas phase experimental<sup>67</sup> and computational<sup>68</sup> data (Figure 3.18) indicate that the stabilization energies are as follows (relative to methyl in kcal/mol):  $\text{CH}_3^+$  (0, 0);  $\text{CH}_3\text{CH}_2^+$  (40, 41),  $(\text{CH}_3)_2\text{CH}^+$  (60, 59);  $(\text{CH}_3)_3\text{C}^+$  (85, 75).

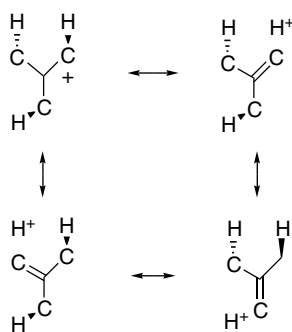


<sup>65</sup> Y. Apeloig and T. Müller in *Dicoordinated Carbocations*, Z. Rappoport and P. J. Stang, eds., John Wiley & Sons, New York, 1997, Chap. 2; J. Abboud, I. Alkorta, J. Z. Davalos, P. Muller, and E. Quintanilla, *Adv. Phys. Org. Chem.*, **37**, 57 (2002).

<sup>66</sup> L. A. Curtiss and J. A. Pople, *J. Chem. Phys.*, **91**, 2420 (1989); W. Koch and G. Frenking, *J. Chem. Phys.*, **93**, 8021 (1990); K. Hashimoto, S. Iwata, and Y. Osamura, *Phys. Chem. Lett.*, **174**, 649 (1990).

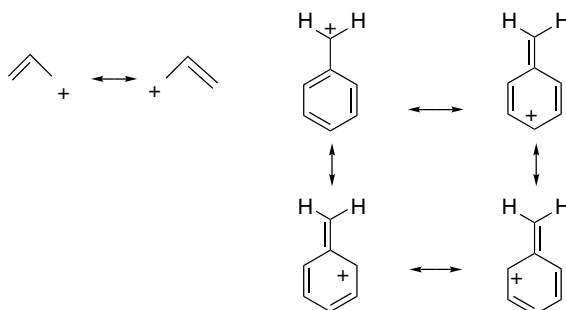
<sup>67</sup> D. H. Aue, in *Dicoordinated Carbocations*, Z. Rappoport and P. J. Stang, eds., John Wiley & Sons, New York, 1997, Chap. 3; D. H. Aue and M. T. Bowers, in *Gas Phase Ion Chemistry*, M. T. Bowers, ed., Academic Press, New York, 1979.

<sup>68</sup> Y. Apeloig and T. Müller, in *Dicoordinated Carbocations*, Z. Rappoport and P. J. Stang, eds., John Wiley & Sons, New York, 1997, Chap. 2.



Resonance Representation of Hyperconjugation

Carbocations that are adjacent to  $\pi$  bonds, as in allylic and benzylic carbocations, are strongly stabilized by delocalization. The stabilization in the gas phase is about 60 kcal/mol for the allyl cation and 75 kcal/mol for benzyl ions, relative to the methyl cation.<sup>67</sup>



Resonance representation of allylic and benzylic stabilization

Total resonance stabilization has been calculated at the MP2/6-31G\* level for a number of conjugated ions, as shown in Table 3.9. One general trend seen in this data is a decrease of the effect of successive phenyl rings in the benzyl, diphenylmethyl, and triphenylmethyl cation series. Two factors are involved. The effect of resonance stabilization is decreased because the successive rings must be twisted from planarity. This factor and related steric repulsions attenuate the effect of each successive phenyl group relative to methyl (see Column B). In the allyl series a 1-phenyl substituent adds 39.4 kcal of stabilization, while a 2-phenyl group adds only 11.4.<sup>69</sup>

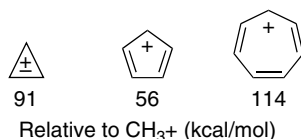
**Table 3.9. Stabilization Energy in kcal/mol for Delocalized Carbocations**

Carbocation	Resonance stabilization	Stabilization relative to $\text{CH}_3^+$
$\text{C}_6\text{H}_5\text{CH}_2^+$	76.4	75.4
$\text{CH}_2=\text{CHCH}_2^+$	53.2	
$(\text{C}_6\text{H}_5)_2\text{CH}^+$	102.7	91.6
$(\text{C}_6\text{H}_5)_3\text{C}^+$	124.8	102.2
$\text{C}_6\text{H}_5\text{C}^+\text{HCH}=\text{CH}_2$	92.6	
$\text{CH}_2=\text{C}(\text{C}_6\text{H}_5)\text{CH}_2^+$	64.6	

a. B. Reindl, T. Clark and P. v. P. Schleyer, *J. Phys. Chem. A*, **102**, 8953 (1998).

<sup>69</sup> B. Reindl, T. Clark, and P. v. R. Schleyer, *J. Phys. Chem. A*, **102**, 8953 (1998).

When the vacant  $p$  orbital is part of a completely conjugated cyclic system, there can be further stabilization resulting from aromaticity. (See Section 8.3 for further discussion.) The cyclopropenylum ion and the cycloheptatrienylium ion fit into this category. When cyclic conjugation is antiaromatic, as in the cyclopentadienylium ion, there is net stabilization relative to a methyl cation, but significantly less than for the aromatic analogs.<sup>70</sup>



Carbocation stability in the gas phase can be measured by mass spectrometry and reported as *hydride affinity*, which is the enthalpy of the reaction:

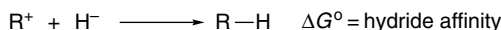


Table 3.10 gives values for the hydride affinity for some carbocations. There is good agreement with the theoretical results shown in Figure 3.18 and the data in Table 3.10.

Substituents such as oxygen and nitrogen that have nonbonding electrons are very strongly stabilizing toward carbocations. This is true both for ether-type oxygen and carbonyl-type oxygen (in acylium ions). Even fluorine and the other halogens are

**Table 3.10. Hydride Affinity of Some Carbocations**

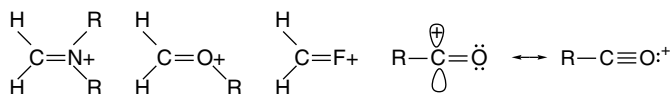
Hydride affinity (kcal/mol)			
	Gas <sup>a</sup>		Gas <sup>a</sup>
CH <sub>3</sub>	314	CH <sub>2</sub> =CHCH <sub>2</sub> <sup>+</sup>	256
CH <sub>3</sub> CH <sub>2</sub> <sup>+</sup> (bridged)	270	CH <sub>2</sub> =CHCC <sup>+</sup> HCH <sub>3</sub>	239
(CH <sub>3</sub> ) <sub>2</sub> CH <sup>+</sup>	252	CH <sub>2</sub> =CHC <sup>+</sup> (CH <sub>3</sub> ) <sub>2</sub>	230
(CH <sub>3</sub> ) <sub>3</sub> C <sup>+</sup>	237	CH <sub>3</sub> CH=CHC + HCH <sub>3</sub>	228
CH <sub>2</sub> =CH <sup>+</sup> (bridged)	288		284
	223 <sup>b</sup>		239
	258 <sup>b</sup>		225
	200 <sup>b</sup>		220 <sup>b</sup>

a. From D. H. Aue in *Dicoordinate Carbocations*, Z. Rappoport and P. J. Stand, eds., John Wiley & Sons, New York, 1997, Chap. 3.

b. From D. H. Aue and M. T. Bowers, in *Gas Phase Ion Chemistry*, M. T. Bowers, ed., Academic Press, New York, 1979.

<sup>70</sup>. Y. Mo, H. Jiao, Z. Lin, and P. v. R. Schleyer, *Chem. Phys. Lett.*, **289**, 383 (1998).

stabilizing by delocalization (but we discuss the opposing polar effect of the halogens below).



The stabilizing effect of delocalization can be seen even with certain functional groups that are normally considered to be electron withdrawing. For example, computations indicate that cyano and carbonyl groups have a stabilizing resonance effect. This is opposed by a polar effect, so the net effect is destabilizing, but the resonance component is stabilizing.

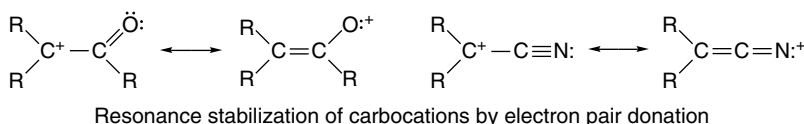


Table 3.11 shows some gas phase stabilization energies computed by various methods. Columns A and B refer to stabilization of substituted methyl (methylium) carbocations, whereas columns C and D are referenced to ethylium ions. Because these values refer to the gas phase, where there is no solvation, the absolute stabilization energies are substantially larger than those found in solution studies. Nevertheless, the results provide a good indication of the relative effect of the various substituents on carbocation stability. Note that of all the substituents included, only  $\text{NO}_2$  is strongly destabilizing. The data for F, Cl, CN, and  $\text{CH}=\text{O}$  indicate small stabilization, reflecting the compensating polar (destabilizing) and delocalization (stabilizing) effects mentioned earlier.

The most wide-ranging and internally consistent computational comparison of substituent effects on carbocation was reported by a group working in The

**Table 3.11. Calculated Substituent Stabilization on Carbocations (in kcal/mol)**

Substituent	$\text{CH}_3^+$		$\text{CH}_3\text{CH}_2^+$	
	PM3 <sup>a</sup>	MP2/6-31G <sup>**b</sup>	MP2/6-311+G( <i>d,p</i> ) <sup>c</sup>	B3LYP/6-311+G( <i>d,p</i> ) <sup>c</sup>
$\text{NH}_2$	80.2			
$\text{CH}_3\text{O}$	57.6			
OH	51.4			
Ph	56.3			
$\text{CH}_2=\text{CH}$	43.3	66.1	30.9	37.3
$\text{CH}_3$	29.0	41.5	17.1	23.4
F	5.5		6.0	7.1
Cl			9.7	10.6
CN	5.0	4.3		
$\text{CH}=\text{O}$	1.7	0.2		
$\text{NO}_2$	-30.8	-22.3		

a. A. M. El-Nahas and T. Clark, *J. Org.Chem.*, **60**, 8023 (1995).

b. X. Creary, X.Y. Wang, and Z. Jiang, *J. Am. Chem. Soc.*, **117**, 3044 (1995).

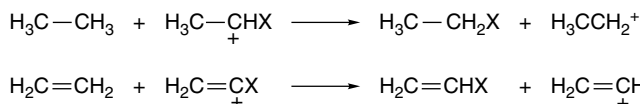
c. K. van Alem, E. J. R. Sudholter, and H. Zuilhof, *J. Phys. Chem. A*, **102**, 10860 (1998).

**Table 3.12. Computed Substituent (De)Stabilization of Carbocation (in kcal/mol)<sup>a</sup>**

X	Ethyl	Vinyl	X	Ethyl	Vinyl
H	0.00	0.00	C≡N	-16.02	-11.71
CH <sub>3</sub>	18.63	25.89	CH=O	-10.25	-4.51
CH <sub>2</sub> OH	15.30	21.69	CO <sub>2</sub> H	-8.41	-5.92
CH <sub>2</sub> CN	-2.10	4.76	H <sub>2</sub> N	64.96	53.69
CH <sub>2</sub> Cl	5.59	12.90	HO	37.43	25.92
CH <sub>2</sub> CF <sub>3</sub>	3.62	9.63	O <sub>2</sub> N	-23.09	-25.44
CH <sub>2</sub> F	4.98	10.89	F	6.95	-9.25
CF <sub>3</sub>	-23.56	-16.41	Cl	9.83	11.17
CH <sub>2</sub> =CH	31.98	25.64	Br	9.52	12.70
HC≡C	18.17	25.64	I	13.32	20.53
C <sub>6</sub> H <sub>5</sub>	36.77	54.10			
<i>c</i> -C <sub>3</sub> H <sub>5</sub>	42.97	47.06			

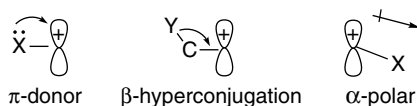
a. K. van Alem, G. Lodder, and H. Zuilhof, *J. Phys. Chem.*, **106**, 10681 (2002).

Netherlands.<sup>71</sup> This study compared MP2/6-311++G(*d,p*), CBS-Q, and B3LYP/6-311+G(*d,p*) calculations and found that the CBS-Q method gave the best correlation with experimental data. There was also good correlation with MP2 and B3LYP results, which could be used to obtain “CBS-Q-like” results when the CBS-Q method was not applicable. Table 3.12 gives some of the computed stabilization (+) and destabilization (-) relative to ethyl and vinyl cations found using isodesmic reactions:



The results show substantial destabilization for CF<sub>3</sub>, CN, CH=O, CO<sub>2</sub>H, and NO<sub>2</sub> groups.

The relative stability, charge distribution, and bond orders obtained by the calculation identified three main factors in carbocation stabilization as  $\pi$ -donation,  $\beta$ -hyperconjugation, and the  $\alpha$ -polar effects.



The  $\pi$ -donor and  $\beta$ -hyperconjugation effects are present for both alkyl and vinyl carbocations. The vinyl carbocations exhibit somewhat larger stabilizations because they are inherently less stable. The vinyl cations also appear to be more sensitive to the  $\alpha$ -polar effect. Note that the F, OH, and NH<sub>2</sub> substituents are less stabilizing of vinyl cations than of alkyl cations. This is believed to be due to the greater sensitivity to the polar effect of the more electronegative *sp* carbon in the vinyl cations. The NPA and bond order characterizations of the carbocations are shown in Table 3.13. The values give the charge associated with the cationic carbon and the bond order between the cationic carbon and the substituent X.

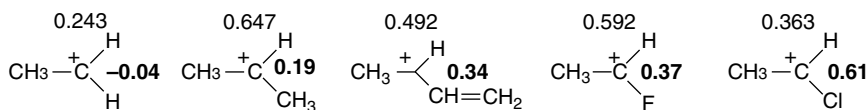
<sup>71</sup> K. van Alem, G. Lodder, and H. Zuilhof, *J. Phys. Chem. A.*, **106**, 10681 (2002).

**Table 3.13. NPA and Bond Order Characterizations of Substituted Carbocations**

X	C(+)		C <sup>+</sup> -X Bond Order	
	Alkyl	Vinyl	Alkyl	Vinyl
CH <sub>3</sub>	0.647	0.585	0.19	0.20
CH <sub>2</sub> OH	0.702	0.568	0.15	0.17
CH <sub>2</sub> CN	0.633	0.598	0.15	0.18
CH <sub>2</sub> Cl	0.719	0.585	0.18	0.16
CH <sub>2</sub> F	0.659	0.577	0.14	0.15
CH <sub>2</sub> CF <sub>3</sub>	0.612	0.601	0.13	0.18
CF <sub>3</sub>	0.666	0.618	-0.07	-0.06
CH <sub>2</sub> =CH	0.492	0.440	0.34	0.27
HC≡C	0.542	0.704	0.28	0.29
C <sub>6</sub> H <sub>5</sub>	0.420	0.383	0.40	0.29
<i>c</i> -C <sub>3</sub> H <sub>5</sub>	0.558	0.525	0.46	0.42
C≡N	0.602	0.572	0.13	0.15
HC=O	0.664	0.656	0.02	-0.03
HO <sub>2</sub> C	0.650	0.587	-0.02	-0.02
H <sub>2</sub> N	0.531	0.394	0.55	0.47
HO	0.242	0.125	0.76	0.67
O <sub>2</sub> N	0.499	0.424	0.02	0.04
F	0.592	0.524	0.37	0.39
Cl	0.363	0.274	0.61	0.60
Br	0.284	0.205	0.67	0.65
I	0.193	0.123	0.74	0.68

a. K. van Alem, G. Lodder, and H. Zuilhof, *J. Phys. Chem. A*, **106**, 10681 (2002).

Except for  $\pi$ -donor substituents, most of the positive charge resides on the cationic carbon. The strongest effect is seen for the halogens, where there is a sharp drop in the positive charge in the order  $F > Cl > Br > I$ . Note from the NPA charge at the cationic carbon that F is more effective than CH<sub>3</sub> in delocalizing the positive charge. However, the net stabilization is much less because the polar effect of the  $\sigma$  C–F bond is strongly destabilizing.<sup>72</sup> The resonance effect is also indicated by increased bond order to the substituent (shown in bold).



Charge on trivalent carbon (upper) and bond order (bold) on carbocation

One feature of the charge distributions in carbocations that deserves attention is the greater positive charge calculated for the trigonal carbon in 2-propyl cation than for ethyl cation. This tendency for more substituted alkyl carbocations to be *more positive* has been found in other calculations<sup>73</sup> and is consistent with the relative <sup>13</sup>C chemical shifts observed in NMR.<sup>74</sup> How does this relationship accord with the very strong *stabilizing* influence on alkyl groups on carbocations? Levy<sup>75</sup> has argued that

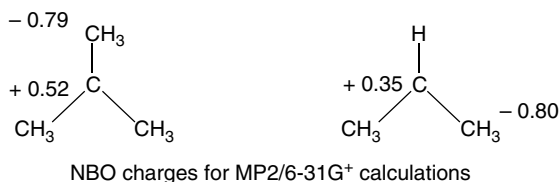
<sup>72</sup> K. van Alem, E. J. R. Sudhölter, and H. Zuilhof, *J. Phys. Chem. A*, **102**, 10860 (1998).

<sup>73</sup> R. Hoffmann, *J. Chem. Phys.*, **40**, 2480 (1964).

<sup>74</sup> G. A. Olah and A. M. White, *J. Am. Chem. Soc.*, **91**, 5801 (1969).

<sup>75</sup> J. B. Levy, *Struct. Chem.*, **10**, 121 (1999).

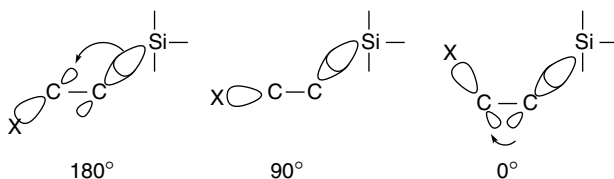
the alternating (+) and (-) charges found in tertiary cations provide the source of the stabilization. The hydrogens bear most of the positive charge according to NPA charge assignment.



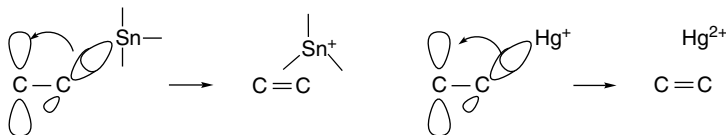
Silicon substitution  $\beta$  to a carbocation is very stabilizing by hyperconjugation.<sup>76</sup>



This stabilization has been shown to be primarily a delocalization effect by demonstrating a strong dependence on the dihedral angle between the Si-C bond and the empty  $p$  orbital of the carbocation. Kinetic rate enhancements of about 1012, 0, and 104 were found for compounds with angles of 180°, 90°, and 0°, respectively. This is consistent with a hyperconjugation mechanism and with analyses of orbital overlap that show considerably stronger overlap for the *anti* (180°) than *syn* (0°) orientations.<sup>77</sup>

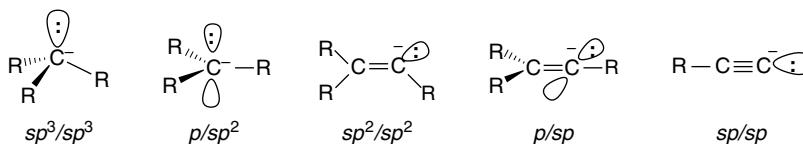


This  $\beta$ -stabilization is even stronger for less electronegative elements such as tin and mercury. In effect, the electron release is complete and elimination occurs. We discuss this kind of reaction further in Section 5.10.5.



### 3.4.2. Carbanions

Carbanions have negative charge on carbon and, as with carbocations, there are several conceivable hybridization schemes.



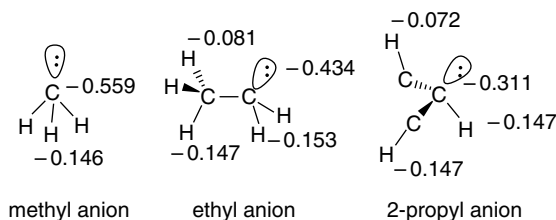
<sup>76</sup> J. B. Lambert, *Tetrahedron*, **46**, 2677 (1996); J. B. Lambert, Y. Zhao, R. W. Emblidge, L. A. Salvador, X. Liu, J. -H. So, and E. C. Chelius, *Acc. Chem. Res.*, **32**, 183 (1999).

<sup>77</sup> A. J. Green, Y. -I. Kuan, and J. M. White, *J. Org. Chem.*, **60**, 2734 (1995).

Because the nonbonding orbital is occupied, stability increases with  $s$  character, the converse of the situation for carbocations. The order of stability of carbanions is  $sp^3 < sp^2 < sp$ . The relative stability of gas phase carbanions can be assessed by the energy of their reaction with a proton, which is called *proton affinity*. The proton affinities of the prototypical hydrocarbons methane, ethene, and ethyne have been calculated at the MP4/6-31+G\* level.<sup>78</sup> The order is consistent with the electronegativity trends discussed in Section 1.1.5, and the larger gap between  $sp$  and  $sp^2$ , as compared to  $sp^2$  and  $sp^3$ , is also evident. The relative acidity of the hydrogen in terminal alkynes is one of the most characteristic features of this group of compounds.

<b>Proton affinity (kcal/mol)</b>		
$R^- + H^+ \longrightarrow R-H$		
$CH_4$	$H_2C=CH_2$	$HC\equiv CH$
419.4	408.7	375.1

The order of gas phase carbanion stability has been calculated as  $Et < Me \sim iso-Pr < tert-Bu$  by both MP2/6-31 + G( $d,p$ ) and B3LYP/6-31 + G( $d,p$ ) calculations.<sup>79</sup> Experimental values in the same order have been recorded.<sup>80</sup> The *pri* < *sec* < *tert* order reflects the ability of the larger groups to disperse the negative charge (polarizability). The  $Et < Me$  order indicates that electron donation by  $CH_3$  (relative to H) slightly destabilizes the ethyl carbanion. However, a larger *tert*-butyl substituent (in the neopentyl anion) has a net stabilizing effect that is evidently due to polarizability. Note that the effect of substitution is *very much smaller* than for carbocations. The range between primary and tertiary carbanions is only about 10 kcal/mol, compared to about 75 kcal/mol for carbocations. The alkyl anions are calculated to be pyramidal, in agreement with the  $sp^3$  hybridization model. The bond angles at the trivalent carbon are as follows:  $CH_3^-$  : 109.4°;  $CH_3CH_2^-$  : 111.0°;  $(CH_3)_2CH^-$  : 109.1°, and  $(CH_3)_3C^-$  : 109.6°.<sup>81</sup> AIM charges were also calculated (B3LYP/6-311 + G\*\*), as shown below, and indicate some  $\sigma$ -delocalization to the  $\beta$ -hydrogens. Note in particular that in the ethyl and 2-propyl anions the *anti* hydrogens are more negative than the *gauche*. Note also the considerable reduction in the charge at carbon as the anion becomes larger. These trends are in accord with dispersal of the negative charge by both hyperconjugation and polarization. Table 3.14 compares proton affinities calculated by several methods with experimental values.



<sup>78</sup> W. H. Saunders, Jr., and J. E. Van Verth, *J. Org. Chem.*, **60**, 3452 (1995).

<sup>79</sup> R. R. Sauers, *Tetrahedron*, **55**, 10013 (1999).

<sup>80</sup> C. H. DePuy, S. Gronert, S. E. Barlow, V. M. Bierbaum, and R. Damrauer, *J. Am. Chem. Soc.*, **111**, 1968 (1989).

<sup>81</sup> P. Burk and K. Sillar, *Theochem*, **535**, 49 (2001).

**Table 3.14. Computational and Experimental Proton Affinities for Small Hydrocarbons (in kcal/mol)**

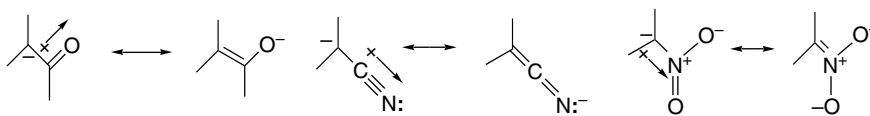
Group	MP2/6-31+G(d,p) <sup>a</sup>	B3LYP/6-311G(3df,2dp) <sup>a</sup>	G2 <sup>b</sup>	Experimental <sup>c</sup>
CH <sub>3</sub> <sup>-</sup>	419.0	414.5	418.4	415–421.5
CH <sub>3</sub> CH <sub>2</sub> <sup>-</sup>	421.8	417.0	420.6	420.1
(CH <sub>3</sub> ) <sub>2</sub> CH <sup>-</sup>	419.6	413.4	418.3	419.4
(CH <sub>3</sub> ) <sub>3</sub> C <sup>-</sup>	412.1	406.9	412.2	413.1
c-(CH <sub>2</sub> ) <sub>2</sub> CH <sup>-</sup>	415.5	411.3		409–413.5

a. R. R. Sauers, *Tetrahedron*, **55**, 10013 (1999).

b. P. Burk and K. Sillar, *Theochem*, **535**, 49 (2001).

c. Range of values includes quoted error ranges.

Electron-withdrawing groups such as carbonyl, cyano, and nitro strongly stabilize carbanions as the result of complementary resonance and polar effects. Table 3.15 gives some computed stabilization energies for various substituent groups.



The stabilization by substituents such as F and OH is presumably due to polar effects. Note that there is considerable discrepancy between the semiempirical and ab initio results, as the former indicate much greater substituent stabilization for the second-row elements C through F. The large stabilizing effect for BH<sub>2</sub> is due to the capacity of the –BH<sub>2</sub> group to accept two electrons. The effect of the heavier substituents, Cl through SiH<sub>3</sub>, is primarily due to polarizability. Very large stabilizations owing to delocalization are seen for the conjugated substituents CH<sub>2</sub>=CH through NO<sub>2</sub>.

Third- and fourth-row substituents such as sulfenyl, sulfinyl, sulfonyl, phosphinyl, and selenenyl stabilize carbanions. Because these substituents have tetrahedral

**Table 3.15. Calculated Stabilization Energies for Methyl Anions (in kcal/mol)**

Substituent	AM1 <sup>a</sup>	AM1 <sub>(H<sub>2</sub>O)</sub> <sup>a</sup>	PM <sup>a</sup>	PM <sub>(H<sub>2</sub>O)</sub> <sup>a</sup>	MP2/6-31G <sup>*b</sup>	MP4SDQ/6-31G <sup>*b</sup>	QCISD(T)/6-31G <sup>*b</sup>
F	19.4	14.4	24.6	21.0	9.09	10.52	10.23
OH	15.9	12.0	19.4	16.4	5.15	5.58	5.70
NH <sub>2</sub>	20.1	13.3	20.9	15.1	-0.67	-0.74	0.46
CH <sub>3</sub>	14.5	4.6	14.7	5.7	3.14	3.32	2.99
BH <sub>2</sub>					57.34	56.83	57.90
Cl					18.13	19.48	19.36
SH					20.98	20.45	20.53
PH <sub>2</sub>					23.45	22.37	22.25
SiH <sub>3</sub>					25.27	24.78	24.79
CH=CH <sub>2</sub>	45.5	29.4	33.0	31.4			
CH=O	62.7		60.3				
CN	55.0	41.2	59.4	49.3			
NO <sub>2</sub>	85.8	69.7	91.9	72.5			
Li					8.95	17.83	24.39
Na					5.04	16.99	21.92

a. M. El-Nahas, *J. Chem. Res. (Synop.)*, 310 (1996).

b. A. M. El-Nahas and P. v. R. Schleyer, *J. Comput. Chem.*, **15**, 596 (1994).

hybridization, the question arises as to whether the stabilization is through delocalization, polar, or polarization effects. The  $\alpha$  substituents increase acidity in the order  $\text{Se} > \text{S} > \text{O}$  and  $\text{Br} > \text{Cl} > \text{F}$ , which indicates that some factor apart from electronegativity (bond polarity) must contribute to the stabilization. The stabilization has been described both in terms of polarization and  $d$  orbital participation for the larger elements. The latter effect, as expressed in resonance terminology, implies shortening of the C–X bond. G2 calculations show very slight shortening for the C–PH<sub>2</sub> and C–SH bonds, but the halogens do not show such a trend.<sup>82</sup> Polarization appears to be the main mechanism for carbanion stabilization by the heavier elements.<sup>83</sup>

Another computational approach to assessing carbanion stabilization by substituents entails calculation of proton affinity. Table 3.16 gives the results of G2 and MP4/6-31G\* computations. The energy given is the energy required to remove a proton from the methyl group. The strong stabilization of the  $\pi$ -electron acceptors, such as BH<sub>2</sub>, CH=O, NO<sub>2</sub>, and CN, is evident. The second-row elements are in the order of electronegativity  $\text{F} > \text{OH} > \text{NH}_2$ , but the effects are comparatively small. The stabilization by third- and fourth-row elements (S, P, Se) are reproduced, and the halogen order,  $\text{F} < \text{Cl} < \text{Br}$ , also suggests that polarization is more important than dipolar stabilization.

These computational studies provide a description of carbanion stabilization effects that is consistent with that developed from a range of experimental observations. The strongest effects come from conjugating EWG substituents that can delocalize the negative charge. Carbon atom hybridization is also a very strong effect. The effect of saturated oxygen and nitrogen substituents is relatively small and seems to be  $\text{O} > \text{N}$ , suggesting a polar effect. This may be opposed by electron-electron repulsion arising from the unshared electrons on nitrogen and oxygen.

**Table 3.16. Gas Phase Proton Affinity of Substituted Methanes (in kcal/mol)**

Compound	G2 <sup>a</sup>	MP4/6-31G <sup>ab</sup>
CH <sub>3</sub> NH <sub>2</sub>	418.8	
CH <sub>3</sub> OH	414.6	417.7 <sup>b</sup>
CH <sub>3</sub> OCH <sub>3</sub>	412.8	
CH <sub>3</sub> PH <sub>2</sub>	393.9	
CH <sub>3</sub> SH	397.6	403.1 <sup>b</sup>
CH <sub>3</sub> SeH		399.3 <sup>b</sup>
CH <sub>3</sub> F	410.4	412.6 <sup>b</sup>
CH <sub>3</sub> Cl	398.2	404.5 <sup>b</sup>
CH <sub>3</sub> Br	393.5	400.3 <sup>b</sup>
CH <sub>3</sub> BH <sub>2</sub>	363.0	
CH <sub>3</sub> CH=O	368.1	367.1 <sup>c</sup>
CH <sub>3</sub> CH=CH <sub>2</sub>		392.5 <sup>c</sup>
CH <sub>3</sub> NO <sub>2</sub>	358.4	
CH <sub>3</sub> CN	375.0	375.9 <sup>c</sup>

a. P. M. Mayer and L. Radom, *J. Phys. Chem. A*, **102**, 4918 (1998).

b. J. E. Van Verth and W. H. Saunders, Jr., *J. Org. Chem.*, **62**, 5743 (1997).

c. W. H. Saunders, Jr., and J. E. Van Verth, *J. Org. Chem.*, **60**, 3452 (1995).

<sup>82</sup> P. M. Mayer and L. A. Radom, *J. Phys. Chem. A*, **102**, 4918 (1998).

<sup>83</sup> P. Speers, K. E. Laidig, and A. Streitwieser, *J. Am. Chem. Soc.*, **116**, 9257 (1994).

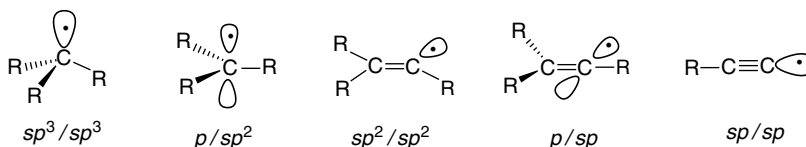
There is also a good deal of information available on carbanion stability in solution.<sup>84</sup> These data are derived from equilibrium measurements analogous to acid dissociation constants, in which the extent of deprotonation of hydrocarbons by strong base is determined:



Only a few hydrocarbon derivatives can be directly measured in aqueous solution, but extensive studies have been done in other solvents, in particular DMSO. We consider this solution data in Chapter 6.

### 3.4.3. Radical Intermediates

Carbon radicals have an unpaired electron in a nonbonding orbital. The possible hybridization schemes are shown below.



The methyl radical is close to planarity.<sup>85</sup> Experimental<sup>86</sup> and computational<sup>87</sup> results indicate that simple alkyl radicals are shallow pyramids with low barriers for inversion, which is consistent with  $p/sp^2$  hybridization. The ethenyl radical is bent with a C–C–H bond angle of 137°.<sup>88</sup> High-level MO calculations arrive at a similar structure.<sup>89</sup> This geometry indicates  $sp^2/sp^2$  hybridization. The alkenyl radicals can readily invert through the linear  $p/sp$  radical as a transition structure.<sup>90</sup> A major structural effect in alkyl (beyond methyl) and alkenyl radicals is a marked weakening of the  $\beta$ -C–H bonds, which occurs by interaction of the  $\beta$ -C–H and the SOMO (singly occupied molecular orbital). According to both computational (CBS-4) and thermodynamic cycles, the strength of the  $\beta$ -C–H bond is only 30–35 kcal/mol.<sup>91</sup> This leads to one of the characteristic bimolecular reactions of alkyl radicals—disproportionation to an alkane and an alkene. Similar values pertain to  $\beta$ -C–H bonds in vinyl radicals.



<sup>84</sup>. E. Buncl and J. M. Dust, *Carbanion Chemistry*, Oxford University Press, Oxford, 2003.

<sup>85</sup>. M. Karplus and G. K. Fraenkel, *J. Chem. Phys.*, **35**, 1312 (1961); L. Andrews and G. C. Pimentel, *J. Chem. Phys.*, **47**, 3637 (1967); E. Hirota, *J. Phys. Chem.*, **87**, 3375 (1983).

<sup>86</sup>. M. Karplus and G. K. Fraenkel, *J. Chem. Phys.*, **35**, 1312 (1961); L. Andrews and G. C. Pimentel, *J. Chem. Phys.*, **47**, 3637 (1967); E. Hirota, *J. Phys. Chem.*, **87**, 3375 (1983); T. J. Sears, P. M. Johnson, P. Jin, and S. Oatis, *J. Phys. Chem.*, **104**, 781 (1996).

<sup>87</sup>. F. M. Bickelhaupt, T. Ziegler, and P. v. R. Schleyer, *Organometallics*, **15**, 1477 (1996); M. N. Paddon-Row and K. N. Houk, *J. Phys. Chem.*, **89**, 3771 (1985); J. Pacansky, W. Koch, and M. D. Miller, *J. Am. Chem. Soc.*, **113**, 317 (1991); H. H. Suter and T. K. Ha, *Chem. Phys.*, **154**, 227 (1991); A. L. L. East and P. R. Bunker, *Chem. Phys. Lett.*, **282**, 49 (1998).

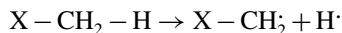
<sup>88</sup>. J. H. Wang, H. -C. Chang, and Y. -T. Chen, *Chem. Phys.*, **206**, 43 (1996).

<sup>89</sup>. L. A. Curtiss and J. A. Pople, *J. Chem. Phys.*, **88**, 7405 (1988); K. A. Peterson and T. H. Dunning, *J. Chem. Phys.*, **106**, 4119 (1997).

<sup>90</sup>. P. R. Jenkins, M. C. R. Symons, S. E. Booth, and C. J. Swain, *Tetrahedron Lett.*, **33**, 3543 (1992).

<sup>91</sup>. X. -M. Zhang, *J. Org. Chem.*, **63**, 1872 (1998).

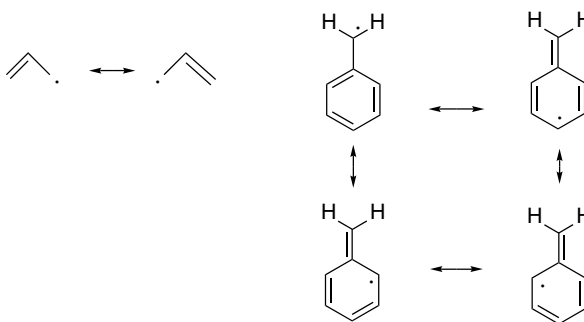
A good place to begin discussion of substituent effects on radicals is by considering the most common measure of radical stability. Radical stabilization is often defined by comparing C–H bond dissociation energies (BDE). For substituted methanes, the energy of the reaction should reflect any stabilizing features in the radical  $X-CH_2\cdot$ .



The BDEs are usually tabulated as the enthalpy change for the reaction at 298 K. The values can be determined experimentally<sup>92</sup> or calculated theoretically. Table 3.2 B (p. 258) gives some C–H BDE for important C–H bonds. The BDEs become smaller in the order  $CH_3 > pri > sec > tert$ . The relatively low enthalpies of the dissociation for forming allyl and benzyl radicals by removal of hydrogen from propene and toluene, respectively, is due to the stabilization of these radicals by delocalization. On the other hand the C–H bond to  $sp^2$  (ethene, benzene) and  $sp$  (ethyne) carbon are substantially stronger than bonds to  $sp^3$  carbon. The BDEs correlate with the ease of formation of the corresponding radicals.<sup>93</sup> The reactivity of C–H groups toward radicals that abstract hydrogen is  $pri < sec < tert$ . Vinyl and phenyl substituents at a reaction site weaken the C–H bond and enhance reactivity. On the other hand, hydrogen abstraction from an  $sp^2$  (vinyl or aryl) C–H bond or from a  $sp$  carbon in a terminal alkyne is difficult because of the increased strength of the corresponding C–H bonds.

The trend of reactivity  $tert > sec > pri$  is consistently observed in various hydrogen atom abstraction reactions, but the range of reactivity is determined by the nature of the reacting radical. The relative reactivity of *pri*, *sec*, and *tert* positions toward hydrogen abstraction by methyl radicals is 1:4.8:61.<sup>94</sup> An allylic or benzylic hydrogen is more reactive toward a methyl radical by a factor of about 9, compared to an unsubstituted C–H. The relative reactivity toward the *t*-butoxy radical is *pri*: 1, *sec*: 10, *tert*: 50.<sup>95</sup> In the gas phase, the bromine atom is much more selective, with relative reactivities of *pri*: 1, *sec*: 250, *tert*: 6300.<sup>96</sup> Data for other types of radicals have been obtained and tabulated.<sup>96</sup>

The stabilizing effects of vinyl groups (in allylic radicals) and phenyl groups (in benzyl radicals) are large and can be described in resonance terminology.



<sup>92</sup> J. Berkowitz, G. B. Ellison, and D. Gutman, *J. Phys. Chem.*, **98**, 2744 (1994).

<sup>93</sup> J. A. Kerr, *Chem. Rev.*, **66**, 465 (1966).

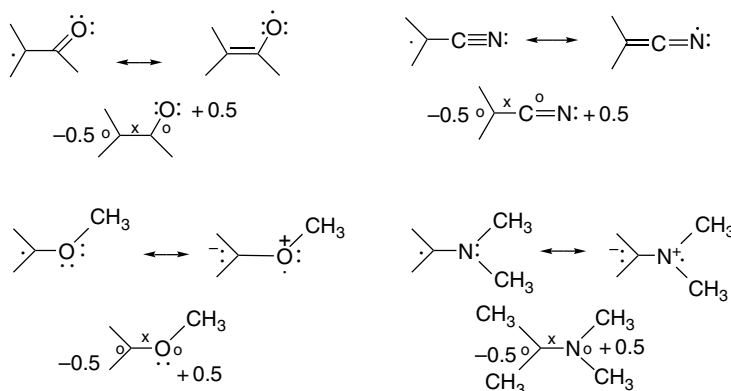
<sup>94</sup> W. A. Pryor, D. L. Fuller, and J. P. Stanley, *J. Am. Chem. Soc.*, **94**, 1632 (1972).

<sup>95</sup> C. Walling and B. B. Jacknow, *J. Am. Chem. Soc.*, **82**, 6108 (1960).

<sup>96</sup> A. F. Trotman-Dickenson, *Adv. Free Radical Chem.*, **1**, 1 (1965).

For the vinyl substituent, the stabilization can be expressed in terms of simple Hückel MO (HMO) theory. The interaction of a  $p$  orbital with an adjacent vinyl group creates the allyl radical. In HMO calculations, the resulting orbitals have energies of  $\alpha + 1.4\beta$ ,  $\alpha$ , and  $\alpha - 1.4\beta$ . Thus the interaction of the  $p$  orbital with both the  $\pi$  and  $\pi^*$  orbitals leaves it at the same energy level, but the  $\pi$  and  $\pi^*$  levels are transformed to  $\psi_1$  and  $\psi_3$  of the allyl radical. There is a net stabilization of  $0.8\beta$  for the two electrons in the more stable  $\psi_1$  orbital. One measure of the stabilization energy is the barrier to rotation at a terminal methylene group. A value of 16.8 kcal/mol has been calculated.<sup>97</sup> The experimental barrier is 15.7 kcal/mol. Another measure of the stabilization is the lowering of the C–H BDE for the allylic bond in propene, which indicates a stabilization of 13.4 kcal/mol.<sup>98</sup>

For radicals, nearly all functional groups are stabilizing. Both EWGs such as carbonyl and cyano and ERGs such as methoxy and dimethylamino have a stabilizing effect on a radical intermediate at an adjacent carbon. The stabilizing role of functional groups can be expressed in resonance terms. Resonance structures depict these interactions as delocalization of the unpaired electron into the substituent group. For unsaturated substituents, the resonance is analogous to the allyl radical. For donor substituents, a dipolar structure is involved. Linnett structures with three-electron bonds are also descriptive of the effect of donor substituents, and imply a degree of charge separation.



The radical-stabilizing effect of both types of substituents also can be described in MO terms. In this case, the issue is how the unpaired electron in a  $p$  orbital interacts with the orbitals of the adjacent substituent, such as vinyl, carbonyl, or methoxy. Figure 3.19 presents a qualitative description of the situation. For unsaturated EWG substituents such as carbonyl, the orbitals are similar to an allyl system, but the energies are lower because of the lower energy of the  $\pi$  and  $\pi^*$  orbitals of the carbonyl group. In the case of an  $\pi$ -electron acceptor there is a lowering of both the  $\psi_1$  orbital and the SOMO containing the unpaired electron, that is, the radical is stabilized. The radical also is more *electrophilic* because the SOMO is lowered in energy. For an electron donor substituent, the strongest interaction is between the unpaired electron in the  $p$  orbital and a nonbonding pair on the electron donor. This interaction results in lowering the energy of the orbital occupied by the electron pair, while raising the energy of the

<sup>97</sup> D. A. Hrovat and W. T. Borden, *J. Phys. Chem.*, **98**, 10460 (1994).

<sup>98</sup> W. R. Roth, F. Bauer, A. Beitat, T. Ebbrecht, and M. Wustefel, *Chem. Ber.*, **124**, 1453 (1991).

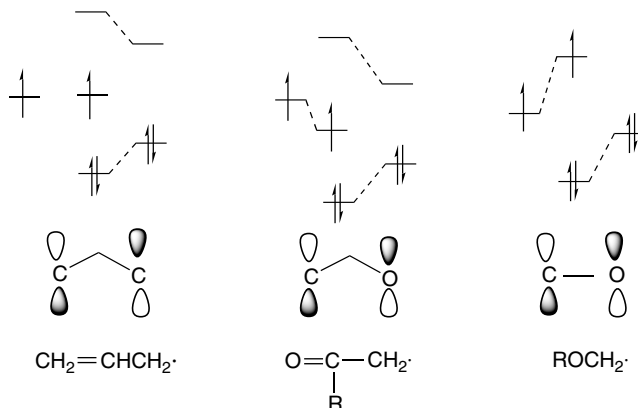


Fig. 3.19. PMO representation of  $p$ -orbital interactions with (a)  $\text{C}=\text{C}$ , (b)  $\text{C}=\text{O}$ , and (c)  $\text{OR}$  substituents. The form of the resulting SOMO is shown at the bottom.

orbital occupied by the single electron. The net effect is stabilizing, since there are two electrons in the stabilized orbital and only one in the destabilized one. The radical center is now more *nucleophilic* because the energy of the SOMO is raised.

Substituent effects on radicals can be expressed as *radical stabilization energies* (RSE). Table 3.17 gives some RSEs determined by one such approach developed by Leroy,<sup>99,100</sup> which can be defined as the difference between the observed enthalpy of atomization  $\Delta H_a$  and the sum of standard bond energies.

$$\text{RSE} = \Delta H_a - \Sigma \text{BE}$$

The  $\Delta H_a$  can be obtained from thermodynamic data or calculated theoretically.<sup>101</sup> These RSE values are generally consistent with chemical experience. For example, the low stability attributed to aryl and vinyl radicals, as opposed to the high stability of benzyl and allyl radicals, is consistent with their respective reactivities. The somewhat less familiar stability of aminoalkyl and acyl radicals is reproduced. The need for care is illustrated by the value for  $\text{Cl}_3\text{C}\cdot$ , which implies considerable *destabilization*. Chemical experience (see Section 11.4.2) shows that  $\text{CCl}_3\cdot$  is a quite accessible species, although it appears in Table 3.17 as one of the most destabilized radicals. The C–H BDE for H– $\text{CCl}_3$  is intermediate between those for *pri* and *tert* C–H bonds. The apparent “destabilization” of  $\text{CCl}_3\cdot$  is due to a “destabilization” that is also present in the reactant  $\text{Cl}_3\text{C}-\text{H}$ . Similarly, the acetyl radical is listed as destabilized, but it, too, is an accessible species. We return to this issue in Topic 11.1. Schemes for assignment of RSE that depend on the definition of standard bond energy terms are subject to the particular definitions that are used. These systems, however, are valuable in providing a basis for comparing substituent effects on a qualitative basis. These approaches can be

<sup>99</sup> G. Leroy, D. Peeters, and C. Wilante, *Theochem*, **5**, 217 (1982); G. Leroy, *Theochem*, **5**, 77 (1988).

<sup>100</sup> Other approaches to radical stabilization energies: C. Ruchardt and H. D. Beckhaus, *Top. Curr. Chem.*, **130**, 1 (1985); F. M. Welle, H.-D. Beckhaus, and C. Ruchardt, *J. Org. Chem.*, **62**, 552 (1997); F. G. Bordwell and X.-M. Zhang, *Acc. Chem. Res.*, **26**, 510 (1993); F. G. Bordwell, X.-M. Zhang, and R. Filler, *J. Org. Chem.*, **58**, 6067 (1993).

<sup>101</sup> J. Espinosa-Garcia and G. Leroy, *Recent Devel. Phys. Chem.*, **2**, 787 (1998).

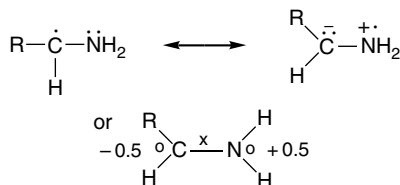
**Table 3.17. Thermochemical Stabilization Energies for Some Substituted Radicals (in kcal/mol)**

	RSE <sup>a</sup>		RSE <sup>a</sup>
CH <sub>3</sub> ·	-1.67	CH <sub>3</sub> (OH)CH·	2.15
CH <sub>3</sub> CH <sub>2</sub> ·	2.11	(NC)FCH·	-2.79
NCCH <sub>2</sub> ·	6.50	F <sub>2</sub> CH·	-4.11
NH <sub>2</sub> CH <sub>2</sub> ·	3.92	(CH <sub>3</sub> ) <sub>3</sub> C·	4.35
CH <sub>3</sub> NHCH <sub>2</sub> ·	12.18	CH <sub>3</sub> Ċ(CN) <sub>2</sub>	3.92
(CH <sub>3</sub> ) <sub>2</sub> NCH <sub>2</sub> ·	14.72	CH <sub>3</sub> Ċ(OH) <sub>2</sub>	0.15
HOCH <sub>2</sub> ·	3.13	CH <sub>3</sub> Ċ(CN)(OH)	2.26
CH <sub>3</sub> OCH <sub>2</sub> ·	3.64	CF <sub>3</sub> ·	-4.17
FCH <sub>2</sub> ·	-1.89	CCl <sub>3</sub> ·	-13.79
(CH <sub>3</sub> ) <sub>2</sub> CH·	2.57	CH <sub>2</sub> =CH-CH <sub>2</sub> ·	13.28
(NC) <sub>2</sub> CH·	5.17	C <sub>6</sub> H <sub>5</sub> -CH <sub>2</sub> ·	12.08
(HO) <sub>2</sub> CH·	-2.05	CH <sub>2</sub> =CH·	-6.16
		HC≡C·	-15.57
		C <sub>6</sub> H <sub>5</sub> ·	-10.27
		C <sub>5</sub> H <sub>5</sub> ·	19.24
		CH <sub>3</sub> Ċ    O	7.10

a. Stabilization energy as defined by G. Leroy, D. Peeters, and C. Wilante, *Theochem*, **5**, 217 (1982).

illustrated by considering the effects on two types of compounds that exhibit significant radical stabilization, namely amines and compounds with captodative stabilization.

The CH bond dissociation energies of amines are particularly interesting and significant. The radical can be stabilized by interaction with the nitrogen unshared pair.

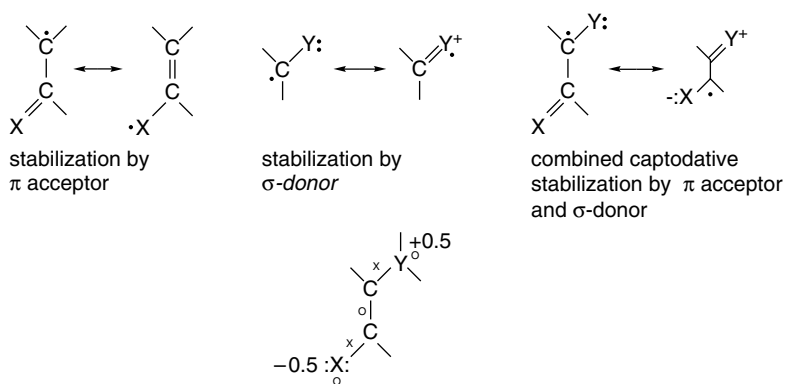


However, the same interaction—hyperconjugation—is present in the parent amine, as revealed by spectroscopic features of the C—H bond (see Section 1.1.8). Recent direct measurements have been made for (CH<sub>3</sub>)<sub>3</sub>N and (CH<sub>3</sub>CH<sub>2</sub>)<sub>3</sub>N, as well as the pyrrolidine and piperidine, among others.<sup>102</sup> The results obtained are shown below. The recommended value for the RSE for the aminomethyl radical is 13 ± 1 kcal/mol. Similar results were obtained using G2(MP2) calculations with isodesmic reactions. Pyrrolidine, the five-membered cyclic amine, has a slightly larger RSE because there is some relief of eclipsing interactions in the radical.

<sup>102</sup>. (a) D. D. M. Wayner, K. B. Clark, A. Rauk, D. Yu, and D. A. Armstrong, *J. Am. Chem. Soc.*, **119**, 8925 (1997); (b) J. Lalevee, X. Allonas, and J.-P. Fouassier, *J. Am. Chem. Soc.*, **124**, 9613 (2002).

<i>pri</i>	BDE	RSE	<i>sec</i>	BDE	RSE	<i>tert</i>	BDE	RSE
H <sub>2</sub> NCH <sub>2</sub> —H	93.9	12.2	(CH <sub>3</sub> ) <sub>2</sub> NH	87.0	12.7	(CH <sub>3</sub> ) <sub>3</sub> N	92.5	12.4
H <sub>2</sub> NCH <sub>2</sub> —H   CH <sub>3</sub>	90.0	13.1		90.0	14.8	Et <sub>3</sub> N	91.0	13.8
H <sub>2</sub> NC(CH <sub>3</sub> ) <sub>2</sub> —H	88.9	12.2		92.0	12.9	Bu <sub>3</sub> N	91.0	13.8

Captodative radicals have both electron donor and electron acceptor substituents at the radical center. The separate stabilizing effects of these substituents appear to have the ability to be synergistic. A Linnett structure gives a similar representation.



The Leroy analysis has been applied to captodative systems.<sup>103</sup> Table 3.18 shows the radical RSE calculated for some captodative radicals. An interesting aspect of the data is the failure of cyano groups to provide captodative stabilization. A significant consequence of the captodative effect is that the C—H bond of  $\alpha$ -amino derivatives of acids, esters, aldehydes, and ketones are expected to be very significantly weakened,

**Table 3.18. Stabilization Energy for Some Captodative Radicals (in kcal/mol)<sup>a</sup>**

HO— $\dot{C}$ H—CN	−3.40
HO— $\dot{C}$ H—CH=O	7.10
HO— $\dot{C}$ H—CO <sub>2</sub> H	5.01
HO— $\dot{C}$ H—NO <sub>2</sub>	0.03
H <sub>2</sub> N— $\dot{C}$ H—CN	0.25
H <sub>2</sub> N— $\dot{C}$ H—CH=O	6.86
H <sub>2</sub> N— $\dot{C}$ H—CO <sub>2</sub> H	7.72
H <sub>2</sub> N— $\dot{C}$ H—NO <sub>2</sub>	3.97

a. From G. Leroy, J. P. Dewispelaere, H. Benkadou, D. R. Tamsamani, and C. Wilante, *Bull. Chim. Soc. Belg.*, **103**, 367 (1994).

<sup>103</sup> G. Leroy, J. P. Dewispelaere, H. Benkadou, D. R. Tamsamani, and C. Wilante, *Bull. Soc. Chim. Belg.*, **103**, 367 (1994); G. Leroy, M. Sana, and C. Wilante, *Theochem*, **234**, 303 (1991).

falling in the range 75–80 kcal, which is weaker than either allylic or benzylic bonds. Because of the prevalence of such bonds in peptides and proteins, the strength of the C–H bonds of  $\alpha$ -amido carboxamides is of substantial biological interest.<sup>104</sup>

The stabilization provided by various functional groups contributes to reduced BDEs for bonds to the stabilized radical center. Computational methods can be used to assess these effects. The BDE can be calculated by comparing the total energy of the dissociated radicals with the reactant. Differences in bond dissociation energies relative to methane ( $\Delta$ BDE) can be taken as a measure of the stabilizing effect of the substituent on the radical. Some computed  $\Delta$ BDE values are given in Table 3.19 and compared with experimental values. As an example of the substituent effect on BDEs, it can be seen that the primary C–H bonds in acetonitrile (12 kcal/mol) and acetone (11 kcal/mol) are significantly weaker than a primary C–H bond in methane. The data show that both electron-releasing and electron-withdrawing functional groups stabilize radicals. The strong bond-weakening effect of amino substituents is noteworthy, both in its size and the apparent underestimation of this effect by the computations. A recent reevaluation of the  $\Delta$ BDE for amines arrived at a value of  $13 \pm 1$  kcal/mol, which is in better agreement with the calculations.<sup>102b</sup>

Theoretical calculations on radical stability entail some issues that are not present in diamagnetic molecules. These complications originate from the need to account for the singly occupied orbital. A comparison assessed the ability of a range of computational methods to reproduce radical stabilization energies.<sup>105</sup> A variant of the CBS-Q method called CBS-RAD was found adequate for calculation of geometry and energy of the  $\text{FCH}_2\cdot$ ,  $\text{CH}_2=\text{CF}\cdot$ , and  $\text{NCCH}_2\cdot$  radicals. This method, along with others,

**Table 3.19. Substituent Stabilization Relative to the Methyl Radical (in kcal/mol)**

Substituent	$\Delta$ BDE <sup>a</sup>	AUMP2 <sup>b</sup>	B3LYP/6-31+G <sup>c</sup>	G3(MP2)RAD <sup>d</sup>	CBS-RAD <sup>d</sup>
H	0.0	0.0	0.0	0.0	0.0
CH <sub>3</sub>	7	3.2	4.8	3.4	3.8
CH <sub>2</sub> =CH	19	12.6	18.8	16.9	17.6
C <sub>6</sub> H <sub>5</sub>	17				
HC=O		9.5		8.3	9.6
CH <sub>3</sub> C=O	11		9.2		
C <sub>6</sub> H <sub>5</sub> C=O	12				
CO <sub>2</sub> C <sub>2</sub> H <sub>5</sub>	10			5.1	6.0
CN	12	6.7	10.4	7.6	8.9
NO <sub>2</sub>	7			2.8	3.3
F	3	5.0		3.0	3.3
CH <sub>3</sub> O	12	8.9(OH)	9.8	7.4	8.2
NH <sub>2</sub>	22	11.1	13.3	10.6	11.6
(CH <sub>3</sub> ) <sub>2</sub> N	21				

a. F. G. Bordwell, X. -M. Zhang, and M. S. Alnajjar, *J. Am. Chem. Soc.*, **114**, 7623 (1992); F. G. Bordwell and X. -M. Zhang, *Acc. Chem. Res.*, **26**, 570 (1993).

b. M. Lehd and F. Jensen, *J. Org. Chem.*, **56**, 884 (1991).

c. B. S. Jursic, J. W. Timberlake, and P. S. Engel, *Tetrahedron Lett.*, **37**, 6473 (1996).

d. D. J. Henry, C. J. Parkinson, P. M. Mayer, and L. Radom, *J. Phys. Chem. A*, **105**, 6750 (2001).

<sup>104</sup>. P. E. M. Siegbahn, M. R. A. Blomberg, and R. H. Crabtree, *Theoretical Chem. Acc.*, **97**, 289 (1997); P. A. Frey, *Annu. Rev. Biochem.*, **70**, 121 (2001); G. Sawyers, *FEMS Microbiological Rev.*, **22**, 543 (1998).

<sup>105</sup>. P. M. Mayer, C. J. Parkinson, D. M. Smith, and L. Radom, *J. Chem. Phys.*, **108**, 604 (1998).

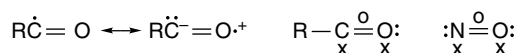
was then applied to a wider range of radicals. G3(MP2), AUMPQ, and B3LYP/6-31+G methods are also satisfactory. Some of these data are included in Table 3.19.

Table 3.20 provides some other comparisons. The first column gives experimental BDEs derived from thermodynamic data. The other columns give  $\Delta H$  calculated for the dissociative reaction, using various computational methods:



The computations that do not include electron correlation (HF) lead to large errors, but the other current methods that are applicable to molecules of this size perform satisfactorily.

Comparison of the thermochemical, kinetic, and computational evaluation of radical substituent effects provides a consistent picture. Delocalization, as in allylic and benzylic systems, provides  $\sim 15$  kcal/mol of stabilization. Conjugated EWGs such as acyl and cyano provide significant stabilization, usually in the range of 5–10 kcal/mol. Oxygen and especially nitrogen groups provide stabilization as well. In contrast, the  $sp^2$  and  $sp$  C–H bonds directly on vinyl, aryl, and alkynyl carbons are difficult to break, and the corresponding radicals are considered to be destabilized. An interesting contrast to these are acyl radicals, which are relatively easily formed from aldehydes by hydrogen atom abstraction (see Section 11.4.3). Stabilization results from conjugation with the oxygen electrons. These radicals are isoelectronic with NO and like NO, a Linnett-type structure can be drawn for acyl radicals. Showing a bond order of 2.5.



**Table 3.20. Comparison of Experimental and Calculated C–H Bond Dissociation Energies for Hydrocarbons and Representative Derivatives (in kcal/mol)**

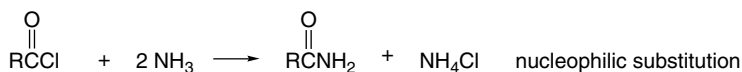
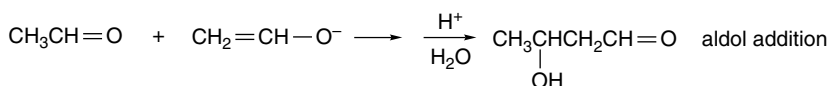
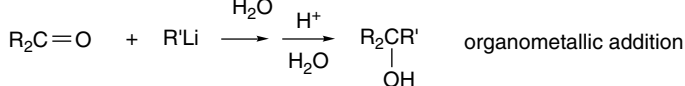
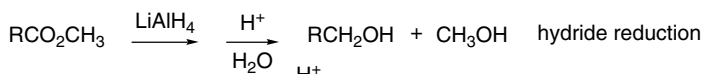
Compound	Experimental BDE (av.) <sup>a</sup>	Theoretical BDE						
		HF/6-31G(d,p)	MP2/6-31G(d,p)	CBS-4 <sup>b</sup>	CBS <sup>b</sup>	G2(MP2) <sup>b</sup>	G2 <sup>b</sup>	B3LYP/6-31G(d,p)
H–H	104.2	79.5	95.8			104.0		106.4
CH <sub>3</sub> –H	104.8	79.4	100.3	103.6	103.3	104.0	104.0	105.8
CH <sub>3</sub> CH <sub>2</sub> –H	101.1	76.8	98.9	99.9	100.0	100.0	100.9	101.1
(CH <sub>3</sub> ) <sub>2</sub> CH–H	97.6	74.5	95.3	97.0	97.4	98.4	98.5	97.1
CH <sub>3</sub> ) <sub>3</sub> C–H	96.5	72.7	93.7					94.0
CH <sub>2</sub> =CHCH <sub>2</sub> –H	84.9	85.0	87.5		87.3			
FCH <sub>2</sub> –H	101.7	77.8	96.0			99.1		
ClCH <sub>2</sub> –H	101.5	76.6	95.0			99.7		
HOCH <sub>2</sub> –H	96.2	74.1	92.3	95.6	95.3	96.2	96.2	95.2
H <sub>2</sub> NCH <sub>2</sub> –H	92.2	67.5	85.0	91.8	91.9	93.1	93.1	87.7
HSCH <sub>2</sub> –H	94.1	74.9	93.1			96.3		
NCCH <sub>2</sub> –H	93.4	69.8	96.2			93.8		
O=CHCH <sub>2</sub> –H	94.2	67.3	93.5			93.4		
CH <sub>3</sub> COCH <sub>2</sub> –H	95.1	69.4	94.4			94.0		
HO <sub>2</sub> CCH <sub>2</sub> –H	96.0	73.7	95.2			97.2		
CH <sub>3</sub> SO <sub>2</sub> CH <sub>2</sub> –H	99.0	80.8	101.2			103.4		
Cl <sub>3</sub> C–H	95.6	71.8	89.4			92.0		

a. H.-G. Korth and W. Sicking, *J. Chem. Soc., Perkin Trans.*, **2**, 715 (1997).

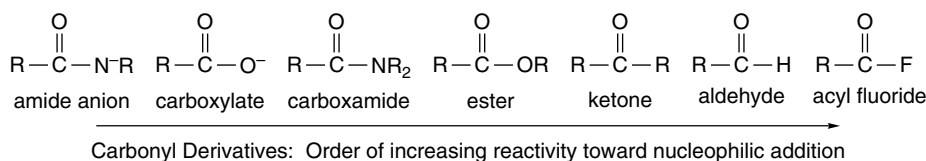
b. J. W. Ochterski, G.A. Petersson, and K. B. Wiberg, *J. Am. Chem. Soc.*, **117**, 11299 (1995).

## 3.4.4. Carbonyl Addition Intermediates

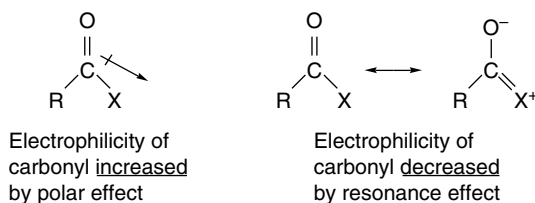
Addition of nucleophiles to carbonyl groups constitutes a very important class of reactions. A wide variety of reactions fall into this category, including hydride reductions, organometallic additions, aldol additions, and the nucleophilic substitution (including, e.g., hydrolysis, esterification, and aminolysis) reactions of carboxylic acid derivatives. We focus attention on the latter group of reactions at this point, because they are familiar from introductory organic chemistry and illustrate important substituent effects on carbonyl group reactivity. Nucleophilic substitution reactions of carboxylic acid derivatives also serve to emphasize the point that substituents can influence reaction rates through effects on reactants as well as on transition states and intermediates.



The major classes of carbonyl compounds include aldehydes, ketones, carboxamides, esters, carboxylic acids and anhydrides, and carbonyl halides (acyl halides). These groups differ in the identity of the substituent X on the carbonyl group. At this point we concentrate on these examples, but a number of other carbonyl derivatives have important roles in synthetic and/or biological reactions. These other compounds include acyl cyanides, acyl azides, *N*-acylimidazoles, *O*-aryl esters, and thioesters. The carbonyl compounds are arranged below in the order of the increasing reactivity toward nucleophilic addition.



At this point we want to consider the relative reactivity of carboxylic acid derivatives and other carbonyl compounds in general terms. We return to the subject in more detail in Chapter 7. Let us first examine some of the salient structural features of the carbonyl compounds. The strong polarity of the C=O bond is the origin of its reactivity toward nucleophiles. The bond dipole of the C–X bond would be expected increase carbonyl reactivity as the group X becomes more electronegative. There is another powerful effect exerted by the group X, which is resonance electron donation.



Substituents with unshared electrons allow electron delocalization, which stabilizes the compound and increases the negative charge on oxygen. This resonance effect stabilizes the carbonyl compound and decreases the reactivity of the carbonyl group toward nucleophiles. The order of electron donation by resonance is  $\text{RN}^- > \text{O}^- > \text{NR}_2 > \text{OR} \sim \text{OH} > \text{F}$ . The trends in the resonance and polar effects of these substituents are *reinforcing* and lead to the overall reactivity trends shown above. The amido group is the strongest resonance donor and weakest polar acceptor, whereas the fluorine is the weakest  $\pi$  donor and strongest  $\sigma$  acceptor.

There have been several attempts to analyze these substituent effects using computational approaches. For example, the isodesmic reaction



yields the results shown in Table 3.21.<sup>106</sup> In this formulation, the total stabilization includes both the differences between the C–X and the C–C bond strength and the resonance stabilization of the substituent. Remember (Section 3.1.2.2) that the C–X bond strength increases because of electronegativity differences. An indication of the extent of the  $\pi$  conjugation can be obtained from the C–X  $\pi$  bond orders shown in Figure 3.20. The  $\text{C}=\text{X}^+$  bond order decreases in the series  $\text{NH}_2(0.28) > \text{OCH}_3(0.22) > \text{F}(0.13)$ . These values can be contrasted to those for  $\text{C}\equiv\text{N}$  and  $\text{CH}_3$ , where there is minimal  $\pi$  delocalization and the  $\pi$  bond orders are around 0.04. Figure 3.20 also shows the atomic charges, as determined by the AIM method.

It is also desirable to separate the resonance component of the total stabilization energy. Wiberg addressed the issue by comparing total stabilization with the rotational barrier, which should be a measure of the resonance contribution.<sup>107</sup> The resonance component for F was assumed to be zero. This analysis provides the order  $\text{NH}_2 > \text{OH}$  for the  $\pi$  stabilization but  $\text{OH} > \text{NH}_2$  for the  $\sigma$  component, as shown in Table 3.22.

**Table 3.21. Carbonyl Substituent Stabilization as Estimated by Isodesmic Replacement by Methyl (in kcal/mol)<sup>a</sup>**

Substituent	$\Delta H_{\text{exp}}$	HF/6-31G*	MP2/6-31G*	MP3/6-311++G**
NH <sub>2</sub>	19.6	20.6	21.2	18.3
OH	23.4	25.5	26.8	22.3
F	17.9	19.0	21.1	16.4
SiH <sub>3</sub>		-13.0	-12.0	-12.6
PH <sub>2</sub>		-6.2	-3.5	-3.9
SH	4.5	4.3	7.3	5.5
Cl	6.6	2.9	7.9	6.7
CN		-11.8	-9.3	-11.0
CF <sub>3</sub>		-11.9	-11.0	-12.4

a. Data from K. B. Wiberg, C. M. Hadad, P. R. Rablen, and J. Cioslowski, *J. Am. Chem. Soc.*, **114**, 8644 (1992).

<sup>106</sup> K. B. Wiberg, C. M. Hadad, P. R. Rablen, and J. Cioslowski, *J. Am. Chem. Soc.*, **114**, 8644 (1992).

<sup>107</sup> K. B. Wiberg, *Acc. Chem. Res.*, **32**, 922 (1999); K. B. Wiberg, *J. Chem. Educ.*, **73**, 1089 (1996).

## (a) Charge density

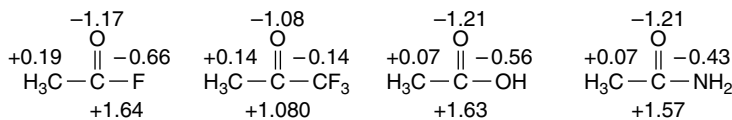
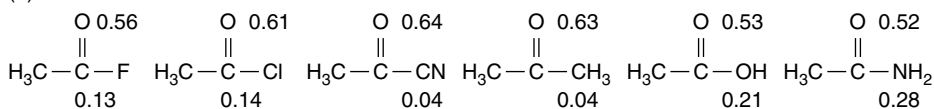
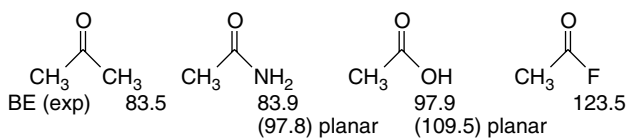
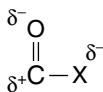
(b)  $\pi$ -Bond order

Fig. 3.20. Charge density (a) and bond orders (b) for carbonyl derivatives.

The bond energies of the  $\text{O}=\text{C}-\text{X}$  bonds increase sharply with electronegativity. For  $\text{NH}_2$  and  $\text{OH}$  there are different values for perpendicular and planar structures, reflecting the resonance contribution to the planar form.



The increasing  $\text{C}-\text{X}$  bond strength (apart from resonance) is attributed to the electrostatic attraction associated with the difference in electronegativity. This is accentuated by the already existing  $\text{C}=\text{O}$  charge separation and leads to a favorable juxtaposition of positive and negative charge.<sup>108</sup>



There have been several attempts<sup>109</sup> to assign relative importance to the polar (including electrostatic) and resonance components of the stabilization carboxylate

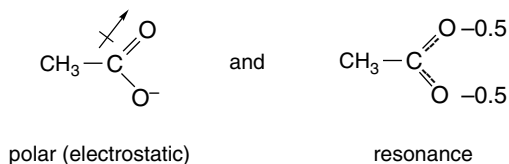
**Table 3.22. Separation of the Resonance Component of the Stabilization Energy**

	Total SE	$\Delta H_{\text{rot}}$	$\Delta H_{\sigma}$
F	16.7	—	16.7
OH	27.7	11.5	16.2
$\text{NH}_2$	19.3	13.9	5.4
Cl	6.8	—	6.8
SH	6.1	8.1	-2.0
$\text{PH}_2$	-3.9	0	-3.9
$\text{SiH}_3$	-12.7	0	-12.7

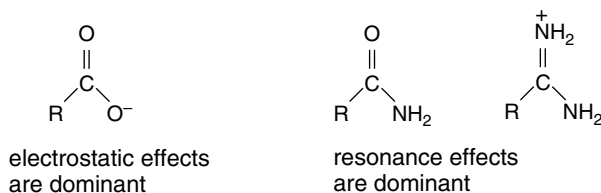
<sup>108</sup>. J. B. Levy, *Struct. Chem.*, **10**, 121 (1999).

<sup>109</sup>. P. C. Hiberty and C. P. Byrman, *J. Am. Chem. Soc.*, **117**, 9875 (1995); R. W. Taft, I. A. Koppel, R. D. Topsom, and F. Anvia, *J. Am. Chem. Soc.*, **112**, 2047 (1990); M. R. F. Siggel, A. Streitwieser, Jr., and T. D. Thomas, *J. Am. Chem. Soc.*, **110**, 8022 (1988).

anions. In a comparison of the acidity of acetic acid ( $pK$  4.7) with that of alcohols ( $pK$  16–18), the issue is the relative importance of the  $C=O$  bond dipole and resonance in stabilizing the carboxylate anion. These approaches have led to estimates ranging from 50 to 80% of the stabilization being polar in origin.



Rablen<sup>110</sup> investigated carbonyl substituent effects by using a series of isodesmic reactions designed to separate resonance and polar effects. He found the oxygen  $\pi$  contributions to be about 6 kcal/mol, as opposed to about 14 kcal/mol for nitrogen. The order of the polar effect is  $F > O > N > C$ , whereas that for the resonance effect is  $N > O > F$ . His analysis suggests that the stabilization in acetate ( $O^-$  donor) is about one-third resonance and two-thirds electrostatic. On the other hand, in amides and amidines, the order is reversed, roughly two-thirds resonance and one-third electrostatic.



A physical property that reflects the electronic character of the carbonyl substituent is the  $^{17}O$  NMR chemical shift. Although the relation of the chemical shift to electronic properties is complex, there is a correlation with the resonance electron-donating ability of the substituent. The  $\pi$ -donor substituents cause large downfield shifts in the order  $Cl \ll F < OCH_3 < NH_2$ . Nonconjugating substituents, such as cyano, trifluoromethyl, and methyl, have much smaller effects (Table 3.23).

**Table 3.23.**  $^{17}O$  Chemical Shifts for  $CH_3COX^a$

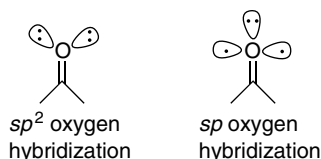
X	$^{17}O$
CN	603 <sup>b</sup>
CF <sub>3</sub>	592
H	592
CH <sub>3</sub>	571
Cl	502
F	374
CH <sub>3</sub> O	361
NH <sub>2</sub>	313

a. H. Dahm and P. A. Carrupt, *Magn. Reson. Chem.*, **35**, 577 (1997).

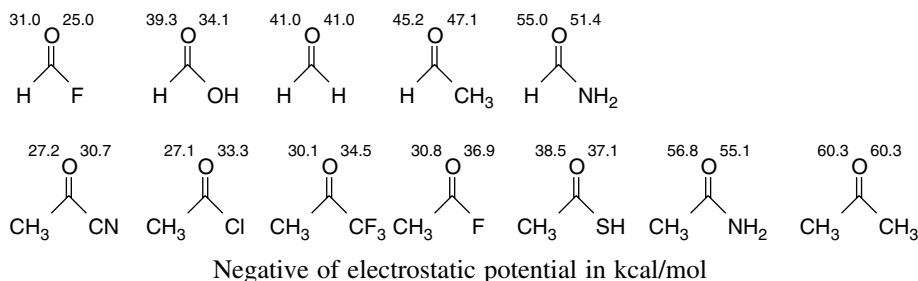
b. J.-C. Zhuo, *Molecules*, **4**, 320 (1999).

<sup>110</sup> P. R. Rablen, *J. Am. Chem. Soc.*, **122**, 357 (2000).

Another important aspect of carbonyl group structure and reactivity is associated with the two pairs of unshared electrons at the oxygen. These are usually formulated as occupying two  $sp^2$ , rather than one  $p$  and one  $sp$  orbital.

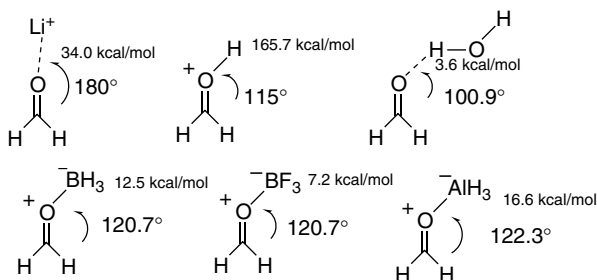


Wiberg and co-workers calculated the electrostatic potential at the carbonyl oxygen for several derivatives at the MP2/6-31 + G\* level.<sup>111</sup> The most negative electrostatic potential is found at angles somewhat greater than  $120^\circ$ , but generally corresponding with the trigonal  $sp^2$  hybridization model.



Note that the unsymmetrical compounds have somewhat different potentials *syn* and *anti* to the substituent. The qualitative order found for the formyl series  $F < OH < H < CH_3 < NH_2$  suggests a mixture of  $\sigma$  polar effects and  $\pi$ -electron donation. The acetyl series also included CN, Cl, and SH. It is interesting that the fluoride is calculated to have a more negative potential at oxygen than the chloride. This indicates a resonance contribution that attenuates the  $\sigma$  polar effect.

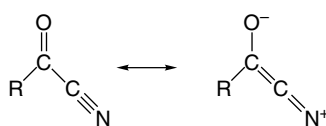
The reactivity of carbonyl groups is strongly influenced by interactions between protons or Lewis acids and the carbonyl oxygen unshared electrons. Wiberg and co-workers computationally probed the interaction of the carbonyl oxygen with  $Li^+$ ,  $H^+$ , and water (hydrogen bonding). Whereas  $Li^+$  prefers a linear structure, indicating that the attraction is primarily electrostatic rather than directional bonding, both protonation and hydrogen bonding favored the trigonal geometry. The same was true for the Lewis acids,  $BH_3$ ,  $BF_3$ , and  $AlH_3$ . The bonding energy was also calculated. Note the wide range of bond strengths from hydrogen bonding (3.6 kcal/mol) to formation of a very strong bond by protonation (165.7 kcal/mol). The calculated bond strengths for the Lewis acids is much smaller.



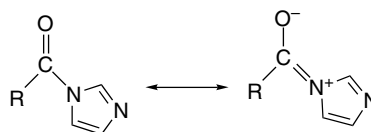
<sup>111</sup> K. B. Wiberg, M. Marquez, and H. Castejon, *J. Org. Chem.*, **59**, 6817 (1994).

Other workers examined hydrogen bonding of HF with carbonyl compounds. There is good correlation between the strength of the hydrogen bond (1–8 kcal/mol) and the electrostatic potential at the carbonyl oxygen.<sup>112</sup> Thus one important factor in carbonyl group reactivity is the potential for interaction with protons and Lewis acids, including metal ions.

We can summarize the structural effects of the substituents at the carbonyl group in terms of the resonance and polar contributions. While there may be variation in the relative weighting assigned to the polar and resonance components, the general trends are clear. Electron pair donors interact with the carbonyl group by resonance and the order of electron donation is  $C:^- > HN^- > O^- > H_2N > RO > F$ . The polar effect owing to substituent electronegativity is in the opposite direction, with  $F > RO > H_2N$ . These effects are *reinforcing* and increase carbonyl reactivity in the order  $C:^- < HN^- < O^- < H_2N < RO < F$ . The consequences of these resonance and polar effects on the carbonyl group can be observed in various ground state, i.e., reactant, properties. Groups such as cyano and imidazolid that have very weak resonance stabilization are dominated by the polar effect of the substituent and are quite reactive toward nucleophiles.



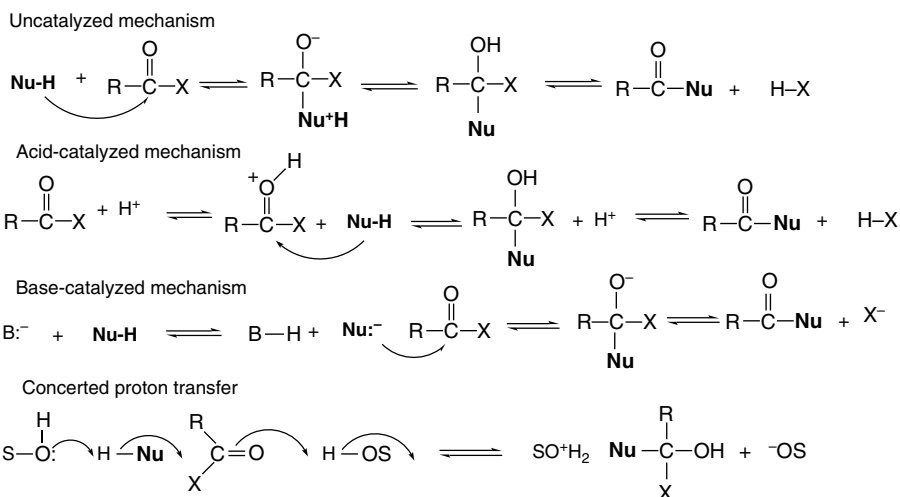
Cyano is very poor  
resonance donor



Imidazole aromaticity minimizes  
resonance donation by nitrogen

Let us now examine how substituent effects in *reactants* influence the rates of nucleophilic additions to carbonyl groups. The most common mechanism for substitution reactions at carbon centers is by an *addition-elimination mechanism*. The adduct formed by the nucleophilic addition step is tetrahedral and has  $sp^3$  hybridization. This adduct may be the product (as in hydride reduction) or an intermediate (as in nucleophilic substitution). For carboxylic acid derivatives, all of the steps can be reversible, but often one direction will be strongly favored by product stability. The addition step can be acid-catalyzed or base-catalyzed or can occur without specific catalysis. In protic solvents, proton transfer reactions can be an integral part of the mechanism. Solvent molecules, the nucleophile, and the carbonyl compound can interact in a concerted addition reaction that includes proton transfer. The overall rate of reaction depends on the reactivity of the nucleophile and the position of the equilibria involving intermediates. We therefore have to consider how the substituent might affect the energy of the tetrahedral intermediate.

<sup>112</sup> P. Bobadova-Parvanova and B. Galabov, *J. Phys. Chem. A.*, **102**, 1815 (1998); J. A. Platts, *Phys. Chem. Phys.*, **2**, 3115 (2000).



Some time ago, J. P. Guthrie derived an energy profile pertaining to the hydrolysis of methyl acetate under acidic, neutral, and basic conditions from kinetic data.<sup>113</sup> These reaction profiles are shown in Figure 3.21. This reaction can serve to introduce the issues of relative reactivity in carbonyl addition reactions. The diagram shows that the reaction is nearly energetically neutral in acidic solution, but becomes exothermic in neutral and basic solutions because of the additional stabilization associated with the carboxylate group. The activation barrier is highest for the neutral reaction. The activation barrier is lowered in acidic solution as a result of the enhanced reactivity of the protonated carbonyl (acid-catalyzed mechanism). The activation barrier for the basic hydrolysis is reduced because hydroxide ion is a more powerful nucleophile than water (base-catalyzed mechanism).

The energy relationships among reactants, transition states, intermediates, and products have been further explored for the base-catalyzed hydrolysis of methyl acetate.<sup>114</sup> The relative energies of the species shown in Figure 3.22 were calculated using

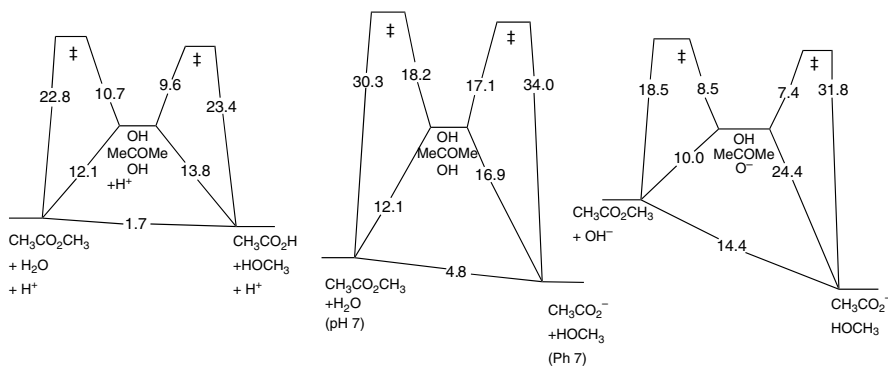


Fig. 3.21. Comparative reaction energy profiles for acidic, neutral, and basic hydrolysis of methyl acetate in water. Adapted from *J. Am. Chem. Soc.*, **95**, 6999 (1973), by permission of the American Chemical Society.

<sup>113</sup> J. P. Guthrie, *J. Am. Chem. Soc.*, **95**, 6999 (1973).

<sup>114</sup> C.-G. Zhan, D. W. Landry, and R. L. Ornstein, *J. Am. Chem. Soc.*, **122**, 1522 (2000).

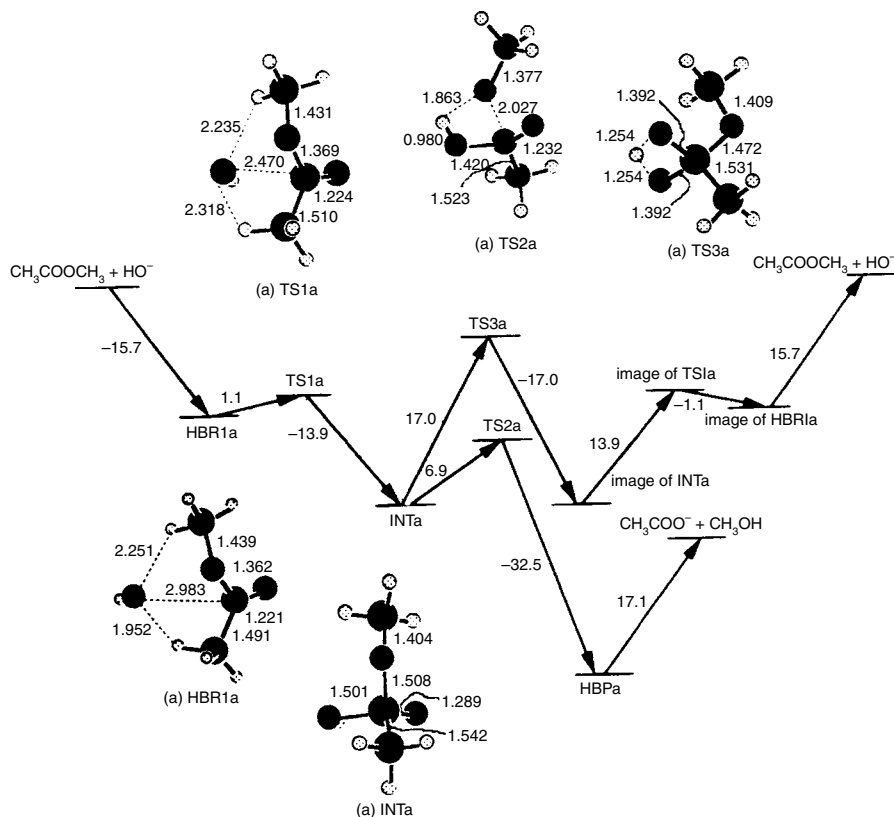
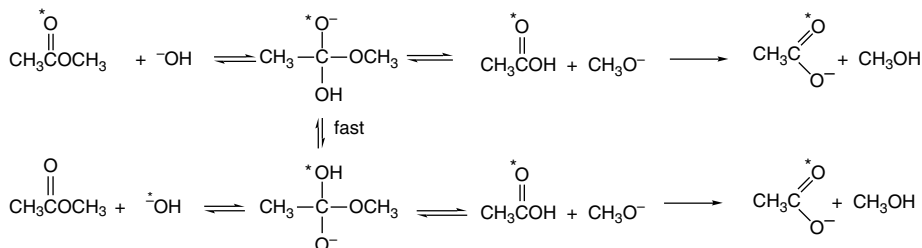


Fig. 3.22. Energy profiles (in kcal/mol) and structures of intermediates and transition states for competing hydrolysis and carbonyl oxygen exchange for methyl acetate and hydroxide ion in the gas phase. Adapted from *J. Am. Chem. Soc.*, **122**, 1522 (2000), by permission of the American Chemical Society.

several MO and DFT computations. The values quoted are for BLYP/6-31++G(*d,p*) level calculations and refer to the gas phase. These energy values describe both the hydrolysis reaction and the carbonyl oxygen exchange reaction, both of which occur through the same tetrahedral addition intermediate. **HBR1a** is a complex between  $\text{HO}^-$  and the reactant. **TS1a** and **INTa** are the TS and tetrahedral intermediate, respectively, resulting from hydroxide addition. **TS2a** is the TS leading to methoxide elimination, which results in the stable complex of methanol and acetate ion. **TS3a** is the TS for proton transfer between the two oxygens, which leads to oxygen exchange via an intermediate that is structurally identical to **TS1a**.



This theoretical examination of carbonyl addition reactions serves to emphasize the enormous role that solvation effects play. As indicated in Figure 3.22 and other studies, gas phase addition of hydroxide ion to esters is calculated to be *exothermic* and to encounter only a very small barrier at **TS1a** and **TS2a**.<sup>115</sup> The major contribution to the activation barrier (18.5 kcal/mol) that is observed in solution is the energy of desolvation of the hydroxide ion.<sup>116</sup> We return to a discussion of solvation effects on carbonyl additions in Section 3.8.

A similar comparison of the gas phase and solution phase reaction of *N,N*-dimethylacetamide was conducted.<sup>117</sup> Energies were calculated at the MP2/6-31+G\*\* level. Solution phase calculations were done using a continuum solvent model. The results are summarized in Figure 3.23 and, as with the ester reaction, the addition is calculated to be exothermic in the gas phase, but to have a barrier in solution. Interestingly, the HF/6-31+G\*\* energy values are somewhat closer to the experimental values than the MP2/6-31+G\*\* results. The solution value is 24.6 kcal/mol.<sup>118</sup>

Similar energy profiles for the other classes of carbonyl compounds would allow us to make broad comparisons in reactivity. Unfortunately, the reactivity covers a very

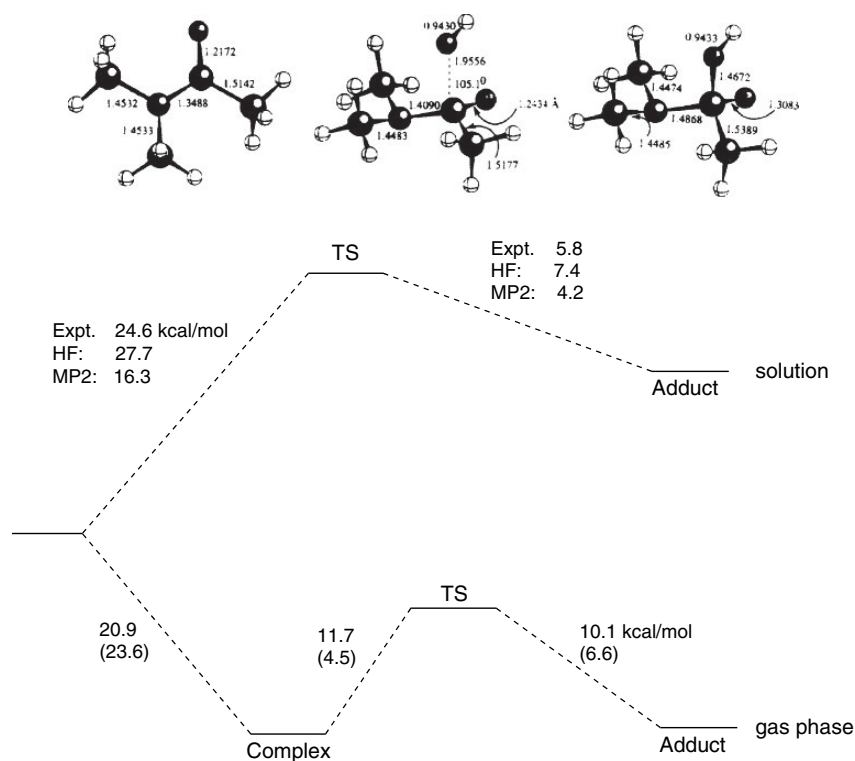


Fig. 3.23. Gas phase and solution reaction energy profiles for addition of hydroxide ion to *N,N*-dimethylacetamide. MP2 values are in paranthese Adapted from *Theochem*, **429**, 41 (1998), by permission of Elsevier.

<sup>115</sup>. K. Hori, *J. Chem. Soc., Perkin Trans.*, **2**, 1629 (1992); I. Lee, D. Lee, and C. K. Kim, *J. Phys. Chem. A*, **101**, 879 (1997); F. Hæfner, C.-H. Hu, T. Brink, and T. Norin, *Theochem*, **459**, 85 (1999).

<sup>116</sup>. M. J. S. Dewar and D. M. Storch, *J. Chem. Soc., Chem. Commun.*, 94 (1985); J. P. Guthrie, *Can. J. Chem.*, **68**, 1643 (1990).

<sup>117</sup>. Y.-J. Zheng and R. L. Ornstein, *Theochem*, **429**, 41 (1998).

<sup>118</sup>. J. P. Guthrie, *J. Am. Chem. Soc.*, **96**, 3608 (1974).

wide range and it is not easy to make direct experimental comparisons. In Scheme 3.2 some available kinetic data are provided that allow at least a qualitative comparison of the reactivity of the most common derivatives. The ratio of reaction toward hydroxide is anhydride > ester > amide, reflecting the expected trend and is dominated by the resonance effect. Acyl chlorides are even more reactive, judging by a comparison of methanolysis and hydrolysis. The data for esters give the nucleophilicity order as  $^-OH > NH_3 > H_2O$ , as expected.

A more extensive and precise set of data has been developed that includes aldehydes and ketones (but not acyl halides), which pertains to the equilibrium constant for hydration.<sup>119</sup>

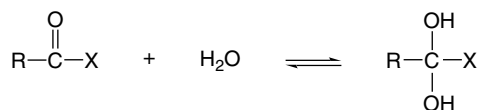


Table 3.24 shows the values for equilibrium constants for nucleophilic addition of both water and hydroxide ion. We can see the following trends in these data: For aldehydes and ketones, the addition is disfavored in the order Ph > alkyl > H. The order  $NH_2 < OR < CH_3 < H$  is indicated by the  $K_{hydr}$  values of  $10^{-13.8}$ ,  $10^{-6.6}$ ,  $10^{0.03}$ , and  $10^{3.36}$  for *N,N*-dimethylformamide, methyl formate, acetaldehyde, and formaldehyde,

**Scheme 3.2. Relative Reactivity Data for Some Carboxylic Acid Derivatives**

	$CH_3-\overset{\text{O}}{\parallel}{C}-Cl$	$(CH_3C)_2O$	$CH_3-\overset{\text{O}}{\parallel}{C}-OR'$	$CH_3-\overset{\text{O}}{\parallel}{C}-N(CH_3)_2$
Hydrolysis ( $^-OH$ )		$8.9 \times 10^2 M^{-1} s^{-1}$ at 25° C (a)	$2.2 \times 10^{-2} M^{-1} s^{-1}$ at 0° C $E_a = 18.5$ (b)	$1.8 \times 10^{-5} M^{-1} s^{-1}$ $E_a = 24.1$ (c)
Hydrolysis ( $H_2O$ )		$2.4 \times 10^{-3} s^{-1}$ at 25° C (a)	$3 \times 10^{-10} s^{-1}$ at 0° C $E_a = 30.2$ kcal(b)	
Methanolysis ( $CH_3OH$ )	$1 \times 10^{-1} s^{-1}$ at 0° C (d)			
Aminolysis ( $NH_3$ )			$2.8 \times 10^{-7} M^{-1} s^{-1}$ in 10 M $H_2O$ in dioxane (e)	$3.7 \times 10^{-7} M^{-1} s^{-1}$ in 5 M $HOCH_2CH_2OH$ in dioxane (f)

a. C. Castro and E. A. Castro, *J. Org. Chem.*, **46**, 2939 (1981); J. F. Kirsch and W. P. Jencks, *J. Am. Chem. Soc.*, **86**, 837 (1964).

b. J. P. Guthrie, *J. Am. Chem. Soc.*, **95**, 6999 (1973).

c. J. P. Guthrie, *J. Am. Chem. Soc.*, **96**, 3608 (1974).

d. T. W. Bentley, G. Llewelyn, and J. A. McAlister, *J. Org. Chem.*, **61**, 7927 (1996).

e. F. H. Wetzel, J. G. Miller, and A. R. Day, *J. Am. Chem. Soc.*, **75**, 1150 (1953).

f. E. M. Arnett, J. G. Miller, and A. R. Day, *J. Am. Chem. Soc.*, **72**, 5635 (1950).

<sup>119</sup> J. P. Guthrie, *J. Am. Chem. Soc.*, **122**, 5529 (2000).

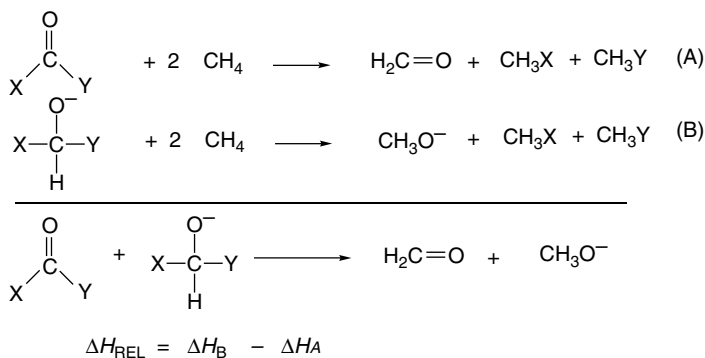
**Table 3.24. Equilibrium Constants for Hydration and Hydroxide Addition for Selected Carbonyl Compounds**

Compounds <sup>a</sup>	log $K_{\text{H}_2\text{O}}$	log $K_{-\text{OH}}$
CH <sub>2</sub> =O	3.36	6.51
CH <sub>3</sub> CH=O	0.03	4.68
(CH <sub>3</sub> ) <sub>2</sub> CHCH=O	-0.21	2.99
PhCH=O	-2.10	2.5
(CH <sub>3</sub> ) <sub>2</sub> C=O	-2.85	2.04
HCO <sub>2</sub> CH <sub>3</sub>	-6.6	1.58
CH <sub>3</sub> CO <sub>2</sub> CH <sub>3</sub>	-8.2	-0.82
(CH <sub>3</sub> ) <sub>2</sub> CHCO <sub>2</sub> CH <sub>3</sub>	-10.42	-1.05
CF <sub>3</sub> CO <sub>2</sub> CH <sub>3</sub>	-0.9	5.53
HCOSC <sub>2</sub> H <sub>5</sub>	-3.5	2.1
CH <sub>3</sub> COSC <sub>2</sub> H <sub>5</sub>	-8.2	-0.92
CF <sub>3</sub> COSC <sub>2</sub> H <sub>5</sub>	-2.8	3.77
HCON(CH <sub>3</sub> ) <sub>2</sub>	-13.8	-3.75
CH <sub>3</sub> CON(CH <sub>3</sub> ) <sub>2</sub>	-14.2	-4.75
CF <sub>3</sub> CON(CH <sub>3</sub> ) <sub>2</sub>	-9.2	-0.13

a. Data from J. P. Guthrie, *J. Am. Chem. Soc.*, **122**, 5529 (2000).

respectively. The hydroxide addition is in the same order but lies much further toward the adduct:  $10^{-3.75}$ ,  $10^{-0.82}$ ,  $10^{4.68}$ , and  $10^{6.5}$ , respectively, as expected for the stronger nucleophile. These data give a good indication of the overall reactivity of carbonyl compounds toward a prototypical nucleophilic addition, but incorporate structural effects pertaining to both the reactant and tetrahedral adduct. For example, the 100-fold difference between benzaldehyde and 2-methylpropanal presumably reflects the extra conjugative stabilization of the aromatic aldehyde. Similarly, the  $10^7$  and  $10^5$  difference between the ethyl esters and *N,N*-dimethylamides of acetic acid and trifluoroacetic acid, respectively, are due to the polar effect of the trifluoromethyl group. Note, however, that the differences are only slightly smaller ( $10^{6.5}$  and  $10^{4.5}$ ) in the anionic hydroxide adducts.

What can we say about substituent effects on the tetrahedral adducts? These have been assessed by comparing hydride affinity of the various derivatives, relative to formaldehyde,<sup>120</sup> using the isodesmic reaction sequence shown below.



<sup>120</sup> R. E. Rosenberg, *J. Am. Chem. Soc.*, **117**, 10358 (1995).

The effect of the same substituents on the adduct was evaluated by another isodesmic reaction:



This analysis permits assignment of hydride affinity to the carbonyl compounds relative to formaldehyde. The stabilization of the carbonyl compound by X relative to H is shown in Table 3.25 as  $\Delta\text{C}=\text{O}$ . The stabilization of the hydride adduct is shown as  $\Delta\text{HCO}^-$ . The difference, the hydride affinity relative to  $\text{CH}_2=\text{O}$ , is listed as  $\Delta\text{HA}$ . The resonance donors  $\text{NH}_2$  and  $\text{CH}_3\text{O}$  have the largest stabilizing effect on the carbonyl starting material, but F also has a very significant stabilizing effect. The stabilization of the tetrahedral adduct is in the order of bond strength  $\text{F} > \text{CH}_3\text{O} > \text{NH}_2 > \text{CH}_3$ . The difference between the two values places the overall substituent effect for reactivity toward hydride in the order  $\text{F} > \text{H} > \text{CH}_3 > \text{OCH}_3 > \text{NH}_2$ , in excellent agreement with experimental data. The polar EWGs CN and  $\text{CF}_3$  strongly favor hydride addition by strong stabilization of the anionic tetrahedral adduct. As a result, they have the largest overall effect on the stability of the hydride adduct, followed by fluoro and formyl.

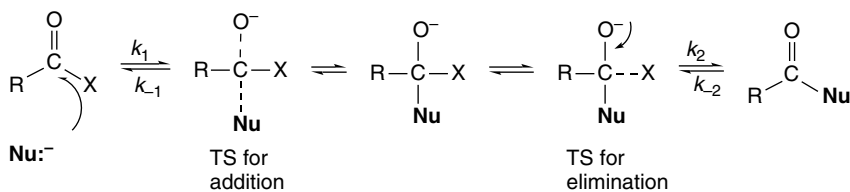
The stability relationships for carbonyl substitution reactions by an anionic nucleophile are summarized in Scheme 3.3. The simplest substitution reactions consist of two reversible steps, the formation of the tetrahedral intermediate and the subsequent elimination of the original substituent. As we discuss in Chapter 7, the mechanism is frequently more complex, often involving proton transfers. However, the stability effects of the carbonyl groups can be illustrated in terms of the simple two-step mechanisms. The stability order of reactants and products is  $\text{F}, \text{Cl} < \text{OR} < \text{NR}_2 < \text{O}^-$ . The order of stability of the *anionic* tetrahedral intermediates is  $\text{F} > \text{RO} > \text{RN}_2 > \text{O}^-$ . The diagram clearly indicates that the reactivity order will be  $\text{F} > \text{RO} > \text{R}_2\text{N} > \text{O}^-$ . Note also that the relative rates for the two possible fates of the tetrahedral intermediate (forward or reverse) are determined by the ease with which either  $\text{X}^-$  or  $\text{Nu}^-$  departs from the tetrahedral intermediate. This order will be  $\text{F}^- > \text{RO}^- > \text{NH}_2^- > \text{O}^{2-}$ , so we expect substitution on acyl fluorides (and other acyl halides) to be fast and irreversible. On the other hand, nucleophilic substitution on carboxylate anions, which is at the other end of the reactivity range, is nearly impossible. (We will see in Section 7.2.2.2 in Part B that organolithium compounds are strong enough nucleophiles to achieve addition with carboxylate groups, at least in the presence of  $\text{Li}^+$ .) The relative stability

**Table 3.25. Substituent Effects on Hydride Affinity of  $\text{XYC}=\text{O}$  by an Isodesmic Reaction Sequence (in kcal/mol by G2(MP2) Calculations)<sup>a</sup>**

X	Y	$\Delta\text{C}=\text{O}$	$\Delta\text{HCO}^-$	$\Delta\text{HA}$
H	H	0	0	0
H	$\text{CH}_3$	11.1	9.6	1.5
H	$\text{NH}_2$	31.5	21.8	9.7
H	$\text{CH}_3\text{O}$	32.8	29.0	3.8
H	F	26.1	38.2	-12.1
H	$\text{CH}=\text{O}$	3.1	19.0	-15.9
H	$\text{CF}_3$	-3.0	23.3	-26.3
H	CN	-2.4	25.9	-28.3

a. R. E. Rosenberg, *J. Am. Chem. Soc.*, **117**, 10358 (1993).

## Scheme 3.3. Summary of Substituent Effects on Carbonyl Substitution Reactions

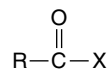
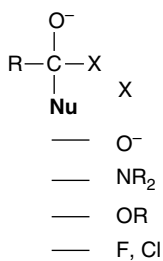


TS for addition  
Based on effect of  
-X on C=O reactivity

— O<sup>-</sup> —  
— R<sub>2</sub>N —  
— RO —  
— F, Cl —

TS for elimination  
Based on leaving group ability  
of X

— O<sup>-</sup>  
— NR<sub>2</sub>  
— OR  
— F, Cl



X

— F, Cl —  
— OR —  
— NR<sub>2</sub> —  
— O<sup>-</sup> —

X

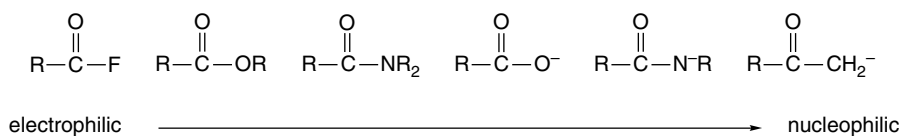
— F, Cl —  
— OR —  
— NR<sub>2</sub> —  
— O<sup>-</sup> —

## SECTION 3.4

*Electronic Substituent  
Effects on Reaction  
Intermediates*

of the carboxylate starting material and the double negative charge on the tetrahedral intermediate make the activation energy for the first step very high. Even if the intermediate is formed, the prospective leaving group O<sup>2-</sup> is very difficult to eliminate, so  $k_{-1} > k_2$  and no substitution is observed.

Perhaps it is worth noting in summary that the series can be extended to include X=NH<sup>-</sup> and X=CH<sub>2</sub><sup>-</sup>. These analogs would be expected to be even less reactive than carboxylate toward nucleophilic addition. The latter species is an *enolate*. We will learn in Section 7.7 that enolates are reactive nucleophiles. Carboxylate and amide anions also are nucleophilic. Even amides are somewhat nucleophilic. Going across the periodic table from F to CH<sub>2</sub><sup>-</sup>, the carbonyl substituent X transforms the carbonyl group from an electrophile to part of a nucleophilic structure in the anionic structures by increasing electron donation.



### 3.5. Kinetic Isotope Effects

A special type of substituent effect that has proved very valuable in the study of reaction mechanisms is the replacement of an atom by one of its isotopes. Isotopic substitution most often involves replacing protium by deuterium (or tritium), but is applicable to nuclei other than hydrogen. The quantitative differences are largest, however, for hydrogen because its isotopes have the largest relative mass differences. Isotopic substitution usually has no effect on the qualitative chemical reactivity of the substrate, but it often has an easily measured effect on the rate, which is called a *kinetic isotope effect (KIE)*. Let us consider how this modification of the rate arises. Initially, the discussion concerns *primary kinetic isotope effects*, those in which a bond to the isotopically substituted atom is broken in the rate-determining step. We use C–H bonds as the specific case for discussion but the same concepts apply for other elements.

Any C–H bond has characteristic vibrations that impart some energy, called the *zero-point energy*, to the molecule. The energy associated with these vibrations is related to the mass of the vibrating atoms. Owing to the greater mass of deuterium, the vibrations associated with a C–D bond contribute less to the zero-point energy than the corresponding C–H bond. For this reason, substitution of protium by deuterium lowers the zero-point energy of a molecule. For a reaction involving cleavage of a bond to hydrogen (or deuterium), a vibrational degree of freedom in the normal molecule is converted to a translational degree of freedom as the bond is broken. The energy difference that is due to this vibration disappears at the transition state. The transition state has the same energy for the protonated and deuterated species. Because the deuterated molecule has the lower zero-point energy, it has a higher activation energy to reach the transition state, as illustrated in Figure 3.24.

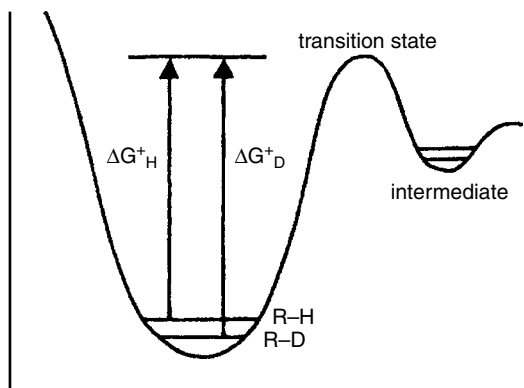
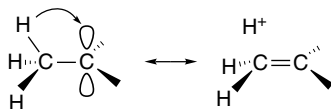


Fig. 3.24. Differing zero-point energies of protium- and deuterium-substituted molecules as the cause of primary kinetic isotope effects.

Just how large the rate difference is depends on the nature of the TSs. The maximum effect occurs when the hydrogen being transferred is bound about equally to two other atoms at the TS. The calculated maximum for the isotope effect  $k_{\text{H}}/k_{\text{D}}$  involving C–H bonds is about 7 at room temperature.<sup>121</sup> When bond breaking is more or less than half complete at the TS, the isotope effect is smaller and can be close to 1 if the TS is very reactant-like or very product-like. Primary isotope effects can provide two very useful pieces of information about a reaction mechanism. First, the existence of a substantial isotope effect, i.e.,  $k_{\text{H}}/k_{\text{D}} > 2$ , is strong evidence that the bond to that particular hydrogen is being broken in the rate-determining step. Second, the magnitude of the isotope effect provides a qualitative indication of where the TS lies with regard to product and reactant. A relatively low primary isotope effect implies that the bond to hydrogen is either only slightly or nearly completely broken at the TS. That is, the TS must occur quite close to reactant or to product. An isotope effect near the theoretical maximum is good evidence that the TS involves strong bonding of the hydrogen to both its new and old bonding partner.

Isotope effects may also be observed when the substituted hydrogen atom is not directly involved in the reaction. Such effects, known as *secondary kinetic isotope effects*, are smaller than primary effects and are usually in the range of  $k_{\text{H}}/k_{\text{D}} = 0.7 - 1.5$ . They may be normal ( $k_{\text{H}}/k_{\text{D}} > 1$ ) or inverse ( $k_{\text{H}}/k_{\text{D}} < 1$ ), and are also classified as  $\alpha$  or  $\beta$ , etc., depending on the location of the isotopic substitution relative to the reaction site. Secondary isotope effects result from a tightening or loosening of a C–H bond at the TS. The strength of the bond may change because of a hybridization change or a change in the extent of hyperconjugation, for example. If an  $sp^3$  carbon is converted to  $sp^2$  as reaction occurs, a hydrogen bound to the carbon will experience decreased resistance to C–H bending. The freeing of the vibration for a C–H bond is greater than that for a C–D bond because the former is slightly longer, and the vibration has a larger amplitude. This will result in a normal isotope effect. Entry 5 in Scheme 3.4 is an example of such a reaction that proceeds through a carbocation intermediate. An inverse isotope effect will occur if coordination at the reaction center increases in the TS. The bending vibration will become more restricted. Entry 4 in Scheme 3.4 exemplifies a case involving conversion of a tricoordinate carbonyl group to a tetravalent cyanohydrin. In this case the secondary isotope effect is 0.73.

Secondary isotope effects at the  $\beta$ -position have been especially thoroughly studied in nucleophilic substitution reactions. When carbocations are involved as intermediates, substantial  $\beta$ -isotope effects are observed because the hyperconjugative stabilization by the  $\beta$ -hydrogens weakens the C–H bond.<sup>122</sup> The observed secondary isotope effects are normal, as would be predicted since the bond is weakened.



Detailed analysis of isotope effects reveals that there are many other factors that can contribute to the overall effect in addition to the dominant change in bond vibrations. There is not a sharp numerical division between primary and secondary effects,

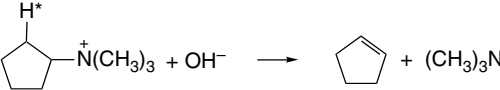
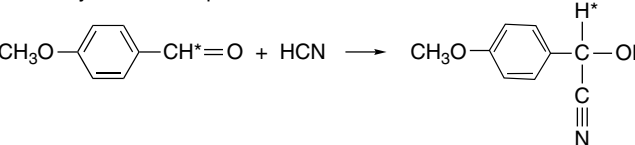
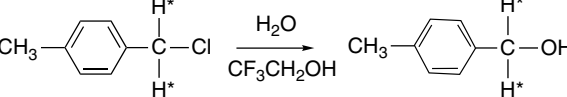
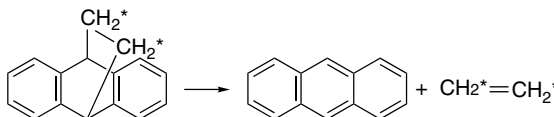
<sup>121</sup>. K. B. Wiberg, *Chem. Rev.*, **55**, 713 (1955); F. H. Westheimer, *Chem. Rev.*, **61**, 265 (1961).

<sup>122</sup>. V. J. Shiner, W. E. Buddenbaum, B. L. Murr, and G. Lamaty, *J. Am. Chem. Soc.*, **90**, 809 (1968); A. J. Kresge and R. J. Preto, *J. Am. Chem. Soc.*, **89**, 5510 (1967); G. J. Karabatsos, G. C. Sonnichsen, C. G. Papaioannou, S. E. Scheppele, and R. L. Shone, *J. Am. Chem. Soc.*, **89**, 463 (1967); D. D. Sunko and W. J. Hehre, *Prog. Phys. Org. Chem.*, **14**, 205 (1983).

## Scheme 3.4. Some Representative Kinetic Isotope Effects

## CHAPTER 3

Structural Effects on  
Stability and Reactivity

	Reaction	$k_H/k_D$ ( $^{\circ}\text{C}$ )
A. Primary kinetic isotope effects		
1 <sup>b</sup>	$\text{PhCH}_2\text{—H}^* + \text{Br}\cdot \longrightarrow \text{Ph—CH}_2\cdot + \text{H}^*\text{—Br}$	4.6 (77)
2 <sup>c</sup>	$(\text{CH}_3)_2\underset{\text{H}^*}{\text{C}}\text{—}\overset{\text{O}}{\parallel}\text{C}\text{—}\underset{\text{H}^*}{\text{C}}(\text{CH}_3)_2 + \text{OH}^- \longrightarrow (\text{CH}_3)_2\underset{\text{H}^*}{\text{C}}\text{—}\overset{\text{O}^-}{\parallel}\text{C}=\text{C}(\text{CH}_3)_2$	6.1 (25)
3 <sup>d</sup>		4.0 (191)
B. Secondary kinetic isotope effects		
4 <sup>e</sup>		0.73 (25)
5 <sup>f</sup>		1.30 (25)
6 <sup>g</sup>		1.37 (50)

a. Temperature of measurement is indicated in parentheses.

b. K. B. Wiberg and L. H. Slauch, *J. Am. Chem. Soc.*, **80**, 3033 (1958).

c. R. A. Lynch, S. P. Vincenti, Y. T. Lin, L. D. Smucker, and S. C. Subba Rao, *J. Am. Chem. Soc.*, **94**, 8351 (1972).

d. W. H. Saunders, Jr., and T. A. Ashe, *J. Am. Chem. Soc.*, **91**, 473 (1969).

e. L. do Amaral, H. G. Bull, and E. H. Cordes, *J. Am. Chem. Soc.*, **94**, 7579 (1972).

f. V. J. Shiner, Jr., M. W. Rapp, and H. R. Pinnick, Jr., *J. Am. Chem. Soc.*, **92**, 232 (1970).

g. M. Taagepera and E. R. Thornton, *J. Am. Chem. Soc.*, **94**, 1168 (1972).

especially in the range between 1 and 2. For these reasons, isotope effects are usually used in conjunction with other criteria in the description of reaction mechanisms.<sup>123</sup>

A new method for determining KIE using compounds of natural isotopic abundance has been developed.<sup>124</sup> This method makes experimental data more readily available. The method is based on the principle that as the reaction proceeds, the amount of the slower reacting isotope, e.g., <sup>2</sup>H or <sup>13</sup>C, is enriched in the remaining reactant. For example, an isotope effect of 1.05 leads to ~25% enrichment of the less reactive isotope at 99% conversion. The extent of enrichment can be measured by <sup>2</sup>H

<sup>123</sup> For more complete discussion of isotope effects see: W. H. Saunders, in *Investigation of Rates and Mechanisms of Reactions*, E. S. Lewis, ed., *Techniques of Organic Chemistry*, 3rd Edition, Vol. VI, Part 1, John Wiley & Sons, New York, 1974, pp. 211–255; L. Melander and W. H. Saunders, Jr., *Reaction Rates of Isotopic Molecules*, Wiley, New York, 1980; W. H. Saunders, in *Investigation of Rates and Mechanisms of Reactions*, C. F. Bernasconi, ed., *Techniques of Organic Chemistry*, 4th Edition, Vol. VI, Part 1, Interscience, New York, 1986, Chap. VIII.

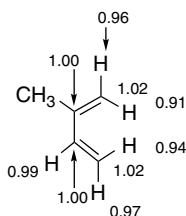
<sup>124</sup> D. A. Singleton and A. A. Thomas, *J. Am. Chem. Soc.*, **117**, 9357 (1995).

or  $^{13}\text{C}$  NMR spectroscopy. The ratio of enrichment is related to the fraction of reaction completed and allows calculation of the KIE.

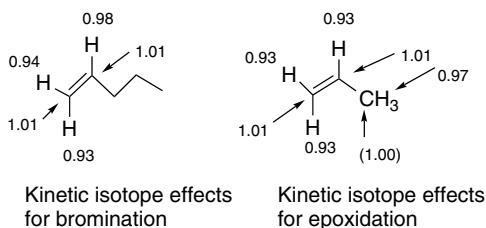
$$\text{KIE} = \frac{\ln(1-F)}{\ln[(1-F)R/R_0]} \quad (3.41)$$

where  $F$  is the fractional completion and  $R/R_0$  is the isotopic enrichment.

The method can be simultaneously applied to each atom of interest. An atom that is expected to have a negligible KIE is selected as an internal standard. For example, with the methyl group as the internal standard, the KIE for every other position in isoprene was determined for the Diels-Alder reaction with maleic anhydride. This method is especially useful for the measurement of carbon isotope effects, where normal methods require synthesis of isotopic labeled reactants.



The experimental KIE can be compared with KIEs calculated from transition structures on the basis of the vibrational frequencies associated with specific bonds. This information is available from computed transition structures,<sup>125</sup> and the comparison can provide a direct experimental means of evaluating the computed transition structures.<sup>126</sup> The method has also been used to measure KIE in reactions such as the bromination of pentene<sup>127</sup> and epoxidation of propene.<sup>128</sup> Those transition structures that are inconsistent with the observed KIE can be excluded.



### 3.6. Linear Free-Energy Relationships for Substituent Effects

#### 3.6.1. Numerical Expression of Linear Free-Energy Relationships

Many important relationships between substituent groups and chemical properties have been developed. For example, in Section 1.2.5 (p. 53), we discussed the effect

<sup>125</sup> M. Saunders, K. E. Laidig, and M. Wolfsberg, *J. Am. Chem. Soc.*, **111**, 8989 (1989).

<sup>126</sup> J. E. Baldwin, V. P. Reddy, B. A. Hess, Jr., and L. J. Schaad, *J. Am. Chem. Soc.*, **110**, 8554 (1988); K. N. Houk, S. M. Gustafson, and K. A. Black, *J. Am. Chem. Soc.*, **114**, 8565 (1992); J. W. Storer, L. Raimondi, and K. N. Houk, *J. Am. Chem. Soc.*, **116**, 9675 (1994).

<sup>127</sup> S. R. Merrigan and D. A. Singleton, *Org. Lett.*, **1**, 327 (1997).

<sup>128</sup> D. A. Singleton, S. R. Merrigan, J. Liu, and K. N. Houk, *J. Am. Chem. Soc.*, **119**, 3385 (1997).

of substituent groups on the acid strength of acetic acid derivatives. It was noted in particular that the presence of groups more electronegative than hydrogen increases the acid strength relative to acetic acid. In Section 3.4, we dealt with substituent effects on carbocation, carbanion, radical, and carbonyl addition intermediates. In many cases, structure-reactivity relationships can be expressed quantitatively in ways that are useful both for interpretation of reaction mechanisms and for prediction of reaction rates and equilibria. The most widely applied of these relationships is the *Hammett equation*, which correlates rates and equilibria for many reactions of compounds containing substituted phenyl groups. It was noted in the 1930s that there is a linear relationship between the acid strengths of substituted benzoic acids and the rates of many other chemical reactions, e.g., the rates of hydrolysis of substituted ethyl benzoates. The correlation is illustrated graphically in Figure 3.25, which shows  $\log k/k_0$ , where  $k_0$  is the rate constant for hydrolysis of ethyl benzoate and  $k$  is the rate constant for the substituted esters plotted against  $\log K/K_0$ , where  $K$  and  $K_0$  are the corresponding acid dissociation constants.

Analogous plots for many other reactions of aromatic compounds show a similar linear correlation with the acid dissociation constants of the corresponding benzoic acids, but with a range of both positive and negative slopes. Neither the principles of thermodynamics nor transition state theory require that there be such linear relationships. In fact, many reaction series fail to show linear correlations. Insight into the significance of the correlations can be gained by considering the relationship between the correlation equation and the free-energy changes involved in the two processes. The line in Figure 3.25 defines an equation in which  $m$  is the slope of the line:

$$m \log \frac{K}{K_0} = \log \frac{k}{k_0} \quad (3.42)$$

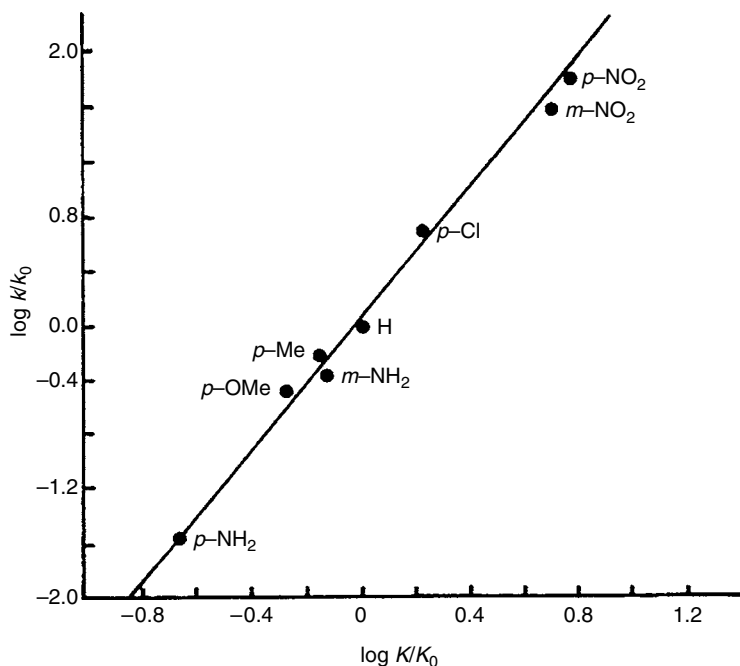


Fig. 3.25. Correlation of acid dissociation constants of benzoic acids with rates of basic hydrolysis of ethyl benzoates.

$$\begin{aligned}
 m(\log K - \log K_0) &= \log k - \log k_0 \\
 m(-\Delta G/2.3RT + \Delta G_0/2.3RT) &= \Delta G^\ddagger/2.3RT + \Delta G_0^\ddagger/2.3RT \\
 m(-\Delta G + \Delta G_0) &= -\Delta G^\ddagger + \Delta G_0^\ddagger \\
 m\Delta\Delta G &= \Delta\Delta G^\ddagger
 \end{aligned}
 \tag{3.43}$$

The linear correlation therefore indicates that the change in  $\Delta G^\ddagger$  on introduction of a series of substituent groups is *directly proportional* to the change in the  $\Delta G$  of ionization that is caused by the same series of substituents on benzoic acid. The correlations arising from such direct proportionality in free-energy changes are called *linear free-energy relationships*.<sup>129</sup>

Since  $\Delta G$  and  $\Delta G^\ddagger$  are combinations of enthalpy and entropy terms, a linear free-energy relationship between two reaction series can result from one of three circumstances: (1)  $\Delta H$  is constant and the  $\Delta S$  terms are proportional for the series; (2)  $\Delta S$  is constant and the  $\Delta H$  terms are proportional; or (3)  $\Delta H$  and  $\Delta S$  are linearly related. Dissection of the free-energy changes into enthalpy and entropy components has often shown the third case to be true.

The Hammett linear free-energy relationship is expressed in the following equations for equilibria and rate data, respectively:

$$\log \frac{K}{K_0} = \sigma\rho \tag{3.44}$$

$$\log \frac{k}{k_0} = \sigma\rho \tag{3.45}$$

The numerical values of the terms  $\sigma$  and  $\rho$  are defined by selection of the reference reaction, the ionization of benzoic acids. This reaction is assigned the *reaction constant*  $\rho = 1$ . The *substituent constant*,  $\sigma$ , can then be determined for a series of substituent groups by measurement of the acid dissociation constant of the substituted benzoic acids. The  $\sigma$  values are then used in the correlation of other reaction series, and the  $\rho$  values of the reactions are thereby determined. The relationship between Equations (3.44) and (3.45) is evident when the Hammett equation is expressed in terms of free energy. For the standard reaction  $\log[K/K_0] = \sigma\rho$ :

$$-\Delta G/2.3RT + \Delta G_0/2.3RT = \sigma\rho = \sigma \tag{3.46}$$

since  $\rho = 1$  for the standard reaction. Substituting into Eq. (3.42):

$$\begin{aligned}
 m\sigma &= -\Delta G^\ddagger/2.3RT + \Delta G_0^\ddagger/2.3RT \\
 m\sigma &= \log k - \log k_0 \\
 m\sigma &= \log \frac{k}{k_0}
 \end{aligned}
 \tag{3.47}$$

<sup>129</sup> A. Williams, *Free-Energy Relationships in Organic and Bio-Organic Chemistry*, Royal Society of Chemistry, Cambridge, UK, 2003.

The value of  $\sigma$  reflects the effect the substituent group has on the  $\Delta G$  of ionization of the substituted benzoic acid, and several factors contribute. A substituent group can affect electron density on the benzene ring by both resonance and polar effects. These changes in charge distribution affect the relative energy of the reactant and product and cause a shift in the equilibrium for the reaction. In the case of a reaction rate, the relative effect on the reactant and the TS determine the change in  $\Delta G^\ddagger$ .

The effect of substituents is illustrated in Figure 3.26. Because substituent effects are a combination of resonance and polar effects, individual substituents may have both electron-donating and electron-withdrawing components (see Scheme 3.1). For example, the methoxy group is a  $\pi$  donor but a  $\sigma$  acceptor. As resonance effects are generally dominant in aromatic systems, the overall effect of a methoxy group is electron release (in the *ortho* and *para* positions). For other groups, such as  $\text{NO}_2$  and  $\text{CN}$ , the resonance and polar effects are reinforcing. The main polar effect seems to be electrostatic<sup>130</sup> (through space) and is sometimes referred to as a *field effect*, to distinguish it from an *inductive effect* (through bonds).

The Hammett equation in the form Equation (3.44) or (3.45) is free of complications owing to steric effects because it is applied only to *meta* and *para* substituents. The geometry of the benzene ring ensures that groups in these positions cannot interact sterically with the site of reaction. The  $\sigma$  values for many substituents have been determined, and some are shown in Table 3.26. Substituent constants are available for a much wider range of substituents.<sup>131</sup> The  $\sigma$  value for any substituent reflects the interaction of the substituent with the reacting site by a combination of resonance and polar interactions. Table 3.26 lists some related substituent constants such as  $\sigma^+$ ,  $\sigma^-$ ,  $\sigma_I$ , and  $\sigma_R$ . We discuss these shortly. Table 3.27 shows a number of  $\rho$  values. The  $\rho$  value reflects the sensitivity of the particular reaction to substituent effects. The examples that follow illustrate some of the ways in which the Hammett equation can be used.

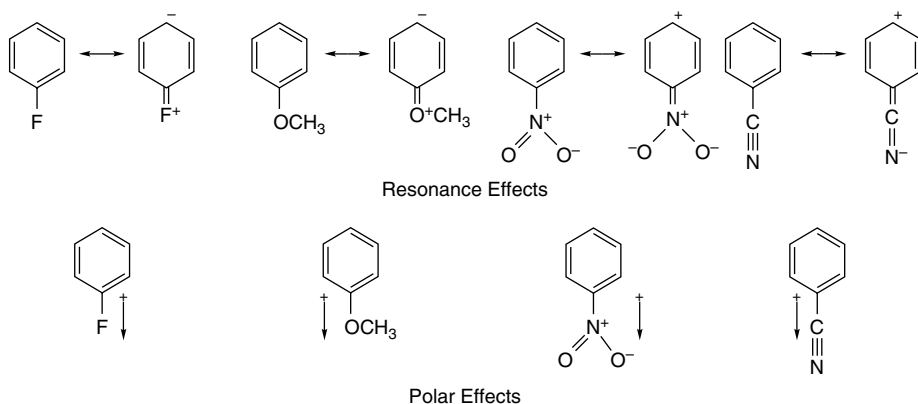


Fig. 3.26. Resonance and polar effects of representative substituents.

<sup>130</sup> K. Bowden and E. J. Grubbs, *Chem. Soc. Rev.*, **25**, 171 (1996).

<sup>131</sup> C. Hansch, A. Leo, and R. W. Taft, *Chem. Rev.*, **91**, 165 (1991); J. Shorter, *Aust. J. Chem.*, **48**, 1453 (1995); J. Shorter, *Pure Appl. Chem.*, **66**, 2451 (1994); J. Shorter, *Aust. J. Chem.*, **51**, 525 (1988); J. Shorter, *Pure Appl. Chem.*, **69**, 2497 (1997).

Table 3.26. Substituent Constants<sup>a</sup>

Substituent	Structure	$\sigma_m$	$\sigma_p$	$\sigma^+$	$\sigma^-$	$\sigma_I$	$\sigma_R$
Acetamido	CH <sub>3</sub> CONH	0.21	0.00	-0.60	0.46	0.28	-0.35
Acetoxy	CH <sub>3</sub> CO <sub>2</sub>	0.37	0.45	0.19		0.38	-0.23
Acetyl	CH <sub>3</sub> CO	0.38	0.50		0.84	0.30	0.20
Amino	NH <sub>2</sub>	-0.16	-0.66	-1.30	-0.15	0.17	-0.80
Bromo	Br	0.37	0.23	0.15	0.25	0.47	-0.25
<i>t</i> -Butyl	(CH <sub>3</sub> ) <sub>3</sub> C	-0.10	-0.20	-0.26	-0.13	-0.01	-0.18
Carboxy	HO <sub>2</sub> C	0.37	0.45	0.42	0.77	0.30	0.11
Chloro	Cl	0.37	0.23	0.11	0.19	0.47	-0.25
Cyano	N≡C	0.56	0.66	0.66	1.00	0.57	0.08
Diazonium	N <sup>+</sup> ≡N	1.76	1.91		3.43		
Dimethylamino	(CH <sub>3</sub> ) <sub>2</sub> N	-0.16	-0.83	-1.70	-0.12	0.13	-0.88
Ethoxy	C <sub>2</sub> H <sub>5</sub> O	0.10	-0.24	-0.81	-0.28	0.28	-0.57
Ethenyl	CH <sub>2</sub> =CH	-0.06	0.04	-0.16		0.11	-0.15
Ethyl	C <sub>2</sub> H <sub>5</sub>	-0.07	-0.15	-0.30	-0.19	-0.01	-0.14
Ethynyl	HC≡C	0.21	0.23	0.18	0.53	0.29	-0.04
Fluoro	F	0.34	0.06	-0.07	-0.03	0.54	-0.48
Hydrogen	H	0.0	0.0	0.0	0.0	0.0	0.0
Hydroxy	HO	0.12	-0.37	-0.92	-0.37	0.24	-0.62
Methanesulfonyl	CH <sub>3</sub> SO <sub>2</sub>	0.60	0.72		1.13	0.59	0.11
Methoxy	CH <sub>3</sub> O	0.12	-0.27	-0.78	-0.26	0.30	-0.58
Methoxycarbonyl	CH <sub>3</sub> OCO	0.37	0.45	0.49	0.74	0.32	0.11
Methyl	CH <sub>3</sub>	-0.07	-0.17	-0.31	-0.17	-0.01	-0.16
Methylthio	CH <sub>3</sub> S	0.15	0.00	-0.60	0.06	0.30	
Nitro	NO <sub>2</sub>	0.71	0.78	0.79	1.27	0.67	0.10
Phenyl	C <sub>6</sub> H <sub>5</sub>	0.06	0.01	-0.18	0.02	0.12	-0.11
Trifluoromethyl	CF <sub>3</sub>	0.43	0.54	0.61	0.65	0.40	0.11
Trimethylammonio	(CH <sub>3</sub> ) <sub>3</sub> N <sup>+</sup>	0.88	0.82	0.41	0.77	1.07	-0.11
Trimethylsilyl	(CH <sub>3</sub> ) <sub>3</sub> Si	-0.04	-0.07	0.02		-0.11	0.12

a. Values of  $\sigma_m$ ,  $\sigma_p$ ,  $\sigma^+$ , and  $\sigma^-$  are from C. Hansch, A. Leo, and R. W. Taft, *Chem. Rev.*, **91**, 165 (1991); Values of  $\sigma_I$  and  $\sigma_R$  are from M. Charton, *Prog. Phys. Org. Chem.*, **13**, 119 (1981).

**Example 3.2** The  $pK_a$  of *p*-chlorobenzoic acid is 3.98; that of benzoic acid is 4.19. Calculate  $\sigma$  for *p*-Cl.

$$\begin{aligned}
 \sigma &= \log \frac{K_{p\text{-Cl}}}{K_H} = \log K_{p\text{-Cl}} - \log K_H \\
 &= -\log K_H - (\log K_{p\text{-Cl}}) \\
 &= pK_{\sigma H} - pK_{\sigma p\text{-Cl}} \\
 &= 4.19 - 3.98 = 0.21
 \end{aligned}$$

**Example 3.3** The  $\rho$  value for alkaline hydrolysis of methyl esters of substituted benzoic acids is 2.38, and the rate constant for hydrolysis of methyl benzoate under the conditions of interest is  $2 \times 10^{-4} M^{-1} s^{-1}$ . Calculate the rate constant for the hydrolysis of methyl *m*-nitrobenzoate.

$$\log \frac{k_{m\text{-NO}_2}}{k_H} = \sigma_{m\text{-NO}_2}(\rho) = (0.71)(2.38) = 1.69$$

Table 3.27. Reaction Constants<sup>a</sup>

Reaction	$\rho$
$\text{ArCO}_2\text{H} \rightleftharpoons \text{ArCO}_2^- + \text{H}^+$ , water	1.00
$\text{ArCO}_2\text{H} \rightleftharpoons \text{ArCO}_2^- + \text{H}^+$ , ethanol	1.57
$\text{ArCH}_2\text{CO}_2\text{H} \rightleftharpoons \text{ArCH}_2\text{CO}_2^- + \text{H}^+$ , water	0.56
$\text{ArCH}_2\text{CH}_2\text{CO}_2\text{H} \rightleftharpoons \text{ArCH}_2\text{CH}_2\text{CO}_2^- + \text{H}^+$ , water	0.24
$\text{ArOH} \rightleftharpoons \text{ArO}^- + \text{H}^+$ , water	2.26
$\text{ArNH}_3^+ \rightleftharpoons \text{ArNH}_2 + \text{H}^+$ , water	3.19
$\text{ArCH}_2\text{NH}_3^+ \rightleftharpoons \text{ArCH}_2\text{NH}_2 + \text{H}^+$ , water	1.05
$\text{ArCO}_2\text{C}_2\text{H}_5 + ^-\text{OH} \longrightarrow \text{ArCO}_2^- + \text{C}_2\text{H}_5\text{OH}$	2.61
$\text{ArCH}_2\text{CO}_2\text{C}_2\text{H}_5 + ^-\text{OH} \longrightarrow \text{ArCH}_2\text{CO}_2^- + \text{C}_2\text{H}_5\text{OH}$	1.00
$\text{ArCH}_2\text{Cl} + \text{H}_2\text{O} \longrightarrow \text{ArCH}_2\text{OH} + \text{HCl}$	-1.31
$\text{ArC}(\text{CH}_3)_2\text{Cl} + \text{H}_2\text{O} \longrightarrow \text{ArC}(\text{CH}_3)_2\text{OH} + \text{HCl}$	-4.48
$\text{ArNH}_2 + \text{PhCOCl} \longrightarrow \text{ArNHCOPh} + \text{HCl}$	-3.21

a. From R. P. Wells, *Linear Free Energy Relationships*, Academic Press, New York, 1968, pp. 12-13.

$$\frac{k_{m-\text{NO}_2}}{k_{\text{H}}} = 49$$

$$k_{m-\text{NO}_2} = 98 \times 10^{-4} \text{ M}^{-1} \text{ s}^{-1}$$

*Example 3.4* Using data in Tables 3.26 and 3.27, calculate how much faster than *p*-nitrobenzyl chloride *p*-bromobenzyl chloride will hydrolyze in water.

$$\log \frac{k_{\text{p-Br}}}{k_{\text{H}}} = (-1.31)(0.23), \quad \log \frac{k_{\text{p-NO}_2}}{k_{\text{H}}} = (-1.31)(0.78)$$

$$\log k_{\text{Br}} - \log k_{\text{H}} = 0.30, \quad \log k_{\text{NO}_2} - \log k_{\text{H}} = -1.02$$

$$\log k_{\text{Br}} + 0.30 = \log k_{\text{H}}, \quad \log k_{\text{NO}_2} + 1.02 = \log k_{\text{H}}$$

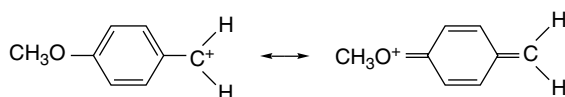
$$\log k_{\text{Br}} + 0.30 = \log k_{\text{NO}_2} + 1.02$$

$$\log k_{\text{Br}} - \log k_{\text{NO}_2} = 0.72$$

$$\log \frac{k_{\text{Br}}}{k_{\text{NO}_2}} = 0.72$$

$$\frac{k_{\text{Br}}}{k_{\text{NO}_2}} = 5.25$$

As we mentioned earlier, not all reaction series can be correlated by a Hammett equation. An underlying reason for the inability of Hammett  $\sigma_m$  and  $\sigma_p$  values to correlate all reaction series is that the substituent effects used to assign  $\sigma$  are a mixture of resonance and polar components. When direct resonance interaction with a reaction site is possible, the extent of the resonance increases and the substituent constants appropriate to the “normal” mix of resonance and polar effects fail. There have been various attempts to develop sets of  $\sigma$  values that take extra resonance interactions into account. In addition to the  $\sigma_m$  and  $\sigma_p$  values used with the classical Hammett equation Table 3.27 lists substituent constants  $\sigma^+$  and  $\sigma^-$ . These are substituent constant sets that reflect enhanced resonance participation. The  $\sigma^+$  values are used for reactions in which there is direct resonance interaction between an electron donor substituent and a cationic reaction center, whereas the  $\sigma^-$  set pertains to reactions in which there is a direct resonance interaction between an electron acceptor and an anionic reaction site. In these cases, the resonance component of the substituent effect is particularly important.



Direct resonance interaction with cationic center



Direct resonance interaction with anionic center

One approach to correct for the added resonance interaction is a modification of the Hammett equation known as the Yukawa-Tsuno equation<sup>132</sup>:

$$\log \frac{k}{k_0} = \rho(\sigma^\circ + r\Delta\bar{\sigma}_{R^+}) \quad (3.48)$$

$$\text{where } \bar{\sigma}_{R^+} = \sigma^+ - \sigma^\circ$$

The additional parameter  $r$  is adjusted from reaction to reaction to optimize the correlation. It reflects the extent of the additional resonance contribution. A large  $r$  corresponds to a reaction with a large resonance component, whereas when  $r$  goes to zero, the equation is identical to the original Hammett equation. When there is direct conjugation with an electron-rich reaction center, an equation analogous to Equation (3.48) can be employed, but  $\sigma^-$  is used instead of  $\sigma^+$ .

A more ambitious goal is to completely separate resonance and polar effects by using independent substituent constants to account for them. The resulting equation, called a *dual-substituent-parameter equation*, takes the form

$$\log \frac{K}{K_0} \quad \text{or} \quad \log \frac{k}{k_0} = \sigma_I \rho_I + \sigma_R \rho_R \quad (3.49)$$

where  $\rho_I$  and  $\rho_R$  are the reaction constants that reflect the sensitivity of the system to polar and resonance effects. The  $\sigma_I$  values have been defined from studies in reaction systems where no resonance component should be present.<sup>133</sup>

<sup>132</sup>. Y. Tsuno and M. Fujio, *Chem. Soc. Rev.*, **25**, 129 (1996).

<sup>133</sup>. M. Charton, *Prog. Phys. Org. Chem.*, **13**, 119 (1981).

In general, the dissection of substituent effects need not be limited to the resonance and polar components that are of special prominence in reactions of aromatic compounds. Any type of substituent interaction with a reaction center might be indicated by a substituent constant characteristic of the particular type of interaction and a reaction parameter indicating the sensitivity of the reaction series to that particular type of interaction. For example, it has been suggested that electronegativity and polarizability can be treated as substituent effects that are separate from polar and resonance effects.<sup>134</sup> This gives rise to the equation

$$\log \frac{k}{k_0} = \sigma_F \rho_F + \sigma_R \rho_R + \sigma_\chi \rho_\chi + \sigma_\alpha \rho_\alpha \quad (3.50)$$

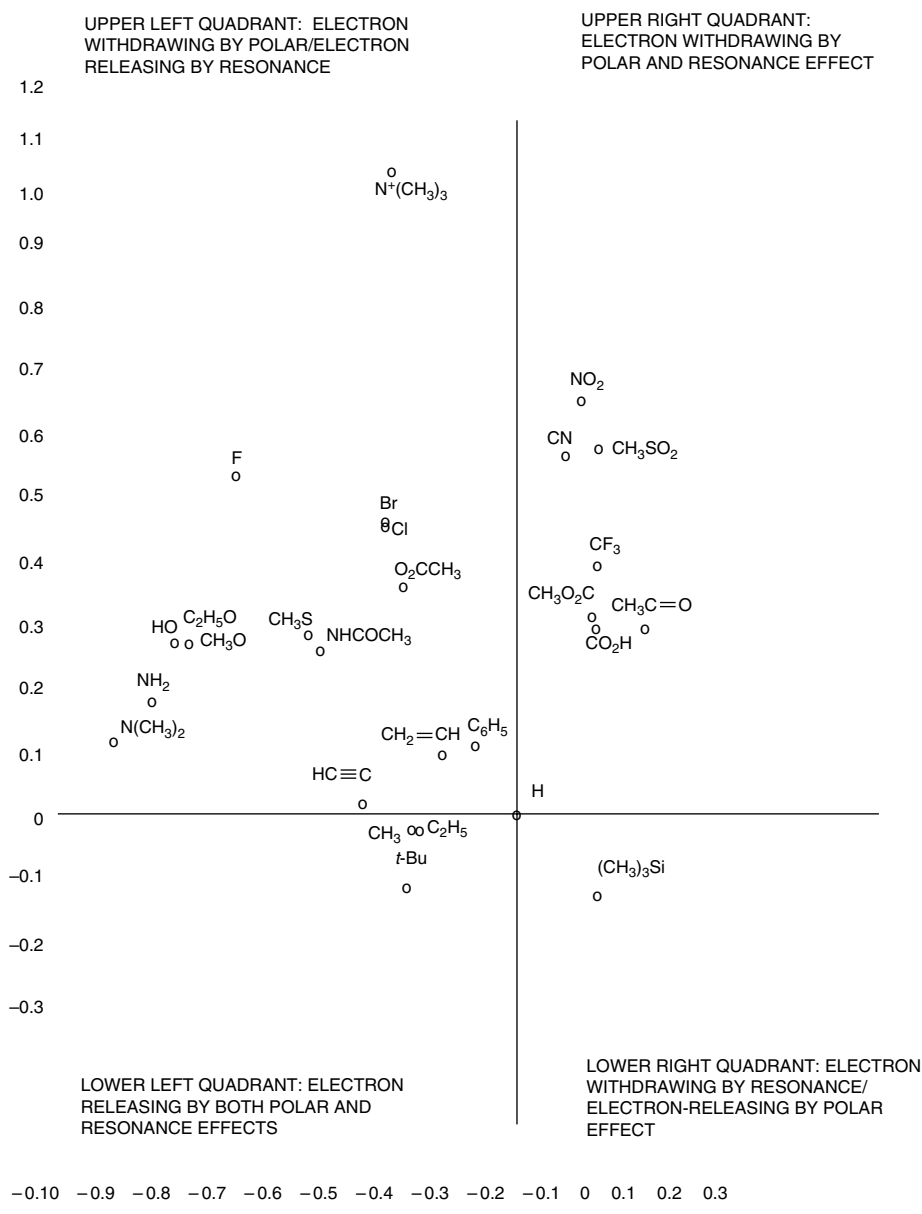
where  $\sigma_F$  is the polar,  $\sigma_R$  is the resonance,  $\sigma_\chi$  is the electronegativity, and  $\sigma_\alpha$  is the polarizability substituent constant. In general, we emphasize the resonance and polar components in our discussion of substituent effects.

The Hammett substituent constants in Table 3.26 provide a more quantitative interpretation of substituent effects than was given in Scheme 3.1, where substituents were simply listed as EWG or ERG with respect to resonance and polar components. The values of  $\sigma_R$  and  $\sigma_I$  provide comparative evaluations of the separate resonance and polar effects. By comparing  $\sigma_R$  and  $\sigma_I$ , individual substituents can be separated into four quadrants, as in Scheme 3.5. Alkyl groups are electron releasing by both resonance and polar effects. Substituents such as alkoxy, hydroxy, and amino, which can act as resonance donors, have negative  $\sigma_p$  and  $\sigma^+$  values, but when polar effects are dominant these substituents act as EWGs, as illustrated by the positive  $\sigma_m$  and  $\sigma_I$  values. A third group of substituents act as EWGs by both resonance and polar interactions. This group includes the carbonyl substituents, such as in aldehydes, ketones, esters, and amides, as well as cyano, nitro, and sulfonyl substituents. Of the common groups, only trialkylsilyl substituents are electron withdrawing by resonance and electron donating by polar effects, and both effects are weak.

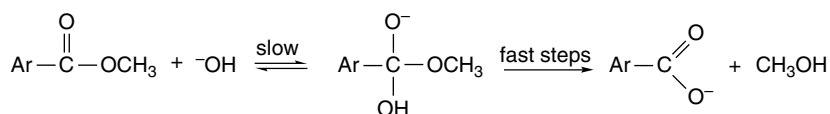
### 3.6.2. Application of Linear Free-Energy Relationships to Characterization of Reaction Mechanisms

Let us now consider how linear free-energy relationships can provide insight into reaction mechanisms. The choice of benzoic acid ionization as the reference reaction for the Hammett equation leads to  $\sigma > 0$  for EWGs and  $\sigma < 0$  for ERGs, since EWGs favor the ionization of the acid and ERGs have the opposite effect. Further inspection of the Hammett equation shows that  $\rho$  will be positive for all reactions that are favored by ERGs and negative for all reactions that are favored by EWGs. If the rates of a reaction series show a satisfactory correlation, both the sign and magnitude of  $\rho$  provide information about the TSs and intermediates for the reaction. In Example 3.3 (p. 340), the  $\rho$  value for hydrolysis of substituted methyl benzoates is +2.38. This indicates that EWGs facilitate the reaction and that the reaction is *more sensitive* ( $\rho > 1$ ) to substituent effects than the ionization of benzoic acids. The observation that the reaction is favored by EWGs is in agreement with the mechanism for ester hydrolysis discussed in Section 3.4.4. The tetrahedral intermediate is negatively charged. Its formation should therefore be favored by substituents that stabilize the developing charge. There is also a ground state effect working in the same direction. EWG substituents make

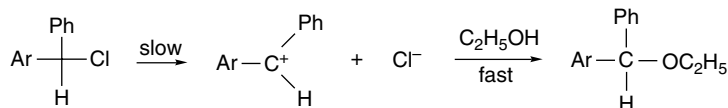
<sup>134</sup> R. W. Taft and R. D. Topsom, *Prog. Phys. Org. Chem.*, **16**, 1 (1987).



the carbonyl group more electrophilic and favor the addition of hydroxide ion in the rate-determining step.



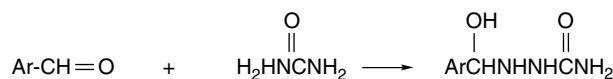
The solvolysis of diarylmethyl chlorides in ethanol correlates with  $\sigma^+$  and shows a  $\rho$  value of  $-4.2$ , indicating that ERGs strongly facilitate the reaction.<sup>135</sup> This  $\rho$  value is consistent with a mechanism involving carbocation formation as the rate-determining step. ERGs facilitate the ionization by a stabilizing interaction with the electron-deficient carbocation that develops as ionization proceeds.



The large  $\rho$  shows that the reaction is very sensitive to substituent effects and implies that there is a relatively large redistribution of charge in going to the TS.

The magnitudes of substituent effects differ in solution and the gas phase. In general, substituent effects are much stronger in the latter because there is no “leveling effect” from solvation. For example, in the ionization of benzoic acids, the substituent effects in terms of  $\Delta H$  are about 11 times larger in the gas phase than in the aqueous phase.<sup>134</sup> The relative importance of direct resonance interactions seems to be greater in aqueous solution. For example, the  $\rho_p$  value of  $\text{NH}_2$  increases from  $-0.17$  in the gas phase to  $-0.39$  in benzene and  $-0.66$  in water. This indicates that the charge separation implied by the resonance structures is facilitated by solvation.

Not all reactions can be described by the Hammett equations or the multiparameter variants. There can be several reasons for this. One possibility is a change in mechanism as substituents vary. In a multistep reaction, for example, one step may be rate determining for EWGs, but a different step may become rate limiting for ERG substituents. The rate of semicarbazone formation of benzaldehydes, for example, shows a nonlinear Hammett plot with  $\rho$  of about 3.5 for ERGs, but  $\rho$  near  $-0.25$  for EWGs.<sup>136</sup> The change in  $\rho$  is believed to be the result of a change in the rate-limiting step.



rate-controlling step for electron-releasing substituents



rate-controlling step for electron-withdrawing substituents

Any reaction that undergoes a major change in mechanism or TS structure over the substituent series would be expected to give a nonlinear Hammett plot.

The development of linear free-energy relationships in aliphatic molecules is complicated because steric and conformation factors come into play along with electronic effects. A number of successful treatments of aliphatic systems have been developed by separating electronic effects from steric effects. We do not discuss these methods in the present work, but there are reviews available that can be consulted for information about this area.<sup>137</sup>

<sup>135</sup> S. Nishida, *J. Org. Chem.*, **32**, 2692 (1967).

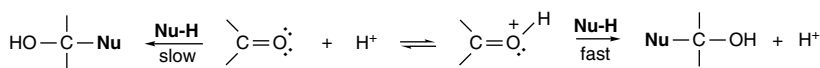
<sup>136</sup> D. S. Noyce, A. T. Bottini and S. G. Smith, *J. Org. Chem.*, **23**, 752 (1958).

<sup>137</sup> M. Charton, *Prog. Phys. Org. Chem.*, **10**, 81 (1973); S. Ehrenson, R. T. C. Brownlee, and R. W. Taft, *Prog. Phys. Org. Chem.*, **10**, 1 (1973).

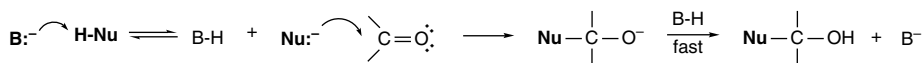
Many chemical reactions involve a *catalyst*. A very general definition of a catalyst is *a substance that makes a reaction path available with a lower energy of activation*. Strictly speaking, a catalyst is not consumed by the reaction, but organic chemists frequently speak of acid-catalyzed or base-catalyzed mechanisms that do lead to overall consumption of the acid or base. Better phrases under these circumstances would be *acid promoted* or *base promoted*. Catalysts can also be described as electrophilic or nucleophilic, depending on the catalyst's electronic nature. Catalysis by Lewis acids and Lewis bases can be classified as electrophilic and nucleophilic, respectively. In free-radical reactions, the *initiator* often plays a key role. An initiator is a substance that can easily generate radical intermediates. Radical reactions often occur by chain mechanisms, and the role of the initiator is to provide the free radicals that start the chain reaction. In this section we discuss some fundamental examples of catalysis with emphasis on proton transfer (Brønsted acid/base) and Lewis acid catalysis.

### 3.7.1. Catalysis by Acids and Bases

A detailed understanding of reaction mechanisms requires knowledge of the role catalysts play in the reaction. Catalysts do not affect the position of equilibrium of a reaction, which is determined by  $\Delta G^\circ$  and is independent of the path (mechanism) of the transformation. Catalysts function by increasing the rate of one or more steps in the reaction mechanism by providing a reaction path having a lower  $E_a$ . The most general family of catalytic processes are those that involve transfer of a proton. Many reactions are strongly catalyzed by proton donors (Brønsted acids) or proton acceptors (Brønsted bases). Catalysis occurs when the conjugate acid or conjugate base of the reactant is more reactive than the neutral species. As we discussed briefly in Section 3.4.4, reactions involving nucleophilic attack at carbonyl groups are often accelerated by acids or bases. Acid catalysis occurs when the conjugate acid of the carbonyl compound, which is much more electrophilic than the neutral molecule, is the kinetically dominant reactant. Base-catalyzed additions occur as a result of deprotonation of the nucleophile, generating a more reactive anion.



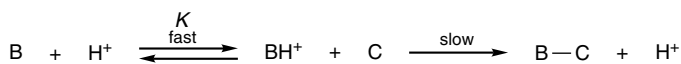
acid catalysis of carbonyl addition by reactant protonation



base catalysis of carbonyl addition by deprotonation of the nucleophile

Many important organic reactions involve carbanions as nucleophiles. The properties of carbanions were introduced in Section 3.4.2, and their reactivity is discussed in more detail in Chapter 6. Most C–H bonds are very weakly acidic and have no tendency to ionize spontaneously to form carbanions. Reactions that involve carbanion intermediates are therefore usually carried out in the presence of a base that can generate the reactive carbanion intermediate. Base-catalyzed addition reactions of carbonyl compounds provide many examples of this type of reaction. The reaction

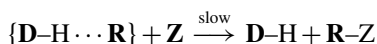
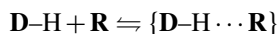




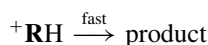
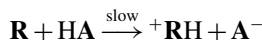
$$\text{Rate} = k_2[\text{BH}^+][\text{C}] = k_2[\text{C}]K[\text{B}][\text{H}^+] = k_{\text{obs}}[\text{H}^+][\text{B}][\text{C}]$$

In the actual experiments, since buffers are used to control pH, the points are extrapolated to zero buffer concentration by making measurements at several buffer concentrations (but at the same pH). Such plots are linear if the reaction is subject to specific acid base catalysis.

Several situations can lead to the observation of general acid catalysis. General acid catalysis can occur as a result of hydrogen bonding between the reactant **R** and a proton donor **D-H** to form a reactive complex  $\{\text{D-H}\cdots\text{R}\}$ , which then undergoes reaction with a reactant **Z**:

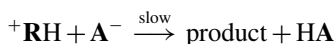
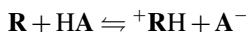


Under these circumstances, a distinct contribution to the overall rate is found for each potential hydrogen bond donor **D-H**. General acid catalysis is also observed when a rate-determining proton transfer occurs from acids other than the solvated proton:



Each acid  $\text{HA}^1$ ,  $\text{HA}^2$ , etc., makes a contribution to the overall rate of the reaction.

General acid catalysis is also observed if a prior equilibrium between the reactant and the acid is followed by rate-controlling proton transfer. Each individual conjugate base  $\text{A}^-$  appears in the overall rate expression:



Note that specific acid catalysis describes a situation where the reactant is in *equilibrium* with regard to proton transfer and proton transfer is not rate-determining. On the other hand, each case that leads to general acid catalysis *involves proton transfer in the rate-determining step*. Because of these differences, the study of rates as a function of pH and buffer concentrations can permit conclusions about the nature of proton transfer processes and their relationship to the rate-determining step in a reaction.

The details of proton transfer processes can also be probed by examination of *solvent isotope effects* by comparing the rates of a reaction in  $\text{H}_2\text{O}$  versus  $\text{D}_2\text{O}$ . The solvent isotope effect can be either normal or inverse, depending on the nature of the proton transfer process.  $\text{D}_3\text{O}^+$  is a stronger acid than  $\text{H}_3\text{O}^+$ . As a result, reactants in  $\text{D}_2\text{O}$  solution are somewhat more extensively protonated than in  $\text{H}_2\text{O}$  at identical acid concentrations. A reaction that involves a rapid equilibrium protonation proceeds *faster* in  $\text{D}_2\text{O}$  than in  $\text{H}_2\text{O}$  because of the higher concentration of the protonated reactant. On the other hand, if proton transfer is part of the rate-determining step, the reaction will be *faster* in  $\text{H}_2\text{O}$  than in  $\text{D}_2\text{O}$  because of the normal primary kinetic isotope effect of the type of reaction.

3.7.1.2. *Brønsted Catalysis Law.* As might be expected, there is a relationship between the effectiveness of general acid catalysts and the acidic strength of a proton donor, as measured by its acid dissociation constant  $K_a$ . The stronger acids are more effective catalysts. This relationship is expressed by the *Brønsted catalysis law*:

$$\log k_{\text{cat}} = \alpha \log K + b \quad (3.51)$$

An analogous equation holds for catalysis by bases. This equation requires that the  $E_a$  for the catalytic step for a series of acids be directly proportional to  $\Delta G$  of dissociation for the same series of acids. The proportionality constant  $\alpha$  is an indication of the sensitivity of the catalytic step to structural changes, relative to the effect of the same structural changes on acid dissociation. It is often found that a single proportionality constant  $\alpha$  is restricted to only structurally similar acids and that linear relationships having  $\alpha$  values of different magnitude apply to each type of acid.

Figure 3.27 is plot of the Brønsted relationship for hydrolysis of a vinyl ether. The plot shows that the effectiveness of the various carboxylic acids as catalysts is related to their dissociation constants. In this particular case, the value of  $\alpha$  is 0.79.<sup>138</sup>

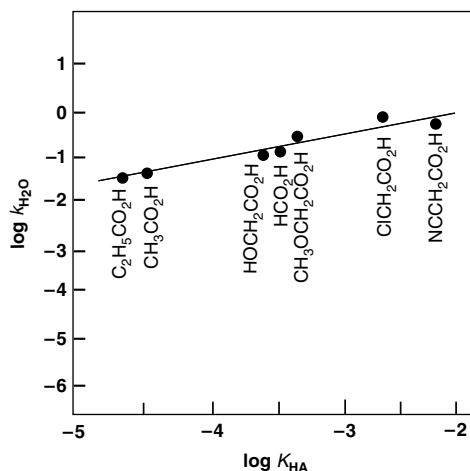
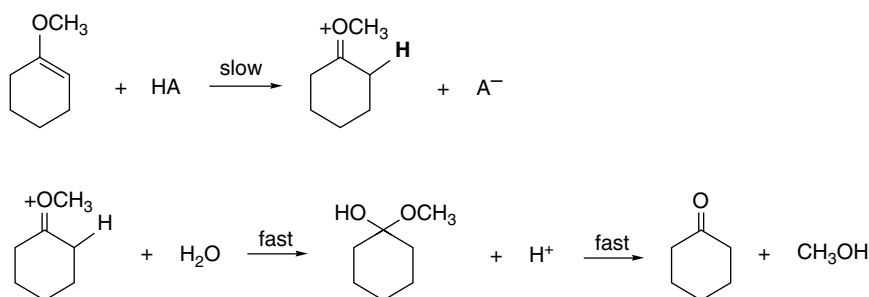
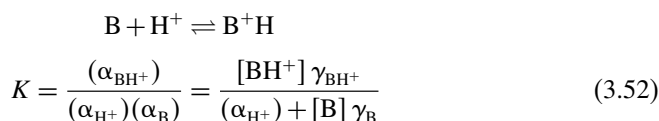


Fig. 3.27. Brønsted relation for the hydrolysis of cyclohexenyl methyl ether. Adapted from *J. Am. Chem. Soc.*, **93**, 413 (1971), by permission of the American Chemical Society.

<sup>138</sup> A. J. Kresge, H. L. Chen, Y. Chiang, E. Murrill, M. A. Payne, and D. S. Sagatys, *J. Am. Chem. Soc.*, **93**, 413 (1971).

Since  $\alpha$  relates the sensitivity of the proton transfer process to that of dissociation of the acid, it is sometimes suggested that the value of  $\alpha$  can be used as an indicator of TS structure. The closer  $\alpha$  approaches unity, the greater the degree of proton transfer in the TS. There are limits to the generality of this interpretation, however.<sup>139</sup>

**3.7.1.3. Acidity Functions.** Some organic reactions require acid concentrations considerably higher than can be accurately measured on the pH scale, which applies to relatively dilute aqueous solutions. For example, concentrated acidic solutions can have formal proton concentrations of 10M or more, but these formal concentrations are not a suitable measure of the *activity* of protons in such solutions. For this reason, *acidity functions* have been developed to measure the proton-donating strength of concentrated acidic solutions. The activity of the hydrogen ion (solvated proton) can be related to the extent of protonation of a series of bases by the equilibrium expression for the protonation reaction:



where  $\gamma$  is the activity coefficient for the base and its conjugate acid. A common measure of acidity is referred to as  $h_0$  and is defined by measuring the extent of protonation of a series of bases for which  $K$  is measured. The relative concentration of the base and its conjugate acid then defines  $h_0$  for any particular acidic solution:

$$h_0 = \frac{[\text{BH}^+] \gamma_{\text{BH}^+}}{K[\text{B}] \gamma_{\text{B}}} \quad (3.53)$$

The quantity  $H_0$  defined as  $-\log h_0$  is commonly tabulated and it corresponds to the pH of very concentrated acidic solutions. The  $H_0$  values are established by making measurements in increasingly acidic solutions with a series of successively weaker bases. The series is begun by measuring a reference base in aqueous solution where  $H_0 \sim \text{pH}$ . This base can then be used to find the  $H_0$  of a somewhat more acidic solution. The  $K$  of a somewhat weaker base is then determined in the more acidic solution. This second base can then be used to extend  $H_0$  into a still more acidic solution. The process is continued by using a series of bases to establish  $H_0$  for successively more acidic solutions.<sup>140</sup> The assumption involved in this procedure is that the ratio of the activity coefficients for the series of base cations does not change from solvent to solvent, that is,

$$\frac{\gamma_{\text{B}_1} [\text{H}^+]}{\gamma_{\text{B}_1}} = \frac{\gamma_{\text{B}_2} [\text{H}^+]}{\gamma_{\text{B}_2}} = \frac{\gamma_{\text{B}_3} [\text{H}^+]}{\gamma_{\text{B}_3}} = \dots \quad (3.54)$$

<sup>139</sup> A. J. Kresge, *J. Am. Chem. Soc.*, **92**, 3210 (1970); R. A. Marcus, *J. Am. Chem. Soc.*, **91**, 7224 (1969); F. G. Bordwell and W. J. Boyle, Jr., *J. Am. Chem. Soc.*, **94**, 3907 (1972); D. A. Jencks and W. P. Jencks, *J. Am. Chem. Soc.*, **99**, 7948 (1977); A. Pross, *J. Org. Chem.*, **49**, 1811 (1984).

<sup>140</sup> For reviews and discussion of acidity functions, see E. M. Arnett, *Prog. Phys. Org. Chem.*, **1**, 223 (1963); C. H. Rochester, *Acidity Functions*, Academic Press, New York, 1970; R. A. Cox and K. Yates, *Can. J. Chem.*, **61**, 225 (1983); C. D. Johnson and B. Stratton, *J. Org. Chem.*, **51**, 4100 (1986).

**Table 3.28.**  $H_0$  as a Function of Composition of Aqueous Sulfuric Acid<sup>a</sup>

% H <sub>2</sub> SO <sub>4</sub>	$H_0$	%H <sub>2</sub> SO <sub>4</sub>	$H_0$
5	0.24	55	-3.91
10	-0.31	60	-4.46
15	-0.66	65	-5.04
20	-1.01	70	-5.80
25	-1.37	75	-6.56
30	-1.72	80	-7.34
35	-2.06	85	-8.14
40	-2.41	90	-8.92
45	-2.85	95	-9.85
50	-3.38	98	-10.41

a. From J. Jorgenson and D. R. Hartter, *J. Am. Chem. Soc.*, **85**, 878 (1963).

Not surprisingly, the results often reveal a dependence on the particular type of base used, so no universal  $H_0$  scale can be established. Nevertheless, this technique provides a very useful measure of the relative hydrogen ion activity of concentrated acid solutions that can be used in the study of reactions that proceed only at high acid concentrations. Table 3.28 gives  $H_0$  values for some water-sulfuric acid mixtures.

**3.7.1.4. pH-Rate Profiles.** pH-Rate profiles are a useful tool for analysis of acid and base catalysis.<sup>141</sup> The rate of the reaction is measured as a function of the pH. Reactions are typically studied under pseudo-first-order conditions so that the rates are first order in the reactant at each pH:

$$\text{Rate} = k_{\text{obs}}[\text{R}]$$

Observed pH rate profiles typically consist of several regions including segments with linear dependence on  $[\text{H}^+]$  or  $[\text{OH}^-]$ , pH-independent, and curved transitions between linear areas. The occurrence of  $[\text{H}^+]$  (or  $[\text{OH}^-]$ ) in the rate expression indicates either that a protonated (or deprotonated) form of the reactant is involved (preequilibrium) or that  $\text{H}^+$  (or  $\text{OH}^-$ ) is involved in the rate-determining step. Figure 3.28 shows some pH dependencies that may be components of a specific profile. Curves (a) and (b) show linear dependence on  $[\text{H}^+]$  and  $[\text{OH}^-]$  that is due to specific acid and base catalysis, respectively. The horizontal portion of the profile corresponds to a reaction that does not involve acid or base catalysis. Usually the slope of the linear part of the curve is  $-1(\text{H}^+)$  or  $+1(\text{OH}^-)$  because there is only one protonation (or deprotonation) step.

The rate expressions for (a) and (b), respectively, would be:

$$(a) \text{ Rate} = k_{\text{H}^+}[\text{R}][\text{H}^+] + k_{\text{H}_2\text{O}}[\text{R}]$$

$$(b) \text{ Rate} = k_{\text{OH}^-}[\text{R}][\text{OH}^-] + k_{\text{H}_2\text{O}}[\text{R}]$$

where  $k_{\text{H}^+}$ ,  $k_{\text{OH}^-}$ , and  $k_{\text{H}_2\text{O}}$  are the rate constants for the acid-catalyzed, base-catalyzed, and uncatalyzed reactions, respectively.

For cases (c) and (d), the rates level off at high  $[\text{H}^+]$  and  $[\text{OH}^-]$ , respectively. This circumstance occurs if the reactant is completely protonated (or deprotonated) so

<sup>141</sup> J. M. Loudon, *J. Chem. Educ.*, **68**, 973 (1991).

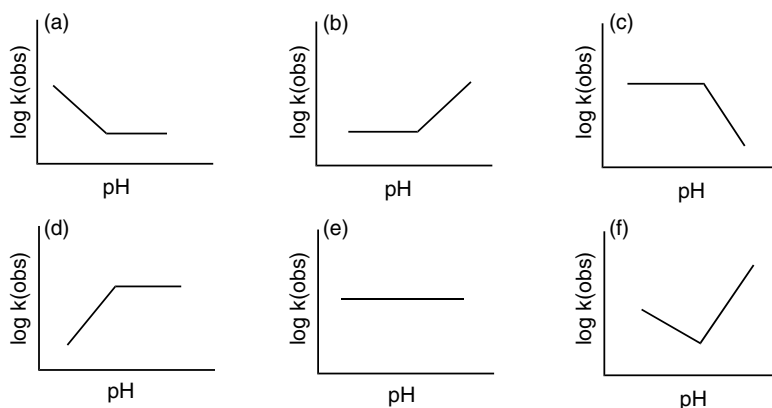


Fig. 3.28. Schematic components of pH rate profiles: (a) acid catalyzed with uncatalyzed component, (b) base catalyzed with uncatalyzed component, (c) acid catalyzed with saturation, (d) base catalyzed with saturation, (e) uncatalyzed reaction, (f) reaction subjected to both acid and base catalysis. Adapted from *J. Chem. Soc., Perkin Trans., 2*, 365 (2000).

that further increase in  $[\text{H}^+]$  or  $[\text{OH}^-]$  causes no further change in the rate. The form of the corresponding rate equations is

$$k_{\text{obs}} = \frac{K_{\text{H}^+}[\text{H}^+]K_{\text{a}}}{K_{\text{a}} + [\text{H}^+]} \quad (3.55)$$

where  $K_{\text{a}}$  is the acid dissociation constant of R.

For base catalysis with saturation, the form is

$$k_{\text{obs}} = \frac{k_{-\text{OH}}K_{\text{w}}}{K_{\text{a}} + [\text{H}^+]} \quad (3.56)$$

The curve in (f) would be observed for a reaction that is catalyzed by both acid and base, for which the rate expression is

$$\text{Rate} = k_{\text{H}^+}[\text{H}^+][\text{R}] + k_{-\text{OH}}[\text{OH}^-][\text{R}] + k_{\text{H}_2\text{O}}[\text{R}] \quad (3.57)$$

In general, there may be a change in mechanism or a change in the rate-limiting step across the range of pH. This results in a pH-rate profile that combines components from the profiles in (a)–(e) of Figure 3.28. There are useful conclusions that can be drawn by inspection of pH profiles. (1) The number of terms in the overall rate expression is one more than the number of upward bends in the profile. (2) upward bends signal a transition to a different mechanism. Each upward bend represents a new mechanism becoming a significant component of the total reaction. For example, in the case of a reaction catalyzed by both acid and base (and also involving an uncatalyzed component), the upward bend in the acidic region corresponds to the acid-catalyzed component and the upward bend in the basic region is the base-catalyzed component, as illustrated in Figure 3.29.

$$k_{\text{obs}} = k_{\text{H}^+}[\text{H}^+] + k_{-\text{OH}}[\text{OH}^-] + k_{\text{H}_2\text{O}} = k_{\text{H}^+}[\text{H}^+] + k_{-\text{OH}}\frac{K_{\text{w}}}{[\text{H}^+]} + k_{\text{H}_2\text{O}} \quad (3.58)$$

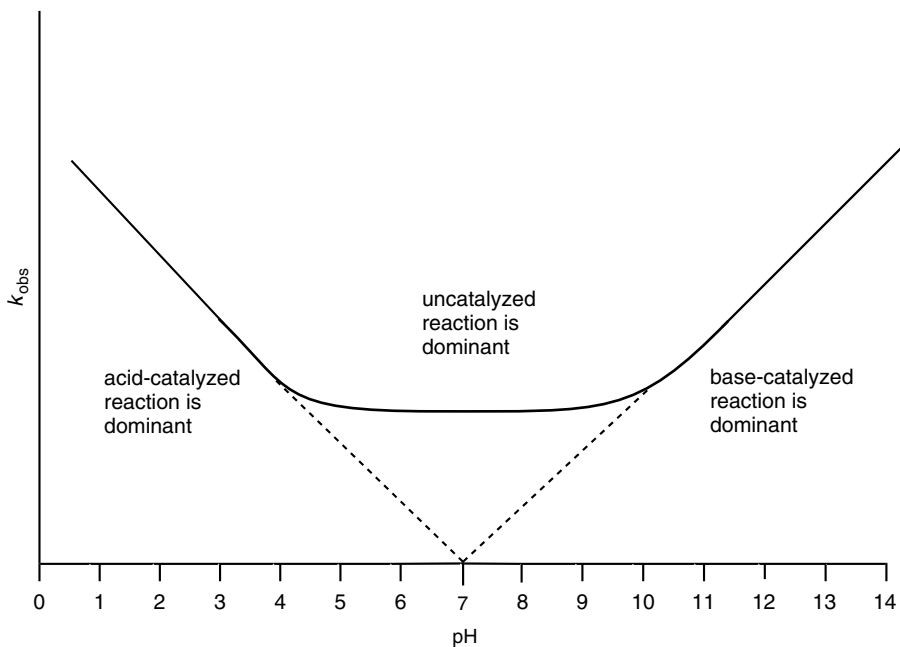
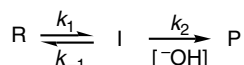
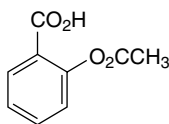


Fig. 3.29. pH-rate profile showing upward bends corresponding to the change from uncatalyzed to acid-catalyzed and base-catalyzed mechanisms.

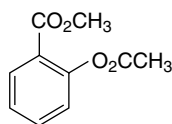
Downward bends in pH profiles occur when there is a change in the rate-limiting step. For example, if there is an unfavorable equilibrium between the reactant and an unstable intermediate, which then undergoes a base-catalyzed reaction, there will be a downward bend. The rate of the equilibrium is pH independent. At low  $[\text{OH}^-]$ , the rate-limiting step will be governed by  $k_2$ . The rate will increase as  $[\text{OH}^-]$  increases until it is no longer rate limiting. At that point  $k_1$  becomes the rate-limiting step,  $[\text{OH}^-]$  no longer affects the observed rate, and the curve bends downward:



We can illustrate the interpretation of pH rate profiles by considering the pH rate profile for the hydrolysis of aspirin. The pH rate profile and that of its methyl ester are shown in Figure 3.30. The methyl ester is a classic case in which there are both acid- and base-catalyzed regions and an uncatalyzed region as described by Equation (3.58). These features are characteristic of the normal ester hydrolysis mechanism outlined on pp. 325–326. Under the reaction conditions, only the more reactive *O*-aryl ester group is hydrolyzed. Aspirin, however, shows a region between pH 2 and pH 9 that reveals one downward and two upward bends. Thus there must be a fourth variant of the mechanism (since there are a total of three upward bends).



aspirin



aspirin methyl ester

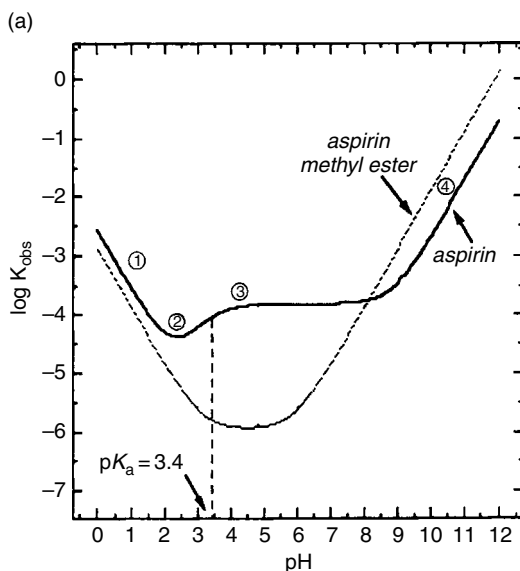
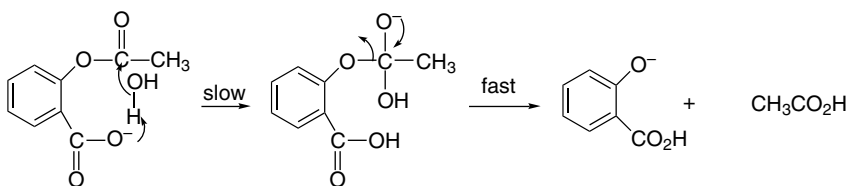


Fig. 3.30. pH rate profile of aspirin and its methyl ester. Reproduced from *J. Chem. Educ.*, **68**, 973 (1991).

The fact that there is a downward bend in the curve at about pH 5 suggests that the  $\text{CO}_2^-$  group in aspirin, which is absent from the methyl ester, might be involved in the reaction. The  $\text{CO}_2^-$  group becomes protonated in this region, which might account for the decreased rate below pH 5. This would require the addition of a fourth term to the rate curve where  $[\text{As}^-]$  is the carboxylate anion of aspirin. The concentration of  $[\text{As}^-]$  is governed by the acid dissociation constant  $K_{\text{as}}$ . This leads to the expression

$$k_{\text{obs}} = k_{\text{H}^+} [\text{H}^+] + \frac{k_{\text{H}_2\text{O}} [\text{H}^+]}{K_{\text{as}} + [\text{H}^+]} + \frac{k_i K_{\text{as}}}{K_{\text{as}} + [\text{H}^+]} + \frac{k_{-\text{OH}} K_{\text{w}}}{[\text{H}^+]}$$

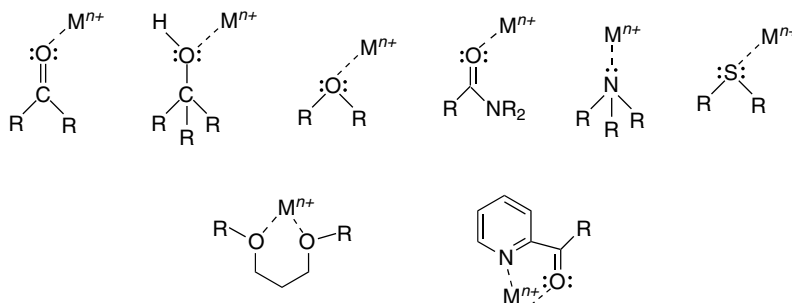
In the region pH 5 to pH 8  $[\text{As}^-]$  is constant, since it is completely deprotonated above pH 5, and the rate is pH independent in this region. Thus the pH-rate profile for aspirin identifies four distinct regions as the pH increases. Regions 1 and 4 correspond to reactions involving a  $\text{H}^+$  and  $^-\text{OH}$  in the rate-determining transition state and are the normal acid- and base-catalyzed mechanisms for ester hydrolysis. Region 2 corresponds to the uncatalyzed reaction and Region 3 is the fourth mechanism, which involves the anion of aspirin or a kinetically equivalent species. Based on other studies, this mechanism has been interpreted as a carboxylate-assisted deprotonation of water leading to rate-determining formation of the tetrahedral intermediate.<sup>142</sup> (See Section 7.5 for discussion of the evidence for this mechanism.)



<sup>142</sup>. A. P. Fresht and A. J. Kirby, *J. Am. Chem. Soc.*, **89**, 4857 (1967).

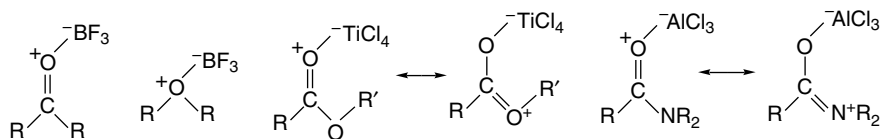
Lewis acids act as electron pair acceptors. The proton is an important special case, but many other compounds catalyze organic reactions by acting as electron pair acceptors. The most important Lewis acids in organic reactions are metal cations and covalent compounds of metals. Metal cations that function as Lewis acids include the alkali metal monocations  $\text{Li}^+$ ,  $\text{Na}^+$ ,  $\text{K}^+$ , di- and trivalent ions such as  $\text{Mg}^{2+}$ ,  $\text{Ca}^{2+}$ ,  $\text{Zn}^{2+}$ ,  $\text{Sc}^{3+}$ , and  $\text{Bi}^{3+}$ ; transition metal cations and complexes; and lanthanide cations, such as  $\text{Ce}^{3+}$  and  $\text{Yb}^{3+}$ . Neutral electrophilic covalent molecules can also act as Lewis acids. The most commonly employed of the covalent compounds include boron trifluoride, aluminum trichloride, titanium tetrachloride, and tin(IV)tetrachloride. Various other derivatives of boron, aluminum, titanium, and tin also are Lewis acid catalysts.

The catalytic activity of metal cations originates in the formation of a donor-acceptor complex between the cation and the reactant, which acts as a Lewis base. As a result of the complexation, the donor atom becomes effectively more electronegative. All functional groups that have unshared electron pairs are potential electron donors, but especially prominent in reaction chemistry are carbonyl oxygens ( $sp^2$ ), hydroxy or ether ( $sp^3$ ) oxygen, as well as similar nitrogen- and sulfur-containing functional groups. For oxygen and nitrogen functional groups, the catalysis generally correlates with hardness, so the smaller and more positively charged ions have the strongest effects. Halogen substituents can act as electron donors to strong Lewis acids. The presence of two potential donor atoms in a favorable geometric relationship permits formation of “bidentate” chelate structures and may lead to particularly strong complexes.



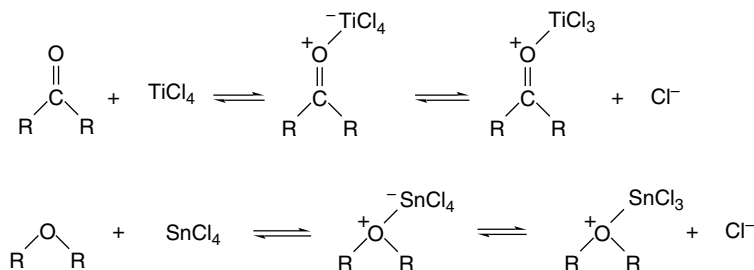
There is a partial transfer of charge to the metal ion from the donor atom, which increases the effective electronegativity of the donor atom. The Lewis acid complexes of carbonyl groups, for example, are more reactive to nucleophilic attack. Hydroxy groups complexed to metal cations are stronger acids and better leaving groups than an uncomplexed hydroxy. Ether or sulfide groups complexed with metal ions are better leaving groups.

Neutral compounds such as boron trifluoride and aluminum trichloride form Lewis acid-base complexes by accepting an electron pair from the donor molecule. The same functional groups that act as electron pair donors to metal cations can form complexes with boron trifluoride, aluminum trichloride, titanium tetrachloride, and related compounds. In this case the complex is formed between two neutral species, it too is neutral, but there is a formal positive charge on the donor atom and a formal negative charge on the acceptor atom.



Complexes of carbonyl oxygen with trivalent boron and aluminum compounds tend to adopt a geometry consistent with directional interaction with one of the oxygen lone pairs. Thus the C–O–M bonds tend to be in the trigonal ( $120^\circ$ – $140^\circ$ ) range and the boron or aluminum is usually close to the carbonyl plane.<sup>143</sup> The structural specificity that is built into Lewis acid complexes can be used to advantage to achieve stereoselectivity in catalysis. For example, use of chiral ligands in conjunction with Lewis acids is frequently the basis for enantioselective catalysts.

Titanium(IV) tetrachloride and tin(IV) tetrachloride can form complexes that are similar to those formed by metal ions and those formed by neutral Lewis acids. Complexation can occur with displacement of a chloride from the metal coordination sphere or by an increase in the coordination number at the Lewis acid.



For example, the crystal structure of the adduct of titanium tetrachloride and the ester formed from ethyl 2-hydroxypropanoate (ethyl lactate) and acrylic acid has been determined.<sup>144</sup> It is a chelate with the oxygen donor atoms incorporated into the titanium coordination sphere along with the four chloride anions, as shown in Figure 3.31.

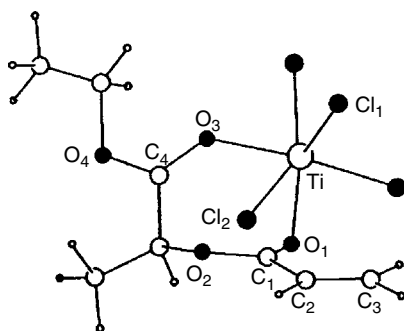
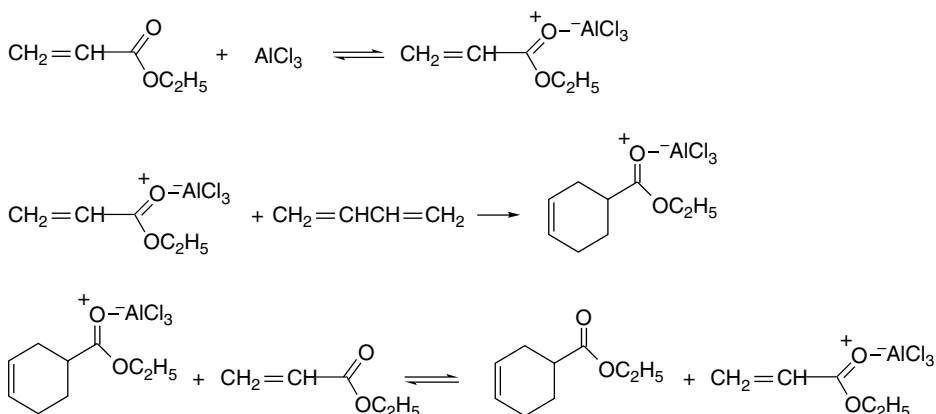


Fig. 3.31.  $\text{TiCl}_4$  complex of ethyl lactate. Reproduced from *Angew. Chem. Int. Ed. Engl.*, **29**, 112, by permission of Wiley-VCH.

<sup>143</sup>. S. Shambayati, W. E. Crowe, and S. L. Schreiber, *Angew. Chem. Int. Ed. Engl.*, **29**, 256 (1990).

<sup>144</sup>. T. Poll, J. O. Melter, and G. Helmchen, *Angew. Chem. Int. Ed. Engl.*, **24**, 112 (1985).

Diels-Alder addition reactions are accelerated by catalytic amounts of a Lewis acid. The complexed ester (ethyl acrylate in the example given) is substantially more reactive than the uncomplexed molecule, and the reaction proceeds through the complex. The reactive complex is regenerated by exchange of the Lewis acid from the adduct. The reaction is accelerated because the dienophile becomes more electrophilic. In MO terminology, the LUMO energy is lowered, resulting in stronger interaction with the diene HOMO.



The strength of the complexation depends on both of the donor atom and the metal ion. The solvent is also an important factor because solvent molecules that are electron donors can compete for the Lewis acid. Qualitative predictions about the strength of donor-acceptor complexation can be made on the basis of the hard-soft-acid-base (HSAB) concept (see Section 1.1.6). The better matched the donor and acceptor, the stronger the complexation. Scheme 3.6 gives an approximate ordering of hardness and softness for some neutral and ionic Lewis acids and bases.

There are more structural variables to consider in catalysis by Lewis acids than in the case of catalysis by protons. In addition to the hard-soft relationship, steric, geometric, and stereoelectronic factors can come into play. This makes the development of an absolute scale of “Lewis acid strength” difficult, since the complexation strength depends on the specific characteristics of the base. There are also variations in the strength of the donor-acceptor bonds. Bond strengths calculated for complexes such as  $\text{H}_3\text{N}^+-\text{BF}_3^-$  (22.0 kcal/mol) and  $(\text{CH}_3)_3\text{N}^+-\text{BH}_3^-$  (41.1 kcal/mol) are substantially

Scheme 3.6. Relative Hardness and Softness

	Lewis acids		Lewis bases	
	Cationic	Neutral	Neutral	Anionic
Hard	$\text{H}^+$	$\text{BF}_3, \text{AlCl}_3$	$\text{H}_2\text{O}$	$\text{F}^-, \text{SO}_4^{2-}$
	$\text{Li}^+, \text{Mg}^{2+}, \text{Ca}^{2+}$	$\text{R}_3\text{B}$	Alcohols	$\text{Cl}^-$
	$\text{Na}^+$		Ketones, ethers	$\text{Br}^-$
	$\text{Zn}^{2+}, \text{Cu}^{2+}$		Amines	$\text{N}_3^-$
	$\text{Pd}^{2+}, \text{Hg}^{2+}, \text{Ag}^+$		Sulfides	$\text{CN}^-$
Soft	$\text{RS}^+, \text{RSe}^+$			$\text{I}^-$
	$\text{I}^+$			$\text{S}^{2-}$

**Table 3.29. Relative Lewis Acidity<sup>a</sup>**

Acid	$\Delta H(\text{kcal/mol})^b$	$\pi^*(\text{eV})^c$	NMR $\Delta\delta^d$	Relative acidity
BCl <sub>3</sub>	-6.6	-2.52	1.35	1.00
AlCl <sub>3</sub>	-25.6	-2.31	1.23	0.91
C <sub>2</sub> H <sub>5</sub> AlCl <sub>2</sub>	-20.0	-2.03	1.15	0.80
BF <sub>3</sub>	+4.1	-1.93	1.17	0.76
(C <sub>2</sub> H <sub>5</sub> ) <sub>2</sub> AlCl	-5.6	-1.82	0.91	0.71
(C <sub>2</sub> H <sub>5</sub> ) <sub>3</sub> Al	-10.1	-1.68	0.63	0.63
SnCl <sub>4</sub>	+10.0	-1.58	0.87	0.61

a. P. Laszlo and M. Teston, *J. Am. Chem. Soc.*, **112**, 8750 (1990).

b. As found by MNDO calculation

c. LUMO  $\pi$  energy in eV.

d. Change of chemical shift of H(3) in butenal.

less than for covalent bonds between similar elements (see also Section 3.4.4). Some Lewis acid-base complexes have weak bonds that are primarily electrostatic in nature (e.g., CH<sub>3</sub>CN<sup>+</sup>-BF<sub>3</sub><sup>-</sup>, 9.1 kcal/mol).<sup>145</sup>

There have been several efforts to develop measures of Lewis acid strength. One indication of Lewis acid strength of a number of compounds commonly used in synthesis is shown in Table 3.29. The relative acidity values given are derived from the LUMO level of the  $\pi^*$  orbital of the compound, with the BCl<sub>3</sub> complex defined as 1.00 and the uncomplexed but-2-enal LUMO energy taken as 0.<sup>146</sup> These values correlate with <sup>1</sup>H-NMR chemical shift of the H(3) proton of butenal.<sup>147</sup> In contrast, the calculated (MNDO) bond strengths ( $\Delta H$ ) do not correlate with the acid strength.

In another study, the <sup>13</sup>C chemical shift for acetone in complexes with various Lewis acids was determined (Table 3.30).<sup>148</sup> One general trend that can be noted is the increasing shift with the formal oxidation state of the metal.

A quite broad range of Lewis acid strengths was evaluated by comparing their effect on the shift of the fluorescence of complexes with *N*-methylacridone.<sup>149</sup> The shifts also correlated with the capacity of the Lewis acid to facilitate the reduction of

**Table 3.30. <sup>13</sup>C Chemical Shifts in Lewis Acid Complexes of Acetone**

Lewis Acid	<sup>13</sup> Chemical Shift
-	210
MgCl <sub>2</sub>	221
ZnCl <sub>2</sub>	227
Sc(O <sub>3</sub> SCF <sub>3</sub> ) <sub>3</sub>	239
AlCl <sub>3</sub>	245
SbF <sub>5</sub>	250

<sup>145</sup>. V. Jonas, G. Frenking, and M. T. Reetz, *J. Am. Chem. Soc.*, **116**, 8741 (1994).

<sup>146</sup>. P. Laszlo and M. Teston, *J. Am. Chem. Soc.*, **112**, 8750 (1990).

<sup>147</sup>. R. F. Childs, D. L. Mulholland, and A. Nixon, *Can. J. Chem.*, **60**, 801 (1982).

<sup>148</sup>. D. H. Barich, J. B. Nicholas, T. Xu, and J. F. Haw, *J. Am. Chem. Soc.*, **120**, 12342 (1998).

<sup>149</sup>. S. Fukuzumi and K. Ohkubo, *J. Am. Chem. Soc.*, **124**, 10270 (2002).

**Table 3.31. Wavelength and Energy Shift in  
N-Methylacridone-Lewis Acid Complexes**

Lewis acid	$\lambda_{\max}$ (nm)	$h\nu_{\text{fl}}$ (eV)
$\text{Fe}(\text{ClO}_4)_3$	478	2.59
$\text{Sc}(\text{O}_3\text{SCF}_3)_3$	474	2.62
$\text{Fe}(\text{ClO}_4)_2$	471	2.63
$\text{Cu}(\text{ClO}_4)_2$	471	2.63
$\text{Yb}(\text{O}_3\text{SCF}_3)_3$	460	2.70
$\text{La}(\text{O}_3\text{SCF}_3)_3$	458	2.71
$\text{Zn}(\text{O}_3\text{SCF}_3)_3$	456	2.72
$\text{Ph}_3\text{SnCl}$	455	2.72
$\text{Bu}_2\text{SnCl}_2$	453	2.72
$\text{Mg}(\text{ClO}_4)_2$	451	2.75
$\text{LiClO}_4$	442	2.81
$\text{NaClO}_4$	437	2.84
Uncomplexed	432	2.87

$\text{O}_2$  to  $\text{O}_2^-$ , which is again a measure of the ability to stabilize anionic charge. The fluorescence shifts are given in Table 3.31 and the correlation is shown in Figure 3.32. The orders  $\text{Li}^+ > \text{Na}^+$  and  $\text{Mg}^{2+} > \text{Ca}^{2+} > \text{Sr}^{2+} > \text{Ba}^{2+}$  show that Lewis acidity decreases with the size of the cation. According to this scale, the tin halides are comparable in acidity to  $\text{Mg}^{2+}$ . The strong Lewis acidity of  $\text{Sc}^{3+}$ ,  $\text{Y}^{3+}$ , and the lanthanides, such as  $\text{La}^{3+}$  and  $\text{Yb}^{3+}$ , has been exploited in various synthetic applications.

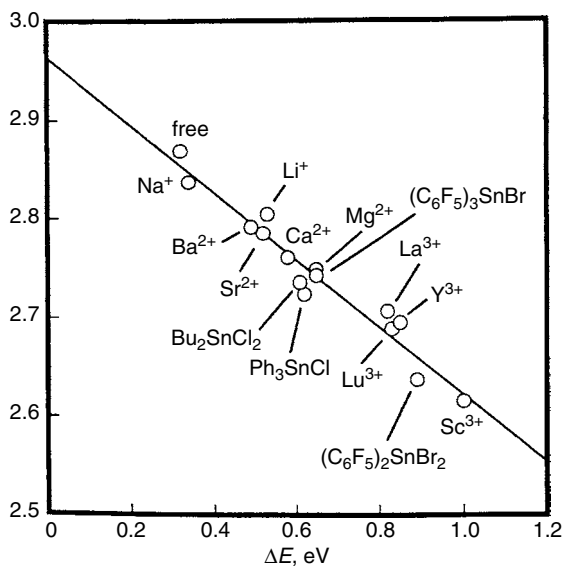


Fig. 3.32. Correlation between fluorescence shift and shift in oxidation energy for several Lewis acids. Reproduced from *J. Am. Chem. Soc.*, **124**, 10270 (2002), by permission of the American Chemical Society.

## 3.8.1. Bulk Solvent Effects

Since most organic reactions are done in solution, it is important to recognize some of the ways that solvents affect the course and rates of reactions. Some of the more common solvents can be roughly classified as in Table 3.32 on the basis of their structure and dielectric constants. There are important differences between *protic solvents*, those which contain hydrogens that form hydrogen bonds and can exchange rapidly (such as those bonded to oxygen, nitrogen, or sulfur), and *aprotic solvents*, in which all hydrogen is bound to carbon. Similarly, *polar solvents*, those that have high dielectric constants, have effects on reaction rates that are different from nonpolar solvent media.

When discussing solvent effects, it is important to distinguish between the macroscopic effects and those that depend upon details of structure. Macroscopic properties refer to properties of the bulk solvent. One example is the dielectric constant, which is a measure of the ability of the solvent to increase the capacitance of a condenser. Dielectric constants increase with molecular dipole moment and polarizability because of the ability of both the permanent and induced molecular dipole to align with the external electric field. An important property of solvent molecules is the response to changes in charge distribution as reaction occurs. The dielectric constant of a solvent is a good indicator of its ability to accommodate separation of charge. It is not the only factor, however, since, being a macroscopic property, it conveys little information about the ability of the solvent molecules to interact with the solute molecules and ions at close range. These direct solute-solvent interactions depend on the specific structures of the molecules.

Solvents that fall into the nonpolar aprotic class are not very effective at stabilizing the development of charge separation. These molecules have small dipole moments and do not have hydrogens capable of forming hydrogen bonds. Reactions that involve charge separation in the TS therefore proceed more slowly in this class of solvents than in protic or polar aprotic solvents. The reverse is true for reactions in which species having opposite charges come together in the TS. In this case the TS is less highly charged than the individual reactants and reaction is favored by weaker solvation that

**Table 3.32. Dielectric Constants ( $\epsilon$ ) and Molecular Dipole Moment ( $\mu$ ) of Some Common Solvents**

Aprotic solvents				Protic solvents				
Nonpolar	$\epsilon$	$\mu$	Polar	$\epsilon$	$\mu$	$\epsilon$	$\mu$	
Hexane	1.9	0	Pyridine	12	2.21	Acetic acid	6.1	1.7
CCl <sub>4</sub>	2.2	0	Acetone	21	2.88	CF <sub>3</sub> CO <sub>2</sub> H	8.6	
Dioxane	2.2	0	HMPA	30		<i>t</i> -Butanol	12.5	1.7
Benzene	2.3	0	Nitromethane	36	3.46	Ammonia	(22)	1.47
Diethyl ether	4.3	1.15	DMF	37	3.82	Ethanol	24.5	1.69
Chloroform	4.8	1.04	Acetonitrile	38	3.92	Methanol	32.7	1.7
THF	7.6	1.75	DMSO	47	3.96	Water	78	1.85

a. Dielectric constants ( $\epsilon$ ) and dipole moments ( $\mu$ ) in debye units from the compilation of solvent properties in J. A. Riddick and W. B. Bunger, eds., *Organic Solvents*, Vol. II of *Techniques of Organic Chemistry*, 3rd Edition, Wiley-Interscience, New York, 1970.

## Scheme 3.7. Effect of Solvent Polarity on Reactions of Various Charge Types

1. Neutralization of charge.	$A^- + B^- \xrightarrow{\delta^- \delta^+} A \cdots B \rightarrow A - B$	Favored by nonpolar solvent
2. Separation of charge.	$A - B \xrightarrow{\delta^- \delta^+} A \cdots B \rightarrow A^- + B^-$	Favored by polar solvent
3. Neutral reactants and products.	$A + B \rightarrow A \cdots B \rightarrow A - B$	Relatively insensitive to solvent polarity
4. Relative concentration of charge.	$[A - B]^+ \xrightarrow{\delta^+ \delta^+} A \cdots B \rightarrow A + B^+$	Slightly favored by polar solvent
5. Relative dispersal of charge.	$A^+ + B \rightarrow A \cdots B \rightarrow [A - B]^+$	Slightly favored by nonpolar solvent

leaves the oppositely charge reactants in a more reactive state. Arguing along these lines, the broad relationships between reactivity and solvent type shown in Scheme 3.7 can be deduced.

Many empirical measures of solvent polarity have been developed.<sup>150</sup> One of the most useful is based on shifts in the absorption spectrum of a reference dye. The position of absorption bands is sensitive to solvent polarity because the electronic distribution, and therefore the polarity, of the excited state is different from that of the ground state. The shift in the absorption maxima reflects the effect of solvent on the energy gap between the ground state and excited state molecules. An empirical solvent polarity measure called  $E_T(30)$  is based on this concept.<sup>151</sup> Some values for common solvents are given in Table 3.33 along with the dielectric constants for the solvents. It can be seen that a quite different order of polarity is given by these two quantities.

**Table 3.33.**  $E_T(30)$ , an Empirical Measure of Solvent Polarity, Compared with Dielectric Constant<sup>a</sup>

	$E_T(30)$	$\epsilon$		$E_T(30)$	$\epsilon$
Water	63.1	78	DMF	43.8	37
Trifluoroethanol	59.5		Acetone	42.2	21
Methanol	55.5	32.7	Dichloromethane	41.1	8.9
80:20 Ethanol-water	53.7		Chloroform	39.1	4.8
Ethanol	51.9	24.5	Ethyl acetate	38.1	6.0
Acetic acid	51.2	6.1	THF	37.4	7.6
2-Propanol	48.6	19.9	Diethyl ether	34.6	4.3
Acetonitrile	46.7	38	Benzene	34.5	2.3
DMSO	45.0	47			

From C. Reichardt, *Angew. Chem. Int. Ed. Engl.*, **18**, 98 (1979)

<sup>150</sup> C. Reichardt, *Angew. Chem. Int. Ed. Engl.*, **18**, 98 (1979); C. Reichardt, *Solvent Effects in Organic Chemistry*, Verlag Chemie, Weinheim, 1990; J. Catalan, V. Lopez, P. Perez, R. Martin-Villamil, and J. G. Rodriguez, *Liebigs Ann.*, 241 (1995); C. Laurance, P. Nicolet, M. T. Dalati, J. L. M. Abboud, and R. Notario, *J. Phys. Chem.*, **98**, 5807 (1994).

<sup>151</sup> C. Reichardt and K. Dimroth, *Fortshr. Chem. Forsch.*, **11**, 1 (1968); C. Reichardt, *Justus Liebigs Ann. Chem.*, **752**, 64 (1971).

As a specific example of a solvent effect, let us consider how the solvent affects the solvolysis of *t*-butyl chloride. Much evidence, which is discussed in detail in Chapter 4, indicates that the rate-determining step of the reaction is ionization of the carbon-chlorine bond to give a carbocation and the chloride ion. The TS reflects some of the charge separation that occurs in the ionization:



Figure 3.33 is a schematic interpretation of the solvation changes that take place during the ionization of *t*-butyl chloride, with S representing surrounding solvent molecules. With the neutral slightly polar reactant, there is only weak solvation. As charge separation develops in the TS, solvent molecules align with the most favorable orientation of the dipoles. The charged ions are strongly solvated.

The bulk dielectric constant may be a poor indicator of the ability of solvent molecules to facilitate the charge separation in the TS. The fact that the carbon and chlorine remain partially bonded at the TS prevents the solvent molecules from actually intervening between the developing centers of charge. Instead, the solvent molecules must stabilize the charge development by acting around the periphery of the activated complex. The nature of this interaction depends upon the detailed structure of the activated complex and solvent. The ability of solvents to stabilize the TS of *t*-butyl chloride ionization has been measured by comparing the rate of the reaction in the different solvent mixtures. The solvents were then assigned *Y* values, with the reference solvent taken as 80:20 ethanol-water. The *Y* value of other solvents is defined by the equation

$$\log \frac{k_{\text{solvent}}}{k_{80\% \text{ ethanol}}} = Y \quad (3.59)$$

Table 3.34 lists the *Y* values for some alcohol-water mixtures and for some other solvents. The *Y* value reflects primarily the ionization power of the solvent. It is largest for polar solvents such as water and formic acid and becomes progressively smaller and eventually negative as the solvent becomes less polar and contains more (or larger) nonpolar alkyl groups. Note that among the solvents listed there is a spread of more than  $10^6$  in the measured rate of reaction between *t*-butyl alcohol ( $Y = -3.2$ ) and water ( $Y = +3.49$ ). This large range of reaction rates demonstrates how important solvent effects can be.

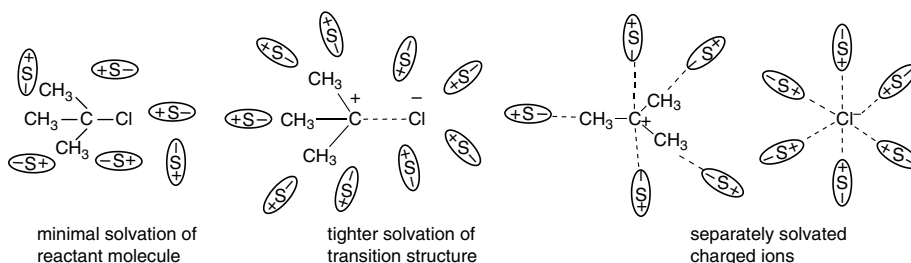


Fig. 3.33. Schematic representation of solvation changes during ionization of *t*-butyl chloride.

Table 3.34.  $Y$  Values for Some Solvent Systems.<sup>a</sup>

CHAPTER 3	Ethanol-water	$Y$	Methanol-water	$Y$	Other solvents	$Y$
<i>Structural Effects on Stability and Reactivity</i>	100:0	-2.03	100:0	-1.09	Acetic acid	-1.64
	80:20	0.00	80:20	0.38	Formic acid	2.05
	50:50	1.65	50:50	1.97	<i>t</i> -Butyl alcohol	-3.2
	20:80	3.05	10:90	3.28	90:10 acetone:water	-1.85
	0:100	3.49			90:10 dioxane:water	-2.03

a. From A. H. Fainberg and S. Winstein, *J. Am. Chem. Soc.*, **78**, 2770 (1956).

Several other treatments of solvent effects on solvolysis rates have been developed.<sup>152</sup> The equations typically include several terms related to: (a) macroscopic nonspecific solvent properties, such as the dipole moment and dielectric constant; (b) empirical polarity criteria, such as  $E_T(30)$ ; (c) solvent electrophilicity and nucleophilicity parameters; and (d) terms related to solvent *cohesivity*. The last term accounts for the difference in work required to disrupt structure within the solvent, when, for example, there is expansion in volume between reactants and the TS.

### 3.8.2. Examples of Specific Solvent Effects

The electrostatic solvent effects discussed in the preceding paragraphs are not the only possible modes of interaction of solvent with reactants and TS. Specific structural effects may cause either the reactants or the TS to be particularly strongly solvated. Figure 3.34 shows how such solvation can affect the relative energies of the ground state and the TS and cause rate variations from solvent to solvent. Unfortunately, no

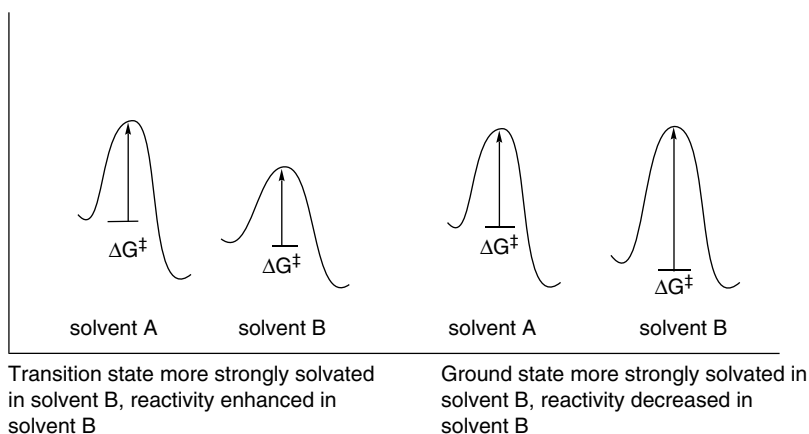


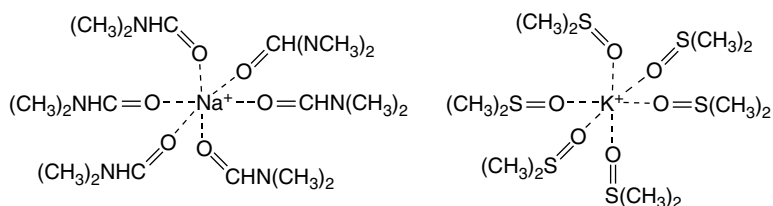
Fig. 3.34. Reaction energy profiles showing effect on  $E_a$  of (a) preferred solvation of the transition state and (b) preferred solvation of reactants.

<sup>152</sup> G. F. Dvorko, A. J. Vasil'kevich, E. A. Ponomareva, and J. V. Koschii, *Russ. J. Gen. Chem.*, **70**, 724 (2000); I. A. Koppel and V. Palm, *Advances in Linear Free Energy Relationships*, N. B. Chapman and J. Shorter, eds., Plenum Press, New York, 1972, Chap. 5.; M. H. Abraham, R. W. Taft, and M. J. Kamlet, *J. Org. Chem.*, **46**, 3053 (1981); M. H. Abraham, R. M. Doherty, M. J. Kamlet, J. M. Harris, and R. W. Taft, *J. Chem. Soc., Perkin Trans.*, **2**, 913 (1987); M. R. C. Goncalves, A. M. N. Simoes, and L. M. P. C. Albuquerque, *J. Chem. Soc., Perkin Trans.*, **2**, 1379 (1990).

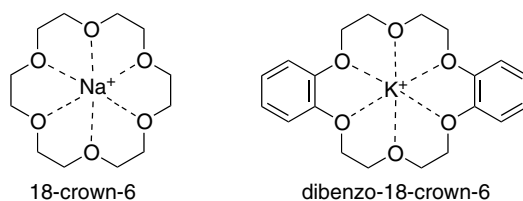
general theory for quantitatively predicting such specific effects has been developed to date. Nevertheless, there are many cases where specific interactions with solvent molecules strongly influence the outcome and/or the rate of reactions.

**3.8.2.1. Enhanced Nucleophilicity in Polar Aprotic Solvents.** An important example of solvent effects is the enhanced nucleophilicity of many anions in polar aprotic solvents as compared with protic solvents.<sup>153</sup> In protic solvents, anions are strongly solvated by hydrogen bonding. This is particularly true for hard anions that have a high concentration of charge on oxygen such as alkoxide ions. Hydrogen-bonding decreases the ability of the nucleophile to act as an electron donor. Stated another way, the energy required to disrupt hydrogen bonding adds to the activation energy of the reaction.

In polar aprotic solvents, no hydrogens suitable for hydrogen bonding are present. As a result, the electrons of the anion are more available for reaction. The anion is at a higher energy level because of the small stabilization by the solvent. The polarity of the aprotic solvents is also important for the solubility of ionic compounds. Dissolved ionic compounds are likely to be present as ion pairs or larger aggregates in which the reactivity of the anion is diminished by the electrostatic interaction with the cation. Energy must be expended against this electrostatic attraction to permit the anion to react as a nucleophile. Metal cations such as  $K^+$  and  $Na^+$  are strongly solvated by polar aprotic solvents such as DMSO and DMF. The oxygen atoms in these molecules act as electron donors toward the cations. The dissolved salts are dissociated, and as a result the anions are more reactive because they are poorly solvated and not associated with cations.

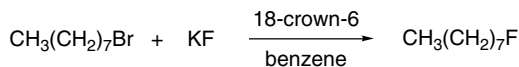


**3.8.2.2. Crown Ether and Phase Transfer Catalysts** Particularly striking examples of the effect of specific solvation occur with the *crown ethers*. These macrocyclic polyethers specifically solvate cations such as  $Na^+$  and  $K^+$ .



<sup>153</sup> A. J. Parker, *Q. Rev. Chem. Soc.*, **16**, 163 (1962); C. D. Ritchie, in *Solute-Solvent Interactions*, J. F. Coetzee and C. D. Ritchie, eds., Marcel Dekker, New York, 1969, Chap. 4; E. Buncl and H. Wilson, *Adv. Phys. Org. Chem.*, **14**, 133 (1977).

When added to nonpolar solvents, the crown ethers increase the solubility of ionic materials. For example, in the presence of 18-crown-6, potassium fluoride is soluble in benzene and acts as a reactive nucleophile:



Ref. 154

In the absence of the polyether, potassium fluoride is insoluble in benzene and unreactive toward alkyl halides. Similar enhancement of solubility and reactivity of other salts is observed in the presence of crown ethers. The solubility and reactivity enhancement results because the ionic compound is dissociated to a tightly complexed cation and a “naked” anion. Figure 3.35 shows the tight coordination that can be achieved with a typical crown ether. The complexed cation, because it is surrounded by the nonpolar crown ether, has high solubility in the nonpolar media. To maintain electroneutrality the anion is also transported into the solvent. The cation is shielded from close interaction with the anion because of the surrounding crown ether molecule. As a result, the anion is unsolvated and at a relatively high energy and therefore highly reactive.

A related solvation phenomenon is the basis for *phase transfer catalysis*.<sup>155</sup> The catalysts here are salts in which one of the ions (usually the cation) has large nonpolar substituent groups that confer good solubility in organic solvents. The most common examples are tetraalkylammonium and tetraalkylphosphonium ions. In two-phase systems consisting of water and a nonpolar organic solvent, these cations are extracted into the organic phase and, as a result of electrostatic forces, anions are transferred to the organic phase. The anions are weakly solvated and display high reactivity. Reactions are carried out between a salt containing the desired nucleophilic anion and

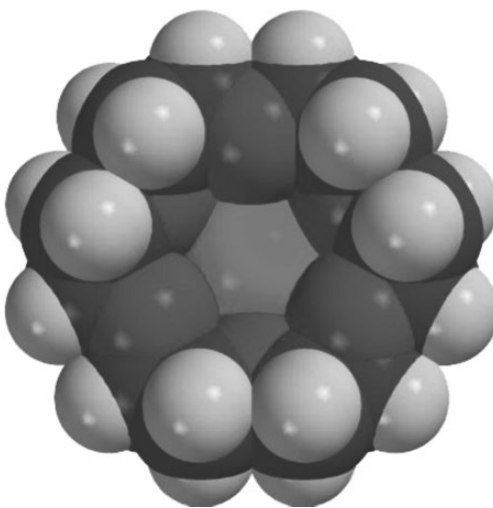
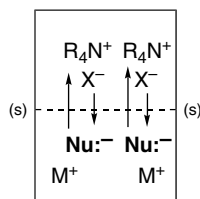


Fig. 3.35. Space-filling molecular model depicting a metal cation complexed by 18-crown-6. (See also color insert.)

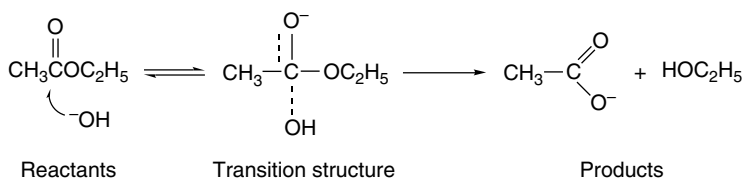
<sup>154</sup> C. Liotta and H. P. Harris, *J. Am. Chem. Soc.*, **96**, 2250 (1974).

<sup>155</sup> C. M. Starks, C. L. Liotta, and M. Halpern, *Phase Transfer Catalysis: Fundamentals: Applications and Industrial Perspectives*, Chapman and Hall, New York, 1994.

an organic reactant, typically in a hydrocarbon or nonpolar halogenated solvent. The addition of phase transfer catalysts causes migration of the anion into the organic phase and, because of its high nucleophilicity, reaction occurs under exceptionally mild conditions.



**3.8.2.3. Differential Solvation of Reactants and Transition States.** It should always be kept in mind that solvent effects can modify the energy of both the reactants and the transition state. It is the *difference* in the solvation that is the basis for changes in activation energies and reaction rates. Thus, although it is common to discuss solvent effects solely in terms of reactant solvation or transition state solvation, this is an oversimplification. A case that illustrates this point is the base-promoted hydrolysis of esters by hydroxide ion.



The reaction is faster in DMSO-water than in ethanol-water. Reactant solvation can be separated from transition state solvation by calorimetric measurement of the heat of solution of the reactants in each solvent system. The data in Figure 3.36 compare the energies of the reactants and TS for ethyl acetate and hydroxide ion reacting in aqueous ethanol versus aqueous DMSO. It can be seen that both the reactants and the TS are more strongly solvated in the ethanol-water medium.<sup>156</sup> The enhancement

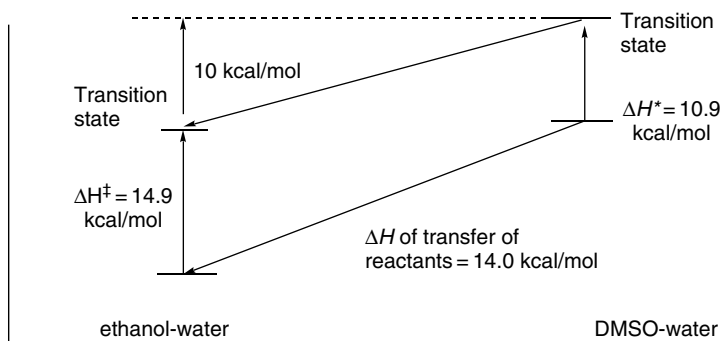
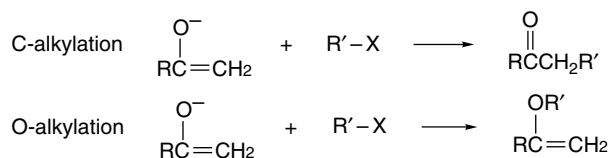


Fig. 3.36. Comparative reactant and transition state solvation in the reaction of ethyl acetate with hydroxide ion in ethanol/water and DMSO. Data from *J. Am. Chem. Soc.*, **94**, 71 (1972).

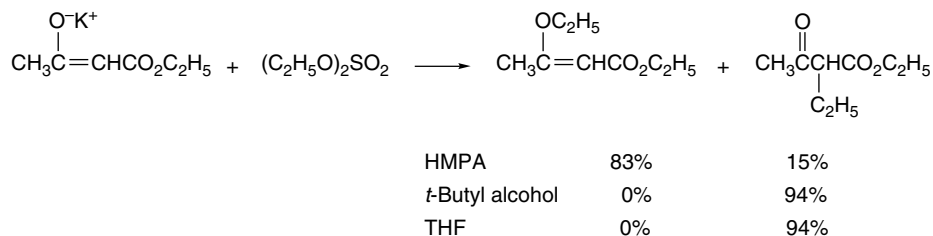
<sup>156</sup> P. Haberfield, J. Friedman, and M. F. Pinkson, *J. Am. Chem. Soc.*, **94**, 71 (1972).

in reaction rate comes from the fact that the difference is greater for the small hard hydroxide ion than for the larger anionic species present at the transition state.<sup>116</sup> It is generally true that solvation forces are strongest for the small, hard anions and decrease with size and softness.

**3.8.2.4. Oxygen versus Carbon Alkylation in Ambident Enolate Anions.** Enolate anions are *ambident nucleophiles*. Alkylation of an enolate can occur at either carbon or oxygen. Since most of the negative charge of an enolate is on the oxygen atom, it might be supposed that O-alkylation would dominate. A number of factors other than charge density affect the C/O-alkylation ratio and it is normally possible to establish reaction conditions that favor alkylation on carbon.



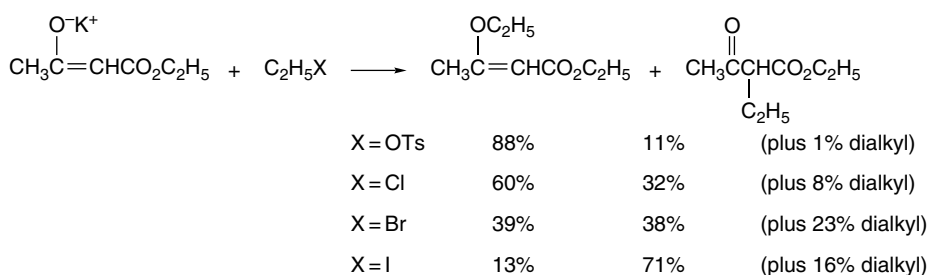
O-Alkylation is most pronounced when the enolate is least solvated. When the potassium salt of ethyl acetoacetate is treated with ethyl sulfate in the polar aprotic solvent HMPA, the major product (83%) results from O-alkylation. In THF, where ion clustering occurs, all of the product is C-alkylated. In *t*-butyl alcohol, where the acetoacetate anion is hydrogen bonded by solvent, again only C-alkylation is observed.<sup>157</sup>



Higher C/O ratios are observed with alkyl halides than with alkyl sulfonates and sulfates. The highest C/O-alkylation ratios are given by alkyl iodides. For ethylation of potassium ethyl acetoacetate in HMPA the product compositions shown below were obtained.<sup>158</sup>

<sup>157</sup> A. L. Kurts, A. Masias, N. K. Genkina, I. P. Beletskaya, and O. A. Reutov, *Dokl. Akad. Nauk. SSSR* (Engl. Transl.), **187**, 595 (1969).

<sup>158</sup> A. L. Kurts, N. K. Genkina, A. Masias, I. P. Beletskaya, and O. A. Reutov, *Tetrahedron*, **27**, 4777 (1971).



Leaving-group effects on the ratio of C- to O-alkylation can be correlated by the HSAB rationale.<sup>159</sup> Of the two nucleophilic sites in an enolate ion, oxygen is harder than carbon. Nucleophilic substitution reactions of the  $S_N2$  type proceed best when the nucleophile and leaving group are either both hard or both soft.<sup>160</sup> Consequently, ethyl iodide, with the soft leaving group iodide, reacts preferentially with the softer carbon site rather than the harder oxygen. Oxygen-leaving groups, such as sulfonate and sulfate, are harder and react preferentially at the hard oxygen site of the enolate. The hard-hard combination is favored by an early transition state where the electrostatic attraction is the most important factor. The soft-soft combination is favored by a later transition state where partial bond formation is the dominant factor. The C-alkylation product is more stable than the O-alkylation product (because the bond energy of  $\text{C}=\text{O} + \text{C}-\text{C}$  is greater than  $\text{C}=\text{C} + \text{C}-\text{O}$ ), as illustrated in Figure 3.37.

Similar effects are also seen with enolates of simple ketones. For isopropyl phenyl ketone, the inclusion of one equivalent of 12-crown-4 in a DME solution of the lithium enolate changes the C:O ratio from 1.2:1 to 1:3, using methyl sulfate as the alkylating agent.<sup>161</sup> The crown ether selectively solvates the  $\text{Li}^+$  ion, leaving the anion in a more

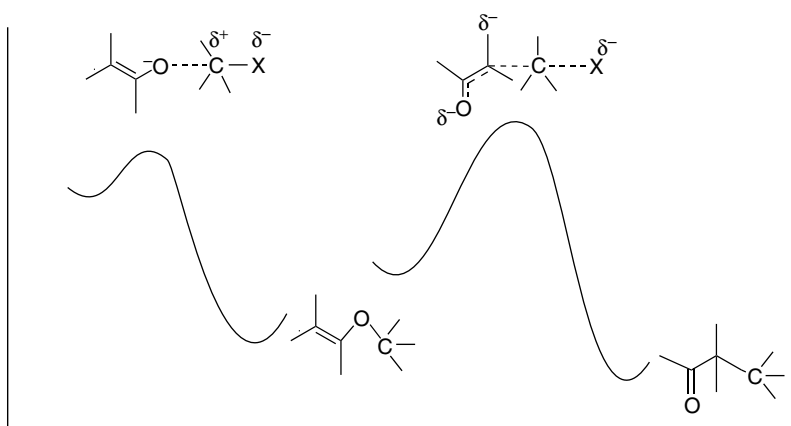


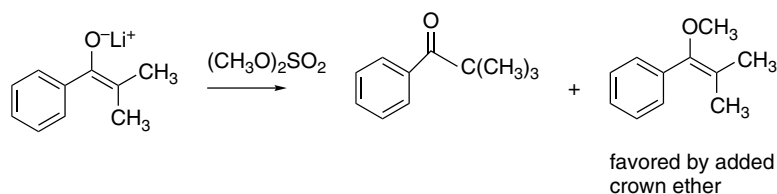
Fig. 3.37. Differential reaction energy profiles for O versus C alkylation of enolates. (a) O-Alkylation is characterized by an early transition state, weak O-solvation, high anion reactivity, and relatively large electrostatic effects. (b) C-Alkylation is characterized by a later transition state with more C–C bond formation and more diffuse charge distribution.

<sup>159</sup>. T. -L. Ho, *Hard and Soft Acids and Bases Principle in Organic Chemistry*, Academic Press, New York (1977).

<sup>160</sup>. R. G. Pearson and J. Songstad, *J. Am. Chem. Soc.*, **89**, 1827 (1967).

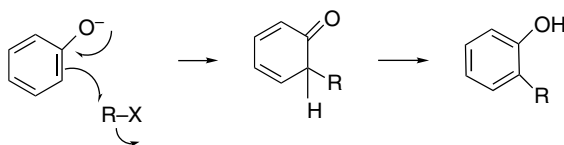
<sup>161</sup>. L. M. Jackman and B. C. Lange, *J. Am. Chem. Soc.*, **103**, 4494 (1981).

reactive state. With methyl iodide as the alkylating agent, C-alkylation is strongly favored with or without 12-crown-4.

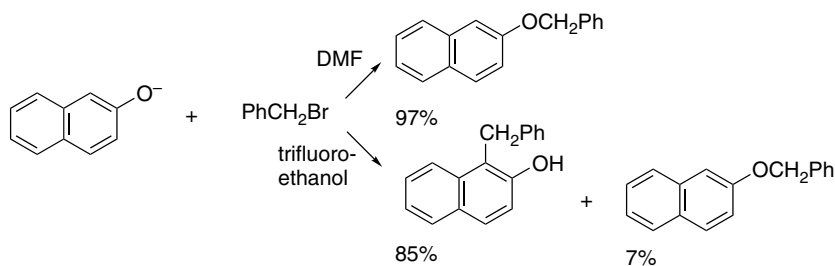


To summarize, the amount of O-alkylation is maximized by use of an alkyl sulfate or alkyl sulfonate in a polar aprotic solvent. The amount of C-alkylation is maximized by using an alkyl halide in a less polar or protic solvent. The majority of synthetic operations involving ketone enolates are carried out in THF or DME using an alkyl bromide or alkyl iodide and C-alkylation is favored.

Phenoxide ions are a special case related to enolate anions and have a strong preference for O-alkylation because C-alkylation disrupts aromatic conjugation.

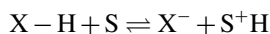


Phenoxides undergo O-alkylation in solvents such as DMSO, DMF, ethers, and alcohols. However, in water and trifluoroethanol there is extensive C-alkylation.<sup>162</sup> These latter solvents form particularly strong hydrogen bonds with the oxygen atom of the phenolate anion. This strong solvation decreases the reactivity at oxygen and favors C-alkylation.



### Topic 3.1. Acidity of Hydrocarbons

One of the fundamental properties of compounds containing hydrogen is their ability to act as proton donors, that is, as *Brønsted acids*.



<sup>162</sup> N. Kornblum, P. J. Berrigan, and W. J. LeNoble, *J. Am. Chem. Soc.*, **85**, 1141 (1963); N. Kornblum, R. Seltzer, and P. Haberfield, *J. Am. Chem. Soc.*, **85**, 1148 (1963).

The concept of acidity was discussed earlier in relation to aqueous solutions and the acidity of carboxylic acids and alcohols (see p. 321–322). The acidity of such compounds can be measured and expressed as the  $pK_a$ .

$$pK_a = -\log K \text{ where } K = \frac{[S^+H][X^-]}{[HX][S]}$$

Determination of the acidity of hydrocarbons is more difficult. As most are very weak acids, very strong bases are required to cause deprotonation. Water and alcohols are far more acidic than most hydrocarbons and are unsuitable solvents for generation of hydrocarbon anions. A strong base deprotonates the solvent rather than the hydrocarbon. For synthetic purposes, aprotic solvents such as ether, THF, and dimethoxyethane are used, but for equilibrium measurements solvents that promote dissociation of ion pairs and ion clusters are preferred. Weakly acidic solvents such as dimethyl sulfoxide (DMSO), dimethylformamide (DMF), and cyclohexylamine are used in the preparation of moderately basic carbanions. The high polarity and cation-solvating ability of DMSO and DMF facilitate dissociation of ion pairs so that the equilibrium data obtained refer to the free ions, rather than to ion aggregates.

The basicity of a base-solvent system can be specified by a basicity constant  $H_-$ . The  $H_-$  is a measure of solution basicity, analogous to the acidity function  $H_0$  (see Section 3.7.1.3). The value of  $H_-$  approximates the pH of strongly basic solutions. The larger the value of  $H_-$ , the greater the proton-abstracting ability of the medium. Use of a series of overlapping indicators permits assignment of  $H_-$  values to base-solvent systems, and allows  $pK$ 's to be determined over a range of 0–30  $pK$  units. Table 3.35 presents  $H_-$  values for some solvent-base systems.

The acidity of a hydrocarbon can be determined in an analogous way.<sup>163</sup> If the electronic spectra of the neutral and anionic forms are sufficiently different, the concentrations of each can be determined directly, and the position of the equilibrium constant is related to  $pK$  by the equation

$$pK_{R-H} = H_- + \log \frac{[R-H]}{[R^-]}$$

A measurement of the ratio  $[RH] : [R^-]$  at a known  $H_-$  yields the  $pK$ . If the electronic spectrum of the hydrocarbon and its anion are not sufficiently different, an indicator is

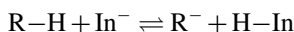
**Table 3.35. Values of  $H_-$  for Some Solvent-Base Systems**

Solvent	$H_-^a$
5M KOH	15.5
10M KOH	17.0
1M KOH	18.5
0.01M NaOMe in 1:1 DMSO-MeOH	15.0
0.01M NaOMe in 10:1 DMSO-MeOH	18.0
0.01M NaOEt in 20:1 DMSO-MeOH	21.0

a. From J. R. Jones, *The Ionization of Carbon Acids*, Academic Press, New York, 1973, Chap. 6.

<sup>163</sup>. D. Dolman and R. Stewart, *Can. J. Chem.*, **45**, 911 (1967); E. C. Steiner and J. M. Gilbert, *J. Am. Chem. Soc.*, **87**, 382 (1965); K. Bowden and R. Stewart, *Tetrahedron*, **21**, 261 (1965).

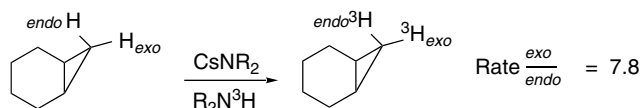
used and its spectrum is monitored. Equilibrium is established between the indicator and hydrocarbon in the basic medium. The relationship



then provides a way to relate the concentrations that are not directly measured—[RH] and [R<sup>-</sup>]<sup>—</sup>to quantities that are—[HIn] and [In<sup>-</sup>].

The p*K* values are influenced by the solvent and other conditions of the measurement. The extent of ion pairing is a function of the ability of the solvent to solvate the ionic species. Ion pairing is greatest in nonpolar solvents such as ethers. In dipolar aprotic solvents, especially DMSO, ion pairing is much less likely to be significant.<sup>164</sup> The identity of the cation present can also have a significant effect if ion pairs are present. Owing to these factors, the numerical p*K* values are not absolute and are specific to the solvent. Nevertheless, they provide a useful measure of relative acidity. The two solvents that have been used for most quantitative measurements on weak carbon acids are cyclohexylamine and DMSO. Some of these values are given in Table 3.36. It is not expected that the values will be numerically identical with aqueous p*K*<sub>a</sub>, but for most compounds the same relative order of acidity is observed for hydrocarbons of similar structural type.

A number of hydrocarbons have been studied in cyclohexylamine using cesium cyclohexylamide as the base. For many of the compounds studied, spectroscopic measurements were used to determine the relative extent of deprotonation of two hydrocarbons and thus establish relative acidity.<sup>165</sup> For other hydrocarbons, the acidity was derived by kinetic measurements. Such studies are usually done by observing the rate of isotopic exchange (deuterium or tritium) at the site of interest. The rate of hydrocarbon exchange can be measured using <sup>3</sup>H NMR spectroscopy.<sup>166</sup> The course of exchange can be followed by the appearance of the <sup>3</sup>H NMR signal corresponding to the hydrogen undergoing exchange. For example, the rates of exchange of both the *exo* and *endo* hydrogens in norcarane can be followed.



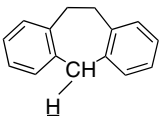
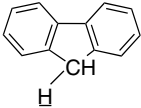
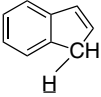
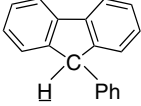
It has been found that there is often a correlation between the rate of proton abstraction (kinetic acidity) and the thermodynamic stability of the carbanion (thermodynamic acidity). Owing to this relationship, kinetic measurements can be used to construct orders of hydrocarbon acidities. These kinetic measurements have the advantage of not requiring the presence of a measurable concentration of the carbanion at any time; instead, the relative ease of carbanion formation is judged from the rate

<sup>164</sup> E. M. Arnett, T. C. Moriarity, L. E. Small, J. P. Rudolph, and R. P. Quirk, *J. Am. Chem. Soc.*, **95**, 1492 (1973); T. E. Hogen-Esch and J. Smid, *J. Am. Chem. Soc.*, **88**, 307 (1966).

<sup>165</sup> A. Streitwieser, Jr., J. R. Murdoch, G. Hafelinger, and C. J. Chang, *J. Am. Chem. Soc.*, **95**, 4248 (1973); A. Streitwieser, Jr., E. Ciuffarin, and J. H. Hammons, *J. Am. Chem. Soc.*, **89**, 63 (1967); A. Streitwieser, Jr., E. Juaristi, and L. L. Nebenzahl, in *Comprehensive Carbanion Chemistry*, Part A, E. Bunce and T. Durst, eds., Elsevier, New York, 1980, Chap. 7.

<sup>166</sup> R. E. Dixon, P. G. Williams, M. Saljoughian, M. A. Long, and A. Streitwieser, *Magn. Res. Chem.*, **29**, 509 (1991).

Table 3.36. Acidity of Some Hydrocarbons

Hydrocarbon	K <sup>+</sup> (DMSO) <sup>a</sup>	Cs <sup>+</sup> (cyclohexylamine) <sup>b</sup>	Cs <sup>+</sup> (THF) <sup>c</sup>
PhCH <sub>2</sub> -H	43	41.2	40.9
Ph <sub>2</sub> CH-H	32.4	33.4	33.3
Ph <sub>3</sub> C-H	30.6	31.4	31.3
		31.2	
	22.6	22.7	22.9
	20.1	19.9	22.9
	17.9	18.5	18.2
	18.1	16.6 <sup>d,e</sup>	

a. F. G. Bordwell, *Acc. Chem. Res.*, **21**, 456, 463 (1988).

b. A. Streitwieser, Jr., J. R. Murdoch, G. Hafelinger, and C. J. Chang, *J. Am. Chem. Soc.*, **95**, 4248 (1973); A. Streitwieser, Jr., and F. Guibe, *J. Am. Chem. Soc.*, **100**, 4532 (1978).

c. M. J. Kaufman, S. Gronert, and A. Streitwieser, Jr., *J. Am. Chem. Soc.*, **110**, 2829 (1988); A. Streitwieser, J. C. Ciula, J. A. Krom, and G. Thiele, *J. Org. Chem.*, **56**, 1074 (1991).

d. A. Streitwieser, Jr., and L. L. Nebenzahl, *J. Am. Chem. Soc.*, **98**, 2188 (1976).

e. The pK of cyclopentadiene in water is 16.0

at which exchange occurs. This method is applicable to very weak acids, for which no suitable base will generate a measurable carbanion concentration. This method was used to extend the scale to hydrocarbons such as toluene, for which the exchange rate, but not equilibrium data, can be obtained.<sup>167</sup>

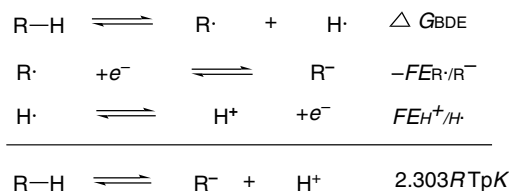
For synthetic purposes, carbanions are usually generated in ether solvents, often THF or dimethoxyethane. There are relatively few quantitative data available on hydrocarbon acidity in such solvents. Table 3.36 contains several entries for Cs<sup>+</sup> salts in THF. The numerical values are scaled with reference to the pK of fluorene of 22.9.<sup>168</sup>

<sup>167</sup>. A. Streitwieser, Jr., M. R. Granger, F. Mares, and R. A. Wolf, *J. Am. Chem. Soc.*, **95**, 4257 (1973).

<sup>168</sup>. M. J. Kaufman, S. Gronert, and A. Streitwieser, Jr., *J. Am. Chem. Soc.*, **110**, 2829 (1988); A. Streitwieser, Jr., J. C. Ciula, J. A. Krom, and G. Thiele, *J. Org. Chem.*, **56**, 1074 (1991).

Allylic conjugation stabilizes carbanions and  $pK$  values of 43 (in cyclohexylamine)<sup>169</sup> and 47–48 (in THF-HMPA)<sup>170</sup> have been determined for propene. On the basis of exchange rates with cesium cyclohexylamide, cyclohexene and cycloheptene have been found to have  $pK$  values of about 45 in cyclohexylamine.<sup>171</sup> The hydrogens on the  $sp^2$  carbons in benzene and ethylene are more acidic than the hydrogens in saturated hydrocarbons. A  $pK$  of 43 has been estimated for benzene on the basis of extrapolation from a series of fluorobenzenes.<sup>172</sup> Electrochemical measurements have been used to establish a lower limit of about 46 for the  $pK$  of ethylene.<sup>170</sup>

For saturated hydrocarbons, exchange is too slow and reference points are so uncertain that direct determination of  $pK$  values by exchange measurements is not feasible. The most useful approach to obtain  $pK$  data for such hydrocarbons involves making a measurement of the electrochemical potential for the one electron reduction of the hydrocarbon radical. From this value and known C–H bond dissociation energies,  $pK$  values can be calculated.



Early application of these methods gave estimates of the  $pK$  of toluene of about 45 and propene of about 48. Methane was estimated to have a  $pK$  in the range of 52–62.<sup>170</sup> More recent electrochemical measurements in DMF provided the results in Table 3.37.<sup>173</sup> These measurements put the  $pK$  of methane at about 48, with benzylic and allylic stabilization leading to values of 39 and 38 for propene and toluene, respectively. The electrochemical values that overlap with the  $pK_{\text{DMSO}}$  scale for compounds such as diphenylmethane and triphenylmethane are in reasonable agreement.

Most of the hydrocarbons included in Tables 3.36 and 3.37 illustrate the effect of *anion stabilization*. Cyclopentadiene is the most striking example. The  $pK$  is similar to that of alcohols. The high relative acidity of cyclopentadiene is due to the *aromatic*

**Table 3.37.  $pK$  Values for Weakly Acidic Hydrocarbons Based on Reduction Potentials in DMF<sup>a</sup>**

	$pK$		$pK$
$\text{CH}_3\text{-H}$	48	$\text{CH}_2=\text{CHCH}_2\text{-H}$	38
$\text{CH}_3\text{CH}_2\text{-H}$	51	$\text{CH}_2=\text{CHC}(\text{CH}_3)\text{-H}$	38
$(\text{CH}_3)_2\text{CH-H}$	50	$\text{HC}\equiv\text{CCH}_2\text{-H}$	38
$(\text{CH}_3)_3\text{C-H}$	49	$\text{PhCH}_2\text{-H}$	39
cyclopentane	49	$\text{Ph}_2\text{CH-H}$	31
cyclohexane	49	$\text{Ph}_3\text{C-H}$	29

a. K. Daasbjerg, *Acta Chem. Scand.*, **49**, 578 (1995).

<sup>169</sup>. D. W. Boerth and A. Streitwieser, Jr., *J. Am. Chem. Soc.*, **103**, 6443 (1981).

<sup>170</sup>. B. Jaun, J. Schwarz, and R. Breslow, *J. Am. Chem. Soc.*, **102**, 5741 (1980).

<sup>171</sup>. A. Streitwieser, Jr., and D. W. Boerth, *J. Am. Chem. Soc.*, **100**, 755 (1978).

<sup>172</sup>. A. Streitwieser, Jr., P. J. Scannon, and H. M. Niemeyer, *J. Am. Chem. Soc.*, **94**, 7936 (1972).

<sup>173</sup>. K. Daasbjerg, *Acta Chem. Scand.*, **49**, 878 (1995).

*stabilization* of the anion. Indene and fluorene derivatives also benefit from stabilization of the cyclopentadienide rings that are incorporated into their structures. The much greater acidity of fluorene relative to dibenzocycloheptatriene (Table 3.36) reflects the aromatic stabilization of the cyclopentadienide ring in the anion of fluorene. Toluene, diphenylmethane, and triphenylmethane anions are also stabilized by delocalization of the negative charge. Note, however, that the third phenyl substituent has only a small effect on the acidity of triphenylmethane, which presumably reflects steric problems that preclude optimal alignment of the rings in the carbanion.

Another factor that influences hydrocarbon acidity is hybridization at the carbon atom. Acidity increases sharply in the order  $sp^3C-H < sp^2C-H < spC-H$ . Terminal alkynes are among the most acidic of the hydrocarbons. For example, in DMSO, phenylacetylene is found to have a  $pK$  near 26.5.<sup>174</sup> In cyclohexylamine, the value is 23.2.<sup>175</sup> An estimate of the  $pK$  in aqueous solution of 20 is based on a Brønsted relationship.<sup>176</sup> The relatively high acidity of alkynes is associated with the high  $s$  character of the C–H bond. The  $s$  character is 50%, as opposed to 25% in  $sp^3$  bonds. The electrons in orbitals with high  $s$  character experience decreased shielding of the nuclear charge. The carbon is therefore effectively more electronegative, as viewed from the proton sharing an  $sp$  hybrid orbital, and hydrogens on  $sp$  carbons exhibit greater acidity. This same effect accounts for the relatively high acidity of the hydrocarbons on cyclopropane and other strained rings that have increased  $s$  character in the C–H bonds.<sup>177</sup> There is a correlation between the coupling constant  $J^{1H-13C}$  and acidity, because the  $J^{1H-13C}$  coupling constant is related to hybridization.<sup>178</sup> The relationship between hybridization and acidity may not be as straightforward as suggested by the correlations for alkynes, alkenes, cyclopropane, and alkanes. Sauers tabulated % $s$  character for 28 hydrocarbons and found relatively poor correlation with % $s$  character.<sup>179</sup>

Cubane has had an interesting place in the discussion of the correlation between C–H acidity and carbon hybridization. Its acidity was measured by the  $^3H$  exchange NMR technique and found to be about  $6.6 \times 10^4$  as reactive as benzene.<sup>180</sup> An experimental gas phase measurement of the proton affinity (PA) as 404 kcal/mol is available.<sup>181</sup> (See Tables 3.14 and 3.38 for comparable data on other hydrocarbons.) Both of these values indicate that cubane is somewhat more acidic than expected on the basis of the carbon hybridization. There appears to be unusual hybridization of the anion in this case. An AIM analysis suggests that the C–C bond paths in the anion are *less than*  $90^\circ$ , suggesting that the bonds bend inward toward the center of the ring. Sauers also noted an *increase* in  $s$  character on going from the hydrocarbon to the anion.<sup>179</sup> Of the 28 deprotonations he examined, only cyclopropane and bicyclo[1.1.1]pentane also showed increased  $s$  character in the anion.

<sup>174</sup>. F. G. Bordwell and W. S. Matthews, *J. Am. Chem. Soc.*, **96**, 1214 (1974).

<sup>175</sup>. A. Streitwieser, Jr., and D. M. E. Reuben, *J. Am. Chem. Soc.*, **93**, 1794 (1971).

<sup>176</sup>. D. B. Dahlberg, M. A. Kuzemko, Y. Chiang, A. J. Kresge, and M. F. Powell, *J. Am. Chem. Soc.*, **105**, 5387 (1983).

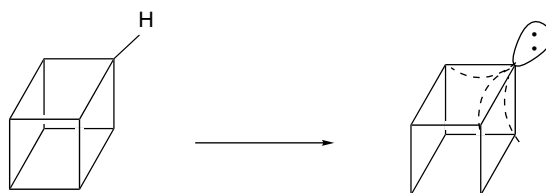
<sup>177</sup>. A. Streitwieser, Jr., R. A. Caldwell, and W. R. Young, *J. Am. Chem. Soc.*, **91**, 529 (1969); G. L. Closs and R. B. Larrabee, *Tetrahedron Lett.*, 287 (1965); M. Randic and Z. Mossic, *Chem. Rev.*, **72**, 43 (1972).

<sup>178</sup>. M. A. Battiste and J. M. Coxon, *The Chemistry of the Cyclopropyl Group*, Z. Rapoport, ed., John Wiley & Sons, New York, 1987, pp. 255–305.

<sup>179</sup>. R. R. Sauers, *Tetrahedron*, **55**, 10013 (1999).

<sup>180</sup>. A. Streitwieser, L. Xie, P. Speers, and P. G. Williams, *Magn. Res. Chem.*, **36**, S509 (1996).

<sup>181</sup>. M. Hare, T. Emrick, P. E. Eaton, and S. R. Kass, *J. Am. Chem. Soc.*, **119**, 237 (1997).



As we discussed in Section 3.4.2, measurements in the gas phase, which eliminate the effect of solvation, show structural trends that parallel measurements in solution but with larger absolute energy differences. Table 3.38 gives  $\Delta H$  of gas phase proton dissociation data for some key hydrocarbons. These data show a correspondence with the hybridization and delocalization effects observed in solution. The very large heterolytic dissociation energies reflect both the inherent instability of the carbanions and also the electrostatic attraction between the oppositely charged carbanion and proton that separate.

There have been several studies aimed at using computations to examine hydrocarbon acidity. The proton affinity values for a number of hydrocarbons were calculated by both *ab initio* and DFT methods.<sup>179</sup> Some of the results are shown in Table 3.39.

Alkorta and Elguero found that there is good correlation between PAs calculated by B3LYP/6-311++G\*\* computations and available gas phase experimental measurements.<sup>182</sup> There was also good correlation with solution *pK* values. Based on these correlations, they made the interesting prediction that the as yet unknown hydrocarbon tetrahedrane would be comparable to water in acidity.

Knowledge of the structure of carbanions is important to understanding the stereochemistry, stability, and reactivity. Theoretical calculations at the *ab initio* level (HF/4-31G) indicate a pyramidal geometry at carbon in the methyl and ethyl anions. The optimum H–C–H angle in these two carbanions was calculated to be 97°–100°. An interesting effect is observed in that the PA (basicity) of methyl anion decreases in a regular manner as the H–C–H angle is decreased.<sup>183</sup> This increase in acidity with decreasing internuclear angle has a parallel in small-ring compounds, in which the acidity of hydrogens is substantially greater than in compounds having tetrahedral geometry at carbon. Pyramidal geometry at carbanions can also be predicted on the

**Table 3.38. Enthalpy of Proton Dissociation for Some Hydrocarbons (Gas Phase)**

Hydrocarbon	Enthalpy (kcal/mol)
Methane	418.8
Ethene	407.5
Cyclopropane	411.5
Benzene	400.8
Toluene	381.0

a. S. T. Gaul and R. R. Squires, *J. Am. Chem. Soc.*, **112**, 2517 (1990).

<sup>182</sup>. I. Alkorta and J. Elguero, *Tetrahedron*, **53**, 9741 (1997).

<sup>183</sup>. A. Streitwieser, Jr., and P. H. Owens, *Tetrahedron Lett.*, 5221 (1973); A. Streitwieser, Jr., P. H. Owens, R. A. Wolf, and J. E. Williams, Jr., *J. Am. Chem. Soc.*, **96**, 5448 (1974); E. D. Jemmis, V. Buss, P. v. R. Schleyer, and L. C. Allen, *J. Am. Chem. Soc.*, **98**, 6483 (1976).

**Table 3.39. Computed Proton Affinity for Some Hydrocarbons in kcal/mol<sup>a</sup>**

Hydrocarbon	MP2/6-31+G(d,p)	B3LYP/6-311++G(2d,p)	Experimental
CH <sub>3</sub> -H	419.0	414.5	417±2
CH <sub>3</sub> CH <sub>2</sub> -H	421.9	417.0	420–421
(CH <sub>3</sub> ) <sub>3</sub> C-H	412.1	406.8	413.1
Cyclopropane	419.6	413.3	411.5
Cyclobutane	415.5	411.5	417.4
Cyclopentane	414.0	409.1	416.1
Bicyclo[1.1.1]-pentane-H(1)	409.4	407.5	411±3.5
Bicyclo[2.2.1]heptane-H(1)	411.3	409.0	
Cubane	407.6	406.5	404±3

TOPIC 3.1  
Acidity of Hydrocarbons

a. R. R. Sauers, *Tetrahedron*, **55**, 10013 (1999).

basis of qualitative considerations of the orbital occupied by the unshared electron pair. In a planar carbanion, the lone pair occupies a *p* orbital. In a pyramidal geometry, the orbital has substantial *s* character. Since the electron pair has lower energy in an orbital with some *s* character, it would be predicted that a pyramidal geometry would be favored.

An effort has been made to dissect the substituent effects in carbanions into their component parts. The energy of the anion was calculated before and after allowing first electronic and then nuclear relaxation. This might be expected to roughly correspond to polar and resonance components, since the nuclear relaxation established the optimal geometry for delocalization (although there may be partial delocalization in the unrelaxed anion). The results are summarized in Table 3.40. Most of the energy change was found at the electronic relaxation stage, but substituents such as formyl and nitro, for which resonance delocalization is expected to be important, showed the largest effect of nuclear relaxation. Interestingly, the cyano group showed only a small nuclear relaxation component, suggesting that its anion-stabilizing effect is mainly of polar origin.

Tuptisyn and co-workers examined several series of hydrocarbons in an effort to confirm the importance of delocalization and hybridization changes as the major factors

**Table 3.40. Electronic and Nuclear Relaxation Components of Carbanion Stabilization<sup>a</sup>**

Substituent	Electronic (kcal/mol)	Nuclear (kcal/mol)
H	67.8	0
NH <sub>2</sub>	61.9	1.0
OH	60.2	1.8
F	61.4	1.6
Cl	59.7	2.6
CH=O	64.5	5.9
C≡N	62.6	1.2
NO <sub>2</sub>	59.5	10.6
CH <sub>3</sub> S	65.9	0.7
CH <sub>3</sub> SO	62.6	2.7
CH <sub>3</sub> SO <sub>2</sub>	60.0	1.4

a. F. Tuptisyn, A. S. Popov, and N. N. Zatssepina, *Russ. J. Gen. Chem.*, **68**, 1314 (1998).

in C–H acidity.<sup>184</sup> Acidity was estimated by using AM1 computations, calibrated to experimental deprotonation energies. For small-ring, bicyclic, and cage compounds, a correlation was found for the  $\Delta E$  for deprotonation and the  $^1\text{H}$ - $^{13}\text{C}$  coupling constant:

$$\Delta E_{\text{deprot}} = 1870(\text{kJ}) - 0.93 J_{\text{H-C}}$$

A similar correlation pertains to cyclic alkenes and dienes in which the deprotonation is from an  $sp^2$  carbon:

$$\Delta E_{\text{deprot}} = 1867(\text{kJ}) - 1.05 J_{\text{H-C}}$$

These correlations suggest that the dominant factor for these compounds is the hybridization of the C–H undergoing deprotonation. For hydrocarbons for which delocalization is expected to be the major factor, e.g., toluene and diphenylmethane, a different kind of correlation was found:

$$\Delta E_{\text{deprot}} = 1640(\text{kJ}) - 0.70\Delta E_{\text{relax}}$$

where  $\Delta E_{\text{relax}}$  is the stabilization found when the carbanion constrained to the geometry of the original structure is allowed to relax to the minimum energy structure. These results support the idea that C–H acidity depends primarily on hybridization and anion stabilization. In addition to the hydrocarbons that show correlations with one of the two factors, some hydrocarbons are correlated by equations that contain terms both terms.

## General References

- C. F. Bernasconi, ed., *Investigation of Rates and Mechanisms: Techniques of Chemistry*, 4th ed. Vol. VI, Part 1, John Wiley & Sons, New York, 1986.
- B. K. Carpenter, *Determination of Organic Reaction Mechanisms*, Wiley-Interscience, New York, 1984.
- K. A. Connors, *Chemical Kinetics*, VCH Publishers, New York, 1990.
- J. D. Cox and G. Pilcher, *Thermochemistry of Organic and Organometallic Compounds*, Academic Press, London, 1970.
- G. G. Hammes, *Principles of Chemical Kinetics*, Academic Press, New York, 1978.
- J. Hine, *Structural Effects on Equilibria in Organic Chemistry*, Wiley-Interscience, New York, 1984.
- C. D. Johnson, *The Hammett Equation*, Cambridge University Press, Cambridge, 1973.
- L. Melander and W. H. Saunders, Jr., *Reaction Rates of Isotopic Molecules*, New York, 1980.
- M. J. Pilling and P. Seakins, *Reaction Kinetics*, 2nd ed. Oxford University Press, Oxford, 1995.
- C. Reichardt, *Solvents and Solvent Effects in Organic Chemistry*, Wiley-VCH, Weinheim, 2003.

## Problems

(References for these problems will be found on page 1158.)

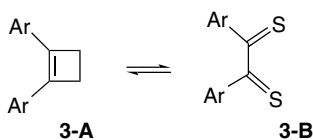
3.1. Use thermochemical relationships to obtain the requested information.

- a. The  $\Delta H_f$  of cyclohexane, cyclohexene, and benzene are, respectively,  $-29.5$ ,  $-1.1$ , and  $+18.9$  kcal/mol. Use this information to estimate the resonance stabilization of benzene.

<sup>184</sup>. I. F. Tupitsyn, A. S. Popov, and N. N. Satsepina, *Russian J. Gen. Chem.*, **67**, 379 (1997).

- b. Calculate  $\Delta H$  for the air oxidation of benzaldehyde to benzoic acid, given that the  $\Delta H_f$  of benzaldehyde and benzoic acid are  $-8.8$  and  $-70.1$  kcal/mol, respectively.
- c. Using the appropriate heats of formation from Table 3.1, calculate the heat of hydrogenation  $\Delta H_{H_2}$  for 2-methyl-1-pentene.

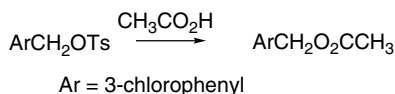
- 3.2. Addition of methylmagnesium bromide to 2-methylcyclohexanone, followed by iodine-catalyzed dehydration of the resulting alcohol gave three alkenes in the ratio A:B:C = 3:31:66. Each alkene gave a mixture of *cis*- and *trans*-1,2-dimethylcyclohexane upon catalytic hydrogenation. When the alkene mixture was heated with a small amount of sulfuric acid, the ratio of A:B:C changed to 0.0:15:85. Assign structures to A, B, and C.
- 3.3. Measurement of the equilibrium constant for the interconversion of the dithiete **3-A** and the dithione **3-B** at several temperatures gave the data below. Calculate  $\Delta G$ ,  $\Delta H$ , and  $\Delta S$ .



Ar - 4-dimethylaminophenyl

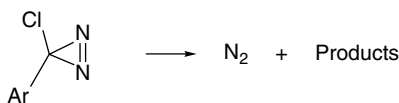
Temperature ( $^{\circ}$ C)	$K$
-2.9	16.9
11.8	11.0
18.1	8.4
21.9	7.9
29.3	6.5
32.0	6.1
34.9	5.7
37.2	5.3
42.5	4.6

- 3.4 a. Calculate the activation parameters ( $\Delta H^{\ddagger}$  and  $\Delta S^{\ddagger}$ ) at  $40^{\circ}$  C for the acetolysis of 3-chlorobenzyl tosylate from the data given below:



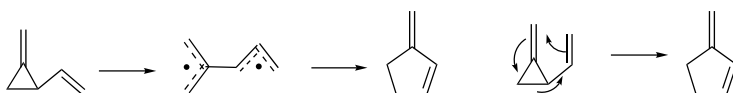
Temperature ( $^{\circ}$ C)	$k \times 10^5 \text{ s}^{-1}$
25.0	0.0136
40.0	0.085
50.1	0.272
58.8	0.726

- b. Calculate the activation parameters ( $E_a$ ,  $\Delta H^\ddagger$ , and  $\Delta S^\ddagger$ ) at 100°C from the data given for the reaction below.

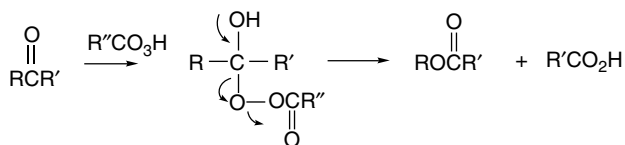


Temperature (°C)	$k \times 10^4 \text{ s}^{-1}$
60.0	0.30
70.0	0.97
75.0	1.79
80.0	3.09
90.0	8.92
95.0	15.90

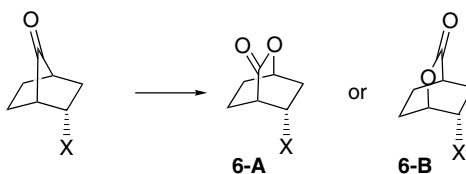
- 3.5. 2-Vinylmethylencyclopropane rearranges thermally to 3-methylene-cyclopentene. In the gas phase, the  $E_a$  is 26.0 kcal/mol, which is close to the estimated energy required for rupture of the C(2)–C(3) bond. Two possible mechanisms for this rearrangement are:



- a. Sketch qualitative reaction energy profiles for each process, based on the information given.
- b. How might an isotopic labeling experiment distinguish between these mechanisms?
- 3.6. The Baeyer-Villiger oxidation of ketones to esters (or lactones) occurs by the following mechanism:

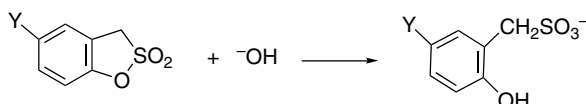


For *endo*-substituted bicyclo[2.2.1]heptan-7-ones, the product ratios shown below are observed. Account for the effect of the substituents.



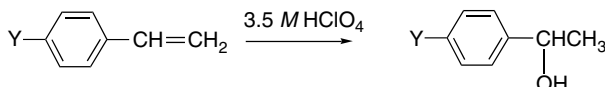
X	6A:6B
CN	100:0
CO <sub>2</sub> CH <sub>3</sub>	77:23
Ph	51:49
<i>p</i> -NO <sub>2</sub> Ph	75:25
<i>p</i> -FPh	52:48
<i>p</i> -CH <sub>3</sub> OPh	39:61

- 3.7 a. Create Hammett plots versus  $\sigma$  and  $\sigma^-$  for the reaction shown below from the data given. Determine the value of  $\rho$  and compare the correlation with the two sets of substituent constants.



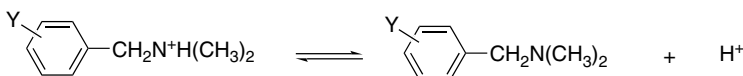
Y	$k M^{-1} s^{-1}$
H	37.4
CH <sub>3</sub> O	21.3
CH <sub>3</sub>	24.0
Br	95.1
NO <sub>2</sub>	1430

- b. The pseudo-first order rate constants for acid-catalyzed hydration of substituted styrenes in 3.5M HClO<sub>4</sub> at 25° C are given. Plot the data against  $\sigma$  and  $\sigma^+$  and determine  $\rho$  and  $\rho^+$ . Interpret the significance of the results.



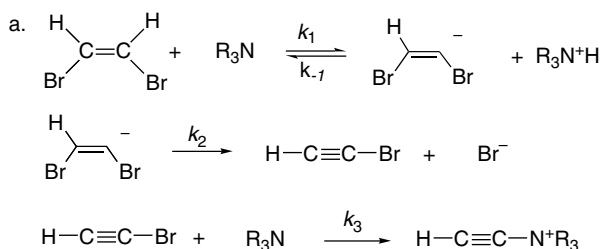
Y	$k \times 10^8 s^{-1}$
4-CH <sub>3</sub> O	488,000
4-CH <sub>3</sub>	16,400
H	811
4-Cl	318
4-NO <sub>2</sub>	1.44

- c. The acidity of a series of substituted benzyldimethylammonium ions has been measured. Determine whether these data are correlated by the Hammett equation using  $\sigma$  and  $\sigma^+$ . What is the value of  $\rho$ ? What interpretation do you put on its sign and magnitude?

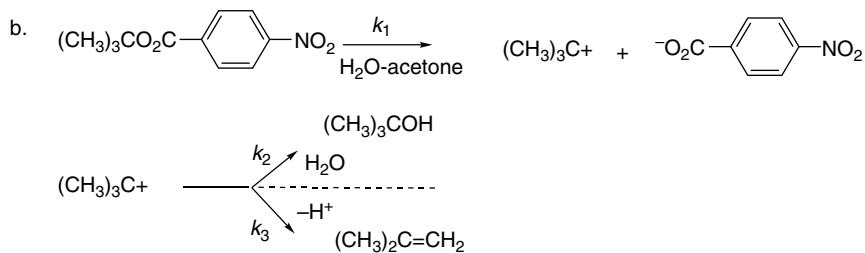


Y	p <i>K<sub>a</sub></i>
4-CH <sub>3</sub> O	9.32
3-CH <sub>3</sub> O	9.04
4-CH <sub>3</sub>	9.22
4-F	8.94
H	9.03
3-NO <sub>2</sub>	8.19
4-NO <sub>2</sub>	8.14
4-Cl	8.83
3-Cl	8.67

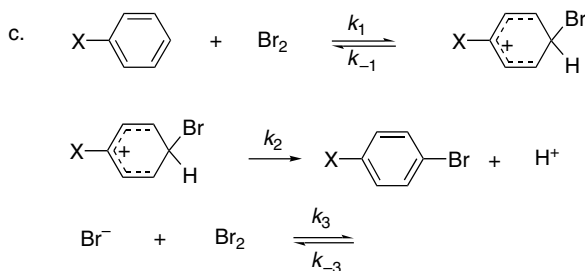
3.8. Write the rate law that would apply to the rate of product formation for each of the following reaction mechanisms.



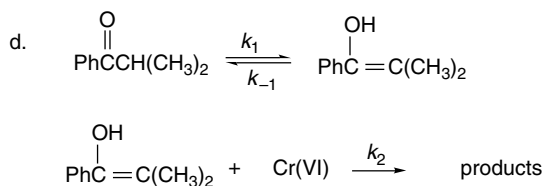
where the second step is rate-determining and the first step is an equilibrium



where the competing product-forming steps are faster than the first step



assuming that the  $\sigma$  complex is a steady state intermediate and that the final step is a rapid equilibrium that converts some of the initial  $\text{Br}_2$  to unreactive  $\text{Br}_3^-$ . What is the form of the rate expression if the intermediate of the first step goes on to product much faster than it reverts to starting material and if the equilibrium constant for  $\text{Br}_3^-$  formation is large.

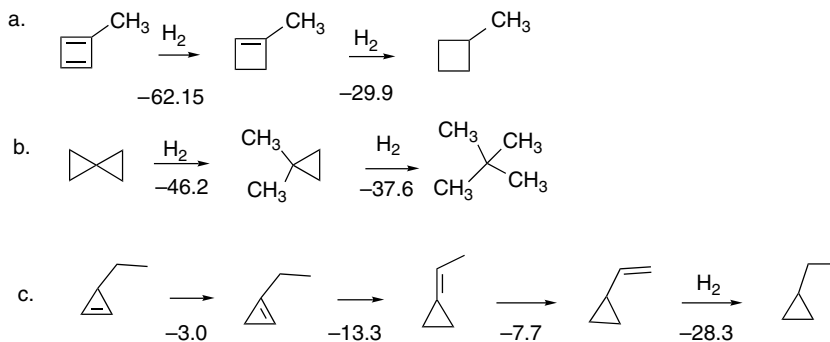


making no assumptions about the relative magnitude of  $k_1$ ,  $k_{-1}$ , or  $k_2$ .

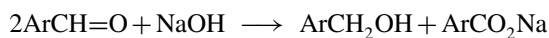
- 3.9. One method of estimating “aromatic stabilization” is to compare the heats of hydrogenation of cyclic conjugated systems with an acyclic molecule having the same number of conjugated bonds and  $\pi$  electrons. The table below gives the AM1 calculated heat of hydrogenation for various cyclic conjugated systems and for the corresponding polyene [ $\Delta H_{\text{H}_2}$  (ref.)] For example, for benzene the comparison would be with 1,3,5-hexatriene. Calculate the aromatic stabilization or antiaromatic destabilization for each system. What conclusions do you draw? Relate your conclusions to HMO theory in Chapter 1. How does this computation deal with “strain?”

System	$\Delta H_{\text{H}_2}$ (ref.)	$\Delta H_{\text{H}_2}$ (cyclic system)
Cyclopropenyl cation	-13.3	10.6
Cyclopropenyl anion	4.7	-59.6
Cyclobutadiene	-50.7	-101.9
Cyclopentadienyl cation	-19.4	-72.9
Cyclopentadienyl anion	-0.3	-2.9
Benzene	-72.2	-45.0
Cycloheptatrienyl cation	-31.4	-23.9
Cycloheptatrienyl anion	-11.4	-26.4

- 3.10. A number of experimentally inaccessible  $\Delta H$  values have been computed at the G2(MP2) level and are given below in kcal/mol. Taking for comparison  $\Delta H_{\text{H}_2}$  of ethene as  $-32.4$  kcal/mol, of 1-butene as  $-30.3$  kcal/mol, and of cyclopropane to propane as  $-38.6$  kcal/mol, indicate what factors lead to the observed differences in each step of the sequences shown.



- 3.11. The Cannizzaro reaction is a disproportionation that takes place in strongly basic solution and converts aromatic aldehydes to the corresponding benzyl alcohol and sodium benzoate.

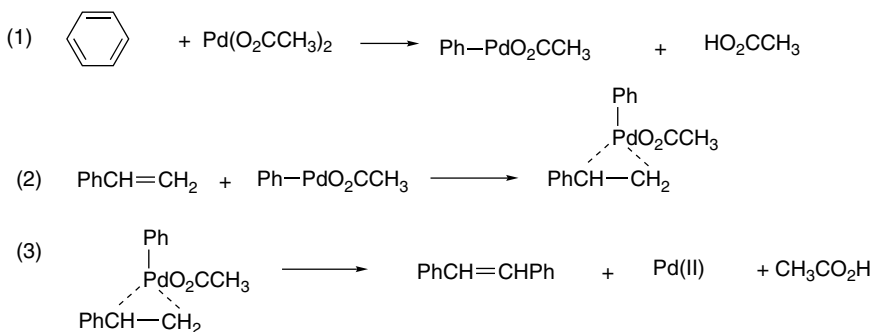


Several mechanisms, all of which involve a hydride transfer as a key step, have been postulated. On the basis of the following information, formulate one or more mechanisms that would be consistent with all the data provided. Indicate the significance of each observation with respect to the mechanism(s) you postulate.

1. When the reaction is carried out in  $D_2O$ , the benzyl alcohol contains no deuterium in the methylene group.
2. When the reaction is carried out in  $H_2^{18}O$ , both the benzyl alcohol and sodium benzoate contain  $^{18}O$ .
3. The overall reaction rate is given by the expression

$$\text{Rate} = k_{\text{obs}}[\text{PhCH=O}]^2[\text{OH}^-]$$

4. The rates of substituted benzaldehydes are correlated by a Hammett LFER with  $\rho = +3.76$ .
  5. The solvent isotope effect  $k_{D_2O}/k_{H_2O} = 1.90$
- 3.12. A mechanism for alkene arylation catalyzed by Pd(II) is outlined below. The isotope effect  $k_H/k_D$  was found to be 5 when benzene- $d_6$  was used. There was no isotope effect when styrene- $\beta-d_2$  was used. Which steps in the reaction mechanism could be rate determining, given this information on isotope effects?



- 3.13. Comparison of the gas phase acidity of substituted benzoic acids with  $pK_a$  values in aqueous solutions reveals some interesting comparisons.
1. The trend in acidity as a function of substituent is the same for both gas phase and aqueous solution, but the substituent effects are much stronger in the gas phase. (The  $\Delta\Delta G$  for any give substituent is about 10 times larger in the gas phase.)
  2. Whereas acetic and benzoic acid are of comparable acidity in water, benzoic acid is considerably more acidic in the gas phase. ( $pK_a$  values are 4.75 and 4.19, respectively; and  $\Delta G$  of ionization is 8.6 kcal/mol more positive for acetic acid.)
  3. While the substituent effect in the gas phase is nearly entirely an enthalpy effect, it is found that in solution, the substituent effect is largely due to changes in  $\Delta S$ .

Discuss how difference between the gas phase and solution can cause these effects.

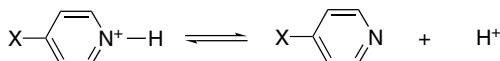
- 3.14. It has been found that the  $^{13}C$  chemical shift of aromatic ring carbons are a good indicator of the intrinsic electron-releasing or electron-withdrawing capacity of substituents, without any perturbation from approaching reagents. Such perturbation is always present when substituent effects are measured on the basis of

reactivity. The changes in chemical shifts of C(4) in some substituted benzenes are given below. Plot these against  $\sigma$ ,  $\sigma^+$ , and  $\sigma^-$ . What conclusions do you draw from these plots in regard to the mix of resonance and polar components in each of the  $\sigma$  values?

X	$\Delta\delta^a$	X	$\Delta\delta^a$
NH <sub>2</sub>	-9.86	CF <sub>3</sub>	3.29
CH <sub>3</sub> O	-7.75	CN	3.80
F	-4.49	CH <sub>3</sub> CO	4.18
Cl	-2.05	CH <sub>3</sub> O <sub>2</sub> C	4.12
Br	-1.62	CH <sub>3</sub> SO <sub>2</sub>	4.64
CH <sub>3</sub>	-2.89	NO <sub>2</sub>	5.53

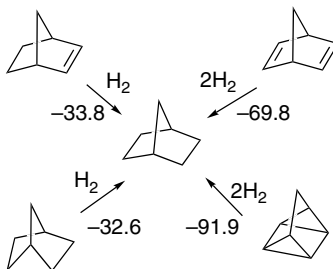
a.  $\delta\Delta$  is the change in chemical shift in ppm relative to benzene in CCl<sub>4</sub> solution.

- 3.15. The ionization constants ( $pK_a$ ) of 4-substituted pyridines have been measured, as have the  $\Delta H$  of ionization at 25° C. Calculate  $\Delta S$  for each ionization. Compare the contribution of  $\Delta H$  and  $\Delta S$  to the free energy of ionization. Test the data for linear free-energy correlations. Are the LFER dominated by the  $\Delta H$  or  $\Delta S$  term?



X	$pK_a$	$\Delta H$ (kcal/mol)	X	$pK_a$	$\Delta H$ (kcal/mol)
H	5.21	4.8	Cl	3.83	3.6
NH <sub>2</sub>	9.12	11.3	Br	3.75	3.5
CH <sub>3</sub> O	6.58	6.8	CN	1.86	1.3
CH <sub>3</sub>	6.03	6.1			

- 3.16 a. Norbornene, norbornadiene, nortricyclane, and quadricyclane can all be hydrogenated to norbornane. The heats of hydrogenation are given in the chart. These data allow calculation of  $\Delta H_f$  for the other derivatives and the results are given as Exp. in the table. The table also gives  $\Delta H_f$  values calculated for each compound by MM and three semiempirical MO methods. Compare the accuracy of the semiempirical methods in predicting the experimental heats of formation.



Heats of Hydrogenation in kcal/mol

Calculated Enthalpies of Formation of Norbornane Analogs<sup>a</sup>

## CHAPTER 3

*Structural Effects on  
Stability and Reactivity*

Compound	MM <sup>b</sup>	MNDO	AM1	PM3	Exp.
Norbornadiene	55.5(30.9)	62.7	67.7	58.8	57.4
Norbornene	19.5(22.7)	25.3	26.0	22.0	21.4
Norbornane	-12.8(18.1)	-10.4	-14.4	-13.7	-12.4
Nortricyclane	19.5(52.6)	27.1	33.8	26.0	20.2
Quadricyclane	79.4(108.1)	79.1	104.4	86.3	79.5

a. In kcal/mol.

b. The calculated strain energies are given in parentheses.

- b. Subsequently, the same compounds were computed by ab initio and DFT methods. Isodesmic reactions were used to compare the  $\Delta H_f$  of the compounds (except for G3(MP2), where atomization energies were used). Compare the ab initio and DFT results with the semiempirical results from Part (a).

Calculated Enthalpies of Formation of Norbornane Analogs<sup>a</sup>

Compound	G2	G2(MP)	G2(MP2, SVP)G3(MP2)	B3LYP
Norbornadiene	56.3	57.0	56.0	66.5
Norbornene	18.5	19.1	18.0	28.9
Norbornane	-14.1	-13.6	-14.7	-3.2
Nortricyclane	16.2	16.9	15.5	24.8
Quadricyclane	79.2	80.1	80.1	83.7

a. In kcal/mol.

- c. Heats of hydrogenation have also been calculated from the semiempirical data. Since the heats of hydrogenation include the  $\Delta H_f$  of H<sub>2</sub>, which is zero, they can be calculated as follows:

$$\Delta H_{\text{H}_2} = \Delta H_{f\text{product}} - \Delta H_{f\text{reactant}}$$

This leads to the calculated  $\Delta H_{\text{H}_2}$  shown below. The  $\Delta H_{\text{H}_2}$  can also be calculated on a strain compensation basis:

$$\Delta H_{\text{H}_2} = \Delta H_{f\text{product}} - \Delta H_{f\text{reactant}} + \text{strain relief}$$

The calculated values are included in the table. Compare the calculated and experimental results.

Calculated Heats of Hydrogenation of Norbornane Analogs<sup>a</sup>

Compound	MM <sup>b</sup>	MNDO	AM1	PM3	Exp.
Norbornadiene	-68.3(1.5)	-73.1(-3.3)	-82.1(-12.3)	-72.5(-2.7)	-69.8
Norbornene	-32.3(1.5)	-35.7(-1.9)	-40.4(-6.6)	-35.7(-1.9)	-33.8
Nortricyclane	-32.3(0.3)	-37.5(-4.9)	-48.2(-15.6)	-33.7(-1.1)	-32.6
Quadricyclane	-92.2(-0.3)	-89.5(2.4)	-118.8(-26.9)	-100.0(-8.1)	-91.9

a. The numbers in parenthesis are the difference with the experimental value on a strain-compensated basis.

- 3.17. The second-order rate constants for the reaction of a number of amines with benzyl chloride are tabulated below. Calculate  $\Delta H^\ddagger$  and  $\Delta S^\ddagger$  from the data.

Compare the reactivity of the various amines. What trends and correlations between reactivity and  $\Delta H^\ddagger$  do you note?

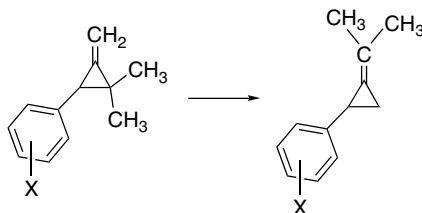
### Rate Constants for the Reaction of Tertiary Amines with Benzyl Chloride

Amine	Rate constants $10^5 k_2 (M^{-1} s^{-1})$								
	20° C	24° C	30° C	40° C	50° C	60° C	70° C	80° C	90° C
(CH <sub>3</sub> ) <sub>3</sub> N	38.2	50.2	72.8						
(C <sub>2</sub> H <sub>5</sub> ) <sub>3</sub> N				1.67	3.07	4.54	7.49		
(C <sub>3</sub> H <sub>7</sub> ) <sub>3</sub> N				0.354	0.633	1.05	1.76	3.04	
(C <sub>4</sub> H <sub>9</sub> ) <sub>3</sub> N				0.471	0.844	1.24	1.94	3.22	
(C <sub>6</sub> H <sub>13</sub> ) <sub>3</sub> N				0.290	0.566	0.860	1.54	2.62	
(C <sub>8</sub> H <sub>17</sub> ) <sub>3</sub> N				0.336	0.570	0.912	1.60	2.73	
PhN(CH <sub>3</sub> ) <sub>2</sub>						0.135	0.233	0.384	0.698
Pyridine				0.168	0.337	0.910	1.55	2.63	
Quinoline					0.051	0.105	0.226	0.457	0.820

3.18. Some data are given below for both gas phase ( $\Delta G$ ) and DMSO (p*K*) acidity of substituted toluenes, phenylacetonitriles, and phenylmalononitriles that illustrate the strongly acidifying effect of the cyano substituent. For each series, plot  $\Delta G$  versus p*K*. Do the plots show any evidence of a solvent attenuation effect; that is, do the substituent effects appear to be weaker in DMSO than in the gas phase?

Group	$\sigma$	Toluenes		Phenylacetonitriles		Phenylmalononitriles	
		$\Delta G_{\text{gas}}$	p <i>K</i>	$\Delta G_{\text{gas}}$	p <i>K</i>	$\Delta G_{\text{gas}}$	p <i>K</i>
H	0.0	373.7	43.0	344.1	21.9	314.3	4.24
4-NO <sub>2</sub>	0.78	345.2	20.4	323.3	12.3	299.5	-1.8
3-NO <sub>2</sub>	0.71	355.7	33.5	330.9	18.1	303.0	1.7
4-CN	0.66	353.6	30.7	327.9	16.0		
3-CN	0.56			332.3	18.7	304.4	2.2
4-SO <sub>2</sub> CF <sub>3</sub>	0.96	340.7	24.1				
4-SO <sub>2</sub> Ph		352.1	29.8				
4-SO <sub>2</sub> CH <sub>3</sub>	0.72	359.3					
4-PhCO	0.43	353.5	26.8				
4-CH <sub>3</sub> CO	0.50	354.9					
4-CF <sub>3</sub> CO	0.80	344.1					
4-CH <sub>3</sub> O <sub>2</sub> C	0.45	355.4					
4-(CH <sub>3</sub> ) <sub>2</sub> NCO	0.36	367.0					
4-CF <sub>3</sub>	0.54			332.9	18.1		
3-CF <sub>3</sub>	0.43			335.3	19.2		
4-Cl	0.23			338.5	20.5	309.0	3.14
3-Cl	0.37			337.5	19.5	308.8	2.7
4-F	0.06			342.4	22.2		
3-F	0.34			344.0	20.0		
4-CH <sub>3</sub> O	-0.27			345.0	23.8	315.4	5.68
3-CH <sub>3</sub> O	0.12			342.8			
4-CH <sub>3</sub>	-0.17			345.0	22.9	315.7	4.85
3-CH <sub>3</sub>	-0.07			344.2			
4-(CH <sub>3</sub> ) <sub>2</sub> N	-0.83			346.6	24.6		

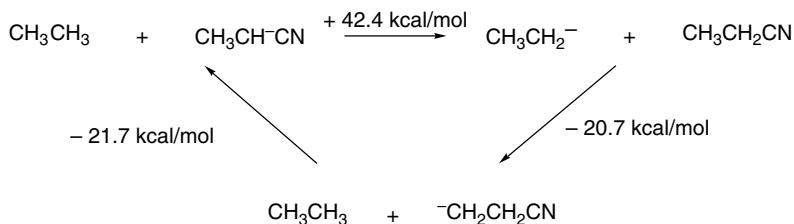
- 3.19. The rate of thermal rearrangement of 3-aryl-2,2-dimethylmethylene-cyclopropanes has been studied as a function of aryl substituents. Some of the data are given below. Examine the rate data for correlation with the Hammett  $\sigma$ -substituent constants. What conclusion do you draw about the mechanism?



Substituent	$10^4 k s^{-1}$	Substituent	$10^4 k s^{-1}$
4-(CH <sub>3</sub> ) <sub>2</sub> N	28.2 <sup>a</sup>	3-CH <sub>3</sub> O	3.40
4-CH <sub>2</sub> =CH	16.7 <sup>a</sup>	3-Cl	3.30
4-NO <sub>2</sub>	13.5 <sup>a</sup>	3-F	3.17
4-CN	10.28	3-CF <sub>3</sub>	3.08
4-Ph	10.3 <sup>a</sup>	4-F	2.98
4-CH <sub>3</sub> S	9.53	3-NO <sub>2</sub>	2.76 <sup>a</sup>
4-CO <sub>2</sub> CH <sub>3</sub>	8.09	3-CN	2.69
4-CH <sub>3</sub> O	6.16		
4-(CH <sub>3</sub> ) <sub>3</sub> Si	5.24		
4-Br	4.88		
4-(CH <sub>3</sub> ) <sub>3</sub> C	4.78		
4-Cl	4.75		
4-CH <sub>3</sub>	4.65		
4-CF <sub>3</sub>	4.25		
3-(CH <sub>3</sub> ) <sub>3</sub> Si	3.87		
3-CH <sub>3</sub>	3.82		
H	3.58		

a. Calculated from relative rate at 80° C in benzene.

- 3.20. The series of isodesmic reactions shown below has been calculated at the MP2/aug-cc-PVDZ level. The results are in good agreement with experimental gas phase proton affinity data.

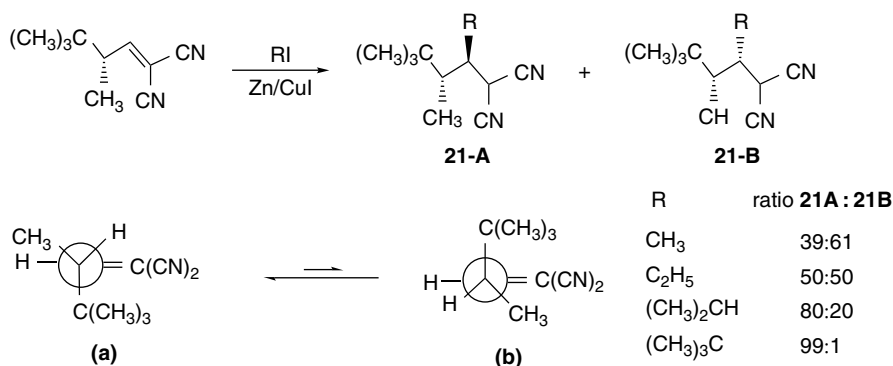


Data are also available for the  $pK_a$  of mono-, di-, and tri-cyanomethane. These data suggest substantially less cumulative drop-off as compared to an acetyl substituent. The first acetyl group causes a substantially *larger* increase in acidity, whereas the second acetyl has a *smaller* effect.

	$\text{CH}_4$	$\text{CH}_3\text{CN}$	$\text{CH}_2(\text{CN})_2$	$\text{CH}(\text{CN})_3$	$\text{CH}_3\overset{\text{O}}{\parallel}\text{CCH}_3$	$\text{CH}_3\overset{\text{O}}{\parallel}\text{CCH}_2\overset{\text{O}}{\parallel}\text{CCH}_3$
p <i>K</i>	49.6	29.4	11.7	-5.1	19.3	8.9

$\beta$ -Cyano substituents also have a quite strong acidifying effect. A value of  $29 \pm 6$  kcal/mol has been estimated, as compared to 42 kcal/mol for  $\alpha$ -cyano. Structural computations find a shortening of the C( $\alpha$ )-CN bond in  $\alpha$ -cyanoethyl anion but a lengthening of the C( $\beta$ )-CN bond in the  $\beta$ -cyanoethyl anion. What structural features of the CN might contribute to its anion stabilizing capacity, as compared with other EWG substituents such as acetyl.

- 3.21. The diastereoselectivity of alkyl radical addition to substituted alkylidene malonitriles is a function of the size of the attacking radical when there is a bulky substituent at the  $\gamma$ -carbon. Conformational analysis of the reactant indicates that it prefers conformation **a** over **b** by 3.0 kcal/mol. Suggest a TS structure, showing reactant conformation and reagent trajectory that is in accord with these results. Use the Curtin-Hammet principle (p. 296) to construct a reaction energy diagram that illustrates the product composition in terms of TS energy.



- 3.22. In the interpretation of substituent effects, consideration must be given as to whether the effect is primarily on the reactant or the product. Some data pertaining to the changes in some substituted benzoic acids, derived from PM3 computations, are given below. The calculated  $\delta\Delta H$  for ionization in the gas phase is given, as are the charges of the H,  $\text{CO}_2\text{H}$ , and  $\text{CO}_2^-$  groups and the energy of the anion HOMO. Construct correlation plots of  $\delta\Delta H$  with each of the structural properties and also against the values of  $\sigma_m$  and  $\sigma_p$  from Table 3.26. What conclusions do you draw about the effects of substituents on H,  $\text{CO}_2\text{H}$ , and  $\text{CO}_2^-$ , and how would these results be reflected in relative acidity?

Substituent	$\delta\Delta H$	$q_{\text{H}}$	$q_{\text{CO}_2\text{H}}$	$q_{\text{CO}_2^-}$	HOMO <sub>(anion)</sub> (eV)
H	0	0.229	-0.0503	-1.237	-4.4549
4-F	-3.68	0.231	-0.0436	-1.229	-4.6395
3-F	-4.02	0.231	-0.0415	-1.224	-4.6487

(Continued)

Substituent	$\delta\Delta H$	$qH$	$qCO_2H$	$qCO_2^-$	HOMO <sub>(anion)</sub> (eV)
4-Cl	-3.11	0.230	-0.0460	-1.227	-4.6383
3-Cl	-3.10	0.230	-0.0440	-1.226	-4.6323
4-CN	-7.95	0.232	-0.0385	-1.215	-4.8765
3-CN	-7.49	0.232	-0.0368	-1.217	-4.8451
4-NO <sub>2</sub>	-12.98	0.234	-0.0297	-1.199	-5.1198
3-NO <sub>2</sub>	-11.14	0.235	-0.0277	-1.207	-5.0247
4-CH <sub>3</sub>	+0.44	0.228	-0.0519	-1.237	-4.4563
3-CH <sub>3</sub>	+0.22	0.228	-0.0514	-1.237	-4.4585
4-OCH <sub>3</sub>	+0.15	0.228	-0.0520	-1.237	-4.5000
3-OCH <sub>3</sub>	-0.36	0.228	-0.0490	-1.230	-4.5047

3.23. From the kinetic data below, calculate  $\Delta H^*$  and  $\Delta S^*$  for each nucleophilic substitution reaction with *n*-butyl tosylate in methanol and DMSO. What trends do you note in  $\Delta H^*$  and how would you explain them? What trends do you note in  $\Delta S^*$  and how would you explain them?

Nucleophile	Solvent	Second-order rate constants (in mol <sup>-1</sup> s <sup>-1</sup> × 10 <sup>4</sup> ) at °C			
		$k_{20}$	$k_{30}$	$k_{40}$	$k_{50}$
Cl <sup>-</sup>	DMSO	5.06	16.7	50.4	
	MeOH	0.00550	0.0226	0.0852	
N <sub>3</sub> <sup>-</sup>	DMSO	16.1	48.3	135	
	MeOH	0.152	0.514	1.66	
Br <sup>-</sup>	DMSO	1.75	5.69	17.8	
	MeOH	0.0191	0.0721	0.250	
SCN <sup>-</sup>	DMSO	0.115	0.365	1.11	
	MeOH	0.0512	0.165	0.481	
I <sup>-</sup>	DMSO		1.75	5.50	16.0
	MeOH	0.0767	0.275	0.956	

3.24. Use the computed values of  $H_{298}$  (in Hartrees) from the reference set below to construct homo desmotic reactions and calculate the stabilization or destabilization (strain) of the following molecules.

- 1,3,5,7-Cyclooctatetraene,  $H_{298} = -308.96286$
- Bicyclo[1.1.0]butane,  $H_{298} = -155.62203$
- Tetracyclo[3.2.0.0<sup>4,9</sup>.0<sup>6,8</sup>]heptane (Quadricyclane),  $H_{298} = -567.74092$

Reference Data<sup>a</sup>

CH <sub>4</sub>	-40.40707	CH <sub>2</sub> =CH <sub>2</sub>	-78.41192	<i>c</i> -C <sub>3</sub> H <sub>6</sub>	-116.37701
C <sub>2</sub> H <sub>6</sub>	-79.62641	CH <sub>3</sub> CH=CH <sub>2</sub>	-117.63998	<i>c</i> -C <sub>4</sub> H <sub>8</sub>	-156.85340
C <sub>3</sub> H <sub>8</sub>	-118.85022	CH <sub>2</sub> =C=CH <sub>2</sub>	-116.41308	C <sub>6</sub> H <sub>6</sub>	-231.77508
C <sub>4</sub> H <sub>10</sub>	-158.07430	(CH <sub>3</sub> ) <sub>2</sub> C=CH <sub>2</sub>	-156.86995		
<i>i</i> -C <sub>4</sub> H <sub>10</sub>	-158.07751	CH <sub>2</sub> =CHCH=CH <sub>2</sub>	-155.65855		

a. L. A. Curtiss, K. Raghavachari, P. C. Refern, and J. A. Pople, *J. Chem. Phys.*, **106**, 1063 (1997)

# Nucleophilic Substitution

## Introduction

Nucleophilic substitution at tetravalent ( $sp^3$ ) carbon is a fundamental reaction of broad synthetic utility and has been the subject of detailed mechanistic study. An interpretation that laid the basis for current understanding was developed in England by C. K. Ingold and E. D. Hughes in the 1930s.<sup>1</sup> Organic chemists have continued to study substitution reactions; much detailed information about these reactions is available and a broad mechanistic interpretation of nucleophilic substitution has been developed from the accumulated data. At the same time, the area of nucleophilic substitution also illustrates the fact that while a broad conceptual framework can outline the general features to be expected for a given system, finer details reveal distinctive aspects that are characteristic of specific systems. As the chapter unfolds, the reader will come to appreciate both the breadth of the general concepts and the special characteristics of some of the individual systems.

## 4.1. Mechanisms for Nucleophilic Substitution

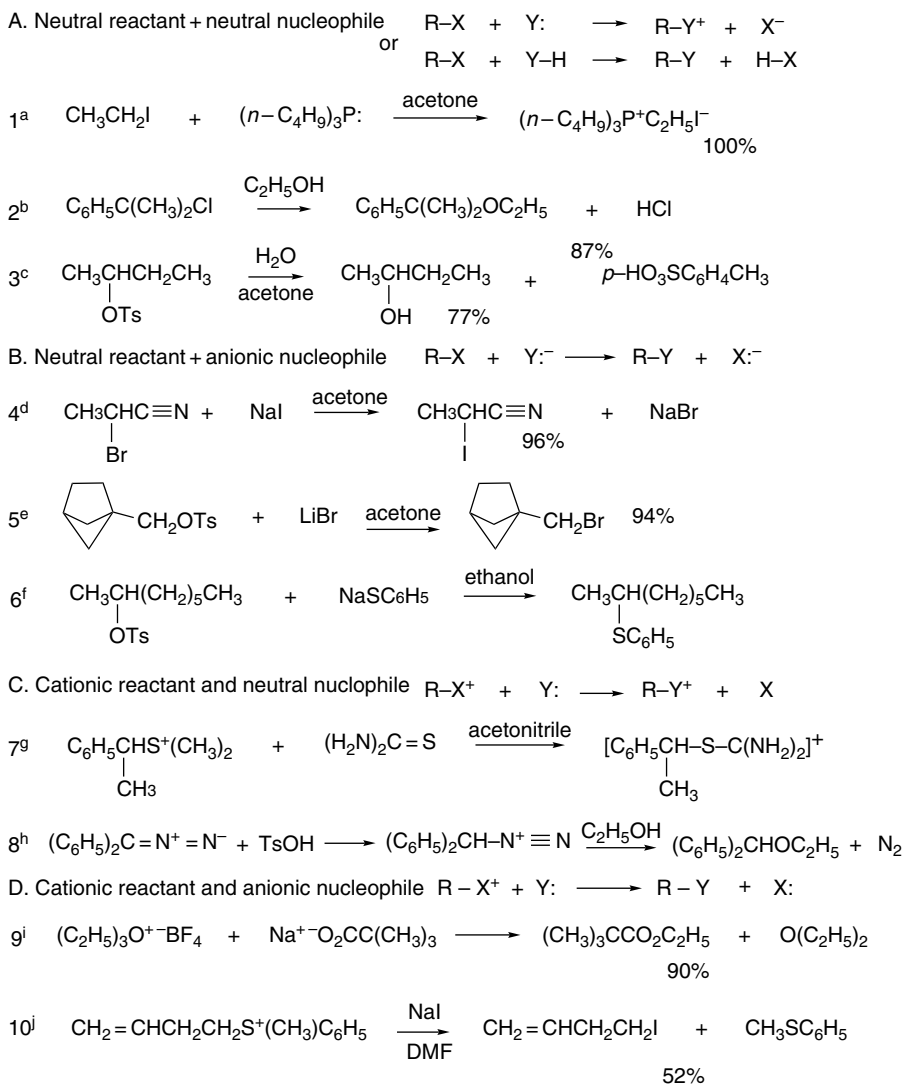
Nucleophilic substitution reactions may involve several different combinations of charged and uncharged species as reactants. The equations in Scheme 4.1 illustrate the four most common charge types. The most common reactants are neutral halides or sulfonates, as illustrated in Parts A and B of the scheme. These compounds can react with either neutral or anionic nucleophiles. When the nucleophile is the solvent, as in Entries 2 and 3, the reaction is called a *solvolysis*. Reactions with anionic nucleophiles, as in Entries 4 to 6, are used to introduce a variety of substituents such as cyanide and azide. Entries 7 and 10 show reactions that involve sulfonium ions, in which a neutral sulfide is the leaving group. Entry 8 involves generation of the diphenylmethyl diazonium ion by protonation of diphenyldiazomethane. In this reaction, the leaving

<sup>1</sup> C. K. Ingold, *Structure and Mechanism in Organic Chemistry*, 2nd Edition, Cornell University Press, Ithaca, NY, 1969.

group is molecular nitrogen. Alkyl diazonium ions can also be generated by nitrosation of primary amines (see Section 4.1.5). Entry 9 is a reaction of an oxonium ion. These ions are much more reactive than sulfonium ions and are usually generated by some in situ process.

The reactions illustrated in Scheme 4.1 show the relationship of reactants and products in nucleophilic substitution reactions, but say nothing about mechanism. In

### Scheme 4.1. Representative Nucleophilic Substitution Reactions



- a. S. A. Buckler and W. A. Henderson, *J. Am. Chem. Soc.*, **82**, 5795 (1960).  
 b. R. L. Buckson and S. G. Smith, *J. Org. Chem.*, **32**, 634 (1967).  
 c. J. D. Roberts, W. Bennett, R. E. McMahon, and E. W. Holroyd, *J. Am. Chem. Soc.*, **74**, 4283 (1952).  
 d. M. S. Newman and R. D. Closson, *J. Am. Chem. Soc.*, **66**, 1553 (1944).  
 e. K. B. Wiberg and B. R. Lowry, *J. Am. Chem. Soc.*, **85**, 3188 (1963).  
 f. H. L. Goering, D. L. Towns, and B. Dittmar, *J. Org. Chem.*, **27**, 736 (1962).  
 g. H. M. R. Hoffmann and E. D. Hughes, *J. Chem. Soc.*, 1259 (1964).  
 h. J. D. Roberts and W. Watanabe, *J. Am. Chem. Soc.*, **72**, 4869 (1950).  
 i. D. J. Raber and P. Gariano, *Tetrahedron Lett.*, 4741 (1971).  
 j. E. J. Corey and M. Jautelat, *Tetrahedron Lett.*, 5787 (1968).

order to develop an understanding of the mechanisms of such reactions, we begin by reviewing the limiting cases as defined by Hughes and Ingold, namely the *ionization mechanism* ( $S_N1$ , substitution-nucleophilic-unimolecular) and the *direct displacement mechanism* ( $S_N2$ , substitution-nucleophilic-bimolecular). We will find that in addition to these limiting cases, there are related mechanisms that have aspects of both ionization and direct displacement.

#### 4.1.1. Substitution by the Ionization ( $S_N1$ ) Mechanism

The ionization mechanism for nucleophilic substitution proceeds by rate-determining heterolytic dissociation of the reactant to a tricoordinate *carbocation*<sup>2</sup> and the *leaving group*. This dissociation is followed by rapid combination of the electrophilic carbocation with a Lewis base (*nucleophile*) present in the medium. A potential energy diagram representing this process for a neutral reactant and anionic nucleophile is shown in Figure 4.1.

The ionization mechanism has several distinguishing features. The ionization step is rate determining and the reaction exhibits first-order kinetics, with the rate of decomposition of the reactant being *independent of the concentration and identity of the nucleophile*. The symbol assigned to this mechanism is  $S_N1$ , for *substitution, nucleophilic, unimolecular*:

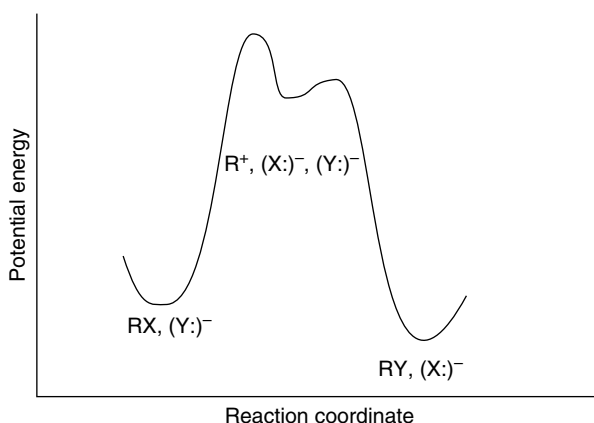
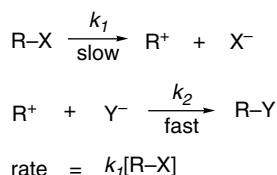


Fig. 4.1. Reaction energy profile for nucleophilic substitution by the ionization ( $S_N1$ ) mechanism.

<sup>2</sup> Tricoordinate carbocations were originally called *carbonium ions*. The terms methyl cation, butyl cation, etc., are used to describe the corresponding tricoordinate cations. *Chemical Abstracts* uses as specific names methylium, ethylium, 1-methylethylum, and 1,1-dimethylethylum to describe the methyl, ethyl, 2-propyl, and *t*-butyl cations, respectively. We use *carbocation* as a generic term for carbon cations. The term *carbonium ion* is now used for pentavalent positively charged carbon species.

As the rate-determining step is endothermic with a late TS, application of *Hammond's postulate* (Section 3.3.2.2) indicates that the TS should resemble the product of the first step, the carbocation intermediate. Ionization is facilitated by factors that lower the energy of the carbocation or raise the energy of the reactant. The rate of ionization depends primarily on reactant structure, including the identity of the leaving group, and the solvent's ionizing power. The most important electronic effects are stabilization of the carbocation by electron release, the ability of the leaving group to accept the electron pair from the covalent bond that is broken, and the capacity of the solvent to stabilize the charge separation that develops in the TS. Steric effects are also significant because of the change in coordination that occurs on ionization. The substituents are spread apart as ionization proceeds, so steric compression in the reactant favors ionization. On the other hand, geometrical constraints that preclude planarity of the carbocation are unfavorable and increase the energy required for ionization.

The ionization process is very sensitive to solvent effects, which are dependent on the charge type of the reactants. These relationships follow the general pattern for solvent effects discussed in Section 3.8.1. Ionization of a neutral substrate results in charge separation, and solvent polarity has a greater effect at the TS than for the reactants. Polar solvents lower the energy of the TS more than solvents of lower polarity. In contrast, ionization of cationic substrates, such as trialkylsulfonium ions, leads to dispersal of charge in the TS and reaction rates are moderately retarded by more polar solvents because the reactants are more strongly solvated than the TS. These relationships are illustrated in Figure 4.2.

Stereochemical information can add detail to the mechanistic picture of the  $S_N1$  substitution reaction. The ionization step results in formation of a carbocation intermediate that is planar because of its  $sp^2$  hybridization. If the carbocation is sufficiently long-lived under the reaction conditions to diffuse away from the leaving group, it becomes symmetrically solvated and gives racemic product. If this condition is not met, the solvation is dissymmetric and product can be obtained with net retention or inversion of configuration, even though an achiral carbocation is formed. The extent of inversion or retention depends on the specific reaction. It is frequently observed that there is net *inversion of configuration*. The stereochemistry can be interpreted in terms of three different stages of the ionization process. The contact ion pair represents

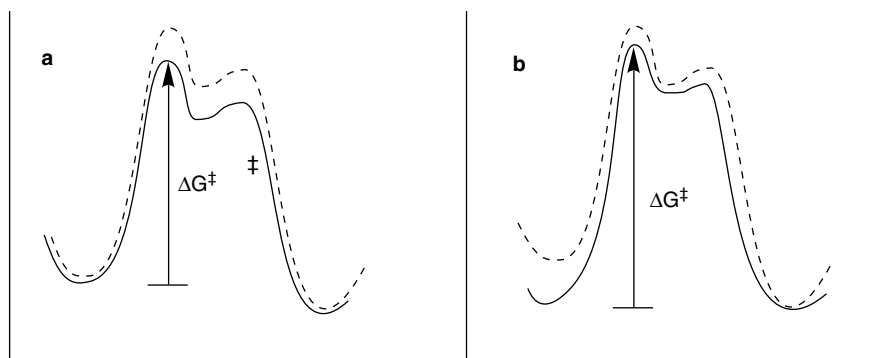
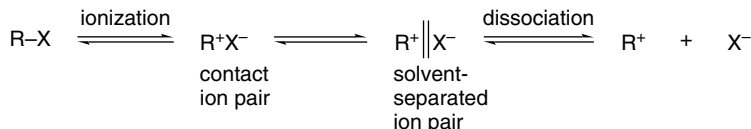


Fig. 4.2. Solid line: polar solvent; dashed line: nonpolar solvent. (a) Solvent effects on  $R-X \rightarrow R^+ + X^-$ . Polar solvents increase the rate by stabilization of the  $R^{\delta+} \cdots X^{\delta-}$  transition state. (b) Solvent effect on  $R-X^+ \rightarrow R^+ + X$ . Polar solvents decrease the rate because stabilization of  $R-\delta^+-X$  transition state is less than for the more polar reactant.

a very close association between the cation and anion formed in the ionization step. The solvent-separated ion pair retains an association between the two ions, but with intervening solvent molecules. Only at the dissociation stage are the ions independent and the carbocation symmetrically solvated. The tendency toward net inversion is believed to be due to electrostatic shielding of one face of the carbocation by the anion in the ion pair. The importance of ion pairs is discussed further in Sections 4.1.3 and 4.1.4.



According to the ionization mechanism, if the same carbocation can be generated from more than one precursor, its subsequent reactions should be independent of its origin. But, as in the case of stereochemistry, this expectation must be tempered by the fact that ionization initially produces an ion pair. If the subsequent reaction takes place from this ion pair, rather than from the completely dissociated and symmetrically solvated ion, the leaving group can influence the outcome of the reaction.

#### 4.1.2. Substitution by the Direct Displacement ( $S_N2$ ) Mechanism

The direct displacement mechanism is concerted and proceeds through a single rate-determining TS. According to this mechanism, the reactant is attacked by a nucleophile from the side opposite the leaving group, with bond making occurring simultaneously with bond breaking between the carbon atom and the leaving group. The TS has trigonal bipyramidal geometry with a pentacoordinate carbon. These reactions exhibit second-order kinetics with terms for both the reactant and nucleophile:

$$\text{rate} = k[\text{R-X}][\text{Nu :}]$$

The mechanistic designation is  $S_N2$  for *substitution, nucleophilic, bimolecular*. A reaction energy diagram for direct displacement is given in Figure 4.3. A symmetric diagram such as the one in the figure would correspond, for example, to exchange of iodide by an  $S_N2$  mechanism.



The frontier molecular orbital approach provides a description of the bonding interactions that occur in the  $S_N2$  process. The frontier orbitals are a filled nonbonding orbital on the nucleophile **Y**: and the  $\sigma^*$  antibonding orbital associated with the carbon undergoing substitution and the leaving group **X**. This antibonding orbital has a large lobe on carbon directed away from the C–X bond.<sup>3</sup> Back-side approach by the nucleophile is favored because the strongest initial interaction is between the filled orbital on the nucleophile and the antibonding  $\sigma^*$  orbital. As the transition state is approached, the orbital at the substitution site has *p* character. The MO picture predicts that the reaction will proceed with inversion of configuration, because the development

<sup>3</sup> L. Salem, *Chem. Brit.*, **5**, 449 (1969); L. Salem, *Electrons in Chemical Reactions: First Principles*, Wiley, New York, 1982, pp. 164–165.

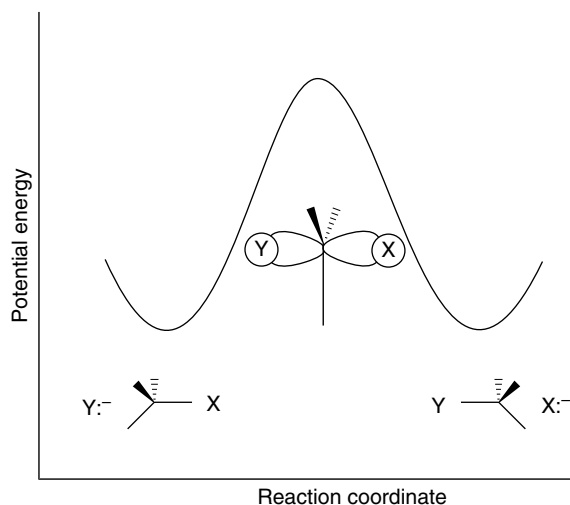
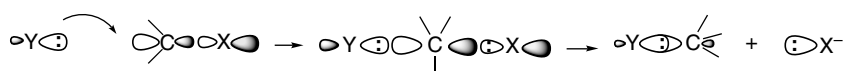
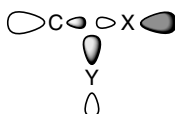


Fig. 4.3. Reaction energy profile for nucleophilic substitution by the direct displacement ( $S_N2$ ) mechanism.

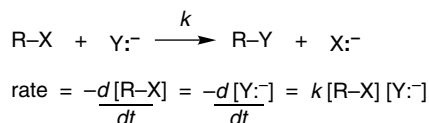
of the TS is accompanied by rehybridization of the carbon to the trigonal bipyramidal geometry. As the reaction proceeds on to product,  $sp^3$  hybridization is reestablished in the product with inversion of configuration.



Front-side approach is disfavored because the density of the  $\sigma^*$  orbital is less in the region between the carbon and the leaving group and, as there is a nodal surface between the atoms, a front-side approach would involve both a bonding and an antibonding interaction with the  $\sigma^*$  orbital.



The direct displacement ( $S_N2$ ) mechanism has both kinetic and stereochemical consequences.  $S_N2$  reactions exhibit second-order kinetics—first order in both reactant and nucleophile. Because the nucleophile is intimately involved in the rate-determining step, not only does the rate depend on its concentration, but the nature of the nucleophile is very important in determining the rate of the reaction. This is in sharp contrast to the ionization mechanism, in which the identity and concentration of the nucleophile do not affect the rate of the reaction.



Owing to the fact that the degree of coordination increases at the reacting carbon atom, the rates of  $S_N2$  reactions are very sensitive to the steric bulk of the substituents.

The optimum reactant from a steric point of view is  $\text{CH}_3\text{-X}$ , because it provides the minimum hindrance to approach of the nucleophile. Each replacement of hydrogen by an alkyl group decreases the rate of reaction. As in the case of the ionization mechanism, the better the leaving group is able to accommodate an electron pair, the faster the reaction. Leaving group ability is determined primarily by the C–X bond strength and secondarily by the relative stability of the anion (see Section 4.2.3). However, since the nucleophile assists in the departure of the leaving group, the leaving group effect on rate is less pronounced than in the ionization mechanism.

Two of the key observable characteristics of  $\text{S}_{\text{N}}1$  and  $\text{S}_{\text{N}}2$  mechanisms are kinetics and stereochemistry. These features provide important evidence for ascertaining whether a particular reaction follows an ionization ( $\text{S}_{\text{N}}1$ ) or direct displacement ( $\text{S}_{\text{N}}2$ ) mechanism. Both kinds of observations have limits, however. Many nucleophilic substitutions are carried out under conditions in which the nucleophile is present in large excess. When this is the case, the concentration of the nucleophile is essentially constant during the reaction and the observed kinetics become *pseudo first order*. This is true, for example, when the solvent is the nucleophile (*solvolysis*). In this case, the kinetics of the reaction provides no evidence as to whether the  $\text{S}_{\text{N}}1$  or  $\text{S}_{\text{N}}2$  mechanism is operating. Stereochemistry also sometimes fails to provide a clear-cut distinction between the two limiting mechanisms. Many substitutions proceed with partial inversion of configuration rather than the complete racemization or inversion implied by the limiting mechanisms. Some reactions exhibit inversion of configuration, but other features of the reaction suggest that an ionization mechanism must operate. Other systems exhibit “borderline” behavior that makes it difficult to distinguish between the ionization and direct displacement mechanism. The reactants most likely to exhibit borderline behavior are secondary alkyl and primary and secondary benzylic systems. In the next section, we examine the characteristics of these borderline systems in more detail.

### 4.1.3. Detailed Mechanistic Description and Borderline Mechanisms

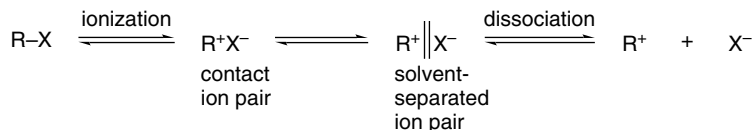
The ionization and direct displacement mechanisms can be viewed as the limits of a mechanistic continuum. At the  $\text{S}_{\text{N}}1$  limit, there is *no covalent interaction* between the reactant and the nucleophile in the TS for cleavage of the bond to the leaving group. At the  $\text{S}_{\text{N}}2$  limit, the bond-formation to the nucleophile is *concerted* with the bond-breaking step. In between these two limiting cases lies the borderline area in which the degree of covalent interaction with the nucleophile is intermediate between the two limiting cases. The concept of ion pairs was introduced by Saul Winstein, who proposed that there are two distinct types of ion pairs involved in substitution reactions.<sup>4</sup> The role of ion pairs is a crucial factor in detailed interpretation of nucleophilic substitution mechanisms.<sup>5</sup>

Winstein concluded that two intermediates preceding the dissociated carbocation were required to reconcile data on kinetics and stereochemistry of solvolysis reactions. The process of ionization initially generates a carbocation and counterion in immediate

<sup>4</sup> S. Winstein, E. Clippinger, A. H. Fainberg, R. Heck, and G. C. Robinson, *J. Am. Chem. Soc.*, **78**, 328 (1956); S. Winstein, B. Appel, R. Baker, and A. Diaz, *Chem. Soc. Spec. Publ.*, No. 19, 109 (1965).

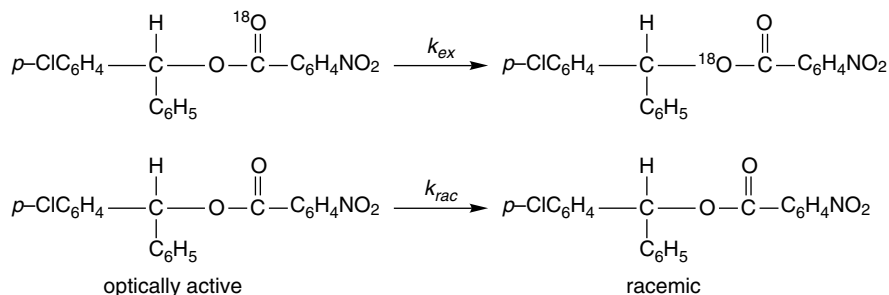
<sup>5</sup> J. M. Harris, *Prog. Phys. Org. Chem.*, **11**, 89 (1984); D. J. Raber, J. M. Harris, and P. v. R. Schleyer, in *Ion Pairs*, M. Szwarc, ed., John Wiley & Sons, New York, 1974, Chap. 3; T. W. Bentley and P. v. R. Schleyer, *Adv. Phys. Org. Chem.*, **14**, 1 (1977); J. P. Richard, *Adv. Carbocation Chem.*, **1**, 121 (1989); P. E. Dietze, *Adv. Carbocation Chem.*, **2**, 179 (1995).

proximity to one another. This species, called a contact ion pair (or intimate ion pair), can proceed to a solvent-separated ion pair in which one or more solvent molecules are inserted between the carbocation and leaving group, but in which the ions are kept together by the electrostatic attraction. The "free carbocation," characterized by symmetrical solvation, is formed by diffusion from the anion, a process known as *dissociation*.



Attack by a nucleophile or the solvent can occur at each stage. Nucleophilic attack on the contact ion pair is expected to occur with inversion of configuration, since the leaving group will shield the front side of the carbocation. At the solvent-separated ion pair stage, the nucleophile can approach from either face, particularly in the case where the solvent is the nucleophile. However, the anionic leaving group may shield the front side and favor attack by external nucleophiles from the back side. Reactions through dissociated carbocations should occur with complete *racemization*. According to this interpretation, the identity and stereochemistry of the reaction products are determined by the extent to which reaction with the nucleophile occurs on the un-ionized reactant, the contact ion pair, the solvent-separated ion pair, or the dissociated carbocation.

Many specific experiments support this general scheme. For example, in 80% aqueous acetone, the rate constant for racemization of *p*-chlorobenzhydryl *p*-nitrobenzoate and the rate of exchange of the  $^{18}\text{O}$  in the carbonyl oxygen can be compared with the rate of racemization.<sup>6</sup> At 100°C,  $k_{\text{ex}}/k_{\text{rac}} = 2.3$ .

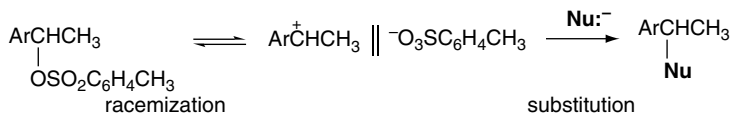


If it is assumed that ionization results in complete randomization of the  $^{18}\text{O}$  label in the carboxylate ion,  $k_{\text{ex}}$  is a measure of the rate of ionization with ion pair return and  $k_{\text{rac}}$  is a measure of the extent of racemization associated with ionization. The fact that the rate of isotopic exchange exceeds that of racemization indicates that ion pair collapse occurs with predominant retention of configuration. This is called *internal return*. When a better nucleophile is added to the system (0.14 M  $\text{NaN}_3$ ),  $k_{\text{ex}}$  is found to be unchanged, but no racemization of reactant is observed. Instead, the intermediate that can racemize is captured by azide ion and converted to substitution product with inversion of configuration. This must mean that the contact ion pair returns to the

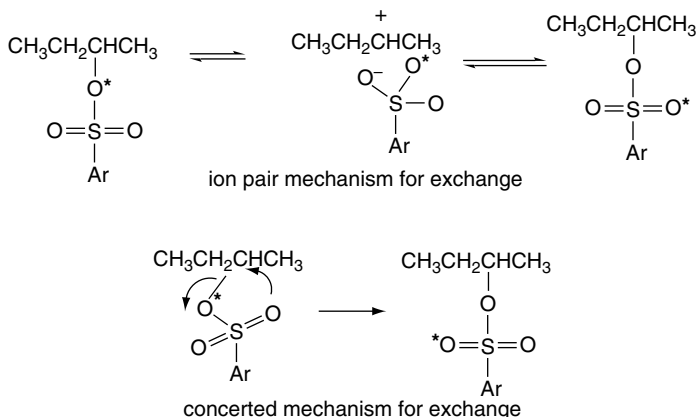
<sup>6</sup> H. L. Goering and J. F. Levy, *J. Am. Chem. Soc.*, **86**, 120 (1964).



The ion pair return phenomenon can also be demonstrated by comparing the rate of racemization of reactant with the rate of product formation. For a number of systems, including 1-arylethyl tosylates,<sup>9</sup> the rate of decrease of optical rotation is greater than the rate of product formation, which indicates the existence of an intermediate that can re-form racemic reactant. The solvent-separated ion pair is the most likely intermediate to play this role.



Racemization, however, does not always accompany isotopic scrambling. In the case of 2-butyl 4-bromobenzenesulfonate, isotopic scrambling occurs in trifluoroethanol solution without any racemization. Isotopic scrambling probably involves a contact ion pair in which the sulfonate can rotate with respect to the carbocation without migrating to its other face. The unlikely alternative is a concerted mechanism, which avoids a carbocation intermediate but requires a front-side displacement.<sup>10</sup>



The idea that ion pairs are key participants in nucleophilic substitution is widely accepted. The energy barriers separating the contact, solvent-separated, and dissociated ions are thought to be quite small. The reaction energy profile in Figure 4.4 depicts the three ion pair species as being roughly equivalent in energy and separated by small barriers.

The gradation from  $S_N1$  to  $S_N2$  mechanisms can be summarized in terms of the shape of the potential energy diagrams for the reactions, as illustrated in Figure 4.5. Curves A and C represent the  $S_N1$  and  $S_N2$  limiting mechanisms. The gradation from the  $S_N1$  to the  $S_N2$  mechanism involves greater and greater nucleophilic participation by the solvent or nucleophile at the transition state.<sup>11</sup> An ion pair with strong nucleophilic participation represents a mechanistic variation between the

<sup>9</sup> A. D. Allen, V. M. Kanagasabapathy, and T. T. Tidwell, *J. Am. Chem. Soc.*, **107**, 4513 (1985).

<sup>10</sup> P. E. Dietze and M. Wojciechowski, *J. Am. Chem. Soc.*, **112**, 5240 (1990).

<sup>11</sup> T. W. Bentley and P. v. R. Schleyer, *Adv. Phys. Org. Chem.*, **14**, 1 (1977).

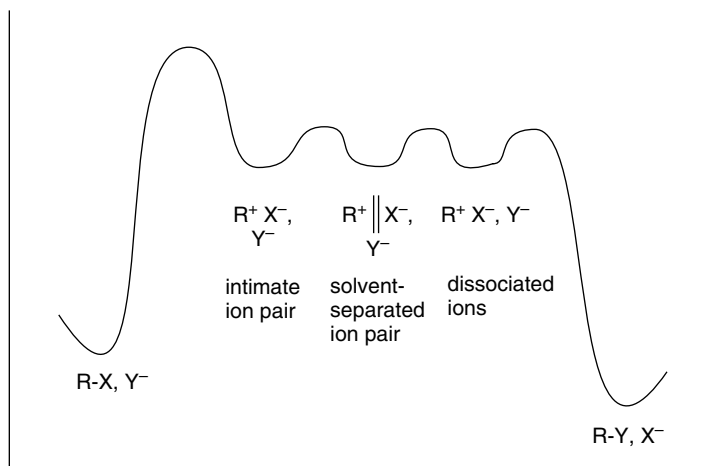
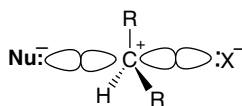


Fig. 4.4. Schematic relationship between reactants, ion pairs, and products in substitution proceeding through ion pairs.

$S_N1$  and  $S_N2$  processes. This mechanism is represented by curve B and designated  $S_N2(\text{intermediate})$ . It pictures a carbocation-like TS, but one that nevertheless requires back-side nucleophilic participation and therefore exhibits second-order kinetics.



Jencks<sup>12</sup> emphasized that the gradation from the  $S_N1$  to the  $S_N2$  mechanism is related to the stability and lifetime of the carbocation intermediate, as illustrated in Figure 4.6. In the  $S_N1(\text{lim})$  mechanism, the carbocation intermediate has a significant lifetime and is equilibrated with solvent prior to capture by a nucleophile. The reaction

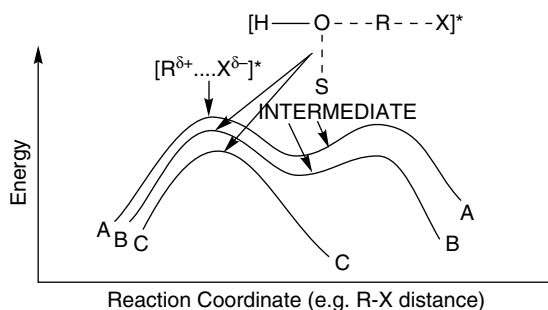


Fig. 4.5. Reaction energy profiles for substitution mechanisms. A is the  $S_N1$  mechanism. B is the  $S_N2$  mechanism with an intermediate ion pair or pentacoordinate species. C is the classical  $S_N2$  mechanism. Reproduced from T. W. Bentley and P. v. R. Schleyer, *Adv. Phys. Org. Chem.*, **14**, 1 (1977), by permission of Academic Press.

<sup>12</sup> W. P. Jencks, *Acc. Chem. Res.*, **13**, 161 (1980).

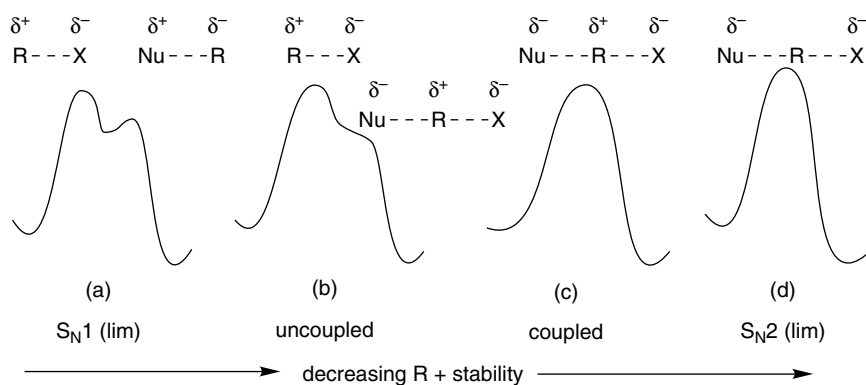
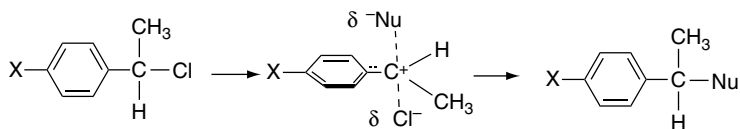


Fig. 4.6. Reaction energy profiles showing decreasing carbocation stability in change from  $S_N1(\text{lim})$  to  $S_N2(\text{lim})$  mechanisms.

is clearly stepwise and the energy minimum in which the carbocation intermediate resides is evident. As the stability of the carbocation decreases, its lifetime becomes shorter. The barrier to capture by a nucleophile becomes less and eventually disappears. This is described as the “uncoupled” mechanism. Ionization proceeds without nucleophilic participation but the carbocation does not exist as a free intermediate. Such reactions exhibit  $S_N1$  kinetics, since there is no nucleophilic participation in the ionization. At still lesser carbocation stability, the lifetime of the ion pair is so short that it always returns to the reactant unless a nucleophile is present to capture it as it is formed. This type of reaction exhibits second-order kinetics, since the nucleophile must be present for reaction to occur. Jencks describes this as the “coupled” substitution process. Finally, when the stability of the (potential) carbocation is so low that it cannot form, the direct displacement mechanism [ $S_N2(\text{lim})$ ] operates. The continuum corresponds to decreasing carbocation character at the TS proceeding from  $S_N1(\text{lim})$  to  $S_N2(\text{lim})$  mechanisms. The degree of positive charge decreases from a full positive charge at a  $S_N1(\text{lim})$  to the possibility of net negative charge on carbon at the  $S_N2(\text{lim})$ .

The reaction of azide ion with substituted 1-phenylethyl chlorides is an example of a coupled displacement. Although it exhibits second-order kinetics, the reaction has a substantially positive  $\rho$  value, indicative of an electron deficiency at the TS.<sup>13</sup> The physical description of this type of activated complex is called the “exploded”  $S_N2$  TS.



For many secondary sulfonates, nucleophilic substitution seems to be best explained by a coupled mechanism, with a high degree of carbocation character at the TS. The bonds to both the nucleophile and the leaving group are relatively weak, and the carbon has a substantial positive charge. However, the carbocation per se has no lifetime, because bond rupture and formation occur concurrently.<sup>14</sup>

<sup>13</sup> J. P. Richard and W. P. Jencks, *J. Am. Chem. Soc.*, **106**, 1383 (1984).

<sup>14</sup> B. L. Knier and W. P. Jencks, *J. Am. Chem. Soc.*, **102**, 6789 (1980); M. R. Skoog and W. P. Jencks, *J. Am. Chem. Soc.*, **106**, 7597 (1984).

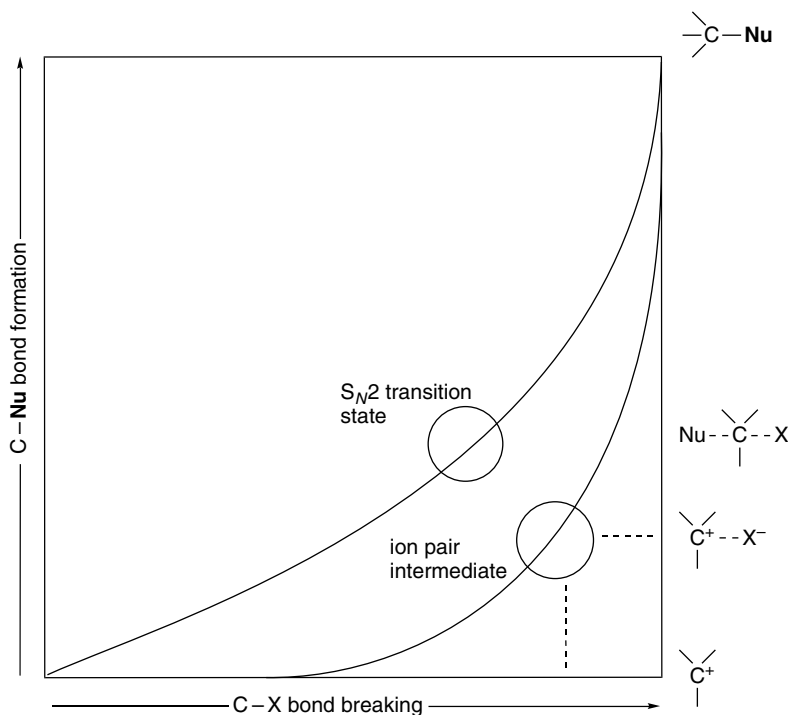


Fig. 4.7. Two-dimensional reaction energy diagram showing concerted, ion pair intermediate, and stepwise mechanisms for nucleophilic substitution.

Figure 4.7 summarizes these ideas using a two-dimensional energy diagram.<sup>15</sup> The  $S_N2(\text{lim})$  mechanism corresponds to the concerted pathway through the middle of the diagram. It is favored by high-energy carbocation intermediates that require nucleophilic participation. The  $S_N1(\text{lim})$  mechanism is the path along the edge of the diagram corresponding to separate bond-breaking and bond-forming steps. An ion pair intermediate mechanism implies a true intermediate, with the nucleophile present in the TS, but at which bond formation has not progressed. The “exploded transition state” mechanism describes a very similar structure, but one that is a transition state, not an intermediate.<sup>16</sup>

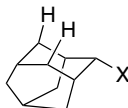
The importance of solvent participation in the borderline mechanisms should be noted. Solvent participation is minimized by high electronegativity and hardness, which reduce the Lewis basicity and polarizability of the solvent molecules. Trifluoroacetic acid and polyfluoro alcohols are among the least nucleophilic of the solvents commonly used in solvolysis studies.<sup>17</sup> These solvents are used to define the characteristics of reactions proceeding with little nucleophilic solvent participation. Solvent nucleophilicity increases with the electron-donating capacity of the molecule. The order trifluoroacetic acid (TFA) < trifluoroethanol (TFE) < acetic acid < water < ethanol gives a qualitative indication of the trend in solvent nucleophilicity. More is said about solvent nucleophilicity in Section 4.2.1.

<sup>15</sup> R. A. More O'Ferrall, *J. Chem. Soc. B*, 274 (1970).

<sup>16</sup> For discussion of the borderline mechanisms, see J. P. Richard, *Adv. Carbocation Chem.*, **1**, 121 (1989); P. E. Dietze, *Adv. Carbocation Chem.*, **2**, 179 (1995).

<sup>17</sup> T. W. Bentley, C. T. Bowen, D. H. Morten, and P. v. R. Schleyer, *J. Am. Chem. Soc.*, **103**, 5466 (1981).

Reactant structure also influences the degree of nucleophilic solvent participation. Solvation is minimized by steric hindrance and the 2-adamantyl system is regarded as being a secondary reactant that cannot accommodate significant back-side nucleophilic participation.



The 2-adamantyl system is used as a model reactant for defining the characteristics of ionization without solvent participation. The degree of nucleophilic participation in other reactions can then be estimated by comparison with the 2-adamantyl system.<sup>18</sup>

#### 4.1.4. Relationship between Stereochemistry and Mechanism of Substitution

Studies of the stereochemistry are a powerful tool for investigation of nucleophilic substitution reactions. Direct displacement reactions by the  $S_N2(\text{lim})$  mechanism are expected to result in complete inversion of configuration. The stereochemical outcome of the ionization mechanism is less predictable, because it depends on whether reaction occurs via an ion pair intermediate or through a completely dissociated ion. Borderline mechanisms may also show variable stereochemistry, depending upon the lifetime of the intermediates and the extent of ion pair recombination.

Scheme 4.2 presents data on some representative nucleophilic substitution processes. Entry 1 shows the use of 1-butyl-1-*d,p*-bromobenzenesulfonate (Bs, brosylate) to demonstrate that primary systems react with inversion, even under solvolysis conditions in formic acid. The observation of inversion indicates a concerted mechanism, even in this weakly nucleophilic solvent. The primary benzyl system in

**Scheme 4.2. Stereochemistry of Nucleophilic Substitution Reactions**

	Reactant <sup>a</sup>	Conditions	Product	Stereochemistry
1 <sup>b</sup>	CH <sub>3</sub> CH <sub>2</sub> CH <sub>2</sub> CHDOBs	HCO <sub>2</sub> H 99° C	CH <sub>3</sub> CH <sub>2</sub> CH <sub>2</sub> CHDO <sub>2</sub> CH	99 ± 6% inv.
2 <sup>c</sup>	C <sub>6</sub> H <sub>5</sub> CHDOTs	CH <sub>3</sub> CO <sub>2</sub> H 25° C	C <sub>6</sub> H <sub>5</sub> CHDO <sub>2</sub> CCH <sub>3</sub>	82 ± 1% inv.
3 <sup>c</sup>	CH <sub>3</sub> CH(CH <sub>2</sub> ) <sub>5</sub> CH <sub>3</sub>   OTs	Et <sub>4</sub> N <sup>+</sup> -O <sub>2</sub> CCH <sub>3</sub> acetone, 56° C	CH <sub>3</sub> CH(CH <sub>2</sub> ) <sub>5</sub> CH <sub>3</sub>   O <sub>2</sub> CCH <sub>3</sub>	100% inv.
4 <sup>d</sup>	CH <sub>3</sub> CH(CH <sub>2</sub> ) <sub>5</sub> CH <sub>3</sub>   OTs	75 % aq. dioxane 65° C	CH <sub>3</sub> CH(CH <sub>2</sub> ) <sub>5</sub> CH <sub>3</sub>   OH	77% inv.
		75 % aq. dioxane 0.06 M NaN <sub>3</sub> , 65° C	CH <sub>3</sub> CH(CH <sub>2</sub> ) <sub>5</sub> CH <sub>3</sub>   OH	22%
			CH <sub>3</sub> CH(CH <sub>2</sub> ) <sub>5</sub> CH <sub>3</sub>   N <sub>3</sub>	78%

(Continued)

<sup>18</sup>. F. L. Schadt, T. W. Bentley, and P. v. R. Schleyer, *J. Am. Chem. Soc.*, **98**, 7667 (1976).

## Scheme 4.2. (Continued)

## SECTION 4.1

Mechanisms for  
Nucleophilic Substitution

5 <sup>e</sup>				
			CH <sub>3</sub> OH, DTBP, 25° C	78% inv.
			C <sub>2</sub> H <sub>5</sub> OH, DTBP, 40° C	55% inv.
			HCO <sub>2</sub> H, DTBP, 0° C	42% inv.
			CF <sub>3</sub> CH <sub>2</sub> OH, DTBP, 25° C	13% ret.
			<i>t</i> -BuOH, 20% H <sub>2</sub> O, 25° C	49% inv.
			dioxane, 20% H <sub>2</sub> O, 25° C	98% inv.
6 <sup>f</sup>		K <sup>+</sup> -O <sub>2</sub> CCH <sub>3</sub> , CH <sub>3</sub> CO <sub>2</sub> H, 50° C		15% inv.
		Et <sub>4</sub> N <sup>+</sup> -O <sub>2</sub> CCH <sub>3</sub> 50% acetone		65% inv.
7 <sup>f</sup>		K <sup>+</sup> -O <sub>2</sub> CCH <sub>3</sub> , CH <sub>3</sub> CO <sub>2</sub> H, 23° C		5 ± 2% inv.
		NaN <sub>3</sub> in CH <sub>3</sub> OH, 65° C		56 ± 1% inv.
				14% inv.
		90% aq, acetone		38% ret.

a. Abbreviations: OBs = *p*-bromobenzenesulfonate; OTs = *p*-toluenesulfonate; OPMB = *p*-nitrobenzoate; DTBP = 2,6-di-*t*-butylpyridine.

b. A. Streitwieser, Jr., *J. Am. Chem. Soc.*, **77**, 1117 (1955).

c. A. Streitwieser, Jr., T. D. Walsh, and J. R. Wolfe, *J. Am. Chem. Soc.*, **87**, 3682 (1965).

d. H. Weiner and R. A. Sneen, *J. Am. Chem. Soc.*, **87**, 287 (1965).

e. P. Muller and J. C. Rosier, *J. Chem. Soc., Perkin Trans.*, **2**, 2232 (2000).

f. J. Steigman and L. P. Hammett, *J. Am. Chem. Soc.*, **59**, 2536 (1937).

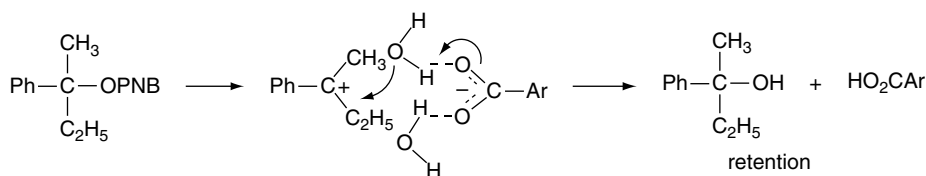
g. L. H. Sommer and F. A. Carey, *J. Org. Chem.*, **32**, 800 (1967).

h. H. L. Goering and S. Chang, *Tetrahedron Lett.* 3607 (1965).

Entry 2 exhibits high, but not complete, inversion for acetolysis, which is attributed to competing racemization of the reactant by ionization and internal return. Entry 3 shows that reaction of a secondary 2-octyl system with the moderately good nucleophile acetate ion occurs with complete inversion. The results cited in Entry 4 serve to illustrate the importance of solvation of ion pair intermediates in reactions of secondary tosylates. The data show that partial racemization occurs in aqueous dioxane but that an added nucleophile (azide ion) results in complete inversion in the products resulting from reaction with both azide ion and water. The alcohol of retained configuration is attributed to an intermediate oxonium ion resulting from reaction of the ion pair



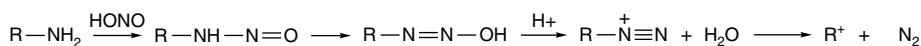
molecule and the anion of the ion pair facilitates capture of a water molecule from the front side of the ion pair.



This selection of stereochemical results points out the relative rarity of the idealized  $S_N1(\text{lim})$  stereochemistry of complete racemization. On the other hand, the predicted inversion of the  $S_N2$  mechanism is consistently observed, and inversion also characterizes the ion pair mechanisms with nucleophile participation. Occasionally net retention is observed. The most likely cause of retention is a double-displacement mechanism, such as proposed for Entry 4, or selective front-side solvation, as in Entry 7c.

#### 4.1.5. Substitution Reactions of Alkyldiazonium Ions

One of the most reactive leaving groups that is easily available for study is molecular nitrogen in alkyl diazonium ions. These intermediates are generated by diazotization of primary amines. Alkyl diazonium ions rapidly decompose to a carbocation and molecular nitrogen. Nucleophilic substitution reactions that occur under diazotization conditions often differ significantly in stereochemistry, as compared with halide or sulfonate solvolysis. Recall the structural description of the alkyl diazonium ions in Section 1.4.3. The nitrogen is a very reactive leaving group and is only weakly bonded to the reacting carbon.



In contrast to an ionization process from a neutral substrate, which initially generates a contact ion pair, deamination reactions generate a cation that does not have a closely associated anion. Furthermore, since the leaving group is very reactive, nucleophilic participation is not needed for bond cleavage. The leaving group, molecular nitrogen, is quite hard, and has no electrostatic attraction to the carbocation. As a result, the carbocations generated by diazonium ion decomposition frequently exhibit rather different behavior from those generated from halides or sulfonates under solvolytic conditions.<sup>21</sup>

Table 4.1 shows the stereochemistry of substitution for five representative systems. Displacement at the primary 1-butyl system occurs mainly by inversion (Entry 1). However, there is also extensive formation of a rearranged product, 2-butanol (not shown in the table). Similarly, the 2-butyl diazonium ion gives 28% inversion in the unrearranged product, but the main product is *t*-butanol (Entry 2). These results indicate competition between concerted rearrangement and dissociation. Several secondary diazonium ions were observed to give alcohol with predominant

<sup>21</sup> C. J. Collins, *Acc. Chem. Res.*, **4**, 315 (1971); A. Streitwieser, Jr., *J. Org. Chem.*, **22**, 861 (1957); E. H. White, K. W. Field, W. H. Hendrickson, P. Dzadzic, D. F. Roswell, S. Paik, and R. W. Mullen, *J. Am. Chem. Soc.*, **114**, 8023 (1992).

Table 4.1. Stereochemistry of Deamination in Acetic Acid

	Amine	Stereochemistry
1 <sup>a</sup>	$\text{CH}_3\text{CH}_2\text{CH}_2\text{CHDNH}_2$	69% inv
2 <sup>b</sup>	$\begin{array}{c} \text{CH}_3\text{CHCH}_2\text{CH}_3 \\   \\ \text{NH}_2 \end{array}$	28% inv
3 <sup>c</sup>	$\begin{array}{c} \text{PhCH}_2\text{CH}_2\text{CHCH}_3 \\   \\ \text{NH}_2 \end{array}$	65% ret
4 <sup>d</sup>	$\begin{array}{c} \text{C}_6\text{H}_5-\text{CHCH}_2\text{CH}_3 \\   \\ \text{NH}_2 \end{array}$	10% ret
5 <sup>e</sup>	$\begin{array}{c} \text{CH}_3 \\   \\ \text{C}_6\text{H}_5-\text{CCH}_2\text{CH}_3 \\   \\ \text{NH}_2 \end{array}$	24% ret

a. D Brosch and W. Kirmse, *J. Org. Chem.*, **56**, 908 (1991).

b. K Banert, M. Bunse, T. Engberts, K.-R. Gassen, A. W. Kurminto, and W. Kirmse, *Recl. Trav. Chim. Pas-Bas*, **105**, 272 (1986).

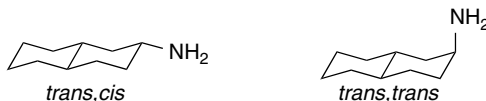
c. N. Ileby, M. Kuzma, L. R. Heggvik, K. Sorbye, and A. Fiksdahl, *Tetrahedron: Asymmetry*, **8**, 2193 (1997).

d. R. Huisgen and C. Ruchardt, *Justus Liebigs Ann. Chem.*, **601**, 21 (1956).

e. E. H. White and J. E. Stuber, *J. Am. Chem. Soc.*, **85**, 2168 (1963).

retention when the reaction was done in acetic acid<sup>22</sup> (Entry 3). However, the acetate esters formed in these reactions is largely racemic. Small net retention was seen in the deamination of 1-phenylpropylamine (Entry 4). The tertiary benzylic amine, 2-phenyl-2-butylamine, reacts with 24% net retention (Entry 5). These results indicate that the composition of the product is determined by collapse of the solvent shell. Considerable solvent dependence has been observed in deamination reactions.<sup>23</sup> Water favors formation of a carbocation with extensive racemization, whereas less polar solvents, including acetic acid, lead to more extensive inversion as the result of solvent participation.

An analysis of the stereochemistry of deamination has also been done using 4-*t*-butylcyclohexylamines and the conformationally rigid 2-decalylamines. The results are summarized in Table 4.2.



In solvent systems containing low concentrations of water in acetic acid, dioxane, or sulfolane, the alcohol is formed by capture of water with net retention of configuration. This result has been explained as involving a solvent-separated ion pair that

<sup>22</sup> N. Ileby, M. Kuzma, L. R. Heggvik, K. Sorbye, and A. Fiksdahl, *Tetrahedron: Asymmetry*, **8**, 2193 (1997).

<sup>23</sup> W. Kirmse and R. Siegfried, *J. Am. Chem. Soc.*, **105**, 950 (1983); K. Banert, M. Bunse, T. Engbert, K.-R. Gassen, A. W. Kurinanto, and W. Kirmse, *Recl. Trav. Chim. Pays-Bas*, **105**, 272 (1986).

Table 4.2. Product Stereochemistry for Deamination of Stereoisomeric Amines

	Product composition <sup>a</sup>			
	Alcohol		Ester	
	Retention	Inversion	Retention	Inversion
<i>Cis</i> -4- <i>t</i> -Butylcyclohexylamine (axial) <sup>b</sup>	33	8	25	33
<i>Trans</i> -4- <i>t</i> -Butylcyclohexylamine (equatorial) <sup>b</sup>	43	2	43	12
<i>Trans,trans</i> -2-Decalylamine (axial) <sup>c</sup>	26	2	32	40
<i>Trans,cis</i> -2-Decalylamine (equatorial) <sup>c</sup>	18	1	55	26

a. Composition of the total of alcohol and acetate ester. Considerable alkene is also formed.

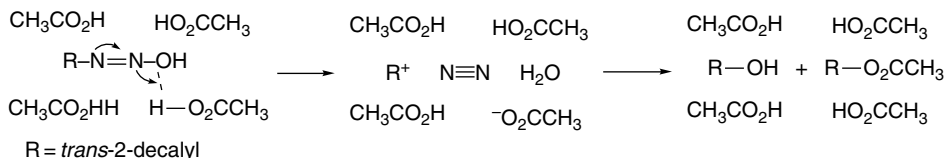
b. H. Maskill and M. C. Whiting, *J. Chem. Soc., Perkin Trans. 2*, 1462 (1976).

c. T. Cohen, A. D. Botelho, and E. Jamnkowski, *J. Org. Chem.*, **45**, 2839 (1980).

SECTION 4.2

Structural and Solvation  
Effects on Reactivity

arises by concerted proton transfer and nitrogen elimination.<sup>24</sup> The water molecule formed in the elimination step is captured preferentially from the front side, leading to net retention of configuration for the alcohol. For the ester product, the extent of retention and inversion is more balanced, although it varies among the four systems.



It is clear from the data in Table 4.2 that the two pairs of stereoisomeric cyclic amines *do not form the same intermediate*. The collapse of the ions to product is evidently so fast that there is not time for relaxation of the initially formed intermediates to reach a common structure. Generally speaking, we can expect similar behavior for all alkyl diazonium ion decompositions. The low activation energy for dissociation and the neutral and hard character of the leaving group result in a carbocation that is free of direct interaction with the leaving group. Product composition and stereochemistry is determined by the details of the collapse of the solvent shell.

## 4.2. Structural and Solvation Effects on Reactivity

### 4.2.1. Characteristics of Nucleophilicity

The term *nucleophilicity* refers to the capacity of a Lewis base to participate in a nucleophilic substitution reaction and is contrasted with *basicity*, which is defined by the position of an equilibrium reaction with a proton donor, usually water. Nucleophilicity is used to describe trends in the rates of substitution reactions that are attributable to properties of the nucleophile. The relative nucleophilicity of a given species may be different toward various reactants and there is not an absolute scale of nucleophilicity. Nevertheless, we can gain some impression of the structural features

<sup>24</sup>. (a) H. Maskill and M. C. Whiting, *J. Chem. Soc., Perkin Trans. 2*, 1462 (1976); (b) T. Cohen, A. D. Botelho, and E. Jankowski, *J. Org. Chem.*, **45**, 2839 (1970).

that govern nucleophilicity and the relationship between nucleophilicity and basicity.<sup>25</sup> As we will see in Section 4.4.3, there is often competition between displacement (nucleophilicity) and elimination (proton removal, basicity). We want to understand how the structure of the reactant and nucleophile (base) affect this competition.

The factors that influence nucleophilicity are best assessed in the context of the limiting  $S_N2$  mechanism, since it is here that the properties of the nucleophile are most important. The rate of an  $S_N2$  reaction is directly related to the effectiveness of the nucleophile in displacing the leaving group. In contrast, relative nucleophilicity has no effect on the rate of an  $S_N1$  reaction. Several properties can influence nucleophilicity. Those considered to be most significant are: (1) the solvation energy of the nucleophile; (2) the strength of the bond being formed to carbon; (3) the electronegativity of the attacking atom; (4) the polarizability of the attacking atom; and (5) the steric bulk of the nucleophile.<sup>26</sup> Let us consider each how each of these factors affect nucleophilicity.

1. Strong solvation lowers the energy of an anionic nucleophile relative to the TS, in which the charge is more diffuse, and results in an increased  $E_a$ . Viewed from another perspective, the solvation shell must be disrupted to attain the TS and this desolvation contributes to the activation energy.
2. Because the  $S_N2$  process is concerted, the strength of the partially formed new bond is reflected in the TS. A stronger bond between the nucleophilic atom and carbon results in a more stable TS and a reduced activation energy.
3. A more electronegative atom binds its electrons more tightly than a less electronegative one. The  $S_N2$  process requires donation of electron density to an antibonding orbital of the reactant, and high electronegativity is unfavorable.
4. Polarizability describes the ease of distortion of the electron density of the nucleophile. Again, because the  $S_N2$  process requires bond formation by an electron pair from the nucleophile, the more easily distorted the attacking atom, the better its nucleophilicity.
5. A sterically congested nucleophile is less reactive than a less hindered one because of nonbonded repulsions that develop in the TS. The trigonal bipyramidal geometry of the  $S_N2$  transition state is sterically more demanding than the tetrahedral reactant so steric interactions increase as the TS is approached.

Empirical measures of nucleophilicity are obtained by comparing relative rates of reaction of a standard reactant with various nucleophiles. One measure of nucleophilicity is the *nucleophilic constant* ( $n$ ), originally defined by Swain and Scott.<sup>27</sup> Taking methanolysis of methyl iodide as the standard reaction, they defined  $n$  as

$$n_{\text{CH}_3\text{I}} = \log(k_{\text{nucl}}/k_{\text{CH}_3\text{OH}}) \text{ in } \text{CH}_3\text{OH}, 25^\circ \text{C}$$

Table 4.3 lists the nucleophilic constants for a number of species according to this definition.

It is apparent from Table 4.3 that nucleophilicity toward methyl iodide does not correlate directly with aqueous basicity. Azide ion, phenoxide ion, and bromide are all

<sup>25</sup> For general reviews of nucleophilicity see R. F. Hudson, in *Chemical Reactivity and Reaction Paths*, G. Klopman, ed., John Wiley & Sons, New York, 1974, Chap. 5; J. M. Harris and S. P. McManus, eds., *Nucleophilicity*, Vol. 215, Advances in Chemistry Series, American Chemical Society, Washington, DC, 1987.

<sup>26</sup> A. Streitwieser, Jr., *Solvolytic Displacement Reactions*, McGraw-Hill, New York, 1962; J. F. Bunnett, *Annu. Rev. Phys. Chem.*, **14**, 271 (1963).

<sup>27</sup> C. G. Swain and C. B. Scott, *J. Am. Chem. Soc.*, **75**, 141 (1953).

**Table 4.3. Nucleophilicity Constants for Various Nucleophiles<sup>a</sup>**

Nucleophile	$n_{\text{CH}_3\text{I}}$	Conjugate acid $\text{p}K_a$
$\text{CH}_3\text{OH}$	0.0	-1.7
$\text{NO}_3^-$	1.5	-1.3
$\text{F}^-$	2.7	3.45
$\text{CH}_3\text{CO}_2^-$	4.3	4.8
$\text{Cl}^-$	4.4	-5.7
$(\text{CH}_3)_2\text{S}$	5.3	
$\text{NH}_3$	5.5	9.25
$\text{N}_3^-$	5.8	4.74
$\text{C}_6\text{H}_5\text{O}^-$	5.8	9.89
$\text{Br}^-$	5.8	-7.7
$\text{CH}_3\text{O}^-$	6.3	15.7
$\text{HO}^-$	6.5	15.7
$\text{NH}_2\text{OH}$	6.6	5.8
$\text{NH}_2\text{NH}_2$	6.6	7.9
$(\text{CH}_3\text{CH}_2)_3\text{N}$	6.7	10.7
$\text{CN}^-$	6.7	9.3
$(\text{CH}_3\text{CH}_2)_3\text{As}$	7.1	
$\text{I}^-$	7.4	-10.7
$\text{HO}_2^-$	7.8	
$(\text{CH}_3\text{CH}_2)_3\text{P}$	8.7	8.7
$\text{C}_6\text{H}_5\text{S}^-$	9.9	6.5
$\text{C}_6\text{H}_5\text{Se}^-$	10.7	
$(\text{C}_6\text{H}_5)_3\text{Sn}^-$	11.5	

a. Data from R. G. Pearson and J. Songstad, *J. Am. Chem. Soc.*, **89**, 1827 (1967); R. G. Pearson, H. Sobel, and J. Songstad, *J. Am. Chem. Soc.*, **90**, 319 (1968); P. L. Bock and G. M. Whitesides, *J. Am. Chem. Soc.*, **96**, 2826 (1974).

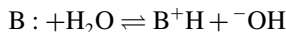
equivalent in nucleophilicity, but differ greatly in basicity. Conversely, azide ion and acetate ion are nearly identical in basicity, but azide ion is 70 times (1.5 log units) more nucleophilic. Among neutral nucleophiles, while triethylamine is 100 times more basic than triethylphosphine ( $\text{p}K_a$  of the conjugate acid is 10.7 versus 8.7), the phosphine is more nucleophilic ( $n$  is 8.7 versus 6.7), by a factor of 100 in the opposite direction. Correlation with basicity is better if the attacking atom is the same. Thus for the series of oxygen nucleophiles  $\text{CH}_3\text{O}^- > \text{C}_6\text{H}_5\text{O}^- > \text{CH}_3\text{CO}_2^- > \text{NO}_3^-$ , nucleophilicity parallels basicity.

Nucleophilicity usually decreases going across a row in the periodic table. For example,  $\text{H}_2\text{N}^- > \text{HO}^- > \text{F}^-$  or  $\text{C}_6\text{H}_5\text{S}^- > \text{Cl}^-$ . This order is primarily determined by electronegativity and polarizability. Nucleophilicity increases going down the periodic table, as, e.g.,  $\text{I}^- > \text{Br}^- > \text{Cl}^- > \text{F}^-$  and  $\text{C}_6\text{H}_5\text{Se}^- > \text{C}_6\text{H}_5\text{S}^- > \text{C}_6\text{H}_5\text{O}^-$ . Three factors work together to determine this order. Electronegativity decreases going down the periodic table. Probably more important is the greater polarizability and weaker solvation of the heavier ions, which have a more diffuse electron distribution. The bond strength effect is in the opposite direction, but is overwhelmed by electronegativity and polarizability.

There is clearly a conceptual relationship between the properties called nucleophilicity and basicity. Both describe processes involving formation of a new bond to an electrophile by donation of an electron pair. The  $\text{p}K_a$  values in Table 4.3 refer to basicity toward a proton. There are many reactions in which a given chemical species might act either as a nucleophile or as a base. It is therefore of great interest to be

able to predict whether a chemical species  $Y^-$  will act as a nucleophile or as a base under a given set of conditions. Scheme 4.3 lists some examples.

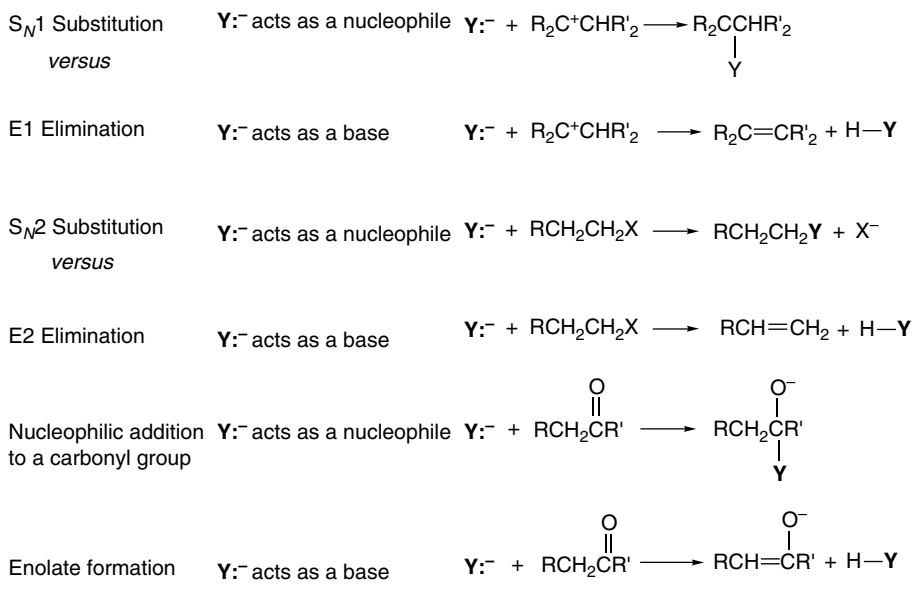
Basicity is a measure of the ability of a substance to attract protons and refers to an *equilibrium* with respect to a proton transfer from solvent:



These equilibrium constants provide a measure of *thermodynamic basicity*, but we also need to have some concept of *kinetic basicity*. For the reactions in Scheme 4.3, for example, it is important to be able to generalize about the rates of competing reactions. The most useful qualitative approach for making predictions is the hard-soft-acid-base (HSAB) concept<sup>28</sup> (see Section 1.1.6), which proposes that reactions occur most readily between species that are matched in hardness and softness. Hard nucleophiles prefer hard electrophiles, whereas soft nucleophiles prefer soft electrophiles.

The HSAB concept can be applied to the problem of competition between nucleophilic substitution and deprotonation as well as to the reaction of anions with alkyl halides. The  $sp^3$  carbon is a soft electrophile, whereas the proton is a hard electrophile. Thus, according to HSAB theory, a soft anion will act primarily as a nucleophile, giving the substitution product, whereas a hard anion is more likely to remove a proton, giving the elimination product. Softness correlates with high polarizability and low electronegativity. The soft nucleophile–soft electrophile combination is associated with a late TS, where the strength of the newly forming bond contributes significantly to the structure and stability of the TS. Species in Table 4.3 that exhibit high nucleophilicity toward methyl iodide include  $CN^-$ ,  $I^-$ , and  $C_6H_5S^-$ . These are soft species. Hardness

#### Scheme 4.3. Examples of Competition between Nucleophilicity and Basicity



<sup>28</sup> R. G. Pearson and J. Songstad, *J. Am. Chem. Soc.*, **89**, 1827 (1967); R. G. Pearson, *J. Chem. Ed.*, **45**, 581, 643 (1968); T. L. Ho, *Chem. Rev.*, **75**, 1 (1975).

**Table 4.4. Hardness and Softness of Some Common Ions and Molecules**

	Bases (Nucleophiles)	Acids (Electrophiles)
Soft	RSH, RS <sup>-</sup> , I <sup>-</sup> , R <sub>3</sub> P <sup>-</sup> C≡N, <sup>-</sup> :C≡O <sup>+</sup> , RCH=CHR benzene	I <sub>2</sub> , Br <sub>2</sub> , RS—X, RSe—X, RCH <sub>2</sub> —X Cu(I), Ag(I), Pd(II), Pt(II), Hg(II) zero-valent metal complexes
Intermediate	Br <sup>-</sup> , N <sub>3</sub> <sup>-</sup> , ArNH <sub>2</sub> pyridine	Cu(II), Zn (II), Sn,(II) R <sub>3</sub> C <sup>+</sup> , R <sub>3</sub> B
Hard	NH <sub>3</sub> , RNH <sub>2</sub> H <sub>2</sub> O, HO <sup>-</sup> , ROH, RO <sup>-</sup> , RCO <sub>2</sub> <sup>-</sup> , Cl <sup>-</sup> F <sup>-</sup> , NO <sub>3</sub> <sup>-</sup>	H—X, Li <sup>+</sup> , Na <sup>+</sup> , R <sub>3</sub> Si—X Mg(II), Ca(II), Al(III), Sn(IV), Ti(IV) H <sup>+</sup>

SECTION 4.2

*Structural and Solvation  
Effects on Reactivity*

reflects a high charge density and is associated with more electronegative elements. The hard nucleophile–hard electrophile combination implies an early TS with electrostatic attraction being more important than bond formation. For hard bases, the reaction pathway is chosen early on the reaction coordinate and primarily on the basis of charge distribution. Examples of hard bases from Table 4.3 are F<sup>-</sup> and CH<sub>3</sub>O<sup>-</sup>. Table 4.4 classifies some representative chemical species with respect to softness and hardness. Numerical values of hardness were presented in Table 1.3.

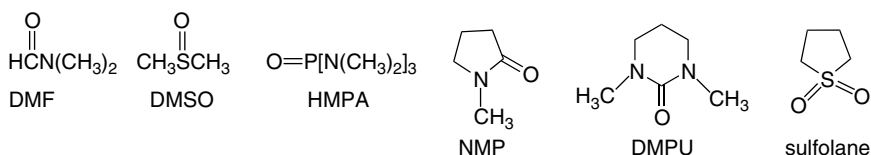
Nucleophilicity is also correlated with oxidation potential for comparisons between nucleophiles involving the same element.<sup>29</sup> Good nucleophilicity correlates with ease of oxidation, as would be expected from the electron-donating function of the nucleophile in S<sub>N</sub>2 reactions. HSAB considerations also suggest that nucleophilicity would be associated with species having relatively high-energy electrons. Remember that soft species have relatively high-lying HOMOs, which implies ease of oxidation.

#### 4.2.2. Effect of Solvation on Nucleophilicity

The nucleophilicity of anions is very dependent on the degree of solvation. Many of the data that form the basis for quantitative measurement of nucleophilicity are for reactions in hydroxylic solvents. In protic hydrogen-bonding solvents, anions are subject to strong interactions with solvent. Hard nucleophiles are more strongly solvated by protic solvents than soft nucleophiles, and this difference contributes to the greater nucleophilicity of soft anions in such solvents. Nucleophilic substitution reactions of anionic nucleophiles usually occur more rapidly in polar aprotic solvents than they do in protic solvents, owing to the fact that anions are weakly solvated in such solvents (see Section 3.8). Nucleophilicity is also affected by the solvation of the cations in solution. Hard cations are strongly solvated in polar aprotic solvents such as *N,N*-dimethylformamide (DMF), dimethyl sulfoxide (DMSO), hexamethylphosphoric triamide (HMPA), *N*-methylpyrrolidone (NMP), *N,N*-dimethylpropyleneurea

<sup>29</sup> M. E. Niyazymbetov and D. H. Evans, *J. Chem. Soc., Perkin Trans. 2*, 1333 (1993); M. E. Niyazymbetov, Z. Rongfeng, and D. H. Evans, *J. Chem. Soc., Perkin Trans. 2*, 1957 (1996).

(DMPU), and sulfolane.<sup>30</sup> As a result, the anions are dissociated from the cations, which enhances their nucleophilicity.



In the absence of the solvation by protic solvents, the relative nucleophilicity of anions changes. Hard nucleophiles increase in reactivity more than soft nucleophiles. As a result, the relative reactivity order changes. In methanol, for example, the relative reactivity order is  $\text{N}_3^- > \text{I}^- > \text{CN}^- > \text{Br}^- > \text{Cl}^-$ . In DMSO the order becomes  $\text{CN}^- > \text{N}_3^- > \text{Cl}^- > \text{Br}^- > \text{I}^-$ .<sup>31</sup> The reactivity order in methanol is dominated by solvation and the more weakly solvated  $\text{N}_3^-$  and  $\text{I}^-$  ions are the most reactive nucleophiles. The iodide ion is large and very polarizable. The anionic charge on the azide ion is dispersed by delocalization. When the effect of solvation is diminished in DMSO, other factors become more important, including the strength of the bond being formed, which accounts for the reversed order of the halides in the two series. There is also evidence that  $\text{S}_\text{N}2$  TSs are better solvated in aprotic dipolar solvents than in protic solvents.

In interpreting many aspects of substitution reactions, particularly solvolysis, it is important to be able to characterize the nucleophilicity of the solvent. Assessment of solvent nucleophilicity can be done by comparing rates of a standard substitution process in various solvents. One such procedure is based on the Winstein-Grunwald equation<sup>32</sup>:

$$\log(k/k_0) = lN + mY$$

where  $N$  and  $Y$  are measures of the solvent nucleophilicity and ionizing power, respectively. The variable parameters  $l$  and  $m$  are characteristic of specific reactions. The value of  $N$ , the indicator of solvent nucleophilicity, can be determined by specifying a standard reactant for which  $l$  is assigned the value 1.00 and a standard solvent for which  $N$  is assigned the value 0.00. The parameters were originally assigned for solvolysis of *t*-butyl chloride. The scale has also been assigned for 2-adamantyl tosylate, in which nucleophilic participation of the solvent is considered to be negligible. Ethanol-water in the ratio 80:20 is taken as the standard solvent. The resulting solvent characteristics are called  $N_{\text{Tos}}$  and  $Y_{\text{Tos}}$ . Some representative values for solvents that are frequently used in solvolysis studies are given in Table 4.5. We see that nucleophilicity decreases from ethanol to water to trifluoroethanol to trifluoroacetic acid as the substituent becomes successively more electron withdrawing. Note that the considerable difference between acetic acid and formic acid appears entirely in

<sup>30</sup> T. F. Magnera, G. Caldwell, J. Sunner, S. Ikuta, and P. Kebarle, *J. Am. Chem. Soc.*, **106**, 6140 (1984); T. Mitsuhashi, G. Yamamoto, and H. Hirota, *Bull. Chem. Soc. Jpn.*, **67**, 831 (1994); K. Okamoto, *Adv. Carbocation Chem.*, **1**, 171 (1989).

<sup>31</sup> R. L. Fuchs and L. L. Cole, *J. Am. Chem. Soc.*, **95**, 3194 (1973); R. Alexander, E. C. F. Ko, A. J. Parker, and T. J. Broxton, *J. Am. Chem. Soc.*, **90**, 5049 (1968); D. Landini, A. Maia, and F. Montanari, *J. Am. Chem. Soc.*, **100**, 2796 (1978).

<sup>32</sup> S. Winstein, E. Grunwald, and H. W. Jones, *J. Am. Chem. Soc.*, **73**, 2700 (1951); F. L. Schadt, T. W. Bentley, and P. v. R. Schleyer, *J. Am. Chem. Soc.*, **98**, 7667 (1976).

**Table 4.5. Solvent Nucleophilicity and Ionization Parameters<sup>a</sup>**

Solvent	<i>t</i> -Butyl chloride		2-Adamantyl tosylate	
	<i>N</i>	<i>Y</i>	<i>N</i> <sub>Tos</sub>	<i>Y</i> <sub>Tos</sub>
Ethanol	+0.09	-2.03	0.00	-1.75
Methanol	+0.01	-1.09	-0.04	-0.92
50% Aqueous ethanol	-0.20	1.66	-0.09	1.29
Water	-0.26	3.49		
Acetic acid	-2.05	-1.64	-2.35	-0.61
Formic acid	-2.05	2.05	-2.35	3.04
Trifluoroethanol	-2.78	1.05	-3.0	1.80
97% (CF <sub>3</sub> ) <sub>2</sub> CHOH-H <sub>2</sub> O	-3.93	2.46	-4.27	3.61
Trifluoroacetic acid	-4.74	1.84	-5.56	4.57

a. From F. L. Schadt, T. W. Bentley, and P. v. R. Schleyer, *J. Am. Chem. Soc.*, **98**, 7667 (1976).

the *Y* terms, which have to do with ionizing power and results from the more polar character of formic acid. The nucleophilicity parameters of formic acid and acetic acid are the same, as might be expected, because the nucleophilicity is associated with the carboxy group.

#### 4.2.3. Leaving-Group Effects

The nature of the leaving group influences the rate of nucleophilic substitution proceeding by either the direct displacement or ionization mechanism. Since the leaving group departs with the pair of electrons from the covalent bond to the reacting carbon atom, a correlation with both bond strength and anion stability is expected. Provided the reaction series consists of structurally similar leaving groups, such relationships are observed. For example, a linear free-energy relationship (*Hammett equation*) has been demonstrated for the rate of reaction of ethyl arenesulfonates with ethoxide ion in ethanol.<sup>33</sup> A qualitative trend of increasing reactivity with the acidity of the conjugate acid of the leaving group also holds for less similar systems, although no generally applicable quantitative system for specifying leaving-group ability has been established.

Table 4.6 lists estimated relative rates of solvolysis of 1-phenylethyl esters and halides in 80% aqueous ethanol at 75°C.<sup>34</sup> The reactivity of the leaving groups generally parallels their electron-accepting capacity. Trifluoroacetate, for example, is about 10<sup>6</sup> times as reactive as acetate and *p*-nitrobenzenesulfonate is about 10 times more reactive than *p*-toluenesulfonate. The order of the halide leaving groups is I<sup>-</sup> > Br<sup>-</sup> > Cl<sup>-</sup> ≫ F<sup>-</sup>. This order is opposite to that of electronegativity and is dominated by the strength of the bond to carbon, which increases from ~55 kcal for the C-I bond to ~110 kcal for the C-F bond (see Table 3.2).

Sulfonate esters are especially useful reactants in nucleophilic substitution reactions in synthesis. They have a high level of reactivity and can be prepared from alcohols by reactions that do not directly involve the carbon atom at which substitution is to be effected. The latter feature is particularly important in cases where the stereochemical and structural integrity of the reactant must be maintained. Trifluoromethanesulfonate (triflate) ion is an exceptionally reactive leaving group and can

<sup>33</sup>. M. S. Morgan and L. H. Cretcher, *J. Am. Chem. Soc.*, **70**, 375 (1948).

<sup>34</sup>. D. S. Noyce and J. A. Virgilio *J. Org. Chem.*, **37**, 2643 (1972).

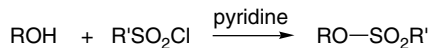
**Table 4.6. Relative Solvolysis Rates of 1-Phenylethyl Esters and Halides<sup>a,b</sup>**

Leaving group	$k_{\text{rel}}$
CF <sub>3</sub> SO <sub>3</sub> <sup>-</sup> (triflate)	1.4 × 10 <sup>8</sup>
<i>p</i> -Nitrobenzenesulfonate (nosylate)	4.4 × 10 <sup>5</sup>
<i>p</i> -Toluenesulfonate (tosylate)	3.7 × 10 <sup>4</sup>
CH <sub>3</sub> SO <sub>3</sub> <sup>-</sup> (mesylate)	3.0 × 10 <sup>4</sup>
I <sup>-</sup>	91
Br <sup>-</sup>	14
CF <sub>3</sub> CO <sub>2</sub> <sup>-</sup>	2.1
Cl <sup>-</sup>	1.0
F <sup>-</sup>	9 × 10 <sup>-6</sup>
<i>p</i> -Nitrobenzoate	5.5 × 10 <sup>-6</sup>
CH <sub>3</sub> CO <sub>2</sub> <sup>-</sup>	1.4 × 10 <sup>-6</sup>

a. From D. S. Noyce and J. A. Virgilio, *J. Org. Chem.*, **37**, 2643 (1972).

b. In 80% ethanol at 75 °C.

be used for nucleophilic substitution reactions on unreactive substrates. Acetolysis of cyclopropyl triflate, for example, occurs 10<sup>5</sup> times faster than acetolysis of cyclopropyl tosylate.<sup>35</sup> Sulfonate esters are usually prepared by reaction of an alcohol with a sulfonyl halide in the presence of pyridine.



Tertiary alcohols are more difficult to convert to sulfonate esters and their high reactivity often makes them difficult to isolate.<sup>36</sup>

It would be anticipated that the limiting S<sub>N</sub>1 and S<sub>N</sub>2 mechanisms would differ in their sensitivity to the nature of the leaving group. The ionization mechanism should exhibit a greater dependence on leaving-group ability because it requires cleavage of the bond to the leaving group without assistance by the nucleophile. Table 4.7 presents data on the variation of the relative leaving-group abilities of tosylate and bromide as a function of reactant structure. The dependence on structure is as expected, with smaller differences in reactivity between tosylate and bromide being observed for systems that react by the S<sub>N</sub>2 mechanism. The largest differences are seen for tertiary systems, where nucleophilic participation is minimal.

**Table 4.7. Tosylate/Bromide Rate Ratios for Solvolysis of RX in 80% Ethanol<sup>a</sup>**

R	$k_{\text{Tos}}/k_{\text{Br}}$
Methyl	11
Ethyl	10
Isopropyl	40
<i>t</i> -Butyl	4000
1-Adamantyl	9750

a. From J. L. Fry, C. J. Lancelot, L. K. M. Lam, J. M. Harris, R. C. Bingham, D. J. Raber, R. E. Hall, and P. v. R. Schleyer, *J. Am. Chem. Soc.*, **92**, 2539 (1970).

<sup>35</sup> T. M. Su, W. F. Sliwinski, and P. v. R. Schleyer, *J. Am. Chem. Soc.*, **91**, 5386 (1969).

<sup>36</sup> H. M. R. Hoffmann, *J. Chem. Soc.*, 6748 (1965).

**Table 4.8. Relative Reactivity of Leaving Groups in S<sub>N</sub>2 Substitution Reactions<sup>a</sup>**

Nucleophile	CH <sub>3</sub> I		CH <sub>3</sub> Br		CH <sub>3</sub> OTs	
	MeOH	DMF	MeOH	DMF	MeOH	DMF
N <sub>3</sub> <sup>-</sup>	8.0 × 10 <sup>-5</sup>	3.2	5.0 × 10 <sup>-5</sup>	4.0 × 10 <sup>-1</sup>	5.0 × 10 <sup>-4</sup>	5.0 × 10 <sup>-2</sup>
NCS <sup>-</sup>	5.0 × 10 <sup>-4</sup>	8.0 × 10 <sup>-2</sup>	2.5 × 10 <sup>-4</sup>	1.3 × 10 <sup>-2</sup>	1.3 × 10 <sup>-4</sup>	8.0 × 10 <sup>-4</sup>
NC <sup>-</sup>	6.4 × 10 <sup>-4</sup>	3.2 × 10 <sup>2</sup>				
ArS <sup>-</sup>	6.4 × 10 <sup>-2</sup>	16			1.6 × 10 <sup>-2</sup>	6.4 × 10 <sup>-1</sup>

a. Bimolecular rate constants at 25°C. Data from the compilation of R. Alexander, E. C. F. Ko, A. J. Parker, and T. J. Broxton, *J. Am. Chem. Soc.*, **90**, 5049 (1968).

SECTION 4.2

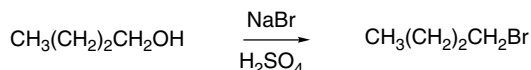
*Structural and Solvation  
Effects on Reactivity*

Leaving-group effects are diminished in S<sub>N</sub>2 reactions, because the nucleophile assists in bond breaking. The mesylate/bromide ratio is compressed from 2 × 10<sup>3</sup> (Table 4.6) to only about 10 for azide ion in methanol, as shown in Table 4.8. In the aprotic dipolar solvent DMF, the leaving-group order is I<sup>-</sup> > Br<sup>-</sup> > <sup>-</sup>O<sub>3</sub>SCH<sub>3</sub> for both azide and thiocyanate anions.

A poor leaving group can be made more reactive by coordination to an electrophile. Hydroxide is a very poor leaving group, so alcohols do not normally undergo direct nucleophilic substitution. It has been estimated that the reaction



is endothermic by 16 kcal/mol.<sup>37</sup> Since the activation energy for the reverse process is about 21 kcal/mol, the reaction would have an  $E_a$  of 37 kcal/mol. As predicted by this  $E_a$ , the reaction is too slow to detect at normal temperature, but it is greatly accelerated in acidic solution. Protonation of the hydroxyl group provides the much better leaving group—water—which is about as good a leaving group as bromide ion. The practical result is that primary alcohols can be converted to alkyl bromides by heating with sodium bromide and sulfuric acid or with concentrated hydrobromic acid.



The reactivity of halides is increased by coordination with Lewis acids. For example, silver ion accelerates solvolysis of methyl and ethyl bromide in 80:20 ethanol water by more than 10<sup>3</sup>.<sup>38</sup> In Section 4.4.1, we will see that the powerful Lewis acids SbF<sub>5</sub> and SbCl<sub>5</sub> also assist in the ionization of halides.

#### 4.2.4. Steric and Strain Effects on Substitution and Ionization Rates

The general trends of reactivity of primary, secondary, and tertiary systems have already been discussed. Reactions that proceed by the direct displacement mechanism are retarded by increased steric repulsions at the TS. This is the principal cause for the relative reactivity of methyl, ethyl, and *i*-propyl chloride, which are in the ratio 93:1:0.0076 toward iodide ion in acetone.<sup>39</sup> A statistical analysis of rate data for a

<sup>37</sup>. R. A. Ogg, Jr., *Trans. Faraday Soc.*, **31**, 1385 (1935).

<sup>38</sup>. L. C. Batman, K. A. Cooper, E. D. Hughes, and C. K. Ingold, *J. Chem. Soc.*, 925 (1940); J. Dostrovsky and E. D. Hughes, *J. Chem. Soc.*, 169 (1946); D. J. Pasto and K. Garves, *J. Org. Chem.*, **32**, 778 (1967).

<sup>39</sup>. J. B. Conant and R. E. Hussey, *J. Am. Chem. Soc.*, **47**, 476 (1925).

**Table 4.9. Rate Constants for Nucleophilic Substitution of Primary Alkyl Bromides and Tosylates<sup>a</sup>**

$k \times 10^5$ for $\text{RCH}_2\text{-X}^b$	R = H	CH <sub>3</sub>	CH <sub>3</sub> CH <sub>2</sub>	(CH <sub>3</sub> ) <sub>2</sub> CH	(CH <sub>3</sub> ) <sub>3</sub> C
RCH <sub>2</sub> Br + LiCl, acetone, 25 °C	600	9.9	6.4	1.5	$2.6 \times 10^{-4}$
RCH <sub>2</sub> I + <i>n</i> -Bu <sub>3</sub> P, acetone, 35 °C	26,000	154	64	4.9	
RCH <sub>2</sub> Br + NaOCH <sub>3</sub> , methanol	8140	906	335	67	
RCH <sub>2</sub> OTs, acetic acid, 70 °C <sup>c</sup>	$5.2 \times 10^{-2}$	$4.4 \times 10^{-2}$		$1.8 \times 10^{-2}$	$4.2 \times 10^{-3}$

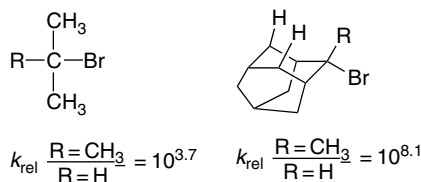
a. M. Charton, *J. Am. Chem. Soc.*, **97**, 3694 (1975).

b.  $\text{M}^{-1} \text{s}^{-1}$

c. pseudo-first order  $\text{s}^{-1}$

number of sets of nucleophilic substitution reactions of substrates of the type  $\text{RCH}_2\text{Y}$ , where Y is a leaving group and R is H or alkyl, indicated that the steric effect of R is the dominant factor in determining rates.<sup>40</sup> Table 4.9 shows some of the data. The first three examples pertain to  $\text{S}_{\text{N}}2$  reactions. Note that the fourth entry, involving solvolysis in acetic acid, shows a diminished sensitivity to steric effects. As acetic acid is a much weaker nucleophile than the other examples, the TS involves less nucleophilic participation.

In contrast to  $\text{S}_{\text{N}}2$  reactions, rates of reactions involving TSs with cationic character increase with substitution. The relative rates of formolysis of alkyl bromides at 100 °C are methyl, 0.58; ethyl, 1.00; *i*-propyl, 26.1; and *t*-butyl 10<sup>8</sup>.<sup>41</sup> This order is clearly dominated by carbocation stability. The effect of substituting a methyl group for hydrogen depends on the extent of nucleophilic participation in the TS. A high  $\text{CH}_3/\text{H}$  rate ratio is expected if nucleophilic participation is weak and stabilization of the cationic nature of the TS is important. A low ratio is expected when nucleophilic participation is strong. The relative rate of acetolysis of *t*-butyl bromide to *i*-propyl bromide at 25 °C is 10<sup>3.7</sup>, whereas that of 2-methyl-2-adamantyl bromide to 2-adamantyl bromide is 10<sup>8.1</sup>.<sup>42</sup>



The reason the adamantyl system is much more sensitive to the  $\text{CH}_3$  for H substitution is that its cage structure precludes solvent participation, whereas the *i*-propyl system allows much greater solvent participation. The electronic stabilizing effect of the methyl substituent is therefore more important in the adamantyl system.

Neopentyl (2,2-dimethylpropyl) systems are resistant to nucleophilic substitution reactions. They are primary and do not form carbocation intermediates; moreover the *t*-butyl substituent hinders back-side displacement. The rate of reaction of neopentyl bromide with iodide ion is 470 times less than that of *n*-butyl bromide.<sup>43</sup> Under solvolysis conditions the neopentyl system usually reacts with rearrangement to the

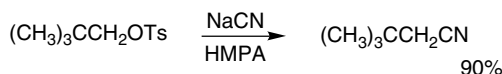
<sup>40</sup>. M. Charton, *J. Am. Chem. Soc.*, **97**, 3694 (1975).

<sup>41</sup>. L. C. Bateman and E. D. Hughes, *J. Chem. Soc.*, 1187 (1937); 945 (1940).

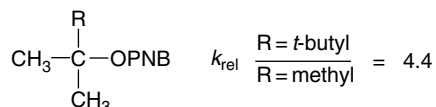
<sup>42</sup>. J. L. Fry, J. M. Harris, R. C. Bingham, and P. v. R. Schleyer, *J. Am. Chem. Soc.*, **92**, 2540 (1970).

<sup>43</sup>. P. D. Bartlett and L. J. Rosen, *J. Am. Chem. Soc.*, **64**, 543 (1942).

*t*-pentyl system, although use of good nucleophiles in polar aprotic solvents permits direct displacement to occur.<sup>44</sup>



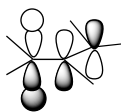
Steric effects of another kind become important in highly branched substrates, and ionization can be facilitated by relief of steric crowding in going from the tetrahedral ground state to the TS for ionization.<sup>45</sup> The relative hydrolysis rates in 80% aqueous acetone of *t*-butyl *p*-nitrobenzoate and 2,3,3-trimethyl-2-butyl *p*-nitrobenzoate are 1:4.4.



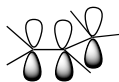
This effect has been called *B-strain* (back strain), and in this example only a modest rate enhancement is observed. As the size of the groups is increased, the effect on rate becomes larger. When all three of the groups in the above example are *t*-butyl, the solvolysis occurs 13,500 times faster than in *t*-butyl *p*-nitrobenzoate.<sup>46</sup>

#### 4.2.5. Effects of Conjugation on Reactivity

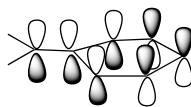
In addition to steric effects, there are other important substituent effects that influence both the rate and mechanism of nucleophilic substitution reactions. As we discussed on p. 302, the benzylic and allylic cations are stabilized by electron delocalization. It is therefore easy to understand why substitution reactions of the ionization type proceed more rapidly in these systems than in alkyl systems. Direct displacement reactions also take place particularly rapidly in benzylic and allylic systems; for example, allyl chloride is 33 times more reactive than ethyl chloride toward iodide ion in acetone.<sup>47</sup> These enhanced rates reflect stabilization of the  $\text{S}_{\text{N}}2$  TS through overlap of the *p*-type orbital that develops at carbon.<sup>48</sup> The  $\pi$  systems of the allylic and benzylic groups provide extended conjugation. This conjugation can stabilize the TS, whether the substitution site has carbocation character and is electron poor or is electron rich as a result of a concerted  $\text{S}_{\text{N}}2$  mechanism.



interaction of  $sp^2$   
hybridized substitution  
center with  $\pi$  LUMO



interaction of empty  $sp^2$   
orbital with  $\pi$  HOMO



interaction of empty  $sp^2$   
orbital of benzyl cation with  
HOMO aromatic  $\pi$  system

<sup>44</sup> B. Stephenson, G. Solladie, and H. S. Mosher, *J. Am. Chem. Soc.*, **94**, 4184 (1972).

<sup>45</sup> H. C. Brown, *Science*, **103**, 385 (1946); E. N. Peters and H. C. Brown, *J. Am. Chem. Soc.*, **97**, 2892 (1975).

<sup>46</sup> P. D. Bartlett and T. T. Tidwell, *J. Am. Chem. Soc.*, **90**, 4421 (1968).

<sup>47</sup> J. B. Conant and R. E. Hussey, *J. Am. Chem. Soc.*, **47**, 476 (1925).

<sup>48</sup> A. Streitwieser, Jr., *Solvolytic Displacement Reactions*, McGraw-Hill, New York, 1962, p. 13; F. Carrion and M. J. S. Dewar, *J. Am. Chem. Soc.*, **106**, 3531 (1984).

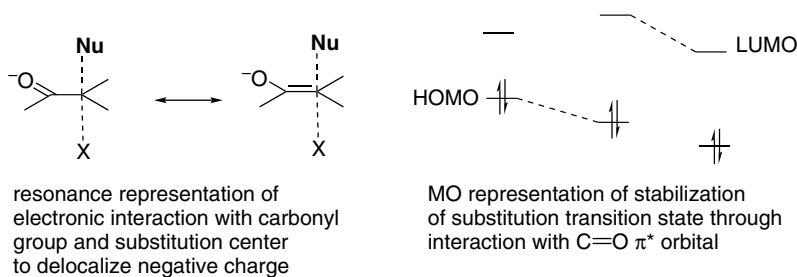
Table 4.10. Substituent Effects of  $\alpha$ -EWG Substituents<sup>a</sup>

$Z-CH_2-Cl + I^- \longrightarrow Z-CH_2-I$			
Z	Relative rate	Z	Relative rate
$CH_3CH_2CH_2$	1	$PhC=O$	$3.2 \times 10^4$
$PhSO_2$	0.25	$N \equiv C$	$3 \times 10^3$
$CH_3C=O$	$3.5 \times 10^4$	$C_2H_5OC=O$	$1.7 \times 10^3$

a. F. G. Bordwell and W. T. Branner, Jr., *J. Am. Chem. Soc.*, **86**, 4645 (1964).

Adjacent carbonyl groups also affect reactivity. Substitution by the ionization mechanism proceeds slowly on  $\alpha$ -halo derivatives of ketones, aldehydes, acids, esters, nitriles, and related compounds. As discussed on p. 304, such substituents destabilize a carbocation intermediate, but substitution by the direct displacement mechanism proceeds especially readily in these systems. Table 4.10 indicates some representative relative rate accelerations.

Steric effects may be responsible for part of the observed acceleration, since an  $sp^2$  carbon, such as in a carbonyl group, offers less steric resistance to the incoming nucleophile than an alkyl group. The major effect is believed to be electronic. The adjacent  $\pi$  LUMO of the carbonyl group can interact with the electron density that builds up at the pentacoordinate carbon in the TS. This can be described in resonance terminology as a contribution from an enolate-like structure to the TS. In MO terminology, the low-lying LUMO has a stabilizing interaction with the developing  $p$  orbital of the TS (see p. 394 for MO representations of the  $S_N2$  transition state).<sup>49</sup>



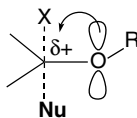
It should be noted that not all electron-attracting groups enhance reactivity. The sulfonyl and trifluoro groups, which cannot participate in this type of  $\pi$  conjugation, retard the rate of  $S_N2$  substitution at an adjacent carbon.<sup>50</sup>

The extent of the rate enhancement of adjacent substituents is dependent on the nature of the TS. The most important factor is the nature of the  $\pi$ -type orbital that develops at the trigonal bipyramidal carbon in the TS. If the carbon is cationic in character, electron donation from adjacent substituents becomes stabilizing. If bond formation at the TS is advanced, resulting in charge buildup at carbon, electron

<sup>49</sup> R. D. Bach, B. A. Coddens, and G. J. Wolber, *J. Org. Chem.*, **51**, 1030 (1986); F. Carrion and M. J. S. Dewar, *J. Am. Chem. Soc.*, **106**, 3531 (1984); S. S. Shaik, *J. Am. Chem. Soc.*, **105**, 4359 (1983); D. McLennon and A. Pross, *J. Chem. Soc., Perkin Trans.*, **2**, 981 (1984); T. I. Yousaf and E. S. Lewis, *J. Am. Chem. Soc.*, **109**, 6137 (1987).

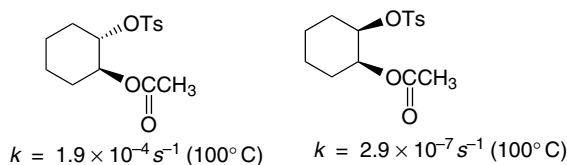
<sup>50</sup> F. G. Bordwell and W. T. Brannen, *J. Am. Chem. Soc.*, **86**, 4645 (1964).

withdrawal is more stabilizing. Thus substituents such as carbonyl have their greatest effect on reactions with strong nucleophiles. Adjacent alkoxy substituents act as  $\pi$  donors and can stabilize  $S_N2$  TSs that are cationic in character. Vinyl and phenyl groups can stabilize either type of TS, and allyl and benzyl systems show enhanced reactivity toward both strong and weak nucleophiles.<sup>51</sup>

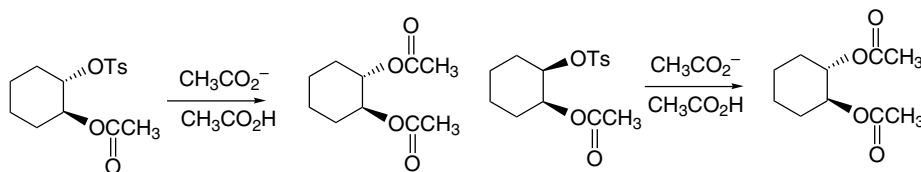


### 4.3. Neighboring-Group Participation

When a molecule that can react by nucleophilic substitution also contains a substituent group that can act as a nucleophile, it is often observed that the rate and stereochemistry of the nucleophilic substitution are strongly affected. The involvement of nearby nucleophilic substituents in a substitution process is called *neighboring-group participation*.<sup>52</sup> A classic example of neighboring-group participation involves the solvolysis of compounds in which an acetoxy substituent is present next to the carbon that is undergoing nucleophilic substitution. For example, the rates of solvolysis of the *cis* and *trans* isomers of 2-acetoxycyclohexyl *p*-toluenesulfonate differ by a factor of about 670, the *trans* compound being more reactive.<sup>53</sup>



Besides the pronounced difference in rate, the isomeric compounds reveal a striking difference in stereochemistry. The diacetate obtained from the *cis* isomer is the *trans* compound (inversion), whereas retention of configuration is observed for the *trans* isomer.



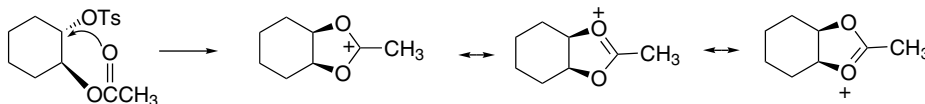
These results can be explained by the participation of the *trans* acetoxy group in the ionization process. The assistance provided by the acetoxy carbonyl group facilitates the ionization of the tosylate group, accounting for the rate enhancement. This kind of back-side participation by the adjacent acetoxy group is both sterically and

<sup>51</sup> D. N. Kost and K. Aviram, *J. Am. Chem. Soc.*, **108**, 2006 (1986).

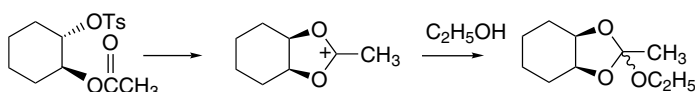
<sup>52</sup> B. Capon, *Q. Rev. Chem. Soc.*, **18**, 45 (1964); B. Capon and S. P. McManus, *Neighboring Group Participation*, Plenum Press, New York, 1976.

<sup>53</sup> S. Winstein, E. Grunwald, R. E. Buckles, and C. Hanson, *J. Am. Chem. Soc.*, **70**, 816 (1948).

energetically favorable. The cation that is formed by participation is stabilized by both acetoxy oxygen atoms and is far more stable than a secondary carbocation. The resulting acetoxonium ion intermediate is subsequently opened by nucleophilic attack with inversion at either of the two equivalent carbons, leading to the observed *trans* product.<sup>54</sup>

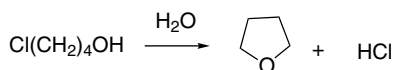


When enantiomerically pure *trans*-2-acetoxycyclohexyl tosylate is solvolyzed, the product is racemic *trans*-diacetate. This result is consistent with the proposed mechanism, because the acetoxonium intermediate is achiral and can only give rise to racemic material.<sup>55</sup> Additional evidence for this interpretation comes from the isolation of a cyclic orthoester when the solvolysis is carried out in ethanol, where the acetoxonium ion is captured by the solvent.

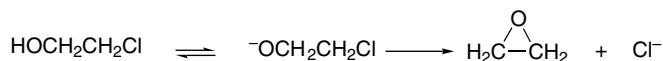


Ref. 56

The hydroxy group can act as an intramolecular nucleophile. Solvolysis of 4-chlorobutanol in water gives tetrahydrofuran as the product.<sup>57</sup> The reaction is much faster than solvolysis of 3-chloropropanol under similar conditions. Participation in the latter case is less favorable because it involves formation of a strained four-membered ring.



The alkoxide ions formed by deprotonation in basic solution are even more effective nucleophiles. In ethanol containing sodium ethoxide, 2-chloroethanol reacts about 5000 times faster than ethyl chloride. The product is ethylene oxide, confirming the involvement of the oxygen atom as a nucleophile.



As would be expected, the effectiveness of neighboring-group participation depends on the ease with which the molecular geometry required for participation can be attained. The rate of cyclization of  $\omega$ -hydroxyalkyl halides, for example, shows a strong dependence on the length of the chain separating the two groups. Some data are given in Table 4.11. The maximum rate occurs for the 4-hydroxybutyl system involving formation of a five-membered ring.

<sup>54</sup> S. Winstein, C. Hanson, and E. Grunwald, *J. Am. Chem. Soc.*, **70**, 812 (1948).

<sup>55</sup> S. Winstein, H. V. Hess, and R. E. Buckles, *J. Am. Chem. Soc.*, **64**, 2796 (1942).

<sup>56</sup> S. Winstein and R. E. Buckles, *J. Am. Chem. Soc.*, **65**, 613 (1943).

<sup>57</sup> H. W. Heine, A. D. Miller, W. H. Barton, and R. W. Greiner, *J. Am. Chem. Soc.*, **75**, 4778 (1953).



Table 4.13. Relative Rates of Cyclization as a Function of Ring Size

Ring size	Lactonization of $\omega$ -bromo carboxylates <sup>a</sup>	$\Delta H^\ddagger$ (kcal/mol)	$\Delta S^\ddagger$ (eu)	Cyclization of $\omega$ -bromoalkylmalonates <sup>b</sup>
3	$8.2 \times 10^{-4}$	22.0	-2.5	
4	0.92	17.7	-5.0	0.58
5	108	15.9	-5.5	833
6	1.00	17.2	-4.1	1.00
7	$3.7 \times 10^{-3}$	17.4	-13.5	$8.7 \times 10^{-3}$
8	$3.8 \times 10^{-5}$	21.7	-9.2	$1.5 \times 10^{-4}$
9	$4.3 \times 10^{-5}$	20.3	-14.0	$1.7 \times 10^{-5}$
10	$1.3 \times 10^{-4}$	17.3	-20.7	$1.4 \times 10^{-6}$
11	$3.3 \times 10^{-4}$	16.4	-22.3	$2.9 \times 10^{-6}$
12	$4.1 \times 10^{-4}$	17.6	-18.0	$4.0 \times 10^{-4}$
13	$1.2 \times 10^{-3}$	15.3	-23.0	$7.4 \times 10^{-4}$
17				$2.9 \times 10^{-3}$
18	$2.0 \times 10^{-3}$	15.2	-21.8	
21				$4.3 \times 10^{-3}$
23	$2.3 \times 10^{-3}$	14.5	-22.3	

a. C. Galli, G. Illuminati, L. Mandolini, and P. Tamborra, *J. Am. Chem. Soc.* **99**, 2591 (1977); L. Mandolini, *J. Am. Chem. Soc.*, **100**, 550 (1978).

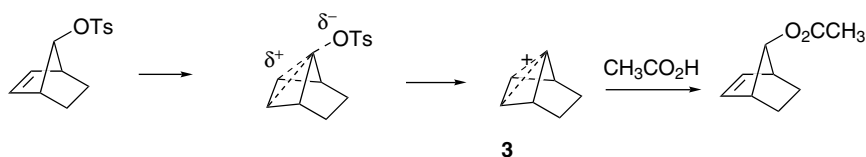
b. M. A. Casadei, C. Galli, and L. Mandolini, *J. Am. Chem. Soc.*, **106**, 1051 (1984).

to lactonization of  $\omega$ -bromocarboxylates. Both reactions occur by direct displacement mechanisms. The dissection of the  $E_a$  of ring-closure reactions into enthalpy and entropy components shows some consistent features. The  $\Delta H^\ddagger$  for formation of three- and four-membered rings is normally higher than for five- and six-membered rings, whereas  $\Delta S^\ddagger$  is least negative for three-membered rings. The  $\Delta S^\ddagger$  is comparable for four-, five-, and six-membered rings and then becomes more negative as the ring size increases above seven. The  $\Delta H^\ddagger$  term reflects the strain that develops in the closure of three-membered rings, whereas the more negative entropy associated with larger rings indicates the decreased probability of encounter of the reaction centers as they get farther apart. Because of the combination of these two factors, the maximum rate is usually observed for the five- and six-membered rings.

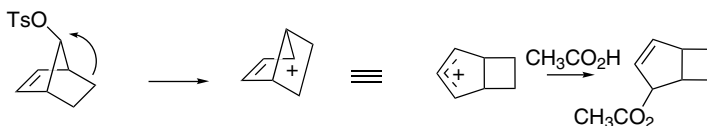
In general, any system that has a nucleophilic substituent situated properly for back-side displacement of a leaving group at another carbon atom of the molecule can be expected to display neighboring-group participation. The extent of the rate enhancement depends on how effectively the group acts as an internal nucleophile. The existence of participation may be immediately obvious from the structure of the product if a derivative of the cyclic intermediate is stable. In other cases, demonstration of kinetic acceleration or stereochemical consequences may provide the basis for identifying nucleophilic participation.

The  $\pi$  electrons of carbon-carbon double bonds can also become involved in nucleophilic substitution reactions. This participation can facilitate the ionization step if it leads to a carbocation having special stability. Solvolysis reactions of the *syn* and *anti* isomers of 7-norbornenyl tosylates provide some dramatic examples of the influence of participation by double bonds on reaction rates and stereochemistry. The *anti*-tosylate is more reactive by a factor of about  $10^{11}$  than the saturated analog toward acetolysis. The reaction product, *anti*-7-acetoxynorbornene, is the product of *retention* of configuration. These results can be explained by participation of the  $\pi$  electrons of the double bond to give the ion **3**, which is stabilized by delocalization of the positive charge.<sup>59</sup>

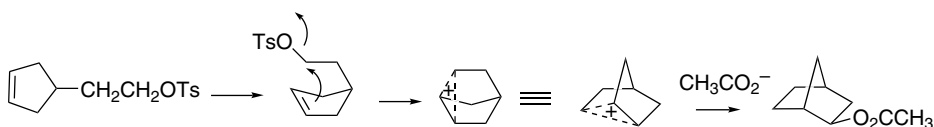
<sup>59</sup> S. Winstein, M. Shavatsky, C. Norton, and R. B. Woodward, *J. Am. Chem. Soc.*, **77**, 4183 (1955); S. Winstein and M. Shavatsky, *J. Am. Chem. Soc.*, **78**, 592 (1956); S. Winstein, A. H. Lewin, and K. C. Pande, *J. Am. Chem. Soc.*, **85**, 2324 (1963).



In contrast, the *syn* isomer, where the double bond is not in a position to participate in the ionization step, reacts  $10^7$  times slower than the *anti* isomer. The reaction product in this case is derived from a rearranged carbocation ion that is stabilized by virtue of being allylic.<sup>60</sup>

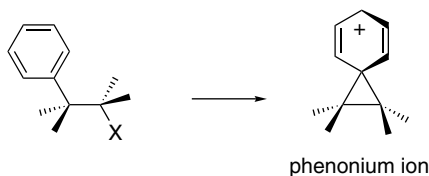


Participation of carbon-carbon double bonds in solvolysis reactions is revealed in some cases by isolation of products with new carbon-carbon  $\sigma$  bonds. A particularly significant case is the formation of the bicyclo[2.2.1]heptane ring during solvolysis of 2-cyclopent-3-enylethyl tosylate.<sup>61</sup>



In this case, the participation leads to the formation of the norbornyl cation, which is captured as the acetate. More is said about this important cation in Section 4.4.5.

A system in which the participation of aromatic  $\pi$  electron has been thoroughly probed is the “phenonium” ions, the species resulting from participation by a  $\beta$ -phenyl group.

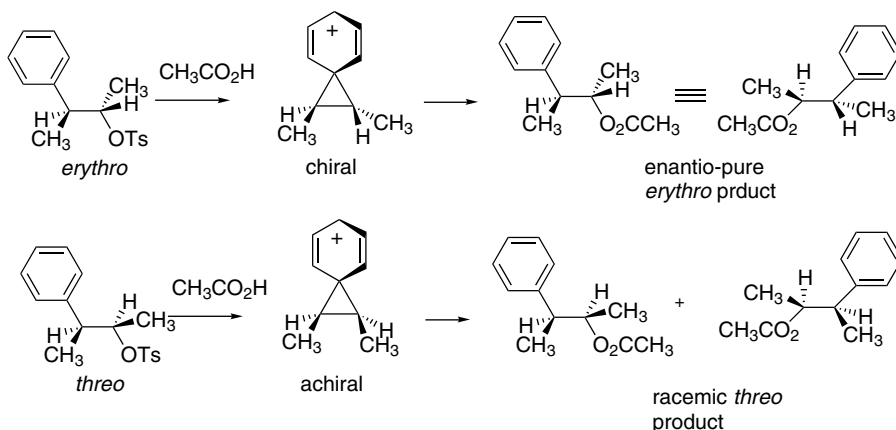


Such participation leads to a bridged carbocation with the positive charge delocalized into the aromatic ring. Evidence for this type of participation was first obtained by a study of the stereochemistry of solvolysis of 3-phenyl-2-butyl tosylates. The *erythro* isomer gave largely retention of configuration, a result that can be explained via a

<sup>60</sup>. S. Winstein and E. T. Stafford, *J. Am. Chem. Soc.*, **79**, 505 (1957).

<sup>61</sup>. R. G. Lawton, *J. Am. Chem. Soc.*, **83**, 2399 (1961).

bridged ion intermediate. The *threo* isomer, where participation leads to an achiral intermediate, gave racemic *threo* product.<sup>62</sup>



The relative importance of aryl participation is a function of the substituents on the ring. The extent of participation can be quantitatively measured by comparing the rate of direct displacement,  $k_s$ , with the rate of aryl-assisted solvolysis, designated  $k_\Delta$ .<sup>63</sup> The relative contributions to individual solvolyses can be distinguished by taking advantage of the higher sensitivity to aryl substituent effects of the assisted mechanism. In systems with EWG substituents, the aryl ring does not participate effectively and only the process described by  $k_s$  contributes to the rate. Such compounds give a Hammett correlation with  $\rho$  values ( $-0.7$  to  $-0.8$ ) characteristic of a weak substituent effect. Compounds with ERG substituents deviate from the correlation line because of the aryl participation. The extent of reaction proceeding through the  $k_s$  process can be estimated from the correlation line for electron-withdrawing substituents.

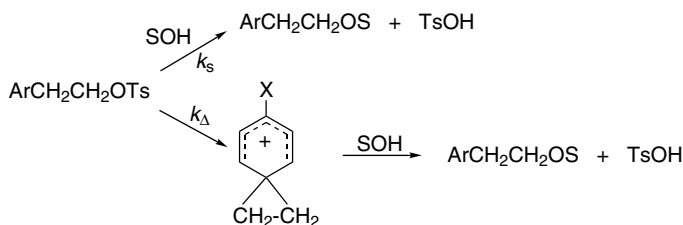


Table 4.14 gives data indicating the extent of aryl rearrangement for several substituents in different solvents. This method of analysis shows that the relative extent of participation of the  $\beta$ -phenyl groups is highly dependent on the solvent.<sup>64</sup> In solvents of good nucleophilicity (e.g., ethanol), the normal solvent displacement mechanism

<sup>62</sup> D. J. Cram, *J. Am. Chem. Soc.*, **71**, 3863 (1949); **74**, 2129 (1952).

<sup>63</sup> A. Diaz, I. Lazdins, and S. Winstein, *J. Am. Chem. Soc.*, **90**, 6546 (1968).

<sup>64</sup> F. L. Schadt, III, C. J. Lancelot, and P. v. R. Schleyer, *J. Am. Chem. Soc.*, **100**, 228 (1978).

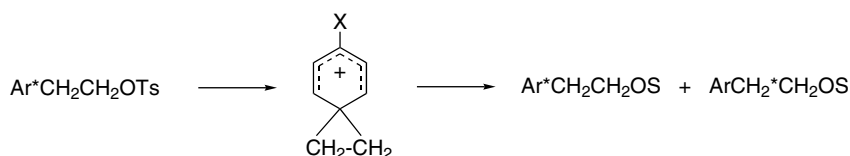
**Table 4.14. Extent of Aryl Rearrangement in 2-Phenylethyl Tosylate Solvolysis**

Substituent	Solvent		
	80% Ethanol <sup>a</sup>	Acetic acid <sup>b</sup>	Formic acid <sup>b</sup>
NO <sub>2</sub>	0	–	–
CF <sub>3</sub>	0	–	–
Cl	7	–	–
H	21	38	78
CH <sub>3</sub>	63	71	94
CH <sub>3</sub> O	93	94	99

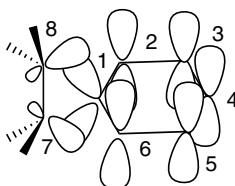
a. D. J. Raber, J. M. Harris, and P. v. R. Schleyer, *J. Am. Chem. Soc.*, **93**, 4829 (1971).

b. C. C. Lancelot and P. v. R. Schleyer, *J. Am. Chem. Soc.*, **91**, 4296 (1969).

makes a larger contribution. As solvent nucleophilicity decreases, the relative extent of aryl participation increases.



The bridged form of the  $\beta$ -phenylethyl cation can be observed in superacid media (see Section 4.4) and characterized by carbon and proton NMR spectra.<sup>65</sup> The bridged ion subsequently rearranges to the more stable  $\alpha$ -methylbenzyl cation with  $E_a$  of about 13 kcal/mol. High-level MO and DFT calculations have been performed on the bridged ion. The bond length to C(1) from C(7) and C(8) is 1.625 Å, whereas the C(7)–C(8) bond length is 1.426 Å. The phenonium ion has a good deal of delocalization of the electron deficiency and the resulting positive charge into the cyclopropane ring.<sup>66</sup> This occurs by overlap of the cyclopropyl orbitals with the  $\pi$  system.



## 4.4. Structure and Reactions of Carbocation Intermediates

### 4.4.1. Structure and Stability of Carbocations

The critical step in the ionization mechanism for nucleophilic substitution is the generation of the carbocation intermediate. For this mechanism to operate, it is essential

<sup>65</sup> G. A. Olah, R. J. Spear, and D. A. Forsyth, *J. Am. Chem. Soc.*, **98**, 6284 (1976).

<sup>66</sup> S. Sieber and P. v. R. Schleyer, *J. Am. Chem. Soc.*, **115**, 6987 (1993); E. Del Rio, M. K. Menendez, R. Lopez, and T. L. Sordo, *J. Phys. Chem. A*, **104**, 5568 (2000); E. del Rio, M. I. Menendez, R. Lopez, and T. L. Sordo, *J. Am. Chem. Soc.*, **123**, 5064 (2001).

that the carbocation not be prohibitively high in energy. Carbocations are inherently high-energy species. The ionization of *t*-butyl chloride is endothermic by 153 kcal/mol in the gas phase.<sup>67</sup>



An activation energy of this magnitude would lead to an unobservably slow reaction at normal temperature. Carbocation formation in solution is feasible because of solvation of the ions that are produced. It is also important to understand the effect structure and substituents have on carbocation stability. We introduced this subject in Section 3.4.1, where we emphasized inherent structural effects in the gas phase, but owing to the important role of solvation in ionization reactions, we have to consider carbocation stability in solution as well. A method that is applicable to highly stabilized cations is to determine the extent of carbocation formation from the parent alcohol in acidic solution. The triarylmethyl cations are stabilized by the conjugation that delocalizes the positive charge. In acidic solution, equilibrium is established between triarylcabinols and the corresponding carbocation:



The relative stability of the carbocation can be expressed in terms of its  $\text{p}K_{\text{R}^+}$ , which is defined as

$$\text{p}K_{\text{R}^+} = \log \frac{[\text{R}^+]}{[\text{ROH}]} + H_{\text{R}}$$

where  $H_{\text{R}}$  is an acidity function defined for the medium.<sup>68</sup> In dilute aqueous solution,  $H_{\text{R}}$  is equivalent to pH, and  $\text{p}K_{\text{R}^+}$  is equal to the pH at which the carbocation and alcohol are present in equal concentrations. The values shown in Table 4.15 were determined by measuring the extent of carbocation formation at several acidities and applying the definition of  $\text{p}K_{\text{R}^+}$ .

The  $\text{p}K_{\text{R}^+}$  values allow for a comparison of the stability of relatively stable carbocations. The data in Table 4.15 show that ERG substituents on the aryl rings stabilize the carbocation (less negative  $\text{p}K_{\text{R}^+}$ ), whereas EWGs such as nitro are destabilizing. This is as expected from the electron-deficient nature of carbocations. The diarylmethyl cations listed in Table 4.14 are 6–7  $\text{p}K_{\text{R}^+}$  units less stable than the corresponding triarylmethyl cations. This indicates that the additional aryl groups have a cumulative, although not necessarily additive, effect on the stability of the carbocation. Primary benzylic cations are generally not sufficiently stable for direct determination of  $\text{p}K_{\text{R}^+}$  values. A value of  $\leq 20$  has been assigned to the benzyl cation based on rate measurements for the forward and reverse reactions.<sup>69</sup> A particularly stable benzylic ion, the 2,4,6-trimethylphenylmethyl cation has a  $\text{p}K_{\text{R}^+}$  of  $-17.4$ . *t*-Alkyl cations have  $\text{p}K_{\text{R}^+}$  values around  $-15$ .

Several very stable carbocations are included in the “Other Carbocations” part of Table 4.15. The tricyclopropylmethyl cation, for example, is more stable than the

<sup>67</sup> D. W. Berman, V. Anicich, and J. L. Beauchamp, *J. Am. Chem. Soc.*, **101**, 1239 (1979).

<sup>68</sup> N. C. Deno, J. J. Jaruzelski, and A. Schriesheim, *J. Am. Chem. Soc.*, **77**, 3044 (1955).

<sup>69</sup> T. L. Amyes, J. P. Richard, and M. Novak, *J. Am. Chem. Soc.*, **114**, 8032 (1992).

Table 4.15. Values of  $pK_{R^+}$  for Some Carbocations<sup>a</sup>

Carbocation	$pK_{R^+}$	Carbocation	$pK_{R^+}$
<i>A. Triarylmethyl</i>			
Triphenyl	-6.63	4, 4', 4''-Tri(dimethylamino)phenyl	+9.36
4, 4', 4''-Trimethyltriphenyl	-3.56	4, 4', 4''-Trichlorotriphenyl	-7.74
4-Methoxytriphenyl	-3.40	4-Nitrotriphenyl	-9.15
4, 4'-Dimethoxytriphenyl	-1.24	4, 4', 4''-Trinitrotriphenyl	-16.27
4, 4', 4''-Trimethoxytriphenyl	+0.82		
<i>B. Diarylmethyl</i>			
Diphenyl	-13.3	2, 2', 4, 4', 6, 6'-Hexamethyldiphenyl	-6.6
4, 4'-Dimethyldiphenyl	-10.4	4, 4'-Dichlorodiphenyl	-13.96
4, 4'-Dimethoxydiphenyl	-5.71		
<i>C. Other Carbocations</i>			
Benzyl <sup>b</sup>	≤ -20	Triphenylcyclopropenyl <sup>c</sup>	+3.1
<i>t</i> -Butyl <sup>c</sup>	-15.5	2,4,6-trimethylbenzyl	-17.4
2-Phenyl-2-propyl <sup>b</sup>	-12.3	Trimethylcyclopropenyl <sup>f</sup>	+7.8
Tropylium (Cycloheptatrienyl)	+4.7	Tricyclopropylcyclopropenyl <sup>g</sup>	+9.7
Tricyclopropylmethyl <sup>d</sup>	-2.3		

SECTION 4.4

Structure and Reactions  
of Carbocation  
Intermediates

a. Unless otherwise indicated, the  $pK_{R^+}$  values are taken from N. C. Deno, J. J. Jaruzelski, and A. Schriesheim, *J. Am. Chem. Soc.*, **77**, 3044 (1955); see also H. H. Freedman in *Carbonium Ions*, vol. IV, G. A. Olah and P. v. R. Schleyer, eds., Wiley-Interscience, New York, 1973, Chap. 28.

b. T. L. Amyes, J. P. Richard, and M. Novak, *J. Am. Chem. Soc.*, **114**, 8032 (1992).

c. R. H. Boyd, R. W. Taft, A. P. Wolf, and D. R. Christman, *J. Am. Chem. Soc.*, **82**, 4729 (1960); E. M. Arnett and T. C. Hofelich, *J. Am. Chem. Soc.*, **105**, 2889 (1983); D. D. M. Wayner, D. J. McPhee, and D. J. Griller, *J. Am. Chem. Soc.*, **110**, 132 (1988).

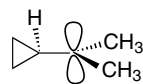
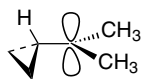
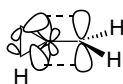
d. N. C. Deno, H. G. Richey, Jr., J. S. Liu, D. N. Lincoln, and J. O. Turner, *J. Am. Chem. Soc.*, **87**, 4533 (1965).

e. R. Breslow, H. Höver, and H. W. Chang, *J. Am. Chem. Soc.*, **84**, 3168 (1962); R. Breslow, J. Lockhart, and H. W. Chang, *J. Am. Chem. Soc.*, **83**, 2367 (1961).

f. J. Ciabattoni and E. C. Nathan, III, *Tetrahedron Lett.*, 4997 (1969).

g. K. Komatsu, I. Tomioka, and K. Okamoto, *Tetrahedron Lett.*, 947 (1980); R. A. Moss and R. C. Munjal, *Tetrahedron Lett.*, 1221 (1980).

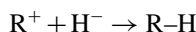
triphenylmethyl cation.<sup>70</sup> The stabilization of carbocations by cyclopropyl substituents results from the interaction of the cyclopropyl bonding orbitals with the vacant carbon *p*-orbital. The electrons in these orbitals are at relatively higher energy than normal  $\sigma$ -electrons and are therefore particularly effective in interacting with the vacant *p*-orbital of the carbocation. This interaction imposes a stereoelectronic preference for the bisected conformation of the cyclopropylmethyl cation in comparison to the perpendicular conformation. Only the bisected conformation aligns the cyclopropyl C–C orbitals for effective overlap.

bisected  
conformationperpendicular  
conformationbisected  
conformationperpendicular  
conformation

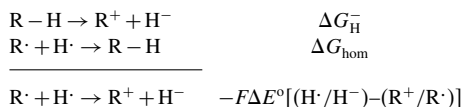
As discussed in Section 3.4.1, carbocation stability can also be expressed in terms of *hydride affinity*. Hydride affinity values based on solution measurements can be

<sup>70</sup> For reviews of cyclopropylmethyl cation see H. G. Richey, Jr., in *Carbonium Ions*, Vol. III, G. A. Olah and P. v. R. Schleyer, eds., Wiley-Interscience, New York, 1972, Chap. 25; G. A. Olah, V. Reddy, and G. K. S. Prakash, *Chem. Rev.*, **92**, 69 (1992); G. A. Olah, V. Reddy, and G. K. S. Prakash, *Chemistry of the Cyclopropyl Group*, Part 2, Z. Rappoport, ed., Wiley, Chichester, 1995, pp. 813–859.

derived from thermodynamic cycles that relate  $pK_a$  and electrochemical potentials. The hydride affinity,  $-\Delta G$ , for the reaction



is a measure of carbocation stability. This quantity can be related to an electrochemical potential by summation with the energy for hydrogen atom removal, i.e., the homolytic bond dissociation energy.



so

$$\Delta G_{\text{H}^-} = \Delta G_{\text{hom}} - -F\Delta E^\circ[(H\cdot/H^-)-R^+/R\cdot]$$

where  $(H\cdot/H^-)$  and  $(R^+/R\cdot)$  are one-electron oxidation potentials for  $H^-$  and  $R\cdot$ .<sup>71</sup> The former potential is about  $-0.55$  V in DMSO. Measurement of  $(R^+/R\cdot)$  can be accomplished by cyclic voltammetry for relatively stable carbocations and by other methods for less stable cations. The values obtained range from 83 kcal/mol for the aromatic tropylium ion to 130 kcal/mol for a benzylic cation destabilized by a EWG substituents. Some of these data are included in Table 4.16. Note that these values are considerably smaller than the corresponding gas phase values, which range from 200 kcal/mol for tropylium ion to 239 kcal/mol for the benzyl cation, although the *difference* in stability is quite similar. This is the result of solvent stabilization.

It is possible to obtain thermodynamic data for the ionization of alkyl chlorides by reaction with  $\text{SbF}_5$ , a strong Lewis acid, in the nonnucleophilic solvent  $\text{SO}_2\text{ClF}$ .<sup>72</sup> The solvation energies of the carbocations in this medium are small and do not differ much from one another, which makes comparison of nonisomeric systems reasonable. As long as subsequent reactions of the carbocation can be avoided, the thermodynamic characteristics of the ionization reactions provide a measure of the relative ease of carbocation formation in solution. There is good correlation between these data and the

**Table 4.16. Solution Hydride Affinity of Some Carbocations<sup>a</sup>**

Carbocation	$\Delta H$ (kcal/mol)	$\Delta H_{\text{gas}}$ (kcal/mol)
Tropylium ion	83	200 <sup>b</sup>
$\text{Ph}_3\text{C}^+$	96	215
$\text{Ph}_2\text{C}^+\text{H}$	105	222
$\text{PhCH}_2^+$	118	238
$p\text{-CH}_3\text{OC}_6\text{H}_4\text{CH}_2^+$	106	227
$p\text{-NCC}_6\text{H}_4\text{CH}_2^+$	122	247

a. J.-P. Cheng, K. L. Handoo, and V. D. Parker, *J. Am. Chem. Soc.*, **115**, 2655 (1993).

b. See Table 3.10.

<sup>71</sup> J.-P. Cheng, K. L. Handoo, and V. D. Parker, *J. Am. Chem. Soc.*, **115**, 2655 (1993).

<sup>72</sup> E. M. Arnett and N. J. Pienta, *J. Am. Chem. Soc.*, **102**, 3329 (1980); E. M. Arnett and T. C. Hofelich, *J. Am. Chem. Soc.*, **105**, 2889 (1983).

gas phase data, in terms of both the stability order and the energy differences between the carbocations. A plot of the ionization enthalpy and gas phase hydride affinity gives a line of slope 1.63 with a correlation coefficient of 0.973. This result is in agreement with the expectation that the gas phase stability would be more sensitive to structure than the solution phase stability. The energy gap between tertiary and secondary ions is about 17 kcal/mol in the gas phase and about 9.5 kcal/mole in the  $\text{SO}_2\text{ClF}$  solution. An independent measurement of the energy difference between secondary and tertiary cations in solution is available from calorimetric measurement of the  $\Delta H$  of isomerization of the *sec*-butyl cation to the *tert*-butyl cation. This value has been found to be 14.5 kcal/mol in  $\text{SO}_2\text{ClF}$  solution.<sup>73</sup> An MP2/6-31G\* computation finds a difference of 14.8 kcal.<sup>74</sup> Some representative data are given in Table 4.17. These data give some basis for comparison of the stability of secondary and tertiary alkyl carbocations with aryl-substituted ions. Note also that the solution data also show that cyclopropyl groups are very stabilizing toward carbocations.

The increase in carbocation stability with additional alkyl substitution is one of the most important and general trends in organic chemistry. This stability relationship is fundamental to understanding many aspects of reactivity, especially nucleophilic substitution. Hyperconjugation is the principal mechanism by which alkyl substituents stabilize carbocations. There is considerable evidence of the importance of hyperconjugation on the structure of carbocations, including NMR data, crystallographic data, and computational studies. The *tert*-butyl cation has been studied by each method. The NMR results indicate shortening of the C–C bonds, as would be predicted by hyperconjugation.<sup>75</sup> The crystal structure gives a value of 1.44 Å.<sup>76</sup> A computational study at the MP2/6-31G\*\* level shows a slight elongation of the C–H bonds aligned with the *p* orbital, and the C–C–H bond angles are slightly reduced (Figure 4.8).<sup>77</sup>

Levy has performed NPA, Mulliken, AIM, and CHELPG charge analyses on the *iso*-propyl, *sec*-butyl, and *tert*-butyl cations using MP2/6-31G\*-level computations.<sup>74</sup> As mentioned briefly in Section 3.4.1, the trivalent carbon atom in *tert*-butyl cation

**Table 4.17.  $\Delta H$  for Ionization of Chlorides and Alcohols in  $\text{SO}_2\text{ClF}$**

Reactant	$\Delta H$ (kcal/mol)	
	X=Cl	X=OH
$(\text{CH}_3)_2\text{CH}-\text{X}$	-15	
$\text{Ph}_2\text{C}(\text{CH}_3)-\text{X}$	-16	
$(\text{CH}_3)_3\text{C}-\text{X}$	-25	-35
$\text{PhC}(\text{CH}_3)_2-\text{X}$	-30	-40
$\text{Ph}_2\text{C}(\text{CH}_3)-\text{X}$		-37.5
$\text{Ph}_3\text{C}-\text{X}$		-49
$(\triangleleft)_3\text{C}-\text{X}$		-59

a. Data from E. M. Arnett and T. C. Hofelich, *J. Am. Chem. Soc.*, **105**, 2889 (1983).

<sup>73</sup> E. W. Bittner, E. M. Arnett, and M. Saunders, *J. Am. Chem. Soc.*, **98**, 3734 (1976).

<sup>74</sup> J. B. Levy, *Struct. Chem.*, **10**, 121 (1999).

<sup>75</sup> C. S. Yannoni, R. D. Kendrick, P. C. Myhre, D. C. Bebout, and B. L. Petersen, *J. Am. Chem. Soc.*, **111**, 6440 (1989).

<sup>76</sup> S. Hollenstein and T. Laube, *J. Am. Chem. Soc.*, **115**, 7240 (1993).

<sup>77</sup> S. Sieber, P. Buzek, P. v. R. Schleyer, W. Koch, and J. W. d. M. Carneiro, *J. Am. Chem. Soc.*, **115**, 259 (1993).

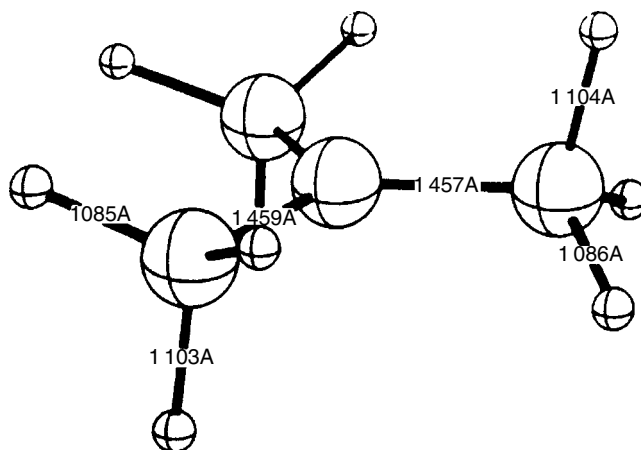
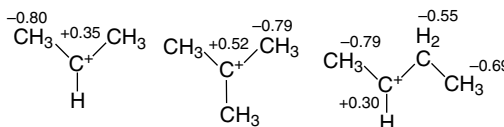
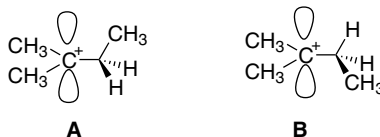


Fig. 4.8. MP2/6-31G\*\* optimized structure of *t*-butyl cation with three hydrogens aligned with the *p* orbital. Reproduced from *J. Am. Chem. Soc.* **115**, 259 (1993), by permission of the American Chemical Society.

is found to be more positive than the carbon in the secondary ions. The adjacent carbons bear negative charges, as a result of electron donation from hydrogen. The charges on hydrogen range from +0.26 to +0.38, averaging +0.32 in the *tert*-butyl cation, according to the NPA analysis. This is consistent with the representation of the stabilizing effect in terms of hyperconjugation. This analysis also suggests that a significant part of the stabilization of the *tert*-butyl cation comes from the favorable electrostatic consequence of alternating positive and negative charges.



The 2-methyl-2-butyl cation provides the opportunity to compare C–C and C–H hyperconjugation. At the MP4/6-31G\*\* level of calculation, little energy difference is found between structures **A** and **B**, which differ in alignment of CH<sub>3</sub> or H with the empty *p* orbital.<sup>78</sup> Structure **A**, however, gives a much closer approximation to the observed <sup>13</sup>C chemical shift and thus seems to be preferred. The calculations also indicate a lengthening of the C(3)–C(4) bond (to 1.58 Å) and a contraction of the C(2)–C(3)–C(4) bond angle to 101.5°, both of which are consistent with C–C hyperconjugation.



A particularly interesting example of the effect of hyperconjugation is found in the 1-methylcyclohexyl carbocation. The NMR spectrum of this cation reveals the presence

<sup>78</sup> P. v. R. Schleyer, J. W. de Carneiro, W. Koch, and D. A. Forsyth, *J. Am. Chem. Soc.*, **113**, 3990 (1991).

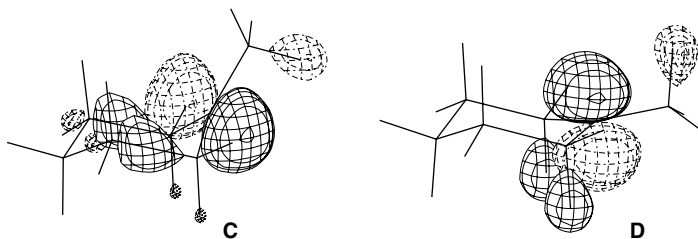
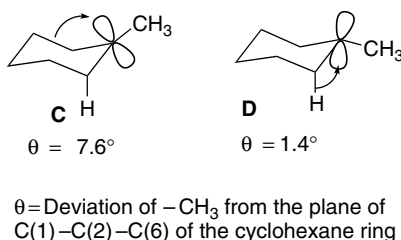


Fig. 4.9. Distribution of LUMO orbitals of isomeric 1-methylcyclohexyl cations showing dominant C–C (**C**) and C–H (**D**) hyperconjugation. Reproduced from *J. Am. Chem. Soc.*, **118**, 3761 (1996), by permission of the American Chemical Society.

of two isomeric cations that are separated by a small barrier. Investigation of the NMR chemical shifts using the MP2-GIAO method points to an axial and equatorial isomer of nearly equal energy. B3LYP/6-31G\* calculations indicate an energy difference of about 0.6 kcal and suggest that the (nearly planar) TS is about 0.9 kcal above the minimum energy structure.<sup>79</sup> The cationic carbon is slightly pyramidalized toward the C–C or C–H bonds involved in hyperconjugation. The reason for the pyramidalization is better alignment with the C–C and C–H bonds that provide hyperconjugative stabilization. The hyperconjugation is also indicated by the differing shapes of the LUMO orbitals for the isomeric ions shown in Figure 4.9.



The 1-adamantyl carbocation provides another example of C–C hyperconjugation. The C $\alpha$ –C $\beta$  bond is shortened by 0.06 Å in the crystal structure.<sup>80</sup> The NMR spectrum also shows characteristics of delocalization of the positive charge. A computational study also indicates delocalization of the positive charge.<sup>81</sup>



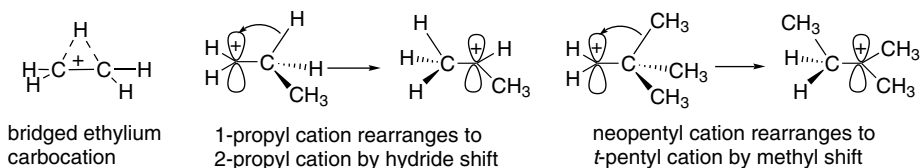
It is important to note the relationship of C–H and C–C hyperconjugation to the *reactivity* as well as the *structure* of carbocations. Hyperconjugation represents electron sharing with an empty orbital and can lead to structural changes or

<sup>79</sup> A. Rauk, T. S. Sorensen, C. Maerker, J. W. d. M. Carneiro, S. Sieber, and P. v. R. Schleyer, *J. Am. Chem. Soc.*, **118**, 3761 (1996); A. Rauk, T. S. Sorensen, and P. v. R. Schleyer, *J. Chem. Soc., Perkin Trans. 2*, 869 (2001).

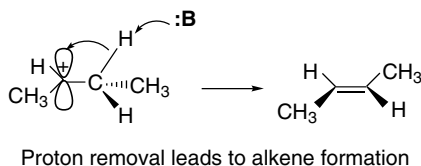
<sup>80</sup> T. Laube, *Angew. Chem. Intl. Ed. Engl.*, **25**, 349 (1986); T. Laube and E. Schaller, *Acta Crystallog. B*, **B51**, 177 (1995).

<sup>81</sup> G. A. Olah, G. K. S. Prakash, J. G. Shih, V. V. Krishnamurthy, G. D. Mateescu, G. Liang, G. Sipos, V. Buss, T. M. Gund, and P. v. R. Schleyer, *J. Am. Chem. Soc.*, **107**, 2764 (1985).

reactions. If the electron density is substantially shared between the two atoms, the structure is *bridged*. If the electron sharing results in a shift of the donor group, *rearrangement* occurs. As we saw in Section 3.4.1, the ethyl cation is bridged. Larger primary cations rearrange to more stable carbocations; for example, the 1-propyl cation rearranges to the 2-propyl cation and a neopentyl cation rearranges to a *t*-pentyl cation. These rearrangements are the culmination of electron donation by formation of a new bond.



Hyperconjugation also makes carbocations susceptible to proton removal, as occurs in elimination reactions. The weakened C–H bond and increased positive charge make hydrogen susceptible to removal as a proton. When we study elimination reactions in Section 5.10, we will find that there is a preference for the removal of the proton from the most highly substituted carbon, which is the one that is most engaged in hyperconjugation.

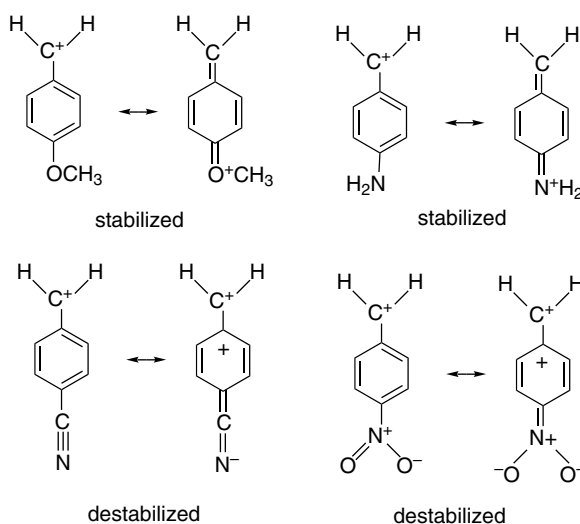


Within any given series of carbocations, substituents affect stability in predictable ways. ERG substituents stabilize carbocations, whereas EWG substituents destabilize them. Careful attention must be paid to both resonance and polar effects. The resonance effect is very strong for substituents directly on the cationic carbon. Benzylic cations are strongly stabilized by resonance interactions with the aromatic ring. Substituent effects can be correlated by the Yukawa-Tsuno equation.<sup>82</sup> For example, gas phase chloride ion affinities correlate with the Yukawa-Tsuno equation with  $\rho = -14.0$  and  $r^+ = 1.29$ , indicating a strong resonance interaction.<sup>83</sup> A molecular orbital calculation estimating the stabilization was done using STO-3G-level basis functions. The electron-donating *p*-amino and *p*-methoxy groups were found to stabilize a benzyl cation by 26 and 14 kcal/mol, respectively. On the other hand, electron-attracting groups such as *p*-cyano and *p*-nitro were destabilizing by 12 and 20 kcal/mol, respectively.<sup>84</sup>

<sup>82</sup> Y. Tsuno and M. Fujio, *Chem. Soc. Rev.*, **25**, 129 (1996).

<sup>83</sup> M. Mishima, K. Arima, H. Inoue, S. Usui, M. Fujio, and Y. Tsuno, *Bull. Chem. Soc. Jpn.*, **68**, 3199 (1995).

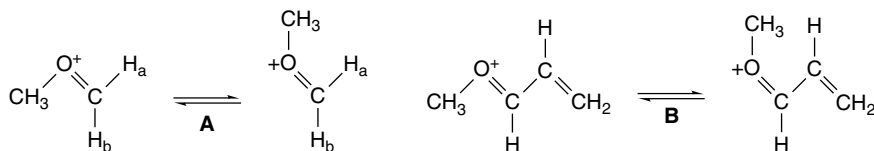
<sup>84</sup> W. J. Hehre, M. Taagepera, R. W. Taft, and R. D. Topsom, *J. Am. Chem. Soc.*, **103**, 1344 (1981).



Adjacent atoms with one or more unshared pairs of electrons strongly stabilize a carbocation. Table 3.11 (p. 304) indicates the stabilization of the methyl cation by such substituents. Alkoxy and dialkylamino groups are important examples of this effect.

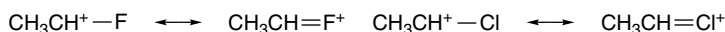


Although these structures have a positive charge on a more electronegative atom, they benefit from an additional bond that satisfies the octet requirement of the tricoordinate carbon. These "carbocations" are best represented by the doubly bonded resonance structures. One indication of the strong participation of adjacent oxygen substituents is the existence of a barrier to rotation about the C–O bonds in this type of carbocation.



The barrier in **A** is about 14 kcal/mole ( $\Delta G^*$ ) as measured by NMR coalescence of the nonidentical vinyl protons.<sup>85</sup> The gas phase barrier is calculated by MO methods to be 26 kcal/mol. The observed barrier for **B** is 19 kcal/mol.<sup>86,87</sup>

Even halogen substituents stabilize carbocations as a result of resonance donation from the halogen electron pairs. A fluorine or chlorine substituent is nearly as stabilizing as a methyl group in the gas phase.<sup>88</sup>



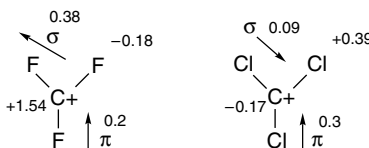
<sup>85</sup> D. Cremer, J. Gauss, R. F. Childs, and C. Blackburn, *J. Am. Chem. Soc.*, **107**, 2435 (1985).

<sup>86</sup> R. F. Childs and M. E. Hagar, *Can. J. Chem.*, **58**, 1788 (1980).

<sup>87</sup> There is another mechanism for equilibration of the cation pairs  $\mathbf{A}_1 \rightleftharpoons \mathbf{A}_2$  and  $\mathbf{B}_1 \rightleftharpoons \mathbf{B}_2$ , namely inversion at oxygen. However, the observed barrier represents at least the *minimum* for the C=O rotational barrier and therefore demonstrates that the C–O bond has double-bond character.

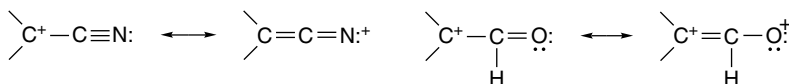
<sup>88</sup> C. H. Reynolds, *J. Am. Chem. Soc.*, **114**, 8676 (1992).

An NPA analysis has been performed on  $F_3C^+$  and  $Cl_3C^+$ .<sup>89</sup> According to this analysis, chlorine is a slightly better  $\pi$  donor than fluorine, and fluorine's polar effect is, of course, stronger. The net result is that the carbon in  $F_3C^+$  is much more positive than the carbon in  $Cl_3C^+$ . Note that even the Cl  $\sigma$  electrons are slightly shifted to the  $sp^2$  carbon. According to this analysis, the positive charge in  $Cl_3C^+$  is carried entirely by the chlorines, whereas in  $F_3C^+$  the positive charge resides entirely on carbon.



Electron-withdrawing groups that are substituted directly on the cationic site are destabilizing. Table 4.18 gives an indication of the relative retardation of the rate of ionization and the calculated destabilization for several substituents.

The trifluoromethyl group, which exerts a powerful polar effect, is strongly destabilizing both on the basis of the kinetic data and the MO calculations. The cyano and formyl groups are less so. In fact, the destabilization of these groups is considerably less than would be predicted on the basis of their polar substituent constants. Both the cyano and formyl groups can act as  $\pi$  donors, even though the effect is to place partial positive charge and electron deficiency on nitrogen and oxygen atoms, respectively.



These resonance structures are the nitrogen and oxygen analogs of the allyl cation. The effect of this  $\pi$  delocalization is to attenuate the polar destabilization by these substituents.<sup>90</sup> These interactions are reflected in MO energies, bond lengths, and charge distributions calculated for such cations<sup>91</sup> (review Section 3.4.1).

**Table 4.18. Destabilization of 2-Substituted *i*-Propyl Cation by EWG Substituents**

Z	Solvolysis rate relative to Z = H	Destabilization HF/4-31G (kcal/mol)
CN	$\sim 10^{-3a}$	9.9 <sup>b</sup>
CF <sub>3</sub>	$\sim 10^{-3c}$	37.3 <sup>b</sup>
CH=O	—	6.1 <sup>b</sup>

a. P. G. Gassman and J. J. Talley, *J. Am. Chem. Soc.*, **102**, 1214 (1980).

b. M. N. Paddon-Row, C. Santiago, and K. N. Houk, *J. Am. Chem. Soc.*, **102**, 6561 (1980).

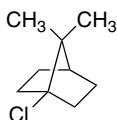
c. K. M. Koshy and T. T. Tidwell, *J. Am. Chem. Soc.*, **102**, 1216 (1980).

<sup>89</sup> G. Frenking, S. Fau, C. M. Marchand, and H. Gruetzmacher, *J. Am. Chem. Soc.*, **119**, 6648 (2000).

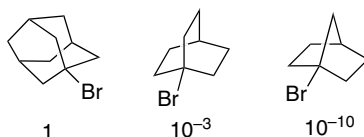
<sup>90</sup> T. T. Tidwell, *Angew. Chem. Int. Ed. Engl.*, **23**, 20 (1984); P. G. Gassman and T. T. Tidwell, *Acc. Chem. Res.*, **16**, 279 (1983); J. L. Holmes and P. M. Mayer, *J. Phys. Chem.*, **99**, 1366 (1995); J. L. Holmes, F. P. Lossing, and P. M. Mayer, *Chem. Phys. Lett.*, **212**, 134 (1993).

<sup>91</sup> D. A. Dixon, P. A. Charlier, and P. G. Gassman, *J. Am. Chem. Soc.*, **102**, 3957 (1980); M. N. Paddon-Row, C. Santiago, and K. N. Houk, *J. Am. Chem. Soc.*, **102**, 6561 (1980); D. A. Dixon, R. A. Eades, R. Frey, P. G. Gassman, M. L. Hendewerk, M. N. Paddon-Row, and K. N. Houk, *J. Am. Chem. Soc.*, **106**, 3885 (1984); X. Creary, Y.-X. Wang, and Z. Jiang, *J. Am. Chem. Soc.*, **117**, 3044 (1995).

Up to this point, we have considered only carbocations in which the cationic carbons are  $sp^2$  hybridized and planar. When this hybridization cannot be achieved, carbocations are of higher energy. In a classic experiment, Bartlett and Knox demonstrated that the tertiary chloride 1-chloroapocamphane was inert to nucleophilic substitution.<sup>92</sup> Starting material was recovered unchanged even after refluxing for 48 h in ethanolic silver nitrate. The unreactivity of this compound is attributed to the structure of the bicyclic system, which prevents rehybridization to a planar  $sp^2$  carbon. Back-side nucleophilic solvent participation is also precluded because of the bridgehead location of the C–Cl bond.



The apocamphyl structure is particularly rigid, and bridgehead carbocations become accessible in more flexible structures. The relative solvolysis rates of the bridgehead bromides 1-bromoadamantane, 1-bromobicyclo[2.2.2]octane, and 1-bromobicyclo[2.2.1]heptane illustrate this trend. The relative rates for solvolysis in 80% ethanol at 25 °C are shown.<sup>93</sup>



The relative reactivity of tertiary bridgehead systems toward solvolysis is well correlated with the increase in strain that results from conversion of the ring structure to a carbocation, as calculated by molecular mechanics.<sup>94</sup> This result implies that the increased energy associated with a nonplanar carbocation is proportional to the strain energy present in the ground state reactant. The solvolysis rates also correlate with bridgehead cation stability measured by gas phase hydride affinity and MP2/6-311G\*\* MO calculations.<sup>95</sup>

Alkenyl carbocations in which the cationic carbon is  $sp$  hybridized are about 15 kcal higher in energy than similar cations in which the cationic center is  $sp^2$  (see Figure 3.18).<sup>96</sup> This is because of the higher electronegativity of the orbital with increasing  $s$ -character. The intermediacy of substituted vinyl cations in solvolysis reactions has been demonstrated, but direct observation has not been possible for simple vinyl cations.<sup>97</sup> Most examples of solvolytic generation of vinyl cations involve very reactive leaving groups, especially trifluoromethanesulfonate (triflates). Typical products include allenes, alkynes, and vinyl esters.<sup>98</sup>

<sup>92</sup> P. D. Bartlett and L. H. Knox, *J. Am. Chem. Soc.*, **61**, 3184 (1939).

<sup>93</sup> For a review of bridgehead carbocations see R. C. Fort, Jr., in *Carbonium Ions*, Vol. IV, G. A. Olah and P. v. R. Schleyer, eds., Wiley-Interscience, New York, 1973, Chap. 32.

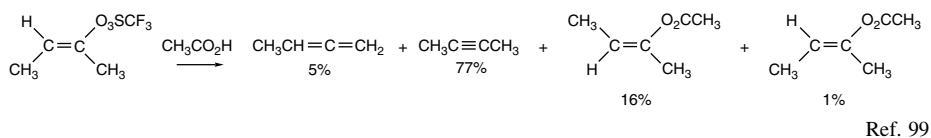
<sup>94</sup> T. W. Bentley and K. Roberts, *J. Org. Chem.*, **50**, 5852 (1985); R. C. Bingham and P. v. R. Schleyer, *J. Am. Chem. Soc.*, **93**, 3189 (1971); P. Müller and J. Mareda, *Helv. Chim. Acta*, **70**, 1017 (1987); P. Müller, J. Mareda, and D. Milin, *J. Phys. Org. Chem.*, **8**, 507 (1995).

<sup>95</sup> E. W. Della and W. K. Janowski, *J. Org. Chem.*, **60**, 7756 (1995); J. L. M. Abboud, O. Castano, E. W. Della, M. Herreros, P. Muller, R. Notario, and J.-C. Rossier, *J. Am. Chem. Soc.*, **119**, 2262 (1997).

<sup>96</sup> V. D. Nefedov, E. N. Sinotova, and V. P. Lebedev, *Russ. Chem. Rev.*, **61**, 283 (1992).

<sup>97</sup> H.-U. Siehl and M. Hanack, *J. Am. Chem. Soc.*, **102**, 2686 (1980).

<sup>98</sup> For reviews of vinyl cations, see Z. Rappoport in *Reactive Intermediates*, R. A. Abramovitch, ed., Vol. 3, Plenum Press, New York, 1983; *Dicoordinated Carbocations*, Z. Rappoport and P. J. Stang, eds., John Wiley & Sons, New York, 1997.



Ref. 99

The phenyl cation is a very unstable cation, as is reflected by the high hydride affinity shown in Figure 3.18. In this case, the ring geometry resists rehybridization so the vacant orbital retains  $sp^2$  character. Since the empty orbital is in the nodal plane of the ring, it receives no stabilization from the  $\pi$  electrons.



Phenyl cations are formed by thermal decomposition of aryldiazonium ions.<sup>100</sup> The cation is so reactive that under some circumstances it can recapture the nitrogen generated in the decomposition.<sup>101</sup> Attempts to observe formation of phenyl cations by ionization of aryl triflates have only succeeded when especially stabilizing groups, such as trimethylsilyl groups are present at the 2- and 6-positions of the aromatic ring.<sup>102</sup>

#### 4.4.2. Direct Observation of Carbocations

A major advance in the study of carbocations occurred during the 1960s when methods for generation of carbocations in superacid media were developed. The term *superacid* refers to media of very high proton-donating capacity, e.g., more acidic than 100% sulfuric acid. A convenient medium for these studies is  $\text{FSO}_3\text{H} - \text{SbF}_5 - \text{SO}_2$ . The fluorosulfonic acid acts as a proton donor and antimony pentafluoride is a powerful Lewis acid that assists ionization. This particular combination has been dubbed “magic acid” because of its powerful protonating ability. The solution is essentially nonnucleophilic, so carbocation of even moderate stability can be generated and observed by NMR spectroscopy.<sup>103</sup> Some examples of these studies are given in Scheme 4.4. Alkyl halides and alcohols, depending on the structure of the alkyl group, react with magic acid and give rise to carbocations. Primary and secondary alcohols are protonated at  $-60^\circ\text{C}$ , but do not ionize. Tertiary alcohols do ionize, giving rise to the corresponding cation. As the temperature is increased, carbocation formation also occurs from secondary alcohols. *sec*-Butyl alcohol ionizes with rearrangement to the

<sup>99</sup> R. H. Summerville, C. A. Senkler, P. v. R. Schleyer, T. E. Dueber, and P. J. Stang, *J. Am. Chem. Soc.*, **96**, 1100 (1974).

<sup>100</sup> C. G. Swain, J. E. Sheats, and K. G. Harbison, *J. Am. Chem. Soc.*, **97**, 783 (1975).

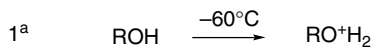
<sup>101</sup> R. G. Bergstrom, R. G. M. Landells, G. W. Wahl, Jr., and H. Zollinger, *J. Am. Chem. Soc.*, **98**, 3301 (1976).

<sup>102</sup> Y. Apeloig and D. Arad, *J. Am. Chem. Soc.*, **107**, 5285 (1985); Y. Himeshima, H. Kobayashi, and T. Sonoda, *J. Am. Chem. Soc.*, **107**, 5286 (1985).

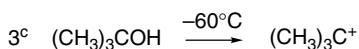
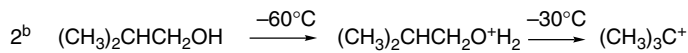
<sup>103</sup> A review of the extensive studies of carbocations in superacid media is available in G. A. Olah, G. K. Surya Prakash, and J. Sommer, *Super Acids*, John Wiley & Sons, New York, 1985.

### Scheme 4.4. Protonation, Ionization, and Rearrangement in Superacid

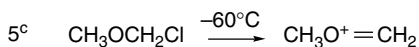
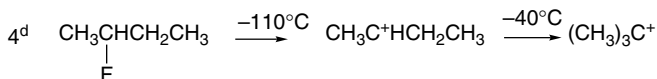
#### A. Alcohols in $\text{FSO}_3\text{H}-\text{SbF}_5-\text{SO}_2$



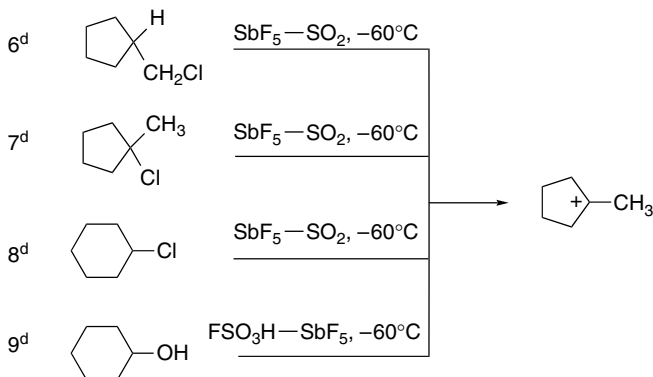
R = methyl, ethyl, *n*-propyl, *i*-propyl, *n*-butyl, *s*-butyl,  
*n*-amyl, *i*-amyl, neopentyl, *n*-hexyl, neohexyl



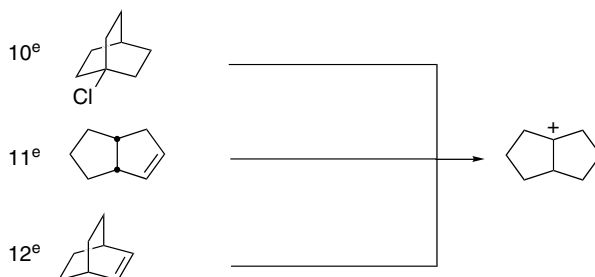
#### B. Alkyl halides in antimony pentafluoride



#### C. Cyclopentyl and Cyclohexyl systems



#### D. Bicyclooctyl systems in $\text{SbF}_5-\text{SO}_2\text{ClF}, -78^\circ\text{C}$



a. G. A. Olah, J. Sommer, and E. Namanworth, *J. Am. Chem. Soc.*, **89**, 3576 (1967).

b. M. Saunders, F. L. Hagen, and J. Rosenfeld, *J. Am. Chem. Soc.*, **90**, 6882 (1968).

c. G. A. Olah and J. M. Bollinger, *J. Am. Chem. Soc.*, **89**, 2993 (1967).

d. G. A. Olah, J. M. Bollinger, C. A. Cupas, and J. Lukas, *J. Am. Chem. Soc.*, **89**, 2692 (1967).

e. G. A. Olah and G. Liang, *J. Am. Chem. Soc.*, **87**, 2998 (1965).

*tert*-butyl cation. At  $-30^{\circ}\text{C}$  the protonated primary isomer, *iso*-butyl alcohol, ionizes, also forming the *tert*-butyl cation. Protonated *n*-butanol is stable to  $0^{\circ}\text{C}$ , at which point it, too, gives rise to the *t*-butyl cation. It is typically observed that ionizations in superacids give rise to the most stable of the isomeric carbocations that can be derived from the alkyl group. The *t*-butyl cation is generated from  $\text{C}_4$  systems, whereas  $\text{C}_5$  and  $\text{C}_6$  alcohols give rise to the *t*-pentyl and *t*-hexyl ions, respectively. Some examples of these studies are given in Scheme 4.4. Entries 6 to 9 and 10 to 12 further illustrate the tendency for rearrangement to the most stable cation to occur. The tertiary 1-methylcyclopentyl cation is the only ion observed from a variety of five- and six-membered ring derivatives. The tertiary bicyclo[3.3.0]octyl cation is formed from all bicyclooctyl ( $\text{C}_8\text{H}_{13}^+$ ) precursors. The tendency to rearrange to the thermodynamically stable ions by multiple migrations is a consequence of the very low nucleophilicity of the solvent system. In the absence of nucleophilic capture by solvent, the carbocations undergo extensive skeletal rearrangement and accumulate as the most stable isomer.

Another important development in permitting structural conclusions from NMR studies on carbocations resulted from the use of theoretical computations of  $^{13}\text{C}$  and  $^1\text{H}$  chemical shifts. Known as the MP2-GIAO method,<sup>104</sup> it has also been applied successfully to allylic, cyclopropylmethyl, and phenonium ions.<sup>105</sup>

Carbocations can also be studied by X-ray crystallography.<sup>106</sup> Early studies involved strongly stabilized cations such as triphenylmethyl<sup>107</sup> and cyclopropylmethyl cations.<sup>108</sup> More recently, the structure of less stable ions, including the *t*-butyl cation, have been obtained.<sup>109</sup> The structure is planar with C–C bonds averaging 1.442 Å. This is substantially less than the  $sp^2$ – $sp^3$  bond length in neutral compounds, which is about 1.50 Å. This finding is consistent with C–H hyperconjugation, although the structure determination did not permit assignment of C–H bond lengths.

#### 4.4.3. Competing Reactions of Carbocations

The product of a substitution reaction that follows the limiting  $\text{S}_{\text{N}}2$  mechanism is determined by the identity of the nucleophile. The nucleophile replaces the leaving group and product mixtures are obtained only if there is competition from several nucleophiles. Product mixtures from ionization mechanisms are often more complex. For many carbocations there are two competing processes that lead to other products: *elimination* and *rearrangement*. We discuss rearrangements in the next section. Here we consider the competition between substitution and elimination under *solvolysis conditions*. We return to another aspect of this competition in Section 5.10, when base-mediated elimination is considered.

The fundamental nature of the substitution-versus-elimination competition is illustrated in Figure 4.10, which is applicable to carbocations such as tertiary alkyl and secondary benzylic that have lifetimes on the order of  $10^{-12}\text{ s}^{-1}$  in hydroxylic solvents (SOH). The carbocation is at a relatively high energy, with very small barriers to either solvent capture ( $k_s$ , substitution product) or proton loss ( $k_e$ , elimination product.) The

<sup>104</sup> J. Gauss, *J. Chem. Phys.*, **99**, 3629 (1993).

<sup>105</sup> P. v. R. Schleyer and C. Maerker, *Pure Appl. Chem.*, **67**, 755 (1995).

<sup>106</sup> T. Laube, *Acc. Chem. Res.*, **28**, 399 (1995).

<sup>107</sup> A. H. Gomes de Mesquita, C. H. MacGillavry, and K. Eriks, *Acta Cryst.*, **18**, 437 (1965).

<sup>108</sup> R. F. Childs, R. Faggiani, C. J. L. Lock, M. Mahendran, and S. D. Zweep, *J. Am. Chem. Soc.*, **108**, 1692 (1986).

<sup>109</sup> S. Hollenstein and T. Laube, *J. Am. Chem. Soc.*, **115**, 7240 (1993).

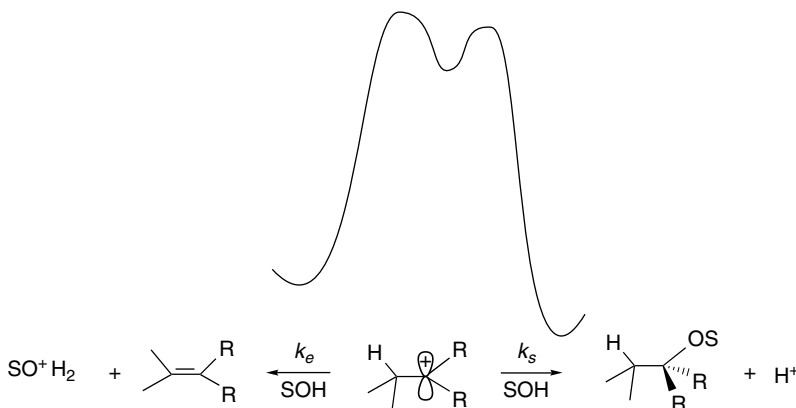
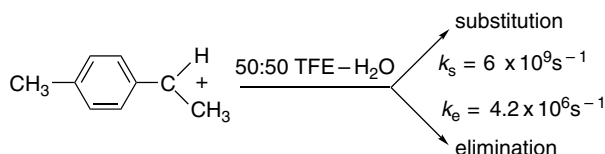


Fig. 4.10. Reaction energy profile illustrating competition between elimination and substitution by solvent for a *tert*-cation.

substitution reaction is more favorable in the thermodynamic sense, since the C–O bond is stronger than the  $\pi$  component of the double bond.

For both tertiary cations and secondary benzylic carbocation, the ratio of substitution to elimination is quite high. For example, for 1-(*p*-tolyl)ethyl cation in 50:50 TFE-water, the ratio is 1400.<sup>110</sup> For the *tert*-butyl cation, the ratio is about 30 in water<sup>111</sup> and 60 in 50:50 TFE-water.<sup>112</sup> These ratios are on the order of  $10^3$  if account is taken of the need for solvent reorganization in the substitution process.<sup>113</sup> The generalization is that *under solvolysis conditions, tert-alkyl and sec-benzyl carbocations prefer substitution to elimination.*



The origin of this preference has been considered by Richard and co-workers. One aspect of the puzzle can be seen by applying Hammond's postulate. Since the competing reactions have early transition states, it is unlikely that the difference in product stability governs the competition. Instead, the substitution process appears to have a smaller *intrinsic barrier* (in the context of the Marcus equation; see Section 3.2.4). The elimination reaction appears to have a barrier that is 3–4 kcal higher, at least for *sec*-benzylic systems.<sup>114</sup> The structural basis of this difference has not been established, but it may be related to the fact that the elimination process has a bond-breaking component, whereas substitution requires only bond formation.

<sup>110</sup> J. P. Richard and W. P. Jencks, *J. Am. Chem. Soc.*, **106**, 1373 (1984); J. P. Richard, T. L. Amyes, and K. B. Williams, *Pure Appl. Chem.*, **70**, 2007 (1998).

<sup>111</sup> I. Dostrovsky and F. S. Klein, *J. Chem. Soc.*, 791 (1955).

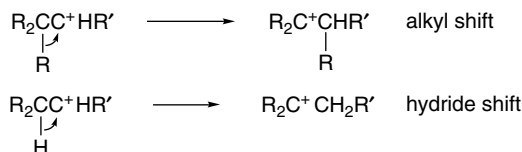
<sup>112</sup> M. M. Toteva and J. P. Richard, *Bioorg. Chem.*, **25**, 239 (1997).

<sup>113</sup> M. M. Toteva and J. P. Richard, *J. Am. Chem. Soc.*, **118**, 11434 (1996).

<sup>114</sup> J. P. Richard, *Tetrahedron*, **51**, 1535 (1995); J. P. Richard, T. L. Amyes, S.-S. Lin, A. M. C. O'Donoghue, M. M. Toteva, Y. Tsuji, and K. B. Williams, *Adv. Phys. Org. Chem.*, **35**, 67 (2000).

## 4.4.4. Mechanisms of Rearrangement of Carbocations

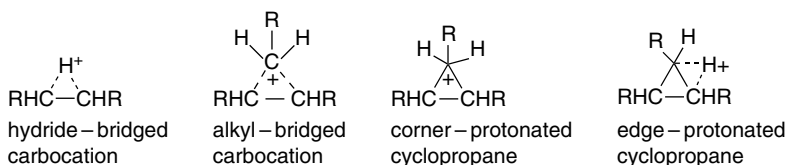
The discussions of the behavior of carbocation intermediates in superacid media and of neighboring-group participation have already provided examples of carbocation rearrangements. This is a characteristic feature of carbocations. Rearrangements can occur by shift of a hydrogen or an alkyl, alkenyl, or aryl group. Rearrangement creates a new carbocation with the positive charge located on the carbon atom from which the migration occurred. 1,2-Shifts are the most common type of rearrangement.<sup>115</sup>



A thermodynamic driving force exists for rearrangement in the direction of forming a more stable carbocation. Activation energies for migrations are small and it is not uncommon to observe overall rearrangements that involve individual steps that proceed from a more stable to a less stable species. Thus, while rearrangement of a tertiary to a secondary cation is endothermic by about 10 kcal/mol, this barrier is not prohibitive if the rearrangement can eventually lead to a more stable cation. Formation of primary cations by rearrangement is less likely to occur, since the primary ions are  $\sim 15$  and  $\sim 25$  kcal/mol higher in energy than secondary and tertiary cations, respectively. Rearrangements can occur through *bridged intermediates or transition structures* that are lower in energy than primary carbocations and comparable to secondary ions. The barriers for conversion to ions of greater (or equal) stability are very low and rearrangements occur very rapidly. For example, in superacid media at  $-160^\circ\text{C}$ , the equilibration of the five methyl groups of the 2,3,3-trimethylbutyl cation by methyl shift is so fast that the barrier must be less than 5 kcal/mol.<sup>116</sup>



While many rearrangements can be formulated as a series of 1,2-shifts, both isotopic tracer studies and computational work have demonstrated the involvement of other species—bridged ions in which hydride or alkyl groups are partially bound to two other carbons. These can be transition structures for hydride and alkyl group shifts, but in some cases they may be intermediates. The alkyl-bridged structures can also be described as “corner-protonated” cyclopropanes, since if the bridging C–C bonds are considered to be fully formed, there is an “extra” proton on the bridging alkyl group. Another possible type of structure is called an “edge-protonated” cyclopropane. The carbon-carbon bonds are depicted as fully formed, with the “extra” proton associated with one of the “bent” bonds.



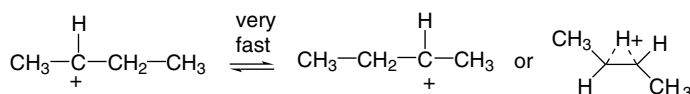
<sup>115</sup>. Reviews: V. G. Shubin, *Top. Current Chem.*, **116–117**, 267 (1984).

<sup>116</sup>. G. A. Olah and A. M. White, *J. Am. Chem. Soc.*, **91**, 5801 (1969).

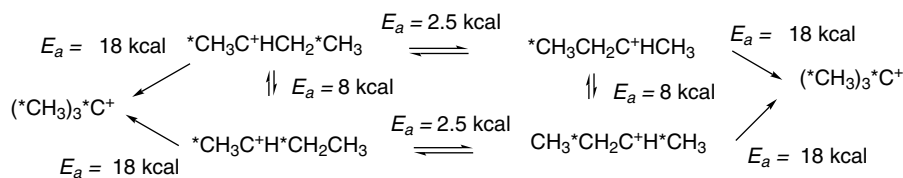
Theoretical calculations, structural studies under stable ion conditions, and product and mechanistic studies of reactions in solution have all been applied to understanding the nature of the intermediates involved in carbocation rearrangements. The energy surface for  $C_3H_7^+$  in the gas phase has been calculated at the MP4/6-311G\*\* level. The 1- and 2-propyl cations and corner- and edge-protonated cyclopropane structures were compared. The secondary carbocation was found to be the most stable structure.<sup>117</sup> Hydrogen migration was found to occur through a process that involves the corner-protonated cyclopropane species. Similar conclusions were drawn at the G2 and B3LYP levels of calculation.<sup>118</sup> Calculations that include an anion change the relative energy of the 1-propyl cation and the protonated cyclopropane. The 1-propyl cation becomes a stable structure in close proximity to an anion.<sup>119</sup> Relative energies of  $[C_3H_7]^+$  cations are shown below.

	$CH_3CH_2CH_2^+$	$CH_3C^+HCH_3$	$\triangle^-H^+$	$\begin{array}{c} H \\   \\ \triangle \\   \\ H \end{array}$
MP4/6-311*	+19.3	0	8.6	7.3
G2		0	8.2	7.2
B3LYP		0	16.0	12.2

The 2-butyl cation has been extensively investigated both computationally and experimentally. The 2-butyl cation can be observed under stable ion conditions. C(2) and C(3) are rapidly interconverted by a hydride shift. The NMR spectrum corresponds to a symmetrical species, which implies either a very rapid hydride shift or a symmetrical H-bridged structure. A maximum barrier of 2.5 kcal/mol for hydride shift can be assigned from the NMR data.<sup>120</sup>



Scrambling of C(3) and C(4) [or C(1) and C(2)] occurs with an  $E_a$  of about 7–8 kcal/mol. The scrambling of C(3) and C(4) can occur via an edge-protonated intermediate. The rearrangement of 2-butyl cation to the *t*-butyl ion is rather slow, occurring with an  $E_a$  of 18 kcal/mol.<sup>121</sup>



<sup>117</sup> W. Koch, B. Liu, and P. v. R. Schleyer, *J. Am. Chem. Soc.*, **111**, 3479 (1989).

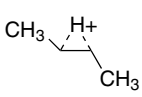
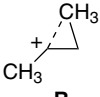
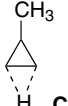
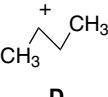
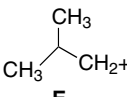
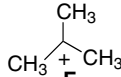
<sup>118</sup> M. V. Frash, V. B. Kazansky, A. M. Rigby, and P. A. van Santen, *J. Phys. Chem. B*, **101**, 5346 (1997).

<sup>119</sup> D. Farcasiu and D. Hancu, *J. Am. Chem. Soc.*, **121**, 7173 (1999); D. Farcasiu and D. Hancu, *J. Phys. Chem. A*, **101**, 8695 (1997).

<sup>120</sup> M. Saunders and M. R. Kates, *J. Am. Chem. Soc.*, **100**, 7082 (1978).

<sup>121</sup> D. M. Brouwer, *Recl. Trav. Chim. Pays-Bas*, **87**, 1435 (1968); D. M. Brouwer and H. Hogeveen, *Prog. Phys. Org. Chem.*, **9**, 179 (1972); M. Boronat, P. Viruela, and A. Corma, *J. Phys. Chem.*, **100**, 633 (1996).

There have been two extensive MO studies of the  $C_4H_9^+$  species. The most stable structure is the *t*-butyl cation. At the MP4/6-311G\*\* level, the H-bridged structure **A** was the next most stable structure and it was 2.3 kcal more stable than the open 2-butyl cation **D**.<sup>122</sup> The methyl-bridged ion **B** is only slightly less stable. The structures were also calculated at the MP4/6-31G\* level of theory.<sup>123</sup> The energies relative to the *t*-butyl cation are similar, although the methyl-bridged ion **B** is found to be slightly more stable than the hydride-bridged ion **A**. Relative energies of  $[C_4H_9]^+$  cations are shown below in kcal/mol.

						
	<b>A</b>	<b>B</b>	<b>C</b>	<b>D</b>	<b>E</b>	<b>F</b>
MP/6-311G*	13.4	13.8	21.9	15.7	33.0	0.0
MP/6-31G**	12.8	12.0	20.5		32.6	0.0

Along with the minimal barrier for hydride shift and the 18 kcal/mol 2-butyl to *t*-butyl rearrangement, these results give the energy profile shown in Figure 4.11, which

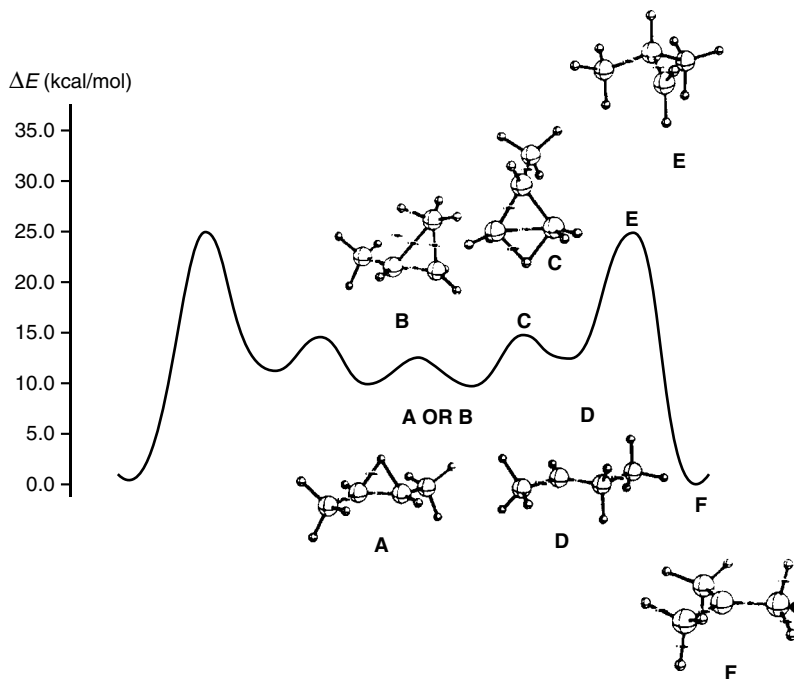
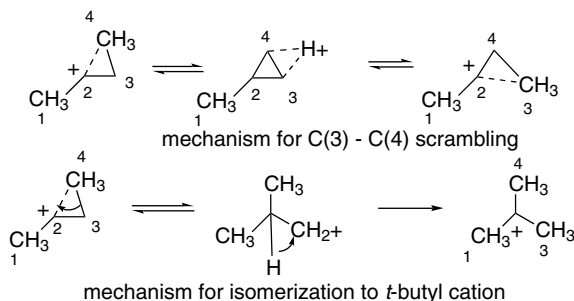


Fig. 4.11. Energy profile for the scrambling and rearrangement of  $C_4H_9^+$  cation. (A) H-bridged; (B) methyl-bridged; (C) edge protonated methylcyclopropane; (D) classical secondary; (E) classical primary; (F) tertiary. Adapted from *J. Am. Chem. Soc.*, **112**, 4064 (1990); *J. Am. Chem. Soc.*, **115**, 259 (1993) and *J. Phys. Chem.*, **100**, 633 (1996), by permission of the American Chemical Society.

<sup>122</sup> J. W. de M. Carneiro, P. v. R. Schleyer, W. Koch, and K. Raghavachari, *J. Am. Chem. Soc.*, **112**, 4064 (1990); S. Sieber, P. Buzek, P. v. R. Schleyer, W. Koch, and J. W. de M. Carneiro, *J. Am. Chem. Soc.*, **115**, 259 (1993).

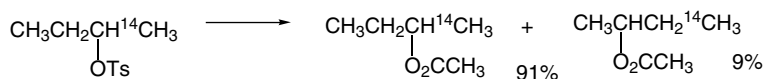
<sup>123</sup> M. Boronat, P. Viruela, and A. Corma, *J. Phys. Chem.*, **100**, 633 (1996).

pertains to the behavior of the carbocation *in the absence of a nucleophile*. This diagram indicates that the mechanism for C(3)–C(4) scrambling in the 2-butyl cation involves the edge-protonated cyclopropane intermediate. The primary cation is an intermediate in the isomerization to *t*-butyl ion, which explains the relatively slow rate of this process.

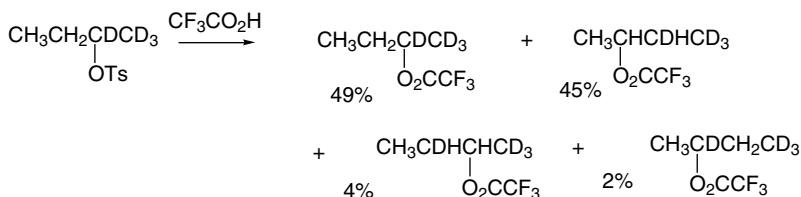


**Visual models, additional information and exercises on C<sub>4</sub>H<sub>9</sub> Carbocations can be found in the Digital Resource available at: [Springer.com/carey-sundberg](http://Springer.com/carey-sundberg).**

The occurrence and extent of rearrangement of the 2-butyl cation *during solvolysis* has been studied using isotopic labeling. When 2-butyl tosylate is solvolyzed in acetic acid, only 9% hydride shift occurs in the 2-butyl acetate that is isolated.<sup>124</sup> Thus, under these conditions most of the reaction proceeds by direct nucleophilic participation of the solvent.



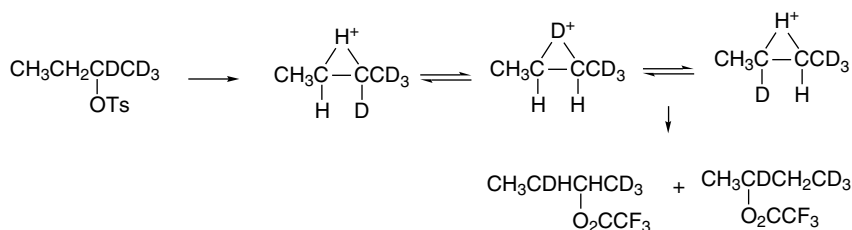
When 2-butyl tosylate is solvolyzed in the less nucleophilic trifluoroacetic acid (TFA), a different result emerges. The extent of migration approaches the 50% that would result from equilibration of the two secondary cations.<sup>125</sup>



<sup>124</sup>. J. D. Roberts, W. Bennett, R. E. McMahon, and E. W. Holroyd, Jr., *J. Am. Chem. Soc.*, **74**, 4283 (1952).

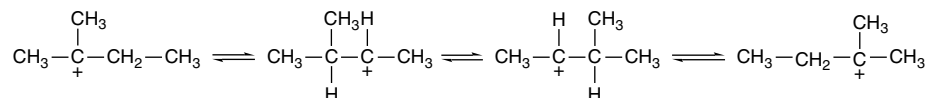
<sup>125</sup>. J. J. Dannenberg, B. J. Goldberg, J. K. Barton, K. Dill, D. H. Weinwurzle, and M. O. Longas, *J. Am. Chem. Soc.*, **103**, 7764 (1981); J. J. Dannenberg, J. K. Barton, B. Bunch, B. J. Goldberg, and T. Kowalski, *J. Org. Chem.*, **48**, 4524 (1983); A. D. Allen, I. C. Ambridge, and T. T. Tidwell, *J. Org. Chem.*, **48**, 4527 (1983).

Two hydride shifts resulting in interchange of the C(2) and C(3) hydrogens can account for the two minor products.



Referring to Figure 4.11, we see that in acetic acid only a small portion of the reaction involves a carbocation. In TFA, the carbocation is formed, but only the H-migration process having an  $E_a$  of  $\sim 2.5$  kcal competes with nucleophilic capture.

Both computational and solvolysis studies have also been done to characterize the  $[C_5H_9]^+$  series of carbocations. The barrier to the hydride and methyl shifts that interconvert the methyl groups in the *t*-pentyl cation is 10–15 kcal/mol.<sup>126</sup> This rearrangement must pass through a secondary ion or related bridged species.



The solvolysis product of 3-methyl-2-butyl tosylate in TFA consists of 98.5% of the ester derived from the rearranged 2-methyl-2-butyl cation and 1.5% of the 3-methyl-2-butyl ester. Even the 1.5% of product retaining the 3-methyl-2-butyl structure has undergone some rearrangement.<sup>127</sup> The gas phase energies of possible intermediates have been calculated at several levels of theory.<sup>128</sup> Relative energies (kcal/mol) assigned to  $[C_5H_9]^+$  cations are shown below.

	B	A			D	H <sup>+</sup>	C	E
MP2/6-31G*	11.7	7.2	0	34.1	17.8	14.4		
B3P86	12.3	10.5	0	35.4	20.4	14.7		
MP4/6-31G*		13.6	0		18.5		9.6	12.4

These results indicate an energy profile for the 3-methyl-2-butyl cation to 2-methyl-2-butyl cation rearrangement in which different rotamers of the open secondary cations are transition structures rather than intermediates, with the secondary cations represented as methyl-bridged **C** (corner-protonated cyclopropanes), as shown in Figure 4.12

The computational investigation of this system was extended to include the effect of a polar medium (dielectric constant = 39) and the effect of the proximity of anions

<sup>126</sup> M. Saunders and E. L. Hagen, *J. Am. Chem. Soc.*, **90**, 2436 (1968).

<sup>127</sup> D. Farcasiu, G. Marino, J. M. Harris, B. A. Hovanes, and C. S. Hsu, *J. Org. Chem.*, **59**, 154 (1994); D. Farcasiu, G. Marino, and C. S. Hsu, *J. Org. Chem.*, **59**, 163 (1994).

<sup>128</sup> M. Boronat, P. Viruela, and A. Corma, *J. Phys. Chem.*, **100**, 16514 (1996); D. Farcasiu and S. H. Norton, *J. Org. Chem.*, **62**, 5374 (1997).

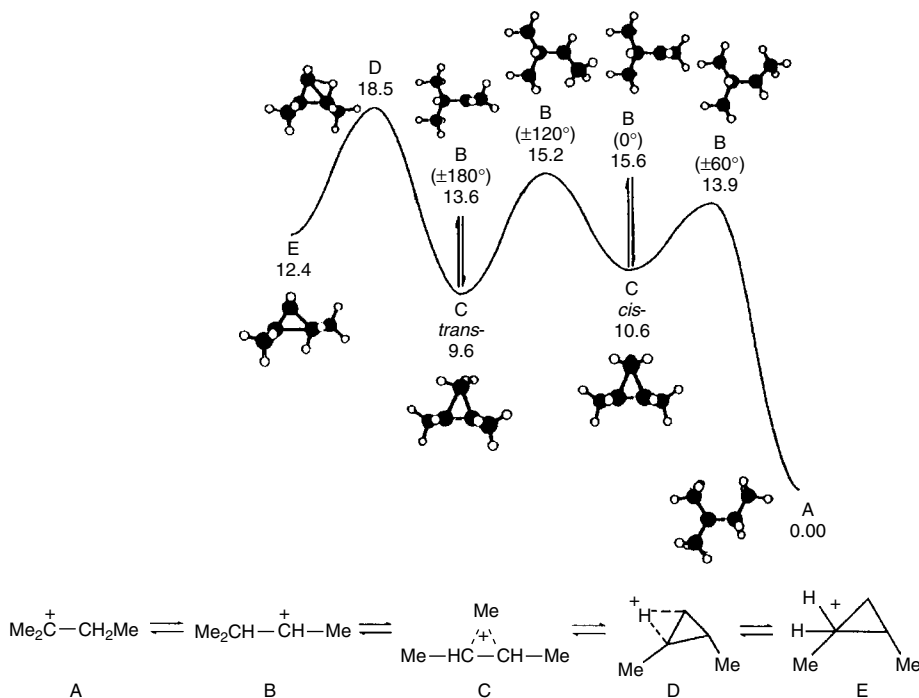
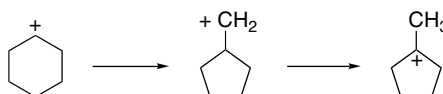


Fig. 4.12. Energy surface for the rearrangement of the 3-methyl-2-butyl cation to the 2-methyl-2-butyl cation. Reproduced from *J. Org. Chem.*, **62**, 5374 (1997), by permission of the American Chemical Society.

on the relative stability of ions **C** and **B**.<sup>129</sup> Whereas a polar medium reduced the energy of **B** relative to the gas phase results, the bridged ion **C** remained more stable than the secondary ion. The proximity of anions changed the situation more dramatically. Anions were modeled using  $[\text{H}-\text{Li}-\text{H}]^-$  and  $[\text{BH}_3\text{F}]^-$ . At distances  $< 3.3 \text{ \AA}$ , the open secondary carbocation **B** is more stable. The energy difference depends on the location of the anion in relation to the cation. Orientations in which the anion approaches hydrogens on C(1) result in elimination to 3-methyl-1-butene, whereas approach to C(3) leads to 2-methyl-2-butene. These computational results present a picture of the elimination process similar to that in the previous section (page 439).

The ring contraction of a cyclohexyl cation to a methylcyclopentyl cation (see Entries 8 and 9 in Scheme 4.4) is thermodynamically favorable, but would require a substantial  $E_a$  if it proceeded through a primary cyclopentylmethyl cation.

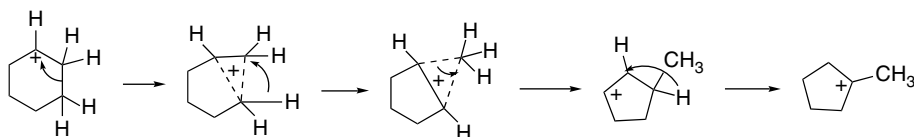


It is believed that a more correct description of the process involves migration through a pentacoordinate *protonated cyclopropane*, in which an alkyl group acts as a bridge in an electron-deficient carbocation structure. The cyclohexyl  $\rightarrow$  methylcyclopentyl rearrangement is postulated to occur by rearrangement between two such structures.<sup>130</sup>

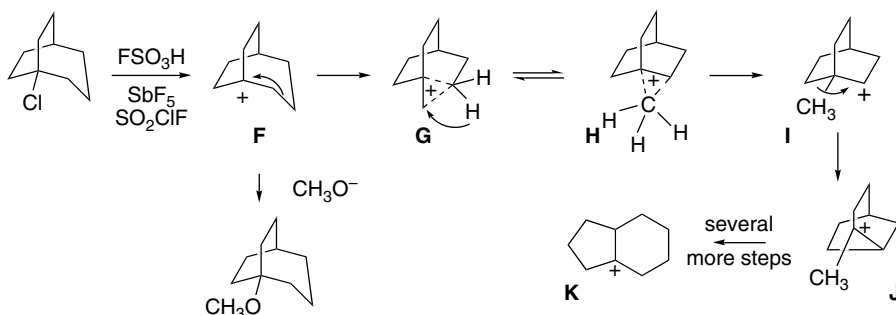
<sup>129</sup>. D. Farcasiu, S. H. Norton, and D. Hancu, *J. Am. Chem. Soc.*, **122**, 668 (2000).

<sup>130</sup>. M. Saunders, P. Vogel, E. L. Hagen, and J. Rosenfeld, *Acc. Chem. Res.*, **6**, 53 (1973).

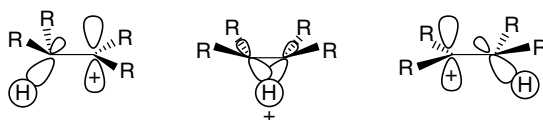
An  $E_a$  of  $7.4 \pm 1$  kcal/mol for the rearrangement has been measured in the gas phase, which is consistent with the protonated cyclopropane mechanism.<sup>131</sup>



In some cases, NMR studies in superacid media have permitted the observation of successive intermediates in a series of rearrangements. An example is the series of  $[C_9H_{15}]^+$  cations originating with the bridgehead ion **F**, generated by ionization of the corresponding chloride. Rearrangement eventually proceeds to the tertiary ion **K**. The bridgehead ion **F** is stable below  $-75^\circ\text{C}$ . The unrearranged methyl ether is obtained if the solution is quenched with sodium methoxide in methanol at  $-90^\circ\text{C}$ . At about  $-65^\circ\text{C}$ , ion **F** rearranges to the tertiary ion **J**. This is believed to involve the methyl-bridged ion **H** as an intermediate. The tertiary ion **J** is stable below  $-30^\circ\text{C}$  but above  $-30^\circ\text{C}$ , **K** is formed. This latter rearrangement involves a sequence of several steps, again including a methyl-bridged species.<sup>132</sup> This multistep sequence terminating in the most stable  $C_9H_{15}^+$  ion is typical of carbocations in superacid media. In the presence of nucleophilic anions or solvent, rearrangement usually does not proceed all the way to the most stable ion, because nucleophilic trapping captures one or more of the rearranged species.



The question of relative preference for rearrangement of different groups, which is sometimes referred to as “migratory aptitude,” is a complex one and there is no absolute order. In general, aryl groups and branched alkyl groups migrate in preference to unbranched alkyl groups, but as the barriers involved are low, selectivity is not high. Often the preferred migration involves the group that is best positioned from a stereoelectronic point of view. The preferred alignment of orbitals for a 1,2-hydride or alkyl shift involves coplanarity of the  $p$ -orbital at the carbocation ion center and the  $\sigma$  orbital of the migrating group.



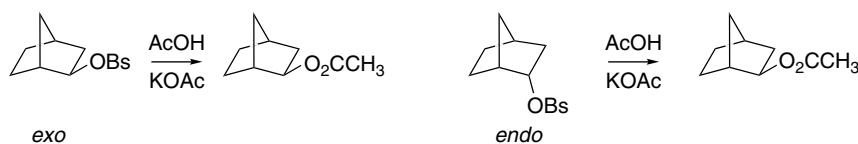
<sup>131</sup> M. Attina, F. Cacace, and A. di Marzio, *J. Am. Chem. Soc.*, **111**, 6004 (1989).

<sup>132</sup> G. A. Olah, G. Liang, J. R. Wiseman, and J. A. Chong, *J. Am. Chem. Soc.*, **94**, 4927 (1972).

The transition structure involves a three-center, two-electron bond and corresponds to a symmetrically bridged structure. As indicated above, the bridged structure may actually be an intermediate in some cases. The migration process can be concerted with the formation of the carbocation; that is, the migration can begin before the bond to the leaving group at the adjacent carbon atom is completely broken. The phenonium ion case discussed in Section 4.3 is one example. The ease of migration is also influenced by strain. In general, a shift that will reduce strain is favored.

#### 4.4.5. Bridged (Nonclassical) Carbocations

In the discussion of carbocation rearrangements, we encountered examples of *bridged ions* that require expansion of bonding concepts beyond the two-center, two-electron bonds that suffice for most stable organic molecules. These bridged carbocations, involve delocalization of  $\sigma$  electrons and formation of three-center, two-electron bonds, and are sometimes called *nonclassical ions*. The recognition of the importance of bridged structures largely originated with a specific structure, the norbornyl cation, and the issue of whether its structure is classical or bridged.<sup>133</sup> The special properties of this intermediate were recognized on the basis of studies by Saul Winstein and his collaborators. The behavior of norbornyl systems in solvolytic displacement reactions was suggestive of neighboring-group participation by a saturated carbon-carbon bond. Evidence for both enhanced rate and unusual stereoselectivity was developed from the study of acetolysis of *exo*-2-norbornyl sulfonates. The acetolyses of both *exo*-2-norbornyl brosylate and *endo*-2-norbornyl brosylate produce exclusively *exo*-2-norbornyl brosylate. The *exo*-brosylate is more reactive than the *endo* isomer by a factor of 350.<sup>134</sup> Furthermore, enantiomerically pure *exo*-brosylate gives completely racemic *exo*-acetate, and the *endo*-brosylate gives acetate that is at least 93% racemic. These results suggest the involvement of an achiral species. Since the secondary norbornyl cation is chiral, it cannot account for the racemization.

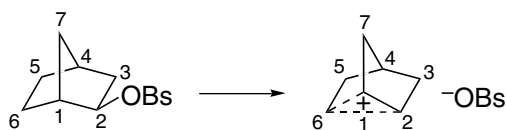


Both acetolyses were considered to proceed by way of a rate-determining formation of a carbocation. The rate of ionization of the *endo*-brosylate was considered normal, since its reactivity was comparable to that of cyclohexyl brosylate. Winstein

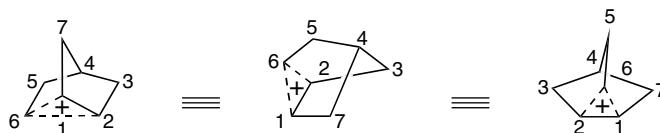
<sup>133</sup>. H. C. Brown, *The Nonclassical Ion Problem*, Plenum Press, New York, 1977; H. C. Brown, *Tetrahedron*, **32**, 179 (1976); P. D. Bartlett, *Nonclassical Ions*, W. A. Benjamin, New York, 1965; S. Winstein, in *Carbonium Ions*, Vol. III, G. A. Olah and P. v. R. Schleyer, eds., Wiley-Interscience, New York, 1972, Chap. 22; G. D. Sargent, *ibid.*, Chap. 24; C. A. Grob, *Angew. Chem. Int. Ed. Engl.*, **21**, 87 (1982); G. M. Kramer and C. G. Scouten, *Adv. Carbocation Chem.*, **1**, 93 (1989).

<sup>134</sup>. S. Winstein and D. S. Trifan, *J. Am. Chem. Soc.*, **71**, 2953 (1949); **74**, 1147, 1154 (1952); S. Winstein, E. Clippinger, R. Howe, and E. Vogelfanger, *J. Am. Chem. Soc.*, **87**, 376 (1965).

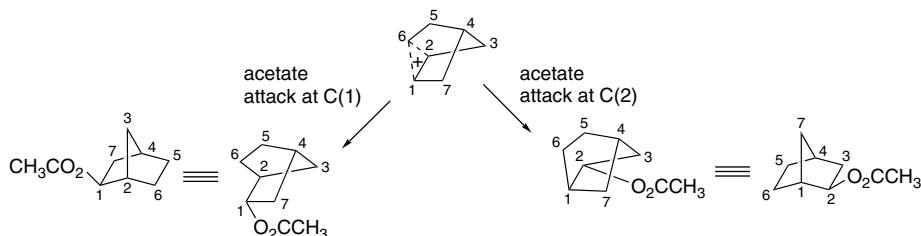
proposed that ionization of the *exo*-brosylate is *assisted* by the C(1)–C(6) bonding electrons and leads directly to the formation of a nonclassical ion as an intermediate.



This intermediate serves to explain the formation of racemic product, since it is achiral. The cation has a plane of symmetry passing through C(4), C(5), C(6), and the midpoint of the C(1)–C(2) bond. The plane of symmetry is seen more easily in an alternative, but equivalent, representation. Carbon 6, which bears two hydrogens, serves as the bridging atom in the cation.



Attack by acetate at C(1) or C(2) is equally likely and results in formation of equal amounts of the enantiomeric *exo*-acetates. The product is *exo* because reaction with acetate occurs from the direction opposite the bridging interaction. The bridged ion can be formed directly only from the *exo*-brosylate because it has the proper *anti* relationship between the C(1)–C(6) bond and the leaving group. The bridged ion can be formed from the *endo*-brosylate only after an unassisted ionization, which explains the rate difference between the *exo* and *endo* isomers.



The description of the nonclassical norbornyl cation developed by Winstein implied that the bridged ion is stabilized relative to a secondary ion by C–C  $\sigma$  bond delocalization. H. C. Brown put forward an alternative interpretation,<sup>135</sup> arguing that all the available data were consistent with describing the intermediate as a rapidly equilibrating classical secondary ion. The 1,2-shift that interconverts the two ions was presumed to be rapid, relative to capture of the nucleophile. Such a rapid rearrangement would account for the isolation of racemic product, and Brown suggested that the rapid migration would lead to preferential approach of the nucleophile from the *exo* direction.



<sup>135</sup> H. C. Brown, *The Transition State*, *Chem. Soc. Spec. Publ.*, No. 16, 140 (1962); *Chem. Brit.*, 199 (1966); *Tetrahedron*, **32**, 179 (1976).

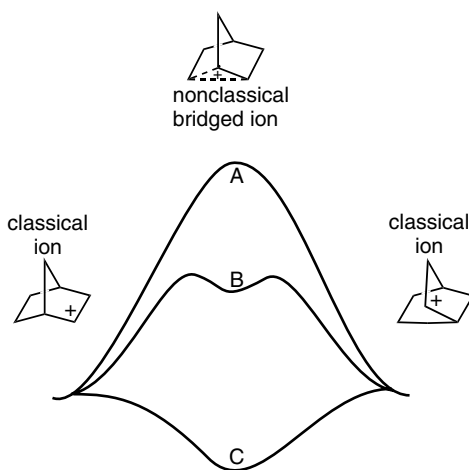


Fig. 4.13. Contrasting energy profiles for stable and unstable bridged norbornyl cation. (A) Bridged ion is a transition structure for rearrangement between classical structures. (B) Bridged ion is an intermediate in rearrangement of one classical structure to the other. (C) Bridged ion is the most stable structure.

The two alternative descriptions of the norbornyl cation were tested very extensively. In essence, the question that is raised has to do with the relative energy of the bridged structure. Is it lower in energy than the classical ion and therefore an *intermediate* to which the classical ion would collapse or is it a transition structure (or higher-energy intermediate) in the rapid isomerization of two classical structures? Figure 4.13 illustrates the energy profiles corresponding to the various possibilities.

When the techniques for direct observation of carbocations became available, the norbornyl cation was subjected to study by those methods. The norbornyl cation was generated in  $\text{SbF}_5\text{-SO}_2\text{-SOF}_2$  and the temperature dependence of the proton magnetic resonance spectrum was examined.<sup>136</sup> Subsequently, the  $^{13}\text{C}$  NMR spectrum was studied and the proton spectrum was determined at higher field strength. These studies excluded rapidly equilibrating classical ions as a description of the norbornyl cation under stable ion conditions.<sup>137</sup> The resonances observed in the  $^{13}\text{C}$  spectrum were assigned. None of the signals appear near the position where the C(2) carbon of the classical secondary 2-propyl cation is found. Instead, the resonances for the norbornyl cation appear at relatively high field and are consistent with the bridged-ion structure.<sup>138</sup> Other NMR techniques were also applied to the problem and confirmed the conclusion that the spectra observed under stable ion conditions could not be the result of averaged spectra of two rapidly equilibrating ions.<sup>139</sup> It was also determined

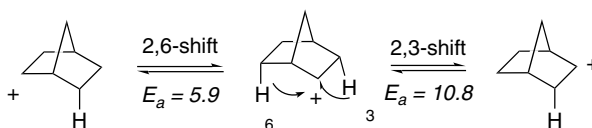
<sup>136</sup> P. v. R. Schleyer, W. E. Watts, R. C. Fort, Jr., M. B. Comisarow, and G. A. Olah, *J. Am. Chem. Soc.*, **86**, 5679 (1964); M. Saunders, P. v. R. Schleyer, and G. A. Olah, *J. Am. Chem. Soc.*, **86**, 5680 (1964).

<sup>137</sup> G. A. Olah, G. K. SuryaPrakash, M. Arvanaghi, and F. A. L. Anet, *J. Am. Chem. Soc.*, **104**, 7105 (1982).

<sup>138</sup> G. A. Olah, G. Liang, G. D. Mateescu, and J. L. Riemenschneider, *J. Am. Chem. Soc.*, **95**, 8698 (1973); G. A. Olah, *Acc. Chem. Res.*, **9**, 41 (1976).

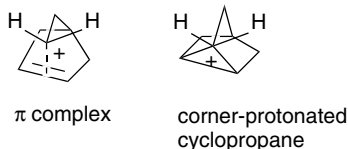
<sup>139</sup> C. S. Yannoni, V. Macho, and P. C. Myhre, *J. Am. Chem. Soc.*, **104**, 7105 (1982); M. Saunders and M. R. Kates, *J. Am. Chem. Soc.*, **102**, 6867 (1980); M. Saunders and M. R. Kates, *J. Am. Chem. Soc.*, **105**, 3571 (1983).

that 3,2- and 6,2-hydride shifts were occurring under stable ion conditions. Activation energies of 10.8 and 5.9 kcal/mol, respectively, were measured for these processes.



These results, which pertain to stable ion conditions, provide a strong case that the most stable structure for the norbornyl cation is the symmetrically bridged ion. How much stabilization does the bridging provide? An estimate based on molecular mechanics calculations and a thermodynamic cycle suggests a stabilization of about  $6 \pm 1$  kcal/mol.<sup>140</sup> A gas phase value based on mass spectrometric measurements is 11 kcal/mol.<sup>141</sup> Gas phase hydride affinity and chloride affinity data also show the norbornyl cation to be especially stable.<sup>142</sup> MO calculations (MP2/6-31G\*) give a bridged structure that is 13.6 kcal more stable than the classical secondary structure and predicts <sup>13</sup>C chemical shifts and coupling in agreement with the experimental results.<sup>143</sup> The C(1)–C(6)=C(2)–C(6) distance is found to be 1.832 Å by an MBPT(2)/DZP computation.<sup>144</sup> The difference in energy between the two structures is reduced only slightly when calculations include the effect of solvation, indicating that the bridged ion would be more stable than the classical ion, even in solution.<sup>145</sup> There is also good agreement between calculated and observed infrared spectra.<sup>146</sup>

Werstiuk and Muchall computed the structure at the B3LYP and QCISD levels. The minimum energy structure was found to be a bridged ion with a C(1)–C(6) distance of 1.892 Å and a C(1)–C(2) distance of 1.389 Å (B3LYP/6-311+G(2d,2p)). They applied AIM concepts to a description of the structure.<sup>147</sup> This analysis resulted in the description of the norbornyl cation as a  $\pi$  complex, consistent with the relatively long C(1)–C(6) and C(2)–C(6) and short C(1)–C(2) distances indicated above. The bond critical points found by the AIM analysis show a T-configuration with the bond from C(6) intersecting with the C(1)–C(2) critical point. There is no bond path directly to C(1) or C(2). Carbon 6 is then best described as tetravalent, with the C(1)–C(2) double bond as the fourth ligand. These computations also examined the effect of bringing C(6) closer to C(1) and C(2) to form the more strongly bridged structure that would be implied by a corner-protonated cyclopropane representation.



<sup>140</sup> P. v. R. Schleyer and J. Chandrasekhar, *J. Org. Chem.*, **46**, 225 (1981).

<sup>141</sup> M. C. Blanchette, J. L. Holmes, and F. P. Lossing, *J. Am. Chem. Soc.*, **109**, 1392 (1987).

<sup>142</sup> R. B. Sharma, D. K. S. Sharma, K. Hiraoka, and P. Kebarle, *J. Am. Chem. Soc.*, **107**, 3747 (1985).

<sup>143</sup> P. v. R. Schleyer and S. Sieber, *Angew. Chem. Int. Ed. Engl.*, **32**, 1606 (1993).

<sup>144</sup> S. A. Perera and R. J. Bartlett, *J. Am. Chem. Soc.*, **118**, 7849 (1996).

<sup>145</sup> P. R. Schreiner, D. L. Severance, W. L. Jorgensen, P. v. R. Schleyer, and H. F. Schaefer, III, *J. Am. Chem. Soc.*, **117**, 2663 (1995).

<sup>146</sup> W. Koch, B. Liu, D. J. DeFrees, D. E. Sunko, and H. Vancik, *Angew. Chem. Int. Ed. Engl.*, **29**, 183 (1990).

<sup>147</sup> N. H. Werstiuk and H. M. Muchall, *J. Phys. Chem. A*, **104**, 2054 (2000); N. H. Werstiuk and H. M. Muchall, *Theochem*, **463**, 225 (1999).

The result is a structure that is 7.5 kcal/mol above the  $\pi$  complex. The  $\pi$  complex structure also gives better agreement with the experimental  $^{13}\text{C}$  and  $^1\text{H}$  NMR chemical shifts than the corner-protonated structure. The preference for the  $\pi$  complex structure persists in computations using a continuum solvent model. The picture that emerges from this analysis is of a primarily electrostatic attraction between a C(1)–C(2) double bond and a carbocation-like C(6).<sup>148</sup> Such a structure would be poised for nucleophilic attack *anti* to C(6), as is observed to occur.

Let us now return to the question of solvolysis and how it relates to the structure under stable ion conditions. To relate the structural data to solvolysis conditions, the primary issues that must be considered are the extent of solvent participation and the nature of solvation of the cationic intermediate. The extent of solvent participation has been probed by comparison of solvolysis characteristics in TFA with acetic acid. The *exo-endo* reactivity ratio in TFA is 1120, compared to 280 in acetic acid. While the *endo* isomer shows solvent sensitivity typical of normal secondary tosylates, the *exo* isomer reveals a reduced sensitivity. This result indicates that the TS for solvolysis of the *exo* isomer possesses a greater degree of charge dispersal, which is consistent with formation of a bridged structure. This fact, along with the rate enhancement of the *exo* isomer, indicates that the  $\sigma$  participation commences prior to ionization, and leads to the conclusion that bridging is a characteristic of the solvolysis TS, as well as of the stable ion structure.<sup>149</sup>

Another line of evidence indicating that bridging is important in solvolysis comes from substituent effects for groups placed at C(4), C(5), C(6), and C(7) in the norbornyl system. The solvolysis rate is most strongly affected by C(6) substituents and the *exo* isomer is more sensitive to these substituents than the *endo* isomer. This implies that the TS for solvolysis is especially sensitive to C(6) substituents, as would be expected if the C(1)–C(6) bond participates in solvolysis.<sup>150</sup>

Computation of the TS using ionization of the protonated *exo* and *endo* alcohols as a model has been done using B3LYP/6-311+G\* calculations.<sup>151</sup> The results confirm that participation occurs during the ionization process and is greater for the *exo* than the *endo* system. However, the stabilization resulting from the participation is considerably less than the full stabilization energy of the bridged carbocation. A difference of 3.7 kcal/mol is calculated between the *exo* and *endo* TSs. Figure 4.14 illustrates the relative energy relationships.

Many other cations besides the norbornyl cation have bridged structures.<sup>152</sup> Scheme 4.5 shows some examples that have been characterized by structural studies or by evidence derived from solvolysis reactions. To assist in interpretation of the bridged structures, the bond representing the bridging electron pair is darkened in a corresponding classical structure. Not surprisingly, the borderline between classical and bridged structures is blurred. There are two fundamental factors that prevent an absolute division: (1) The energies of the two (or more) possible structures may

<sup>148</sup>. N. H. Werstiuk, H. M. Muchall, and S. Noury, *J. Phys. Chem. A*, **104**, 11601 (2000).

<sup>149</sup>. J. E. Nordlander, R. R. Gruetzmacher, W. J. Kelly, and S. P. Jindal, *J. Am. Chem. Soc.*, **96**, 181 (1974).

<sup>150</sup>. F. Fusco, C. A. Grob, P. Sawlewicz, and G. W. Yao, *Helv. Chim. Acta*, **69**, 2098 (1986); P. Flury and C. A. Grob, *Helv. Chim. Acta*, **66**, 1971 (1983).

<sup>151</sup>. P. R. Schreiner, P. v. R. Schleyer, and H. F. Schaefer, III, *J. Org. Chem.*, **62**, 4216 (1997).

<sup>152</sup>. V. A. Barkhash, *Top. Current Chem.*, **115–117**, 1 (1984); G. A. Olah and G. K. SuryaPrakash, *Chem. Brit.*, **19**, 916 (1983).

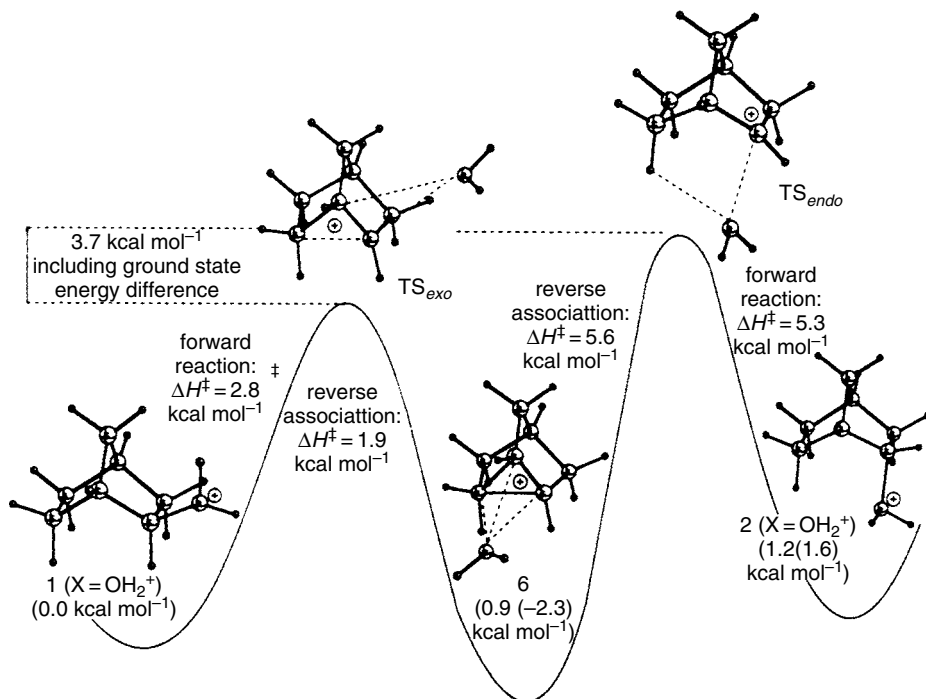
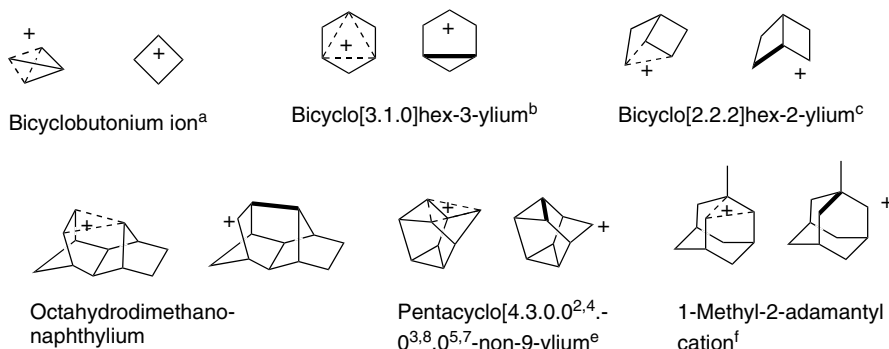


Fig. 4.14. Computational energy diagram (B3LYP)/6-311+G\*) for intermediates and transition states in ionization and rearrangement of protonated 2-norbornanol. Reproduced from *J. Org. Chem.*, **62**, 4216 (1997), by permission of the American Chemical Society.

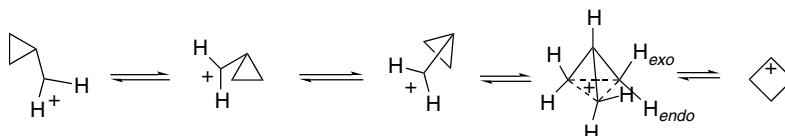
### Scheme 4.5. Examples of Bridged Carbocations



- a. M. Saunders and H.-U. Siehl, *J. Am. Chem. Soc.*, **102**, 6868 (1980); J. S. Starat, J. D. Roberts, G. K. S. Prakash, D. J. Donovan, and G. A. Olah, *J. Am. Chem. Soc.*, **100**, 8016, 8018 (1978); W. Koch, B. Liu, and D. J. De Frees, *J. Am. Chem. Soc.*, **110**, 7325 (1988); M. Saunders, K. E. Laidig, K. B. Wiberg, and P. v. R. Schleyer, *J. Am. Chem. Soc.*, **110**, 7652 (1988); P. C. Myhre, G. C. Webb, and C. Y. Yannoni, *J. Am. Chem. Soc.*, **112**, 8992 (1990).
- b. G. A. Olah, G. K. S. Prakash, T. N. Rawdah, D. Whittaker, and J. C. Rees, *J. Am. Chem. Soc.*, **101**, 3935 (1979); K. J. Szabo, E. Kraka, and D. Cremer, *J. Org. Chem.*, **61**, 2783 (1996).
- c. R. N. McDonald and C. A. Curi, *J. Am. Chem. Soc.*, **101**, 7116, 7118 (1979).
- d. S. Winstein and R. L. Hansen, *Tetrahedron Lett.*, No. 25, 4 (1960).
- e. R. M. Coates and E. R. Fretz, *J. Am. Chem. Soc.*, **99**, 297 (1977); H. C. Brown and M. Ravindranathan, *J. Am. Chem. Soc.*, **99**, 299 (1977).
- f. J. E. Nordlander and J. E. Haky, *J. Am. Chem. Soc.*, **103**, 1518 (1981).

be so close as to prevent a clear distinction as to stability. (2) The molecule may adopt a geometry that is intermediate between a classical geometry and a symmetrical bridged structure. Computational studies (MP2/6-311G\*\*) have been carried out on several nonclassical carbocations.<sup>153</sup> The results show structural features similar to the norbornyl cation, with relatively long ( $\sim 1.8 \text{ \AA}$ ) bonds to the bridging carbon and a much shorter ( $1.39 \text{ \AA}$ ) bond between the bridged carbons. The bond path from the bridging carbon is directed between the two bridged carbons, with a bond order of  $\sim 0.48$ , whereas the bridged bond order is  $\sim 1.2$ .

The  $\text{C}_4\text{H}_7^+$  cation shown as the first entry in Scheme 4.5 is a particularly interesting case. It can be described as a bridged structure that is isomeric with cyclopropylmethyl and cyclobutyl ions.



NMR studies show that all three methylene groups are equivalent, but the *exo* and *endo* sets of hydrogen do not exchange. The barrier for exchange among the three  $\text{CH}_2$  groups is  $< 2$  kcal. MO calculations at the MP4SDTQ/6-31G\* level indicate that both the cyclopropylmethyl and the bridged (bicyclobutonium) cations are energy minima, differing by only 0.26 kcal. The secondary cyclobutyl cation is about 12 kcal higher in energy.<sup>154</sup> The bridged structure is a tetracyclic cation in which each of the methylene groups is pentacoordinate.<sup>155</sup>

To summarize, bridged structures are readily attainable intermediates or transition structures for many cations and are intimately involved in rearrangement processes. In some cases, such as the norbornyl cation, the bridged structure is the most stable one. As a broad generalization, tertiary cations are nearly always more stable than related bridged ions and therefore have classical structures. Primary carbocations can be expected to undergo rearrangement to more stable secondary or tertiary ions, with bridged ions being likely transition structures (or intermediates) on the rearrangement path. Recall that the ethylium ion,  $\text{C}_2\text{H}_5^+$ , is an H-bridged structure in the gas phase. Unlike other primary carbocations, it cannot rearrange to a more stable secondary structures. The energy balance between classical secondary structures and bridged structures is close and depends on the individual system. Bridged structures are most likely to be stable where a strained bond can participate in bridging or where solvation of the positive charge is difficult. Because of poor solvation, bridged structures are particularly likely to be favored in superacid media and in the gas phase. In the cases examined so far, proximity to anions favors classical structures in relation to bridged structures.

<sup>153</sup>. I. Alkorta, J. L. M. Abboud, E. Quintanilla, and J. Z. Davalos, *J. Phys. Org. Chem.*, **16**, 546 (2003).

<sup>154</sup>. M. Saunders, K. E. Laidig, K. B. Wiberg, and P. v. R. Schleyer, *J. Am. Chem. Soc.*, **110**, 7652 (1988); S. Sieber, P. v. R. Schleyer, A. H. Otto, J. Gauss, F. Reichel, and D. Cremer, *J. Phys. Org. Chem.*, **6**, 445 (1993).

<sup>155</sup>. For further discussion of this structure see R. F. W. Bader and K. E. Laidig, *Theochem*, **261**, 1 (1992).

### Topic 4.1. The Role Carbocations and Carbonium Ions in Petroleum Processing

Petroleum refining is a basic industry in the modern world. The industry provides fuels for transportation, industrial energy, and residential heat, as well as petrochemicals for the manufacture of a wide range of products. The largest consumption of petroleum is for transportation fuels. The fundamental technology of petroleum refining involves distillation to remove nonvolatile materials and separate the hydrocarbons on the basis of boiling range. The gasoline b.p. range is approximately 30–200 °C, and the fuel oil range is 200–300 °C. There are also processes that modify the chemical composition, which include *cracking*, *hydrocracking*, and *catalytic reforming*. In cracking and hydrocracking, larger hydrocarbons are converted to hydrocarbons in the gasoline range; catalytic reforming involves isomerization to increase the fraction of branched chain, cyclic, and aromatic hydrocarbons in the gasoline product. The objective of catalytic reforming is to improve gasoline performance. One of the measures of performance is the *octane number*, which is a measure of the degree of engine knocking observed for a particular hydrocarbon or hydrocarbon mixture. The scale is calibrated with *n*-heptane as 0.0 and 2,2,4-trimethylpentane as 100.0. Table 4.19 shows some *research octane numbers* (RON) for the heptane and octane isomers. There is a second scale, *motor octane number* that is also used. Note that chain branching leads to improved octane numbers.

The chemical basis for engine performance is related to the rates of reaction of the peroxy radicals involved in the combustion process. Components with high octane numbers have relatively low rates of chain branching, which reduces the premature ignition that causes poor engine performance.<sup>156</sup> Engine performance can also be improved by gasoline additives. Tetraethyllead was used for this purpose for many years before it became apparent that the accumulating lead in the environment had many adverse consequences. Lead also interferes with the catalytic converters required

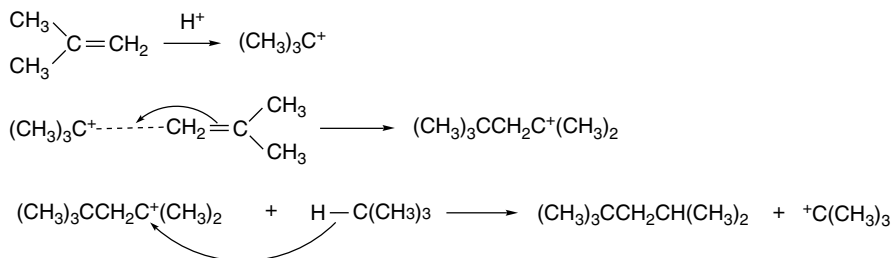
**Table 4.19. Octane Numbers for Some Hydrocarbons**

Heptanes	RON	Octanes	RON
<i>n</i> -Heptane	0.0	<i>n</i> -Octane	–19.0
2-Methylhexane	42.4	2-Methylheptane	21.7
3-Methylhexane	52.0	3-Methylheptane	36.8
3-Ethylpentane	65.0	4-Methylheptane	26.7
2,2-Dimethylpentane	92.8	3-Ethylhexane	33.5
2,3-Dimethylpentane	91.1	2,2-Dimethylhexane	72.5
2,4-Dimethylpentane	83.1	2,3-Dimethylhexane	71.5
3,3-Dimethylpentane	80.8	2,4-Dimethylhexane	65.2
2,2,3-Trimethylpentane	112.1	2,5-Dimethylhexane	55.5
		3,3-Dimethylhexane	75.5
		3,4-Dimethylhexane	76.3
		2-Methyl-3-ethylpentane	87.3
		3-Methyl-3-ethylpentane	80.8
		2,2,3-Trimethylpentane	109.6
		2,2,4-Trimethylpentane	100.0
		2,3,3-Trimethylpentane	106.1
		2,3,4-Trimethylpentane	102.7

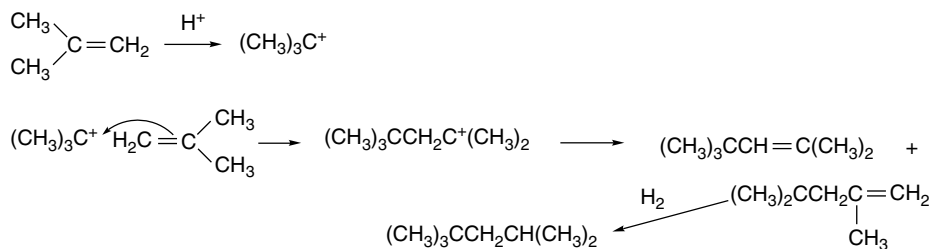
<sup>156</sup> C. Morley, *Combust. Sci. Technol.*, **55**, 115 (1987).

to reduce pollution from partial combustion. In the 1980s methyl *t*-butyl ether (MTBE) was introduced as a major antiknock component, but it was soon discovered that MTBE contaminated groundwater as a result of leakage and spillage.<sup>157</sup> It is being phased out as a gasoline performance enhancer.<sup>158</sup> As a result, new emphasis has been placed on catalytic reforming as a means of meeting engine performance requirements.

A possible replacement for MTBE is the mixture of branched C<sub>8</sub> hydrocarbons prepared by dimerization of C<sub>4</sub> compounds.<sup>159</sup> This is economically attractive since the C<sub>4</sub> compounds are by-products of other stages of petroleum refining. Isobutane and isobutene react with strong acid to give C<sub>8</sub> products.<sup>160</sup> The reaction involves intermolecular hydride transfers.



The same kind of product can be obtained by acid-catalyzed dimerization of isobutene, followed by hydrogenation.



The hydrocarbon mixtures formed by these processes have octane numbers ranging from 90 to 95.

Cracking, which is done at high temperatures (480–550 °C) in flow reactors with short contact times (seconds), converts high-boiling components of petroleum to hydrocarbons in the gasoline-boiling range. The catalysts are rapidly degraded and are regenerated by high-temperature (700 °C) exposure to air.<sup>161</sup> The product mixture is complex but is enriched in hydrocarbons in the gasoline range. Low-boiling hydrocarbons such as methane and ethane are produced as by-products. Reactivity toward cracking increases with molecular weight and branching. Carbocations are intermediates in the cracking process, which leads to isomerizations.

<sup>157</sup> S. Fiorenza, M. P. Suarez, and H. S. Rifai, *J. Envir. Eng.*, **128**, 773 (2002); S. Erdal and B. D. Goldstein, *Ann. Rev. Energy Environ.*, **25**, 765 (2000).

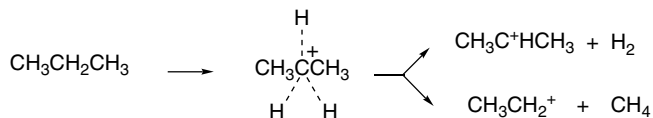
<sup>158</sup> A. K. Kolah, Q. Zhiwen, and S. M. Mahajani, *Chem. Innovation*, **31**, 15 (2001).

<sup>159</sup> J. M. Meister, S. M. B. Black, B. S. Muldoon, D. H. Wei, and C. M. Roessler, *Hydrocarbon Process.*, **79**, 63 (2000).

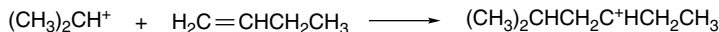
<sup>160</sup> G. A. Olah, P. Batamack, D. Deffieux, B. Toeroek, Q. Wang, A. Molnar, and G. K. S. Prakash, *Appl. Catal. A*, **146**, 107 (1996).

<sup>161</sup> Y. V. Kissin, *J. Catal.*, **126**, 600 (1990); Y. V. Kissin, *Catal. Rev.*, **43**, 85 (2001).

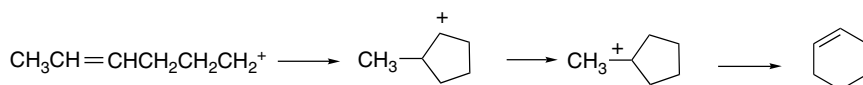
Cracking over acidic catalysts occurs through pentacovalent *carbonium ions*. The basic reactions are also observed with small hydrocarbons such as propane. Both the C–H and the C–C bond can be broken.



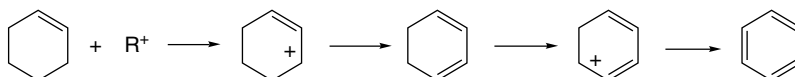
Alkenes are also formed and can react with trivalent carbocations to give alkylation products.



Intermediates with both a double bond and a carbocation can cyclize and rearrange.



Once cyclization has occurred, aromatization can occur through abstraction of hydride.



One process that occurs by these mechanisms, called the *Cyclar process*, uses a gallium-modified zeolite catalyst.<sup>162</sup> The gallium increases the rate of the early cracking steps that generate alkenes. The Cyclar process can convert butane, propane, and ethane to mixtures of benzene, toluene, and the isomeric xylenes. The reactivity order is butane > propane > ethane.

Hydrocracking is used to convert high-boiling crude petroleum having a high content of nitrogen and sulfur and relatively low hydrogen content to material suitable for use as fuel.<sup>163</sup> Hydrocracking is also used in the processing of very heavy crude petroleum such as that obtained from tar sands and shale oil.<sup>164</sup> The chemical transformations include reductive removal of nitrogen and sulfur (forming ammonia and hydrogen sulfide) and cracking to smaller molecules. These processes are normally carried out in separate reaction chambers. The catalysts include transition metals capable of hydrogenation and zeolites that catalyze cracking. The final product composition can be influenced by reactor temperature and catalyst composition.

Reforming catalysts usually involve both transition metals, often platinum, and minerals, particularly zeolites modified with various metals; the zeolites are aluminum silicates. Depending on the exact structure, there are a number of anionic sites, which must be neutralized by metal cations or protons. The protonic forms are strongly acidic. The zeolites have distinctive pore sizes and are selective for certain molecular sizes or shapes.<sup>165</sup> For example, pore size can be a factor in determining the ratio of the *o*-, *m*-, and *p*-isomers of xylenes, with narrower pores favoring the last. Under normal

<sup>162</sup> M. Guisnet, N. S. Gnep, and F. Alario, *Appl. Catal. A*, **89**, 1 (1992).

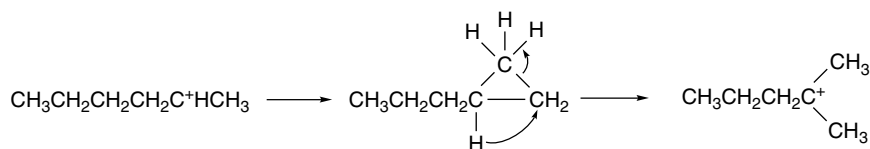
<sup>163</sup> J. W. Ward, *Fuel Proc. Technol.*, **35**, 55 (1993).

<sup>164</sup> J. F. Kriz, M. Ternan, and J. M. Denis, *J. Can. Pet. Technol.*, **22**, 29 (1983).

<sup>165</sup> C. R. Marcilly, *Top. Catal.*, **13**, 357 (2000).

operating conditions, the catalysts incorporate sulfur, which modifies the catalytic properties and tends to enhance rearrangement and aromatization.<sup>166</sup>

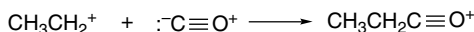
There is rapid interconversion of alkenes and carbocations over acidic zeolite catalysts, and the carbocations permit skeletal rearrangements and hydride transfer reactions. These reactions proceed in the direction of formation of more stable isomers.<sup>161</sup> The rearrangements probably proceed through protonated cyclopropanes (see Section 4.4.4).



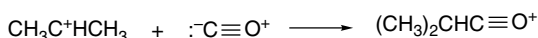
An important advance in understanding the mechanisms of reactions of alkanes with acidic catalysts resulted from study of the reactions of alkanes with superacids. This work demonstrated that both C–H and C–C bonds can be protonated, leading to fragmentation and formation of alkanes and carbocations.<sup>167</sup>



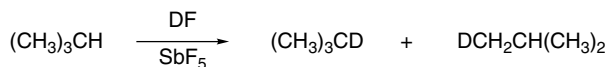
The reactions of propane and isobutene with HF-SbF<sub>5</sub> have been studied using C≡O to trap the carbocation intermediates.<sup>168</sup>



and



The C–C bond of propane is more reactive than the C–H bonds, in accord with its lower bond strength. With isobutane, however, the reaction occurs with both the primary and tertiary C–H bonds, leading to hydrogen exchange.



The carbocation intermediates can also alkylate alkanes, leading to chain lengthening.

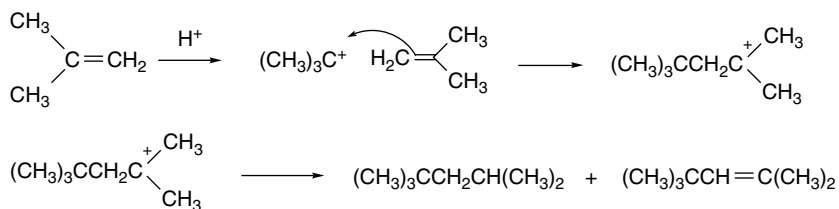


<sup>166</sup> P. G. Mennon and Z. Paal, *Ind. Eng. Chem. Res.*, **36**, 3282 (1997).

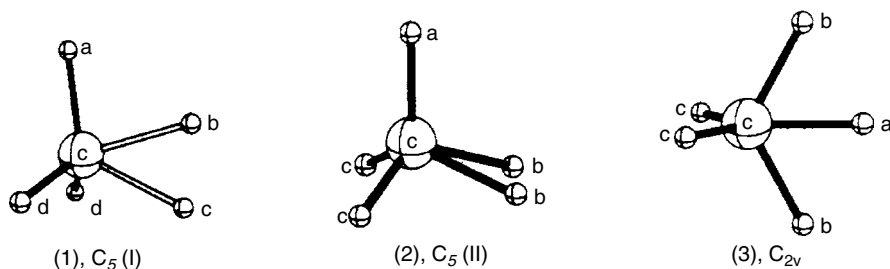
<sup>167</sup> G. A. Olah, Y. Halpern, J. Shen, and Y. K. Mo, *J. Am. Chem. Soc.*, **95**, 4960 (1973).

<sup>168</sup> J. Sommer and J. Bukala, *Acc. Chem. Res.*, **26**, 370 (1993).

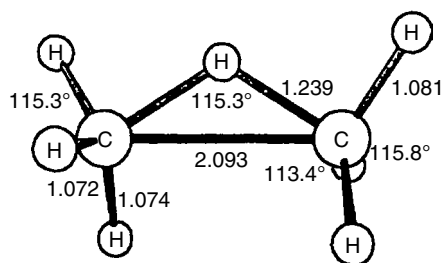
Similar reactions are observed over other strongly acidic catalysts, such as  $\text{AlCl}_3$  and  $\text{SbF}_5$ .<sup>169</sup> The acidic catalysts also promote dimerization and oligomerization of alkenes by mechanisms that are well known in the solution chemistry of carbocations.<sup>170</sup>



The structure of pentacovalent carbonium ions has been investigated by ab initio MO (CCSD(T)) methods. The  $\text{CH}_5^+$  molecule is fluxional with facile conversion among closely related geometries.<sup>171</sup>



SD(Q)CI + DZP calculations find a bridged structure as the most stable form of  $\text{C}_2\text{H}_7^+$ .



BLYP/6-311G\*\* calculations have also been done on  $\text{CH}_5^+$  and  $\text{C}_2\text{H}_7^+$ .<sup>172</sup>

Hydrocarbon protonations by catalysts have been modeled theoretically.<sup>173</sup> BLYP/6-31G\*\* calculations suggest protonation of the C–C bonds, followed by collapse to alkane and alkene. The acidic catalyst site is regenerated by transfer of a proton to an adjacent oxygen. This model, which is summarized in Figure 4.15, undoubtedly oversimplifies the picture, but probably contains the fundamental aspects of the catalysis.

<sup>169</sup> G. A. Fuentes and B. C. Gates, *J. Catal.*, **76**, 440 (1982); G. A. Fuentes, J. V. Boegel, and B. C. Gates, *J. Catal.*, **78**, 436 (1982).

<sup>170</sup> J. P. G. Pater, P. A. Jacobs, and J. A. Martens, *J. Catal.*, **184**, 262 (1999).

<sup>171</sup> P. R. Schreiner, S. J. Kim, H. F. Schaefer, III, and P. v. R. Schleyer, *J. Chem. Phys.*, **99**, 3716 (1993).

<sup>172</sup> S. J. Collins and P. J. O'Malley, *Chem. Phys. Lett.*, **228**, 246 (1994).

<sup>173</sup> S. J. Collins and P. J. O'Malley, *J. Catal.*, **153**, 94 (1995); S. J. Collins and P. J. O'Malley, *Chem. Phys. Lett.*, **246**, 555 (1995).

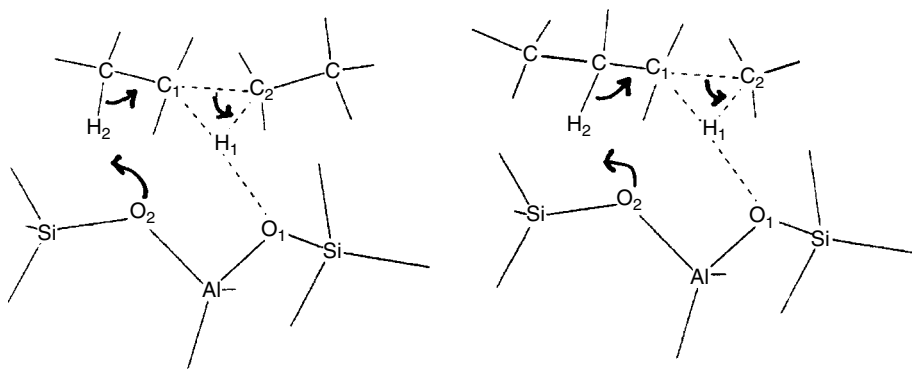


Fig. 4.15. Representation of C(2)–C(3) and C(1)–C(2) protonation and fragmentation to an alkane and alkene. Adapted from *Chem. Phys. Lett.*, **246**, 555 (1995).

## General References

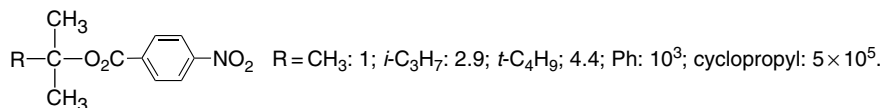
- S. P. McManus and C. U. Pittman, Jr., in *Organic Reaction Intermediates*, S. P. McManus, ed., Academic Press, New York, 1973, Chap. 4.  
 G. A. Olah and P. v. R. Schleyer, eds., *Carbonium Ions*, Vols. I–IV, Wiley-Interscience, New York, 1968–1973.  
 A. Streitwieser, Jr., *Solvolytic Displacement Reactions*, McGraw-Hill, New York, 1962.  
 E. R. Thornton, *Solvolysis Mechanisms*, Ronald Press, New York, 1964.

## Problems

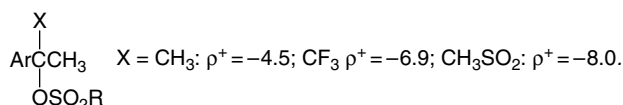
(References for these problems will be found on page 1159.)

4.1. Provide an explanation for the relative reactivity relationships revealed by the following data.

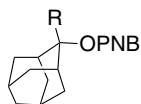
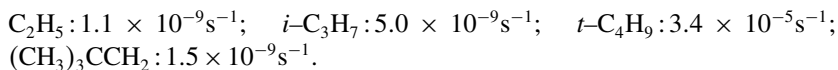
a. The relative rates of solvolysis in aqueous acetone of several tertiary *p*-nitrobenzoate esters:



b. For solvolysis of *a*-substituted 1-aryl-1-ethyl sulfonates, the value of  $\rho^+$  varies with the substituent.



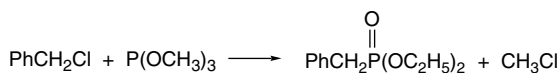
c. The rates of solvolysis for a series of 2-alkyl-2-adamantyl *p*-nitrobenzoates in 80% aqueous acetone at 25 °C are: R = CH<sub>3</sub>: 1.4 × 10<sup>-10</sup> s<sup>-1</sup>;



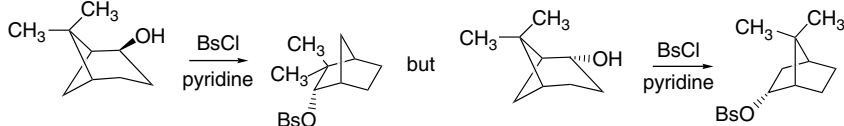
- d. The relative rates of methanolysis of a series of *w*-phenylthioalkyl chlorides depend on the chain length:  $n = 1 : 3.3 \times 10^4$ ;  $n = 2 : 1.5 \times 10^2$ ;  $n = 3 : 1$ ;  $n = 4 : 1.3 \times 10^2$ ;  $n = 5 : 4.3$ .

4.2. Suggest reasonable mechanisms for each of the following reactions. The starting materials are racemic, unless otherwise stated.

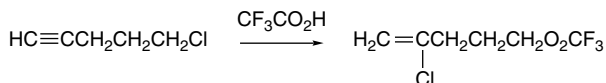
a.



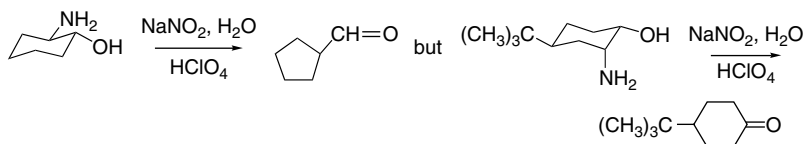
b.



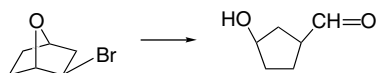
c.



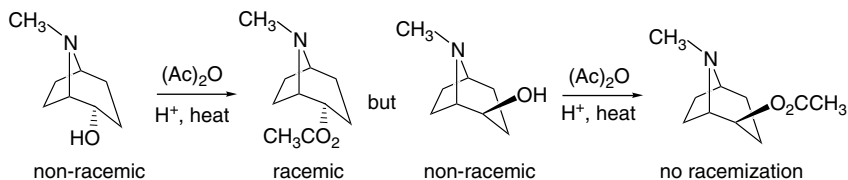
d.



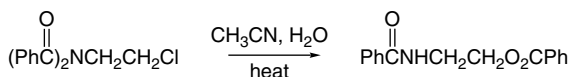
e.



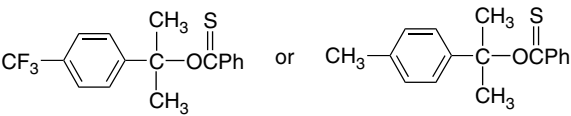
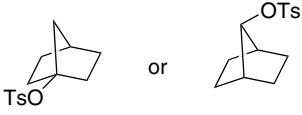
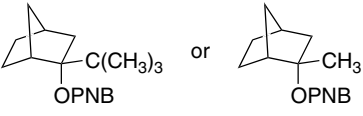
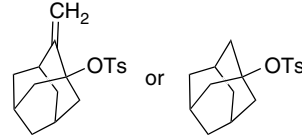
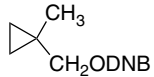
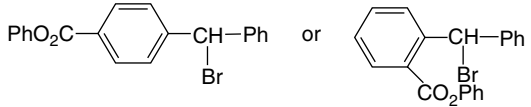
f.



g.



4.3. Which reaction in each pair would be expected to be faster? Explain.

- a.  $\text{Ar}-\overset{\text{CH}_3}{\text{C}}\text{HOSO}_2\text{CH}_3$  or  $\text{Ar}-\overset{\text{CH}_3}{\text{C}}\text{HOSO}_2\text{CH}_2\text{CF}_3$  solvolysis in 80% ethanol  
Ar = 3, 5-bis-(trifluoromethyl)phenyl
- b.  solvolysis in 100% ethanol
- c.  solvolysis in acetic acid
- d.  solvolysis in aqueous acetone
- e.  solvolysis in acetic acid
- f.  $\text{PhSO}_2\text{CH}_2\text{CH}_2\text{CH}_2\text{Cl}$  or  $\text{PhSO}_2\text{CH}_2\text{Cl}$  reaction with KI
- g.  $(\text{CH}_3)_3\text{CCH}_2\text{ODNB}$  or  solvolysis in aqueous dioxane
- h.  solvolysis in acetic acid
- i.  $\text{PhS}(\text{CH}_2)_3\text{Cl}$  or  $\text{PhS}(\text{CH}_2)_4\text{Cl}$  Solvolysis in methanol
- j.  solvolysis in acetic acid

4.4. The solvolysis of 2*R*,3*S*-3-(4-methoxyphenyl)but-2-yl tosylate in acetic acid can be followed by several kinetic measurements: (a) rate of decrease of observed rotation ( $k_\alpha$ ); rate of release of the leaving group ( $k_t$ ); and (c) when  $^{18}\text{O}$ -labeled sulfonate is used, the rate of equilibration of the sulfonate oxygens in the reactant ( $k_{ex}$ ). At 25°C the rate constants are:

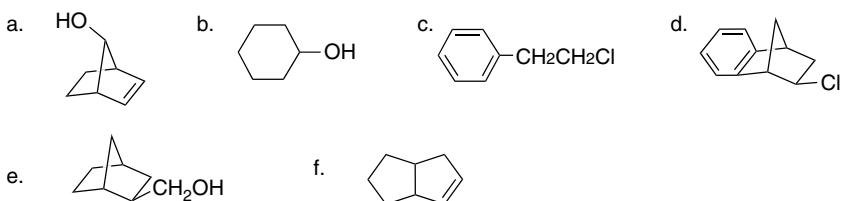
$$k_\alpha = 25.5 \times 10^{-6} \text{ s}^{-1}; k_t = 5.5 \times 10^{-6} \text{ s}^{-1}; k_{ex} 17.2 \times 10^{-6} \text{ s}^{-1}$$

Indicate the nature of the process that is measured by each of these rate constants and devise an overall mechanism that includes each of these processes. Rationalize the order of the rates  $k_\alpha > k_{ex} > k_t$ .

- 4.5. Both *endo*- and *exo*-norbornyl brosylates react with  $R_4P^+N_3^-$  (R is a long-chain alkyl) in toluene to give azides of inverted configuration. The yield from the *endo* and *exo* reactant is 95 and 80%, respectively. The remainder of the *exo* reactant is converted to nortricyclane (tricyclo[2.2.1.0<sup>2,6</sup>]heptane.) The measured rates of azide formation are first order in both reactant and azide ion. The *endo* isomer reacts about twice as fast as the *exo* isomer. Both react considerably more slowly than cyclohexyl brosylate under the same conditions. No rearrangement of deuterium is observed when deuterium-labeled reactants are used. What conclusions about the mechanism of the substitution process can you draw from these results? How do the reaction conditions relate to the mechanism you have suggested? How is the nortricyclane formed?
- 4.6 The following observations have been made concerning the reaction of *Z*-1-phenyl-1,3-butadiene (**6-A**) and *Z*-4-phenyl-3-buten-2-ol (**6-B**) in 3-7M  $H_2SO_4$  and 0.5-3M  $HClO_4$
- Both compounds are converted to a mixture of the corresponding *E*-isomers with the rate governed by  $\text{Rate} = k[\text{reactant}][H^+]$ , where  $[H^+]$  is measured by the  $H_0$  acidity function.
  - The rate of isomerization of **6-A** is slower in deuterated ( $D_2SO_4$ - $D_2O$ ) media by a factor of 2 to 3. For **6-B**, the rate of isomerization is faster in by a factor of 2.5.
  - When  $^{18}O$ -labeled **6-B** is used, the rate of loss of  $^{18}O$  to the solvent is equal to the rate of isomerization.
  - The measured activation energies for **6-A** is  $19.5 \pm 1$  kcal/mol and  $22.9 \pm 0.7$  kcal/mol for **6-B**.

Write a mechanism that encompasses both isomerizations and is consistent with the information given.

- 4.7 Treatment of 2-(4-hydroxyphenyl)ethyl bromide with basic alumina produces a white solid, mp, 40-43 °C; IR 1640  $cm^{-1}$ ;  $UV_{\max}$  282 nm in  $H_2O$ ; NMR two singlets of equal intensity at 1.69 and 6.44 ppm from TMS; anal: C 79.98% H, 6.71%. Suggest a possible structure for this product and explain how it could be formed.
- 4.8. In the discussion of the *syn*- and *anti*-norborn-2-en-7-yl tosylates (p. 422-423) it was pointed out that, relative to the saturated norborn-7-yl tosylate, the reactivities of the *syn* and *anti* isomers were  $10^4$  and  $10^{11}$ , respectively. Whereas the *anti* isomer gives a product of retained configuration, the *syn* isomer gives a bicyclo[3.2.0]hept-2-enyl derivative. The high reactivity of the *anti* isomer was attributed to participation of the carbon-carbon bond. What explanation can you offer for the  $10^4$  acceleration of the *syn* isomer relative to the saturated system?
- 4.9. Indicate the structure of the final stable ion that would be formed from each of the following reactants in superacid media.



- 4.10. A series of  $^{18}\text{O}$ -labeled sulfonate esters was studied to determine the extent of  $^{18}\text{O}$  scrambling that accompanies solvolysis. The rate of  $^{18}\text{O}$  exchange was compared with that of solvolysis and the results are shown below. Discuss the variation in the ratio  $k_{\text{sol}} : k_{\text{exch}}$  and offer an explanation for the absence of exchange in the 3,3-dimethyl-2-butyl case.

R	$k_{\text{sol}}$	$k_{\text{exch}}$
<i>i</i> -propyl	$3.6 \times 10^{-5}$	$7.9 \times 10^{-6}$
cyclopentyl	$3.8 \times 10^{-3}$	$8.5 \times 10^{-4}$
2-adamantyl	$1.5 \times 10^{-3}$	$1.8 \times 10^{-3}$
3,3-dimethyl-2-butyl <sup>a</sup>	$7.3 \times 10^{-3}$	Negligible

a. Solvolysis product is 2,3-dimethyl-2-butyl trifluoroacetate.

- 4.11. The relative stabilities of 1-phenylvinyl cations can be measured by determining the gas phase basicity of the corresponding alkynes. The table below gives data on free energy of protonation for substituted phenyethynes and phenylpropynes. These data give rise to the corresponding Yukawa-Tsuno relationships:

$$\text{For ArC}\equiv\text{CH} : \delta\Delta G^\circ = -14.1(\sigma^\circ + 1.21\sigma_{\text{R}}^+)$$

$$\text{For ArC}\equiv\text{CCH}_3 : \delta\Delta G^\circ = -13.3(\sigma^\circ + 1.12\sigma_{\text{R}}^+)$$

How do you interpret the values of  $\rho$  and  $r$  in these equations? Which system is more sensitive to the aryl substituents? How do you explain the difference in sensitivity? Sketch the resonance, polar, and hyperconjugative interactions that contribute to these substituent effects. What geometric constraints do these interactions place on the ions?

Substituent	$\delta\Delta G$ (kcal/mol)	
	Arylethynes	Arylpropynes
4-CH <sub>3</sub> O	11.8	13.0
3-Cl-4-CH <sub>3</sub> O	7.9	9.1
4-CH <sub>3</sub>	4.7	5.5
3-CH <sub>3</sub>	1.9	2.2
4-Cl	-0.5	0.1
3-F	-5.1	-5.6
3-Cl	-4.5	-5.1
3-CF <sub>3</sub>	-6.5	-6.6
3,5-diF	-8.4	
H	0	0

a.  $\delta\Delta$  is the change in free energy relative to the unsubstituted compound.

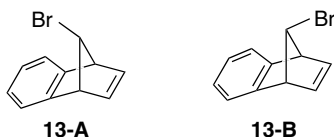
- 4.12. Studies of the solvolysis of 1-phenylethyl chloride and its 4-substituted derivatives in aqueous trifluoroethanol containing azide anion provide information relative to the mechanism of nucleophilic substitution in this system.
- a. The reaction rate is independent of the azide ion concentration for substituents that have  $\sigma^+$  values more negative than  $-0.3$ , but is first order in  $[\text{N}_3^-]$  for substituents with  $\sigma^+$  less negative than  $-0.08$ .

- b. When other good nucleophiles, e.g.,  $C_3H_7SH$ , are present, they can compete with azide ion. The reactants that are zero order in  $[N_3^-]$  show little selectivity among competing nucleophiles.
- c. For reactants that solvolyze at rates independent of  $[N_3^-]$ , the ratio of 1-arylethyl azide to 1-arylethanol in the product increases as  $\sigma^+$  of the substituent becomes more negative.
- d. The major product in reactions that are first order in  $[N_3^-]$  are 1-arylethyl azides.

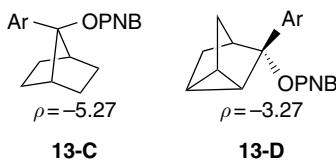
Consider these results in relation to the mechanism outlined in Figure 4.6 (p. 400). On the basis of the data given above, delineate the types of 1-arylethyl chlorides that react with azide ion according to those mechanistic types.

4.13. Offer a mechanistic interpretation of the following observations.

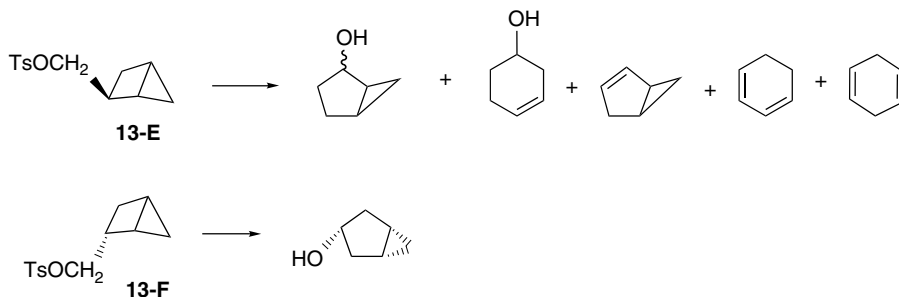
- a. Although there is a substantial difference in the rate at which **13-A** and **13-B** solvolyze (**13-A** reacts  $4.4 \times 10^4$  times faster than **13-B** in acetic acid), both compounds give products of completely retained configuration.



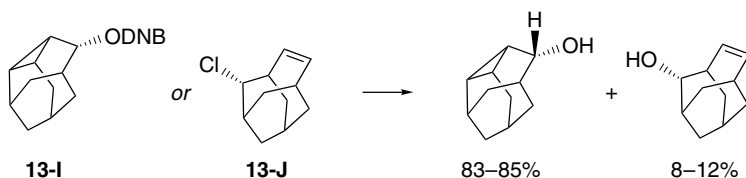
- b. The solvolysis of **13-C** is much more sensitive to aryl substituent effects than that of **13-D**.



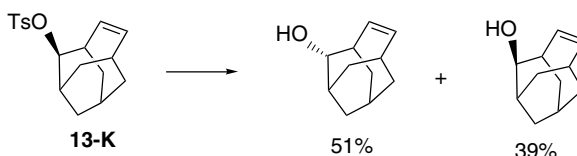
- c. Although stereoisomers **13-E** and **13-F** solvolyze in aqueous acetone at similar rates, the reaction products are quite different.



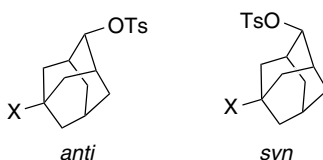
- d. Solvolysis of compounds **13-I** and **13-J** exhibits rate enhancement relative to a homoadamantane analog and gives product mixtures that are quite similar for both reactants.



On the other hand, compound **13-K** is less reactive than the saturated analog and gives a different product mixture.



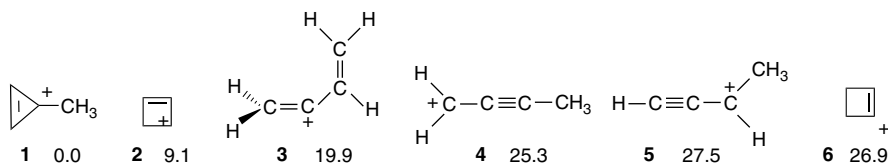
- e. The solvolysis of both stereoisomers of 5-fluoro- and 5-trimethylstannyl-2-adamantyl tosylate has been examined and the two have been compared. The relative rates and stereochemistry are summarized below.



X	<i>anti</i>		<i>syn</i>	
	Rate <sup>a</sup>	Stereochemistry	Rate	Stereochemistry
F	$2.5 \times 10^{-6}$	4% net ret.	$5 \times 10^{-4}$	100% ret.
(CH <sub>3</sub> ) <sub>3</sub> Sn	10	100% ret.	15	63% net inv.

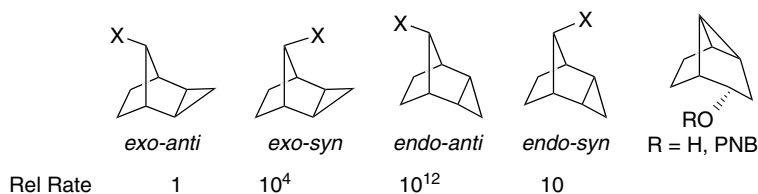
a. Rate is relative to unsubstituted system.

- 4.14. The six structures below are all found to be minima on the [C<sub>4</sub>H<sub>5</sub>]<sup>+</sup> energy surface. The relative energies from MP2/6-311G(*d,p*) calculations are shown in kcal/mol. Comment on the stabilizing features that are present in each of these cations.

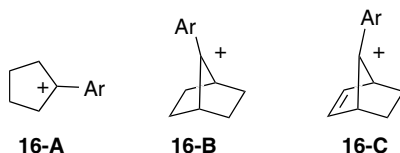


- 4.15. The rates of solvolysis of four stereoisomeric tricyclo[3.2.1.0<sup>2,4</sup>]octan-8-yl systems have been determined. After accounting for leaving group and temperature, the relative rates are as shown. In aqueous dioxane, the *endo-anti* isomer

gives a product mixture consisting of the rearranged alcohol and the corresponding PNB ester (from leaving-group capture). The other isomers gave complex product mixtures that were not fully characterized. Explain the trend in rates and discuss the reason for the stereochemical outcome in the case of the *endo-anti* isomer.

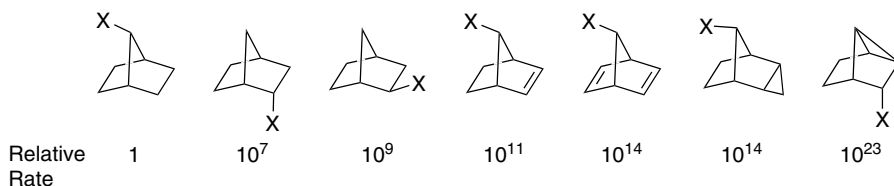


- 4.16. The  $^{13}\text{C}$ -NMR chemical shift of the trivalent carbon is a sensitive indicator of carbocation structure. Generally, the greater the chemical shift value, the lower the electron density at the carbon. Data for three different cations with aryl substituents are given below. How do you explain the close similarity of the trend for the first two series and the opposite trend of the third?



Aryl substituent	Chemical shift (ppm)		
	16-A	16-B	16-C
3, 5-diCF <sub>3</sub>	287	283	73
4-CF <sub>3</sub>	284	278	81
H	272	264	109
4-CH <sub>3</sub>	262	252	165
4-OCH <sub>3</sub>	235	230	220

- 4.17. Relative rate data are available for a wide range of reactivities for rings related to the bicyclo[2.2.1]heptyl (norbornyl) system. Offer a discussion of the structural effects that are responsible for the observed relative rates.



- 4.18. Fujio and co-workers studied the reaction of pyridine with a wide range of 1-arylethyl bromides in acetonitrile. By careful analysis of the kinetic data, they were able to dissect each reaction into a first-order and a second-order component, as shown in the table below. The first-order components were correlated by a Yukawa-Tsuno equation:  $\log k/k_o = 5.0(\sigma^o + 1.15\bar{\sigma}^+)$ . The second-order component gave a curved plot, as shown in Figure 4.P18. Analyze the responses of the reaction to the aryl substituents in terms of transition state structures.

Substituent	$10^5 k_1 (\text{s}^{-1})$	$10^5 k_2 (M^{-1} \text{s}^{-1})$	Substituent	$10^5 k_1 (\text{s}^{-1})$	$10^5 k_2 (M^{-1} \text{s}^{-1})$
4-CH <sub>3</sub> O	1660	2820	2-Naphthyl	0.28	11.6
4-CH <sub>3</sub> S	103	215	3-CH <sub>3</sub>	0.055	7.29
4-C <sub>6</sub> H <sub>5</sub> O	41.5	119	H	0.032	5.54
3-Cl-4-CH <sub>3</sub> O	21.2	79.0	4-Cl		4.37
2-Fluorenyl	18.3	59.5	3-Cl		2.085
3,4,5-tri-CH <sub>3</sub>	8.56	41.1	3-CF <sub>3</sub>		1.77
3,4-di-CH <sub>3</sub>	3.67	28.3	3-NO <sub>2</sub>		1.21
4-CH <sub>3</sub>	1.46	19.2	4-NO <sub>2</sub>		1.19
4-(CH <sub>3</sub> ) <sub>3</sub> C	0.82	15.2	3,5-di-CF <sub>3</sub>		0.651

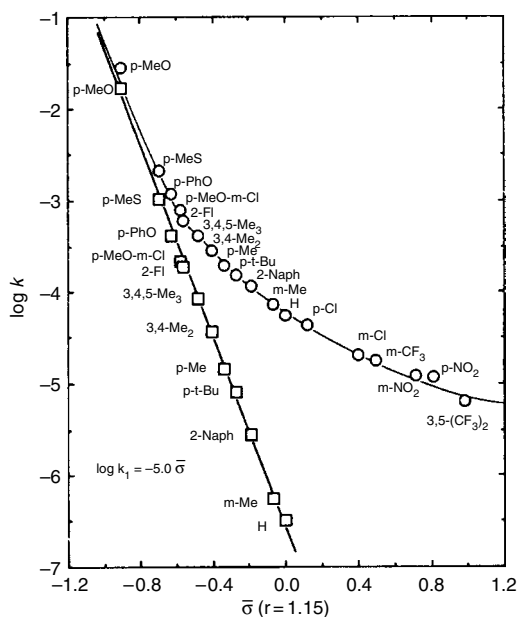
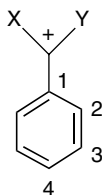


Fig. 4.P18. Substituent effects on the rates of reaction of pyridine with 1-arylethyl bromides in acetonitrile at 35 °C. Squares are the first-order rates and open circles are the second-order rates. Reproduced from *Tetrahedron Lett.* **38**, 3243 (1997), by permission of Elsevier.

4.19 The Yukawa-Tsuno equation  $r$  values have been measured for the solvolysis reactions of substituted benzyl cations and  $\alpha$ -substituted analogs. HF/6-31G\* charges and bond orders have been calculated for the presumed cationic intermediates. Analyze the data for relationships between  $r$  and the structural parameters.



X,Y	H,H	CH <sub>3</sub> , H	CH <sub>3</sub> , CH <sub>3</sub>	CF <sub>3</sub> , H
<i>r</i>	1.28	1.15	1.00	1.51
Mulliken Charge				
C(1)	-0.0024	-0.050	-0.068	-0.211
C(2)	+0.189	+0.164	+0.140	+0.053
C(3)	+0.051	+0.046	+0.043	+0.053
C(4)	+0.213	+0.190	+0.171	+0.233
Bond Order				
C(1)-C(7)	1.584	1.465	1.363	1.622
C(1)-C(2)	1.158	1.193	1.225	1.134
C(2)-C(3)	1.167	1.543	1.524	1.585
C(3)-C(4)	1.343	1.361	1.375	1.329

4.20. Reactions of substituted cumyl benzoates in 50:50 trifluoroethanol-water show no effect of  $[\text{NaN}_3]$  on the rate of reaction between 0 and 0.5M for either EWG or ERG substituents. The product ratio, however, as shown in the figure, is highly dependent on the cumyl substituent. ERG substituents favor azide formation, whereas EWG groups result in more solvent capture. Formulate a reaction mechanism that is consistent with these observations.

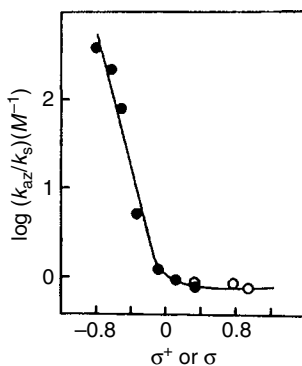
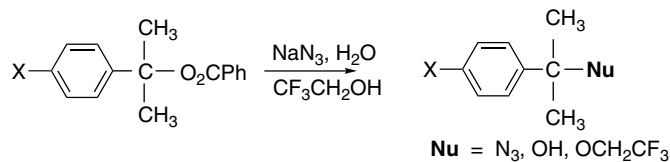


Fig. 4.P20. Log of product selectivity  $(k_{\text{az}}/k_{\text{s}})\text{M}^{-1}$  versus  $\sigma^+$ . Solid circles are substituted benzoate leaving groups and open circles are chloride. Reproduced from *J. Am. Chem. Soc.*, **113**, 5 871 (1991), by permission of the American Chemical Society.

4.21. The comparison of activation parameters for reactions in different solvents requires consideration of solvation differences of both the reactants and the transition states. The comparison can be done by using potential energy diagrams, such as that illustrated below for two different solvents A and B. It is possible to measure  $\Delta H_{\text{transfer}}$  values, which correspond to the enthalpy change associated with transfer of a solute from one solvent to another.

— TS in A  
— TS in B  
reactants in A —  
reactants in B —

$\Delta H_{\text{transfer}}$  data for *n*-hexyl tosylate and several nucleophilic anions are given in Table 4.P1.21. In Table 4.P2.21, the activation parameters for  $S_N2$  displacement reactions with *n*-hexyl tosylate are given. Use these data to construct a potential energy comparison for each of the nucleophiles. Use these diagrams to interpret the relative reactivity data given in Table 4.P3.21. Discuss the following aspects of the data.

- Why is  $\text{Cl}^-$  more reactive than  $\text{Br}^-$  in DMSO, whereas the reverse is true in methanol?
- Why does the rate of thiocyanate ( $\text{SCN}^-$ ) ion change the least of the five nucleophiles on going from methanol to DMSO?
- Why does thiocyanate have the most negative entropy of activation?

**Table 4.P1.21. Enthalpies of Transfer of Ions and *n*-Hexyl Tosylate From Methanol to DMSO at 25° C**

Reactant	$\Delta H_{\text{transfer}}$ (kcal/mol)
<i>n</i> -C <sub>6</sub> H <sub>13</sub> OTs	-0.4
$\text{Cl}^-$	6.6
$\text{N}_3^-$	3.6
$\text{Br}^-$	2.3
$\text{NCS}^-$	1.0
$\text{I}^-$	-1.1

**Table 4.P2.21. Activation Parameters for Nucleophilic Displacement Reactions of *n*-Hexyl Tosylate**

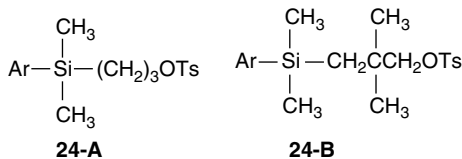
Nu <sup>-</sup>	Solvent	$\Delta H^\ddagger$ (kcal/mol)	$\Delta S^\ddagger$ (eu)	$\Delta G^\ddagger$ (kcal/mol)
$\text{Cl}^-$	MeOH	24.3	-4.2	25.5
	DMSO	20.2	-4.4	21.6
$\text{N}_3^-$	MeOH	21.2	-8.2	23.5
	DMSO	18.6	-7.8	21.0
$\text{Br}^-$	MeOH	22.9	-6.4	24.9
	DMSO	20.5	-5.6	22.0
$\text{NCS}^-$	MeOH	19.8	-15.8	24.2
	DMSO	20.0	-12.4	23.7
$\text{I}^-$	MeOH	22.4	-6.0	23.9
	DMSO	20.9	-5.8	22.8

Table 4.P3.21. Rates of Nucleophilic Substitution on *n*-Hexyl Tosylate<sup>a</sup>

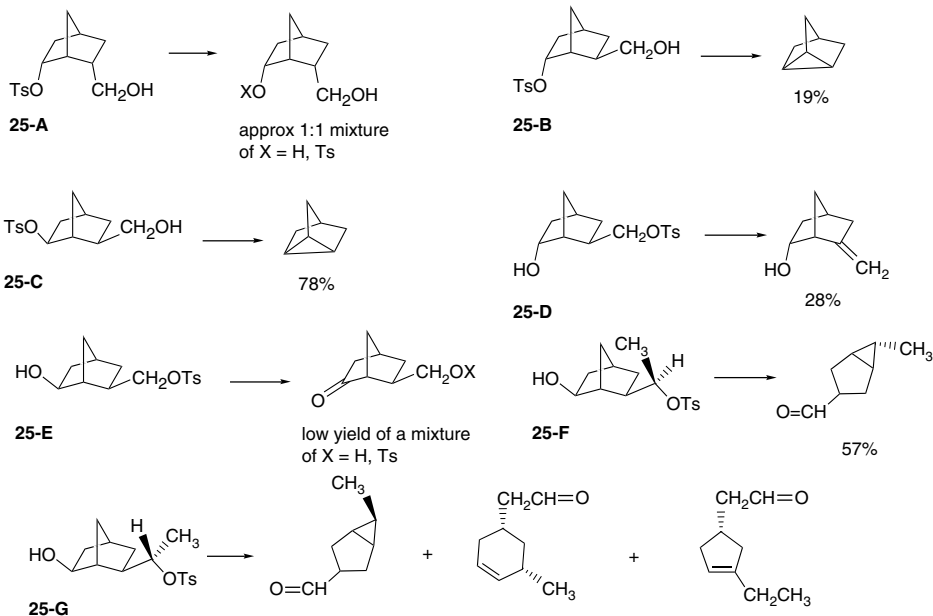
Nu: <sup>-</sup>	Solvent	<i>k</i> (40 °C)	<i>k</i> (30 °C)	<i>k</i> (20 °C)
Cl <sup>-</sup>	MeOH	0.0852	0.0226	0.00550
	DMSO	50.5	16.7	5.06
N <sub>3</sub> <sup>-</sup>	MeOH	1.66	0.514	0.152
	DMSO	135	48.3	16.1
Br <sup>-</sup>	MeOH	0.250	0.0721	0.0191
	DMSO	17.8	5.60	1.75
NCS <sup>-</sup>	MeOH	0.481	0.165	0.0512
	DMSO	1.11	0.365	0.115
I <sup>-</sup>	MeOH	0.956	0.275	0.0767
	DMSO	5.50	1.75	16.0 (50 °C)

a.  $k_2 \times 10^4 \text{ M}^{-1}\text{s}^{-1}$ .

- d. Is there any correlation between softness (which is in the order  $\text{I}^- > ^-\text{SCN} > \text{N}_3^- > \text{Br}^- > \text{Cl}^-$ ) and the effect of the solvent change on the rate of the reaction?
- 4.22. The Yukawa-Tsuno parameter  $r^+$  has been measured for several solvolysis reactions. What relationship do you see among the properties of the reactants, the likely nature of the transition structures, and the observed value of  $r^+$ ?
- Solvolysis of benzyl tosylates in acetic acid;  $r^+ = 1.3$  compared to solvolysis of 1-aryl-2,2,2-trifluoroethyl tosylates in 80% aqueous acetone;  $r^+ = 1.39$
  - Aryl-assisted solvolysis of 2-aryl-2-(trifluoromethyl)ethyl *m*-nitrobenzoates in 80% aqueous trifluoroethanol;  $r^+ = 0.77$  compared to aryl-assisted solvolysis of 2-arylethyl tosylates;  $r^+ = 0.6$
- 4.23. Comparison of several series of solvolysis reactions that proceed via carbocation intermediates revealed that an  $\alpha$ -cyano substituent is rate retarding by a factor of about  $10^{-3}$ . A  $\beta$ -cyano is even more rate retarding, with the difference being as much as  $10^{-7}$ . Why are both  $\alpha$ - and  $\beta$ -cyano rate retarding and why might the  $\beta$ -substituent have a stronger effect?
- 4.24. Several substituted propyl tosylates with  $\gamma$ -silicon groups have been studied. For the 2,2-dimethyl derivatives **24-B**, the solvolysis rates are  $10^3$  to  $10^4$  greater than for the nonsilyl analogs. The products are rearranged 1,1-dimethyl derivatives. The reaction shows modest sensitivity to substituents in the aryl group, correlating with a Hammett  $\rho$  value of  $-1.0$ . When the parent system **24-A** (without the 2,2-dimethyl substituents) was studied in the nonnucleophilic solvent 97% TFE, cyclopropane was formed, ranging in yield from 0% with EWG ( $\text{CF}_3$ ) to 100% with ERG ( $\text{CH}_3\text{O}$ ). The Hammett correlation gave  $\rho = -1.1$  for cyclopropane formation but no significant substituent effect for substitution. Describe a mechanism that is consistent with this information.



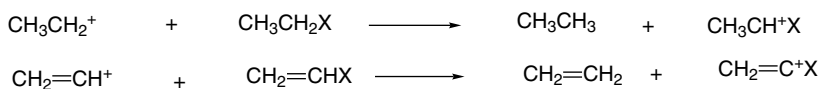
4.25. The reaction of several monotosylates derived from 6-hydroxy-2-(hydroxymethyl)norbornane were studied under conditions where alkoxide formation would be expected at the nontosylated hydroxy. Compounds **25-C** and **25-F** showed highly specific product formation, whereas the other compounds gave slower reactions and more complex product mixtures. Identify the structural features that make the observed pathways particularly favorable for **25-C** and **25-F**. Offer a mechanistic rationale for the formation of the products shown for the other reactants.



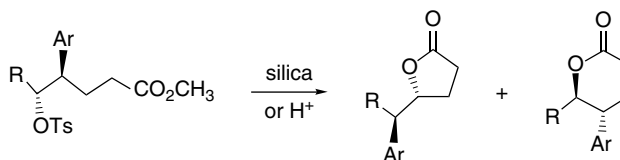
4.26. Table 4.P26 shows stabilization (+) and destabilization (–) of  $\alpha$ -substituted ethyl and vinyl cations as determined by the isodesmic reactions shown below. Comment on the following trends in the data.

**Table 4.P26. Stabilization of Ethyl and Vinyl Carbocations by  $\alpha$ -Substituent**

Substituent	$\text{C}_2\text{H}_5^+$	$\text{CH}_2=\text{CH}^+$	Substituent	$\text{C}_2\text{H}_5^+$	$\text{CH}_2=\text{CH}^+$
H	0.00	0.00	CN	–16.02	–11.71
$\text{CH}_3$	18.83	25.89	$\text{CH}=\text{O}$	–10.25	–4.51
$\text{CH}_2\text{Cl}$	5.59	12.90	F	6.95	–9.25
$\text{CH}_2\text{Br}$	8.66	14.00	Cl	9.83	11.17
$\text{CH}_2\text{OH}$	15.30	21.69	Br	9.52	12.70
$\text{CH}_2\text{CN}$	–2.10	4.76	I	13.32	20.53
$\text{CH}_2\text{CF}_3$	3.62	9.63	$\text{NH}_2$	64.96	53.69
$\text{CH}_2\text{F}$	4.98	10.89	OH	37.43	25.92
$\text{CF}_3$	–23.56	–16.41	SH	36.39	38.21
$\text{CH}_2=\text{CH}$	31.98	32.55	$\text{NO}_2$	–23.09	–25.44
$\text{HC}\equiv\text{C}$	18.17	25.64	$(\text{CH}_3)_3\text{Si}$	17.30	34.21
$\text{C}_6\text{H}_5$	36.77	54.10			
<i>c</i> - $\text{C}_3\text{H}_5$	42.97	47.06			



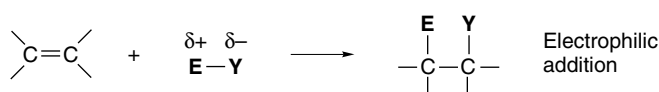
- The stabilization of vinyl cations tends to be somewhat larger than for the corresponding ethyl cation.
  - F, OH, and NH<sub>2</sub> provide less stabilization of vinyl cations than of ethyl cations.
  - CF<sub>3</sub> and CN are less destabilizing of vinyl cations than of ethyl cations.
  - What factors dominate the effect of the CH<sub>2</sub>-X substituents?
  - Compare the π-donor and polar effects of the OH, NH<sub>2</sub>, and SH substituents.
- 4.27. 4-Aryl-5-tosyloxyhexanoates are converted to mixtures of lactones when exposed to silica or heated with *p*-toluenesulfonic acid in various solvents. The aryl ring must have an EWG for the reaction to proceed. A similar reaction occurs with 4-aryl-5-tosyloxyhexanoates, but in this case only γ-lactones are formed. Suggest a mechanism that accounts for both the observed regioselectivity and stereoselectivity and the requirement for an EWG on the aryl ring.



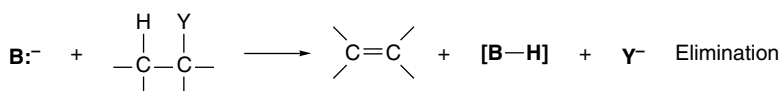
# Polar Addition and Elimination Reactions

## Introduction

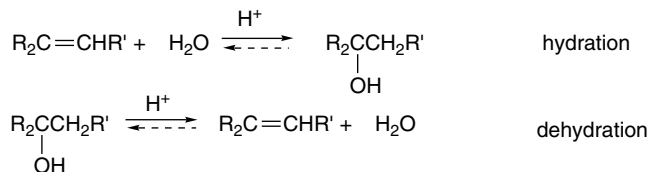
In this chapter, we discuss reactions that either add adjacent (*vicinal*) groups to a carbon-carbon double bond (*addition*) or remove two adjacent groups to form a new double bond (*elimination*). The discussion focuses on addition reactions that proceed by electrophilic polar (*heterolytic*) mechanisms. In subsequent chapters we discuss addition reactions that proceed by *radical (homolytic)*, *nucleophilic*, and *concerted* mechanisms. The electrophiles discussed include protic acids, halogens, sulfonyl and selenenyl reagents, epoxidation reagents, and mercuric and related metal cations, as well as diborane and alkylboranes. We emphasize the relationship between the regio- and stereoselectivity of addition reactions and the reaction mechanism.



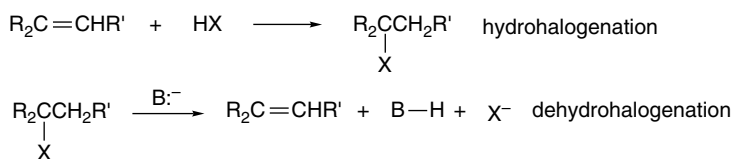
The discussion of elimination reactions considers the classical E2, E1, and E1cb eliminations that involve removal of a hydrogen and a leaving group. We focus on the kinetic and stereochemical characteristics of elimination reactions as key indicators of the reaction mechanism and examine how substituents influence the mechanism and product composition of the reactions, paying particular attention to the nature of transition structures in order to discern how substituent effects influence reactivity. We also briefly consider reactions involving trisubstituted silyl or stannyl groups. Thermal and concerted eliminations are discussed elsewhere.



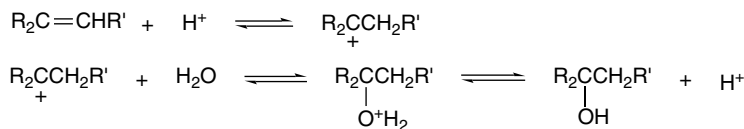
Addition and elimination processes are the formal reverse of one another, and in some cases the reaction can occur in either direction. For example, acid-catalyzed hydration of alkenes and dehydration of alcohols are both familiar reactions that constitute an addition-elimination pair.



Another familiar pair of addition-elimination reactions is hydrohalogenation and dehydrohalogenation, although these reactions are not reversible under normal conditions, because the addition occurs in acidic solution, whereas the elimination requires a base.



When reversible addition and elimination reactions are carried out under similar conditions, they follow the same mechanistic path, but in opposite directions. The *principle of microscopic reversibility* states that the mechanism of a reversible reaction is the same in the forward and reverse directions. The intermediates and transition structures involved in the addition process are the same as in the elimination reaction. Under these circumstances, mechanistic conclusions about the addition reaction are applicable to the elimination reaction and vice versa. The reversible acid-catalyzed reaction of alkenes with water is a good example. Two intermediates are involved: a carbocation and a protonated alcohol. The direction of the reaction is controlled by the conditions, which can be adjusted to favor either side of the equilibrium. Addition is favored in aqueous solution, whereas elimination can be driven forward by distilling the alkene from the reaction solution. The reaction energy diagram is shown in Figure 5.1.



Several limiting general mechanisms can be written for polar additions. Mechanism A involves prior dissociation of the electrophile and implies that a carbocation is generated that is free of the counterion  $\text{Y}^-$  at its formation. Mechanism B also involves a carbocation intermediate, but it is generated in the presence of an anion and exists initially as an ion pair. Depending on the mutual reactivity of the two ions, they might or might not become free of one another before combining to give product. Mechanism C leads to a bridged intermediate that undergoes addition in a second step in which the ring is opened by a nucleophile. Mechanism C implies stereospecific *anti* addition. Mechanisms A, B, and C are all  $\text{A}_{\text{E}}2$  reactions; that

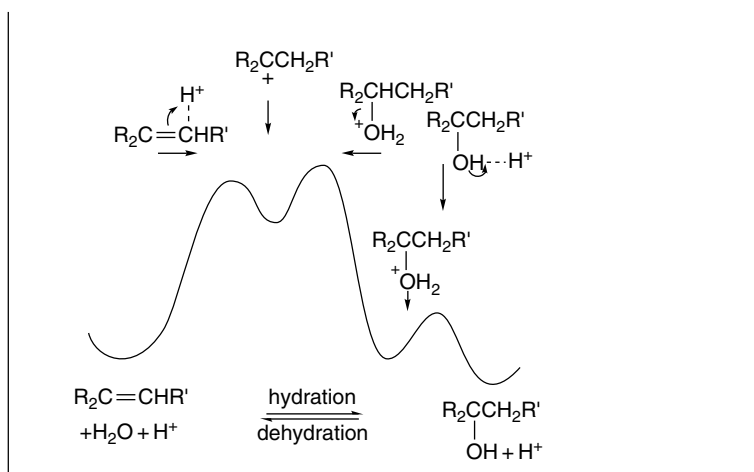
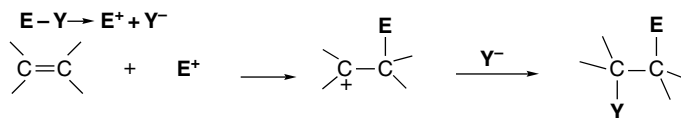


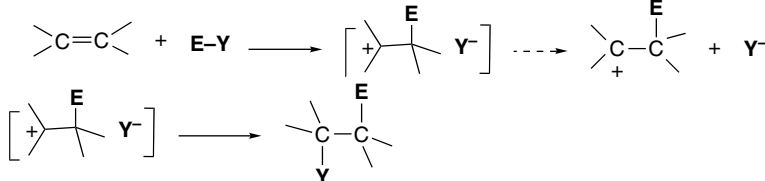
Fig. 5.1. Conceptual representation of the reversible reaction path for the hydration-dehydration reaction pair.

is, they are *bimolecular electrophilic additions*. Mechanism D is a process that has been observed for several electrophilic additions and implies concerted transfer of the electrophilic and nucleophilic components of the reagent from two separate molecules. It is a *termolecular electrophilic addition*,  $Ad_E3$ , a mechanism that implies formation of a complex between one molecule of the reagent and the reactant and also is expected to result in *anti* addition. Each mechanism has two basic parts, the electrophilic interaction of the reagent with the alkene and a step involving reaction with a nucleophile. Either formation of the bond to the electrophile or nucleophilic capture of the cationic intermediate can be rate controlling. In mechanism D, the two stages are concurrent.

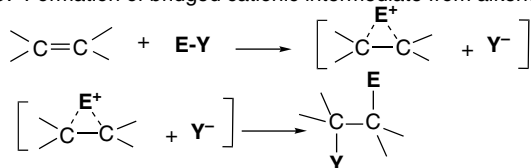
A. Prior dissociation of electrophile and formation of carbocation intermediate



B. Formation of carbocation ion pair from alkene and electrophile

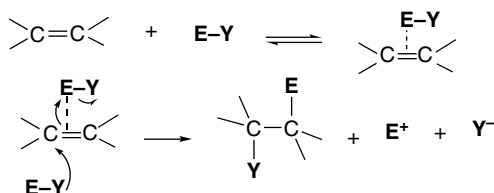


C. Formation of bridged cationic intermediate from alkene and electrophile



(Continued)

## D. Concerted addition of electrophile and nucleophile in a termolecular reaction



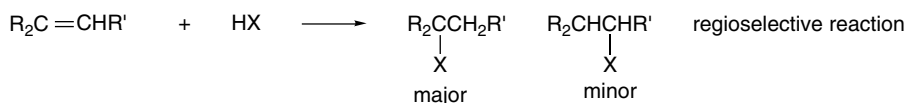
All of these mechanisms are related in that they involve electrophilic attack on the  $\pi$  bond of the alkene. Based on the electron distribution and electrostatic potential maps of alkenes (Section 1.4.5), the initial attack is expected to be perpendicular to the plane of the double bond and near the midpoint of the  $\pi$  bond. The mechanisms differ in the relative stability of the carbocation or bridged intermediates and in the timing of the bonding to the nucleophile. Mechanism A involves a prior dissociation of the electrophile, as would be the case in protonation by a strong acid. Mechanism B can occur if the carbocation is fairly stable and  $E^+$  is a poor bridging group. The lifetime of the carbocation may be very short, in which case the ion pair would react faster than it dissociates. Mechanism C is an important general mechanism that involves bonding of  $E^+$  to both carbons of the alkene and depends on the ability of the electrophile to function as a bridging group. Mechanism D avoids a cationic intermediate by concerted formation of the C-E and C-Y bonds.

The nature of the electrophilic reagent and the relative stabilities of the intermediates determine which mechanism operates. Because it is the hardest electrophile and has no free electrons for bridging, the proton is most likely to react via a carbocation mechanism. Similarly, reactions in which  $E^+$  is the equivalent of  $F^+$  are unlikely to proceed through bridged intermediates. Bridged intermediates become more important as the electrophile becomes softer (more polarizable). We will see, for example, that bridged halonium ions are involved in many bromination and chlorination reactions. Bridged intermediates are also important with sulfur and selenium electrophiles. Productive termolecular collisions are improbable, and mechanism D involves a prior complex of the alkene and electrophilic reagent. Examples of each of these mechanistic types will be encountered as specific reactions are dealt with in the sections that follow. The discussion focuses on a few reactions that have received the most detailed mechanistic study. Our goal is to see the common mechanistic features of electrophilic additions and recognize some of the specific characteristics of particular reagents.

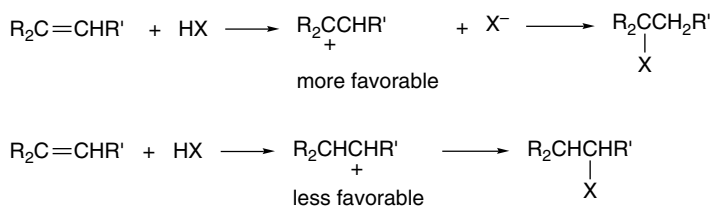
## 5.1. Addition of Hydrogen Halides to Alkenes

The addition of hydrogen halides to alkenes has been studied from a mechanistic perspective for many years. One of the first aspects of the mechanism to be established was its regioselectivity, that is, the direction of addition. A reaction is described as *regioselective* if an unsymmetrical alkene gives a predominance of one of the two isomeric addition products.<sup>1</sup>

<sup>1</sup> A. Hassner, *J. Org. Chem.*, **33**, 2684 (1968).



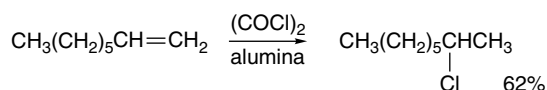
In the addition of hydrogen halides to alkenes, it is usually found that the nucleophilic halide ion becomes attached to the more-substituted carbon atom. This general observation is called *Markovnikov's rule*. The basis for this regioselectivity lies in the relative ability of the carbon atoms to accept positive charge. The addition of hydrogen halide is initiated by protonation of the alkene. The new C–H bond is formed from the  $\pi$  electrons of the carbon-carbon double bond. It is easy to see that if a carbocation is formed as an intermediate, the halide will be added to the more-substituted carbon, since protonation at the less-substituted carbon atom provides the more stable carbocation intermediate.



As is indicated when the mechanism is discussed in more detail, discrete carbocations are not always formed. Unsymmetrical alkenes nevertheless follow the Markovnikov rule, because the partial positive charge that develops is located predominantly at the carbon that is better able to accommodate an electron deficiency, which is the more-substituted one.

The regioselectivity of addition of hydrogen bromide to alkenes can be complicated if a free-radical chain addition occurs in competition with the ionic addition. The free-radical chain reaction is readily initiated by peroxidic impurities or by light and leads to the *anti* Markovnikov addition product. The mechanism of this reaction is considered more fully in Chapter 11. Conditions that minimize the competing radical addition include use of high-purity alkene and solvent, exclusion of light, and addition of a radical inhibitor.<sup>2</sup>

The order of reactivity of the hydrogen halides is  $\text{HI} > \text{HBr} > \text{HCl}$ , and reactions of simple alkenes with HCl are quite slow. The reaction occurs more readily in the presence of silica or alumina and convenient preparative methods that take advantage of this have been developed.<sup>3</sup> In the presence of these adsorbents, HBr undergoes exclusively ionic addition. In addition to the gaseous hydrogen halides, liquid sources of hydrogen halide such as  $\text{SOCl}_2$ ,  $(\text{COCl})_2$ ,  $(\text{CH}_3)_3\text{SiCl}$ ,  $(\text{CH}_3)_3\text{SiBr}$ , and  $(\text{CH}_3)_3\text{SiI}$  can be used. The hydrogen halide is generated by reaction with water and/or hydroxy group on the adsorbent.



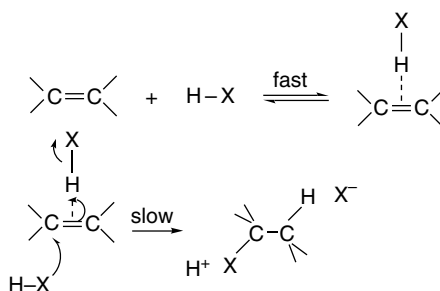
<sup>2</sup> D. J. Pasto, G. R. Meyer, and B. Lepeska, *J. Am. Chem. Soc.*, **96**, 1858 (1974).

<sup>3</sup> P. J. Kropp, K. A. Daus, M. W. Tubergen, K. D. Kepler, V. P. Wilson, S. C. Craig, M. M. Baillargeon, and G. W. Breton, *J. Am. Chem. Soc.*, **115**, 3071 (1993).

Studies aimed at determining mechanistic details of hydrogen halide addition to alkenes have focused on the kinetics and stereochemistry of the reaction and on the effect of added nucleophiles. Kinetic studies often reveal rate expressions that indicate that more than one process contributes to the overall reaction rate. For addition of hydrogen bromide or hydrogen chloride to alkenes, an important contribution to the overall rate is often made by a third-order term.

$$\text{Rate} = k[\text{alkene}][\text{HX}]^2$$

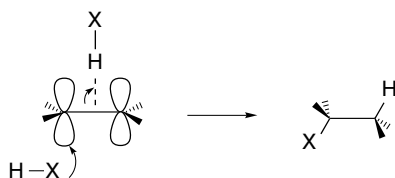
Among the cases in which this type of kinetics has been observed are the addition of HCl to 2-methyl-1-butene, 2-methyl-2-butene, 1-methylcyclopentene,<sup>4</sup> and cyclohexene.<sup>5</sup> The addition of HBr to cyclopentene also follows a third-order rate expression.<sup>2</sup> The TS associated with the third-order rate expression involves proton transfer to the alkene from one hydrogen halide molecule and capture of the halide ion from the second, and is an example of general mechanism D ( $\text{Ad}_{\text{E}3}$ ). Reaction occurs through a complex formed by the alkene and hydrogen halide with the second hydrogen halide molecule.



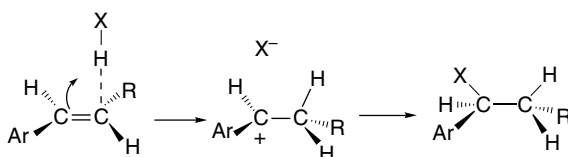
The stereochemistry of addition of hydrogen halides to unconjugated alkenes is usually *anti*. This is true for addition of HBr to 1,2-dimethylcyclohexene,<sup>6</sup> cyclohexene,<sup>7</sup> 1,2-dimethylcyclopentene,<sup>8</sup> cyclopentene,<sup>2</sup> *Z*- and *E*-2-butene,<sup>2</sup> and 3-hexene,<sup>2</sup> among others. *Anti* stereochemistry is also dominant for addition of hydrogen chloride to 1,2-dimethylcyclohexene<sup>9</sup> and 1-methylcyclopentene.<sup>4</sup> Temperature and solvent can modify the stereochemistry, however. For example, although the addition of HCl to 1,2-dimethylcyclohexene is *anti* near room temperature, *syn* addition dominates at  $-78^\circ\text{C}$ .<sup>10</sup>

*Anti* stereochemistry is consistent with a mechanism in which the alkene interacts simultaneously with a proton-donating hydrogen halide and a source of halide ion, either a second molecule of hydrogen halide or a free halide ion. The *anti* stereochemistry is consistent with the expectation that the attack of halide ion occurs from the opposite side of the  $\pi$ -bond to which the proton is delivered.

- <sup>4</sup> Y. Pocker, K. D. Stevens, and J. J. Champoux, *J. Am. Chem. Soc.*, **91**, 4199 (1969); Y. Pocker and K. D. Stevens, *J. Am. Chem. Soc.*, **91**, 4205 (1969).
- <sup>5</sup> R. C. Fahey, M. W. Monahan, and C. A. McPherson, *J. Am. Chem. Soc.*, **92**, 2810 (1970).
- <sup>6</sup> G. S. Hammond and T. D. Nevitt, *J. Am. Chem. Soc.*, **76**, 4121 (1954).
- <sup>7</sup> R. C. Fahey and R. A. Smith, *J. Am. Chem. Soc.*, **86**, 5035 (1964); R. C. Fahey, C. A. McPherson, and R. A. Smith, *J. Am. Chem. Soc.*, **96**, 4534 (1974).
- <sup>8</sup> G. S. Hammond and C. H. Collins, *J. Am. Chem. Soc.*, **82**, 4323 (1960).
- <sup>9</sup> R. C. Fahey and C. A. McPherson, *J. Am. Chem. Soc.*, **93**, 1445 (1971).
- <sup>10</sup> K. B. Becker and C. A. Grob, *Synthesis*, 789 (1973).

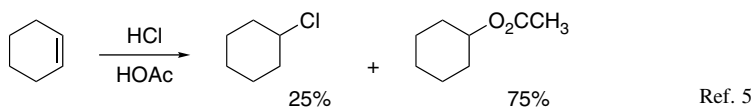
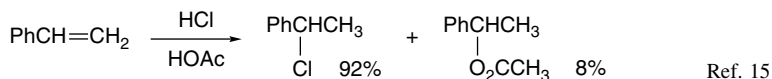


A change in the stereoselectivity is observed when the double bond is conjugated with a group that can stabilize a carbocation intermediate. Most of the specific cases involve an aryl substituent. Examples of alkenes that give primarily *syn* addition are *Z*- and *E*-1-phenylpropene,<sup>11</sup> *cis*- and *trans*- $\beta$ -*t*-butylstyrene,<sup>12</sup> 1-phenyl-4-*t*-butylcyclohexene,<sup>13</sup> and indene.<sup>14</sup> The mechanism proposed for these reactions features an ion pair as the key intermediate. Owing to the greater stability of the benzylic carbocations formed in these reactions, concerted attack by halide ion is not required for protonation. If the ion pair formed by alkene protonation collapses to product faster than rotation takes place, *syn* addition occurs because the proton and halide ion are initially on the same face of the molecule.



Kinetic studies of the addition of hydrogen chloride to styrene support the conclusion that an ion pair mechanism operates. The reaction is first order in hydrogen chloride, indicating that only one molecule of hydrogen chloride participates in the rate-determining step.<sup>15</sup>

There is a competing reaction with solvent when hydrogen halide additions to alkenes are carried out in nucleophilic solvents.



This result is consistent with the general mechanism for hydrogen halide additions. These products are formed because the solvent competes with halide ion as the nucleophilic component in the addition. Solvent addition can occur via a concerted mechanism or by capture of a carbocation intermediate. Addition of a halide salt increases the likelihood of capture of a carbocation intermediate by halide ion. The effect of added halide salt can be detected kinetically. For example, the presence of tetramethylammonium chloride increases the rate of addition of hydrogen chloride to cyclohexene.<sup>9</sup> Similarly, lithium bromide increases the rate of addition of hydrogen bromide to cyclopentene.<sup>8</sup>

<sup>11</sup> M. J. S. Dewar and R. C. Fahey, *J. Am. Chem. Soc.*, **85**, 3645 (1963).

<sup>12</sup> R. J. Abraham and J. R. Monasterios, *J. Chem. Soc., Perkin Trans. 2*, 574 (1975).

<sup>13</sup> K. D. Berlin, R. O. Lyerla, D. E. Gibbs, and J. P. Devlin, *J. Chem. Soc., Chem. Commun.*, 1246 (1970).

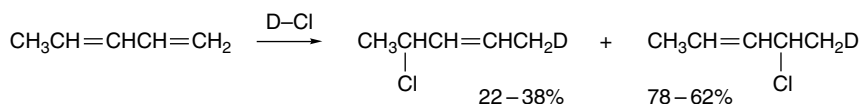
<sup>14</sup> M. J. S. Dewar and R. C. Fahey, *J. Am. Chem. Soc.*, **85**, 2248 (1963).

<sup>15</sup> R. C. Fahey and C. A. McPherson, *J. Am. Chem. Soc.*, **91**, 3865 (1969).

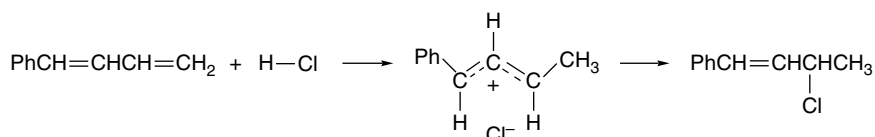


ionization, as discussed in Chapter 4. The prevalence of nucleophilic capture by  $\text{Br}^-$  over  $\text{CF}_3\text{CO}_2^-$  reflects relative nucleophilicity and is also dependent on  $\text{Br}^-$  concentration. Competing elimination is also consistent with the pattern of the solvolytic reactions.

The addition of hydrogen halides to dienes can result in either 1,2- or 1,4-addition. The extra stability of the allylic cation formed by proton transfer to a diene makes the ion pair mechanism more favorable. Nevertheless, a polar reaction medium is required.<sup>17</sup> 1,3-Pentadiene, for example, gives a mixture of products favoring the 1,2-addition product by a ratio of from 1.5:1 to 3.4:1, depending on the temperature and solvent.<sup>18</sup>

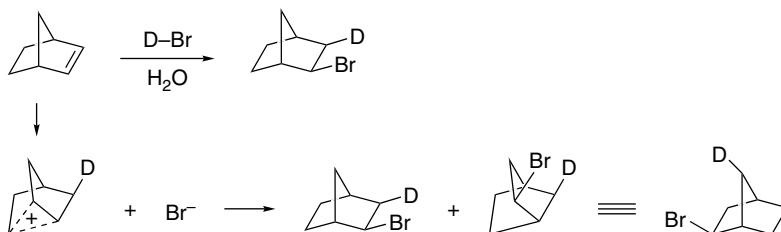


With 1-phenyl-1,3-butadiene, the addition of HCl is exclusively at the 3,4-double bond. This reflects the greater stability of this product, which retains styrene-type conjugation. Initial protonation at C(4) is favored by the fact that the resulting carbocation benefits from both allylic and benzylic stabilization.



The kinetics of this reaction are second order, as would be expected for the formation of a relatively stable carbocation by an  $\text{A}_{\text{D}}\text{E}_2$  mechanism.<sup>19</sup>

The additions of HCl or HBr to norbornene are interesting cases because such factors as the stability and facile rearrangement of the norbornyl cation come into consideration. (See Section 4.4.5 to review the properties of the 2-norbornyl cation.) Addition of deuterium bromide to norbornene gives *exo*-norbornyl bromide. Degradation to locate the deuterium atom shows that about half of the product is formed via the bridged norbornyl cation, which leads to deuterium at both the 3- and 7-positions.<sup>20</sup> The *exo* orientation of the bromine atom and the redistribution of the deuterium indicate the involvement of the bridged ion.



Similar studies have been carried out on the addition of HCl to norbornene.<sup>21</sup> Again, the chloride is almost exclusively the *exo* isomer. The distribution of deuterium

<sup>17</sup> L. M. Mascavage, H. Chi, S. La, and D. R. Dalton, *J. Org. Chem.*, **56**, 595 (1991).

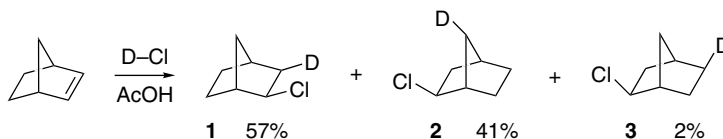
<sup>18</sup> J. E. Nordlander, P. O. Owuor, and J. E. Haky, *J. Am. Chem. Soc.*, **101**, 1288 (1979).

<sup>19</sup> K. Izawa, T. Okuyama, T. Sakagami, and T. Fueno, *J. Am. Chem. Soc.*, **95**, 6752 (1973).

<sup>20</sup> H. Kwart and J. L. Nyce, *J. Am. Chem. Soc.*, **86**, 2601 (1964).

<sup>21</sup> J. K. Stille, F. M. Sonnenberg, and T. H. Kinstle, *J. Am. Chem. Soc.*, **88**, 4922 (1966).

in the product was determined by NMR. The fact that **1** and **2** are formed in unequal amounts excludes the possibility that the symmetrical bridged ion is the only intermediate.<sup>22</sup>

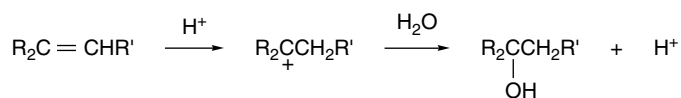


The excess of **1** over **2** indicates that some *syn* addition occurs by ion pair collapse before the bridged ion achieves symmetry with respect to the chloride ion. If the amount of **2** is taken as an indication of the extent of bridged ion involvement, one can conclude that 82% of the reaction proceeds through this intermediate, which must give equal amounts of **1** and **2**. Product **3** results from the C(6)  $\rightarrow$  C(2) hydride shift that is known to occur in the 2-norbornyl cation with an activation energy of about 6 kcal/mol (see p. 450).

From these examples we see that the mechanistic and stereochemical details of hydrogen halide addition depend on the reactant structure. Alkenes that form relatively unstable carbocations are likely to react via a termolecular complex and exhibit *anti* stereospecificity. Alkenes that can form more stable cations can react via rate-determining protonation and the structure and stereochemistry of the product are determined by the specific properties of the cation.

## 5.2. Acid-Catalyzed Hydration and Related Addition Reactions

The formation of alcohols by acid-catalyzed addition of water to alkenes is a fundamental reaction in organic chemistry. At the most rudimentary mechanistic level, it can be viewed as involving a carbocation intermediate. The alkene is protonated and the carbocation then reacts with water.

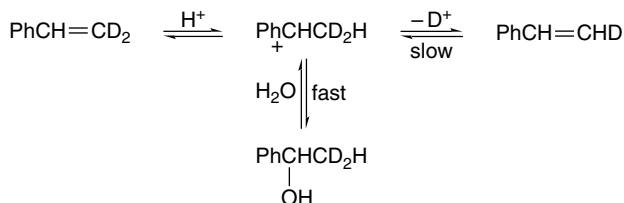


This mechanism explains the formation of the more highly substituted alcohol from unsymmetrical alkenes (Markovnikov's rule). A number of other points must be considered in order to provide a more complete picture of the mechanism. Is the protonation step reversible? Is there a discrete carbocation intermediate, or does the nucleophile become involved before proton transfer is complete? Can other reactions of the carbocation, such as rearrangement, compete with capture by water?

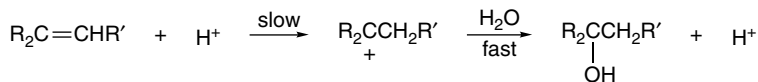
Much of the early mechanistic work on hydration reactions was done with conjugated alkenes, particularly styrenes. Owing to the stabilization provided by the phenyl group, this reaction involves a relatively stable carbocation. With styrenes, the rate of hydration is increased by ERG substituents and there is an excellent correlation

<sup>22</sup> H. C. Brown and K.-T. Liu, *J. Am. Chem. Soc.*, **97**, 600 (1975).

with  $\sigma^+$ .<sup>23</sup> A substantial solvent isotope effect  $k_{\text{H}_2\text{O}}/k_{\text{D}_2\text{O}}$  equal to 2 to 4 is observed. Both of these observations are in accord with a rate-determining protonation to give a carbocation intermediate. Capture of the resulting cation by water is usually fast relative to deprotonation. This has been demonstrated by showing that in the early stages of hydration of styrene deuterated at C(2), there is no loss of deuterium from the unreacted alkene that is recovered by quenching the reaction. The preference for nucleophilic capture over elimination is also consistent with the competitive rate measurements under solvolysis conditions, described on p. 438–439. The overall process is reversible, however, and some styrene remains in equilibrium with the alcohol, so isotopic exchange eventually occurs.



Alkenes lacking phenyl substituents appear to react by a similar mechanism. Both the observation of general acid catalysis<sup>24</sup> and solvent isotope effect<sup>25</sup> are consistent with rate-limiting protonation of alkenes such as 2-methylpropene and 2,3-dimethyl-2-butene.



Relative rate data in aqueous sulfuric acid for a series of alkenes reveal that the reaction is strongly accelerated by alkyl substituents. This is as expected because alkyl groups both increase the electron density of the double bond and stabilize the carbocation intermediate. Table 5.1 gives some representative data. The  $1 : 10^7 : 10^{12}$  relative rates for ethene, propene, and 2-methylpropene illustrate the dramatic rate enhancement by alkyl substituents. Note that styrene is intermediate between monoalkyl and dialkyl alkenes. These same reactions show solvent isotope effects consistent with the reaction proceeding through a rate-determining protonation.<sup>26</sup> Strained alkenes show enhanced reactivity toward acid-catalyzed hydration. *trans*-Cyclooctene is about 2500 times as reactive as the *cis* isomer,<sup>27</sup> which reflects the higher ground state energy of the strained alkene.

Other nucleophilic solvents can add to alkenes in the presence of strong acid catalysts. The mechanism is analogous to that for hydration, with the solvent replacing water as the nucleophile. Strong acids catalyze the addition of alcohols

<sup>23</sup> W. M. Schubert and J. R. Keefe, *J. Am. Chem. Soc.*, **94**, 559 (1972); W. M. Schubert and B. Lamm, *J. Am. Chem. Soc.*, **88**, 120 (1966); W. K. Chwang, P. Knittel, K. M. Koshy, and T. T. Tidwell, *J. Am. Chem. Soc.*, **99**, 3395 (1977).

<sup>24</sup> A. J. Kresge, Y. Chiang, P. H. Fitzgerald, R. S. McDonald, and G. H. Schmid, *J. Am. Chem. Soc.*, **93**, 4907 (1971); H. Slebocka-Tilk and R. S. Brown, *J. Org. Chem.*, **61**, 8079 (1998).

<sup>25</sup> V. Gold and M. A. Kessick, *J. Chem. Soc.*, 6718 (1965).

<sup>26</sup> V. J. Nowlan and T. T. Tidwell, *Acc. Chem. Res.*, **10**, 252 (1977).

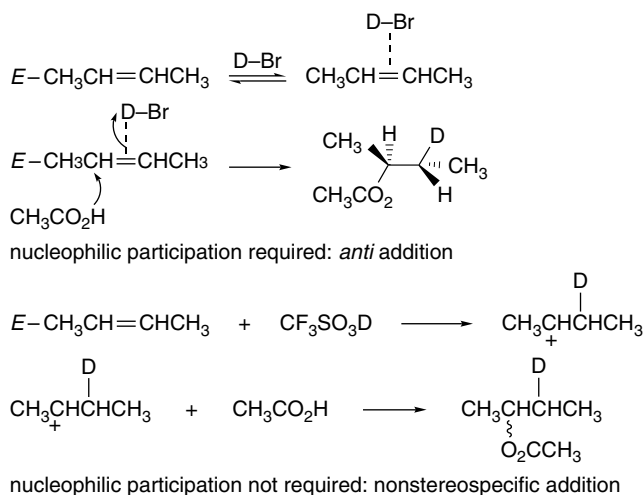
<sup>27</sup> Y. Chiang and A. J. Kresge, *J. Am. Chem. Soc.*, **107**, 6363 (1985).

**Table 5.1. Rates of Alkene Hydration in Aqueous Sulfuric Acid<sup>a</sup>**

Alkene	$k_2 (M^{-1}s^{-1})$	$k_{rel}$
$CH_2=CH_2$	$1.56 \times 10^{-15}$	1
$CH_3CH=CH_2$	$2.38 \times 10^{-8}$	$1.6 \times 10^7$
$CH_3(CH_2)_3CH=CH_2$	$4.32 \times 10^{-8}$	$3.0 \times 10^7$
$(CH_3)_2C=CHCH_3$	$2.14 \times 10^{-3}$	$1.5 \times 10^{12}$
$(CH_3)_2C=CH_2$	$3.71 \times 10^{-3}$	$2.5 \times 10^{12}$
$PhCH=CH_2$	$2.4 \times 10^{-6}$	$1.6 \times 10^9$

a. W. K. Chwang, V. J. Nowlan, and T. T. Tidwell, *J. Am. Chem. Soc.*, **99**, 7233 (1977).

to alkenes to give ethers, and the mechanistic studies that have been done indicate that the reaction closely parallels the hydration process.<sup>28</sup> The strongest acid catalysts probably react via discrete carbocation intermediates, whereas weaker acids may involve reaction of the solvent with an alkene-acid complex. In the addition of acetic acid to *Z*- or *E*-2-butene, the use of DBr as the catalyst results in stereospecific *anti* addition, whereas the stronger acid  $CF_3SO_3H$  leads to loss of stereospecificity. This difference in stereochemistry can be explained by a stereospecific  $Ad_E3$  mechanism in the case of DBr and an  $Ad_E2$  mechanism in the case of  $CF_3SO_3D$ .<sup>29</sup> The dependence of stereochemistry on acid strength reflects the degree to which nucleophilic participation is required to complete proton transfer.



Trifluoroacetic acid adds to alkenes without the necessity of a stronger acid catalyst.<sup>30</sup> The mechanistic features of this reaction are similar to addition of water catalyzed by strong acids. For example, there is a substantial isotope effect when  $CF_3CO_2D$  is used ( $k_H/k_D = 4.33$ )<sup>31</sup> and the reaction rates of substituted styrenes are

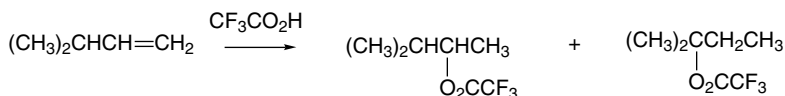
<sup>28</sup> N. C. Deno, F. A. Kish, and H. J. Peterson, *J. Am. Chem. Soc.*, **87**, 2157 (1965).

<sup>29</sup> D. J. Pasto and J. F. Gadberry, *J. Am. Chem. Soc.*, **100**, 1469 (1978).

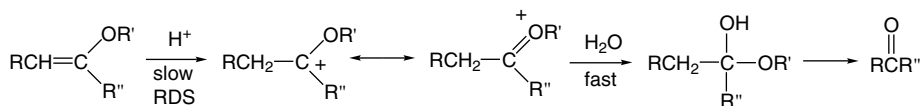
<sup>30</sup> P. E. Peterson and G. Allen, *J. Am. Chem. Soc.*, **85**, 3608 (1963); A. D. Allen and T. T. Tidwell, *J. Am. Chem. Soc.*, **104**, 3145 (1982).

<sup>31</sup> J. J. Dannenberg, B. J. Goldberg, J. K. Barton, K. Dill, D. M. Weinwurzel, and M. O. Longas, *J. Am. Chem. Soc.*, **103**, 7764 (1981).

correlated with  $\sigma^+$ .<sup>32</sup> 2-Methyl-1-butene and 2-methyl-2-butene appear to react via the 2-methylbutyl cation, and 3-methyl-1-butene gives the products expected for a carbocation mechanism, including rearrangement. These results are consistent with rate-determining protonation.<sup>33</sup>



The reactivity of carbon-carbon double bonds toward acid-catalyzed addition of water is greatly increased by ERG substituents. The reaction of vinyl ethers with water in acidic solution is an example that has been carefully studied. With these reactants, the initial addition products are unstable hemiacetals that decompose to a ketone and alcohol. Nevertheless, the protonation step is rate determining, and the kinetic results pertain to this step. The mechanistic features are similar to those for hydration of simple alkenes. Proton transfer is rate determining, as demonstrated by general acid catalysis and solvent isotope effect data.<sup>34</sup>



### 5.3. Addition of Halogens

Alkene chlorinations and brominations are very general reactions, and mechanistic study of these reactions provides additional insight into the electrophilic addition reactions of alkenes.<sup>35</sup> Most of the studies have involved brominations, but chlorinations have also been examined. Much less detail is known about fluorination and iodination. The order of reactivity is  $\text{F}_2 > \text{Cl}_2 > \text{Br}_2 > \text{I}_2$ . The differences between chlorination and bromination indicate the trends for all the halogens, but these differences are much more pronounced for fluorination and iodination. Fluorination is strongly exothermic and difficult to control, whereas for iodine the reaction is easily reversible.

The initial step in bromination is the formation of a complex between the alkene and  $\text{Br}_2$ . The existence of these relatively weak complexes has long been recognized. Their role as intermediates in the addition reaction has been established more recently.

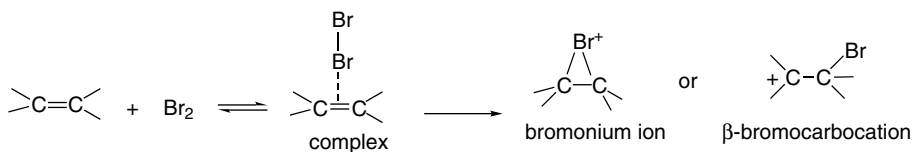
<sup>32</sup> A. D. Allen, M. Rosenbaum, N. O. L. Seto, and T. T. Tidwell, *J. Org. Chem.*, **47**, 4234 (1982).

<sup>33</sup> D. Farcasiu, G. Marino, and C. S. Hsu, *J. Org. Chem.*, **59**, 163 (1994).

<sup>34</sup> A. J. Kresge and H. J. Chen, *J. Am. Chem. Soc.*, **94**, 2818 (1972); A. J. Kresge, D. S. Sagatys, and H. L. Chen, *J. Am. Chem. Soc.*, **99**, 7228 (1977).

<sup>35</sup> Reviews: D. P. de la Mare and R. Bolton, in *Electrophilic Additions to Unsaturated Systems*, 2nd Edition, Elsevier, New York, 1982, pp. 136–197; G. H. Schmidt and D. G. Garratt, in *The Chemistry of Double Bonded Functional Groups*, Supplement A, Part 2, S. Patai, ed., Wiley-Interscience, New York, 1977, Chap. 9; M.-F. Ruasse, *Adv. Phys. Org. Chem.*, **28**, 207 (1993); M.-F. Ruasse, *Industrial Chem. Library*, **7**, 100 (1995); R. S. Brown, *Industrial Chem. Library*, **7**, 113 (1995); G. Bellucci and R. Bianchini, *Industrial Chem. Library*, **7**, 128 (1995); R. S. Brown, *Acc. Chem. Res.*, **30**, 131 (1997).

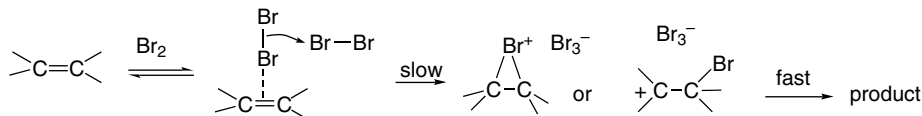
The formation of the complex can be observed spectroscopically, and they subsequently disappear at a rate corresponding to the formation of bromination product.<sup>36,37</sup> The second step in bromination involves formation of an ionic intermediate, which can be either a bridged bromonium ion or a  $\beta$ -bromocarocation. Whether a bridged intermediate or a carbocation is formed depends on the stability of the potential cation. Aliphatic systems normally react through the bridged intermediate but styrenes are borderline cases. When the phenyl ring has an ERG substituent, there is sufficient stabilization to permit carbocation formation, whereas EWGs favor the bridged intermediate.<sup>38</sup> Because this step involves formation of charged intermediates, it is strongly solvent dependent. Even a change from  $\text{CCl}_4$  to 1,2-dichloroethane accelerates the reaction (with cyclohexene) by a factor of  $10^5$ .<sup>39</sup>



The kinetics of bromination reactions are often complex, with at least three terms making contributions under given conditions.

$$\text{Rate} = k_1[\text{alkene}][\text{Br}_2] + k_2[\text{alkene}][\text{Br}_2]^2 + k_3[\text{alkene}][\text{Br}_2][\text{Br}^-]$$

In methanol, pseudo-second-order kinetics are observed when a high concentration of  $\text{Br}^-$  is present.<sup>40</sup> Under these conditions, the dominant contribution to the overall rate comes from the third term of the general expression. In nonpolar solvents, the observed rate is frequently described as a sum of the first two terms in the general expression.<sup>41</sup> The mechanism of the third-order reaction is similar to the process that is first order in  $\text{Br}_2$ , but with a second  $\text{Br}_2$  molecule replacing solvent in the rate-determining conversion of the complex to an ion pair.



There are strong similarities in the second- and third-order reaction in terms of magnitude of  $\rho$  values and product distribution.<sup>41b</sup> In fact, there is a quantitative correlation between the rate of the two reactions over a broad series of alkenes, which can be expressed as

$$\Delta G_3^\ddagger = \Delta G_2^\ddagger + \text{constant}$$

<sup>36</sup> S. Fukuzumi and J. K. Kochi, *J. Am. Chem. Soc.*, **104**, 7599 (1982).

<sup>37</sup> G. Bellucci, R. Bianchi, and R. Ambrosetti, *J. Am. Chem. Soc.*, **107**, 2464 (1985).

<sup>38</sup> M.-F. Ruasse, A. Argile, and J. E. Dubois, *J. Am. Chem. Soc.*, **100**, 7645 (1978).

<sup>39</sup> M.-F. Ruasse and S. Motallebi, *J. Phys. Org. Chem.*, **4**, 527 (1991).

<sup>40</sup> J.-E. Dubois and G. Mouvier, *Tetrahedron Lett.*, 1325 (1963); *Bull. Soc. Chim. Fr.*, 1426 (1968).

<sup>41</sup> (a) G. Bellucci, R. Bianchi, R. A. Ambrosetti, and G. Ingrosso, *J. Org. Chem.*, **50**, 3313 (1985); G. Bellucci, G. Berti, R. Bianchini, G. Ingrosso, and R. Ambrosetti, *J. Am. Chem. Soc.*, **102**, 7480 (1980); (b) K. Yates, R. S. McDonald, and S. Shapiro, *J. Org. Chem.*, **38**, 2460 (1973); K. Yates and R. S. McDonald, *J. Org. Chem.*, **38**, 2465 (1973); (c) S. Fukuzumi and J. K. Kochi, *Int. J. Chem. Kinetics*, **15**, 249 (1983).

Table 5.2. Relative Reactivity of Alkenes toward Halogenation

Alkene	Relative reactivity		
	Chlorination <sup>a</sup>	Bromination <sup>b</sup>	Bromination <sup>c</sup>
Ethene		0.01	0.0045
1-Butene	1.00	1.00	1.00
3,3-Dimethyl-1-butene	1.15	0.27	1.81
Z-2-Butene	63	27	173
E-2-Butene	50	17.5	159
2-Methylpropene	58	57	109
2-Methyl-2-butene	$1.1 \times 10^4$	$1.38 \times 10^4$	
2,3-Dimethyl-2-butene	$4.3 \times 10^5$	$19.0 \times 10^4$	

a. M. L. Poutsma, *J. Am. Chem. Soc.*, **87**, 4285 (1965), in excess alkene.

b. J. E. Dubois and G. Mouvier, *Bull. Chim. Soc. Fr.*, 1426 (1968), in methanol.

c. A. Modro, G. H. Schmid, and K. Yates, *J. Org. Chem.*, **42**, 3673 (1977), in  $\text{ClCH}_2\text{CH}_2\text{Cl}$ .

SECTION 5.3

Addition of Halogens

where  $\Delta G_3^\ddagger$  and  $\Delta G_2^\ddagger$  are the free energies of activation for the third- and second-order processes, respectively.<sup>41c</sup> These correlations suggest that the two mechanisms must be very similar.

Observed bromination rates are very sensitive to common impurities such as  $\text{HBr}$ <sup>42</sup> and water, which can assist in formation of the bromonium ion.<sup>43</sup> It is likely that under normal preparative conditions, where these impurities are likely to be present, these catalytic mechanisms may dominate.

Chlorination generally exhibits second-order kinetics, first-order in both alkene and chlorine.<sup>44</sup> The relative reactivities of some alkenes toward chlorination and bromination are given in Table 5.2. The reaction rate increases with alkyl substitution, as would be expected for an electrophilic process. The magnitude of the rate increase is quite large, but not as large as for protonation. The relative reactivities are solvent dependent.<sup>45</sup> Quantitative interpretation of the solvent effect using the Winstein-Grunwald *Y* values indicates that the TS has a high degree of ionic character. The Hammett correlation for bromination of styrenes is best with  $\sigma^+$  substituent constants, and gives  $\rho = -4.8$ .<sup>46</sup> All these features are in accord with an electrophilic mechanism.

Stereochemical studies provide additional information pertaining to the mechanism of halogenation. The results of numerous stereochemical studies can be generalized as follows: For brominations, *anti* addition is preferred for alkenes lacking substituent groups that can strongly stabilize a carbocation intermediate.<sup>47</sup> When the alkene is conjugated with an aryl group, the extent of *syn* addition increases and can become the dominant pathway. Chlorination is not as likely to be as stereospecific as bromination, but tends to follow the same pattern. Some specific results are given in Table 5.3.

<sup>42</sup>. C. J. A. Byrnell, R. G. Coombes, L. S. Hart, and M. C. Whiting, *J. Chem. Soc., Perkin Trans. 2*, 1079 (1983); L. S. Hart and M. C. Whiting, *J. Chem. Soc., Perkin Trans. 2*, 1087 (1983).

<sup>43</sup>. V. V. Smirnov, A. N. Miroshnichenko, and M. I. Shilina, *Kinet. Catal.*, **31**, 482, 486 (1990).

<sup>44</sup>. G. H. Schmid, A. Modro, and K. Yates, *J. Org. Chem.*, **42**, 871 (1977).

<sup>45</sup>. F. Garnier and J.-E. Dubois, *Bull. Soc. Chim. Fr.*, 3797 (1968); F. Garnier, R. H. Donnay, and J.-E. Dubois, *J. Chem. Soc., Chem. Commun.*, 829 (1971); M.-F. Ruisse and J.-E. Dubois, *J. Am. Chem. Soc.*, **97**, 1977 (1975); A. Modro, G. H. Schmid, and K. Yates, *J. Org. Chem.*, **42**, 3673 (1977).

<sup>46</sup>. K. Yates, R. S. McDonald, and S. A. Shapiro, *J. Org. Chem.*, **38**, 2460 (1973).

<sup>47</sup>. J. R. Chretien, J.-D. Coudert, and M.-F. Ruisse, *J. Org. Chem.*, **58**, 1917 (1993).

Table 5.3. Stereochemistry of Alkene Halogenation

Alkene	Solvent	Ratio <i>anti:syn</i>
A. Bromination		
Z-2-Butene <sup>a</sup>	CH <sub>3</sub> CO <sub>2</sub> H	> 100 : 1
E-2-Butene <sup>a</sup>	CH <sub>3</sub> CO <sub>2</sub> H	> 100 : 1
Cyclohexene <sup>b</sup>	CCl <sub>4</sub>	Very large
Z-1-Phenylpropene <sup>c</sup>	CCl <sub>4</sub>	83:17
E-1-Phenylpropene <sup>c</sup>	CCl <sub>4</sub>	88:12
Z-2-Phenylbutene <sup>a</sup>	CH <sub>3</sub> CO <sub>2</sub> H	68:32
E-2-Phenylbutene <sup>a</sup>	CH <sub>3</sub> CO <sub>2</sub> H	63:37
<i>cis</i> -Stilbene <sup>d</sup>	CCl <sub>4</sub>	> 10 : 1
	CH <sub>3</sub> NO <sub>2</sub> <sup>d</sup>	1:9
B. Chlorination		
Z-2-Butene <sup>e</sup>	None	> 100 : 1
	CH <sub>3</sub> CO <sub>2</sub> H <sup>f</sup>	> 100 : 1
E-2-Butene <sup>e</sup>	None	> 100 : 1
	CH <sub>3</sub> CO <sub>2</sub> H <sup>f</sup>	> 100 : 1
Cyclohexene <sup>g</sup>	None	> 100 : 1
E-1-Phenylpropene <sup>f</sup>	CCl <sub>4</sub>	45:55
	CH <sub>3</sub> CO <sub>2</sub> H <sup>f</sup>	41:59
Z-1-Phenylpropene <sup>f</sup>	CCl <sub>4</sub>	32:68
	CH <sub>3</sub> CO <sub>2</sub> H <sup>f</sup>	22:78
<i>Cis</i> -Stilbene <sup>h</sup>	ClCH <sub>2</sub> CH <sub>2</sub> Cl	8:92
<i>Trans</i> -Stilbene <sup>h</sup>	ClCH <sub>2</sub> CH <sub>2</sub> Cl	35:65

a. J. H. Rolston and K. Yates, *J. Am. Chem. Soc.*, **91**, 1469, 1477 (1969).

b. S. Winstein, *J. Am. Chem. Soc.*, **64**, 2792 (1942).

c. R. C. Fahey and H.-J. Schneider, *J. Am. Chem. Soc.*, **90**, 4429 (1968).

d. R. E. Buckles, J. M. Bader, and R. L. Thurmaier, *J. Org. Chem.*, **27**, 4523 (1962).

e. M. L. Poutsma, *J. Am. Chem. Soc.*, **87**, 2172 (1965).

f. R. C. Fahey and C. Schubert, *J. Am. Chem. Soc.*, **87**, 5172 (1965).

g. M. L. Poutsma, *J. Am. Chem. Soc.*, **87**, 2161 (1965).

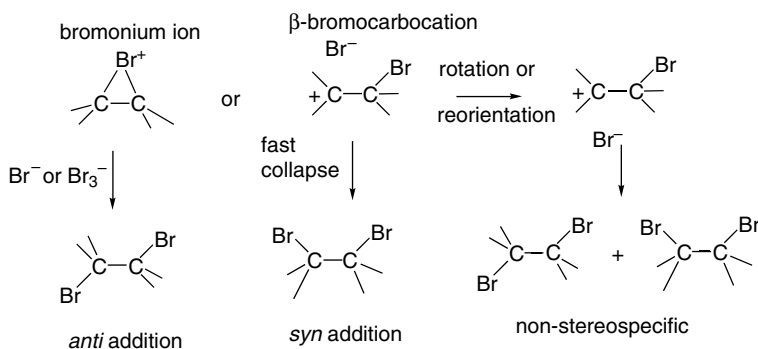
h. R. E. Buckles and D. F. Knaack, *J. Org. Chem.*, **25**, 20 (1960).

Interpretation of reaction stereochemistry has focused attention on the role played by bridged halonium ions. When the reaction with Br<sub>2</sub> involves a bromonium ion, the *anti* stereochemistry can be readily explained. Nucleophilic ring opening occurs by back-side attack at carbon, with rupture of one of the C–Br bonds, giving overall *anti* addition. On the other hand, a freely rotating open β-bromo carbocation can give both the *syn* and *anti* addition products. If the principal intermediate is an ion pair that collapses faster than rotation occurs about the C–C bond, *syn* addition can predominate. Other investigations, including kinetic isotope effect studies, are consistent with the bromonium ion mechanism for unconjugated alkenes, such as ethene,<sup>48</sup> 1-pentene,<sup>49</sup> and cyclohexene.<sup>50</sup>

<sup>48</sup>. T. Koerner, R. S. Brown, J. L. Gainsforth, and M. Klobukowski, *J. Am. Chem. Soc.*, **120**, 5628 (1998).

<sup>49</sup>. S. R. Merrigan and D. A. Singleton, *Org. Lett.*, **1**, 327 (1999).

<sup>50</sup>. H. Slebocka-Tilk, A. Neverov, S. Motallebi, R. S. Brown, O. Donini, J. L. Gainsforth, and M. Klobukowski, *J. Am. Chem. Soc.*, **120**, 2578 (1998).

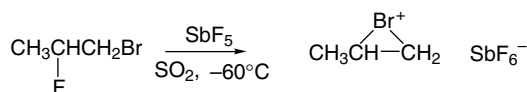


Substituent effects on stilbenes provide examples of the role of bridged ions versus nonbridged carbocation intermediates. In aprotic solvents, stilbene gives clean *anti* addition, but 4,4'-dimethoxystilbene gives a mixture of the *syn* and *anti* addition products indicating a carbocation intermediate.<sup>51</sup>

Nucleophilic solvents compete with bromide, but *anti* stereoselectivity is still observed, except when ERG substituents are present. It is proposed that *anti* stereoselectivity can result not only from a bridged ion intermediate, but also from very fast capture of a carbocation intermediate.<sup>52</sup> Interpretation of the ratio of capture by competing nucleophiles has led to the estimate that the bromonium ion derived from cyclohexene has a lifetime on the order of 10<sup>-10</sup> s in methanol, which is about 100 times longer than for secondary carbocations.<sup>53</sup>

The stereochemistry of chlorination also can be explained in terms of bridged versus open cations as intermediates. Chlorine is a somewhat poorer bridging group than bromine because it is less polarizable and more resistant to becoming positively charged. Comparison of the data for *E*- and *Z*-1-phenylpropene in bromination and chlorination confirms this trend (see Table 5.3). Although *anti* addition is dominant for bromination, *syn* addition is slightly preferred for chlorination. Styrenes generally appear to react with chlorine via ion pair intermediates.<sup>54</sup>

There is direct evidence for the existence of bromonium ions. The bromonium ion related to propene can be observed by NMR when 1-bromo-2-fluoropropane is subjected to superacid conditions.



Ref. 55

A bromonium ion also is formed by electrophilic attack on 2,3-dimethyl-2-butene by a species that can generate a positive bromine.

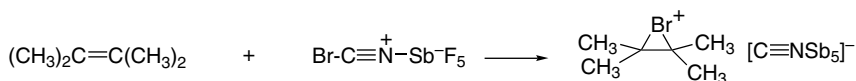
<sup>51</sup> G. Bellucci, C. Chiappe, and G. Lo Moro, *J. Org. Chem.*, **62**, 3176 (1997).

<sup>52</sup> M.-F. Ruasse, G. Lo Moro, B. Galland, R. Bianchini, C. Chiappe, and G. Bellucci, *J. Am. Chem. Soc.*, **119**, 12492 (1997).

<sup>53</sup> R. W. Nagorski and R. S. Brown, *J. Am. Chem. Soc.*, **114**, 7773 (1992).

<sup>54</sup> K. Yates and H. W. Leung, *J. Org. Chem.*, **45**, 1401 (1980).

<sup>55</sup> G. A. Olah, J. M. Bollinger, and J. Brinich, *J. Am. Chem. Soc.*, **90**, 2587 (1968).



Ref. 56

The highly hindered alkene adamantylideneadamantane forms a bromonium ion that crystallizes as a tribromide salt. This particular bromonium ion does not react further because of extreme steric hindrance to back-side approach by bromide ion.<sup>57</sup> Other very hindered alkenes allow observation of both the initial complex with  $\text{Br}_2$  and the bromonium ion.<sup>58</sup> An X-ray crystal structure has confirmed the cyclic nature of the bromonium ion species (Figure 5.2).<sup>59</sup>

Crystal structures have also been obtained for the corresponding chloronium and iodonium ions and for the bromonium ion with a triflate counterion.<sup>60</sup> Each of these structures is somewhat unsymmetrical, as shown by the dimensions below. The significance of this asymmetry is not entirely clear. It has been suggested that the bromonium ion geometry is affected by the counterion and it can be noted that the triflate salt is more symmetrical than the tribromide. On the other hand, the dimensions of the unsymmetrical chloronium ion, where the difference is considerably larger, has been taken as evidence that the bridging is inherently unsymmetrical.<sup>61</sup> Note that the C—C bond lengthens considerably from the double-bond distance of 1.35 Å.

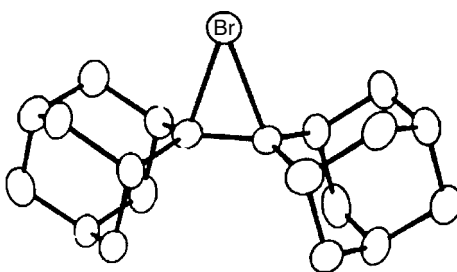
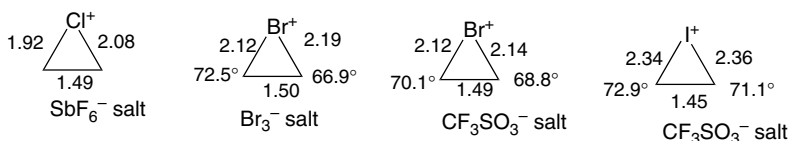


Fig. 5.2. X-ray crystal structure of the bromonium ion from adamantylideneadamantane. Reproduced from *J. Am. Chem. Soc.*, **107**, 4504 (1985), by permission of the American Chemical Society.

<sup>56</sup> G. A. Olah, P. Schilling, P. W. Westerman, and H. C. Lin, *J. Am. Chem. Soc.*, **96**, 3581 (1974).

<sup>57</sup> R. S. Brown, *Acc. Chem. Res.*, **30**, 131 (1997).

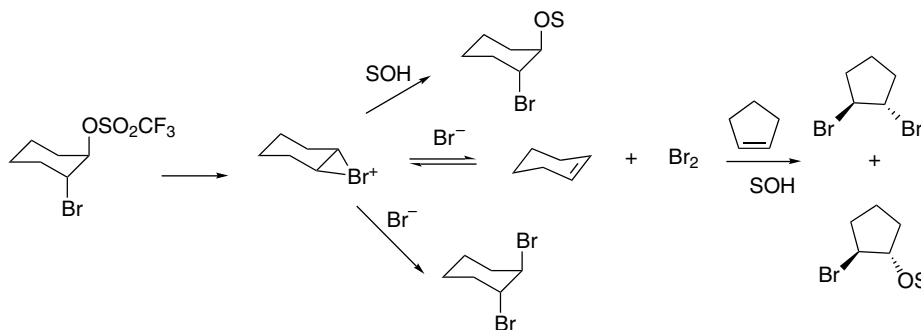
<sup>58</sup> G. Bellucci, R. Bianchini, C. Chiappe, F. Marioni, R. Ambrosetti, R. S. Brown, and H. Slebocka-Tilk, *J. Am. Chem. Soc.*, **111**, 2640 (1989); G. Bellucci, C. Chiappe, R. Bianchini, D. Lenoir, and R. Herges, *J. Am. Chem. Soc.*, **117**, 12001 (1995).

<sup>59</sup> H. Slebocka-Tilk, R. G. Ball, and R. S. Brown, *J. Am. Chem. Soc.*, **107**, 4504 (1985).

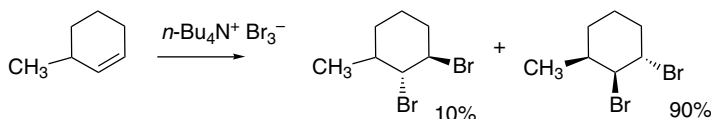
<sup>60</sup> R. S. Brown, R. W. Nagorski, A. J. Bennet, R. E. D. McClung, G. H. M. Aarts, M. Klobukowski, R. McDonald, and B. D. Santarisiero, *J. Am. Chem. Soc.*, **116**, 2448 (1994).

<sup>61</sup> T. Mori, R. Rathore, S. V. Lindeman, and J. K. Kochi, *Chem. Commun.*, 1238 (1998); T. Mori and R. Rathore, *Chem. Commun.*, 927 (1998).

Another aspect of the mechanism is the reversibility of formation of the bromonium ion. Reversibility has been demonstrated for highly hindered alkenes,<sup>62</sup> and attributed to a relatively slow rate of nucleophilic capture. However, even the bromonium ion from cyclohexene appears to be able to release Br<sub>2</sub> on reaction with Br<sup>-</sup>. The bromonium ion can be generated by neighboring-group participation by solvolysis of *trans*-2-bromocyclohexyl triflate. If cyclopentene, which is more reactive than cyclohexene, is included in the reaction mixture, bromination products from cyclopentene are formed. This indicates that free Br<sub>2</sub> is generated by reversal of bromonium ion formation.<sup>63</sup> Other examples of reversible bromonium ion formation have been found.<sup>64</sup>



Bromination also can be carried out with reagents that supply bromine in the form of the Br<sub>3</sub><sup>-</sup> anion. One such reagent is pyridinium bromide tribromide. Another is tetrabutylammonium tribromide.<sup>65</sup> These reagents are believed to react via the Br<sub>2</sub>-alkene complex and have a strong preference for *anti* addition.



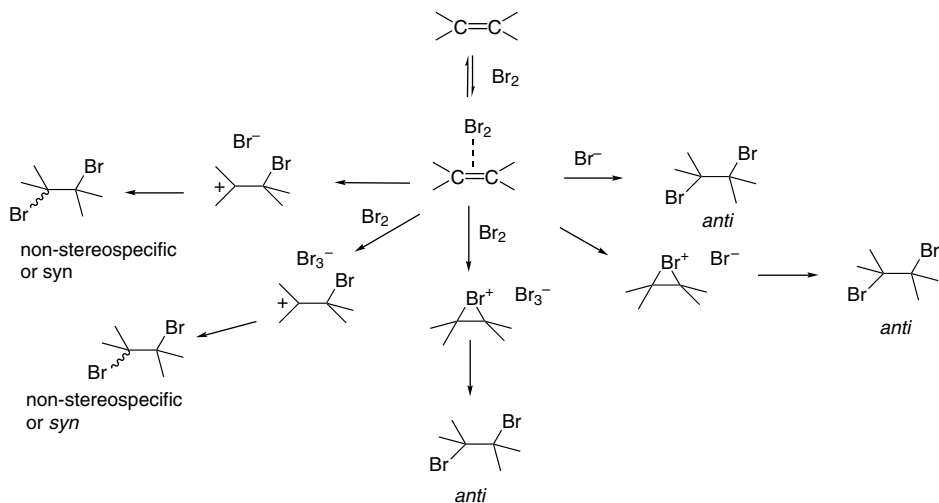
In summary, it appears that bromination usually involves a complex that collapses to an ion pair intermediate. The ionization generates charge separation and is assisted by solvent, acids, or a second molecule of bromine. The cation can be a β-carbocation, as in the case of styrenes, or a bromonium ion. Reactions that proceed through bromonium ions are stereospecific *anti* additions. Reactions that proceed through open carbocations can be *syn* selective or nonstereospecific.

<sup>62</sup> R. S. Brown, H. Slebocka-Tilk, A. J. Bennet, G. Belluci, R. Bianchini, and R. Ambrosetti, *J. Am. Chem. Soc.*, **112**, 6310 (1990); G. Bellucci, R. Bianchini, C. Chiappe, F. Marioni, R. Ambrosetti, R. S. Brown, and H. Slebocka-Tilk, *J. Am. Chem. Soc.*, **111**, 2640 (1989).

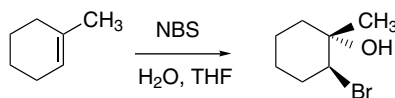
<sup>63</sup> C. Y. Zheng, H. Slebocka-Tilk, R. W. Nagorski, L. Alvarado, and R. S. Brown, *J. Org. Chem.*, **58**, 2122 (1993).

<sup>64</sup> R. Rodebaugh and B. Fraser-Reid, *Tetrahedron*, **52**, 7663 (1996).

<sup>65</sup> J. Berthelot and M. Founier, *J. Chem. Educ.*, **63**, 1011 (1986); J. Berthelot, Y. Benammar, and C. Lange, *Tetrahedron Lett.*, **32**, 4135 (1991).

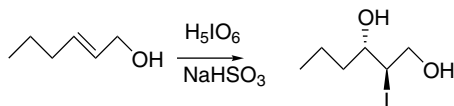


The cationic intermediates also can be captured by solvent. Halogenation with solvent capture is a synthetically important reaction, especially for the preparation of chlorohydrins and bromohydrins.<sup>66</sup> Chlorohydrins can be prepared using various sources of electrophilic chlorine. Chloroamine T is a convenient reagent for chlorohydrin formation.<sup>67</sup> Bromohydrins are prepared using NBS and an aqueous solvent mixture with acetone or THF. DMSO has also been recommended as a solvent.<sup>68</sup> These reactions are regioselective, with the nucleophile water introduced at the more-substituted position.



Ref. 69

Iodohydrins can be prepared using iodine or phenyliodonium di-trifluoroacetate.<sup>70</sup> Iodohydrins can be prepared in generally good yield and high *anti* stereoselectivity using  $\text{H}_5\text{IO}_6$  and  $\text{NaHSO}_3$ .<sup>71</sup> These reaction conditions generate hypoiodous acid. In the example shown below, the hydroxy group exerts a specific directing effect, favoring introduction of the hydroxyl at the more remote carbon.



<sup>66</sup> J. Rodriguez and J. P. Dulcere, *Synthesis*, 1177 (1993).

<sup>67</sup> B. Damin, J. Garapon, and B. Sillion, *Synthesis*, 362 (1981).

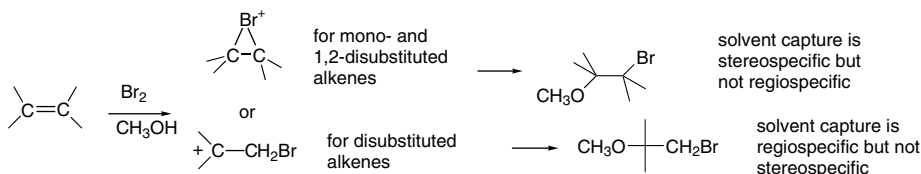
<sup>68</sup> J. N. Kim, M. R. Kim, and E. K. Ryu, *Synth. Commun.*, **22**, 2521 (1992); V. L. Heasley, R. A. Skidgel, G. E. Heasley, and D. Strickland, *J. Org. Chem.*, **39**, 3953 (1974); D. R. Dalton, V. P. Dutta, and D. C. Jones, *J. Am. Chem. Soc.*, **90**, 5498 (1988).

<sup>69</sup> D. J. Porter, A. T. Stewart, and C. T. Wigal, *J. Chem. Educ.*, **72**, 1039 (1995).

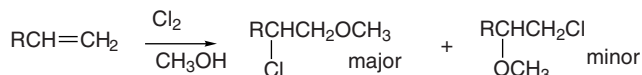
<sup>70</sup> A. R. De Corso, B. Panunzi, and M. Tingoli, *Tetrahedron Lett.*, **42**, 7245 (2001).

<sup>71</sup> H. Masuda, K. Takase, M. Nishio, A. Hasegawa, Y. Nishiyama, and Y. Ishii, *J. Org. Chem.*, **59**, 5550 (1994).

A study of several substituted alkenes in methanol developed some generalizations pertaining to the capture of bromonium ions by methanol.<sup>72</sup> For both *E*- and *Z*-disubstituted alkenes, the addition of both methanol and Br<sup>-</sup> was completely *anti* stereospecific. The reactions were also completely regioselective, in accordance with Markovnikov's rule, for disubstituted alkenes, *but not for monosubstituted alkenes*. The lack of high regioselectivity of the addition to monosubstituted alkenes can be interpreted as competitive addition of solvent at both the mono- and unsubstituted carbons of the bromonium ion. This competition reflects conflicting steric and electronic effects. Steric factors promote addition of the nucleophile at the unsubstituted position, whereas electronic factors have the opposite effect.

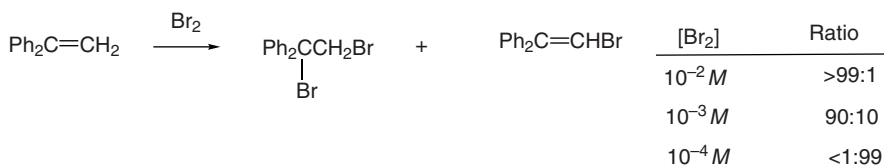


Similar results were obtained for chlorination of several of alkenes in methanol.<sup>73</sup> Whereas styrene gave only the Markovnikov product, propene, hexene, and similar alkenes gave more of the *anti* Markovnikov product. This result is indicative of strong bridging in the chloronium ion.



We say more about the regioselectivity of opening of halonium ions in Section 5.8, where we compare halonium ions with other intermediates in electrophilic addition reactions.

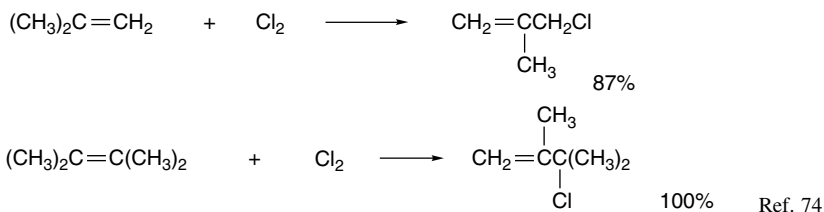
Some alkenes react with halogens to give substitution rather than addition. For example, with 1,1-diphenylethene, substitution is the main reaction at low bromine concentration. Substitution occurs when loss of a proton is faster than capture by bromide.



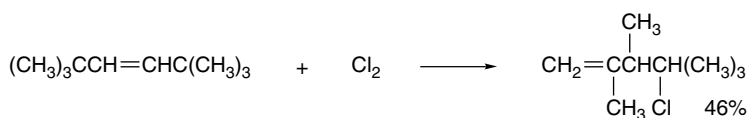
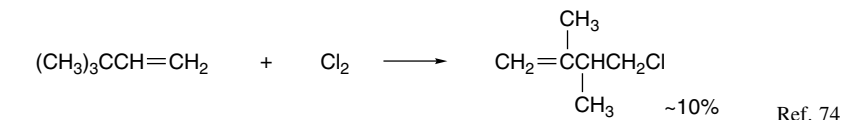
Similarly, in chlorination, loss of a proton can be a competitive reaction of the cationic intermediate. 2-Methylpropene and 2,3-dimethyl-2-butene give products of this type.

<sup>72</sup> J. R. Chretien, J.-D. Coudert, and M.-F. Ruasse, *J. Org. Chem.*, **58**, 1917 (1993).

<sup>73</sup> K. Shinoda and K. Yasuda, *Bull. Chem. Soc. Jpn.*, **61**, 4393 (1988).



Alkyl migrations can also occur.



Ref. 75

These reactions are characteristic of carbocation intermediates. Both proton loss and rearrangement are more likely in chlorination than in bromination because of the weaker bridging by chlorine.

There have been several computational investigations of bromonium and other halonium ions. These are gas phase studies and so do not account for the effect of solvent or counterions. In the gas phase, formation of the charged halonium ions from halogen and alkene is energetically prohibitive, and halonium ions are not usually found to be stable by these calculations. In an early study using PM3 and HF/3-21G calculations, bromonium ions were found to be unsymmetrical, with weaker bridging to the more stabilized carbocation.<sup>76</sup> Reynolds compared open and bridged  $[\text{CH}_2\text{CH}_2\text{X}]^+$  and  $[\text{CH}_3\text{CHCHXCH}_3]^+$  ions.<sup>77</sup> At the MP2/6-31G\*\* level, the bridged haloethyl ion was favored slightly for X= F and strongly for X= Cl and Br. For the 3-halo-2-butyl ions, open structures were favored for F and Cl, but the bridged structure remained slightly favored for Br. The relative stabilities, as measured by hydride affinity are given below.

X	$\triangle^+\text{X}$	$+\text{CH}_2\text{CH}_2\text{X}$	$\text{CH}_3-\text{CH}(\text{CH}_3)-\text{CH}^+\text{CH}_3$	$\text{CH}_3-\text{CH}(\text{CH}_3)-\text{CH}(\text{CH}_3)-\text{X}$
F	274.3	278.6	249.9	227.6
Cl	253.4	277.8	233.8	230.6
Br	239.9	270.8	221.6	225.0

Hydride affinity in kcal/mol

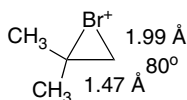
<sup>74</sup> M. L. Poutsma, *J. Am. Chem. Soc.*, **87**, 4285 (1965).

<sup>75</sup> R. C. Fahey, *J. Am. Chem. Soc.*, **88**, 4681 (1966).

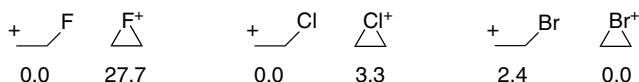
<sup>76</sup> S. Yamabe and T. Minato, *Bull. Chem. Soc. Jpn.*, **66**, 3339 (1993).

<sup>77</sup> C. H. Reynolds, *J. Am. Chem. Soc.*, **114**, 8676 (1992).

The computed structure of bromonium ions from alkenes such as 2-methylpropene are highly dependent on the computational method used and inclusion of correlation is essential.<sup>78</sup> CISD/DZV calculations gave the following structural characteristics.

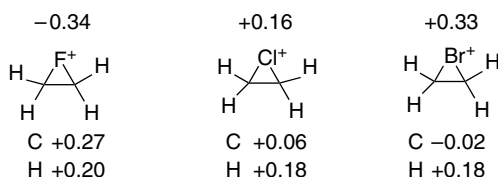


Another study gives some basis for comparison of the halogens.<sup>79</sup> QCISD(T)/6-311(*d, p*) calculations found the open carbocation to be the most stable for  $[\text{C}_2\text{H}_4\text{F}]^+$  and  $[\text{C}_2\text{H}_4\text{Cl}]^+$  but the bridged ion was more stable for  $[\text{C}_2\text{H}_4\text{Br}]^+$ . The differences were small for Cl and Br.

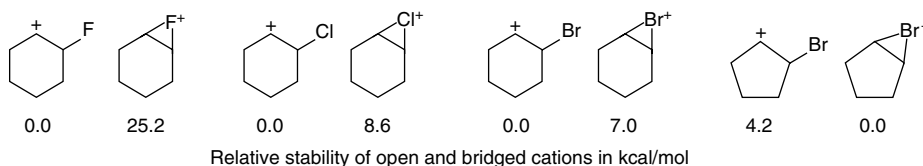


Relative energy in kcal/mol of open and bridged  $[\text{C}_2\text{H}_4\text{X}]^+$  ions

AIM charges for the bridged ions were as follows (MP2/6-311G(*d, p*)). Note the very different net charge for the different halogens.



MP2/6-311G(*d, p*) calculations favored open carbocations for the ions derived from cyclohexene. On the other hand, the bridged bromonium ion from cyclopentene was found to be stable relative to the open cation.



Ref. 79

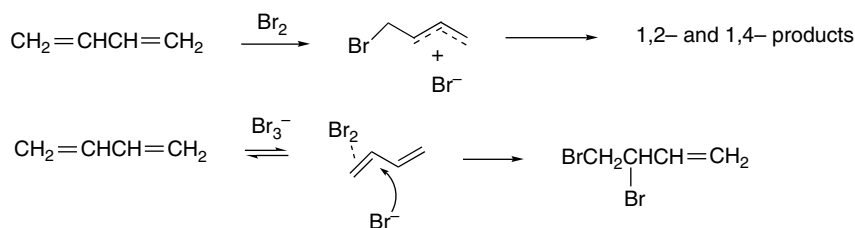
This result is in qualitative agreement with an NMR study under stable ion conditions that found that the bromonium ion from cyclopentene could be detected, but not the one from cyclohexene.<sup>80</sup> Broadly speaking, the computational results agree with the  $\text{F} < \text{Cl} < \text{Br}$  order in terms of bridging, but seem to underestimate the stability of the bridged ions, at least as compared to solution behavior.

<sup>78</sup> M. Klobukowski and R. S. Brown, *J. Org. Chem.*, **59**, 7156 (1994).

<sup>79</sup> R. Damrauer, M. D. Leavell, and C. M. Hadad, *J. Org. Chem.*, **63**, 9476 (1998).

<sup>80</sup> G. K. S. Prakash, R. Aniszefeld, T. Hashimoto, J. W. Bausch, and G. A. Olah, *J. Am. Chem. Soc.*, **111**, 8726 (1989).



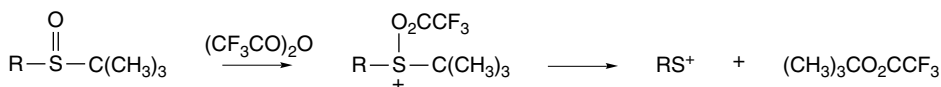


The stereochemistry of both chlorination and bromination of several cyclic and acyclic dienes has been determined. The results show that bromination is often stereospecifically *anti* for the 1,2-addition process, whereas *syn* addition is preferred for 1,4-addition. Comparable results for chlorination show much less stereospecificity.<sup>90</sup> It appears that chlorination proceeds primarily through ion pair intermediates, whereas in bromination a stereospecific *anti*-1,2-addition may compete with a process involving a carbocation intermediate. The latter can presumably give *syn* or *anti* product.

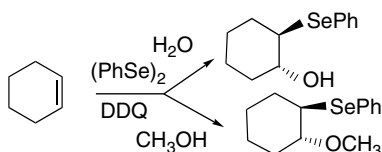
## 5.4. Sulfonylation and Selenenylation

Electrophilic derivatives of both sulfur and selenium can add to alkenes. A variety of such reagents have been developed and some are listed in Scheme 5.1. They are characterized by the formulas  $\text{RS}-\text{X}$  and  $\text{RSe}-\text{X}$ , where X is a group that is more electronegative than sulfur or selenium. The reactivity of these reagents is sensitive to the nature of both the R and the X group.

Entry 4 is a special type of sulfonylation agent. The sulfoxide fragments after O-acylation, generating a sulfonyl electrophile.



Entries 12 to 14 are examples of oxidative generation of selenenylation reagents from diphenyldiselenide. These reagents can be used to effect hydroxy- and methoxyseleenylation.



Ref. 91

Entry 15 shows *N*-(phenylselenyl)phthalimide, which is used frequently in synthetic processes.

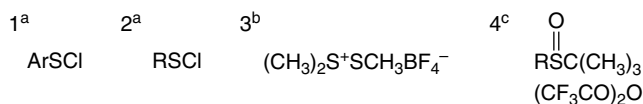
<sup>90</sup> G. E. Heasley, D. C. Hayes, G. R. McClung, D. K. Strickland, V. L. Heasley, P. D. Davis, D. M. Ingle, K. D. Rold, and T. L. Ungermann, *J. Org. Chem.*, **41**, 334 (1976).

<sup>91</sup> M. Tiecco, L. Testaferrri, A. Temperini, L. Bagnoli, F. Marini, and C. Santi, *Synlett*, 1767 (2001).

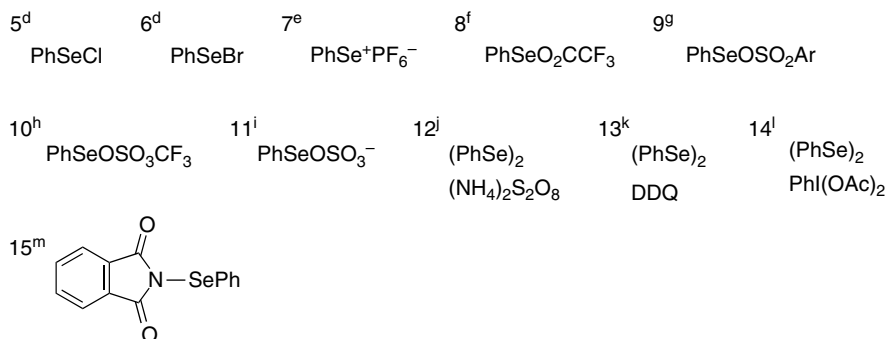
## CHAPTER 5

Polar Addition  
and Elimination  
Reactions

## A. Sulfonylation Reagents



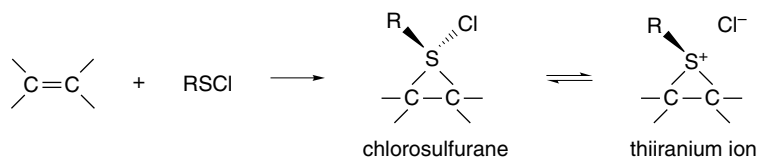
## B. Selenenylation Reagents



- a. G. Capozzi, G. Modena, and L. Pasquato, in *The Chemistry of Sulphenic Acids and Their Derivatives*, S. Patai, editor, Wiley, Chichester, 1990, Chap. 10.  
 b. B. M. Trost, T. Shibata, and S. J. Martin, *J. Am. Chem. Soc.*, **104**, 3228 (1982).  
 c. M.-H. Brichard, M. Musick, Z. Janousek, and H. G. Viehe, *Synth. Commun.*, **20**, 2379 (1990).  
 d. K. B. Sharpless and R. F. Lauer, *J. Org. Chem.*, **39**, 429 (1974). e. W. P. Jackson, S. V. Ley, and A. J. Whittle, *J. Chem. Soc., Chem. Commun.*, 1173 (1980).  
 f. H. J. Reich, *J. Org. Chem.*, **39**, 428 (1974).  
 g. T. G. Back and K. R. Muralidharan, *J. Org. Chem.*, **58**, 2781 (1991).  
 h. S. Murata and T. Suzuki, *Tetrahedron Lett.*, **28**, 4297, 4415 (1987).  
 i. M. Tiecco, L. Testaferri, M. Tingoli, L. Bagnoli, and F. Marini, *J. Chem. Soc., Perkin Trans. 1*, 1989 (1993).  
 j. M. Tiecco, L. Testaferri, M. Tingoli, D. Chianelli, and D. Bartoli, *Tetrahedron Lett.*, **30**, 1417 (1989).  
 k. M. Tiecco, L. Testaferri, A. Temperini, L. Bagnoli, F. Marini, and C. Santi, *Synlett*, 1767 (2001).  
 l. M. Tingoli, M. Tiecco, L. Testaferri, and A. Temperini, *Synth. Commun.*, **28**, 1769 (1998).  
 m. K. C. Nicolaou, N. A. Petasis, and D. A. Claremon, *Tetrahedron*, **41**, 4835 (1985).

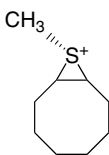
## 5.4.1. Sulfonylation

By analogy with halogenation, *thiiranium ions* can be intermediates in electrophilic sulfonylation. However, the corresponding tetravalent sulfur compounds, which are called *sulfuranes*, may also lie on the reaction path.<sup>92</sup>

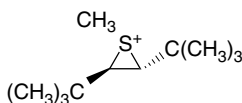


The sulfur atom is a stereogenic center in *both* the sulfurane and the thiiranium ion, and this may influence the stereochemistry of the reactions of stereoisomeric alkenes. Thiiranium ions can be prepared in various ways, and several have been characterized, such as the examples below.

<sup>92</sup> M. Fachini, V. Lucchini, G. Modena, M. Pasi, and L. Pasquato, *J. Am. Chem. Soc.*, **121**, 3944 (1999).

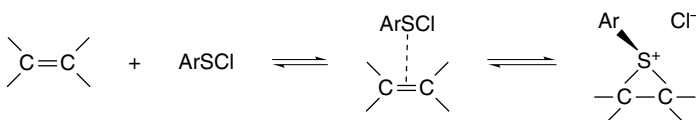


Ref. 93



Ref. 94

Perhaps the closest analog to the sulfonyl chlorides is chlorine, in the sense that both the electrophilic and nucleophilic component of the reagent are third-row elements. However, the sulfur is less electronegative and is a much better bridging element than chlorine. Although sulfonylation reagents are electrophilic in character, they are much less so than chlorine. The extent of rate acceleration from ethene to 2,3-dimethyl-2-butene is only  $10^2$ , as compared to  $10^6$  for chlorination and  $10^7$  for bromination (see Table 5.2). The sulfur substituent can influence reactivity. The initial complexation is expected to be favored by EWGs, but if the rate-determining step is ionization to the thiiranium ion, ERGs are favored.



As sulfur is less electronegative and more polarizable than chlorine, a strongly bridged intermediate, rather than an open carbocation, is expected for alkenes without ERG stabilization. Consistent with this expectation, sulfonylation is weakly regioselective and often shows a preference for *anti*-Markovnikov addition<sup>95</sup> as the result of steric factors. When bridging is strong, nucleophilic attack occurs at the less-substituted position. Table 5.4 gives some data for methyl- and phenyl- sulfonyl chloride. For bridged intermediates, the stereochemistry of addition is *anti*. Loss of stereospecificity with strong regioselectivity is observed when highly stabilizing ERG substituents are present on the alkene, as in 4-methoxyphenylstyrene.<sup>96</sup>

Similar results have been observed for other sulfonylating reagents. The somewhat more electrophilic trifluoroethylsulfonyl group shows a shift toward Markovnikov regioselectivity but retains *anti* stereospecificity, indicating a bridged intermediate.<sup>97</sup>

<sup>93</sup> D. J. Pettit and G. K. Helmkamp, *J. Org. Chem.*, **28**, 2932 (1963).

<sup>94</sup> V. Lucchini, G. Modena, and L. Pasquato, *J. Am. Chem. Soc.*, **113**, 6600 (1991); R. Destro, V. Lucchini, G. Modena, and L. Pasquato, *J. Org. Chem.*, **65**, 3367 (2000).

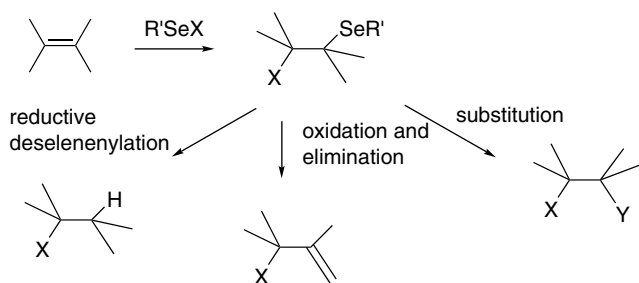
<sup>95</sup> W. H. Mueller and P. E. Butler, *J. Am. Chem. Soc.*, **88**, 2866 (1966).

<sup>96</sup> G. H. Schmid and V. J. Nowlan, *J. Org. Chem.*, **37**, 3086 (1972); I. V. Bodrikov, A. V. Borisov, W. A. Smit, and A. I. Lutsenko, *Tetrahedron Lett.*, **25**, 4983 (1984).

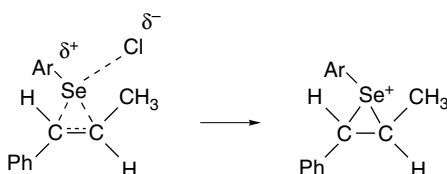
<sup>97</sup> M. Redon, Z. Janousek, and H. G. Viehe, *Tetrahedron*, **53**, 15717 (1997).



can undergo substitution reactions.  $\alpha$ -Selenenylation of carbonyl compounds has been particularly important and we consider this reaction in Section 4.7.2 of Part B.

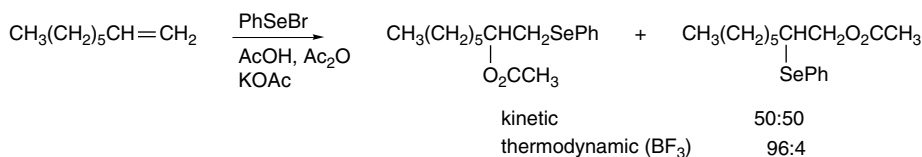


The various selenenylation reagents shown in Part B of Scheme 5.1 are characterized by an areneselenenyl group substituted by a leaving group. Some of the fundamental mechanistic aspects of selenenylation were established by studies of the reaction of *E*- and *Z*-1-phenylpropene with areneselenenyl chlorides.<sup>100</sup> The reaction is accelerated by an ERG in the arylselenenides. These data were interpreted in terms of a concerted addition with ionization of the Se–Cl bond leads C–Se bond formation. This accounts for the favorable effect of ERG substituents. Bridged seleniranium ions are considered to be intermediates.



As shown in Table 5.5, alkyl substitution enhances the reactivity of alkenes, but the effect is very small in comparison with halogenation (Table 5.2). Selenenylation seems to be particularly sensitive to steric effects. Note that a phenyl substituent is *rate retarding for selenenylation*. This may be due to both steric factors and alkene stabilization. The Hammett correlation with  $\sigma^+$  gives a  $\rho$  value of  $-0.715$ , also indicating only modest electron demand at the TS.<sup>101</sup> Indeed, positive values of  $\rho$  have been observed in some cases.<sup>102</sup>

Terminal alkenes show anti-Markovnikov regioselectivity, but rearrangement is facile.<sup>103</sup> The Markovnikov product is thermodynamically more stable (see Section 3.1.2.2).



Ref. 104

<sup>100</sup>. G. H. Schmid and D. G. Garratt, *J. Org. Chem.*, **48**, 4169 (1983).

<sup>101</sup>. C. Brown and D. R. Hogg, *J. Chem. Soc. B*, 1262 (1968).

<sup>102</sup>. I. V. Bodrikov, A. V. Borisov, L. V. Chumakov, N. S. Zefirov, and W. A. Smit, *Tetrahedron Lett.*, **21**, 115 (1980).

<sup>103</sup>. D. Liotta and G. Zima, *Tetrahedron Lett.*, 4977 (1978); P. T. Ho and R. J. Holt, *Can. J. Chem.*, **60**, 663 (1982); S. Raucher, *J. Org. Chem.*, **42**, 2950 (1977).

<sup>104</sup>. L. Engman, *J. Org. Chem.*, **54**, 884 (1989).

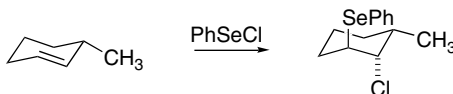
**Table 5.5. Relative Reactivity of Some Alkenes toward 4-Chlorophenylsulfenyl Chloride and Phenylselenenyl Chloride<sup>a</sup>**

Alkene	<i>p</i> -ClPhSeCl <i>k</i> <sub>rel</sub>	PhSeCl <i>k</i> <sub>rel</sub>
Ethene	1.00	1.00
Propene	3.15	8.76
1-Butene	3.81	6.67
<i>Z</i> -2-Butene	20.6	3.75
<i>E</i> -2-Butene	6.67	2.08
<i>Z</i> -3-Hexene	54.8	5.24
<i>E</i> -3-Hexene	5.96	2.79
2-Methylpropene	8.46	6.76
2-Methyl-2-butene	46.5	3.76
2,3-Dimethyl-2-butene	119	2.46
Styrene	0.95	0.050
<i>Z</i> -1-Phenylpropene	0.66	0.010
<i>E</i> -1-Phenylpropene	1.82	0.016

a. G. H. Schmid and D. G. Garratt, in *The Chemistry of Double-Bonded Functional Groups, Supplement A, Part 2*, S. Patai, ed., Wiley, New York, 1977, Chap. 9.

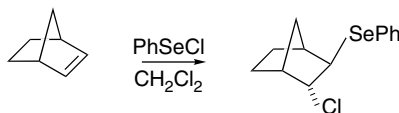
Styrene, on the other hand, is regioselective for the Markovnikov product, with the nucleophilic component bonding to the aryl-substituted carbon as is the result of weakening of the bridging by the phenyl group.

Selenenylation is a stereospecific *anti* addition with acyclic alkenes.<sup>105</sup> Cyclohexenes undergo preferential diaxial addition.



Ref. 106

Norbornene gives highly stereoselective *exo-anti* addition, pointing to an *exo* bridged intermediate.



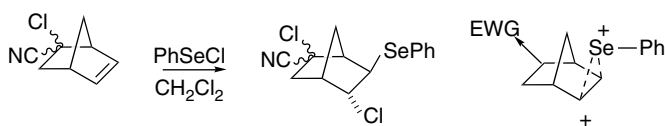
Ref. 107

The regiochemistry of addition to substituted norbornenes appears to be controlled by polar substituent effects.

<sup>105</sup> H. J. Reich, *J. Org. Chem.*, **39**, 428 (1974).

<sup>106</sup> D. Liotta, G. Zima, and M. Saindane, *J. Org. Chem.*, **47**, 1258 (1982).

<sup>107</sup> D. G. Garratt and A. Kabo, *Can. J. Chem.*, **58**, 1030 (1980).



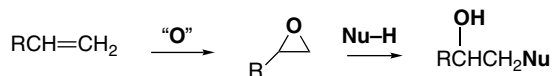
This regioselectivity is consistent with an unsymmetrically bridged seleniranium intermediate in which the more positive charge is remote from the EWG substituent. The directive effect is contrary to regiochemistry being dominated by the chloride ion approach, since chloride addition should be facilitated by the dipole of an EWG.

There has been some computational modeling of selenenylation reactions, particularly with regard to enantioselectivity of chiral reagents. The enantioselectivity is attributed to the relative ease of nucleophilic approach on the seleniranium ion intermediate, which is consistent with viewing the intermediate as being strongly bridged.<sup>108</sup> With styrene, a somewhat unsymmetrical bridging has been noted and the regiochemistry (Markovnikov) is attributed to the greater positive charge at C(1).<sup>109</sup>

Broadly comparing sulfur and selenium electrophiles to the halogens, we see that they are *less electrophilic* and characterized by *more strongly bridged intermediates*. This is consistent with reduced sensitivity to electronic effects in alkenes (e.g., alkyl or aryl substituents) and an increased tendency to anti-Markovnikov regiochemistry. The strongly bridged intermediates favor *anti* stereochemistry.

## 5.5. Addition Reactions Involving Epoxides

Epoxidation is an electrophilic addition. It is closely analogous to halogenation, sulfenylation, and selenenylation in that the electrophilic attack results in the formation of a three-membered ring. In contrast to these reactions, however, the resulting epoxides are neutral and stable and normally can be isolated. The epoxides are susceptible to nucleophilic ring opening so the overall pattern results in the addition of  $\text{OH}^+$  and a nucleophile at the double bond. As the regiochemistry of the ring opening is usually controlled by the ease of nucleophilic approach, *the oxygen is introduced at the more-substituted carbon*. We concentrate on peroxidic epoxidation reagents in this chapter. Later, in Chapter 12 of Part B, transition metal-mediated epoxidations are also discussed.



### 5.5.1. Epoxides from Alkenes and Peroxidic Reagents

The most widely used reagents for conversion of alkenes to epoxides are peroxy-carboxylic acids.<sup>110</sup> *m*-Chloroperoxybenzoic acid<sup>111</sup> (MCPBA) is a common reagent.

<sup>108</sup>. M. Spichy, G. Fragale, and T. Wirth, *J. Am. Chem. Soc.*, **122**, 10914 (2000); X. Wang, K. N. Houk, and M. Spichy, *J. Am. Chem. Soc.*, **121**, 8567 (1999).

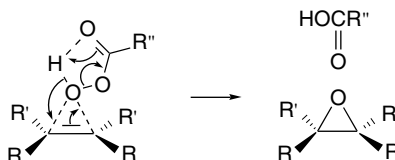
<sup>109</sup>. T. Wirth, G. Fragale, and M. Spichy, *J. Am. Chem. Soc.*, **120**, 3376 (1998).

<sup>110</sup>. D. Swern, *Organic Peroxides*, Vol. II, Wiley-Interscience, New York, 1971, pp. 355–533; B. Plesnicar, in *Oxidation in Organic Chemistry*, Part C, W. Trahanovsky, ed., Academic Press, New York, 1978, pp. 211–253.

<sup>111</sup>. R. N. McDonald, R. N. Steppel, and J. E. Dorsey, *Org. Synth.*, **50**, 15 (1970).

The magnesium salt of monoperoxyphthalic acid is an alternative.<sup>112</sup> Peroxyacetic acid, peroxybenzoic acid, and peroxytrifluoroacetic acid also are used frequently for epoxidation. All of the peroxycarboxylic acids are potentially explosive materials and require careful handling. Potassium hydrogen persulfate, which is sold commercially as Oxone<sup>®</sup>,<sup>113</sup> is a convenient reagent for epoxidations that can be done in aqueous solution.<sup>114</sup>

It has been demonstrated that no ionic intermediates are involved in the epoxidation of alkenes. The reaction rate is not very sensitive to solvent polarity.<sup>115</sup> Stereo-specific *syn* addition is consistently observed. The oxidation is considered to be a concerted process, as represented by the TS shown below. The plane including the peroxide bond is approximately perpendicular to the plane of the developing epoxide ring, so the oxygen being transferred is in a *spiro* position.



The rate of epoxidation of alkenes is increased by alkyl groups and other ERG substituents, and the reactivity of the peroxy acids is increased by EWG substituents.<sup>116</sup> These structure-reactivity relationships demonstrate that the peroxy acid acts as an electrophile in the reaction. Low reactivity is exhibited by double bonds that are conjugated with strongly EWG substituents, and very reactive peroxy acids, such as trifluoroperoxyacetic acid, are required for oxidation of such compounds.<sup>117</sup> Strain increases the reactivity of alkenes toward epoxidation. Norbornene is about twice as reactive as cyclopentene toward peroxyacetic acid.<sup>118</sup> *trans*-Cyclooctene is 90 times more reactive than cyclohexene.<sup>119</sup> Shea and Kim found a good correlation between relief of strain, as determined by MM calculations, and the epoxidation rate.<sup>120</sup> There is also a correlation with ionization potentials of the alkenes.<sup>121</sup> Alkenes with aryl substituents are *less reactive* than unconjugated alkenes because of ground state stabilization and this is consistent with a lack of carbocation character in the TS.

The stereoselectivity of epoxidation with peroxycarboxylic acids has been studied extensively.<sup>122</sup> Addition of oxygen occurs preferentially from the less hindered side of nonpolar molecules. Norbornene, for example, gives a 96:4 *exo:endo* ratio.<sup>123</sup> In molecules where two potential modes of approach are not greatly different, a mixture

<sup>112</sup> P. Brougham, M. S. Cooper, D. A. Cummerson, H. Heaney, and N. Thompson, *Synthesis*, 1015 (1987).

<sup>113</sup> Oxone is a registered trademark of E.I. du Pont de Nemours and company.

<sup>114</sup> R. Bloch, J. Abecassis, and D. Hassan, *J. Org. Chem.*, **50**, 1544 (1985).

<sup>115</sup> N. N. Schwartz and J. N. Blumbergs, *J. Org. Chem.*, **29**, 1976 (1964).

<sup>116</sup> B. M. Lynch and K. H. Pausacker, *J. Chem. Soc.*, 1525 (1955).

<sup>117</sup> W. D. Emmons and A. S. Pagano, *J. Am. Chem. Soc.*, **77**, 89 (1955).

<sup>118</sup> J. Spanget-Larsen and R. Gleiter, *Tetrahedron Lett.*, **23**, 2435 (1982); C. Wipff and K. Morokuma, *Tetrahedron Lett.*, **21**, 4445 (1980).

<sup>119</sup> K. J. Burgoine, S. G. Davies, M. J. Peagram, and G. H. Whitham, *J. Chem. Soc., Perkin Trans. 1*, 2629 (1974).

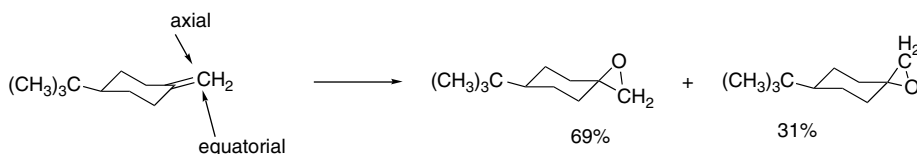
<sup>120</sup> K. J. Shea and J. -S. Kim, *J. Am. Chem. Soc.*, **114**, 3044 (1992).

<sup>121</sup> C. Kim, T. G. Traylor, and C. L. Perrin, *J. Am. Chem. Soc.*, **120**, 9513 (1998).

<sup>122</sup> V. G. Dryuk and V. G. Kartsev, *Russ. Chem. Rev.*, **68**, 183 (1999).

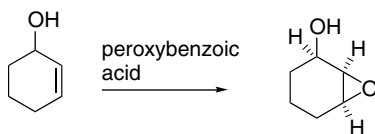
<sup>123</sup> H. Kwart and T. Takeshita, *J. Org. Chem.*, **28**, 670 (1963).

of products is formed. For example, the unhindered exocyclic double bond in 4-*t*-butylmethylene cyclohexane gives both stereoisomeric products.<sup>124</sup>

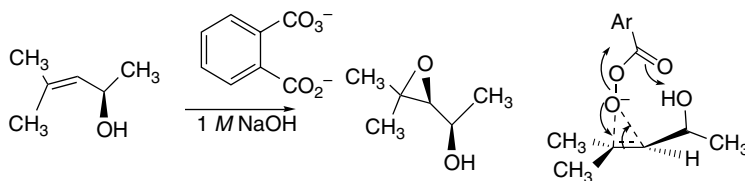


Several other conformationally biased methylenecyclohexanes have been examined and the small preference for axial attack is quite general, unless a substituent sterically encumbers one of the faces.<sup>125</sup>

Hydroxy groups exert a directive effect on epoxidation and favor approach from the side of the double bond closest to the hydroxy group.<sup>126</sup> Hydrogen bonding between the hydroxy group and the peroxidic reagent evidently stabilizes the TS.



This is a strong directing effect that can exert stereochemical control even when steric effects are opposed. Other substituents capable of hydrogen bonding, in particular amides, also exert a *syn*-directing effect.<sup>127</sup> The hydroxy-directing effect also operates in alkaline epoxidation in aqueous solution.<sup>128</sup> Here the alcohol group can supply a hydrogen bond to assist the oxygen transfer.



The hydroxy-directing effect has been carefully studied with allylic alcohols.<sup>129</sup> The analysis begins with the reactant conformation, which is dominated by allylic strain.

<sup>124</sup>. R. G. Carlson and N. S. Behn, *J. Org. Chem.*, **32**, 1363 (1967).

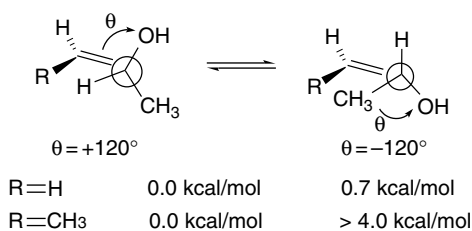
<sup>125</sup>. A. Sevin and J. -N. Cense, *Bull. Chim. Soc. Fr.*, 964 (1974); E. Vedejs, W. H. Dent, III, J. T. Kendall, and P. A. Oliver, *J. Am. Chem. Soc.*, **118**, 3556 (1996).

<sup>126</sup>. H. B. Henbest and R. A. L. Wilson, *J. Chem. Soc.*, 1958 (1957).

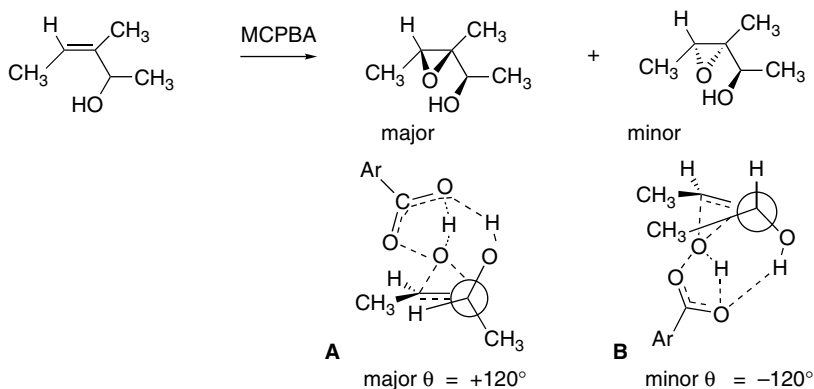
<sup>127</sup>. F. Mohamadi and M. M. Spees, *Tetrahedron Lett.*, **30**, 1309 (1989); P. G. M. Wuts, A. R. Ritter, and L. E. Pruitt, *J. Org. Chem.*, **57**, 6696 (1992); A. Jenmalm, W. Berts, K. Luthman, I. Csoregh, and U. Hackzell, *J. Org. Chem.*, **60**, 1026 (1995); P. Kocovsky and I. Stary, *J. Org. Chem.*, **55**, 3236 (1990); A. Armstrong, P. A. Barsanti, P. A. Clarke, and A. Wood, *J. Chem. Soc., Perkin Trans., 1*, 1373 (1996).

<sup>128</sup>. D. Ye, F. Finguelli, O. Piermatti, and F. Pizzo, *J. Org. Chem.*, **62**, 3748 (1997); I. Washington and K. N. Houk, *Org. Lett.*, **4**, 2661 (2002).

<sup>129</sup>. W. Adam and T. Wirth, *Acc. Chem. Res.*, **32**, 703 (1999).

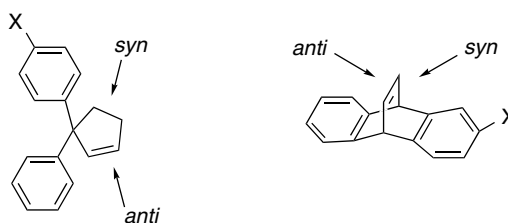


The epoxidation of goes through TSA, with 9:1 diastereoselectivity.<sup>130</sup>



The preference is the result of the CH<sub>3</sub>-CH<sub>3</sub> steric interaction that is present in TSB. The same stereoselectivity is exhibited by other reagents influenced by hydroxy-directing effects.<sup>131</sup>

There has been considerable interest in finding and interpreting electronic effects in sterically unbiased systems. (See Topic 2.4 for the application of this kind of study to ketones.) The results of two such studies are shown below. Generally, EWGs are *syn* directing, whereas ERGs are *anti* directing, but the effects are not very large.



X	<i>syn:anti</i>
NO <sub>2</sub>	73:27
Br	57:43
Cl	57:43
H	50:50
CH <sub>3</sub> O	48:52

Ref. 132

X	<i>syn:anti</i>
NO <sub>2</sub>	77:23
F	58:42
H	50:50
CH <sub>3</sub> O	48:52

Ref. 133

<sup>130</sup> W. Adam and B. Nestler, *Tetrahedron Lett.*, **34**, 611 (1993).

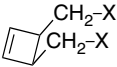
<sup>131</sup> W. Adam, H.-G. Degen, and C. R. Saha-Moller, *J. Org. Chem.*, **64**, 1274 (1999).

<sup>132</sup> R. L. Halterman and M. A. McEvoy, *Tetrahedron Lett.*, **33**, 753 (1992).

<sup>133</sup> T. Ohwada, I. Okamoto, N. Haga, and K. Shudo, *J. Org. Chem.*, **59**, 3975 (1994).

Whether these electronic effects have a stereoelectronic or an electrostatic origin is an open question. In either case, there would be a more favorable electronic environment *anti* to the ERG substituents and *syn* to the EWGs.

A related study of 3,4-disubstituted oxymethylcyclobutenes showed moderate *syn*-directive effects on MCPBA epoxidation.<sup>134</sup> In this case, the effect was attributed to interaction of the relatively electron-rich peroxide oxygens with the positively charged methylene hydrogens, but the electrostatic effect of the bond dipoles would be in the same direction.



X	<i>syn:anti</i>
H	55:45
OH	67:33
OCH <sub>3</sub>	62:38
O <sub>2</sub> CCH <sub>3</sub>	72:28
OSO <sub>2</sub> CH <sub>3</sub>	79:21
OSO <sub>2</sub>	70:30
(cyclic sulfite)	

There have been several computational studies of the peroxy acid–alkene reaction. The proposed spiro TS has been supported in these studies for alkenes that do not present insurmountable steric barriers. The spiro TS has been found for ethene (B3LYP/6-31G\*),<sup>135</sup> propene and 2-methylpropene (QCISD/6-31G\*),<sup>136</sup> and 2,3-dimethylbutene and norbornene (B3LYP/6-311+G(*d, p*)).<sup>137</sup> These computational studies also correctly predict the effect of substituents on the  $E_a$  and account for these effects in terms of less synchronous bond formation. This is illustrated by the calculated geometries and  $E_a$  (B3LYP/6-31G\*) of the TS for ethene, propene, methoxyethene, 1,3-butadiene, and cyanoethene, as shown in Figure 5.3. Note that the TSs become somewhat unsymmetrical with ERG substituents, as in propene, methoxyethene, and butadiene. The TS for acrylonitrile with an EWG substituent is even more unsymmetrical and has a considerably shorter C(3)–O bond, which reflects the electronic influence of the cyano group. In this asynchronous TS, the nucleophilic character of the peroxidic oxygen toward the  $\beta$ -carbon is important. Note also that the  $E_a$  is increased considerably by the EWG.

**Visual images and additional information available at: [springer.com/cary-sundberg](http://springer.com/cary-sundberg)**

Another useful epoxidizing agent is dimethyldioxirane (DMDO).<sup>138</sup> This reagent is generated by an in situ reaction of acetone and peroxymonosulfate in buffered aqueous solution. Distillation gives an  $\sim 0.1 M$  solution of DMDO in acetone.<sup>139</sup>

<sup>134</sup> M. Freccero, R. Gandolfi, and M. Sarzi-Amade, *Tetrahedron*, **55**, 11309 (1999).

<sup>135</sup> K. N. Houk, J. Liu, N. C. DeMello, and K. R. Condroski, *J. Am. Chem. Soc.*, **119**, 10147 (1997).

<sup>136</sup> R. D. Bach, M. N. Glukhovtsev, and C. Gonzalez, *J. Am. Chem. Soc.*, **120**, 9902 (1998).

<sup>137</sup> M. Freccero, R. Gandolfi, M. Sarzi-Amade, and A. Rastelli, *J. Org. Chem.*, **67**, 8519 (2002).

<sup>138</sup> R. W. Murray, *Chem. Rev.*, **89**, 1187 (1989); W. Adam and L. P. Hadjarapoglou, *Topics Current Chem.*, **164**, 45 (1993); W. Adam, A. K. Smerz, and C. G. Zhao, *J. Prakt. Chem., Chem. Zeit.*, **339**, 295 (1997).

<sup>139</sup> R. W. Murray and R. Jeyaraman, *J. Org. Chem.*, **50**, 2847 (1985); W. Adam, J. Bialas, and L. Hadjarapoglou, *Chem. Ber.*, **124**, 2377 (1991).

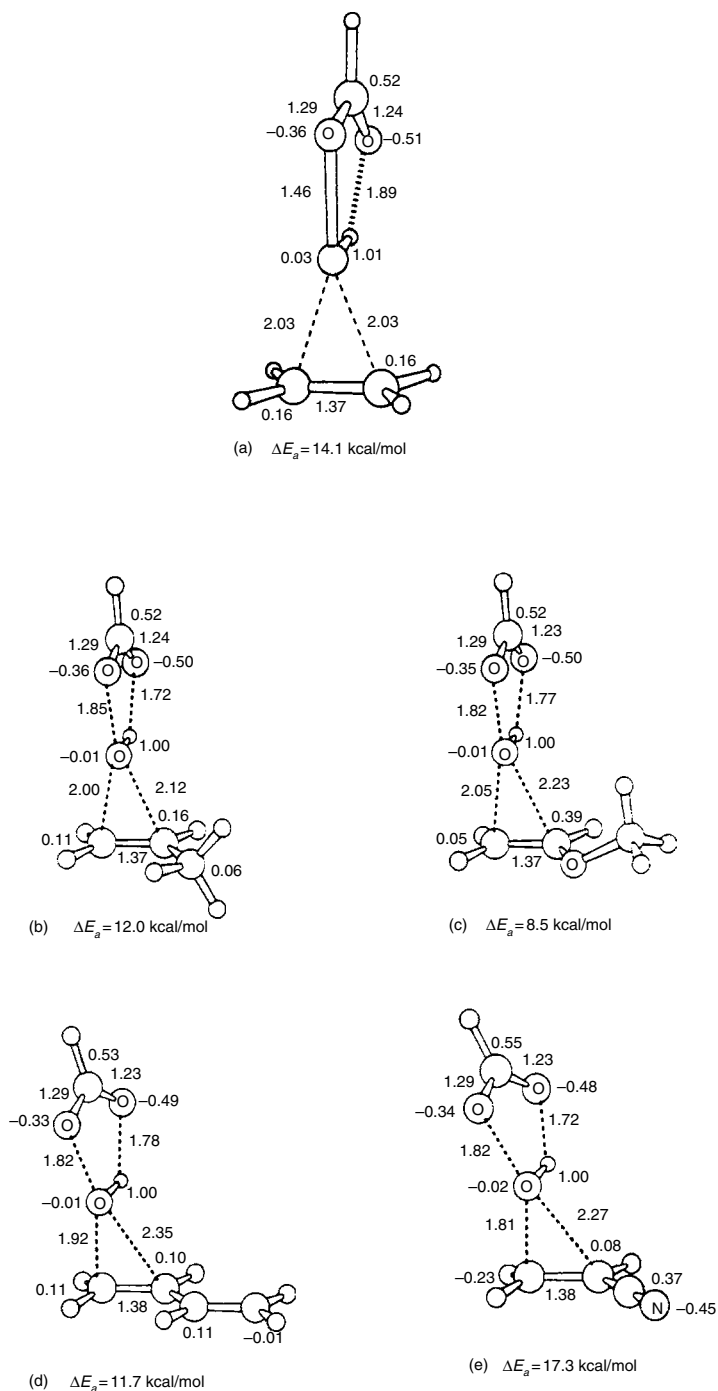
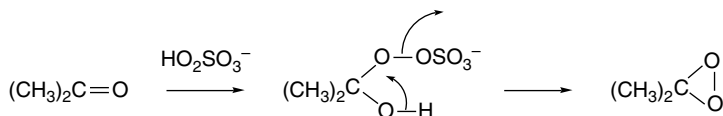
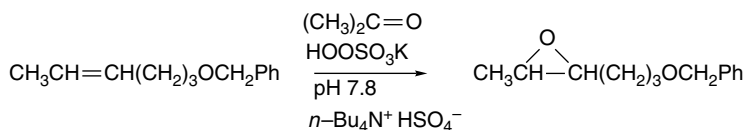


Fig. 5.3. Comparison of B3LYP/6-31G\* TS structures and  $E_a$  for epoxidation by  $\text{HCO}_3\text{H}$  for: (a) ethene; (b) propene; (c) methoxyethene; (d) 1,3-butadiene, and (e) cyanoethene. Reproduced from *J. Am. Chem. Soc.*, **119**, 10147 (1997), by permission of the American Chemical Society.

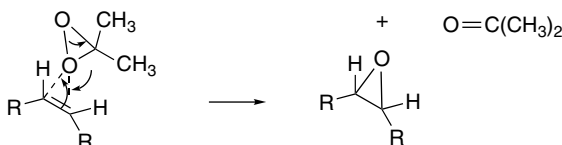


Higher concentrations of DMDO can be obtained by extraction of a 1:1 aqueous dilution of the distillate by  $\text{CH}_2\text{Cl}_2$ ,  $\text{CHCl}_3$ , or  $\text{CCl}_4$ .<sup>140</sup> Other improvements in convenience have been described,<sup>141</sup> including in situ generation of DMDO under phase transfer conditions.<sup>142</sup>

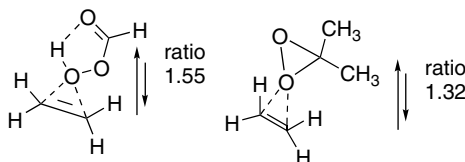


The yields and rates of oxidation by DMDO under these in situ conditions depend on pH and other reaction conditions.<sup>143</sup>

Various computational models of the TS show that the reaction occurs by a concerted mechanism that is quite similar to that for peroxy acids.<sup>144</sup> Kinetics and isotope effects are consistent with this mechanism.<sup>145</sup>



For example, the NPA charges for the DMDO and performic oxidations of ethene have been compared.<sup>146</sup> The ratio of the electrophilic interaction involving electron density transfer from the alkene to the O–O  $\sigma^*$  orbitals can be compared with the nucleophilic component involving back donation from the oxidant to the alkene  $\pi^*$  orbital. By this comparison, performic acid is somewhat more electrophilic.



<sup>140</sup> M. Gilbert, M. Ferrer, F. Sanchez-Baeza, and A. Messeguer, *Tetrahedron*, **53**, 8643 (1997).

<sup>141</sup> W. Adam, J. Bialoas, and L. Hadjjaropoglou, *Chem. Ber.*, **124**, 2377 (1991).

<sup>142</sup> S. E. Denmark, D. C. Forbes, D. S. Hays, J. S. DePue, and R. G. Wilde, *J. Org. Chem.*, **60**, 1391 (1995).

<sup>143</sup> M. Frohn, Z.-X. Wang, and Y. Shi, *J. Org. Chem.*, **63**, 6425 (1998); A. O'Connell, T. Smyth, and B. K. Hodnett, *J. Chem. Tech. Biotech.*, **72**, 60 (1998).

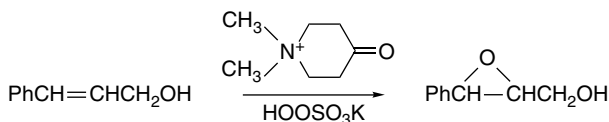
<sup>144</sup> R. D. Bach, M. N. Glukhovtsev, C. Gonzalez, M. Marquez, C. M. Estevez, A. G. Baboul, and H. Schlegel, *J. Phys. Chem.*, **101**, 6092 (1997); M. Freccero, R. Gandolfi, M. Sarzi-Amade, and A. Rastelli, *Tetrahedron*, **54**, 6123 (1998); J. Liu, K. N. Houk, A. D'Ino, C. Fusco, and R. Curci, *J. Org. Chem.*, **63**, 8565 (1998).

<sup>145</sup> W. Adam, R. Paredes, A. K. Smerz, and L. A. Veloz, *Liebigs Ann. Chem.*, 547 (1997); A. L. Baumstark, E. Michalenabaez, A. M. Navarro, and H. D. Banks, *Heterocycl. Commun.*, **3**, 393 (1997); Y. Angelis, X. J. Zhang, and M. Orfanopoulos, *Tetrahedron Lett.*, **37**, 5991 (1996).

<sup>146</sup> D. V. Deubel, G. Frenking, H. M. Senn, and J. Sundermeyer, *J. Chem. Soc., Chem. Commun.*, 2469 (2000).



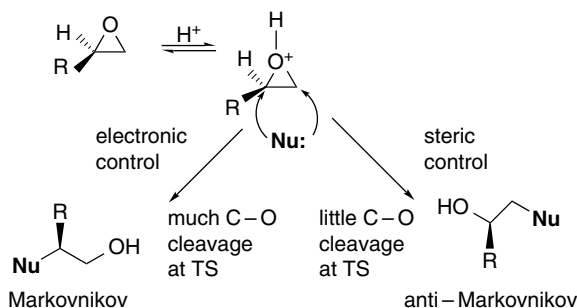
epoxidation.<sup>156</sup> The positively charged quaternary nitrogen enhances the reactivity of the carbonyl group toward nucleophilic addition and also makes the dioxirane intermediate more reactive.



### 5.5.2. Subsequent Transformations of Epoxides

Epoxides are useful synthetic intermediates and the conversion of an alkene to an epoxide is often part of a more extensive overall transformation.<sup>157</sup> Advantage is taken of the reactivity of the epoxide ring to introduce additional functionality. As epoxide ring opening is usually stereospecific, such reactions can be used to establish stereochemical relationships between adjacent substituents. Such two- or three-step operations can achieve specific oxidative transformations of an alkene that might not be easily accomplished in a single step.

Ring opening of epoxides can be carried out under either acidic or basic conditions. The regiochemistry of the ring opening depends on whether steric or electronic factors are dominant. Base-catalyzed reactions in which the nucleophile provides the driving force for ring opening usually involve breaking the epoxide bond at the less-substituted carbon, since this is the position most accessible to nucleophilic attack (*steric factor dominates*).<sup>158</sup> The situation in acid-catalyzed reactions is more complicated. The bonding of a proton to the oxygen weakens the C–O bonds and facilitates rupture of the ring by weak nucleophiles. If the C–O bond is largely intact at the TS, the nucleophile will become attached to the less-substituted position for the same steric reasons that were cited for nucleophilic ring opening. If, on the other hand, C–O rupture is more complete when the TS is reached, the opposite orientation is observed. This results from the ability of the more-substituted carbon to stabilize the developing positive charge (*electronic factor dominates*). *Steric control corresponds to anti-Markovnikov regioselectivity, whereas electronic control leads to Markovnikov regioselectivity.*

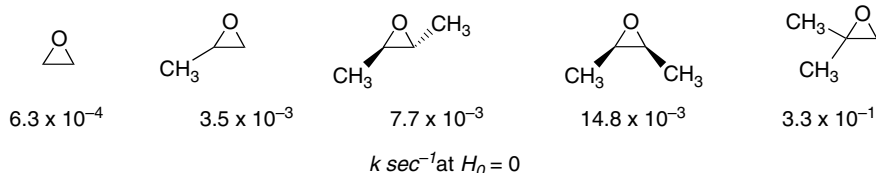


<sup>156</sup> S. E. Denmark, D. C. Forbes, D. S. Hays, J. S. DePue, and R. G. Wilde, *J. Org. Chem.*, **60**, 1391 (1995).

<sup>157</sup> J. G. Smith, *Synthesis*, 629 (1984).

<sup>158</sup> R. E. Parker and N. S. Isaacs, *Chem. Rev.*, **59**, 737 (1959).

These fundamental aspects of epoxide ring opening were established by kinetic and isotopic labeling studies.<sup>159</sup> The dominant role of bond cleavage in acidic hydrolysis is indicated by the increase in rates with additional substitution. Note in particular that the 2,2-dimethyl derivative is much more reactive than the *cis* and *trans* disubstituted derivative, as expected for an intermediate with carbocation character.



The pH-rate profiles of hydrolysis of 2-methyloxirane and 2,2-dimethyloxirane have been determined and interpreted.<sup>160</sup> The profile for 2,2-dimethyloxirane, shown in Figure 5.4, leads to the following rate constants for the acid-catalyzed, uncatalyzed, and base-catalyzed reactions.

$$k_{H^+} = 25.8 \pm 1.7 M^{-1} s^{-1}$$

$$k_{H_2O} = 2.19 \pm 10^{-6} M^{-1} s^{-1}$$

$$k_{-OH} = 1.95 \pm 10^{-4} M^{-1} s^{-1}$$

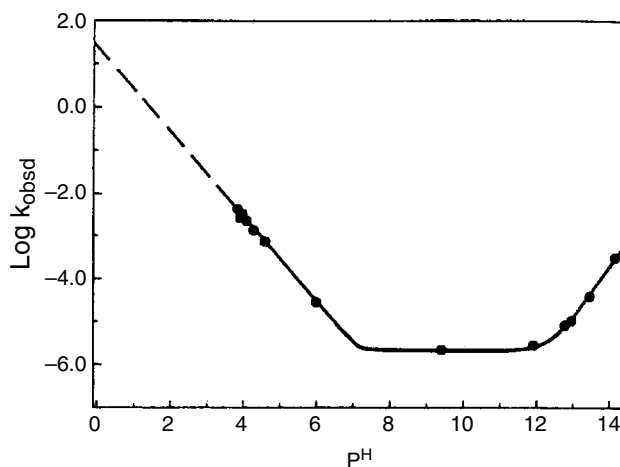
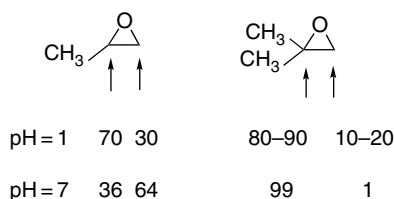


Fig. 5.4. pH-Rate profile for hydrolysis of 2,2-dimethyloxirane. Reproduced from *J. Am. Chem. Soc.*, **110**, 6492 (1988), by permission of the American Chemical Society.

<sup>159</sup> J. G. Pritchard and F. A. Long, *J. Am. Chem. Soc.*, **78**, 2667, 6008 (1956); F. A. Long, J. G. Pritchard, and F. E. Stafford, *J. Am. Chem. Soc.*, **79**, 2362 (1957).

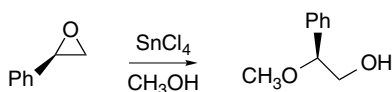
<sup>160</sup> Y. Pocker, B. P. Ronald, and K. W. Anderson, *J. Am. Chem. Soc.*, **110**, 6492 (1988).

Nucleophilic attack occurs at both the more-substituted and the less-substituted carbon, as determined by isotopic labeling.<sup>161</sup>

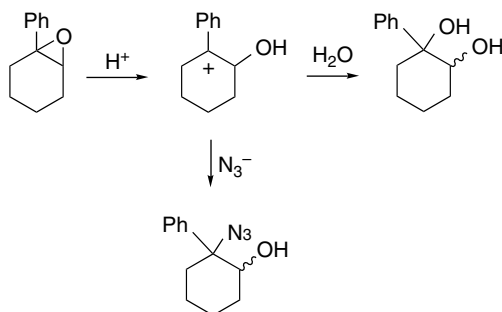


The opening of *cis*- and *trans*-2,3-dimethyloxirane in methanol or acetic acid is a stereospecific *anti* addition.<sup>162</sup>

The presence of an aryl substituent favors cleavage of the benzylic C–O bond. The case of styrene oxide hydrolysis has been carefully examined. Under acidic conditions the bond breaking is exclusively at the benzylic position (electronic control). Under basic conditions, ring opening occurs at both epoxide carbons.<sup>163</sup> Styrene also undergoes highly regioselective ring opening in the presence of Lewis acids. For example, methanolysis is catalyzed by SnCl<sub>4</sub>; it occurs with more than a 95% attack at the benzyl carbon and with high *inversion of configuration*.<sup>164</sup> Similar results are observed with BF<sub>3</sub>.<sup>165</sup> The stereospecificity indicates a concerted nucleophilic opening of the complexed epoxide, with bond-weakening factors (electronic control) determining the regiochemistry.



In the case of epoxides of 1-arylcyclohexene, there is direct evidence for a carbocation intermediate.<sup>166</sup> The hydrolysis product can be diverted by addition of azide ion as a competing nucleophile. As expected for a carbocation intermediate, both the *cis* and *trans* diols are formed.



<sup>161</sup> F. A. Long and J. G. Pritchard, *J. Am. Chem. Soc.*, **78**, 2663, 2667 (1956); F. A. Long, J. G. Pritchard, and F. E. Stafford, *J. Am. Chem. Soc.*, **79**, 2362 (1957).

<sup>162</sup> V. F. Shvets, N. N. Lebedev, and O. A. Tyukova, *Zh. Org. Khim.*, **7**, 1851 (1971).

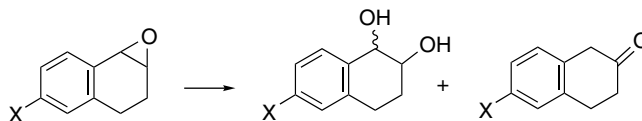
<sup>163</sup> B. Lin and D. L. Whalen, *J. Org. Chem.*, **59**, 1638 (1994); J. J. Blumenstein, V.C. Ukachukwu, R. S. Mohan, and D. L. Whalen, *J. Org. Chem.*, **58**, 924 (1993).

<sup>164</sup> C. Moberg, L. Rakos, and L. Tottie, *Tetrahedron Lett.*, **33**, 2191 (1992).

<sup>165</sup> Y. J. Liu, T. Y. Chu, and R. Engel, *Synth. Commun.*, **22**, 2367 (1992).

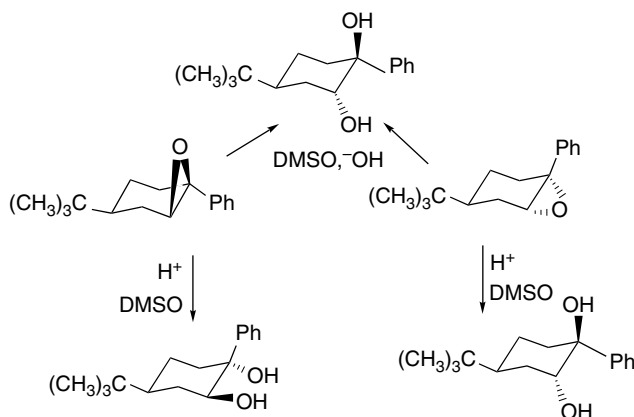
<sup>166</sup> L. Doan, K. Bradley, S. Gerdes, and D. L. Whalen, *J. Org. Chem.*, **64**, 6227 (1999).

Similarly, comparison of the epoxide of 1,2-dihydronaphthalene and its 6-methoxy analog provided interesting contrasts. The product was partitioned into the components formed by the acid-catalyzed and uncatalyzed mechanisms.<sup>167</sup> The unsubstituted compound gives the *trans* diol exclusively, indicating participation of the nucleophile in the ring opening. The 6-methoxy derivative gives a substantial amount of a rearrangement product and the diol is a mixture of the *cis* and *trans* stereoisomers. These differences indicate that the more stabilized carbocation has a significant lifetime.



X	<i>cis</i>	<i>trans</i>	
H			
H <sup>+</sup> - catalyzed	6	94	0
uncatalyzed	0	100	0
CH <sub>3</sub> O			
H <sup>+</sup> - catalyzed	81	19	<1
uncatalyzed	17	7	76

The conformationally biased *cis*- and *trans*-4-*t*-butyl derivatives were examined. The stereochemistry of both acid- and base-catalyzed reactions was investigated in 85:15 DMSO-H<sub>2</sub>O. Under acidic conditions the epoxides give *anti* ring opening and the reaction is stereospecific. The base-catalyzed reactions involve *trans*-diaxial ring opening. The acid-catalyzed reactions occur by preferential opening of the benzylic bond with inversion.<sup>168</sup>

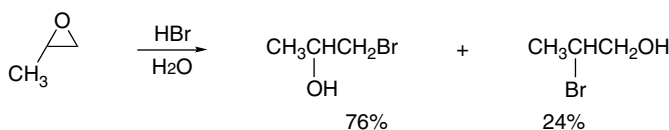


When saturated epoxides such as propylene oxide react with hydrogen halides, the dominant mode of reaction introduces halide at the less-substituted primary carbon (*anti*-Markovnikov).<sup>169</sup>

<sup>167</sup> R. E. Gillilan, T. M. Pohl, and D. L. Whalen, *J. Am. Chem. Soc.*, **104**, 4481 (1982).

<sup>168</sup> G. Berti, B. Macchia, and F. Macchia, *Tetrahedron Lett.*, 3421 (1965).

<sup>169</sup> C. A. Stewart and C. A. VanderWerf, *J. Am. Chem. Soc.*, **76**, 1259 (1954).

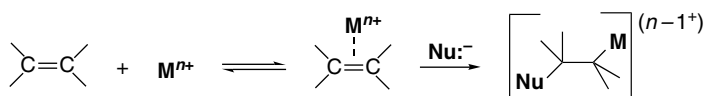


Substituents that further stabilize a carbocation intermediate lead to reversal of the mode of addition.<sup>170</sup> To summarize, because they are stable compounds, both the stereochemistry and regiochemistry of epoxides can be controlled by the reaction conditions. Ring opening that is dominated by the nucleophilic reagent is determined by steric access. Ring opening that is electrophilic in character introduces the nucleophile at the position that has the largest cationic character.

## 5.6. Electrophilic Additions Involving Metal Ions

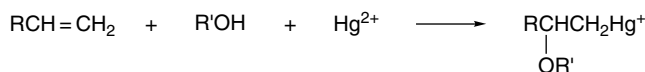
Visual images and additional information available at: [springer.com/cary-sundberg](http://springer.com/cary-sundberg)

Certain metal cations promote addition by electrophilic attack on alkenes. Addition is completed when a nucleophile adds to the alkene-cation complex. The nucleophile may be the solvent or a ligand from the metal ion's coordination sphere. The same process occurs for other transition metal cations, especially for  $\text{Pd}^{2+}$ , but the products often go on to react further. Synthetically important reactions involving  $\text{Pd}^{2+}$  are discussed in Section 8.2 of Part B. The mercuration products are stable, and this allows study of the addition reaction itself. We also consider reactions of the  $\text{Ag}^+$  ion, which give complexes, but usually do not proceed to adducts.



### 5.6.1. Solvomercuration

The best characterized of these reactions involve the mercuric ion,  $\text{Hg}^{2+}$ , as the cation.<sup>171</sup> The usual nucleophile is the solvent. The term *oxymercuration* is used to refer to reactions in which water or an alcohol acts as the nucleophile. The adducts can be isolated as halide salts, but in synthetic applications the mercury is often replaced by hydrogen (*oxymercuration reduction*; see below).



The reactivity of mercury salts is a function of both the solvent and the counterion.<sup>172</sup> Mercuric chloride, for example, is unreactive and mercuric acetate is the most commonly used reagent, but the trifluoroacetate, trifluoromethanesulfonate, nitrate, or perchlorate salts are preferable in some applications.

<sup>170</sup>. S. Winstein and L. L. Ingraham, *J. Am. Chem. Soc.*, **74**, 1160 (1952).

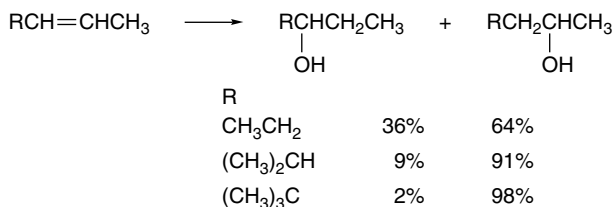
<sup>171</sup>. W. Kitching, *Organomet. Chem. Rev.*, **3**, 61 (1968); R. C. Larock, *Solvomercuration/Demercuration Reactions in Organic Synthesis*, Springer-Verlag, New York, 1986.

<sup>172</sup>. H. C. Brown, J. T. Kurek, M.-H. Rei, and K. L. Thompson, *J. Org. Chem.*, **49**, 2551 (1984).

The reactivity of different alkenes toward mercuration spans a considerable range and is governed by a combination of steric and electronic factors.<sup>173</sup> In contrast to protonation and halogenation reactions, the oxymercuration reaction is not always accelerated by alkyl substituents on the alkene. Dialkyl terminal alkenes are more reactive than monosubstituted ones, but internal disubstituted alkenes are less reactive. For example, 1-pentene is about ten times more reactive than *Z*-2-pentene and 40 times more reactive than *E*-2-pentene.<sup>174</sup> This reversal of reactivity is due to steric effects, which generally outweigh the normal electron-releasing effect of alkyl substituents.<sup>175</sup> The relative reactivity data for some pentene derivatives are given in Table 5.6.

As expected for an electrophilic reaction, the  $\rho$  values for oxymercuration of styrene ( $-3.16$ )<sup>176</sup> and  $\alpha$ -methylstyrene ( $-3.12$ )<sup>177</sup> derivatives are negative. The positive deviation of the methoxy substituent, when treated by the Yukawa-Tsuno equation, is indicative of a modestly enhanced resonance component. The additional methyl substituent in  $\alpha$ -methylstyrene is slightly activating and indicates that its electron-donating effect outweighs any adverse steric effect.

The addition of the nucleophile follows Markovnikov's rule and the regioselectivity of oxymercuration is ordinarily very high. Terminal alkenes are usually more than 99% regioselective and even disubstituted alkenes show significant regioselectivity, which is enhanced by steric effects.



Ref. 178

**Table 5.6. Relative Reactivity of Some Alkenes in Oxymercuration**

Alkene	Relative reactivity <sup>a</sup>
1-Pentene	6.6
2-Methyl-1-pentene	48
<i>Z</i> -2-Pentene	0.56
<i>E</i> -2-Pentene	0.17
2-Methyl-2-pentene	1.24
Cyclohexene	1.00

a. H. C. Brown and P. J. Geoghegan, Jr., *J. Org. Chem.*, **37**, 1937 (1972).

<sup>173</sup> H. C. Brown and P. J. Geoghegan, Jr., *J. Org. Chem.*, **37**, 1937 (1972); H. C. Brown, P. J. Geoghegan, Jr., G. J. Lynch, and J. T. Kurek, *J. Org. Chem.*, **37**, 1941 (1972); H. C. Brown, P. J. Geoghegan, Jr., and J. T. Kurek, *J. Org. Chem.*, **46**, 3810 (1981).

<sup>174</sup> H. C. Brown and P. J. Geoghegan, Jr., *J. Org. Chem.*, **37**, 1937 (1972).

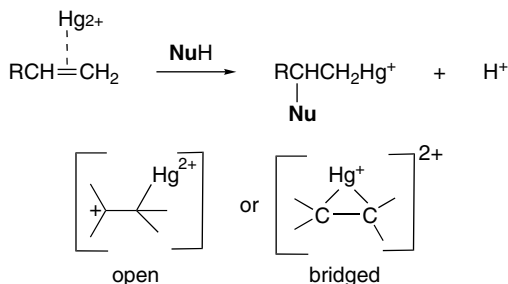
<sup>175</sup> S. Fukuzumi and J. K. Kochi, *J. Am. Chem. Soc.*, **103**, 2783 (1981).

<sup>176</sup> A. Lewis and J. Azoro, *J. Org. Chem.*, **46**, 1764 (1981); A. Lewis, *J. Org. Chem.*, **49**, 4682 (1984).

<sup>177</sup> I. S. Hendricks and A. Lewis, *J. Org. Chem.*, **64**, 7342 (1999).

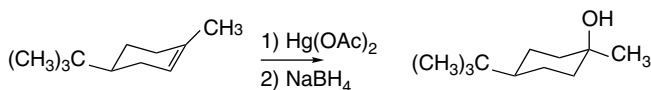
<sup>178</sup> H. C. Brown and J. P. Geoghegan, Jr., *J. Org. Chem.*, **35**, 1844 (1970).

In analogy with other electrophilic additions, the mechanism of the oxymercuration reaction can be discussed in terms of a cationic intermediate.<sup>179</sup> The cationic intermediate can be bridged (*mercurinium ion*) or open, depending on the structure of the particular alkene. The intermediates can be detected by NMR in nonnucleophilic solvents.<sup>180</sup> The addition is completed by attack of a nucleophile at the more positive carbon.

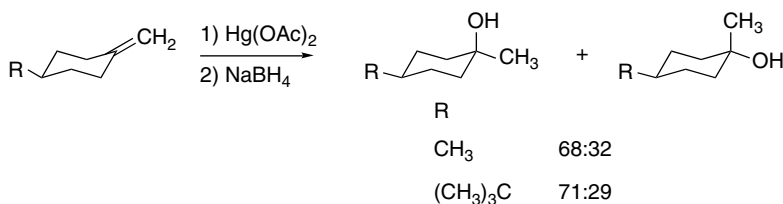


After the addition step is complete, the mercury is usually replaced by hydrogen, using a reducing agent. The net result is the addition of hydrogen and the nucleophile to the alkene, and the reaction is known as *oxymercuration reduction*. The regioselectivity is in the same sense as is observed for proton-initiated additions.<sup>181</sup>

Oxymercuration of unhindered alkenes is usually a stereospecific *anti* addition. This result is consistent with the involvement of a mercurinium ion intermediate that is opened by nucleophilic attack.<sup>182</sup> Conformationally biased cyclic alkenes such as 4-*t*-butylcyclohexene and 4-*t*-butyl-1-methylcyclohexene give exclusively the product of *anti*-diaxial addition.<sup>181, 183</sup>



Methylenecyclohexenes are not very stereoselective, showing a small preference for the axial alcohol, which corresponds to mercuration from the equatorial face.<sup>184</sup>



<sup>179</sup> S. J. Cristol, J. S. Perry, Jr., and R. S. Beckley, *J. Org. Chem.*, **41**, 1912 (1976); D. J. Pasto and J. A. Gontarz, *J. Am. Chem. Soc.*, **93**, 6902 (1971).

<sup>180</sup> G. A. Olah and P. R. Clifford, *J. Am. Chem. Soc.*, **95**, 6067 (1973); G. A. Olah and S. H. Yu, *J. Org. Chem.*, **40**, 3638 (1975).

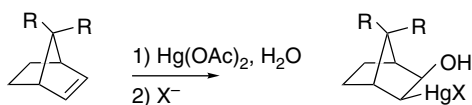
<sup>181</sup> H. C. Brown and P. J. Geoghegan, Jr., *J. Org. Chem.*, **35**, 1844 (1970); H. C. Brown, J. T. Kurek, M.-H. Rei, and K. L. Thompson, *J. Org. Chem.*, **49**, 2511 (1984); H. C. Brown, J. T. Kurek, M.-H. Rei, and K. L. Thompson, *J. Org. Chem.*, **50**, 1171 (1985).

<sup>182</sup> H. B. Vardhan and R. D. Bach, *J. Org. Chem.*, **57**, 4948 (1992).

<sup>183</sup> H. C. Brown, G. J. Lynch, W. J. Hammar, and L. C. Liu, *J. Org. Chem.*, **44**, 1910 (1979).

<sup>184</sup> Y. Senda, S. Kamiyama, and S. Imaizumi, *J. Chem. Soc., Perkin Trans. 1*, 530 (1978).

In contrast to the *anti* addition observed with acyclic and monocyclic alkenes, bicyclic alkenes frequently show *syn* addition. Norbornene gives exclusively *exo-syn* addition. Even 7,7-dimethylnorbornene gives the *exo-syn* product, in sharp contrast to the usual *endo*-directing effects of 7-substitution. These results are difficult to reconcile with a bridged mercurinium ion and suggest that intramolecular transfer of the nucleophile from mercury occurs. In norbornene derivatives, the competing *anti* addition is sterically restricted by the *endo* bridge.

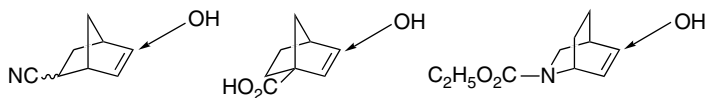


R = H Ref. 185

R = CH<sub>3</sub> Ref. 186

Other bicyclic alkenes have been observed to give largely or exclusively *syn* addition.<sup>187</sup>

Oxymercuration shows considerable sensitivity to polar substituents. Several early examples set the pattern, which is for the nucleophile to add at the carbon that is more remote from a polar EWG substituent.



Ref. 188

Ref. 188

Ref. 189

In considering the basis of this effect, Factor and Traylor<sup>188</sup> suggested that the EWGs “make the unsymmetrical TS having less positive charge near the substituted position the one of lowest energy.” Mayo and colleagues carried out a systematic study of the effect, including comparison of *exo* and *endo* substituents.<sup>190</sup> Some of the results of that study are shown below. The directive effect was found for both *exo* and *endo* substituents, but was somewhat stronger for *exo* groups.



X	5:6 ( <i>exo</i> )	5:6 ( <i>endo</i> )
CH <sub>2</sub> OTBS	1:1	1:1
CO <sub>2</sub> CH <sub>3</sub>	5:1	5:1
OH	6:1	3:1
OCH <sub>2</sub> Ph	9:1	6:1
O <sub>2</sub> CCH <sub>3</sub>	14:1	9:1

<sup>185</sup> T. G. Traylor and A. W. Baker, *J. Am. Chem. Soc.*, **85**, 2746 (1963).

<sup>186</sup> H. C. Brown and J. H. Kawakami, *J. Am. Chem. Soc.*, **95**, 8665 (1973).

<sup>187</sup> T. N. Sokolova, V. R. Kartashov, O. V. Vasil'eva, and Y. K. Grishin, *Russ. Chem. Bull.*, **42**, 1583 (1993).

<sup>188</sup> A. Factor and T. G. Traylor, *J. Org. Chem.*, **33**, 2607 (1968).

<sup>189</sup> G. Krow, R. Rodebaugh, M. Grippi, and R. Carosin, *Synth. Commun.*, **2**, 211 (1972).

<sup>190</sup> P. Mayo, G. Orlova, J. D. Goddard, and W. Tam, *J. Org. Chem.*, **66**, 5182 (2001).

These workers used B3PW91/LanL2DZ DFT calculations to probe the TS using  $\text{Hg}(\text{O}_2\text{CH})_2$  as the reagent. Using ethene as the reactant, they found a symmetrical bridged structure to be a stable prereaction complex. The TS for addition is very unsymmetrical with partial bonding by one of the formate ligands. The TS for addition to norbornenes was somewhat looser and the addition corresponded to a four-center *syn* mechanism. These gas phase computations may bias the ethene TS toward *syn* addition by virtue of the attachment of the nucleophile to  $\text{Hg}^{2+}$ . However, the results with both ethene and norbornene suggest that there is no strong prohibition against a *syn* addition, in agreement with the experimental results.

The regioselectivity in substituted norbornenes is the result of polarization of the double bond, with the  $\text{Hg}^{2+}$  attacking the more negative carbon. The NPA charges calculated for the TS show that this polarization becomes much larger as the C–Hg bond is formed and the TS is approached. The substituent effect results from an initial polarization of the double bond that is enhanced as the TS is approached. Figure 5.5 shows the TS for C(5) and C(6) for the *endo* hydroxyl reactant. The  $\Delta E^\ddagger$  for the two TSs differ by 1.6 kcal and in the direction of the observed preferred addition of Hg at C(6).

**Visual models, additional information and exercises on Oxymercuration can be found in the Digital Resource available at: [Springer.com/carey-sundberg](http://Springer.com/carey-sundberg).**

The effect of remote polar substituents was also probed with substituted 7-methylenenorbornanes.<sup>191</sup> The substituents are located in the *endo* position and cannot interact directly with the approaching reagent. Ester groups are strongly *syn*

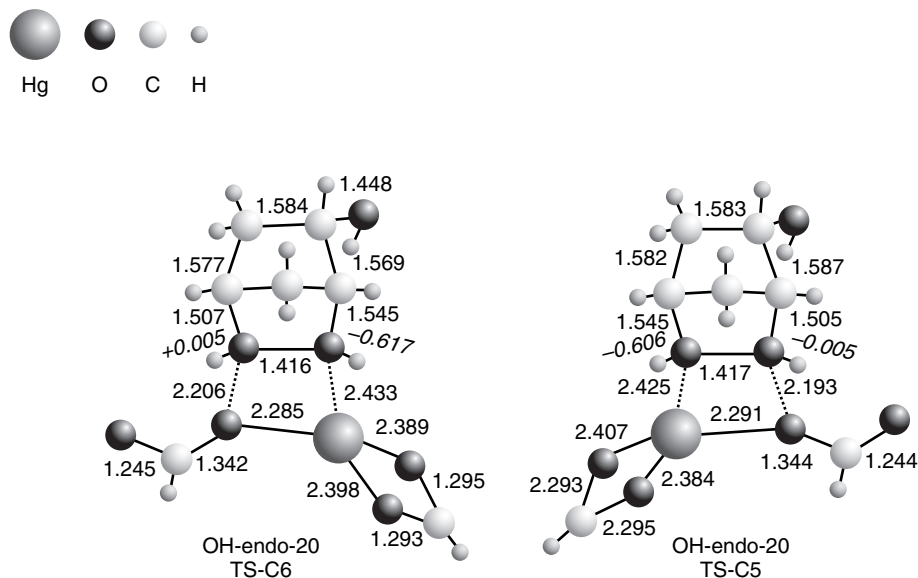
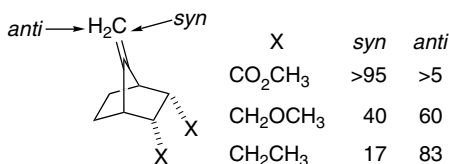


Fig. 5.5. Transition structures for C(6) and C(5) mercuration of the *endo* hydroxy derivative of norbornene. Italic numbers give the NPA charges at the reacting carbons. Reproduced from *J. Org. Chem.*, **66**, 5182 (2001), by permission of the American Chemical Society.

<sup>191</sup>. G. Mehta and F. A. Khan, *J. Chem. Soc., Chem. Commun.*, 18 (1991).

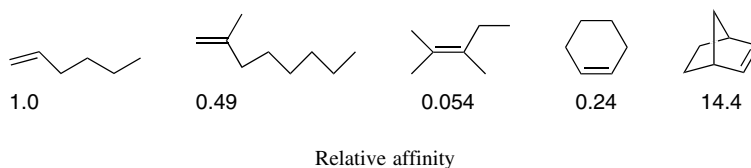
directing, whereas ethyl groups are *anti* directing. These results were attributed to differential polarization of the faces of the  $\pi$  bond (see Section 2.4). Similar, but much weaker, directive effects are seen for epoxidation and hydroboration.



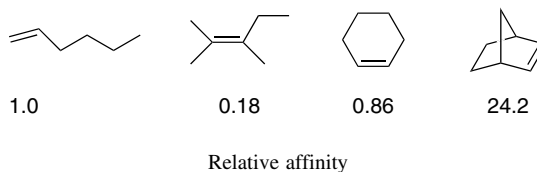
A broad mechanistic interpretation that can encompass most of these results suggests that the  $\text{Hg}^{2+}$  ion is rather loosely bound prior to the rate-determining nucleophilic addition. The bonding is weaker at the carbon best able to accommodate positive charge, resulting in Markovnikov regioselectivity. If there is little steric hindrance, *anti* addition of a nucleophile is preferred, but the *syn* mechanism is available. The *syn* mechanism, at least as modeled in the gas phase, seems to involve migration of a ligand from  $\text{Hg}^{2+}$  to carbon. It is *the nucleophilic capture that determines the regiochemistry and stereochemistry of the product*, since the mercuriation step is reversible. It should also be noted that oxymercuration has a different electronic pattern from most of the other electrophilic additions in that the Hg-substituted carbon becomes *negatively charged* as bonding occurs (see Figure 5.5). This is also true in hydroboration, although less so, whereas halogenation, sulfenylation, and selenylation result in placing a more electronegative substituent on *both* carbons of the double bond.

### 5.6.2. Argentation—the Formation of Silver Complexes

Several analytical and separation techniques are based on the reversible formation of complexes between alkenes and  $\text{Ag}^+$  ions.<sup>192</sup> Analytical methods for terpenes, unsaturated acids and esters, and other unsaturated nonpolar compounds are based on the use of  $\text{Ag}^+$ -impregnated materials for thin-layer (TLC) and high-pressure (HPLC) as well as gas-liquid (GLC) chromatography. GLC measurements done some years ago suggest that the affinity decreases with additional substituents, but increases with strain.<sup>193</sup>



An NMR study in methanol showed a similar trend in relative stability of the  $\text{Ag}(\text{I})$  complexes.<sup>194</sup>



<sup>192</sup> G. Dobson, W. W. Christie, and B. Nikolovadamyanova, *J. Chromatogr. B*, **671**, 197 (1995); C. M. Williams and L. N. Mander, *Tetrahedron*, **57**, 425 (2001).

<sup>193</sup> M. A. Muhs and F. T. Weiss, *J. Am. Chem. Soc.*, **84**, 4697 (1962).

<sup>194</sup> H. B. Varhan and R. D. Bach, *J. Org. Chem.*, **57**, 4948 (1992).

In contrast to Hg(II), Ag(I) does not normally induce intermolecular nucleophilic addition to alkenes. However, internal nucleophiles can sometimes be captured, leading to cyclization reactions.

The structure and stability of alkene-Ag<sup>+</sup> complexes has also been examined by computation.<sup>195</sup> MP2/SBK(*d*) calculations indicate that three ethene molecules are accommodated at Ag<sup>+</sup> with  $\Delta E$  of  $-30 \pm 3$  kcal/mol, but subsequent ethenes are less strongly bound. The computations find stronger complexation with alkyl-substituted alkenes in the gas phase, which is in contrast to the trend in the solution stabilities. This might be the result of the greater importance of solvation in the liquid phase, whereas polarization might be the dominant factor in the gas phase.

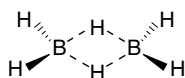
	Solution <sup>a</sup>	$\Delta E$ (gas phase) <sup>b</sup> kcal/mol
Ethene	1.32	-33.7
Propene	0.98	-36.6
Z-2-Butene	0.49	-38.0
E-2-Butene	0.27	-38.3
2-Methylpropene	0.16	-41.3
2,3-Dimethyl-2-butene	0.04	-43.5

a. T. A. van Beek and D. Suburtova, *Phytochem. Anal.*, **6**, 1 (1995).  
A solution relative affinity value based on chromatographic measurements.

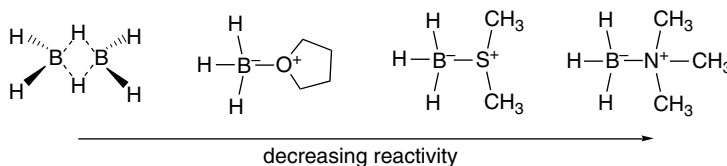
b. J. Kaneti, L. P. C. M. de Smet, R. Boom, H. Zuilhof, and E. J. R. Sudholter, *J. Phys. Chem. A*, **106**, 11197 (2002).

## 5.7. Synthesis and Reactions of Alkylboranes

Alkenes react with borane, BH<sub>3</sub>, and a number of its derivatives to give synthetically useful alkylboranes. Borane is an electron-deficient molecule and in its pure form exists as a hydrogen-bridged dimer.



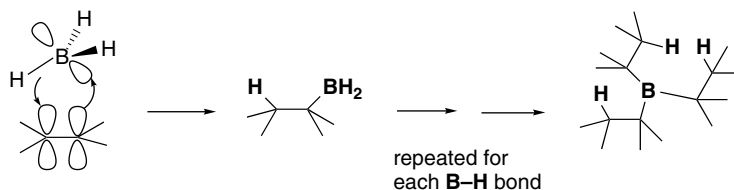
Borane reacts with electron pair donors to form Lewis acid-base complexes. The most common forms for use in synthesis are the THF and dimethyl sulfide complexes. Stronger bases, particularly amines, form less reactive adducts.



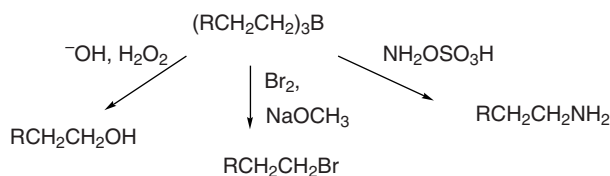
The addition of borane to alkenes is an electrophilic process, but it is concerted. The alkene donates electron density to the borane but a hydrogen shifts to carbon,

<sup>195</sup> J. Kaneti, L. C. P. M. de Smet, R. Boom, H. Zuilhof, and E. J. R. Sudholter, *J. Phys. Chem. A*, **106**, 11197 (2002).

resulting in an overall *syn* addition. In MO terms, the addition is viewed as taking place by interaction of the alkene  $\pi$  orbital with the vacant  $p$  orbital on boron, accompanied by concerted C–H bond formation by interaction with the empty  $\pi^*$  orbital.<sup>196</sup> Unhindered alkenes proceed to the trialkylborane stage by three successive additions.



As a result of a combination of steric and electronic factors, hydroboration is highly regioselective, with boron becoming bonded to the *less-substituted carbon*. The boron can eventually be replaced by hydroxy, carbonyl, amino, or halogen substituents. These reactions occur with retention of configuration. The overall transformations occur by *syn* addition with anti-Markovnikov regiochemistry.



### 5.7.1. Hydroboration

The synthetic applications of the hydroboration reaction are highly developed, largely through the work of H. C. Brown and his associates.<sup>197</sup> Hydroboration is one of the most widely applied of the alkene addition reactions for synthesis on a laboratory scale. Several aspects of the reaction are complementary to the reactions discussed earlier in this chapter. Hydroboration can be used to make alcohols and halides, and these reactions usually lead to the opposite (*anti*-Markovnikov) regiochemistry from reactions that proceed through cationic intermediates. Moreover, since there are no carbocation intermediates, there is no competition from rearrangement or elimination. The reactions are also stereospecific *syn* additions, as compared to the *anti* stereoselectivity for many reactions proceeding through cationic intermediates. On the basis of these contrasts, we might be inclined to think that hydroboration is fundamentally different from the other electrophilic addition reactions discussed in this chapter, but there are many similarities. At its outset, the hydroboration reaction involves an *electrophilic attack* on the  $\pi$  electrons of the alkene, just as is the case of the other reactions. The reaction is diverted to *syn* addition by the presence of the potentially

- <sup>196</sup> D. J. Pasto, B. Lepeska, and T.-C. Cheng, *J. Am. Chem. Soc.*, **94**, 6083 (1972); P. R. Jones, *J. Org. Chem.*, **37**, 1886 (1972); S. Nagase, K. N. Ray, and K. Morokuma, *J. Am. Chem. Soc.*, **102**, 4536 (1980); X. Wang, Y. Li, Y.-D. Wu, M. N. Paddon-Row, N. G. Rondan, and K. N. Houk, *J. Org. Chem.*, **55**, 2601 (1990); N. J. R. van Eikema Hommes and P. v. R. Schleyer, *J. Org. Chem.*, **56**, 4074 (1991).
- <sup>197</sup> G. Zweifel and H. C. Brown, *Org. React.*, **13**, 1 (1963); H. C. Brown, *Organic Synthesis via Boranes*, Wiley, New York, 1975; A. Pelter, K. Smith, and H. C. Brown, *Borane Reagents*, Academic Press, New York, 1988.

nucleophilic hydrogen on boron. As the electron-deficient boron bonds to one carbon, the hydrogen with two electrons shifts to the other carbon. The addition occurs through a four-center TS. Both the new C–B and C–H bonds are thus formed from the same side of the double bond.

Hydroboration is highly regioselective. The boron becomes bonded predominantly to the *less-substituted* carbon atom of the alkene. A *combination of steric and electronic effects* favors this orientation. Borane is an electrophilic reagent. The reaction with substituted styrenes exhibits a negative  $\rho$  value ( $-0.5$ ).<sup>198</sup> Compared with bromination ( $\rho^+ = -4.3$ ),<sup>199</sup> this is a weak substituent effect, but it does favor addition of the electrophilic boron at the more nucleophilic end of the double bond. In contrast to the case of addition of protic acids to alkenes, it is boron, not hydrogen, that is the more electrophilic atom. This electronic effect is reinforced by steric factors. Hydroboration is usually done under conditions in which the borane eventually reacts with three alkene molecules to give a trialkylborane. The second and third alkyl groups encounter severe steric repulsion if the boron is added at the internal carbon.

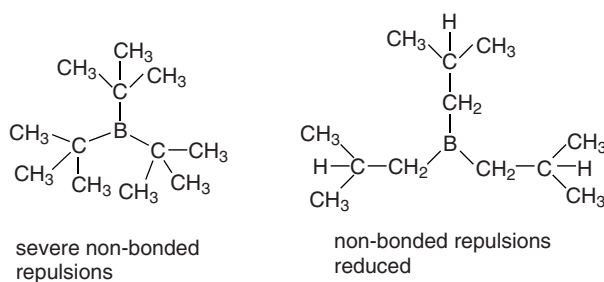


Table 5.7 provides some data on the regioselectivity of the addition of diborane and several of its derivatives to representative alkenes.

**Table 5.7. Regioselectivity of Diborane and Derivatives toward Representative Alkenes**

Hydroborating Reagent	Percent added at less-substituted carbon			
	1-Hexene	2-Methyl-1-Butene	4-Methyl-2-Pentene	Styrene
Diborane <sup>a</sup>	94	99	57	80
Chloroborane-dimethylsulfide <sup>b</sup>	99	99.5	—	98
Disiamylborane <sup>a</sup>	99	—	97	98
Thexylborane <sup>c</sup>	94	—	66	95
Chlorothexylborane-dimethylsulfide <sup>d</sup>	99	99	97	99
9-Borabicyclo[3.3.1]nonane (9-BBN) <sup>e</sup>	99.9	99.8 <sup>f</sup>	99.8	98.5

a. G. Zweifel and H. C. Brown, *Org. React.*, **13**, 1 (1963).

b. H. C. Brown, N. Ravindran, and S. U. Kulkarni, *J. Org. Chem.*, **44**, 2417 (1969); H. C. Brown and U. S. Racherla, *J. Org. Chem.*, **51**, 895 (1986).

c. H. C. Brown and G. Zweifel, *J. Am. Chem. Soc.*, **82**, 4708 (1960).

d. H. C. Brown, J. A. Sikorski, S. U. Kulkarni, and H. D. Lee, *J. Org. Chem.* **45**, 4540 (1980).

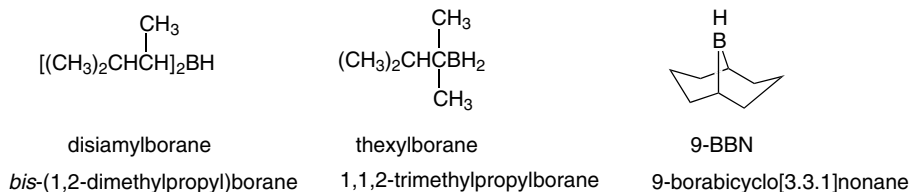
e. H. C. Brown, E. F. Knight, and C. G. Scouten, *J. Am. Chem. Soc.*, **96**, 7765 (1974).

f. Data for 2-methyl-1-pentene.

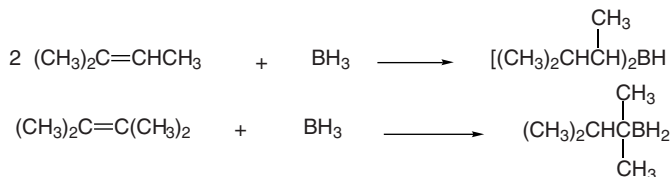
<sup>198</sup>. L. C. Vishwakarma and A. Fry, *J. Org. Chem.*, **45**, 5306 (1980).

<sup>199</sup>. J. A. Pincock and K. Yates, *Can. J. Chem.*, **48**, 2944 (1970).

Table 5.7 includes data for some mono- and dialkylboranes that show even higher regioselectivity than diborane itself. These derivatives are widely used in synthesis and are frequently referred to by the shortened names shown with the structures.



These reagents are prepared by hydroboration of the appropriate alkene, using control of stoichiometry to achieve the desired degree of alkylation. 9-BBN is prepared from 1,4-cyclooctadiene



As is true for most addition reactions, there is a preference for approach of the borane from the less hindered face of the double bond. Since diborane itself is a relatively small molecule, the stereoselectivity is not high for unhindered molecules. Table 5.8 gives some data comparing the direction of approach for three cyclic alkenes. The products in all cases result from *syn* addition, but the mixtures result from both the low regioselectivity and from addition to both faces of the double bond. Even 7,7-dimethylnorbornene shows only a modest preference for *endo* addition with diborane. The selectivity is much enhanced with the bulkier reagent 9-BBN.

The haloboranes  $\text{BH}_2\text{Cl}$ ,  $\text{BH}_2\text{Br}$ ,  $\text{BHCl}_2$ , and  $\text{BHBr}_2$  are also useful hydroborating reagents.<sup>200</sup> These compounds are somewhat more regioselective than borane itself, but otherwise show similar reactivity. The halogen(s) can be replaced by hydride and a second hydroboration step can then be carried out. This allows for preparation of unsymmetrically substituted boranes.

**Table 5.8. Stereoselectivity of Hydroboration with Cyclic Alkenes<sup>a</sup>**

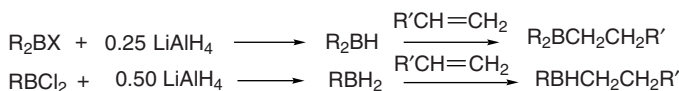
Hydroboration Reagent	Product composition <sup>b</sup>								
	3-Methyl- cyclopentene			3-Methyl- cyclohexene				7,7-Dimethyl norbornene	
	<i>trans</i> -2	<i>cis</i> -3	<i>trans</i> -3	<i>cis</i> -2	<i>trans</i> -2	<i>cis</i> -3	<i>trans</i> -3	<i>exo</i>	<i>endo</i>
Diborane	45		55	16	34	18	32	22 <sup>c</sup>	78 <sup>c</sup>
Disiamylborane	40		60	18	30	27	25	–	–
9-BBN	25	50	25	0	20	40	40	3	97

a. Data from H. C. Brown, R. Liotta, and L. Brenner, *J. Am. Chem. Soc.*, **99**, 3427 (1977), except where noted otherwise.

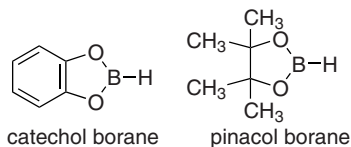
b. Product composition refers to the alcohols formed by subsequent oxidation.

c. H. C. Brown, J. H. Kawakami, and K.-T. Liu, *J. Am. Chem. Soc.*, **95**, 2209 (1973).

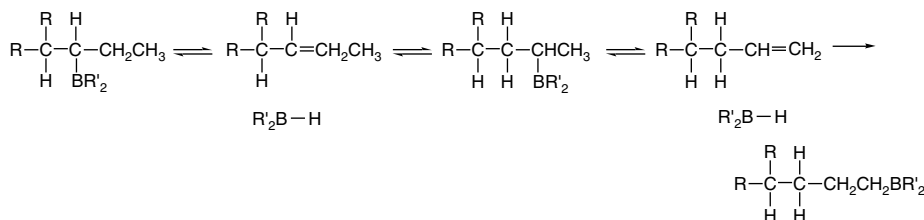
<sup>200</sup> H. C. Brown and S. U. Kulkarni, *J. Organomet. Chem.*, **239**, 23 (1982).



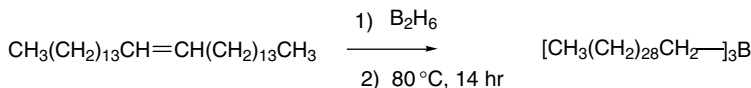
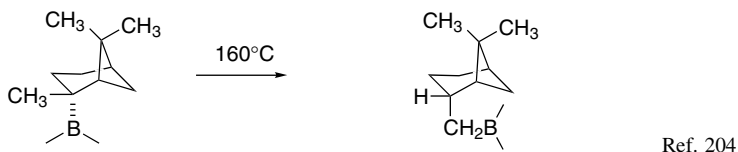
Catecholborane<sup>201</sup> and pinacolborane,<sup>202</sup> in which the boron has two oxygen substituents, are much less reactive hydroborating reagents than alkyl or haloboranes. The boron electron deficiency is attenuated by the oxygen atoms. Nevertheless, they are useful reagents for certain applications. The reactivity of catecholborane has been found to be substantially enhanced by addition of 10–20% of *N,N*-dimethylacetamide to  $CH_2Cl_2$ .<sup>203</sup>



Hydroboration is thermally reversible. At 160°C and above, B–H moieties are eliminated from alkylboranes, but the equilibrium is still in favor of the addition products. This provides a mechanism for migration of the boron group along the carbon chain by a series of eliminations and additions.



Migration cannot occur past a quaternary carbon, however, since the required elimination is blocked. At equilibrium, the major trialkylborane is the least-substituted terminal isomer that is accessible, because it is the one that minimizes unfavorable steric interactions. The availability of the isomerization provides a means for *thermodynamic control* of the hydroboration reaction.



Ref. 205

201. H. C. Brown and S. K. Gupta, *J. Am. Chem. Soc.*, **97**, 5249 (1975); H. C. Brown and J. Chandrasekharan, *J. Org. Chem.*, **48**, 5080 (1983).

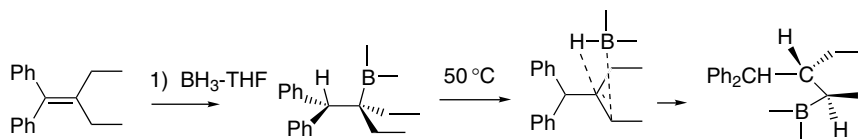
202. C. E. Tucker, J. Davidson, and P. Knochel, *J. Org. Chem.*, **57**, 3482 (1992).

203. C. E. Garrett and G. C. Fu, *J. Org. Chem.*, **61**, 3224 (1996).

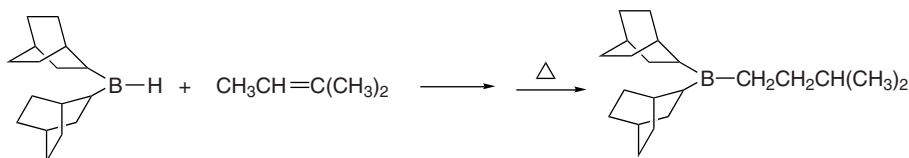
204. G. Zweifel and H. C. Brown, *J. Am. Chem. Soc.*, **86**, 393 (1964).

205. K. Maruyama, K. Terada, and Y. Yamamoto, *J. Org. Chem.*, **45**, 737 (1980).

Migrations are especially facile for *tetra*-substituted alkenes; they occur at 50–60°C and exhibit both regio- and stereoselectivity. The course of the reactions is dictated by the relative energy of the reversibly formed borane alkene complexes.<sup>206</sup>

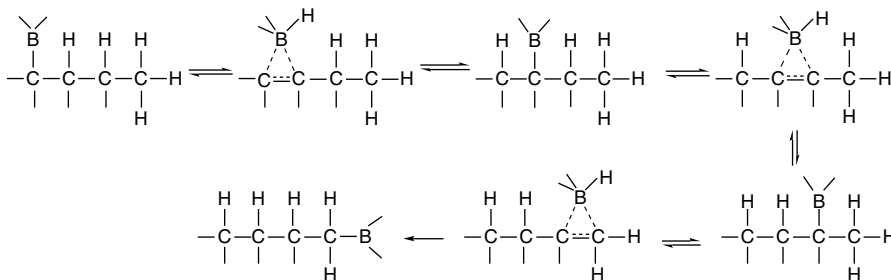


Unstrained bicyclic rings have little tendency to rearrange. *bis*-Bicyclo[2.2.2]octanylborane has been found to be particularly useful for formation and isomerization of monoalkyl derivatives.



Ref. 207

There is evidence that boron migration occurs *intramolecularly*.<sup>208</sup> A TS that describes this process has been located computationally (Figure 5.6).<sup>209</sup> It involves an electron-deficient  $\pi$ -complex about 20–25 kcal above the trialkylborane. These structures are analogous to the bridged carbocations in carbocation rearrangements. The boron can migrate to the end of the chain through a series of such structures.



### 5.7.2. Reactions of Organoboranes

Alkylboranes are very useful intermediates in organic synthesis. In this section we discuss methods by which the boron atom can be efficiently replaced by hydroxy,

<sup>206</sup> L. O. Bromm, H. Laaziri, F. Lhermitte, K. Harms, and P. Knochel, *J. Am. Chem. Soc.*, **122**, 10218 (2000).

<sup>207</sup> H. C. Brown and U. S. Racherla, *J. Am. Chem. Soc.*, **105**, 6506 (1983).

<sup>208</sup> S. E. Wood and B. Rickborn, *J. Org. Chem.*, **48**, 555 (1983).

<sup>209</sup> N. J. R. van Eikema Hommes and P. v. R. Schleyer, *J. Org. Chem.*, **56**, 4074 (1991).

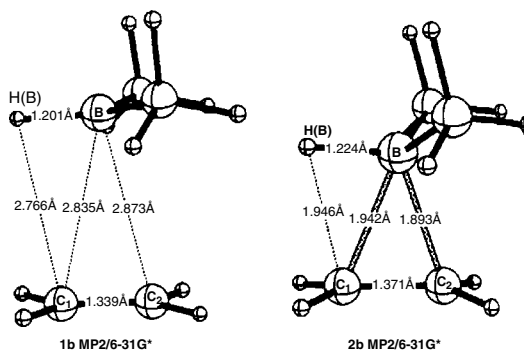
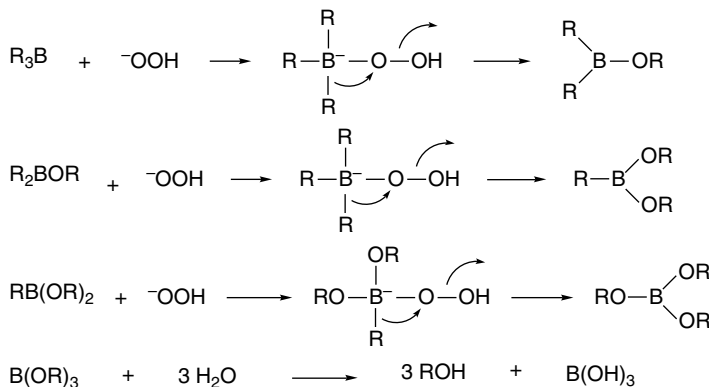


Fig. 5.6. Geometries (MP2/6-31G\*) of (a)  $\pi$  complex and (b) transition state in reaction of ethene and dimethylborane. Reproduced from *J. Org. Chem.*, **56**, 4074 (1991), by permission of the American Chemical Society.

halogen, or amino groups. There are also important processes that use alkylboranes in the formation of new carbon-carbon bonds, and these reactions are discussed in Chapter 9 of Part B. The most widely used reaction of organoboranes is the oxidation to alcohols. Alkaline hydrogen peroxide is the reagent usually employed to effect the oxidation. The trialkylborane is converted to a trialkoxyborane (trialkyl borate) by a series of B  $\rightarrow$  O migrations. The R–O–B bonds are hydrolyzed in the alkaline aqueous solution, generating the alcohol. The mechanism is outlined below.



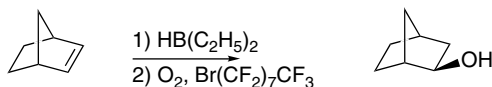
The stereochemical outcome is replacement of the C–B bond by a C–O bond with retention of configuration. In combination with the stereospecific *syn* hydroboration, this allows the structure and stereochemistry of the alcohols to be predicted with confidence. The preference for boronation at the less-substituted carbon of a double bond results in the alcohol being formed with regiochemistry that is complementary to that observed by direct hydration or oxymercuration, i.e., anti-Markovnikov.

Conditions that permit oxidation of organoboranes to alcohols using other oxidants, including molecular oxygen,<sup>210</sup> sodium peroxycarbonate,<sup>211</sup> or amine

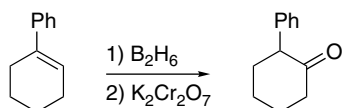
<sup>210</sup>. H. C. Brown, M. M. Midland, and G. W. Kabalka, *J. Am. Chem. Soc.* **93**, 1024 (1971).

<sup>211</sup>. G. W. Kabalka, P. P. Wadgaonkar, and T. M. Shoup, *Tetrahedron Lett.*, **30**, 5103 (1989).

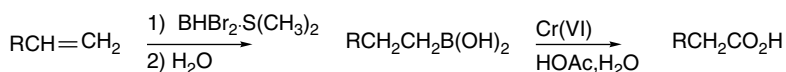
oxides<sup>212</sup> have been developed. Oxone<sup>®</sup> has been recommended for oxidations done on a large scale.<sup>213</sup> The reaction with molecular oxygen is particularly effective in perfluoroalkane solvents.<sup>214</sup>



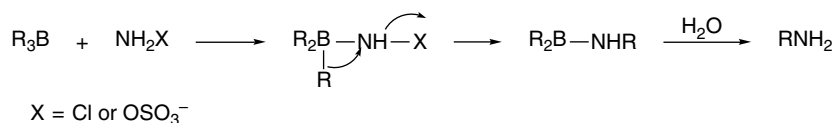
More vigorous oxidizing agents such as Cr(VI) reagents effect replacement of boron with oxidation to the carbonyl level.<sup>215</sup>



An alternative procedure for oxidation to ketones involves treatment of the alkylborane with a quaternary ammonium perruthenate salt and an amine oxide.<sup>216</sup> Use of dibromoborane-dimethyl sulfide for hydroboration of terminal alkenes followed by hydrolysis and Cr(VI) oxidation gives carboxylic acids.<sup>217</sup>



The boron atom can also be replaced by an amino group.<sup>218</sup> The reagents that effect this conversion are chloramine or hydroxylamine-*O*-sulfonic acid. The mechanisms of these reactions are very similar to that of the hydrogen peroxide oxidation of organoboranes. The nitrogen-containing reagent initially reacts as a nucleophile by adding at boron; then a B → N shift occurs with expulsion of chloride or sulfate. As in the oxidation, the migration step occurs with retention of configuration. The amine is freed from the borane by hydrolysis.



Secondary amines are formed by reaction of boranes with alkyl or aryl azides. The most efficient borane reagents are monoalkyldichloroboranes, which are generated by

<sup>212</sup> G. W. Kabalka and H. C. Hedgecock, Jr., *J. Org. Chem.*, **40**, 1776 (1975); R. Koster and Y. Monta, *Justus Liebigs Ann. Chem.*, **704**, 70 (1967).

<sup>213</sup> D. H. B. Ripin, W. Cai, and S. T. Brenek, *Tetrahedron Lett.*, **41**, 5817 (2000).

<sup>214</sup> I. Klement and P. Knochel, *Synlett*, 1004 (1996).

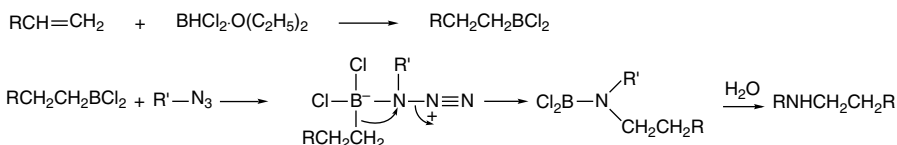
<sup>215</sup> H. C. Brown and C. P. Garg, *J. Am. Chem. Soc.*, **83**, 2951 (1961); H. C. Brown, C. Rao, and S. Kulkarni, *J. Organomet. Chem.*, **172**, C20 (1979).

<sup>216</sup> M. H. Yates, *Tetrahedron Lett.*, **38**, 2813 (1997).

<sup>217</sup> H. C. Brown, S. V. Kulkarni, V. V. Khanna, V. D. Patil, and U. S. Racherla, *J. Org. Chem.*, **57**, 6173 (1992).

<sup>218</sup> M. W. Rathke, N. Inoue, K. R. Varma, and H. C. Brown, *J. Am. Chem. Soc.*, **88**, 2870 (1966); G. W. Kabalka, K. A. R. Sastry, G. W. McCollum, and H. Yoshioka, *J. Org. Chem.*, **46**, 4296 (1981).

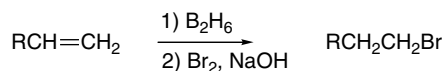
the reaction of an alkene with  $\text{BHCl}_2 \cdot \text{Et}_2\text{O}$ .<sup>219</sup> The entire sequence of steps and the mechanism of the final stages are summarized by the equation below.



Secondary amines can also be made using the *N*-chloro derivatives of primary amines.<sup>220</sup>

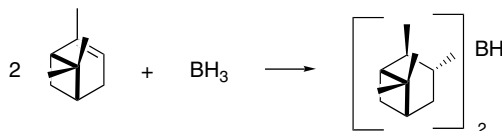


Organoborane intermediates can also be used to synthesize alkyl halides. Replacement of boron by iodine is rapid in the presence of base.<sup>221</sup> The best yields are obtained using sodium methoxide in methanol.<sup>222</sup> If less basic conditions are desirable, the use of iodine monochloride and sodium acetate gives good yields.<sup>223</sup> As is the case in hydroboration-oxidation, the regioselectivity of hydroboration-halogenation is opposite to that observed with direct ionic addition of hydrogen halides to alkenes. Terminal alkenes give primary halides.



### 5.7.3. Enantioselective Hydroboration

Several alkylboranes are available in enantiomerically enriched or pure form and they can be used to prepare enantiomerically enriched alcohols and other compounds from organoborane intermediates.<sup>224</sup> The most thoroughly investigated of these boranes is *bis*-(isopinocampheyl)borane,  $(\text{Ipc})_2\text{BH}$ , which can be prepared in 100% enantiomeric purity from the readily available terpene  $\alpha$ -pinene.<sup>225</sup> Both enantiomers are available.



<sup>219</sup>. H. C. Brown, M. M. Midland, and A. B. Levy, *J. Am. Chem. Soc.*, **95**, 2394 (1973).

<sup>220</sup>. G. W. Kabalka, G. W. McCollum, and S. A. Kunda, *J. Org. Chem.*, **49**, 1656 (1984).

<sup>221</sup>. H. C. Brown, M. W. Rathke, and M. M. Rogic, *J. Am. Chem. Soc.*, **90**, 5038 (1968).

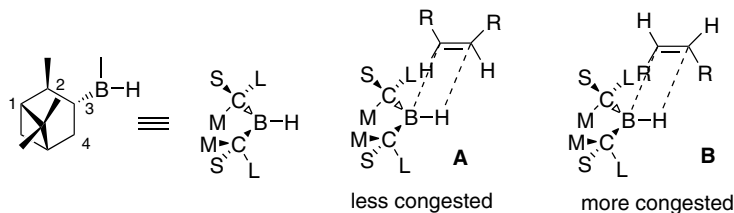
<sup>222</sup>. N. R. De Lue and H. C. Brown, *Synthesis*, 114 (1976).

<sup>223</sup>. G. W. Kabalka and E. E. Gooch, III, *J. Org. Chem.*, **45**, 3578 (1980).

<sup>224</sup>. H. C. Brown and B. Singaram, *Acc. Chem. Res.*, **21**, 287 (1988); D. S. Matteson, *Acc. Chem. Res.*, **21**, 294 (1988).

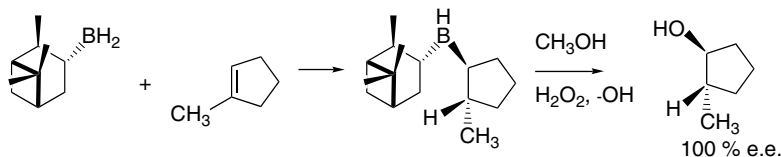
<sup>225</sup>. H. C. Brown, P. K. Jadhav, and A. K. Mandal, *Tetrahedron*, **37**, 3547 (1981); H. C. Brown and P. K. Jadhav, in *Asymmetric Synthesis*, Vol. 2, J. D. Morrison, ed., Academic Press, New York, 1983, Chap. 1.

(*Ip*c)<sub>2</sub>BH adopts a conformation that minimizes steric interactions. This conformation can be represented schematically, where the *S*, *M*, and *L* substituents are, respectively, the 3-H, 4-CH<sub>2</sub>, and 2-CHCH<sub>3</sub> groups of the carbocyclic structure. The steric environment at boron in this conformation is such that *Z*-alkenes encounter less steric encumbrance in TS **A** than in **B**.

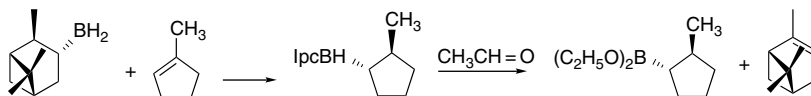


*Z*-2-Butene undergoes hydroboration with 98% enantioselectivity with (*Ip*c)<sub>2</sub>BH.<sup>226</sup> Other *Z*-disubstituted alkenes give good enantioselectivity (75–90%) but *E*-alkenes and simple cycloalkenes give low enantioselectivity (5–30%).<sup>227</sup>

Monoisopinocampheylborane (*Ip*cBH<sub>2</sub>) can be prepared in enantiomerically pure form by purification of its TMEDA adduct.<sup>228</sup> When this monoalkylborane reacts with a prochiral alkene, one of the diastereomeric products is normally formed in excess and can be obtained in high enantiomeric purity by an appropriate separation.<sup>229</sup> Oxidation of the borane then provides the corresponding enantiomerically enriched alcohol.



As direct oxidation also converts the original chiral terpene-derived group to an alcohol, it is not directly reusable as a chiral auxiliary. Although this is not a problem with inexpensive materials, the overall efficiency of generation of enantiomerically pure product is improved by procedures that can regenerate the original terpene. This can be done by heating the dialkylborane intermediate with acetaldehyde. The  $\alpha$ -pinene is released and a diethoxyborane is produced.<sup>230</sup> The usual oxidation conditions then convert this boronate ester to an alcohol.<sup>231</sup>



<sup>226</sup> H. C. Brown, M. C. Desai, and P. K. Jadhav, *J. Org. Chem.*, **47**, 5065 (1982).

<sup>227</sup> H. C. Brown, P. K. Jadhav, and A. K. Mandal, *J. Org. Chem.*, **47**, 5074 (1982).

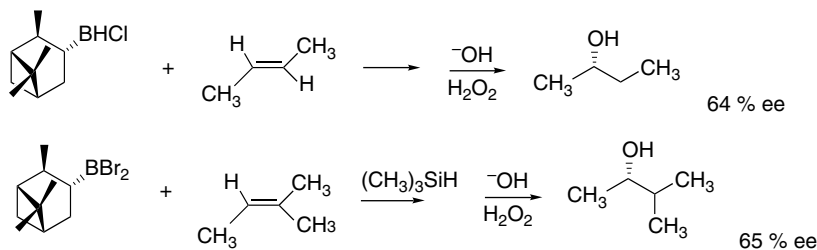
<sup>228</sup> H. C. Brown, J. R. Schwier, and B. Singaram, *J. Org. Chem.*, **43**, 4395 (1978); H. C. Brown, A. K. Mandal, N. M. Yoon, B. Singaram, J. R. Schwier, and P. K. Jadhav, *J. Org. Chem.*, **47**, 5069 (1982).

<sup>229</sup> H. C. Brown and B. Singaram, *J. Am. Chem. Soc.*, **106**, 1797 (1984); H. C. Brown, P. K. Jadhav, and A. K. Mandal, *J. Org. Chem.*, **47**, 5074 (1982).

<sup>230</sup> H. C. Brown, B. Singaram, and T. E. Cole, *J. Am. Chem. Soc.*, **107**, 460 (1985); H. C. Brown, T. Imai, M. C. Desai, and B. Singaram, *J. Am. Chem. Soc.*, **107**, 4980 (1985).

<sup>231</sup> D. S. Matteson and K. M. Sadhu, *J. Am. Chem. Soc.*, **105**, 2077 (1983).

The corresponding haloboranes are also useful for enantioselective hydroboration. Isopinocampheylchloroborane can achieve 45–80% e.e. with representative alkenes.<sup>232</sup> The corresponding bromoborane achieves 65–85% enantioselectivity with simple alkenes when used at  $-78^{\circ}\text{C}$ .<sup>233</sup>



## 5.8. Comparison of Electrophilic Addition Reactions

In this section, we make some broad comparisons among the electrophilic addition reactions that have been discussed. We have presented data on substituent effects, regioselectivity, and stereochemistry for protonation, halogenation, sulfenylation and selenenylation, epoxidation, mercuration, and hydroboration. What general trends and insights can be gained by comparing these reactions? There have been several efforts at elucidating correlations among the different reactions. Fukuzumi and Kochi showed that when steric effects are considered in a quantitative way, there is a strong correlation between bromination and mercuration rates.<sup>234</sup> Nelson and co-workers examined most of the reaction series and found correlations between the reactivity of various alkenes and the IP of the alkene. For some of these correlations, there were separate lines for mono-, di-, and trisubstituted alkenes, reflecting different steric environments.<sup>235</sup> We take a similar but less detailed look at relative reactivity of several representative alkenes. Figure 5.7 is a graph of the relative reactivity (with ethene as the standard) for the various reactions. The log of the relative reactivity, as shown in Table 5.9, is plotted against alkene IP. A separate symbol is used for each reaction. The alkenes are in order of decreasing IP.

We make comparisons based on these data in very broad terms. Looking first at protonation, represented in Figure 5.7 by circles, we see that reactivity rises sharply with substitution from ethene to propene to 2-methylpropene, but 2-methyl-2-butene and 2,3-dimethyl-2-butene have rates roughly similar to 2-methylpropene. *The degree of substitution at the more-substituted carbon is the major factor in reactivity.* We can surmise from this trend that *carbocation stability* is the major factor in determining the protonation rates. Note also that styrene is *more reactive* than propene, again consistent with carbocation stability as the major influence on reactivity. In terms of the Hammond postulate, the carbocation is a good model of the TS because the protonation step is substantially *endothermic* and the TS is late.

<sup>232</sup>. U. P. Dhokte, S. V. Kulkarni, and H. C. Brown, *J. Org. Chem.*, **61**, 5140 (1996).

<sup>233</sup>. U. P. Dhokte and H. C. Brown, *Tetrahedron Lett.*, **37**, 9021 (1996).

<sup>234</sup>. S. Fukuzumi and J. K. Kochi, *J. Am. Chem. Soc.*, **103**, 2783 (1981).

<sup>235</sup>. (a) D. J. Nelson and R. Soundararajan, *Tetrahedron Lett.*, **29**, 6207 (1988); (b) D. J. Nelson, P. J. Cooper, and R. Soundararajan, *J. Am. Chem. Soc.*, **111**, 1414 (1989); (c) D. J. Nelson, R. Li, and C. N. Brammer, *J. Org. Chem.*, **66**, 2422 (2001).

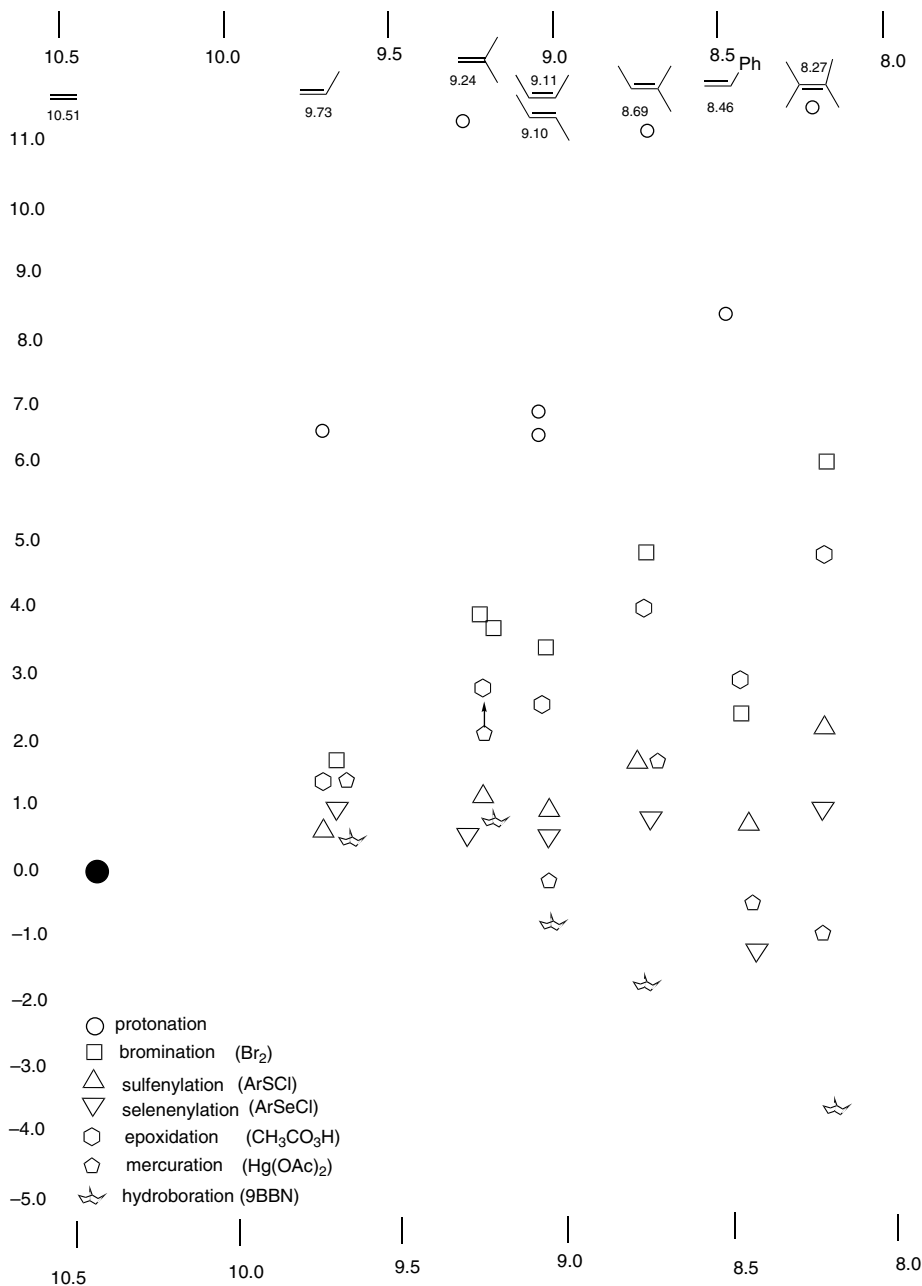


Fig. 5.7. Relationship between reactivity and IP for several alkenes.

Moving to bromination, represented by squares in the figure, we again see an increase of reactivity with alkyl substitution. Now, however, the *total number of substituents is important*. The rate continues to increase as substitution increases from ethene through 2,3-dimethyl-2-butene. This pattern is consistent with the more symmetrical (bridged) nature of the rate-determining TS. All of the substituents contribute to stabilization.

Table 5.9. Log of Relative Reactivity of Representative Alkenes.

Alkene	IP(ev) <sup>a</sup>	H <sup>+b</sup>	Br <sub>2</sub> <sup>c</sup>	ArSCl <sup>d</sup>	ArSeCl <sup>d</sup>	RCO <sub>3</sub> H <sup>e</sup>	Hg <sup>2+f</sup>	9-BBN <sup>g</sup>
Ethene	10.51	0	0	0	0	0	0	—
Propene	9.73	6.2	1.8	0.50	0.94	1.3	1.3	0.3
2-Methylpropene	9.24	11.5	3.7	0.93	0.83	2.5	>2	0.6
Z-2-Butene	9.11	6.0	3.4	1.30	0.57	2.3	0.04	-1.0
E-2-Butene	9.10	6.4	3.2	0.82	0.32	2.3	-0.5	
Z-3-Hexene	9.0 <sup>h</sup>							-1.2
E-3-Hexene	9.0 <sup>h</sup>							-1.5
Cyclohexene	8.95	7.5				2.8	0.0	
2-Methyl-2-butene	8.69	11.2	5.1	1.6	0.57	3.8	1.6	-2.0
Styrene	8.46	8.2	2.4 <sup>i</sup>	-0.03	-1.3	2.7	-0.6	
2,3-Dimethyl-2-butene	8.27	11.3	6.0	2.1	0.39	4.8	-1.2	-4.2

a. D. R. Lide, ed., *Handbook of Chemistry and Physics*, 83rd Edition, CRC Press, Boca Raton, FL, 2002, Sec. 10.

b. W. W. Chwang, V. J. Nowlan, and T. T. Tidwell, *J. Am. Chem. Soc.*, **99**, 7233 (1977); P. Knittel and T. T. Tidwell, *J. Am. Chem. Soc.* **99**, 3408 (1977)

c. J. E. Dubois and G. Mouvier, *Bull. Soc. Chim. Fr.*, 1426 (1968).

d. G. H. Schmid and D. G. Garratt, in *The Chemistry of Double-Bonded Functional Groups*, Supplement A, Part 2, S. Patai, ed., Wiley, New York, 1977, Chap. 9.

e. M. H. Khalil and W. Pritzkow, *J. Prakt. Chem.*, **315**, 58 (1973); The 2-butene data is for Z- and E-2-pentene.

f. R. C. Larock, *Solvolmercurat/Demercurat Reactions in Organic Synthesis*, Springer-Verlag, Berlin, 1986, pp. 86–87.

g. D. J. Nelson, P. J. Cooper, and R. Soundararajan, *J. Am. Chem. Soc.*, **111**, 1414 (1989). The relative rates for ethene, propene and 2-methylpropene are not available. The relative rate of propene was taken as equal to that of 1-hexene and estimated as 0.5. The value listed for 2-methylpropene is that given for 2-methyl-2-pentene.

h. Estimated from the tabulated value for the 2-hexene isomers.

i. M.-F. Ruasse, J. E. Dubois, and A. Argile, *J. Org. Chem.*, **44**, 1173 (1979).

The most noteworthy feature of the sulfenylation and selenenylation rates (represented by the triangles) is their much diminished sensitivity to substitution. This reflects both smaller electron demand in the TS and increased sensitivity to steric factors. The relatively low rate of styrene toward selenenylation is somewhat of an anomaly, and may reflect both ground state stabilization and steric factors in the TS. The epoxidation data (CH<sub>3</sub>CO<sub>3</sub>H, hexagons) show a trend similar to bromination, but with a reduced slope. There is no evidence of a rate-retarding steric component. One indicator of a strong steric component is decreased reactivity of the E-isomer in an E,Z-disubstituted alkene pair, but the rates for the 2-butene isomers toward epoxidation are very similar (Table 5.9).

Mercurat exhibits a carbocation-like pattern, but with the superposition of a large steric effect. For unsubstituted terminal carbons, the rate increases from ethene to propene to 2-methylpropene. This trend also holds for internal alkenes, as 2-methyl-2-butene is more reactive than 2-butene. However, steric effects become dominant for 2,3-dimethylbutene. This incursion of steric effects in oxymercurat has long been recognized and is exemplified by the results of Nelson and co-workers, who found separate correlation lines for mono- and disubstituted alkenes.<sup>235b</sup> Hydroborat by 9-BBN (structures) shows a different trend: steric effects are dominant and reactivity decreases with substitution. Similar trends apply to rates of addition of dibromoborane<sup>236</sup> and disiamylborane.<sup>237</sup> The importance of steric factors is no doubt due in part to the relatively bulky nature of these boranes. However, it also reflects a decreased electron demand in the hydroborat TS.

<sup>236</sup>. H. C. Brown and J. Chandrasekharan, *J. Org. Chem.*, **48**, 644 (1983).

<sup>237</sup>. J. Chandrasekharan and H. C. Brown, *J. Org. Chem.*, **50**, 518 (1985).

An overall perspective of the data in Table 5.9 and Figure 5.7 can be gained by simply comparing the relative rates of ethene and 2,3-dimethyl-2-butene. These go from very large for protonation ( $10^{11.4}$ ) to small ( $10^{-4.2}$ ) for hydroboration by 9-BBN as the dominance of carbocation stability effects for protonation is replaced by dominant steric effects for hydroboration by 9-BBN.

Another useful perspective from which to compare the electrophilic addition reactions is to focus on structure of the TS and intermediates. Figure 5.8 arranges the

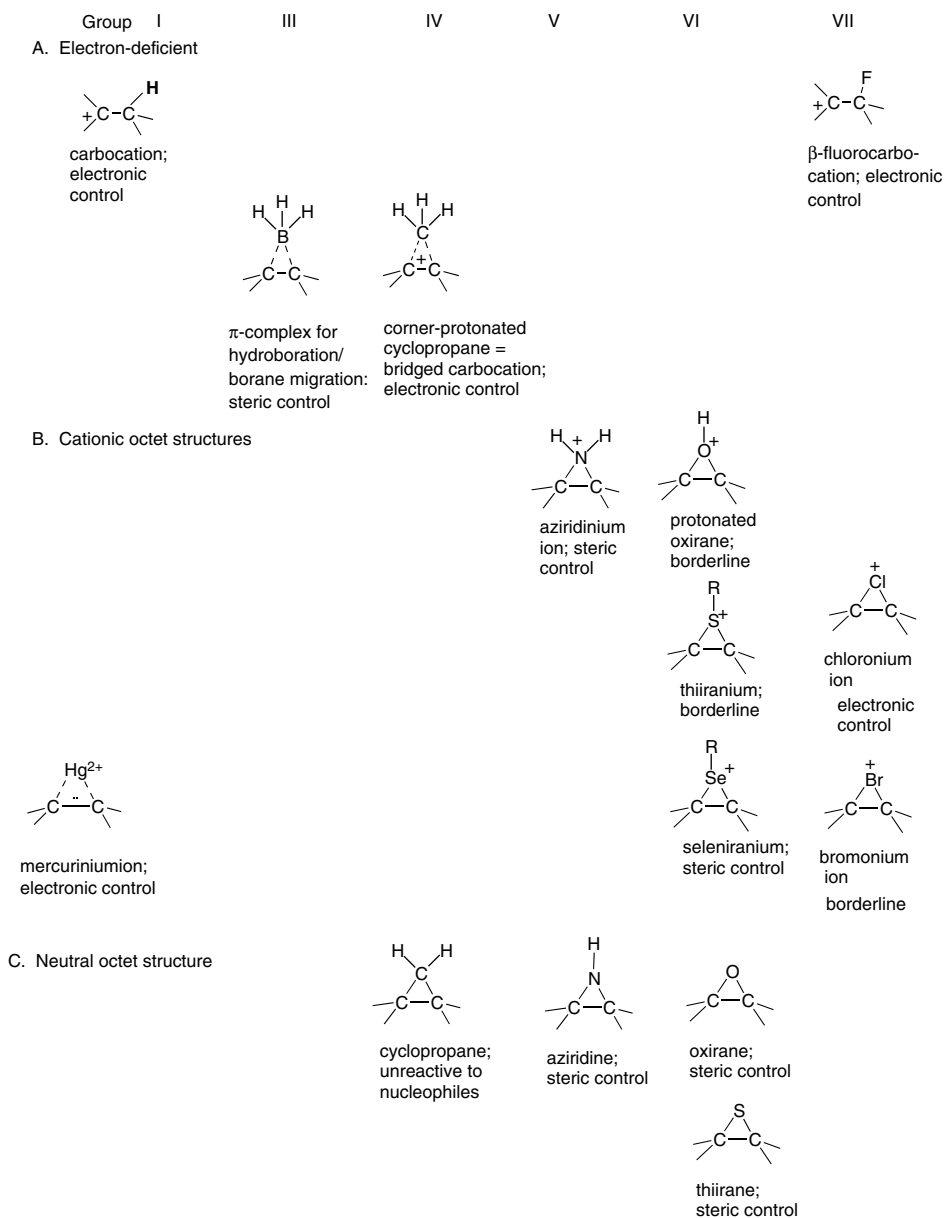
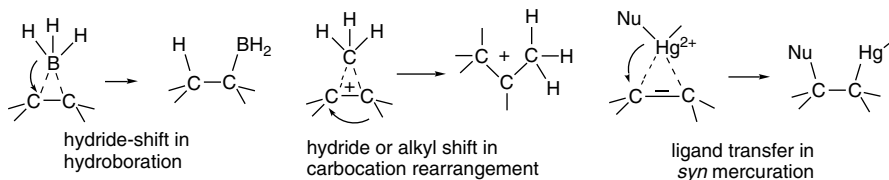


Fig. 5.8. Relationship between small ring structures and regiochemistry of addition reactions.

cationic and neutral species in relation to the periodic table. Some of these structures are stable products, others are reaction intermediates, and still other are transition structures. If the bridged and open versions of a species are comparable in energy, both are shown.

Taking the view that protonation of alkenes gives open carbocations, at least in solution, gives us a starting point for comparing the various addition reaction intermediates. From the discussion of carbocations in Chapter 4, we know the reactions that are characteristic of carbocations, namely nucleophilic capture, elimination of a proton, and rearrangement. These reactions are controlled by *electronic factors*, as illustrated by Markovnikov regioselectivity for nucleophile capture and Saytzeff regiochemistry for elimination. (see Section 4.4.3) The TSs for hydroboration and protonated cyclopropanes are related to open carbocations in being *electron deficient*. The hydroboration TS collapses by a hydride shift from boron to carbon that is driven by both electronegativity and steric factors. Corner-protonated cyclopropanes are converted to the carbocation best able to support positive charge. It is also clear from the mercuriation reaction that a ligand transfer process is available when *anti*-nucleophilic addition is sterically hindered. The *syn* addition is similar to the hydride migration that occurs during hydroboration. The regiochemistry of the migration is dictated by electronic factors.



Moving to the right in the periodic table, aziridinium ions and protonated epoxides are no longer electron deficient, although they are electrophilic. Ring opening of aziridinium ions is normally controlled by *steric access*, because of the need for nucleophilic participation.<sup>238</sup> The regioselectivity of solvo-fluorination, by contrast, is subject to electronic control and strictly follows Markovnikov's rule because of the carbocationic character of the species (see p. 496). An O-protonated or Lewis acid-activated oxirane is borderline, with instances of both Markovnikov and anti-Markovnikov ring opening (see Section 5.5.2).

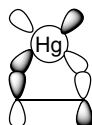
When we drop down to the next two rows of the periodic table, bridging becomes more important. For chloronium ions and bromonium ions (as in halohydrin formation; see p. 492), Markovnikov orientation (electronic control) usually prevails because the bridging bonds are relatively weak. However, the mixed regiochemistry of methoxybromination in methanol is an exception (see p. 493). For sulfenylation and selenenylation, the bridging bonds are stronger and anti-Markovnikov regiochemistry is frequently observed because nucleophilic engagement (steric access) is a critical feature for ring opening (see p. 499, 502). For the neutral small rings, cyclopropane is resistant to nucleophilic attack. Aziridines and epoxides are successively more reactive toward nucleophiles, but the regiochemistry is controlled by steric approach factors.

The proton that initiates acid-catalyzed addition processes is a hard acid and has no unshared electrons. It can form either a carbocation or a hydrogen-bridged cation. Both species are *electron deficient* and highly reactive. The formation of the cationic

<sup>238</sup> C. M. Rayner, *Synlett*, 11 (1997).

intermediate is rate determining and nucleophilic capture is fast. The positive bromine in a bromonium ion intermediate is a softer electrophile and also has unshared electron pairs that permit a total of *four electrons* to participate in the bonding. The bromonium ion can be represented as having two covalent bonds to bromine and is *electrophilic* but not *electron deficient*. This results in a more strongly bridged and more stable species than is possible for the proton.

Where do mercuriation reactions fit into this picture? A mercurinium ion has both similarities and differences, as compared with the intermediates that have been described for other electrophilic additions. The electrophile in oxymercuration reactions,  $^+\text{HgX}$  or  $\text{Hg}^{2+}$ , is a soft Lewis acid and polarizes the  $\pi$ -electrons of an alkene to the extent that a three-center two-electron bond is formed between mercury and the two carbons of the double bond. However, there is also back bonding from  $\text{Hg}^{2+}d$  orbitals to the alkene  $\pi^*$  orbital. There is weaker bridging in the mercurinium ion than in the three-center four-electron bonding of the bromonium ion.



Cremer and Kraka have provided another perspective on the nature of some the cyclic structures represented in Figure 5.9 by focusing on the bond paths for the three-membered ring.<sup>239</sup> (See p. 63 to review the discussion of bond paths.) Neutral cyclopropane, aziridine, and oxirane rings are well described by the bent bond model, but the C–O bonds are somewhat less bent than those in cyclopropane. On the other hand, in protonated oxirane, the bonds begin to bend inward. For the bridged-fluorine species, there is no longer a ring; instead the structure is that of a  $\pi$  complex. (Remember, however, from p. 495 that a bridged fluoronium ion is unstable relative to the corresponding carbocation.) The differences in the nature of the bonds result from the relative ability of the bridging atom to donate electron density to the ring-forming orbitals, which is in the order  $\text{CH}_2 > \text{NH} > \text{O} > \text{O}^+\text{H} > \text{F}^+$ . These ideas are summarized in Figures 5.9.

## 5.9. Additions to Alkynes and Allenes

Reactions of alkynes with electrophiles are generally similar to those of alkenes. Since the HOMO of alkynes is also a  $\pi$  type orbital, it is not surprising that there is a good deal of similarity to the reactivity of alkenes.<sup>240</sup> The fundamental questions about additions to alkynes include the following: How reactive are alkynes in comparison with alkenes? What is the stereochemistry of additions to alkynes? What is the regiochemistry of additions to alkynes? The important role of bridged ions in addition reactions of alkenes raises the question of whether similar species are involved with alkynes, where the ring includes a double bond and bridged intermediates and would be expected to be substantially more strained.

<sup>239</sup> D. Cremer and E. Kraka, *J. Am. Chem. Soc.*, **107**, 3800 (1985).

<sup>240</sup> G. H. Schmid, *The Chemistry of the Carbon-Carbon Triple Bond*, Part. 1, S. Patai, ed., Wiley, New York, 1978, Chap. 3.

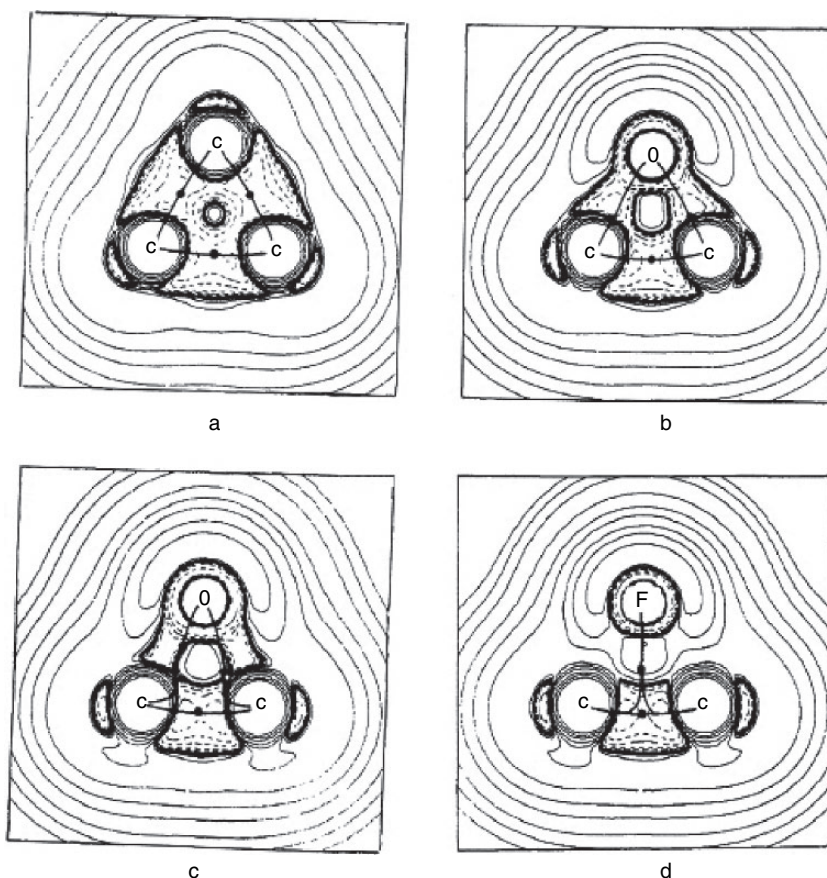
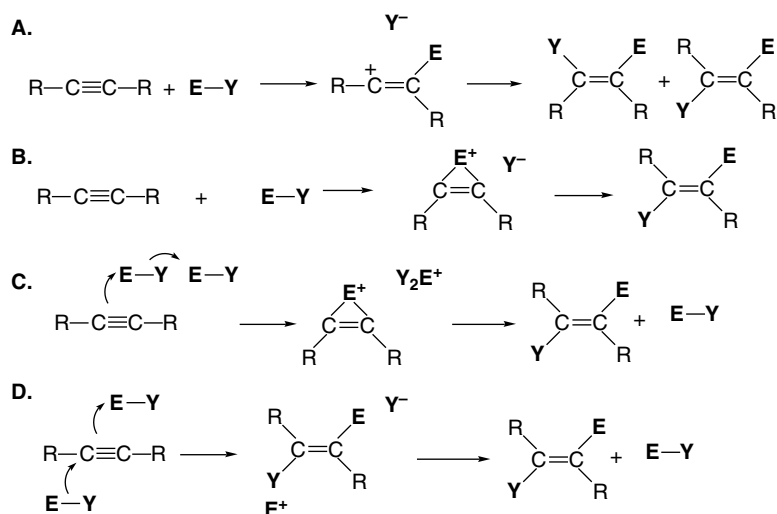


Fig. 5.9. Molecular graphs showing the Laplacian  $-\nabla^2\rho(\mathbf{r})$  and bond paths. Bond paths are shown as solid lines and bond critical points as dots. Dashed contours show areas of electronic charge concentration and solid contours show regions of charge depletion. (a) cyclopropane, (b) oxirane, (c) protonated oxirane, and (d) fluorine-bridged cation. Reproduced from *J. Am. Chem. Soc.*, **107**, 3800 (1985), by permission of the American Chemical Society.



The basic mechanisms that are considered to be involved in electrophilic additions to alkynes are outlined below. The first involves a discrete vinyl cation. In general, this reaction will lead to a mixture of the two stereoisomeric addition products. Mechanisms **B** and **C** depict bridged intermediates formed without (**B**) or with (**C**) participation of a second electrophilic molecule. Mechanisms **B** and **C** should lead to *anti* addition. Mechanism **D** is a termolecular process that would be expected to be a stereospecific *anti* addition. Mechanisms **A** and **B** are of the  $\text{Ad}_E2$  type, whereas **C** and **D** are classified as  $\text{Ad}_E3$ . Each of these mechanisms may involve a prior complex formation between the alkyne and an electrophile.



In general, alkynes are somewhat less reactive than alkenes toward many electrophiles. A major reason for this difference in reactivity is the substantially higher energy of the vinyl cation intermediate that is formed by an electrophilic attack on an alkyne. It is estimated that vinyl cations are about 10 kcal/mol less stable than an alkyl cation with similar substitution (see p. 300). For additions that proceed through bridged intermediates, the alkynes are also less reactive because of additional strain in the intermediate. The differences in the rate of addition between alkenes and alkynes depends upon the specific electrophile and the reaction conditions.<sup>241</sup> Table 5.10 summarizes some specific rate comparisons. These results show large differences for bromination and chlorination but relatively small differences for protonation. The presence of a carbocation-stabilizing phenyl group reduces the difference for bromination and chlorination.

### 5.9.1. Hydrohalogenation and Hydration of Alkynes

Hydrogen chloride adds to aryl alkynes in acetic acid to give mixtures of  $\alpha$ -chlorostyrenes and the corresponding vinyl acetate.<sup>242</sup> A vinyl cation, which is stabilized by the aryl substituent, is believed to be an intermediate. The ion pair formed by

**Table 5.10. Relative Reactivity of Alkenes and Alkynes<sup>a</sup>**

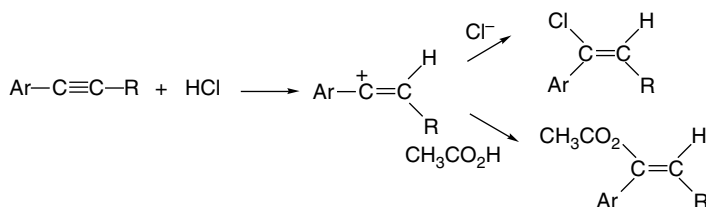
Alkene/alkyne pair	Bromination, HOAc	Chlorination, HOAc	Acid-catalyzed hydration
1-Hexene/1-hexyne	$1.8 \times 10^5$	$5.3 \times 10^5$	3.6
<i>E</i> -3-Hexene/3-hexyne	$3.4 \times 10^5$	$\sim 1 \times 10^5$	16.6
Styrene/phenylethyne	$2.6 \times 10^3$	$7.2 \times 10^2$	0.65

a. From data tabulated in ref. 241.

<sup>241</sup> K. Yates, G. H. Schmid, T. W. Regulski, D. G. Garratt, H.-W. Leung, and R. McDonald, *J. Am. Chem. Soc.*, **95**, 160 (1973).

<sup>242</sup> R. C. Fahey and D.-J. Lee, *J. Am. Chem. Soc.*, **90**, 2124 (1968).

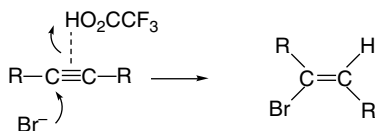
protonation can either collapse to give the vinyl halide or capture solvent to give the acetate. Aryl-substituted acetylenes give mainly the *syn* addition product.



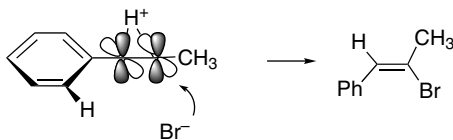
Alkyl-substituted acetylenes can react with HCl by either the  $Ad_E3$  or the  $Ad_E2$  mechanism. The  $Ad_E3$  mechanism leads to *anti* addition. The preference for one or the other mechanism depends on the reactant structure and the reaction conditions. Added halide ion promotes the  $Ad_E3$  mechanism and increases the overall rate of reaction.<sup>243</sup> Reaction of 4-octyne with TFA in  $CH_2Cl_2$  containing 0.1–1.0 M  $Br^-$  leads mainly to *Z*-4-bromo-4-octene by an *anti* addition. The presence of  $Br^-$  greatly accelerates the reaction as compared to reaction with TFA alone, indicating the involvement of the  $Br^-$  in the rate-determining protonation step.<sup>244</sup>



1-Octyne and 2-octyne also give more than 95% *anti* addition under these conditions. The reactions are formulated as concerted  $Ad_E3$  processes, involving bromide attack on an alkene-acid complex.



Under these conditions, 1-arylalkynes react by a mixture of  $Ad_E2$  and  $Ad_E3$  mechanisms with the proportion of  $Ad_E3$  reaction increasing with increasing bromide concentration and decreasing effective acidity.<sup>245</sup> The  $Ad_E3$  reaction of 1-phenylpropyne gives the anti-Markovnikov product. This is believed to be due to a steric effect of the phenyl group.



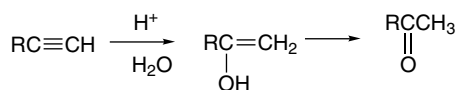
Compared to alkene additions carried out under similar conditions, there is less likely to be involvement of a cationic intermediate because of the higher energy of the vinyl cation (see Section 3.4.1).

<sup>243</sup>. R. C. Fahey, M. T. Payne, and D.-J. Lee, *J. Org. Chem.*, **39**, 1124 (1974).

<sup>244</sup>. H. M. Weiss and K. M. Touchette, *J. Chem. Soc., Perkin Trans. 2*, 1523 (1998).

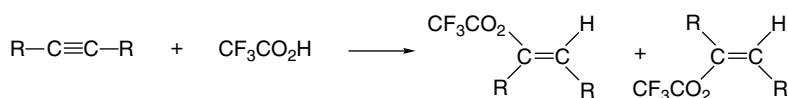
<sup>245</sup>. H. M. Weiss, K. M. Touchette, F. Andersen, and D. Iskhakov, *Org. Biomol. Chem.*, **1**, 2148 (2003);  
H. M. Weiss, K. M. Touchette, S. Angell, and J. Khan, *Org. Biomol. Chem.*, **1**, 2152 (2003).

Alkynes can be hydrated in concentrated aqueous acid solutions. The initial product is an enol, which isomerizes to the more stable ketone.



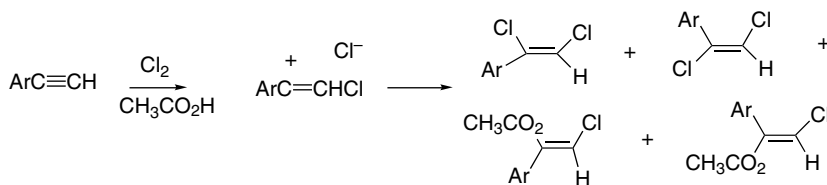
Alkynes are somewhat less reactive than alkenes. For example, 1-butene is 20 times more reactive than 1-butyne in 8.24 M H<sub>2</sub>SO<sub>4</sub>.<sup>246</sup> Alkyne reactivity increases with the addition of ERG substituents. Solvent isotope effects are indicative of a rate-determining protonation.<sup>247</sup> These reactions are believed to proceed by rate-determining proton transfer to give a vinyl cation. Reactions proceeding through a vinyl cation would not be expected to be stereospecific, since the cation will adopt *sp* hybridization (see Section 3.4.1).

Alkynes react when heated with TFA to give addition products. Mixtures of *syn* and *anti* addition products are obtained.<sup>248</sup> Similar addition reactions occur with trifluoromethanesulfonic acid.<sup>249</sup> These reactions are analogous to acid-catalyzed hydration and proceed through a vinyl cation intermediate.



## 5.9.2. Halogenation of Alkynes

Alkynes undergo addition reactions with halogens. In the presence of excess halogen, tetrahaloalkanes are formed but mechanistic studies can be carried out with a limited amount of halogen so that the first addition step can be characterized. In general, halogenation of alkynes is slower than for the corresponding alkenes. We consider the reason for this later. The reaction shows typical characteristics of an electrophilic reaction. For example, the rates of chlorination of substituted phenylacetylenes are correlated by  $\sigma^+$  with  $\rho = -4.2$ . In acetic acid, the reaction is overall second order, first order in both reactants. The addition is not very stereoselective and a considerable amount of solvent capture product is formed. All of these features are consistent with the reaction proceeding through a vinyl cation intermediate.<sup>250</sup>



<sup>246</sup> A. D. Allen, Y. Chiang, A. J. Kresge, and T. T. Tidwell, *J. Org. Chem.*, **47**, 775 (1982).

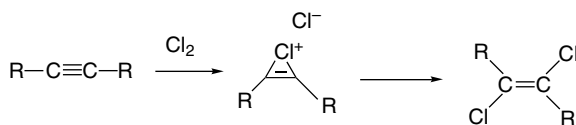
<sup>247</sup> P. Cramer and T. T. Tidwell, *J. Org. Chem.*, **46**, 2683 (1981).

<sup>248</sup> P. E. Peterson and J. E. Dudley, *J. Am. Chem. Soc.*, **88**, 4990 (1966); R. H. Summerville and P. v. R. Schleyer, *J. Am. Chem. Soc.*, **96**, 1110 (1974).

<sup>249</sup> P. J. Stang and R. H. Summerville, *J. Am. Chem. Soc.*, **91**, 4600 (1969); R. H. Summerville, C. A. Senkler, P. v. R. Schleyer, T. E. Dueber, and P. J. Stang, *J. Am. Chem. Soc.*, **96**, 100 (1974); R. H. Summerville and P. v. R. Schleyer, *J. Am. Chem. Soc.*, **96**, 1110 (1974); G. I. Crisp and A. G. Meyer, *Synthesis*, 667 (1974).

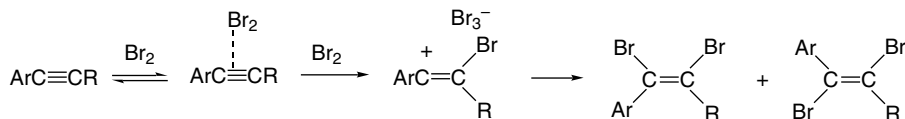
<sup>250</sup> K. Yates and T. A. Go, *J. Org. Chem.*, **45**, 2377, 2385 (1980).

For alkyl-substituted alkynes, there is a difference in stereochemistry between mono- and disubstituted derivatives. The former give *syn* addition, whereas the latter react by *anti* addition. The disubstituted (internal) compounds are considerably ( $\sim 100$  times) more reactive than the monosubstituted (terminal) ones. This result suggests that the TS of the rate-determining step is stabilized by *both* alkyl substituents and points to a bridged structure. This interpretation is consistent with the *anti* stereochemistry of the reaction for internal alkynes.

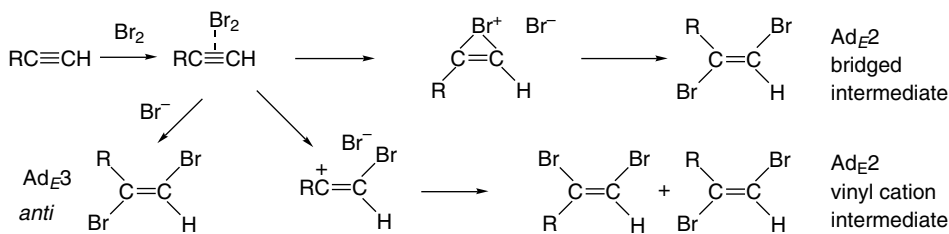


The monosubstituted intermediates do not seem to be effectively bridged, since *syn* addition predominates. A very short-lived vinyl cation appears to be the best description of the intermediate in this case.<sup>251</sup>

The stereochemistry of bromination is usually *anti* for alkyl-substituted alkynes.<sup>252</sup> A series of substituted arylalkynes has been examined in dichloroethane.<sup>253</sup> As with alkenes, a  $\pi$ -complex intermediate was observable. The  $\Delta H$  for formation of the complex with 1-phenylpropyne is about  $-3.0$  kcal/mol. The overall kinetics are third order, as for an  $\text{Ad}_{\text{E}}3$  mechanism. The rate-determining step is the reaction of  $\text{Br}_2$  with the  $\pi$  complex to form a vinyl cation, and both *syn* and *anti* addition products are formed.



For the aryl-substituted alkynes, the reaction stereochemistry is sensitive to the aryl substitution. With EWG substituents ( $\text{NO}_2$ ,  $\text{CN}$ ) the reaction becomes stereospecifically *anti* and the same is true for 2-hexyne, reflecting the diminished stability of the vinyl cation in these cases. Aryl-substituted alkynes can be shifted toward *anti* addition by including a bromide salt in the reaction medium. Under these conditions, a species preceding the vinyl cation must be intercepted by a bromide ion. This intermediate is presumably the complex of molecular bromine with the alkyne. An overall mechanistic summary is shown in the following equations.



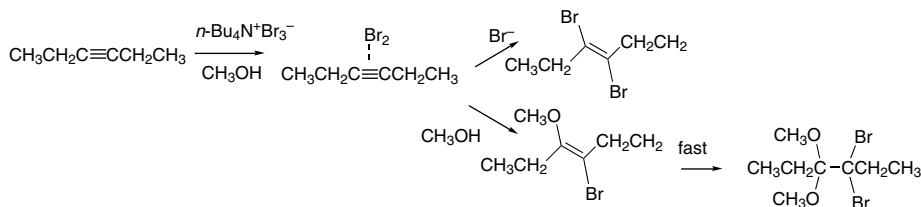
<sup>251</sup>. K. Yates and T. A. Go, *J. Org. Chem.*, **45**, 2385 (1980).

<sup>252</sup>. J. A. Pincock and K. Yates, *Can. J. Chem.*, **48**, 3332 (1970).

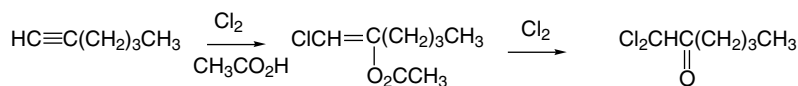
<sup>253</sup>. R. Bianchini, C. Chiappe, G. Lo Moro, D. Lenoir, P. Lemmen, and N. Goldberg, *Chem. Eur. J.*, **1570** (1999).

This scheme shows an alkyne-bromine complex as an intermediate in all alkyne brominations, which is analogous to the case of alkenes. The complex may dissociate to a vinyl cation when the cation is sufficiently stable, as is the case when there is an aryl substituent. It may collapse to a bridged bromonium ion or undergo reaction with a nucleophile. The latter is the dominant reaction for alkyl-substituted alkynes and leads to stereospecific *anti* addition. Reactions proceeding through vinyl cations are nonstereospecific.

As for alkenes, the alkyne- $\text{Br}_2$  complex can be intercepted by nucleophilic solvent. Alkynes react with  $n\text{-Bu}_4\text{N}^+\text{Br}_3^-$  in methanol to give a mixture of dimethoxydibromo and *E*-dibromo products. A key aspect of this reaction is the high reactivity of the methoxybromo intermediate, which is more reactive than the starting material. Evidently, the dibromo intermediate is unreactive toward  $\text{Br}_3^-$ .<sup>254</sup>



Chlorination of 1-hexyne in acetic acid gives mainly to 1,1-dichlorohexan-2-one via chlorination and deacetylation of the initial product, 2-acetoxy-1-chlorohexene.



The corresponding intermediate, *E*-3-acetoxy-4-chlorohexene can be isolated from 3-hexyne.<sup>255</sup>

The rates of bromination of a number of alkynes have been measured under conditions that permit comparison with the corresponding alkenes. The rate of bromination of styrene exceeds that of phenylacetylene by about  $10^3$ .<sup>256</sup> For dialkylacetylene-disubstituted alkene comparisons, the ratios range from  $10^3$  to  $10^7$ , being greatest in the least nucleophilic solvents.<sup>257</sup> Bromination of alkyl-substituted alkynes shows rate enhancement by both alkyl substituents, and this indicates that the TS has bridged character.<sup>258</sup> Remember (p. 512) that alkene bromination was similar in this respect. The lower reactivity of the alkynes is probably due to a combination of factors including greater strain in the bridged TS and reduced electron-donating capacity of alkynes. The IP of 2-butyne (9.6 eV), for example, is considerably higher than that of 2-butene (9.1 eV).

MP2/6-311+G\*\* and B3LYP/6-311+G\*\* computations have been used to compare the stability of the  $\text{Br}_2$  complexes with ethene, ethyne, and allene. The computed

<sup>254</sup> J. Berthelot, Y. Benammar, and B. Desmazieres, *Synth. Commun.*, **27**, 2865 (1997).

<sup>255</sup> G. E. Heasley, C. Codding, J. Sheehy, K. Gering, V. L. Heasley, D. F. Shellhamer, and T. Rempel, *J. Org. Chem.*, **50**, 1773 (1985).

<sup>256</sup> M.-F. Ruasse and J.-E. Dubois, *J. Org. Chem.*, **42**, 2689 (1977).

<sup>257</sup> K. Yates, G. H. Schmid, T. W. Regulski, D. G. Garratt, H.-W. Leung, and R. McDonald, *J. Am. Chem. Soc.*, **95**, 160 (1973); J. M. Kornprobst and J.-E. Dubois, *Tetrahedron Lett.*, 2203 (1974); G. Modena, F. Rivetti, and U. Tonellato, *J. Org. Chem.*, **43**, 1521 (1978).

<sup>258</sup> G. H. Schmid, A. Modro, and K. Yates, *J. Org. Chem.*, **45**, 665 (1980).

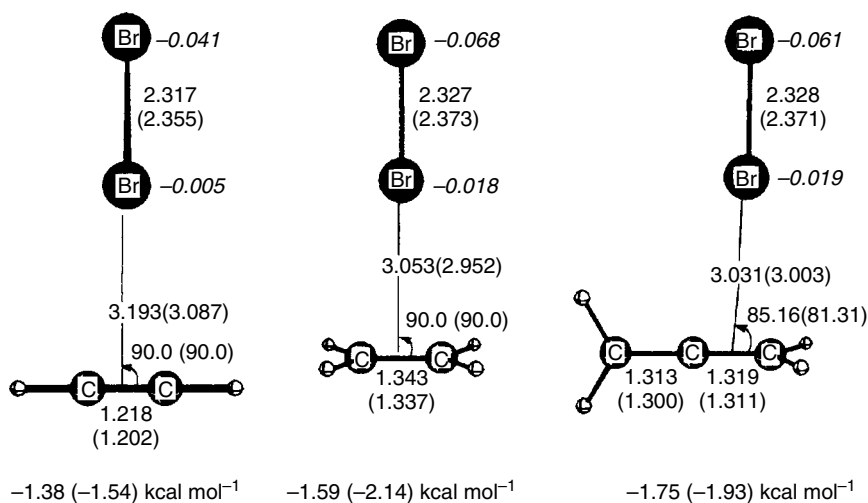
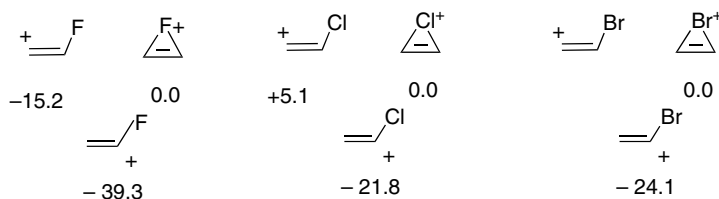


Fig. 5.10. Optimized structures and  $\Delta E$  for formation of (a) ethyne-Br<sub>2</sub>, (b) ethene-Br<sub>2</sub>, and (c) allene-Br<sub>2</sub> complexes. Values of  $\Delta E$  from MP2/6-311+G\*\* and B3LYP/6-311G\*\* (the latter in parentheses). Reproduced from *Chem. Eur. J.*, 967 (2002), by permission of Wiley-VCH.

structures and  $\Delta E$  for formation of the complex are shown in Figure 5.10.<sup>259</sup> The structures and energies are quite similar. This indicates that it is the formation of the cationic intermediate that is more difficult for alkynes.

Calculations comparing the open  $\beta$ -halovinyl and bridged cations have been reported using MP2/6-311G++(3df,3pd)- and B3LYP/6-31+G(d)-level computations.<sup>260</sup> The bridged ions are found to be favored for chlorine and bromine but the open ion is favored for fluorine. The  $\beta$ -chloro and  $\beta$ -bromovinyl cations are found not to be minima. They rearrange to the much more stable  $\alpha$ -halovinyl cations by a hydride shift. The bridged ions tend to be more strongly stabilized by solvation than the open ions. As was noted for the halonium ions derived from alkenes (p. 495), the charge on halogen is positive for Cl and Br, but negative for F.



When a methyl group is added, the vinyl cation is favored. The open cation was also favored for ions derived from 2-butyne.

Computational studies have also explored the issue of how the  $\pi$  complex is converted to the intermediate and several potential mechanisms have been described.<sup>261</sup>

<sup>259</sup> C. Chiappe, A. de Rubertis, H. Detert, D. Lenoir, C. S. Wannere, and P. v. R. Schleyer, *Chem. Eur. J.*, 967 (2002).

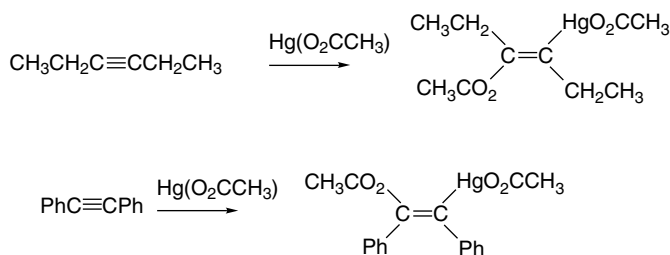
<sup>260</sup> T. Okazaki and K. K. Laali, *J. Org. Chem.*, **70**, 9139 (2005).

<sup>261</sup> R. Herges, A. Papafiliopoulos, K. Hess, C. Chiappe, D. Lenoir, and H. Detert, *Angew. Chem. Int. Ed.*, **44**, 1412 (2005); M. Zabalov, S. S. Karlov, D. A. Le menovskii, and G. S. Zaitseva, *J. Org. Chem.*, **70**, 9175 (2005).

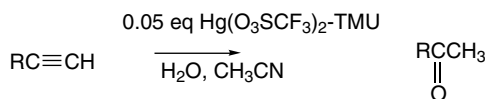
A salient result of these studies is that ionization is energetically prohibitive, at least in the gas phase. This finding is consistent with experimental studies that indicate strong acceleration in polar solvents or in the presence of acids that can facilitate ionization.

### 5.9.3. Mercuration of Alkynes

Alkynes react with mercuric acetate in acetic acid to give addition products. For 3-hexyne the product has *E*-stereochemistry but the *Z*-isomer is isolated from diphenylacetylene.<sup>262</sup> The kinetics of the addition reactions are first order in both alkyne and mercuric acetate.<sup>263</sup>



The most common synthetic application of mercury-catalyzed addition to alkynes is the conversion of alkynes to ketones. This reaction is carried out under aqueous conditions, where the addition intermediate undergoes protonation to regenerate  $\text{Hg}^{2+}$ . Mercuric triflate has been found to be a useful reagent for this reaction.<sup>264</sup>



### 5.9.4. Overview of Alkyne Additions

We can understand many of the general characteristics of electrophilic additions to alkynes by recognizing the possibility for both bridged ions and vinyl cations as intermediates. Reactions proceeding through vinyl cations are expected to be nonstereospecific, with the precise stereochemistry depending upon the lifetime of the vinyl cation and the identity and concentration of the potential nucleophiles. Stereospecific *anti* addition is expected from processes involving nucleophilic attack on either a bridged ion intermediate or an alkyne-electrophile complex. These general mechanisms also explain the relative reactivity of alkenes and alkynes in comparable addition processes. In general, reactions that proceed through vinyl cations, such as those involving rate-determining protonation, are only moderately slower for alkynes as compared to similar alkenes. This is attributed to the somewhat higher energy of vinyl cations compared to cations with  $sp^2$  hybridization. It has been estimated that this difference for secondary ions is around 10–15 kcal/mol, a significant but not an

<sup>262</sup> R. D. Bach, R. A. Woodard, T. J. Anderson, and M. D. Glick, *J. Org. Chem.*, **47**, 3707 (1982).

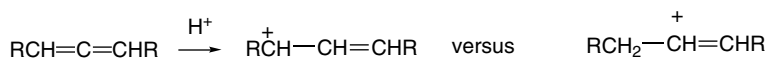
<sup>263</sup> M. Bassetti and B. Floris, *J. Org. Chem.*, **51**, 4140 (1986).

<sup>264</sup> M. Nishizawa, M. Skwarczynski, H. Imagawa, and T. Sugihara, *Chem. Lett.*, 12 (2002).

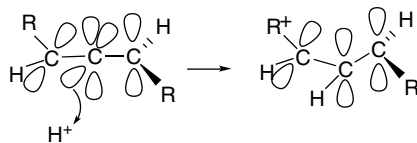
enormous difference,<sup>265</sup> which is partially compensated by the higher ground state energy of the alkynes. Reactions that proceed through TSs leading to bridged intermediates typically show much greater rate retardation for the alkyne addition. Bromination is the best studied example of this type. The lower rate reflects the greater strain of bridged species in the case of alkynes. Bridged intermediates derived from alkynes must incorporate a double bond in the three-membered ring.<sup>266</sup> The activation energies for additions to alkynes through bridged intermediates are thus substantially greater than for alkenes.

### 5.9.5. Additions to Allenes

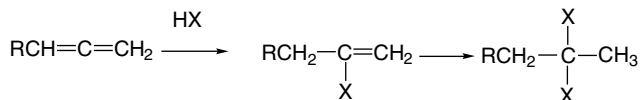
Electrophilic additions to allenes represent an interesting reaction type that is related to additions to both alkenes and alkynes.<sup>267</sup> An allene could, for example, conceivably be protonated at either a terminal  $sp^2$  carbon or the central  $sp$  carbon.



The allylic carbocation resulting from protonation of the center carbon might seem the obvious choice but, in fact, the kinetically favored protonation at a  $sp^2$  carbon leads to the vinyl cation intermediate. The reason for this is stereoelectronic. The allene structure is nonplanar, so that a protonation of the center carbon leads to a twisted structure that lacks of allylic conjugation. This twisted cation is calculated to be about 36–38 kcal/mol higher in energy than the cation formed by protonation at a terminal carbon.<sup>268</sup>



Consistent with this generalization, addition of hydrogen halides to terminal allenes initially gives the vinyl halide; if the second double bond reacts, a geminal dihalide is formed.<sup>269</sup> The regioselectivity of the second step is consistent with Markovnikov's rule because a halogen atom can stabilize a carbocation by resonance (see Section 3.4.1).



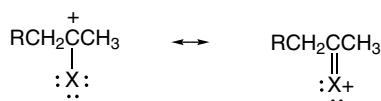
<sup>265</sup> Z. Rappoport, in *Reactive Intermediates*, Vol. 3, R. A. Abramovitch, ed., Plenum Press, New York, 1985, Chap. 7; Y. Apeloig and T. Muller, in *Dicoordinated Carbocations*, Z. Rappoport and P. J. Stang, eds., John Wiley & Sons, New York, 1997, Chap. 2.

<sup>266</sup> G. Melloni, G. Modena, and U. Tonellato, *Acc. Chem. Res.*, **8**, 227 (1981).

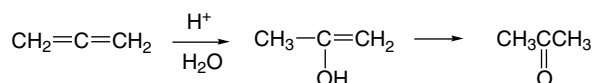
<sup>267</sup> For a review of electrophilic additions to allenes, see W. Smadja, *Chem. Rev.*, **83**, 263 (1983).

<sup>268</sup> K. B. Wiberg, C. M. Breneman, and T. J. Le Page, *J. Am. Chem. Soc.*, **112**, 61 (1990); A. Gobbi and G. Frenking, *J. Am. Chem. Soc.*, **116**, 9275 (1994).

<sup>269</sup> T. L. Jacobs and R. N. Johnson, *J. Am. Chem. Soc.*, **82**, 6397 (1960); R. S. Charleston, C. K. Dalton, and S. R. Schraeder, *Tetrahedron Lett.*, 5147 (1969); K. Griesbaum, W. Naegle, and G. G. Wanless, *J. Am. Chem. Soc.*, **87**, 3151 (1965).

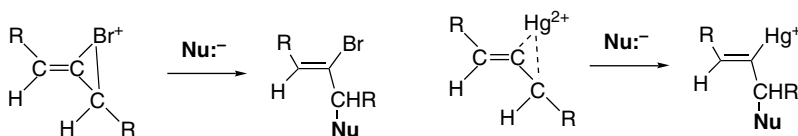


Strong acids in aqueous solution convert allenes to ketones via an enol intermediate. This process also involves protonation at a terminal carbon.



The kinetic features of this reaction, including the solvent isotope effect, are consistent with a rate-determining protonation to form a vinyl cation.<sup>270</sup>

Allenes react with other typical electrophiles such as the halogens and mercuric ion. In systems where bridged ion intermediates would be expected, nucleophilic capture generally occurs at the allylic position. This pattern is revealed, for example, in the products of solvent capture in halogen additions<sup>271</sup> and by the structures of mercuration products.<sup>272</sup>



## 5.10. Elimination Reactions

Elimination reactions involve the removal of another molecule from a reactant. In this section we focus on polar elimination reactions involving heterolytic bond breaking. A fundamental example involves deprotonation in conjunction with expulsion of a good leaving group, such as dehydrohalogenation. Elimination reactions can be classified according to the structural relationship between the proton and the leaving group. The products of  $\alpha$  eliminations are unstable divalent carbon species called carbenes, which are discussed in Chapter 10 of Part B. Here attention is focused on  $\beta$ -elimination reactions that lead to formation of carbon-carbon double bonds.<sup>273</sup>

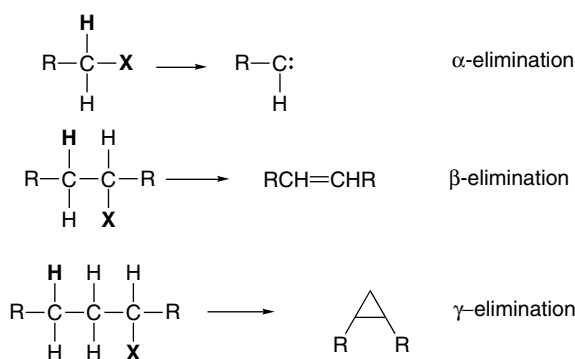
<sup>270</sup> P. Cramer and T. T. Tidwell, *J. Org. Chem.*, **46**, 2683 (1981).

<sup>271</sup> H. G. Peer, *Recl. Trav. Chim. Pays-Bas*, **81**, 113 (1962); W. R. Dolbier, Jr., and B. H. Al-Sader, *Tetrahedron Lett.*, 2159 (1975).

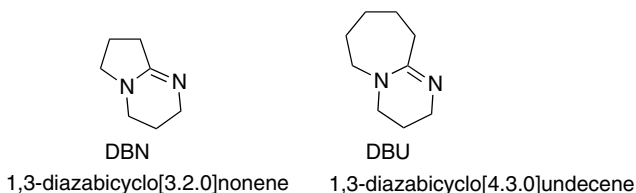
<sup>272</sup> W. Waters and E. F. Kieter, *J. Am. Chem. Soc.*, **89**, 6261 (1967).

<sup>273</sup> Reviews: J. R. Gandler, in *The Chemistry of Double-bonded Functional Groups*, S. Patai, ed., Wiley-Interscience, New York, 1989, Chap. 12; E. Baciocchi, in *Chemistry of Halides, Pseudo-Halides and Azides*, Part 2, S. Patai and Z. Rappoport, eds., Wiley-Interscience, New York, 1983, Chap. 23; W. H. Saunders, Jr., and A. F. Cockerill, *Mechanisms of Elimination Reactions*, Wiley, New York, 1973; D. J. McLennan, *Tetrahedron*, **31**, 2999 (1975).

Eliminations of  $\gamma$ - and higher leaving groups result in *cyclization*; mechanistically they are intramolecular nucleophilic displacements.



Some representative examples of  $\beta$ -elimination reactions are given in Scheme 5.2. Entry 1 is a typical dehydrohalogenation that involves no issue of regioselectivity or stereoselectivity. With primary reactants, the main competing reaction is substitution. The base used in Entry 1 ( $\text{K}^+ \cdot^- \text{O-}t\text{-Bu}$ ) favors elimination over substitution, as compared with less branched alkoxides. Entry 2 illustrates the issues of regiochemistry and stereochemistry that can arise, even with a relatively simple reactant and also shows that substitution can compete with elimination in unhindered systems. Entry 3 shows the use of a very hindered alkoxide to favor the less-substituted product. The strong organic bases DBU<sup>274</sup> and DBN<sup>275</sup> can also effect dehydrohalogenation, as illustrated by Entry 4. These bases are particularly effective for reactants that are easily ionized, such as tertiary halides.



Entry 5 is a case in which the carbanion-stabilizing effect of a carbonyl group facilitates elimination by a relatively weak base and controls regiochemistry by favoring deprotonation of the  $\alpha$ -carbon. Entries 6 and 7 are tosylate eliminations. Generally speaking, tosylates give a higher proportion of substitution than do halides.<sup>276</sup> Entries 8 and 9 are examples of the *Hofmann elimination reaction*, which is a case where the relatively poor and bulky leaving group (trimethylamine) leads to a preference for formation of the less-substituted alkene (see Section 5.10.2).

In the sections that follow, we discuss the mechanisms of these and related reactions and explore the relationship between mechanism and regio-/stereoselectivity. We also look at some examples that illustrate how choice of reactant, reagent, and solvent can influence the outcome of the reaction.

<sup>274</sup>. H. Oediger and F. Moeller, *Angew. Chem. Int. Ed. Engl.*, **6**, 76 (1967); P. Wolkoff, *J. Org. Chem.*, **47**, 1944 (1982).

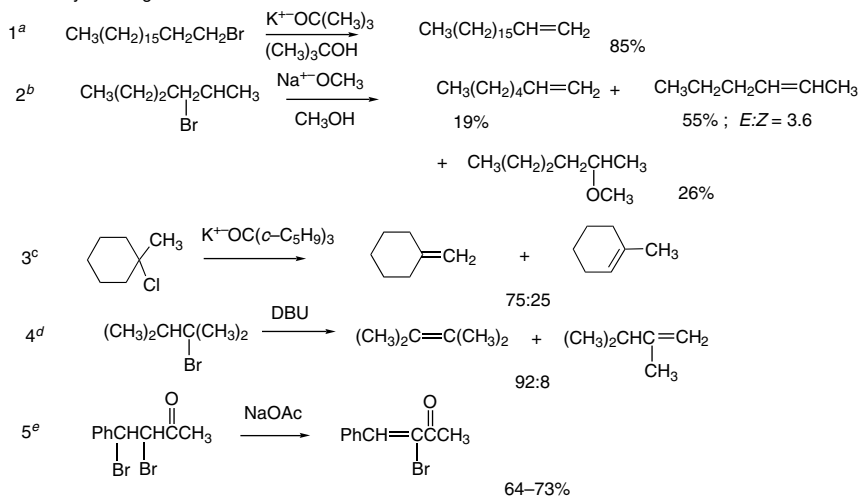
<sup>275</sup>. H. Oediger, H. J. Kabbe, F. Moeller, and K. Eiter, *Chem. Ber.*, **99**, 2012 (1966).

<sup>276</sup>. P. Veeravagu, R. T. Arnold, and E. W. Eigenmann, *J. Am. Chem. Soc.*, **86**, 3072 (1964).

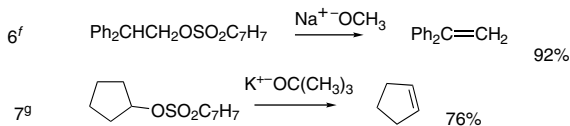
## CHAPTER 5

Polar Addition  
and Elimination  
Reactions

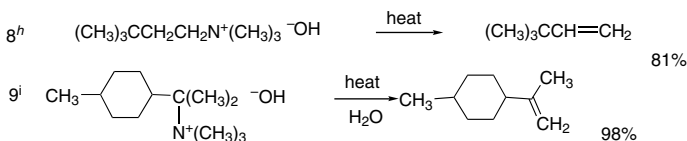
## A. Dehydrohalogenation



## B. Dehydrosulfonation



## C. Eliminations of Quaternary Ammonium Hydroxides

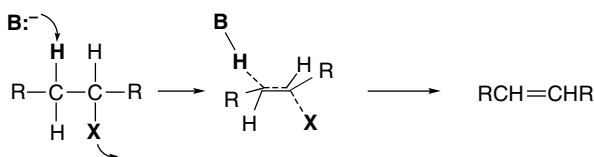


- a. P. Veeragu, R. T. Arnold, and E. W. Eigemann, *J. Am. Chem. Soc.*, **86**, 3072 (1964).  
 b. R. A. Bartsch and J. F. Bunnett, *J. Am. Chem. Soc.*, **90**, 408 (1968).  
 c. S. A. Acharya and H. C. Brown, *J. Chem. Soc., Chem. Commun.*, 305 (1968).  
 d. P. Wolkoff, *J. Org. Chem.*, **47**, 1944 (1982).  
 e. N. H. Cromwell, D. J. Cram, and C. E. Harris, *Org. Synth.*, **III**, 125 (1953).  
 f. P. J. Hamrick, Jr., and C. R. Hauser, *J. Org. Chem.*, **26**, 4199 (1961).  
 g. C. H. Snyder and A. R. Soto, *J. Org. Chem.*, **29**, 742 (1964).  
 h. A. C. Cope and D. L. Ross, *J. Am. Chem. Soc.*, **83**, 3854 (1961).  
 i. L. C. King, L. A. Subluskey, and E. W. Stern, *J. Org. Chem.*, **21**, 1232 (1956).

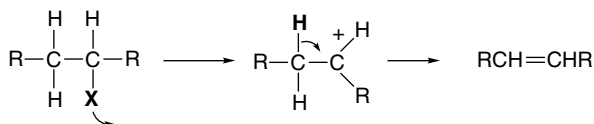
## 5.10.1. The E2, E1 and E1cb Mechanisms

The  $\beta$ -eliminations can be subdivided on the basis of the mechanisms involved. Three distinct limiting mechanisms are outlined below.

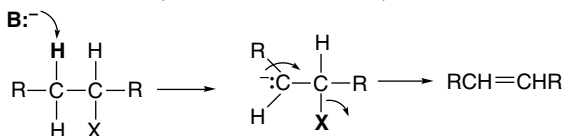
## E2 Mechanism (concerted)



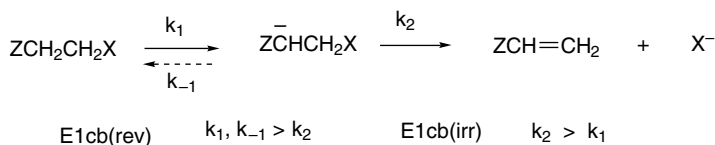
E1 Mechanism (carbocation intermediate)



E1cb Mechanism (carbanion intermediate)



The E2 mechanism involves a bimolecular TS in which removal of a proton  $\beta$  to the leaving group is concerted with departure of the leaving group. The rate-determining step in the E1 mechanism is the unimolecular ionization of the reactant to form a carbocation intermediate. This is the same process as the rate-determining step in the  $S_N1$  mechanism. Elimination is completed by removal of a  $\beta$ -proton. The E1cb mechanism, like the E1, involves two steps, but the order is reversed. Deprotonation, forming a carbanion intermediate, precedes expulsion of the leaving group. E1cb mechanisms can be subdivided into E1cb<sub>(irr)</sub> and E1cb<sub>(rev)</sub>, depending on whether the formation of the carbanion intermediate is or is not rate determining. If the anion is formed reversibly it may be possible to detect proton exchange with the solvent (E1cb<sub>(rev)</sub>). This is not the case if formation of the carbanion is the rate-determining step (E1cb<sub>(irr)</sub>).



The correlation of many features of  $\beta$ -elimination reactions is facilitated by recognition that these three mechanisms represent *variants of a continuum of mechanistic possibilities*. Many  $\beta$ -elimination reactions occur via mechanisms that are intermediate between the limiting mechanistic types. This idea, called the *variable E2 transition state theory*, is outlined in Figure 5.11.

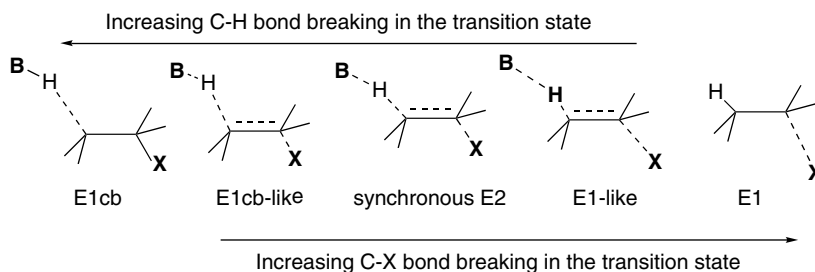
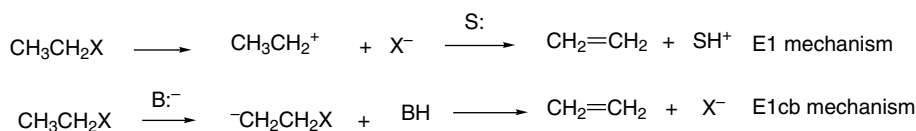


Fig. 5.11. Variable transition state theory of elimination reactions. J. F. Bunnett, *Angew. Chem. Int. Ed. Engl.*, **1**, 225 (1962); J. F. Bunnett, *Survey Prog. Chem.*, **5**, 53 (1969); W. H. Saunders, Jr., and A. F. Cockerill, *Mechanisms of Elimination Reactions*, John Wiley & Sons, New York, 1973, pp. 48–55; W. H. Saunders, Jr., *Acc. Chem. Res.*, **9**, 19 (1976).

The variable transition state theory allows discussion of reactions proceeding through TSs of intermediate character in terms of the limiting mechanistic types. These are called “E1cb-like” and “E1-like,” as illustrated in Figure 5.11. The most important factors to be considered are: (1) the nature of the leaving group, (2) electronic and steric effect of substituents in the reactant molecule, (3) the nature of the base, and (4) solvent effects.

The ideas embodied in the variable transition state theory of elimination reactions can be depicted in a two-dimensional potential energy diagram.<sup>277</sup> If we consider the case of an ethyl halide, both stepwise reaction paths require the formation of high-energy intermediates. The E1 mechanism requires formation of a primary carbocation, whereas the E1cb proceeds via a carbanion intermediate.



In the absence of stabilizing substituent groups, both a primary carbocation and a primary carbanion are highly unstable intermediates. If we construct a reaction energy diagram in which progress of C–H bond breaking is one dimension, progress of C–X bond breaking is the second, and the energy of the reacting system is the third, we obtain a diagram such as the one in Figure 5.12. In Figure 5.12A only the two horizontal (bond-breaking) dimensions are shown. We see that the E1 mechanism corresponds to complete C–X cleavage before C–H cleavage begins, whereas the E1cb mechanism corresponds to complete C–H cleavage before C–X cleavage begins. In Figure 5.12B the energy dimension is added. The front-right and back-left corners correspond to the E1 and E1cb intermediates, respectively. Because of the high energy of both the E1 and E1cb intermediates, the lowest-energy path is the concerted E2 path, more or less diagonally across the energy surface. This pathway is of lower energy because the partially formed double bond provides some compensation for the energy required to break the C–H and C–X bonds and the high-energy intermediates are avoided.

The presence of a substituent on the ethyl group that stabilizes the carbocation intermediate lowers the right-front corner of the diagram, which corresponds

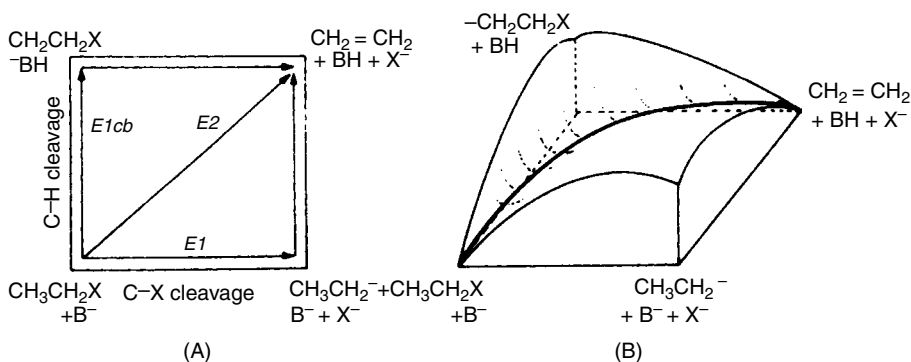


Fig. 5.12. Two-dimensional potential energy diagrams depicting E1, E2, and E1cb mechanisms.

<sup>277</sup> R. A. More O'Ferrall, *J. Chem. Soc. B*, 274 (1970).

to the energy of the carbocation intermediate. Similarly, a substituent that stabilizes a carbanion intermediate lowers the back-left corner of the diagram. As a result, substituents that stabilize carbocation character move the E2 TS to a point that more closely resembles the E1 TS. A structural change that stabilizes carbanion character shifts the E2 TS to be more similar to the E1cb TS. In the E1-like TS, C–X bond cleavage is more advanced than C–H cleavage, whereas in the E1cb-like TS, the C–H bond breaking is more advanced. Figure 5.13 depicts these changes.

The variable transition state concept can be used to discuss specific structural effects that influence the possible mechanisms of elimination reactions. We have background that is pertinent to the structure-reactivity effects in E1 reactions from the discussion of  $S_N1$  reactions in Chapter 4. Ionization is favored by: (1) electron-releasing groups that stabilize the positive charge in the carbocation intermediate; (2) readily ionized, i.e., “good,” leaving groups; and (3) solvents that facilitate ionization. The base plays no role in the rate-determining step in the E1 mechanism, but its identity cannot be ignored. After ionization, the cationic intermediate is subject to two competing reactions: nucleophilic capture ( $S_N1$ ) or proton removal (E1). Remember from Section 4.4.3 (p. 437) that there is an inherent preference for substitution. The reaction can be diverted to elimination by bases. Stronger and harder bases favor the E1 path over the  $S_N1$  path.

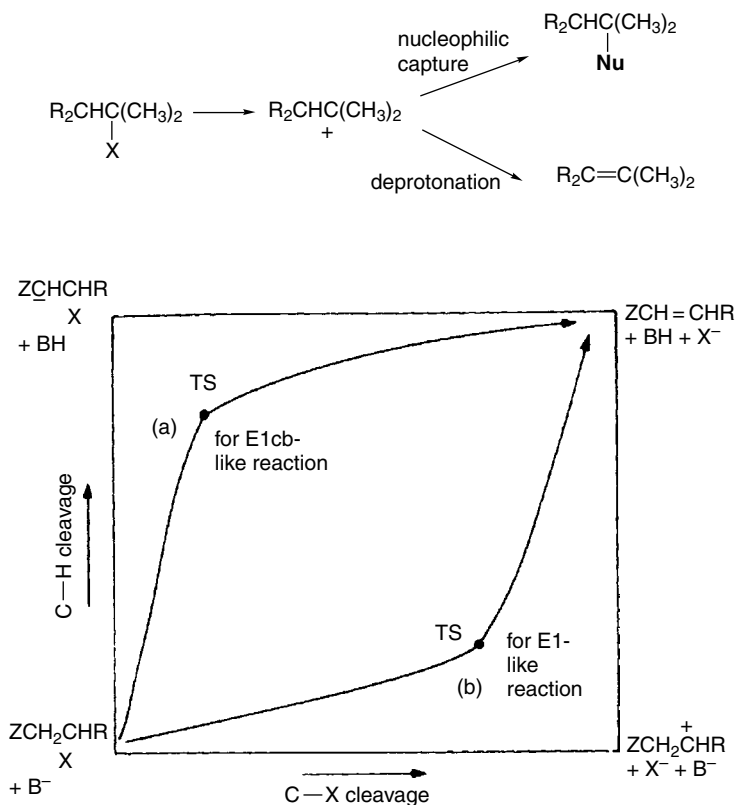


Fig. 5.13. Representation of changes in transition state character in the E2 elimination reaction as a result of substituent effects: (a) substituent Z stabilizes carbanion character of E1cb-like TS; (b) substituent R stabilizes carbocation character of E1-like TS.

E2 reactions are distinguished from E1 reactions in that the base is present in the TS for the rate-determining step. The reactions therefore exhibit overall second-order kinetics. The precise nature of the TS is a function of variables such as the strength of the base, the identity of the leaving group, reactant structure, and the solvent. For example, an elimination reaction proceeding by an E2 TS will be moved in the E1cb direction by an increase in base strength or by a change to a poorer leaving group. On the other hand, a good leaving group in a highly ionizing solvent will result in an E2 TS that resembles an E1 process, with greater weakening of the bond to the leaving group. Reactions that proceed by the E1cb mechanism require substituents that can stabilize the carbanion intermediate. This mechanism is not observed with simple alkyl halides or sulfonates. It is more likely to be involved when the leaving group is  $\beta$  to a carbonyl, nitro, cyano, sulfinyl, or other carbanion-stabilizing group. Poorer leaving groups move the E2 TS in the E1cb direction, since they require greater buildup of negative charge at the  $\beta$ -carbon. Scheme 5.3 summarizes some of the characteristic features of the E1, E2, and E1cb mechanisms.

Scheme 5.4 shows some examples of reactions for which the mechanisms have been characterized. From these data, we can conclude that E1cb reactions generally require *both* carbanion stabilization and a relatively poor leaving group. For example, simple 2-arylethyl halides and tosylates react by the E2 mechanism and only when a *p*-nitro group is present is there clear evidence of an E1cb mechanism (Entry 1). Entry 2 illustrates one of the distinguishing characteristics of E2 reactions. Both the  $\alpha$ - and  $\beta$ -carbons show isotope effects because rehybridization occurs at both carbons. Entry 3 illustrates some of the kinetic features that characterize E2 reactions. In addition to second-order kinetics, the concerted mechanism results in kinetic isotope effects at both the  $\beta$ -hydrogen and the leaving group. The substantial Br > Cl ratio also

### Scheme 5.3. Distinguishing Features of Elimination Mechanisms

---

**A. E1 Mechanism**

First Order Kinetics: rate =  $k[\text{RX}]$

LFER indicate cationic character of the TS

Strong dependence on leaving group

**B. E2 Mechanism**

Second Order Kinetics: rate =  $k[\text{RX}][\text{base}]$

Leaving group effect is normally  $\text{I} > \text{Br} > \text{Cl} \gg \text{F}$  because bond-breaking occurs in RDS.

Kinetic isotope effect for both  $\beta$ -C-H and leaving group.

Kinetic isotope effect for both  $\alpha$ - and  $\beta$ -carbons.

**C. E1cb(rev)**

Second Order Kinetics: rate =  $k[\text{RX}][\text{base}]$

Exchange of  $\beta$ -H with protic solvent

LFER indicate anionic character in TS

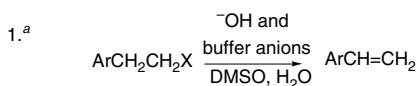
**D. E1cb(irr)**

Second Order Kinetics: rate =  $k[\text{RX}][\text{base}]$

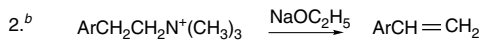
Leaving group effect may be  $\text{F} > \text{Cl} > \text{Br} > \text{I}$ , since C-X bond-breaking is not involved in RDS.

LFER indicates anionic character in TS

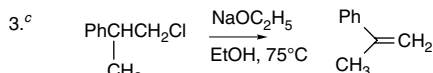
---



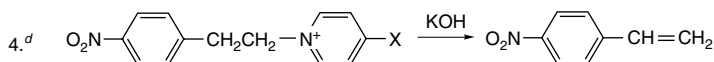
E2 for X = TsO<sup>-</sup>, Br<sup>-</sup>, and quinuclidinium, except for Ar = *p*-nitrophenyl and X = quinuclidinium: based on variation of sensitivity to base (Bronsted β) and LFER relationships.



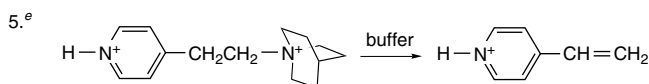
E2: based on k<sup>12</sup>C/k<sup>14</sup>C isotope effects for both C(1) and C(2)



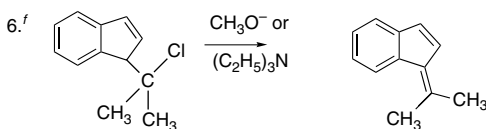
E2; based on k<sup>35</sup>Cl:k<sup>37</sup>Cl = 1.0059; k<sub>H</sub>/k<sub>D</sub> = 5.37, and k<sub>Br</sub>/k<sub>Cl</sub> = 52



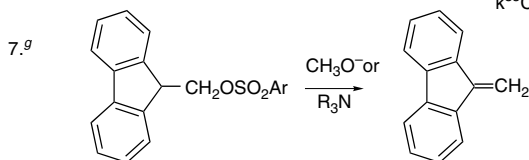
E1cb: based on kinetics and Bronsted dependence on substituent X; shifts from E1cb(irr) to E1cb(rev) as X becomes ERG



E1cb(rev): based on observation of CH solvent exchange and solvent isotope effect



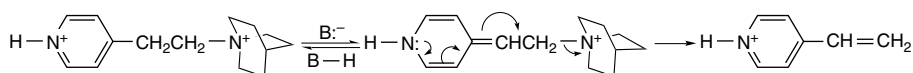
E2: based on both CH and Cl kinetic isotope effects: k<sub>H</sub>/k<sub>D</sub> = 7.1 (CH<sub>3</sub>O<sup>-</sup>); 8.4 ((C<sub>2</sub>H<sub>5</sub>)<sub>3</sub>N)  
k<sup>35</sup>Cl:k<sup>37</sup>Cl = 1.0086 (CH<sub>3</sub>O<sup>-</sup>); 1.0101 ((C<sub>2</sub>H<sub>5</sub>)<sub>3</sub>N)



E2 with transition to E1cb for ERG in Ar based on curved LFER (Hammett) relationships

- a. J. R. Gandler and W. P. Jencks, *J. Am. Chem. Soc.*, **104**, 1937 (1982).  
 b. J. R. I. Eubanks, L. B. Sims, and A. Fry, *J. Am. Chem. Soc.*, **113**, 8821 (1991).  
 c. H. F. Koch, D. McLennan, J. G. Koch, W. Tumas, B. Dobson, and N. H. Koch, *J. Am. Chem. Soc.*, **105**, 1930 (1983).  
 d. J. W. Bunting and J. P. Kanter, *J. Am. Chem. Soc.*, **113**, 6950 (1991).  
 e. S. Alunni, A. Conti and R. P. Erico, *J. Chem. Soc., Perkin Trans.*, **2**, 453 (2000); S. Alunni, A. Conti, and R. P. Errico, *Res. Chem. Inter.*, **27**, 635 (2001).  
 f. J. S. Jia, J. Rudzinski, P. Paneth, and A. Thibblin, *J. Org. Chem.*, **67**, 177 (2002).  
 g. F. G. Larkin, R. A. More O'Ferrall, and D. G. Murphy, *Coll. Czech. Chem. Commun.*, **64**, 1833 (1999).

shows that the bond to the leaving group is involved in the rate-determining step. The pyridinium system in Entry 5 is an interesting case. Kinetic studies have shown that the reaction occurs through the *conjugate acid* of the reactant. The protonation of the pyridine ring enhances the acidity of the C–H bond. The reaction occurs with exchange, indicating that the proton removal is reversible.



The indenyl (Entry 6) and fluorenyl (Entry 7) ring systems have been studied carefully. Note that these are cases where (aromatic) anionic stabilization could potentially stabilize an anionic intermediate. However, the elimination reactions show E2 characteristics. The reaction in Entry 7 shifts to an E1cb mechanism if the leaving group is made less reactive.

Because of their crucial role in the ionization step, solvents have a profound effect on the rates of E1 reactions. These rates for a number of tertiary halides have been determined in a variety of solvents. For *t*-butyl chloride there are huge differences in the rates in water ( $\log k = -1.54$ ), ethanol ( $\log k = -7.07$ ), and diethyl ether ( $\log k = -12.74$ ).<sup>278</sup> Similarly, the rates of the E1 reaction of 1-methylcyclopentyl bromide range from  $1 \times 10^{-3} \text{ s}^{-1}$  in methanol to  $2 \times 10^{-9} \text{ s}^{-1}$  in hexane. Polar aprotic solvents such as DMSO ( $k = 2 \times 10^{-4} \text{ s}^{-1}$ ) and acetonitrile ( $k = 9 \times 10^{-5} \text{ s}^{-1}$ ) are also conducive for ionization.<sup>279</sup> The solvent properties that are most important are polarity and the ability to assist leaving group ionization. These, of course, are the same features that favor S<sub>N</sub>1 reactions, as we discussed in Section 3.8.

The details of the mechanism as well as the stereochemistry and regiochemistry also depend on the identity and degree of aggregation of the base. This is affected by variables such as the nature of the solvent, the cationic counterions, and the presence of coordinating ligands.<sup>280</sup> Under given reaction conditions, there may be an equilibrium involving a number of different species, which, in turn, have different rates for inducing elimination. The nature of the TS in elimination reactions also controls the regiochemistry of β-elimination for compounds in which the double bond can be introduced at one of several positions. These effects are discussed in the next section.

### 5.10.2. Regiochemistry of Elimination Reactions

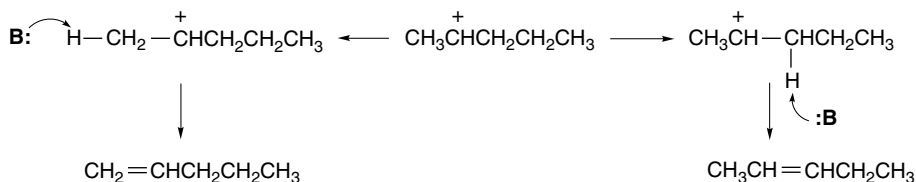
Useful generalizations and predictions regarding regioselectivity in elimination reactions can be drawn from the variable transition state theory. As we saw earlier in Figure 5.11, this theory proposes that the TSs in E2 reactions can vary over a mechanistic range between the E1 and E1cb extremes. When the base is present at the TS, the reaction will exhibit second-order kinetics and meet the other criteria of an E2 mechanism. There is no intermediate. The cleavage of the C–H and the C–X bonds is concerted, but not necessarily synchronous. The relative extent of the breaking of the two bonds at the TS may differ, depending on the nature of the leaving group X and the ease of removal of the β-hydrogen as a proton. If there are several nonequivalent β-hydrogens, competition among them determines which one is removed and the regiochemistry and stereochemistry of the reaction. If one compares E1 and E1cb eliminations, it is seen that quite different structural features govern the direction of elimination. The variable transition state theory suggests that E2 elimination proceeding through an “E1-like” TS will have the regiochemistry of E1 eliminations, whereas E2 eliminations proceeding through an “E1cb-like” TS will show regioselectivity similar to E1cb reactions. It is therefore instructive to consider these limiting mechanisms before discussing the E2 case.

<sup>278</sup> M. H. Abraham, R. M. Doherty, M. J. Kamlet, J. M. Harris, and R. W. Taft, *J. Chem. Soc., Perkin Trans. 2*, 913 (1987).

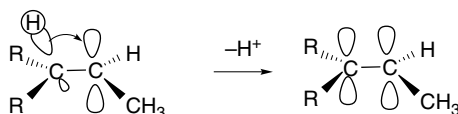
<sup>279</sup> E. A. Ponomareva, I. V. Koshchii, T. L. Pervishko, and G. F. Dvorko, *Russ. J. Gen. Chem.*, **70**, 907 (2000).

<sup>280</sup> R. A. Bartsch and J. Zavada, *Chem. Rev.*, **80**, 453 (1980).

In the E1 mechanism, the leaving group is completely ionized before C–H bond breaking occurs. The direction of the elimination therefore depends on the structure of the carbocation and the identity of the base involved in the proton transfer that follows C–X heterolysis. Because of the high energy of the carbocation intermediate, quite weak bases can effect proton removal. The solvent can serve this function. The counterion formed in the ionization step can also act as the proton acceptor.



The product composition of the alkenes formed in E1 elimination reaction usually favors the more-substituted alkene, and therefore the more stable one. This indicates that the energies of the *product-determining TSs parallel those of the isomeric alkenes*. However, since the activation energy for proton removal from a carbocation is low, the TS should resemble the carbocation intermediate much more than the alkene product (Hammond postulate; Section 3.3.2.2). In the carbocation there is hyperconjugation involving each  $\beta$ -hydrogen.<sup>281</sup> Since the hyperconjugation structures possess some double-bond character, the interaction with hydrogen is greatest at more highly substituted carbons; that is, there will be greater weakening of C–H bonds and more double-bond character at more highly substituted carbon atoms. This structural effect in the carbocation intermediate governs the direction of elimination and leads to the *preferential formation of the more highly substituted alkene*, as illustrated in Figure 5.14.



In the E1cb mechanism, the direction of elimination is governed by the *kinetic acidity* of the individual  $\beta$ -protons, which in turn is determined by the polar and

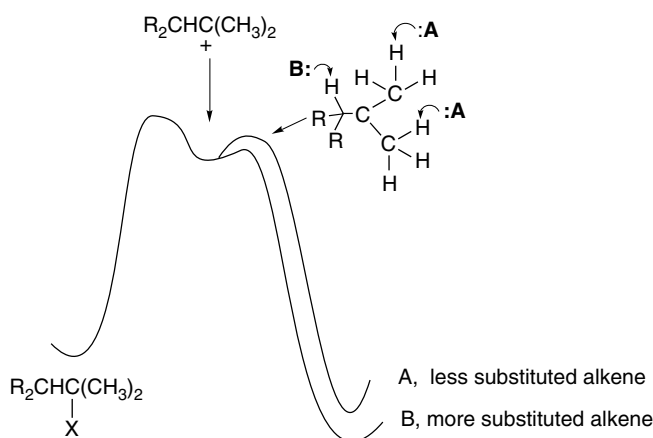


Fig. 5.14. Potential energy profile for product-determining step for E1 elimination.

<sup>281</sup> P. B. D. de la Mare, *Pure Appl. Chem.*, **56**, 1755 (1984).

resonance effects of adjacent substituents, and by the degree of steric hindrance to approach of base to the proton. Alkyl substituents tend to retard proton abstraction both electronically and sterically. Preferential proton abstraction from less-substituted carbons leads to the formation of the less-substituted alkene. Carbanion-stabilizing substituents control the regiochemistry of E1cb eliminations by favoring deprotonation at the most acidic carbon.

The preferred direction of elimination via the E2 mechanism depends on the precise nature of the TS. The two extreme TSs for the E2 elimination resemble the E1 and E1cb mechanisms in their orientational effects. At the “E1cb-like” end of the E2 range, a highly developed bond is present between the proton and the base. The leaving group remains tightly bound to carbon, and there is relatively little development of the carbon-carbon double bond. *When the TS of an E2 reaction has E1cb character, the direction of the elimination is governed by the ease of proton removal.* In this case, the less-substituted alkene usually dominates. At the “E1-like” end of the E2 spectrum, the TS is characterized by well-advanced cleavage of the C–X bond and a largely intact C–H bonds. An “E1-like” TS for E2 reactions leads to formation of the more highly substituted of the possible alkenes. In a more synchronous E2 reaction, the new double bond is substantially formed at the TS with partial rupture of both the C–H and C–X bonds. E2 eliminations usually give mainly the more-substituted alkene. This is because the TSs leading to the isomeric alkenes reflect the partial double-bond character and the greater stability of the more-substituted double bond. Concerted E2 reactions are also subject to the stereoelectronic requirement that the reacting C–H and C–X bond be antiperiplanar. This requirement makes reactant conformation a factor in determining the outcome of the reaction.

Prior to development of the mechanistic ideas outlined above, it was recognized by experience that some types of elimination reactions give the more substituted alkene as the major product. Such eliminations are said to follow the *Saytzeff rule*. This behavior is characteristic of E1 reactions and E2 reactions involving relatively good leaving groups, such as halides and sulfonates. These are now recognized as reactions in which C–X cleavage is well advanced in the TS. E2 reactions involving poor leaving groups, particularly those with quaternary ammonium salts, are said to follow the *Hofmann rule* and give primarily the less-substituted alkene. We now recognize that such reactions proceed through TSs with E1cb character.

The data recorded in Table 5.11 for the 2-hexyl system illustrate two general trends that have been recognized in other systems as well. First, poorer leaving groups favor elimination according to the Hofmann rule, as shown, for example, by the increasing amount of terminal olefin in the halogen series as the leaving group is changed from iodide to fluoride. Poorer leaving groups move the TS in the E1cb direction. A higher negative charge must build up on the  $\beta$ -carbon to induce loss of the leaving group. This charge increase is accomplished by more complete proton abstraction.

Comparison of the data for methoxide with those for *t*-butoxide in Table 5.11 illustrates a second general trend. Stronger bases favor formation of the less-substituted alkene.<sup>282</sup> A stronger base leads to an increase in the carbanion character at the TS and, thus, shifts it in the E1cb direction. A correlation between the strength of the

<sup>282</sup> (a) D. H. Froemsdorf and M. D. Robbins, *J. Am. Chem. Soc.*, **89**, 1737 (1967); I. N. Feit and W. H. Saunders, Jr., *J. Am. Chem. Soc.*, **92**, 5615 (1970); (b) R. A. Bartsch, G. M. Pruss, B. A. Bushaw, and K. E. Wieggers, *J. Am. Chem. Soc.*, **95**, 3405 (1973); (c) R. A. Bartsch, K. E. Wieggers, and D. M. Guritz, *J. Am. Chem. Soc.*, **96**, 430 (1974).

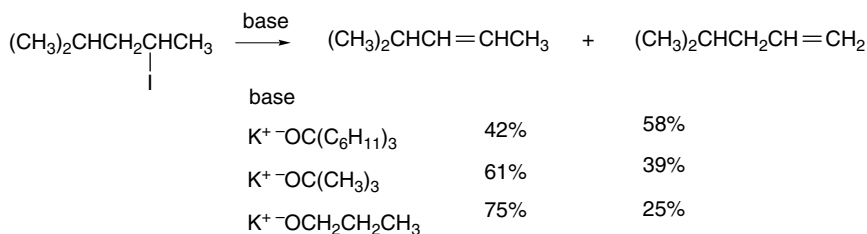
**Table 5.11. Product Ratios for Some Elimination Reactions of 2-Hexyl Systems**

Leaving group	Base/solvent	Product Composition		
		1-Hexene	<i>E</i> -2-Hexene	<i>Z</i> -2-Hexene
I	MeO <sup>-</sup> /MeOH	19	63	18
Cl	MeO <sup>-</sup> /MeOH	33	50	17
F	MeO <sup>-</sup> /MeOH	69	21	9
OSO <sub>2</sub> C <sub>7</sub> H <sub>7</sub>	MeO <sup>-</sup> /MeOH	33	44	23
I	<i>t</i> -BuO <sup>-</sup> / <i>t</i> -BuOH	78	15	7
Cl	<i>t</i> -BuO <sup>-</sup> / <i>t</i> -BuOH	91	5	4
F	<i>t</i> -BuO <sup>-</sup> / <i>t</i> -BuOH	97	2	1
OSO <sub>2</sub> C <sub>7</sub> H <sub>7</sub>	<i>t</i> -BuO <sup>-</sup> / <i>t</i> -BuOH	83	4	14

a. R. A. Bartsch and J. F. Bunnett, *J. Am. Chem. Soc.*, **91**, 1376 (1967).

base and the difference in  $\Delta G^\ddagger$  for the formation of 1-butene versus 2-butene has been established.<sup>282b</sup> Some of the data are given in Table 5.12.

The direction of elimination is also affected by steric effects, and if both the base and the reactant are highly branched, steric factors may lead to preferential removal of the less hindered hydrogen.<sup>283</sup> Thus, when 4-methyl-2-pentyl iodide reacts with very hindered bases such as potassium tricyclohexylmethoxide, there is preferential formation of the terminal alkene. In this case, potassium *t*-butoxide favors the internal alkene, although by a smaller ratio than for less branched alkoxides.

**Table 5.12. Orientation of E2 Elimination as a Function of Base Strength**

Base (K <sup>+</sup> salt)	p <i>K</i> (DMSO)	Percent 1-butene	
		2-Iodobutane <sup>a</sup>	2-Butyl tosylate <sup>b</sup>
<i>p</i> -Nitrobenzoate	8.9	5.8	c
Benzoate	11.0	7.2	c
Acetate	11.6	7.4	c
Phenolate	16.4	11.4	30.6
Trifluoroethoxide	21.6	14.3	46.0
Methoxide	29.0	17.0	c
Ethoxide	29.8	17.1	56.0
<i>t</i> -Butoxide	32.2	20.7	58.5

a. R. A. Bartsch, G. M. Pruss, B. A. Bushaw, and K. E. Wiegers, *J. Am. Chem. Soc.*, **95**, 3405 (1973).

b. R. A. Bartsch, R. A. Read, D. T. Larsen, D. K. Roberts, K. J. Scott, and B. R. Cho, *J. Am. Chem. Soc.*, **101**, 1176 (1979).

c. Not reported.

<sup>283</sup>. R. A. Bartsch, R. A. Read, D. T. Larsen, D. K. Roberts, K. J. Scott, and B. R. Cho, *J. Am. Chem. Soc.*, **101**, 1176 (1979).

**Table 5.13. Orientation of Elimination from 2-Butyl Systems under E2 Conditions**

CHAPTER 5	Leaving group	Base/solvent	1-Butene (%)	2-Butene (%)
<i>Polar Addition and Elimination Reactions</i>	I <sup>a</sup>	PhCO <sub>2</sub> <sup>-</sup> /DMSO	7	93
	I <sup>a</sup>	C <sub>2</sub> H <sub>5</sub> O <sup>-</sup> /DMSO	17	83
	I <sup>b</sup>	<i>t</i> -C <sub>4</sub> H <sub>9</sub> O <sup>-</sup> /DMSO	21	79
	Br <sup>b</sup>	<i>t</i> -C <sub>4</sub> H <sub>9</sub> O <sup>-</sup> /DMSO	33	67
	Cl <sup>b</sup>	<i>t</i> -C <sub>4</sub> H <sub>9</sub> O <sup>-</sup> /DMSO	43	57
	Br <sup>c</sup>	C <sub>2</sub> H <sub>5</sub> O <sup>-</sup> /DMSO	19	81
	OSO <sub>2</sub> C <sub>7</sub> H <sub>7</sub> <sup>d</sup>	C <sub>2</sub> H <sub>5</sub> O <sup>-</sup> /DMSO	35	65
	OSO <sub>2</sub> C <sub>7</sub> H <sub>7</sub> <sup>d</sup>	<i>t</i> -C <sub>4</sub> H <sub>9</sub> O <sup>-</sup> /DMSO	61	39
	S <sup>+</sup> (CH <sub>3</sub> ) <sub>2</sub> <sup>e</sup>	C <sub>2</sub> H <sub>5</sub> O <sup>-</sup> /DMSO	74	26
	N <sup>+</sup> (CH <sub>3</sub> ) <sub>3</sub> <sup>f</sup>	OH <sup>-</sup>	95	5

a. R. A. Bartsch, B. M. Pruss, B. A. Bushaw, and K. E. Wiegers, *J. Am. Chem. Soc.*, **95**, 3405 (1973).

b. D. L. Griffith, D. L. Megees, and H. C. Brown, *J. Chem. Soc. Chem. Commun.*, 90 (1968).

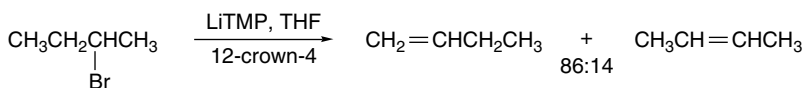
c. M. L. Dahr, E. D. Hughes, and C. K. Ingold, *J. Chem. Soc.*, 2058 (1948).

d. D. H. Froemsdorf and M. D. Robbins, *J. Am. Chem. Soc.*, **89**, 1737 (1967).

e. E. D. Hughes, C. K. Ingold, G. A. Maw, and L. I. Woolf, *J. Chem. Soc.*, 2077 (1948).

f. A. C. Cope, N. A. LeBel, H.-H. Lee, and W. R. Moore, *J. Am. Chem. Soc.*, **79**, 4720 (1957).

Branched amide bases can also control the regiochemistry of elimination on the basis of steric effects. For example LiTMP favors formation of 1-butene from 2-bromobutane.

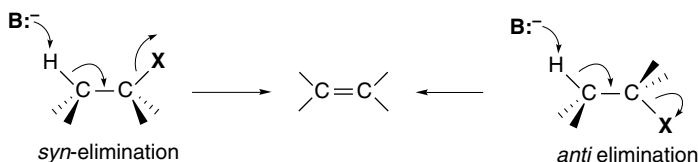


Ref. 284

The leaving group also affects the amount of internal versus terminal alkene that is formed. The poorer the leaving group, the more E1cb-like the TS. This trend is illustrated for the case of the 2-butyl system by the data in Table 5.13. Positively charged leaving groups, such as in dimethylsulfonium and trimethylammonium salts, may also favor a more E1cb-like TS because their inductive and field effects increase the acidity of the β-protons.

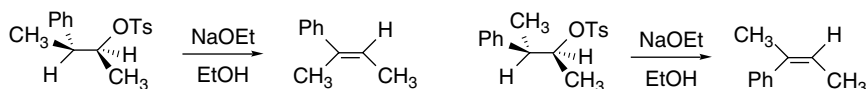
### 5.10.3. Stereochemistry of E2 Elimination Reactions

In this section we focus primarily on the stereochemistry of the concerted E2 mechanism. The most familiar examples are dehydrohalogenation and dehydrosulfonation reactions effected by strong bases. In principle, elimination can proceed with either *syn* or *anti* stereochemistry. For acyclic systems, there is a preference for *anti* elimination, but this can be overridden if conformational factors favor a *syn* elimination. The *anti* TS maximizes orbital overlap and avoids the eclipsing that is present in the *syn* TS.

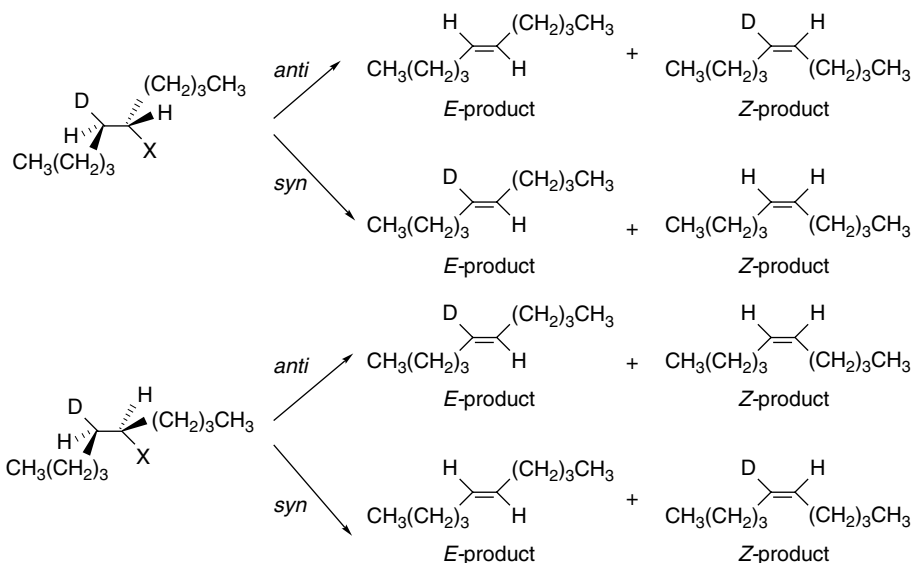


<sup>284</sup> I. E. Kopka, M. A. Nowak, and M. W. Rathke, *Synth. Commun.*, **16**, 27 (1986).

In acyclic systems, the extent of *anti* versus *syn* elimination can be determined by use of either stereospecifically deuterated reactants or diastereomeric reactants that give different products by *syn* and *anti* elimination. The latter approach showed that elimination from 3-phenyl-2-butyl tosylate is a stereospecific *anti* process.<sup>285</sup>



The extent of *syn* elimination in 5-decyl systems was measured using diastereomeric deuterium-labeled substrates. Stereospecifically deuterated 5-substituted decane derivatives were prepared and subjected to various elimination conditions. By comparison of the amount of deuterium in the *E*- and *Z*-isomers of the product, it is possible to determine the extent of *syn* and *anti* elimination.<sup>286</sup>



Data obtained for three different leaving groups are shown in Table 5.14. The results demonstrate that *syn* elimination is extensive for quaternary ammonium salts. With better leaving groups, the extent of *syn* elimination is small in the polar solvent DMSO but quite significant in benzene. The factors that promote *syn* elimination are discussed below. Table 5.15 summarizes some data on *syn* versus *anti* elimination in other acyclic systems.

The general trend revealed by these and other data is that *anti* stereochemistry is normally preferred for reactions involving good leaving groups such as bromide and tosylate. With poorer leaving groups (e.g., fluoride, trimethylamine), *syn* elimination becomes important. The amount of *syn* elimination is small in the 2-butyl system, but it becomes a major pathway with 3-hexyl compounds and longer chains.

In cyclic systems, the extent of *anti* and *syn* elimination depends on ring size, among other factors. Cyclohexyl systems have a very strong preference for *anti* elimination via

<sup>285</sup> W.-B. Chiao and W. H. Saunders, *J. Org. Chem.*, **45**, 1319 (1980).

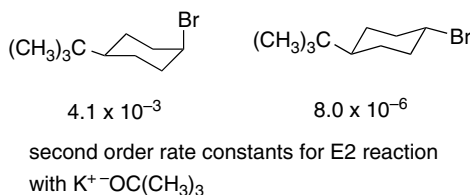
<sup>286</sup> M. Pankova, M. Svoboda, and J. Zavada, *Tetrahedron Lett.*, 2465 (1972). The analysis of the data also requires that account be taken of (a) isotope effects and (b) formation of 4-decene. The method of analysis is described in detail by J. Sicher, J. Zavada, and M. Pankova, *Coll. Czech. Chem. Commun.*, **36**, 3140 (1971).

**Table 5.14. Extent of *syn* Elimination as a Function of the Leaving Group in the 5-Decyl System<sup>a</sup>**

Leaving group	Percent <i>syn</i> elimination			
	E-product		Z-product	
	DMSO	Benzene	DMSO	Benzene
Cl	6	62	7	39
OTs	4	27	4	16
(CH <sub>3</sub> ) <sub>3</sub> N <sup>+</sup>	93	92	76	84

a. M. Pankova, M. Svoboda, and J. Zavada, *Tetrahedron Lett.*, 2465 (1972); the base used was potassium *t*-butoxide.

conformations in which both the departing proton and the leaving group occupy axial positions. This orientation permits alignment of the orbitals so that concerted *anti* elimination can occur. For example, *cis*-4-*t*-butylcyclohexyl bromide undergoes E2 elimination at a rate about 500 times greater than the *trans* isomer because only the *cis* isomer permits *anti* elimination from the favored chair conformation.<sup>287</sup>



Other cyclic systems are not so selective. In the decomposition of *N,N,N*-trimethyl-cyclobutylammonium hydroxide, elimination is 90% *syn*.<sup>288</sup> The cyclobutyl ring resists the conformation required for *anti* elimination. The more flexible five-membered ring analog undergoes about 50% *syn* elimination. Elimination from the

**Table 5.15. Stereochemistry of E2 Elimination for Some Acyclic Systems**

Reactant	Base/solvent	% <i>anti</i>	% <i>syn</i>
2-Bromobutane <sup>a</sup>	K <sup>+</sup> OC(CH <sub>3</sub> ) <sub>3</sub> / <i>t</i> -BuOH	100	0
2-Butyl tosylate <sup>b</sup>	K <sup>+</sup> OC(CH <sub>3</sub> ) <sub>3</sub> / <i>t</i> -BuOH	> 98	< 2
<i>N,N,N</i> -trimethyl-2-butylammonium <sup>c</sup>	K <sup>+</sup> OC(CH <sub>3</sub> ) <sub>3</sub> /DMSO	100	0
3-Fluorohexane <sup>d</sup>	K <sup>+</sup> OC(CH <sub>3</sub> ) <sub>3</sub> / <i>t</i> -BuOH	32	68
<i>N,N,N</i> -trimethyl-4-octylammonium <sup>e</sup>	K <sup>+</sup> OC(CH <sub>3</sub> ) <sub>3</sub> /DMSO	24	76
5-Decyl tosylate <sup>f</sup>	K <sup>+</sup> OC(CH <sub>3</sub> ) <sub>3</sub> / <i>t</i> -BuOH	93	7
5-Decyl chloride <sup>g</sup>	K <sup>+</sup> OC(CH <sub>3</sub> ) <sub>3</sub> /benzene	62	38
5-Decyl fluoride <sup>g</sup>	K <sup>+</sup> OC(CH <sub>3</sub> ) <sub>3</sub> /benzene	< 20	> 80
5-Decyl chloride <sup>g</sup>	K <sup>+</sup> OC(CH <sub>3</sub> ) <sub>3</sub> /DMSO	93	7
5-Decyl fluoride <sup>g</sup>	K <sup>+</sup> OC(CH <sub>3</sub> ) <sub>3</sub> , DMSO	80	20

a. R. A. Bartsch, *J. Am. Chem. Soc.*, **93**, 3683 (1971).

b. D. H. Froemsdorf, W. Dowd, W. A. Gifford, and S. Meyerson, *J. Chem. Soc., Chem. Commun.*, 449 (1968).

c. D. H. Froemsdorf, H. R. Pinnick, Jr., and S. Meyerson, *J. Chem. Soc., Chem. Commun.*, 1600 (1968).

d. J. K. Borchardt, J. C. Swanson, and W. H. Saunders, Jr., *J. Am. Chem. Soc.*, **96**, 3918 (1974).

e. J. Sicher, J. Zavada, and M. Pankova, *Collect. Czech. Chem. Commun.*, **36**, 3140 (1971).

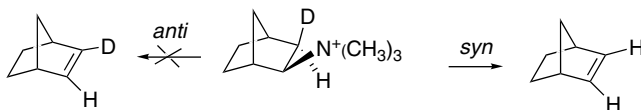
f. J. Zavada, M. Pankova, and J. Sicher, *J. Chem. Soc., Chem. Commun.*, 1145 (1968).

g. M. Pankova, M. Svoboda, and J. Zavada, *Tetrahedron Lett.*, 2465 (1972).

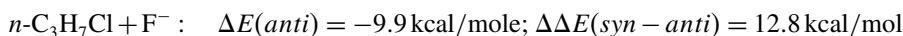
<sup>287</sup> J. Zavada, J. Krupicka, and J. Sicher, *Coll. Czech. Chem. Commun.*, **33**, 1393 (1968).

<sup>288</sup> M. P. Cooke, Jr., and J. L. Coke, *J. Am. Chem. Soc.*, **90**, 5556 (1968).

*N,N,N*-trimethylnorbornylammonium ion is exclusively *syn*.<sup>289</sup> This is another case where the rigid ring prohibits attainment of an *anti*-elimination process. There is also a steric effect operating against removal of an *endo* proton, which is required for *anti* elimination. *Syn* elimination is especially prevalent in the medium-sized ring compounds.<sup>290</sup>



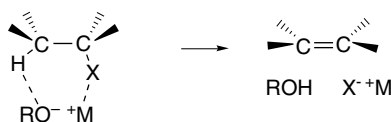
The energy difference between the *anti* and *syn* transition structures has been examined computationally using fluoride as the base and alkyl chlorides as the reactants. Simple primary and secondary chlorides show no barriers for *anti* elimination at the MP4SDQ/6-31+G\*\* level. The *syn* TSs show positive barriers and the total difference between the *syn* and *anti* TSs is on the order of 13 kcal/mol.<sup>291</sup>



The preferred TS for *syn* elimination is not periplanar, but rather has a torsion angle of about 30°. The *syn* TS has more E1cb character than the *anti*.

MP2/6-31+G\*\* computations have been used to compare cyclopentyl and cyclohexyl systems.<sup>292</sup> As noted above, cyclohexyl systems have a much stronger preference for the *anti* stereochemistry.<sup>293</sup> The optimum TSs are shown in Figure 5.15. Both the *anti* and *syn* TSs have negative barriers in the cyclopentyl system (−10.2 and −0.9 kcal/mol), whereas the *syn* system shows a positive barrier in the cyclohexyl system (−10.9 and +5.4 kcal/mol).

The factors that determine whether *syn* or *anti* elimination predominates are complex.<sup>294</sup> One factor that is believed to be important is whether the base is free or present as an ion pair.<sup>295</sup> The evidence suggests that an ion pair promotes *syn* elimination of anionic leaving groups. This effect can be explained by a TS in which the anion functions as a base and the cation assists in the departure of the leaving group.



This interpretation is in agreement with the solvent effect that is evident for the 5-decyl system data in Table 5.15. The extent of *syn* elimination is much higher in the nondissociating solvent benzene than in DMSO. The ion pair interpretation is also supported by the fact that addition of specific metal ion-complexing agents (crown

<sup>289</sup> J. P. Coke and M. P. Cooke, *J. Am. Chem. Soc.*, **89**, 6701 (1967).

<sup>290</sup> J. Sicher, *Angew. Chem. Int. Ed. Engl.*, **11**, 200 (1972).

<sup>291</sup> S. Gronert, *J. Am. Chem. Soc.*, **113**, 6041 (1991); *J. Am. Chem. Soc.*, **115**, 652 (1993).

<sup>292</sup> S. Gronert, *J. Org. Chem.*, **59**, 7046 (1994).

<sup>293</sup> C. H. DePuy, G. F. Morris, J. S. Smith, and R. J. Smat, *J. Am. Chem. Soc.*, **87**, 2421 (1965).

<sup>294</sup> R. A. Bartsch and J. Zavada, *Chem. Rev.*, **80**, 453 (1980).

<sup>295</sup> R. A. Bartsch, G. M. Pruss, R. L. Buswell, and B. A. Bushaw, *Tetrahedron Lett.*, 2621 (1972); J. K. Borchardt, J. C. Swanson, and W. H. Saunders, Jr., *J. Am. Chem. Soc.*, **96**, 3918 (1974).

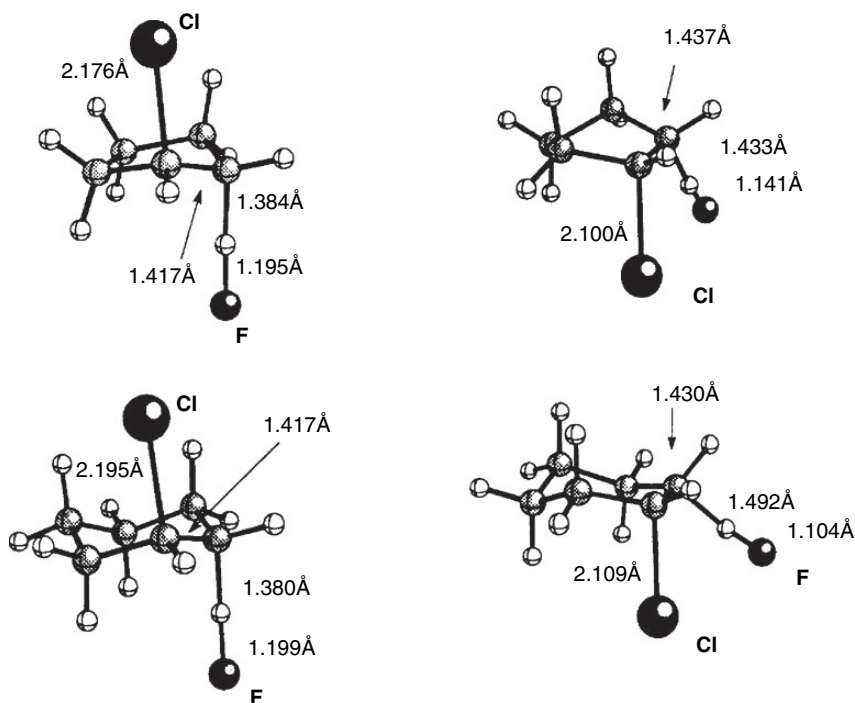
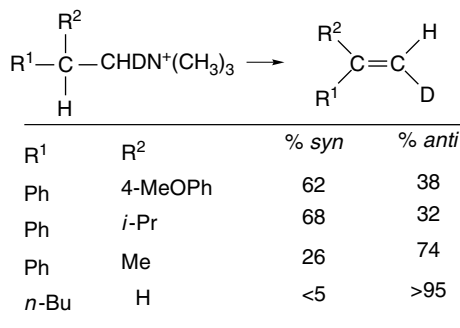


Fig. 5.15. *Anti* and *syn* transition states for fluoride-induced E2 elimination in (a) cyclopentyl and (b) cyclohexyl systems. Reproduced from *J. Org. Chem.*, **59**, 7046 (1994), by permission of the American Chemical Society.

ethers) that promote dissociation of the ion pair leads to diminished amounts of *syn* elimination.<sup>296</sup> Another factor that affects the *syn:anti* ratio is the strength of the base. Strong bases exhibit a higher proportion of *syn* elimination.<sup>297</sup>

Steric and conformational effects also play a significant role in determining the *syn:anti* ratio. With *N*-( $\beta,\beta$ -disubstituted-ethyl)-*N,N,N*-trimethylammonium ions, *syn* elimination is more prevalent when the  $\beta$ -substituents are aryl or branched. As the  $\beta$ -groups become less bulky, the amount of *syn* elimination decreases. This effect is illustrated by the data below.<sup>298</sup>

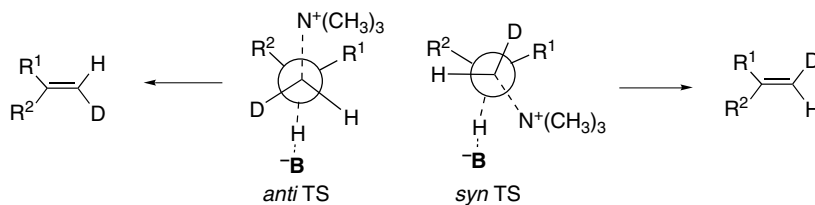


<sup>296</sup> R.A. Bartsch, E. A. Mintz, and R. M. Parلمان, *J. Am. Chem. Soc.*, **96**, 3918 (1974).

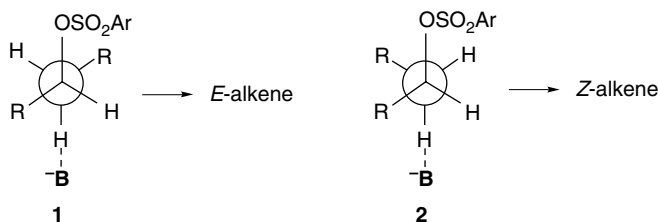
<sup>297</sup> K. C. Brown and W. H. Saunders, Jr., *J. Am. Chem. Soc.*, **92**, 4292 (1970); D. S. Bailey and W. H. Saunders, Jr., *J. Am. Chem. Soc.*, **92**, 6904 (1970).

<sup>298</sup> Y.-T. Tao and W. H. Saunders, Jr., *J. Am. Chem. Soc.*, **105**, 3183 (1983).

The steric dependence is imposed by the bulky trimethylamine leaving group. In the TS for *anti* elimination, steric repulsion is increased as R<sup>1</sup> and R<sup>2</sup> increase in size. When the repulsion is sufficiently large, the TS for *syn* elimination is preferred.



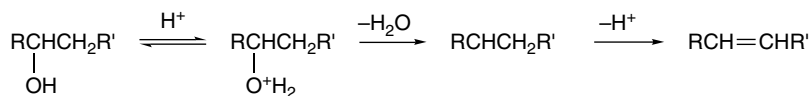
Another aspect of the stereochemistry of elimination reactions is the ratio of *E*- and *Z*-products. The proportion of *Z*- and *E*-isomers of disubstituted internal alkenes formed during elimination reactions depends on the identity of the leaving group. Halides usually give mainly the *E*-alkenes.<sup>299</sup> Bulkier groups, particularly arenesulfonates, give higher proportions of the *Z*-alkene. Sometimes, more *Z*-isomer is formed than *E*-isomer. The preference for *E*-alkene probably reflects the unfavorable steric repulsions present in the E2 transition state leading to *Z*-alkene. High *Z*:*E* ratios are attributed to a second steric effect that becomes important only when the leaving group is large. The conformations leading to *E*- and *Z*-alkene by *anti* elimination are depicted below.



When the leaving group and base are both large, conformation **2** is favored because it permits the leaving group to occupy a position removed from the  $\beta$ -alkyl substituents, while also maintaining an *anti* relationship to the  $\alpha$ -hydrogen. *Anti* elimination through a TS arising from conformation **2** gives *Z*-alkene.

#### 5.10.4. Dehydration of Alcohols

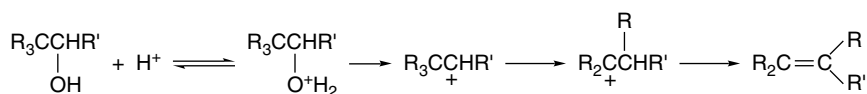
The dehydration of alcohols is an elimination reaction that takes place under acidic rather than basic conditions and involves an E1 mechanism.<sup>300</sup> The function of the acidic reagent is to convert the hydroxyl group to a better leaving group by protonation.



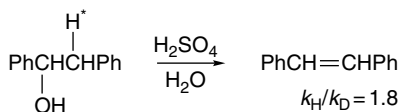
<sup>299</sup>. H. C. Brown and R. L. Kliminsch, *J. Am. Chem. Soc.*, **87**, 5517 (1965); I. N. Feit and W. H. Saunders, Jr., *J. Am. Chem. Soc.*, **92**, 1630 (1970).

<sup>300</sup>. D. V. Banthorpe, *Elimination Reactions*, Elsevier, New York, 1963, pp. 145–156.

This elimination reaction is the reverse of acid-catalyzed hydration, which was discussed in Section 5.2. Since a carbocation or closely related species is the intermediate, the elimination step is expected to favor the more-substituted alkene. The E1 mechanism also explains the trends in relative reactivity. Tertiary alcohols are the most reactive, and reactivity decreases going to secondary and primary alcohols. Also in accord with the E1 mechanism is the fact that rearranged products are found in cases where a carbocation intermediate would be expected to rearrange.



For some alcohols, exchange of the hydroxyl group with solvent competes with dehydration.<sup>301</sup> This exchange indicates that the carbocation can undergo  $S_N1$  capture in competition with elimination. Under conditions where proton removal is rate determining, it would be expected that a significant isotope effect would be seen, which is, in fact, observed.

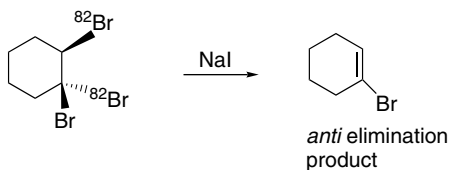


Ref. 302

### 5.10.5. Eliminations Reactions Not Involving C–H Bonds

The discussion of elimination processes thus far has focused on reactions that involve removal of a proton bound to a  $\beta$ -carbon, but it is the electrons in the C–H  $\sigma$  bond that are essential to the elimination process. Compounds bearing other substituents that can release electrons undergo  $\beta$ -eliminations. Many such reactions are known, and they are frequently stereospecific.

Vicinal dibromides can be debrominated by certain reducing agents, including iodide ion. The stereochemical course in the case of 1,1,2-tribromocyclohexane was determined using a  $^{82}\text{Br}$ -labeled sample prepared by *anti* addition of  $^{82}\text{Br}_2$  to bromocyclohexene. Exclusive *anti* elimination gave unlabeled bromocyclohexene, whereas  $^{82}\text{Br}$ -labeled product resulted from *syn* elimination. Debromination with sodium iodide was found to be cleanly an *anti* elimination.<sup>303</sup>

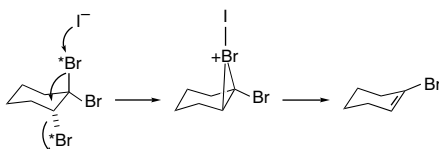


<sup>301</sup> C. A. Bunton and D. R. Llewellyn, *J. Chem. Soc.*, 3402 (1957); J. Manassen and F. S. Klein, *J. Chem. Soc.*, 4203 (1960).

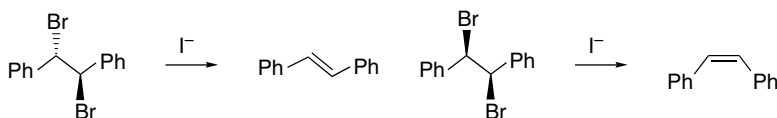
<sup>302</sup> D. S. Noyce, D. R. Hartter, and R. M. Pollack, *J. Am. Chem. Soc.*, **90**, 3791 (1968).

<sup>303</sup> C. L. Stevens and J. A. Valicenti, *J. Am. Chem. Soc.*, **87**, 838 (1965).

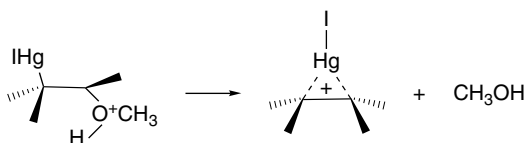
The iodide-induced reduction is essentially the reverse of a halogenation. Application of the principle of microscopic reversibility suggests that the reaction proceeds through a bridged intermediate.<sup>304</sup>



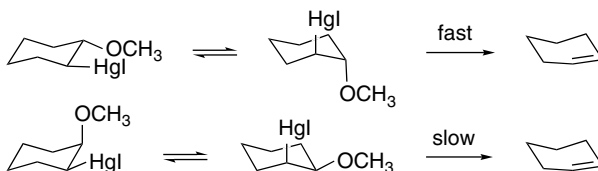
The rate-determining expulsion of bromide ion through a bridged intermediate requires an *anti* orientation of the two bromides. The nucleophilic attack of iodide at one bromide enhances its nucleophilicity and permits formation of the bridged ion. The stereochemical preference in noncyclic systems is also *anti*, as indicated by the fact that *meso*-stilbene dibromide yields *trans*-stilbene, whereas *d,l*-stilbene dibromide gives mainly *cis*-stilbene under these conditions.<sup>94</sup>



Structures of type M—C—C—X in which M is a metal and X is a leaving group are very prone to elimination with formation of a double bond. One example is acid-catalyzed deoxymercuration.<sup>305</sup> The  $\beta$ -oxyorganomercurials are more stable than similar reagents derived from more electropositive metals, but are much more reactive than simple alcohols. For example,  $\text{CH}_3\text{CH}(\text{OH})\text{CH}_2\text{HgI}$  is converted to propene under acid-catalyzed conditions at a rate that is  $10^{11}$  times greater than dehydration of 2-propanol under the same conditions. These reactions are believed to proceed through a bridged mercurinium ion by a mechanism that is the reverse of oxymercuration (see Section 5.6).



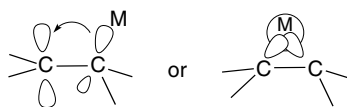
One of the pieces of evidence supporting this mechanism is the fact that the  $\Delta H^\ddagger$  for deoxymercuration of *trans*-2-methoxycyclohexylmercuric iodide is about 8 kcal/mol less than for the *cis* isomer. Only the *trans* isomer can undergo elimination by an *anti* process through a chair conformation.



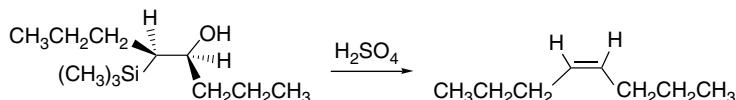
<sup>304</sup>. C. S. T. Lee, I. M. Mathai, and S. I. Miller, *J. Am. Chem. Soc.*, **92**, 4602 (1970).

<sup>305</sup>. M. M. Kreevoy and F. R. Kowitz, *J. Am. Chem. Soc.*, **82**, 739 (1960).

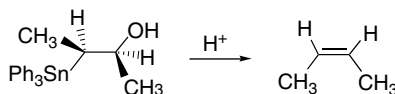
Comparing the rates of acid-catalyzed  $\beta$ -elimination of compounds of the type  $MCH_2CH_2OH$  yields the reactivity order for  $\beta$ -substituents  $IHg \sim Ph_3Pb \sim Ph_3Sn > Ph_3Si > H$ . The relative rates are within a factor of ten for the first three, but these are  $10^6$  greater than for  $Ph_3Si$  and  $10^{11}$  greater than for a proton. There are two factors involved in these very large rate accelerations. One is bond energies. The relevant values are  $Hg-C = 27 < Pb-C = 31 < Sn-C = 54 < Si-C = 60 < H-C = 96 \text{ kcal/mol}$ .<sup>306</sup> The metal substituents also have a very strong stabilizing effect for carbocation character at the  $\beta$ -carbon. This stabilization can be pictured either as an orbital-orbital interaction in which the carbon-metal bond donates electron density to the adjacent  $p$  orbital, or as formation of a bridged species.



There are a number of synthetically valuable  $\beta$ -elimination processes involving organosilicon<sup>307</sup> and organotin<sup>308</sup> compounds. Treatment of  $\beta$ -hydroxyalkylsilanes or  $\beta$ -hydroxyalkylstannanes with acid results in stereospecific *anti* eliminations that are much more rapid than for compounds lacking the group IV substituent.

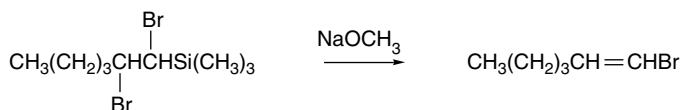


Ref. 309



Ref. 310

$\beta$ -Halosilanes also undergo facile elimination when treated with methoxide ion.



Ref. 311

<sup>306</sup> D. D. Davis and H. M. Jacobs, III, *J. Organomet. Chem.*, **206**, 33 (1981).

<sup>307</sup> A. W. P. Jarvie, *Organomet. Chem. Rev. Sect. A*, **6**, 153 (1970); W. P. Weber, *Silicon Reagents for Organic Synthesis*, Springer-Verlag, Berlin, 1983; E. W. Colvin, *Silicon in Organic Synthesis*, Butterworths, London, 1981.

<sup>308</sup> M. Pereyre, J. -P. Quintard, and A. Rahm, *Tin in Organic Synthesis*, Butterworths, London, 1987.

<sup>309</sup> P. F. Hudrlick and D. Peterson, *J. Am. Chem. Soc.*, **97**, 1464 (1975).

<sup>310</sup> D. D. Davis and C. E. Gray, *J. Org. Chem.*, **35**, 1303 (1970).

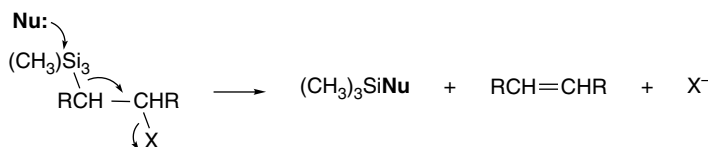
<sup>311</sup> A. W. P. Jarvie, A. Holt, and J. Thompson, *J. Chem. Soc. B*, 852 (1969); B. Miller and G. J. McGarvey, *J. Org. Chem.*, **43**, 4424 (1978).

Fluoride-induced  $\beta$ -elimination of silanes having leaving groups in the  $\beta$ -position are important processes in synthetic chemistry, as, for example, in the removal of  $\beta$ -trimethylsilyloxy groups.

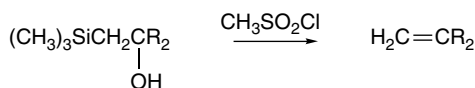


Ref. 312

These reactions proceed by alkoxide or fluoride attack at silicon that results in C–Si bond cleavage and elimination of the leaving group from the  $\beta$ -carbon. These reactions are stereospecific *anti* eliminations.

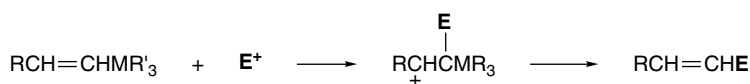


$\beta$ -Elimination reactions of this type can also be effected by converting a  $\beta$ -hydroxy group to a better leaving group. For example, conversion of  $\beta$ -hydroxyalkylsilanes to the corresponding methanesulfonates leads to rapid elimination.<sup>313</sup>



$\beta$ -Trimethylsilylalkyl trifluoroacetates also undergo facile *anti* elimination.<sup>314</sup>

The ability to promote  $\beta$ -elimination and the electron-donor capacity of the  $\beta$ -metalloid substituents can be exploited in a very useful way in synthetic chemistry.<sup>315</sup> Vinylstannanes and vinylsilanes react readily with electrophiles. The resulting intermediates then undergo elimination of the stannyl or silyl substituent, so that the net effect is replacement of the stannyl or silyl group by the electrophile. The silyl and stannyl substituents are crucial to these reactions in two ways. In the electrophilic addition step, they act as electron-releasing groups that promote addition and control the regiochemistry. A silyl or stannyl substituent strongly stabilizes carbocation character at the  $\beta$ -carbon atom and thus directs the electrophile to the  $\alpha$ -carbon.



Computational investigations indicate that there is a ground state interaction between the alkene  $\pi$  orbital and the carbon-silicon bond that raises the energy of the  $\pi$

<sup>312</sup> P. Sieber, *Helv. Chim. Acta*, **60**, 2711 (1977).

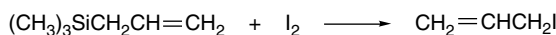
<sup>313</sup> F. A. Carey and J. R. Toler, *J. Org. Chem.*, **41**, 1966 (1976).

<sup>314</sup> M. F. Connil, B. Jousseane, N. Noiret, and A. Saux, *J. Org. Chem.*, **59**, 1925 (1994).

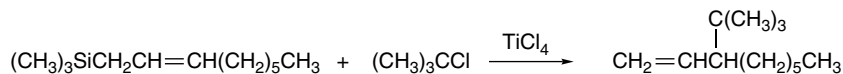
<sup>315</sup> T. H. Chan and I. Fleming, *Synthesis*, 761 (1979); I. Fleming, *Chem. Soc. Rev.*, **10**, 83 (1981).

HOMO and enhances reactivity.<sup>316</sup> MP3/6-31G\* calculations indicate a stabilization of 38 kcal/mol, which is about the same as the value calculated for an  $\alpha$ -methyl group.<sup>317</sup> Furthermore, this stereoelectronic interaction favors attack of the electrophile *anti* to the silyl substituent. The reaction is then completed by the elimination step in which the carbon-silicon or carbon-tin bond is broken.

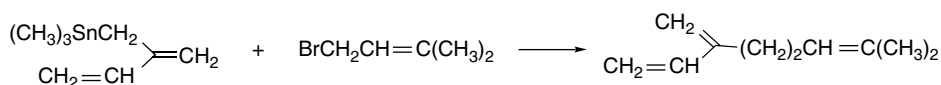
Allyl silanes and allyl stannanes are also reactive toward electrophiles and usually undergo a concerted elimination of the silyl substituent.



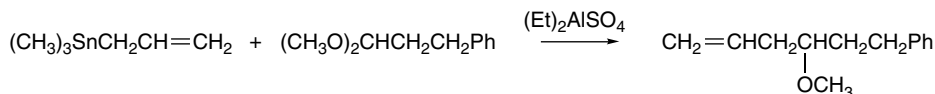
Ref. 318



Ref. 319

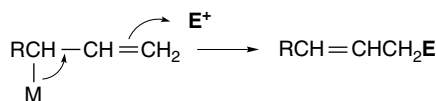


Ref. 320



Ref. 321

The common mechanistic pattern in these reactions involves electron release toward the developing electron deficiency on the C(2) of the double bond. Completion of the reaction involves loss of the electron-donating group and formation of the double bond. Further examples of these synthetically useful reactions can be found in Section 9.3 in Part B.



<sup>316</sup> S. D. Kahn, C. F. Pau, A. R. Chamberlin, and W. J. Hehre, *J. Am. Chem. Soc.*, **109**, 650 (1987).

<sup>317</sup> S. E. Wierschke, J. Chandrasekhar, and W. L. Jorgensen, *J. Am. Chem. Soc.*, **107**, 1496 (1985).

<sup>318</sup> D. Grafstein, *J. Am. Chem. Soc.*, **77**, 6650 (1955).

<sup>319</sup> I. Fleming and I. Paterson, *Synthesis*, 445 (1979).

<sup>320</sup> J. P. Godschalx and J. K. Stille, *Tetrahedron Lett.*, **24**, 1905 (1983).

<sup>321</sup> A. Hosomi, H. Iguchi, M. Endo, and H. Sakurai, *Chem. Lett.*, 977 (1979).

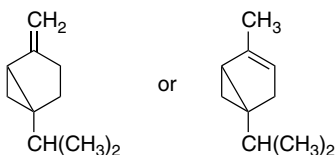
- G. V. Boyd, in *The Chemistry of Triple-Bonded Functional Groups*, Supplement 2, S. Patai, ed., John Wiley & Sons, New York, 1994, Chap. 6.
- A. F. Cockerill and R. G. Harrison, *The Chemistry of Double-Bonded Functional Groups*, Part 1, S. Patai, ed., John Wiley & Sons, New York, 1977, Chap. 4.
- P. B. de la Mare and R. Bolton, *Electrophilic Additions to Unsaturated Systems*, 2nd Edition, Elsevier, New York, 1982.
- J. G. Gandler, in *The Chemistry of Double-Bonded Functional Groups*, Supplement A, Vol. 2, S. Patai, ed., John Wiley & Sons, New York, 1989, Chap. 12.
- G. H. Schmid, in *The Chemistry of Double-Bonded Functional Groups*, Supplement A, Vol. 2, S. Patai, ed., John Wiley & Sons, New York, 1989, Chap. 11.
- P. J. Stang and F. Diederich, eds., *Modern Acetylene Chemistry*, VCH Publishers, Weinheim, 1995.
- W. H. Saunders, Jr., and A. F. Cockerill, *Mechanisms of Elimination Reactions*, John Wiley & Sons, New York, 1973.

## Problems

(References for these problems will be found on page 1160.)

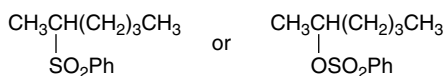
5.1 Which compound of each pair will react faster with the specified reagent? Explain your answer.

- 1-hexene or *E*-3-hexene with bromine in acetic acid.
- cis*- or *trans*-4-(*t*-butyl)cyclohexylmethyl bromide with  $\text{KOC}(\text{CH}_3)_3$  in *t*-butyl alcohol.
- 2-phenylpropene or 4-(1-methylethenyl)benzoic acid with sulfuric acid in water.
- 



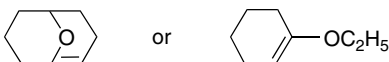
toward acid-catalyzed hydration.

e.



with  $\text{KOC}(\text{CH}_3)_3$  in *t*-butyl alcohol.

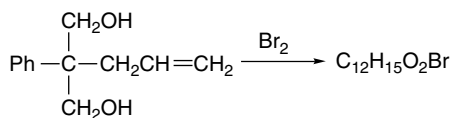
- 4-bromophenylacetylene or 4-methylphenylacetylene with  $\text{Cl}_2$  in acetic acid.
- 



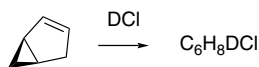
toward acid-catalyzed hydration.

5.2. Predict the structure, including stereochemistry, of the product(s) expected for the following reactions. If more than one product is shown, indicate which is major and which is minor.

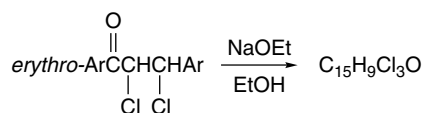
a.



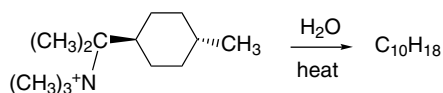
b.



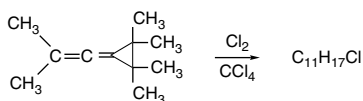
c.



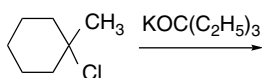
d.



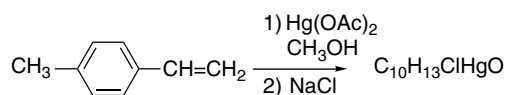
e.



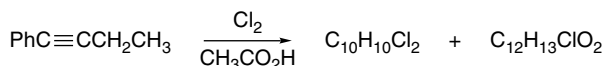
f.



g.



h.

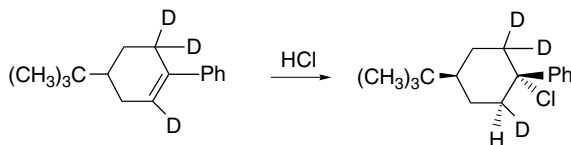


- 5.3. The reaction of the *cis* and *trans* isomers of *N,N,N*-trimethyl-(4-*t*-butylcyclohexyl)ammonium chloride with  $\text{K}^+\text{-O-}t\text{-Bu}$  in *t*-butyl alcohol have been compared. The *cis* isomer gives 90% 4-*t*-butylcyclohexene and 10% *N,N*-dimethyl-(4-*t*-butylcyclohexyl)amine, whereas the *trans* isomer gives only the latter product in quantitative yield. Explain the different behavior of the two isomers.
- 5.4. For E2 eliminations in 2-phenylethyl systems with several different leaving groups, both the primary kinetic isotope effect and Hammett  $\rho$  have been determined. Deduce information about the nature and location (early, late) of the TS in the variable E2 spectrum. How does the identity of the leaving group affect the nature and location of the TS?

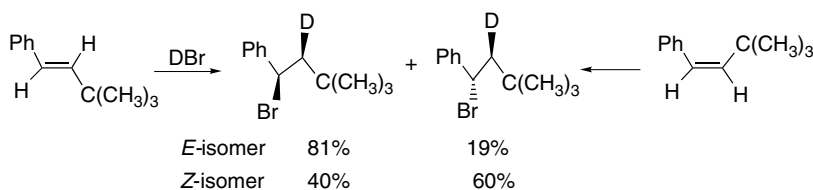
X	$k_{\text{H}}/k_{\text{D}}$	$\rho$
Br	7.11	2.1
OTs	5.66	2.3
$^+\text{S}(\text{CH}_3)_2$	5.07	2.7
$^+\text{N}(\text{CH}_3)_3$	2.98	3.7

- 5.5. Predict the effect on the 1-butene, *Z*-2-butene, and *E*-2-butene product ratio when the E2 elimination (KOEt, EtOH) of *erythro*-3-deuterio-2-bromobutane is compared with 2-bromobutane. Which alkene(s) will increase in relative amount and which will decrease in relative amount? Explain the basis of your answer.
- 5.6. Arrange the following compounds in order of increasing rate of acid-catalyzed hydration: ethene, propene, 2-cyclopropylpropene, 2-methylpropene, 1-cyclopropyl-1-methoxyethene. Explain the basis of your answer.
- 5.7. Discuss the factors that are responsible for the regiochemistry and stereochemistry observed for the following reactions.

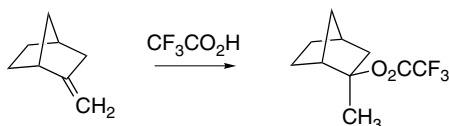
a.



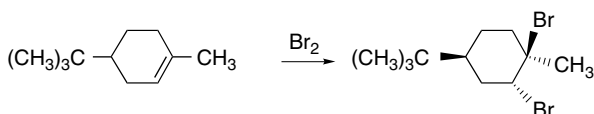
b.



c.

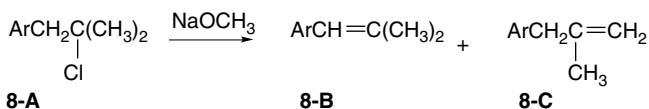


d.

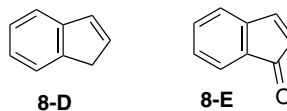


5.8. Explain the mechanistic basis of the following observations and discuss how the observation provides information about the reaction mechanism.

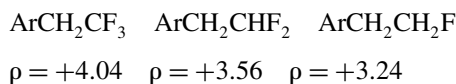
- a. When 1-aryl-2-methyl-2-propyl chlorides (**8-A**) react with  $\text{NaOCH}_3$ , roughly 1:1 mixtures of internal (**8-B**) and terminal alkene (**8-C**) are formed. By using the product ratios, the overall reaction rate can be dissected into the rates for formation of **8-B** and **8-C**. The rates are found to be substituent dependent for **8-B** ( $\rho = +1.4$ ) but not for **8-C** ( $\rho = -0.1 \pm 0.1$ ). All the reactions are second order, first order in reactant and first order in base.



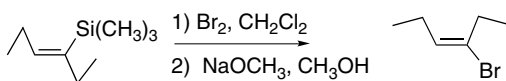
- b. When 1,3-pentadiene reacts with  $\text{DCl}$ , more *E*-4-chloro-5-deuterio-2-pentene (60–75%) is formed than *E*-4-chloro-1-deuterio-2-pentene (40–25%).
- c. When indene (**8-D**) is brominated in  $\text{CCl}_4$ , it gives some 15% *syn* addition, but indenone (**8-E**) gives only *anti* addition under these conditions. When the halogenation of indenone is carried out using  $\text{Br}-\text{Cl}$ , the product is *trans*-2-bromo-3-chloroindenone.



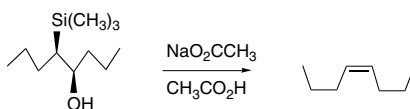
- d. The acid-catalyzed hydration of allene gives acetone, not allyl alcohol or propanal.
- e. In the addition of  $\text{HCl}$  to cyclohexene in acetic acid, the ratio of cyclohexyl acetate to cyclohexyl chloride drops significantly when tetramethylammonium chloride is added in increasing concentrations. The rate of the reaction is also accelerated. These effects are not observed with styrene.
- f. The  $\rho$  value for elimination of  $\text{HF}$  using  $\text{K}^+\text{O}^-t\text{-Bu}$  from a series of 1-aryl-2-fluoroethanes increases from the mono- to di- and trifluoro derivatives, as indicated below.



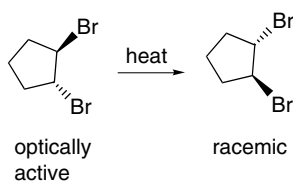
a.



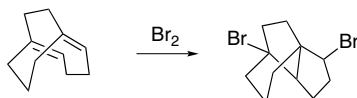
b.



c.

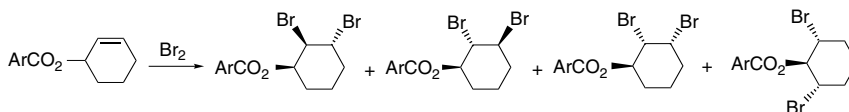


d.

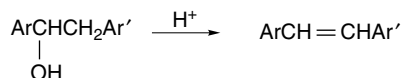


5.10. The rates of bromination of internal alkynes are roughly 100 times greater than the corresponding terminal alkynes. For hydration, however, the rates are less than 10 times greater for the disubstituted compounds. Account for this difference by comparison of the mechanisms for bromination and hydration.

5.11. The bromination of 3-aryloxycyclohexenes gives rise to a mixture of stereoisomeric and regioisomeric products. The product composition for Ar = phenyl is shown. Account for the formation of each of these products.



5.12. The Hammett correlation of the acid-catalyzed dehydration of 1,2-diaryl ethanols has been studied. The correlation resulting from substitution on both the 1- and 2-aryl rings is:  $\log k = -3.78(\sigma_{\text{Ar}}^+ + 0.23\sigma_{\text{Ar}'}) - 3.18$ . Rationalize the form of this correlation equation. What information does it give about the involvement of the Ar' ring in the rate-determining step of the reaction?

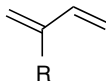


- 5.13. The addition of HCl to alkenes such as 2-methyl-1-butene and 2-methyl-2-butene in nitromethane follow a third-order rate expression:

$$\text{Rate} = k[\text{HCl}]^2[\text{alkene}]$$

It has also been established that there is no incorporation of deuterium into the reactant at 50% completion when DCl is used. Added tetraalkylammonium chloride retards the reaction, but the corresponding perchlorate salt does not. Propose a reaction mechanism that is consistent with these observations.

- 5.14. In the bromination of substituted styrenes, a  $\rho\sigma^+$  plot is noticeably curved. If the extremes of the curve are taken to represent straight lines, the curve can be resolved into two Hammett relationships with  $\rho = -2.8$  for EWG substituents and  $\rho = -4.4$  for ERG substituents. The corresponding  $\beta$ -methylstyrenes give a similarly curved plot. The stereoselectivity of the reaction of the  $\beta$ -methylstyrenes is also dependent on the substituents. The reaction is stereospecifically *anti* for strong EWGs, but is only weakly stereoselective, e.g., 63% *anti*:37% *syn*, for methoxy. Discuss a possible mechanistic basis for the curved Hammett plots and the relationship to the observed stereochemistry.
- 5.15. The second-order rate constants and solvent kinetic isotope effects for acid-catalyzed hydration are given below for several 2-substituted 1,3-butadienes. The products are a mixture of 1,2- and 1,4-addition. What information do these data provide about the mechanism of the reaction?



R	$k_2(M^{-1}s^{-1})$	$k_H^+/k_D^+$
c-C <sub>3</sub> H <sub>5</sub>	$1.22 \times 10^{-2}$	1.2
CH <sub>3</sub>	$3.19 \times 10^{-5}$	1.8
Cl	$2.01 \times 10^{-8}$	1.4
H	$3.96 \times 10^{-8}$	1.8
C <sub>2</sub> H <sub>5</sub> O	60	-

- 5.16. The reaction of both *E*- and *Z*-2-butene with acetic acid to give 2-butyl acetate is catalyzed by various strong acids. With DBr, DCl, and CH<sub>3</sub>SO<sub>3</sub>H in CH<sub>3</sub>CO<sub>2</sub>D, the reaction proceeds with largely ( $84 \pm 2\%$ ) *anti* addition. If the reaction is stopped short of completion, there is no incorporation of deuterium into unreacted alkene, nor any interconversion of the *E*- and *Z*-isomers. When the catalyst is changed to CF<sub>3</sub>SO<sub>3</sub>H, the recovered butene shows small amounts of 1-butene and interconversion of the 2-butene stereoisomers. The stereoselectivity of the reaction drops to 60–70% *anti* addition. How can you account for the changes that occur when CF<sub>3</sub>SO<sub>3</sub>H is used as the catalyst, as compared with the other acids?
- 5.17. A comparison of rate and product composition of the products from reaction of *t*-butyl chloride with NaOCH<sub>3</sub> in methanol and methanol-DMSO mixtures has been reported. Some of the data are shown below. Interpret the changes in rates and product composition as the amount of DMSO in the solvent mixture is increased.

[NaOMe] <i>M</i>	100% MeOH			36.8% DMSO			64.2% DMSO		
	Rate $k \times 10^4 \text{s}^{-1}$	Product comp.(%)		Rate $k \times 10^4 \text{s}^{-1}$	Product comp.(%)		Rate $k \times 10^4 \text{s}^{-1}$	Product comp.(%)	
		Ether	Alkene		Ether	Alkene		Ether	Alkene
0.00	2.15	73.8	26.2	0.81	50	50	0.24	24	76
0.20	2.40			1.52			5.3		
0.25	2.30	62.9	32.1						
0.30	2.26			1.90	10.5	89.5	10.3	0	100
0.40	2.36			2.65			17.5	0	100
0.50	2.56	58.6	41.4				24.2	0	100
0.70				4.11	1.1	98.9			
0.75	2.58	51.7	48.3						
0.80				4.59					
0.90	2.64			6.16	4.1	95.9			
1.00	2.74	52.2	47.8	6.81	3.8	96.2			

5.18 a. The gas phase basicity of substituted  $\alpha$ -methyl styrenes follows the Yukawa-Tsuno equation with  $r^+ = 1.0$ . The corresponding  $r^+$  for 1-phenylpropyne is 1.12 and for phenylacetylene it is 1.21. How are these values related to the relative stability of the carbocations formed by protonation?

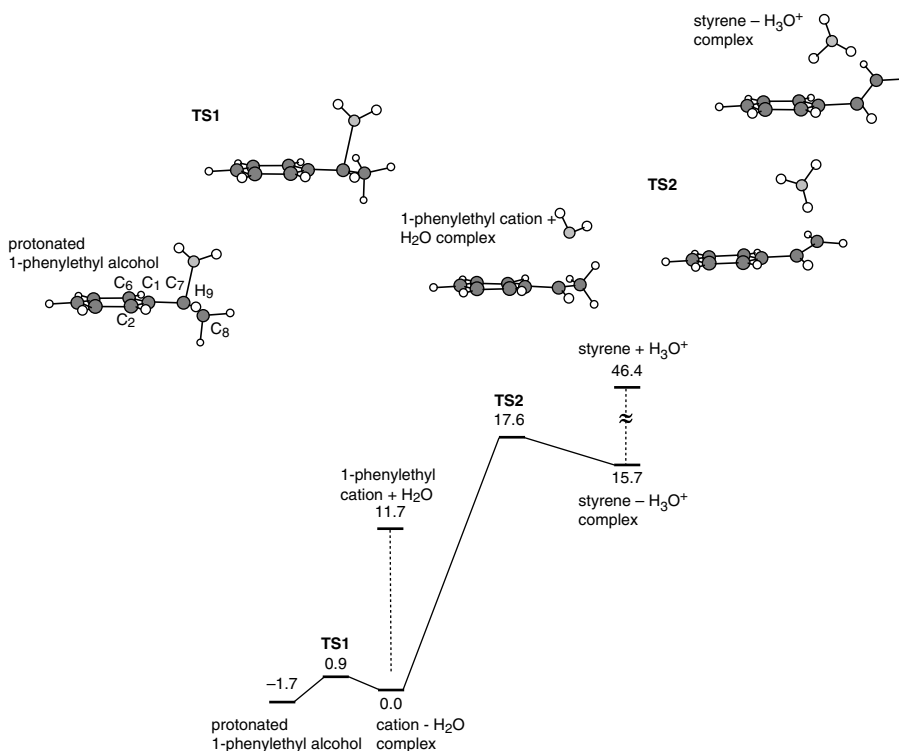


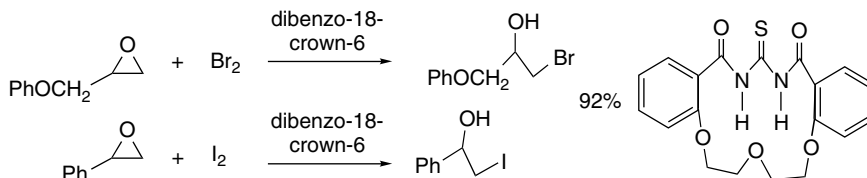
Fig. 5.P18b. Reaction profile for ionization and protonation routes to 1-phenylethyl cation. Relative energies are in kcal/mol. Reproduced from the *Bulletin of the Chemical Society of Japan.*, **71**, 2427 (1998).

**Table 5.P18b. Selected Structural Parameters, Charge Densities, and Energies of Reactants and Transition States for Formation of a 1-Phenylethyl Cation**

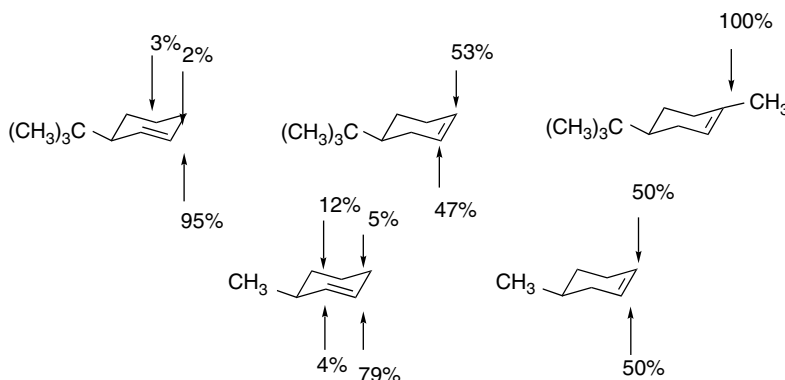
Bond length	Protonated Alcohol	TS1	Phenylethyl Cation-H <sub>2</sub> O Complex	TS2	Styrene-H <sub>3</sub> O <sup>+</sup> Complex	Styrene
C(1)-C(7)	1.474	1.420	1.395	1.457	1.478	1.472
C(7)-C(8)	1.500	1.481	1.469	1.367	1.353	1.343
C(7)-O	1.641	2.077	2.639			
C(8)-C(10)	1.093	1.091	1.098	1.608	2.118	
Charge on Ph	0.225	0.369	0.468	0.196	0.111	-0.002
Relative energy	-1.7	0.9	0.0	17.6	15.7	46.4

b. The acid-catalyzed hydration of styrene and the dissociation of protonated 1-phenylethanol provide alternative routes to the 1-phenylethyl cation. The resonance component ( $r^+$ ) of the Yukawa-Tsuno equations are 0.70 and 1.15, respectively. The reactions have been modeled using MP2/6-31G\* calculations and Figure 5.P18b gives the key results. Table 5.P18b lists some of the structural features of the reactants, TSs, and products. Interpret and discuss these results.

5.19. Crown ethers have been found to catalyze the ring opening of epoxides by I<sub>2</sub> and Br<sub>2</sub>. The catalysts also improve the regioselectivity, favoring addition of the halide at the less-substituted position. A related structure (shown on the right) is an even better catalyst. Indicate a mechanism by which these catalytic effects can occur.

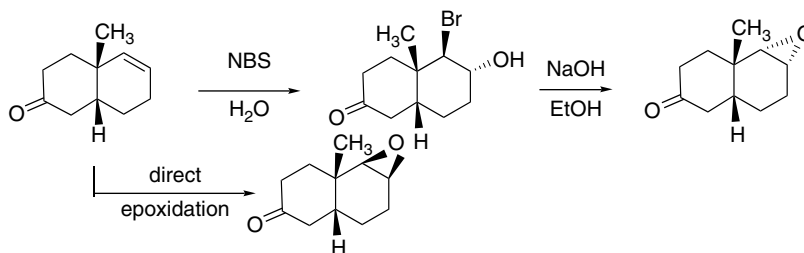


5.20. The chart below shows the regio- and stereoselectivity observed for oxymercuration reduction of some 3- and 4-alkylcyclohexenes. Provide an explanation for the product ratios in terms of the general mechanism for oxymercuration discussed in Section 5.6.1.

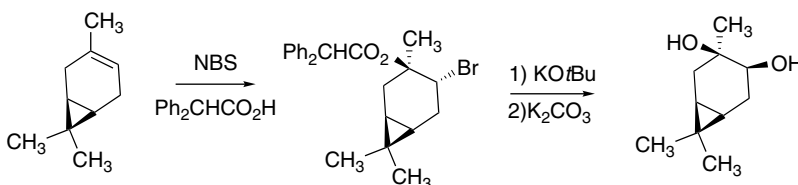


5.21. Solvolhalogenation can be used to achieve both regio- and stereochemical control for synthetic purposes in alkene addition reactions. Some examples are shown below. Discuss the factors that lead to the observed regio- or stereochemical outcome.

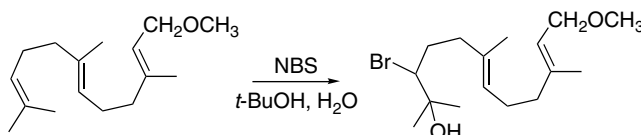
a. Control of the stereochemistry of an epoxide:



b. Formation of *cis*-diols:



c. Chemoselective functionalization of polyalkenes:



# Carbanions and Other Carbon Nucleophiles

## Introduction

This chapter is concerned with carbanions, which are the conjugate bases (in the Brønsted sense) formed by deprotonation at carbon atoms. Carbanions are very important in synthesis because they are good nucleophiles and formation of new carbon-carbon bonds often requires a nucleophilic carbon species. Carbanions vary widely in stability, depending on the hybridization of the carbon atom and the ability of substituent groups to stabilize the negative charge. In the absence of a stabilizing substituent, removal of a proton from a C–H bond is difficult. There has therefore been much effort devoted to study of the methods of generating carbanions and understanding substituent effects on stability and reactivity. Fundamental aspects of carbanion structure and stability were introduced in Section 3.4.2. In this chapter we first consider the measurement of hydrocarbon acidity. We then look briefly at the structure of organolithium compounds, which are important examples of carbanionic character in organometallic compounds. In Section 6.3 we study carbanions that are stabilized by functional groups, with emphasis on carbonyl compounds. In Section 6.4 the neutral nucleophilic enols and enamines are considered. Finally in Section 6.5 we look at some examples of carbanions as nucleophiles in  $S_N2$  reactions.

## 6.1. Acidity of Hydrocarbons

In the discussion of the relative acidity of carboxylic acids in Chapter 1 (p. 53–54), the thermodynamic acidity, expressed as the acid dissociation constant in aqueous solution, was taken as the measure of acidity. Determining the dissociation constants of carboxylic acids in aqueous solution by measuring the titration curve with a pH-sensitive electrode is straightforward, but determination of the acidity of hydrocarbons is more difficult. As most are quite weak acids, very strong bases are required

to effect deprotonation. Water and alcohols are far more acidic than nearly all hydrocarbons and are unsuitable solvents for the generation of anions from hydrocarbons. Any strong base will deprotonate the solvent rather than the hydrocarbon. For synthetic purposes, aprotic solvents such as diethyl ether, THF, and DME are used, but for equilibrium measurements solvents that promote dissociation of ion pairs and ion clusters are preferred. Weakly acidic solvents such as dimethyl sulfoxide (DMSO) and cyclohexylamine are used in the preparation of strongly basic carbanions. The high polarity and cation-solvating ability of DMSO facilitates dissociation of ion pairs so that the equilibrium data refer to the solvated dissociated ions, rather than to ion aggregates.

The basicity of a base-solvent system can be specified by a basicity function  $H_-$ . The value of  $H_-$  corresponds essentially to the pH of strongly basic nonaqueous solutions. The larger the value of  $H_-$ , the greater the proton-abstracting ability of the medium. The process of defining a basicity function is analogous to that described for acidity functions in Section 3.7.1.3. Use of a series of overlapping indicators permits assignment of  $H_-$  values to base-solvent systems, and allows  $pK$ 's to be determined over a range of 0–35  $pK$  units.<sup>1</sup> The indicators employed include substituted anilines and arylmethanes that have significantly different electronic (UV–VIS) spectra in their neutral and anionic forms. Table 6.1 presents  $H_-$  values for some representative solvent-base systems.

The acidity of a hydrocarbon can be determined in an analogous way.<sup>2</sup> If the electronic spectra of the neutral and anionic forms are sufficiently different, the concentration of each can be determined directly in a solution of known  $H_-$ ; the equilibrium constant for



is related to  $pK_{\text{RH}}$  by the equation

$$pK_{\text{RH}} = H_- + \log \frac{[\text{RH}]}{[\text{R}^-]} \quad (6.1)$$

**Table 6.1. Values of  $H_-$  for Some Representative Solvent-Base Systems**

Solution	$H_-^a$
1 M KOH	14.0
5 M KOH	15.5
10 M KOH	17.0
1.0 M NaOMe in MeOH	17.0
5.0 M NaOMe in MeOH	19.0
0.01 M NaOMe in 1:1 DMSO-MeOH	15.0
0.01 M NaOMe in 10:1 DMSO-MeOH	18.0
0.01 M NaOEt in 20:1 DMSO-EtOH	21.0

a. Selected values from J. R. Jones, *The Ionization of Carbon Acids*, Academic Press, New York, 1973, Chap. 6, are rounded to the nearest 0.5 pH unit.

- <sup>1</sup> We will restrict the use of  $pK_a$  to acid dissociation constants in aqueous solution. The designation  $pK$  refers to the acid dissociation constant under other conditions.
- <sup>2</sup> D. Dolman and R. Stewart, *Can. J. Chem.*, **45**, 911 (1967); E. C. Steiner and J. M. Gilbert, *J. Am. Chem. Soc.*, **87**, 382 (1965); K. Bowden and R. Stewart, *Tetrahedron*, **21**, 261 (1965).



that a linear relationship between exchange rates and equilibrium acidity be established for representative examples of the compounds under study. A satisfactory correlation provides a basis for using kinetic acidity data for compounds of that structural type.

The nature of the solvent in which the extent or rate of deprotonation is determined has a significant effect on the apparent acidity of the hydrocarbon. In general, the extent of ion aggregation is primarily a function of the ability of the solvent to solvate the ionic species. In THF, DME, and other ethers, there is usually extensive ion aggregation. In dipolar aprotic solvents, especially dimethyl sulfoxide, ion pairing is less significant.<sup>6</sup> The identity of the cation also has a significant effect on the extent of ion pairing. Hard cations promote ion pairing and aggregation. Because of these factors, the numerical  $pK$  values are not absolute and are specific to the solvent and cation. Nevertheless, they provide a useful measure of relative acidity. The two solvents that have been used for most quantitative measurements on hydrocarbons are dimethyl sulfoxide and cyclohexylamine.

A series of hydrocarbons has been studied in cyclohexylamine, using cesium cyclohexylamide as base. For many of the compounds studied, spectroscopic measurements were used to determine the relative extent of deprotonation of two hydrocarbons and thus establish relative acidity.<sup>7</sup> For other hydrocarbons, the acidity was derived by kinetic measurements. It was shown that the rate of tritium exchange for a series of related hydrocarbons is linearly related to the equilibrium acidities of these hydrocarbons in the solvent system. This method was used to extend the scale to hydrocarbons such as toluene for which the exchange rate, but not equilibrium data, can be obtained.<sup>8</sup> Representative values of some hydrocarbons with  $pK$  values ranging from 16 to above 40 are given in Table 6.2. The  $pK$  values of a wide variety of organic compounds have been determined in DMSO,<sup>9</sup> and some of these values are listed in Table 6.2 as well. It is not expected that these values will be numerically identical with those in other solvents, but for most compounds the same relative order of acidity is observed. For synthetic purposes, carbanions are usually generated in ether solvents, often THF or DME. There are relatively few quantitative data available on hydrocarbon acidity in such solvents. Table 6.2 contains a few entries for  $Cs^+$  salts. The numerical values are scaled with reference to the  $pK$  of 9-phenylfluorene.<sup>10</sup> The acidity trends are similar to those in cyclohexylamine and DMSO.

Some of the relative acidities in Table 6.2 can be easily understood. The order of decreasing acidity  $Ph_3CH > Ph_2CH_2 > PhCH_3$ , for example, reflects the ability of each successive phenyl group to stabilize the negative charge on carbon. This stabilization is a combination of both resonance and the polar EWG effect of the phenyl groups. The much greater acidity of fluorene relative to dibenzocycloheptatriene (Entries 5 and 6) is the result of the aromaticity of the cyclopentadienide ring in the anion of fluorene. Cyclopentadiene (Entry 9) is an exceptionally acidic hydrocarbon, comparable in acidity to simple alcohols, owing to the aromatic stabilization of the anion. Some more subtle effects are seen as well. Note that fusion of a benzene ring *decreases* the acidity

<sup>6</sup> E. M. Arnett, T. C. Moriarity, L. E. Small, J. P. Rudolph, and R. P. Quirk, *J. Am. Chem. Soc.*, **95**, 1492 (1973); T. E. Hogen-Esch and J. Smid, *J. Am. Chem. Soc.*, **88**, 307 (1966).

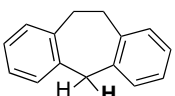
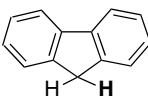
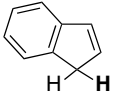
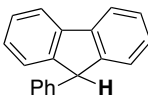
<sup>7</sup> A. Streitwieser, Jr., J. R. Murdoch, G. Hafelinger, and C. J. Chang, *J. Am. Chem. Soc.*, **95**, 4248 (1973); A. Streitwieser, Jr., E. Ciuffarin, and J. H. Hammons, *J. Am. Chem. Soc.*, **89**, 63 (1967); A. Streitwieser, Jr., E. Juaristi, and L. L. Nebenzahl, in *Comprehensive Carbanion Chemistry*, Part A, E. Buncl and T. Durst, ed., Elsevier, New York, 1980, Chap. 7.

<sup>8</sup> A. Streitwieser, Jr., M. R. Granger, F. Mares, and R. A. Wolf, *J. Am. Chem. Soc.*, **95**, 4257 (1973).

<sup>9</sup> F. G. Bordwell, *Acc. Chem. Res.*, **21**, 456 (1988).

<sup>10</sup> D. A. Bors, M. J. Kaufman, and A. Streitwieser, Jr., *J. Am. Chem. Soc.*, **107**, 6975 (1985).

Table 6.2. Acidity of Some Hydrocarbons

Entry	Hydrocarbon	Cs <sup>+</sup> (CHA) <sup>a</sup>	Cs <sup>+</sup> (THF) <sup>b</sup>	K <sup>+</sup> (DMSO) <sup>c</sup>
1	PhCH <sub>2</sub> —H	41.2	40.9	43
2	(CH <sub>3</sub> —  —) <sub>2</sub> CH—H	35.1	33.1	
3	(Ph <sub>2</sub> )CH—H	33.4	33.3	32.3
4	(Ph) <sub>3</sub> C—H	31.4	31.3	30.6
5		31.2		
6		22.7	22.9	22.6
7		19.9		20.1
8		18.5	18.2	17.9
9		16.6		18.1

a. A. Streitwieser, Jr., J. R. Murdoch, G. Hafelinger, and C. J. Chang, *J. Am. Chem. Soc.*, **93**, 4248 (1973); A. Streitwieser, Jr., E. Ciuffarin, and J. H. Hammons, *J. Am. Chem. Soc.*, **89**, 93 (1967); A. Streitwieser, Jr., and F. Guibe, *J. Am. Chem. Soc.*, **100**, 4523 (1978).

b. M. J. Kaufman, S. Gronert, and A. Streitwieser, *J. Am. Chem. Soc.*, **110**, 2829 (1988); A. Streitwieser, J. C. Ciula, J. A. Krom, and G. Thiele, *J. Org. Chem.*, **56**, 1074 (1991).

c. F. G. Bordwell, *Acc. Chem. Res.*, **21**, 456, 463 (1988).

of cyclopentadiene, as illustrated by comparing Entries 6, 7, and 9. (This relationship is considered in Problem 6.3)

Allylic conjugation stabilizes carbanions and  $pK$  values of 43 (in cyclohexylamine)<sup>11</sup> and 47–48 (in THF-HMPA)<sup>12</sup> were determined for propene. On the basis of exchange rates with cesium cyclohexylamide, cyclohexene and cycloheptene were found to have  $pK$  values of about 45 in cyclohexylamine.<sup>13</sup> These data indicate that allylic positions have  $pK \sim 45$ . The hydrogens on the  $sp^2$  carbons in benzene and ethene are more acidic than the hydrogens in saturated hydrocarbons. A  $pK$  of 45 has been estimated for benzene on the basis of extrapolation from a series of halogenated

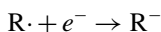
<sup>11</sup>. D. W. Boerth and A. Streitwieser, Jr., *J. Am. Chem. Soc.*, **103**, 6443 (1981).

<sup>12</sup>. B. Jaun, J. Schwarz, and R. Breslow, *J. Am. Chem. Soc.*, **102**, 5741 (1980).

<sup>13</sup>. A. Streitwieser, Jr., and D. W. Boerth, *J. Am. Chem. Soc.*, **100**, 755 (1978).

benzenes.<sup>14</sup> Electrochemical measurements have been used to establish a lower limit of about 46 for the  $pK$  of ethene.<sup>12</sup>

For saturated hydrocarbons, exchange is too slow and reference points are so uncertain that determination of  $pK$  values by exchange measurements is not feasible. The most useful approach for obtaining  $pK$  data for such hydrocarbons involves making a measurement of the electrochemical potential for the reaction:



From this value and known C–H bond dissociation energies, we can calculate the  $pK$  values. Early application of these methods gave estimates of the  $pK$  of toluene of about 45 and of propene of about 48. Methane was estimated to have a  $pK$  in the range of 52–62.<sup>12</sup> Electrochemical measurements in DMF have given the results in Table 6.3.<sup>15</sup> These measurements put the  $pK$  of methane at about 48, with benzylic and allylic stabilization leading to values of 39 and 38 for propene and toluene, respectively. These values are several units smaller than those determined by other methods. The electrochemical values overlap with the  $pK_{\text{DMSO}}$  scale for compounds such as diphenylmethane and triphenylmethane, and these values are also somewhat lower than those found by equilibrium studies.

Terminal alkynes are among the most acidic of the hydrocarbons. For example, in DMSO, phenylacetylene is found to have a  $pK$  near 26.5.<sup>16</sup> In cyclohexylamine, the value is 23.2.<sup>17</sup> An estimate of the  $pK$  in aqueous solution of 20 is based on a Brønsted relationship (see p. 348).<sup>18</sup> The relatively high acidity of acetylenes is associated with the large degree of  $s$  character of the C–H bond. The  $s$  character is 50%, as opposed to 25% in  $sp^3$  bonds. The electrons in orbitals with high  $s$  character experience decreased shielding from the nuclear charge. The carbon is therefore effectively *more electronegative*, as viewed from the proton sharing an  $sp$  hybrid orbital, and hydrogens on  $sp$  carbons exhibit greater acidity. (See Section 1.1.5 to review carbon hybridization-electronegativity relationships.) This same effect accounts for the relatively high acidity

**Table 6.3.  $pK$  Values for Less Acidic Hydrocarbons**

Hydrocarbon	$pK(\text{DMF})^a$
Methane	48
Ethane	51
Cyclopentane	49
Cyclohexane	49
Propene	38
Toluene	39
Diphenylmethane	31
Triphenylmethane	29

a. K. Daasbjerg, *Acta Chem. Scand.*, **49**, 878 (1995).

<sup>14</sup> M. Stratakis, P. G. Wang, and A. Streitwieser, Jr., *J. Org. Chem.*, **61**, 3145 (1996).

<sup>15</sup> K. Daasbjerg, *Acta Chem. Scand.*, **49**, 878 (1995).

<sup>16</sup> F. G. Bordwell and W. S. Matthews, *J. Am. Chem. Soc.*, **96**, 1214 (1974).

<sup>17</sup> A. Streitwieser, Jr., and D. M. E. Reuben, *J. Am. Chem. Soc.*, **93**, 1794 (1971).

<sup>18</sup> D. B. Dahlberg, M. A. Kuzemko, Y. Chiang, A. J. Kresge, and M. F. Powell, *J. Am. Chem. Soc.*, **105**, 5387 (1983).

of the hydrogens on cyclopropane rings and other strained hydrocarbons that have increased  $s$  character in the C–H bonds. The relationship between hybridization and acidity can be expressed in terms of the  $s$  character of the C–H bond.<sup>19</sup>

$$\text{p}K_a = 83.1 - 1.3(\%s)$$

The correlation can also be expressed in terms of the NMR coupling constant  $J^{13}\text{C-H}$ , which is related to hybridization.<sup>20</sup> These numerical relationships break down when applied to a wider range of molecules, where other factors contribute to carbanion stabilization.<sup>21</sup>

Knowledge of the structure of carbanions is important to understanding the stereochemistry of their reactions. Ab initio (HF/4-31G) calculations indicate a pyramidal geometry at carbon in the methyl and ethyl anions. The optimum H–C–H angle in these two carbanions is calculated to be 97°–100°. An interesting effect is found in that the proton affinity (basicity) of methyl anion decreases in a regular manner as the H–C–H angle is decreased.<sup>22</sup> This increase in acidity with decreasing internuclear angle parallels the trend in small-ring compounds, in which the acidity of hydrogens is substantially greater than in compounds having tetrahedral geometry at carbon. Pyramidal geometry at carbanions can also be predicted on the basis of qualitative considerations of the orbital occupied by the unshared electron pair. In a planar carbanion, the lone pair would occupy a  $p$  orbital. In a pyramidal geometry, the orbital has more  $s$  character. Because the electron pair is of lower energy in an orbital with some  $s$  character, it is predicted that a pyramidal geometry will be favored. Qualitative VSEPR considerations also predict pyramidal geometry (see p. 7).

As was discussed in Section 3.8, measurements in the gas phase, which eliminate the effect of solvation, show structural trends that parallel measurements in solution but have much larger absolute energy differences. Table 6.4 gives some data for key hydrocarbons for the  $\Delta H$  of proton dissociation. These data show a correspondence with

**Table 6.4. Enthalpy of Proton Dissociation for Some Hydrocarbons (Gas Phase)<sup>a</sup>**

Hydrocarbon	$\Delta H(\text{kcal/mol})^a$
Methane	418.8
Ethene	407.5
Cyclopropane	411.5
Benzene	400.8
Toluene	381

a. S. T. Graul and R. R. Squires, *J. Am. Chem. Soc.*, **112**, 2517 (1990).

<sup>19</sup> Z. B. Maksic and M. Eckert-Maksic, *Tetrahedron*, **25**, 5113 (1969); M. Randic and Z. Maksic, *Chem. Rev.*, **72**, 43 (1972).

<sup>20</sup> A. Streitwieser, Jr., R. A. Caldwell, and W. R. Young, *J. Am. Chem. Soc.*, **91**, 529 (1969); S. R. Kass and P. K. Chou, *J. Am. Chem. Soc.*, **110**, 7899 (1988); I. Alkorta and J. Elguero, *Tetrahedron*, **53**, 9741 (1997).

<sup>21</sup> R. R. Sauer, *Tetrahedron*, **55**, 10013 (1999).

<sup>22</sup> A. Streitwieser, Jr., and P. H. Owens, *Tetrahedron Lett.*, 5221 (1973); A. Streitwieser, Jr., P. H. Owens, R. A. Wolf, and J. E. Williams, Jr., *J. Am. Chem. Soc.*, **96**, 5448 (1974); E. D. Jemmis, V. Buss, P. v. R. Schleyer, and L. C. Allen, *J. Am. Chem. Soc.*, **98**, 6483 (1976).

hybridization and delocalization effects observed in solution. The very large heterolytic dissociation energies reflect both the inherent instability of the carbanions and the electrostatic attraction between the oppositely charged carbanion and proton. By way of comparison, enthalpy measurements in DMSO using  $K^+ \cdot O-t-Bu$  or  $KCH_2SOCH_3$  as base give values of  $-15.4$  and  $-18.2$  kcal/mol, respectively, for fluorene, a hydrocarbon with a  $pK$  of about 20.<sup>23</sup>

Aqueous phase acidity for a number of hydrocarbons has been computed theoretically. A continuum dielectric solvation model was used and B3LYP/6-311++G(*d, p*) and MP2/G2 computations were employed.<sup>24</sup> Some of the results are given in Table 6.5. There is good agreement with experimental estimates for most of the compounds, although cyclopropane is somewhat less acidic than anticipated.

Tupitsyn and co-workers dissected the energies of deprotonation into two factors—the C–H bond energy and the structural reorganization of the carbanion—by calculating the energy of the carbanion at the geometry of the reactant hydrocarbon and then calculating the energy of relaxation to the minimum energy structure using AM1 computations.<sup>25</sup> It was found that strained ring compounds were dominated by the first factor, whereas compounds such as propene and toluene that benefit from carbanion delocalization were dominated by the second term. Benzene has a very low relaxation energy, consistent with a carbanion localized in an  $sp^2$  orbital. The broad general picture that emerges from this analysis is that there are two major factors that influence the acidity of hydrocarbons. One is the inherent characteristics of the C–H bond resulting from hybridization and strain and the other is anion stabilization, which depends on delocalization of the charge.

The stereochemistry observed in proton exchange reactions of carbanions is dependent on the conditions under which the anion is formed and trapped by proton transfer. The dependence on solvent, counterion, and base is the result of the importance of ion pairing effects. The base-catalyzed cleavage of **1** is illustrative. The anion of **1** is cleaved at elevated temperatures to 2-butanone and 2-phenyl-2-butyl anion, which under the conditions of the reaction is protonated by the solvent. Use of resolved

**Table 6.5. Computed Aqueous  $pK$  Values for Some Hydrocarbons**

Hydrocarbon	B3LYP	MP2/G2
Ethyne	24.7	25.1
Cyclopentadiene	17.8	19.1
Cyclopropane	52.2	52.3
Toluene	42.1	42.4
Ethane	53.8	55.0

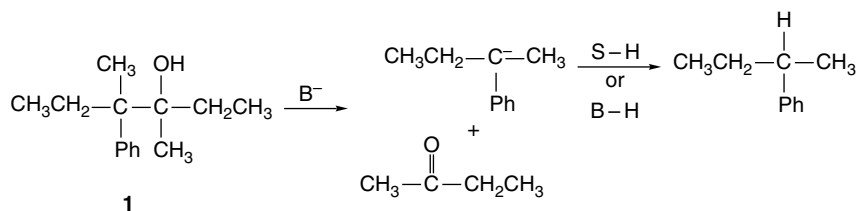
a. I. A. Topol, G. J. Tawa, R. A. Caldwell, M. A. Eisenstat, and S. K. Burt, *J. Phys. Chem. A*, **104**, 9619 (2000).

<sup>23</sup> E. M. Arnett and K. G. Venkatasubramanian, *J. Org. Chem.*, **48**, 1569 (1983).

<sup>24</sup> I. A. Topol, G. J. Tawa, R. A. Caldwell, M. A. Eisenstat, and S. K. Burt, *J. Phys. Chem. A*, **104**, 9619 (2000).

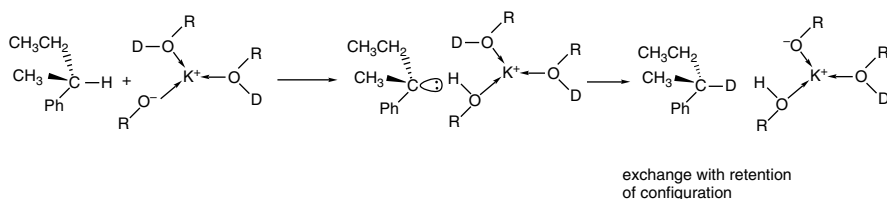
<sup>25</sup> I. F. Tupitsyn, A. S. Popov, and N. N. Zatsepina, *Russian J. Gen. Chem.*, **67**, 379 (1997).

**1** allows the stereochemical features of the anion to be probed by measuring the enantiomeric purity of the 2-phenylbutane product.



Retention of configuration was observed in nonpolar solvents, while increasing amounts of inversion occurred as the proton-donating ability and the polarity of the solvent increased. Cleavage of **1** with potassium *t*-butoxide in benzene gave 2-phenylbutane with 93% net retention of configuration. The stereochemical course changed to 48% net inversion of configuration when potassium hydroxide in ethylene glycol was used. In DMSO using  $\text{K}^+\cdot\text{O}-t\text{-Bu}$  as base, completely racemic 2-phenylbutane was formed.<sup>26</sup> The retention in benzene presumably reflects a short lifetime for the carbanion in a tight ion pair. Under these conditions, the carbanion does not become symmetrically solvated before proton transfer from either the protonated base or the ketone. The solvent benzene is not an effective proton donor and the most likely proton source is *t*-butanol. In ethylene glycol, the solvent provides a good proton source and since net inversion is observed, the protonation must occur on an unsymmetrically solvated species that favors back-side protonation. The racemization that is observed in DMSO indicates that the carbanion has a sufficient lifetime to become symmetrically solvated. The stereochemistry observed in the three solvents is in good accord with their solvating properties. In benzene, reaction occurs primarily through ion pairs. Ethylene glycol provides a ready source of protons and fast proton transfer accounts for the observed inversion. DMSO promotes ion pair dissociation and equilibration, as indicated by the observed racemization.

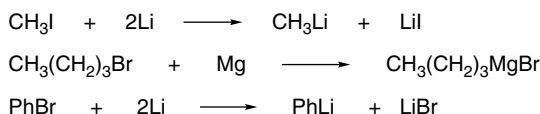
The stereochemistry of hydrogen-deuterium exchange at the chiral carbon in 2-phenylbutane shows a similar trend. When potassium *t*-butoxide is used as the base, the exchange occurs with retention of configuration in *t*-butanol, but racemization occurs in DMSO.<sup>27</sup> The retention of configuration is visualized as occurring through an ion pair in which a solvent molecule coordinated to the metal ion acts as the proton donor. In DMSO, symmetrical solvation is achieved prior to protonation and there is complete racemization.



<sup>26</sup> D. J. Cram, A. Langemann, J. Allinger, and K. R. Kopecky, *J. Am. Chem. Soc.*, **81**, 5740 (1959).

<sup>27</sup> D. J. Cram, C. A. Kingsbury, and B. Rickborn, *J. Am. Chem. Soc.*, **83**, 3688 (1961).

The organometallic derivatives of lithium, magnesium, and other strongly electropositive metals have some of the properties expected for salts of carbanions. Owing to the low acidity of most hydrocarbons, organometallic compounds usually cannot be prepared by proton transfer reactions. Instead, the most general preparative methods start with the corresponding halogen compound.



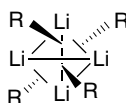
There are other preparative methods, which are considered in Chapter 7 of Part B.

Organolithium compounds derived from saturated hydrocarbons are extremely strong bases and react rapidly with any molecule having an  $-\text{OH}$ ,  $-\text{NH}$ , or  $-\text{SH}$  group by proton transfer to form the hydrocarbon. Accurate  $pK$  values are not known, but range upward from the estimate of  $\sim 50$  for methane. The order of basicity  $\text{CH}_3\text{Li} < \text{CH}_3(\text{CH}_2)_3\text{Li} < (\text{CH}_3)_3\text{CLi}$  is due to the electron-releasing effect of alkyl substituents and is consistent with increasing reactivity in proton abstraction reactions in the order  $\text{CH}_3\text{Li} < \text{CH}_3(\text{CH}_2)_3\text{Li} < (\text{CH}_3)_3\text{CLi}$ . Phenyl-, methyl-, *n*-butyl-, and *t*-butyllithium are all stronger bases than the anions of the hydrocarbons listed in Table 6.2. Unlike proton transfers from oxygen, nitrogen, or sulfur, proton removal from carbon atoms is usually not a fast reaction. Thus, even though *t*-butyllithium is thermodynamically capable of deprotonating toluene, the reaction is quite slow. In part, the reason is that the organolithium compounds exist as tetramers, hexamers, and higher aggregates in hydrocarbon and ether solvents.<sup>28</sup>

In solution, organolithium compounds exist as aggregates, with the degree of aggregation depending on the structure of the organic group and the solvent. The nature of the species present in solution can be studied by low-temperature NMR. *n*-Butyllithium in THF, for example, is present as a tetramer-dimer mixture.<sup>29</sup> The tetrameric species is dominant.



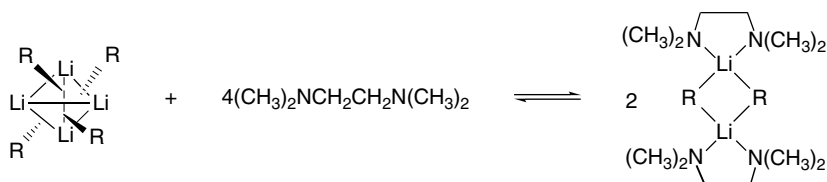
Tetrameric structures based on distorted cubic structures are also found for  $(\text{CH}_3\text{Li})_4$  and  $(\text{C}_2\text{H}_5\text{Li})_4$ ,<sup>30</sup> and they can be represented as tetrahedral of lithium ions with each face occupied by a carbanion ligand.



- <sup>28</sup> G. Fraenkel, M. Henrichs, J. M. Hewitt, B. M. Su, and M. J. Geckle, *J. Am. Chem. Soc.*, **102**, 3345 (1980); G. Fraenkel, M. Henrichs, M. Hewitt, and B. M. Su, *J. Am. Chem. Soc.*, **106**, 255 (1984).  
<sup>29</sup> D. Seebach, R. Hassig, and J. Gabriel, *Helv. Chim. Acta*, **66**, 308 (1983); J. F. McGarrity and C. A. Ogle, *J. Am. Chem. Soc.*, **107**, 1805 (1984).  
<sup>30</sup> E. Weiss and E. A. C. Lucken, *J. Organomet. Chem.*, **2**, 197 (1964); E. Weiss and G. Hencken, *J. Organomet. Chem.*, **21**, 265 (1970); H. Koester, D. Thoennes, and E. Weiss, *J. Organomet. Chem.*, **160**, 1 (1978); H. Dietrich, *Acta Crystallogr.*, **16**, 681 (1963); H. Dietrich, *J. Organomet. Chem.*, **205**, 291 (1981).

The THF solvate of lithium *t*-butylacetylide is another example of a tetrameric structure.<sup>31</sup> In solutions of *n*-propyllithium in cyclopropane at 0°C, the hexamer is the main species, but higher aggregates are present at lower temperatures.<sup>20</sup>

The reactivity of the organolithium compounds is increased by adding molecules capable of solvating the lithium cations. Tetramethylethylenediamine (TMEDA) is commonly used for organolithium reagents. This tertiary diamine can chelate lithium. The resulting complexes generally are able to effect deprotonation at accelerated rates.<sup>32</sup> In the case of phenyllithium, NMR studies show that the compound is tetrameric in 1:2 ether-cyclohexane, but dimeric in 1:9 TMEDA-cyclohexane.<sup>33</sup>



X-ray crystal structure determinations have been done on both dimeric and tetrameric structures. A dimeric structure crystallizes from hexane containing TMEDA.<sup>34</sup> This structure is shown in Figure 6.1a. A tetrameric structure incorporating four ether molecules forms from ether-hexane solution.<sup>35</sup> This structure is shown in Figure 6.1b. There is a good correspondence between the structures that crystallize and those indicated by the NMR studies.

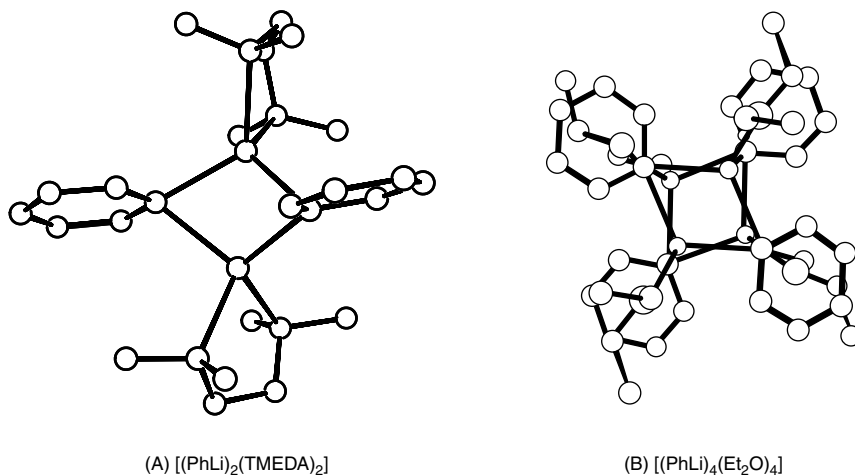


Fig. 6.1. Crystal structures of phenyllithium: (a) dimeric structure incorporating tetramethylethylenediamine; (b) tetrameric structure incorporating diethyl ether. Reproduced from *Chem. Ber.*, **111**, 3157 (1978) and *J. Am. Chem. Soc.*, **105**, 5320 (1983), by permission of Wiley-VCH and the American Chemical Society, respectively.

<sup>31</sup> W. Neuberger, E. Weiss, and P. v. R. Schleyer, quoted in Ref. 37.

<sup>32</sup> G. G. Eberhardt and W. A. Butte, *J. Org. Chem.*, **29**, 2928 (1964); R. West and P. C. Jones, *J. Am. Chem. Soc.*, **90**, 2656 (1968).

<sup>33</sup> L. M. Jackman and L. M. Scarmoutzos, *J. Am. Chem. Soc.*, **106**, 4627 (1984).

<sup>34</sup> D. Thoennes and E. Weiss, *Chem. Ber.*, **111**, 3157 (1978).

<sup>35</sup> H. Hope and P. P. Power, *J. Am. Chem. Soc.*, **105**, 5320 (1983).

Crystal structure determination has also been done on several complexes of *n*-butyllithium. A 4:1 *n*-BuLi:TMEDA complex is a tetramer accommodating two TMEDA molecules, which, rather than chelating a lithium, links the tetrameric units. The 2:2 *n*-BuLi:TMEDA complex has a structure similar to  $[\text{PhLi}]_2\text{:}[\text{TMEDA}]_2$ . Both 1:1 *n*-BuLi:THF and 1:1 *n*-BuLi:DME complexes are tetrameric with ether molecules coordinated at each lithium (Figure 6.2).<sup>36</sup> These and many other organolithium structures have been discussed in a review of this topic.<sup>37</sup>

There has been extensive computational study of the structure of organolithium compounds.<sup>38</sup> The structures of the simple monolithium compounds are very similar to the corresponding hydrocarbons. The gas phase structure of monomeric methyl lithium has been determined to be tetrahedral with an H–C–H bond angle of  $106^\circ$ .<sup>39</sup> These structural parameters are close to those calculated at the MP2/6-311G\* level of theory.<sup>40</sup> Ethyllithium, and vinyl lithium are also structurally similar to the corresponding

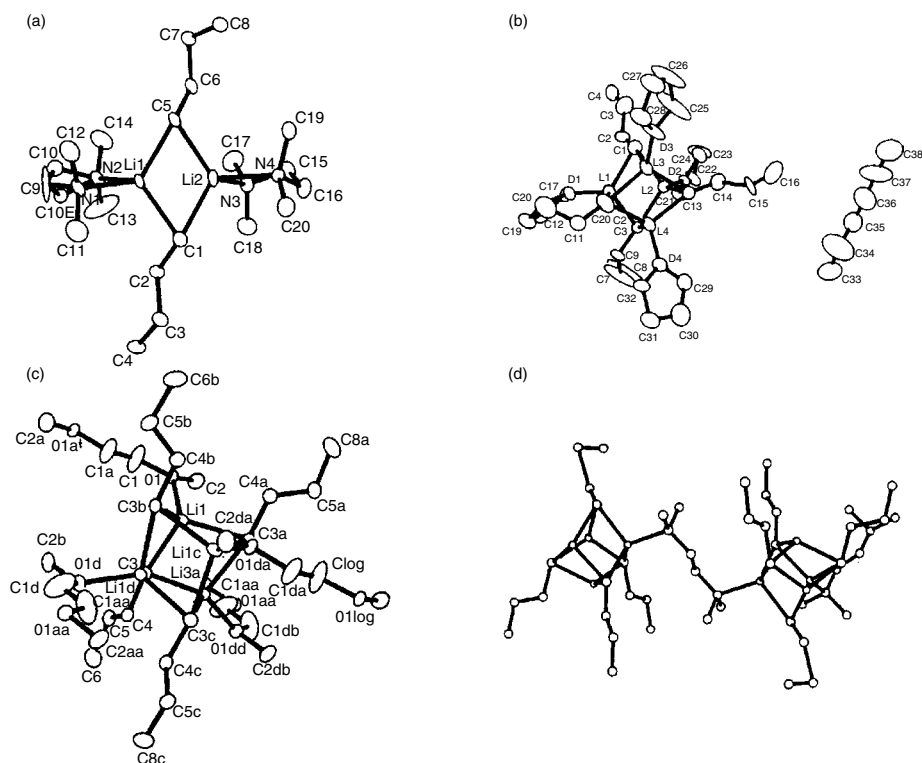


Fig. 6.2. Crystal structures of *n*-butyllithium: (a)  $[(n\text{-BuLi-TMEDA})_2]_2$ ; (b)  $[(n\text{-BuLi-THF})_4]\text{hexane}$ ; (c)  $[(n\text{-BuLi-DME})_4]$ ; (d)  $[(n\text{-BuLi})_4]\cdot\text{TMEDA}$ . Reproduced from *J. Am. Chem. Soc.*, **115**, 1568, 1573 (1993), by permission of the American Chemical Society.

<sup>36</sup> M. A. Nichols and P. G. Williard, *J. Am. Chem. Soc.*, **115**, 1568 (1993); N. D. R. Barnett, R. E. Mulvey, W. Clegg, and P. A. O'Neil, *J. Am. Chem. Soc.*, **115**, 1573 (1993).

<sup>37</sup> W. N. Setzer and P. v. R. Schleyer, *Adv. Organomet. Chem.*, **24**, 353 (1985).

<sup>38</sup> A. Streitwieser, S. M. Bachrach, A. Dorigo, and P. v. R. Schleyer, in *Lithium Chemistry*, A. M. Sapsee and P. v. R. Schleyer, eds., Wiley, New York, 1995, pp. 1–43.

<sup>39</sup> D. B. Grotjahn, T. C. Pesch, J. Xin, and L. M. Ziurys, *J. Am. Chem. Soc.*, **119**, 12368 (1997).

<sup>40</sup> E. Kaufman, K. Raghavachari, A. E. Reed, and P. v. R. Schleyer, *Organometallics*, **7**, 1597 (1988).

hydrocarbon. This fact, along with the relatively high solubility of simple lithium compounds in nonpolar solvents, has given rise to the idea that the C–Li bond is largely covalent. However, AIM analysis of simple alkyllithium compounds indicates that the bonds are largely ionic. The charges on lithium in methyl- and vinyl lithium are  $+0.91e$  and  $+0.92e$ , respectively.<sup>41</sup> The ionic character is also evident in the structure of allyllithium. The lithium is centered above the allyl anion, indicating an ionic structure.<sup>42</sup> The good solubility in nonpolar solvents is perhaps due to the cluster-type structures, which place the organic groups on the periphery of the cluster.

The relative slowness of the abstraction of protons from carbon acids by organolithium reagents is probably also due to the compact character of the carbon-lithium clusters. Since the electrons associated with the carbanion are tightly associated with the cluster of lithium cations, some activation energy is required to break the bond before the carbanion can act as a base. This kinetic sluggishness of organometallic compounds as bases permits important reactions in which the organometallic species acts as a *nucleophile* in preference to functioning as a strong base. The addition reactions of organolithium and organomagnesium compounds to carbonyl groups in aldehydes, ketones, and esters are important examples. As will be seen in the next section, carbonyl compounds are much more acidic than hydrocarbons. Nevertheless, in most cases, the proton transfer reaction of organometallic reagents is *slower than nucleophilic attack at the carbonyl group*. It is this feature of the reactivity of organometallics that permits the very extensive use of organometallic compounds in organic synthesis. The reactions of organolithium and organomagnesium compounds with carbonyl compounds is discussed in a synthetic context in Chapter 7 of Part B.

### 6.3. Carbanions Stabilized by Functional Groups

Electron-withdrawing substituents cause very large increases in the acidity of C–H bonds. Among the functional groups that exert a strong stabilizing effect on carbanions are carbonyl, nitro, sulfonyl, and cyano. Both polar and resonance effects are involved in the ability of these functional groups to stabilize the negative charge. Perhaps the best basis for comparing these groups is the data on the various substituted methanes. Bordwell and co-workers determined the relative acidities of the substituted methanes with reference to aromatic hydrocarbon indicators in DMSO.<sup>43</sup> The data are given in Table 6.6, which established the ordering  $\text{NO}_2 > \text{C}=\text{O} > \text{CO}_2\text{R} \sim \text{SO}_2 \sim \text{CN} > \text{CONR}_2$  for anion stabilization.

Carbanions derived from carbonyl compounds are often referred to as *enolates*, a name derived from the enol tautomer of carbonyl compounds. The resonance-stabilized enolate anion is the conjugate base of both the keto and enol forms of carbonyl compounds. The anions of nitro compounds are called *nitronates* and are also resonance stabilized. The stabilization of anions of sulfones is believed to be derived primarily from polar and polarization effects.

<sup>41</sup> J. P. Richie and S. M. Bachrach, *J. Am. Chem. Soc.*, **109**, 5909 (1987).

<sup>42</sup> T. Clark, C. Rohde, and P. v. R. Schleyer, *Organometallics*, **2**, 1344 (1983).

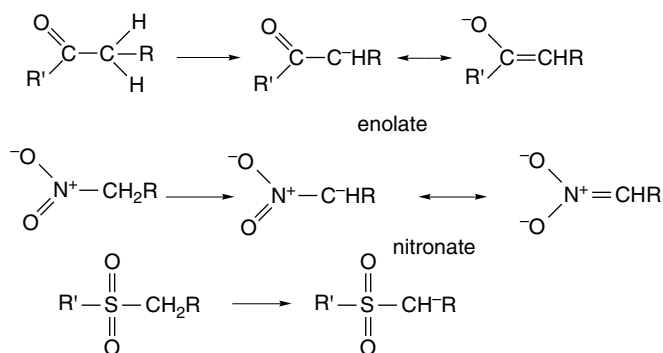
<sup>43</sup> F. G. Bordwell and W. S. Matthews, *J. Am. Chem. Soc.*, **96**, 1216 (1974); W. S. Matthews, J. E. Bares, J. E. Bartmess, F. G. Bordwell, F. J. Cornforth, G. E. Drucker, Z. Margolin, R. J. McCallum, G. J. McCollum, and N. R. Vanier, *J. Am. Chem. Soc.*, **97**, 7006 (1975).

**Table 6.6. Equilibrium Acidities of Substituted Methanes in Dimethyl Sulfoxide<sup>a</sup>**

Compound	pK
CH <sub>3</sub> NO <sub>2</sub>	17.2
CH <sub>3</sub> COPh	24.7
CH <sub>3</sub> COCH <sub>3</sub>	26.5
CH <sub>3</sub> SO <sub>2</sub> Ph	29.0
CH <sub>3</sub> CO <sub>2</sub> C <sub>2</sub> H <sub>5</sub>	30.5 <sup>b</sup>
CH <sub>3</sub> SO <sub>2</sub> CH <sub>3</sub>	31.1
CH <sub>3</sub> CN	31.3
CH <sub>3</sub> CON(C <sub>2</sub> H <sub>5</sub> ) <sub>2</sub>	34.5 <sup>b</sup>

a. Except as noted otherwise, from W. S. Matthews, J. E. Bares, J. E. Bartmess, F. G. Bordwell, F. J. Cornforth, G. E. Drucker, Z. Margolin, R. J. McCallum, G. J. McCollum, and N. R. Vanier, *J. Am. Chem. Soc.*, **97**, 7006 (1975).

b. F. G. Bordwell and H. E. Fried, *J. Org. Chem.*, **46**, 4327 (1981).



The presence of two EWGs further stabilizes the negative charge. Pentane-2,4-dione, for example, has a pK around 9 in water. Most β-diketones are sufficiently acidic that their carbanions can be generated using the conjugate bases of hydroxylic solvents such as water or alcohols, which have pK values of 15–20. Stronger bases are required for compounds that have a single stabilizing functional group. Alkali metal salts of ammonia or amines and sodium hydride are sufficiently strong bases to form carbanions from most ketones, aldehydes, and esters. The Li<sup>+</sup> salt of diisopropylamine (LDA) is a popular strong base for use in synthetic procedures. It is prepared by reaction of *n*-BuLi with diisopropylamine. Lithium, sodium, and potassium salts of hexamethyldisilylamide (LiHMDS, NaHMDS, KHMDS) are also important.<sup>44</sup> The generation of carbanions stabilized by electron-attracting groups is very important from a synthetic point of view; the synthetic aspects of the chemistry of these carbanions is discussed in Chapters 1 and 2 of Part B. Table 6.7 gives experimental pK data for some representative compounds in DMSO.

There have been numerous studies of the rates of deprotonation of carbonyl compounds. These data are of interest not only because they define the relationship

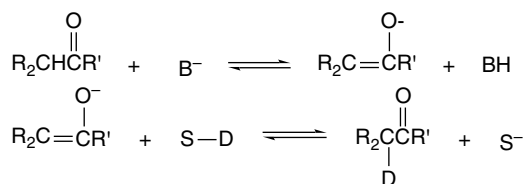
<sup>44</sup> T. L. Rathman, *Spec. Chem. Mag.*, **9**, 300 (1989).

Table 6.7.  $pK$  Values for Other Representative Compounds in DMSO<sup>a</sup>

Ketones	$pK$	Esters	$pK$
	26.5	PhCH <sub>2</sub> CO <sub>2</sub> C <sub>2</sub> H <sub>5</sub>	22.6
	24.7	PhSCH <sub>2</sub> CO <sub>2</sub> C <sub>2</sub> H <sub>5</sub>	21.4
	19.9		25.2
	18.7	Ketoesters	
	25.8		14.2
	26.4	Diesters	
	16.95	CH <sub>2</sub> (CO <sub>2</sub> C <sub>2</sub> H <sub>5</sub> ) <sub>2</sub>	16.4
Diketones			7.3
	13.3	Nitroalkanes	
	13.35	CH <sub>3</sub> NO <sub>2</sub>	17.2
	11.2	PhCH <sub>2</sub> NO <sub>2</sub>	12.3
			16.0
			17.9

a. F. G. Bordwell, *Acc. Chem. Res.*, **21**, 456 (1988).

between thermodynamic and kinetic acidity for these compounds, but also because they are necessary for understanding mechanisms of reactions in which enolates are involved as intermediates. Rates of enolate formation can be measured conveniently by following isotopic exchange using either deuterium or tritium.



An older technique is to measure the rate of halogenation of the carbonyl compound. Ketones and aldehydes in their carbonyl forms do not react rapidly with the halogens but the enolate is rapidly attacked. The rate of halogenation is therefore a measure of the rate of deprotonation.

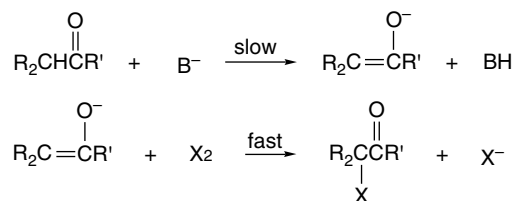


Table 6.8 gives data on the rates of deuteration of some alkyl ketones. From these data, the order of reactivity toward deprotonation is  $\text{CH}_3 > \text{RCH}_2 > \text{R}_2\text{CH}$ . Steric hindrance to the approach of the base is the major factor in establishing this order. The importance of steric effects can be seen by comparing the  $\text{CH}_2$  group in 2-butanone with the more hindered  $\text{CH}_2$  group in 4,4-dimethyl-2-pentanone. The two added methyl groups on the adjacent carbon decrease the rate of proton removal by a factor of about 100. The rather slow rate of exchange at the  $\text{CH}_3$  group of 4,4-dimethyl-2-pentanone must also reflect a steric factor arising from the bulky nature of the neopentyl group. If bulky groups

**Table 6.8. Relative Rates and  $E_a$  for Base-Catalyzed Deuteration of Some Ketones**

Ketone	Relative Rate <sup>a</sup>	$E_a^b$
$\text{CH}_3\overset{\text{O}}{\parallel}\text{CCH}_2\text{—H}$	100	11.9
$\text{CH}_3\overset{\text{O}}{\parallel}\text{CCHCH}_3$	41.5	12.1
$\text{H—CH}_2\overset{\text{O}}{\parallel}\text{CCH}_2\text{CH}_3$	45	
$\text{CH}_3\overset{\text{O}}{\parallel}\text{C}(\text{CH}_3)_2$	<0.1	
$\text{H—CH}_2\overset{\text{O}}{\parallel}\text{CCH}(\text{CH}_3)_2$	45	12.3
$\text{CH}_3\overset{\text{O}}{\parallel}\text{CCH}(\text{CH}_3)_3$	0.45	
$\text{H—CH}_2\overset{\text{O}}{\parallel}\text{CCH}_2\text{C}(\text{CH}_3)_3$	5.1	

a. In aqueous solution with sodium carbonate as the base. The data of C. Rappe and W. H. Sachs, *J. Org. Chem.*, **32**, 4127 (1967), given on a per-group basis have been converted to a per-hydrogen basis.

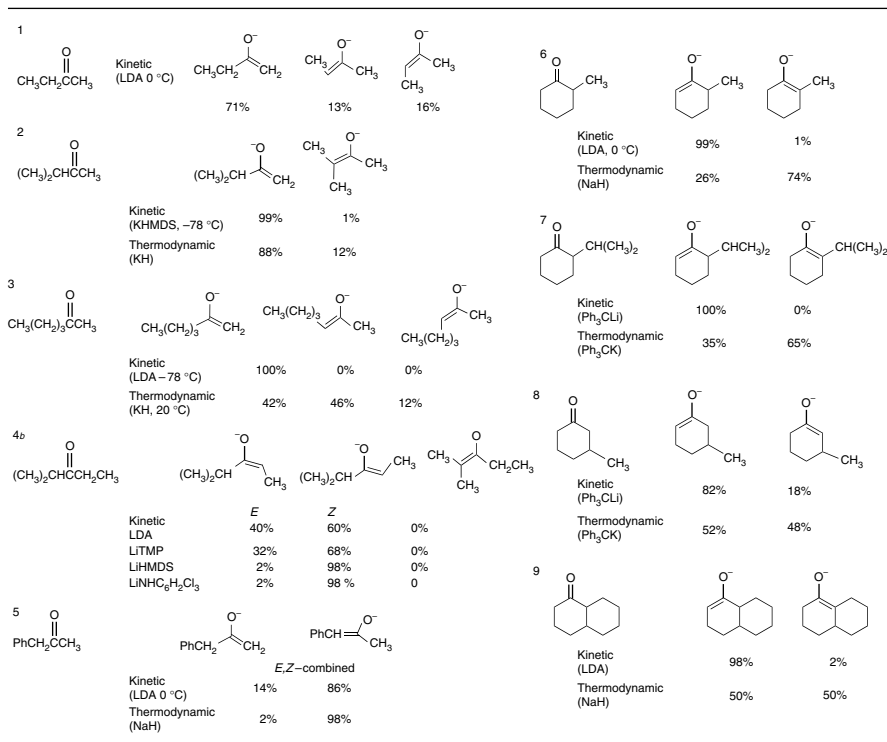
b.  $\text{CH}_3\text{O}^-$ -catalyzed exchange in  $\text{CH}_3\text{OD}$ . T. Niya, M. Yukawa, H. Morishita, H. Ikeda, and Y. Goto, *Chem. Pharm. Bull.*, **39**, 2475 (1991).

interfere with effective solvation of the developing negative charge on oxygen, the rate of proton abstraction is reduced. The observed activation energies parallel the rates.<sup>45</sup>

Structural effects on the rates of deprotonation of ketones have also been studied using very strong bases under conditions where complete conversion to the enolate occurs. In solvents such as THF or DME, bases such as LDA and KHMDS give solutions of the enolates that reflect the relative rates of removal of the different protons in the carbonyl compound (*kinetic control*). The least hindered proton is removed most rapidly under these conditions, so for unsymmetrical ketones the major enolate is the less-substituted one. Scheme 6.1 shows some representative data. Note that for many ketones, both *E*- and *Z*-enolates can be formed.

The equilibrium ratios of enolates for several ketone-enolate systems are also shown in Scheme 6.1. Equilibrium among the various enolates of a ketone can be established by the presence of an excess of the ketone, which permits reversible proton transfer. Equilibration is also favored by the presence of dissociating additives such as HMPA. As illustrated by most of the examples in Scheme 6.1, the kinetic enolate is formed by removal of the least hindered hydrogen. The composition of the equilibrium enolate mixture is usually more closely balanced than for kinetically

**Scheme 6.1. Composition of Enolate Mixtures Formed under Kinetic and Thermodynamic Control<sup>a</sup>**



a. Selected from a more complete compilation by D. Caine, in *Carbon-Carbon Bond Formation*, R. L. Augustine, ed., Marcel Dekker, New York, 1979.

b. C. H. Heathcock, C. T. Buse, W. A. Kleschick, M. C. Pirrung, J. E. Sohn, and J. Lampe, *J. Org. Chem.*, **45**, 1066 (1980); L. Xie, K van Landeghem, K. M. Isenberger, and C. Bernier, *J. Org. Chem.*, **68**, 641 (2003).

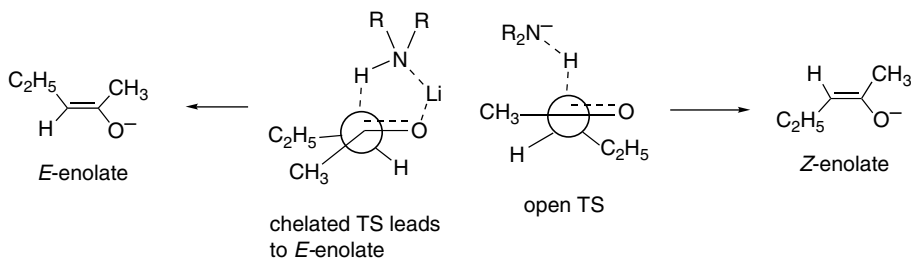
<sup>45</sup> T. Niiya, M. Yukawa, H. Morishita, H. Ikeda, and Y. Goto, *Chem. Pharm. Bull.*, **39**, 2475 (1991).

controlled conditions. In general, the more highly substituted enolate is the preferred isomer, but if the alkyl groups are sufficiently branched as to interfere with solvation of the enolate there are exceptions. This factor, along with  $\text{CH}_3/\text{CH}_3$  repulsion, presumably accounts for the higher stability of the less-substituted enolate from 3-methyl-2-butanone (Entry 2). The acidifying effect of an adjacent phenyl group outweighs steric effects in the case of 1-phenyl-2-propanone, and as a result the conjugated enolate is favored by both kinetic and thermodynamic conditions (Entry 5).

The synthetic importance of the LDA and LiHMDS type of deprotonation has led to studies of enolate composition under various conditions. Deprotonation of 2-pentanone was examined with LDA in THF, with and without HMPA. C(1)-deprotonation was favored under both conditions, but the *Z:E* ratio for C(3) deprotonation was sensitive to the presence of HMPA (0.75 *M*).<sup>46</sup> More *Z*-enolate is formed when HMPA is present.

Conditions	Ratio C(1):C(3) deprotonation	Ratio <i>Z:E</i> for C(3) deprotonation
0°C, THF alone	7.9	0.20
-60°C, THF alone	7.1	0.15
0°C, THF – HMPA	8.0	1.0
-60°C, THF – HMPA	5.6	3.1

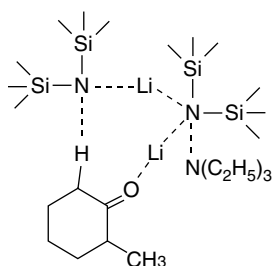
These and other related enolate ratios are interpreted in terms of a tight, reactant-like TS with Li chelation in THF and a looser TS in the presence of HMPA. The chelated TS favors the *E*-enolate, whereas the open TS favors the *Z*-enolate. The effect of the HMPA is to solvate the  $\text{Li}^+$  ion, reducing the importance of  $\text{Li}^+$  coordination with the carbonyl oxygen.<sup>47</sup>



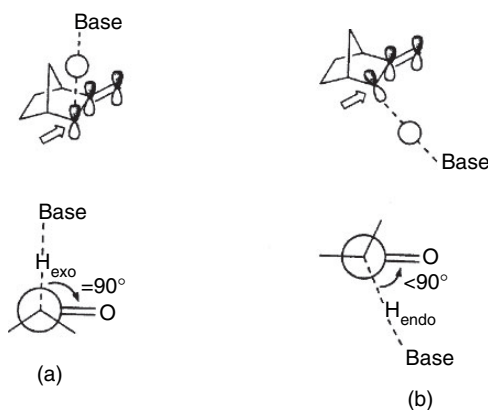
Very significant acceleration of the rate of deprotonation of 2-methylcyclohexanone by LiHMDS was observed when triethylamine was included in enolate-forming reactions in toluene. The rate enhancement is attributed to a TS containing LiHMDS dimer and triethylamine. This is an example of how modification of conditions can be used to affect rates and selectivity of deprotonation.

<sup>46</sup> L. Xie and W. H. Saunders, Jr., *J. Am. Chem. Soc.*, **113**, 3123 (1991).

<sup>47</sup> R. E. Ireland, R. H. Mueller, and A. K. Willard, *J. Am. Chem. Soc.*, **98**, 2868 (1972); R. E. Ireland, P. Wipf, and J. D. Armstrong, III, *J. Org. Chem.*, **56**, 650 (1991).



Structural effects on deprotonation rates have also been probed computationally.<sup>48</sup> In cyclic ketones, a stereoelectronic factor can be important in determining the rate of deprotonation. For the norbornanone ring, for example, the *exo* proton is more favorably aligned with the carbonyl group than the *endo* hydrogen. Computational investigation (B3LYP/6-31G\*) of the TS for deprotonation by an  $\text{OH}^-:\text{H}_2\text{O}$  complex found a difference of 3.8 kcal/mol favoring *exo* deprotonation.



A similar factor is found for deprotonation of cyclohexanone. There is a 2.8 kcal preference for removal of an axial proton because of the better stereoelectronic alignment and less torsional strain, as depicted in Figure 6.3.

Nitroalkanes show an interesting relationship between kinetic and thermodynamic acidity. Additional alkyl substituents on nitromethane retard the rate of proton removal, although the equilibrium is more favorable for the more highly substituted derivatives.<sup>49</sup> The alkyl groups have a strong stabilizing effect on the nitronate ion but unfavorable steric effects are dominant at the TS for proton removal. As a result, kinetic and thermodynamic acidity show opposite responses to alkyl substitution.

Nitroalkane	Kinetic acidity $k(M^{-1}\text{min}^{-1})$	Thermodynamic acidity ( $\text{p}K_{\text{a}}$ )
$\text{CH}_3\text{NO}_2$	238	10.2
$\text{CH}_3\text{CH}_2\text{NO}_2$	39.1	8.5
$(\text{CH}_3)_2\text{CHNO}_2$	2.08	7.7

<sup>48</sup>. S. M. Behnam, S. E. Benham, K. Ando, N. S. Green, and K. N. Houk, *J. Org. Chem.*, **65**, 8970 (2000).

<sup>49</sup>. F. G. Bordwell, W. J. Boyle, Jr., and K. C. Yee, *J. Am. Chem. Soc.*, **92**, 5926 (1970).

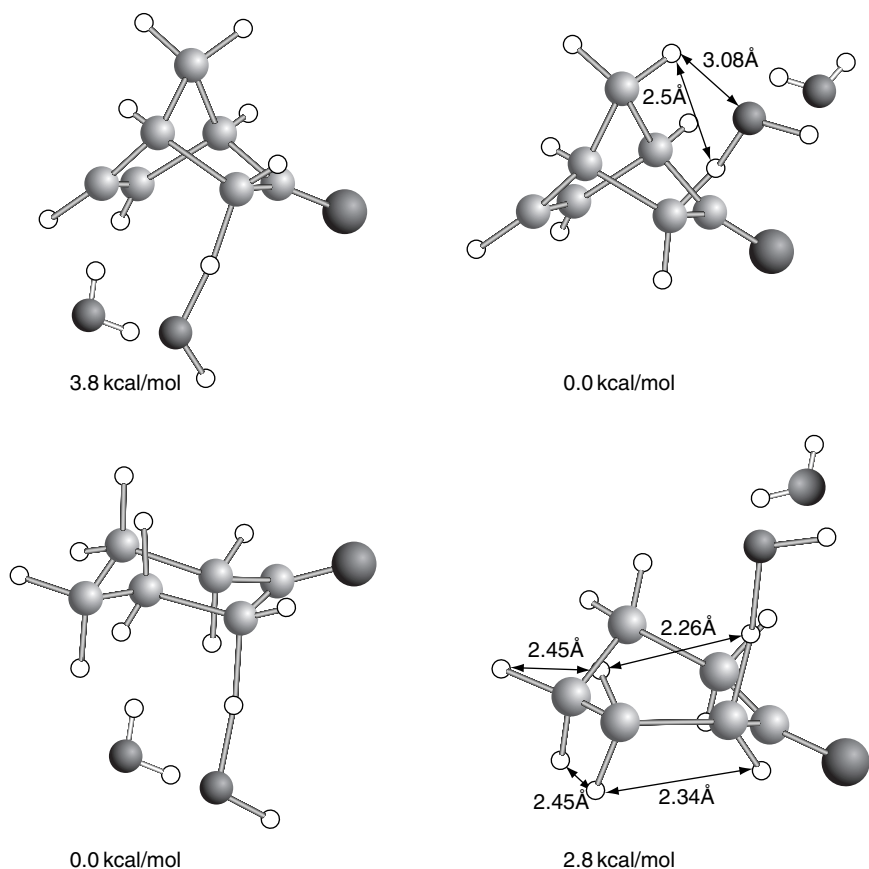


Fig. 6.3. Comparison of transition structures for deprotonation of 2-norbornanone (top) and cyclohexanone (bottom). In 2-norbornanone, *exo* deprotonation is favored by 3.8 kcal/mol. In cyclohexanone, axial deprotonation is favored by 2.8 kcal/mol. Reproduced from *J. Org. Chem.*, **65**, 8970 (2000), by permission of the American Chemical Society.

The cyano group is also effective at stabilizing negative charge on carbon. The minimal steric demands of the cyano group have made it possible to synthesize a number of hydrocarbon derivatives that are very highly substituted with cyano groups. Table 6.9 gives  $pK$  values for some of these compounds. As can be seen, the highly substituted derivatives are very strong acids.

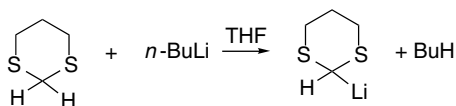
**Table 6.9. Acidities of Some Cyanohydrocarbons<sup>a</sup>**

Compound	$pK$
$\text{CH}_3\text{CN}$	> 25
$\text{NCCH}_2\text{CN}$	11.2
$(\text{NC})_3\text{CH}$	-5.6
$(\text{NC})_2\text{C}=\text{C}(\text{CN})\text{CH}(\text{CN})_2$	< -8.5
Pentacyanocyclopentadiene	< -11.0

a. Selected from data in Tables 5.1 and 5.2 in J. R. Jones, *The Ionization of Carbon Acids*, Academic Press, New York, 1973, pp. 64,65.

Third-row elements, particularly phosphorus and sulfur, stabilize adjacent carbanions. The  $pK$ 's of some pertinent compounds are given in Table 6.10.

The conjugate base of 1,3-dithiane has proven valuable in synthetic applications as a nucleophile (Part B, Chap.3). The anion is generated by deprotonation using *n*-butyllithium.



The  $pK$  of 1,3-dithiane is 36.5 ( $\text{Cs}^+$  ion pair in THF).<sup>50</sup> The value for 2-phenyl-1,3-dithiane is 30.5. There are several factors that can contribute to the anion-stabilizing effect of sulfur substituents. Bond dipole effects may contribute but cannot be the dominant factor since oxygen does not have a comparable stabilizing influence. Polarizability of sulfur can also stabilize the carbanion. Delocalization can be described as involving  $3d$  orbitals on sulfur or hyperconjugation with the  $\sigma^*$  orbital of the C–S bond.<sup>51</sup> An experimental study of the rates of deprotonation of phenylthiomethane indicates that sulfur polarizability is the major factor.<sup>52</sup> Whatever the structural basis, there is no question that thio substituents enhance the acidity of hydrogens on the adjacent carbons. The phenylthio group increases the acidity of hydrocarbons by at least 15  $pK$  units. The effect is from 5–10  $pK$  units in carbanions stabilized by other EWGs.<sup>53</sup>

**Table 6.10. Acidities of Some Compounds with Sulfur and Phosphorus Substituents**

Compound	$pK(\text{DMSO})$
$\text{PhCH}_2\text{SPh}^{\text{a}}$	30.8
$\text{PhSO}_2\text{CH}_3^{\text{b}}$	29.0
$\text{PhSO}_2\text{CH}_2\text{Ph}^{\text{b}}$	23.4
$\text{PhCH}(\text{SPh})_2^{\text{a}}$	23.0
$(\text{PhS})_2\text{CH}_2^{\text{a}}$	38.0
$\text{PhSO}_2\text{CH}_2\text{SPh}^{\text{b}}$	20.3
$\text{PhSO}_2\text{CH}_2\text{PPh}_2^{\text{b}}$	20.2
$\text{C}_2\text{H}_5\text{O}_2\text{CCH}_2\text{PPh}_2^{\text{d}}$	9.2 <sup>c</sup>
$\text{PhCOCH}_2\text{PPh}_2^{\text{d}}$	6.0 <sup>c</sup>

a. F. G. Bordwell, J. E. Bares, J. E. Bartmess, G. E. Drucker, J. Gerhold, G. J. McCollum, M. Van Der Puy, N. R. Vanier, and W. S. Matthews, *J. Org. Chem.*, **42**, 326 (1977).

b. F. G. Bordwell, W. S. Matthews, and N. R. Vanier, *J. Am. Chem. Soc.*, **97**, 442 (1975).

c. In methanol.

d. A. J. Speziale and K. W. Ratts, *J. Am. Chem. Soc.*, **85**, 2790 (1963).

<sup>50</sup> L. Xie, D. A. Bors, and A. Streitwieser, *J. Org. Chem.*, **57**, 4986 (1992).

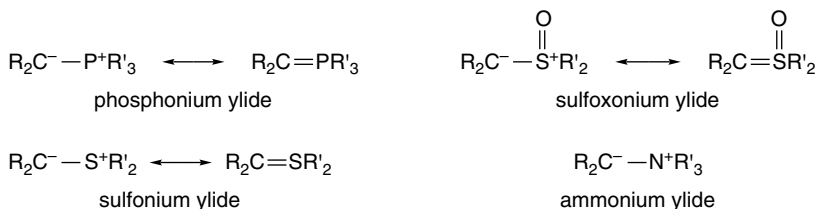
<sup>51</sup> W. T. Borden, E. R. Davidson, N. H. Andersen, A. D. Deniston, and N. D. Epiotis, *J. Am. Chem. Soc.*, **100**, 1604 (1978); A. Streitwieser, Jr., and S. P. Ewing, *J. Am. Chem. Soc.*, **97**, 190 (1975); A. Streitwieser, Jr., and J. E. Williams, Jr., *J. Am. Chem. Soc.*, **97**, 191 (1975); N. D. Epiotis, R. L. Yates, F. Bernardi, and S. Wolfe, *J. Am. Chem. Soc.*, **98**, 5435 (1976); J.-M. Lehn and G. Wipff, *J. Am. Chem. Soc.*, **98**, 7498 (1976); D. A. Bors and A. Streitwieser, Jr., *J. Am. Chem. Soc.*, **108**, 1397 (1986).

<sup>52</sup> C. F. Bernasconi and K. W. Kittredge, *J. Org. Chem.*, **63**, 1944 (1998).

<sup>53</sup> F. G. Bordwell, J. E. Bares, J. E. Bartmess, G. E. Drucker, J. Gerhold, G. J. McCollum, V. Van Der Puy, N. R. Vanier, and W. S. Matthews, *J. Org. Chem.*, **42**, 326 (1977); F. G. Bordwell, M. Van Der Puy, and N. R. Vanier, *J. Org. Chem.*, **41**, 1885 (1976).

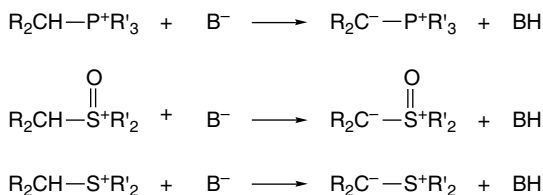
Trialkyl and triarylsilyl substituents have a modest carbanion-stabilizing effect that is attributed mainly to polarizability and is somewhat greater for the triarylsilyl substituents. This stabilization results in a reduced  $pK$  by 1 (trimethylsilyl) to 4 (triphenylsilyl) log units in fluorenes and 3 to 7.5, respectively, in sulfones.<sup>54</sup>

Another important group of nucleophilic carbon species consists of the phosphorus and sulfur ylides. *Ylide* is the name given to molecules in which one of the contributing resonance structures has opposite charges on adjacent atoms when both atoms have octets of electrons. Since we are dealing with nucleophilic carbon species, our interest is in ylides with a negative charge on the carbon. These are of great synthetic importance, and their reactivity is considered in some detail in Chapter 2 of Part B. Here, we discuss the structures of some of the best-known ylides. The three groups of primary synthetic importance are phosphonium, sulfoxonium, and sulfonium ylides. Ylides of ammonium ions also have some synthetic significance.



The question of which resonance structure is the principal contributor has been a point of discussion. Since the uncharged *ylene* resonance structures have ten electrons at the phosphorus or sulfur atom, they imply participation of *d* orbitals on the heteroatoms. Such resonance structures are not possible for ammonium ylides. Structural studies indicate that the dipolar ylide structure is the main contributor.<sup>55</sup> The stabilizing effect of phosphonium and sulfonium substituents is primarily the result of dipolar and polarization effects.<sup>56</sup>

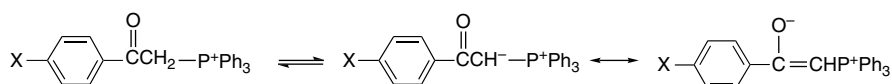
The ylides are formed by deprotonation of the corresponding “onium salts.”



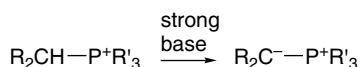
The stability of the ylide is increased by substituent groups that can stabilize the electron-rich carbon.<sup>57</sup> Phosphonium ions with acylmethyl substituents, for example,

- <sup>54</sup> S. Zhang, X.-M. Zhang, and F. G. Bordwell, *J. Am. Chem. Soc.*, **117**, 602 (1995); A. Streitwieser, L. Xie, P. Wang, and S. M. Bachrach, *J. Org. Chem.*, **58**, 1778 (1993).  
<sup>55</sup> H. Schmidbaur, W. Buchner, and D. Scheutzwow, *Chem. Ber.*, **106**, 1251 (1973); D. G. Gilheany, in *The Chemistry of Organophosphorus Compounds*, F. R. Hartley, ed., Wiley, New York, 1994, pp. 1–44; S. M. Bachrach and C. I. Nitsche, in *The Chemistry of Organophosphorus Compounds*, F. R. Hartley, ed., Wiley, New York, 1994, pp. 273–302.  
<sup>56</sup> X.-M. Zhang and F. G. Bordwell, *J. Am. Chem. Soc.*, **116**, 968 (1994).  
<sup>57</sup> M. Schlosser, T. Jenny, and B. Schaub, *Heteroatom. Chem.*, **1**, 151 (1990).

are quite acidic. A series of aryloymethyl phosphonium ions has  $pK$  values of 4–7, with the precise value depending on the aryl substituents.<sup>58</sup>



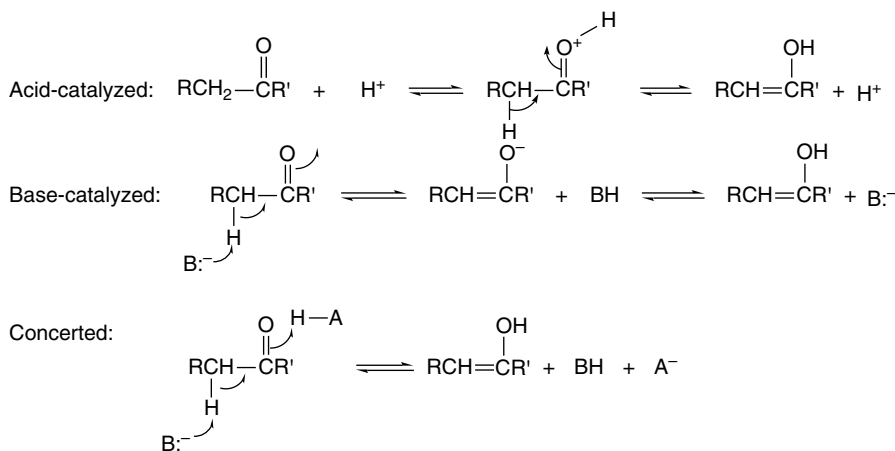
In the absence of the carbonyl or similar stabilizing group, the onium salts are less acidic. The  $pK_{\text{DMSO}}$  of methyltriphenylphosphonium ion is estimated to be 22. Strong bases such as amide ion or the anion of DMSO are required to deprotonate alkylphosphonium salts.



Similar considerations apply to the sulfoxonium and sulfonium ylides, which are formed by deprotonation of the corresponding positively charged sulfur-containing cations. The additional electronegative oxygen atom in the sulfoxonium salts stabilizes these ylides considerably, relative to the sulfonium ylides.<sup>59</sup>

## 6.4. Enols and Enamines

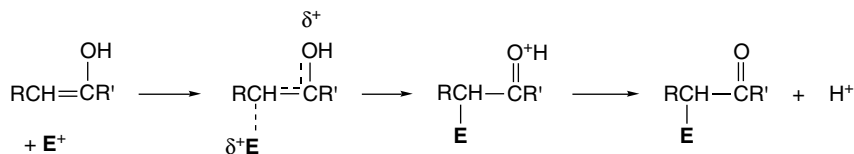
Carbonyl compounds can act as carbon nucleophiles in the presence of *acid catalysts*, as well as bases. The nucleophilic reactivity of carbonyl compounds in acidic solution is due to the presence of the *enol tautomer*. The equilibrium between carbonyl compounds and the corresponding enol can be acid- or base-catalyzed and can also occur by a concerted mechanism in which there is concurrent protonation and deprotonation. As we will see shortly, the equilibrium constant is quite small for monocarbonyl compounds, but the presence of the enol form permits reactions that do not occur from the carbonyl form.



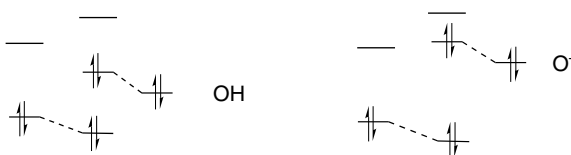
<sup>58</sup>. S. Fliszar, R. F. Hudson, and G. Salvadori, *Helv. Chim. Acta*, **46**, 1580 (1963).

<sup>59</sup>. E. J. Corey and M. Chaykovsky, *J. Am. Chem. Soc.*, **87**, 1353 (1965).

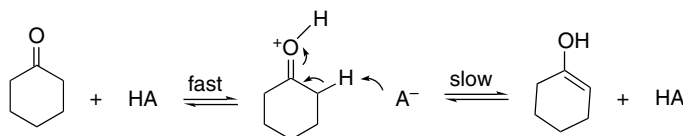
Like simple alkenes, enols are nucleophilic by virtue of their  $\pi$  electrons. Enols are much more reactive than simple alkenes, however, because the hydroxy group participates as an electron donor during the reaction process. The oxygen is deprotonated and the strong C=O bond is formed, providing a favorable energy contribution.



Enols are not as reactive as enolate anions, however. This lower reactivity reflects the presence of the additional proton in the enol, which decreases the electron density of the enol relative to the enolate. In MO terminology, the  $-\text{OH}$  and  $-\text{O}^-$  donor substituents both raise the energy of the  $\pi$ -HOMO, but the  $\text{O}^-$  group is the better donor.



A number of studies of the acid-catalyzed mechanism of enolization have been done, and the case of cyclohexanone is illustrative.<sup>60</sup> The reaction is catalyzed by various carboxylic acids and substituted ammonium ions. The effectiveness of these proton donors as catalysts correlates with their  $\text{p}K_a$  values. When plotted according to the Brønsted catalysis law (Section 3.6.1) the value of the slope  $\alpha$  is 0.74. When deuterium or tritium is introduced in the  $\alpha$ -position, there is a marked decrease in the rate of acid-catalyzed enolization:  $k_{\text{H}}/k_{\text{D}} \sim 5$ . This kinetic isotope effect indicates that the C–H bond cleavage is part of the rate-determining step. The generally accepted mechanism for acid-catalyzed enolization pictures the rate-determining step as deprotonation of the protonated ketone.



It is possible to measure the rate of enolization by isotopic exchange. NMR spectroscopy provides a very convenient method for following hydrogen-deuterium exchange. Data for several ketones are given in Table 6.11.

A point of contrast with the data for base-catalyzed removal of a proton (see Table 6.8) is the tendency for acid-catalyzed enolization to result in preferential formation of the *more-substituted enol*. For 2-butanone, the ratio of exchange at  $\text{CH}_2$  to that at  $\text{CH}_3$  is 4.2:1, after making the statistical correction for the number of hydrogens. The preference for acid-catalyzed enolization to give the more-substituted enol is the result of the stabilizing effect that alkyl groups have on carbon-carbon double bonds. To the extent that the TS resembles product,<sup>61</sup> alkyl groups stabilize the

<sup>60</sup> G. E. Lienhard and T.-C. Wang, *J. Am. Chem. Soc.*, **91**, 1146 (1969).

<sup>61</sup> C. G. Swain, E. C. Stivers, J. F. Reuwer, Jr., and L. J. Schaad, *J. Am. Chem. Soc.*, **80**, 5885 (1958).

**Table 6.11. Relative Rates of Acid-Catalyzed Enolization of some Ketones<sup>a</sup>**

Ketone	Relative rate
$\begin{array}{c} \text{O} \\ \parallel \\ \text{CH}_3\text{CCH}_2\text{—H} \end{array}$	100
$\begin{array}{c} \text{O} \\ \parallel \\ \text{CH}_3\text{CCHCH}_3 \\   \\ \text{H} \end{array}$	220
$\begin{array}{c} \text{O} \\ \parallel \\ \text{H—CH}_2\text{CCH}_2\text{CH}_3 \end{array}$	76
$\begin{array}{c} \text{O} \\ \parallel \\ \text{CH}_3\text{CCHCH}_2\text{CH}_3 \\   \\ \text{H} \end{array}$	171
$\begin{array}{c} \text{O} \\ \parallel \\ \text{CH}_3\text{CC}(\text{CH}_3)_2 \\   \\ \text{H} \end{array}$	195
$\begin{array}{c} \text{O} \\ \parallel \\ \text{H—CH}_2\text{CCH}(\text{CH}_3)_2 \end{array}$	80
$\begin{array}{c} \text{O} \\ \parallel \\ \text{CH}_3\text{CCHC}(\text{CH}_3)_3 \\   \\ \text{H} \end{array}$	46
$\begin{array}{c} \text{O} \\ \parallel \\ \text{H—CH}_2\text{CCH}_2\text{C}(\text{CH}_3)_3 \end{array}$	105

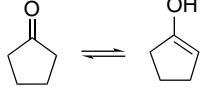
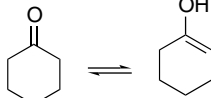
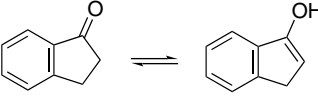
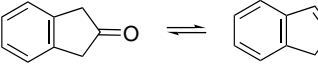
a. In D<sub>2</sub>O-dioxane with DCl catalyst. The data of C. Rappe and W. H. Sachs, *J. Org. Chem.*, **32**, 3700 (1967), given on a per group basis have been converted to a per-hydrogen basis.

more branched TS. There is an opposing steric effect that appears to be significant for 4,4-dimethyl-2-pentanone, in which the methylene group that is flanked by a *t*-butyl group is less reactive than the methyl group. The overall range of reactivity differences in acid-catalyzed exchange is much less than for base-catalyzed exchange, however (compare Tables 6.8 and 6.11). This is consistent with the C-deprotonation of the O-protonated compound having an earlier TS.

There are extensive data on the equilibrium constant for enolization. Table 6.12 gives data on the amount of enol present at equilibrium for some representative compounds. For simple aldehydes, the  $K_{\text{enol}}$  is in the range  $10^{-4}$  to  $10^{-5}$ . Ketones have *smaller* enol content, with  $K_{\text{enol}}$  around  $10^{-8}$ . For esters and amides, where the carbonyl form is resonance stabilized, the  $K_{\text{enol}}$  drops to  $10^{-20}$ . Somewhat surprisingly, 1-aryl substituents do not have a large effect on enol content, as in acetophenone, probably because there is conjugation in the ketone as well as in the enol. On the other hand, there is a large difference when the aryl group is  $\beta$  to the carbonyl, as in 2-indanone, which has a much higher enol content than 1-indanone.

The amount of enol present at equilibrium is influenced by other substituent groups. In the case of compounds containing a single ketone, aldehyde, or ester

Table 6.12. Equilibrium Constants for Enolization of Some Carbonyl Compounds

	Enolization equilibrium	<i>K</i> enol/keto
1 <sup>b</sup>	$\text{CH}_3\text{CH}=\text{O} \rightleftharpoons \text{CH}_2=\text{CHOH}$	$10^{-5}$
2 <sup>c</sup>	$(\text{CH}_3)_2\text{CHCH}=\text{O} \rightleftharpoons (\text{CH}_3)_2\text{C}=\text{CHOH}$	$1.4 \times 10^{-4}$
3 <sup>d</sup>	$\text{PhCH}_2\text{CH}=\text{O} \rightleftharpoons \text{PhCH}=\text{CHOH}$	$8.5 \times 10^{-4}$
4 <sup>e</sup>	$\text{CH}_3\overset{\text{O}}{\parallel}\text{CCH}_3 \rightleftharpoons \text{CH}_2=\overset{\text{OH}}{\text{C}}\text{CH}_3$	$1.3 \times 10^{-8}$
5 <sup>e</sup>	$\text{CH}_3\text{CH}_2\overset{\text{O}}{\parallel}\text{CCH}_2\text{CH}_3 \rightleftharpoons \text{CH}_3\text{CH}=\overset{\text{OH}}{\text{C}}\text{CH}_2\text{CH}_3$	$3.7 \times 10^{-8}$
6 <sup>e</sup>	$(\text{CH}_3)_2\text{CHC}\overset{\text{O}}{\parallel}\text{CH}(\text{CH}_3)_2 \rightleftharpoons (\text{CH}_3)_2\text{C}=\overset{\text{OH}}{\text{C}}\text{CH}(\text{CH}_3)_2$	$3.0 \times 10^{-8}$
7 <sup>e</sup>	$\text{PhC}\overset{\text{O}}{\parallel}\text{CH}_3 \rightleftharpoons \text{PhC}=\overset{\text{OH}}{\text{C}}\text{H}_2$	$1.1 \times 10^{-8}$
8 <sup>e</sup>	$\text{PhC}\overset{\text{O}}{\parallel}\text{CH}(\text{CH}_3)_2 \rightleftharpoons \text{PhC}=\overset{\text{OH}}{\text{C}}(\text{CH}_3)_2$	$3.3 \times 10^{-7}$
9 <sup>e</sup>		$1.2 \times 10^{-8}$
10 <sup>e</sup>		$4.2 \times 10^{-7}$
11 <sup>f</sup>	$\text{CH}_3\overset{\text{O}}{\parallel}\text{COCH}_3 \rightleftharpoons \text{CH}_2=\overset{\text{OH}}{\text{C}}\text{OCH}_3$	$3.2 \times 10^{-19}$
12 <sup>f</sup>	$\text{CH}_3\overset{\text{O}}{\parallel}\text{CNH}_2 \rightleftharpoons \text{CH}_2=\overset{\text{OH}}{\text{C}}\text{NH}_2$	$6.3 \times 10^{-20}$
13 <sup>g</sup>		$3.3 \times 10^{-8}$
14 <sup>h</sup>		$1.5 \times 10^{-4}$
15 <sup>i</sup>	$\text{CH}_3\overset{\text{O}}{\parallel}\text{CCH}_2\overset{\text{O}}{\parallel}\text{CCH}_3 \rightleftharpoons \text{CH}_3\overset{\text{OH}}{\text{C}}=\overset{\text{O}}{\text{C}}\text{CH}_3$	$2.3 \times 10^{-1}$ (H <sub>2</sub> O)
16 <sup>j</sup>		29 (CCl <sub>4</sub> )
17 <sup>i</sup>	$\text{CH}_3\overset{\text{O}}{\parallel}\text{CCH}_2\overset{\text{O}}{\parallel}\text{COC}_2\text{H}_5 \rightleftharpoons \text{CH}_3\overset{\text{OH}}{\text{C}}=\overset{\text{O}}{\text{C}}\text{OC}_2\text{H}_5$	$7 \times 10^{-2}$ (H <sub>2</sub> O)
18 <sup>j</sup>		$3 \times 10^{-1}$ (CCl <sub>4</sub> )
19 <sup>i</sup>	$\text{CH}_3\overset{\text{O}}{\parallel}\text{CCH}_2\overset{\text{O}}{\parallel}\text{CNH}_2 \rightleftharpoons \text{CH}_3\overset{\text{OH}}{\text{C}}=\overset{\text{O}}{\text{C}}\text{NH}_2$	1.3 (H <sub>2</sub> O)

(Continued)

Table 6.12. (Continued)

	Enolization equilibrium	K enol/keto
20 <sup>j</sup>		20 (H <sub>2</sub> O) 0.05 (CHCl <sub>3</sub> )
21 <sup>k</sup>		> 50(CCl <sub>4</sub> )
22 <sup>l</sup>		5.4 x 10 <sup>-2</sup> (H <sub>2</sub> O)

a. In water unless otherwise noted.

b. J. P. Guthrie and P. A. Cullimore, *Can. J. Chem.*, **57**, 240 (1979).

c. Y. Chiang, A. J. Kresge, and P. A. Walsh, *J. Am. Chem. Soc.*, **108**, 6314 (1986).

d. Y. Chiang, A. J. Kresge, P. A. Walsh, and Y. Yin, *J. Chem. Soc., Chem. Commun.*, 869 (1989).

e. J. R. Keefe, A. J. Kresge, and N. P. Schepp, *J. Am. Chem. Soc.*, **112**, 4862 (1990).

f. J. P. Richard, G. Williams, A. M. C. O'Donoghue, and T. L. Amyes, *J. Am. Chem. Soc.*, **124**, 2957 (2002).

g. E. A. Jefferson, J. R. Keefe, and A. J. Kresge, *J. Chem. Soc. Perkin Trans. 2*, 2041 (1995).

h. J. R. Keefe, A. J. Kresge, and Y. Yin, *J. Am. Chem. Soc.*, **110**, 8201 (1988).

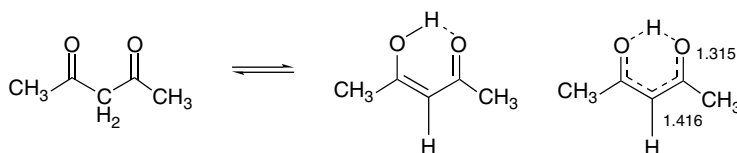
i. J. W. Bunting and J. P. Kanter, *J. Am. Chem. Soc.*, **115**, 11705 (1993).

j. S. G. Mills and P. Beak, *J. Org. Chem.*, **50**, 1216 (1985).

k. E. W. Garbisch, *J. Am. Chem. Soc.*, **85**, 1696 (1963).

l. J. A. Chang, A. J. Kresge, V. A. Nikolaev, and V. V. Popik, *J. Am. Chem. Soc.*, **125**, 6478 (2003).

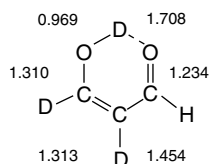
function, very little of the enol is present at equilibrium. When two such groups are close to one another, particularly if they are separated by a single carbon atom, the enol may be the major form. The enol forms of  $\beta$ -diketones and  $\beta$ -ketoesters are stabilized by intramolecular hydrogen bonds and by conjugation of the carbon-carbon double bond with the carbonyl group. The structural data given below for the enol form of 2,4-pentanedione were obtained by an electron diffraction study.<sup>62</sup> In this case the data pertain to the time-averaged structure resulting from proton transfer between the two hydrogen-bonded oxygens.



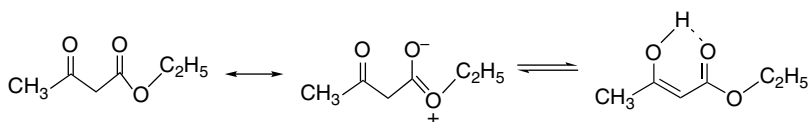
The simplest compound with this type of enolic structure is malonaldehyde. The structures determined by microwave spectroscopy on a deuterated analog have provided

<sup>62</sup>. A. H. Lowrey, C. George, P. D'Antonio, and J. Karle, *J. Am. Chem. Soc.*, **93**, 6399 (1971).

the bond length data shown below.<sup>63</sup> The barrier for shift of the enolic hydrogen (or deuterium) between the two oxygen atoms is about 4–5 kcal.<sup>64</sup>

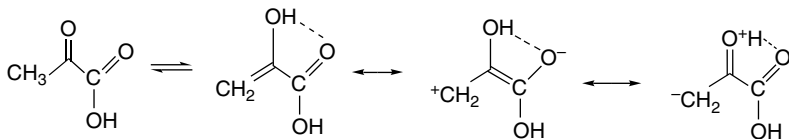


The extent of enolization at equilibrium is also solvent dependent.<sup>65</sup> The hydrogen-bonding capacity of the solvent is especially important. For example, for ethyl acetoacetate, the amount of enol is higher (15–30%) in nonpolar solvents such as carbon tetrachloride or benzene than in more polar solvents such as water or acetone (5% enol in acetone, 1% enol in water).<sup>66</sup> The strong intramolecular hydrogen bond in the enol form minimizes the molecular dipole by reducing the negative charge on the oxygen of the carbonyl group. In more polar solvents this stabilization is less important, and in protic solvents such as water, hydrogen bonding by the solvent is dominant.



This relationship is reversed in compounds where intramolecular hydrogen bonding is not possible. (See the entry for 5,5-dimethylcyclohexane-1,3-dione in Table 6.12.)

$\alpha$ -Dicarbonyl compounds also have an enhanced tendency toward enolization, although it is not as pronounced as for  $\beta$ -dicarbonyl compounds. The  $K_{\text{enol}}$  for pyruvic acid is about  $10^{-3}$ .<sup>67</sup> There is resonance stabilization between the enol double bond and the ester carbonyl as well as a contribution from hydrogen bonding.



Enols of simple ketones can be generated in high concentrations as metastable species by special techniques.<sup>68</sup> Vinyl alcohol, the enol of acetaldehyde, can be generated by very careful hydrolysis of any of several ortho ester derivatives in which the group  $\text{RCO}_2^-$  is acetic acid or a chloroacetic acid.<sup>69</sup>

<sup>63</sup> S. L. Baughcum, R. W. Duerst, W. F. Rowe, Z. Smith, and E. B. Wilson, *J. Am. Chem. Soc.*, **103**, 6296 (1981).

<sup>64</sup> S. L. Baughcum, Z. Smith, E. B. Wilson, and R. W. Duerst, *J. Am. Chem. Soc.*, **106**, 2260 (1984).

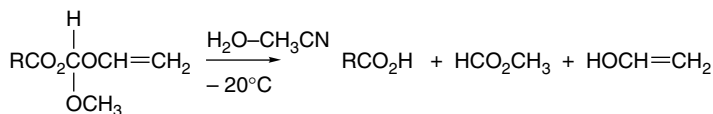
<sup>65</sup> J. Elmsley and N. J. Freeman, *J. Mol. Struct.*, **161**, 193 (1987); J. N. Spencer, E. S. Holcombe, M. R. Kirshenbaum, D. W. Firth, and P. B. Pinto, *Can. J. Chem.*, **60**, 1178 (1982).

<sup>66</sup> K. D. Grande and S. M. Rosenfeld, *J. Org. Chem.*, **45**, 1626 (1980); S. G. Mills and P. Beak, *J. Org. Chem.*, **50**, 1216 (1985).

<sup>67</sup> Y. Chiang, A. J. Kresge, and P. Pruszyński, *J. Am. Chem. Soc.*, **114**, 3103 (1992); J. Damitio, G. Smith, J. E. Meany, and Y. Pocker, *J. Am. Chem. Soc.*, **114**, 3081 (1992).

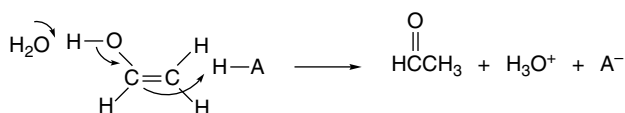
<sup>68</sup> B. Capon, B. Z. Guo, F. C. Kwok, A. F. Siddhanta, and C. Zucco, *Acc. Chem. Res.*, **21**, 135 (1988).

<sup>69</sup> B. Capon, D. S. Rycroft, T. W. Watson, and C. Zucco, *J. Am. Chem. Soc.*, **103**, 1761 (1981).

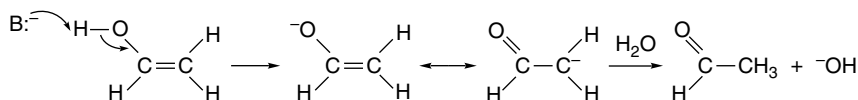


The enol can be observed by NMR and at  $-20^\circ\text{C}$  has a half-life of several hours. At  $+20^\circ\text{C}$  the half-life is only 10 min. The presence of bases causes very rapid isomerization to acetaldehyde via the enolate. Solvents have a significant effect on the lifetime of such unstable enols. Solvents such as DMF or DMSO, which are known to slow the rate of proton exchange by hydrogen bonding, increase the lifetime of unstable enols.<sup>70</sup>

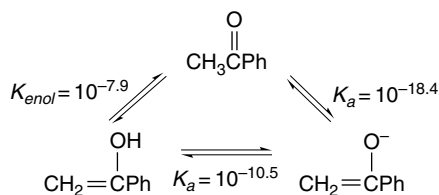
Solutions of unstable enols of simple ketones and aldehydes can also be generated in water by the addition of a solution of the enolate.<sup>71</sup> The initial protonation takes place on oxygen, generating the enol, which is then ketonized at a rate that depends on the solution pH. The ketonization exhibits both acid and base catalysis.<sup>72</sup> Acid catalysis involves C-protonation with concerted O-deprotonation. In agreement with expectation for a rate-determining proton transfer, the reaction shows general acid catalysis.



Base-catalyzed ketonization occurs by C-protonation of the enolate.



As would be expected on the basis of electronegativity arguments, enols are much more acidic than the corresponding keto form. It has been possible to determine the  $pK$  of the enol form of acetophenone as being 10.5 in water. The  $pK$  of the keto form is 18.4.<sup>73</sup> Since the enolate is the same for both equilibria, the difference in the  $pK$  values is equal to the enol  $\rightleftharpoons$  keto equilibrium constant,  $K_{\text{enol}}$ .



Similar measurements have been made for the equilibria involving acetone and its enol, 2-hydroxypropene.<sup>74</sup> In this case, the activation parameters were also determined and are shown below.<sup>75</sup>

<sup>70</sup> E. A. Schmidt and H. M. R. Hoffmann, *J. Am. Chem. Soc.*, **94**, 7832 (1972).

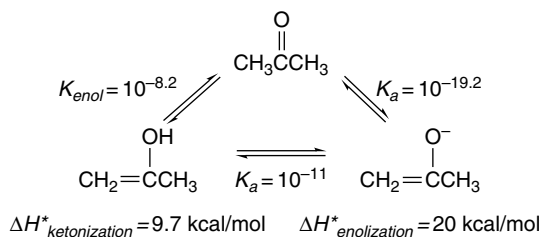
<sup>71</sup> Y. Chiang, A. J. Kresge, and P. A. Walsh, *J. Am. Chem. Soc.*, **104**, 6122 (1982); Y. Chiang, A. J. Kresge, and P. A. Walsh, *J. Am. Chem. Soc.*, **108**, 6314 (1986).

<sup>72</sup> B. Capon and C. Zucco, *J. Am. Chem. Soc.*, **104**, 7567 (1982).

<sup>73</sup> Y. Chiang, A. J. Kresge, and J. Wirz, *J. Am. Chem. Soc.*, **106**, 6392 (1984).

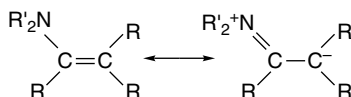
<sup>74</sup> Y. Chiang, A. J. Kresge, Y. S. Tang, and J. Wirz, *J. Am. Chem. Soc.*, **106**, 460 (1984).

<sup>75</sup> Y. Chiang, A. J. Kresge, and N. P. Schepp, *J. Am. Chem. Soc.*, **111**, 3977 (1989).

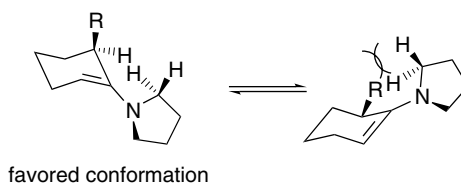


The accessibility of enols and enolates, respectively, in acidic and basic solutions of carbonyl compounds makes possible a wide range of reactions that depend on their nucleophilicity. These reactions are discussed in Chapter 7 and in Chapters 1 and 2 of Part B.

Amino substituents on a carbon-carbon double bond enhance the nucleophilicity of the  $\beta$ -carbon to an even greater extent than the hydroxy group in enols because of the greater electron-donating power of nitrogen. Such compounds are called *enamines*.<sup>76</sup>



An interesting and useful property of enamines of 2-alkylcyclohexanone is the substantial preference for the less-substituted isomer to be formed. This tendency is especially pronounced for enamines derived from cyclic secondary amines such as pyrrolidine, a preference that can be traced to  $A^{1,3}$  allylic strain. In order to maximize conjugation between the nitrogen lone pair and the carbon-carbon double bond, the nitrogen substituent must be coplanar with the double bond. This creates a steric repulsion when the enamine bears a  $\beta$ -substituent and leads to a preference for the unsubstituted enamine. Because of the same preference for coplanarity in the enamine system,  $\alpha$ -alkyl substituents adopt an axial conformation to minimize steric interaction with the amino group.

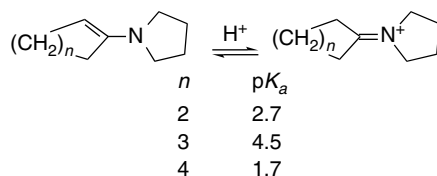


These steric factors are also indicated by the relative basicity of enamines derived from five-, six-, and seven-membered ketones.<sup>77</sup> The five- and seven-membered enamines

<sup>76</sup> A. G. Cook, *Enamines*, 2nd Edition, Marcel Dekker, New York, 1988, Chap. 1; Z. Rappoport, ed., *Chemistry of Enamines*, Wiley, Chichester, 1994.

<sup>77</sup> A. G. Cook, M. L. Absi, and V. F. Bowden, *J. Org. Chem.*, **60**, 3169 (1995).

are considerably stronger bases, indicating better conjugation between the nitrogen lone pair and the double bond. The reduced basicity of the cyclohexanone enamines is related to the preference for *exo* and *endo* double bonds in six-membered rings.



The preparation of enamines is discussed in Chapter 7, and their application as carbon nucleophiles in synthesis is dealt with in Chapter 1 of Part B.

## 6.5. Carbanions as Nucleophiles in $S_N2$ Reactions

Carbanions are very useful intermediates in the formation of carbon-carbon bonds. This is true for both unstabilized structures found in organometallic reagents and stabilized structures such as enolates. Carbanions can participate as nucleophiles in both addition and substitution reactions. At this point we consider aspects of the reactions of carbanions as nucleophiles in reactions that proceed by the  $S_N2$  mechanism. Other synthetic applications of carbanions are discussed more completely in Chapter 7 and in Chapters 1 and 2, Part B.

### 6.5.1. Substitution Reactions of Organometallic Reagents

Carbanions are classified as soft nucleophiles. They are expected to be good nucleophiles in  $S_N2$  reactions and this is generally true. The reactions of aryl-, alkenyl-, and allyl lithium reagents with primary alkyl halides and tosylates appear to proceed by  $S_N2$  mechanisms. Similar reactions occur between arylmagnesium halides (Grignard reagents) and alkyl sulfates and sulfonates. Some examples of these reactions are given in Scheme 6.2.

Note that all the examples in Scheme 6.2 involve either  $sp^2$  or stabilized organometallic reagents. Evidence for an  $S_N2$ -type mechanism in the reaction of allyl and benzyl lithium reagents has been obtained from stereochemical studies. With 2-bromobutane, both of these reagents react with complete inversion of configuration.<sup>78</sup> *n*-Butyllithium, however, gives largely racemic product, indicating that some competing process must also be occurring.<sup>79</sup> A general description of the mechanism for the reaction of organolithium compounds with alkyl halides must take account of the structure of the organometallic compound. It is known that halide anions are accommodated into typical organolithium cluster structures and can replace solvent molecules as ligands. A similar process in which the alkyl halide became complexed

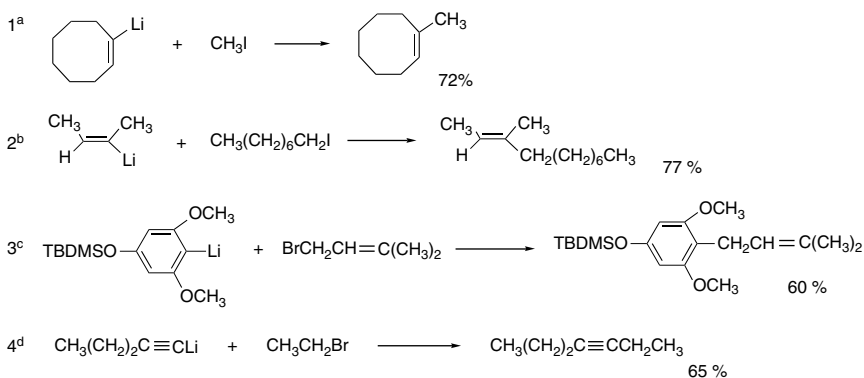
<sup>78</sup> L. H. Sommer and W. D. Korte, *J. Org. Chem.*, **35**, 22 (1970).

<sup>79</sup> H. D. Zook and R. N. Goldey, *J. Am. Chem. Soc.*, **75**, 3975 (1953).

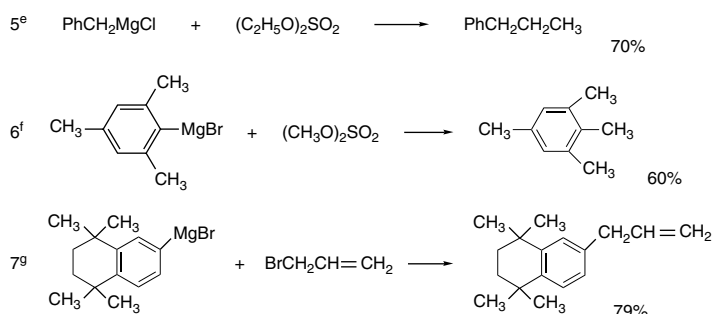
## CHAPTER 6

Carbanions and Other  
Carbon Nucleophiles

## A. Organolithium Reagents

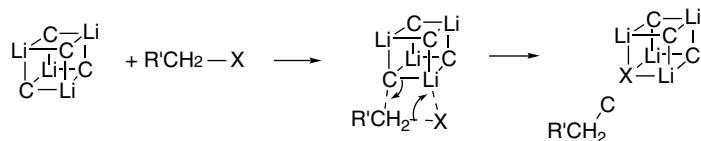


## B. Organomagnesium reagents

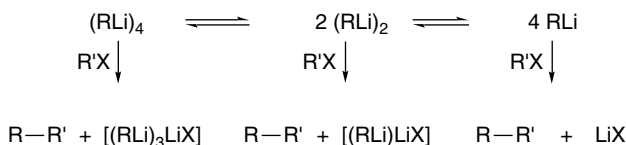


- a. H. Neumann and D. Seebach, *Chem. Ber.*, **111**, 2785 (1978).  
 b. J. Millon, R. Lorne, and G. Linstumelle, *Synthesis*, 434 (1975).  
 c. T. L. Shih, M. J. Wyratt, and H. Mroziak, *J. Org. Chem.*, **52**, 2029 (1987).  
 d. A. J. Quillinan and F. Schienman, *Org. Synth.*, **58**, 1 (1978).  
 e. H. Gilman and W. E. Catlin, *Org. Synth.*, **1**, 360 (1943).  
 f. L. I. Smith, *Org. Synth.*, **II**, 360 (1943).  
 g. J. Eustache, J. M. Bernardon, and B. Shroot, *Tetrahedron Lett.*, **28**, 4681 (1987).

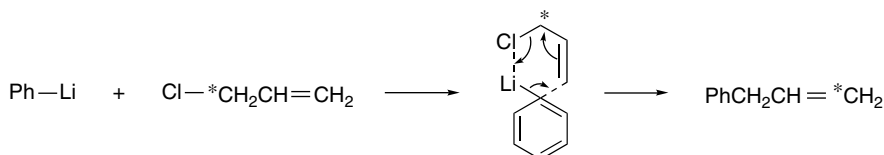
at lithium would provide an intermediate structure that could account for the subsequent alkylation. This process is represented below for a tetrameric structure, with the organic group simply represented by C.



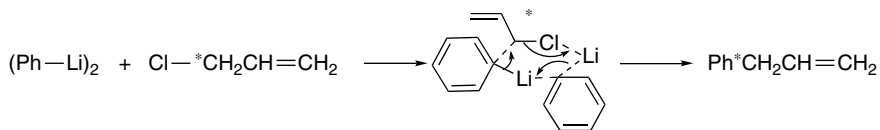
In general terms, the reactions of organolithium reagents with alkylating agents might occur at any of the aggregation stages present in solution and there could be reactivity differences among them. There has been little detailed mechanistic study that would distinguish among these possibilities.



The reaction of phenyllithium and allyl chloride using  $^{14}\text{C}$  label reveals the occurrence of allylic transposition. About three-fourths of the product results from bond formation at C(3) rather than C(1), which can be accounted for by a cyclic mechanism.<sup>80</sup>



The portion of the product formed by reaction at C(1) in allylic systems may form by direct substitution, but it has also been suggested that a cyclic TS involving an aryllithium dimer might be involved.



These mechanisms ascribe importance to the Lewis acid–Lewis base interaction between the allyl halide and the organolithium reagent. When substitution is complete, the halide ion is incorporated into the lithium cluster in place of one of the carbon ligands.

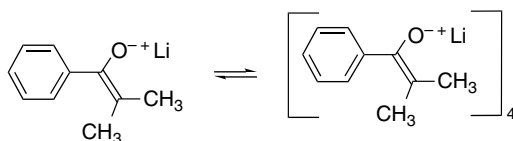
From a synthetic point of view, direct alkylation of lithium and magnesium organometallic compounds has been largely supplanted by transition metal–catalyzed processes. We discuss these reactions in Chapter 8 of Part B.

### 6.5.2. Substitution Reactions of Enolates

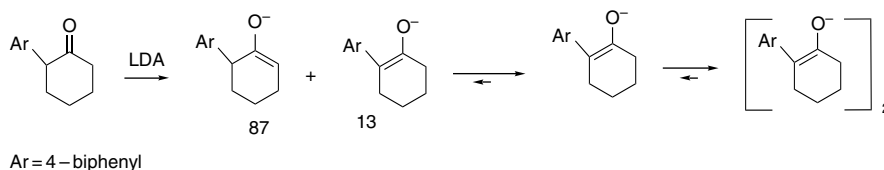
The alkylation reactions of enolate anions of both ketones and esters have been extensively utilized in synthesis. Both stable enolates, such as those derived from  $\beta$ -ketoesters,  $\beta$ -diketones, and malonate esters, as well as less stable enolates of monofunctional ketones, esters, nitriles, etc., are reactive. Many aspects of the relationships among reactivity, stereochemistry, and mechanism have been clarified. The starting point for the discussion of these reactions is the structure of the enolates. Studies of ketone enolates in solution indicate that both tetrameric and dimeric clusters can exist. THF, a solvent in which many synthetic reactions are performed, favors tetrameric structures for the lithium enolate of isobutyrophenone, for example.<sup>81</sup>

<sup>80</sup> R. M. Magid and J. G. Welch, *J. Am. Chem. Soc.*, **90**, 5211 (1968); R. M. Magid, E. C. Nieh, and R. D. Gandour, *J. Org. Chem.*, **36**, 2099 (1971).

<sup>81</sup> L. M. Jackman and N. Szeverenyi, *J. Am. Chem. Soc.*, **99**, 4954 (1977); L. M. Jackman and B. C. Lange, *Tetrahedron*, **33**, 2737 (1977).



Detailed investigation of the degree of aggregation in solution has been applied to several alkyl aryl ketones.<sup>82</sup> The lithium enolate of 4-(4-biphenyl)-2-methyl-1-propanone in THF exhibits a monomer-tetramer equilibrium.<sup>83</sup> The  $K_{\text{eq}}$  for tetramerization is estimated as  $5 \times 10^8 M^3$ , which corresponds to 1.3% of the enolate being present as the monomer. The kinetics of the alkylation reaction with benzyl bromide indicates that the *monomer is the reactive nucleophile*. Related studies were carried out with 2-(4-biphenyl)cyclohexanone. In this case, an initial 87:13 mixture of the regioisomeric enolates is completely converted to the conjugated enolate at equilibrium. There is an equilibrium between monomer and dimer, with  $K_{\text{eq}} = 4.3 \times 10^3 M$ . Again, the monomer is more reactive in the alkylation reaction. This is attributed to less electrostatic stabilization by a single  $\text{Li}^+$  than by two or four in the aggregates.



The structures of several lithium enolates of ketones have been determined by X-ray crystallography and reveal aggregated structures in which oxygen and lithium occupy alternating corners of distorted cubes. Figure 6.4 illustrates some of the observed structures. Figure 6.4a shows an unsolvated enolate of methyl *t*-butyl ketone (pinacolone).<sup>84</sup> The structures in Figures 6.4b and 6.4c are THF solvates of the enolates of methyl *t*-butyl ketone and cyclopentanone, respectively.<sup>85</sup> Each of these structures consists of clusters of four enolate anions and four lithium cations arranged with lithium and oxygen at alternating corners of a distorted cube. The structure in Figure 6.4d includes only two enolate anions. Four lithium ions are present, along with two di-*i*-propylamide ion. A significant feature of this structure is the coordination of the remote silyloxy oxygen atom to one of the lithium cations.<sup>86</sup> This is an example of the Lewis acid–Lewis base interactions that are frequently involved in organizing TS structure in the reactions of lithium enolates. A common feature of all four of the structures is the involvement of the enolate oxygen in multiple contacts with lithium cations in the cluster. An approaching electrophile will clearly be somewhat hindered from direct contact with oxygen in such structures, whereas the nucleophilic carbon is somewhat more exposed.

<sup>82</sup> A. Streitwieser and D. Z.-R. Wang, *J. Am. Chem. Soc.*, **121**, 6213 (1999).

<sup>83</sup> A. Abbotto, S. S.-W. Leung, A. Streitwieser, and K. V. Kilway, *J. Am. Chem. Soc.*, **120**, 10807 (1998).

<sup>84</sup> P. G. Williard and G. B. Carpenter, *J. Am. Chem. Soc.*, **107**, 3345 (1985).

<sup>85</sup> R. Amstutz, W. B. Schweizer, D. Seebach, and J. D. Dunitz, *Helv. Chim. Acta*, **64**, 2617 (1981).

<sup>86</sup> P. G. Williard and M. J. Hintze, *J. Am. Chem. Soc.*, **109**, 5539 (1987).

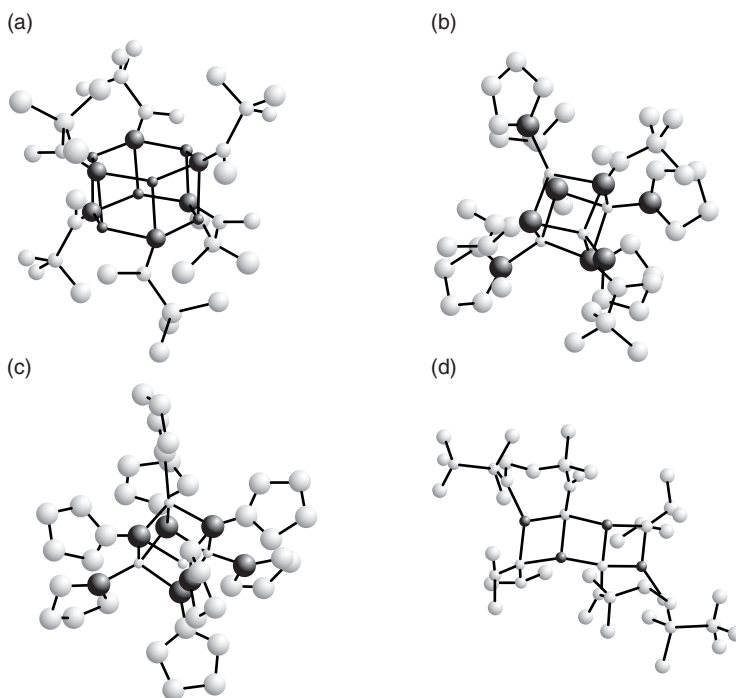


Fig. 6.4. Crystal structures of some enolates of ketones: (a) unsolvated hexameric enolate of methyl *t*-butyl ketone; (b) THF solvate of tetrameric enolate of methyl *t*-butyl ketone; (c) THF solvate of tetrameric enolate of cyclopentanone; and (d) dimeric enolate of 3,3-dimethyl-4-(*t*-butyl)dimethylsilyloxy-2-pentanone. Adapted from *J. Am. Chem. Soc.*, **107**, 3345 (1985); *Helv. Chim. Acta*, **64**, 2617 (1981); *J. Am. Chem. Soc.*, **107**, 5403 (1985); and *J. Am. Chem. Soc.*, **109**, 5539 (1987), by permission of the American Chemical Society and Wiley-VCH.

Several ester enolates have also been examined by X-ray crystallography.<sup>87</sup> The enolates of *t*-butyl propionate and *t*-butyl 3-methylpropionate were obtained as TMEDA solvates of enolate dimers. Methyl 3,3-dimethylbutanoate was obtained as a THF-solvated tetramer.

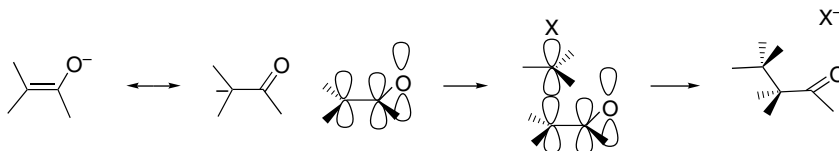
Most of the structural features of enolates are correctly modeled using B3LYP/6-31+G\* computations with dimethyl ether as the solvent molecule.<sup>88</sup> Computational methods also indicate the stability of aggregated structures. Both *ab initio* and semiempirical calculations of the structure of the lithium enolate of methyl isobutyrate have been reported.<sup>89</sup> Although semiempirical PM3 calculations give adequate representations of the geometries of the aggregates, the energy values are not accurate. Dimeric and tetrameric structures give calculated <sup>13</sup>C chemical shifts in agreement with the experimental values.

<sup>87</sup>. D. Seebach, R. Amstutz, T. Laube, W. B. Schweizer, and J. D. Dunitz, *J. Am. Chem. Soc.*, **107**, 5403 (1985).

<sup>88</sup>. A. Abbotto, A. Streitwieser, and P. v. R. Schleyer, *J. Am. Chem. Soc.*, **119**, 11255 (1997).

<sup>89</sup>. H. Weiss, A. V. Yakimansky, and A. H. E. Mueller, *J. Am. Chem. Soc.*, **118**, 8897 (1996).

Because of the delocalized nature of enolates, an electrophile can attack either at oxygen or at carbon. Soft electrophiles prefer carbon and it is found experimentally that most alkyl halides react to give C-alkylation. Because of the  $\pi$  character of the HOMO of the anion, there is a stereoelectronic preference for attack of the electrophile approximately perpendicular to the plane of the enolate. The frontier orbital is  $\psi_2$  with electron density mainly at O and C(2). The TS for an  $S_N2$  alkylation of an enolate can be represented as below.



One of the general features of the reactivity of enolate anions is the sensitivity of both the reaction rate and the ratio of C versus O alkylation to the degree of aggregation of the enolate. For example, addition of HMPA frequently increases the rate of enolate alkylation reactions.<sup>90</sup> Use of a dipolar aprotic solvent such as DMF or DMSO in place of THF also leads to rate acceleration.<sup>91</sup> These effects are attributed, at least in part, to dissociation of the enolate aggregates. Similar effects are observed when crown ethers or other cation-complexing agents are added to reaction mixtures.<sup>92</sup> The order of enolate reactivity also depends on the metal cation that is present. The general order is  $\text{BrMg} < \text{Li} < \text{Na} < \text{K}$ , which is also in the order of greater dissociation of the enolate-cation ion pairs and ion aggregates. Carbon-13 chemical shift data provide an indication of electron density at the nucleophilic carbon in enolates. These shifts have been found to be both cation and solvent dependent. Apparent electron density is in the order  $\text{K}^+ > \text{Na}^+ > \text{Li}^+$  and  $\text{THF/HMPA} > \text{DME} > \text{THF} > \text{ether}$ .<sup>93</sup> There is a good correlation with observed reactivity under the corresponding conditions.

The leaving group in the alkylating reagent has a major effect on whether C- or O-alkylation occurs. The C- versus O-alkylation ratio has been studied for the potassium salt of ethyl acetoacetate as a function of both solvent and leaving group.<sup>94</sup>

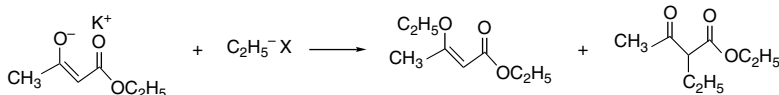
<sup>90</sup> L. M. Jackman and B. C. Lange, *J. Am. Chem. Soc.*, **103**, 4494 (1981); C. L. Liotta and T. C. Caruso, *Tetrahedron Lett.*, **26**, 1599 (1985).

<sup>91</sup> H. D. Zook and J. A. Miller, *J. Org. Chem.*, **36**, 1112 (1971); H. E. Zaugg, J. F. Ratajczyk, J. E. Leonard, and A. D. Schaeffer, *J. Org. Chem.*, **37**, 2249 (1972); H. E. Zaugg, *J. Am. Chem. Soc.*, **83**, 837 (1961).

<sup>92</sup> A. L. Kurts, S. M. Sakembaeva, J. P. Beletskaya, and O. A. Reutov, *Zh. Org. Khim. SSSR*, (Engl. Transl.), **10**, 1588 (1974).

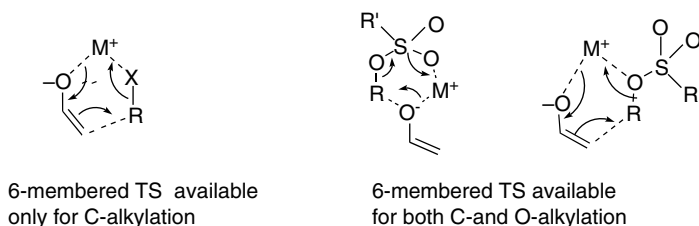
<sup>93</sup> H. O. House, A. V. Prabhu, and W. V. Phillips, *J. Org. Chem.*, **41**, 1209 (1976).

<sup>94</sup> A. L. Kurts, A. Macias, N. K. Genkina, I. P. Beletskaya, and O. A. Reutov, *Dokl. Akad. Nauk, SSSR* (Engl. Trans.), **187**, 595 (1969); A. L. Kurts, N. K. Genkina, A. Macias, I. P. Beletskaya, and O. A. Reutov, *Tetrahedron*, **27**, 4777 (1971).



Leaving group X	Solvent	C:O ratio	Leaving group X	Solvent	C:O ratio
OSO <sub>2</sub> OC <sub>2</sub> H <sub>5</sub>	THF	100:0	OSO <sub>2</sub> C <sub>7</sub> H <sub>7</sub>	HMPA	12:88
OSO <sub>2</sub> OC <sub>2</sub> H <sub>5</sub>	<i>t</i> -BuOH	100:0	Cl	HMPA	40:60
OSO <sub>2</sub> OC <sub>2</sub> H <sub>5</sub>	EtOH	92:8	Br	HMPA	61:39
OSO <sub>2</sub> OC <sub>2</sub> H <sub>5</sub>	CH <sub>3</sub> CN	68:32	I	HMPA	87:13
OSO <sub>2</sub> OC <sub>2</sub> H <sub>5</sub>	DMSO	30:70			
OSO <sub>2</sub> OC <sub>2</sub> H <sub>5</sub>	DMF	21:79			
OSO <sub>2</sub> OC <sub>2</sub> H <sub>5</sub>	HMPA	17:83			

These data show that a change from a hard leaving group (sulfonate, sulfate) to a softer leaving group (bromide, iodide) favors carbon alkylation. Another possible factor in C:O ratios may be the ability of sulfonates to form a six-membered cyclic TS for both modes of reaction, whereas halides can form such structures only for C-alkylation.<sup>83</sup>



The data for ethyl acetoacetate alkylation also show a shift from C-alkylation in THF and alcohols to dominant O-alkylation in DMSO, DMF, and HMPA. This reflects the more dissociated and weakly solvated state of the enolate in the aprotic dipolar solvents.

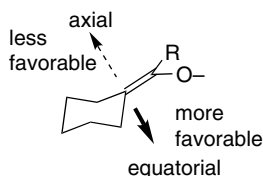
Another major influence on the C:O ratios is presumably the degree of aggregation. The reactivity at oxygen should be enhanced by dissociation since the electron density is less tightly associated with the cation. With the lithium enolate of acetophenone, for example, C-alkylation is the major product with methyl iodide but C-alkylation and O-alkylation occur to approximately equal extents with dimethyl sulfate. The C:O ratio is shifted more to O-alkylation by addition of HMPA or other cation-complexing agents. Thus, with four equivalents of HMPA the C:O ratio for methyl iodide drops from more than 200:1 to 10:1, whereas with dimethyl sulfate the C:O ratio changes from 1.2:1 to 0.2:1 when HMPA is added.<sup>95</sup>

Steric and stereoelectronic effects control the direction of approach of an electrophile to the enolate. Electrophiles approach from the side of the enolate that is less hindered. Many examples of such effects have been observed.<sup>96</sup> In ketone and ester enolates that are exocyclic to a conformationally biased cyclohexane ring there is a small preference for the electrophile to approach from the equatorial

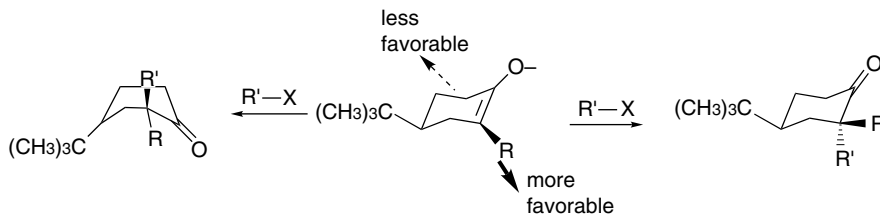
<sup>95</sup> L. M. Jackman and B. C. Lange, *J. Am. Chem. Soc.*, **103**, 4494 (1981).

<sup>96</sup> Reviews: D. A. Evans, in *Asymmetric Synthesis*, Vol. 3, J. D. Morrison, ed., Academic Press, New York, 1984, Chap. 1; D. Caine, in *Carbon-Carbon Bond Formation*, R. L. Augustine, ed., Marcel Dekker, New York, 1979.

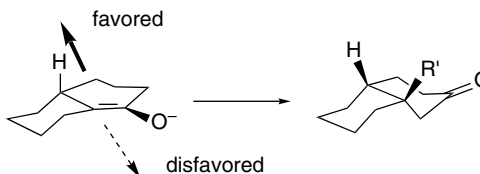
direction.<sup>97</sup> If the axial face is further hindered by the addition of a substituent, the selectivity is increased.



Endocyclic cyclohexanone enolates with 2-alkyl groups show a small preference (1:1–5:1) for approach of the electrophile from the direction that permits maintenance of the chair conformation.<sup>98</sup>



The 1(9)-enolate of 1-decalone exhibits a preference for alkylation to form a *cis* ring juncture.



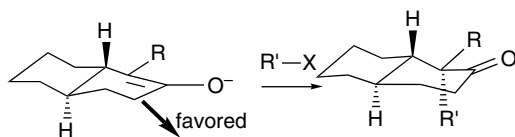
This is the result of a steric differentiation with of the electrophile approaching from the side of the enolate occupied by the smaller hydrogen, rather than the ring methylene group at the C(10) position.

The 2(1)-enolate of *trans*-2-decalone is preferentially alkylated by an axial approach of the electrophile. The stereoselectivity is enhanced if there is an alkyl substituent at C(1). The factors operating in this case are similar to those described for 4-*t*-butylcyclohexanone. The *trans*-decalone framework is conformationally rigid. Axial attack from the lower face leads directly to the chair conformation of the product. The 1-alkyl group enhances this stereoselectivity because a steric interaction with the solvated enolate oxygen distorts the enolate in such a way as to favor the axial attack.<sup>99</sup>

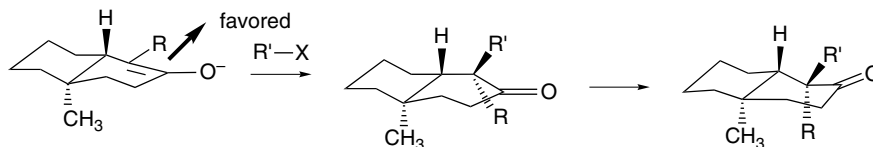
<sup>97</sup> A. P. Krapcho and E. A. Dundulis, *J. Org. Chem.*, **45**, 3236 (1980); H. O. House and T. M. Bare, *J. Org. Chem.*, **33**, 943 (1968).

<sup>98</sup> H. O. House, B. A. Tefertiller, and H. D. Olmstead, *J. Org. Chem.*, **33**, 935 (1968); H. O. House and M. J. Umen, *J. Org. Chem.*, **38**, 1000 (1973); J. M. Conia and P. Briet, *Bull. Soc. Chim. France*, 3881, 3886 (1966); C. Djerassi, J. Burakevich, J. W. Chamberlin, D. Elad, T. Toda, and G. Stork, *J. Am. Chem. Soc.*, **86**, 465 (1964); C. Agami, J. Levisalles, and B. Lo Cicero, *Tetrahedron*, **35**, 961 (1979).

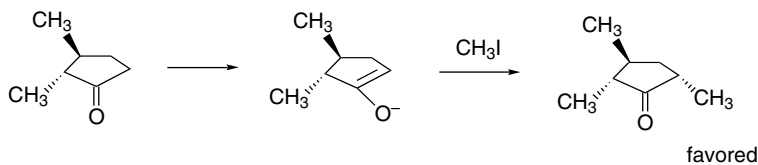
<sup>99</sup> R. S. Mathews, S. S. Grigenti, and E. A. Folkers, *J. Chem. Soc., Chem. Commun.*, 708 (1970); P. Lansbury and G. E. DuBois, *Tetrahedron Lett.*, 3305 (1972).



The placement of an axial methyl group at C(10) in a 2(1)-decalone enolate introduces a 1,3-diaxial interaction with the approaching electrophile. The preferred alkylation product results from approach on the other side of the enolate.

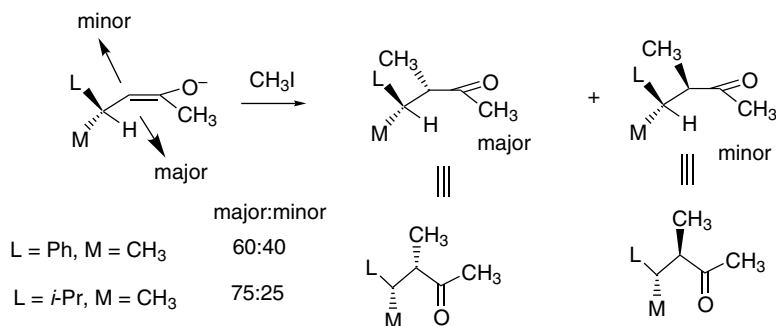


Houk and co-workers have emphasized the role of torsional effects in the stereoselectivity of enolate alkylation.<sup>100</sup> This analysis can explain the preference for C(5)-alkylation *syn* to the 2-methyl group in *trans*-2,3-dimethylcyclopentanone.



The *syn* TS is favored by about 1 kcal/mol, owing to reduced eclipsing, as illustrated in Figure 6.5. An experimental study using the kinetic enolate of 3-(*t*-butyl)-2-methylcyclopentanone in an alkylation reaction with benzyl iodide gave an 85:15 preference for the predicted *cis*-2,5-dimethyl derivative.

In acyclic systems, the enolate conformation comes into play. In unfunctionalized systems, alkylation usually takes place *anti* to the larger substituent, but with rather modest stereoselectivity.



Ref. 101

<sup>100</sup>. K. Ando, N. S. Green, Y. Li, and K. N. Houk, *J. Am. Chem. Soc.*, **121**, 5334 (1999).

<sup>101</sup>. I. Fleming and J. J. Lewis, *J. Chem. Soc., Perkin Trans. 1*, 3257 (1992).

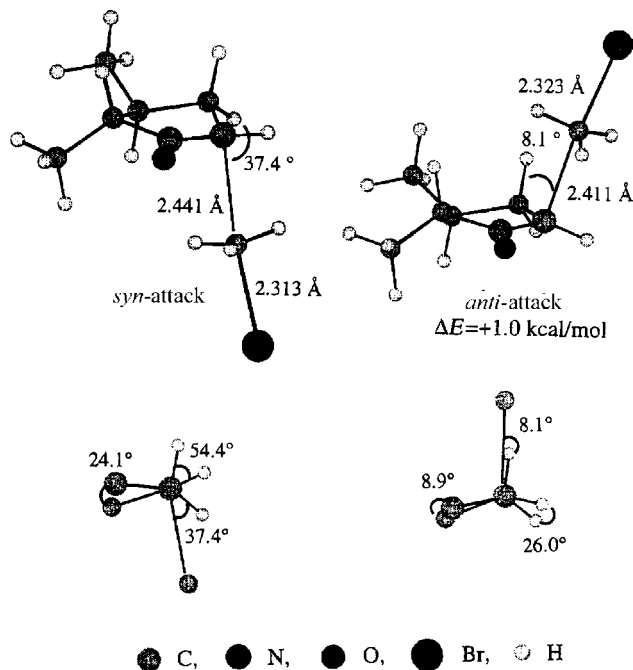
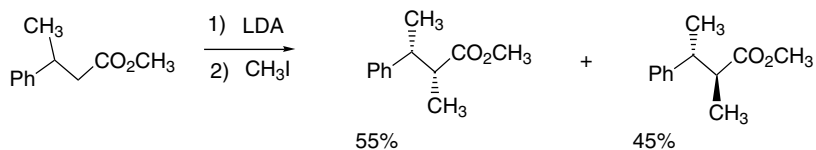
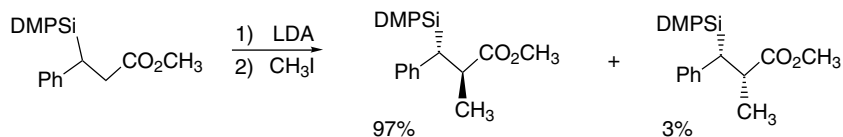


Fig. 6.5. Transition structures for *syn* and *anti* attack on the kinetic enolate of *trans*-2,3-dimethylcyclopentanone showing the staggered versus eclipsed nature of the newly forming bond. Reproduced from *J. Am. Chem. Soc.*, **121**, 5334 (1999), by permission of the American Chemical Society.

The enolate of the corresponding methyl ester gives a similar result.



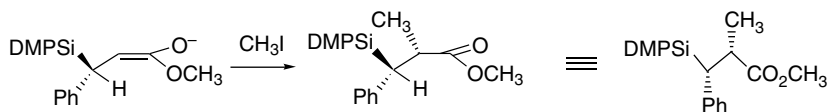
When a silyl substituent is present, the reaction becomes much more selective.



Ref. 102

<sup>102</sup> R. A. N. C. Crump, I. Fleming, J. H. M. Hill, D. Parker, N. L. Reddy, and D. Waterson, *J. Chem. Soc., Perkin Trans. 2*, 3277 (1992).

This result is due to a dominant steric effect of the large silyl substituent.<sup>103</sup>



In general, the stereoselectivity of enolate alkylation can be predicted and interpreted on the basis of the stereoelectronic requirement for an approximately perpendicular approach to the enolate with minimal torsional strain in combination and preference between the two faces on the basis of steric factors.

## General References

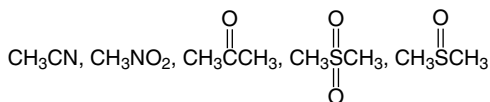
- E. Buncl, *Carbanions: Mechanistic and Isotopic Aspects*, Elsevier, Amsterdam, 1975.  
 E. Buncl and T. Durst, eds., *Comprehensive Carbanion Chemistry*, Elsevier, New York, 1981.  
 D. J. Cram, *Fundamentals of Carbanion Chemistry*, Academic Press, New York, 1965.  
 J. R. Jones, *The Ionization of Carbon Acids*, Academic Press, New York, 1973.  
 E. M. Kaiser and D. W. Slocum, in *Organic Reactive Intermediates*, S. P. McManus, ed., Academic Press, New York, 1973, Chap. 5.  
 Z. Rappoport, ed., *The Chemistry of Enols*, Wiley, New York, 1990.  
 M. Szwarc, *Ions and Ion Pairs in Organic Reactions*, Wiley, New York, 1972.  
 J. Toullec, *Adv. Phys. Org. Chem.*, **18**, 1 (1982).

## Problems

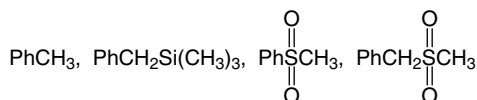
(References for these problems will be found on page 1161.)

6.1. Predict the order of increasing thermodynamic acidity in each series of compounds and explain the basis of your prediction.

- a. benzene, 1,4-cyclohexadiene, cyclopentadiene, cyclohexane  
 b.

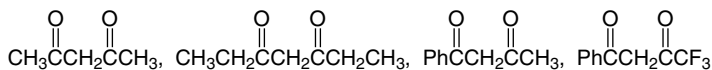


c.



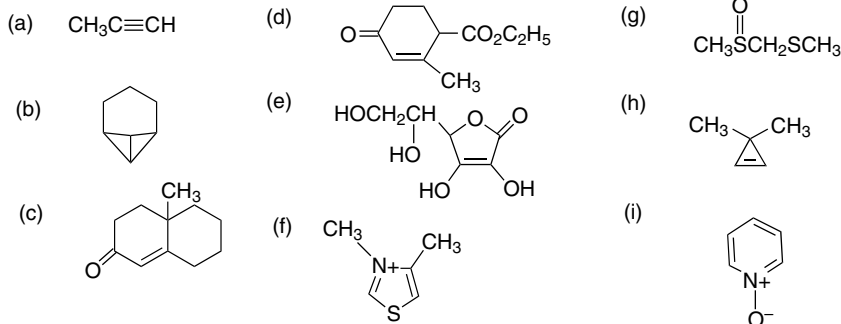
<sup>103</sup>. I Fleming, *J. Chem. Soc., Perkin Trans. 1*, 3363 (1992).

d.



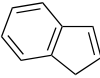
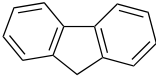
e. 9-(*m*-chlorophenyl)fluorene, 9-(*p*-methoxyphenyl)fluorene,  
9-phenylfluorene, 9-(*m*-methoxyphenyl)fluorene,  
9-(*p*-methylphenyl)fluorene.

6.2. Indicate the most acidic hydrogen in each of the following molecules. Explain your reasoning.

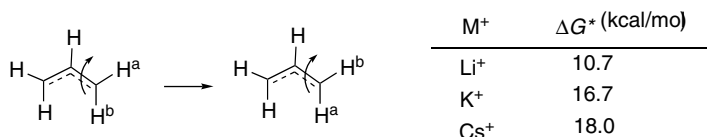


6.3. Offer an explanation for the following observations.

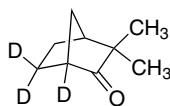
- Base-catalyzed exchange rates indicate that the hydrocarbon cubane is much more acidic than cyclobutane, and even more acidic than cyclopropane.
- Cyclopropyl phenyl ketone ( $pK = 28.2$ ) is less acidic than acetophenone ( $pK = 24.7$ ) and undergoes C–H exchange more slowly than phenyl *i*-propyl ketone, despite the fact that its most acidic hydrogen is located on a cyclopropyl ring.
- The order of acidity for cyclopentadiene, indene, and fluorene in DMSO is indicated below. The gas phase acidity is in the opposite direction, as measured by the proton affinity. Why does the fusion of benzene rings *decrease* the solution acidity relative to cyclopentadiene?

			
$pK_{\text{DMSO}}$	18.0	20.1	22.6
$PA_{\text{gas}}$	347.8	344.6	343.9

d. The rotational barrier of the allyl anion in THF, as measured by NMR, is dependent on the identity of the cation present.



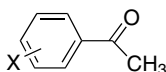
- 6.4 a. The relative rates of hydroxide ion-catalyzed deuterium exchange at C(3) have been measured for bicyclo[2.1.1]hexan-2-one, bicyclo[2.2.1]heptan-2-one, and bicyclo[2.2.2]octan-2-one. What factor(s) could account for the much smaller rate of exchange for bicyclo[2.1.1]hexan-2-one?
- b. Treatment of (+)-camphenilone with  $K^+ \cdot ^-O-t-Bu$  in  $t-BuOD$  at  $185^\circ C$  results in incorporation of D, as indicated below. Racemization occurs at the same rate. Suggest a mechanism that could account for these observations.



- 6.5. Using data from Tables 6.1 (p. 580) and 6.2 (p. 583), estimate the extent of deprotonation for each hydrocarbon-base combination below. Discuss the uncertainties that could affect the calculation.
- indene by  $0.01 M NaOCH_3$  in 1:1 DMSO- $C_2H_5OH$
  - fluorene by  $0.01 M NaOC_2H_5$  in 20:1 DMSO- $C_2H_5OH$
  - triphenylmethane by  $5 M KOCH_3$  in  $CH_3OH$
- 6.6. The rates of removal of axial and equatorial protons from 4- $t$ -butylcyclohexanone in NaOD/dioxane have been compared by an NMR technique. The rate of removal of an axial proton is 5.5 times faster than for an equatorial proton. How do you explain the difference?
- 6.7. The following table gives exchange rates in methanolic  $NaOCH_3$  and  $pK$  values for some hydrocarbons. Determine if there is a correlation between the kinetic and thermodynamic acidity.

Compound	$k_{\text{exchange}}$ $M^{-1}s^{-1} (\times 10^4)$	$pK$
9-Phenylfluorene	173	18.5
Indene	50	19.9
3,4-Benzofluorene	90.3	19.75
1,2-Benzofluorene	31.9	20.3
2,3-Benzofluorene	2.15	23.5
Fluorene	3.95	22.7

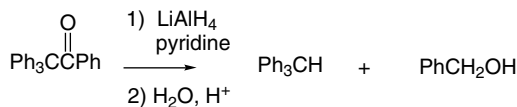
- 6.8. The acidity of various substituted acetophenones in DMSO is given below. Would you expect the  $\rho$  value to correlate best with  $\sigma$ ,  $\sigma^+$ , or  $\sigma^-$ ? Explain, considering each of the  $\sigma$  parameters explicitly. Do a plot of the  $pK/pK_0$  values for each  $\sigma$  parameter.



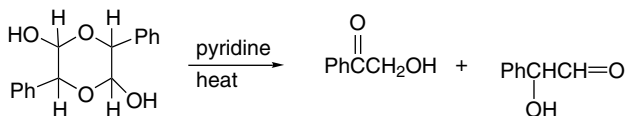
X	pK	X	pK	X	pK
<i>p</i> -(CH <sub>3</sub> ) <sub>2</sub> N	27.48	H	24.70	<i>m</i> -Cl	23.18
<i>p</i> -CH <sub>3</sub> O	25.70	<i>p</i> -F	24.45	<i>m</i> -Br	23.19
<i>m</i> -(CH <sub>3</sub> ) <sub>2</sub> N	25.32	<i>m</i> -CH <sub>3</sub> O	24.52	<i>m</i> -CF <sub>3</sub>	22.76
<i>p</i> -CH <sub>3</sub>	25.19	<i>p</i> -Br	23.81	<i>p</i> -CF <sub>3</sub>	22.69
<i>m</i> -CH <sub>3</sub>	24.95	<i>p</i> -Cl	23.78	<i>p</i> -CN	22.04
<i>p</i> -Ph	24.51	<i>m</i> -F	23.45		

6.9. Suggest mechanisms for the following reactions:

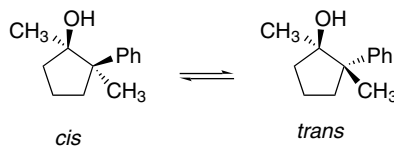
a.



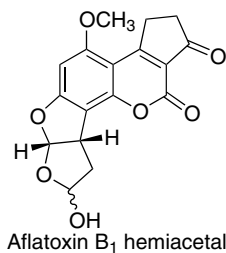
b.



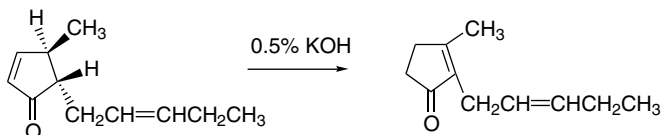
c. Treatment of the *cis* and *trans* isomers of 1,2-dimethyl-2-phenylcyclopentanol with 0.25 M NaCH<sub>2</sub>SOCH<sub>3</sub> in DMSO leads to an 72:28 equilibrium mixture favoring the *trans* isomer.



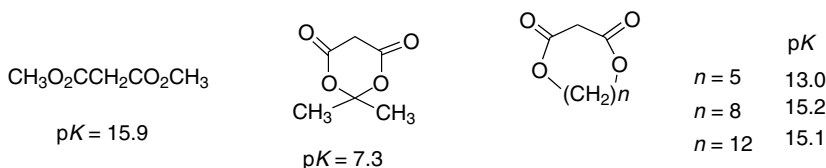
d. Aflatoxin B<sub>1</sub> hemiacetal racemizes readily in basic solution.



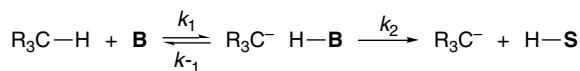
e. 4,5-Disubstituted cyclopent-2-enones can rearrange to 2,3-disubstituted cyclopent-2-enones in basic solution.



6.10. Meldrum's acid,  $pK = 7.3$ , is exceptionally acidic in comparison with acyclic analogs, such as dimethyl malonate ( $pK = 15.9$ ). 5,5-Dimethyl-1,3-cyclohexadione is only moderately more acidic than pentane-2,4-dione. ( $pK = 11.2$  versus 13.43). (All  $pK$  values in DMSO). It is found that the enhanced acidity of Meldrum's acid derivatives decreases as the ring size increases, with the larger ring compounds being similar in acidity to dimethyl malonate. Analyze the factors that contribute to the enhanced acidity of Meldrum's acid.



6.11. In some solvents, such as  $\text{K}^+\text{-OR-DMSO}$ , it can be shown that the *internal return* equilibrium characterized by  $k_1/k_{-1}$  is fast relative to the dissociation process characterized by  $k_2$ . In this process, the base returns the proton to the carbanion faster than the proton donor exchanges with other molecules from solution. If internal return is important under a given set of conditions, how might that affect the correlation between observed kinetic and thermodynamic acidity? How can the occurrence of internal return be detected experimentally?

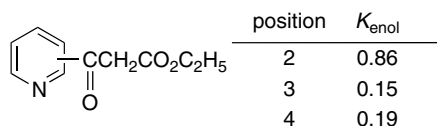


6.12. Discuss the following comparison of the enol content at equilibrium based on data given in Table 6.12. Discuss the reason for the differing enol content of the pairs of compounds in question.

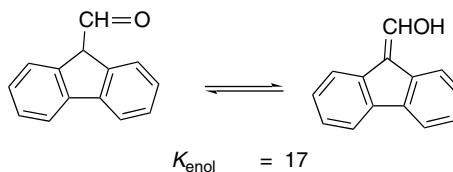
- Why does cyclohexanone have a somewhat higher enol content than cyclopentanone?
- Why do methyl acetate and acetamide have much lower enol content than acetone?
- Why does 2-indanone have a much higher enol content than 1-indanone?
- Why does 5,5-dimethyl-1,3-cyclohexa-1,3-dione have a higher enol content than acyclic diones such as acetylacetone, even though intramolecular hydrogen bonding is not possible?

6.13. Identify the structural factors that lead to the special stabilization of the enol form noted in each example.

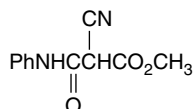
- The enol content of the 2-isomer of 3-(x-pyridyl)-3-oxopropanoate esters is higher than for the 3- and 4-isomers.



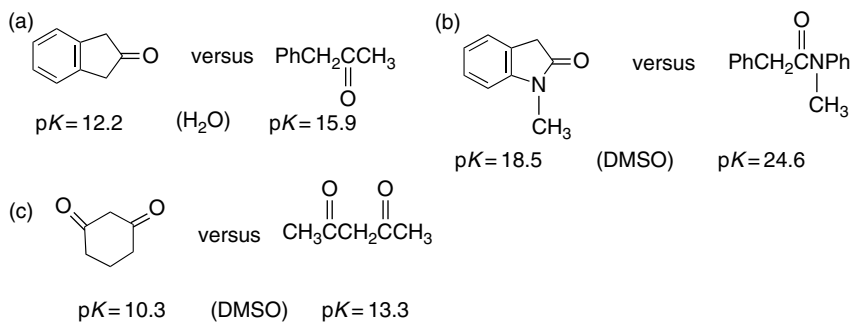
- b. The  $K_{\text{enol}}$  of 9-formylfluorene is 17, that is, the enol form is favored at equilibrium.



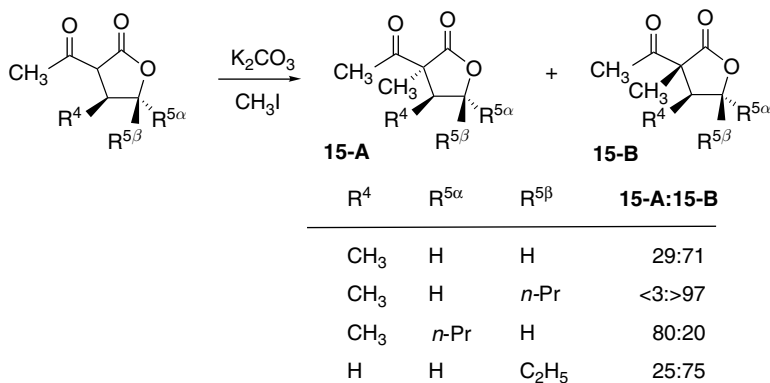
- c. Monoanilides of 2-cyanopropane-1,3-dicarboxyate monoesters exist in an enolic form in the solid state and in halogenated solvents.



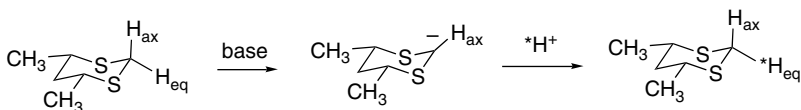
- 6.14. Certain cyclic compounds exhibit enhanced acidity relative to acyclic models. Offer an explanation for the examples given below.



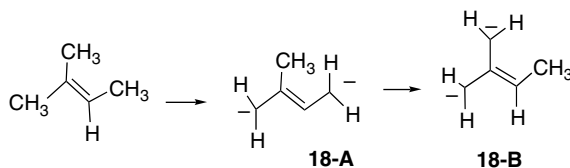
- 6.15. The stereoselectivity of alkylation of 3-acetylbutyrolactones is influenced by alkyl substituents at C(4) and C(5). Analyze possible conformations of the enolate and develop an explanation of the observed stereoselectivity.



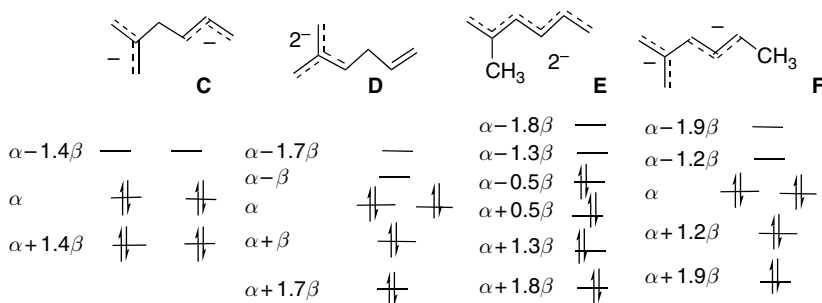
- 6.16. Metal ions such as  $\text{Zn}^{2+}$ ,  $\text{Ni}^{2+}$ , and  $\text{Cu}^{2+}$  enhance the rate of general base-catalyzed enolization of 2-acetylpyridine by a several orders of magnitude. Account for this effect.
- 6.17. The C(2) equatorial hydrogen is selectively removed when 1,3-dithianes are deprotonated. Furthermore, if the resulting carbanion is protonated, there is a strong preference for equatorial protonation, even though it leads to the less stable axial orientation for the 2-substituent. Discuss the relevance of these observations to the structure of the sulfur-stabilized carbanion in MO terminology.



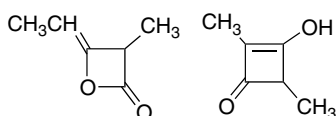
- 6.18. a. It is found that when 2-methyl-2-butene is converted to a dianion, it first gives the 2-methylbutadiene dianion **18-A**, but this is converted to the more stable anion **18-B**, which can be referred to as a “methyltrimethylenemethane dianion. Does simple HMO theory offer an explanation for this result?



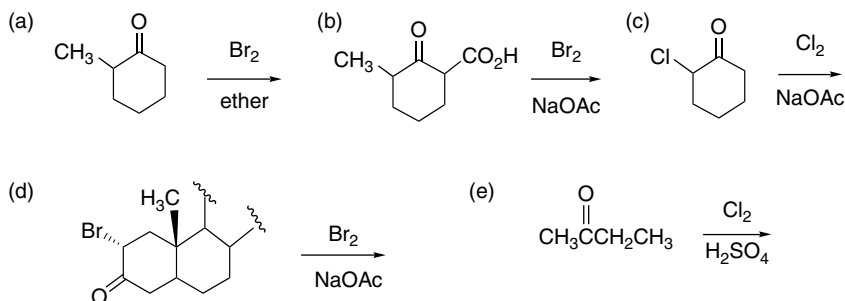
- b. The HMO diagrams of several conceivable dianions that might be formed from double deprotonation of 2-methyl-1,5-hexadiene are given. On the basis of these diagrams, which dianion would be expected to be most stable?



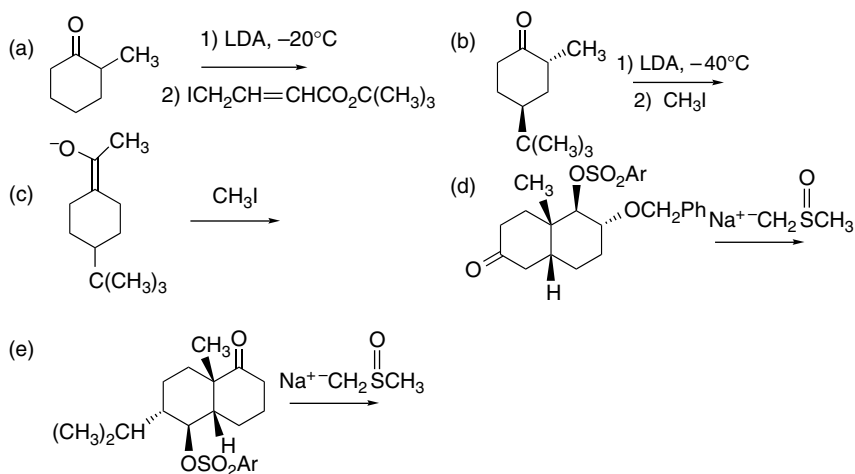
- 6.19. Which of the two possible structures for the dimer of methylketene is in best accord with the observed  $\text{p}K$  of 2.8? Explain.



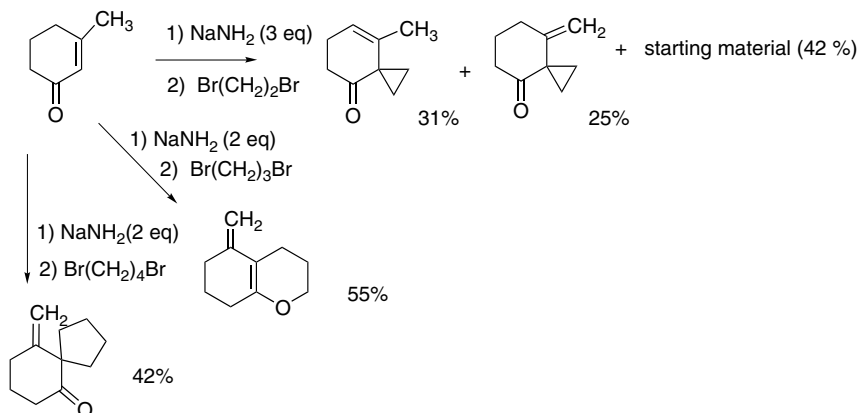
6.20. Predict the products of each of the following halogenation reactions.



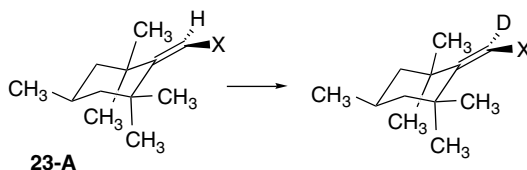
6.21. Predict the structure and stereochemistry of the products that would be obtained under the specified reaction conditions. Explain the basis of your prediction.



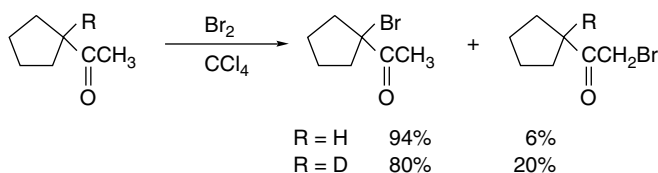
6.22. The alkylation of 3-methylcyclohex-2-enone with several dibromides led to the products shown below. Discuss the outcome of each reaction and suggest an explanation for the dependence of the product structure on the identity of the dihalide.



6.23. The stereochemistry of base-catalyzed deuterium exchange has been examined for **23-A**, where X = CN and COPh. When X = CN, the exchange occurs with 99% retention of configuration, but with X = COPh, only about 30% net retention is observed. Explain these contrasting results.

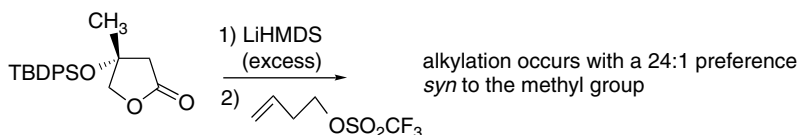


6.24. The distribution of  $\alpha$ -bromoketones formed in the reaction of acetylcyclopentane with bromine shows an altered product ratio when the 1-position of the ring is deuterated. Assuming that acid-catalyzed enolization is the rate-determining step in bromination, calculate the primary isotope effect.

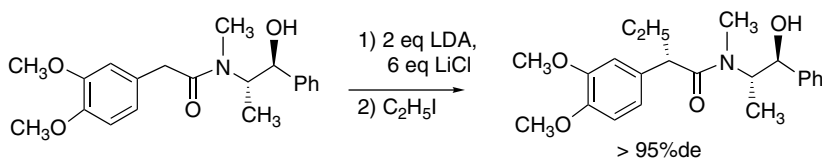


6.25. Analyze the mechanisms and transition structures for the following alkylation reactions in order to determine the factors that lead to the observed stereoselectivity.

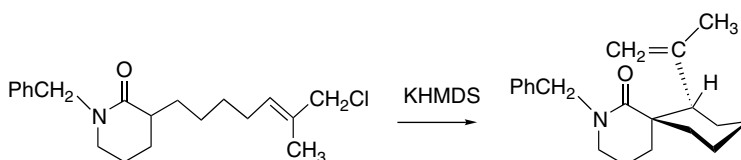
a.



b.



c.



6.26. Several dialkyl malate esters were alkylated with a benzylic bromide. The dimethyl and diethyl esters show a 8:1 and 9:1 selectivity for **26-A** (*si* face, respectively). The diastereoselectivities are shown for several more bulky esters. Figure 6.P26 gives the HF/6-31G\* structures of the corresponding enolates. Explain the observed stereoselectivity on the basis of structural features present in these enolates.

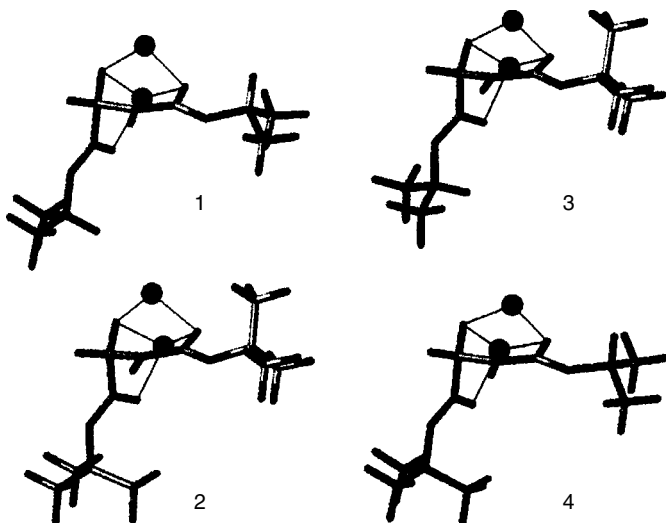
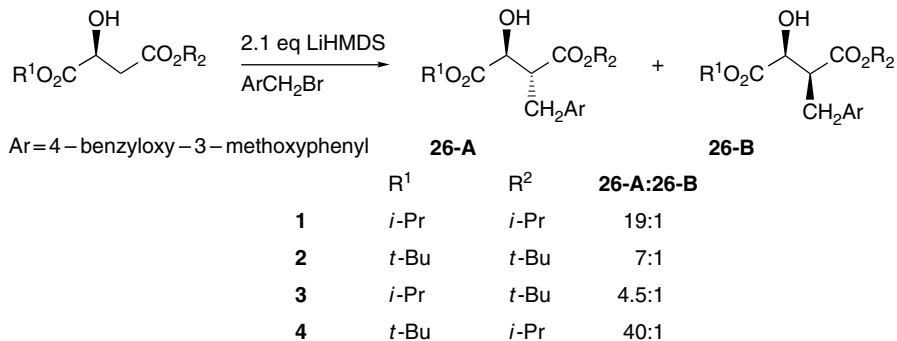


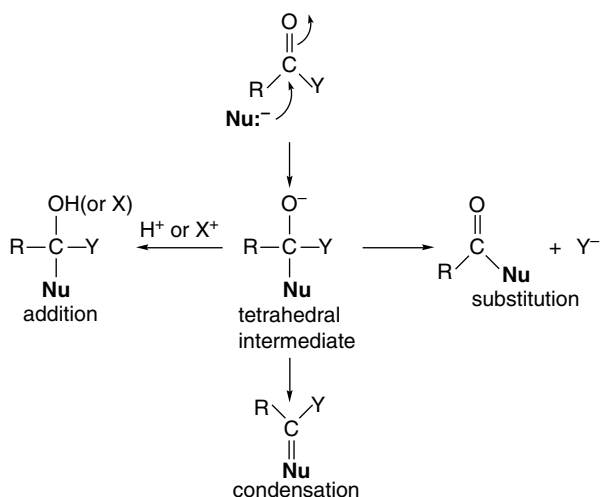
Fig. 6.P26. HF/6-31G\* structures of enolates **1-4**. Reproduced from *Helv. Chim. Acta*, **85**, 4216 (2002), by permission of Wiley-VCH.

# Addition, Condensation and Substitution Reactions of Carbonyl Compounds

## Introduction

The carbonyl group is one of the most prevalent of the functional groups and is involved in many synthetically important reactions. Reactions involving carbonyl groups are also particularly important in biological processes. Most of the reactions of aldehydes, ketones, esters, carboxamides, and the other carboxylic acid derivatives directly involve the carbonyl group. We discussed properties of enols and enolates derived from carbonyl compounds in Chapter 6. In the present chapter, the primary topic is the mechanisms of addition, condensation and substitution reactions at carbonyl centers. We deal with the use of carbonyl compounds to form carbon-carbon bonds in synthesis in Chapters 1 and 2 of Part B.

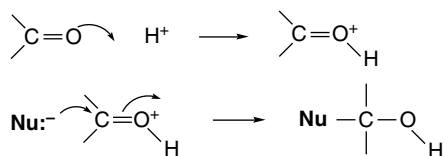
In many reactions at carbonyl groups, a key step is the addition of a nucleophile, which generates a tetracoordinate carbon atom. The overall course of the reaction is then determined by the fate of this tetrahedral intermediate. *Addition* occurs when the tetrahedral intermediate goes directly on to product. *Condensation* occurs if the carbonyl oxygen is eliminated and a double bond is formed. *Substitution* results when one of the groups is eliminated from the tetrahedral intermediate to re-form a carbonyl group.



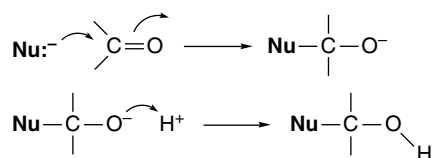
The reaction patterns of the specific classes of carbonyl compounds are related by the decisive importance of tetrahedral intermediates, and differences in reactivity can often be traced to structural features present in those intermediates. In Section 3.4.4, we considered some of the fundamental substituent effects on the stability of both carbonyl compounds and tetrahedral intermediates. These relationships will be important as we discuss the reactions in this chapter.

In broad terms, there are three possible mechanisms for addition of a nucleophile and a proton to give a tetrahedral intermediate in a carbonyl addition reaction.

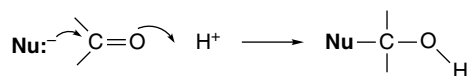
(a) Protonation followed by nucleophilic attack on the protonated carbonyl group:



(b) Nucleophilic addition at the carbonyl group followed by protonation:



(c) Concerted proton transfer and nucleophilic attack:

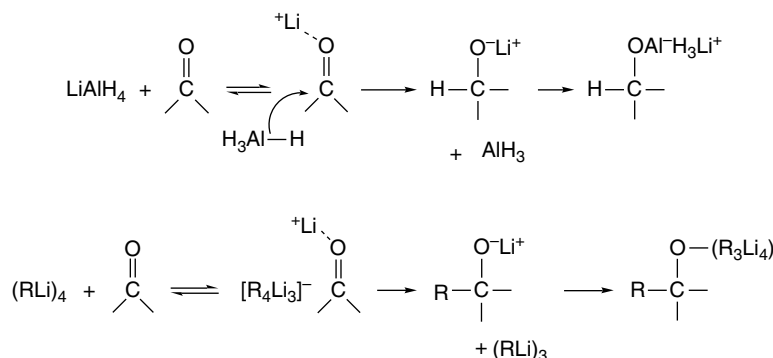


The nucleophile is shown as an anion, but can also be a neutral species, in which case a proton is subsequently lost.

There are carbonyl addition reactions that are examples of each of the general mechanisms, and a two-dimensional potential energy diagram provides a useful framework within which to consider specific addition reactions. The breakdown of a tetrahedral intermediate involves the same processes but operates in the opposite direction, so the principles that are developed also apply to the reactions of the tetrahedral intermediates. Let us examine the three general mechanistic cases in relation to the energy diagram in Figure 7.1.

Case (a) is favored for weak nucleophiles. The protonated carbonyl compound is more reactive toward such nucleophiles. The nucleophile may be neutral or a weakly basic anion. This mechanism is most likely to operate in relatively acidic conditions. Case (b) is favored for strongly basic nucleophiles. For example, carbanions cannot generally exist under acidic conditions, so carbanion additions occur under strongly basic conditions. These nucleophiles are more basic than carbonyl oxygens and are protonated in preference to the carbonyl group. In such systems, proton donors diminish the overall reaction rate by decreasing the amount of anionic nucleophile that is available for reaction. The concerted mechanism, case (c), is observed for less basic nucleophiles. The simultaneous transfer of the proton at the carbonyl oxygen facilitates addition by species that are not sufficiently nucleophilic to react by mechanism (b). The general pattern is that the weaker and less basic the nucleophile, the more important the partial or complete protonation of the carbonyl group. If we consider the reverse process, the same general relationships will hold. Good leaving groups (which are poor nucleophiles) can be expected to follow path (a); poor leaving groups will follow path (b); and intermediate cases are likely to react by the concerted mechanism (c).

Metal cations and other Lewis acids can replace protons as reagents/catalysts for carbonyl addition reactions. Metal cations, for example, are involved in hydride and organometallic addition reactions. Metal cations and Lewis acids are also key reagents in the aldol-type reactions that are considered in Section 7.7.



It is useful to recognize that the dissociation of tetrahedral intermediates in carbonyl chemistry is closely related to the generation of carbocations by ionization processes. The protonated carbonyl compounds or iminium ions that

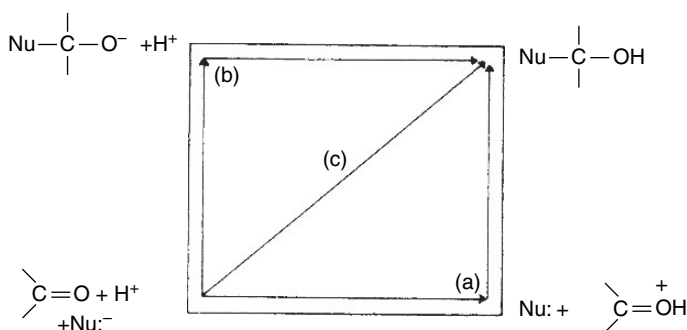
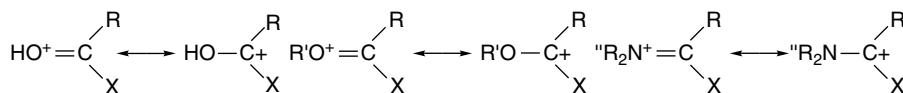


Fig. 7.1. Two-dimensional potential energy diagram for addition of a proton and nucleophile to a carbonyl group. (a) Proton transfer complete before nucleophilic addition begins; (b) nucleophilic addition complete before proton transfer begins; (c) concerted proton transfer and nucleophilic addition.

are generated by breakdown of tetrahedral intermediates are resonance-stabilized carbocations.



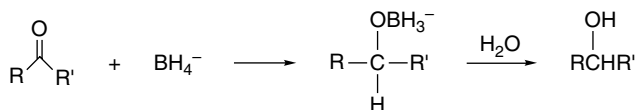
The question of which substituent on a tetrahedral intermediate is the best leaving group is similar to comparing  $\text{S}_{\text{N}}1$  reactants on the basis of leaving-group ability. Poorer leaving groups such as alkoxides can function as leaving groups in the case of tetrahedral intermediates because of the assistance provided by the remaining oxygen or nitrogen substituents. Keeping these relationships in mind should be helpful in understanding the reactivity of tetrahedral intermediates.

## 7.1. Reactivity of Carbonyl Compounds toward Addition

At this point we consider some general relationships concerning the reactivity of carbonyl compounds toward addition of nucleophiles. Several factors influence the overall rate of a reaction under various conditions. Among the crucial factors are: (1) structural features of the carbonyl compound; (2) the role of protons or other Lewis acids in activating the carbonyl group toward nucleophilic attack; (3) the reactivity of the nucleophilic species and its influence on subsequent steps; and (4) the stability of the tetrahedral intermediate and the extent to which it proceeds to product rather than reverting to starting material.

We focus first on the inherent reactivity of the carbonyl compound itself. An irreversible processes in which the addition product is stable is the most direct means of comparing the reactivity of carbonyl compounds. In these circumstances, the relative rate of reaction of different carbonyl compounds can be directly compared. One such reaction is hydride reduction. In particular, reductions by sodium borohydride in protic

solvents are fast, irreversible reactions that provide a convenient basis for comparing the reactivity of different carbonyl compounds.<sup>1</sup>



The reaction is second-order overall, with the rate equal to  $k[\text{R}_2\text{C}=\text{O}][\text{NaBH}_4]$ . The interpretation of the rates is complicated somewhat by the fact that the alkoxyborohydrides produced by the first addition can also function as reducing agents by successive hydride transfers, but this has little apparent effect on the relative reactivity of the carbonyl compounds. Table 7.1 presents some of the rate data obtained from these studies.

Reductions by  $\text{NaBH}_4$  are characterized by low enthalpies of activation (8 to 13 kcal/mol) and large negative entropies of activation ( $-28$  to  $-40$  eu). These data suggest an early TS with considerable organization. Aldehydes are substantially more reactive than ketones, as can be seen by comparing benzaldehyde and acetophenone. This relative reactivity is characteristic of nearly all carbonyl addition reactions. The lower reactivity of ketones is due primarily to steric effects. Not only does the additional substituent increase the steric restrictions to approach of the nucleophile, but it also causes greater steric interaction in the tetrahedral adduct as the hybridization changes from trigonal to tetrahedral. Alkyl substituents also act as electron donors toward carbonyl groups by hyperconjugation (see Section 2.2.1).

Among the cyclic ketones shown in Table 7.1, the reactivity of cyclobutanone is enhanced because of the strain of the four-membered ring, which is decreased on going from  $sp^2$  to  $sp^3$  hybridization. The higher reactivity of cyclohexanone compared to cyclopentanone is quite general for carbonyl addition reactions. The major factor responsible for the difference in this case is the change in torsional strain as addition occurs. As the hybridization goes from  $sp^2$  to  $sp^3$ , the torsional strain is *increased* in cyclopentanone. The opposite is true for cyclohexanone. The

**Table 7.1. Rates of Reduction of Aldehydes and Ketones by Sodium Borohydride**

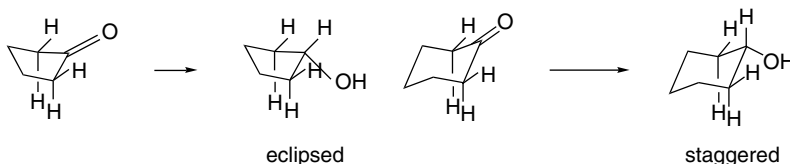
Carbonyl compound	$k \times 10^4 M^{-1} s^{-1a}$
Benzaldehyde	12,400 <sup>b</sup>
Benzophenone	1.9
Acetophenone	2.0
Acetone	15.1
Cyclobutanone	264
Cyclopentanone	7
Cyclohexanone	161

a. In isopropanol at 0°C.

b. Extrapolated from data at lower temperatures.

<sup>1</sup>. H. C. Brown, O. H. Wheeler, and K. Ichikawa, *Tetrahedron*, **1**, 214 (1957); H. C. Brown and K. Ichikawa, *Tetrahedron*, **1**, 221 (1957).

equatorial hydrogens are nearly eclipsed with the carbonyl oxygen in cyclohexanone, but the chair structure of cyclohexanol allows all bonds to attain staggered arrangements.



The borohydride reduction rate data are paralleled by many other carbonyl addition reactions. In fact, for a series of ketones, most of which are cyclic, a linear free-energy correlation of the form

$$\log k = A \log k_0 + B$$

exists for nucleophiles such as  $\text{NH}_2\text{OH}$ ,  $\text{CN}^-$ ,  $\text{HOCH}_2\text{CH}_2\text{S}^-$ , and  $\text{HSO}_3^-$ .<sup>2</sup> These nucleophiles span a wide range of reactivity and include nitrogen, carbon, and sulfur nucleophiles. This free-energy relationship implies that in this series of ketones the same structural features govern reactivity toward each of the nucleophiles. To a good approximation the parameter  $A = 1$ , which reduces the correlation to

$$\log (k/k_0) = B$$

This equation implies that the *relative reactivity is independent of the specific nucleophile* and is insensitive to changes in position of the transition state. Table 7.2 lists some of the  $B$  values for some representative ketones. The parameter  $B$  indicates relative reactivity on a log scale. Cyclohexanone is seen to be a particularly reactive ketone, being almost as reactive as cyclobutanone and more than ten times as reactive as acetone.

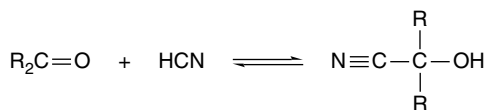
The same structural factors come into play in determining the position of equilibria in reversible additions to carbonyl compounds. An example of such equilibrium processes is the addition of cyanide to give cyanohydrins.

**Table 7.2. Relative Reactivity of Some Ketones toward Addition of Nucleophiles**

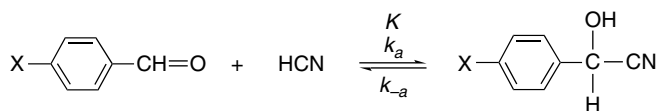
Ketone	$B^a$
Cyclobutanone	0.09
Cyclohexanone	0.00
4- <i>t</i> -Butylcyclohexanone	-0.008
Adamantanone	-0.46
Cycloheptanone	-0.95
Cyclopentanone	-1.18
Acetone	-1.19
Norbornan-2-one	-1.48
3,3,5,5-Tetramethylcyclohexanone	-1.92

a. A. Finiels and P. Geneste, *J. Org. Chem.*, **44**, 1577 (1979); reactivity relative to cyclohexanone.

<sup>2</sup> A. Finiels and P. Geneste, *J. Org. Chem.*, **44**, 1577 (1979).



The equilibrium constants in Table 7.3 illustrate some of the broad trends in carbonyl group reactivity. Alkyl substitution decreases the extent of addition. Aromatic carbonyl compounds are somewhat less reactive toward addition than similar alkyl compounds because the carbonyl group is stabilized by conjugation with the aromatic ring. Strong electron-attracting groups, such as trifluoromethyl, favor addition by enhancing the electrophilicity of the carbonyl group. For cyclopentanone, cyclohexanone, and cycloheptanone the  $K$ 's for addition of  $\text{CN}^-$  are 48, 1000, and  $8\text{ M}^{-1}$ , respectively.<sup>3</sup> For aromatic aldehydes, the equilibria are affected by the electronic nature of the aryl substituent. Electron donors disfavor addition by stabilizing the aldehyde, whereas electron-accepting substituents have the opposite effect. The Hammett correlation with  $\sigma^+$  gives  $\rho = +1.01$ .



Ref. 4

There are large differences in the reactivity of the various carboxylic acid derivatives, such as amides, esters, and acyl chlorides. One important factor is the resonance stabilization provided by the heteroatom substituent, which is in the order  $\text{N} > \text{O} > \text{Cl}$ . Electron delocalization reduces the electrophilicity of the carbonyl group and the corresponding stabilization is lost in the tetrahedral intermediate.

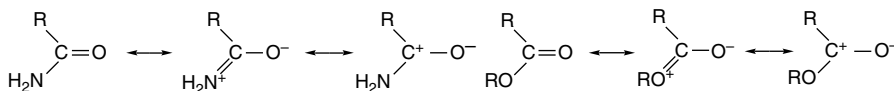


**Table 7.3. Equilibrium Constants for Cyanohydrin Formation<sup>a</sup>**

$\text{R}_2\text{C}=\text{O}$	$\log K$
$\text{CH}_2=\text{O}$	7.48
$\text{CH}_3\text{CH}=\text{O}$	2.29
$(\text{CH}_3)_2\text{C}=\text{O}$	-1.84
$\text{PhCH}=\text{O}$	0.74 <sup>b</sup>
$\text{PhCOCF}_3$	3.98 <sup>c</sup>

a. Except where otherwise noted the data are from G. Schlesinger and S. L. Miller, *J. Am. Chem. Soc.*, **85**, 3729 (1973).

b. W. M. Ching and R. G. Kallen, *J. Am. Chem. Soc.*, **100**, 6119 (1978).

c. C. D. Ritchie, *J. Am. Chem. Soc.*, **106**, 7087 (1984).

<sup>3</sup>. V. Prelog and M. Kobelt, *Helv. Chim. Acta*, **32**, 1187 (1949).

<sup>4</sup>. W.-M. Ching and R. G. Kallen, *J. Am. Chem. Soc.*, **100**, 6119 (1978); V. Gold and W. N. Wassef, *J. Chem. Soc., Perkin Trans. 2*, 1431 (1984).

The high reactivity of the acyl chlorides also reflects the polar electron-withdrawing effect of the chlorine, which more than outweighs its small  $\pi$ -donor effect. Another factor that strongly affects the reactivity of these carboxylic acid derivatives is the leaving-group ability of the substituents. The order is  $\text{Cl} > \text{OAr} > \text{OR} > \text{NR}_2 > \text{O}^-$  so that not only is it easier to form the tetrahedral intermediate in the order  $\text{Cl} > \text{OAr} > \text{OR} > \text{NR}_2 > \text{O}^-$ , but the tendency for subsequent elimination to occur is also in the same order. As the two factors work together, there are large differences in reactivity toward the nucleophiles. (See Scheme 3.3 for some specific data.)

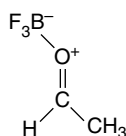
**Approximate Relative Reactivity toward  
Hydrolysis**

RCOCl	$10^{11}$
$\text{RCO}_2\text{R}'$	1
$\text{RCONR}'_2$	$10^{-3}$
$\text{RCO}_2^-$	$\ll 1$

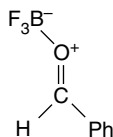
Many carbonyl addition and substitution reactions are carried out under acidic conditions or in the presence of Lewis acids. Qualitatively, protonation or complexation increases the electrophilicity of the carbonyl group. The structural effects of protonation have been examined for formaldehyde, acetaldehyde, acetone, formamide, and formyl fluoride. These effects should correspond to those in more complex carbonyl compounds. Protonation results in a substantial lengthening of the  $\text{C}=\text{O}$  bond.<sup>5</sup> The calculated [B3LYP/ 6-31++G(*d, p*)] gas phase proton affinities reflect the trend of increasing basicity with donor groups ( $\text{CH}_3$ ,  $\text{NH}_2$ ) and decreased basicity for fluorine.

	$\text{CH}_2=\text{O}$	$\text{CH}_3\text{CH}=\text{O}$	$(\text{CH}_3)_2\text{C}=\text{O}$	$\text{H}_2\text{NCH}=\text{O}$	$\text{FCH}=\text{O}$
$r_{\text{C}=\text{O}}$	1.209	1.214	1.219	1.219	1.186
$r_{\text{C}=\text{OH}^+}$	$\text{CH}_2=\text{O}^+\text{H}$	$\text{CH}_3\text{CH}=\text{O}^+\text{H}$	$(\text{CH}_3)_2\text{C}=\text{O}^+\text{H}$	$\text{H}_2\text{NCH}=\text{O}^+\text{H}$	$\text{FCH}=\text{O}^+\text{H}$
	1.252	1.270	1.282	1.294	1.252
PA in kcal/mol	168.9	184.4	195.7	198.0	156.2

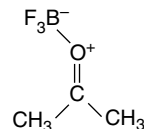
The effect of Lewis acids has also been examined computationally. In agreement with crystal structure determinations,<sup>6</sup> Lewis acids such as  $\text{BF}_3$  normally adopt an *anti* structure for aldehydes. Despite the unfavorable steric effect in acetone, the calculated (MP2/6-31G) energy of complexation with  $\text{BF}_3$  is nearly as high as for acetaldehyde, presumably owing to the additional electron donation by the methyl groups.<sup>7</sup>



$\Delta E$       -11.9



-13.0



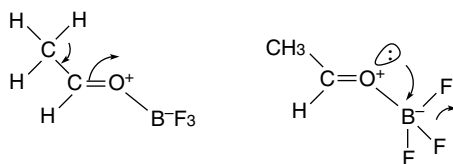
-10.3

<sup>5</sup> A. K. Chandra, M. T. Nguyen, and T. Zeegers-Huyskens, *Chem. Phys.*, **255**, 149 (2000).

<sup>6</sup> M. T. Reetz, M. Hullmann, W. Massa, S. Berger, P. Rademacher, and P. Heymanns, *J. Am. Chem. Soc.*, **108**, 2405 (1986).

<sup>7</sup> B. W. Gung and M. A. Wolf, *J. Org. Chem.*, **57**, 1370 (1992).

It is believed that two significant hyperconjugative effects result from complexation with a Lewis acid. The donor effect of alkyl substituents is enhanced by the greater electrophilicity of the carbonyl oxygen. There is also believed to be an interaction of the remaining unshared oxygen electrons with the  $\sigma^*$  orbital of the B–F bond. The interaction lowers the energy of both the  $\pi$  and  $\pi^*$  orbitals and enhances the reactivity toward nucleophiles, as indicated in Figure 7.2.<sup>8</sup>



Several factors, then, are important in assessing relative reactivity of carbonyl compounds. Electronegative substituents enhance reactivity by a polar effect, but if they are also  $\pi$  donors, there is a resonance effect in the opposite direction. Alkyl and aryl substituents decrease reactivity relative to hydrogen by a combination of steric and electronic effects. Protonation or complexation with a Lewis acid at the carbonyl oxygen enhances reactivity.

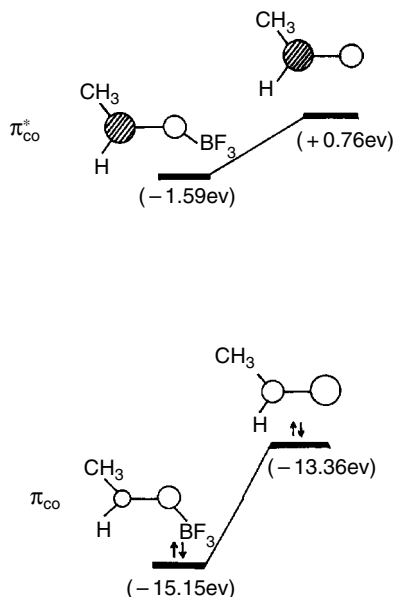


Fig. 7.2. Effect of  $\text{BF}_3$  complexation of HOMO and LUMO in acetaldehyde. From MNDO calculations, *J. Am. Chem. Soc.*, **108**, 2405 (1986).

<sup>8</sup> K. N. Houk and R. W. Strozier, *J. Am. Chem. Soc.*, **95**, 4094 (1973).

The reactivity of carbonyl compounds toward hydration parallels the order indicated in Section 7.1. For most carbonyl compounds, the equilibrium constant for addition of water to the carbonyl group is unfavorable.



Formaldehyde is an exception and is nearly completely hydrated in aqueous solution. Unhindered aliphatic aldehydes are approximately 50% hydrated in water. Aryl groups disfavor hydration by conjugative stabilization of the carbonyl group. Ketones are much less extensively hydrated than aldehydes. Aldehydes and ketones with highly electronegative substituents such as trichloroacetaldehyde and hexafluoroacetone are extensively hydrated.  $\alpha$ -Dicarbonyl compounds, such as biacetyl and ethyl pyruvate, are also significantly hydrated. Table 7.4 gives the  $K_{\text{hydr}}$  for a number of carbonyl compounds. Data on other compounds are available in Table 3.23.

Although the equilibrium constant for hydration is usually unfavorable, the equilibrium between an aldehyde or ketone and its hydrate is established rapidly and can be detected by isotopic exchange, using water labeled with  $^{17}\text{O}$ , for example.<sup>9</sup> For

**Table 7.4. Equilibrium Constants for Hydration of Carbonyl Compounds**

Carbonyl compound	$K$ (in water, 25°C) <sup>a</sup>
$\text{CH}_2\text{O}$	$2.28 \times 10^3$ <sup>b</sup>
$\text{CH}_3\text{CHO}$	1.06 <sup>b</sup>
$\text{CH}_3\text{CH}_2\text{CHO}$	0.85 <sup>b</sup>
$(\text{CH}_3)_2\text{CHCHO}$	0.61 <sup>b</sup>
$(\text{CH}_3)_3\text{CCCHO}$	0.23 <sup>b</sup>
$\text{CF}_3\text{CHO}$	$2.9 \times 10^4$ <sup>b</sup>
$\text{C}_6\text{H}_5\text{CHO}$	$8 \times 10^{-3}$ <sup>c</sup>
$\text{CH}_3\text{COCH}_3$	$1.4 \times 10^{-3}$ <sup>b</sup>
$\text{FCH}_2\text{COCH}_3$	0.11 <sup>c</sup>
$\text{ClCH}_2\text{COCH}_3$	0.11 <sup>b</sup>
$\text{CF}_3\text{COCH}_3$	35 <sup>b</sup>
$\text{CF}_3\text{COCF}_3$	$1.2 \times 10^6$ <sup>b</sup>
$\text{C}_6\text{H}_5\text{COCH}_3$	$9.3 \times 10^{-6}$ <sup>c</sup>
$\text{C}_6\text{H}_5\text{COCF}_3$	78 <sup>b</sup>
$\text{CH}_3\text{COCOCH}_3$	0.6 <sup>d</sup>
$\text{CH}_3\text{COCO}_2\text{CH}_3$	0.8 <sup>d</sup>

a.  $K = [\text{hydrate}][\text{carbonyl}] = K_{\text{eq}}[\text{H}_2\text{O}] = 55.5 K_{\text{eq}}$

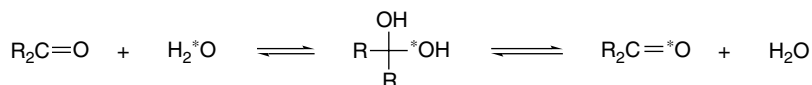
b. J. P. Guthrie, *Can. J. Chem.*, **53**, 898 (1975).

c. J. P. Guthrie, *Can. J. Chem.*, **56**, 962 (1978).

d. T. J. Burkey and R. C. Fahey, *J. Am. Chem. Soc.*, **105**, 868 (1983).

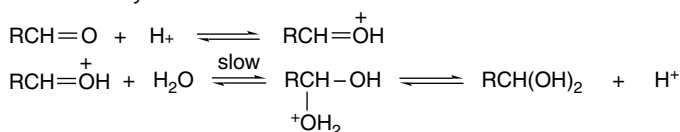
<sup>9</sup> P. Greenzaid, Z. Luz, and D. Samuel, *Trans. Faraday Soc.*, **64**, 2780, 2787 (1968).

acetaldehyde, the half-life of the exchange reaction is on the order of 1 min under neutral conditions, but is considerably faster in acidic or basic solution. The second-order rate constant for acid-catalyzed hydration of acetaldehyde is about  $500 M^{-1}s^{-1}$ .<sup>10</sup>

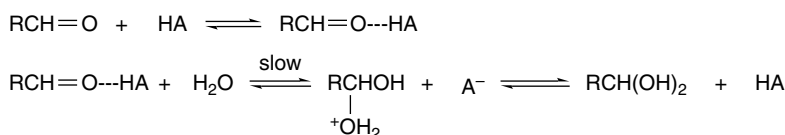


The hydration reaction is the mechanistic prototype for many reactions at carbonyl centers that involve more complex molecules.<sup>11</sup> Acid catalysis involves either protonation or hydrogen-bonding at the carbonyl oxygen. Both specific and general acid catalysis can be observed.<sup>12</sup> (Review Section 3.7.1.1 for the discussion of specific and general acid catalysis.)

*Specific acid-catalyzed mechanism*

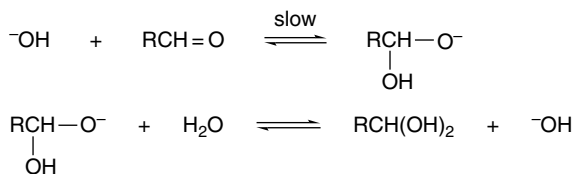


*General acid-catalyzed hydration*

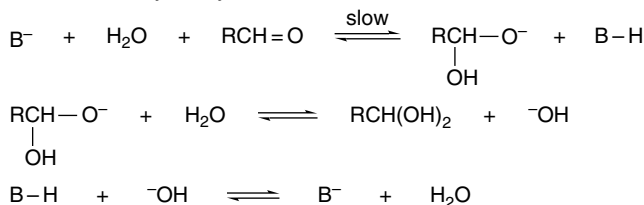


Hydroxide ion addition results in specific base-catalyzed hydration. General base catalysts function by deprotonating water to give the more nucleophilic hydroxide ion.

*Specific base-catalyzed hydration*



*General base-catalyzed hydration*

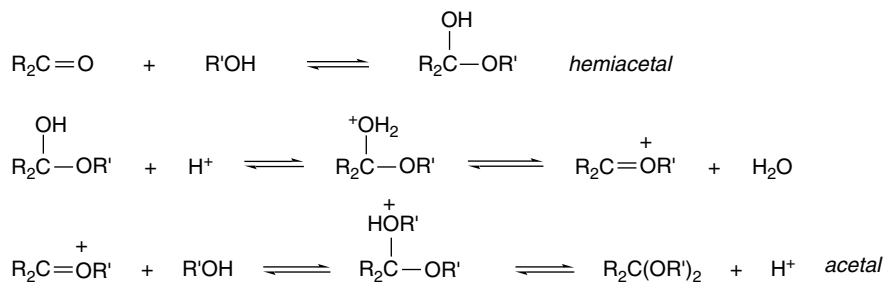


<sup>10</sup> P. Greenzaid, Z. Luz, and D. Samuel, *J. Am. Chem. Soc.*, **89**, 756 (1967).

<sup>11</sup> R. P. Bell, *Adv. Phys. Org. Chem.*, **4**, 1 (1966); W. P. Jencks, *Chem. Rev.*, **72**, 705 (1972).

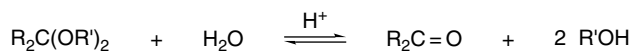
<sup>12</sup> L. H. Funderburk, L. Aldwin, and W. P. Jencks, *J. Am. Chem. Soc.*, **100**, 5444 (1978); R. A. McClelland and M. Coe, *J. Am. Chem. Soc.*, **105**, 2718 (1983).

Aldehydes and ketones undergo reversible addition reactions with alcohols. The product of addition of one molecule of alcohol to an aldehyde or ketone is referred to as a *hemiacetal*. Dehydration followed by addition of a second molecule of alcohol gives an *acetal*.<sup>13</sup> This second phase of the process can be catalyzed only by acids because a necessary step is elimination of hydroxide (as water) from the tetrahedral intermediate. There is no low-energy mechanism for base assistance of this elimination step, so acetals are stable toward hydrolysis in alkaline aqueous solution but are hydrolyzed rapidly in acidic solution.



The equilibrium constants for addition of alcohols to carbonyl compounds to give hemiacetals show the same response to structural features as the hydration reaction. Equilibrium constants for addition of methanol to acetaldehyde in both water and chloroform solution are near  $0.8 \text{ M}^{-1}$ . The structural effects of the alcohol group have been examined.<sup>14</sup> Steric effects result in an order of  $\text{CH}_3 \sim \text{C}_2\text{H}_5 > (\text{CH}_3)_2\text{CH} > (\text{CH}_3)_3\text{C}$  for acetaldehyde hemiacetals. EWG substituents in the alcohol disfavor hemiacetal formation and this trend is believed to reflect the decreasing  $n \rightarrow \pi^*$  hyperconjugation (anomeric effect, see Topic 1.2) as the substituents become more electron withdrawing.

The overall equilibrium constant for formation of the dimethyl acetal of acetaldehyde is  $1.58 \text{ M}^{-1}$ . The comparable value for the addition of water is about  $0.02 \text{ M}^{-1}$ .<sup>15</sup> Because the position of the equilibrium does not strongly favor product, the synthesis of acetals is carried out in such a way as to drive the reaction to completion. One approach is to use a dehydrating reagent or azeotropic distillation so that the water that is formed is irreversibly removed from the system. Because of the unfavorable equilibrium constant and the relative facility of the hydrolysis, acetals are rapidly converted back to aldehydes and ketones in acidic aqueous solution. The facile hydrolysis makes acetals useful carbonyl protecting groups (see Part B, Section 3.5.3).

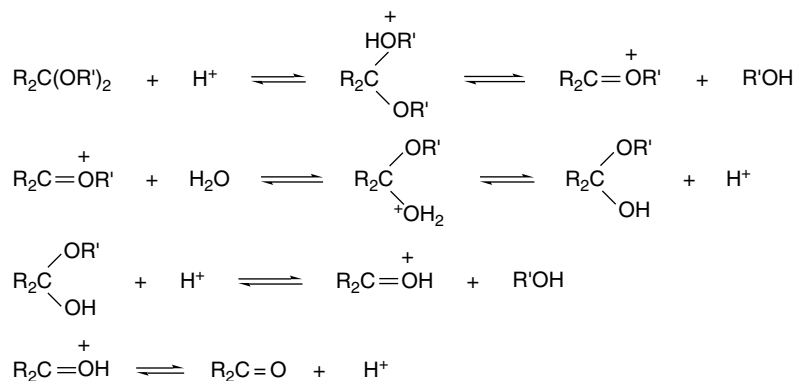


<sup>13</sup>. Sometimes these derivatives of ketones are called hemiketals and ketals, respectively.

<sup>14</sup>. Y.-H. Fan and J. Haseltine, *Tetrahedron Lett.*, **37**, 9279 (1996).

<sup>15</sup>. R. Bone, P. Cullis, and R. Wolfenden, *J. Am. Chem. Soc.*, **105**, 1339 (1983).

The mechanism of this hydrolysis reaction has been studied in great detail.<sup>16</sup> The mechanism is the reverse of that for acetal formation. Acetal protonation is followed by elimination of an alcohol molecule. The resulting intermediate is a stabilized carbocation. Addition of water and a second acid-catalyzed elimination lead to the product.



Some of the evidence that has helped to establish the general mechanism is as follows:

1. Isotopic-labeling experiments have established that C—O bond rupture occurs between the carbonyl carbon and oxygen; substitution at the alcohol C—O bond is not involved.
2. For most acetals, the reaction is *specific acid catalyzed*, which is consistent with the existence of a preequilibrium in which the acetal is protonated. The proton assists the departure of the alkoxy group by converting it to a better leaving group. In essence, this cleavage step is an  $\text{S}_{\text{N}}1$  reaction with the remaining alkoxy group stabilizing the carbocation formed by ionization.
3. Hammett treatments show good correlations with large negative  $\rho$  values for the hydrolysis of acetals of aromatic aldehydes, which is consistent with the development of a positive charge at the carbonyl center in the rate-determining step.
4. Solvent isotope effects are usually in the range  $k_{\text{D}_2\text{O}}/k_{\text{H}_2\text{O}} = 2\text{--}3$ . These values reflect the greater equilibrium acidity of deuterated acids (see Section 3.7.1.1) and indicate that the initial protonation is a fast preequilibrium.

Acetal hydrolyses usually exhibit specific acid catalysis, in agreement with a mechanism involving rate-determining cleavage of the conjugate acid of the reactant. However, general acid catalysis is observed in certain acetals and ketals in which special structural features reduce the energy required for C—O bond cleavage.<sup>17</sup> Thus, hydrolysis of each of the acetals shown in Scheme 7.1 exhibits general acid catalysis, and each acetal has a structural feature that facilitates C—O bond heterolysis. Reducing the energy requirement for C—O bond cleavage permits the proton transfer step to become partially rate determining and results in the observation of general acid catalysis.

<sup>16</sup> E. H. Cordes and H. G. Bull, *Chem. Rev.*, **74**, 581 (1974).

<sup>17</sup> T. H. Fife, *Acc. Chem. Res.*, **5**, 264 (1972).

	Acetal	Structural feature promoting hydrolysis
1 <sup>a</sup>		Very stable oxonium ion intermediate; stabilized by aromaticity.
2 <sup>b</sup>		Resonance-stabilized phenolic leaving group.
3 <sup>c</sup>		Especially acidic alcohol is good leaving group.
4 <sup>d</sup>		Ring strain is relieved in bond-breaking step
5 <sup>e</sup>	(Ar) <sub>2</sub> C(OC <sub>2</sub> H <sub>5</sub> ) <sub>2</sub>	Aryl substituents stabilize oxonium ion.
6 <sup>f</sup>	PhCH[OC(CH <sub>3</sub> ) <sub>3</sub> ] <sub>2</sub>	Aryl stabilization of oxonium ion and relief of steric strain.

a. E. Anderson and T. H. Fife, *J. Am. Chem. Soc.*, **91**, 7163 (1969).

b. T. H. Fife and L. H. Brod, *J. Am. Chem. Soc.*, **92**, 1681 (1970).

c. J. L. Jensen and W. B. Wuhrman, *J. Org. Chem.*, **48**, 4686 (1983).

d. R. F. Atkinson and T. C. Bruice, *J. Am. Chem. Soc.*, **96**, 819 (1974).

e. R. H. DeWolfe, K. M. Ivanetich, and N. F. Perry, *J. Org. Chem.*, **34**, 848 (1969).

f. E. Anderson and T. H. Fife, *J. Am. Chem. Soc.*, **93**, 1701 (1971).

Two-dimensional potential energy diagrams can be used to evaluate structural effects on the reactivity of carbonyl compounds and the tetrahedral intermediates. These reactions involve the formation or breaking of two separate bonds. This is the case in the first stage of acetal hydrolysis, which involves both a proton transfer and breaking of a C–O bond. The overall reaction might take place in several ways, but there are two stepwise mechanistic extremes.

1. The proton can be completely transferred and then the departing alcohol molecule can leave to form a carbocation in a distinct second step. This is the specific acid-catalyzed mechanism.
2. The acetal can undergo ionization with formation of an alkoxide ion and a carbocation. The alkoxide is protonated in a second step. This mechanism is extremely rare, if not impossible, because an alkoxide ion is a poor leaving group. An alternative mechanism involves general acid catalysis, in which the proton transfer and the C–O bond rupture occur as a *concerted process*. The concerted process need not be perfectly synchronous; that is, proton transfer

might be more complete at the TS than C–O rupture, or vice-versa. These ideas are represented in the two-dimensional energy diagram in Figure 7.3.

The two paths around the edge of the diagram represent the stepwise processes described as the mechanistic extremes 1 and 2. We know that Process 2 represented by path (a) is a high-energy process so the upper-left corner of the diagram would have a very high energy. The lines designated (b) and (c) indicate concerted but nonsynchronous mechanisms in which there is both partial proton transfer and partial C–O bond rupture at the transition state. In path (b) C–O cleavage is more complete than proton transfer at the transition state, whereas the reverse is true for path (c). Both these paths represent concerted, general acid-catalyzed processes. Path (d) represents the specific acid-catalyzed process in which proton transfer precedes C–O cleavage.

If it is possible to estimate or calculate the energy of the reacting system at various stages, the energy dimension can be added as in Figure 7.4 and can be shown as contours. The actual mechanism is the process that proceeds over the lowest energy barrier. The diagram in Figure 7.4 shows the initial ionization to an alkoxide and carbocation as very high in energy. The stepwise path of protonation followed by ionization is shown with smaller barriers with the protonated ketal as an intermediate. The lowest energy path is shown as a concerted process represented by the dashed line. The TS, which lies at the highest energy point on this line, would exhibit more complete proton transfer than C–O cleavage.

Structural and substituent effects can be discussed by considering how they affect the position of the TS on the potential energy surface. The stepwise path via the protonated acetal is preferred in the case of alcohols that are poor leaving groups. If the alcohol is more acidic, its conjugate base is a better leaving group and the TS shifts to a point where C–O bond breaking begins before proton transfer is complete. This means that the mechanism is concerted, although the TS still has much of the character of a carbocation. Two-dimensional reaction energy diagrams can be used to describe how structural changes affect the nature of the TS. Just as potential energy diagrams give

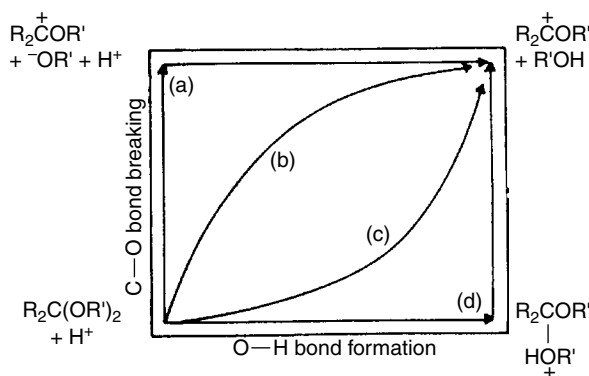


Fig. 7.3. Representation of mechanism for the first stage of acetal hydrolysis: (a) stepwise mechanism with initial C–O bond breaking; (b) concerted mechanism with C–O bond breaking leading O–H bond formation; (c) concerted mechanism with proton transfer leading C–O bond breaking; and (d) stepwise mechanism with initial proton transfer.

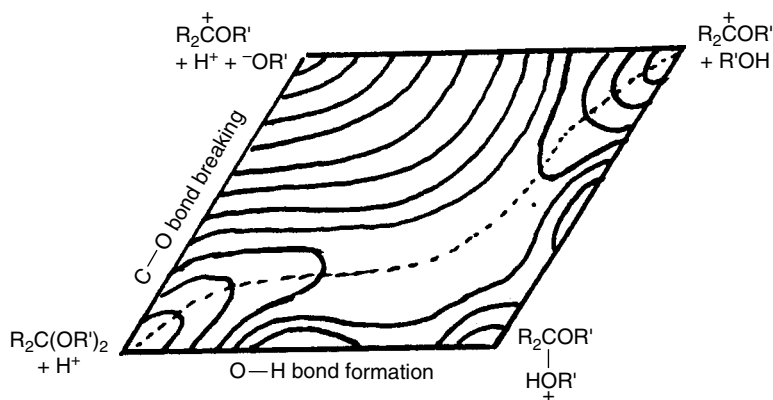
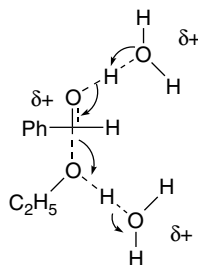


Fig. 7.4. Contour plot showing a favored concerted mechanism for the first step in acetal hydrolysis, with proton transfer more advanced at the transition state than C–O bond breaking.

meaning to such phrases as an “early” or a “late” TS, the two-dimensional diagrams are illustrative of statements such as “C–O cleavage is more advanced than proton transfer.”

Consideration of the types of acetals shown in Scheme 7.1, which exhibit general acid catalysis, indicates why the concerted mechanism operates in these molecules. The developing aromatic character of the cation formed in the case of Entry 1 lowers the energy requirement for C–O bond rupture. The bond can begin to break before protonation is complete. Entries 2 and 3 are cases where a better leaving group reduces the energy requirement for C–O bond cleavage. In Entry 4, the four-membered ring is broken in the reaction. Cleavage in this case is facilitated by release of strain energy. Entries 5 and 6 are similar to Entry 1 because the aryl groups provide stabilization for developing cationic character.

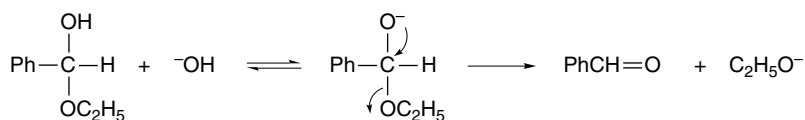
The second step in acetal hydrolysis is conversion of the hemiacetal to the carbonyl compound. The mechanism of this step is similar to that of the first step. Usually the second step is faster than the initial one.<sup>18</sup> Hammett  $\sigma$ – $\rho$  plots and solvent isotope effects both indicate that the TS has less cationic character than is the case for the first step. These features of the mechanism suggest that a concerted removal of the proton at the hydroxyl group occurs as the alcohol is eliminated.



<sup>18</sup> Y. Chiang and A. J. Kresge, *J. Org. Chem.*, **50**, 5038 (1985); R. A. McClelland, K. M. Engell, T. S. Larsen, and P. O. Sorensen, *J. Chem. Soc., Perkin Trans. 2*, 2199 (1994).

The positive charge is dispersed over several atoms and this diminishes the sensitivity of the reaction to substituent effects. The  $\rho$  values that are observed are consistent with this interpretation. Whereas  $\rho$  is  $-3.25$  for hydrolysis of aryl acetals, it is only  $-1.9$  for hemiacetal hydrolysis.<sup>19</sup>

In contrast to acetals, which are base stable, hemiacetals undergo base-catalyzed hydrolysis. In the alkaline pH range the mechanism shifts toward a base-catalyzed elimination.



There are two opposing substituent effects on this reaction. Electron-attracting aryl substituents favor the deprotonation but disfavor the elimination step. The observed substituent effects are small, and under some conditions the Hammett plots are nonlinear.<sup>20</sup>

### 7.3. Condensation Reactions of Aldehydes and Ketones with Nitrogen Nucleophiles

The mechanistic pattern of hydration and alcohol addition reactions of ketones and aldehydes is followed in reactions of carbonyl compounds with amines and related nitrogen nucleophiles. These reactions involve addition and elimination steps proceeding through tetrahedral intermediates. These steps can be either acid catalyzed or base catalyzed. The rates of the reactions are determined by the energy and reactivity of the tetrahedral intermediates. With primary amines, C=N bond formation ultimately occurs. These reactions are reversible and the position of the overall equilibrium depends on the nitrogen substituents and the structure of the carbonyl compound.



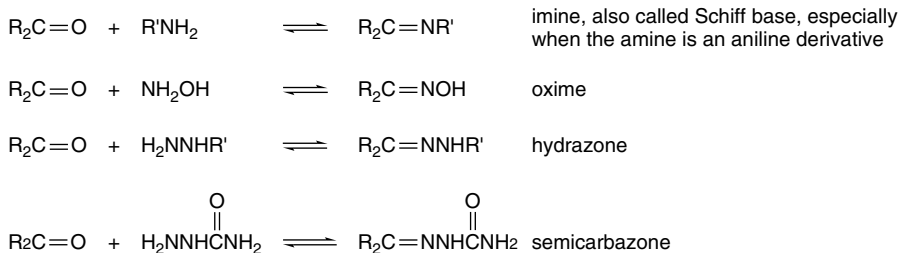
Scheme 7.2 lists some familiar types of such reactions. In general, these reactions are reversible and mechanistic information can be obtained by study of either the forward or the reverse process.

<sup>19</sup>. T. J. Przystas and T. H. Fife, *J. Am. Chem. Soc.*, **103**, 4884 (1981).

<sup>20</sup>. R. L. Finley, D. G. Kubler, and R. A. McClelland, *J. Org. Chem.*, **45**, 644 (1980).

## CHAPTER 7

Addition, Condensation  
and Substitution  
Reactions of Carbonyl  
Compounds



For simple alkyl amines, the  $K$  for imine formation in aqueous solution is defined as

$$K = \frac{[\text{imine}][H_2O]}{[\text{aldehyde}][\text{amine}]}$$

The value of  $K$  has been measured for several amines with 2-methylpropanal.<sup>21</sup> The effect of the structure of the alkyl group is quite small, although the trifluoroethyl group significantly reduces imine stability.

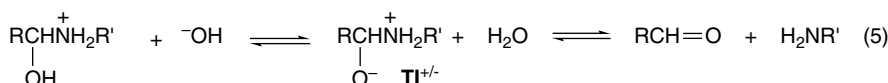
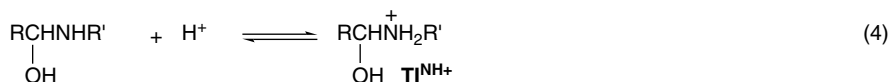
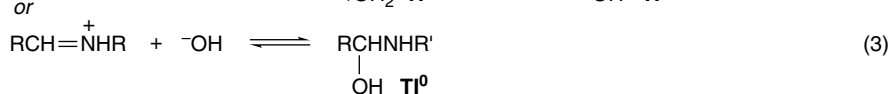
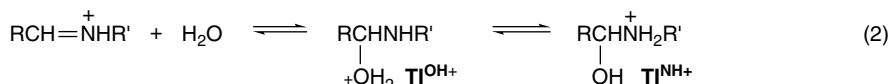
**Equilibrium Constants for Imines  
Formation with 2-Methylpropanal**

Amine	$K$
$CH_3NH_2$	$4.98 \times 10^3$
$CH_3CH_2NH_2$	$3.49 \times 10^3$
$CH_3CH_2CH_2NH_2$	$4.18 \times 10^3$
$(CH_3)_2CHNH_2$	$1.84 \times 10^3$
$PhCH_2NH_2$	$2.50 \times 10^3$
$CF_3CH_2NH_2$	$2.38 \times 10^2$
$CH_3OCH_2CH_2NH_2$	$2.06 \times 10^3$

The hydrolysis of simple imines occurs readily in aqueous acid, and has been studied in detail by kinetic methods. The precise mechanism is a function of the reactant structure and the pH of the solution. The overall mechanism consists of an addition of water to the C=N bond, followed by expulsion of the amine from a tetrahedral intermediate.<sup>22</sup> There are at least four variants of the tetrahedral intermediate that differ in the extent and site of protonation. In the general mechanism below, the neutral intermediate is labeled **TI**<sup>0</sup> and the zwitterionic form is labeled **TI**<sup>+/-</sup>. There are two possible monoprotonated forms, one protonated on oxygen (**TI**<sup>OH+</sup>) and one protonated on nitrogen (**TI**<sup>NH+</sup>).

<sup>21</sup> J. Hine and C. Y. Yeh, *J. Am. Chem. Soc.*, **89**, 2669 (1967); J. Hine, C. Y. Yeh, and F. C. Schmalstieg, *J. Org. Chem.*, **35**, 340 (1970).

<sup>22</sup> (a) J. Hine, J. C. Craig, Jr., J. G. Underwood, II, and F. A. Via, *J. Am. Chem. Soc.*, **92**, 5194 (1970); (b) E. H. Cordes and W. P. Jencks, *J. Am. Chem. Soc.*, **85**, 2843 (1963).



The rates of the various steps are a function of the pH of the solution, the basicity of the imine, and the reactivity of the aldehyde. Imine protonation enhances reactivity toward either water or hydroxide ion as nucleophiles. *N*-Protonation in the tetrahedral intermediate makes the amine a better leaving group. The zwitterionic intermediate  $\text{TI}^{+/-}$  is more reactive toward elimination of the amine than  $\text{TI}^{\text{NH}+}$  because of the assistance of the anionic oxygen. In the alkaline range, the rate-determining step is usually nucleophilic attack by hydroxide ion on the protonated C=N bond (Step 3). At intermediate pH values, water replaces hydroxide as the dominant nucleophile (Step 2). In acidic solution, the rate-determining step is the breakdown of the tetrahedral intermediate (Step 5). A mechanism of this sort, in which the observed rate is sensitive to pH, can be usefully studied by constructing a pH-rate profile, which is a plot of the observed rate constants versus pH. (See Section 3.7.1.4 to review pH-rate profiles.) Figure 7.5 is an example of the pH-rate profile for hydrolysis of a series of imines derived from substituted aromatic aldehydes and *t*-butylamine. The form of pH-rate profiles can be predicted on the basis of the detailed mechanism of the reaction. The value of the observed rates can be calculated as a function of pH if a sufficient number of the individual rate constants and the acid dissociation constants of the participating species are known. Agreement between the calculated and observed pH-rate profiles serves as a sensitive test of the adequacy of the postulated mechanism. Alternatively, one may begin with the experimental pH-rate profile and deduce details of the mechanism from it.

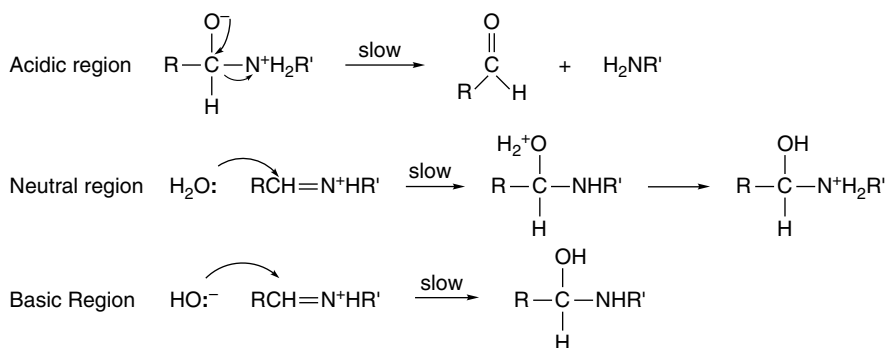
Complete understanding of the shape of the curves in Figure 7.5 requires a kinetic expression somewhat more complicated than we wish to deal with here. However, the nature of the extremities of the curve can be understood on the basis of qualitative arguments. The rate decreases with pH in the acidic region because formation of the zwitterionic tetrahedral intermediate  $\text{TI}^{+/-}$  is required for expulsion of the amine (Step 5). The concentration of the zwitterionic species decreases with increasing acidity, since its concentration is governed by an acid-base equilibrium.

$$K = \frac{[\text{H}^+][\text{TI}^{+/-}]}{[\text{TI}^{\text{NH}+}]}$$

Note also that in the acidic region, EWG substituents accelerate the reaction, owing to a more favorable equilibrium for the hydration step. In the alkaline region, the rate is pH independent. In this region, the rate-controlling step is attack of the

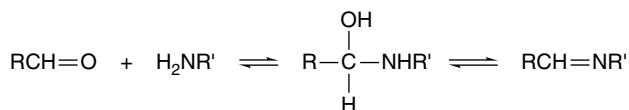
hydroxide ion on the protonated imine (Step 3). The concentration of both of these species is pH dependent, but in opposite, compensating, ways. The overall rate is therefore pH independent in the alkaline range. (Work problem 7.26 to establish that this is so.) Note that in this region the substituent effect is considerably smaller and is in the opposite sense from the acidic portion of the profile. This is due to the enhanced basicity of the ERG-substituted imines. At any given pH, more of the protonated imine is present for the ERG substituents.

The pH-rate profile for the hydrolysis of the *N*-methylimine of 2-methylpropanal is shown in Figure 7.6. The curve is similar to that for aromatic ketones with EWG substituents. The rate increases in the pH range 0–4.5, where decomposition of the zwitterionic intermediate is rate controlling. In the pH range 4.5–8, the rate decreases and then levels off. This corresponds to the transformation of the protonated imine to the less reactive neutral form. Above pH 8, the rate is again constant, as the increase in  $[\text{OH}^-]$  is compensated by the decrease in the amount of protonated imine.



G2 computations have been used to model the formation of the imine between methylamine and formaldehyde and to study the effect of water on the process.<sup>23</sup> The computations lead to the TS structures and energy profiles shown in Figure 7.7. The results point to the importance of the proton transfer steps in the overall energy requirement of the reaction. The inclusion of one or two water molecules leads to cyclic TS for proton transfer. This corresponds to concerted addition and elimination of water through six- and eight-membered cyclic hydrogen-bonded structures. The addition of water molecules substantially lowers the energy of the TS for each step of the reaction, while having relatively modest effects on the energy of the products. This is because the TSs involve considerably more charge separation than the products.

The formation of imines takes place by a mechanism that is the reverse of hydrolysis. Preparative procedures often ensure completion of the reaction by removing water by azeotropic distillation or by the use of an irreversible dehydrating agent.



The other C=N systems included in Scheme 7.2 are more stable to aqueous hydrolysis than the imines. The equilibrium constants for oxime formation are high, even in

<sup>23</sup> N. E. Hall and B. I. Smith, *J. Phys. Chem. A*, **102**, 4930 (1998).

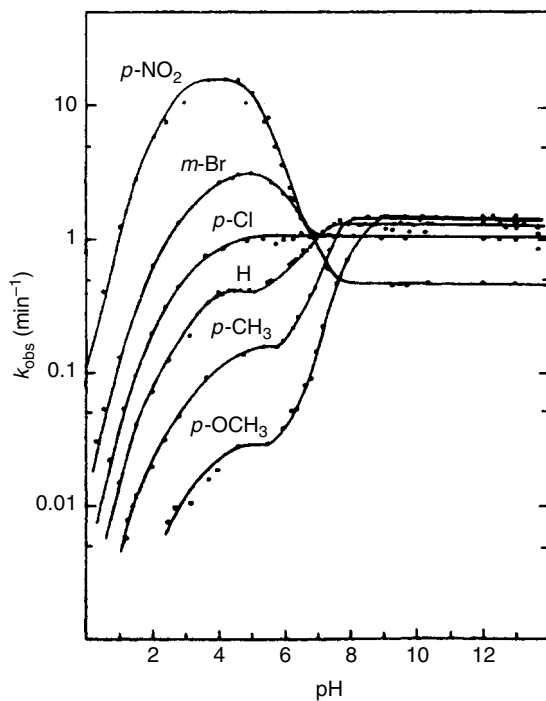


Fig. 7.5. pH-Rate profile for the hydrolysis of substituted benzylidene-1,1-dimethylethylamines. Reproduced from *J. Am. Chem. Soc.*, **85**, 2843 (1963), by permission of the American Chemical Society.

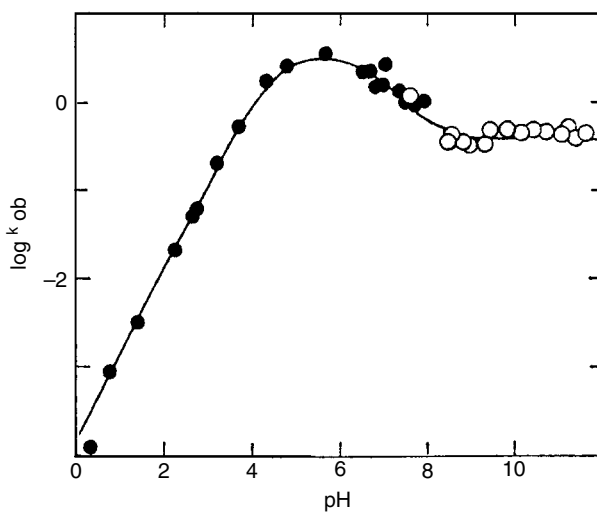


Fig. 7.6. pH-Rate profile for hydrolysis of *N*-methyl-2-methylpropanimine in water at 35°C. Solid points are from the hydrolysis reaction and open points are from the formation of the imine. Reproduced from *J. Am. Chem. Soc.*, **92**, 5194 (1970), by permission of the American Chemical Society.

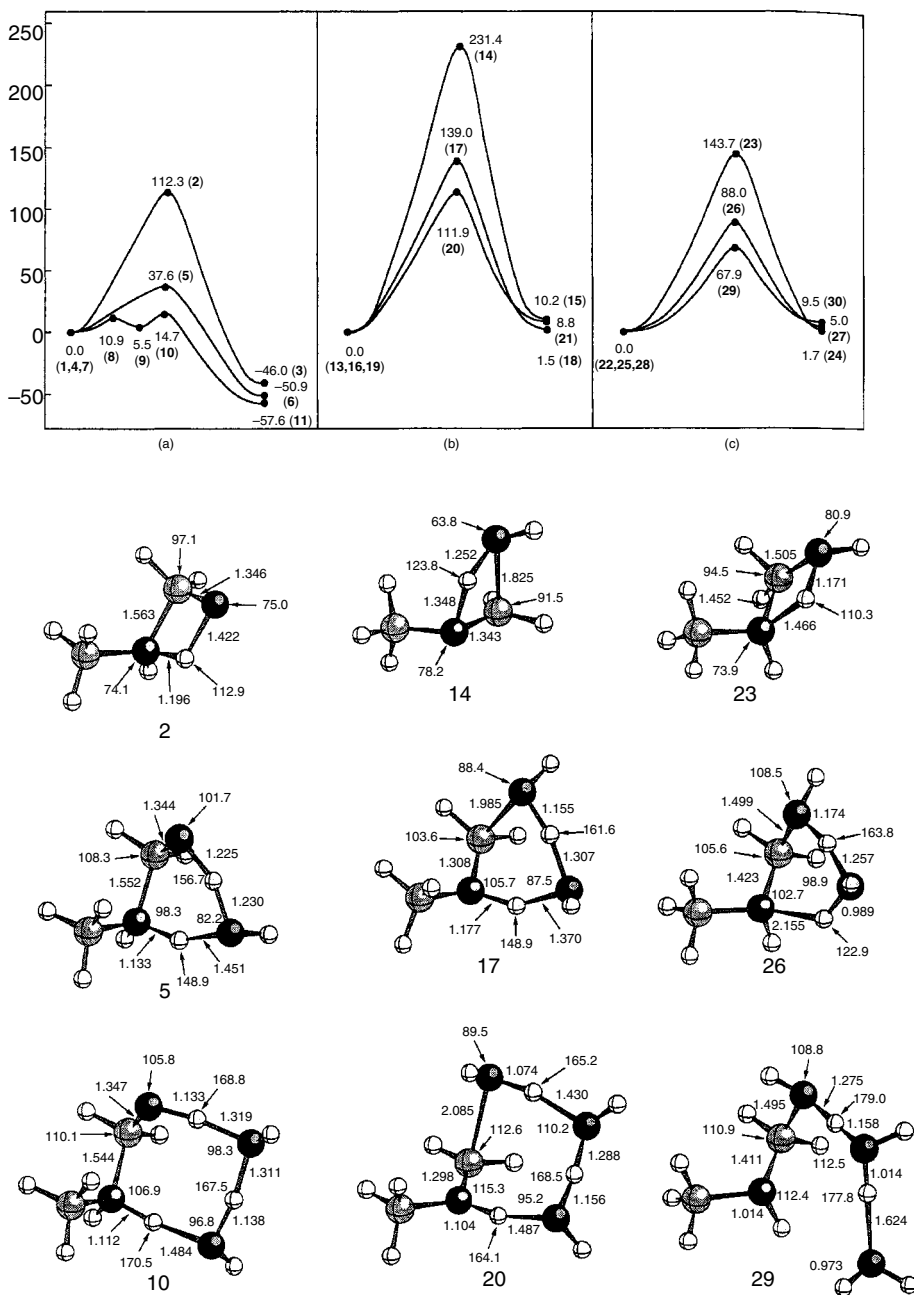


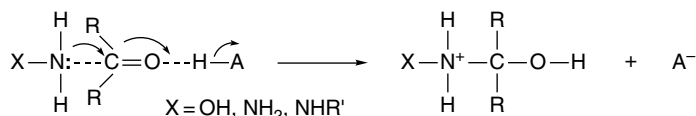
Fig. 7.7. Upper panel: Energy profiles from G2 computations for: (a) carbinolamine formation, (b) imine formation, and (c) iminium ion formation with zero, one, and two water molecules. Lower panel: Transition structures for carbinolamine, imine, and iminium ion formation with zero, one, and two water molecules and showing selected bond lengths and angles. Reproduced from *J. Phys. Chem. A*, **102**, 4930 (1998), by permission of the American Chemical Society.

aqueous solution. For example, the values for acetone ( $4.7 \times 10^5 M^{-1}$ ), 3-pentanone ( $7.7 \times 10^4 M^{-1}$ ), and cyclopentanone ( $4.0 \times 10^5 M^{-1}$ ) have been measured.<sup>24</sup> Traditionally, the additional stability was attributed to the participation of the atom adjacent to the nitrogen in delocalized bonding.

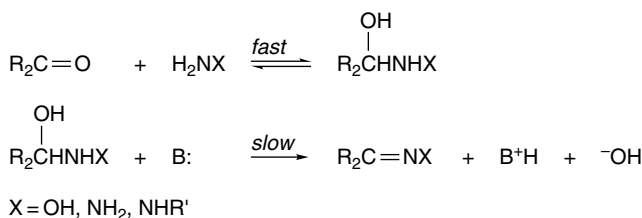


However, analysis based on HF/6-31G\* computations suggests that reduction of the lone pair repulsions that are present in hydroxylamine and hydrazine reactants may be more important.<sup>25</sup>

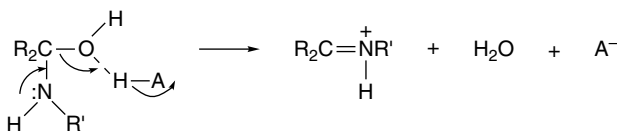
The formation of oximes and hydrazones is usually catalyzed by both general acids and general bases. The acid-catalyzed addition step can be depicted as concerted proton transfer and nucleophilic addition.<sup>26</sup>



General base catalysis of dehydration of the tetrahedral intermediate involves nitrogen deprotonation concerted with elimination of hydroxide ion.<sup>27</sup>



General acid catalysis of the breakdown of the carbinolamine intermediate occurs by assistance of the expulsion of water.



As with imines, the identity of the rate-limiting step changes with solution pH. As the pH decreases, the rate of addition decreases because protonation of the amino compound reduces the concentration of the nucleophilic unprotonated form. Thus, while the dehydration step is normally rate determining in neutral and basic solutions, addition becomes rate determining in acidic solutions. Figure 7.8 shows the pH-rate profiles for oximation of benzaldehyde and acetone. The acetone profile shows a region from pH 8 to 10 that is pH independent and corresponds to catalysis by water. The profile for benzaldehyde shows only a very slight contribution from a pH-independent reaction.

<sup>24</sup> J. Hine, J. P. Zeigler, and M. Johnston, *J. Org. Chem.*, **44**, 3540 (1979).

<sup>25</sup> K. B. Wiberg and R. Glaser, *J. Am. Chem. Soc.*, **114**, 841 (1992).

<sup>26</sup> C. G. Swain and J. C. Worosz, *Tetrahedron Lett.*, 3199 (1965).

<sup>27</sup> W. P. Jencks, *Prog. Phys. Org. Chem.*, **2**, 63 (1964); J. M. Sayer, M. Peskin, and W. P. Jencks, *J. Am. Chem. Soc.*, **95**, 4277 (1973).

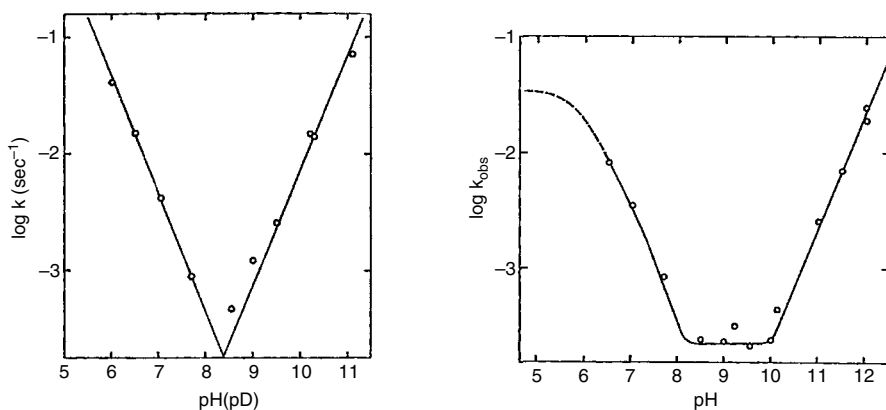


Fig. 7.8. pH-Rate profiles for formation of oximes of benzaldehyde (left) and acetone (right). The solid lines are the theoretical lines of slope  $-1$ ,  $0$ , and  $+1$ . Reproduced from *J. Am. Chem. Soc.*, **88**, 2508 (1966), by permission of the American Chemical Society.

The  $\rho$  values for both the addition and elimination steps in oxime formation of aromatic aldehydes have been determined.<sup>28</sup> For addition,  $\rho$  is  $+1.21$  (and the best correlation is with  $\sigma^+$ ). This is due to the decreased reactivity of aldehydes having direct conjugation with donor substituents. For the dehydration step,  $\rho$  is  $-0.85$ , which is the result of stabilization of the developing  $C=N$  bond by conjugation with donor substituents.

The mechanism of semicarbazone formation is similar to that for oximes.<sup>29</sup> The rate-limiting step at neutral pH is acid-catalyzed dehydration of the tetrahedral intermediate. Comparison of the semicarbazone and oxime formation reactions with those for imines has shown that there are differences in the details, such as the pH ranges associated with the different steps. The less basic amines, including aromatic amines and semicarbazide, undergo the addition step through concerted general acid catalysis. That is, the activation of the carbonyl group by simultaneous interaction with a proton donor is important.<sup>30</sup> For the more nucleophilic primary amines and hydroxylamine, the proton transfer associated with the addition step can be accomplished by the solvent, without an external proton source. Note that this relationship between amine nucleophilicity and the nature of proton transfer are consistent with the broad concepts indicated in Figure 7.1.

Certain reactions between carbonyl compounds and nucleophiles are catalyzed by amines. Some of these reactions are of importance for forming carbon-carbon bonds and these are discussed in Section 2.2.3 of Part B. The mechanistic principle can be illustrated by considering the catalysis of the reaction between ketones and hydroxylamine by aniline derivatives.<sup>31</sup>



<sup>28</sup> M. Calzadilla, A. Malpica, and T. Cordova, *J. Phys. Org. Chem.*, **12**, 708 (1999).

<sup>29</sup> W. P. Jencks, *J. Am. Chem. Soc.*, **81**, 475 (1959); B. M. Anderson and W. P. Jencks, *J. Am. Chem. Soc.*, **82**, 1773 (1960).

<sup>30</sup> R. B. Martin, *J. Phys. Chem.*, **68**, 1369 (1964).

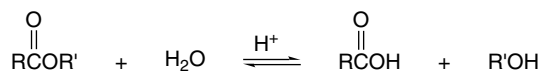
<sup>31</sup> E. H. Cordes and W. P. Jencks, *J. Am. Chem. Soc.*, **84**, 826 (1962); J. Hine, R. C. Dempsey, R. A. Evangelista, E. T. Jarvi, and J. M. Wilson, *J. Org. Chem.*, **42**, 1593 (1977).



Substitution reactions of carboxylic acid derivatives are among the most fundamental reactions in organic chemistry. The most common derivatives include acyl halides, anhydrides, esters, and carboxamides. Both synthesis and hydrolysis of esters and amides are examples of these substitution reactions. Most of these substitution reactions involve the formation and breakdown of a tetrahedral intermediate. The structural features of the carboxylic acid derivatives and related tetrahedral intermediates are discussed in Section 3.4.4. The fundamental difference in the chemistry of the carboxylic acid derivatives, as compared to ketones and aldehydes, is the presence of a potential leaving group at the carbonyl carbon. The order of reactivity as leaving groups is  $\text{Cl, Br} > \text{O}_2\text{CR} > \text{OR} > \text{NHR} > \text{O}^- > \text{N}^-\text{R}$ . The broad reactivity trends among the carboxylic acid derivatives can be recognized by taking account of the *effect of the substituents on the stability of the carbonyl center and the ability of the various substituents to act as leaving groups from the tetrahedral intermediate*. The detailed mechanisms of these reactions also depend on the site and extent of protonation in the tetrahedral intermediate.

#### 7.4.1. Ester Hydrolysis and Exchange

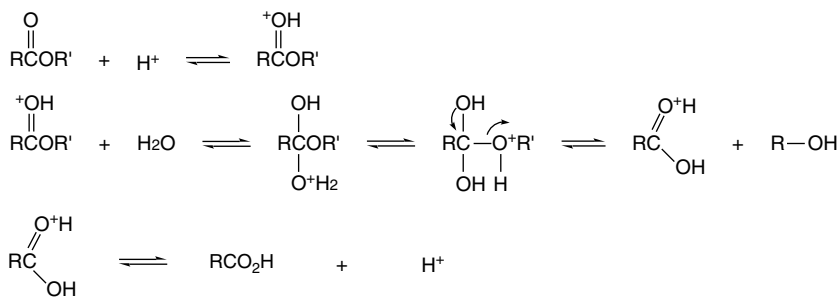
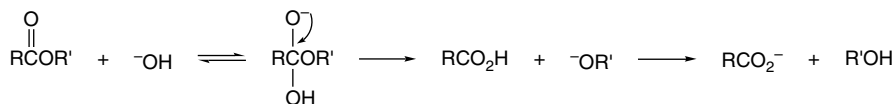
Esters can be hydrolyzed in either basic or acidic solution. In acidic solution, the reaction is reversible. The position of the equilibrium depends on the relative concentration of water and the alcohol. In aqueous solution, hydrolysis occurs. In alcoholic solution, the equilibrium is shifted in favor of the ester.



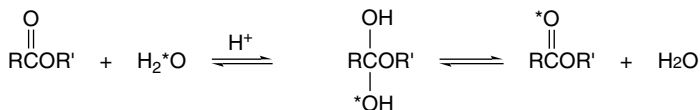
In alkaline aqueous solution, ester hydrolysis is essentially irreversible.



The carboxylic acid is converted to its anion under these conditions, and the position of the equilibrium lies far to the right. The mechanistic designations  $A_{\text{AC}2}$  and  $B_{\text{AC}2}$  are given to the acid- and base-catalyzed hydrolysis mechanisms, respectively. The A denotes acid catalysis and B indicates base catalysis. The subscript AC designation indicates that acyl-oxygen bond cleavage occurs. The digit 2 has its usual significance, indicating the bimolecular nature of the rate-determining step.

A<sub>AC</sub>2 mechanismB<sub>AC</sub>2 mechanism

Esters without special structural features can hydrolyze by either of these mechanisms. Among the evidence supporting these mechanisms are kinetic studies that show the expected dependence on hydrogen ion or hydroxide ion concentration and isotopic-labeling studies that prove it is the acyl-oxygen bond, not the alkyl-oxygen bond, that is cleaved during hydrolysis.<sup>33</sup> Acid-catalyzed hydrolysis of esters is accompanied by some exchange of oxygen from water into the carbonyl group. This exchange occurs by way of the tetrahedral intermediate because loss of water is competitive with expulsion of the alcohol.



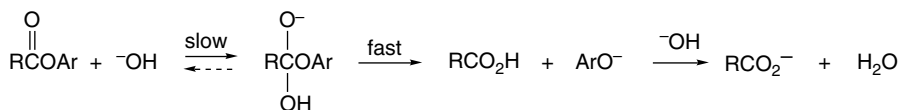
Alkyl benzoate esters give only a small amount of exchange under basic hydrolysis conditions. This means that reversal of the hydroxide addition must be slow relative to the forward breakdown of the tetrahedral intermediate.<sup>34</sup>

Substituent effects come into play at several points in the ester hydrolysis mechanism. In the base-catalyzed reaction, EWG substituents in either the acyl or alkoxy group facilitate hydrolysis. If the carbonyl group is conjugated with an ERG, reactivity is decreased by ground state stabilization. Since the rate-determining tetrahedral intermediate is negatively charged, the corresponding TS is stabilized by an EWG. The partitioning of the tetrahedral intermediate between reversion to starting material by loss of hydroxide ion and formation of product by expulsion of the alkoxide is strongly affected by substituents in the alkoxy group. An EWG on the alkoxy group shifts the partitioning to favor loss of the alkoxide and accelerates hydrolysis. For this reason, exchange of carbonyl oxygen with solvent does not occur in basic hydrolyses when the alkoxy group is a good leaving group. This has been demonstrated, for example, for esters of phenols. As phenols are stronger acids than alcohols,

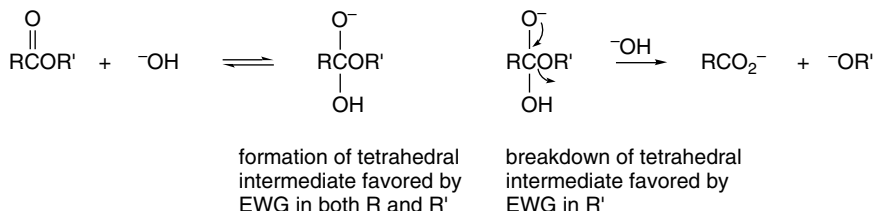
<sup>33</sup> M. I. Bender, *Chem. Rev.*, **60**, 53 (1960); S. L. Johnson, *Adv. Phys. Org. Chem.*, **5**, 237 (1967); D. P. N. Satchell and R. S. Satchell, in *Chemistry of Carboxylic Acid Derivatives*, Vol. 2, Part 1, S. Patai, ed., Wiley, New York, 1992, pp. 747–802.

<sup>34</sup> R. A. McClelland, *J. Am. Chem. Soc.*, **106**, 7579 (1984).

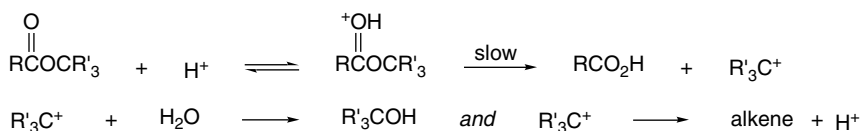
their conjugate bases are better leaving groups than alkoxide ions. Aryl esters are hydrolyzed faster than alkyl esters, without observable exchange of carbonyl oxygen with solvent.



These substituent effects can be summarized for the  $B_{AC}2$  mechanism by noting the effect of substituents on each step of the mechanism.



Structural changes in the reactant can shift ester hydrolysis away from the usual  $A_{AC}2$  or  $B_{AC}2$  mechanisms. When the ester is derived from a tertiary alcohol, acid-catalyzed hydrolysis often occurs by a mechanism involving *alkyl oxygen fission*. The change in mechanism is due to the stability of the tertiary carbocation that can be formed by alkyl-oxygen cleavage.<sup>35</sup> When this mechanism occurs, alkenes as well as alcohols are produced, because the carbocation can react by either substitution or elimination. This mechanism is referred to as  $A_{AL}1$ , indicating the cleavage of the alkyl-oxygen bond and the unimolecular character of the rate-determining step.

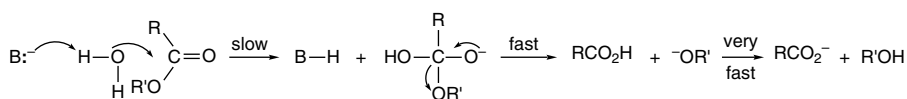


The facile  $A_{AL}1$  mechanism of tertiary alkyl esters is valuable in synthetic methodology because it permits tertiary esters to be hydrolyzed selectively. The usual situation involves the use of *t*-butyl esters, which can be cleaved to carboxylic acids by the action of acids such as *p*-toluenesulfonic acid or trifluoroacetic acid under anhydrous conditions where other esters are stable.

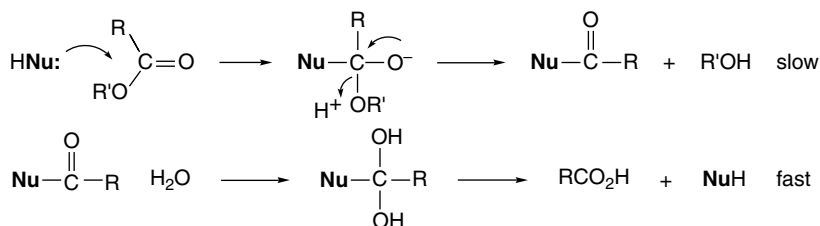
The ester hydrolysis mechanisms discussed in the preceding paragraphs pertained to aqueous solutions of strong acids and strong bases, in which specific acid or base catalysis is dominant. In media where other acids or bases are present, general acid-catalyzed and general base-catalyzed hydrolysis can occur. General base catalysis has been observed in the case of esters in which the acyl group carries EWG substituents.<sup>36</sup> The TS for esters undergoing hydrolysis by a general base-catalyzed mechanism involves partial proton transfer from the attacking water molecule to the general base during formation of the tetrahedral intermediate.

<sup>35</sup> A. G. Davies and J. Kenyon, *Q. Rev. Chem. Soc.*, **9**, 203 (1955).

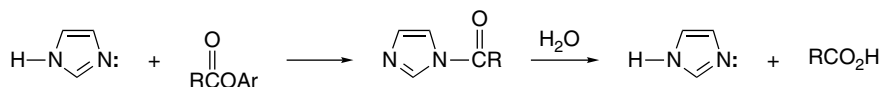
<sup>36</sup> W. P. Jencks and J. Carriuolo, *J. Am. Chem. Soc.*, **83**, 1743 (1961); D. Stefanidis and W. P. Jencks, *J. Am. Chem. Soc.*, **115**, 6045 (1993).



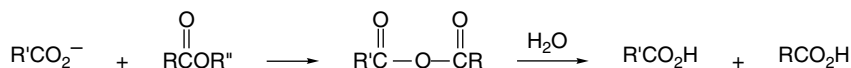
Ester hydrolysis can also occur by *nucleophilic catalysis*. If a component of the reaction system is a more effective nucleophile toward the carbonyl group than water under a given set of conditions, an acyl transfer reaction can take place to form the acyl derivative of the catalytic nucleophile. If this acyl intermediate, in turn, is more rapidly attacked by water than the original ester, the overall reaction will be faster in the presence of the nucleophile than in its absence. These are the requisite conditions for nucleophilic catalysis.



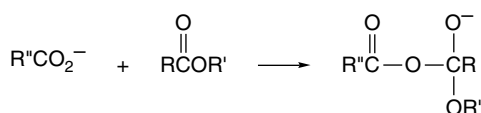
Esters of relatively acidic alcohols (in particular phenols) are hydrolyzed by the nucleophilic catalysis mechanism in the presence of imidazole.<sup>37</sup> The acylimidazolides are inherently quite reactive and protonation of the second nitrogen can facilitate the hydrolysis.



Carboxylate anions can also serve as nucleophilic catalysts.<sup>38</sup> In this case, an anhydride is the reactive intermediate.



The nucleophilic catalysis mechanism only operates when the alkoxy group being hydrolyzed is not substantially more basic than the nucleophilic catalyst. This requirement can be understood by considering the tetrahedral intermediate generated by attack of the potential catalyst on the ester.



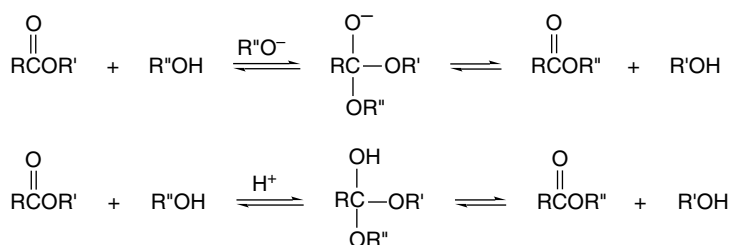
The relative leaving-group abilities of  $\text{R}'\text{O}^-$  and  $\text{R}''\text{CO}_2^-$  are strongly correlated with the basicity of the two anions. If  $\text{R}''\text{CO}_2^-$  is a much better leaving group than  $\text{R}'\text{O}^-$ , it will be eliminated preferentially from the tetrahedral intermediate and no catalysis will occur.

<sup>37</sup> T. C. Bruice and G. L. Schmir, *J. Am. Chem. Soc.*, **79**, 1663 (1967); M. L. Bender and B. W. Turnquest, *J. Am. Chem. Soc.*, **79**, 1652, 1656 (1957); P. Menegheli, J. P. S. Farah, and O. A. El Seoud, *Ber. Bunsenges. Phys. Chem.*, **95**, 1610 (1991).

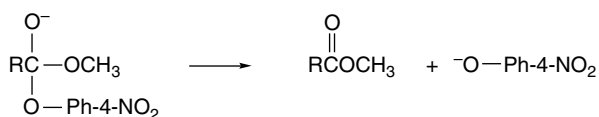
<sup>38</sup> V. Gold, D. G. Oakenfull, and T. Riley, *J. Chem. Soc., Perkin Trans. B*, 515 (1968).

The preceding discussion has touched on the most fundamental aspects of ester hydrolysis mechanisms. Much effort has been devoted to establishing some of the finer details, particularly concerning proton transfers during the formation and breakdown of the tetrahedral intermediates. These studies have been undertaken in part because of the importance of hydrolytic reactions in biological systems, which are catalyzed by enzymes. The detailed mechanistic studies of ester hydrolysis laid the groundwork for understanding the catalytic mechanisms of the hydrolytic enzymes. Discussions of the biological mechanisms and their relationship to the fundamental mechanistic studies are available in several books that discuss enzyme catalysis in terms of molecular mechanisms.<sup>39</sup>

Esters react with alcohols in either acidic or basic solution to exchange alkoxy groups (ester interchange) by a mechanism that parallels hydrolysis. The alcohol or alkoxide acts as the nucleophile.



As in the case of hydrolysis, there has been a good deal of study of substituent effects, solvent effects, isotopic exchange, kinetics, and the catalysis of these processes.<sup>40</sup> In contrast to hydrolysis, the alcoholysis reaction is reversible in both acidic and basic solutions. The key intermediate is the tetrahedral adduct. Its fate is determined mainly by the relative basicity of the two alkoxy groups. A tetrahedral intermediate generated by addition of methoxide ion to a *p*-nitrophenyl ester, for example, breaks down exclusively by elimination of the much less basic *p*-nitrophenoxide ion.

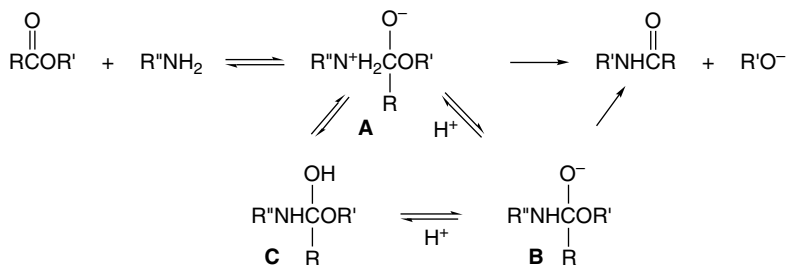


In general, the equilibrium in a base-catalyzed alcohol exchange reaction lies in the direction of incorporation of the less acidic alcohol in the ester. This is a reflection both of the kinetic factor, the more acidic alcohol being a better leaving group, and the greater stabilization provided to the carbonyl group by the more electron-rich alkoxy substituent.

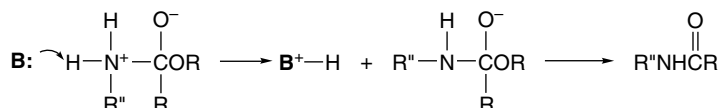
- <sup>39</sup> T. C. Bruice and S. J. Benkovic, *Bioorganic Mechanisms*, Vol. 1, W. A. Benjamin, New York, 1966, pp. 1–258; W. P. Jencks, *Catalysis in Chemistry and Enzymology*, McGraw-Hill, New York, 1969; M. L. Bender, *Mechanisms of Homogeneous Catalysis from Protons to Proteins*, Wiley-Interscience, New York, 1971; C. Walsh, *Enzymatic Reaction Mechanisms*, W. H. Freeman, San Francisco, 1979; A. Fersht, *Enzyme Structure and Mechanism*, 2nd Edition, W. H. Freeman, New York, 1985.
- <sup>40</sup> C. G. Mitton, R. L. Schowen, M. Gresser, and J. Shapely, *J. Am. Chem. Soc.*, **91**, 2036 (1969); C. G. Mitton, M. Gresser, and R. L. Schowen, *J. Am. Chem. Soc.*, **91**, 2045 (1969).

## 7.4.2. Aminolysis of Esters

Esters react with ammonia and amines to give amides. The mechanism involves nucleophilic attack of the amine at the carbonyl group, followed by expulsion of the alkoxy group from the tetrahedral intermediate. The identity of the rate-determining step depends primarily on the leaving-group ability of the alkoxy group.<sup>41</sup> With relatively good leaving groups such as phenols or trifluoroethanol, the slow step is expulsion of the oxygen leaving group from a zwitterionic tetrahedral intermediate **A**. With poorer leaving groups, breakdown of the tetrahedral intermediate occurs only after formation of the anionic species **B**.



Aminolysis of esters often exhibits general base catalysis in the form of reaction rate terms that are second order in the amine. The amine is believed to assist deprotonation of the zwitterionic tetrahedral intermediate.<sup>42</sup> Deprotonation of the nitrogen facilitates breakdown of the tetrahedral intermediate because the increased electron density at nitrogen favors expulsion of an alkoxide ion.

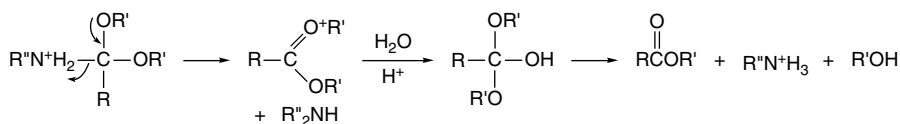


Detailed mechanistic studies have been carried out on aminolysis of substituted aryl acetates and aryl carbonates.<sup>43</sup> Aryl esters are considerably more reactive than alkyl esters because phenoxide ions are better leaving groups than alkoxide ions. The tetrahedral intermediate formed in aminolysis can exist in several forms that differ in the extent and the site of protonation.

- <sup>41</sup> F. M. Menger and J. H. Smith, *J. Am. Chem. Soc.*, **94**, 3824 (1972); A. C. Satterthwait and W. P. Jencks, *J. Am. Chem. Soc.*, **96**, 7018 (1974).  
<sup>42</sup> W. P. Jencks and M. Gilchrist, *J. Am. Chem. Soc.*, **88**, 104 (1966); J. F. Kirsch and A. Kline, *J. Am. Chem. Soc.*, **91**, 1841 (1969); A. S. Shawali and S. S. Biechler, *J. Am. Chem. Soc.*, **89**, 3020 (1967); J. F. Bunnett and G. T. Davis, *J. Am. Chem. Soc.*, **82**, 665 (1961).  
<sup>43</sup> W. P. Jencks and M. Gilchrist, *J. Am. Chem. Soc.*, **90**, 2622 (1968); A. Satterthwait and W. P. Jencks, *J. Am. Chem. Soc.*, **96**, 7018 (1974); A. Satterthwait and W. P. Jencks, *J. Am. Chem. Soc.*, **96**, 7031 (1974); M. J. Gresser and W. P. Jencks, *J. Am. Chem. Soc.*, **99**, 6970 (1977).

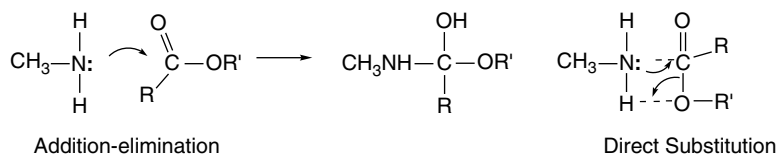


In acidic solution, the protonated nitrogen is a better leaving group, and also loses its ability to assist in the elimination of the alkoxide. Under these circumstances, nitrogen elimination is favored.



In analyzing the behavior of these types of tetrahedral intermediates, it should be kept in mind that proton transfer reactions are usually fast relative to other steps. This circumstance permits the possibility that a minor species in equilibrium with the major species may be the kinetically dominant intermediate. Detailed studies of kinetics, solvent isotope effects, and catalysis are the best tools for investigating the various possibilities.

Recent computational work has suggested the existence of a mechanism for aminolysis that bypasses the tetrahedral intermediates. Transition structures corresponding to both stepwise addition-elimination through a tetrahedral intermediate and direct substitution were found for the reaction of methylamine with methyl acetate and phenyl acetate.<sup>45</sup> There is considerable development of charge separation in the direct displacement mechanism because proton transfer lags rupture of the C–O bond.



The direct substitution reaction becomes progressively more favorable as the alcohol becomes a better leaving group. According to the computations, the two mechanisms are closely competitive for alkyl esters, but the direct substitution mechanism is favored for aryl esters. These results refer to the gas phase.

#### Computed Activation Energy (kcal/mol)

	Addition-elimination	Direct substitution
CH <sub>3</sub> CO <sub>2</sub> CH <sub>3</sub>	35.5	36.2
CH <sub>3</sub> CO <sub>2</sub> C <sub>6</sub> H <sub>5</sub>	32.1	26.6
CH <sub>3</sub> CO <sub>2</sub> C <sub>6</sub> H <sub>4</sub> NO <sub>2</sub>		~1.7

A direct substitution mechanism was indicated for the 2-pyridone catalysis of aminolysis of methyl acetate by methylamine.<sup>46</sup> This mechanism is represented in Figure 7.9. It avoids a tetrahedral intermediate and describes a concerted displacement process that is facilitated by proton transfer involving 2-pyridone. Two very closely related TSs involving either the 2-hydroxypyridine or 2-pyridone tautomers were found. These TSs show extensive cleavage of the C–O bond (2.0–2.2 Å) and formation

<sup>45</sup> H. Zipse, L.-h. Wang, and K. N. Houk, *Liebigs Ann.*, 1511 (1996).

<sup>46</sup> L.-h. Wang and H. Zipse, *Liebigs Ann.*, 1501 (1996).

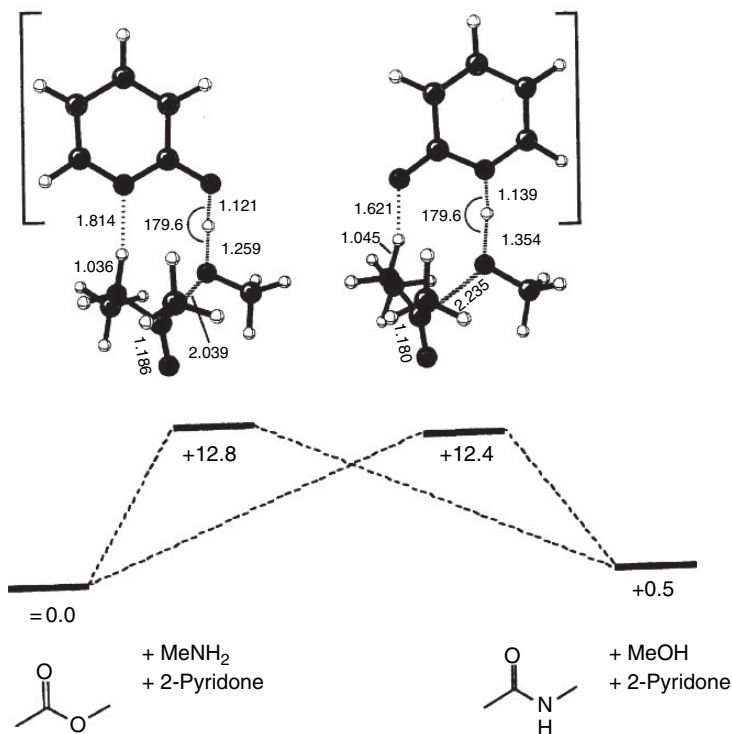
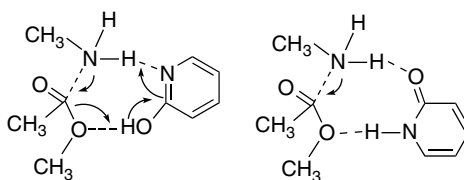


Fig. 7.9. Concerted mechanism for 2-pyridone-catalyzed reaction of methylamine with methyl acetate. TS energies (kcal/mol) are from B3LYP/6-31G\*\* calculations. Reproduced from *Liebigs Ann.*, 1501 (1996), by permission of Wiley-VCM.

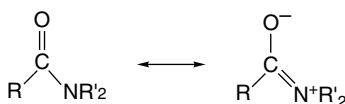
of the C–N bond. O-Protonation is also advanced, but N-deprotonation is minimal. Experimentally, it was found that catalytic efficiency could be improved by a factor of about 2500 by use of the more acidic 4-cyano-2-pyridone.



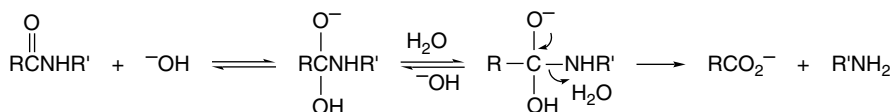
### 7.4.3. Amide Hydrolysis

The hydrolysis of amides to carboxylic acids and amines requires considerably more vigorous conditions than ester hydrolysis.<sup>47</sup> The reason is that the electron-releasing nitrogen imparts a very significant ground state stabilization that is lost in the TS leading to the tetrahedral intermediate.

<sup>47</sup> C. O'Connor, *Q. Rev. Chem. Soc.*, **24**, 553 (1970).

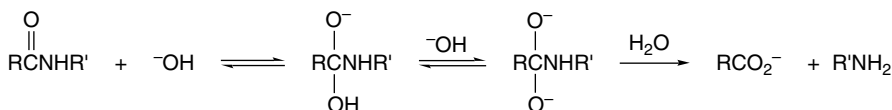


In basic solution, a B<sub>AC</sub>2 mechanism similar to the that for ester hydrolysis is believed to operate.<sup>48</sup>



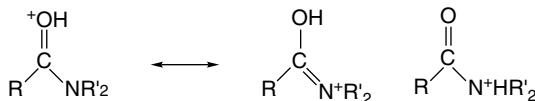
The principal difference lies in the poorer ability of amide anions to act as leaving groups, compared to alkoxides. As a result, protonation at nitrogen is required for dissociation of the tetrahedral intermediate. Exchange between the carbonyl oxygen and water is extensive because reversal of the tetrahedral intermediate to reactants is faster than decomposition to products.

In some amide hydrolyses, the rupture of the tetrahedral intermediate in the forward direction requires formation of a dianion.<sup>49</sup>



This variation from the ester hydrolysis mechanism also reflects the poorer leaving ability of amide ions, as compared to alkoxide ions. The evidence for the involvement of the dianion comes from kinetic studies and from solvent isotope effects that suggest that a rate-limiting proton transfer is involved.<sup>50</sup> The reaction is also higher than first order in hydroxide ion under these circumstances, which is consistent with the dianion mechanism.

The mechanism for acid-catalyzed hydrolysis of amides involves attack by water on the protonated amide. Amides are weak bases with p*K<sub>a</sub>* values in the range from 0 to -2.<sup>51</sup> An important feature of the chemistry of amides is that the most basic site is the carbonyl oxygen. Very little of the N-protonated form is present.<sup>52</sup> The major factor that favors the O-protonated form is the retention of π-electron delocalization over the O-C-N system. No such delocalization is possible in the N-protonated form.



<sup>48</sup>. M. L. Bender and R. J. Thomas, *J. Am. Chem. Soc.*, **83**, 4183 (1961); R. S. Brown, A. J. Bennet, and H. Slebocka-Tilk, *Acc. Chem. Res.*, **25**, 481 (1992).

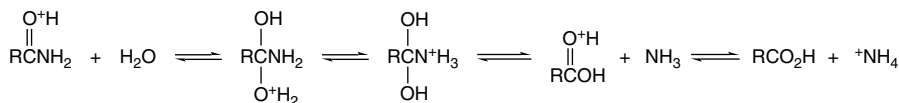
<sup>49</sup>. R. M. Pollack and M. L. Bender, *J. Am. Chem. Soc.*, **92**, 7190 (1970).

<sup>50</sup>. R. L. Schowen, H. Jayaraman, L. Kershner, and G. W. Zuorick, *J. Am. Chem. Soc.*, **88**, 4008 (1966).

<sup>51</sup>. R. A. Cox, L. M. Druet, A. E. Klausner, T. A. Modro, P. Wan, and K. Yates, *Can. J. Chem.*, **59**, 1568 (1981); A. Bagno, G. Lovato, and G. Scorrano, *J. Chem. Soc., Perkin Trans. 2*, 1091 (1993).

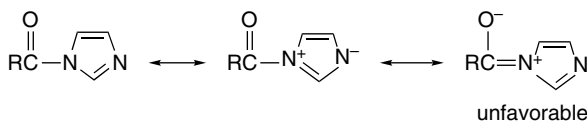
<sup>52</sup>. R. J. Gillespie and T. Birchall, *Can. J. Chem.*, **41**, 148, 2642 (1963); A. R. Fersht, *J. Am. Chem. Soc.*, **93**, 3504 (1971); R. B. Martin, *J. Chem. Soc., Chem. Commun.*, 793 (1972); A. J. Kresge, P. H. Fitzgerald, and Y. Chiang, *J. Am. Chem. Soc.*, **96**, 4698 (1974).

The usual hydrolysis mechanism in strongly acidic solutions involves addition of water to the O-protonated amide followed by dissociation of the tetrahedral intermediate.



There is almost no exchange of oxygen with water during acid-catalyzed hydrolysis of amides.<sup>53</sup> Since a tetrahedral intermediate is involved, the lack of exchange means that it must react exclusively by elimination of the nitrogen substituent. This result is reasonable, because the amino group is the most basic site and is the preferred site of protonation in the tetrahedral intermediate. The protonated amine is a much better leaving group than the hydroxide ion.

Acyimidazoles and related amides in which the nitrogen atom is part of an aromatic ring hydrolyze much more rapidly than aliphatic amides. A major factor is the decreased resonance stabilization of the carbonyl group, which is opposed by the participation of the nitrogen lone pair in the aromatic sextet.

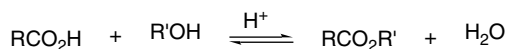


The acid-catalyzed hydrolysis of imidazolides is accelerated by protonation of N(3), which increases the leaving-group ability of the ring,<sup>54</sup> and accumulation of additional nitrogens in the ring (triazoles, tetrazoles) further increased that ability.<sup>55</sup>

#### 7.4.4. Acylation of Nucleophilic Oxygen and Nitrogen Groups

The conversion of alcohols to esters by O-acylation and of amines to amides by N-acylation are fundamental organic reactions that are the reverse of the hydrolyses discussed in the preceding sections. In Section 3.4 of Part B we discuss these reactions from the point of view of synthetic applications and methods.

Although the previous two sections of this chapter emphasized hydrolytic processes, two mechanism that led to O or N-acylation were considered. In the discussion of acid-catalyzed ester hydrolysis, it was pointed out that this reaction is reversible (p. 654). Thus it is possible to acylate alcohols by acid-catalyzed reaction with a carboxylic acid. This is called the *Fischer esterification* method. To drive the reaction forward, the alcohol is usually used in large excess, and it may also be necessary to remove water as it is formed. This can be done by azeotropic distillation in some cases.



<sup>53</sup> R. A. McClelland, *J. Am. Chem. Soc.*, **97**, 5281 (1975); For cases in which some exchange does occur, see H. Slebocka-Tilk, R. S. Brown, and J. Olekszyk, *J. Am. Chem. Soc.*, **109**, 4620 (1987); A. J. Bennet, H. Slebocka-Tilk, R. S. Brown, J. P. Guthrie, and A. J. Jodhan, *J. Am. Chem. Soc.*, **112**, 8497 (1990).

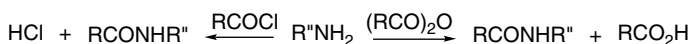
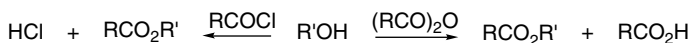
<sup>54</sup> T. H. Fife, *Acc. Chem. Res.*, **26**, 325 (1993).

<sup>55</sup> J. F. Patterson, W. P. Huskey, and J. L. Hoggs, *J. Org. Chem.*, **45**, 4675 (1980); B. S. Jursic and Z. Zdravkovski, *Theochem*, **109**, 177 (1994).

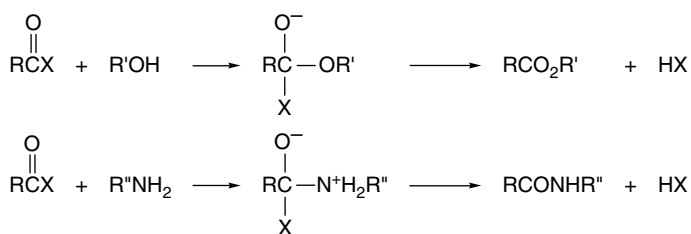
The second reaction that should be recalled is the aminolysis of esters (p. 659), which leads to the formation of amides by N-acylation. The equilibrium constant for this reaction is ordinarily favorable, but the reactions are rather slow.



The most common O- and N-acylation procedures use acylating agents that are more reactive than carboxylic acids or their esters. Acyl chlorides and anhydrides react rapidly with most unhindered alcohols and amines to give esters and amides, respectively.

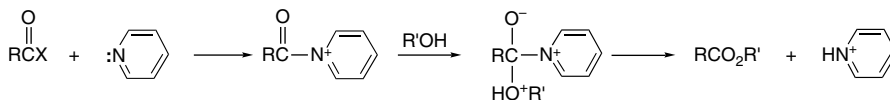


The general features of the mechanisms are well established.<sup>56</sup> The nucleophilic species undergoes addition at the carbonyl group, followed by elimination of the halide or carboxylate group. Acyl halides and anhydrides are reactive acylating reagents because of a combination of the polar effect of the halogen or oxygen substituent, which enhances the reactivity of the carbonyl group, and the ease with which the tetrahedral intermediate can expel these relatively good leaving groups.



X = halide or carboxylate

Acylation of alcohols is often performed in the presence of an organic base such as pyridine. The base serves two purposes: it neutralizes the protons generated in the reaction and prevents the development of high acid concentrations. Pyridine also becomes directly involved in the reaction as a *nucleophilic catalyst* (see p. 657).



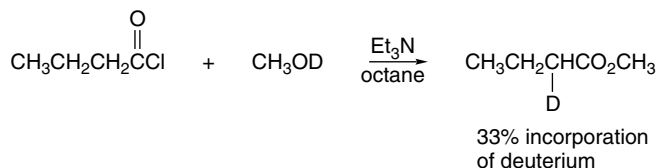
X = halide or carboxylate

Pyridine is more nucleophilic than an alcohol toward the carbonyl center of an acyl chloride. The product that results, an acylpyridinium ion, is, in turn, more reactive toward an alcohol than the original acyl chloride. The conditions required for nucleophilic catalysis therefore exist, and acylation of the alcohol by acid chloride is faster in the presence of pyridine than in its absence. Among the evidence that supports this

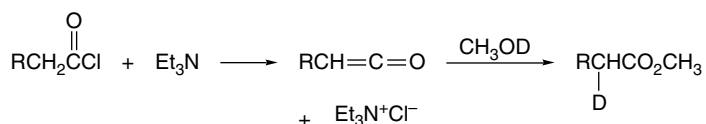
<sup>56</sup> D. P. N. Satchell, *Q. Rev. Chem. Soc.*, **17**, 160 (1963).

mechanism is spectroscopic observation of the acetylpyridinium ion intermediate.<sup>57</sup> An even more effective catalyst is 4-dimethylaminopyridine (DMAP), which functions in the same way, but is more reactive because of the ERG dimethylamino substituent.<sup>58</sup>

With more strongly basic tertiary amines such as triethylamine, another mechanism can come into play. It has been found that when methanol deuterated on oxygen reacts with acyl chlorides in the presence of triethylamine, some deuterium is introduced  $\alpha$  to the carbonyl group in the ester.

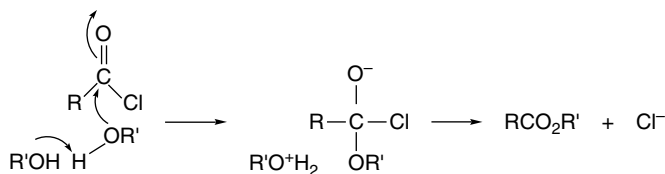


This finding suggests that some of the ester is formed via a ketene intermediate.<sup>59</sup>



Ketenes undergo rapid addition by nucleophilic attack at the *sp*-carbon atom. The reaction of tertiary amines and acyl halides in the absence of nucleophiles is a general preparation for ketenes for other purposes.<sup>60</sup>

Kinetic studies of the reaction of alcohols with acyl chlorides in polar solvents in the absence of basic catalysts generally reveal terms of both first and second order in alcohol.<sup>61</sup> Transition structures in which the second alcohol molecule acts as a proton acceptor have been proposed.



There is an alternative to the addition-elimination mechanism for nucleophilic substitution of acyl chlorides. Certain acyl chlorides react with alcohols by a dissociative mechanism in which *acylium ions* are intermediates. This mechanism is observed with aroyl halides having ERG substituents.<sup>62</sup> Other acyl halides show

<sup>57</sup> A. R. Fersht and W. P. Jencks, *J. Am. Chem. Soc.*, **92**, 5432, 5442 (1970).

<sup>58</sup> E. F. V. Scriven, *Chem. Soc. Rev.*, **12**, 129 (1983).

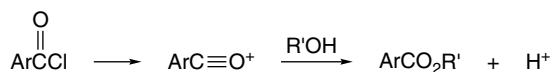
<sup>59</sup> W. E. Truce and P. S. Bailey, *J. Org. Chem.*, **34**, 1341 (1969).

<sup>60</sup> R. N. Lacey, in *The Chemistry of Alkenes*, S. Patai, ed., Interscience Publishers, New York, 1964, pp. 1168–1170; W. E. Hanford and J. C. Sauer, *Org. React.*, **3**, 108 (1947).

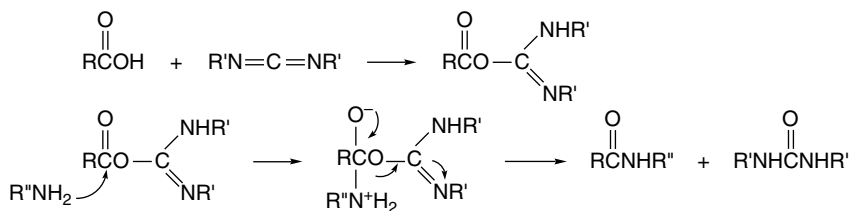
<sup>61</sup> D. N. Kevill and F. D. Foss, *J. Am. Chem. Soc.*, **91**, 5054 (1969); S. D. Ross, *J. Am. Chem. Soc.*, **92**, 5998 (1970).

<sup>62</sup> M. L. Bender and M. C. Chen, *J. Am. Chem. Soc.*, **85**, 30 (1963); T. W. Bentley, H. C. Harris, and I. S. Koo, *J. Chem. Soc., Perkin Trans. 2*, 783 (1988); B. D. Song and W. P. Jencks, *J. Am. Chem. Soc.*, **111**, 8470 (1989).

reactivity indicative of mixed or borderline mechanisms.<sup>63</sup> The existence of the  $S_N1$ -like dissociative mechanism reflects the relative stability of acylium ions.

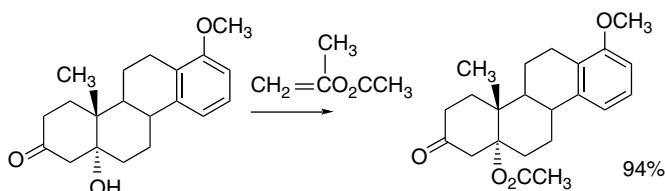


In addition to acyl chlorides and acid anhydrides, there are a number of other types of compounds that are reactive acylating agents. Many have been developed to facilitate the synthesis of polypeptides, for which mild conditions and high selectivity are required (see Part B, Section 3.4). The carbodiimides, such as dicyclohexylcarbodiimide, make up an important group of reagents for converting carboxylic acids to active acylating agents. The mechanism for carbodiimide-promoted amide bond formation is shown below.



The first step is addition of the carboxylic acid to the  $\text{C}=\text{N}$  bond of the carbodiimide, which generates an  $\text{O}$ -acylated urea derivative. This is a reactive acylating agent because there is a strong driving force for elimination of the very stable urea carbonyl group.<sup>64</sup> The amine reacts with the active acylating agent. In the absence of an amine, the acid is converted to the anhydride, with a second molecule of the carboxylic acid serving as the nucleophile.

Enol esters are another type of acylating agent. The acetate of the enol form of acetone, isopropenyl acetate, is the most commonly used example. In the presence of an acid catalyst, they act as acylating agents and are reactive toward weak nucleophiles such as hindered hydroxy groups.



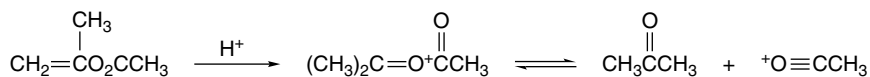
Ref. 65

The active acylating agent is presumably the  $\text{C}$ -protonated enol ester. This species is highly reactive owing to the presence of a positively charged oxygen. An alternative possibility is that the protonated enol ester dissociates to acetone and the acetylum ion, which then acts as the acylating agent.

<sup>63</sup> T. W. Bentley, I. S. Koo, and S. J. Norman, *J. Org. Chem.*, **56**, 1604 (1991); T. W. Bentley and B. S. Shim, *J. Chem. Soc., Perkin Trans. 2*, 1659 (1993).

<sup>64</sup> D. F. DeTar and R. Silverstein, *J. Am. Chem. Soc.*, **88**, 1013, 1020 (1966).

<sup>65</sup> W. S. Johnson, J. Ackerman, J. F. Eastham, and H. A. DeWalt, Jr., *J. Am. Chem. Soc.*, **78**, 6302 (1956).

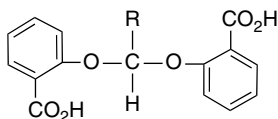


Other examples of synthetically useful acylating reagents are given in Section 3.4 of Part B.

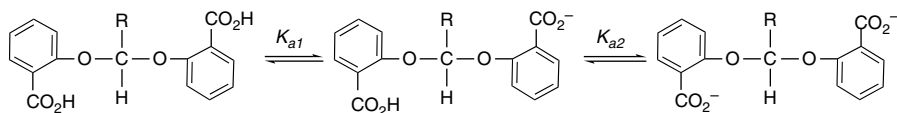
## 7.5. Intramolecular Catalysis of Carbonyl Substitution Reactions

The reactions of carbonyl compounds have provided an important testing ground for developing an understanding of *intramolecular catalysis*, which is a neighboring-group interaction that accelerates a reaction. Studies in intramolecular catalysis have been designed to determine how much more efficiently a given functional group can act as a catalyst when it is part of the reacting molecule and located in a position that enables an encounter between the catalytic group and the reaction center. These studies are relevant to understanding biological mechanisms, because enzymes achieve exceedingly efficient catalysis by bringing together at the “active site” combinations of basic, acidic, and nucleophilic groups in a geometry that is particularly favorable for reaction. The present section illustrates some of the facts that have emerged from these studies and the mechanistic conclusions that have been drawn.

It was pointed out in the mechanistic discussion concerning acetal hydrolysis (see p. 641) Usually, specific acid catalysis operates. The question of whether general acid catalysis can be observed in intramolecular reactions has been of interest because intramolecular general acid catalysis is thought to play a part in the mechanism of action of the enzyme lysozyme, which hydrolyzes the acetal linkage present in certain polysaccharides. One group of molecules that has been examined as a model system are acetals derived from *o*-hydroxybenzoic acid (salicylic acid).<sup>66</sup>



The pH-rate profile for hydrolysis of the benzaldehyde acetal (see Figure 7.10) indicates that of the species that are available, the *monoanion* of the acetal is the most reactive. The reaction is fastest in the pH range where the concentration of the monoanion is at a maximum. The neutral molecule decreases in concentration with increasing pH and the converse is true for the dianion.



<sup>66</sup> E. Anderson and T. H. Fife, *J. Am. Chem. Soc.*, **95**, 6437 (1973).

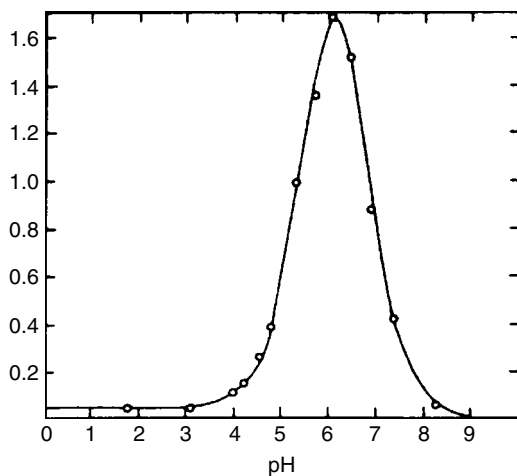
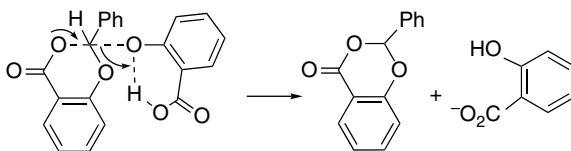
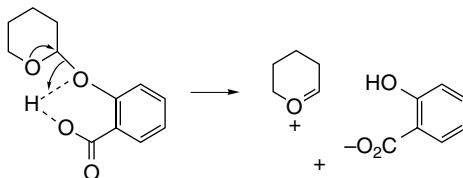


Fig. 7.10. pH-Rate profile for release of salicylic acid from benzaldehyde disalicyl acetal. Reproduced from *J. Am. Chem. Soc.*, **95**, 6437 (1973), by permission of the American Chemical Society.

The TS for the rapid hydrolysis of the monoanion is depicted as involving an intramolecular general acid catalysis by the carboxylic acid group, with participation by the anionic carboxylate group, which becomes bound at the developing electrophilic center. The un-ionized carboxylic acid group acts as a *general acid catalyst* and the carboxylate as a *nucleophilic catalyst*.



A mixed acetal of benzaldehyde, tetrahydropyranol, and salicylic acid has also been studied.<sup>67</sup> It, too, shows a marked rate enhancement attributable to intramolecular general acid catalysis. In this case the pH-rate profile (Figure 7.11) shows a plateau in the region Ph 2–5. As the carboxy group becomes protonated below pH 6, it provides an increment owing to intramolecular general acid catalysis.



The case of intramolecular carboxylate participation in ester hydrolysis has been extensively studied using acetylsalicylic acid (aspirin) and its derivatives. The kinetic data show that the anion is hydrolyzed more rapidly than the neutral species, indicating

<sup>67</sup> T. H. Fife and E. Anderson, *J. Am. Chem. Soc.*, **93**, 6610 (1971).

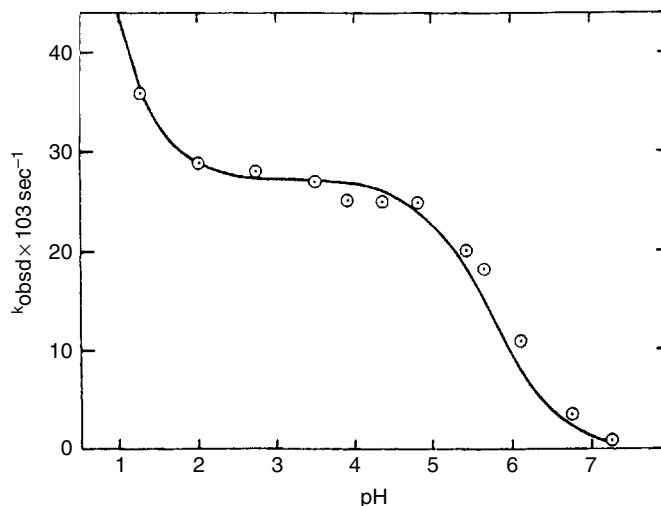
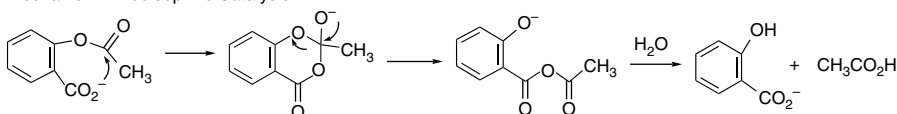


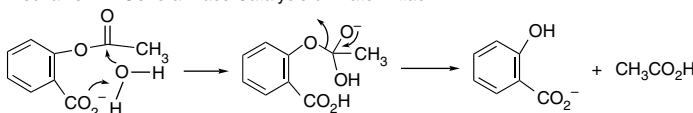
Fig. 7.11. pH-Rate profile for hydrolysis of 2-(*o*-carboxyphenoxy)tetrahydropyran in 50% dioxane-water at 15°C. Reproduced from *J. Am. Chem. Soc.*, **93**, 6610 (1971), by permission of the American Chemical Society.

that the carboxylate group becomes involved in the reaction in some way. Three mechanisms can be considered.

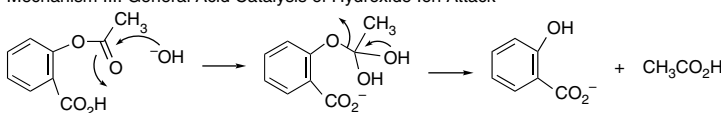
Mechanism I. Nucleophilic Catalysis



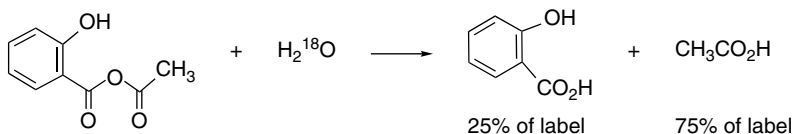
Mechanism II. General Base Catalysis of Water Attack



Mechanism III. General Acid Catalysis of Hydroxide Ion Attack



Mechanism I was ruled out by an isotopic-labeling experiment. The mixed anhydride of salicylic acid and acetic acid is an intermediate if nucleophilic catalysis occurs by Mechanism I. This molecule, which can be prepared independently, hydrolyzes in water with about 25% incorporation of solvent water into the salicylic acid.



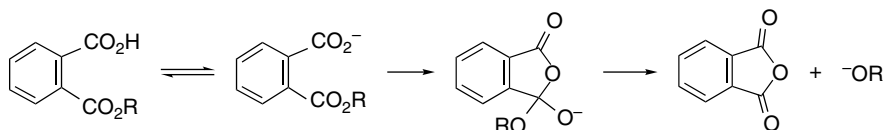
Hydrolysis of aspirin in  $\text{H}_2^{18}\text{O}$  does not lead to incorporation of  $^{18}\text{O}$  into the product salicylic acid, ruling out the anhydride as an intermediate and thereby excluding

Mechanism I.<sup>68</sup> Mechanism III cannot be distinguished from the first two on the basis of kinetics alone, because the reactive species shown is in rapid equilibrium with the anion and therefore equivalent to it in terms of reaction kinetics. The general acid catalysis of Mechanism III can be eliminated on the basis of failure of other nucleophiles to show evidence for general acid catalysis by the neighboring carboxylic acid group. Since there is no reason to believe hydroxide should be special in this way, Mechanism III is ruled out. Thus Mechanism II, general base catalysis of water attack, is believed to be the correct description of the hydrolysis of aspirin.

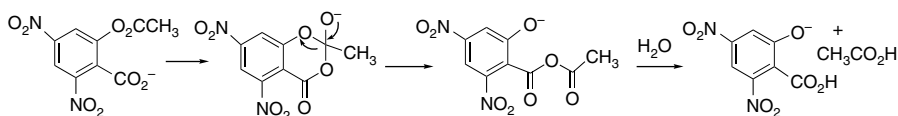
The extent to which intramolecular nucleophilic catalysis of the type depicted in Mechanism I is important is a function of the leaving ability of the alkoxy group. This has been demonstrated by the study of the hydrolysis of a series of monoesters of phthalic acid.



Nucleophilic participation is important only for esters of alcohols that have  $pK_a < 13$ . Specifically, phenyl and trifluoroethyl esters exhibit nucleophilic catalysis, but methyl and 2-chloroethyl esters do not.<sup>69</sup> This result reflects the fate of the tetrahedral intermediate that results from nucleophilic participation. For relatively acidic alcohols, the alkoxide group can be eliminated, leading to hydrolysis via nucleophilic catalysis.



For less acidic alcohols, nucleophilic participation is ineffective because of the low tendency of such alcohols to function as leaving groups. The tetrahedral intermediate formed by intramolecular addition simply returns to starting material because the carboxylate is a much better leaving group than the alkoxide. A similar observation is made for salicylate esters. In contrast to aspirin itself, acetyl salicylates with EWG groups (*o*- and *p*-nitro analogs) hydrolyze via the nucleophilic catalysis mechanism in which the phenolates act as leaving groups from the cyclic intermediate.<sup>70</sup> The difference, in comparison with aspirin, is the improved leaving group capacity of the phenolate.



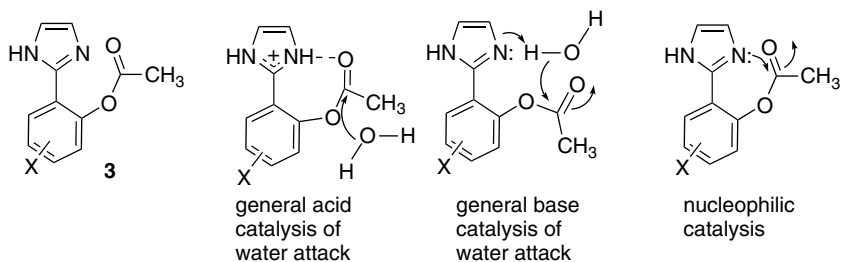
Intramolecular catalysis of ester hydrolysis by nitrogen nucleophiles is also important. The role of imidazole rings in intramolecular catalysis has received particularly close scrutiny. There are two reasons for this. One is that the imidazole ring of

<sup>68</sup> A. R. Fersht and A. J. Kirby, *J. Am. Chem. Soc.*, **89**, 4857 (1967).

<sup>69</sup> J. W. Thanassi and T. C. Bruice, *J. Am. Chem. Soc.*, **88**, 747 (1966).

<sup>70</sup> A. R. Fersht and A. J. Kirby, *J. Am. Chem. Soc.*, **89**, 5960 (1967); *J. Am. Chem. Soc.*, **90**, 5818 (1968).

the histidine residue in proteins is involved in enzyme-catalyzed hydrolyses. Secondly, the imidazole ring has several possible catalytic functions, which include acting as a general acid in the protonated form, acting as a general base, or acting as a nucleophile in the neutral form. A study of a number of derivatives of Structure **3** was undertaken to distinguish between these various possible mechanisms as a function of pH.<sup>71</sup>



The relative importance of the potential catalytic mechanisms depends on pH, which also determines the concentration of the other participating species such as water, hydronium ion, and hydroxide ion. The change in mechanism with pH gives rise to the pH-rate profile shown in Figure 7.12.

The rates at the extremities  $\text{pH} < 2$  and  $\text{pH} > 9$  are proportional to  $[\text{H}^+]$  and  $[\text{OH}^-]$ , respectively, and represent the specific proton-catalyzed and hydroxide-catalyzed mechanisms. In the absence of an intramolecular catalytic mechanisms, the  $\text{H}^+$ - and  $\text{OH}^-$ -catalyzed reactions would decrease in proportion to the concentration of the catalytic species and intersect at a minimum value representing the “uncatalyzed water hydrolysis.” An estimate of the effectiveness of the intramolecular mechanisms can be made by extrapolating the lines that are proportional to  $[\text{H}^+]$  and  $[\text{OH}^-]$ . The extent to which the actual rate lies above these extrapolated lines in the pH range 2–8 represents the contribution from the intramolecular catalysis. The region at pH 2–4 is the area where intramolecular general acid catalysis operates. Comparison with similar systems where intramolecular proton transfer is not available suggests a 25–100 fold rate enhancement. At pH 6–8 the intramolecular general base catalysis mechanism is

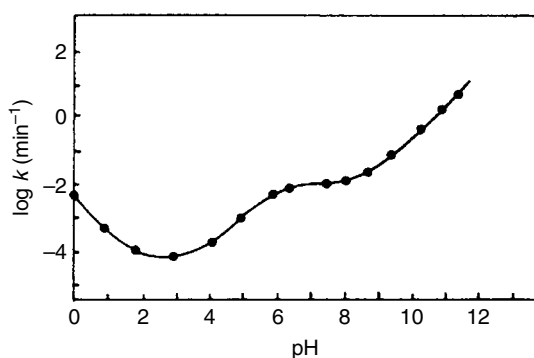
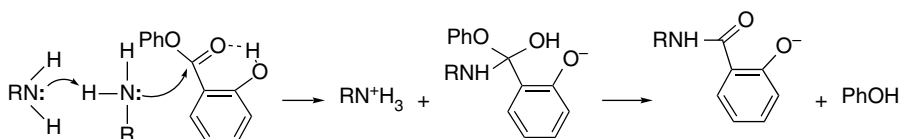


Fig. 7.12. pH-rate profile for hydrolysis of Compound **3**. Reproduced from *J. Am. Chem. Soc.*, **96**, 2463 (1974), by permission of the American Chemical Society.

<sup>71</sup> G. A. Rogers and T. C. Bruice, *J. Am. Chem. Soc.*, **96**, 2463 (1974).

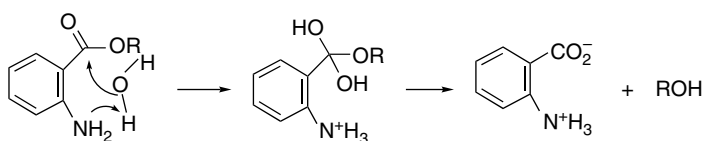
dominant. Analysis of the kinetic data indicates an acceleration of about  $10^4$ . Although the nucleophilic catalysis mechanism was not observed in the parent compound, it did occur in certain substituted derivatives.

Intramolecular participation of the *o*-hydroxy group in aminolysis of phenyl salicylate has been established by showing that such compounds are more reactive than analogs lacking the hydroxyl substituent. This reaction exhibits overall third-order kinetics, second order in the reacting amine. Similar kinetics are observed in the aminolysis of simple esters (see p. 659) Both intermolecular general base catalysis (by the second amine molecule) and intramolecular general acid catalysis (by the hydroxyl group) apparently occur.<sup>72</sup>

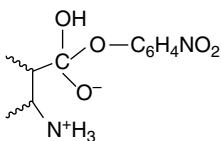


This mechanism can reduce the overall activation energy of the reaction in at least two ways. The partial transfer of a proton to the carbonyl oxygen increases its electrophilicity. Likewise, partial deprotonation of the amino group increases its nucleophilicity.

Intramolecular general base-catalyzed water attack has also been observed for phenyl 2-aminobenzoate.<sup>73</sup>



Similar results have been obtained with  $\beta$ -aminoalkyl 4-nitrophenolates, with observed rate enhancements of  $\sim 10^4$ .<sup>74</sup> Besides the general base-catalyzed mechanism, it has been suggested that the kinetically equivalent electrostatic stabilization of the tetrahedral intermediate by the protonated amino group might be involved.



Neither of these systems is likely to react by direct nucleophilic catalysis, because that would require formation of a four-membered ring. The pH-rate profiles for these reactions are shown in Figure 7.13. Note that the plateau region for the aromatic amines occurs at lower pH than for the alkylamines, reflecting the difference in the basicity of the two types of amino groups.

Certain molecules that can permit concerted proton transfers are efficient catalysts for reaction at carbonyl centers. An example is the catalytic effect that 2-pyridone

<sup>72</sup> F. M. Menger and J. H. Smith, *J. Am. Chem. Soc.*, **91**, 5346 (1969).

<sup>73</sup> T. H. Fife, R. Singh, and R. Bembi, *J. Org. Chem.*, **67**, 3179 (2002).

<sup>74</sup> M. I. Page, D. Pender, and G. Bernath, *J. Chem. Soc., Perkin Trans. 2*, 867 (1986).

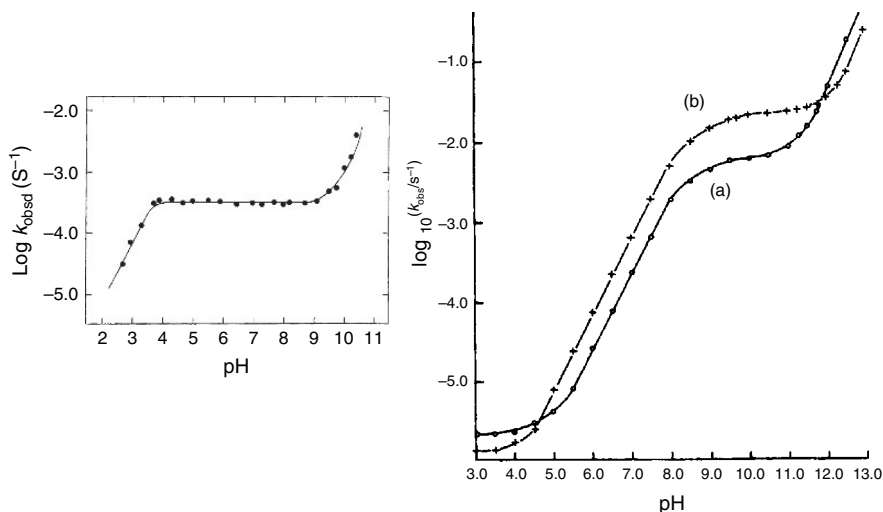
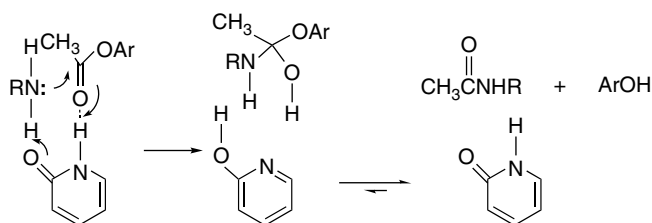
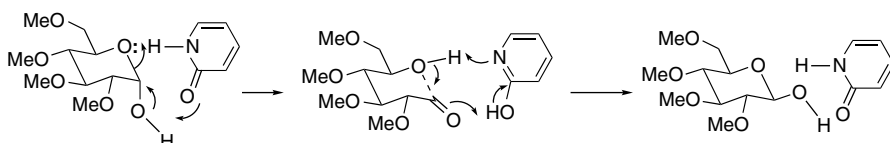


Fig. 7.13. pH-Rate profiles for phenyl *o*-aminobenzoates (left, 50°C) and  $\beta$ -aminoalkyl 4-nitrophenolates (right, 30°C). Reproduced from *J. Org. Chem.*, **67**, 3179 (2002) and *J. Chem. Soc., Perkin Trans.*, **2**, 867 (1986), respectively, by permission of the American Chemical Society and the Royal Society of Chemistry.

has on the aminolysis of esters (see also p. 661–662). Although neither a strong base ( $\text{p}K_{\text{aH}^+} = 0.75$ ) nor a strong acid ( $\text{p}K_{\text{a}} = 11.6$ ), 2-pyridone is an effective catalyst of the reaction of *n*-butylamine with 4-nitrophenyl acetate.<sup>75</sup> The overall rate is more than 500 times greater when 2-pyridone acts as the catalyst than when a second molecule of butylamine (acting as a general base) is present in the TS. 2-Pyridone has been called a *tautomeric catalyst* to emphasize its role in proton transfer. Such molecules are also called *bifunctional catalysts*, since two atoms in the molecule are involved in the proton transfer process.



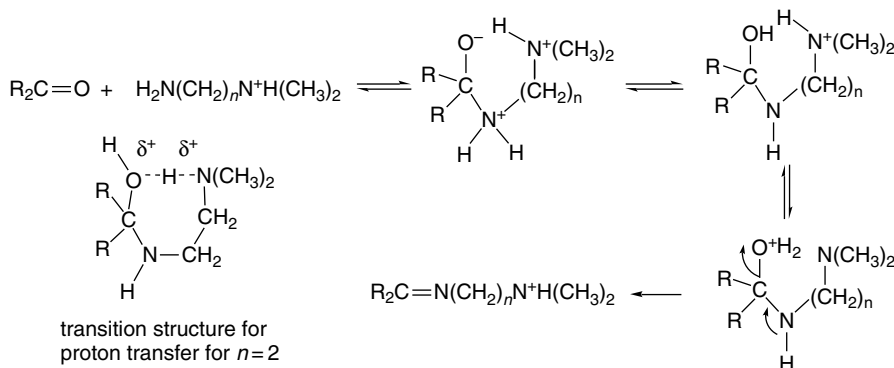
2-Pyridone also catalyzes epimerization of the anomeric position of the tetramethyl ether of glucose. The mechanism involves two double-proton transfers. The first leads to a ring-opened intermediate and the second results in ring closure to the isomerized product.



<sup>75</sup> P. R. Rony, *J. Am. Chem. Soc.*, **91**, 6090 (1969).

Other compounds such as benzoic acid and pyrazole, which can effect similar concerted proton transfer and avoid charged species, also catalyze this and related reactions.<sup>76</sup>

Another type of bifunctional catalysis has been noted with  $\alpha$ ,  $\omega$ -diamines in which one of the amino groups is primary and the other tertiary. These substituted diamines are from several times to as much as 1000 times more reactive toward imine formation than monofunctional amines.<sup>77</sup> This is attributed to a catalytic intramolecular proton transfer.



The rate enhancement is greatest for  $n = 2$  (1000) but still significant for  $n = 3$  (a factor of 10). As the chain is lengthened to  $n = 4$  and  $n = 5$ , the rate enhancement, if any, is minor. This relationship reflects the fact that when  $n = 4$  or  $5$ , the TS for the intramolecular proton transfer would have to involve rings of nine and ten atoms, respectively, which is not structurally advantageous. The particularly rapid reaction when  $n = 2$  corresponds to the possibility of a proton transfer via a seven-membered cyclic TS. If the assumption is that the proton is transferred in a colinear fashion through a hydrogen bond, this represents a favorable TS geometry.

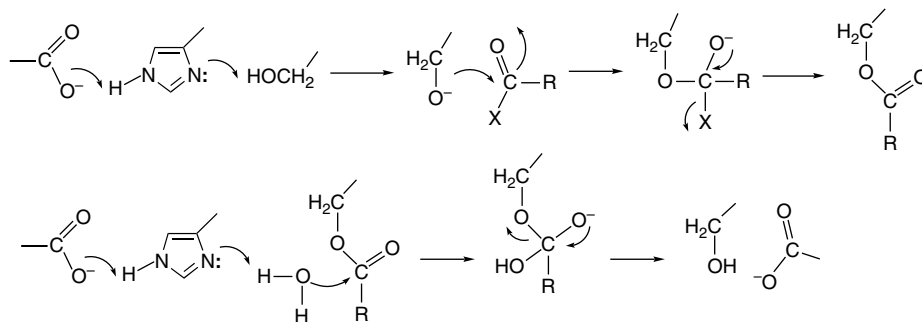
These examples serve to illustrate the concept of intramolecular catalysis and the idea that favorable juxtaposition of acidic, basic, or nucleophilic sites can markedly accelerate some of the common reactions of carbonyl compounds. Nature has used optimal placement of functional groups to achieve the catalytic activity of enzymes. The functional groups employed to accomplish this are those present on the amino acid residues found in proteins. The acidic sites available include phenolic (tyrosine) or carboxylic acid groups (glutamic acid and aspartic acid). Basic sites include the imidazole ring (histidine) and the  $\epsilon$ -amino group of lysine. This latter group and the guanidine group in arginine are normally protonated at physiological pH and can stabilize nearby anionic centers by electrostatic effects. Thiol (cysteine) and hydroxyl (threonine and serine) groups and the deprotonated carboxyl groups of glutamic and aspartic acids are potential nucleophilic sites.

A good example of an enzyme active site is the "catalytic triad" found in various hydrolytic enzymes. The active sites of these enzymes contain a hydroxyl group (from serine), a carboxylate group (from glutamic or aspartic acid), and an imidazole ring (from histidine). The three groups are aligned in such a way that the carboxylate group assists a proton transfer from the serine hydroxyl to the imidazole. This enhances the nucleophilicity of the serine toward the carbonyl group of the substrate undergoing

<sup>76</sup> P. R. Rony, *J. Am. Chem. Soc.*, **90**, 2824 (1968).

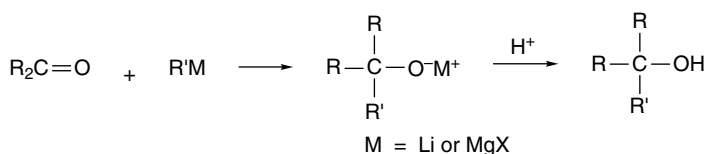
<sup>77</sup> J. Hine, R. C. Dempsey, R. A. Evangelista, E. T. Jarvi, and J. M. Wilson, *J. Org. Chem.*, **42**, 1593 (1977); J. Hine and Y. Chou, *J. Org. Chem.*, **46**, 649 (1981).

hydrolysis. The acyl group is transferred to the serine through a tetrahedral intermediate. Breakdown of the tetrahedral intermediate is accompanied by transfer of a proton back to the leaving group. Subsequently, a water molecule is activated by the same mechanism to cleave the acyl enzyme intermediate.<sup>78</sup>

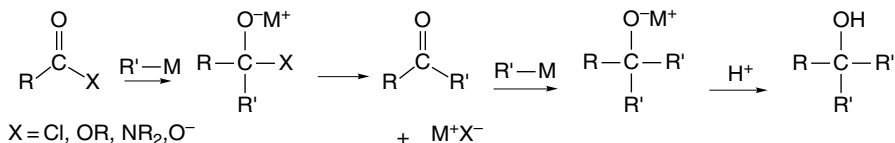


## 7.6. Addition of Organometallic Reagents to Carbonyl Groups

The addition of carbon nucleophiles, such as organometallic compounds, to carbonyl groups is one of the main methods of formation of carbon-carbon bonds. Such reactions are extremely important in synthesis and are discussed extensively in Chapter 7 of Part B. Here, we examine some of the fundamental mechanistic aspects of the addition of organometallic reagents to carbonyl groups. Organolithium and organomagnesium reagents are highly reactive toward most carbonyl compounds. With aldehydes and ketones, the tetrahedral adduct is stable and alcohols are isolated after protonation of the adduct.



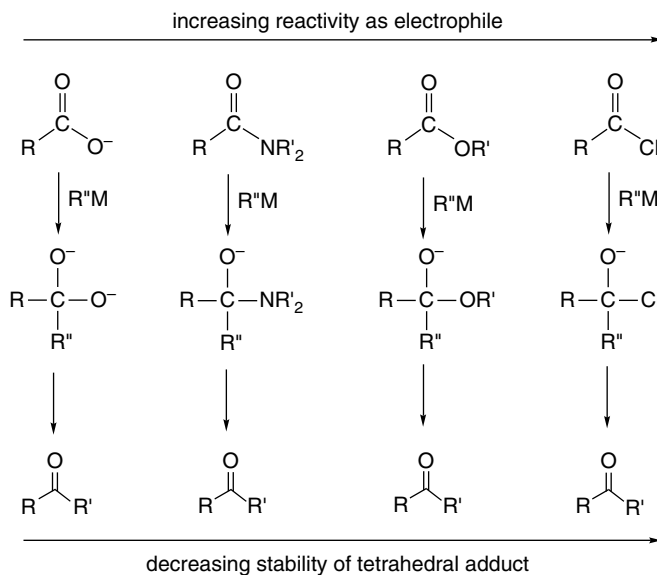
For acyl chlorides, anhydrides, esters, carboxamides, and carboxylate anions, the tetrahedral adduct can undergo elimination. The elimination forms a ketone, permitting a second addition step to occur.



The rate at which dissociation of the tetrahedral adduct occurs depends on the reactivity of the heteroatom substituent as a leaving group. The order of stability of the tetrahedral

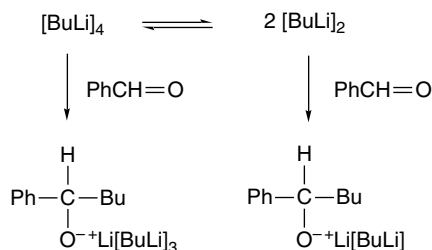
<sup>78</sup> D. M. Blow, *Acc. Chem. Res.*, **9**, 145 (1976); R. M. Garavito, M. G. Rossman, P. Argos, and W. Eventoff, *Biochemistry*, **16**, 5065 (1977); M. L. Bender, R. J. Bergeron, and M. Komiyama, *The Bioorganic Chemistry of Enzymatic Catalysis*, Wiley, New York, 1984, pp. 121–123; C.-H. Hu, T. Brinck, and K. Hult, *Int. J. Quantum Chem.*, **69**, 89 (1998).

adducts is shown in the diagram below. In some cases, the product can be controlled by the choice of reaction conditions. Ketones are isolated under conditions where the tetrahedral intermediate is stable until hydrolyzed, whereas tertiary alcohols are formed when the tetrahedral intermediate decomposes while unreacted organometallic reagent remains. Ketones can also be obtained with certain organometallic reagents that react only with acyl halides.



### 7.6.1. Kinetics of Organometallic Addition Reactions

The reactions of organolithium reagents with simple carbonyl compounds are very fast and there is relatively little direct kinetic evidence concerning the details of the reaction. It is expected that one important factor in determining reactivity is the degree of aggregation of the organolithium reagent (see p. 588). It is possible to follow the reaction of benzaldehyde with *n*-butyllithium at  $-85^\circ\text{C}$ , using NMR techniques that are capable of monitoring fast reactions. The reaction occurs over a period of 50–300 ms. It has been concluded that the dimer of *n*-butyllithium is more reactive than the tetramer by a factor of about 10. As the reaction proceeds, the product alkoxide ion is incorporated into butyllithium aggregates, which gives rise to additional species with different reactivities.<sup>79</sup>



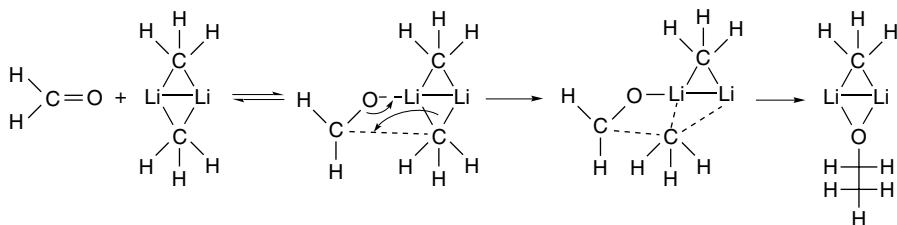
<sup>79</sup> J. F. McGarrity, C. A. Ogle, Z. Brich, and H.-R. Loosli, *J. Am. Chem. Soc.*, **107**, 1810 (1985).

The rates for the reaction of several aromatic ketones with alkyllithium reagents have been examined. The reaction of 2,4-dimethyl-4'-(methylthio)benzophenone with methyl lithium in ether exhibits the rate expression

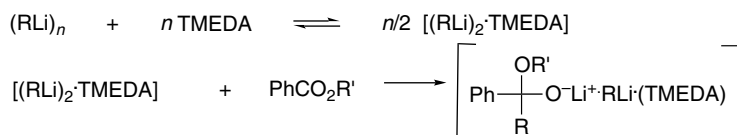
$$\text{Rate} = k[\text{MeLi}]^{1/4} [\text{ketone}]$$

This is consistent with a mechanism in which monomeric methyl lithium, in equilibrium with the tetramer, is the reactive nucleophile.<sup>80</sup> Most other studies have indicated considerably more complex behavior. The rate data for reaction of 3-methyl-1-phenyl-1-butanone with *s*-butyllithium and *n*-butyllithium in cyclohexane can be fit to a mechanism involving product formation both through a complex of the ketone with alkyllithium aggregate and by reaction with dissociated alkyllithium.<sup>81</sup> Initial formation of a complex is indicated by a shift in the carbonyl absorption band in the infrared spectrum. Complex formation presumably involves a Lewis acid-base interaction between the lithium ions and carbonyl oxygen in the alkyllithium cluster. In general terms, it appears likely that alkyllithium reagents have the possibility of reacting through any of several aggregated forms.

MO modeling (HF/3-21G) of the reaction of organolithium compounds with carbonyl groups has examined the interaction of formaldehyde with the dimer of methyl lithium. The reaction is predicted to proceed by initial complexation of the carbonyl group at lithium, followed by a rate-determining formation of the new carbon-carbon bond. The cluster then reorganizes to incorporate the newly formed alkoxide ion.<sup>82</sup> The TS is reached very early in the second step with only slight formation of the C—C bond. This feature is consistent with the fast and exothermic nature of the addition step.



The kinetics of addition of alkyllithium reagents to esters has been studied using a series of ethyl benzoates.<sup>83</sup> The rates show a rather complex dependence on both alkyllithium concentration and the nature of aryl substituents. The rapid formation of an initial ester-alkyllithium complex can be demonstrated. It is believed that product can be formed by reaction with aggregated or monomeric alkyllithium reagent. *N,N,N,N*-Tetramethylethylenediamine greatly accelerates the reaction, presumably by dissociating the organometallic aggregate (see Section 6.1).



<sup>80</sup> S. G. Smith, L. F. Charbonneau, D. P. Novak, and T. L. Brown, *J. Am. Chem. Soc.*, **94**, 7059 (1972).

<sup>81</sup> M. A. Al-Aseer and S. G. Smith, *J. Org. Chem.*, **49**, 2608 (1984).

<sup>82</sup> E. Kaufmann, P. v. R. Schleyer, K. N. Houk, and Y.-D. Wu, *J. Am. Chem. Soc.*, **107**, 5560 (1985).

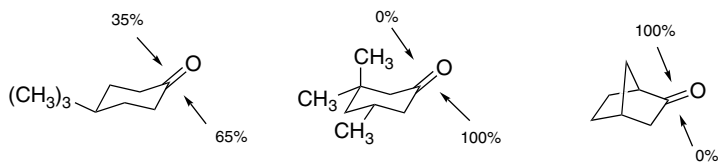
<sup>83</sup> M. A. Al-Aseer, B. D. Allison, and S. G. Smith, *J. Org. Chem.*, **50**, 2715 (1985).



## CHAPTER 7

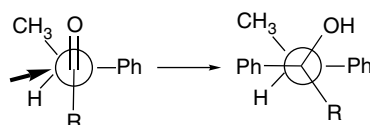
Addition, Condensation  
and Substitution  
Reactions of Carbonyl  
Compounds

The stereochemistry of organometallic additions with carbonyl compounds fits into the general pattern for nucleophilic attack discussed in Chapter 2. With 4-*t*-butylcyclohexanone there is a preference for equatorial approach, but the selectivity is low. Enhanced steric factors promote stereoselective addition.



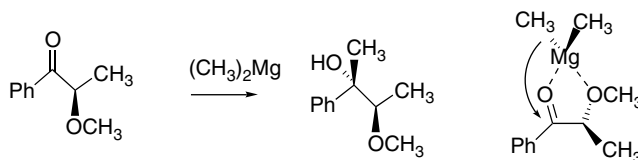
Ref. 88

The stereochemistry of organometallic additions in acyclic carbonyl compounds has also been examined. Additions of Grignard reagents to ketones and aldehydes was one of the reactions that led to the formulation of Cram's rule (see p. 179).<sup>89</sup> Many ketones and aldehydes have subsequently been subjected to studies to determine the degree of stereoselectivity. Cram's rule is obeyed when no special complexing functional groups are present near the reaction site. One series of studies is summarized in Table 7.5. These data show consistent agreement with Cram's rule and the Felkin TS, as discussed in Section 2.4.1.2.



Felkin Transition Structure Model

The role of chelation has been investigated both experimentally and computationally. In experimental studies, it was found that an  $\alpha$ -methoxy group increases the rate of addition of dimethylmagnesium to propiophenone approximately 2000-fold.<sup>90</sup> The rate acceleration indicates that chelation not only controls stereochemistry but also facilitates the addition step. The methyl group adds from the less hindered face of the chelate. The reaction gives a greater than 99:1 preference for chelation-controlled addition.



<sup>88</sup> E. C. Ashby and S. A. Noding, *J. Org. Chem.*, **44**, 4371 (1979).

<sup>89</sup> D. J. Cram and F. A. Abd Elhafez, *J. Am. Chem. Soc.*, **74**, 5828 (1952); D. J. Cram and J. D. Knight, *J. Am. Chem. Soc.*, **74**, 5835 (1952); F. A. Abd Elhafez and D. J. Cram, *J. Am. Chem. Soc.*, **74**, 5846 (1952).

<sup>90</sup> S. V. Frye, E. L. Eliel, and R. Cloux, *J. Am. Chem. Soc.*, **109**, 1862 (1987); X. Chen, E. R. Hortelano, E. L. Eliel, and S. V. Frye, *J. Am. Chem. Soc.*, **112**, 6130 (1990).

**Table 7.5. Stereoselectivity in Addition of Organometallic Reagents to Some Chiral Aldehydes and Ketones<sup>a</sup>**

R	L	M	S	R'M	Percent of major product
H	Ph	CH <sub>3</sub>	H	CH <sub>3</sub> MgBr	71
H	Ph	CH <sub>3</sub>	H	PhMgBr	78
H	<i>t</i> -C <sub>4</sub> H <sub>9</sub>	CH <sub>3</sub>	H	PhMgBr	98
CH <sub>3</sub>	Ph	CH <sub>3</sub>	H	C <sub>2</sub> H <sub>5</sub> Li	93
CH <sub>3</sub>	Ph	CH <sub>3</sub>	H	C <sub>2</sub> H <sub>5</sub> MgBr	88
CH <sub>3</sub>	Ph	CH <sub>3</sub>	H	<i>t</i> -C <sub>4</sub> H <sub>9</sub> MgBr	96
C <sub>2</sub> H <sub>5</sub>	Ph	CH <sub>3</sub>	H	CH <sub>3</sub> MgBr	86
C <sub>2</sub> H <sub>5</sub>	Ph	CH <sub>3</sub>	H	CH <sub>3</sub> Li	94
C <sub>2</sub> H <sub>5</sub>	Ph	CH <sub>3</sub>	H	PhLi	85
<i>i</i> -C <sub>3</sub> H <sub>7</sub>	Ph	CH <sub>3</sub>	H	CH <sub>3</sub> MgBr	90
<i>i</i> -C <sub>3</sub> H <sub>7</sub>	Ph	CH <sub>3</sub>	H	CH <sub>3</sub> Li	96
<i>i</i> -C <sub>3</sub> H <sub>7</sub>	Ph	CH <sub>3</sub>	H	PhLi	96
<i>t</i> -C <sub>4</sub> H <sub>9</sub>	Ph	CH <sub>3</sub>	H	CH <sub>3</sub> MgBr	96
<i>t</i> -C <sub>4</sub> H <sub>9</sub>	Ph	CH <sub>3</sub>	H	CH <sub>3</sub> Li	97
<i>t</i> -C <sub>4</sub> H <sub>9</sub>	Ph	CH <sub>3</sub>	H	PhLi	98
Ph	Ph	CH <sub>3</sub>	H	CH <sub>3</sub> MgBr	87
Ph	Ph	CH <sub>3</sub>	H	CH <sub>3</sub> Li	97
Ph	Ph	CH <sub>3</sub>	H	<i>t</i> -C <sub>4</sub> H <sub>9</sub> MgBr	96

a. Data from O. Arjona, R. Perez-Ossorio, A. Perez-Rubalcaba, and M. L. Quiroga, *J. Chem. Soc., Perkin Trans. 2*, 587 (1981); C. Alvarez-Ibarra, P. Perz-Ossorio, A. Perez-Rubalcaba, M. L. Quiroga, and M. J. Santestanes, *J. Chem. Soc. Perkin Trans. 2*, 1645 (1983).

An  $\alpha$ -benzyloxy group was found to cause rate acceleration of more than 100, relative to a nonchelating  $\alpha$ -trimethylsiloxy group. On the other hand, a 4-benzyloxy group in 2-butanone ( $\beta$ -substitution) caused only a 20% rate increase.

Computational studies were carried out on the addition reaction of dimethylmagnesium to several  $\alpha$ - and  $\beta$ -substituted carbonyl compounds, including methoxyacetaldehyde, methoxyacetone, and 3-methoxypropanal. MP2/6-31+G\* energies were computed for structures minimized with HF/3-31G calculations.<sup>91</sup> Some of the salient features of this study are summarized in Figure 7.14, which compares relative energy of reactants, prereaction complexes, TS, and products. In Panel A, the energies of acetone (A), methoxyacetone (B), and methoxyacetaldehyde (C) are shown. Both of the chelated TSs have lower  $\Delta H$  than for acetone, in agreement with the experimental finding of rate acceleration by an  $\alpha$ -methoxy substituent. The structures of the TS for the chelated reactants also indicate an earlier TS than for acetone. Furthermore, IRC analysis indicates that chelation is maintained throughout the course of the reaction. Use of a continuum solvent model ( $\epsilon = 7.58$ ) resulted in only small changes in the computed  $\Delta H^\ddagger$ . These results are all consistent with chelation control of reagent approach for  $\alpha$ -methoxy substituents.

The results for the  $\beta$ -methoxy substituents in 3-methoxypropanal (D) and 4-methoxy-2-butanone (E) are less clear. There are two chelated TSs of comparable energy, and only the chairlike TS suggests strong diastereoselectivity. There is also a qualitative difference in regard to the experimental kinetic studies. The

<sup>91</sup> S. Mori, M. Nakamura, E. Nakamura, N. Koga, and K. Morokuma, *J. Am. Chem. Soc.*, **117**, 5055 (1995).

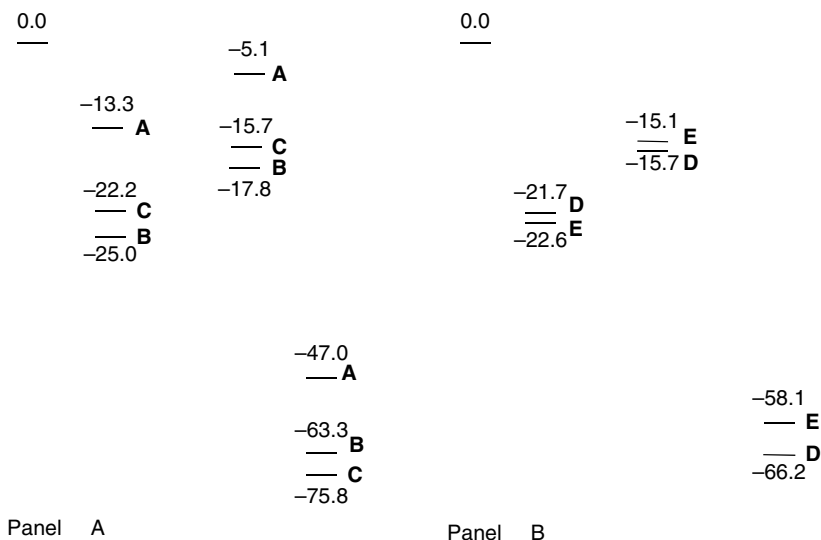
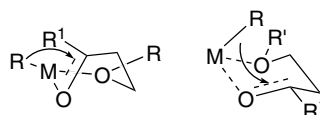


Fig. 7.14. Panel A: Relative  $\Delta H$  of reactant complex, transition structure, and products at  $0^\circ\text{C}$  (including ZPE correction) for acetone (**A**), methoxyacetone (**B**), and methoxyacetaldehyde (**C**). Panel B: Relative  $\Delta H$  at  $0^\circ\text{C}$  (including ZPE correction) for 3-methoxypropanal (**D**) and 4-methoxy-2-butanone (**E**). Data from *J. Am. Chem. Soc.*, **117**, 5055 (1995).

calculated activation barriers for  $\beta$ -methoxy groups are similar to those for  $\alpha$ -methoxy substituents, whereas the experimental kinetic studies indicate that  $\beta$ -substituents are much less activating.

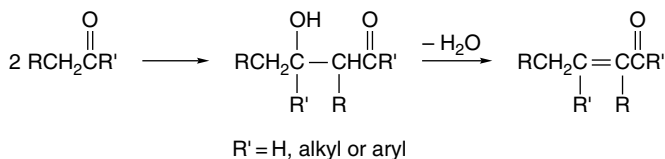


## 7.7. Addition of Enolates and Enols to Carbonyl Compounds: The Aldol Addition and Condensation Reactions

### 7.7.1. The General Mechanisms

The prototypical *aldol addition reaction* is the acid- or base-catalyzed dimerization of a ketone or aldehyde.<sup>92</sup> Under certain conditions, the reaction product may undergo dehydration leading to an  $\alpha,\beta$ -unsaturated aldehyde or ketone. This variant can be called the *aldol condensation*.

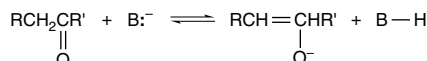
<sup>92</sup> A. T. Nielsen and W. J. Houlihan, *Org. React.*, **16**, 1 (1968); R. L. Reeves, in *Chemistry of the Carbonyl Group*, S. Patai, ed., Interscience, New York, 1966, pp. 580–593; H. O. House, *Modern Synthetic Reactions*, 2nd Edition, W. A. Benjamin, Menlo Park, CA, 1972, pp. 629–682; C. H. Heathcock, in *Asymmetric Synthesis*, Vol 2, J. D. Morrison, ed., 1984; C. H. Heathcock, in *Comprehensive Carbanion Chemistry*, E. Bunce and T. Durst, eds., Elsevier, Amsterdam, 1984, Chap. 6.



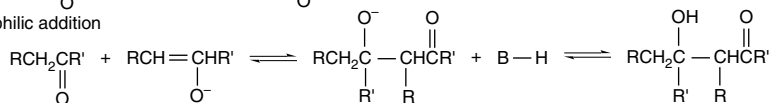
The mechanism of the base-catalyzed reaction involves equilibrium formation of the enolate ion, followed by addition of the enolate to the carbonyl group of the aldehyde or ketone. These reactions of aldehydes occur in dilute basic solution at or below room temperature. Under somewhat more vigorous conditions, such as higher temperature or increased base concentration, the elimination step occurs.

### 1. Addition phase

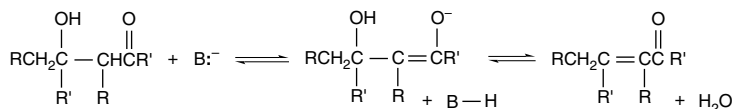
#### a. Enolate formation



#### b. Nucleophilic addition



### 2. Dehydration phase

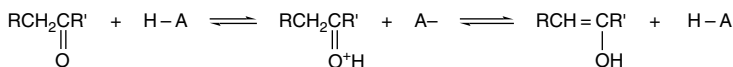


It is also possible to carry out the aldol condensation under acidic conditions. The mechanism was established in detail for acetaldehyde.<sup>93</sup> Under conditions of acid catalysis, it is the enol form of the aldehyde or ketone that functions as the nucleophile. The carbonyl group is activated toward nucleophilic attack by O-protonation.

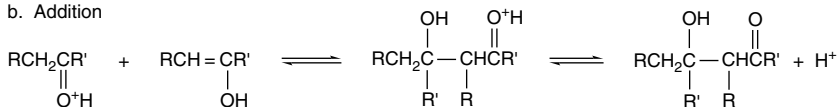
### *Acid-Catalyzed Mechanism*

#### 1. Addition phase

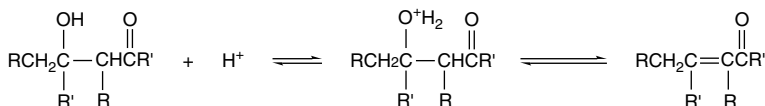
##### a. Enolization



##### b. Addition



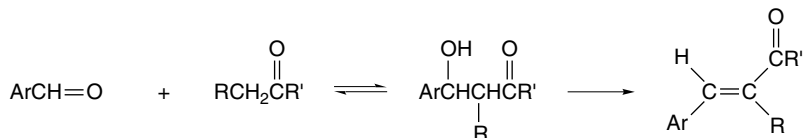
#### 2. Dehydration phase



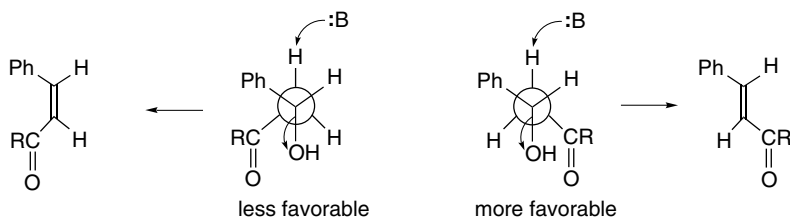
<sup>93</sup> L. M. Baigrie, R. A. Cox, H. Slebocka-Tilk, M. Tencer, and T. T. Tidwell, *J. Am. Chem. Soc.*, **107**, 3640 (1985).



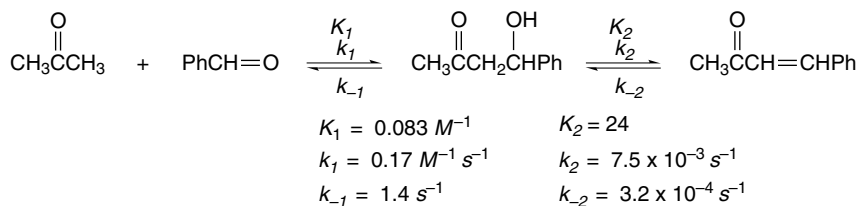
Aldol addition and condensation reactions involving two different carbonyl compounds are called *mixed aldol reactions*. To be useful as a method for synthesis there must be some basis for controlling which carbonyl component serves as the electrophile and which acts as the enolate precursor. One of the most general mixed aldol condensations involves the use of aromatic aldehydes with alkyl ketones or aldehydes. There are numerous examples of both acid- and base-catalyzed mixed aldol condensations involving aromatic aldehydes. The reaction is sometimes referred to as the *Claisen-Schmidt condensation*. Aromatic aldehydes are incapable of enolization and cannot function as the nucleophilic component. Furthermore, dehydration is especially favorable because the resulting enone is conjugated with the aromatic ring.



There is a pronounced preference for the formation of a *trans* double bond in the Claisen-Schmidt condensation of methyl ketones. This stereoselectivity arises in the dehydration step. In the TS for elimination to a *cis* double bond, an unfavorable steric interaction develops between the substituent (R) and the phenyl group. This interaction is absent in the TS for elimination to the *trans* double bond.



The dehydration reactions require somewhat higher activation energies than the addition step. Detailed studies have provided rate and equilibrium constants for the individual steps in a few cases. The results for the acetone-benzaldehyde system in the presence of hydroxide ion are given below. Note that  $K_2$  is sufficiently large to drive the first equilibrium forward.



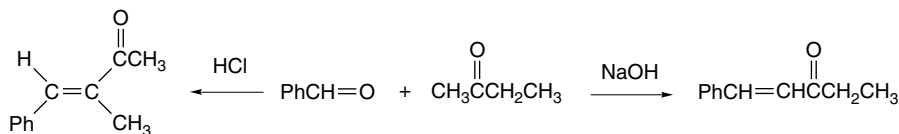
Ref. 94

Additional insight into the factors affecting product structure was obtained by study of the condensation of 2-butanone with benzaldehyde.<sup>95</sup> When catalyzed by base,

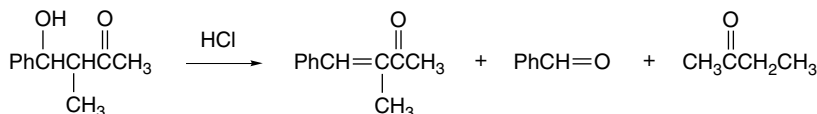
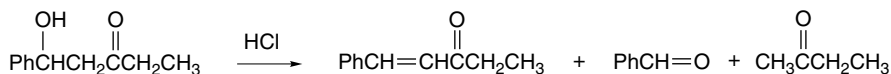
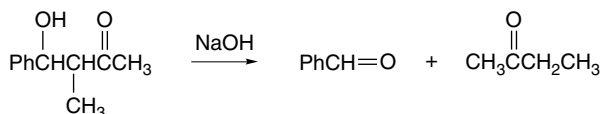
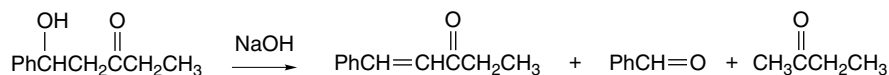
<sup>94</sup> J. P. Guthrie, J. Cossar, and K. F. Taylor, *Can. J. Chem.*, **62**, 1958 (1984).

<sup>95</sup> M. Stiles, D. Wolf, and G. V. Hudson, *J. Am. Chem. Soc.*, **81**, 628 (1959); D. S. Noyce and W. A. Pryor, **81**, 618 (1959); D. S. Noyce and L. R. Snyder, **81**, 620 (1959); D. S. Noyce and W. L. Reed, *J. Am. Chem. Soc.*, **81**, 624 (1959).

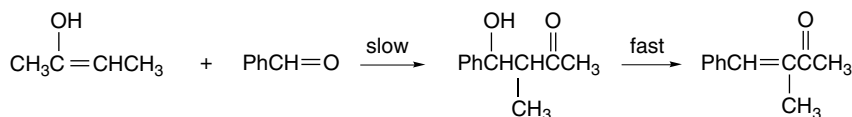
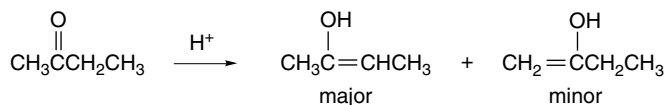
2-butanone reacts with benzaldehyde at the methyl group to give 1-phenylpent-1-en-3-one. Under acid-catalyzed conditions the product is the result of condensation at the methylene group, namely 3-methyl-4-phenylbut-3-en-2-one.



The results indicate that the product ratio is determined by the competition among the various reaction steps. Under the reaction conditions used, it is not possible to isolate the intermediate ketols because the addition step is rate limiting. These intermediates can be prepared by alternative methods and they behave as shown in the following equations.



These results establish that the base-catalyzed dehydration is slow relative to the reverse of the addition step for the branched-chain isomer. The reason for selective formation of the straight-chain product under conditions of base catalysis is then apparent. In base, the straight-chain ketol is the only intermediate that is dehydrated. The branched-chain ketol reverts to starting material. Under acid conditions, both intermediates are dehydrated. However, under acid-catalyzed conditions the branched-chain ketol is formed most rapidly because of the preference for acid-catalyzed enolization to give the more-substituted enol (see Section 6.3).



In general, the product ratio of a mixed aldol condensation depends upon the individual reaction rates in the equilibrium process. Most methyl ketones show a pattern similar

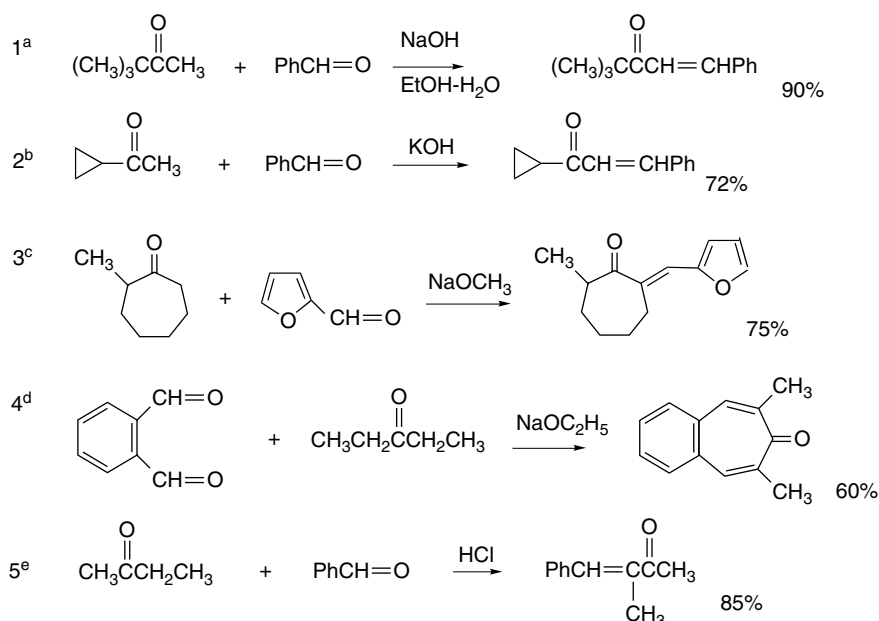
to 2-butanone in reactions with aromatic aldehydes. Base catalysis favors reaction at a methyl position over a methylene group, whereas acid catalysis gives the opposite preference.

Scheme 7.4 presents some representative examples of Claisen-Schmidt reactions. Entries 1 and 2 are typical base-catalyzed condensations at methyl groups. Entry 3 illustrates the use of a cyclic ketone, and reaction occurs at the methylene group, where dehydration is possible. The stereochemistry presumably places the furan ring *trans* to the carbonyl group for maximum conjugation. Entry 4 shows the use of phthalaldehyde to effect a cyclization. Entry 5 illustrates the preference for condensation at the more-substituted position under acidic conditions.

### 7.7.3. Control of Regiochemistry and Stereochemistry of Aldol Reactions of Ketones

The wide synthetic applicability of the aldol reaction depends on the ability to achieve both versatility in reactants and control of regiochemistry and stereochemistry. The term *directed aldol addition*<sup>96</sup> is applied to reaction conditions that are designed to achieve specific regio- and stereochemical outcomes. Control of product structure requires that one reactant act exclusively as the electrophile and the other exclusively

**Scheme 7.4. Mixed Aldol Condensation Reactions of Ketones and Aromatic Aldehydes**



a. G. A. Hill and G. Bramann, *Org. Synth.*, **I**, 81 (1941).

b. S. C. Bunce, H. J. Dorsman, and F. D. Popp, *J. Chem. Soc.*, 303 (1963).

c. A. M. Islam and M. T. Zenaity, *J. Am. Chem. Soc.*, **79**, 6023 (1957).

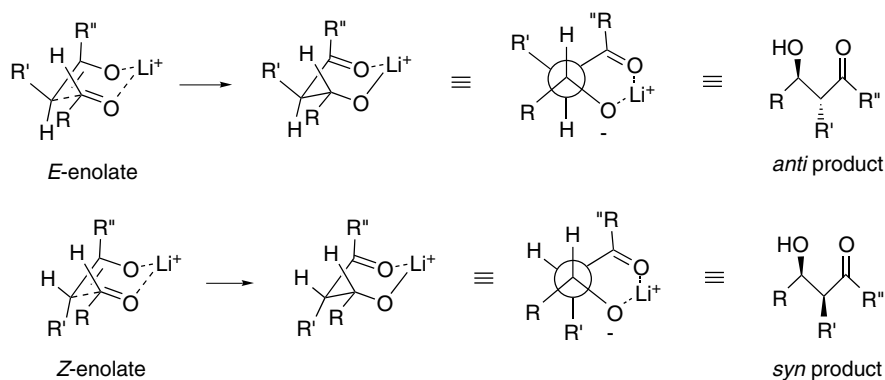
d. D. Meuche, H. Strauss, and E. Heilbronner, *Helv. Chim. Acta*, **41**, 2220 (1958).

e. M. E. Kronenberg and E. Havinga, *Recl. Trav. Chim. Pays-Bas*, **84**, 17 (1965).

<sup>96</sup> T. Mukaiyama, *Org. React.*, **28**, 203 (1982).

as the nucleophile. This can be achieved by preforming the reactive nucleophilic enolate and ensuring that the addition step is fast relative to proton exchange between the nucleophilic and electrophilic reactants. These reactions are under *kinetic control*, both at the stage of forming the enolate and at the addition step. The enolate that is to serve as the nucleophile is generated stoichiometrically, usually with lithium as the counterion in an aprotic solvent. Under these conditions enolates do not equilibrate with the other regio- or stereoisomeric enolates that can be formed from the ketone (see Section 6.3). The electrophilic carbonyl compound is then added. The structure of the reaction product is determined primarily by two factors: (1) the *E*- or *Z*-configuration of the initial enolate and (2) the structure of the TS for addition to the electrophilic carbonyl group.

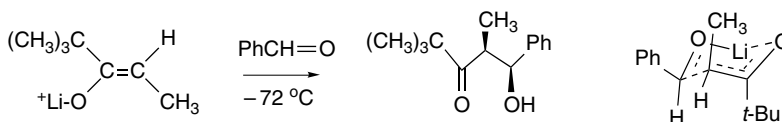
The fundamental mechanistic concept for stereochemical control of an aldol reaction under conditions of kinetic control is based on a cyclic TS in which both the carbonyl and enolate oxygen are coordinated to a Lewis acid.<sup>97</sup> This Lewis acid promotes reaction by enhancing the carbonyl group electrophilicity and by bringing the reactants together in the TS. It is further assumed that the structure of this TS is sufficiently similar to that of chair cyclohexane that the conformational concepts for cyclohexane derivatives can be applied. We use the  $\text{Li}^+$  cation in our initial discussion, but other metal cations and electrophilic atoms can play the same role. We discuss reactions of boron, titanium, and tin enolates shortly. In the structures below, the reacting aldehyde is shown with R rather than H in the equatorial-like position. The orientation of the aldehyde substituent establishes the degree of facial selectivity. A consequence of the cyclic TS is that the reaction is *stereospecific* with respect to the *E*- or *Z*-configuration of the enolate. The *E*-enolate will give the *anti*-aldol product whereas the *Z*-enolate will give the *syn*-aldol.



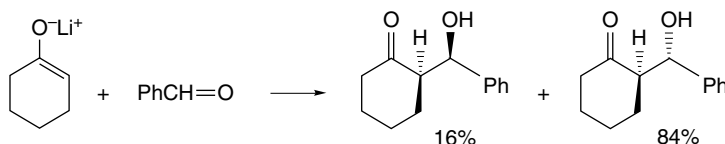
Owing to the dependence of the product stereochemistry on enolate configuration, control of the stereochemistry of enolate formation is important. For ketones with one relatively bulky group, the *Z*-enolate is favored, resulting in formation of the *syn*-aldol product. This is the case, for example, in the reaction of 2,2-dimethyl-3-pentanone and

<sup>97</sup> H. E. Zimmerman and M. D. Traxler, *J. Am. Chem. Soc.*, **79**, 1920 (1957); C. H. Heathcock, C. T. Buse, W. A. Kleschick, M. C. Pirrung, J. E. Sohn, and J. Lampe, *J. Org. Chem.*, **45**, 1066 (1980).

benzaldehyde.<sup>97</sup> The product stereochemistry is correctly predicted if the aldehyde is in a conformation with the phenyl substituent in an equatorial position in the cyclic TS.



The enolates derived from cyclic ketones are necessarily *E*-isomers. The enolate of cyclohexanone reacts with benzaldehyde to give both possible stereoisomeric products under kinetically controlled conditions. The stereoselectivity is about 6:1 in favor of the *anti* isomer under optimum conditions.<sup>98</sup>



While ketones with one tertiary alkyl substituent give mainly the *Z*-enolate, less highly substituted ketones usually give mixtures of *E*- and *Z*-enolates.<sup>99</sup> Therefore efforts aimed at expanding the scope of stereoselective aldol condensations have been directed at two facets of the problem: (1) control of enolate stereochemistry, and (2) enhancement of the degree of stereoselectivity in the addition step. The *E*:*Z* ratio can be modified by the precise conditions for formation of the enolate. For example, the *E*:*Z* ratio for 3-pentanone and 2-methyl-3-pentanone can be increased by use of a 1:1 lithium tetramethylpiperidide-LiBr mixture for kinetic enolization.<sup>100</sup> The precise mechanism of this effect is not clear, but it is probably due to an aggregate species containing bromide acting as the base.<sup>101</sup> Relatively weakly basic lithium anilides, specifically lithium 2,4,5-trichloroanilide and lithium diphenylamide, give high *Z*:*E* ratios.<sup>102</sup> On the other hand, lithium *N*-trimethylsilyl-*iso*-propylamide and lithium *N*-trimethylsilyl-*tert*-butylamide give selectivity for the *E*-enolate.<sup>103</sup>

*E* : *Z* Stereoselectivity

R	LDA	LiHMDS	LiTMP	LiTMP-LiBr	LiTMSN <i>t</i> Bu	LiNHAr
Ethyl	77:33	34:66	83:17	98:2	92:8	11:89
Isopropyl	63:37	2:98	66:34	95:5	94:6	2:98
<i>t</i> -Butyl	1:99	>2:98	<5:>95	<5:95	11:89	0:100

<sup>98</sup>. M. Majewski and D. M. Gleave, *Tetrahedron Lett.*, **30**, 5681 (1989).

<sup>99</sup>. R. E. Ireland, R. H. Mueller, and A. K. Willard, *J. Am. Chem. Soc.*, **98**, 2868 (1976); W. A. Kleschick, C. T. Buse, and C. H. Heathcock, *J. Am. Chem. Soc.*, **99**, 247 (1977); Z. A. Fataftah, I. E. Kopka, and M. W. Rathke, *J. Am. Chem. Soc.*, **102**, 3959 (1980).

<sup>100</sup>. P. L. Hall, J. H. Gilchrist, and D. B. Collum, *J. Am. Chem. Soc.*, **113**, 9571 (1991).

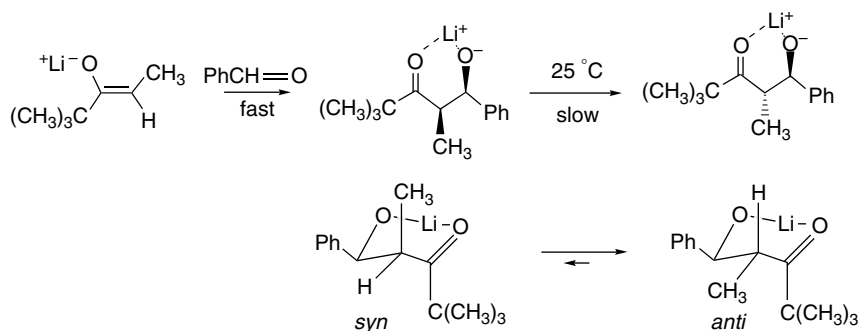
<sup>101</sup>. F. S. Mair, W. Clegg, and P. A. O'Neil, *J. Am. Chem. Soc.*, **115**, 3388 (1993).

<sup>102</sup>. L. Xie, K. Vanlandeghem, K. M. Isenberger, and C. Bernier, *J. Org. Chem.*, **68**, 641 (2003).

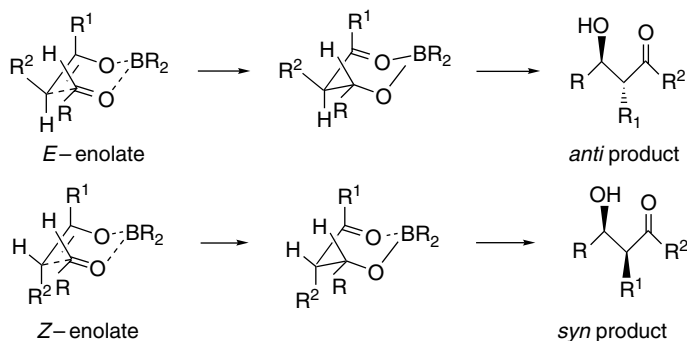
<sup>103</sup>. L. Xie, K. M. Isenberger, G. Held, and L. M. Dahl, *J. Org. Chem.*, **62**, 7516 (1997).

Under other reaction conditions, the product can result from *thermodynamic control*. Aldol reactions can be effected for many compounds using less than a stoichiometric amount of base. In these circumstances, the aldol reaction is reversible and the product ratio is determined by the relative stability of the various possible products. Thermodynamic conditions also permit equilibration among all the enolates of the nucleophile. The conditions that lead to equilibration include higher reaction temperatures, the presence of protic or dissociating polar solvents, and the use of less tightly coordinating cations.

When the aldol addition reaction is carried out under thermodynamic conditions, the difference in stability of the stereoisomeric *anti* and *syn* products determines the product composition. In the case of lithium enolates, the adducts can be equilibrated by keeping the reaction mixture at room temperature. This has been done, for example, for the product from the reaction of the enolate of ethyl *t*-butyl ketone and benzaldehyde. The greater stability of the *anti* isomer is attributed to the pseudoequatorial position of the methyl group in the chairlike product chelate. With larger substituent groups, the thermodynamic preference for the *anti* isomer is still greater.<sup>104</sup>



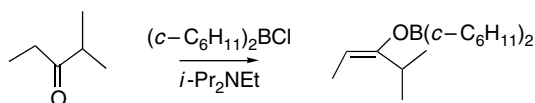
Another important version of the aldol reaction involves the use of boron enolates.<sup>105</sup> A cyclic TS similar to that for lithium enolates is involved and the same relationship exists between enolate geometry and product stereochemistry. In general, the stereoselectivity is higher than for lithium enolates. The O–B bond distances are shorter than those in lithium enolates, and this leads to a more compact TS and magnifies the steric interactions that control facial stereoselectivity. As with lithium enolates, the enolate stereochemistry controls diastereoselectivity.



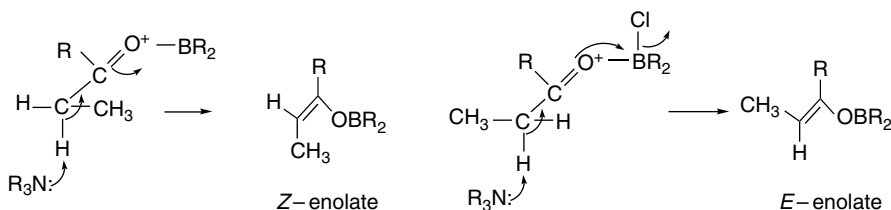
<sup>104</sup> C. H. Heathcock and J. Lampe, *J. Org. Chem.*, **48**, 4330 (1983).

<sup>105</sup> C. J. Cowden and I. A. Paterson, *Org. React.*, **51**, 1 (1997); E. Tagliavini, C. Trombini, and A. Umami-Ronchi, *Adv. Carbanion Chem.*, **2**, 111 (1996).

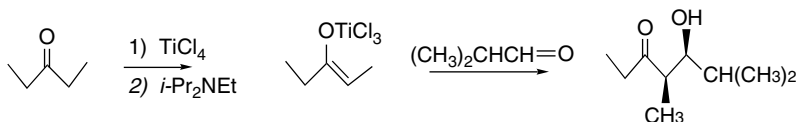
Boron enolates can be prepared by reaction of the ketone with a dialkylboron trifluoromethanesulfonate (triflate) and a tertiary amine.<sup>106</sup> Use of boron triflates with a hindered amine favors the *Z*-enolate. The resulting aldol products are predominantly the *syn* stereoisomers. The *E*-boron enolates of some ketones can be preferentially obtained by using dialkylboron chlorides.<sup>107</sup>



The contrasting stereoselectivity of the boron triflates and chlorides has been discussed in terms of reactant conformation and the stereoelectronic requirement for perpendicular alignment of the hydrogen with the carbonyl group  $\pi$  orbital.<sup>108</sup> The distinction between the two types of borylation reagents seems to lie in the extent of dissociation of the leaving group. The triflate is likely present as an ion pair, whereas with the less reactive chloride, the deprotonation may be a concerted ( $E2$ -like) process. The difference between trigonal and tetrahedral coordination of boron affects the steric interactions and reactant conformation. The two proposed TSs are shown below.



Titanium enolates can be prepared from lithium enolates by reaction with a trialkoxytitanium(IV) chloride, such as tri-(isopropoxy)titanium chloride.<sup>109</sup> Titanium enolates can also be prepared directly from ketones by reaction with  $\text{TiCl}_4$  and a tertiary amine.<sup>110</sup>



<sup>106</sup>. D. A. Evans, E. Vogel, and J. V. Nelson, *J. Am. Chem. Soc.*, **101**, 6120 (1979); D. A. Evans, J. V. Nelson, E. Vogel, and T. R. Taber, *J. Am. Chem. Soc.*, **103**, 3099 (1981).

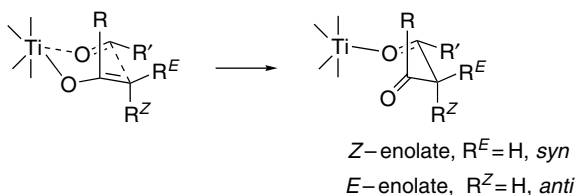
<sup>107</sup>. H. C. Brown, R. K. Dhar, R. K. Bakshi, P. K. Pandiarajan, and B. Singaram, *J. Am. Chem. Soc.*, **111**, 3441 (1989); H. C. Brown, R. K. Dhar, K. Ganesan, and B. Singaram, *J. Org. Chem.*, **57**, 499 (1992); H. C. Brown, R. K. Dhar, K. Ganesan, and B. Singaram, *J. Org. Chem.*, **57**, 2716 (1992); H. C. Brown, K. Ganesan, and R. K. Dhar, *J. Org. Chem.*, **58**, 147 (1993); K. Ganesan and H. C. Brown, *J. Org. Chem.*, **58**, 7162 (1993).

<sup>108</sup>. J. M. Goodman and I. Paterson, *Tetrahedron Lett.*, **33**, 7223 (1992); E. J. Corey and S. S. Kim, *J. Am. Chem. Soc.*, **112**, 4976 (1990).

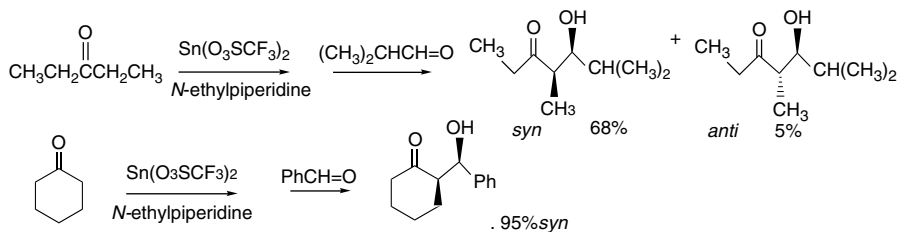
<sup>109</sup>. C. Siegel and E. R. Thornton, *J. Am. Chem. Soc.*, **111**, 5722 (1989).

<sup>110</sup>. D. A. Evans, D. L. Rieger, M. T. Bilodeau, and F. Urpi, *J. Am. Chem. Soc.*, **113**, 1047 (1991).

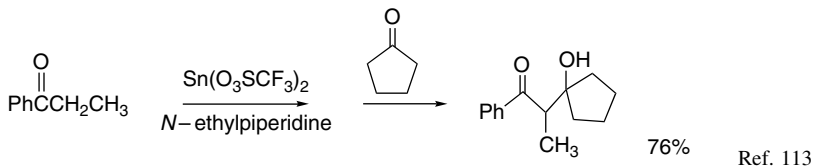
Under these conditions, the *Z*-enolate is formed and the aldol adducts have *syn* stereochemistry. The addition proceeds through a cyclic TS assembled around titanium.



Tin enolates can be generated from ketones and  $\text{Sn}(\text{O}_3\text{SCF}_3)_2$  in the presence of tertiary amines.<sup>111</sup> The subsequent aldol addition is *syn* selective.<sup>112</sup>



Tin(II) enolates prepared in this way also show good reactivity toward ketones as the carbonyl component.



#### 7.7.4. Aldol Reactions of Other Carbonyl Compounds

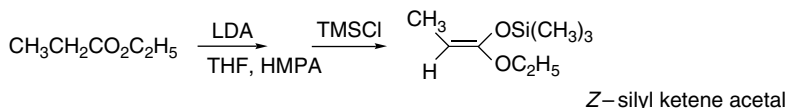
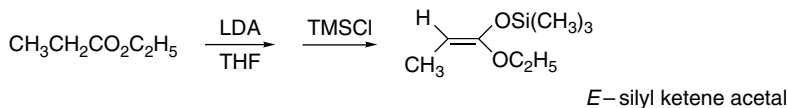
The enolates of other carbonyl compounds can be used in mixed aldol condensations. Extensive use has been made of the enolates of esters, thioesters, and amides. Of particular importance are several modified amides, such as those derived from oxazolidinones, that can be used as chiral auxiliaries. The methods for formation of these enolates are similar to those for ketones. Lithium, boron, tin, and titanium derivatives have all been used. Because of their usefulness in aldol additions and other synthetic methods (see especially Section 6.4.2.3, Part B), there has been a good deal of interest in the factors that control the stereoselectivity of enolate formation from esters. For simple esters such as ethyl propanoate, the *E*-enolate is preferred under kinetic conditions using a strong base such as LDA in THF solution. Inclusion of a

<sup>111</sup> T. Mukaiyama, N. Isawa, R. W. Stevens, and T. Haga, *Tetrahedron*, **40**, 1381 (1984); T. Mukaiyama and S. Kobayahi, *Org. React.*, **46**, 1 (1994); I. Shibata and A. Babu, *Org. Prep. Proc. Int.*, **26**, 85 (1994).

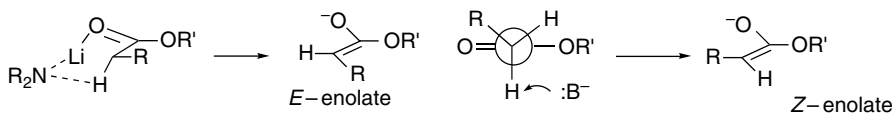
<sup>112</sup> T. Mukaiyama, R. W. Stevens, and N. Iwasawa, *Chem. Lett.*, 353 (1982).

<sup>113</sup> R. W. Stevens, N. Iwasawa, and T. Mukaiyama, *Chem. Lett.*, 1459 (1982).

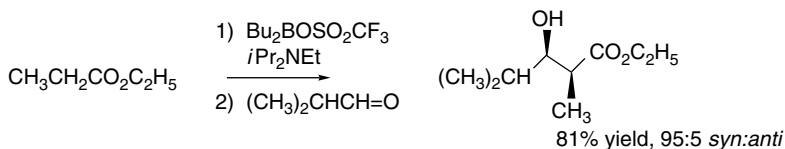
strong cation-solvating cosolvent, such as HMPA or DMPU favors the *Z*-enolate.<sup>114</sup> The enolates are often trapped as the corresponding silyl ethers, which are called *silyl ketene acetals*.



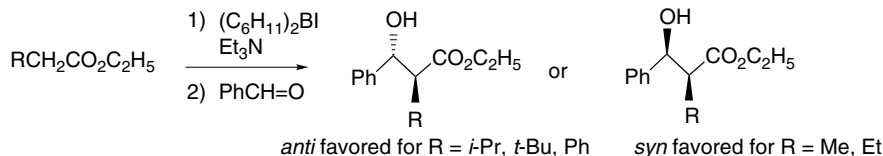
These observations are explained in terms of a cyclic TS for the LDA/THF conditions and a more open TS in the presence of an aprotic dipolar solvent.



Boron enolates can also be obtained from esters<sup>115</sup> and amides<sup>116</sup> and undergo aldol addition reactions. Various combinations of borylating reagents and amines have been used and the *E*:*Z* ratios are dependent on the reagents and conditions. In most cases esters give *Z*-enolates, which lead to *syn* adducts, but there are exceptions. For example, branched-chained esters give mainly *anti* adducts when the enolates are formed using dicyclohexylidoborane.



Ref. 117



Ref. 115

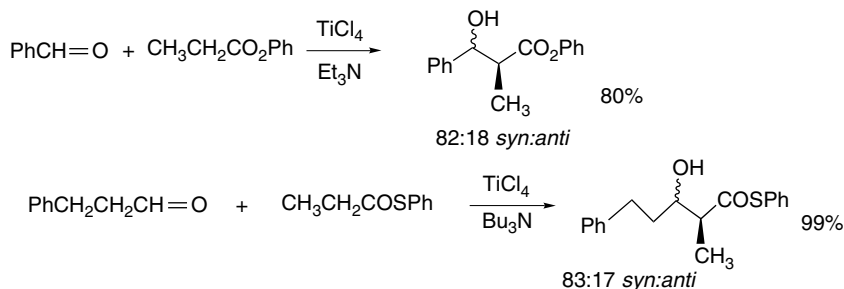
<sup>114</sup>. R. E. Ireland, P. Wipf, and J. D. Armstrong, III, *J. Org. Chem.*, **56**, 650 (1991).

<sup>115</sup>. K. Ganesan and H. C. Brown, *J. Org. Chem.*, **59**, 2336 (1994).

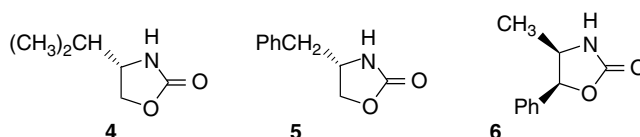
<sup>116</sup>. K. Ganesan and H. C. Brown, *J. Org. Chem.*, **59**, 7346 (1994).

<sup>117</sup>. A. Abiko, J.-F. Liu, and S. Masamune, *J. Org. Chem.*, **61**, 2590 (1996).

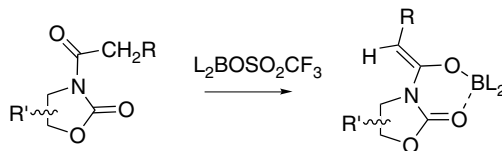
Phenyl and phenylthio esters have proven to be advantageous in  $\text{TiCl}_4$ -mediated additions, perhaps because they are slightly more acidic than the alkyl analogs. The reactions show *syn* diastereoselectivity.<sup>118</sup>



The methods that we have just discussed can be used to control the ratio of *syn* and *anti* diastereomeric products. It is often desired to also control the reaction to provide a *specific enantiomer*. Nearby stereocenters in either the carbonyl compound or the enolate can impose facial selectivity. Chiral auxiliaries can achieve the same effect. Finally, use of chiral Lewis acids as catalysts can also achieve enantioselectivity. Much effort has also been devoted to the use of chiral auxiliaries and chiral catalysts to effect enantioselective aldol reactions.<sup>119</sup> A very useful approach for enantioselective aldol additions is based on the oxazolidinones **4**, **5**, and **6**.



These compounds are readily available in enantiomerically pure form. They can be acylated and converted to the lithium or boron enolates by the same methods applicable to ketones and esters. When they are converted to boron enolates using di-*n*-butylboron triflate and triethylamine, the enolates are the *Z*-stereoisomers.<sup>120</sup> The carbonyl oxygen of the oxazolidinone ring is bonded to the boron.



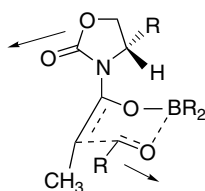
Reaction occurs through a cyclic TS in which the aldehyde displaces the oxazolidinone oxygen as a boron ligand. The oxazolidinone substituents direct the approach of the aldehyde. The conformation of the addition TS for boron enolates is believed to have

<sup>118</sup>. Y. Tanabe, N. Matsumoto, S. Funakoshi, and N. Mantra, *Synlett*, 1959 (2001).

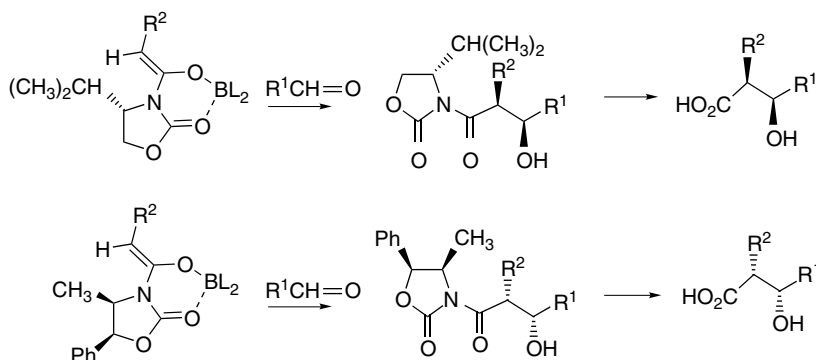
<sup>119</sup>. M. Braun and H. Sacha, *J. prakt. Chem.*, **335**, 653 (1993); S. G. Nelson, *Tetrahedron: Asymmetry*, **9**, 357 (1998); E. Carreira, in *Catalytic Asymmetric Synthesis*, 2nd Edition, I. Ojima, ed., Wiley-VCH, 2000, pp. 513–541.

<sup>120</sup>. D. A. Evans, J. Bartroli, and T. L. Shih, *J. Am. Chem. Soc.*, **103**, 2127 (1981).

the oxazolidinone ring oriented with opposed dipoles of the ring and the aldehyde carbonyl groups.

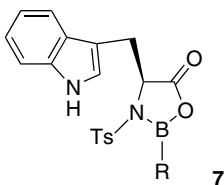


Because of the opposite steric encumbrance provided by **4** and **6**, the products, both of which are *syn*, result from opposite facial selectivity and have opposite absolute configuration. The acyl oxazolidinones are solvolyzed in water or alcohols to give the enantiomeric  $\beta$ -hydroxy acid or ester. Alternatively, they can be reduced to aldehydes or alcohols.



We discuss other chiral auxiliaries and other strategies for controlling facial selectivity in Section 2.1.3 of Part B.

There are also several catalysts that can effect enantioselective aldol addition. The reactions generally involve enolate equivalents, such as silyl enol ethers, that are unreactive toward the carbonyl component alone, but can react when activated by a Lewis acid. The tryptophan-based oxaborazolidinone **7** has proven to be a useful catalyst<sup>121</sup> that induces preferential *re* facial attack on simple aldehydes.



The enantioselectivity appears to involve the shielding of the *si* face by the indole ring, through a  $\pi$ -stacking interaction, as indicated in Fig. 7.15.<sup>122</sup>

<sup>121</sup>. E. J. Corey, C. L. Cywin, and T. D. Roper, *Tetrahedron Lett.*, **33**, 6907 (1992); E. J. Corey, T.-P. Loh, T. D. Roper, M. D. Azimioara, and M. C. Noe, *J. Am. Chem. Soc.*, **114**, 8290 (1992).

<sup>122</sup>. The model is from S. G. Nelson, *Tetrahedron: Asymmetry*, **9**, 357 (1998).

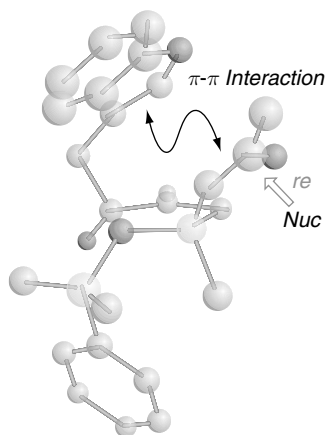
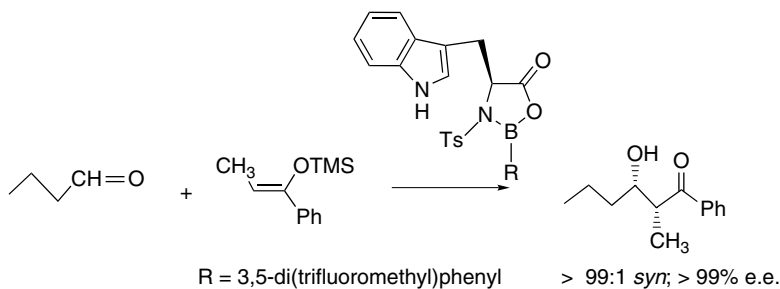
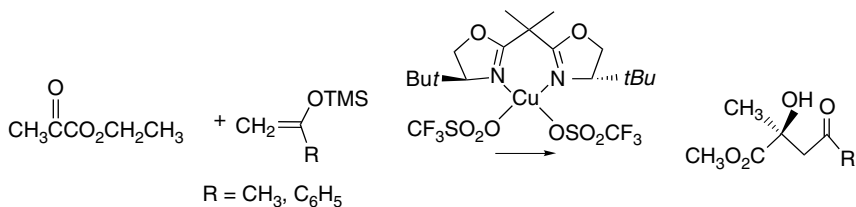


Fig. 7.15. Facial selectivity of 3-indolylmethylboronate ester catalyst. Reproduced from *Tetrahedron Asymmetry*, **9**, 357 (1998), by permission of Elsevier. (See also color insert.)

The *B*-3,5-di(trifluoromethyl)phenyl derivative was found to be a very effective catalyst.<sup>123</sup>

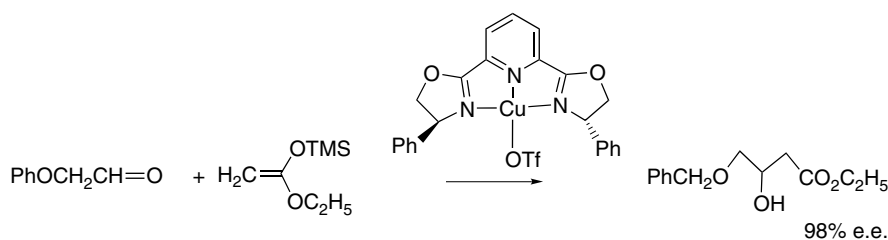


Another effective group of catalysts is made up of the copper *bis*-oxazolines.<sup>124</sup>



<sup>123</sup> K. Ishihara, S. Kondo, and H. Yamamoto, *J. Org. Chem.*, **65**, 9125 (2000).

<sup>124</sup> D. A. Evans, J. A. Murry, and M. C. Kozlowski, *J. Am. Chem. Soc.*, **118**, 5814 (1996).



These catalysts function as Lewis acids at the carbonyl oxygen. The chiral ligands promote facial selectivity.<sup>126</sup> Figure 7.16 shows a representation of the reactant complex.

In summary, several factors determine the stereochemical outcome of aldol addition reactions. The diastereochemical preference of the *syn* or *anti* isomer is determined by the configuration of the enolate and the orientation of the aldehyde within the TS. Chirality in either reactant introduces another stereochemical influence. The use of chiral auxiliaries can promote high facial selectivity in the approach of the aldehyde and thus permit the preparation of enantiomerically enriched products. The same outcome can be achieved using chiral Lewis acids as reaction catalysts.

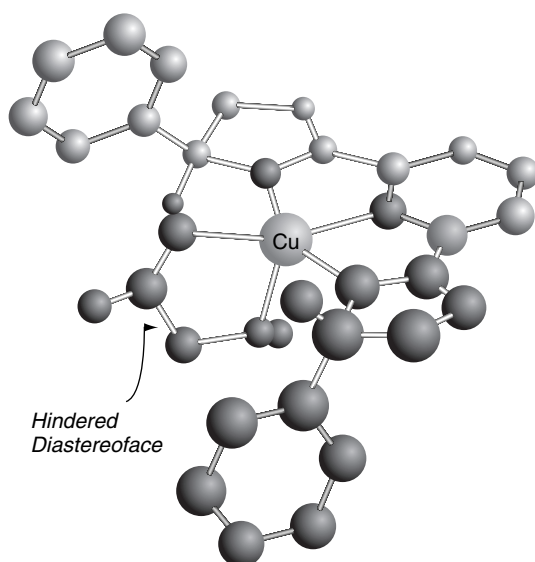


Fig. 7.16. Facial selectivity of diphenyl pyridine-*bis*-oxazoline catalysts. Reproduced from *Tetrahedron Asymmetry*, **9**, 357 (1998), by permission of Elsevier.

<sup>125</sup>. D. A. Evans, D. W. C. MacMillan, and K. R. Campos, *J. Am. Chem. Soc.*, **119**, 10859 (1997); D. A. Evans, M. C. Kozlowski, C. S. Burgey, and D. W. C. MacMillan, *J. Am. Chem. Soc.*, **119**, 7893 (1997).

<sup>126</sup>. The model is from S. G. Nelson, *Tetrahedron: Asymmetry*, **9**, 357 (1998).

## CHAPTER 7

Addition, Condensation  
and Substitution  
Reactions of Carbonyl  
Compounds

- M. L. Bender, *Mechanisms of Homogeneous Catalysis from Protons to Proteins*, Wiley-Interscience, New York, 1971.
- T. C. Bruice and S. J. Benkovic, *Bioorganic Mechanisms*, W. A. Benjamin, New York, 1966.
- H. Dugas and C. Penney, *Bioorganic Chemistry: A Chemical Approach to Enzyme Action*, 3rd Edition, Springer-Verlag, New York, 1996.
- W. P. Jencks, *Catalysis in Chemistry and Enzymology*, McGraw-Hill, New York, 1969.
- A. J. Kirby and A. R. Fersht, *Progress in Bioorganic Chemistry*, Vol. 1, E. T. Kaiser and R. J. Kezdy, eds., Wiley-Interscience, New York, 1971, pp. 1–82.
- S. Patai, ed., *The Chemistry of Acid Derivatives*, Suppl. B, Vol. 2, Wiley, New York, 1992.
- S. Patai, ed., *The Chemistry of the Carbonyl Group*, Wiley-Interscience, New York, 1969.
- S. Patai, ed., *The Chemistry of Carboxylic Acids and Esters*, Wiley-Interscience, New York, 1969.
- J. E. Zabricky, ed., *The Chemistry of Amides*, Wiley-Interscience, New York, 1970.

## Problems

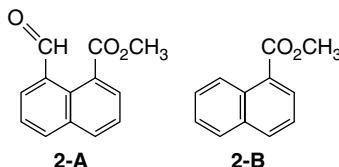
(References for these problems will be found on page 1162.)

- 7.1. The hydrates of aldehydes and ketones are considerably more acidic than alcohols (pK 16–19). Some values are shown below. How do you account for this enhanced acidity? Explain the relative order of acidity for the compounds in the list.

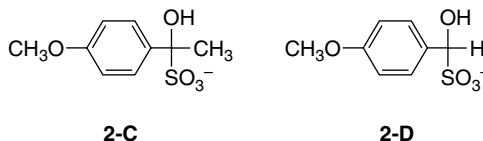
Hydrate	pK
$\text{CH}_2(\text{OH})_2$	13.3
$\text{CH}_3\text{CH}(\text{OH})_2$	13.6
$\text{Cl}_3\text{CCH}(\text{OH})_2$	10.0
$\text{PhC}(\text{CF}_3)(\text{OH})_2$	10.0
$3\text{-NO}_2\text{PhC}(\text{CF}_3)(\text{OH})_2$	9.2

- 7.2. Suggest explanations for each of the following observations:

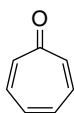
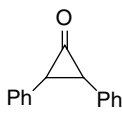
- The equilibrium constant for cyanohydrin formation for 3,3-dimethyl-2-butanone (pinacolone) is 40 times larger than for acetophenone.
- The ester **2-A** undergoes alkaline hydrolysis 8300 faster than the unsubstituted analog **2-B**.



- Under comparable conditions, the general base-catalyzed elimination of bisulfite ion from **2-C** is about 10 times faster than for **2-D**.



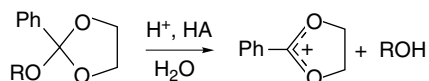
- d. The rates of isotopic exchange of the carbonyl oxygen in troponone (**2-E**) and 2,3-diphenyl-cyclopropanone (**2-F**) are much less than for acetophenone.

**2-E****2-F**

- 7.3. Arrange each series of compounds in order of decreasing rate of acid-catalyzed hydrolysis of the corresponding diethyl acetals. Explain your reasoning.
- acetaldehyde, chloroacetaldehyde, buten-2-al
  - acetaldehyde, formaldehyde, acetone
  - cyclopentanone, cyclohexanone, camphor
  - acetone, 3,3-dimethyl-2-butanone, 4,4-dimethyl-2-butanone
  - benzaldehyde, 4-methoxybenzaldehyde, butanal

- 7.4 The acid-catalyzed hydrolysis of 2-alkoxy-2-phenyl-1,3-dioxolane exhibits general acid catalysis of the initial rate-determining cleavage under some circumstances, as is indicated by the rate law:

$$k_{\text{obs}} = k_{\text{H}^+}[\text{H}^+] + k_{\text{H}_2\text{O}}[\text{H}_2\text{O}] + k_{\text{HA}}[\text{HA}]$$



The Brønsted relationship (see Section 3.7.1.2 to review the Brønsted catalysis law) shows a correlation with the identity of the alkoxy group. The alkoxy groups derived from more acidic alcohols have lower Brønsted coefficients  $\alpha$ .

Alcohol	p <i>K</i>	$\alpha$
Cl <sub>2</sub> CHCH <sub>2</sub> OH	12.9	0.69
ClCH <sub>2</sub> CH <sub>2</sub> OH	14.3	0.80
CH <sub>3</sub> OCH <sub>2</sub> CH <sub>2</sub> OH	14.8	0.85
CH <sub>3</sub> OH	15.7	0.90

What information about the reaction mechanism does this correlation provide? Interpret the results in terms of a More O'Ferrall-Jencks two-dimensional potential energy diagram.

- 7.5 Each of the following molecules is capable of some form of intramolecular catalysis of ester hydrolysis. For each reactant, indicate one or more possible mechanisms for intramolecular catalysis. Indicate the relationship that you would expect to exist between the catalytic mechanism and the pH. Determine if that relationship is consistent with the experimental pH-rate profile shown in Fig. 7.P5. Depict a mechanism showing the proposed catalysis.

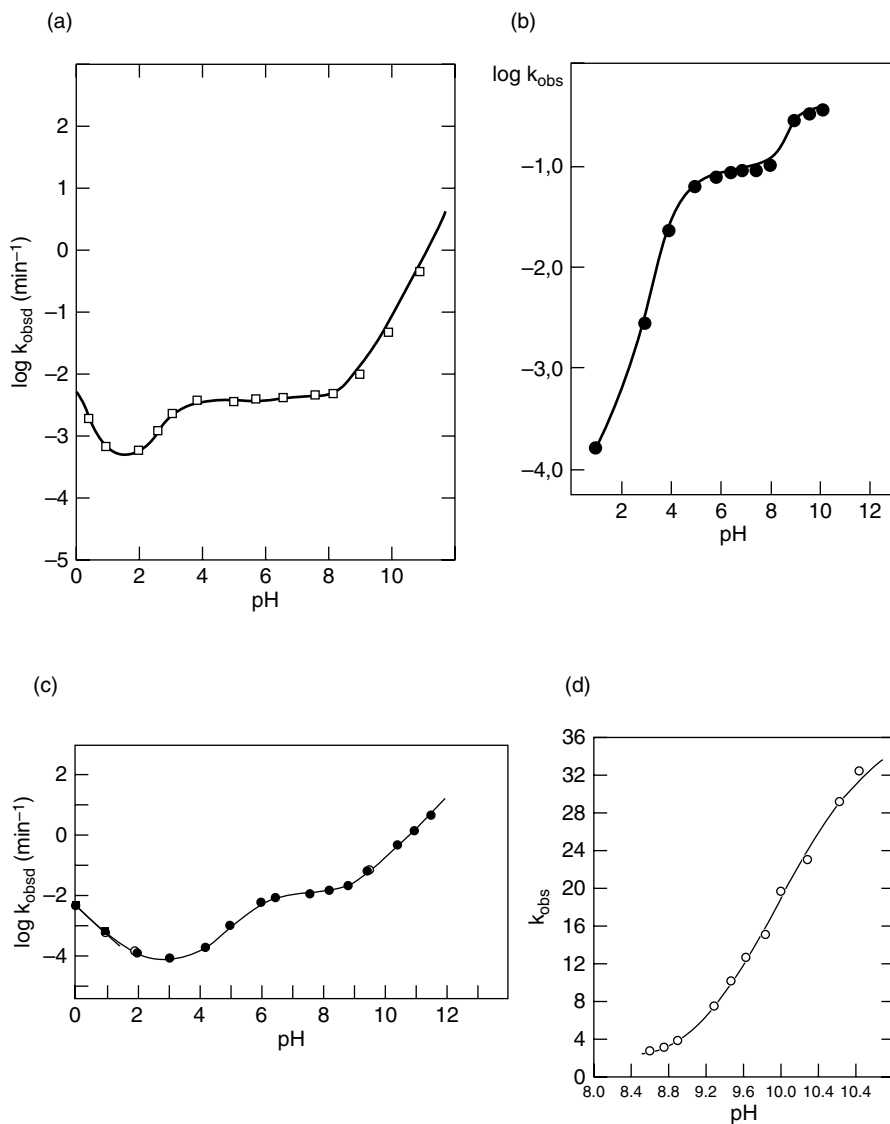
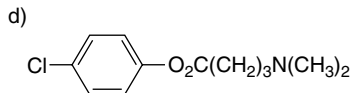
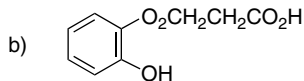
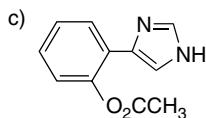
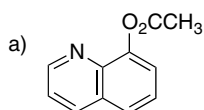
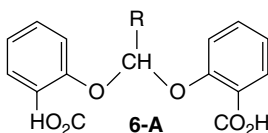


Fig. 7.P5. Reproduced from problem references 5 a–d by permission of the American Chemical Society.

7.6 Derive the general expression for the observed rate of hydrolysis of compound **6-A** as a function of pH. Assume that intramolecular general acid catalysis outweighs specific acid catalysis in the region between pH 3 and pH 9.

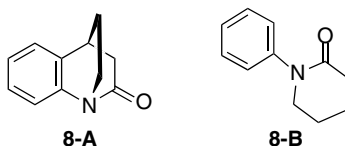
Does the form of the rate expression agree with the shape of the pH-rate profile in Figure 7.10?



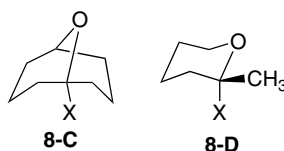
7.7. Enantiomerically pure dipeptide is obtained when the 4-nitrophenyl ester of *N*-benzoyl-L-leucine is coupled with ethyl glycinate in ethyl acetate. If, however, the leucine ester is treated with 1-methylpiperidine in chloroform for 30 min prior to coupling, the dipeptide is formed in nearly completely racemized. Treatment of the leucine ester with 1-methylpiperidine leads to formation of a crystalline material of composition  $C_{13}H_{15}NO_2$ , which has strong IR bands at  $1832$  and  $1664\text{ cm}^{-1}$ . Explain how racemization occurs and suggest a reasonable structure for the crystalline material.

7.8 Provide an explanation in terms of structure and mechanism for the following observations:

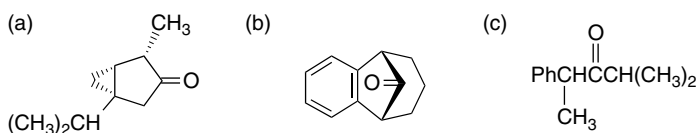
a. The bicyclic lactam **8-A** hydrolyzes  $10^7$  times faster than the related monocyclic compound **8-B**



b. Leaving groups X solvolyze from the bicyclic structure **8-C** at a rate that is  $10^{-13}$  less than for the monocyclic analog **8-D**.



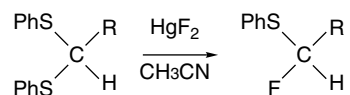
7.9. Analyze the factors that determine the stereoselectivity of the addition of organometallic compounds to the following ketones. Predict the stereochemistry of the major product.



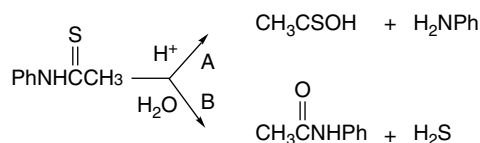
7.10. Indicate which of the compounds of each of the following pairs will have the more negative free-energy change for hydrolysis at pH 7. Explain your reasoning.



such questions as: (1) is the reaction an  $S_N1$  or  $S_N2$  process? Would NaF cause the same reaction? Why is only one of the phenylthio groups replaced?



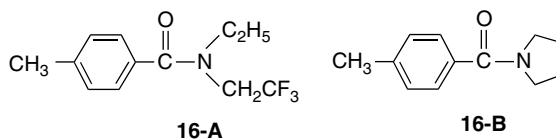
7.15. The acid-catalyzed hydrolysis of thioacetanilide can follow two different courses.



The product composition is a function of acid concentration, as shown below. Provide a mechanism that accounts for the change in product composition as a function of acid concentration.

$\text{H}_2\text{SO}_4$ (% by weight)	1.1	3.2	6.1	12	18	36	48
% formed by path A	20	50	55	65	75	96	100

7.16. A comparison of the kinetics of hydrolysis and isotopic exchange of amides **16-A** and **16-B** gave the data below for reactions conducted in 0.1–1.0  $M$   $[\text{OH}^-]$ . An interesting observation is that there is more  $\text{C}=\text{O}$  exchange for **16-A** than for **16-B**. From this information and the other data given, propose a stepwise mechanism for hydrolysis of each amide. Make a qualitative comparison of the behavior of the substituent effects on the various steps in the mechanisms.



$k_{\text{ex/hydrolysis}}$	(1.0 $M$ $\text{OH}^-$ in $\text{D}_2\text{O}$ )	35.6	0.04
$k_{\text{ex}}$	(100 $^\circ\text{C}$ ; 1.0 $M$ $\text{OH}^-$ in $\text{D}_2\text{O}$ )	$1.09 \times 10^{-3} \text{ s}^{-1}$	$1.53 \times 10^{-5} \text{ s}^{-1}$
$k_{\text{hydrolysis}}$	(100 $^\circ\text{C}$ ; 1.0 $M$ $\text{OH}^-$ in $\text{D}_2\text{O}$ )	$3.06 \times 10^{-5} \text{ s}^{-1}$	$3.85 \times 10^{-4} \text{ s}^{-1}$
$\Delta G_{\text{ex}}^*$	(100 $^\circ\text{C}$ )	26.5 kcal/mol	27.1 kcal/mol
$\Delta G_{\text{hydrolysis}}^*$	(100 $^\circ\text{C}$ )	29.6 kcal/mol	24.4 kcal/mol

7.17. Data pertaining to substituent effects on the acid-catalyzed hydrolysis of mixed aryl-methyl acetals of benzaldehyde are given below. The reactions exhibited general acid catalysis, and the Brønsted  $\alpha$  values are tabulated for a series of substituents in both the benzaldehyde ring and the phenoxy group. Discuss the information that these data provide about the nature of the TS for the first hydrolysis step, making reference to a three-dimensional energy diagram.

Series I, substituent in Ar			Series II, substituent in Ar'		
X	$k_{\text{cat}}^a$	$\alpha$	X	$k_{\text{cat}}^a$	$\alpha$
<i>m</i> -NO <sub>2</sub>	$2.7 \times 10^{-4}$	1.05	<i>m</i> -NO <sub>2</sub>	$8.85 \times 10^{-2}$	0.49
<i>m</i> -F	$2.2 \times 10^{-3}$	0.92	<i>m</i> -Br	$4.7 \times 10^{-2}$	0.65
<i>m</i> -CH <sub>3</sub> O	$9.6 \times 10^{-3}$	0.78	<i>m</i> -F	$2.45 \times 10^{-2}$	0.67
H	$1.3 \times 10^{-2}$	0.77	<i>m</i> -CH <sub>3</sub> O	$2.55 \times 10^{-2}$	0.71
<i>p</i> -CH <sub>3</sub>	$1.1 \times 10^{-1}$	0.72	H	$1.3 \times 10^{-2}$	0.77
<i>p</i> -CH <sub>3</sub> O	$2.8 \times 10^{-1}$	0.68	<i>p</i> -CH <sub>3</sub>	$1.3 \times 10^{-2}$	0.88
			<i>p</i> -CH <sub>3</sub> O	$1.65 \times 10^{-2}$	0.96

a. Rate constant in s<sup>-1</sup> for catalysis by acetic acid.

- 7.18. The introduction of an additional carboxy function into the structure of aspirin results in a significant rate enhancement of hydrolysis. The hydrolysis is 6300 times faster than for the monoanion of aspirin. 3-Hydroxyphthalic anhydride is an observable intermediate. The pH-rate profile is shown in Figure 7.P18. Suggest a mechanism to account for the accelerated hydrolysis involving both of the carboxy derivatives.

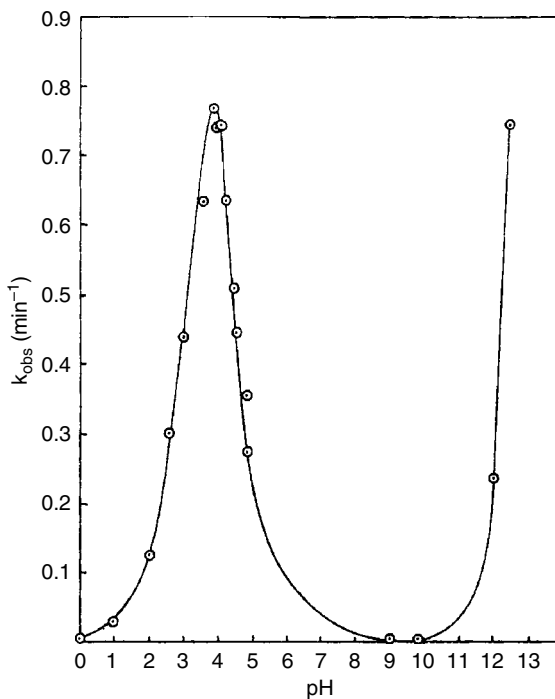
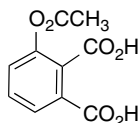


Fig. 7.P18. pH-Rate profile for hydrolysis of 3-acetoxyphthalic acid. Reproduced from *J. Am. Chem. Soc.*, **90**, 5833 (1968), by permission of the American Chemical Society.

7.19. The hydrolysis of the lactone **19-A** shows catalysis by acetate ion, with the rate expression being

$$k_{\text{obs}} = 1.6 \times 10^{-6} + 6.4 \times 10^{-4}[\text{H}^+] + 2.08 \times 10^{-5}[\text{OAc}^-] + 49[\text{OH}^-] \text{ s}^{-1}$$

This expression results in a pH-rate profile shown in Figure 7.P19, with acetate catalysis being significant in the pH range 3–6. The reaction shows a solvent isotope effect of 2.65. Discuss how the catalysis by acetate might occur. What are the likely mechanisms for hydrolysis at pH < 1 and pH > 7, where the rates are linearly dependent on  $[\text{H}^+]$  and  $[\text{OH}^-]$ , respectively?

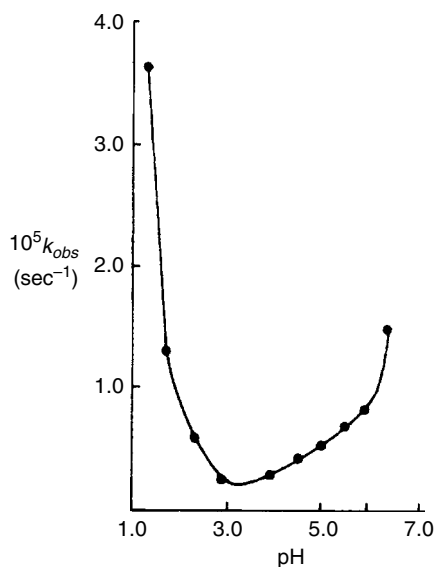
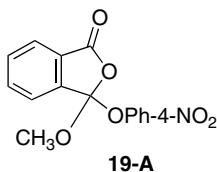
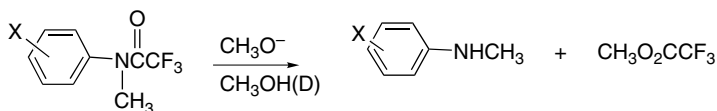


Fig. 7.P19. pH-Rate profile for hydrolysis of **19-A** in acetate buffer solution. Reproduced from *J. Am. Chem. Soc.*, **103**, 3555 (1981), by permission of the American Chemical Society.

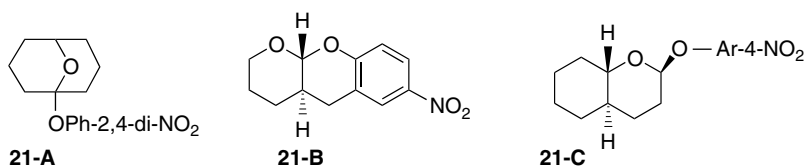
7.20. Some data on substituent effects for the reaction of trifluoroacetanilides with methoxide ion in methanol and methanol-OD are given below. Calculate the isotope effect for each reactant. Plot the rate data against appropriate Hammett substituent constants. What facets of the data are in specific agreement with the normal addition-intermediate mechanism proceeding through a tetrahedral intermediate? What facets of the data suggest other complications? Propose a mechanism that is consistent with the data given.



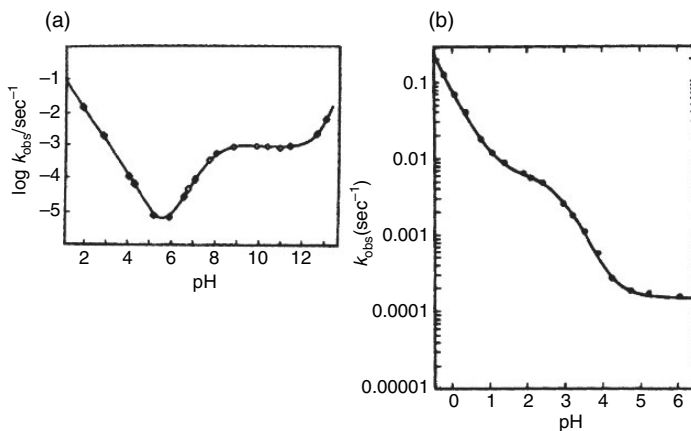
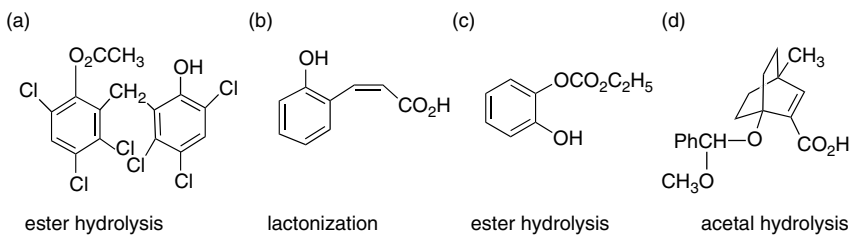
X	$k_{\text{CH}_3\text{OH}}$	$k_{\text{CH}_3\text{OD}}$
<i>m</i> -NO <sub>2</sub>	5.75	8.13
<i>m</i> -Br	0.524	0.464
<i>p</i> -Cl	0.265	0.274
<i>p</i> -Br	0.349	0.346
<i>m</i> -Cl	0.513	0.430
<i>m</i> -OCH <sub>3</sub>	0.110	0.101
H	0.104	0.0899
<i>m</i> -CH <sub>3</sub>	0.0833	0.0595
<i>p</i> -CH <sub>3</sub>	0.0729	0.0451
<i>p</i> -OCH <sub>3</sub>	0.0564	0.0321

a. Second-order rate constants in  $M^{-1} s^{-1}$ .

- 7.21. The order of the reactivity of the cyclic acetals toward hydrolysis is **21-A**  $\ll$  **21-B**  $\ll$  **21-C**. Offer an explanation for the large differences in reactivity of these acetals.



- 7.22. Examine the structure of the following reactants and the corresponding pH-rate profiles. Offer mechanisms for each reaction that is consistent with the pH-rate profile. Indicate the most likely mechanism corresponding to each feature of the profile.



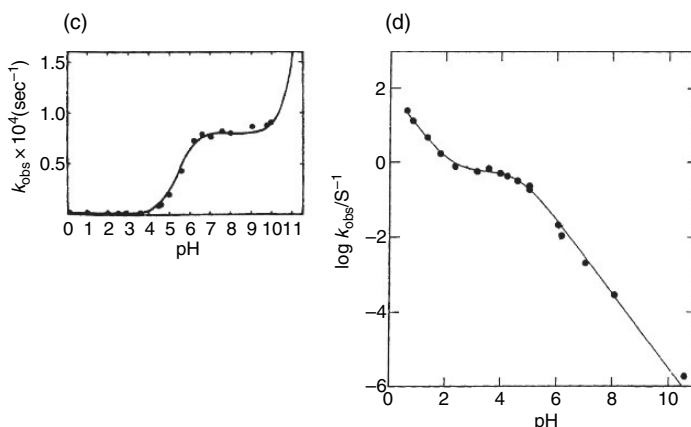
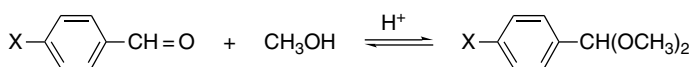
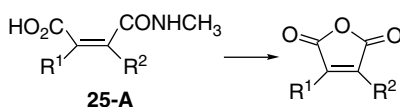


Fig. 7.P22. Reproduced from problem references 22a–c, by permission of the American Chemical Society and reference 22d by permission of the Royal Society of Chemistry.

- 7.23. The pH-rate profiles for 2-carboxy- and 4-carboxy benzylidene acetals of the *trans*-1,2-cyclohexanediol are shown in Figure 7.P23a (page 708). Figure 7.P23b is the pH-rate profile of 3-(*trans*-2-hydroxycyclohexyloxy) phthalide, an intermediate isolated from the 2-carboxy derivative. Interpret both the relative rates and the form of the pH-rate profiles.
- 7.24. The rates of both formation and hydrolysis of dimethyl acetals of *p*-substituted benzaldehydes are substituent dependent. Do you expect the rate of formation to increase or decrease with the increasing EWG strength of the substituent? How do you expect the rate of hydrolysis to respond to the nature of the substituent? The equilibrium constant for acetal formation is determined by these two rates. How do you expect  $K$  to vary with substitution?



- 7.25. Figure 7.P25 (page 709) gives the pH-rate profile for conversion of the acid **25-A** to the anhydride in aqueous solution. Note that the rate of the reaction increases with the size of the alkyl substituent, and, although not shown, the compound with both  $\text{R}^1$  and  $\text{R}^2 = \text{CH}_3$  is still more reactive. Suggest a mechanism for the reaction, including the structure of any intermediate. How do you account for the effect of the alkyl substituents on the reaction rate?



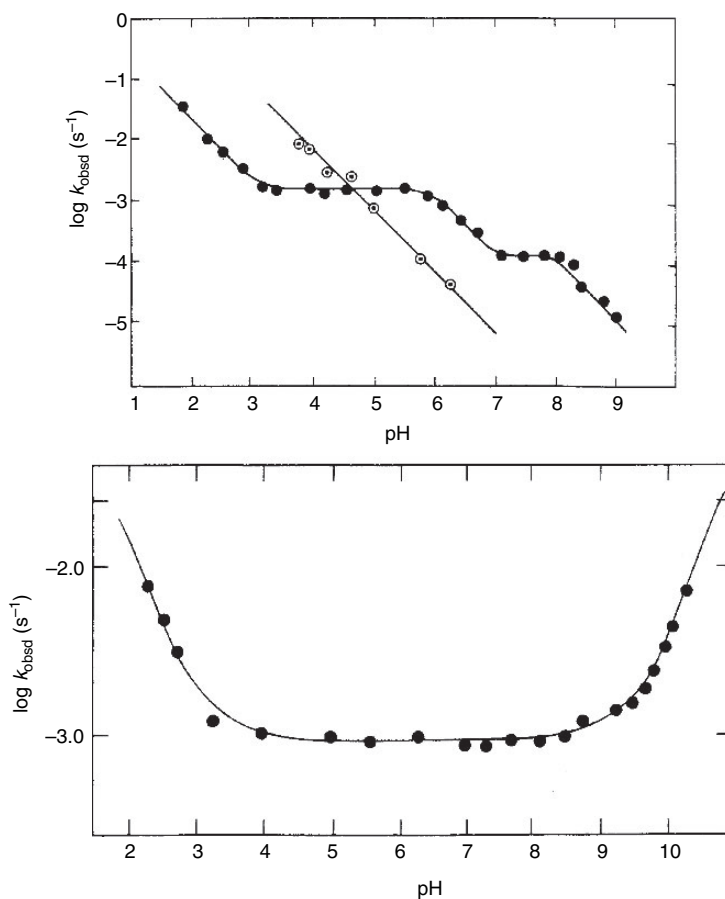


Fig. 7.P23. (a) pH-Rate profile for hydrolysis of 2-carboxy (solid circles) and 4-carboxy (open circles) benzylidene acetals of *trans*-1,2-cyclohexanediol. (b) pH-Rate profile for 3-(*trans*-2-hydroxycyclohexyloxy)phthalide, an intermediate isolated from the 2-carboxy derivative. Reproduced from *J. Am. Chem. Soc.*, **118**, 12956 (1996), by permission of the American Chemical Society.

- 7.26. Assume that the general mechanism for imine hydrolysis described on p. 647–648 is operative. Assume that a steady state approximation can be applied to the tetrahedral intermediate. Derive the kinetic expression for the observed rate of imine hydrolysis. What variables have to be determined to construct the pH-rate profile? What simplifying assumptions can be justified at very high and very low pH values? What are the kinetic expressions that result from these assumptions?
- 7.27. Give the expected structure, including stereochemistry if appropriate, for the products of the following reactions:

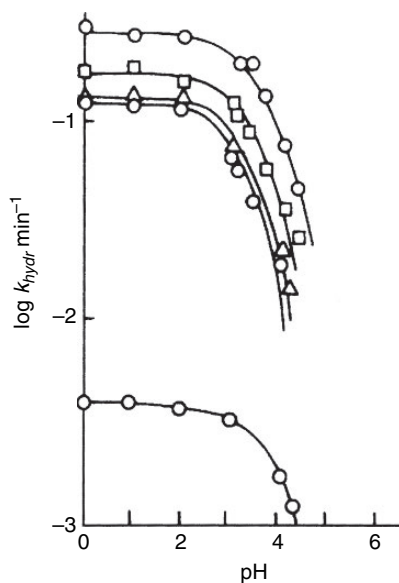
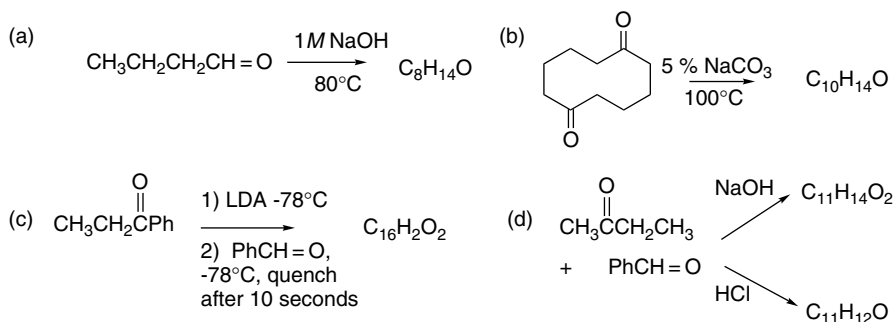
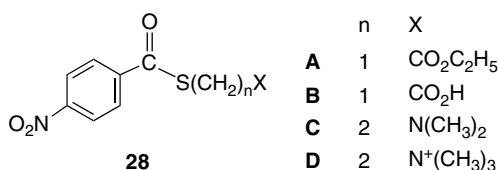


Fig. 7.P25. pH-Rate profile for the hydrolysis of alkyl *N*-methylmaleamic acids at 39°C. The order of increasing reactivity is  $R^1 = H < Me < Et < i\text{-Pr} << t\text{-Bu}$ . Reproduced from *J. Chem. Soc., Perkin Trans. 2*, 1206 (1972), by permission of the Royal Society of Chemistry.



7.28. Figure 7.P28 (page 710) gives the pH-rate profile for the hydrolysis of thioesters **28-A-D** and indicates differing dependence on pH, depending on the thiol substituents. Propose a mechanism that would account for the observed pH dependence in each case.



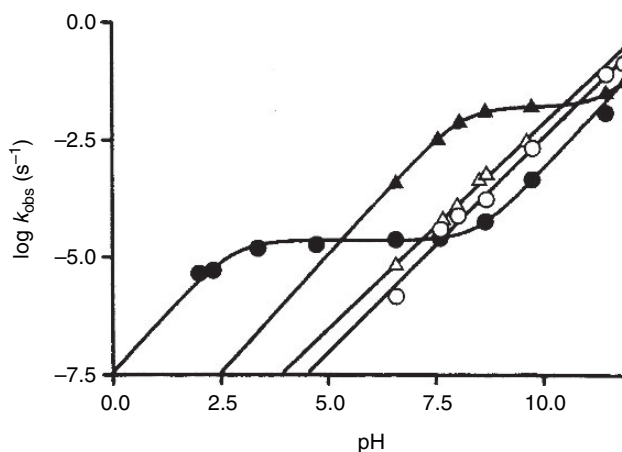


Fig. 7.P28. pH-Rate plots for thioesters **28-A** (○), **28-B** (●), **28-C** (▲) and **28-D** (△). Reproduced from *J. Org. Chem.*, **62**, 4816 (1997), by permission of the American Chemical Society.

- 7.29. Figure 7.P29 gives the pH-rate profile for alkaline hydrolysis of two substituted salicylate amides, as compared with benzamide. Consider whether the pH-rate profiles for the salicylamides are more consistent with mechanism (A), intramolecular basic catalysis of water attack, or (B), intramolecular acid catalysis of hydroxide ion attack.

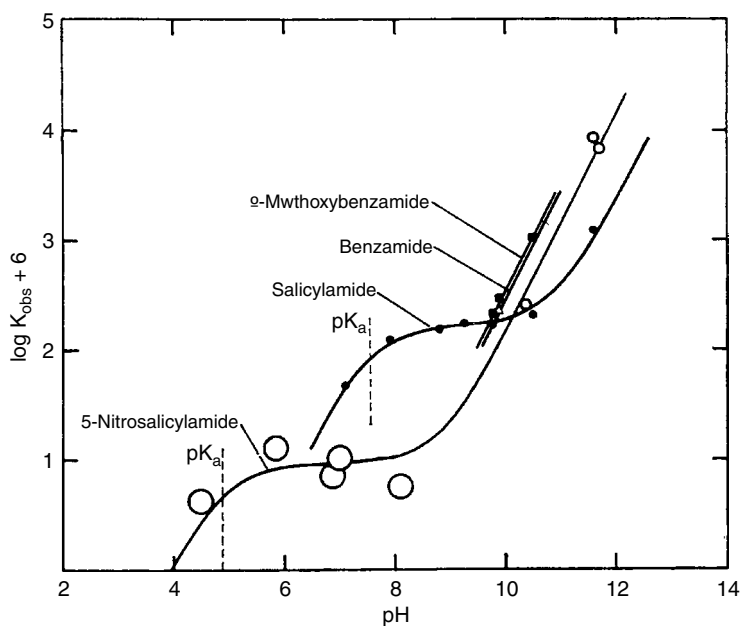
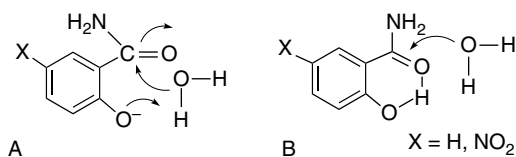


Fig. 7.P29. pH-Rate profiles for substituted salicylamides compared to benzamide in water at 100°C. The rate constants are in  $\text{min}^{-1}$ . Reproduced from *J. Org. Chem.*, **30**, 1668 (1965), by permission of the American Chemical Society.



- 7.30. The hydrolysis of the ester group in 2-acetoxybenzaldehyde is accelerated by about  $10^4$ , relative to the 4-isomer. The rate of hydrolysis in the pH range 6.0–8.5 follows the rate expression

$$\text{Rate} = k_0 + k[\text{OH}^-]$$

Both the  $k_0$  and  $k[\text{OH}^-]$  terms are larger than for the 4-isomer. When the hydrolysis is carried out in  $^{18}\text{O}$ -labeled water, the acetic acid contains 50%  $^{18}\text{O}$ . Suggest a mechanism that is consistent with these observations.

- 7.31. The pH-rate profile for the hydrolysis of 4-nitrophenyl 2-aminobenzoate is given in Figure 7.13 (p. 674). The reaction exhibits a solvent isotope effect of  $\sim 0.5$  in  $\text{D}_2\text{O}$ . Suggest possible mechanisms for the reaction, based on the shape of the pH-rate profile and chemical structure considerations. Derive the kinetic expression for the most likely mechanism.

# Aromaticity

## Introduction

The meaning of the word *aromaticity* has evolved as understanding of the special properties of benzene and other aromatic molecules has deepened.<sup>1</sup> Originally, aromaticity was associated with a specific chemical reactivity. The aromatic hydrocarbons undergo substitution reactions in preference to addition. Later, the idea of special stability became more important. Benzene can be shown to be much lower in enthalpy than predicted by summation of the normal bond energies for the C=C, C–C, and C–H bonds in the Kekule representation of benzene (see p. 265). Aromaticity is now generally associated with this property of special stability of certain completely conjugated cyclic molecules. A major contribution to the stability of aromatic systems comes from the delocalization of  $\pi$  electrons in these molecules, which also imparts other properties that are characteristic of aromaticity, especially a diamagnetic ring current.

Aromaticity is usually described in MO terminology. Cyclic structures that have a particularly stable arrangement of occupied  $\pi$  molecular orbitals are called aromatic. *Hückel's rule*, a familiar expression of the relationship between an MO description of structure and aromaticity, is derived from Hückel molecular orbital (HMO) theory and states that *planar monocyclic completely conjugated hydrocarbons will be aromatic when the ring contains  $(4n + 2)\pi$  electrons*. HMO calculations assign the  $\pi$ -orbital energies of the cyclic unsaturated systems of ring size three to nine as shown in Figure 8.1. (See Section 1.5, p. 27 to review HMO theory.)

Orbitals below the dotted reference line in the figure are bonding orbitals; when they are filled, the molecule is stabilized. The orbitals that fall on the reference line are nonbonding; electrons in these orbitals are neither stabilizing nor destabilizing. The orbitals above the reference line are antibonding; electrons in these orbitals

<sup>1</sup> M. Glukhovtsev, *J. Chem. Ed.*, **74**, 132 (1997); D. Lloyd, *J. Chem. Inf. Comput. Sci.*, **36**, 442 (1996), Z. Zhou, *Int. Rev. Phys. Chem.*, **11**, 243 (1992); J. P. Snyder, *Nonbenzenoid Aromatics*, Vol. 1, Academic Press, New York, 1969, Chap. 1. A series of reviews on many aspects of aromaticity is published in *Chem. Rev.*, **101**, 1115–1566 (2001).

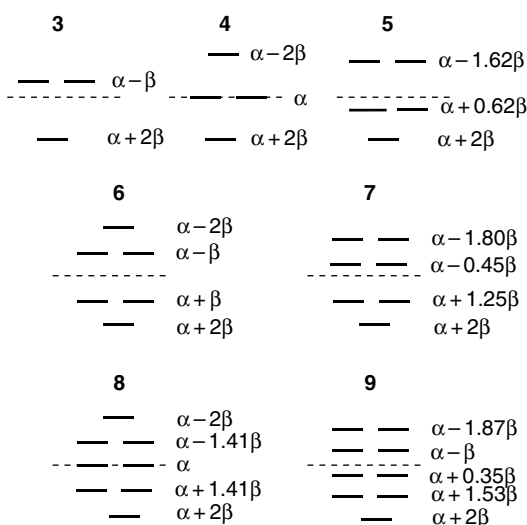
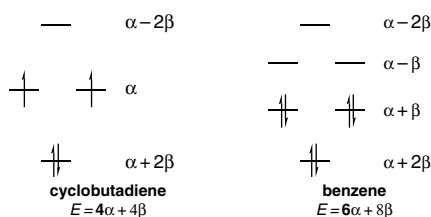


Fig. 8.1. HMO energies for conjugated planar ring systems of three to nine carbon atoms.

destabilize the molecule. The dramatic difference in properties of cyclobutadiene (extremely unstable) and benzene (very stable) are explicable in terms of these HMO diagrams.



Cyclobutadiene has two bonding electrons, but the other two electrons are unpaired because of the degeneracy of the two nonbonding orbitals. The two electrons in the nonbonding levels do not contribute to the stabilization of the molecule. The total HMO energy is  $4\alpha + 4\beta$ , which is the same as for two isolated double bonds. Furthermore, as these electrons occupy a high-energy orbital, they are particularly available for chemical reactions. As we shall see shortly, experimental evidence indicates that cyclobutadiene is rectangular rather than square. This modifies somewhat the orbital picture from the simple HMO pattern, which applies to a square geometry. The two nonbonding levels are no longer degenerate, so cyclobutadiene is not predicted to have unpaired electrons. Nevertheless, higher-level calculations agree with the Hückel concept in predicting cyclobutadiene to be an extremely unstable molecule with a high-lying HOMO. We will see that several methods of analysis indicate that cyclobutadiene is not only highly reactive, but is also *less stable* than an isolated diene. Cyclobutadiene is called *antiaromatic*.<sup>2</sup>

Simple Hückel calculations on benzene, in contrast, place all the  $\pi$  electrons in bonding MOs. The  $\pi$ -electron energy of the benzene molecule is calculated by

<sup>2</sup> R. Breslow, *Acc. Chem. Res.*, **6**, 393 (1973).

summing the energies of the six  $\pi$ -electrons, which is  $6\alpha + 8\beta$ , lower by  $2\beta$  than the value of  $6\alpha + 6\beta$  for three isolated double bonds. Thus the HMO method predicts a special stabilization for benzene.

The eight-electron cyclic conjugated polyene is 1,3,5,7-cyclooctatetraene, which was first synthesized in 1911.<sup>3</sup> Cyclooctatetraene is not much different in reactivity and stability from noncyclic conjugated polyenes. It has no aromatic characteristics. Structural studies determined that cyclooctatetraene is nonplanar, and its most stable structure is tub-shaped. This reduces the overlap between the  $\pi$  bonds, and since the molecule is not planar, the HMO orbital pattern does not apply. Cyclooctatetraene is neither aromatic nor antiaromatic.

The pattern for planar conjugated systems established for cyclobutadiene, benzene, and cyclooctatetraene persists for larger rings. All  $4n + 2$  systems are predicted to have all electrons paired in bonding MOs with net stabilization relative to isolated double bonds. In contrast, planar systems containing  $4n$   $\pi$  electrons are predicted to have two degenerate orbitals, each with one unpaired electron. This pattern is the theoretical basis of the Hückel rule.

## 8.1. Criteria of Aromaticity

HMO theory and Hückel's rule make a good starting point for considering the two molecules, benzene and cyclobutadiene, that are at opposite extremes of aromaticity. There are many other structures that can be described as aromatic and antiaromatic. In this section, we discuss various criteria of aromaticity and its effect on the properties of a few prototypical compounds. In the sections that follow, we look at various specific compounds, including charged rings and homoaromatic systems, as well as polycyclic and heterocyclic rings. We apply these criteria to evaluating aromaticity. We consider three types of criteria: (1) *energy data* indicating thermodynamic stabilization or destabilization; (2) *structural information*, particularly as it relates to bond lengths indicating delocalized structures; and (3) *electronic properties*, including energy levels, electron distribution, and polarizability. The third group of properties includes the response of the electrons to a magnetic field, which can be observed through NMR and magnetic susceptibility measurements. For the most part we use benzene, naphthalene, anthracene, and phenanthrene as examples of aromatic molecules, cyclobutadiene as an example of an antiaromatic molecule, and 1,3,5,7-cyclooctatetraene as a nonaromatic molecule.

### 8.1.1. The Energy Criterion for Aromaticity

One approach to evaluation of the aromaticity of a molecule is to determine the extent of thermodynamic stabilization. Attempts to describe stabilization of a given aromatic molecule in terms of simple HMO calculations have centered on the *delocalization energy*. The total  $\pi$ -electron energy of a molecule is expressed in terms of the energy parameters  $\alpha$  and  $\beta$  that are used in HMO calculations. This energy value can be compared to that for a hypothetical localized version of the same molecule. The HMO energy for the  $\pi$  electrons of benzene is  $6\alpha + 8\beta$ . The same quantity for

<sup>3</sup> R. Willstätter and E. Waser, *Ber.*, **44**, 3423 (1911); R. Willstätter and M. Heidelberger, *Ber.*, **46**, 517 (1913); A. C. Cope and C. G. Overberger, *J. Am. Chem. Soc.*, **70**, 1433 (1948).

the hypothetical localized model cyclohexatriene is  $6\alpha + 6\beta$ , the sum of three isolated C=C bonds. The difference of  $2\beta$  is called the *delocalization energy* or *resonance energy*. Although this quantity can be used for comparing related systems, it is not a measurable physical quantity; rather, it is a comparison between a real molecule and a hypothetical one and depends on the definition of the reference point.

There have been two general approaches to determining the amount of stabilization that results from aromatic delocalization. One is to use experimental thermodynamic measurements. Bond energies, as we discussed in Chapter 3, are nearly additive when there are no special interactions among the various bond types. Thus it is possible to assign such quantities as the heat of combustion or heat of hydrogenation of “cyclohexatriene” by assuming that it is a compound with no interaction between the conjugated double bonds. For example, a very simple calculation of the heat of hydrogenation for cyclohexatriene would be to multiply the heat of hydrogenation of cyclohexene by 3, i.e.,  $3 \times 28.6 = 85.8$  kcal/mol. The actual heat of hydrogenation of benzene is 49.8 kcal/mol, suggesting a total stabilization or delocalization energy of 36 kcal/mol. The difference between the calculated and corresponding measured thermodynamic property of benzene is taken to be the aromatic stabilization. There are other, more elaborate, ways of approximating the thermodynamic properties of the hypothetical cyclohexatriene. There are also other possible reference points. Most estimates of the thermodynamic stabilization of benzene are in the range 20–40 kcal/mol, but the stabilization cannot be determined in an absolute sense since it depends on the choice of the reference molecules and the properties ascribed to them.

The second general approach to estimating aromatic stabilization is to use computational methods. This has already been illustrated by the discussion of benzene according to HMO theory, which assigns the stabilization energy as  $2\beta$  units. More advanced MO and DFT methods can assign the stabilization energy in a more quantitative way. The most successful method is to perform calculations on the aromatic compound and on a linear, conjugated polyene containing the same number of double bonds.<sup>4</sup> This method assigns a resonance stabilization of zero to the polyene, even though it is known by thermodynamic criteria that conjugated polyenes do have some stabilization relative to isomeric compounds with isolated double bonds. In effect, this method defines the stabilization *over and above that present in the conjugated polyene*. With this definition, semiempirical MO calculations assign a value of about 20 kcal/mol to the resonance energy of benzene, relative to 1,3,5-hexatriene. The use of polyenes as reference compounds gives better agreement with experimental trends in stability than comparison with the sums of isolated double bonds. It is very significant that MO calculations indicate a *destabilization* of certain conjugated cyclic polyenes, cyclobutadiene in particular. This conclusion has recently been supported experimentally. The technique of photoacoustic calorimetry provided the first experimental thermodynamic data on cyclobutadiene. The  $\Delta H_f$  value of  $114 \pm 11$  kcal/mol leads to a total destabilization of 87 kcal/mol, of which 32 kcal/mol is attributed to ring strain and 55 kcal/mol to antiaromaticity.<sup>5</sup>

The isodesmic reaction method (see Section 1.2.6) has also been applied to the calculation of the resonance stabilization of benzene. *Homodesmotic reactions*, a special version of isodesmic reactions, can also be used.<sup>6</sup> Homodesmotic reactions

<sup>4</sup> M. J. S. Dewar and C. de Llano, *J. Am. Chem. Soc.*, **91**, 789 (1969).

<sup>5</sup> A. A. Deniz, K. S. Peters, and G. J. Snyder, *Science*, **286**, 1119 (1999).

<sup>6</sup> P. George, M. Trachtman, C. W. Bock, and A. M. Brett, *J. Chem. Soc., Perkin Trans. 2*, 1222 (1976); P. George, M. Trachtman, C. W. Bock, and A. M. Brett, *Tetrahedron*, **32**, 1357 (1976).

not only balance the bond types, but also match the hybridization of all atoms on both sides of the equation. For example, the stabilization of benzene, relative to 1,3-butadiene, can be calculated by the reaction below, which has 12  $sp^2$  carbons on each side of the equation.

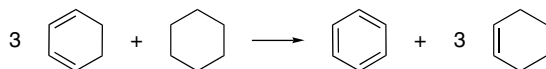


Isodesmic and homodesmotic reactions can use either experimental thermochemical data or energies obtained by MO or DFT calculations. There have been many specific reaction schemes and computational methods applied to calculation of stabilization energies.<sup>7</sup> With the above homodesmotic sequence, calculations at the MP4(SDTQ)/6-31G( $d,p$ ) level give the following stabilization ( $\Delta E$ ) values.<sup>8</sup>

	$\Delta E$	$\Delta E/\pi$ Electron
Cyclobutadiene	-75.1	-18.8
Benzene	25.3	4.3
Cyclooctatetraene(planar)	-28.3	-3.6

The destabilization of cyclobutadiene is estimated to include 33.5 kcal/mol of strain. Planar cyclooctatetraene would also have some strain resulting from expansion of the bond angles. Because the calculations are referenced to butadiene, the stabilization is in addition to the stabilization of butadiene by conjugation. If the stabilization energy of butadiene is assigned as zero, the above reaction gives the resonance energy of benzene as 25.3 kcal/mol. If butadiene is considered to have a delocalization energy of 4.5 kcal/mol (see Section 3.1.2.3), the benzene stabilization energy is 29.8 kcal/mol. B3LYP/6-311+G\*\* calculations on the same homodesmotic reaction led to a stabilization energy of 29.3 kcal/mol.<sup>9</sup>

This particular calculation may *underestimate* the relative stabilization, since it uses *trans*-1,3-butadiene as the model, rather than the *cis* geometry that is incorporated into cyclic structures.<sup>10</sup> For example, the homodesmotic reaction below gives a stabilization energy of 30.5 kcal/mol *relative to cyclohexadiene*.<sup>11</sup> A feature of this scheme is that it incorporates many of the structural features of the system, such as ring strain, into both sides of the equation so that they should largely cancel. The net stabilization has been called the *aromatic stabilization energy*.



Another refinement of the isodesmic approach to defining aromatic stabilization is to compare methyl-substituted aromatics with the corresponding

<sup>7</sup> A. Skanke, R. Hosmane, and J. F. Liebman, *Acta Chem. Scand.*, **52**, 967 (1998).

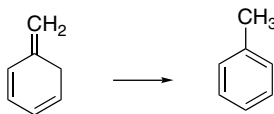
<sup>8</sup> M. N. Glukhovtsev, R. D. Bach, and S. Laiter, *Theochem*, **417**, 123 (1997).

<sup>9</sup> P. v. R. Schleyer, H. Jiao, N. J. R. van Eikema Hommes, V. G. Malkin, and O. L. Malkina, *J. Am. Chem. Soc.*, **119**, 12669 (1997).

<sup>10</sup> M. K. Cyranski, P. v. R. Schleyer, T. M. Krygowski, H. Jiao, and G. Hohlneicher, *Tetrahedron*, **59**, 1657 (2003).

<sup>11</sup> P. v. R. Schleyer, M. Manoharan, H. Jiao, and F. Stahl, *Org. Lett.*, **3**, 3643 (2001).

*exo*-methylene polyene analogs. For example, toluene can be compared with 5-methylene-1,3-cyclohexadiene. This reaction gives a stabilization of 33.2 kcal/mol using B3LYP/6-311+G\*\* calculations.<sup>12</sup>



This sequence is not a suitable one for using experimental data, since the *exo*-methylene analogs are seldom available, but it is practical for computational approaches.

Although the stabilization of aromatic compounds is frequently associated with the delocalization of the  $\pi$  electrons, it is important to recognize that there are other large energy contributions to the difference between localized and delocalized structures, because the *nuclear positions are also different*. The method of separation of nuclear-nuclear, electron-electron, and nuclear-electron forces (see Topic 1.1) has been applied to cyclobutadiene and benzene.<sup>13</sup> According to this analysis, nuclear-nuclear interactions are destabilizing in both cyclobutadiene and benzene. Electron-electron forces are also destabilizing in benzene, but a very favorable nuclear-electron interaction is responsible for the net stabilization.

#### Net Stabilization of Delocalized Structure Relative to Localized Model

	Cyclobutadiene	Benzene
$V_{ee}$	+16.4	-84.4
$V_{nn}$	-43.4	-78.7
$V_{ne}$	-1.7	+168.7

These various approaches for comparing the thermodynamic stability of aromatic compounds with reference compounds all indicate that there is a large stabilization of benzene and an even greater destabilization of cyclobutadiene. These compounds are the best examples of aromaticity and antiaromaticity, and in subsequent discussions of other systems we compare their stabilization or destabilization to that of benzene and cyclobutadiene.

### 8.1.2. Structural Criteria for Aromaticity

Benzene is a perfectly hexagonal molecule with a bond length (1.39 Å) that is intermediate between single and double bonds between  $sp^2$  carbons. Cyclobutadiene, on the other hand, adopts a rectangular shape. This contrasting behavior suggests that *bond length alternation* might be a useful criterion for assessing aromaticity, and several such schemes have been developed. One such system, called HOMA (for harmonic oscillator model for aromaticity), developed by Krygowski and co-workers,<sup>14</sup> takes

<sup>12</sup>. P. v. R. Schleyer and F. Puhlhofer, *Org. Lett.*, **4**, 2873 (2002).

<sup>13</sup>. Z. B. Maksic, D. Baric, and I. Petanjek, *J. Phys. Chem. A*, **104**, 10873 (2000).

<sup>14</sup>. J. Kruszewski and T. M. Krygowski, *Tetrahedron Lett.*, 3839 (1972).

both bond length alternation and bond stretching into consideration. The aromaticity index HOMA is formulated as

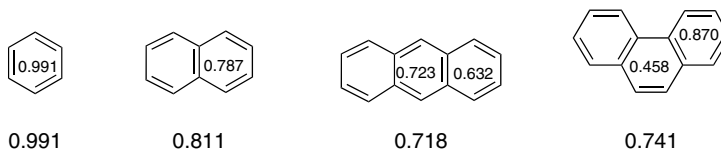
$$\text{HOMA} = 1 - [\alpha(R_{\text{opt}} - R_{\text{av}})^2 + \frac{\alpha}{n} \sum (R_{\text{av}} - R_i)^2] \quad (8.1)$$

where  $R_{\text{av}}$  is average bond length,  $R_{\text{opt}}$  is the optimum bond length,  $R_i$  is an individual bond length,  $n$  is the number of bonds, and  $\alpha$  is a constant such that HOMA is equal to zero for a single localized structure. The HOMA equation can be rewritten as

$$\text{HOMA} = 1 - \frac{\alpha}{n} \sum [R_{\text{opt}} - R_i]^2 \quad (8.2)$$

The  $R_{\text{opt}}$  values are derived from butadiene, which is thereby the implicit standard of the definition. For C–C bonds,  $\alpha = 257.7 \text{ \AA}^{-2}$  and  $R_{\text{opt}} = 1.388 \text{ \AA}$ . Further definition of bond lengths is required for structures with heteroatoms.

In the formulation in Equation (8.1), the first term, the deviation from the optimum length, accounts for the energy associated with bond length effects, and the second term, which reflects deviation from the average, accounts for bond alternation. The HOMA energy and alternation terms have been calculated for many aromatic compounds.<sup>15</sup> The values for benzene, naphthalene, anthracene, and phenanthrene are shown below.<sup>16</sup> Note the decrease as the molecules get larger. HOMA indices can also be assigned to the individual rings in polycyclic structures. A relatively low HOMA is assigned to the center ring in phenanthrene. We will see later that this is in accord with other properties of phenanthrene. In contrast, the center ring in anthracene has a slightly higher index than the terminal rings.



Another aromaticity index based on bond lengths was devised by Bird.<sup>17</sup> The input into the index are bond order values derived from bond lengths. (See Section 1.4.6 to review the relationship between bond length and bond order.) The formulation of the index is

$$I = 100(1 - \frac{V}{V_k})V = \frac{100}{\bar{N}} \sqrt{\frac{\sum (N - \bar{N})^2}{n}} \text{ and } N = \frac{a}{R_2} - b \quad (8.3)$$

where  $\bar{N}$  is the arithmetic mean of bond orders.  $V_k$  is the value of  $V$  for the corresponding localized structures, and  $a$  and  $b$  are constants for each bond type.

The index  $I_A$  is assigned as 100 for benzene. The values are scaled for ring size and ring fusions, and increase with ring size so that naphthalene (142) and anthracene (206) have higher indices than benzene. This method is particularly useful for comparing heterocyclic compounds with hydrocarbons (see Section 8.6).

<sup>15</sup> T. M. Krygowski and M. Cyranski, *Tetrahedron*, **52**, 1713 (1996).

<sup>16</sup> M. K. Cyranski, B. T. Stepien, and T. M. Krygowski, *Tetrahedron*, **56**, 9663 (2000).

<sup>17</sup> C. W. Bird, *Tetrahedron*, **41**, 1409 (1985); C. W. Bird, *Tetrahedron*, **48**, 335 (1992); C. W. Bird, *Tetrahedron*, **52**, 9945 (1996); C. W. Bird, *Tetrahedron*, **54**, 4641 (1998).

### 8.1.3. Electronic Criteria for Aromaticity

As discussed in the Introduction, Hückel's rule is an electronic criterion for aromaticity, and is based on the configuration of the  $\pi$  electrons. Another characteristic of aromatic compounds is a relatively large HOMO-LUMO gap, which indicates the absence of high-energy, reactive electrons, in agreement with the reduced reactivity of aromatic compounds to electrophilic reagents. This facet of electronic configuration can be expressed in terms of hardness (see p. 96 for the definition of hardness in terms of DFT theory).<sup>18</sup>

$$\eta = (\epsilon_{\text{HOMO}} - \epsilon_{\text{LUMO}})/2$$

The numerical value of hardness obtained by HMO calculations correlates with the stability of aromatic compounds.<sup>19</sup> The energy gap can also be compared with polyene reference molecules to give "relative hardness." By this measure, the relative hardness of benzene is 0.765 $\beta$  when butadiene is assigned as 0. MNDO calculations have also been used in this context.<sup>20</sup>

The correlation can be given an experimental basis when hardness is related to molar refractivity<sup>21</sup>:

$$\eta = \frac{19.6}{(R_D)^3} \quad (8.4)$$

Molar refractivity is easily derived from the refractive index. Hardness measured in this way correlates with other aromaticity criteria such as resonance energy per electron for a variety of hydrocarbons and heterocyclic molecules (see p. 747).<sup>22</sup>

An experimental measure of the HOMO-LUMO gap is the reduction and oxidation potential of the ring.<sup>23</sup> A range of benzenoid and nonbenzenoid reduction potentials correlates with the LUMO energy, as calculated by a modified HMO method.<sup>24</sup>

NMR spectroscopy also provides an experimental tool capable of assessing aromaticity. Aromatic compounds exhibit a *diamagnetic ring current*. Qualitatively, this ring current can be viewed as the result of migration of the delocalized  $\pi$  electrons under the influence of the magnetic field in an NMR spectrometer. The ring current results in a large magnetic anisotropy in aromatic compounds. The induced ring current gives rise to a local magnetic field that is opposed to the direction of the applied magnetic field. Nuclei in a region above or below the plane of an aromatic ring are shielded by the induced field and appear at relatively high field in the NMR spectrum, whereas nuclei in the plane of the ring—i.e., the atoms bound directly to the ring—occur at downfield positions. Antiaromatic compounds have a *paramagnetic ring current* and show opposite effects. These chemical shifts are evidence of *magnetic anisotropy*.<sup>25</sup> The detailed analysis of <sup>1</sup>H and <sup>13</sup>C chemical shifts is complicated.

<sup>18</sup> F. De Proft and P. Geerlings, *Chem. Rev.*, **101**, 1451 (2001).

<sup>19</sup> Z. Zhou and R. G. Parr, *J. Am. Chem. Soc.*, **111**, 7371 (1989).

<sup>20</sup> Z. Zhou and H. V. Navangul, *J. Phys. Org. Chem.*, **3**, 784 (1990); Z. Zhou, *Int. Rev. Phys. Chem.*, **11**, 243 (1992).

<sup>21</sup> L. Komorowski, *Structure and Bonding*, **80**, 45 (1993).

<sup>22</sup> C. W. Bird, *Tetrahedron*, **53**, 3319 (1997).

<sup>23</sup> A. J. Fry and P. C. Fox, *Tetrahedron*, **42**, 5255 (1986).

<sup>24</sup> A. Streitwieser, *J. Am. Chem. Soc.*, **82**, 4123 (1960).

<sup>25</sup> R. C. Haddon, *J. Am. Chem. Soc.*, **101**, 1722 (1979); J. Aihara, *J. Am. Chem. Soc.*, **103**, 5704 (1981); R. C. Haddon and K. Raghavachari, *J. Am. Chem. Soc.*, **107**, 289 (1985); S. Kuwajima and Z. G. Soos, *J. Am. Chem. Soc.*, **109**, 107 (1987).

The  $^1\text{H}$  and  $^{13}\text{C}$  shifts are also strongly dependent on carbon hybridization. In aromatic compounds, the ring current makes a significant contribution to the overall chemical shift, but does not appear to be the dominant factor.<sup>26</sup> Figure 8.2 is a representation of the shielding and deshielding areas of the benzene ring.

The relationship between chemical shift phenomena and aromaticity can be put on a numerical basis by calculation of the magnetic field at the center of the ring. These values, called the *nucleus independent chemical shift* (NICS), show good correlation with other manifestations of aromaticity.<sup>27</sup> Benzenoid hydrocarbons such as benzene, naphthalene, and anthracene show values of about  $-9$  to  $-10$  ppm. Heteroaromatic five-membered rings show somewhat more negative values (pyrrole,  $-15.1$ ; thiophene,  $-13.6$ ; furan,  $-12.3$ ). Aromatic ions such as cyclopentadienide ( $-14.3$ ) and cycloheptatrienylium ( $-7.6$ ) are also negative. Antiaromatic species, including cyclobutadiene ( $+27.6$ ) and borole ( $+17.5$ ) are positive. Saturated compounds such as cyclohexane have values near zero. It is also possible to calculate NICS values for individual rings in a polycyclic system. The NICS value can be affected by other structural features that are not directly related to the aromatic ring current. The maximum for the ring current is located somewhat above the ring and other factors are reduced at this location, so that calculation of the NICS  $1.0 \text{ \AA}$  above and below the ring is useful.<sup>28</sup>

Several other methods have been devised to analyze the ring current effect. One approach is to isolate the individual orbitals that have  $\pi$  character and use them for the NICS computation.<sup>29</sup> Another quantity that relates anisotropic shielding to aromaticity is called the ARCS, *aromatic ring current shielding*.<sup>30</sup> As with NICS, it is computed

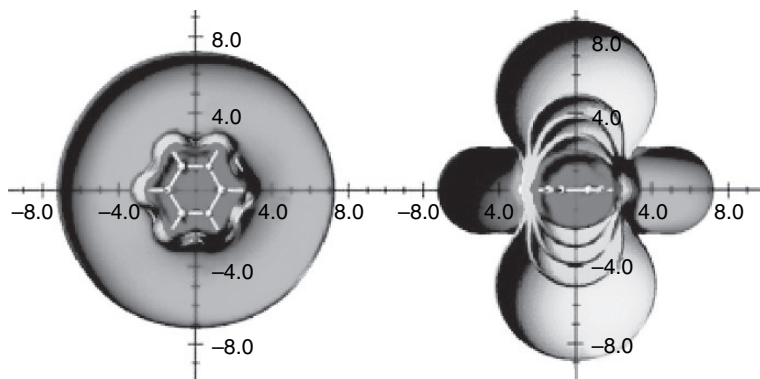


Fig. 8.2. Areas of shielding and deshielding in and perpendicular to the plane of the benzene ring. Reproduced from *J. Chem. Soc., Perkin Trans. 2*, 1893 (2001), by permission of the Royal Society of Chemistry. (See also color insert.)

- <sup>26</sup> U. Fleischer, W. Kutzelnigg, P. Lazzeretti, and V. Muehlenkamp, *J. Am. Chem. Soc.*, **116**, 5298 (1994); S. Klod and E. Kleinpeter, *J. Chem. Soc., Perkin Trans. 2*, 1893 (2001); C. S. Wannere and P. v. R. Schleyer, *Org. Lett.*, **5**, 605 (2003).
- <sup>27</sup> P. v. R. Schleyer, C. Maerker, A. Dransfeld, H. Jiao, and N. J. P. van Eikema Hommes, *J. Am. Chem. Soc.*, **118**, 6317 (1996).
- <sup>28</sup> P. v. R. Schleyer, H. Jiao, N. J. R. van Eikema Hommes, V. G. Malkin, and O. L. Malkina, *J. Am. Chem. Soc.*, **119**, 12669 (1997); P. v. R. Schleyer, M. Manoharan, Z. -X. Wang, B. Kiran, H. Jiao, R. Puchta, and N. J. R. van Eikema Hommes, *Org. Lett.*, **3**, 2465 (2001).
- <sup>29</sup> C. Corminboeuf, T. Heine, and J. Weber, *Phys. Chem. Chem. Phys.*, **5**, 246 (2003).
- <sup>30</sup> J. Juselius and D. Sundholm, *Phys. Chem. Chem. Phys.*, **1**, 3429 (1999).

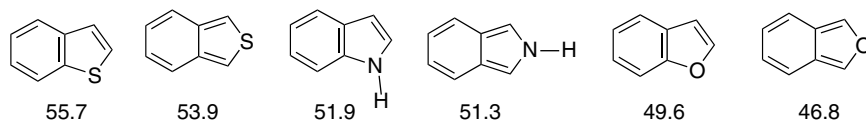
theoretically and defined in such a way that it can be used to compare different rings. The units are nanoamperes (nA), and the calculated ring currents are found to increase in more electron-rich systems, as is the case with NICS. Whereas benzene is 32 nA, pyrrole is 41.4 nA and cyclopentadienide is 72.2 nA. Conversely, it is lower for the cycloheptatrienyl cation (26.1 nA); thiophene (32.1 nA) is very similar to benzene; and nonaromatic compounds such as cyclohexane or 1,4-cyclohexadiene have much smaller values (2.1 and 1.7 nA, respectively).

Another electronic property associated with aromaticity is *magnetic susceptibility*, which is determined by measuring the force exerted on the sample by a magnetic field.<sup>31</sup> Magnetic susceptibility is closely related to polarizability and is different in the plane and perpendicular to the plane of the ring. It can be determined by various spectroscopic measurements,<sup>32</sup> as well as by using an NMR spectrometer.<sup>33</sup> It is observed that aromatic compounds have enhanced magnetic susceptibility, called *exaltation* ( $\Lambda$ ), relative to values predicted on the basis of the localized structural components.<sup>34</sup>

**Magnetic Susceptibility Exaltation for Some Aromatic Hydrocarbons**

Compound	$\Lambda$
Benzene	13.7
Naphthalene	30.5
Anthracene	48.6
Phenanthrene	46.2
Azulene	29.6

Magnetic susceptibility can also be calculated by computational methods; calculation by the B3LYP method correctly reproduces some of the trends in stability among the benzo[b]- and benzo[c]- derivatives of five-membered heterocycles.<sup>35</sup> The benzenoid benzo[b]- isomers are much more stable compounds than the quinoid benzo[c] isomers.



Because all of these electronic aspects of aromaticity are ultimately derived from the electron distribution, we might ask whether representations of electron density reveal any special features in aromatic compounds. The electron density of the  $\pi$  electrons can be mapped through the MESP (molecular electrostatic potential, see Section 1.4.5).<sup>36</sup> The MESP perpendicular to the ring is completely symmetrical for benzene, as would be expected for a delocalized structure and is maximal at about

<sup>31</sup> E. A. Boudreaux and R. R. Gupta, in *Physical Methods in Heterocyclic Chemistry*, R. R. Gupta, ed., Wiley-Interscience, New York, 1984, pp. 281–311.

<sup>32</sup> W. H. Flygare, *Chem. Rev.*, **74**, 653 (1974).

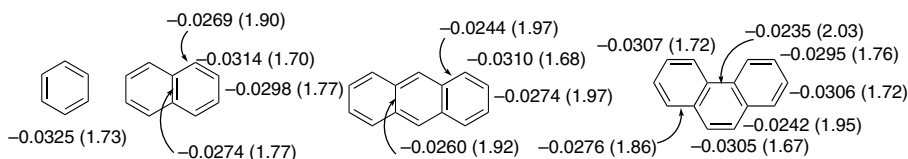
<sup>33</sup> K. Frei and H. J. Bernstein, *J. Chem. Phys.*, **37**, 1891 (1962).

<sup>34</sup> H. J. Dauben, J. D. Wilson, and J. L. Laity, *J. Am. Chem. Soc.*, **90**, 811 (1968); P. v. R. Schleyer and H. Jiao, *Pure Appl. Chem.*, **68**, 209 (1996); P. Friedman and K. F. Ferris, *Int. J. Quantum Chem.*, **24**, 843 (1990).

<sup>35</sup> B. S. Jursic, *J. Heterocycl. Chem.*, **33**, 1079 (1996).

<sup>36</sup> C. H. Suresh and S. R. Gadre, *J. Org. Chem.*, **64**, 2505 (1999).

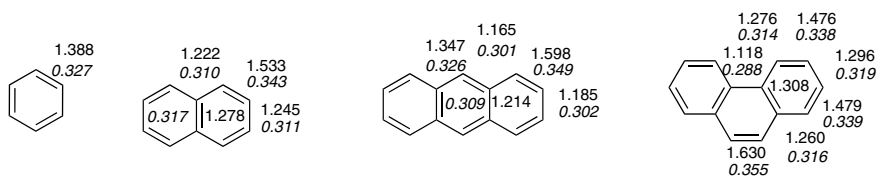
1.73 Å above and below the ring. In naphthalene, there are different values for the different bond types and also shifts in the position of the maxima. The 1,2-bonds, which have higher double-bond character, have more negative MESP than the 2,3-, 8a-1, or 4a,8a-bonds. The maximum in the MESP is also closer to the ring for these bonds. The trend continues for anthracene and is particularly accentuated for phenanthrene. The 9,10-bond in phenanthrene has the closest maxima with respect to the ring, which suggests considerable localization of the 9,10-bond in phenanthrene.



Value of MESP and distance of maxima.

These data are consistent with both the bond order concept (see p. 76) and the idea that benzenoid structures are preferred to quinoid structures (see p. 724).

Atoms in molecules (AIM) concepts have also been applied to analysis of electron density distribution in benzene and several polycyclic hydrocarbons.<sup>37</sup> (See Section 1.4.3 to review AIM electron density indicators.) A correlation was found between the charge density at the bond critical point and bond lengths. Shorter bonds had higher  $\rho_c$  and more negative  $-L(\nabla^2\rho_c)$ , which is also true for other types of bonds. The shorter bonds also have greater ellipticity. Matta and Hernandez-Trujillo found that bond lengths were related to  $\rho_c$  for a series of aromatic molecules<sup>38</sup> They determined the delocalization indices, which indicate the number of electrons shared by adjacent atoms, for a number of rings. These values are 0.99, 1.39, and 1.89, respectively, for ethane, benzene, and ethene, the numbers reflecting the additional electron density associated with the multiple bonds. These values were also calculated for several fused-ring systems, as shown below. The bond ellipticity was also calculated and is given with the structures (italic numbers). Bond ellipticity increases with bond order, reflecting the accumulation of  $\pi$ -electron density.



These values faithfully capture both structural and reactivity variations among the ring systems. The highest bond orders are found at the 1,2-bond of naphthalene and in anthracene. For phenanthrene, the highest bond order is between the 9,10 positions in the center ring. There is substantially less bond alteration around the periphery of phenanthrene than in anthracene. A pictorial representation of this information is given in Figure 8.3. The overall molecular shape is represented by the 0.001 au isodensity

<sup>37</sup>. S. T. Howard and T. M. Krygowski, *Can. J. Chem.*, **75**, 1174 (1997).

<sup>38</sup>. C. F. Matta and J. Hernandez-Trujillo, *J. Phys. Chem. A*, **107**, 7496 (2003).

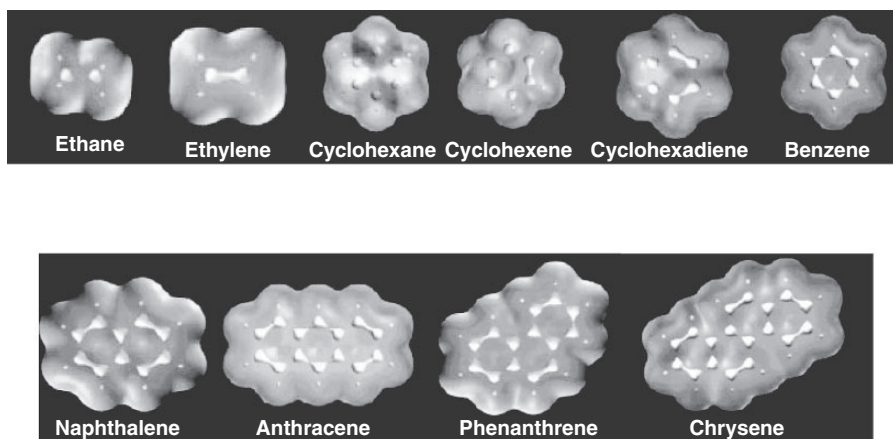
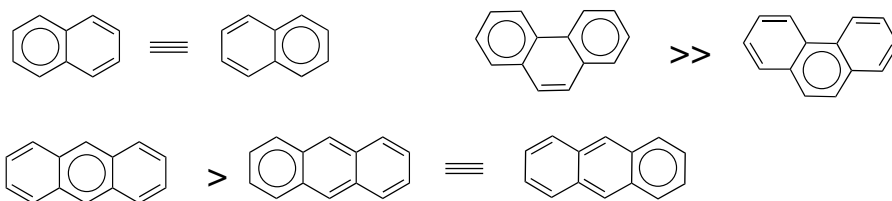


Fig. 8.3. Comparison of electron density as a function of bond order. See text for discussion. Reproduced from *J. Phys. Chem. A*, **107**, 7496 (2003), by permission of the American Chemical Society. (See also color insert.)

surface (gray). The inner lighter surface uses the 0.3274 au surface, which corresponds to the  $\rho_c$  for benzene. Bonds with higher  $\rho_c$  and higher bond order show merged density at this level. Bonds with lower  $\rho_c$  show separation of density at this level between the atoms.

The picture is also consistent with the intuitive idea that the best structure for any given polycyclic molecule is the one with the maximum number of benzene-like rings.<sup>39</sup> According to this concept the two rings in naphthalene are identical, but less aromatic than the benzene ring. The external rings in phenanthrene are more aromatic than the central ring, whereas the central ring is more aromatic in anthracene.



#### 8.1.4. Relationship among the Energetic, Structural, and Electronic Criteria of Aromaticity

It has been argued that there are two fundamental aspects of aromaticity, one reflecting the structural and energetic facets and the other related to electron mobility.<sup>40</sup> Parameters of aromaticity such as bond length and stabilization energy appear to be largely separate from the electronic criteria, such as diamagnetic ring current. However, there is often a correlation between the two kinds of measurements. The

<sup>39</sup> E. Clar, *The Aromatic Sextet*, John Wiley & Sons, London, 1972.

<sup>40</sup> A. R. Katritzky, P. Barczynski, G. Musumarra, D. Pisano, and M. Szafran, *J. Am. Chem. Soc.*, **111**, 7 (1989); A. R. Katritzky, M. Karelson, S. Sild, T. M. Krygowski, and K. Jug, *J. Org. Chem.*, **63**, 5228 (1998); V. I. Minkin, M. N. Glukhovtsev, and B. Ya. Simkin, *Aromaticity and Antiaromaticity*, Wiley, New York, 1994.

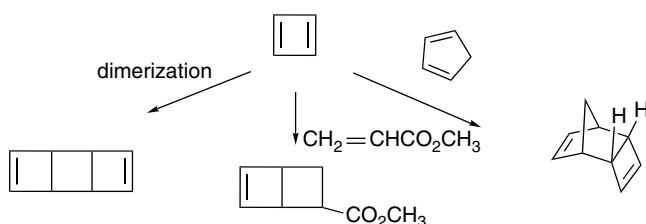
more stabilized compounds exhibit the greatest magnetic susceptibility.<sup>41</sup> The various criteria all correlate, although there may be variation in the degree of correlation for different types of compounds.<sup>42</sup> Aromaticity is thus best conceived of as a single characteristic owing to structural factors that results in both stabilization and the phenomena associated with electron mobility.

## 8.2. The Annulenes

The term *annulene* refers to completely conjugated monocyclic polyenes.<sup>43</sup> The synthesis and study of annulenes has been extended well beyond the first several members of the series, cyclobutadiene, benzene, and cyclooctatetraene, which were described in the Introduction. The generality and limits of the Hückel rule can be tested by considering the properties of the annulene series. In this section, we consider the properties of the annulenes and related compounds in the context of aromaticity.

### 8.2.1. Cyclobutadiene

Although several derivatives of cyclobutadiene are known and are discussed shortly, cyclobutadiene itself has been observed only as a *matrix-isolated species*, that is trapped at very low temperature in a frozen inert gas. The first successful synthesis of cyclobutadiene was achieved by release from a stable iron complex.<sup>44</sup> Various trapping agents react with cyclobutadiene to give Diels-Alder adducts, indicating that it is reactive as both a diene and a dienophile.<sup>45</sup> Dehalogenation of *trans*-3,4-dibromocyclobutene gave the same reaction products.<sup>46</sup>



In the absence of trapping agents, a characteristic dimer is produced, which is the result of one cyclobutadiene molecule acting as a diene and the other as a dienophile in a Diels-Alder reaction. This dimerization is an extremely fast reaction and limits the lifetime of cyclobutadiene, except at extremely low temperatures.

<sup>41</sup> P. v. R. Schleyer, P. K. Freeman, H. Jiao, and B. Goldfuss, *Angew. Chem. Int. Ed. Engl.*, **34**, 337 (1995); C. W. Bird, *Tetrahedron*, **52**, 9945 (1996).

<sup>42</sup> M. K. Cyranski, T. M. Krygowski, A. R. Katritzky, and P. v. R. Schleyer, *J. Org. Chem.*, **67**, 1333 (2002).

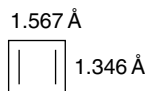
<sup>43</sup> F. Sondheimer, *Pure Appl. Chem.*, **28**, 331 (1971); *Acc. Chem. Res.*, **5**, 81 (1972).

<sup>44</sup> L. Watts, J. D. Fitzpatrick, and R. Pettit, *J. Am. Chem. Soc.*, **87**, 3253 (1965).

<sup>45</sup> L. Watts, J. D. Fitzpatrick, and R. Pettit, *J. Am. Chem. Soc.*, **88**, 623 (1966); J. C. Barborak, L. Watts, and R. Pettit, *J. Am. Chem. Soc.*, **88**, 1328 (1966); D. W. Whitman and B. K. Carpenter, *J. Am. Chem. Soc.*, **102**, 4272 (1980).

<sup>46</sup> E. K. G. Schmidt, L. Brener, and R. Pettit, *J. Am. Chem. Soc.*, **92**, 3240 (1970).

Cyclobutadiene can also be prepared by photolysis of several different precursors at very low temperature in solid inert gases.<sup>47</sup> These methods provide cyclobutadiene in a form that is amenable for spectroscopic study. Analysis of the infrared spectrum of the product and deuterated analogs generated from labeled precursors have confirmed the theoretical conclusion that cyclobutadiene is a rectangular molecule.<sup>48</sup>



A number of alkyl-substituted cyclobutadienes have been prepared by related methods.<sup>49</sup> Increasing alkyl substitution enhances the stability of the compounds. The tetra-*t*-butyl derivative is stable up to at least 150°C, but is very reactive toward oxygen.<sup>50</sup> This reactivity reflects the high energy of the HOMO. The chemical behavior of the cyclobutadienes is in excellent accord with that expected from the theoretical picture of the structure of these compounds.

While simple HMO theory assumes a square geometry for cyclobutadiene, most MO methods predict a rectangular structure as the minimum-energy geometry.<sup>51</sup> The rectangular structure is calculated to be strongly destabilized (antiaromatic) with respect to a polyene model.<sup>52</sup> With HF/6-31G\* calculations, for example, cyclobutadiene is found to have a negative resonance energy of -54.7 kcal/mol, relative to 1,3-butadiene. Furthermore, 30.7 kcal of strain is found, giving a total destabilization of 85.4 kcal/mol.<sup>53</sup> G2 and MP4/G-31(*d,p*) calculations arrive at an antiaromatic destabilization energy of about 42 kcal/mol.<sup>54</sup> A homodesmotic reaction incorporating polyradicals gives a value of 40.3 as the antiaromatic destabilization at the MP4(SDQ)/6-31G(*d,p*) level.<sup>55</sup> Recently, the technique of photoacoustic calorimetry provided the first experimental thermodynamic data on cyclobutadiene. The  $\Delta H_f$  value of  $114 \pm 11$  kcal/mol that was found leads to a total destabilization of 87 kcal/mol, of which 32 kcal/mol is attributed to ring strain and 55 kcal/mol to antiaromaticity.<sup>56</sup>

<sup>47</sup> G. Maier and M. Scheider, *Angew. Chem. Int. Ed. Engl.*, **10**, 809 (1971); O. L. Chapman, C. L. McIntosh, and J. Pancansky, *J. Am. Chem. Soc.*, **95**, 614 (1973); O. L. Chapman, D. De La Cruz, R. Roth, and J. Pancansky, *J. Am. Chem. Soc.*, **95**, 1337 (1973); C. Y. Lin and A. Krantz, *J. Chem. Soc., Chem. Commun.*, 1111 (1972); G. Maier, H. G. Hartan, and T. Sayrac, *Angew. Chem. Int. Ed. Engl.*, **15**, 226 (1976); H. W. Lage, H. P. Reisenauer, and G. Maier, *Tetrahedron Lett.*, **23**, 3893 (1982).

<sup>48</sup> S. Masamune, F. A. Souto-Bachiller, T. Machiguchi, and J. E. Bertie, *J. Am. Chem. Soc.*, **100**, 4889 (1978).

<sup>49</sup> G. Maier, *Angew. Chem. Int. Ed. Engl.*, **13**, 425 (1974); S. Masamune, *Tetrahedron*, **36**, 343 (1980).

<sup>50</sup> G. Maier, S. Pfriem, U. Schafer, and R. Matusch, *Angew. Chem. Int. Ed. Engl.*, **17**, 520 (1978).

<sup>51</sup> J. A. Jafri and M. D. Newton, *J. Am. Chem. Soc.*, **100**, 5012 (1978); W. T. Borden, E. R. Davidson, and P. Hart, *J. Am. Chem. Soc.*, **100**, 388 (1978); H. Kollmar and V. Staemmler, *J. Am. Chem. Soc.*, **99**, 3583 (1977); M. J. S. Dewar and A. Komornicki, *J. Am. Chem. Soc.*, **99**, 6174 (1977); B. A. Hess, Jr., P. Carsky, and L. J. Schaad, *J. Am. Chem. Soc.*, **105**, 695 (1983); H. Kollmar and V. Staemmler, *J. Am. Chem. Soc.*, **100**, 4304 (1978); C. van Wullen and W. Kutzelnigg, *Chem. Phys. Lett.*, **205**, 563 (1993).

<sup>52</sup> M. N. Glukhovtsev, S. Laiter, and A. Pross, *J. Phys. Chem.*, **99**, 6828 (1995).

<sup>53</sup> B. A. Hess, Jr., and L. J. Schaad, *J. Am. Chem. Soc.*, **105**, 7500 (1983).

<sup>54</sup> M. N. Glukhovtsev, R. D. Bach, and S. Laiter, *Theochem*, **417**, 123 (1997).

<sup>55</sup> C. H. Suresh and N. Koga, *J. Org. Chem.*, **67**, 1965 (2002).

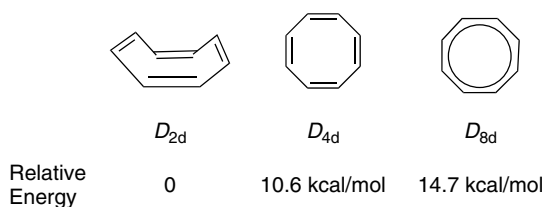
<sup>56</sup> A. A. Deniz, K. S. Peters, and G. J. Snyder, *Science*, **286**, 1119 (1999).

### 8.2.2. Benzene

[6]Annulene is benzene. Its properties are so familiar to students of organic chemistry that not much need be said here. It is the parent compound of a vast series of derivatives. As we indicated in Section 8.2.1, benzene exhibits all the properties associated with aromaticity. It shows exceptional thermodynamic stability and its perfectly hexagonal structure sets the standard for bond uniformity. Benzene is much less reactive than conjugated polyenes toward electrophiles, which is in line with the energy of the HOMO of benzene being lower than that for the HOMO of a conjugated polyene. Benzene also exhibits NMR and magnetic susceptibility criteria consistent with aromaticity.

### 8.2.3. 1,3,5,7-Cyclooctatetraene

The next higher annulene, cyclooctatetraene, is nonaromatic.<sup>57</sup> It is readily isolable and the chemical reactivity is normal for a polyene. X-ray structure determination shows that the molecule is tub-shaped,<sup>19</sup> and therefore is not a planar system to which the Hückel rule applies. The bond lengths around the ring alternate as expected for a polyene. The C=C bonds are 1.33 Å, whereas the C–C bonds are 1.462 Å in length.<sup>58</sup> Thermodynamic analysis provides no evidence of any special stability.<sup>59</sup> There have been both experimental and theoretical studies aimed at estimating the relative stability of the planar form of cyclooctatetraene.<sup>60</sup> HF/6-31G\* calculations find the completely delocalized  $D_{8h}$  structure to be about 4.1 kcal higher in energy than the conjugated planar  $D_{4h}$  structure, suggesting that delocalization leads to destabilization.<sup>61</sup> Similar results are obtained using MP2/CASSCF calculations.<sup>62</sup>



These two energies are, respectively, comparable to the experimental activation energies for conformation inversion of the tub conformer and bond shifting, suggesting that the two planar structures might represent the transition states for those processes. The  $E_a$  have been measured for several substituted cyclooctatetraenes. According to

<sup>57</sup> G. Schroeder, *Cyclooctatetraene*, Verlag Chemie, Weinheim, 1965; G. I. Fray and R. G. Saxton, *The Chemistry of Cyclooctatetraene and Its Derivatives*, Cambridge University Press, Cambridge, 1978.

<sup>58</sup> M. Traetteberg, *Acta Chem. Scand.*, **20**, 1724 (1966).

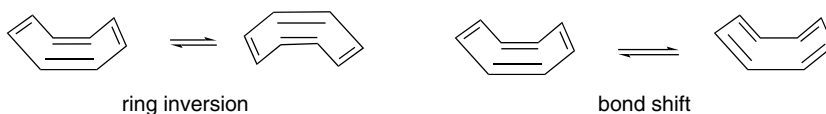
<sup>59</sup> R. B. Turner, B. J. Mallon, M. Tichy, W. v. E. Doering, W. Roth, and G. Schroeder, *J. Am. Chem. Soc.*, **95**, 8605 (1973).

<sup>60</sup> L. A. Paquette, *Acc. Chem. Res.*, **26**, 57 (1993).

<sup>61</sup> D. A. Hrovat and W. T. Borden, *J. Am. Chem. Soc.*, **114**, 5879 (1992); P. Politzer, J. S. Murray, and J. M. Seminario, *Int. J. Quantum Chem.*, **50**, 273 (1994).

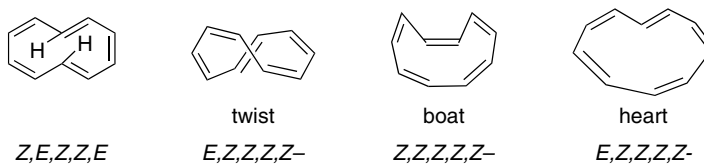
<sup>62</sup> J. L. Andres, D. Castano, A. Morreale, R. Palmeiro, and R. Gomperts, *J. Chem. Phys.*, **108**, 203 (1998).

these studies the ring inversion TS is usually about 2 kcal/mol below the bond shift TS.<sup>60</sup> This result implies a small destabilization of the delocalized structure.



#### 8.2.4. [10]Annulenes—1,3,5,7,9-Cyclodecapentaene Isomers

Larger annulenes permit the incorporation of *trans* double bonds into the rings, and isomeric structures are possible beginning with [10]annulene. According to the Hückel rule, [10]annulene would be aromatic if it were planar. However, all the 1,3,5,7,9-cyclodecapentaene isomers suffer serious steric strain that prevents the planar geometry from being adopted. The *Z,E,Z,Z,E*-isomer, which has minimal bond angle strain, suffers a severe nonbonded repulsion between the two internal hydrogens. The most stable structures are called the twist, boat, and heart.

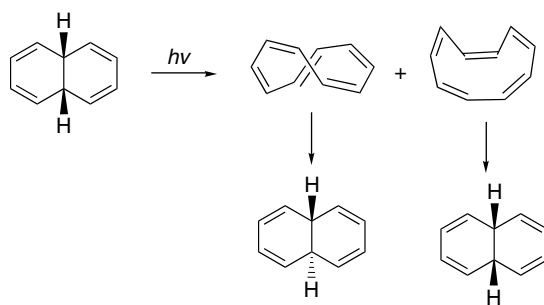


The *Z,Z,Z,Z,Z*-isomer is required by geometry to have bond angles of 144° to maintain planarity and would therefore be destabilized by distortion of the normal trigonal bond angle. According to CCSD(T)/TZ2P-level calculations, the most stable structure is the twist form of the *E,Z,Z,Z,Z*-isomer.<sup>63</sup> This isomer also has the closest agreement between calculated and observed NMR chemical shifts.<sup>64</sup> All of the isomers prepared to date are quite reactive, but whether the most stable isomer has been observed is uncertain. Two isomeric [10]annulenes, as well as other products, are formed by photolysis of *cis*-9,10-dihydronaphthalene.<sup>65</sup> Neither compound exhibits properties that would suggest aromaticity. The NMR spectra are consistent with polyene structures. Both compounds are thermally unstable and revert back to stereoisomeric dihydronaphthalenes. The stereochemistry of the products is consistent with assigning the *E,Z,Z,Z,Z*- and *Z,Z,Z,Z,Z*-configurations. These results indicate that [10]annulene is sufficiently distorted from planarity that little aromatic stabilization is achieved.

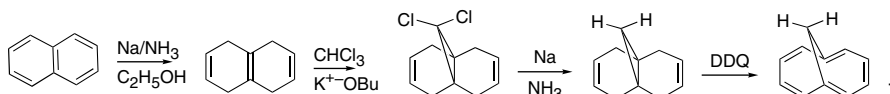
<sup>63</sup> R. A. King, T. D. Crawford, J. F. Stanton, and H. F. Schaefer, III, *J. Am. Chem. Soc.*, **121**, 10788 (1999).

<sup>64</sup> D. R. Price and J. F. Stanton, *Org. Lett.*, **4**, 2809 (2002).

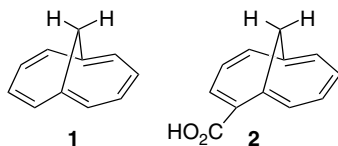
<sup>65</sup> S. Masamune, K. Hojo, G. Gigam, and D. L. Rabenstein, *J. Am. Chem. Soc.*, **93**, 4966 (1971); S. Masamune and N. Darby, *Acc. Chem. Res.*, **5**, 272 (1972).



A number of structures have been prepared that avoid the steric problems associated with the 1,3,5,7,9-cyclodecapentaenes. 1,6-Methano[10]annulene (**1**) can be prepared from naphthalene in multigram quantities in four steps.<sup>66</sup>



Quite a number of substituted derivatives have also been prepared. In compound **1** the steric problem is avoided with only a modest loss of planarity in the  $\pi$  system.<sup>67</sup>



The results of X-ray crystal structure determinations on **1**<sup>68</sup> and its carboxylic acid derivative **2**<sup>69</sup> are shown in Figure 8.4. Both reveal a pattern of bond lengths that is similar to that in naphthalene (see p. 18).<sup>70</sup>

The NMR spectrum of compound **1** shows a diamagnetic ring current of the type expected in an aromatic system.<sup>71</sup> The NICS calculated for **1** is  $-17.7$ , which indicates aromaticity.<sup>72</sup> Both spectroscopic data and MO (MP2/DZV\*\*) and DFT (B3LYP/6-31G) calculations indicate that the ground state of **1** is delocalized.<sup>73</sup> Thus while the  $\pi$  system in **1** is not completely planar, it appears to be sufficiently close to provide a delocalized 10-electron  $\pi$  system. A stabilization energy of 17.2 kcal has been obtained on the basis of an experimental heat of hydrogenation.<sup>74</sup>

<sup>66</sup> E. Vogel, W. Klug, and A. Breuer, *Org. Synth.*, **VI**, 731 (1988).

<sup>67</sup> E. Vogel and H. D. Roth, *Angew. Chem. Int. Ed. Engl.*, **3**, 228 (1964).

<sup>68</sup> R. Bianchi, T. Pilati, and M. Simonetta, *Acta Crystallogr.*, Sect. B, **B36**, 3146 (1980).

<sup>69</sup> M. Dobler and J. D. Dunitz, *Helv. Chim. Acta*, **48**, 1429 (1965).

<sup>70</sup> O. Bastainens and P. N. Skancke, *Adv. Chem. Phys.*, **3**, 323 (1961).

<sup>71</sup> E. Vogel, *Pure Appl. Chem.*, **20**, 237 (1969).

<sup>72</sup> M. Nendel, K. N. Houk, L. M. Tolbert, E. Vogel, H. Jiao, and P. v. R. Schleyer, *J. Phys. Chem. A*, **102**, 7191 (1998).

<sup>73</sup> C. Gellini, P. R. Salvi, and E. Vogel, *J. Phys. Chem. A*, **104**, 3110 (2000); R. Seiler and B. Dick, *Angew. Chem. Int. Ed. Engl.*, **48**, 4020 (2001); L. Catani, C. Gellini, and P. R. Salvi, *J. Phys. Chem. A*, **102**, 1945 (1998).

<sup>74</sup> W. R. Roth, M. Bohm, H. W. Lennartz, and E. Vogel, *Angew. Chem. Int. Ed. Engl.*, **22**, 1007 (1983); W. R. Roth, F.-G. Klarner, G. Siepert, and H.-W. Lennartz, *Chem. Ber. Recueil.*, **125**, 217 (1992).

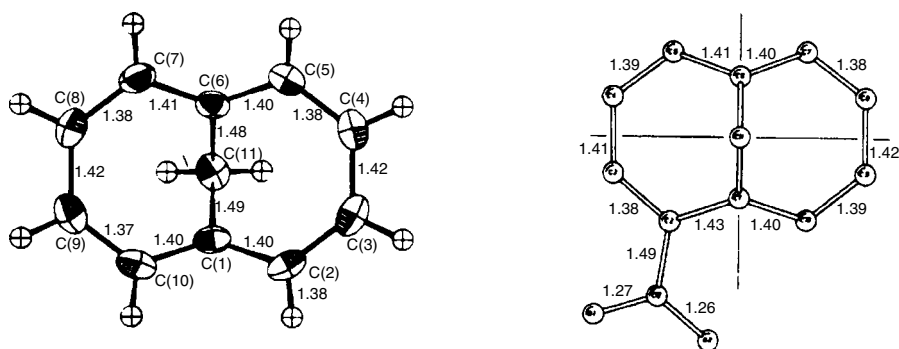
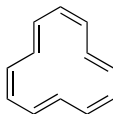


Fig. 8.4. X-ray crystal structure of 1,6-methanocyclodeca-1,3,5,7,9-pentaene (left) and 1,6-methanocyclodeca-1,3,5,7,9-pentaene-2-carboxylic acid (right). Reproduced from *Acta Crystallogr. B*, **36**, 3146 (1980) and *Helv. Chim. Acta*, **48**, 1429 (1965), by permission of the International Union of Crystallography and Wiley-VCH, respectively.

The deviation from planarity that is present in a structure such as **1** raises the question of how severely a conjugated system can be distorted from the ideal coplanar alignment of  $p$  orbitals and still retain aromaticity. This problem has been analyzed by determining the degree of rehybridization necessary to maximize  $p$ -orbital overlap in **1**.<sup>75</sup> A quantitative VB treatment also finds the periphery of conjugated bonds to be delocalized and the orbitals are quite similar to those in naphthalene.<sup>76</sup> Thus a relatively small amount of rehybridization greatly improves orbital overlap in the twisted system and stabilizes the structure.

### 8.2.5. [12], [14], and [16]Annulenes

[12]Annulene is a very unstable compound that undergoes cyclization to bicyclic isomers and can be kept only at very low temperature.<sup>77</sup> The NMR spectrum has been studied at low temperature.<sup>78</sup> Apart from indicating the  $Z,E,Z,E,Z,E$ -double-bond geometry shown in the structure, the spectrum reveals a *paramagnetic ring current*, the opposite from what is observed for aromatic systems. This feature is characteristic of the  $[4n]$ annulenes and has been useful in characterizing the aromaticity or lack of it in annulenes.<sup>79</sup>



[14]Annulene was first prepared in 1960.<sup>80</sup> Its NMR spectrum has been investigated and shows that two geometric isomers are in equilibrium.<sup>81</sup>

<sup>75</sup> R. C. Haddon, *Acc. Chem. Res.*, **21**, 243 (1988).

<sup>76</sup> M. Sironi, M. Raimondi, D. L. Cooper, and J. Gerratt, *Theochem*, **338**, 257 (1995).

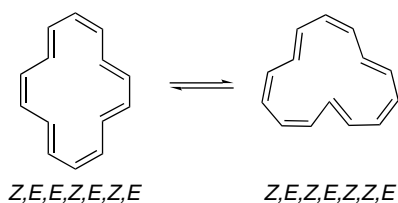
<sup>77</sup> J. F. M. Oth, H. Rottele, and G. Schroeder, *Tetrahedron Lett.*, 61 (1970).

<sup>78</sup> J. F. M. Oth, J.-M. Gilles, and G. Schroeder, *Tetrahedron Lett.*, 67 (1970).

<sup>79</sup> R. C. Haddon, *Tetrahedron*, **28**, 3613, 3635 (1972).

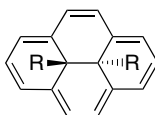
<sup>80</sup> F. Sondheimer and Y. Gaoni, *J. Am. Chem. Soc.*, **82**, 5765 (1960).

<sup>81</sup> J. F. M. Oth, *Pure Appl. Chem.*, **25**, 573 (1971).



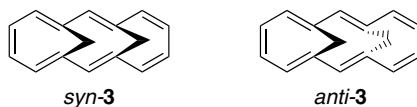
The spectrum also reveals a significant diamagnetic (aromatic) ring current. The internal hydrogens [C(3), C(6), C(10), C(13)] are very far upfield ( $\delta = -0.61$  ppm).<sup>86</sup> The interconversion of the two forms involves a configurational change from *E* to *Z* of at least one double bond, and the  $E_a$  for this process is about 10 kcal/mol. The crystal structure for [14]annulene shows the *Z,E,E,Z,E,Z,E*-form to be present in the solid.<sup>82</sup> The bond lengths around the ring range from 1.35 to 1.41 Å, but do not show the alternating pattern of short and long bonds expected for a localized polyene. There is some distortion from planarity, especially at carbon atoms 3, 6, 10, and 13, which is caused by nonbonded repulsions between the internal hydrogens. MP2/6-31G\* and B3LYP/6-31G\* calculations find the delocalized structure as the only minimum.<sup>83</sup>

A 14-electron  $\pi$  system can be generated in circumstances in which the steric problem associated with the internal hydrogens of [14]annulene can be avoided. This can be achieved in 10b,10c-dihydropyrene systems, in which the annulene ring is built around a saturated core.



Several derivatives of this ring system have been synthesized.<sup>84</sup> The properties of these compounds indicate that the conjugated system has aromatic character. They exhibit NMR shifts characteristic of a diamagnetic ring current. Typical aromatic substitution reactions can be carried out.<sup>85</sup> An X-ray crystal structure ( $R = C_2H_5$ ) shows that the bond lengths are in the aromatic range (1.39–1.40 Å), and there is no strong alternation around the ring.<sup>86</sup> The peripheral atoms are not precisely planar, but the maximum deviation from the average plane is only 0.23 Å. The dimethyl derivative is essentially planar with bond lengths between 1.38 and 1.40 Å.

Another family of 14  $\pi$ -electron systems is derived from structure **3**.<sup>87</sup>



<sup>82</sup> C. C. Chiang and I. C. Paul, *J. Am. Chem. Soc.*, **94**, 4741 (1972).

<sup>83</sup> C. H. Choi, M. Kertesz, and A. Karpfen, *J. Am. Chem. Soc.*, **119**, 11994 (1997).

<sup>84</sup> (a) R. H. Mitchell and V. Boekelheide, *J. Am. Chem. Soc.*, **96**, 1547 (1974); (b) V. Boekelheide and T. A. Hylton, *J. Am. Chem. Soc.*, **92**, 3669 (1970); (c) H. Blaschke, C. E. Ramey, I. Calder, and V. Boekelheide, *J. Am. Chem. Soc.*, **92**, 3675 (1970); (d) V. Boekelheide and J. B. Phillips, *J. Am. Chem. Soc.*, **89**, 1695 (1967); (e) R. H. M. Mitchell, V. S. Iyer, N. Khalifa, R. Mahadevan, S. Venugopalan, S. A. Weerawarna, and P. Zhou, *J. Am. Chem. Soc.*, **117**, 1514 (1995).

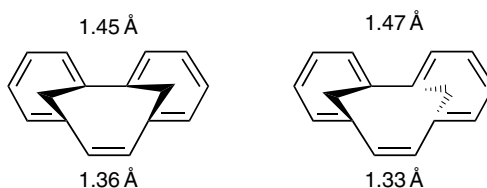
<sup>85</sup> J. B. Phillips, R. J. Molyneux, E. Sturm, and V. Boekelheide, *J. Am. Chem. Soc.*, **89**, 1704 (1967).

<sup>86</sup> A. W. Hanson, *Acta Crystallogr.*, **23**, 476 (1967).

<sup>87</sup> E. Vogel, *Pure Appl. Chem.*, **28**, 355 (1971).

The *syn* isomer can achieve a conjugated system with angles of up to  $35^\circ$  between adjacent *p* orbitals. The *anti* isomer is much more twisted.<sup>88</sup> An X-ray crystal structure determination has been done on the *syn* isomer and is illustrated in Figure 8.5. It shows C–C bond lengths between 1.368 and 1.418 Å for the conjugated system.<sup>89</sup> The spectroscopic properties of the *syn* isomer are consistent with considering it to be a delocalized annulene.<sup>90</sup> B3LYP/6-31G\* calculations indicate that both the *syn* and *anti* structures are stabilized by delocalization, the *syn* (17.6 kcal/mol) more so than the *anti* (8.1 kcal).<sup>91</sup>

An isomeric system is related to the benzenoid hydrocarbon phenanthrene. Both the *syn* and *anti* stereoisomers have been synthesized.<sup>92</sup>



The *syn* isomer shows evidence of a diamagnetic ring current, from both the relatively low field position of the vinylic hydrogens and the upfield shift of the methylene hydrogens. The *anti* isomer shows much less pronounced shifts. The X-ray crystal structure (Figure 8.6) of the *syn* isomer shows a moderate level of bond alternation, ranging from 1.36 to 1.45 Å. In the *anti* isomer bond alternation is more pronounced with the double bond in the center ring being essentially a localized double bond.

The Hückel rule predicts nonaromaticity for [16]annulene. The compound has been synthesized and characterized.<sup>93</sup> The bond lengths show significant alternation in length (C=C, 1.34 Å; C–C, 1.46 Å), and the molecule is less planar

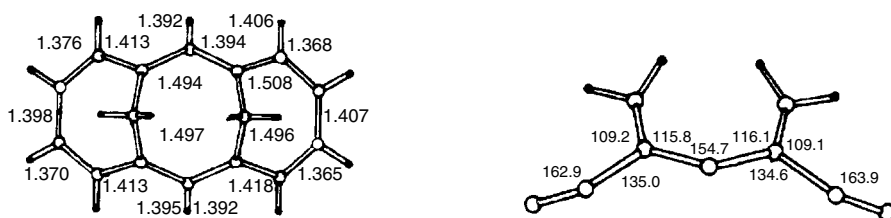


Fig. 8.5. Carbon framework from X-ray crystal structure of *syn*-tricyclo[8.4.1.1<sup>3,8</sup>]hexadeca-1,3,5,7,9,11,13-heptaene (left). Side view showing deviation from planarity of the annulene ring (right). Reproduced from *Acta Crystallogr. B*, **33**, 940 (1977), by Permission of the International Union of Crystallography.

- <sup>88</sup> E. Vogel, J. Sombroek, and W. Wagemann, *Angew. Chem. Int. Ed. Engl.*, **14**, 564 (1975); E. Vogel, U. Haberland, and H. Gunther, *Angew. Chem. Int. Ed. Engl.*, **9**, 513 (1970).
- <sup>89</sup> R. Destro, T. Pilati, and M. Simonetta, *Acta Crystallogr.*, **B**, **33**, 940 (1977).
- <sup>90</sup> J. Dewey, H. M. Deger, W. Froehlich, B. Dick, K. A. Klingensmith, G. Hohlneicher, E. Vogel, and J. Michl, *J. Am. Chem. Soc.*, **102**, 6412 (1980).
- <sup>91</sup> M. Nendel, K. N. Houk, L. M. Tolbert, E. Vogel, H. Jiao, and P. v. R. Schleyer, *Angew. Chem. Int. Ed. Engl.*, **36**, 748 (1997).
- <sup>92</sup> E. Vogel, W. Puttmann, W. Duchatsch, T. Schieb, H. Schmickler, and J. Lex, *Angew. Chem. Int. Ed. Engl.*, **25**, 720 (1986); E. Vogel, T. Schieb, W. H. Schulz, K. Schmidt, H. Schmickler, and J. Lex, *Angew. Chem. Int. Ed. Engl.*, **25**, 723 (1986).
- <sup>93</sup> I. Calder, Y. Gaoni, and F. Sondheimer, *J. Am. Chem. Soc.*, **90**, 4946 (1968); G. Schroeder and J. F. M. Oth, *Tetrahedron Lett.*, 4083 (1966).

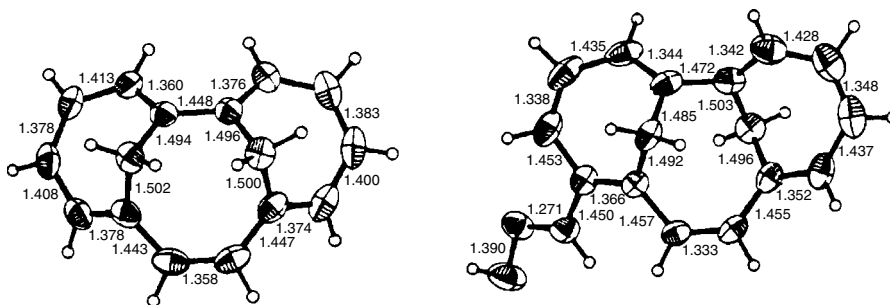
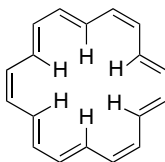


Fig. 8.6. X-ray structure of *syn*-tricyclo[8.4.1.1<sup>4,9</sup>]hexadeca-2,4,6,8,10,12,14-heptaene (left). X-ray crystal structure of *anti* isomer of tricyclo[8.4.1.1<sup>4,9</sup>]hexadeca-2,4,6,8,10,12,14-heptaene-5-carbaldehyde oxime (right). Reproduced from *Angew. Chem. Int. Ed. Engl.*, **25**, 720, 723 (1986), by permission of Wiley-VCH.

than [14]annulene.<sup>94</sup> Experimental combustion data indicate that [16]annulene is less stable than cyclooctatetraene.<sup>95</sup> Computational studies and NMR spectra of deuterated [16]annulene indicate that there are several conformations that differ in relative placement of the internal hydrogens.<sup>96</sup> These structural data are consistent with regarding [16]annulene as being nonaromatic.

### 8.2.6. [18]Annulene and Larger Annulenes

[18]Annulene offers a particularly significant test of the Hückel rule. The internal cavity in [18]annulene is large enough to minimize steric interaction between the internal hydrogens in a geometry that is free of angle strain. Most MO calculations find the delocalized structure to be more stable than the polyene.<sup>97</sup> Both MP/6-31G\* and B3LYP/6-311G\* calculations find a delocalized structure with  $D_{6h}$  symmetry as the minimum energy. The bond lengths are 1.39–1.42 Å, and a stabilization of 18 kcal/mol is indicated.<sup>98</sup>



The properties of [18]annulene are consistent with its being aromatic. The X-ray crystal structure shows the molecule to be close to planarity, with the maximum deviation from the plane being 0.085 Å.<sup>99</sup> The bond lengths are in the range 1.385–1.405 Å, and

<sup>94</sup> S. M. Johnson and I. C. Paul, *J. Am. Chem. Soc.*, **90**, 6555 (1968).

<sup>95</sup> G. R. Stevenson and B. E. Forch, *J. Am. Chem. Soc.*, **102**, 5985 (1980).

<sup>96</sup> J. M. Hernando, J. J. Quirante, and F. Enriquez, *Collect. Czech. Chem. Commun.*, **57**, 1 (1992);

C. D. Stevenson and T. L. Kurth, *J. Am. Chem. Soc.*, **122**, 722 (2000).

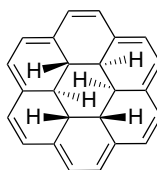
<sup>97</sup> J. M. Shulman and R. L. Disch, *Theochem.*, **80**, 213 (1991); K. Yoshizawa, T. Kato, and T. Yamabe, *J. Phys. Chem.*, **100**, 5697 (1996).

<sup>98</sup> K. K. Baldridge and J. S. Siegel, *Angew. Chem. Int. Ed. Engl.*, **36**, 745 (1997); C. H. Choi, M. Kertesz, and A. Karpfen, *J. Am. Chem. Soc.*, **119**, 11994 (1997).

<sup>99</sup> J. Bregman, F. L. Hirshfeld, D. Rabinovich, and G. M. J. Schmidt, *Acta Crystallogr.*, **19**, 227 (1965); F. L. Hirshfeld and D. Rabinovich, *Acta Crystallogr.*, **19**, 235 (1965); S. Gorter, E. Rutten-Keulemans, M. Krever, C. Romers, and D. W. J. Cruickshank, *Acta Cryst.*, **B51**, 1036 (1995).

the pattern is short, short, long, rather than alternating. The NMR spectrum indicates an aromatic ring current.<sup>100</sup> The chemical reactivity of the molecule also justifies its classification as aromatic.<sup>101</sup>

There are also examples of [18]annulene systems constructed around a saturated central core, such as in compound **4**.<sup>102</sup> In this compound, the internal protons are at very high field (−6 to −8 ppm), whereas the external protons are far downfield (~ 9.5 ppm).

**4**

The chemical shift data can be used as the basis for calculating the diamagnetic ring current by comparing the value with the maximum ring current expected for a completely delocalized  $\pi$  system. By this criterion, the flexible [18]annulene maintains only about half (0.56) of the maximum ring current, whereas the rigid ring in **4** gives a value of 0.88, indicating more effective conjugation in this system.

The synthesis of annulenes has been carried forward to larger rings as well. [20]Annulene,<sup>103</sup> [22]annulene,<sup>104</sup> and [24]annulene<sup>105</sup> have all been reported. The NMR spectra of these compounds are consistent with regarding [22]annulene as aromatic, whereas the [20] and [24] analogs are not. The dominant structure for [24]annulene has a repeating *Z,E,E*-motif of double bonds. The internal hydrogens are at lower field in the <sup>1</sup>H-NMR spectrum than the external ones, which is consistent with a paramagnetic ring current. There is another minor conformation that has the same configuration of the double bonds. There is also evidence for a bond shift process that interchanges single and double bonds. This process occurs with a  $\Delta G^\ddagger$  of about 10 kcal/mol.<sup>106</sup> Although the properties of these molecules have not been studied as completely as for the smaller systems, they are consistent with the predictions of the Hückel rule.

<sup>100</sup>. Y. Gaoni, A. Melera, F. Sondheimer, and R. Wolovsky, *Proc. Chem. Soc.*, 397 (1965).

<sup>101</sup>. I. C. Calder, P. J. Garratt, H. C. Longuet-Higgins, F. Sondheimer, and R. Wolovsky, *J. Chem. Soc. C*, 1041 (1967).

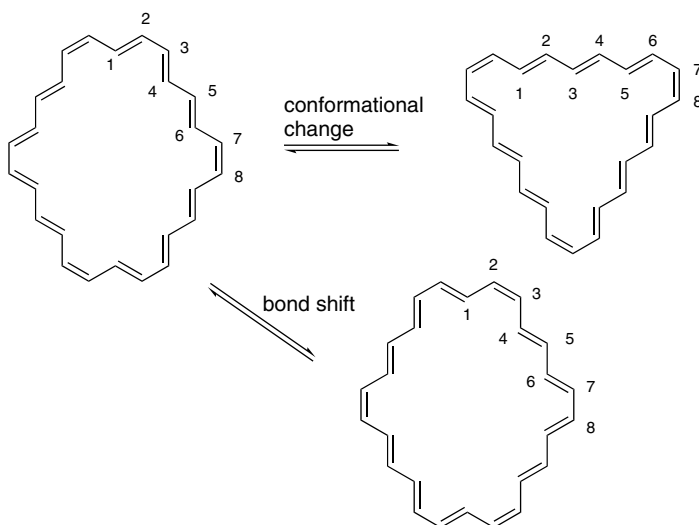
<sup>102</sup>. T. Otsubo, R. Gray, and V. Boekelheide, *J. Am. Chem. Soc.*, **100**, 2449 (1978).

<sup>103</sup>. B. W. Metcalf and F. Sondheimer, *J. Am. Chem. Soc.*, **93**, 6675 (1971).

<sup>104</sup>. R. M. McQuilkin, B. W. Metcalf, and F. Sondheimer, *J. Chem. Soc., Chem. Commun.*, 338 (1971).

<sup>105</sup>. I. C. Calder and F. Sondheimer, *J. Chem. Soc., Chem. Commun.*, 904 (1966).

<sup>106</sup>. J. F. M. Oth and Y. de J. de Zelicourt, *Helv. Chim. Acta*, **82**, 435 (1999).



Theoretical calculations indicate that the tendency to be aromatic decreases as ring size increases.<sup>107</sup> For example, the NICS value decreases from  $-15.0$  and  $-14.7$  for [14] and [18]annulene, respectively, to  $-5.6$  at [42]annulene and  $-1.2$  at [66]annulene. The delocalized structures are computed to be more stable, however, leveling off at 22–23 kcal/mol at [30]annulene.<sup>108</sup> Of course, on a per electron basis, this means a decrease in relative stability.

### 8.2.7. Other Related Structures

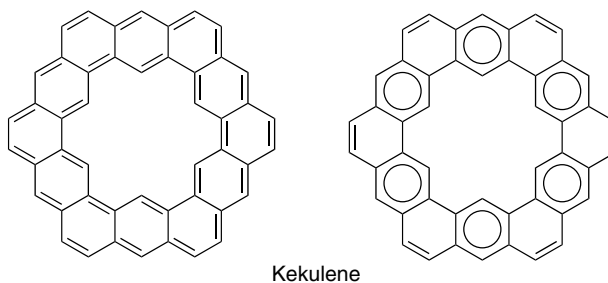
Both clever synthesis and energetic processes leading to stable compounds have provided other examples of structures for which aromaticity might be important. Kekulene was synthesized in 1978.<sup>109</sup> How aromatic is this substance? By both energy and magnetic criteria, it appears that it is primarily benzenoid in character. Its energy is close to that expected from isodesmic reactions summing smaller aromatic components. Magnetic criteria, too, indicate that it is similar to the smaller polycyclic benzenoid hydrocarbons, such as phenanthrene and anthracene.<sup>110</sup> Kekulene seems best represented by a structure that emphasizes the aromaticity of alternating rings, similar to the structure of phenanthrene (see p. 772). (See Problem 8.15 to consider this issue more thoroughly.)

<sup>107</sup> C. H. Choi and M. Kertesz, *J. Chem. Phys.*, **108**, 6681 (1998).

<sup>108</sup> C. S. Wannere and P. v. R. Schleyer, *Org. Lett.*, **5**, 865 (2003).

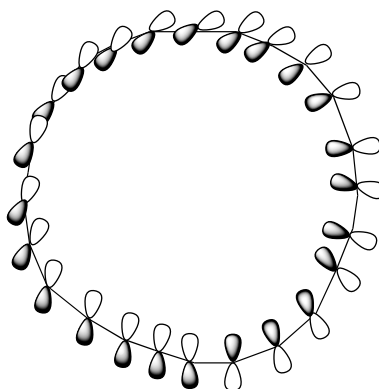
<sup>109</sup> H. A. Staab and F. Diedrich, *Angew. Chem. Int. Ed. Engl.*, **17**, 372 (1978); H. A. Staab and F. Diedrich, *Chem. Ber.*, **116**, 3487 (1983).

<sup>110</sup> H. Jiao and P. v. R. Schleyer, *Angew. Chem. Int. Ed. Engl.*, **35**, 2383 (1996).



Fullerene,  $C_{60}$ , is a spherical form of carbon that is produced by processes such as laser vaporization of graphite.<sup>111</sup> The structure consists of hexagons and pentagons, corresponding to the pattern of a soccer ball. There is bond length variation with the bonds shared by the hexagonal rings being shorter ( $1.40 \pm 0.01 \text{ \AA}$ ) than those of the pentagons ( $1.46 \pm 0.01 \text{ \AA}$ ). Unlike benzene, with its two-Kekule structure, there is only one valence bond structure for  $C_{60}$ . It has double bonds at all hexagon-hexagon edges and single bonds at the pentagonal edges. An isodesmic energy computation suggests that the  $\pi$  system is substantially less stable than for benzene on an atom-by-atom comparison.<sup>112</sup> Calculated chemical shift parameters suggest that the five-membered rings are antiaromatic, whereas the hexagonal rings are aromatic.<sup>113</sup> Thus it appears that fullerene is a delocalized molecule, but with both stabilizing and destabilizing components, which are partially compensating in terms of stabilization energy.

It was pointed out that a different array of atomic orbitals might be conceived of in large conjugated rings. The array, called a *Mobius twist*, results in there being one point in the ring at which the atomic orbitals have a phase reversal (node).<sup>114</sup>



If the ring were sufficiently large that the twist between individual orbitals was small, such a system would not necessarily be less stable than the normal array of atomic orbitals. This same analysis points out that in such an array the Hückel rule is reversed and aromaticity is predicted for the  $4n$   $\pi$ -electron systems.

<sup>111</sup> H. W. Kroto, J. P. Heath, S. C. O'Brien, R. F. Curl, and R. E. Smalley, *Nature*, **318**, 162 (1985).

<sup>112</sup> P. W. Fowler, D. J. Collins, and S. J. Austin, *J. Chem. Soc., Perkin Trans. 2*, 275 (1993).

<sup>113</sup> P. v. R. Schleyer, C. Maerker, A. Dransfeld, H. Jiao, and N. J. R. van Eikema Hommes, *J. Am. Chem. Soc.*, **118**, 6317 (1996).

<sup>114</sup> E. Helibronner, *Tetrahedron Lett.*, 1923 (1964).

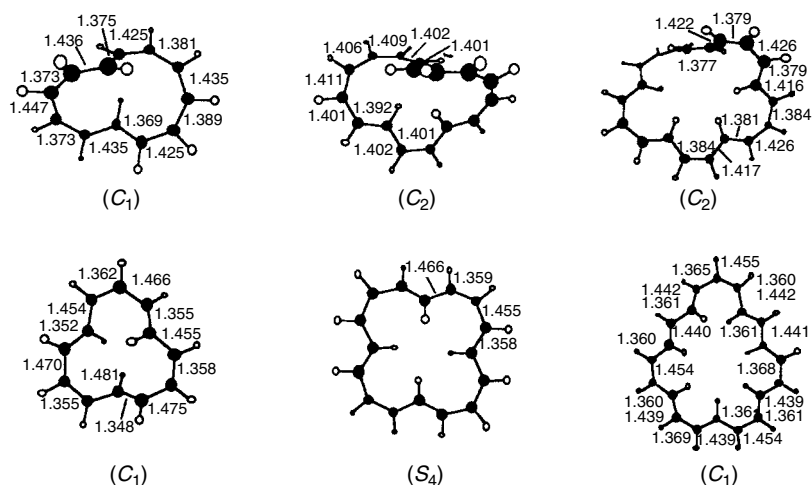


Fig. 8.7. Most stable (top) and most aromatic (bottom) Mobius structures for [12], [16], and [20]annulene. Reproduced from *Org. Lett.*, **4**, 3431 (2002), by permission of the American Chemical Society.

The possibility of Mobius conjugation in [12], [16], and [20]annulene has been explored using B3LYP/6-31G\* calculations.<sup>115</sup> The most stable and most aromatic structures are shown in Figure 8.7. The most aromatic Mobius isomer of [12]annulene is found about 4.4 kcal/mol above the most stable structure. It shows an NICS of  $-14.6$  and relatively little bond length alternation, despite angles deviating as much as  $53.6^\circ$  from the alignment of the  $p$  orbitals. The most stable structure does not have aromatic characteristics, showing a positive NICS. For [16]annulene, the most aromatic Mobius structure is 15.8 kcal/mol above the most stable structure. The most aromatic structure for [20]annulene is 6.2 kcal/mol above the most stable structure. Thus, although it appears that there are energy minima corresponding to Mobius structures, they all lie above nonaromatic structures in energy.

#### Comparison of Properties of “Most Stable” and “Most Aromatic” Structure for [12], [16], and [20]annulenes

	[12]		[16]		[20]	
	Most stable	Best Mobius	Most stable	Best Mobius	Most stable	Best Mobius
Relative energy <sup>a</sup>	0.0	4.4	0.0	15.8	0.0	6.2
$\Delta$ in bond length <sup>b</sup>	0.133	0.078	0.097	0.019	0.095	0.049
NICS	+3.2	$-14.6$	+10.9	$-14.5$	+12.1	$-10.2$
$\chi$	$-65.0$	$-101.5$	$-63.9$	$-176.8$	$-75.6$	$-170.8$
Max angle of twist	$62.4^\circ$	$53.6^\circ$	$32.6^\circ$	$29.1^\circ$	$29.5^\circ$	$29.9^\circ$

a. kcal/mol.

b. Difference between shortest and longest bond lengths in Å.

So far, no ground state molecule in which the twisted conjugation exists has been made. Whatever stabilization is associated with aromaticity in the Mobius structures is

<sup>115</sup> C. Castro, C. Isborn, W. L. Karney, M. Mauksch, and P. v. R. Schleyer, *Org. Lett.*, **4**, 3431 (2002).

counterbalanced by bond angle and other strain, so the prediction of Möbius aromaticity remains to be verified experimentally. Its correctness is strongly suggested, however, by the fact that transition structures with twisted orbital arrays appear to be perfectly acceptable in many organic reactions.<sup>116</sup> We return to this topic in Section 10.1. The rules for aromaticity can be generalized to include Möbius orbital arrays:

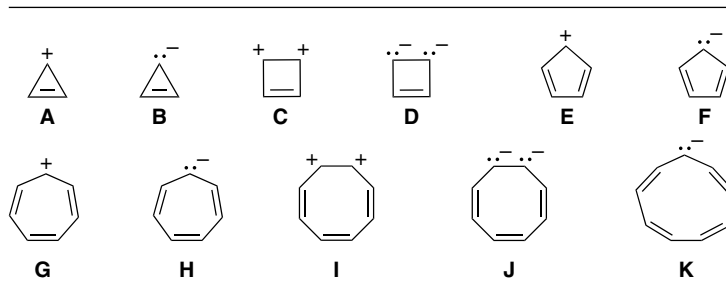
Hückel Orbital Array	Möbius Orbital Array
$4n + 2 = \text{Aromatic}$	$4n = \text{Aromatic}$
$4n = \text{Antiaromatic}$	$4n + 2 = \text{Antiaromatic}$

### 8.3. Aromaticity in Charged Rings

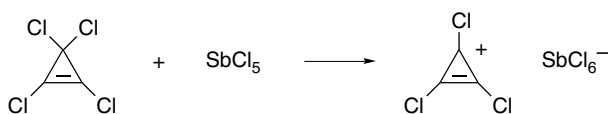
There are striking stability relationships owing to aromaticity in charged ring systems. The HMO energy levels that apply to fully conjugated planar three- to nine-membered rings were shown earlier in Figure 8.1 (p. 714). These energy levels are applicable to ions as well as to the neutral annulenes. A number of cations and anions that are completely conjugated planar structures are shown in Scheme 8.1. Among these species, the Hückel rule predicts aromatic stability for cyclopropenium ion (**A**), cyclobutadiene dication (**C**), cyclobutadiene dianion (**D**), cyclopentadienide anion (**F**), cycloheptatrienyl cation (tropylium ion, **G**), the dications and dianions derived from cyclooctatetraene (**I**, **J**) and the cyclononatetraenide anion (**K**). The other species shown, which have  $4n \pi$  electrons, are expected to be quite unstable. These include cyclopropenide anion (**B**), cyclopentadienyl cation (**E**), and cycloheptatrienide (**H**). Let us examine what is known about the chemistry of some of these systems.

There is a good deal of information about the cyclopropenium ion that supports the idea that it is exceptionally stable. It and a number of derivatives can be generated by ionization procedures.

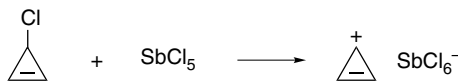
Scheme 8.1. Conjugated Cyclic Cations and Anions



<sup>116</sup> H. E. Zimmerman, *J. Am. Chem. Soc.*, **88**, 1566 (1966); H. E. Zimmerman, *Acc. Chem. Res.*, **4**, 272 (1971).



Ref. 117

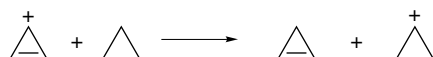


Ref. 118

The 1,2,3-tri-*t*-butylcyclopropenium cation is so stable that the perchlorate salt can be recrystallized from water.<sup>119</sup> An X-ray study of triphenylcyclopropenium perchlorate has verified the existence of the carbocation as a discrete ion.<sup>120</sup> Quantitative estimation of the stability of the unsubstituted cyclopropenium ion can be made in terms of its  $pK_{R^+}$  value of  $-7.4$ , which is intermediate between such highly stabilized ions as triphenylmethyl cation and the *bis*-(4-methoxyphenyl)methyl cation.<sup>121</sup> (See Section 4.4.1 for the definition of  $pK_{R^+}$ ). An HF/6-31G\* MO calculation on the following isodesmic reaction:



yields a  $\Delta H$  of  $+38.2$  kcal/mol, whereas experimental data on the heats of formation of the various species give  $\Delta H = +31$  kcal/mol.<sup>122</sup> Both values imply that the cyclopropenium ion is much more stable than the allyl cation. G2 calculations indicate total aromatic stabilization of  $59.1$  kcal/mol based on the reaction<sup>123</sup>



A radical-based homodesmotic reaction gives a value of  $30.4$  kcal/mol, which compares with  $29.1$  kcal/mol for benzene by the same approach.<sup>124</sup> The gas phase heterolytic bond dissociation energy to form cyclopropenium ion from cyclopropene is  $225$  kcal/mol. This compares with  $256$  kcal/mol for formation of the allyl cation from propene and  $268$  kcal/mol for the 1-propyl cation from propane.<sup>125</sup> It is clear that the cyclopropenyl cation is highly stabilized.

In contrast, the less strained four  $\pi$ -electron cyclopentadienyl cation is quite unstable, being calculated to have a negative stabilization of  $56.7$  kcal/mol.<sup>126</sup> The

<sup>117</sup> S. W. Tobey and R. West, *J. Am. Chem. Soc.*, **86**, 1459 (1964); R. West, A. Sado, and S. W. Tobey, *J. Am. Chem. Soc.*, **88**, 2488 (1966).

<sup>118</sup> R. Breslow, J. T. Groves, and G. Ryan, *J. Am. Chem. Soc.*, **89**, 5048 (1967).

<sup>119</sup> J. Ciabattoni and E. C. Nathan, III, *J. Am. Chem. Soc.*, **91**, 4766 (1969).

<sup>120</sup> M. Sundaralingam and L. H. Jensen, *J. Am. Chem. Soc.*, **88**, 198 (1966).

<sup>121</sup> R. Breslow and J. T. Groves, *J. Am. Chem. Soc.*, **92**, 984 (1970).

<sup>122</sup> L. Radom, P. C. Hariharan, J. A. Pople, and P. v. R. Schleyer, *J. Am. Chem. Soc.*, **98**, 10 (1976).

<sup>123</sup> M. N. Glukhovtsev, S. Laiter, and A. Pross, *J. Phys. Chem.*, **100**, 17801 (1996).

<sup>124</sup> C. H. Suresh and N. Koga, *J. Org. Chem.*, **67**, 1965 (2002).

<sup>125</sup> F. P. Lossing and J. L. Holmes, *J. Am. Chem. Soc.*, **106**, 6917 (1984).

<sup>126</sup> P. v. R. Schleyer, P. K. Freeman, H. Jiao, and B. Goldfuss, *Angew. Chem. Int. Ed. Engl.*, **34**, 337 (1995); B. Reidl and P. v. R. Schleyer, *J. Comput. Chem.*, **19**, 1402 (1998).

cyclopentadienyl cation is also calculated to be antiaromatic by magnetic susceptibility and chemical shift criteria.<sup>127</sup> Its  $pK_{R^+}$  has been estimated as  $-40$ , using an electrochemical cycle.<sup>128</sup> The heterolytic bond dissociation energy to form the cation from cyclopentadiene is 258 kcal/mol, which is substantially more than for formation of an allylic cation from cyclopentene but only slightly more than the 252 kcal/mol required for formation of an unstabilized secondary carbocation.<sup>64</sup> The high energy of the cyclopentadienyl cation is also indicated by ionization studies in solution. A rate retardation of  $10^{-14}$  relative to cyclopentyl analogs has been estimated from solvolytic rate data.<sup>129</sup> Solvolysis of cyclopentadienyl halides assisted by silver ion is extremely slow, even though the halide is doubly allylic.<sup>130</sup> When cyclopentadienyl bromide and antimony pentafluoride react at  $-78^\circ\text{C}$ , an EPR spectrum is observed, which indicates that the cyclopentadienyl cation is a triplet.<sup>131</sup> Similar studies indicate that the pentaisopropyl<sup>132</sup> and pentachlorocyclopentadienyl cation are also triplets, but the ground state of the pentaphenyl derivative is a singlet.

The relative stability of the anions derived from cyclopropene and cyclopentadiene by deprotonation is just the reverse of the situation for the cations. Cyclopentadiene is one of the most acidic hydrocarbons known, with a  $pK_a$  of 16.0.<sup>133</sup> The  $pK$ 's of triphenylcyclopropene and trimethylcyclopropene have been estimated as 50 and 62, respectively, using electrochemical cycles<sup>134</sup> (see Section 6.1). The unsubstituted compound would be expected to fall somewhere between and thus must be about 40 powers of 10 less acidic than cyclopentadiene. MP2/6-311+G(2df,2pd) and B3LYP/6-311+G(2df,2pd) calculations indicate a small destabilization of the cyclopropenyl anion, relative to the cyclopropyl anion.<sup>135</sup> Thus the six  $\pi$ -electron cyclopentadienide anion is enormously stabilized relative to the four  $\pi$ -electron cyclopropenide ion, in agreement with the Hückel rule.

The Hückel rule predicts aromaticity for the six  $\pi$ -electron cation derived from cycloheptatriene by hydride abstraction and antiaromaticity for the planar eight  $\pi$ -electron anion that would be formed by deprotonation. The cation is indeed very stable, with a  $pK_{R^+}$  of  $+4.7$ .<sup>136</sup> Salts containing the cation can be isolated as a result of a variety of preparative procedures.<sup>137</sup> On the other hand, the  $pK$  of cycloheptatriene has been estimated at 36.<sup>134</sup> This value is similar to normal 1,4-dienes and does not indicate strong destabilization. The seven-membered eight  $\pi$ -electron anion is probably nonplanar. This would be similar to the situation in the nonplanar eight  $\pi$ -electron hydrocarbon, cyclooctatetraene.

<sup>127</sup> H. Jiao, P. v. R. Schleyer, Y. Mo, M. A. McAllister, and T. T. Tidwell, *J. Am. Chem. Soc.*, **119**, 7075 (1997).

<sup>128</sup> R. Breslow and S. Mazur, *J. Am. Chem. Soc.*, **95**, 584 (1975).

<sup>129</sup> A. D. Allen, M. Sumonja, and T. T. Tidwell, *J. Am. Chem. Soc.*, **119**, 2371 (1997).

<sup>130</sup> R. Breslow and J. M. Hoffman, Jr., *J. Am. Chem. Soc.*, **94**, 2110 (1972).

<sup>131</sup> M. Saunders, R. Berger, A. Jaffe, J. M. McBride, J. O'Neill, R. Breslow, J. M. Hoffman, Jr., C. Perchonock, E. Wasserman, R. S. Hutton, and V. J. Kuck, *J. Am. Chem. Soc.*, **95**, 3017 (1973).

<sup>132</sup> H. Sitzmann, H. Bock, R. Boese, T. Dezember, Z. Havlas, W. Kaim, M. Moscherosch, and L. Zantry, *J. Am. Chem. Soc.*, **115**, 12003 (1993).

<sup>133</sup> A. Streitwieser, Jr., and L. L. Nebenzahl, *J. Am. Chem. Soc.*, **98**, 2188 (1976).

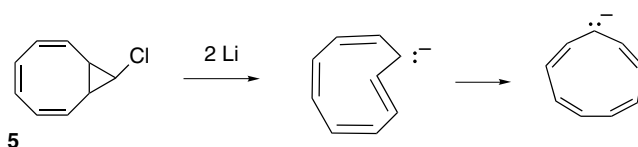
<sup>134</sup> R. Breslow and W. Chu, *J. Am. Chem. Soc.*, **95**, 411 (1973).

<sup>135</sup> G. N. Merrill and S. R. Kass, *J. Am. Chem. Soc.*, **119**, 12322 (1997).

<sup>136</sup> W. v. E. Doering and L. H. Knox, *J. Am. Chem. Soc.*, **76**, 3203 (1954).

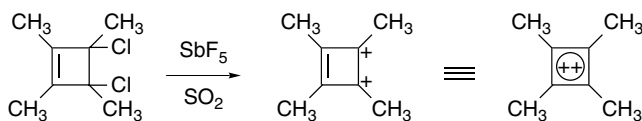
<sup>137</sup> T. Nozoe, *Prog. Org. Chem.*, **5**, 132 (1961); K. M. Harmon, in *Carbonium Ions*, Vol. IV, G. A. Olah and P. v. R. Schleyer, eds., Wiley-Interscience, New York, 1973, Chap. 2.

The cyclononatetraenide anion is generated by treatment of the halide **5** with lithium metal.<sup>138</sup>

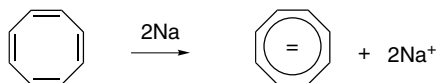


An isomeric form of the anion that is initially formed is converted to the all-*cis* system rapidly at room temperature.<sup>139</sup> Data on the equilibrium acidity of the parent hydrocarbon are not available, so the stability of the anion cannot be judged quantitatively. The NMR spectrum of the anion, however, is indicative of aromatic character.<sup>139b</sup>

Several doubly charged ions are included in Scheme 8.1; some have been observed experimentally. Ionization of 3,4-dichloro-1,2,3,4-tetramethylcyclobutene in  $\text{SbF}_5\text{-SO}_2$  at  $-75^\circ\text{C}$  results in an NMR spectrum attributed to the tetramethyl derivative of the cyclobutadienyl dication.<sup>140</sup>



It is difficult to choose a reference compound against which to judge the stability of the dication. That it can be formed at all, however, is suggestive of special stabilization associated with the two  $\pi$ -electron system. The dianion formed by adding two electrons to the  $\pi$  system of cyclobutadiene also meets the  $4n + 2$  criterion. In this case, however, four of the six electrons would occupy HMO nonbonding orbitals, so high reactivity could be expected. There is some evidence that this species may have a finite existence.<sup>141</sup> Reaction of 3,4-dichlorocyclobutene with sodium naphthalenide, followed a few minutes later by methanol-*O-d* gives a low yield of 3,4-di-deuterocyclobutene. The inference is that the dianion  $[\text{C}_4\text{H}_4^{2-}]$  is present, but there has not yet been direct experimental observation of this species. Cyclooctatetraene is reduced by alkali metals to a dianion.



The NMR spectrum is indicative of a planar aromatic structure.<sup>142</sup> The NICS value (MP2/6-31G\*) is  $-19.9$ .<sup>143</sup> It has been demonstrated that the dianion is more stable

<sup>138</sup>. T. J. Katz and P. J. Garratt, *J. Am. Chem. Soc.*, **86**, 5194 (1964); E. A. LaLancette and R. E. Benson, *J. Am. Chem. Soc.*, **87**, 1941 (1965).

<sup>139</sup>. (a) G. Boche, D. Martens, and W. Danzer, *Angew. Chem. Inter. Ed. Engl.*, **8**, 984 (1969); (b) S. Fliszar, G. Cardinal, and M. Bernaldin, *J. Am. Chem. Soc.*, **104**, 5287 (1982); S. Kuwajima and Z. G. Soos, *J. Am. Chem. Soc.*, **108**, 1707 (1986).

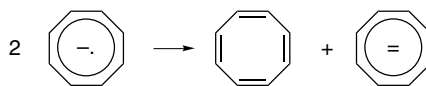
<sup>140</sup>. G. A. Olah, J. M. Bollinger, and A. M. White, *J. Am. Chem. Soc.*, **91**, 3667 (1969); G. A. Olah and G. D. Mateescu, *J. Am. Chem. Soc.*, **92**, 1430 (1970).

<sup>141</sup>. J. S. McKennis, L. Brener, J. R. Schweiger, and R. Pettit, *J. Chem. Soc., Chem. Commun.*, 365 (1972).

<sup>142</sup>. T. J. Katz, *J. Am. Chem. Soc.*, **82**, 3784 (1960).

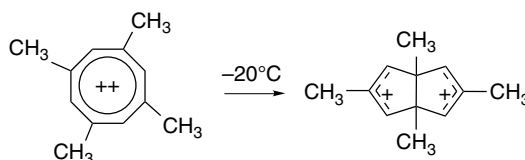
<sup>143</sup>. P. v. R. Schleyer, C. Maerker, A. Dransfeld, H. Jiao, and J. R. van Eikema Hommes, *J. Am. Chem. Soc.*, **118**, 6317 (1996).

than the radical anion formed by one-electron reduction, since the radical anion disproportionates to cyclooctatetraene and the dianion.

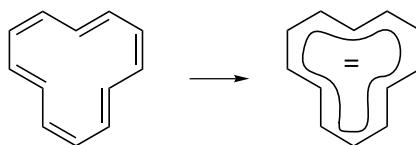


The crystal structure of the potassium salt of 1,3,5,7-tetramethylcyclooctatetraene dianion has been determined by X-ray diffraction.<sup>144</sup> The eight-membered ring is planar, with “aromatic” C–C bond lengths of about 1.41 Å without significant alternation. Spectroscopic and structural studies lead to the conclusion that the cyclooctatetraene dianion is a stabilized delocalized structure.

A dication derived from 1,3,5,7-tetramethylcyclooctatetraene is formed at  $-78^{\circ}\text{C}$  in  $\text{SO}_2\text{Cl}$  by reaction with  $\text{SbF}_5$ . Both the proton and carbon NMR spectra indicate that the ion is a symmetrical, diamagnetic species, and the chemical shifts are consistent with an aromatic anisotropy. At about  $-20^{\circ}\text{C}$ , this dication undergoes a chemical transformation to a more stable diallylic dication.<sup>145</sup>



Reduction of the nonaromatic polyene [12]annulene, either electrochemically or with lithium metal, generates a 14  $\pi$ -electron dianion.<sup>146</sup>



The NMR spectrum of the resulting dianion shows chemical shifts indicative of aromatic character, even though steric interactions among the internal hydrogens must prevent complete coplanarity. In contrast to the neutral [12]annulene, which is thermally unstable above  $-50^{\circ}\text{C}$ , the dianion remains stable at  $30^{\circ}\text{C}$ . The dianion of [16]annulene has also been prepared, and shows properties consistent with its being regarded as aromatic.<sup>147</sup>

The pattern of experimental results on charged species with cyclic conjugated systems is summarized in Table 8.1. It is consistent with the applicability of Hückel's rule to charged, as well as neutral, conjugated planar cyclic structures.

<sup>144</sup> S. Z. Goldberg, K. N. Raymond, C. A. Harmon, and D. H. Templeton, *J. Am. Chem. Soc.*, **96**, 1348 (1974).

<sup>145</sup> G. A. Olah, J. S. Staral, G. Liang, L. A. Paquette, W. P. Melega, and M. J. Carmody, *J. Am. Chem. Soc.*, **99**, 3349 (1977).

<sup>146</sup> J. F. M. Oth and G. Schroeder, *J. Chem. Soc. B*, 904 (1971).

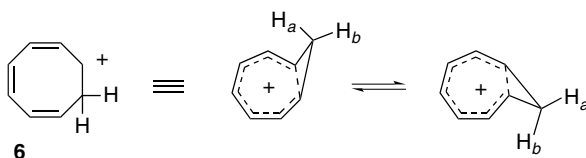
<sup>147</sup> J. F. M. Oth, G. Anthoine, and J. -M. Gilles, *Tetrahedron Lett.*, 6265 (1968).

**Table 8.1. Hückel's Rule Relationships for Charged Species**

Compound	$\pi$ Electrons
Aromatic	
Cyclopropenylum ion	2
Cyclopentadienide anion	6
Cycloheptatrienylum ion	6
Cyclooctatetraene dianion	10
Cyclononatetraenide anion	10
[12]Annulene dianion	14
Antiaromatic	
Cyclopropenide anion	4
Cyclopentadienylum ion	4
Nonaromatic	
Cycloheptatrienide anion	8

## 8.4. Homoaromaticity

*Homoaromaticity* is a term used to describe systems in which a stabilized cyclic conjugated system is formed by bypassing one saturated atom.<sup>148</sup> One would expect the resulting stabilization to be reduced because of poorer overlap of the orbitals, but the properties of several such cationic species suggest that there is substantial stabilization. The cyclooctatrienyl cation (homotropylium **6**) is an example.



A significant feature of the NMR spectrum of this cation is the fact that the protons *a* and *b* exhibit sharply different chemical shifts. Proton *a* is 5.8 ppm upfield of *b*, indicating the existence of a diamagnetic ring current.<sup>149</sup> The fact that the two protons exhibit separate signals also establishes that there is a substantial barrier for the conformational process that interchanges  $H_a$  and  $H_b$ . The  $\Delta G^\ddagger$  for this process is 22.3 kcal/mol.<sup>150</sup> MO (MP3/6-31G\*) calculations that include the effects of electron correlation indicate that the homoconjugated structure is a good description of the cation and find that there is a strong aromatic ring current.<sup>151</sup> MP4(SDQ)/6-31G(*d*) calculations were used to compare the homoaromatic structure with a planar model. The computations indicate that the total energy difference between the two structures includes a homoaromatic stabilization of about 4 kcal/mol and that additional strain in

<sup>148</sup>. S. Winstein, *Q. Rev. Chem. Soc.*, **23**, 141 (1969); L. A. Paquette, *Angew. Chem. Int. Ed. Engl.*, **17**, 106 (1978); R. V. Williams, *Adv. Phys. Org. Chem.*, **29**, 273 (1994); R. V. Williams, *Chem. Rev.*, **101**, 1185 (2001).

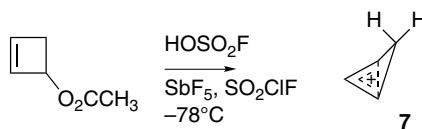
<sup>149</sup>. (a) P. Warner, D. L. Harris, C. H. Bradley, and S. Winstein, *Tetrahedron Lett.*, 4013 (1970); C. E. Keller and R. Pettit, *J. Am. Chem. Soc.*, **88**, 604, 606 (1966); R. F. Childs, *Acc. Chem. Res.*, **17**, 347 (1984); (b) R. C. Haddon, *J. Am. Chem. Soc.*, **110**, 1108 (1988).

<sup>150</sup>. S. Winstein, C. G. Kreiter, and J. I. Brauman, *J. Am. Chem. Soc.*, **88**, 2047 (1966).

<sup>151</sup>. R. C. Haddon, *J. Am. Chem. Soc.*, **110**, 1108 (1988).

the planar structure accounts for most of the difference.<sup>152</sup> A higher estimate of the homoaromatic stabilization of 13.4 kcal/mol results from a calculation that assigns the difference in strain as 10.1 kcal/mol.<sup>153</sup>

The cyclobutenyl cation **7** is the homoaromatic analog of the very stable cyclopropenium cation. This ion can be prepared from 3-acetoxycyclobutene using “superacid” conditions.<sup>154</sup>



The homoaromatic cyclobutenylium ion is calculated to be 10.3 kcal/mol less stable than the isomeric methylcyclopropenylium ion, but the barrier for interconversion is high.<sup>155</sup> The temperature-dependent NMR spectrum of the ion can be analyzed to show that there is a barrier (8.4 kcal/mol) for the ring flip that interchanges the two hydrogens of the methylene group. The <sup>13</sup>C-NMR chemical shift is also compatible with the homoaromatic structure. MO (MP3/6-31G\*) calculations are successful in reproducing the structural and spectroscopic characteristics of the cation and are consistent with a homoaromatic structure.<sup>156</sup> Analysis of electron density did not find a bond critical point between C(1) and C(3), but the electron density is equivalent to a bond order of about 0.45. The electron density contours are shown in Figure 8.8.

The existence of stabilizing homoconjugation in anions has been more difficult to establish. Much of the discussion has revolved about anion **8**. The species was proposed to have aromatic character on the basis of the large upfield shift of the CH<sub>2</sub> group, which would lie in the shielding region generated by a diamagnetic ring current.<sup>157</sup> The <sup>13</sup>C-NMR spectrum can also be interpreted in terms of homoaromaticity.<sup>158</sup> Both

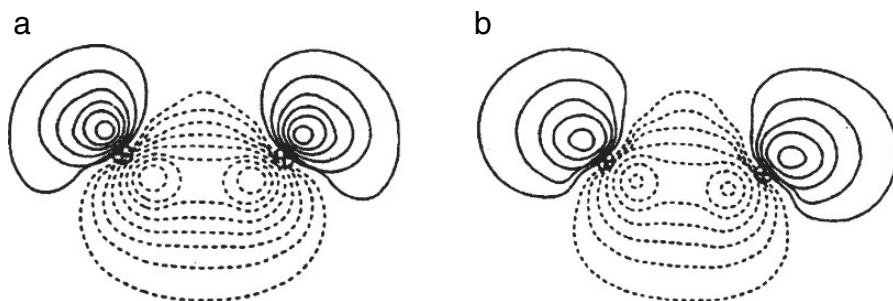


Fig. 8.8. Electron density contours for C(1)–C(3) bridging in homoaromatic cations: (a) cyclobutenylium ion; (b) cyclooctatrienylium ion. Reproduced from *J. Phys. Org. Chem.*, **6**, 445 (1993).

<sup>152</sup> D. Cremer, F. Reichel, and E. Kraka, *J. Am. Chem. Soc.*, **113**, 9459 (1991).

<sup>153</sup> B. Reindl, T. Clark, and P. v. R. Schleyer, *J. Phys. Chem. A*, **102**, 8953 (1998).

<sup>154</sup> G. A. Olah, J. S. Staral, R. J. Spear, and G. Liang, *J. Am. Chem. Soc.*, **97**, 5489 (1975).

<sup>155</sup> A. Cunje, C. F. Rodriguez, M. H. Lien, and A. C. Hopkinson, *J. Org. Chem.*, **61**, 5212 (1996).

<sup>156</sup> R. C. Haddon and K. Raghavachari, *J. Am. Chem. Soc.*, **105**, 1188 (1983); M. Schindler, *J. Am. Chem. Soc.*, **109**, 1020 (1987); S. Sieber, P. v. R. Schleyer, A. H. Otto, J. Gauss, F. Reichel, and D. Cremer, *J. Phys. Org. Chem.*, **6**, 445 (1993).

<sup>157</sup> S. Winstein, M. Ogliaruso, M. Sakai, and J. M. Nicholson, *J. Am. Chem. Soc.*, **89**, 3656 (1967).

<sup>158</sup> M. Cristl, H. Leininger, and D. Brueckner, *J. Am. Chem. Soc.*, **105**, 4843 (1983).

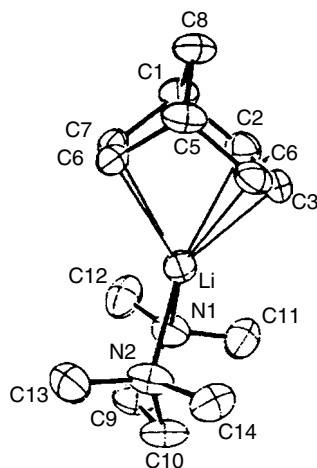
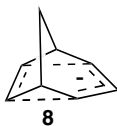


Fig. 8.9. Crystal structure of the TMEDA complex of lithium bicyclo[3.2.1]octa-2,6-dienide. Reproduced from *Angew. Chem. Int. Ed. Engl.*, **25**, 468 (1986), by permission of Wiley-VCH.

gas phase and solution measurements suggest that the parent hydrocarbon is more acidic than would be anticipated if there were no special stabilization of the anion.<sup>159</sup> An X-ray crystal structure of the lithium salt has been done.<sup>160</sup> The structure is a monomeric TMEDA complex (Fig. 8.9). The lithium is not symmetrically disposed toward the anion but is closer to one carbon of the allyl system. There is no indication of flattening of the homoconjugated atoms and the C(6)–C(7) bond distance is in the normal double-bond range (1.354 Å).

In contrast to the homoaromatic cations **6** and **7**, MO calculations fail to reveal substantial stabilization of the anion **8**.<sup>161</sup> There does not seem to be any diamagnetic ring current associated with the anion.<sup>162</sup> The weight of the evidence seems to be against significant homoaromatic stabilization in **8**.



## 8.5. Fused-Ring Systems

Many completely conjugated hydrocarbons can be built up from benzene, the other annulenes and related structural fragments. Scheme 8.2 gives the structures, names, and stabilization energies of a variety of such hydrocarbons. Derivatives of

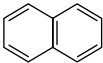
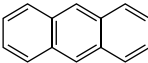
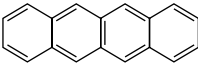
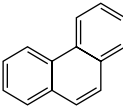
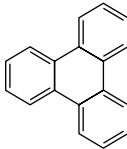
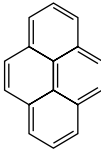
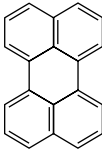
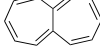
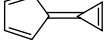
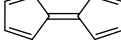
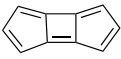
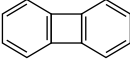
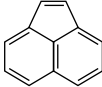
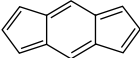
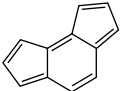
<sup>159</sup> R. E. Lee and R. R. Squires, *J. Am. Chem. Soc.*, **108**, 5078 (1986); W. N. Washburn, *J. Org. Chem.*, **48**, 4287 (1983).

<sup>160</sup> N. Hertkorn, F. H. Kohler, G. Mueller, and G. Reber, *Angew. Chem. Int. Ed. Engl.*, **25**, 468 (1986).

<sup>161</sup> J. B. Grutzner and W. L. Jorgenson, *J. Am. Chem. Soc.*, **103**, 1372 (1981); E. Kaufman, H. Mayr, J. Chandrasekhar, and P. v. R. Schleyer, *J. Am. Chem. Soc.*, **103**, 1375 (1981); R. Lindh, B. O. Roos, G. Jonsall, and P. Ahlberg, *J. Am. Chem. Soc.*, **108**, 6554 (1986).

<sup>162</sup> N. H. Werstiuk and J. Ma, *Can. J. Chem.*, **77**, 752 (1999).

Scheme 8.2. Stabilization Energies of Some Polycyclic Hydrocarbons<sup>a</sup>

				
	Benzene	Naphthalene	Anthracene	Naphthacene
HMO	2.00	3.698	5.31	6.93
HMO'	0.39	0.55	0.66	0.76
RE	0.38	0.59	0.71	0.83
SCF-MO	0.869 eV	1.323 eV	1.600 eV	1.822 eV
				
	Phenanthrene	Triphenylene	Pyrene	Perylene
HMO	5.44	7.27	6.50	8.24
HMO'	0.72	1.01	0.82	0.96
RE	0.85	1.13	0.95	1.15
SCF-MO	1.933 eV	2.654 eV	2.10 eV	2.619 eV
				
	Butalene	Pentalene	Azulene	Heptalene
HMO	1.66	2.45	3.25	3.61
HMO'	-0.48	-0.14	0.23	-0.04
RE	-0.34	-0.09	0.27	-0.01
SCF-MO	-0.28 eV	-0.006 eV	0.169 eV	-0.004 eV
				
	Methylene-cyclopropene	Fulvene	Calicene	Fulvalene
HMO	0.96	1.46	-	2.80
HMO'	0.02	-0.012	0.34	-0.33
RE		-0.01	0.39	-0.29
SCF-MO				
				
	Benzo-cyclobutadiene		Biphenylene	Acenaphthene
HMO	2.38	-	4.50	4.61
HMO'	-0.22	-0.22	0.32	0.47
RE	-0.16	-	0.42	0.57
SCF-MO	-	-	1.346 eV	1.335 eV
				
	s-indacene	as-indacene		
HMO'	0.110	-0.249		

a. Stabilization energies are from the following sources: HMO: C. A. Coulson, A. Streitwieser, Jr., M. D. Poole, and J. I. Brauman, *Dictionary of  $\pi$ -Electron Calculations*, W. H. Freeman, San Francisco, 1965.

HMO': B. A. Hess, Jr., and L. J. Schaad, Jr., *J. Am. Chem. Soc.*, **93**, 305, 2413 (1971); *J. Org. Chem.*, **36**, 3418 (1971); *J. Org. Chem.*, **37**, 4179 (1972).

RE: A. Moyano and J. C. Paniagua, *J. Org. Chem.*, **51**, 2250 (1986).

SCF-MO: M. J. S. Dewar and C. de Llano, *J. Am. Chem. Soc.*, **91**, 789 (1969); 1 eV = 23 kcal/mol.

these hydrocarbons having heteroatoms in place of one or more carbon atoms constitute another important class of organic compounds and are discussed in Section 8.6. It is of interest to be able to predict the stability of such fused-ring compounds. Because Hückel's rule applies only to monocyclic systems, it cannot be applied to the fused-ring compounds, but there have been many efforts to develop relationships that would predict their stability. The underlying concepts are the same as for monocyclic systems; stabilization results from a particularly favorable arrangement of MOs, whereas instability is associated with unpaired electrons or electrons in high-energy orbitals.

The same approximations discussed in Section 1.5 permit calculation of the HMO for conjugated systems of the type shown in Scheme 8.2, and many of the results have been tabulated.<sup>163</sup> However, attempts to correlate stability with the Hückel delocalization energy relative to isolated double bonds give poor correlation with the observed chemical properties of the compounds.

Much better agreement between calculated stabilization energy and experimental chemical properties is achieved when a polyene is chosen as the reference state.<sup>164</sup> A series of energy terms corresponding to the structural units in the reference polyene was established empirically by Hess and Schaad.<sup>165</sup> The difference between the energy of the conjugated hydrocarbon by HMO calculations and the sum of the appropriate structural units gives a stabilization energy. For azulene, for example, the HMO calculation gives an energy of  $10\alpha + 13.36\beta$ . The energy for the polyene reference is obtained by summing contributions for the component bond types:  $3(\text{CH}=\text{CH}) + 2(\text{HC}=\text{C}) + 3(\text{HC}-\text{CH}) + 1(\text{C}-\text{C}) = 13.13\beta$ . The difference,  $0.23\beta$ , is the stabilization or resonance energy assigned to azulene by this method. For comparison of nonisomeric molecules, the Hess-Schaad treatment uses resonance energy per electron, which is obtained by dividing the calculated stabilization energy by the number of  $\pi$  electrons. Although the resulting stabilization energies are based on a rudimentary HMO calculation, they are in good qualitative agreement with observed chemical stability. The stabilizations have been calculated for most of the molecules in Scheme 8.2 and are listed as HMO'.

The energy parameters assigned to the reference polyene used by Hess and Schaad were developed on an empirical basis. Subsequently Moyano and Paniagua developed an alternative set of reference bond energies on a theoretical basis,<sup>166</sup> and these values are shown along with the Hess-Schaad values in Table 8.2. The stabilizations calculated for the various hydrocarbons using this point of reference in Scheme 8.2 are those listed as RE (for resonance energy). The Hess-Schaad HMO' and the RE values are in generally good agreement with observed stability. Both calculations give negative stabilization for benzocyclobutadiene, for example.<sup>167</sup>

The values listed in Scheme 8.2 as SCF-MO are from an early semiempirical SCF calculation, which was the first instance in which a polyene was chosen as the reference state.<sup>164</sup>

<sup>163</sup> E. Heilbronner and P. A. Straub, *Hückel Molecular Orbitals*, Springer-Verlag, Berlin, 1966; C. A. Coulson and A. Streitwieser, *Dictionary of  $\pi$ -Electron Calculations*, W. H. Freeman, San Francisco, 1965.

<sup>164</sup> M. J. S. Dewar and C. de Llano, *J. Am. Chem. Soc.*, **91**, 789 (1969).

<sup>165</sup> B. A. Hess, Jr., and L. J. Schaad, *J. Am. Chem. Soc.*, **93**, 305, 2413 (1971); *J. Org. Chem.*, **36**, 3418 (1971); *J. Org. Chem.*, **37**, 4179 (1972).

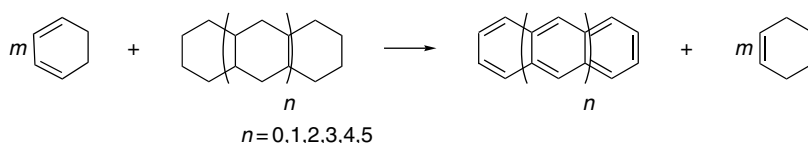
<sup>166</sup> A. Moyano and J. C. Paniagua, *J. Org. Chem.*, **51**, 2250 (1986).

<sup>167</sup> There are a number of other systems for comparing the stability of conjugated cyclic compounds with reference polyenes. For example, see L. J. Schaad and B. A. Hess, Jr., *Pure Appl. Chem.*, **54**, 1097 (1982); J. Aihara, *Pure Appl. Chem.*, **54**, 1115 (1982); K. Jug, *J. Org. Chem.*, **48**, 1344 (1983); W. Gründler, *Monatsch. Chem.*, **114**, 155 (1983).

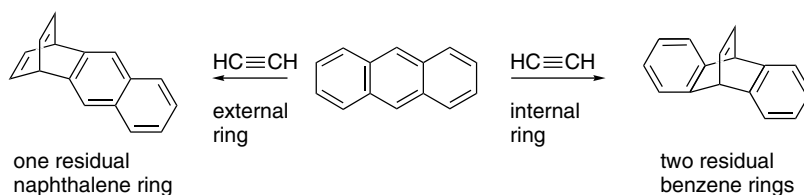
Table 8.2. Energy Values for Reference Bond Types

Bond type	Hess-Schaad value ( $\beta$ )	Bond type	Moyano-Paniagua value ( $\beta$ )
$\text{H}_2\text{C}=\text{CH}$	2.000	$\text{H}_2\text{C}=\text{CH}-\text{CH}=\text{}$	2.2234
$\text{HC}=\text{CH}$	2.070	$\text{H}_2\text{C}=\text{CH}-\text{C}=\text{}$	2.2336
$\text{H}_2\text{C}=\text{C}$	2.000	$=\text{CH}-\text{CH}=\text{CH}-\text{CH}=\text{}$	2.5394
$\text{HC}=\text{C}$	2.108	$=\text{CH}-\text{CH}=\text{CH}-\text{C}=\text{}$	2.5244
$\text{C}=\text{C}$	2.172	$=\text{C}-\text{CH}=\text{CH}-\text{C}=\text{}$	2.4998
$\text{HC}-\text{CH}$	0.466	$\text{H}_2\text{C}=\text{C}-$	2.4320
$\text{HC}-\text{C}$	0.436	$-\text{CH}=\text{CH}-$	2.7524
$\text{C}-\text{C}$	0.436	$-\text{C}=\text{C}-$	2.9970

All these approaches agree that benzene and the structures that can be built up by fusing benzenoid rings together are strongly stabilized relative to the reference polyenes. The larger rings tend to have lower resonance energies per  $\pi$  electron than does benzene. This feature is in agreement with experimental trends in reactivity.<sup>168</sup> Schleyer and co-workers have applied some of the criteria of aromaticity to this series of compounds.<sup>169</sup> With application of the isodesmic equation below, the stabilization per electron was found to increase on going from benzene to naphthalene and then to remain approximately constant.



Another manifestation of aromatic stability is resistance to addition reactions. For example, the  $E_a$  and  $\Delta H$  for cycloaddition with ethyne were calculated, and the results are shown as in Table 8.3. The internal rings have greater exothermicity and lower  $E_a$ .



A similar trend is observed for the rates of Diels-Alder addition reactions of anthracene, naphthalene, and pentacene, in which three, four, and five rings, respectively, are linearly fused. The rate data are shown in Table 8.4. The same trend can be seen in the  $E_a$  and the gain in resonance energy when cycloreversion of the adducts **9–12** yields the aromatic compound, as shown in Scheme 8.3.

<sup>168</sup> D. Biermann and W. Schmidt, *J. Am. Chem. Soc.*, **102**, 3163, 3173 (1980).

<sup>169</sup> P. v. R. Schleyer, M. Manoharan, H. Jiao, and F. Stahl, *Org. Lett.*, **3**, 3643 (2001).

**Table 8.3. Calculated Barriers and Reaction Energy for Cycloaddition of Ethyne with Polycyclic Hydrocarbons**

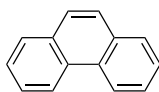
Compound	$E_a$	$\Delta H$
Benzene	43.8	6.1
Naphthalene	36.8	-8.7
Anthracene (external ring)	34.3	-13.9
Anthracene (center ring)	29.4	-26.2
Naphthacene (external ring)	33.3	-16.1
Naphthacene (internal ring)	26.8	-32.6
Pentacene (external ring)	32.7	-17.3
Pentacene (internal ring)	25.5	-35.4
Pentacene (center ring)	24.0	-39.5

**Table 8.4. Rates of Diels-Alder Additions of Linear Polycyclic Aromatic Hydrocarbons<sup>a</sup>**

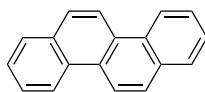
Dienophile	$k(M^{-1}s^{-1})$ in toluene at 80°C		
	Anthracene	Naphthacene	Pentacene
Benzoquinone		44	181
Maleic anhydride	5	294	4710
<i>N</i> -Phenylmaleimide	10	673	19,280

a. V. D. Samuilov, V. G. Uryadov, L. F. Uryadova, and A. J. Konolova, *Zh. Org. Khim.* (Engl. Trans.), **21**, 1137 (1985).

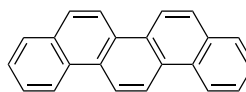
Benzene rings can also be fused in angular fashion, as in phenanthrene, chrysene, and picene. These compounds, while quite reactive toward additions in the center ring, retain most of the REPE stabilization of benzene and naphthalene.<sup>170</sup>



phenanthrene



chrysene



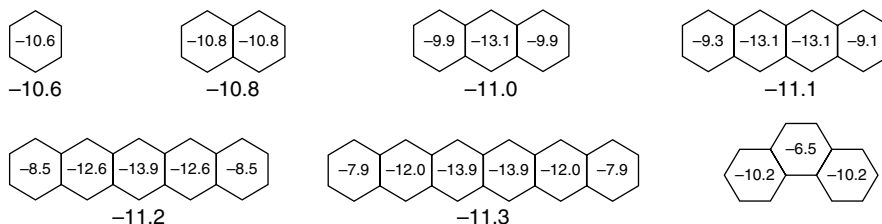
picene

**Scheme 8.3. Correlation between  $E_a$  for Retro-Diels-Alder Reaction and Change in Resonance Stabilization of Polycyclic Hydrocarbons**

	<b>9</b>	<b>10</b>	<b>11</b>	<b>12</b>
	↓	↓	↓	↓
	benzene	naphthalene	anthracene	naphthacene
$E_a$ (kcal/mol)	16	20	29	31
$\Delta RE$ (kcal/mol)	40	30	17	11

<sup>170</sup> K. B. Wiberg, *J. Org. Chem.*, **62**, 5720 (1997).

The NICS values for the linear polycyclic arenes show a pattern of increasing negativity (aromaticity) toward the center ring. In contrast, for phenanthrene, the center ring has the lowest NICS, consistent with the more localized nature of this ring.<sup>171</sup>



Average (beneath the structure) and individual ring (inside each ring) NICS values for polycyclic hydrocarbons. Except for phenanthrene the values are 1 Å above the ring.

The HOMO-LUMO gap decreases as the number of fused rings increases. The decreasing gap is reflected in the hardness values shown in Scheme 8.4, as assigned by Zhou and Parr.<sup>172</sup> The values for phenanthrene and acenaphthene, which have more localized double bonds, are 0.315 and 0.151, respectively. Similarly, the nonbenzenoid hydrocarbon azulene is calculated to be softer.

There is evidence that aromatic circuits can exist within a larger conjugated unit resulting in an aromatic segment in conjugation with a “localized” double bond. For example, in acenaphthene, the double bond in the five-membered ring is both structurally and chemically similar to a normal localized double bond. The resonance energy given in Scheme 8.2,  $0.57\beta$ , is slightly less than that for naphthalene ( $0.59\beta$ ). The additional double bond of acenaphthene has only a small effect on the stability of the conjugated system. The molecular structure determined at 80 K by neutron diffraction shows bond lengths for the aromatic portion that are quite similar to those

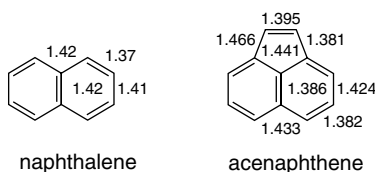
**Scheme 8.4. HOMO-LUMO Gaps and Hardness for Polycyclic Hydrocarbons**

HMO gap ( $\beta$ )	2.000	1.3360	0.8284	0.5900
Rel Hardness	0.482	0.264	0.151	0.088
HMO gap ( $\beta$ )	0.8775	0.9221	1.2104	
Rel Hardness	0.253	0.206	0.315	

<sup>171</sup> P. v. R. Schleyer, M. Manoharan, H. Jiao, and F. Stahl, *Org. Lett.*, **3**, 3643 (2001).

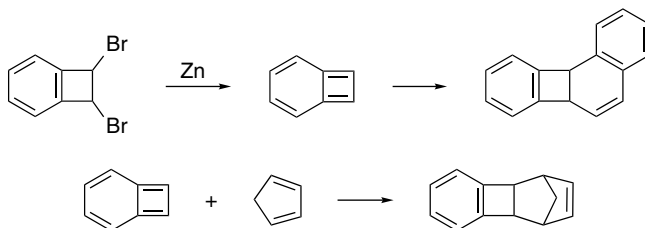
<sup>172</sup> Z. Zhou and R. G. Parr, *J. Am. Chem. Soc.*, **111**, 7371 (1989).

of naphthalene.<sup>173</sup> The double bond is somewhat longer than a normal double bond, but this may reflect the strain imposed on it by the naphthalene framework.



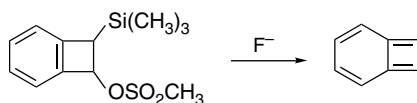
The predictions of relative stability by the various approaches diverge more widely when nonbenzenoid systems are considered. The simple Hückel method using total  $\pi$  delocalization energies relative to an isolated double-bond reference energy ( $\alpha + \beta$ ) fails. This approach predicts stabilization of the same order of magnitude for such unstable systems as pentalene and fulvalene as it does for much more stable aromatics. The HMO', RE, and SCF-MO methods, which use polyene reference energies, do much better. All show drastically reduced stabilization for such systems and, in fact, indicate destabilization of systems such as butalene and pentalene (Scheme 8.2).

It is of interest to consider at this point some of the specific molecules in Scheme 8.2 and compare their chemical properties with the calculated stabilization energies. Benzocyclobutadiene has been generated in a number of ways, including dehalogenation of dibromobenzocyclobutene.<sup>174</sup> Chemically, benzocyclobutadiene reacts as a polyene having a quinodimethane structure and is a reactive diene in Diels-Alder cycloadditions, dimerizing or polymerizing readily.<sup>175</sup>



Ref. 176

Generation of benzocyclobutadiene by fluoride-induced elimination has permitted the NMR spectrum to be observed under flow conditions.<sup>177</sup> All the peaks are somewhat upfield of the aromatic region, suggesting polyene character.



<sup>173</sup> R. A. Wood, T. R. Welberry, and A. D. Rae, *J. Chem. Soc., Perkin Trans. 2*, 451 (1985).

<sup>174</sup> M. P. Cava and D. R. Napier, *J. Am. Chem. Soc.*, **78**, 500 (1956); *J. Am. Chem. Soc.*, **79**, 1701 (1957).

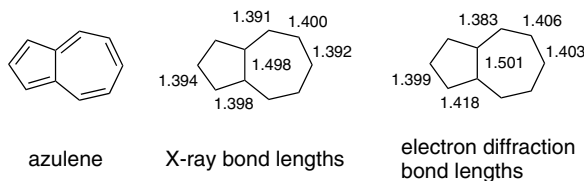
<sup>175</sup> (a) M. P. Cava and M. J. Mitchell, *Cyclobutadiene and Related Compounds*, Academic Press, New York, 1967, pp. 192–216; (b) M. K. Shepherd, *Cyclobutarenes: Chemistry of Benzocyclobutene, Biphenylene and Related Compounds*, Elsevier, New York, 1991; W. S. Trahanovsky and K. B. Arvidson, *J. Org. Chem.*, **61**, 9528 (1996); P. Gandhi, *J. Sci. Ind. Res.*, **41**, 495 (1982); M. P. Cava and D. R. Napier, *J. Am. Chem. Soc.*, **80**, 2255 (1958); M. P. Cava and M. J. Mitchell, *J. Am. Chem. Soc.*, **81**, 5409 (1959); A. K. Sadana, R. K. Saini, and W. E. Billups, *Chem. Rev.*, **103**, 1539 (2003).

<sup>176</sup> M. P. Cava and M. J. Mitchell, *J. Am. Chem. Soc.*, **81**, 5409 (1959).

<sup>177</sup> W. S. Trahanovsky and D. R. Fischer, *J. Am. Chem. Soc.*, **112**, 4971 (1990).

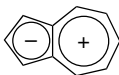
The ring current in benzocyclobutadiene has been analyzed in detail.<sup>178</sup> The main ring current is associated with the four-membered ring and is paramagnetic. This is consistent with the calculated NICS values, which are  $-2.5$  for the six-membered ring and  $22.5$  for the four-membered ring.<sup>179</sup> The fusion of the cyclobutadiene ring to benzene greatly diminishes the aromatic character of the benzenoid ring. The implication of a nonaromatic structure is that the combination of ring strain and the antiaromaticity associated with the four-membered ring results in a localized system.<sup>180</sup>

Azulene is one of the few nonbenzenoid hydrocarbons that appear to have appreciable aromatic stabilization. There is some divergence on this point between the SCF-MO and HMO' results in Scheme 8.2. The latter estimates a resonance energy about half that for the isomeric naphthalene, whereas the SCF-MO method assigns a resonance energy that is only about one-seventh that of naphthalene. Naphthalene is thermodynamically more stable than azulene by about 38.5 kcal/mol. Molecular mechanics calculations attribute about 12.5 kcal/mol of the difference to strain and about 26 kcal/mol to greater resonance stabilization of naphthalene.<sup>181</sup> Based on heats of hydrogenation, the stabilization energy of azulene is about 16 kcal/mol.<sup>182</sup> The parent hydrocarbon and many of its derivatives are well-characterized compounds with considerable stability. The structure of azulene has been determined by both X-ray crystallography and electron-diffraction measurements.<sup>183</sup> The peripheral bond lengths are in the aromatic range and show no regular alternation. The bond shared by the two rings is significantly longer, indicating that it has predominantly single-bond character, which indicates that the conjugated system more closely resembles [10]annulene than naphthalene. Theoretical calculations indicate that the molecule has  $C_{2v}$  symmetry, suggesting delocalization of the  $\pi$  electrons.<sup>184</sup>



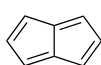
An interesting structural question involves the contribution of a dipolar structure that pictures the molecule as the fusion of a cyclopentadienide anion and a cycloheptatrienyl cation.

- <sup>178</sup> A. Soncini, R. W. A. Havenith, P. W. Fowler, L. W. Jenneskens, and E. Steiner, *J. Org. Chem.*, **67**, 4753 (2002); R. W. A. Havenith, F. Lugli, P. W. Fowler, and E. Steiner, *J. Phys. Chem. A*, **106**, 5703 (2002).
- <sup>179</sup> P. v. R. Shleyer, C. Maerker, A. Dransfeld, H. Jiao, and N. J. R. van Eikema Hommes, *J. Am. Chem. Soc.*, **118**, 6317 (1996).
- <sup>180</sup> P. B. Karadakov, J. Gerratt, D. L. Cooper, M. Raimondi, and M. Sironi, *Int. J. Quantum Chem.*, **60**, 545 (1996); M. O. Jensen, T. Thorsteinsson, and A. E. Hansen, *Intl. J. Quantum Chem.*, **90**, 616 (2002).
- <sup>181</sup> N. L. Allinger and Y. H. Yu, *Pure Appl. Chem.*, **55**, 191 (1983).
- <sup>182</sup> W. R. Roth, M. Boehm, H. W. Lennartz, and E. Vogel, *Angew. Chem. Int. Ed. Engl.*, **22**, 1007 (1983).
- <sup>183</sup> A. W. Hanson, *Acta Crystallogr.*, **19**, 19 (1965); O. Bastiansen and J. L. Derissen, *Acta Chem. Scand.*, **20**, 1319 (1966).
- <sup>184</sup> (a) C. Glidewell and D. Lloyd, *Tetrahedron*, **40**, 4455 (1984); (b) R. C. Haddon and K. Raghavachari, *J. Am. Chem. Soc.*, **104**, 3516 (1982); (c) S. Grimme, *Chem. Phys. Lett.*, **201**, 67 (1993); (d) S. J. Mole, X. Zhou, J. G. Wardeska, and R. Liu, *Spectrochim. Acta A*, **52**, 1211 (1996); (e) B.-C. Wang, Y.-S. Lin, J.-C. Chang, and P.-Y. Wang, *Can. J. Chem.*, **78**, 224 (2000); (f) I. Bandyopadhyay, *Theochem*, **618**, 59 (2002).

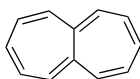


Azulene does have an appreciable dipole moment (0.8 D).<sup>185</sup> B3LYP/6-31G\* and MP2/6-31G\* computations calculate the dipole moment as about 1.0 D.<sup>184c,d</sup> The essentially single-bond nature of the shared bond indicates, however, that the conjugation is principally around the periphery of the molecule.

The significant resonance stabilization of azulene can be contrasted with pentalene and heptalene, both of which are indicated to be destabilized relative to a reference polyene.

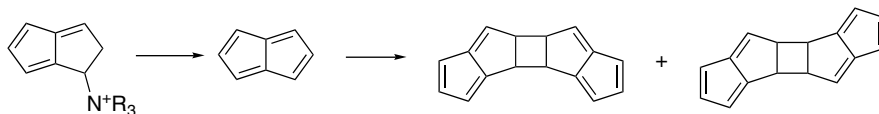


pentalene

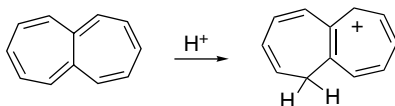


heptalene

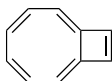
Preparation of pentalene is followed by immediate dimerization.<sup>186</sup> Low-temperature photolysis produces a new species believed to be pentalene, but the compound reverts to dimer at  $-100^{\circ}\text{C}$ . The matrix-isolated monomer has been characterized spectroscopically,<sup>187</sup> and the results are in accord with the predicted lack of stabilization.<sup>188</sup>



Heptalene readily polymerizes and is sensitive to oxygen. The NMR spectrum does not indicate the presence of an aromatic ring current. The conjugate acid of heptalene, however, is very stable (even at pH 7 in aqueous solution), reflecting the stability of the cation, which is a substituted tropylium ion.<sup>189</sup>



Another structure with a ten electron conjugated system is bicyclo[6.2.0]deca-1,3,5,7,9-pentaene. The crystal structure of the 9,10-diphenyl derivative shows the conjugated system to be nearly planar,<sup>190</sup> but there is significant bond alternation.



<sup>185</sup>. H. J. Tobler, A. Bauder, and H. H. Günthard, *J. Mol. Spectrosc.*, **18**, 239 (1965); G. W. Wheland and D. E. Mann, *J. Chem. Phys.*, **17**, 264 (1949).

<sup>186</sup>. K. Hafner, R. Donges, E. Goedecke, and R. Kaiser, *Angew. Chem. Int. Ed. Engl.*, **12**, 337 (1973); S. You and M. Neuenschwander, *Chimia*, **50**, 24 (1996).

<sup>187</sup>. T. Bally, S. Chai, M. Neuenschwander, and Z. Zhu, *J. Am. Chem. Soc.*, **119**, 1869 (1997).

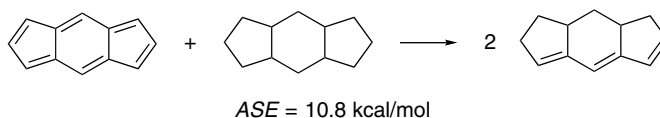
<sup>188</sup>. T. K. Zywiets, H. Jiao, P. v. R. Schleyer, and A. de Meijere, *J. Org. Chem.*, **63**, 3417 (1998).

<sup>189</sup>. H. J. Dauben, Jr., and D. J. Bertelli, *J. Am. Chem. Soc.*, **83**, 4657, 4659 (1961).

<sup>190</sup>. C. Kabuto and M. Oda, *Tetrahedron Lett.*, 103 (1980).

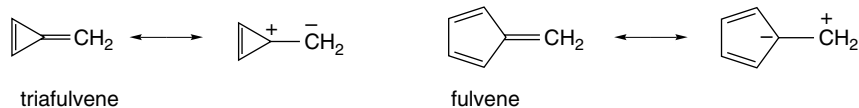
The bond at the ring fusion is quite long. A molecular mechanics calculation on this molecule, which includes an SCF-MO treatment of the planar conjugated system, concluded that the molecule is slightly destabilized (4 kcal/mol) relative to a polyene reference.<sup>191</sup> HF/STO-3G calculations found a small stabilization.<sup>192</sup> An experimental determination of  $\Delta H_{H_2}$  also suggests a small (3.7 kcal/mol) stabilization.<sup>193</sup>

The tricyclic fused systems known as *s*-indacene and *as*-indacene have also been of interest in assessing the range of aromaticity. *s*-Indacene derivatives have bond lengths varying from 1.39 to 1.44 Å in the crystal structure.<sup>194</sup> MO and DFT calculations vary in predicting the relative energy of localized and delocalized structures.<sup>195</sup> B3LYP/6-31G\* calculations place the structures within 0.1 kcal/mol of one another.<sup>196</sup> An aromatic stabilization of 10.8 kcal/mol is calculated based on the following isodesmic reaction, which is much less than for anthracene.<sup>197</sup> The NICS values for both rings are positive and indicate a paramagnetic ring current.



The possibility of extra stabilization in systems that have conjugated components exocyclic to the ring has also been examined. Such substituents complete conjugated rings but are not part of the cyclic system. Some representative structures are shown in Scheme 8.5.

Cyclopropenes and cyclopentadienes with exocyclic double bonds provide the possibility of dipolar resonance structures that suggest aromatic character in the cyclic structure.



For methylenecyclopropene, a microwave structure determination has established bond lengths that show the strong alternation anticipated for a localized structure.<sup>198</sup> The molecule does have a significant (1.90 D) dipole moment, implying a contribution from the dipolar resonance structure. The net stabilization calculated at the MP/6-31G\* level is small and comparable to the stabilization of 1,3-butadiene. The molecular geometry

<sup>191</sup> N. L. Allinger and Y. H. Yuh, *Pure Appl. Chem.*, **55**, 191 (1983).

<sup>192</sup> D. Cremer, T. Schmidt, and C. W. Bock, *J. Org. Chem.*, **50**, 2684 (1985).

<sup>193</sup> W. Roth, H. -W. Lennartz, E. Vogel, M. Leiendecker, and M. Oda, *Chem. Ber.*, **119**, 837 (1986).

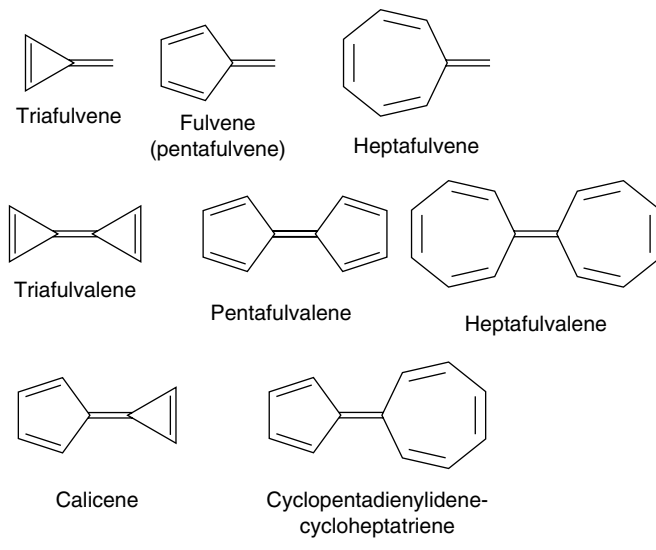
<sup>194</sup> K. Hafner, B. Stowasser, H. -P. Krimmer, S. Fischer, M. C. Böhm, and H. J. Lindner, *Angew. Chem. Intl. Ed. Engl.*, **25**, 6201 (1986); J. D. Dunitz, C. Kruger, H. Ingartinger, E. F. Maverick, Y. Wang, and M. Nixdorf, *Angew. Chem. Intl. Ed. Engl.*, **27**, 387 (1988).

<sup>195</sup> C. Gellini, G. Cardini, P. R. Salvi, G. Marconi, and K. Hafner, *J. Phys. Chem.*, **97**, 1286 (1993); R. H. Hertwig, M. C. Holthausen, W. Koch, and Z. B. Maksic, *Angew. Chem. Intl. Ed. Engl.*, **33**, 1192 (1994); R. H. Hertwig, M. C. Holthausen, and W. Koch, *Intl. J. Quantum Chem.*, **54**, 147 (1995).

<sup>196</sup> M. Nendel, B. Goldfuss, B. Beno, K. N. Houk, K. Hafner, and H.-J. Lindner, *Pure Appl. Chem.*, **71**, 221 (1999).

<sup>197</sup> M. Nendel, B. Goldfuss, K. N. Houk, and K. Hafner, *Theochem*, **461-2**, 23 (1999).

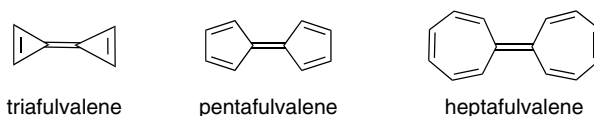
<sup>198</sup> T. D. Norden, S. W. Staley, W. H. Taylor, and M. D. Harmony, *J. Am. Chem. Soc.*, **108**, 7912 (1986).

**Scheme 8.5. Completely Conjugated Hydrocarbons Incorporating Exocyclic Double Bonds**


of dimethylfulvene has been examined by electron diffraction methods. Strong bond length alternation indicative of a localized structure was found.<sup>199</sup>



The fulvalene systems are not predicted to be aromatic by any of the theoretical estimates of stability. Even simple resonance considerations would suggest polyene behavior, since only dipolar resonance structures can be drawn in addition to the single nonpolar structure.



Triafulvalene (cyclopropenylidene-cyclopropene) has not been isolated. A substantial number of pentafulvalene derivatives have been prepared.<sup>200</sup> The chemical properties of these molecules are those of reactive polyenes. The NMR spectrum of pentafulvalene is characteristic of a localized system.<sup>201</sup> Heptafulvalene (cycloheptatrienylidene-cycloheptatriene) is a well-characterized compound with the properties expected for a polyene.<sup>202</sup>

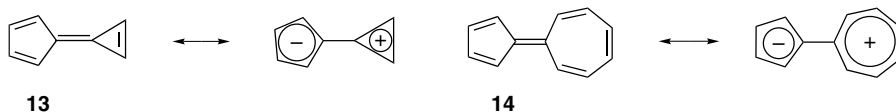
<sup>199</sup>. J. F. Chiang and S. H. Bauer, *J. Am. Chem. Soc.*, **92**, 261 (1970).

<sup>200</sup>. E. D. Bergmann, *Chem. Rev.*, **68**, 41 (1968).

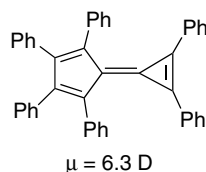
<sup>201</sup>. E. Escher, P. Bönzli, A. Otter, and M. Neuenschwander, *Mag. Reson. Chem.*, **24**, 350 (1986).

<sup>202</sup>. T. Nozoe and I. Murata, *Int. Rev. Sci., Org. Chem. Ser. Two*, **3**, 197 (1976).

Because the five-membered ring is a substituted cyclopentadienide anion in some dipolar resonance structures, it might be expected that exocyclic groups that could strongly stabilize a positive charge might lead to a larger contribution from dipolar structures and enhanced stability. Structures **13** and **14** are cases in which a large dipolar contribution would be feasible.

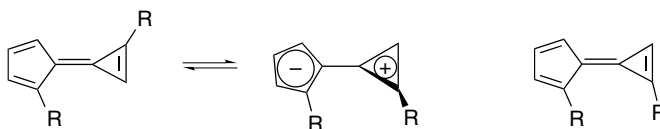


The stability of such dipolar systems depends on the balance between the increase in energy required to separate unlike charges and the aromaticity associated with Hückel  $4n + 2$  systems. The parent compound, tripentafulvalene, is unknown, but BLYP/6-31G\* and MP2/6-31G\* calculations suggest some delocalization and a substantial dipole moment.<sup>203</sup> Phenyl-substituted analogs are known, and the large measured dipole moments suggest considerable charge separation.



Ref. 204

Some alkyl derivatives have been prepared. Their chemical behavior is that of highly reactive polyenes. One interesting property does appear in the NMR spectra, which reveal a reduced barrier to rotation about the double bond between the two rings.<sup>205</sup> This property suggests that rotation about this bond takes place easily through a TS in which the two charged aromatic rings are twisted out of conjugation.



MO calculations (HF/STO-3G and HF/3-21G) indicate a rotational barrier that is substantially reduced relative to the corresponding barrier in ethene. The TS for the rotation is calculated to have a charge separation of the type suggested by the dipolar resonance structure.<sup>206</sup>

Agranat, Radom, and co-workers surveyed the fulvene and fulvalene combinations including three-, five-, and seven-membered rings. Structures and energies were calculated at the BLYP/6-31G\* and MP2/6-31G\* levels.<sup>203</sup> A large destabilization was found for triafulvalene on the basis of homodesmotic reactions. The potentially

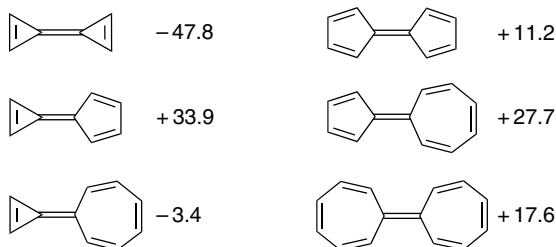
<sup>203</sup> A. P. Scott, I. Agranat, P. U. Biedermann, N. V. Riggs, and L. Radom, *J. Org. Chem.*, **62**, 2026 (1997).

<sup>204</sup> E. D. Bergmann and I. Agranat, *J. Chem. Soc. Chem. Commun.*, 512 (1965).

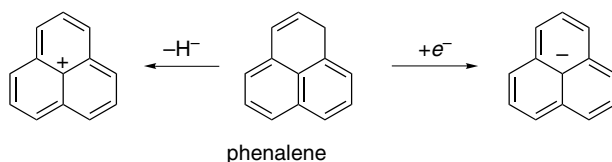
<sup>205</sup> A. S. Kende, P. T. Izzo, and W. Fulmer, *Tetrahedron Lett.*, 3697 (1966); H. Prinzbach, *Pure Appl. Chem.*, **28**, 281 (1971).

<sup>206</sup> B. A. Hess, Jr., L. J. Schaad, C. S. Ewig, and P. Carsky, *J. Comput. Chem.*, **4**, 53 (1982).

favorable three-five and five-seven combinations showed somewhat larger stabilizations than the five-five and seven-seven combinations.



The hydrocarbon phenalene is the precursor of a highly stabilized anion and cation. The HMO diagram is shown in Figure 8.10. The single orbital at the nonbonding level is the LUMO in the cation and the HOMO in the anion. The stabilization energy calculated is the same for both and is  $0.41\beta$  by the HMO' comparison.<sup>207</sup> The  $pK$  for conversion of phenalene to its anion is 19.<sup>208</sup> The cation is estimated to have a  $pK_{R+}$  of about 0–2.<sup>209</sup> Several methods for generating the phenalenyl cation have been developed.<sup>210</sup> Since the center carbon is part of the conjugated system, the Hückel rule, which applies only to *monocyclic* conjugated systems, cannot be applied to just the peripheral conjugation. The nature of the phenalenyl system is considered further in Problem 8.12.



The general conclusion is that the HMO', RE, and SCF methods based on comparison with conjugated polyenes make reasonably accurate predictions about the stabilization in conjugated molecules. The stabilization is general for benzenoid compounds, but quite restricted in nonbenzenoid systems. Since the HMO' method of estimating stability is based on the ideas of HMO theory, its success vindicates the ability of this very simplified MO approach to provide insight into the structural nature of the annulenes and other conjugated polyenes. Of course, more sophisticated MO methods are now accessible and can be applied for more detailed analyses of the structures of these molecules.

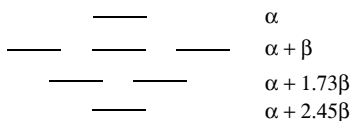


Fig. 8.10. Hückel molecular orbitals for phenalenyl.

<sup>207</sup> J. Aihara, *Bull. Chem. Soc. Japan*, **51**, 3540 (1978); P. Ilic and N. Trinjastic, *J. Org. Chem.*, **45**, 1738 (1980).

<sup>208</sup> A. Streitwieser, Jr., J. M. Word, F. Guibe, and J. S. Wright, *J. Org. Chem.*, **46**, 2588 (1981); R. A. Cox and R. Stewart, *J. Am. Chem. Soc.*, **98**, 488 (1976).

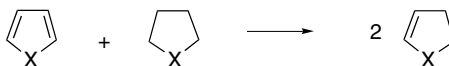
<sup>209</sup> D. Menche, H. Strauss, and E. Heilbronner, *Helv. Chim. Acta*, **41**, 57 (1958).

<sup>210</sup> I. Murata, in *Topics in Nonbenzenoid Aromatic Chemistry*, T. Nozoe, R. Breslow, K. Hafner, S. Ito, and I. Murata, ed., Hirokawa, Tokyo, 1976, pp. 159–190.

## 8.6. Heteroaromatic Systems

Certain structural units containing heteroatoms can be inserted into aromatic systems in such a way that the system remains conjugated and isoelectronic with the original hydrocarbon. The most common examples are  $-\text{CH}=\text{N}-$  and  $-\text{N}=\text{N}-$  double bonds and divalent  $sp^2$   $-\text{O}-$ ,  $-\text{S}-$ , and  $-\text{NR}-$  units. Each of these structural fragments can replace  $-\text{CH}=\text{CH}-$  in an aromatic ring and contribute two  $\pi$  electrons.<sup>211</sup> These compounds are called *heteroaromatic* to recognize both their heterocyclic and aromatic nature. Scheme 8.6 gives some of the common structures that are isoelectronic with benzene and naphthalene.

Various approaches have been taken to estimate the aromaticity of these compounds. The Hess-Schaad HMO' values are available,<sup>212</sup> as are SCF comparisons with polyene models.<sup>213</sup> Generally speaking, the various approaches suggest that the aromatic stabilization of pyridine is similar to that of benzene. This is in agreement with thermochemical estimates of the pyridine stabilization energy.<sup>214</sup> Typically, the five-membered compounds are found to be somewhat less stabilized than benzene with resonance energies in the range of 0.5 to 0.75 of that for benzene.<sup>215</sup> Theoretical calculations at the MP2/6-31G\* and B3LYP/6-31G\*\* have provided aromatic stabilization energies (ASE; see p. 717).



The ASE values correlate with magnetic susceptibility for the five-membered heteroaromatic compounds.<sup>216</sup> Magnetic and polarizability criteria put the order of aromaticity as thiophene > pyrrole > furan.<sup>215a,c</sup> The other criteria of aromaticity discussed in Section 8.2 are also applicable to heterocyclic compounds. HOMO-LUMO gaps<sup>217</sup> and Fukui functions<sup>218</sup> (see Topic 1.5) have been calculated for compounds such as indole, benzofuran, and benzo thiophene and are in accord with the known reactivity patterns of these heterocycles.

Additional heteroaromatic structures can be built up by fusing benzene rings to the aromatic heterocyclic rings or by fusing heterocyclic rings together. Examples of the former type are included in Scheme 8.6. When benzene rings are fused to the heterocyclic five-membered rings, the structures from fusion at the 2,3-positions are much more stable than those from fusion at the 3,4-positions. The  $\pi$ -electron system in the 3,4-fused compounds is more similar to a peripheral 10  $\pi$ -electron system than

<sup>211</sup> B. Ya. Simkin, V. I. Minkin, and M. N. Glukhovtsev, *Adv. Heterocycl. Chem.*, **56**, 303 (1993).

<sup>212</sup> B. A. Hess, L. S. Schaad, and C. W. Holyoke, *Tetrahedron*, **31**, 295 (1975); B. A. Hess and L. S. Schaad, *J. Am. Chem. Soc.*, **95**, 3907 (1973).

<sup>213</sup> M. J. S. Dewar, A. J. Harget, N. Trinjastic, and S. D. Worley, *Tetrahedron*, **28**, 4505 (1970).

<sup>214</sup> K. B. Wiberg, D. Nakaji, and K. M. Morgan, *J. Am. Chem. Soc.*, **115**, 3527 (1993).

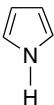
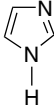
<sup>215</sup> (a) M. Stolze and D. H. Sutter, *Z. Naturforsch. A*, **42**, 49 (1987); (b) L. Nyulaszi, P. Varnai, and T. Veszpremi, *Theochem*, **358**, 55 (1995); (c) A. Hincliffe and H. J. Soscun, *Theochem*, **331**, 109 (1995); (d) P. Friedman and K. F. Ferris, *Int. J. Quantum Chem., Symposium* **24**, 843 (1990); (e) G. P. Bean, *J. Org. Chem.*, **63**, 2497 (1998).

<sup>216</sup> P. v. R. Schleyer, P. K. Freeman, H. Jiao, and B. Goldfuss, *Angew. Chem. Int. Ed. Engl.*, **34**, 337 (1995); M. K. Cyranski, P. v. R. Schleyer, T. M. Krygowski, H. Jiao, and G. Hohlneicher, *Tetrahedron*, **59**, 1657 (2003).

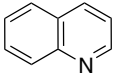
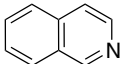
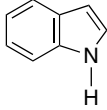
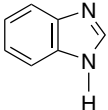
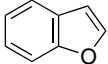
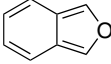
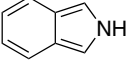
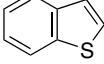
<sup>217</sup> B. S. Jursic, *J. Heterocycl. Chem.*, **33**, 1079 (1996); B. S. Jursic, *Theochem*, **468**, 171 (1999).

<sup>218</sup> R. Salcedo, A. Martinez, and L. E. Sansores, *Tetrahedron*, **57**, 8759 (2001); A. Martinewz, M.-V. Vazquez, J. L. Carreon-Macedo, L. E. Sansores, and R. Salcedo, *Tetrahedron*, **59**, 6415 (2003).

**Scheme 8.6. Stabilization Energy and Index of Aromaticity for Heteroaromatic Compounds Isolelectronic with Benzene and Naphthalene**
**A. Structures isolelectronic with benzene**

					
	Pyridine	Pyrimidine	Pyrazine	Pyridazine	s-Triazine
SE	43.3	40.6	40.9	32.7	44.9
HMO'	0.35	0.30	0.29		
SCF-MO	20.9	20.2	14.6		
AM1	25.6	25.0	24.6	22.6	
IA	86	84	89	79	100
					
	Furan	Pyrrole	Thiophene	Imidazole	Thiazole
SE	27.2	40.4	43.0	48.3	42.0
HMO'			0.19	15.4	
SCF-MO	1.6	8.5			
AM1	12.1	22.5	16.5		
IA	53	90	81.5	79	79

**B. Structures isolelectronic with naphthalene**

				
	Quinoline	Isoquinoline	Indole	Benzimidazole
SE	81.0	81.0	73.8	78.9
HMO'	0.51	0.52		30.9
SCF-MO	32.9			
IA	134	133	146	148
				
	Benzofuran	Isobenzofuran	Isoindole	Benzothiophene
SE	55.4			0.44
HMO'				
SCF-MO	20.3			
IA	94			

SE: Thermochemical stabilization in kcal/mol based on the difference between  $\Delta H_f$  and summation of standard bond energies. Benzene = 45.8 kcal/mol. C. W. Bird, *Tetrahedron*, **48**, 335 (1992); *Tetrahedron*, **52**, 9945 (1996).

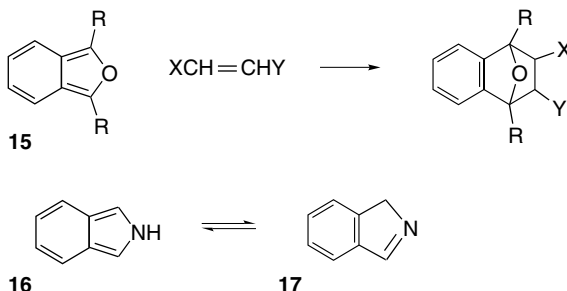
HMO': HMO stabilization in  $\beta$  relative to localized bond model. Benzene = 0.39; B. A. Hess, Jr., L.J. Schaad, and C. W. Holyoke, *J. Org. Chem.*, **31**, 295 (1975); B. A. Hess, Jr. and L. J. Schaad, *J. Am. Chem. Soc.*, **95**, 3907 (1973).

SCF-MO: Difference in total energy in kcal/mol relative to polyene model; Benzene = 20 kcal/mol. M. J. S. Dewar, A. J. Harget, and N. Trinajstić, *J. Am. Chem. Soc.*, **91**, 6321 (1969).

AM1: Stabilization in kcal/mol relative to localized model using AM1 semiempirical calculations; M. J. S. Dewar and A. J. Holder, *Heterocycles*, **28**, 1135 (1989).

IA: Index of aromaticity based on bond length variation. Benzene = 100.

to the 10 electron system for naphthalene. As a result these compounds have a strong tendency to undergo reactions that restore benzene conjugation in the carbocyclic ring. The isobenzofuran structure **15** is known to be an exceptionally reactive diene, for example. Isoindole, **16**, readily tautomerizes to the benzenoid imine **17**.



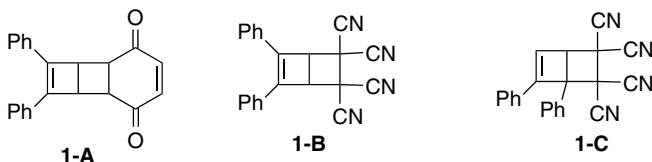
## General References

- E. Clar, *Polycyclic Hydrocarbons*, Academic Press, New York, 1964.  
 P. J. Garratt, *Aromaticity*, Wiley, New York, 1986.  
 I. Gutman and S. J. Cyvin, *Introduction to the Theory of Benzenoid Hydrocarbons*, Springer-Verlag, Berlin, 1989.  
 D. Lloyd, *Nonbenzenoid Conjugated Carbocyclic Compounds*, Elsevier, Amsterdam, 1984.  
 V. I. Minkin, M. N. Glukhovtsev and B. Y. Simkin, *Aromaticity and Anti-aromaticity*, Wiley, New York, 1994.  
 M. Sainsbury, *Aromatic Chemistry*, Oxford University Press, Oxford, 1992.

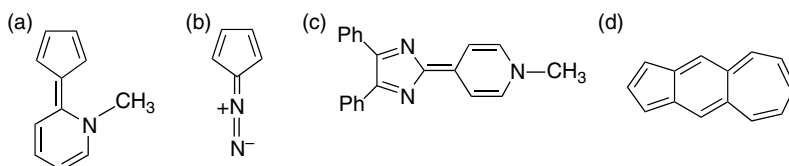
## Problems

(References for these problems will be found on page 1163.)

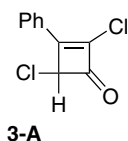
- 8.1. The reaction of 1,2-diphenylcyclobutadiene (generated in situ by oxidation of its iron tricarbonyl complex) with *p*-benzoquinone yields adduct **1-A** as the exclusive product. A completely analogous structure is obtained using maleimide as the dienophile. However, with the more reactive dienophiles tetracyanoethylene and dicyanomaleimide, two isomeric adducts of type **1-B** and **1-C** are found in a 1:7 ratio in each case. Discuss these results and explain how they relate to the issue of a square versus a rectangular structure for the cyclobutadiene ring.



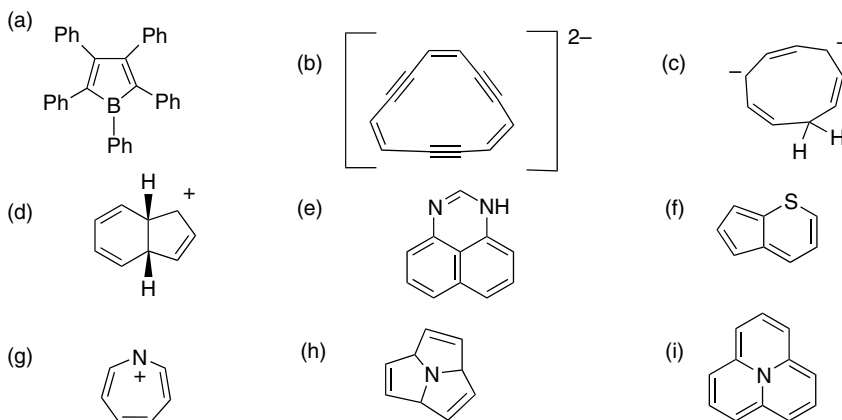
- 8.2. A single resonance structures is shown below for each of several molecules. Consider other resonance structures and identify those that would be expected to make a major stabilizing contribution to the molecule in question.



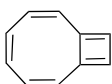
- 8.3. a. A synthesis of tropone (cycloheptatrienone) entails treating 1-methoxy-1,3,5-cycloheptatriene with bromine. A salt is produced that yields tropone on treatment with aqueous  $\text{NaHCO}_3$ . What is a likely structure for the salt? Write a mechanism for its formation and for the formation of tropone on hydrolysis.
- b. The optically active dichlorophenylcyclobutenone **3-A** undergoes racemization in acetic acid at  $100^\circ\text{C}$ . Suggest an experiment to determine if the enol (a hydroxycyclobutadiene) is an intermediate.



- 8.4. Predict whether or not the following structures would show strong delocalization and stabilization (aromatic), weak stabilization by conjugation (nonaromatic), or strong destabilization (antiaromatic) relative to acyclic model structures. Explain the basis for your prediction.



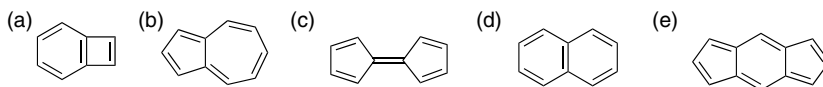
- 8.5. Bicyclo[6.2.0]deca-2,4,6,8,10-pentaene has been synthesized, and a number of MO and MM calculations have been performed to assess its aromaticity or antiaromaticity. Consider the structure and discuss the points below.



- a. What aspects of the structure suggest that antiaromaticity might be observed?
- b. What aspects of the structure suggest that aromaticity might be observed?

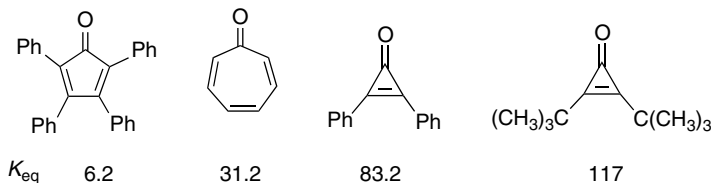
c. What are some of the experimental and computational criteria that could be applied to assess aromaticity or antiaromaticity? Cite at least three such probes and indicate the nature of the observation and interpretation.

8.6. Using the empirically chosen energy equivalents for bond types given on p. 748 and a standard compilation of HMO calculations, determine the resonance energies of the following molecules by the Hess-Schaad procedure (p. 747). Do you find any discrepancies between the predicted and observed properties, as described in Section 8.5?



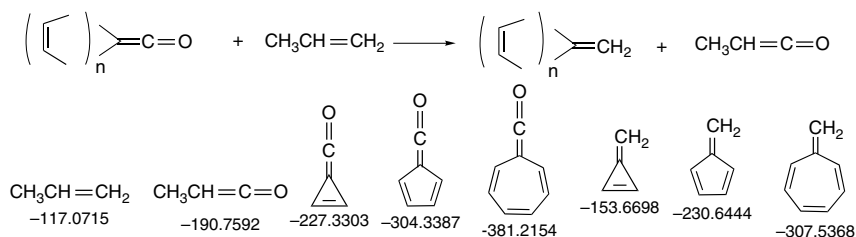
8.7. The completely conjugated cyclic polyenones have attracted considerable interest. Consider the following aspects of their properties:

a. The relative basicity of carbonyl oxygens can be measured by studying the strength of hydrogen bonding with a hydrogen donor such as phenol. The  $K_{eq}$  for 1:1 complexation of the following substituted cycloenones was determined. What conclusions do you draw from these data?

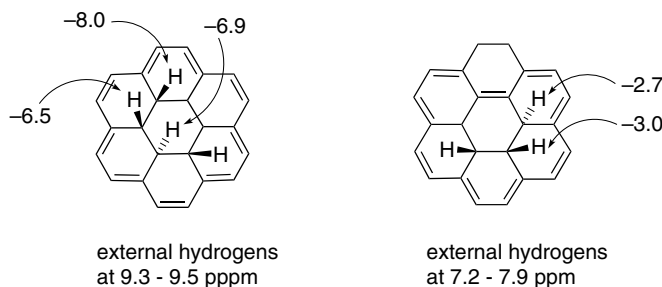


b. There have been extensive physical and chemical studies on cyclopropenone, cyclopentadienone, and cycloheptatrienone (tropone). The results of these studies can be briefly summarized as follows: (a) cyclopropenone appears to be stabilized by  $20 \pm 5$  kcal/mol, relative to localized model structures; (b) cyclopentadienone is a kinetically unstable molecule; (c) tropone is estimated to be stabilized by less than 10 kcal/mol, relative to localized models. It is nonplanar and rather reactive. Rationalize these results in terms of MO concepts.

8.8. The isodesmic reaction series shown below has been used to compare the stabilities of the cyclopolyene ketenes. The total energies (HF/6-31G\*) are given in hartrees. Calculate the stabilization found for each cyclopolyene ketene for  $n = 1-3$ . Account for the differences in stabilization and compare the results of these exocyclic ketenes to the corresponding cyclopolyenones (Problem 8.7).

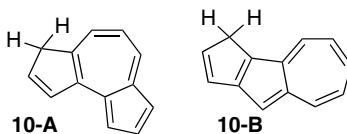


- 8.9. One criterion of aromaticity is the diamagnetic ring current, which is indicated by a substantial chemical shift difference between hydrogens in the plane of a conjugated system and those above or below the plane. The chemical shifts of two isomeric hydrocarbons are given below. In qualitative terms, which compound appears to be more aromatic? (Because the chemical shift owing to ring current depends on the detailed geometry, a quantitative calculation would be necessary to confirm the correctness of the qualitative assessment.) Does HMO theory predict a difference in the aromaticity of these two compounds?

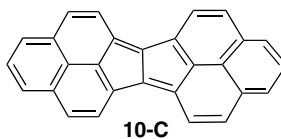


- 8.10. Offer an explanation for the following observations:

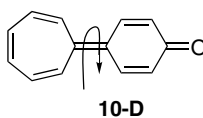
- a. Hydrocarbon **10-A** ( $pK \approx 14$ ) is considerably more acidic than **10-B** ( $pK \approx 22$ ).



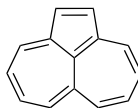
- b. Hydrocarbon **10-C** has an unusually small separation of its oxidation and reduction potentials, as established by electrochemical measurements. It is both easily reduced and easily oxidized. Both mono- and dication and mono- and dianions can be readily formed.



- c. The barrier for rotation about the marked bond in **10-D** is only about 14 kcal/mol.



- d. The hydrocarbon **10-E** is easily reduced to a dianion. The  $^1\text{H}$ NMR spectrum of the dianion shows an average downfield shift relative to the hydrocarbon. The central carbon shows a large upfield shift in the  $^{13}\text{C}$ -NMR spectrum.

**10-E**

- 8.11. The HMOs for acenaphthene are shown below. The atomic coefficients for the orbital that is the LUMO in the neutral compound and the HOMO in the dianion are given at the right.

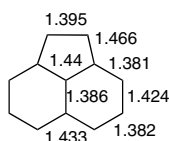
—	-2.36	
—	-1.92	
=	-1.43	
=	-1.31	
—	-1.00	
—	-0.28	
—	+0.63	
—	+0.83	
—	+1.00	
— —	+1.69	
—	+2.47	

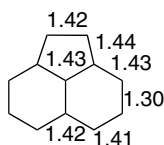
	+0.322	-0.322	
	+0.230	-0.230	
-0.388	8	8a	2a
-0.120	7	5a	4
	+0.422	-0.422	+0.388

Comment on the aromaticity, antiaromaticity, or nonaromaticity of acenaphthene and its dianion on the basis of the following physical measurements:

- a. The bond lengths of acenaphthene are given below. Compare them with the bond lengths for naphthalene given on p. 18. What conclusions can you draw about the aromaticity of acenaphthene?



- b. Both X-ray crystallography and NMR data indicate that the C(1)–C(2) bond lengthens significantly in the dianion, as indicated below (X-ray data). There is also a different pattern of bond length alternation. What conclusions can you draw about the aromaticity of the acenaphthene dianion?



- c. The  $^1\text{H}$ - and  $^{13}\text{C}$ -NMR shifts for acenaphthene and its dianion ( $\text{Na}^+$  counterion) are given below. What conclusions about charge density and aromaticity can be drawn from these data?

		1,2	3,8	4,7	5,6	2a,8a	5a	8b
$^1\text{H}$	Neutral	7.04	7.65	7.50	7.78			
	Dianion	4.49	4.46	5.04	3.34			
$^{13}\text{C}$	Neutral	129.9	124.7	128.3	127.8	140.7	129.1	129.3
	Dianion	86.1	97.0	126.8	82.6	123.4	149.3	137.7

- 8.12. The  $^1\text{H}$ -NMR and  $^{13}\text{C}$ -NMR spectra of both the anion and cation derived from phenalene have been observed. The HMO pattern for phenalene is given below.

atom	Energy( $\beta$ )	HMO coefficients					
	2.44949	1.73205	1.73205	1.00000	1.0000	1.0000	0.0000
1	0.22361	0.35355	0.20412	-0.00473	-0.35355	-0.27382	-0.40825
2	0.18257	0.	0.00000	-0.00947	-0.00000	-0.54764	-0.20000
9a	0.36515	0.20412	0.35355	-0.00473	-0.35355	0.27382	0.00000
9b	0.44721	0.00000	0.00000	-0.40811	0.00000	0.37215	0.00000
9	0.22361	-0.00000	0.40825	0.41134	0.00000	0.17549	0.40825
8	0.18257	-0.20412	0.035355	0.40661	0.35355	-0.09833	0.00000
7	0.22361	-0.35355	0.20412	-0.00473	0.35355	-0.27382	-0.40825
6a	0.36515	-0.40825	0.00000	-0.41434	0.00000	-0.17549	-0.00000

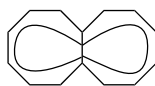
The chemical shifts observed for the cation and anion are given below.

	$^1\text{H}$ -NMR		$^{13}\text{C}$ -NMR			
	C(1)	C(2)	C(1)	C(2)	C(9b)	C(3a)
[Cation]	9.38	8.55	155.5	133.7	123.7	133.7
[Anion]	5.36	6.10	103.4	128.0	139.6	145.0

What conclusions can be drawn about electron distribution in the cation and anion from the NMR data and how does it relate to the HMO pattern?

- 8.13. The  $^{13}\text{C}$ -NMR spectrum of octalene (**13-A**, **13-B**, or **13-C**) is temperature dependent. At  $-150^\circ\text{C}$ , there are signals for 14 different carbons. At  $-100^\circ\text{C}$ , these collapse to seven different signals. Above  $80^\circ\text{C}$ , all but one of the remaining signals become broad. Although not attained experimentally, because of decomposition, it would be expected that only four different signals would be obtained at still higher temperature. (1) Show that these data rule out structures **13-A** and **13-B** for the room temperature structure of octalene, and favor structure **13-C**. (2) What is the nature of the dynamic process that converts the 14-line spectrum

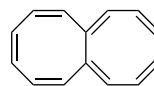
to a 7-line spectrum? (3) What would be the nature of the process that converts the 7-line spectrum to a 4-line spectrum?



13-A



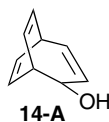
13-B



13-C

8.14. When alcohol **14-A** is dissolved in  $\text{FSO}_3\text{H}$  at  $-136^\circ\text{C}$  and then brought to  $-110^\circ\text{C}$ , it gives rise to a  $^{13}\text{C}$ -NMR spectrum having five lines in the intensity ratio 2:1:2:2:2.

a. Suggest several possible structures for this cation and discuss stabilizing features that might favor a particular structure.



14-A

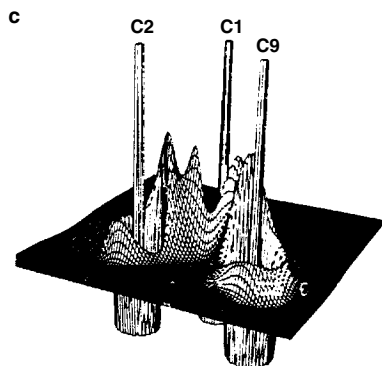
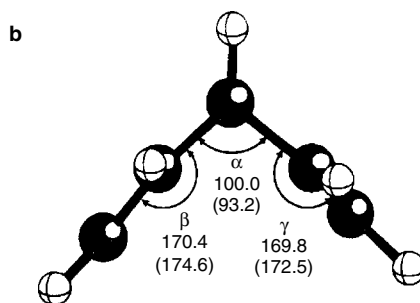
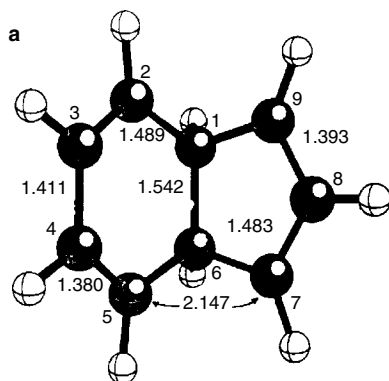


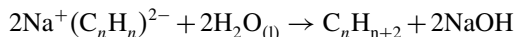
Fig. 8.P14. (a) Bond lengths and (b) inter-ring angles for minimum-energy cation; (c)  $-\nabla^2\rho(\mathbf{r})$  in the  $\text{C}(1)\text{--C}(2)\text{--C}(9)$  plane. Reproduced by permission of the American Chemical Society  
 Bond Orders: 1,2: 1.04; 2,3:1.59; 3,4: 1.57; 1,6:0.94; 1,9: 1.04; 8,9:1.56; 2,9:0.34.

b. Figure 8.P14(a, b) gives the computed minimum-energy structure at the MP4(SDQ)/6-31G(d) level. Diagram (c) is the  $-\nabla^2\rho(\mathbf{r})$  in the C(1)–C(2)–C(9) plane. Does this structure correspond to any of those you have suggested in Part (a)? What structural representation would be most consistent with the calculated minimum-energy structure?

- 8.15. a. The heats of combustion ( $\Delta H_c$ ) and heats of hydrogenation ( $\Delta H_{H_2}$ ) for addition of 1 mol of  $H_2$  and the estimated stabilization energy (SE) for benzene and cyclooctatetraene (in kcal/mol) are given below. The  $\Delta H_c$  and  $\Delta H_{H_2}$  are also given for [16]annulene. Compare the stabilization energy of [16]annulene with benzene and cyclooctatetraene on a per CH basis.

	Benzene	Cyclooctatetraene	[16]Annulene
$\Delta H_c$	781	1086	2182
$\Delta H_{H_2}$	-5.16	25.6	28.0
SE	36	4	?

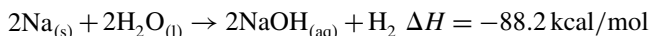
- b. The enthalpies of the reaction of the cyclooctatetraene and [16]annulene dianions with water have been measured.



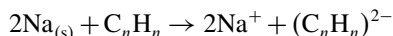
$$\Delta H = -33.33 \text{ kcal/mol for cyclooctatetraene}$$

$$\Delta H = -10.9 \text{ kcal/mol for [16]annulene.}$$

Using these data and the enthalpy of the reaction of sodium with water:

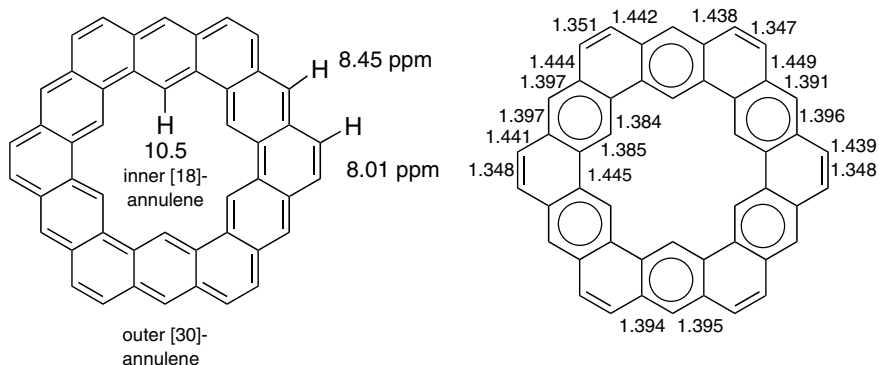


calculate  $\Delta H$  for the reaction:

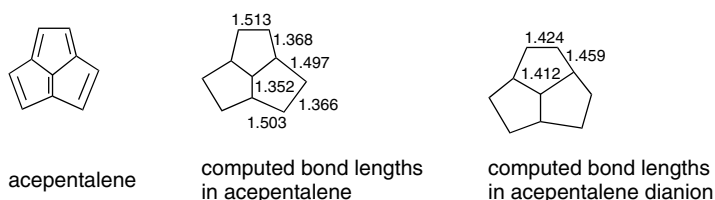


Why might the reaction of  $[C_{16}H_{16}]^{2-}$  with water be less exothermic than for  $[C_8H_8]^{2-}$ ? How do you interpret the difference in the heat of reaction of the two hydrocarbons to form the respective dianions?

- 8.16. Consider the two structures shown for kekulene, one suggesting inner and outer annulenes and the other a series of phenanthrene-like units.  $^1H$ -NMR and bond length data are given. The NICS values are calculated as  $-4.3$  for the angularly fused rings and  $-10.8$  for the linearly fused rings. Indicate properties that you would expect to be associated with each structure. Do you consider the properties to be more consistent with the double-annulene or the phenanthrene-like structures?



8.17. Acepentalene is a rather unstable molecule, but its dianion can be formed quite readily. The structure and properties of acepentalene and its dianion and dication have been calculated (B3LYP/6-31G\*) and are given below. The computed lowest-energy structure is slightly pyramidal, with an inversion barrier of 7.1 kcal/mol. The structure of the lithium salt of the dianion is given in the Figure 8.P17. The calculated inversion barrier for the dianion is 5.4 kcal/mol. The chemical shift of the  $^1\text{H}$  signal in the dianion is at  $-8.2$ .



- a. What evidence in terms of aromaticity/antiaromaticity can you offer for the apparently greater stability of the  $12\pi$ -electron dianion as compared with the  $10\pi$ -electron neutral? What accounts for the pyramidal as opposed to planar structures for the neutral and dianion?

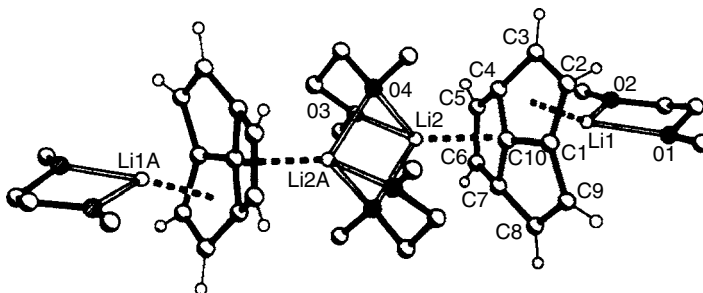


Fig. 8.P17. Crystal structure of  $\text{Li}_2(\text{DME})_2\text{acepentalenediide}$ . Reproduced from *Angew. Chem. Int. Ed. Engl.*, **34**, 1492 (1995), by permission of Wiley-VCH.

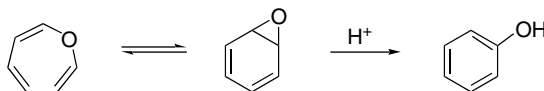
	NICS*	NICS <sub>(in)</sub> <sup>a</sup>	NICS <sub>(out)</sub> <sup>a</sup>	$\chi$	$\Lambda$
Acepentalene	+42.3	50.0	31.0	-62.4	23.1
Dianion	-32.7	-42.3	-27.9	-141.0	-43.1
Dication	+10.2	-24.9	2.4	-72.9	-18.8

a. The NICS values are relative to positions 0.5 Å inside and outside the pyramidal structure. NICS\* is the sum for all rings.

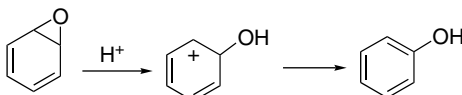
b. The HMO orbitals of acepentalene are given below. How do the predictions of HMO theory accord with the experimental and B3LYP results?

—	-2.086
— —	-1.879
—	-1.000
— —	+0.347
—	+0.572
— —	+1.532
—	+2.514

8.18. Arene oxides are important intermediates in the metabolism of aromatic compounds. Although they are highly reactive, both valence tautomerism to oxepins and acid-catalyzed ring opening to phenols can be observed and studied.

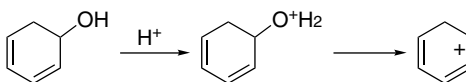


Surprisingly, the rate of acid-catalyzed ring opening is less than that for dehydration of “2,4-cyclohexadienol” even though they lead to similar cations. Normally, epoxide ring opening is much faster than alcohol dehydration. For example, the epoxide of cyclohexadiene is about 10<sup>7</sup> more reactive than cyclohexenol.



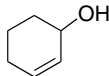
$$k[\text{H}^+][\text{oxide}] = 32 \text{ M}^{-1}\text{s}^{-1}$$

$$\Delta H_r = -57 \text{ kcal/mol}$$



$$k[\text{H}^+][\text{dien-ol}] = 190 \text{ M}^{-1}\text{s}^{-1}$$

$$\Delta H_r = -39 \text{ kcal/mol}$$



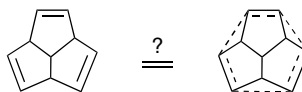
$$k[\text{H}^+][\text{oxide}] = 1.1 \times 10^4 \text{ M}^{-1}\text{s}^{-1} \quad k[\text{H}^+][\text{en-ol}] = 10^{-3} \text{ M}^{-1}\text{s}^{-1}$$

What might account for the apparent kinetic stability of the arene oxide toward acid-catalyzed ring opening?

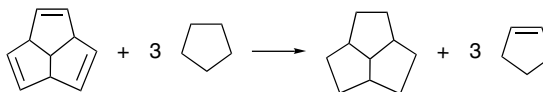
- 8.19. Using isodesmic reactions and the G2(MP2) energies given below, determine if 1,2,3-trichlorocyclopropenium ion is more or less stable than the *tert*-butyl carbocation. Are the chlorine substituents stabilizing or destabilizing with respect to cyclopropenium ion?

Substance	G2(MP2) energy (hartrees)
Trichlorocyclopropenium	-1492.916633
Cyclopropenium ion	-115.492839
<i>tert</i> -Butyl carbocation	-157.169332
1,2,3,3-tetrachlorocyclopropene	-1952.950661
3-Chlorocyclopropene	-575.525577
<i>tert</i> -Butyl chloride	-617.226718

- 8.20. Triquinacene is a hydrocarbon that might be stabilized by homoaromaticity.



The calculated (B3LYP/6-3111+G\*)  $\Delta H_{H_2}$  for the successive double bond are -27.6, -27.3, and -26.8 kcal/mol. The  $\Delta H_{H_2}$  for cyclopentene is -26.9 kcal/mol. The existence of homoaromatic stabilization of triquinacene might be assessed by the following homodesmotic reaction, where  $\Delta E = -0.8$  kcal/mol:



$$\Delta E = -0.8 \text{ kcal/mol}$$

Do these data indicate homoaromatic stabilization of triquinacene? Why or why not?

# Aromatic Substitution

## Introduction

The introduction or replacement of substituents on aromatic rings by substitution reactions is one of the most fundamental transformations in organic chemistry. On the basis of the reaction mechanism, these substitution reactions can be divided into (a) electrophilic, (b) nucleophilic, (c) radical, and (d) transition metal catalyzed. In this chapter we consider the electrophilic and nucleophilic substitution mechanisms. Radical substitutions are dealt with in Chapter 11 and transition metal-catalyzed reactions are discussed in Chapter 9 of Part B.

## 9.1. Electrophilic Aromatic Substitution Reactions

Electrophilic aromatic substitution (abbreviated EAS in this chapter) reactions are important for synthetic purposes and are also among the most thoroughly studied classes of organic reactions from a mechanistic point of view. The synthetic aspects of these reactions are considered in Chapter 9 of Part B. This section focuses on the mechanisms of several of the most completely studied reactions. These mechanistic ideas are the foundation for the structure-reactivity relationships in aromatic electrophilic substitution that are discussed in Section 9.2.

A wide variety of electrophiles can effect aromatic substitution. Usually, it is a substitution of some other group for hydrogen that is of interest, but this is not always the case. For example, both silicon and mercury substituents can be replaced by electrophiles. Scheme 9.1 lists some of the specific electrophiles that are capable of carrying out substitution of hydrogen. Some indication of the relative reactivity of the electrophiles is given as well. Many of these electrophiles are not treated in detail until Part B. Nevertheless, it is important to recognize the very broad scope of electrophilic aromatic substitution.

The reactivity of a particular electrophile determines which aromatic compounds can be successfully substituted. The electrophiles grouped in the first category are sufficiently reactive to attack almost all aromatic compounds, even those having strongly

EWG substituents. Those in the second group react readily with benzene and derivatives having ERG substituents but are not generally reactive toward aromatic rings with EWG substituents. Those classified in the third group are reactive only toward aromatic compounds that are much more reactive than benzene. These groupings can provide a general guide to the feasibility of a given EAS reaction.

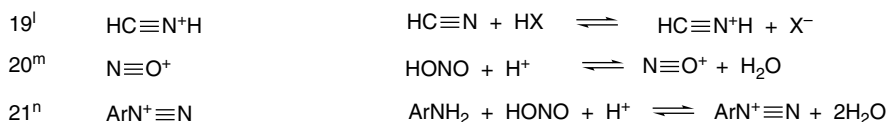
Despite the wide range of electrophilic species and aromatic ring systems that can undergo substitution, a single broad mechanistic picture encompasses most EAS reactions. The identity of the rate-determining step and the shape of the reaction energy profile are specific to individual reactions, but the sequence of steps and the nature of the intermediates are very similar across a wide range of reactivity. This permits discussion of EAS reactions in terms of the general mechanism that is outlined in Scheme 9.2.

A complexation of the electrophile with the  $\pi$  electron system of the aromatic ring is the first step. This species, called the  $\pi$  complex, may or may not be involved

### Scheme 9.1. Electrophiles Active in Aromatic Substitution

	Electrophile	Typical means of generation
A. Electrophiles capable of substituting both activated and deactivated aromatic rings		
1 <sup>a</sup>	$\text{O}=\text{N}^+=\text{O}$	$2 \text{H}_2\text{SO}_4 + \text{HNO}_3 \rightleftharpoons \text{NO}_2^+ + 2 \text{HSO}_4^- + \text{H}_3\text{O}^+$
2 <sup>b</sup>	$\text{Br}_2$ or $\text{Br}_2-\text{MX}_n$	$\text{Br}_2 + \text{MX}_n \rightleftharpoons \text{Br}_2-\text{MX}_n$
3 <sup>b</sup>	$\text{BrO}^+\text{H}_2$	$\text{BrOH} + \text{H}_3\text{O}^+ \rightleftharpoons \text{BrO}^+\text{H}_2$
4 <sup>b</sup>	$\text{Cl}_2$ or $\text{Cl}_2-\text{MX}_n$	$\text{Cl}_2 + \text{MX}_n \rightleftharpoons \text{Cl}_2-\text{MX}_n$
5 <sup>b</sup>	$\text{ClO}^+\text{H}_2$	$\text{ClOH} + \text{H}_3\text{O}^+ \rightleftharpoons \text{ClO}^+\text{H}_2$
6 <sup>c</sup>	$\text{SO}_3$ or $\text{SO}_2\text{O}^+\text{H}$	$\text{H}_2\text{S}_2\text{O}_7 \rightleftharpoons \text{HSO}_4^- + \text{SO}_2\text{O}^+\text{H}$
7 <sup>d</sup>	$\text{RSO}_2^+$	$\text{RSO}_2\text{Cl} + \text{AlCl}_3 \rightleftharpoons \text{RSO}_2^+ + \text{AlCl}_4^-$
B. Electrophiles capable of substituting activated but not deactivated aromatic rings		
8 <sup>e</sup>	$\text{R}_3\text{C}^+$	$\text{R}_3\text{CX} + \text{MX}_n \rightleftharpoons \text{R}_3\text{C}^+ + [\text{MX}_{n+1}]^-$
9 <sup>f</sup>	$\text{R}_3\text{C}^+$	$\text{R}_3\text{COH} + \text{H}^+ \rightleftharpoons \text{R}_3\text{C}^+ + \text{H}_2\text{O}$
10 <sup>g</sup>	$\text{R}_2\text{C}^+\text{CHR}'_2$	$\text{R}_2\text{C}=\text{CR}'_2 + \text{H}^+ \rightleftharpoons \text{R}_2\text{C}^+\text{CHR}'_2$
11 <sup>e</sup>	$\text{RCH}_2\text{X}-\text{MX}_n$	$\text{RCH}_2\text{X} + \text{MX}_n \rightleftharpoons \text{RCH}_2\text{X}-\text{MX}_n$
12 <sup>h</sup>	$\text{RC}\equiv\text{O}^+$	$\text{RCOX} + \text{MX}_n \rightleftharpoons \text{RC}\equiv\text{O}^+ + [\text{MX}_{n+1}]^-$
13 <sup>h</sup>	$\text{RCOX}-\text{MX}_n$	$\text{RCOX} + \text{MX}_n \rightleftharpoons \text{RCOX}-\text{MX}_n$
14 <sup>i</sup>	$\text{RC}^+=\text{O}^+\text{H}$	$\text{RCOX} + \text{MX}_n + \text{H}^+ \rightleftharpoons \text{RC}^+=\text{O}^+\text{H} + [\text{MX}_{n+1}]^-$
15 <sup>j</sup>	$\text{H}^+$	$\text{HX} \rightleftharpoons \text{H}^+ + \text{X}^-$
16 <sup>k</sup>	$\text{R}_2\text{C}=\text{O}^+\text{H}$	$\text{R}_2\text{C}=\text{O} + \text{H}^+ \rightleftharpoons \text{R}_2\text{C}=\text{O}^+\text{H}$
17 <sup>k</sup>	$\text{R}_2\text{C}=\text{O}^+-\text{M}-\text{X}_n$	$\text{R}_2\text{C}=\text{O} + \text{MX}_n \rightleftharpoons \text{R}_2\text{C}=\text{O}^+-\text{M}-\text{X}_n$
18 <sup>i</sup>	$\text{HC}^+=\text{N}^+\text{H}_2$	$\text{HC}\equiv\text{N} + 2\text{H}^+ \rightleftharpoons \text{HC}^+=\text{N}^+\text{H}_2$

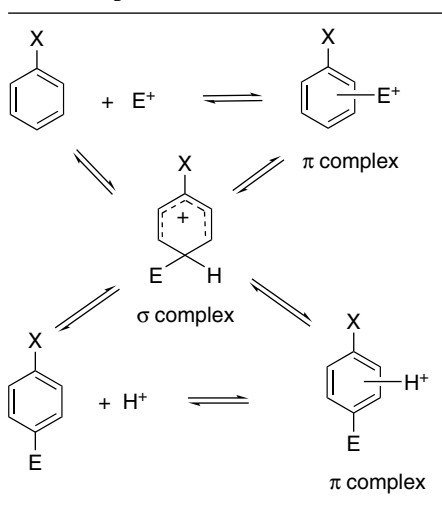
## C. Electrophiles capable of substitution only strongly activated aromatic rings



- a. G. A. Olah and S. J. Kuhn, in *Friedel-Crafts and Related Reactions*, Vol. III, G. A. Olah, ed., Interscience, New York, 1964, Chapter XLIII.
- b. H. P. Braendlin and E. T. McBee, in *Friedel-Crafts and Related Reactions*, Vol. III, G. A. Olah, ed., Interscience, New York, 1964, Chapter XLVI.
- c. K. L. Nelson, in *Friedel-Crafts and Related Reactions*, Vol. III, G. A. Olah, ed., Interscience, New York, 1964, Chapter XLVII.
- d. F. R. Jensen and G. Goldman, in *Friedel-Crafts and Related Reactions*, Vol. III, G. A. Olah, ed., Interscience, New York, 1964, Chapter XL.
- e. F. A. Drahowzal, in *Friedel-Crafts and Related Reactions*, Vol. II, G. A. Olah, ed., Interscience, New York, 1964, Chapter XVII.
- f. A. Schreisheim, in *Friedel-Crafts and Related Reactions*, Vol. II, G. A. Olah, ed., Interscience, New York, 1964, Chapter XVIII.
- g. S. H. Patinkin and B. S. Friedman, in *Friedel-Crafts and Related Reactions*, Vol. II, G. A. Olah, ed., Interscience, New York, 1964, Chapter XIV.
- h. P. H. Gore, in *Friedel-Crafts and Related Reactions*, Vol. III, G. A. Olah, ed., Interscience, New York, 1964, Chapter XXXI.
- i. Y. Sato, M. Yato, T. Ohwada, S. Saito, and K. Shudo, *J. Am. Chem. Soc.*, **117**, 3037 (1995).
- j. R. O. C. Norman and R. Taylor, *Electrophilic Substitution in Benzenoid Compounds*, Elsevier, New York, 1965, Chapter 8.
- k. J. E. Hofmann and A. Schreisheim, in *Friedel-Crafts and Related Reactions*, Vol. II, G. A. Olah, ed., Interscience, New York, 1964, Chapter XIX.
- l. W. Ruske, in *Friedel-Crafts and Related Reactions*, Vol. III, G. A. Olah, ed., Interscience, New York, 1964, Chapter XXXII.
- m. B. C. Challis, R. J. Higgins, and A. J. Lawson, *J. Chem. Soc., Perkin Trans.*, **2**, 1831 (1972).
- n. H. Zollinger, *Azo and Diazo Chemistry*, transl. H. E. Nursten, Interscience, New York, 1961, Chapter 10.

directly in the substitution mechanism.  $\pi$  Complex formation is, in general, rapidly reversible and in many cases the equilibrium constant is small. The  $\pi$  complex is a donor-acceptor type of complex with the  $\pi$  electrons of the aromatic ring donating electron density to the electrophile. Although these complexes are readily observed by spectroscopic measurements, they generally are of only modest stability. Only recently

**Scheme 9.2. Generalized Mechanism for Electrophilic Aromatic Substitution**



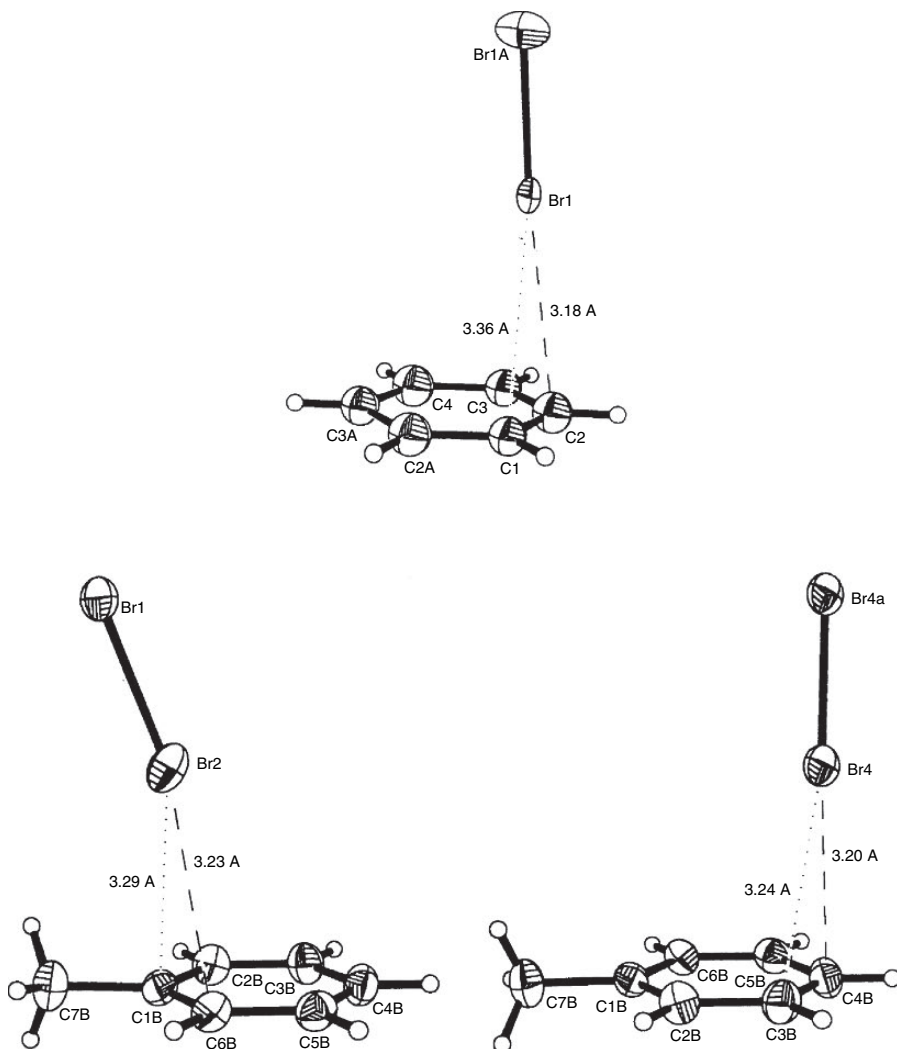


Fig. 9.1. Structures of benzene-Br<sub>2</sub> (top) and toluene-Br<sub>2</sub> (bottom) complexes. Reproduced from *Chem. Commun.*, 909 (2001), by permission of the Royal Society of Chemistry.

has structural data become available. The structures of the Br<sub>2</sub> complexes with benzene and toluene have been examined by X-ray crystallography at low temperature. The Br<sub>2</sub> molecule is nearly perpendicular to the ring and located between two specific carbons, as opposed to being associated with the delocalized  $\pi$  electron density. For toluene, there are two complexes with the Br<sub>2</sub> being associated with the *ortho* and *para* carbons.<sup>1</sup> This is significant because these are also the preferred sites for substitution, and the structures indicate that an aspect of position selectivity is present at the  $\pi$  complex stage. These structures are shown in Figure 9.1.

Structural information is also available on the complex between mesitylene and the nitrosonium ion, NO<sup>+</sup>.<sup>2</sup> In this case there appears to be a high degree of charge transfer and the complex is essentially between the aromatic radical cation and the NO

<sup>1</sup> A. V. Vasilyev, S. V. Lindeman, and J. K. Kochi, *Chem. Commun.*, 909 (2001); S. V. Rosokha and J. K. Kochi, *J. Org. Chem.*, **67**, 1727 (2002).

<sup>2</sup> E. K. Kim and J. K. Kochi, *J. Am. Chem. Soc.*, **113**, 4962 (1991).

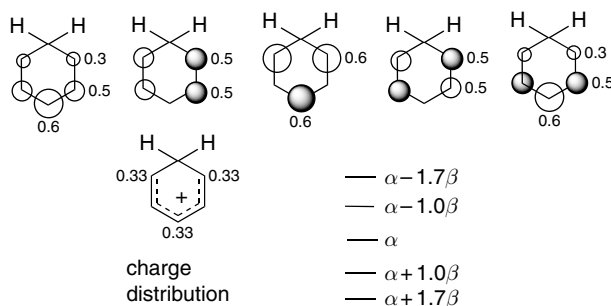
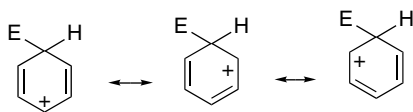


Fig. 9.2.  $\pi$  Molecular orbitals and energy levels for the cyclohexadienylum ion.

molecule, which is located centrally with respect to the aromatic ring. The N–O bond distance is 1.07 Å and the C–C bond distances are similar to those observed for the radical cation.<sup>3</sup> There are probably similar complexes in other EAS reactions. Recent computational studies of the nitration of benzene describe the earliest energy minimum as  $\text{NO}_2^+$  approaches benzene (in the gas phase) as being directed at the midpoint of a particular C–C bond, as opposed to the center of the ring.<sup>4</sup>

In order for a substitution to occur, a “ $\sigma$  complex” must be formed. The term  $\sigma$  complex is used to describe a *cationic intermediate* in which the carbon at the site of substitution is bonded to both the electrophile and the hydrogen that is being displaced. As the term implies, a  $\sigma$  bond is formed at the site of substitution. The intermediate is a *cyclohexadienylum cation*. Its fundamental electronic characteristics can be described in simple MO terms, as shown in Figure 9.2. The intermediate is a  $4\pi$  electron delocalized system that is electronically equivalent to a pentadienyl cation. There is no longer cyclic conjugation. The LUMO has nodes at C(2) and C(4) of the pentadienyl structure and these correspond to the positions *meta* to the site of substitution on the aromatic ring. As a result, the positive charge of the cation is located at the positions *ortho* and *para* to the site of substitution. These electronic features of the  $\sigma$ -complex intermediate are also shown by resonance structures.

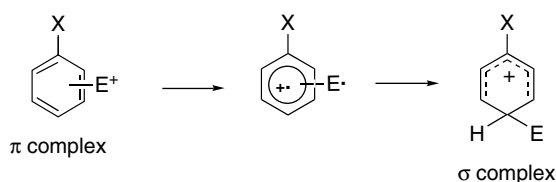


As we will see in Section 9.2, this pattern of charge distribution leads to the *o,p*- or *m*-directing characteristics of various ring substituents.

There is considerable interest in the mechanism for conversion of the  $\pi$  complex into the  $\sigma$  complex. In particular, the question arises as to whether an electron transfer occurs to yield a discrete cation radical–radical pair.

<sup>3</sup> S. V. Rosokha and J. K. Kochi, *J. Am. Chem. Soc.*, **123**, 8985 (2001).

<sup>4</sup> H. Xiao, L. Chen, X. Ju, and G. Li, *Science in China B*, **46**, 453 (2003); P. M. Esteves, J. W. de Carneiro, S. P. Cardoso, A. G. H. Barbosa, K. K. Laali, G. Rasul, G. K. S. Prakash, and G. A. Olah, *J. Am. Chem. Soc.*, **125**, 4836 (2003).



This mechanism implies that a considerable change in the structure of the electrophile occurs prior to  $\sigma$ -bond formation. These structural changes could account in large part for the energy barrier to formation of the  $\sigma$  complex.<sup>5</sup> Moreover, this mechanism implies that the cation radical–radical pair might play a key role in determining the isomeric (*ortho*, *meta*, *para*) product composition. These issues have been investigated most closely for nitration and bromination and are considered further when those reactions are discussed.

Formation of the  $\sigma$  complex can be reversible. The partitioning of the  $\sigma$  complex forward to product or back to reactants depends on the ease with which the electrophile can be eliminated, relative to a proton. For most electrophiles, it is easier to eliminate the proton, in which case the formation of the  $\sigma$  complex is essentially irreversible. The electrophiles in group A of Scheme 9.1 are the least likely to be reversible, whereas those in group C are most likely to undergo reversible  $\sigma$ -complex formation. Formation of the  $\sigma$  complex is usually, but not always, the rate-determining step in EAS. There may also be a  $\pi$  complex involving the aromatic ring and the departing electrophile. This would be expected on the basis of the principle of microscopic reversibility, but there is little direct evidence on this point.<sup>6</sup>

Let us now consider some of the evidence for this general mechanism. Such evidence has, of course, been gathered by study of specific reaction mechanisms. Only some of the most clear-cut cases are cited here. Additional evidence is mentioned when individual mechanisms are discussed in Section 9.4. A good example of studies that have focused on the identity and mode of generation of the electrophile is aromatic nitration. Primarily on the basis of kinetic studies, it has been shown that the active electrophile in nitration is often the nitronium ion,  $\text{NO}_2^+$ , which is formed by the reaction of nitric acid with concentrated sulfuric. Several other lines of evidence support the role of the nitronium ion. It can be detected spectroscopically and the freezing-point depression of the solution is consistent with the following equation:



Solid salts in which the nitronium ion is the cation can be prepared with unreactive anion such as for  $\text{NO}_2^+\text{BF}_4^-$  and  $\text{NO}_2^+\text{PF}_6^-$ . These salts act as nitrating reagents.

Two types of rate expressions have been found to describe the kinetics of many aromatic nitration reactions. With relatively unreactive substrates, second-order kinetics, first order in the nitrating reagent and first order in the aromatic, are observed. This second-order relationship corresponds to rate-limiting attack of the electrophile on the aromatic reactant. With more reactive aromatics, this step can be faster than formation of the active electrophile. In these cases, the generation of the electrophile

<sup>5</sup> S. V. Rosokha and J. K. Kochi, *J. Org. Chem.*, **67**, 1727 (2002).

<sup>6</sup> For additional discussion of the role of  $\sigma$  and  $\pi$  complexes in aromatic substitution, see G. A. Olah, *Acc. Chem. Res.*, **4**, 240 (1971); J. H. Ridd, *Acc. Chem. Res.*, **4**, 248 (1971).

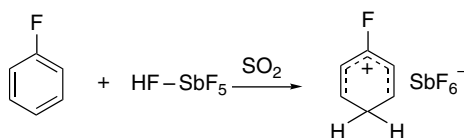
is the rate-determining step. When formation of the active electrophile is the rate-determining step, the concentration of the aromatic reactant no longer appears in the observed rate expression. Under these conditions, different aromatic substrates undergo nitration at the same rate, corresponding to the rate of formation of the active electrophile.

An important general point to be drawn from the specific case of nitration is that the active electrophile is usually some species that is more reactive than the added reagents. The active electrophile is formed from the reagents by a subsequent reaction, often involving a Brønsted or Lewis acid. One goal of mechanistic study is to determine the identity of the active electrophile, the formation of which may or may not be the rate-determining step. Scheme 9.1 indicates the structure of some of the electrophilic species that are involved in EAS processes and the reactions involved in their formation.

There are several lines of evidence pointing to formation of  $\sigma$  complexes as intermediates in EAS. One approach involves measurement of isotope effects on the rate of substitution. If removal of the proton at the site of substitution is concerted with the introduction of the electrophile, a primary isotope effect is expected when electrophilic attack on the ring is rate determining. This is not the case for nitration. Nitration of aromatic substrates partially labeled by tritium shows no selectivity between protium- and tritium-substituted sites.<sup>7</sup> Similarly, the rate of nitration of nitrobenzene is identical to that of penta-deuterio-nitrobenzene.<sup>8</sup>

The lack of a primary isotope effect indicates that the proton is lost in a fast step following the rate-determining step, which means that proton loss must occur from some intermediate that is formed before the cleavage of the C–H bond begins. The  $\sigma$ -complex intermediate fits this requirement. There are some electrophilic aromatic substitution reactions that show  $k_{\text{H}}/k_{\text{D}}$  values between 1 and 2 and there are a few others that are in the range indicating a primary isotope effect.<sup>9</sup> The existence of these isotope effects is compatible with the general mechanism if the proton removal is rate limiting (or partially rate limiting). Many of the modest kinetic isotope effects ( $k_{\text{H}}/k_{\text{D}} \sim 1.2 - 2.0$ ) have been interpreted in terms of comparable rates for formation and deprotonation of the  $\sigma$ -complex intermediate.

The case for the cyclohexadienyl cation intermediates is further strengthened by numerous studies showing that such cations can exist as stable entities under suitable conditions. Substituted cyclohexadienyl cations can be observed by NMR under stable ion conditions. They are formed by protonation of the aromatic reactant.<sup>10</sup>



Ref. 11

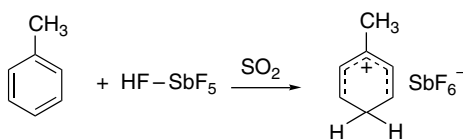
<sup>7</sup> L. Melander, *Acta Chem. Scand.*, **3**, 95 (1949); *Arkiv Kemi.*, **2**, 211 (1950).

<sup>8</sup> T. G. Bonner, F. Bower, and G. Williams, *J. Chem. Soc.*, 2650 (1953).

<sup>9</sup> H. Zollinger, *Adv. Phys. Org. Chem.*, **2**, 163 (1964).

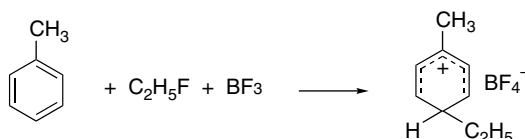
<sup>10</sup> G. A. Olah, R. H. Schlosberg, R. D. Porter, Y. K. Mo, D. P. Kelly, and G. Mateescu, *J. Am. Chem. Soc.*, **94**, 2034 (1972).

<sup>11</sup> G. A. Olah and T. E. Kiovsky, *J. Am. Chem. Soc.*, **89**, 5692 (1967).



Ref. 12

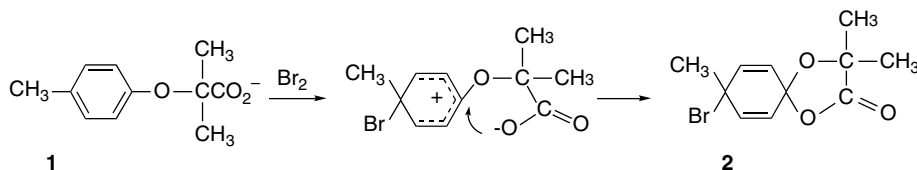
Cations formed by alkylation of benzene derivatives have also been characterized.



Ref. 13

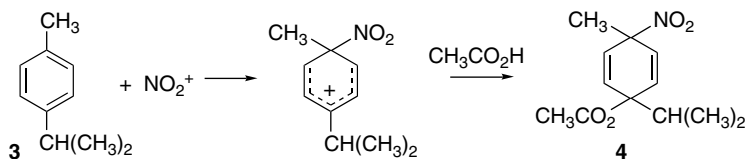
Under normal conditions of electrophilic substitution, these cyclohexadienyl ions are short-lived intermediates. The fact that the structures are stable in nonnucleophilic media clearly demonstrates the feasibility of such intermediates.

The existence of  $\sigma$ -complex intermediates can be inferred from experiments in which they are trapped by nucleophiles in special circumstances. For example, treatment of the acid **1** with bromine gives the cyclohexadienyl lactone **2**. This product results from intramolecular nucleophilic capture of the  $\sigma$  complex by the carboxylate group.



Ref. 14

A number of examples of intramolecular nucleophilic capture of cyclohexadienyl intermediates have also been uncovered in the study of nitration of alkylated benzenes in acetic acid. For example, nitration of **3** at 0°C leads to formation of **4** with acetate serving as the nucleophile.<sup>15</sup>



This type of addition process is particularly likely to be observed when the electrophile attacks a position that is already substituted, since facile rearomatization by deprotonation is then blocked. Attack at a substituted position is called *ipso* attack. Addition

<sup>12</sup> G. A. Olah, *J. Am. Chem. Soc.*, **87**, 1103 (1965).

<sup>13</sup> G. A. Olah and S. J. Kuhn, *J. Am. Chem. Soc.*, **80**, 6541 (1958).

<sup>14</sup> E. J. Corey, S. Barcza, and G. Klotmann, *J. Am. Chem. Soc.*, **91**, 4782 (1969).

<sup>15</sup> R. C. Hahn and D. L. Strack, *J. Am. Chem. Soc.*, **96**, 4335 (1974).

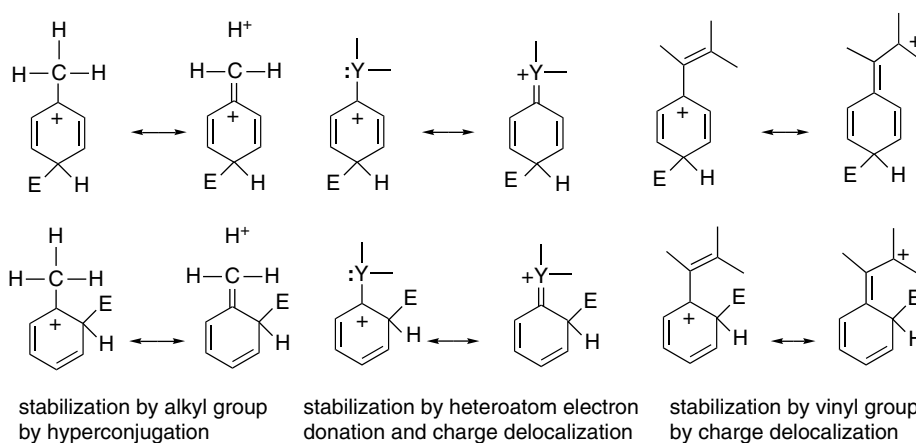
products have also been isolated when initial electrophilic attack has occurred at an unsubstituted position. The extent of addition in competition with substitution increases on going to naphthalene and the larger polycyclic aromatic ring systems.<sup>16</sup>

The general mechanistic framework outlined in this section can be elaborated by other details to more fully describe the mechanisms of the individual electrophilic substitutions. The question of the identity of the active electrophile in each reaction is important. We have discussed the case of nitration in which, under many circumstances, the electrophile is the nitronium ion. Similar questions about the structure of the active electrophile arise in most of the other substitution processes. Another issue that is important is the ability of the electrophile to select among the alternative positions on a substituted aromatic ring (*position selectivity*). The relative reactivity and selectivity of substituted benzenes toward various electrophiles is important in developing a firm understanding of EAS. The next section considers some of the structure-reactivity relationships that have proven to be informative.

## 9.2. Structure-Reactivity Relationships for Substituted Benzenes

### 9.2.1. Substituent Effects on Reactivity

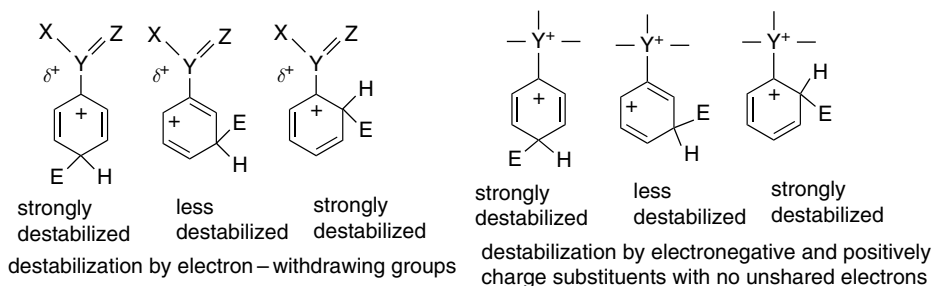
The effect that existing substituents have on EAS reactions has been studied since about 1870. The classification of substituents as *activating* and *ortho-para* directing or *deactivating* and *meta* directing became clear from these early studies. An understanding of the origin of these substituent effects became possible when ideas about electronic interactions and resonance theory were developed. Activating, *ortho-para*-directing substituents are those that can serve as electron donors and stabilize the TS leading to  $\sigma$ -complex formation. Saturated and unsaturated hydrocarbon groups and substituents having an unshared electron pair on the atom adjacent to the ring fall into this group. The stabilizing effects of these types of substituents can be expressed in terms of resonance and hyperconjugation. Direct resonance stabilization is only possible when the substituent is *ortho* or *para* to the incoming electrophile. As a result the TSs for *ortho* and *para* substitution are favored over that for *meta* substitution.



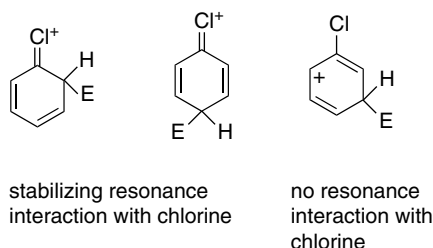
<sup>16</sup> P. B. de la Mare, *Acc. Chem. Res.*, **7**, 361 (1974).

As the substituent groups have a direct resonance interaction with the charge that develops in the  $\sigma$  complex, quantitative substituent effects exhibit a high-resonance component. Hammett equations usually correlate best with the  $\sigma^+$ -substituent constants (see Section 3.5).<sup>17</sup>

EWGs retard electrophilic substitution. The classification of specific substituents given in Scheme 3.1 (p. 299) indicates the ones that are electron attracting. Substituents in this group include those in which a carbonyl group is directly attached to the ring and substituents containing electronegative elements that do not have an unshared pair on an atom adjacent to the ring. Owing to the greater destabilization at the *ortho* and *para* positions, electrophilic attack occurs primarily at the *meta* position, which is *less deactivated* than the *ortho* and *para* positions.



A few substituents, most notably the halogens, decrease the rate of reaction, but nevertheless direct incoming electrophiles to the *ortho* and *para* positions. This is the result of the opposing influence of polar and resonance effects for these substituents. The halogens are more electronegative than carbon, and the carbon-halogen bond dipole opposes the development of positive charge in the ring. Overall reactivity toward electrophiles is therefore reduced. However, the unshared electron pairs on the halogen can preferentially stabilize the *ortho* and *para* TSs by resonance. As a result the substituents are deactivating but nevertheless *ortho-para* directing.

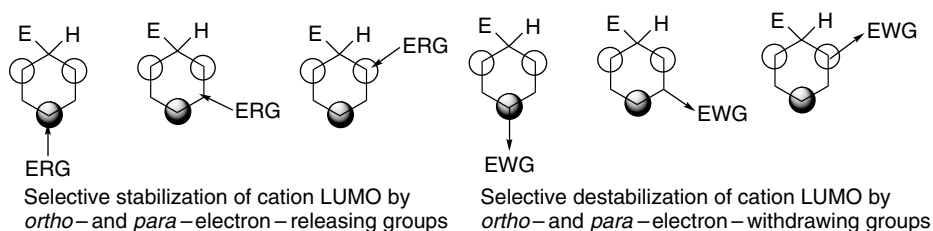


The *o,p*-directing and activating versus *m*-directing and deactivating effect of substituents can also be described in MO terminology. The discussion can focus either on the  $\sigma$  complex or on the aromatic reactant. According to the Hammond postulate, it would be most appropriate to focus on the intermediate in the case of reactions that have relatively high  $E_a$  and a late TS. In such cases, the TS should closely resemble the cyclohexadienylium intermediate. For highly reactive electrophiles, where the  $E_a$  is low, it may be more appropriate to regard the TS as closely resembling the

<sup>17</sup> H. C. Brown and Y. Okamoto, *J. Am. Chem. Soc.*, **80**, 4979 (1958).

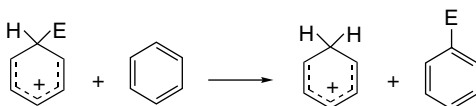
reactant aromatic. Let us examine the MO description of substituent effects from both these perspectives.

The TS resembles the intermediate, a substituted cyclohexadienyl cation. The electrophile has localized one pair of electrons to form the new  $\sigma$  bond. The Hückel orbitals are the same as for the pentadienyl system, as shown in Figure 9.2. A substituent can stabilize the cation by electron donation. The LUMO is  $\psi_3$ . This orbital has its highest coefficients at carbons 1, 3, and 5 of the pentadienyl system, which are the positions that are *ortho* and *para* to the position occupied by the electrophile. EWG substituents at the 2 and 4 (*meta*) positions stabilize the system much less, because of the nodes at these carbons in the LUMO. If we consider a  $\pi$ -acceptor substituent, we see that such a substituent strongly destabilizes the system when it occupies the 1, 3, or 5 position on the pentadienyl cation. The destabilizing effect is less at the 2 or 4 position. The conclusions drawn by this MO interpretation are the same as from resonance arguments. ERG substituents will be *most stabilizing* in the TS leading to *ortho-para* substitution. EWG substituents will be *least destabilizing* in the TS leading to *meta* substitution.



The effect of the bond dipole associated with EWG groups can also be expressed in terms of its interaction with the cationic  $\sigma$  complex. The atoms with the highest coefficient of the LUMO  $\psi_3$  are the most positive. The unfavorable interaction of the bond dipole will therefore be greatest at these positions. This effect operates with substituents such as carbonyl, cyano, and nitro. With alkoxy and amino substituents, the unfavorable dipole interaction is outweighed by the stabilizing delocalization effect of the electron pair donation.

The effect of substituents was probed by MO calculations at the HF/STO-3G level.<sup>18</sup> An isodesmic reaction corresponding to transfer of a proton from a substituted  $\sigma$  complex to an unsubstituted one indicates the stabilizing or destabilizing effect of the substituent. The results are given in Table 9.1.



The calculated energy differences give a good correlation with Hammett  $\sigma^+$  values. The  $\rho$  parameter ( $\rho = -17$ ) is considerably larger than that observed experimentally for proton exchange ( $\rho \sim -8$ ). A physical interpretation of this difference is that the computational results pertain to the gas phase, where substituents are at a maximum because of the absence of any leveling effect owing to solvation. Note that the numerical results parallel the conclusions from qualitative application of resonance

<sup>18</sup> J. M. McKelvey, S. Alexandratos, A. Streitwieser, Jr., J.-L. M. Abboud, and W. J. Hehre, *J. Am. Chem. Soc.*, **98**, 244 (1976).

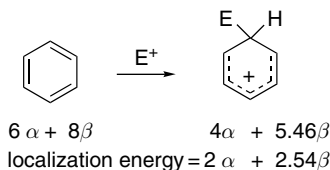
**Table 9.1. Energy Changes for Isodesmic Proton-Transfer Reactions of Substituted Benzenes<sup>a</sup>**

Substituent	$\Delta E(\text{kcal/mol})$	
	<i>meta</i>	<i>para</i>
NO <sub>2</sub>	-17.9	-22.1
CN	-14.0	-13.8
CF <sub>3</sub>	-7.5	-8.4
F	-7.5	3.7
CH <sub>3</sub>	2.0	8.5
OCH <sub>3</sub>		15.7
OH	-5.3	16.0
NH <sub>2</sub>	0.6	27.2

a. From HF/STO-3G calculations reported by J. M. McKelvey, S. Alexandratos, A. Streitwieser, Jr., J.-L. M. Abboud, and W. H. Hehre, *J. Am. Chem. Soc.*, **98**, 244 (1976).

and MO arguments. Strong EWGs are more destabilizing at the *ortho* and *para* position than at the *meta* position. Methyl is stabilizing at both positions, but more so at *para*. Methoxy and amino are very stabilizing at the *para* position. Fluoro is slightly stabilizing at the *para* position, but strongly destabilizing at the *meta* position, in agreement with its competing resonance and polar effects.

Both HMO calculations and more elaborate MO methods can be applied to the issue of the position selectivity in EAS. The most direct approach is to calculate the *localization energy*, which is the energy difference between the aromatic molecule and the cyclohexadienylum intermediate. In simple HMO calculations, the localization energy is just the difference between the energy calculated for the initial  $\pi$  system and that remaining after two electrons and the carbon atom at the site of substitution are removed from the conjugated system.



Comparison of localization energies has been applied to prediction of the relative positional reactivity in polycyclic aromatic hydrocarbons. Simple HMO calculations are only marginally success; CNDO/2 and SCF calculations give results that show good correlation with experimental data on the rate of proton exchange.<sup>19</sup>

Now let us turn to the case of a highly reactive electrophile, where we expect an early TS. In this case the charge density distribution and coefficients of the HOMO characteristic of the aromatic reactant are expected to be major factors governing the orientation of electrophilic attack. The TS should resemble the reactants and, according to frontier orbital theory, the electrophile will attack the position with the largest coefficient of the HOMO. The case of methoxybenzene (anisole) can be taken as an example of a reactive molecule. MO calculations place the lone-pair oxygen orbital lower in energy than the  $\psi_2$  and  $\psi_3$  orbitals, leading to the MO diagram in Figure 9.3.

<sup>19</sup> A. Streitwieser, Jr., P. C. Mowery, R. G. Jesaitis, and A. Lewis, *J. Am. Chem. Soc.*, **92**, 6529 (1970).

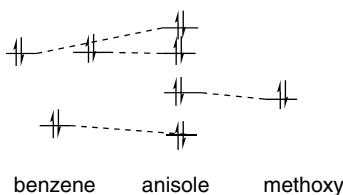


Fig. 9.3. MO diagram for anisole (methoxybenzene) showing effects of methoxy substituent.

The degeneracy of the two highest-lying occupied  $\pi$  orbitals is broken because the methoxy group interacts preferentially with one of them. The other has a node at the site of methoxy substitution.

Figure 9.4 gives the coefficients for the two highest-occupied  $\pi$  orbitals, as calculated by the CNDO method. We see that the HOMO has its highest coefficients at the *ipso*, *ortho*, and *para* positions. As indicated in Figure 9.3, the energy of this orbital is raised by its interaction with the electron donor substituent. Figure 9.5 shows the distribution of  $\pi$  electrons from all the orbitals, based on HF/STO-3G calculations.<sup>20</sup> The ERG substituents show increased electron density at the *ortho* and *para* positions. Both the HOMO coefficients and the total charge distribution predict preferential attack by the electrophile *ortho* and *para* to donor substituents.

Figures 9.4 and 9.5 also show some examples of EWG substituents, which, as expected, lower the energies of the  $\pi$  orbitals, but the HOMO distribution remains highest at the *para* position. The total charge distribution shows greater depletion at the *ortho* and *para* position than at the *meta* position. The lower energy of the HOMO is consistent with decreased reactivity for rings with an EWG substituent. However, if frontier orbital theory is used, the distribution of the HOMO in Figure 9.4

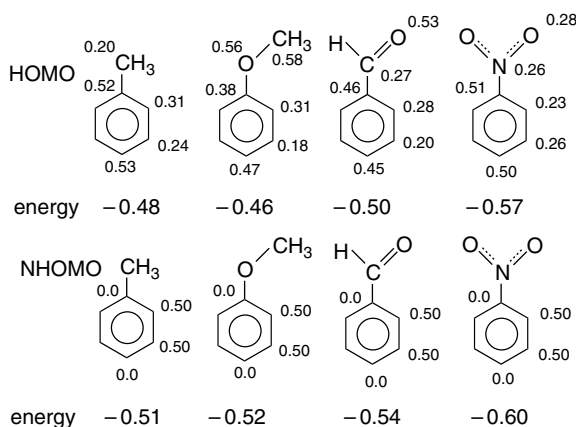
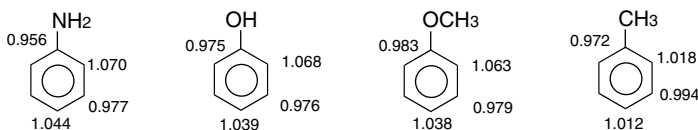


Fig. 9.4. Orbital coefficients for HOMO and next highest  $\pi$  MO for some substituted benzenes (from CNDO/2 calculations). The individual *ortho* and *meta* coefficients have been averaged in the case of the unsymmetrical methoxy and formyl substituents. Orbital energies are in atomic units.

<sup>20</sup> W. J. Hehre, L. Radom, and J. A. Pople, *J. Am. Chem. Soc.*, **94**, 1496 (1972).

## Electron-releasing substituents



## Electron-attracting substituents

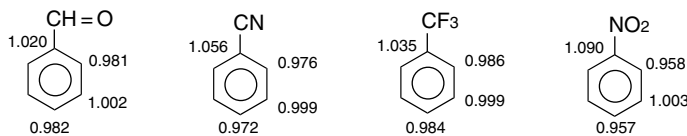


Fig. 9.5. Total  $\pi$ -electron density for some substituted benzenes. From HF/STO-3G calculations.

erroneously predicts *para* substitution.. Aromatic rings with EWG substituents are relatively unreactive and therefore will not have early TSs. For such compounds, considerations of the stability of the cyclohexadienylum intermediate, which correctly predict *meta* substitution, are more appropriate.

Prediction of reactivity toward EAS on the basis of MO computations can be improved by considering hybrid MOs rather than the conventional aromatic MOs. Orbitals called *reactive hybrid orbitals* can be defined to combine the contributions of all MOs to the reactivity at each site. The properties of these orbitals can be computed on the basis of the extent of electron transfer to a proton located 1.5 Å above each ring position.<sup>21</sup> The properties of these orbitals correlate well not only with the position selectivity of the substituents, but also with relative reactivity. Figure 9.6 shows a correlation between the energy of interaction and the partial rate factors (a measure of relative reactivity; see p. 786–787) for several reactions.

Substituents that are not directly bound to the aromatic ring also influence the course of EAS. Several alkyl groups bearing EWG substituents are *meta* directing and deactivating. Some examples are given in Table 9.2. In these molecules, stabilization of the *ortho* and *para*  $\sigma$  complex by electron release from the alkyl group is opposed by the polar effect of the electronegative substituent. Both the reduced electron density at the alkyl substituent and the bond dipoles in the substituent reduce electron donation by the methylene group. From the examples in Table 9.2 we see that  $\text{CH}_2\text{CO}_2\text{C}_2\text{H}_5$ ,  $\text{CHCl}_2$ , and  $\text{CH}_2\text{CCl}_3$  remain *o-p* directing, but with reduced selectivity. The stronger EWGs,  $\text{CH}_2\text{NO}_2$ ,  $\text{CCl}_3$ , and  $\text{CH}_2\text{N}^+(\text{CH}_3)_3$ , lead to predominantly *meta* substitution.

The relationships between substituents and the typical electrophilic substitution reactions, such as those listed in Scheme 9.1, can be summarized as follows:

1. The hydroxy and amino groups are highly activating *ortho-para* directing. Such compounds are attacked by all the electrophilic reagents tabulated in Scheme 9.1 (p. 772). With some electrophilic reagents, all available *ortho* and *para* positions are rapidly substituted.
2. The alkyl, amido, and alkoxy groups are activating and *ortho-para* directing, but not as strongly so as hydroxyl or amino groups. Synthetically useful conditions for selective substitution are available for essentially all the electrophiles in Scheme 9.1 except for very weak electrophiles such as  $\text{NO}^+$  or  $\text{PhN}_2^+$ .

<sup>21</sup> H. Hirao and T. Ohwada, *J. Phys. Chem. A*, **107**, 2875 (2003).

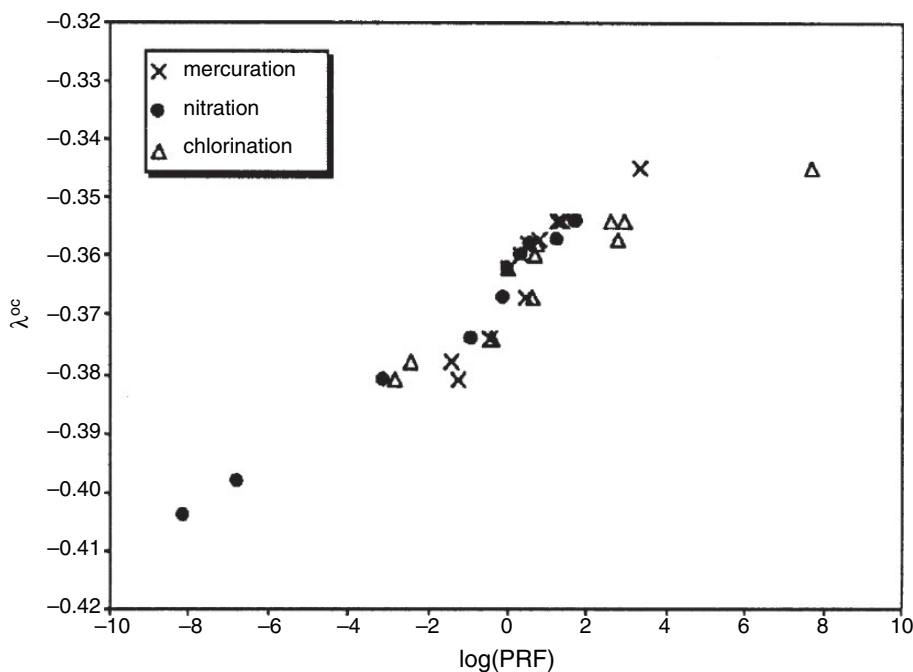


Fig. 9.6. Correlation between the interaction energy  $\lambda^{oc}$  and the log of partial rate factors for mercuration, nitration, and chlorination. Reproduced from *J. Phys. Chem. A*, **107**, 2875 (2003), by permission of the American Chemical Society.

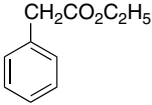
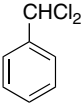
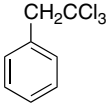
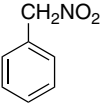
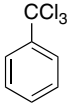
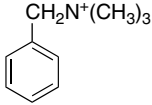
3. The halobenzenes, are unusual substituents, being deactivating but *ortho-para* directing. In general, halogenated aromatics react successfully with electrophiles listed in categories A and B.
4. The carbonyl group in aldehydes, ketones, acids, esters, and carboxamides is deactivating and *meta* directing. There are limitations on the type of substitution reactions that are satisfactory for these deactivating substituents. In general, only those electrophiles in category A in Scheme 9.1 react readily.
5. The cyano, nitro, and quaternary ammonium groups are strongly deactivating and *meta* directing. Electrophilic substitutions of compounds with these substituents require vigorous conditions, and fail completely with the less reactive electrophiles.

Nitration has been studied over a wide variety of aromatic compounds, which makes it a useful reaction for illustrating the directing effect of substituent groups. Table 9.3 presents some of the data. A range of reaction conditions is represented, so direct comparison is not always valid, but the trends are nevertheless clear. It is important to remember that other electrophiles, while following the same qualitative trends, show large quantitative differences in position selectivity.

The groups in the top half of the table are *meta* directing. Note that the carbonyl and cyano groups give rise to relatively high ratios of *ortho* product. This may be due to intramolecular process in which the nitronium ion initially bonds at the functional group.<sup>22</sup> The halogens show *o-p*-directing effects with fluorine being much less favorable to *ortho* substitution, because of the stronger C–F dipole, which results

<sup>22</sup> G. S. Hammond, F. J. Modic, and R. M. Hedges, *J. Am. Chem. Soc.*, **75**, 1388 (1953); P. Kovacic and J. J. Hillier, Jr., *J. Org. Chem.*, **30**, 2871 (1985).

**Table 9.2. Percent *meta* Nitration for Some Alkyl Groups with Electron-Withdrawing Substituents<sup>a</sup>**

					
11%	34%	37%	55 %	64%	85 %

a. From C. K. Ingold, *Structure and Mechanism in Organic Chemistry*, 2nd Edition, Cornell University Press, Ithaca, 1969, pp. 275, 281; F. De Sarlo, A. Rici, and J. H. Ridd, *J. Chem. Soc. B*, 719 (1971).

in both electrostatic and polarization effects that destabilize the *ortho* TS.<sup>23</sup> The trichloromethyl and trifluoromethyl groups are *meta* directing. Similarly to some of the groups in Scheme 9.2, the CH<sub>2</sub>CN and CH<sub>2</sub>NO<sub>2</sub> groups are also *meta* directing. The alkyl and methoxy groups are strongly *o-p* directing.

The effect of substituents on electrophilic substitution can be placed on a quantitative basis by use of *partial rate factors*. The reactivity of each position in a substituted aromatic compound can be compared with benzene by measuring the overall

**Table 9.3. Isomer Proportions in the Nitration of Some Substituted Benzenes<sup>a</sup>**

Substituent	Product (%)		
	<i>ortho</i>	<i>meta</i>	<i>para</i>
N <sup>+</sup> H <sub>3</sub>	3–5	35–50	50–60
N <sup>+</sup> (CH <sub>3</sub> ) <sub>3</sub>	0	89	11
CH <sub>2</sub> N <sup>+</sup> (CH <sub>3</sub> ) <sub>3</sub>	0	85	15
S <sup>+</sup> (CH <sub>3</sub> ) <sub>2</sub>	4	90	6
NO <sub>2</sub>	5–8	91–93	0–2
CO <sub>2</sub> H	15–20	75–85	~1
CN	15–17	81–83	~2
CO <sub>2</sub> C <sub>2</sub> H <sub>5</sub>	24–28	66–73	1–6
COCH <sub>3</sub>	26	72	0–2
F	9–13	0–1	86–91
Cl	30–35	~1	64–70
Br	36–43	1	56–62
I	38–45	1–2	54–60
CCl <sub>3</sub>	7	64	29
CF <sub>3</sub>	6	91	3
CH <sub>2</sub> CN	24	20	56
CH <sub>2</sub> NO <sub>2</sub>	22	55	23
CH <sub>2</sub> OCH <sub>3</sub>	51	7	42
CH <sub>3</sub>	56–63	2–4	34–41
CH <sub>2</sub> CH <sub>3</sub>	46–59	2–4	46–51
OCH <sub>3</sub>	30–40	0–2	60–70

a. Data are from Tables 9.1, 9.2, 9.3, 9.4, 9.5, and 9.6 in J. G. Hoggett, R. B. Moodie, J. R. Penton, and K. Schofield, *Nitration and Aromatic Reactivity*, Cambridge University Press, Cambridge, 1971.

<sup>23</sup> P. Laszlo and P. Penntreau, *J. Org. Chem.*, **52**, 2407 (1987); J. Rosenthal and D. I. Schuster, *J. Chem. Educ.*, **80**, 679 (2003).

rate relative to benzene and dividing the total rate among the *ortho*, *meta*, and *para* products. Correction for the statistical factor arising from the relative number of available positions permits the partial rate factors to provide comparisons at positions on a substituted ring with a single position on benzene.

$$\text{Partial rate factor} = f = \frac{6(k_{\text{subs}})(\text{Fraction of product})}{y(k_{\text{benz}})} \quad (9.1)$$

where  $y$  is the number of equivalent positions. A partial rate factor calculation for nitration of toluene is given in Example 9.1.

*Example 9.1.* The nitration of toluene is 23 times as fast as for benzene in nitric acid–acetic anhydride. The product ratio is 63% *ortho*, 34% *para*, and 3% *meta*. Calculate the partial rate factor at each position.

$$f_o = \frac{6}{2} \times \frac{23}{1} \times 0.63 = 43.5$$

$$f_m = \frac{6}{2} \times \frac{23}{1} \times 0.03 = 2.1$$

$$f_p = \frac{6}{1} \times \frac{23}{1} \times 0.34 = 46.9$$

Partial rate factors give insight into two related aspects of reactivity and reveal the selectivity of a given electrophile for different *reactants*. Some electrophiles exhibit high *reactant selectivity*; that is, there are large differences in the rate of reaction depending on the identity of the ring substituent. In general, low reactant selectivity is correlated with high electrophile reactivity and vice versa. Clearly, when reactant selectivity is high, the partial rate factors for the substituted aromatic compound will be very different from unity. The partial rate factors also reveal *positional selectivity* within the substituted aromatic, which also varies for different electrophiles and provides some insight into the mechanism. In general, there is a correlation between position and reactant selectivity. High reactant selectivity is accompanied by high position selectivity. Electrophiles that show high reactant selectivity generally exhibit low *ortho:para* ratios and negligible amounts of *meta* substitution. Very reactive electrophiles tend to show low position and reactant selectivity. Table 9.4 gives some data on the selectivity of some EAS reactions. The most informative data in terms of reactant is  $f_p$ , since the partial rate factors for *ortho* substitution contain variable steric components. With  $f_p$  as the criterion, halogenation and Friedel-Crafts acylation exhibit high selectivity, protonation and nitration are intermediate, and Friedel-Crafts alkylation shows low selectivity.

### 9.2.2. Mechanistic Interpretation of the Relationship between Reactivity and Selectivity

Reactivity and selectivity are largely determined by the position of the TS on the reaction coordinate. With highly reactive electrophiles, the TS will come early on the reaction coordinate as in Figure 9.7a. The TS then resembles the reactants more closely than the intermediate. The positive charge on the ring is small, and, as a result, the interaction with the substituent group is relatively weak. However, the substituent also effects electron distribution in the reactant, which can cause position selectivity.

**Table 9.4. Selectivity in Some Electrophilic Aromatic Substitution Reactions<sup>a</sup>**

Reaction	Partial rate factors for toluene		
	$f_o$	$f_m$	$f_p$
Nitration			
HNO <sub>3</sub> (CH <sub>3</sub> NO <sub>2</sub> )	38.9	1.3	45.7
Halogenation			
Cl <sub>2</sub> (CH <sub>3</sub> CO <sub>2</sub> H)	617	5	820
Br <sub>2</sub> (CH <sub>3</sub> CO <sub>2</sub> H, H <sub>2</sub> O)	600	5.5	2420
Protonation			
H <sub>2</sub> SO <sub>4</sub> -H <sub>2</sub> O	83	1.9	83
H <sub>2</sub> SO <sub>4</sub> , CF <sub>3</sub> CO <sub>2</sub> H, H <sub>2</sub> O	350	7.2	313
Acylation			
PhCOCl (AlCl <sub>3</sub> , PhNO <sub>2</sub> )	32.6	5.0	831
CH <sub>3</sub> COCl (AlCl <sub>3</sub> , ClCH <sub>2</sub> CH <sub>2</sub> Cl)	4.5	4.8	749
Alkylation			
CH <sub>3</sub> Br (GaBr <sub>3</sub> )	9.5	1.7	11.8
(CH <sub>3</sub> ) <sub>2</sub> CHBr (GaBr <sub>3</sub> )	1.5	1.4	5.0
PhCH <sub>2</sub> Cl (AlCl <sub>3</sub> )	4.2	0.4	10.0

a. From L. M. Stock and H. C. Brown, *Adv. Phys. Org. Chem.*, **1**, 35 (1963).

With a less reactive electrophile, the TS is reached later, as in Figure 9.7b. The bond to the electrophile is more completely formed and a substantial positive charge is present on the ring. This situation results in stronger substituent effects. These arguments follow the general lines of Hammond's postulate (Section 3.3.2.2). MO calculations at the HF/STO-3G level reproduce these qualitative expectations by revealing greater stabilization of the *ortho* and *para* positions in toluene with a closer approach of an electrophile.<sup>24</sup>

Hammett correlations also permit some insight into the reactivity and selectivity of electrophiles in EAS reactions. In general, the standard Hammett  $\sigma$  substituent constants lead to poor correlations with EAS reactions. The  $\sigma^+$  values, which reflect an increased importance of direct resonance interaction (see Section 3.6) give better correlations and, indeed, were developed as a result of the poor correlations observed with  $\sigma$  in EAS. It has been suggested that the position of a TS on the reaction coordinate can be judged from the slope,  $\rho$ , of the correlation line between the rate of substitution and  $\sigma^+$ .<sup>25</sup> The rationale is the following: A numerically large value for  $\rho$  suggests a strong substituent effect, that is, a late TS that resembles the intermediate. A small value indicates a weak substituent effect and implies an early TS. Table 9.5 gives some of the  $\rho$  values for typical EAS reactions. The data indicate that the halogenation reactions show the characteristics of a highly selective electrophile, nitration and Friedel-Crafts acylation represent reactions of intermediate selectivity, and Friedel-Crafts alkylation is an example of low selectivity. This is in general agreement with the selectivity trend as measured by  $f_p$ , indicated in Table 9.4.

Isotope effects provide insight into other aspects of the mechanisms of individual electrophilic aromatic substitution reactions. In particular, since primary isotope effects are expected only when the deprotonation of the  $\sigma$  complex to product is rate determining, the observation of a substantial  $k_H/k_D$  points to a rate-determining

<sup>24</sup>. C. Santiago, K. N. Houk, and C. L. Perrin, *J. Am. Chem. Soc.*, **101**, 1337 (1979).

<sup>25</sup>. P. Rys, P. Skrabal, and H. Zollinger, *Angew. Chem. Int. Ed. Engl.*, **11**, 874 (1972).

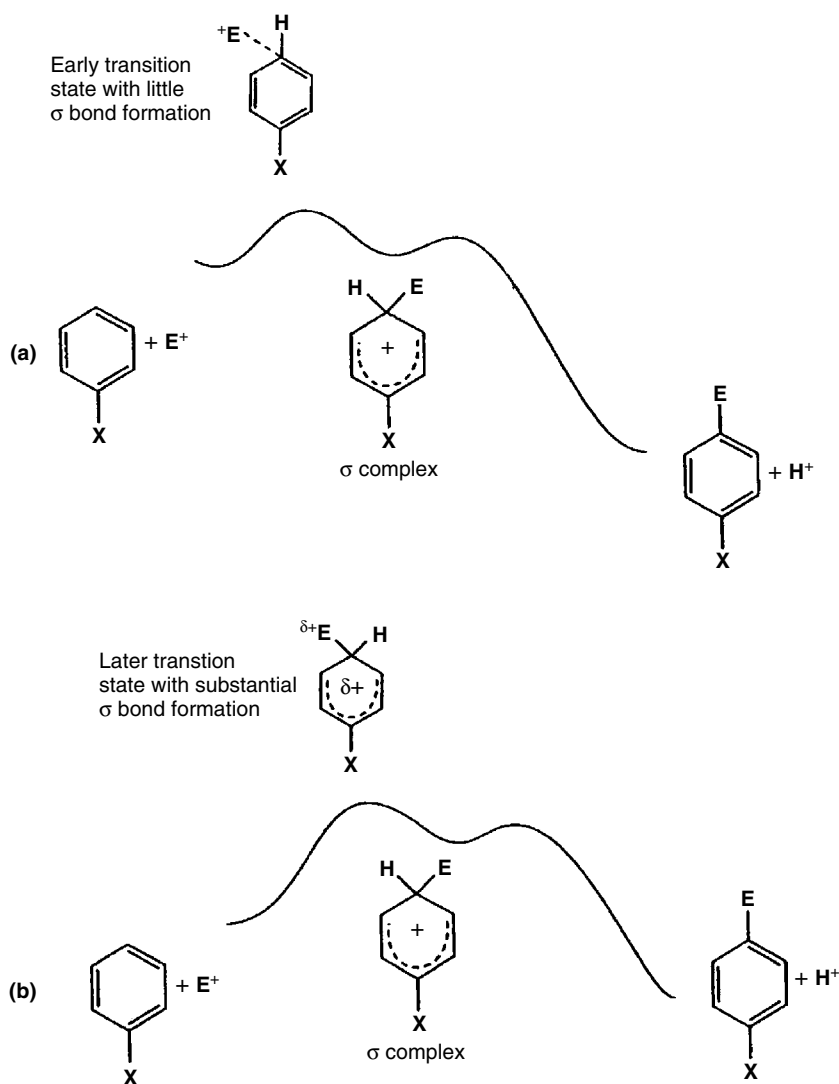


Fig. 9.7. Relation between transition state character and reaction energy profiles for highly reactive (a) and less reactive (b) electrophiles.

deprotonation. Some typical isotope effects are summarized in Table 9.6. Although isotope effects are seldom observed for nitration and halogenation, Friedel-Crafts acylation, sulfonation, nitrosation, and diazo coupling provide examples in which the rate of proton loss can affect the rate of substitution. Only in the case of the reactions involving weak electrophiles, namely nitrosation and diazo coupling, are isotope effects in the range expected for a fully rate-controlling deprotonation. Even for weak electrophiles, some factor that retards deprotonation is required for deprotonation to become rate determining. For example, in the two diazotizations cited, the steric hindrance associated with the C(8)-sulfonic acid group leads to the observation of a primary isotope effect, whereas in the unhindered four-isomer there is no isotope effect.

**Table 9.5. Values of  $\rho$  for some Electrophilic Aromatic Substitution Reactions<sup>a</sup>**

Reaction	$\rho$
Bromination (CH <sub>3</sub> CO <sub>2</sub> H)	-13.3
Chlorination (CH <sub>3</sub> NO <sub>2</sub> )	-13.0
Chlorination (CH <sub>3</sub> CO <sub>2</sub> H, H <sub>2</sub> O)	-8.8
Protonation (H <sub>2</sub> SO <sub>4</sub> , CF <sub>3</sub> CO <sub>2</sub> H, H <sub>2</sub> O)	-8.6
Acetylation (CH <sub>3</sub> COCl, AlCl <sub>3</sub> , C <sub>2</sub> H <sub>4</sub> Cl <sub>2</sub> )	-8.6
Nitration (HNO <sub>3</sub> , H <sub>2</sub> SO <sub>4</sub> )	-6.4
Chlorination (HOCl, H <sup>+</sup> )	-6.1
Alkylation (C <sub>2</sub> H <sub>5</sub> Br, GaBr <sub>3</sub> )	-2.4

a. From P. Rys, P. Skrabal, and H. Zollinger, *Angew. Chem. Intl. Ed. Engl.*, **11**, 874 (1972).

Figure 9.8 summarizes the general ideas presented in this section. At least four types of energy profiles can exist for individual EAS reactions. Case A is the rate-determining generation of the electrophile and is most readily identified by kinetics. A rate law independent of the concentration of the aromatic is diagnostic of this case. Case B represents rate-determining  $\sigma$  complex formation, with an electrophile of low selectivity. The rate law in such a case should have terms in both the electrophile and the aromatic. Furthermore, low selectivity, as indicated by low  $\rho$  values and low partial rate factors, is expected when this energy profile is applicable. Case C is rate-determining  $\sigma$  complex formation with a more selective electrophile having a

**Table 9.6. Kinetic Isotope Effects for some Electrophilic Aromatic Substitution Reactions**

Reaction and reactants	Reagent	$k_H/k_D$ or $k_H/k_T$
Nitration		
Benzene- <i>r</i> <sup>a</sup>	HNO <sub>3</sub> -H <sub>2</sub> SO <sub>4</sub>	<1.2
Toluene- <i>r</i> <sup>a</sup>	HNO <sub>3</sub> -H <sub>2</sub> SO <sub>4</sub>	<1.2
Nitrobenzene- <i>d</i> <sub>5</sub> <sup>a</sup>	HNO <sub>3</sub> -H <sub>2</sub> SO <sub>4</sub>	1
Halogenation		
Benzene- <i>d</i> <sub>6</sub> <sup>a</sup>	HOBr, HClO <sub>4</sub>	1
Methoxybenzene- <i>d</i> <sup>a</sup>	Br <sub>2</sub>	1.05
Acylation		
Benzene- <i>d</i> <sub>6</sub> <sup>b</sup>	CH <sub>3</sub> CO <sup>+</sup> SbF <sub>6</sub> <sup>-</sup> , CH <sub>3</sub> NO <sub>2</sub>	2.25
Benzene- <i>d</i> <sub>6</sub> <sup>b</sup>	PhCO <sup>+</sup> SbF <sub>6</sub> <sup>-</sup> , CH <sub>3</sub> NO <sub>2</sub>	1.58
Sulfonation		
Benzene- <i>d</i> <sub>6</sub> <sup>c</sup>	ClSO <sub>3</sub> H, CH <sub>3</sub> NO <sub>2</sub>	1.7
Benzene- <i>d</i> <sub>6</sub> <sup>c</sup>	ClSO <sub>3</sub> H, CH <sub>2</sub> Cl <sub>2</sub>	1.6
Nitrobenzene- <i>d</i> <sub>5</sub> <sup>a</sup>	H <sub>2</sub> SO <sub>4</sub> , SO <sub>3</sub>	1.6-1.7
Nitrosation		
Benzene- <i>d</i> <sub>6</sub> <sup>d</sup>	HNO <sub>2</sub> , D <sub>2</sub> SO <sub>4</sub>	8.5
Diazo coupling		
1-Naphthol-4-sulfonic acid <sup>a</sup>	PhN <sub>2</sub> <sup>+</sup>	1.0
2-Naphthol-8-sulfonic acid <sup>a</sup>	PhN <sub>2</sub> <sup>+</sup>	6.2

a. From a more extensive compilation by H. Zollinger, *Adv. Phys. Org. Chem.*, **2**, 163 (1964).

b. G. A. Olah, J. Lukas, and E. Lukas, *J. Am. Chem. Soc.*, **91**, 5319 (1969).

c. M. P. van Albada, and H. Cerfontain, *Rec. Trav. Chim.*, **91**, 499 (1972).

d. B. C. Challis, R. J. Higgins, and A. J. Lawson, *J. Chem. Soc., Perkin Trans. 2*, 1831 (1972).

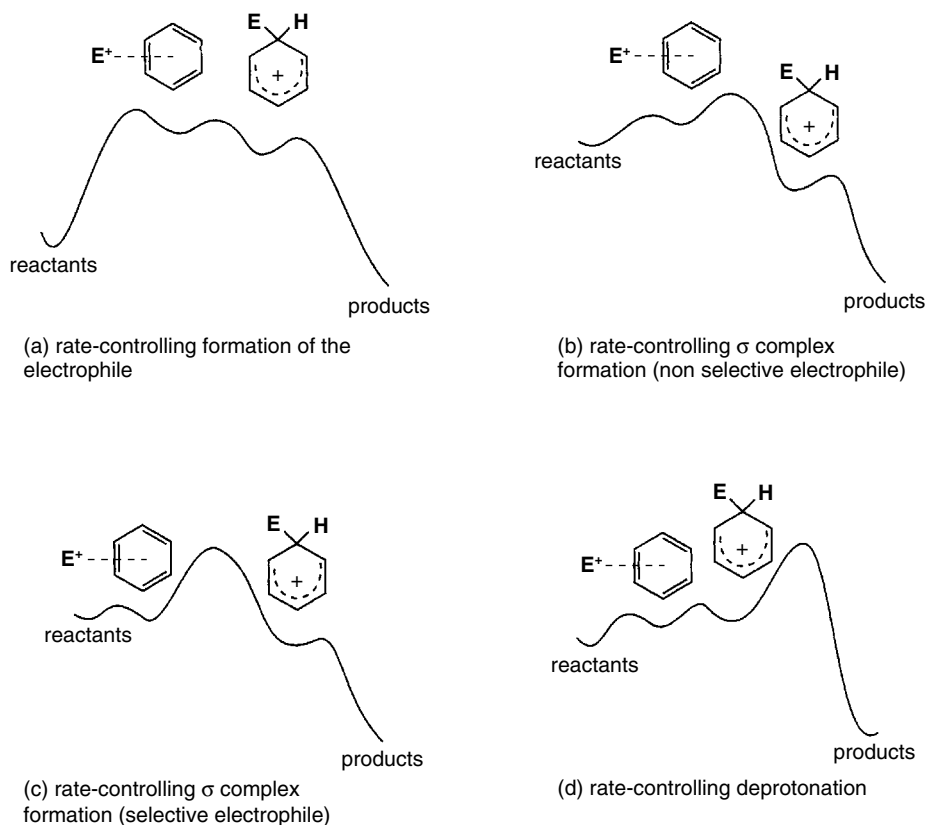
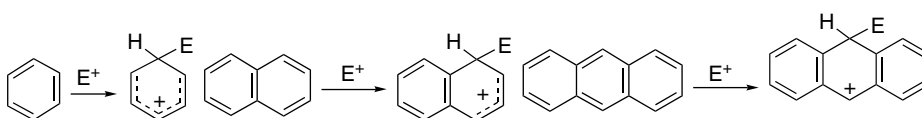


Fig. 9.8. Reaction energy profiles for electrophilic aromatic substitution showing variation in rate-determining step and electrophile selectivity.

later TS. Finally, there is case D, in which the proton removal and rearomatization are rate limiting. This case can be recognized by the observation of a primary kinetic isotope effect at the site of substitution.

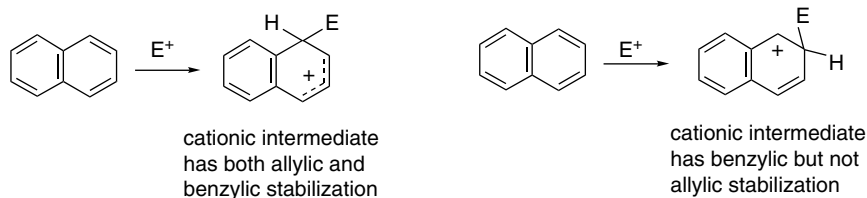
### 9.3. Reactivity of Polycyclic and Heteroaromatic Compounds

The polycyclic aromatic hydrocarbons such as naphthalene, anthracene, and phenanthrene undergo the various types of EAS and are generally more reactive than benzene. One reason for this is that the localization energy for formation of the cationic intermediate is lower than for benzene because more of the initial resonance stabilization is retained in intermediates that have a fused benzene ring. CNDO calculations provide estimates of the localization energies. For benzene, naphthalene, and anthracene, these are, respectively, 36.3, 15.4, and 8.3 kcal/mol.<sup>26</sup>



<sup>26</sup> A. Streitwieser, Jr., P. C. Mowery, R. G. Jesaitis, and A. Lewis, *J. Am. Chem. Soc.*, **92**, 6529 (1970).

The relative stability of the TSs determines the position of substitution under kinetically controlled conditions. For naphthalene, the preferred site for electrophilic attack is the 1-position, which is the result of the greater stability of the cationic intermediate for 1-substitution.



The more rapid substitution at C(1) of naphthalene can be demonstrated by following the incorporation of deuterium under acidic conditions. Figure 9.9 shows that the  $^1\text{H}(\text{C}1)$  signal disappears more rapidly than the  $^1\text{H}(\text{C}2)$  signal. As reaction continues to equilibrium, the extent of deuteration becomes the same at both positions (about 80% in this example), because there is no difference in the thermodynamic stability of the two deuterated products.<sup>27</sup>

Two factors can result in substitution at the 2-position. If the electrophile is very bulky, the hydrogen on the adjacent ring may cause a steric preference for attack at C(2). Under conditions of reversible substitution, where relative thermodynamic stability is the controlling factor, 2-substitution is frequently preferred. An example of this behavior is in sulfonation, where low-temperature reaction gives the 1-isomer, but at elevated temperatures the 2-isomer is formed.<sup>28</sup>

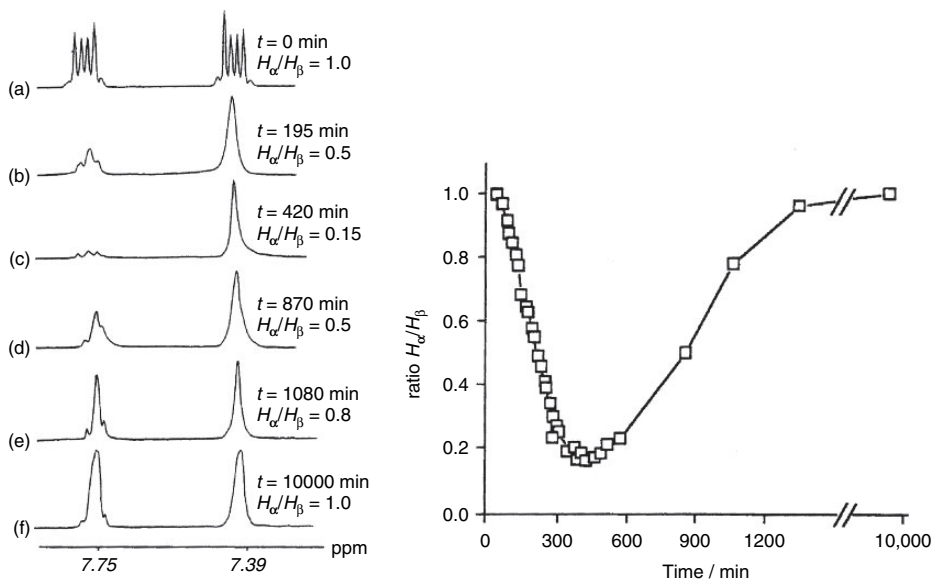
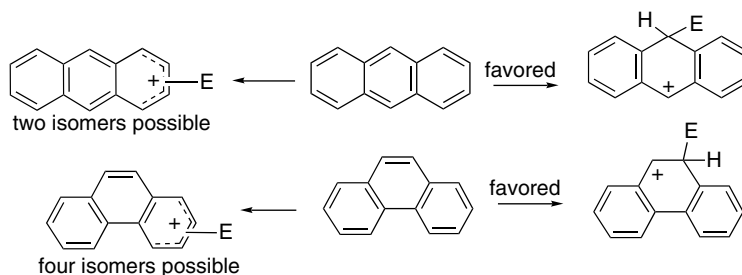


Fig. 9.9. Changes in  $^1\text{H}$ -NMR spectrum of naphthalene heated with  $\text{CF}_3\text{CO}_2\text{D}$  in the presence of  $(\text{CF}_3\text{CO})_2\text{O}$  and  $\text{Al}(\text{O}_2\text{CCF}_3)_3$  (left). Ratio of  $^1\text{H}$  level at C(1)/C(2) (right). Reproduced from *J. Chem. Educ.*, **76**, 1246 (1999), by permission of the journal.

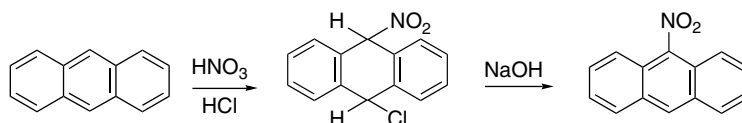
<sup>27</sup> L. D. Field, S. Sternhell, and H. V. Wilton, *J. Chem. Educ.*, **76**, 1246 (1999).

<sup>28</sup> H. Cerfontain, *Mechanistic Aspects in Aromatic Sulfonation and Desulfonation*, Interscience, New York, 1968, pp. 68–69.

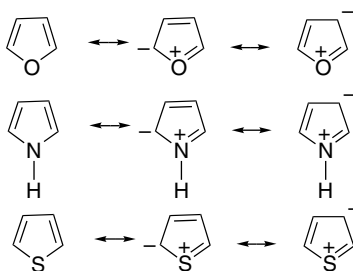
Phenanthrene and anthracene both react preferentially in the center ring. This behavior is consistent with resonance considerations. The  $\sigma$  complexes that result from substitution in the center ring have two intact benzene rings. The total resonance stabilization of these intermediates is larger than that of a naphthalene system that results if substitution occurs at one of the terminal rings.<sup>29</sup>



Both phenanthrene and anthracene have a tendency to undergo addition reactions under the conditions involved in certain electrophilic substitutions.<sup>30</sup> For example, an addition product can be isolated in the nitration of anthracene in the presence of hydrochloric acid.<sup>31</sup> This is a result of the relatively close balance in resonance stabilization to be regained by elimination (giving an anthracene ring) or addition (resulting in two benzene rings).



The heteroaromatic compounds can be divided into two broad groups, called  $\pi$  *excessive* and  $\pi$  *deficient*, depending on whether the heteroatom acts as an electron donor or electron acceptor. Furan, pyrrole, and thiophene, as well as other heterocyclics incorporating an oxygen, nitrogen, or sulfur atom that contributes two  $\pi$  electrons are in the  $\pi$ -excessive group. This classification is indicated by resonance structures and has been confirmed by various MO methods.<sup>32</sup>



<sup>29</sup> D. Z. Wang and A. Streitwieser, *Theor. Chim. Acta*, **102**, 78 (1999).

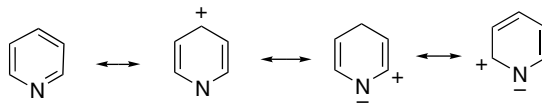
<sup>30</sup> P. B. D. de la Mare and J. H. Ridd, *Aromatic Substitution*, Academic Press, New York, 1959, p. 174.

<sup>31</sup> C. E. Braun, C. D. Cook, C. Merritt, Jr., and J. E. Rousseau, *Org. Synth.*, **IV**, 711 (1965).

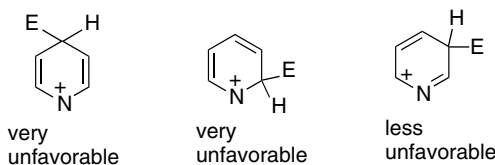
<sup>32</sup> N. D. Epiotis, W. P. Cherry, F. Bernardi, and W. J. Hehre, *J. Am. Chem. Soc.*, **98**, 4361 (1976); W. Adam and A. Grimison, *Theor. Chem. Acta*, **7**, 342 (1967); D. W. Genson and R. E. Christoffersen, *J. Am. Chem. Soc.*, **94**, 6904 (1972); N. Bodor, M. J. S. Dewar, and A. J. Harget, *J. Am. Chem. Soc.*, **92**, 2929 (1970).

The reactivity order is pyrrole > furan > thiophene, which indicates the order  $N > O > S$  in electron-donating capacity.<sup>33</sup> The  $N > O$  order is as expected on the basis of electronegativity, and  $O > S$  probably reflects the better overlap of the oxygen  $2p$  orbital than the sulfur  $3p$  orbital with the carbon  $2p$  orbitals of the ring.

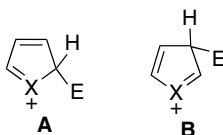
Structures such as pyridine that incorporate the  $-N=CH-$  unit are called  $\pi$  deficient and are deactivated to electrophilic attack. Again a resonance interpretation is evident. The nitrogen, being more electronegative than carbon, is a net acceptor of  $\pi$ -electron density, especially at C(2) and C(4).



There is another important factor in the low reactivity of pyridine derivatives toward EAS. The  $-N=CH-$  unit is basic because the electron pair on nitrogen is not part of the aromatic  $\pi$  system. The nitrogen is protonated or complexed with a Lewis acid under many of the conditions typical of EAS reactions. The formal positive charge present at nitrogen in such species further reduces the reactivity toward electrophiles. For pyridine, the reactivity toward electrophilic substitution is  $3 > 4, 2$ . The ring nitrogen acts as a strongly destabilizing “internal” electron-withdrawing substituent in the 2- and 4- intermediates. The nitrogen also deactivates the 3-position, but less so than the 2- and 4-positions. These unfavorable effects are enhanced if the nitrogen is protonated or complexed with a Lewis acid.



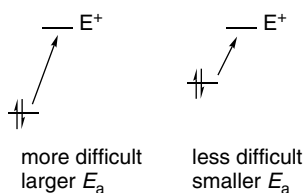
The position selectivity for electrophilic substitution in the five-membered heteroaromatic rings is usually  $2 > 3$ , which reflects the more favorable conjugation in intermediate **A** than in intermediate **B**. In structure **A** the remaining  $C=C$  bond can delocalize the positive charge more effectively than in **B**, but substituents on the ring can override this directive influence.



Reactivity and orientation in EAS can also be related to the concept of hardness (see Section 8.1.3). Ionization potential is a major factor in determining hardness and is also intimately related to EAS. In MO terms, hardness is related to the gap between

<sup>33</sup> S. Clementi, F. Genel, and G. Marino, *Chem. Commun.*, 498 (1967).

the LUMO and HOMO,  $\eta = (\epsilon_{\text{LUMO}} - \epsilon_{\text{HOMO}})/2$ .<sup>34</sup> Thus the harder a reactant ring system is, the more difficult it is for an electrophile to complete  $\sigma$ -bond formation.



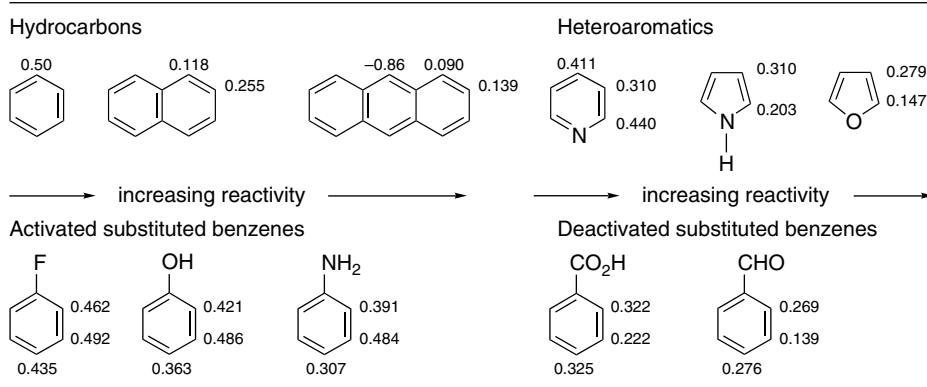
This idea can be quantitatively expressed by defining *activation hardness* as the difference in the LUMO-HOMO gap for the reactant and the cationic intermediate<sup>35</sup>:

$$\Delta\eta^* = \beta[(\chi_{\text{LUMO}}^{\text{R}} - \chi_{\text{HOMO}}^{\text{R}}) - (\chi_{\text{LUMO}}^{\sigma} - \chi_{\text{HOMO}}^{\sigma})]/2$$

where  $\chi^{\text{R}}$  and  $\chi^{\sigma}$  are the orbitals of the reactant and cationic intermediate.

Simple HMO theory has been used to calculate  $\Delta\eta^*$  for several benzenoid hydrocarbons, substituted benzenes, and heterocycles. The resulting values are in qualitative agreement with reactivity trends. Scheme 9.3 gives some of the data. The less positive the number, the more reactive the position. Although there are some discrepancies between structural groups, within groups the  $\Delta\eta^*$  values correlate well with position selectivity. The most glaring discrepancy is the smaller activation hardness for deactivated compared with activated benzenes. In particular, benzaldehyde and benzoic acid have  $\Delta\eta^*$  values that are lower than that of benzene, which is counter to their relative reactivity. However, the preference for *meta* substitution of the deactivated benzenes is predicted correctly. The deactivation of pyridine, relative to benzene, is also not indicated by the  $\Delta\eta^*$  value.

**Scheme 9.3. Activation Hardness for Aromatic and Heteroaromatic Compounds<sup>a</sup>**



a. Z. Zhou and R. G. Parr, *J. Am. Chem. Soc.*, **112**, 5720 (1990).

<sup>34</sup>. R. G. Pearson, *Proc. Natl. Acad. Sci. USA*, **83**, 8440 (1986).

<sup>35</sup>. Z. Zhou and R. G. Parr, *J. Am. Chem. Soc.*, **112**, 5720 (1990).

## 9.4. Specific Electrophilic Substitution Reactions

At this point, we focus on specific electrophilic substitution reactions. The kinds of data that have been especially pertinent in elucidating mechanistic detail include linear free-energy relationships, kinetic studies, isotope effects, and selectivity patterns. In general, the basic questions to be asked about each mechanism are: (1) What is the active electrophile? (2) Which step in the general mechanism for EAS is rate determining? (3) What are the orientation and selectivity patterns?

### 9.4.1. Nitration

A substantial body of data including reaction kinetics, isotope effects, and structure-reactivity relationships is available for aromatic nitration.<sup>36</sup> As anticipated from the general mechanism for electrophilic substitution, there are three distinct steps. Conditions under which each of the first two steps is rate determining have been recognized. The third step is usually very fast.

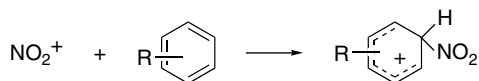
#### 1. Generation of the electrophile



or



#### 2. Attack on the aromatic ring forming the cationic intermediate



#### 3. Deprotonation



The existence of the nitronium ion in sulfuric-nitric acid mixtures can be demonstrated by both cryoscopic measurements and spectroscopy. An increase in the strong acid concentration increases the rate of reaction by shifting the equilibrium of Step 1 to the right. Addition of a nitrate salt has the opposite effect by suppressing the preequilibrium dissociation of nitric acid. It is possible to prepare crystalline salts of nitronium ions such as nitronium tetrafluoroborate. Solutions of these salts in organic solvents nitrate aromatic compounds rapidly.<sup>37</sup>

There are three general types of kinetic situations that have been observed for aromatic nitration. Aromatics of modest reactivity exhibit second-order kinetics in mixtures of nitric acid with the stronger sulfuric or perchloric acid.<sup>38</sup> Under these

<sup>36</sup> J. G. Hoggett, R. B. Moodie, J. R. Penton, and K. Schofield, *Nitration and Aromatic Reactivity*, Cambridge University Press, Cambridge, 1971; L. M. Stock, *Prog. Phys. Org. Chem.*, **12**, 21 (1976); G. A. Olah, R. Malhotra, and S. C. Narang, *Nitration*, VCH Publishers, New York, 1989.

<sup>37</sup> S. J. Kuhn and G. A. Olah, *J. Am. Chem. Soc.*, **83**, 4564 (1961); G. A. Olah and S. J. Kuhn, *J. Am. Chem. Soc.*, **84**, 3684 (1962); C. M. Adams, C. M. Sharts, and S. A. Shackelford, *Tetrahedron Lett.*, **34**, 6669 (1993); C. L. Dwyer and C. W. Holzapfel, *Tetrahedron*, **54**, 7843 (1998).

<sup>38</sup> J. G. Hoggett, R. B. Moodie, J. R. Penton, and K. Schofield, *Nitration and Aromatic Reactivity*, Cambridge University Press, Cambridge, 1971, Chap. 02.

conditions, the formation of the nitronium ion is a fast preequilibrium and Step 2 of the nitration mechanism is rate controlling. If nitration is conducted in inert organic solvents, such as nitromethane or carbon tetrachloride in the absence of a strong acid, the rate of formation of nitronium ion is slower and becomes rate limiting.<sup>39</sup> Finally, some very reactive aromatics, including alkylbenzenes, can react so rapidly under conditions where nitronium ion concentration is high that the rate of nitration becomes governed by encounter rates. Under these circumstances mixing and diffusion control the rate of reaction and no differences are observed between the reactants.<sup>40</sup>

With very few exceptions, the final step in the nitration mechanism, the deprotonation of the  $\sigma$  complex, is fast and has no effect on the observed kinetics. The fast deprotonation can be confirmed by the absence of an isotope effect when deuterium or tritium is introduced at the substitution site. Several compounds such as benzene, toluene, bromobenzene, and fluorobenzene were subjected to this test and did not exhibit isotope effects during nitration.<sup>41</sup> The only case where a primary isotope effect has been seen is with 1,3,5-tri-*t*-butylbenzene, where steric hindrance evidently makes deprotonation the slow step.<sup>42</sup>

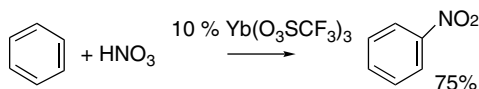
There are several other synthetic methods for aromatic nitration. Nitric acid in acetic anhydride is a potent nitrating agent and effects nitration at higher rates than nitric acid in inert organic solvents. Acetyl nitrate is formed and it is the nitrating agent.



A very convenient synthetic procedure for nitration involves the mixing of a nitrate salt with trifluoroacetic anhydride.<sup>43</sup> This generates trifluoroacetyl nitrate, which is even more reactive than acetyl nitrate.



Benzene, toluene, and aromatics of similar reactivity can be nitrated using  $\text{Yb}(\text{O}_3\text{SCF}_3)_3$  and 69% nitric acid in an inert solvent.<sup>44</sup> The catalyst remains active and can be reused. The active nitrating agent under these conditions is uncertain but must be some complex of nitrate with the oxyphilic lanthanide.



<sup>39</sup> E. D. Hughes, C. K. Ingold, and R. I. Reed, *J. Chem. Soc.*, 2400 (1950); R. G. Coombes, *J. Chem. Soc. B*, 1256 (1969).

<sup>40</sup> R. G. Coombes, R. B. Moodie, and K. Schofield, *J. Chem. Soc. B*, 800 (1968); H. W. Gibbs, L. Main, R. B. Moodie, and K. Schofield, *J. Chem. Soc., Perkin Trans. 2*, 848 (1981).

<sup>41</sup> G. A. Olah, S. J. Kuhn, and S. H. Flood, *J. Am. Chem. Soc.*, **83**, 4571, 4581 (1961); H. Suhr and H. Zollinger, *Helv. Chim. Acta*, **44**, 1011 (1961); L. Melander, *Acta Chem. Scand.*, **3**, 95 (1949); *Arkiv Kemi.*, **2**, 211 (1950).

<sup>42</sup> P. C. Myhre, M. Beug, and L. L. James, *J. Am. Chem. Soc.*, **90**, 2105 (1968).

<sup>43</sup> J. V. Crivello, *J. Org. Chem.*, **46**, 3056 (1981).

<sup>44</sup> F. J. Waller, A. G. M. Barrett, D. C. Braddock, and D. Ramprasad, *Chem. Commun.*, 613 (1997).

The identification of a specific nitrating species can be approached by comparing selectivity with that of nitration under conditions known to involve the nitronium ion. Examination of Part B of Table 9.7 shows that the position selectivity exhibited by acetyl nitrate toward toluene and ethylbenzene is not very different from that observed with nitronium ion. The data for *i*-propylbenzene suggest a lower *ortho:para* ratio for acetyl nitrate nitrations, which could indicate a larger steric factor for nitration by acetyl nitrate.

Relative reactivity data for nitration must be treated with special caution because of the possibility of encounter control. An example of this can be seen in Part A of Table 9.7, where no difference in reactivity between mesitylene and xylene is found in  $\text{H}_2\text{SO}_4\text{-HNO}_3$  nitration, whereas in  $\text{HNO}_3\text{-CH}_3\text{NO}_2$  the rates differ by a factor of more than 2. Encounter-control prevails in the former case. In general, nitration is a relatively unselective reaction with toluene  $f_p$  being about 50–60, as shown in

**Table 9.7. Relative Reactivity and Position Selectivity for Nitration of Some Aromatic Compounds**

A. Relative Reactivity of Some Hydrocarbons									
Reactant	$\text{H}_2\text{SO}_4\text{-HNO}_3\text{-H}_2\text{O}^a$			$\text{HNO}_3\text{-CH}_3\text{NO}_2^b$			$\text{HNO}_3\text{-(CH}_3\text{CO)}_2\text{O}^c$		
Benzene	1			1			1		
Toluene	17			25			27		
<i>p</i> -Xylene	38			139			92		
<i>m</i> -Xylene	38			146			—		
<i>o</i> -Xylene	38			139			—		
Mesitylene	36			400			1750		
B. Partial Rate Factors for Some Monoalkylbenzenes									
Reactant	$\text{HNO}_3\text{-H}_2\text{SO}_4\text{(sulfolane)}^d$			$\text{HNO}_3\text{-CH}_3\text{NO}_2^{e,f}$			$\text{HNO}_3\text{(CH}_3\text{CO)}_2\text{O}^g$		
	$f_o$	$f_m$	$f_p$	$f_o$	$f_m$	$f_p$	$f_o$	$f_m$	$f_p$
Toluene	52.1	2.8	58.1	49	2.5	56	49.7	1.3	60.0
Ethylbenzene	36.2	2.6	66.4	32.7	1.6	67.1	31.4	2.3	69.5
<i>i</i> -Propylbenzene	17.9	1.9	43.3	—	—	—	14.8	2.4	71.6
<i>t</i> -Butylbenzene	—	—	—	5.5	3.7	71.4	4.5	3.0	75.5
C. Relative Reactivity and Isomer Distribution for Nitrobenzene and the Nitrotoluenes <sup>h</sup>									
Reactant	Relative reactivity			Product composition (%)					
				<i>ortho</i>	<i>meta</i>	<i>para</i>			
Nitrobenzene	1			7	92	1			
<i>o</i> -Nitrotoluene	545			29	1	70			
<i>m</i> -Nitrotoluene	138			38	1	60			
<i>p</i> -Nitrotoluene	217			100	0	—			

a. R. G. Coombes, R. B. Moodie, and K. Schofield, *J. Chem. Soc. B*, 800 (1968).

b. J. G. Hoggett, R. B. Moodie, and K. Schofield, *J. Chem. Soc. B*, 1 (1969).

c. A. R. Cooksey, K. J. Morgan, and D. P. Morrey, *Tetrahedron*, **26**, 5101 (1970).

d. G. A. Olah, S. J. Kuhn, S. H. Flood, and J. C. Evans, *J. Am. Chem. Soc.*, **84**, 3687 (1962).

e. L. M. Stock, *J. Org. Chem.*, **26**, 4120 (1961).

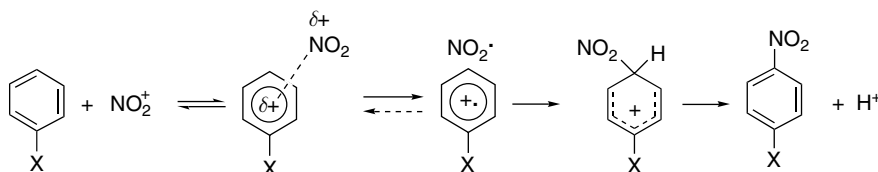
f. G. A. Olah and H. C. Lin, *J. Am. Chem. Soc.*, **96**, 549 (1974).

g. J. R. Knowles, R. O. C. Norman, and G. K. Radda, *J. Chem. Soc.*, 4885 (1960).

h. G. A. Olah and H. C. Lin, *J. Am. Chem. Soc.*, **96**, 549 (1974); *o*, *m*, and *p* designations for the toluenes are in relation to the methyl group.

Table 9.7. When the aromatic reactant carries an EWG, the selectivity increases, since the TS occurs later. For example, while toluene is about 20 times more reactive than benzene, *p*-nitrotoluene is about 200 times more reactive than nitrobenzene. The effect of the methyl substituent is magnified as a result of the later TS.

An aspect of aromatic nitration that has received attention is the role of charge transfer complexes and electron transfer intermediates on the path to the  $\sigma$ -complex intermediate. For some  $\text{NO}_2\text{-X}$  nitrating reagents, the mechanism may involve formation of a distinct electron transfer intermediate prior to the formation of the  $\sigma$  complex.<sup>45</sup>



The existence of charge transfer complexes can be demonstrated for several reaction combinations that eventually lead to nitration, but the crucial question is whether a complete electron transfer to a cation radical–radical pair occurs as a distinct step in the mechanism. This has been a matter of continuing discussion, both pro<sup>46</sup> and con.<sup>47</sup> One interesting fact that has emerged about nitration is that the product composition from toluene is virtually invariant at  $4 \pm 2\%$  *meta*,  $33 \pm 3\%$  *para*, and  $65 \pm 5\%$  *ortho*, that is, close to a statistical *o:p* ratio over a wide range of nitrating species.<sup>48</sup> This argues for a common product-forming step, and one interpretation is that this step is a collapse of a  $\text{NO}_2\text{-cation}$  radical pair, as in the electron transfer mechanism. If the  $\sigma$ -complex were formed in a single step from different  $\text{NO}_2\text{-X}$  reagents, some variation of the product composition for different X would be expected.

The mechanism of aromatic nitration has been studied by computational methods. Various structures resulting from interaction of benzene with  $\text{NO}_2^+$  were found by B3LYP/6-311++G\*\* computations.<sup>49</sup> Three of the key intermediates are shown in Fig. 9.10. In structure **A** the  $\text{NO}_2$  unit is associated with a single carbon atom with a C–N bond distance is 1.997 Å. This structure is only slightly more stable than **B**, in which the  $\text{NO}_2$  group is located equidistant between two carbon atoms. The  $\text{NO}_2$  group in both structures is significantly bent and resembles the neutral  $\text{NO}_2$  molecule, suggesting that a substantial degree of electron transfer has occurred. CHELPG charge analysis is consistent with this conclusion. Various complexes with the linear  $\text{NO}_2^+$  ion associated more generally with the ring are at considerably higher energies. Note that these structures are similar to the  $\text{Br}_2$ -benzene and  $\text{Br}_2$ -toluene complexes described on p. 774. The nitrocyclohexadienylum ion intermediate **C** is about 1 kcal/mol more stable than these oriented complexes. These results pertain to the gas phase.

<sup>45</sup> C. L. Perrin, *J. Am. Chem. Soc.*, **99**, 5516 (1977).

<sup>46</sup> J. K. Kochi, *Acc. Chem. Res.*, **25**, 39 (1992); T. M. Bockman and J. K. Kochi, *J. Phys. Org. Chem.*, **7**, 325 (1994); A. Peluso and G. Del Re, *J. Phys. Chem.*, **100**, 5303 (1996); S. V. Rosokha and J. K. Kochi, *J. Org. Chem.*, **67**, 1727 (2002).

<sup>47</sup> L. Ebersson and F. Radner, *Acc. Chem. Res.*, **20**, 53 (1987); L. Ebersson, M. P. Hartshorn, and F. Radner, *Acta Chem. Scand.*, **48**, 937 (1994); M. Lehnig, *J. Chem. Soc., Perkin Trans. 2*, 1943 (1996).

<sup>48</sup> E. K. Kim, K. Y. Lee, and J. K. Kochi, *J. Am. Chem. Soc.*, **114**, 1756 (1992).

<sup>49</sup> P. M. Esteves, J. W. de Carneiro, S. P. Cardoso, A. G. H. Barbosa, K. K. Laali, G. Rasul, G. K. S. Prakash, and G. A. Olah, *J. Am. Chem. Soc.*, **125**, 4836 (2003).

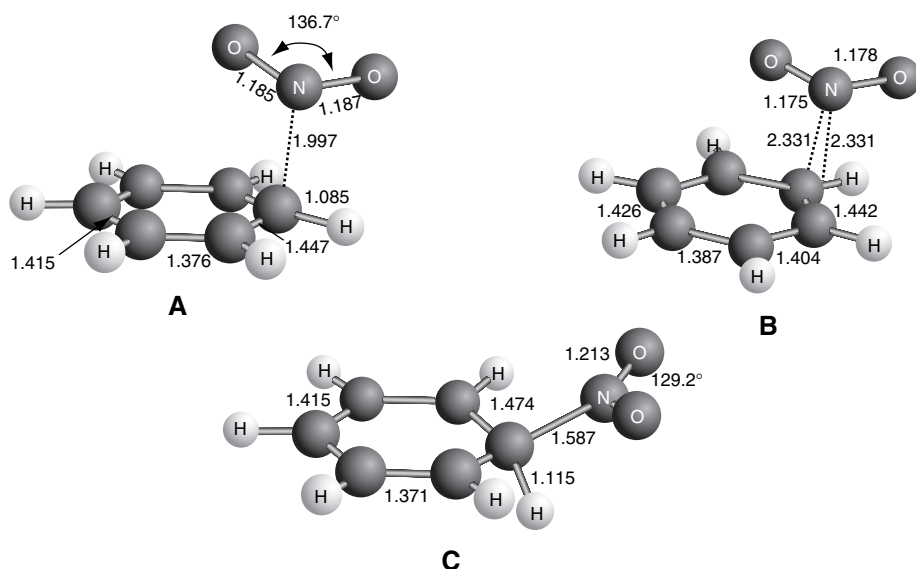


Fig. 9.10. Oriented complexes and nitrocyclohexadienylum intermediate in the nitration of benzene. Adapted from *J. Am. Chem. Soc.*, **125**, 4836 (2003), by permission of the American Chemical Society.

The nitration mechanism also has been modeled by B3LYP/6-311G\*\* computations using a continuum solvent model.<sup>50</sup> Structures corresponding to an oriented  $\pi$  complex and the TS and  $\sigma$  complex intermediate were identified. Computations were done at several solvent dielectrics,  $\epsilon$ , ranging from 0 (vacuum) to 78.5 (water). The barrier for  $\sigma$  complex formation is small and decreases as  $\epsilon$  increases. The reaction is calculated to occur without a barrier at  $\epsilon > 50$ . These computational results are consistent with an electron transfer mechanism for nitration of benzene. The reaction occurs through a complex that allows charge transfer to form a radical cation–NO<sub>2</sub>· pair, which is followed by collapse to the nitrocyclohexadienylum intermediate. The product distribution is determined at this latter stage. This feature of the mechanism explains the relatively constant position selectivity of nitration because only the NO<sub>2</sub> group is in intimate contact with the substrate at that point.

**Visual models, additional information and exercises on Nitration of Benzene can be found in the Digital Resource available at: [Springer.com/carey-sundberg](http://Springer.com/carey-sundberg).**

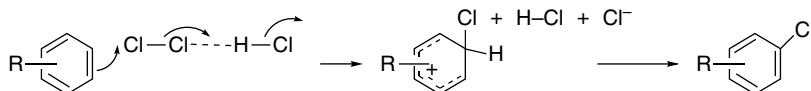
### 9.4.2. Halogenation

Substitution for hydrogen by halogen is a synthetically important electrophilic aromatic substitution reaction. The reactivity of the halogens increases in the order I<sub>2</sub> < Br<sub>2</sub> < Cl<sub>2</sub> < F<sub>2</sub>. Halogenation reactions are normally run in the presence of Lewis acids, in which case a complex of the halogen with the Lewis acid is probably the active electrophile. The molecular halogens are reactive enough to halogenate activated aromatics. Bromine and iodine form stable complexes with the corresponding halide

<sup>50</sup> H. Xiao, L. Chen, X. Ju, and G. Ji, *Science in China B*, **46**, 453 (2003).

ions. These anionic trihalide ions are less reactive than the free halogen, but are capable of substituting highly reactive rings. This factor can complicate kinetic studies, since the concentration of halide ion increases during the course of halogenation and successively more of the halogen is present as the trihalide ion.

Molecular chlorine is believed to be the active electrophile in uncatalyzed chlorination of reactive aromatic compounds. Second-order kinetics are observed in acetic acid.<sup>51</sup> The reaction is much slower in nonpolar solvents such as dichloromethane and carbon tetrachloride, and chlorination in nonpolar solvents is catalyzed by added acid. The catalysis by acids is probably the result of assistance by proton transfer in the cleavage of the Cl–Cl bond.<sup>52</sup>

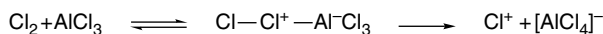


Chlorination in acetic acid is characterized by a large  $\rho$  value ( $\sim -9$  to  $-10$ ) and a high partial rate factor for toluene,  $f_p = 820$ . Both values indicate a late TS that resembles the  $\sigma$  complex intermediate.

For preparative purposes, a Lewis acid such as  $\text{AlCl}_3$  or  $\text{FeCl}_3$  is often used to catalyze chlorination. Chlorination of benzene using  $\text{AlCl}_3$  is overall third order.<sup>53</sup>

$$\text{Rate} = k[\text{ArH}][\text{Cl}_2][\text{AlCl}_3]$$

This rate law is consistent with formation of a  $\text{Cl}_2\text{-AlCl}_3$  complex that acts as the active halogenating agent but is also consistent with a rapid equilibrium involving formation of  $\text{Cl}^+$ .

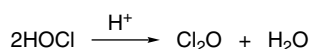


There is, however, no direct evidence for the formation of  $\text{Cl}^+$ , and it is much more likely that the complex is the active electrophile. The substrate selectivity under catalyzed conditions ( $k_{\text{tol}} = 160k_{\text{benz}}$ ) is lower than in uncatalyzed chlorinations, as would be expected for a more reactive electrophile. The effect of the Lewis acid is to weaken the Cl–Cl bond and lower the activation energy for  $\sigma$  complex formation.

Hypochlorous acid is a weak chlorinating agent. In acidic solution, it is converted to a much more active chlorinating agent. Although early mechanistic studies suggested that  $\text{Cl}^+$  might be formed under these conditions, it was shown that this is not the case. Detailed kinetic analysis of the chlorination of methoxybenzene revealed a rather complex rate law.<sup>54</sup>

$$\text{Rate} = k_1[\text{HOCl}]^2 + k_2[\text{H}_3\text{O}^+][\text{HOCl}]^2 + k_3[\text{ArH}][\text{H}_3\text{O}^+][\text{HOCl}]$$

Some of the terms are independent of the concentration of the aromatic reactant. This rate law can be explained in terms of the formation of  $\text{Cl}_2\text{O}$ , the anhydride of hypochlorous acid.



<sup>51</sup> L. M. Stock and F. W. Baker, *J. Am. Chem. Soc.*, **84**, 1661 (1962).

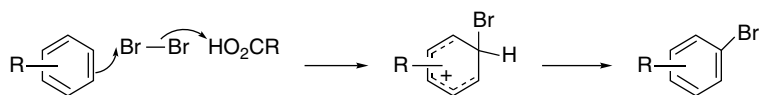
<sup>52</sup> L. J. Andrews and R. M. Keefer, *J. Am. Chem. Soc.*, **81**, 1063 (1959); R. M. Keefer and L. J. Andrews, *J. Am. Chem. Soc.*, **82**, 4547 (1960).

<sup>53</sup> S. Y. Caille and R. J. P. Corriu, *Tetrahedron*, **25**, 2005 (1969).

<sup>54</sup> C. G. Swain and D. R. Crist, *J. Am. Chem. Soc.*, **94**, 3195 (1972).

Both  $\text{Cl}_2\text{O}$  and  $[\text{H}_2\text{OCl}]^+$  apparently are active electrophiles under these conditions. The terms involving  $\text{Cl}_2\text{O}$  are zero order in the aromatic reactant because formation of  $\text{Cl}_2\text{O}$  is the rate-limiting step. Thermodynamic considerations argue strongly against rate-determining cleavage of  $[\text{H}_2\text{OCl}]^+$  to  $\text{H}_2\text{O}$  and  $\text{Cl}^+$ . The estimated equilibrium constant for this dissociation is so small that the concentration of  $\text{Cl}^+$  would be far too low to account for the observed reaction rate.<sup>55</sup>

Molecular bromine is thought to be the reactive brominating agent in uncatalyzed brominations. The bromination of benzene and toluene are first order in both bromine and the aromatic reactant in trifluoroacetic acid solution,<sup>56</sup> but becomes more complicated in the presence of water.<sup>57</sup> The bromination of benzene in aqueous acetic acid exhibits a first-order dependence on bromine concentration when bromide ion is present. The observed rate is dependent on bromide ion concentration, decreasing with increasing concentration. The acids presumably assist in the rate-determining step, as in the case of chlorination. The detailed kinetics are consistent with a rate-determining formation of the  $\sigma$  complex when bromide ion concentration is low, but with a shift to reversible formation of the  $\sigma$  complex with rate-determining deprotonation at high bromide ion concentration.<sup>58</sup>



The issue of involvement of an electron-transfer step in the formation of the intermediate has been investigated both experimentally and computationally. As noted in Section 9.1, discrete complexes of bromine with aromatic hydrocarbons have been characterized structurally for benzene and toluene.<sup>59</sup> Kinetic studies show that the rate of disappearance of the complexes is identical to the rate of formation of the bromination product, but this alone does not prove that the complex is an intermediate.<sup>60</sup> Computational studies are consistent with formation of a benzene radical cation– $[\text{Br}_2]^-$  radical pair as an intermediate. The calculated  $\Delta H^\ddagger$  is about 10 kcal/mol less than for a mechanism leading directly to a cyclohexadienyl cation intermediate.<sup>61</sup>

Bromination is characterized by high reactant selectivity.<sup>62</sup> The data in Table 9.4 showed that for toluene  $f_p$  is around 2500, as compared to about 50 for nitration. The very large stabilizing effect of ERG substituents is also evident in the large negative  $\rho$  value ( $-12$ ).<sup>63</sup> The fact that substituents can strongly influence both the rate and the orientation implies that the TS comes late in the reaction and resembles the intermediate cyclohexadienyl cation.

<sup>55</sup> E. Berliner, *J. Chem. Ed.*, **43**, 124 (1966).

<sup>56</sup> H. C. Brown and R. A. Wirkkala, *J. Am. Chem. Soc.*, **88**, 1447 (1966).

<sup>57</sup> W. M. Schubert and D. F. Gurka, *J. Am. Chem. Soc.*, **91**, 1443 (1969).

<sup>58</sup> E. Berliner and J. C. Powers, *J. Am. Chem. Soc.*, **83**, 905 (1961); W. M. Schubert and J. L. Dial, *J. Am. Chem. Soc.*, **97**, 3877 (1975).

<sup>59</sup> A. V. Vasilyev, S. V. Lindeman, and J. K. Kochi, *Chem. Commun.*, 909 (2001); S. V. Rosokha and J. K. Kochi, *J. Org. Chem.*, **67**, 1727 (2002).

<sup>60</sup> S. Fukuzumi and J. K. Kochi, *J. Org. Chem.*, **46**, 4116 (1981); S. Fukuzumi and J. K. Kochi, *J. Am. Chem. Soc.*, **103**, 7240 (1981).

<sup>61</sup> W. B. Smith, *J. Phys. Org. Chem.*, **16**, 34 (2003).

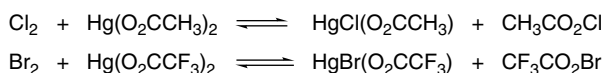
<sup>62</sup> L. M. Stock and H. C. Brown, *Adv. Phys. Org. Chem.*, **1**, 35 (1963).

<sup>63</sup> H. C. Brown and L. M. Stock, *J. Am. Chem. Soc.*, **79**, 1421 (1957).

Bromination has been shown not to exhibit a primary kinetic isotope effect in the case of benzene,<sup>64</sup> bromobenzene,<sup>65</sup> toluene,<sup>66</sup> or methoxybenzene.<sup>67</sup> There are several examples of reactants that do show significant isotope effects, including substituted anisoles,<sup>46</sup> *N,N*-dimethylanilines,<sup>68</sup> and 1,3,5-trialkylbenzenes.<sup>69</sup> The observation of isotope effects in highly substituted systems seems to be the result of steric factors that can operate in two ways. There may be resistance to the bromine taking up a position coplanar with adjacent substituents in the aromatization step, which would favor return of the  $\sigma$  complex to reactants. In addition, the steric bulk of several substituents may hinder solvent or other base from assisting in proton removal. Either factor could allow deprotonation to become rate controlling.

Bromination is catalyzed by Lewis acids, and a study of the kinetics of bromination of benzene and toluene in the presence of aluminum chloride has been reported.<sup>70</sup> Toluene is found to be about 35 times more reactive than benzene under these conditions. The catalyzed reaction thus shows a good deal less substrate selectivity than the uncatalyzed reaction, as would be expected on the basis of the greater reactivity of the aluminum chloride-bromine complex.

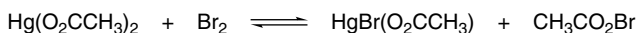
Halogenation is also effected by acyl hypohalites, such as acetyl hypochlorite and trifluoroacetyl hypobromite.<sup>71</sup>



The latter is an extremely reactive species. Trifluoroacetate is a good leaving group and facilitates cleavage of the O–Br bond. The acyl hypohalites are also the active halogenating species in solutions of the hypohalous acids in carboxylic acids, where they exist in equilibrium. Acetyl hypobromite is considered to be the active halogenating species in solutions of hypobromous acid in acetic acid:



This reagent can also be formed by reaction of bromine with mercuric acetate:



Both of the above equilibria lie to the left, but acetyl hypobromite is sufficiently reactive that it is the principal halogenating species in both solutions. The reactivity of the acyl hypohalites as halogenating agents increases with the ability of the carboxylate to function as a leaving group. This is, of course, correlated with the acidity of the carboxylic acid. The estimated order of reactivity of  $\text{Br}_2$ ,  $\text{CH}_3\text{CO}_2\text{Br}$ , and  $\text{CF}_3\text{CO}_2\text{Br}$  is

<sup>64</sup>. P. B. D. de la Mare, T. M. Dunn, and J. T. Harvey, *J. Chem. Soc.*, 923 (1957).

<sup>65</sup>. L. Melander, *Acta Chem. Scand.*, **3**, 95 (1949); *Arkiv Kemi.*, **2**, 211 (1950).

<sup>66</sup>. R. Josephson, R. M. Keefer, and L. J. Andrews, *J. Am. Chem. Soc.*, **83**, 3562 (1961).

<sup>67</sup>. J.-J. Aaron and J.-E. Dubois, *Bull. Soc. Chim. Fr.*, 603 (1971).

<sup>68</sup>. J.-E. Dubois and R. Uzan, *Bull. Soc. Chim. Fr.*, 3534 (1968); A. Nilsson, *Acta Chem. Scand.*, **21**, 2423 (1967); A. Nilsson and K. Olsson, *Acta Chem. Scand.*, **23**, 2317 (1969).

<sup>69</sup>. P. C. Myhre, *Acta Chem. Scand.*, **14**, 219 (1969).

<sup>70</sup>. S. Y. Caille and R. J. P. Corriu, *Tetrahedron*, **25**, 2005 (1969).

<sup>71</sup>. (a) A. L. Henne and W. F. Zimmer, *J. Am. Chem. Soc.*, **73**, 1362 (1951); (b) P. B. D. de la Mare, I. C. Hilton, and S. Varma, *J. Chem. Soc.*, 4044 (1960); (c) P. B. D. de la Mare and J. L. Maxwell, *J. Chem. Soc.*, 4829 (1962); (d) Y. Hatanaka, R. M. Keefer, and L. J. Andrews, *J. Am. Chem. Soc.*, **87**, 4280 (1965); (e) J. R. Bennett, L. J. Andrews, and R. M. Keefer, *J. Am. Chem. Soc.*, **94**, 6129 (1972).

1:10<sup>6</sup>:10<sup>10</sup>.<sup>71b,e</sup> It is this exceptionally high reactivity of the hypobromites that permits them to be the reactive halogenating species in solutions where they are present in relatively low equilibrium concentration.

Molecular iodine is not a very powerful halogenating agent. Only very reactive aromatics such as anilines or phenolate anions are reactive toward iodine. Iodine monochloride can be used as an iodinating agent. The greater electronegativity of the chlorine makes the iodine the electrophilic entity in the substitution reaction. Iodination by iodine monochloride is catalyzed by Lewis acids, such as ZnCl<sub>2</sub>.<sup>72</sup> Iodination can also be carried out with acetyl hypoiodite and trifluoroacetyl hypoiodite. The methods of formation of these reagents are similar to those for the hypobromites.<sup>73</sup>

Direct fluorination of aromatics is not a preparatively important laboratory reaction because it can occur with explosive violence. Mechanistic studies have been done at very low temperatures and with low fluorine concentrations. For toluene, the  $f_p$  and  $f_m$  values are 8.2 and 1.55, respectively, indicating that fluorine is a very unselective electrophile. The  $\rho$  value in a Hammett correlation with  $\sigma^+$  is  $-2.45$ . Thus, fluorination exhibits the characteristics that would be expected for a very reactive electrophile.<sup>74</sup> A number of reagents in which fluorine is bound to a very electronegative group also serve as fluorinating agents, including CF<sub>3</sub>OF, CF<sub>3</sub>CO<sub>2</sub>F, CH<sub>3</sub>CO<sub>2</sub>F, and HOSO<sub>2</sub>OF.<sup>75</sup> The synthetic applications of these reagents are discussed in Section 11.1.2 of Part B.

### 9.4.3. Protonation and Hydrogen Exchange

Hydrogen exchange resulting from reversible protonation of an aromatic ring can be followed by the use of isotopic labels. Either deuterium or tritium can be used and the experiment can be designed to follow either the incorporation or the release of the isotope. The study of the mechanism of electrophilic hydrogen exchange is somewhat simplified by the fact that the proton is the active electrophile. The principle of microscopic reversibility implies that the TS occurs on a symmetrical potential energy surface, since the attacking electrophile is chemically identical to the displaced proton. The TS involves partial transfer of a proton to (or from) a solvent molecule(s) to the aromatic ring. The intermediate  $\sigma$  complex is a cyclohexadienylum cation.

Partial rate factors for exchange for a number of substituted aromatic compounds have been measured. They reveal activation of *ortho* and *para* positions by ERGs. Some typical data are given in Table 9.8. The  $k_{\text{tol}}/k_{\text{benz}}$  ratio of around 300 indicates considerable substrate selectivity. The  $f_p$  value for toluene varies somewhat, depending on the reaction medium, but is generally about 10<sup>2</sup>.<sup>76</sup> The  $\rho$  value for hydrogen exchange in H<sub>2</sub>SO<sub>4</sub>-CF<sub>3</sub>CO<sub>2</sub>H-H<sub>2</sub>O is  $-8.6$ .<sup>77</sup> A similar  $\rho$  value of  $-7.5$  has been observed in aqueous sulfuric acid.<sup>78</sup> As seen for other electrophilic aromatic substitution reactions, the best correlation is with  $\sigma^+$ . These  $\rho$  values put protonation in the intermediate range of selectivity.

<sup>72</sup> R. M. Keefer and L. J. Andrews, *J. Am. Chem. Soc.*, **78**, 5623 (1956).

<sup>73</sup> E. M. Chen, R. M. Keefer, and L. J. Andrews, *J. Am. Chem. Soc.*, **89**, 428 (1967).

<sup>74</sup> F. Cacace, P. Giacomello, and A. P. Wolff, *J. Am. Chem. Soc.*, **102**, 3511 (1980).

<sup>75</sup> A. Haas and M. Lieb, *Chimia*, **39**, 134 (1985).

<sup>76</sup> L. M. Stock and H. C. Brown, *Adv. Phys. Org. Chem.*, **1**, 35 (1963).

<sup>77</sup> P. Rys, P. Skrabal, and H. Zollinger, *Angew. Chem. Int. Ed. Engl.*, **11**, 874 (1972).

<sup>78</sup> S. Clementi and A. R. Katritzky, *J. Chem. Soc., Perkin Trans. 2*, 1077 (1973).

**Table 9.8. Partial Rate Factors for Hydrogen Exchange for Some Substituted Aromatic Compounds**

Substituent	$f_o$	$f_m$	$f_p$
CH <sub>3</sub> <sup>a</sup>	330	7.2	313
F <sup>b</sup>	0.136	-	1.70
Cl <sup>b</sup>	0.035	-	0.161
OPh <sup>c</sup>	6900	~0.1	31,000
Ph <sup>d</sup>	133	< 1	143

a. C. Eaborn and R. Taylor, *J. Chem. Soc.*, 247 (1961).

b. C. Eaborn and R. Taylor, *J. Chem. Soc.*, 2388 (1961).

c. R. Baker and C. Eaborn, *J. Chem. Soc.*, 5077 (1961).

d. C. Eaborn and R. Taylor, *J. Chem. Soc.*, 1012 (1961).

Among the many experimental results pertaining to hydrogen exchange, a most important one is that general acid catalysis has been demonstrated,<sup>79</sup> a finding that is in accord with a rate-limiting proton transfer step. Since proton removal is partially rate determining, hydrogen exchange exhibits an isotope effect. A series of experiments using both deuterium and tritium labels arrived at  $k_H/k_D = 9.0$  for the proton-loss step for 1,3,5-trimethoxybenzene.<sup>80</sup> A substantial isotope effect has also been observed for the exchange process with azulene.<sup>81</sup>

#### 9.4.4. Friedel-Crafts Alkylation and Related Reactions

The Friedel-Crafts reaction is a very important method for introducing alkyl substituents on an aromatic ring by generation of a carbocation or related electrophilic species. The usual method of generating these electrophiles involves reaction between an alkyl halide and a Lewis acid. The most common Friedel-Crafts catalyst for preparative work is AlCl<sub>3</sub>, but other Lewis acids such as SbF<sub>5</sub>, TiCl<sub>4</sub>, SnCl<sub>4</sub>, and BF<sub>3</sub> can also promote reaction. Alternative routes to alkylating species include reaction of alcohols or alkenes with strong acids.

There are relatively few kinetic data on the Friedel-Crafts reaction. Alkylation of benzene or toluene with methyl bromide or ethyl bromide with gallium bromide as the catalyst is first order in each reactant and in the catalyst.<sup>82</sup> With aluminum bromide as the catalyst, the rate of reaction changes with time, apparently because of heterogeneity of the reaction mixture.<sup>83</sup> The initial rate data fit the following kinetic expression:

$$\text{Rate} = k[\text{EtBr}][\text{benzene}][\text{AlBr}_3]^2$$

<sup>79</sup> A. J. Kresge and Y. Chiang, *J. Am. Chem. Soc.*, **83**, 2877 (1961); A. J. Kresge, S. Slae, and D. W. Taylor, *J. Am. Chem. Soc.*, **92**, 6309 (1970).

<sup>80</sup> A. J. Kresge and Y. Chiang, *J. Am. Chem. Soc.*, **89**, 4411 (1967).

<sup>81</sup> L. C. Gruen and F. A. Long, *J. Am. Chem. Soc.*, **89**, 1287 (1967).

<sup>82</sup> S. U. Choi and H. C. Brown, *J. Am. Chem. Soc.*, **85**, 2596 (1963).

<sup>83</sup> B. J. Carter, W. D. Covey, and F. P. DeHaan, *J. Am. Chem. Soc.*, **97**, 4783 (1975); cf. S. U. Choi and H. C. Brown, *J. Am. Chem. Soc.*, **81**, 3315 (1959); F. P. DeHaan and H. C. Brown, *J. Am. Chem. Soc.*, **91**, 4844 (1969); H. Jungk, C. R. Smoot, and H. C. Brown, *J. Am. Chem. Soc.*, **78**, 2185 (1956).

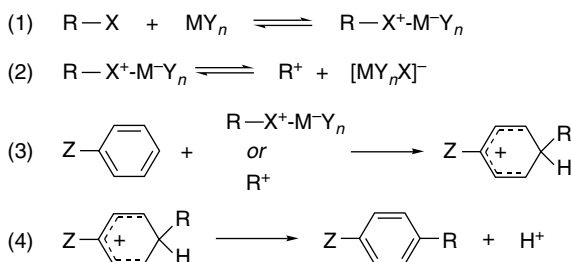
The reaction rates of toluene and benzene with *i*-propyl chloride<sup>84</sup> or *t*-butyl chloride<sup>85</sup> in nitromethane can be fit to a third-order rate law.

$$\text{Rate} = k[\text{AlCl}_3][i\text{-PrCl}][\text{ArH}]$$

Rates that are *independent* of aromatic substrate concentration have been found for reaction of benzyl chloride catalyzed by  $\text{TiCl}_4$  or  $\text{SbF}_5$  in nitromethane.<sup>86</sup> This can be interpreted as resulting from rate-determining formation of the electrophile, presumably a benzyl ion pair. The reaction of benzyl chloride and toluene shows a second-order dependence on the titanium chloride concentration under conditions where there is a large excess of hydrocarbon.<sup>87</sup> This is attributed to reaction through a 1:2 benzyl chloride- $\text{TiCl}_4$  complex, with the second  $\text{TiCl}_4$  molecule assisting in the ionization reaction:

$$\text{Rate} = k[\text{PhCH}_2\text{Cl}][\text{TiCl}_4]^2$$

All these kinetic results can be accommodated by a general mechanistic scheme that incorporates the following fundamental components: (1) complexation of the alkylating agent and the Lewis acid; in some systems, there may be an ionization of the complex to yield a discrete carbocation; (2) electrophilic attack on the aromatic reactant to form the cyclohexadienylum ion intermediate; and (3) deprotonation. The formation of carbocations accounts for the fact that rearrangement of the alkyl group is observed frequently during Friedel-Crafts alkylation.



Absolute rate data for the Friedel-Craft reactions are difficult to obtain. The reaction is very sensitive to the effects of moisture and heterogeneity. For this reason, most of the structure-reactivity trends have been developed using competitive methods, rather than by direct measurements. Relative rates are established by allowing the electrophile to compete for an excess of the two reactants. The product ratio establishes

<sup>84</sup> F. P. DeHaan, G. L. Delker, W. D. Covey, J. Ahn, R. L. Cowan, C. H. Fong, G. Y. Kim, A. Kumar, M. P. Roberts, D. M. Schubert, E. M. Stoler, Y. J. Suh, and M. Tang, *J. Org. Chem.*, **51**, 1587 (1986).

<sup>85</sup> F. P. DeHaan, W. H. Chan, J. Chang, D. M. Ferrara, and L. A. Wamschel, *J. Org. Chem.*, **51**, 1591 (1986).

<sup>86</sup> F. P. DeHaan, G. L. Delker, W. D. Covey, J. Ahn, M. S. Anisman, E. C. Brehm, J. Chang, R. M. Chicz, R. L. Cowan, D. M. Ferrara, C. H. Fong, J. D. Harper, C. D. Irani, J. Y. Kim, R. W. Meinhold, K. D. Miller, M. P. Roberts, E. M. Stoler, Y. J. Suh, M. Tang, and E. L. Williams, *J. Am. Chem. Soc.*, **106**, 7038 (1984); F. P. DeHaan, W. H. Chan, J. Chang, T. B. Chang, D. A. Chiriboga, M. M. Irving, C. R. Kaufmann, G. Y. Kim, A. Kumar, J. Na, T. T. Nguyen, D. T. Nguyen, B. R. Patel, N. P. Sarin, and J. H. Tidwell, *J. Am. Chem. Soc.*, **112**, 356 (1990).

<sup>87</sup> F. P. DeHaan, W. D. Covey, R. L. Ezelle, J. E. Margetan, S. A. Pace, M. J. Sollenberger, and D. S. Wolfe, *J. Org. Chem.*, **49**, 3954 (1984).

the relative reactivity. These studies indicate low reactant and position selectivity for the Friedel-Crafts alkylation reaction.

A study of alkylations with a group of substituted benzyl halides and a range of Friedel-Crafts catalysts provided insight into the trends in selectivity and orientation that accompany changes in both the alkyl group and the catalysts.<sup>88</sup> There is a marked increase in selectivity on going from *p*-nitrobenzyl chloride to *p*-methoxybenzyl chloride. For example, with TiCl<sub>4</sub> as the catalyst,  $k_{\text{tol}}/k_{\text{benz}}$  increases from 2.5 to 97. This increase in reactant selectivity is accompanied by an increasing preference for *para* substitution. With *p*-nitrobenzyl chloride, the *o*:*p* ratio is close to the statistically expected 2:1 ratio, whereas with the *p*-methoxy compound, the *para* product dominates by 2.5:1. There is a clear trend within the family of substituted benzyl chlorides of increasing selectivity with the increasing ERG capacity of the benzyl substituent. All of the reactions, however, remain in a region that constitutes rather low selectivity. Therefore it seems that the TS for substitution by a benzylic cation comes quite early. The substituents on the ring undergoing substitution have a relatively weak orienting effect on the attacking electrophile. With benzylic cations stabilized by donor substituents, the TS comes later and the selectivity is somewhat higher.

Toluene-benzene reactivity ratios under a number of Friedel-Crafts conditions are recorded in Table 9.9. As would be expected on the basis of the low substrate selectivity, position selectivity is also modest. The amount of *ortho* product is often comparable to the *para* product. Steric effects play a major role in determining the *o*:*p* ratio in Friedel-Crafts alkylations. The amount of *ortho* substitution of toluene

**Table 9.9. Reactant and Position Selectivity in Friedel-Crafts Alkylation Reactions**

	Electrophilic reagent	$k_{\text{tol}}/k_{\text{benz}}$	Toluene <i>o</i> : <i>p</i> ratio
1	CH <sub>3</sub> Br-AlBr <sub>3</sub> <sup>a</sup>	2.5–4.1	1.9
2	C <sub>2</sub> H <sub>5</sub> Br-GaBr <sub>3</sub> <sup>b</sup>	6.5	—
3	(CH <sub>3</sub> ) <sub>2</sub> CHBr-AlCl <sub>3</sub> <sup>c</sup>	1.9	1.2
4	(CH <sub>3</sub> ) <sub>2</sub> CHCl-AlCl <sub>3</sub> <sup>d</sup>	2.0	1.5
5	(CH <sub>3</sub> ) <sub>3</sub> CCl-AlCl <sub>3</sub> <sup>e</sup>	25	0
6	(CH <sub>3</sub> ) <sub>3</sub> CBr-SnCl <sub>4</sub> <sup>f</sup>	16.6	0
7	(CH <sub>3</sub> ) <sub>3</sub> CBr-AlCl <sub>3</sub> <sup>f</sup>	1.9	0
8	PhCH <sub>2</sub> Cl-AlCl <sub>3</sub> <sup>g</sup>	3.2	0.82
9	PhCH <sub>2</sub> Cl-AlCl <sub>3</sub> <sup>h</sup>	2–3	0.9
10	PhCH <sub>2</sub> Cl-TiCl <sub>4</sub> <sup>i</sup>	6.3	0.74
11	<i>p</i> -CH <sub>3</sub> OC <sub>6</sub> H <sub>4</sub> CH <sub>2</sub> Cl-TiCl <sub>4</sub> <sup>i</sup>	97	0.40
12	<i>p</i> -NO <sub>2</sub> C <sub>6</sub> H <sub>4</sub> CH <sub>2</sub> Cl-TiCl <sub>4</sub> <sup>i</sup>	2.5	1.7

a. H. C. Brown and H. Jungk, *J. Am. Chem. Soc.*, **77**, 5584 (1955).

b. S. U. Choi and H. C. Brown, *J. Am. Chem. Soc.*, **85**, 2596 (1963).

c. G. A. Olah, S. H. Flood, S. J. Kuhn, M. E. Moffatt, and N. A. Overchuck, *J. Am. Chem. Soc.*, **86**, 1046 (1964).

d. F. P. DeHaan, G. L. Delker, W. D. Covey, J. Ahn, R. L. Cowan, C. H. Fong, G. Y. Kim, A. Kumar, M. P. Roberts, D. M. Schubert, E. M. Stoler, Y. J. Suh, and M. Tang, *J. Org. Chem.*, **51**, 1587 (1986).

e. F. P. DeHaan, W. H. Chan, J. Chang, D. M. Ferrara, and L. A. Wainschel, *J. Org. Chem.*, **51**, 1591 (1986).

f. G. A. Olah, S. H. Flood, and M. E. Moffatt, *J. Am. Chem. Soc.*, **86**, 1060 (1964).

g. G. A. Olah, S. J. Kuhn, and S. H. Flood, *J. Am. Chem. Soc.*, **84**, 1688 (1962).

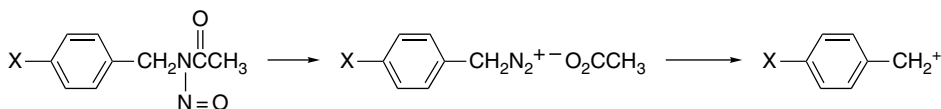
h. F. P. DeHaan, W. D. Covey, R. L. Ezelle, J. E. Margetan, S. A. Pace, M. J. Sollenberger, and D. S. Wolf, *J. Org. Chem.*, **49**, 3954 (1984).

i. G. A. Olah, S. Kobayashi, and M. Tashiro, *J. Am. Chem. Soc.*, **94**, 7448 (1972).

<sup>88</sup>. G. A. Olah, S. Kobayashi, and M. Tashiro, *J. Am. Chem. Soc.*, **94**, 7448 (1972).

decreases as the size of the entering alkyl group increases along the series methyl, ethyl, *i*-propyl.<sup>89</sup> No *ortho* product is found when the entering group is *t*-butyl.<sup>90</sup>

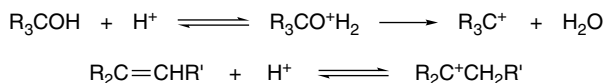
Selectivity by substituted benzyl cations has also been investigated using cations generated from benzyldiazonium ion intermediates.<sup>91</sup> This system removes potential complications of direct involvement of the Lewis acid in the substitution.



Toluene/benzene selectivity decreases in the order  $\text{X} = \text{CH}_3 > \text{H} \sim \text{Cl} > \text{NO}_2$ , in agreement with the expectation that the least stable (and most reactive) carbocation would be the least selective. These reactions also show low position selectivity.

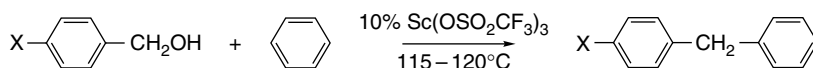
A good deal of experimental care is often required to ensure that the product mixture at the end of a Friedel-Crafts reaction is determined by *kinetic control*. The strong Lewis acid catalysts can catalyze the isomerization of alkylbenzenes and, if isomerization takes place, the product composition is not informative about the position selectivity of electrophilic attack. Isomerization increases the amount of the *meta* isomer in the case of dialkylbenzenes because this isomer is thermodynamically the most stable.<sup>92</sup>

Alcohols and alkenes can also serve as sources of electrophiles in Friedel-Crafts reactions in the presence of strong acids.



The generation of carbocations from these sources is well documented (see Section 4.4). The reaction of aromatics with alkenes in the presence of Lewis acid catalysts is the basis for the industrial production of many alkylated aromatic compounds. Styrene, for example, is prepared by dehydrogenation of ethylbenzene, which is made from benzene and ethylene.

Benzyl and allyl alcohols that can generate stabilized carbocations give Friedel-Crafts alkylation products with mild Lewis acid catalysts such as  $\text{Sc}(\text{O}_3\text{SCF}_3)_3$ .<sup>93</sup>



<sup>89</sup> R. H. Allen and L. D. Yats, *J. Am. Chem. Soc.*, **83**, 2799 (1961).

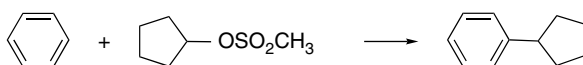
<sup>90</sup> G. A. Olah, S. H. Flood, and M. E. Moffatt, *J. Am. Chem. Soc.*, **86**, 1060 (1964).

<sup>91</sup> E. H. White, R. W. Darbeau, Y. Chen, S. Chen, and D. Chen, *J. Org. Chem.*, **61**, 7986 (1996); E. H. White, *Tetrahedron Lett.*, **38**, 7649 (1997); R. W. Darbeau and E. H. White, *J. Org. Chem.*, **65**, 1121 (2000).

<sup>92</sup> D. A. McCaulay and A. P. Lien, *J. Am. Chem. Soc.*, **74**, 6246 (1952).

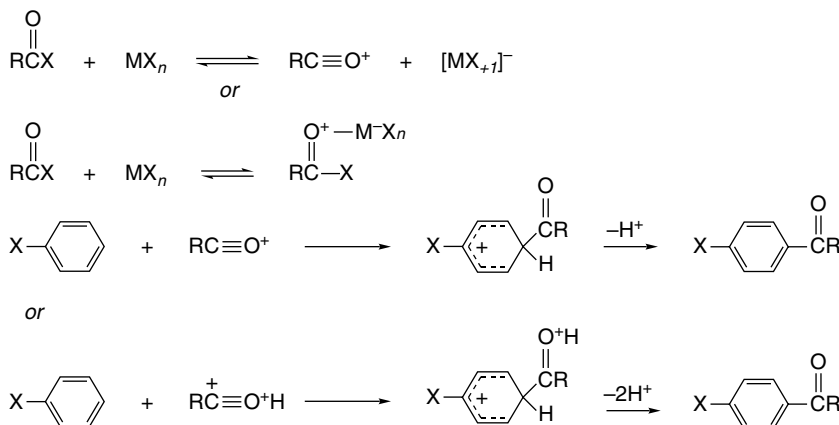
<sup>93</sup> T. Tsuchimoto, K. Tobita, T. Hiyama, and S. Fukuzawa, *Synlett*, 557 (1996); T. Tsuchimoto, K. Tobita, T. Hiyama, and S. Fukuzawa, *J. Org. Chem.*, **62**, 6997 (1997).

Scandium triflate, copper triflate, and lanthanide triflates catalyze alkylation by secondary methanesulfonates.<sup>94</sup>



### 9.4.5. Friedel-Crafts Acylation and Related Reactions

Friedel-Crafts acylation usually involves the reaction of an acyl halide, a Lewis acid catalyst, and the aromatic reactant. Several species may function as the active electrophile, depending on the reactivity of the aromatic compound. For activated aromatics, the active electrophile can be a discrete positively charged acylium ion or a complex formed between the acyl halide and the Lewis acid catalyst. For benzene and less reactive aromatics, it is believed that the active electrophile is a protonated acylium ion or an acylium ion complexed by a Lewis acid.<sup>95</sup> Reactions using acylium salts are slow with toluene or benzene as the reactant and do not proceed with chlorobenzene. The addition of triflic acid accelerates the reactions with benzene and toluene and permits reaction with chlorobenzene. These results suggest that a protonation step must be involved.



The formation of acyl halide–Lewis acid complexes can be demonstrated readily. Acetyl chloride, for example, forms both 1:1 and 1:2 complexes with  $\text{AlCl}_3$  that can be observed by NMR.<sup>96</sup> Several Lewis acid complexes of acyl chlorides have been characterized by low-temperature X-ray crystallography.<sup>97</sup> For example, the crystal structures of  $\text{PhCOCl-SbCl}_5$  and  $\text{PhCOCl-GaCl}_3$  and  $[\text{PhCOCl-TiCl}_4]_2$  have been determined. In all of these complexes, the *Lewis acid is bound to the carbonyl oxygen*. Figure 9.11 shows two examples.

Acylium salts are generated at slightly higher temperatures or with more reactive acyl halides. For example, both 4-methylbenzoyl chloride and 2,4,6-trimethylbenzoyl

<sup>94</sup> H. Kotsuki, T. Oshisi, and M. Inoue, *Synlett*, 2551 (1998); R. P. Singh, R. M. Kamble, K. L. Chandra, P. Saravanan, and V. K. Singh, *Tetrahedron*, **57**, 241 (2000).

<sup>95</sup> M. Vol'pin, I. Akhrem, and A. Orlinikov, *New J. Chem.*, **13**, 771 (1989); Y. Sato, M. Yato, T. Ohwada, S. Sato, and K. Shudo, *J. Am. Chem. Soc.*, **117**, 3037 (1995).

<sup>96</sup> B. Glavincevski and S. Brownstein, *J. Org. Chem.*, **47**, 1005 (1982).

<sup>97</sup> M. G. Davlieva, S. V. Lindeman, I. S. Neretin, and J. K. Kochi, *J. Org. Chem.*, **70**, 4013 (2005).

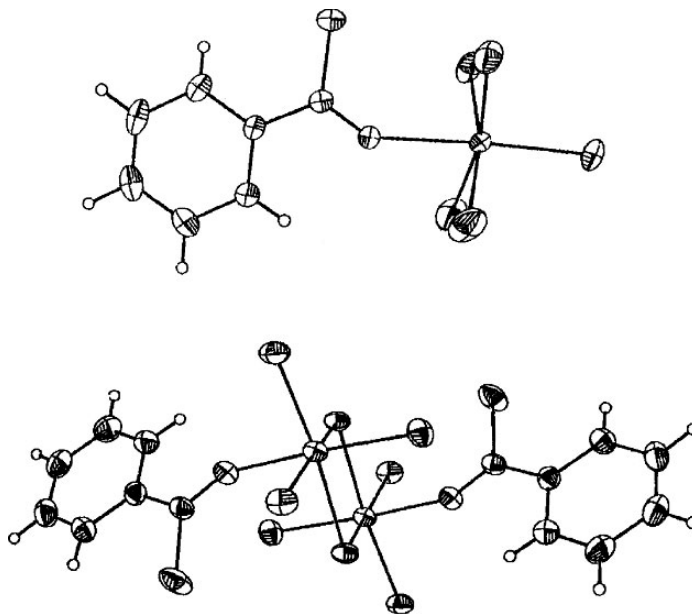
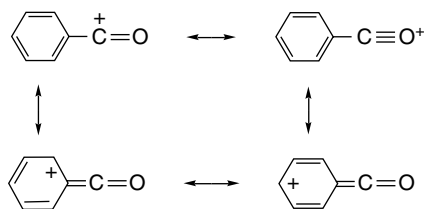


Fig. 9.11. X-Ray crystal structures of PhCOCl-SbCl<sub>5</sub> (top) and [PhCOCl-TiCl<sub>4</sub>]<sub>2</sub> (bottom). Reproduced from *J. Org. Chem.*, **70**, 4013 (2005), by permission of the American Chemical Society.

chloride give acylium salts with SbCl<sub>5</sub>. Acylium salts are also formed from benzoyl fluoride and SbF<sub>5</sub>. The structure of other acylium ions has been demonstrated by X-ray diffraction. For example, crystal structure determinations have been reported for *p*-methylphenylacylium<sup>98</sup> and acetylium<sup>99</sup> ions as SbF<sub>6</sub><sup>-</sup> salts. There is also evidence from NMR measurements that demonstrates that acylium ions can exist in nonnucleophilic solvents.<sup>100</sup> The positive charge on acylium ions is delocalized onto the oxygen atom.<sup>101</sup> This delocalization is demonstrated by the short O–C bond length in acylium ions, which implies a major contribution from the structure having a triple bond.



Aryl acylium ions are also stabilized by charge delocalization into the aromatic ring.



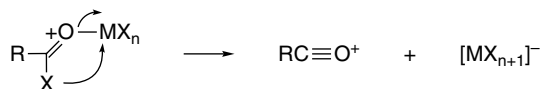
<sup>98</sup>. B. Chevrier, J.-M. LeCarpentier, and R. Weiss, *J. Am. Chem. Soc.*, **94**, 5718 (1972).

<sup>99</sup>. F. P. Boer, *J. Am. Chem. Soc.*, **90**, 6706 (1968).

<sup>100</sup>. N. C. Deno, C. U. Pittman, Jr., and M. J. Wisotsky, *J. Am. Chem. Soc.*, **86**, 4370 (1964); G. A. Olah and M. B. Comisarow, *J. Am. Chem. Soc.*, **88**, 4442 (1966).

<sup>101</sup>. T. Xu, D. H. Barich, P. D. Torres, J. B. Nicholas, and J. F. Haw, *J. Am. Chem. Soc.*, **119**, 396 (1997).

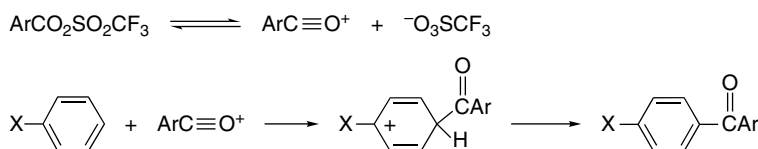
These acylium ions react rapidly with aromatic hydrocarbons such as pentamethylbenzene to give the Friedel-Crafts acylation products. Thus, the mechanisms consists of formation of the complex, ionization to an acylium ion, and substitution via a cyclohexadienylium ion intermediate.<sup>97</sup> The most likely mechanism for formation of the acylium ion is by an intramolecular transfer of the halide to the Lewis acid.



As is the case with Friedel-Crafts alkylations, direct kinetic measurements are difficult, and not many data are available. Rate equations of the form

$$\text{Rate} = k_1[\text{RCOCl}\text{-AlCl}_3][\text{ArH}] + k_2[\text{RCOCl}\text{-AlCl}_3]^2[\text{ArH}]$$

have been reported for the reaction of benzene and toluene with both acetyl and benzoyl chloride.<sup>102</sup> The available kinetic data usually do not permit unambiguous conclusions about the identity of the active electrophile. Direct kinetic evidence for acylium ions acting as electrophiles has been obtained using aroyl triflates, which can ionize without assistance from a Lewis acid.<sup>103</sup> Either formation of the acylium ion or formation of the  $\sigma$  complex can be rate determining, depending on the reactivity of the substrate.



Selectivity in Friedel-Crafts acylation with regard to both reactant selectivity and position selectivity is moderate. Some representative data are collected in Table 9.10. It can be seen that the toluene:benzene reactivity ratio is generally between 100 and 200. A progression from low substrate selectivity (Entries 5 and 6) to higher substrate selectivity (Entries 8 and 9) has been demonstrated for a series of aroyl halides.<sup>104</sup> EWGs on the aroyl chloride lead to low selectivity, presumably because of the increased reactivity of such electrophiles. ERGs diminish reactivity and increase selectivity. For the more selective electrophiles, the selectivity for *para* substitution is unusually high. Friedel-Crafts acylation is generally a more selective reaction than Friedel-Crafts alkylation. The implication is that acylium ions are less reactive electrophiles than the cationic intermediates involved in the alkylation process.

Steric factors clearly enter into determining the *o:p* ratio. The hindered 2,4,6-trimethylbenzoyl group is introduced with a 50:1 preference for the *para* position.<sup>77</sup> Similarly, in the benzoylation of alkylbenzenes by benzoyl chloride–aluminum chloride, the amount of *ortho* product decreases (10.3, 6.0, 3.1, and 0.6%, respectively) as the branching of the alkyl group is increased along the series methyl, ethyl, *i*-propyl, *t*-butyl.<sup>105</sup>

<sup>102</sup> R. Corriu, M. Dore, and R. Thomassin, *Tetrahedron*, **27**, 5601, 5819 (1971).

<sup>103</sup> F. Effenberger, J. K. Ebehard, and A. H. Maier, *J. Am. Chem. Soc.*, **118**, 12572 (1996).

<sup>104</sup> G. A. Olah and S. Kobayashi, *J. Am. Chem. Soc.*, **93**, 6964 (1971).

<sup>105</sup> G. A. Olah, J. Lukas, and E. Lukas, *J. Am. Chem. Soc.*, **91**, 5319 (1969).

**Table 9.10. Reactant and Position Selectivity in Friedel-Crafts Acylation Reactions**

	Electrophilic reagents	$k_{\text{tol}}/k_{\text{benz}}$	Toluene <i>o</i> : <i>p</i> ratio
1	CH <sub>3</sub> COCl-AlCl <sub>3</sub> <sup>a</sup>	134	0.012
2	CH <sub>3</sub> CH <sub>2</sub> COCl-AlCl <sub>3</sub> <sup>b</sup>	106	0.033
3	CH <sub>3</sub> C≡O <sup>+</sup> SbF <sub>6</sub> <sup>-c</sup>	125	0.014
4	HCOF-BF <sub>3</sub> <sup>d</sup>	35	0.82
5	2,4-Dinitrobenzoyl chloride-AlCl <sub>3</sub> <sup>d</sup>	29	0.78
6	Pentafluorobenzoyl chloride-AlCl <sub>3</sub> <sup>d</sup>	16	0.61
7	PhCOCl-AlCl <sub>3</sub> <sup>d</sup>	153	0.09
8	<i>p</i> -Toluoyle chloride-AlCl <sub>3</sub> <sup>d</sup>	164	0.08
9	<i>p</i> -Methoxybenzoyl chloride-AlCl <sub>3</sub> <sup>d</sup>	233	0.2

a. G. A. Olah, M. E. Moffatt, S. J. Kuhn, and B. A. Hardie, *J. Am. Chem. Soc.*, **86**, 2198 (1964).

b. G. A. Olah, J. Lukas, and E. Lukas, *J. Am. Chem. Soc.*, **91**, 5139 (1969).

c. G. A. Olah, S. J. Kuhn, S. H. Flood, and B. A. Hardie, *J. Am. Chem. Soc.*, **86**, 2203 (1964).

d. G. A. Olah and S. Kobayashi, *J. Am. Chem. Soc.*, **93**, 6964 (1972).

One other feature of the data in Table 9.10 is worthy of further comment. Note that alkyl- (acetyl-, propionyl-)substituted acylium ions exhibit a smaller *o*:*p* ratio than the various aryl systems. If steric factors were dominating the position selectivity, one would expect the opposite result. A possible explanation for this feature of the data is that the aryl compounds are reacting via free acylium ions, whereas the alkyl systems may involve more bulky acid-chloride catalyst complexes.

Friedel-Crafts acylation sometimes shows a modest kinetic isotope effect.<sup>106</sup> This observation suggests that the proton removal is not much faster than the formation of the cyclohexadienylium ion and that its formation may be reversible under some conditions. It has been shown that the *o*:*p* ratio can depend on the rates of deprotonation of the  $\sigma$  complex. With toluene, for example, aryl triflates give higher ratios of *ortho* product when a base, (2,4,6-tri-*t*-butylpyridine) is present.<sup>107</sup> This is because in the absence of base, reversal of acylation leads to reaction through the more easily deprotonated *para* intermediate. Steric effects on deprotonation have also been surmised to be a factor in the 1- versus 2-acylation of naphthalene by acetyl chloride-AlCl<sub>3</sub>.<sup>108</sup> The two competing reactions show different concentration dependence, with 1-acylation being second order in acylating agent, whereas 2-acylation is first order:

$$\text{Rate (1-acylation)} = k_1[\text{naphth}][\text{CH}_3\text{COCl-AlCl}_3]^2$$

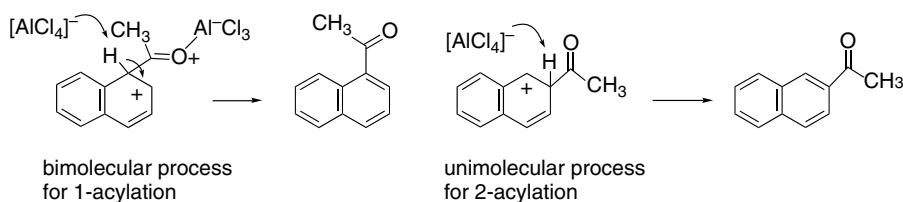
$$\text{Rate (2-acylation)} = k_2[\text{naphth}][\text{CH}_3\text{COCl-AlCl}_3]$$

The 2-acylation also showed a much larger H/D isotope effect ( $\sim 5.4$  versus 1.1). The postulated mechanism suggests that breakdown of the more hindered  $\sigma$  complex for 1-acylation is bimolecular, whereas a unimolecular deprotonation process occurs for 2-acylation.

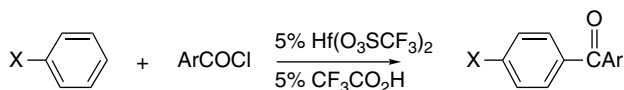
<sup>106</sup> G. A. Olah, S. J. Kuhn, S. H. Flood, and B. A. Hardie, *J. Am. Chem. Soc.*, **86**, 2203 (1964); D. B. Denney and P. P. Klemchuk, *J. Am. Chem. Soc.*, **80**, 3285, 6014 (1958).

<sup>107</sup> F. Effenberger and A. H. Maier, *J. Am. Chem. Soc.*, **123**, 3429 (2001).

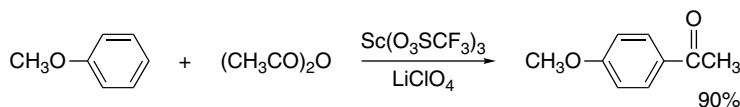
<sup>108</sup> D. Dowdy, P. H. Gore, and D. N. Walters, *J. Chem. Soc., Perkin Trans. I*, 1149 (1991).



Although the Lewis acids used as co-reagents in Friedel-Crafts acylations are often referred to as “catalysts,” they are in fact consumed in the reaction with the generation of strong acids. There has been interest in finding materials that could function as true catalysts.<sup>109</sup> Considerable success has been achieved using lanthanide triflates.<sup>110</sup>



These reactions are presumed to occur through aroyl triflate intermediates that dissociate to aryl acylium ions. Lithium perchlorate and scandium triflate also promote acylation.<sup>111</sup>



A number of variations of the Friedel-Crafts reaction conditions are possible. Acid anhydrides can serve as the acylating agent in place of acyl chlorides, and the carboxylic acid can be used directly, particularly in combination with strong acids. For example, mixtures of carboxylic acids with polyphosphoric acid in which a mixed anhydride is presumably formed in situ are reactive acylating agents.<sup>112</sup> Similarly, carboxylic acids dissolved in trifluoromethanesulfonic acid can carry out Friedel-Craft acylation. The reactive electrophile under these conditions is believed to be the protonated mixed anhydride.<sup>113</sup> In these procedures, the leaving group from the acylating agent is different, but other aspects of the reaction are similar to those under the usual conditions. Synthetic applications of Friedel-Crafts acylation are discussed further in Chapter 11 of Part B.

#### 9.4.6. Aromatic Substitution by Diazonium Ions

Among the reagents that are classified as weak electrophiles, the best studied are the aryl diazonium ions. These reagents react only with aromatic substrates having strong ERG substituents, and the products are azo compounds. The aryl diazonium

<sup>109</sup>. K. Smith, *J. Chem. Tech. Biotech.*, **68**, 432 (1997).

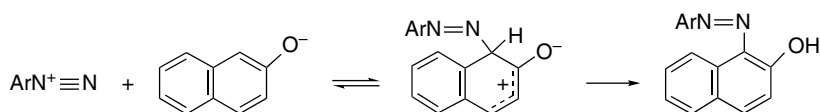
<sup>110</sup>. I. Hachiya, K. Morikawa, and S. Kobayashi, *Tetrahedron Lett.*, **36**, 409 (1995); S. Kobayashi and S. Iwamoto, *Tetrahedron Lett.*, **39**, 4697 (1998).

<sup>111</sup>. A. Kawada, S. Mitamura, and S. Kobayashi, *Chem. Commun.*, 183 (1996).

<sup>112</sup>. T. Katuri and K. M. Damodaran, *Can. J. Chem.*, **47**, 1529 (1969).

<sup>113</sup>. R. M. G. Roberts and A. R. Sardi, *Tetrahedron*, **39**, 137 (1983).

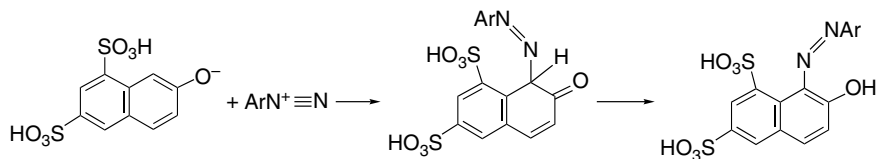
ions are usually generated by diazotization of aromatic amines. The mechanism of diazonium ion formation is discussed more completely in Section 11.2.1 of Part B.



Aryl diazonium ions are stable in solution only near or below room temperature, and this also limits the range of compounds that can be successfully substituted by diazonium ions.

Kinetic investigations revealed second-order kinetic behavior for substitution by diazonium ions in a number of instances. In the case of phenols, it is the *conjugate base* that undergoes substitution.<sup>114</sup> This finding is entirely reasonable, since the deprotonated oxy group is a better electron donor than the neutral hydroxy substituent. The reactivity of the diazonium ion depends on the substituent groups that are present. Reactivity is increased by EWG and decreased by ERG.<sup>115</sup>

An unusual feature of the mechanism for diazonium coupling is that in some cases proton loss can be demonstrated to be the rate-determining step. This feature is revealed in two ways. First, diazonium couplings of several naphthalenesulfonate ions exhibit primary isotope effects in the range 4–6 when deuterium is present at the site of substitution, clearly indicating that cleavage of the C–H bond is rate determining. Second, these reactions can also be shown to be general base catalyzed. This, too, implies that proton removal is rate determining.<sup>116</sup>



Because of the limited range of aromatic compounds that react with diazonium ions, selectivity data comparable to those discussed for other electrophilic substitutions are not available. Diazotization, since it involves a weak electrophile, would be expected to reveal high substrate and position selectivity.

#### 9.4.7. Substitution of Groups Other than Hydrogen

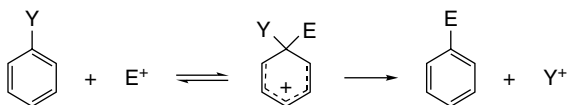
The general mechanism for EAS suggests that groups other than hydrogen could be displaced, provided that the electrophile attacked at the substituted carbon. Substitution at a site already having a substituent is called *ipso* substitution and has been observed in a number of circumstances. The ease of removal of a substituent depends on its ability to accommodate a positive charge. This factor determines whether the

<sup>114</sup> R. Wistar and P. D. Bartlett, *J. Am. Chem. Soc.*, **63**, 413 (1941).

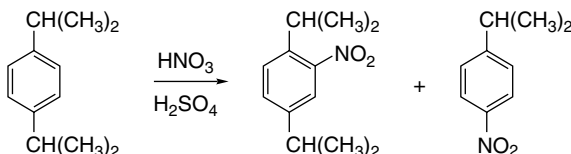
<sup>115</sup> A. F. Hegarty, in *The Chemistry of the Diazonium and Diazo Groups*, S. Patai, ed., John Wiley & Sons, New York, 1978, Chap. 12; H. Mayr, M. Hartnagel, and K. Grimm, *Liebigs Ann.*, 55 (1997).

<sup>116</sup> H. Zollinger, *Azo and Diazo Chemistry*, transl. H. E. Nursten, Interscience, New York, 1961, Chap. 10; H. Zollinger, *Adv. Phys. Org. Chem.*, **2**, 163 (1964); H. Zollinger, *Helv. Chim. Acta*, **38**, 1597 (1955).

newly attached electrophile or the substituent is eliminated from the intermediate on rearomatization.



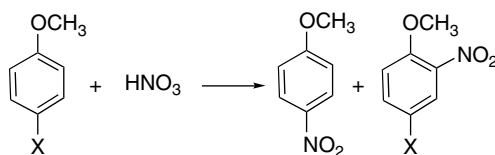
One type of substituent replacement involves cleavage of a highly branched alkyl substituent. The alkyl group is expelled as a carbocation, so substitution is most common for branched alkyl groups. The nitration 1,4-*bis*-(*i*-propyl)benzene provides an example.



Ref. 117

Cleavage of *t*-butyl groups has been observed in halogenation reactions. Minor amounts of dealkylated products are formed during chlorination and bromination of *t*-butylbenzene.<sup>118</sup> The amount of dealkylation increases greatly in the case of 1,3,5-tri-*t*-butylbenzene, and the principal product of bromination is 3,5-dibromo-*t*-butylbenzene.<sup>119</sup>

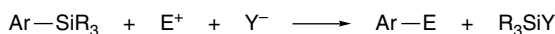
The replacement of bromine and iodine during aromatic nitration has also been observed. *p*-Bromoanisole and *p*-iodoanisole, for example, both give 30–40% of *p*-nitroanisole, a product resulting from displacement of halogen on nitration.



Ref. 120

Owing to the greater resistance to elimination of chlorine as a positively charged species, *p*-chloroanisole does not undergo dechlorination under similar conditions.

The most general type of aromatic substitution involving replacement of a substituent group in preference to a hydrogen is the electrophilic substitution of arylsilanes.



The silyl group directs electrophiles to the substituted position; that is, it is an *ipso*-directing group. Because of the polarity of the carbon-silicon bond, the substituted

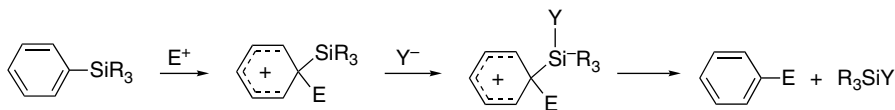
<sup>117</sup> G. A. Olah and S. J. Kuhn, *J. Am. Chem. Soc.*, **86**, 1067 (1964).

<sup>118</sup> P. B. D. de la Mare and J. T. Harvey, *J. Chem. Soc.*, 131 (1957); P. B. D. de la Mare, J. T. Harvey, M. Hassan, and S. Varma, *J. Chem. Soc.*, 2756 (1958).

<sup>119</sup> P. D. Bartlett, M. Roha, and R. M. Stiles, *J. Am. Chem. Soc.*, **76**, 2349 (1954).

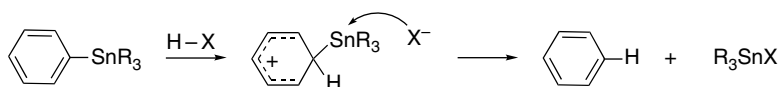
<sup>120</sup> C. L. Perrin and G. A. Skinner, *J. Am. Chem. Soc.*, **93**, 3389 (1971).

position is relatively electron rich. The ability of silicon substituents to stabilize carbocation character at  $\beta$ -carbon atoms (see Section 5.10.5, p. 564) also promotes *ipso* substitution. A silicon substituent is easily removed from the intermediate by reaction with a nucleophile. The desilylation step probably occurs through a pentavalent silicon species.



The reaction exhibits other characteristics typical of an electrophilic aromatic substitution.<sup>121</sup> Examples of electrophiles that can effect substitution for silicon include protons and the halogens, as well as acyl, nitro, and sulfonyl groups.<sup>122</sup> The fact that these reactions occur very rapidly has made them attractive for situations where substitution must be done under very mild conditions.<sup>123</sup> One example is the introduction of radioactive iodine for use in tracer studies.<sup>124</sup>

Trialkyltin substituents are also powerful *ipso*-directing groups. The overall electronic effects are similar to those in silanes but the tin substituent is more metallic and less electronegative. The electron density at carbon is increased, as is the stabilization of  $\beta$ -carbocation character. Acidic cleavage of arylstannanes is an electrophilic aromatic substitution proceeding through an *ipso*-oriented  $\sigma$ -complex.<sup>125</sup>



## 9.5. Nucleophilic Aromatic Substitution

Neither of the major mechanisms for nucleophilic substitution in saturated compounds is accessible for substitution on aromatic rings. A back-side  $S_N2$ -type reaction is precluded by the geometry of the benzene ring. The back lobe of the  $sp^2$  orbital is directed toward the center of the ring. An inversion mechanism is precluded by the geometry of the ring. An  $S_N1$  mechanism is very costly in terms of energy because a cation directly on a benzene ring is very unstable. From the data in Figure 3.18 (p. 300) it is clear that a phenyl cation is less stable than even a primary carbocation, which is a consequence of the geometry and hybridization of the aromatic

<sup>121</sup> F. B. Deans and C. Eaborn, *J. Chem. Soc.*, 2299 (1959).

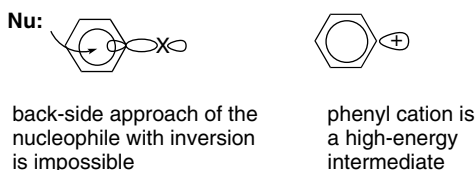
<sup>122</sup> F. B. Deans, C. Eaborn, and D. E. Webster, *J. Chem. Soc.*, 3031 (1959); C. Eaborn, Z. Lasocki, and D. E. Webster, *J. Chem. Soc.*, 3034 (1959); C. Eaborn, *J. Organomet. Chem.*, **100**, 43 (1975); J. D. Austin, C. Eaborn, and J. D. Smith, *J. Chem. Soc.*, 4744 (1963); F. B. Deans and C. Eaborn, *J. Chem. Soc.*, 498 (1957); R. W. Bott, C. Eaborn, and T. Hashimoto, *J. Chem. Soc.*, 3906 (1963).

<sup>123</sup> S. R. Wilson and L. A. Jacob, *J. Org. Chem.*, **51**, 4833 (1986).

<sup>124</sup> E. Orstad, P. Hoff, L. Skattebol, A. Skretting, and K. Breistol, *J. Med. Chem.*, **46**, 3021 (2003).

<sup>125</sup> C. Eaborn, I. D. Jenkins, and D. R. M. Walton, *J. Chem. Soc., Perkin Trans. 2*, 596 (1974).

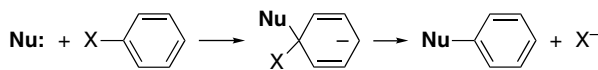
carbon atoms. An aryl carbocation is localized in an  $sp^2$  orbital that is orthogonal to the  $\pi$  system so there is no stabilization available from the  $\pi$  electrons.



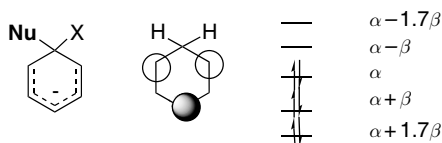
There are several mechanisms by which net nucleophilic aromatic substitution can occur. In this section we discuss the addition-elimination mechanism and the elimination-addition mechanisms. The  $S_{RN}1$  mechanism, which involves radical intermediates, is discussed in Chapter 11. Substitutions via organometallic intermediates and via aryl diazonium ions are considered in Chapter 11 of Part B.

### 9.5.1. Nucleophilic Aromatic Substitution by the Addition-Elimination Mechanism

The addition-elimination mechanism<sup>126</sup> uses one of the vacant  $\pi^*$  orbitals for bonding interaction with the nucleophile. This permits addition of the nucleophile to the aromatic ring without displacing any of the existing substituents. If attack occurs at a position occupied by a potential leaving group, net substitution can occur by a second step in which the leaving group is expelled.



The addition intermediate is isoelectronic with a pentadienyl anion.



The HOMO is  $\psi_3$ , which has its electron density primarily at the carbons *ortho* and *para* to the position of substitution. The intermediate is therefore strongly stabilized by an EWG *ortho* or *para* to the site of substitution. Such substituents activate the ring to nucleophilic substitution. The most powerful effect is exerted by a nitro group, but cyano and carbonyl groups are also favorable. Generally speaking, nucleophilic aromatic substitution is an energetically demanding reaction, even when electron-attracting substituents are present. The process disrupts the aromatic  $\pi$  system. Without an EWG present, nucleophilic aromatic substitution occurs only under extreme reaction conditions.

The role of the leaving group in determining the reaction rate is somewhat different from  $S_N2$  and  $S_N1$  substitution at alkyl groups. In those cases, the bond strength is

<sup>126</sup> Reviews: C. F. Bernasconi, in *MTP Int. Rev. Sci., Organic Series One*, Vol. 3, H. Zollinger, ed., Butterworths, London, 1973; J. A. Zoltewicz, *Top. Curr. Chem.*, **59**, 33 (1975); J. Miller, *Aromatic Nucleophilic Substitution*, Elsevier, Amsterdam, 1968.

usually the dominant factor, so the order of reactivity of the halogens is  $I > Br > Cl > F$ . In nucleophilic aromatic substitution, the formation of the addition intermediate is usually the rate-determining step, so the ease of  $C-X$  bond breaking does not affect the rate. When this is the case, the order of reactivity is often  $F > Cl > Br > I$ .<sup>127</sup> This order is the result of the polar effect of the halogen. The stronger bond dipoles associated with the more electronegative halogens favor the addition step and thus increase the overall rates of reaction.

The broad features of these experimental results, which pertain to solution reactions, are paralleled by computational results on the gas phase reactions.<sup>128</sup> The barriers for direct halide exchange reactions for  $Cl^-$ ,  $Br^-$ , and  $I^-$  in unsubstituted rings were calculated to be  $27 \pm 1$  kcal/mol, with little difference among the halides. These reactions are calculated to proceed through a single-stage process, without a stable addition intermediate. The situation is quite different for  $F^-$  exchange. The  $\sigma$  intermediate in this case is calculated to be 3.7 kcal/mol more stable than the reactants, but the barrier for  $F^-$  elimination is only 1.5 kcal/mol. The addition of one, two, or three nitro groups lowers the  $Cl^-$  exchange barrier by 22, 39, and 70 kcal/mol, so that the latter two reactions are also calculated to have negative barriers. These reactions all show addition intermediates. Figure 9.12 depicts the contrasting energy profiles for these systems. Besides indicating the important effect of EWGs, these calculations emphasize the special reactivity of the fluoride derivative.

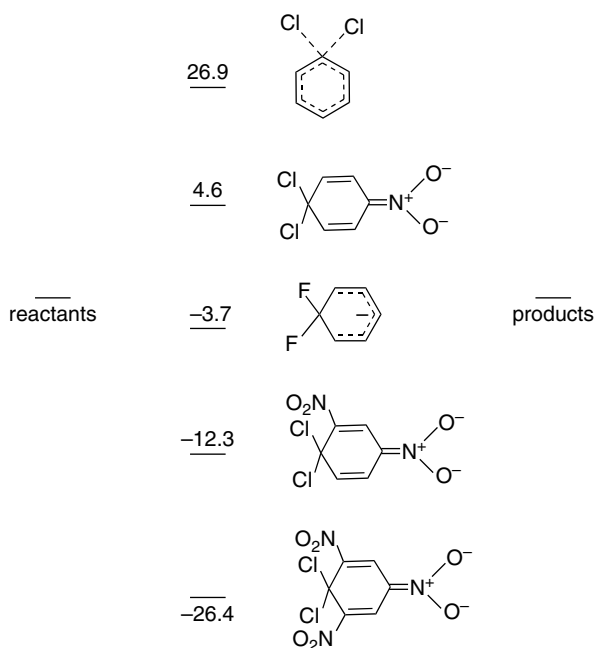
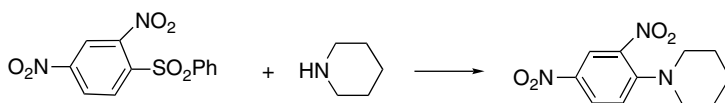


Fig. 9.12. Computed [B3LYP/6-31+G(d)] energy barriers for halide exchange by nucleophilic aromatic substitution. Data from *J. Org. Chem.*, **62**, 4036 (1997).

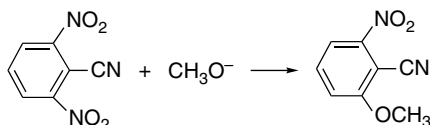
<sup>127</sup> G. P. Briner, J. Miller, M. Liveris, and P. G. Lutz, *J. Chem. Soc.*, 1265 (1954); J. F. Bunnett, E. W. Garbisch, Jr., and K. M. Pruitt, *J. Am. Chem. Soc.*, **79**, 585 (1957); G. Bartoli and P. E. Todesco, *Acc. Chem. Res.*, **10**, 125 (1977).

<sup>128</sup> M. N. Glukhovtsev, R. D. Bach, and S. Laiter, *J. Org. Chem.*, **62**, 4036 (1997).

Groups other than halogen can serve as leaving groups. Alkoxy groups are very poor leaving groups in  $S_N2$  reactions but can act as leaving groups in aromatic substitution. The reason is the same as for the inverted order of reactivity for the halogens. The rate-determining step is the addition, and the alkoxide can be eliminated in the energetically favorable rearomatization. Nitro<sup>129</sup> and sulfonyl<sup>130</sup> groups can also be displaced.

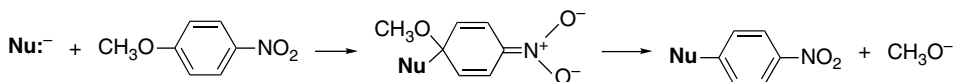


Ref. 131



Ref. 132

The addition intermediates, which are known as *Meisenheimer complexes*, can often be detected spectroscopically and can sometimes be isolated.<sup>133</sup> Especially in the case of adducts stabilized by nitro groups, the intermediates are often strongly colored.



The range of nucleophiles that can participate in nucleophilic aromatic substitution is similar to the range of those that participate in  $S_N2$  reactions and includes alkoxides,<sup>134</sup> phenoxides,<sup>135</sup> sulfides,<sup>136</sup> fluoride ion,<sup>137</sup> and amines.<sup>138</sup> For reaction with aromatic amines with 1-chloro-2,4-dinitrobenzene, the value of  $\rho$  is  $-4.0$ , indicating a substantial buildup of positive charge at nitrogen in the TS.<sup>139</sup> Substitution by carbanions is somewhat less common. This may be because there are frequently

<sup>129</sup> J. R. Beck, *Tetrahedron*, **34**, 2057 (1978).

<sup>130</sup> A. Chisari, E. Maccarone, G. Parisi, and G. Perrini, *J. Chem. Soc., Perkin Trans. 2*, 957 (1982).

<sup>131</sup> J. F. Bunnett, E. W. Garbisch, Jr., and K. M. Pruitt, *J. Am. Chem. Soc.*, **79**, 385 (1957).

<sup>132</sup> J. R. Beck, R. L. Sobczak, R. G. Suhr, and J. A. Vahner, *J. Org. Chem.*, **39**, 1839 (1974).

<sup>133</sup> E. Buncel, A. R. Norris, and K. E. Russel, *Q. Rev. Chem. Soc.*, **22**, 123 (1968); M. J. Strauss, *Chem. Rev.*, **70**, 667 (1970); C. F. Bernasconi, *Acc. Chem. Res.*, **11**, 147 (1978).

<sup>134</sup> J. P. Idoux, M. L. Madenwald, B. S. Garcia, D. L. Chu, and J. T. Gupton, *J. Org. Chem.*, **50**, 1876 (1985).

<sup>135</sup> R. O. Brewster and T. Groening, *Org. Synth.*, **II**, 445 (1943).

<sup>136</sup> M. T. Bogert and A. Shull, *Org. Synth.*, **I**, 220 (1941); N. Kharasch and R. B. Langford, *Org. Synth.*, **V**, 474 (1973); W. P. Reeves, T. C. Bothwell, J. A. Rudis, and J. V. McClusky, *Synth. Commun.*, **12**, 1071 (1982).

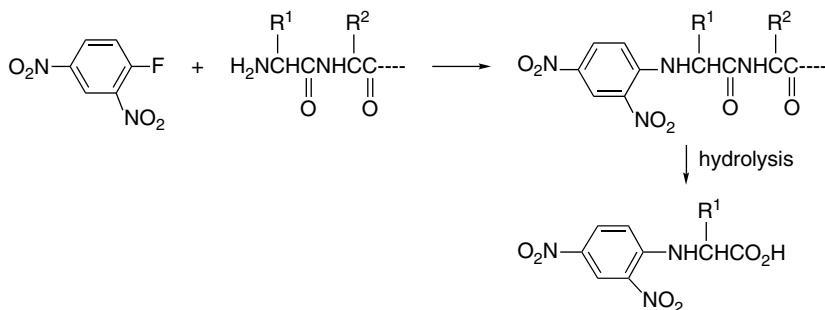
<sup>137</sup> W. M. S. Berridge, C. Crouzel, and D. Comar, *J. Labelled Compd. Radiopharm.*, **22**, 687 (1985).

<sup>138</sup> H. Bader, A. R. Hansen, and F. J. McCarty, *J. Org. Chem.*, **31**, 2319 (1966); F. Pietra and F. Del Cima, *J. Org. Chem.*, **33**, 1411 (1968); J. F. Pilichowski and J. C. Gramain, *Synth. Commun.*, **14**, 1247 (1984).

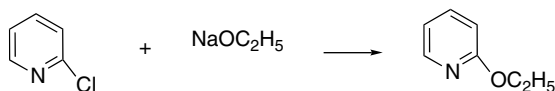
<sup>139</sup> T. M. Ikramuddeen, N. Chandrasekara, K. Ramarajan, and K. S. Subramanian, *J. Indian Chem. Soc.*, **66**, 342 (1989).

complications resulting from electron transfer processes with nitroaromatics. Solvent effects on nucleophilic aromatic substitutions are similar to those discussed for  $S_N2$  reactions (see Section 3.8). Dipolar aprotic solvents,<sup>140</sup> crown ethers,<sup>141</sup> and phase transfer catalysts<sup>142</sup> all can enhance the rate of substitution by providing the nucleophile in a reactive state with weak solvation.

One of the most historically significant examples of aromatic nucleophilic substitution is the reaction of amines with 2,4-dinitrofluorobenzene. This reaction was used by Sanger<sup>143</sup> to develop a method for identification of the N-terminal amino acid in proteins, and the process opened the way for structural characterization of proteins and other biopolymers.



2-Halopyridines and other  $\pi$ -deficient nitrogen heterocycles are excellent reactants for nucleophilic aromatic substitution.<sup>144</sup>



Ref. 145

Substitution reactions also occur readily for other heterocyclic systems, such as 2-haloquinolines and 1-haloisoquinolines, in which a potential leaving group is adjacent to a pyridine-type nitrogen. 4-Halopyridines and related heterocyclic compounds can also undergo substitution by addition-elimination, but are somewhat less reactive.

A variation of the aromatic nucleophilic substitution process in which the leaving group is part of the entering nucleophile has been developed and is known as *vicarious nucleophilic aromatic substitution*. These reactions require a strong EWG substituent

<sup>140</sup> F. Del Cima, G. Biggi, and F. Pietra, *J. Chem. Soc., Perkin Trans. 2*, 55 (1973); M. Makosza, M. Jagusztyn-Grochowska, M. Ludwikow, and M. Jawdosiuk, *Tetrahedron*, **30**, 3723 (1974); M. Prato, U. Quintily, S. Salvagno, and G. Scorrano, *Gazz. Chim. Ital.*, **114**, 413 (1984).

<sup>141</sup> J. S. Bradshaw, E. Y. Chen, R. H. Holes, and J. A. South, *J. Org. Chem.*, **37**, 2051 (1972); R. A. Abramovitch and A. Newman, Jr., *J. Org. Chem.*, **39**, 2690 (1974).

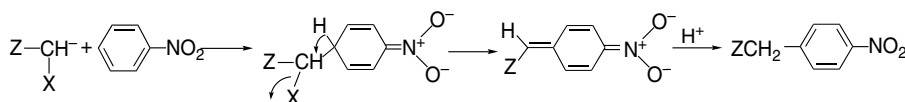
<sup>142</sup> M. Makosza, M. Jagusztyn-Grochowska, M. Ludwikow, and M. Jawdosiuk, *Tetrahedron*, **30**, 3723 (1974).

<sup>143</sup> F. Sanger, *Biochem. J.*, **45**, 563 (1949).

<sup>144</sup> H. E. Mertel, in *Heterocyclic Chemistry*, Vol 14, Part 2, E. Klingsberg, ed., Interscience, New York, 1961; M. M. Boudakian, in *Heterocyclic Compounds*, Vol 14, Part 2, Supplement, R. A. Abramovitch, ed., Wiley-Interscience, New York, 1974; B. C. Uff, in *Comprehensive Heterocyclic Chemistry*, Vol. 2A, A. J. Boulton and A. McKillop, eds., Pergamon Press, Oxford, 1984, Chap. 2.06.

<sup>145</sup> N. Al-Awadi, J. Ballam, R. R. Hemblade, and R. Taylor, *J. Chem. Soc., Perkin Trans. 2*, 1175 (1982).

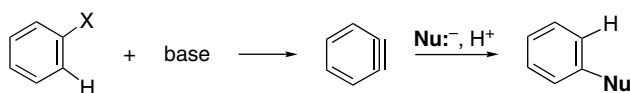
such as a nitro group but do not require a halide or other leaving group. The reactions proceed through addition intermediates.<sup>146</sup>



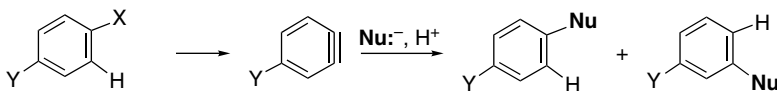
The combinations  $Z = \text{CN}, \text{RSO}_2, \text{CO}_2\text{R}, \text{SR}$  and  $X = \text{F}, \text{Cl}, \text{Br}, \text{I}, \text{ArO}, \text{ArS}$ , and  $(\text{CH}_3)_2\text{NCS}_2$  are among those that have been demonstrated.<sup>147</sup>

### 9.5.2. Nucleophilic Aromatic Substitution by the Elimination-Addition Mechanism

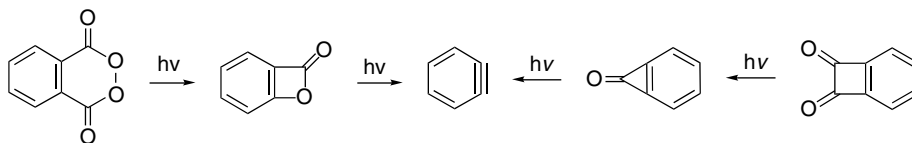
The elimination-addition mechanism involves a highly unstable intermediate, known as *dehydrobenzene* or *benzyne*.<sup>148</sup>



A characteristic feature of this mechanism is the substitution pattern in the product. The entering nucleophile need not always enter at the carbon to which the leaving group was bound, since it can add to either of the triply bound carbons.



Benzyne can be observed spectroscopically in an inert matrix at very low temperatures.<sup>149</sup> For these studies the molecule is generated photolytically.



The bonding in benzyne is considered to be similar to benzene, but with an additional weak bond in the plane of the ring formed by overlap of the two  $sp^2$  orbitals.<sup>150</sup>

<sup>146</sup>. M. Makosza, T. Lemek, A. Kwast, and F. Terrier, *J. Org. Chem.*, **67**, 394 (2002); M. Makosza and A. Kwast, *J. Phys. Org. Chem.*, **11**, 341 (1998).

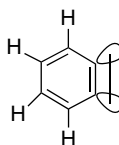
<sup>147</sup>. M. Makosza and J. Winiarski, *J. Org. Chem.*, **45**, 1574 (1980); M. Makosza, J. Golinski, and J. Baron, *J. Org. Chem.*, **49**, 1488 (1984); M. Makosza and J. Winiarski, *J. Org. Chem.*, **49**, 1494 (1984); M. Makosza and J. Winiarski, *J. Org. Chem.*, **49**, 5272 (1984); M. Makosza and J. Winiarski, *Acc. Chem. Res.*, **20**, 282 (1987); M. Makosza and K. Wojcienchowski, *Liebigs Ann. Chem./Recueil*, 1805 (1997).

<sup>148</sup>. R. W. Hoffmann, *Dehydrobenzene and Cycloalkynes*, Academic Press, New York (1967); H. H. Wenk, M. Winkler, and W. Sander, *Angew. Chem. Int. Ed. Engl.*, **42**, 502 (2003).

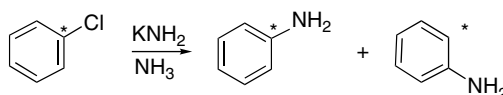
<sup>149</sup>. O. L. Chapman, K. Mattes, C. L. McIntosh, J. Pacansky, G. V. Calder, and G. Orr, *J. Am. Chem. Soc.*, **95**, 6134 (1973); J. W. Laing and R.S. Berry, *J. Am. Chem. Soc.*, **98**, 660 (1976); J. G. Rasdziszewski, B. A. Hess, Jr., and R. Zahradnik, *J. Am. Chem. Soc.*, **114**, 52 (1992).

<sup>150</sup>. H. E. Simmons, *J. Am. Chem. Soc.*, **83**, 1657 (1961).

Comparison of the NMR characteristics<sup>151</sup> with MO calculations indicates that the  $\pi$  conjugation is maintained and the benzyne is a strained but aromatic molecule.<sup>152</sup>

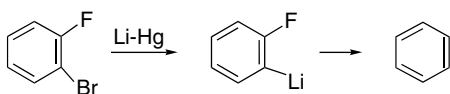


An early case in which the existence of benzyne as an intermediate was established was the reaction of chlorobenzene with potassium amide. <sup>14</sup>C-label in the starting material was found to be distributed between C(1) and the *ortho* position in the aniline, consistent with a benzyne intermediate.<sup>153</sup>



The elimination-addition mechanism is facilitated by structural effects that favor removal of a hydrogen from the ring by strong base. Relative reactivity also depends on the halide. The order  $\text{Br} > \text{I} > \text{Cl} > \text{F}$  has been established in the reaction of aryl halides with  $\text{KNH}_2$  in liquid ammonia.<sup>154</sup> This order has been interpreted as representing a balance between two effects. The polar order favoring proton removal would be  $\text{F} > \text{Cl} > \text{Br} > \text{I}$ , but this is largely overwhelmed by the order of leaving-group ability  $\text{I} > \text{Br} > \text{Cl} > \text{F}$ , which reflects bond strengths.

Benzyne can also be generated from *o*-dihaloaromatics. Reaction of lithium-amalgam or magnesium results in formation of a transient organometallic compound that decomposes with elimination of lithium halide. 1-Bromo-2-fluorobenzene is the usual starting material in this procedure.<sup>155</sup>



With organometallic compounds as bases in aprotic solvents, the acidity of the *ortho* hydrogen is the dominant factor and the reactivity order, owing to the bond polarity effect, is  $\text{F} > \text{Cl} > \text{Br} > \text{I}$ .<sup>156</sup>

<sup>151</sup> R. Warmuth, *Angew. Chem. Int. Ed. Engl.*, **36**, 1347 (1997).

<sup>152</sup> H. Jiao, P.v.R. Schleyer, B. R. Beno, K. N. Houk, and R. Warmuth, *Angew. Chem. Int. Ed. Engl.*, **36**, 2761 (1997).

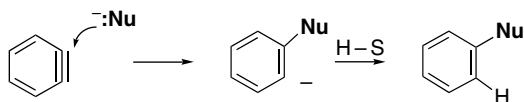
<sup>153</sup> J. D. Roberts, D. A. Semenov, H. E. Simmons, Jr., and L. A. Carlsmith, *J. Am. Chem. Soc.*, **78**, 601 (1956).

<sup>154</sup> F. W. Bergstrom, R. E. Wright, C. Chandler, and W. A. Gilkey, *J. Org. Chem.*, **1**, 170 (1936).

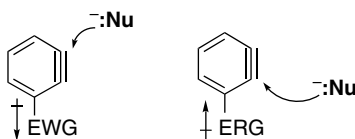
<sup>155</sup> G. Wittig and L. Pohmer, *Chem. Ber.*, **89**, 1334 (1956); G. Wittig, *Org. Synth.*, **IV**, 964 (1963).

<sup>156</sup> R. Huisgen and J. Sauer, *Angew. Chem.*, **72**, 91 (1960).

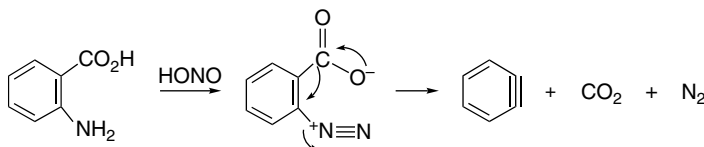
Addition of nucleophiles such as ammonia or alcohols or their conjugate bases to benzyne takes place very rapidly. These nucleophilic additions are believed to involve capture of the nucleophile, followed by protonation to give the substituted benzene.<sup>157</sup>



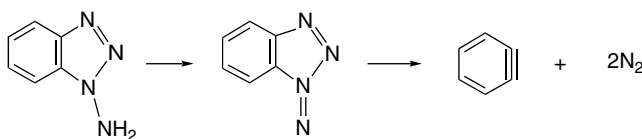
The regiochemistry of the nucleophilic addition is influenced by ring substituents. EWGs tend to favor addition of the nucleophile at the more distant end of the “triple bond,” since this permits maximum stabilization of the developing negative charge. ERGs have the opposite effect. These directive effects probably arise mainly through interaction of the substituent with the electron pair that is localized on the *ortho* carbon by the addition step. Selectivity is usually not high, however, and formation of both possible products from monosubstituted benzyne is common.<sup>158</sup>



There are several methods for generation of benzyne in addition to base-catalyzed elimination of hydrogen halide from a halobenzene, and some of these are more generally applicable for preparative work. Probably the most convenient method is diazotization of *o*-aminobenzoic acids.<sup>159</sup> Concerted loss of nitrogen and carbon dioxide follows diazotization and generates benzyne, which can be formed in the presence of a variety of compounds with which it reacts rapidly.



Oxidation of 1-aminobenzotriazole also serves as a source of benzyne under mild conditions. An oxidized intermediate decomposes with loss of two molecules of nitrogen.<sup>160</sup>



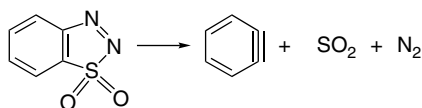
<sup>157</sup>. J. F. Bunnett, D. A. R. Happer, M. Patsch, C. Pyun, and H. Takayama, *J. Am. Chem. Soc.*, **88**, 5250 (1966); J. F. Bunnett and J. K. Kim, *J. Am. Chem. Soc.*, **95**, 2254 (1973).

<sup>158</sup>. E. R. Biehl, E. Nieh, and K. C. Hsu, *J. Org. Chem.*, **34**, 3595 (1969).

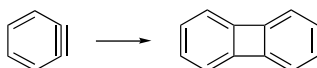
<sup>159</sup>. M. Stiles, R. G. Miller, and U. Burckhardt, *J. Am. Chem. Soc.*, **85**, 1792 (1963); L. Friedman and F. M. Longullo, *J. Org. Chem.*, **34**, 3595 (1969); P. C. Buxton, M. Fensome, F. Heaney, and K. G. Mason, *Tetrahedron*, **51**, 2959 (1995).

<sup>160</sup>. C. D. Campbell and C. W. Rees, *J. Chem. Soc. C*, 742, 745 (1969).

Another heterocyclic molecule that can serve as a benzyne precursor is benzothiadiazole-1,1-dioxide, which decomposes with elimination of sulfur dioxide and nitrogen.<sup>161</sup>



Benzyne dimerizes to biphenylene when generated in the absence of either a nucleophile or a reactive unsaturated compound.<sup>162</sup> The lifetime of benzyne is estimated to be on the order of a few seconds in solution near room temperature.<sup>163</sup>



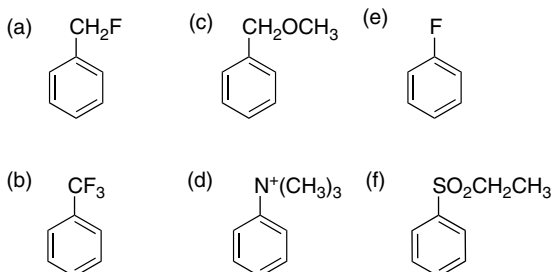
## General References

- L. F. Albright, R. V. C. Carr and R. J. Schmitt, *Nitration: Recent Laboratory and Industrial Developments*, American Chemical Society, Washington, DC, 1996.
- R. W. Hoffman, *Dehydrobenzene and Cycloalkynes*, Academic Press, New York, 1967.
- J. G. Hoggett, R. B. Moodie, J. R. Penton and K. S. Schofield, *Nitration and Aromatic Reactivity*, Cambridge University Press, Cambridge, 1971.
- C. K. Ingold, *Structure and Mechanism in Organic Chemistry*, Cornell University Press, Ithaca, 1969, Chapter VI.
- R. O. C. Norman and R. Taylor, *Electrophilic Substitution in Benzenoid Compounds*, Elsevier, Amsterdam, 1965.
- G. A. Olah, *Friedel Crafts Chemistry*, Wiley, New York, 1973.
- S. Patai, (ed.), *The Chemistry of Diazonium and Diazo Groups*, Wiley, New York, 1978.
- R. M. Roberts and A. A. Khalaf, *Friedel-Crafts Alkylation Chemistry*, Marcel Dekker, New York, 1984.
- R. Taylor, *Electrophilic Aromatic Substitution*, Wiley, Chichester, 1990.
- F. Terrier, *Nucleophilic Aromatic Substitution*, VCH Publishers, New York, 1991.

## Problems

(References for these problems will be found on page 1164)

9.1. Predict qualitatively the isomer ratio for nitration of each of the following compounds:

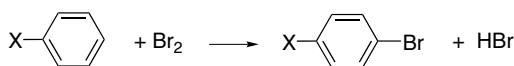


<sup>161</sup> G. Wittig and R. W. Hoffmann, *Org. Synth.*, **47**, 4 (1967); G. Wittig and R. W. Hoffmann, *Chem. Ber.*, **95**, 2718, 2729 (1962).

<sup>162</sup> F. M. Logullo, A. H. Seitz, and L. Friedman, *Org. Synth.*, **48**, 12 (1968).

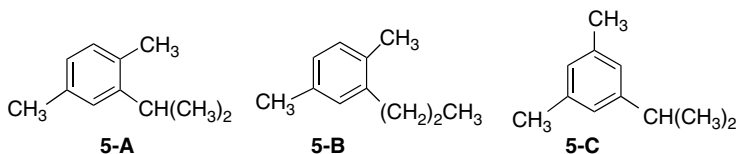
<sup>163</sup> F. Gavina, S. V. Luis, and A. M. Costero, *Tetrahedron*, **42**, 155 (1986).

- 9.2. Although *N,N*-dimethylaniline is extremely reactive toward electrophilic aromatic substitution and is readily substituted by weak electrophiles, such as diazonium and nitrosonium ions, this reactivity is greatly diminished by introduction of an alkyl substituent in an *ortho* position. Explain.
- 9.3. Toluene is 28 times more reactive than benzene, whereas isopropylbenzene is 14 times more reactive than benzene toward nitration in the organic solvent sulfolane. The *o*:*m*:*p* ratio for toluene is 62:3:35. For isopropylbenzene, the ratio is 43:5:52. Calculate the partial rate factors for each position in toluene and isopropylbenzene. Discuss the significance of the partial rate factors. Compare the reactivity at each position of the molecules, and explain any significant differences.
- 9.4. Some bromination rate constants are summarized below. Compare the correlation of the data with both  $\sigma$  and  $\sigma^+$  substituent constants. What is the value of  $\rho$ ? What information do the results provide about the mechanism of bromination?



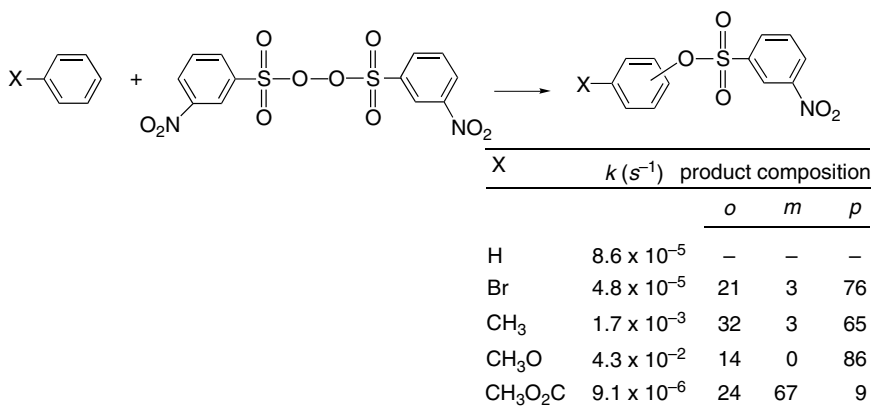
X	$k (M^{-1}s^{-1})$
H	$2.7 \times 10^{-6}$
CH <sub>3</sub>	$1.5 \times 10^{-2}$
OCH <sub>3</sub>	$9.8 \times 10^3$
OH	$4.0 \times 10^4$
N(CH <sub>3</sub> ) <sub>2</sub>	$2.2 \times 10^8$

- 9.5. Compare the product distribution results given below for the alkylation of *p*-xylene at two different temperatures after 2 h. The ratio of aromatic reagent:halide:AlCl<sub>3</sub> was 1.0:0.5:0.1.

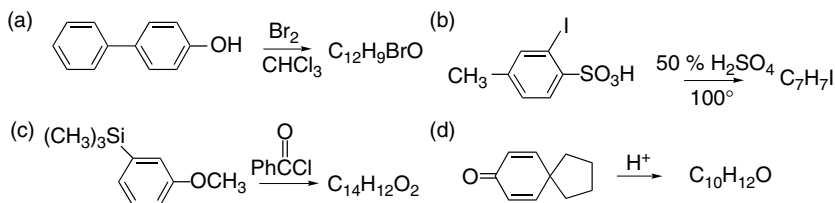


alkyl chloride	temp	Product Composition (%)		
		5-A	5-B	5-C
<i>n</i> -propyl	0°C	34	66	0
<i>n</i> -propyl	50°C	31	53	16
<i>i</i> -propyl	0°C	100	0	0
<i>i</i> -propyl	50°C	62	0	38

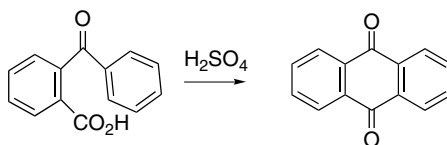
- 9.6. The table below gives first order-rate constants for the reaction of substituted benzenes with *m*-nitrobenzenesulfonyl peroxide. From these data, calculate the relative reactivity and partial rate factors. Does this reaction fit the pattern of an electrophilic aromatic substitution? If so, does the active electrophile exhibit low, intermediate, or high reactant and position selectivity?



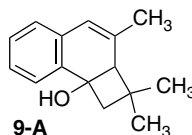
9.7. Propose a structure for the products of the following reactions:



9.8. In 100% H<sub>2</sub>SO<sub>4</sub> the cyclization shown below occurs. If one of the *ortho* hydrogens is replaced by deuterium, the rate of cyclization drops from  $1.56 \times 10^{-4}$  to  $1.38 \times 10^{-4} s^{-1}$ . Calculate the kinetic isotope effect. The product from such a reaction contains 60% of the original deuterium. Write a mechanism for this reaction that is consistent with both the magnitude of the kinetic isotope effect and the deuterium retention data.

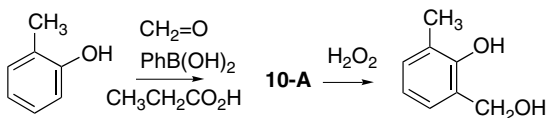


9.9. Reaction of 3,5,5-trimethylcyclohex-2-en-1-one with NaNH<sub>2</sub> (3 equiv) in THF generates an enolate. When bromobenzene is added to this solution and stirred for 4 h, a product **9-A** is isolated in 30% yield. Formulate a mechanism for this reaction.

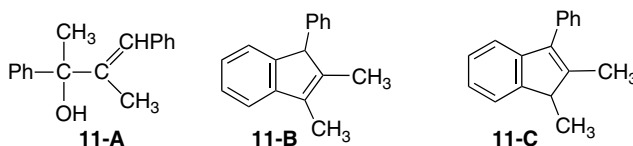


9.10. Several phenols can be selectively hydroxymethylated at the *ortho* position by heating with paraformaldehyde and phenylboronic acid in propanoic acid. An intermediate **10-A** having the formula C<sub>14</sub>H<sub>13</sub>O<sub>2</sub>B can be isolated in the case

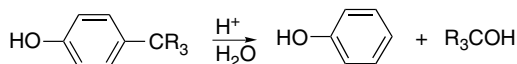
of 2-methylphenol. Propose a structure for the intermediate and indicate the role of phenylboronic acid in the reaction.



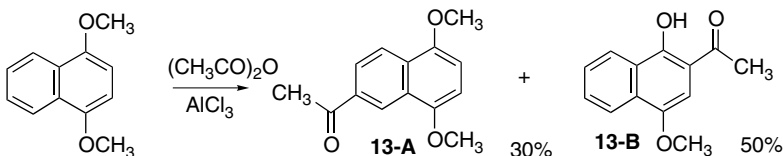
- 9.11. When compound **11-A** is dissolved in  $\text{FSO}_3\text{H}$  at  $-78^\circ\text{C}$ , the NMR spectrum shows that a carbocation is formed. If the solution is then allowed to warm to  $-10^\circ\text{C}$ , a different carbocation is formed. When the acidic solution is quenched with 15% NaOH, the first carbocation gives product **11-B**, whereas the second gives **11-C**. What are the likely structures of the two carbocations?



- 9.12. Alkyl groups that are *para* to strong ERG substituents such as hydroxy or methoxy can be removed from aromatic rings under acidic conditions if they can form stable carbocations. A comparison of the cases  $\text{R} = \text{CH}_3$  and  $\text{R} = \text{Ph}$  showed strikingly different solvent isotope effects. For  $\text{R} = \text{CH}_3$   $k_{\text{H}}/k_{\text{D}} \sim 0.1$ , whereas for  $\text{R} = \text{Ph}$ ,  $k_{\text{H}}/k_{\text{D}} = 4.3$ . How do you account for the difference in the solvent isotope effects in the two systems? What accounts for the inverse isotope effect in the case of  $\text{R} = \text{CH}_3$ ?

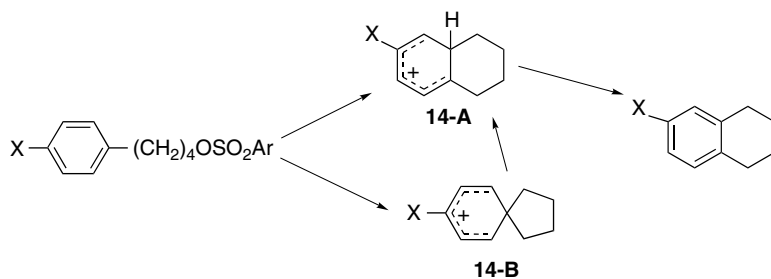


- 9.13. Acylation of 1,4-dimethoxynaphthalene with acetic anhydride (1.2 equiv) and  $\text{AlCl}_3$  (2.2 equiv) in dichloroethane at  $60^\circ\text{C}$  leads to two products, as shown below. Suggest a rationalization for the formation of these two products. What might account for the demethylation observed in product **13-B**?



- 9.14. The solvolysis of 4-arylbutyl arenesulfonates in nonnucleophilic media leads to formation of tetralins. Two  $\sigma$  intermediates, **14-A** and **14-B**, are conceivable.

**14-A** would lead directly to product on deprotonation, whereas **14-B** would give product by rearrangement to **14-A**, followed by deprotonation.



Suggest an experiment that could determine how much of the product was formed via each of the two paths. How would you expect the relative importance of the two routes to vary with the substituent group X?

- 9.15. The kinetic expression for chlorination of anisole by HOCl given on p. 799 becomes simpler for both less reactive and more reactive reactants. For benzene the expression is

$$\text{Rate} = k[\text{benzene}][\text{HOCl}][\text{H}^+]$$

and for 1,4-dimethoxybenzene it is

$$\text{Rate} = k[\text{HOCl}][\text{H}^+]$$

Why does the form of the rate expression depend on the reactivity of the aromatic compound? What conclusions can be drawn about the mechanism of chlorination of benzene and 1,4-dimethoxybenzene under these conditions?

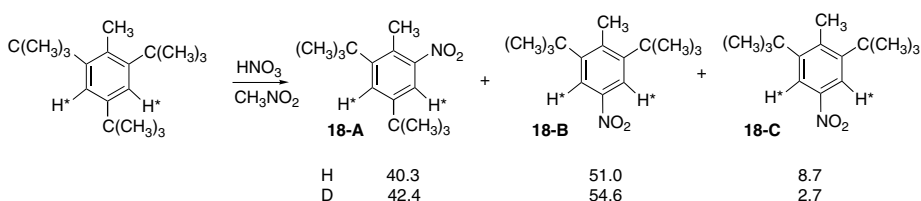
- 9.16. Relative reactivity and product distribution data for nitration of the halobenzenes is given below. Calculate the partial rate factors for each position for each halogen. What insight into the substituent activating/directing effects of the halogens can you draw from this data?

Halogen	Rel rate	%ortho	%meta	%para
F	0.15	13	0	87
Cl	0.033	30	1	69
Br	0.03	37	1	62
I	0.18	38	2	60

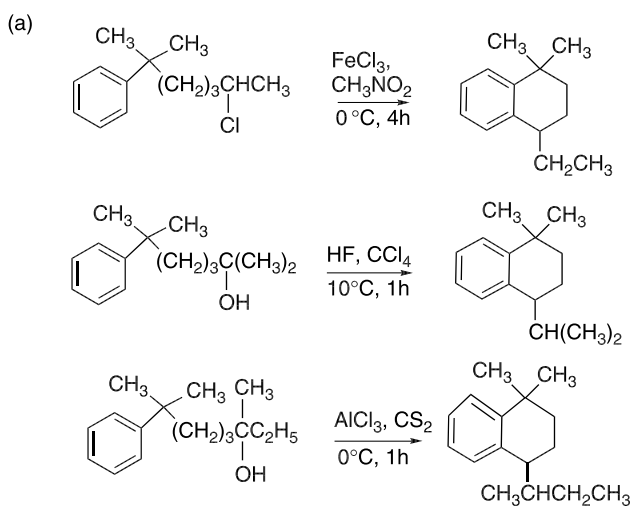
- 9.17. *Ips*o substitution is relatively rare in electrophilic aromatic substitution and was not explicitly covered in Section 9.2 in the discussion of substituent effects on reactivity and selectivity. Using qualitative concepts, discuss the effect of the following types of substituents on the TS and intermediate for *ip*s<sub>o</sub> substitution.
- A  $\pi$ -donor substituent that is more electronegative than carbon, e.g., methoxy.
  - A  $\pi$ -acceptor substituent that is more electronegative than carbon, e.g., cyano or nitro.

- c. A very polar EWG that does not have  $\pi$ -conjugation capacity, e.g.,  $N^+(CH_3)_3$ .
- d. A group without strong  $\pi$ -conjugating capacity that is less electronegative than carbon, e.g.,  $Si(CH_3)_3$ .

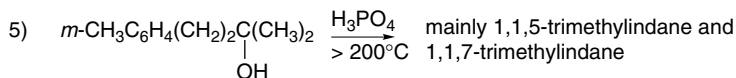
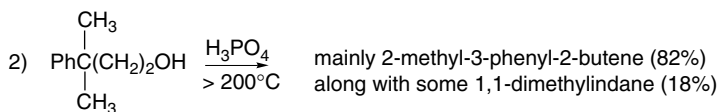
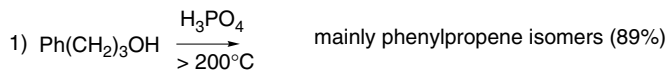
9.18. The nitration of 2,4,6-*tris*-(*t*-butyl)toluene gives rise to three products. The product distribution changes when the 3-position and the 5-position are deuterated, as shown by the data below. Indicate a mechanism for formation of each product. Show why the isotopic labeling results in a change in product composition. Calculate the isotope effect. Does this appear to be a primary isotope effect? Is an isotope effect of this magnitude consistent with your proposed mechanism?



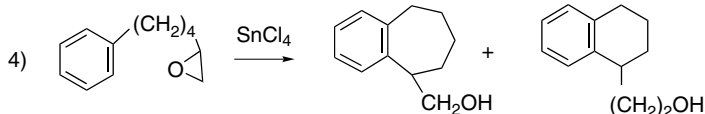
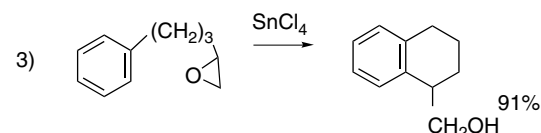
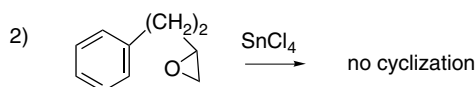
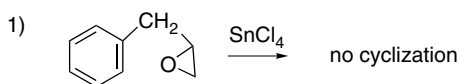
9.19. Analyze the results of the studies of intramolecular electrophilic substitution that are described below. Write mechanisms for each of the cyclizations and comment on the relation between ring size and the outcome of cyclization.



(b)

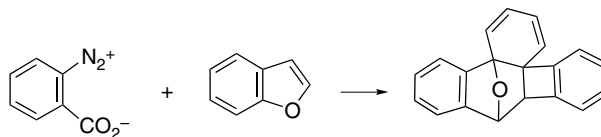


(c)

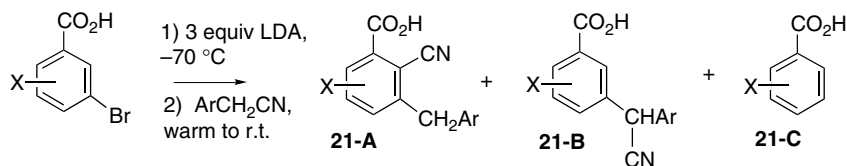


9.20. Explain the outcome of the following reactions by a mechanism showing how the product could be formed.

- 2,6-Di-(*t*-butyl)phenoxide reacts with *o*-nitroaryl halides in NaOH/DMSO at 80°C to give 2,6-di-(*t*-butyl)-4-(2-nitrophenyl)phenol in 60–90% yield. Under similar conditions, 1,4-dinitrobenzene gives 2,6-di-(*t*-butyl)-4-(4-nitrophenyl)phenol.
- 2-(3-Chlorophenyl)-4,4-dimethyloxazoline reacts with alkyl lithium reagents to give 2-(2-alkylphenyl)-4,4-dimethyloxazolines.
- Nitrobenzene reacts with cyanomethyl phenyl sulfide in NaOH/DMSO to give a mixture of 2- and 4-nitrophenylacetonitrile.
- The following transformation occurs:



- e. Reaction of benzene with 3,3,3-trifluoropropene in the presence of  $\text{BF}_3$  gives 3,3,3-trifluoropropylbenzene.
- f. 3-Chloronitrobenzene reacts with 4-amino-1,2,4-triazole in  $\text{K}^+ \cdot \text{O}-t\text{-Bu}/\text{DMSO}$  to give 2-chloro-4-nitroaniline.
- g. Good yields of tetralone can be obtained from 4-phenylbutanoic acid or the corresponding acyl chloride in the presence of the strongly acidic resin Nafion-H. With 3-phenylpropanoic acid, only the acyl chloride gives a cyclization product.
- 9.21. Reaction of several 3-bromobenzoic acids with excess LDA at  $-70^\circ\text{C}$ , followed by addition of benzyl cyanide and warming, gives the product mixtures shown below. Suggest a mechanism for formation of products **21-A** and **21-B** under these conditions.



X	Ar	<b>21-A</b>	<b>21-B</b>	<b>21-C</b>
4- $\text{CH}_3\text{O}$	Ph	56	9	11
4- $\text{CH}_3\text{O}$	4- $\text{CH}_3\text{Ph}$	70	8	12
4- $\text{CH}_3\text{O}$	2- $\text{CH}_3\text{Ph}$	44	5	10
4- $\text{CH}_3$	Ph	53	<2	7
4- $\text{CH}_3$	4- $\text{CH}_3\text{Ph}$	43	<2	8

# Concerted Pericyclic Reactions

## Introduction

*Concerted reactions* occur without an intermediate. The transition structure involves both bond breaking and bond formation, although not necessarily to the same degree. There are numerous examples of both unimolecular and bimolecular concerted reactions. A particularly important group consists of the *concerted pericyclic reactions*,<sup>1</sup> which are characterized by a continuous reorganization of electrons through *cyclic transition structures*. Furthermore, the cyclic TS must correspond to an arrangement of the participating orbitals that can maintain a bonding interaction between the reacting atoms throughout the course of the reaction. We shall see shortly that these requirements make pericyclic reactions predictable in terms of relative reactivity, regioselectivity, and stereoselectivity.

A key to understanding the mechanisms of the concerted pericyclic reactions was the recognition by Woodward and Hoffmann that the pathway of such reactions is determined by the symmetry properties of the orbitals that are directly involved.<sup>2</sup> Specifically, they stated the requirement for *conservation of orbital symmetry*. The idea that the symmetry of each participating orbital must be conserved during the reaction process dramatically transformed the understanding of concerted pericyclic reactions and stimulated much experimental work to test and extend their theory.<sup>3</sup> The Woodward and Hoffmann concept led to other related interpretations of orbital properties that are also successful in predicting and interpreting the course of concerted

<sup>1</sup>. R. B. Woodward and R. Hoffmann, *The Conservation of Orbital Symmetry*, Academic Press, New York, 1970.

<sup>2</sup>. R. B. Woodward and R. Hoffmann, *J. Am. Chem. Soc.*, **87**, 395 (1965).

<sup>3</sup>. For reviews of several concerted reactions within the general theory of pericyclic reactions, see A. P. Marchand and R. E. Lehr, eds., *Pericyclic Reactions*, Vols. I and II, Academic Press, New York, 1977.

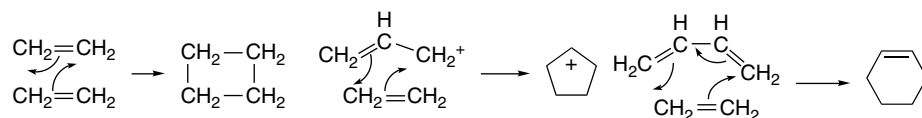
pericyclic reactions.<sup>4</sup> These various approaches conclude that TSs with certain orbital alignments are energetically favorable (allowed), whereas others lead to high-energy (forbidden) TSs. The stabilized TSs share certain electronic features with aromatic systems, whereas the high-energy TSs are more similar to antiaromatic systems.<sup>4b,c</sup> As we will see shortly, this leads to rules similar to the Hückel and Möbius relationships for aromaticity (see Section 8.1) that allow prediction of the outcome of the reactions on the basis of the properties of the orbitals of the reactants. Because these reactions proceed through highly ordered cyclic transition structures with specific orbital alignments, the concerted pericyclic reactions often have characteristic and predictable stereochemistry. In many cases, the reactions exhibit regioselectivity that can be directly related to the effect of orbital interactions on TS structure. Similarly, substituent effects on reactivity can be interpreted in terms of the effect of the substituents on the interacting orbitals.

A great deal of effort has been expended to model the transition structures of concerted pericyclic reactions.<sup>5</sup> All of the major theoretical approaches, semiempirical MO, ab initio MO, and DFT have been applied to the problem and some comparisons have been made.<sup>6</sup> The conclusions drawn generally parallel the orbital symmetry rules in their prediction of reactivity and stereochemistry and provide additional insight into substituent effects.

We discuss several categories of concerted pericyclic reactions, including Diels-Alder and other *cycloaddition reactions*, *electrocyclic reactions*, and *sigmatropic rearrangements*. The common feature is a concerted mechanism involving a cyclic TS with continuous electronic reorganization. The fundamental aspects of these reactions can be analyzed in terms of orbital symmetry characteristics associated with the TS. For each major group of reactions, we examine how regio- and stereoselectivity are determined by the cyclic TS.

## 10.1. Cycloaddition Reactions

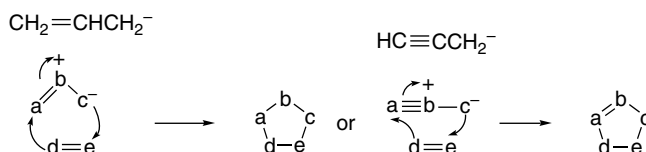
Cycloaddition reactions involve the combination of two molecules to form a new ring. Concerted pericyclic cycloadditions involve reorganization of the  $\pi$ -electron systems of the reactants to form two new  $\sigma$  bonds. Examples might include cyclodimerization of alkenes, cycloaddition of allyl cation to an alkene, and the addition reaction between alkenes and dienes (Diels-Alder reaction).



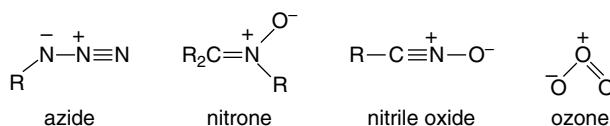
- <sup>4</sup> (a) H. C. Longuet-Higgins and E. W. Abrahamson, *J. Am. Chem. Soc.*, **87**, 2045 (1965); (b) M. J. S. Dewar, *Angew. Chem. Int. Ed. Engl.*, **10**, 761 (1971); M. J. S. Dewar, *The Molecular Orbital Theory of Organic Chemistry*, McGraw-Hill, New York, 1969; (c) H. E. Zimmerman, *Acc. Chem. Res.*, **4**, 272 (1971); (d) K. N. Houk, Y. Li, and J. D. Evanseck, *Angew. Chem. Int. Ed. Engl.*, **31**, 682 (1992).
- <sup>5</sup> O. Wiest, D. C. Montiel, and K. N. Houk, *J. Phys. Chem. A*, **101**, 8378 (1997).
- <sup>6</sup> D. Sperling, H. U. Reissig, and J. Fabian, *Liebigs Ann. Chem.*, 2443 (1997); B. S. Jursic, *Theochem*, **358**, 139 (1995); H.-Y. Yoo and K. N. Houk, *J. Am. Chem. Soc.*, **119**, 2877 (1997); V. Aviente, H. Y. Yoo, and K. N. Houk, *J. Org. Chem.*, **62**, 6121 (1997); K. N. Houk, B. R. Beno, M. Nendal, K. Black, H. Y. Yoo, S. Wilsey, and J. K. Lee, *Theochem*, **398**, 169 (1997); J. E. Carpenter and C. P. Sosa, *Theochem*, **311**, 325 (1994); B. Jursic, *Theochem*, **423**, 189 (1998); V. Brachadell, *Int. J. Quantum Chem.*, **61**, 381 (1997).

The cycloadditions can be characterized by specifying the number of  $\pi$  electrons involved for each species, and for the above three cases, this would be  $[2+2]$ ,  $[2+2]$ , and  $[2+4]$ , respectively. Some such reactions occur readily, whereas others are not observed. We will learn, for example, that of the three reactions above, only the alkene-diene cycloaddition occurs readily. The pattern of reactivity can be understood by application of the principle of conservation of orbital symmetry.

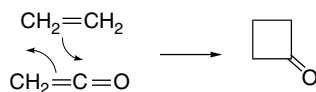
The most important of the concerted cycloaddition reactions is the *Diels-Alder reaction* between a diene and an alkene derivative to form a cyclohexene. The alkene reactant usually has a substituent and is called the *dienophile*. We discuss this reaction in detail in Section 10.2. Another important type of  $[2+4]$  cycloaddition is *1,3-dipolar cycloaddition*. These reactions involve heteroatomic systems that have four  $\pi$  electrons and are electronically analogous to the allyl or propargyl anions.



Many combinations of atoms are conceivable, among them azides, nitrones, nitrile oxides, and ozone. As these systems have four  $\pi$  electrons, they are analogous to dienes, and cycloadditions with alkenes and alkynes are allowed  $[4+2]$  reactions. These are discussed in Section 10.3.



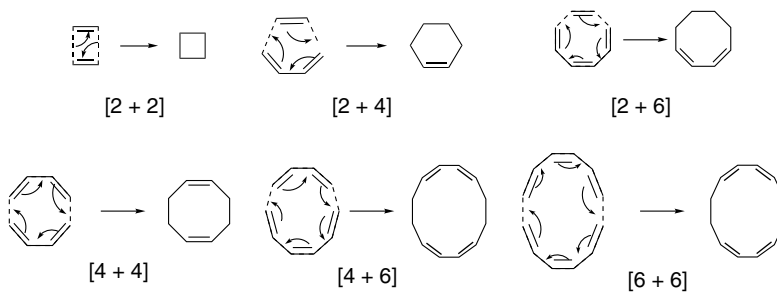
In a few cases  $[2+2]$  cycloadditions are feasible, particularly with ketenes, and these reactions are dealt with in Section 10.4.



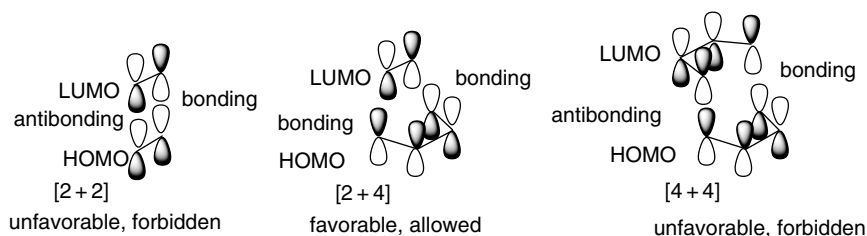
We begin the discussion of concerted cycloaddition reactions by exploring how the orbital symmetry requirements distinguish between reactions that are favorable and those that are unfavorable. Cycloaddition reactions that occur through a pericyclic concerted mechanism can be written as a continuous rearrangement of electrons. If we limit consideration to conjugated systems with from two to six  $\pi$  electrons, the reactions shown in Scheme 10.1 are conceivable.

We recognize immediately that some of these combinations would encounter strain and/or entropic restrictions. However, orbital symmetry considerations provide a fundamental insight into the electronic nature of the cycloaddition reactions and allow us to see that some of the TS structures are electronically favorable, whereas others are not. Woodward and Hoffmann formulated the orbital symmetry principles for cycloaddition reactions in terms of the frontier orbitals. An energetically accessible TS requires overlap of the frontier orbitals to permit smooth formation of the new

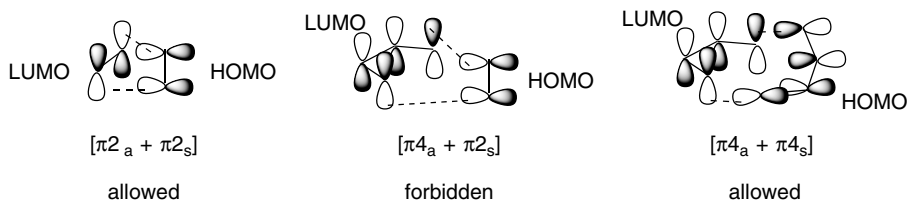
## Scheme 10.1. Possible Combinations for Cycloaddition Reactions of Conjugated Polyenes



$\sigma$  bonds. If it is assumed that the reactants approach one another face-to-face, as would be expected for reactions involving  $\pi$  orbitals, the requirement for bonding interactions between the HOMO and LUMO are met for  $[2 + 4]$  but not for  $[2 + 2]$  or  $[4 + 4]$  cycloadditions. (See Section 1.2 to review the MOs of conjugated systems.) More generally, systems involving  $4n + 2$   $\pi$  electrons are favorable (allowed), whereas systems with  $4n$   $\pi$  electrons are not.



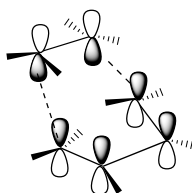
There is another aspect of cycloaddition TS structure that must be considered. It is conceivable that some systems might react through an arrangement with Möbius rather than Hückel topology (see p. 716). Möbius systems can also be achieved by addition to opposite faces of the  $\pi$  system. This mode of addition is called *antarafacial* and the face-to-face addition is called *suprafacial*. In order to specify the topology of cycloaddition reactions, subscripts *s* and *a* are added to the numerical classification. For systems of Möbius topology, as for aromaticity,  $4n$  combinations are favored and  $4n + 2$  combinations are unfavorable.<sup>4c</sup>



The generalized Woodward-Hoffmann rules for cycloaddition are summarized below.

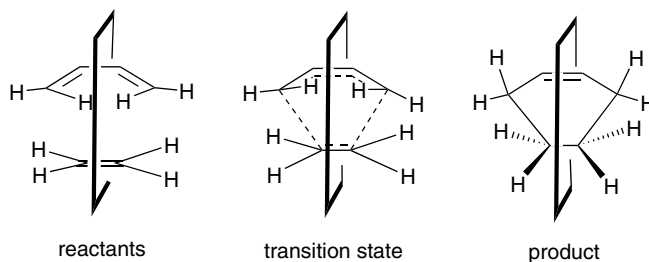
$m + n$	Orbital Symmetry Rules for $m + n$ Cycloaddition		
	Supra/supra	Supra/antara	Antara/antara
$4n$	Forbidden	Allowed	Forbidden
$4n + 2$	Allowed	Forbidden	Allowed

The selection rules for  $[\pi 4_s + \pi 2_s]$  and other cycloaddition reactions can also be derived from consideration of the aromaticity of the TS.<sup>4b,c</sup> In this approach, the basis set  $p$  orbitals are aligned to correspond with the orbital overlaps that occur in the TS. The number of nodes in the array of orbitals is counted. If the number is zero or even, the system is classified as a Hückel system. If the number is odd, it is a Möbius system. Just as was the case for ground state molecules (see p. 716), Hückel systems are stabilized with  $4n + 2$  electrons, whereas Möbius systems are stabilized with  $4n$  electrons. For the  $[\pi 4 + \pi 2]$  suprafacial-suprafacial cycloaddition the transition state is aromatic.



Basis set orbitals for *supra,supra*  $[\pi 2 + \pi 4]$  cycloaddition. Six electrons, zero nodes: aromatic

The orbital symmetry principles can also be applied by constructing an *orbital correlation diagram*.<sup>4a</sup> Let us construct a correlation diagram for the addition of butadiene and ethene to give cyclohexene. For concerted addition to occur, the diene must adopt an *s-cis* conformation. Because the electrons that are involved are the  $\pi$  electrons in both the diene and dienophile, the reaction occurs via a face-to-face rather than an edge-to-edge orientation. When this orientation of the reacting complex and TS is adopted, it can be seen that a plane of symmetry perpendicular to the planes of the reacting molecules is maintained during the course of the cycloaddition.



An orbital correlation diagram can be constructed by examining the symmetry of the reactant and product orbitals with respect to this plane, as shown in Figure 10.1. An additional feature must be taken into account in the case of cyclohexene. The cyclohexene orbitals  $\sigma_1$ ,  $\sigma_2$ ,  $\sigma_1^*$ , and  $\sigma_2^*$  are called *symmetry-adapted orbitals*. We might be inclined to think of the  $\sigma$  and  $\sigma^*$  orbitals as being localized between specific pairs of carbon atoms, but this is not the case for the MO treatment because localized

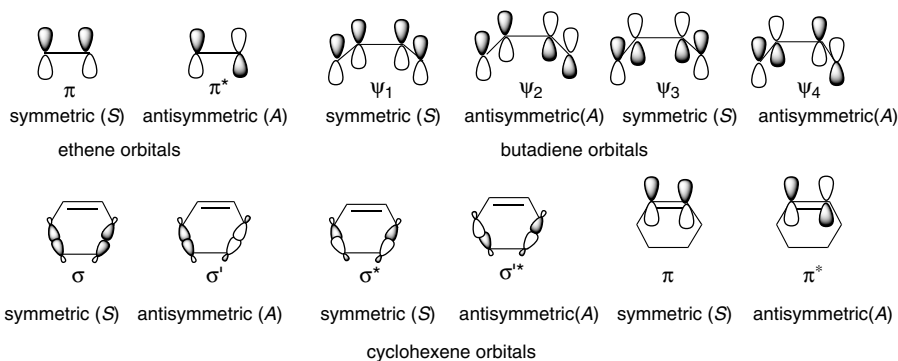


Fig. 10.1. Symmetry properties of ethene, butadiene, and cyclohexene orbitals with respect to a plane bisecting the reacting system.

orbitals would fail the test of being either symmetric or antisymmetric with respect to the plane of symmetry (see p. 37). In the construction of orbital correlation diagrams, *all* of the orbitals involved must be either symmetric or antisymmetric with respect to the element of symmetry being considered.

When the orbitals have been classified with respect to symmetry, they are arranged according to energy and the correlation lines are drawn as in Figure 10.2. From the orbital correlation diagram, it can be concluded that the thermal concerted cycloaddition reaction between butadiene and ethylene is allowed. All bonding levels of the reactants correlate with product ground state orbitals. Extension of orbital correlation analysis to cycloaddition reactions with other numbers of  $\pi$  electrons leads to the conclusion that suprafacial-suprafacial addition is allowed for systems with  $[4n + 2]$   $\pi$  electrons but forbidden for systems with  $4n$   $\pi$  electrons.

The frontier orbital analysis, basis set orbital aromaticity, and orbital correlation diagrams can be applied to a particular TS geometry to determine if the reaction is symmetry allowed. These three methods of examining TS orbital symmetry are equivalent and interchangeable. The orbital symmetry rules can be generalized from conjugated polyenes to any type of conjugated  $\pi$  system. Conjugated anions and cations such as allylic and pentadienyl systems fall within the scope of the rules. The orbital symmetry considerations can also be extended to isoelectronic systems

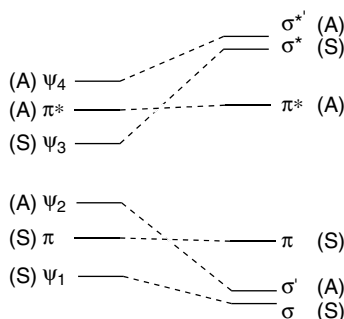
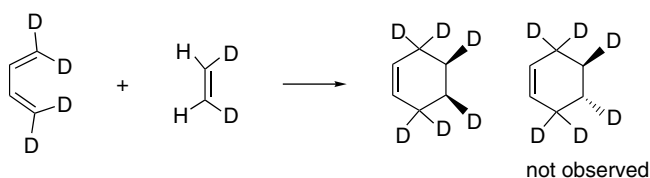


Fig. 10.2. Orbital symmetry correlation diagram for  $[\pi 2_s + \pi 4_s]$  cycloaddition of ethene and 1,3-butadiene.

## 10.2. The Diels-Alder Reaction

### 10.2.1. Stereochemistry of the Diels-Alder Reaction

The  $[\pi 4_s + \pi 2_s]$  cycloaddition of alkenes and dienes is a very useful method for forming substituted cyclohexenes. This reaction is known as the Diels-Alder (abbreviated D-A in this chapter) reaction.<sup>7</sup> The transition structure for a concerted reaction requires that the diene adopt the *s-cis* conformation. The diene and substituted alkene (called the *dienophile*) approach each other in approximately parallel planes. This reaction has been the object of extensive mechanistic and computational study, as well as synthetic application. For most systems, the reactivity pattern, regioselectivity, and stereoselectivity are consistent with a concerted process. In particular, the reaction is a stereospecific *syn* (suprafacial) addition with respect to both the alkene and the diene. This stereospecificity has been demonstrated with many substituted dienes and alkenes and also holds for the simplest possible example of the reaction, ethene with butadiene, as demonstrated by isotopic labeling.<sup>8</sup>



The issue of the concertedness of the D-A reaction has been studied and debated extensively. It has been argued that there might be an intermediate that is diradical in character.<sup>9</sup> D-A reactions are almost always stereospecific, which implies that if an intermediate exists, it cannot have a lifetime sufficient to permit rotation or inversion. The prevailing opinion is that the majority of D-A reactions are concerted reactions and most theoretical analyses agree with this view.<sup>10</sup> It is recognized that in reactions between unsymmetrical alkenes and dienes, bond formation might be more advanced at one pair of termini than at the other. This is described as being an *asynchronous*

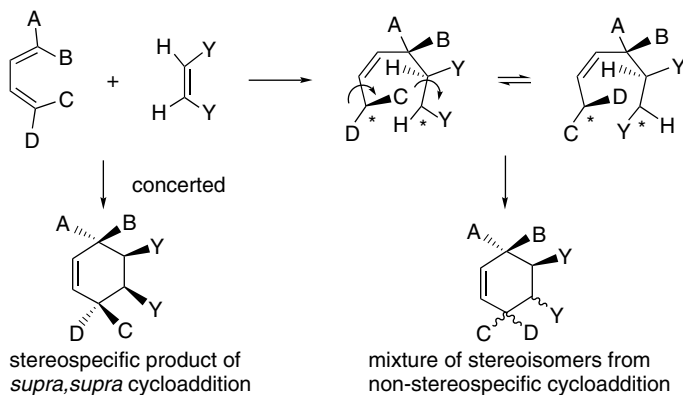
<sup>7</sup> L. W. Butz and A. W. Rytina, *Org. React.*, **5**, 136 (1949); M. C. Kloetzel, *Org. React.*, **4**, 1 (1948); A. Wasserman, *Diels-Alder Reactions*, Elsevier, New York (1965); R. Huisgen, R. Grashey, and J. Sauer, in *Chemistry of Alkenes*, S. Patai, ed., Interscience, New York, 1964, pp. 878–928; J. G. Martin and R. K. Hill, *Chem. Rev.*, **61**, 537 (1961); J. Hamer, ed., *1,4-Cycloaddition Reactions: The Diels-Alder Reaction in Heterocyclic Syntheses*, Academic Press, New York, 1967; J. Sauer and R. Sustmann, *Angew. Chem. Int. Ed. Engl.*, **19**, 779 (1980); R. Gleiter and M. C. Boehm, *Pure Appl. Chem.*, **55**, 237 (1983); R. Gleiter and M. C. Boehm, in *Stereochemistry and Reactivity of Systems Containing  $\pi$  Electrons*, W. H. Watson, ed., Verlag Chemie, Deerfield Beach, FL, 1983; F. Fringuelli and A. Taticchi, *The Diels-Alder Reaction: Selected Practical Methods*, Wiley, Chichester, 2002.

<sup>8</sup> K. N. Houk, Y.-T. Lin, and F. K. Brown, *J. Am. Chem. Soc.*, **108**, 554 (1986).

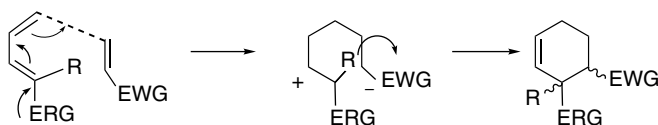
<sup>9</sup> M. J. S. Dewar, S. Olivella, and J. P. Stewart, *J. Am. Chem. Soc.*, **108**, 5771 (1986).

<sup>10</sup> J. J. Gajewski, K. B. Peterson, and J. R. Kagel, *J. Am. Chem. Soc.*, **109**, 5545 (1987); K. N. Houk, Y.-T. Lin, and F. K. Brown, *J. Am. Chem. Soc.*, **108**, 554 (1986); E. Goldstein, B. Beno, and K. N. Houk, *J. Am. Chem. Soc.*, **118**, 6036 (1996); V. Branchadell, *Int. J. Quantum Chem.*, **61**, 381 (1997).

process. Loss of stereospecificity is expected only if there is an intermediate in which one bond is formed and the other is not, permitting rotation or inversion at the unbound termini.

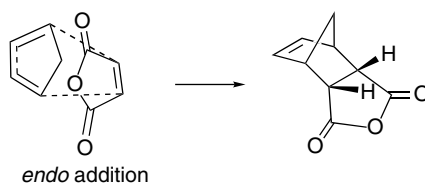


Loss of stereospecificity is observed when ionic intermediates are involved. This occurs when the reactants are of very different electronic character, with one being strongly electrophilic and the other strongly nucleophilic. Usually more than one substituent of each type is required for the ionic mechanism to occur.



For a substituted dienophile, there are two possible stereochemical orientations with respect to the diene. In the *endo* TS the reference substituent on the dienophile is oriented toward the  $\pi$  orbitals of the diene. In the *exo* TS the substituent is oriented away from the  $\pi$  system. The two possible orientations are called *endo* and *exo*, as illustrated in Figure 10.3.

For many substituted butadiene derivatives, the two TSs lead to two different stereoisomeric products. The *endo* mode of addition is usually preferred when an EWG substituent such as a carbonyl group is present on the dienophile. This preference is called the *Alder rule*. Frequently a mixture of both stereoisomers is formed and sometimes the *exo* product predominates, but the Alder rule is a useful initial guide to prediction of the stereochemistry of a D-A reaction. The *endo* product is often the more sterically congested. For example, the addition of dienophiles to cyclopentadiene usually favors the *endo*-stereoisomer, even though this is the sterically more congested product.



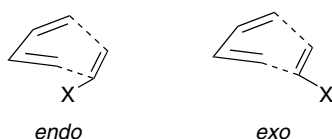
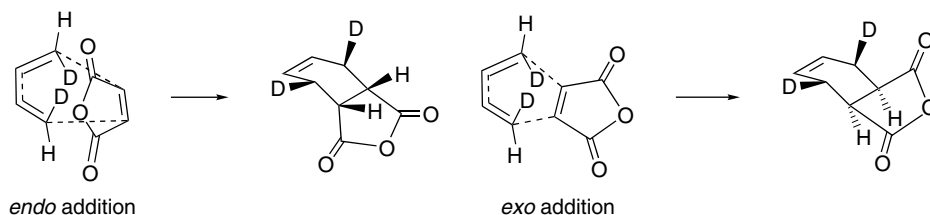
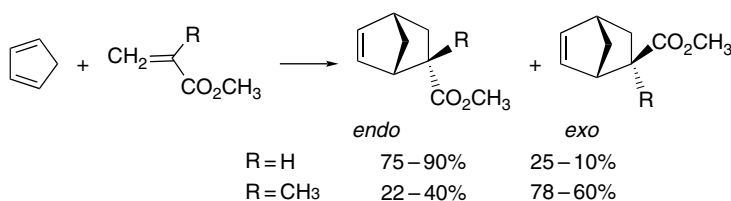


Fig. 10.3. *Exo* and *endo* transition structures for the Diels-Alder reaction.

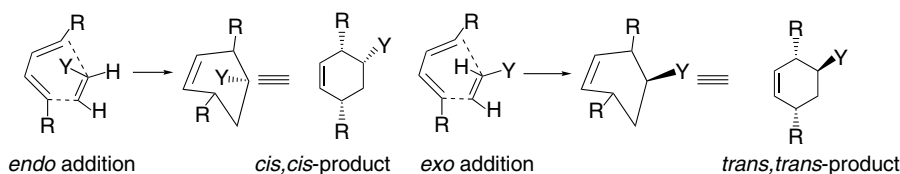
The preference for the *endo* mode of addition is not restricted to cyclic dienes such as cyclopentadiene. By using deuterium labels it has been shown that in the addition of 1,3-butadiene and maleic anhydride, 85% of the product arises from the *endo* TS.<sup>11</sup>



The stereoselectivity predicted by the Alder rule is independent of the requirement for suprafacial-suprafacial cycloaddition because both the *endo* and *exo* TSs meet this requirement. There are many exceptions to the Alder rule and in most cases the preference for the *endo* isomer is relatively modest. For example, although cyclopentadiene reacts with methyl acrylate in decalin solution to give mainly the *endo* adduct (75%), the ratio is solvent sensitive and ranges up to 90% *endo* in methanol. When a methyl substituent is added to the dienophile (methyl methacrylate) the *exo* product predominates.<sup>12</sup>



Stereochemical predictions based on the Alder rule are made by aligning the diene and dienophile in such a way that the unsaturated substituent on the dienophile overlaps the diene  $\pi$  system.



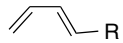
There are probably several factors that contribute to determining the *endo:exo* ratio in any specific case, including steric effects, electrostatic interactions, and London

<sup>11</sup> L. M. Stephenson, D. E. Smith, and S. P. Current, *J. Org. Chem.*, **47**, 4170 (1982).

<sup>12</sup> J. A. Berson, Z. Hamlet, and W. A. Mueller, *J. Am. Chem. Soc.*, **84**, 297 (1962).

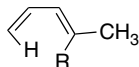
dispersion forces.<sup>13</sup> Molecular orbital interpretations emphasize *secondary orbital interactions* between the  $\pi$  orbitals on the dienophile substituent(s) and the developing  $\pi$  bond between C(2) and C(3) of the diene.

D-A cycloadditions are sensitive to steric effects. Bulky substituents on the dienophile or on the termini of the diene can hinder the approach of the two components to each other and decrease the rate of reaction. This effect can be seen in the relative reactivity of 1-substituted butadienes toward maleic anhydride.<sup>14</sup>

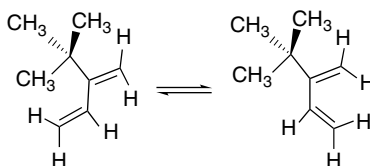
	R	$k_{\text{rel}}$ (25°C)
	H	1
	CH <sub>3</sub>	4.2
	C(CH <sub>3</sub> ) <sub>3</sub>	<0.05

Substitution of hydrogen by methyl results in a slight rate *increase* as a result of the electron-releasing effect of the methyl group. A *t*-butyl substituent produces a large rate *decrease* because the steric effect is dominant.

Another type of steric effect has to do with interactions between diene substituents. Adoption of the *s-cis* conformation of the diene in the TS brings the *cis*-oriented 1- and 4-substituents on diene close together. *trans*-1,3-Pentadiene is 10<sup>3</sup> times more reactive than 4-methyl-1,3-pentadiene toward the very reactive dienophile tetracyanoethene, owing to the unfavorable steric interaction between the additional methyl substituent and the C(1) hydrogen in the *s-cis* conformation.<sup>15</sup>

	R	$k_{\text{rel}}$
	H	1
	CH <sub>3</sub>	10 <sup>-3</sup>

Relatively small substituents at C(2) and C(3) of the diene exert little steric influence on the rate of D-A addition. 2,3-Dimethylbutadiene reacts with maleic anhydride about ten times faster than butadiene because of the electron-releasing effect of the methyl groups. 2-*t*-Butyl-1,3-butadiene is 27 times more reactive than butadiene. The *t*-butyl substituent favors the *s-cis* conformation because of the steric repulsions in the *s-trans* conformation.



<sup>13</sup> Y. Kobuke, T. Sugimoto, J. Furukawa, and T. Funco, *J. Am. Chem. Soc.*, **94**, 3633 (1972); K. L. Williamson and Y.-F. L. Hsu, *J. Am. Chem. Soc.*, **92**, 7385 (1970).

<sup>14</sup> D. Craig, J. J. Shipman, and R. B. Fowler, *J. Am. Chem. Soc.*, **83**, 2885 (1961).

<sup>15</sup> C. A. Stewart, Jr., *J. Org. Chem.*, **28**, 3320 (1963).

The presence of a *t*-butyl substituent on *both* C(2) and C(3), however, prevents attainment of the *s-cis* conformation, and D-A reactions of 2,3-di-(*t*-butyl)-1,3-butadiene have not been observed.<sup>16</sup>

### 10.2.2. Substituent Effects on Reactivity, Regioselectivity and Stereochemistry

There is a strong electronic substituent effect on the D-A cycloaddition. It has long been known that the reaction is particularly efficient and rapid when the dienophile contains one or more EWG and is favored still more if the diene also contains an ERG. Thus, among the most reactive dienophiles are quinones, maleic anhydride, and nitroalkenes.  $\alpha,\beta$ -Unsaturated esters, ketones, and nitriles are also effective dienophiles. The D-A reaction between unfunctionalized alkenes and dienes is quite slow. For example, the reaction of cyclopentadiene and ethene occurs at around 200°C.<sup>17</sup> These substituent effects are illustrated by the data in Table 10.1. In the case of the diene, reactivity is increased by ERG substituents. Data for some dienes are given in Table 10.2. Note that ERG substituents at C(1) have a larger effect than those at C(2). Scheme 10.2 gives some representative examples of dienophiles activated by EWG substitution.

It is significant that if an electron-poor diene is utilized, the preference is reversed and electron-rich alkenes, such as vinyl ethers and enamines, are the best dienophiles. Such reactions are called *inverse electron demand Diels-Alder reactions*, and the reactivity relationships are readily understood in terms of frontier orbital theory. Electron-rich dienes have high-energy HOMOs that interact strongly with the LUMOs of electron-poor dienophiles. When the substituent pattern is reversed and the diene is electron poor, the strongest interaction is between the dienophile HOMO and the diene LUMO. The FMO approach correctly predicts both the relative reactivity and regioselectivity of the D-A reaction for a wide range of diene-dienophile combinations.

**Table 10.1. Relative Reactivity toward Cyclopentadiene in the Diels-Alder Reaction**

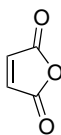
Dienophile	Relative rate <sup>a</sup>
Tetracyanoethene	43,000,000
1,1-Dicyanoethene	450,000
Maleic anhydride	56,000
<i>p</i> -Benzoquinone	9,000
<i>Z</i> -1,2-Dicyanoethene	91
<i>E</i> -1,2-Dicyanoethene	81
Dimethyl fumarate	74
Dimethyl maleate	0.6
Methyl acrylate	1.2
Cyanoethene	1.0

a. From second-order rate constants in dioxane at 20°C, as reported by J. Sauer, H. Wiest, and A. Mielert, *Chem. Ber.*, **97**, 3183 (1964).

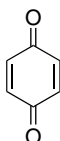
<sup>16</sup> H. J. Backer, *Rec. Trav. Chim. Pays-Bas*, **58**, 643 (1939).

<sup>17</sup> J. Meinwald and N. J. Hudak, *Org. Synth.*, **IV**, 738 (1963).

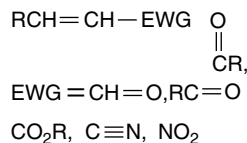
## A. Substituted Alkenes.

1<sup>a</sup>

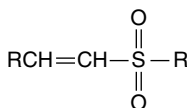
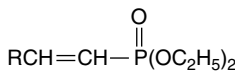
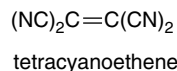
Maleic anhydride

1<sup>b</sup>

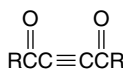
Benzoquinone

3<sup>c</sup>

$\alpha,\beta$ -unsaturated aldehydes,  
ketones, esters, nitriles and  
nitro compounds

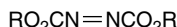
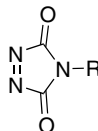
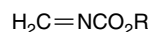
4<sup>d</sup> $\alpha,\beta$ -unsaturated  
sulfones5<sup>e</sup> $\alpha,\beta$ -unsaturated  
phosphonates6<sup>f</sup>

## B. Substituted Alkynes

7<sup>g</sup>Esters of acetylene-  
dicarboxylic acid8<sup>h</sup>Dibenzoyl-  
acetylene9<sup>i</sup>

Dicyanoethyne

## C. Heteroatomic dienophiles

10<sup>j</sup>Esters of azodicarboxylic  
acids11<sup>k</sup>*N*-substituted 1,2,4-  
triazoline-3,5-diones12<sup>l</sup>

iminocarbonates

a. M. C. Kloetzel, *Org. React.*, **4**, 1 (1948).b. L. W. Butz and A. W. Rytina, *Org. React.*, **5**, 136 (1949).c. H. L. Holmes, *Org. React.*, **4**, 60 (1948).d. J. C. Phillips and M. Oku, *J. Org. Chem.*, **37**, 4479 (1972).e. W. M. Daniewski and C. E. Griffin, *J. Org. Chem.*, **31**, 3236 (1966).f. E. Ciganek, W. J. Linn, and O. W. Webster, *The Chemistry of the Cyano Group*, Z. Rappoport, ed., John Wiley & Sons, New York, 1970, pp. 423–638.g. J. Sauer, H. Wiest, and A. Mielert, *Chem. Ber.*, **97**, 3183 (1964).h. J. D. White, M. E. Mann, H. D. Kirshenbaum, and A. Mitra, *J. Org. Chem.*, **36**, 1048 (1971).i. C. D. Weis, *J. Org. Chem.*, **28**, 74 (1963).j. B. T. Gillis and P. E. Beck, *J. Org. Chem.*, **28**, 3177 (1963).k. B. T. Gillis and J. D. Hagarty, *J. Org. Chem.*, **32**, 330 (1967).l. M. P. Cava, C. K. Wilkins, Jr., D. R. Dalton, and K. Bessho, *J. Org. Chem.*, **30**, 3772 (1965); G. Krow, R. Rodebaugh, R. Carmosin, W. Figures, H. Panella, G. De Vicaris, and M. Grippi, *J. Am. Chem. Soc.*, **95**, 5273 (1973).

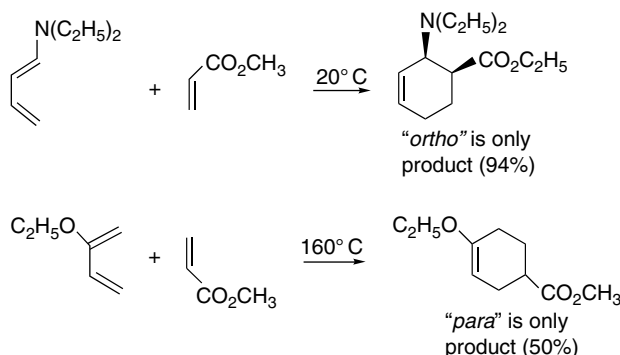
The question of regioselectivity arises when both the diene and alkene are unsymmetrically substituted. Generally, there is a preference for the “*ortho*” and “*para*” orientations, respectively, as in the examples shown.<sup>18</sup>

<sup>18</sup> J. Sauer, *Angew. Chem. Int. Ed. Engl.*, **6**, 16 (1967).

**Table 10.2. Relative Reactivity of Some Substituted Butadienes in the Diels-Alder Reaction<sup>a</sup>**

Diene Substituents	Dienophile	
	Tetracyanoethene	Maleic anhydride
None	1	1
1-Methyl	103	3.3
2-Methyl	45	2.3
1,4-Dimethyl	1,660	
1-Phenyl	385	1.65
2-Phenyl	191	8.8
1-Methoxy	50,900	12.4
2-Methoxy	1,750	
1,4-Dimethoxy	49,800	
Cyclopentadiene	2,100,000	1,350

a. C. Rücker, D. Lang, J. Sauer, H. Friege, and R. Sustmann, *Chem. Ber.*, **113**, 1663 (1980).



The regioselectivity of the D-A reaction is determined by the nature of the substituents on the diene and dienophile. FMO theory has been applied by calculating the energy and orbital coefficients of the frontier orbitals.<sup>19</sup> When the dienophile bears an EWG and the diene an ERG, the strongest interaction is between the HOMO of the diene and the LUMO of the dienophile, as indicated in Figure 10.4. The reactants are preferentially oriented with the carbons having the highest coefficients of the two frontier orbitals aligned for bonding. Scheme 10.3 shows the preferred regiochemistry for various substitution patterns. The combination of an electron donor in the diene and an electron acceptor in the dienophile gives rise to cases **A** and **B**. Inverse electron demand D-A reactions give rise to combinations **C** and **D**. In reactions of types **A** and **B**, the frontier orbitals will be the diene HOMO and the dienophile LUMO. The strongest interaction is between  $\psi_2$  and  $\pi^*$  because the donor substituent on the diene raises the diene orbitals in energy, whereas the acceptor substituent lowers the dienophile orbitals. In reaction types **C** and **D**, the pairing of the diene LUMO and dienophile HOMO is the strongest interaction.

The regiochemical relationships summarized in Scheme 10.3 can be understood by considering the atomic coefficients of the frontier orbitals. Figure 10.5 gives the approximate energies and orbital coefficients for the various classes of dienes and dienophiles. 1-ERG substituents (X:) raise the HOMO level and increase the coefficient

<sup>19</sup> K. N. Houk, *J. Am. Chem. Soc.*, **95**, 4092 (1973).

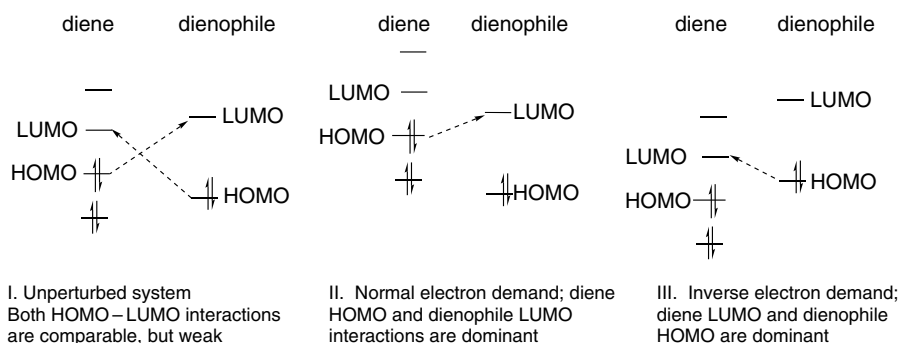
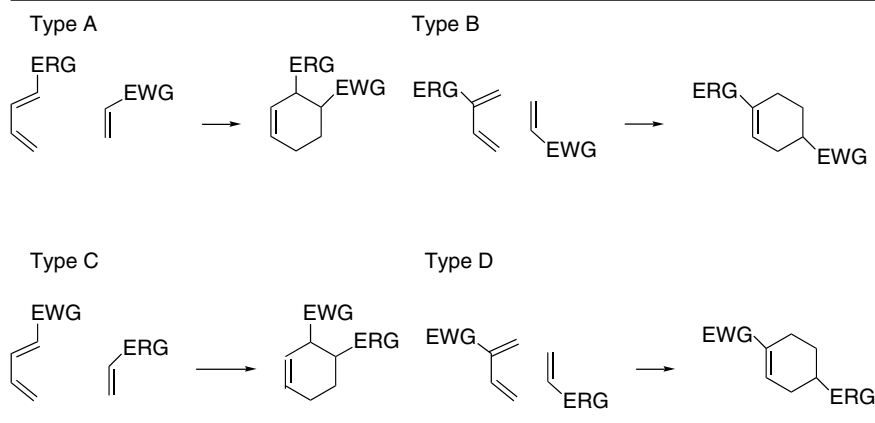


Fig. 10.4. Frontier orbital interactions in Diels-Alder reactions.

on C(4) of the diene. 2-ERG substituents raise the HOMO and result in the largest HOMO coefficient at C(1). For EWG substituents, the HOMO and LUMO are lowered in energy. For dienophiles, the largest LUMO coefficient is at C(2).

The regiochemistry can be predicted by the generalization that the strongest interaction is between the centers on the frontier orbitals having the largest orbital coefficients. For dienophiles with EWG substituents,  $\pi^*$  has its largest coefficient on the  $\beta$ -carbon atom. For dienes with ERG substituents at C(1) of the diene, the HOMO has its largest coefficient at C(4). This is the case designated **A** in Scheme 10.3, and is the observed regiochemistry for the type **A** Diels-Alder addition. A similar analysis of each of the other combinations in Scheme 10.3 using the orbitals in Figure 10.5 leads to the prediction of the favored regiochemistry. Note that in the type **A** and **C** reactions this leads to preferential formation of the more sterically congested 1,2-disubstituted cyclohexene. The predictive capacity of these frontier orbital relationships for D-A reactions is excellent.<sup>20</sup>

## Scheme 10.3. Regioselectivity of the Diels-Alder Reaction



<sup>20</sup> For discussion of the development and application of frontier orbital concepts in cycloaddition reactions, see K. N. Houk, *Acc. Chem. Res.*, **8**, 361 (1975); K. N. Houk, *Topics Current Chem.*, **79**, 1 (1979); R. Sustmann and R. Schubert, *Angew. Chem. Int. Ed. Engl.*, **11**, 840 (1972); J. Sauer and R. Sustmann, *Angew. Chem. Int. Ed. Engl.*, **19**, 779 (1980).

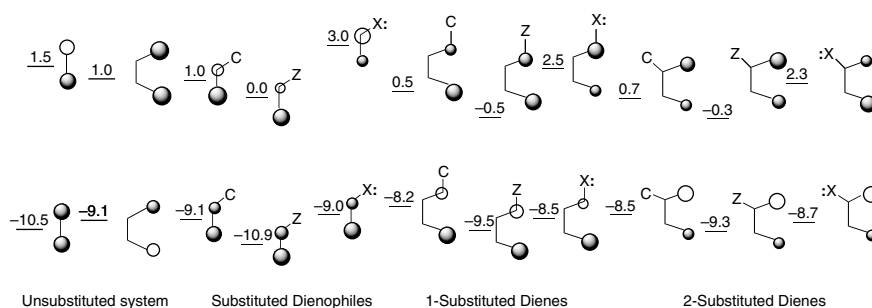


Fig. 10.5. Coefficients and relative energies of dienophile and diene frontier MOs. Orbital energies are given in eV. The sizes of the circles give a relative indication of the orbital coefficient. Z stands for a conjugated EWG, e.g., C=O, C≡N, NO<sub>2</sub>; C is a conjugated substituent without strong electronic effect, e.g., phenyl, vinyl; X is a conjugated ERG, e.g., OCH<sub>3</sub>, NH<sub>2</sub>. From *J. Am. Chem. Soc.*, **95**, 4092 (1973).

From these ideas, we see that for substituted dienes and dienophiles there is *charge transfer* in the process of formation of the TS. The more electron-rich reactant acts as an electron donor (*nucleophilic*) and the more electron-poor reactant accepts electron density (*electrophilic*). It also seems from the data in Tables 10.1 and 10.2 that reactions are faster, the *greater the extent of charge transfer*. The reactivity of cyclopentadiene increases with the electron-acceptor capacity of the dienophile. Note also that the very strongly electrophilic dienophile, tetracyanoethene, is more sensitive to substituent effects in the diene than the more moderately electrophilic dienophile, maleic anhydride. These relationships can be understood in terms of FMO theory by noting that the electrophile LUMO and nucleophile HOMO *are closer in energy the stronger the substituent effect*, as illustrated schematically in Figure 10.6.

The FMO considerations are most reliable when one component is clearly more electrophilic and the other more nucleophilic. When a diene with a 2-EWG substituent

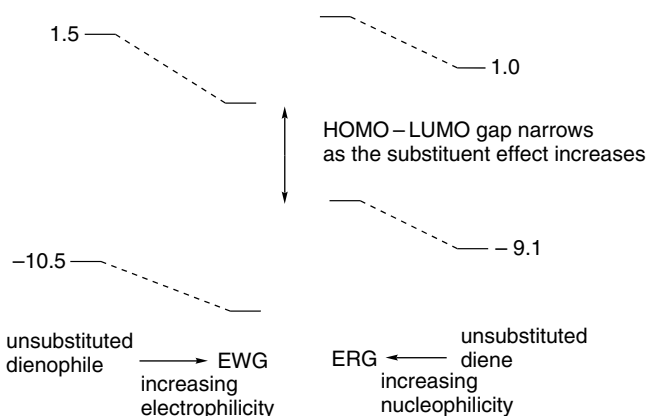
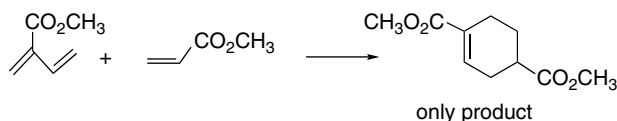
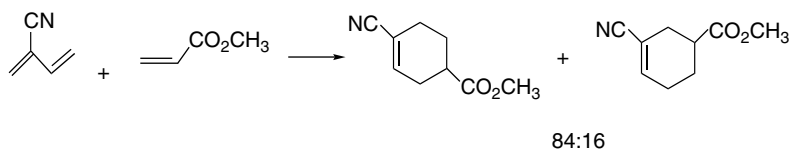


Fig. 10.6. Schematic diagram illustrating substituent effect on reactivity in terms of FMO theory. HOMO-LUMO gap narrows, transition state is stabilized, and reactivity is increased in normal electron-demand Diels-Alder reaction as the nucleophilicity of diene and the electrophilicity of dienophile increase.

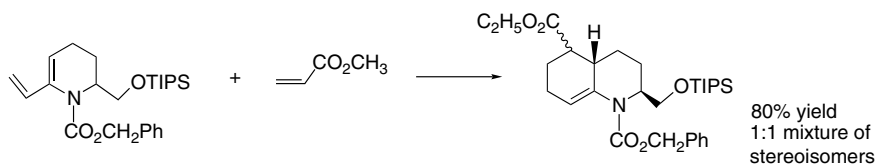
reacts with an electrophilic dienophile, the major product is the *para* product, even though simple resonance consideration would suggest that the *meta* product might be preferred.



Ref. 21

Ref. 22

Another case that goes contrary to simple resonance or FMO predictions are reactions of 2-amido-1,3-dienes. The main product has a *meta* rather than a *para* orientation. These reactions also show little *endo:exo* stereoselectivity.

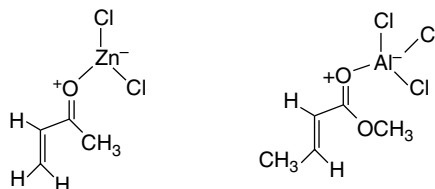


Ref. 23

Thus, there seems to be reason for caution in application of simple resonance or FMO predictions to 2-substituted dienes. We say more about this Topic 10.1.

### 10.2.3. Catalysis of Diels-Alder Reactions by Lewis Acids

Diels-Alder reactions are catalyzed by many Lewis acids, including  $\text{SnCl}_4$ ,  $\text{ZnCl}_2$ ,  $\text{AlCl}_3$ , and derivatives of  $\text{AlCl}_3$  such as  $(\text{CH}_3)_2\text{AlCl}$  and  $(\text{C}_2\text{H}_5)_2\text{AlCl}$ .<sup>24</sup> A variety of other Lewis acids are effective catalysts. The types of dienophiles that are subject to catalysis are typically those with carbonyl substituents. Lewis acids form complexes at the carbonyl oxygen and this increases the electron-withdrawing capacity of the carbonyl group. The basic features are well modeled by HF/3-21G level computations on the TS structures.<sup>25</sup>



<sup>21</sup> T. Inukai and T. Kojima, *J. Org. Chem.*, **36**, 924 (1971).

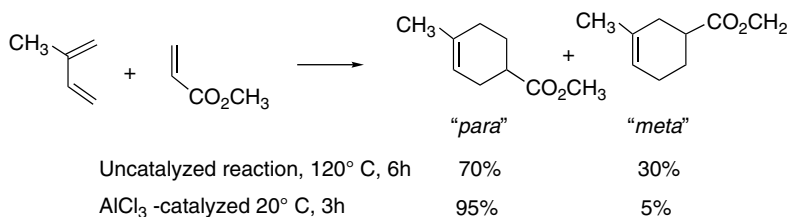
<sup>22</sup> C. Spino, J. Crawford, Y. Cui, and M. Gugelchuk, *J. Chem. Soc., Perkin Trans. 2*, 1499 (1998).

<sup>23</sup> J. D. Ha, C. H. Kang, K. A. Belmore, and J. K. Cha, *J. Org. Chem.*, **63**, 3810 (1998).

<sup>24</sup> P. Laszlo and J. Lucche, *Actual. Chim.*, 42 (1984).

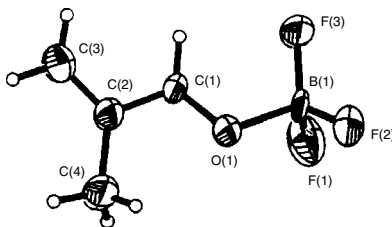
<sup>25</sup> D. M. Birney and K. N. Houk, *J. Am. Chem. Soc.*, **112**, 4127 (1990); M. I. Menendez, J. Gonzalez, J. A. Sordo, and T. L. Sordo, *Theochem*, **120**, 241 (1994).

This complexation accentuates both the energy and orbital distortion effects of the substituent and enhances both the reactivity and selectivity of the dienophile relative to the uncomplexed compound.<sup>26</sup> Usually, both regioselectivity and *exo,endo* stereoselectivity increase. Part of this may be due to the lower reaction temperature. However, the catalysts also shift the reaction toward a higher degree of charge transfer by making the EWG substituent more electrophilic.

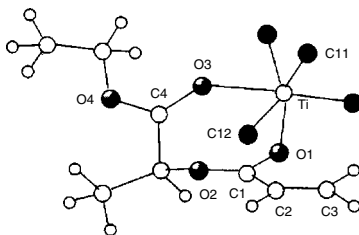


Ref. 27

The stereoselectivity of any particular D-A reaction depends on the details of the TS structure. The structures of several enone–Lewis acid complexes have been determined by X-ray crystallography.<sup>28</sup> The site of complexation is the carbonyl oxygen, which maintains a trigonal geometry, but with somewhat expanded angles (130°–140°). The Lewis acid is normally *anti* to the larger carbonyl substituent. Boron trifluoride complexes are tetrahedral, but Sn(IV) and Ti(IV) complexes can be trigonal bipyramidal or octahedral. The structure of the 2-methylpropenal–BF<sub>3</sub> complex is illustrative.<sup>29</sup>



Chelation can favor a particular structure. For example, *O*-acryloyl lactates adopt a chelated structure with TiCl<sub>4</sub>.<sup>30</sup>



<sup>26</sup> K. N. Houk and R. W. Strozier, *J. Am. Chem. Soc.*, **95**, 4094 (1973).

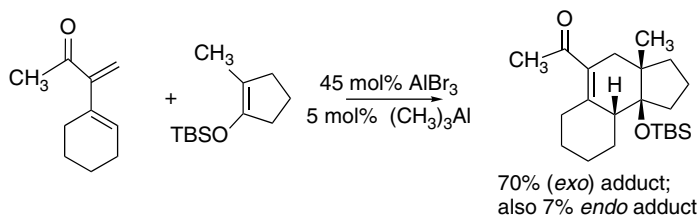
<sup>27</sup> T. Inukai and T. Kojima, *J. Org. Chem.*, **31**, 1121 (1966).

<sup>28</sup> S. Shambayati, W. E. Crowe, and S. L. Schreiber, *Angew. Chem. Int. Ed. Engl.*, **29**, 256 (1990).

<sup>29</sup> E. J. Corey, T.-P. Loh, S. Sarshar, and M. Azimioara, *Tetrahedron Lett.*, **33**, 6945 (1992).

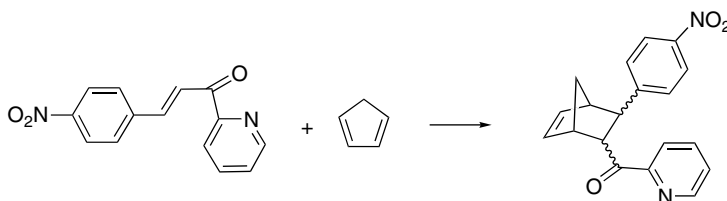
<sup>30</sup> T. Poll, J. O. Metter, and G. Helmchen, *Angew. Chem. Int. Ed. Engl.*, **24**, 112 (1985).

Lewis acid catalysis can also be applied to inverse electron demand D-A reactions, but with the proviso that the strongest interaction must be with the diene in this case.



Ref. 31

Metal cations can catalyze reactions of certain dienophiles. For example,  $\text{Cu}^{2+}$  strongly catalyzes addition reactions of 2-pyridyl styryl ketones, presumably through a chelate.<sup>32</sup> DFT (B3LYP/6-31G\*) computations indicate that this reaction shifts to a stepwise ionic mechanism in the presence of the Lewis acid.<sup>33</sup>



Solvent	Rate ( $M^{-1}s^{-1}$ )	Relative Rate
Acetonitrile	$1.3 \times 10^{-5}$	1
Ethanol	$3.8 \times 10^{-5}$	2.9
Water	$4.0 \times 10^{-5}$	310
Water + 0.01 M $\text{Cu}(\text{NO}_3)_2$	3.25	250,000

The solvent also has an important effect on the rate of D-A reactions. The traditional solvents were nonpolar organic solvents such as aromatic hydrocarbons. However, water and other highly polar solvents, such as ethylene glycol and formamide, accelerate a number of D-A reactions.<sup>34</sup> The accelerating effect of water is attributed to “enforced hydrophobic interactions.”<sup>35</sup> That is, the strong hydrogen-bonding network in water tends to exclude nonpolar solutes and forces them together, resulting in higher effective concentrations. There may also be specific stabilization of the developing TS.<sup>36</sup> For example, hydrogen bonding with the TS can contribute to the rate acceleration.<sup>37</sup>

<sup>31</sup> M. E. Jung and P. Davidov, *Angew. Chem. Int. Ed. Engl.*, **41**, 4125 (2002).

<sup>32</sup> S. Otto and J. B. F. N. Engberts, *Tetrahedron Lett.*, **36**, 2645 (1995).

<sup>33</sup> L. R. Domingo, J. Andres, and C. N. Alves, *Eur. J. Org. Chem.*, 2557 (2002).

<sup>34</sup> D. Rideout and R. Breslow, *J. Am. Chem. Soc.*, **102**, 7816 (1980); R. Breslow and T. Guo, *J. Am. Chem. Soc.*, **110**, 5613 (1988); T. Dunams, W. Hoekstra, M. Pentaleri, and D. Liotta, *Tetrahedron Lett.*, **29**, 3745 (1988).

<sup>35</sup> S. Otto and J. B. F. N. Engberts, *Pure Appl. Chem.*, **72**, 1365 (2000).

<sup>36</sup> R. Breslow and C. J. Rizzo, *J. Am. Chem. Soc.*, **113**, 4340 (1991).

<sup>37</sup> W. Blokzijl, M. J. Blandamer, and J. B. F. N. Engberts, *J. Am. Chem. Soc.*, **113**, 4241 (1991); W. Blokzijl and J. B. F. N. Engberts, *J. Am. Chem. Soc.*, **114**, 5440 (1992); S. Otto, W. Blokzijl, and J. B. F. N. Engberts, *J. Org. Chem.*, **59**, 5372 (1994); A. Meijer, S. Otto, and J. B. F. N. Engberts, *J. Org. Chem.*, **65**, 8989 (1998); S. Kong and J. D. Evanseck, *J. Am. Chem. Soc.*, **122**, 10418 (2000).

The idea of complementary electronic interactions between the diene and dienophile provides a reliable qualitative guide to the regio- and stereoselectivity of the D-A reaction. Structural and substituent effects can be explored in more detail by computational analysis of TS structure and energy. Comparison of the relative energy of competing TSs allows prediction and interpretation of the course of the reaction. Ab initio HF calculations often can be relied on to give the correct order of isomeric TS structures. Accurate  $E_a$  estimates require a fairly high-level treatment of electron correlation. Reliable results have been achieved with B3LYP/6-31G\*, MP3/6-31G\*, and CCSD(T)/6-31G\* computations.<sup>38</sup> These calculations permit prediction and interpretation of relative reactivity and regio- and stereoselectivity by comparison of competing TSs. There are other aspects of TS character that can be explored, including the degree of asynchronicity in bond formation and the nature of the electronic reorganization within the TS. Kinetic isotope effects can be calculated from the TS and provide a means of validation of TS characteristics by comparison with experimental results.<sup>39</sup>

A range of quantum chemical computations were applied to Diels-Alder reactions as the methods were developed. The consensus that emerged is illustrated by typical recent studies.<sup>25,40</sup> For symmetrical dienes and dienophiles without strong EWG substituents, the reaction is *synchronous*, that is the degree of bond making of the C(1)–C(1') and C(4)–C(2') bonds is the same. As we will see shortly, this does not always seem to be the case for strongly electrophilic dienophiles, even when they are symmetric. The TS displays aromaticity, as indicated by the computed NICS value (see Section 8.1.3),<sup>41</sup> which implies that there is enhanced delocalization of the six electrons that participate in bonding changes. Fradera and co-workers have used the AIM localization and delocalization parameters  $\lambda$  and  $\delta$  to investigate the electron distribution in the TS for ethene/butadiene cycloaddition.<sup>42</sup> At the HF/6-31G\* level, the delocalization indices are about 0.4 for all the reacting bonds (plus 1.0 for the residual bonds). There is stronger delocalization between the *para* than the *meta* positions. Both of these parameters are very similar to those found for benzene.<sup>43</sup> These similarities support the idea that the electronic distribution in the TS for the D-A reaction resembles that of the  $\pi$  system of benzene, an idea that goes back to the 1930s.<sup>44</sup>

<sup>38</sup> T. C. Dinadayalane, R. Vijaya, A. Smitha, and G. N. Sastry, *J. Phys. Chem. A*, **106**, 1627 (2002); B. R. Beno, S. Wilsey, and K. N. Houk, *J. Am. Chem. Soc.*, **121**, 4816 (1999).

<sup>39</sup> B. R. Beno, K. N. Houk, and D. A. Singleton, *J. Am. Chem. Soc.*, **118**, 9984 (1996); E. Goldstein, B. Beno, and K. N. Houk, *J. Am. Chem. Soc.*, **118**, 6036 (1996).

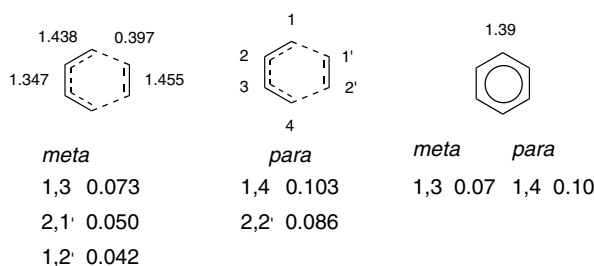
<sup>40</sup> S. Sakai, *J. Phys. Chem. A*, **104**, 922 (2000); R. D. J. Froese, J. M. Coxon, S. C. West, and K. Morokuma, *J. Org. Chem.*, **62**, 6991 (1997).

<sup>41</sup> H. Jiao and P. v. R. Schleyer, *J. Phys. Org. Chem.*, **11**, 655 (1998).

<sup>42</sup> J. Poater, M. Sola, M. Duran, and X. Fradera, *J. Phys. Chem. A*, **105**, 2052 (2001).

<sup>43</sup> X. Fradera, M. A. Austen, and R. F. W. Bader, *J. Phys. Chem. A*, **103**, 304 (1999).

<sup>44</sup> M. G. Evans, *Trans. Faraday Soc.*, **35**, 824 (1939).



The TS of D-A reactions can also be characterized with respect to *synchronicity*. If both new bonds are formed to the same extent the reaction is synchronous, but if they differ it is asynchronous. Synchronicity has been numerically defined in terms of Wiberg bond order indices.<sup>45</sup>

$$S_y^1 = 1 - \frac{\sum_{i=1}^n |\delta B_i - \delta B_{av}|}{2n - 2} \delta B_{av} \quad (10.1)$$

where  $n$  is the number of bonds directly involved in the reaction,  $\delta B_i$  is the relative variation in the  $B_i$  at the TS. The terms  $\delta B_i$  and  $\delta B_{av}$  are defined as follows:

$$\delta B_i = \frac{B_i^{TS} - B_i^R}{B_i^P - B_i^R} \quad (10.2)$$

$$\delta B_{av} = n^{-1} \sum_{i=1}^n \delta B_i \quad (10.3)$$

Computations have also been applied to the analysis of *exo:endo* ratios. The computed differences in energies of the *exo* and *endo* TS are often small and are subject to adjustments when solution models are used.<sup>46</sup> Cyclopentadiene has been a common subject, since there is more experimental data for this compound than for any other. MP3/6-31G\*-level computations were used to compare the *exo* and *endo* TS  $E_a$  for the reactions with acrylonitrile and but-2-en-3-one (methyl vinyl ketone), and ZPE and thermal corrections were included in the calculations.<sup>47</sup> Good qualitative agreement was achieved with the experimental results, which is little stereoselectivity for acrylonitrile and *endo* stereoselectivity for but-3-en-2-one.

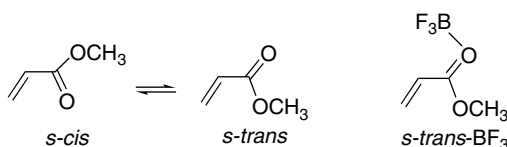
	Acrylonitrile		But-3-en-2-one	
	$E_a$	$\Delta G^\ddagger$	$E_a$	$G^\ddagger$
<i>exo</i>	18.49	31.72	16.16	29.86
<i>endo</i>	18.53	31.69	15.92	29.42
Difference	-0.04	+0.03	+0.24	+0.44

<sup>45</sup> A. Moyano, M. A. Pericas, and E. Valenti, *J. Org. Chem.*, **54**, 573 (1989); B. Lecea, A. Arrieta, G. Roa, F. P. Ugalde, and F. P. Cossio, *J. Am. Chem. Soc.*, **116**, 9613 (1994).

<sup>46</sup> M. F. Ruiz-Lopez, X. Assfeld, J. I. Garcia, J. A. Mayoral, and L. Salvatella, *J. Am. Chem. Soc.*, **115**, 8780 (1993).

<sup>47</sup> W. L. Jorgensen, D. Lim, and J. F. Blake, *J. Am. Chem. Soc.*, **115**, 2936 (1993).

Computational studies have revealed some of the distinctive effects of Lewis acid catalysis on TS structure. MO (HF/6-31G\*, MP2/6-31G\*) and DFT (B3LYP/6-311+G(2d,p)) calculations have been used to compare the structure and energy of four possible TSs for the D-A reaction of the BF<sub>3</sub> complex of methyl acrylate with 1,3-butadiene. The results are summarized in Figure 10.7. The uncatalyzed reaction favors the *exo-cis* TS by 0.38 kcal/mol over the *endo-cis* TS. For the catalyzed reaction, the *endo* TS with the *s-trans* conformation of the dienophile is preferred to the two *exo* TSs by about 0.8 kcal/mol.<sup>48</sup> Part of the reason for the shift in preferred TS is the difference in the ground state dienophile conformation. The *s-trans* conformation minimizes repulsions with the BF<sub>3</sub> group. There is also a significant difference in the degree of charge transfer between the uncatalyzed and catalyzed reactions, as reflected by the NPA  $\delta$  values. The catalyzed reaction has a much larger net transfer of electron density to the dienophile. The catalyzed reactions are less synchronous than the uncatalyzed reactions, as can be seen by comparing the differences in the lengths of the forming bonds.



Relative Transition State Energies					
Uncatalyzed reaction			BF <sub>3</sub> -catalyzed reaction		
	Rel <i>E</i>	NPA $\delta$		Rel <i>E</i>	NPA $\delta$
<i>s-cis</i> Acrylate	0.00	–	<i>s-cis</i> Acrylate-BF <sub>3</sub>	1.71	–
<i>s-trans</i> Acrylate	0.65	–	<i>s-trans</i> Acrylate-BF <sub>3</sub>	0.00	–
<i>endo-cis</i> TS	0.38	0.005	<i>endo-cis</i> BF <sub>3</sub> TS	2.23	0.276
<i>endo-trans</i> TS	1.65	0.005	<i>endo-trans</i> BF <sub>3</sub> TS	0.00	0.225
<i>exo-cis</i> TS	0.00	0.006	<i>exo-cis</i> BF <sub>3</sub> TS	0.82	0.260
<i>exo-trans</i> TS	1.44	0.006	<i>exo-trans</i> BF <sub>3</sub> TS	0.83	0.216

**Visual models, additional information and exercises on the Diels-Alder Reaction can be found in the Digital Resource available at: [Springer.com/carey-sundberg](http://Springer.com/carey-sundberg).**

Similar calculations have been done for propenal.<sup>49</sup> For the uncatalyzed reaction, the *endo-cis* TS is slightly favored over the *exo-cis*; the two *trans* TSs are more than 1 kcal/mol higher. The order is the same for the catalyzed reaction, but the differences are accentuated. The TSs for the catalyzed reactions are considerably more asynchronous than those for the uncatalyzed reactions. For example, for the reaction of butadiene and acrolein, the asynchronicity was measured as the difference in bond length of the two forming bonds.

$$\Delta d = [C(1)-C(1'')] - [C(4)-C(2')]$$

<sup>48</sup> J. I. Garcia, J. A. Mayoral, and L. Salvatella, *Tetrahedron*, **53**, 6057 (1997).

<sup>49</sup> J. I. Garcia, J. A. Mayoral, and L. Salvatella, *J. Am. Chem. Soc.*, **118**, 11680 (1996); J. I. Garcia, V. Martinez-Merino, J. A. Mayoral, and L. Salvatella, *J. Am. Chem. Soc.*, **120**, 2415 (1998).

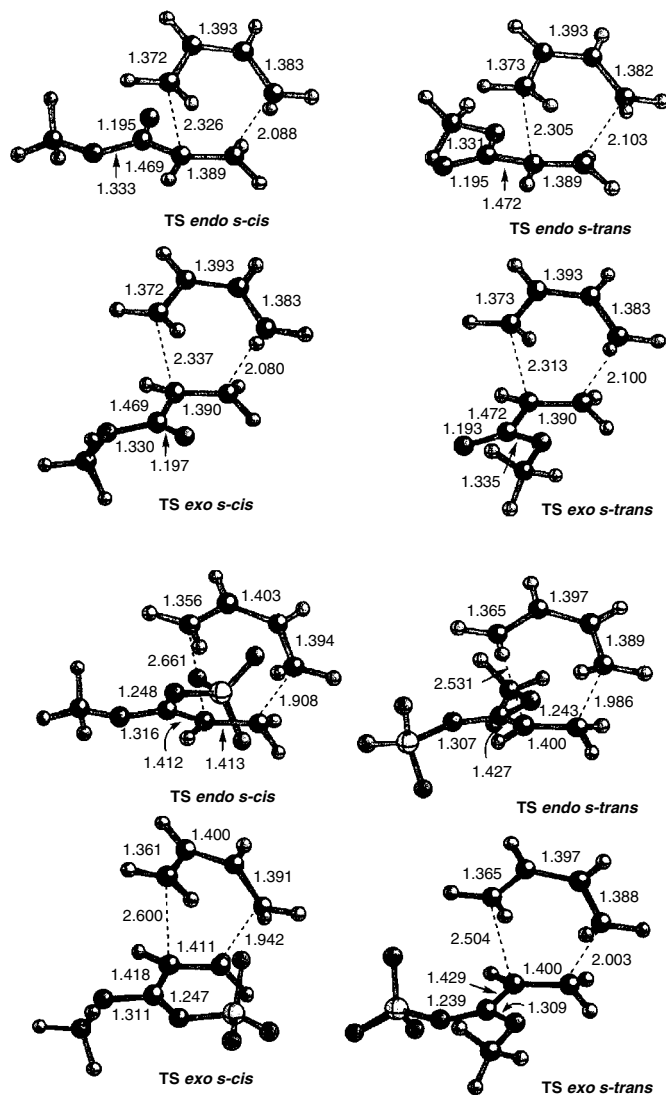


Fig. 10.7. Computed transition structures for uncatalyzed and  $\text{BF}_3$ -catalyzed Diels-Alder reaction of 1,3-butadiene with methyl acrylate. Reproduced from *Tetrahedron*, **53**, 6057 (1997), by permission of Elsevier.

The value of  $\Delta d$  increases from 0.617 to 0.894 going from the uncatalyzed to the  $\text{BF}_3$ -catalyzed reaction.

Another feature of the catalyzed TS is stronger interaction between the diene and the complexed EWG by a type of secondary orbital interaction. For example, in the butadiene-acrolein/ $\text{BH}_3$  catalytic complex,<sup>50</sup> there is a quite close approach of diene C(1) to the complexed carbonyl carbon.<sup>51</sup> This aspect of the TS was examined for the  $\text{BF}_3$ -catalyzed reaction by comparing the electron density between C(1) and

<sup>50</sup> D. M. Birney and K. N. Houk, *J. Am. Chem. Soc.*, **112**, 4127 (1990).

<sup>51</sup> D. A. Singleton, *J. Am. Chem. Soc.*, **114**, 6563 (1992).

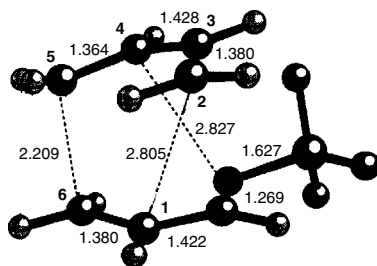
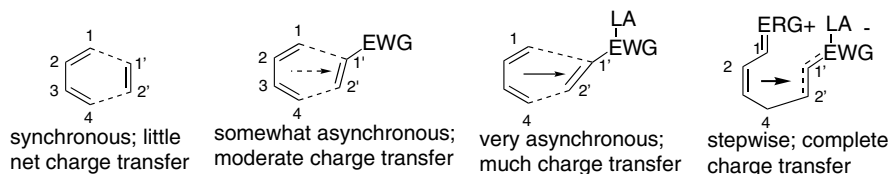


Fig. 10.8. Secondary orbital interaction between carbonyl oxygen and butadiene in  $\text{BF}_3$ -catalyzed transition structure. Reproduced from *J. Am. Chem. Soc.*, **120**, 2415 (1998), by permission of the American Chemical Society.

the carbonyl carbon as shown in Figure 10.8. Significant bonding was noted and is represented by the second dashed line in the TS structure.<sup>49</sup>

The extent of this interaction is different in the *endo* and *exo* TSs and contributes to the enhanced *endo* stereoselectivity that is observed in catalyzed reactions. This structural feature is consistent with the catalyzed reaction having more extensive charge transfer, owing to the more electrophilic character of the complexed dienophile. In the limiting case, the reaction can become a stepwise ionic process.



One might expect that a D-A reaction of butadiene with any *symmetrical* dienophile would have a synchronous TS, since the new bonds that are being formed are *identical*. However, that does not seem to be the case, at least for highly electrophilic dienophiles. For example, highly asynchronous TSs are found for maleic acid<sup>52</sup> and 1,2,4-triazoline, as shown in Figure 10.9.<sup>53</sup>

There is, however, disagreement in the case of the results for another very reactive dienophile, dimethyl acetylenedicarboxylate. Froese and co-workers also found the TS of cyclopentadiene and dimethyl acetylenedicarboxylate to be unsymmetrical by B3LYP/6-31G computation,<sup>54</sup> but another group discovered that a symmetrical TS was favored for 1,3-butadiene.<sup>55</sup> These unsymmetrical TSs seem to reflect the same trend noted in comparing Lewis acid-catalyzed reactions with uncatalyzed reactions.

<sup>52</sup> D. A. Singleton, B. E. Schulmeier, C. Hang, A. A. Thomas, S.-W. Leung, and S. R. Merrigan, *Tetrahedron*, **57**, 5149 (2001).

<sup>53</sup> J. S. Chen, K. N. Houk, and C. S. Foote, *J. Am. Chem. Soc.*, **120**, 12303 (1998).

<sup>54</sup> R. D. J. Froese, J. M. Coxon, S. C. West, and K. Morokuma, *J. Org. Chem.*, **62**, 6991 (1997).

<sup>55</sup> L. R. Domingo, M. Arno, R. Contreras, and P. Perez, *J. Phys. Chem. A*, **106**, 952 (2002).

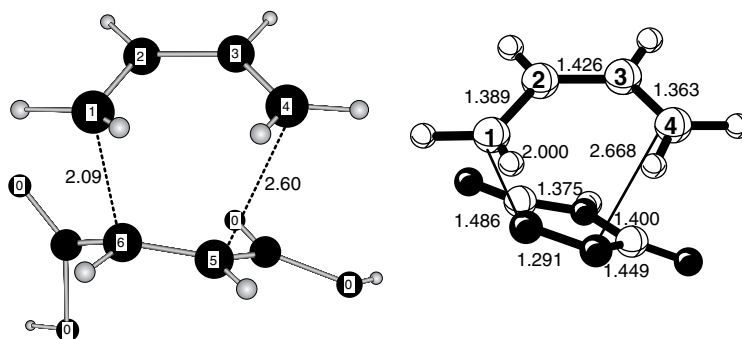
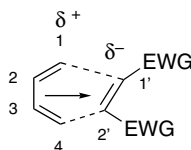
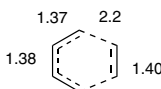


Fig. 10.9. Asynchronous transition structures for Diels-Alder reactions of butadiene with maleic acid and 1,2,4-triazoline using B3LYP/6-31G\* calculations. Reproduced from *Tetrahedron*, **57**, 5149 (2001) and *J. Am. Chem. Soc.*, **120**, 12303 (1998), by permission of Elsevier and the American Chemical Society, respectively.

The asynchronous TS results from an increase in the extent of charge transfer, leading to partial ionic character in the TS.



There seems to be another element of asynchronicity associated with bond formation in D-A reactions. The formation of the new double bond and the lengthening of the reacting dienophile bond seem to *run ahead* of the formation of the new  $\sigma$  bonds. For example, in the MP4SDTQ/6-31G\* TS for the reaction of butadiene and ethene, the new  $\sigma$  bonds are only 22% formed at the TS. The same picture emerges by following the transformations of the orbitals during the course of the reaction.<sup>56</sup> The transfer of  $\pi$ -electronic characteristics from the dienophile  $\pi$  bond to the product  $\pi$  bond seems to occur ahead of the reorganization of electrons to form the two new  $\sigma$  bonds.



**Visual models, additional information and exercises on the Diels-Alder Reaction can be found in the Digital Resource available at: [Springer.com/carey-sundberg](http://Springer.com/carey-sundberg).**

A wide variety of diene substituents were surveyed using B3LYP/6-31G(*d,p*) calculations to determine the effect on the  $E_a$  for D-A addition with ethene.<sup>57</sup> There was stabilization of the TS by EWG substituents, which was accompanied by a small positive charge (NPA) on ethene. This indicates that the electronic interaction involves

<sup>56</sup> C. Spino, M. Pesant, and Y. Dory, *Angew. Chem. Int. Ed. Engl.*, **37**, 3262 (1998).

<sup>57</sup> R. Robiette, J. Marchand-Brynaert, and D. Peeters, *J. Org. Chem.*, **67**, 6823 (2002).

the diene as a net electron acceptor; that is, the reactions are diene LUMO-controlled inverse electron demand reactions. The size of the stabilization and the charge transfer correlated reasonably well with a *combination* of the polar and resonance substituent constants. A polarization effect was also noted in several series. In each instance, the stabilization *increased* with substituent size and polarizability ( $F < Cl < Br$ ;  $CH_3 < CF_3 < CCl_3 < CBr_3$ ;  $OCH_3 < SCH_3 < SeCH_3$ ).

Computation on TS structure may be useful in predicting and interpreting trends in reactivity, regioselectivity, and stereoselectivity. To the extent observed trends are in agreement with the computations, the validity of the TS structure is supported. One experimental measurement that can be directly connected to TS structure is the kinetic isotope effect (review Section 3.5), which can be measured with good experimental accuracy as well as calculated from the TS structure.<sup>58</sup> Comparisons can be used to examine TS structure at a very fine level of detail. The computed TS for the  $(CH_3)_2AlCl$ -catalyzed reaction of isoprene with acrolein, ethyl acrylate, and but-3-en-2-one indicated highly asynchronous TSs and gave calculated isotope effects in agreement with experiment.<sup>59</sup> For example, the study of the  $(CH_3)_2AlCl$ -catalyzed D-A reaction of isoprene with propenal found good agreement between observed and computed isotope effects, except at one position. A later study located an alternative TS that gave better agreement with the isotope effect at this position.<sup>60</sup> This structure incorporates a formyl H bond, as postulated in other Lewis acid-catalyzed reactions of aldehydes.<sup>61</sup> Although this structure was computed to be slightly higher in energy, it was favored when a PCM solvent model was used. The TSs are shown in Figure 10.10.

Several studies have looked at the TS of D-A reactions in which the extent of aromaticity increases or decreases in going from reactants to products. For example, aromaticity is enhanced with *o*-quinodimethanes, where a new benzene ring is formed. The benzo[*c*] fused heterocycles contain an *o*-quinoid structure. The aromaticity of the heterocyclic ring is lost, but a new benzenoid ring is formed by cycloaddition. When polycyclic aromatic compounds undergo D-A reactions, the aromaticity of the reacting central ring is lost, but the peripheral rings have increased aromaticity per carbon.

Calculated  $E_a$ 's in several cases are in accord with the experimental trends.<sup>62</sup> Quinodimethanes are more reactive than benzo[*c*]heterocycles and the reactivity of the linear polycyclic hydrocarbons increases with the number of rings. The changes in the NICS values for the rings is consistent with the changing aromaticity. In the case of polycyclic hydrocarbons, the aromaticity in the peripheral rings increases. The aromaticity of the center ring is transformed to the aromaticity of the TS and then diminishes as the reaction is completed.<sup>63</sup>

<sup>58</sup> B. R. Beno, K. N. Houk, and D. A. Singleton, *J. Am. Chem. Soc.*, **118**, 9984 (1996); E. Goldstein, B. Beno, and K. N. Houk, *J. Am. Chem. Soc.*, **118**, 6036 (1996).

<sup>59</sup> D. A. Singleton, S. R. Merrigan, B. R. Beno, and K. N. Houk, *Tetrahedron Lett.*, **40**, 5817 (1999).

<sup>60</sup> O. Acevedo and J. D. Evanseck, *Org. Lett.*, **5**, 649 (2003).

<sup>61</sup> E. J. Acevedo Corey, J. J. Rohde, A. Fischer, and M. D. Alimiora, *Tetrahedron Lett.*, **38**, 33 (1997).

<sup>62</sup> C. Di Valentin, M. Freccero, M. Sarzi-Amade, and R. Zanaletti, *Tetrahedron*, **56**, 2547 (2000).

<sup>63</sup> M. Manoharan, F. De Proft, and P. Geerlings, *J. Chem. Soc., Perkin Trans. 2*, 1767 (2000); M.-F. Cheng and W.-K. Li, *Chem. Phys. Lett.*, **368**, 630 (2003).

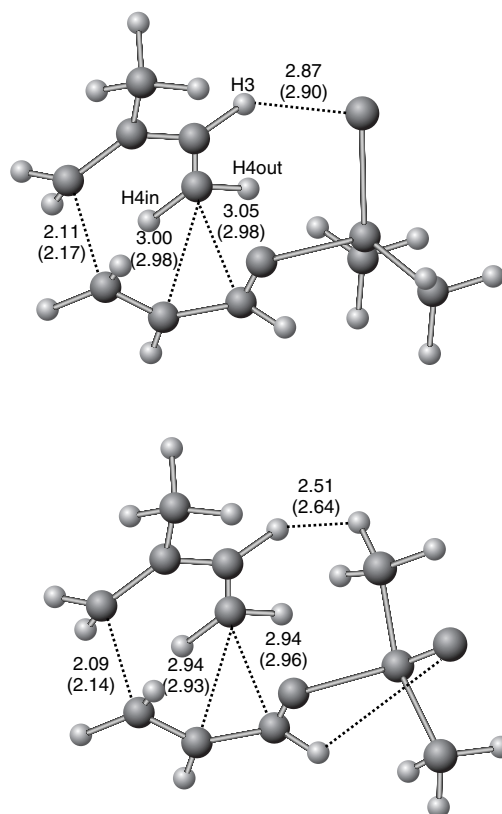
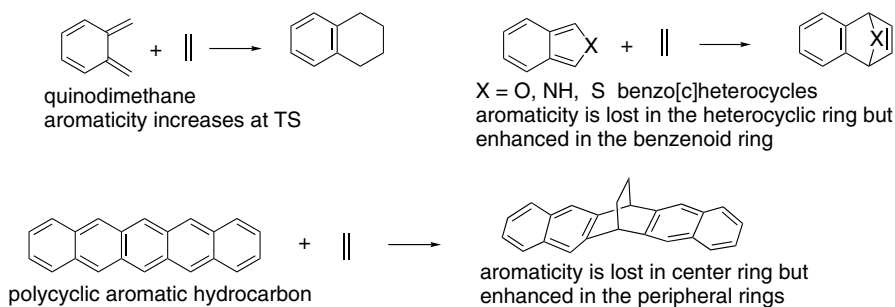
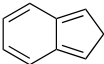
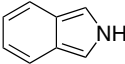
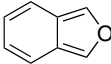
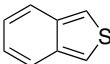


Fig. 10.10. Alternate transition structures for Diels-Alder reaction of isoprene with propenal: (a) structure without formyl hydrogen bond; (b) structure with formyl hydrogen bond. Dimensions are from B3LYP/6-31G(*d*) computations in the gas phase and in PMC with  $\epsilon = 4.335$  (shown in parentheses). Adapted from *Org. Lett.*, **5**, 649 (2003), by permission of the American Chemical Society.

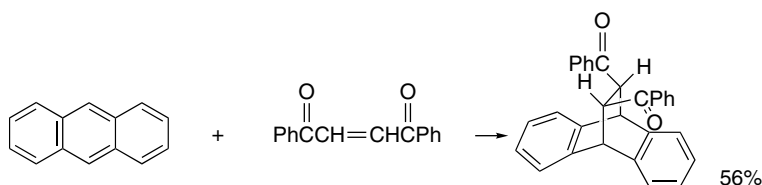


In the case of the benzo[*c*] heterocycles, the  $\Delta E$ ,  $E_a$ , and degree of charge transfer in the TS were calculated. The  $E_a$  correlated with the exothermicity of the reaction for the second-row elements. The extent of charge transfer at the TS increased from carbon to oxygen to nitrogen, but was low for the benzo[*c*]thiophene.<sup>64</sup>

<sup>64</sup> T. C. Dinadayalane and G. N. Sastry, *J. Chem. Soc., Perkin Trans. 2*, 1902 (2002).

				
$E_a$	10.8	21.4	15.4	24.7
$\Delta E$	-48.8	-16.2	-29.8	-27.1
c.t.	0.022	0.092	0.043	0.001

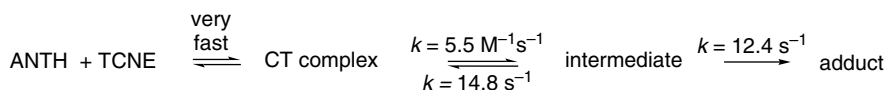
These results are consistent with experimental results. Polycyclic aromatic hydrocarbons are moderately reactive as the diene component of Diels-Alder reactions. Although benzene and naphthalene show no reactivity toward maleic anhydride at 90° C, anthracene does give an adduct.<sup>65</sup> A variety of dienophiles react with anthracene, including benzoquinone, dimethyl fumarate, nitroethene, and phenyl vinyl sulfoxide.<sup>66</sup> The addition occurs at the center ring. There is no net loss of resonance stabilization, since the anthracene ring (resonance energy = 1.60 eV) is replaced by two benzenoid rings (total resonance energy =  $2 \times 0.87 = 1.74$  eV).<sup>67</sup>



Ref. 68

A B3LYP/6-31+G(*d,p*) computational investigation of the reaction between anthracene and tetracyanoethene indicates that the reaction proceeds through a charge transfer complex.<sup>69</sup> Mulliken population analysis was used to follow the transfer of charge at the various stages of the reaction. At the CT complex, 0.20 electron had been transferred. This increased to 0.46 electron at the TS, but then dropped to 0.32 electron in the product. There is partial pyramidalization of both the dienophile and anthracene in the CT complex. This distortion is believed to make the transformation of the reactants to the TS more facile. The formation of the CT complex also begins the process of decreasing the aromaticity of the center ring, which makes the distortion of the ring toward the TS easier.

In the case of the reaction of anthracene with tetracyanoethene, there is kinetic evidence for an intermediate that is distinct from the rapidly formed charge transfer complex.<sup>70</sup> The intermediate is proposed to be a tight complex with a geometry favorable for formation of the adduct. The formation of the charge transfer complex is fast and reversible and may also lie on the overall reaction path.



65. B. Biermann and W. Schmidt, *J. Am. Chem. Soc.*, **102**, 3163 (1980).

66. J. C. C. Atherton and S. Jones, *Tetrahedron*, **59**, 9039 (2003).

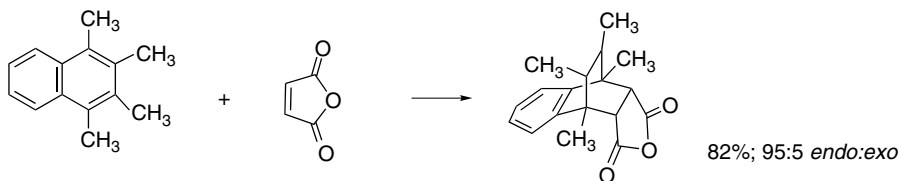
67. M. J. S. Dewar and C. de Llano, *J. Am. Chem. Soc.*, **91**, 789 (1969).

68. D. M. McKinnon and J. Y. Wong, *Can. J. Chem.*, **49**, 3178 (1971).

69. K. E. Wise and R. A. Wheeler, *J. Phys. Chem. A*, **103**, 8279 (1999).

70. K. L. Handoo, Y. Lu, and V. D. Parker, *J. Am. Chem. Soc.*, **125**, 9381 (2003).

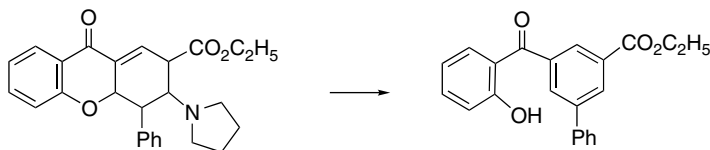
The naphthalene ring is much less reactive. Polymethylnaphthalenes are more reactive than the parent molecule and 1,2,3,4-tetramethylnaphthalene gives an adduct with maleic anhydride in 82% yield. Reaction occurs exclusively in the substituted ring because it is more electron rich.<sup>71</sup> The steric repulsions between the methyl groups, which are relieved in the nonplanar adduct, may also exert an accelerating effect.



### 10.2.5. Scope and Synthetic Applications of the Diels-Alder Reaction

Examples of some compounds that exhibit a high level of reactivity as dienophiles are shown in Scheme 10.2 (p. 844). Scheme 10.4 presents some typical uncatalyzed D-A reactions. Part A shows normal electron demand reactions. Each of the reactive dienophiles has at least one strongly electron-attracting substituent on the carbon-carbon double or triple bond. Part B shows several inverse electron demand D-A reactions. Ethene, ethyne, and their alkyl derivatives are poor dienophiles and react only under vigorous conditions.

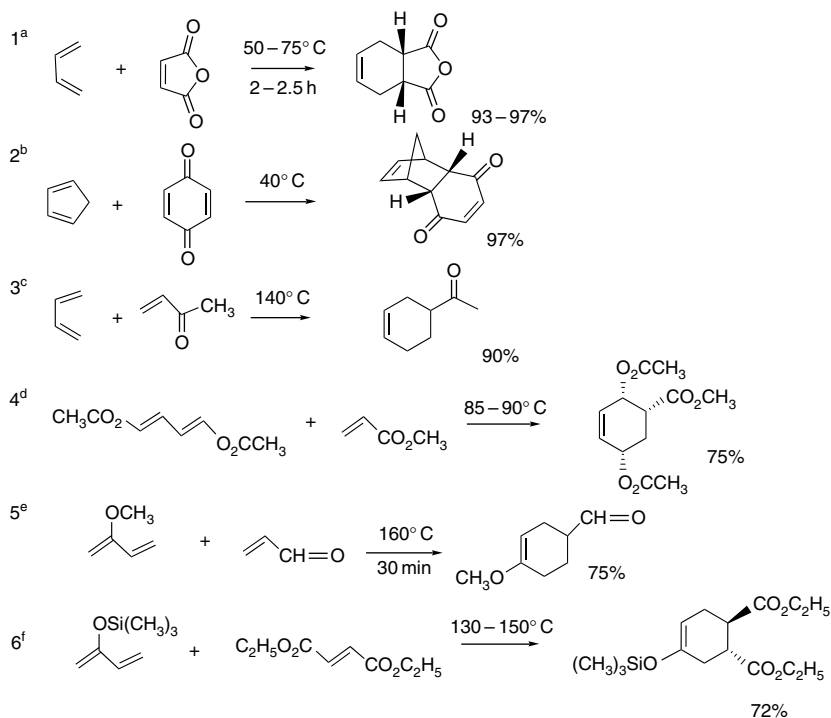
Entries 1 to 3 are classical examples of D-A reactions between simple dienes and electrophilic dienophiles. Note the *endo* stereoselectivity in Entry 2. Entries 4 to 6 are examples with dienes having activating ERG substituents. There is no regiochemical issue with the symmetrical diene in Entry 4, but the all-*cis* stereochemistry results from an *endo* TS. Entry 5 exhibits the expected regiochemistry, with C(1) of the diene bonded to the more electrophilic  $\beta$ -carbon of the dienophile. Entries 7 and 8 are inverse electron demand reactions with ERGs in the dienophiles and an EWG in the diene. The reaction in Entry 8 leads to formation of an aromatic ring by elimination of pyrrolidine and opening of the pyrone ring.



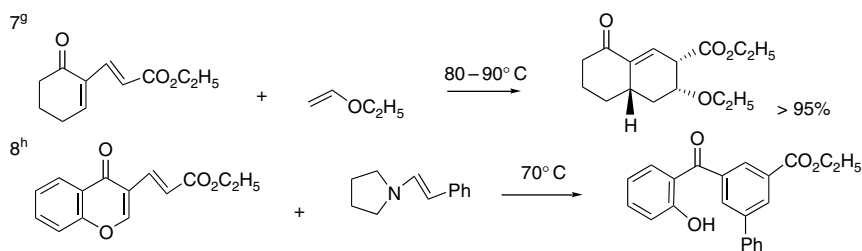
The regiochemistry of this reaction is consistent with expectation. The more nucleophilic  $\beta$ -carbon of the enamine bonds to C(2) of the pyrone ring, which is activated by both the C(4) ring carbonyl and the ester substituent.

<sup>71</sup> A. Oku, Y. Ohnishi, and F. Mashio, *J. Org. Chem.*, **37**, 4264 (1972).

## A. Normal Electron Demand



## B. Inverse Electron Demand



a. A. C. Cope and E. C. Herrichy, *Org. Synth.*, **IV**, 890 (1963).

b. A. Wasserman, *J. Chem. Soc.*, 1511 (1935).

c. W. K. Johnson, *J. Org. Chem.*, **29**, 864 (1959).

d. R. McCrindle, K. H. Overton, and R. A. Raphael, *J. Chem. Soc.*, 1560 (1960); R. K. Hill and G. R. Newkome, *Tetrahedron Lett.*, 1851 (1968).

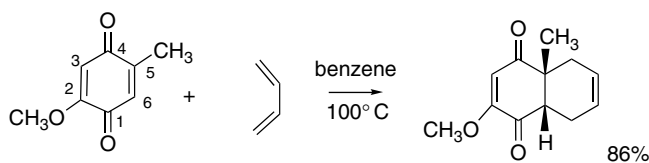
e. J. I. DeGraw, L. Goodman, and B. R. Baker, *J. Org. Chem.*, **26**, 1156 (1961).

f. M. E. Jung and C. A. McCombs, *Org. Synth.*, **VI**, 445 (1988).

g. G. J. Bodwell and Z. Pi, *Tetrahedron Lett.*, **38**, 309 (1997).

h. G. J. Bodwell, K. M. Hawco, and R. P. da Silva, *Synlett*, 179 (2003).

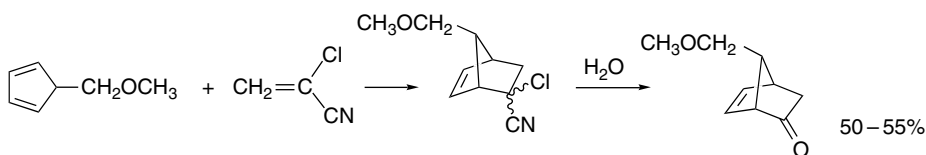
**10.2.5.1. Dienophiles** There are many examples of synthetic applications of D-A reactions where it is necessary to have additional substituents. The reaction of a substituted benzoquinone and 1,3-butadiene, for example, was the first step in early syntheses of steroids. The angular methyl group was introduced via the quinone and the other functional groups were used for further elaboration.



Ref. 72

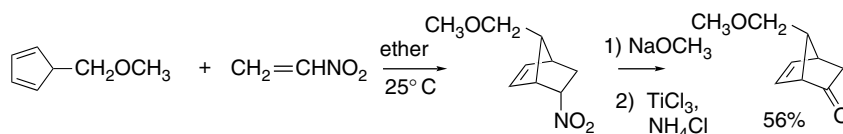
Note that the unsymmetrically substituted quinone exhibits excellent regioselectivity. The stronger donor effect of the methoxy group deactivates the C(4) carbonyl relative to the C(1) carbonyl, making the C(5)–C(6) double bond the more reactive dienophile.

The synthetic utility of the D-A reaction can be expanded by the use of dienophiles that contain *masked functionality* and are the *synthetic equivalent* of unreactive or inaccessible species. For example,  $\alpha$ -chloroacrylonitrile shows satisfactory reactivity as a dienophile. The  $\alpha$ -chloronitrile functionality in the adduct can be hydrolyzed to a carbonyl group, so  $\alpha$ -chloroacrylonitrile can function as the equivalent of ketene,  $\text{CH}_2=\text{C}=\text{O}$ .<sup>73</sup> Ketene itself is not a suitable dienophile because it reacts with dienes by [2 + 2] cycloaddition, rather than in the desired [4 + 2] fashion.



Ref. 74

Nitroalkenes are good dienophiles and the variety of transformations that are available for nitro groups makes them versatile intermediates.<sup>75</sup> Nitro groups can be converted to carbonyl groups by reductive hydrolysis, so nitroethene can also be used as a ketene equivalent.<sup>76</sup>



Ref. 77

The adducts from both the  $\alpha$ -chloroacrylonitrile and nitroethene and 5-methoxymethylcyclopentadiene are intermediates for the synthesis of prostaglandins.

Vinyl sulfones are useful dienophiles. The sulfonyl group can be removed reductively with sodium amalgam. In this two-step reaction sequence, the vinyl sulfone functions as an ethene equivalent. The sulfonyl group also allows for alkylation of the

<sup>72</sup> R. B. Woodward, F. Sondheimer, D. Taub, K. Heusler, and W. M. McLamore, *J. Am. Chem. Soc.*, **74**, 4223 (1952).

<sup>73</sup> V. K. Aggarwal, A. Ali, and M. P. Coogan, *Tetrahedron*, **55**, 293 (1999).

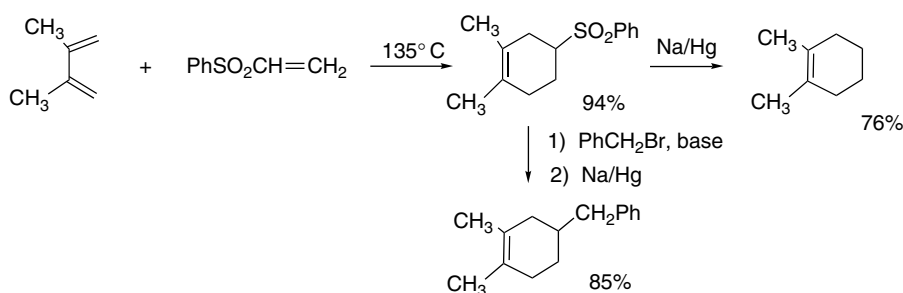
<sup>74</sup> E. J. Corey, N. M. Weinshenker, T. K. Schaaf, and W. Huber, *J. Am. Chem. Soc.*, **91**, 5675 (1969).

<sup>75</sup> D. Ranganathan, C. B. Rao, S. Ranganathan, A. K. Mehrotra, and R. Iyengar, *J. Org. Chem.*, **45**, 1185 (1980).

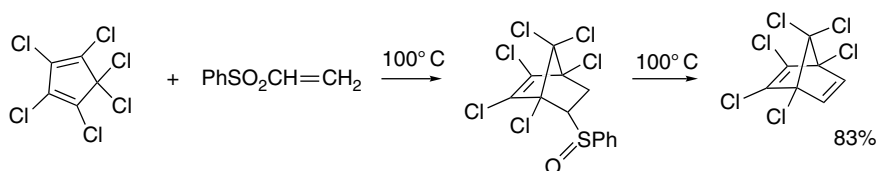
<sup>76</sup> For a review of ketene equivalents, see S. Ranganathan, D. Ranganathan, and A. K. Mehrotra, *Synthesis*, 289 (1977).

<sup>77</sup> S. Ranganathan, D. Ranganathan, and A. K. Mehrotra, *J. Am. Chem. Soc.*, **96**, 5261 (1974).

adduct, via the carbanion. This three-step sequence permits the vinyl sulfone to serve as the synthetic equivalent of a terminal alkene.<sup>78</sup>

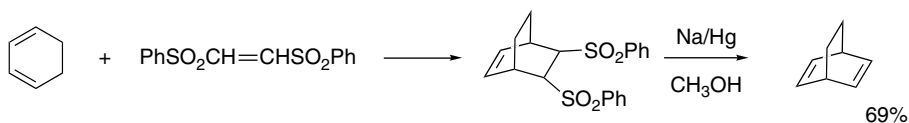


Phenyl vinyl sulfonate can serve as an ethyne equivalent. Its Diels-Alder adducts can undergo thermal elimination of benzenesulfenic acid.



Ref. 79

*E*- and *Z*-bis-(benzenesulfonyl)ethene are also ethyne equivalents. The two sulfonyl groups undergo reductive elimination on reaction with sodium amalgam.



Ref. 80

Vinylphosphonium salts are reactive as dienophiles as a result of the electron-withdrawing capacity of the phosphonium substituent. The D-A adducts can be deprotonated to give ylides that undergo the Wittig reaction to introduce an exocyclic double bond (see Part B, Section 2.4.1). This sequence of reactions corresponds to a D-A reaction employing allene ( $\text{CH}_2=\text{C}=\text{CH}_2$ ) as the dienophile.<sup>81</sup>



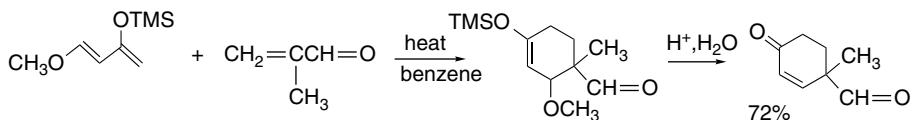
<sup>78</sup> R. V. C. Carr and L. A. Paquette, *J. Am. Chem. Soc.*, **102**, 853 (1980); R. V. C. Carr, R. V. Williams, and L. A. Paquette, *J. Org. Chem.*, **48**, 4976 (1983); W. A. Kinney, G. O. Crouse, and L. A. Paquette, *J. Org. Chem.*, **48**, 4986 (1983).

<sup>79</sup> L. A. Paquette, R. E. Moerck, B. Harirchian, and P. D. Magnus, *J. Am. Chem. Soc.*, **100**, 1597 (1978).

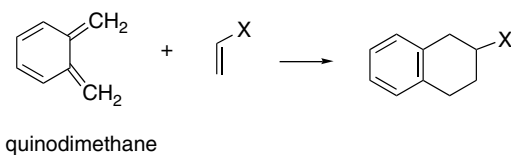
<sup>80</sup> O. DeLucchi, V. Lucchini, L. Pasquato, and G. Modena, *J. Org. Chem.*, **49**, 596 (1984).

<sup>81</sup> R. Bonjouklian and R. A. Buden, *J. Org. Chem.*, **42**, 4095 (1977).

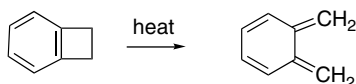
10.2.5.2. *Dienes* Simple dienes react readily with good dienophiles in D-A reactions. Functionalized dienes are also important in organic synthesis. One example that illustrates the versatility of such reagents is 1-methoxy-3-trimethylsiloxy-1,3-butadiene (*Danishefsky's diene*).<sup>82</sup> Its D-A adducts are trimethylsilyl enol ethers that can be readily hydrolyzed to ketones. The  $\beta$ -methoxy group is often eliminated during hydrolysis, leading to an enone.



Unstable dienes can be generated in situ in the presence of a dienophile. Among the most useful examples of this type of diene are the quinodimethanes.<sup>83</sup> These compounds are especially reactive as dienes because the cycloaddition reestablishes a benzenoid ring and results in aromatic stabilization (see p. 858).

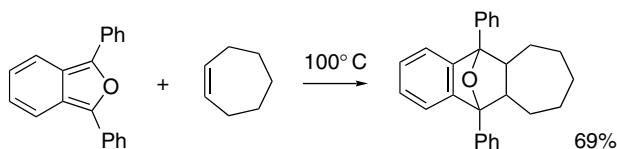


There are several possible routes to quinodimethanes, including pyrolysis of benzocyclobutenes.<sup>84</sup>



The reaction is accelerated by ERG substituents, particularly trialkylsiloxy groups, on the cyclobutene ring.<sup>85</sup> Quinodimethanes have been especially useful in intramolecular Diels-Alder reactions, as is illustrated in Section 10.2.7.

Another group of dienes with extraordinarily high reactivity is made up of the derivatives of benzo[*c*]furan (isobenzofuran).<sup>86</sup> Here again, the high reactivity can be traced to the gain of aromatic stabilization in the adduct.



Ref. 87

<sup>82</sup> S. Danishefsky and T. Kitahara, *J. Am. Chem. Soc.*, **96**, 7807 (1974).

<sup>83</sup> W. Oppolzer, *Angew. Chem. Int. Ed. Engl.*, **16**, 10 (1977); T. Kametani and K. Fukumoto, *Heterocycles*, **3**, 29 (1975); J. J. McCulloch, *Acc. Chem. Res.*, **13**, 270 (1980); W. Oppolzer, *Synthesis*, 793 (1978); J. L. Charlton and M. M. Alauddin, *Tetrahedron*, **43**, 2873 (1987); H. N. C. Wong, K.-L. Lau, and K. F. Tam, *Top. Curr. Chem.*, **133**, 85 (1986); P. Y. Michellys, H. Pellissier, and M. Santelli, *Org. Prep. Proc. Int.*, **28**, 545 (1996); J. L. Segura and N. Martin, *Chem. Rev.*, **99**, 3199 (1999).

<sup>84</sup> M. P. Cava and M. J. Mitchell, *Cyclobutadiene and Related Compounds*, Academic Press, New York, 1967, Chap. 6; I. L. Klundt, *Chem. Rev.*, **70**, 471 (1970); R. P. Thummel, *Acc. Chem. Res.*, **13**, 70 (1980); G. Mehta and S. Kotha, *Tetrahedron*, **57**, 625 (2001); A. K. Sadana, R. K. Saini, and W. E. Billups, *Chem. Rev.*, **103**, 1539 (2003).

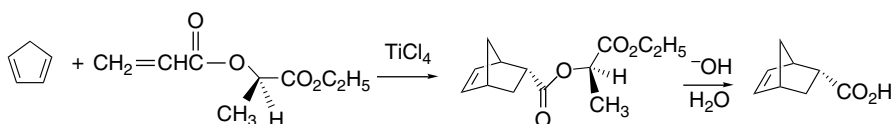
<sup>85</sup> J. G. Allen, M. F. Hentemann, and S. J. Danishefsky, *J. Am. Chem. Soc.*, **122**, 571 (2000).

<sup>86</sup> M. J. Haddadin, *Heterocycles*, **9**, 865 (1978); W. Friedrichsen, *Adv. Heterocycl. Chem.*, **26**, 135 (1980).

<sup>87</sup> G. Wittig and T. F. Burger, *Liebigs Ann. Chem.*, **632**, 85 (1960).

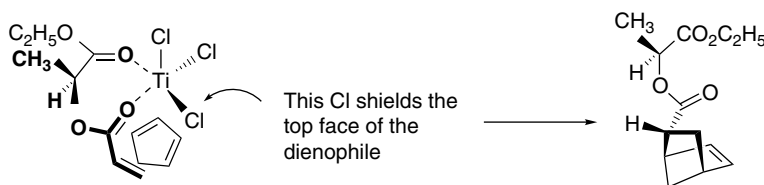
## 10.2.6. Enantioselective Diels-Alder Reactions

**10.2.6.1. Chiral Auxiliaries for Diels-Alder Reactions** The highly ordered cyclic TS of the Diels-Alder reaction permits design of reactants and catalysts that lead to a preference between diastereomeric or enantiomeric adducts. (See Section 2.4) to review the principles of diastereoselectivity and enantioselectivity.) One way to achieve diastereoselectivity is to install a chiral auxiliary.<sup>88</sup> The cycloaddition proceeds to give two diastereomeric products that can be separated and purified. Because of the lower temperature and the greater stereoselectivity, the best diastereoselectivity is often observed in Lewis acid-catalyzed reactions. Chiral esters and amides of acrylic acid are particularly useful because the chiral auxiliary can be easily recovered by hydrolysis of the purified adduct to give the enantiomerically pure carboxylic acid.



Ref. 89

Prediction and analysis of diastereoselectivity is based on steric, stereoelectronic, and chelating interactions in the TS.<sup>90</sup> For example, the facial selectivity of the reaction above is governed by a chloride ligand on titanium, which shields one face of the dienophile.



The lactone of 2,4-dihydroxy-3,3-dimethylpentanoic acid (known as pantolactone) has been successfully employed as a chiral auxiliary in several D-A reactions. For example, in conjunction with  $\text{TiCl}_4$ , it provides a 92% de in the reaction of 2,3-dimethylbutadiene with  $\alpha$ -cyanocinnamic acid.<sup>91</sup> The diastereoselectivity is consistent with a chelated structure similar to that shown above for acryloyl lactate. In the absence of  $\text{TiCl}_4$ , this same ester gives a 64% de of the opposite configuration. This

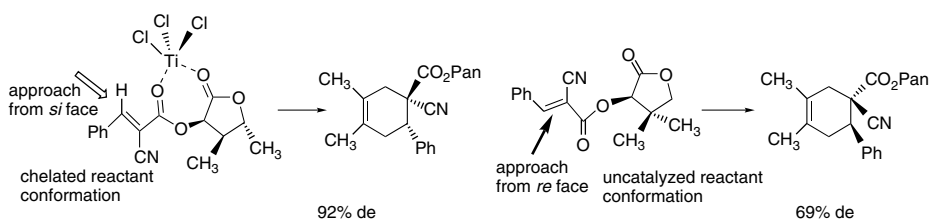
<sup>88</sup> W. Oppolzer, *Angew. Chem. Int. Ed. Engl.*, **23**, 876 (1984); M. J. Tascher, in "Organic Synthesis, Theory and Applications," Vol. 1, T. Hudlicky, ed., JAI Press, Greenwich, CT, 1989, pp. 1–101; H. B. Kagan and O. Riant, *Chem. Rev.*, **92**, 1007 (1992); K. Narasaka, *Synthesis*, 16 (1991).

<sup>89</sup> T. Poll, G. Helmchen, and B. Bauer, *Tetrahedron Lett.*, **25**, 2191 (1984).

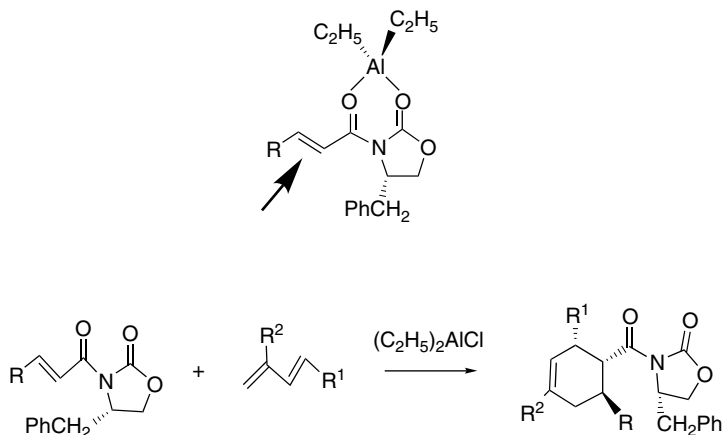
<sup>90</sup> For example, see T. Poll, A. Sobczak, H. Hartmann, and G. Helmchen, *Tetrahedron Lett.*, **26**, 3095 (1985).

<sup>91</sup> A. Avenoza, C. Cativiela, J. A. Mayoral, and J. M. Peregrina, *Tetrahedron: Asymmetry*, **3**, 913 (1992); C. Cativiela, J. A. Mayoral, A. Avenoza, J. M. Peregrina, F. J. Lahoz, and S. Gimeno *J. Org. Chem.*, **57**, 4664 (1992).

result suggests that the uncatalyzed reaction goes through a conformation in which the two carbonyl groups are *anti* to one another.



$\alpha$ ,  $\beta$ -Unsaturated derivatives of chiral oxazolidinones have proven to be especially useful for enantioselective D-A additions.<sup>92</sup> Reaction occurs at low temperatures in the presence of such Lewis acids as  $\text{SnCl}_4$ ,  $\text{TiCl}_4$ , and  $(\text{C}_2\text{H}_5)_2\text{AlCl}$ .<sup>93</sup> Both the 4-isopropyl (derived from valine) and the 4-benzyl (derived from phenylalanine) derivative are frequently used. Both carbonyl oxygens are coordinated with the Lewis acid and the oxazolidinone substituent provides steric shielding of one face of the dienophile. We discuss a number of other chiral auxiliaries for D-A reactions in Section 6.1.5 of Part B.



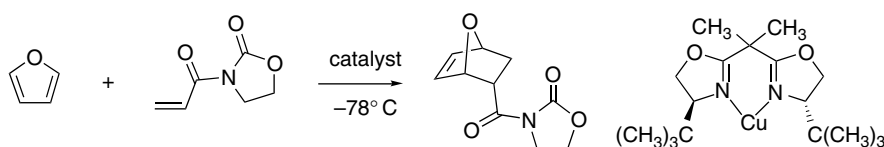
R	R <sup>1</sup>	R <sup>2</sup>	Yield (%)	dr
H	H	CH <sub>3</sub>	85	95:5
H	CH <sub>3</sub>	H	84	>100:1
CH <sub>3</sub>	H	CH <sub>3</sub>	83	94:6
CH <sub>3</sub>	CH <sub>3</sub>	H	77	95:5

<sup>92</sup> D. J. Ager, J. Prakash, and D. R. Schaad, *Chem. Rev.*, **96**, 835 (1996); D. J. Ager, J. Prakash, and D. R. Schaad, *Aldrichimica Acta*, **30**, 3 (1997).

<sup>93</sup> D. A. Evans, K. T. Chapman, and J. Bisaha, *J. Am. Chem. Soc.*, **110**, 1238 (1988).

10.2.6.2. *Enantioselective Catalysts for Diels-Alder Reactions* Enantioselectivity can also be achieved with chiral catalysts.<sup>94</sup> Many of the most efficient catalysts involve a chiral ligand in conjunction with a metal ion that acts as a Lewis acid. The metal ion provides the electron-attracting capacity and in conjunction with the ligand establishes a chiral environment at the catalytic site. Several boron compounds are also good catalysts, with the boron playing the role of the Lewis acid. The ligands typically have bulky substituents, often substituted aromatic rings. The ligands are usually derived from readily available chiral substances, such as amino acids. In addition to the Lewis acid complexation and steric effects,  $\pi$  stacking and hydrogen bonding can contribute to the structure of the catalytic complex. The effectiveness of the catalyst is related to the proximity of the chiral features to the reaction center. If the chiral environment is too remote from the catalytic site, it does not control the enantioselectivity effectively. This proposition was tested for a number of catalysts for the D-A reaction and generally found to be true.<sup>95</sup>

One group of chiral catalysts consists of metal ion complexes, usually  $\text{Cu}^{2+}$ ,<sup>96</sup> of *bis*-oxazolines (referred to as box catalysts).<sup>97</sup>



Ref. 98

Based on a crystal structure of the catalyst and PM3 modeling of the complex, the reaction is proposed to proceed preferentially from the *re* face as a result of steric shielding by a *t*-butyl group, as shown in Figure 10.11.

Chiral oxazaborolidines have also been found to be useful catalysts in D-A reactions. The tryptophan-derived catalyst shown in TS **A**, for example, can achieve 99% enantioselectivity in the D-A reaction between 5-benzyloxymethyl-1,3-cyclopentadiene and 2-bromopropenal. The adduct is an important intermediate in the synthesis of prostaglandins.<sup>99</sup> The aldehyde is bound to the catalyst by a Lewis interaction. There is also believed to be a hydrogen bond between the formyl C–H and the oxygen bound to boron. This type of hydrogen bonding has been recognized in several Lewis acid complexes of aldehydes.<sup>100</sup> The upper face of the aldehyde is shielded by the indole ring. The benzyloxymethyl substituent provides a steric differentiation of the two faces of the cyclopentadiene ring, as shown in TS **A**.

<sup>94</sup> Y. Hayashi, in *Cycloaddition Reactions in Organic Synthesis*, S. Kobayashi and K. A. Jorgensen, eds., Wiley-VCH, Weinheim, 2002, pp. 5–55.

<sup>95</sup> K. B. Lipkowitz, C. A. D'Hue, T. Sakamoto, and J. N. Stack, *J. Am. Chem. Soc.*, **124**, 14255 (2002).

<sup>96</sup> D. A. Evans, S. J. Miller, and T. Lectka, *J. Am. Chem. Soc.*, **115**, 6460 (1993); D. A. Evans, J. P. Murry, P. von Matt, R. D. Norcross, and S. J. Miller, *Angew. Chem. Int. Ed. Engl.*, **34**, 798 (1995); J. S. Johnson and D. A. Evans, *Acc. Chem. Res.*, **33**, 325 (2000).

<sup>97</sup> A. K. Ghosh, P. Mathivanan, and J. Cappiello, *Tetrahedron: Asymmetry*, **9**, 1 (1998).

<sup>98</sup> D. A. Evans and D. M. Barnes, *Tetrahedron Lett.*, **38**, 57 (1997).

<sup>99</sup> E. J. Corey and T. P. Loh, *J. Am. Chem. Soc.*, **113**, 8966 (1991).

<sup>100</sup> E. J. Corey, J. J. Rohde, A. Fischer, and M. D. Azimioara, *Tetrahedron Lett.*, **38**, 33 (1997).

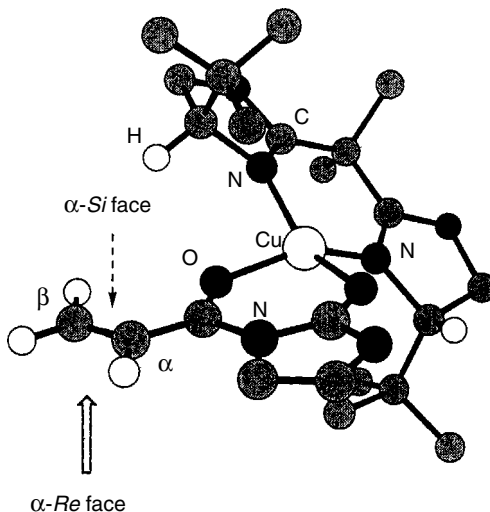
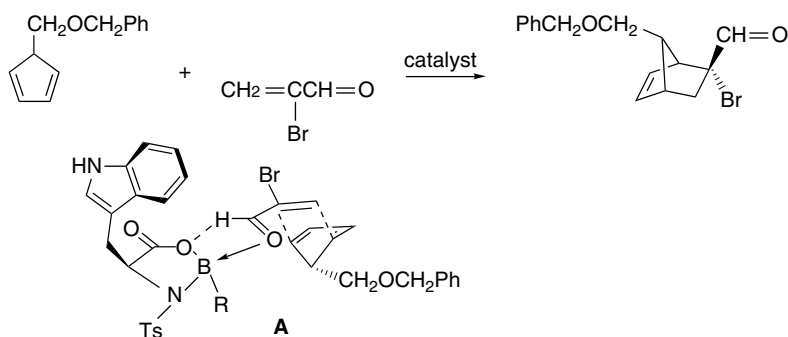


Fig. 10.11. Model of Cu(*S,S*-*t*-BuBox) catalyst with *N*-acryloyloxazolidinone showing facial stereodifferentiation. Reproduced from *J. Am. Chem. Soc.*, **121**, 7559 (1999), by permission of the American Chemical Society.



Other enantioselective catalysts for the D-A reactions have been developed. The chiral ligands used include the TADDOLs ( $\alpha, \alpha, \alpha, \alpha$ -tetraaryl-1,3-dioxolane-4,5-dimethanols)<sup>101</sup> and BINOL derivatives.<sup>102</sup> These are discussed in Section 6.4 of Part B.

### 10.2.7. Intramolecular Diels-Alder Reactions

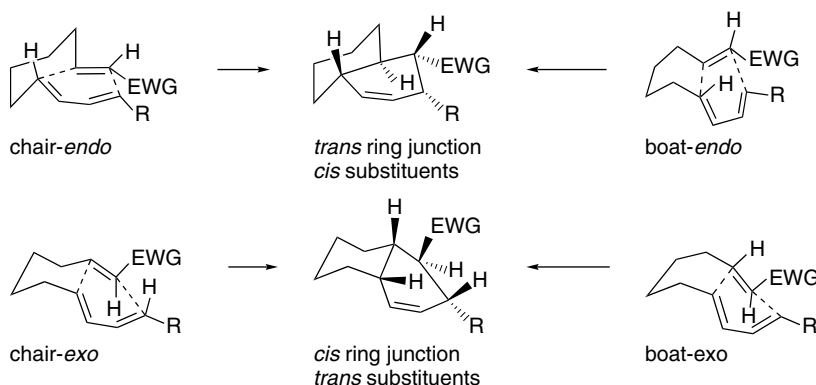
Intramolecular Diels-Alder (IMDA) reactions are very useful in the synthesis of polycyclic compounds.<sup>103</sup> Two new rings are created by the reaction, and the stereochemistry of the ring junction is determined by TS geometry. In addition to the *exo*

<sup>101</sup> D. Seebach, A. K. Back, and A. Heckel, *Angew. Chem. Intl. Ed. Engl.*, **40**, 93 (2001).

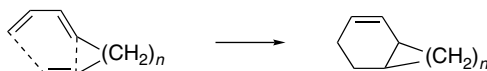
<sup>102</sup> K. Ishihara, H. Kurihara, M. Matsumoto, and H. Yamamoto, *J. Am. Chem. Soc.*, **120**, 6920 (1995); S. Kobayashi, M. Araki, and I. Hachiya, *J. Org. Chem.*, **59**, 3758 (1994); S. Kobayashi, M. Sugiura, H. Kitagawa, and W.-L. Lam, *Chem. Rev.*, **102**, 2227 (2002).

<sup>103</sup> W. Oppolzer, *Angew. Chem. Intl. Ed. Engl.*, **16**, 10 (1977); G. Brieger and J. N. Bennett, *Chem. Rev.*, **80**, 63 (1980); E. Ciganek, *Org. React.*, **32**, 1 (1984); D. F. Taber, *Intramolecular Diels-Alder and Alder Ene Reactions*, Springer-Verlag, Berlin, 1984.

and *endo* relationships present in intermolecular D-A reactions, the conformation of the intervening linkage influences the stereochemistry. For example, in the case of an *E,E*-undeca-1,7,9-trienes with 1-EWG substituents, four TSs are possible. Two lead to a *trans* ring junction with *cis* orientation of the substituents, whereas the other two lead to a *cis* ring junction and *trans* orientation of the substituents. As for intermolecular D-A reactions, the reaction is stereospecific with respect to the diene and dienophile substituents, so that the *Z,E*-, *E,Z*-, and *Z,Z*-reactants also give specific stereoisomers.



One of the factors that affect TS structure is the length of the connecting chain. Sastry and co-workers looked systematically at this factor in the unsubstituted triene system with from one to four linking  $\text{CH}_2$  groups.<sup>104</sup> Single-point B3LYP/6-31G\* energies were calculated at the PM3 structural minima. Because of strain, a *cis* ring junction is strongly favored for  $n = 1$  and  $n = 2$  and slightly for  $n = 3$ . The *trans* ring junction is favored somewhat for  $n = 4$ . The effect of strain is reflected in the energy of both the TS and the product and indicates the rudimentary features associated with the linking group. The  $E_a$  and reaction energies are given below and are plotted in Figure 10.12. The synchronicity of the reaction was computed. (See p. 852 for the numerical definition of synchronicity.) Synchronicity was quite high for  $n = 2$  to  $n = 4$ , but was lower (0.669) for  $n = 1$  (*cis*), where the formation of the peripheral bond is leading. According to these results, formation of a bicyclo[4.3.0]non-2-ene ring system ( $n = 3$ ) is slightly preferred kinetically to a bicyclo[4.4.0]dec-2-ene ring for both *cis* and *trans* ring junctions.



$n$	$E_{\text{act}}$		$\Delta E_{\text{react}}$		Synchronicity	
	<i>cis</i>	<i>trans</i>	<i>cis</i>	<i>trans</i>	<i>cis</i>	<i>trans</i>
1	35.7	57.2	-11.0	+25.6	0.6692	0.8987
2	37.0	41.1	-18.2	-4.3	0.9816	0.9730
3	17.9	19.6	-40.9	-38.8	0.9248	0.9473
4	26.1	23.3	-41.8	-47.7	0.9267	0.9054

<sup>104</sup> R. Vijaya and G. N. Sastry, *Theochem*, **618**, 201 (2002).

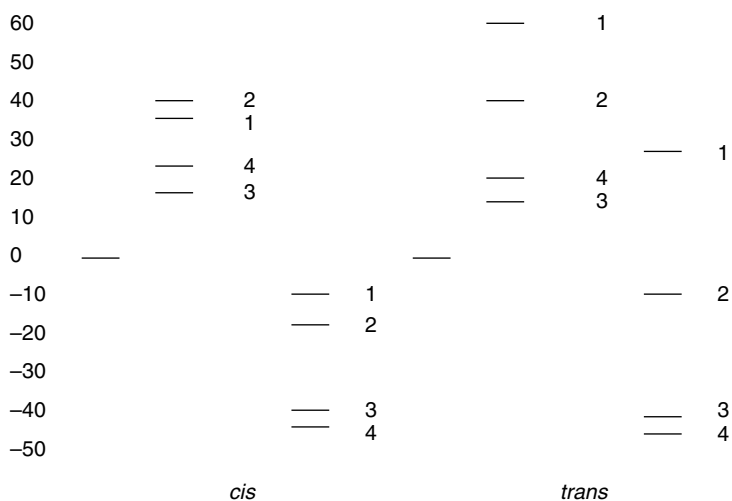
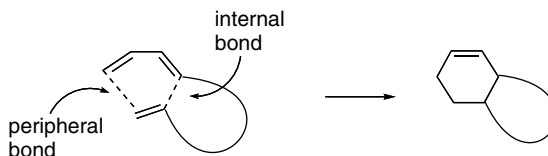


Fig. 10.12. Activation and reaction energies (B3LYP/6-31G\*) in kcal/mol for intramolecular Diels-Alder reactions of  $\text{CH}_2=\text{CH}(\text{CH}_2)_n\text{CH}=\text{CHCH}=\text{CH}_2$  for  $n = 1$  to 4. Adapted from *Theochem*, **618**, 201 (2002).

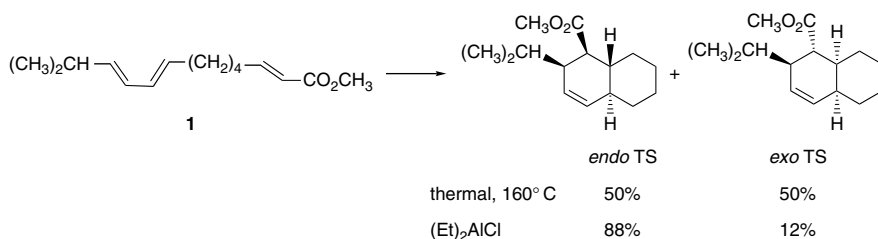
In several IMDA reactions involving substituted systems, the direction of the asynchronicity appears to be controlled by steric and torsional, rather than electronic, factors. Often the internal bond formation is more advanced than the peripheral bond, regardless of the location and electronic characteristics of the substituents.<sup>105</sup> This is presumably due to the proximity (entropic) factor and is in contrast to intermolecular D-A reactions, where electronic effects are dominant.



Lewis acid catalysis usually substantially improves the stereoselectivity of IMDA reactions, just as it does in intermolecular cases. For example, the thermal cyclization of **1** at 160° C gives a 50:50 mixture of two stereoisomers, but the use of  $(\text{C}_2\text{H}_5)_2\text{AlCl}$  as a catalyst permits the reaction to proceed at room temperature, and *endo* addition is favored by 7:1.<sup>106</sup>

<sup>105</sup> C. I. Turner, R. M. Williamson, M. N. Paddon-Row, and M. S. Sherburn, *J. Org. Chem.*, **66**, 3963 (2001); T. N. Cayzer, L. S. M. Wong, P. Turner, M. N. Paddon-Row, and M. S. Sherburn, *Chem. Eur. J.*, **8**, 739 (2002).

<sup>106</sup> W. R. Roush and H. R. Gillis, *J. Org. Chem.*, **47**, 4825 (1982).

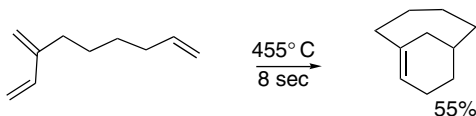


The general pattern of IMDA stereoselectivity suggests that although electronic interactions govern the regioselectivity, conformational effects are the main factors in determining stereoselectivity.<sup>107</sup> Because the conformational interactions depend on the substituent pattern in the specific case, no general rules for stereoselectivity can be put forward. Molecular modeling can frequently identify the controlling structural features.<sup>108</sup>

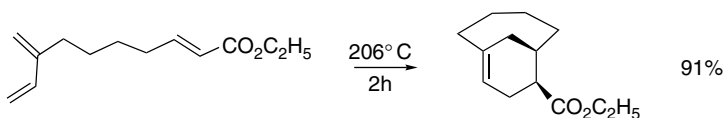
A less common type of IMDA reaction leads to bicyclic rings with bridgehead double bonds.<sup>109</sup>



Both activated and unactivated systems have been observed to react, and the reaction is subject to Lewis acid catalysis.



Ref. 110



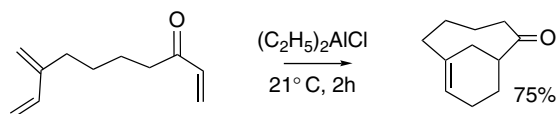
Ref. 110

<sup>107</sup>. W. R. Roush, A. I. Ko, and H. R. Gillis, *J. Org. Chem.*, **45**, 4264 (1980); R. K. Boeckman, Jr., and S. S. Ko, *J. Am. Chem. Soc.*, **102**, 7146 (1980); W. R. Roush and S. E. Hall, *J. Am. Chem. Soc.*, **103**, 5200 (1981); J. A. Marshall, J. E. Audia, and J. Grote, *J. Org. Chem.*, **49**, 5277 (1984); T.-C. Wu and K. N. Houk, *Tetrahedron Lett.*, **26**, 2293 (1985); K. A. Parker and T. Iqbal, *J. Org. Chem.*, **52**, 4369 (1987); W. R. Roush, A. P. Eisenfeld, and J. S. Warmus, *Tetrahedron Lett.*, **28**, 2447 (1987).

<sup>108</sup>. K. J. Shea, L. D. Burke, and W. P. England, *J. Am. Chem. Soc.*, **110**, 860 (1988); L. Raimondi, F. K. Brown, J. Gonzalez, and K. N. Houk, *J. Am. Chem. Soc.*, **114**, 4796 (1992); D. P. Dolata and L. M. Harwood, *J. Am. Chem. Soc.*, **114**, 10738 (1992); F. K. Brown, U. C. Singh, P. A. Kollman, L. Raimondi, K. N. Houk, and C. W. Bock, *J. Org. Chem.*, **57**, 4862 (1992); J. D. Winkler, H. S. Kim, S. Kim, K. Ando, and K. N. Houk, *J. Org. Chem.*, **62**, 2957 (1997).

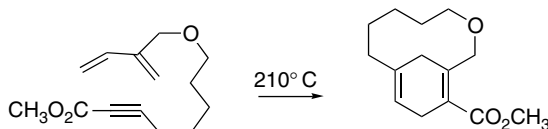
<sup>109</sup>. B. R. Bear, S. M. Sparks, and K. J. Shea, *Angew. Chem. Int. Ed. Engl.*, **40**, 821 (2001).

<sup>110</sup>. K. J. Shea, S. Wise, L. D. Burke, P. D. Davis, J. W. Gilman, and A. C. Greeley, *J. Am. Chem. Soc.*, **104**, 5708 (1982).



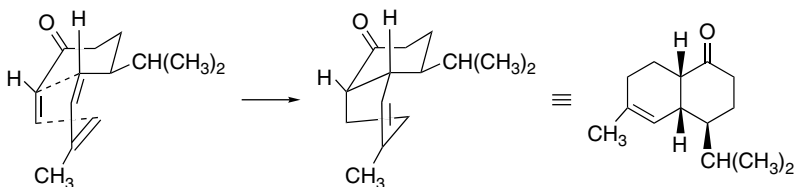
Ref. 111

Alkynes give cyclohexadienes.

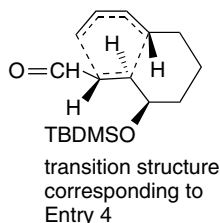


Ref. 112

We can illustrate some of the features of the IMDA reaction by considering some specific examples given in Scheme 10.5. In Entry 1 the dienophilic portion bears a carbonyl substituent and cycloaddition occurs easily. Two stereoisomeric products are formed, but both have *cis* ring fusion, which is the stereochemistry expected for an *endo* TS.



In Entry 2 a similar triene that lacks the activating carbonyl group undergoes reaction, but a much higher temperature is required. In this case the ring junction is *trans*. This corresponds to an *exo*-transition state and may reflect the absence of secondary orbital interaction between the diene and dienophile. Entry 3 is an example of the use of a benzocyclobutene to generate a quinodimethane intermediate. The IMDA reaction creates the steroidal skeleton.<sup>113</sup> Entries 4 and 5 illustrate the use of Lewis acid catalysts in IMDA. The *trans* ring junctions arise from *endo* TSs.

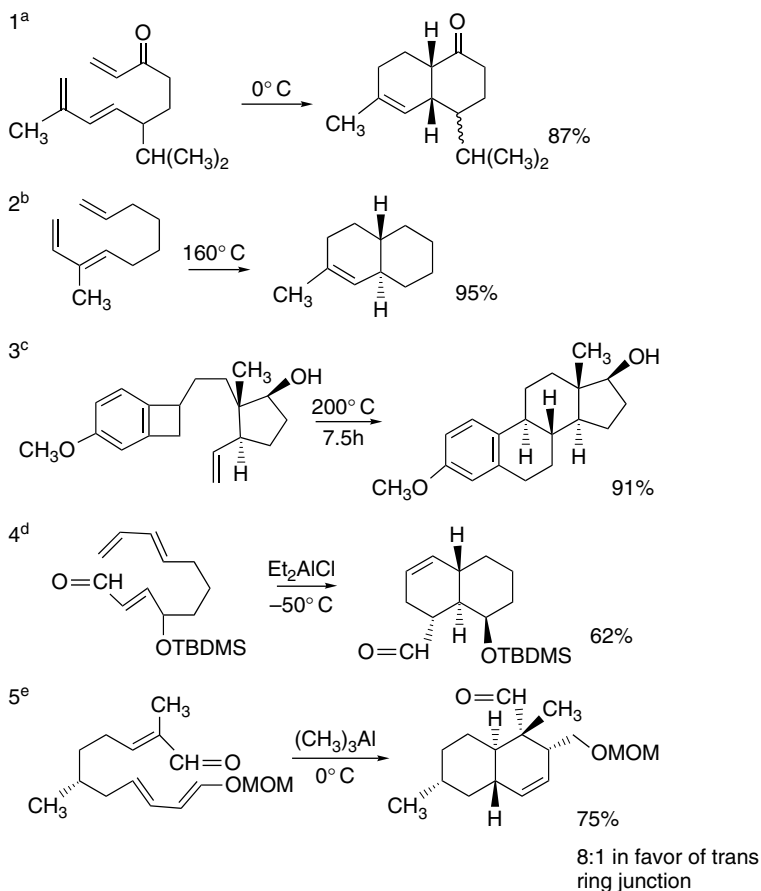


Note that all the reactions are stereospecific with respect to the configuration at the diene and dienophile double bonds.

<sup>111</sup>. K. J. Shea and J. W. Gilman, *Tetrahedron Lett.*, **24**, 657 (1983).

<sup>112</sup>. K. J. Shea, L. D. Burke, and W. P. England, *J. Am. Chem. Soc.*, **110**, 860 (1988).

<sup>113</sup>. H. Nemoto and K. Fukumoto, *Tetrahedron*, **54**, 5425 (1998).

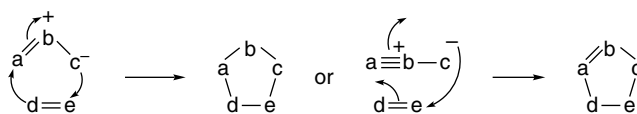


- a. D. F. Taber and B. P. Gunn, *J. Am. Chem. Soc.*, **101**, 3992 (1979); T. Kitahara, H. Kurata, T. Matsuoka, and K. Mori, *Tetrahedron*, **41**, 5475 (1985).  
 b. S. R. Wilson and D. T. Mao, *J. Am. Chem. Soc.*, **100**, 6289 (1978).  
 c. P. A. Grieco, T. Takigawa, and W. J. Schilling, *J. Org. Chem.*, **45**, 2247 (1980).  
 d. J. A. Marshall, J. E. Audia, and J. Grote, *J. Org. Chem.*, **49**, 5277 (1984).  
 e. K. Yuki, M. Shindo, and K. Shishido, *Tetrahedron Lett.*, **42**, 2517 (2001).

### 10.3. 1,3-Dipolar Cycloaddition Reactions

There is a large class of reactions known as *1,3-dipolar cycloaddition reactions* (1,3-DPCA) that are analogous to the Diels-Alder reaction in that they are concerted  $[\pi 4_s + \pi 2_s]$  cycloadditions.<sup>114</sup> 1,3-DPCA reactions can be represented as shown in the following diagram. The entity *a-b-c* is called the *1,3-dipole* and *d-e* is the *dipolarophile*.

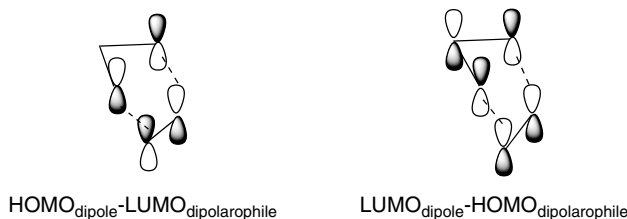
<sup>114</sup>. (a) R. Huisgen, *Angew. Chem. Int. Ed. Engl.*, **2**, 565 (1963); (b) R. Huisgen, R. Grashey, and J. Sauer, in *The Chemistry of the Alkenes*, S. Patai, ed., Interscience, London, 1965, pp. 806–878; (c) G. Bianchi, C. DeMicheli, and R. Gandolfi, in *The Chemistry of Double Bonded Functional Groups*, Part I, Supplement A, S. Patai, ed., Wiley-Interscience, New York, 1977, pp. 369–532; (e) A. Padwa, ed., *1,3-Dipolar Cycloaddition Chemistry*, Wiley, New York, 1984; (d) For a review of intramolecular 1,3-dipolar cycloaddition reactions, see A. Padwa, *Angew. Chem. Int. Ed. Engl.*, **15**, 123 (1976).



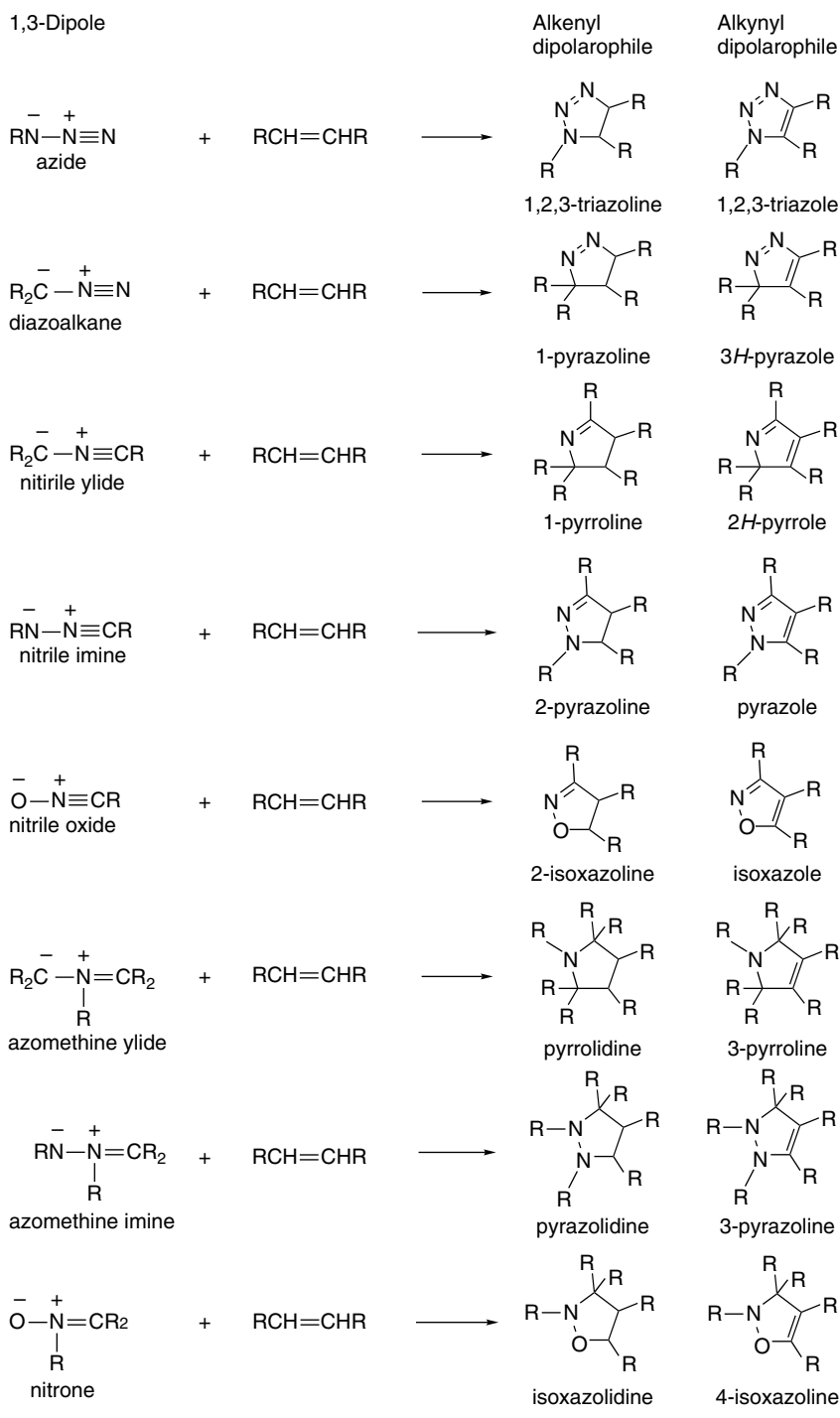
The 1,3-dipoles have a  $\pi$ -electron system consisting of two filled and one empty orbital and are analogous with the allyl or propargyl anion. Each 1,3-dipole has at least one charge-separated resonance structure with opposite charges in a 1,3-relationship. It is this structural feature that leads to the name 1,3-dipole for this class of reactants. The dipolarophiles are typically substituted alkenes or alkynes but all that is essential is a  $\pi$  bond, and other multiply bonded functional groups such as carbonyl, imine, azo, and nitroso can also act as dipolarophiles. The reactivity of dipolarophiles depends both on the substituents present on the  $\pi$  bond and on the nature of the 1,3-dipole involved in the reaction. Owing to the wide range of structures that can serve either as a 1,3-dipole or as a dipolarophile, the 1,3-DPCA is a very useful reaction for the construction of five-membered heterocyclic rings. Scheme 10.6 gives some examples using both ethenyl and ethynyl dipolarophiles. Some of the structures shown can undergo hydrogen shifts to more stable heterocyclic molecules, if there is one or more  $R = H$ .

### 10.3.1. Relative Reactivity, Regioselectivity, Stereoselectivity, and Transition Structures

The bonding changes for 1,3-DPCA reactions involve four  $\pi$  electrons from the 1,3-dipole and two from the dipolarophile. In most cases, the reaction is a concerted  $[\pi 2_s + \pi 4_s]$  cycloaddition.<sup>115</sup> As in the D-A reaction, the reactants approach one another in parallel planes. There is interaction between the complementary HOMO-LUMO combinations, and depending on the combination, either reactant can be the electrophilic or the nucleophilic component. Generally speaking, the reactant 1,3-dipoles are more polar than the TS or the reaction product. The rate of reaction is not strongly sensitive to solvent polarity.



<sup>115</sup> P. K. Kadaba, *Tetrahedron*, **25**, 3053 (1969); R. Huisgen, G. Szeimes, and L. Mobius, *Chem. Ber.*, **100**, 2494 (1967); P. Scheiner, J. H. Schomaker, S. Deming, W. J. Libbey, and G. P. Nowack, *J. Am. Chem. Soc.*, **87**, 306 (1965).



There have been many computational analyses of 1,3-DPCA TSs, and they are generally regarded to be aromatic in character. Typical TSs are characterized by aromatic NICS values.<sup>116</sup> The ring current associated with this aromaticity is primarily due to the six electrons undergoing bonding changes.<sup>117</sup> The orbital interactions in the cyclic TS serve as the focal point for discussion of relative reactivity, regioselectivity, and stereoselectivity of 1,3-DPCA reactions.

The most widely applied interpretation of substituent effects on relative reactivity is based on FMO theory. According to FMO theory, interacting orbitals are most stabilized when they are closest in energy. Substituent effects on dipolar cycloadditions can be interpreted in terms of matching of HOMO and LUMO orbitals of the two reactants.<sup>118</sup> This is the same concept used in applying FMO theory to D-A reactions (see p. 844–848). In the D-A reaction, it is fairly clear which reactant is electrophilic and which is nucleophilic, and the interpretation of substituent effects follows directly. This choice is not always so obvious for 1,3-DPCA reactions. In fact, for several of the 1,3-dipoles both EWGs and ERGs in the dipolarophile enhance reactivity. These 1,3-dipoles are called *ambiphilic*. Let us look carefully to see why they have this property.

Much of the relative reactivity data on 1,3-DPCA reactions has been tabulated and discussed in reviews by R. Huisgen, a pioneer researcher in the field.<sup>114b</sup> Some representative data are presented in Table 10.3. The dipolarophiles are shown in decreasing order of electrophilicity. The data from these monosubstituted dipolarophiles should be relatively free of steric influences on reactivity. Note that for phenyl azide and benzonitrile oxide, reactivity is at a minimum for unfunctionalized alkenes and is increased by both donor and acceptor substituents.

**Table 10.3. Representative Relative Rate Data for 1,3-Dipolar Cycloadditions<sup>a</sup>**

CH <sub>2</sub> =CHX	Ph <sub>2</sub> CN <sub>2</sub> <sup>b</sup>	PhN <sub>3</sub> <sup>c</sup>	PhC≡NO <sup>d</sup>	PhCH=NCH <sub>3</sub> <sup>e</sup>	PhC≡NNPh <sup>f</sup>	CH <sub>2</sub> N <sub>2</sub> <sup>g</sup>
Dimethyl fumarate	996	31	94	18.3	283	
Dimethyl maleate	27.8	1.25	1.61	6.25	7.94	
Ethyl acrylate	288	36.5	66	11.1	48.2	175
Ethyl crotonate	1.0	1.0	1.0	1.0	1.0	1.0
Norbornene	1.15	700	97	0.13	3.12	3.3 × 10 <sup>-2</sup>
1-Alkene		0.8	2.6	0.072	0.146	6.9 × 10 <sup>-4</sup>
Styrene	0.57	1.5	9.3	0.32	1.60	6.9 × 10 <sup>-2</sup>
Cyclopentene		6.9	1.04	0.022	0.128	4.2 × 10 <sup>-4</sup>
Cyclohexene			0.055		0.011	1.6 × 10 <sup>-5</sup>
Vinyl ether		1.5	15			8.5 × 10 <sup>-6</sup>
Vinyl amine		~ 1 × 10 <sup>5</sup>				

a. Relative to ethyl crotonate as tabulated in Ref. 114b.

b. R. Huisgen, H. Stangl, H. J. Sturm, and H. Wagenhofer, *Angew. Chem.*, **73**, 170 (1961).

c. R. Huisgen, G. Szeimies, and L. Mobius, *Chem. Ber.*, **100**, 2494 (1967).

d. K. Bast, M. Christl, R. Huisgen, and W. Mack, *Chem. Ber.*, **106**, 3312 (1973).

e. R. Huisgen, H. Seidl, and I. Brunig, *Chem. Ber.*, **102**, 1102 (1969).

f. E. Eckell, R. Huisgen, R. Sustmann, D. Wallbillich, D. Grashey, and E. Spindler, *Chem. Ber.*, **100**, 2192 (1967).

g. J. Geitner, R. Huisgen, and R. Sustmann, *Tetrahedron Lett.*, 881 (1977).

<sup>116</sup> F. P. Cossio, I. Marao, H. Jiao, and P. v. R. Schleyer, *J. Am. Chem. Soc.*, **121**, 6737 (1999).

<sup>117</sup> I. Marao, B. Lecea, and F. P. Cossio, *J. Org. Chem.*, **62**, 7033 (1997); I. Marao and F. P. Cossio, *J. Org. Chem.*, **64**, 1868 (1999).

<sup>118</sup> R. Sustmann and H. Trill, *Angew. Chem. Int. Ed. Engl.*, **11**, 838 (1972); R. Sustmann, *Pure Appl. Chem.*, **40**, 569 (1974).

In addition to the electronic effects of substituents, several other structural features affect the reactivity of dipolarophiles. Strain increases reactivity. Norbornene, for example, is consistently more reactive than cyclopentene in 1,3-dipolar cycloadditions. Cyclopentene is also more reactive than cyclohexene. Conjugating substituents, such as the phenyl group in styrene, usually increase reactivity of dipolarophiles (compare styrene with 1-alkenes in Table 10.3).

An interesting series of compounds for which a fairly broad range of data exists is diazomethane, methyl diazoacetate, and diethyl diazomalonate, in which each additional ester group should make the 1,3-dipole successively more electrophilic. The data are given in Table 10.4. We see that diazomethane is primarily nucleophilic in character, dropping sharply in reactivity from electrophilic to nucleophilic dipolarophiles. The other two reactants clearly show an ambiphilic reactivity. These reagents show increased reactivity with both EWG and ERG dipolarophiles, with the diazomalonate shifted somewhat more toward electrophilic character.

Sustmann and Trill<sup>118</sup> summarized these and related reactivity relationships in terms of FMO theory and pointed out that 1,3-DPCA reactions could be of three types, depending on relative placement of the frontier orbitals: (A) HOMO<sub>dipole</sub>-LUMO<sub>dipolarophile</sub> dominant; (B) LUMO<sub>dipole</sub>-HOMO<sub>dipolarophile</sub> dominant; (C) both HOMO-LUMO interactions are significant. The first type should be accelerated by ERG in the dipole and EWG in the dipolarophile. The second type should be facilitated by an EWG in the dipole and an ERG in the dipolarophile. These relationships suggest a parabolic substituent effect as the Type C reactions shift from LUMO<sub>dipolarophile</sub> to mixed to HOMO<sub>dipolarophile</sub> controlled. Figure 10.13 illustrates this relationship for aryl azides. The Hammett  $\rho$  is positive for reaction with nucleophilic enamines but negative for the electrophilic dipolarophile maleic anhydride, showing that the direction of the substituent effect depends on the relative importance of the two HOMO-LUMO interactions. The unfunctionalized alkenes cyclopentene and norbornene are nucleophilic in character, but less so than the enamine. Using a wider range of reactants, Sustmann and Trill demonstrated a parabolic rate relationship and developed a mathematical treatment in terms of FMO theory that provided a semiquantitative explanation of relative reactivity.<sup>118</sup> We pursue the application of FMO theory to the regiochemistry of the 1,3-DPCA reaction in more detail below.

As with the D-A reaction, the concerted pericyclic mechanism can account for many aspects of the stereochemistry and regiochemistry of the 1,3-DPCA reaction. Most 1,3-DPCA reactions are highly *stereospecific* with respect to the dipolarophile. In one case, it was established that a pair of isomeric dipolarophiles both reacted

**Table 10.4. Relative Reactivity for Diazo Compounds**

CH <sub>2</sub> =CHX	CH <sub>2</sub> N <sub>2</sub> <sup>a</sup>	RO <sub>2</sub> CCHN <sub>2</sub> <sup>b</sup>	(RO <sub>2</sub> C) <sub>2</sub> CN <sub>2</sub> <sup>c</sup>
Acrylate	250,000	930	35
1-Alkene	1	1	1
Styrene	100	2.5	1.5
Vinyl ether	0.02	0.1	0.15
Vinyl amine	0.07	470	620

a. J. Geittner, R. Huisgen, and R. Sustmann, *Tetrahedron Lett.*, 881 (1977).

b. W. Bihlmaier, R. Huisgen, H.-U. Reissig and S. Voss, *Tetrahedron Lett.*, 2621 (1979).

c. H. U. Reissig, Ph. D. Thesis, University of Munich, 1978, as quoted in Ref. 114b.

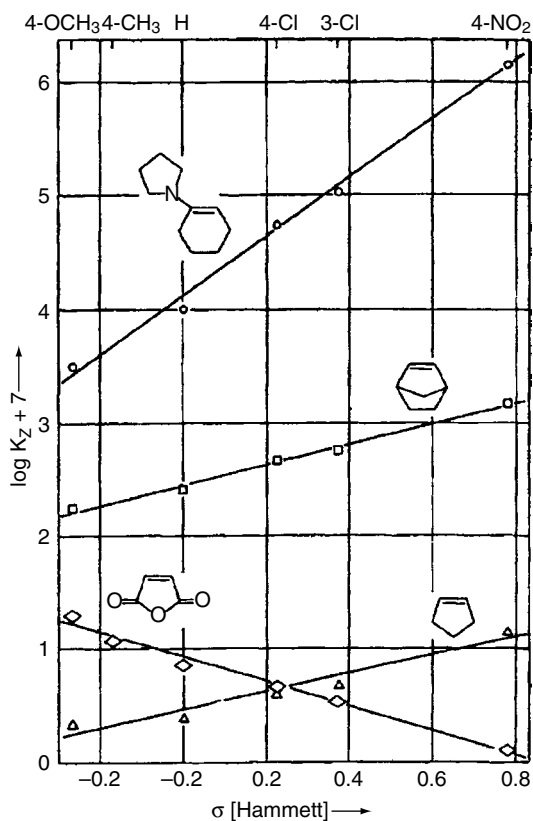
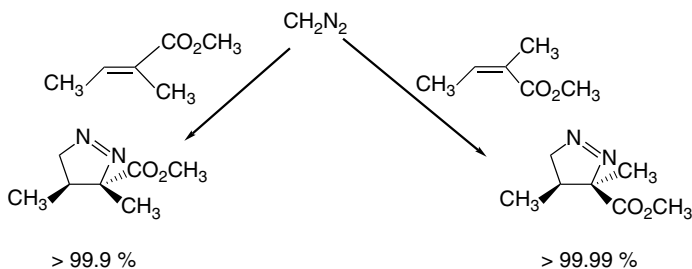


Fig. 10.13. Hammett plots of cycloaddition rates of substituted aryl azides with nucleophilic, electrophilic, and unsubstituted alkenes showing the ambiphilic character of the azide cycloaddition. Reaction with maleic anhydride (electrophilic) is favored by donor substituents. Reaction with pyrrolidinocyclohexene (nucleophilic) is favored by acceptor substituents. Reactions with cyclopentene and norbornene are modestly favored by acceptor substituents. Reproduced from *Chem. Ber.*, **100**, 2494 (1967), by permission of Wiley-VCH.

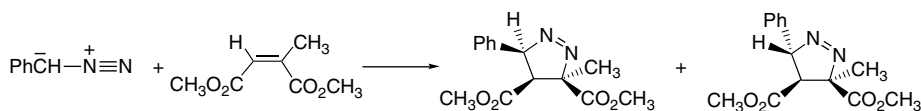
with more than 99.9% stereospecificity, and there are numerous other examples of stereospecific additions.



Ref. 119

With some 1,3-dipoles, two possible stereoisomers can be formed. These products result from two differing orientations of the reacting molecules and are analogous to

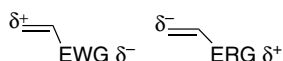
<sup>119</sup> W. Bihlmaier, J. Geitner, R. Huisgen, and H. U. Reissig, *Heterocycles*, **10**, 147 (1978).



Ref. 120

For unsymmetrical dipolarophiles, two regioisomeric products are also possible. The prediction and interpretation of the stereo- and regioselectivity of 1,3-DPCA reactions have been of ongoing interest. The issues are the same as in the D-A reaction. The reactions are usually under kinetic control, so TS energy is the controlling factor. As the reactants come together, charge transfer and polarization occur, with one reactant donating electron density to the other. As the TS is reached, the degree of bond formation and electron delocalization are important. The TS can be characterized by the extent of orbital interaction, charge transfer, and the degree of bond formation.<sup>121</sup> Reactant conformation may also be a factor in distinguishing between *exo* and *endo* TSs. For any given reaction, computational comparison of TS energies can be informative, but there is also a need for qualitative understanding of the factors that contribute to TS energy and therefore to regio- and stereocontrol.

The polarity of the common dipolarophiles can be recognized from the nature of the substituent.



When both the 1,3-dipole and the dipole are unsymmetrical, there are two possible orientations for addition. Both steric and electronic factors play a role in determining the regioselectivity of the addition. The most generally satisfactory interpretation of the regiochemistry of 1,3-DPCA is based on frontier orbital concepts.<sup>122</sup> As with the D-A reaction, the most favorable orientation is the one that gives the strongest interaction between the frontier orbitals of the 1,3-dipole and the dipolarophile. Most 1,3-DPCA are of the type in which the frontier orbitals are the LUMO of the dipolarophile and the HOMO of the 1,3-dipole. There are a number of systems in which the relationship is reversed, as well as some in which the two possible HOMO-LUMO interactions are of comparable magnitude.

The analysis of the regioselectivity of a 1,3-dipolar cycloaddition by FMO theory requires information about the energy and atomic coefficients of the frontier orbitals of the 1,3-dipole and the dipolarophile. Most of the more common 1,3-dipoles have been examined using CNDO/2 calculations.<sup>122b</sup> Figure 10.14 gives estimates of the energies of the HOMO and LUMO orbitals of some representative 1,3-dipoles. By using these orbital coefficients and calculating or estimating the relative energies

<sup>120</sup> R. Huisgen and P. Eberhard, *Tetrahedron Lett.*, 4343 (1971).

<sup>121</sup> P. Merino, J. Revuelta, T. T. Tejero, U. Chiacchio, A. Rescifina, and G. Romeo, *Tetrahedron*, **59**, 3581 (2003).

<sup>122</sup> (a) R. Sustmann and H. Trill, *Angew. Chem. Int. Ed. Engl.*, **11**, 838 (1972); (b) K. N. Houk, J. Sims, B. E. Duke, Jr., R. W. Strozier, and J. K. George, *J. Am. Chem. Soc.*, **95**, 7287 (1973); (c) R. Sustmann, *Pure Appl. Chem.*, **40**, 569 (1974); (d) I. Fleming, *Frontier Orbitals and Organic Chemical Reactions*, Wiley, New York, 1977; (e) K. N. Houk, in *Pericyclic Reactions*, Vol. II, A. P. Marchand and R. E. Lehr, eds., Academic Press, New York, 1977, pp. 181–271; (f) K. N. Houk, *Top. Curr. Chem.*, **79**, 1 (1979).

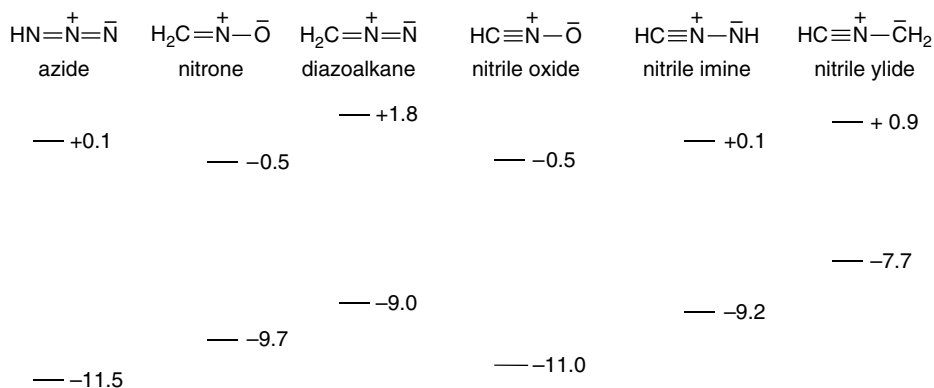


Fig. 10.14. Estimated energies (eV) of frontier  $\pi$  MOs for some 1,3-dipoles. Data from *J. Am. Chem. Soc.*, **95**, 7287 (1973).

of the interacting orbitals, it is possible to make predictions of the regiochemistry of 1,3-DPCA reactions. The most important dipolarophiles are the same types of compounds that are dienophiles in the D-A reaction. The orbital coefficients given in Figure 10.5 can be used in analyses of 1,3-DPCA reactions. In conjunction with the orbital coefficients given in Figure 10.15, this information allows conclusions as to which HOMO-LUMO combination will interact most strongly for a given pair of reactants.

This procedure is illustrated for two specific cases in Figure 10.16. The reaction of a nitrile oxide with an alkene is considered on the left. The smallest energy gap is for the alkene HOMO and the 1,3-dipole LUMO. This is qualitatively reasonable in that the atoms in the 1,3-dipole are more electronegative than those in the dipolarophile. Reference to Figure 10.15 shows that the LUMO coefficient is largest at carbon for the nitrile oxide group. The largest coefficient for a terminal alkene HOMO is at C(1). The matching of the largest coefficients of the 1,3-dipole LUMO and the dipolarophile HOMO leads to the predicted (and observed) product. The same procedure can be applied to the case shown at the right of Figure 10.16. In this case, the 1,3-dipole is the nucleophile and the dipolarophile is the electrophile. The largest coefficient of the nitron HOMO is at oxygen and the largest coefficient for the acrylate ester LUMO is at the  $\beta$ -carbon.

Although the FMO approach provides a good foundation for understanding the regioselectivity of 1,3-cycloadditions, there are many specific cases in which it fails to provide a complete understanding. Steric factors are not considered by the FMO analysis and in many instances steric factors control regiochemistry. 1,3-DPCA can be broadly classified as *sterically controlled* or *electronically controlled*. There may also be specific interactions in the TSs that are not considered by the FMO analysis.

There have been many studies of individual systems by MO and DFT methods and these provide further insight into the factors that control regio- and stereoselectivity. For example, there are two possible regioisomers from the reaction of diazomethane and methyl vinyl ether, but only the 3-methoxy isomer is formed. Calculations at several levels of theory (AM1, HF/6-31G, and MP2/6-31G\*) found lower activation

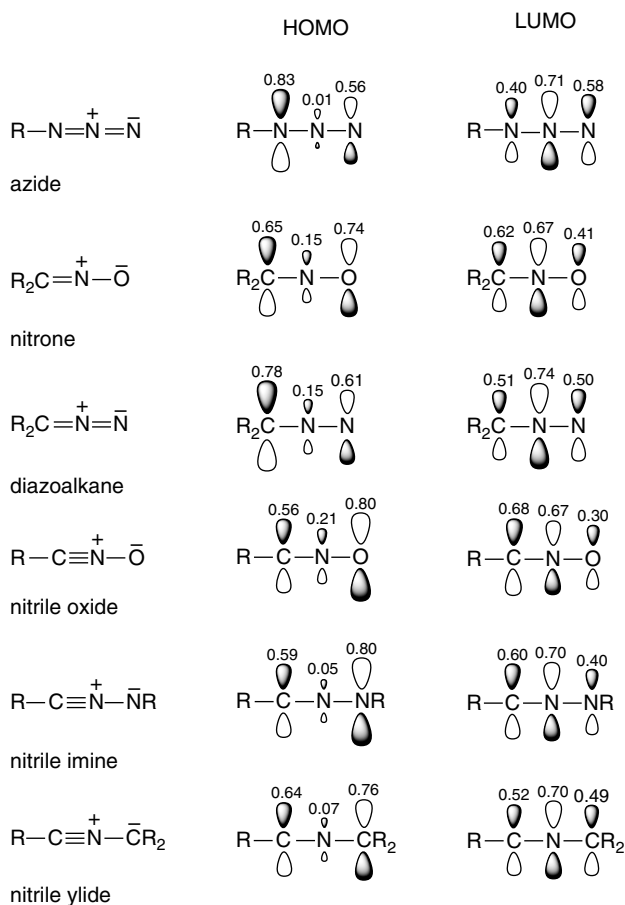


Fig. 10.15. Orbital coefficients for HOMO and LUMO of some common 1,3-dipoles. Data from *J. Am. Chem. Soc.*, **95**, 7287 (1973).

energies for the TS leading to the observed product.<sup>123</sup> The energies (MP2/6-31G\*) of the four different TSs are shown in Figure 10.17.

To dissect the factors involved, the TSs were approached in stepwise fashion and the energies associated with each step were assessed. The steps were: (a) deformation of the reactants to their TS geometry; (b) approach of the reactants to the TS geometry; and (c) bond formation. The picture that emerged was that the *earliest* TS had the lowest  $E_a$ . Although the total binding energy was less in this looser TS, there was a smaller cost in terms of deformations and repulsions for bringing the reactants together. The favored TS was also characterized by the lowest dipole moment and reflects a favorable alignment of the electrostatic features of the reactants. Finally, bond formation was favored in this TS by a relatively strong donor-acceptor interaction between the HOMO of the electron-rich vinyl ether and the LUMO of the dipolarophile, in agreement with the qualitative FMO analysis.

<sup>123</sup> Y. L. Pascal, J. Chanet-Ray, R. Vessiere, and A. Zeroual, *Tetrahedron*, **48**, 7197 (1992); A. Rastelli, M. Bagatti, R. Gandolfi, and M. Burdisso, *J. Chem. Soc., Faraday Trans.*, **90**, 1077 (1994).



X	$E_a$	Degree of Asynchronicity
N=O	-1.4	0.309
C≡N	+1.4	0.198
Cl	+10.1	0.107
OH	+13.2	0.154
CH <sub>3</sub>	+14.3	0.025

Note that there is no barrier for the (hypothetical) reaction with dinitrosoethene. For X = N=O and C≡N, shallow energy minima for prereaction complexes were identified. The conclusion that can be drawn from this study is that stronger EWGs in the dipolarophile lead to greater electrophile/nucleophile character and higher reactivity. This is the same qualitative trend noted for D-A reactions (see p. 847). The nitrile ylide is clearly an electron donor in these reactions, which is consistent with the relatively high energy of the HOMO, as indicated in Figure 10.14.

Computations were also applied to representative 1,3-dipoles in reaction with ethene.<sup>125</sup> The  $E_a$  and  $\Delta E$  for the reactions were calculated using CCSD(T)/6-311G\*\* energies at B3LYP/6-31G\* structural minima.

1,3-Dipole	$E_a$	$\Delta E$	Leading bond (Å)
H-C≡N <sup>+</sup> -CH <sub>2</sub> <sup>-</sup>	+6.9	-72.1	2.443
H-C≡N <sup>+</sup> -NH <sup>-</sup>	+6.9	-62.6	2.326
H-C≡N <sup>+</sup> -O <sup>-</sup>	+11.4	-45.9	2.235
N≡N <sup>+</sup> -CH <sub>2</sub> <sup>-</sup>	+14.3	-37.0	2.225
N≡N <sup>+</sup> -NH <sup>-</sup>	+17.2	-26.2	2.143
N≡N <sup>+</sup> -O <sup>-</sup>	+23.5	-10.7	2.036

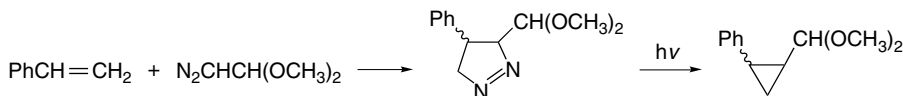
A number of factors appear to be involved here. There is an Bell-Evans-Polyani type correlation with the most stable products (most negative  $\Delta E$ ) having the lowest  $E_a$ . There is also a trend toward a later TS with the slower reactions, as indicated by the length of the leading bond in the TS. This is consistent with the Hammond postulate, with the smaller  $E_a$  correlating with an early TS. Within the 1,3-dipoles, there is a negative correlation with electronegativity. The most electrophilic 1,3-dipoles are the least reactive in this case. This trend suggests a dominant HOMO<sub>dipole</sub>-LUMO<sub>dipolarophile</sub> interaction, but it also may reflect the strength of the bonds being formed, which decreases in the same direction.

In broad terms, there is similarity in the reactivity and regiochemistry relationships for 1,3-DPCA and those of the D-A reaction. The most favorable reactions are those with the most complementary electronic character, that is, high nucleophilicity in one reactant with high electrophilicity in the other. Such reactions have high charge transfer character, early TS, and lower TS energy. Bond formation is more advanced in the TS between the most complementary pair of reaction centers and asynchronicity is high. The best match between HOMO and LUMO predicts the preferred regiochemistry. Relative reactivity trends should also be governed by these criteria, but as yet no broad quantitative analyses of relative reactivity have been developed.

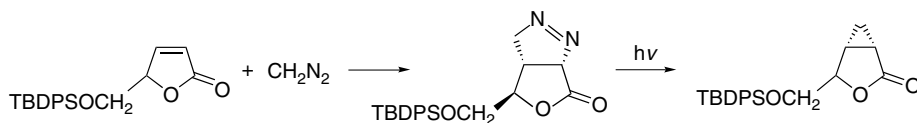
<sup>125</sup> M.-D. Su, H.-L. Liao, W.-S. Chung, and S.-Y. Chu, *J. Org. Chem.*, **64**, 6710 (1999).

## 10.3.2. Scope and Applications of 1,3-Dipolar Cycloadditions

As can be judged from Scheme 10.6, a wide variety of five-membered heterocyclic compounds can be made by the 1,3-DPCA reaction. Sometimes, these products are not the final target but rather intermediates for preparation of other compounds. Pyrazolines, which are formed from alkenes and diazo compounds, for example, can be pyrolyzed or photolyzed to give cyclopropanes.

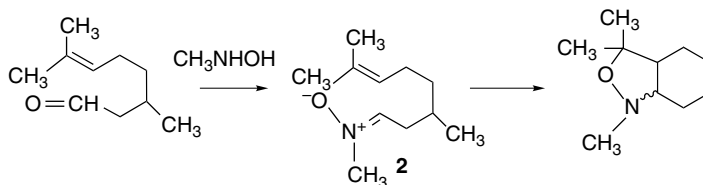


Ref. 126



Ref. 127

The addition of nitrones to alkenes serves both to form a carbon-carbon bond and to introduce oxygen and nitrogen functionality.<sup>128</sup> The products are isoxazolines and the oxygen-nitrogen bond can be cleaved by reduction, leaving both an amino and a hydroxy function in place. A number of imaginative syntheses have employed this strategy. Intramolecular 1,3-dipolar cycloaddition has proven to be especially useful in synthesis. The nitron **2** is generated by condensation of the aldehyde group with *N*-methylhydroxylamine and then goes on to product by intramolecular cycloaddition.



Ref. 129

Scheme 10.7 gives some other examples of 1,3-DPCA reactions. Entries 1 to 3 are typical intermolecular 1,3-DPCA. The 1,3-dipoles in each instance are isolatable compounds. Entries 4 and 5 are intramolecular nitron cycloadditions. The product from Entry 5 was used in the synthesis of the alkaloid pseudotropine. The proper stereochemical orientation of the hydroxyl group is ensured by the structure of the isoxazoline from which it is formed.

An interesting variation of the 1,3-DPCA involves generation of 1,3-dipoles from three-membered rings. As an example, aziridines **3** and **4** give adducts derived from apparent formation of 1,3-dipoles **5** and **6**, respectively.<sup>130</sup>

<sup>126</sup> P. Carrie, *Heterocycles*, **14**, 1529 (1980).

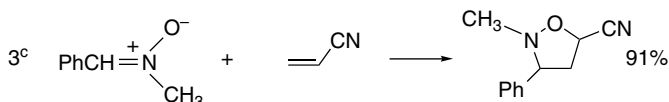
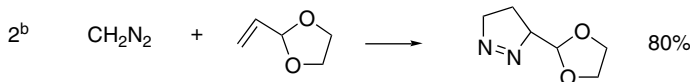
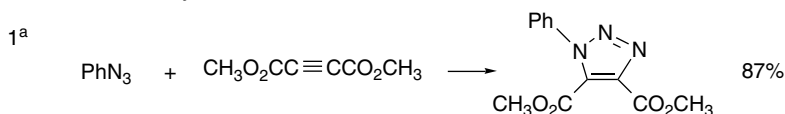
<sup>127</sup> M. Martin-Vila, N. Hanafi, J. M. Jimenez, A. Alvarez-Larena, J. F. Piniella, V. Branchadell, A. Oliva, and R. M. Ortuno, *J. Org. Chem.*, **63**, 3581 (1998).

<sup>128</sup> For reviews of nitron cycloadditions, see D. St. C. Black, R. F. Crozier, and V. C. Davis, *Synthesis*, 205 (1975); J. J. Tufariello, *Acc. Chem. Res.*, **12**, 396 (1979); P. N. Confalone and E. M. Huie, *Org. React.*, **36**, 1 (1988).

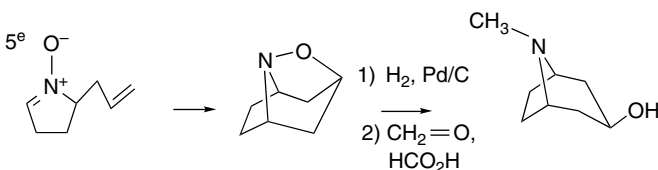
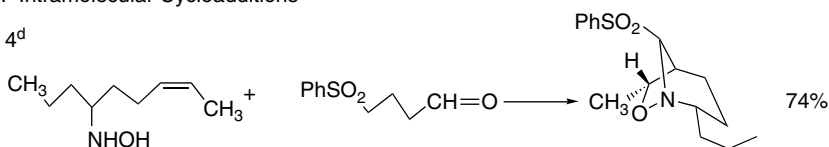
<sup>129</sup> N. LeBel and D. Hwang, *Org. Synth.*, **58**, 106 (1978).

<sup>130</sup> R. Huisgen and H. Maeder, *J. Am. Chem. Soc.*, **93**, 1777 (1971).

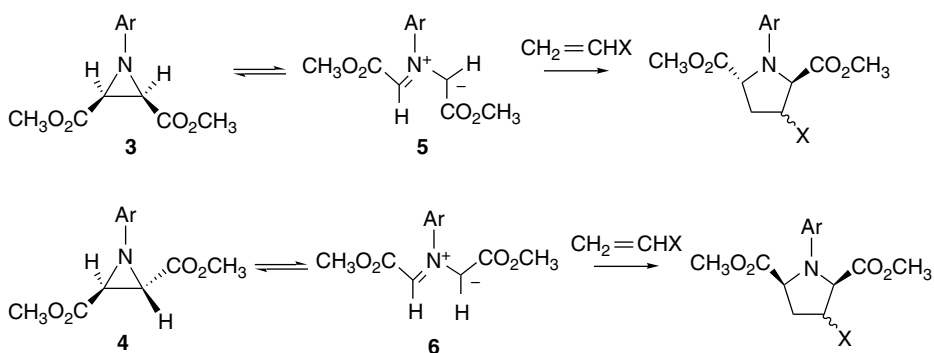
## A. Intermolecular Cycloadditions



## B. Intramolecular Cycloadditions



- a. R. Huisgen, R. Knorr, L. Mobius, and G. Szeimies, *Chem. Ber.*, **98**, 4014 (1965).  
 b. J. M. Stewart, C. Carlisle, K. Kem, and G. Lee, *J. Org. Chem.*, **35**, 2040 (1970).  
 c. R. Huisgen, H. Hauck, R. Grashey, and H. Seidl, *Chem. Ber.*, **101**, 2568 (1968).  
 d. N. A. LeBel and N. Balasubramanian, *J. Am. Chem. Soc.*, **111**, 3363 (1989).  
 e. J. J. Tufariello, G. B. Mullen, J. J. Tegler, E. J. Trybulski, S. C. Wong, and S. A. Ali, *J. Am. Chem. Soc.*, **101**, 2435 (1979).

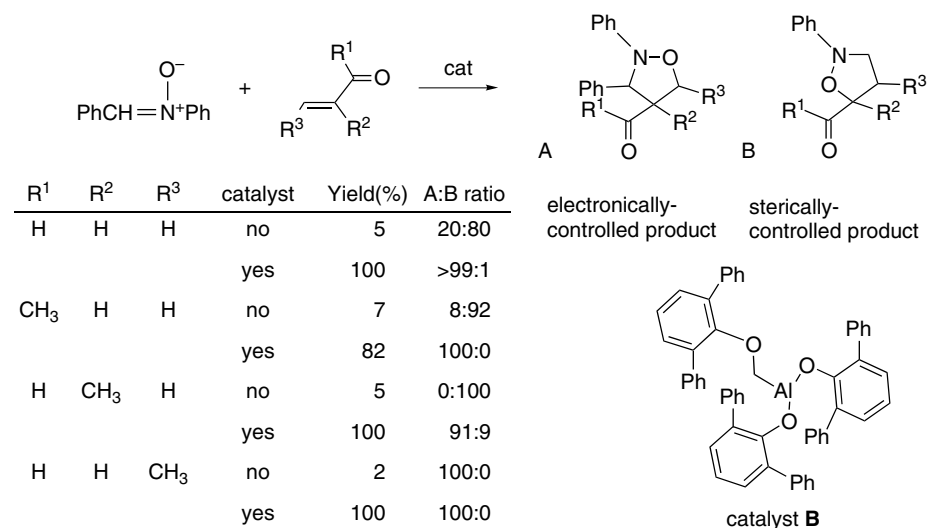


Ring opening is most facile for aziridines that have an EWG to stabilize the carbanion center in the dipole. The evidence for the involvement of 1,3-dipoles as discrete intermediates includes the observation that the reaction rates are independent of dipolarophile concentration. This fact indicates that the ring opening is the

rate-determining step in the reaction. Note that the ring opening is a stereospecific electrocyclic process. (The stereochemistry of electrocyclic ring opening is discussed in Section 10.5).

### 10.3.3. Catalysis of 1,3-Dipolar Cycloaddition Reactions

The role of catalysts in 1,3-DPCA reactions is similar to that in D-A reactions. Most catalysts are Lewis acids. Effective catalysts include  $\text{Yb}(\text{O}_3\text{SCF}_3)_3$  with BINOL,<sup>131</sup>  $\text{Mg}^{2+}$ -*bis*-oxazolines,<sup>132</sup> and oxazaborolidines.<sup>133</sup> Intramolecular nitronc cycloadditions can be facilitated by Lewis acids such as  $\text{ZnCl}_2$ .<sup>134</sup> The catalysts function by enhancing the reactivity of the *more electrophilic component of the reaction*. Although the diene is often nonpolar and inert to Lewis acids in D-A reactions, that is not the case for 1,3-DPCA. Consideration of catalysts must include the potential interaction with both the dipole and dipolarophile. Catalyst interaction with the 1,3-dipole is likely to be detrimental if the dipole is the more nucleophilic component of the reaction. For example, with nitrones and enones, formation of a Lewis acid adduct with the nitronc in competition with the enone is detrimental. One approach to this problem is to use highly substituted catalysts that are selective for the less substituted reactant. Bulky aryloxyaluminum compounds are excellent catalysts for nitronc cycloaddition and also enhance regioselectivity.<sup>135</sup> The reaction of diphenylnitronc with enones is usually subject to steric regiochemical control. With the catalyst **B** high *electronic regiochemical control* is achieved and reactivity is greatly enhanced, but the catalyst does not strongly influence the *exo:endo* selectivity, which is 23:77 for propenal.



<sup>131</sup> M. Kawamura and S. Kobayashi, *Tetrahedron Lett.*, **40**, 3213 (1999).

<sup>132</sup> G. Desimoni, G. Faita, A. Mortoni, and P. Righetti, *Tetrahedron Lett.*, **40**, 2001 (1999); K. V. Gothelf, R. G. Hazell, and K. A. Jorgensen, *J. Org. Chem.*, **63**, 5483 (1998).

<sup>133</sup> J. P. G. Seerden, M. M. M. Boeren, and H. W. Scheeren, *Tetrahedron*, **53**, 11843 (1997).

<sup>134</sup> J. Marcus, J. Brussee, and A. van der Gen, *Eur. J. Org. Chem.*, 2513 (1998).

<sup>135</sup> S. Kanemasa, N. Ueno, and M. Shirahase, *Tetrahedron Lett.*, **43**, 657 (2002).

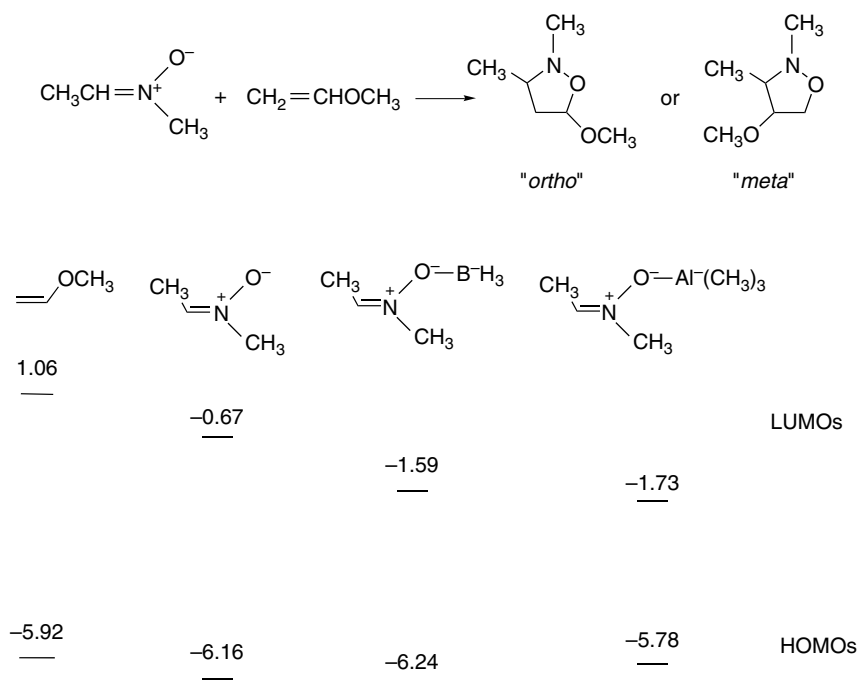


Fig. 10.18. Shift in FMO energy levels (in eV) (B3LYP/6-31G\*) on complexation with  $\text{BH}_3$  or  $(\text{CH}_3)_3\text{Al}$  with nitronium reactant. Data from *Eur. J. Org. Chem.*, 2265 (2000).

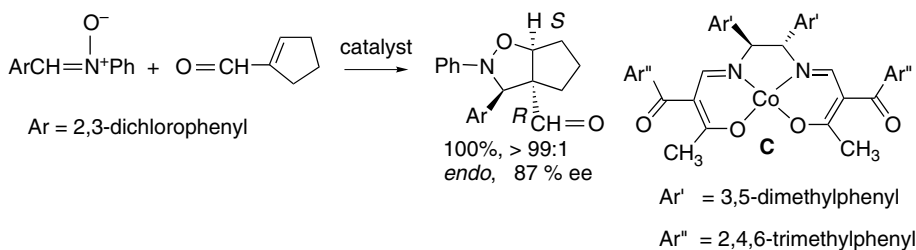
Domingo examined computationally the effect of Lewis acid catalysis in the reaction of a nitronium ion with a vinyl ether, a combination in which the nitronium ion is the electrophilic reagent.<sup>136</sup> The results are summarized in Figure 10.18. The Lewis acid, modeled by  $\text{BH}_3$  or  $\text{Al}(\text{CH}_3)_3$ , is attached at the nitronium oxygen. The Lewis acid decreases the  $E_a$  for "ortho" addition, while increasing it for "meta" addition. The catalyst also increases the selectivity for the *exo* TS. These results are consistent with the energy changes of the FMO of the reactants. The catalyst lowers the energy of the nitronium LUMO, enhancing its interaction with the vinyl ether HOMO. The reaction takes on enhanced charge transfer character in the presence of the catalyst. These overall effects are similar to those found in D-A reactions catalyzed by Lewis acids.

As with D-A reactions, it is possible to achieve enantioselective cycloaddition in the presence of chiral catalysts.<sup>137</sup> Many of the catalysts are similar to those used in enantioselective D-A reactions. The catalysis usually results from a lowering of the LUMO energy of the dipolarophile, which is analogous to the Lewis acid catalysis of D-A reactions. The more organized TS, incorporating a metal ion and associated ligands, then enforces a preferred orientation of the reagents. For example, the bulky aryl groups in the catalyst **C** favor one direction of approach of the nitronium reactant.<sup>138</sup>

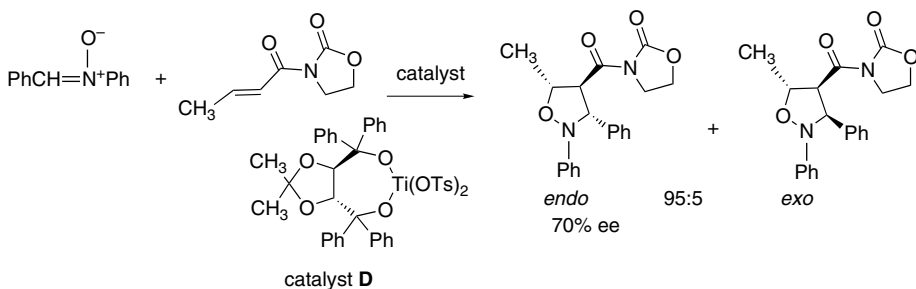
<sup>136</sup> L. R. Domingo, *Eur. J. Org. Chem.*, 2265 (2000).

<sup>137</sup> K. V. Gothelf and K. A. Jorgensen, *Chem. Rev.*, **98**, 863 (1998); M. Frederickson, *Tetrahedron*, **53**, 403 (1997).

<sup>138</sup> T. Mita, N. Ohtsuki, T. Ikeno, and T. Yamada, *Org. Lett.*, **4**, 2457 (2002).



The Ti(IV) TADDOL catalyst **D** leads to moderate to high enantioselectivity in nitrene cycloaddition with *N*-acyloxazolidinones.<sup>139</sup>



## 10.4. [2 + 2] Cycloaddition Reactions

As indicated in the Introduction, [2 + 2] cycloadditions are forbidden for the  $[\pi 2_s + \pi 2_s]$  topology but allowed for the  $[\pi 2_a + \pi 2_s]$  topology.<sup>140</sup> One example of  $[2\pi_s + 2\pi_a]$  cycloaddition involves ketenes.<sup>141</sup> An alternative description of the orbital array for this reaction is a  $[\pi 2_s + (\pi 2_s + \pi 2_s)]$  addition.<sup>142</sup> The basis set orbital arrays for both arrangements are shown in Figure 10.19. The  $[\pi 2_a + \pi 2_s]$  system has Möbius topology, whereas the  $[\pi 2_s + (\pi 2_s + \pi 2_s)]$  system has Hückel topology with six  $\pi$  electrons involved and is an allowed process.

The TS found for the latter mode of addition is very asynchronous with a strong initial interaction of the ketene *sp* carbon with both carbons of the alkene and considerable polar character.<sup>143</sup> Analysis of the electronic interactions at the TS by NPA shows substantial charge transfer from ethene to ketene, as would be expected on the

<sup>139</sup> K. V. Gothelf and K. A. Jorgensen, *Acta Chem. Scand.*, **50**, 652 (1996); K. B. Jensen, K. V. Gothelf, R. G. Hazell, and K. A. Jorgensen, *J. Org. Chem.*, **62**, 2471 (1997); K. B. Jensen, K. V. Gothelf, and K. A. Jorgensen, *Helv. Chim. Acta*, **80**, 2039 (1997).

<sup>140</sup> R. B. Woodward and R. Hoffmann, *Angew. Chem. Int. Ed. Engl.*, **8**, 781 (1969).

<sup>141</sup> W. T. Brady and R. Roe, *J. Am. Chem. Soc.*, **93**, 1662 (1971); W. T. Brady, in *The Chemistry of Ketenes, Allenes and Related Compounds*, S. Patai, ed., John Wiley, Chichester, 1980, Chap. 8.

<sup>142</sup> E. Valenti, M. A. Pericas, and A. Moyano, *J. Org. Chem.*, **55**, 3582 (1990).

<sup>143</sup> L. A. Burke, *J. Org. Chem.*, **50**, 3149 (1985); X. Wang and K. N. Houk, *J. Am. Chem. Soc.*, **112**, 1754 (1990); S. Yamabe, T. Minato, and Y. Osamura, *J. Chem. Soc., Chem. Commun.*, 53 (1993); S. Yamabe, K. Kuwata, and T. Minato, *Theo. Chem. Acc.*, **102**, 139 (1999).

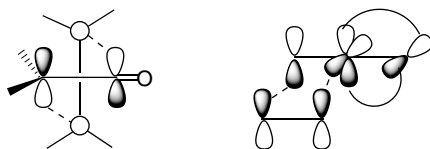


Fig. 10.19.  $[\pi 2_a + \pi 2_s]$  and  $[\pi 2_s + (\pi 2_s + \pi 2_s)]$  orbital arrays for alkene-ketene [2+2] cycloaddition.

basis of relative electrophilicity.<sup>144</sup> Figure 10.20 gives the bond distances and NPA charges as determined by DFT (BP86/III) computations.

Predictions of stereoselectivity and reactivity based on the  $[\pi 2_s + (\pi 2_s + \pi 2_s)]$  TS are in better accord with experimental results than predictions derived from the  $[\pi 2_s + \pi 2_a]$  TS.<sup>145</sup> Minimization of interaction between the substituents leads to a cyclobutanone in which the substituents at C(2) and C(3) are *cis*, which is the stereochemistry usually observed in these reactions. For example, *E*- and *Z*-2-butene give stereoisomeric products with ethoxyketene.<sup>146</sup>

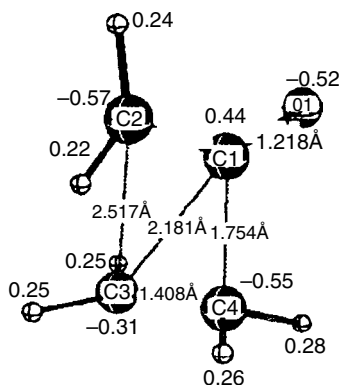
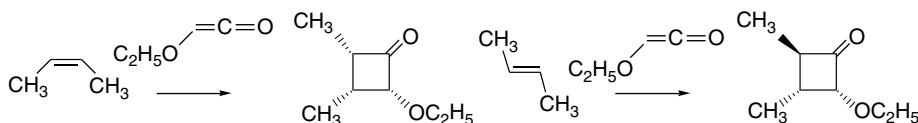


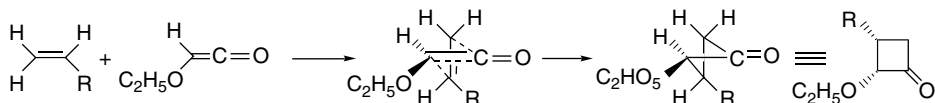
Fig. 10.20. Bond distances and NPA charges for the DFT (BP86/III) transition structure for addition between ketene and ethene. Reproduced from *J. Phys. Chem. A*, **106**, 431 (2002), by permission of the American Chemical Society.

<sup>144</sup>. D. V. Deubel, *J. Phys. Chem., A*, **106**, 431 (2002).

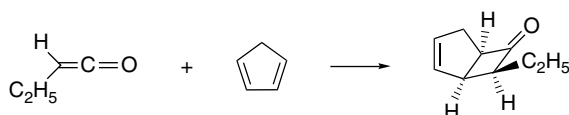
<sup>145</sup>. D. J. Pasto, *J. Am. Chem. Soc.*, **101**, 37 (1979).

<sup>146</sup>. T. DoMinh and O. P. Strausz, *J. Am. Chem. Soc.*, **92**, 1766 (1970).

For monosubstituted alkenes, the substituent is vicinal and *cis* to the ethoxy group in the cyclobutanone product, a structure that maximizes the separation of the alkyl and ethoxy substituents in the TS.



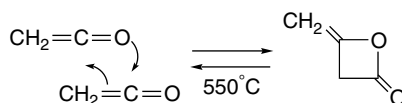
Similarly, ethyl ketene reacts with cyclopentadiene to give the ethyl group in the *endo* position.



Ref. 147

Note also the preference for [2 + 2] rather than [2 + 4] cycloaddition with cyclopentadiene. A computational comparison of the [2 + 2] and [2 + 4] modes of reaction between cyclopentadiene and ketene found the former to have a lower  $E_a$  (by about 10 kcal/mol).<sup>148</sup>

The best yields are obtained when the ketene has an electronegative substituent, such as halogen. Simple ketenes are not very stable and are usually generated in situ. The most common method for generating ketenes for synthesis is by dehydrohalogenation of acyl chlorides, which is usually done with an amine such as triethylamine.<sup>149</sup> Ketene itself and certain alkyl derivatives can be generated by pyrolysis of carboxylic anhydrides.<sup>150</sup> Ketene can also be generated by pyrolysis of acetone.<sup>151</sup> Ketene forms a dimer, from which it can be regenerated at 550°C.<sup>152</sup>



Intramolecular ketene cycloadditions are possible if the ketene and alkene functionalities can achieve an appropriate orientation.<sup>153</sup>

<sup>147</sup> M. Rey, S. M. Roberts, A. S. Dreiding, A. Roussel, H. Vanlierde, S. Toppet, and L. Ghosez, *Helv. Chim. Acta*, **65**, 703 (1982).

<sup>148</sup> U. Salzner and S. M. Bachrach, *J. Org. Chem.*, **61**, 237 (1996).

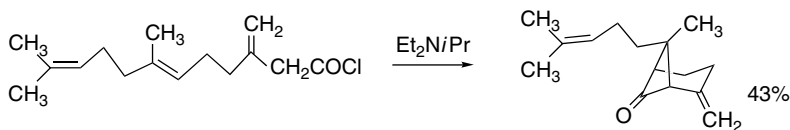
<sup>149</sup> K. Shishido, T. Azuma, and M. Shibuya, *Tetrahedron Lett.*, **31**, 219 (1990).

<sup>150</sup> G. J. Fisher, A. F. MacLean, and A. W. Schnizer, *J. Org. Chem.*, **18**, 1055 (1953).

<sup>151</sup> C. D. Hurd, *Org. Synth.*, **1**, 330 (1941).

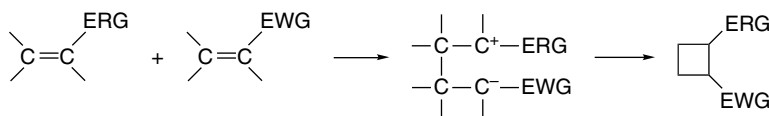
<sup>152</sup> S. Andreades and H. D. Carlson, *Org. Synth.*, **V**, 679 (1973).

<sup>153</sup> B. B. Snider, R. A. H. F. Hui, and Y. S. Kulkarni, *J. Am. Chem. Soc.*, **107**, 2194 (1985); B. B. Snider and R. A. H. F. Hui, *J. Org. Chem.*, **50**, 5167 (1985); W. T. Brady and Y. F. Giang, *J. Org. Chem.*, **50**, 5177 (1985).

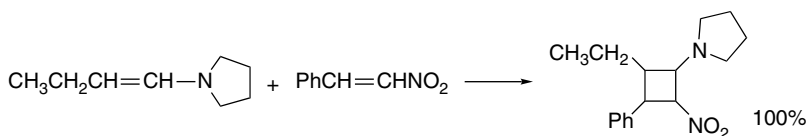


Ref. 154

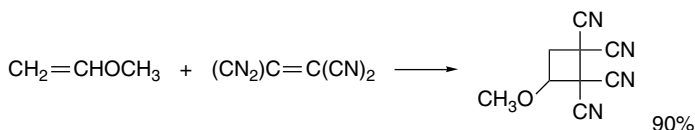
Cyclobutanes can also be formed by nonconcerted processes involving zwitterionic intermediates. The combination of an electron-rich alkene (enamine, vinyl ether) and an electrophilic one (nitro- or polycyanoalkene) is required for such processes.



Below are two examples of this reaction type.



Ref. 155



Ref. 156

The stereochemistry of these reactions depends on the lifetime of the dipolar intermediate, which, in turn, is influenced by the polarity of the solvent. In the reactions of enol ethers with tetracyanoethylene, the stereochemistry of the vinyl ether portion is retained in nonpolar solvents. In polar solvents, cycloaddition is nonstereospecific as a result of a longer lifetime for the zwitterionic intermediate.<sup>157</sup>

The [2+2] cycloaddition of ketenes and imines is an important route to the  $\beta$ -lactam ring (azetidinone),<sup>158</sup> which is a crucial structural feature of the penicillin class of antibiotics. A number of theoretical treatments of this reaction indicate that in solution phase this is a two-step reaction, with the second step being rate determining.<sup>159</sup> The stepwise nature of the reaction is accommodated by the relative stability of both charged moieties, an iminium cation and an enolate anion.

<sup>154</sup> E. J. Corey and M. C. Desai, *Tetrahedron Lett.*, **26**, 3535 (1985).

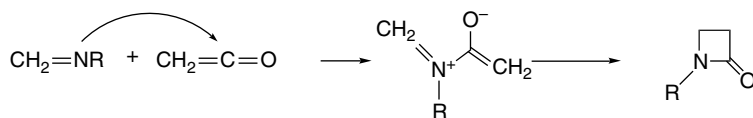
<sup>155</sup> M. E. Kuehne and L. Foley, *J. Org. Chem.*, **30**, 4280 (1965).

<sup>156</sup> J. K. Williams, D. W. Wiley, and B. C. McKusick, *J. Am. Chem. Soc.*, **84**, 2210 (1962).

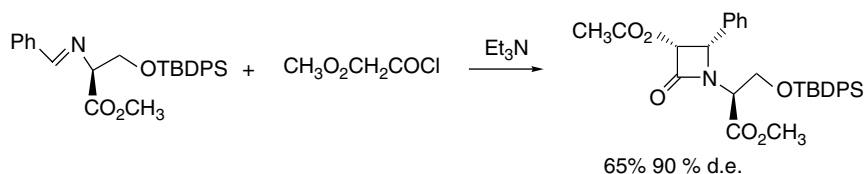
<sup>157</sup> R. Huisgen, *Acc. Chem. Res.*, **10**, 117, 199 (1977).

<sup>158</sup> C. Palomo, J. M. Aizpurua, I. Ganboa, and M. Oiarbide, *Eur. J. Org. Chem.*, 3223 (1999); I. Ojima and F. Dalalogue, *Chem. Soc. Rev.*, **26**, 377 (1997).

<sup>159</sup> X. Assfeld, J. A. Sordo, J. Gonzalez, M. F. Ruiz-Lopez, and T. L. Sordo, *Theochem*, **106**, 193 (1993); X. Assfeld, M. F. Ruiz-Lopez, J. Gonzalez, R. Lopez, J. A. Sordo, and T. L. Sordo, *J. Comput. Chem.*, **15**, 479 (1994); T. N. Truong, *J. Phys. Chem. B*, **102**, 7877 (1998).



In addition to its application in the synthesis of  $\beta$ -lactams, this reaction has been used for stereoselective synthesis of the side chain of the taxol class of antitumor agents.

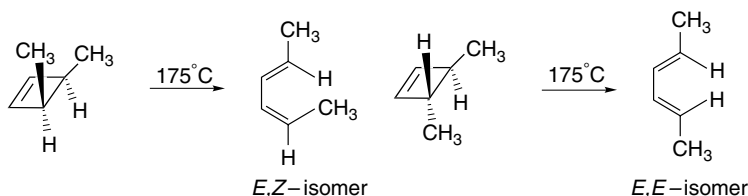


Ref. 160

## 10.5. Electrocyclic Reactions

### 10.5.1. Overview of Electrocyclic Reactions

An electrocyclic reaction is defined as the formation of a single bond between the terminal atoms of a linear conjugated system of  $\pi$  electrons and the reverse process. One example is the thermal ring opening of cyclobutenes to butadienes.



Ref. 161

It is not surprising that thermolysis of cyclobutenes leads to ring opening because the strain in the four-membered ring is relieved. The ring opening of cyclobutene to 1,3-butadiene is exothermic by 11 kcal/mol. The  $E_a$  for simple alkyl-substituted cyclobutene is in the range of 30–35 kcal/mol.<sup>162</sup> What is particularly significant about these reactions is that they are stereospecific. *cis*-3,4-Dimethylcyclobutene is converted to *E,Z*-2,4-hexadiene, whereas *trans*-3,4-dimethylcyclobutene yields the *E,E*-isomer. The level of stereospecificity is very high. In the ring opening of *cis*-3,4-dimethylcyclobutene, for example, only 0.005% of the minor product *E,E*-2,4-hexadiene is formed, even though it is more stable than the *E,Z*-isomer.<sup>163</sup>

The reason for the stereospecificity is that the groups bonded to the breaking bond rotate in the same sense during the ring-opening process. Such motion, in which all

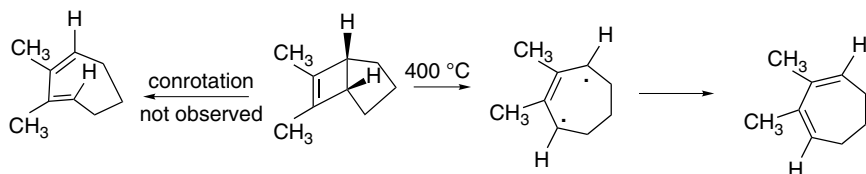
<sup>160</sup> V. Farina, S. I. Hauck, and D. G. Walker, *Synlett*, 761 (1992).

<sup>161</sup> R. F. K. Winter, *Tetrahedron Lett.*, 1207 (1965).

<sup>162</sup> W. Kirmse, N. G. Rondan, and K. N. Houk, *J. Am. Chem. Soc.*, **106**, 7989 (1984).

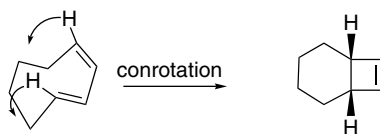
<sup>163</sup> J. I. Brauman and W. C. Archie, Jr., *J. Am. Chem. Soc.*, **94**, 4262 (1972).

the substituents rotate either clockwise or counterclockwise, is called the *conrotatory* mode. When the conrotatory motion is precluded by some structural feature, ring opening requires a much higher temperature. In the bicyclo[3.2.0]hept-6-ene example shown below, the five-membered ring prevents a conrotatory ring opening because it would lead to the very strained *Z,E*-cycloheptadiene. The reaction takes place only at very high temperature, 400°C, and probably involves the diradical shown as an intermediate.



Ref. 164

The *principle of microscopic reversibility* (see p. 275) requires that the reverse process, ring closure of a butadiene to a cyclobutene, also be conrotatory. Usually this is thermodynamically unfavorable, but a case in which the ring closure is energetically favorable is conversion of *E,Z*-1,3-cyclooctadiene to *cis*-bicyclo[4.2.0]oct-7-ene. The ring closure is favorable in this case because of the strain associated with the *E*-double bond. The ring closure occurs by a conrotatory process.



Ref. 165

Electrocyclic reactions of 1,3,5-trienes lead to 1,3-cyclohexadienes. Note that only the 3-*Z*-isomer can attain a conformation suitable for cyclization. The ring closure is normally the favored direction of reaction for conjugated trienes because of the greater thermodynamic stability of the cyclic compound, which has six  $\sigma$  bonds and two  $\pi$  bonds, whereas the triene has five  $\sigma$  and three  $\pi$  bonds. The closure of *Z*-1,3,5-hexatriene to cyclohexa-1,3-diene is exothermic by 16.4 kcal/mol.<sup>166</sup> The  $E_a$  is about 30 kcal/mol.<sup>167</sup> These ring closure reactions also exhibit a high degree of stereospecificity, illustrated with octatrienes **7** and **8**. *E,Z,E*-2,4,6-Octatriene (**7**) cyclizes only to *cis*-5,6-dimethyl-1,3-cyclohexadiene, whereas the *E,Z,Z*-2,4,6-octatriene (**8**) leads exclusively to the *trans* cyclohexadiene isomer.<sup>168</sup> A point of particular importance regarding the stereochemistry of this reaction is that the groups at the termini of the triene system rotate in the opposite sense during the cyclization process, a mode of electrocyclic reaction known as *disrotatory*.

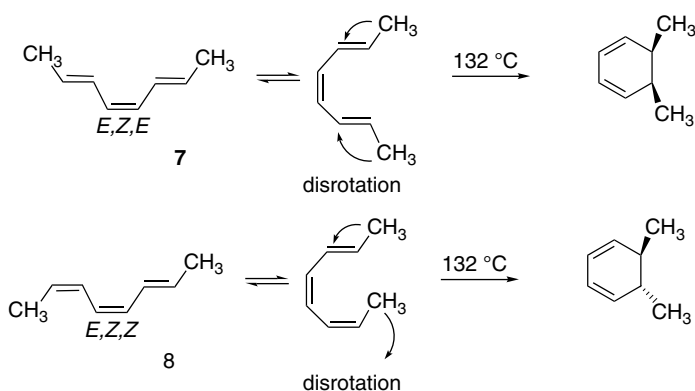
<sup>164</sup> R. Criegee and H. Furr, *Chem. Ber.*, **97**, 2949 (1964).

<sup>165</sup> K. M. Schumate, P. N. Neuman, and G. J. Fonken, *J. Am. Chem. Soc.*, **87**, 3996 (1965); R. S. H. Liu, *J. Am. Chem. Soc.*, **89**, 112 (1967).

<sup>166</sup> R. B. Turner, B. J. Mallon, M. Tichy, W. von E. Doering, W. R. Roth, and G. Schroeder, *J. Am. Chem. Soc.*, **95**, 8605 (1973); W. R. Roth, O. Adamczak, R. Breuckmann, H.-W. Lennartz, and R. Boese, *Chem. Ber.*, **124**, 2499 (1991).

<sup>167</sup> K. E. Lewis and H. Steiner, *J. Chem. Soc.*, 3080 (1964).

<sup>168</sup> E. N. Marvell, G. Caple, and B. Schatz, *Tetrahedron Lett.*, 385 (1965); E. Vogel, W. Grimme, and E. Dinne, *Tetrahedron Lett.*, 391 (1965); J. E. Baldwin and V. P. Reddy, *J. Org. Chem.*, **53**, 1129 (1988).



### 10.5.2. Orbital Symmetry Basis for the Stereospecificity of Electrocyclic Reactions

A mechanistic description of electrocyclic reactions must explain not only the high degree of stereospecificity, but also why four  $\pi$ -electron systems undergo conrotatory reactions, whereas six  $\pi$ -electron systems undergo disrotatory reactions. Woodward and Hoffmann proposed that the stereochemistry of the reactions is controlled by the symmetry properties of the highest occupied molecular orbital (HOMO) of the reacting system.<sup>169</sup> The idea that the HOMO should control the course of the reaction is another example of *frontier molecular orbital theory* (FMO), which holds that it is the electrons of highest energy, i.e., those in the HOMO, that are of prime importance in determining the course of the reaction (see p. 43).<sup>170</sup>

Why do the symmetry properties of the HOMO determine the stereochemistry of the electrocyclic reaction? For convenience, let us examine the microscopic reverse of the ring opening. The stereochemical features of the reaction are the same in both the forward or reverse directions. For conjugated dienes, the HOMO is  $\psi_2$ . For bonding to occur between C(1) and C(4), the positive lobe on C(1) must overlap with the positive lobe on C(4) (or negative with negative, since the signs are interchangeable). This overlap of lobes of the same sign can be accomplished only by a conrotatory motion. Disrotatory motion causes overlap of orbitals of opposite sign, leading to an antibonding overlap that would preclude bond formation. Other conjugated dienes have identical orbital symmetries, so the conrotatory mode is preferred for all thermal electrocyclic processes of 1,3-dienes. The conrotatory process is illustrated in Figure 10.21.

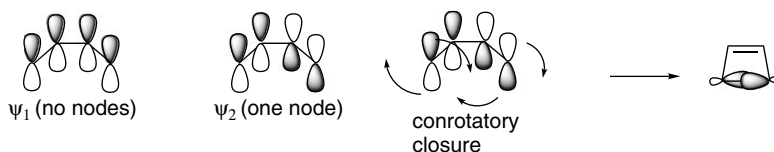


Fig. 10.21. Symmetry properties of the occupied  $\pi$  orbitals of a conjugated diene.

<sup>169</sup> R. B. Woodward and R. Hoffmann, *J. Am. Chem. Soc.*, **87**, 395 (1965).

<sup>170</sup> K. Fukui and H. Fujimoto, in *Mechanisms of Molecular Migrations*, Vol. 2, B. S. Thyagarajan, ed., Interscience, New York, 1968, p. 117; K. Fukui, *Acc. Chem. Res.*, **4**, 57 (1971); K. Fukui, *Angew. Chem. Int. Ed. Engl.*, **21**, 801 (1982).

The analysis for the 1,3,5-triene system according to FMO theory proceeds in the same way as for a diene, but leads to the conclusion that a bonding interaction between C(1) and C(6) of the triene will require a disrotatory motion. This is because the HOMO,  $\psi_3$ , has positive lobes on the same face of the  $\pi$  system and these must overlap to permit bond formation. The symmetry properties of other six  $\pi$ -electron conjugated triene systems are the same, so disrotatory ring closure (or opening) is general for conjugated trienes. The  $\pi$  orbitals for the hexatriene system are shown in Figure 10.22.

When we recall the symmetry patterns for linear polyenes that were discussed in Chapter 1 (see p. 29), we can further generalize the predictions based on the symmetry of the polyene HOMO. The HOMOs of the  $4n$  systems are like those of 1,3-dienes in having opposite phases at the terminal atoms. The HOMOs of other  $4n + 2$  systems are like trienes and have the same phase at the terminal atoms. Systems with  $4n$   $\pi$  electrons will undergo electrocyclic reactions by conrotatory motion, whereas systems with  $4n + 2$   $\pi$  electrons will react by the disrotatory mode.

The analysis of electrocyclic reactions can also be done using *orbital correlation diagrams*.<sup>171</sup> This approach focuses attention on the orbital symmetries of both reactants and products and considers the symmetry properties of all the orbitals. In any concerted process, the orbitals of the starting material must be smoothly transformed into orbitals of product having the same symmetry. If this process of orbital conversion leads to the ground state electronic configuration of the product, the process will have a relatively low activation energy and be an *allowed* process. If, on the other hand, the orbitals of the reactant are transformed into a set of orbitals that does not correspond to the ground state of the product, a high-energy TS occurs and the reaction is *forbidden*, since it would lead to an excited state of the product.

The cyclobutene-butadiene interconversion can serve as an example of the construction of an orbital correlation diagram. For this reaction to occur, the four  $\pi$  orbitals of butadiene must be converted smoothly into the two  $\pi$  and two  $\sigma$  orbitals of the ground state of cyclobutene. The  $\pi$  orbitals of butadiene are  $\psi_1$ ,  $\psi_2$ ,  $\psi_3$ , and  $\psi_4$ . For cyclobutene, the four orbitals are  $\sigma$ ,  $\pi$ ,  $\sigma^*$ , and  $\pi^*$ , with each of them classified with respect to the symmetry elements that are maintained in the course of the transformation. The relevant symmetry features depend on the structure of the reacting system. The most common elements of symmetry to be considered are planes of symmetry and rotation axes. An orbital is classified as symmetric, *S*, if it is unchanged by reflection in a plane of symmetry or by rotation about an axis of symmetry. If the orbital changes sign (phase) at each lobe as a result of the symmetry operation, it is called antisymmetric, *A*. Proper molecular orbitals must be either symmetric or antisymmetric. If an orbital is neither *S* nor *A*, it must be adapted by combination with other orbitals to meet this requirement.

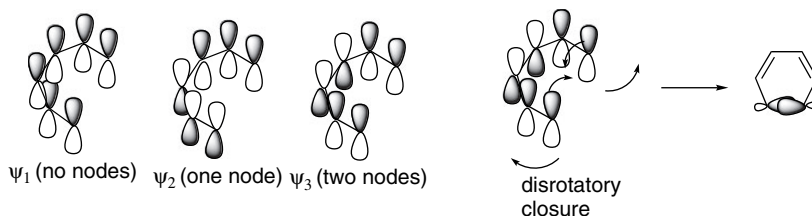
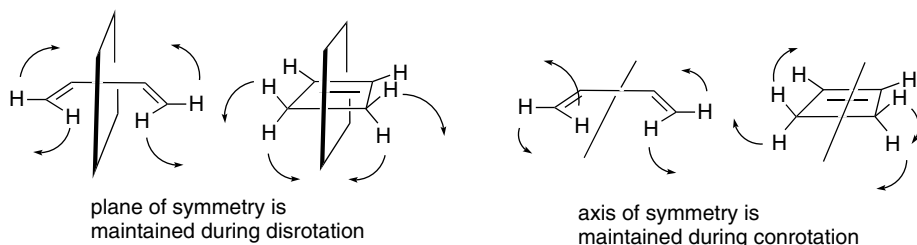


Fig. 10.22. Symmetry properties of the occupied  $\pi$  orbitals of a conjugated triene.

<sup>171</sup> H. C. Longuet-Higgins and E. W. Abrahamson, *J. Am. Chem. Soc.*, **87**, 2045 (1965).

Figure 10.23 illustrates the classification of the MOs of butadiene and cyclobutene. There are two elements of symmetry that are common to both *s-cis*-butadiene and cyclobutene: a plane of symmetry and a twofold axis of rotation. The plane of symmetry is maintained during a disrotatory transformation of butadiene to cyclobutene. In the conrotatory transformation, the axis of rotation is maintained throughout the process. Therefore to analyze the disrotatory process, the orbitals must be classified with respect to the plane of symmetry, and to analyze the conrotatory process, they must be classified with respect to the axis of rotation.



Both the disrotatory and the conrotatory process can be analyzed by comparing the symmetry classification of reactant and product orbitals given in Figure 10.23. The orbitals are arranged according to energy in Figure 10.24, and the states of like symmetry for the disrotatory process are connected. It is seen that in the disrotatory process, not all of the ground state orbitals of cyclobutene correlate with ground state orbitals of butadiene. The bonding  $\pi$  orbital of cyclobutene is transformed into an antibonding orbital ( $\psi_3$ ) of butadiene. In the reverse process,  $\psi_2$  of butadiene is transformed into the antibonding  $\pi^*$  orbital of cyclobutene. Because of the failure of the orbitals of the ground state molecules to correlate, the transformation would lead to a high-energy TS, and the disrotatory reaction is said to be *symmetry forbidden*.

Analysis of the conrotatory process is carried out in exactly the same way. In this case the element of symmetry that is maintained throughout the reaction process is the twofold rotation axis. The resulting correlation diagram is shown in Figure 10.24. The conrotatory reaction is *symmetry allowed*, since the bonding orbitals of butadiene correlate with the bonding orbitals of cyclobutene and vice versa. Figure 10.25 is a pictorial representation of the orbital in the reactant, transition structure, and product.

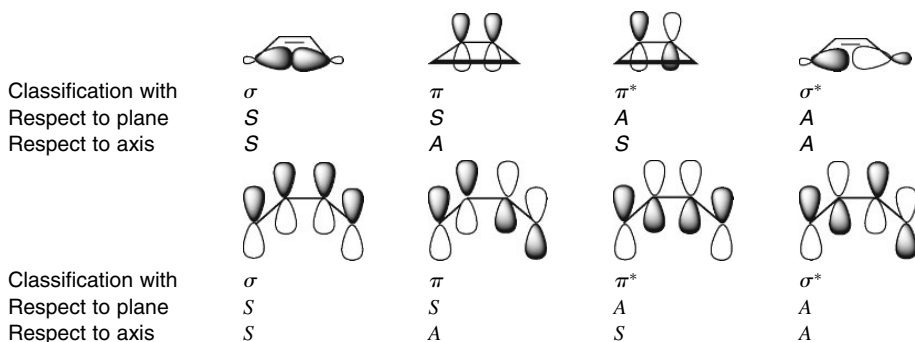


Fig. 10.23. Elements of symmetry for and classification of orbitals for disrotatory and conrotatory interconversion of 1,3-butadiene and cyclobutene.

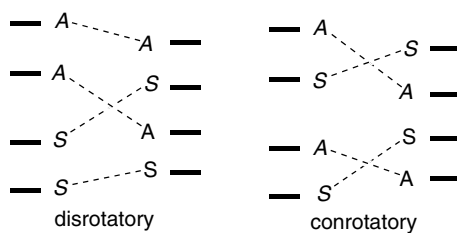


Fig. 10.24. Correlation diagrams for interconversion of cyclobutene and 1,3-butadiene: (left) symmetry forbidden disrotatory reaction; (right) symmetry allowed conrotatory reaction.

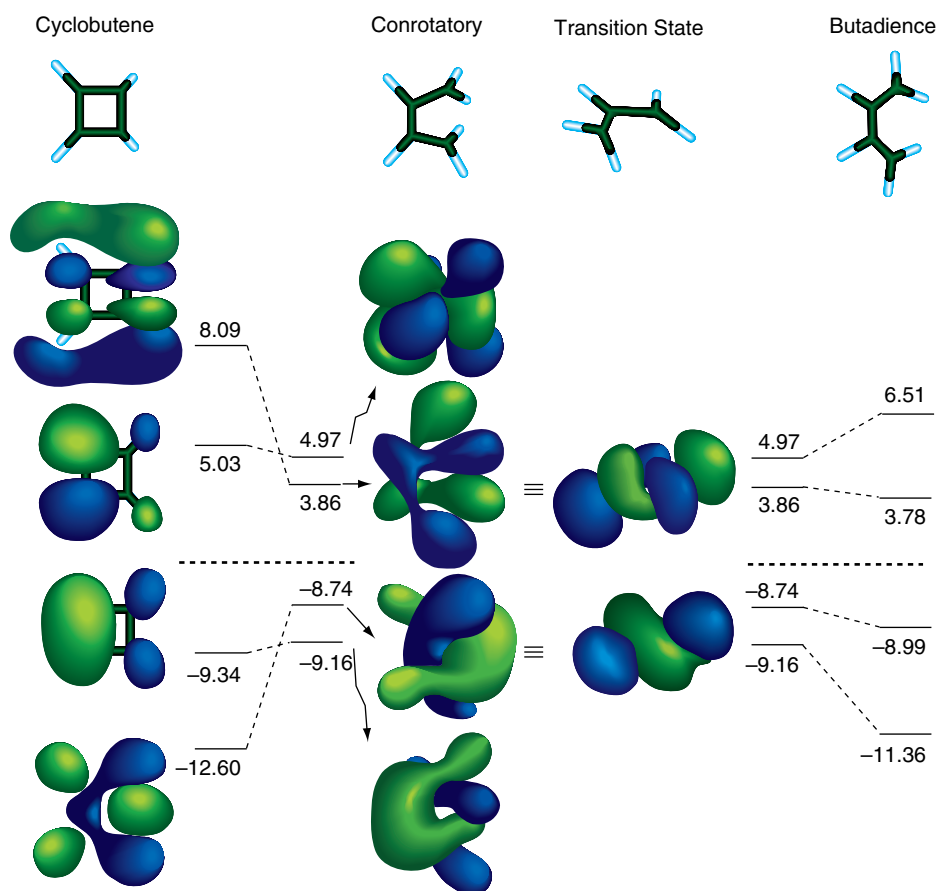
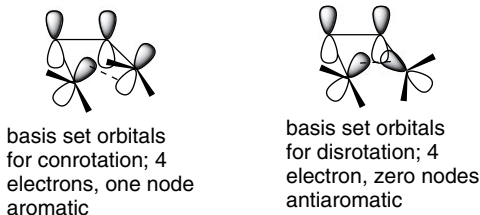


Fig. 10.25. Correlation of orbitals of cyclobutene with the conrotatory transition state and the product, 1,3-butadiene. Energies (in eV) are from HF/6-31G(d) computations. Reproduced from *J. Am. Chem. Soc.*, **125**, 5072 (2003), by permission of the American Chemical Society.

Correlation diagrams can be constructed in an analogous manner for the disrotatory and conrotatory modes for interconversion of 1,3,5-hexatriene and cyclohexadiene. They lead to the prediction that the disrotatory mode is an allowed process, whereas the conrotatory reaction is forbidden, which is in agreement with the experimental results on this reaction. Other electrocyclizations can be analyzed by the same method. Substituted derivatives of polyenes obey the orbital symmetry rules, even in cases where the substitution pattern does not correspond in symmetry to that of the orbital system. It is the symmetry of the participating orbitals, not of the molecule as a whole, that is crucial to the analysis.

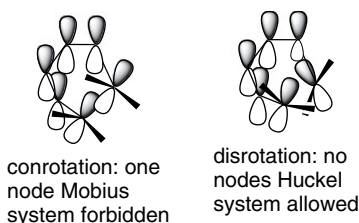
Electrocyclic reactions can also be analyzed on the basis of the idea that transition states can be classified as aromatic or antiaromatic, just as is the case for ground state molecules.<sup>172</sup> A stabilized aromatic TS results in a low activation energy, i.e., an allowed reaction. An antiaromatic TS has a high energy barrier and corresponds to a forbidden process. The analysis of electrocyclizations by this process consists of examining the array of basis set orbitals that is present in the transition structure and classifying the system as aromatic or antiaromatic. For the butadiene-cyclobutene interconversion, the TSs for conrotatory and disrotatory interconversion are shown below. The array of orbitals represents the *basis set orbitals*, that is, the complete set of  $2p$  orbitals involved in the reaction process, not the individual molecular orbitals. The tilt at C(1) and C(4) as the butadiene system rotates toward the TS is different for the disrotatory and conrotatory modes. The dashed line represents the  $\sigma$  bond that is being broken (or formed).



For the cyclobutene-butadiene TS, the conrotatory closure results in a Möbius system, whereas a disrotatory TS gives a Hückel system. The same rules of aromaticity apply as for ground state molecules. A Hückel system is aromatic when it has  $4n + 2$  electrons. A Möbius system is aromatic when it has  $4n$  electrons. In the case of the cyclobutene-butadiene interconversion, which involves four electrons, it is the conrotatory Möbius TS that is the favored aromatic transition state.

Basis set orbital analysis of the hexatriene-cyclohexadiene system leads to the conclusion that the disrotatory process will be favored. The basis set orbitals for the conrotatory and disrotatory transition states are shown below. Here, with six electrons involved, it is the disrotatory mode (Hückel system) that gives a stabilized TS.

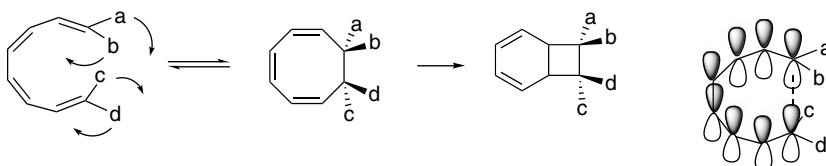
<sup>172</sup> H. E. Zimmerman, *Acc. Chem. Res.*, **4**, 272 (1971); M. J. S. Dewar, *Angew. Chem. Int. Ed. Engl.*, **10**, 761 (1971).



There have been a number of computational studies of the 1,3-butadiene-cyclobutene electrocyclozation.<sup>173</sup> The approaches usually involve location of the minimum energy TS (as described in Section 3.2.2.3) and evaluation of its characteristics. These computational approaches confirm the preference for the conrotatory process, and DFT and CI-MO calculations can provide good estimates of  $E_a$ .<sup>174</sup> The aromaticity of the TS structures can also be evaluated computationally. The criteria are the same as for ground state molecules, namely energy, bond lengths, and magnetic properties.<sup>175</sup>

A number of theoretical analyses of the 1,3,5-hexatriene electrocyclozation support the preference for the disrotatory mode. For example, MP2/CAS/6-311+G(*d,p*) calculations found the TSs for both modes of cyclization, as shown in Figure 10.26. The disrotatory mode is 11 kcal/mol lower in energy.<sup>176</sup>

For conjugated tetraenes,  $n = 8$ , conrotation should be preferred. The expectation that cyclization of eight  $\pi$ -electron systems will be conrotatory has been confirmed by study of isomeric 2,4,6,8-decatetraenes. Electrocyclic reaction occurs near room temperature. The unsubstituted system, has an  $E_a$  of 17.0 kcal/mol and  $\Delta H$  of  $-11.2$  kcal/mol.<sup>177</sup> At slightly higher temperatures, the cyclooctatriene system that is formed undergoes a subsequent disrotatory cyclization, establishing equilibrium with the corresponding bicyclo[4.2.0]octa-2,4-diene.<sup>178</sup>



MO calculations (MP2/6-31G\*) on the TS confirmed that it is helical and conforms to the expected conrotatory mode.<sup>179</sup> This is a Möbius type TS. The NICS and magnetic properties attributed to the TS by MO calculation also indicate that it has aromatic character.<sup>180</sup>

<sup>173</sup>. N. G. Rondan and K. N. Houk, *J. Am. Chem. Soc.*, **107**, 2099 (1985); J. Breulet and H. F. Schaefer, III, *J. Am. Chem. Soc.*, **106**, 1221 (1984); O. Wiest, D. C. Montiel, and K. N. Houk, *J. Phys. Chem. A*, **101**, 8378 (1997).

<sup>174</sup>. L. O. Deng and T. Ziegler, *J. Phys. Chem.*, **99**, 612 (1995); S. Sakai, *Theochem*, **461**, 283 (1999).

<sup>175</sup>. H. Jiao and P. v. R. Schleyer, *J. Phys. Org. Chem.*, **11**, 655 (1998).

<sup>176</sup>. S. Sakai and S. Takane, *J. Phys. Chem. A*, **103**, 2878 (1999).

<sup>177</sup>. G. Desimoni, G. Faita, S. Guidetti, and P. P. Righetti, *Eur. J. Org. Chem.*, 1921 (1999).

<sup>178</sup>. R. Huisgen, A. Dahmen, and H. Huber, *Tetrahedron Lett.*, 1461 (1969); R. Huisgen, A. Dahmen, and H. Huber, *J. Am. Chem. Soc.*, **89**, 7130 (1967); A. Dahmen and R. Huisgen, *Tetrahedron Lett.*, 1465 (1969).

<sup>179</sup>. B. E. Thomas, IV, J. D. Evanseck, and K. N. Houk, *J. Am. Chem. Soc.*, **115**, 4165 (1993); B. E. Thomas, J. D. Evanseck, and K. N. Houk, *Isr. J. Chem.*, **33**, 287 (1993).

<sup>180</sup>. H. Jiao and P. v. R. Schleyer, *J. Chem. Soc., Perkin Trans. 2*, 407 (1994).

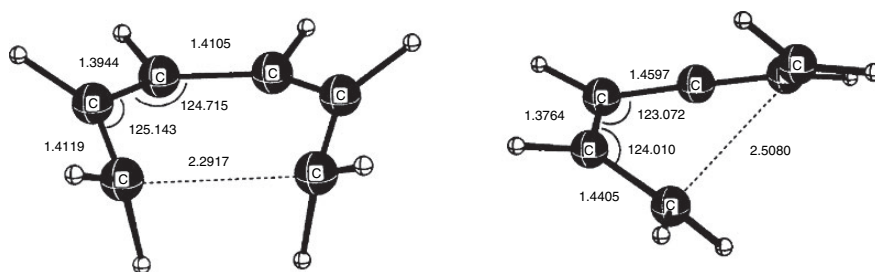


Fig. 10.26. Disrotatory (left) and conrotatory (right) transition structures for 1,3,5-hexatriene electrocycyclization from MP2/CAS/6-311+G(*d,p*) calculations. Reproduced from *J. Phys. Chem. A*, **103**, 2878 (1999), by permission of the American Chemical Society.

We have considered three viewpoints from which thermal electrocyclic processes can be analyzed: symmetry characteristics of the frontier orbital, orbital correlation diagrams, and transition state aromaticity. All arrive at the same conclusions about the stereochemistry of electrocyclic reactions. *Reactions involving  $4n + 2$  electrons are disrotatory and involve a Hückel-type transition structure, whereas those involving  $4n$  electrons are conrotatory and the orbital array are of the Möbius type.* These general principles serve to explain and correlate many specific experimental observations. The chart that follows summarizes the relationship between transition structure topology, the number of electrons, and the feasibility of the reaction.

Orbital Symmetry Rules for Electrocyclic Reactions		
Electrons	Hückel (disrotatory)	Möbius (conrotatory)
2	Aromatic	Antiaromatic
4	Antiaromatic	Aromatic
6	Aromatic	Antiaromatic
8	Antiaromatic	Aromatic

Figure 10.27 summarizes the energy relationships for the four-, six-, and eight-electron systems relative to the polyenes. We see that for cyclobutene-1,3-butadiene, ring opening is favored and the  $E_a$  is 32 kcal/mol. The  $E_a$  is similar for the 1,3,5-triene cyclization (30 kcal/mol), but ring closure is favored. The  $E_a$  drops to 17.0 kcal/mol for the *Z,Z*-1,3,5,7-octatriene to 1,3,5-cyclooctatriene cyclization, whereas the  $E_a$  for the reverse reaction is 28.2 kcal/mol.

For cyclobutenes, there is another interesting aspect to the stereochemistry of the electrocyclic reactions. There are two stereochemically distinct possibilities for the conrotatory process. A substituent group at C(3) might move away from or toward the breaking bond.

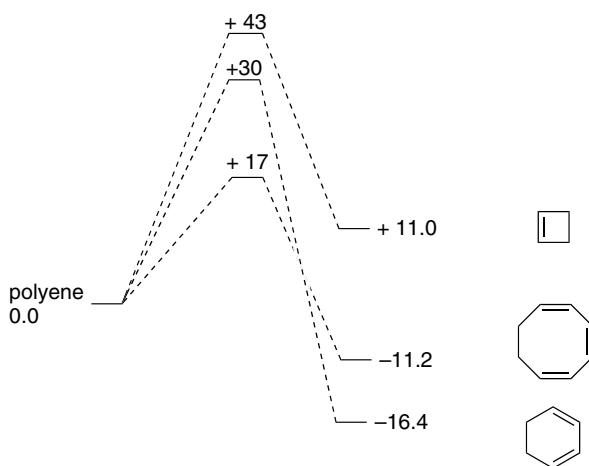
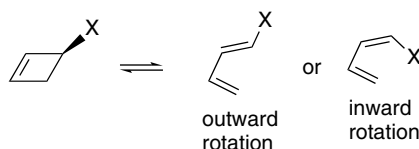
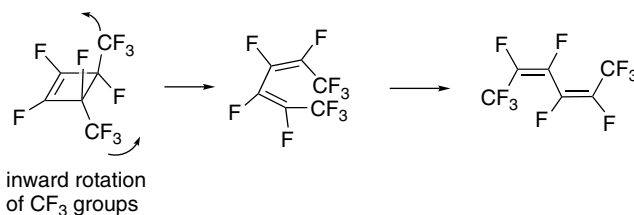


Fig. 10.27. Summary of relative  $E_a$  and  $\Delta H$  relationships in kcal/mol for electrocyclic reactions of conjugated dienes, trienes, and tetraenes.



Steric factors should cause a preference for the larger group to move outward. It was observed, however, that in the case of 1,2,3,4-tetrafluoro-*trans*-3,4-bis-(trifluoromethyl)cyclobutene, ring opening occurred with an inward rotation of the trifluoromethyl groups, leading to the *Z,Z*-product.<sup>181</sup>



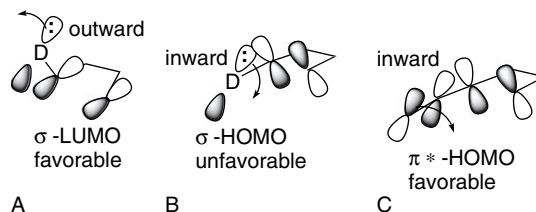
MO calculations (HF/6-21G) for the case of  $Y = \text{CH}=\text{O}$  found that the formyl group preferred to rotate inward and this was confirmed experimentally.<sup>182</sup> A general theoretical analysis indicates that the preference is for donor substituents to rotate outward, whereas acceptor substituents prefer to rotate inward.<sup>183</sup> A qualitative understanding of this stereoselectivity is based on analysis of the interaction of the substituents with the C(3)–C(4)  $\sigma$  bond that is breaking. The  $\sigma$  and  $\sigma^*$  orbitals of the reacting bond become much closer in energy in the TS, making them better donors and acceptors, respectively, in interactions with substituents. The orbital orientations

<sup>181</sup> W. R. Dolbier, Jr., H. Koroniak, D. J. Burton, and P. Heinze, *Tetrahedron Lett.*, **27**, 4387 (1986).

<sup>182</sup> K. Rudolf, D. C. Spellmeyer, and K. N. Houk, *J. Org. Chem.*, **52**, 3708 (1987).

<sup>183</sup> D. C. Spellmeyer and K. N. Houk, *J. Am. Chem. Soc.*, **110**, 3412 (1988); W. R. Dolbier, Jr., H. Koroniak, K. N. Houk, and C. Sheu, *Acc. Chem. Res.*, **29**, 471 (1996).

are such that donors interact with the LUMO best by outward rotation (**A**) while leading to a repulsive interaction with the HOMO by inward rotation (**B**). In contrast, acceptor substituents stabilize the HOMO in the TS best by inward rotation because a  $\pi^*$ -substituent orbital can provide a stabilizing interaction with the C(3)–C(4) HOMO (**C**). The largest outward preferences are for strong donor groups such as  $O^-$  and  $NH_2$ , whereas  $CH=O$  and  $CH=NH_2^+$  favor inward rotation.



The rotational preferences for a number of groups have been analyzed by HF/6-31G\* computation of TS energies. The trends agree with the rotational preference that is observed experimentally.<sup>184</sup> Some of the substituents have also been examined by DFT [B3LYP/6-31G(*d*)] computations.<sup>185</sup> Some of the data are given in Table 10.5.

The acetyl group is calculated to have a slight preference for outward rotation. Lewis acids increase the tendency toward inward rotation by making the substituent more electrophilic.<sup>186</sup> In accordance with this expectation, a Lewis acid ( $ZnI_2$ ) changes the ratio from 2:1 favoring outward rotation to 5:1 favoring inward rotation.

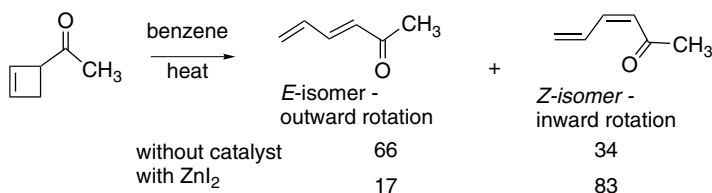


**Table 10.5. Directive Effect of Substituents on Inward/Outward Conrotation in Cyclobutene Ring Opening**

	Donor substituent $\Delta_{in-out}^a$		Acceptor substituent $\Delta_{in-out}^a$	
	HF/6-31G* <sup>a</sup>	B3LYP/6-311G* <sup>c</sup>	HF/6-31G* <sup>b</sup>	B3LYP/6-31G* <sup>c</sup>
$O^-$	24.4		$CH=O$	-4.6
$NH_2$	17.5	14.7	$CH=NH_2^+$	-10.1
$OH$	17.2		$NO_2$	7.3
$F$	16.9		$N=O$	-2.6
$Cl$	13.6		$CF_3$	2.6
$CH_3$	6.8	6.5	$CN$	4.3

a.  $\Delta_{in-out}$  is energy difference in kcal/mol between transition states for inward and outward rotation.

b. S. Niwayama, E. A. Kallel, D. C. Spellmeyer, C. M. Sheu and K. N. Houk, *J. Org. Chem.*, **61**, 2813 (1996).

c. P. S. Zhang, and K. N. Houk, *J. Am. Chem. Soc.*, **125**, 5072 (2003).

<sup>184</sup>. E. A. Kallel, Y. Wang, D. C. Spellmeyer, and K. N. Houk, *J. Am. Chem. Soc.*, **112**, 6759 (1990); S. Niwayama, E. A. Kallel, D. C. Spellmeyer, C. Sheu, and K. N. Houk, *J. Org. Chem.*, **61**, 2813 (1996); W. R. Dolbier, Jr., H. Koroniak, K. N. Houk, and C. Sheu, *Acc. Chem. Res.*, **29**, 471 (1996).

<sup>185</sup>. P. S. Lee, X. Zhang, and K. N. Houk, *J. Am. Chem. Soc.*, **125**, 5072 (2003).

<sup>186</sup>. S. Niwayama and K. N. Houk, *Tetrahedron Lett.*, **34**, 1251 (1993); S. Niwayama, *J. Org. Chem.*, **61**, 640 (1996).

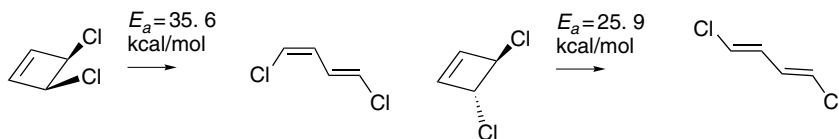
Table 10.6. Effect of Substituents on  $E_a$  for Outward or Inward Rotation.

Strong outward		Moderate outward		Inward		Deactivating (both)	
$O^-Li^+$	-17.2	$NO_2$	-3.3	$BH_2$	-24.5	$CF_3$	+3.5 (out)
$NH_2$	-14.6	Cl	-3.0	$CH=N^+H_2$	-19.5	$CF_3$	+5.4(in)
OH	-9.3	$CH_3C=O$	-2.6	$C^+(OH)_2$	-18.3	$NH_3^+$	+0.5 (out)
F	-6.1	CN	-2.3	N=O	-7.1	$NH_3^+$	+8.2(in)
				CH=O	-6.9		

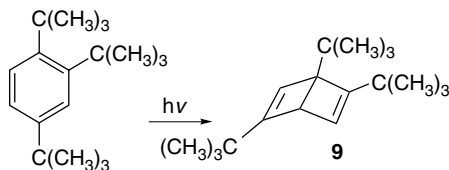
These substituents also have an effect on the reaction rate, which is indicated by the  $E_a$ , relative to the unsubstituted compound, as shown in Table 10.6. The strongly outwardly directing donor substituents decrease the  $E_a$  more for outward rotation, whereas the inward-directing groups preferentially stabilize the TS for inward rotation. A few substituents, e.g.,  $CF_3$  and  $NH_3^+$ , are destabilizing toward both types of TS.

### 10.5.3. Examples of Electrocyclic Reactions

In addition to the 3,4-dimethylcyclobutene case discussed in Section 10.5.1, there are many other examples of electrocyclic ring opening of cyclobutenes, and *cis*- and *trans*-3,4-dichlorocyclobutene have been examined carefully. The products are those expected for conrotation.<sup>187</sup> In the case of the *trans*-isomer, the product results from outward rotation of both chlorine atoms, in agreement with the calculated substituent effect. The *cis*-isomer, in which one of the chlorines must rotate inward, has a substantially higher  $E_a$ .



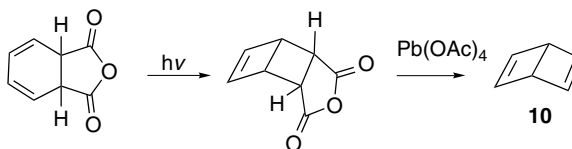
A particularly interesting case involves the bicyclo[2.2.0]hexa-2,5-diene system. This ring system is a valence isomer of the benzene ring and is often referred to as *Dewar benzene*. Attempts prior to 1960 to prepare Dewar benzene derivatives failed, and the pessimistic opinion was that such efforts would be fruitless because Dewar benzene would be so unstable as to immediately revert to benzene. Then in 1962, van Tamelen and Pappas isolated a stable Dewar benzene derivative **9** by photolysis of 1,2,4-tri-(*t*-butyl)benzene.<sup>188</sup> The compound was reasonably stable, reverting to the aromatic starting material only on heating. Part of the stability of this particular derivative can be attributed to steric factors. The *t*-butyl groups are farther apart in the Dewar benzene structure than in the aromatic structure.



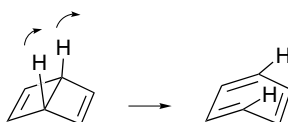
<sup>187</sup> R. Criegee, D. Seebach, R. E. Winter, B. Boerretzen, and H. Brune, *Chem. Ber.*, **98**, 2339 (1963); G. Maier and A. Bothur, *Eur. J. Org. Chem.*, 2063 (1998).

<sup>188</sup> E. E. van Tamelen, S. P. Pappas, and K. L. Kirk, *J. Am. Chem. Soc.*, **93**, 6092 (1971); this paper contains references to the initial work and describes subsequent studies.

The unsubstituted Dewar benzene **10** was successfully prepared in 1963.



This compound is less stable than **9** and reverts to benzene with a half-life of about 2 days at 25°C, with  $\Delta H^\ddagger = 23$  kcal/mol.<sup>189</sup> Nevertheless, the relative kinetic stability of Dewar benzene is surprisingly high when one considers that its conversion to benzene is exothermic by 71 kcal/mol. Furthermore, the central bond is not only strained but also *bis*-allylic. The kinetic stability of Dewar benzene is related to the orbital symmetry requirements for concerted electrocyclic transformations. The concerted thermal pathway would be conrotatory, since the reaction is the ring opening of a cyclobutene and therefore leads not to benzene, but to a highly strained *Z,Z,E*-cyclohexatriene. A disrotatory process, which would lead directly to benzene, is forbidden.



There have been several computational studies of the process.<sup>190</sup> CAS-SCF/6-311G++ calculations found a TS that leads from Dewar benzene to benzene without the intermediacy of the *Z,Z,E*-isomer. Both a conrotatory and a disrotatory TS were found, as shown in Figure 10.28. The conrotatory TS is calculated to be about 22.9 kcal/mol above Dewar benzene and 99.3 kcal/mol less stable than benzene.<sup>191</sup> Thus, although a route for ring opening exists, the energy barrier is sufficient to permit the isolation of Dewar benzene.

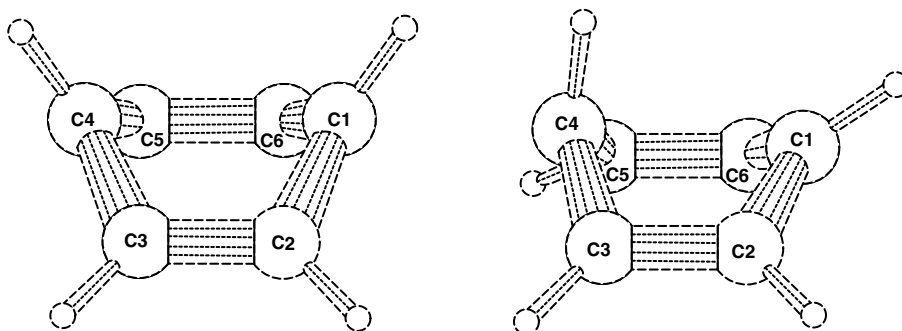


Fig. 10.28. Disrotatory (left) and conrotatory (right) transition structures for conversion of *cis*-bicyclo[2.2.0]hexa-2,5-diene (Dewar benzene) to benzene. The conrotatory TS is 6.6 kcal/mol lower in energy than the disrotatory TS. Reproduced from *Theochem*, **492**, 217 (1999), by permission of Elsevier.

<sup>189</sup>. M. J. Goldstein and R. S. Leight, *J. Am. Chem. Soc.*, **99**, 8112 (1977).

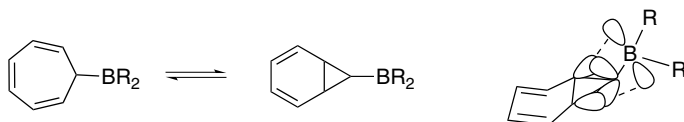
<sup>190</sup>. R. P. Johnson and K. J. Daoust, *J. Am. Chem. Soc.*, **118**, 7381 (1996).

<sup>191</sup>. R. W. A. Havenith, L. W. Jenneskens, and J. H. van Lenthe, *Theochem*, **492**, 217 (1999).

There are numerous examples of interconversion of 1,3,5-trienes and 1,3-cyclohexadiene systems by the electrocyclic mechanism.<sup>192</sup> An especially interesting case of hexatriene-cyclohexadiene interconversion is the equilibrium between cycloheptatrienes and bicyclo[4.1.0]hepta-2,4-dienes.<sup>193</sup>



The energy requirement for this electrocyclic transformation is so low that the process occurs at room temperature, as determined by NMR measurements. Low-temperature NMR measurements give a  $E_a$  value of about 7 kcal/mol when  $R = \text{CO}_2\text{CH}_3$ .<sup>194</sup> This transformation is an example of *valence tautomerism*, a rapid process involving only reorganization of bonding electrons. The reason the reaction is much more rapid than electrocyclization of acyclic trienes is that the ring holds the reacting termini together, reducing the negative entropy of activation. In contrast to the ring opening of Dewar benzene, disrotatory opening of bicyclo[4.1.0]hepta-2,4-diene involves six electrons, is allowed by orbital symmetry rules, and is easily accommodated by the ring geometry. For unsubstituted bicyclo[4.1.0]hepta-2,4-diene the equilibrium constant for ring closure is small, about  $3 \times 10^{-3}$  at 100°C. Alkyl groups do not have much of an effect on the position of equilibrium but EWGs such as cyano and trifluoromethyl shift the equilibrium more in favor of the bicyclic ring.<sup>195</sup> A boron derivative has been studied both experimentally and computationally.<sup>196</sup> The experimental  $\Delta G^\ddagger$  is 8.2 kcal/mol. The *exo*-bicyclic structure is stabilized by interaction of the cyclopropyl  $\sigma$  orbitals with the empty boron  $p$  orbital. This interaction is analogous to the one that stabilizes the cyclopropylcarbinyl cation (see p. 427)



Synthetic applications of electrocyclic reactions are normally designed to take advantage of their stereospecificity, especially for the construction of *Z*-double bonds. Scheme 10.8. shows some examples. Entries 1 and 2 illustrate the inward rotation of formyl groups in cyclobutenes to generate *Z*-enals. The product in Entry 3 results from outward rotation of the substituents. Although they are EWGs, their reduced electrophilicity and enhanced steric demands favor outward rotation. Entries 4 to 6 illustrate the formation of cyclohexadienes by triene electrocyclization. Note that in Entry 6, there has also been a hydrogen migration, presumably by a 1,5-hydrogen shift (see Section 10.6).

<sup>192</sup>. V. A. Bakulev, *Russ. Chem. Rev.*, **64**, 99 (1995).

<sup>193</sup>. G. Maier, *Angew. Chem. Int. Ed. Engl.*, **6**, 402 (1967).

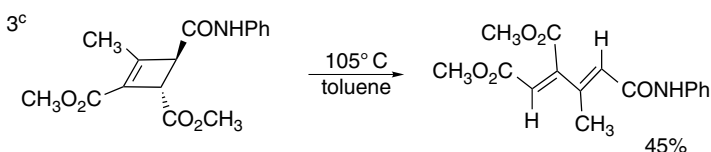
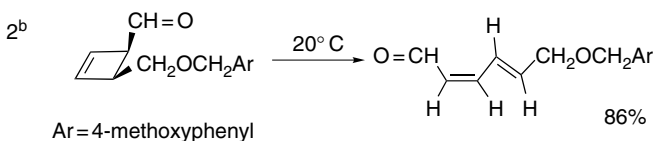
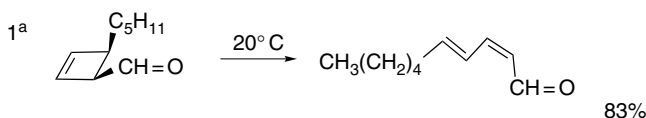
<sup>194</sup>. M. Gorlitz and H. Gunther, *Tetrahedron*, **25**, 4467 (1969).

<sup>195</sup>. P. Warner and S.-L. Lu, *J. Am. Chem. Soc.*, **95**, 5099 (1973); P. M. Warner and S.-L. Lu, *J. Am. Chem. Soc.*, **102**, 331 (1980); K. Takeuchi, H. Fujimoto, and K. Okamoto, *Tetrahedron Lett.*, **22**, 4981 (1981); T.-H. Tang, C. S. Q. Lew, Y.-P. Cui, B. Capon, and I. G. Csizmadia, *Theochem*, **305**, 49 (1994); Y. Guzel, E. Saripinar, and L. Yildirim, *Monatsh. Chem.*, **123**, 513 (1996).

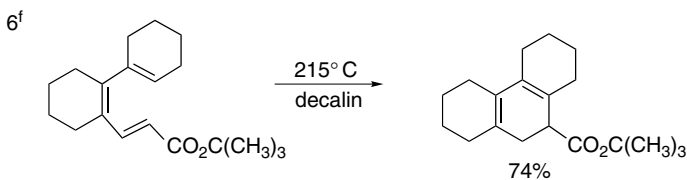
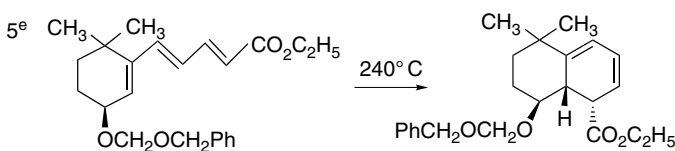
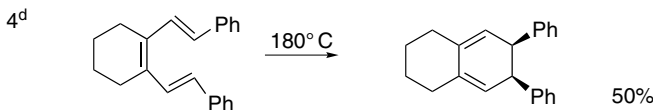
<sup>196</sup>. I. D. Gridnev, O. L. Tok, N. A. Gridneva, Y. N. Bubnov, and P. R. Schreiner, *J. Am. Chem. Soc.*, **120**, 1034 (1998).

## Scheme 10.8. Electrocyclic Reactions

## A. Electrocyclic Ring-Opening of Cyclobutenes



## B. Electrocyclization of Substituted 1,3,5-hexatrienes.

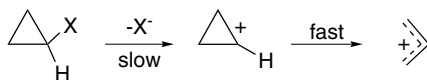


- a. K. J. Hodgetts, S. T. Saengchantara, C. J. Wallis, and T. W. Wallace, *Tetrahedron Lett.*, **34**, 6321 (1993).  
 b. F. Binns, R. Hayes, S. Ingham, S. T. Saengchantara, R. W. Turner, and T. W. Wallace, *Tetrahedron*, **48**, 515 (1992).  
 c. I. Yavari and S. Asghari, *Tetrahedron*, **55**, 11853 (1999).  
 d. K. Voigt, P. von Zezschwitz, K. Rosauer, A. Lansky, A. Adams, O. Reiser, and A. de Meijere, *Eur. J. Org. Chem.*, 1521 (2001).  
 e. H. Venkataraman and J. K. Cha, *J. Org. Chem.*, **54**, 2505 (1989).  
 f. P. von Zezschwitz, F. Petry, and A. de Meijere, *Chem. Eur. J.*, **7**, 4035 (2001).

## 10.5.4. Electrocyclic Reactions of Charged Species

The Woodward-Hoffmann orbital symmetry rules are not limited in application to the neutral polyene systems that have been discussed up to this point. They also apply to charged systems, just as the Hückel aromaticity rule can be applied to charged ring systems. The conversion of a cyclopropyl cation to an allyl cation is the simplest

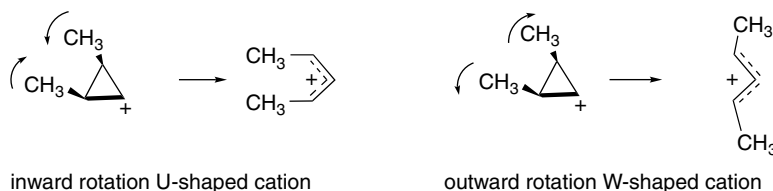
possible case of an electrocyclic process because it involves only two  $\pi$  electrons.<sup>197</sup> Owing to the strain imposed by the cyclopropyl ring, cyclopropyl cations do not form easily, and cyclopropyl halides and sulfonates are quite unreactive under ordinary solvolytic conditions. For example, solvolysis of cyclopropyl tosylate in acetic acid requires a temperature of 180°C. The product is allyl acetate rather than cyclopropyl acetate.<sup>198</sup> This transformation might occur by formation of the cyclopropyl cation, followed by ring opening to the allyl cation or (see below) the reaction might occur in a single step.



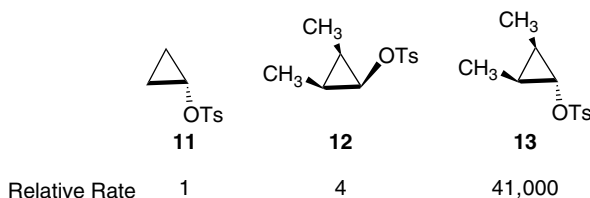
Formation of allylic products is characteristic of solvolytic reaction of other cyclopropyl halides and sulfonates. Similarly, diazotization of cyclopropylamine in aqueous solution gives allyl alcohol.<sup>199</sup>

The ring opening of a cyclopropyl cation is an electrocyclic process of the  $4n + 2$  type, where  $n$  equals zero, and should therefore be a disrotatory process. CCSD(T)/6-311G(2d) and B3LYP/6-31G(2d) computations on the reaction indicate that the cyclopropyl cation is not a stable intermediate and that there is no barrier to electrocyclic ring opening.<sup>200</sup> This result implies that the ring opening occurs as a concerted process in conjunction with rupture of the bond to the leaving group.

As with cyclobutenes, there are two possible directions for the allowed disrotation in substituted cyclopropyl cations. For a *cis*-2,3-dimethylcyclopropyl cation, for example, two different disrotatory modes are possible, leading to structurally distinct allyl cations.



The W-shaped allylic cation should be formed in preference to the sterically less favorable U-shaped cation. This issue was investigated by comparing the rates of solvolysis of the cyclopropyl tosylates **11** to **13**.



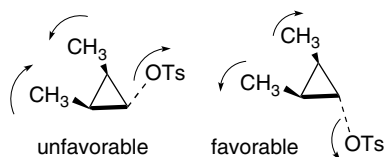
<sup>197</sup>. P. v. R. Schleyer, W. F. Sliwinski, G. W. Van Dine, U. Schollkopf, J. Paust, and K. Fellenberger, *J. Am. Chem. Soc.*, **94**, 125 (1972); W. F. Sliwinski, T. M. Su, and P. v. R. Schleyer, *J. Am. Chem. Soc.*, **94**, 133 (1972).

<sup>198</sup>. J. D. Roberts and V. C. Chambers, *J. Am. Chem. Soc.*, **73**, 5034 (1951).

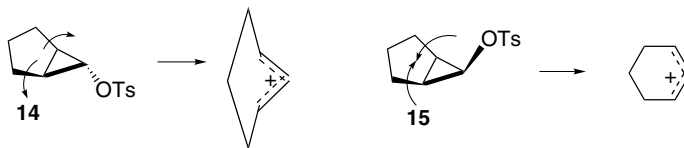
<sup>199</sup>. P. Lipp, J. Buchkremer, and H. Seeles, *Justus Liebigs Ann. Chem.*, **499**, 1 (1932); E. J. Corey and R. F. Atkinson, *J. Org. Chem.*, **29**, 3703 (1964).

<sup>200</sup>. P. A. Arnold and B. K. Carpenter, *Chem. Phys. Lett.*, **328**, 90 (2000).

Some very significant conclusions can be drawn from the data. If formation of the cyclopropyl cation were the rate-determining step, **12** would be more reactive than **13** because the steric interaction between the tosylate leaving group and the methyl substituents in **12** is relieved as ionization occurs. Since **12** is 10,000 times less reactive than **13**, some other factor must be determining the relative rates of reaction and it is doubtful that rate-limiting ionization to a cyclopropyl cation is occurring. The results can be explained, as proposed by DePuy,<sup>201</sup> if the ionization and ring opening are part of a single, concerted process. In such a process, the ionization is assisted by the electrons in the breaking C(2)–C(3) bond, which provide maximum assistance when positioned toward the back side of the leaving group. This, in turn, requires that the substituents *anti* to the leaving group rotate outward as the ionization proceeds. This concerted process explains why **12** reacts more slowly than **13**. In **12** such a rotation moves the methyl groups together, resulting in increased steric interaction and the formation of the U-shaped allylic anion. In **13**, the methyl groups move away from one another and form the W-shaped allylic ion.



This interpretation is supported by results on the acetolysis of the bicyclic tosylates **14** and **15**. With **14**, after 3 months in acetic acid at 150°C, 90% of the starting material is recovered. This means that both ionization to a cyclopropyl cation and a concerted ring opening are extremely slow. The preferred disrotatory ring-opening process would lead to an impossibly strained structure, the *trans*-cyclohexenyl cation. In contrast, the stereoisomer **15** reacts at least  $2 \times 10^6$  more rapidly, since it can proceed to a stable *cis*-cyclohexenyl cation.<sup>197</sup>



Pentadienyl cations can undergo electrocyclization to cyclopentenyl cations. As this is a four  $\pi$ -electron system, it should occur by conrotation. Based on gas phase ion stability data, the reaction is exothermic by 18 kcal/mol.<sup>202</sup>



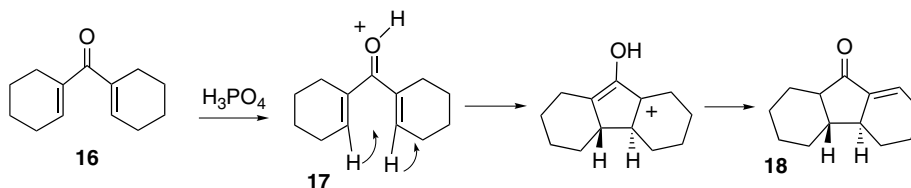
This cyclization has been employed synthetically and is known as the *Nazarov reaction*.<sup>203</sup> An example of preferred conrotatory cyclization of four  $\pi$ -electron cation systems can be found in the acid-catalyzed cyclization of the dienone **16**, which

<sup>201</sup> C. H. DePuy, *Acc. Chem. Res.*, **1**, 33 (1968).

<sup>202</sup> F. P. Lossing and J. L. Holmes, *J. Am. Chem. Soc.*, **106**, 6917 (1984).

<sup>203</sup> K. L. Habermas, S. E. Denmark, and T. K. Jones, *Org. React.*, **45**, 1 (1994).

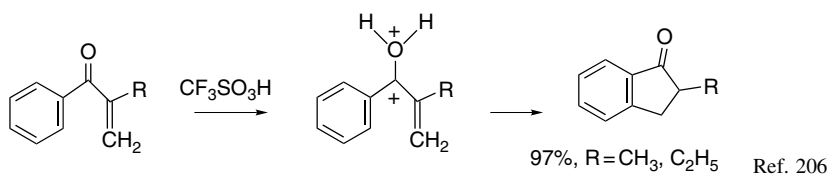
proceeds through the 3-hydroxypentadienyl cation **17**. The final product **18** arises from ketonization and deprotonation, and the stereochemistry is that expected for a conrotatory process.<sup>204</sup>



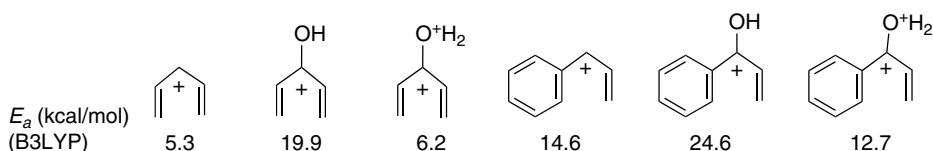
Although most synthetic examples of this cyclization have involved protonation of divinyl ketones to give 3-hydroxy-1,4-pentadienyl cations, computational studies suggest that the cyclization would occur even more readily with alternative substituents at C(3).<sup>205</sup> For example, the parent ( $\text{X} = \text{H}$ ) and the boron derivative ( $\text{X} = \text{BH}_2$ ) are calculated to be more reactive.



Experimental support for this idea comes from the study of cyclization of 1-arylprop-2-en-1-ones to 1-indanones by strong acid.



The acidity dependence of this reaction suggests that it passes through the *diprotonated intermediate* shown. B3LYP/6-31G\* and MP2/6-31G\* calculations find the  $E_a$  to be considerably smaller for the dication than for the corresponding monocation.



There are also examples of electrocyclic processes involving anionic species. Since the pentadienyl anion is a six  $\pi$ -electron system, thermal cyclization to a cyclopentenyl anion should be disrotatory. Examples of this electrocyclic reaction are rare. NMR studies of pentadienyl anions indicate that they are stable and do not tend to cyclize.<sup>207</sup> Cyclooctadienyllithium provides an example where cyclization does occur,

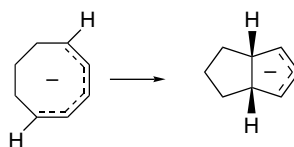
<sup>204</sup>. R. B. Woodward, in *Aromaticity*, Chemical Society Special Publication No. 21, 217 (1969).

<sup>205</sup>. D. A. Smith and C. W. Ulmen, *J. Org. Chem.*, **62**, 5110 (1997).

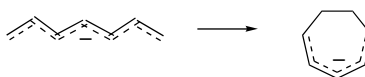
<sup>206</sup>. T. Suzuki, T. Ohwada, and K. Shudo, *J. Am. Chem. Soc.*, **119**, 6774 (1997).

<sup>207</sup>. R. B. Bates, D. W. Gosselink, and J. A. Kaczynski, *Tetrahedron Lett.*, 199, 205 (1967); R. B. Bates and D. A. McCombs, *Tetrahedron Lett.*, 977 (1969); R. B. Bates, S. Brenner, C. M. Cole, E. W. Davidson, G. D. Forsythe, D. A. McCombs, and A. S. Roth, *J. Am. Chem. Soc.*, **95**, 926 (1973).

with the first-order rate constant being  $8.7 \times 10^{-3} \text{ min}^{-1}$ . The stereochemistry of the ring closure is consistent with the expected disrotatory nature of the reaction.

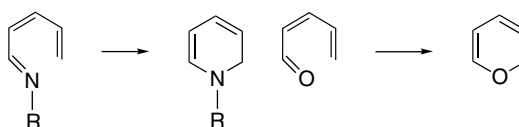


In contrast to pentadienyl anions, heptatrienyl anions cyclize readily to cycloheptadienyl anions.<sup>208</sup> The transformation of heptatrienyl anion to cycloheptadienyl anion proceeds with a half-life of 13 min at  $-13^\circ\text{C}$ . The Woodward-Hoffmann rules predict that this would be a conrotatory closure.<sup>209</sup>



### 10.5.5. Electrocyclization of Heteroatomic Trienes

Electrocyclization can also occur when heteroatoms are incorporated into diene, triene, or polyene systems. Most attention has focused on 1-azatriene and 1-oxatrienes, which lead to dihydropyridines and pyrans, respectively.



Comparison of the energy requirements of these reactions with the all-carbon system indicates reduced barriers for the aza and oxa systems, but because of the loss of the C=O bond, the 1-oxahexatriene electrocyclization is slightly endothermic.<sup>210</sup> Marvell and co-workers estimated the acceleration as being a factor of  $10^5$  to  $10^6$ .<sup>211</sup> This result suggests a change in mechanism for the heteroatom cases.

A computational study has examined these effects.<sup>212</sup> The reaction energy comparisons are given in Figure 10.29 and the transition structure for 1-aza-1,3,5-hexatriene is shown in Figure 10.30. NPA analysis indicates that an unshared pair of the heteroatom participates in the reaction, which leads to a strong preference for outward rotation of the N–H or N–R group in the azatrienes. There is also a change of the TS geometry, relative to 1,3,5-hexatriene. Whereas the C(2)X(1)C(6)C(5) dihedral angle is nearly  $0^\circ$  for X=C, it increases to  $30^\circ$ – $40^\circ$  for X=O or N. It is the involvement of unshared electrons on oxygen and nitrogen that lowers the energy barrier.

<sup>208</sup> E. A. Zuech, D. L. Crain, and R. F. Kleinschmidt, *J. Org. Chem.*, **33**, 771 (1968); R. B. Bates, W. H. Deines, D. A. McCombs, and D. E. Potter, *J. Am. Chem. Soc.*, **91**, 4608 (1969).

<sup>209</sup> S. W. Staley, in *Pericyclic Reactions*, Vol. 1, A. P. Marchand and R. E. Lehr, eds., Academic Press, New York, 1977, Chap. 4.

<sup>210</sup> J. Rodriguez-Otero, *J. Org. Chem.*, **64**, 6842 (1999).

<sup>211</sup> E. N. Marvell, G. Caple, T. A. Gosink, and G. Zimmer, *J. Am. Chem. Soc.*, **88**, 619 (1966).

<sup>212</sup> M. J. Walker, B. N. Hietbrink, B. E. Thomas, IV, K. Nakamura, E. A. Kallel, and K. N. Houk, *J. Org. Chem.*, **66**, 6669 (2001).

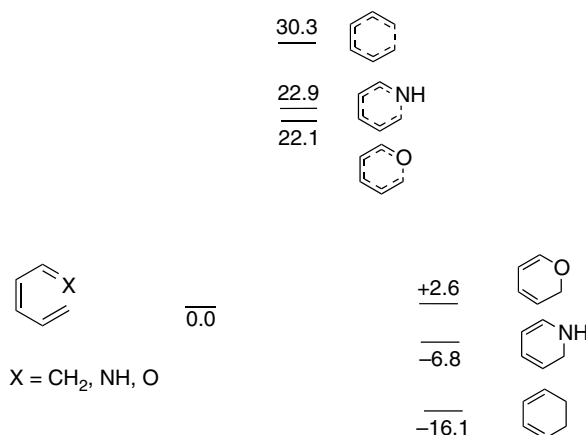


Fig. 10.29. Energy comparisons for electrocyclization of 1-aza- and 1-oxa-1,3,5-hexatriene to 1,3,5-hexatriene in kcal/mol.

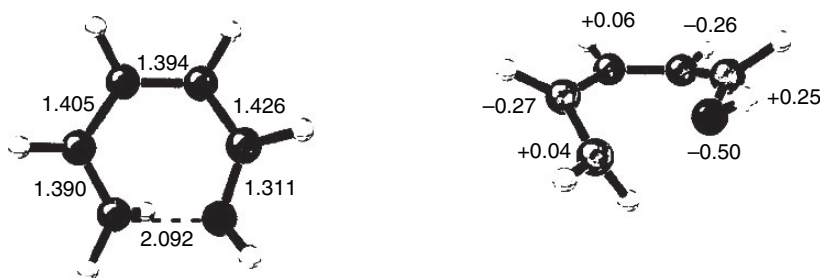


Fig. 10.30. Bond lengths and CHELPG charges of transition structure for electrocyclization of 1-aza-1,3,5-hexatriene. Reproduced from *J. Org. Chem.*, **66**, 6669 (2001) by permission of the American Chemical Society.

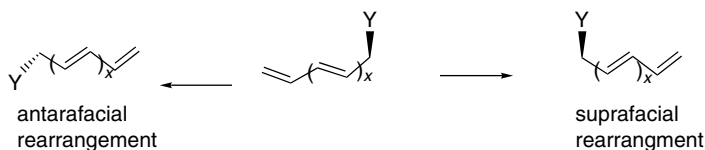
## 10.6. Sigmatropic Rearrangements

### 10.6.1. Overview of Sigmatropic Rearrangements

*Sigmatropic rearrangements* constitute another important class of concerted pericyclic reactions governed by orbital symmetry.<sup>213</sup> They involve a reorganization of electrons during which a group attached by a  $\sigma$  bond migrates to the other terminus of a conjugated  $\pi$ -electron system, with a simultaneous shift of the  $\pi$  electrons. Sigmatropic rearrangements are described by stating the relationship between the reacting centers in the migrating fragment and the  $\pi$  system. The order  $[i, j]$  specifies the number of atoms in the migrating fragment and in the  $\pi$  system, respectively. As with other concerted reactions, the topology of the interacting orbitals determines the facility and the stereochemistry of each sigmatropic rearrangement. There are two topologically distinct processes by which a sigmatropic migration can occur. If the migrating group remains associated with the same face of the conjugated  $\pi$  system throughout the reaction, the migration is termed *suprafacial*. In the alternative

<sup>213</sup> R. B. Woodward and R. Hoffmann, *J. Am. Chem. Soc.*, **87**, 2511 (1965).

mode, called *antarafacial*, the migrating group moves to the opposite face of the  $\pi$  system during the course of the migration. There is another important element of stereochemistry for the migration of alkyl groups. The migrating group can retain its original configuration (retention) or undergo inversion. The stereochemical features and the number of electrons involved determine whether a reaction is allowed or forbidden.



The generalized orbital symmetry selection rules<sup>213</sup> are given below. The bases of these rules are discussed for each of the major classes of sigmatropic rearrangements.

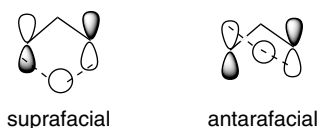
#### Generalized Orbital Symmetry Rules for Sigmatropic Processes

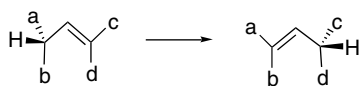
	Supra/ Retention	Supra/ Inversion	Antara/ Retention	Antara/ Inversion
Order $[1, j]$ $1 + j$				
$4n$	Forbidden	Allowed	Allowed	Forbidden
$4n + 2$	Allowed	Forbidden	Forbidden	Allowed
	Supra/Supra	Supra/Antara	Antara/Antara	
Order $[i, j]$ $i + j$				
$4n$	Forbidden	Allowed	Forbidden	
$4n + 2$	Allowed	Forbidden	Allowed	

Several important types of sigmatropic reactions are listed in Scheme 10.9. We first discuss shifts of hydrogen and alkyl groups, concentrating on [1,3]-, [1,5]-, and [1,7]-shifts. There is also a large and synthetically important group of [3,3]-sigmatropic shifts, which include the Cope and Claisen rearrangements that are dealt with in Section 10.6.3. Finally, [2,3]-sigmatropic shifts are considered in Section 10.6.4.

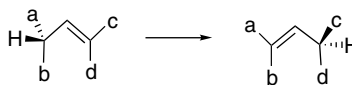
### 10.6.2. [1,3]-, [1,5]-, and [1,7]-Sigmatropic Shifts of Hydrogen and Alkyl Groups

The orbital symmetry requirements of sigmatropic reactions can be analyzed by considering the interactions between the frontier orbitals of the  $\pi$  system and those of the migrating fragment. The simplest case, 1,3-sigmatropic shift of a hydrogen is illustrated in the first entry in Scheme 10.9. An FMO analysis of this process treats the system as a hydrogen atom interacting with an allyl radical. The frontier orbitals are the hydrogen  $1s$  and the allyl  $\psi_2$  orbitals. These interactions are depicted below for both the suprafacial and antarafacial modes.

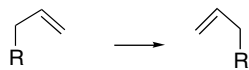




[1,3]-suprafacial shift of hydrogen



[1,3]-antarafacial shift of hydrogen



[1,3]-sigmatropic alkyl shift



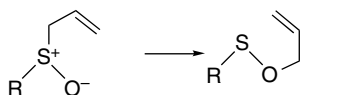
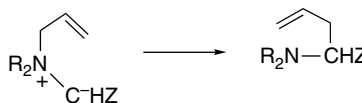
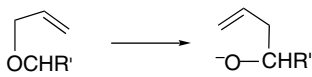
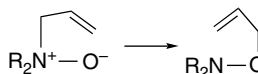
[1,5]-sigmatropic alkyl shift



[1,7]-sigmatropic hydrogen shift



[1,7]-sigmatropic alkyl shift

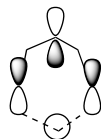
[3,3]-sigmatropic rearrangement of  
1,5-hexadiene (Cope rearrangement)[3,3]-sigmatropic rearrangement of  
allyl vinyl ether (Claisen rearrangement)[2,3]-sigmatropic rearrangement of  
allyl sulfoxide[2,3]-sigmatropic rearrangement of  
*N*-allyl ammonium ylide[2,3]-sigmatropic rearrangement of  
allyloxy carbanion (Wittig rearrangement)[2,3]-sigmatropic shift of *N*-allyl  
amine oxide

A bonding interaction can be maintained only in the antarafacial mode. The 1,3-suprafacial shift of hydrogen is therefore forbidden by orbital symmetry considerations. The antarafacial process is symmetry allowed, but it involves such a contorted geometry that this shift, too, would be expected to be energetically difficult. As a result, orbital symmetry considerations indicate that concerted [1,3]-shifts of hydrogen are unlikely processes. Computational studies also find that the 1,3-shift of hydrogen should be antarafacial, but in agreement with expectations based on molecular geometry, the TS that is found is so energetic that it is close to a stepwise bond dissociation process.<sup>214,215</sup>

<sup>214</sup>. B. A. Hess, Jr., L. J. Schaad, and J. Pancir, *J. Am. Chem. Soc.*, **107**, 149 (1985).

<sup>215</sup>. F. Bernardi, M. A. Robb, H. B. Schlegel, and G. Tonachini, *J. Am. Chem. Soc.*, **106**, 1198 (1984).

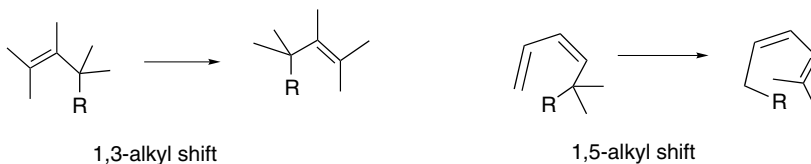
Orbital symmetry analysis of the 1,5-sigmatropic shift of hydrogen leads to the opposite conclusion. The relevant frontier orbitals in this case are the hydrogen  $1s$  and  $\psi_3$  of the pentadienyl radical. The suprafacial mode is allowed, whereas the antarafacial mode is forbidden. The suprafacial shift corresponds to a geometrically favorable six-membered ring.



allowed [1,5]-suprafacial  
hydrogen shift in 1,3-pentadiene

An alternative analysis of sigmatropic reactions involves drawing the basis set atomic orbitals and classifying the resulting system as Hückel or Möbius in character. When this classification has been done, the electrons involved in the process are counted to determine if the TS is aromatic or antiaromatic. The conclusions reached are the same as for the frontier orbital approach. The suprafacial 1,3-shift of hydrogen is forbidden but the suprafacial 1,5-shift is allowed. Analysis of a 1,7-shift of hydrogen shows that the antarafacial shift is allowed. This analysis is illustrated in Figure 10.31. These conclusions based on orbital symmetry considerations are supported by HF/6-31G\* calculations, which conclude that 1,5-shifts should be suprafacial, whereas 1,7-shifts should be antarafacial.<sup>214</sup>

Sigmatropic migration involving alkyl group shifts can also occur.



When an alkyl group migrates, there is an additional stereochemical feature to consider. The shift can occur with retention or inversion at the migrating center. The analysis of sigmatropic shifts of alkyl groups is illustrated in Figure 10.32. The allowed processes include the suprafacial 1,3-shift with inversion and the suprafacial 1,5-shift with retention.

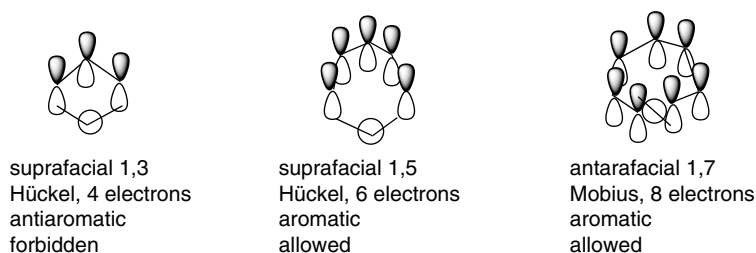


Fig. 10.31. Classification of sigmatropic hydrogen shifts with respect to basis set orbitals.

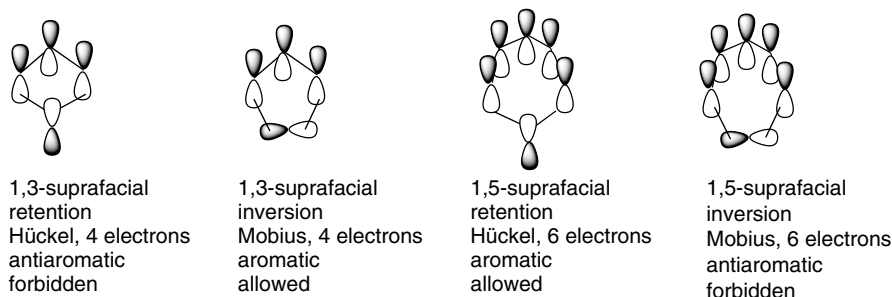


Fig. 10.32. Classification of sigmatropic shifts of alkyl groups with respect to basis set orbitals.

**10.6.2.1. Computational Characterization of Transition Structures for [1,3]-, [1,5]-, and [1,7]-Sigmatropic Shifts** There have been a number of computational studies aimed at providing information about the TSs of the sigmatropic rearrangements. Chamorro and co-workers characterized the TS for prototypical [1,3]-sigmatropic shifts of hydrogen and methyl.<sup>216</sup> The 1,3-hydrogen shift is an antarafacial process, whereas the methyl migration is a suprafacial process that occurs with inversion at the alkyl group. The corresponding nuclear positions are depicted in Figure 10.33.

Computational studies on [1,5]-sigmatropic hydrogen shifts are also in agreement with the qualitative predictions based on orbital symmetry relationships. The TS shows aromatic character. Activation energies are calculated<sup>217</sup> to be in the range 35–37 kcal/mol, in good agreement with the experimental value of 36.3.<sup>218</sup>

Lee and co-workers compared the activation barrier and TS structure for suprafacial migration of  $\text{BH}_2$ ,  $\text{CH}_3$ , and  $\text{NH}_2$  at several levels of theory.<sup>219</sup>

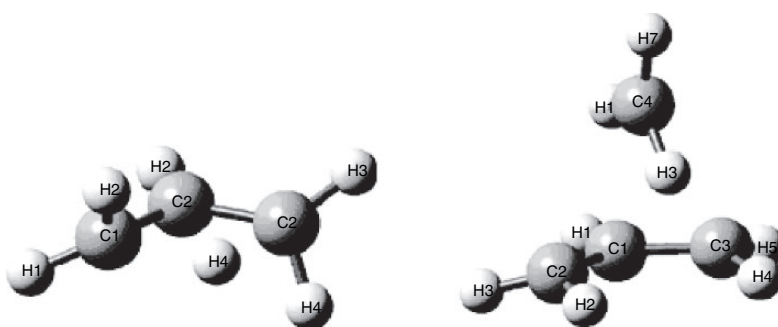


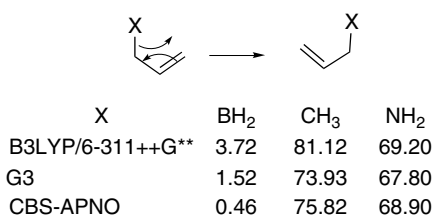
Fig. 10.33. Nuclear positions and for antarafacial [1,3]-sigmatropic migration of hydrogen and for suprafacial [1,3]-sigmatropic migration of methyl with inversion (B3LYP/6-311++G(d,p)), Reproduced from *J. Phys. Chem. A*, **106**, 11533 (2002), by permission of the American Chemical Society.

<sup>216</sup> E. Chamorro, J. C. Santos, B. Gomez, R. Contreras, and P. Fuentealba, *J. Phys. Chem. A*, **106**, 11533 (2002).

<sup>217</sup> I. Alkorta and J. Elguero, *J. Chem. Soc., Perkin Trans.*, **2**, 2497 (1998); B. S. Jursic, *Theochem*, **423**, 189 (1998); N. J. Saettel and O. Wiest, *J. Org. Chem.*, **65**, 2331 (2000).

<sup>218</sup> W. R. Roth and J. König, *Liebigs Ann. Chem.*, **699**, 24 (1966).

<sup>219</sup> J. Y. Choi, C. K. Kim, C. K. Kim, and I. Lee, *J. Phys. Chem. A*, **106**, 5709 (2002).



The barrier for boron migration is very low, but for X = CH<sub>3</sub> and NH<sub>2</sub>, the barriers are close to the bond dissociation energies, indicating that the reaction would be stepwise. No antarafacial pathways were found. The suprafacial migration is facile for BH<sub>2</sub> because the empty *p* orbital is available. Figure 10.34 shows the lowest-energy (QCISD/6-311G\*\*) TS and the NPA bond orders associated with them. We see that the vacant *p* orbital allows for continuous bonding during the migration of BH<sub>2</sub>, whereas the absence of such an orbital for CH<sub>3</sub> and NH<sub>2</sub> results in electronic repulsion and a much higher-energy TS. Note the much greater bond lengths of the allyl fragment. In the case of X = CH<sub>3</sub> and NH<sub>2</sub>, these bonds are close to single-bond lengths, indicating substantial loss of the  $\pi$  bond. It is also worth noting that the allylborane system is isoelectronic with the nonclassical C<sub>4</sub>H<sub>7</sub><sup>+</sup> carbocation (see p. 453). The computed TS for BH<sub>2</sub> migration corresponds in structure to the bicyclobutenyl carbocation.

*10.6.2.2. Examples of Sigmatropic Shifts of Hydrogen and Alkyl Groups* With the generalized selection rules as a unifying theoretical framework (see p. 912), we can consider specific examples of sigmatropic rearrangements. In accordance with the orbital symmetry concepts, there are many examples of sigmatropic [1,5]-hydrogen migrations in molecules that incorporate a pentadienyl fragment. The activation energies for such reactions are usually in the vicinity of 35 kcal/mol, so the reactions require moderately elevated temperatures.<sup>220</sup> Two examples are given below. The first rearrangement is detected by migration of the isotopic label. The second results in transformation to a more stable diene.

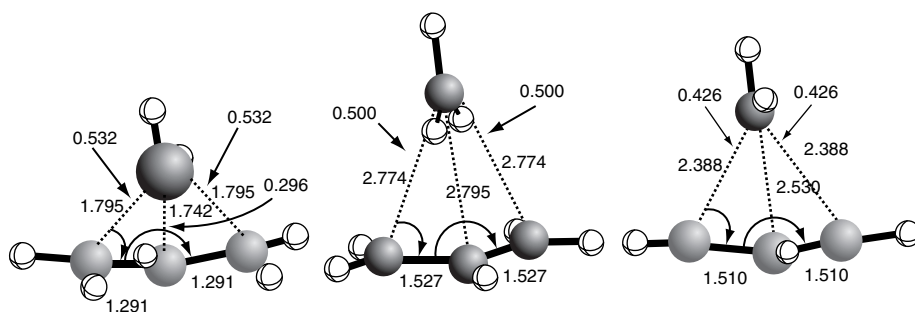
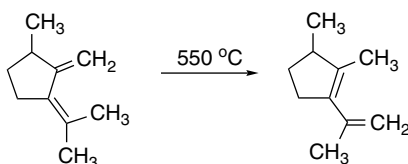


Fig. 10.34. Transition structures for suprafacial 1,3-migrations of BH<sub>2</sub> (left), CH<sub>3</sub> (center), and NH<sub>2</sub> (right) at the QCISD/6-311+G\*\* level. Bond distances and NPA bond orders are shown. Adapter from *J. Phys. Chem. A*, **106**, 5709 (2002), by permission of the American Chemical Society.

<sup>220</sup> W. R. Roth and J. Koenig, *Liebigs Ann. Chem.*, **699**, 24 (1966).

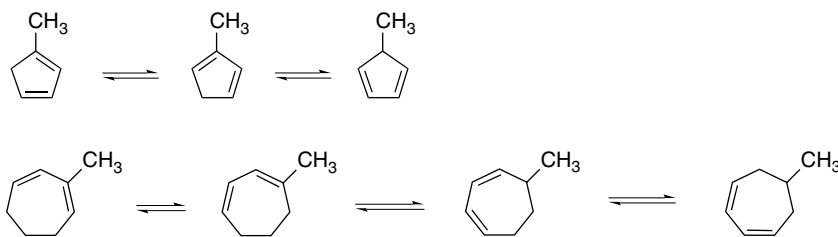


Ref. 221



Ref. 222

Sigmatropic shifts of hydrogens have been systematically examined in cyclic systems. Early studies demonstrated equilibration among the methylcyclopentadienes<sup>223</sup> and methylcycloheptadienes by 1,5-hydrogen shift.<sup>224</sup>



Computational studies (B3LYP/6-31G\*) have been carried out on cyclopentadiene ( $E_a = 27$  kcal/mol),<sup>225</sup> 1,3-cyclohexadiene ( $E_a = 41.9$  kcal/mol),<sup>226</sup> 1,3-cycloheptatriene ( $E_a = 32.7$ – $35.3$  kcal/mol),<sup>227</sup> and 1,3-cyclooctadiene ( $E_a = 32.2$  kcal/mol).<sup>226</sup> In each case, there is reasonable agreement with experimental data. The energy requirement depends on the structure of the TS, which is influenced by the ring geometry. For example, in methyl-substituted 1,3-cycloheptadienes, there are seven minima and seven TS for [1,5]-sigmatropic shifts. The  $E_a$  range from 29.6 (4→TS34) to 35.3 (2→TS34) kcal/mol. These energy relationships are depicted in Figure 10.35.

Like the thermal 1,3-hydrogen shift, a 1,7-hydrogen shift is allowed when antarafacial but forbidden when suprafacial. Because a  $\pi$  system involving seven carbon atoms is more flexible than one involving only three carbon atoms, the geometrical restrictions on the antarafacial TS are not as severe as in the 1,3-case. For the conversion of *Z,Z*-1,3,5-octatriene to *Z,Z,E*-2,4,6-octatriene, the  $E_a$  is 20.2 kcal/mol.

221. A. P. ter Borg, H. Kloosterziel, and N. Van Meurs, *Proc. Chem. Soc.*, 359 (1962).

222. J. Wolinsky, B. Chollar, and M. D. Baird, *J. Am. Chem. Soc.*, **884**, 2775 (1962).

223. V. A. Mironov, E. V. Sobolev, and A. N. Elizarova, *Tetrahedron*, **19**, 1939 (1963).

224. V. A. Mironov, O. S. Chizhov, I. M. Kimelfeld, and A. A. Akhrem, *Tetrahedron Lett.*, 499 (1969).

225. I. Alkorta and J. Elguero, *J. Chem. Soc., Perkin Trans. 2*, 2497 (1998).

226. B. A. Hess, Jr., and J. E. Baldwin, *J. Org. Chem.*, **67**, 6025 (2002).

227. B. A. Hess, Jr., *Int. J. Quantum Chem.*, **90**, 1064 (2002).

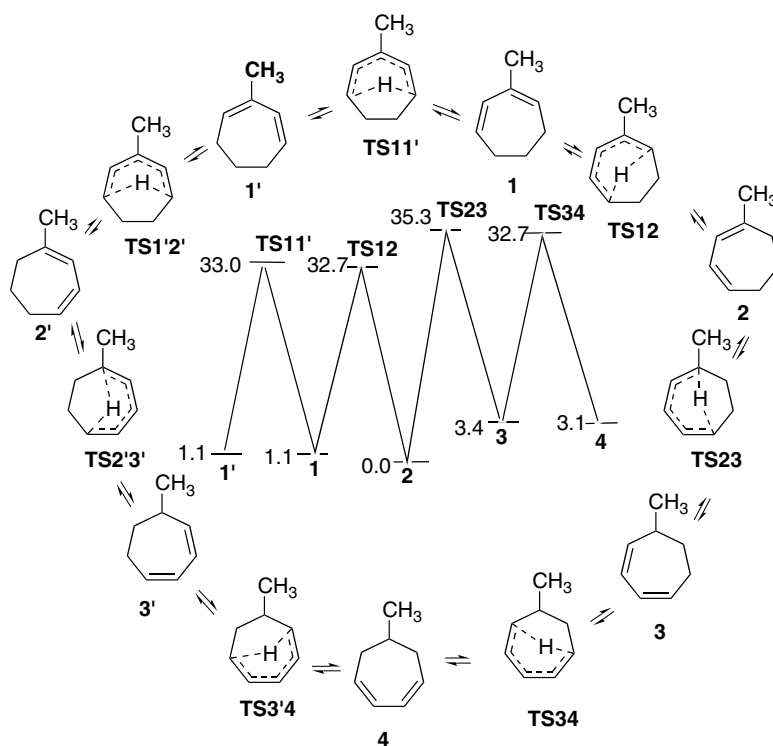
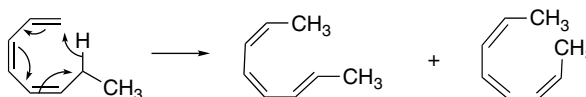


Fig. 10.35. Structures and relative energies of isomeric methyl-1,3-cycloheptatrienes and TS for [1,5]-sigmatropic hydrogen shift between them. Data from *Int. J. Quantum Chem.*, **90**, 1064 (2002).

The *Z,Z,Z*-isomer is also formed, but with a slightly higher activation energy. The kinetic isotope for the transferred hydrogen is around 7, consistent with C–H bond-breaking being involved in the rate-determining step.<sup>228</sup> A similar  $E_a$  has been measured for the unsubstituted *Z,Z*-1,3,5-heptatriene.<sup>229</sup>

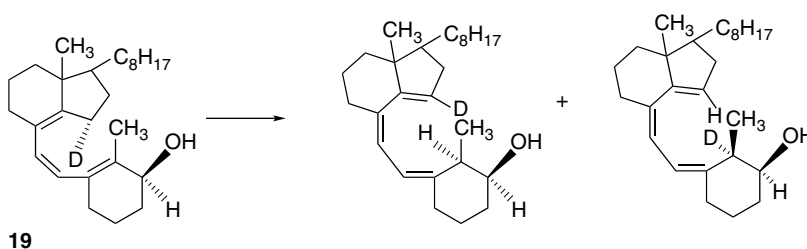


More complex structures such as **19** exhibit similar activation energies. This compound was used to demonstrate that the stereochemistry is *antarafacial*, as predicted by the general selection rules.<sup>230</sup>

<sup>228</sup> J. E. Baldwin and V. P. Reddy, *J. Am. Chem. Soc.*, **109**, 8051 (1987).

<sup>229</sup> M. Gurski, I. D. Gridnev, Y. V. Il'ichev, A. V. Ignatenko, and Y. N. Bubnov, *Angew. Chem. Int. Ed. Engl.*, **31**, 781 (1992).

<sup>230</sup> C. A. Hoeger, A. D. Johnston, and W. H. Okamura, *J. Am. Chem. Soc.*, **109**, 4690 (1987); W. H. Okamura, C. A. Hoeger, K. J. Miller, and W. Reischl, *J. Am. Chem. Soc.*, **110**, 973 (1988).



An especially important case of 1,7-hydrogen shift is the thermal equilibrium between precalciferol (previtamin D<sub>3</sub>, **20**) and calciferol (vitamin D<sub>3</sub>, **21**).<sup>231, 232</sup> This reaction has an  $E_a$  of 19.2 kcal/mol.

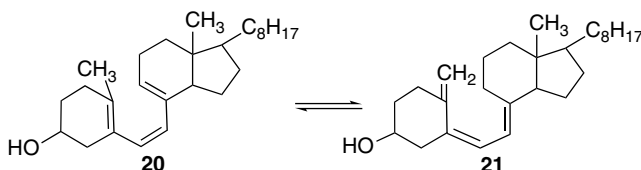


Figure 10.36 summarizes the comparative  $E_a$  for [1,3]-, [1,5]-, and [1,7]-hydrogen shifts.

### 10.6.3. Overview of [3,3]-Sigmatropic Rearrangements

[3,3]-Sigmatropic rearrangements are very important and useful reactions. The most important [3,3]-sigmatropic rearrangement from the synthetic point of view are those that form new carbon-carbon bonds. The [3,3]-sigmatropic rearrangement of 1,5-hexadienes is called the *Cope rearrangement*.

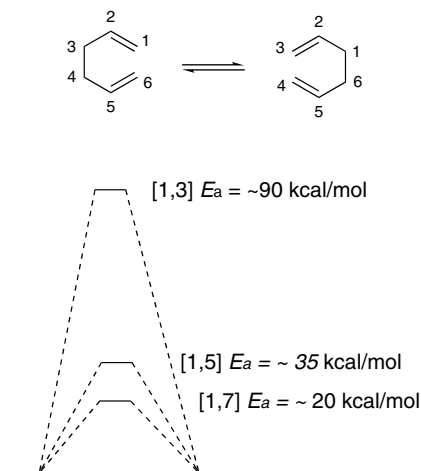
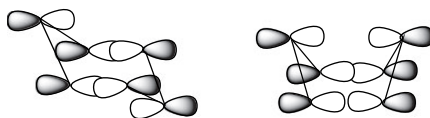


Fig. 10.36. Schematic comparison of  $E_a$  for 1,3-, 1,5-, and 1,7-sigmatropic hydrogen shifts.

<sup>231</sup>. J. L. M. A. Schlatmann, J. Pot, and E. Havinga, *Rec. Trav. Chim.*, **83**, 1173 (1964).

<sup>232</sup>. For a historical review of this reaction, see L. Fieser and M. Fieser, *Steroids*, Reinhold, New York, 1959, Chap. 4.

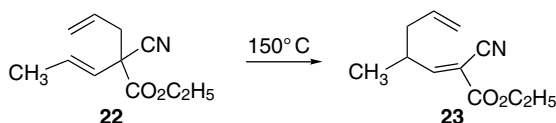
The TS for [3,3]-sigmatropic rearrangements can be considered to be two interacting allyl fragments. When the process is suprafacial in both groups, an aromatic orbital array results and the process is thermally allowed. Usually a chairlike TS is involved but a boatlike conformation is also possible.<sup>233</sup>



chair transition structure    boat transition structure  
Basis set orbitals for chair and boat transition structures  
for [3,3]-sigmatropic shifts. 6  $\pi$  electrons, Hückel, aromatic

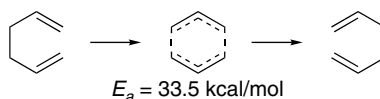
Heteroatoms can be present in the conjugated system or as substituents. From a synthetic point of view, the most important cases have oxygen or nitrogen at position 3. The oxygen case is known as the *Claisen rearrangement*. Oxygen and nitrogen substituents at C(2) or C(3) also provide important variations of [3,3]-sigmatropic rearrangements. Scheme 10.10 gives the structural pattern and names of some of the most important [3,3]-sigmatropic rearrangements. We discuss these variations in the sections that follow.

**10.6.3.1. Cope Rearrangements** The thermal [3,3]-sigmatropic rearrangement of 1,5-dienes is called the *Cope rearrangement*. Cope rearrangements are reversible reactions and as there is no change in the number or in the types of bonds, to a first approximation the total bond energy is unchanged. The reaction is under thermodynamic control and establishes equilibrium between the two 1,5-dienes. The position of the final equilibrium is governed by the relative stability of the starting material and product. The conversion of **22** to **23** is an example. The equilibrium in this case is controlled by the conjugation with the carbonyl and cyano groups in the product.



Ref. 234

The rearrangement of the simplest possible case, 1,5-hexadiene, has been studied using deuterium labeling. The  $E_a$  is 33.5 kcal/mol and the entropy of activation is  $-13.8$  eu.<sup>235</sup> The substantially negative entropy reflects the formation of the cyclic TS.

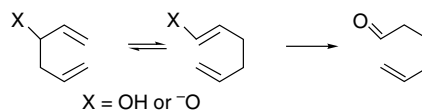
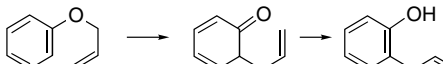
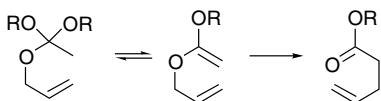
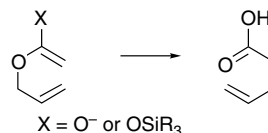
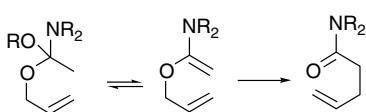
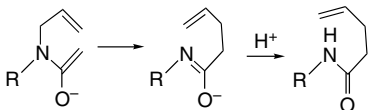
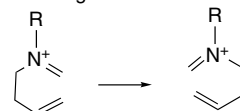


The Cope rearrangement usually proceeds through a chairlike TS. The stereochemistry of the reaction can be predicted and analyzed on the basis of a chair TS that minimizes steric interactions between the substituents. The reaction is both

<sup>233</sup> K. J. Shea, G. J. Stoddard, W. P. England, and C. D. Haffner, *J. Am. Chem. Soc.*, **114**, 2635 (1992).

<sup>234</sup> A. C. Cope and E. M. Hardy, *J. Am. Chem. Soc.*, **62**, 441 (1940).

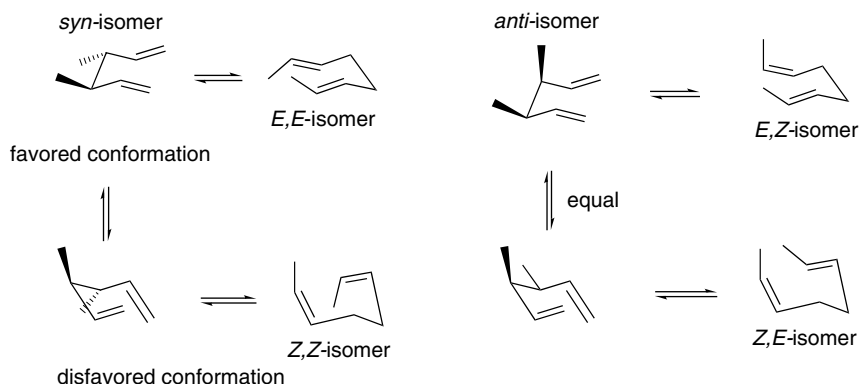
<sup>235</sup> W. v. E. Doering, V. G. Tascano, and G. H. Beasley, *Tetrahedron*, **27**, 5299 (1971); K. A. Black, S. Wilsey, and K. N. Houk, *J. Am. Chem. Soc.*, **120**, 5622 (1998).

1. Cope Rearrangement<sup>a</sup>2. Oxy-Cope and Anionic Oxy-Cope Rearrangement<sup>b</sup>3. Claisen Rearrangement of Vinyl Ethers<sup>c</sup>4. Claisen Rearrangement of Aryl Ethers<sup>d</sup>5. Orthoester Claisen Rearrangement<sup>e</sup>6. Ester enolate and Ireland-Claisen Rearrangement<sup>f</sup>7. *N,N*-Dialkyl Ketene Aminal Rearrangement<sup>g</sup>8. *O*-Allyl Imidate Rearrangement<sup>h</sup>9. *N*-Allyl Amide Enolate Rearrangement10. Azonia-Cope Rearrangement<sup>i</sup>a. S. J. Rhoads and N. R. Raulins, *Org. React.*, **22**, 1 (1975).b. J. A. Berson and M. Jones, Jr., *J. Am. Chem. Soc.*, **86**, 5019 (1964); D. A. Evans and A. M. Golob, *J. Am. Chem. Soc.*, **97**, 4765 (1975).c. A. M. M. Castro, *Chem. Rev.*, **104**, 2939 (2004).d. D. S. Tarbel, *Org. React.*, **2**, 1 (1944).e. W. S. Johnson, L. Wethermann, W. R. Bartlett, T. J. Brocksom, T. Li, D. J. Faulkner, and M. R. Petersen, *J. Am. Chem. Soc.*, **92**, 741 (1970).f. R. E. Ireland and R. H. Mueller, *J. Am. Chem. Soc.*, **94**, 5898 (1972); R. E. Ireland, R. H. Mueller, and A. K. Willard, *J. Am. Chem. Soc.*, **98**, 2868 (1976).g. D. Felix, K. Gschwend-Steen, A. E. Wick, and A. Eschenmoser, *Helv. Chim. Acta*, **52**, 1030 (1969).h. L. E. Overman, *Acc. Chem. Res.*, **13**, 218 (1980).i. U. Nubbemeyer, *Synthesis*, 961 (2003).j. L. E. Overman, *Acc. Chem. Res.*, **13**, 218 (1980).

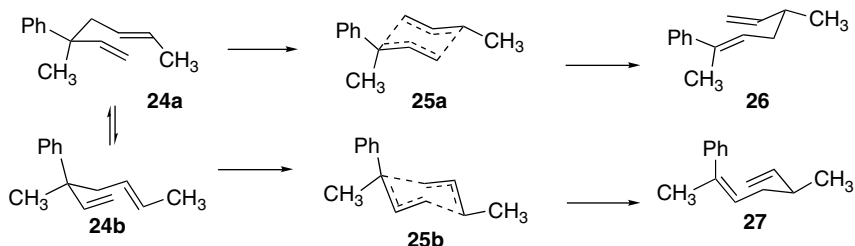
stereospecific and stereoselective. It is stereospecific in that a *Z*- or *E*-configurational relationship at either double bond is maintained in the TS and governs the stereochemical relationship at the newly formed single bond in the product.<sup>236</sup> However, the relationship depends upon the conformation of the TS. When a chair TS is favored the *E,E*- and *Z,Z*-dienes lead to *anti*-3,4-diastereomers, whereas the *E,Z*- and *Z,E*-isomers give the 3,4-*syn* product. The reaction is stereoselective with respect to the configuration of the newly formed double bond. If both *E*- and *Z*- stereoisomers

236. W. v. E. Doering and W. R. Roth, *Tetrahedron*, **18**, 67 (1962).

are possible for the product, the product ratio reflects product (and TS) stability. Thus an *E*-arrangement is normally favored for the newly formed double bonds. The stereochemical aspects of the Cope rearrangements for relatively simple reactants are consistent with a chairlike TS in which the larger substituent at C(3) or C(4) adopts an equatorial-like conformation.



Because of the concerted mechanism, chirality at C(3) or C(4) leads to enantiospecific formation of the new stereocenters at C(1) or C(6).<sup>237</sup> These relationships are illustrated in the example below. Both the configuration of the new stereocenter and the new double bond are those expected on the basis of a chairlike TS. Since there are two stereogenic centers, the double bond and the asymmetric carbon, there are four possible stereomers of the product. Only two are formed. The *E*-isomer has the *S*-configuration at C(4), whereas the *Z*-isomer has the *R* configuration. The stereochemistry of the new double bond is determined by the relative stability of the two chair TSs. TS **25b** is less favorable than **25a** because of the axial placement of the larger phenyl substituent. Thus compound **24** reacts primarily through TS **25a** to give **26** as the major product. Minor product **27** is formed through the less sterically favorable TS **25b**.



When enantiomerically pure **24** is used, the product has an e.e. >95% and the configuration shown above. This result establishes that chirality is maintained throughout the course of the reaction. This stereospecificity is a general feature of [3,3]-sigmatropic shifts and has made them valuable reactions in enantiospecific syntheses.<sup>238</sup>

There is a second possible TS for the Cope rearrangement having a boatlike geometry. The products corresponding to a boatlike TS are usually not observed for

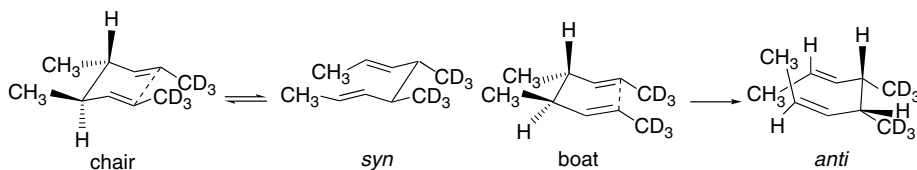
<sup>237</sup> R. K. Hill and N. W. Gilman, *Chem. Commun.*, 619 (1967).

<sup>238</sup> R. K. Hill, in *Asymmetric Synthesis*, Vol. 3, J. D. Morrison, ed., 1984, Chap. 8; D. Enders, M. Knopp and R. Schiffrs, *Tetrahedron: Asymmetry*, **7**, 1847 (1996).

acyclic dienes. However, this TS is allowed by orbital symmetry rules and if steric factors make a boat TS preferable to a chair, reaction proceeds through a boat.

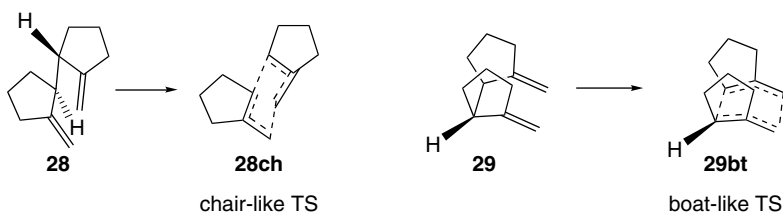


It is generally agreed that the boat TS is higher in energy than the chair TS. There have been several studies aimed at determining the energy difference between the two. One study involved 1,1,1,8,8,8-*deuterio*-4,5-dimethyloctadienes. The chair and boat TSs predict different stereoisomeric products.



Although the process is further complicated by *cis-trans* isomerizations not considered in the above structures, by analysis of the product ratio it was possible to determine that the boat TS is about 6 kcal/mol less stable than the chair.<sup>239</sup> Related experiments on deuterated 1,5-hexadiene itself indicated a difference of 5.8 kcal in  $\Delta G^\ddagger$  for the chair and boat TSs.<sup>240</sup>

Another approach to determining the energy difference between the chair and boat TSs is based on measurement of the activation parameters for the isomeric alkenes **28** and **29**.<sup>241</sup> These two compounds are diastereomeric. Whereas **28** can attain a chairlike TS **28ch**, **29** can achieve bonding between the 1,6-carbons only in a boatlike TS, **29bt**.



Comparison of the rate of rearrangement of **28** and **29** showed **28** to react faster by a factor of 18,000. This corresponds to a difference of about 14 kcal/mol in the measured  $\Delta H^\ddagger$ , but is partially compensated for by a more favorable  $\Delta S^\ddagger$  for **29**. In the corresponding methylenecyclohexane analogs, the  $\Delta H^\ddagger$  favors the chairlike TS by 16 kcal/mol.

The TS involves six partially delocalized electrons being transformed from one 1,5-diene system to another. Theoretical calculations on reactions with delocalized TSs, such as [3,3]-sigmatropic rearrangements, require special care. Correlation effects are especially important and either CI or DFT calculations are required.<sup>242</sup> The most

<sup>239</sup> J. J. Gajewski, C. W. Benner, and C. M. Hawkins, *J. Org. Chem.*, **52**, 5198 (1987).

<sup>240</sup> M. J. Goldstein and M. S. Benzon, *J. Am. Chem. Soc.*, **94**, 7147 (1972).

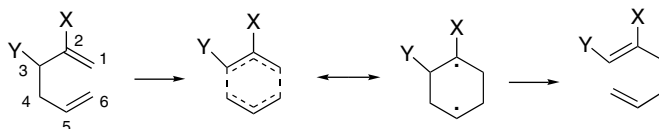
<sup>241</sup> K. J. Shea and R. B. Phillips, *J. Am. Chem. Soc.*, **102**, 3156 (1980).

<sup>242</sup> O. Wiest, D. C. Montiel, and K. N. Houk, *J. Phys. Chem.*, **101**, 8378 (1997).

advanced MO and DFT calculations support the idea of an aromatic TS.<sup>243</sup> The TS can range in character from a 1,4-cyclohexadiyl diradical to two nearly independent allyl radicals, depending on whether bond making or bond breaking is more advanced.<sup>244</sup> The *electrons remain paired* in either case, however, and the two representations are best considered to be resonance structures. The energy surface in the transition region seems to be quite flat; that is, there does not seem to be a strong difference in the energy over the range from 1.64 to 2.19 Å.<sup>245</sup>

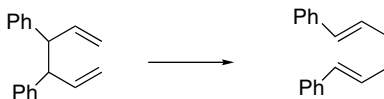


Substituent effects provide other insights into the nature of the TS for the Cope rearrangement. Conjugated substituents at C(2), C(3), C(4), or C(5) accelerate the reaction.<sup>246</sup> Donor substituents at C(2) and C(3) have an accelerating effect.<sup>247</sup> The net effect on the reaction rate of any substituent is determined by the relative stabilization of the TS and ground state.<sup>248</sup> The effect of substituents on the stabilization of the TS can be analyzed by considering their effect on two interacting allyl systems. We consider the case of phenyl substituents in detail.



As shown in Table 10.7, phenyl substituents at positions 2 and 3 reduce the  $\Delta H^\ddagger$ . On the other hand, a 1-substituent, which is conjugated in the reactant but not the product, increases the  $\Delta H^\ddagger$ .

The first step in interpreting these substituent effects is to recognize how they affect the reactant and product energy. Substituents that are conjugated, such as cyano and phenyl, are more stabilizing on a double bond than at a saturated carbon. For example, the rearrangement of 3,4-diphenyl-1,5-hexadiene to 1,6-diphenyl-1,5-hexadiene is exothermic by 10.2 kcal/mol, indicating about 5 kcal/mol of stabilization at each conjugated double bond.



<sup>243</sup> D. A. Hrovat, W. T. Borden, R. L. Vance, N. G. Rondan, K. N. Houk, and K. Morokuma, *J. Am. Chem. Soc.*, **112**, 2018 (1990); D. A. Hrovat, K. Morokuma, and W. T. Borden, *J. Am. Chem. Soc.*, **116**, 1072 (1994); O. Wiest, K. A. Black and K. N. Houk, *J. Am. Chem. Soc.*, **116**, 10336 (1994); M. D. Davidson, I. H. Hillier, and M. A. Vincent, *Chem. Phys. Lett.*, **246**, 536 (1995); S. Yamada, S. Okumoto, and T. Hayashi, *J. Org. Chem.*, **61**, 6218 (1996); W. T. Borden and E. R. Davidson, *Acc. Chem. Res.*, **29**, 57 (1995); P. M. Kozlowski, M. Dupuis, and E. R. Davidson, *J. Am. Chem. Soc.*, **117**, 774 (1995); K. N. Houk, B. R. Beno, M. Nendel, K. Block, H.-Y. Yoo, S. Wilsey, and J. K. Lee, *Theochem*, **398**, 169 (1997); E. R. Davidson, *Chem. Phys. Lett.*, **284**, 301 (1998).

<sup>244</sup> J. J. Gajewski and N. D. Conrad, *J. Am. Chem. Soc.*, **100**, 6268, 6269 (1978); J. J. Gajewski and K. E. Gilbert, *J. Org. Chem.*, **49**, 11 (1984).

<sup>245</sup> P. M. Kozlowski, M. Dupuis, and E. R. Davidson, *J. Am. Chem. Soc.*, **117**, 774 (1995); E. R. Davidson, *J. Phys. Chem.*, **100**, 6161 (1996).

<sup>246</sup> M. J. S. Dewar and L. E. Wade, *J. Am. Chem. Soc.*, **95**, 290 (1972); *J. Am. Chem. Soc.*, **99**, 4417 (1977); R. Wehrli, H. Schmid, D. E. Bellus, and H. J. Hansen, *Helv. Chim. Acta*, **60**, 1325 (1977).

<sup>247</sup> M. Dollinger, W. Henning, and W. Kirmse, *Chem. Ber.*, **115**, 2309 (1982).

<sup>248</sup> For analysis of substituent effects in molecular orbital terminology, see B. K. Carpenter, *Tetrahedron*, **34**, 1877 (1978); F. Delbecq and N. T. Anh, *Nouv. J. Chim.*, **7**, 505 (1983).

**Table 10.7. Effect of Phenyl Substituents on Activation Enthalpy of Cope Rearrangements**

R <sup>1</sup>	R <sup>2</sup>	R <sup>3</sup>	R <sup>4</sup>	R <sup>5</sup>	R <sup>6</sup>	$\Delta H^\ddagger(\text{calc.})^a$	$\Delta H^\ddagger(\text{exp})$
H	H	H	H	H	H	33.2	33.5 <sup>b</sup>
Ph	H	H	H	H	H	36.2	—
H	Ph	H	H	H	H	29.4	29.3 <sup>c</sup>
H	H	Ph	H	H	H	28.4	28.1 <sup>c</sup>
Ph	H	Ph	H	H	H	30.2	30.5 <sup>d</sup>
Ph	H	H	Ph	H	H	29.2	29.9 <sup>c</sup>
H	Ph	H	Ph	H	H	24.6	26.7 <sup>c</sup>
H	Ph	H	H	Ph	H	21.3	21.3 <sup>f</sup>
H	H	Ph	Ph	H	H	—	24.0 <sup>g</sup>
Ph	H	Ph	H	Ph	H	29.2	27.8 <sup>d</sup>
Ph	H	Ph	Ph	H	Ph	19.1	21.3 <sup>g</sup>

a. Calculated from D. A. Hrovat, J. Chen, K. N. Houk, and W. T. Borden, *J. Am. Chem. Soc.*, **122**, 7456 (2000)

b. W. v. E. Doering, V. G. Toscano, and G. H. Beasley, *Tetrahedron*, **27**, 5299 (1971).

c. M. J. S. Dewar and L. E. Wade, Jr., *J. Am. Chem. Soc.*, **99**, 4417 (1977).

c. E. G. Foster, A. C. Cope, and F. Daniels, *J. Am. Chem. Soc.*, **69**, 1893 (1947).

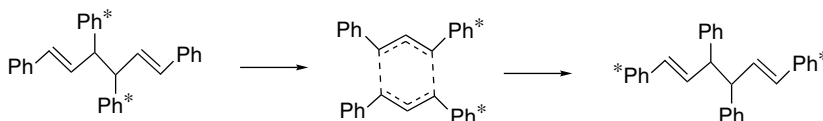
d. W. von E. Doering and Y. Wang, *J. Am. Chem. Soc.*, **121**, 10112 (1999).

e. W. von E. Doering, L. Birladeanu, K. Sarma, J. H. Teles, F.-G. Klaerner, and J.-S. Gehrke, *J. Am. Chem. Soc.*, **110**, 4289 (1994).

f. W. R. Roth, H.-W. Lennartz, W. v. E. Doering, L. Birladeanu, C. A. Guyton, and T. Kitagawa, *J. Am. Chem. Soc.*, **112**, 1722 (1990).

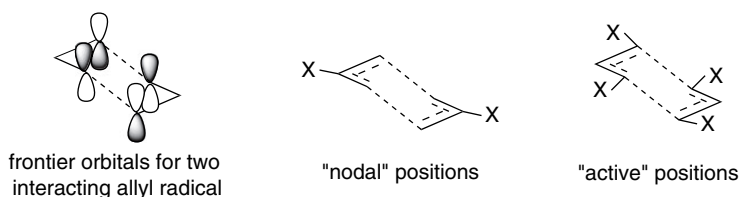
g. W. von E. Doering, L. Birladeanu, K. Sarma, G. Blaschke, U. Scheidemantel, R. Boese, J. Benet-Buchholz, F.-G. Klärner, J. S. Zimny, R. Sustmann, and H.-G. Korth, *J. Am. Chem. Soc.*, **122**, 193 (2000).

On the other hand, the degenerate rearrangement of *syn*-1,3,4,6-tetraphenyl-1,6-hexadiene is equi-energetic.



The next step is to understand how the *position* of the substitution influences the direction and magnitude of the rate effect and TS structure. If the TS is best represented by two loosely interacting allyl radicals, substituents at the 1, 3, 4, and 6 positions should have the strongest influence. This is because the 2 and 5 positions are at nodes of the frontier orbitals in allyl radicals and should not strongly influence radical stability. On the other hand, a cyclohexadienyl diradical intermediate should be affected most strongly by 2- and 5-substituents. The 1, 3, 4, and 6 positions have been called “active” and the 3 and 5 positions “nodal” to distinguish their relationship to the allyl HOMO orbitals.<sup>249</sup> It was suggested that substituents at the “active” positions would move the TS toward the diallyl radical structure (by preferentially stabilizing that structure), whereas substituents at the “nodal” positions would favor the 1,4-cyclohexadienyl structure.

<sup>249</sup>. (a) W. v. E. Doering and Y. Wang, *J. Am. Chem. Soc.*, **121**, 10112 (1999); (b) W. von E. Doering, L. Birladeanu, K. Sarma, G. Blaschke, U. Scheidemantel, R. Boese, J. Benet-Buchholz, F.-G. Klaerner, J. S. Gehrke, B. U. Zimny, R. Sustmann, and H.-G. Korth, *J. Am. Chem. Soc.*, **122**, 193 (2000).



Borden, Houk, and co-workers evaluated the various phenyl-substituted cases using B3LYP/6-31G\* calculations.<sup>250</sup> They found that the TS structure did indeed respond to the placement of phenyl substituents. Phenyl groups at the 2 and 5 positions resulted in a tighter, more 1,4-cyclohexadiyl TS, whereas 1- and 4-phenyl substituents resulted in a looser, more diallylic TS. When several substituents of the same type (matched) were present, the effects were reinforced. On the other hand, 1,5-diphenyl-1,3,5-hexatriene, where the substituents are of different types (unmatched) led to little change from the unsubstituted system. The bond lengths for some of the relevant systems are shown in Figure 10.37. The C–C bond length in the TS for 1,3,4,6-tetraphenyl-1,3,5-hexatriene corresponds to a bond order of only 0.06.

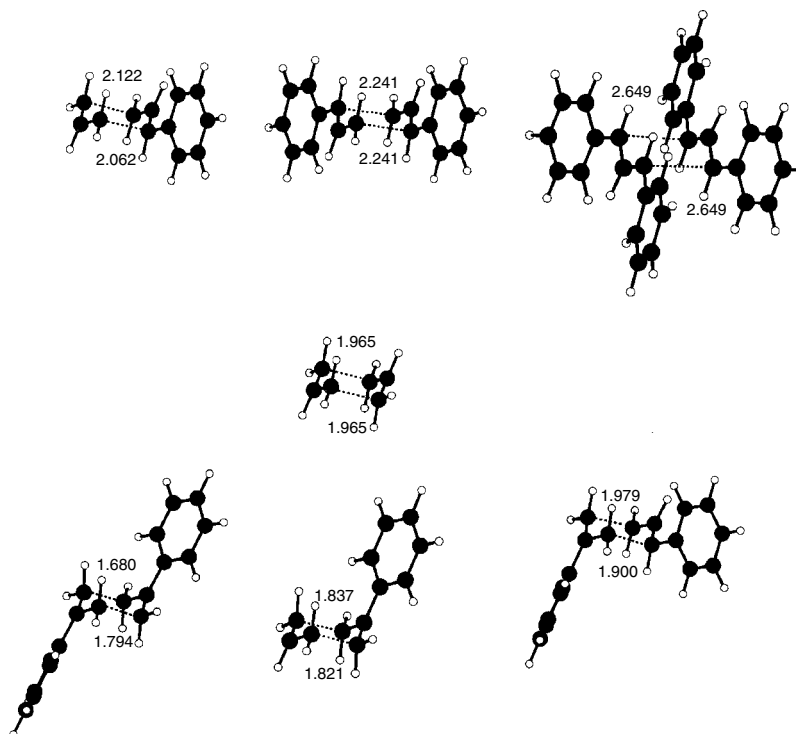


Fig. 10.37. Changes in bond length at the TS for [3,3]-sigmatropic rearrangement of phenyl-substituted 1,3,5-hexatrienes. (a) Top: cumulative loosening of the TS with one, two, and four phenyl groups in "active" positions. (b) Center: unsubstituted system. (c) Lower Left: cumulative tightening of TS by 2- and 2,5-phenyl substitution. (d) Lower Right: "unmatched" 2- and 4-substituents are competitive, leading to little structural change. Reproduced from *J. Am. Chem. Soc.*, **122**, 7456 (2000), by permission of the American Chemical Society.

<sup>250</sup> D. A. Hrovat, J. Chen, K. N. Houk, and W. T. Borden, *J. Am. Chem. Soc.*, **122**, 7456 (2000).

In the case of the 2,5-diphenyl derivative, the bond distance corresponds to a bond order of 0.94. Thus these TS structures span a range from nearly “diallylic” to nearly “cyclohexadiyl” character. The substituent effects are also reflected in TS energies. An additional “matched” phenyl substituent lowers TS energy more than an addition “unmatched” substituent.

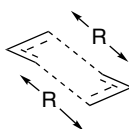
**Effect of Phenyl Substitution on  $E_a$  (kcal/mol) for  
Rearrangement of 1,3,5-Hexatrienes**

Unsubstituted	1-Phenyl	1,4-Diphenyl	1,3,4,6-Tetraphenyl
33.2	36.2	29.2	19.1 (matched)
	2-Phenyl	2,5-Diphenyl	
	29.4	21.3 (matched)	
	2-Phenyl	2,4-Diphenyl	
	29.4	27.1 (unmatched)	

The role of cyano substituents has also been explored in detail. The symmetrical “matched” 2,5- and 1,3,4,6-systems and the unmatched (but still symmetrical) 1,3,5-cyano system were investigated.<sup>251</sup> The effect of the substituents on TS energy was examined, as were the 1–6 and 3–4 bond distances. The energies of the TSs were evaluated relative to two allyl radicals by an isodesmic reaction.



Several levels of calculations were performed with the 6-31\* basis set using a type of CAS-SCF computation. Cyano substituents at both positions were stabilizing, but more so at 2,5 than at 1,3,4,6. The energetic and geometric effects are similar to those in the phenyl-substituted compounds. The TS is tightened (cyclohexadiyl-like) by 2,5-substituents, but loosened (diallyl-like) by 1,3,4,6-substitution. The 2,5-cyano substituents provide the highest TS stabilization. The distribution of unpaired electron density was used to assess radical character. In contrast to the significant energy and geometry differences, there was little change in the radical character of the TS with substitution.



**Effect of Cyano Substituents on Transition State Energy and  
Structure**

Substitution	R(1, 6) = (3, 4) Å	$\Delta E$ (isodesmic) kcal/mol
None	1.9661	–22.7
2,5-	1.7524	–41.0
1,3,5-	2.1062	–32.1
1,3,4,6-	2.4670	–29.4

<sup>251</sup> V. N. Staroverov and E. R. Davidson, *J. Am. Chem. Soc.*, **122**, 7377 (2000).

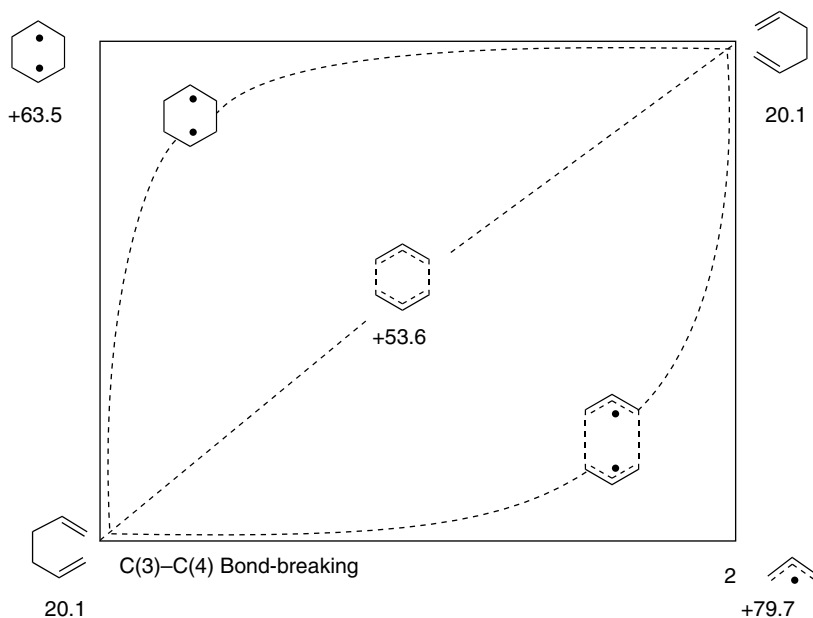
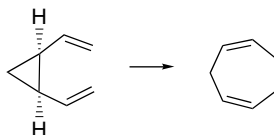


Fig. 10.38. More-O'Ferrall-Jencks diagram representing the variable transition structure for the Cope rearrangement. Energies (in kcal/mol) are from thermodynamic data, as quoted by D. A. Hrovat, J. Chen, K. N. Houk, and W. T. Borden, *J. Am. Chem. Soc.*, **122**, 7456 (2000).

The idea that the nature of the Cope rearrangement TS is variable can be expressed in terms of a More-O'Ferrall-Jencks energy diagram, as in Figure 10.38.<sup>252</sup> The 1,4-cyclohexadiyl diradical is believed to have a  $\Delta H_f$  of 63.5 kcal/mol, which is 43.4 kcal/mol above 1,5-hexadiene. Two separate allyl radicals are at 79.7 kcal/mol, which is 59.6 kcal/mol above the reactant.<sup>249a</sup> The unsubstituted TS is at 53.6 kcal/mol, which is well below either the 1,4-diyl radicals or two allyl radicals, and the reaction proceeds by a concerted process. For the unsubstituted compound, there is a nearly equal amount of bond making and bond breaking at the TS, with a C(1)–C(6) and C(3)–C(4) bond order of 0.49.<sup>250</sup> The substituent effects can be interpreted by analyzing how they affect reactant and product energies and how they change TS character.

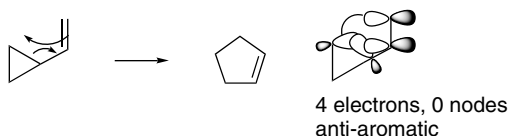
When strain is relieved, Cope rearrangements can occur at much lower temperatures and with complete conversion to ring-opened products. Some particularly striking examples of Cope rearrangement can be found in the rearrangement of *cis*-divinylcyclopropanes. An example is the conversion of *cis*-divinylcyclopropane to 1,4-cycloheptadiene, a reaction that occurs readily at temperatures below  $-40^\circ\text{C}$ .<sup>253</sup>



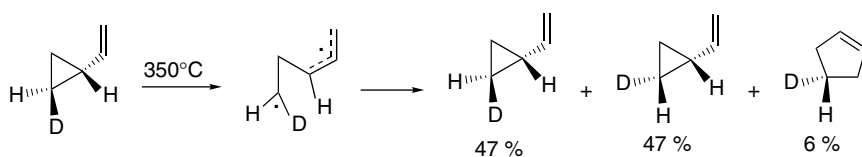
<sup>252</sup> J. J. Gajewski, *Acc. Chem. Res.*, **13**, 142 (1980); K. N. Houk, S. M. Gustafson, and K. A. Black, *J. Am. Chem. Soc.*, **114**, 8565 (1992); J. J. Gajewski, *Acc. Chem. Res.*, **30**, 219 (1997).

<sup>253</sup> W. v. E. Doering and W. R. Roth, *Tetrahedron*, **19**, 715 (1963).

Before we go into these reactions in detail, let us examine vinylcyclopropane itself, which rearranges at high temperature to cyclopentene.<sup>254</sup>

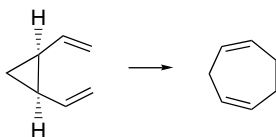


The most geometrically accessible TS corresponds to a forbidden 1,3-suprafacial alkyl shift with retention of configuration. The rearrangement requires a temperature of at least 200°–300° C.<sup>255</sup> The measured  $E_a$  is about 50 kcal/mol, which is consistent with a stepwise reaction beginning with rupture of a cyclopropane bond and formation of an allylic fragment.<sup>256</sup> Support for a nonconcerted mechanism comes from the observation that *cis*-*trans* isomerization occurs faster than the rearrangement. This isomerization presumably occurs by reversible cleavage of the C(1)–C(2) cyclopropane bond.



When this prior stereoisomerization is accounted for, the rearrangement is found to have resulted from a mixture of all possible suprafacial, antarafacial, inversion, and retention combinations in roughly equal amounts, indicating lack of stereoselectivity.<sup>258</sup> Thus, the rearrangement of vinylcyclopropane occurs with nearly complete bond rupture. Computational modeling of the reaction finds no intermediate, and the TS is diradical in character.<sup>259</sup>

A dramatic difference in reactivity is evident when *cis*-divinylcyclopropane is compared with vinylcyclopropane.<sup>260</sup> *cis*-Divinylcyclopropane can only be isolated at low temperature because it very rapidly undergoes Cope rearrangement to 1,4-cycloheptatriene.<sup>261</sup> At 0°C  $\Delta H^\ddagger$  is 18.8 kcal/mol and  $\Delta S^\ddagger$  is  $-9.4$  eu.



<sup>254</sup>. C. G. Overberger and A. E. Borchert, *J. Am. Chem. Soc.*, **82**, 1007 (1960).

<sup>255</sup>. T. Hudlicky, T. M. Kutchan, and S. M. Naqui, *Org. React.*, **33**, 247 (1984); T. Hudlicky and J. D. Price, *Chem. Rev.*, **89**, 1467 (1989); J. E. Baldwin, in *Chemistry of the Cyclopropyl Group*, Vol. 2, Z. Rapoport, ed., Wiley, 1995, pp. 469–494.

<sup>256</sup>. D. K. Lewis, D. J. Charney, B. L. Kalra, A. M. Plate, M. H. Woodard, S. J. Cianciosi, and J. E. Baldwin, *J. Phys. Chem.*, **101**, 4097 (1997).

<sup>257</sup>. M. R. Willcott and V. H. Cargle, *J. Am. Chem. Soc.*, **89**, 723 (1967).

<sup>258</sup>. J. J. Baldwin, K. A. Villarica, D. I. Freedberg, and F. A. L. Anet, *J. Am. Chem. Soc.*, **116**, 10845 (1994).

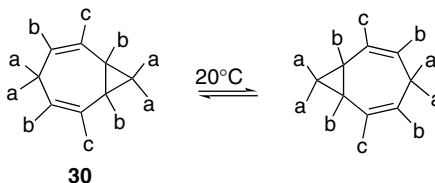
<sup>259</sup>. E. R. Davidson and J. J. Gajewski, *J. Am. Chem. Soc.*, **119**, 10543 (1997); K. N. Houk, M. Nendal, O. Wiest, and J. W. Storer, *J. Am. Chem. Soc.*, **119**, 10545 (1997); J. E. Baldwin, *J. Comput. Chem.*, **19**, 222 (1998).

<sup>260</sup>. T. Hudlicky, R. Fan, J. W. Reed, and K. G. Gadamasetti, *Org. React.*, **41**, 1 (1992).

<sup>261</sup>. J. M. Brown, B. T. Bolding, and J. F. Stofko, Jr., *Chem. Commun.*, 319 (1973); M. Schneider, *Angew. Chem. Int. Ed. Engl.*, **14**, 707 (1975); M. P. Schneider and A. Rau, *J. Am. Chem. Soc.*, **101**, 4426 (1979).

Owing to unfavorable molecular geometry, the corresponding rearrangement of *trans*-divinylcyclopropane to cycloheptatriene cannot be concerted and requires temperatures on the order of 190°C. The very low energy requirement for the Cope rearrangement of *cis*-divinylcyclopropane reflects several favorable circumstances. The *cis*-orientation facilitates interaction of the diene termini, so the loss in entropy in going to the TS is smaller than for an acyclic diene. The breaking bond is strained and this reduces the  $E_a$ . The importance of the latter factor can be appreciated by comparison with *cis*-divinylcyclobutane and *cis*-divinylcyclopentane. The former compound has  $\Delta H^\ddagger = 23$  kcal/mol for rearrangement to cyclooctadiene.<sup>262</sup> *cis*-Divinylcyclopentane does not rearrange to cyclononadiene, even at 250°C.<sup>263</sup> In the latter case, the rearrangement is presumably thermodynamically unfavorable, since there is no strain release from ring opening.

Divinylcyclopropane rearrangements can proceed with even greater ease if the  $\Delta S^\ddagger$  is made less negative by incorporating both vinyl groups into a ring. An example of this is found in the degenerate homotropilidene rearrangement. A *degenerate rearrangement* is a reaction process in which no overall change in structure occurs, and the product of rearrangement is structurally identical to the starting material. Depending on the rate at which the reaction occurs, the existence of a degenerate rearrangement can be detected by use of isotopic labels or by interpretation of the temperature dependence of NMR spectra. In the case of homotropilidene, **30**, the occurrence of a dynamic equilibrium is evident from the NMR spectrum. At low temperature the rate of interconversion is slow and the spectrum indicates the presence of four vinyl protons, two allylic protons, and two pairs of cyclopropyl protons. As the temperature is raised and the rate of the rearrangement increases, it is observed that two of the vinyl protons remain essentially unchanged with respect to their chemical shift, whereas the other two coalesce with one of the pairs of cyclopropyl protons. Coalescence is also observed between the allylic protons and the other two cyclopropyl protons.<sup>264</sup> The sets of protons that coalesce undergo sufficiently rapid interchange with one another to result in an averaged signal (see p. 155).



Many other examples of this type of rearrangement are known. Another interesting case is bullvalene, which is converted into itself with a first-order rate constant of  $3.4 \times 10^3 \text{ s}^{-1}$  at 25°C.<sup>265</sup> At 10°C, the <sup>1</sup>H-NMR spectrum of bullvalene exhibits a single peak at 4.22 ppm, which indicates the “fluxional” nature of the molecule. Owing to the threefold axis of symmetry present in bullvalene, the degenerate rearrangement results in all of the carbons having an identical averaged environment. This is illustrated in the

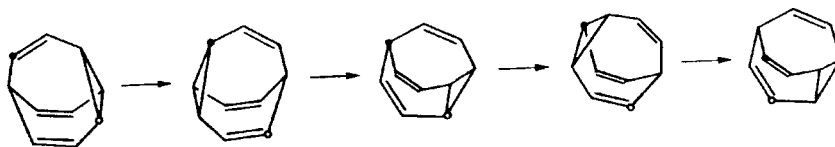
<sup>262</sup> E. Vogel, *Justus Liebigs Ann. Chem.*, **615**, 1 (1958); G. S. Hammond and C. D. DeBoer, *J. Am. Chem. Soc.*, **86**, 899 (1964).

<sup>263</sup> E. Vogel, W. Grimme, and E. Dinne, *Angew. Chem.*, **75**, 1103 (1963).

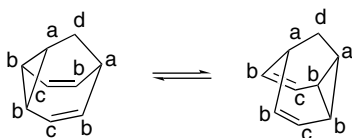
<sup>264</sup> G. Schroeder, J. F. M. Oth, and R. Merenyi, *Angew. Chem. Int. Ed. Engl.*, **4**, 752 (1965); H. Gunther, J. B. Pawliczek, J. Ulmen, and W. Grimme, *Angew. Chem. Int. Ed. Engl.*, **11**, 517 (1972); W. v. E. Doering and W. R. Roth, *Tetrahedron*, **19**, 715 (1963).

<sup>265</sup> G. Schroeder and J. F. M. Oth, *Angew. Chem. Int. Ed. Engl.*, **6**, 414 (1967).

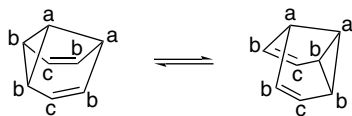
diagram below by the interchanging environments of the labeled carbons. The  $E_a$  for the rearrangement has been determined to be 13.9 kcal/mol.<sup>266</sup> Substituted bullvalenes have also been studied.<sup>267</sup>



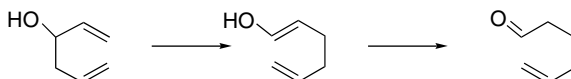
Other degenerate rearrangements have been discovered that are even faster than that of bullvalene. Barbaralane rearranges to itself with a rate constant of  $1.7 \times 10^7 \text{ s}^{-1}$  at  $25^\circ \text{C}$ .<sup>268</sup> The  $E_a$  of this rearrangement is only 7.7 kcal/mol. The lowered energy requirement is attributed to an increase in ground state energy owing to strain. Barbaralane is less symmetrical than bullvalene. There are four different kinds of carbons and protons in the averaged structure. Only the methylene group labeled “d” is unaffected by the degenerate rearrangement.



A further reduction in the barrier and increase in rate is seen with semibullvalene in which strain is increased still more. The  $\Delta G^\ddagger$  for this rearrangement is 5.5 kcal/mol at  $-143^\circ \text{C}$ .<sup>269</sup>



When there is a hydroxy substituent at C(3) of the diene system, the Cope rearrangement product is an enol that is subsequently converted to the corresponding carbonyl compound. This is called the *oxy-Cope* rearrangement.<sup>270</sup> The formation of the carbonyl compound provides a net driving force for the reaction.<sup>271</sup>



<sup>266</sup> R. Poupko, H. Zimmerman, and Z. Luz, *J. Am. Chem. Soc.*, **106**, 5391 (1984).

<sup>267</sup> R. Poupko, H. Zimmermann, K. Muller, and Z. Luz, *J. Am. Chem. Soc.*, **118**, 7995 (1996).

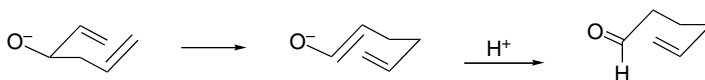
<sup>268</sup> W. v. E. Doering, B. M. Ferrier, E. T. Fossel, J. H. Hartenstein, M. Jones, Jr., G. Klumpp, R. M. Rubin, and M. Saunders, *Tetrahedron*, **23**, 3943 (1967); H. Gunther, J. Runsink, H. Schmickler, and P. Schmitt, *J. Org. Chem.*, **50**, 289 (1985).

<sup>269</sup> A. K. Cheng, F. A. L. Anet, J. Mioduski, and J. Meinwald, *J. Am. Chem. Soc.*, **96**, 2887 (1974); D. Moskau, R. Aydin, W. Leber, H. Gunther, H. Quast, H.-D. Martin, K. Hassenruck, L. S. Miller, and K. Grohmann, *Chem. Ber.*, **122**, 925 (1989).

<sup>270</sup> S. R. Wilson, *Org. React.*, **43**, 93 (1993); L. A. Paquette, *Angew. Chem. Int. Ed. Engl.*, **29**, 609 (1990); L. A. Paquette, *Tetrahedron*, **53**, 13971 (1997).

<sup>271</sup> A. Viola, E. J. Iorio, K. K. N. Chen, G. M. Glover, U. Nayak, and P. J. Kocienski, *J. Am. Chem. Soc.*, **89**, 3462 (1967).

There is a very powerful substituent effect for dienes having anionic oxygen substituents at C(3), a reaction known as the *anionic oxy-Cope reaction*.<sup>272</sup> When the C(3) hydroxyl group is converted to its alkoxide, the reaction is accelerated by factors of  $10^{10}$ – $10^{17}$ .<sup>273</sup>



The rates of anionic oxy-Cope rearrangements depend on the degree of cation coordination at the oxy anion. The reactivity trend is  $K^+ > Na^+ > Li^+$ . Crown ethers catalyze reaction by promoting ion pair dissociation.<sup>274</sup> Catalytic amounts of *tetra-n*-butylammonium salts lead to accelerated rates in some cases. This presumably results from the dissociation of less reactive ion pair species promoted by the *tetra-n*-butylammonium ion.<sup>275</sup> As with other [3,3]-sigmatropic rearrangements, the stereochemistry of the anionic oxy-Cope rearrangement depends on TS conformation. There is no strong stereochemical preference associated with the C–O<sup>−</sup> bond, and in the absence of other controlling steric factors, products arising from both equatorial and axial orientations are formed.<sup>276</sup>

The origin of the rate acceleration has been explored by computation. The B3LYP/6-31+G\* computational results give a  $\Delta G^\ddagger$  of 6.3 kcal/mol, some 30 kcal/mol less than the unsubstituted system.<sup>277</sup> Another study found the barrier to be only 8.3 kcal/mol in the gas phase. This is raised substantially (to 31.8 kcal/mol) by coordination of an Li<sup>+</sup> cation at the oxygen.<sup>278</sup> As shown in Figure 10.39, the TS for the anionic oxy-Cope reaction is much more asynchronous than for the parent system. The TS is much looser and closer to two dissociated fragments. Note that the C(3)–C(4) bond has lengthened substantially in the TS, whereas the C(1)–C(6) bond distance is still quite long. Several factors probably contribute to the large rate acceleration. The anionic oxy substituent substantially weakens the C(3)–C(4) bond.<sup>279</sup> The delocalization of the negative charge in the enolate is also likely a factor, in view of the dissociative nature of the TS.

3-Amino groups also accelerate the Cope rearrangement.<sup>280</sup> The products are enamines and subsequent reactions of the enamine are feasible, such as  $\alpha$ -alkylation.

<sup>272</sup> L. A. Paquette, *Angew. Chem. Int. Ed. Engl.*, **29**, 609 (1990).

<sup>273</sup> D. A. Evans and A. M. Golob, *J. Am. Chem. Soc.*, **97**, 4765 (1975); D. A. Evans, D. J. Baillargeon, and J. V. Nelson, *J. Am. Chem. Soc.*, **100**, 2242 (1978).

<sup>274</sup> J. J. Gajewski and K. R. Gee, *J. Am. Chem. Soc.*, **113**, 967 (1991).

<sup>275</sup> M. George, T.-F. Tam, and B. Fraser-Reid, *J. Org. Chem.*, **50**, 5747 (1985).

<sup>276</sup> L. A. Paquette and G. D. Maynard, *J. Am. Chem. Soc.*, **114**, 5018 (1992); E. Lee, Y. R. Lee, B. Moon, O. Kwon, M. S. Shim, and J. S. Yun, *J. Org. Chem.*, **59**, 1444 (1994).

<sup>277</sup> H. Bauman and P. Chen, *Helv. Chim. Acta*, **84**, 124 (2001).

<sup>278</sup> F. Haeffner, K. N. Houk, S. M. Schulze, and J. K. Lee, *J. Org. Chem.*, **68**, 2310 (2003).

<sup>279</sup> (a) M. L. Steigerwald, W. A. Goddard, III, and D. A. Evans, *J. Am. Chem. Soc.*, **101**, 1994 (1979); (b) H. Y. Yoo, K. N. Houk, J. K. Lee, M.A. Scialdone, and A. I. Meyers, *J. Am. Chem. Soc.*, **120**, 205 (1998).

<sup>280</sup> R. W. Jemison, W. D. Ollis, I. O. S. Sutherland, and J. Tannock, *J. Chem. Soc., Perkin Trans. 1*, 1462 (1980); J. P. Hagen, K. D. Lewis, S. W. Lovell, P. Rossi, and A. Z. Tescan, *J. Org. Chem.*, **60**, 7471 (1995).

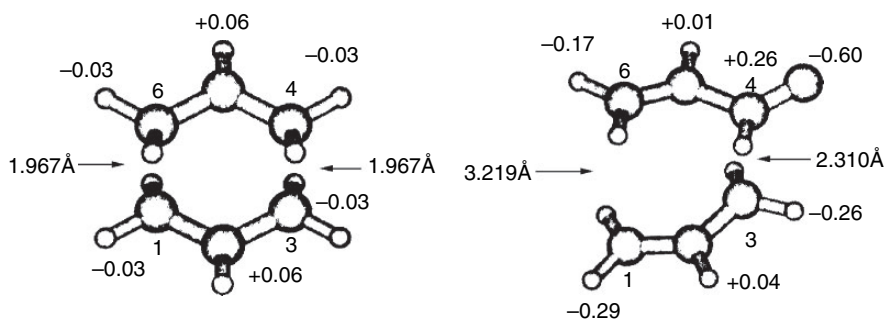
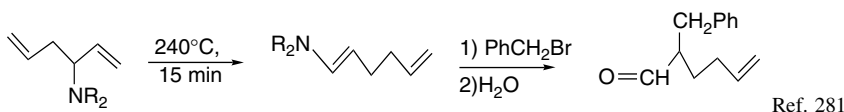
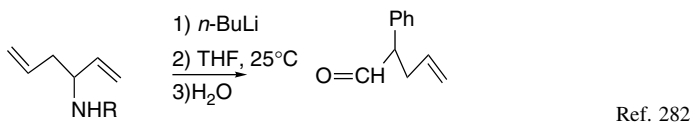


Fig. 10.39. Comparison of transition structure geometry for anionic oxy-Cope (right) rearrangement with Cope rearrangement (left) showing atom separation distances and Mulliken charges (B3LYP/6-311G\*). Reproduced from *Helv. Chim. Acta*, **84**, 124 (2001), by permission of Wiley-VCH.



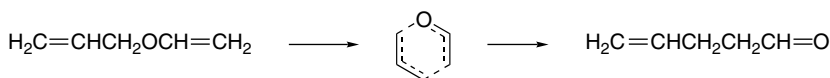
When secondary amines are used, an anionic version of the reaction occurs when the amine is deprotonated by *n*-BuLi.



However, as implied by computations on the anionic amino-Cope reaction,<sup>279b</sup> a dissociative pathway is competitive and can complicate the outcome of the reaction.<sup>283</sup>

### 10.6.3.2. [3,3]-Sigmatropic Rearrangement in Triene Systems Containing Oxygens

The [3,3]-sigmatropic reaction pattern is quite general for other systems that incorporate one or more heteroatoms in place of carbon in the 1,5-hexadiene unit. The most synthetically useful and widely studied of these reactions is the Claisen rearrangement, in which an oxygen atom is present at position 3.<sup>284</sup> The simplest example of a Claisen rearrangement is the thermal conversion of allyl vinyl ether to 4-pentenal.



This reaction occurs with an  $E_a$  of 30.6 kcal/mol and an  $\Delta S^\ddagger$  of  $-7.7$  eu at 180°C.<sup>285</sup> Both computational modeling of the TS and analysis of kinetic isotope effects are in accord with a concerted mechanism in which C–O bond cleavage is more advanced

<sup>281</sup>. S. M. Allin, M. A. C. Button, and S. J. Shuttleworth, *Synlett*, 725 (1997).

<sup>282</sup>. S. M. Allin, M. A. C. Button, and R. D. Baird, *Synlett*, 1117 (1998).

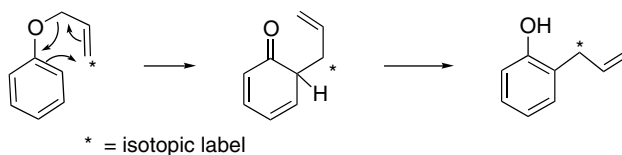
<sup>283</sup>. S. M. Allin and M. A. C. Button, *Tetrahedron Lett.*, **40**, 3801 (1999).

<sup>284</sup>. G. B. Bennett, *Synthesis*, 589 (1977); S. J. Rhoads and N. R. Raulins, *Org. React.*, **22**, 1 (1975).

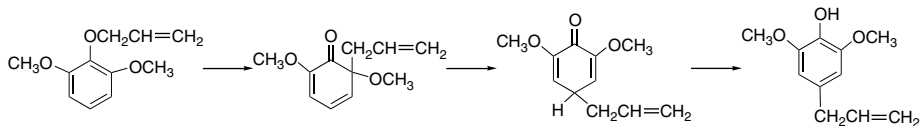
<sup>285</sup>. F. W. Schuler and G. W. Murphy, *J. Am. Chem. Soc.*, **72**, 3155 (1950).

than C–C bond formation.<sup>286</sup> Claisen rearrangements show a considerable sensitivity to solvent polarity, with reaction rates increasing with solvent polarity.<sup>287</sup> Water is an especially favorable solvent.<sup>288</sup> The solvent effect is believed to be due to differential solvation of the reactants and TS. Hydrogen bonding contributes to stabilization of the TS.<sup>289</sup>

Allyl ethers of phenols undergo [3,3]-sigmatropic rearrangements and some aspects of the mechanism were developed by studying these compounds.<sup>290</sup> For example, an important clue as to the mechanism of the Claisen rearrangement was obtained by use of <sup>14</sup>C-labeled allyl phenyl ether. It was found that the rearrangement was specific as to which carbon atom of the allyl group became bonded to the ring, which is consistent with a cyclic mechanism.<sup>291</sup>



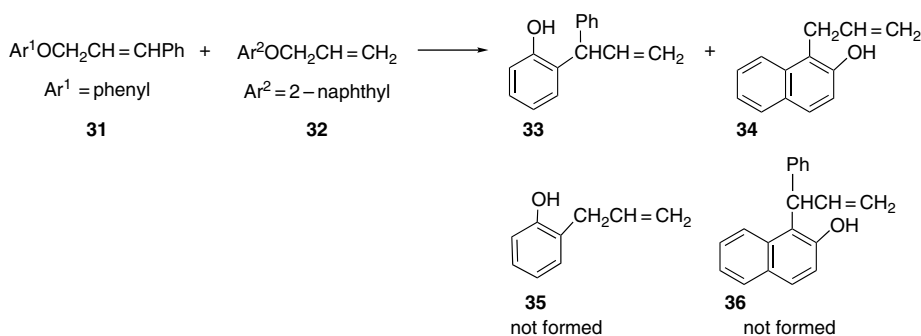
If both *ortho*-positions are substituted, the allyl group undergoes a second migration, giving the *para*-substituted phenol.



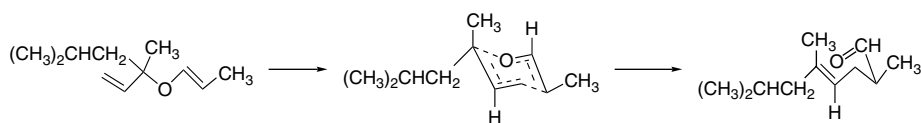
Ref. 292

The intramolecular nature of the rearrangement was established by a crossover experiment in which **31** and **32** were heated simultaneously and found to yield the same products as when they were heated separately. There was no evidence for the formation of the crossover products **35** and **36**,<sup>293</sup> which indicates that the rearrangement must be intramolecular.

- <sup>286</sup> J. J. Gajewski and N. D. Conrad, *J. Am. Chem. Soc.*, **101**, 6693 (1979); R. L. Vance, N. G. Rondan, K. N. Houk, H. F. Jensen, W. T. Borden, A. Komornicki, and E. Winner, *J. Am. Chem. Soc.*, **110**, 2314 (1988); L. Kupczyk-Subotkowska, W. H. Saunders, Jr., H. J. Shine, and W. Subotkowski, *J. Am. Chem. Soc.*, **115**, 5957 (1993); M. P. Meyer, A. J. Del Monte, and D. A. Singleton, *J. Am. Chem. Soc.*, **121**, 10865 (1999).
- <sup>287</sup> B. Ganem, *Angew. Chem. Int. Ed. Engl.*, **35**, 937 (1996).
- <sup>288</sup> P. A. Grieco, E. B. Brandes, S. McCann, and J. D. Clark, *J. Org. Chem.*, **54**, 5849 (1989); A. Lubineau, J. Auge, N. Bellanger, and S. Caillebourdin, *J. Chem. Soc., Perkin Trans. 2*, 1631 (1992).
- <sup>289</sup> D. L. Severance and W. L. Jorgensen, *J. Am. Chem. Soc.*, **114**, 10966 (1992); M. M. Davidson and I. H. Hillier, *J. Phys. Chem.*, **99**, 6748 (1995); J. J. Gajewski, *Acc. Chem. Res.*, **30**, 219 (1997).
- <sup>290</sup> D. S. Tarbell, *Org. React.*, **2**, 1 (1944); S. J. Rhoads, in *Molecular Rearrangements*, Vol. 1, P. de Mayo, ed., Interscience, New York, 1963, pp. 655–684.
- <sup>291</sup> J. P. Ryan and P. R. O'Connor, *J. Am. Chem. Soc.*, **74**, 5866 (1952).
- <sup>292</sup> I. A. Pearl, *J. Am. Chem. Soc.*, **70**, 1746 (1948).
- <sup>293</sup> C. D. Hurd and L. Schmerling, *J. Am. Chem. Soc.*, **59**, 107 (1937).

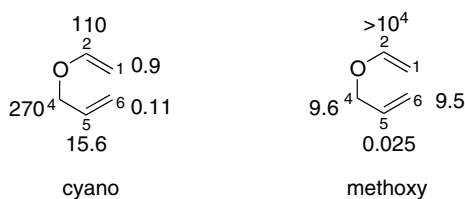


The stereochemical features of the Claisen rearrangement are very similar to those described for the Cope rearrangement, and stereochemical predictions can be made on the basis of the preference for a chairlike TS. The major product has the *E*-configuration at the newly formed double bond because of the preference for placing the larger substituent in the pseudoequatorial position in the TS.<sup>294</sup>



Studies of chiral substrates have also demonstrated that chirality is maintained in the reaction.<sup>295</sup> Examples of the synthetic application of the Claisen rearrangement are discussed in Section 6.4.2.1 of Part B.

Like the Cope rearrangement, the Claisen rearrangement is sensitive to substituents on the reacting system. Cyano groups promote the rearrangement by a factor of  $10^2$  at positions 2 and 4 and have smaller effects at the other positions, as shown in the diagram below.<sup>296</sup> Experimental data are also available for methoxy groups at positions 2, 4, 5, and 6.<sup>297</sup> The methoxy substituent is very activating at C(2). These substituents set the pattern for  $\pi$ -conjugated EWG and  $\sigma$ -donor substituents, respectively.



Relative rate effect of cyano and methoxy substituents

As in the case of the Cope rearrangement, the interpretation of these substituent effects is best approached by considering the effect on TS stability. The effect on

<sup>294</sup>. R. Marbet and G. Saucy, *Helv. Chim. Acta*, **50**, 2095 (1967); A. W. Burgstahler, *J. Am. Chem. Soc.*, **82**, 4681 (1960); C. L. Perrin and D. J. Faulkner, *Tetrahedron Lett.*, 2783 (1969).

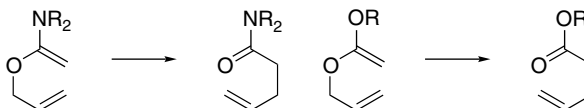
<sup>295</sup>. H. L. Goering and W. I. Kimoto, *J. Am. Chem. Soc.*, **87**, 1748 (1965).

<sup>296</sup>. C. J. Burrows and B. K. Carpenter, *J. Am. Chem. Soc.*, **103**, 6983 (1981).

<sup>297</sup>. R. M. Coates, B. D. Rogers, S. J. Hobbs, D. R. Peck, and D. P. Curran, *J. Am. Chem. Soc.*, **109**, 1160 (1987).

the TS for the Claisen rearrangement by hydroxy substituents has been probed using both HF/6-31G\* and B3LYP/6-31G\* calculations.<sup>298</sup> The effect of cyano, amino, and trifluoromethyl groups has also been calculated.<sup>299</sup> The effect of methoxy groups has been examined using a combination AM1-MM method. The predicted changes in  $E_a$ , as summarized in Table 10.8, are in qualitative agreement with experimental results.

These substituent effects can be analyzed by considering the effect on reactants, products, and the TS. For example, the large accelerating effect of 2-alkoxy and 2-amino substituents is due in substantial part to the amide and ester resonance stabilization that develops in the products.



The analysis can be done in terms of the Marcus theory by considering the effect on overall reaction energy  $\Delta E_{\text{rxn}}$  and  $\Delta E_0^\ddagger$ , the *intrinsic barrier*, using a version of the Marcus equation.<sup>300</sup> (See Section 3.3.2.3 to review the Marcus equation.)

$$\Delta E^\ddagger = \Delta E_0^\ddagger + \frac{1}{2}\Delta E_{\text{rxn}} + (\Delta E_{\text{rxn}})^2/16(\Delta E_0^\ddagger)$$

For the HF/6-31G\* calculations, the barriers were separated into effects owing to changes in reaction energy and changes in TS energy.<sup>299b</sup> Changes in TS energy can be analyzed in terms of radical stabilization effects, as was done for the Cope rearrangement. (see p. 924ff). In addition, there may be variation in the extent of the polar character at the TS. The TS for the Claisen rearrangement has some ionic character, resembling an enolate for C(1), C(2), and O(3) and allyl cation for C(4), C(5), C(6). For the parent reaction, charge transfer is calculated to be  $0.21e$ . The stabilizing effect of the 4- and 6-oxy substituents may be due to stabilization of the cationic fragment, as indicated by the charge distribution below.

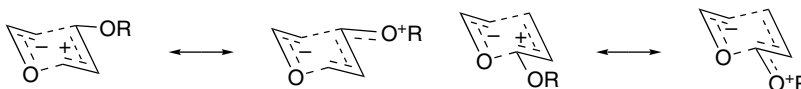


**Table 10.8. Calculated Substituent Effects on  $E_a$  in kcal/mol for Claisen Rearrangement**

Position	OH <sup>a</sup>	CN <sup>b</sup>	NH <sub>2</sub> <sup>b</sup>	CF <sub>3</sub> <sup>b</sup>	OCH <sub>3</sub> <sup>c</sup>
1	-2.7	+0.1	-5.5	+1.1	
2	-9.1	-3.8	-6.7	-3.8	-9.1
4	-1.0	-4.8	-8.6	-1.2	-4.7
5	+5.0	-2.4	+4.5	-1.8	+4.0
6	-0.6	+2.6	-2.3	+1.6	-1.2

a. HF/6-31G\*: H. Y. Yoo and K. N. Houk, *J. Am. Chem. Soc.*, **119**, 2877 (1997);

b. B3LYP/6-31G\*: V. Aviyente and K. N. Houk, *J. Phys. Chem. A*, **105**, 383 (2001).

c. AM1-MM: A. Sehgal, L. Shao, and J. Gao, *J. Am. Chem. Soc.*, **117**, 11337 (1995).

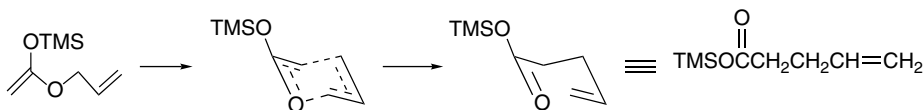
<sup>298</sup> H. Y. Yoo and K. N. Houk, *J. Am. Chem. Soc.*, **119**, 2877 (1997).

<sup>299</sup> (a) V. Aviyente, H. Y. Yoo, and K. N. Houk, *J. Org. Chem.*, **62**, 6121 (1997); (b) V. Aviyente and K. N. Houk, *J. Phys. Chem. A*, **105**, 383 (2001).

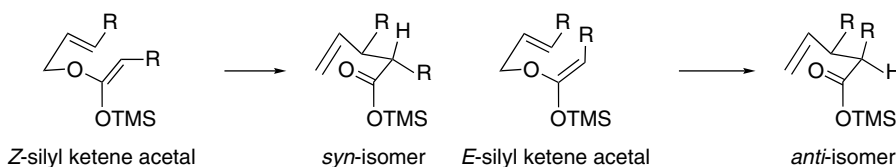
<sup>300</sup> M. Y. Chen and J. R. Murdoch, *J. Am. Chem. Soc.*, **106**, 4735 (1984).

The decelerating effect of the 5-substituent is primarily on TS energy and is reflected in the intrinsic barrier. Structurally, this may be due to a repulsive interaction between the 5-oxy substituent and the ring oxygen.

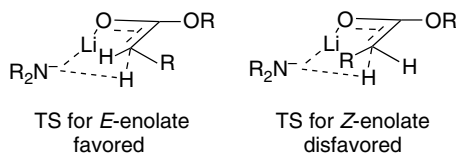
Other donor substituents, e.g., trimethylsilyloxy, at C(2) are strongly accelerating.<sup>301</sup> This effect is the basis of the synthetic importance of ester enolate Claisen rearrangements, in which enolates or silyl ketene acetals of allylic esters are rearranged into 4-pentenoate esters.<sup>302</sup> This reaction is known as the *Ireland-Claisen rearrangement*.



The stereoselectivity of the Ireland-Claisen rearrangement is controlled by the configuration of the double bonds in both the allylic alcohol and the silyl ketene acetal. The chair TS model predicts that the configuration at the newly formed C–C bond will be determined by the *E*- or *Z*-configuration of the silyl ketene acetal.



The stereochemistry of the silyl ketene acetal can be controlled by the conditions of preparation. The base that is usually used for enolate formation is lithium diisopropylamide (LDA). If the enolate is prepared in pure THF, the *E*-enolate is generated and this stereochemistry is maintained in the silyl derivative. The preferential formation of the *E*-enolate can be explained in terms of a cyclic TS in which the proton is abstracted from the stereoelectronically preferred orientation, more or less perpendicular to the carbonyl plane. Steric interaction between the base and the  $\alpha$ -substituent disfavors the TS for the *Z*-enolate.



If HMPA is included in the solvent, the *Z*-enolate predominates.<sup>303</sup> DMPU also favors the *Z*-enolate. The switch to the *Z*-enolate with HMPA or DMPU is attributed to a looser, perhaps acyclic, TS being favored as the result of strong solvation of the lithium ion by the cosolvent. The steric factors favoring the *E*-TS are therefore diminished.<sup>304</sup>

<sup>301</sup> J. J. Gajewski and J. Emrani, *J. Am. Chem. Soc.*, **106**, 5733 (1984); S. E. Denmark and M. A. Harmata, *J. Am. Chem. Soc.*, **104**, 4972 (1982).

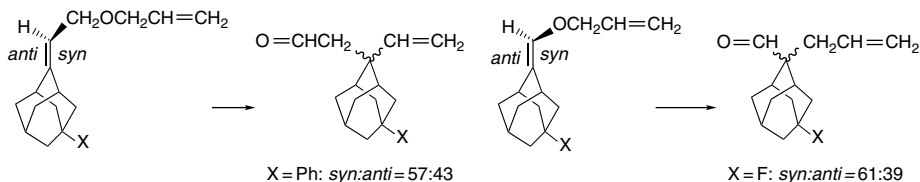
<sup>302</sup> S. Pereira and M. Srebnik, *Aldrichimica Acta*, **26**, 17 (1993).

<sup>303</sup> R. E. Ireland, R. H. Mueller, and A. K. Willard, *J. Am. Chem. Soc.*, **98**, 2868 (1972); R. E. Ireland and A. K. Willard, *Tetrahedron Lett.*, 3975 (1975); R. E. Ireland, P. Wipf, and J. Armstrong, III, *J. Org. Chem.*, **56**, 650 (1991).

<sup>304</sup> C. H. Heathcock, C. T. Buse, W. A. Kleschick, M. C. Pirrung, J. E. Sohn, and J. Lampe, *J. Org. Chem.*, **45**, 1066 (1980).

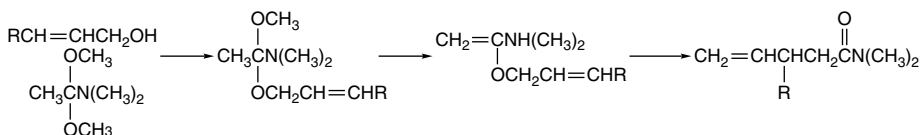
These general principles of solvent control of enolate stereochemistry are applicable to other systems.<sup>305</sup>

The sensitivity of the Claisen rearrangement to remote substituent effects has been examined using 2-adamantyl vinyl ethers and allyl 2-adamantylidene ethers.<sup>306</sup>  $\sigma$ -EWG substituents favor formation of the *syn*-isomer.



The conclusion drawn is that the TS is relatively electron deficient and is preferentially stabilized by the more electron rich (unsubstituted) of the two adamantyl bonds. A significant feature of this interpretation is that it applies to *both* the cationic and enolate fragments. Although the ionic character of both fragments is relatively small, it appears that the ability to interact with electrons from alkyl groups stabilizes both fragments. This result is consistent with the radical character of the two fragments. A similar facial selectivity was observed in the anionic oxy-Cope rearrangements.<sup>307</sup> In this case, the TS bears a *negative charge*, but is still stabilized by the better donor bond.

**10.6.3.3. [3,3]-Sigmatropic Rearrangement of Trienes Containing Nitrogen** A reaction that is closely related to the orthoester Claisen rearrangement utilizes an amide acetal, such as dimethylacetamide dimethyl acetal, in the exchange reaction with allylic alcohols and gives amides of  $\gamma$ ,  $\delta$ -unsaturated carboxylic acids.<sup>308</sup> The stereochemistry of the reaction is analogous to the other variants of the [3,3]-sigmatropic rearrangement.<sup>309</sup>



O-allyl imidate esters undergo [3,3]-sigmatropic rearrangements to *N*-allyl amides. This is sometimes referred to as an *aza-Claisen rearrangement* and the resonance stabilization of the amide bond that is formed provides a thermodynamic driving force. Trichloromethyl imidates can be easily made from allylic alcohols by reaction with trichloroacetonitrile. The rearrangement then provides trichloroacetamides of *N*-allylamines.<sup>310</sup> Yields in the reaction are sometimes improved by inclusion of  $K_2CO_3$  in the reaction mixture.<sup>311</sup>

<sup>305</sup> J. Corset, F. Froment, M.-F. Lautie, N. Ratovelomanana, J. Seyden-Penne, T. Strzalko, and M. C. Roux-Schmitt, *J. Am. Chem. Soc.*, **115**, 1684 (1993).

<sup>306</sup> A. Mukherjee, Q. Wu, and W. J. le Noble, *J. Org. Chem.*, **59**, 3270 (1994).

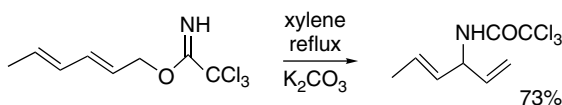
<sup>307</sup> M.-H. Lin, W. H. Watson, R. P. Kashyap, and W. J. le Noble, *J. Org. Chem.*, **55**, 3597 (1990).

<sup>308</sup> A. E. Wick, D. Felix, K. Steen, and A. Eschenmoser, *Helv. Chim. Acta*, **47**, 2425 (1964); D. Felix, K. Gschwend-Steen, A. E. Wick, and A. Eschenmoser, *Helv. Chim. Acta*, **52**, 1030 (1969).

<sup>309</sup> W. Sucrow, M. Slopianka, and P. P. Calderia, *Chem. Ber.*, **108**, 1101 (1975).

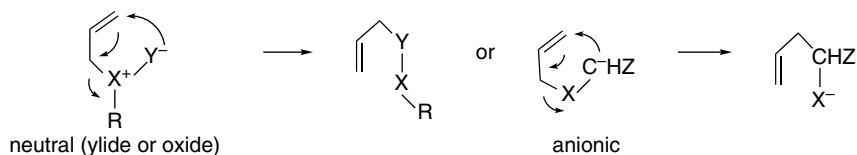
<sup>310</sup> L. E. Overman, *J. Am. Chem. Soc.*, **98**, 2901 (1976); L. E. Overman, *Acc. Chem. Res.*, **13**, 218 (1980).

<sup>311</sup> T. Nishikawa, M. Asai, N. Ohyabu, and M. Isobe, *J. Org. Chem.*, **63**, 188 (1998).



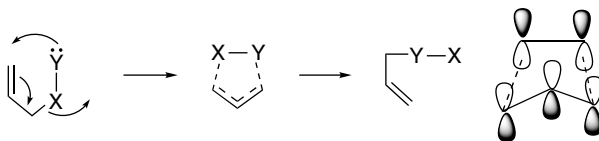
#### 10.6.4. [2,3]-Sigmatropic Rearrangements

**10.6.4.1. Mechanism of [2,3]-Sigmatropic Rearrangements** There are also concerted rearrangements that exhibit a [2,3]-sigmatropic reactivity pattern. The [2,3]-sigmatropic class of rearrangements is represented by two generic charge types, one involving ylides or oxides and the other those of anions.



One requirement for a facile [2,3]-sigmatropic process is that the atom X at the allylic position be able to act as a leaving group as the adjacent atom Y begins bonding to the allyl system, so X is normally an electronegative element. The reaction is most facile in systems where the atoms X and Y bear formal charges, as in the case of ylides and oxides. The most well developed of these reactions are rearrangements of allyl sulfoxides<sup>312</sup> and selenoxides<sup>313</sup> and of ammonium<sup>314</sup> and sulfonium<sup>315</sup> ylides. In the anionic variation, the group Z must be able to facilitate formation of the carbanion. The most useful examples of the anionic type are rearrangements of carbanions of allyl ethers. Scheme 10.11 outlines these kinds of [2,3]-sigmatropic rearrangements.

The TS for 2,3-sigmatropic shifts is viewed as involving an allylic system and the migrating fragment. There are six participating electrons in a Hückel-type array, so the TS is aromatic.



There have been several computational studies of [2,3]-sigmatropic rearrangements. MP3/3-21G\*-level calculations of the allyl sulfoxide rearrangement reproduce the stereoselectivity and activation energies.<sup>316</sup> This and several related rearrangements exhibit TS aromaticity in terms of magnetic criteria (NICS and magnetic susceptibility).<sup>317</sup> The mechanism of the anionic [2,3]-sigmatropic Wittig rearrangement has

<sup>312</sup>. D. A. Evans and G. C. Andrews, *Acc. Chem. Res.*, **7**, 147 (1974).

<sup>313</sup>. K. B. Sharpless and R. F. Lauer, *J. Am. Chem. Soc.*, **95**, 2697 (1973); D. L. J. Clive, *Tetrahedron*, **34**, 1049 (1978); Y. Nishibayashi and S. Uemura, *Top. Curr. Chem.*, **208**, 201 (2000).

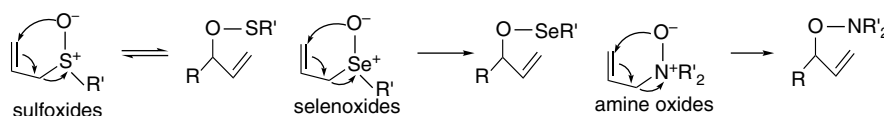
<sup>314</sup>. E. Vedejs, J. P. Hagen, B. L. Roach, and K. L. Spear, *J. Org. Chem.*, **43**, 1185 (1978).

<sup>315</sup>. B. M. Trost and L. S. Melvin, Jr., *Sulfur Ylides*, Academic Press, New York, 1975.

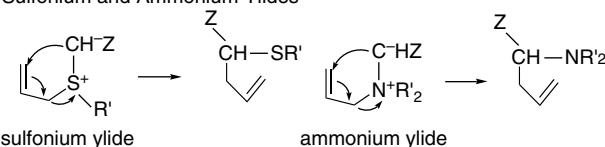
<sup>316</sup>. D. K. Jones-Hertzog and W. L. Jorgensen, *J. Am. Chem. Soc.*, **117**, 9077 (1995); D. K. Jones-Hertzog and W. L. Jorgensen, *J. Org. Chem.*, **60**, 6682 (1995); B. S. Jursic, *Theochem*, **338**, 131 (1995).

<sup>317</sup>. F. P. Cossio, I. Morao, H. Jiao, and P. v. R. Schleyer, *J. Am. Chem. Soc.*, **121**, 6737 (1999); A. A. Fonkin, A. O. Kushko, A. V. Kirij, A. G. Yurchenko, and P. v. R. Schleyer, *J. Org. Chem.*, **65**, 2984 (2000).

## A. Allylic Sulfoxides, Selenoxides and Amine Oxides.



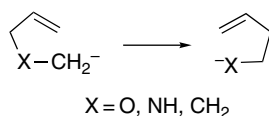
## B. Sulfonium and Ammonium Ylides



## C. Anions of Allyl Ethers

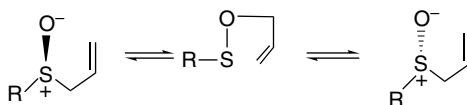


been probed by B3LYP/6-31+G\* computations and comparisons made for carbon, nitrogen, and oxygen prototypes.<sup>318</sup>



Computation in the gas phase did not locate a concerted TS, but indicated instead that the reactions proceed by dissociation-reassociation. The reassociation process has no barrier, whereas the dissociation has a very small one (2.4–2.6 kcal/mol). For the oxy anion, inclusion of a  $Li^+$  counterion resulted in a concerted process with a barrier of about 12 kcal/mol. Since this more closely approximates solution conditions, it suggests that a concerted mechanism is feasible in solution. The dissociation mechanism is favored for both nitrogen and carbon.

*10.6.4.2. [2,3]-Sigmatropic Rearrangements of Oxides and Ylides* The rearrangement of allylic sulfoxides to allylic sulfenates first received attention in connection with the mechanism of racemization of allyl aryl sulfoxides.<sup>319</sup> Although the allyl sulfoxide structure is strongly favored at equilibrium, rearrangement through the achiral allyl sulfenate provides a low-energy pathway for racemization.

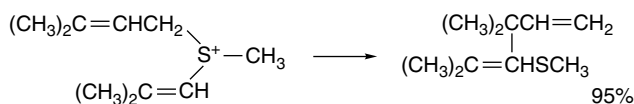


<sup>318</sup> F. Haeffner, K. N. Houk, S. M. Schulze, and J. K. Lee, *J. Org. Chem.*, **68**, 2310 (2003).

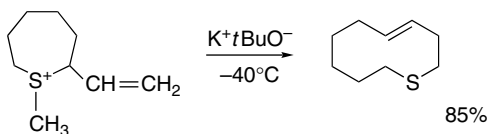
<sup>319</sup> R. Tang and K. Mislow, *J. Am. Chem. Soc.*, **92**, 2100 (1970).



Allylic sulfonium ylides readily undergo [2,3]-sigmatropic rearrangement.<sup>324</sup>

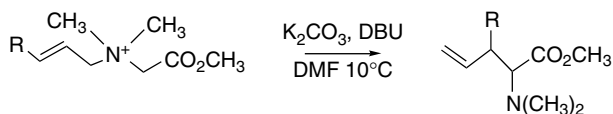


This reaction results in formation of a new carbon-carbon bond. The reaction proceeds best when the ylide has a carbanion-stabilizing substituent. It has found synthetic application in ring-expansion sequences for generation of medium-sized rings.

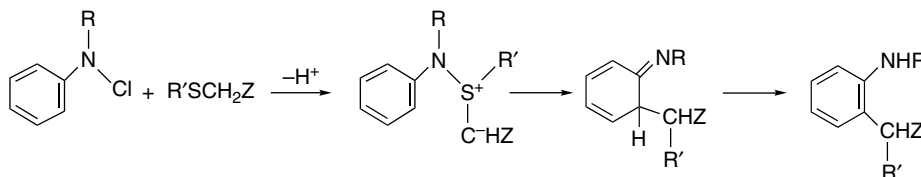


Ref. 325

The corresponding ammonium ylides can also be generated when one of the nitrogen substituents has an anion-stabilizing group on the  $\alpha$ -carbon. For example, quaternary salts of *N*-allyl  $\alpha$ -aminoesters readily rearrange to  $\alpha$ -allyl products.<sup>326</sup>



A useful method for *ortho*-alkylation of aromatic amines is based on [2,3]-sigmatropic rearrangement of *S*-anilinosulfonium ylides. These ylides are generated from anilinosulfonium ions, which can be prepared from *N*-chloroanilines and sulfides.<sup>327</sup>



This method is the basis for synthesis of nitrogen-containing heterocyclic compounds when Z is a carbonyl-containing group that can undergo cyclization with the amino group.<sup>328</sup>

**10.6.4.3. [2,3]-Sigmatropic Rearrangements of Anions** The [2,3]-sigmatropic rearrangement pattern is also observed with anionic species. The most important case

<sup>324</sup> J. E. Baldwin, R. E. Hackler, and D. P. Kelly, *Chem. Commun.*, 537 (1968).

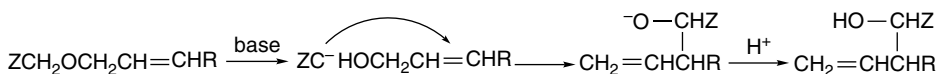
<sup>325</sup> V. Cere, C. Paolucci, S. Pollicino, E. Sandri, and A. Fava, *J. Org. Chem.*, **43**, 4826 (1978).

<sup>326</sup> I. Coldham, M. L. Middleton, and P. L. Taylor, *J. Chem. Soc., Perkin Trans. 1*, 2951 (1997); I. Coldham, M. L. Middleton, and P. L. Taylor, *J. Chem. Soc., Perkin Trans. 1*, 2817 (1998).

<sup>327</sup> P. G. Gassman and G. D. Gruetzmacher, *J. Am. Chem. Soc.*, **96**, 5487 (1974); P. G. Gassman and H. R. Drewes, *J. Am. Chem. Soc.*, **100**, 7600 (1978).

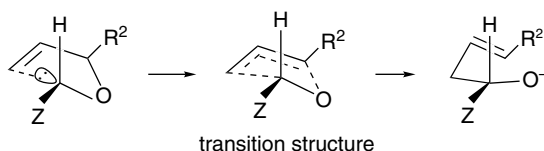
<sup>328</sup> P. G. Gassman, T. J. van Bergen, D. P. Gilbert, and B. W. Cue, Jr., *J. Am. Chem. Soc.*, **96**, 5495 (1974); P. G. Gassman and T. J. van Bergen, *J. Am. Chem. Soc.*, **96**, 5508 (1974); P. G. Gassman, G. Gruetzmacher, and T. J. van Bergen, *J. Am. Chem. Soc.*, **96**, 5512 (1974).

for synthetic purposes is the *Wittig rearrangement*, in which a strong base converts allylic ethers to  $\alpha$ -allyl alkoxides.<sup>329</sup>

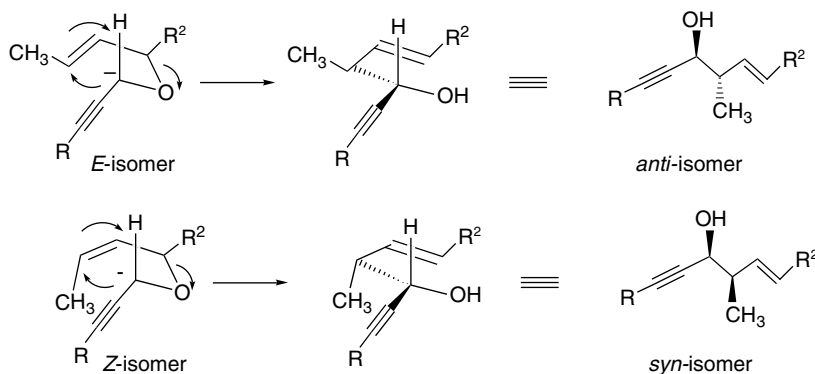


As the deprotonation at the  $\alpha'$ -carbon must compete with deprotonation of the  $\alpha$ -carbon in the allyl group, most examples involve a conjugated or electron-withdrawing substituent Z that can facilitate deprotonation.<sup>330</sup> In addition to direct deprotonation, there are other means of generating the anions of allyl ethers.<sup>331,332</sup>

The stereochemistry of the Wittig rearrangement can be predicted in terms of a cyclic TS in which the  $\alpha$ -substituent R<sup>2</sup> prefers an equatorial orientation.<sup>333</sup>



A consistent feature of the stereochemistry is a preference for *E*-stereochemistry at the newly formed double bond, but the reaction can also show stereoselectivity at the newly formed single bond. This stereoselectivity has been carefully studied for the case where the substituent Z is an acetylenic group.



The preferred stereochemistry arises from the TS that minimizes interaction between the alkynyl and R<sup>2</sup> substituents. This stereoselectivity is exhibited in the rearrangement of **37** to **38**.

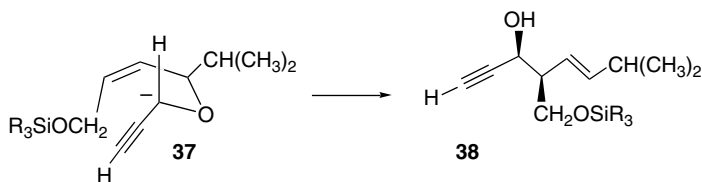
<sup>329</sup> J. Kallmarten, in *Stereoselective Synthesis, Houben Weyl Methods in Organic Chemistry*, R. W. Hoffmann, J. Mulzer, and E. Schaumann, eds., G. Thieme Verlag, Stuttgart, 1996, pp. 3810; T. Nakai and K. Mikami, *Org. Reactions*, **46**, 105 (1994).

<sup>330</sup> For reviews of [2,3]-sigmatropic rearrangement of allyl ethers, see T. Nakai and K. Mikami, *Chem. Rev.*, **86**, 885 (1986).

<sup>331</sup> W. C. Still and A. Mitra, *J. Am. Chem. Soc.*, **100**, 1927 (1978).

<sup>332</sup> K. Hioki, K. Kono, S. Tani, and M. Kunishima, *Tetrahedron Lett.*, **39**, 5229 (1998).

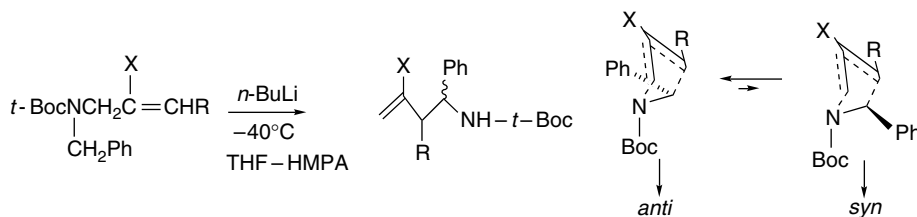
<sup>333</sup> R. W. Hoffmann, *Angew. Chem. Int. Ed. Engl.*, **18**, 563 (1979); K. Mikami, Y. Kimura, N. Kishi, and T. Nakai, *J. Org. Chem.*, **48**, 279 (1983); K. Mikami, K. Azuma, and T. Nakai, *Tetrahedron*, **40**, 2303 (1984); Y.-D. Wu, K. N. Houk, and J. A. Marshall, *J. Org. Chem.*, **55**, 1421 (1990).



Ref. 334

The effect of substituents on the TS has been explored using MP3/6-31+G\* computations.<sup>335</sup> An alkynyl group at C(5) results in a much later TS than in the unsubstituted case and the TS has greater cyclic character. This tighter TS would be expected to be more sensitive to the steric effects that lead to stereoselectivity. These computations also indicated a preference for carbonyl substituents to adopt an *s-trans-endo* conformation that leads to the observed *syn* stereoselectivity. Inclusion of a Li<sup>+</sup> cation leads to a chelated TS, again in accord with observed stereochemistry. These TSs are depicted in Figure 10.40.  $\alpha$ -Carboxy substituents also lead to reaction through chelated TSs.<sup>336</sup>

[2,3]-Sigmatropic rearrangements of anions of *N*-allyl amines have also been observed and are known as aza-Wittig rearrangements.<sup>337</sup> The reaction requires anion-stabilizing substituents and is favored by *N*-benzyl and by silyl or sulfenyl substituents on the allyl group.<sup>338</sup> The reaction is further facilitated by *N*-acyl groups and by EWGs on the amide nitrogen.<sup>339</sup> These groups all facilitate the initial deprotonation and the charge redistribution that accompanies rearrangement. The steric interactions between the benzyl group and allyl substituent govern the stereoselectivity, which markedly improved in the trimethylsilyl derivatives.<sup>340</sup>



R	X	<i>syn:anti</i>
CH <sub>3</sub>	H	3:2
C <sub>2</sub> H <sub>5</sub>	H	1:1
(CH <sub>3</sub> ) <sub>2</sub> CH	H	4:3
CH <sub>3</sub>	Si(CH <sub>3</sub> ) <sub>3</sub>	<1:20
C <sub>2</sub> H <sub>5</sub>	Si(CH <sub>3</sub> ) <sub>3</sub>	1:18
(CH <sub>3</sub> ) <sub>2</sub> CH	Si(CH <sub>3</sub> ) <sub>3</sub>	1:11

<sup>334</sup> M. M. Midland and J. Gabriel, *J. Org. Chem.*, **50**, 1143 (1985).

<sup>335</sup> K. Mikami, T. Uchida, T. Hirano, Y.-D. Wu, and K. N. Houk, *Tetrahedron*, **50**, 5917 (1994).

<sup>336</sup> T. Okajima and Y. Fukazawa, *Chem. Lett.*, 81 (1997).

<sup>337</sup> C. Vogel, *Synthesis*, 497 (1997).

<sup>338</sup> J. C. Anderson, S. C. Smith, and M. E. Swarbrick, *J. Chem. Soc., Perkin Trans. 1*, 1517 (1997).

<sup>339</sup> J. C. Anderson, A. Flaherty, and M. E. Swarbrick, *J. Org. Chem.*, **65**, 9152 (2000).

<sup>340</sup> J. C. Anderson, D. C. Siddons, S. C. Smith, and M. E. Swarbrick, *J. Org. Chem.*, **61**, 4820 (1996).

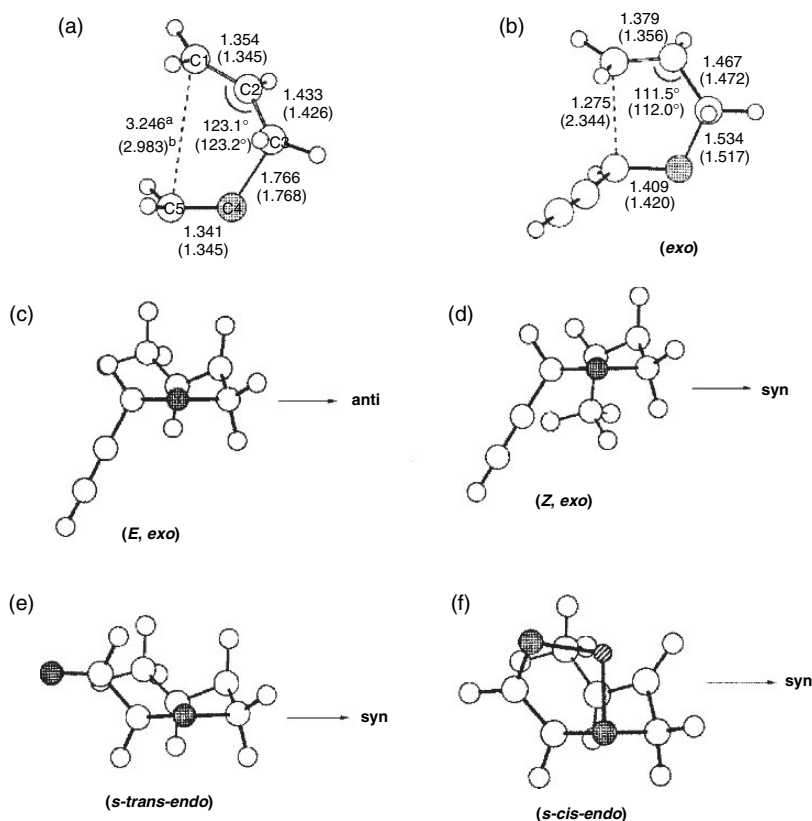


Fig. 10.40. Relationship between TS structure and stereoselectivity in [2,3]-sigmatropic rearrangement of allyloxycarbanions: (a) early TS for unsubstituted allyloxymethyl anion; (b) tighter cyclic TS for stabilized allyloxypropargyl anion; (c,d) preferred conformation of *E*- and *Z*-crotyloxypropargyl anions leading to the *E*  $\rightarrow$  *anti* and *Z*  $\rightarrow$  *syn* stereoselectivity; (e,f) unchelated and chelated TSs for  $\alpha$ -crotyloxy ethanal enolate leading to the *E*  $\rightarrow$  *syn* stereoselectivity. Reproduced from *Tetrahedron*, **50**, 5917 (1994), by permission of Elsevier.

## Topic 10.1. Application of DFT Concepts to Reactivity and Regiochemistry of Cycloaddition Reactions

Recently, attempts have been made to understand both the relative reactivity and regioselectivity of the Diels-Alder reaction in terms of the DFT concepts of hardness and softness. Several DFT parameters have been examined as potential indicators of D-A reactivity. (See Topic 1.5 to review the DFT concepts of hardness, softness, Fukui functions, and global electrophilicity.) The D-A reaction can be thought of as having two components in the overall electronic reorganization, corresponding to initial charge transfer between the diene and dienophile, followed by electronic reconfiguration to generate the new bonds. These ideas parallel FMO theory, but DFT considers the total electron density rather than the distribution of the frontier orbitals.

Table 10.9. DFT Global Electrophilicity of Representative Dienes and Dienophiles<sup>a</sup>

CHAPTER 10	Primarily Electrophilic		Balanced	Primarily Nucleophilic		
<i>Concerted Pericyclic Reactions</i>	(NC) <sub>2</sub> C=C(CN) <sub>2</sub>	5.96	CH <sub>3</sub> CO <sub>2</sub> CH=CHCH=CH <sub>2</sub>	1.10	CH <sub>3</sub> OCH=CHCH=CH <sub>2</sub>	0.77
	Maleic anhydride	3.24	CH <sub>2</sub> =CHCH=CH <sub>2</sub>	1.05	CH <sub>2</sub> =CH <sub>2</sub>	0.73
	CH <sub>2</sub> =CHCH=O <sup>+</sup> B <sup>-</sup> H <sub>3</sub>	3.20	CH <sub>2</sub> =CCH=CH <sub>2</sub>	0.94	TMSOCH=CHCH=CH <sub>2</sub>	0.73
	CH <sub>2</sub> =C(CN) <sub>2</sub>	2.82	CH <sub>3</sub>		Furan	0.59
	CH <sub>2</sub> =CHNO <sub>2</sub>	2.61	CH <sub>3</sub> CH=CHCH=CH <sub>2</sub>	0.93	(CH <sub>3</sub> ) <sub>2</sub> NCH=CHCH=CH <sub>2</sub>	0.57
	CH <sub>3</sub> O <sub>2</sub> CC≡CCO <sub>2</sub> CH <sub>3</sub>	2.27	H <sub>2</sub> C=CCH=CH <sub>2</sub>	0.88	HC≡CH	0.54
	CH <sub>2</sub> =C(CO <sub>2</sub> CH <sub>3</sub> ) <sub>2</sub>	1.93	OTMS		2-Methylfuran	0.52
	CH <sub>2</sub> =CHCH=O	1.84	(CH <sub>3</sub> ) <sub>2</sub> C=CHCH=CH <sub>2</sub>	0.86		
	CH <sub>2</sub> =CHCN	1.74	Cyclopentadiene	0.83	CH <sub>3</sub> OCH=CH	0.42
	CH <sub>2</sub> =CHCOCH <sub>3</sub>	1.65			Pyrrrole	0.31
	HC≡CCO <sub>2</sub> CH <sub>3</sub>	1.52			(CH <sub>3</sub> ) <sub>2</sub> NCH=CH <sub>2</sub>	0.27
	CH <sub>2</sub> =CHCO <sub>2</sub> CH <sub>3</sub>	1.50				

a. From L. R. Domingo, M. Aurell, P. Perez, and R. Contreras, *Tetrahedron*, **58**, 4417 (2002).

Domingo investigated the *global electrophilic parameter*,  $\omega$ , as an indicator of relative reactivity.<sup>341</sup> Table 10.9 gives the value of this parameter calculated for a number of dienes and dienophiles.

This parameter gives an ordering that is in good qualitative agreement with the reactivity trends that would be expected on the basis of polar and resonance substituent interactions, although the parent molecules, ethene and ethyne, are somewhat more toward the nucleophilic side of the scale than might have been anticipated. The electrophilic group includes the traditional dienophiles such as acrolein and acrylonitrile. Dienes with donor substituents, such as 1-methoxy-1,3-butadiene, exhibit the anticipated nucleophilic characteristics. Note that a 1-ERG seems to have a stronger effect than a 2-ERG (compare the isomeric trimethylsiloxy-1,3-butadienes). This is consistent with the greater reactivity of 1-methoxy-1,3-butadiene than the 2-isomer (see Table 10.2). Methoxyethene and dimethylaminoethene are among the most nucleophilic dienophiles in the list. It should be noted that  $\omega$  is a *global* parameter; that is, it pertains to the molecule as a whole. Thus, it gives no indication of the regioselectivity of the reaction, but is an indicator of the direction and extent of electron transfer between the reactants. The idea that increased charge transfer increases reactivity suggests that mutual reactivity will be highest for compounds that have the largest difference in  $\omega$ . This is equivalent to the FMO concept that the strongest donors and strongest acceptors will have the highest mutual reactivity.

The issue of regiochemistry can be addressed by identifying sites of *local electrophilicity* and *local nucleophilicity*. This was done by calculation of a *local electrophilicity index*.<sup>342</sup> The index of nucleophilicity can be taken as  $f^-$ , the local Fukui function for electrophilic attack. The regiochemistry is then predicted by matching the highest local electrophilicity in the electrophilic component with the largest  $f^-$  for the nucleophilic component. Table 10.10 gives some values of representative dienes and dienophiles.

We see that a terminal ERG on the diene leads to  $f^-_{(1)} > f^-_{(4)}$ , that is, the carbon at the *end* of the conjugated system is the most nucleophilic. For example, compare the  $f^-$  values for the substituted (4) and unsubstituted (1) atoms for 1,3-pentadiene, and

<sup>341</sup> L. R. Domingo, M. J. Aurell, P. Perez, and R. Contreras, *Tetrahedron*, **58**, 4417 (2002).

<sup>342</sup> L. R. Domingo, M. J. Aurell, P. Perez, and R. Contreras, *J. Phys. Chem. A*, **106**, 6871 (2002).

**Table 10.10. Local Electrophilicity and Fukui Functions for Some Dienes and Dienophiles<sup>a</sup>**

Dienes		C(1)		C(4)	
1	4	$\omega$	$f^-$	$\omega$	$f^-$
CH <sub>2</sub> = CHCH = CH <sub>2</sub>		0.355	0.338	0.355	0.338
CH <sub>2</sub> = CHCH = CHCH <sub>3</sub>		0.300	0.309	0.282	0.2296
CH <sub>2</sub> = CCH = CH <sub>2</sub>		0.316	0.380	0.354	0.289
$\begin{array}{c}   \\ \text{CH}_3 \\ \text{CH}_2 = \text{CHC} = \text{C}(\text{CH}_3)_2 \end{array}$		0.277	0.273	0.234	0.277
CH <sub>2</sub> = CHCH = CHOCH <sub>3</sub>		0.240	0.217	0.251	0.290
CH <sub>2</sub> = CHCH = CHOSi(CH <sub>3</sub> ) <sub>3</sub>		0.232	0.264	0.217	0.218
CH <sub>2</sub> = CCH = CH <sub>2</sub>		0.240	0.465	0.315	0.212
$\begin{array}{c}   \\ \text{OSi}(\text{CH}_3)_3 \\ \text{CH}_2 = \text{CHCH} = \text{CHN}(\text{CH}_3)_2 \end{array}$		0.173	0.304	0.230	0.117
Dienophiles		C(1)		C(2)	
1	2	$\omega$	$f^+$	$\omega$	$f^+$
CH <sub>2</sub> = CH = O <sup>+</sup> - B <sup>-</sup> H <sub>3</sub>		1.144	0.357	0.253	0.079
CH <sub>2</sub> = C(CN) <sub>2</sub>		1.407	0.499	0.589	0.209
CH <sub>2</sub> = CHNO <sub>2</sub>		0.726	0.279	0.200	0.077
CH <sub>2</sub> = CHCH = O		0.685	0.372	0.253	0.137
CH <sub>2</sub> = CHCN		0.816	0.469	0.461	0.265
CH <sub>2</sub> = CHCOCH <sub>3</sub>		0.579	0.351	0.250	0.152
CH <sub>2</sub> = CHCO <sub>2</sub> CH <sub>3</sub>		0.617	0.409	0.300	0.199
CH <sub>2</sub> = CH <sub>2</sub>		0.365	0.500	0.365	0.500
CH $\equiv$ CH		0.268	0.500	0.268	0.500
CH <sub>2</sub> = CHOCH <sub>3</sub>		0.183	0.435	0.194	0.463
CH <sub>2</sub> = CHN(CH <sub>3</sub> ) <sub>2</sub>		0.108	0.399	0.119	0.442

a. From L. R. Domingo, M. J. Aurell, P. Perez, and R. Contreras, *J. Phys. Chem. A*, **106**, 6871 (2002).

for the cases substituted by methoxy, trimethylsilyloxy, and dimethylamino groups. This implies that the *unsubstituted* terminal carbon will be the most nucleophilic site of the diene, which is the same prediction that is made by resonance or FMO treatment of terminally substituted butadienes. For dienophiles having EWG substituents, the  $\omega_{(\text{local})}$  or  $f^+$  parameters can indicate relative electrophilicity. For such dienophiles, the  $\beta$ -(unsubstituted)carbon is more electrophilic than the  $\alpha$ -(substituted)carbon, again consistent with resonance and FMO conclusions. The local electrophilicity of ethene (0.365) is less than for EWG-substituted derivatives, in agreement with its lower reactivity as a dienophile.

In all the cases studied by this approach so far, the diene is the nucleophile and the dienophile is the electrophile. For this combination, the dienophile  $\omega_{(\text{global})}$  shows a correlation with reactivity, whereas comparison of the  $f^+$  between C(1) and C(2) gives an indication of the regioselectivity. Dienophiles with EWG substituents have higher  $f^+$  at the unsubstituted carbon, in agreement with observed regioselectivity. For ERG cases (methoxyethene and dimethylaminoethene) the  $\omega$  value is small and the highest  $f^+$  value shifts to the substituted carbon. For the dienes, the position with the largest  $f^-$  is predicted to be the most nucleophilic. The challenging case of dienes with 2-EWG groups (see p. 844) has not yet been addressed by DFT analysis.

Another DFT-based approach to regioselectivity focused on softness. It has been suggested, based on the DFT definitions, that maximum reactivity should occur when

the local softness of reacting positions is matched.<sup>343</sup> This proposal has been explored in a quantitative way.<sup>344</sup> Local softness values were calculated for a number of substituted dienes and dienophiles. Then the alternative regioisomers were evaluated by comparing the alternative pairs:

$$\text{Ortho regioisomer} = (s^-_1 - s^+_{1'})^2 + (s^-_4 - s^+_{2'})^2 \quad (10.4)$$

$$\text{Meta regioisomer} = (s^-_1 - s^+_{2'})^2 + (s^-_4 - s^+_{1'})^2 \quad (10.5)$$

where  $s^-$  and  $s^+$  are the local softness values for nucleophilic and electrophilic reactivity, as appropriate for the reaction of a nucleophilic diene with and electrophilic dienophile.

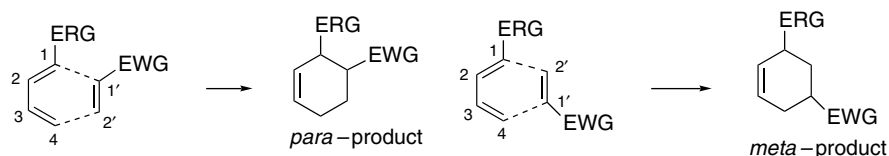


Table 10.11 gives the value of the local softness for some representative diene and dienophiles.

Qualitatively comparing these numbers to the traditional polar and resonance substituent effects, we see that for a donor substituent  $s^-_4 > s^-_1$ . EWG substituents make  $s^+_{2'} > s^+_{1'}$ . However, the trend that dominates the sum of the differences in

**Table 10.11. Local Softness Parameters for Dienes and Dienophiles<sup>a</sup>**

Dienes				
1-Substituent	$s^+_1$	$s^-_1$	$s^+_4$	$s^-_4$
CH <sub>3</sub>	0.266	0.277	0.309	0.282
CH <sub>3</sub> O	0.363	0.193	0.293	0.201
C <sub>2</sub> H <sub>5</sub> O	0.369	0.177	0.294	0.198
(CH <sub>3</sub> ) <sub>2</sub> N	0.413	-0.137	0.321	0.193
(C <sub>2</sub> H <sub>5</sub> ) <sub>2</sub> N	0.396	-0.298	0.281	0.103
CO <sub>2</sub> H	0.271	0.118	0.224	0.131
CN	0.416	0.354	0.264	0.319
Dienophiles				
1-Substituent	$s^+_{1'}$	$s^-_{1'}$	$s^+_{2'}$	$s^-_{2'}$
CO <sub>2</sub> H	0.167	0.073	0.306	0.150
CO <sub>2</sub> CH <sub>3</sub>	0.166	0.077	0.300	0.139
CH = O	0.030	0.024	0.309	0.276
CH <sub>3</sub> CO	0.038	0.101	0.327	0.188
CN	0.296	-0.014	0.278	0.140
NO <sub>2</sub>	-0.53	-0.073	0.291	0.258

a. From J. Damoun, G. Van de Woude, F. Mendez, and P. Geerlings, *J. Phys. Chem. A*, **101**, 886 (1997).

<sup>343</sup>. J. L. Gazquez and F. Mendez, *J. Phys. Chem.*, **98**, 4591 (1994).

<sup>344</sup>. J. Damoun, G. Van de Woude, F. Mendez, and P. Geerlings, *J. Phys. Chem. A*, **101**, 886 (1997).

Equations (10.4) and (10.5) is the fact that the more remote positions (4 and 2') *change less than the substituted positions*. Local softness parameters have also been calculated by a bond electronegativity equalization approach.<sup>345</sup> All the computations reported to date refer to diene (HOMO)-dienophile (LUMO) combination pairs, so it is not possible to see if this approach successfully predicts the case in which both the diene and the dienophile carry EWG substituents.

By comparing the FMO and DFT analyses, we see that most combinations of diene and dienophiles lead to the same prediction. The underlying physical basis of the predictions is also quite similar. In FMO theory it is the closeness in energy of the FMOs that is considered to be the origin of relative reactivity. Regioselectivity is attributed to maximum orbital overlap, as judged by the FMO coefficients. In the DFT approach, the extent of charge transfer (as measured by the global electrophilicity and nucleophilicity parameters) is considered to be the indicator of reactivity and local softness is considered to govern regioselectivity. The physical picture of the D-A reaction that emerges is one of *complementary electronic interactions* between the diene and dienophile that reduce the electron-electron repulsions that are otherwise dominant in the early stages of the reaction. Although both approaches can provide predictive relationships for a range of diene-dienophile combinations, neither has yet developed quantitative predictions of relative rates over a wide range of reactant combinations. This, of course, would be inherently difficult for combinations in which steric effects are significant, since neither FMO coefficients nor the DFT parameters take account of steric effects directly. It would be interesting to know, however, perhaps with cyanoethenes and cyanoethynes, if some combination of the local electrophilicity and softness parameters could account for relative reactivity.

Domingo and co-workers applied the DFT concepts of electrophilicity and softness in a study of all the possible cyanoethenes in reaction with cyclopentadiene, calculating the TS geometries, energies, and charge transfer at the B3LYP/6-31G\* level.<sup>346</sup> Both gas phase and benzene solution  $E_a$  values were calculated. The geometries indicated that the TS is slightly earlier in benzene. For symmetrically substituted ethenes, the reactions are nearly synchronous, whereas for unsymmetrical dienophiles they are asynchronous. The global and local  $\omega$  parameters were determined and the local electrophilicity parameter  $\omega_2$  was found to correlate with the number of cyano substituents, as would be expected.

Substitution	$\omega$	$\omega_1$	$f^+_{1}$	$\omega_2$	$f^+_{2}$
1-CN	1.74	0.46	0.266	0.82	0.469
1,1-diCN	2.82	0.59	0.209	1.41	0.499
<i>E</i> -1,2-diCN	3.08	0.92	0.300	0.92	0.300
<i>Z</i> -1,2-diCN	3.01	0.92	0.306	0.92	0.306
1,1,2-triCN	4.38	1.03	0.236	1.46	0.333
1,1,2,2-tetraCN	5.96	1.53	0.257	1.53	0.257

The calculated  $E_a$  decreased with the value of  $\omega$ , whereas the extent of charge transfer at the TS increased.

<sup>345</sup> Y. Cong, Z. Z. Yang, C. S. Wang, X. C. Liu, and Y. H. Bao, *Chem. Phys. Lett.*, **357**, 59 (2002).

<sup>346</sup> L. R. Domingo, M. J. Aurell, P. Perez, and R. Contreras, *J. Org. Chem.*, **68**, 3884 (2003).

Substitution	$E_a(\text{gas})$	$E_a(\text{benzene})$	Charge transfer
1-CN	17.5	16.7	0.15
1,1-diCN	10.5	8.7	0.28
<i>E</i> -1,2-diCN	15.2	14.3	0.25
<i>Z</i> -1,2-diCN	16.3	14.5	0.24
1,1,2-triCN	11.3	9.0	0.36
1,1,2,2-tetraCN	11.5	8.7	0.43

The extent of charge transfer is more closely related to the total number of CN substituents rather than their position, i.e., 1,1-  $\sim$  *E*-1,2-  $\sim$  *Z*-1,2, but CN < diCN < triCN < tetraCN. On the other hand, the  $E_a$  is more sensitive to the placement of the substituents with those reactants with 1,1-diCN substitution having  $E_a$  near 9 kcal/mol, whereas those with 1-CN substitution are near 15 kcal/mol. Note that the decrease of  $E_a$  is also somewhat greater in benzene for the 1,1-diCN cases. These trends suggest that ability to accept negative charge at a 1,1-disubstituted carbon facilitates the reaction. It is also worth noting that according to these calculations, tetracyanoethene *does not* have an asynchronous TS, in contrast to several other very electrophilic dienophiles such as dimethyl acetylene dicarboxylate and maleic acid (see p. 855)

The application of DFT concepts to interpretation of relative reactivity and regioselectivity of 1,3-DPCA is being explored.<sup>347</sup> DFT recognizes both charge transfer interactions between the reactants and electron redistribution in the TS as key parts of the reaction process.<sup>348</sup> As discussed earlier for D-A reactions, DFT theory can also be

**Table 10.12. Global Electrophilicity and  $\Delta N_{\text{max}}$  Parameters for 1,3-Dipoles<sup>a</sup>**

Strongly Electrophilic		Moderately Electrophilic		Marginally Electrophilic				
$\omega$	$\Delta N_{\text{max}}$	$\omega$	$\Delta N_{\text{max}}$	$\omega$	$\Delta N_{\text{max}}$			
$\text{O}=\overset{+}{\text{O}}-\overset{-}{\text{O}}$	6.10	1.73	$\text{H}_2\text{C}=\overset{+}{\text{N}}=\overset{-}{\text{N}}$	1.40	0.77	$\text{HC}\equiv\overset{+}{\text{N}}-\overset{-}{\text{O}}$	0.73	0.43
$\text{HN}=\overset{+}{\text{O}}-\overset{-}{\text{O}}$	4.18	1.39	$\text{N}\equiv\overset{+}{\text{N}}-\overset{-}{\text{O}}$	1.37	0.56	$\text{H}_2\text{C}=\overset{+}{\text{N}}-\overset{-}{\text{NH}}$	0.72	0.54
$\text{HN}=\overset{+}{\text{O}}-\overset{-}{\text{NH}}$	2.88	1.17	$\text{HN}=\overset{+}{\text{N}}-\overset{-}{\text{NH}}$	1.22	0.66	$\text{HN}=\overset{+}{\text{N}}=\overset{-}{\text{N}}$	0.66	0.40
$\text{H}_2\text{C}=\overset{+}{\text{O}}-\overset{-}{\text{O}}$	2.43	1.08	$\text{H}_2\text{C}=\overset{+}{\text{N}}-\overset{-}{\text{O}}$	1.06	0.62	$\text{H}_2\text{C}=\overset{+}{\text{N}}-\overset{-}{\text{NH}}$	0.37	0.41
$\text{O}=\overset{+}{\text{N}}-\overset{-}{\text{O}}$	2.38	0.86	$\text{H}_2\text{C}=\overset{+}{\text{N}}-\overset{-}{\text{O}}$	1.06	0.62	$\text{H}_2\text{C}=\overset{+}{\text{N}}-\overset{-}{\text{NH}}$	0.37	0.41
$\text{HN}=\overset{+}{\text{N}}-\overset{-}{\text{O}}$	1.70	0.74	$\text{CH}_2=\overset{+}{\text{O}}-\overset{-}{\text{CH}_2}$	0.93	0.70	$\text{HC}\equiv\overset{+}{\text{N}}-\overset{-}{\text{NH}}$	0.28	0.28
$\text{H}_2\text{C}=\overset{+}{\text{O}}-\overset{-}{\text{NH}}$	1.65	0.91						

a. From P. Perez, I. R. Domingo, M. J. Aurell, and R. Contreras, *Tetrahedron*, **39**, 3117 (2003).

<sup>347</sup> P. Geerlings and F. De Proft, *Int. J. Quantum Chem.*, **80**, 227 (2000).

<sup>348</sup> F. Mendez, J. Tamariz, and P. Geerlings, *J. Phys. Chem. A*, **102**, 6292 (1998).

applied to interpretation of the regiochemistry of 1,3-dipolar cycloaddition reactions.<sup>349</sup> The DFT concept of local softness (see Topic 1.5) has been applied to regioselectivity. Chandra and co-workers have emphasized in particular that softness matching may be a determining factor in regiochemistry.<sup>350</sup> As discussed in connection with the D-A reaction, the global electrophilicity parameter  $\omega$ , as defined in DFT,<sup>341</sup> can provide some insight into relative reactivity of 1,3-dipoles. Domingo and co-workers have calculated  $\omega$  and  $\Delta N_{\max}$  for representative 1,3-dipoles are given in Table 10.12.

There are some anomalies in Table 10.12; for example, the nitro group is listed as strongly electrophilic, but in fact is not reactive at all in normal 1,3-dipolar cycloadditions. The  $\omega$  scale is also applicable only to the reactions in which the dipolarophile is acting as the electrophilic component; that is, in FMO terminology, the  $\text{LUMO}_{\text{dipole}}-\text{HOMO}_{\text{dipolarophile}}$  interaction is dominant.

## Problems

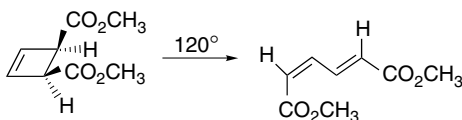
(References for these problems will be found on page 1165.)

10.1. Show, by construction of both a TS orbital array and an orbital symmetry correlation diagram, which of the following electrocyclizations are allowed.

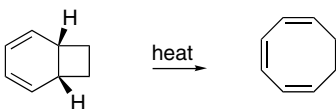
- disrotatory cyclization of the pentadienyl cation to the cyclopent-2-enyl cation.
- disrotatory cyclization of the pentadienyl anion to the 3-cyclopentenyl anion.
- disrotatory cyclization of the heptatrienyl anion to the cyclohepta-3,5-dienyl anion.

10.2. Which of the following reactions are allowed according to orbital symmetry conservation rules? Explain. Discuss any special structural features that might influence the facility of the reaction.

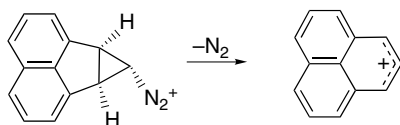
a.



b.



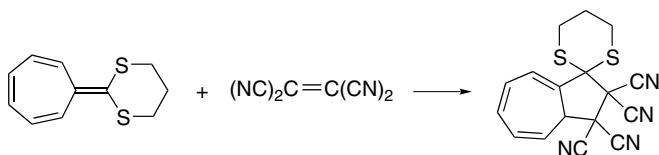
c.



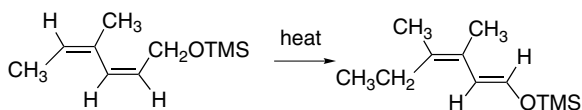
<sup>349</sup> F. Mendez, J. Tamariz, and P. Geerlings, *J. Phys. Chem. A*, **102**, 6292 (1998); A. K. Chandra and M. T. Nguyen, *J. Comput. Chem.*, **19**, 195 (1998).

<sup>350</sup> J. Korchowiec, A. K. Chandra, and T. Uchimaru, *Theochem.*, **572**,193 (2001).

d.



e.



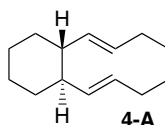
10.3. *Z,Z,Z,Z*-1,3,5,7-cyclononatetraene undergoes a spontaneous electrocyclic ring closure at 25°C. Predict the most likely structure for this cyclization product. Describe an alternative, symmetry-allowed electrocyclic reaction that would lead to an isomeric product. Explain why this alternate reaction pathway is not followed.

10.4. Offer a mechanistic explanation for each of the following reactions:

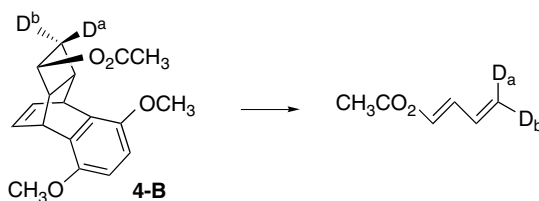
a. The 3,5-dinitrobenzoate esters of the stereoisomeric bicyclo[2.1.0]pentan-2-ols shown below both yield cyclopent-3-enol on hydrolysis in dioxane-water. The relative rates, however, differ by a factor of 10 million! Which is more reactive and why?



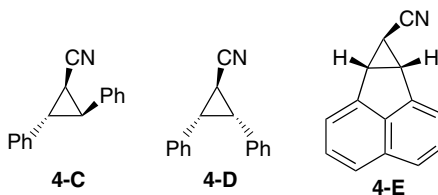
b. Optically active **4-A** racemizes on heating at 50°C with a half-life of 24 h.



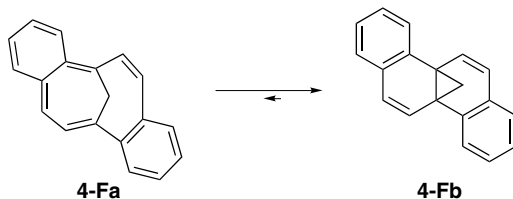
c. On being heated to 320°–340°C, compound **4-B** produces 1,4-dimethoxynaphthalene and 1-acetoxybutadiene. Furthermore, deuterium labeling has shown that the reaction is stereospecific as indicated.



- d. It has been found that compounds **4-C** and **4-D** are opened at  $-25^{\circ}\text{C}$  to allylic anions in the presence of strong bases such as lithium *t*-butylamide. In contrast, **4-E**, opens only slowly at  $25^{\circ}\text{C}$ .

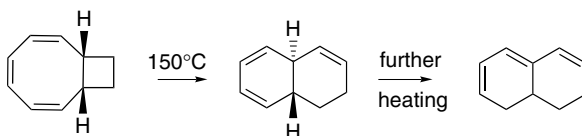


- e. When the 1,6-methano-1,3,5,7,9-pentaene structure is modified by fusion of two benzene rings as shown in **4-Fa**, a valence isomer **4-Fb** is the dominant structure.

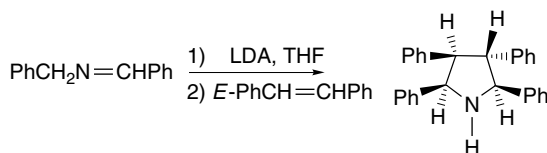


- 10.5. Suggest a mechanism by which each transformation could occur. More than one step may be involved.

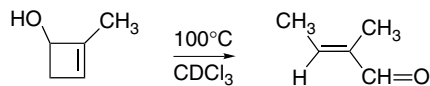
a.



b.



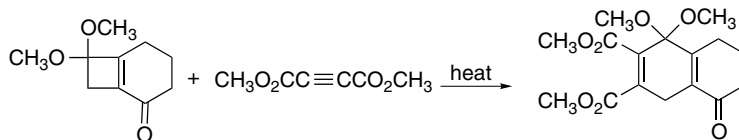
c.



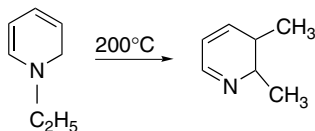
d.



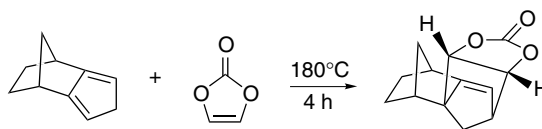
e.



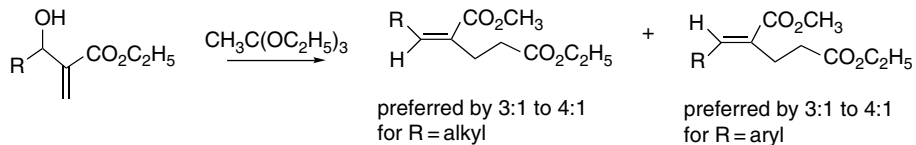
f.



g.



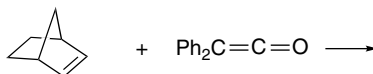
10.6. It has been found that 3-substituted methyl 3-hydroxy-2-methylene alkanooates give rise to a preference for the *Z*-isomer if R is alkyl, but for the *E*-isomer if R is aryl under the conditions of the thermal orthoester Claisen rearrangement.



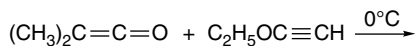
Analyze the transition structure for the reaction in terms of steric interactions and suggest a reason for the difference in stereoselectivity.

10.7. Give the structure, including stereochemistry, of the product expected for the following reactions:

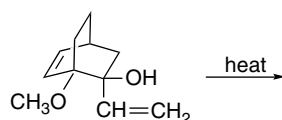
a.



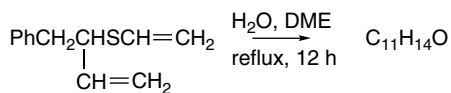
b.



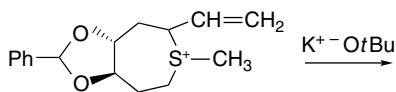
c.



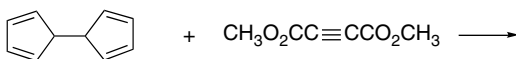
d.



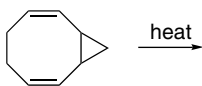
e.



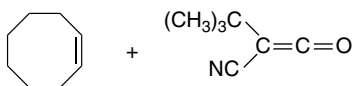
f.



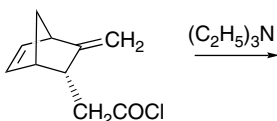
g.



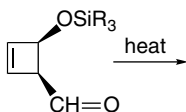
h.



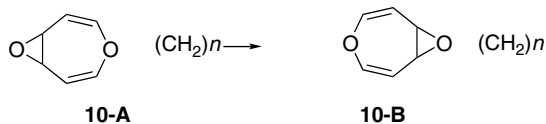
i.



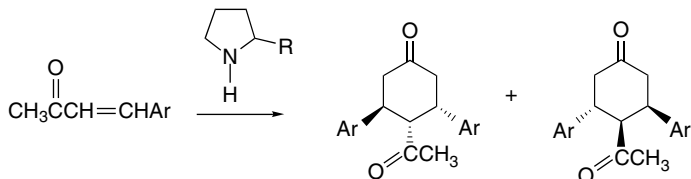
j.



10.8. In the series of bicyclic oxepins **10-A** ( $n = 3, 4, 5$ ), only the compound with  $n = 5$  undergoes rearrangement (at  $60^\circ\text{C}$ ) to the isomeric oxepin **10-B**. The other two compounds ( $n = 3$  or  $4$ ) are stable, even at much higher temperature. When **10-B** ( $n = 3$ ) was synthesized by another route, it showed no tendency to revert to **10-A** ( $n = 3$ ). Offer an explanation for these observations.

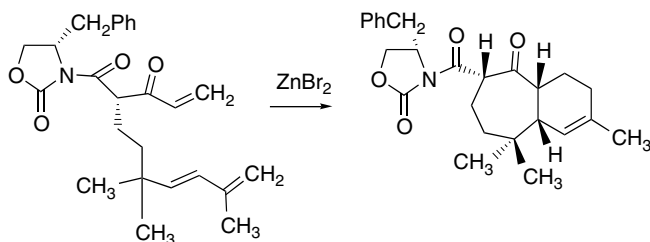


- 10.9. Bromocyclooctatetraene rearranges to *E*- $\beta$ -bromostyrene. The rate of the rearrangement is solvent dependent, with the first-order rate constant increasing from about  $10^{-7} \text{ s}^{-1}$  in cyclohexane to about  $10^{-3} \text{ s}^{-1}$  in acetonitrile at  $80^\circ\text{C}$ . In the presence of lithium iodide, the product is *E*- $\beta$ -iodostyrene, although *E*- $\beta$ -bromostyrene is unaffected by lithium iodide under the reaction conditions. Suggest a mechanism for the rearrangement.
- 10.10. Pyrrolidine derivatives catalyze the formation of 3,5-diaryl-4-acetylcyclohexanones from 4-arylbut-3-en-2-ones. A Diels-Alder reaction is believed to be involved. Suggest a mechanism.

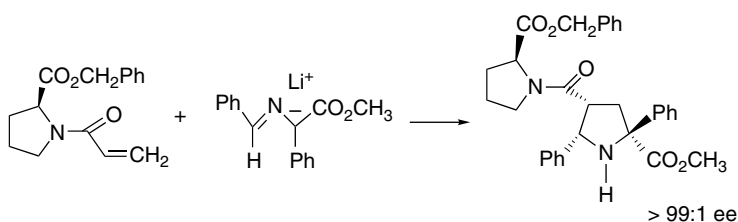


- 10.11. Propose a transition structure that would account for the stereochemistry observed in each of the following reactions:

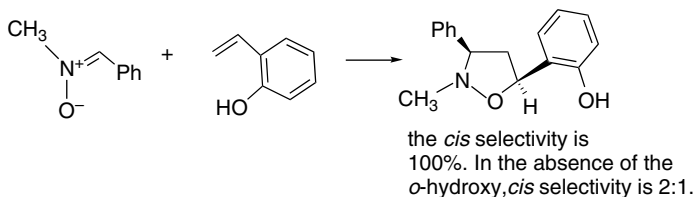
a.



b.

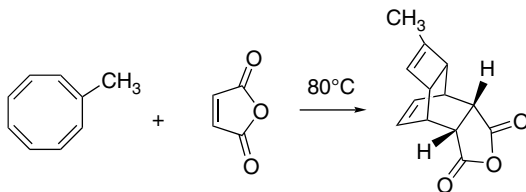


c.

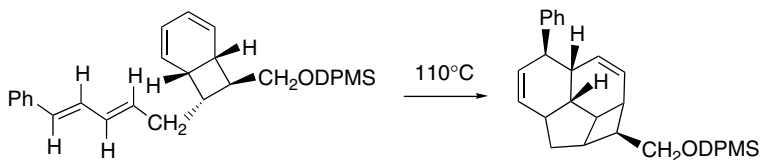


- 10.12. Classify the following reactions as electrocyclizations, sigmatropic rearrangement, cycloaddition, etc., and give the correct symbolism for the electrons involved in each process. Some of the reactions proceed in two steps.

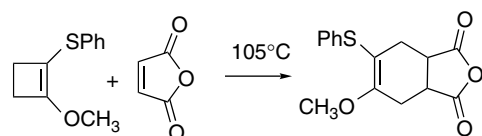
a.



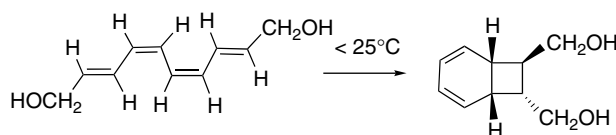
b.



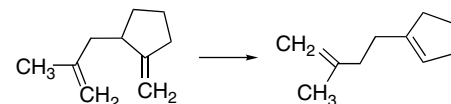
c.



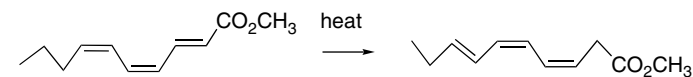
d.



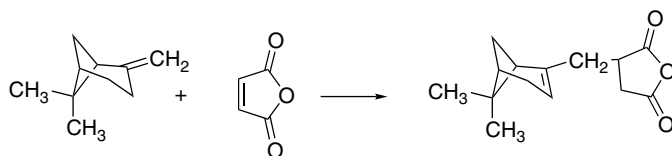
e.



f.



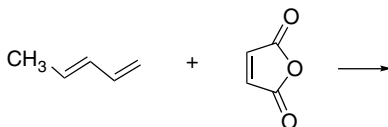
10.13. The “ene” reaction is a concerted reaction in which addition of an alkene and an electrophilic olefin occurs with transfer of a hydrogen to the electrophile and with a double-bond shift. For example:



Depict the orbital array through which this reaction can occur as a concerted process.

10.14. Predict the regiochemistry and stereochemistry of the following cycloaddition reactions and indicate the basis for your prediction.

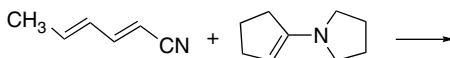
a.



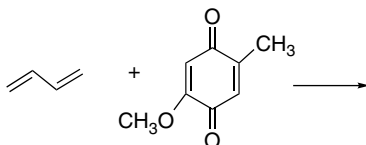
b.



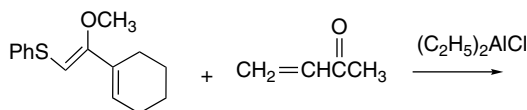
c.



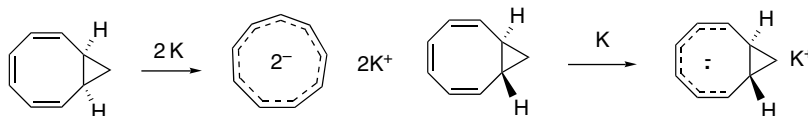
d.



e.

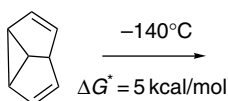


10.15. On treatment with potassium metal, *cis*-bicyclo[6.1.0]nona-2,4,6-triene gives a monocyclic aromatic dianion. The *trans* isomer under similar conditions give a bicyclic radical anion that does not undergo further reduction. Explain how the stereochemistry of the ring junction can control the course of these reductions.

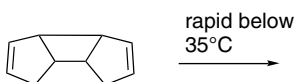


10.16. The following compounds are capable of degenerate rearrangement at the temperature given. Identify reaction processes that are consistent with the temperature and would lead to a degenerate rearrangement. Indicate by an appropriate labeling scheme the carbons and hydrogens that become equivalent as a result of the rearrangement process you have suggested.

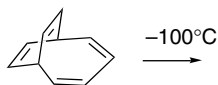
a.



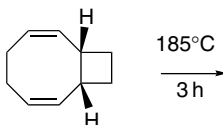
b.



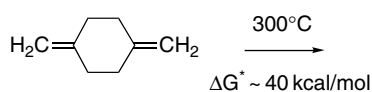
c.



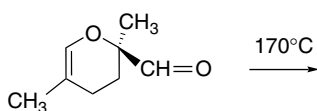
d.



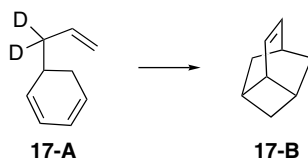
e.



f.



- 10.17. On heating at 225°C, 5-allylcyclohexa-1,3-diene, **17-A**, undergoes intramolecular cycloaddition to give the tricyclononene **17-B**. The same product is predicted for both [2+2] and [2+4] cycloaddition. The mechanism of the reaction has been probed by using the deuterium-labeled derivative, as shown. Indicate the position of the deuterium labeling in the product if the reaction proceeds by (a) a [2+2] cycloaddition or (b) a [2+4] cycloaddition.



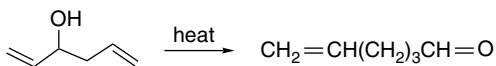
- 10.18. Computations on the cyclization of pentadienyl cations to cyclopentenyl cations has indicated increasing reactivity in the order  $X = \text{NH}_2 < \text{OH} < \text{H} < \text{O}^+\text{H}_2$ .



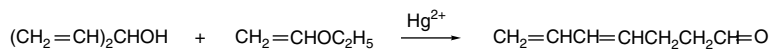
Based on these results, indicate which of the following types of groups would be favorable relative to the unsubstituted system: (a) alkyl; (b)  $\pi$ -conjugated EWGs, e.g., CN, CH=O; (c)  $\sigma$ -EWGs, e.g.,  $\text{CF}_3$ ,  $\text{CF}_3\text{SO}_2$ .

10.19. Suggest mechanisms for the following reactions. Classify the orbital symmetry character of the process as completely as you can.

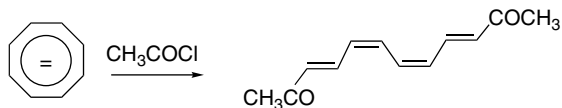
a.



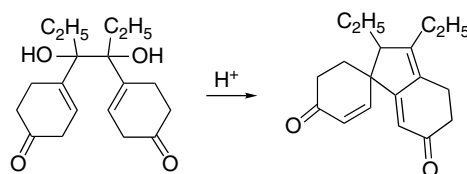
b.



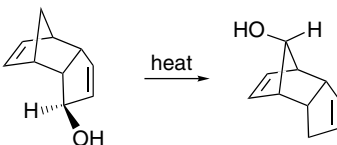
c.



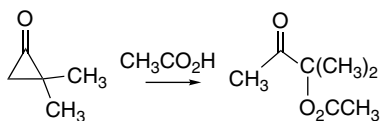
d.



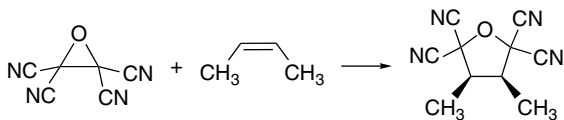
e.



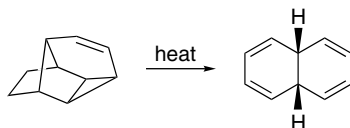
f.



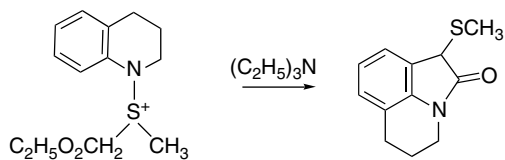
g.



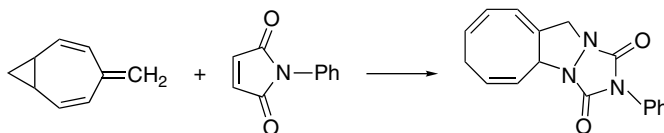
h.



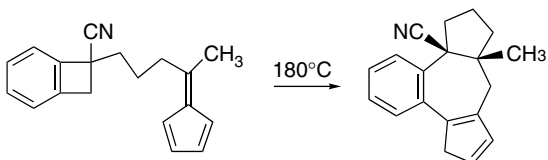
i.



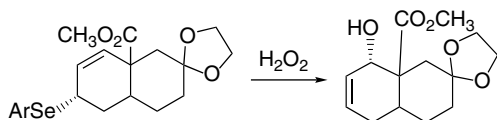
j.



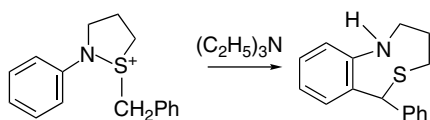
k.



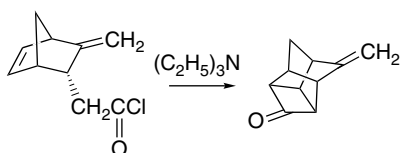
l.



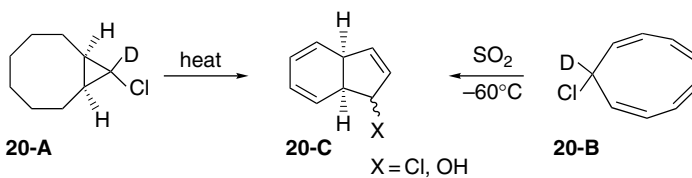
m.



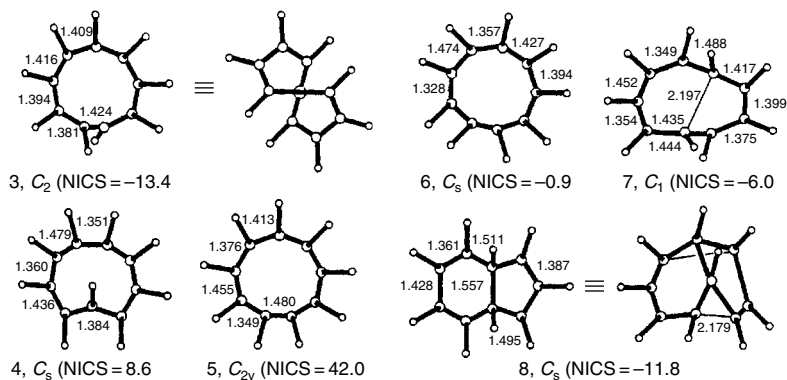
n.



- 10.20. Both compounds **20-A** and **20-B** undergo solvolysis in polar solvents at low temperature. The isolated product is **20-C**. When **20-B** is labeled with deuterium it is found that there is complete scrambling of label *equally among all positions* in the product.



It has been suggested that the cyclononatetraenyl cation might be an intermediate, and several  $[C_9H_9]^+$  structures have been compared computationally to determine their relative energy. Structure **3** has the lowest energy among the monocations. It has an *E*-configuration at one double bond. Structure **4** is also an energy minimum, but it is 21.6 kcal/mol higher in energy than **3**. The calculated relative energy and nucleus independent chemical shift (NICS) values are given for several structures, including structure **6**, which gives rise to the observed product. Formulate a mechanism that is in accord with the experimental observation of label scrambling. Discuss the role of structure **3** in the mechanism.



10.21. Reaction of ketene with cyclopentadiene proceeds in a  $[2+2]$  rather than a  $[2+4]$  manner. A number of potential TSs have been characterized computationally. The diagrams below show product and TS energy, TS bond orders, and TS NPA

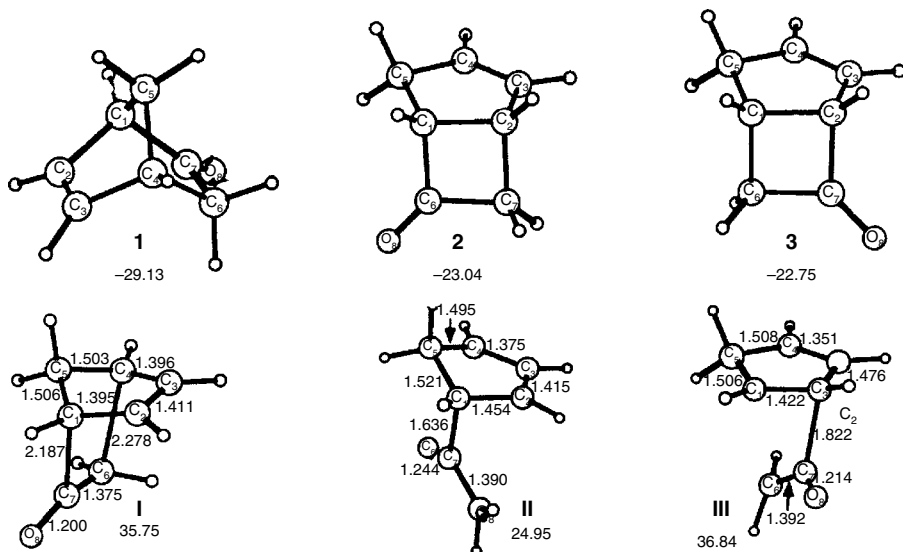


Fig. 10.P21a.  $\Delta E$  and  $E_a$  (MP4SDQ/6-31G\* + ZPE) for products **1** to **3** and the corresponding lowest-energy transition structures **I**, **II**, and **III**. Reproduced by Permission of the American Chemical Society.

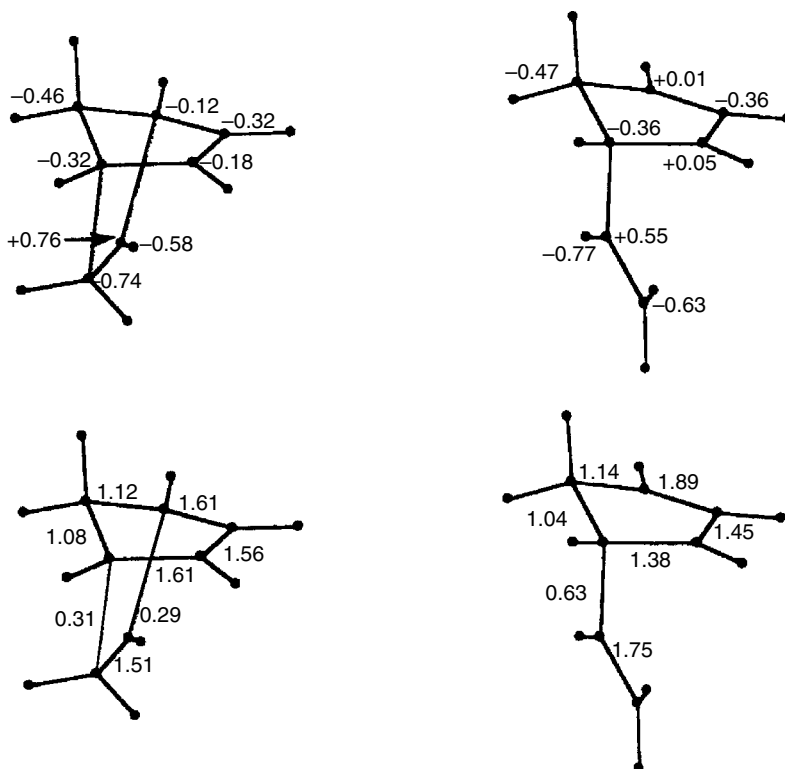


Fig. 10.P21b. NPA charges and bond orders for TS I and II. Reproduced by Permission of the American Chemical Society.

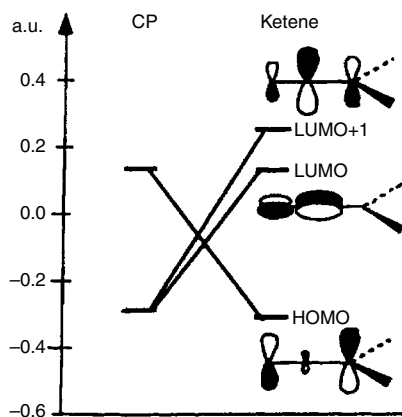
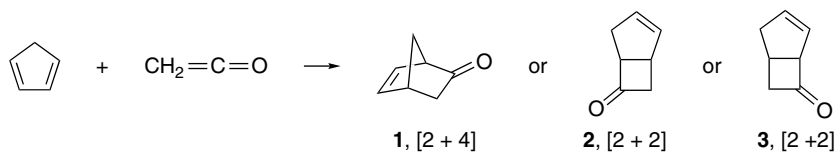


Fig. 21Pc. Relative energy (in au) of cyclopentadiene HOMO and LUMO and ketene  $\pi$ ,  $\pi_{C=O}^*$ , and  $\pi^*$  orbitals. Reproduced by permission of the American Chemical Society.

charges from MP4SDQ/6-31G\* + ZPE computations. Analyze the computational output in order to answer the following questions:

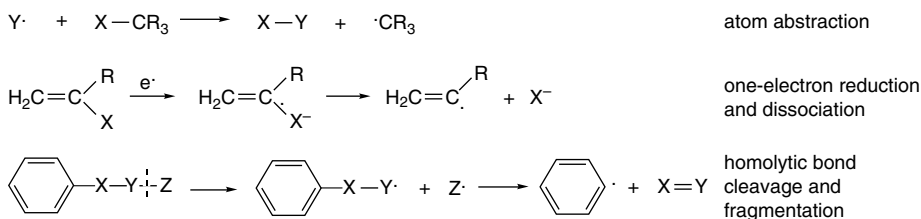


- In very broad terms, why is the [2 + 2] product **2** favored over the other possible products? Draw a reaction potential energy diagram to illustrate your conclusion.
- More specifically, why is product **2** preferred to product **3**? What structural features account for this preference?
- What structural features of TS **1** make it less favorable than TS **2**?

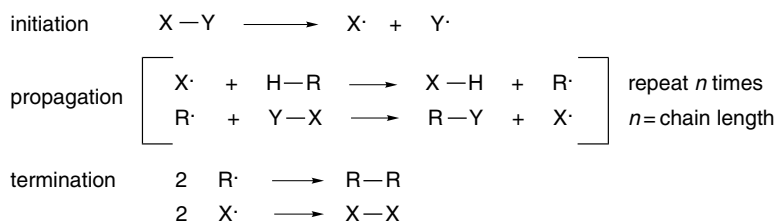
# Free Radical Reactions

## Introduction

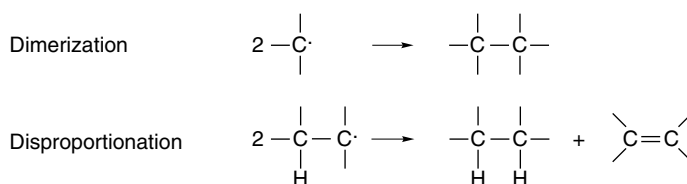
A free radical reaction involves molecules having unpaired electrons. The radical can be a starting compound or a product, but radicals are usually intermediates in reactions. Most of the reactions discussed to this point have been *heterolytic processes* involving polar intermediates and/or transition structures *in which all electrons remained paired throughout the course of the reaction*. In radical reactions, *homolytic bond cleavages* occur, with each fragment retaining one of the bonding electrons. The generalized reactions below illustrate the formation of alkyl, vinyl, and aryl free radicals by homolytic processes.



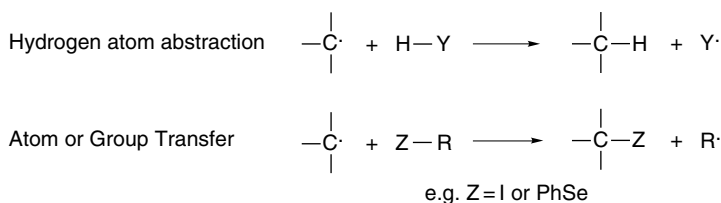
Free radicals are often involved in *chain reactions*. The overall mechanism consists of a series of reactions that regenerates a radical that can begin a new cycle of reactions. This sequence of reactions is called the *propagation phase*. Free radicals are usually highly reactive and the individual steps in a chain reaction typically have high absolute rate constants. However, the concentrations of the intermediates are low. The overall rates of reaction depend on the balance between the *initiation* and *termination* phases of the reaction, which start and end the chain sequence. The *chain length* is an important characteristic of free radical reactions. It specifies the average number of propagation sequences that occur per initiation step.



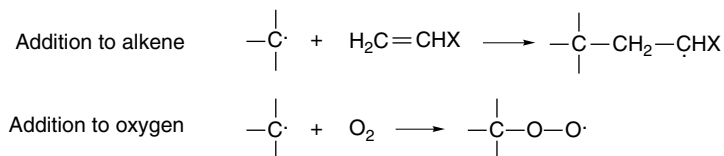
The effect of substituents on radical stability was introduced in Section 3.4.3. Most organic free radicals have very short lifetimes and dimerize or disproportionate at a diffusion-controlled rate. The usual disproportionation process for alkyl radicals involves transfer of a hydrogen from the  $\beta$ -carbon to the radical site, leading to formation of an alkane and an alkene. Disproportionation is facilitated by the weak  $\beta$ -C-H bond (see p. 311)



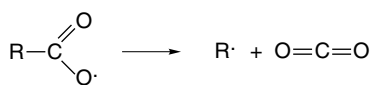
There are several fundamental types of radical reactions. Radicals can abstract hydrogen or other atoms from many types of solvents and reagents. This is a particularly important example of an *atom or group transfer reaction*.



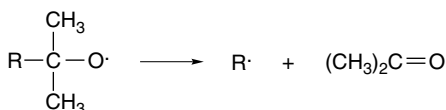
Radicals are also capable of addition reactions. For synthetic purposes, additions to alkenes are particularly important. Most radicals are highly reactive toward  $O_2$ .



Radicals also undergo fragmentation reactions. Most of these are  $\beta$ -scission reactions, such as illustrated by decarboxylation and fragmentation of alkoxy radicals, but decarbonylation, an  $\alpha$ -cleavage, is also facile.



decarboxylation

 $\beta$ -fragmentation of alkoxy radical

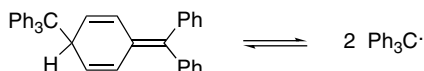
decarbonylation

As we discuss specific reaction mechanisms, we will see that they are combinations of a relatively small number of reaction types that are applicable to a number of different reactants and reaction sequences.

## 11.1. Generation and Characterization of Free Radicals

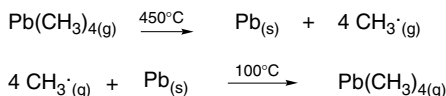
### 11.1.1. Background

Two early studies have special historical significance in the development of the concept of free radical reactions. The work of Gomberg around 1900 provided evidence that when triphenylmethyl chloride was treated with silver metal, the resulting solution contained  $\text{Ph}_3\text{C} \cdot$  in equilibrium with a less reactive molecule. Eventually it was shown that the dimeric product is a cyclohexadiene derivative.<sup>1</sup>



The dissociation constant is small, only about  $2 \times 10^{-4} M$  at room temperature. The presence of the small amount of the radical at equilibrium was deduced from observation of reactions that could not reasonably be attributed to a normal hydrocarbon.

The second set of experiments was carried out in 1929 by Paneth. The decomposition of tetramethyllead was accomplished in such a way that the products were carried by an inert gas over a film of lead metal. The lead was observed to disappear with re-formation of tetramethyllead. The conclusion reached was that methyl radicals must exist long enough in the gas phase to be transported from the point of decomposition to the lead film, where they are reconverted to tetramethyllead.



Since these early experiments, a great deal of additional information about the structure and properties of free radical intermediates has been developed. In this chapter, we discuss the structure of free radicals and some of the special features associated with free radical reactions. We also consider some of the key chemical reactions that involve free radical intermediates.

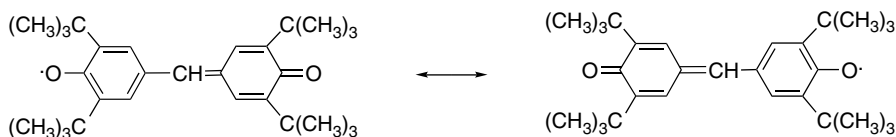
<sup>1</sup> H. Lankamp, W. Th. Nauta, and C. MacLean, *Tetrahedron Lett.*, 249 (1968); J. M. McBride, *Tetrahedron*, **30**, 2009 (1974); K. J. Skinner, H. S. Hochster, and J. M. McBride, *J. Am. Chem. Soc.*, **96**, 4301 (1974).

## 11.1.2. Long-Lived Free Radicals

Radicals that have long lifetimes and are resistant to dimerization, disproportionation, and other routes to self-annihilation are called *persistent free radicals*. Scheme 11.1 gives some examples of long-lived free radicals. A few free radicals are indefinitely stable, such as Entries 1, 3, and 6, and are just as stable to ordinary conditions of temperature and atmosphere as typical closed-shell molecules. Entry 2 is somewhat less stable to oxygen, although it can exist indefinitely in the absence of oxygen. The structures shown in Entries 1, 2, and 3 all permit extensive delocalization of the unpaired electron into aromatic rings. These highly delocalized radicals show little tendency toward dimerization or disproportionation. The radical shown in Entry 3 is unreactive under ordinary conditions and is thermally stable even at 300°C.<sup>2</sup>

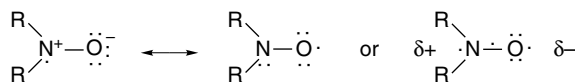
The *bis*-(*t*-butyl)methyl radical shown in Entry 4 has only alkyl substituents and yet has a significant lifetime in the absence of oxygen. The *tris*-(*t*-butyl)methyl radical has an even longer lifetime with a half-life of about 20 min at 25°C.<sup>3</sup> The steric hindrance provided by the *t*-butyl substituents greatly retards the rates of dimerization of these radicals. Moreover, they lack  $\beta$ -hydrogens, precluding the normal disproportionation reaction. They remain highly reactive toward oxygen, however. The extended lifetimes have more to do with kinetic factors than with inherent stability.<sup>4</sup> Entry 5 is a sterically hindered perfluorinated radical that is even more long-lived than similar alkyl radicals.

Certain radicals are stabilized by synergistic conjugation involving two or more functional groups. Entries 6 and 7 are examples. Galvinoxyl, the compound shown in Entry 6 benefits not only from delocalization over the two aromatic rings, but also from the equivalence of the two oxygens, which is illustrated by the resonance structures. The hindered nature of the oxygens also contributes to persistence.



Entry 7 also benefits from interaction between the ester and amino groups, as is discussed in Section 11.1.6.

There are only a few functional groups that contain an unpaired electron and yet are stable in a wide range of structural environments. The best example is the nitroxide group illustrated in Entry 8. There are numerous specific nitroxide radicals that have been prepared and characterized. The unpaired electron is delocalized between nitrogen and oxygen in a structure with a N–O bond order of 1.5.

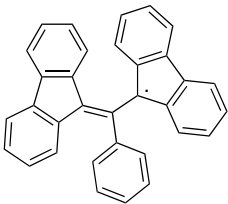
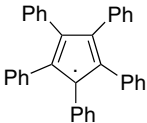
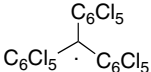
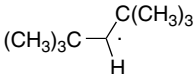
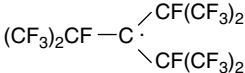
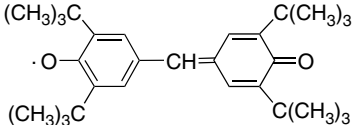
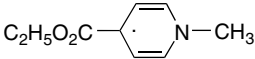
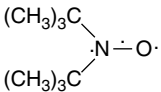


Many nitroxides are stable under normal conditions, and heterolytic reactions can be carried out on other functional groups in the molecule without affecting the nitroxide

<sup>2</sup> M. Ballester, *Acc. Chem. Res.*, **18**, 380 (1985).

<sup>3</sup> G. D. Mendenhall, D. Griller, D. Lindsay, T. T. Tidwell, and K. U. Ingold, *J. Am. Chem. Soc.*, **96**, 2441 (1974).

<sup>4</sup> For a review of various types of persistent radicals, see D. Griller and K. U. Ingold, *Acc. Chem. Res.*, **9**, 13 (1976).

Structure	Stability
<p>1<sup>a</sup></p> 	Indefinitely stable as a solid, even in the presence of air
<p>2<sup>b</sup></p> 	Crystalline substance is not rapidly attacked by oxygen, although solutions are air-sensitive. The compound is stable to high temperature in the absence of air.
<p>3<sup>c</sup></p> 	Stable in solution for days, even in the presence of air. Indefinitely stable in the solid state. Thermally stable up to 300°C.
<p>4<sup>d</sup></p> 	Persistent in dilute solution ( $<10^{-5} M$ ) below $-30^{\circ}\text{C}$ in the absence of oxygen; $t_{1/2}$ of 50 s at $25^{\circ}\text{C}$ .
<p>5<sup>e</sup></p> 	Thermally stable to $70^{\circ}\text{C}$ ; stable to $\text{O}_2$ .
<p>6<sup>f</sup></p> 	Stable to oxygen; stable to extended storage as a solid. Slowly decomposes in solution.
<p>7<sup>g</sup></p> 	Stable distillable liquid that is only moderately sensitive to $\text{O}_2$ .
<p>8<sup>h</sup></p> 	Stable to oxygen, even above $100^{\circ}\text{C}$

a. C. F. Koelsch, *J. Am. Chem. Soc.*, **79**, 4439 (1957).

b. K. Ziegler and B. Schnell, *Liebigs Ann. Chem.*, **445**, 266 (1925).

c. M. Ballester, J. Riera, J. Castaner, C. Badia, and J. M. Monso, *J. Am. Chem. Soc.*, **93**, 2215 (1971).

d. G. D. Mendenhall, D. Griller, D. Lindsay, T. T. Tidwell, and K. U. Ingold, *J. Am. Chem. Soc.*, **96**, 2441 (1974).

e. K. V. Scherer, Jr., T. Ono, K. Yamanouchi, R. Fernandez, and P. Henderson, *J. Am. Chem. Soc.*, **107**, 718 (1985).

f. G. M. Coppinger *J. Am. Chem. Soc.*, **79**, 501 (1957); P. D. Bartlett and T. Funahashi, *J. Am. Chem. Soc.*, **84**, 2596 (1962).

g. J. Hermolin, M. Levin, and E. M. Kosower, *J. Am. Chem. Soc.*, **103**, 4808 (1981).

h. A. K. Hoffmann and A. T. Henderson, *J. Am. Chem. Soc.*, **83**, 4671 (1961).

group.<sup>5</sup> Nitroxides are very useful in biochemical studies by being easily detected paramagnetic probes.<sup>6</sup>

Although the existence of stable and persistent free radicals is of significance in establishing that free radicals can have extended lifetimes, most free radical reactions involve highly reactive intermediates that have fleeting lifetimes and are present at very low concentrations. The techniques for the study of radicals under these conditions are the subject of the next section.

### 11.1.3. Direct Detection of Radical Intermediates

The distinguishing characteristic of free radicals is the presence of an unpaired electron. Species with an unpaired electron are *paramagnetic*, that is, they have a nonzero electronic spin. The most useful method for detecting and characterizing unstable radical intermediates is *electron spin resonance* (ESR) spectroscopy,<sup>7</sup> also known as *electron paramagnetic resonance* (EPR) spectroscopy. ESR spectroscopy detects the transition of an electron between the energy levels associated with the two possible orientations of electron spin in a magnetic field. An ESR spectrometer records the absorption of energy when an electron is excited from the lower to the higher state. The energy separation is very small on an absolute scale and corresponds to the energy of microwaves. ESR spectroscopy is a highly specific tool for detecting radical species because only molecules with unpaired electrons give rise to ESR spectra. As with other spectroscopic methods, detailed analysis of the absorption spectrum can provide structural information. One feature that is determined is the *g* value, which specifies the separation of the two spin states as a function of the magnetic field strength of the spectrometer:

$$h\nu = E = g\mu_B H \quad (11.1)$$

where  $\mu_B$  is the Bohr magneton (a constant equal to 9.273 ergs/gauss) and  $H$  is the magnetic field in gauss. The measured value of  $g$  is a characteristic of the particular type of radical, just as the line position in NMR spectra is characteristic of the absorbing nucleus.

More detailed structural information can be deduced from the *hyperfine splitting* in ESR spectra. The origin of this splitting is closely related to the factors that cause spin-spin splitting in <sup>1</sup>H-NMR spectra. Certain nuclei have a magnetic moment, and among those of greatest interest in organic chemistry are <sup>1</sup>H, <sup>13</sup>C, <sup>14</sup>N, <sup>19</sup>F, and <sup>31</sup>P. Interaction of the electron with one or more of these nuclei splits the signal arising from the unpaired electron. The number of lines is given by the equation

$$\text{Number of lines} = 2nI + 1 \quad (11.2)$$

where  $I$  is the nuclear spin quantum number and  $n$  is the number of equivalent interacting nuclei. For <sup>1</sup>H, <sup>13</sup>C, <sup>19</sup>F, and <sup>31</sup>P,  $I = 1/2$ . so a single hydrogen splits a

<sup>5</sup>. For reviews of the preparation, reactions and uses of nitroxide radicals, see J. F. W. Keana, *Chem. Rev.*, **78**, 37 (1978); L. J. Berliner, ed., *Spin-Labeling*, Vol. 2, Academic Press, New York, 1979; S. Banerjee and G. K. Trivedi, *J. Sci. Ind. Res.*, **54**, 623 (1995); L. B. Volodarsky, V. A. Reznikov, and V. I. Ovcharenko, *Synthetic Chemistry of Stable Nitroxides*, CRC Press, Boca Raton, FL, 1994.

<sup>6</sup>. G. L. Millhauser, W. R. Fiori, and S. M. Miick, *Methods Enzymol.*, **246**, 589 (1995).

<sup>7</sup>. B. Mile, *Current Org. Chem.*, **4**, 55 (2000); F. Gerson and W. Huber, *Electron Spin Resonance of Organic Radicals*, Wiley-VCH, Weinheim, 2003.

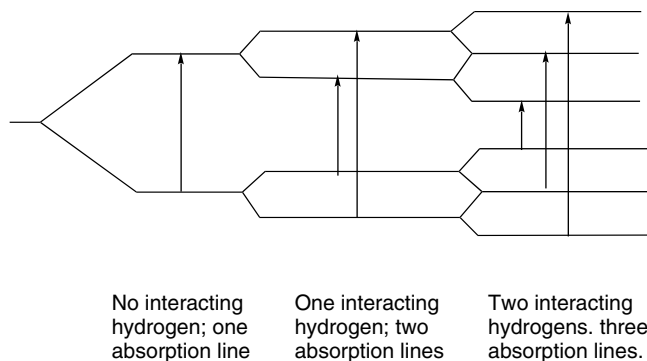


Fig. 11.1. Hyperfine splitting in ESR spectra.

signal into a doublet. Interaction with three equivalent hydrogens, as in a methyl group, gives splitting into four lines. This splitting is illustrated in Figure 11.1. Nitrogen ( $^{14}\text{N}$ ) with  $I = 1$  splits each energy level into three lines. Neither  $^{12}\text{C}$  nor  $^{16}\text{O}$  has a nuclear magnetic moment, and just as they cause no signal splitting in NMR spectra, they have no effect on the multiplicity in ESR spectra.

A great deal of structural information can be obtained by analysis of the hyperfine splitting pattern of a free radical. If we limit our discussion for the moment to radicals without heteroatoms, the number of lines indicates the number of interacting hydrogens, and the magnitude of the splitting, given by the hyperfine splitting constant  $a$ , is a measure of the unpaired electron density in the hydrogen  $1s$  orbital. For planar conjugated systems in which the unpaired electron resides in a  $\pi$ -orbital system, the relationship between electron spin density and the splitting constant is given by the McConnell equation<sup>8</sup>:

$$a = \rho Q \quad (11.3)$$

where  $a$  is the hyperfine coupling constant for a proton,  $Q$  is a proportionality constant (about 23 G), and  $\rho$  is the spin density on the carbon to which the hydrogen is attached. For example, taking  $Q = 23.0\text{G}$ , the hyperfine splitting in the benzene radical anion can be readily calculated by taking  $\rho = 1/6$ , because the one unpaired electron must be distributed equally among the six carbon atoms. The calculated value of  $a = 3.83$  is in good agreement with the observed value. The spectrum (Figure 11.2a) consists of seven lines separated by a coupling constant of 3.75 G.<sup>9</sup> Note that EPR spectra, unlike NMR and IR spectra, are displayed as the derivative of absorption rather than as absorption.

The ESR spectrum of the ethyl radical shown in Figure 11.2b is readily interpreted, and the results are of interest with respect to the distribution of unpaired electron density in the molecule.<sup>10</sup> The 12-line spectrum is a triplet of quartets resulting from unequal coupling of the electron spin to the  $\alpha$ - and  $\beta$ -hydrogens. The two coupling constants,  $a_\alpha = 22.4\text{G}$  and  $a_\beta = 26.9\text{G}$ , imply extensive delocalization of spin density through the  $\sigma$  bonds.

<sup>8</sup>. H. M. McConnell, *J. Chem. Phys.*, **24**, 764 (1956).

<sup>9</sup>. J. R. Bolton, *Mol. Phys.*, **6**, 219 (1963).

<sup>10</sup>. R. W. Fessenden and R. M. Shuler, *J. Chem. Phys.*, **33**, 935 (1960); *J. Phys. Chem.*, **39**, 2147 (1963).

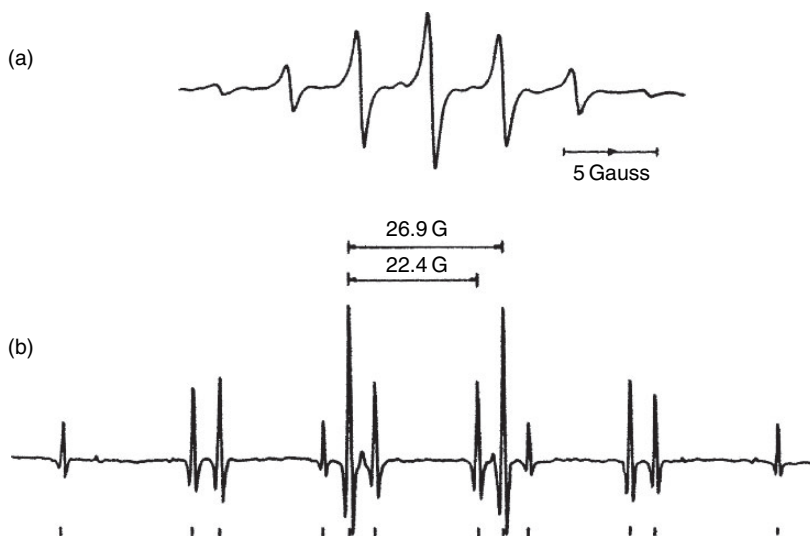
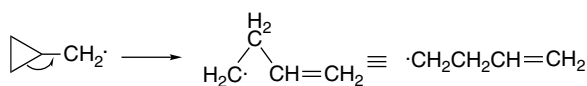
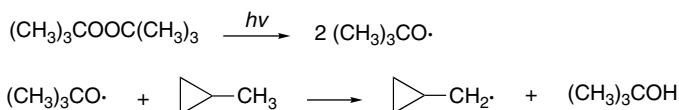


Fig. 11.2. Some EPR spectra of small radicals: (a) Spectrum of the benzene radical anion. From *Mol. Phys.*, **6**, 219 (1963); (b) Spectrum of the ethyl radical. From *J. Chem. Phys.*, **33**, 935 (1960); *J. Phys. Chem.* **39**, 2147 (1963). Reproduced by permission of Taylor and Francis, Ltd, and the American Institute of Physics, respectively.

ESR spectra have been widely used in the study of reactions to detect free radical intermediates. An important example involves the cyclopropylmethyl radical. Much chemical experience has indicated that this radical is unstable, rapidly giving rise to the 3-butenyl radical after being generated.



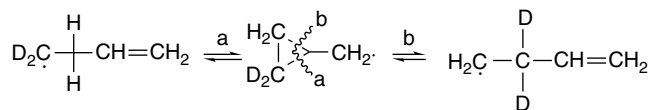
The radical was generated by photolytic decomposition of di-*t*-butyl peroxide in methylcyclopropane, a process that leads to selective abstraction of a methyl hydrogen.



Below  $-140^\circ\text{C}$ , the ESR spectrum observed was that of the cyclopropylmethyl radical. If the photolysis was done above  $-140^\circ\text{C}$ , however, the spectrum of a second species was seen, and above  $-100^\circ\text{C}$ , this was the only spectrum observed. This second spectrum was shown to be that of the 3-butenyl radical.<sup>11</sup> This study also established that the 3-butenyl radical does not revert to the cyclopropylmethyl radical on being cooled back to  $-140^\circ\text{C}$ . The conclusion is that the ring opening of the cyclopropyl radical is a very facile process and its lifetime above  $-100^\circ\text{C}$  is very short. Even

<sup>11</sup> J. K. Kochi, P. J. Krusic, and D. R. Eaton, *J. Am. Chem. Soc.*, **91**, 1877 (1969).

though the equilibrium favors the 3-butenyl radical, the reversible ring closure can be detected by an isotopic-labeling experiment that reveals the occurrence of deuterium exchange.

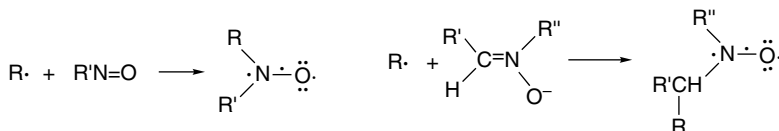


The rate of both the ring opening ( $k = 1 \times 10^8 \text{ s}^{-1}$  at  $25^\circ\text{C}$ ) and the ring closure ( $k = 3 \times 10^3 \text{ s}^{-1}$ ) have been measured and confirm that only a very small amount of the cyclopropylmethyl radical is present at equilibrium, in agreement with the ESR results.<sup>12</sup>

Several MO and DFT computations on the energetics of the ring opening of the cyclopropylmethyl radical have been carried out. The computed energy profile shown in Figure 11.3 is derived from CCSD(T)/cc-pvTZ-level calculations.<sup>13</sup> A barrier of 8.5 kcal/mol is calculated for the ring opening, along with smaller barriers associated with rotations in the reactant and product. A value of 7.2 kcal/mol has been obtained from CBS-RAD calculations.<sup>14</sup> The experimental barrier is about 7.5 kcal/mol. It is worth noting that the rotational process is analogous to the interconversion of the perpendicular and bisected conformations of the cyclopropylmethyl cation. The radical rotamers differ by less than 3 kcal/mol, whereas the difference is nearly 30 kcal/mol in the cation (see Section 4.4.1).

It is important to emphasize that direct studies such as those carried out on the cyclopropylmethyl radical can be done with *low steady state concentrations of the radical*. In the case of the study of the cyclopropylmethyl radical, removal of the source of irradiation leads to rapid disappearance of the ESR spectrum because the radicals react rapidly and are not replaced by continuing radical formation. Under many conditions, the steady state concentration of a radical intermediate may be too low to permit direct detection. Therefore, failure to observe an ESR signal cannot be taken as conclusive evidence against a radical intermediate.

A technique called *spin trapping* can also be used to study radicals. A diamagnetic molecule that reacts rapidly with radicals to give a stable paramagnetic species is introduced into the reaction system being studied. As radical intermediates are generated, they are trapped by the reactive molecule to give more stable radicals that are detectable. The most useful spin traps are nitrones and nitroso compounds, which react rapidly with radicals to give stable nitroxides.<sup>15</sup> Analysis of the ESR spectrum of the nitroxide can provide information about the structure of the original radical.



<sup>12</sup> A. Effio, D. Griller, K. U. Ingold, A. L. J. Beckwith, and A. K. Serelis, *J. Am. Chem. Soc.*, **102**, 1734 (1980); L. Mathew and J. Warkentin, *J. Am. Chem. Soc.*, **108**, 7981 (1986); M. Newcomb and A. G. Glenn, *J. Am. Chem. Soc.*, **111**, 275 (1989); A. L. J. Beckwith and V. W. Bowry, *J. Org. Chem.*, **54**, 2681 (1989); D. C. Nonhebel, *Chem. Soc. Rev.*, **22**, 347 (1993).

<sup>13</sup> A. L. Cooksy, H. F. King, and W. H. Richardson, *J. Org. Chem.*, **68**, 9441 (2003).

<sup>14</sup> D. M. Smith, A. Nicolaidis, B. T. Golding, and L. Radom, *J. Am. Chem. Soc.*, **120**, 10223 (1998).

<sup>15</sup> E. G. Janzen, *Acc. Chem. Res.*, **4**, 31 (1971); E. G. Janzen, in *Free Radicals in Biology*, Vol. 4, W. A. Pryor, ed., Academic Press, New York, 1980, pp. 115–154.

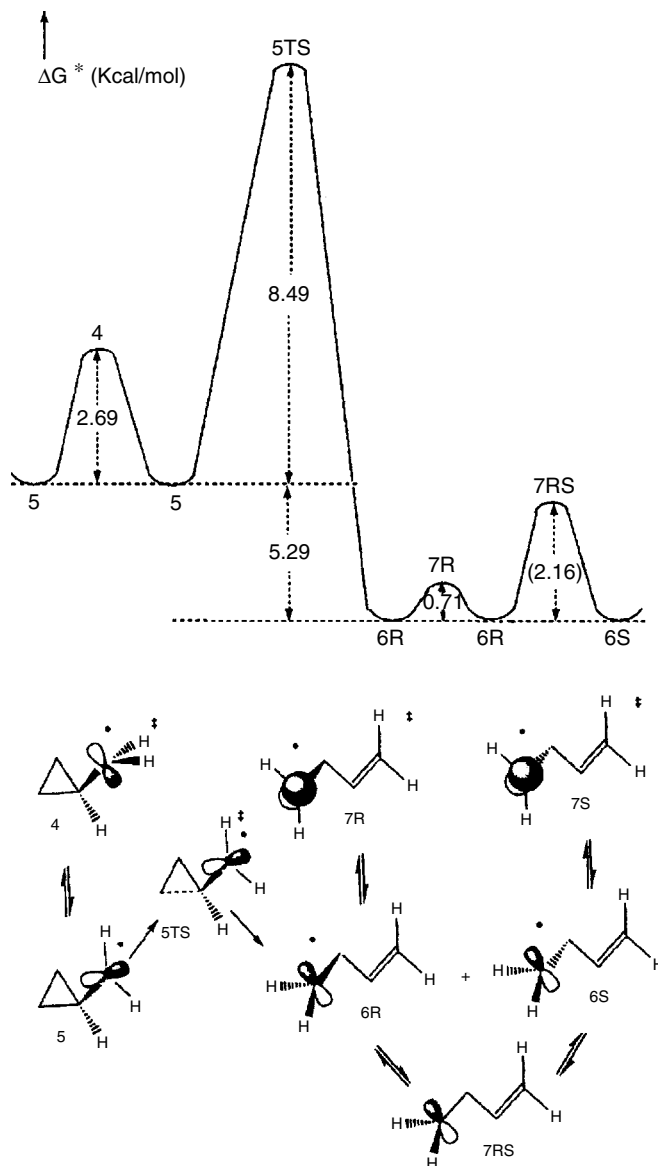


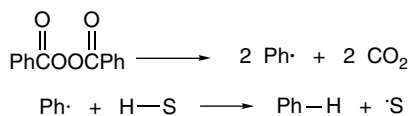
Fig. 11.3. Energy profile for rotation and ring opening of the cyclopropyl methyl radical derived from CCSD(T)/cc-pvTZ computations. Reproduced from *J. Org. Chem.*, **68**, 9441 (2003), by permission of the American Chemical Society.

Another technique that is specific for radical processes is known as CIDNP, an abbreviation for *chemically induced dynamic nuclear polarization*.<sup>16</sup> The instrumentation required for such studies is an NMR spectrometer. CIDNP is observed as a strong perturbation of the intensity of NMR signals in products formed in certain types of free radical reactions. The variation in intensity results when the normal population of

<sup>16</sup> H. R. Ward, *Acc. Chem. Res.*, **5**, 18 (1972); R. G. Lawler, *Acc. Chem. Res.*, **5**, 25 (1972).

nuclear spin states dictated by the Boltzmann distribution is disturbed by the presence of an unpaired electron. The magnetic moment associated with an electron causes a redistribution of the nuclear spin states. Molecules can become overpopulated in either the lower or upper spin state. If the lower state is overpopulated an enhanced absorption signal is observed. If the upper state is overpopulated, an emission signal is observed. The CIDNP method is not as general as EPR spectroscopy because not all free radical reactions can be expected to exhibit the phenomenon.<sup>17</sup>

Figure 11.4 shows the observation of CIDNP during the decomposition of benzoyl peroxide in cyclohexanone.



The emission signal corresponding to benzene confirms that it is formed by a free radical process. As in steady state ESR experiments, the enhanced emission and absorption are observed only as long as the reaction is proceeding. When the reaction is complete or is stopped in some way, the signals return to their normal intensity because equilibrium population of the two spins states is rapidly reached.

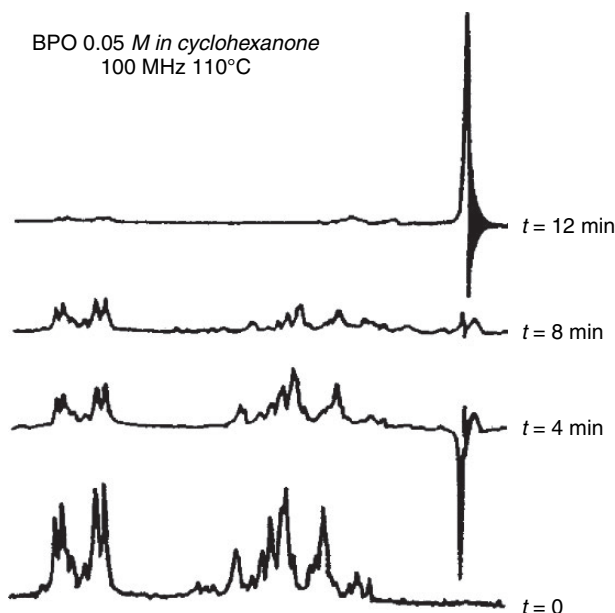
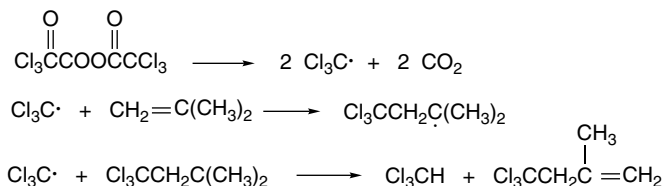


Fig. 11.4. NMR spectra recorded during decomposition of dibenzoyl peroxide. The upfield signal is due to benzene; the other signals are due to dibenzoyl peroxide. Reproduced from *Acc. Chem. Res.*, **2**, 110 (1969), by permission of the American Chemical Society.

<sup>17</sup> For a discussion of the theory of CIDNP and the conditions under which spin polarization occurs, see G. L. Closs, *Adv. Mag. Res.*, **7**, 157 (1974); R. Kaptein, *Adv. Free Radical Chem.*, **5**, 318 (1975); G. L. Closs, R. J. Miller, and O. D. Redwine, *Acc. Chem. Res.*, **18**, 196 (1985).

One aspect of both EPR and CIDNP studies that should be kept in mind is that either is capable of detecting very small amounts of radical intermediates. Although this sensitivity makes both techniques very useful, it can also present a pitfall. The most prominent features of either ESR or CIDNP spectra may actually be due to radicals that account for only minor amounts of the total reaction process. An example of this was found in a study of the decomposition of trichloroacetyl peroxide in alkenes.



In addition to the emission signals of  $\text{CHCl}_3$  and  $\text{Cl}_3\text{CCH}_2\text{C}(\text{CH}_3)=\text{CH}_2$ , which are the major products, a strong emission signal for  $\text{Cl}_3\text{CCHCl}_2$  was identified. However, this compound is a very minor product of the reaction and when the signals have returned to their normal intensity,  $\text{Cl}_3\text{CCHCl}_2$  is present in such a small amount that it cannot be detected.<sup>18</sup>

#### 11.1.4. Generation of Free Radicals

There are several reactions that are used frequently to generate free radicals, both to study radical structure and reactivity and in synthetic processes. Some of the most general methods are outlined here. These methods will be encountered again when we discuss specific examples of free radical reactions. For the most part, we defer discussion of the reactions of the radicals until that point.

Peroxides are a common source of radical intermediates. Commonly used initiators include benzoyl peroxide, *t*-butyl peroxybenzoate, di-*t*-butyl peroxide, and *t*-butyl hydroperoxide. Reaction generally occurs at relatively low temperature (80° – 100°C). The oxygen-oxygen bond in peroxides is weak (~ 30 kcal/mol) and activation energies for radical formation are low. Dialkyl peroxides decompose thermally to give two alkoxy radicals.<sup>19</sup>



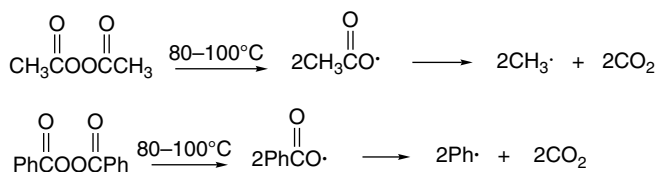
Diacyl peroxides are sources of alkyl radicals because the carboxyl radicals that are initially formed lose  $\text{CO}_2$  very rapidly.<sup>20</sup> In the case of aroyl peroxides, products can be derived from either the carboxyl radical or the radical formed by decarboxylation.<sup>21</sup> The decomposition of peroxides can also be accomplished by photochemical excitation.

<sup>18</sup> H. Y. Loken, R. G. Lawler, and H. R. Ward, *J. Org. Chem.*, **38**, 106 (1973).

<sup>19</sup> W. A. Pryor, D. M. Huston, T. R. Fiske, T. L. Pickering, and E. Ciuffarin, *J. Am. Chem. Soc.*, **86**, 4237 (1964).

<sup>20</sup> J. C. Martin, J. W. Taylor, and E. H. Drew, *J. Am. Chem. Soc.*, **89**, 129 (1967); F. D. Greene, H. P. Stein, C.-C. Chu, and F. M. Vane, *J. Am. Chem. Soc.*, **86**, 2080 (1964).

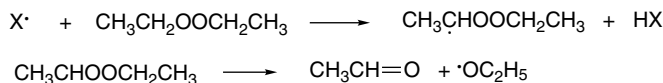
<sup>21</sup> D. F. DeTar, R. A. J. Long, J. Rendleman, J. Bradley, and P. Duncan, *J. Am. Chem. Soc.*, **89**, 4051 (1967).



Peroxyesters are also sources of radicals. The acyloxy portion normally loses carbon dioxide, so peroxyesters yield an alkyl (or aryl) and alkoxy radical.<sup>22</sup>



The thermal decompositions described above are unimolecular reactions that should exhibit first-order kinetics. Peroxides often decompose at rates faster than expected for unimolecular thermal decomposition and with more complicated kinetics. This behavior is known as *induced decomposition* and occurs when part of the peroxide decomposition is the result of bimolecular reactions with radicals present in solution, as illustrated specifically for diethyl peroxide.



The amount of induced decomposition that occurs depends on the concentration and reactivity of the radical intermediates and the susceptibility of the reactant to radical attack. The radical  $\text{X}\cdot$  may be formed from the peroxide, but it can also be derived from subsequent reactions with the solvent. For this reason, both the structure of the peroxide and the nature of the reaction medium are important in determining the extent of induced decomposition relative to unimolecular homolysis. All of the peroxides are used in relatively dilute solution. Many peroxides are explosive, and due precautions must be taken.

Alkyl hydroperoxides give alkoxy radicals and the hydroxyl radical. *t*-Butyl hydroperoxide is often used as a radical source. Detailed studies on the mechanism of the decomposition indicate that it is a more complicated process than simple unimolecular decomposition.<sup>23</sup> The alkyl hydroperoxides are sometimes used in conjunction with a transition metal salt. Under these conditions, an alkoxy radical is produced, but the hydroxyl portion appears as hydroxide ion as the result of one-electron reduction by the metal ion.<sup>24</sup>



A technique that provides a convenient source of radicals for study by ESR involves photolysis of a mixture of di-*t*-butyl peroxide, triethylsilane, and the alkyl bromide corresponding to the radical to be studied.<sup>25</sup> Photolysis of the peroxide gives

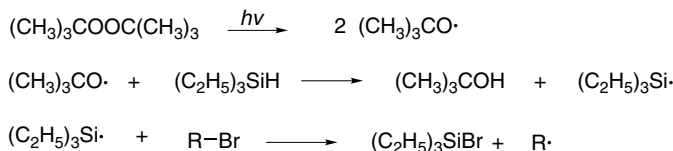
<sup>22</sup> P. D. Bartlett and R. R. Hiatt, *J. Am. Chem. Soc.*, **80**, 1398 (1958).

<sup>23</sup> R. Hiatt, T. Mill, and F. R. Mayo, *J. Org. Chem.*, **33**, 1416 (1968), and accompanying papers.

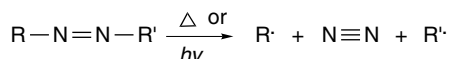
<sup>24</sup> W. H. Richardson, *J. Am. Chem. Soc.*, **87**, 247 (1965).

<sup>25</sup> A. Hudson and R. A. Jackson, *Chem. Commun.*, 1323 (1969); D. J. Edge and J. K. Kochi, *J. Am. Chem. Soc.*, **94**, 7695 (1972).

*t*-butoxy radicals, which selectively abstract hydrogen from the silane. This reactive silicon radical in turn abstracts bromine, generating the alkyl radical at a steady state concentration suitable for ESR study.



Another quite general source of free radicals is the decomposition of azo compounds. The products are molecular nitrogen and the radicals are derived from the substituent groups.

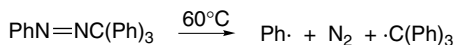


Both symmetrical and unsymmetrical azo compounds can be made, so a single radical or two different ones can be generated. The energy for the decomposition can be either thermal or photochemical.<sup>26</sup> The temperature at which decomposition occurs depends on the nature of the substituent groups. Azomethane does not decompose to methyl radicals and nitrogen until temperatures above 400°C are reached. Azo compounds that generate relatively stable radicals decompose at much lower temperatures. Azo compounds derived from allyl groups decompose somewhat above 100°C.



Ref. 27

Unsymmetrical azo compounds must be used to generate phenyl radicals because azobenzene is very stable thermally. Phenylazotriphenylmethane decomposes readily because of the stability of the triphenylmethyl radical.



Ref. 28

Azo compounds with functional groups that stabilize the radical are especially reactive. The stabilizing effect of the cyano substituent is responsible for the easy decomposition of azoisobutyronitrile (AIBN), which is frequently used as an initiator in radical reactions.

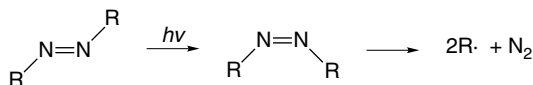


<sup>26</sup> P. S. Engel, *Chem. Rev.*, **80**, 99 (1980).

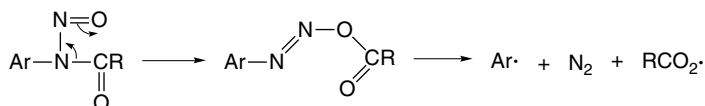
<sup>27</sup> K. Takagi and R. J. Crawford, *J. Am. Chem. Soc.*, **93**, 5910 (1971).

<sup>28</sup> R. F. Bridger and G. A. Russell, *J. Am. Chem. Soc.*, **85**, 3754 (1963).

Many azo compounds also generate radicals when photolyzed. This occurs by a thermal decomposition of the *cis*-azo compounds that are formed in the photochemical step.<sup>29</sup> The *cis* isomers are thermally much more labile than the *trans* isomers.



*N*-Nitrosoanilides are a convenient source of aryl radicals. There is a close mechanistic relationship to the decomposition of azo compounds. The *N*-nitrosoanilides rearrange to intermediates having a nitrogen-nitrogen double bond. The intermediate then decomposes to generate aryl and acyloxy radicals.<sup>30</sup>

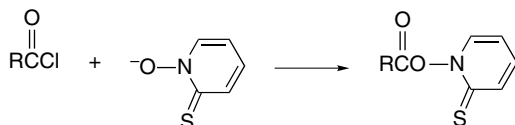


Triethylboron<sup>31</sup> and 9-borabicyclo[3.3.1]nonane<sup>32</sup> (9-BBN) are good radical sources for certain synthetic procedures. The reactions involve oxidation of the borane.



These initiators can be used in conjunction with stannanes and halides, as well as other reagents that undergo facile chain reactions. The reaction can be initiated at temperatures as low as  $-78^\circ\text{C}$ .<sup>33</sup>

The acyl derivatives of *N*-hydroxypyridine-2-thione are a versatile source of free radicals.<sup>34</sup> These compounds are readily prepared from reactive acylating agents, such as acyl chlorides, and a salt of the *N*-hydroxypyridine-2-thione.



Radicals react at the sulfur and decomposition ensues, generating an acyloxy radical. The acyloxy radical undergoes decarboxylation. Usually the radical then gives product and another radical that can continue a chain reaction. The process can be illustrated by the reactions with tri-*n*-butylstannane and bromoform.

<sup>29</sup> M. Schmittel and C. Rüchardt, *J. Am. Chem. Soc.*, **109**, 2750 (1987).

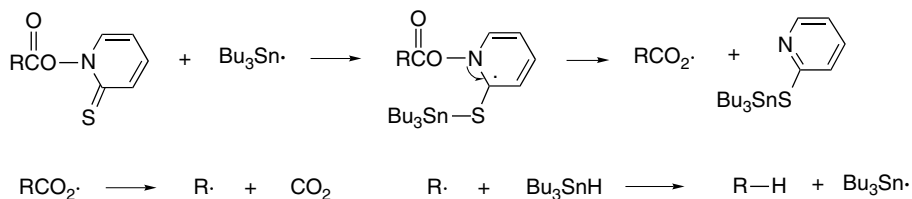
<sup>30</sup> C. Rüchardt and B. Freudenberg, *Tetrahedron Lett.*, 3623 (1964); J. I. G. Cadogan, *Acc. Chem. Res.*, **4**, 186 (1971).

<sup>31</sup> K. Nozaki, K. Oshima, and K. Utimoto, *J. Am. Chem. Soc.*, **109**, 2547 (1987).

<sup>32</sup> V. T. Perchyonok and C. H. Schiesser, *Tetrahedron Lett.*, **39**, 5437 (1998).

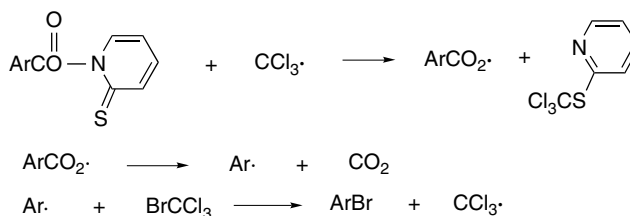
<sup>33</sup> K. Miura, Y. Ichinose, K. Nozaki, K. Fugami, K. Oshima, and K. Utimoto, *Bull. Chem. Soc. Jpn.*, **62**, 143 (1989).

<sup>34</sup> D. H. R. Barton, D. Crich, and W. B. Motherwell, *Tetrahedron*, **41**, 3901 (1985).

a. Reductive decarboxylation by reaction with tri-*n*-butylstannane.

Ref. 35

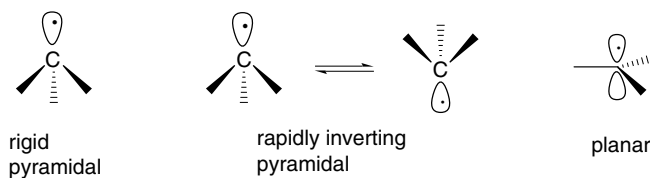
## b. Conversion of arenecarboxylic acid to aryl bromide by reaction with bromotrichloromethane.



Ref. 36

## 11.1.5. Structural and Stereochemical Properties of Free Radicals

ESR studies and other physical methods have provided insight into the geometry of free radicals.<sup>37</sup> Deductions about structure can also be drawn from the study of the stereochemistry of reactions involving radical intermediates. Several structural possibilities can be considered. If discussion is limited to alkyl radicals, the possibilities include a rigid pyramidal structure, rapidly inverting pyramidal structures, or a planar structure.



Precise description of the pyramidal structures also requires that the bond angles be specified. The ESR spectrum of the methyl radical leads to the conclusion that its structure could be either planar or a shallow pyramid with a very low barrier to inversion.<sup>38</sup> The IR spectrum of methyl radical at very low temperature in frozen argon puts a maximum of about 5° on the deviation from planarity.<sup>39</sup> A microwave study has also indicated the methyl radical is planar.<sup>40</sup> Various MO calculations indicate a planar structure.<sup>41</sup>

<sup>35</sup> D. H. R. Barton, D. Crich, and W. B. Motherwell, *J. Chem. Soc., Chem. Commun.*, 939 (1983).

<sup>36</sup> D. H. R. Barton, B. Lacher, and S. Z. Zard, *Tetrahedron Lett.*, **26**, 5939 (1985).

<sup>37</sup> For a review, see J. K. Kochi, *Adv. Free Radicals*, **5**, 189 (1975).

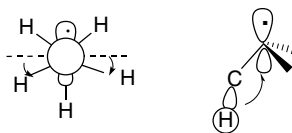
<sup>38</sup> M. Karplus and G. K. Fraenkel, *J. Chem. Phys.*, **35**, 1312 (1961).

<sup>39</sup> L. Andrews and G. C. Pimentel, *J. Chem. Phys.*, **47**, 3637 (1967).

<sup>40</sup> E. Hirota, *J. Phys. Chem.*, **87**, 3375 (1983).

<sup>41</sup> F. M. Bickelhaupt, T. Ziegler, and P. v. R. Schleyer, *Organometallics*, **15**, 1477 (1996).

Simple alkyl radicals are generally pyramidal, although the barrier to inversion is very small. According to MP2/6-311G\*\* and MM computations, substituted alkyl radicals become successively more pyramidal in the order ethyl < *i*-propyl < *t*-butyl.<sup>42</sup> The *t*-butyl radical has been studied extensively, and both experimental and theoretical calculations indicate a pyramidal structure.<sup>43</sup> The pyramidal geometry results from interaction of the SOMO and alkyl group hydrogens. There is a hyperconjugative interaction between the half-filled orbital and the hydrogen that is aligned with it. The pyramidalization also leads to a staggered conformation. The hyperconjugation is stronger in the conformation in which the pyramidalization is in the same direction as to minimize eclipsing.<sup>42a,44</sup> The C–H bonds *anti* to the unpaired electron are longer than those that are *gauche*. The *anti* hydrogens have maximum hyperconjugation with the orbital containing the unpaired electron and make a higher contribution to the SOMO orbital. There is also a shortening of the C–C bond, which is consistent with hyperconjugation.<sup>45</sup> Note that this hyperconjugative interaction accounts for the substantial hyperfine coupling with the  $\beta$ -H that was discussed in Section 11.1.3. The  $\beta$ -C–H bond is also greatly weakened by the hyperconjugation. MP4/6-311G(*d,p*) calculations assign a bond energy of only about 36 kcal/mol.<sup>46</sup>



hyperconjugation in pyramidal radicals

Radical geometry is also significantly affected by substituent groups that can act as  $\pi$  donors. Addition of a fluorine or oxygen substituent favors a pyramidal structure. Analysis of the ESR spectra of the mono-, di-, and trifluoromethyl radicals indicate a progressive distortion from planarity.<sup>43d,47</sup> Both ESR and IR studies of the trifluoromethyl radical show it to be pyramidal.<sup>48</sup> The basis of this structural effect has been probed by MO calculations and is considered to result from interactions of both the  $\sigma$  and  $\pi$  type. There is a repulsive interaction between the singly occupied  $p$  orbital and the filled orbitals occupied by unshared electrons on the fluorine or oxygen substituents. This repulsive interaction is reduced by adoption of a pyramidal geometry.

42. (a) J. Pacansky, W. Koch, and M. D. Miller, *J. Am. Chem. Soc.*, **113**, 317 (1991); (b) R. Liu and N. L. Allinger, *J. Comput. Chem.*, **15**, 283 (1994).

43. (a) D. E. Wood, C. F. Williams, R. F. Sprecher, and W. A. Lathan, *J. Am. Chem. Soc.*, **94**, 6241 (1972); (b) T. Koenig, T. Balle, and W. Snell, *J. Am. Chem. Soc.*, **97**, 662 (1975); (c) P. J. Krusic and P. Meakin, *J. Am. Chem. Soc.*, **98**, 228 (1976); (d) P. J. Krusic and R. C. Bingham, *J. Am. Chem. Soc.*, **98**, 230 (1976); (e) L. Bonazzola, N. Leray, and J. Roncin, *J. Am. Chem. Soc.*, **99**, 8348 (1977); (f) D. Griller, K. U. Ingold, P. J. Krusic, and H. Fischer, *J. Am. Chem. Soc.*, **100**, 6750 (1978); (g) J. Pacansky and J. S. Chang, *J. Phys. Chem.*, **74**, 5539 (1978); (g) B. Schrader, J. Pacansky, and U. Pfeiffer, *J. Phys. Chem.*, **88**, 4069 (1984).

44. M. N. Paddon-Row and K. N. Houk, *J. Am. Chem. Soc.*, **103**, 5046 (1981).

45. M. N. Paddon-Row and K. N. Houk, *J. Phys. Chem.*, **89**, 3771 (1985).

46. J. A. Seetula, *J. Chem. Soc., Faraday Trans.*, **94**, 1933 (1998).

47. F. Bernardi, W. Cherry, S. Shaik, and N. D. Epiotis, *J. Am. Chem. Soc.*, **100**, 1352 (1978).

48. R. W. Fessenden and R. H. Schuler, *J. Chem. Phys.*, **43**, 2704 (1965); G. A. Carlson and G. C. Pimentel, *J. Chem. Phys.*, **44**, 4053 (1966).

The tendency for pyramidal geometry is reinforced by an interaction between the  $p$  orbital on carbon and the  $\sigma^*$  antibonding orbitals associated with the C–F or C–O bonds. The interaction increases electron density on the more electronegative fluorine or oxygen atom. This stabilizing  $p$ - $\sigma^*$  interaction is increased by pyramidal geometry.



pyramidalization reduces electron-electron repulsion and enhances  $p$ - $\sigma^*$  interaction

Computations on the  $\text{FCH}_2\cdot$ ,  $\text{F}_2\text{CH}\cdot$ , and  $\text{F}_3\text{C}\cdot$  radicals indicate successively greater pyramidalization.<sup>49</sup> Chlorinated methyl radicals and mixed chlorofluoro radicals show the same trend toward increasing pyramidalization,<sup>50</sup> as illustrated in Figure 11.5.

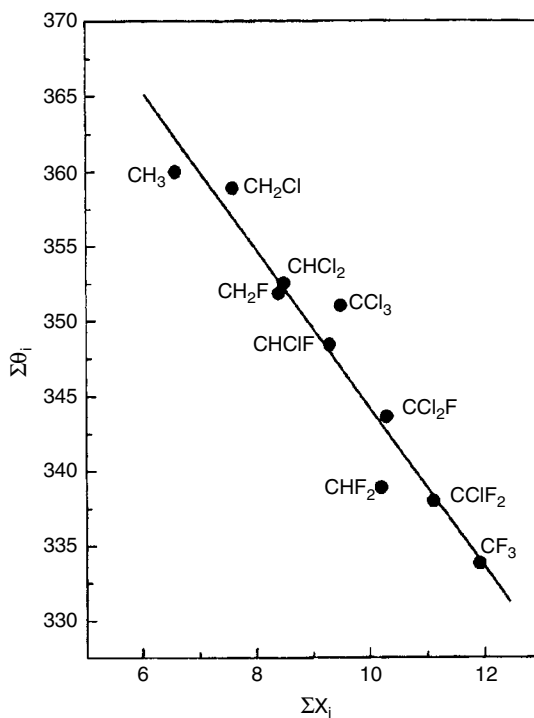


Fig. 11.5. Degree of pyramidalization of halogenated methyl radicals. The sum of the bond angles  $\Sigma\theta$  is plotted against the sum of the electronegativity ( $\Sigma\chi_i$ ) of the substituents.  $\Sigma\theta = 360^\circ$  for planar and  $323.7^\circ$  for tetrahedral geometry. Reproduced from *J. Chem. Phys.*, **118**, 557 (2003), by permission of the American Institute of Physics.

<sup>49</sup> Q.-S. Li, J.-F. Zhao, Y. Xie, and H. F. Schaefer, III, *Mol. Phys.*, **100**, 3615 (2002).

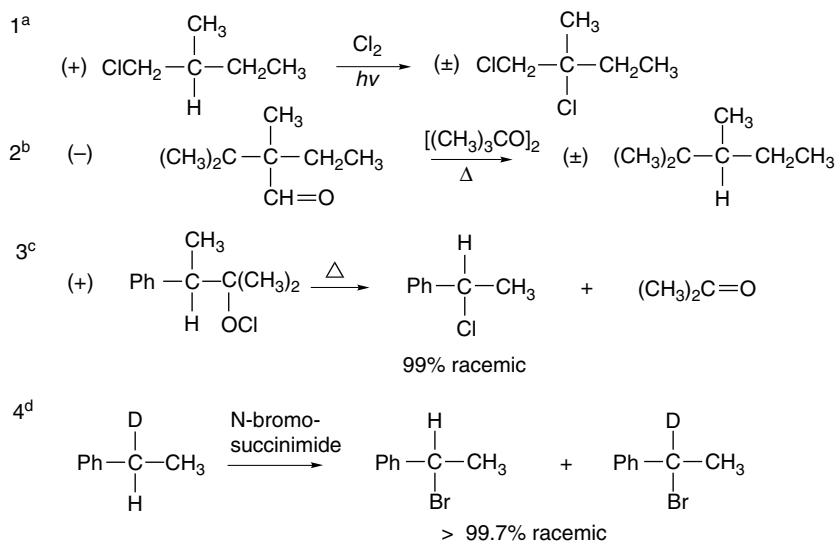
<sup>50</sup> M. Schwartz, L. R. Peebles, R. J. Berry, and P. Marshall, *J. Chem. Phys.*, **118**, 557 (2003).

There have been many studies aimed at deducing the geometry of radical sites by examining the stereochemistry of radical reactions. The most direct kind of study involves the generation of a radical at a carbon that is a stereogenic center. A planar or rapidly inverting radical leads to racemization, whereas a rigid pyramidal structure would lead to product of retained configuration. Some examples of reactions that have been subjected to this kind of study are shown in Scheme 11.2. In each case racemic product is formed, indicating that alkyl radicals do not retain the tetrahedral geometry of their precursors.

Entry 1 is a chlorination at a stereogenic tertiary center and proceeds with complete racemization. In Entry 2, a tertiary radical is generated by loss of  $C\equiv O$ , again with complete racemization. In Entry 3, an  $\alpha$ -methylbenzyl radical is generated by a fragmentation and the product is again racemic. Entry 4 involves a benzylic bromination by NBS. The chirality of the reactant results from enantiospecific isotopic labeling of ethylbenzene. The product, which is formed via an  $\alpha$ -methylbenzyl radical intermediate, is racemic.

Cyclic molecules permit deductions about stereochemistry without the necessity of using resolved chiral compounds. The stereochemistry of a number of reactions of 4-substituted cyclohexyl radicals has been investigated.<sup>51</sup> In general, reactions starting from pure *cis* or *trans* stereoisomers give mixtures of *cis* and *trans* products. This result indicates that the radical intermediates do not retain the stereochemistry of the precursor. Radical reactions involving *t*-butylcyclohexyl radicals are usually not very stereoselective, but some show a preference for formation of the *cis* product. This has been explained in terms of a torsional effect. The pyramidalization of the radical is

**Scheme 11.2. Stereochemistry of Radical Reactions at Stereogenic Carbon Centers**



a. H. C. Brown, M. S. Kharasch, and T. H. Chao, *J. Am. Chem. Soc.*, **62**, 3435 (1940).

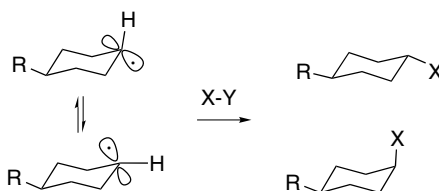
b. W. v. E. Doering, M. Farber, M. Sprecher, and K. B. Wiberg, *J. Am. Chem. Soc.*, **74**, 3000 (1952).

c. F. D. Greene, *J. Am. Chem. Soc.*, **81**, 2688 (1959); D. B. Denney and W. F. Beach, *J. Org. Chem.*, **24**, 108 (1959).

d. H. J. Dauben, Jr., and L. L. McCoy, *J. Am. Chem. Soc.*, **81**, 5404 (1959).

<sup>51</sup> F. R. Jensen, L. H. Gale, and J. E. Rodgers, *J. Am. Chem. Soc.*, **90**, 5793 (1968).

expected to be in the direction favoring axial attack.<sup>52</sup> Structural evidence suggests that the cyclohexyl radical is somewhat pyramidal with an equatorial hydrogen.<sup>53</sup> Equatorial attack leading to *trans* product causes the hydrogen at the radical site to become eclipsed with the two neighboring equatorial hydrogens. Axial attack does not suffer from this strain, since the hydrogen at the radical site moves away from the equatorial hydrogens toward the staggered conformation that is present in the chair conformation of the ring.

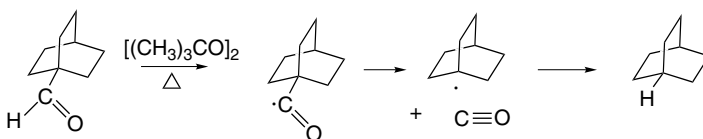


The inversion of the cyclohexyl radical can occur by a conformational process. This is expected to have a higher barrier than the radical inversion, since it involves bond rotations very similar to the ring inversion in cyclohexane. An  $E_a$  of 5.6 kcal/mol has been measured for the cyclohexyl radical.<sup>54</sup> A measurement of the rate of inversion of a tetrahydropyranyl radical ( $k = 5.7 \times 10^8 \text{ s}^{-1}$  at 22°C) has been reported.<sup>55</sup>



It can be concluded from these data that radical inversion is also fast in cyclic systems.

Another approach to obtaining information about the geometric requirements of free radicals has been to examine bridgehead systems. Recall that small bicyclic rings strongly resist formation of carbocations at bridgehead centers because the skeletal geometry prevents attainment of the preferred planar geometry. There is significant rate retardation for reactions in which the norbornyl radical is generated in a rate-determining step.<sup>56</sup> Typically, such reactions proceed 500 to 1000 times slower than the corresponding reaction generating the *t*-butyl radical. This is a much smaller rate retardation than the  $10^{-14}$  found in  $S_N1$  solvolysis (see p. 435). Rate retardation is still smaller for less strained bicyclic systems. The decarbonylation of less strained bridgehead aldehydes was found to proceed without special difficulty.<sup>57</sup>



<sup>52</sup> W. Damm, B. Giese, J. Hartung, T. Hasskerl, K. N. Houk, O. Huter, and H. Zipse, *J. Am. Chem. Soc.*, **114**, 4067 (1992).

<sup>53</sup> J. E. Freitas, H. J. Wang, A. B. Ticknor, and M. A. El-Sayed, *Chem. Phys. Lett.*, **183**, 165 (1991); A. Hudson, H. A. Hussain, and J. N. Murrell, *J. Chem. Soc., A*, 2336 (1968).

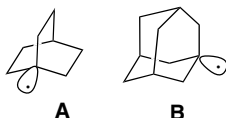
<sup>54</sup> B. P. Roberts and A. J. Steel, *J. Chem. Soc., Perkin Trans. 2*, 2025 (1992).

<sup>55</sup> A. J. Buckmelter, A. I. Kim, and S. D. Rychnovsky, *J. Am. Chem. Soc.*, **122**, 9386 (2000).

<sup>56</sup> A. Oberlinner and C. Rüchardt, *Tetrahedron Lett.*, 4685 (1969); L. B. Humphrey, B. Hodgson, and R. E. Pincock, *Can. J. Chem.*, **46**, 3099 (1968); D. E. Applequist and L. Kaplan, *J. Am. Chem. Soc.*, **87**, 2194 (1965).

<sup>57</sup> W. v. E. Doering, M. Farber, M. Sprecher, and K. B. Wiberg, *J. Am. Chem. Soc.*, **74**, 3000 (1952).

Conclusions about radical structure can also be drawn from analysis of ESR spectra. The ESR spectra of the bridgehead radicals **A** and **B** are consistent with pyramidal geometry at the bridgehead carbon atoms.<sup>58</sup>



The ESR spectra of a number of bridgehead radicals have been determined and the hyperfine couplings measured (see Section 11.1.3). Both the  $H_\alpha$  and  $^{13}\text{C}_\beta$  couplings are sensitive to the pyramidal geometry of the radical.<sup>59</sup> The reactivity of bridgehead radicals increases with increased pyramidal character.<sup>60</sup>

Radical	$H_\alpha$	$^{13}\text{C}_\beta$	$\Phi^a$
Adamantyl	6.58	132	113.6
Bicyclo[2.2.2]octyl	6.64	143	113.2
Bicyclo[2.2.1]heptyl	2.35	151	112.9
Bicyclo[2.1.1]hexyl	0	174	111.9
Bicyclo[1.1.1]pentyl	-1.2	223	110.3

a.  $\Phi$  = the C–C–C bond angle at the bridgedhead radical.

The broad conclusion of all these studies is that alkyl radicals except methyl are pyramidal, but the barrier to inversion is low. Radicals also are able to tolerate some geometric distortion associated with strained ring systems.

The allyl radical would be expected to be planar in order to maximize  $\pi$  delocalization. Structure parameters have been obtained from ESR, IR, and electron diffraction measurements and confirm that the radical is planar.<sup>61</sup> The vinyl radical,  $\text{CH}_2 = \text{CH}\cdot$ , is found by both experiment and theory to be bent with a C–C–H bond angle of about  $137^\circ$ .<sup>62</sup> Substituents affect the preferred geometry of vinyl radicals. Conjugation with  $\pi$ -acceptor substituents favors a linear geometry, whereas  $\sigma$ -donor substituents favor a bent geometry.<sup>63</sup> For  $\sigma$ -donors the barriers for isomerization are in the order  $\text{CH}_3(3.1) < \text{OH}(13.3) < \text{F}(19.5)$  kcal/mol, according to BLYP/6-311G(2d,2p) calculations. Although these barriers have not been measured experimentally, reaction stereoselectivity is in agreement with the results. For the  $\pi$ -acceptor substituents, the preferred geometry is one in which the substituent is aligned with the singly occupied  $p$  orbital, not the  $\pi$  bond.

<sup>58</sup> P. J. Krusic, T. A. Rettig, and P. v. R. Schleyer, *J. Am. Chem. Soc.*, **94**, 995 (1972).

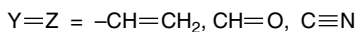
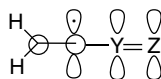
<sup>59</sup> C. J. Rhodes, J. C. Walton, and E. W. Della, *J. Chem. Soc., Perkin Trans. 2*, 2125 (1993); G. T. Binmore, J. C. Walton, W. Adcock, C. I. Clark, and A. R. Krstic, *Mag. Resonance Chem.*, **33**, Supplement S53 (1995).

<sup>60</sup> F. Recupero, A. Bravo, H. R. Bjorsvik, F. Fontana, F. Minisci, and M. Piredda, *J. Chem. Soc., Perkin Trans. 2*, 2399 (1997); K. P. Dockery and W. G. Bentrude, *J. Am. Chem. Soc.*, **119**, 1388 (1997).

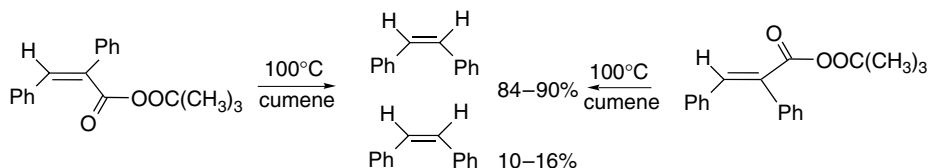
<sup>61</sup> R. W. Fessenden and R. H. Schuler, *J. Chem. Phys.*, **39**, 2147 (1963); A. K. Maltsev, V. A. Korolev, and O. M. Nefedov, *Izv. Akad. Nauk SSSR, Ser. Khim.*, 555 (1984); E. Vajda, J. Tremmel, B. Rozandai, I. Hargittai, A. K. Maltsev, N. D. Kagramanov, and O. M. Nefedov, *J. Am. Chem. Soc.*, **108**, 4352 (1986).

<sup>62</sup> J. H. Wang, H.-C. Chang, and Y.-T. Chen, *Chem. Phys.*, **206**, 43 (1996).

<sup>63</sup> C. Galli, A. Guarnieri, H. Koch, P. Mencarelli, and Z. Rappoport, *J. Org. Chem.*, **62**, 4072 (1997).

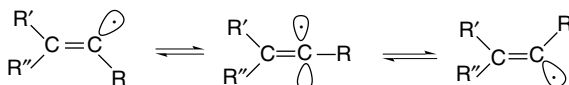


The stereochemistry of reactions involving substituted alkenyl free radicals indicates that radicals formed at trigonal centers rapidly undergo interconversion with the geometric isomer.<sup>64</sup> Reactions proceeding through alkenyl radical intermediates usually give rise to the same mixture from both the *E*- and *Z*-precursor. In the example given below, more *cis*- than *trans*-stilbene is formed, which is attributed to the steric effects of the  $\beta$ -phenyl group causing the H-abstraction to occur *anti* to the substituent.



Ref. 65

In this particular case, there is evidence from EPR spectra that the radical is not linear in its ground state, but is an easily inverted bent species.<sup>66</sup> The barrier to inversion is very low (0~2 kcal), so that the lifetime of the individual isomers is very short ( $\sim 10^{-9}$  s). The TS for inversion approximates *sp* hybridization.<sup>67</sup>



### 11.1.6. Substituent Effects on Radical Stability

The basic concepts of radical substituent effects were introduced in Section 3.4.1, where we noted that both donor and acceptor substituents can stabilize radicals. The extent of stabilization can be expressed in terms of the radical stabilization energy (RSE). The stabilization resulting from conjugation with unsaturated groups, such as in allyl and benzyl radicals, was also discussed. These substituent effects can sometimes cause synergistic stabilization. Allylic and benzylic radicals are also stabilized by both acceptor and donor substituents. Calculations at the AUMP2/6-31G\* level indicate that substituents at the 2-position are only slightly less effective than 1-substituents in the stabilization of allylic radicals (Table 11.1). This is somewhat surprising in that the SOMO has a node at the 2-position. However,  $\psi_1$  is also stabilized by interaction with the 2-substituent. Calculations have also been done on the stabilizing effect of *p*

<sup>64</sup> For reviews of the structure and reactivity of vinyl radicals, see W. G. Bentrude, *Annu. Rev. Phys. Chem.*, **18**, 283 (1967); L. A. Singer, in *Selective Organic Transformations*, Vol. II, B. S. Thyagarajan, ed., John Wiley, New York, 1972, p. 239; O. Simamura, *Top. Stereochem.*, **4**, 1 (1969).

<sup>65</sup> L. A. Singer and N. P. Kong, *J. Am. Chem. Soc.*, **88**, 5213 (1966); J. A. Kampmeier and R. M. Fantazier, *J. Am. Chem. Soc.*, **88**, 1959 (1966).

<sup>66</sup> R. W. Fessenden and R. H. Schuler, *J. Chem. Phys.*, **39**, 2147 (1963).

<sup>67</sup> P. R. Jenkins, M. C. R. Symons, S. E. Booth, and C. J. Swain, *Tetrahedron Lett.*, **33**, 3543 (1992).

**Table 11.1. Substituent Effects on the Stability of Allylic and Benzylic Radical from Calculation of Radical Stabilization Energy**

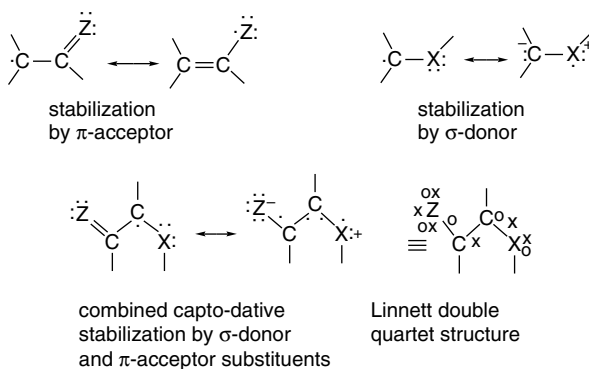
Substituent	Relative Stabilization in kcal/mol		
	Allylic <sup>a</sup>		Benzylic <sup>b</sup>
	1-position	2-position	<i>p</i> -position
H	0	0	0
CH <sub>3</sub>	5.6	4.3	0.3
CN	9.9	3.0	1.4
CH=O	11.7	11.6	
F	8.3	11.0	-0.1
HO	12.8	12.6	
CH <sub>3</sub> O			0.7
H <sub>2</sub> N	13.7	9.4	
(CH <sub>3</sub> ) <sub>2</sub> N			1.8

a. AUMP2/6-31G\* calculation from M. Lehd and F. Jensen, *J. Org. Chem.*, **56**, 884 (1991).

b. BLYP/6-31G\* calculations from Y.-D. Wu, C.-L. Wong, K. W. K. Chan, G.-Z. Ji, and X.-K. Jang, *J. Org. Chem.*, **61**, 746 (1996).

substituents on benzylic radicals, and the results indicate that both donor and acceptor substituents are stabilizing. The effects are greatly attenuated in the case of the benzyl substituents, owing to the leveling effect of the delocalization in the ring.

Radicals are particularly strongly stabilized when both an electron-attracting and an electron-donating substituent are present at the radical site. This has been called “*mero-stabilization*”<sup>68</sup> or “*capto-dative stabilization*,”<sup>69</sup> and results from mutual reinforcement of the two substituent effects.<sup>70</sup> The bonding in capto-dative radicals can be represented by resonance or Linnett-type structures (see p. 8).

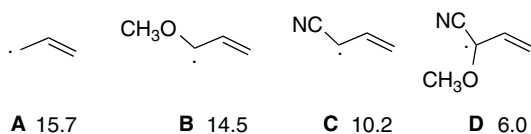


A comparison of the rotational barriers in allylic radicals **A** to **D** provides evidence for the stabilizing effect of the capto-dative combination.

<sup>68</sup> R. W. Baldock, P. Hudson, A. R. Katritzky, and F. Soti, *J. Chem. Soc., Perkin Trans. 1*, 1422 (1974).

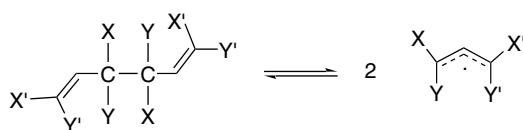
<sup>69</sup> H. G. Viehe, R. Merenyi, L. Stella, and Z. Janousek, *Angew. Chem. Int. Ed. Engl.*, **18**, 917 (1979).

<sup>70</sup> R. Sustmann and H.-G. Korth, *Adv. Phys. Org. Chem.*, **26**, 131 (1990).



The decreasing barrier at the formal single bond along the series **A** to **D** implies decreasing  $\pi$ -allyl character in this bond. The decrease in the importance of the  $\pi$  bonding in turn reflects a diminished degree of interaction of the radical center with the adjacent double bond. The fact that the decrease from **C**  $\rightarrow$  **D** is greater than for **A**  $\rightarrow$  **B** indicates a synergistic effect, as implied by the capto-dative formulation. The methoxy group is more stabilizing when it can interact with the cyano group than as an isolated substituent.<sup>71</sup>

The capto-dative effect has also been demonstrated by studying the bond dissociation process in a series of 1,5-dienes substituted at C(3) and C(4).



X	Y	X'	Y'	$\Delta H$
CO <sub>2</sub> R	CO <sub>2</sub> R	CO <sub>2</sub> R	CO <sub>2</sub> R	38.1
CO <sub>2</sub> R	CO <sub>2</sub> R	CO <sub>2</sub> R	OR'	28.2
CN	OR'	CN	OR'	24.5
CN	NR <sub>2</sub>	CN	NR <sub>2</sub>	8.1

When the combinations X,Y and X',Y' are of the capto-dative type, as is the case for an alkoxy and ester group, the enthalpy of bond dissociation is 10–15 kcal lower than when all four groups are electron attracting. When the capto-dative combination CN/NR<sub>2</sub> occupies both X,Y and X'Y' positions, the enthalpy for dissociation of the C(3)–C(4) bond is less than 10 kcal/mol.<sup>72</sup> Scheme 11.3 gives some information on the stability of other examples of this type of radical.

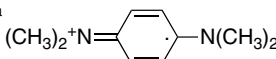
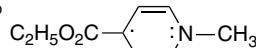
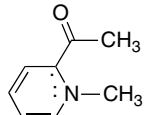
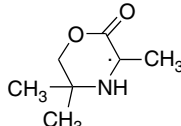
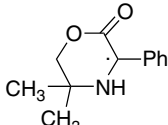
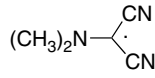
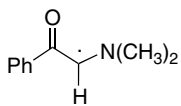
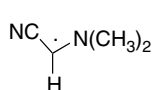
### 11.1.7. Charged Radicals

Unpaired electrons can be present in ions as well as in the neutral systems that have been considered up to this point. There are many such *radical cations* and *radical anions*, and we consider some representative examples in this section. Various aromatic and conjugated polyunsaturated hydrocarbons undergo one-electron reduction by alkali metals.<sup>73</sup> Benzene and naphthalene are examples. The ESR spectrum of the benzene radical anion was shown earlier in Figure 11.2a. These reductions must be carried out in aprotic solvents, and ethers are usually used for that purpose. The ease of formation of the radical anion increases as the number of fused rings increases. The electrochemical reduction potentials of some representative compounds are given in

<sup>71</sup> H.-G. Korth, P. Lommes, and R. Sustmann, *J. Am. Chem. Soc.*, **106**, 663 (1984).

<sup>72</sup> M. Van Hoecke, A. Borghese, J. Penelle, R. Merenyi, and H. G. Viehe, *Tetrahedron Lett.*, **27**, 4569 (1986).

<sup>73</sup> D. E. Paul, D. Lipkin, and S. I. Weissman, *J. Am. Chem. Soc.*, **78**, 116 (1956); T. R. Tuttle, Jr., and S. I. Weissman, *J. Am. Chem. Soc.*, **80**, 5342 (1958).

1 <sup>a</sup> 	Wurster's salts. Generated by one-electron oxidation of the corresponding diamine. Indefinitely stable to normal conditions.
2 <sup>b</sup> 	Generated by one-electron reduction of the corresponding pyridinium salt. Thermally stable to distillation and only moderately reactive toward oxygen.
3 <sup>c</sup> 	Stable to distillation. A small amount of the dimer is present in equilibrium with the radical.
4 <sup>d</sup> 	In equilibrium with the dimer Sensitive to oxygen.
5 <sup>e</sup> 	Generated by spontaneous dissociation of the dimer. Stable for several days at room temperature, but sensitive to oxygen.
6 <sup>f</sup> 	Generated spontaneously from dimethylamino-malonitrile at room temperature. Observed to be persistent over many hours by ESR.
7 <sup>g</sup> 	Radical stabilization energy of 19.6 kcal/mol implies about 10 kcal/mol of excess stabilization relative to the combined substituents. The CH-N(CH <sub>3</sub> ) <sub>2</sub> rotational barrier is >17 kcal/mol, indicating a strong resonance interaction.
8 <sup>h</sup> 	Synergistic stabilization of about 6.3 kcal/mol, based on thermodynamics of dimerization.

a. A. R. Forrester, J. M. Hay, and R. H. Thompson, *Organic Chemistry of Stable Free Radicals*, Academic Press, New York, 1968, pp. 254–261.

b. J. Hermolin, M. Levin, and E. M. Kosower, *J. Am. Chem. Soc.*, **103**, 4808 (1981).

c. J. Hermolin, M. Levin, Y. Ikegami, M. Sawayangai, and E. M. Kosower, *J. Am. Chem. Soc.*, **103**, 4795 (1981).

d. T. H. Koch, J. A. Oleson, and J. DeNiro, *J. Am. Chem. Soc.*, **97**, 7285 (1975).

e. J. M. Burns, D. L. Wharry, and T. H. Koch, *J. Am. Chem. Soc.*, **103**, 849 (1981).

f. L. de Vries, *J. Am. Chem. Soc.*, **100**, 926 (1978).

g. F. M. Welle, H.-D. Beckhaus, and C. Rüchardt, *J. Org. Chem.*, **62**, 552 (1997).

h. F. M. Welle, S. P. Verevkin, H.-D. Beckhaus and C. Rüchardt, *Liebigs Ann. Chem.*, 115 (1997).

Table 11.2. The potentials correlate with the energy of the LUMO as calculated by simple Hückel MO theory.<sup>74</sup> Note that polycyclic aromatics are easier both to reduce and to oxidize than benzene. This is because the HOMO-LUMO gap decreases with

<sup>74</sup> E. S. Pysh and N. C. Yang, *J. Am. Chem. Soc.*, **85**, 2124 (1963); D. Bauer and J. P. Beck, *Bull. Soc. Chim. Fr.*, 1252 (1973); C. Madec and J. Courtot-Coupez, *J. Electroanal. Chem. Interfacial Electrochem.*, **84**, 177 (1977).

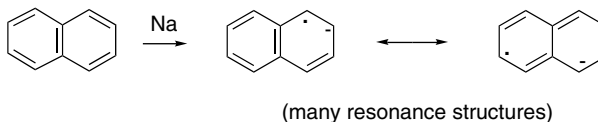
**Table 11.2. Oxidation and Reduction Potentials for Some Aromatic Hydrocarbons<sup>a</sup>**

Hydrocarbon	Ar-H $\rightarrow$ [Ar-H] <sup>-</sup>	Ar-H $\rightarrow$ [Ar-H] <sup>+</sup>
Benzene	-3.42 <sup>b</sup>	+2.06
Naphthalene	-2.95	+1.33
Phenanthrene	-2.87	+1.34
Anthracene	-2.36	+0.89
Tetracene	-1.92	+0.57

a. Except where noted otherwise, the data are from C. Madec and J. Courtot-Coupez, *J. Electroanal. Chem., Interfacial Electrochem.*, **84**, 177 (1977).

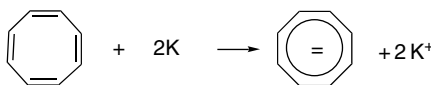
b. J. Mortensen and J. Heinze, *Angew. Chem. Int. Ed. Engl.* **13**, 84 (1984).

the size of the molecule, with the HOMO being higher in energy and the LUMO lower than in benzene. A correlation that includes a more extensive series of compounds can be observed using somewhat more sophisticated MO methods.<sup>75</sup>



In the presence of a proton source, the radical anion is protonated and further reduction occurs (Birch reduction; Part B, Section 5.6.2). In general, when no proton source is present, it is relatively difficult to add a second electron. Solutions of the radical anions of aromatic hydrocarbons can be maintained for relatively long periods in the absence of oxygen or protons.

Cyclooctatetraene provides a significant contrast to the preference of aromatic hydrocarbons for one-electron reduction. It is converted to a diamagnetic dianion by addition of two electrons.<sup>76</sup> It is easy to understand the ease with which the cyclooctatetraene radical accepts a second electron because of the aromaticity of the ten  $\pi$ -electron aromatic system that results (see Section 8.3).



Radical cations can be derived from aromatic hydrocarbons or alkenes by one-electron oxidation. Antimony trichloride and pentachloride are among the chemical oxidants that have been used.<sup>77</sup> Photodissociation or  $\gamma$ -radiation can generate radical cations from aromatic hydrocarbons.<sup>78</sup> Most radical cations derived from hydrocarbons

<sup>75</sup> C. F. Wilcox, Jr., K. A. Weber, H. D. Abruna, and C. R. Cabrera, *J. Electroanal. Chem. Interfacial Electrochem.*, **198**, 99 (1986).

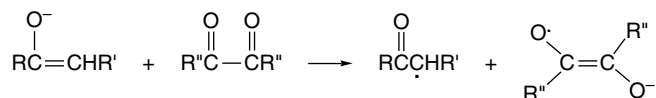
<sup>76</sup> T. J. Katz, *J. Am. Chem. Soc.*, **82**, 3784 (1960).

<sup>77</sup> I. C. Lewis and L. S. Singer, *J. Chem. Phys.*, **43**, 2712 (1965); R. M. Dessau, *J. Am. Chem. Soc.*, **92**, 6356 (1970).

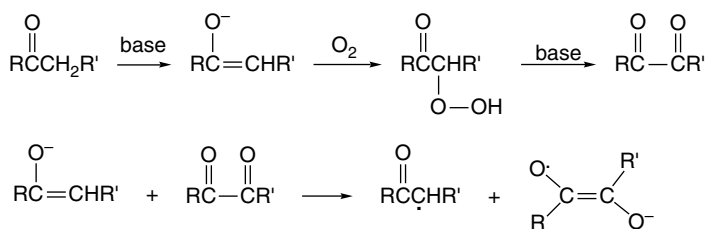
<sup>78</sup> R. Gschwind and E. Haselbach, *Helv. Chim. Acta*, **62**, 941 (1979); T. Shida, E. Haselbach, and T. Bally, *Acc. Chem. Res.*, **17**, 180 (1984); M. C. R. Symons, *Chem. Soc. Rev.*, **13**, 393 (1984).



Reductants such as zinc or sodium dithionite generate the semidiones from diketones. Electrolytic reduction can also be used. Enolates can reduce diones to semidiones by electron transfer.



The radicals that are formed from the enolate are rapidly destroyed so only the stable semidione radical remains detectable for ESR study. Semidiones can also be generated oxidatively from ketones by reaction with oxygen in the presence of base.<sup>82</sup>



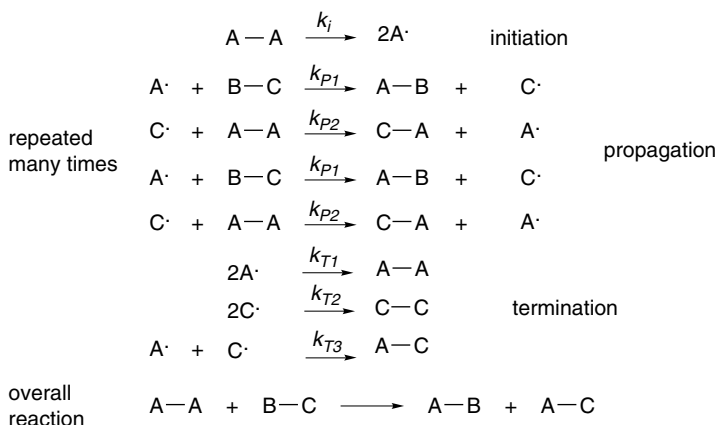
The diketone is presumably generated oxidatively and then reduced to the semidione via reduction by the enolate derived from the original ketone. The ESR spectra of semidione radical anions can provide information on the spin density at the individual atoms. The semidione derived from butane-2,3-dione, for example, has a spin density of 0.22 at each oxygen and 0.23 at each carbonyl carbon. The small amount of remaining spin density is associated with the methyl groups. This extensive delocalization is consistent with the resonance picture of the semidione radical anion.

## 11.2. Characteristics of Reactions Involving Radical Intermediates

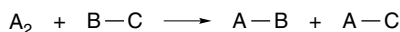
### 11.2.1. Kinetic Characteristics of Chain Reactions

Certain kinetic aspects of free radical reactions are unique in comparison with other reaction types that have been considered to this point. The underlying difference is that many free radical reactions are chain reactions. The reaction mechanism consists of a cycle of repetitive steps that form many product molecules for each initiation event. The hypothetical mechanism below illustrates a chain reaction.

<sup>82</sup> G. A. Russell and E. T. Strom, *J. Am. Chem. Soc.*, **86**, 744 (1964).



The step in which the radical intermediate, in this case  $A\cdot$ , is generated is called the *initiation step*. In the next four equations of the example, a sequence of two reactions is repeated; this is the *propagation phase*. Chain reactions are characterized by a *chain length*, which is the number of propagation steps that take place per initiation step. Finally, there are *termination steps*, which include all reactions that destroy one of the reactive intermediates necessary for the propagation of the chain. Clearly, the greater the frequency of termination steps, the smaller the chain length will be. The stoichiometry of a free radical chain reaction is independent of the initiating and termination steps because the reactants are consumed and products are formed almost entirely in the propagation steps.



The rate of a chain process is determined by the rates of initiation, propagation, and termination reactions. Analysis of the kinetics of chain reactions normally depends on application of the steady state approximation (see Section 3.2.3) to the radical intermediates. Such intermediates are highly reactive, and their concentrations are low and nearly constant through the course of the reaction. A result of the steady state condition is that the overall rate of initiation must equal the total rate of termination. The application of the steady state approximation and the resulting equality of the initiation and termination rates permits formulation of a rate law for the reaction mechanism above.

The overall reaction rate is given by

$$\text{Rate} = \frac{d[A-B]}{dt} = \frac{d[A-C]}{dt} = \frac{-d[A_2]}{dt} = \frac{-d[B-C]}{dt}$$

Setting the rate of initiation equal to the rate of termination and assuming that  $k_{t2}$  is the dominant termination process gives

$$k_i[A_2] = 2k_{t2}[C\cdot]^2$$

$$[C\cdot] = \left(\frac{k_i}{2k_{t2}}\right)^{1/2} [A_2]^{1/2}$$

Termination reactions involving coupling or disproportionation of two radicals ordinarily occurs at diffusion-controlled rates. Since the concentration of the reactive

intermediates is very low and these steps involve the reactants, which are present at much higher concentrations, the overall rate of termination is low enough that the propagation steps can compete. The rate of the overall reaction is that of either propagation step:

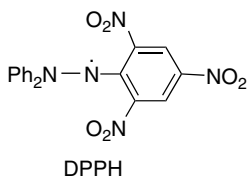
$$\text{Rate} = k_{p2}[\text{C}\cdot][\text{A}_2] = k_{p1}[\text{A}\cdot][\text{B} - \text{C}]$$

After the steady state approximation, both propagation steps must proceed at the same rate or the concentration of  $\text{A}\cdot$  or  $\text{C}\cdot$  would build up. By substituting for the concentration of the intermediate  $\text{C}\cdot$ , we obtain

$$\text{Rate} = k_{p2} \left( \frac{k_i}{2k_{t2}} \right)^{1/2} [\text{A}_2]^{3/2} = k_{\text{obs}}[\text{A}_2]^{3/2}$$

The observed rate law is then three-halves order in the reagent  $\text{A}_2$ . In most real systems, the situation is somewhat more complicated because more than one termination reaction makes a contribution to the total termination rate. A more complete discussion of the effect of termination steps on the form of the rate law is given by Huyser.<sup>83</sup>

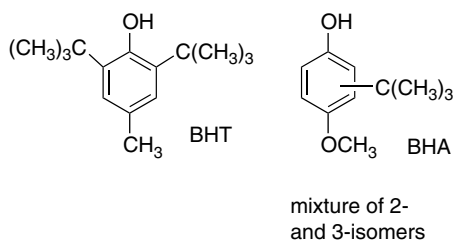
The overall rates of chain reactions can be greatly modified by changing the rate at which initiation or termination steps occur. The idea of initiation was touched on in Section 11.1.4, where sources of free radicals were discussed. Many radical reactions of interest in organic chemistry depend on the presence of an *initiator*, which serves as a source of free radicals to start chain sequences. Peroxides are frequently used as initiators, since they give radicals by thermal decomposition at relatively low temperatures. Azo compounds are another very useful class of initiators, with azoisobutyronitrile, AIBN, being the most commonly used compound. Initiation by irradiation of a photosensitive compound that generates radical products is also a common procedure. Conversely, chain reactions can be retarded by *inhibitors*. A compound can act as an inhibitor if it is sufficiently reactive toward a radical involved in the chain process that it effectively traps the radical, thus terminating the chain. Certain stable free radicals, for example, galvinoxyl (Scheme 11.1, Entry 6) and the hydrazinyl radical diphenylpicrylhydrazyl (DPPH) are used in this way. As they contain an unpaired electron, they are usually very reactive toward radical intermediates. The sensitivity of the rates of free radical chain reactions to both initiators and inhibitors can be used in mechanistic studies to distinguish radical chain reactions from polar or concerted processes.



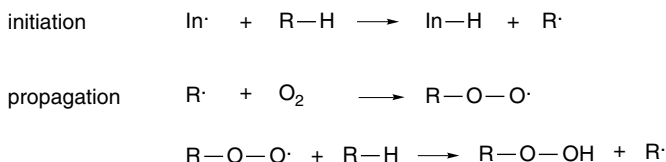
Free radical chain inhibitors are of considerable economic importance. The term *antioxidant* is commonly applied to inhibitors that retard the free radical chain oxidations that can cause deterioration of many commercial materials derived from organic molecules, including foodstuffs, petroleum products, and plastics. The substituted

<sup>83</sup> E. S. Huyser, *Free Radical Chain Reactions*, Wiley-Interscience, New York, 1970, pp. 39–54.

phenols BHT, “butylated hydroxytoluene,” and BHA, “butylated hydroxyanisole,” are used in many commercial foodstuffs.



The chain mechanism for autoxidation of hydrocarbons is:



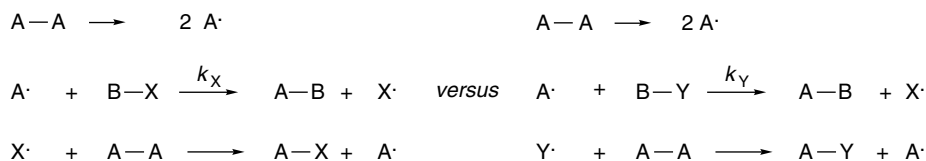
The function of an antioxidant is to divert the peroxy radicals and thus prevent a chain process. The hydroperoxides generated by autoxidation are themselves potential chain initiators, so autoxidations have the potential of being autocatalytic. Some antioxidants function by reducing hydroperoxides and thereby preventing their accumulation. Other antioxidants function by reacting with potential initiators, and retard oxidative degradation by preventing the initiation of autoxidation chains.

The presence of oxygen can modify the course of a free radical chain reaction if a radical intermediate is diverted by reaction with molecular oxygen. The oxygen molecule, with its two unpaired electrons, is extremely reactive to most free radical intermediates. The product that is formed is a reactive peroxy radical that can propagate a chain reaction leading to oxygen-containing products:



### 11.2.2. Determination of Reaction Rates

Structure-reactivity relationships can be probed by measurements of rates and equilibria, as was discussed in Chapter 3. Direct comparison of reaction rates is used relatively less often in the study of radical reactions than for heterolytic reactions. Instead, *competition methods* have frequently been used. The basis of a competition method lies in the rate expression for a reaction, and the results can be just as valid a comparison of relative reactivity as directly measured rates, *provided the two competing processes are of the same kinetic order*. Suppose we want to compare the reactivity of two related compounds, B-X and B-Y, in a hypothetical sequence:



The data required are the relative magnitudes of  $k_x$  and  $k_y$ . When both B–X and B–Y are present in the reaction system, they will be consumed at rates that are a function of their reactivity and concentration.

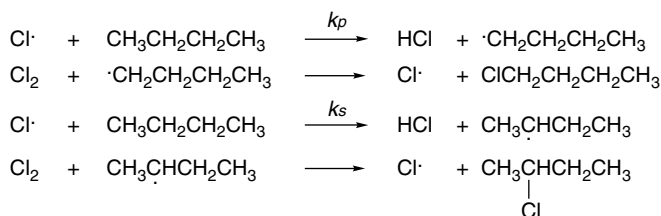
$$\begin{aligned}\frac{-d[\text{B}-\text{X}]}{dt} &= k_x[\text{A}\cdot][\text{B}-\text{X}] \\ \frac{-d[\text{B}-\text{Y}]}{dt} &= k_y[\text{A}\cdot][\text{B}-\text{Y}] \\ \frac{k_x}{k_y} &= \frac{d[\text{B}-\text{X}]/[\text{B}-\text{X}]}{d[\text{B}-\text{Y}]/[\text{B}-\text{Y}]}\end{aligned}$$

Integration of this expression with the limits  $[\text{B}-\text{X}] = [\text{B}-\text{X}]_{\text{in}}$  to  $[\text{B}-\text{X}]_t$ , where  $t$  is a point in time during the course of the reaction gives

$$\frac{k_x}{k_y} = \frac{\ln([\text{B}-\text{X}]_{\text{in}}/[\text{B}-\text{X}]_t)}{\ln([\text{B}-\text{Y}]_{\text{in}}/[\text{B}-\text{Y}]_t)}$$

This relationship permits the measurement of the ratio  $k_x/k_y$ . The initial concentrations  $[\text{B}-\text{X}]_{\text{in}}$  and  $[\text{B}-\text{Y}]_{\text{in}}$  are known from the conditions of the experiment. The reaction can be stopped at some point when some of both B–X and B–Y remain unreacted, or an excess of B–X and B–Y can be used so that neither is completely consumed when A–A has reacted completely. Determination of  $[\text{B}-\text{X}]_t$  and  $[\text{B}-\text{Y}]_t$  then provides the information needed to calculate  $k_x/k_y$ . It is clear that the reactions being compared must be of the same kinetic order. If they are not, division of the two rate expressions would leave uncanceled concentration terms.

Another experiment of the competition type involves the comparison of the reactivity of different atoms in the same molecule. For example, gas phase chlorination of butane can lead to 1- or 2-chlorobutane. The relative reactivity ( $k_p/k_s$ ) of the primary and secondary hydrogens is the sort of information that helps to characterize the details of the reaction process.



The value of  $k_p/k_s$  can be determined by measuring the ratio of the products 1-chlorobutane:2-chlorobutane during the course of the reaction. A statistical correction must be made to take account of the fact that the primary hydrogens outnumber the secondary ones by 3:2. This calculation provides the relative reactivity of chlorine atoms toward the primary and secondary hydrogens in butane:

$$\frac{k_p}{k_s} = \frac{2[1\text{-chlorobutane}]}{3[2\text{-chlorobutane}]}$$

Techniques for measuring the rates of very fast reactions have permitted absolute rates to be measured for fundamental types of free radical reactions.<sup>84</sup> Some examples

<sup>84</sup> M. Newcomb, *Tetrahedron*, **49**, 1151 (1993).

of absolute rates and  $E_a$  are given in Table 11.3. The examples include hydrogen abstraction (Section A), addition (Section B), ring closure and opening (Section C), and other types of reactions such as fragmentation and halogen atom abstraction (Section D). In the sections that follow, we discuss some of the reactivity relationships revealed by these data.

**Table 11.3. Absolute Rates for Some Free Radical Reactions<sup>a</sup>**

	Reaction	Rate/ $E_a$	Reference
A. Hydrogen abstraction reactions			
1	$\text{Ph}\cdot + \text{C}_4\text{H}_8\text{O} \longrightarrow \text{Ph-H} + \cdot\text{C}_4\text{H}_7\text{O}$	$4.8 \times 10^6 \text{ M}^{-1}\text{s}^{-1}$	b
2	$(\text{CH}_3)_3\text{CO}\cdot + (\text{CH}_3)_2\underset{\text{H}}{\text{C}}\text{Ph} \longrightarrow (\text{CH}_3)_3\text{COH} + (\text{CH}_3)_2\dot{\text{C}}\text{Ph}$	$8.7 \times 10^5 \text{ M}^{-1}\text{s}^{-1}$	c
3	$(\text{CH}_3)_3\text{CO}\cdot + \text{C}_4\text{H}_8\text{O} \longrightarrow (\text{CH}_3)_3\text{COH} + \cdot\text{C}_4\text{H}_7\text{O}$	$8.3 \times 10^6 \text{ M}^{-1}\text{s}^{-1}$	c
4	$\text{Cl}\cdot + \text{C}_5\text{H}_{10} \longrightarrow \text{H-Cl} + \cdot\text{C}_5\text{H}_9$ (free)	$4.7 \times 10^9 \text{ M}^{-1}\text{s}^{-1}$	d
5	$\text{Cl}\cdot + \text{C}_5\text{H}_{10} \longrightarrow \text{H-Cl} + \cdot\text{C}_5\text{H}_9$ (benzene complex)	$4.3 \times 10^7 \text{ M}^{-1}\text{s}^{-1}$	d
6	$\text{CH}_3\cdot + \text{Bu}_3\text{SnH} \longrightarrow \text{CH}_4 + \text{Bu}_3\text{Sn}\cdot$	$1.0 \times 10^7 \text{ M}^{-1}\text{s}^{-1}$ $E_a = 3.2 \text{ kcal/mol}$	e
7	$(\text{CH}_3)_3\text{C}\cdot + \text{Bu}_3\text{SnH} \longrightarrow (\text{CH}_3)_3\text{CH} + \text{Bu}_3\text{Sn}\cdot$	$1.8 \times 10^7 \text{ M}^{-1}\text{s}^{-1}$ $E_a = 2.95 \text{ kcal/mol}$	e
8	$\text{Ph}\cdot + \text{Bu}_3\text{SnH} \longrightarrow \text{C}_6\text{H}_6 + \text{Bu}_3\text{Sn}\cdot$	$7.8 \times 10^8 \text{ M}^{-1}\text{s}^{-1}$	f
9	$\text{CF}_3\text{CF}_2\text{CF}_2\cdot + \text{Bu}_3\text{SnH} \longrightarrow \text{CF}_3\text{CF}_2\text{CF}_2\text{H} + \text{Bu}_3\text{Sn}\cdot$	$2.0 \times 10^9 \text{ M}^{-1}\text{s}^{-1}$	g
10	$\text{PhCH}_2\cdot + \text{PhSH} \longrightarrow \text{PhCH}_3 + \text{PhS}\cdot$	$3.1 \times 10^5 \text{ M}^{-1}\text{s}^{-1}$	h
11	$\text{RCH}_2\cdot + (\text{CH}_3)_3\text{CSH} \longrightarrow \text{RCH}_3 + (\text{CH}_3)_3\text{CS}\cdot$	$8 \times 10^6 \text{ M}^{-1}\text{s}^{-1}$	i
12	$\text{Cyclopropyl-CH}_2\cdot + \text{PhSeH} \longrightarrow \text{Cyclopropyl-CH}_3 + \text{PhSe}\cdot$	$2.1 \times 10^9 \text{ M}^{-1}\text{s}^{-1}$	j
13	$(\text{CH}_3)_3\text{CC}=\text{O} + \text{Bu}_3\text{SnH} \longrightarrow (\text{CH}_3)_3\text{CCH}=\text{O} + \text{Bu}_3\text{Sn}\cdot$	$3.0 \times 10^5 \text{ M}^{-1}\text{s}^{-1}$	k
14	$\text{RC}=\text{O} + \text{Bu}_3\text{SnH} \longrightarrow \text{RCH}=\text{O} + \text{Bu}_3\text{Sn}\cdot$	$1.3 \times 10^6 \text{ M}^{-1}\text{s}^{-1}$	l
15	$\text{Ph}_2\text{C}=\dot{\text{C}}\text{Ph} + \text{Bu}_3\text{SnH} \longrightarrow \text{Ph}_2\text{C}=\text{CHPh} + \text{Bu}_3\text{Sn}\cdot$	$7.5 \times 10^8 \text{ M}^{-1}\text{s}^{-1}$	m
16	$\text{RCH}_2\cdot + [(\text{CH}_3)_3\text{Si}]_3\text{SiH} \longrightarrow \text{RCH}_3 + [(\text{CH}_3)_3\text{Si}]_3\text{Si}\cdot$	$1.0 \times 10^5 \text{ M}^{-1}\text{s}^{-1}$	n
17	$\text{Ph}_2\text{C}=\dot{\text{C}}\text{Ph} + [(\text{CH}_3)_3\text{Si}]_3\text{SiH} \longrightarrow \text{Ph}_2\text{C}=\text{CHPh} + [(\text{CH}_3)_3\text{Si}]_3\text{Si}\cdot$	$1.6 \times 10^9 \text{ M}^{-1}\text{s}^{-1}$	m
18	$\text{RC}=\text{O} + [(\text{CH}_3)_3\text{Si}]_3\text{SiH} \longrightarrow \text{RCH}=\text{O} + [(\text{CH}_3)_3\text{Si}]_3\text{Si}\cdot$	$1.0 \times 10^5 \text{ M}^{-1}\text{s}^{-1}$	l

(Continued)

Table 11.3. (Continued)

B. Additions to Alkenes and Aromatic Rings			
19	$\text{CH}_3\cdot + \text{H}_2\text{C}=\text{CHPh} \longrightarrow \text{CH}_3\text{CH}_2\dot{\text{C}}\text{HPh}$	$2.6 \times 10^5 \text{ M}^{-1}\text{s}^{-1}$ $E_a = 4.9 \text{ kcal/mol}$	o
20	$\text{CH}_3\cdot + \text{H}_2\text{C}=\text{CHCN} \longrightarrow \text{CH}_3\text{CH}_2\dot{\text{C}}\text{HCN}$	$6.1 \times 10^5 \text{ M}^{-1}\text{s}^{-1}$	o
21	$\text{CF}_3\cdot + \text{H}_2\text{C}=\text{CHPh} \longrightarrow \text{CF}_3\text{CH}_2\dot{\text{C}}\text{HPh}$	$5.3 \times 10^6 \text{ M}^{-1}\text{s}^{-1}$	p
22	$\text{Ph}\cdot + \text{CH}_2=\text{CHPh} \longrightarrow \text{PhCH}_2\dot{\text{C}}\text{HPh}$	$1.1 \times 10^8 \text{ M}^{-1}\text{s}^{-1}$	b
23	$\text{Ph}\cdot + \text{C}_6\text{H}_6 \longrightarrow \text{Ph-C}_6\text{H}_5\cdot$	$2.1 \times 10^7 \text{ M}^{-1}\text{s}^{-1}$	q
24	$\text{PhCH}_2\cdot + \text{H}_2\text{C}=\text{C}(\text{CH}_3)_2 \longrightarrow \text{PhCH}_2\text{CH}_2\dot{\text{C}}(\text{CH}_3)_2$	$18 \text{ M}^{-1}\text{s}^{-1}$	r
25	$(\text{CH}_3)_2\dot{\text{C}}\text{CN} + \text{CH}_2=\text{CHPh} \longrightarrow (\text{CH}_3)_2\text{C}(\text{CN})\dot{\text{C}}\text{H}_2\text{CHPh}$	$7.0 \times 10^4 \text{ M}^{-1}\text{s}^{-1}$ $E_a = 6.4 \text{ kcal/mol}$	s
26	$\text{CH}_3\cdot + \text{C}_6\text{H}_6 \longrightarrow \text{C}_6\text{H}_5\text{CH}_3$	$46 \text{ M}^{-1}\text{s}^{-1}$ $E_a = 8.9 \text{ kcal/mol}$	t
27	$\text{Ph}\cdot + \text{C}_6\text{H}_6 \longrightarrow \text{C}_6\text{H}_5\text{Ph}$	$4.5 \times 10^5 \text{ M}^{-1}\text{s}^{-1}$	b
28	$(\text{CH}_3)_3\text{CO}\cdot + \text{H}_2\text{C}=\text{CH}(\text{CH}_2)_5\text{CH}_3 \longrightarrow (\text{CH}_3)_3\text{COCH}_2\dot{\text{C}}\text{H}(\text{CH}_2)_5\text{CH}_3$	$1.5 \times 10^6 \text{ M}^{-1}\text{s}^{-1}$	c
29	$\text{PhS}\cdot + \text{CH}_2=\text{CHPh} \longrightarrow \text{PhSCH}_2\dot{\text{C}}\text{HPh}$	$2.0 \times 10^7 \text{ M}^{-1}\text{s}^{-1}$	u
C. Cyclization and Ring-Opening			
30	$\text{Cyclopropyl}\cdot \longrightarrow \text{propene}$	$9.4 \times 10^7 \text{ s}^{-1}$ $E_a = 7-7.5 \text{ kcal/mol}$	v
31	$\text{1,1-dimethylcyclopropyl}\cdot \longrightarrow \text{2-methylpropene}$	$1.8 \times 10^7 \text{ s}^{-1}$	w
32	$\text{Ph-CH=CH-CH}_2\cdot \xrightleftharpoons{K=80} \text{Ph-CH}_2\dot{\text{C}}\text{H-CH}_2\text{Cyclopropyl}$	$5.4 \times 10^6 \text{ s}^{-1}$	x
33	$\text{CH}_2=\text{CH-CH}_2\text{CH}_2\text{CH}_2\cdot \longrightarrow \text{cyclopentyl}\cdot$	$2.4 \times 10^5 \text{ s}^{-1}$ $E_a = 6.2 \text{ kcal/mol}$	e, y
34	$\text{X-CH}_2\text{CH}_2\text{CH}_2\text{CH}(\text{Ph})\cdot \longrightarrow \text{cyclopentane ring with Ph and X substituents}$	X = H $4 \times 10^7 \text{ s}^{-1}(20^\circ\text{C})$ X = CH <sub>3</sub> $2 \times 10^7 \text{ s}^{-1}(20^\circ\text{C})$ X = OCH <sub>3</sub> $4 \times 10^7 \text{ s}^{-1}(20^\circ\text{C})$ X = CO <sub>2</sub> C <sub>2</sub> H <sub>5</sub> $5.4 \times 10^7 \text{ s}^{-1}(20^\circ\text{C})$	z
35	$\text{Cyclohex-1-en-1-yl}\cdot \longrightarrow \text{bicyclic product}$	$4 \times 10^8 \text{ s}^{-1}$ $E_a = 3.6 \text{ kcal/mol}$	aa
36	$\text{Cyclohex-1-en-1-yl}\cdot \longrightarrow \text{bicyclic product}$	$1.5 \times 10^5 \text{ s}^{-1}$ $E_a = 7.3 \text{ kcal/mol}$	bb
37	$\text{Cyclohex-1-en-1-yl}\cdot \longrightarrow \text{bicyclic product}$	$2 \times 10^{-1} \text{ s}^{-1}$ $E_a = 16.3 \text{ kcal/mol}$	cc

(Continued)

Table 11.3. (Continued)

SECTION 11.2

Characteristics of  
Reactions Involving  
Radical Intermediates

38		$2.8 \times 10^4 \text{ s}^{-1}$ $E_a = 8.3 \text{ kcal/mol}$	dd
39		$4.2 \times 10^8 \text{ s}^{-1}$	ee
40		$1.4 \times 10^5 \text{ s}^{-1}$ $9.1 \times 10^7 \text{ s}^{-1}$ $E_a = 6.8 \text{ kcal/mol}$	ff
41		$2.5 \times 10^5 \text{ s}^{-1}$ $E_a = 5.4 \text{ kcal/mol}$	gg
D. Other Reactions			
42	$(\text{CH}_3)_3\text{C}\cdot + \text{O}_2 \longrightarrow (\text{CH}_3)_3\text{C}-\text{O}-\text{O}\cdot$	$4.9 \times 10^9 \text{ M}^{-1}\text{s}^{-1}$	gg
43	$\text{PhCH}_2\cdot + \text{O}_2 \longrightarrow \text{PhCH}_2-\text{O}-\text{O}\cdot$	$2.4 \times 10^9 \text{ M}^{-1}\text{s}^{-1}$	k
44		$4 \times 10^5 \text{ s}^{-1}$ 10.2 kcal/mol	hh
45	$(\text{CH}_3)_3\text{CC}=\text{O} \longrightarrow (\text{CH}_3)_3\text{C}\cdot + \text{C}\equiv\text{O}$	$3.0 \times 10^5 \text{ s}^{-1}$	ii
46	$\text{PhCH}_2\text{C}=\text{O} \longrightarrow \text{PhCH}_2\cdot + \text{C}\equiv\text{O}$	$5.2 \times 10^7 \text{ s}^{-1}$ $E_a = 7.2 \text{ kcal/mol}$	jj
47		$5.2 \times 10^5 \text{ s}^{-1}$ $E_a = 10.0 \text{ kcal/mol}$	aa
48		$11 \times 10^7 \text{ s}^{-1}$	kk
49	$\text{PhC}(\text{CH}_3)_2\text{O}\cdot \longrightarrow \text{PhC}(\text{O})\text{CH}_3 + \text{CH}_3\cdot$	$7 \times 10^5 \text{ s}^{-1}$	ll
50	$\text{Ph}\cdot + \text{CCl}_4 \longrightarrow \text{PhCl} + \cdot\text{CCl}_3$	$2.3 \times 10^6 \text{ M}^{-1}\text{s}^{-1}$	kk
51	$\text{CH}_3(\text{CH}_2)_3\cdot + \text{BrCCl}_3 \longrightarrow \text{CH}_3(\text{CH}_2)_3\text{Br} + \cdot\text{CCl}_3$	$2.6 \times 10^8 \text{ M}^{-1}\text{s}^{-1}$ (80°C)	mm
52	$\text{Ph}\cdot + \text{BrCCl}_3 \longrightarrow \text{PhBr} + \cdot\text{CCl}_3$	$1.6 \times 10^9 \text{ M}^{-1}\text{s}^{-1}$	nn
53	$\text{CH}_2=\text{CHCH}_2\cdot + \text{ClOC}(\text{CH}_3)_3 \longrightarrow \text{CH}_2=\text{CHCH}_2\text{Cl} + (\text{CH}_3)_3\text{CO}\cdot$	$2.6 \times 10^9 \text{ M}^{-1}\text{s}^{-1}$	nn
54	$\text{C}_8\text{H}_{19}\cdot + \text{PhSeCH}_2\text{CO}_2\text{C}_2\text{H}_5 \longrightarrow \text{C}_8\text{H}_{19}\text{SePh} + \cdot\text{CH}_2\text{CO}_2\text{C}_2\text{H}_5$	$1.0 \times 10^5 \text{ M}^{-1}\text{s}^{-1}$	oo
55	$\text{C}_8\text{H}_{19}\cdot + \text{PhSeC}(\text{CO}_2\text{C}_2\text{H}_5)_2 \longrightarrow \text{C}_8\text{H}_{19}\text{SePh} + \text{CH}_3\text{C}(\text{CO}_2\text{C}_2\text{H}_5)_2$	$8 \times 10^5 \text{ M}^{-1}\text{s}^{-1}$	oo

a. Unless otherwise noted, the rates are for temperatures near 25°C. The reference should be consulted for precise temperature and other conditions.

b. J. Scaiano and L. C. Stewart, *J. Am. Chem. Soc.*, **105**, 3609 (1983).

c. A. Baignee, J. A. Howard, J. C. Scaiano, and L. C. Stewart, *J. Am. Chem. Soc.*, **105**, 6120 (1983).

d. N. J. Bunce, K. U. Ingold, J. P. Landers, J. Luszyk, and J. Scaiano, *J. Am. Chem. Soc.*, **107**, 564 (1985).

e. C. Chatgililoglu, K. U. Ingold, and J. C. Scaiano, *J. Am. Chem. Soc.*, **103**, 7739 (1981).

f. S. J. Garden, D. V. Avila, A. L. J. Beckwith, V. W. Bowry, K. U. Ingold, and J. Luszyk, *J. Org. Chem.* **61**, 805 (1996).

g. D. V. Avila, K. U. Ingold, J. Luszyk, W. R. Dolbier, Jr., H.-Q. Pan and M. Muir, *J. Am. Chem. Soc.*, **116**, 99 (1994).

h. J. A. Franz, N. K. Suleman, and M. S. Alnajjar, *J. Org. Chem.*, **51**, 19 (1986).

i. M. Newcomb, A. G. Glenn, and M. B. Manek, *J. Org. Chem.*, **54**, 4603 (1989).

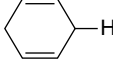
- j. M. Newcomb, T. R. Varick, C. Ha, B. Manek, and X. Yue, *J. Am. Chem. Soc.*, **114**, 8158 (1992).  
k. C. E. Brown, A. G. Neville, D. M. Raynner, K. U. Ingold, and J. Luszytk, *Aust. J. Chem.*, **48**, 363 (1995).  
l. C. Chatgililoglu and M. Lucarini, *Tetrahedron Lett.*, **36**, 1299 (1995).  
m. B. Branchi, C. Galli, and P. Gentili, *Eur. J. Org. Chem.*, 2844 (2002).  
n. C. Chatgililoglu, J. Dickhaut, and B. Giese, *J. Org. Chem.*, **56**, 6399 (1991).  
o. T. Zytowski and H. Fischer, *J. Am. Chem. Soc.*, **118**, 437 (1996).  
p. D. V. Avila, K. U. Ingold, J. Luszytk, W. R. Dolbier, Jr., and H.-Q. Pan, *Tetrahedron*, **52**, 12351 (1996).  
q. D. Weldon, S. Holland, and J. C. Scaiano, *J. Org. Chem.*, **61**, 8544 (1996).  
r. K. Heberger, M. Walbinder, and H. Fischer, *Angew. Chem. Int. Ed. Engl.* **31**, 635 (1992).  
s. K. Heberger and H. Fischer, *Int. J. Chem. Kinet.*, **25**, 249 (1993).  
t. T. Zytowski and H. Fischer, *J. Am. Chem. Soc.*, **119**, 12869 (1997).  
u. O. Ito, S. Tamura, K. Murakami, and M. Matsuda, *J. Org. Chem.*, **53**, 4758 (1988).  
v. M. Mewcomb and A. G. Glenn, *J. Am. Chem. Soc.*, **111**, 275 (1989); A. L. J. Beckwith and V.W. Bowry, *J. Org. Chem.*, **54**, 2681 (1989); V. W. Bowry, J. Luszytk, and K. U. Ingold, *J. Am. Chem. Soc.*, **113**, 5687 (1991).  
w. P. S. Engel, S.-L. He, J. T. Banks, K. U. Ingold, and J. Luszytk, *J. Org. Chem.*, **62**, 1210 (1997).  
x. T. A. Halgren, J. D. Roberts, J. H. Horner, F. N. Martinez, C. Tronche, and M. Newcomb, *J. Am. Chem. Soc.*, **122**, 2988 (2000).  
y. A. L. J. Beckwith, C. J. Easton, T. Lawrence, and A. K. Serelis, *Aust. J. Chem.* **36**, 545 (1983).  
z. C. Ha, J. H. Horner, M. Newcomb, T. R. Varick, B. R. Arnold, and J. Luszytk, *J. Org. Chem.*, **58**, 1194 (1993); M. Newcomb, J. H. Horner, M. A. Filipowski, C. Ha, and S.-U. Park, *J. Am. Chem. Soc.*, **117**, 3674 (1995).  
aa. L. J. Johnson, J. Luszytk, D. D. M. Wayner, A. N. Abeywickreyma, A. L. J. Beckwith, J. C. Scaiano, and K. U. Ingold, *J. Am. Chem. Soc.*, **107**, 4594 (1985).  
bb. J. A. Franz, R. D. Barrows, and D. M. Camaioni, *J. Am. Chem. Soc.*, **106**, 3964 (1984).  
cc. J. A. Franz, M. S. Alnajjar, R. D. Barrows, D. L. Kaisaki, D. M. Camaioni, and N. K. Suleman, *J. Org. Chem.*, **51**, 1446 (1986).  
dd. A. L. J. Beckwith and C. H. Schiesser, *Tetrahedron Lett.*, **26**, 373 (1985).  
ee. A. Annunziata, C. Galli, M. Marinelli, and T. Pau, *Eur. J. Org. Chem.* 1323 (2001).  
ff. A. L. J. Beckwith and B. P. Hay, *J. Am. Chem. Soc.*, **111**, 230 (1989).  
gg. A. L. J. Beckwith and B. P. Hay, *J. Am. Chem. Soc.*, **111**, 2674 (1989).  
hh. H. Misawa, K. Sawabe, S. Takahara, H. Sakuragi, and K. Tokumaru, *Chem. Lett.*, 357 (1988).  
ii. B. Maillard, K. U. Ingold, and J. C. Scaiano, *J. Am. Chem. Soc.*, **105**, 5095 (1983).  
jj. C. Chatgililoglu, C. Ferreri, M. Lucarini, P. Pedrielli, and G. Pedulli, *Organometallics*, **14**, 2672 (1995); O. A. Kurnysheva, N. P. Gritsan, and Y. P. Tsentlovich, *Phys. Chem. Chem. Phys.*, **3**, 3677 (2001).  
kk. R. Han and H. Fischer, *Chem. Phys.*, **172**, 131 (1993).  
ll. E. Baciocchi, M. Bietti, M. Salamone, and S. Steenken, *J. Org. Chem.*, **67**, 2266 (2002).  
mm. L. Mathew and J. Warkentin *Can. J. Chem.*, **66**, 11 (1988).  
nn. J. M. Tanko and J. F. Blackert, *J. Chem. Soc., Perkin Trans. 2*, 1175 (1996).  
oo. D. P. Curran, A. A. Martin-Esker, S.-B. Ko, and M. Newcomb, *J. Org. Chem.*, **58**, 4691 (1993).

### 11.2.3. Structure-Reactivity Relationships

**11.2.3.1. Hydrogen Abstraction Reactions** In hydrogen atom abstraction reactions, the strength of the bond to the reacting hydrogen is a major determinant of the rate at which reaction occurs. Table 11.4 gives some bond dissociation energies (BDE) that are particularly relevant to free radical reactions.

Generally, the ease of hydrogen atom abstraction parallels the BDE. Several of the trends, such as those for hydrocarbons and alkyl halides were discussed in Sections 3.1.2 and 3.4.3. The general tendency for functional groups to weaken  $\alpha$ -CH bond is illustrated by the values for methanol, diethyl ether, acetone, and acetonitrile. The bond order relationship  $\text{Si-H} > \text{Ge-H} > \text{Sn-H}$  is particularly important in free radical chemistry. Entries 16 and 18 in Table 11.3 provide abstraction rates for silanes. The comparison between Entries 6 and 16 and 14 and 18 shows that silanes are somewhat less reactive than stannanes. Trisubstituted stannanes are among the most reactive hydrogen atom donors. As indicated by Entries 6 to 8, hydrogen abstractions from stannanes proceed with rates higher than  $10^7 \text{ M}^{-1}\text{s}^{-1}$  and have very low activation energies. This high reactivity correlates with the low bond strength of the Sn-H bond (78 kcal). For comparison, Entries 1 to 3 give the rates of hydrogen abstraction from two of the more reactive C-H hydrogen atom donors, tetrahydrofuran and isopropylbenzene. For the directly comparable reaction with the phenyl radical

Table 11.4. Selected Bond Dissociation Energies (kcal/mol)<sup>a</sup>

Bond	BDE	Bond	BDE
CH <sub>3</sub> -H	105.0	CH <sub>3</sub> S-H	87
CH <sub>3</sub> CH <sub>2</sub> -H	100.5	PhS-H	83
(CH <sub>3</sub> ) <sub>2</sub> CH-H	98.1	(CH <sub>3</sub> ) <sub>3</sub> Si-H	93
(CH <sub>3</sub> ) <sub>3</sub> C-H	95.7	(CH <sub>3</sub> ) <sub>3</sub> Ge-H	87
CH <sub>2</sub> =CH-H	111	(C <sub>4</sub> H <sub>9</sub> ) <sub>3</sub> Sn-H	78
	106		
	76	[CH <sub>3</sub> C(=O)O-] <sub>2</sub>	30
HOCH <sub>2</sub> -H	96	(CH <sub>3</sub> ) <sub>3</sub> CO-OH	44
C <sub>2</sub> H <sub>5</sub> OCH(CH <sub>3</sub> )-H	93	CH <sub>3</sub> S-SCH <sub>3</sub>	65
CH <sub>3</sub> C(=O)CH <sub>2</sub> -H	96	C <sub>2</sub> H <sub>5</sub> -F	113
N-CCH <sub>2</sub> -H	96	C <sub>2</sub> H <sub>5</sub> -Cl	84
F <sub>3</sub> C-H	107	C <sub>2</sub> H <sub>5</sub> -Br	70
Cl <sub>3</sub> C-H	94	C <sub>2</sub> H <sub>5</sub> -I	56
F-H	136	F-F	38
Cl-H	102	Cl-Cl	57
Br-H	87	Br-Br	45
I-H	71	I-I	36

SECTION 11.2

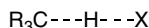
Characteristics of  
Reactions Involving  
Radical Intermediates

a. From Y.-R. Luo, *Bond Dissociation Energies of Organic Compounds*, CRC Press, Boca Raton, FL, 2003.

(Entries 1 and 8), tri-*n*-butylstannane is about 100 times more reactive than tetrahydrofuran as a hydrogen atom donor. Thiols are also quite reactive as hydrogen atom donors, as indicated by Entries 10 and 11. Phenylselenol is an even more reactive hydrogen atom donor than tri-*n*-butylstannane (see Entry 12).

Entries 4 and 5 point to another important aspect of free radical reactivity. The data given indicate that the observed reactivity of the chlorine atom is strongly influenced by the presence of benzene. Evidently a complex is formed that attenuates the reactivity of the chlorine atom. Another case is chlorination in bromomethene, where the *pri*:*sec*:*tert* selectivity increases to 1:8.8:38.<sup>85</sup> This is probably a general feature of radical chemistry, but there are relatively few data available on solvent effects on either absolute or relative reactivity of radical intermediates.

The TS for hydrogen atom abstraction is pictured as having the hydrogen partially bonded to the donor carbon and the abstracting radical. Generally, theoretical models of such reactions indicate a linear alignment, although there are exceptions:



The Bell-Evans-Polanyi relationship and the Hammond postulate (see Section 3.3) provide a basic framework within which to discuss structure-reactivity relationships. The Bell-Evans-Polanyi equation implies that there will be a linear relationship between  $E_a$  and the C-H BDE.

$$E_a = \alpha \Delta H_r + E_0 \quad (11.4)$$

<sup>85</sup>. A. Dneprovskii, D. V. Kuznetsov, E. V. Eliseenkov, B. Fletcher, and J. M. Tanko, *J. Org. Chem.*, **63** 8860 (1998).

$$E_a = \alpha(BDE) + \beta \quad (11.5)$$

We would therefore expect the  $E_a$  to decrease as the reacting C–H bond becomes weaker. The Hammond postulate relates position on the reaction coordinate to TS structure. Hydrogen atom abstractions with early TS will be reactant-like and those with late TS will be radical-like. We expect highly exothermic atom transfers to have early TSs and to be less sensitive to radical stability factors. Energy neutral reactions should have later TSs.

Table 11.5 summarizes some activation energies and relative reactivity data for some of the types of radicals that we are discussing, including alkyl, allyl, phenyl, benzyl, halomethyl, and hydroxyl radicals, and halogen atoms. These data provide confirmation of the widely recognized reactivity order *tert* > *sec* > *pri* for formation of alkyl radicals by hydrogen atom abstraction. They also provide some examples of the *reactivity-selectivity principle*, which is the premise that the most reactive radicals are the least selective and vice versa. The halogens are a familiar example of this idea. Chlorine atom selectivity is low, corresponding to very small  $E_a$  values and an early TS. Bromine, by contrast, has a significant  $E_a$  and is quite selective. The hydroxyl and alkoxy radicals are only modestly selective, whereas the  $\text{CF}_3\cdot$  and  $\text{CCl}_3\cdot$  radicals have higher  $E_a$  and greater selectivity.

Relative reactivity information such as that in Table 11.5 can be used in interpreting and controlling reactivity. For example, the high selectivity of the  $\text{CBr}_3\cdot$  and  $\text{CCl}_3\cdot$  is the basis for a recently developed halogenation procedure that is especially

**Table 11.5. Activation Energies (kcal/mol) and Approximate Selectivity Ratios for Hydrogen Atom Abstraction Reactions**

Radical	$\text{CH}_3\text{-H}$	$\text{CH}_3\text{CH}_2\text{-H}$	$(\text{CH}_3)_2\text{CH-H}$	$(\text{CH}_3)_3\text{C-H}$	$\text{PhCH}_2\text{-H}$	$\text{CH}_2=\text{CHCH}_2\text{-H}$	<i>pri:sec:tert</i>
$\text{CH}_3^{\cdot,a,b,c}$	14.0	11.6	9.6	8.1	9.5	7.7	1.0:4.8:61
$\text{C}_2\text{H}_5^{\cdot,d}$		13.3	11.4	10.0	9.3		
$(\text{CH}_3)_2\text{CH}^{\cdot,d}$				$10 \pm 2$			
$(\text{CH}_3)_3\text{C}^{\cdot,d}$				10.5	10.3		
$\text{Ph}^{\cdot,d,e,f}$	10.3	4.4		3.0	2.0		1:8.5:40
$\text{PhCH}_2^{\cdot,d}$					17.0		
$\text{HC}\equiv\text{C}^{\cdot,g}$	$\sim 2.5$	0	0	0			
$\text{CF}_3^{\cdot,a}$	10.9	8.0	6.5	4.9	5.8		
$\text{CCl}_3^{\cdot,c}$	17.9	14.2	10.6	7.7			
$\text{F}^{\cdot,c}$	1–1.5	< 1		< 1			
$\text{Cl}^{\cdot,c}$	3.4	1.1					1:2.8:2.1
$\text{Br}^{\cdot,g}$	17.5	13.0	9.5	6.9			1:250:6300
$\text{HO}^{\cdot,c}$	3.6	1.0	0.6	0.3			
$\text{CH}_3\text{O}^{\cdot,a}$	10.1	7.1		2.4			
$(\text{CH}_3)_3\text{CO}^{\cdot,c}$					3.5 <sup>h</sup>		1:12:50

a. B. P. Roberts and A. J. Steel, *J. Chem. Soc., Perkin Trans. 2*, 2155 (1994).

b. N. Kobko and J. J. Dannenberg, *J. Phys. Chem. A*, **105**, 1944 (2001).

c. A. A. Fokin and P. Schreiner, *Chem. Rev.*, **102**, 1551 (2002); see also P. A. Hooshiyar and H. Niki, *Int. J. Chem. Kinetics*, **27**, 1197 (1995).

d. A. A. C. C. Pais, L. G. Armut, and S. J. Formosinho, *J. Chem. Soc., Perkin Trans. 2*, 2577 (1998).

e. J. Park, D. Chakraborty, D. M. Bhusari, and M. C. Lin, *J. Phys. Chem. A*, **103**, 4002 (1999). T. Yu and M. C. Lin, *J. Phys. Chem.*, **99**, 8599 (1995).

f. B. Ceursters, H. M. T. Nguyen, J. Peeters and M. T. Nguyen, *Chem. Phys. Lett.*, **329**, 412 (2000). R. J. Hoobler, B. J. Opansky, and S. R. Leone, *J. Phys. Chem. A*, **101**, 1338 (1997). J. Parks, S. Gheyas, and M. C. Lin, *Int. J. Chem. Kinetics*, **33**, 64 (2001).

g. A. F. Trotman-Dickenson, *Adv. Free Radical Chem.*, **1**, 1 (1965).

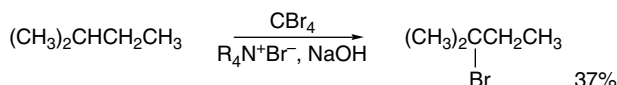
h. M. Finn, R. Friedline, N. K. Suleman, G. J. Wohl, and J. M. Tanko, *J. Am. Chem. Soc.*, **126**, 7578 (2004).

applicable to polycyclic hydrocarbons such as cubane, which do not react cleanly by direct halogenation. The reactions are carried out under phase transfer conditions using  $\text{CBr}_4$  or  $\text{CCl}_4$  as the halogen source and the  $\text{CBr}_3\cdot$  and  $\text{CCl}_3\cdot$  as the chain carriers. The reactions are initiated by electron transfer from hydroxide ion.

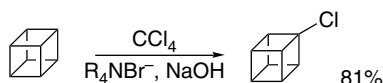
Initiation



Propagation

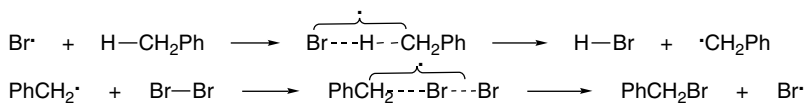


Ref. 86



Ref. 87

Many free radical reactions respond to introduction of polar substituents, just as do heterolytic processes that involve polar or ionic intermediates. The case of toluene bromination can be used to illustrate this point.



The substituent effects on toluene bromination are correlated by the Hammett equation, which gives a  $\rho$  value of  $-1.4$ , indicating that the benzene ring acts as an electron donor in the TS.<sup>88</sup> Other radicals, for example, the *t*-butyl radical, show a positive  $\rho$  for hydrogen abstraction reactions involving toluene,<sup>89</sup> which indicates that radicals can exhibit either electrophilic or nucleophilic character. Why do free radical reactions involving neutral reactants and intermediates respond to substituent changes that modify electron distribution? One explanation is based on the idea that there is some polar character in the TS because of the electronegativity differences of the reacting atoms.<sup>90</sup>



<sup>86</sup> P. R. Schreiner, O. Lauenstein, I. V. Kolomitsyn, S. Nadi, and A. A. Fokin, *Angew. Chem. Int. Ed. Engl.*, **37**, 1895 (1998).

<sup>87</sup> A. A. Fokin, O. Lauenstein, P. A. Gunchenko, and P. R. Schreiner, *J. Am. Chem. Soc.*, **123**, 1842 (2001).

<sup>88</sup> J. Hradil and V. Chvalovsky, *Collect. Czech. Chem. Commun.*, **33**, 2029 (1968); S. S. Kim, S. Y. Choi, and C. H. Kong, *J. Am. Chem. Soc.*, **107**, 4234 (1984); G. A. Russell, C. DeBoer, and K. M. Desmond, *J. Am. Chem. Soc.*, **85**, 365 (1963); C. Walling, A. L. Rieger, and D. D. Tanner, *J. Am. Chem. Soc.*, **85**, 3129 (1963).

<sup>89</sup> W. A. Pryor, F. Y. Tang, R. H. Tang, and D. F. Church, *J. Am. Chem. Soc.*, **104**, 2885 (1982); R. W. Henderson and R. O. Ward, Jr., *J. Am. Chem. Soc.*, **96**, 7556 (1974); W. A. Pryor, D. F. Church, F. Y. Tang, and R. H. Tang, *Frontiers of Free Radical Chemistry*, W. A. Pryor, ed., Academic Press, New York, 1980, pp. 355–380.

<sup>90</sup> E. S. Huyser, *Free Radical Chain Reactions*, Wiley-Interscience, New York, 1970, Chap. 4; G. A. Russell, in *Free Radicals*, Vol. 1, J. Kochi, ed., Wiley, New York, 1973, Chap. 7.

This idea receives support from the fact that the most negative  $\rho$  values are found for more electronegative radicals such as  $\text{Br}\cdot$ ,  $\text{Cl}\cdot$ , and  $\text{Cl}_3\text{C}\cdot$ . There is, however no simple correlation with a single property and this probably reflects the fact that the *selectivity* of the radicals is also different. Furthermore, in hydrogen abstraction reactions, where many of the quantitative measurements have been done, the C–H bond dissociation energy is also subject to a substituent effect.<sup>91</sup> Thus the extent of bond cleavage and formation at the TS may be different for various radicals. Successful interpretation of substituent effects in radical reactions therefore requires consideration of factors such as the electronegativity and polarizability of the radicals as well as the bond energy of the reacting C–H bond. The relative importance of these effects may vary from system to system. As a result, substituent effect trends in radical reactions can appear to be more complicated than those for heterolytic reactions, where substituent effects are usually dominated by the electron-releasing or electron-donating capacity of the substituent.<sup>92</sup>

*11.2.3.2. Addition Reactions* Section B of Table 11.3 gives some rates of addition reactions involving carbon-carbon double bonds and aromatic rings. Comparison of Entries 23 and 24 shows that the phenyl radical is much more reactive toward addition to alkenes than the benzyl radical. Comparison of Entries 26 and 27 shows the same effect on additions to an aromatic ring. Delocalized benzyl and cumyl radicals have somewhat reduced reactivity.<sup>93</sup> Additions to aromatic rings are much slower than additions to alkenes (compare Entries 23 and 27). This kinetic relationship shows that it is more difficult to disrupt an aromatic ring than an alkene  $\pi$  bond.

Despite their overall electrical neutrality, carbon-centered radicals can show pronounced electrophilic or nucleophilic character, depending on the substituents present.<sup>94</sup> This electrophilic or nucleophilic character is reflected in rates of reaction with nonradical species, for example, in additions to substituted alkenes. Alkyl radicals and  $\alpha$ -alkoxyalkyl radicals are distinctly nucleophilic in character and react most rapidly with alkenes having EWG substituents. Even methyl radicals with a single EWG, such as *t*-butoxycarbonyl or cyano are weakly nucleophilic.<sup>95</sup> Radicals having two EWGs, such as those derived from malonate esters, react preferentially with double bonds having ERG substituents.<sup>96</sup> Perfluoro radicals are electrophilic and are about  $10^3$  more reactive than alkyl radicals.<sup>97</sup>

These substituent effects are consistent with an FMO interpretation with a dominant SOMO-LUMO interaction.<sup>98</sup> As shown in Figure 11.6, ERG substituents will raise the energy of the radical SOMO and increase the strength of interaction with the relatively low-lying LUMO of alkenes having electron-withdrawing groups. When

<sup>91</sup> A. A. Zavitsas and J. A. Pinto, *J. Am. Chem. Soc.*, **94**, 7390 (1972); W. M. Nau, *J. Phys. Org. Chem.*, **10**, 445 (1997).

<sup>92</sup> W. H. Davis, Jr., and W. A. Pryor, *J. Am. Chem. Soc.*, **99**, 6365 (1972); W. H. Davis, Jr., J. H. Gleason, and W. A. Pryor, *J. Org. Chem.*, **42**, 7 (1977); W. A. Pryor, G. Gojon, and D. F. Church, *J. Org. Chem.*, **43**, 793 (1978).

<sup>93</sup> M. Walbiner, J. Q. Wu, and H. Fischer, *Helv. Chim. Acta*, **78**, 910 (1995).

<sup>94</sup> B. Giese, *Angew. Chem. Int. Ed. Engl.*, **22**, 753 (1983); H. Fischer and L. Radom, *Angew. Chem. Int. Ed. Engl.*, **40**, 1340 (2001).

<sup>95</sup> K. Heberger and A. Lopata, *J. Org. Chem.*, **63**, 8646 (1998).

<sup>96</sup> B. Giese, H. Horler, and M. Leising, *Chem. Ber.*, **119**, 444 (1986).

<sup>97</sup> D. V. Avila, K. U. Ingold, J. Luszytk, W. R. Dolbier, and H. Q. Pan, *J. Am. Chem. Soc.*, **115**, 1577 (1993).

<sup>98</sup> U. Berg, E. Butkus, and A. Stoncius, *J. Chem. Soc., Perkin Trans. 2*, 97 (1995); M. W. Wong, A. Pross, and L. Radom, *J. Am. Chem. Soc.*, **116**, 6284 (1994).

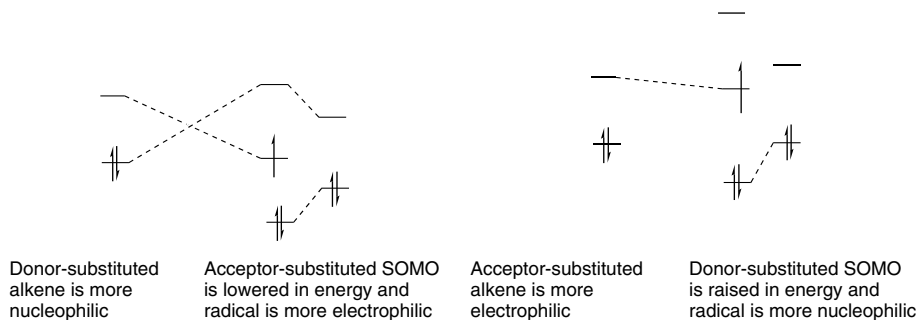


Fig. 11.6. Frontier orbital interactions between different combinations of substituted radicals and alkenes showing enhanced interaction relative to unsubstituted systems.

the radical site is substituted by an electron-attracting group, the SOMO is lower. A complementary interaction between the radical and alkene is possible.

The TS for radical additions is quite early and correlates with ground state characteristics of the reactant alkene. In particular there is a strong correlation between relative reactivity and the LUMO energy of the reactant alkene for addition reactions of the *t*-butyl radical, as shown in Figure 11.7.<sup>99</sup> The rate constants range over ten ln exponents and the correlation coefficient is 0.971.  $\pi$ -Donor substituents

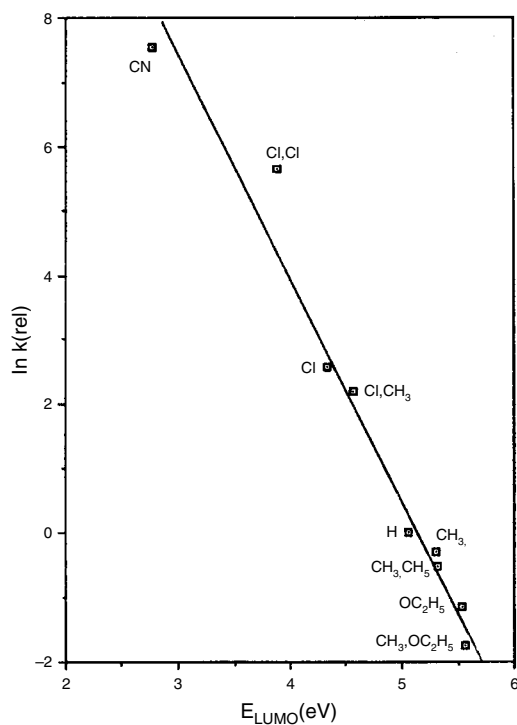


Fig. 11.7. Correlation between relative rates of addition reactions of *t*-butyl radicals and  $E_{LUMO}$  for alkenes. Reproduced from *J. Org. Chem.*, **57**, 1139 (1992), by permission of the American Chemical Society.

<sup>99</sup> D. J. Pasto, *J. Org. Chem.*, **57**, 1139 (1992).

(e.g., OR) retard reaction, whereas EWGs (e.g., CN) accelerate reaction, which is in agreement with the classification of alkyl radicals as nucleophilic. A relationship was also found between reactivity and the ground state stabilization of the alkene. Certain substituent combinations (e.g., CN,CN or Cl,Cl) significantly destabilize the alkene, and these compounds are highly reactive toward alkyl radicals. On the other hand, the (OC<sub>2</sub>H<sub>5</sub>, CH<sub>3</sub>) combination stabilizes the alkene and such compounds are less reactive toward alkyl radicals. These results are consistent with an early TS for radical addition controlled by SOMO-LUMO interactions. The regiochemistry, which generally involves addition at the β-carbon, also correlates with the coefficient of the LUMO, as would be expected for an FMO-controlled reaction.

Some other representative rate data are given in Table 11.6. Methyl radicals are somewhat more reactive toward alkenes bearing EWG substituents than with ERG substituents. Secondary cyclohexyl radicals show a stronger trend in this direction. Some of this effect can be attributed to the stabilizing influence that these substituents have on the product radical. There is a strong correlation of reaction rate with the overall exothermicity of the reaction.<sup>100</sup>

Related trends are seen in data for radicals with functional group substituents. Hydroxymethyl and 2-hydroxy-2-propyl radicals show nucleophilic character.<sup>101</sup> The hydroxymethyl radical shows a slightly enhanced rate toward acrylonitrile and acrolein, but a sharply decreased rate toward ethyl vinyl ether. The more electrophilic cyanomethyl radical shows reactivity enhancement not only with radical-stabilizing EWGs, but also with ERGs. Table 11.7 gives some of the reactivity data.

α-Fluoro substituents enhance reactivity toward alkene addition. The effect of polyfluorination is more than cumulative. The rates of RCH<sub>2</sub>· (1); RCHF· (3.5); RCF<sub>2</sub>·

**Table 11.6. Relative Rates of Radical Additions as a Function of Alkene Substitution<sup>a</sup>**

A. Addition to substituted ethenes, CH<sub>2</sub>=CH-X

X	CH <sub>3</sub> ·	CH <sub>3</sub> CH <sub>2</sub> ·	c-C <sub>6</sub> H <sub>11</sub> ·
CN	2.2	5.1	24
COCH <sub>3</sub>	2.3		13
CO <sub>2</sub> CH <sub>3</sub>	1.3	1.9	6.7
Ph	1.0	1.0	1.0
O <sub>2</sub> CCH <sub>3</sub>		0.05	0.016

B. Additions to α-substituted styrenes, CH<sub>2</sub>=CXPh

X	c-C <sub>6</sub> H <sub>11</sub> ·	·CH(CO <sub>2</sub> C <sub>2</sub> H <sub>5</sub> ) <sub>2</sub>
CN	122	
CO <sub>2</sub> C <sub>2</sub> H <sub>5</sub>	11.7	0.28
Ph	1.0	1.0
CH <sub>3</sub>	0.28	1.06
CH <sub>3</sub> O		0.78
(CH <sub>3</sub> ) <sub>2</sub> N		6.6

a. Data from B. Giese, H. Horler, and M. Leising, *Chem. Ber.*, **119**, 444 (1986); B. Giese, *Angew. Chem. Int. Ed. Engl.*, **22**, 753 (1983).

<sup>100</sup> M. W. Wong, A. Pross, and L. Radom, *J. Am. Chem. Soc.*, **115**, 11050 (1993); R. Arnaud, N. Bugaud, V. Vetere, and V. Barone, *J. Am. Chem. Soc.*, **120**, 5733 (1998).

<sup>101</sup> J. Q. Wu and H. Fischer, *Int. J. Chem. Kinetics*, **27**, 167 (1995); S. N. Batchelor and H. Fischer, *J. Chem. Phys.*, **100**, 9794 (1996).

**Table 11.7. Absolute Rates of Addition Reactions of Methyl, Cyanomethyl, and Hydroxymethyl Radicals toward Substituted Alkenes, CH<sub>2</sub>=CHX**

X	$k (M^{-1} s^{-1})$		
	$\cdot\text{CH}_3^a$	$\cdot\text{CH}_2\text{CN}^b$	$\cdot\text{CH}_2\text{OH}^c$
H	$3.5 \times 10^3$	$3.3 \times 10^3$	$4.1 \times 10^2$
Ph	$2.6 \times 10^5$	$3.8 \times 10^3$	$2.3 \times 10^4$
CN	$6.1 \times 10^5$	$1.1 \times 10^5$	$1.1 \times 10^6$
CH=O	$7.4 \times 10^5$	$2.5 \times 10^4$	$2.1 \times 10^6$
CO <sub>2</sub> CH <sub>3</sub>	$3.4 \times 10^5$	$1.1 \times 10^5$	$7.1 \times 10^5$
OC <sub>2</sub> H <sub>5</sub>	$1.4 \times 10^4$	$1.2 \times 10^4$	$1.8 \times 10^2$
CH <sub>3</sub>	$4.3 \times 10^3$	$1.2 \times 10^4$	$2.7 \times 10^2$

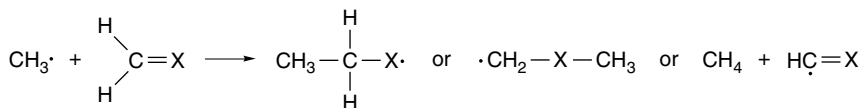
a. T. Zytowski and H. Fischer, *J. Am. Chem. Soc.*, **118**, 437 (1996); T. Zytowski and H. Fischer, *J. Am. Chem. Soc.*, **119**, 12869 (1997).

b. J. Q. Wu and H. Fischer, *Int. J. Chem. Kinet.*, **27**, 167 (1995).

c. J. Q. Wu, I. Beranek, and H. Fischer, *Helv. Chim. Acta*, **78**, 194 (1995).

(20); and CF<sub>3</sub>· (300) show this trend.<sup>102</sup> Further accumulation of fluorine enhances this effect still further and the perfluoro-*t*-butyl radical is typically eight to ten times more reactive than CF<sub>3</sub>· toward alkenes.

Computational studies have also compared some of the fundamental substituent effects on addition reactions for other functional groups. The relative barriers for addition and hydrogen abstraction were compared for ethene, formaldehyde, methylene imine, and formaldehyde nitrene. The data shown below are the result of B3LYP/6-311+G(2df,p) calculations, but G2 and CBS calculations were carried out in some cases.<sup>103</sup>



X	Addition at C		Addition at X		H Abstraction	
	$\Delta H$	$\Delta H^\ddagger$	$\Delta H$	$\Delta H^\ddagger$	$\Delta H$	$\Delta H^\ddagger$
=CH <sub>2</sub>	-20	+7	-20	+7	+5	+15
=O	-13	+4.5	-7.4	+15	-17	+5
=NH	-18	+6.5	-19	+9.5	-18	+4
=N <sup>+</sup> (O <sup>-</sup> )H	-44	+1.7	+6.2	+22	-34	-1

Addition is preferred to hydrogen atom abstraction for alkenes. Addition at carbon and hydrogen abstraction are competitive for aldehydes and imines. Both addition at carbon and hydrogen abstraction reactions are very exothermic for nitrenes and are calculated to have low barriers. There are two possible modes of addition for the unsymmetrical systems. For the carbonyl and nitrene groups, addition at the carbon is preferred. The same is true for imines, but the balance is much closer. The activation

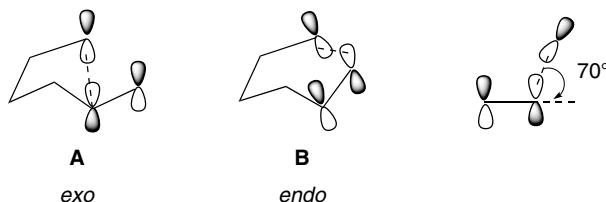
<sup>102</sup>. D. V. Avila, K. U. Ingold, J. Luszyk, W. R. Dolbier, Jr., and H.-Q. Pan, *J. Org. Chem.*, **61**, 2027 (1996); D. Avila, K. U. Ingold, J. Luszyk, W. R. Dolbier, Jr., and H.-Q. Pan, *Tetrahedron*, **52**, 12351 (1996).

<sup>103</sup>. S. L. Boyd and R. J. Boyd, *J. Phys. Chem. A*, **105**, 7096 (2001).



the stabilization by a phenyl substituent shifts the cyclopropyl  $\rightleftharpoons$  butenyl equilibrium to favor the cyclic form.

The cyclization of the 5-hexenyl radical to cyclopentylmethyl (Entry 33) is a commonly observed reaction. The  $E_a$  is 6 kcal/mol. The cyclization shows a preference for *exo* cyclization to a five-membered ring over *endo* cyclization to a six-membered ring,<sup>106</sup> even though it results in formation of a less stable primary radical. The cause for this preference has been traced to stereoelectronic effects. In order for a bonding interaction to occur, the radical center must interact with the  $\pi^*$  orbital of the alkene. According to MO calculations, the preferred direction of attack is from an angle of about  $70^\circ$  with respect to the plane of the double bond.<sup>107</sup>



When this stereoelectronic requirement is included with a calculation of the steric and angle strain imposed on the TS, as determined by MM-type calculations, preferences of the *exo* versus *endo* modes of cyclization are predicted to be as summarized in Table 11.8.

The observed results agree with the calculated trend. Relative rates of cyclization are in the order *5-exo* > *6-endo*  $\sim$  *6-exo* > *7-endo*.<sup>108</sup> The relationship holds only for terminal double bonds. An additional alkyl substituent at either end of the double bond reduces the relative reactivity by a steric effect. The underlying conformational and stereoelectronic effects can be modified by both steric and electronic effects of substituents. For example, a 5-methoxycarbonyl substituent promotes the *6-endo* mode of cyclization by an electronic effect.<sup>109</sup> The reactivity of the  $\beta$ -carbon is enhanced by the substituent.

**Table 11.8. Regioselectivity of Radical Cyclization as a Function of Ring Size<sup>a</sup>**

Ring size	<i>exo:endo</i> Ratio	
	Calculated	Found
5:6	10:1	50:1
6:7	> 100 : 1	10:1
7:8	1:5.8	< 1 : 100

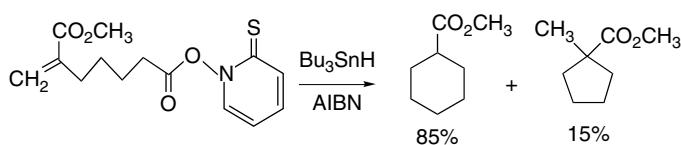
a. D. C. Spellmeyer and K. N. Houk, *J. Org. Chem.*, **52**, 959 (1987).

<sup>106</sup>. A. L. J. Beckwith, C. J. Eaton, and A. K. Serelis, *J. Chem. Soc., Chem. Commun.*, 482 (1980); A. L. J. Beckwith, T. Lawrence, and A. K. Serelis, *J. Chem. Soc., Chem. Commun.*, 484 (1980); A. L. J. Beckwith, *Tetrahedron*, **37**, 3073 (1981).

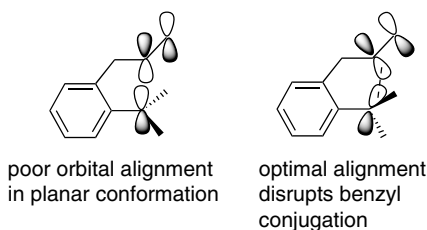
<sup>107</sup>. M. J. S. Dewar and S. Olivella, *J. Am. Chem. Soc.*, **100**, 5290 (1978); D. C. Spellmeyer and K. N. Houk, *J. Org. Chem.*, **52**, 959 (1987).

<sup>108</sup>. A. L. J. Beckwith and C. H. Schiesser, *Tetrahedron*, **41**, 3925 (1985).

<sup>109</sup>. E. W. Della, C. Kostakis, and P. A. Smith, *Org. Lett.*, **1**, 363 (1999).



The relatively low rate and high activation energy noted for Entry 37 of Table 11.3 also reflects a stereoelectronic effect. The preference for delocalization at the radical center requires coplanarity of the substituents at the radical site, which results in poor alignment. In view of the restrictions on the mode of approach of the radical to the double bond, significant strain develops in the TS and requires rotation of the benzylic methylene group out of its preferred coplanar alignment.<sup>110</sup>



Several computational studies have explored the cyclization of the 5-hexenyl radical. CBS-RAD(B3LYP) calculations provided thermochemical and kinetic parameters that are in good agreement with experiment.<sup>111</sup> Similar results were obtained with UB3LYP/6-31G(d) calculations.<sup>112</sup>

	5- <i>exo</i>	6- <i>endo</i>
$\Delta G$	-13.7 kcal/mol	-16.5 kcal/mol
$\Delta G^\ddagger$	9.3 kcal/mol	12.0 kcal/mol
$E_a$	6.3 kcal/mol	8.7 kcal/mol
$k_{\text{gas}}$	$1.2 \times 10^7 \text{ s}^{-1}$	$2.7 \times 10^5 \text{ s}^{-1}$
$k_{\text{benzene}}$	$8.2 \times 10^6 \text{ s}^{-1}$	$1.6 \times 10^5 \text{ s}^{-1}$

Cyclization of 5-hexenyl radicals has been compared computationally (BLYP/31+G\*\*) with 2-oxo-5-hexenyl radicals.<sup>113</sup> Several methyl-substituted analogs

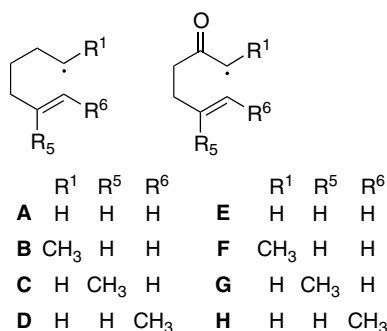
<sup>110</sup> J. A. Franz, N. K. Suleman, and M. S. Alnajjar, *J. Org. Chem.*, **51**, 19 (1986).

<sup>111</sup> B. J. Maxwell, B. J. Smith, and J. Tsanaktsidis, *J. Chem. Soc., Perkin Trans. 2*, 425 (2000).

<sup>112</sup> B. S. Jursic, *Theochem*, **492**, 285 (1999).

<sup>113</sup> A. G. Leach, R. Wang, G. E. Wohlhieter, S. I. Khan, M. E. Jung, and K. N. Houk, *J. Am. Chem. Soc.*, **125**, 4271 (2003).

were included in the study. There is a change to a preference from 5-*exo* to 6-*endo* with the introduction of the 2-oxo group.



Experimentally, it is found that the hexenyl radicals prefer the 5-*exo* route, whereas the  $\alpha$ -keto radicals prefer the 6-*endo* path. This effect is mirrored in the calculations, which find the 5-*exo* route strongly favored in the 5-hexenyl system (except for the 5-methyl derivative **C**), whereas for the  $\alpha$ -keto radicals the 6-*endo* TS is preferred, although again the steric effect of a 6-methyl group somewhat disfavors this mode. Figure 11.9 shows various TSs. The conjugation present in the  $\alpha$ -keto radicals imparts a planarity to the radical that favors the *endo* structure.<sup>114</sup>

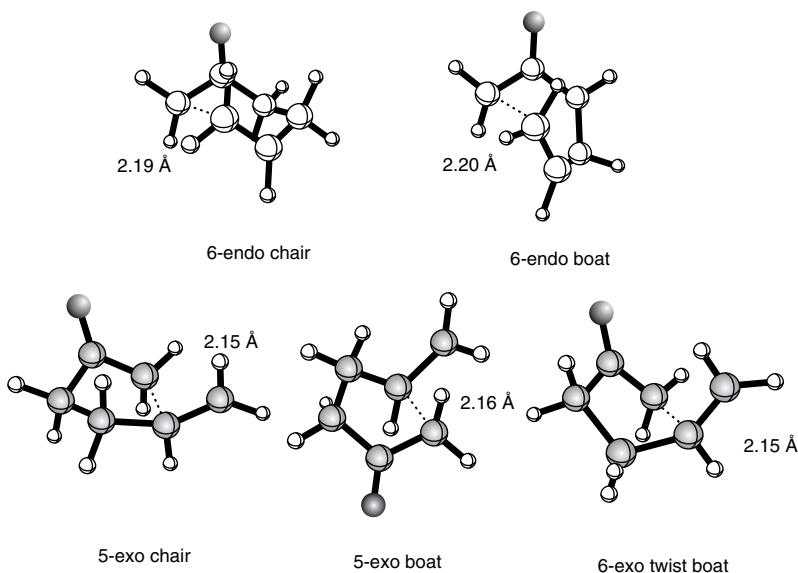
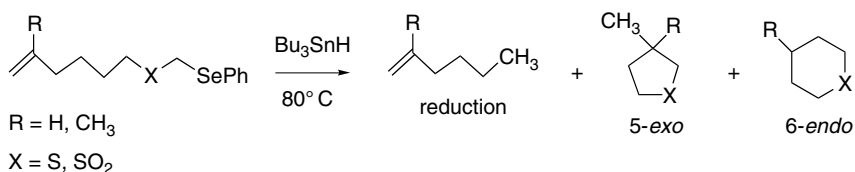


Fig. 11.9. Structures for various conformations of the radical cyclization transition structures for 2-oxo-5-hexenyl radical. Reproduced from *J. Am. Chem. Soc.*, **125**, 4271 (2003), by permission of the American Chemical Society.

<sup>114</sup> J. L. Broecker and K. N. Houk, *J. Org. Chem.*, **56**, 3651 (1991).

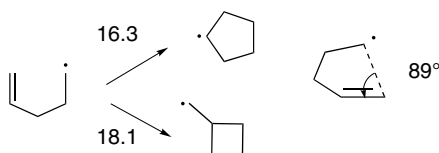
	Computed Transition Structure Energy (kcal/mol)				
	5-exo(chair)	5-exo(boat)	6-endo(chair)	6-endo(boat)	endo:exo ratio
<b>A</b>	<b>6.4</b>	8.1	9.1	11.6	1:99
<b>B</b>	<b>7.0</b>	8.7	9.6	12.2	1:99
<b>C</b>	9.1	10.3	<b>8.4</b>	10.7	75:25
<b>D</b>	<b>6.5</b>	8.1	9.8	12.5	1:99
<b>E</b>	13.3	12.6	<b>10.0</b>	16.5	98:2
<b>F</b>	15.9	14.4	<b>12.6</b>	19.1	95:5
<b>G</b>	15.8	14.7	<b>8.6</b>	15.2	> 99 : 1
<b>H</b>	12.7	12.1	<b>10.9</b>	17.2	84:16

Competition between 5-*exo* and 6-*endo* has also been examined for the 2-thia and 2-sulfonyl analogs of the 5-hexenyl radicals.<sup>115</sup> As in the case of the parent radical, a 5-methyl substituent favors the 6-*endo* mode and this is reinforced in the case of the sulfonyl substituent, where the electrophilic radical prefers the more electron-rich alkene position.



R	X	Product composition		
		Reduction	5-exo	6-endo
H	S	17.1	70.1	12.8
H	SO <sub>2</sub>	3.8	73.1	23.1
CH <sub>3</sub>	S	38.6	7.1	54.3
CH <sub>3</sub>	SO <sub>2</sub>	3.9	2.5	93.6

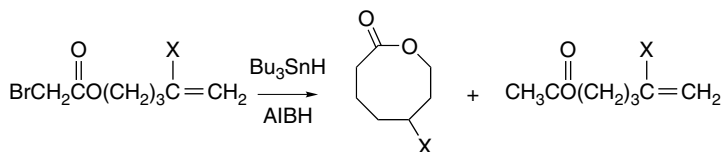
The 4-pentenyl radical can undergo 4-*exo* or 5-*endo* cyclization. UB3LYP/6-31G\* calculations find a preference of 1.8 kcal/mol for the 5-*endo* TS. The angle to approach to the double bond is found to be about 89°.<sup>116</sup>



<sup>115</sup> E. W. Della and S. D. Graney, *Org. Lett.*, **4**, 4065 (2002); E. W. Della and S. D. Graney, *J. Org. Chem.*, **69**, 3824 (2004).

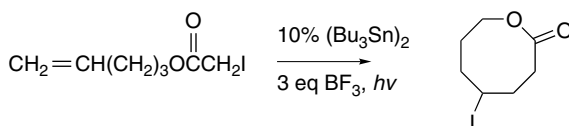
<sup>116</sup> P. S. Engel, S. L. He, and W. B. Smith, *J. Am. Chem. Soc.*, **119**, 6059 (1997); C. Chatgililoglu, C. Ferreri, M. Guerra, V. Timokhin, G. Froudakis, and T. Gimisis, *J. Am. Chem. Soc.*, **124**, 10765 (2002).

Reactions of 4-substituted 4-pentenyl bromoacetates with tri-*n*-butylstannane resulted in modest yields of eight-membered *endo*-cyclization products, along with reduction products.<sup>117</sup>



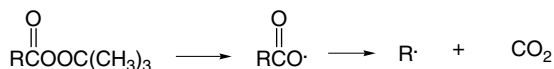
X	Product yield	
	Cyclization	Reduction
H	38%	31%
CH <sub>3</sub>	38%	18%
(CH <sub>3</sub> ) <sub>3</sub> Si	54%	32%

This type of cyclization can be further improved by use of a BF<sub>3</sub> catalyst.<sup>118</sup>



Systems with the potential for forming nine-, ten-, or sixteen-membered rings gave only reduction. The relatively favorable formation of eight-membered rings is attributed to the *s-trans* conformation of the ester group. The relative energies of the 8-*endo* and 7-*exo* TS were calculated for both the *s-trans* and *s-cis* conformations by ROHF/MP2/3-21G computations.<sup>117</sup> The most favorable TS is the 8-*endo-cis* structure. The relative energies are shown in Figure 11.10. The general pattern that emerges from these experimental and computational results is that trajectory of approach, steric effects, and reactant conformation are the controlling factors in the ring size selectivity for radical cyclizations.

**11.2.3.4. Other Radical Reactions** Section D of Table 11.3 includes several examples of *radical fragmentation reactions*. Entries 44, 48, and 49 are examples of *β-scission reactions*. The facile decarboxylation of acyloxy radicals is an example.



<sup>117</sup> E. Lee, C. H. Yoon, T. H. Lee, S. Y. Kim, T. J. Ha, Y. Sung, S.-H. Park, and S. Lee, *J. Am. Chem. Soc.*, **120**, 7469 (1998).

<sup>118</sup> J. Wang and C. Li, *J. Org. Chem.*, **67**, 1271 (2002).

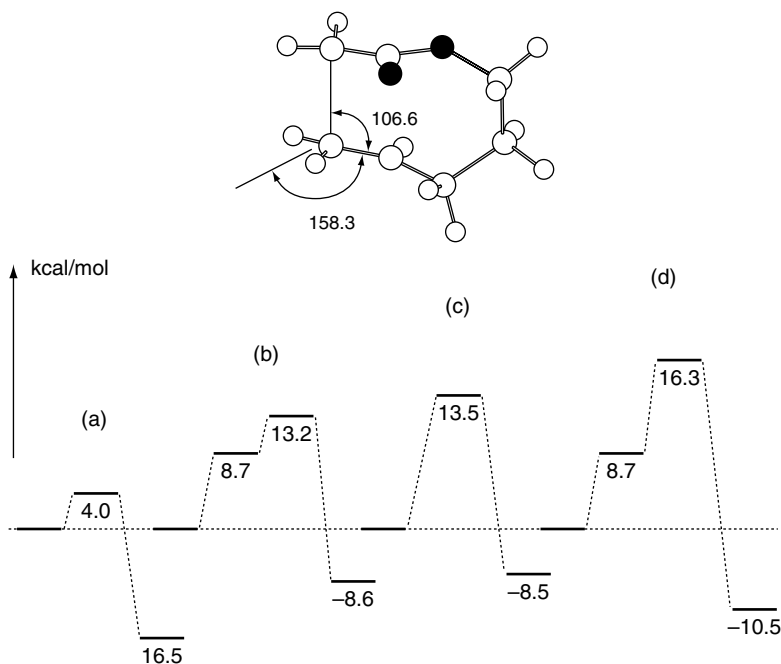
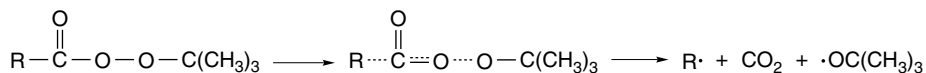


Fig. 11.10. Comparison of energies of (a) 8-endo-s-cis, (b) 8-endo-s-trans, (c) 7-exo-s-cis, and (d) 7-exo-s-trans transition structures. Reproduced from *J. Am. Chem. Soc.*, **120**, 7469 (1998), by permission of the American Chemical Society.

The rate of decarboxylation of aryloxy radicals is about  $10^6 \text{ s}^{-1}$  near room temperature.<sup>119</sup> Decarboxylation of alkanoyloxy radicals is even faster. Thus only very rapid reactions can compete with decarboxylation. Hydrogen abstraction from very reactive hydrogen atom donors, such as triethylsilane, can compete with decarboxylation at moderate temperatures.

These radical stability effects can be observed in the *rates of formation of radicals as well as their lifetimes*. It has already been indicated that radical structure and stability determines the temperature at which azo compounds undergo decomposition with elimination of nitrogen (see Section 11.1.4). Similar trends have been established in other radical-forming reactions. Rates of thermal decomposition of *t*-butyl peroxyesters, for example, vary over a wide range, depending on the structure of the carbonyl substituent.<sup>120</sup> These data clearly indicate that the bonding changes involved in the rate-determining step are not localized in the O–O bond. Radical character must also be developing at the alkyl group by partial cleavage of the alkyl-carbonyl bond.



<sup>119</sup> J. Chateaufneuf, J. Luszytk, and K. U. Ingold, *J. Am. Chem. Soc.*, **110**, 2886 (1988); H. Misawa, K. Sawabe, S. Takahara, H. Sakuragi, and K. Tokumaru, *Chem. Lett.*, 357 (1988).

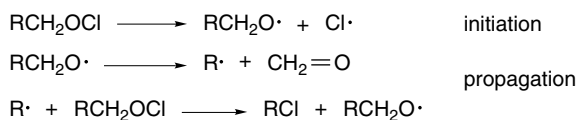
<sup>120</sup> P. D. Bartlett and R. R. Hiatt, *J. Am. Chem. Soc.*, **80**, 1398 (1958).

R	Relative rate at 60°C
CH <sub>3</sub>	1
C <sub>6</sub> H <sub>5</sub>	17
PhCH <sub>2</sub>	290
(CH <sub>3</sub> ) <sub>3</sub> C	1,700
Ph <sub>2</sub> CH	19,300
Ph(CH <sub>3</sub> ) <sub>2</sub> C	41,500
PhCHCH=CH <sub>2</sub>	125,000

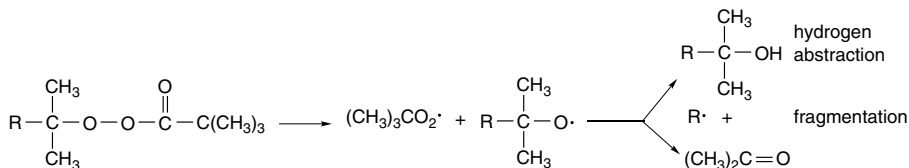
Another common fragmentation reaction is the cleavage of an alkoxy radical to an alkyl radical and a carbonyl compound.<sup>121</sup>



This type of fragmentation is involved in the chain decomposition of alkyl hypochlorites.<sup>122</sup> In this reaction, too, the stability of the radical being eliminated is the major factor in determining the rate of fragmentation.



Radical trapping by a nitroxide was used to determine the ratio between  $\beta$ -fragmentation and hydrogen abstraction by alkoxy radicals generated by thermal decomposition of peroxy pivalate esters.<sup>123</sup> The ratio of fragmentation:hydrogen abstraction increased sharply with radical substitution and stability.



R	Fragmentation relative to CH <sub>3</sub>	Rate of decomposition (60°C, $\times 10^{-5} \text{ s}^{-1}$ )
CH <sub>3</sub>	1	2.95
CH <sub>3</sub> CH <sub>2</sub>	252	3.51
CH <sub>3</sub> CH <sub>2</sub> CH <sub>2</sub>	254	3.37
(CH <sub>3</sub> ) <sub>3</sub> CCH <sub>2</sub>	2670	6.18
(CH <sub>3</sub> ) <sub>2</sub> CH	3300	5.14
Cyclohexyl	28000	5.72
(CH <sub>3</sub> ) <sub>3</sub> C	86400	9.10
PhCH <sub>2</sub>		9.91
Ph		10.32

<sup>121</sup>. P. Gray and A. Williams, *Chem. Rev.*, **59**, 239 (1959).

<sup>122</sup>. F. D. Greene, M. L. Savitz, F. D. Osterholtz, H. H. Lau, W. N. Smith, and P. M. Zanet, *J. Org. Chem.*, **28**, 55 (1963); C. Walling and A. Padwa, *J. Am. Chem. Soc.*, **85**, 1593, 1597 (1963).

<sup>123</sup>. T. Nakamura, Y. Watanabe, S. Suyama, and H. Tezuka, *J. Chem. Soc., Perkin Trans. 2*, 1364 (2002).

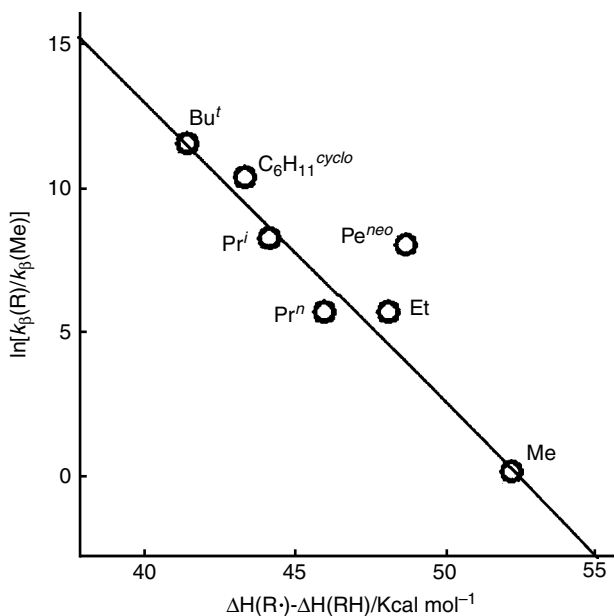
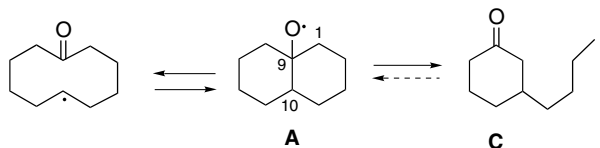


Fig. 11.11. Correlation between fragmentation of 2-alkyl-2-propoxy radicals and radical stability as measured by  $\Delta H(R\cdot) - \Delta H(R-H)$ . Reproduced from *J. Chem. Soc., Perkin Trans. 2*, 1364 (2002), by permission of the Royal Society of Chemistry.

As shown in Figure 11.11, there is a strong correlation between the ratio and radical stability, as measured by the difference in the enthalpy of formation. The outlying value for neopentyl can be improved by a correction for steric strain. On the other hand, the *rate of decomposition of the peroxy ester* is nearly independent of the nature of R, even for the stabilized benzyl or destabilized phenyl cases.<sup>124</sup> This is in marked contrast to a strong dependence on the structure of the acyl group (see above) and indicates that the fragmentation of the alkoxy radical is not concerted with the peroxy bond cleavage, but must be a separate step.

In cyclic systems the fragmentation of alkoxy radicals can be a reversible process. The 9-decalyloxy radical can undergo fragmentation of either the 1–9 or the 9–10 bond:

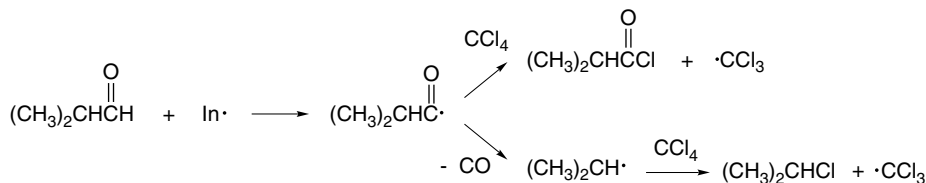


By using various trapping reagents it has been deduced that the transannular fragmentation is rapidly reversible. The cyclization of the fragmented radical C is less favorable and it is trapped at rates that exceed recyclization under most circumstances.<sup>125</sup>

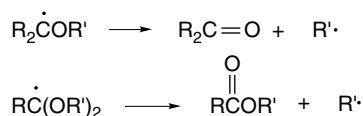
<sup>124</sup> T. Nakamura, W. K. Busfield, I. D. Jenkins, O. Rizzardo, S. H. Thang, and S. Suyama, *J. Org. Chem.*, **65**, 16 (2000).

<sup>125</sup> A. L. J. Beckwith, R. Kazlauskas, and M. R. Syner-Lyons, *J. Org. Chem.*, **48**, 4718 (1983).

Acyl radicals can fragment by loss of carbon monoxide. Decarbonylation is slower than decarboxylation, but the rate also depends on the stability of the radical that is formed.<sup>126</sup> For example, rates for decarbonylations giving tertiary benzylic radicals are on the order of  $10^8 \text{ s}^{-1}$ , whereas the benzoyl radical decarbonylates to phenyl radical with a rate on the order of  $1 \text{ s}^{-1}$  (see also Table 11.3, Entries 45 to 48). When reaction of isobutyraldehyde with carbon tetrachloride is initiated by *t*-butyl peroxide, both isopropyl chloride and isobutyroyl chloride are formed, indicating that decarbonylation is competitive with the chlorine atom transfer.

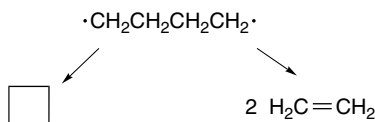


Radicals derived from ethers and acetals by hydrogen abstraction are subject to  $\beta$ -scission, with formation of a ketone or ester, respectively.

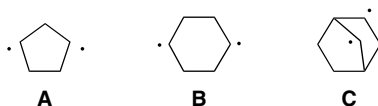


These fragmentations are sufficiently slow that the initial radicals can undergo reactions such as addition to alkenes at rates that are competitive with fragmentation.

A special case of fragmentation is that of 1,4-diradicals, where it can lead to two alkene molecules. In the case of 1,4-diradicals without functional group stabilization, reclosure to cyclobutanes is competitive with fragmentation to two molecules of alkene. The most recent of many detailed computational studies indicates that there is no barrier between the diradical and either the cyclization or fragmentation products.<sup>127</sup>



A study of the lifetimes of the triplet biradicals **A**, **B**, and **C**, which were generated from the corresponding photoexcited azo compounds, gave the order of lifetime **A** > **B** > **C**. The lifetime of **A** is about  $2.6 \times 10^{-7} \text{ s}$ , which is quite long for a 1,4-diradical.<sup>128</sup>

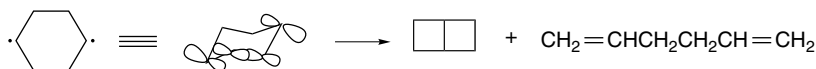


<sup>126</sup> D. E. Applequist and L. Kaplan, *J. Am. Chem. Soc.*, **87**, 2194 (1965); W. H. Urry, D. J. Trecker, and H. D. Hartzler, *J. Org. Chem.*, **29**, 1663 (1964); H. Fischer and H. Paul, *Acc. Chem. Res.*, **20**, 200 (1987).

<sup>127</sup> E. Ventura, M. Dallos, and H. Lischka, *J. Chem. Phys.*, **118**, 10963 (2003).

<sup>128</sup> W. Adam, K. Hannemann, and R. M. Wilson, *J. Am. Chem. Soc.*, **106**, 7646 (1984); W. Adam, K. Hannemann, and R. M. Wilson, *Angew. Chem. Int. Ed. Engl.*, **24**, 1071 (1985); W. Adam, H. Platsch, J. Sendelbach, and J. Wirz, *J. Org. Chem.*, **58**, 1477 (1993).

The major factor identified in controlling the lifetimes of these diradicals is the orientation of the singly occupied orbitals with respect to one another. One factor determining the lifetime is the rate of conversion (intersystem crossing) to the singlet biradical. The rate of conversion is dependent on the orientation of the orbitals having the unpaired electrons. In **A** the orbitals are essentially parallel, which is a poor orientation for intersystem crossing. Diradical **B** is more flexible and the triplet is converted more rapidly to the singlet diradical, which reacts rapidly to give the cyclization and fragmentation products.



The geometry of the bicyclic ring system in radical **C** directs the half-filled orbitals toward one another and its lifetime is less than  $1 \times 10^{-10}$  s.<sup>129</sup>

### 11.3. Free Radical Substitution Reactions

#### 11.3.1. Halogenation

The basic reactivity and selectivity relationships for halogenation of alkanes can be understood in terms of bond dissociation energies. Bond dissociation energies such as those in Part B of Table 3.2 can be used to estimate the energy balance in individual steps in a free radical reaction sequence. This is an important factor in assessing the feasibility of chain reaction sequences because only reactions with low activation energies are fast enough to sustain a chain process. If individual steps are identified as being endothermic by more than a few kcal, it is unlikely that a chain mechanism can operate.

*Example 11.1* Calculate the enthalpy for each step in the bromination of ethane by bromine atoms from molecular bromine. Determine the overall enthalpy of the reaction.

				bond energy (kcal/mol)
initiation	$\text{Br}-\text{Br}$	$\longrightarrow$	$2 \text{ Br}\cdot$	$\text{Br}-\text{Br}$ +45
propagation	$\text{Br}\cdot + \text{CH}_3\text{CH}_3$	$\longrightarrow$	$\text{H}-\text{Br} + \text{CH}_3\text{CH}_2\cdot$	$\text{H}-\text{Br}$ -87
				$\text{H}-\text{C}$ +100.5
				+13.5
	$\text{CH}_3\text{CH}_2\cdot + \text{Br}-\text{Br}$	$\longrightarrow$	$\text{CH}_3\text{CH}_2\text{Br} + \text{Br}\cdot$	$\text{Br}-\text{Br}$ +45
				$\text{Br}-\text{C}$ -70
				-25
				total -11.5

The enthalpy of the reaction is given by the sum of the propagation steps and is  $-11.5$  kcal/mol. Analysis of the enthalpy of the individual steps indicates that the first step is somewhat endothermic (+13.5 kcal). This endothermicity is the lower limit of the  $E_a$  for the step. An  $E_a$  of  $14.0 \pm 0.25$  kcal/mol has been reported.<sup>130</sup>

Radical chain processes depend on a series of fast steps that maintain the reactive intermediates at low concentration. Since termination reactions are usually very fast,

<sup>129</sup> W. Adam, S. Grabowski, and R. M. Wilson, *Acc. Chem. Res.*, **23**, 165 (1990).

<sup>130</sup> K. D. King, D. M. Golden, and S. W. Benson, *Trans. Faraday Soc.*, **66**, 2794 (1970).

the presence of an endothermic step in a chain sequence means that the chains will be short. The value for ethane is borderline, which suggests that radical bromination of ethane will exhibit only short chain lengths. As the enthalpy of the corresponding steps for abstraction of secondary or tertiary hydrogen is less positive, the bromination selects for tertiary > secondary > primary in compounds with more than one type of hydrogen. Enthalpy calculations cannot give a direct evaluation of the activation energy of either exothermic or endothermic steps, since these depend on the energy of the TS. The bond dissociation energies can therefore provide only permissive, not definitive, conclusions. For single atom abstraction reactions such as these involved in hydrocarbon halogenation, the enthalpy correlates with  $E_a$  for both steps.

—	CH <sub>4</sub> (105.0)	+18.0
—	C <sub>2</sub> H <sub>6</sub> (100.5)	+13.5
—	(CH <sub>3</sub> ) <sub>2</sub> CH <sub>2</sub> (98.1)	+11.1
—	(CH <sub>3</sub> ) <sub>3</sub> CH(95.7)	+9.7

The thermochemistry of radical chain halogenations varies strongly with the halogens. Fluorination is strongly exothermic and difficult to control. Iodination is endothermic and cannot sustain a chain reaction. Both chlorination and bromination are moderately exothermic and chain reactions with hydrocarbons are feasible. Figure 11.12 summarizes these energies for reaction with methane, ethane, propane, and isobutane. By tracking each hydrocarbon-halogen combination, the energy profile can be obtained. From these data we can, for example, determine and compare the minimum  $E_a$  for chlorination and bromination at C(2) in propane.

Cl<sub>2</sub> : H abstraction  $\Delta H = -4.9$  kcal/mol    Cl abstraction  $\Delta H = -23$  kcal/mol

Br<sub>2</sub> : H abstraction  $\Delta H = +11.1$  kcal/mol    Br abstraction  $\Delta H = -26.5$  kcal/mol

The two energy profiles are significantly different in that bromination, but not chlorination, has an endothermic step.

Free radical bromination is an important method of selective functionalization of hydrocarbons.<sup>131</sup> The reaction is often initiated by photolysis of bromine. The hydrogen atom abstraction step is rate limiting and the product composition is governed by the selectivity of the hydrogen abstraction step. Based on BDE (see Table 3.2, p. 258), the enthalpy requirements for abstraction of hydrogen from methane, ethane (primary), propane (secondary), and isobutane (tertiary) by bromine atoms are +18.0, +13.5, +11.1, and +9.7 kcal/mol, respectively (see Figure 11.12).<sup>132</sup> These differences are reflected in the  $E_a$  and there is a substantial kinetic preference for hydrogen abstraction in the order tertiary > secondary > primary. Substituents that promote radical stability, such as phenyl, vinyl, or carbonyl groups, also lead to kinetic selectivity in radical brominations. Bromination at benzylic positions is a particularly efficient process.

In addition to Br<sub>2</sub>, *N*-bromosuccinimide is an important reagent for radical chain bromination, especially at allylic and benzylic positions. Mechanistic investigations have established that Br<sub>2</sub> is the active halogenating agent under the conditions used

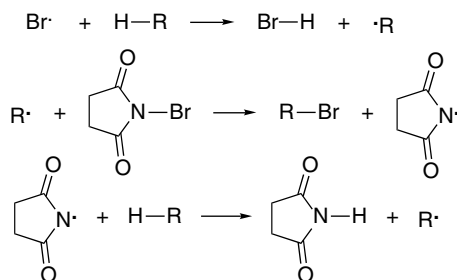
<sup>131</sup> W. A. Thaler, *Meth. Free Radical Chem.*, **2**, 121 (1969); A. Nechvatal, *Adv. Free Radicals*, **4**, 175 (1972).

<sup>132</sup> E. S. Huyser, *Free Radical Chain Reactions*, Wiley-Interscience, New York, 1970, p. 91.

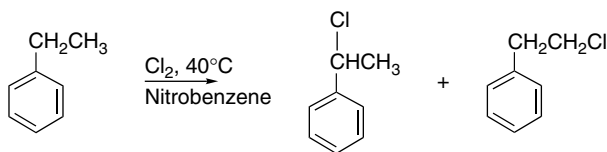


The fact that the  $\text{Br}_2$  concentration remains at very low levels is important to the success of the allylic halogenation process. The allylic bromination of alkenes must compete with polar addition of bromine via a bromonium ion intermediate. The reactions differ in their dependence on bromine concentration. The allylic substitution is one-half order in bromine, whereas the addition reaction follows a first- or second-order dependence on  $[\text{Br}_2]$  (see Section 5.3). Therefore a low concentration of  $\text{Br}_2$  favors substitution over addition.<sup>134</sup>

NBS can also be used to brominate alkanes. For example, cyclopropane, cyclopentane, and cyclohexane give the corresponding bromides when irradiated with NBS in dichloromethane.<sup>135</sup> Under these conditions, the succinimidyl radical appears to be involved as the hydrogen-abstracting intermediate.



Significant differences are seen with the reactions of the other halogens relative to bromination. In the case of chlorination, although the same chain mechanism is operative, there is a key difference in the *diminished selectivity of the chlorination*. For example, the *pri:tert* selectivity in 2,3-dimethylbutane for chlorination is 1:3.6 in typical solvents.<sup>136</sup> Owing to the greater reactivity of the chlorine atom, abstractions of primary, secondary, and tertiary hydrogens are all *exothermic* (see Figure 11.12). As a result of this exothermicity, the stability of the product radical has less influence on the  $E_a$ . In terms of the Hammond postulate (Section 3.3.2.2), the TS is expected to be more *reactant-like*. As an example of the low selectivity, ethylbenzene is chlorinated at both the methyl and the methylene positions, despite the much greater stability of the benzyl radical.<sup>137</sup>



(4.25:1, ratio is solvent dependent)

Isotope effect and relative rate studies also suggest an early TS for benzylic chlorination and bromination. The benzylic position is only moderately activated toward uncomplexed chlorine atoms. Relative to ethane, toluene reactivity is increased only by a factor of 3.3.<sup>137</sup> The kinetic isotope effect observed for bromination<sup>138</sup> and chlorination<sup>139</sup> of toluene suggest little rehybridization at the TS.

<sup>134</sup>. C. C. Wamser and L. T. Scott, *J. Chem. Educ.*, **62**, 650(1985); D. W. McMillen and J. B. Grutzner, *J. Org. Chem.*, **59**, 4516 (1994).

<sup>135</sup>. J. G. Traynham and Y.-S. Lee, *J. Am. Chem. Soc.*, **96**, 3590 (1974).

<sup>136</sup>. K. D. Raner, J. Luszyk, and K. U. Ingold, *J. Org. Chem.*, **53**, 5220 (1988).

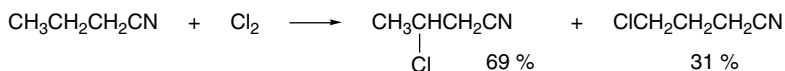
<sup>137</sup>. G. A. Russell, A. Ito, and D. G. Hendry, *J. Am. Chem. Soc.*, **85**, 2976 (1963).

<sup>138</sup>. R. P. Hanzlik, A. R. Schaefer, J. B. Moon, and C. M. Judson, *J. Am. Chem. Soc.*, **109**, 4926 (1987).

<sup>139</sup>. K. B. Wiberg and L. H. Slaugh, *J. Am. Chem. Soc.*, **80**, 3033 (1958).

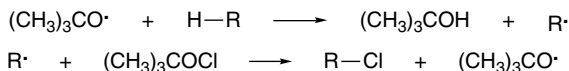
The selectivity of chlorination is influenced by solvents. For example, the chlorination of 2,3-dimethylbutane shows increased preference for the tertiary position in benzene.<sup>140</sup> The complexation with solvent attenuates the reactivity of chlorine atoms. Halogenated solvents also give evidence of complex formation. Brominated solvents lead to greater selectivity.<sup>141</sup>

Radical chlorination shows a substantial polar effect. Positions substituted by EWG are relatively unreactive toward chlorination, even though the substituents are capable of stabilizing the radical intermediate.<sup>142</sup> For example, butanonitrile is chlorinated at C(3) and C(4), but not at C(2), despite the greater stability of the C(2) radical.



Similarly, carboxylic acid and ester groups tend to direct chlorination to the  $\beta$ - and  $\gamma$ -positions, because attack at the  $\alpha$ -position is electronically disfavored. The polar effect is attributed to the fact that the chlorine atom is an electrophilic species, and the relatively electron-poor methylene group adjacent to the EWG is avoided. Because the chlorine atom is highly reactive, the reaction is expected to have a very early TS and the electrostatic effect predominates over the stabilizing effect of the substituent on the intermediate. The electrostatic effect is the dominant factor in the *kinetic selectivity* of the reaction and the relative stability of the radical intermediate has relatively little influence.

Another reagent that effects chlorination by a radical mechanism is *t*-butyl hypochlorite. The hydrogen-abstracting species in the chain mechanism is the *t*-butoxy radical.



For this reason, selectivity and product composition is different from direct chlorination. The *t*-butoxy radical is intermediate in selectivity between chlorine and bromine atoms. The selectivity is also solvent and temperature dependent. A typical ratio in chlorobenzene as the solvent is *tert:sec:pri* = 60:10:1.<sup>143</sup>

Radical substitution reactions by iodine are not practical because the abstraction of hydrogen from hydrocarbons by iodine is endothermic, even for stable radicals. The enthalpy of the overall reaction is also slightly endothermic (see Figure 11.12). Thus, both because of the kinetic problem precluding a chain reaction and an unfavorable equilibrium constant for substitution, iodination does not proceed by a radical chain mechanism.

Fluorination presents problems at the other extreme. Both steps in the substitution chain reaction are exothermic and the reaction is violent if not performed under

<sup>140</sup> G. A. Russell, *J. Am. Chem. Soc.*, **80**, 4987, 4997, 5002 (1958); C. Walling and M. F. Mayahi, *J. Am. Chem. Soc.*, **81**, 1485 (1959).

<sup>141</sup> A. S. Dneprovskii, D. V. Kuznetsov, E. V. Eliseenkov, B. Fletcher, and J. M. Tanko, *J. Org. Chem.*, **63**, 8860 (1998).

<sup>142</sup> A. Bruylants, M. Tits, C. Dieu, and R. Gauthier, *Bull. Soc. Chim. Belg.*, **61**, 266 (1952); A. Bruylants, M. Tits, and R. Danby, *Bull. Soc. Chim. Belg.*, **58**, 210 (1949); M. S. Kharasch and H. C. Brown, *J. Am. Chem. Soc.*, **62**, 925 (1940).

<sup>143</sup> C. Walling and P. J. Wagner, *J. Am. Chem. Soc.*, **86**, 3368 (1964).

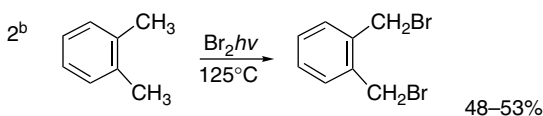
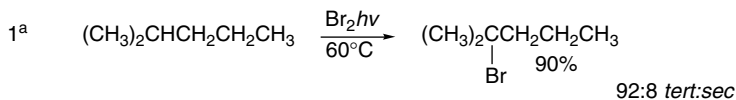
carefully controlled conditions. Furthermore, fluorine atoms are capable of cleaving carbon-carbon bonds.



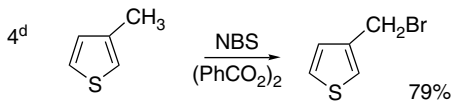
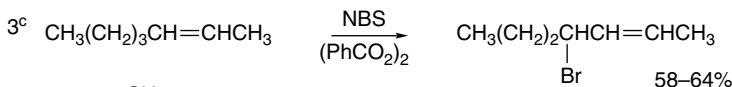
Saturated hydrocarbons such as neopentane, norbornane, and cyclooctane have been converted to the corresponding perfluoro derivatives in 10–20% yield by reaction

### Scheme 11.4. Radical Chain Halogenation

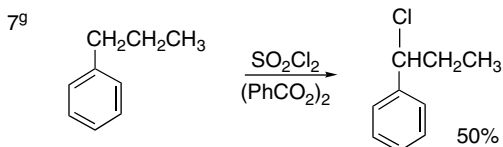
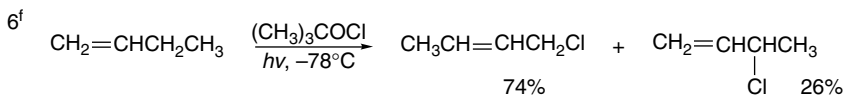
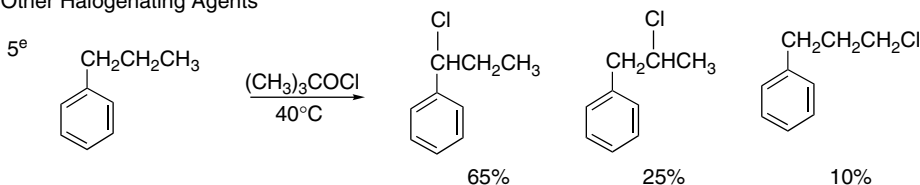
#### Molecular Bromine



#### N-Bromosuccinimide



#### Other Halogenating Agents



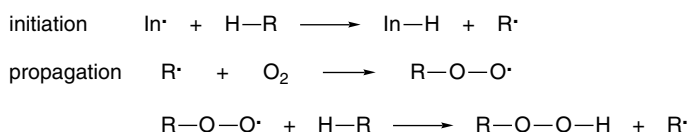
- a. G. A. Russell and H. C. Brown, *J. Am. Chem. Soc.*, **77**, 4025 (1955).  
 b. E. F. M. Stephenson, *Org. Synth.*, **IV**, 984 (1963).  
 c. F. L. Greenwood, M. D. Kellert, and J. Sedlak, *Org. Synth.*, **IV**, 108 (1963).  
 d. E. Campaigne and B. F. Tullar, *Org. Synth.*, **IV**, 921 (1963).  
 e. C. Walling and B. B. Jacknow, *J. Am. Chem. Soc.*, **82**, 6108 (1960).  
 f. C. Walling and W. Thaler, *J. Am. Chem. Soc.*, **83**, 3877 (1961).  
 g. H. C. Brown and A. B. Ash, *J. Am. Chem. Soc.*, **77**, 4019 (1955).

with fluorine gas diluted with helium at  $-78^{\circ}\text{C}$ .<sup>144</sup> Simple ethers can be completely fluorinated under similar conditions.<sup>145</sup> Crown polyethers can be fluorinated by passing a  $\text{F}_2/\text{He}$  stream over a solid mixture of sodium fluoride and the crown ether.<sup>146</sup> Liquid phase fluorination of hydrocarbons has also been observed, but the reaction is believed to be ionic, rather than radical, in character.<sup>147</sup>

Scheme 11.4 illustrates some representative halogenation reactions. The reaction in Entry 1 was conducted by slow addition of bromine to excess 2-methylpentane at  $60^{\circ}\text{C}$ , with irradiation from a tungsten light bulb. The reaction in Entry 2 is a typical benzylic bromination, carried out at  $125^{\circ}\text{C}$  with irradiation from a sun lamp. Entries 3 and 4 are examples of NBS bromination using benzoyl peroxide as the initiator. Entry 3 is interesting in that none of the allylic isomer 2-bromo-3-heptene is found. Entries 5 and 6 are examples of chlorination by *t*-butyl hypochlorite in which the *t*-butoxy radical is the chain carrier. Note that in Entry 6, both the primary and secondary allylic products are formed. The reaction in Entry 7 uses sulfuryl chloride as the halogenation reagent. Note that in contrast to chlorination with  $\text{Cl}_2$  (see p. 1021), the reaction shows selectivity for the benzylic position.

### 11.3.2. Oxygenation

Free radical chain oxidation of organic molecules by molecular oxygen is often referred to as *autoxidation*. The general mechanism is outlined below.



The reaction of oxygen with most radicals is very fast because of the triplet character of molecular oxygen (see Table 11.2, Entries 42 and 43). The ease of autoxidation is therefore governed by the rate of hydrogen abstraction in the second step of the propagation sequence. The alkylperoxyl radicals that act as the chain carriers are fairly selective. Positions that are relatively electron rich or provide particularly stable radicals are the most easily oxidized. Benzylic, allylic, and tertiary positions are the most susceptible to oxidation. This selectivity makes radical chain oxidation a preparatively useful reaction in some cases.

The reactivity of a series of hydrocarbons toward oxygen measured under a standard set of conditions gives some indication of the susceptibility of various structural units to autoxidation.<sup>148</sup> Table 11.9 gives the results for a series of hydrocarbons. These data indicate the activating effect of alkyl, vinyl, and phenyl substituents.

<sup>144</sup> N. J. Maraschin, D. B. Catsikis, L. H. Davis, G. Jarvinen, and R. J. Lagow, *J. Am. Chem. Soc.*, **97**, 513 (1975).

<sup>145</sup> D. F. Persico, H.-N. Huang, R. J. Lagow, Jr., and L. C. Clark, Jr., *J. Org. Chem.*, **50**, 5156 (1985).

<sup>146</sup> W.-H. Lin, W. I. Bailey, Jr., and R. J. Lagow, *J. Chem. Soc., Chem. Commun.*, 1350 (1985).

<sup>147</sup> C. Gal and S. Rozen, *Tetrahedron Lett.*, **25**, 449 (1984).

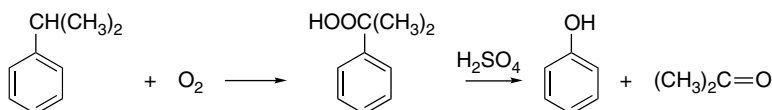
<sup>148</sup> G. A. Russell, *J. Am. Chem. Soc.*, **78**, 1047 (1956).

**Table 11.9. Relative Reactivities of Some Aromatic Hydrocarbons toward Oxygen**

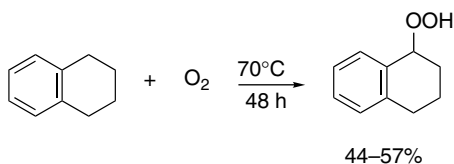
PhCH(CH <sub>3</sub> ) <sub>2</sub>	1.0	PhCH <sub>2</sub> CH <sub>3</sub>	0.18
PhCH <sub>2</sub> CH=CH <sub>2</sub>	0.8	PhCH <sub>3</sub>	0.015
Ph <sub>2</sub> CH <sub>2</sub>	0.35		

a. Data from G. A. Russell, *J. Am. Chem. Soc.*, **78**, 1047 (1956).

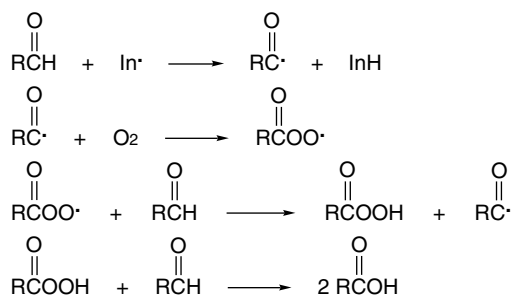
The best preparative results from autoxidation are obtained when only one relatively reactive hydrogen is available for abstraction. The oxidation of isopropylbenzene (cumene) is carried out on an industrial scale with the ultimate products being acetone and phenol.



The benzylic position in tetralin can be selectively oxidized to the hydroperoxide.<sup>149</sup>

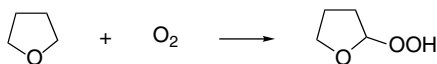


Functional groups that stabilize radicals are expected to increase susceptibility to autoxidation. This is illustrated by two cases that have been relatively well studied. Aldehydes, in which abstraction of the formyl hydrogen is facile, are easily autoxidized. The autoxidation initially forms a peroxyacid, but usually the corresponding carboxylic acid is isolated because the peroxy acid oxidizes additional aldehyde in a parallel heterolytic reaction. The final step is an example of the Baeyer-Villiger reaction, which is discussed in Section 12.5.2.1 of Part B.



Similarly, the  $\alpha$ -position in ethers is autoxidized quite readily to give  $\alpha$ -hydroperoxy ethers.

<sup>149</sup> H. B. Knight and D. Swern, *Org. Synth.*, **IV**, 895 (1963).



This reaction is the cause of a widely recognized laboratory hazard. The peroxides formed from several commonly used ethers such as diethyl ether and tetrahydrofuran are explosive. Appreciable amounts of such peroxides can build up in ether samples that have been exposed to air. Since the hydroperoxides are less volatile than the ethers, they are concentrated by evaporation or distillation and the concentrated peroxide solutions may explode. For this reason, storage of ethers that have been exposed to oxygen is extremely hazardous.

## 11.4. Free Radical Addition Reactions

### 11.4.1. Addition of Hydrogen Halides

As with halogen substitution, thermochemical relationships impose limits on free radical chain addition reactions of the hydrogen halides. These relationships are summarized in Figure 11.13. There are significant endothermic steps for HF and HI and a slightly endothermic step for HCl. Radical chain additions of hydrogen fluoride and hydrogen iodide to alkenes are not observed. In the case of hydrogen iodide, the addition of an iodine atom to an alkene is an endothermic process and is too slow to permit a chain reaction, even though the hydrogen abstraction step is favorable. In the case of hydrogen fluoride, the abstraction of hydrogen from hydrogen fluoride is energetically prohibitive. Only in the case of HBr is the thermochemistry consistent with a radical chain process. The HBr addition has one thermal neutral step and an

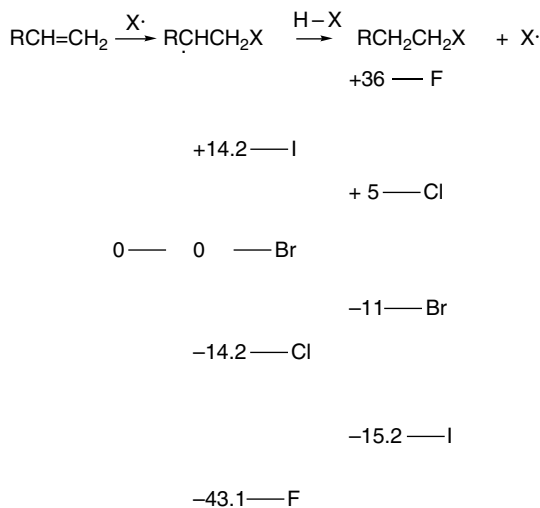
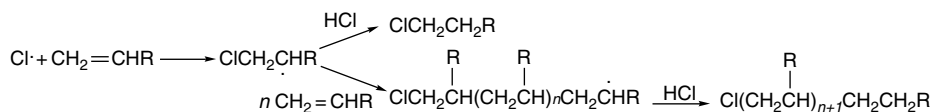
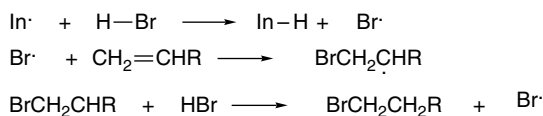


Fig. 11.13. Thermochemistry for the steps in radical chain additions of the hydrogen halides to alkenes. The C=C and C-H bond energies were taken as 70 and 98 kcal/mol, respectively, and primary C-X bond energies were used.

exothermic step. Because of the relatively slow second step, polymerization competes with addition of the hydrogen halide in the case of HCl.

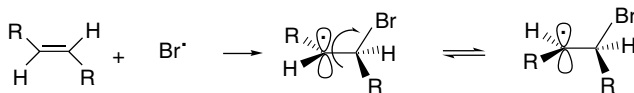


The reaction with HBr is also significant in terms of regiochemistry. The reaction results in the anti-Markovnikov orientation, with the bromine adding to the less-substituted carbon of the double bond. The anti-Markovnikov addition of HBr to alkenes was one of the earliest free radical reactions to be put on a firm mechanistic basis. In the presence of a suitable initiator, such as a peroxide, a radical chain mechanism becomes competitive with the ionic mechanism for addition of HBr.



The bromine atom adds to the less-substituted carbon of the double bond, generating the more stable radical intermediate. The regioselectivity of radical chain hydrobromination is opposite to that of ionic addition. (See Section 5.3 for discussion of the ionic mechanism.) The early work on the radical mechanism of addition of HBr was undertaken to understand why Markovnikov's rule was violated under certain circumstances. The cause was found to be conditions that initiated the radical chain process, such as peroxide impurities or light. Some examples of radical chain additions of hydrogen bromide to alkenes are discussed in Section 11.4.5.

The stereochemistry of radical addition of hydrogen bromide to alkenes has been studied with both acyclic and cyclic alkenes.<sup>150</sup> *Anti* addition is favored.<sup>151,152</sup> This is contrary to what would be expected if the  $sp^2$  carbon of the radical intermediate was rapidly rotating or inverting with respect to the remainder of the molecule, which should result in stereorandomization and a mixture of *syn* and *anti* products.



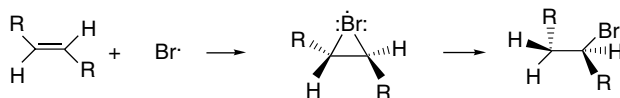
The stereoselectivity of the radical addition can be explained in terms of a bridged structure similar to that involved in ionic bromination of alkenes.<sup>153</sup>

<sup>150</sup>. B. A. Bohm and P. I. Abell, *Chem. Rev.*, **62**, 599 (1962).

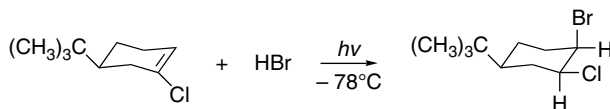
<sup>151</sup>. P. S. Skell and P. K. Freeman, *J. Org. Chem.*, **29**, 2524 (1964).

<sup>152</sup>. H. L. Goering and D. W. Larsen, *J. Am. Chem. Soc.*, **81**, 5937 (1959).

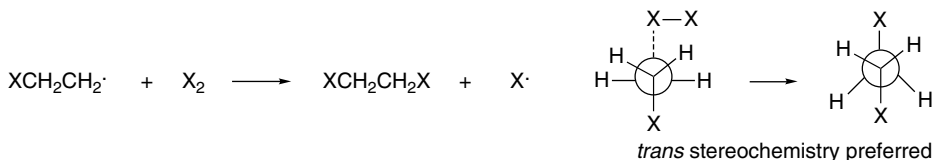
<sup>153</sup>. P. S. Skell and J. G. Traynham, *Acc. Chem. Res.*, **17**, 160 (1984).



*trans*-Diaxial addition is the preferred stereochemical mode for addition to cyclohexene and its derivatives.<sup>154</sup> This stereochemistry, too, can be explained in terms of a bromine-bridged intermediate.



The issue of the role of bridged radicals in the stereochemistry of halogenation has recently been examined computationally and a new interpretation offered.<sup>155</sup> The structure, rotational barriers, and  $E_a$  for halogen atom abstraction for  $\beta$ -haloethyl radicals were studied. For the reactions where  $X=\text{Cl}$  or  $\text{Br}$ , the halogen atom abstraction reaction shows a preference for a *trans* TS.



The results also indicate that the chlorine and bromine abstraction steps are faster than rotational equilibration, so the stereochemistry can be explained without requiring a bridged radical.

The nature of bridging and migration involving chlorine has been explored computationally for the 3-chloro-2-butyl radical.<sup>156</sup> B3LYP/aug-cc-pVD2 calculations found an open radical to be the most stable form. The symmetrically bridged radical is a TS for chlorine atom migration. The energy of the TS varied from 2.4 to 7.0 kcal/mol, depending on the computational method. The methods also give differing values for the barrier to single-bond rotation. The chlorine has considerable negative charge ( $-0.351e$ ) in the bridged radical, compared to the open radical ( $-0.189e$ ) by NPA analysis. The spin density also increases at chlorine in the TS. These results suggest partial heterolytic character for the migration. The energy profile for rotation and migration derived from the B3LYP energies is given in Figure 11.14.

In contrast to the  $\beta$ -chloro radical, bromine-bridged radicals are calculated to be stable relative to open radicals at the MP2/6-31G\*\* and B3LYP/6-31G\*\* level of computation.<sup>157</sup> The 2-fluoroethyl radical shows no bridging and only a low barrier to single-bond rotation ( $<0.5$  kcal/mol). Bridging was also found to be unfavorable for the other second-row substituents OH and  $\text{NH}_2$ .<sup>158</sup> These computational results suggest that significant bridging is to be expected in  $\beta$ -bromo radicals, whereas  $\beta$ -chloro radicals should be subject to facile 1,2-migration.

<sup>154</sup> H. L. Goering and L. L. Sims, *J. Am. Chem. Soc.*, **77**, 3465 (1955); N. A. LeBel, R. F. Czaja, and A. DeBoer, *J. Org. Chem.*, **34**, 3112 (1969); P. D. Readio and P. S. Skell, *J. Org. Chem.*, **31**, 753 (1966); H. L. Goering, P. I. Abell, and B. F. Aycock, *J. Am. Chem. Soc.*, **74**, 3588 (1952).

<sup>155</sup> Z.-H. Li, K.-N. Fan, and M. W. Wong, *J. Phys. Chem. A*, **105**, 10890 (2001).

<sup>156</sup> B. Neumann and H. Zipse, *Org. Biomol. Chem.*, **1**, 168 (2003).

<sup>157</sup> H. Ihee, A. H. Zewail, and W. A. Goddard, III, *J. Phys. Chem. A*, **103**, 6638 (1999).

<sup>158</sup> M. Guerra, *J. Am. Chem. Soc.*, **114**, 2077 (1992).

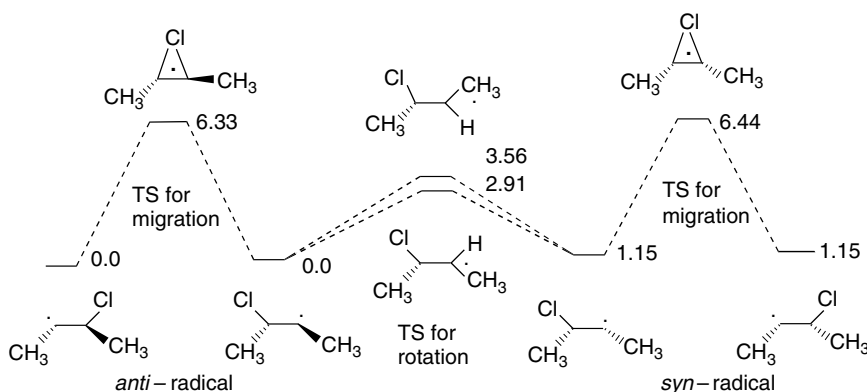
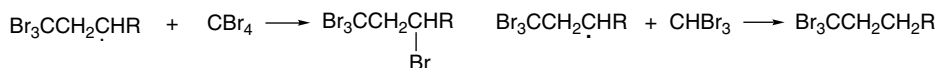
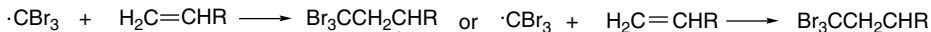
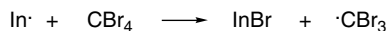


Fig. 11.14. Energy profile for chlorine migration and rotation in the 3-chloro-2-butyl radical.

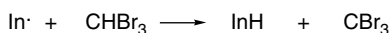
### 11.4.2. Addition of Halomethanes

One of the oldest preparative free radical reactions is the addition of polyhalomethanes to alkenes. Examples of addition of carbon tetrabromide, carbon tetrachloride, and bromoform have been recorded.<sup>159</sup> The reactions are chain processes that depend on facile abstraction of halogen or hydrogen from the halomethane.

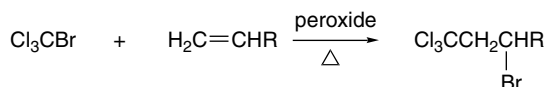
#### ADDITION OF TETRABROMOMETHANE



#### ADDITION OF TRIBROMOMETHANE

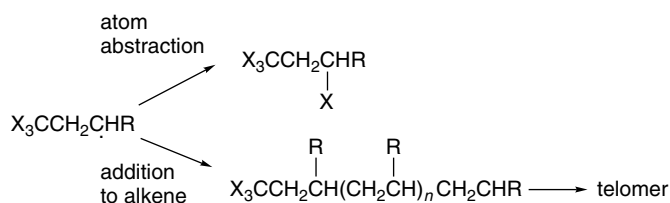


Bromotrichloromethane can also be used effectively in the addition reaction. Because of the preferential abstraction of bromine, a trichloromethyl unit is added to the less-substituted carbon atom of the alkene.

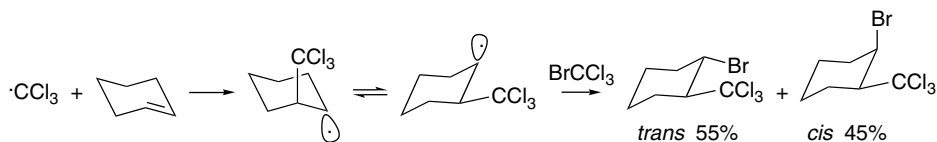


The order of reactivity of the halomethanes is  $\text{CBr}_4 > \text{CBrCl}_3 > \text{CCl}_4 > \text{CH}_2\text{Cl}_2 > \text{CHCl}_3$ . The efficiency of 1:1 addition for a given alkene also depends on the ease with which it undergoes radical chain polymerization, since polymerization can compete with the halogen atom abstraction step in the chain mechanism. Polymerization is usually most rapid for terminal alkenes bearing stabilizing substituents such as a phenyl or ester group.

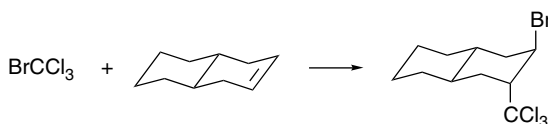
<sup>159</sup> E. Sosnovsky, *Free Radical Reactions in Preparative Organic Chemistry*, Macmillan, New York, 1964, Chap. 2.



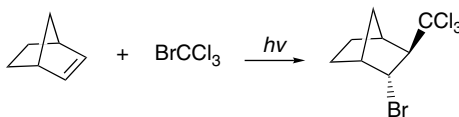
The addition of bromotrichloromethane to cyclohexene gives a nearly 1:1 mixture of the two possible stereoisomers.<sup>160</sup>



This result indicates that the initially added trichloromethyl group has little influence on the stereochemistry of the subsequent bromine atom abstraction. The intermediate 2-(trichloromethyl)cyclohexyl radical presumably relaxes to the equatorial conformation faster than the occurrence of bromine atom abstraction, and there is little preference for axial or equatorial approach. In contrast, with  $\Delta^{2,3}$ -octahydronaphthalene, the addition is exclusively *trans*-diaxial.



The *trans*-fused decalin system is conformationally rigid and the stereochemistry of the product indicates that the initial addition of the trichloromethyl radical is from an axial direction. This is expected on stereoelectronic grounds because the radical should initially interact with the  $\pi^*$  orbital. The axial trichloromethyl group then shields the adjacent radical position and directs the bromine abstraction in the *trans* sense. Addition of bromotrichloromethane to norbornene is also *anti*. This is again the result of steric shielding by the trichloromethyl group, which causes the bromine atom to be abstracted from the *endo* face of the intermediate radical.

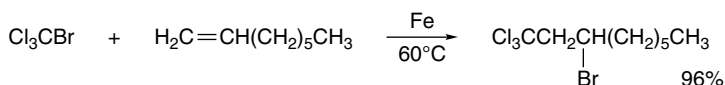


The addition of bromotrichloromethane to terminal alkenes occurs in reasonable yield in THF without the addition of a specific initiator.<sup>161</sup> Bromotrichloromethane additions are effectively catalyzed by Fe(0), which acts as an initiator by one-electron reduction.<sup>162</sup>

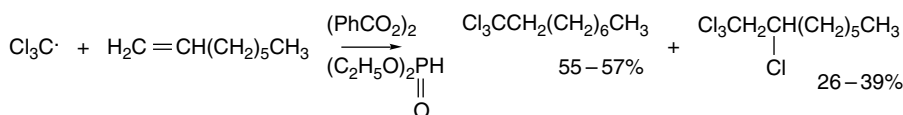
<sup>160.</sup> J. G. Traynham, A. G. Lane, and N. S. Bhacca, *J. Org. Chem.*, **34**, 1302 (1969).

<sup>161.</sup> M. Heintz, G. L. Ny, and J. Y. Nedelec, *Tetrahedron Lett.*, **25**, 5767 (1984).

<sup>162.</sup> F. Bellesia, L. Forti, F. Ghelfi, and U. M. Pagnoni, *Synth. Commun.*, **27**, 961 (1997).

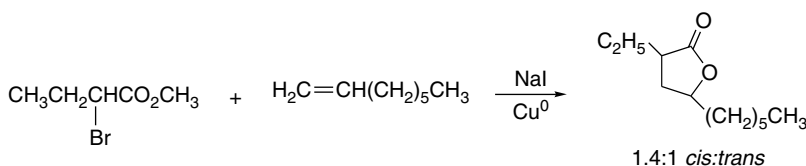


The combination of  $\text{CCl}_4$  and diethyl phosphite with a peroxide initiator gives competitive addition of  $\text{H}-\text{CCl}_3$ . In this case the phosphite acts as a hydrogen donor.<sup>163</sup>



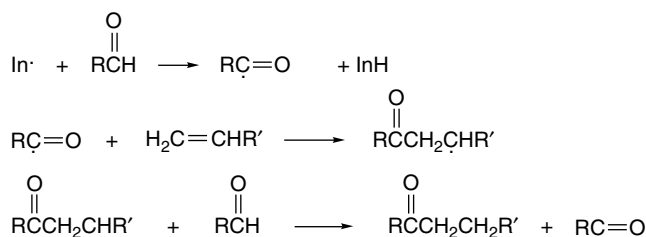
Section 11.4.5 provides some other examples of additions of tetrahalomethanes.

There are examples of other halomethanes that can undergo radical addition.  $\alpha$ -Haloesters have been successfully added to alkenes in the presence of copper metal. The copper serves as an electron transfer initiator. The  $\gamma$ -haloester adduct cyclizes to a lactone. The reaction works best when  $\text{NaI}$  is also used to convert the bromide to the more reactive iodide.<sup>164</sup>



### 11.4.3. Addition of Other Carbon Radicals

Other functional groups provide sufficient stabilization of radicals to permit successful chain additions to alkenes. Acyl radicals are formed by abstraction of the formyl hydrogen from aldehydes. As indicated in Table 3.17 (p. 315), the acyl radicals are somewhat stabilized. The  $\text{C}-\text{H}$  BDE for acetaldehyde, which is 88.3 kcal/mol, decreases slightly with additional substitution but increases for  $\text{CF}_3$ .<sup>165</sup> The chain process results in formation of a ketone by addition of the aldehyde to an alkene



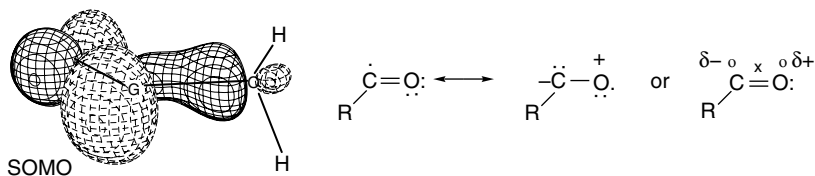
Acyl radicals are strongly bent with a nearly trigonal angle, according to MP2/6-31G\* computations. The  $\text{C}=\text{O}$  bond length is just under 1.200 Å, somewhat shorter than a normal carbonyl bond. The SOMO orbital is in the plane of the molecule and

<sup>163</sup>. J. M. Barks, B. C. Gilbert, A. F. Parsons, and B. Upeandran, *Synlett*, 1719 (2001).

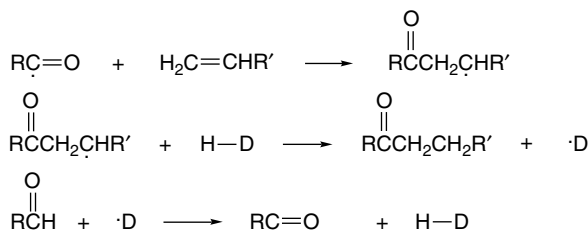
<sup>164</sup>. J. O. Metzger, R. Mahler, and G. Franke, *Liebigs Ann. Recueil*, 2303 (1997).

<sup>165</sup>. B. Viskolcz and T. Berces, *Phys. Chem. Chem. Phys.*, **2**, 5430 (2000); C. W. Bauschlicher, Jr., *J. Chem. Phys.*, **98**, 2564 (1994).

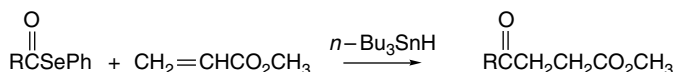
centered mainly on carbon, but also on the oxygen.<sup>166</sup> Acyl radicals are *nucleophilic*, based on their reactivity toward protonated heterocyclic molecules.<sup>167</sup> The acyl radical is isoelectronic with  $\text{N}=\ddot{\text{O}}$  and a similar Linnett structure can be drawn.



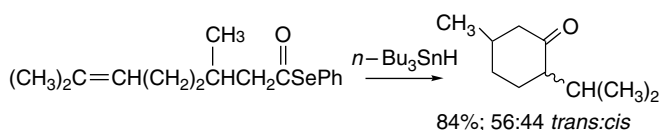
The efficiency of aldehyde additions can be improved by adding an alternative hydrogen atom donor, such as methyl thioglycolate or *N*-hydroxysuccinimide.<sup>168</sup>



Acyl radicals can also be generated from acyl selenides and *tri-n*-butylstannane.<sup>166</sup>



Intramolecular versions of this reaction have been used to form both common and macrocyclic rings.



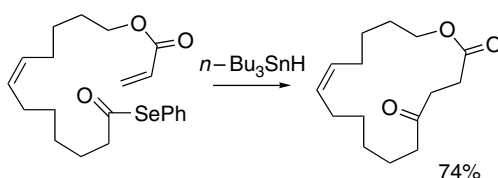
The latter reactions are carried out under high-dilution conditions and require an activating EWG substituent.<sup>169</sup>

<sup>166</sup> D. L. Boger and R. J. Mathvink, *J. Org. Chem.*, **57**, 1429 (1992).

<sup>167</sup> M. Bellatti, T. Caronna, A. Citterio, and F. Minisci, *J. Chem. Soc., Perkin Trans. 2*, 1835 (1976); F. Minisci, *Top. Current Chem.*, **62**, 1 (1976).

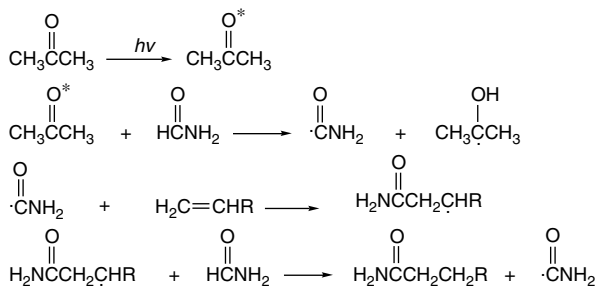
<sup>168</sup> V. Paul, B. P. Roberts, and C. R. Willis, *J. Chem. Soc., Perkin Trans. 2*, 1953 (1989); S. Tsujimoto, I. Iwahama, S. Sakaguchi, and Y. Ishii, *Chem. Commun.*, 2352 (2001); S. Tsujimoto, S. Sakaguchi, and Y. Ishii, *Tetrahedron Lett.*, **44**, 5601 (2003).

<sup>169</sup> D. L. Boger and R. J. Mathvink, *J. Am. Chem. Soc.*, **112**, 4008 (1990).



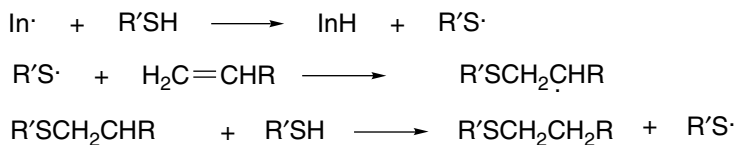
Some other examples of acyl radical additions are discussed in Section 11.4.5.

The chain addition of formamide to alkenes is a closely related reaction and results in the formation of primary amides.<sup>170</sup> The reaction is carried out with irradiation in acetone. The photoexcited acetone initiates the chain reaction by abstracting hydrogen from formamide.



#### 11.4.4. Addition of Thiols and Thiocarboxylic Acids

The addition of S–H compounds to alkenes by a radical chain mechanism is a quite general and efficient reaction.<sup>171</sup> The mechanism is analogous to that for hydrogen bromide addition. The energetics of both the hydrogen abstraction and addition steps are favorable. The reaction exhibits anti-Markovnikov regioselectivity.



The preferred stereochemistry of addition to cyclic alkenes is *anti*,<sup>172</sup> but the additions are not as highly stereoselective as for hydrogen bromide addition.

#### 11.4.5. Examples of Radical Addition Reactions

Scheme 11.5 gives some examples of these radical addition reactions. Entries 1 to 3 show anti-Markovnikov addition of HBr. The reaction in Entry 1 was carried out by passing HBr gas into the alkene, using benzoyl peroxide as the initiator, apparently near room temperature. Entry 2 is an example of anti-Markovnikov addition to

<sup>170</sup>. D. Elad and J. Rokach, *J. Org. Chem.*, **29**, 1855 (1964).

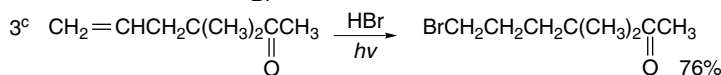
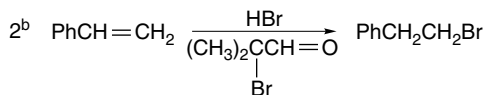
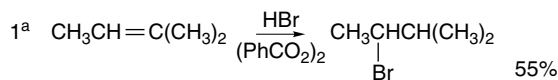
<sup>171</sup>. K. Griesbaum, *Angew. Chem. Int. Ed. Engl.*, **9**, 273 (1970).

<sup>172</sup>. N. A. LeBel, R. F. Czaja, and A. DeBoer, *J. Org. Chem.*, **34**, 3112 (1969); P. D. Readio and P. S. Skell, *J. Org. Chem.*, **31**, 759 (1966); F. G. Bordwell, P. S. Landis, and G. S. Whitney, *J. Org. Chem.*, **30**, 3764 (1965); E. S. Huyser, H. Benson, and H. J. Sinnige, *J. Org. Chem.*, **32**, 622 (1962).

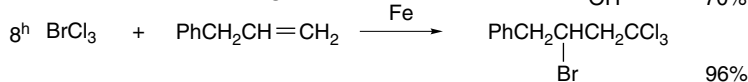
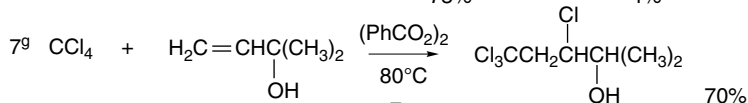
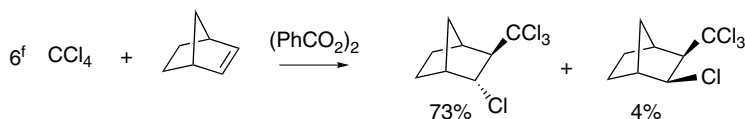
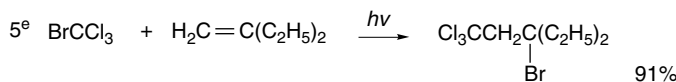
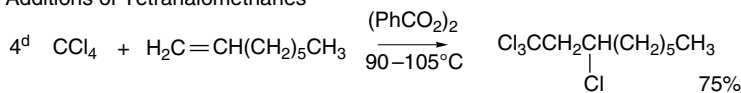
styrene. The  $\alpha$ -bromoaldehyde additive was shown to increase the regioselectivity. A similar effect has been noted for  $\text{PBr}_3$ ,<sup>173</sup> but the mechanistic basis is not established in either case. The reaction in Entry 3 was carried out under irradiation from

### Scheme 11.5. Free Radical Additions to Alkenes

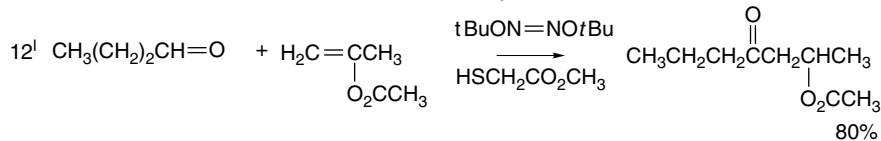
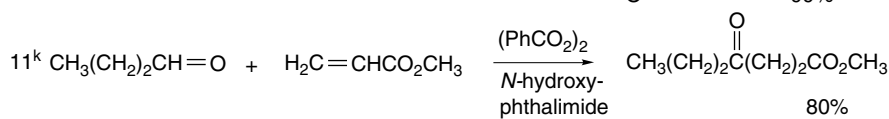
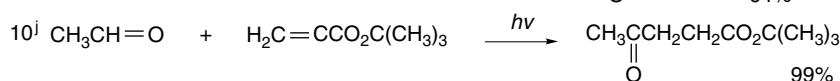
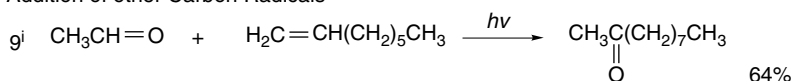
#### A. Addition of Hydrogen Bromide



#### B. Additions of Tetrahalomethanes

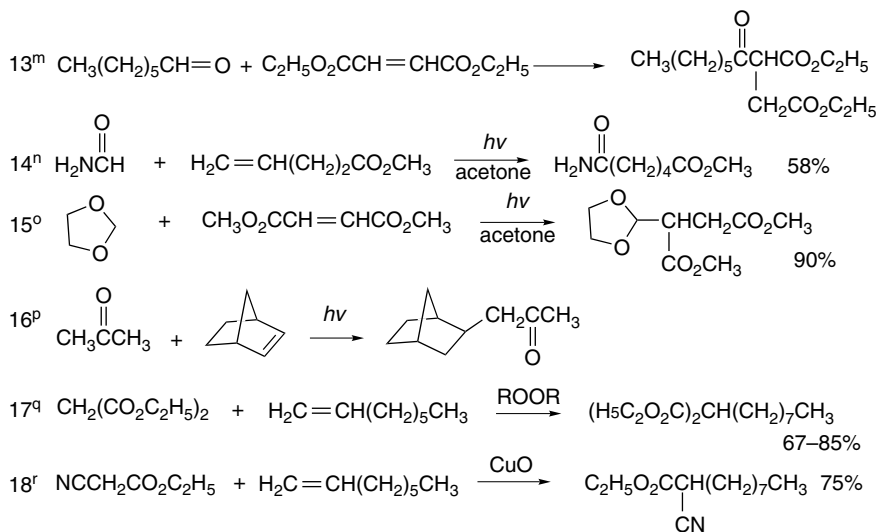


#### C. Addition of other Carbon Radicals

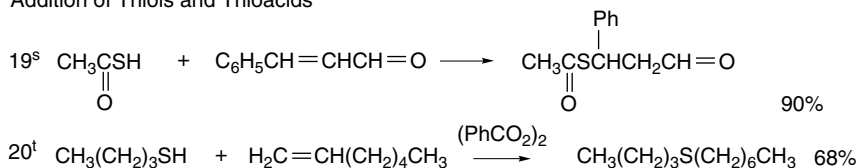


(Continued)

<sup>173</sup> G. A. Olah and T. R. Hockswender, Jr., *J. Org. Chem.*, **39**, 3478 (1974).



## D. Addition of Thiols and Thioacids

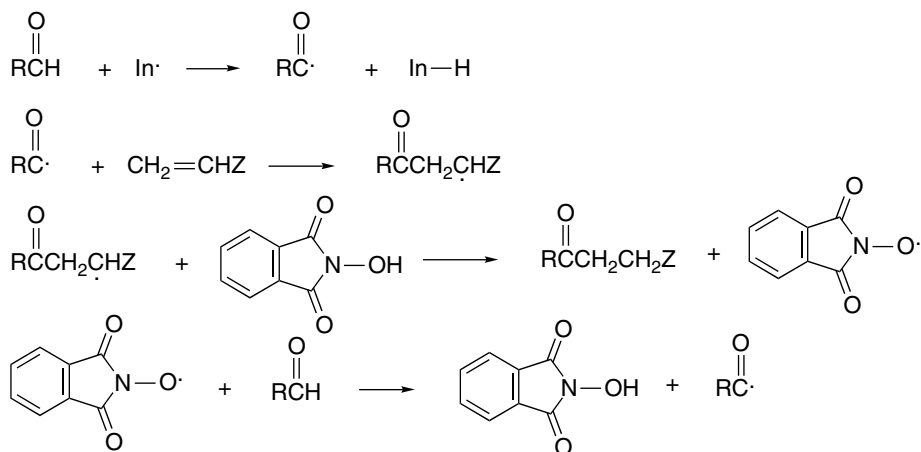


- a. W. J. Bailey and S. S. Hirsch, *J. Org. Chem.*, **28**, 2894 (1963).  
 b. R. Neumann, F. de la Vega, and A. Bar-On, *J. Org. Chem.*, **60**, 1315 (1995).  
 c. H. O. House, C.-Y. Chu, W. V. Phillips, T. S. B. Sayer, and C.-C. Yau, *J. Org. Chem.*, **42**, 1709 (1977).  
 d. M. S. Kharasch, E. W. Jensen, and W. H. Urry, *J. Am. Chem. Soc.*, **69**, 1100 (1947).  
 e. M. S. Kharasch and M. Sage, *J. Org. Chem.*, **14**, 537 (1949).  
 f. C. L. Osborn, T. V. Van Auken, and D. J. Trecker, *J. Am. Chem. Soc.*, **90**, 5806 (1968).  
 g. P. D. Klemmensen, H. Kolind-Andersen, H. B. Madsen, and A. Svendsen, *J. Org. Chem.*, **44**, 416 (1979).  
 h. F. Bellesia, L. Forti, F. Ghelfi, and U. M. Pagnoni, *Synth. Commun.*, **27**, 961 (1997).  
 i. M. S. Kharasch, W. H. Urry, and B. M. Kuderna, *J. Org. Chem.*, **14**, 248 (1949).  
 j. E. C. Macias, J. M. G. Molinillo, G. M. Massanet, and F. Rodriguez-Luis, *Tetrahedron*, **48**, 3345 (1992).  
 k. S. Tsushimoto, S. Sakaguchi, and Y. Ishii, *Tetrahedron Lett.*, **44**, 5601 (2003).  
 l. H.-S. Dang and B. P. Roberts, *J. Chem. Soc. Perkin Trans. 1*, 67 (1998).  
 m. T. M. Patrick, Jr., and F. B. Erickson, *Org. Synth.*, **IV**, 430 (1963).  
 n. D. Elad and J. Rokach, *J. Org. Chem.*, **29**, 1855 (1964).  
 o. I. Rosenthal and D. Elad, *J. Org. Chem.*, **33**, 805 (1968).  
 p. W. Reusch, *J. Org. Chem.*, **27**, 1882 (1962).  
 q. J. C. Allen, J. I. G. Cadogan, B. W. Harris, and D. H. Hey, *J. Chem. Soc.*, 4468 (1962).  
 r. A. Hajek and J. Malek, *Synthesis*, 454 (1977).  
 s. R. Brown, W. E. Jones, and A. R. Pinder, *J. Chem. Soc.*, 2123 (1951).  
 t. D. W. Grattan, J. M. Locke, and S. R. Wallis, *J. Chem. Soc., Perkin Trans. 1*, 2264 (1973).

a mercury lamp. Entries 4 to 8 involve additions of tetrahalomethanes. In Entry 4 the ratio of reactants was 1.00  $\text{CCl}_4$ , 0.33 alkene, and 0.02 peroxide. Similar ratios were used in Entries 6 and 7. Entry 5 was done with irradiation from a mercury lamp. Entry 6 demonstrates the exclusive *exo* addition of the trichloromethyl radical and dominant *endo* abstraction of chlorine. Entry 8 is an example of a recently developed procedure in which iron powder acts both as an initiator and catalyst.

Entries 9 to 16 show additions of various carbon radicals. Entry 9 involves addition of acetaldehyde to a terminal alkene. The reaction was done under mercury

lamp irradiation and the conversion was rather low. Higher yields were obtained using heptanal. Entries 10 and 11 demonstrate that alkenes with EWG substituents are suitable reactants, which is consistent with the nucleophilic character of acyl radicals. The reaction in Entry 10 was carried out under irradiation from a mercury lamp. These reactions were found to be facilitated by  $O_2$ , which is thought to be involved in the initiation phase of the reaction. Entry 11 uses *N*-hydroxyphthalimide as the chain transfer agent in a process called *polarity reversal catalysis*. The adduct radical abstracts hydrogen from *N*-hydroxyphthalimide. The resulting radical is much more reactive toward hydrogen abstraction from the aldehyde than is the adduct radical. In the example cited, the ratio of reactants used was aldehyde 7.5, alkene 1.0, *N*-hydroxyphthalimide 0.1, benzoyl peroxide 0.1.



The reaction in Entry 12 is related and uses thioglycolate esters as a chain transfer agent. In this particular reaction involving an electron-rich alkene, the yield is only 8% in the absence of the thioglycolate. Entry 13 is another example of the addition of an acyl radical to relatively electrophilic alkene. Entry 14, involving the addition of formamide was done with acetone photosensitization. The 2-dioxolanyl radical involved in Entry 15 would be expected to be nucleophilic in character and higher yields were obtained with diethyl maleate than with typical terminal alkenes. The addition of 1,3-dioxolane to various enones has been done using benzophenone sensitization.<sup>174</sup> The radicals in Entries 17 and 18 are electrophilic in character. Entries 19 and 20 are examples of thiol additions.

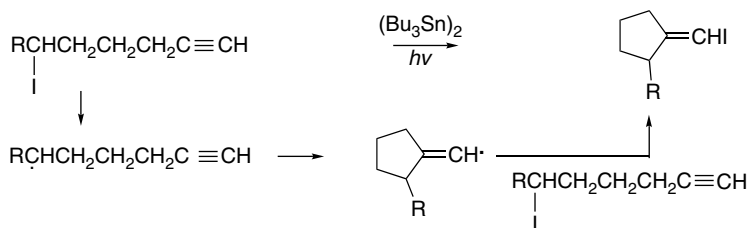
Intramolecular addition reactions are quite common when radicals are generated in molecules with unsaturation in a sterically favorable position.<sup>175</sup> We will encounter several examples of intramolecular additions in the next section. Cyclization reactions based on intramolecular addition of radical intermediates are synthetically useful and several specific cases are considered in Section 10.3.3 of Part B.

<sup>174</sup> C. Manfrotto, M. Mella, M. Freccero, M. Fagnoni, and A. Albini, *J. Org. Chem.*, **64**, 5024 (1999).

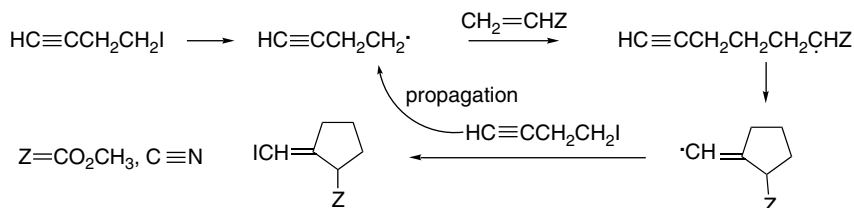
<sup>175</sup> A. L. J. Beckwith, *Tetrahedron*, **37**, 3073 (1981).



The chain is propagated by abstraction of iodine by the cyclized vinyl radical intermediate. This sequence of reactions benefits from the high reactivity of the intermediate alkenyl reaction in the iodine transfer step.

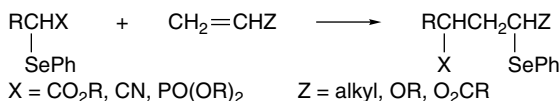


The hexabutyldistannane used in this reaction is not involved in the propagation sequence but may be involved in initiation or scavenging of potential chain termination radicals. With 4-iodobutyne, the intermediate radicals can be trapped by activated alkenes, which leads to cyclized products.<sup>180</sup>



For all of these reactions, the reagents and reaction conditions must be chosen to meet the fundamental requirement for successful chain reactions. Each step in the sequence must be fast and exothermic to permit chain propagation.<sup>181</sup>

Aryl selenides have also proven to be excellent reagents in group transfer reactions.<sup>182</sup> Photolysis of selenides in an inert solvent such as benzene can initiate chain reactions. Various substituted radicals can be generated in this manner by using  $\alpha$ -selenenyl derivatives of esters,<sup>183</sup> nitriles,<sup>184</sup> malonates,<sup>185</sup>  $\beta$ -ketoesters,<sup>183</sup>  $\alpha$ -methoxyesters,<sup>186</sup> and phosphonates.<sup>187</sup> The resulting radicals undergo addition to alkenes to generate  $\gamma$ -seleno derivatives.



<sup>180</sup> D. P. Curran and M.-H. Chen, *J. Am. Chem. Soc.*, **109**, 6558 (1987).

<sup>181</sup> D. P. Curran, *Synthesis*, 417, 511 (1988); C. P. Jasperse, D. P. Curran, and T. L. Fervig, *Chem. Rev.*, **91**, 1237 (1991).

<sup>182</sup> L. Castle and M. J. Perkins, in *The Chemistry of Organic Selenium and Tellurium Compounds*, Part 2, S. Patai, ed., Wiley, Chichester, 1987, Chap. 16.

<sup>183</sup> J. H. Byers and B. C. Harper, *Tetrahedron Lett.*, **33**, 6953 (1992).

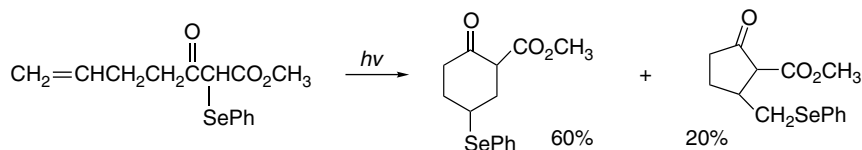
<sup>184</sup> D. P. Curran and G. Thoma, *J. Am. Chem. Soc.*, **114**, 4436 (1992).

<sup>185</sup> J. H. Byers and G. C. Lane, *J. Org. Chem.*, **58**, 3355 (1993).

<sup>186</sup> P. Renaud and S. Abazi, *Synthesis*, 253 (1996).

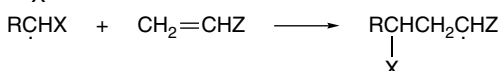
<sup>187</sup> P. Balczewski, W. M. Pietrzykowski, and M. Mikolajczyk, *Tetrahedron*, **51**, 7727 (1995); J. H. Byers, J. G. Thissell, and M. A. Thomas, *Tetrahedron Lett.*, **36**, 6403 (1995).

Appropriately substituted selenides can undergo cyclization reactions via a group transfer process.<sup>188</sup>

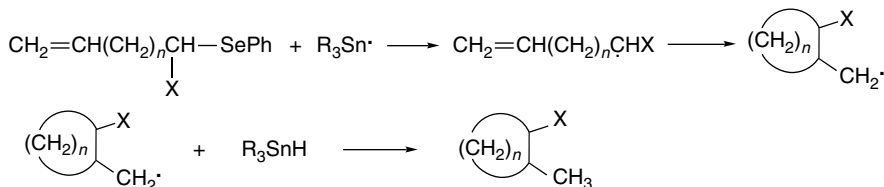


If selenide additions are carried out in the presence of tri-*n*-butylstannane, the radical generated by addition is reduced by hydrogen abstraction. The chain is then continued by selenide abstraction by the stannyl radical, which leads to reduced addition and cyclization products.

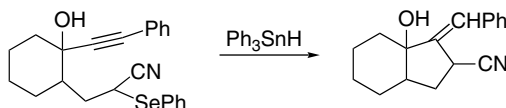
*Intermolecular addition:*



*Intramolecular addition:*

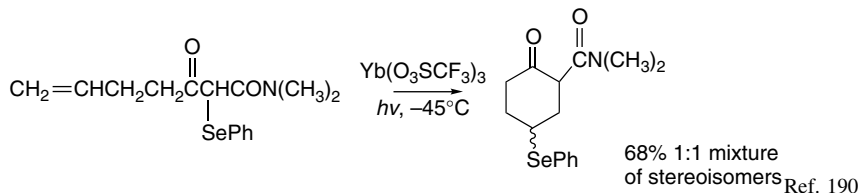


This reaction can also be applied to alkynes.



Ref. 189

Certain of these phenylselenenyl radical transfer reactions are catalyzed by Lewis acids. The regioselectivity depends on reactant structure, and related compounds give *5-exo* and *7-endo* products. The catalysis is believed to be the result of complexation at the carbonyl, which enhances the electrophilicity of the radical.



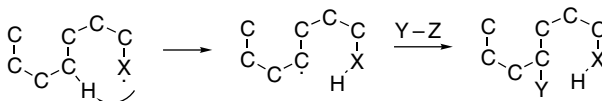
<sup>188</sup>. J. H. Byers, T. G. Gleason, and K. S. Knight, *J. Chem. Soc., Chem. Commun.*, 354 (1991).

<sup>189</sup>. D. J. L. Clive, T. L. B. Boivin, and A. G. Angoh, *J. Org. Chem.*, **52**, 4943 (1982).

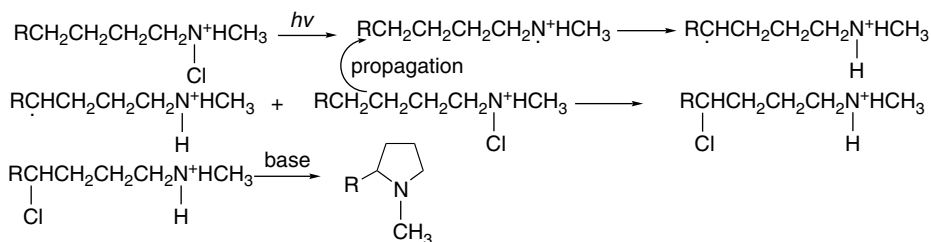
<sup>190</sup>. D. Yang, Q. Gao, and O.-Y. Lee, *Org. Lett.*, **4**, 1239 (2002).

## 11.5.2. Intramolecular Hydrogen Atom Transfer Reactions

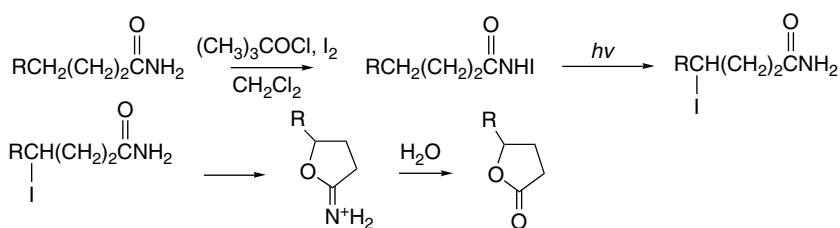
We have seen that substitution, addition, and group transfer reactions can occur intramolecularly. Intramolecular substitution reactions that involve hydrogen abstraction have some unique synthetic applications because they permit functionalization of carbon atoms relatively remote from the initial reaction site.<sup>191</sup> The preference for a six-membered cyclic TS in the hydrogen abstraction step imparts position selectivity to the process.



There are several reaction sequences that involve such intramolecular hydrogen abstraction steps. One example is the photolytically initiated decomposition of *N*-haloamines in acidic solution, which is known as the *Hofmann-Loeffler reaction*.<sup>192</sup> The reaction leads to  $\gamma$ -haloamines, but these are usually converted to pyrrolidines by intramolecular nucleophilic substitution.



There are related procedures involving *N*-haloamides that lead to lactones via iminolactone intermediates.<sup>193</sup>



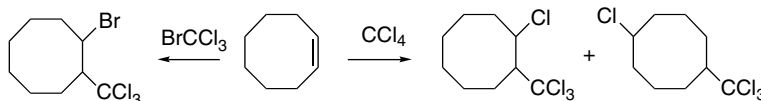
Intramolecular hydrogen abstraction reactions have also been observed in medium-sized rings. The reaction of cyclooctene with carbon tetrachloride and bromotrichloromethane is an interesting case. As shown in the equations below,

<sup>191</sup> G. Majetich and K. Wheless, *Tetrahedron*, **51**, 7095 (1995).

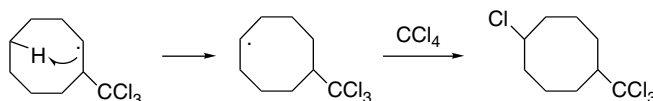
<sup>192</sup> M. E. Wolff, *Chem. Rev.*, **63**, 55 (1963).

<sup>193</sup> D. H. R. Barton, A. L. J. Beckwith, and A. Goosen, *J. Chem. Soc.*, 181 (1965); R. S. Neale, N. L. Marcus, and R. G. Schepers, *J. Am. Chem. Soc.*, **88**, 3051 (1966).

bromotrichloromethane adds in a completely normal manner, but carbon tetrachloride gives some 4-chloro-1-trichloromethylcyclooctane, as well as the expected product.<sup>194</sup>



In the case of carbon tetrachloride, the radical intermediate undergoes two competing reactions; transannular hydrogen abstraction is competitive with abstraction of a chlorine atom from carbon tetrachloride. The former reaction leads to the 1,5-disubstituted product.

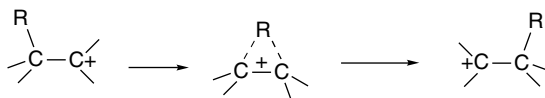


No product derived from the transannular hydrogen abstraction is observed in the addition of bromotrichloromethane because bromine atom transfer is sufficiently fast to prevent effective competition from the intramolecular hydrogen abstraction.

The selectivity observed in most intramolecular functionalizations depends on the preference for a six-membered TS in the hydrogen atom transfer step. Appropriate molecules can be constructed in which steric or conformational effects dictate a preference for selective abstraction of a hydrogen that is more remote from the reactive radical.

### 11.5.3. Rearrangement Reactions of Free Radicals

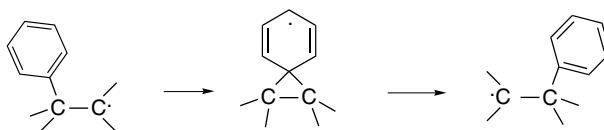
Compared with carbocations, rearrangements of radical intermediates are much less common. However, migrations can occur for specific structural types. The groups that are usually involved in migration in free radical intermediates include aryl, vinyl, acyl, and other unsaturated substituents. Migration of saturated groups is unusual and there is a simple structural reason for this. With carbocations, migration occurs through a bridged TS (or intermediate) that involves a three-center two-electron bond.



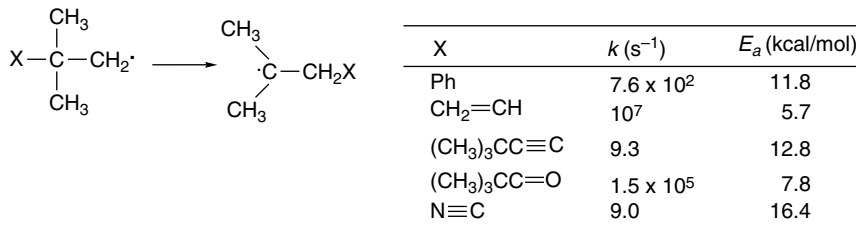
In a free radical, there is a third electron in the system that cannot occupy the same orbital as the other two electrons and must instead be in an antibonding level. As a result, the TS for migration is much less favorable than for the corresponding carbocation. The more facile migration of aryl and other unsaturated groups involves

<sup>194</sup> J. G. Traynham, T. M. Couvillon, and N. S. Bhacca, *J. Org. Chem.*, **32**, 529 (1967); J. G. Traynham and T. M. Couvillon, *J. Am. Chem. Soc.*, **87**, 5806 (1965); J. G. Traynham and T. M. Couvillon, *J. Am. Chem. Soc.*, **89**, 3205 (1967).

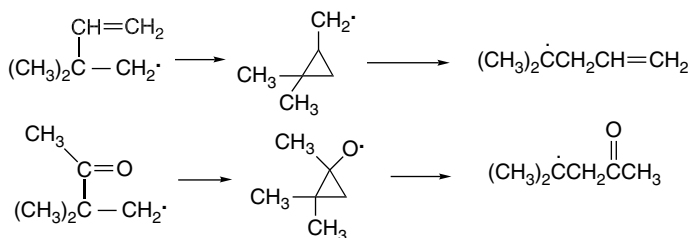
bridged radicals formed by an addition process. In the case of aryl migration, the bridged intermediate is a cyclohexadienyl radical.



It has been possible to measure absolute rates and  $E_a$  for rearrangement in a series of 2-substituted 2,2-dimethylethyl radicals. The rates at 25° C and the  $E_a$  for several substituents are as indicated below.<sup>195</sup>



The rapid rearrangement of vinyl and acyl substituents can be explained as proceeding through cyclopropyl intermediates.



The vinyl rearrangement is an example of reversible cyclopropylcarbinyl radical formation and ring opening. The acyl migration occurs through cyclopropoxy radicals. The energy profile of the cyclopropoxy radical has been compared computationally to that of the cyclopropylcarbinyl radical (see Section 11.1.3 and Figure 11.3). At the UMP3/6-31G\* level, the cyclopropoxy radical is a TS, rather than an intermediate.<sup>196</sup> The energy profile for the formation of the 2-oxocyclopentylmethyl radical and its rearrangement to the 3-oxocyclohexyl radical by acyl migration has been explored,<sup>197</sup> and the results are shown in Figure 11.15. The rearrangement is found to be exothermic and the calculated barrier for the rearrangement is 20.3 kcal/mol, which is slightly less than that for the initial cyclization. This calculation, too, indicates that the cyclopropoxy radical fragments with no barrier.

Aryl migration is considerably slower because of the diminished susceptibility of the aryl ring to radical addition. Aryl migrations are promoted by steric crowding at the initial radical site. This trend is illustrated by data from the thermal decomposition

<sup>195</sup> D. A. Lindsay, J. Luszyk, and K. U. Ingold, *J. Am. Chem. Soc.*, **106**, 7087 (1984).

<sup>196</sup> A. L. Cooksy, H. F. King, and W. H. Richardson, *J. Org. Chem.*, **68**, 9441 (2003).

<sup>197</sup> I. Ryu, H. Fukushima, T. Okuda, K. Matsu, N. Kombe, N. Sonada, and M. Komatsu, *Synlett*, 1265 (1997).

	$E_a$	$E_b$	$E_c$	$E_d$	$E_e$
UMP3/6-31G*/UMP3/3-21G	30.7	20.3	17.0	16.4	-4.8

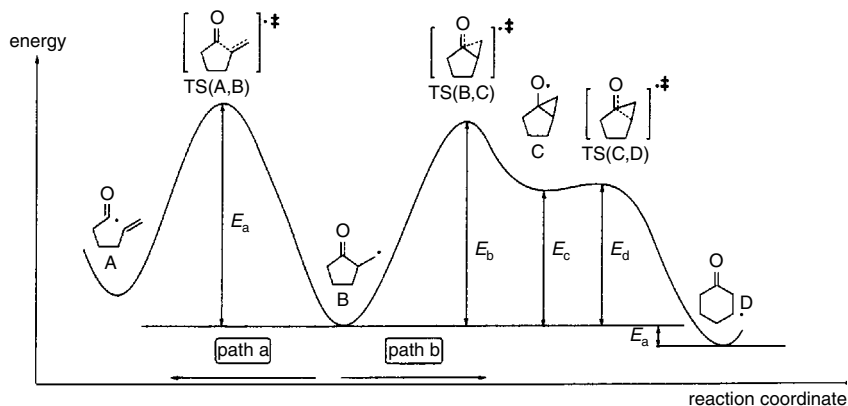
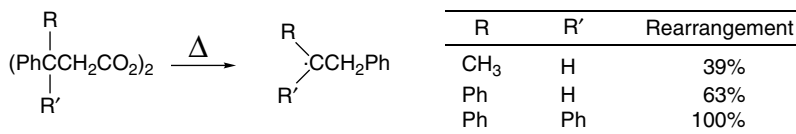


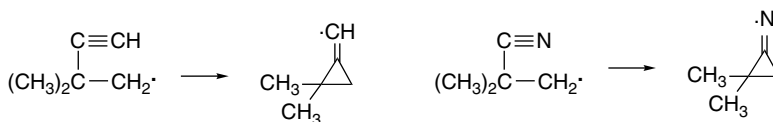
Fig. 11.15. Relative energies of the 5-hexenoyl, 2-oxocyclopentylmethyl, and 3-oxocyclohexyl radicals and the transition structures separating them. Reproduced from *Synlett*, 1265 (1997), by permission of G. Thieme Verlag.

of a series of diacyl peroxides. The amount of product derived from rearrangement increases with the size and number of the substituents.<sup>198</sup>



The aryl migration has been modeled computationally at the UB3PW91/G-31G(*d,p*) level.<sup>199</sup> The bridged cyclohexadienyl radical is found to be a short-lived intermediate that is 10.1 kcal/mol above the open radical. The barrier for return to the open radical is 4.0 kcal/mol. The relative stability of the bridged radical is increased by most *para*-substituents, since they provide stabilization of the cyclohexadienyl radical.

The much slower rearrangement of alkynyl and cyano substituents can be attributed to the reduced stability of the intermediate derived by cyclization of the triply bound substituents.

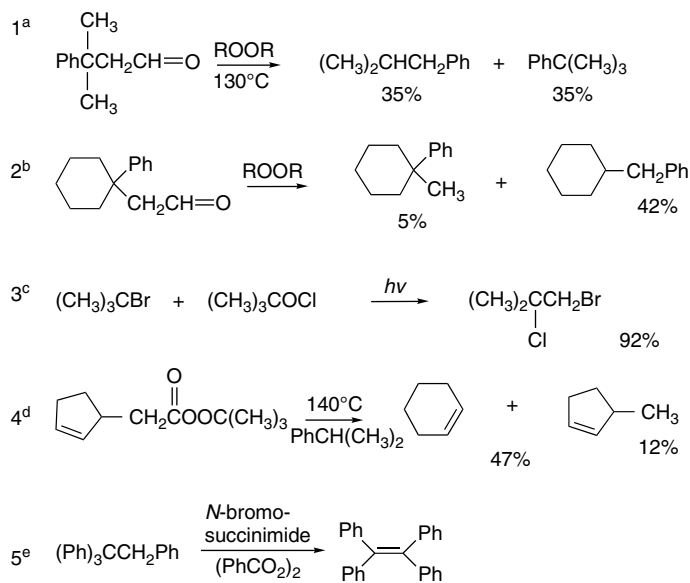


Scheme 11.6 gives some examples of reactions in which free radical rearrangements have been observed. Entries 1 and 2 are phenyl group migrations in primary alkyl radicals generated by decarbonylation. The migration is competitive with the

<sup>198</sup>. W. Rickatson and T. S. Stevens, *J. Chem. Soc.*, 3960 (1963).

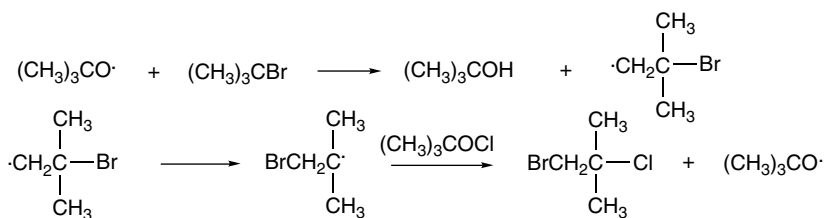
<sup>199</sup>. A. Asensio and J. J. Dannenberg, *J. Org. Chem.*, **66**, 5996 (2001).

## Scheme 11.6. Free Radical Rearrangements



- a. S. Winstein and F. H. Seubold, Jr., *J. Am. Chem. Soc.*, **69**, 2916 (1947).  
 b. J. W. Wilt and H. P. Hogan, *J. Org. Chem.*, **24**, 441 (1959).  
 c. P. S. Skell, R. G. Allen, and N. D. Gilmour, *J. Am. Chem. Soc.*, **83**, 504 (1961).  
 d. L. H. Slaugh, *J. Am. Chem. Soc.*, **87**, 1522 (1965).  
 e. H. Meislich, J. Constanza, and J. Strelitz, *J. Org. Chem.*, **33**, 3221 (1968).

hydrogen abstraction reaction that gives unrearranged product. The reaction in Entry 3 occurs by hydrogen abstraction followed by bromine migration.



Entry 4 is an alkenyl migration that presumably occurs through a bicyclic radical.

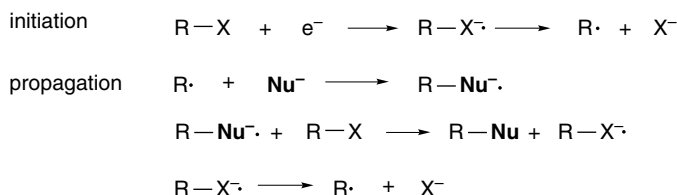


The reaction in Entry 5 involves a phenyl migration. The rearranged radical undergoes hydrogen atom elimination rather than the usual abstraction of bromine.

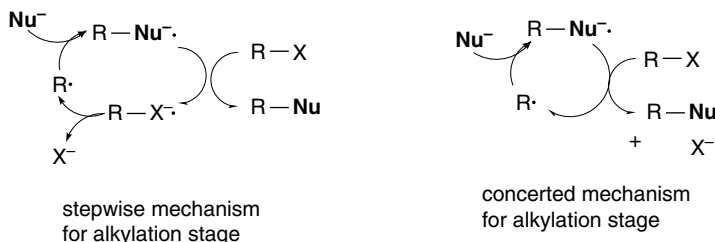
## 11.6. $S_{RN}1$ Substitution Processes

The mechanistic description  $S_{RN}1$  refers to a nucleophilic substitution via a radical intermediate that proceeds by unimolecular decomposition of a radical anion derived from the reactant. There are two families of such reactions that have been developed

to a stage of solid mechanistic understanding as well as synthetic utility. The common mechanistic pattern of  $S_{RN}1$  involves electron transfer to the reactant that generates a radical anion, which then expels the leaving group. A chain process occurs if the radical generated by expulsion of the leaving group can react with the nucleophile to give a radical anion capable of sustaining a chain reaction.



A key to the efficiency of  $S_{RN}1$  reactions is the electron transfer to the alkylating reagent.<sup>200</sup> This process can be stepwise if the radical anion that is formed is sufficiently stable, but can also be concerted. The concerted path is the most likely one for alkyl halides. The combination reaction between the radical and nucleophile is very fast.



The  $S_{RN}1$  reaction was first discovered and developed for nitroalkane anions, but it is applicable to several other types of nucleophiles. The  $S_{RN}1$  reaction is applicable to various aryl and tertiary alkyl halides and has also been extended to other leaving groups. The reaction has found a number of synthetic applications, especially in substitution of aryl and bridgehead alkyl halides that are resistant to other substitution mechanisms.<sup>201</sup>

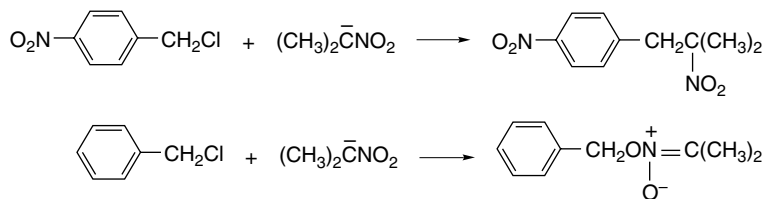
### 11.6.1. $S_{RN}1$ Substitution Reactions of Alkyl Nitro Compounds

The  $S_{RN}1$  mechanism of this type permits substitution of certain aromatic and aliphatic nitro compounds by a variety of nucleophiles. These reactions were discovered as the result of efforts to understand the mechanistic basis for high-yield carbon alkylation of the 2-nitropropane anion by *p*-nitrobenzyl chloride. The corresponding

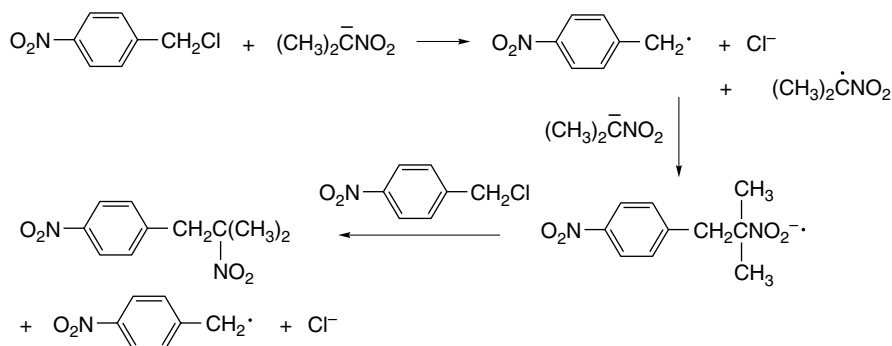
<sup>200</sup> J.-M. Saveant, *J. Phys. Chem.*, **98**, 3716 (1994); R. A. Rossi, A. B. Pierini, and G. L. Borosky, *J. Chem. Soc., Perkin Trans. 2*, 2577 (1994).

<sup>201</sup> R. A. Rossi, *Current Org. Chem.*, **7**, 747 (2003); R. A. Rossi, A. B. Pierini, and A. N. Santiago, *Org. React.*, **54**, 1 (1999); R. A. Rossi, A. B. Pierini and A. B. Penenory, *Chem. Rev.*, **103**, 71 (2003).

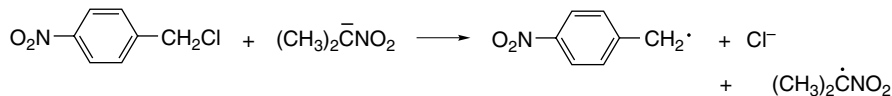
bromide and iodide, as well as benzyl halides that do not contain a nitro substituent give mainly the unstable oxygen alkylation product with this ambident anion.<sup>202</sup>



A mixture of carbon and oxygen alkylation would be expected for an  $\text{S}_{\text{N}}2$  substitution process. The high preference for carbon alkylation suggested that a different mechanism operates with *p*-nitrobenzyl chloride. This conclusion was further strengthened by the fact that the chloride is more reactive than would be predicted by application of the usual  $\text{I} > \text{Br} > \text{Cl}$  reactivity trend for leaving groups in  $\text{S}_{\text{N}}2$  reactions. The involvement of a free radical process was indicated by ESR studies and by demonstrating that typical free radical inhibitors decrease the rate of the carbon alkylation process. The mechanism proposed is a free radical chain process initiated by electron transfer from the nitronate anion to the nitroaromatic compound.<sup>203</sup> This process is the dominant reaction only for the chloride, because, with the better leaving groups bromide and iodide, a direct  $\text{S}_{\text{N}}2$  process is faster.



The absolute rate of dissociation of the *p*-nitrobenzyl chloride radical anion has been measured as  $4 \times 10^3 \text{ s}^{-1}$ . The *m*-nitro isomer does not undergo a corresponding reaction,<sup>204</sup> owing to the fact that the *m*-nitro group does not provide any resonance stabilization of the benzylic radical. The kinetics of the overall reaction supports a concerted electron transfer involving dissociation at the stage of electron transfer from the nitronate to the benzylic halide.<sup>205</sup>



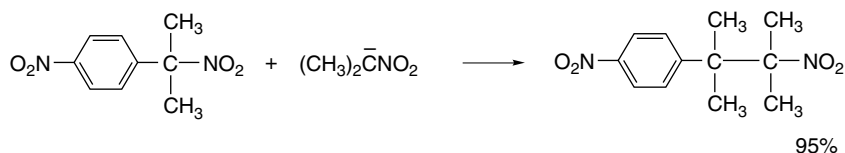
<sup>202</sup> N. Kornblum, *Angew. Chem. Int. Ed. Engl.*, **14**, 734 (1975); N. Kornblum, in *The Chemistry of Amino, Nitroso and Nitro Compounds and Their Derivatives*, S. Patai, ed., Interscience, New York, 1982, Chap. 10.

<sup>203</sup> N. Kornblum, R. E. Michel, and R. C. Kerber, *J. Am. Chem. Soc.*, **88**, 5662 (1966); G. A. Russell and W. C. Danen, *J. Am. Chem. Soc.*, **88**, 5663 (1966).

<sup>204</sup> R. K. Norris, S. D. Baker, and P. Neta, *J. Am. Chem. Soc.*, **106**, 3140 (1984).

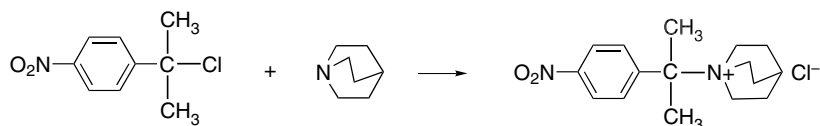
<sup>205</sup> C. Costentin, P. Hapiot, M. Medebielle, and J.-M. Saveant, *J. Am. Chem. Soc.*, **121**, 4451 (1999).

The synthetic value of the  $S_{RN}1$  substitution reaction was developed from this mechanistic understanding. The reaction is capable of providing highly substituted carbon skeletons that would be inaccessible by normal  $S_N2$  processes. For example, tertiary *p*-nitrocumyl halides can act as alkylating agents in high yield. The nucleophile need not be a nitroalkane anion, but can be anions such as thiolate, phenolate, or a carbanion such as those derived from malonate esters.<sup>206</sup> The same mechanism operates as for the nitronate anion. Furthermore, the leaving group need not be a halide. Displacement of nitrite ion from  $\alpha, p$ -nitrocumene occurs with good efficiency.<sup>207</sup>



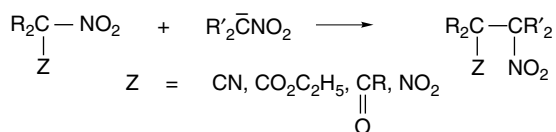
Azido, sulfonyl, and quaternary nitrogen groups can also be displaced by this mechanism.

An  $S_{RN}1$  mechanism has been proposed for the alkylation of amines by *p*-nitrocumyl chloride.<sup>208, 209</sup>



Clearly, the tertiary nature of the chloride would make a  $S_N2$  mechanism highly unlikely. Furthermore, the nitro substituent is essential to the success of these reactions. Cumyl chloride itself undergoes elimination of HCl on reaction with amines.

A related process constitutes a method of carrying out alkylation reactions to give highly branched alkyl chains that cannot easily be formed by an  $S_N2$  mechanism. The alkylating agent must contain a nitro group and a second EWG. These compounds react with nitronate anions to effect displacement of the nitro group.<sup>210</sup>



When radical scavengers are added, the reaction is greatly retarded, which indicates that a chain reaction is involved. The mechanism shown below indicates that one of the steps in the chain process is an electron transfer and that none of the steps involves

<sup>206</sup> N. Kornblum, T. M. Davies, G. W. Earl, N. L. Holy, R. C. Kerber, M. T. Musser, and D. H. Snow, *J. Am. Chem. Soc.*, **89**, 725 (1967); N. Kornblum, L. Cheng, T. M. Davies, G. W. Earl, N. L. Holy, R. C. Kerber, M. M. Kestner, J. W. Manthey, M. T. Musser, H. W. Pinnick, D. H. Snow, F. W. Stuchal, and R. T. Swiger, *J. Org. Chem.*, **52**, 196 (1987).

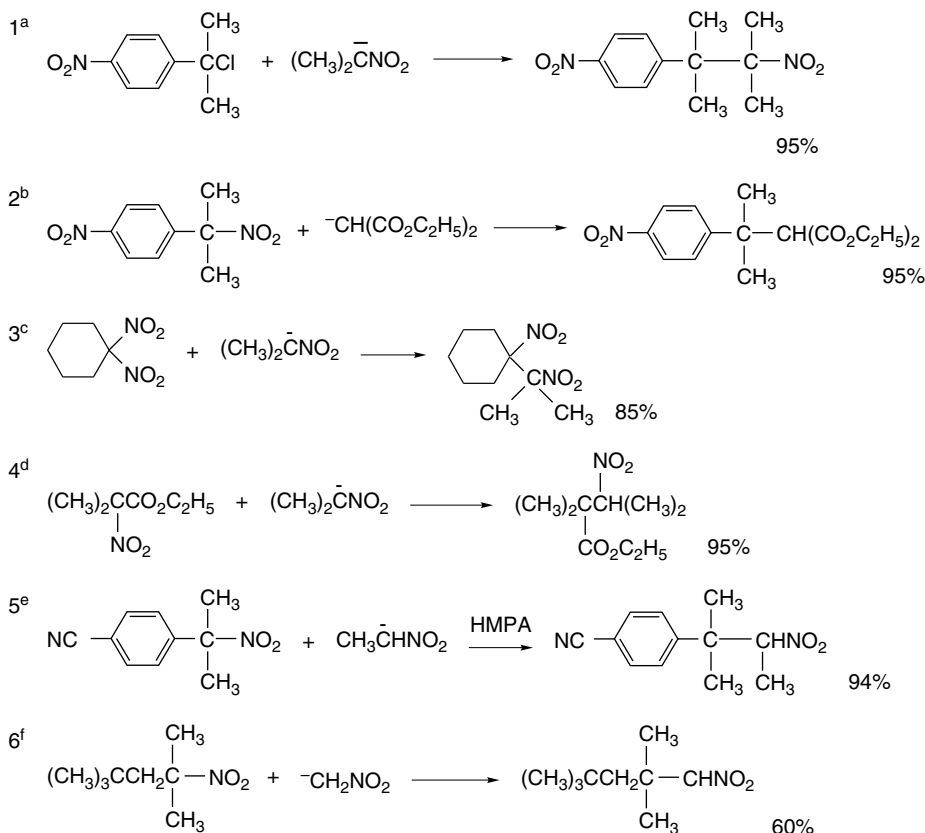
<sup>207</sup> N. Kornblum, T. M. Davis, G. W. Earl, G. S. Greene, N. L. Holy, R. C. Kerber, J. W. Manthey, M. T. Musser, and D. H. Snow, *J. Am. Chem. Soc.*, **89**, 5714 (1967).

<sup>208</sup> N. Kornblum and F. W. Stuchal, *J. Am. Chem. Soc.*, **92**, 1804 (1970).

<sup>209</sup> W. R. Bowman, *Chem. Soc. Rev.*, **17**, 283 (1988).

<sup>210</sup> N. Kornblum and S. D. Boyd, *J. Am. Chem. Soc.*, **92**, 5784 (1970).





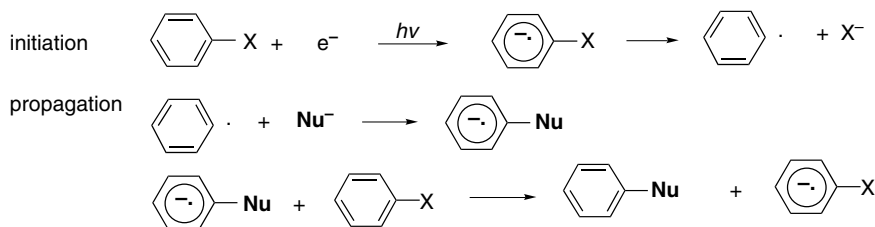
a. N. Kornblum, T. M. Davies, G. W. Earl, N. L. Holy, R. C. Kerber, M. T. Musser, and D. H. Snow, *J. Am. Chem. Soc.*, **89**, 725 (1967).

b. N. Kornblum, T. M. Davies, G. W. Earl, G. S. Greene, N. L. Holy, R. C. Kerber, J. W. Manthey, M. T. Musser, and D. H. Snow, *J. Am. Chem. Soc.*, **89**, 5714 (1967).

c. N. Kornblum, S. D. Boyd, and F. W. Stuchal, *J. Am. Chem. Soc.*, **92**, 5783 (1970).

d. N. Kornblum, S. C. Carlson, J. Widmer, N. Fifolt, B. N. Newton, and R. G. Smith, *J. Org. Chem.*, **43**, 1394 (1978).

e. N. Kornblum and A. S. Erickson, *J. Org. Chem.*, **46**, 1037 (1984).

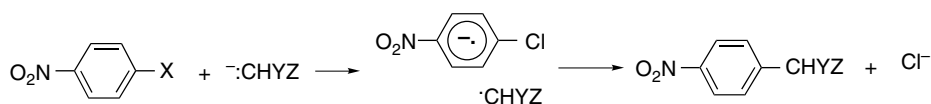


The reactions can also be initiated by a strong chemical reductant or electrochemically.<sup>215</sup> There are several lines of evidence that support the operation of a chain

<sup>215</sup> C. Amatore, J. Chaussard, J. Pinson, J.-M. Saveant, and A. Thiebault, *J. Am. Chem. Soc.*, **101**, 6012 (1979).

mechanism, one of the most general observations being that the reactions are stopped or greatly retarded by radical traps. The reactions are not particularly sensitive to the aromatic ring substituents. Both ERGs (such as methoxy) and EWGs (such as benzoyl) can be present.<sup>216</sup> Groups that easily undergo one electron reduction, especially the nitro group, cause the reaction to fail. The nucleophiles that have been used successfully include sulfide and phosphide anions, dialkyl phosphite anions, and certain enolates. Kinetic studies have shown that the enolate and phosphorus nucleophiles react at about the same rate.<sup>217</sup> This suggests that the step directly involving the nucleophile (Step 2 of the propagation sequence) occurs at essentially the diffusion-controlled rate, since there is little selectivity among the individual nucleophiles.<sup>218</sup> The combination of aryl radicals with diethyl phosphate anion has been measured at about  $10^9 M^{-1} s^{-1}$ .<sup>219</sup>

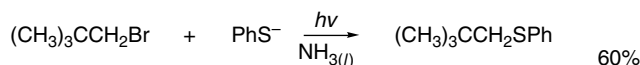
A related mechanism has been suggested for nitroarylation of enolates. An impetus for considering other mechanisms is the fact that the by-products that might be expected from aryl radicals, such as reduction products from hydrogen abstraction from the solvent or biaryls from coupling, are not observed. The alternative is that rather than being a chain process, the radicals may combine (*cage recombination*) more rapidly than they separate.



The kinetics of the reaction of *p*-nitrochlorobenzene with the sodium enolate of ethyl cyanoacetate is consistent with this mechanism. Moreover, radical scavengers have no effect on the reaction, contrary to what would be expected for a chain mechanism in which aryl radicals must encounter the enolate in a propagation step. However, the reactant, *p*-nitrophenyl chloride, is one that might also react by the addition-elimination mechanism (see Section 9.5) and the postulated mechanism is essentially the stepwise electron transfer version of the latter. The question then becomes whether the postulated radical pair is a distinct intermediate.

The synthetic value of the  $S_{RN}1$  arylation lies in the fact that other substituents that activate the halide to substitution are not required, in contrast to aromatic nucleophilic substitution that proceeds by an addition-elimination mechanism (see Section 9.5). Scheme 11.8 illustrates some typical reactions.

Substitution of hindered alkyl halides by the  $S_{RN}1$  mechanism have also been documented.<sup>220</sup> Some examples are shown below.



Ref. 221

<sup>216</sup> J. F. Bunnett and J. E. Sundberg, *Chem. Pharm. Bull.*, **23**, 2620 (1975); R. A. Rossi, R. H. deRossi, and A. F. Lopez, *J. Org. Chem.*, **41**, 3371 (1976).

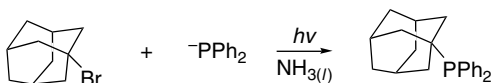
<sup>217</sup> X.-M. Zhang, D.-L. Yang, X.-Q. Jia, and Y.-C. Liu, *J. Org. Chem.*, **58**, 7350 (1993).

<sup>218</sup> C. Galli and J. F. Bunnett, *J. Am. Chem. Soc.*, **103**, 7140 (1981); R. G. Scamehorn, J. M. Hardacre, J. M. Lukanich, and L. R. Sharpe, *J. Org. Chem.*, **49**, 4881 (1984).

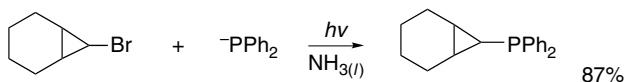
<sup>219</sup> A. Annunziata, C. Galli, M. Marinelli, and T. Pau, *Eur. J. Org. Chem.*, 1323 (2001).

<sup>220</sup> S. M. Palacios, A. N. Santiago, and R. A. Rossi, *J. Org. Chem.*, **49**, 4609 (1984).

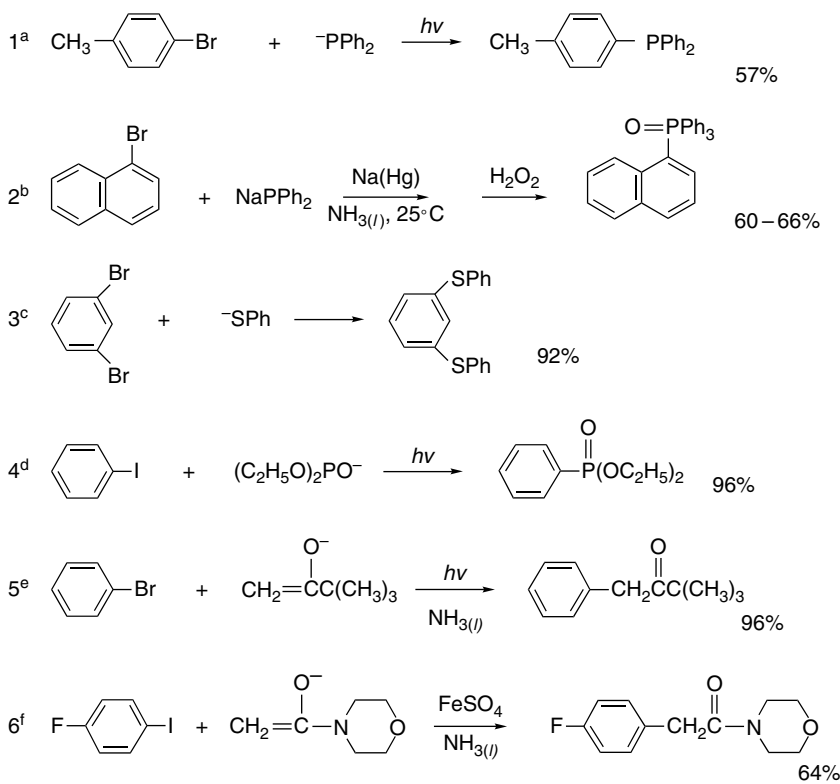
<sup>221</sup> A. B. Pierini, A. B. Penenory, and R. A. Rossi, *J. Org. Chem.*, **50**, 2739 (1985).



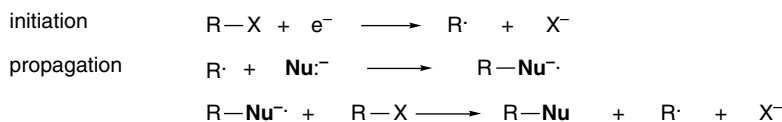
Ref. 222



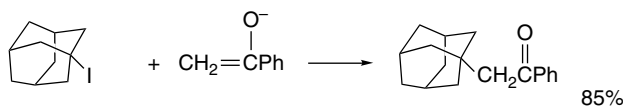
Ref. 223

**Scheme 11.8. Aromatic Substitution by the S<sub>RN</sub>1 Mechanism**
a. J. E. Swartz and J. F. Bunnett, *J. Org. Chem.*, **44**, 340 (1979).b. P. G. Mabzo, S. M. Palacios, R. A. Alonso, and R. A. Rossi, *Org. Prep. Proc. Int.*, **27**, 660 (1995).c. J. E. Bunnett and X. Creary, *J. Org. Chem.*, **39**, 3611 (1974).d. J. E. Bunnett and X. Creary, *J. Org. Chem.*, **39**, 3612 (1974).e. M. F. Semmelhack and T. Bargar, *J. Am. Chem. Soc.*, **102**, 7765 (1980).f. M. van Leeuwen and A. McKillop, *J. Chem. Soc., Perkin Trans. 1*, 2433 (1993).222. R. A. Rossi, S. M. Palacios, and A. N. Santiago, *J. Org. Chem.*, **47**, 4654 (1982).223. R. A. Rossi, A. N. Santiago, and S. M. Palacios, *J. Org. Chem.*, **49**, 3387 (1984).

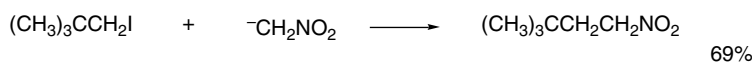
The mechanism is the same as for aryl halides, but the dissociation of the halide is probably concerted with the electron transfer.



Acetophenone enolate and nitromethane anions have also been used successfully in alkyl substitution.



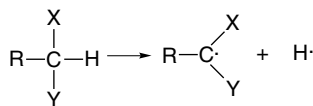
Ref. 224



Ref. 225

### Topic 11.1. Relationships between Bond and Radical Stabilization Energies

In Section 3.4.3, we discussed substituent effects on radicals in terms of radical stabilization energies (RSE). These values are defined in terms of standard bond dissociation energies. These RSE values provide a numerical assessment of some well-recognized effects, such as increasing radical stability in the order methyl < primary < secondary < tertiary and the strong stabilization of benzylic and allylic radicals. However, there are some RSE values that are less consistent with chemical experience. For example, the  $\text{CCl}_3\cdot$  radical is assigned a negative RSE of 13.79 kcal/mol, although it has a prominent place in radical chemistry. There is a general issue that pertains to radical stabilization energies from both thermochemical and computational BDE when they are defined as  $\Delta H$  for the reaction



This formulation includes any stabilization of the reactant in the value of the BDE and resulting RSE. Thus the “inherent” strength of the C–H bond is considered to be decreased to the extent that the product radical is stabilized. Further interpretation requires subdividing the BDE into its “inherent” and “extra stabilization” factors. To

<sup>224</sup> M. A. Nazareno and R. A. Rossi, *J. Org. Chem.*, **61**, 1645 (1996).

<sup>225</sup> A. B. Peneory and R. A. Rossi, *Gazz. Chem. Ital.*, **125**, 605 (1995).

do this, structural features that strengthen or weaken the bond *in the reactant* must be accounted for. The AIM approach (see Section 1.4.3) provides the basis for one such scheme. The intrinsic bond energy  $BE_i$  was defined in terms of the AIM energy  $E_i(r_{\text{BCP}})$  and charge density  $\rho_i(r_{\text{BCP}})$ :

$$BE_i = c_1^{\text{AB}} E_i(r_{\text{BCP}}) / [c_2^{\text{AB}} + \rho_i(r_{\text{BCP}})] - c_3^{\text{AB}} \Delta R \quad (11.6)$$

where  $c_1^{\text{AB}}$ ,  $c_2^{\text{AB}}$ , and  $c_3^{\text{AB}}$  are empirical characteristics of bond types and  $\Delta R$  is the difference between the length of the AIM bond path and the internuclear distance.<sup>226</sup>

This concept of inherent bond energy was extended by Exner and Schleyer to a wider range of structures.<sup>227</sup> The approach reproduced atomization energies for typical alkanes and alkenes with a standard deviation of about 4.6 kcal/mol, i.e., within about 1%, although some molecules, e.g., allene and cyclopropene, fell well outside those limits. The calculated intrinsic bond energies  $BE_i$  were then compared with BDE, the energy required for homolytic dissociation. This analysis suggested that most of the dependence of BDE on structure can be attributed to the “extra stabilization” of the radicals, rather than to inherent differences in bond strength. Table 11.10 includes experimental bond energies, computed (G2) bond dissociation energies, the  $BE_i$  resulting from application of Equation (11.6), and the resulting RSE.

The data conform to familiar qualitative trends. We see the methyl < *pri* < *sec* < *tert* trend for alkyl groups. The strong stabilization of allyl radicals is evident in the value C(3)–H bond energy for propene, whereas the positive RSE for ethene, ethyne, and benzene reflect the low stability of radicals at  $sp^2$  and  $sp$  carbons. Also apparent in these data is the relative strength of C–H bonds in strained-ring compounds (cyclopropane). These results are also in accord with the concept of assigning most of the change in the BDE to radical stabilization or destabilization. The intrinsic bond energies,  $BE_i$ , show much less variation with substitution than the BDE.

**Table 11.10. Comparison of Experimental, Computational, and Calculated C–H Bond Dissociation Energies (kcal/mol)<sup>a</sup>**

Compound	BDE (exp)	BDE (G2)	$BE_i$	RSE <sup>b</sup>
Methane	104.9	105.8	103.9	+1.0
Ethane	101.4	102.6	104.1	–2.7
Propane	98.6	100.3	100.3	–5.7
Isobutane	96.5	98.8	104.4	–7.9
Cyclopropane	106.3	113.0	105.8	+0.5
Cyclobutane	96.5	102.1	104.3	–7.8
Cyclopentane	94.5		103.9	–9.4
Cyclohexane	94.5		103.5	–9.0
Ethene	112.2	112.0	106.0	+5.2
Ethyne	132.8	135.0	110.4	+22.4
Propene	88.2	88.7	103.2	–15.0
Benzene	111.2		106.5	+4.7

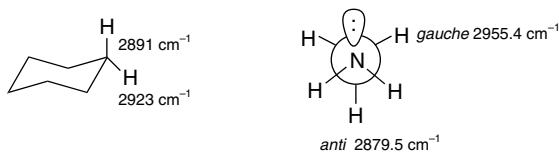
a. K. Exner and P. v. R. Schleyer, *J. Phys. Chem. A.*, **105**, 3407 (2001).

b. Apparent radical stabilization from BDE (exp) –  $BE_i$  [Equation ( 11.6)]

<sup>226</sup>. S. Grimme, *J. Am. Chem. Soc.*, **118**, 1529 (1996).

<sup>227</sup>. K. Exner and P. v. R. Schleyer, *J. Phys. Chem. A.*, **105**, 3407 (2001)

Larson and Cremer have explored another approach to dissecting BDE into inherent and RSE effects.<sup>228</sup> There is a relationship between C–H BDE and the vibrational frequencies of the bonds.<sup>229</sup> Furthermore, the vibrations can be determined for C–H bonds in specific conformations, for example, the equatorial and axial bonds in cyclohexanes or the *anti* and *gauche* bonds in amines.



Ref. 230

Ref. 231

Variation in vibrational frequencies of stereochemically distinct bonds

The measurement of the vibrational frequencies provides a means to compare the relative stabilization in radicals with effects already present in the reactant molecules. Following up on experimental work that demonstrated that spectroscopic C–H-bond-stretching frequencies correlate with bond strength,<sup>229</sup> Larson and Cremer developed reliable computation methods for calculating C–H frequencies and from them inherent (or ideal) bond energies. The difference is the radical stabilization (or destabilization energy), as indicated in Figure 11.16.

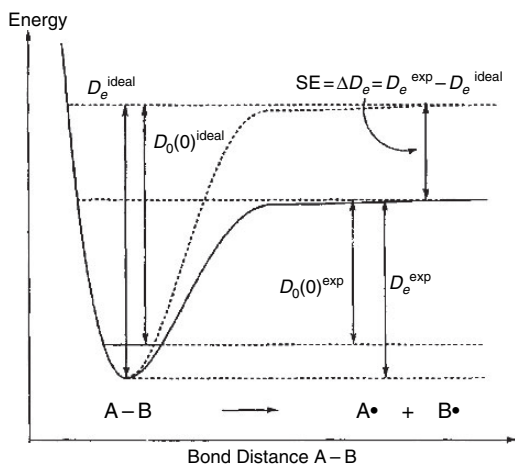


Fig. 11.16. Determination of fragment stabilization energy (SE) by comparison of  $D_e$  (exp) with  $D_e$  (ideal).  $D_0$  includes correction for zero point energy. Reproduced from *J. Mol. Struct.*, **485/486**, 385 (1999), by permission of Elsevier.

<sup>228</sup> J. A. Larson and D. Cremer, *J. Mol. Struct.*, **485/486**, 385 (1999).

<sup>229</sup> D. C. McKean, *Chem. Soc. Rev.*, **7**, 399 (1978); D. C. McKean, *Int. J. Chem. Kinetics*, **21**, 445 (1989).

<sup>230</sup> J. Caillod, O. Saur, and J.-C. Lavalley, *Spectrochim Acta*, **36A**, 185 (1980).

<sup>231</sup> J. L. Duncan, D. C. McKean, J. Torto, A. Brown, and A. M. Ferguson, *J. Chem. Soc., Faraday Trans.*, **II**, **84**, 1423 (1988).

**Table 11.11. Radical Stabilization Energy (SE) as Defined in Figure 11.16**

Structure	BE <sub>exp</sub>	BE <sub>i</sub>	SE
CH <sub>3</sub> -H	112.9	112.3	0.5
CH <sub>3</sub> CH <sub>2</sub> -H	109.0	109.2	-0.1
CH <sub>3</sub> CH <sub>2</sub> CH <sub>2</sub> -H	105.6	108.5	-2.9
(CH <sub>3</sub> ) <sub>2</sub> CH-H	102.9	106.4	-3.4
FCH <sub>2</sub> -H	107.5	110.0	-3.4
HOCH <sub>2</sub> -H	101.2	103.6	-2.3
H <sub>2</sub> NCH <sub>2</sub> -H	103.3	96.0	7.3
ClCH <sub>2</sub> -H	108.6	113.4	-4.7
O=CH-H	95.1	95.4	-0.2
O=CHCH <sub>2</sub> -H	101.2	107.2	-6.0
CH <sub>3</sub> C(=O)-H	95.6	95.9	-0.3
NCCH <sub>2</sub> -H	102.3	112.1	-9.8
H <sub>2</sub> C=CH-H	118.8	118.2	0.5
HC≡C-H	140.1	140.2	-0.1
HC≡CCH <sub>2</sub> -H	97.0	110.9	-13.9
C <sub>6</sub> H <sub>5</sub> -H	118.0	118.6	-0.6
H <sub>2</sub> C=CHC(=O)-H	93.4	93.7	-0.3
O=C=CH-H	111.9	123.7	-11.7

TOPIC 11.1

*Relationships between  
Bond and Radical  
Stabilization Energies*

The RSEs found for several groups by this approach are given in Table 11.11. Among the noteworthy features of this analysis is the disappearance of the “negative stabilization energies” associated with phenyl, ethenyl, and ethynyl radicals. Nearly all the observed high BDEs in these compounds is attributed to the inherent strength of the C–H bond in the reactant. On the other hand, the stabilization of acyl radicals (see H<sub>2</sub>C=O and CH<sub>3</sub>CH=O) also disappear, because in this case the bonds in the reactant are inherently weaker. The various  $\pi$ -conjugating substituents such as propargyl, cyanomethyl, and the  $\alpha$ -acyl radicals show significant stabilization (a negative number by this definition). The halogens and hydroxyl groups have modest stabilizing effects according to this analysis, but an  $\alpha$ -amino group has a destabilizing effect. This is because the C–H bond in the reactant is particularly *weak*, not because the aminoalkyl radicals are unstable. The ketene ( $\cdot\text{CH}=\text{C}=\text{O}$ ) radical shows a large stabilization, but only because the reactant bond is strong and the BDE is high, so one would not expect facile reaction, despite the apparent stabilization.

Where does this leave us in terms of understanding substituent effects on radicals? The most general statement to be made is that the BDE, not the RSE, is the best indicator of reactivity of the C–H bond. This is evident in the relationship allyl  $\sim$  benzyl  $<$  *tert*  $<$  *sec*  $<$  *pri*  $<$  methyl  $<$  ethenyl  $\sim$  phenyl  $<$  ethynyl bonds to hydrogen. We also note that the statement “all substituents weaken adjacent C–H bonds” is generally true. The traditional RSE values, however, result from two substituent effects, those in the reactant and those in the radical, and ultimately depend on the definition of the inherent bond strength. The clearest guide to reactivity is the experimental BDE or its computational equivalent. We discuss the *rates of hydrogen abstraction reactions* in more detail in Topic 11.2.

## Topic 11.2. Structure-Reactivity Relationships in Hydrogen Abstraction Reactions

*Hydrogen abstraction reactions* are of considerable importance in several contexts. They play a role in determining the kinetics of combustion, which determines fuel characteristics, e.g., octane number. The rates of hydrogen abstraction reactions are also important in understanding the role of hydrocarbons and halogenated hydrocarbons in such environmental issues such as air pollution and polar ozone depletion. Hydrogen abstraction reactions are also of importance in understanding the relationship between bond dissociation energies and reactivity. The order allyl  $\sim$  benzyl  $>$  *tert*  $>$  *sec*  $>$  *pri*  $>$  aryl  $\sim$  vinyl for C–H bond reactivity is one of the fundamental structure-reactivity relationships that is developed in introductory organic chemistry. In this section we explore the empirical relationship between the rates and  $E_a$  for some hydrogen abstraction reactions from small hydrocarbons and halogenated hydrocarbons by some radicals of fundamental importance, such as the halogen atoms and hydroxyl radical. We consider some empirical, analytical, and computational approaches to understanding hydrogen atom abstraction reactions.

Owing to the importance of hydrogen abstraction reactions, there have been several approaches to developing empirical relationships that can be used to predict activation energies. These efforts are kinetic analogs of the group equivalent approach to thermodynamic properties, in that experimental data are taken as the base and predictive relationships are derived from the data. An example of an empirical approach has been reported by Ranzi et al.<sup>232</sup> From thermodynamic and kinetic data pertaining to radicals such as alkyl, hydroxyl, hydroperoxyl, methoxyl, and chlorine atoms, characteristic values corresponding to the  $A$  and  $E_a$  components of the Arrhenius equation were tabulated. Each reactant species was also assigned a correction factor. These characteristic values are then put into an equation that uses the reference Arrhenius parameters and correction factors to compute  $E_a$ :

$$E_a = E_x^o + E_{R-H}^C \left( \frac{E_x^o}{13500} \right)^{0.333} - \left[ 1 - \left( \frac{E_R^o}{13500} \right)^{0.333} \right] E_{X-H} \quad (11.7)$$

where  $E_x^o$  and  $E_R^o$  are the tabulated energy terms and  $E^C$  is the correction term. This equation has no theoretical basis beyond the Arrhenius equation and essentially assumes that each reactant and radical has transferable characteristics. The relative simplicity of the hydrogen atom transition state perhaps contributes to the existence of transferability. Figure 11.17 shows the correlation between calculated and experimental rate constants.

Roberts and Steel investigated the applicability of an extended Bell-Evans-Polyani relationship to a series of hydrogen abstraction reactions. They developed a correlation equation that incorporated additional terms for electronegativity differences and for radical stabilization effects:

$$E_a = E_o f + \alpha \Delta H^o (1 - d) + \beta \Delta \chi_{AB}^2 + \gamma (s_A + s_B) \quad (11.8)$$

where  $f = (\text{BDE}_{\text{AH}} \times \text{BDE}_{\text{BH}}) / \text{BDE}_{\text{H}_2}$ ,  $d$  is a parameter added for delocalized radicals,  $\beta$  and  $\gamma$  are parameters derived from the correlation,  $\chi$  is electronegativity, and  $s$  is a parameter that is characteristic of the atoms A and B. The inclusion of the various

<sup>232</sup> E. Ranzi, M. Dente, T. Faravelli, and G. Pennati, *Combust. Sci. and Tech.*, **95**, 1 (1994).

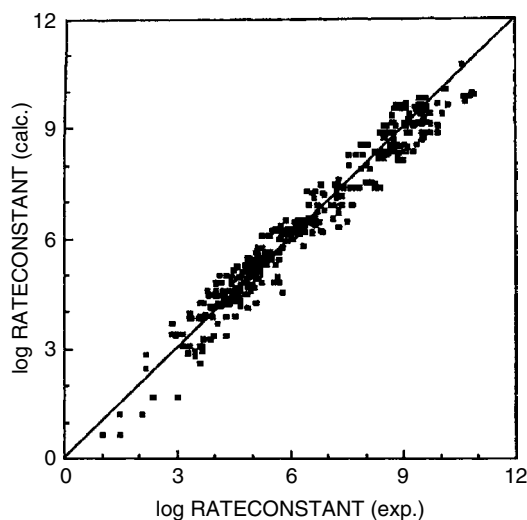
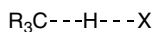


Fig. 11.17. Correlation of experimental hydrogen abstraction rates with rates calculated by Equation (11.7). Reproduced from *Combust. Sci. and Tech.*, **95**, 1 (1994) by permission of Taylor and Francis

terms has conceptual justifications; for example, the electronegativity term accounts for the increased strength of bonds between elements of differing electronegativity and the parameter  $d$  is related to the stabilization associated with delocalized radicals. For the set of 65 reactions examined, the  $E_a$  averaged to within 0.5 kcal/mol of the experimental value. The value of such an approach is that it provides for prediction of relative reactivity (in the form of  $E_a$ ) on the basis of existing BDE and electronegativity data. The numerical values of the parameters are determined by the correlation equation.<sup>233</sup>

Another kind of approach is based on estimates from first principles. The fundamental concept of these approaches is that the  $E_a$  of a hydrogen abstraction reaction will be determined mainly by the strength of the C–H and H–X bonds and by repulsions between  $R_3C$  and X in the transition state.



The problem is to formulate these relationships quantitatively. One approach, called the *interacting state model* (ISM) uses the Morse curves for the C–H and H–X bonds as the starting point and describes the TSs in terms of the length of the C–H and C–X bonds at the TS.<sup>234</sup> The total bond order is taken to be 1.0 unless one of the radicals has extra (e.g., resonance) stabilization, in which case a parameter is added to the formulation. These assumptions lead to a formula that gives the TS energy from the bond lengths and force constants of the C–H and H–X bonds. These structural characteristics are available from experiment or computation. There are other methods

<sup>233</sup> B. P. Roberts and A. J. Steel, *J. Chem. Soc., Perkin Trans. 2*, 2155 (1994); B. P. Roberts, *J. Chem. Soc., Perkin Trans. 2*, 2719 (1996).

<sup>234</sup> L. G. Arnaut, A. A. C. C. Pais, and S. J. Formosinho, *J. Mol. Struct.*, **563**, 1 (2001).

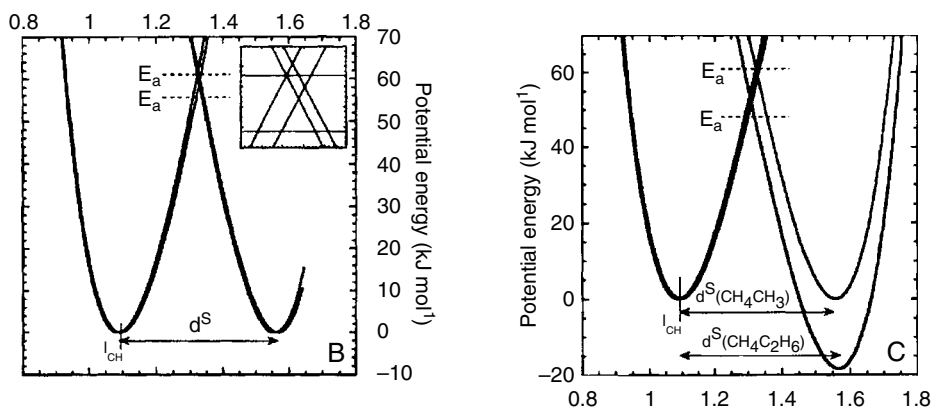


Fig. 11.18. Comparison of Morse curves from: (a)  $\text{CH}_3 \cdot + \text{CH}_4$  and  $\text{C}_2\text{H}_5 \cdot + \text{C}_2\text{H}_6$  thermoneutral; and (b)  $\text{CH}_3 \cdot + \text{C}_2\text{H}_6$  exothermic hydrogen atom transfer reactions. Reproduced from *J. Mol. Struct.*, **563**, 1 (2001), by permission of Elsevier.

of estimating or calculating  $E_a$  that use the C–H and H–X bond energies as the principal determinant of  $E_a$ .<sup>235</sup>

The qualitative interpretation of the ISM method can be illustrated by Figure 11.18. Figure 11.18a shows the equi-energy curves that pertain to the transfer of H between methyl and methane and ethyl and ethane. The curves nearly overlap, but the slightly weaker C–H bond in ethane is characterized by a smaller force constant and leads to a somewhat smaller barrier. The calculated barriers are 14.6 and 14.3 kcal/mol, respectively. The methyl-ethane reaction, shown in Figure 11.18b, is exothermic and there is a much more substantial shift in the curves. The calculated barrier is 12.4 kcal, compared with the experimental value of 11.5. Thus, the calculation moves the barriers in the right direction, although it does not reproduce the entire effect that is observed experimentally.

There have also been computational approaches using both semiempirical and ab initio MO and DFT methods. As in the treatment of isolated radicals, computational methods applied to radical transition states must use methods that are applicable for systems having unpaired electrons.<sup>236</sup> In one study, reactant, product, and TS energies were calculated using the PM3 method.<sup>237</sup> These were then compared with the corresponding experimental data. Figure 11.19 shows the PM3 representation of the SOMO distribution for the TS for hydrogen abstraction from propene (allylic hydrogen) by ethyl radical. Note that there is some delocalization of the SOMO distribution into the propene double bond, which is consistent with the idea that the stabilization of the allylic radical will contribute to the TS structure and lower the  $E_a$ . When the PM3 computations were applied to about 40 hydrocarbons, including some 10 benzylic and related conjugated structures, a good linear correlation was found between experimental and calculated  $E_a$ . The calculated  $E_a$  values tended to be too high by several kcal, but calibration of the linear correlation provided an average deviation of 1.5 kcal. The correlation was even better if the hydrocarbons were subdivided into structurally related groups.

<sup>235</sup> H. S. Johnston and C. Parr, *J. Am. Chem. Soc.*, **85**, 2544 (1963); N. Agmon and R. D. Levine, *Chem. Phys. Lett.*, **52**, 197 (1977); R. D. Gilliom, *J. Am. Chem. Soc.*, **99**, 8399 (1977); A. A. Zavitsas and C. Chatgililoglu, *J. Am. Chem. Soc.*, **117**, 10645 (1995).

<sup>236</sup> Y. Y. Chuang, E. L. Coitino, and D. G. Truhlar, *J. Phys. Chem. A*, **104**, 446 (2000).

<sup>237</sup> X. Ma and H. H. Schobert, *Ind. Eng. Chem. Res.*, **40**, 743 (2001).

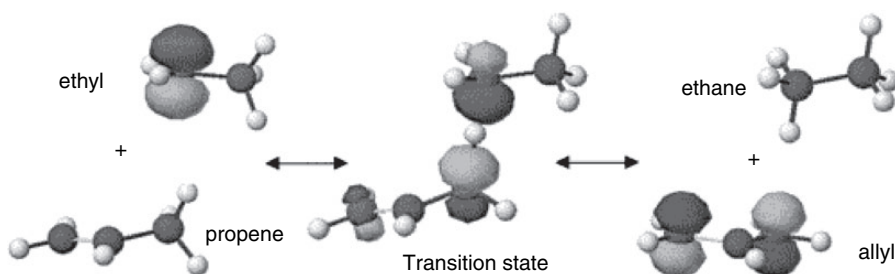


Fig. 11.19. PM3 representation of reactants, transition state, and products showing optimal geometry and distribution of SOMO orbital. Reproduced from *Int. Eng. Chem. Res.*, **40**, 743 (2001), by permission of the American Chemical Society.

These results extend those of an earlier study using AM1 and PM3 computations that showed excellent correlations within structurally similar groups, e.g., *tert*, *sec*, *pri*, and conjugated.<sup>238</sup> These studies also showed that the barrier for identity hydrogen atom transfers (e.g., ethyl/ethane) *increased* with conjugation. This result, which at first might seem surprising, reflects the fact that there is greater conjugative stabilization in the radicals than in the transition state. Table 11.12 lists some of the computed barriers. The trend toward an increased barrier with conjugation should not be confused with the *greater* reactivity of allylic and benzylic C–H toward more reactive alkyl radicals. For example, the data for hydrogen atom abstraction from toluene and propene by the methyl radical in Table 11.5 show barriers of 9.5 and 7.7 kcal/mol, respectively.

There has been a good deal of study of the polyhalogenated methanes in hydrogen atom abstraction reactions toward hydroxyl (HO·) and chlorine radicals.<sup>239</sup> These reactions are involved in both the atmospheric destruction of such compounds as well as their involvement in ozone depletion. Information is needed about these reactions to model the environmental impact of the compounds.

The reactions of halogenated methanes with HO· are characterized by a low activation barrier and early TS. In one study the reactants, products, and TS were calculated at the 6-311G(2*d*,2*p*) level using the PMP4(SDTQ) method to remove spin contamination.<sup>240</sup> Table 11.13 gives the calculated rates,  $E_a$ , and the derived atmospheric lifetimes for the halogenated methanes based on the reaction with HO·. The atmospheric lifetimes are computed in relation to the known rate for CH<sub>3</sub>CCl<sub>3</sub>.

**Table 11.12. Computed Barriers for Identity Hydrogen Atom Abstraction Reactions**

Saturated		Conjugated	
R	$E_a$	R	$E_a$
CH <sub>3</sub> ·	15.8	CH <sub>2</sub> =CHCH <sub>2</sub> ·	15.7
CH <sub>3</sub> CH <sub>2</sub> ·	10.1	(CH <sub>2</sub> =CH) <sub>2</sub> CH·	20.0
(CH <sub>3</sub> ) <sub>2</sub> CH·	8.3	PhCH <sub>2</sub> ·	15.7
(CH <sub>3</sub> ) <sub>3</sub> C·	10.9 <sup>a</sup>	Ph <sub>2</sub> CH·	19.3

a. This value is believed to be overestimated by the PM3 method.

<sup>238</sup>. D. M. Camioni, S. T. Autrey, T. B. Salinas, and J. A. Franz, *J. Am. Chem. Soc.*, **118**, 2013 (1996).

<sup>239</sup>. R. Atkinson, *Chem. Rev.*, **86**, 69 (1986).

<sup>240</sup>. F. Louis, C. A. Gonzalez, R. E. Huie, and M. J. Kurylo, *J. Phys. Chem. A*, **105**, 1599 (2001).

**Table 11.13. Computed Rates,  $E_a$ , and Atmospheric Lifetimes for Halomethanes<sup>a</sup>**

Compound	Number	$k_{298} \times 10^{-15}$	$E_a/R$	Lifetime (years)
CH <sub>3</sub> F	2	21	1340	6.37
CH <sub>3</sub> Cl	5	189	1015	1.55
CH <sub>3</sub> Br	8	100	1190	2.47
CH <sub>2</sub> F <sub>2</sub>	3	23	1595	3.59
CH <sub>2</sub> FCl	11	80	1160	1.68
CH <sub>2</sub> Cl <sub>2</sub>	6	433	510	0.43
CH <sub>2</sub> ClBr	16	304	590	0.54
CH <sub>2</sub> Br <sub>2</sub>	8	247	690	0.57
CHF <sub>3</sub>	4	0.28	2640	397
CHF <sub>2</sub> Cl	12	9.1	1540	13.16
CHF <sub>2</sub> Br	15	15	1375	6.03
CHFCl <sub>2</sub>	13	115	765	1.18
CHCl <sub>3</sub>	7	870	10	0.15
CH <sub>2</sub> FBr	17	30	1440	1.88
CHFBr <sub>2</sub>	17	100	825	0.49
CHFCIBr	20	68	920	0.73
CHCl <sub>2</sub> Br	18	264	330	0.16
CHClBr <sub>2</sub>	19	346	250	0.12

a. F. Louis, C. A. Gonzalez, R. E. Huie, and M. J. Kurylo, *J. Phys. Chem. A*, **105**, 1599 (2001).

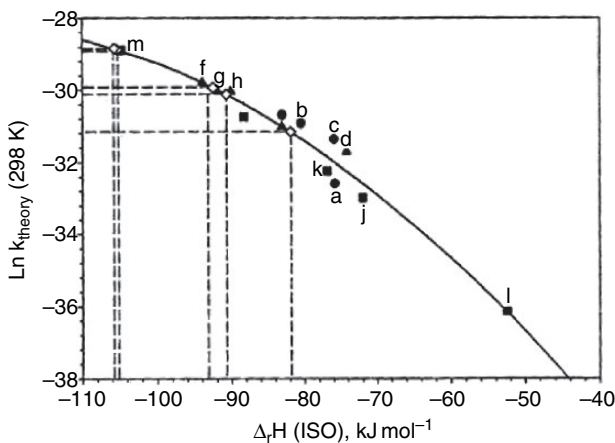


Fig. 11.20. Quadratic Evans-Polanyi relationship  $\ln k(298) = -1.368 \times 10^{-3} \Delta H_r^2 - 0.354 \Delta H_r - 50.96$ : (a) CH<sub>3</sub>F, (b) CH<sub>3</sub>Cl, (c) CH<sub>3</sub>Br, (d) CH<sub>2</sub>F<sub>2</sub>, (e) CH<sub>2</sub>FCl, (f) CH<sub>2</sub>Cl<sub>2</sub>, (g) CH<sub>2</sub>ClBr, (h) CH<sub>2</sub>Br<sub>2</sub>, (i) CHF<sub>3</sub>, (j) CHF<sub>2</sub>Cl, (k) CHF<sub>2</sub>Br, (l) CHFCl<sub>2</sub>, (m) CHCl<sub>3</sub>. From *J. Phys. Chem. A*, **105**, 1599 (2001).

**Table 11.14. Comparison of Computed and Observed  $E_a$  (kcal/mol) for Reaction of Halomethanes with Cl.**

Compound	$E_a$ (MP4/6-31G**) (kcal/mol)	$E_a$ (observed) (kcal/mol)
CH <sub>3</sub> F	3.4	1.54 ± 1.0
CH <sub>2</sub> F <sub>2</sub>	3.7	3.26 ± 1.0
CHF <sub>3</sub>	9.7	7.62 ± .16
CH <sub>3</sub> Cl	3.9	2.50 ± 0.4
CH <sub>2</sub> Cl <sub>2</sub>	1.6	2.7 ± 1.0
CHCl <sub>3</sub>	0.6	2.48 ± 1.0
CH <sub>2</sub> CF	2.6	2.78 ± 1.0
CHClF <sub>2</sub>	5.4	4.51 ± 1.0
CHCl <sub>2</sub> F	2.3	

The purpose of this study was to test the reliability of theoretical rate calculations to predict the atmospheric lifetime, an important property of these compounds:



These kinetic data lead to a quadratic rather than linear Bell-Evans-Polyani relationship:

$$\ln k_{298} = 1.368 \times 10^{-3} \Delta H^2 - 0.354 \Delta H - 50.96$$

The corresponding plot is shown in Figure 11.20.

A quadratic relationship between  $E_a$  and  $\Delta H$  was also noted for the reactions of Cl $\cdot$  and some of the same halomethanes.<sup>241</sup> Table 11.14 shows the computed and experimental  $E_a$  and Figure 11.21 shows the Evans-Polyani relationship. The

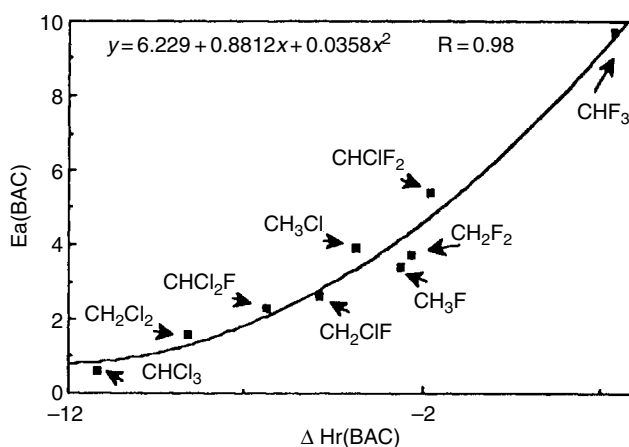


Fig. 11.21. Quadratic Evans Polyani relationship between  $E_a$  and BDE for Cl $\cdot$  and halomethanes. From *J. Phys. Chem.*, **98**, 111342 (1994).

<sup>241</sup> M.-T. Rayez, J.-C. Rayez, and J.-P. Sawerysyn, *J. Phys. Chem.*, **98**, 11342 (1994).

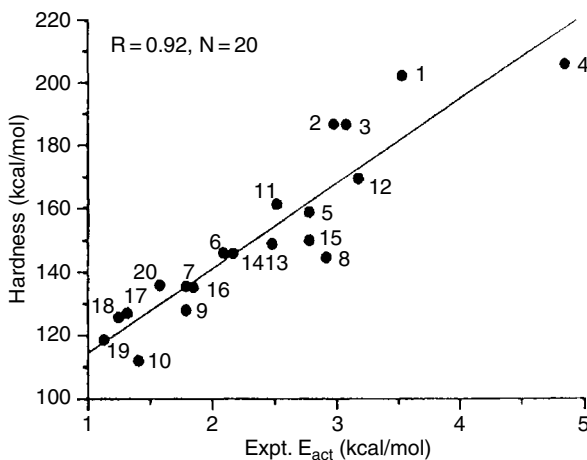


Fig. 11.22. Correlation between hardness and  $E_a$  for reaction of halomethanes with hydroxyl radical. Compounds are identified in Table 11.13. Reproduced from *Chem. Phys. Lett.*, **318**, 69 (2000), by permission of Elsevier.

observation of quadratic relationships is related to the concept of intrinsic barriers as formulated in the Marcus theory (see Section 3.3.2.3).

Chandra et al. considered the reactivity trends of the halomethanes toward  $\text{HO}\cdot$  in the DFT/hardness context.<sup>242</sup> There is a good correlation with the global hardness parameter. For  $X=\text{Cl}$  or  $\text{Br}$ , hardness decreases as more  $\text{Cl}$  and  $\text{Br}$  substituents are added. For fluorine the hardness trend is  $\text{CH}_3\text{F}=\text{CH}_2\text{F}_2 < \text{CH}_4 < \text{CHF}_3$ . This is in qualitative agreement with the rate data shown in Table 11.14. For the halomethanes, electron transfer to  $\cdot\text{OH}$  is exothermic, and  $\cdot\text{OH}$  is expected to be electrophilic in its reactions with the halomethanes. The trend of decreased reactivity with increased hardness can then be interpreted as decreased electron donation in the TS. Figure 11.22 shows the correlation between global hardness and the  $E_a$ .

## General References

### Reactions and Mechanisms

- A. L. J. Beckwith and K. U. Ingold, in *Rearrangements in Ground and Excited States*, P. de Mayo, ed., Academic Press, New York, 1980, Chap. 4.
- M. Birkhofer, H.-D. Beckhaus, and C. Rüdhardt, *Substituent Effects in Radical Chemistry*, Reidel, Boston, 1986.
- J. Fossey, D. Lefort, and J. Sorba, *Free Radicals in Organic Chemistry*, Wiley, Chichester, 1995.
- B. Giese, *Radicals in Organic Synthesis: Formation of Carbon-Carbon Bonds*, Pergamon Press, Oxford, 1986.
- E. S. Huyser, *Free Radical Chain Reactions*, Wiley-Interscience, New York, 1970.
- J. E. Leffler, *An Introduction to Free Radicals*, Wiley, New York, 1993.
- W. B. Motherwell and D. Crich, *Free Radical Chain Reactions in Organic Synthesis*, Academic Press, London, 1992.
- W. H. Pryor, *Free Radicals*, McGraw-Hill, New York, 1966.

<sup>242</sup> A. K. Chandra, T. Uchimaru, M. Sugie, and A. Sekiya, *Chem. Phys. Lett.*, **318**, 69 (2000).

## Spectroscopic Methods

M. Bersohn and J. C. Baird, *An Introduction to Electron Paramagnetic Resonance*, W. A. Benjamin, New York, 1966.

N. Hirota and H. Ohya-Nishiguchi, in *Investigation of Rates and Mechanisms of Reactions*, C. Bernasconi, ed., *Techniques of Chemistry*, 4th Edition, Vol. VI, Part 2, Wiley-Interscience, New York, Chapter XI.

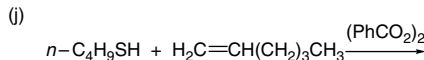
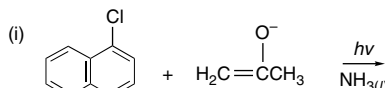
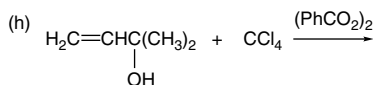
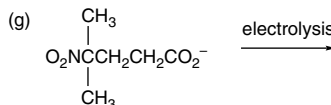
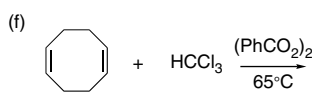
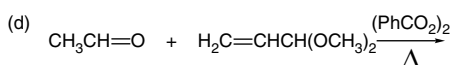
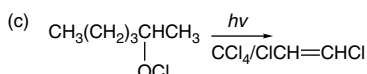
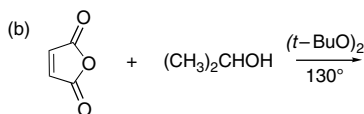
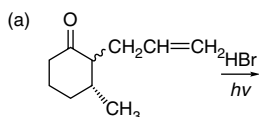
A. G. Lawler and H. R. Ward, in *Determination of Organic Structures by Physical Methods*, Vol 5, F. C. Nachod and J. J. Zuckerman, eds., Academic Press, New York, 1973, Chap. 3.

F. Gerson and W. Huber, *Electron Spin Resonance of Organic Radicals*, Wiley-VCH, Weinheim, 2003.

## Problems

(References for these problems will be found on page 1167.)

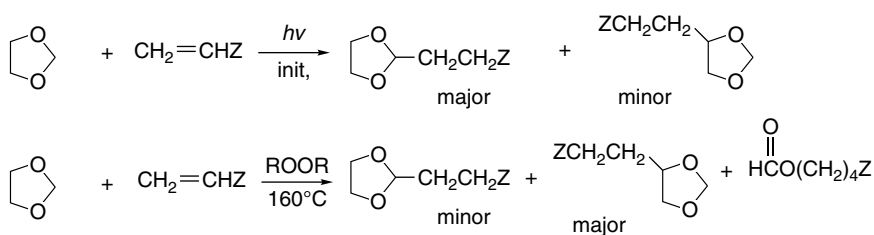
11.1. Predict the structure of the products of the following reactions.



11.2. Using the data in Table III of Problem ref 11.2, calculate the expected product composition from gas phase chlorination and bromination of 3-methylpentane under conditions (excess hydrocarbon) that minimize polyhalogenation.

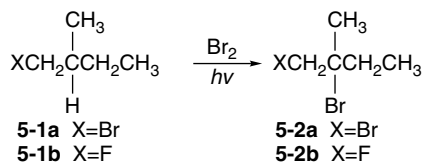
11.3. A careful study of the photoinitiated addition of HBr to 1-hexene established the following facts: (1) The chain length is about 400. (2) The products are 1-bromohexane, 2-bromohexane, and 3-bromohexane. The amounts of 2- and 3-bromohexane formed are always nearly identical and increase from about 8% at 4°C to about 22% at 63°C. (3) During the course of the reaction, a small amount of 2-hexene can be detected. Write a mechanism that is consistent with these results.

11.4. The irradiation of 1,3-dioxolane in the presence of alkenes and an initiator leads to 2-alkyldioxolanes along with small amounts of 4-alkyldioxolanes. The reaction is particularly effective with EWG-substituted alkenes such as diethyl maleate. When the reaction is done thermally with a peroxide initiator at 160°C, the product mixture is more complex and more of the 4-substituted dioxolane is formed. Account for the change in product ratio with increasing temperature.

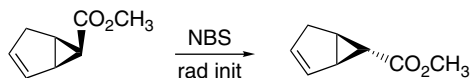


11.5. Provide a detailed mechanistic explanation for the following results.

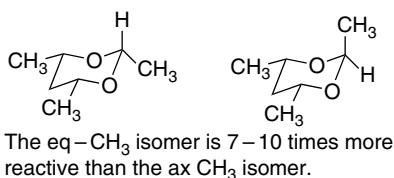
- a. Photochemically initiated bromination of resolved **5-1a**,  $\alpha_D + 4.21$ , affords **5-2a** which retains optical activity,  $\alpha_D - 3.23$ , but **5-1b** under the same conditions gives racemic **5-2b**.



- b. The stereoisomerization shown below proceeds efficiently, with no other chemical change occurring at a comparable rate, when the compound is warmed with *N*-bromosuccinimide and a radical chain initiator.



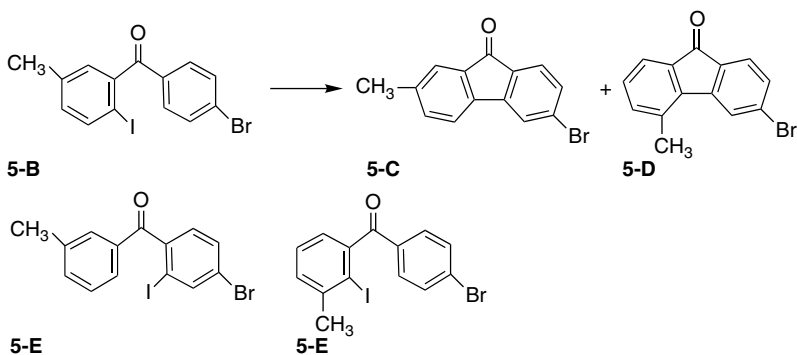
- c. There is a substantial difference in the reactivity of the two stereoisomeric compounds shown below toward abstraction of the hydrogen atom at C(2) by the *t*-butoxy radical.



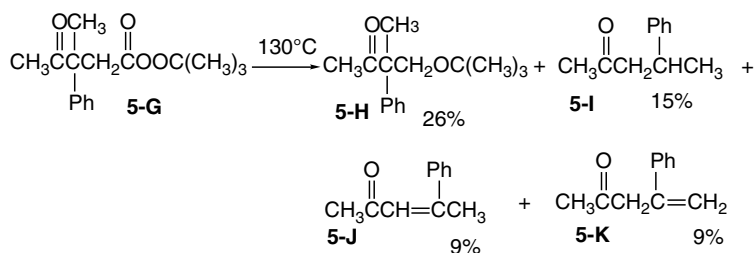
- d. Free radical chain chlorination of enantiomerically resolved 1-chloro-2-methylbutane yields six dichloro derivatives, of which four are optically active and two are not. Identify the products that are expected to fall in each group. Indicate the mechanistic significance of the identity of the optically active and inactive compounds.
- e. Irradiation of the hydrocarbon **5-A** in the presence of di-*t*-butyl peroxide generates a radical that can be identified as the 2-phenylethyl radical by its ESR spectrum. This is the only radical identified, even when the photolysis is carried out at  $-173^\circ\text{C}$ .



- f. Among the products from heating 1,6-heptadiene with 1-iodoperfluoropropane in the presence of AIBN are two saturated 1:1 adducts. Both adducts give the same product on dehydroiodination, and it can be shown by spectroscopic means to contain a  $=\text{CH}_2$  unit. Indicate structures for the two adducts and propose a mechanism for their formation.
- g. Photolysis of the iodide **5-B** gives not only the expected cyclization product **5-C** but also **5-D**. During the course of the photolysis halides **5-E** and **5-F** are also formed.

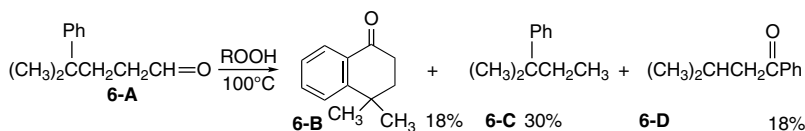


- h. Thermal decomposition of **5-G** gives products **5-H** to **5-K**:

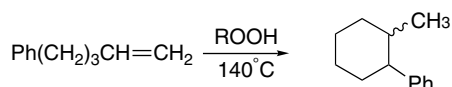


11.6. Write mechanisms for the following reactions:

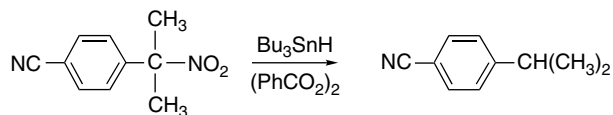
a.



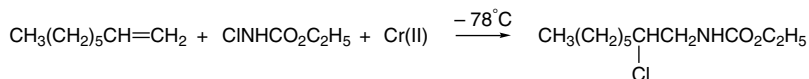
b.



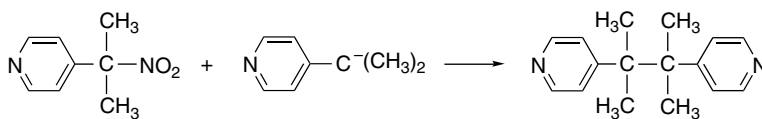
c.



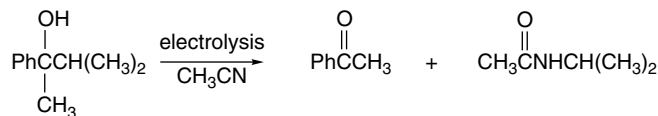
d.



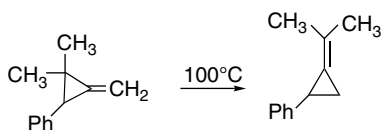
e.



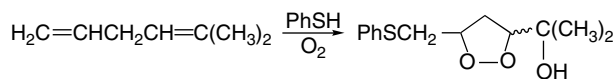
f.



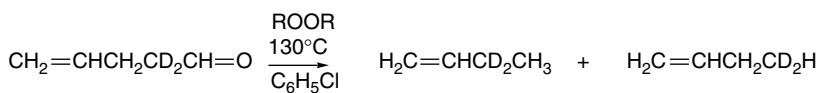
g.



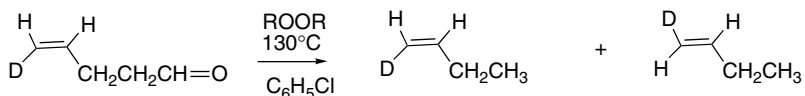
h.



11.7. The decarbonylation of the two isotopically labeled pentenals shown below have been studied. Explain why the distribution of deuterium found in the products is affected by solution concentration.

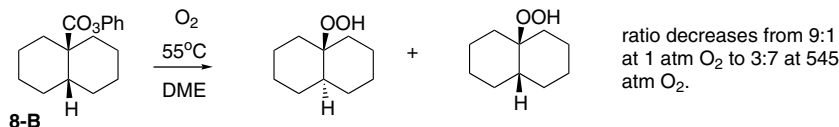
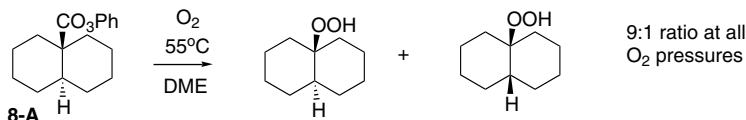


1:1 ratio in dilute solution increasing to 1:1.5 in concentrated solution.

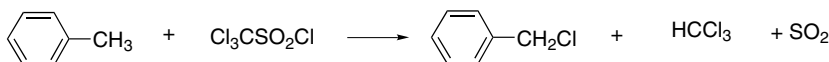


1:1 ratio in dilute solution increasing to 1:1.4 in concentrated solution.

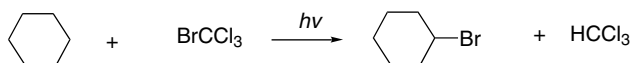
- 11.8. Decomposition of the *trans*-decyl peroxyester **8-A** gives a 9:1 ratio of *trans*- and *cis*-hydroperoxides at all the oxygen pressures studied. The product ratio from the *cis*-peroxyester **8-B** is dependent on oxygen pressure. At 1 atm O<sub>2</sub> it is 9:1 *trans*:*cis*, identical to the *trans* isomer, but the ratio decreases and eventually inverts with increasing O<sub>2</sub> pressure. At 545 atm, the ratio is 7:3, favoring the *cis*-hydroperoxide. What deductions about the stereochemistry of the 9-decyl radical can be made from these observations?



- 11.9 a. Trichloromethanesulfonyl chloride can chlorinate hydrocarbons as described in the stoichiometric equation below. The reaction occurs by a free radical chain process. Write at least two possible sequences for chain propagation.



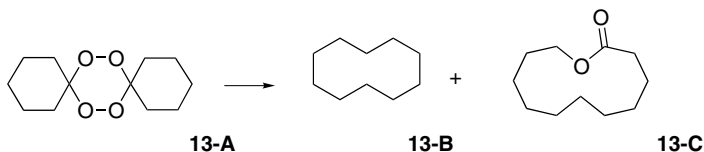
- b. The chlorination has been compared with bromination by BrCCl<sub>3</sub> carried out under radical chain conditions. In this reaction, cyclohexane is about one-fifth as reactive as toluene, but in the chlorination by trichloromethanesulfonyl chloride, cyclohexane is about three times more reactive than toluene. Does this information permit a choice between the chain sequences you have written in part (a)?



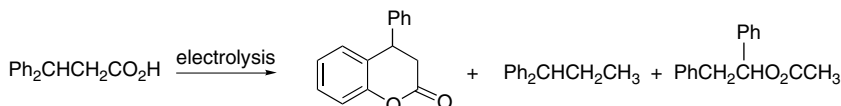
- 11.10. A highly selective photochemical chlorination of esters, amides, and alcohols can be carried out in 70–90% H<sub>2</sub>SO<sub>4</sub> using *N*-chlorodialkylamines as the



- 11.13. The *spiro* peroxide **13-A**, which is readily prepared from cyclohexanone and hydrogen peroxide, decomposes thermally to give substantial amounts of cyclodecane (**13-B**) and 11-undecanolactone (**13-C**). Account for the efficient formation of these macrocyclic compounds.

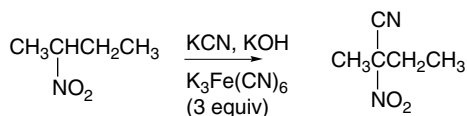


- 11.14. Methylcyclopropane shows strikingly different reactivity toward chlorine and bromine under radical chain conditions in  $\text{CH}_2\text{Cl}_2$  solution. The main product with chlorine is chloromethylcyclopropane (56%), along with smaller amounts of 1,3-dichlorobutane and 1,3-dichloro-2-methylpropane. Bromine gives only 1,3-dibromobutane. Offer a mechanistic explanation.
- 11.15. Electrolysis of 3,3-diphenylpropanoic acid in acetic acid–sodium acetate solution gives the products shown below. Propose mechanisms for the formation of each product.

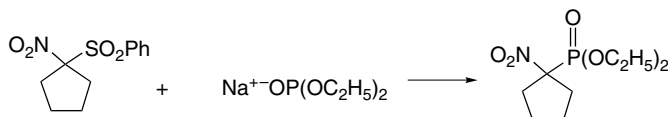


- 11.16. Write a mechanism to account for the observed product of each of the following reactions:

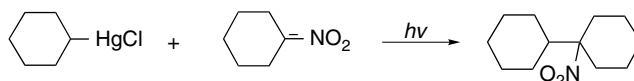
a.



b.

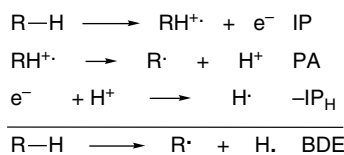


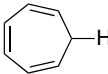
c.



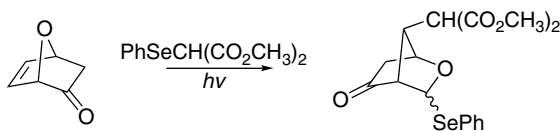
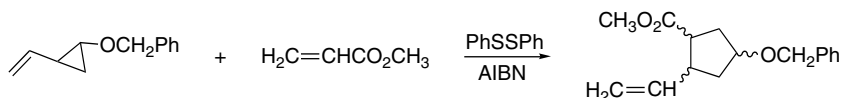
- 11.17. The *N*-benzoyl methyl esters of the amino acids glycine, alanine, and valine have been shown to react with *N*-bromosuccinimide to give the  $\alpha$ -bromo derivatives. The order of reactivity is glycine > alanine > valine in the ratio 23:8:1. Account for the formation of the products and the order of the reactivity.

11.18. By measurement in an ion cyclotron resonance mass spectrometer, it is possible to measure the proton affinity (PA) of free radicals. These data can be combined with ionization potential (IP) data according to the scheme below to determine the bond dissociation energy (BDE) of the corresponding C–H bond. The ionization potential of the H atom is 313.6 kcal/mol. Use the data given below to determine the relative stabilization of the various radicals relative to methyl, for which the BDE is 104 kcal/mol. Compare the BDE determined in this way with the comparable values given in Table 3.20.



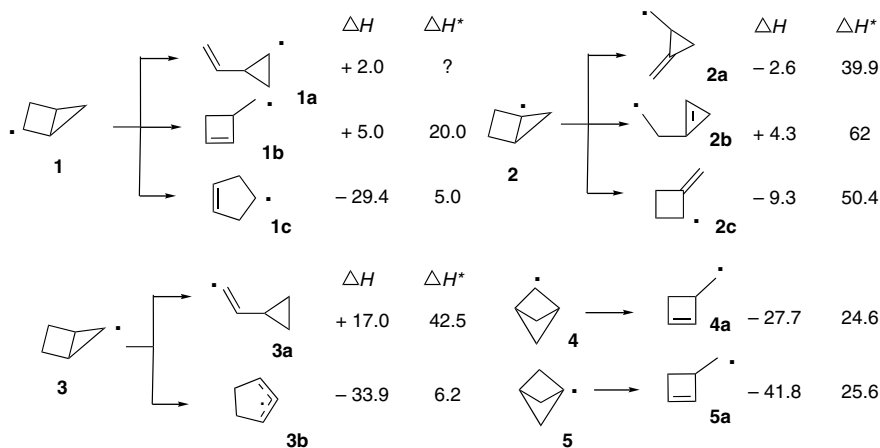
	IP	PA
PhCH <sub>2</sub> –H	203	198
	190	200
	198	199
	224	180
CH <sub>2</sub> =CHCH <sub>2</sub> –H	224	180
	232	187
CH <sub>2</sub> =CH–H	242	183

11.19. Provide stepwise mechanisms for the following reactions:

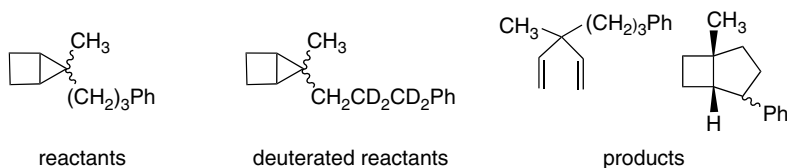


11.20. The energy of some free radicals derived from small strained hydrocarbons has been calculated at the MINDO/3 level. The  $\Delta H$  and  $\Delta H^\ddagger$  were calculated for several possible fragmentations and are given below. Consider the stereoelectronic and steric

factors involved in the various fragmentations. Explain the large variations in  $\Delta H$  and  $\Delta H^\ddagger$  and identify structural features that lead to facile fragmentation.



- 11.21. The pyrolysis of a mixture of the two stereoisomers of 5-methyl-5-(3-phenylpropyl)bicyclo[2.1.0]pentane leads to a mixture of three products. The two reactants equilibrate under the reaction conditions at a rate that exceeds product formation. When deuterium is introduced into the propyl side chain, there is no intermolecular deuterium scrambling. Write a mechanism for formation of each product and indicate how the deuterium results help to define the mechanism. What can be said about the lifetime of the intermediates in your mechanism?



# Photochemistry

## Introduction

The photochemical reactions of organic compounds attracted great interest beginning in the 1960s. As a result, many useful and fascinating reactions were uncovered and photochemistry is now an important synthetic tool in organic chemistry. A firm basis for mechanistic descriptions of many photochemical reactions has been developed. Some of the more general types of photochemical reactions are discussed in the present chapter. In Section 12.2, the photochemistry of alkenes, dienes, and polyenes is considered, including the relationship of photochemical reactions to orbital symmetry principles. Important reaction types include *cis-trans* isomerization, electrocyclic reactions, photocycloadditions, and rearrangements. In subsequent sections, characteristic photochemical reactions of carbonyl compounds and aromatic rings are introduced.

## 12.1. General Principles

We begin by summarizing the basic elements of photochemical reactions. The first condition that must be met is that the reactant absorb light emitted by the source. For light to be absorbed, the compound must have an energy level that corresponds to the energy of the radiation. Organic photochemical reactions usually involve excited electronic states. Depending on functionality, organic compounds can have electronic absorption bands in the ultraviolet and/or the visible region of the spectrum. Most of the photochemistry we discuss involves unsaturated groups, mainly alkenes, carbonyl compounds, and arenes, in which an electron is promoted to an antibonding  $\pi^*$  orbital. These excited states involve promotion of electrons in valence shell orbitals. The excited states can be singlets or triplets. In a *singlet excited state* the excited electrons retain opposite spins, whereas in *triplet excited states* they have parallel spins. The photoexcitation of organic molecules can also involve *Rydberg states*, which involve excitation of an electron from the valence level to a higher shell, typically  $3s$  and  $3p$  for organic molecules. The Rydberg states are similar to a radical cation in the

valence shell but with an additional diffuse distribution of the excited electron. In many molecules, there is mixing of character of valence shell excited states with Rydberg states, and the latter can decay to valence shell excited states.

Table 12.1 lists the general regions of absorption for the classes of organic molecules that are discussed in this chapter. A number of light sources can be used, the most common for preparative scale work being mercury vapor lamps, which emit mainly at 214, 254, 313, and 366 nm. The composition of the radiation reaching the sample can be controlled by filters. For example, if the system is constructed so that light passes through standard glass, only wavelengths longer than 300–310 nm reach the sample because the glass absorbs below this wavelength. Pure fused quartz, which transmits down to 200 nm, must be used if the 254-nm radiation is desired. Other glasses have cutoff points between those of quartz and standard glass. Filter solutions that absorb in specific wavelength ranges can also be used to control the energy of the light reaching the sample.<sup>1</sup> Mechanistic studies are frequently done using lasers, which permits intense radiation at specific wavelengths and for brief periods of time.

The energy supplied by a particular wavelength of light can be calculated from the fundamental equation

$$E = hv \quad (12.1)$$

The energy in kcal/mole is

$$E = 2.86 \times 10^4 / \lambda$$

where  $\lambda$  is wavelength in nm. Thus, light of  $\lambda = 254$  nm equals 112.6 kcal/mol, an energy sufficient to rupture most single bonds. The energy is also often expressed in terms of the frequency of the light:

$$E(\text{cm}^{-1}) = 349.8 \text{ cm}^{-1} / \text{kcal/mol}$$

Energy is also some times expressed in eV, where 1 eV = 23.14 kcal/mol.

When a quantum of light is absorbed, the electronic configuration changes to correspond to an excited state. Three general points about this process should be emphasized:

**Table 12.1. Approximate Wavelength Ranges for Lowest-Energy Absorption Band of Representative Organic Compounds**

Reactant	Absorption maxima (nm)
Monoalkenes	190–200
Acyclic dienes	220–250
Cyclic dienes	250–270
Aryl-substituted alkenes	270–300
Saturated ketones	270–280
$\alpha$ , $\beta$ -Unsaturated ketones	310–330
Benzene derivatives	250–280
Aromatic ketones and aldehydes	280–300

<sup>1</sup> Detailed information on the emission characteristics of various sources and the transmission properties of glasses and filter solutions can be found in A. J. Gordon and R. A. Ford, *The Chemist's Companion*, Wiley-Interscience, New York, 1972, pp. 348–368 and in S. L. Murov, I. Carmichael, and G. L. Hug, *Handbook of Photochemistry*, 2nd Edition, Marcel Dekker, New York, 1993.

1. The excitation promotes an electron from a filled orbital to an empty one. In many cases, the promotion is from the HOMO to the LUMO, which is usually an antibonding orbital. Higher excited states, can also be populated. In any case, photoexcitation involves *unpairing of electrons* but at the instant of excitation they still have opposite spins.
2. At the instant of excitation, only electrons are reorganized. The nuclei retain their ground state geometry. The excitation is called a *vertical transition*, and the statement of this condition is referred to as the *Frank-Condon principle*. A consequence is that the initial excited state is in a nonminimal energy geometry. The excited state then attains its minimum energy structure extremely rapidly, with release of excess energy.
3. The electrons do not undergo spin inversion at the instant of excitation. Inversion is forbidden by quantum mechanical selection rules, which require that there be conservation of spin during the excitation process. Although a subsequent spin state change may occur, it is a separate step from excitation. In the initial excited state the unpaired electrons have opposite spins in a *singlet state*.

Thus, in the very short time ( $10^{-15}$  s) required for excitation, the molecule does not undergo changes in nuclear position or in the spin state of the promoted electron. After the excitation, however, these changes can occur very rapidly. There may be a minimum, usually shallow, close to the initial Franck-Condon geometry. Such states are attained very rapidly (<50 ps). The ultimate minimum energy geometry associated with the excited state is rapidly achieved by vibrational processes that transfer thermal energy to the solvent. This process, called *internal conversion*, results in formation of the minimum energy structure of the singlet excited state. The rate of transformation between different excited states depends on their similarity in structure and energy.<sup>2</sup> The more similar in structure and energy, the faster the transition. Often, the excited state attains its minimum energy without passing any barrier. Sometimes, chemical reactions of the excited molecule are fast relative to this vibrational relaxation, but this is unusual in solution. When reaction proceeds more rapidly than vibrational relaxation, the reaction is said to involve a *hot excited state*, that is, one with excess vibrational energy. The excited state can also undergo *intersystem crossing*, the inversion of spin of an electron in a half-filled orbital to give a *triplet state*, in which both unpaired electrons have the same spin. The triplet state also adopts a new minimum energy molecular geometry. Photochemical transitions can also be described as *diabatic* and *adiabatic*. A diabatic process involves a shift from one energy surface to another without a geometric change. An adiabatic process occurs on one energy surface by geometric reorganization.

Intersystem crossing must also occur when triplet excited states return to singlet ground states. A prominent factor in the rate of such processes is *spin-orbit coupling*, which depends on the structure of the triplet state and strongly affects the rate of intersystem crossing. The extent of spin-orbit coupling and the rate of intersystem crossing decrease with increasing separation of the orbitals containing the unpaired electrons.<sup>3</sup> There is also a preference for perpendicular orientation of the orbitals.

<sup>2</sup>. L. Landau, *Phys.Z. Sowjet.*, **2**, 46 (1932); L. Zener, *Proc. Royal Soc. London*, **A137**, 696 (1932).

<sup>3</sup>. L. Salem and C. Rowland, *Angew. Chem. Int. Ed. Engl.*, **11**, 92 (1972); L. Carlucci, C. Doubleday, Jr., T. R. Furlani, H. F. King, and J. W. McIver, Jr., *J. Am. Chem. Soc.*, **109**, 5323 (1987); C. Doubleday, Jr., N. J. Turro, and J.-F. Wang, *Acc. Chem. Res.*, **22**, 199 (1989); M. Klessinger, *Theor. Org. Chem.*, **5**, 581 (1998).

Spin-orbit coupling also increases with the degree of ionic character of the singlet state. The presence of a heavy element, e.g., bromine, also promotes intersystem crossing.

The overall situation can be represented for a hypothetical molecule using a potential energy diagram. The designations  $S$  and  $T$  are used for singlet and triplet states, respectively. The excitation is a vertical transition; that is, it involves no distortion of the molecular geometry. Horizontal displacement on the diagram corresponds to motion of the atoms relative to one another. Since the potential energy surfaces of the excited states are displaced from that of the ground state, the species formed by excitation is excited both electronically and vibrationally. The energy wells corresponding to the triplet states also correspond to a different minimum energy molecular geometry. *Nonradiative decay*, also called *internal conversion*, results in dissipation of the vibrational energy as the molecule moves to the bottom of any particular energy well. One of the central issues in the description of any photochemical reaction is the question of whether a singlet or triplet excited state is involved, and this depends on the rate of intersystem crossing in comparison with the rate of chemical reaction of the singlet excited state. If intersystem crossing is fast relative to reaction, reaction will occur through the triplet excited state. If reaction is faster than intersystem crossing, the reaction will occur from the singlet state. The processes that can occur after photochemical excitation are summarized in Figure 12.1.

*Photosensitization* is an important alternative to direct excitation of molecules and this method usually results in reaction occurring via a triplet excited state. If a reaction is to be carried out by photosensitization, a substance known as the *sensitizer* is present in the system. Each sensitizer has a characteristic energy,  $E_T$ , that it can transfer to a reactant. The sensitizer is chosen to meet the following criteria: (1) It must be excited by the irradiation to be used. (2) It must be present in sufficient concentration and absorb more strongly than the other reactants under the conditions

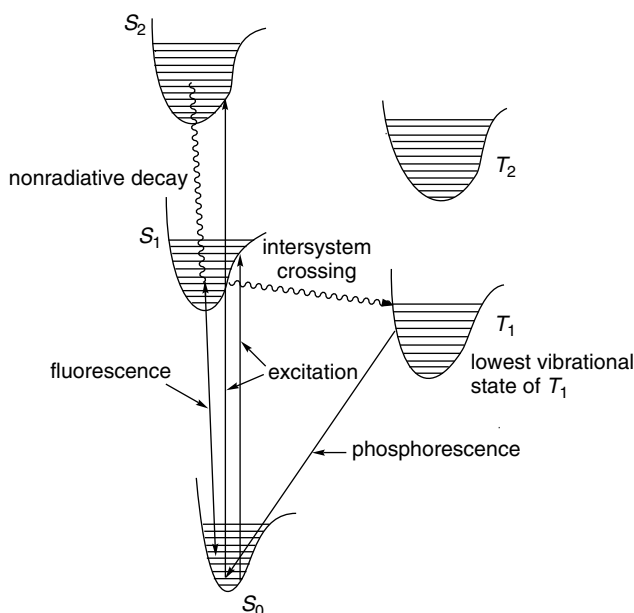
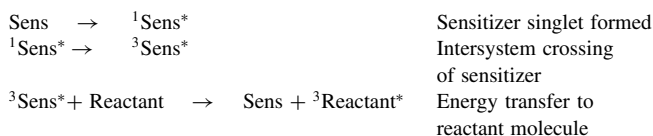


Fig. 12.1. Energy level diagram and summary of photochemical processes.

of the experiment so that it is the major light absorber. (3) Its intersystem crossing rate must be faster than energy transfer to the reactant or solvent from the singlet excited state. (4) The energy of its triplet state must be greater than that of the reactant; if this condition is not met, the energy transfer becomes endothermic and cannot compete with other transformations. (5) The triplet excited sensitizer must be able to transfer energy to the desired reactant.

The transfer of energy proceeds with net conservation of spin. In the usual case, the reactant molecule is a ground state singlet, and its reaction with the triplet excited state of the sensitizer produces a triplet state of the reactant. The mechanism for triplet photosensitization is as follows:



Sensitization can occur from singlet excited states, but for most cases we discuss, triplet sensitization operates.

When an excited state of the reactant has been formed, either by direct or sensitized energy transfer, the stage is set for a photochemical reaction. There are, however, competitive processes that can occur and result in the return of unreacted starting material. The excited state can decay to the ground state by emission of light, a *radiative transition*. The rate of emission can be very fast ( $k = 10^5 - 10^9 \text{ s}^{-1}$ ) for transitions between electronic states of the same multiplicity, but is somewhat slower ( $k = 10^3 - 10^5 \text{ s}^{-1}$ ) between states of different multiplicities. The two processes are known as *fluorescence* and *phosphorescence*, respectively. When energy has been emitted as light, the reactant is no longer excited, of course, and a photochemical reaction does not occur. Excited states can also be *quenched*. Quenching is the same physical process as sensitization, but the term “quenched” is used when a photoexcited state of the reactant is deactivated by transferring its energy to another molecule in solution. This substance is called a *quencher*. Finally, *nonradiative decay* can occur. In this process, the energy of the excited state is transferred to the surrounding molecules as vibrational (thermal) energy without light emission.

Owing to the existence of these competing processes, not every molecule that is excited undergoes a photochemical reaction. The fraction of molecules that react relative to those that are excited is called the *quantum yield*,  $\Phi$ , which is a measure of the efficiency of the absorption of light in producing reaction product. A quantum yield of 1 means that each molecule excited (which equals the number of quanta of light absorbed) goes to product. If the quantum yield is 0.01, then only 1 out of 100 of the molecules that are excited undergoes photochemical reaction. The quantum yield can vary widely, depending on the structure of the reactants and the reaction conditions. The quantum yield can be greater than 1 in a chain reaction, in which a single photoexcitation initiates a series of repeating reactions leading to many molecules of product per initiation step.

As photochemical processes are very fast, special techniques are required to obtain rate measurements. One method is flash photolysis, in which the excitation is effected by a short pulse of light in an apparatus designed to monitor very fast spectroscopic

changes. The rate characteristics of the reactions following radiation can be determined from these spectroscopic changes. Various other techniques have been developed to follow the exceedingly fast changes that occur immediately after excitation. Some of them can detect changes that occur over 10–100 fs ( $10^{-15}$  s).

A useful technique for indirectly determining the rates of certain reactions involves measuring the quantum yield as a function of quencher concentration. A plot of the inverse of the quantum yield versus quencher concentration is then made (*Stern-Volmer plot*). As the quantum yield indicates the fraction of excited molecules that go on to product, it is a function of the rates of the processes that result in other fates for the excited molecule. These processes are described by the rate constants  $k_q$  (quenching) and  $k_n$  (other nonproductive decay to ground state):

$$\Phi = \frac{k_r}{k_r + k_q[Q] + k_n} \quad (12.2)$$

A plot of  $1/\Phi$  versus  $[Q]$  then gives a line with the slope  $k_q/k_r$ . It is often possible to assume that quenching is diffusion controlled, permitting assignment of a value to  $k_q$ . The rate of photoreaction,  $k_r$ , for the excited intermediate can then be calculated.

In the sections that follow, the discussion centers on the reactions of excited states, rather than on the other routes available for dissipation of excitation energy. The chemical reactions of photoexcited molecules are of interest for several reasons:

1. Excited states have excess energy and can therefore undergo reactions that would be highly endothermic if initiated from the ground state. For example, from the relationship  $E = h\nu$  we can calculate that excitation by 350-nm light corresponds to 82 kcal/mol in energy transfer.
2. The population of one or more antibonding orbitals in the excited state allows the occurrence of chemical transformations that are electronically forbidden to ground state species.
3. Both singlet and triplet excited states have unpaired electrons, whereas closed-shell species are involved in most thermal processes (free radical reaction being an exception). This permits the formation of intermediates that are unavailable under thermal conditions.

Another important distinction between ground state and excited state reactions involves the relative rates of conformational interconversion. In thermal reactions, as stated by the Curtin Hammett principle (p. 296) conformers are normally in equilibrium, but the position of the equilibrium does not determine the reaction pathway. Many steps in photochemical reactions occur sufficiently rapidly that various conformers are not in equilibrium. This is the principle of *nonequilibrium of excited rotamers* (NEER).<sup>4</sup> Thus in analyses of photochemical reactions, it is often necessary to consider conformational issues in order to interpret the reaction. *Reaction dynamics* refers to the conformational and other geometrical aspects of the reactions.

As we describe photochemical reactions, we note repeatedly that photochemical reactions involve unpairing and re-pairing of electrons. Frequently, atom and group migrations occur prior to the final electron re-pairing. Although discerning these unpairing/re-pairing schemes is a first step in understanding photochemical mechanisms, we also want to consider the structure of excited states and reaction intermediates. As is the case for transition structures in thermal reactions, computational approaches have provided a new level of insight.

<sup>4</sup> H. J. C. Jacobs and E. Havinga, *Adv. Photochem.*, **11**, 305 (1979).

The mechanisms of photochemical reactions can be presented at several levels of detail. The most basic level is to recognize the unpairing/re-pairing sequence that is associated with bond breaking and bond forming. These processes can be further described by depicting the orbitals that are involved. Just as in thermal reactions, orbital symmetry and/or stereoelectronic effects can be recognized in this way. Photochemical reactions can also be described by potential energy diagrams, similar to those we have used for thermal reactions. For a photochemical reaction, the diagram represents transitions between the excited structures and aims to trace the path from excitation to photoproduct. As for thermal reactions, the path depicted is the minimum energy path across a potential energy surface. Photochemical reactions, however, can involve several excited states, each with its own potential energy surface, so there are several energy plots representing these surfaces. Two-dimensional representations can depict progress in one structural change, such as a twist about a bond or a bond breaking. Alternatively, the reaction progress may be viewed as a composite of all the structural changes that take place among reactant, excited state, and product. Figure 12.2 is such a diagram, depicting transitions between excited states and, eventually, the ground state surface of the products. The diagram shows excitation to both  $S_1$  and  $S_2$ , the first and second singlet excited states. Molecules drop to the  $S_1$  surface at point C. Singlet excited molecules return to the ground state at point A and may return to reactant or proceed to product  $P_1$ . Intersystem crossing occurs at points B or D and provides the triplet excited state, which gives product  $P_2$ .

Reactions in which structural change is simultaneously occurring in more than one structural parameter can be depicted as interaction between surfaces with coordinates described by the structural parameters. For many photochemical reactions it has been found that transfer from an excited to a ground state involves a *conical intersection* (CI), which can be thought of as a funnel that permits transition from one energy surface (state) to another. The efficiency of the transformation depends on the structural similarity between the excited state and the corresponding ground state molecular ensemble. There can be a number of CIs for the excited states of a typical polyatomic molecule. The transition occurs without luminescence. Conical

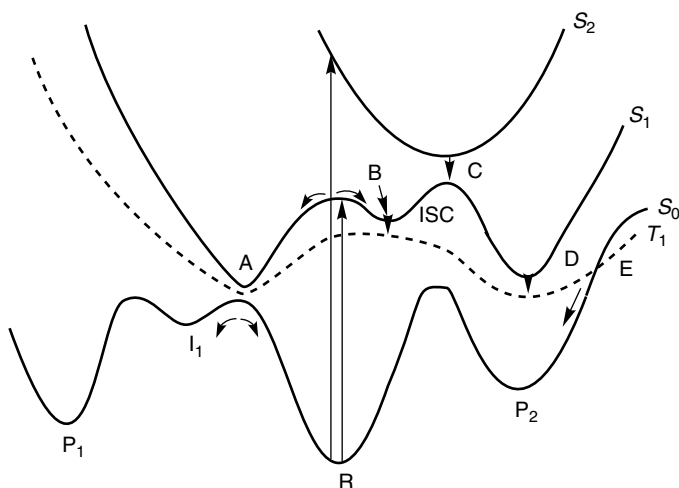


Fig. 12.2. A schematic representation of several transitions between excited states leading to photochemical reaction products.

intersections are analogous to transition states in thermal reactions in that they are points at which the electronic transition from the excited to the ground state is very fast.<sup>5</sup> In a transition structure there is an imaginary vibrational frequency corresponding to the reaction coordinate (Section 3.2.1). Conical intersections can proceed along any direction in a plane and can reach more than one minimum (product). The ultimate outcome of the reaction is influenced by dynamic factors at the CI. Thus motion toward a particular product may be associated with dynamic factors, e.g., direction of rotation at a preceding stage of the reaction. As in the case of thermal TSs, the structure of a CI can be described on the basis of computation.<sup>6</sup> Figure 12.3 is a representation of a conical intersection showing divergent paths to two different products,  $P_1$  and  $P_2$ , resulting from different components of motion along the  $X_1$  and  $X_2$  coordinates.

We discuss some prototypical reactions, such as *cis-trans* isomerization, electrocyclic reactions, and cycloadditions in terms of the structures of excited states and conical intersections. For most other reactions, we represent the reaction changes in terms of structures that depict the unpairing and re-pairing events. Such representations identify key structural features that influence the outcome of the reaction, even though they may leave much uncertainty about the detailed structure of the excited states and intermediates. For several reactions, the mechanism is discussed in terms of the structure and reaction paths for CIs. Structures of specific CIs derived from computation are depicted. At this time, it is perhaps too early to fully judge the accuracy of these structural representations. However, just as for depiction of TS structures, visualization of the CI can help understand the course of a photochemical reaction.

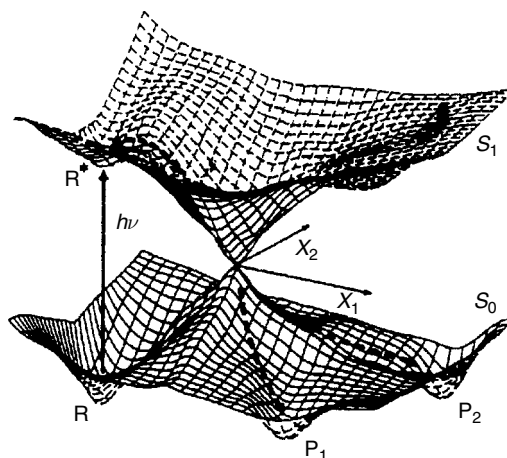


Fig. 12.3. Schematic representation of the potential energy surfaces of the ground ( $S_0$ ) and excited ( $S_1$ ) state in a nonadiabatic photochemical reaction. Two reaction channels lead from the conical intersection to products  $P_1$  and  $P_2$ . The trajectories entering the conical intersection determine which reaction channel is followed. Reproduced from *Angew. Chem. Int. Ed. Engl.*, **34**, 549 (1995), by permission of Wiley-VCH.

<sup>5</sup> Y. Haas and S. Zilberg, *J. Photochem. Photobiol.*, **144**, 221 (2001); M. Klessinger, *Angew. Chem. Int. Ed. Engl.*, **34**, 549 (1995).

<sup>6</sup> F. Bernardi, M. Olivucci, and M. A. Robb, *J. Photochem. Photobiol. A*, **105**, 365 (1997).

We begin by discussing two fundamental types of photochemical reactions of alkenes and dienes. One is *cis-trans* isomerization and the others fall into the category of pericyclic reactions, including electrocyclic reactions and cycloadditions. As indicated in Chapter 10, there is a broad dichotomy between thermal and photochemical pericyclic reactions. Thermally forbidden processes are typically allowed photochemically and vice versa. Although the interpretation and prediction of the stereoselectivity of pericyclic thermal reactions is generally possible within the framework of the Woodward-Hoffmann rules, we will find several complicating factors when we consider photochemical reactions. We also examine a number of unimolecular photochemical rearrangements of alkenes and polyenes. Cycloadditions are considered further, from a synthetic viewpoint, in Section 6.3.2 of Part B.

### 12.2.1. *cis-trans* Isomerization

Interconversion of *cis* and *trans* isomers is a characteristic photochemical reaction of alkenes. Usually, the *trans* isomer is thermodynamically more stable, but photolysis can establish a mixture that is richer in the *cis* isomer. Irradiation therefore provides a means of converting a *trans* alkene to the *cis* isomer. The composition of the photostationary state depends on the absorption spectra of the isomeric alkenes. A hypothetical case is illustrated in Figure 12.4. Assume that the vertical line at 265 nm is the lower limit for light reaching the system. This wavelength can be controlled by use of appropriate sources and filters. Because of the shift of its spectrum toward longer wavelengths and higher extinction coefficients, the *trans* isomer absorbs substantially more light than the *cis* isomer. The relative amount of light absorbed at any wavelength is proportional to the extinction

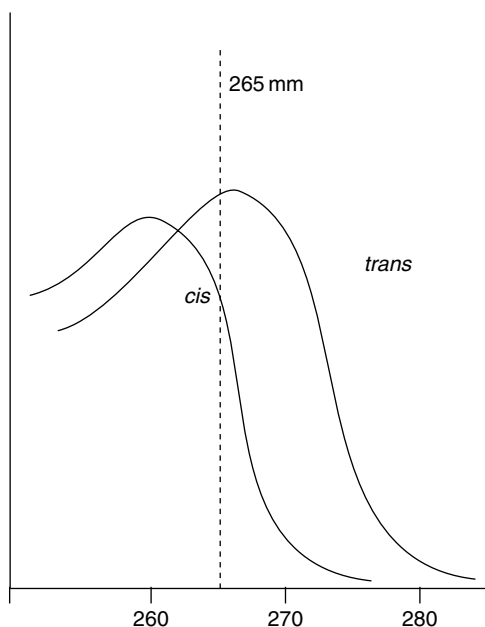


Fig. 12.4. Absorption spectra of a *cis-trans* isomer pair.

coefficients at that wavelength. If we assume that the quantum yield for conversion of *cis*→*trans* is approximately equal to that for *trans*→*cis*, the conversion of *trans* alkene to *cis* will occur faster than the converse process when the two isomers are in equal concentrations. On continued photolysis, a photostationary state will be achieved when the rate of *trans*→*cis* is equal to that of *cis*→*trans*. At this point the concentration of the *cis* isomer will be greater than that of the *trans* isomer. The relationship can be expressed quantitatively for monochromatic light as

$$\frac{[trans]}{[cis]} = \left( \frac{\epsilon_c}{\epsilon_t} \right) \left( \frac{\Phi_{c \rightarrow t}}{\Phi_{t \rightarrow c}} \right) \quad (12.3)$$

The *cis-trans* isomerization of alkenes is believed to take place via an excited state in which the two *sp*<sup>2</sup> carbons are twisted by about 90° with respect to one another. This twisted geometry is believed to be the minimum energy geometry for both the singlet and triplet excited states. The twisted geometry is an *energy maximum* on the ground state surface. The twisted geometry for the excited state permits the possibility of returning to either the *cis* or *trans* configuration of the ground state. The return from the singlet excited state to the ground state involves re-pairing of the electrons by a nonradiative process. Return from the triplet state requires intersystem crossing.

*12.2.1.1. Photoisomerization of Ethene and Styrene* We consider the excited states of ethene and styrene in some detail. These molecules do not exist as *cis* and *trans* isomers unless they are isotopically labeled. However, they are prototypes of isolated and conjugated alkenes and have been studied extensively. The excited states of ethene have been studied both by experiment and computation. The *S*<sub>1</sub> and *T*<sub>1</sub> excited states have been described by MP4(SDTQ)/6-311G\*\* computations.<sup>7</sup> At this level of computation the energy of *T*<sub>1</sub> is 2.92 eV and *S*<sub>1</sub> is 5.68 eV. The *T*<sub>1</sub> state is calculated to have a perpendicular structure with extension of the C–C bond to 1.455 Å. The *S*<sub>1</sub> state is also twisted and is very strongly pyramidalized at one carbon. The C–C bond distance is 1.360 Å. This state is believed to have a large degree of zwitterionic character, with the negative charge at the pyramidalized carbon. These structures are depicted in Figure 12.5.

The excited state lifetime of ethene is very short (<10<sup>-13</sup> s). Both the valence and Rydberg excited states return to the ground state through a conical intersection. The CIs of the *S*<sub>1</sub> state have been examined using quantum dynamics calculations.<sup>8,9</sup> Return from an excited state to the ground state involves both twisting at the C–C bond and pyramidalization. Another conical intersection, which is similar in structure to the carbene ethylidene, occurs at a similar energy. These structures are shown in Figure 12.6. As we explore alkene photochemistry, we will see that the excited states and CIs depicted in Figures 12.5 and 12.6 are prototypical of the structures that are involved in the photochemistry of alkenes. The triplet *T*<sub>1</sub> state of alkenes can be represented as a twisted triplet diradical. The *S*<sub>1</sub> state is often referred to as a zwitterionic state and can be thought of as having cationic character at one carbon and carbanionic character at the other. The *S*<sub>1</sub> excited state is quite similar to the strongly

<sup>7</sup> S. El-Taher, P. Hilal, and T. A. Albright, *Int. J. Quantum Chem.*, **82**, 242 (2001); V. Molina, M. Merchan, B. O. Roos, and P.-A. Malmqvist, *Phys. Chem. Chem. Phys.*, **2**, 2211 (2000).

<sup>8</sup> M. Ben-Nun and T. J. Martinez, *Chem. Phys. Lett.*, **298**, 57 (1998); M. Ben-Nun, J. Quenneville, and T. J. Martinez, *J. Chem. Phys. A*, **104**, 5161 (2000); J. Quenneville, M. Ben-Nun, and T. J. Martinez, *J. Photochem. Photobiol.*, **144**, 229 (2001).

<sup>9</sup> M. Ben-Nun and T. J. Martinez, *Chem. Phys.*, **259**, 237 (2000).

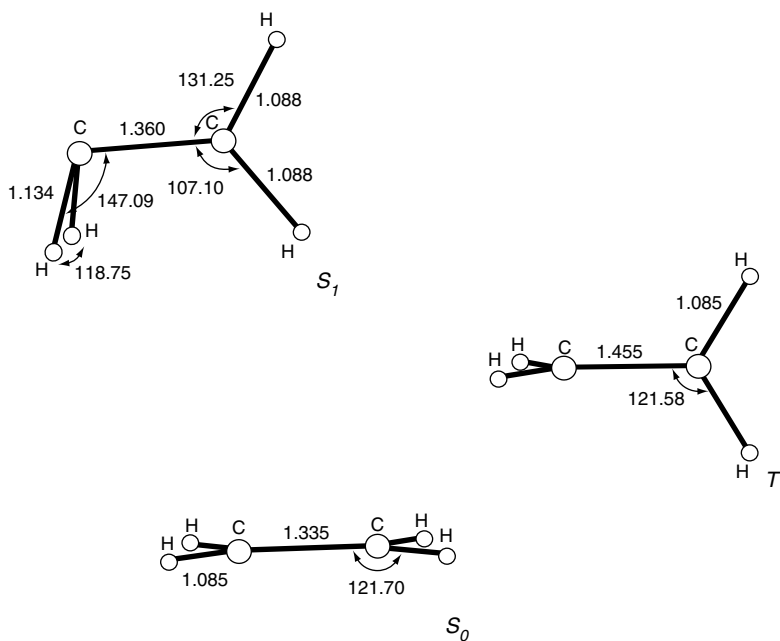
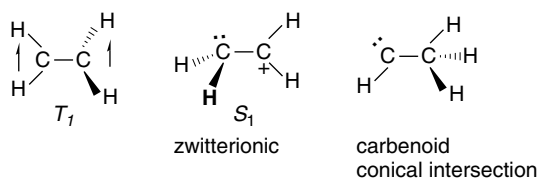


Fig. 12.5. Minimum energy structures (MP2/6-31G\*) for  $S_0$ ,  $S_1$ , and  $T_1$  states of ethene. Reproduced from *Int. J. Quantum Chem.*, **82**, 242 (2001), by permission of Wiley-VCH.

pyramidalized CI in Figure 12.6. The CI with carbene character is also a common feature of alkene chemistry and can be considered to form by hydride migration from the zwitterionic excited state. Similar structures involving carbon migration are also found for substituted alkenes.



There are two relatively low-lying singlet states for styrene.  $S_1$  is associated primarily with the benzene ring, whereas  $S_2$  is a singlet quinoid structure. The  $S_1$  state

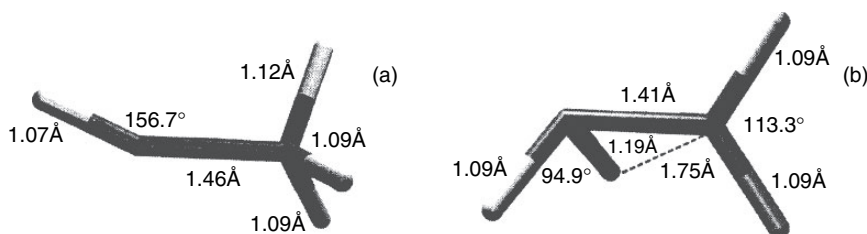
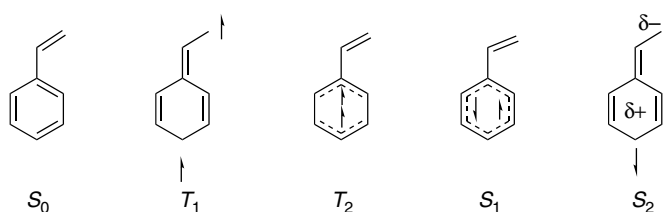


Fig. 12.6. Structures of lowest-energy conical intersections for the singlet excited state of ethene: (a) ethylidene-like structure; (b) twisted and pyramidalized structure. Reproduced from *Chem. Phys.*, **259**, 237 (2000), by permission of Elsevier.

is believed to be planar with a barrier to rotation of the double bond with respect to the ring of at least 3–4 kcal/mol.<sup>10</sup> The decay time for the  $S_1$  styrene is in the nanosecond range, which is considerably longer than for ethene.<sup>11</sup> The  $S_2$  excited state of styrene is a zwitterionic structure similar to the  $S_1$  state for ethene. In this case, as might be expected, the terminal methylene group is pyramidalized, with the cationic character associated with the phenyl-substituted carbon. The  $T_1$  state is quinoid in character with a shortened bond between the benzene ring and the double bond.  $T_2$  involves a triplet configuration of the benzene  $\pi$  electrons. Valence bond representations are shown below.



Valence Bond Representation of Excited States of Styrene

The geometries and energetics of the styrene excited states have been calculated at the CAS-SCF/6-31G\* level using all the  $\pi$  orbitals of styrene and are given in Figure 12.7.<sup>12</sup> The changes in bond length relative to the ground state indicate the nature of the excited states. Figure 12.7 shows the computed structures and energies of the excited states and indicates the singlet-singlet and singlet-triplet intersections. The  $T_2 \rightarrow T_1$  internal conversion, which involves transfer of triplet character from the benzene ring to the ethylene bond, is efficient. The  $T_1 \rightarrow S_0$  intersection, labeled  $ISC_c$ , is considered to be inefficient because of small spin-orbit coupling. This conversion is believed to occur in time range 20–100 ns.<sup>13</sup> This appears to be the slowest step in the decay sequence from the triplet excited state. Return to the ground state in the singlet manifold can occur from the  $ISC_b$  intersection. The styrene conical intersection appears to be similar to that for ethene and to involve both twisting and pyramidalization.<sup>14</sup> As Figure 12.7 suggests, there is considerable complexity to the styrene excited state surface. The introduction of the second chromophore, the benzene ring, introduces new issues

<sup>10</sup> J. I. Seeman, V. H. Grassian, and E. R. Bernstein, *J. Am. Chem. Soc.*, **110**, 8542 (1988); V. H. Grassian, E. R. Bernstein, H. V. Secor, and J. I. Seeman, *J. Phys. Chem.*, **93**, 3470 (1989); J. A. Syage, F. Al Adel, and A. H. Zewail, *Chem. Phys. Lett.*, **103**, 15 (1983).

<sup>11</sup> D. A. Condirston and J. D. Lapos, *Chem. Phys. Lett.*, **63**, 313 (1979).

<sup>12</sup> M. J. Bearpack, M. Olivucci, S. Wilsey, F. Bernardi, and M. A. Robb, *J. Am. Chem. Soc.*, **117**, 6944 (1995).

<sup>13</sup> R. Bonneau, *J. Photochem.*, **10**, 439 (1979); R. A. Caldwell, L. D. Jacobs, T. R. Furlani, E. A. Nalley, and J. Laboy, *J. Am. Chem. Soc.*, **114**, 1623 (1992).

<sup>14</sup> V. Molina, M. Merchan, B. O. Roos, and P.-A. Malmqvist, *Phys. Chem. Chem. Phys.*, **2**, 2211 (2000).

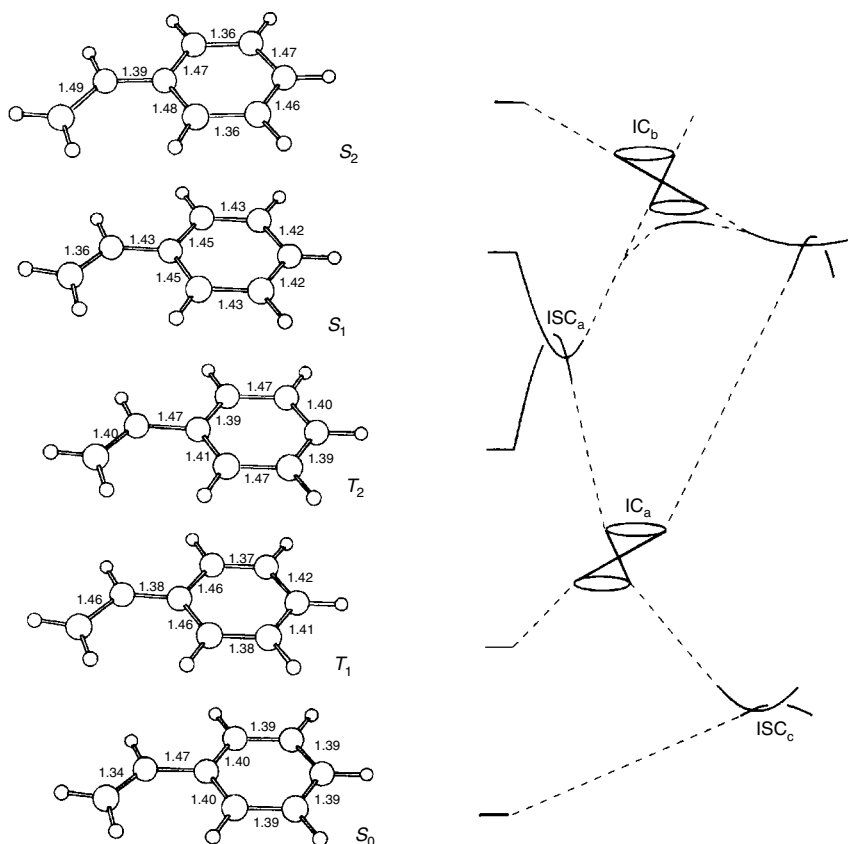


Fig. 12.7. Structures for the excited states  $T_1$ ,  $T_2$ ,  $S_1$ , and  $S_2$  of styrene. Singlet-singlet conical intersections are labeled IC (internal conversion). Singlet-triplet intersections are labeled ISC (inter-system crossing). Adapted from *J. Am. Chem. Soc.*, **117**, 6944 (1995), by permission of the American Chemical Society.

concerning energy transfer between the chromophores. However, the fundamental aspects of the double-bond rotation seem to be structurally similar to those for ethene.

**12.2.1.2. Photoisomerization of Stilbene** Especially detailed study of the mechanism of photochemical configurational isomerism has been done on *Z*- and *E*-stilbene.<sup>15</sup> The isomerization involves a twisted singlet state that can be attained from either the *Z*- or the *E*-isomer. Spectroscopic data have established the energies of the singlet and triplet states of both *Z*- and *E*-stilbene and of the twisted excited states that are formed from both isomers. Some features of the potential energy diagram are due to structural

<sup>15</sup> J. Saltiel, J. T. D'Agostino, E. D. Megarity, L. Metts, K. R. Neuberger, M. Wrighton, and O. C. Zafiriow, *Org. Photochem.*, **3**, 1 (1973); J. Saltiel and J. L. Charlton, in *Rearrangements in Ground and Excited States*, Vol. 3, P. de Mayo, ed., Academic Press, New York, 1980, Chap. 14; D. H. Waldeck, *Chem. Rev.*, **91**, 415 (1991); U. Mazzucato, G. A. Aloisi, G. Bartocci, F. Elisei, G. Galianzo, and A. Spalletti, *Med. Biol. Environ.*, **23**, 69 (1995); H. Gerner and H. J. Kuhn, *Adv. Photochem.*, **19**, 1 (1995).

differences in the ground state molecules.<sup>16</sup> Although the double bond in *E*-stilbene can be assumed to be planar, the phenyl groups can rotate with respect to the plane of the double bond. In the solid state, the molecule is nearly planar, but in solution or gas phase the molecule is probably somewhat twisted. For the *Z*-isomer, steric interactions between the phenyl rings require their rotation from coplanarity. A rotation of 43° has been found in the gas phase. This steric effect makes the *Z*-isomer somewhat less stable than the *E*-isomer. Computed minimum energy ground state structures are shown in Figure 12.8.<sup>17</sup>

As shown in Figure 12.9, the absorption spectra of *Z*- and *E*-stilbene differ substantially, with the *E*-isomer absorbing more strongly at  $\lambda > 260$  nm. Thus the

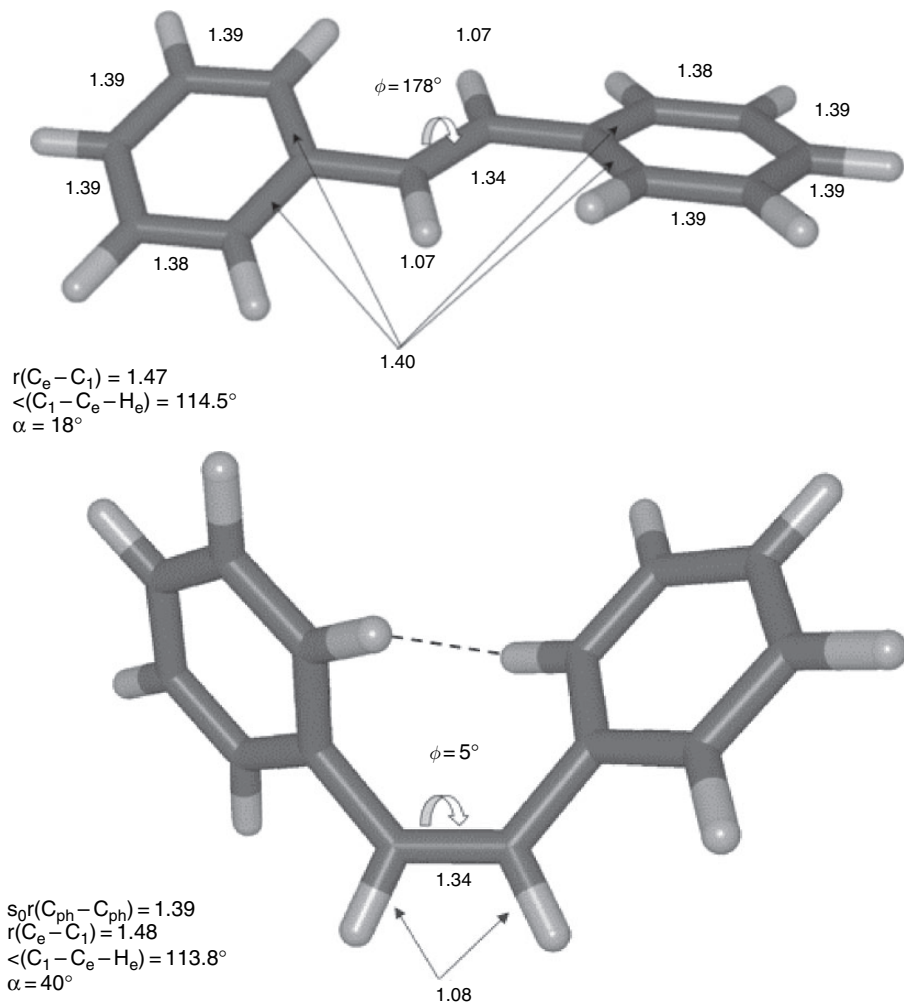


Fig. 12.8. Computed ground state geometries of *E*- and *Z*-stilbene. Reproduced from *J. Phys. Chem. A*, **107**, 829 (2003), by permission of the American Chemical Society.

<sup>16</sup> H. Meier, *Angew. Chem. Int. Ed. Engl.*, **31**, 1399 (1992).

<sup>17</sup> J. Quenneville and T. J. Martinez, *J. Phys. Chem. A*, **107**, 829 (2003).

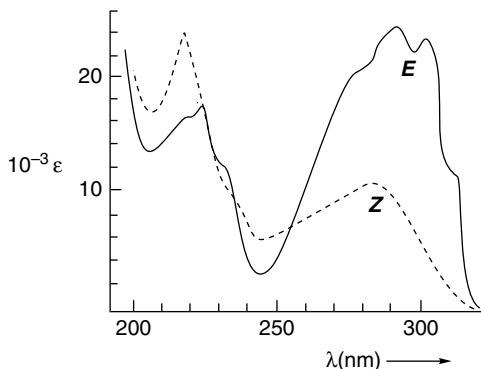


Fig. 12.9. UV spectra of *E*- and *Z*-stilbene in hexane at room temperature. Reproduced from *Angew. Chem. Int. Ed. Engl.*, **31**, 1399 (1992), by permission of Wiley-VCH.

photostationary state composition can be controlled by the wavelength of the irradiation, as indicated by the general examples and Equation (12.3) on p. 1082.<sup>18</sup>

Direct irradiation leads to isomerization via singlet state intermediates.<sup>19</sup> This involves a HOMO→LUMO excitation that involves primarily the ethylenic bond. Among the pieces of evidence indicating that a triplet intermediate is not involved in direct irradiation is the fact that azulene, which is known to intercept stilbene triplets, has only a minor effect on the efficiency of the direct photoisomerization.<sup>20</sup> Some aspects of this process can be described in terms of the two-dimensional energy diagram shown in Figure 12.10, which shows the relative energies and shapes of the  $S_0$ ,  $T_1$ ,  $S_1$ , and  $S_2$  states with respect to twisting at the double bond. The temperature dependence of the isomerization reveals that the process of formation of the twisted state from  $S_1$  involves a small activation energy. This energy is required for conversion of the initial excited state to the twisted geometry associated with the  $S_1$  state. The energy barrier is greater from the *E*-isomer than from the *Z*-isomer. Note, however, that the large energy gap between the twisted excited and ground states implies a low probability of direct interconversion.

The photoisomerization can also be carried out by photosensitization. Under these conditions, the composition of the photostationary state depends on the triplet energy of the sensitizer. With sensitizers having triplet energies above 60 kcal/mol,  $[Z]/[E]$  is slightly more than 1, but a range of sensitizers having triplet energies of 52–58 kcal/mol affords much higher *Z*:*E* ratios in the photostationary state.<sup>21</sup> The high *Z*:*E* ratio in this region results from the fact that the energy required for excitation of *E*-stilbene is less than for *Z*-stilbene. Thus sensitizers in the range 52–58 kcal/mol selectively excite the *E*-isomer. Since the rate of conversion of *E*→*Z* is increased, the composition of the photostationary state is enriched in *Z*-isomer.

<sup>18</sup>. J. Saltiel, A. Marinari, D. W.-L. Chang, J. C. Mitchener, and E. D. Megarity, *J. Am. Chem. Soc.*, **101**, 2982 (1979).

<sup>19</sup>. J. Saltiel, *J. Am. Chem. Soc.*, **89**, 1036 (1967); **90**, 6394 (1968).

<sup>20</sup>. J. Saltiel, E. D. Megarity, and K. G. Kneipp, *J. Am. Chem. Soc.*, **88**, 2336 (1966); J. Saltiel and E. D. Megarity, *J. Am. Chem. Soc.*, **91**, 1265 (1969).

<sup>21</sup>. G. S. Hammond, J. Saltiel, A. A. Lamola, N. J. Turro, J. S. Bradshaw, D. O. Cowan, R. C. Counsell, V. Vogt, and C. Dalton, *J. Am. Chem. Soc.*, **86**, 3197 (1964); S. Yamauchi and T. Azumi, *J. Am. Chem. Soc.*, **95**, 2709 (1973).

Photosensitizer <sup>a</sup>	$E_T$	[Z:E]
Acetophenone	73.6	1.2
Benzophenone	68.5	1.2
2-Acetylnaphthalene	59.3	2.6
1-Naphthyl phenyl ketone	57.5	2.8
Benzil	53.7	4.6
Fluorenone	52.3	8.3
Pyrene	48.7	4.6
3-Acetylpyrene	45	2.8

a. From *J. Am. Chem. Soc.*, **86**, 3197 (1964).

Further insight into the stilbene  $E \rightarrow Z$  photoisomerization has been obtained by computational studies. The  $S_1$  state is considered to be a  $\pi \rightarrow \pi^*$  state with considerable zwitterionic character. The transfer from the singlet photoexcited state of stilbene to the ground state is observed to be very fast and involves a CI. There have been two computational studies aimed at characterization of the CI. A CAS-SCF(STDQ-CI) study examined five filled and seven vacant  $\pi$  orbitals.<sup>22</sup> The CI was characterized by considering primarily the singlet and doublet HOMO  $\rightarrow$  LUMO excitations. The CI is described as two PhCH fragments that are twisted with respect to one another. The structure of the CI has also been investigated by CAS-SCF-CASPT2 methods,<sup>17</sup> and is shown in Figure 12.11. The qualitative characteristics of the CI are very similar to

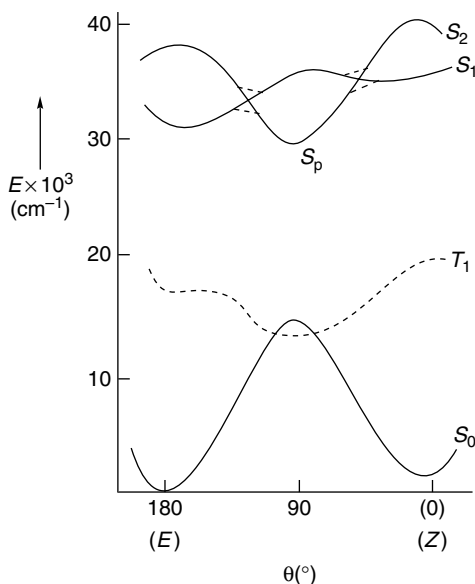


Fig. 12.10. Schematic potential energy profile for the  $E \rightarrow Z$  isomerization of stilbene. The reaction coordinate is the torsion angle  $\theta$  about the double bond. Reproduced from *Angew. Chem. Int. Ed. Engl.*, **31**, 1399 (1992), by permission of Wiley-VCH.

<sup>22</sup> V. Molina, M. Merchan, and B. O. Roos, *J. Phys. Chem. A*, **101**, 3478 (1997); V. Molina, M. Merchan, and B. O. Roos, *Spectrochim Acta A*, **55**, 433 (1999).

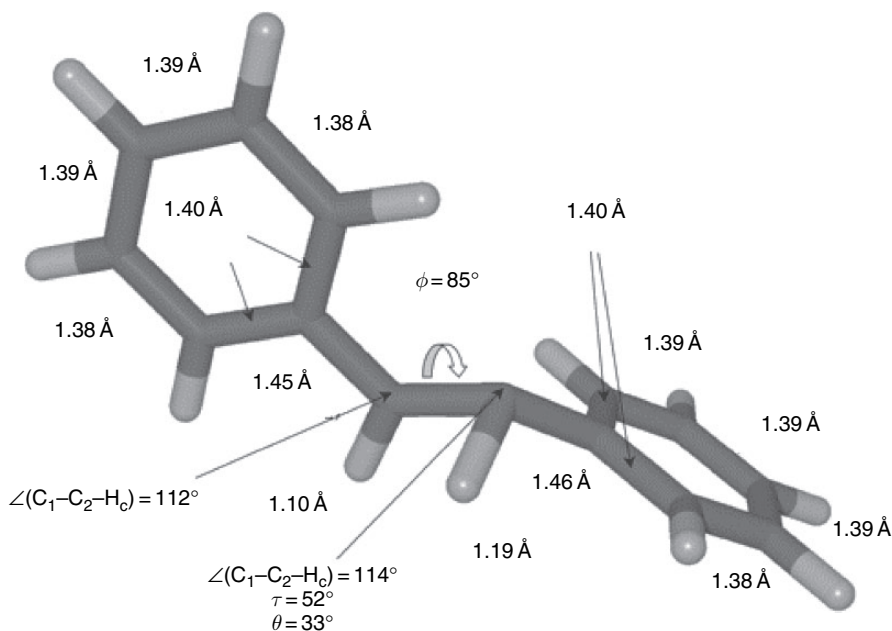


Fig. 12.11. The minimum energy structure for the  $S_0/S_1$  conical intersection for stilbene. The geometrical parameters are from SA-2-CAS(2/2) level computations. Reproduced from *J. Phys. Chem. A*, **107**, 829 (2003), by permission of the American Chemical Society.

those described earlier for ethene and styrene. The structure is both twisted and pyramidalized, and is a mix of zwitterionic and (singlet) diradical character. Figure 12.12 depicts the singlet energy surface for stilbene as a function of both torsion at the ethylenic bond and pyramidalization.

The common feature of the ethene, styrene, and stilbene  $S_1 \rightarrow S_0$  transformations is that double-bond isomerization involves not only twisting at the double bond but also pyramidalization. The pyramidalization modifies the energies that are depicted in Figure 12.10, which considers only the bond rotation, and lowers the energy of the  $S_p$  state sufficiently to permit rapid internal conversion.

The stilbene *cis-trans* isomerization has also been explored using DFT calculations.<sup>23</sup> The potential energy as a function of rotation of the single bond for the  $S_0$ ,  $T_1$ ,  $S_1$ , and  $S_2$  states is as shown in Figure 12.13. The  $S_0$  maximum at  $90^\circ$  is characterized as a singlet diradical with the electrons delocalized in the adjacent phenyl ring, *i.e.*, two benzylic radicals. The central bond is essentially a single bond. This structure is 44.9 kcal/mol above the ground state *trans* ( $180^\circ$ ) minimum. The rotational potential for  $T_1$  is very flat and nearly intersects the  $S_0$  curve near  $90^\circ$ , at an energy of 46.5 kcal/mol. There is essentially no barrier to rotation at the  $T_1$  surface. This structure is a triplet diradical. The vertical energy to the  $T_1$  state is slightly higher for *cis*-stilbene than for *E*-stilbene, and proceeds without a barrier to the twisted minimum. The  $S_1$  state shows a small maximum near  $90^\circ$ . There is a very shallow minimum slightly displaced from the vertical  $180^\circ$  (*trans*) structure. There is also a shallow minimum

<sup>23</sup> W.-G. Han, T. Lovell, T. Liu, and L. Noodleman, *Chem. Phys. Chem.*, **3**, 167 (2002).

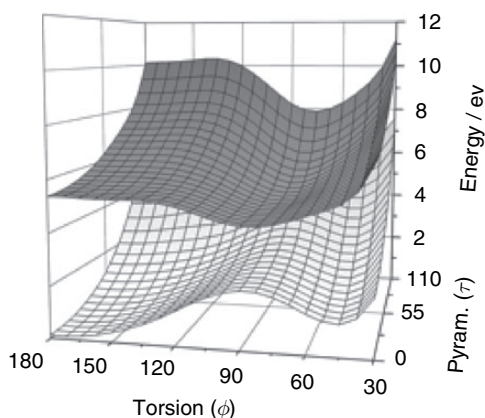


Fig. 12.12. Potential energy surfaces for  $S_0$  and  $S_1$  for stilbene computed at the SA-2-CAS(2/2) level as a function of C=C twist and pyramidalization  $\tau$  with other dimensions held constant. The  $S_0$  minima correspond to the  $E$ -isomer ( $180^\circ$ ) and  $Z$ -isomer ( $45^\circ$ ). Reproduced from *J. Phys. Chem. A*, **107**, 829 (2003), by permission of the American Chemical Society.

on  $S_1$  at about  $45^\circ$  beginning from the  $Z$ -vertical state. At  $90^\circ$ , the  $S_1$  state is about 70 kcal/mol above ground state  $E$ -stilbene. The twisted structure is a neutral diradical, but in contrast to  $T_1$  and the  $S_0$  maximum, there is nearly equal distribution of each

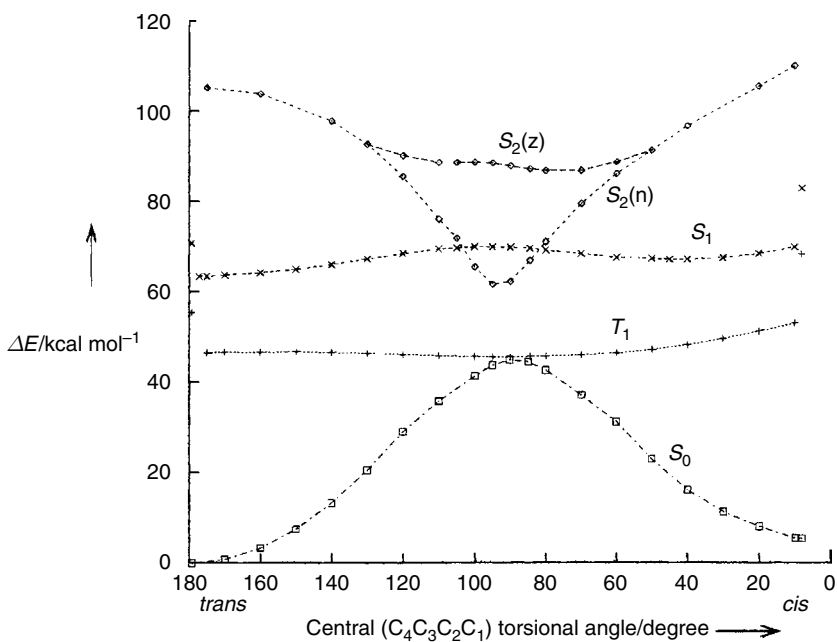
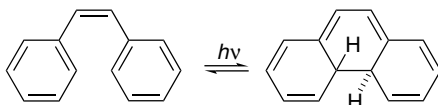


Fig. 12.13. DFT computation of the rotational energy profile of stilbene, beginning at the *trans* ( $180^\circ$ ) and *cis* ( $0^\circ$ ) geometries. Both neutral ( $n$ ) and zwitterionic ( $z$ ) versions of  $S_2$  were computed. Reproduced from *Chem. Phys. Chem.*, **3**, 167 (2002), by permission of the Royal Society of Chemistry.

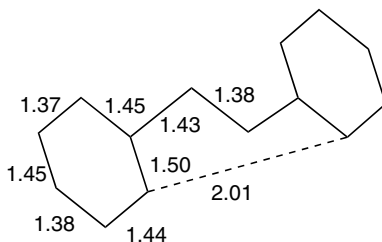
electron over both rings. The  $S_2$  state shows a minimum at  $90^\circ$ , about 18 kcal above  $T_1$  and  $S_0$  at this geometry. The  $S_2$  curve encounters small barriers from the vertical transitions (6.6 kcal/mol for *trans* and 2.2 for *cis*), in agreement with experimental conclusions. The main difference between the DFT and MO calculations is that the DFT computation describes the  $S_2$  minimum as primarily a singlet diradical, rather than a zwitterionic, structure.

In addition to *cis-trans* isomerization, *Z*-stilbene also undergoes photocyclization to 4a,4b-dihydrophenanthrene via an electrocyclicization.<sup>24</sup>



The cyclization product is thermally unstable relative to *cis*-stilbene and reverts to starting material unless trapped by an oxidizing agent.<sup>25</sup> The extent of cyclization is solvent dependent, with nonpolar solvents favoring cyclization more than polar ones.<sup>26</sup> The quantum yield for *cis-trans* isomerization is nearly constant at about 0.35, but the cyclization quantum yield is in the range of 0.15–0.18 in hydrocarbons, as compared with 0.05–0.08 in acetonitrile or methanol. The detailed interpretation of the system involves the effect of solvent on the lifetime and dynamics of the excited states.<sup>27</sup> Figure 12.14 incorporates the reaction coordinate for cyclization into the *cis-trans* energy diagram.

The cyclization has been investigated by computation and can be described in terms of a CI involving interaction between the two phenyl rings.<sup>28</sup> The structural features are similar to the CI involved in electrocyclicization of *Z*-1,3,5-hexatrienes to cyclohexadienes described on p. 1142.



### 12.2.2. Photoreactions of Other Alkenes

Direct photochemical excitation of unconjugated alkenes requires light with  $\lambda < 220$  nm. A study of *Z*- and *E*-2-butene diluted with neopentane demonstrated that *cis-trans* isomerization was competitive with the photochemical  $[2\pi + 2\pi]$

<sup>24</sup> T. Wismonski-Knittel, G. Fischer, and E. Fischer, *J. Chem. Soc., Perkin Trans. 2*, 1930 (1974).

<sup>25</sup> L. Liu, B. Yang, T. J. Katz, and M. K. Poindexter, *J. Org. Chem.*, **56**, 3769 (1991).

<sup>26</sup> J.-M. Rodier and A. B. Myers, *J. Am. Chem. Soc.*, **115**, 10791 (1993).

<sup>27</sup> R. J. Senson, S. T. Repinec, A. Z. Szarka, and R. M. Hochstrasser, *J. Phys. Chem.*, **98**, 6291 (1993).

<sup>28</sup> M. J. Bearpark, F. Bernardi, S. Clifford, M. Olivucci, M. A. Robb, and T. Vreven, *J. Phys. Chem. A*, **101**, 3841 (1997).

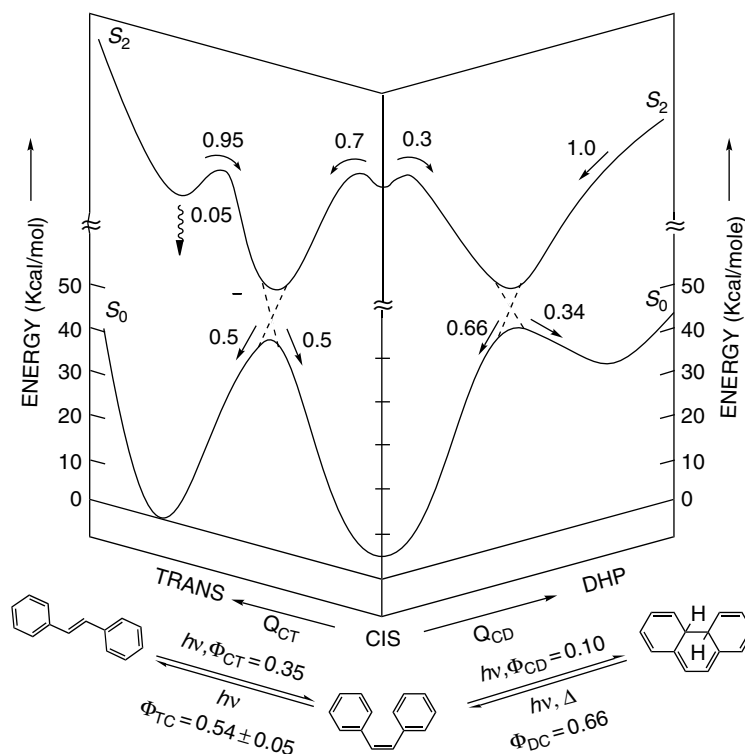
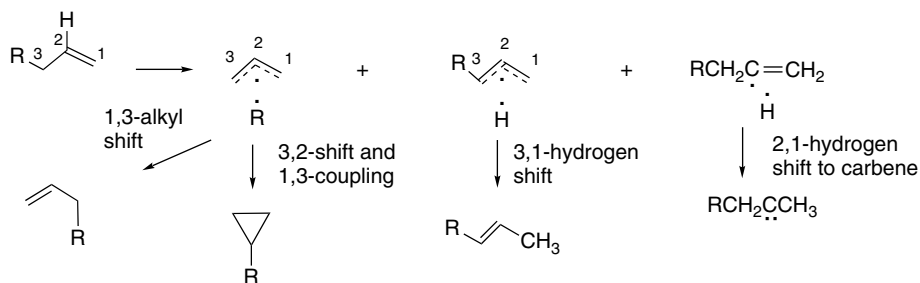


Fig. 12.14. Schematic representation of the potential energy surface for  $S_2$  and  $S_0$  of stilbene including the photocyclization reaction. Approximate branching ratios and quantum yields are indicated. Reproduced from *J. Phys. Chem.*, **98**, 6291 (1993), by permission of the American Chemical Society.

cycloaddition that occurs in pure liquid alkene.<sup>29</sup> We discuss the cycloaddition further in the next section. As the ratio of neopentane to butene increased, the amount of cycloaddition decreased, relative to *cis-trans* isomerization. This effect presumably is the result of the very short lifetime of the intermediate responsible for cycloaddition. When the alkene is diluted by inert hydrocarbon, the rate of encounter of a second alkene molecule is reduced, and the unimolecular isomerization becomes the dominant reaction. Rearrangement reactions are also observed, including 1,2-hydrogen shifts (to carbenes), 1,3-hydrogen and alkyl shifts, and cyclopropane formation. These reactions can occur from CIs that have the character of hydrogen or alkyl groups associated with an allyl or vinyl radical.<sup>30</sup> The vertical excitation energy for unconjugated alkenes is in the range of 150 kcal/mol, and these CIs are at  $100 \pm 20$  kcal/mol. This is similar to the energy required for the dissociation of allylic C–H and C–C bonds, and dissociation is one of the pathways open to excited state alkenes.

<sup>29</sup> H. Yamazaki and R. J. Cventanovic, *J. Am. Chem. Soc.*, **91**, 520 (1969); H. Yamazaki, R. J. Cventanovic, and R. S. Irwin, *J. Am. Chem. Soc.*, **98**, 2198 (1976).

<sup>30</sup> F. Bernardi, M. Olivucci, M. A. Robb, and G. Tonachini, *J. Am. Chem. Soc.*, **114**, 5805 (1992); S. Wilsey and K. N. Houk, *J. Am. Chem. Soc.*, **122**, 2651 (2000).



Simple alkenes can be isomerized using triplet sensitizers and this often avoids the competing rearrangement reactions. Aromatic compounds such as benzene, toluene, xylene, and phenol can photosensitize *cis-trans* interconversion of simple alkenes.<sup>31</sup> This is a case where the sensitization process must be somewhat endothermic because of the energy relationships between the excited states of the alkene and the sensitizers. The photostationary state obtained under these conditions favors the less strained of the alkene isomers. The explanation for this effect can be summarized with reference to Figure 12.15. Isomerization takes place through a twisted triplet state that is achieved by a combination of energy transfer from the sensitizer and thermal activation. Because the *cis* isomer is somewhat higher in energy, its requirement for activation to the excited state is somewhat less than for the *trans* isomer. If it is also assumed that the excited state forms the *cis* and *trans* isomers with equal ease, the rate of *cis*→*trans* exceeds that for *trans*→*cis* conversion ( $k_{c\rightarrow t} > k_{t\rightarrow c}$ ) at the photostationary state and therefore  $[\textit{trans}] > [\textit{cis}]$ .<sup>32</sup>

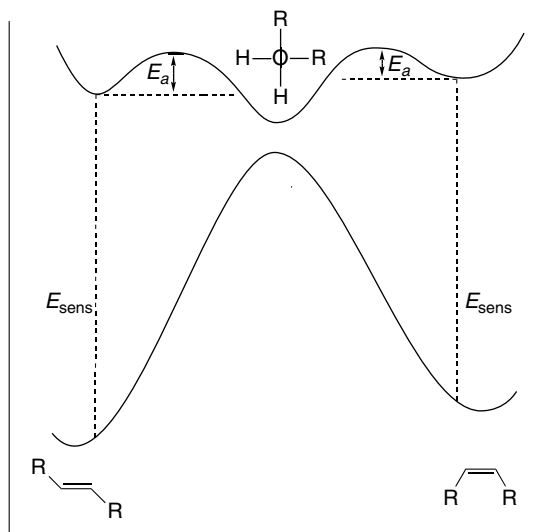
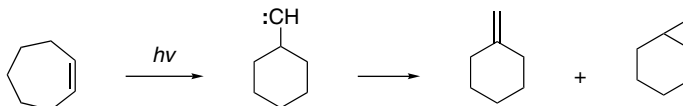


Fig. 12.15. Schematic potential energy diagram illustrating differential in energy required for triplet-sensitized photoisomerization of *cis* and *trans* isomers.

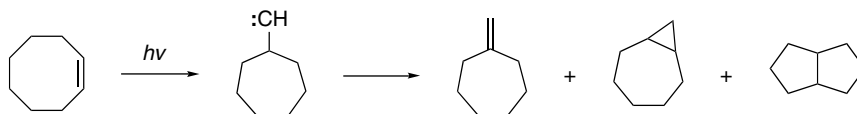
<sup>31</sup> M. Tonaka, T. Terao, and S. Sato, *Bull. Chem. Soc. Jpn.*, **38**, 1645 (1965); G. A. Haninger and E. K. C. Lee, *J. Phys. Chem.*, **71**, 3104 (1967).

<sup>32</sup> J. J. Snyder, F. P. Tise, R. D. Davis, and P. J. Kropp, *J. Org. Chem.*, **46**, 3609 (1981).

Photoexcitation of cycloalkenes introduces additional features because the ring limits the extent to which the double bond can twist. Cyclohexene, cycloheptene, and cyclooctene give rise to ring contraction and carbene insertion products.



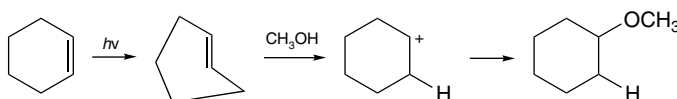
Ref. 33



Ref. 34

It has been possible to observe the processes that occur within 100 fs after excitation of cyclohexene to the  $\pi\text{-}\pi^*$  and  $\pi, 3s(\text{R})$  states (200 nm). This time scale is too short to allow for intermolecular reactions, even in solution. The products are methylenecyclopentane and bicyclo[3.1.0]hexane. The processes are summarized in Figure 12.16.<sup>35</sup> The process designated  $\tau_1$  (20 fs) is believed to follow the relaxation of the vertical  $\pi\text{-}\pi^*$  and  $\pi, 3s(\text{R})$  states to the equilibrium geometry on the  $\pi\text{-}\pi^*$  surface. The process designated  $\tau_2$  represents the start of 1,3-H migration. At  $\tau_3$  the isomerization to the carbenoid structure is complete. The C–C bond shift corresponds to  $\tau_4$ . The carbene can then return to the ground state surface by forming cyclohexene, bicyclo[3.1.0]hexane, or methylenecyclopentane. Some *E*-cyclohexene is formed and can be trapped by hydroxylic solvents.<sup>36</sup>

The reaction course taken by photoexcited cycloalkenes in hydroxylic solvents depends on ring size.<sup>37</sup> Cyclohexene, cycloheptene, cyclooctene, 1-methylcyclohexene, 1-methylcycloheptene, and 1-methylcyclooctene all add methanol, but neither 1-methylcyclopentene nor norbornene does so. The key intermediate in the addition reaction is believed to be the highly reactive *E*-isomer of the cycloalkene. The *E*-cycloalkenes can be protonated exceptionally easily because of the enormous relief of strain that accompanies protonation.<sup>36, 38</sup>



The *E*-cycloheptene and cyclooctene isomers can be observed and *E*-cyclooctene can be isolated.

<sup>33</sup> Y. Inoue, S. Takamuka, and H. Sakurai, *J. Chem. Soc., Chem. Commun.*, 577 (1975).

<sup>34</sup> P. J. Kropp, J. D. Mason, and G. F. H. Smith, *Can. J. Chem.*, **63**, 1845 (1985).

<sup>35</sup> W. Fuss, W. E. Schmid, and S. A. Trushin, *J. Am. Chem. Soc.*, **123**, 7101 (2001).

<sup>36</sup> P. J. Kropp, E. J. Reardon, Jr., Z. L. F. Gaibel, K. F. Williard, and J. H. Hattaway, Jr., *J. Am. Chem. Soc.*, **95**, 7058 (1973).

<sup>37</sup> T. Mori and Y. Inoue, *CRC Handbook of Photochemistry and Photobiology*, W. Horspool and F. Lenci, ed., CRC Press, Boca Raton, FL, 2004, Section 16.

<sup>38</sup> J. A. Marshall, *Acc. Chem. Res.*, **2**, 33 (1969).

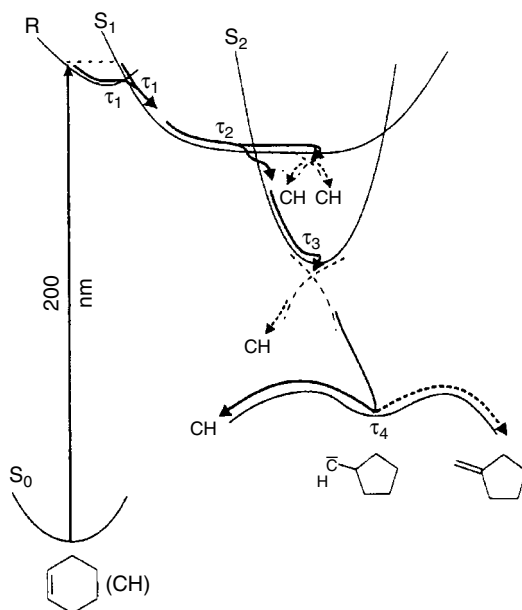
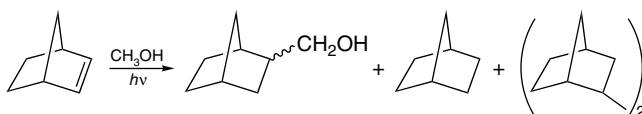
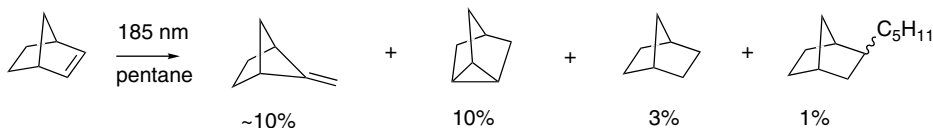
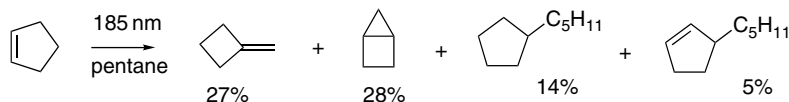


Fig. 12.16. Sequential events in the excitation and return to ground state for cyclohexene. Reproduced from *J. Am. Chem. Soc.*, **123**, 7101 (2001), by permission of the American Chemical Society.

The *trans* isomers of cyclopentene and norbornene are too strained to be formed. Rather, they give products in methanol that result from hydrogen abstraction and other radical-like processes.<sup>39</sup>



Photolysis in hydrocarbon solvents leads to rearranged products similar to those from other cycloalkenes, as well as hydrogen abstraction and coupling products.<sup>40</sup>



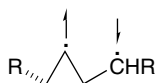
The nature of the excited states involved in formation of the carbene intermediates has been explored using CAS-SCF/6-31G\* computations including the  $\sigma$ ,  $\sigma^*$ ,  $\pi$ , and

<sup>39</sup> P. J. Kropp, *J. Am. Chem. Soc.*, **91**, 5783 (1969).

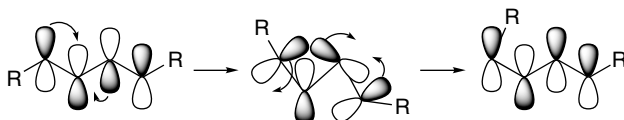
<sup>40</sup> R. Srinivasan and K. H. Brown, *J. Am. Chem. Soc.*, **100**, 4602 (1978); Y. Inoue, T. Mukai, and T. Hakushi, *Chem. Lett.*, 1045 (1982).



(See p. 1138 for a discussion of the role of this structure in the  $S_2$  excited state of 1,3-butadiene.)



Orbital symmetry control of subsequent ring opening could account for isomerization at only one of the double bonds. Taking  $\psi_3$  as the controlling frontier orbital, it can be seen that a concerted return to  $\psi_2$  leads to rotation at only one terminus of the diene.



The conclusion from these studies is that singlet *cis-trans* isomerization of substituted conjugated dienes such as 2,4-hexatriene must proceed through a structure that is free to rotate at only one terminus, whereas sensitized (triplet) isomerization involves a structure that can rotate at both termini.

The discussion of *cis-trans* photoisomerization of alkenes, styrene, stilbene, and dienes has served to introduce some important ideas about the interpretation of photochemical reactions. We see that thermal barriers are usually low, so that reactions are very fast. Because excited states are open-shell species, they present new kinds of structures, such as the twisted and pyramidalized CIs that are associated with both isomerization and rearrangement of alkenes. However, we will also see familiar structural units as we continue our discussion of photochemical reactions. Thus the triplet diradical involved in photosensitized isomerization of dienes is not an unanticipated species, given what we have learned about the stabilization of allylic radicals.

#### 12.2.4. Orbital Symmetry Considerations for Photochemical Reactions of Alkenes and Dienes

The photochemistry of alkenes, dienes, and conjugated polyenes in relation to orbital symmetry relationships has been the subject of extensive experimental and theoretical study.<sup>44</sup> The analysis of concerted pericyclic reactions by the principles of orbital symmetry leads to a complementary relationship between photochemical and thermal reactions. A process that is forbidden thermally is allowed photochemically and vice versa. The complementary relationship between thermal and photochemical reactions can be illustrated by considering some of the reaction types discussed in Chapter 10 and applying orbital symmetry considerations to the photochemical mode of reaction. The case of  $[2\pi + 2\pi]$  cycloaddition of two alkenes, which was classified as a forbidden thermal reaction (see Section 10.1), can serve as an example. The correlation diagram (Figure 12.17) shows that the ground state molecules would lead to a doubly excited state of cyclobutane, and would therefore involve a prohibitive thermal activation energy.

How does the situation change when a photochemical reaction involving one ground state alkene and one excited state alkene is considered? If we assume a

<sup>44</sup> B. H. O. Cook and W. J. Leigh, in *Chemistry of Dienes and Polyenes*, Vol. 2, Z. Rappoport, ed. John Wiley, Chichester, 2000, pp. 197–255.

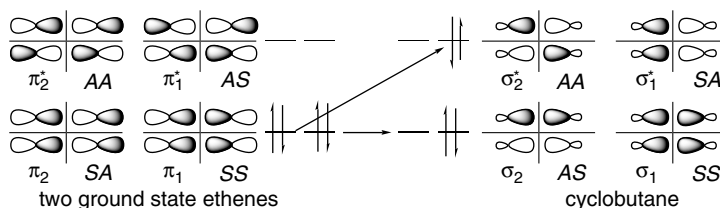


Fig. 12.17. Orbital correlation for two ground state ethenes and cyclobutane. The symmetry designations apply, respectively, to the horizontal and vertical planes for two ethene molecules approaching one another in parallel planes.

symmetrical approach as in the thermal reaction, then the same array of orbitals is involved, but the occupation of the orbitals is different: the  $\pi_1$  ( $SS$ ) orbital is doubly occupied, but  $\pi_2$  ( $SA$ ) and  $\pi_2^*$  ( $AA$ ) are singly occupied. The reaction is therefore allowed in the sense that there is no high-energy barrier. Although the correlation diagram illustrated in Figure 12.18 might suggest that the product would initially be formed in an excited state, this is not necessarily the case. The concerted process can involve a transformation of the reactant excited state to the ground state of product. The nature of this transformation is discussed shortly.

Consideration of the HOMO-LUMO interactions also indicates that the  $[2\pi + 2\pi]$  addition is allowed photochemically. The HOMO in this case is the excited alkene  $\pi^*$  orbital. The LUMO is the  $\pi^*$  of the ground state alkene, and a bonding interaction is present between both pairs of carbons where new bonds must be formed. Similarly, the concept of aromatic transition states shows that the reaction has an antiaromatic  $4\pi$  combination of basis set orbitals, which predicts an *allowed photochemical reaction*. Thus, orbital symmetry considerations indicate that photochemical  $[2\pi + 2\pi]$  cycloaddition of alkenes is feasible.

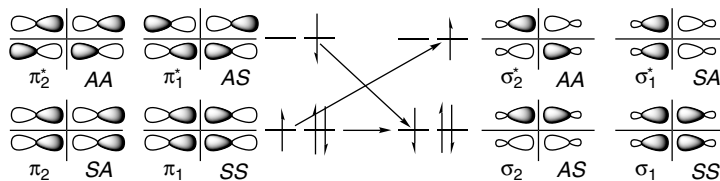
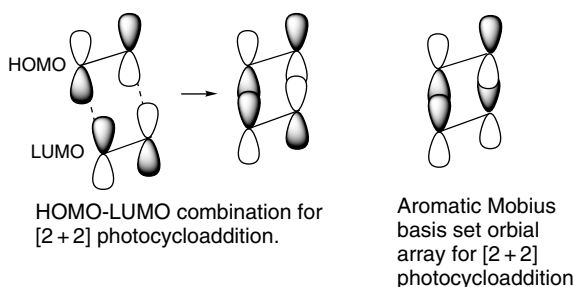
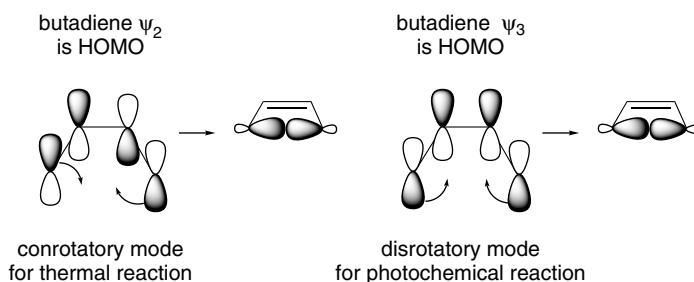


Fig. 12.18. Orbital correlation diagram for one ground state ethene and one ethene in an excited state. The symmetry designations apply, respectively, to the horizontal and vertical planes for two ethene molecules approaching one another in parallel planes.

It is a general result that the Woodward-Hoffmann rules predict that photochemical reactions will be complementary to thermal reactions. What is allowed photochemically is forbidden thermally, and vice versa. *The physical basis for this complementary relationship is that the high barrier associated with forbidden thermal reactions provides a point for strong interaction of the ground state and excited state species.* As the two states are close in energy and of the same symmetry, they “mix” and allow the excited molecule to reach the ground state. This interaction is necessary for efficient photochemical reactions.<sup>45</sup>

Let us now consider photochemical electrocyclic reactions. In Chapter 10, we described the distinction between the conrotatory and disrotatory modes of reaction as a function of the number of electrons in the system. Striking illustrations of the relationship between orbital symmetry considerations and the outcome of photochemical reactions are found in the stereochemistry of electrocyclic reactions. Orbital symmetry predicts that photochemical electrocyclic reactions will show a reversal of stereochemistry relative to thermal reactions.<sup>46</sup> One way of making this prediction is to construct an electronic energy state diagram for the reactant and product molecule and observe the correlation between the states.<sup>47</sup> The reactions in which the reacting state correlates with a state of the product that is not appreciably higher in energy are permitted.<sup>48</sup> The orbitals involved in the photochemical butadiene-to-cyclobutene conversion are  $\psi_1$ ,  $\psi_2$ , and  $\psi_3$  of the first excited state of butadiene and  $\sigma$ ,  $\pi$ , and  $\pi^*$  for cyclobutene. The appropriate elements of symmetry are the plane of symmetry for the conrotatory and the axis of symmetry for the disrotatory process. The correlation diagram for this reaction is shown in Figure 12.19. This analysis shows that disrotatory cyclization is allowed, whereas conrotation would lead to a highly excited  $\sigma^1$ ,  $\pi^2$ ,  $\sigma^{*1}$  configuration of cyclobutene. The same conclusion is reached if it is assumed that the frontier orbital will govern reaction stereochemistry.



Although orbital symmetry provides a starting point for analyses of photochemical reactions of conjugated dienes and polyenes, experimental studies have identified a number of additional facets of the problem, some of which have to do with the fundamental assumptions of the orbital symmetry analysis. One of the underlying

<sup>45</sup> H. E. Zimmerman, *J. Am. Chem. Soc.*, **88**, 1566 (1966); W. Th. A. M. van der Lugt and L. J. Oosterhoff, *Chem. Commun.*, 1235 (1968); W. Th. A. M. van der Lugt and L. J. Oosterhoff, *J. Am. Chem. Soc.*, **91**, 6042 (1969); R. C. Dougherty, *J. Am. Chem. Soc.*, **93**, 7187 (1971); J. Michl, *Top. Current Chem.*, **46**, 1 (1974); J. Michl, *Photochem. Photobiol.*, **25**, 141 (1977).

<sup>46</sup> R. B. Woodward and R. Hoffmann, *J. Am. Chem. Soc.*, **87**, 395 (1965).

<sup>47</sup> H. C. Longuet-Higgins and E. W. Abrahamson, *J. Am. Chem. Soc.*, **87**, 2045 (1965).

<sup>48</sup> R. B. Woodward and R. Hoffmann, *The Conservation of Orbital Symmetry*, Academic Press, New York, 1970.

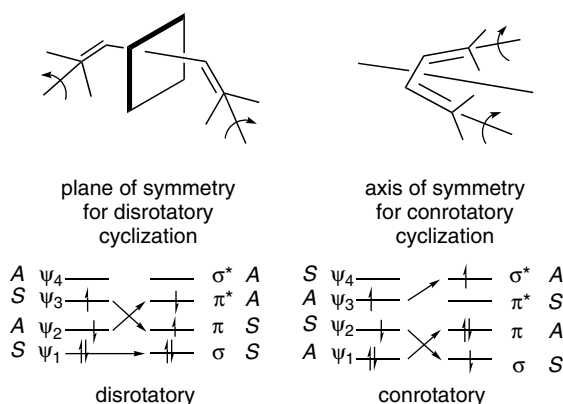


Fig. 12.19. Orbital correlation diagram for the states involved in the photochemical interconversion of butadiene and 1,3-butadiene.

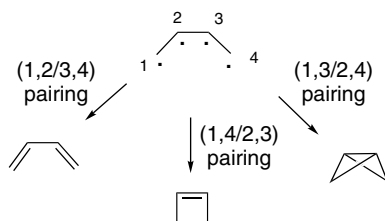
assumptions is that the processes are *concerted*. Although the criteria for concertedness are fairly clear in thermal reactions (the existence or nonexistence of an intermediate), the case for photochemical reactions is not so clear. Several excited state transformations and CIs can appear on the overall reaction path, but there may be no significant barrier. The orbital symmetry analysis also makes assumptions about the *geometry of the interacting molecules*, usually choosing the most symmetrical arrangement. We have to consider whether this assumption is justified. Another difference between the thermal and photochemical reactions is that the *principle of microscopic reversibility applies to the former, but not to the latter*. Concerted thermal pericyclic reactions traverse the same minimum energy pathway in the forward and reverse directions. In photochemical processes, the initial reactant geometries are different, and owing to the NEER principle (see p. 1078) these differences may persist in excited states and influence their reactivity. We first consider some of the experimental observations for dienes and then look at the mechanistic interpretations that have been developed. Computational studies have been applied to the structure of CIs, as was discussed for alkene *cis-trans* isomerization, and these have provided new insights into the photochemical reactions of conjugated dienes and polyenes.

### 12.2.5. Photochemical Electrocyclic Reactions

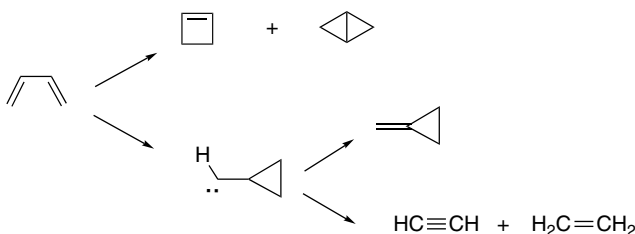
The case of butadiene-cyclobutene interconversion, which one might expect to provide a straightforward example illustrating the stereoselectivity of photochemical electrocyclic cyclization, is actually quite complex, especially when substituted systems are involved. We first consider experimental outcomes from the photolysis of butadiene and substituted derivatives, as well as the reverse reaction, the photochemical ring-opening reactions of cyclobutenes. We then examine the 1,3,5-hexatriene system in the same way.

In addition to cyclobutene, bicyclo[1.1.0]butane, methylenecyclopropane, and the fragmentation products ethene and ethyne are formed in the direct photolysis of butadiene. These results can be interpreted in terms of CIs related to those described for ethene and other alkenes. Formation of cyclobutene and bicyclobutane can be attributed to different re-pairing schemes that correlate with different motions into and

out of the area of a CI that can be described as a tetraradicaloid. (1,2/3,4)-pairing leads to 1,3-butadiene, (1-4/2-3)-pairing leads to cyclobutene, and (1,3/2,4)-pairing leads to bicyclo[1.1.0]butane.



The rearrangement and fragmentation products are thought to arise from a carbene intermediate.

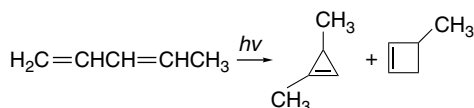


After excitation to the  $S_2$  surface and transition to  $S_1$ , the CI leads to partitioning to products and starting material. These processes occur on the femtosecond time scale. Lifetimes have been assigned to several of the transformations, as illustrated in Figure 12.20.<sup>49</sup>

Electrocyclization of conjugated dienes occurs in competition with *cis-trans* isomerization. The cyclization occurs from the *s-cis* conformation of the diene.<sup>50</sup> Cyclobutene formation is favored in cyclic dienes and for other dienes where the *s-cis* diene conformation is dominant.<sup>51</sup> For several dienes, the quantum yield in nonpolar solvents at 257 nm is about 0.1.<sup>52</sup> As the cyclized alkenes do not absorb at this wavelength, the reaction can give substantial preparative yields, despite the competing *cis-trans* isomerization.



On direct irradiation of 1,3-pentadiene, *cis-trans* isomerization is accompanied by cyclization to 1,3-dimethylcyclopropene and 3-methylcyclobutene.<sup>53</sup>



<sup>49</sup> W. Fuss, W. E. Schmid, and S. A. Trushin, *Chem. Phys. Lett.*, **342**, 91 (2001).

<sup>50</sup> M. E. Squillacote and T. C. Semple, *J. Am. Chem. Soc.*, **112**, 5546 (1990).

<sup>51</sup> W. J. Leigh, K. Zheng, and K. B. Clark, *J. Org. Chem.*, **56**, 1574 (1991); W. H. Laarhoven, *Org. Photochem.*, **9**, 129 (1987).

<sup>52</sup> R. Srinivasan, *J. Am. Chem. Soc.*, **84**, 4141 (1982).

<sup>53</sup> S. Boué and R. Srinivasan, *J. Am. Chem. Soc.*, **92**, 3226 (1970).

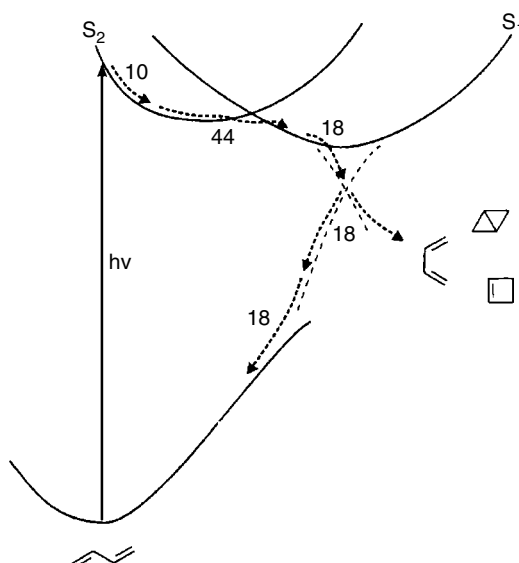
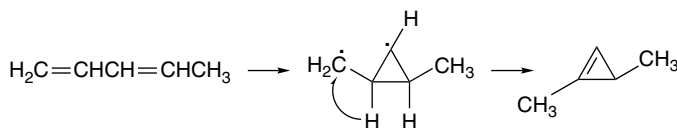
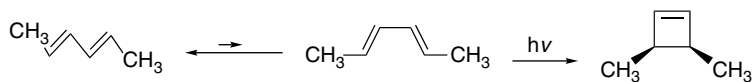


Fig. 12.20. Representation of the 1,3-butadiene potential energy surface based on experimental observations. The broken arrows show the path for return to the ground state reactant and other products. Lifetimes are given in femtoseconds. The dashed lines indicate a conical intersection for partitioning between products. Adapted from *Chem. Phys. Lett.*, **342**, 91 (2001).

The latter product is an example of a photochemically allowed electrocyclic reaction. The cyclopropene arises from (2,4)-pairing and hydrogen migration.



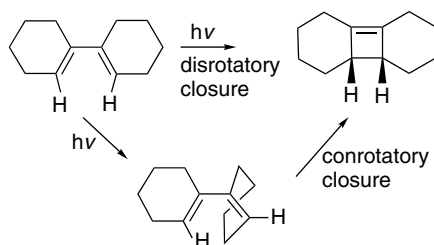
For *E,E*-2,4-hexadiene, the cycloaddition reaction is stereospecific and in accord with the Woodward-Hoffmann predictions.<sup>54</sup>



Cyclic dienes can give cyclobutenes by either direct photochemical electrocyclic cyclization or by isomerization to the *E*-isomer in one ring, followed by [2+2] cycloaddition. The latter process can be intercepted by methanol (see p. 1094).<sup>55</sup>

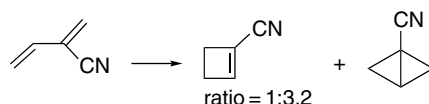
<sup>54</sup> R. Srinivasan, *J. Am. Chem. Soc.*, **90**, 4498 (1968).

<sup>55</sup> Y. Daino, S. Hagiwara, T. Hakushi, Y. Inoue, and A. Tai, *J. Chem. Soc., Perkin Trans. 2*, 275 (1989).

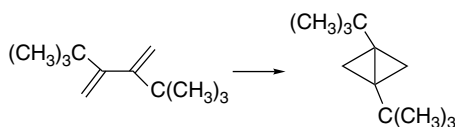


Ref. 56

Substituents can affect the partitioning among the competing reaction paths. The formation of the bicyclo[1.1.0]butane product is favored by radical-stabilizing substituents.<sup>57</sup>

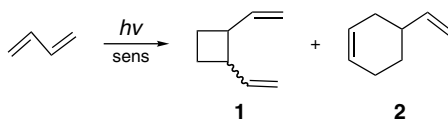


The steric effect of 2,3-di-*t*-butyl groups causes the cyclization to the bicyclo[1.1.0]butane to become the dominant reaction.<sup>58</sup>



Ref. 59

Reactions of conjugated dienes can also occur through the triplet state generated by photosensitization. 1,3-Butadiene gives a mixture of *cis*- and *trans*-1,2-divinylcyclobutane (**1**) and 4-vinylcyclohexene (**2**).



The ratio of divinylcyclobutanes to cyclohexene product depends on the  $E_T$  of the sensitizer that is used. With sensitizer  $E_T > 60$  kcal/mol, either the *s-trans* (dominant) or *s-cis* conformation can be excited. With  $E_T \sim 55$  kcal/mol, the *s-cis* is preferentially excited (see Figure 12.15). The excited *s-trans* conformer can give only cyclobutanes, whereas the excited *s-cis* structure can also form the cyclohexene product.<sup>60</sup> Isoprene shows a similar effect with cyclohexene formation being at a maximum with  $E_T$  at 46–54 kcal/mol.

<sup>56</sup> J. Saltiel, G. R. Marchand, and R. Bonneau, *J. Photochem.*, **28**, 367 (1987).

<sup>57</sup> D. M. Gale, *J. Org. Chem.*, **35**, 970 (1970); M. Olivucci, F. Bernardi, S. Ottani, and M. A. Robb, *J. Am. Chem. Soc.*, **116**, 2034 (1994).

<sup>58</sup> M. Garavelli, B. Frabboni, M. Fato, P. Celani, F. Bernardi, M. A. Robb, and M. Olivucci, *J. Am. Chem. Soc.*, **121**, 1537 (1999).

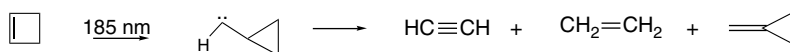
<sup>59</sup> H. Hopf, H. Lipka, and M. Traetteberg, *Angew. Chem. Int. Ed. Engl.*, **33**, 204 (1994).

<sup>60</sup> R. S. H. Liu, N. J. Turro, Jr., and G. S. Hammond, *J. Am. Chem. Soc.*, **87**, 3406 (1965).

Sensitizer	$E_T$	Product composition	
		1	2
Acetophenone	73.6	97	3
Benzophenone	68.5	92	2
Flavone	62.0	93	7
2-Acetylnaphthalene	59.6	92	8
1-Acetylnaphthalene	56.4	80	20
Benzil	53.7	55	45
Fluorenone	53.3	57	43
Benzanthrone	47	65	35
3-Acetylpyrene	45	55	45
Anthracene	42.5	85	15

Summarizing these experimental results on conjugated dienes, we find that the singlet state electrocyclozation to cyclobutenes generally follows the Woodward-Hoffmann expectation and are disrotatory. There are competing reactions, including formation of bicyclo[1.1.0]butanes and rearrangement products. With direct excitation, the *cis-trans* isomerization occurs by rotation at only one double bond. In contrast, for triplet-sensitized reactions, isomerization can occur at both double bonds (see Section 12.1.2.4). Considerable dimerization is observed in the triplet state reactions. The difference in outcomes of the singlet and triplet processes has been ascribed to differences in the structure of the two excited states. In the singlet state, there is a very close interaction among all of the carbons of the diene system. Transformations of the singlet species are also very fast. The  $T_1$  state is more flexible and longer-lived, which allows the triplet to capture ground state butadiene, leading to dimerization.<sup>61</sup>

Let us now turn to the *photochemical ring opening of cyclobutenes to 1,3-dienes*. This reaction requires excitation with light of  $\lambda < 200\text{ nm}$ . Interpretation of the resonance Raman spectra of cyclobutene following photoexcitation provides insight into the dynamics of ring opening and is consistent with the predicted disrotatory stereochemistry.<sup>62</sup> Cyclobutene gives ethene, ethyne, and methylenecyclopropane in addition to butadiene.<sup>63</sup> These competing reactions are believed to occur by ring contraction to a carbene, followed by rearrangement or fragmentation.<sup>64</sup> This species is also formed by excitation of butadiene.



Surprisingly, the ring opening of *cis-* and *trans*-3,4-dimethylcyclobutene is not stereospecific.<sup>65</sup> When irradiated with far-UV light, alkyl-substituted cyclobutenes,

<sup>61</sup> M. Klessinger and J. Michl, *Excited States and Photochemistry of Organic Molecules*, VCH Publishers, New York, 1995, pp. 339–341.

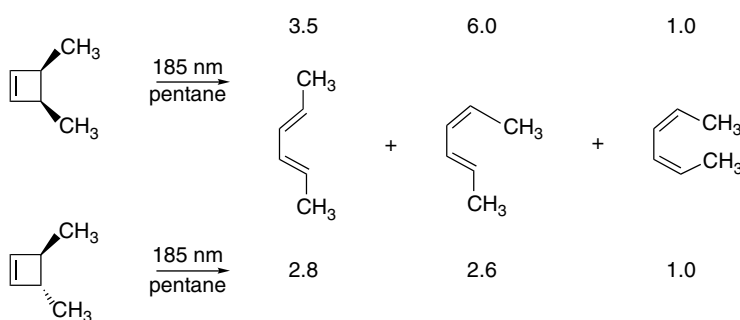
<sup>62</sup> M. K. Lawless, S. D. Wickham, and R. A. Mathies, *J. Am. Chem. Soc.*, **116**, 1593 (1994).

<sup>63</sup> W. Adam, T. Oppenlander, and G. Zang, *J. Am. Chem. Soc.*, **107**, 3921 (1985).

<sup>64</sup> W. J. Leigh, K. Zheng, N. Nguyen, N. H. Werstiuk, and J. Ma, *J. Am. Chem. Soc.*, **113**, 4993 (1993).

<sup>65</sup> K. B. Clark and W. J. Leigh, *J. Am. Chem. Soc.*, **109**, 6086 (1987).

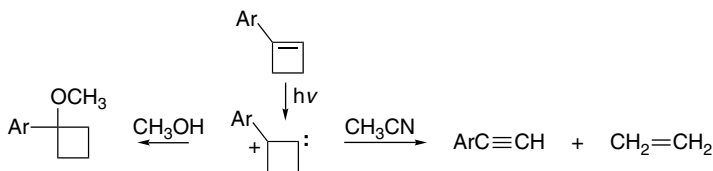
give mixtures of stereoisomers.<sup>66</sup> All of the corresponding butadiene stereoisomers are formed but in different ratios from the stereoisomeric reactants.



A number of other nonstereospecific photolytic ring openings of substituted cyclobutenes have been reported.<sup>67</sup>

These results are not consistent with a concerted disrotatory mechanism for the ring opening and several descriptions of the mechanism have been provided.<sup>64,68</sup> One possibility is that the ring opening proceeds stereospecifically to an *excited state* of the diene, which then decays to the ground state with a stereoselectivity that is independent of the stereochemistry of the original cyclobutene.<sup>69</sup> The transformations are believed to occur via a twisted CI in which all of the  $\pi$  electrons are unpaired, similar to that from singlet excited 1,3-butadiene. Passage through the CI can lead to mixture of stereoisomers.<sup>68</sup> The composition is governed by dynamic and steric factors.

1-Aryl substituted cyclobutenes undergo cycloreversion to arylalkynes but can also give addition products in hydroxylic solvents.<sup>70</sup> These reactions are singlet state processes. The aryl derivatives of cyclobutene do not open to 1,3-butadienes, and based on substituent effects, the excited states appear to have zwitterionic character. These results suggest that the aryl substituent favors the formation of a zwitterionic excited state.



The cyclohexadiene-hexatriene photochemical interconversion is predicted by orbital symmetry considerations to involve conrotatory motion. Cyclohexadiene derivatives undergo photochemical electrocyclic ring opening. The photostationary state

<sup>66</sup> W. J. Leigh, *Can. J. Chem.*, **71**, 147 (1993); W. J. Leigh, *Chem. Rev.*, **93**, 487 (1993); W. J. Leigh, K. Zheng, and K. B. Clark, *Can. J. Chem.*, **68**, 1988 (1990).

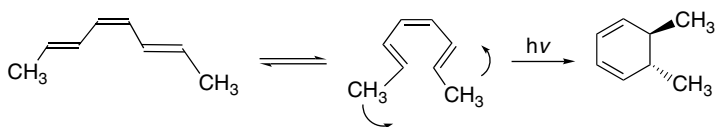
<sup>67</sup> W. G. Dauben and J. E. Haubrich, *J. Org. Chem.*, **53**, 600 (1988); W. J. Leigh and K. Zhang, *J. Am. Chem. Soc.*, **113**, 2163 (1985); G. Maier and A. Bothur, *Eur. J. Org. Chem.*, 2063 (1998).

<sup>68</sup> F. Bernardi, M. Olivucci, and M. A. Robb, *Acc. Chem. Res.*, **23**, 405 (1990); F. Bernardi, M. Olivucci, I. N. Ragazos, and M. A. Robb, *J. Am. Chem. Soc.*, **114**, 2752 (1992).

<sup>69</sup> W. J. Leigh, J. A. Postigo, and K. C. Zheng, *Can. J. Chem.*, **74**, 951 (1996).

<sup>70</sup> W. J. Leigh and J. A. Postigo, *Can. J. Chem.*, **73**, 191 (1995).

favors the triene, and the reaction is highly stereospecific.<sup>71</sup> *E,Z,E*-Octa-2,4,6-triene gives *trans*-5,6-dimethylcyclohexene.<sup>72</sup>



Ring opening of more highly substituted cyclohexadienes also follows the Woodward-Hoffmann rules.

The conrotatory electrocyclic ring opening of 1,3-cyclohexadiene can be observed by several ultrafast techniques.<sup>73</sup> It is believed that the first step after excitation is attainment of a planar geometry, which occurs within  $10^{-11}$  s.<sup>74</sup> The observations are consistent with an excitation followed by return to the ground state via a CI that permits formation of either reactant or *Z*-1,3,5-hexatriene. The lifetimes of the two excited states are both shorter than 100 fs, and the product is formed within 200 fs.<sup>75</sup> These results are summarized in Figure 12.21.

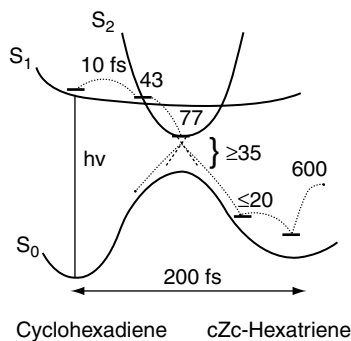
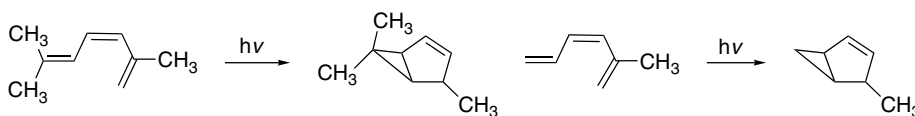


Fig. 12.21. Lifetime in femtoseconds for regions on the potential energy surface for isomerization of 1,3-cyclohexadiene to 1,3,5-hexatriene. Reproduced from *Chem. Phys.*, **232**, 161 (1998) by permission of Elsevier.

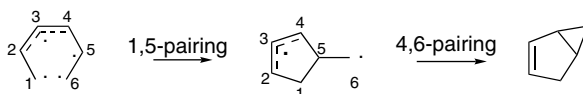
- <sup>71</sup> H. J. C. Jacobs and E. Havinga, *Adv. Photochem.*, **11**, 305 (1979); H. J. C. Jacobs and W. H. Laarhoven, in *CRC Press Handbook of Organic Photochemistry and Biology*, W. H. Horspool, ed., CRC Press, Boca Raton, FL, 1995, pp. 155–164.
- <sup>72</sup> G. J. Fonken, *Tetrahedron Lett.*, 549 (1962).
- <sup>73</sup> H. Ihee, V. A. Lebastov, U. M. Gomez, B. M. Goodson, R. Srinivasan, C.-Y. Ruan, and A. H. Zewail, *Science*, **291**, 458 (2001); W. Fuss, W. E. Schmid, and S. A. Trushin, *J. Chem. Phys.*, **112**, 8347 (2000); S. A. Trushin, W. Fuss, T. Schikavski, W. E. Schmid, and K. L. Kompa, *J. Chem. Phys.*, **106**, 9386 (1997); S. H. Pullen, N. A. Anderson, L. A. Walker, II, and R. J. Sension, *J. Chem. Phys.*, **108**, 556 (1998).
- <sup>74</sup> P. J. Reid, M. K. Lawless, S. D. Wickham, and R. A. Mathies, *J. Phys. Chem.*, **98**, 5597 (1994); W. Fuss, T. Hofer, P. Hering, K. L. Kompa, S. Lochbrunner, T. Schikarski, and W. E. Schmid, *J. Phys. Chem.*, **100**, 921 (1996).
- <sup>75</sup> W. Fuss, S. Lochbrunner, A. M. Mueller, T. Schikarski, W. E. Schmid, and S. A. Trushin, *Chem. Phys.*, **232**, 161 (1998).

Particularly interesting photoproducts from hexatrienes are the bicyclo[3.1.0]hex-2-enes.

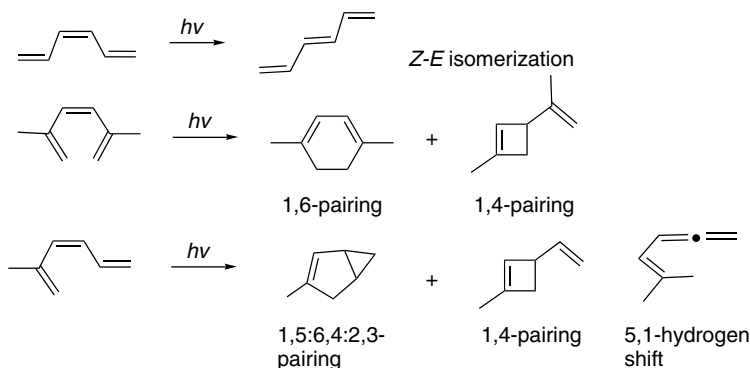


Ref. 76

These products can be formulated as occurring from a tetra-radicaloid CI via a diradical intermediate by (1,5/4,6)-pairing.<sup>77</sup>



The partitioning among *cis-trans* isomerization, closure to cyclohexadiene, and formation of bicyclo[3.1.0]hexenes-2-enes is believed to depend on the conformation of the ground state triene.<sup>78</sup> An extended conformation, as in 1,3,5-hexatriene, is not favorable to cyclization. A conformation that is *s-cis* at both C(2)–C(3) and C(4)–C(5) as well as *Z* at C(3)–C(4) is favorable to electrocyclicization. An *s-cis* conformation at C(2)–C(3) and *Z*-configuration at C(3)–C(4) favors formation of the bicyclo[3.1.0]hexene structure.



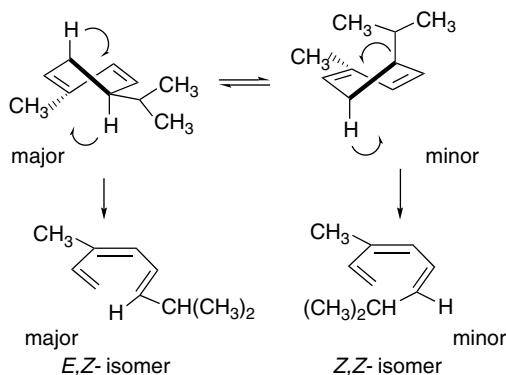
The stereochemistry of the product from ring opening is also dependent on the ground state conformation of the cyclohexadiene. For example, the composition of

<sup>76</sup> P. Courtot, R. Rumin, and J.-Y. Salaun, *Pure Appl. Chem.*, **49**, 317 (1977); P. Courtot and R. Rumin, *Tetrahedron*, **32**, 441 (1976).

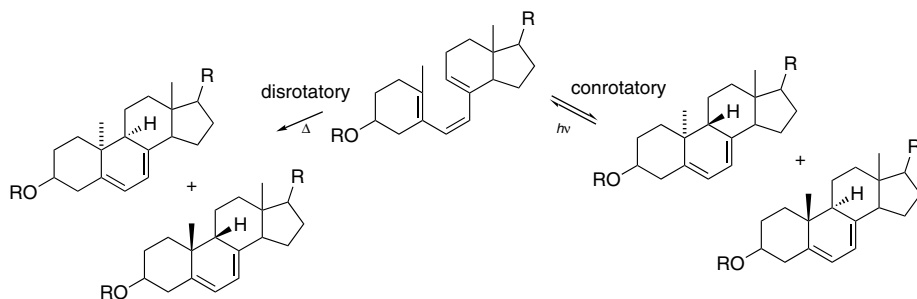
<sup>77</sup> M. Garavelli, R. Celani, M. Fato, M. J. Bearpark, B. R. Smith, M. Olivucci, and M. A. Robb, *J. Phys. Chem. A*, **101**, 2023 (1997).

<sup>78</sup> P. J. Vroegop, J. Lugtenburg, and E. Havinga, *Tetrahedron*, **29**, 1393 (1973); E. Havinga, *Experientia*, **29**, 1181 (1973).

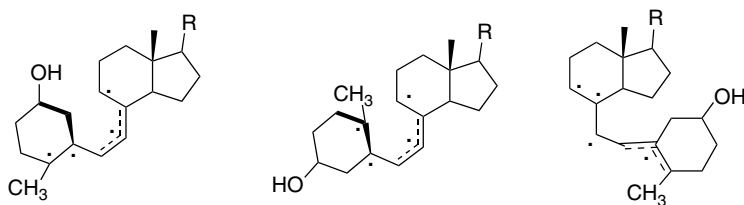
the conrotatory ring-opening products from photolysis of  $\alpha$ -phellandrene mirrors the ground state conformational equilibrium.<sup>79</sup>



These results are in accord with orbital symmetry principles. Indeed, examples found in the study of vitamin D provided the initial examples of the dichotomy between thermal and photochemical processes that led to development of the concepts underlying the Woodward-Hoffmann rules for photochemical reaction.<sup>80</sup> It was found that the triene precalciferol gave ergosterol on photocyclization, but the stereoisomer lumisterol on heating.



The vitamin D photochemical system can also be interpreted in terms of CIs with tetraradicaloid character. Three such structures have been identified by computation, and they account for the observed products.<sup>81</sup>



Thus, looking broadly over these results on electrocyclic reactions of conjugated systems, we find that the picture is in general accord with orbital symmetry considerations, *except for the nonstereospecific ring opening of cyclobutenes*. The results also

<sup>79</sup> J. E. Baldwin and S. M. Krueger, *J. Am. Chem. Soc.*, **91**, 6444 (1969).

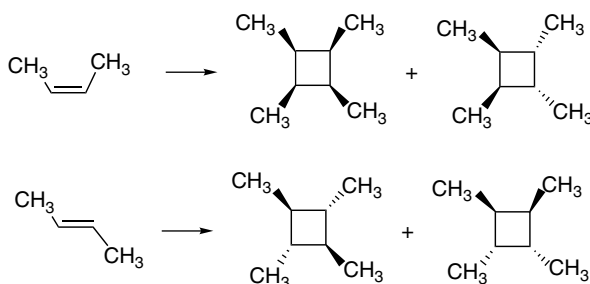
<sup>80</sup> R. B. Woodward, in *Aromaticity*, Chemical Society Special Publication No. 21, 217 (1967); E. Havinga and J. L. M. A. Schlatmann, *Tetrahedron*, **16**, 146 (1961); J. A. Berson, *Tetrahedron*, **48**, 3 (1992).

<sup>81</sup> F. Bernardi, M. Olivucci, I. N. Ragazos, and M. A. Robb, *J. Am. Chem. Soc.*, **114**, 8211 (1992).

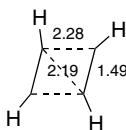
indicate the importance of reactant conformation in influencing the reaction outcome. By contrast, the ring opening of cyclobutenes is more complex. In Topic 12.1 we take a look at the computational interpretation of these results.

### 12.2.6. Photochemical Cycloaddition Reactions

As described on p. 1098, the original orbital symmetry interpretation of alkene  $[2\pi + 2\pi]$  cycloaddition was in terms of a suprafacial transition structure with a rectangular geometry. This arrangement leads to a photochemical process that is allowed by orbital symmetry criteria. Early experimental work also provided examples of stereospecific  $[2\pi + 2\pi]$  cycloadditions, lending support to a concerted reaction path. For example, dimerization of *Z*-2-butene gives two products that retain *cis*-methyl groups. The adducts from *E*-2-butene have *trans*-methyl groups.<sup>82</sup> This establishes that the configuration is retained at both alkene double bonds during the formation of the dimers.



The prototypical ethene + ethene cycloaddition has been explored computationally and a somewhat different picture has emerged.<sup>83</sup> The CI for ethene dimerization is calculated to be rhomboid.<sup>84</sup>



These computations lead to an energy surface featuring the rhomboid CI, which can lead to formation of cyclobutane or separation into two ethene molecules, as shown in Figure 12.22. Point *E* is the rhomboid CI that permits rapid return to the ground state surface. The process is expected to be very fast and this is consistent with the observed retention of alkene stereochemistry in substituted cases. In contrast to the pathway through the rhomboid CI, a completely symmetrical rectangular approach does not lead to minima.

<sup>82</sup> H. Yamazaki and R. J. Cvetanovic, *J. Am. Chem. Soc., Chem. Commun.*, **91**, 520 (1969).

<sup>83</sup> F. Bernardi, S. De, M. Olivucci, and M. A. Robb, *J. Am. Chem. Soc.*, **112**, 1737 (1990); F. Bernardi, A. Bottini, M. Olivucci, A. Venturini, and M. A. Robb, *J. Chem. Soc., Faraday Trans.*, **90**, 1617 (1994).

<sup>84</sup> F. Bernardi, M. Olivucci, and M. A. Robb, *Pure Appl. Chem.*, **67**, 17 (1995).

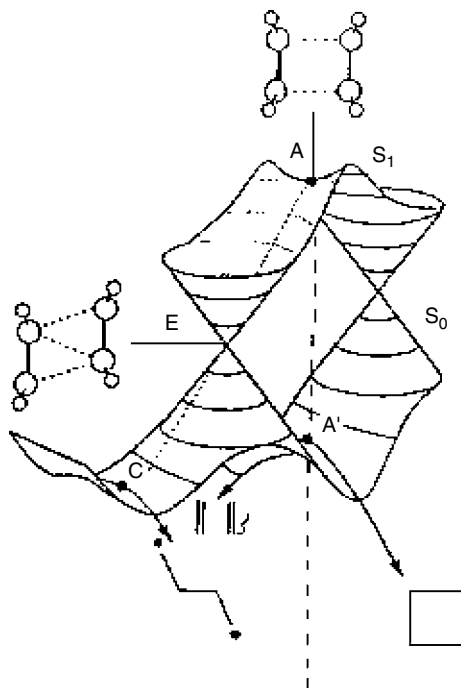
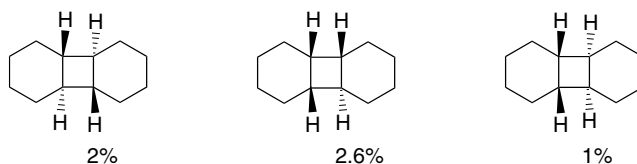
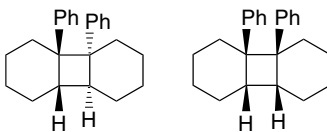


Fig. 12.22. Energy surface depicting the  $S_1$  and  $S_0$  potential energy surfaces for singlet state photodimerization of ethene. Adapted from *J. Photochem. Photobiol.*, **105**, 365 (1997), by permission of Elsevier.

Photodimerization of cyclohexene sensitized by xylene gives a low yield of a mixture of stereoisomers. The reaction was interpreted as a  $Z \rightarrow E$  isomerization followed by a nonstereospecific ground state  $[2\pi + 2\pi]$  addition.<sup>85</sup>



1-Phenylcyclohexene can be photodimerized by irradiation at  $\lambda > 280 \text{ nm}$ .<sup>86</sup> *E*-2-Phenylcyclohexene is generated under these conditions and can be trapped in methanol. The fact that the tail-to-tail products are formed from both singlet and triplet excited states indicates an intermediate with diradical character.

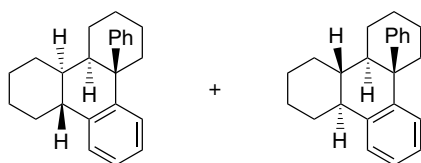


With high-intensity (laser) irradiation, the reaction also gives stereoisomeric  $[2 + 4]$  dimers. These products are believed to be formed by dimerization of the *E*-isomer.

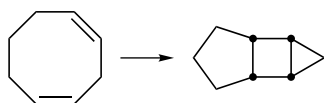
<sup>85</sup> P. J. Kropp, J. J. Snyder, P. C. Rawlings, and H. G. Fravel, Jr., *J. Org. Chem.*, **45**, 4471 (1980).

<sup>86</sup> D. J. Unett, R. A. Caldwell, and D. C. Hrcir, *J. Am. Chem. Soc.*, **118**, 1682 (1996).

Under low intensity, the concentration of the *E*-isomer is too low to permit this reaction.

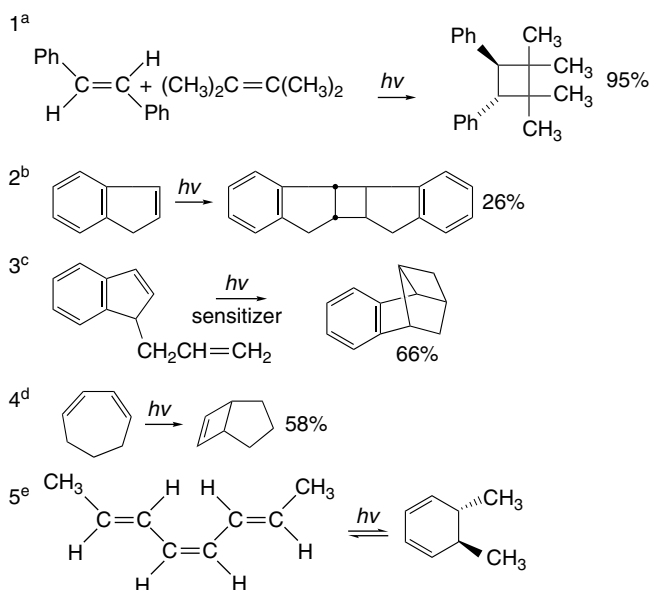


Intramolecular cycloaddition is observed for 1,4-cyclooctadiene.<sup>87</sup>



The most useful intermolecular  $[2\pi + 2\pi]$  cycloadditions from a synthetic point of view involve alkenes and cyclic  $\alpha,\beta$ -unsaturated carbonyl compounds. These reactions are discussed in more detail in Section 6.3.2 of Part B. Scheme 12.1 lists some examples of photochemical cycloaddition and electrocyclic reactions of the type that are consistent with the predictions of orbital symmetry considerations.

**Scheme 12.1. Examples of Electrocyclic Reactions and Cycloadditions**

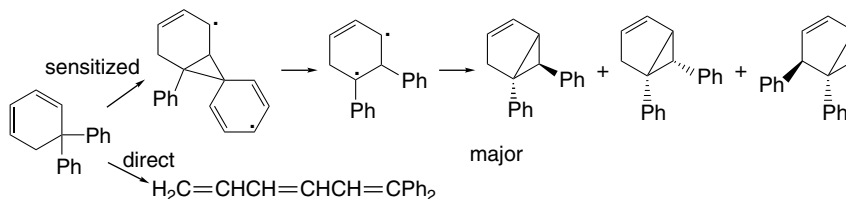


- a. O. L. Chapman and W. R. Adams, *J. Am. Chem. Soc.*, **99**, 2333 (1968).  
 b. A. G. Anastassiou, F. L. Setliff, and G. W. Griffin, *J. Org. Chem.*, **31**, 2705 (1966).  
 c. A. Padwa, S. Goldstein, and M. Pulwer, *J. Org. Chem.*, **47**, 3893 (1982).  
 d. O. L. Chapman, D. J. Pasto, G. W. Borden, and A. A. Griswold, *J. Am. Chem. Soc.*, **84**, 1220 (1962).  
 e. G. J. Fonken, *Tetrahedron Lett.*, 549 (1962).

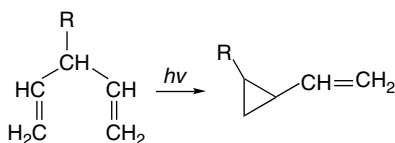
<sup>87</sup>. S. Moon and C. R. Ganz, *Tetrahedron Lett.*, 6275 (1968).

## 12.2.7. Photochemical Rearrangements Reactions of 1,4-Dienes

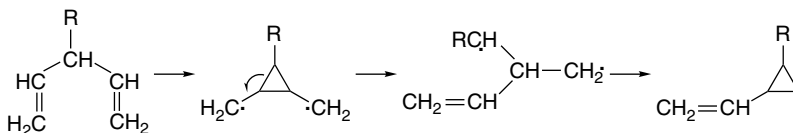
In addition to the electrocyclic and cycloaddition reactions described earlier, certain dienes undergo interesting rearrangements. For example, 5,5-diphenylcyclohexa-1,3-diene shows divergent photochemical behavior, depending on whether the reaction is induced by direct irradiation or by photosensitization. On direct irradiation, the electrocyclic ring opening to 1,1-diphenylhexatriene is dominant, whereas a rearrangement involving migration one of the aromatic rings is the major reaction of the triplet excited state formed by photosensitization.<sup>88</sup>



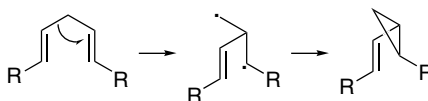
The latter reaction is an example of the *di- $\pi$ -methane rearrangement*,<sup>89</sup> which is a quite general reaction for 1,4-dienes and other systems that have two  $\pi$  systems separated by an  $sp^3$ -carbon atom. The  $\pi$  systems can be a double bond, an aromatic ring, or, as we will see in Section 12.3, a carbonyl group.



The transformation can be formulated in terms of bonding between C(2) and C(4) involving formation of a cyclopropyl diradical intermediate. This diradical can fragment to form a new 1,3-diradical that gives the cyclic product.



An alternative mechanism involves a direct migration of one of the vinyl groups, followed by formation of the ring.<sup>90</sup>

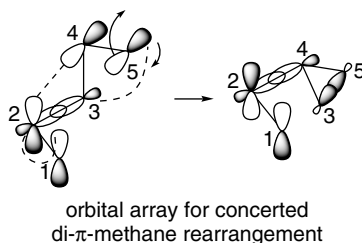


<sup>88</sup> H. E. Zimmerman and G. A. Epling, *J. Am. Chem. Soc.*, **94**, 8749 (1972); J. S. Swenton, J. A. Hyatt, T. J. Walker, and A. L. Crumrine, *J. Am. Chem. Soc.*, **93**, 4808 (1971); M.-D. Su, *J. Org. Chem.*, **60**, 6621 (1995).

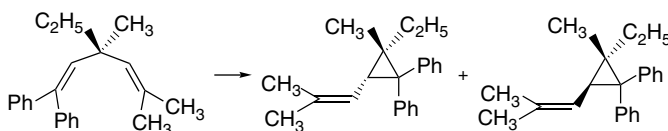
<sup>89</sup> For reviews of the di- $\pi$ -methane rearrangement, see S. S. Hixson, P. S. Mariano, and H.E. Zimmerman, *Chem. Rev.*, **73**, 531 (1973); H. E. Zimmerman, in *Rearrangements in Ground and Excited States*, Vol. 3, P. de Mayo, ed., Academic Press, New York, 1980, Chap. 16; H. E. Zimmerman, in *Organic Photochemistry and Photobiology*, W. H. Horspool and P.-S. Song, eds., CRC Press, Boca Raton, FL, 1995, pp. 184–193; H. E. Zimmerman and D. Armesto, *Chem. Rev.*, **96**, 3065 (1996).

<sup>90</sup> L. A. Paquette and E. Bay, *J. Org. Chem.*, **47**, 4597 (1982).

In some cases, the di- $\pi$ -methane rearrangement can proceed through either a singlet or a triplet excited state.<sup>91</sup> The singlet reaction can be formulated as a concerted process, and this mechanism is followed in the case of some acyclic dienes and for cyclic systems in which a concerted process is sterically feasible. Note that the orbital array is of the Möbius topology with a phase change depicted between the C(1) and C(2) positions. This corresponds to an allowed photochemical process since there are six electrons involved in bonding changes and this is an antiaromatic system.



The di- $\pi$ -methane rearrangement is a stereospecific reaction. There are several elements of stereochemistry to be considered. It is known that the double bond that remains uncyclized retains the *E*- or *Z*-configuration present in the starting material. This result excludes any intermediate with a freely rotating terminal radical. The concerted mechanism implies that C(3) would undergo inversion of configuration since the new C(3)–C(5) bond is formed using the back lobe of the C(2)–C(3)  $\sigma$ -bond. This inversion of configuration has been confirmed.<sup>92</sup>



Thus the TS depicted above for the concerted reaction correctly predicts the stereochemical course of the di- $\pi$ -methane rearrangement, as does the computational analysis discussed below.

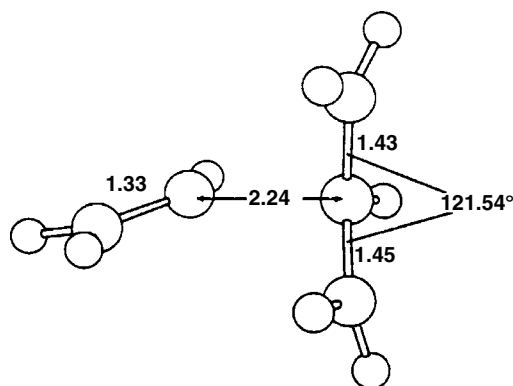
The di- $\pi$ -methane rearrangement of 1,4-pentadiene has been modeled using CAS-SCF/4-31G calculations. The results indicate that a singlet 1,3-diradical is the key intermediate.<sup>93</sup> This species can be reached from the excited state via a CI that involves vinyl migration. It consists of a vinyl group associated with the central carbon of an allylic system and is similar in structure to the CI involved in alkene sigmatropic rearrangements (see p. 1093). The structure of the CI is also consistent with the

<sup>91</sup> H. E. Zimmerman and P. S. Mariano, *J. Am. Chem. Soc.*, **91**, 1718 (1969); P. S. Mariano, R. B. Steitle, D. G. Watson, M. J. Peters, and E. Bay, *J. Am. Chem. Soc.*, **98**, 5899 (1976).

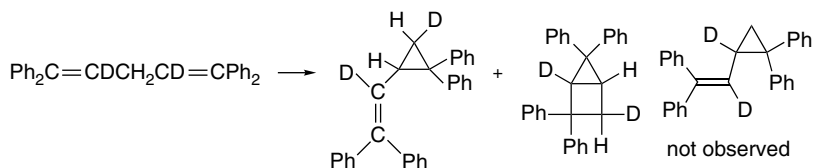
<sup>92</sup> H. E. Zimmerman, J. D. Robbins, R. D. McKelvey, C. J. Samuel, and L. R. Sousa, *J. Am. Chem. Soc.*, **96**, 1974, 4630 (1974).

<sup>93</sup> M. Reguero, F. Bernardi, H. Jones, M. Olivucci, I. N. Ragazos, and M. A. Robb, *J. Am. Chem. Soc.*, **115**, 2073 (1993).

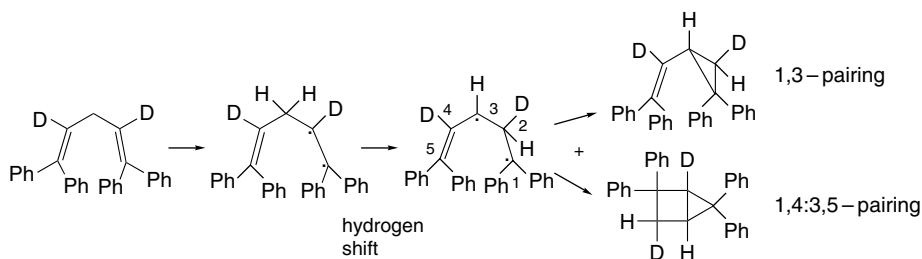
observed stereochemistry of the reaction. It remains to be seen if this mechanism applies to the more highly substituted systems that have been studied experimentally.



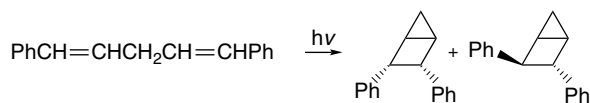
The di- $\pi$ -methane rearrangement has been studied in a sufficient number of cases to recognize some of the substituent effects. When the central  $sp^3$ -carbon is unsubstituted, the di- $\pi$ -methane path becomes less favorable. The case of 1,1,5,5-tetraphenyl-1,4-pentadiene is illustrative. Although one of the products has the expected structure for di- $\pi$ -methane rearrangement, labeling with deuterium proves that an alternative mechanism operates.



The cyclopropane ring is formed only after hydrogen atom migration. The driving force for this migration may be the fact that it produces a more stable allylic radical. The resulting 1,3-diradical can re-pair to give the observed products.



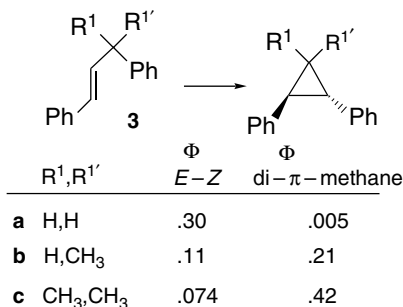
Photolysis of 1,5-diphenyl-1,4-pentadiene is another example where a compound undergoes cycloaddition in preference to di- $\pi$ -methane rearrangement.<sup>94</sup>



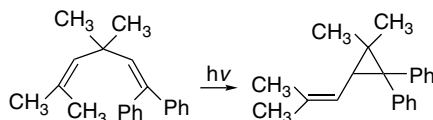
<sup>94</sup> E. Block and H. W. Orf, *J. Am. Chem. Soc.*, **94**, 8438 (1972).

The resistance of the 3-unsubstituted system to the di- $\pi$ -methane rearrangement probably occurs at the stage of the vinyl rearrangement.<sup>95</sup> If the central carbon is unsubstituted this step results in the formation of a primary radical and would be energetically unfavorable.

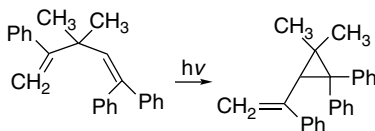
Kinetic studies of **3a**, **3b**, and **3c** have provided experimental evidence that a cyclopropyl diradical is an intermediate.<sup>96</sup> The product composition reveals a temperature dependence that implicates an intermediate. These compounds undergo both *cis-trans* isomerization and di- $\pi$ -methane rearrangement on direct irradiation and mainly *cis-trans* isomerization when photosensitized (triplet) by benzophenone. The quantum yield of the di- $\pi$ -methane rearrangement increases dramatically with substitution at the allylic position.



The groups at the termini of the 1,4-pentadiene system also affect the efficiency and direction of the di- $\pi$ -methane reaction. The general trend is that cyclization occurs at the diene terminus that best stabilizes radical character. Thus, a terminus substituted with aryl groups will cyclize in preference to an unsubstituted or alkyl-substituted terminus.



Ref. 97



Ref. 98

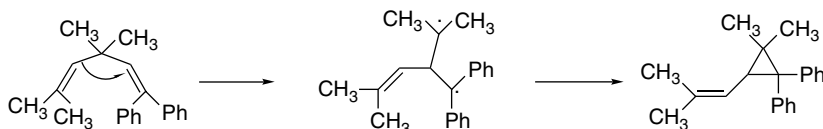
<sup>95</sup> H. E. Zimmerman and J. A. Pincock, *J. Am. Chem. Soc.*, **95**, 2957 (1973).

<sup>96</sup> F. D. Lewis, X. Zuo, R. S. Kalgutkar, M. A. Miranda, E. Font-Sanchis, and J. Perez-Prieto, *J. Am. Chem. Soc.*, **122**, 8571 (2000); F. D. Lewis, X. Zuo, R. S. Kalgutkar, J. M. Wagner-Brennan, M. A. Miranda, E. Font-Sanchis, and J. Perez-Prieto, *J. Am. Chem. Soc.*, **123**, 11883 (2001).

<sup>97</sup> H. E. Zimmerman and A. C. Pratt, *J. Am. Chem. Soc.*, **92**, 1409 (1970).

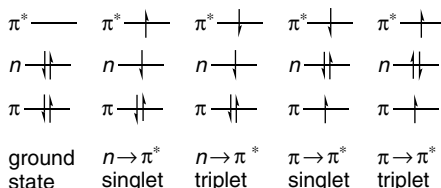
<sup>98</sup> H. E. Zimmerman and A. A. Baum, *J. Am. Chem. Soc.*, **93**, 3646 (1971).

This result can be rationalized in terms of the vinyl migration mechanism by noting that rearrangement will occur to give the more stable of the two possible 1,3-diradicals.<sup>99</sup> The cyclopropane ring in the final product will then incorporate this terminus.



### 12.3. Photochemistry of Carbonyl Compounds

The photochemistry of carbonyl compounds has been extensively studied, both in solution and in the gas phase. There are major differences between the two phases. In the gas phase, the energy transferred by excitation is not lost rapidly by collision, whereas in the liquid phase the excess vibrational energy is rapidly transferred to the solution. We emphasize solution photochemistry here because both mechanistic study and preparative applications of organic reactions usually involve solution processes. The reactive excited state of alkyl ketones is usually the  $n-\pi^*$  state. On excitation, an electron from an oxygen nonbonding orbital is transferred to the  $\pi$ -antibonding orbital of the carbonyl group. The singlet excited state is formed initially, but intersystem crossing to the triplet can occur. For saturated ketones, the singlet and the triplet lie, respectively, about 80–85 and 75–80 kcal/mol above the ground state. The first excited singlet ( $S_1$ ) and triplet ( $T_1$ ) can be described structurally from spectroscopic data available for formaldehyde, which is the simplest analog. In both excited states, the molecule is pyramidal, the C–O bond is lengthened, and the dipole moment is reduced.<sup>100</sup> The reduction of the dipole moment results from the transfer of electron density from an orbital localized on oxygen to one that also encompasses the carbon atom. An alternative excited state involves promotion of a bonding  $\pi$  electron to the antibonding  $\pi^*$  orbital. This is called the  $\pi-\pi^*$  excited state and is most likely to be involved when the carbonyl group is conjugated with an extended  $\pi$ -bonding system, as is the case for aryl ketones. The excited carbonyl groups have radical character at both carbon and oxygen, and the oxygen is rather similar in its reactivity to alkoxy radicals. The MO diagrams for the  $n-\pi^*$  and  $\pi-\pi^*$  states are depicted below.



MP2/6-311G calculations have described the geometric and charge distribution of the excited state of formaldehyde as summarized below.<sup>101</sup> Three valence shell

<sup>99</sup> H. E. Zimmerman and A. C. Pratt, *J. Am. Chem. Soc.*, **92**, 6259, 6267 (1970).

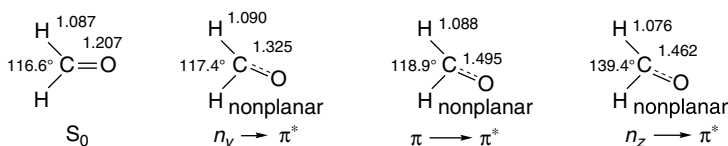
<sup>100</sup> J. C. D. Brand and D. G. Williamson, *Adv. Phys. Org. Chem.*, **1**, 365 (1963); D. E. Freeman and W. Klemperer, *J. Chem. Phys.*, **45**, 52 (1966).

<sup>101</sup> C. M. Hadad, J. B. Foresman, and K. B. Wiberg, *J. Phys. Chem.*, **97**, 4293 (1993).

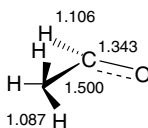
excited states corresponding to  $n_y \rightarrow \pi^*$ ,  $\pi \rightarrow \pi^*$ , and  $n_z \rightarrow \pi^*$  have been described, and there are several Rydberg states as well. The atomic populations and bond orders were calculated using the AIM method.

State	$E$ (eV)	Atomic population						Bond order			
		C		O		H		C–O		C–H	
		$\pi$	Total	$\pi$	Total	$\pi$	Total	$\pi$	Total	$\pi$	Total
$S_0$	0.00	0.431	4.833	1.541	9.207	0.014	0.980	0.664	1.43	0.006	0.958
$n_y \rightarrow \pi^*$	4.58	1.025	5.438	1.890	8.821	0.043	0.871	0.094	0.871	0.000	0.886
$\pi \rightarrow \pi^*$	9.19	0.521	5.170	1.425	9.063	0.028	0.883	0.171	0.957	0.011	0.867
$n_z \rightarrow \pi^*$	9.97	1.069	5.467	1.844	8.674	0.043	0.930	0.263	0.797	0.041	0.943

According to these results the  $n_y \rightarrow \pi^*$  shows  $0.39e$  and  $0.11e$  lost from O and H, respectively, whereas C gains  $0.61e$  compared to the ground state. The  $\pi \rightarrow \pi^*$  state shows a smaller loss from both O ( $0.140e$ ) and from H ( $0.10$ ). The  $\pi$  bond order in all the excited states is decreased by the population of an antibonding  $\pi^*$  orbital. The charge shifts in the  $\sigma$  and  $\pi$  systems are in opposite senses, but the overall effect is that the O becomes less electron rich and takes on the character of an electrophilic radical. The excited states are nonplanar. Some of the computed bond distances and angles are shown below.<sup>102</sup>



The excited states of other saturated carbonyl compounds are similar. Alkyl groups somewhat stabilize the excited state and reduce the excitation energy. In acetaldehyde, the conformation of the  $n \rightarrow \pi^*$  state changes from the H–O eclipsed structure in the ground state (see p. 148) to an H–O staggered conformation.<sup>103</sup>



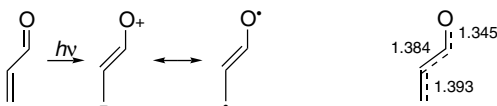
For conjugated carbonyl compounds, such as  $\alpha,\beta$ -enones, the orbital diagram is similar, except that the HOMO of the ground state is  $\psi_2$  of the enone system, rather than an oxygen unshared pair orbital. In the  $\pi\text{-}\pi^*$  state, the C=O and C=C bonds lengthen and the C(1)–C(2) bond shortens.<sup>104</sup> Population of the  $\pi^*$  orbital shifts

<sup>102</sup>. M. Dallos, T. Muller, H. Lischka, and R. Shepard, *J. Chem. Phys.*, **114**, 746 (2001).

<sup>103</sup>. J. M. Price, J. A. Mack, G. v. Helden, X. Yang, and A. M. Wodtke, *J. Phys. Chem.*, **98**, 1791 (1994).

<sup>104</sup>. C. S. Page and M. Olivucci, *J. Comput. Chem.*, **24**, 298 (2003).

electron density from oxygen to carbon. The excited state can be represented as a hybrid with dipolar and diradical structures.



Although Lewis structures of this type are not entirely adequate descriptions of the excited states, they do correspond to the MO picture by indicating polarization of charge and the presence of polar radical-like centers. In addition to the increased energy content, the high reactivity of the excited states is associated with the presence of half-filled orbitals. The two SOMO orbitals in the excited states have enhanced radical, cationic, or anionic character.

For aromatic carbonyl compounds, as for styrene (see p. 1084), there are excited states associated with the aromatic ring. The absorption spectrum of benzaldehyde, for example, is believed to include two triplet levels and at least five singlet bands.<sup>105</sup>

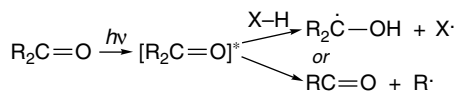
—	6.23	
—	5.98	$1(\pi - \pi^*)$
—	4.89	
—	4.33	
—	3.71	$1(n - \pi^*)$
—	3.49	$3(\pi - \pi^*)$
—	3.40	$3(n - \pi^*)$

Computed absorption  
levels in eV for benzaldehyde

For acetophenone, the  $S_1$  state, like acetaldehyde adopts a H-C-C-O staggered conformation, whereas  $T_1$  retains the eclipsed conformation found in the ground state.<sup>106</sup>

### 12.3.1. Hydrogen Abstraction and Fragmentation Reactions

One of the most common reactions of photoexcited carbonyl groups is hydrogen atom abstraction from solvent or some other hydrogen donor. A second common reaction is cleavage of the carbon-carbon bond adjacent to the carbonyl group, which is called  $\alpha$ -cleavage.

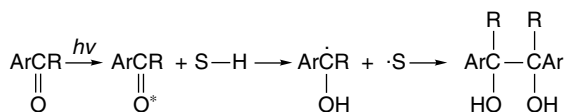


The hydrogen atom abstraction can be either intramolecular or intermolecular. The intermediates that are generated are free radicals. If these radicals come to thermal equilibrium, they have the same structure and reactivity as radicals generated by

<sup>105</sup> V. Molina and M. Merchan, *J. Phys. Chem. A*, **105**, 3745 (2001).

<sup>106</sup> J. L. Tomer, L. H. Spanler, and D. W. Pratt, *J. Am. Chem. Soc.*, **110**, 1615 (1988).

thermal processes. Many aromatic ketones react by hydrogen atom abstraction and the stable products are diols formed by coupling of the resulting  $\alpha$ -hydroxybenzyl radicals.



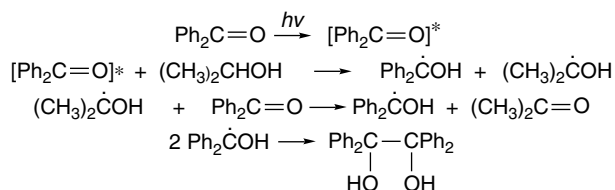
These reactions usually occur via the triplet excited state  $T_1$ . The intersystem crossing of the initially formed singlet excited state is so fast ( $k \sim 10^{10} \text{ s}^{-1}$ ) that reactions of the  $S_1$  state are usually not observed. The reaction of the benzophenone  $T_1$  state has been particularly closely studied. Some of the facts that have been established in support of the general mechanism outlined above are as follows:

1. For a given hydrogen donor S—H, replacement by S—D leads to a decreased rate of reduction, relative to nonproductive decay to the ground state.<sup>107</sup> This decreased rate is consistent with a primary isotope effect in the hydrogen abstraction step.
2. The photoreduction can be quenched by known triplet quenchers. The effective quenchers are those that have  $T_1$  states less than 69 kcal/mol above  $S_0$ . Quenchers with higher triplet energies are ineffective because the benzophenone  $\pi$ - $\pi^*$  triplet is not sufficiently energetic to effect energy transfer.
3. The intermediate diphenylhydroxymethyl radical has been detected after generation by flash photolysis.<sup>108</sup> Photolysis of benzophenone in benzene solution containing potential hydrogen donors results in the formation of two intermediates that are detectable, and their rates of decay have been measured. One intermediate is the  $\text{Ph}_2\dot{\text{C}}\text{OH}$  radical, which disappears by dimerization in a second-order process. A much shorter-lived species disappears with first-order kinetics in the presence of excess amounts of various hydrogen donors. The pseudo-first-order rate constants vary with the structure of the donor; with 2,2-diphenylethanol, for example,  $k = 2 \times 10^6 \text{ s}^{-1}$ . The rate is much less with poorer hydrogen atom donors. The rapidly reacting intermediate is the triplet excited state of benzophenone.
4. In 2-propanol, the quantum yield for dimeric conversion of benzophenone to the dimeric reduction product is 2.0.<sup>109</sup> The reason is that the radical remaining after abstraction of a hydrogen atom from 2-propanol transfers a hydrogen atom to ground state benzophenone in a nonphotochemical reaction. Because of this process, two molecules of benzophenone are reduced for each one that is photoexcited. These results suggest the following mechanism:

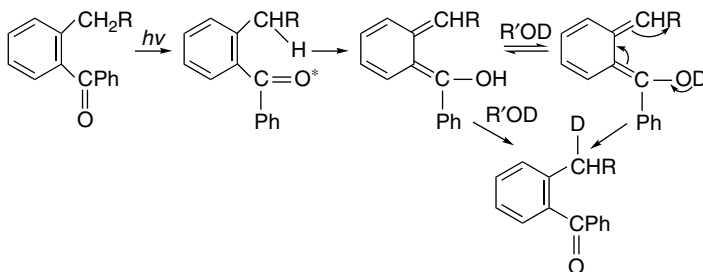
<sup>107</sup>. W. M. Moore, G. S. Hammond, and R. P. Foss, *J. Am. Chem. Soc.*, **83**, 2789 (1961); G. S. Hammond, W. P. Baker, and W. M. Moore, *J. Am. Chem. Soc.*, **83**, 2795 (1961).

<sup>108</sup>. J. A. Bell and H. Linschitz, *J. Am. Chem. Soc.*, **85**, 528 (1963).

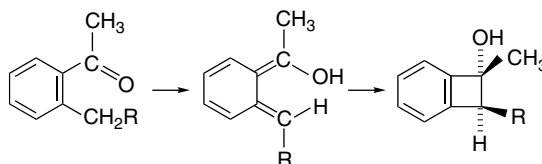
<sup>109</sup>. N. J. Turro, *Molecular Photochemistry*, W. A. Benjamin, New York, 1965, pp. 143, 144.



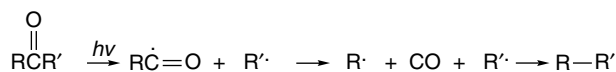
The efficiency of photoreduction of benzophenone derivatives is greatly diminished when an *ortho* alkyl substituent is present because a new photoreaction, intramolecular hydrogen atom transfer, becomes the dominant process. Hydrogen abstraction takes place from the benzylic position on the adjacent alkyl chain, giving an unstable enol that can revert to the original benzophenone without photoreduction. This process, known as *photoenolization*,<sup>110</sup> can be detected by photolysis in deuterated hydroxylic solvents even though there is no net transformation of the reactant. The proton of the enolic hydroxyl is rapidly exchanged with solvent, so deuterium is introduced at the benzylic position. Deuterium is also introduced if the enol is protonated at the benzylic carbon by solvent.



The reactive dienols can also undergo thermal electrocyclicization to cyclobutenols.<sup>111</sup>



The dominant photochemical reaction of ketones in the gas phase is cleavage of one of the carbonyl substituents, which is followed by decarbonylation and subsequent reactions of the free radicals that are formed. The initial cleavage occurs within 100 fs of excitation. There is an activation barrier for decarbonylation (see Table 11.2), so decarbonylation can be relatively slow with excitation at 270 nm.<sup>112</sup> At shorter wavelengths, there may be sufficient excess energy for rapid decarbonylation. This reaction is referred to as the *Type-I* or  $\alpha$ -cleavage reaction of carbonyl compounds.

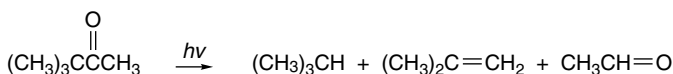


<sup>110</sup> P. G. Sammes, *Tetrahedron*, **32**, 405 (1976).

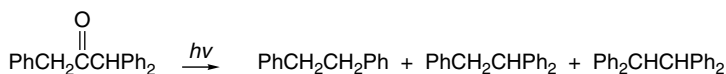
<sup>111</sup> P. J. Wagner, D. Subrahmayam, and B.-S. Park, *J. Am. Chem. Soc.*, **113**, 709 (1991).

<sup>112</sup> S. K. Kim and A. H. Zewail, *Chem. Phys. Lett.*, **250**, 279 (1996); E. W. G. Diau, C. Kotting, T. I Solling, and A. H. Zewail, *Chem. Phys. Chem.*, **3**, 57 (2000); A. P. Baronavski and J. C. Owrutsky, *Chem. Phys. Lett.*, **33**, 36 (2001).

The energetics of  $\alpha$ -cleavage and decarbonylation depend on the structure of the ketone. For acetone, the  $S_1$  and  $T_1$  states are 88 and 80 kcal/mol above the ground state, respectively. For acetone, both  $\alpha$ -cleavage and decarbonylation are slightly endothermic, owing to the low stability of the methyl radical.<sup>113</sup> However, the reaction is exothermic with radical-stabilizing substituents, as illustrated in Figure 12.23.



Ref. 115



Ref. 114

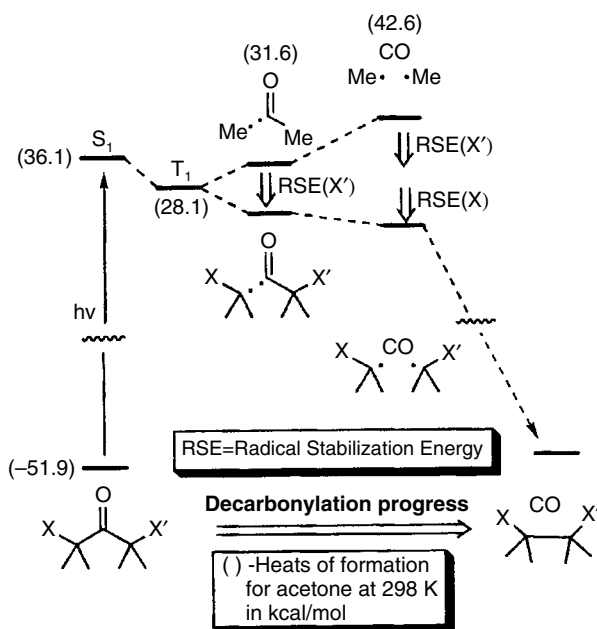


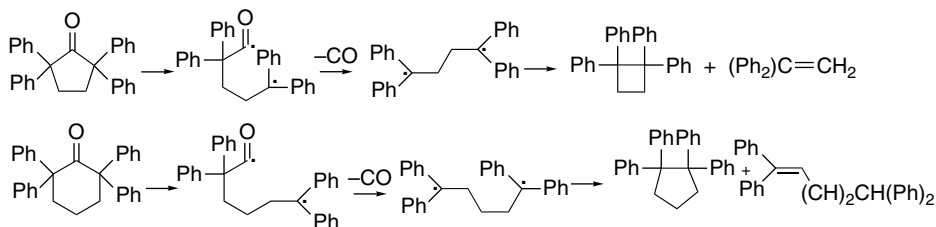
Fig. 12.23. Energetics for  $\alpha$ -cleavage and decarbonylation of acetone showing the effect of radical stabilization. Reproduced from *J. Org. Chem.*, **67**, 3749 (2002), by permission of the American Chemical Society.

<sup>113</sup> L. M. Campos, H. Dang, D. Ng, Z. Yang, H. L. Martinez, and M. A. Garcia-Garibay, *J. Org. Chem.*, **67**, 3749 (2002).

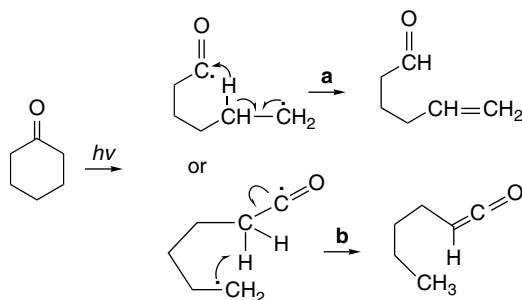
<sup>114</sup> G. Quinkert, K. Opitz, W. W. Wiersdorff, and J. Weinlich, *Tetrahedron Lett.*, 1863 (1963).

<sup>115</sup> N. C. Yang and E. D. Feit, *J. Am. Chem. Soc.*, **90**, 504 (1968).

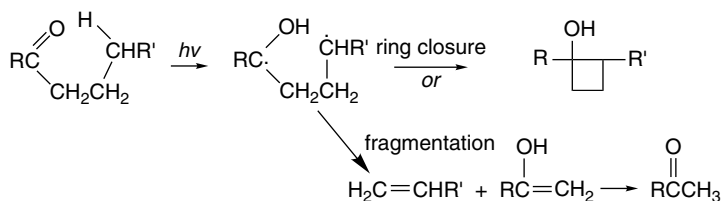
Ketones such as 2,2,5,5-tetraphenylcyclopentanone and 2,2,6,6-tetraphenylcyclohexanone decarbonylate readily because of the stabilization afforded by the phenyl groups. The products result from recombination, disproportionation, or fragmentation of the diradical intermediate.<sup>116</sup>



With some cyclic ketones, the  $\alpha$ -cleavage can also be followed by intramolecular hydrogen abstraction that eventually leads to an unsaturated ring-opened aldehyde.<sup>117</sup> An alternative reaction path involves formation of a ketene. The competition between these two reactions is determined by the effect of substituents on the conformation and reactivity of the diradical intermediate.<sup>118</sup>



For ketones having propyl or longer alkyl groups as a carbonyl substituent, intramolecular hydrogen abstraction can be followed by either cleavage of the bond between the  $\alpha$ - and  $\beta$ -carbon atoms or by formation of a cyclobutanol.



Cleavage between  $C_\alpha$  and  $C_\beta$  is referred to as *Type-II photoelimination* to distinguish it from  $\alpha$ -cleavage. Type-II photoeliminations are observed for both aryl and allyl ketones.<sup>119</sup> Studies aimed at establishing the identity of the reactive excited state

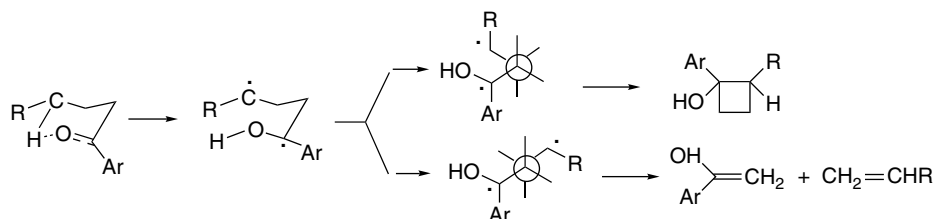
<sup>116</sup>. D. H. R. Barton, B. Charpiot, K. U. Ingold, L. J. Johnston, W. B. Motherwell, J. C. Scaiano, and S. Stanforth, *J. Am. Chem. Soc.*, **107**, 3607 (1985).

<sup>117</sup>. W. C. Agosta and W. L. Schreiber, *J. Am. Chem. Soc.*, **93**, 3947 (1971); P. J. Wagner and R. W. Spierke, *J. Am. Chem. Soc.*, **91**, 4437 (1969).

<sup>118</sup>. P. J. Wagner, *Top. Curr. Chem.*, **61**, 1 (1976).

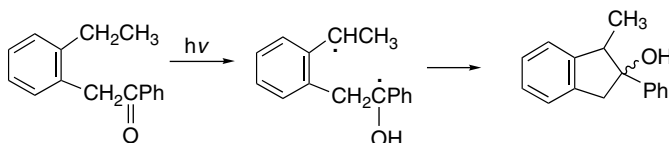
<sup>119</sup>. P. J. Wagner and P. Klan, in *CRC Handbook of Photochemistry and Photobiology*, W. Horspod and F. Lenci, eds., CRC Press, Boca Raton, FL, 2004, Chap 52.

indicate that both  $S_1$  and  $T_1$  are involved for allyl ketones, but when one of the carbonyl substituents is aryl, intersystem crossing is very fast and  $T_1$  is the reactive state. Theoretical analysis indicates that the hydrogen abstraction involves an in-plane ( $n$ ) orbital on oxygen, rather than a  $\pi$  orbital. Usually, cleavage is the dominant reaction, with cyclobutanol yields being rather low, but there are exceptions. Activation energies for the hydrogen abstraction process from a methylene group are about 4 kcal, whereas the activation energy for carbon-carbon bond cleavage is 8–12 kcal. The competition between these two processes can be understood in terms of the structure and conformation of the diradical intermediates.<sup>120</sup> The hydrogen abstraction reaction is believed to occur through a chairlike conformation. The diradical can give cyclobutanol from the *gauche* conformation or fragment through the *anti* conformation.

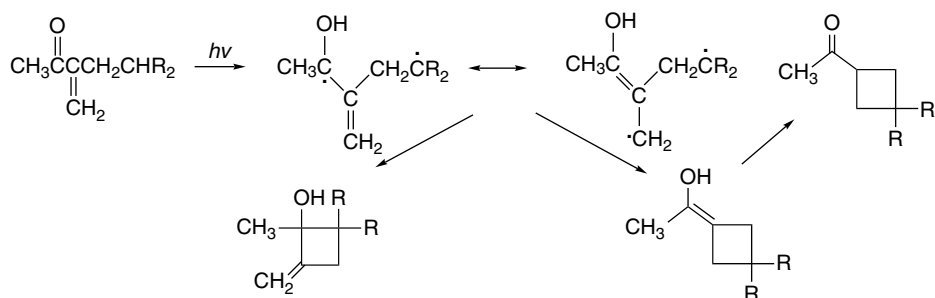


The nature of substituents on the aryl ring can affect the balance between the competing reactions.<sup>121</sup>

With aryl benzyl ketones, indanols can be formed.<sup>122</sup> This is a particularly favorable case because of the benzylic stabilization of both radical sites.



Intramolecular hydrogen atom abstraction is also an important process for acyclic  $\alpha,\beta$ -unsaturated ketones.<sup>123</sup> The intermediate diradical then cyclizes to give the enol of a cyclobutyl ketone. Among the by-products of such photolyses are methylenecyclobutanols resulting from alternative modes of cyclization of the diradical intermediate.



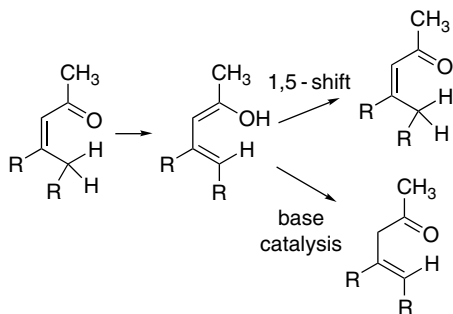
<sup>120</sup>. P. J. Wagner, *Acc. Chem. Res.*, **4**, 168 (1971).

<sup>121</sup>. M. V. Encina, E. A. Lissi, E. Lemp, A. Zanocco, and J. C. Scaiano, *J. Am. Chem. Soc.*, **105**, 1856 (1983).

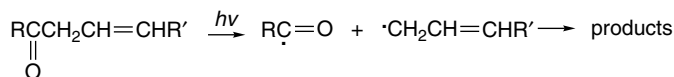
<sup>122</sup>. P. J. Wagner, A. Zand, and B.-S. Park, *J. Am. Chem. Soc.*, **118**, 12856 (1996).

<sup>123</sup>. R. A. Cormier, W. L. Schreiber, and W. C. Agosta, *J. Am. Chem. Soc.*, **95**, 4873 (1973); R. A. Cormier and W. C. Agosta, *J. Am. Chem. Soc.*, **96**, 618 (1974).

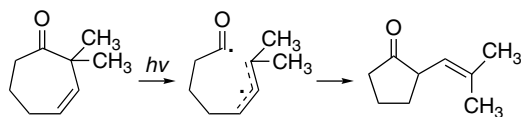
$\alpha,\beta$ -Unsaturated ketones with  $\gamma$ -hydrogens can undergo hydrogen atom transfer resulting in formation of a dienol. Because the hydrogen atom transfer occurs through a cyclic TS, the originally formed dienol has *Z*-stereochemistry. The dienol is unstable and two separate processes have been identified for ketonization: a [1,5]-sigmatropic shift of hydrogen leading back to the conjugated enone and a base-catalyzed proton transfer that leads to the  $\beta,\gamma$ -enone.<sup>124</sup> The deconjugated enone is formed because of a kinetic preference for reprotonation of the dienolate at the  $\alpha$ -carbon. Photochemical deconjugation is a synthetically useful way of effecting isomerization of  $\alpha,\beta$ -unsaturated ketones and esters to the  $\beta,\gamma$ -isomers.



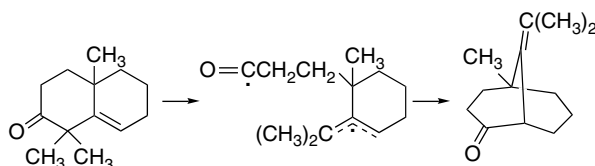
Ketones in which the double bond is located in the  $\beta,\gamma$ -position are likely candidates for  $\alpha$ -cleavage because of the stability of the allyl radical that is formed. This is an important process in direct irradiation. Products then arise by recombination of the radicals before or after decarbonylation.



For cyclic ketones, the diradical intermediates can recombine, leading to isomerized ketones.



Ref. 125



Ref. 126

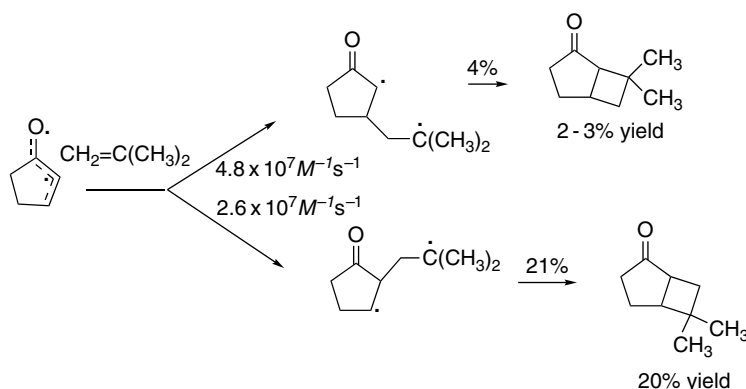
<sup>124</sup> R. Ricard, P. Sauvage, C. S. K. Wan, A. C. Weedon, and D. F. Wong, *J. Org. Chem.*, **51**, 62 (1986).

<sup>125</sup> H. Sato, N. Furutachi, and K. Nakanishi, *J. Am. Chem. Soc.*, **94**, 2150 (1972); L. A. Paquette, R. F. Eizember, and O. Cox, *J. Am. Chem. Soc.*, **90**, 5153 (1968).

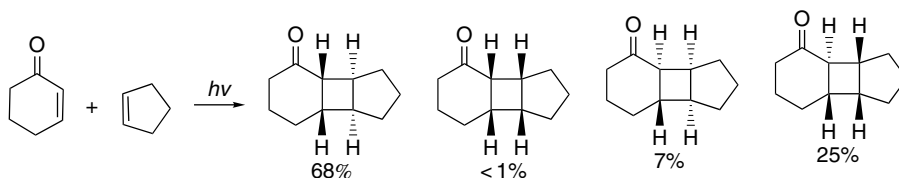
<sup>126</sup> P. S. Engel and M. A. Schnexnyder, *J. Am. Chem. Soc.*, **97**, 145 (1975).

### 12.3.2. Cycloaddition and Rearrangement Reactions of Cyclic Unsaturated Ketones

Cyclic  $\alpha,\beta$ -unsaturated ketones present a rich array of photochemical reactions, some of which are of considerable synthetic value (see Part B, Section 6.3.2.2). Generally, noncyclic enones relax rapidly by *cis-trans* interconversion and do not undergo intermolecular photochemical reactions. One useful reaction of cyclic enones is photochemical addition of alkenes.<sup>127</sup> The reaction involves the  $\pi-\pi^*$  triplet excited state and 1,4-diradical intermediates.<sup>128</sup> Both the regiochemistry and stereochemistry of the reaction are determined by the properties of the diradical intermediate. It appears that initial bonding can occur at either C(2) or C(3) of the excited enone system. The alkene reacts at its less-substituted terminus, generating the more stable radical. The regiochemistry is determined by the relative efficiency of cyclization to product versus fragmentation back to reactants. In the case of cyclopentenone and isobutene, both the relative rates of addition and the fraction proceeding on to product have been determined. The preferred regioisomer results from a larger fraction of cyclization for the intermediate with radical character at the  $\beta$ -carbon.<sup>129</sup>



Significantly, both *cis* and *trans* ring junctures are formed.<sup>130</sup> Cyclohexenone and cyclopentene, for example, give four adducts with about a 2:1 *cis:trans* ratio.<sup>131</sup>



<sup>127</sup> P. de Mayo, *Acc. Chem. Res.*, **4**, 41 (1971); D. I. Schuster, G. Lem, and N. A. Kaprinidis, *Chem. Rev.*, **93**, 3 (1993).

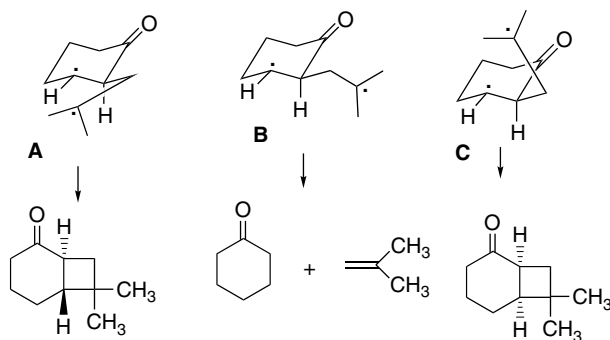
<sup>128</sup> D. I. Schuster, D. A. Dunn, G. E. Heibel, P. B. Brown, J. M. Rao, J. Woning, and R. Bonneau, *J. Am. Chem. Soc.*, **113**, 6245 (1991).

<sup>129</sup> D. Andrew, D. J. Hastings, D. L. Oldroyd, A. Rudolph, A. C. Weedon, D. F. Wong, and B. Zhang, *Pure Appl. Chem.*, **64**, 1327 (1992); D. Andrew, D. J. Hastings, and A. C. Weedon, *J. Am. Chem. Soc.*, **116**, 10870 (1994); D. Andrew and A. C. Weedon, *J. Am. Chem. Soc.*, **117**, 5647 (1995).

<sup>130</sup> E. J. Corey, J. D. Bass, R. Le Mahieu, and R. B. Mitra, *J. Am. Chem. Soc.*, **86**, 5570 (1964).

<sup>131</sup> D. I. Schuster, N. Kaprinidis, D. J. Wink, and J. C. Dewan, *J. Org. Chem.*, **56**, 561 (1991).

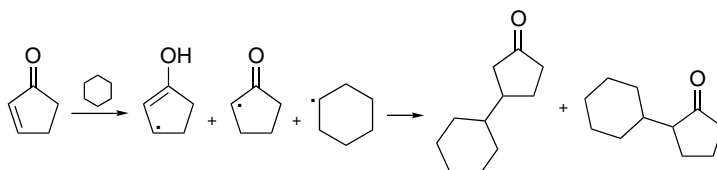
The *trans* products obviously are more strained. The stereochemistry can be traced to conformational factors in the diradical. For example, the diradical from cyclohexenone and isobutene can be formed in several conformations.



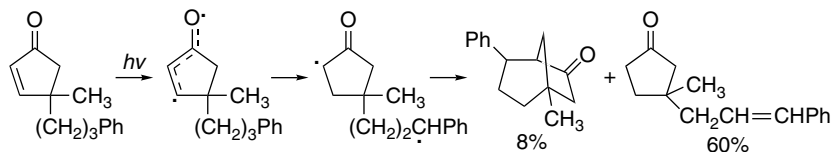
The extended radical **B** is likely to fragment. The *gauche* radicals **A** and **C** lead to *trans* and *cis* ring junctions, respectively. In this particular case, it has been proposed that there is less steric repulsion to cyclization of radical **A**, resulting in a preference for formation of the *trans* ring closure.<sup>132</sup> In general, the competing modes of attack of alkene and the ease of cyclization of the diradical govern the stereochemistry of the ring juncture.

In hydrocarbon solvents, the principal products from cyclopentenones result from hydrogen abstraction processes. Irradiation of cyclopentenone in cyclohexane gives a mixture of 2- and 3-cyclohexylcyclopentanone.<sup>133</sup> These products can be formed by intermolecular hydrogen abstraction, followed by recombination of the resulting radicals.

It is interesting that as in the alkene cycloaddition reaction, reactivity is observed at both C(2) and C(3) of the excited enone system.



If a substituent chain is present on the cyclopentenone ring, an intramolecular hydrogen abstraction can take place.

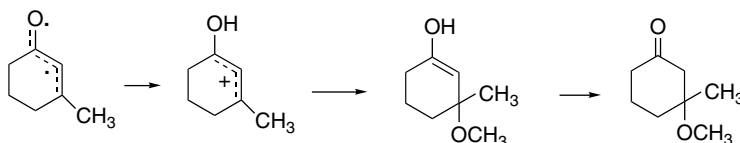


The bicyclic product is formed by coupling of the two radical sites, whereas the unsaturated side chain results from an intramolecular hydrogen atom transfer. These reactions can be sensitized by aromatic ketones and quenched by typical triplet quenchers, and are therefore believed to proceed via triplet excited states.

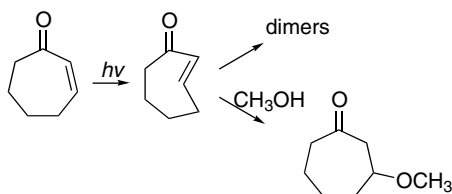
<sup>132</sup> P. G. Bauslaugh, *Synthesis*, 287 (1970).

<sup>133</sup> S. Wolff, W. L. Schreiber, A. B. Smith, III, and W. C. Agosta, *J. Am. Chem. Soc.*, **94**, 7797 (1972).

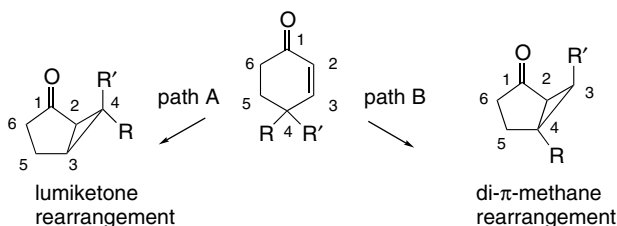
Cyclohexenones can add methanol in an acid-catalyzed reaction. This is thought to involve protonation of the  $\pi$ - $\pi^*$  excited state.<sup>134</sup>



In the case of cycloheptenone and larger rings, the main initial photoproducts are the *trans*-cycloalkenones produced by photoisomerization. In the case of the seven- and eight-membered rings, the *trans*-double bonds are sufficiently strained that rapid reactions follow. In nonnucleophilic solvents dimerization takes place, whereas in nucleophilic solvents addition reactions occur.<sup>135</sup>



There are also important rearrangement reactions for cyclic enones. For cyclohexenones two prominent reactions are the *lumiketone rearrangement* (Path A) and the *di- $\pi$ -methane rearrangement* (Path B). The di- $\pi$ -methane rearrangement pathway is restricted to 4-aryl or 4-vinyl cyclohexenones. 4,4-Dialkylcyclohexenones undergo the lumiketone rearrangement, which involves the shift of the C(4)–C(5) bond to C(3) and formation of a new C(2)–C(4) bond.<sup>136</sup>

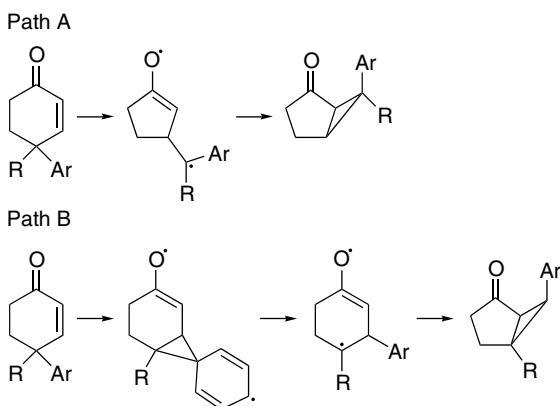


Both reactions proceed via triplet excited species and to some extent depend on whether the  $\pi$ - $\pi^*$  or  $n$ - $\pi^*$  states are involved. At the most basic level of mechanism, the reactions can be depicted as involving the following steps.

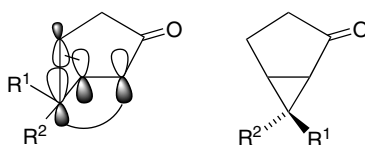
<sup>134</sup>. D. I. Schuster, J.-M. Yang, J. Woning, T. A. Rhodes, and A. W. Jensen, *Can. J. Chem.*, **73**, 2004 (1995).

<sup>135</sup>. H. Hart, B. Chen, and M. Jeffares, *J. Org. Chem.*, **44**, 2722 (1979).

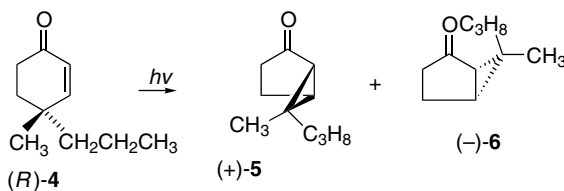
<sup>136</sup>. For a review of this reaction, see D. I. Schuster, in *Rearrangements in Ground and Excited States*, Vol. 3, P. de Mayo, ed., Academic Press, New York, 1980, Chap. 17.



The lumiketone rearrangement is stereospecific and can be described as a  $[\pi 2_a + \sigma 2_a]$  cycloaddition. This mechanism requires that inversion of configuration occur at C(4) as the new  $\sigma$  bond is formed at the back lobe of the reacting C(4)–C(5)  $\sigma$  bond.

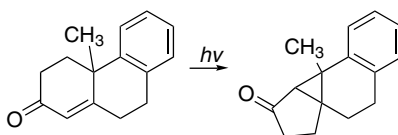


It has been demonstrated in several systems that the reaction is in fact stereospecific with the expected inversion occurring at C(4). The ketone **4** provides a specific example. The stereoisomeric products **5** and **6** are both formed, but in each product inversion has occurred at C(4).



Ref. 137

The lumiketone rearrangement also proceeds in the case of some 4-alkyl-4-arylcyclohexenones.



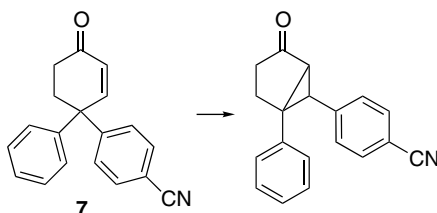
Ref. 138

With 4,4-diarylcyclohexenones, the di- $\pi$ -methane rearrangement is the preferred reaction. For compounds in which the two aryl groups are substituted differently, it

<sup>137</sup>. D. I. Schuster and J. M. Rao, *J. Org. Chem.*, **46**, 1515 (1981); D. I. Schuster, R. H. Brown, and B. M. Resnick, *J. Am. Chem. Soc.*, **100**, 4504 (1978).

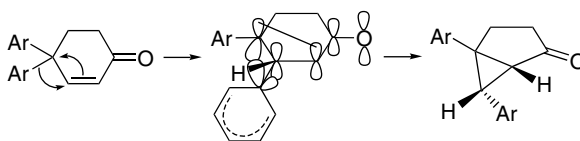
<sup>138</sup>. O. L. Chapman, J. B. Sieja, and W. J. Welstead, Jr., *J. Am. Chem. Soc.*, **88**, 161 (1966).

is found that substituents that stabilize radical character favor migration. Thus the *p*-cyanophenyl substituent migrates in preference to the phenyl substituent in **7**.

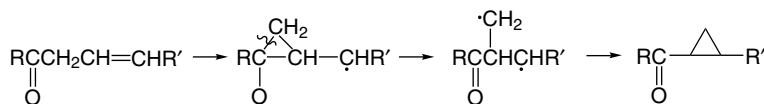


Ref. 139

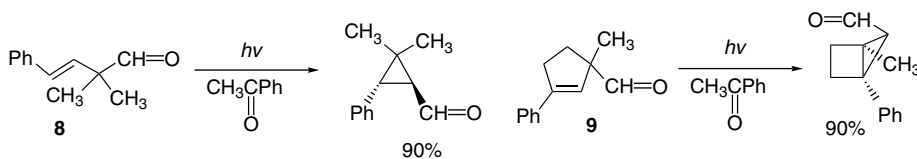
As described on p. 1113, di- $\pi$ -methane rearrangement can be considered to occur via a TS in which C(2)–C(4) bridging is accompanied by a 4  $\rightarrow$  3 aryl migration.<sup>140</sup> Note that the *endo* product is predicted by the concerted mechanism. It is the major product, even though it is sterically more congested than the *exo* isomer. This stereospecificity is characteristic of the reaction.



Excitation of acyclic  $\beta,\gamma$ -unsaturated ketones by triplet photosensitization can give cyclopropyl ketones.<sup>141</sup> This reaction is known as the *oxadi- $\pi$ -methane rearrangement*.



Oxadi- $\pi$ -methane rearrangements have been observed by both direct and triplet-sensitized excitation. The reaction is generally associated with the  $\pi$ - $\pi^*$  excited state, but there are also examples that involve other levels. The most favorable cases for the rearrangement involve conjugation at the  $\gamma$ -carbon (e.g., aryl) and disubstitution or a bulky substituent at the  $\alpha$ -carbon. The reaction is also favored by more or less rigid cyclic systems. The features are present in reactants such as **8** and **9**, which give particularly high yields.<sup>142</sup>



As with other reactions involving triplet excited states, the efficiency of intersystem crossing appears to be a major factor in the outcome of the reaction.<sup>143</sup> The

<sup>139</sup> H. E. Zimmerman, R. D. Rieke, and J. R. Scheffer, *J. Am. Chem. Soc.*, **89**, 2033 (1967).

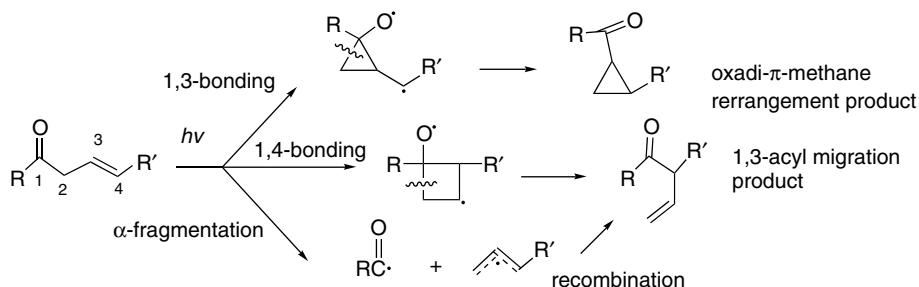
<sup>140</sup> H. E. Zimmerman, *Tetrahedron*, **30**, 1617 (1974).

<sup>141</sup> W. G. Dauben, M. S. Kellog, J. I. Seeman, and W. A. Spitzer, *J. Am. Chem. Soc.*, **92**, 1786 (1970).

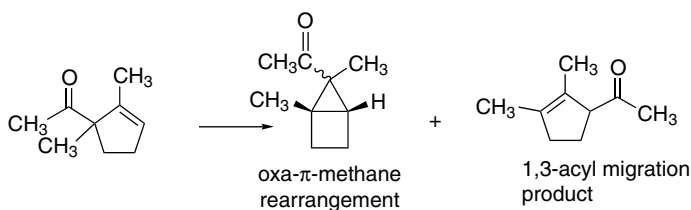
<sup>142</sup> D. Armesto, M. J. Ortiz, and S. Romano, *Tetrahedron Lett.*, **36**, 965 (1995).

<sup>143</sup> B. Reimann, D. E. Sadler, and K. Schaffner, *J. Am. Chem. Soc.*, **108**, 5527 (1986); M.-D. Su, *J. Org. Chem.*, **61**, 3080 (1996).

reaction pathway has been modeled computationally (MC-SCF/6-31G\*) using the simplest  $\beta,\gamma$ -unconjugated carbonyl compound, but-3-en-1-one.<sup>144</sup> The results suggest that two short-lived diradical intermediates are involved, one leading to oxadi- $\pi$ -methane rearrangement and the other to 1,3-acyl migration. These structures are closely related to CIs that provide efficient crossing to the ground state. The computations suggest that both the singlet and triplet states are energetically comparable. A dissociation-recombination mechanism is also available for the 1,3-shift. It appears that individual structural differences can favor any of the competing reaction paths.



This conclusion is in general agreement with experimental studies that indicate that several excited states can lead to oxadi- $\pi$ -methane rearrangement and the related reactions.<sup>145</sup> For example, 1,2-dimethylcyclopent-2-enyl methyl ketone reacts by all three pathways. In the gas phase about 25% of the 1,3-acyl migration occurs by a dissociation mechanism, as indicated by the ability of NO and O<sub>2</sub> to divert a part but not all of the intermediate.<sup>143</sup>



Other conjugated carbonyl compounds that have received a great deal of attention are the cyclohexadienones.<sup>146</sup> The main photolysis product of 4,4-diphenylcyclohexadienone, for example, is **10**.<sup>147</sup> Quenching and photosensitization

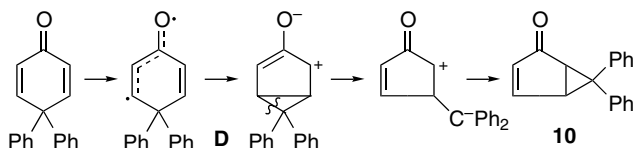
<sup>144</sup> S. Wilsey, M. J. Bearpark, F. Bernardi, M. Olivucci, and M. A. Robb, *J. Am. Chem. Soc.*, **118**, 176 (1996).

<sup>145</sup> T. J. Eckersley, S. D. Parker, and N. A. J. Rogers, *Tetrahedron*, **40**, 3749 (1984); T. J. Eckersley and N. A. J. Rogers, *Tetrahedron*, **40**, 3759 (1984); M. J. C. M. Koppes and H. Cerfontain, *Rec. Trav. Chim. Pays-Bas*, **107**, 549 (1988).

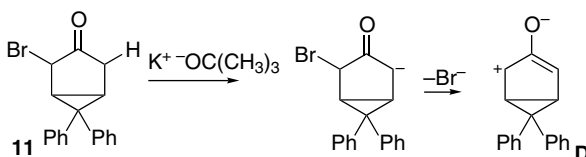
<sup>146</sup> H. E. Zimmerman, *Angew. Chem. Int. Ed. Engl.*, **8**, 1 (1969); K. Schaffner and M. Demuth, in *Rearrangements in Ground and Excited States*, Vol. 3, P. de Mayo, ed., Academic Press, New York, 1980, Chap. 18; D. I. Schuster, *Acc. Chem. Res.*, **11**, 65 (1978).

<sup>147</sup> H. E. Zimmerman and D. I. Schuster, *J. Am. Chem. Soc.*, **83**, 4486 (1961).

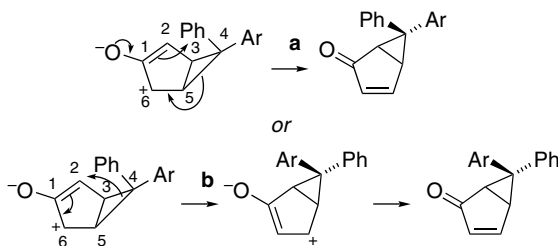
experiments have indicated that the reaction proceeds through a triplet excited state. A scheme that delineates the bonding changes is outlined below.



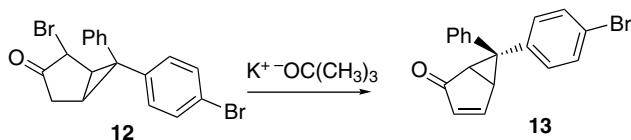
It is believed that a reactive ground state species, the zwitterion **D**, is an intermediate and that it rearranges to the observed product.<sup>148</sup> To test this mechanism, generation of species **D** by nonphotochemical means was undertaken.<sup>149</sup>  $\alpha$ -Haloketones, when treated with strong base, ionize to such dipolar intermediates. Thus, the bromoketone **11** is a potential precursor of intermediate **D**.



The zwitterion prepared by this route did indeed lead to **10**, as required if it is an intermediate in the photochemical reaction. Further study of this process established another aspect of the reaction mechanism. The product could be formed by a process involving inversion at C(4) (Path a) or by one involving a pivot about the bond C(3)–C(4) (Path b).



The two mechanisms predict the formation of stereochemically different products when the aryl groups at C(4) are different. When the experiment was carried out on **12** only **13** the product corresponding to inversion of configuration at C(4) was observed.<sup>150</sup>

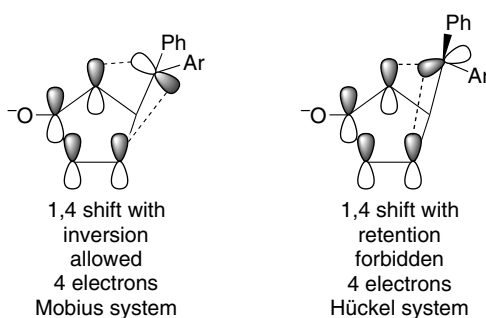


The rearrangement step is a ground state thermal process and may be classified as a [1,4]-sigmatropic shift of carbon across the face of a 2-oxybutenyl cation. The Woodward-Hoffmann rules require a sigmatropic shift of this type to proceed with inversion of configuration. The orbitals involved in a [1,4]-sigmatropic shift are shown below.

<sup>148</sup>. H. E. Zimmerman and J. S. Swenton, *J. Am. Chem. Soc.*, **89**, 906 (1967).

<sup>149</sup>. H. E. Zimmerman, D. Döpp, and P. S. Huyffer, *J. Am. Chem. Soc.*, **88**, 5352 (1966).

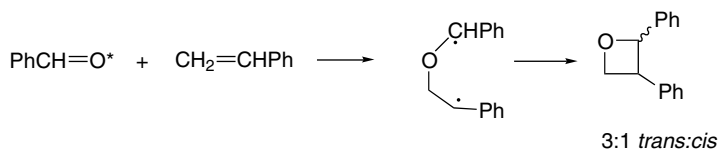
<sup>150</sup>. H. E. Zimmerman and D. S. Crumrine, *J. Am. Chem. Soc.*, **90**, 5612 (1968).



As is clear from the preceding examples, there are a variety of overall reactions that can be initiated by photolysis of ketones. The course of photochemical reactions of ketones is very dependent on the structure of the reactant. Despite the variety of overall processes that can be observed, the number of individual steps involved is limited. For ketones, the most important are inter- and intramolecular hydrogen abstraction,  $\alpha$ -cleavage at the carbonyl group, and substituent migration to the  $\beta$ -carbon atom of  $\alpha,\beta$ -unsaturated ketones. Reexamination of the mechanisms illustrated in this section will reveal that most of the reactions of carbonyl compounds that have been described involve combinations of these fundamental processes. The final products usually result from re-bonding of reactive intermediates generated by these steps.

### 12.3.3. Cycloaddition of Carbonyl Compounds and Alkenes

Ketones and aldehydes can undergo photochemical [2+2] cycloaddition reactions with alkenes to give oxetanes. This is called the *Paterno-Buchi reaction*. For alkyl carbonyl compounds both singlet and triplet excited states seem to be involved, but for aromatic compounds the reaction occurs through the triplet state.<sup>151</sup> The regiochemistry can usually be accounted for on the basis of formation of the most stable 2-oxa-1,4-diradical. For example, styrene and benzaldehyde give 2,3- not 2,4-diphenyloxetane.<sup>152</sup>

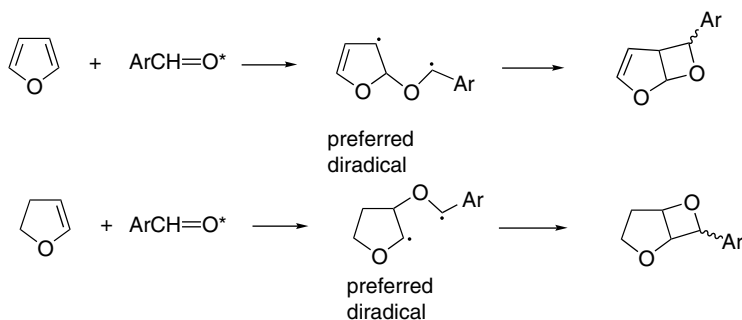


The same generalization can also account for the reversal of orientation between furan and dihydrofuran.<sup>153</sup>

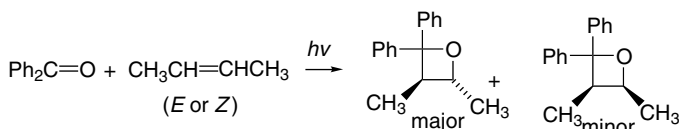
<sup>151</sup> R. A. Caldwell, G. W. Sovocool, and R. P. Gajewski, *J. Am. Chem. Soc.*, **95**, 2549 (1973).

<sup>152</sup> S. A. Fleming and J. J. Gao, *Tetrahedron Lett.*, **38**, 5407 (1997).

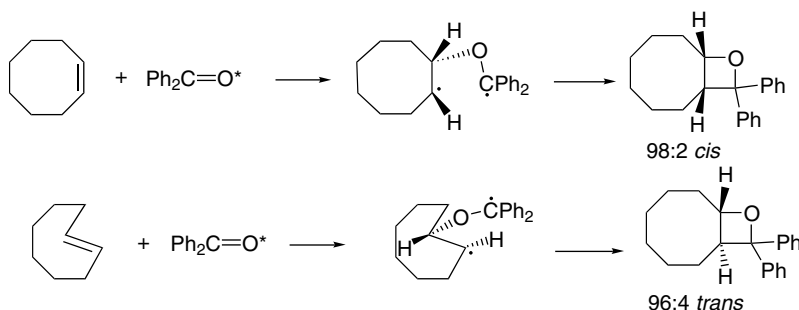
<sup>153</sup> A. G. Griesbeck and S. Stadtmüller, *Chem. Ber.*, **123**, 357 (1990).



The Paterno-Buchi reaction is ordinarily not stereospecific, but instead favors the more stable adduct for either alkene isomer, indicating the involvement of a relatively a long-lived diradical intermediate.<sup>154</sup>



An exception to this generalization has been noted for *E*- and *Z*-cyclooctene.<sup>155</sup> This reaction is nearly stereospecific at low temperature. This result is attributed to conformationally distinct 1,4-diradical intermediates that undergo intersystem crossing and cyclization faster than stereochemical interconversion.



At higher temperature, some stereorandomization occurs as the result of competition between rotational processes and fragmentation of the 1,4-diradical intermediate.

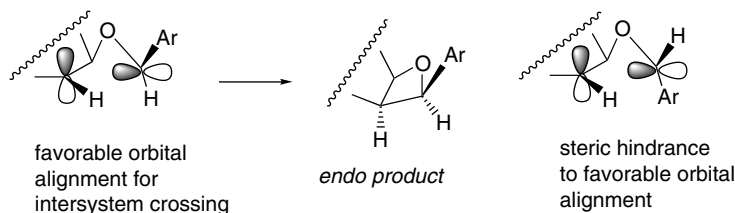
Many of the details of both regio- and stereoselectivity of the Paterno-Buchi reaction can be understood in terms of the conformation and lifetime of the 1,4-diradical intermediates. Griesbeck and co-workers have proposed that the relative lifetime of the radicals, and whether they cyclize or revert to reactants, is governed by the rate of intersystem crossing, which in turn depends on the efficiency of spin-orbit coupling.<sup>156</sup> With cyclic alkenes, for example, the *endo* stereoisomer is often preferred. This can be explained by noting that the conformation leading to *exo* product is not well oriented for the perpendicular orbital interaction that favors intersystem crossing (see p. 1075).

<sup>154</sup>. D. R. Arnold, R. L. Hinman, and A. H. Glick, *Tetrahedron Lett.*, 1425 (1964).

<sup>155</sup>. W. Adam, V. R. Stegmann, and S. Weinkotz, *J. Am. Chem. Soc.*, **123**, 2452 (2001); W. Adam and V. R. Stegmann, *J. Am. Chem. Soc.*, **124**, 3600 (2002).

<sup>156</sup>. A. G. Griesbeck and S. Stadtmueller, *J. Am. Chem. Soc.*, **112**, 1281 (1990); A. G. Griesbeck, H. Mauder, and S. Stadtmueller, *Acc. Chem. Res.*, **27**, 70 (1994).

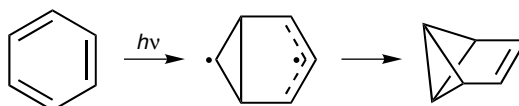
Computational modeling of orbital interactions supports this proposal.<sup>157</sup>



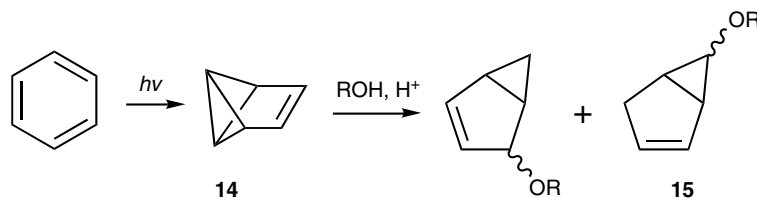
The Paterno-Buchi reaction, particularly its synthetic application,<sup>158</sup> is considered in more detail in Section 6.3.2.3 of Part B.

## 12.4. Photochemistry of Aromatic Compounds

Irradiation of benzene and certain of its derivatives results in bond reorganization and formation of nonaromatic products.<sup>159</sup> Irradiation of liquid benzene with light  $\lambda = 254\text{ nm}$  wavelength results in the accumulation of fulvene and a very small amount of tricyclo[3.1.0.0<sup>2,6</sup>]hex-3-ene, also known as benzvalene.<sup>160</sup> The maximum conversion to this product in liquid benzene is about 0.05%. The key intermediate is believed to be a diradical formed by 1,3-bonding.



Because of the low photostationary concentration of benzvalene, photolysis is not an efficient way of accumulating this compound. However, the highly reactive molecule can be trapped if it is generated in the presence of other molecules with which it reacts. Irradiation of benzene in acidic hydroxylic solvents gives products resulting from 1,3-bonding in the benzene ring and addition of a molecule of solvent. The compounds of structure **15** arise by solvolysis of, the initial photoproduct benzvalene.<sup>161</sup>



<sup>157</sup> A. G. Kutateladze, *J. Am. Chem. Soc.*, **123**, 9279 (2001).

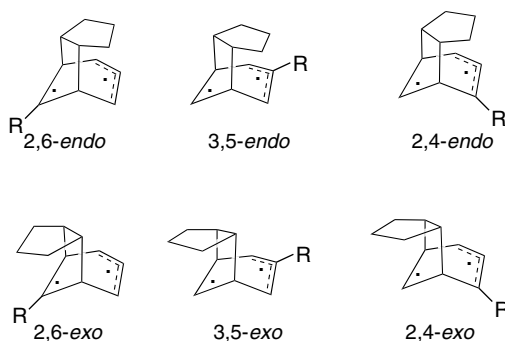
<sup>158</sup> T. Bach, *Synthesis*, 683 (1998).

<sup>159</sup> D. Bryce-Smith and A. Gilbert, *Tetrahedron*, **32**, 1309 (1976); A. Gilbert, in *Organic Photochemistry and Photobiology*, W. M. Horspool and P.-S. Song, eds., CRC Press, Boca Raton, FL, 1995, pp. 229–236.

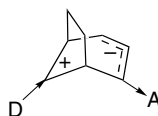
<sup>160</sup> K. E. Wilzbach, J. S. Ritscher, and L. Kaplan, *J. Am. Chem. Soc.*, **89**, 1031 (1967).

<sup>161</sup> L. Kaplan, D. J. Rausch, and K. E. Wilzbach, *J. Am. Chem. Soc.*, **94**, 8638 (1972).

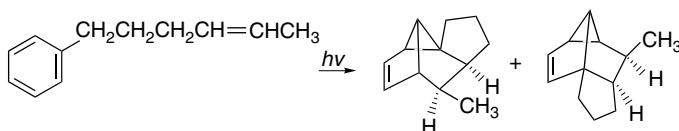




Donor substituents favor the 2,6-regioisomer, whereas EWGs favor the 2,4-orientation.<sup>165</sup> These results suggest that there is considerable polar character to the reaction between the excited aromatic and the alkene. Acceptor substituents at C(3) can stabilize the negative charge at C(3) and C(5), whereas donor substituents can stabilize the positive charge at C(1).<sup>166</sup>



Addition of alkenes and aromatic rings has also been realized intramolecularly when the distance between the alkene and phenyl substituent is sufficient to permit bonding.



The photocycloaddition of ethene and benzene has been studied by CAS-SCF computation using the 6-31G\* basis set for energies and 4-31G orbitals for structural minimization.<sup>167</sup> The structure of the CI is shown in Figure 12.24. The *ortho* and *meta* cycloaddition processes proceed through alternate electron-pairing schemes from a single CI without barriers. For unsubstituted alkenes, the *meta* CI is lower in energy than the *ortho*, whereas the *ortho* CI is stabilized by alkenes with ERG and EWG substituents. Product compositions tend to reflect these differences.<sup>168</sup>

<sup>165</sup> P. de Vaal, E. M. Osselton, E. S. Krijnen, G. Lodder, and J. Cornelisse, *Rec. Trav. Chim. Pays-Bas*, **107**, 407 (1988).

<sup>166</sup> D. Bryce-Smith, B. Foulger, J. Forrester, A. Gilbert, B. H. Orger, and H. M. Tyrrell, *J. Chem. Soc., Perkin Trans. 1*, 55 (1980); G. Weber, J. Runsink, and J. Mattay, *J. Chem. Soc., Perkin Trans.*, **1**, 2333 (1987); V. Y. Merritt, J. Cornelisse, and R. Srinivasan, *J. Am. Chem. Soc.*, **95**, 8250 (1973).

<sup>167</sup> S. Clifford, M. J. Bearpark, F. Bernardi, M. Olivucci, M. A. Robb, and B. R. Smith, *J. Am. Chem. Soc.*, **118**, 7353 (1996).

<sup>168</sup> A. Gilbert and P. Yianni, *Tetrahedron*, **37**, 3275 (1981); J. Mattay, *Tetrahedron*, **41**, 2405 (1985).

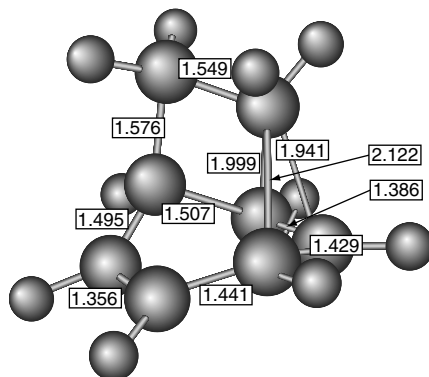
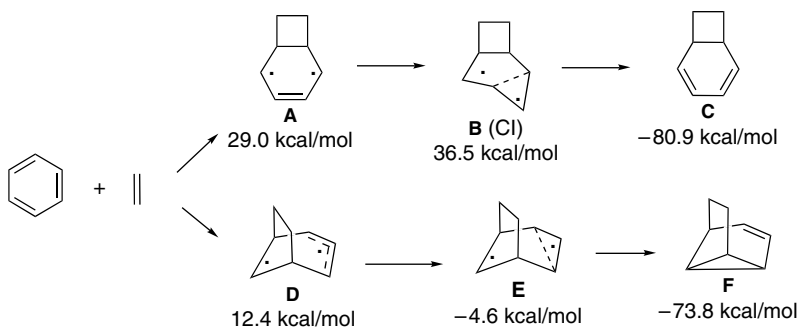


Fig. 12.24. Structure of conical intersection for benzene + ethene addition from *J. Am. Chem. Soc.*, **118**, 7353 (1996), by permission of the American Chemical Society.



## Topic 12.1. Computational Interpretation of Diene and Polyene Photochemistry

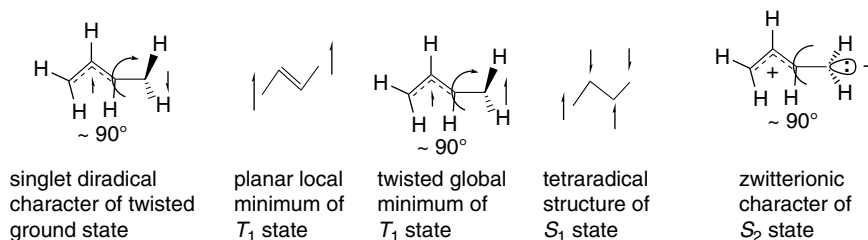
As a starting point for the mechanistic discussion, it is useful to review the structural features of the excited states. The first singlet excited state of butadiene,  $S_1$ , can be approximated as the  $\psi_2 \rightarrow \psi_3$ /HOMO  $\rightarrow$  LUMO  $\pi$ - $\pi^*$  transition.<sup>169</sup> The lack of fluorescence from this excited state indicates that a very facile path exists for nonradiative energy transfer. The  $S_2$  state has doubly excited character and relaxes to a structure with ionic character that can rotate at the pyramidal carbon but not at the allyl fragment. The minimum energy of the  $T_1$  state corresponds to the allyl-methylene diradical with a nearly  $90^\circ$  twist and slight pyramidalization at the methylene carbon. In substituted systems, one or the other of the zwitterion structures (e.g., allyl cation versus allyl anion) may be favored.<sup>170</sup>

<sup>169</sup>. K. B. Wiberg, C. M. Hadad, G. B. Ellison, and J. B. Foresman, *J. Phys. Chem.*, **97**, 13586 (1993).

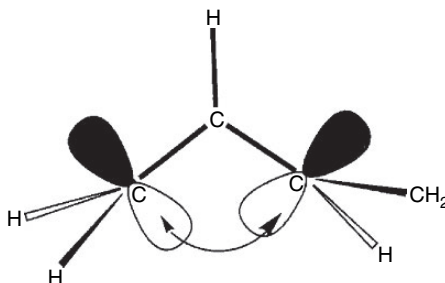
<sup>170</sup>. M. E. Squillacote and T. C. Semple, *J. Am. Chem. Soc.*, **109**, 892 (1987).

As computational methods for describing excited states have been refined, additional understanding of the structures has developed. Relatively early computational studies provided some indication of the geometries associated with the butadiene excited states.<sup>171</sup> The ground state has a maximum at a twist of  $90^\circ$  about the C(1)–C(2) bond. This structure, which can be approximately described as a singlet methylene-allyl diradical, is found at about 2.3 eV and is more stable than a structure with  $90^\circ$  twist at both terminal groups (3.1 eV). There is no major pyramidalization of the methylene groups in this second structure. The spectroscopic (Franck-Condon)  $T_1$  state is about 3.5 eV above  $S_0$ . A *local planar minimum* is found to have a shortened C(2)–C(3) bond and lengthened C(1)–C(2) and C(3)–C(4) bonds. The energy of this structure is about 2.7 eV. The C(2)–C(3) bond distance is 1.36 Å, so the bond has considerable double-bond character. This local minimum can be represented as a 1,4-but-2-enyl diradical. The *global minimum* on the  $T_1$  surface is a twisted triplet allyl-methylene diradical that is at about 2.3 eV. This structure is very similar in geometry to the singlet diradical on the ground state surface.

The *initial*  $S_1$  state has all bonds lengthened and both ends are able to rotate. The most stable geometry for this state is twisted and pyramidalized at both ends. The energy is about 5.5 eV, but is slightly higher (5.7 eV) when only one end is twisted  $90^\circ$ . All the C–C bonds are around 1.48 Å, and the structure can be described as a completely unpaired singlet tetradical. The  $S_2$  state also has a *local planar minimum* and has considerable  $3p$  (Rydberg) character in this geometry. The  $S_2$  *global minimum* energy structure has one end twisted  $90^\circ$ ; this end is strongly pyramidalized and the structure has considerable zwitterionic character. Approximate representations of these are given below, and this representation of the excited states in terms of energy is given in Figure 12.25.



As we shall see shortly, the singlet state often gives rise to products with 1,3-bridging, which suggests that there is a pronounced C(1)–C(3) interaction.<sup>172</sup>



<sup>171</sup> M. Aoyagi, Y. Osamura, and S. Iwata, *J. Chem. Phys.*, **83**, 1140 (1985); P. G. Szalay, A. Karpfen, and H. Lischka, *Chem. Phys.*, **130**, 219 (1989).

<sup>172</sup> M. Ito and I. Ohmine, *J. Phys. Chem.*, **106**, 3159 (1997).

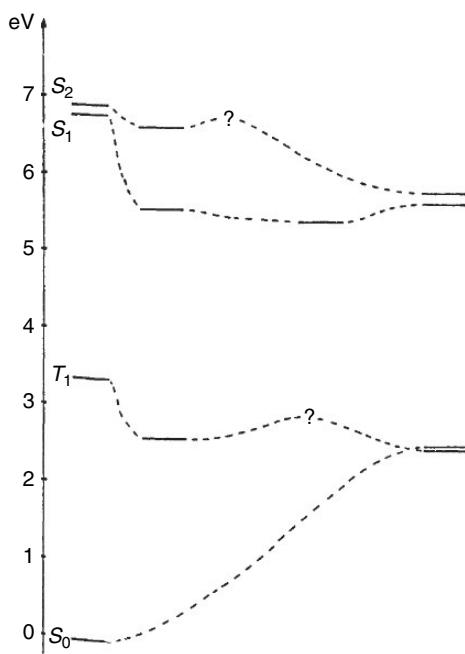


Fig. 12.25. Energy level diagram for the low-lying states of *trans*-1,3-butadiene. The left-hand levels correspond to the vertical excitation energies; the intermediate levels correspond to planar structures resulting from relaxation of bond lengths; and the right-hand levels are the 90° twist structures. Reproduced from *J. Phys. Chem.* **83**, 1140 (1985), by permission of the American Chemical Society.

More recent studies have refined these structural representations. The excited states can be attained by excitation of either the *s-trans* or *s-cis* conformers of 1,3-butadiene, and the excited state structure depends on the original conformation. The structures of the *initial* excited states have been calculated at the MC-SCF/4-31G level.<sup>173</sup> Two slightly different structures were found for each of the conformations. The lower-energy structures are shown in Figure 12.26. Both structures show stretching and twisting about the C=C, indicating loss of electron pairing. These excited state structures can continue to twist at the C(2)–C(3) bond to reach the global minima.<sup>174</sup>

The singlet photochemistry of 1,3-butadiene is believed to be dominated by the  $S_2$  state, which is rapidly reached from the  $S_1$  state by rotation.  $S_1$  and  $S_2$  are, respectively, singly and doubly excited  $\pi \rightarrow \pi^*$  states. The return to ground state is believed to involve an  $S_2$ - $S_0$  CI. The  $S_2$  energy surface of butadiene has been modeled by a computation that combines molecular mechanics and a valence bond structural

<sup>173</sup>. (a) M. Olivucci, I. N. Ragazos, F. Bernardi, and M. A. Robb, *J. Am. Chem. Soc.*, **115**, 3710 (1993); (b) M. Olivucci, F. Bernardi, S. Ottani, and M. A. Robb, *J. Am. Chem. Soc.*, **116**, 2034 (1994); (c) F. Bernardi, M. Olivucci, and M. A. Robb, *J. Photochem. Photobiol.*, **105**, 365 (1997); (d) M. Garavelli, F. Bernardi, P. Celani, M. A. Robb, and M. Olivucci, *J. Photochem. Photobiol.*, **114**, 109 (1998).

<sup>174</sup>. V. Bonacic-Koutecky, M. Persico, D. Dohnert, and A. Sevin, *J. Am. Chem. Soc.*, **104**, 6900 (1982); M. Aoyagi, Y. Osamura, and S. Iwata, *J. Chem. Phys.*, **83**, 1140 (1985).

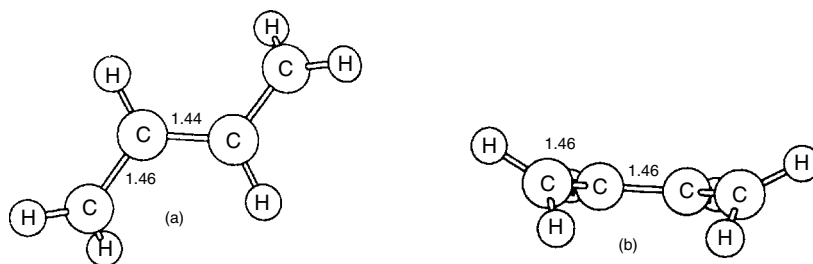


Fig. 12.26. Computed initial excited state structures of butadiene. (a) *s-trans*  $S_1$ ; (b) *s-cis*  $S_1$ . Reproduced from *J. Am. Chem. Soc.*, **115**, 3710 (1993), by permission of the American Chemical Society.

representation.<sup>173a</sup> The structural parameters that were followed were the rotations of the C(1)–C(2) ( $\alpha$ ), C(2)–C(3) ( $\beta$ ), and C(3)–C(4) ( $\alpha'$ ) bonds. The structures that were located were then refined using MC-SCF/4-31G calculations. The excited state near the CI involves rotation at all three bonds and can be represented as having all four  $\pi$  electrons unpaired.

Comparison of the disrotatory and conrotatory paths for electrocyclicization indicates that the disrotatory path can proceed without a barrier. Figure 12.27 is a cross section of the  $S_2$  and  $S_0$  surfaces and depicts the formation of the observed products via transition from  $S_2$  to the ground state surface. Figure 12.28 is a “reaction cube” in which each of the edges represents rotation about one of the bonds. The shaded central area is near 90-90-90 and is the region in which the CIs are located. Figure 12.29 shows the structures of three CIs found in this area.

There are also higher-energy CIs, which resemble the H migration carbenoid structures found for ethene.<sup>175</sup> (See Figure 12.29) These structures have also been located

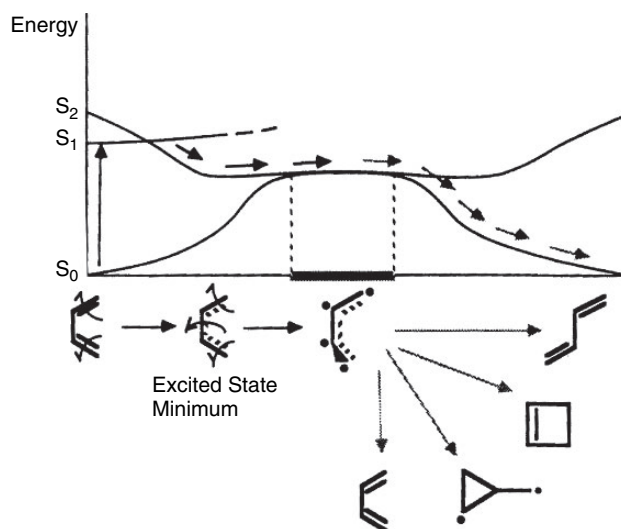


Fig. 12.27. Cross section of energy surface indicating re-pairing of  $S_2$  to reactant and other products. Reproduced from *J. Am. Chem. Soc.*, **115**, 3710 (1993), by permission of the American Chemical Society.

<sup>175</sup> S. Wilsey and K. N. Houk, *Photochem. Photobiol.*, **76**, 616 (2002).

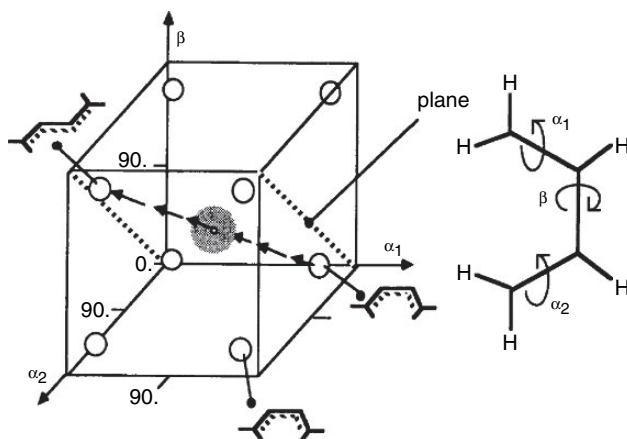


Fig. 12.28. Reaction cube locating the butadiene conical intersection in relation to rotation at each of the bonds. The shaded area in the center represents the location of the conical intersection with all bond rotations near  $90^\circ$ . The open circles represent initial excited states. The energy surface in Figure 12.27 represents the diagonal plane bisecting the cube. Reproduced from *J. Am. Chem. Soc.*, **115**, 3710 (1993), by permission of the American Chemical Society.

at the MC-SCF/4-31G level of computation.<sup>173a</sup> CASPT2 theory, which is appropriate for excited states with large ionic character,<sup>176</sup> gives a similar description of the CI.<sup>177</sup> Other descriptions of the butadiene excited surface have also been developed,<sup>178,179</sup> including explicit consideration of the formation of bicyclo[1.1.0]butane by 1,3-bonding.<sup>180</sup>

The energy profile in Figure 12.30 compares the disrotatory and conrotatory paths for cyclization. There is no barrier on the disrotatory path but the conrotatory path

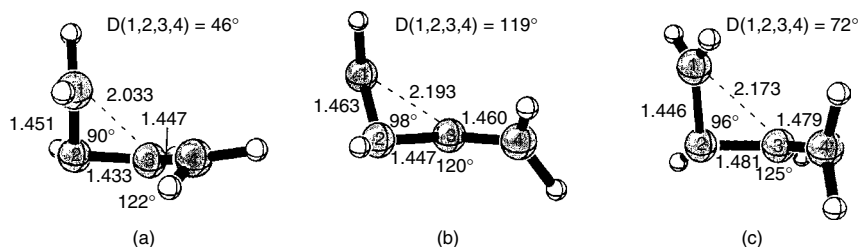


Fig. 12.29. Structure of the 1,3-butadiene conical intersections from CAS(6,6)/6-31G\* computations: (a) cisoid, (b) transoid, (c) central. Reproduced from *Photochem. Photobiol.*, **76**, 616 (2002), by permission of Elsevier.

<sup>176</sup>. C. S. Page and M. Olivucci, *J. Comput. Chem.*, **24**, 298 (2003).

<sup>177</sup>. B. Ostojic and W. Domcke, *Chem. Phys.*, **269**, 1 (2001); R. P. Krawczyk, K. Malsch, G. Hohlneicher, R. C. Gillen, and W. Domcke, *Chem. Phys. Lett.*, **320**, 535 (2000).

<sup>178</sup>. S. Saki, *Chem. Phys. Lett.*, **287**, 263 (1998); R. P. Krawczyk, K. Malsch, G. Hohlneicher, R. C. Gillen, and W. Domcke, *Chem. Phys. Lett.*, **320**, 535 (2000).

<sup>179</sup>. M. Olivucci, I. N. Ragazos, F. Bernardi, and M. A. Robb, *J. Am. Chem. Soc.*, **115**, 3710 (1993); M. Olivucci, F. Bernardi, S. Ottani, and M. A. Robb, *J. Am. Chem. Soc.*, **116**, 2034 (1994).

<sup>180</sup>. S. Sakai, *Chem. Phys. Lett.*, **319**, 687 (2000).

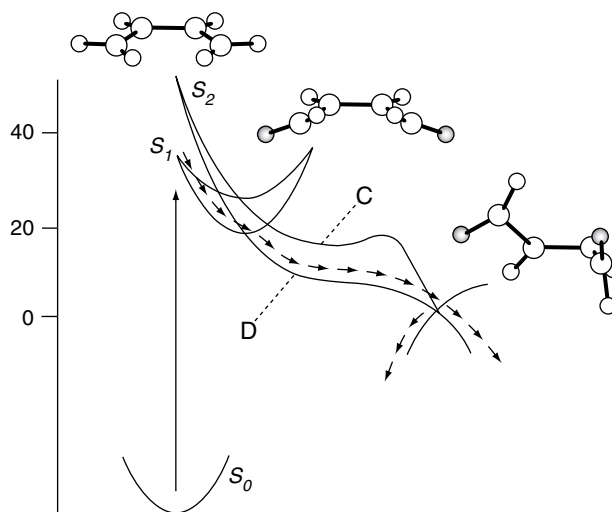
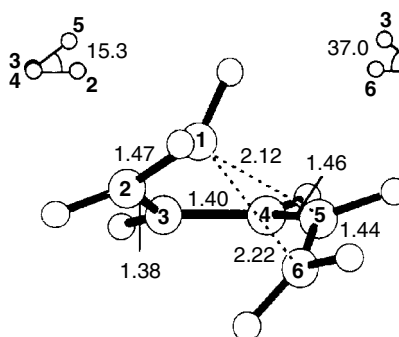


Fig. 12.30. Comparison of disrotatory (D) and conrotatory (C) minimum energy paths for photocyclization of 1,3-butadiene. The disfavored conrotatory motion encounters a barrier. Reproduced from *J. Photochem. Photobiol.*, **105**, 365 (1997), by permission of Elsevier.

encounters a small barrier. The reverse reaction, opening of cyclobutene to butadiene, has also been explored computationally, using CAS-SCF/double  $\zeta$  calculations. The disrotatory pathway is found to be favored, although the interpretation is somewhat more complex than the simplest Woodward-Hoffmann formulation. Computational quantum dynamics calculations have been used to model the very early stages of the photoreaction of cyclobutene (<50 fs).<sup>181</sup> The C=C bond stretches and the CH<sub>2</sub>–CH<sub>2</sub> bond weakens as the CH<sub>2</sub> groups move toward  $sp^2$  hybridization. The motion is in agreement with the predicted (Woodward-Hoffmann) disrotatory motion.<sup>182</sup> It can be shown that a CI exists for the disrotatory but not the conrotatory mode.<sup>183</sup>

The 1,3,5-hexatriene-1,3-cyclohexadiene system has also been studied by computation. A CI connecting the excited state to the ground state has been located. The CI can be described as a tetraradical.<sup>182</sup> The structure is shown below.

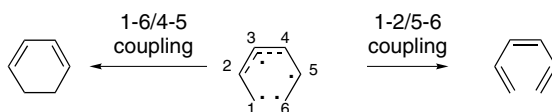


<sup>181</sup> M. Ben-Nun and T. J. Martinez, *J. Am. Chem. Soc.*, **122**, 6299 (2000).

<sup>182</sup> M. Garavelli, F. Bernardi, M. Olivucci, T. Vreven, S. Klein, P. Celani, and M. A. Robb, *Faraday Discussions*, **110**, 51 (1998); P. Celani, S. Offani, M. Olivucci, F. Bernardi, and M. A. Robb, *J. Am. Chem. Soc.*, **116**, 10141 (1994).

<sup>183</sup> Y. Haas and S. Zilberg, *J. Photochem. Photobiol.*, **144**, 221 (2001).

In this structure C(1) is actually a bit closer to C(5) than to C(6). The C(2,3,4) fragment resembles an allyl radical. There are recoupling patterns that can lead either to cyclohexadiene or to *Z*-1,3,5-hexatriene.



The minimum energy reaction path after transit through the CI has also been investigated.<sup>184</sup> Two major reaction channels were identified that lead to the two products. These channels are sufficiently comparable in terms of their topological features that product formation can occur along both routes in approximately equal amounts. It would be expected that substituents that favored one or the other pathway would alter the relative yields of the two types of products. There is also a minor channel that can lead to formation of the bicyclo[3.1.0]hex-2-ene ring system. This situation is represented schematically in Figure 12.31.

Another kind of tetradicaloid CI has been invoked and computationally characterized for photoisomerization of cyclooctatetraene.<sup>185</sup> Photoexcitation leads to return to reactant, double-bond shift, and formation of semibullvalene. The tetradicaloid

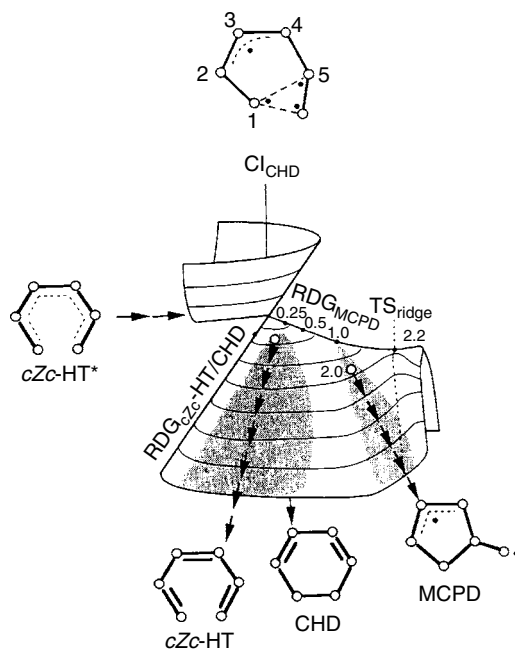
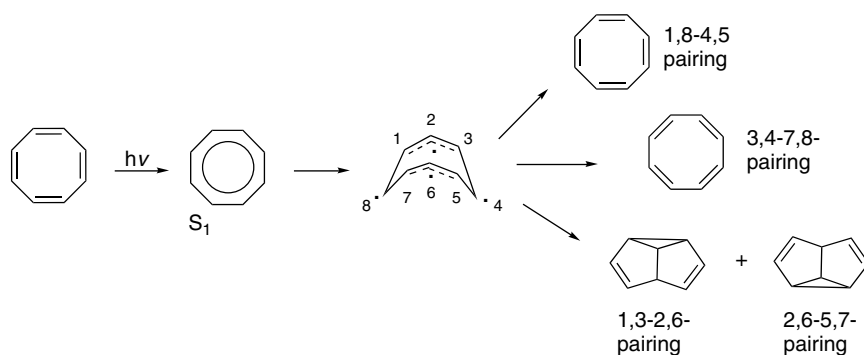


Fig. 12.31. Schematic representation of conical intersection showing partitioning between 1,3,5-hexatriene, 1,3-cyclohexadiene, and bicyclo[3.1.0]hex-2-ene products. Reproduced from *J. Phys. Chem. A*, **101**, 2023 (1997), by permission of the American Chemical Society.

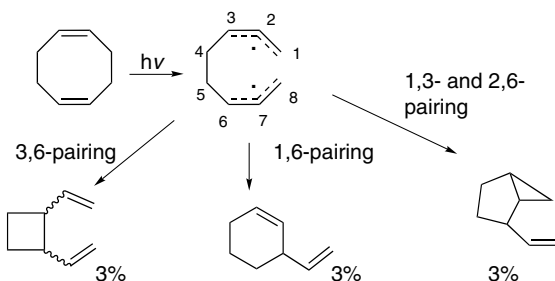
<sup>184</sup>. M. Garavelli, P. Celani, M. Fato, M. J. Bearpark, B. R. Smith, M. Olivucci, and M. A. Robb, *J. Phys. Chem. A*, **101**, 2023 (1997).

<sup>185</sup>. M. Garavelli, F. Bernardi, V. Molino, and M. Olivucci, *Angew. Chem. Int. Ed. Engl.*, **40**, 1466 (2001).

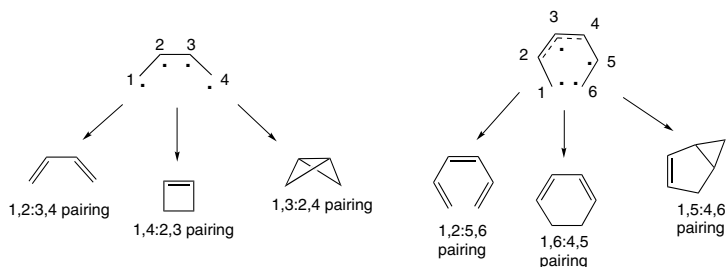
CI consist of two allyl fragments and two localized unpaired electrons. Alternate re-pairing schemes lead to the observed products.



Photolysis of both acyclic and cyclic 1,5-dienes leads to both 1,3-sigmatropic shifts and formation of allylcyclopropanes by 1,2-shift followed by cyclization.<sup>186</sup> The product mixture from 1,5-cyclooctadiene illustrates these reaction patterns.



The pattern that emerges from the experimental and computational studies of the conjugated dienes and trienes is the involvement of CIs having certain features in common. The singlet CI for the dienes appears to be a tetradicaloid with the potential for several re-bonding schemes. In the absence of steric problems, it is structurally compact. The hexatriene-cyclohexadiene system also appears to involve a tetradicaloid structure, one component of which is an allylic system. These structures can account for the major product types in both systems.



These results, as well as those from cyclooctatetraene and 1,5-cyclooctadiene, indicate that structures with isolated and allylic unpaired electrons play a key role in diene

<sup>186</sup> T. D. R. Manning and P. J. Kropp, *J. Am. Chem. Soc.*, **103**, 889 (1981).

and polyene photochemistry. For triplet excited states of dienes, the minimum energy corresponds to a twisted diradical that consists of an allylic radical and a localized radical. The pattern continues for higher polyenes with the excited states consisting of components similar to those recognized for simple alkenes and dienes.

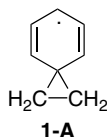
## General References

- D. R. Arnold, N. C. Baird, J. R. Bolton, J. C. D. Brand, P. W. M. Jacobs, P. de Mayo, and W. R. Ware, *Photochemistry; An Introduction*, Academic Press, New York, 1974.
- D. O. Cowan and R. L. Drisko, *Elements of Organic Photochemistry*, Plenum Press, New York, 1976.
- J. M. Coxon and B. Halton, *Organic Photochemistry*, Cambridge University Press, Cambridge, 1974.
- A. Gilbert and J. Baggott, *Essentials of Molecular Photochemistry*, CRC Press, Boca Raton, FL, 1991.
- W. Horspool and D. Armester, *Organic Photochemistry: A Comprehensive Treatment*, Ellis Horwood/Prentice-Hall, Chichester, 1992.
- W. H. Horspool and P.-S. Song, eds., *Organic Photochemistry and Photobiology*, CRC Press, Boca Raton, FL, 1995.
- W. Horspool and F. Lenci, eds., *CRC Handbook of Organic Photochemistry and Photobiology*, 2nd Edition, CRC Press, Boca Raton, FL, 2004.
- J. Kagan, *Organic Photochemistry: Principles and Applications*, Academic Press, San Diego, 1993.
- M. Klessinger and J. Michl, *Excited States and Photochemistry of Organic Molecules*, VCH, New York, 1995.
- J. Kopecky, *Organic Photochemistry*, VCH, New York, 1992.
- P. de Mayo, ed., *Rearrangements in Ground and Excited States*, Vol. 3, Academic Press, New York, 1980.
- J. Michl and V. Bonacic-Kouteky, *Electronic Aspects of Organic Photochemistry*, John Wiley, New York, 1990.
- N. J. Turro, *Modern Molecular Photochemistry*, Benjamin-Cummings, Menlo Park, CA, 1978.
- A. West, *Flash and Laser Photolysis in Investigation of Rates and Mechanisms of Reactions*, C. F. Bernasconi, ed., *Techniques of Chemistry*, Vol. VI, Part 2, Wiley-Interscience, New York, 1986.
- H. E. Zimmerman, "Topic in Photochemistry," *Top. Curr.Chem.*, **100**, 45 (1982).

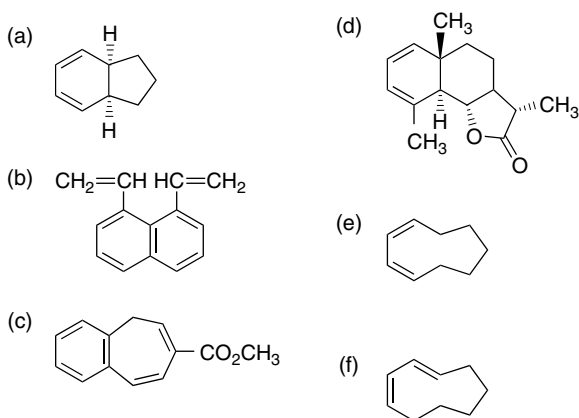
## Problems

(References for these problems will be found on page 1168.)

- 12.1. The bridged radical **1-A** has been suggested as a possible intermediate in the photochemical decarbonylation of 3-phenylpropanal. Suggest an experiment to test this hypothesis.

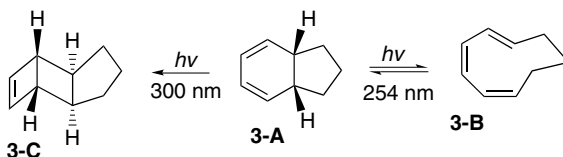


- 12.2. Predict the structure, including all aspects of the stereochemistry, based on orbital symmetry principles for the following photochemical electrocyclic and cycloaddition reactions.

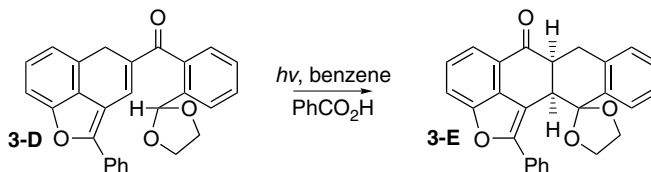


12.3. Suggest reasonable mechanisms for the following observations:

- The optically active allene, 2,3-pentadiene, is racemized under toluene-sensitized photolysis.
- Direct photolysis of diene **3-A** at 254 nm produces a photostationary state containing about 30% **3-A** and 70% **3-B**. When photolysis is carried out at 300 nm, photocyclization to **3-C** occurs and little **3-B** is present in the mixture.

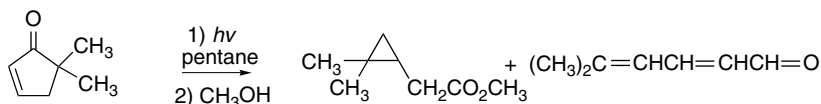


- Photocyclization of the acetal **3-D** to **3-E** is catalyzed by benzoic acid.

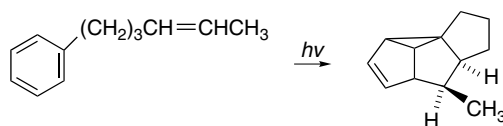


12.4. Provide a mechanistic rationalization for each of the following reactions:

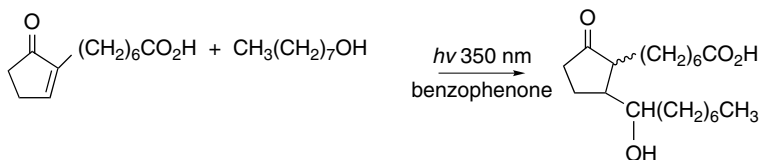
a.



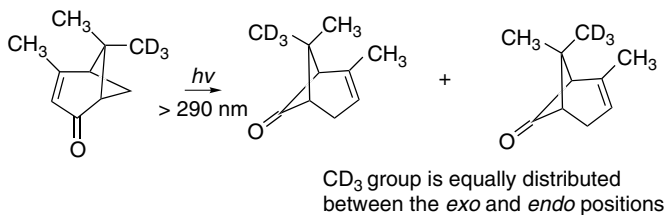
b.



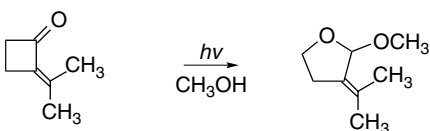
c.



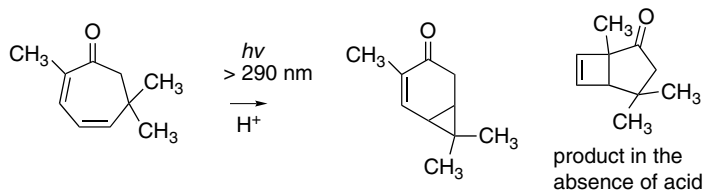
d.



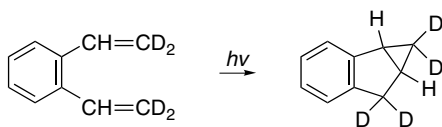
e.



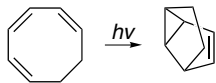
f.



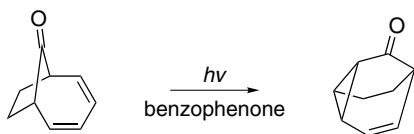
g.



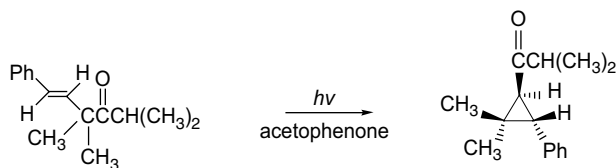
h.



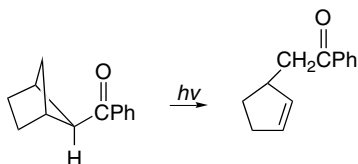
i.



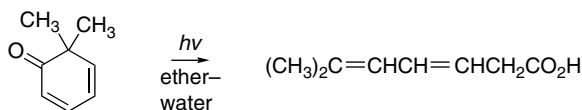
j.



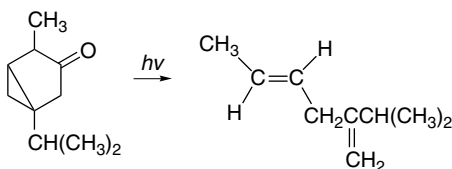
k.



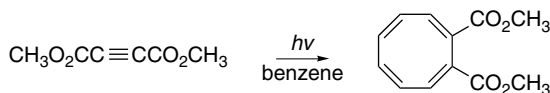
l.



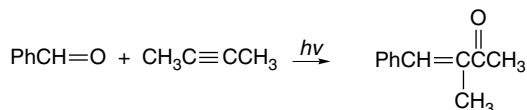
m.



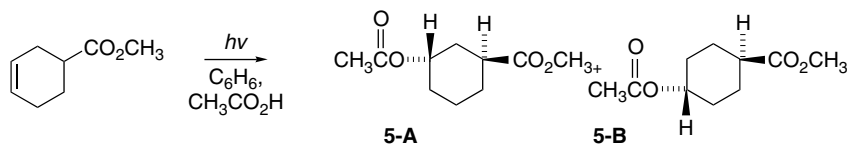
n.



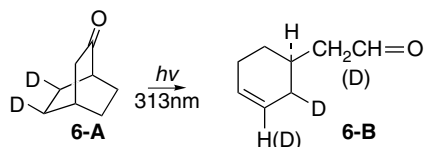
o.



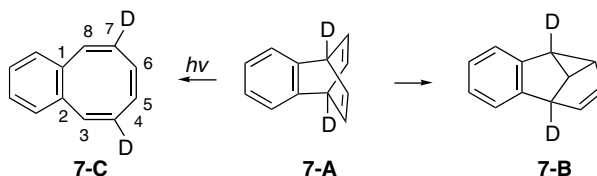
- 12.5. Benzene-sensitized photolysis of methyl 3-cyclohexene-1-carboxylate in acetic acid leads to addition of acetic to the double bond. Only the *trans* adducts are formed. What factor(s) might be responsible for this stereoselectivity? Which of the two regioisomers do you expect to be the major product?



- 12.6. Photolysis of bicyclo[2.2.2]octan-2-one (**6-A**) gives **6-B** in good yield. When **6-A** is labeled as shown, the aldehyde group carries 48.3% of the deuterium. Write a mechanism to account for the overall transformation. Calculate the isotope effect for the hydrogen abstraction step. What mechanistic conclusion do you draw from the magnitude of the isotope effect?

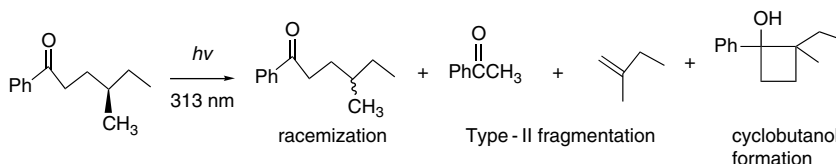


- 12.7. The photolysis of benzobarrelene **7-A** has been studied in considerable detail. Direct photolysis gives **7-C** (benzocyclooctatetraene), but when acetone is used as a photosensitizer, the di- $\pi$ -methane rearrangement product **7-B** (benzosemibullvalene) is formed. A deuterium-labeling study gave the results shown. What mechanistic conclusions do you draw from these results? Is there a feasible mechanism that would have resulted in a different isotopic label distribution in **7-B**?



(A small amount of D is at C-3,8.)

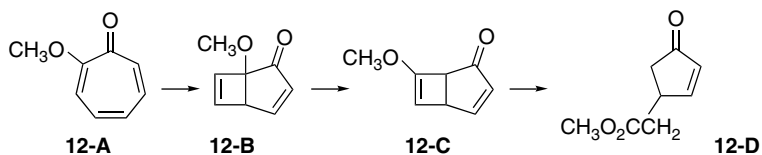
- 12.8. Quantum yield data for three competing processes that occur on photolysis of *S*-methyl-1-phenyl-1-hexanone at 313 nm in benzene have been determined and are tabulated below. When the reaction is run in *t*-butanol, the racemization is entirely suppressed and the Type-II fragmentation is the major reaction. What information do these data provide about the mechanism operating under these conditions?



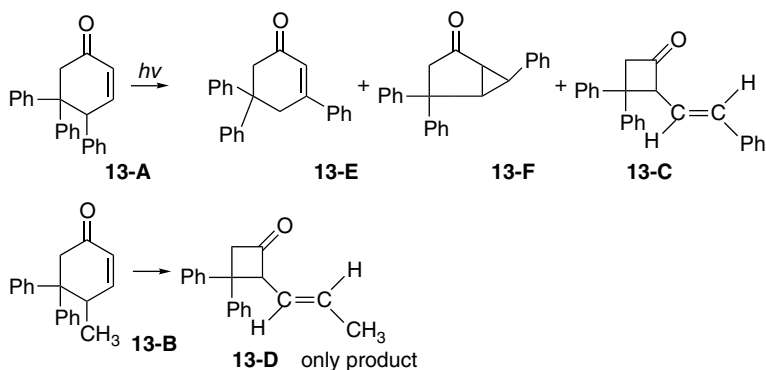
Process	Quantum yield	
	Benzene	<i>t</i> -Butanol
Type-II fragmentation	0.23	0.94
Cyclobutanol formation	0.03	0.05
Racemization	0.78	0.0

- 12.9. Show by means of an energy diagram the reason that the energy of light emitted from an excited electronic state by fluorescence or phosphorescence

- is of lower energy than the exciting radiation. Would you expect the shift in energy to be more pronounced for fluorescence or phosphorescence? Explain?
- 12.10. *cis*-2-Propyl-4-*t*-butylcyclohexanone undergoes cleavage to 4-*t*-butylcyclohexanone on photolysis. The *trans* isomer does not undergo fragmentation directly, but is converted to the *cis* isomer, which then fragments. The *trans*  $\rightarrow$  *cis* isomerization is quenched by 1,3-pentadiene, but the photofragmentation is not. Offer an explanation of this pronounced stereochemical effect.
- 12.11. The quantum yield for formation of 3-methylcyclobutene from *E*-1,3-pentadiene by 254 nm radiation is ten times greater than for cyclization of the *Z*-isomer. 1,3-Dimethylcyclopropene is also formed but the difference in  $\Phi$  for these reactions is only a factor of two. Offer an explanation for these differences in terms of energy surfaces that are involved.
- 12.12. The irradiation of 2-methoxytropone (**12-A**) leads to methyl 4-oxo-2-cyclopentenylacetate (**12-D**). The course of the reaction can be followed by gas chromatography and two intermediates are observed, which have structures **12-B** and **12-C**. Indicate a mechanism for the three successive reactions. The first two are photochemical, whereas the third is probably an acid-catalyzed reaction that does not require light.

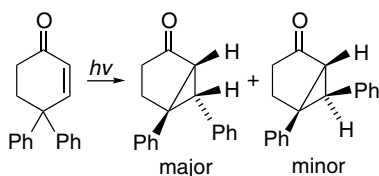


- 12.13. When an aryl substituent is placed at C(5) of a 4-substituted cyclohexenone, a new product type involving formation of a cyclobutanone ring is formed.

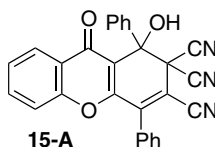


The reaction products are the same for both direct irradiation and acetophenone sensitization. When reactant **13-B** is used in enantiomerically pure form, the product **13-D** is nearly racemic (6% e.e.). Relate the formation of the cyclobutanone to the more normal products of 4-substituted cyclohexenones.

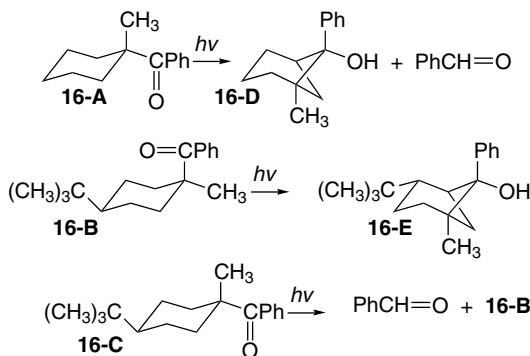
- 12.14. In the rearrangement of 4,4-diphenylcyclohex-2-en-1-one to 5,6-diphenylbicyclo[3.1.0]hexan-2-one, there is a strong preference for formation of the *endo* phenyl stereoisomer. Offer an explanation for this stereoselectivity.



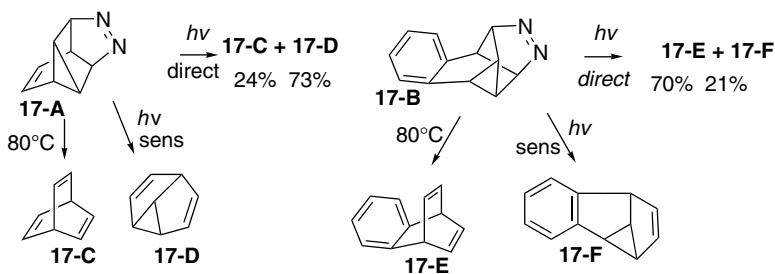
- 12.15. Compound **15-A** is photochromic; that is, it becomes colored on exposure to light. The process is reversible, giving back the starting material in the dark. Suggest a structure for the colored photoisomer.



- 12.16. The photolysis of **16-A**, **16-B**, and **16-C** has been studied. **16-A** gives both **16-D** and the cleavage product benzaldehyde. **16-B** gives only **16-E**. **16-C** gives **16-B** and benzaldehyde. Discuss how the presence of the *t*-butyl group and its stereochemistry can influence the reaction outcome.

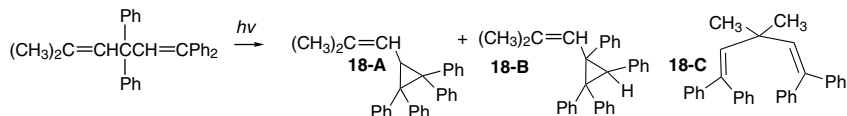


- 12.17. The azo compounds **17-A** and **17-B** were prepared and the thermal and photochemical behavior of these materials was investigated. The results are summarized in the Formulas below. It is also known that triplet photosensitization converts **17-C** to **17-D** and **17-E** to **17-F**, respectively. Discuss how these results relate to the mechanism of the di- $\pi$ -methane rearrangement.

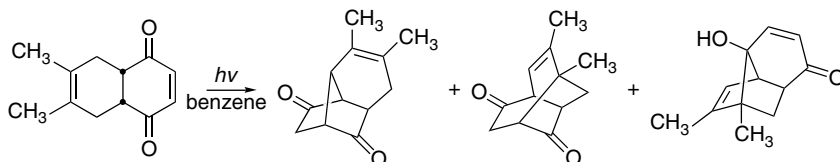


- 12.18. Direct irradiation of 1,1,3,3-tetraphenyl-5-methyl-1,4-hexadiene gives the products **18-A** and **18-B** shown below. When the reaction is carried out by

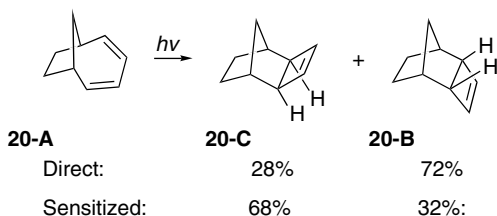
photosensitization, only **18-A** is formed. Suggest mechanisms for formation of **18-A** and **18-B**. A minor product **18-C** is formed only in the photosensitized reaction. What other products might have been expected? Can you explain the preference for the observed products?



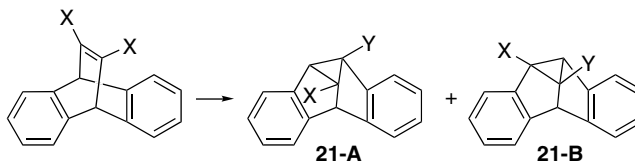
12.19. Suggest a mechanistic pathway for formation of each of the products formed on irradiation of the Diels-Alder adduct of 2,3-dimethylbutadiene and quinone.



12.20. The direct irradiation of **20-A** gives predominantly **20-B**, but the photosensitized reaction gives more **20-C**. Explain these observations.

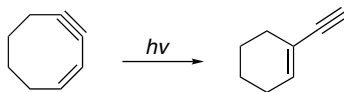


12.21. 9,10-Ethanoanthracenes undergo the di- $\pi$ -methane rearrangement. Analyze the substituent effects that are observed in this reaction.

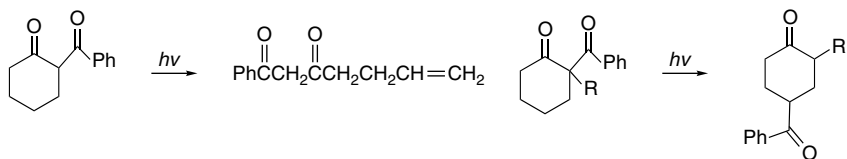


Substituent X	Substituent Y	% <b>21-A</b>	% <b>21-B</b>
H	CO <sub>2</sub> CH <sub>3</sub>	0	100
H	CON(CH <sub>3</sub> ) <sub>2</sub>	0	100
CON(CH <sub>3</sub> ) <sub>2</sub>	CO <sub>2</sub> CH <sub>3</sub>	3	97
CO <sub>2</sub> CH <sub>3</sub>	CSOCH <sub>3</sub>	0	100
CH <sub>3</sub>	CO <sub>2</sub> CH <sub>3</sub>	0	100
Ph	CO <sub>2</sub> CH <sub>3</sub>	100	0

12.22. Formulate a mechanism for the following reaction.



12.23. The photochemistry of 2-benzoylcyclohexanone and its 2-alkyl derivatives diverges. The unsubstituted compound undergoes ring cleavage, whereas the substituted compounds result in migration of the benzoyl substituent to the 4-position of the ring. Suggest mechanisms for both reactions and account for the effect of the alkyl substituent.



# References for Problems

## Chapter 1

- 1a. H. Prinzbach, *Pure Appl. Chem.*, **28**, 281 (1971).
- b. E. S. Gould, *Mechanism and Structure in Organic Chemistry*, Holt-Dryden, New York, 1959, pp. 69–70.
- c. K. E. Laidig, P. Speers, and A. Streitwieser, *Can. J. Chem.*, **74**, 1215 (1996).
- 2a. R. L. Reeves and W. F. Smith, *J. Am. Chem. Soc.*, **85**, 724 (1963).
- b. R. B. Martin, *J. Chem. Soc., Chem. Commun.*, 793 (1972).
- c, d. J. A. Joule and G. F. Smith, *Heterocyclic Chemistry*, Van Nostrand Reinhold, London, 1972; c: pp 194–195; d: p. 64.
- 3a. H. L. Ammon and G. L. Wheeler, *J. Am. Chem. Soc.*, **97**, 2326 (1975).
- b. R. Breslow, T. Eicher, A. Krebs, R. A. Peterson, and J. Posner, *J. Am. Chem. Soc.*, **87**, 1320 (1965).
- c. R. B. Woodward, *J. Am. Chem. Soc.*, **63**, 1123 (1941).
- 4a. E. D. Glendening and J. A. Hrabal, II, *J. Am. Chem. Soc.*, **119**, 12940 (1997).
- b. B. B. Ross and N. S. True, *J. Am. Chem. Soc.*, **106**, 2451 (1984).
- c. H. Slebocka-Tilk and R. S. Brown, *J. Org. Chem.*, **52**, 805 (1987); V. Somayaji and R. S. Brown, *J. Org. Chem.*, **51**, 2676 (1986).
5. S. Cunha and A. Kascheres, *Theochem.*, **364**, 45 (1996).
6. B. Jursic, *Tetrahedron*, **53**, 13285 (1997).
7. K. B. Wiberg and F. H. Walker, *J. Am. Chem. Soc.*, **104**, 5239 (1982).
8. R. B. Turner, B. J. Mallon, M. Tichy, W. v. E. Doering, W. R. Roth, and G. Schroeder, *J. Am. Chem. Soc.*, **95**, 8605 (1973).
9. D. W. Rogers and F. J. McLafferty, *J. Org. Chem.*, **66**, 1157 (2001).
10. A. M. Toth, M. D. Liptak, D. L. Phillips, and G. C. Shields, *J. Chem. Phys.*, **114**, 4595 (2001).
11. J. B. Lambert, R. G. Keske, R. E. Carhart, and A. P. Jovanovich, *J. Am. Chem. Soc.*, **89**, 3761 (1967); P. J. Krueger and J. Jan, *Can. J. Chem.*, **48**, 3236 (1970).
- 12a. R. C. Bingham, *J. Am. Chem. Soc.*, **98**, 535 (1976).
- b. W. L. Jorgensen and L. Salem, *The Organic Chemist's Book of Orbitals*, Academic Press, New York, 1973, pp. 179–184.
- c. H. Stafast and H. Bock, *Tetrahedron*, **32**, 855 (1976).
- d. L. Libit and R. Hoffmann, *J. Am. Chem. Soc.*, **96**, 1370 (1974).
- e. I. Fleming, *Frontier Orbitals and Organic Chemical Reactions*, Wiley-Interscience, New York, 1976, pp. 51–57.
- f. W. J. Hehre, L. Radom, and J. A. Pople, *J. Am. Chem. Soc.*, **94**, 1496 (1972).
13. K. B. Wiberg and K. E. Laidig, *J. Org. Chem.*, **57**, 5092 (1992); M. A. McAllister and T. T. Tidwell, *J. Org. Chem.*, **59**, 4506 (1994).

14. K. N. Houk, N. G. Rondan, M. N. Paddon-Row, C. W. Jefford, P. T. Huy, P. D. Burrow, and K. N. Jordan, *J. Am. Chem. Soc.*, **105**, 5563 (1983).
15. C. A. Coulson and A. Streitwieser, Jr., *Dictionary of  $\pi$ -Electron Calculations*, W. H. Freeman, San Francisco, 1965, p. 184.
16. T. Ohwada and K. Shudo, *J. Am. Chem. Soc.*, **111**, 34 (1989).
17. C. A. Coulson and A. Streitwieser, *Dictionary of  $\pi$ -Electron Calculations*, W. H. Freeman, San Francisco, 1965.
18. R. D. Bertrand, D. M. Grant, E. L. Allred, J. C. Hinshaw, and A. B. Strong, *J. Am. Chem. Soc.*, **94**, 997 (1972); R. Boese, D. Blaeser, K. Gomann, and U. H. Brinker, *J. Am. Chem. Soc.*, **111**, 1501 (1989); L. B. Krivdin, *Magn. Res. Chem.*, **41**, 91 (2003).
- 19a. C. H. DePuy, V. M. Bierbaum, and R. Damrauer, *J. Am. Chem. Soc.*, **106**, 4051 (1984); C. H. DePuy, S. Gronert, S. E. Barlow, V. M. Bierbaum, and R. Damrauer, *J. Am. Chem. Soc.*, **111**, 1968 (1989).
- b. P. C. Redfern, J. S. Murray, and P. Politzer, *Can. J. Chem.*, **70**, 636 (1992).
- c. C. F. Rodriguez, S. Sirois, and A. C. Hopkinson, *J. Org. Chem.*, **57**, 4869 (1992).
- 20a. R. Breslow and J. M. Hoffmann, Jr., *J. Am. Chem. Soc.*, **94**, 2110 (1972).
- b. R. Breslow and P. Dowd, *J. Am. Chem. Soc.*, **85**, 2729 (1963); J. E. Bartmess, J. Kester, W. T. Borden, and H. G. Koser, *Tetrahedron Lett.*, **27**, 5931 (1986).
- c. R. Breslow and J. M. Hoffmann, *J. Am. Chem. Soc.*, **94**, 2110 (1972); M. Saunders, R. Berger, A. Jaffe, M. McBride, J. O'Neill, R. Breslow, J. M. Hoffmann, Jr., C. Perchonock, E. Wasserman, R. S. Hutton, and V. J. Kuck, *J. Am. Chem. Soc.*, **95**, 3017 (1973); R. Breslow and S. Mazur, *J. Am. Chem. Soc.*, **95**, 584 (1973).
21. W. Kirmse, K. Kund, E. Pitzer, A. Dorigo, and K. N. Houk, *J. Am. Chem. Soc.*, **108**, 6045 (1986).
22. M. A. McAllister and T. T. Tidwell, *J. Chem. Soc., Perkin Trans. 2*, 2239 (1994).
23. P. M. Deya, A. Frontera, G. A. Sunier, D. Quinonero, C. Garau, A. Costa, and P. Ballester, *Theor. Chem. Acc.*, **108**, 157 (2002).

## Chapter 2

- 2a. J. A. Pettus, Jr., and R. E. Moore, *J. Am. Chem. Soc.*, **93**, 3087 (1971).
- b. K. T. Black and H. Hope, *J. Am. Chem. Soc.*, **93**, 3053 (1971).
- c. J. Dillon and K. Nakanishi, *J. Am. Chem. Soc.*, **96**, 4055 (1974).
- d. M. Miyano and C. R. Dorn, *J. Am. Chem. Soc.*, **95**, 2664 (1973).
- e. M. Koreeda, G. Weiss, and K. Nakanishi, *J. Am. Chem. Soc.*, **95**, 239 (1973).
- f. P. A. Apgar and M. L. Ludwig, *J. Am. Chem. Soc.*, **94**, 964 (1972).
- g. M. R. Jones and D. J. Cram, *J. Am. Chem. Soc.*, **96**, 2183 (1974).
- 3a. J. W. deHaan and L. J. M. van den Ven, *Tetrahedron Lett.*, 2703 (1971).
- b. T. Sone, S. Terashima, and S. Yamada, *Synthesis*, 725 (1974).
- c. B. Witkop and C. M. Foltz, *J. Am. Chem. Soc.*, **79**, 197 (1957).
- d. S. Iwaki, S. Marumo, T. Saito, M. Yamada, and K. Katagiri, *J. Am. Chem. Soc.*, **96**, 7842 (1974).
- e. E. W. Yankee, B. Spencer, N. E. Howe, and D. J. Cram, *J. Am. Chem. Soc.*, **95**, 4220 (1973).
- f. R. S. Lenox and J. A. Katzenellenbogen, *J. Am. Chem. Soc.*, **95**, 957 (1973).
- g. R. Bausch, B. Bogdanovic, H. Dreeskamp, and J. B. Koster, *Liebigs Ann. Chem.*, 1625 (1974).
5. N. L. Allinger and M. T. Tribble, *Tetrahedron Lett.*, 3259 (1971); E. L. Eliel and M. Manoharan, *J. Org. Chem.*, **46**, 1959 (1981); D. J. Hodgson, U. Rychlewska, E. L. Eliel, M. Manoharan, D. E. Knox, and E. M. Olefirowicz, *J. Org. Chem.*, **50**, 4838 (1985).
6. K. B. Wiberg, *J. Am. Chem. Soc.*, **108**, 5817 (1986).
- 7a. H. C. Brown, J. H. Kawakami, and S. Ikegami, *J. Am. Chem. Soc.*, **92**, 6914 (1970).
- b. B. Waegell and C. W. Jefford, *Bull. Soc. Chim. Fr.*, 844 (1964).
- c. H. C. Brown and J. H. Kawakami, *J. Am. Chem. Soc.*, **92**, 1990 (1970).
- d. L. A. Spurlock and K. P. Clark, *J. Am. Chem. Soc.*, **94**, 5349 (1972).
- e. W. P. Griffith and J. M. Jolliffe, *J. Chem. Soc., Dalton Trans.*, 3483 (1992); although the *exo* stereochemistry is not expressly stated in this reference, it can be assumed from the well-documented stereochemistry of  $\text{KMnO}_4$  dihydroxylation, e.g., J. E. Taylor, *Synthesis*, 1142 (1985).
- f. H. C. Brown, J. H. Kawakami, and S. Ikegami, *J. Am. Chem. Soc.*, **92**, 6914 (1970).
- g. E. C. Asby and S. A. Noding, *J. Am. Chem. Soc.*, **98**, 2010 (1976).
- 8a, b. A. L. Verma, W. F. Murphy, and H. J. Bernstein, *J. Phys. Chem.*, **60**, 1540 (1974); R. L. Lipnick and E. W. Garbisch, Jr., *J. Am. Chem. Soc.*, **95**, 6375 (1973); L. Lunazzi, D. Macciantelli, F. Bernardi,

- and K. U. Ingold, *J. Am. Chem. Soc.*, **99**, 4573 (1977); E. Osawa, H. Shirahama, and T. Matsumoto, *J. Am. Chem. Soc.*, **101**, 4824 (1979); K. B. Wiberg and M. A. Murcko, *J. Am. Chem. Soc.*, **110**, 8029 (1988); D. S. Maxwell, J. Tirado-Rives, and W. L. Jorgensen, *J. Comput. Chem.*, **16**, 984 (1995).
- c. B. Rickborn and M. T. Wuesthoff, *J. Am. Chem. Soc.*, **92**, 6894 (1970).
9. D. K. Dalling and D. M. Grant, *J. Am. Chem. Soc.*, **94**, 5318 (1972).
10. A. Bienvenue, *J. Am. Chem. Soc.*, **95**, 7345 (1973).
11. D. J. Cram and F. A. Abd Elhafez, *J. Am. Chem. Soc.*, **74**, 5828 (1952).
12. M. J. Burk, J. G. Allen, and W. F. Kiesman, *J. Am. Chem. Soc.*, **120**, 657 (1998).
- 14a. Y.-F. Cheung and C. Walsh, *J. Am. Chem. Soc.*, **98**, 3397 (1976).
- b. D. M. Jerina, H. Selander, H. Yagi, M. C. Wells, J. F. Davey, V. Magadevan, and D. T. Gibson, *J. Am. Chem. Soc.*, **98**, 5988 (1976).
- c. R. K. Hill, S. Yan, and S. M. Arfin, *J. Am. Chem. Soc.*, **95**, 7857 (1973).
- d. F. C. Huang, L. F. H. Lee, R. S. D. Mittal, P. R. Ravikumar, J. A. Chan, C. J. Sih, E. Capsi, and C. R. Eck, *J. Am. Chem. Soc.*, **97**, 4144 (1975).
15. J. Dominguez, J. D. Dunitz, H. Gerlach, and V. Prelog, *Helv. Chim. Acta*, **45**, 129 (1962); H. Gerlach and V. Prelog, *Liebigs Ann. Chem.*, **669**, 121 (1963); B. T. Kilbourn, J. D. Dunitz, L. A. R. Pioda, and W. Simon, *J. Molec. Biol.*, **30**, 559 (1967).
- 16a. R. K. Hill and T.-H. Chan, *Tetrahedron*, **21**, 2015 (1965).
- b. M. Raban, S. K. Lauderback, and D. Kost, *J. Am. Chem. Soc.*, **97**, 5178 (1975).
17. E. Eliel and S. H. Schroeter, *J. Am. Chem. Soc.*, **87**, 5031 (1965).
18. S. E. Denmark, M. S. Dappen, N. L. Sear, and R. T. Jacobs, *J. Am. Chem. Soc.*, **112**, 3466 (1990).
19. E. Ghera, Y. Gaoni, and S. Shoua, *J. Am. Chem. Soc.*, **98**, 3627 (1976).
20. H. W. Gschwend, *J. Am. Chem. Soc.*, **94**, 8430 (1972).
21. J. K. Thottanil, C. Przybyla, M. Malley, and J. Z. Gougoutas, *Tetrahedron Lett.*, **27**, 1533 (1986).
22. T. Varnali, V. Aviyente, B. Terry, and M. F. Ruiz-Lopez, *Theochem*, **280**, 169 (1993).
- 23a. G. Bartoli, M. Bosco, E. Marcantoni, M. Massaccesi, S. Rinaldi, and L. Sambri, *Eur. J. Org. Chem.*, 4679 (2001).
- b. M. Shimagaki, A. Suzuki, T. Nakata, and T. Oishi, *Chem. Pharm. Bull.*, **36**, 3138 (1988).
- 24a. J. W. Hilborn, Z.-H. Lu, A. R. Jurgens, Q. K. Fang, P. Byers, S. A. Wald, and C. H. Senanayake, *Tetrahedron Lett.*, **42**, 8919 (2001).
- 25a. b. M. Kainosho, K. Akjisaka, W. H. Pirkle, and S. D. Beare, *J. Am. Chem. Soc.*, **94**, 5924 (1972).
- c. M. Rabin and K. Mislou, *Tetrahedron Lett.*, 3961 (1966).
- d. R. K. Hill, S. Yan, and S. M. Arfin, *J. Am. Chem. Soc.*, **95**, 7857 (1973).
- e. V. J. Morlino and R. B. Martin, *J. Am. Chem. Soc.*, **89**, 3107 (1967).
- f. J. A. Elvidge and R. G. Foster, *J. Chem. Soc.*, 981 (1964); L. S. Rattet and J. H. Goldstein, *Org. Magn. Reson.*, **1**, 229 (1969).
- 26a. G. Helmchen and G. Staiger, *Angew. Chem., Int. Ed. Engl.*, **16**, 116 (1977).
- b. M. Farina and C. Morandi, *Tetrahedron*, **30**, 1819 (1974).
- c. D. T. Longone and M. T. Reetz, *J. Chem. Soc., Chem. Commun.*, 46 (1967).
- d. I. T. Jacobson, *Acta Chem. Scand.*, **21**, 2235 (1967).
- e. R. J. Ternansky, D. W. Balogh, and L. A. Paquette, *J. Am. Chem. Soc.*, **104**, 4503 (1982).
- f. C. Ganter and K. Wicker, *Helv. Chim. Acta*, **53**, 1693 (1970).
- g. M. S. Newman and D. Lednicer, *J. Am. Chem. Soc.*, **78**, 4765 (1956).
- h. T. Otsubo, R. Gray, and V. Boekelheide, *J. Am. Chem. Soc.*, **100**, 2449 (1978).
- i. J. H. Brewster and R. S. Jones, Jr., *J. Org. Chem.*, **34**, 354 (1969).
- j. H. Gerlach, *Helv. Chim. Acta*, **51**, 1587 (1968).
- k. l. H. Gerlach, *Helv. Chim. Acta*, **68**, 1815 (1985).
- m. R. K. Hill, G. H. Morton, J. R. Peterson, J. A. Walsh, and L. A. Paquette, *J. Org. Chem.*, **50**, 5528 (1985).
27. H. C. Kolb, M. S. Van Nieuwenhze, and K. B. Sharpless, *Chem. Rev.*, **94**, 2483 (1994).
- 28a. J. V. B. Kanth and H. C. Brown, *Tetrahedron*, **58**, 1069 (2002); B. Jiang, Y. Feng, and J. Zheng, *Tetrahedron Lett.*, **41**, 10281 (2000).
- b. Y. Hanzawa, K. Kawagoe, and Y. Kobayashi, *Chem. Pharm. Bull.*, **35**, 2609 (1987).
- c. J. G. Hill and K. B. Sharpless, *Org. Synth.*, **63**, 66 (1985).
- 29a. E. J. Ebberts, B. J. M. Plam, G. J. A. Ariaans, B. Kaptein, Q. B. Broxterman, A. Bruggink, and B. Zwanenburg, *Tetrahedron Asymmetry*, **8**, 4047 (1997).
- b. B. S. Lakshmi, P. Kanguano, Y. Guo, Y. Z. Chen, and P. Gautam, *Biocatal. Biotrans.*, **17**, 475 (2000); M. Trani, A. Ducret, P. Pepin, and R. Lortie, *Biotech. Lett.*, **17**, 1095 (1995).

- c. R. Bushan and J. Martens, *Biomed. Chromatogr.*, **12**, 309 (1998).
- d. T. Uemura, X. Zhang, K. Matsumura, N. Sayo, H. Kumobayashi, T. Ohta, K. Nozaki, and H. Takaya, *J. Org. Chem.*, **61**, 5510 (1996).
- e. H. Ishibashi, M. Maeki, J. Yagi, M. Ohba, and T. Kanai, *Tetrahedron*, **55**, 6075 (1999).
- f. M. Cleij, A. Archelas, and R. Furstoss, *J. Org. Chem.*, **64**, 5029 (1999).
30. A. Pross, L. Radom, and N. V. Riggs, *J. Am. Chem. Soc.*, **102**, 2252 (1980); L. Goodman, T. Kundu, and J. Leszczynski, *J. Am. Chem. Soc.*, **117**, 2082 (1995).
31. J.-F. Cavalier, F. Fotiadu, R. Verger, and G. Buono, *Synlett*, 73 (1998).
32. H. C. Brown, W. J. Hammar, J. H. Kawakami, I. Rothberg, and D. L. Vander Jagt, *J. Am. Chem. Soc.*, **89**, 6381 (1967).
33. L. Brener and H. C. Brown, *J. Org. Chem.*, **42**, 2702 (1977).
34. J. R. Del Valle and M. Goodman, *J. Org. Chem.*, **68**, 3923 (2003).

### Chapter 3

2. N. L. Allinger and N. A. Pamphilis, *J. Org. Chem.*, **38**, 316 (1973).
3. W. Kusters and P. de Mayo, *J. Am. Chem. Soc.*, **96**, 3502 (1974).
- 4a. A. Streitwieser, H. A. Hammond, R. H. Jagow, R. M. Williams, R. G. Jesaitis, C. J. Chang, and R. Wolf, *J. Am. Chem. Soc.*, **92**, 5141 (1970).
- b. M. T. H. Liu, and D. H. T. Chien, *J. Chem. Soc., Perkin Trans. 2*, 937 (1974).
5. W. E. Billups, K. H. Leavell, E. S. Lewis, and S. Vanderpool, *J. Am. Chem. Soc.*, **95**, 8096 (1973); J. C. Gilbert and D. P. Higley, *Tetrahedron Lett.*, 2075 (1973); E. R. Davidson, J. J. Gajewski, C. A. Shook, and T. Cohen, *J. Am. Chem. Soc.*, **112**, 8495 (1995).
6. G. Mehta and N. Mohal, *J. Chem. Soc., Perkin Trans. 1*, 505 (1998).
- 7a. O. R. Zaborsky and E. T. Kaiser, *J. Am. Chem. Soc.*, **92**, 860 (1970).
- b. W. M. Schubert and J. R. Keefe, *J. Am. Chem. Soc.*, **94**, 559 (1972).
- c. D. H. Rosenblatt, L. A. Hull, D. C. DeLuca, G. T. Davis, R. C. Weglein, and H. K. R. Williams, *J. Am. Chem. Soc.*, **89**, 1158 (1967).
- 8a. W. K. Kwok, W. G. Lee, and S. I. Miller, *J. Am. Chem. Soc.*, **91**, 468 (1969).
- b. H. C. Brown and E. N. Peters, *J. Am. Chem. Soc.*, **95**, 2400 (1973).
- c. W. M. Schubert and D. F. Gurka, *J. Am. Chem. Soc.*, **91**, 1443 (1969).
- d. J. Rocek and A. Riehl, *J. Am. Chem. Soc.*, **88**, 4749 (1966).
9. B. S. Jursic, *Theochem*, **468**, 171 (1999).
10. D. W. Rogers, F. J. McLafferty, and A. V. Podosenin, *J. Phys. Chem.*, **102**, 1209 (1998).
11. C. G. Swain, A. L. Powell, W. A. Sheppard, and C. R. Morgan, *J. Am. Chem. Soc.*, **101**, 3576 (1979).
12. R. S. Shue, *J. Am. Chem. Soc.*, **93**, 7116 (1971).
13. T. B. McMahon and P. Kebarle, *J. Am. Chem. Soc.*, **99**, 2222 (1977).
14. J. Bromilow, R. T. C. Brownlee, V. O. Lopez, and R. W. Taft, *J. Org. Chem.*, **44**, 4766 (1979).
15. A. Fischer, W. J. Galloway, and J. Vaughn, *J. Chem. Soc.*, 3591 (1964); C. Liotta, E. M. Perdue, and H. P. Hopkins, *J. Am. Chem. Soc.*, **96**, 7308 (1974).
- 16a. D. W. Rogers, F. J. McLafferty, W. Fang, Q. Yang, and Y. Zhao, *Struct. Chem.*, **3**, 53 (1992).
- b. D. W. Rogers and F. J. McLafferty, *J. Phys. Chem. A*, **103**, 8733 (1999).
17. T. T. Wang and T.-C. Huang, *Chem. Eng. J.*, **53**, 1076 (1993).
18. I. A. Koppel, J. Koppel, V. Pihl, I. Leito, M. Mishima, V. M. Vlasov, L. M. Yagupolskii, and R. W. Taft, *J. Chem. Soc., Perkin Trans. 2*, 1125 (2000).
19. X. Creary, *J. Org. Chem.*, **45**, 280 (1980); X. Creary, M. E. Mehrsheikh-Mohammadi, and S. McDonald, *J. Org. Chem.*, **52**, 3254 (1987).
20. J. P. Richard, G. Williams, and J. Gao, *J. Am. Chem. Soc.*, **121**, 715 (1999); G. N. Merrill, G. D. Dahlke, and S. R. Kass, *J. Am. Chem. Soc.*, **118**, 4462 (1996).
21. M. Roth, W. Damm, and B. Giese, *Tetrahedron Lett.*, **37**, 351 (1996).
22. A. Ponti and A. Gamba, *Gazz. Chim. Ital.*, **127**, 151 (1997).
23. R. Fuchs and L. L. Cole, *J. Am. Chem. Soc.*, **95**, 3194 (1973).
- 24a. O. Castano, R. Notario, J.-L. M. Abboud, R. Palmeiro, and J. L. Andres, *J. Phys. Chem. A*, **102**, 4949 (1998).
- b. J. E. Walker, P. A. Adamson, and S. R. Davis, *Theochem*, **487**, 145 (1999).

- 1a. H. C. Brown and E. N. Peters, *J. Am. Chem. Soc.*, **99**, 1712 (1977).
- b. X. Creary, M. E. Mehrsheikh-Mohammadi, and M. D. Eggers, *J. Am. Chem. Soc.*, **109**, 2435 (1987).
- c. J. L. Fry, E. M. Engler, and P. v. R. Schleyer, *J. Am. Chem. Soc.*, **94**, 4628 (1972).
- d. F. G. Bordwell and W. T. Brannen, *J. Am. Chem. Soc.*, **86**, 4645 (1964).
- 2b. P. v. R. Schleyer, W. E. Watts, and C. Cupas, *J. Am. Chem. Soc.*, **86**, 2722 (1964).
- c. P. E. Peterson and J. E. Duddey, *J. Am. Chem. Soc.*, **85**, 2865 (1963).
- d. M. Cherest, H. Felkin, J. Sicher, F. Sipos, and M. Tichy, *J. Chem. Soc.*, 2513 (1965).
- e. J. C. Martin and P. D. Bartlett, *J. Am. Chem. Soc.*, **79**, 2533 (1957).
- f. S. Archer, T. R. Lewis, M. R. Bell, and J. W. Schulenberg, *J. Am. Chem. Soc.*, **83**, 2386 (1961).
- g. D. A. Tomalia and J. N. Paige, *J. Org. Chem.*, **38**, 422 (1973).
- 3a. R. K. Crossland, W. E. Wells, and V. J. Shiner, Jr., *J. Am. Chem. Soc.*, **93**, 4217 (1971).
- b. R. L. Buckson and S. G. Smith, *J. Org. Chem.*, **32**, 634 (1967).
- c. C. J. Norton, Ph.D. Thesis, Harvard University, 1955; cited by P. v. R. Schleyer, W. E. Watts, R. C. Fort, Jr., M. B. Comisarow, and G. A. Olah, *J. Am. Chem. Soc.*, **86**, 5679 (1964); P. Mueller and J. Mareda, *Helv. Chim. Acta*, **70**, 1017 (1987).
- d. E. N. Peters and H. C. Brown, *J. Am. Chem. Soc.*, **97**, 2892 (1975).
- e. B. R. Ree and J. C. Martin, *J. Am. Chem. Soc.*, **92**, 1660 (1970).
- f. F. G. Bordwell and W. T. Brannen, Jr., *J. Am. Chem. Soc.*, **86**, 4645 (1964).
- g. D. D. Roberts, *J. Org. Chem.*, **34**, 285 (1969).
- h. R. G. Lawton, *J. Am. Chem. Soc.*, **83**, 2399 (1961).
- i. F. G. Bordwell and W. T. Brannen, Jr., *J. Am. Chem. Soc.*, **86**, 4645 (1964).
- j. S. Kim, S. S. Friedrich, L. J. Andrews, and R. M. Keefer, *J. Am. Chem. Soc.*, **92**, 5452 (1970).
4. H. L. Goering and B. E. Jones, *J. Am. Chem. Soc.*, **102**, 1628 (1980).
5. K. Banert and W. Kirmse, *J. Am. Chem. Soc.*, **104**, 3766 (1982); C. A. Grob, R. Hanreich, and A. Waldner, *Tetrahedron Lett.*, **22**, 3231 (1981).
6. Y. Pocker and M. J. Hill, *J. Am. Chem. Soc.*, **93**, 691 (1971).
7. R. Baird and S. Winstein, *J. Am. Chem. Soc.*, **85**, 567 (1963).
8. S. Winstein and E. T. Stafford, *J. Am. Chem. Soc.*, **79**, 505 (1957).
- 9a. M. Brookhart, A. Diaz, and S. Winstein, *J. Am. Chem. Soc.*, **88**, 3135 (1966); M. Bremer, K. Schoetz, P. v. R. Schleyer, U. Fleischer, M. Schindler, W. Kutzelnigg, W. Koch, and P. Palay, *Angew. Chem. Int. Ed. Engl.*, **28**, 1042 (1989).
- b. G. A. Olah, J. M. Bollinger, C. A. Cupas, and J. Lukas, *J. Am. Chem. Soc.*, **89**, 2692 (1967).
- c. G. A. Olah and R. D. Porter, *J. Am. Chem. Soc.*, **92**, 7627 (1970).
- d. G. A. Olah and G. Liang, *J. Am. Chem. Soc.*, **97**, 2236 (1975).
- e.f. G. A. Olah and G. Liang, *J. Am. Chem. Soc.*, **93**, 6873 (1971).
10. C. Paradisi and J. F. Bunnett, *J. Am. Chem. Soc.*, **103**, 946 (1981).
11. S. Kobayashi, T. Matsumoto, H. Taniguchi, M. Mishima, M. Fujio, and Y. Tsuno, *Tetrahedron Lett.*, **34**, 5903 (1993).
12. J. P. Richard and W. P. Jencks, *J. Am. Chem. Soc.*, **106**, 1373, 1383 (1984).
- 13a. J. Wilt and P. J. Chenier, *J. Am. Chem. Soc.*, **90**, 7366(1968); S. J. Cristol and G. W. Nachtigall, *J. Am. Chem. Soc.*, **90**, 7132, 7133 (1968).
- b. H. C. Brown and E. N. Peters, *J. Am. Chem. Soc.*, **97**, 1927 (1975).
- c. P. G. Gassman and W. C. Pike, *J. Am. Chem. Soc.*, **90**, 1250 (1975).
- d. J. M. Harris, J. R. Moffatt, M. G. Case, F. W. Clarke, J. S. Polley, T. K. Morgan, Jr., T. M. Ford, and R. K. Murray, Jr., *J. Org. Chem.*, **47**, 2740 (1982).
- e. M. Xie and W. J. le Noble, *J. Org. Chem.*, **54**, 3839 (1989).
14. A. Cunje, C. F. Rodriguez, M. H. Lien, and A. C. Hopkinson, *J. Org. Chem.*, **61**, 5212 (1996).
15. J. S. Haywood-Farmer and R. E. Pincock, *J. Am. Chem. Soc.*, **91**, 3020 (1969).
16. G. A. Olah, A. L. Berrier, M. Arvanaghi, and G. K. S. Prakash, *J. Am. Chem. Soc.*, **103**, 1122 (1981).
17. J. J. Tufariello and R. J. Lorence, *J. Am. Chem. Soc.*, **91**, 1546 (1969); J. Lhomme, A. Diaz, and S. Winstein, *J. Am. Chem. Soc.*, **91**, 1548 (1969).
18. C. Lim, S.-H. Kim, S.-D. Yoh, M. Fujio, and Y. Tsuno, *Tetrahedron Lett.*, **38**, 3243 (1997).
19. K. Nataka, M. Fujio, Y. Saeki, M. Mishima, Y. Tsuno, and K. Nishimoto, *J. Phys. Org. Chem.*, **9**, 561 (1996).

20. J. P. Richard, T. L. Amyes, and T. Vontor, *J. Am. Chem. Soc.*, **113**, 5871 (1991).
21. R. Fuchs and L. L. Cole, *J. Am. Chem. Soc.*, **95**, 3194 (1973).
22. Y. Tsuno and M. Fujio, *Chem. Soc. Rev.*, **25**, 129 (1996).
- 22a. M. Fujio, M. Goto, S. Suzuki, M. Mishima, and Y. Tsuno, *J. Phys. Org. Chem.*, **3**, 449 (1990); M. Mishima, H. Inoue, S. Itai, M. Fujio, and Y. Tsuno, *Bull. Chem. Soc. Jpn.*, **69**, 3273 (1996).
- 22b. M. Okamura, K. Hazama, M. Ohra, K. Kato, T. Horaguci, and A. Ohno, *Chem. Lett.*, 973 (1997); M. Fujio, K. Funatsu, M. Goto, Y. Seki, M. Mishima, and Y. Tsuno, *Bull. Chem. Soc. Jpn.*, **60**, 1091 (1987).
23. P. G. Gassman and K. Saito, *Tetrahedron Lett.*, **22**, 1311 (1981).
24. T. Nakashima, R. Fujiyama, M. J. Fujio, and Y. Tsuno, *Bull. Chem. Soc. Jpn.*, **72**, 741, 1043 (1999); T. Nakashima, R. Fujiyama, H.-J. Kim, M. Fujio, and Y. Tsuno, *Bull. Chem. Soc. Jpn.*, **73**, 429 (2000).
25. P. M. F. M. Bastiaansen, J. B. P. A. Wijnberg, and A. deGroot, *J. Org. Chem.*, **60**, 4240 (1995).
26. K. van Alem, G. Lodder, and H. Zuilhof, *J. Phys. Chem. A*, **106**, 10681 (2002).
27. S. Nagumo, T. Furukawa, M. Ono, and H. Akita, *Tetrahedron Lett.*, **38**, 2849 (1997); S. Nagumo, T. Hisano, Y. Kakimoto, N. Kawahara, M. Ono, T. Furukawa, S. Takeda, and H. Akita, *Tetrahedron Lett.*, **39**, 8109 (1998).

## Chapter 5

- 1a. K. Yates, G. H. Schmid, T. W. Regulski, D. G. Garratt, H.-W. Leung, and R. McDonald, *J. Am. Chem. Soc.*, **95**, 160 (1973).
- b. J. F. King and M. J. Coppen, *Can. J. Chem.*, **49**, 3714 (1971).
- c. N. C. Deno, F. A. Kish, and H. J. Peterson, *J. Am. Chem. Soc.*, **87**, 2157 (1965).
- d. M. A. Cooper, C. M. Holden, P. Loftus, and D. Whittaker, *J. Chem. Soc., Perkin Trans. 2*, 665 (1973).
- e. R. A. Bartsch and J. F. Bunnett, *J. Am. Chem. Soc.*, **91**, 1376 (1969).
- f. K. Yates and T. A. Go, *J. Org. Chem.*, **45**, 2377 (1980).
- g. C. B. Quinn and J. R. Wiseman, *J. Am. Chem. Soc.*, **95**, 1342 (1973).
- 2a. H. Wong, J. Chapuis, and I. Monkovic, *J. Org. Chem.*, **39**, 1042 (1974).
- b. P. K. Freeman, F. A. Raymond, and M. F. Grostic, *J. Org. Chem.*, **32**, 24 (1967).
- c. T. I. Crowell, R. T. Kemp, R. E. Lutz, and A. A. Wall, *J. Am. Chem. Soc.*, **90**, 4638 (1968).
- d. L. C. King, L. A. Subluskey, and E. W. Stern, *J. Org. Chem.*, **21**, 1232 (1956).
- e. M. L. Poutsma and P. A. Ibarbia, *J. Am. Chem. Soc.*, **93**, 440 (1971).
- f. S. P. Acharya and H. C. Brown, *J. Chem. Soc., Chem. Commun.*, 305 (1968).
- g. K. Yates and T. A. Go, *J. Org. Chem.*, **45**, 2377 (1980).
3. D. Y. Curtin, R. D. Stolow, and W. Maya, *J. Am. Chem. Soc.*, **81**, 3330 (1959).
4. W. H. Saunders and A. F. Cockerill, *Mechanisms of Elimination Reactions*, John Wiley & Sons, New York, 1973, pp. 79–80.
5. R. A. Bartsch, *J. Am. Chem. Soc.*, **93**, 3683 (1971).
6. K. Oyama and T. T. Tidwell, *J. Am. Chem. Soc.*, **98**, 947 (1976).
- 7a. K. D. Berlin, R. O. Lyster, D. E. Gibbs, and J. P. Devlin, *J. Chem. Soc., Chem. Commun.*, 1246 (1970).
- b. R. J. Abraham and J. R. Monasterios, *J. Chem. Soc. Perkin Trans. 2*, 574 (1975).
- c. H. C. Brown and K.-T. Liu, *J. Am. Chem. Soc.*, **97**, 2469 (1975).
- d. D. J. Pasto and J. A. Gontarz, *J. Am. Chem. Soc.*, **93**, 6902 (1971).
- 8a. J. F. Bunnett and S. Sridharan, *J. Org. Chem.*, **44**, 1458 (1979); L. F. Blackwell, A. Fischer, and J. Vaughan, *J. Chem. Soc. B*, 1084 (1967).
- b. J. E. Nordlander, P. O. Owuor, and J. E. Haky, *J. Am. Chem. Soc.*, **101**, 1288 (1979).
- c. G. E. Heasley, T. R. Bower, K. W. Dougharty, J. C. Easdon, V. L. Heasley, S. Arnold, T. L. Carter, D. B. Yeager, B. T. Gipe, and D. F. Shellhamer, *J. Org. Chem.*, **45**, 5150 (1980).
- d. P. Cramer and T. T. Tidwell, *J. Org. Chem.*, **46**, 2683 (1981).
- e. R. C. Fahey and C. A. McPherson, *J. Am. Chem. Soc.*, **91**, 3865 (1969); R. C. Fahey, M. W. Mohahan, and C. A. McPherson, *J. Am. Chem. Soc.*, **92**, 2810 (1970).
- f. C. H. DePuy and A. L. Schultz, *J. Org. Chem.*, **39**, 878 (1974).
- 9a. R. B. Miller and G. McGarvey, *J. Org. Chem.*, **44**, 4623 (1979).
- b. P. F. Hudrlik and D. Peterson, *J. Am. Chem. Soc.*, **97**, 1464 (1975).
- c. G. Bellucci, A. Marsili, E. Mastroilli, I. Morelli, and V. Scartoni, *J. Chem. Soc., Perkin Trans. 2*, 201 (1974).

- d. K. J. Shea, A. C. Greeley, S. Nguyen, P. D. Beauchamp, D. H. Aue, and J. S. Witzeman, *J. Am. Chem. Soc.*, **108**, 5901 (1986).
10. G. H. Schmid, A. Modro, and K. Yates, *J. Org. Chem.*, **45**, 665 (1980); A. D. Allen, Y. Chiang, A. J. Kresge, and T. T. Tidwell, *J. Org. Chem.*, **47**, 775 (1982).
11. G. Bellucci, R. Bianchi, and S. Vecchiani, *J. Org. Chem.*, **52**, 3355 (1987).
12. D. S. Noyce, D. R. Hartter, and F. B. Miles, *J. Am. Chem. Soc.*, **90**, 3794 (1968).
13. Y. Pocker, K. D. Stevens, and J. J. Champoux, *J. Am. Chem. Soc.*, **91**, 4199 (1969).
14. M. F. Ruisse, A. Argile, and J. E. Dubois, *J. Am. Chem. Soc.*, **100**, 7645 (1978).
15. W. K. Chwang, P. Knittel, K. M. Koshy, and T. T. Tidwell, *J. Am. Chem. Soc.*, **99**, 3395 (1977).
16. D. J. Pasto and J. F. Gadberry, *J. Am. Chem. Soc.*, **100**, 1469 (1978).
17. J. F. Bunnett and C. A. Migdal, *J. Org. Chem.*, **54**, 3037 (1989).
- 18a. S. Kobayashi, T. Matsumoto, H. Taniguchi, M. Mishima, M. Fujio, and Y. Tsuno, *Tetrahedron Lett.*, **34**, 5903 (1993); M. Mishima, H. Nakamura, K. Nakata, M. Fujio, and Y. Tsuno, *Chem. Lett.*, 1607 (1994).
- b. M. Mishima and H. Yamataka, *Bull. Chem. Soc. Jpn.*, **71**, 2427 (1998).
19. H. Sharghi, A. R. Massah, H. Eshghi, and K. Niknam, *J. Org. Chem.*, **63**, 1455 (1998).
20. D. J. Pasto and J. A. Gontarz, *J. Am. Chem. Soc.*, **93**, 6902 (1971); H. C. Brown, G. J. Lynch, W. J. Hammar, and L. C. Liu, *J. Org. Chem.*, **44**, 1910 (1979).
- 21a. C. H. Heathcock, R. A. Badger, and J. W. Patterson, Jr., *J. Am. Chem. Soc.*, **89**, 4133 (1967).
- b. J. -P. Dulcere and J. Rodriguez, *Synlett*, 347 (1992).
- c. J. Rodriguez and J. -P. Dulcere, *Synthesis*, 1177 (1993).

## Chapter 6

- 1b. F. G. Bordwell, *Acc. Chem. Res.*, **21**, 456 (1988).
- c. A. Streitwieser, L. Xie, P. Wang, and S. M. Bachrach, *J. Org. Chem.*, **58**, 1778 (1993).
- d. J. R. Jones and S. P. Patel, *J. Am. Chem. Soc.*, **96**, 574 (1974); J. R. Jones and S. P. Patel, *J. Chem. Soc., Perkin Trans. 2*, 1231 (1975).
- e. A. F. Cockerill and J. E. Lamper, *J. Chem. Soc. B*, 503 (1971).
- 2b. G. L. Closs and L. E. Closs, *J. Am. Chem. Soc.*, **85**, 2022 (1963).
- c. R. A. Lee, C. M. Andrews, K. M. Patel, and W. Reusch, *Tetrahedron Lett.*, 965 (1973).
- d. J. D. White and W. L. Sung, *J. Org. Chem.*, **39**, 2323 (1974); D. Nasipuri, M. Mitra, and S. Venkataraman, *J. Chem. Soc., Perkin Trans. 1*, 1836 (1972).
- f. R. Breslow, *J. Am. Chem. Soc.*, **79**, 1762 (1957).
- g. K. Ogura and G. Tsuchihashi, *Tetrahedron Lett.*, 3151 (1971).
- h. G. L. Closs and R. B. Larabee, *Tetrahedron Lett.*, 287 (1965); A. Fattah, R. E. McCarthy, M. R. Ahmad, and S. R. Kass, *J. Am. Chem. Soc.*, **125**, 11746 (2003).
- i. J. A. Zoltewicz, G. M. Kaufmann, and C. L. Smith, *J. Am. Chem. Soc.*, **90**, 5939 (1968).
- 3a. T.-Y. Luh and L. M. Stock, *J. Am. Chem. Soc.*, **96**, 3712 (1974); A. Streitwieser, L. Xie, D. Speere, and P. G. Williams, *Magn. Res. Chem.*, **36**, S509 (1996); M. Hare, T. Emrich, P. E. Eaton, and S. R. Kass, *J. Am. Chem. Soc.*, **119**, 237 (1997); R. R. Sauers, *Tetrahedron*, **55**, 10013 (1999).
- b. H. W. Amburn, K. C. Kaufman, and H. Shechter, *J. Am. Chem. Soc.*, **91**, 530 (1969); F. G. Bordwell, J. C. Branca, C. R. Johnson, and N. R. Vanier, *J. Org. Chem.*, **45**, 3884 (1980).
- c. F. G. Bordwell, G. E. Drucker, and H. E. Fried, *J. Org. Chem.*, **46**, 632 (1981); E. M. Arnett and K. G. Venkatasubramanian, *J. Org. Chem.*, **48**, 1569 (1983); K. Daasbjerg, *Acta Chem. Scand.*, **49**, 878 (1995).
- d. T. B. Thompson and W. T. Ford, *J. Am. Chem. Soc.*, **101**, 5459 (1979).
- 4a. G. A. Abad, S. P. Jindal, and T. T. Tidwell, *J. Am. Chem. Soc.*, **95**, 6326 (1973).
- b. A. Nickon and J. L. Lambert, *J. Am. Chem. Soc.*, **84**, 4604 (1962).
6. G. B. Trimitis and E. M. Van Dam, *J. Chem. Soc., Chem. Commun.*, 610 (1974).
7. A. Streitwieser, Jr., W. B. Hollyhead, A. H. Pudjaatmaka, P. H. Owens, T. L. Kruger, P. A. Rubenstein, R. A. MacQuarrie, M. L. Brokaw, W. K. C. Chu, and H. M. Niemeyer, *J. Am. Chem. Soc.*, **93**, 5088 (1971).
8. F. G. Bordwell and F. J. Cornforth, *J. Org. Chem.*, **43**, 1763 (1978).
- 9a. P. T. Lansbury, *J. Am. Chem. Soc.*, **83**, 429 (1961).
- b. D. W. Griffiths and C. D. Gutsche, *J. Am. Chem. Soc.*, **93**, 4788 (1971).
- c. T. D. Hoffman and D. J. Cram, *J. Am. Chem. Soc.*, **91**, 1000 (1969).

- d. G. Buchi, D. M. Foulkes, M. Kurono, G. F. Mitchell, and R. S. Schneider, *J. Am. Chem. Soc.*, **89**, 6745 (1967).
- e. G. Stork, G. L. Nelson, F. Rouessac, and O. Grignone, *J. Am. Chem. Soc.*, **93**, 3091 (1971).
10. S. Danishefsky and R. K. Singh, *J. Am. Chem. Soc.*, **97**, 3239 (1975); E. M. Arnett, S. G. Maroldo, S. L. Schilling, and J. A. Harrelson, *J. Am. Chem. Soc.*, **106**, 6759 (1984); E. M. Arnett and J. A. Harrelson, Jr., *J. Am. Chem. Soc.*, **109**, 809 (1987).
11. A. Streitwieser, Jr., R. G. Lawler, and C. Perrin, *J. Am. Chem. Soc.*, **87**, 5383 (1965); J. E. Hofmann, A. Schriesheim, and R. E. Nichols, *Tetrahedron Lett.*, 1745 (1965).
- 13a. J. W. Bunting and J. P. Kanter, *J. Am. Chem. Soc.*, **115**, 11705 (1993).
- b. M. P. Harcourt and R. A. More O'Ferrall, *Bull. Soc. Chim. Fr.*, 407 (1988).
- c. J. K. Mukhopadaya, S. Sklenak, and Z. Rappoport, *J. Org. Chem.*, **65**, 6856 (2000).
- 14a. J. R. Keefe, A. J. Kresge, and Y. Yin, *J. Am. Chem. Soc.*, **110**, 1982 (1988); S. Eldin, R. M. Pollack, and D. L. Whalen, *J. Am. Chem. Soc.*, **113**, 1344 (1991); E. Eldin, D. L. Whalen, and R. M. Pollack, *J. Org. Chem.*, **58**, 3490 (1993).
- b. F. G. Bordwell and H. E. Fried, *J. Org. Chem.*, **56**, 4218 (1991).
- c. E. M. Arnett, S. G. Maroldo, S. L. Schilling, and J. A. Harrelson, **106**, 6759 (1984).
15. T. J. Sprules and J.-F. Lavalley, *J. Org. Chem.* **60**, 5041 (1995).
16. B. G. Cox, *J. Am. Chem. Soc.* **96**, 6823 (1974).
17. E. L. Eliel, A. A. Hartmann, and A. G. Abatjoglou, *J. Am. Chem. Soc.*, **96**, 1807 (1974); J.-M. Lehn and G. Wipff, *J. Am. Chem. Soc.*, **98**, 7498 (1976).
- 18a. N. S. Mills, J. Shapiro, and M. Hollingsworth, *J. Am. Chem. Soc.*, **103**, 1263 (1981).
- b. N. S. Mills, *J. Am. Chem. Soc.*, **104**, 5689 (1982).
19. R. B. Woodward and G. Small, Jr., *J. Am. Chem. Soc.*, **72**, 1297 (1950).
- 20a. E. J. Corey, T. H. Hopie, and W. A. Wozniak, *J. Am. Chem. Soc.*, **77**, 5415 (1955).
- b. E. W. Garbisch, Jr., *J. Org. Chem.*, **30**, 2109 (1965).
- c. F. Cajouille and D. Q. Quan, *C. R. Acad. Sci. C*, **265**, 269 (1967).
- d. C. W. P. Crowne, R. M. Evans, G. F. H. Green, and A. G. Long, *J. Chem. Soc.*, 4351 (1956).
- e. N. C. Deno and R. Fishbein, *J. Am. Chem. Soc.*, **95**, 7445 (1973).
- 21a. P. L. Stotter and K. A. Hill, *J. Am. Chem. Soc.*, **96**, 6524 (1974).
- b. B. J. L. Huff, F. N. Tuller, and D. Caine, *J. Org. Chem.*, **34**, 3070 (1969).
- c. H. O. House and T. M. Bare, *J. Org. Chem.*, **33**, 943 (1968).
- d. C. H. Heathcock, R. A. Badger, and J. W. Patterson, Jr., *J. Am. Chem. Soc.*, **89**, 4133 (1967).
- e. J. E. McMurry, *J. Am. Chem. Soc.*, **90**, 6821 (1968).
22. M. S. Newman, V. De Vries, and R. Darlak, *J. Org. Chem.*, **31**, 2171 (1966).
23. H. M. Walborsky and L. M. Turner, *J. Am. Chem. Soc.*, **94**, 2273 (1972); J. F. Arnett and H. M. Walborsky, *J. Org. Chem.*, **37**, 3678 (1972).
24. Y. Jator, M. Gaudry, and A. Marquet, *Tetrahedron Lett.*, 53 (1976).
- 25a. J. Uenishi, Y. Tatsumi, N. Kobayashi, and O. Yonemitsu, *Tetrahedron Lett.*, **36**, 5909 (1995).
- b. A. G. Myers, B. H. Yang, H. Chen, L. McKinstry, D. J. Kopecky, and J. L. Gleason, *J. Am. Chem. Soc.*, **119**, 6496 (1997); J. L. Vicario, D. Badia, E. Dominguez, and L. Carrillo, *J. Org. Chem.*, **64**, 4610 (1999).
- c. D. Kim, W. J. Choi, J. Y. Hong, I. Y. Park, and Y. B. Kim, *Tetrahedron Lett.*, **37**, 1433 (1996).
26. M. Sefkow, A. Koch, and E. Kleinpeter, *Helv. Chim. Acta*, **85**, 4216 (2002).

## Chapter 7

1. R. P. Bell, *Adv. Phys. Org. Chem.*, **4**, 1 (1966).
- 2a. A. Lapworth and R. H. F. Manske, *J. Chem. Soc.*, 1976 (1930).
- b. K. Bowden and A. M. Last, *J. Chem. Soc., Chem. Commun.* 1315 (1970).
- c. P. R. Young and W. P. Jencks, *J. Am. Chem. Soc.*, **99**, 1206 (1977).
- d. H. Dahn and M.-N. Ung-Truong, *Helv. Chim. Acta*, **70**, 2130 (1987).
- 3a,b. M. M. Kreevoy and R. W. Taft, Jr., *J. Am. Chem. Soc.*, **77**, 5590 (1955).
- c,d. M. M. Kreevoy, C. R. Morgan, and R. W. Taft, Jr., *J. Am. Chem. Soc.*, **82**, 3064 (1960).
- e. T. H. Fife and L. H. Brod, *J. Org. Chem.*, **33**, 4136 (1968).
4. R. G. Bergstrom, M. J. Cashen, Y. Chiang, and A. J. Kresge, *J. Org. Chem.*, **44**, 1639 (1979).
- 5a. S. M. Felton and T. C. Bruice, *J. Am. Chem. Soc.*, **91**, 6721 (1969); T. Maugh, II, and T. C. Bruice, *J. Am. Chem. Soc.*, **93**, 3237 (1971).

- b. L. E. Ebersson and L.-A. Svensson, *J. Am. Chem. Soc.*, **93**, 3827 (1971).
- c. G. A. Rogers and T. C. Bruice, *J. Am. Chem. Soc.*, **96**, 2463 (1974).
- d. T. C. Bruice and S. J. Benkovic, *J. Am. Chem. Soc.*, **85**, 1 (1963).
6. E. Anderson and T. H. Fife, *J. Am. Chem. Soc.*, **95**, 6437 (1973).
7. M. W. Williams and G. T. Young, *J. Chem. Soc.*, 3701 (1964).
- 8a. V. Somayaji and R. S. Brown, *J. Org. Chem.*, **51**, 2676 (1986).
- b. A. J. Briggs, C. M. Evans, R. Glenn, and A. J. Kirby, *J. Chem. Soc., Perkin Trans. 2*, 1637 (1983); C. B. Quin and J. R. Wiseman, *J. Am. Chem. Soc.*, **95**, 1342 (1973).
- 9a. N. S. Nudelman, Z. Gatto, and L. Bohe, *J. Org. Chem.*, **49**, 1540 (1984).
- b. P. Baierwick, D. Hoell, and K. Mueller, *Angew. Chem. Int. Ed. Engl.*, **24**, 972 (1985).
- c. C. Alvarez-Ibarra, P. Perez-Ossorio, A. Perez-Rubalcaba, M. L. Quiroga, and M. J. Santemases, *J. Chem. Soc., Perkin Trans. 2*, 1645 (1983).
10. H. R. Mahler and E. H. Cordes, *Biological Chemistry*, Harper and Row, New York, 1966, p. 201.
11. J. Hajdu and G. M. Smith, *J. Am. Chem. Soc.*, **103**, 6192 (1981).
12. T. Okuyama, H. Shibuya, and T. Fueno, *J. Am. Chem. Soc.*, **104**, 730 (1982).
13. R. P. Bell, M. H. Rand, and K. M. A. Wynne-Jones, *Trans. Faraday Soc.*, **52**, 1093 (1956).
14. S. T. Purrington and J. H. Pittman, *Tetrahedron Lett.*, **28**, 3901 (1987).
15. J. T. Edwards and S. C. Wong, *J. Am. Chem. Soc.*, **101**, 1807 (1979).
16. H. Slebocka-Tilk, A. J. Bennet, J. W. Keillor, R. S. Brown, J. P. Guthrie, and A. Jodhan, *J. Am. Chem. Soc.*, **112**, 8507 (1990); H. Slebocka-Tilk, A. J. Bennet, H. J. Hogg, and R. S. Brown, *J. Am. Chem. Soc.*, **113**, 1288 (1991).
17. B. Capon and K. Nimmo, *J. Chem. Soc., Perkin Trans. 2*, 1113 (1975).
18. A. R. Fersht and A. J. Kirby, *J. Am. Chem. Soc.*, **90**, 5833 (1968).
19. D. P. Weeks and D. B. Whitney, *J. Am. Chem. Soc.*, **103**, 3555 (1981).
20. R. L. Schowen, C. R. Hopper, and C. M. Bazikian, *J. Am. Chem. Soc.*, **94**, 3095 (1972).
21. C. M. Evans, R. Glenn, and A. J. Kirby, *J. Am. Chem. Soc.*, **104**, 4706 (1982).
- 22a. T. Higuchi, H. Takeshi, I. H. Pitman, and H.-L. Fung, *J. Am. Chem. Soc.*, **93**, 539 (1971); T. C. Bruice and I. Oka, *J. Am. Chem. Soc.*, **96**, 4500 (1974).
- b. R. Hershfield and G. L. Schmir, *J. Am. Chem. Soc.*, **95**, 7359 (1973).
- c. T. H. Fife and J. E. C. Hutchins, *J. Am. Chem. Soc.*, **94**, 2837 (1972).
- d. C. J. Brown and A. J. Kirby, *J. Chem. Soc. Perkin Trans. 2*, 1081 (1997).
23. T. H. Fife, R. Bembi, and R. Natarajan, *J. Am. Chem. Soc.*, **118**, 12956 (1996).
24. T. S. Davis, P. D. Feil, D. G. Kubler, and D. J. Wells Jr., *J. Org. Chem.*, **40**, 1478 (1975).
25. A. J. Kirby and P. W. Lancaster, *J. Chem. Soc., Perkin Trans. 2*, 1206 (1972).
26. E. H. Cordes and W. P. Jencks, *J. Am. Chem. Soc.*, **85**, 2843 (1963).
- 27a. M. Hausermann, *Helv. Chim. Acta*, **34**, 1482 (1951).
- b. A. C. Anderson and J. A. Nelson, *J. Am. Chem. Soc.*, **73**, 232 (1951).
- c. W. A. Kleschick, C. T. Buse, and C. H. Heathcock, *J. Am. Chem. Soc.*, **99**, 247 (1977); C. H. Heathcock, C. T. Buse, W. A. Kleschick, M. C. Pirrung, J. E. Sohn, and J. Lampe, *J. Org. Chem.*, **45**, 1066 (1980).
- d. A. T. Nielsen and W. J. Houlihan, *Org. React.*, **16**, 1 (1968).
28. R. S. Brown and A. Aman, *J. Org. Chem.*, **62**, 4816 (1997).
29. T. C. Bruice and D. W. Tanner, *J. Org. Chem.*, **30**, 1668 (1965).
30. J. A. Walder, R. S. Johnson, and I. M. Klotz, *J. Am. Chem. Soc.*, **100**, 5156 (1978).
31. T. H. Fife, R. Singh, and R. Bembi, *J. Org. Chem.*, **67**, 3179 (2002).

## Chapter 8

1. P. Reeves, T. Devon, and R. Pettit, *J. Am. Chem. Soc.*, **91**, 5890 (1969).
- 2a. H. L. Ammon and G. L. Wheeler, *J. Am. Chem. Soc.*, **97**, 2326 (1975).
- b. W. v. E. Doering and C. H. DePuy, *J. Am. Chem. Soc.*, **75**, 5955 (1953).
- c. J. H. M. Hill, *J. Org. Chem.*, **32**, 3214 (1967).
- d. D. J. Bertelli, *J. Org. Chem.*, **30**, 891 (1965).
- 3a. W. v. E. Doering and F. L. Detert, *J. Am. Chem. Soc.*, **73**, 876 (1951).
- b. E. F. Jenny and J. D. Roberts, *J. Am. Chem. Soc.*, **78**, 2005 (1956).
- 4a. J. J. Eisch, J. E. Galle, and S. Kozima, *J. Am. Chem. Soc.*, **108**, 379 (1986).
- b. P. J. Garratt, N. E. Rowland, and F. Sondheimer, *Tetrahedron*, **27**, 3157 (1971).

- c. R. Concepcion, R. C. Reiter, and G. R. Stevenson, *J. Am. Chem. Soc.*, **105**, 1778 (1983).  
 d. G. Jonsall and P. Ahlberg, *J. Am. Chem. Soc.*, **108**, 3819 (1986).  
 e. J. M. Hebert, P. D. Woodgate, and W. A. Denny, *J. Med. Chem.*, **30**, 2081 (1987).  
 f. R. F. X. Klein and V. Horak, *J. Org. Chem.*, **51**, 4644 (1986).  
 g. D. A. Smith and J. Bitar, *J. Org. Chem.*, **58**, 6 (1993).  
 h. T. K. Zywiets, H. Jiao, P. v. R. Schleyer, and A. de Meijere, *J. Org. Chem.*, **63**, 3417 (1998).  
 i. M. J. S. Dewar and N. Trinajstic, *J. Chem. Soc. A*, 1754 (1969).  
 5. D. Cremer, T. Schmidt, and C. W. Bock, *J. Org. Chem.*, **50**, 2684 (1985).  
 6. B. A. Hess, Jr., and L. J. Schaad, *J. Am. Chem. Soc.*, **93**, 305 (1971).  
 7a. D. Bostwick, H. F. Henneike, and Jr. H. P. Hopkins, *J. Am. Chem. Soc.*, **97**, 1505 (1975).  
 b. A. Greenberg, R. P. T. Tomkins, M. Dobrovolny, and J. E. Liebman, *J. Am. Chem. Soc.*, **105**, 6855 (1983); F. Gavina, A. M. Costero, P. Gil, and S. V. Luis, *J. Am. Chem. Soc.*, **106**, 2077 (1984).  
 8. M. A. McAllister and T. T. Tidwell, *J. Am. Chem. Soc.*, **114**, 5362 (1992).  
 9. T. Otsuba, R. Gray, and V. Boekelheide, *J. Am. Chem. Soc.*, **100**, 2449 (1978).  
 10a. Z. Yoshida, M. Shibata, and T. Sugimoto, *Tetrahedron Lett.*, **24**, 4585 (1983); *J. Am. Chem. Soc.*, **106**, 6383 (1984).  
 b. K. Nakasuji, K. Yoshida, and I. Murata, *J. Am. Chem. Soc.*, **105**, 5136 (1983).  
 c. K. Takahashi, T. Nozoe, K. Takase, and T. Kudo, *Tetrahedron Lett.*, **25**, 77 (1984).  
 d. A. Minsky, A. Y. Meyers, K. Hafner, and M. Rabinovitz, *J. Am. Chem. Soc.*, **105**, 3975 (1983).  
 11. R. A. Wood, T. R. Welberry, and A. D. Rae, *J. Chem. Soc., Perkin Trans. 2*, 451 (1985); W. E. Rhine, J. H. Davis, and G. Stucky, *J. Organomet. Chem.*, **134**, 139 (1977); Y. Cohen, N. H. Roelofs, G. Reinhardt, L. T. Scott, and M. Rabinovitz, *J. Org. Chem.*, **52**, 4207 (1987); B. Eliasson and H. Edlund, *J. Chem. Soc., Perkin Trans. 2*, 1837 (1983); B. C. Becker, W. Huber, C. Schneiders, and K. Mueller, *Chem. Ber.*, **116**, 1573 (1983); A. Minsky, A. Y. Meyers, K. Hafner, and M. Rabinovitz, *J. Am. Chem. Soc.*, **105**, 3975 (1983); C. Glidewell and D. Lloyd, *J. Chem. Res.*, 283 (1989).  
 12. H. Prinzbach, V. Freudenberger, and U. Scheidegger, *Helv. Chim. Acta*, **50**, 1087 (1967); B. Eliasson, D. Johnels, I. Sethson, U. Edlund, and K. Mueller, *J. Chem. Soc. Perkin Trans. 2*, 897 (1990); I. Sethson, D. Johnels, U. Edlund, and A. Sygula, *J. Chem. Soc., Perkin Trans. 2*, 1339 (1990); C. Glidewell and D. Lloyd, *J. Chem. Res.*, 106 (1986).  
 13. J. F. M. Oth, K. Muller, H.-V. Runzheimer, P. Mues, and E. Vogel, *Angew. Chem. Int. Ed. Engl.*, **16**, 872 (1977). For computational studies on the conformations of octalene, see: G. Favini, G. Moro, R. Todeschini, and M. Simonetta, *J. Comput. Chem.*, **5**, 343 (1984); S. Koseki, M. Kataoka, M. Hanamara, T. Nakajima, and A. Toyota, *J. Org. Chem.*, **49**, 2988 (1984).  
 14. G. Jonsall and P. Ahlberg, *J. Am. Chem. Soc.*, **108**, 3819 (1986); P. Svensson, F. Reichel, P. Ahlberg, and D. Cremer, *J. Chem. Soc., Perkin Trans. 2*, 1463 (1991); D. Cremer, P. Svensson, E. Kraka, Z. Konkoli, and P. Ahlberg, *J. Am. Chem. Soc.*, **115**, 7457 (1993).  
 15. G. R. Stevenson and B. E. Forch, *J. Am. Chem. Soc.*, **102**, 5985 (1980).  
 16. H. A. Staab, F. Diedrich, C. Krieger, and D. Schwitzer, *Chem. Ber.*, **116**, 3504 (1983); H. Jiao and P. v. R. Schleyer, *Angew. Chem. Int. Ed. Engl.*, **35**, 2383 (1996).  
 17. T. K. Zywiets, H. Jiao, P. v. R. Schleyer, and A. de Meijere, *J. Org. Chem.*, **63**, 3417 (1998); R. Haag, R. Fleischer, D. Stalke, and A. de Meijere, *Angew. Chem. Int. Ed. Engl.*, **34**, 1492 (1995).  
 18. S. N. Rao, R. A. More O'Ferrall, S. C. Kelly, D. R. Boyd, and R. Agarwal, *J. Am. Chem. Soc.*, **115**, 5458 (1993); Z. S. Jia, P. Brandt, and A. Thibblin, *J. Am. Chem. Soc.*, **123**, 10147 (2001).  
 19. J.-L. M. Abboud, O. Castano, M. Herreros, I. Leito, R. Notario, and K. Sak, *J. Org. Chem.*, **63**, 8995 (1998).  
 20. S. P. Verevkin, H.-D. Beckhaus, C. Ruchardt, R. Haag, S. I. Kozhushkov, T. Zywiets, A. de Meijere, H. Jiao, and P. v. R. Schleyer, *J. Am. Chem. Soc.*, **120**, 11130 (1998).

## Chapter 9

- 1a. C. K. Ingold and E. H. Ingold, *J. Chem. Soc.* 2249 (1928).  
 b. R. J. Albers and E. C. Kooyman, *Recl. Trav. Chim.*, **83**, 930 (1964).  
 c. J. R. Knowles and R. O. C. Norman, *J. Chem. Soc.*, 1938 (1961).  
 d. A. Gastaminza, T. A. Modro, J. H. Ridd, and J. H. P. Utley, *J. Chem. Soc. B*, 534 (1968).  
 e. J. R. Knowles, R. O. C. Norman, and G. K. Radda, *J. Chem. Soc.*, 4885 (1960).  
 f. F. L. Riley and E. Rothstein, *J. Chem. Soc.*, 3860 (1964).

2. T. C. van Hock, P. E. Verkade, and B. M. Wepster, *Recl. Trav. Chim.*, **77**, 559 (1958); A. van Loon, P. E. Verkade, and B. M. Wepster, *Recl. Trav. Chim.*, **79**, 977 (1960).
3. G. Olah, S. J. Kuhn, S. H. Flood, and J. C. Evans, *J. Am. Chem. Soc.*, **84**, 3687 (1962).
4. J. E. Dubois, J. A. Aaron, P. Alcais, J. P. Doucet, F. Rothenberg, and R. Uzan, *J. Am. Chem. Soc.*, **94**, 6823 (1972).
5. R. M. Roberts and D. Shiengthong, *J. Am. Chem. Soc.*, **86**, 2851 (1964).
6. R. L. Dannley, J. E. Gagen, and K. Zak, *J. Org. Chem.*, **38**, 1 (1973); R. L. Dannley and W. R. Knipple, *J. Org. Chem.*, **38**, 6 (1973).
- 7a. C. D. Gutsche and K. H. No, *J. Org. Chem.*, **47**, 2708 (1982).
- b. G. D. Figuly and J. C. Martin, *J. Org. Chem.*, **45**, 3728 (1980).
- c. K. Dey, C. Eaborn, and D. R. M. Walton, *Organomet. Chem. Synth.*, **1**, 151 (1970-1971).
- d. S. Winstein and R. Baird, *J. Am. Chem. Soc.*, **79**, 756 (1957).
8. D. S. Noyce, P. A. Kittle, and E. H. Bannitt, *J. Org. Chem.*, **33**, 1500 (1958).
9. M. Essiz, G. Guillaumet, J.-J. Brunet, and P. Caubere, *J. Org. Chem.*, **45**, 240 (1980).
10. W. Nagata, K. Okada, and T. Akoi, *Synthesis*, 365 (1979).
11. W. G. Miller and C. U. Pittman, Jr., *J. Org. Chem.*, **39**, 1955 (1974).
12. T. A. Modro and K. Yates, *J. Am. Chem. Soc.*, **98**, 4247 (1976).
13. A. V. R. Rao, V. H. Desphande, and N. L. Reddy, *Tetrahedron Lett.*, **23**, 4373 (1982).
14. L. M. Jackman and V. R. Haddon, *J. Am. Chem. Soc.*, **96**, 5130 (1974); M. Gates, D. L. Frank, and W. C. von Felten, *J. Am. Chem. Soc.*, **96**, 5138 (1974).
15. C. K. Ingold, *Structure and Mechanism in Organic Chemistry*, 2nd Edition, Cornell University Press, Ithaca, 1969, pp. 340-344; C. G. Swain and D. R. Crist, *J. Am. Chem. Soc.*, **94**, 3195 (1972).
16. J. Rosenthal and D. I. Schuster, *J. Chem. Ed.*, **80**, 679 (2003).
17. R. B. Moodie and K. Schofield, *Acc. Chem. Res.*, **9**, 287 (1976).
18. P. C. Myhre, M. Beug, and L. L. James, *J. Am. Chem. Soc.*, **90**, 2105 (1968).
- 19a. L. R. C. Barclay, B. A. Ginn, and C. E. Milligan, *Can. J. Chem.*, **42**, 579 (1964).
- b. A. A. Khalaf and R. M. Roberts, *J. Org. Chem.*, **34**, 3571 (1969); A. A. Khalaf, *Rev. Chim. (Bucharest)*, **19**, 1373 (1974).
- c. S. K. Taylor, G. H. Hockerman, G. L. Karrick, S. B. Lyle, and S. B. Schramm, *J. Org. Chem.*, **48**, 2449 (1983).
- 20a. G. P. Stahly, *J. Org. Chem.*, **50**, 3091 (1985).
- b. A. I. Meyers and P. D. Pansegrau, *Tetrahedron Lett.*, **24**, 4935 (1983).
- c. M. Makosza and J. Winiarski, *J. Org. Chem.*, **49**, 1494 (1984).
- d. I. J. Anthony and D. Wege, *Aust. J. Chem.*, **37**, 1283 (1984).
- e. Y. Konayashi, T. Nagai, I. Kumadaki, M. Takahashi, and T. Yamauchi, *Chem. Pharm. Bull.*, **32**, 4382 (1984); P. C. Myhre and G. D. Andrews, *J. Am. Chem. Soc.*, **92**, 7596 (1970).
- f. A. R. Katritzky and K. S. Laurenzo, *J. Org. Chem.*, **51**, 5039 (1986).
- g. T. Yamato, G. Hideshima, G. K. Surya Prakash, and G. A. Olah, *J. Org. Chem.*, **56**, 3955 (1991).
21. A. Wang, J. A. Maquire and E. Biehl, *J. Org. Chem.*, **63**, 2451 (1998).

## Chapter 10

- 1a. R. B. Woodward and R. Hoffmann, *Angew. Chem. Int. Ed. Engl.*, **8**, 781 (1969); O. N. Faza, C. S. Lopez, R. Alvarez, and A. R. de Lera, *Chem. Eur. J.*, **10**, 4324 (2004).
- b. R. B. Woodward and R. Hoffmann, *J. Am. Chem. Soc.*, **87**, 395 (1965); D. R. Williams and J. T. Reeves, *J. Am. Chem. Soc.*, **126**, 3434 (2004).
- c. R. Hoffmann and R. A. Olofson, *J. Am. Chem. Soc.*, **88**, 943 (1966); R. B. Bates, W. H. Deines, D. A. McCombs, and D. E. Potter, *J. Am. Chem. Soc.*, **91**, 4608 (1969).
- 2a. E. Vogel, *Liebigs Ann. Chem.*, **615**, 14 (1958).
- b. A. C. Cope, A. C. Haven, Jr., F. L. Ramp, and E. R. Turnbull, *J. Am. Chem. Soc.*, **74**, 4867 (1952).
- c. R. Pettit, *J. Am. Chem. Soc.*, **82**, 1972 (1960).
- d. K. M. Rapp and J. Daub, *Tetrahedron Lett.*, 2011 (1976).
- e. E. J. Corey and D. K. Herron, *Tetrahedron Lett.*, 1641 (1971).
3. A. G. Anastassiou, V. Orfanos, and J. H. Gebrian, *Tetrahedron Lett.*, 4491 (1969); P. Radlick and G. Alford, *J. Am. Chem. Soc.*, **91**, 6529 (1969).
- 4a. K. B. Wiberg, V. Z. Williams, Jr., and L. E. Friedrich, *J. Am. Chem. Soc.*, **90**, 5338 (1968).
- b. P. S. Wharton and R. A. Kretschmer, *J. Org. Chem.*, **33**, 4258 (1968).

- c. d. R. K. Hill and M. G. Bock, *J. Am. Chem. Soc.*, **100**, 637 (1978).  
d. M. Newcomb and W. T. Ford, *J. Am. Chem. Soc.*, **95**, 7186 (1973).  
e. R. K. Hill, C. B. Giberson, and J. V. Silverton, *J. Am. Chem. Soc.*, **110**, 497 (1988).  
5a. S. W. Staley and T. J. Henry, *J. Am. Chem. Soc.*, **93**, 1292 (1971).  
b. T. Kaufmann and E. Koppelman, *Angew. Chem. Int. Ed. Engl.*, **11**, 290 (1972).  
c. C. W. Jefford, A. F. Boschung, and C. G. Rimbault, *Tetrahedron Lett.*, 3387 (1974).  
d. M. F. Semmelhack, H. N. Weller, and J. S. Foos, *J. Am. Chem. Soc.*, **99**, 292 (1977).  
e. R. K. Boeckman, Jr., M. H. Delton, T. Nagasaka, and T. Watanabe, *J. Org. Chem.*, **42**, 2946 (1977);  
M. F. Semmelhack, H. N. Weller, and J. Clardy, *J. Org. Chem.*, **43**, 3791 (1978).  
f. I. Hasan and F. W. Fowler, *J. Am. Chem. Soc.*, **100**, 6696 (1978).  
g. R. Subramanyam, P. D. Bartlett, G. Y. M. Iglesias, W. H. Watson, and J. Galloy, *J. Org. Chem.*, **47**, 4491 (1982).  
6. C. Basavaiah, S. Pandiaraju, and M. Krishnamacharyulu, *Synlett*, 747 (1996).  
7a. L. A. Feiler, R. Huisgen, and P. Koppitz, *J. Am. Chem. Soc.*, **96**, 2270 (1974).  
b. H. H. Wasserman, J. U. Piper, and E. V. Dehmlow, *J. Org. Chem.*, **38**, 1451 (1973).  
c. D. A. Evans and A. M. Golob, *J. Am. Chem. Soc.*, **97**, 4765 (1975).  
d. K. Oshima, H. Takahashi, H. Yamamoto, and H. Nozaki, *J. Am. Chem. Soc.*, **95**, 2693 (1973).  
e. V. Cere, E. Dalcanale, C. Paolucci, S. Pollicino, E. Sandri, L. Lunazzi, and A. Fava, *J. Org. Chem.*, **47**, 3540 (1982).  
f. L. A. Paquette and M. J. Wyvratt, *J. Am. Chem. Soc.*, **96**, 4671 (1974); D. McNeil, B. R. Vogt, J. J. Sudol, S. Theodoropoulos, and E. Hedaya, *J. Am. Chem. Soc.*, **96**, 4673 (1974).  
g. W. Grimme, *J. Am. Chem. Soc.*, **95**, 2381 (1973).  
h. W. Weyler, Jr., L. R. Byrd, M. C. Caserio, and H. W. Moore, *J. Am. Chem. Soc.*, **94**, 1027 (1972).  
i. M. Nakazaki, K. Naemura, H. Harada, and H. Narutaki, *J. Org. Chem.*, **47**, 3470 (1982).  
j. F. Binns, R. Hayes, K. J. Hodgetts, S. T. Saengchantara, T. W. Wallace, and C. J. Wallis, *Tetrahedron*, **52**, 3631 (1996).  
8. W. H. Rastetter and T. J. Richard, *J. Am. Chem. Soc.*, **101**, 3893 (1979).  
9. R. Huisgen and W. E. Konz, *J. Am. Chem. Soc.*, **92**, 4102 (1970).  
10. D. B. Ramachary, N. S. Chowdari, and C. F. Barbas, III, *Tetrahedron Lett.*, **43**, 6743 (2002).  
11a. D. A. Evans, D. H. B. Ripin, J. S. Johnson, and E. A. Shaughnessy, *Angew. Chem. Int. Ed. Engl.*, **36**, 2119 (1997).  
b. H. Waldman, E. Blaeser, M. Jansen, and H.-P. Letschert, *Chem. Eur. J.*, **1**, 150 (1995).  
c. U. Chiacchio, F. Casuscelli, A. Corsaro, A. Rescifina, G. Romeo, and N. Uccella, *Tetrahedron*, **50**, 6671 (1994).  
12a. L. A. Paquette and R. S. Beckley, *J. Am. Chem. Soc.*, **97**, 1084 (1975).  
b. K. C. Nicolaou, N. A. Petasis, R. E. Zipkin, and J. Uenishi, *J. Am. Chem. Soc.*, **104**, 5555 (1982).  
c. B. M. Trost and A. J. Bridges, *J. Am. Chem. Soc.*, **98**, 5017 (1976).  
d. K. C. Nicolaou, N. A. Petasis, R. E. Zipkin, and J. Uenishi, *J. Am. Chem. Soc.*, **104**, 5555 (1982).  
e. K. J. Shea and R. B. Phillips, *J. Am. Chem. Soc.*, **100**, 654 (1978).  
f. J. G. Millar, *Tetrahedron Lett.*, **38**, 7971 (1997).  
13. R. K. Hill, J. W. Morgan, R. V. Shetty, and M. E. Synerholm, *J. Am. Chem. Soc.*, **96**, 4201 (1974);  
H. M. R. Hoffmann, *Angew. Chem. Int. Ed. Engl.*, **8**, 556 (1969).  
14a. T. J. Brocksom and M. G. Constantino, *J. Org. Chem.*, **47**, 3450 (1982).  
b. L. E. Overman, G. F. Taylor, K. N. Houk, and L. N. Domelsmith, *J. Am. Chem. Soc.*, **100**, 3182 (1978).  
c. P. W. Tang and C. A. Maggiulli, *J. Org. Chem.*, **46**, 3429 (1981).  
d. R. B. Woodward, F. Sondheimer, D. Taub, K. Heusler, and W. M. McLamore, *J. Am. Chem. Soc.*, **74**, 4223 (1952).  
e. T. Cohen and Z. Kosarych, *J. Org. Chem.*, **47**, 4005 (1982).  
15a. S. V. Ley and L. A. Paquette, *J. Am. Chem. Soc.*, **96**, 6670 (1974).  
16a. A. K. Cheng, F. A. L. Anet, J. Mioduski, and J. Meinwald, *J. Am. Chem. Soc.*, **96**, 2887 (1974).  
b. J. S. McKennis, L. Brener, J. S. Ward, and R. Pettit, *J. Am. Chem. Soc.*, **93**, 4957 (1971).  
c. W. Grimme, H. J. Riebel, and E. Vogel, *Angew. Chem. Int. Ed. Engl.*, **7**, 823 (1968).  
d. W. Grimme, *J. Am. Chem. Soc.*, **94**, 2525 (1972).  
e. J. J. Gajewski, L. K. Hoffman, and C. N. Shih, *J. Am. Chem. Soc.*, **96**, 3705 (1974).  
f. D. P. Lutz and J. D. Roberts, *J. Am. Chem. Soc.*, **83**, 2198 (1961).  
17. A. Krantz, *J. Am. Chem. Soc.*, **94**, 4020 (1972).  
18. D. A. Smith and C. W. Ulmer, II, *J. Org. Chem.*, **62**, 5110 (1997); T. Suzuki, T. Ohwada, and K. Shudo, *J. Am. Chem. Soc.*, **119**, 6774 (1997).  
19a. A. Viola and L. Levasseur, *J. Am. Chem. Soc.*, **87**, 1150 (1965).

- b. S. F. Reed, Jr., *J. Org. Chem.*, **30**, 1663 (1965).
- c. T. S. Cantrell and H. Schecter, *J. Am. Chem. Soc.*, **89**, 5868 (1967).
- d. R. B. Woodward, R. E. Lehr, and H. H. Inhoffen, *Liebigs Ann. Chem.*, **714**, 57 (1968).
- e. R. B. Woodward and T. J. Katz, *Tetrahedron*, **5**, 70 (1959).
- f. N. J. Turro and W. B. Hammond, *Tetrahedron*, **24**, 6029 (1968).
- g. W. J. Linn and R. E. Benson, *J. Am. Chem. Soc.*, **87**, 3657 (1965).
- h. M. Jones, Jr., S. D. Reich, and L. T. Scott, *J. Am. Chem. Soc.*, **92**, 3118 (1970).
- i. P. G. Gassman, J. J. Roos, and S. J. Lee, *J. Org. Chem.*, **49**, 717 (1984).
- j. V. Glock, M. Wette, and F.-G. Klärner, *Tetrahedron Lett.*, **26**, 1441 (1985).
- k. Y. N. Gupta, M. J. Don, and K. N. Houk, *J. Am. Chem. Soc.*, **104**, 7336 (1982).
- l. P. A. Zoretic, R. J. Chambers, G. D. Marbury, and A. A. Riebiro, *J. Org. Chem.*, **50**, 2981 (1985).
- m. S. Sato, K. Tomita, H. Fujita, and Y. Sabo, *Heterocycles*, **22**, 1045 (1984).
- n. M. Nakazaki, K. Naemura, H. Harada, and H. Narutaki, *J. Org. Chem.*, **47**, 3470 (1982).
20. A. G. Anastassiou and E. Yakali, *J. Chem. Soc., Chem. Commun.*, 92 (1972); M. Mauksch, V. Gogonea, H. Jiao, and P. v. R. Schleyer, *Angew. Chem. Int. Ed. Engl.*, **37**, 2395 (1998).
21. U. Salzner and S. M. Bachrach, *J. Org. Chem.*, **61**, 237 (1996).

## Chapter 11

- 1a. H. O. House, C.-Y. Chu, W. V. Phillips, T. S. B. Sayer, and C.-C. Yau, *J. Org. Chem.*, **42**, 1709 (1977).
- b. K. Fukunishi, Y. Inoue, Y. Kishimoto, and F. Mashio, *J. Org. Chem.*, **40**, 628 (1975).
- c. C. Walling and D. Bristol, *J. Org. Chem.*, **37**, 3514 (1972).
- d. D. H. Miles, P. Loew, W. S. Johnson, A. F. Kluge, and J. Meinwald, *Tetrahedron Lett.*, 3019 (1972).
- e. K. Pederson, P. Jakobsen, and S.-O. Lawesson, *Org. Synth.*, **V**, 70 (1973).
- f. R. Dowbenko, *Org. Synth.*, **V**, 93 (1973).
- g. W. H. Sharkey and C. M. Langkammerer, *Org. Synth.*, **V**, 445 (1973).
- h. P. D. Klemmensen, H. Kolind-Andersen, H. B. Madsen, and A. Svendsen, *J. Org. Chem.*, **44**, 416 (1979).
- i. R. A. Rossi, R. H. deRossi, and A. F. Lopez, *J. Am. Chem. Soc.*, **98**, 1252 (1976).
- j. D. W. Grattan, J. M. Locke, and S. R. Wallis, *J. Chem. Soc., Perkin Trans. 1*, 2264 (1973).
2. W. A. Pryor, D. L. Fuller, and J. P. Stanley, *J. Am. Chem. Soc.*, **94**, 1632 (1972).
3. L. H. Gale, *J. Am. Chem. Soc.*, **88**, 4661 (1961).
4. I. Rosenthal and D. Elad, *J. Org. Chem.*, **33**, 825 (1968); R. Lalande, B. Maillard, and M. Cazaux, *Tetrahedron Lett.*, 745 (1969).
- 5a. D. D. Tanner, H. Yabuuchi, and E. V. Blackburn, *J. Am. Chem. Soc.*, **93**, 4802 (1971); Z.-H. Li, K.-N. Fan, and M. W. Wong, *J. Phys. Chem. A*, **105**, 10890 (2001).
- b. E. Mueller, *Tetrahedron Lett.*, 1835 (1974).
- c. A. L. J. Beckwith and C. J. Easton, *J. Am. Chem. Soc.*, **103**, 615 (1981).
- d. H. C. Brown, M. S. Kharasch, and T. H. Caho, *J. Am. Chem. Soc.*, **62**, 3435 (1940).
- e. A. Effio, D. Griller, K. U. Ingold, J. C. Scaiano, and S. J. Sheng, *J. Am. Chem. Soc.*, **102**, 6063 (1980).
- f. N. O. Brace, *J. Am. Chem. Soc.*, **86**, 523 (1964).
- g. J. M. Cummins, U.-H. Dolling, A. W. Douglas, S. Karady, W. R. Leonard, Jr., and B. F. Marcume, *Tetrahedron Lett.*, **40**, 6153 (1999).
- h. C. L. Karl, E. J. Maas, and W. Reusch, *J. Org. Chem.*, **37**, 2834 (1972).
- 6a. W. H. Urry, D. R. Trecker, and H. D. Hartzler, *J. Org. Chem.*, **29**, 1663 (1964).
- b. H. Pines, N. C. Sih, and D. B. Rosenfeld, *J. Org. Chem.*, **31**, 2255 (1966).
- c. D. D. Tanner, E. V. Blackburn, and G. E. Diaz, *J. Am. Chem. Soc.*, **103**, 1557 (1981).
- d. H. Driquez, J. M. Pantan, and J. Lessard, *Can. J. Chem.*, **55**, 700 (1977).
- e. H. Feuer, J. Doty, and J. P. Lawrence, *J. Org. Chem.*, **38**, 417 (1973).
- f. E. A. Mayeda, *J. Am. Chem. Soc.*, **97**, 4012 (1975).
- g. X. Creary, *J. Org. Chem.*, **45**, 280 (1980).
- h. A. L. J. Beckwith and R. D. Wagner, *J. Am. Chem. Soc.*, **101**, 7099 (1979).
7. L. K. Montgomery and J. W. Matt, *J. Am. Chem. Soc.*, **89**, 6556 (1967).
8. P. D. Bartlett, R. E. Pincock, J. H. Rolston, W. G. Schindel, and L. A. Singer, *J. Am. Chem. Soc.*, **87**, 2590 (1965).
9. E. S. Huysen and B. Giddings, *J. Org. Chem.*, **27**, 3391 (1962).

10. N. C. Deno, W. E. Billups, R. Fishbein, C. Pierson, R. Whalen, and J. C. Wyckoff, *J. Am. Chem. Soc.*, **93**, 438 (1971).
- 11a. D. H. Levy and R. J. Myers, *J. Chem. Phys.*, **41**, 1062 (1964).
- b. J. K. Kochi and P. J. Krusic, *J. Am. Chem. Soc.*, **90**, 7157 (1968).
- 12a. S. Winstein and F. H. Seubold, Jr., *J. Am. Chem. Soc.*, **69**, 2916 (1947).
- b. J. W. Wilt and H. P. Hogan, *J. Org. Chem.*, **24**, 441 (1959).
- c. P. S. Skell, R. G. Allen, and N. D. Gilmour, *J. Am. Chem. Soc.*, **83**, 504 (1961).
- d. L. H. Slaugh, *J. Am. Chem. Soc.*, **87**, 1522 (1965).
- e. H. Meislich, J. Constanza, and J. Strelitz, *J. Am. Chem. Soc.*, **33**, 3221 (1968).
13. P. R. Story, D. D. Denson, C. E. Bishop, B. C. Clark, Jr., and J.-C. Farine, *J. Am. Chem. Soc.*, **90**, 817 (1968).
14. K. J. Shea and P. S. Skell, *J. Am. Chem. Soc.*, **95**, 6728 (1973).
15. W. A. Bonner and F. D. Mango, *J. Org. Chem.*, **29**, 430 (1964).
- 16a. N. Kornblum, H. K. Singh, and W. J. Kelly, *J. Org. Chem.*, **48**, 332 (1983).
- b. G. A. Russell, F. Ros, J. Hershberger, and H. Tashtoush, *J. Org. Chem.*, **47**, 1480 (1982).
- c. G. A. Russell, J. Hershberger, and K. Owens, *J. Am. Chem. Soc.*, **101**, 1312 (1979).
17. S. S. D. Brown, J. J. Colquhoun, W. McFarlane, M. Murray, I. D. Salfer, and V. Sik, *J. Chem. Soc., Chem. Commun.*, 53 (1986).
18. D. J. DeFrees, R. J. McIver, and W. J. Hehre, *J. Am. Chem. Soc.*, **102**, 3334 (1980); J. D. Roberts, A. Streitwieser, and C. M. Regan, *J. Am. Chem. Soc.*, **74**, 4579 (1952).
- 19a. K. S. Feldman, A. L. Romanelli, R. E. Ruckle, Jr., and G. Jean, *J. Org. Chem.*, **57**, 100 (1992).
- b. J. P. Vionnet and P. Renaud, *Helv. Chim. Acta*, **77**, 1781 (1994).
20. J. R. Bews, C. Glidewell, and J. C. Walton, *J. Chem. Soc., Perkin Trans. 2*, 1447 (1982). M.-S. Lee, D. A. Hrovat, and W. T. Borden, *J. Am. Chem. Soc.*, **117**, 10353 (1995).
21. T. H. Peterson and B. K. Carpenter, *J. Am. Chem. Soc.*, **114**, 1496 (1992).

## Chapter 12

1. C. C. Lee and D. Unger, *Can. J. Chem.*, **50**, 593 (1972).
- 2a. E. Vogel, W. Grimme, and E. Dinne, *Tetrahedron Lett.*, 391 (1965); W. G. Dauben and M. S. Kellogg, *J. Am. Chem. Soc.*, **102**, 4456 (1980).
- b. J. Meinwald and J. W. Young, *J. Am. Chem. Soc.*, **93**, 725 (1971).
- c. D. M. Madigan and J. S. Swenton, *J. Am. Chem. Soc.*, **93**, 6316 (1971).
- d. E. J. Corey and A. G. Hortmann, *J. Am. Chem. Soc.*, **85**, 4033 (1963).
- e.f. K. M. Shumate, P. N. Neumann, and G. J. Fonken, *J. Am. Chem. Soc.*, **87**, 3996 (1965); K. M. Shumate and G. J. Fonken, *J. Am. Chem. Soc.*, **88**, 1073 (1966).
- 3a. O. Rodriguez and H. Morrison, *J. Chem. Soc. Chem. Commun.*, 679 (1971).
- b. W. G. Dauben and M. S. Kellogg, *J. Am. Chem. Soc.*, **102**, 4456 (1980).
- c. D. H. R. Barton, D. L. J. Clive, P. D. Magnus, and G. Smith, *J. Chem. Soc. C*, 2193 (1971).
- 4a. W. C. Agosta and A. B. Smith, III, *J. Am. Chem. Soc.*, **93**, 5513 (1971).
- b. W. Ferree, Jr., J. B. Grutzner, and H. Morrison, *J. Am. Chem. Soc.*, **93**, 5502 (1971).
- c. A. Wissner, *J. Org. Chem.*, **42**, 356 (1977).
- d. G. W. Shaffer and M. Pesaro, *J. Org. Chem.*, **39**, 2489 (1974).
- e. D. R. Morton and N. J. Turro, *J. Am. Chem. Soc.*, **95**, 3947 (1973).
- f. H. Hart and A. F. Naples, *J. Am. Chem. Soc.*, **94**, 3256 (1972).
- g. M. Pomerantz and G. W. Gruber, *J. Am. Chem. Soc.*, **93**, 6615 (1971).
- h. O. L. Chapman, G. W. Borden, R. W. King, and B. Winkler, *J. Am. Chem. Soc.*, **86**, 2660 (1964); A. Padwa, L. Brodsky, and S. Clough, *J. Am. Chem. Soc.*, **94**, 6767 (1972).
- i. D. I. Schuster and C. W. Kim, *J. Am. Chem. Soc.*, **96**, 7437 (1974).
- j. W. G. Dauben, M. S. Kellogg, J. I. Seeman, and W. A. Spitzer, *J. Am. Chem. Soc.*, **92**, 1786 (1970).
- k. A. Padwa and W. Eisenberg, *J. Am. Chem. Soc.*, **92**, 2590 (1970).
- l. D. H. R. Barton and G. Quinkert, *J. Chem. Soc.*, 1 (1960); J. Griffiths and H. Hart, *J. Am. Chem. Soc.*, **90**, 5296 (1968).
- m. R. S. Cooke and G. D. Lyon, *J. Am. Chem. Soc.*, **93**, 3840 (1971).
- n. D. Bryce-Smith and J. E. Lodge, *J. Chem. Soc.*, 695 (1963); E. Grovenstein and D. V. Rao, *Tetrahedron Lett.*, 148 (1961).
- o. L. E. Friedrich and J. D. Bower, *J. Am. Chem. Soc.*, **95**, 6869 (1973).

5. T.-Y. Leong, I. Imagawa, K. Kimoto, and M. Kawanishi, *Bull. Chem. Soc. Jpn.*, **46**, 596 (1973).
6. W. B. Hammond and T. S. Yeung, *Tetrahedron Lett.*, 1173 (1975).
7. H. E. Zimmerman, R. S. Givens, and R. M. Pagni, *J. Am. Chem. Soc.*, **90**, 6096 (1968).
8. P. J. Wagner, P. A. Kelso, and R. G. Zepp, *J. Am. Chem. Soc.*, **94**, 7480 (1972).
10. N. J. Turro and D. S. Weiss, *J. Am. Chem. Soc.*, **90**, 2185 (1968).
11. S. Boue and R. Srinivasan, *J. Am. Chem. Soc.*, **92**, 3226 (1970); J. Saltiel et al., *Org. Photochem.*, **3**, 1 (1973).
12. W. G. Dauben, K. Koch, S. L. Smith, and O. L. Chapman, *J. Am. Chem. Soc.*, **85**, 2616 (1963).
13. H. E. Zimmerman and R. D. Solomon, *J. Am. Chem. Soc.*, **108**, 6276 (1986).
14. H. E. Zimmerman, *Angew. Chem. Int. Ed. Engl.*, **8**, 1 (1969).
15. K. R. Huffman, M. Burger, W. H. Henderson, Jr., M. Loy, and E. F. Ullman, *J. Org. Chem.*, **34**, 2407 (1969).
16. F. D. Lewis, R. W. Johnson, and D. E. Johnson, *J. Am. Chem. Soc.*, **96**, 6090 (1974).
17. H. E. Zimmerman, R. J. Boettcher, N. E. Buehler, G. E. Keck, and M. G. Steinmetz, *J. Am. Chem. Soc.*, **98**, 7680 (1976).
18. H. E. Zimmerman, R. J. Boettcher, and W. Braig, *J. Am. Chem. Soc.*, **95**, 2155 (1973).
19. J. R. Scheffer, K. S. Bhandari, R. E. Gayler, and R. A. Wostradowski, *J. Am. Chem. Soc.*, **97**, 2178 (1975).
20. C. W. Jefford and F. Delay, *J. Am. Chem. Soc.*, **97**, 2272 (1975).
21. G. Rattray, J. Yang, A. D. Gudmundsdottir, and J. R. Scheffer, *Tetrahedron Lett.*, **34**, 35 (1993).
22. H. Meier and P. Konig, *Nouv. J. Chem.*, **10**, 437 (1986); M. Zheng, K. J. DiRico, M. M. Kirchoff, K. M. Phillips, L. M. Cuff, and R. P. Johnson, *J. Am. Chem. Soc.*, **115**, 12167 (1993).
23. T. Hasegawa, Y. Yang, and M. Yoshioka, *Bull. Chem. Soc. Jpn.*, **64**, 3488 (1991).

# Index

- ab initio, *see* MO Theory
- absorption bands
  - comparison of a *cis-trans* isomer pair, 1081
  - of *E*- and *Z*-stilbene, 1087
  - wavelength ranges for organic compounds, 1074
- acenaphthacene
  - bond lengths of, 751
- acetaldehyde
  - conformation, 148
  - hydration, 638
- acetals
  - conformation, 83, 231–232
  - formation of, 640
  - hydrolysis of, 641–645
    - general acid catalysis of, 641–644, 669
    - nucleophilic catalysis in, 669
    - solvent isotope effect in, 641
    - specific acid catalysis of, 641
  - of salicylic acid
    - mechanism of hydrolysis, 668–669
- acetic acid derivatives
  - acidity of, 13, 53, 102–103
- acetone
  - aldol reaction of, 685
  - enolization of, 608
- acetophenone
  - enolization of, 607
- acetylene, *see* ethyne
- acidity
  - of alcohols, 104
  - of carbonyl compounds, 591–597
  - of carboxylic acids, 13, 53–54, 102–103, 105
  - of cyano compounds, 598
  - of halogenated alcohols, 105
  - of hydrides of second and third row elements, 103–104
  - of hydrocarbons, computation of, 56–57
  - of nitroalkanes, 591, 597
  - of phosphorus ylides, 600–601
  - of representative compounds, table, 593
- acidity functions, 349–350
- acids, *see also* carboxylic acids
  - strong, gas phase ionization energies, 57
- acrolein, *see* propenal
- acryloyl lactates
  - as dienophiles, 849
- acylases
  - as catalysts for esterification, 223
- acylation
  - of alcohols, 664–667
  - of amines, 667
  - in Friedel-Crafts reactions, 809–813
- acyl halides
  - in Friedel-Crafts reactions, 772, 809–813
  - Lewis acid complexes of, 810
  - relative reactivity of, 328
- acylium ion
  - as intermediates
    - in alcohol acylation, 666
    - in Friedel-Crafts acylation, 809–813
- acyloxy radicals
  - decarboxylation of, 967, 980, 1013
- acyl radicals
  - addition reactions of, 1032–1033
  - decarbonylation of, 967, 1017, 1122
  - generation of, 1031–1032
    - from acyl selenides, 1032
    - from aldehydes, 1031
  - SOMO of, 1031
  - stabilization of, 318, 1055
- adamantane
  - derivatives, in nucleophilic substitution, 402, 412–413, 416

- adamantane (*cont.*)  
halides, substitution reactions, 1052  
structure of, 166
- adamantanone  
polar effects in reduction of, 238–239
- AIBN, *see* azoisobutyronitrile
- AIM, *see* atoms in molecules approach
- Albery-More O'Ferrall-Jencks diagram, *see*  
potential energy diagram, two-dimensional
- alcohol dehydrogenase  
enantiospecificity of, 135
- alcohols  
acetal formation, 640  
acidity of, 104–105  
acylation of, 664–667  
acylium ions as intermediates, 664–665  
carbodiimides in, 667  
allylic  
enantioselective epoxidation of, 196–199  
dehydration of, 474, 563–564  
esterification of, 664–668  
nucleophilic catalysis in, 665  
synthesis using organoboranes, 527–528
- aldehydes, *see also* carbonyl compounds  
addition reactions of, 629–632  
conformation of, 148  
cyanohydrins from, 635  
imine formation from, 645–650  
radical addition reactions of, 1031–1034
- Alder rule, 840–841
- aldol reaction, 682  
acid-catalyzed mechanism, 683  
analysis by Marcus equation, 283–285  
base-catalyzed mechanism, 683  
directed, 687  
kinetic control in, 688–689  
stereochemistry of, 688–692  
enantioselective catalysts for, 695–697  
examples of, 682  
kinetics of, 284–5, 685  
mixed aldol reaction, 685–686  
regioselectivity of, 686  
stereoselectivity of, 685  
silyl ketene acetals as nucleophiles in, 697  
silyl ketene thioacetals as nucleophiles in, 697  
thermodynamic control in, 690
- alkanes  
bond orders for, 77  
computation of enthalpy of formation by MO  
methods, 52  
conformation of, 142–145  
molecular graphs for, 64
- alkenes  
bridgehead, synthesis by intramolecular  
Diels-Alder reactions, 871  
bromination, 482–497  
bromonium ion intermediates in, 486  
mechanism of, 492  
reagents for, 491  
stereospecificity of, 183–185, 487–489
- chlorination, 487–488  
rearrangement during, 494  
configuration of, 113  
conformation of, 145–148  
bisected, definition, 145  
eclipsed, definition, 145  
cyclic, photoreactions of, 1094  
cycloaddition reactions with enones, 1125–1126  
dihydroxylation of, 186  
computational model for, 202–203  
enantioselective, 200–203  
electrophilic addition reactions of, 473–476  
comparison of, 531–536  
mechanisms for, 474–478  
enthalpy of formation, 256–257  
epoxidation, 186–187, 503–511  
by dimethyldioxirane, 507–510
- fluorination  
reagents for, 496
- halogenation, 485–497  
relative rate in, table, 487  
stereochemistry of, 487–488
- hydration of, 474, 482–484  
relative rates of, table, 484
- hydroboration of, 521–526  
electrophilic character of, 522  
mechanism of, 522  
reagents for, 521, 524–525  
regioselectivity of, table, 523  
steric effects in, 523  
thermal reversibility of, 524–525
- hydroboration-oxidation of, 187–188
- hydrobromination, radical  
examples of, 1036  
regiochemistry of, 1027  
stereochemistry, 1027–1028
- hydrohalogenation, 474, 476–482  
by radical addition, 1026–1028  
stereochemistry of, 478–479
- oxymercuration of, 515–520  
relative rates for, table, 516  
substituent effects in, 518–520
- photochemical cycloadditions, 1109–1111  
with aromatic compounds, 1135–1137  
with carbonyl compounds, 1132–1134
- photochemical isomerization of, 1081–1090  
composition of photostationary state, 1082  
of ethene, 1082–1083  
of stilbene, 1085–1090  
of styrene, 1083–1085
- photochemical reactions of, 1091–1096,  
1109–1111  
examples, 1111
- radical addition reactions, 1004–1008  
of aldehydes, 1031, 1034  
examples, 1033–1036  
of formamide, 1032–1033  
of halomethanes, 1029–1031

- of hydrogen halides, 1026–1028
- substituent effects on rates, 1004–1006
- of thiols and thiocarboxylic acids, 1033
- relative reactivity of, summary, 531–535
  - with trifluoroacetic acid, 484–485
  - with trifluoromethanesulfonic acid, 484
- selenenylation, 497, 498, 500–503
  - relative reactivity of, 501
- silver complexes of, 520–521
- stabilization by substituents, 52
- sulfenylation, 497–500
  - relative reactivity of, 501
- alkoxyl radicals
  - formation from alkyl hypochlorites, 1015
  - fragmentation of, 1114–1116
- alkylboranes, *see* boranes, alkyl
- alkyl groups
  - as electron donating groups, 13
  - electronegativity of, 13, 102–103
- alkyl halides
  - bridgehead, reactivity of, 435
  - $S_{RN}1$  substitution reactions, 1051
  - $S_{RN}1$  substitution reactions of, 1048–1052
  - synthesis
    - using organoboranes, 529
- 1,3-allylic strain, definition, 147
- in alkylidene cyclohexanes, 161
- alkyl radicals
  - disproportionation of, 966
  - halo-substituted
    - Structure of, 981–982
    - structure of, 980–984
- alkynes
  - Acidity of, 584
  - electrophilic addition reactions of, 537–545
  - halogenation, 540–544
  - hydration of, 538, 544
  - hydrohalogenation of, 539–540
  - mercuration of, 545
- allenes
  - chirality of, 129
  - electrophilic addition reactions of, 545–546
  - hybridization in, 6
- allyl cation
  - cycloaddition with alkenes, 48
  - from cyclopropyl cation, 907–908
  - MOs of, 48
  - stabilization of, 302
- allyl phenyl ethers
  - Claisen rearrangement of, 934
- allyl radical
  - resonance in, 312–313, 985
  - structure of, 985
  - substituent effects on, 986–987
- allyl vinyl ether
  - Claisen rearrangement of, 273, 933–934
- AlpineHydride®
  - in enantioselective reduction of ketones, 193
- aluminum trichloride
  - in Friedel-Crafts reaction, 809–813
  - as Lewis acid catalyst, 354
- AM1 MO method, 32
- amides
  - hydrolysis, 662–664
    - mechanism of, 327
  - protonation of, 663–664
  - resonance in, 320–322
- amine oxides
  - allyl, [2,3]-sigmatropic rearrangements of, 941
- amines
  - alkylation by  $S_{RN}1$  substitution reactions, 1047
  - bifunctional, intramolecular catalysis by, 675
  - bond energies in, 317, 1054
  - configuration and inversion of, 129
  - diazotization of, 405
  - hyperconjugation in, 315, 1054
  - N*-allyl, aza Wittig rearrangement of, 944
  - synthesis using organoboranes, 528–529
- aminolysis
  - of esters, 659–662
  - of salicylate esters, 673
- anhydrides, *see* carboxylic acid anhydrides
- annulenes, 715–718
  - [10]annulene, 728–730
  - [12]annulene, 730
    - dianion of, 742
    - Mobius topology, 737
  - [14]annulene, 730–732
  - [16]annulene, 732–733
    - Mobius topology, 737
  - [18]annulene, 733–734
  - [20]annulene, 734
    - Mobius topology, 737
  - [22]annulene, 734
  - [24]annulene, 734
  - Hückel MOs for, 30
  - large ring, 734–735
    - NICS values for, 735
- anomeric effect, *see also* hyperconjugation
  - in acyclic molecules, 81–85
  - computational analysis of, 231–232
  - in conformation of disubstituted methanes, 81–85
  - in cyclic ethers, 227–233
  - electrostatic effects in, 230–231
  - hyperconjugation in, 230–231
  - MO interpretation, 82
  - role in nucleoside conformation, 233–234
  - solvent effects on, 231–232
  - in tetrahydropyrans, 228–233
- anthracene, 749
  - Diels-Alder reaction with tetracyanoethene, 859
  - electrophilic aromatic substitution in, 793
- antiaromatic, definition, 714
- antioxidants, 994–995
- ARCS, *see* aromatic ring current shielding
- aromatic compounds
  - fused ring systems, 745–758

- aromatic compounds (*cont.*)
- Diels-Alder reactions of, 748–749, 857–858
  - examples of, 746
  - halogenation of, 800–804
  - hardness of, 750, 795
  - heterocyclic, 758–760
  - nitration of, 796–800
  - photochemistry of, 1134–1137
  - redox potentials of, 990
- aromaticity
- of charged rings, 32, 738–743
  - examples of, 738
  - criteria for, 714
  - bond length alternation, 718–719
  - electronic, 720–724
  - in fused ring systems, 747–748
  - stabilization energy, 715–718
  - of cyclopropenium ions, 738–739
  - of fused ring systems, 745–758
  - Huckel rule for, 31, 713
  - of transition state in Diels-Alder reaction, 851
- aromatic ring current shielding
- as a criterion of aromaticity, 721
- aromatic stabilization energy,
- definition, 717
  - of heteroaromatic compounds, 758
  - of indacene, 754
- aromatic substitution, *see* electrophilic, nucleophilic etc.
- Arrhenius equation, 272
- aryl halides
- benzynes from, 821–822
  - $S_{RN}1$  substitution reactions, 1048–1052
  - examples of, 1051
  - mechanism of, 1049, 1052
- aryl radicals
- from *N*-acyloxypyridine-2-thiones, 980
  - from *N*-nitrosoacetanilides, 979
- ASE, *see* aromatic stabilization energy
- aspirin, *see* salicylic acid esters
- 1,2-asymmetric induction, 171
- Cieplak model for, 180
  - Cram's rule for, 179
  - Felkin-Ahn model for, 179
- 1,3-asymmetric induction
- in hydride reduction of ketones, 181
- atomic charge, *see also* electron density distribution
- definition, 27, 713
- atoms in molecules approach, 62–69
- for aromatic compounds, 723–724
- atom transfer reactions, definition, 966
- Aufbau principle, 35
- autoxidation, 1024
- of aldehydes, 1025
  - of ethers, 1026
  - of hydrocarbons, 995, 1025
  - relative rates, 1025
  - of isopropylbenzene, 1025
- azetidiones
- formation by [2+2] cycloadditions of imines, 890–891
- azides
- as 1,3-dipoles, 875
  - aryl, as ambiphilic 1,3-dipoles, 876–878
  - frontier orbitals of, 880–881
- azo compounds
- configuration of, 121
  - as sources of radicals, 978
- azoisobutyronitrile
- as radical source, 978
- azomethine imines
- as 1,3-dipoles, 875
- azomethine ylides
- as 1,3-dipoles, 875
  - generation from aziridines, 885
- azulene
- dipole moment of, 753
  - stabilization of, 747, 752
  - structure of, 752
- B3LYP computational method, 55
- 9-BBN, *see* 9-borabicyclo[3.3.1]nonane
- Baeyer-Villiger reaction, 1025
- basicity function
- $H_{-}$ , 580
- basis sets, definition, 26–27
- abbreviations for, table, 34
  - characteristics of, 33–35
- Bell-Evans-Polyani relationship, 288–289
- in 1,3-dipolar cycloaddition reactions of ethene, 883
  - for hydrogen abstraction reactions, 1001–1002, 1056–1057
  - quadratic, for reaction of hydroxyl radical with halomethanes, 1060
- benzaldehyde
- excited state of, 1118
- benzene
- acidity of, 583
  - electron density in, 57–58
  - Hückel MO diagram for, 714
  - photocycloaddition with alkenes, 1135–1137
  - photoisomerization of, 1135
  - photoproducts of, 1134
  - radical anion of, 990
  - ESR spectrum of, 972
  - resonance in, 18, 62
  - stabilization in, 716–718, 727
- benzocyclobutadiene
- generation of, 751
  - properties of, 751–2
- benzophenone
- reductive photodimerization of, 1119–1120
- benzvalene, *see* tricyclo[3.1.0.0<sup>2,6</sup>]hex-3-ene
- benzyl cation
- in Friedel-Crafts alkylation reactions, 806, 808

- resonance in, 62  
 substituent effects on, 432–433
- benzyl radical  
 resonance in, 312–313  
 substituent effects on, 986–987
- benzyne  
 additions to, 823  
 generation of, 821–824
- biaryls  
 chirality of, 129–130
- bicyclo[1.1.0]butane, 87–88  
 reaction with halogens, 87
- bicyclo[1.1.1]pentane, 87–88
- bicyclo[2.2.0]hexa-2,5-diene  
 conversion to benzene, transition structures for, 904  
 derivatives of, 904  
 kinetic stability of, 904  
 synthesis of, 904
- bicyclo[4.1.0]hepta-2,4-dienes  
 electrocyclic reactions of, 905
- bicyclo[5.2.0]octa-3,5-diene  
 Cope rearrangement of, 927
- bicyclo[6.2.0]deca-1,3,5,7,9-pentaene, 753–4
- BINAP, *see* *bis*-2,2'-(diphenylphosphinyl)-1,1'-binaphthalene
- 1,1'-binaphthalene-2,2'-diol  
 chirality of, 130  
 derivatives as catalysts for enantioselective Diels-Alder reactions, 868
- 1,1'-binaphthyl derivatives  
 chirality of, 129–130
- BINOL, *see* 1,1'-binaphthalene-2,2'-diol
- biphenylene, 824
- bis*-2,2'-(diphenylphosphinyl)-1,1'-binaphthalene  
 chirality of, 130  
 as ligand in enantioselective hydrogenation, 190
- bis*-oxazoline catalysts  
 for aldol reaction, 696  
 for enantioselective Diels-Alder reactions, 867–868
- bond angles  
 in relation to hybridization, 4–5, 87
- bond critical point, AIM definition, 63
- bond dipole, 10
- bond dissociation energy, 257–258  
 computation of, 318  
 electronegativity effect on, 14, 259–260  
 of halogens, 258–259  
 relationship to radical stability, 312–313, 317, 1052–1055  
 relation to hybridization, 259–260  
 in relation to hydrogen abstraction reactions, 1001  
 table of, 258, 1053
- bond energy, *see also* bond dissociation energy  
 intrinsic, 1053  
 in substituted carbonyl compounds, 321
- bond length  
 computation by MO methods, 51  
 as a criterion of aromaticity, 718–719
- bond order  
 in carbonyl compounds, 320–321  
 as a criterion of aromaticity, 723–724  
 of hydrocarbons, 77  
 relation to electron density, 76–77
- bond path  
 AIM definition, 63
- bonds, *see* chemical bonds
- 9-borabicyclo[3.3.1]borane  
 formation of, 188  
 hydroboration by, 524, 533
- boranes  
 alkyl  
 chiral, 529–531  
 formation of, 188  
 halogenation of, 529  
 hydroboration by, 524  
 oxidation of, 527–528  
 reactions of, 526–529  
 reduction of ketones by, 193–194
- allyl, facile 1,3-sigmatropic shift  
 in, 916
- chloro  
 reduction of ketones by, 193–194
- halo  
 hydroboration by, 524, 531  
 as radical sources, 979
- borohydrides, alkyl  
 in reduction of ketones, 193
- boron enolates  
 in aldol reactions, 690–691  
 of amides, 693  
 of esters, 693  
 of *N*-acyloxazolidinones  
 in aldol reactions, 694–695
- boron trifluoride  
 complex with 2-methylpropenal, 849  
 as Lewis acid catalyst, 354
- BOX catalysts, *see bis*-oxazolines
- BPE, *see* phosphines
- bromination, *see also* halogenation  
 of alkenes  
 mechanism of, 486–489  
 reagents for, 491  
 stereospecificity of, 183–185
- allylic, 1020–1021  
 of aromatic compounds, 802–803  
 substituent effects on, 290–293  
 of butene, kinetic isotope effect, 335  
 by *N*-bromosuccinimide, 1020–1  
 by radical substitution, 1018–24  
 examples, 1002–4  
 of dienes, 496–497
- bromohydrins  
 formation of, 492

- bromonium ions  
in bromination of alkenes, 185, 486, 535  
characterization of, 489–491  
computational modeling, 494–495
- bromotrichloromethane, *see* halomethanes
- Brønsted catalysis law, 348, 602
- 1,3-butadiene and derivatives  
2,3-*bis*-(*t*-butyl)  
photoproducts from, 1103
- 2,3-dimethyl  
photocyclization of, 1101
- 2-cyano  
photoproducts from, 1103
- conformation of, 149–51
- electron density distribution in, 21, 73–74
- electrostatic potential surface of, 73–74
- excited states for  
computational modeling, 1137–1142
- photochemical reactions of, 1100–1101
- photodimerization of, 1103–4  
effect of photosensitizers, 1104
- photoisomerization of, 1096–1097
- resonance in, 20, 62
- stabilization of, 262
- but-3-enyl radical  
from ring opening of cyclopropylmethyl radical,  
972
- butane  
chlorination of, 996  
conformation of, 143–144  
rotational barrier in, 80
- 2-butanone  
conformation of, 149
- 1-butene  
kinetic isotope effect in bromination, 335  
kinetic isotope effect in epoxidation, 335
- 2-butene  
photochemical cycloaddition of, 1109
- t*-butyl carbocation  
structure of, 430
- t*-butyl hydroperoxide  
as a radical source, 977  
in Sharpless asymmetric epoxidation, 197
- t*-butyl hypochlorite, 1022
- 2-butylium cation  
rearrangement of, 441–444
- Cahn-Ingold-Prelog priority rules, 120, 122
- capto-dative stabilization of radicals, 316, 987–988
- carbanions  
[12]annulene dianion, 742  
additions to carbonyl compounds, 676–682,  
687–692  
bicyclo[3.2.1]octa-2,6-dienide, 744–745  
charge distribution in, 308  
cyclononatetraenide, aromaticity of, 741  
cyclooctatetraene dianion, aromaticity of, 741  
cyclopentadienide, aromaticity of, 740
- hybridization of, 307  
as nucleophiles, 609–619  
organometallic compounds, relation to, 588–591  
phenalenyl, 757  
proton affinity of, 308  
table, 310  
stabilization by substituents, 307–311, 591–601  
computation of, 309–311  
phosphorus-containing, 599  
sulfur-containing, 599  
structure of, 307, 585
- carbocations  
[C<sub>3</sub>H<sub>7</sub>]<sup>+</sup> isomers, 441  
[C<sub>4</sub>H<sub>7</sub>]<sup>+</sup> isomers, 453  
[C<sub>4</sub>H<sub>9</sub>]<sup>+</sup> isomers, 441–443  
[C<sub>5</sub>H<sub>11</sub>]<sup>+</sup> isomers, 444–445
- 2-butyl  
rearrangements of, 441–444
- adamantylum, 431
- alkenyl, 435–436
- allyl  
from cyclopropyl cation by ring opening,  
907–908  
stabilization of, 302
- aromatic, 303
- aryl, 436
- benzylic, 302, 439  
substituent effects on, 432–433
- bicyclic, rearrangement of, 446
- bicyclobutonium, 453, 744  
electron density for, 744
- bridged, 301, 432, 440, 447–453  
examples, 452
- t*-butyl, 430
- charge distribution in, 306–307, 429–430
- computational characterization of, 305–306
- cycloheptatrienyl, 740
- cyclohexadienyl  
Huckel MO diagram for, 775  
observation of, 777–778  
role in electrophilic aromatic substitution,  
775–776  
trapping of, 778
- cyclohexyl, rearrangement of, 445–446
- cyclooctatrienyl, 743–745
- cyclopentadienyl, 739–740
- cyclopropenyl, 738–739
- cyclopropyl, ring opening of, 907–908
- cyclopropylmethyl, 427
- elimination versus substitution, 437–439
- from diazonium ions, 405–407
- hybridization of, 300
- hydride affinity of, 303, 314  
table, 303, 314
- hyperconjugation in, 301, 305, 307, 429, 432  
as intermediates  
in electrophilic addition reactions, 479, 480  
in Friedel-Crafts alkylation, 806, 808  
in nucleophilic substitution, 391–393

- methyl, 300  
  electron distribution in, 65  
methylcyclohexyl, 430–431  
norbornyl, 422, 448–452  
observation of, 436–438  
pentadienyl  
  electrocyclization of, 908–909  
in petroleum processing, 454–459  
phenalenyl, 757  
phenonium, 425  
phenyl, 436, 817  
rearrangement of, 440–447, 480  
resonance in, 22, 301–302, 433  
stability of, 300, 426–429  
  table, 427  
structure of, 430–433  
substituent effects on, 304–305,  
  432–434, 632  
substitution versus elimination, 437–439  
trichloromethyl, 434  
trifluoromethyl, 434  
vinyl, 435–436  
   $\alpha$ -alkoxy, 22
- carbodiimides  
  in acylation reactions, 667
- carbon  
  electronegativity of, 12–14  
carbonium ions, 456–458  
  structure of, 458
- carbon monoxide  
  electron density by Laplacian function, 94
- carbon tetrachloride, *see* halomethanes
- carbonyl addition reactions  
  acid and base catalysis of, 345, 630  
  mechanisms of, 325–327  
  nucleophilic, intermediates in, 319–331  
  radical, comparison of rates with alkenes,  
    1007–1008  
  tetrahedral intermediate in  
    evaluation of relative stability, 329–30
- carbonyl compounds, *see also* aldehydes, esters,  
  ketones, etc.  
  acetal formation, 640  
  addition reactions of, 629–632  
    with enolates and enols, 682–697  
    with organometallic reagents, 676–682  
  condensation reactions of, 629, 645–653  
    with nitrogen nucleophiles, 645–653  
  conformation of, 148–149  
  cyanohydrin formation from, 635  
  enolization of, 601–608  
  excited states of, 1116–1117  
    charge distribution and bond order, 1117  
    structure, 1116–1117  
  hydration of, 638–639  
    acid and base catalysis of, 639  
    equilibrium constants for, table, 329, 638  
  interaction with Lewis acids, 323, 636–637,  
    848–849
- photochemical reactions of, 1116–1132  
  cycloaddition with alkenes, 1132–1134  
  type-II cleavage, proton affinity of, 636  
   $\alpha$ -cleavage, 1118, 1120–1122, 1124  
  reactions with organometallic reagents, 676–682  
  stereoselectivity of, 680–682  
  reduction, 176–179  
    by sodium borohydride, 633–634  
    enantioselective, 193–196  
  relative reactivity of, 319–323, 632–637  
  resonance effects in, 320–321  
  substituent effects in, 320–322  
  substitution reactions of, 629, 654–668  
    acylation of alcohols, 664–667  
    amide hydrolysis, 662–664  
    ester aminolysis, 659–662  
    ester hydrolysis, 654–658  
    intramolecular catalysis of, 668–676  
  tetrahedral intermediates in, 630  
  unsaturated  
    conformation of, 151  
    excited states of, 1117–1118  
    photocycloaddition reactions with alkenes,  
      1125–1126  
    photoreactions of, 1123–1124  
    resonance of, 21
- carboxylic acid anhydrides  
  rate of hydrolysis, 328
- carboxylic acid derivatives, *see also* acyl chloride,  
  acid anhydrides, etc.  
  acylation reactions of, 664–668  
  reactivity toward organometallic compounds, 677  
  relative reactivity of, 636  
  substitution reactions of, 654–668
- carboxylic acids  
  acid dissociation constants, computation of, 53  
  derivatives, relative reactivity of, 328  
  substituent effects on acidity, 13, 53–54, 105,  
    322
- CAS MO method, 36
- catalysis, 345–358  
  by acids and bases, 345–353  
  by Lewis acids, 354–358  
  intramolecular in carbonyl substitution reactions,  
    668–676  
  nucleophilic  
    in ester hydrolysis, 657
- catalytic hydrogenation, *see* hydrogenation
- catalytic reforming, 454–456
- catalytic triad in enzymatic hydrolysis, 675–676
- catechol borane  
  hydroboration by, 525
- CBS catalysts, *see also* oxazaborolidines  
  for enantioselective reduction of ketones,  
    194–196
- CBS MO method, 36
- CD, *see* circular dichroism
- chain reaction, definition, 965  
  chain length of, 965, 993

- chain reaction, definition (*cont.*)  
initiation of, 965, 993  
kinetic characteristics of, 992–995  
propagation phase, 965, 993  
termination of, 965, 993
- charge distribution, *see* electron density distribution
- chelation control  
in hydride reduction of ketones, 181–182  
in organometallic additions to carbonyl compounds, 680–682  
computational modeling of, 681–682
- chemical bonds  
bent, in cyclopropanes, 85  
polarity of, 10
- chemical kinetics, *see* kinetics
- chemically induced dynamic nuclear polarization  
in decomposition of benzoyl peroxide, 975  
in decomposition of trichloroacetyl peroxide, 976  
for detection of radicals, 974–975
- chemical potential, definition, 95
- chiral auxiliaries  
in control of stereoselectivity, 207–208  
for Diels-Alder reactions, 865–866
- chirality, definition, 122  
relationship to molecular symmetry, 131–133
- chiral selectors, in capillary electrophoresis, 214
- chiral shift reagents, 208–211
- chiral stationary phase  
brush type, 213  
chiracels as, 212  
for enantiomeric separation, 211–213
- chiraphos, *see* phosphines
- chlorination, *see also* halogenation  
of alkenes, 487–488  
of alkynes, 540–543  
of aromatic compounds, 800–804  
of butane, 996  
by radical chain substitution  
substituent effects on, 1022  
by *t*-butyl hypochlorite, 1022
- chlorohydrins  
formation of, 492
- chloronium ions, 490, 535  
computational modeling, 494–495
- chrysene, 749
- $\alpha$ -chymotrypsin  
in resolution of  $\alpha$ -amino esters, 222
- CIDNP, *see* chemically induced dynamic nuclear polarization
- Cieplak model, 180, 234
- circular dichroism, definition, 125
- Claisen rearrangements, 933–937  
activation parameters for, 273, 933  
of allyl aryl ethers, 934–935  
of allyl vinyl ether, 933  
Marcus theory treatment of, 936  
stereochemistry of, 935  
substituent effect on, 935–938
- Claisen-Schmidt condensation, 685–686  
examples of, 687
- CNDO MO method, 32
- concerted pericyclic reaction, definition, 833
- configuration, definition, 117  
specification of in Fischer projection formulas, 127  
at tetrahedral atoms, 122
- conformation, definition, 117  
of 1,3-butadiene, 149–151  
of 1-butene, 147  
of 2-butanone, 149  
of 3-pentanone, 149  
of acyclic compounds, 142–151  
of aldehydes, 148  
of alkanes, 142–145  
of alkenes, 145–147  
of butane, 80, 143–144  
of chlorocyclohexane, 155–156  
of cycloalkanes, 161–166  
of cyclobutane derivatives, 161  
of cyclodecane, 165–166  
of cycloheptane, 163–164  
of cyclohexane derivatives, 152–161  
of cyclohexanones, 161  
of cyclohexene, 160  
of cyclooctane, 164–165  
of cyclopentane derivatives, 162–163  
of disubstituted methanes, 81–85  
of ethane, 142–143  
of iodocyclohexane, 156–157  
of ketones, 148–149  
of large ring hydrocarbons, 166  
of methanol, 145  
of methylamine, 145  
of propenal, 148, 151
- conformational free energy, definition, 156  
measurement of, 156–158  
table of values, 158
- conical intersections in photochemical reactions, 1080  
of 1,3,5-hexatriene  
computational modeling of, 1142–1144  
of 1,3-butadiene  
computational modeling of, 1140–1142  
of photocycloaddition of benzene and ethane, 1136–1137  
potential energy surface for, 1080  
of stilbene, 1089–1090
- connectivity, 1
- conrotatory, definition, 893
- conservation of orbital symmetry  
for concerted pericyclic reactions, 833
- constitution, molecular, 1
- Cope rearrangement, 920–931  
activation energy for, 920  
of barbaralane, 931  
of bulvalene, 930–931

- chair versus boat transition structure for, 923  
computational modeling of, 926–927  
cyano substituents, effect on, 927  
of divinylcyclopropane, 929  
effect of strain on, 928  
More-O’Ferrall-Jencks diagram for, 928  
of semibullvalene, 931  
stereochemistry of, 922–923  
substituent effects on, 924–928
- covalent radii, 24  
definition within DFT, 97  
table of, 25, 98
- Crabtree catalyst, 174  
cracking, 454–456  
Cram’s rule, 179  
critical micellar concentration, definition, 219  
critical point, in electron density distribution, 63  
for substituted methanes, 66–68  
crown ether catalysts, 364–365  
CSP, *see* chiral stationary phase
- cubane  
acidity of, 373–374  
halogenation of, 1003
- Curtin-Hammett principle, 296–297
- cyano groups  
anion stabilization by, 598
- cyanohydrins  
formation from carbonyl compounds, 635
- cycloaddition reactions, 834–892  
[2+2] of ketenes, 835, 888–892  
azetidiones from, 891–892  
intramolecular, 890–891  
orbital array for, 888–889  
stereoselectivity of, 890  
transition structure for, 889
- 1,3-dipolar cycloaddition as, *see also* 1,3-dipolar  
cycloaddition, 834  
antarafacial and suprafacial modes of, 836  
application of DFT concepts to regiochemistry,  
945–951  
Diels-Alder as, *see also* Diels-Alder reaction,  
834  
as examples of concerted pericyclic reactions,  
834  
Huckel versus Mobius topology of, 836  
of ozone with ethene, 49–50  
photochemical, of alkenes, 1125–1126  
Woodward-Hoffmann rules for, 836–837
- cycloalkanes  
configuration of, 121  
conformation of, 161–166  
molecular symmetry of, 133  
strain in, 161–166
- cycloalkenes  
chirality of, 130  
*E*-cycloalkenes, racemization of, 131  
photochemistry of, 1094–1096
- 1,3-cyclobutadiene  
antiaromaticity of, 714, 718, 726  
destabilization of, 718, 726  
generation of, 725  
Huckel MO diagram for, 714  
reactions of, 725  
structure of, 726
- 1,3-cyclohexadiene derivatives  
electrocyclic ring opening of, 1108–1109  
photoproducts from, 1106, 1112
- cyclobutane derivatives  
conformation of, 162  
formation by cycloaddition, 891
- cyclobutenes  
1-aryl  
photoproducts from, 1105  
electrocyclic ring opening of, 892–893  
3,4-dichlorocyclobutene, 903  
inward versus outward rotation during,  
901–903  
stereochemistry of, 896–897  
photochemical reactions of, 1104–1105
- cyclodecane  
conformation of, 165–166
- cycloheptane  
conformation of, 163–164
- cycloheptatrienes  
electrocyclic reactions of, 905  
sigmatropic shift of hydrogen in, 917–918
- cycloheptatrienyl cation  
aromaticity of, 32, 740
- cycloheptene  
photoreactions of, 1094
- 1,5-cyclohexadienone  
4,4-diphenyl, photochemistry of, 1130–1132
- cyclohexane derivatives  
alkyl, conformation of, 157–159  
chloro-  
conformational half-life of, 153–154  
conformation of, 152–161  
iodo- conformation by NMR, 156–157  
kinetics of ring inversion, 152–156
- cyclohexanone derivatives  
conformation of, 161  
stereoselective reduction of, 176–179
- cyclohexene  
1-phenyl  
photodimerization of, 1110–1111  
conformation of, 170  
photoreactions of, 1094–1095, 1110
- cyclohexyl radical  
structure of, 984
- 1,3-cyclooctadiene  
photocyclization of, 1101
- 1,4-cyclooctadiene  
photocyclization of, 1111
- 1,5-cyclooctadiene  
photochemistry of, 1145
- cyclooctane  
conformation of, 164–165
- cyclooctatrienyl cation, 743

- 1,3,5,7-cyclooctatetraene  
dianion of, 741–742, 990  
dication of, 742  
photochemistry of, 1144  
properties of, 727–728
- cyclooctene  
*E*-isomer, chirality of, 131  
photoreactions of, 1094
- cyclopentadiene  
acidity of, 740  
derivatives, sigmatropic shifts in, 917  
Diels-Alder reactions of, 840–841, 843
- cyclopentadienyl anion  
aromaticity of, 32, 740
- cyclopentadienyl cation, 739–740
- cyclopentane derivatives  
conformation of, 162–163  
pseudorotation in, 163
- cyclopentene  
photocycloaddition with cyclohexenone,  
1125–1126  
photoreactions of, 1095
- cyclopentenone  
photochemical reactions of, 1125
- cyclopropane  
bonding in, 85–87  
divinyl, Cope rearrangement, 929  
electron delocalization in, 86–87  
hybridization in, 86  
protonated  
in carbocation rearrangements,  
441–443  
structure of, 162  
vinyl, thermal rearrangement, 929
- cyclopropenium cation, 738–739
- cyclopropyl cation  
electrocyclic ring opening of, 907–908
- cyclopropyl halides  
 $S_{RN}1$  substitution reactions, 1051
- cyclopropylmethyl cation, 427
- cyclopropylmethyl radical  
generation of, 972  
potential energy profile for, 974  
ring opening of, 973–974, 1008–1009
- decahydronaphthalene, *see* decalin
- decalin  
conformations of, 159–160
- decarbonylation  
of acyl radicals, 967  
of ketones, photochemical, 1120–1122
- decarboxylation  
Of acyloxy radicals, 967, 979–980
- degenerate rearrangements, 930–931
- dehalogenation  
stereochemistry of, 564–565
- dehydration  
of alcohols, 474, 564–565
- in aldol reactions, 683–685
- delocalization energy, definition, 19  
as a criteria of aromaticity, 715  
estimation of, 30
- density functional theory  
application to properties and reactivity, 94–105  
B3LYP method, 55–57  
concepts, application to cycloaddition reactions,  
947–951  
electron density functionals, 54–57  
interpretation of substituent effects by, 100–105  
Kohn-Sham equation, 54
- Dewar benzene, *see* bicyclo[2.2.0]hexa-2,5-diene
- DFT, *see* density functional theory
- DHQ, *see* quinoline alkaloids
- DHQD, *see* quinoline alkaloids
- diamines  
intramolecular catalysis by, 675
- diaminomethane, conformation, 84
- diamond lattice, as conformational framework, 166
- diastereomers, definition, 126–127
- diastereotopic, definition, 134  
relationship to NMR spectra, 134–135
- diazoalkanes  
as 1,3-dipoles, 875, 878–879  
relative reactivity of, table, 877  
frontier orbitals of, 880–881
- diazonium ions  
alkyl  
nucleophilic substitution reactions of, 405–407  
stability of, 68  
aryl  
as electrophiles in aromatic substitution,  
813–814  
benzyl, in electrophilic aromatic substitution, 808  
methyl, charge distribution in, 66
- $\alpha$ -dicarbonyl compounds  
enolization of, 606
- $\beta$ -dicarbonyl compounds  
acidity of, 592  
enolization of, 603–606
- Diels-Alder reaction, 839–873  
as an indicator of aromatic stabilization, 748–749  
application of DFT concepts to reactivity,  
945–950  
in comparison with frontier MO theory, 949  
softness matching for regioselectivity, 948  
catalysis by Lewis acids, 356, 848–850  
chiral auxiliaries for, 865–866  
enantioselective, 865–868  
examples of, 861  
intramolecular, 868–873  
conformational factors in, 869–870  
examples of, 872–873  
inverse electron demand, 843  
of isobenzofuran derivatives, 760, 858, 864  
kinetic isotope effect in, 335  
of polycyclic aromatic hydrocarbons, 748–749,  
857–858

- regioselectivity of, 844–848  
  frontier MO analysis of, 844–847  
stereochemistry of, 839  
  Alder rule for, 840–841  
  computational analysis of, 852–853  
  Lewis acids, effect on, 853  
  secondary orbital interactions in, 842, 854–855  
substituent effects on, 843–848  
synthetic applications of, 860–864  
transition structures for, 840–841  
  aromaticity of, 851  
  charge transfer character in, 847, 857–858, 950  
  computational characterization of, 851–860  
  synchronicity of, 852, 855–856  
water, as solvent for, 850
- 1,4-dienes  
  photochemical reactions of, 1112–1116
- 1,5-dienes  
  [3,3]-sigmatropic rearrangements of, 920–930  
  substituted, BDE for, table, 988
- dienes, *see also* specific dienes e.g. 1,3-butadiene  
addition reactions  
  bromination of, 496–497  
  with hydrogen halides, 481  
conformation of, 149–151  
  in Diels-Alder reactions, 842  
Danishefsky's diene, 864  
in Diels-Alder reactions, 839  
  2-substituted, 847–848  
  effect of conformation, 842  
  effect of substituents on rate, 842–848  
electrocyclic reactions of, 892–893  
global electrophilicity of, table, 946  
local electrophilicity of, 947  
local nucleophilicity of, 947  
local softness of, 948  
photochemical reactions of, 1100–1104  
  computational interpretation, 1137–1145  
photoisomerization of, 1096–7  
quinodimethanes as, 857, 864
- dienophiles, 839  
chiral acrylate esters as, 865–866  
effect of substituents on reactivity, 843–848  
examples of, 844  
frontier orbitals of, 846–847  
global electrophilicity of, 946  
local electrophilicity of, 947  
local nucleophilicity of, 947  
local softness of, 948  
nitroethene as, 862  
quinones as, 862  
vinylphosphonium salts as, 863  
vinyl sulfones as, 863  
vinyl sulfoxides as, 863
- dihydroxylation of alkenes  
  enantioselective, 200–203  
  computational model for, 202–203  
  reagent control of, 206–207
- diisopinocampheylborane  
  in enantioselective reduction of ketones, 194  
  hydroboration by, 529–531
- dimethoxymethane  
  conformation, 83  
  stabilization of, 262–263
- dimethyl sulfoxide  
  as solvent, 363, 411–412
- 2,4-dinitrofluorobenzene  
  nucleophilic substitution reactions of, 820
- dinitrogen, *see* Nitrogen, molecular
- DIOP, *see* phosphines
- dioxoles  
  anomeric effects in, 233
- DIPAMP, *see* phosphines
- 1,2-diphenylethane-1,2-diamine  
  as chiral shift additive for NMR, 210
- diphenylpicrylhydrazyl, as radical inhibitor, 994
- 1,3-dipolar cycloaddition reactions, 873–888  
  application of DFT concepts to, 950–951  
  Bell-Evans-Polyani relation in, 883  
  catalysis of, 886–888  
  computational modeling of, 887  
  *tris*-aryloxyaluminum as, 886  
  comparison with Diels-Alder reaction, 883  
  computational model of, 880–883  
  examples of, 885  
  frontier MO interpretation of, 874–882  
  intramolecular, 884  
  regiochemistry, 880–883  
  effect of catalysts, 886–888  
  electronic versus steric control, 880, 886  
  stereochemistry of, 877–879  
  synchronicity of, 882  
  synthetic applications of, 884–886
- 1,3-dipoles  
  characteristics of, 874  
  examples of, 875  
  frontier orbitals of, 880–881  
  global electrophilicity of, 950
- dipolarophiles  
  frontier orbitals of, 845–847  
  relative reactivity of, table, 876  
  with ethene, 883
- dipole moment  
  computation of, 53
- diradicals  
  photochemical generation, 1123  
  structural effect on lifetimes, 1017–1018
- disiamylborane  
  formation of, 188  
  hydroboration by, 524
- dispersion forces, 24
- disrotatory, definition, 893
- dithianes  
  acidity of, 599  
  anomeric effects in, 233

- di- $\pi$ -methane rearrangement, 1112–1116  
   conical intersection, computational model, 1113–1114  
   of cyclohexenones, 1127–1129  
   mechanism of, 1112–1113  
   orbital array for, 1129  
   stereochemistry of, 1113  
   substituent effects in, 1114–1115  
 DMF, *see* *N,N*-dimethylformamide  
 DMSO, *see* dimethyl sulfoxide  
 double stereodifferentiation  
   in aldol reactions, 205  
   examples of, 204–207  
   in organozinc addition reactions, 205–206  
   reactant control in, 206  
   substrate control in, 206  
 DPPH, *see* diphenylpicrylhydrazyl  
 dual substituent parameter equation, 341  
 DuPHOS, *see* phosphines
- EA, *see* electron affinity  
 eclipsed, definition, 142  
 EHT MO method, 32  
 electrocyclic reactions, 892–911  
   of [10]annulene, 728–729  
   of 1,3,5-trienes, 893–894  
     computational analysis of, 899–900  
     heteroatom analogs of, 910–911  
   of 1,3-dienes, 892–893  
     computational modeling of, 1140–1142  
   of 2,4,6,8-decatetraene, 899  
   of charged species, 906–910  
   as concerted pericyclic reactions, 834  
   of cyclopropyl cation  
     stereochemistry of, 907–908  
   examples of, 903–906  
   frontier MO interpretation of, 894–895  
   inward versus outward rotation in, 901–903  
   orbital correlation diagrams for, 895–897  
   orbital symmetry rules for, 900  
   of pentadienyl cations, 908–909  
     substituent effects on, 909  
   photochemical, 1099–1100  
   of photoenols, 1120  
   stereospecificity of, 892–4  
   summary of thermodynamics for, 901  
   transition state  
     aromaticity of, 898  
     orbitals for, 897  
 electron affinity, 9, 95  
 electron correlation  
   treatments in MO calculations, 34–35  
 electron density distribution  
   1,3,5-hexatriene, 19  
   in 1,3-butadiene, 20, 48, 74  
   in ammonia, 92  
   in aromatic compounds, 723–724  
     in relation to electrophilic substitution, 784  
     in benzene, 57–58, 723–724  
     in bicyclobutonium ion, 744  
     in carbanions, 308  
     in carbon monoxide, 94  
     critical point of, 63  
     in cyclooctatrienyl ion, 744  
     in cyclopropane, 86–87, 537  
     deformation electron density, definition, 57  
     ellipticity of, 58, 64–65  
     in ethane, 94  
     in ethenamine, 48, 74  
     in ethene, 93–94  
     in formaldehyde, 59, 61, 70, 94  
       excited state, 1117  
     in formamide, 71  
     in hydrides of second row elements, table, 66  
     in hydrogen molecule, 3–4, 6  
     in methoxide ion, 68–69  
     in methyl cation, 65  
     in methyl derivatives, 68–69  
     Mulliken population analysis of, 60–61  
     in nitrogen, 94  
     in oxirane and conjugate acid, 537  
     in propenal, 21, 48, 60, 74  
     in propene, 23  
     representation of, 57–77  
       by Laplacian function, 92–94  
     in substituted ethenes, 71–73, 75  
 electronegativity, 8–11  
   absolute, 9  
   of alkyl groups, 13  
   Allred-Rochow, 9  
   of carbon, 12–14  
   Luo-Benson, 9, 95  
   Mulliken, 9, 95  
   Pauling, 9  
     correlation with hardness, 96  
   in relation to bond strength, 14  
   spectroscopic determination of, 9  
   of substituent groups, 260  
 electronegativity equalization, 11–12, 95, 260  
 electron paramagnetic resonance, *see* electron spin resonance  
 electron spin resonance, 970–972  
   of bridgehead radicals, 985  
   in detection and characterization of radicals, 970–972  
   hyperfine splitting in, 970–971  
 electron transfer  
   in aromatic nitration, 799–800  
   in initiation of  $S_{RN}1$  substitution reactions, 1048–1049  
   in organometallic addition reactions, 679  
 electrophilic aromatic substitution  
   bromination, *see* halogenation  
   chlorination, *see also* halogenation  
     kinetics of, 801  
   cyclohexadienyl cation as intermediates in, 775–778

- diazonium coupling, 813–814  
examples of, 772–773  
Friedel-Crafts acylation, 809–813  
Friedel-Crafts alkylation, 805–809  
  position selectivity, 807  
general mechanism for, 772–779  
halogenation, 800–804  
Hammett reaction constants for  
  Table, 790  
of heteroaromatic compounds, 793–794  
HOMO distribution in relation to, 783  
*Ips*o substitution in, 778, 814–816  
kinetic isotope effects in, 777  
  table, 790  
localization energy in, 782, 791  
nitration, 796–800  
partial rate factors for, 786–787  
  table, 788  
of polycyclic hydrocarbons, 791–793  
position selectivity in, 787–791  
proton exchange as, 804–805  
  of naphthalene, 792  
reactivity-selectivity relationships for, 787–791  
role of  $\pi$  complexes in, 773–775  
role of  $\sigma$  complexes in, 775–776  
substituent effects in, 779–787  
  MO interpretation of, 780–781  
  summary of, 784–785
- electrostatic effects  
  in reduction of substituted ketones, 238
- elimination reactions, 473–474, 546–568  
  computational modeling, 561–562  
  examples of, 548  
  kinetic isotope effects in, 552  
  mechanisms of, 548–554  
    distinguishing features of, 552  
    E1, 548  
    E1cb, 549  
    E2, 548  
  of organomercury compounds, 565–566  
  reductive, 564–5  
  regiochemistry of, 554–558  
    effect of base strength, 556–557  
    effect of leaving group, 557–558  
    Hofmann rule for, 556  
    Saytzeff rule for, 556  
  solvent effects on, 554  
  stereochemistry of, 558–563  
    anti versus syn, 558–562  
    leaving group effect, 559–561  
    steric effects on, 562–563  
  variable transition state theory for, 549–551
- enamines, 608–609  
  formation of, 653  
  hydrolysis of, 653  
  nucleophilicity of, 608–609  
  resonance in, 22, 608–609
- enantiomeric excess, definition, 123–124  
  determination of, 208–211
- enantiomeric mixtures  
  analysis and separation by capillary  
    electrophoresis, 213–215  
  analysis of, 208–211  
  separation of by chromatography, 211–213
- enantiomers  
  properties of, 123, 127  
  resolution of, 136–141
- enantioselective catalysts for  
  1,3-dipolar cycloaddition reactions, 887–888  
  aldol reaction, 695–696  
  Diels-Alder reactions, 867–868  
  dihydroxylation, 200–203  
  epoxidation, 196–199  
  hydroboration, 529–531
- enantioselective reactions, 189–203  
  dihydroxylation of alkenes, 200–203  
  examples of, 189–203  
  hydrogenation, 189–193  
  reduction of ketones, 193–196
- enantiotopic, definition, 133
- energy dependence of light wavelength, 1074
- energy of atomization, definition, 257  
  calculation of, 265–267
- enolates, 591  
  alkylation of, 614–619  
    stereoselectivity of, 615–619  
  arylation by, substitution reactions, examples,  
    1051
- boron  
  in aldol reactions, 691–692
- composition of, 595–596  
  effect of base on, 689
- computational characterization, 613
- C- versus O-alkylation, 366–368, 614–615
- of esters  
  aldol reactions of, 692–693  
  formation of, 592–595  
  kinetic control of formation, 287, 595, 689  
  nucleophilicity of, 331–332  
  structure of, 612–613  
  substitution reactions of, 611–618
- tin  
  in aldol reactions, 692
- titanium  
  in aldol reactions, 691–692
- enol esters  
  in acylation reactions, 667–668
- enols, 601–608  
  equilibrium constants for, table, 604  
  formation of, 607  
  nucleophilicity of, 602
- enthalpy of formation, definition, 254  
  calculation using group equivalents, 261–262  
  calculation using molecular mechanics, 263–264  
  computation by MO and DFT methods, 265–267  
  determination of, 255  
  of hydrocarbons, 256

- enthalpy of reaction, 253  
  calculation of, 258–259  
  determination of, 271  
  examples of, 273  
  relation to reaction rates, 269–270
- entropy of reaction, 253  
  determination of, 271  
  examples of, 273–274  
  for solvolysis of *t*-butyl chloride, 273
- enzymes  
  alcohol dehydrogenase, 135  
  epoxide hydrolases, 224–227  
  hydrolytic, 875–876  
  lipases, 216–221  
  proteases, 222–224  
  in resolution of enantiomers, 215–227  
  stereoselective reactions of, 133–136
- epoxidation  
  of alkenes, 503–511  
    by dimethyldioxirane, 507–510  
    hydroxy group directing effects in, 505–506  
    mechanism of, 504  
    reagents for, 503–504, 510–511  
    substituent effect on, 504, 506–508  
    transition structures for, 507–508  
  Sharpless asymmetric, 196–199  
  computational model for, 198–199
- epoxides  
  enzymatic hydrolysis of, 224–227  
  ring-opening of, 186–187, 511–512  
  pH-rate profile for, 512  
  regioselectivity of, 511–512, 515  
  stereochemistry of, 513–515
- ESR, *see* electron spin resonance
- esterases, *see also* hydrolases  
  pig liver esterase  
    in resolution of enantiomers, 217–220  
    selectivity model for, 217–220  
  in resolution of enantiomers, 216–221
- esterification  
  by acylation of alcohols, 664–668  
  enzymes as catalysts for, 216, 223
- esters  
  aminolysis, 659–662  
  catalysis by 2-pyridone, 661–662, 673–674  
  general base catalysis of, 659  
  leaving group effects on, 661  
  rate of, 328
- enolates of  
  in aldol reactions, 692–694  
  boron, 693  
  formation of, 937  
  solvent effects on, 937
- formation  
  by Fischer esterification, 664  
  from acid anhydrides, 665  
  from acyl halides, 665–666
- hydrolysis, 654–656  
  A<sub>AC</sub>2 mechanism, 654
- A<sub>AL</sub>1 mechanism, 656
- B<sub>AC</sub>2 mechanism, 654
- computational model for, 325–326
- intramolecular catalysis of, 670–674
- leaving group effects on, 655
- mechanism of, 324–326, 654–656
- nucleophilic catalysis of, 657
- solvent effects on, 365–366
- of tertiary alcohols, 656
- rate of hydrolysis, 328
- reactions with organometallic compounds, 678  
  effect of TMEDA, 678
- E<sub>T</sub>(30), as measure of solvent polarity, 360
- ethane  
  conformation of, 78–81, 142–143  
  electron density by Laplacian function, 93–94  
  rotational barrier in, 78–81
- ethenamine  
  electron density distribution in, 73–74  
  electrostatic potential surface for, 73–74  
  MOs of, 47  
  resonance in, 22
- ethene  
  electron density by Laplacian function, 93  
  MOs of, 39–42, 46–47  
  photocycloaddition with benzene  
    computational modeling of, 1136–1137  
  photodimerization of  
    computational modeling, 1109–1110  
  photoexcited states of, 1082–1083  
  reaction with ozone, 49–50  
  stabilization by substituents, 52  
  substituted  
    electron density distribution, 71–73  
    electrostatic potential surface, 74–75
- ethers  
  allyl phenyl, sigmatropic rearrangement of, 934–935  
  allyl vinyl, sigmatropic rearrangement of, 273, 933  
  autoxidation, 1026  
  neighboring group participation, 421  
  α-halo, effect of hyperconjugation on reactivity, 84–85
- ethylene, *see* ethene
- ethyl radical  
  ESR spectrum of, 971
- ethyne  
  electron density by Laplacian function, 93
- excited states of  
  1,3-cyclohexadiene, 1106  
  benzaldehyde, 1118  
  ethene, 1082–1083  
  stilbene, 1085–1090  
  styrene, 1083–1085
- Felkin-Ahn model, 179, 234  
  for addition reactions with carbonyl compounds, 680

- field effect, 338  
 Fischer projection formulas, 127  
 fluorescence, 1077  
 fluorination, *see also* halogenation  
   of alkenes  
     reagents for, 496  
   of aromatic compounds, 804  
   of hydrocarbons, 1023  
 fluoromethanol, conformation, 83  
 fluoromethylamine, conformation, 84  
 FMO, *see* frontier molecular orbital theory  
 formaldehyde  
   electron density distribution in, 59, 61, 70, 94  
   excited states of, 1116–1117  
   Fukui functions of, 99–100  
   MOs of, 43–46  
 formamide  
   electron density distribution in, 71  
   radical addition to alkenes, 1032–1033  
   resonance in, 62  
 formate anion  
   resonance in, 62  
 fragmentation reactions  
   photochemical, 1118  
   of radicals, 1013–1017  
 Frank-Condon principle, 1075  
 free energy  
   of activation, 254, 270, 271  
   of reaction, 253, 270  
 free radicals, *see* radicals  
 Friedel-Crafts acylation, 809–813  
   of naphthalene, 812–813  
   selectivity in, 812  
 Friedel-Crafts alkylation, 805–809  
 frontier molecular orbitals, 29, 43, 99  
   of cycloaddition reactions, 837, 844–847  
   of Diels-Alder reactions, 844–847  
   of electrocyclic reactions, 894–895  
   of electrophilic aromatic substitution, 783–784  
   of radical substituent effects, 1004–1006  
   in sigmatropic rearrangements, 912–915, 920  
 Frost's circle, 31  
 Fukui functions, 97–100  
 fulvalenes, 755–757  
 fulvene, 754–755  
 functional groups, 2  
 furan  
   aromatic stabilization of, 758–759  
   electrophilic aromatic substitution of, 793–794  
  
 G2 MO method, 36  
*gauche*, definition, 143–144  
   increments for in enthalpy calculation, 261  
   interactions  
     in butane, 144  
     in *cis*- and *trans*-decalin, 159  
     in cyclohexane derivatives, 154  
 general acid catalysis, 346  
 general base catalysis, 347  
 glyceraldehyde, as reference for configuration, 127  
   in radical reactions, 1037–1039  
 Grignard reagents, *see* magnesium  
 group transfer reactions, definition, 966  
  
 halides, *see* alkyl halides, aryl halides etc.  
 halogenation, *see also* bromination, chlorination  
   etc.  
   of alkenes, 485–497  
   of alkynes, 540–544  
     intermediates in, 542–543  
   aromatic, 800–804  
     reagents for, 803  
   of hydrocarbons by radical mechanisms,  
     1002–1004  
 halomethanes  
   atmospheric lifetimes of, table, 1060  
   radical addition reactions of, 1029–1031  
     to cyclooctene, 1041  
   reactions with hydroxyl radical, 1059–1062  
     correlation with global hardness, 1061–1062  
   relative reactivity of, 1029  
 halonium ions  
   computational comparison, 494–495  
 Hammett equation, 335–342  
   non-linear, 344  
   reaction constant for, 337  
     examples of, 340  
   substituent constant for, 337  
     table of, 339  
 Hammond's postulate, 289–293  
   application in electrophilic aromatic substitution,  
     788  
   application in radical halogenation, 1021  
 hardness, definition, 14, 96  
   as an indicator of aromaticity, 720, 750  
   of metal ions, 14  
   of methyl halides, 16  
   principle of maximum hardness, 15–16  
   relationship to HOMO-LUMO gap, 15  
   in relation to electrophilic aromatic substitution,  
     794–795  
 hard-soft-acid-base theory, 14–17, 105  
   principle of maximum hardness, 15–16  
   in relation to nucleophilicity, 410  
 harmonic oscillator model for aromaticity, 718–719  
 heat of formation, *see* enthalpy of formation  
 hemiacetals, 640  
 heptafulvalene, 755–757  
 heptalene, 753  
 heptatrienyl anion, 740  
   electrocyclization of, 910  
 heteroaromatic compounds, 758–760  
   electrophilic aromatic substitution in, 793–794  
 heterotropic, definition, 133  
 hex-5-enoyl radical rearrangement  
   energetics of, 1042–1043

- 2,4-hexadiene  
  photocyclization of, 1102
- hexahelicene  
  chirality of, 130
- hexamethylphosphoric triamide  
  effect on enolate alkylation, 616  
  effect on enolate composition, 596
- 1,3,5-hexatriene derivatives  
  electrocyclization reactions of, 895, 899–900  
  photochemical, 1106–1107  
  excited states  
    computational modeling of, 1142–1144  
    Hückel MO orbitals for, 29
- 5-hexenyl radical  
  cyclization of, 1009–1011
- high performance liquid chromatography  
  in separation of enantiomers, 211–213
- HMPA, *see* hexamethylphosphoric triamide
- Hofmann-Loeffler reaction, 1040
- Hofmann rule, 556
- HOMA, *see* harmonic oscillator model for aromaticity
- HOMO, 15, 29, 44, 97  
  distribution, in relation to electrophilic aromatic substitution, 783  
  in cyclooctatrienyl cation, 743
- homoaromaticity, 743–745  
  in cyclooctatrienyl cation, 743
- homodesmotic reactions, 265–267  
  in estimation of aromatic stabilization, 716–717
- HOMO-LUMO gap, 750  
  relationship to hardness, 15
- homolytic bond cleavage, definition, 965  
  examples, 965
- homotropilidene, *see* bicyclo[5.2.0]octa-3,5-diene
- homotropylium ion, *see* cyclooctatrienyl cation
- HPLC, *see* high performance liquid chromatography
- HSAB theory, *see* hard-soft acid-base theory
- Hückel's rule, 713, 738  
  application to charged rings, 742–743
- Hückel MO Method, 27–32
- hybridization, 4–7  
  in allene, 6  
  in cyclopropane, 85–86  
  effect on electronegativity of carbon, 12–13  
  effect on hydrocarbon acidity, 373, 376, 584–585  
     $sp$ , 5  
     $sp^2$ , 5  
     $sp^3$ , 5
- hydration  
  of alkenes, 474, 482–484  
  of carbonyl compounds, 329, 638–639
- hydrazone, 646  
  mechanism of formation, 651
- hydride affinity  
  of carbocation, 303  
  of carbonyl compound  
    table, 330
- hydroboration, 521–526  
  electrophilic character of, 522  
  enantioselective, 529–531  
  mechanism of, 522  
  reagents for, 521, 524–525  
  regioselectivity of, table, 523  
  stereoselectivity, 187–188  
  steric effects in, 523
- hydrocarbons, *see also* alkanes, alkenes, etc.  
  acidity of, 368–376, 579–587  
    computation of, 56–57, 586  
    effect of anion delocalization, 375  
    electrochemical determination of, 372, 584  
    gas phase, 585–586  
    hybridization effect on, 373, 376, 584–585  
    measurement of, 580–584  
    in relation to anion aromaticity, 740  
    table of, 371, 583
- aromatic  
  fused ring systems, 745–758  
  hardness of, 750, 795  
  photochemical reactions of, 1134–1137  
  redox potentials for, 990  
  stability comparisons for, 715–718, 746–748
- autoxidation of, 995
- bond dissociation energies for, 1053
- bond orders for, 77
- bromination of  
  Bell-Evans-Polyani relationship for, 288  
  by free radical substitution, 1018–1020, 1022  
  computation of enthalpy of formation by MO methods, 52  
  enthalpy of formation, table, 256  
  calculation by MO and DFT methods, 265–269  
  calculation using group equivalents, 29  
  relation to structure, 256
- fluorination of, 1023
- halogenation of  
  by radical substitution, 1018–1024  
  by tetrahalomethanes, 1003
- octane numbers of, 454
- polycyclic aromatic  
  aromaticity of, 749–751  
  electrophilic substitution of, 791–793  
  strained, bonding in, 87–89
- hydrocracking, 454–456
- hydrogenation, catalytic  
  catalysts for, 173–174  
  enantioselective, 189–193  
    of  $\alpha$ ,  $\beta$ -unsaturated carboxylic acids, 190  
    of  $\alpha$ -amidoacrylic acids, 191–192
- heterogeneous catalysis, 172
- homogeneous catalysis, 172
- mechanism of, 172, 174, 189–192
- stereoselectivity of, 170–176
- substituent directive effects in, 171–176
- hydrogen atom abstraction reactions, 1001–1004  
  by bromine atoms, 288

- by *t*-butoxy radical, 289, 1022  
interacting state model for, 1057–1058  
effect of bond energies on, 1001  
intramolecular, 1040–1041  
photochemical, 1118–1121  
intramolecular, 1122, 1123, 1126  
reactivity-selectivity relationship for, 1002  
structure-reactivity relationships for, 1056–1062  
Bell-Evans-Polyani relationship for, 1056–1057  
transition state, computational model for, 1058
- hydrogen bonding  
in enols, 605–606
- hydrolases  
epoxide, 224–227  
mechanism of, 216–217  
in resolution of enantiomers, 216–221
- hydrolysis  
of acetals, 641–645  
of amides, 662–664  
of enamines, 653  
of enol ethers, 485  
of esters, 654–658  
of imines, 647–649  
of vinyl ethers, 485
- hydroxy group  
directing effect in epoxidation, 194–197  
directing effect in hydrogenation, 174–176  
neighboring group participation by, 420–421
- hydroxyl radical  
reaction with halomethanes, 1059–1060
- hyperconjugation, 22–24  
of alkyl groups, 23  
in amines, 315, 1054  
anomeric effect, relation to, 230–231  
in carbocations, 301, 305, 307, 429  
in disubstituted methanes, 81–85  
of heteroatoms, 81–85  
in natural population analysis, 62  
in radicals, 981–982  
in regiochemistry of E1 reactions, 555–556  
in relation to alkene conformation, 146–7  
in relation to rotational barriers, 78–81  
role in kinetic isotope effects, 333  
role in substitution effects, 297–8
- IA, *see* index of aromaticity
- imidazole derivatives  
in catalytic triad of enzymes, 675–676  
intramolecular catalysis by, 671–672  
*N*-acyl, 324  
reactivity of, 664  
nucleophilic catalysis by, 656
- imines, 646  
[2+2] cycloaddition reactions with ketenes, 891–892  
configuration of, 121  
equilibrium constants for formation, table, 646  
hydrolysis of, 648–649  
intramolecular catalysis of formation, 675  
mechanism of formation, 646–650  
pH-rate profile for formation and hydrolysis, 647–649  
potential energy diagram for, 648–650  
computation of, 648–650
- indacene  
stability of, 754  
1-indanones, formation by Nazarov reaction, 909  
index of aromaticity, 719  
induced decomposition of peroxides, 977  
inductive effect, 12, 338  
intermediates  
in reaction mechanisms, 253  
internal return  
in hydrocarbon deprotonation, 581–582  
in nucleophilic substitution, 396–398  
intersystem crossing, 1075  
intrinsic barrier, in Marcus equation, 293  
intrinsic reaction coordinate, 279  
in computational modeling of chelation control, 681  
iodination, *see also* halogenation  
of aromatic compounds, 804  
iodohydrins  
formation of, 492  
ion pairs  
in nucleophilic substitution, 395–398, 404  
IP, *see* ionization potential  
ionization potential, 9, 95  
(*Ip*)<sub>2</sub>BH, *see* diisopinocampheylborane  
*Ips*o substitution, 778, 814–816  
Ireland-Claisen rearrangement, 937–938  
stereoselectivity of, 937  
effect of solvent on, 937  
isobenzofuran  
as Diels-Alder diene, 760, 858, 864  
isobutene  
acid-catalyzed dimerization, 455  
isodesmic reactions  
definition, 51  
for determining hydrocarbon stability, 265  
for evaluation of carbonyl addition  
intermediates, 329–330  
for evaluation of stabilization of carbonyl  
compounds, 320–321  
isoindole  
stability of, 760  
isopinocampheylborane  
hydroboration by, 530  
isotope effects, *see* kinetic isotope effects  
isotopic labeling  
in detection of internal return, 396–398  
in hydrolysis of aspirin, 670–671  
in racemization of benzhydrol  
*p*-nitrobenzoates, 396  
in solvolysis of sulfonate esters, 395–396

- kekulene, 735–736
- ketenes
- [2+2] cycloaddition reactions of, 835
    - intramolecular, 890–891
    - orbital array for, 888–889
    - stereoselectivity of, 890
    - transition structure for, 889
  - formation from acyl halides, 666
  - synthetic equivalents for in Diels-Alder reaction, 862
- ketones, *see also* carbonyl compounds
- acidity of, 592–593
  - acyclic
    - conformation of, 148–149
    - stereoselective reduction of, 179–182
  - addition reactions of, 629–632
    - alcohols, 640
    - hydride reducing agents, 176–181, 633–634
    - of organometallic reagents, 680–682
  - cyclic
    - relative reactivity of, 634–635
    - stereoselective reduction of, 176–179
  - enantioselective reduction of, 193–196
  - enolate formation from, 592–595
    - kinetic control of, 287, 595
    - stereoselectivity of, 597
  - enolization of, 601–608
    - equilibrium constants for, table, 604
  - hydration, 638–639
  - photochemical reactions of, 1116–1132
    - decarbonylation, 1120–1122
    - photoenolization, formation of
      - benzocyclobutenols by, 1120
    - type-II cleavage, 1122
    - $\alpha$ -cleavage, 1118, 1120–1122, 1124
  - reactions with organometallic compounds, 676–682
    - chelation in, 680–682
    - stereoselectivity of, 680–682
  - reduction of
    - electrostatic effects in, 238
    - polar effects on, 234–239
  - reductive photodimerization, 1119–1120
  - relative reactivity of, 633–634
    - towards  $\text{NaBH}_4$ , 633
  - synthesis
    - by hydration of alkynes, 544
    - using organoboranes, 528
  - unsaturated
    - conformation of, 151–152
    - cyclic, photochemical reactions of, 1125–1129
    - photochemical cycloaddition reactions, 1125–1126
    - photochemical deconjugation of, 1124
- ketyl radicals, 991
- kinetic acidity, 581
- kinetic control of product composition, 285–287
  - of enolate formation, 287
- kinetic isotope effect, 332–335
  - in benzylic bromination, 1021–1022
  - determination of, 334–335
  - in diazonium coupling, 814
  - in Diels-Alder reaction, 851
  - in electrophilic aromatic substitution, 777
    - bromination, 803
    - table of, 790
  - in elimination reactions, 552
    - examples of, 334
    - primary, 332–333
    - secondary, 333
    - solvent, 347
- kinetics
- of chain reactions, 992–995
  - integrated rate expressions, 280–285
  - Michaelis-Menten, 140
  - rate expressions
    - for addition of hydrogen halides to alkenes, 478
    - for aldol reactions, 284–285, 685
    - aromatic chlorination, 801
    - for bromination of alkenes, 486
    - chain reactions, 993–994
    - examples of, 283–285
    - for Friedel-Crafts acylation, 811
    - for Friedel-Crafts alkylation, 805–806
    - for nitration, 796–797
    - for nucleophilic substitution, 391, 393–394
  - reaction order, 280
  - steady state approximation, 282, 993
- Kohn-Sham equation, 54
- $\beta$ -lactams, *see* azetidinones
- lactones
- formation by 8-*endo* cyclization, 1014
  - ring size effect in formation, 422
- lanthanides
- as chiral shift reagents, 208–209
- Laplacian representation of electron density, 92–94
  - in cyclopropane, 86–87
- LCAO, *see* linear combination of atomic orbitals
- leaving groups
- in aromatic nucleophilic substitution, 817–819
  - in elimination reactions, 558
  - in nucleophilic substitution
    - reactivity of, 413–415
    - table of, 414, 415
  - in relation to enolate alkylation, 614–615
- Lewis acids
- as catalysts, 355–358
    - in 1,3-dipolar cycloaddition, 886–888
    - in aromatic nitration, 797
    - in Diels-Alder reactions, 848–850
    - in radical cyclization, 1013, 1039
  - effect on carbonyl  $^{13}\text{C}$  chemical shifts, 357
  - empirical measures of, 357–358

- in Friedel-Crafts acylation reaction, 809–813  
 in Friedel-Crafts alkylation reaction, 805–809  
 hardness and softness of, 354  
 interaction with carbonyl compounds, 323  
 metal ions as, 354  
 relative strength of, 357–358
- linear combination of atomic orbitals,  
 definition of, 26
- linear free energy relationships, 298, 335–343  
 application of in characterization of mechanisms,  
 343–344
- Linnert structures, 8  
 of radicals, 313, 315–318, 968, 987
- lipases, *see also* enzymes  
 from *Pseudomonas*, 220–221  
 kinetic resolution by, 141, 216–221  
 porcine pancreatic lipase  
 in resolution of enantiomers, 219–220  
 selectivity model for, 219–220
- lithium  
 hexamethyldisilylamide  
 as a strong base, 592  
 organolithium compounds  
 addition to carbonyl compounds, 676–682  
 kinetics of addition reactions, 677–679  
 structure of, 588–591
- localization energy  
 for electrophilic aromatic substitution, 782  
 for polycyclic hydrocarbons, 791
- lumiketone rearrangement, 1127–1128  
 orbital array for, 1128  
 stereochemistry of, 1128
- LUMO, 15, 29, 44, 97  
 of alkenes, correlation with radical addition  
 rates, 1005  
 distribution of 1-methylcyclohexyl cation, 431
- magic acid, 436
- magnesium, organo- compounds of  
 addition to carbonyl compounds, 676–682
- magnetic anisotropy, *see also* ring current  
 as a criterion of aromaticity, 720
- magnetic susceptibility  
 as a criterion of aromaticity, 722
- malonate anions  
 $\omega$ -halo, cyclization of, 422
- Marcus equation, 293–296  
 application to Cope rearrangement, 936
- McConnell equation, 971
- Meisenheimer complexes, 819
- mercuration, *see* oxymercuration
- mercurinium ion  
 as intermediate in oxymercuration, 517, 536
- mercury, organo compounds of  
 elimination reactions of, 565–566  
 formation by addition reactions, 515–520
- mero stabilization, *see* capto-dative stabilization
- MESP, *see* molecular electrostatic potential
- metal ions  
 as catalysts for Diels-Alder reactions, 850  
 hardness of, 14  
 role in hydride reductions of ketones, 181
- methane  
 derivatives, hyperconjugation in, 81–85  
 Laplacian representation of electron density, 92  
 MOs of, 37–39
- methanol  
 rotational barrier of, 81
- methoxide ion  
 electron density in, 68–69
- methyl acrylate  
 as dienophile, transition structures for, 853–854
- methylamine  
 rotational barrier of, 81
- methyl anion  
 electron distribution in, 308  
 structure of, 308  
 substituent effects on stability, 310
- methyl cation  
 electron density of, 65  
 substituent effects on stability, 304
- methyl derivatives  
 electron distribution of by AIM method, table, 69  
 halides, hardness of, 16  
 of second row elements, electron population in, 61
- methyl radical  
 structure of, 311, 980–981
- Michaelis-Menten kinetics, 140
- microscopic reversibility, 275–276, 475  
 non-applicability in photochemical reactions,  
 1100
- MM, *see* molecular mechanics
- MNDO MO method, 32
- Mobius topology  
 in relation to aromaticity, 736–737  
 in transition structures for  
 [2 + 2]-photocycloaddition of alkenes, 1098  
 1,7 hydrogen shift in trienes, 914, 918  
 cyclohexadienone photorearrangement,  
 1131–1132  
 di- $\pi$ -methane photorearrangement, 1113
- molecular electrostatic potential  
 CHELPG method for calculation, 73  
 as a criterion of aromaticity, 722–723  
 for representation of electron density, 73–76  
 of 1,3-butadiene, 73–74  
 of carbonyl compounds, 323  
 of ethenamine, 73–74  
 of propenal, 73–74
- molecular graph, 63–64  
 of alkanes, 64
- molecular mechanics, 166–169  
 calculation of enthalpy of formation using,  
 263–264  
 composite calculations with MO/DFT, 169
- molecular orbitals  
 of 1,3-butadiene, 46–47

- molecular orbitals (*cont.*)  
of aromatic compounds, 31–32  
of cyclopropane, 85–86  
of ethenamine, 46–47  
of ethene, 39–42, 46–47  
of formaldehyde, 43–46  
frontier, 29, 44  
Hückel, 27–31  
of methane, 37–39  
pictorial representation of, 35–41  
of polyenes, 27–30  
of propenal, 46–47  
reactive hybrid orbitals, 784  
symmetry adapted, 837–838  
symmetry of, 35–37
- molecular orbital theory, *see* MO theory
- molecular structure  
computation by DFT methods, 55–56  
computation by MO methods, 51
- molecular symmetry  
center of, 132  
of cycloalkanes, 133  
*meso* compounds, 131–134  
plane of, 131  
relationship to chirality, 131–133
- More O'Ferrall diagram, *see* potential energy diagram, two-dimensional
- Mosher reagent, 209
- MO theory, 26–54  
ab initio methods, 32–35  
characteristics of, summary, 36  
application of, 41–54  
in electrophilic aromatic substitution, 780–782  
computation of enthalpy of formation of hydrocarbons, 52, 264–269  
computation of structure by, 51  
Hückel, 27–32  
numerical applications, 50–54  
perturbational, 41–50  
pictorial representation, 35–41  
PMO theory, *see* MO theory, perturbational  
qualitative application, 41–50  
semi-empirical methods, 32  
solvation treatment in, 50–51
- Mulliken electronegativity, 9, 95  
correlation with acidity of carboxylic acids, 105
- Mulliken population analysis, 60–61
- N,N*-dimethylformamide  
As solvent, 363, 411–412
- naphthalene  
bond lengths, 18, 751  
as a Diels-Alder diene, 858–859  
Friedel-Crafts acylation of, 812–813  
proton exchange in, 792  
radical anion of, 990
- natural bond orbitals, 61–62  
natural population analysis, 61–62
- Nazarov reaction, 908–909
- NB-Enantride©  
in enantioselective reduction of ketones, 193
- NEER, *see* nonequilibrium of excited rotamers
- neighboring group participation, 419–425  
by acetoxy groups, 419–420  
by alkoxy groups, 421  
by aryl groups, 423–425  
by carbon-carbon double bonds, 422–423  
by hydroxy group, 420–421  
ring size effects on, 421–422
- Newman projection formulas, 128
- N*-fluoro-*N,N*-dimethylamine, conformation, 84
- N*-haloamides  
radical reactions of, 1040
- N*-hydroxyphthalimide  
in polarity reversal catalysis of radical addition, 1034
- N*-hydroxypyridine-2-thione  
acyl derivatives as radical sources, 979
- NICS, *see* nucleus independent chemical shift
- nitration, aromatic, 796–800  
computational modeling of, 799–800  
electron transfer mechanism for, 799  
isomer distribution for substituted benzenes, table, 786  
Lewis acid catalysis of, 797  
mechanism of, 796, 799–800  
reagents for, 797
- nitrile imines  
as 1,3-dipoles, 875  
frontier orbitals of, 880–881
- nitrile oxides  
as 1,3-dipoles, 875  
frontier orbitals of, 880–881
- nitrile ylides  
as 1,3-dipoles, 875  
substituent effects on, 882–883  
frontier orbitals of, 880–881
- nitro compounds  
acidity of, 597  
in aromatic nucleophilic substitution, 817–820  
reductive denitration by thiolates, 1048  
in  $S_{RN}1$  substitution reactions, 1045–1048  
examples of, 1049
- nitroethene  
as dienophile and ketene synthetic equivalent, 862
- nitrogen, molecular  
electron density by Laplacian function, 94
- nitronates, 591  
 $S_{RN}1$  substitution reactions, 1045–1048
- nitrones  
as 1,3-dipoles, 875  
frontier orbitals of, 880–881
- nitronium ion  
role in electrophilic aromatic substitution, 776

- nitroxide radicals  
 formation by spin trapping, 973  
 stability of, 968
- NMR spectra  
<sup>17</sup>O chemical shifts in carbonyl compounds, 322  
 aromaticity, in relation to, 720–722  
 calculation by MP2–GIAO, 431, 437  
 in characterization of carbocations, 436–438  
 norbornyl cation, 449–450  
 in determining enantiomeric purity, 208–211  
 chiral additive for, 209  
 in determining kinetic acidity of hydrocarbons, 370, 581  
 diastereotopicity in, 134–135  
 in monitoring enolization, 602–603  
 in relation to conformational equilibria, 154–155
- N*-Nitrosoanilides  
 as a source of aryl radicals, 979
- nonactin  
 chirality of, 132
- nonclassical carbocations, *see* carbocations, bridged
- nonequilibrium of excited rotamers, 1078
- nonradiative decay, 1076
- nonsteroidal anti-inflammation drugs  
 enantioselective synthesis of, 203
- norbornanones  
 stereoselective hydride reduction, 177–178
- norbornene  
 addition reactions of  
 with hydrogen halides, 481–482  
 with phenylselenenyl chloride, 502  
 with polyhalomethanes, 1030  
 photoreactions of, 1095–1096
- norbornyl cation, *see also* carbocations  
 formation of, 422  
 in solvolysis reactions, 447–448  
 structure of, 448–452
- NSAIDs, *see* nonsteroidal anti-inflammation drugs
- nucleophilic aromatic substitution  
 addition-elimination mechanism, 817–821  
 computational modeling of, 818  
 elimination-addition mechanism, 821–824  
 leaving groups in, 819  
 mechanisms for, 816–817  
 nucleophiles for, 819  
 vicarious, 820–821
- nucleophilic catalysis  
 in ester hydrolysis, 657  
 in esterification, 665
- nucleophilicity  
 characteristics of, 407–411  
 measurement of, 408–409  
 relations to hardness, softness, 410–411  
 table of, 411  
 solvent effects on, 411–413
- nucleophilic substitution  
 adamantyl derivatives in, 402, 412–413, 416  
 borderline mechanisms, 395–402  
 carbocation intermediates in, 391–393  
 in competition with elimination, 437–439  
 conjugation, effect on, 427–29  
 direct displacement (*S<sub>N</sub>2*) mechanism, 393–5  
 MO interpretation, 393–394  
 rate expression for, 393–394  
 examples of, 389  
 ionization (*S<sub>N</sub>1*) mechanism, 391–393  
 rate expression for, 391  
 ion pairs in, 395–398, 404  
 leaving groups in, 413–415  
 table, 414, 415  
 mechanisms of, 389–391  
 solvent effects, 392–393, 401, 411–413  
 solvolysis, 389, 395  
 stereochemistry of, 403–405, 406–407  
 steric effects in, 415–417  
 substituent effects on, 418–419
- nucleus independent chemical shift  
 as an indicator of transition state  
 aromaticity, 851  
 as a criterion of aromaticity, 721  
 of polycyclic arenes, 750
- octet rule, 3  
 1,3,5-octatriene  
 1,7-sigmatropic hydrogen shift in, 917–918  
 2,4,6-octatriene  
 photocyclization of, 1106
- optical activity, definition, 123
- optical purity, *see* enantiomeric excess
- optical rotatory dispersion, 124–125
- orbital correlation diagram  
 for [2+4] cycloaddition, 837–838  
 for electrocyclic reactions, 895–897  
 for photochemical addition of alkenes, 1098  
 for photochemical electrocyclic reactions, 1100
- orbitals, *see* molecular orbitals
- ORD, *see* optical rotatory dispersion
- organolithium compounds, *see* lithium
- organomercury compounds, *see* mercury
- organometallic compounds  
 addition to carbonyl compounds, 676–682  
 electron transfer mechanism for, 679  
 carbanion character of, 588–591  
 substitution reactions of, 609–611  
 examples, 610  
 mechanism of, 609–611
- osmium tetroxide  
 as catalyst for dihydroxylation of alkenes, 200–203
- oxadi- $\pi$ -methane rearrangement, 1129
- oxazaborolidines  
 as catalysts for  
 aldol reaction, 695–696  
 Diels-Alder reaction, 867–868  
 enantioselective reduction of ketones, 194–196  
 computational model for, 196

- oxazolidinones
  - boron enolates of, 694–695
  - as chiral auxiliaries, 207–208, 694–695
  - for Diels-Alder reactions, 866
- 2-oxo-5-hexenyl radical
  - cyclization in comparison with 5-hexenyl radical, 1010–1012
- oximes, 646, 651
  - configuration of, 121
  - formation of, 651–653
  - catalysis of, 653
  - pH-rate profiles for, 651–652
  - stability of, 651
- oxy-Cope rearrangement, 931–932
  - anionic, 932
  - origin of rate acceleration in, 932
  - transition structure for, 933
- oxygen
  - origin of paramagnetism, 7
  - reaction with radicals, 1024–1026
- oxymercuration
  - of alkenes, 515–520
  - reagents for, 515
  - relative rate for, 516
  - stereochemistry of, 517–518
  - substituent effects in, 518–520
- ozone
  - MOs of, 49
  - reaction with ethene, 49–50
- PA, *see* proton affinity
- pantolactone
  - as chiral auxiliary for Diels-Alder reaction, 865–866
- partial rate factors
  - for electrophilic aromatic substitution, 786–787
  - bromination, 802
  - hydrogen exchange, 804–805
  - nitration, 798
  - table of, 788
- Paterno-Buchi reaction, 1132–1134
  - regiochemistry of, 1132–1133
- Pauli exclusion principle, 7, 35
  - in relation to rotational barriers, 78–81
- 1,3-pentadiene
  - photoproducts from, 1101–1102
- 1,4-pentadiene
  - 1,1,5,5-tetraphenyl, photoproducts from, 1114
  - 1,5-diphenyl, photoproducts from, 1114
- pentafulvalene, 755–757
- pentalene, 753
- 3-pentanone
  - conformation of, 149
- 4-pentenyl radical
  - cyclization of, 1012
- pericyclic reactions, *see* concerted pericyclic reactions
- peroxides
  - as radical sources, 976–978
- peroxycarboxylic acids
  - epoxidation of alkenes by, 504–506
- peroxy esters
  - as radical sources, 977
  - structural effects on rate of decomposition, 1015–1016
- perturbational molecular orbital theory, 41–50
- phase transfer catalysts
  - effect on nucleophilicity, 363–364
- phenalene
  - anion, 757
  - cation, 757
  - Hückel MO diagram for, 757
- phenanthrene, 749
  - electrophilic aromatic substitution in, 793
- phenols
  - solvent effect on alkylation, 368
- phenonium ion, 423–425
  - structure of, 425
- phenyl cation, 436, 817
- phosphines
  - BPE, 192
  - chirality of, 129
  - chiraphos, 192
  - DIPAMP, 192
  - DuPHOS, 192
  - as ligand in enantioselective hydrogenation, 190–192
- phosphorescence, 1077
- phosphorus-containing groups
  - carbanion stabilization by, 599
  - ylides, 599–600
- photochemical reactions, *see also* photoexcitation
  - adiabatic and diabatic transitions, 1075
  - alkene photocycloaddition, 1109–1111
  - alkene photoisomerization, 1081–1090
    - of 1,3-butadienes, 1096–1097
    - of ethene, 1082–1083
    - of stilbene, 1085–1090
    - of styrene, 1083–1085
  - conical intersection, definition, 1080
  - of cyclic alkenes, 1094–6
  - cycloaddition of alkenes
    - computational modeling of, 1109–1110
    - with aromatic compounds, 1136–1137
  - of dienes, 1100–1104
    - computational modeling of, 1137–1145
  - di- $\pi$ -methane rearrangement, 1112–1116
    - conical intersection, computational model, 1113–1114
    - mechanism of, 1112–1115
    - stereochemistry of, 1113
  - electrocyclic reactions, 1099–1100
  - fluorescence, 1077
  - Frank-Condon principle, 1075
  - general principles, 1073–1080
  - internal conversion, 1076
  - intersystem crossing, 1075

- nonequilibrium of excited rotamers (NEER), 1078
- nonradiative decay, 1076
- orbital symmetry considerations for, 1097–1100
- phosphorescence, 1077
- potential energy diagram for, 1079
- quantum yield, 1077
- quenching, 1077
- Rydberg states, 1073
- singlet excited states, 1073
- Stern-Volmer plot, 1078
- triplet excited states, 1073
- photoexcitation, *see also* photosensitization
- of 1,3-cyclohexadiene, 1106
  - energy equivalence of, 1074
  - of ethene, 1082–1083
  - schematic potential energy diagram for, 1076
  - of stilbene, 1085–1090
  - of styrene, 1083–1085
  - of trienes, 1106–1108
- photosensitization, 1076–1077
- of 1,3-butadiene dimerization, 1103–1104
  - mechanism of, 1077
  - of stilbene photoisomerization, 1087–1088
- pH-rate profiles, 350–353
- for hydrolysis of 2,2-dimethyloxirane, 512
  - for hydrolysis of salicylic acid acetals, 669
  - for hydrolysis of salicylic acid esters, 670
  - for imine formation and hydrolysis, 647–649
  - for oxime formation, 649–650
- picene, 749
- pinacol borane
- hydroboration by, 525
- Pirkle alcohol, *see*
- 2,2,2-trifluoro-1-(9-anthryl)ethanol
- PM3 MO method, 32
- PMO theory, *see* perturbation molecular orbital theory
- polarity reversal catalysis, 1034
- polarizability, 14–18
- correlation with softness, 96
- polycyclic aromatic hydrocarbons, 745–758
- as Diels-Alder dienes, 748–749, 857
  - electrophilic aromatic substitution in, 791–793
  - redox potentials for, table, 990
- polyenes
- cyclic
    - Hückel MO diagrams for, 30, 713
    - stability criteria for, 747–748  - cycloaddition reactions of, 836
  - Hückel MO diagrams for, 28
  - as a reference for aromatic stabilization, 716, 747–748
- porcine pancreatic lipase, 219–221
- potassium
- hexamethyldisilylamide, as a strong base, 592
- potential energy diagrams
- for 1,3-butadiene photoexcitation, 1102
  - for alkene photoisomerization, 1093
  - for carbonyl addition reactions, 631
  - for cyclohexadiene photoreactions, 1106
  - for cyclohexene photoreactions, 1095
  - for electrophilic aromatic substitution, 791
  - for elimination reactions, 550–551
  - for hex-5-enoyl radical cyclization, 1043
  - for hydration of alkenes, 475
  - for hydrolysis of methyl acetate, 324–326
  - for imine formation and hydrolysis, 648–650
  - for nucleophilic substitution, 391, 394, 399–400
  - for a photochemical reaction, 1079
  - for rearrangement of 2-butyl cation, 442
  - for rearrangement of 3-methyl-2-butyl cation, 445
  - relation to Hammond's postulate, 290
  - relation to reaction mechanism, 274–276
  - relation to transition state theory, 263–64, 273–280
  - for stilbene excited states, 1088, 1090
  - for styrene excited states, 1085
  - three-dimensional, 277–279
  - two-dimensional, 276–277
    - acetal hydrolysis, 643
    - Cope rearrangement, 928
    - elimination reactions, 550–551
    - nucleophilic addition to carbonyl groups, 631
    - nucleophilic substitution, 401
- PPL, *see* porcine pancreatic lipase
- priority rules, *see* Cahn-Ingold-Prelog priority rules
- prochiral centers, definition, 133
- projection formulas
- Fischer, 127
  - Newman, 128
- prop-2-en-1-one
- 1-aryl, cyclization by strong acid, 909
- [1.1.1]propellane, 87–88
- reactivity of, 90–91
  - structure of, 89
- propenal
- 3-methyl, BF<sub>3</sub> complex, structure of, 849
  - conformation of, 148–149, 151
  - as dienophile, transition structures for, 853–854
  - electron density distribution in, 21, 48, 60–74
  - electrostatic potential surface for, 73–74
  - resonance in, 20–21
- propene
- acidity of, 583
  - conformation of, 147
  - electron density distribution in, 22
  - hyperconjugation in, 22–23
- proteases
- in resolution of enantiomers, 222–224
- proton affinity
- of hydrocarbon anions, 374–375
- proton transfer
- in acetal hydrolysis, 644
  - in carbonyl addition reactions, 630

- pseudorotation  
 in relation to cyclopentane conformations, 163
- pyrans  
 formation by electrocyclization, 910–911
- pyridine derivatives  
 aromaticity of, 758  
 dihydro by electrocyclization, 910–911  
 electrophilic aromatic substitution of, 794  
 nucleophilic aromatic substitution of, 820
- 2-pyridone  
 catalysis of carbohydrate anomerization, 674  
 catalysis of ester aminolysis by, 661–662, 673–674
- pyrrole  
 aromatic stabilization of, 758–760  
 electrophilic aromatic substitution of, 793–794
- quantum yield, 1077
- quenching, 1077
- quinodimethanes  
 as Diels-Alder dienes, 857, 864
- quinoline alkaloids  
 as chiral shift additives, 210  
 DHQ, 200  
 DHQD, 200  
 as ligands in alkene dihydroxylation, 200–203
- racemate, *see* racemic mixture
- racemic mixture  
 properties of, 123–124
- racemization  
 of allylic sulfoxides, 940  
 during nucleophilic substitution, 396, 398  
 during radical reactions, 983–984  
 of *E*-cyclooctene, 131
- radical anions, 988  
 from naphthalene, 990  
 in  $S_{RN}1$  substitution, 1045–1052
- radical cations, 988
- radical reactions  
 addition reactions  
 of aldehydes, 1031, 1034  
 comparison of, by computation, 1007–1008  
 examples of, 1033–1036  
 of halomethanes, 1029–1031, 1036, 1041  
 of hydrogen halides, 1026–1028  
 rates of, 1004–1008  
 substituent effects on, 1004–1006
- atom transfer, 966
- chain length, 965
- cyclization, 1008–1013  
 8-endo cyclization to lactones, 1013–1014  
 atom and group transfer reactions in, 1037–1039  
 computational modeling, 1010–1012  
 rates of, 1008–1013  
 regiochemistry in relation to ring size, 1009–1010  
 stereoelectronic effects on, 1009–1010
- disproportionation, 966
- group transfer reactions, 1037–1039
- halogenation, 1002–1004, 1018–1024  
 energetics of, 1018–1020  
 selectivity of, 1019–1020  
 substituent effects on, 1003–1004
- hydrogen atom abstraction, 1001–1004
- inhibitors for, 994–5
- initiation, 965
- iodine atom transfer, 1037–1038
- kinetics of, 992–995
- propagation, 965
- rates of, 995–1000  
 competition methods for, 995–996  
 table of, 997–1000
- rearrangement, 1041–1044  
 of cyclopent-2-enylmethyl radical, 1044  
 examples, 1044  
 of hex-5-enoyl radical, 1042–1043
- selenyl group transfer reactions, 1038–1039  
 Lewis acid catalysis of, 1039
- spin trapping of, 973
- stereochemistry of, 983–986  
 examples of, 983
- substitution by  $S_{RN}1$  processes, 1044–1052  
 mechanisms for, 1044–1045  
 of nitro compounds, 1045–1048
- termination, 965
- with oxygen, 1023–1026
- $\beta$ -scission, 966–7, 1013
- radicals, *see also* alkyl, aryl, vinyl etc.
- 9-decalyloxy  
 fragmentation of, 1016
- acyl  
 decarbonylation of, 967, 1017
- acyloxy  
 decarboxylation of, 967
- alkoxy  
 formation from alkyl hypochlorites, 1015
- alkyl  
 disproportionation, 966
- allyl  
 resonance of, 312–313  
 substituent effects on, 985–987
- bridgehead, 984–985  
 ESR parameters for, 985
- capto-dative, 316, 987–988  
 examples, 989
- charged, 988–992
- cyclization of unsaturated, 1008–1013, 1037–1039
- cyclohexyl  
 structure of, 984
- delocalized, 312–313
- detection of, 966–976  
 by CIDNP, 974–975  
 by ESR spectroscopy, 970–971  
 by spin trapping, 973

- electrophilic versus nucleophilic character of, 1004  
   frontier MO interpretation of, 1004–1006  
 generation of, 976–80  
   from azo compounds, 978–979  
   from boranes, 979  
   from *N*-acyloxy pyridine-2-thiones, 979–980  
   from *N*-nitrosoacetanilides, 979  
   from peroxides, 976–978  
 group transfer reactions of, 1037–1039  
 halogen bridging in, 1028  
 hybridization of, 311  
 long-lived, 968–970  
   examples of, 969  
 methyl, 967  
   structure of, 980–981  
 nitroxide, 968, 973  
 persistent, 968  
 reaction with oxygen, 1023  
 rearrangements of, 1041–1044  
   of acyl groups, 1042  
   of aryl groups, 1042–1043  
   of cyano groups, 1042–1043  
   hex-5-enoyl radical, 1042–1043  
   of vinyl groups, 1042  
 stabilization of, 312–313, 317, 1052–1055  
 structure of, 311, 980–982  
 substituent effects on, 317–318  
   table, 317, 1055  
 trifluoromethyl  
   structure of, 981–982  
 triphenylmethyl, 967  
 unsaturated, cyclization of, 1008–1013,  
   1037–1039  
 vinyl, 986  
    $\alpha$ -amino, 315  
 radical stabilization energy, definition, 314  
   relation to bond dissociation energy, 312–313,  
   317, 1052–1055  
   table, 315, 1055  
 rate determining step, 276  
 RE, *see* resonance energy  
 reaction constant, in Hammett equation, 338  
   for electrophilic aromatic substitution, 790  
   table of, 341  
 reaction cube, *see* potential energy diagram,  
   three-dimensional  
 reaction rates, *see also* kinetics  
   relation to thermodynamic stability, 285–287  
 reactivity-selectivity relationships  
   for electrophilic aromatic substitution, 787–791  
 rearrangements  
   of carbocations, 440–447  
   during addition of hydrogen chloride to alkenes,  
   448–450  
   during chlorination of alkenes, 494  
   of radicals, 1041–1044  
 refractive index  
   relationship to polarizability, 17  
   regioselective, definition, 476  
   resolution of enantiomers, 136–141  
   chromatographic, 137  
   dynamic, 215  
   enzymatic, 215–227  
     by epoxide hydrolases, 225–226  
     selectivity in, 140–141  
   kinetic, 138–141  
     chemical, 139  
     enzymatic, 140–141  
 resolving agents  
   examples of, 136–137  
 resonance, 18–22  
   in 1,3-butadiene, 20, 62  
   in allyl radicals, 312–313  
   in amides, 320–322  
   in benzene, 18, 62  
   in carbocations, 22, 433  
   in carbonyl compounds, evaluation of, 320–321  
   in enamines, 22  
   in formamide, 62  
   in formate anion, 62  
   in naphthalene, 18  
   natural bond orbital representation, 62  
   in propenal, 20–21  
   in substituent effects, role of, 297–298  
   in vinyl ethers, 21–22  
 resonance energy, definition, 19  
   as a criterion of aromaticity, 715–716  
 ring current  
   as an indicator of aromaticity, 720  
 rotational barriers, definition, 143  
   in butane, 79–80  
   in ethane, 78–79  
   origin of, 78–81  
 Rydberg excited states, 1073  
   of ethene, 1082  
 salicylic acid  
   acetals of  
     hydrolysis, 668–669  
   acetate ester (aspirin), 352–353  
   esters, hydrolysis of  
     leaving group effects, 671  
     mechanism, 669–671  
     pH-rate profile for, 670  
 SCF, *see* self-consistent field  
 Schrödinger equation, 26  
 selectivity  
   in aromatic electrophilic substitution, 787–791  
 selenenylation  
   of alkenes, 500–503  
   regioselectivity of, 502  
 self-consistent field, definition, 26, 32  
 semicarbazones, 646  
   mechanism of formation, 652  
 semidiones, 991–992  
 semiquinones, 991

- sequence rule, *see* Cahn-Ingold Prelog rules
- Sharpless asymmetric epoxidation, 196–199
- computational model for, 198–199
  - double stereodifferentiation in, 207
- [2,3]-sigmatropic rearrangements, 939–945
- of allylic selenoxides, 941
  - of allylic sulfoxides, 940–941
  - aza-Wittig, 944
  - examples of, 940
  - of *N*-allyl amine oxides, 941
  - transition structures for, 939–940
  - Wittig, of allylic ethers, 943–944
  - stereoselectivity of, 945
- [3,3]-sigmatropic rearrangements, 919–939
- of allyl vinyl ether, 933
  - Marcus theory treatment of, 936
  - remote substituent effects, 938
  - stereochemistry of, 935
  - of amide acetals, 938
  - Claisen rearrangements, 933–937
    - of allyl aryl ethers, 934–935  - Cope rearrangement, 920–31
    - activation energy for, 920
    - of barbaralane, 931
    - of bullvalene, 930–931
    - chair versus boat transition structure for, 923
    - computational modeling of, 926–927
    - cyano substituents, effect on, 927
    - of divinylcyclopropane, 929
    - effect of strain on, 928
    - More-O'Ferrall-Jencks diagram for, 928
    - of semibullvalene, 931
    - stereochemistry of, 922–923
    - substituent effects on, 924–928  - examples of, 921
  - Ireland-Claisen rearrangement, 937–938
    - stereoselectivity of, 937  - of *O*-allyl imidate esters, 938
  - oxy-Cope rearrangement, 931–932
  - transition structures for, 920
- sigmatropic rearrangements, 911–945
- of alkyl groups, 914–916
    - stereochemistry of, 914–915  - antarafacial versus suprafacial, 914–915
  - classification of, 911–912
  - in equilibrium of precalciferol and calciferol, 919
  - as example of concerted pericyclic reactions, 934
  - examples of, 913
    - for hydrogen and alkyl group shifts, 916–919
    - of hydrogen, 912–914
    - summary of thermodynamics, 919  - orbital symmetry selection rules for, 912
  - transition structures
    - computational models of, 915–916
- silanes
- allyl
    - electrophilic substitution reactions of, 568  - aryl
    - electrophilic substitution of, 815–816
- $\beta$ -halo
    - elimination reactions of, 566  - $\beta$ -hydroxy
    - elimination reactions of, 566–568
- silyl substituent groups
- stabilization of carbocations by, 299, 307
  - steric effects in enolate alkylation, 618–619
- sodium
- hexamethyldisilylamide, as a strong base, 592
- softness, definition, 14, 96
- in regioselectivity of Diels-Alder reaction, 947–949
  - relation to nucleophilicity, 410–411
- solvent effects, 359–362
- on acidity of carboxylic acids, 53
  - on anomeric equilibria, 228–232
  - on elimination reactions, 554
  - empirical measures of, 360–361
  - on enolate alkylation, 615
  - on enolate composition, 596, 937
  - examples of, 362–368
  - in MO theory, 50–51
  - on  $S_N1$  substitution, 392–393
  - on solvolysis of *t*-butyl chloride, 361
- solvent isotope effect, 347
- in acetal hydrolysis, 641
- solvents
- dielectric constant of, table, 359
  - dipolar aprotic
    - effect on nucleophilicity, 363  - dipole moment of, table, 359
- solvolysis, 389, 395
- SOMO, 313
- substituent effects on, 313–314, 1004–1006
- specific acid catalysis, 346–347
- in acetal hydrolysis, 641
- specific base catalysis, 347
- specific rotation, definition, 123
- spin trapping, 973
- spiro[2.2]pentane, 87–88
- spiro compounds
- chirality of, 130
- stacking,  $\pi$ – $\pi$  of aromatic ring
- in enantioselective oxidation of alkenes, 202
- staggered, definition, 142
- stannanes
- allyl
    - electrophilic substitution reactions of, 568  - aryl
    - electrophilic substitution reactions of, 816
- stannic chloride, *see* tin tetrachloride
- stannyl groups
- stabilization of carbocations by, 307
- steady state approximation, 282
- stereoelectronic effect
- hyperconjugation, 24
  - on radical cyclization reactions, 1009–1010
    - computational modeling of, 1010–1012  - on stability of reaction intermediates, 297–298

- stereoisomer, definition, 117
- stereoselective reactions
- 1,3-dipolar cycloaddition, 878–879
  - catalytic hydrogenation, 170–176
  - Diels-Alder reaction, 839–842
  - enolate alkylation, 615–619
  - examples of, 170–182
  - hydride reduction of ketones, 176–179
  - hydroboration, 188, 524–525
  - nucleophilic addition to acyclic ketones, 179–182
- stereoselectivity, 119, 169
- stereospecificity, 169
- stereospecific reactions
- 1,3-dipolar cycloaddition, 877–8
  - bromination of alkenes, 183–185
  - Diels-Alder reaction, 839–840
  - examples of, 183–188
- steric approach control, definition, 177
- in additions to acyclic ketones, 180
  - in hydride reduction of cyclic ketones, 177–178
- steric effects
- in Diels-Alder reactions, 843
  - in enolate alkylation, 615–619
  - in Friedel-Crafts acylation, 812
  - in nucleophilic substitution, 415–417
  - on reactivity, 297
  - on regiochemistry of elimination reactions, 562–563
- stilbene
- E* and *Z* isomers
    - absorption spectra, 1087
    - ground state structure, 1086
- photocyclization of, 1091
  - photoisomerization of, 1085–1090
  - rotational energy profile for excited states, 1090
- strain
- 1,3-allylic, 147
  - in cycloalkanes, 86–88, 161–166
  - from molecular mechanics, 167–168
  - torsional, 143, 153
  - van der Waals, 78, 143–144, 154
- styrene and derivatives
- excited states of, 1083–1085
  - hydration reactions of, 482–483
  - reactivity toward selenenylation, 501
- substituent constants, Hammett, 338–339
- table, 340
- substituent effects
- on [3,3]-sigmatropic rearrangements, 924–927, 932, 937
  - on carbanion stability, 309–311, 591–594
  - on carbocation stability, 304–305, 432–434
  - comparison of gas phase and solution phase, 344
  - DFT formulation of, 100–105
  - in Diels-Alder reactions, 843–848
  - directive, in catalytic hydrogenation, 171–176
  - in electrophilic aromatic substitution, 779–787
  - on nucleophilic substitution, 418–419
  - on radical reactivity, 1004–1007
  - on radical stability, 311–318, 986–988
  - on reaction intermediates, 297–299
- substituent groups
- electronegativity of, table, 102, 260
  - hardness of, table, 102
- subtilisin
- enzymatic resolution by, 141, 222
- sulfonylation of alkenes, 497–500
- regioselectivity of, 499
- sulfides
- as nucleophiles in  $S_{RN}1$  reactions, 1050
- sulfinyl substituents, 299
- sulfonate groups
- internal return in solvolysis, 397–398
  - as leaving groups in nucleophilic substitution, 413–414
- sulfones
- vinyl as dienophiles and synthetic equivalents, 862–863
- sulfonium ylides
- allylic, [2,3]-sigmatropic rearrangement of, 942
- sulfonyl group
- effect on cyclization of 5-hexenyl radical, 1012
  - substituent effect of, 299
- sulfoxides
- acidity of, 589
  - allylic
    - 2,3-sigmatropic rearrangement of, 940
- chirality of, 129
  - vinyl, as dienophiles, 863
- sulfuranes
- as intermediates in sulfonylation of alkenes, 498
- sulfur-containing groups
- carbanion stabilization by, 599
  - ylides, 600–601
- sultams
- camphor, as chiral auxiliaries, 207–208
- suprafacial, definition, 911–912
- symmetry, *see* orbital symmetry, molecular symmetry
- synchronicity
- of 1,3-dipolar cycloadditions, 882
  - definition, 852
  - of Diels-Alder reaction, 852
- synthetic equivalent, definition, 862
- TADDOLS, *see*
- tetraaryl-1,3-dioxolane-4,5-dimethanols
- tartrate esters
- as chiral ligands for enantioselective epoxidation, 197–199
- termination, in radical reactions, 965, 992–994
- tetraaryl-1,3-dioxolane-4,5-dimethanols derivatives
- as enantioselective catalysts
    - for 1,3-dipolar cycloaddition, 868
    - for Diels-Alder reactions, 888
- tetrabromomethane, *see* halomethanes
- tetrahedral intermediate

- tetrahedral intermediate (*cont.*)  
 in ester aminolysis, 660–661  
 in imine formation and hydrolysis, 646–650  
 in reactions of carbonyl compounds,  
 325–331, 630
- tetrahydropyrans  
 anomeric effect in, 228–232  
 radical conformation, 984
- tetramethylethylenediamine (TMEDA)  
 affect on organolithium compounds, 589–590  
 in reactions with esters, 678
- thermodynamic control of product composition,  
 285–287  
 in aldol addition, 690
- thermodynamic stability, 253–270
- thexylborane  
 formation of, 188  
 hydroboration by, 524
- thiiranium ions  
 as intermediates in sulfonylation of alkenes, 498
- thiophene  
 aromatic stabilization of, 758–759  
 electrophilic aromatic substitution of, 793–794
- three electron bond  
 in radicals, 313, 315, 316, 318
- tin tetrachloride  
 as Lewis acid catalyst, 354–355
- titanium tetrachloride  
 as Lewis acid catalyst, 354–355, 849  
 in enantioselective Diels-Alder reactions,  
 865–866
- TMEDA, *see* tetramethylethylenediamine
- torsional barrier, *see* rotational barrier
- torsional effects  
 in enolate alkylation, 617
- torsional strain, *see* strain, torsional
- transition state, definition, 253
- transition state theory, 270–272
- transition structure  
 computational characterization of, 279–80  
 definition, 270
- triafulvene, 754–757
- tricyclo[3.1.0.0<sup>2,6</sup>]hex-3-ene, from photolysis of  
 benzene, 1134
- 1,3,5-trienes  
 electrocyclic reactions of, 893–894  
 heteroatom analogs of, electrocyclization,  
 910–911  
 photochemical reactions, 1106–1107
- triflate, *see* trifluoromethanesulfonate
- 2,2,2-trifluoro-1-(9-anthryl)ethanol  
 as chiral additive for NMR spectra, 210
- trifluoroacetic acid, addition to alkenes, 484–485
- trifluoroethanol, as solvent, 368, 412
- trifluoromethanesulfonic acid, addition to  
 alkenes, 484
- trifluoromethylsulfonate, as leaving group,  
 413–414
- triphenylmethyl cation, 426–427
- triphenylmethyl radical, 967
- triplet state, 1073, 1076–1077
- tropylium ion, *see* cycloheptatrienyl cation
- valence, 2  
 valence bond theory, 3  
 valence shell electron pair repulsion, 7  
 valence tautomerism, definition, 905
- van der Waals radii, 24–26  
 definition within DFT, 97  
 table of, 26
- van der Waals strain  
 in cyclohexane derivatives, 154  
 in relation to butane conformation, 143–144  
 in relation to rotational barriers, 78–80
- vicarious nucleophilic aromatic substitution,  
 820–821
- vinyl amines, *see* enamines, ethenamine
- vinyl cations, 301, 435–436
- vinylcyclopropane  
 thermal rearrangement of, 929
- vinyl ethers  
 cycloaddition with diazomethane, 880–882  
 hydrolysis of, 485  
 resonance in, 21–22
- vinyl radicals  
 structure of, 985–986  
 substituent effects on, 985–986
- VSEPR, *see* valence shell electron pair repulsion
- water  
 effect on mechanism of imine formation,  
 648–650  
 Laplacian of electron density, 92  
 as solvent for Diels-Alder reaction, 850
- Wilkinson's catalyst, 174
- Winstein-Grunwald equation, 412
- Wittig rearrangement, 943–944
- Woodward-Hoffmann rules  
 for concerted cycloaddition, 836–837  
 for electrocyclic reactions, 900  
 in relation to photochemical reactions, 1099  
 for sigmatropic rearrangements, 912
- X-ray crystal structures  
 ( $\pm$ ) and ( $-$ ) forms of  
 2,5'-diazabicyclo[2.2.2]octane-3,6,6-dione,  
 1123–1124  
 1,6-methanocyclodeca-1,3,5,7,9-pentaene-3-  
 carboxylic acid,  
 773–780  
 1,6-methanocyclodeca-1,3,5,7,9-pentaene, 730  
 2-methylpropenal-BF<sub>3</sub> complex, 849  
 3,3-dimethyl-4-(*t*-butyldimethylsilyl)-2-  
 pentanone enolate,  
 613  
 benzoyl chloride-SbCl<sub>5</sub> complex, 810  
 benzoyl chloride-TiCl<sub>4</sub> dimeric complex, 810

- bromonium ion from  
  adamantylideneadamantane, 490  
*n*-butyllithium-DME tetrameric complex, 590  
*n*-butyllithium-THF tetrameric complex, 590  
*n*-butyllithium-TMEDA dimeric complex, 590  
*n*-butyllithium-TMEDA tetrameric complex, 590  
*t*-butyl methyl ketone enolate hexamer, 613  
*t*-butyl methyl ketone enolate-THF tetrameric complex, 613  
cyclopentanone enolate-THF tetrameric complex, 613  
ethyl acryloyllactate-TiCl<sub>4</sub> complex, 849  
lithium bicyclo[3.2.1]octa-2,6-dienide, 745  
phenyllithium-diethyl ether tetrameric complex, 589  
phenyllithium-TMEDA dimeric complex, 589  
*syn*-tricyclo[8.4.1.1<sup>3,8</sup>]hexadeca-1,3,5,7,9,11,13-heptaene, 732  
*syn*-tricyclo[8.4.1.1<sup>4,9</sup>]hexadeca-2,4,6,8,10,12,14-heptaene, 732
- ylides, 600  
  [2,3]-sigmatropic rearrangements of, 940–942  
  acidity of, 600–601  
  ammonium, *N*-allyl  
    [2,3]-sigmatropic rearrangement of, 942  
  phosphonium, 600–601  
  *S*-anilinosulfonium  
    [2,3]-sigmatropic rearrangement of, 942  
  sulfonium  
    Allylic, [2,3]-sigmatropic rearrangement of, 942
- Yukawa-Tsuno equation, 341  
  application in oxymercuration reaction, 516  
  application to benzyl cations, 432
- zero point energy  
  correction for in computation of enthalpy, 265  
  role of isotope effect, 332